NUCLEAR SCIENCE ABSTRACTS

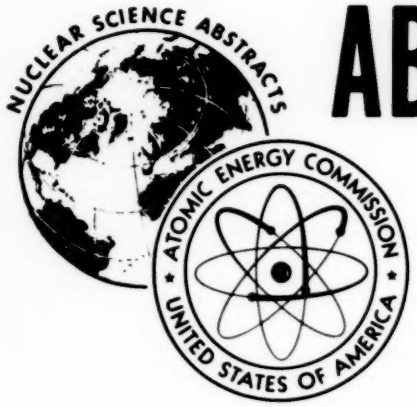

Volume 25 Number 13

Abstracts 28912-31763

July 15, 1971

UNITED STATES ATOMIC ENERGY COMMISSION
Division of Technical Information

REPORT COLLECTIONS IN THE UNITED STATES

The libraries listed below purchase and maintain microfiche collections of USAEC and foreign reports that are abstracted in *NSA*. Their collections also include *NSA* and its indexes, AEC's Technical Progress Reviews, AEC-sponsored translations, conference proceedings published by AEC, and various bibliographic tools. Most of these libraries have microfiche reader-printers or other photocopy facilities with which to reproduce enlarged copies from microfiche. Charges for reproduction services vary.

ALABAMA
Auburn, Auburn University
Tuskegee Institute, Tuskegee Institute

ALASKA
College, University of Alaska

ARIZONA
Tucson, University of Arizona

ARKANSAS
Fayetteville, University of Arkansas

CALIFORNIA
Davis, University of California
Los Angeles, University of California

COLORADO
Boulder, University of Colorado

DISTRICT OF COLUMBIA
Washington, Library of Congress (by deposit)

FLORIDA
Gainesville, University of Florida

GEORGIA
Atlanta, Georgia Institute of Technology

HAWAII
Honolulu, University of Hawaii

IDAHO
Pocatello, Idaho State University

ILLINOIS
Evanston, Northwestern University
Urbana, University of Illinois

INDIANA
Lafayette, Purdue University

IOWA
Ames, Iowa State University

KANSAS
Manhattan, Kansas State University

KENTUCKY
Lexington, University of Kentucky
Louisville, University of Louisville

LOUISIANA
Baton Rouge, Louisiana State University
New Orleans, Tulane University

MARYLAND
Baltimore, Johns Hopkins University
College Park, University of Maryland

MASSACHUSETTS
Cambridge, Massachusetts Institute of Technology
Worcester, Worcester Polytechnic Institute

MICHIGAN
Ann Arbor, University of Michigan

MISSISSIPPI
State College, Mississippi State University

MISSOURI
Kansas City, Linda Hall Library

NEVADA
Las Vegas, University of Nevada

NEW JERSEY
Princeton, Princeton University

NEW MEXICO
Albuquerque, University of New Mexico

NEW YORK
Albany, New York State Library
Albany, State University at Albany
Buffalo, State University of New York at Buffalo
Ithaca, Cornell University
New York, Columbia University
Rochester, University of Rochester
Syracuse, Syracuse University
Troy, Rensselaer Polytechnic Institute

NORTH CAROLINA
Raleigh, North Carolina State University

OHIO
Cincinnati, University of Cincinnati
Cleveland, Cleveland Public Library
Columbus, Ohio State University
Toledo, University of Toledo

OKLAHOMA
Norman, University of Oklahoma

PENNSYLVANIA
Philadelphia, University of Pennsylvania
Pittsburgh, Carnegie Library
University Park, Pennsylvania State University

PUERTO RICO
San Juan, University of Puerto Rico

SOUTH CAROLINA
Columbia, University of South Carolina

TENNESSEE
Knoxville, University of Tennessee
Nashville, Joint University Libraries
Oak Ridge, Oak Ridge Associated Universities

TEXAS
Austin, University of Texas
College Station, Texas A & M University
Houston, Rice University

UTAH
Salt Lake City, University of Utah

VIRGINIA
Blacksburg, Virginia Polytechnic Institute
Charlottesville, University of Virginia

WASHINGTON
Pullman, Washington State University
Seattle, University of Washington

WEST VIRGINIA
Morgantown, West Virginia University

WISCONSIN
Madison, University of Wisconsin

WYOMING
Laramie, University of Wyoming

The following governmental and international organizations offer for sale USAEC reports abstracted in *Nuclear Science Abstracts*:

National Technical Information Service, U. S. Department of Commerce
Springfield, Virginia 22151
International Atomic Energy Agency, Vienna, Austria
National Lending Library, Boston Spa, England

XUM

Volume 25, Number 13, July 15, 1971

NUCLEAR SCIENCE ABSTRACTS

A semimonthly publication of the USAEC Division of Technical Information, Edward J. Brunenkant, Director, Published by the USAEC Division of Technical Information Extension, Robert L. Shannon, Extension Manager.

Nuclear Science Abstracts provides the only comprehensive abstracting and indexing coverage of international nuclear science literature. *Nuclear Science Abstracts* covers scientific and technical reports of the U. S. Atomic Energy Commission and its contractors, other U. S. Government agencies, other governments, universities, and industrial and research organizations. In addition, books, conference proceedings, individual conference papers, patents, and journal literature on a worldwide basis are abstracted and indexed. Each issue of *Nuclear Science Abstracts* includes four indexes: subject, personal author, corporate author, and report number.

The following organizations scan and abstract the nuclear science literature in their respective countries:

Atomic Energy of Canada Limited
Australian Atomic Energy Commission
Danish Atomic Energy Commission
Finnish Atomic Energy Commission
French Atomic Energy Commission
Japan Atomic Energy Bureau–Atomic Energy Research Institute
Institutt for Atomenergi (Norway)
Aktiebolaget Atomenergi (Sweden)
United Kingdom Atomic Energy Authority

Numerous organizations, societies, and publishers throughout the world provide *Nuclear Science Abstracts* with advance page-proof copy of their publications, e.g., in the United States the American Institute of Physics provides page-proof copy of its publications.

A list of the journals scanned regularly and the abbreviations used appears in Issue 1 (January 15) of each volume of *Nuclear Science Abstracts* and is supplemented in Issues 7, 13, and 19. Issue 1 of each volume also describes the scope and arrangement of the subject matter covered in *Nuclear Science Abstracts*. The subject matter covered is also described in TID-4552, *Subject Scope of Nuclear Science Abstracts*, available free from the USAEC Division of Technical Information Extension, P.O. Box 62, Oak Ridge, Tennessee 37830. An outline of the subject categories appears in the Contents of each issue.

AVAILABILITY OF PUBLICATIONS ABSTRACTED

Public availability of all U. S. Atomic Energy Commission reports is indicated in the report number indexes. The availability of other reports, when known, is also indicated. The availability of some unnumbered reports is given in the abstract.

Dissertations abstracted in *Dissertation Abstracts* and included in *Nuclear Science Abstracts* are available from University Microfilms, Inc., 315 N. First Street, Ann Arbor, Michigan 48103.

Information on the availability of the published literature and unpublished conference papers abstracted in *Nuclear Science Abstracts* can be obtained from the USAEC Division of Technical Information Extension, P.O. Box 62, Oak Ridge, Tennessee 37830.

HOW TO OBTAIN NUCLEAR SCIENCE ABSTRACTS

Nuclear Science Abstracts is available to the public on a subscription basis from the Superintendent of Documents, U. S. Government Printing Office, Washington, D. C. 20402.

For the 24 regular issues, the yearly rate is $42.00 for domestic subscribers and $52.50 for foreign subscribers. A single issue costs $1.75, domestic rates, or $2.19, foreign rates. Domestic rates apply to the United States, Canada, Mexico, and Central and South American countries except Argentina, Brazil, Guyana, French Guiana, Surinam, and British Honduras.

For a yearly subscription to the cumulative indexes, the rates are $38.00 for domestic subscribers and $47.50 for foreign subscribers.

The following cumulative indexes are available:

From Johnson Reprint Corporation, 111 Fifth Avenue, New York, N. Y. 10003:
Vols. 1–4, Subjects and Authors (1948–1950), $30.00.

From Superintendent of Documents, U. S. Government Printing Office, Washington, D. C. 20402:

Vols. 5–10, Subjects and Authors (1951–1956), $5.25.

Vols. 11–15, Subjects (1957–1961), $19.00.
Vols. 11–15, Personal Authors (1957–1961), $14.25.
Vols. 11–15, Corporate Authors (1957–1961), $2.50.

Vols. 16–20, Subjects (1962–1966), $36.00.
Vols. 16–20, Personal Authors (1962–1966), $22.50.
Vols. 16–20, Corporate Authors (1962–1966), $3.75.

Vol. 21, Subjects and Authors (1967), $16.00.
Vol. 22, Subjects and Authors (1968), $26.00.
Vol. 23, Subjects and Authors (1969), $25.75.
Vol. 24, Subjects and Authors (1970), $22.50.

Cumulative Report Number Index, Vols. 1-15 Revised, $4.00.
Cumulative Report Number Index, Vols. 16-20 Revised, $5.50.
Cumulative Report Number Index, Vols. 21-24, $4.25.

Nuclear Science Abstracts is available on an exchange basis to universities, research institutions, industrial firms, and publishers of scientific information. Government agencies may obtain *NSA* free of charge. Inquiries should be directed to the USAEC Division of Technical Information Extension, P. O. Box 62, Oak Ridge, Tennessee 37830.

XUM

INDEXES TO NSA

Comprehensive indexes appear in each issue and are cumulated quarterly and annually. Multivolume cumulations have been issued as indicated above.

All documents abstracted are indexed by subjects and personal authors. Report literature is indexed also by corporate author and report number. Each of these indexes in every issue is preceded by an introduction explaining in detail the organization of the index and the principles by which it is compiled. The reader is referred to these explanations for information not found in the brief summary below.

Personal Authors

Each author's name is indexed in the form appearing on the document abstracted:

ISHIHARA, T., Accumulation of fallout ^{137}Cs in newborn infants, 23:50538
ISHIHARA, Toyokuki, Shielding effect of paraffin, water, soil, concrete, Fe, and Pb for high-energy neutrons, 23:51748

Subjects

The subject index consisting of specific materials, objects, and processes is arranged alphabetically. Modifying phrases specific to these subjects in turn are arranged alphabetically under the subjects.

MELPHALAN
  effects on proliferation of cultured antigen-stimulated spleen cells from mice, dose-response curve for, 23:50820
MEMBRANE FILTERS
  design for removal of cell-free Streptococcus faecalus from bacteria cultures in fermentation tank, 23:49996 (UCRL-18667, pp 322-9)
MENDELEVIUM
  separation from einsteinium and fermium by electrolysis, 23:49772 (UCRL-18667, pp 277-312)
  separation from sodium acetate solutions by solvent extraction using sodium amalgam, 23:49772 (UCRL-18667, pp 277-312)
  stability of divalent state of, 23:49772 (UCRL-18667, pp 277-312)

Corporate Authors

Technical report literature is indexed from the name of the organization or institution responsible for the issuance of the report.

51093 (LA-4164) FABRICATION OF BORON CARBIDE RINGS AND DISKS. Sheinberg, H.; Herrera, T.; Kostacopoulos, J. **(Los Alamos Scientific Lab., N. Mex.).** Apr. 25, 1969. Contract W-7405-eng-36. 11p. Dep. CFSTI.

is indexed as:

LOS ALAMOS SCIENTIFIC LAB., N. MEX.
  Fabrication of boron carbide rings and disks, 23:51093 (LA-4164)

Report Numbers

Technical report literature is also indexed by report numbers. This index includes information on where individual reports may be obtained. While not reports, patents and conference papers are indexed here as a matter of convenience.

JPRS-	**(Non-AEC)**	
46949	23-51587	CFSTI
48330	23-52305	CFSTI
48331	23-52451	CFSTI
48481	23-50889	CFSTI
48743	23-51034	CFSTI
49025	23-51706	CFSTI (U. S. Sales Only)
JUL-	**(German)**	
571-RG	23-52269	Dep
578-PP	23-51624	Dep. CFSTI (U. S. Sales Only)
581-FN	23-51079	Dep. CFSTI (U. S. Sales Only)
584-RG	23-52313	Dep
586-FN	23-51035	Dep. CFSTI (U. S. Sales Only)
K-		
1777	23-50987	Dep. CFSTI
1778	23-50988	Dep. CFSTI
KFK-	**(German)**	
743	23-52461	Dep
743	23-52447	For translation see EURFNR-613
781/I	23-52462	Dep
824	23-52397	Dep. CFSTI (U. S. Sales Only)

TABLE OF CONTENTS

Volume 25, Number 13, July 15, 1971

Category	Page
CHEMISTRY	2855
Analytical Chemistry	2855
Chemical and Spectral Procedures	2855
Isotope Dilution Procedures	2861
Radiometric and Radiochemical Procedures	2861
Activation Procedures	2864
Inorganic, Organic, and Physical Chemistry	2866
Chemical Properties	2866
Isotope Effects and Exchange	2867
Physical Chemistry	2871
Radiation and Nuclear Chemistry	2873
Radiation Effects	2873
Radiation Processes	2874
Radiolysis	2877
Radioisotope Production	2881
Recoil Production and Reactions	2881
Radiochemistry	2882
Separation Processes	2882
EARTH SCIENCES	2885
Geology and Hydrology	2885
Meteorology	2886
Mineralogy and Exploration	2887
Oceanography	2889
Seismology	2889
ENGINEERING	2890
Nuclear Explosions	2890
Facilities and Equipment	2890
Heat Transfer and Fluid Flow	2892
Isotope Technology	2893
Materials Testing	2894
Protective Structures	2897
Radioactive Material Handling	2897
Vacuum Engineering	2898
INSTRUMENTATION	2899
Radiation Detection Instruments	2899
General Detectors and Monitors	2899
Nuclear Spectroscopic Instrumentation	2901
High Energy Physics Instrumentation	2902
Radiation Dosimeters	2904
Radiometric Instruments	2904
Miscellaneous Instruments and Components	2905
Radiation Effects on Instruments and Instrument Components	2906
LIFE SCIENCES	2907
Biochemistry, Physiology, and Molecular Biology	2907
Basic Processes	2907
Metabolism, Physiology, and Toxicology	2907
Radiation Effects	2912
Immunology	2914
Ecology	2914
Genetics and Cytogenetics	2915
Health Physics and Safety	2917
Radioactive Contamination and Decontamination	2917
Dosimetry and Monitoring	2918
Radiation Protection	2919
Safety Procedures	2920

Category	Page
LIFE SCIENCES (Cont'd.)	
Civil Defense	2921
Legal Aspects	2921
Medicine	2921
Protective Substances	2921
Radiation Sickness and Injuries	2924
Radiodiagnosis	2924
Radiotherapy	2926
Radiation Effects on Animals	2927
Invertebrates	2928
Vertebrates	2929
Man	2935
Radiation Effects on Plants	2937
Radiation Effects on Microorganisms	2938
Radiosterilization and Radiopreservation	2939
METALS, CERAMICS, AND OTHER MATERIALS	2945
Metals and Alloys	2945
Corrosion and Erosion	2945
Preparation and Fabrication	2947
Properties Evaluations	2950
Structure and Phase Studies	2956
Radiation Effects	2958
Ceramics and Cermets	2960
Corrosion and Erosion	2960
Preparation and Fabrication	2960
Properties Evaluations	2962
Structure and Phase Studies	2966
Radiation Effects	2969
Plastics and Other Materials	2970
PHYSICS (GENERAL)	2973
Astrophysics and Cosmology	2973
Cosmic Ray Exposure Ages	2973
Stars	2973
Quasi-Stellar, Radio, and X-Ray Sources	2980
Solar Phenomena	2984
Galaxies	2987
Cosmology	2989
Planetary Phenomena	2992
Atomic and Molecular Physics	2992
Atomic, Electron, Ion, and Molecular Beams and Their Reactions	2992
Atomic and Molecular Properties	2993
Positronium, Muonium, and Mesic Atoms and Molecules	2994
Collision Phenomena	2994
Atomic Theory	2997
Cosmic Radiation	2997
Direct Energy Conversion	3000
Fluid Physics	3001
Geophysics (Upper Atmosphere)	3002
Low-Temperature Physics and Cryogenic Equipment	3008
Superfluidity	3008
Superconductivity	3008
Equipment and Devices	3011
Plasma and Thermonuclear Physics	3012
Confinement and Heating	3012
Diagnostics	3014

XUM

TABLE OF CONTENTS (continued)

Category	Page
PHYSICS (GENERAL) (Cont'd.)	
Kinetics (General)	3016
Kinetics (Experimental)	3017
Kinetics (Theoretical)	3018
Production	3021
Stability	3021
Thermonuclear Processes	3022
Wave Phenomena	3028
Shielding	3030
Solid-State Physics	3032
Radiation Effects	3032
Physical Properties	3033
Moessbauer Effects and NMR	3036
Theory	3037
Theoretical Physics	3037
PHYSICS (HIGH-ENERGY)	3039
Particle Interactions and Properties (Experimental)	3039
Electromagnetic	3039
Weak	3039
Strong (Baryon-Induced)	3040
Strong (Meson-Induced)	3041
Particle Interactions and Properties (Theoretical)	3042
General	3042
Electromagnetic	3043
Weak	3046
Strong (General)	3047
Strong (Baryon No. = 0)	3049
Strong (Baryon No. = 1)	3051
Strong (Baryon No. ≥ 2)	3053
Particle Invariance Principles and Symmetries	3055
General	3055
Applications (Electromagnetic and Weak)	3056
Applications (Strong)	3057
Field Theories	3057
General	3057
Quantum Field Theory	3057
Gravitation and General Relativity	3061
Scattering Theory	3063
Particle Accelerators	3065
PHYSICS (NUCLEAR)	3081
Neutron Interactions with Matter	3081
Nuclear Properties and Reactions, $A \leq 5$	3083

Category	Page
PHYSICS (NUCLEAR) (Cont'd.)	
Nuclear Properties and Reactions, $6 \leq A \leq 19$	3085
Nuclear Properties and Reactions, $20 \leq A \leq 89$	3089
Nuclear Properties and Reactions, $A \geq 90$	3094
Nuclear Theory	3102
REACTOR TECHNOLOGY	3109
Commercial Power Reactors	3109
Operation and Economics	3109
Safety and Siting	3110
Steam and Power Conversion Systems	3113
Power Reactor Development	3113
Kinetics and Dynamics	3114
Control Systems	3114
Cooling Systems	3114
Fuels	3117
Auxiliary and Emergency Systems	3118
Operation and Economics	3119
Safety and Siting	3119
Power Conversion Systems	3124
Research and Test Reactors	3124
Rocket and Space Reactors	3126
Marine and Portable Power Reactors	3126
Production Reactors	3126
Reactor Theory	3126
Kinetics	3127
Dynamics	3128
Experimental Applications	3128
Reactor Components, Fuels, and Accessories	3128
GENERAL	3131
CORPORATE AUTHOR INDEX	INDEX-1
PERSONAL AUTHOR INDEX	INDEX-12
SUBJECT INDEX	INDEX-71
REPORT NUMBER INDEX	INDEX-171
JOURNAL LIST	APPENDIX-1

STAFF OF NUCLEAR SCIENCE ABSTRACTS

John W. Norris
Managing Editor

Donald D. Davis
Assistant Managing Editor

David E. Bost
Production Manager

Sidney F. Lanier
Subject Heading Specialist

J. Paul Meredith
Descriptive Cataloging Specialist

Frederick E. Marsh, Jr.
Computer Index Coordinator

Clara L. Fox
Corporate Author Specialist

Helen W. White
Report Number Specialist

Section Editors

Everett J. Hoffman
Chemistry

Robert C. Kelly
Engineering; Earth Sciences; Metals, Ceramics, and Other Materials

Lee M. Thompson
General Physics

Charles E. Stuber
High Energy Physics; Instrumentation

Donald D. Davis
Life Sciences

Lawrence T. Whitehead
Nuclear Physics

James M. Jacobs
Reactor Technology

Evaluators

Thomas S. Chapman
Rose V. Jermain
John H. Mitchell
Mary H. Newman
Polly C. Summers

Abstractors

F. S. Armstrong*
Ellis R. Bedford
Mary M. Brown
Jane G. Buchanan
D. Lamar Cason
Gloria M. Caton
David C. Cunningham
James R. Dulaney
Helga B. Gerstner
Mary C. Grissom
Phyllis C. Hansen
Carolyn D. Houston
Elaine E. Huber
Rose V. Jermain
W. Hugh Kinser, Jr.
Lisbeth C. Lieberman
Betty L. McDowell
Patricia B. McEwen
Fay M. Martin
William D. Matheny
Dora H. Moneyhun
Jean F. Peckham
Henry D. Raleigh
Mona H. Raridon
Julia S. Redford
Jessie W. Rushing
Robert W. Rutkowski
Francis L. Sachs
Lila B. Smith
Anne G. Ward
Helen L. Ward
Milton O. Whitson
Juanita Wilson

*Atomic Energy of Canada, Ltd.

Charles R. Bruce
Publishing Coordinator

Communication concerning the editorial policy and content of *Nuclear Science Abstracts* should be addressed to the Managing Editor, *Nuclear Science Abstracts*, USAEC Division of Technical Information Extension, P. O. Box 62, Oak Ridge, Tennessee 37830.

Use of funds for printing this publication approved by the Director of the Bureau of the Budget, June 26, 1969.

XUM

Volume 25, Number 13 July 15, 1971

NUCLEAR SCIENCE ABSTRACTS

CHEMISTRY

Analytical Chemistry

Refer also to abstract 29400.

Chemical and Spectral Procedures

Refer also to abstract 29155.

28912 (BARC–500) DETERMINATION OF TOTAL HYDROGEN CONTENT OF UO_2 PELLETS. Bhat, R. K.; Karnik, S. G.; Krishnamoorthy, T. S.; Venkateswarlu, Ch. (Bhabha Atomic Research Centre, Bombay (India)). 1970. 12p. Dep. NTIS (U. S. Sales Only).

UO_2 pellets are heated at 1000°C under high vacuum. The gases released are passed over uranium at 1000°C. The hydrogenous compounds decompose giving elemental hydrogen. The hydrogen content is determined by oxidizing it to H_2O and measuring the decrease in pressure on selectively condensing H_2O at −96°C. (auth)

28913 (BARC–508) LITHIUM ISOTOPIC ANALYSIS ON RECORDING FABRY–PEROT SPECTROMETER. Ahmad, S. A.; Saksena, G. D. (Bhabha Atomic Research Centre, Bombay (India)). 1970. 26p. Dep. NTIS (U. S. Sales Only).

A method was developed for isotopic analysis of lithium samples by recording the isotopic structure of the lithium resonance line at 6708 Å on the Recording Fabry–Perot Spectrometer using a hollow cathode source. In order to obtain the true intensity ratio of the isotopic components (i.e., to render the effects of the self-absorption negligible) optimum experimental conditions were worked out. By using only 2 μgm of lithium (as Li_2SO_4) in the hollow cathode and exciting it at 10 mA of current, the effects due to self-absorption are practically eliminated. By this method the concentration of ^6Li in a natural lithium sample was found to be 7.4 ± 0.3%. (auth)

28914 (BARC–515) WATER CHEMISTRY STUDIES: CHEMICAL ANALYSIS MANUAL FOR MODERATOR AND COOLANT WATER SYSTEMS. Mathur, P. K.; Gokhale, A. S.; Venkateswarlu, K. S. (Bhabha Atomic Research Centre, Bombay (India)). 1970. 31p. Dep. NTIS (U. S. Sales Only).

The specifications of high-purity water employed in water-moderated and water-cooled power reactors are very stringent. A strict control and regular monitoring of some of the specific dissolved impurities is essential. Procedures for the quantitative determination of submicrogram amounts of dissolved oxygen (<10 ppB), F^-, Cl^-, NO_3^-, boric acid, Al^{3+}, Cr^{3+}, Fe^{3+}, Ni^{2+}, Cu^{2+}, and Zr^{4+} in high-purity water were developed and standardized, and are presented. (auth)

28915 (BARC–517) CHEMICAL SEPARATION AND SPECTROGRAPHIC DETERMINATION OF TRACE AMOUNTS OF RARE EARTH ELEMENTS IN URANIUM. Joshi, B. D.; Patel, B. M. (Bhabha Atomic Research Centre, Bombay (India)). 1970. 34p. Dep. NTIS (U. S. Sales Only).

An emission spectrographic method was developed for determination of rare earth elements at submicrogram levels after their separation from uranium using a cellulose column and an ether–nitric acid mixture separation procedure. A mixture of 25% LiF, 25% AgCl, and 50% graphite powder was used as carrier. The samples were excited by a dc are carrying 13 amp using a Stallwood jet in an atmosphere of 80% argon and 20% oxygen at flow rate of 20 liters/minute and were photographed in the 3880 to 4440 Å region. Thulium was used as the internal standard. The detection limits by this procedure in μg are: Ce, Pr, Nd, Sm, Gd, Lu, 0.1; Eu, 0.01; Tb, 0.25; Dy, Ho, Er, 0.05; Yb, 0.001. The influence of uranium and thorium on the estimation of rare earths was investigated. Up to 20 μg each of uranium and thorium on the electrode the detection limits and estimation of rare earths were not affected to a considerable extent. The method is suitable for the estimation of rare earths in the presence of 20 μg each of uranium and thorium. The percentage standard deviation of this method ranges from 3 to 30% for different elements. (auth)

28916 (CEA-R–4071) STUDY OF IMPURITIES DISTRIBUTION IN A METAL (PLUTONIUM): REALIZATION AND STUDY OF REFERENCE SAMPLES TO BE USED IN ANALYTICAL CHEMISTRY. Billon, Jean-Pierre; Buffereau, Michel; Deniaud, Suzanne; (and others) (Commissariat a l'Energie Atomique, Bruyeres-le-Chatel (France). Centre d'Etudes. Commissariat a l'Energie Atomique, Valduc (France). Centre d'Etudes). Jan 1971. 59p. (In French). Dep. NTIS (U. S. Sales Only).

The distribution of impurities in a natural metal (plutonium) that has been remelted under vacuum was studied. Elements present at significant levels were found to be fairly homogeneously distributed. However, these metals could not be used as reference standards. A technique was used in which metallic powders were added to the metal. After melting and homogenization treatment, the metal was cut according to a convenient method for a statistical study and analyzed. Analysis of the plutonium for added elements was performed by mass spectrometry, spectrography, and spectrophotometry. The feasibility of preparing reference standards by this method is discussed. (J.G.B.)

28917 (CONF-701044–(Sect.3)) PAPERS OF THE V. CONGRESS ON MATERIAL TESTING. III. SECTION. SPECTROCHEMICAL ANALYSIS, BUDAPEST, 19–24 OCTOBER 1970. (Scientific Society of Mechanical Engineers, Budapest (Hungary)). 229p. (In English and German).

Separate abstracts were prepared for 9 papers included in Section III. (M.C.G.)

For abstracts of individual papers see: 28943–28951.

28918 (NIM–951) COLORIMETRIC DETERMINATION OF MINOR QUANTITIES OF NITRATE IN URANIUM COMPOUNDS. Laboratory Method No. 7/2. Steele, T. W.; King, R. H.; Stoch, H. (National Inst. for Metallurgy, Johannesburg (South Africa)). 11 Jun 1970. 3p. Dep. NTIS (U. S. Sales Only).

After the sample is leached in dilute H_2SO_4, the 2,4-xylenol complex is developed and extracted into toluene. The yellow nitrate compound is extracted into NaOH solution and the nitrate determined colorimetrically. The procedure is suitable for uranium compounds having a nitrate content between 0.001 and 5.0% and for solutions having a nitrate content of from 1 ppM to 10 g/l. (M.C.G.)

28919 DETERMINATION AND DISTRIBUTION OF VARIOUS TRACE ELEMENTS IN NATURAL WATERS BY X-RAY FLUORESCENCE SPECTROSCOPY. Armitage, Donald Bruce. Honolulu, Hawaii; Univ. of Hawaii (1970). 86p. University Microfilms Order No. 71-4934.

Thesis.

A method was developed for the analysis, consecutively, of six trace metals, uranium, copper, nickel, cobalt, iron, and manganese, in a sample of fresh water and seawater through a combi-

XUM

nation of solvent extraction with an 8-hydroxyquinoline–chloroform mixture and x-ray fluorescence spectrometry. The primary concentration step, which may be carried out on board ship, requires only three reagents and minimal equipment, thus reducing the risk of contamination and chemical changes due to storage. In addition, the method is nondestructive and extracted samples evaporated on filter paper may be stored for future reference. A precision of 10% or better was obtained for the six elements with a sample volume of 500 ml. The analysis was applied to seawater and fresh water samples obtained from various sources. Coastal seawater trace element content was found to be lower than that from mid-ocean. What appears to be significant differences in the trace element levels were found in the water masses studied but little variation with latitude was detected. Several of the elements, notably uranium, displayed an increase in concentration with depth. Examination of fresh water samples indicated that biological activity is related to the extractable trace metal content in that increased activity was accompanied by higher content of trace metals. This view has as yet not been substantiated by biological studies. Other samples showed evidence of differences that may be associated with the water source and pollution. (Diss. Abstr. Int., B)

28920 STABILITY CONSTANTS OF THE MOLYBDENUM(VI) COMPLEXES OF DTPA AND TTHA. Lund, Walter (Univ. of Oslo). Anal. Chim. Acta; 53: 295-302(Feb 1971).

The complex formation of molybdenum(VI) with diethylenetriaminepentaacetic acid (DTPA) and with triethylenetetraminehexaacetic acid (TTHA) was studied by means of potentiometric pH titrations. The presence of five molybdenum(VI)–DTPA complexes, as well as eight Mo(VI)–TTHA complexes was established. The stability constants of the series of protonated mononuclear and binuclear complexes were calculated by means of a least-squares method, utilizing a high-speed digital computer. (auth)

28921 ANALYTICAL METHODS IN OCEANOGRAPHY. I. INORGANIC METHODS. Spencer, Derek W.; Brewer, Peter G. (Woods Hole Oceanographic Institution, Mass.). CRC Crit. Rev. Solid State Sci.; 1: 409-78(Sep 1970).

The analytical chemistry involved in the determination of the major ions, trace elements, nutrients, dissolved gases, and radionuclides present in seawater is discussed. Particular attention is paid to recent developments and to the techniques that are actively in use in oceanographic laboratories. Seawater sampling and storage methods are reviewed, and tables of the trace elements and radionuclides that have been determined in the ocean are given. (332 references.) (auth)

28922 RADIONUCLIDE X-RAY FLUORESCENCE ANALYSIS. III. EXAMPLES OF PRACTICAL APPLICATION. Varga, Stefan. Chem. Listy; 65: 113-27(Feb 1971). (In Czech).

A number of examples are used to demonstrate the utilization and the importance of radionuclide fluorescence analysis as a method of instrumental analysis. (auth)

28923 SENSITIVITY OF THE FLUORIDE-SELECTIVE ELECTRODE BELOW THE MICROMOLAR-RANGE. Baumann, Elizabeth W. (E. I. du Pont de Nemours and Co., Aiken, S. C.). Anal. Chim. Acta; 54: 189-97(Apr 1971).

In the presence of fluoride-complexing cations, the lanthanum fluoride electrode responds theoretically to free fluoride one to three decades below 10^{-6} M, the accepted limit in non-complexing solutions. Experimentally determined fluoride concentrations were compared with values calculated from literature stability quotients for the thorium, zirconium, lanthanum, and hydrogen systems. The limit suggests the presence of background fluoride. Dissolution of the lanthanum fluoride crystal, determined by neutron activation analyses and electrode measurements, could supply the required level of background fluoride in bulk solution. Contribution of fluoride from reagents was not significant. (auth)

28924 SPECTROPHOTOMETRIC DETERMINATION OF SILICON BY A STANDARD ADDITION PROCEDURE. Pakalns, P. (Australian Atomic Energy Commission Research Establishment, Lucas Heights). Anal. Chim. Acta; 54: 281-94(Apr 1971).

The pH ranges suitable for the development of yellow molybdosilicate in sulfuric, hydrochloric, nitric, and perchloric acids were established, and the effect of sodium salts of these acids, fluoride–boric acid mixtures, zirconium–fluoride and titanium–fluoride system on the pH various acid media has been studied. A method is given for calculating the required minimum pH in mixed acid systems. Procedures are described for determining silicon in steels, aluminum, nickel–silicon, uranium–silicon, potassium hydrogen difluoride, and titanium sponge by a standard addition procedure. (auth)

28925 DEWAR TUBE SAMPLE CELL ASSEMBLY FOR LOW-TEMPERATURE FLUORIMETRY. Kirkbright, G. F.; Mayne, P. J.; West, T. S. (Imperial Coll. of Science and Tech., London). Anal. Chim. Acta; 54: 353-7(Apr 1971).

The construction and performance of a sample compartment and cell assembly based on a Dewar tube is described for fluorescence measurements at liquid N_2 temperatures. The assembly, which is designed to reduce problems from noise, liquid N_2 contamination, and irreproducible sample cell positioning, was constructed from fused silica tubing. The sample cell contains three sections; one at the base to permit passage of cold N_2 gas, a middle compartment for the sample solution, and a top compartment above the sample compartment for a fluorescence standard. The sample tube fits into an Aminco phosphoroscope attachment. Fluorescence spectra for U(VI) in 6 M HCl at very low temperatures measured with the cell are reported. (B.L.M.)

28926 DIANTIPYRINYLMETHANE PYROCATECHOLATE COMPLEX OF MOLYBDENUM AND ITS ANALYTICAL APPLICATION. Tananaiko, M. M.; Gorenshtein, L. I.; Zhidik, L. G. (Kiev State Univ.). Ukr. Khim. Zh.; 36: 703-6(Jul 1970). (In Russian).

The molybdenum compound with pyrocatechol forms a salt with organic bases, such as pyridine. The property of these salts of being soluble in chloroform may be used for analytical determinations, but the technique is rendered difficult by the requirement that the pH must be carefully adjusted to a value between 4 and 6. The experiments carried out indicated that introduction of diantipyrinyl hydrochloride into a system containing the compound of Mo(VI) with pyrocatechol results in the formation of a strongly colored complex that may be easily extracted with chloroform or dichloroethane. The salt is stable in strong acid solutions, which makes it easier to use for analytical determinations. The compound was prepared by using ammonium molybdate as the starting material. Determination of the absorption spectrum of the compound revealed that it has two maxima at λ = 440 and 640 nm. The complex may be used for the photometric determination of Mo in the concentration range of 5 to 90 μg per 10 ml of extract. Details of the analytical technique are described. (TTT)

28927 IMPROVEMENT IN ISOTOPIC RATIO MEASUREMENT OF URANIUM. Komori, Takuji; Tamura, Syuzo; Gunji, Katsubumi; Tamura, Kimiko (Japan Atomic Energy Research Inst., Tokai). Shitsuryo Bunseki; 18: 1270-4(Dec 1970). (In Japanese).

A study was made on the precise measurement of the isotopic ratio of uranium using a surface ionization mass spectrometer (CEC 21–702 B) equipped with an expanded scale recorder. By stabilizing the ion current and controlling the measuring conditions, such as sample mounting and filament heating, the relative standard deviation was improved to 0.1% for observed $^{236}U/^{238}U$ ratio in a reference sample of uranium. Time variations of $^{235}U/^{238}U$ ratio during one run were investigated. (auth) (Japan)

28928 FLUORESCENCE DETERMINATION OF COPPER. Zel'tser, L. E.; Maksimycheva, Z. T.; Talipov, Sh. T. Dokl. Akad. Nauk Uzb. SSR; No. 3, 30-1(1969). (In Russian).

A reaction between H_2O_2 and 1-(2-hydroxypropyl)anabasine (I) produces a compound that fluoresces green (max. at 525 nm) when exposed to uv radiation; in the presence of Cu^{2+} at pH 9 to 11, the fluorescence maximum is displaced to a shorter wavelength, with a simultaneous decrease in the intensity of fluorescence. Optimum conditions for determining 0.05 to 0.5 μg of Cu are as follows—pH 10 to 11 (borate buffer soln.); concentration of I, 3mM; concentration of H_2O_2, 2.5 mM; duration of reaction, 10 min. Many cations do not interfere in concentrations up to 10 μg per ml, but UO_2^{2+} and Pd^{2+} do. The method was used to determine Cu in alkali-metal chlorides water and acids. (Referativnyi Zh.)

28929 INTERFEROMETRIC DETERMINATION OF SMALL QUANTITIES OF D_2O AND H_2O. Mercea, Judith (Inst. for Atomic Physics, Cluj). Jena Rev.: No. 1, 34-5(1971).

A layer of D_2O specimens is placed under homogeneous H_2O or D_2O in a glass cell or a layer of H_2O placed above it. The difference between the refractive indices of the two liquids was decisive and sufficient for effecting a shifting of more than 150 interference fringes. Small quantities of D_2O and H_2O can be determined by this method. (M.C.G.)

28930 EXTRACTIONS WITH LONG-CHAIN AMINES. III. COLORIMETRIC DETERMINATION OF MOLYBDENUM AS THIOGLYCOLLATE. Pribil, R. (Heyrovsky Polarographic Inst., Prague); Adam, J. Talanta; 18: 349-54(Mar 1971).

A highly selective and sensitive colorimetric determination of molybdenum(VI) based on its extraction with a chloroform solution of trioctylamine from solutions of acetic and thioglycollic acid (TGA) is described. The yellow chloroform extract containing the molybdenum-TGA complex is measured at 370 nm. With a single extraction it is possible to determine small amounts of molybdenum in the presence of very large concentrations of al-

most all metals. Only bismuth, mercury, and tungsten interfere. (auth) (UK)

28931 COLORIMETRIC DETERMINATION OF TELLURIUM WITH SODIUM PYROSULFITE. Gromakova, Z. I.; Gorokhova, L. G.; Buketov, E. A. Tr. Khim.-Met. Inst., Akad. Nauk Kaz. SSR; No. 7, 155-7(1969). (In Russian).

A method for determining tellurium by colloid color without selenium separation is described. Sensitivity is 0.05 mg in 50 ml. of solution. The method is used for analysis of alkaline soda–sulfide solutions and copper electrolyte slags. (Referativnyi Zh.)

28932 ORGANIC REAGENTS IN THE ANALYTICAL CHEMISTRY OF ZIRCONIUM AND HAFNIUM. VI. ZIRCONIN AS A REAGENT FOR ZIRCONIUM. Mustafin, I. S.; Shchukina, V. S. Tr. Kom. Anal. Khim. Akad. Nauk SSSR; 17: 345-51(1969). (In Russian).

A study is presented of the reaction of Zr with zirconin (the disodium salt of 7-dimethylamino-3,4-dihydroxy-3-sulfo-3H-phenoxazine-1-carboxylic acid), which is prepared by sulfonating gallocyanine (C.I. Mordant Blue 10). Zirconin is recommended for the direct spectrophotometric determination of Zr in alloys of Mg, Al, Ni or Cu, and for the determination of 70 to 99% of Zr in Zr-base alloys by difference spectrophotometry. (Referativnyi Zh.)

28933 DETERMINATION OF SELENIUM, TELLURIUM, GOLD, AND SILVER IN COPPER ELECTROLYSIS SLIMES. Polukarov, A. N.; Makhmetov, M. Tr. Khim.-Met. Inst., Akad. Nauk Kaz. SSR; No. 9, 85-95(1969). (In Russian).

Determination of Se and Te in Au-containing Cu electrolysis slimes is based on decomposition of slimes in HCl (2 +1) with 2 to 3 ml. HNO_3, and separation of Se and Au from Te in HCl solution by simultaneous addition of $NH_2OH \cdot HCl$ and mercaptobenzothiazole. Te is determined iodometrically. Se and Au precipitate is dissolved in $HCl-HNO_3$, the solution is made alkaline, and Au is precipitated with NH_2OH. The filtrate is neutralized with HNO_3 and urea, and Se is determined iodometrically. The determination of Au and Ag in Au-containing Cu electrolysis slimes and Ag-Au alloy is based on the decomposition of the material in H_2SO_4 at 260 to 300°C. The mixture is diluted with water, boiled, and filtered, and Ag is determined in the filtrate gravimetrically or titrimetrically with SCN^-. The precipitate on the filter is extracted with hot chloride mixture to dissolve Au, which is determined iodometrically or gravimetrically by precipitation with N_2H_4. For determination of Au and Ag, the Ag-Au alloy is decomposed with H_2SO_4 at 180 to 250°. After diluting with water, the solution is decanted, and the Au precipitate is rinsed with water, calcined, and weighed. Ag is determined in the solution, the same as for electrolysis slimes. (Referativnyi Zh.)

28934 SPECTROPHOTOMETRIC DETERMINATION OF URANIUM(VI) BY SOLVENT EXTRACTION OF THE URANIUM (VI)-ALIZARIN RED S-1,3-DIPHENYLGUANIDINIUM ASSOCIATED COMPLEX. Otomo, Makoto (Nagoya Inst. of Tech., Japan). Nippon Kagaku Zasshi; 92: 171-4(Feb 1971). (In Japanese).

The extraction of the uranium(M)-Alizarin Red S(ARS) chelate with 1-butanol in the presence of 1,3-diphenylguanidinium(DPG) salt was investigated spectrophotometrically. The extracted species has an absorption maximum at about 580 mμ, with a constant absorbance in the pH range from 4.6 to 4.9. The 1:1 uranium(M)–ARS chelate anion is extracted from aqueous solution in a 1:1 molar ratio with the DPG cation. The infrared spectrum of the associated complex implies that the metal is probably chelated to the two phenolic oxygen atoms of the ARS. For the absorbance of the associated complex under the optimum conditions of pH, reagent concentrations, and shaking time, Beer's law is obeyed up to 5.0×10^{-6} mol./l uranium(M) in aqueous phase. The molar absorptivity was calculated to be about 6500 at 580 mμ. The effect of diverse ions was also examined. Calcium(II)–CyDTA complex can be used as a masking agent for many interfering metal ions. (auth)

28935 RADIONUCLIDE X-RAY-FLUORESCENCE ANALYSIS. I. EXCITATION OF FLUORESCENT X RADIATION USING NUCLEAR RADIATION. Varga, Stefan (Slovenian Coll. of Tech., Bratislava). Chem. Listy; 64: 1253-65(Dec 1970). (In Slovak).

On the basis of a review of the literature (68 references, mostly English or Western European languages), the principal radionuclides that excite fluorescent x rays are listed and their use in analytical chemistry is discussed. The theory of x-ray-fluorescence analysis is presented, and the relatively low-atomic-number elements suitable for such determination are listed together with the energies and wavelengths of their $K_{\alpha 1}$ rays. Tabulations are also presented of gamma-emitting radionuclides suitable for producing x rays and of x-ray emitters. Beta and gamma emitters as inducers of fluorescent x rays are discussed along with source-target configurations. (TTT)

28936 RAPID DETERMINATION OF HYDROGEN IN METALS BY THE ARGON GAS CARRIER FUSION-GAS CHROMATOGRAPHIC METHOD. Goto, Hidehiro; Hosoya, Minoru (Tohoku Univ., Sendai). J. Jap. Inst. Metals; 35: 16-20(Jan 1971). (In Japanese).

A rapid determination of hydrogen in metals was designed by applying the carrier gas fusion–gas chromatographic technique. The sample was melted in the stream of argon at a flow rate of 150 mL/min, by using a graphite crucible and a reaction tube of small-size. The extracted hydrogen was passed through a molecular-sieve 5 A column to separate from the other gases. Measurement was carried out with a cathetometer and an integrator. The accuracy of the proposed method was equal to that obtained with the hot extraction method (using an argon carrier-Pd osmosis tube), but the analytical time could be reduced to about ¼ (about 5 to 7 min). The present method was applied to the determination of hydrogen in various metal samples such as stainless steel, rare earths, V–H, Zr–H, Nb–H, Ta–H, Al, and Cu with satisfactory results. (auth)

28937 COMPARISON OF A MODIFIED KJELDAHL AND A VACUUM FUSION TECHNIQUE FOR DETERMINATION OF NITROGEN IN TANTALUM ALLOYS. Davis, Warren F.; Graab, Judson W.; Merkle, Emery J. (Lewis Research Center, Cleveland). Talanta; 18: 263-72(Mar 1971).

Results obtained for determination of nitrogen in the tantalum alloys T-111 (Ta–8W–2Hf) and T-222 (Ta–10W–2.5 Hf–0.1C) by Kjeldahl and vacuum fusion procedures are compared. Results obtained by each technique are shown for the determination of nitrogen in the MAB T-111 sample, two commercial T-111 samples and a commercial sample of T-222 alloy. In the 5 to 25 ppM range, the relative standard deviation was 3 to 9% by the Kjeldahl procedure and 4 to 8% by vacuum fusion. This is a measure of the homogeneity of the material as well as of the reproducibility of the results. The agreement of the results obtained by these two techniques increases confidence in the vacuum fusion results for nitrogen in tantalum. (auth)

28938 SUITABILITY OF VITREOUS CARBON AS A MORTAR MATERIAL FOR SPECTROCHEMICAL ANALYSIS. Findeisen, Berndt; Schuffenhauer, Werner (Instituteil fur Metallische Spezialwerkstoffe, Dresden). Neue Huette; 16: 47-50(Jan 1971). (In German).

The suitability of the vitreous carbon was tested using ZrO_2, SiO_2 and Al_2O_3. Optimum conditions, impurities introduced into the sample by the carbon, and properties of the product material are discussed. (M.C.G.)

28939 EFFECT OF MULTIPLY SCATTERED γ-RADIATION IN THE X-RAY RADIOMETRIC METHOD. Mitov, V. N.; Yanshevskii, Yu. P.; Marenkov, O. S.; Ochkur, A. P.; Leman, E. P. Vop. Razved. Geofiz.; No. 11, 59-63(1969). (In Russian).

The effect was studied of multiply scattered γ radiation on the spectrum of secondary radiation of alabaster model samples containing 0 and 5% Pb. ^{57}Co, ^{75}Se, and ^{139}Ce were used as sources of the primary radiation. A probe with Pb shielding was equipped with a NaI(Tl) detector and collimators with the diameter of 10 and 8 mm for the primary and secondary radiation, respectively. With the angle between the collimators increasing from 20 to 120°, an inflection point becomes more significant in the secondary spectrum of the Pb-free sample. This is caused by multiply scattered γ quanta, especially by those twice Compton-scattered in the plane coinciding with the axes of the collimators. At an energy of the primary radiation of >100 keV, effective atomic number of the sample of 12, and average density, of the sample of 1.6 g/cm³, the contribution of the multiply scattered γ radiation to the secondary spectrum is 7 to 10%. The effect of the effective atomic number change of the sample on the excited radiation to background ratio is negligible at the angle between the collimators of 110 to 20°. The contribution of the multiply scattered radiation relative to the total albedo value can be as high as 30% and decreases with increasing effective atomic number and decreasing average density of the sample, with decreasing probe length and with increasing distance between the primary source and sample surface. (Selenium-Tellurium Abstr.)

28940 X-RAY RADIOMETRIC DETERMINATION OF LEAD IN SAMPLES WITH A ^{75}Se SOURCE. Mitov, V. N. Vop. Razved. Geofiz.; No. 11, 26-32(1969). (In Russian).

To avoid the effect of sample composition on determination of Pb and Ba in ores, a nomogram must be constructed for each given SiO_2/Pb/Ba ratio. The nomogram correlates the Pb and Ba contents with the measured intensity-to-background ratio of 75-keV x rays and of scattered 105-keV γ radiation. One single

nomogram can be used for different deposits if only Pb is to be determined. The determination of Pb and Ba in mineral polycomponent samples is only slightly affected by the average density of the sample. The saturation layer of ore samples with the density of 1.5 to 1.7 g/cm^3 is <4 cm for both 75- and 105-keV channels and at any concentration of Pb. In measuring in the energy regions 75 ± 3.5 and 105 ± 3.5 keV (NaI(Tl) detector) and using samples with a particle size of 1 mm, the accuracy of the determination is better than, equal to, and is lower than that of a chemical analysis for Pb contents of 0 to 6, 0.25 to 0.5, and 0.05 to 0.25%, respectively. Samples containing >10% Pb must be diluted with quartz sand; 120 to 50 determinations can be performed in 7 hr. (Selenium-Tellurium Abstr.)

28941 APPLICATION OF KINETICS FOR QUANTITATIVE CHEMICAL ANALYSIS OF MIXTURES. Worthington, James Brian. Lafayette, Ind.; Purdue Univ. (1970). 195p. University Microfilms Order No. 71-2716.

Thesis.

The kinetics of the Ru-catalyzed reaction between Ce(IV) and As(III) were investigated. The rate of chemical reaction was measured by following the decrease in Ce(IV) absorbance as a function of time. Initial rates were computed from response curves using appropriate calibration factors. The reaction rate dependency on Ce(IV), As(III), As(V), Ce(III) and Ru was investigated. A dependence on the order of addition of reagents was observed and investigated under a wide range of reagent concentrations. For Ce(IV) concentrations below 5×10^{-3}M, the reaction rates for Ce(IV), added to a As(III) – Ru(VIII) mixture are slower than the rates for As(III) added to a Ce(IV) – Ru(VIII) mixture. Above this Ce(IV) concentration the rates are almost equal for both methods of reagent addition. The reaction rate was found to be independent of Ce(III) and As(V) for concentrations tenfold greater than the reactant concentrations and for both methods of reagent addition. The rate dependency on Ce(IV) concentration has two distinct types of behavior. At low Ce(IV) concentrations ($<5 \times 10^{-4}$M) the reaction is first order in Ce(IV) while at high Ce(IV) concentrations ($>2 \times 10^{-3}$M) the reaction is second order in Ce(IV). This Ce(IV) dependency is found to hold for [As(III)] to [Ce(IV)] ratios as low as 0.1. This dependence is also observed for both methods of reagent addition. The rate dependency on As(III) is a function of the absolute Ce(IV) concentration. At 1×10^{-2}M Ce(IV) and [As(III)] to [Ce(IV)] ratios below 0.5, the reaction is half order in As(III). At lower Ce(IV) concentrations, the As(III) dependency is less than half order. A small As(III) concentration dependency is observed for [As(III)] to [Ce(IV)] ratios greater than unity. At low Ce(IV) concentrations and substoichiometric As(III), the reaction rate is independent of As(III) for Ce(IV) added to As(III) – Ru(VIII) mixture. The reaction is first order in Ru(VIII) under all conditions investigated. The use of ruthenium chloride compounds as catalysts results in irreproducible rates. A rate expression is presented that fits the experimental data for As(III) added to Ce(IV) – Ru(VIII) mixtures to within 10% in most cases. The information from this study is used to define reaction conditions for the combined analysis of Ru and Os without a prior separation. Kinetic differences between the catalyzed reactions are exploited for this analysis. The determination of mixtures of osmium and ruthenium tetroxides at 10^{-9}M is reported with accuracies of 1 to 3%, and relative standard deviations of 1 to 4%. The development and application of a data reduction system for the graphical extrapolation method used in differential kinetic analysis is described. The system is demonstrated for the determination of mixtures of rare earths using a ligand exchange reaction. (Diss. Abstr. Int., B)

28942 SAMPLE INPUT SYSTEM. (to Atomic Energy of Canada Ltd.). British Patent 1,226,823. 31 Mar 1971. Priority date 21 Jun 1967, Canada.

A sample delivery device is described for use with a water analyzer, which compares water samples with a reference to determine isotopic purity by means of ir spectral measurements. The delivery system serves to supply both the reference water and the samples to the ir cell at substantially identical temperatures and pressures. The device includes means for storing the reference water and at least two supplies of samples, equilibration tubing passing through a controlled temperature bath, and connections to a single source of pneumatic pressure for driving quantities of the selected materials to the isotopic-purity-measuring device. (B.L.M.)

28943 SPECTRAL ANALYTICAL DETERMINATION OF TELLURIUM TRACES IN CAST IRON. Peter, L.; Szopory, B. pp 47-52 of Papers of the V. Congress on Material Testing. III. Budapest; Scientific Society of Mechanical Engineers (1970). (In German.)

From fifth congress on material testing; Budapest, Hungary (19 Oct 1970). See CONF-701044–(Sect.3).

The tellerium content of cast iron can be determined by spectral analysis in amounts on the order of 10 ppM. After bending most of the iron on an ion exchanger, a radial electrode method and copper as the reference element were used. (M.C.G.)

28944 SPECTROCHEMICAL ANALYSIS OF HARD METALS BY A ROTATING DISC SOLUTION TECHNIQUE. Kantor, T.; Erdey, L.; Szabo, Zs. pp 81-7 of Papers of the V. Congress on Material Testing. III. Budapest; Scientific Society of Mechanical Engineers (1970).

From fifth congress on material testing; Budapest, Hungary (19 Oct 1970). See CONF-701044–(Sect.3).

A spectrographic method was developed for the simultaneous determination of the constituents W, Co, Ti, Ta, and Nb, and contaminants Fe, Ni, Cr, Mn, Mg, Ca in hard metals. The samples were dissolved in Hf and HNOs and the solutions stabilized with citric acid. Graphite discs were waterproofed in order to ensure controllability of solution introduction into the source. For the types of hard metal samples studied no inter-element effect was observed. Titanium was also determined using a double-beam optical spectrometer. (auth)

28945 DIRECT SPECTRAL DETERMINATION OF RHENIUM IN MOLYBDENUM AND COPPER CONCENTRATES. Krasnobaeva, N.; Nedyalkova, N. pp 99-103 of Papers of the V. Congress on Material Testing. III. Budapest; Scientific Society of Mechanical Engineers (1970).

From fifth congress on material testing; Budapest, Hungary (19 Oct 1970). See CONF-701044–(Sect.3).

A method for determination of rhenium in molybdenum concentrates was developed. The concentration range is 60 to 1000 grams/ton, with a precision $V_c = 6\%$. A method for determination of rhenium in copper concentrates is described. It has a sensitivity of 1×10^{-4}%. No systematic errors were found. (M.C.G.)

28946 PROBLEMS IN THE QUANTITATIVE SPECTRAL ANALYSIS OF RARE EARTH METAL TRACES. II. SELECTION OF OPTIMAL ANALYSIS LINE PAIRS FOR DETERMINATION OF RARE EARTHS IN BAUXITE. Zimmer, K.; Toth, M.; Koller, L. pp 123-39 of Papers of the V. Congress on Material Testing. III. Budapest; Scientific Society of Mechanical Engineers (1970). (In German).

From fifth congress on material testing; Budapest, Hungary (19 Oct 1970). See CONF-701044–(Sect.3).

The analysis line pairs were chosen from the wavelength region 360 to 440 nm. Studies were made of the correlation coefficient, the regression coefficient, and other parameters. Experimental conditions were evaluated and detection limits determined. Results are presented in tables for La, Eu, Nd, and Gd. (M.C.G.)

28947 SPECTROGRAPHIC DETERMINATION OF IMPURITIES IN VANADIUM PENTOXIDE AND HIGH PURITY LEAD. Tripkovic, M.; Dmitrovic, M. pp 145-51 of Papers of the V. Congress on Material Testing. III. Budapest; Scientific Society of Mechanical Engineers (1970).

From fifth congress on material testing; Budapest, Hungary (19 Oct 1970). See CONF-701044–(Sect.3).

Two groups of methods for spectrographic analysis of vanadium are described. The first group is based on separation of matrix material from impurities and the second on direct spectrographic methods. Determination of Mo, Ni, Fe, Al, Cr, Mn, Sb, As, Zn, and Ag is reported. A method for spectrographic analysis of high-purity lead is also reported. (M.C.G.)

28948 DEVELOPMENT OF DRILLED ELECTRODES OF SYNTHETIC MATERIALS AND THEIR USE FOR DETERMINATION OF RARE EARTH OXIDE TRACES IN RARE EARTHS. Papp, L.; Szarvas, P. pp 159-63 of Papers of the V. Congress on Material Testing. III. Budapest; Scientific Society of Mechanical Engineers (1970). (In German).

From fifth congress on material testing; Budapest, Hungary (19 Oct 1970). See CONF-701044–(Sect.3).

A compressed electrode system of synthetic materials was developed for the spark excitation method and evaluated for spectrographic and spectroscopic determination of rare earth oxides and analysis of rare earth oxides for impurities. (M.C.G.)

28949 EXPERIENCE WITH SPECTRAL ANALYSIS OF NUCLEAR MATERIALS WITH THE LASER MICROPROBE. Tlalka, R. pp 179-97 of Papers of the V. Congress on Material Testing. III. Budapest; Scientific Society of Mechanical Engineers (1970). (In German).

From fifth congress on material testing; Budapest, Hungary (19 Oct 1970). See CONF-701044–(Sect.3).

The apparatus and the materials to be analyzed are reviewed.

Materials include: U_3O_8, UO_2, ThO_2, zirconium alloys, and steels. A ruby laser was used. (M.C.G.)

28950 USE OF THE MEDIUM METHOD OF TWO STANDARDS TAKEN FROM UNIFORMLY NORMALIZED CALIBRATION CURVES IN SPECTROMETRIC STEEL ANALYSIS. I. ANALYSIS OF LOW-ALLOY STEEL. Paksy, L. pp 203-8 of Papers of the V. Congress on Material Testing. III. Budapest; Scientific Society of Mechanical Engineers (1970). (In German).

From fifth congress on material testing; Budapest, Hungary (19 Oct 1970). See CONF-701044-(Sect.3).

Principles of the method, experimental conditions, and analytical results for C, Mn, Si, S, P, Cr, Ni, Cu, Mo, W, and V are given. (M.C.G.)

28951 INVESTIGATION OF THE DETECTION LIMITS OF IODINE WITH THE HOLLOW CATHODE LAMP. Szilvassy-Vamos, Zs. pp 221-5 of Papers of the V. Congress on Material Testing. III. Budapest; Scientific Society of Mechanical Engineers (1970). (In German).

From fifth congress on material testing; Budapest, Hungary (19 Oct 1970). See CONF-701044-(Sect.3).

Improvements are reported in the construction of hollow-cathode discharge tubes and their uses for emission spectral analysis for detection of halogens considered. Optimal parameters for iodine determination were investigated and a method developed for determination of iodine to 0.01%. (tr-auth)

28952 SPECTRAL ISOTOPIC ANALYSIS OF ELEMENTS IN THE MIDDLE PART OF MENDELEEV PERIODIC TABLE. Zhiglinskii, A. G.; Polyanskii, V. A.; Turkin, Yu. I.; Fafurina, E. N.; Khlopina, T. N. Vestn. Leningrad. Univ., No. 10, Fiz., Khim.; No. 2, 62-8(May 1970). (In Russian).

The resolution of the spectral lines of isotopes is calculated for 41 elements in the middle part of the periodic table. It is shown that for 27 elements the resolution has a value that is found sufficient to develop a new method of spectral isotopic analysis. The correctness of values obtained is confirmed experimentally. For the first time the isotopic composition of Ne, Cu, Rb, and Eu is obtained by methods of spectral analysis. The results of spectral and mass-spectrometric measurements are shown to have ±2% difference in the value. (auth)

28953 SEPARATION OF PERRHENATE, MOLYBDATE, AND SELENITE IONS ON SILICA GEL. Phipps, Alan M. (Raytheon Co., Waltham, Mass.). Anal. Chem.; 43: 467-9(Mar 1971).

A wide separation between rhenium and molybdenum is rapidly obtained on silica gel-coated polyester sheets with methanolic HCl or HNO_3 solvents. The influence of solvent composition on the R_f values of the anions, ReO_4^-, SeO_3^{2-}, and MoO_4^{-2} on silica gel were investigated because separation with this solvent is not observed on silica gel-coated glass plates. The method is useful for the rapid identification of rhenium in alloys containing molybdenum and/or tungsten. (D.P.O.)

28954 OPTIMIZATION OF EXPERIMENTAL CONDITIONS FOR SPECTROFLUORIMETRIC DETERMINATION OF EUROPIUM, SAMARIUM, AND TERBIUM AS THEIR HEXAFLUOROACETYLACETONE-TRIOCTYLPHOSPHINE OXIDE COMPLEXES. Fisher, R. P.; Winefordner, J. D. (Univ. of Florida, Gainesville). Anal. Chem.; 43: 454-5(Mar 1971).

The effect of pH on the fluorescence of the hexafluoroacetylacetone-triactylphosphine oxide complexes of the rare earths was investigated. Only europium, samarium, and terbium yielded analytically useful fluorescent chelates and a pH of 3 was found to be the most suitable for measurements of the three rare earths. (D.P.O.)

28955 QUANTITATIVE CATION EXCHANGE SEPARATION OF ZIRCONIUM AND HAFNIUM IN FORMIC ACID MEDIA. Qureshi, Mohsin; Husain, Khadim (Aligarh Muslim Univ., India). Anal. Chem.; 43: 447-9(Mar 1971).

The adsorption behavior of zirconium and hafnium on ion exchangers in dilute as well as concentrated formic acid solutions and the quantitative separation of zirconium from hafnium in varying ratios are described. (D.P.O.)

28956 POTENTIOMETRIC STUDIES WITH AN ION PERMSELECTIVE MEMBRANE. Lal, Sudarshan; Christian, Gary D. (Univ. of Kentucky, Lexington). Anal. Chem.; 43: 410-21(Mar 1971).

A dithizone-containing membrane is described, which shows varying degrees of permselectivity to a large number of cations and anions, including mono-, di-, and trivalent ions. It was used successfully for the potentiometric monitoring of precipitation, chelometric, redox, acid-base, and nonaqueous titrations. Relative selectivities of the membrane toward different ions are used to interpret different shapes of titration curves. Effects of sample concentration, organic solvents, and extraneous salts on the shapes of titration curves are reported. The effect of the membrane plasticizer on permselectivity to different ions and on titration curves was studied. The membrane is stable for several months, except when used in purely nonaqueous solvents. (auth)

28957 MULTIVARIABLE ANALYSIS OF QUANTITATIVE X-RAY EMISSION DATA. THE SYSTEM ZIRCONIUM OXIDE-ALUMINUM OXIDE-SILICON OXIDE-CALCIUM OXIDE-CERIUM OXIDE. Stephenson, Donald A. (Corning Glass Works, N. Y.). Anal. Chem.; 43: 310-18(Mar 1971).

Guidelines for the correct use of statistical methods for quantitative x ray-emission analysis of multicomponent systems are set forth, and a general review and discussion of the technique is presented. The regression model first proposed by Alley and Myers is the only model, among many, that seems both physically and statistically adequate for general application, and its use is recommended before more elaborate models are tried. A new procedure for the selection of synthetic reference standards covering any region of interest in any n-component system in a homogeneous fashion is described and applied to the standardization of part of the system ZrO_2 (35 to 85 wt %)-Al_2O_3 (5 to 55 wt %)-SiO_2 (1 to 10 wt %)-CaO (5 to 15 wt %)-CeO_2 (5 to 15 wt %). The residual error in the prediction of the composition of the synthetic standards is around 1 to 2% relative, which compares favorably with other methods of analysis. (auth)

28958 USE OF CUPFERRON FOR THE POTENTIOMETRIC DETERMINATION OF THORIUM AND CERIUM WHEN PRESENT TOGETHER. Kovalenko, P. N.; Ivanova, Z. I.; Poyarkova, I. F. Tr. Kom. Anal. Khim. Akad. Nauk SSSR; 17: 381-3(1969). (In Russian).

The method described is based on the fact that, at pH 4, the sum of Th and Ce is titrated with cupferron solution whereas only Th is titrated at pH 2 and in the presence of sulfosalicylic acid. (Referativnyi Zh.)

28959 DETERMINATION OF ARSENIC AND TELLURIUM IN GASEOUS MEDIA. Polukarov, A. N.; Makhmetov, M. Tr. Khim.-Met. Inst., Akad. Nauk Kaz. SSR; No. 9, 105-9(1968). (In Russian).

Determination of As and Te in a gaseous medium is based on low temperature combustion of S, which allows complete concentra- of As and Te from any sample in a small residue. Te and As are easily transferred into solution after treating the S with boiling HNO_3. The nitrate solution is evaporated to appearance of H_2SO_4 vapors and diluted with H_2O, and Te is precipitated with $SnCl_2$ and determined iodometrically; As is determined in the filtrate by the hypophosphite dichromatic method. (Referativnyi Zh.)

28960 SPECTROPHOTOMETRIC DETERMINATION OF SMALL AMOUNTS OF RUTHENIUM AND OSMIUM IN MINERALS AND INDUSTRIAL SAMPLES. Khvostova, V. P.; Shlenskaya, V. I. Tr. Tsent. Nauch.-Issled. Gornorazved. Inst.; 86: 154-60 (1969). (In Russian).

To determine both these elements in platinum containing chromite, boil the sample in a distillation flask with 15 ml of 57% of $HClO_4$, then add 5 ml of $HClO_4$ and distil off OsO_4 and RuO_4 during 40 min. (pass a stream of air through the solution during the distillation); absorb the RuO_4 and OsO_4 in 7 ml of 4N NaSCN. To the contents of the receiver add 2.5 ml of 0.01N $HClO_4$, heat on a water bath for 10 min., cool, dilute to 25 ml with water, and measure the extinction at 470 and 590 nm (10-cm cell). Calculate the contents of Ru and Os from the extinction at 590 nm (for Ru) and from the difference between the extinctions at 470 and 590 nm (for Os). (Referativnyi Zh.)

28961 X-RAY EXCITED OPTICAL LUMINESCENCE ANALYSIS OF TRACE RARE EARTHS IN HIGH-PURITY YTTRIUM AND GADOLINIUM OXIDES. Sato, Matsuji; Matsui, Hiroshi; Matsubara, Tadao (Shinetsu Chemical Industry Co. Ltd., Takefu Japan). Jap. Anal.; 20: 70-8(Jan 1971). (In Japanese).

Analysis by x-ray excited optical luminescence was applied to the determination of trace amounts of rare earths as impurities in yttrium and gadolinium oxides. In order to establish fundamental conditions, studies were made on the method of purification of base materials, the effects of temperature and time of ignition of test specimens and mutual interferences of different rare earths and (or) non-rare earth metals. An internal standard was employed for the compensation of the self-quenching of emission spectra. Yttrium and gadolinium oxides used for the base materials were purified by ion exchange to 7-nines purity with respect to the rare earth contents. They were further purified twice by homogeneous precipitation to remove non-rare earth impurities. The ignition of the oxalates into oxides were done at 1200°C for 4

XUM

hours. The self-quenching effect in emission spectra of rare earth impurities increased with the amounts of other rare earths, especially of terbium and (or) praseodymium. The effect was much larger in gadolinium oxide than in yttrium oxide. The use of praseodymium and dysprosium as the internal standard elements respectively for the analyses of yttrium and gadolinium oxides eliminated the influences of those impurities. The coefficients of variation in the results of analysis were 6.6 to 8.6% for 2 ppM of terbium, europium, and dysprosium in yttrium oxide and 5.2 to 8.2% for 2 ppM of terbium, europium, and praseodymium in gadolinium oxide. (auth) (Japan)

28962 ACCURACY AND APPLICABILITY OF X-RAY FLUORESCENCE FOR DETERMINATION OF THE CONCENTRATION OF THE ELEMENTS PHOSPHORUS TO URANIUM IN SOLUTION. Magyar, B. (Eidgenoessiche Technische Hochschule, Zurich). Talanta, 18: 27-38(Jan 1971). (In German).

X-ray fluorescence spectroscopy was used for the determination in solution of elements of atomic number greater than 14. Inter-element effects were investigated, and the use of internal (neighboring element) standards and of external standards was compared. In dilute solutions (less than 5×10^{-3}M) matrix effects can be ignored. The sources of error and their effect on the choice of operating conditions and the optimum concentration range are discussed. (auth) (UK)

28963 FLUOROMETRIC DETERMINATION OF SUBMICROGRAM QUANTITIES OF ZIRCONIUM. Filer, T. D. (Atomic Energy Commission, Idaho Falls, Idaho). Anal. Chem.; 43: 469-73(Mar 1971).

This method uses 3, 4, 7-trihydroxyflavone as the fluorometric reagent, and the fluorescence is measured in a sulfuric acid solution that permits use of peposulfate fusion as the method of sample dissolution. The advantage of the present procedure is that many of the common elements associated with zirconium alloys and ores do not interfere in milligram quantities, thus making the direct determination of zirconium possible. (D.P.O.)

28964 EMISSION SPECTROCHEMICAL DETERMINATION OF TANTALUM IN CURIUM OXIDE. Gaddy, R. H. (E. I. du Pont de Nemours and Co., Aiken, S. C.). Contract AT(07-2)-1. Anal. Chem.; 43: 475-6(Mar 1971).

The potassium carbonate leaching of tantalum from curium oxide, the methyl isobutyl ketone extraction of the tantalum, and its spectrographic determination are described. The limit of detection is approximately 1 μg of tantalum in 10 mg of curium oxide. Interferences in the method were not tested. (D.P.O.)

28965 EMISSION SPECTROGRAPHIC DETERMINATION OF RARE EARTH ELEMENTS IN LANTHANUM. Kaneko, Keiji. Denki Shikensho Iho; 34: 920-6(1970). (In Japanese).

A copper spark excitation method using an internal standard was applied successfully to the spectrographic determination of cerium, praseodymium, neodymium, samarium, gadolinium, dysprosium, europium, and yttrium in lanthanum. A series of standard solutions covering 0.15 to 15 and 1.5 to 150 μg per milliliter of the above rare earth elements is prepared in hydrochloric acid solutions. The standard solution is transferred to a pair of copper electrodes, and evaporated gently to dryness by heating at 90°C for complete conversion into chloride. The samples are treated exactly in the same manner as the standards. Chromium is used as the internal standard for the determination of rare earth elements. The spectrographic conditions are as follows: sample weight-3 mg; Shimadzu Littrow type spectrograph; Shimadzu Faussner source unit for emission, primary 70 V, 6 A, L = 0.8 mH, C = 0.006 μF; slit width 15 μ and duration of exposure 40 sec. The variation coefficient for 0.005 to 10% of rare earth elements in lanthanum is less than 6%. (auth)

28966 DETERMINATION OF THE COMPOSITIONS OF THIN FILM COMPOUNDS BY USING THE ELECTRON-PROBE X-RAY MICROANALYZER. I. ANALYSIS OF NITRIDE THIN FILMS. Itoh, Akio; Misawa, Shunji. Denki Shikensho Iho; 34: 927-35 (1970). (In Japanese).

For the purpose of establishing precise relationships between electrical characteristics and chemical compositions of such binary systems as refractory nitrides of transition metals, e.g., Ta_2N, TaN, TiN, ZrN, etc., a convenient method is proposed for determining the compositions of thin films of both Ti–N system and Zr–N system, prepared by evaporation synthesis and reactive sputtering, by using the electron-probe x-ray microanalyzer. The error in this analysis is several percent or less. Data of the film composition determined by this process have been adopted to feature each resistivity and temperature coefficient of resistivity–composition curves of Zr–N system and Ti–N system, respectively. (auth)

28967 ION SPECIFIC DETECTION OF INTERNAL STANDARDS LABELLED WITH STABLE ISOTOPES. Gaffney, Thomas E.; Hammar, Carl-Gustaf; Holmstedt, Bo; McMahon, Robert E. (Karolinska Institutet, Stockholm. Lilly Research Labs., Indianapolis). Anal. Chem.; 43: 307-10(Mar 1971).

The purpose of an internal standard in quantitative analytical techniques is to permit the analyst to correct for losses of the compound under study. This requires chemical similarity between the internal standard and the compound in question. When conventional gas chromatographic detector systems are used, there must at the same time be sufficient dissimilarity so that the peaks from the compound and the standard can be resolved. However, in the study described in which the mass spectrometer is used as the detector for a gas chromatographic effluent, there is no need for any chemical differences, and mass differences alone are sufficient to discriminate between the compound being analyzed and the standard. This allows the use of the ideal internal standard, namely the actual compound under study modified to contain an increased mass by the introduction of stable isotopes. Examples of the use of ^{15}N-and/or deuterium-labeled compounds as internal standards are given. (auth)

28968 SAMPLE PREPARATION FOR PRECISION CARBON ISOTOPIC ANALYSIS. Maass, I.; Geissler, C. (Zentralinstitut fuer Isotopen- und Strahlentechnik, Leipzig). Isotopenpraxis; 7: 14-17(Jan 1971). (In German).

Experimental details of processes used in sample preparations for precision carbon isotopic analysis of solid, liquid, and gaseous hydrocarbons and of carbonates are described. (auth)

28969 ORGANICHESKIE REAGENTY V ANALITICHESKOI KHIMII TSIRKONIYA. (Organic Reagents in the Analytical Chemistry of Zirconium). Ermakov, A. N. (ed.). Moscow; Izdatel'stvo Nauka (1970). 144p.

Ten papers are included on chemical determination of zirconium. Some of the papers cover the use of various organic reagents in the analytical chemistry of zirconium (including spectrophotometry and extraction chemistry). Colorimetric and complexometric determination of Zr in Nb-base alloys is reviewed as well as determination of Zr by Arsenazo III and various new types of reagents. (R.V.J.)

28970 AMPEROMETRIC, CONDUCTOMETRIC, CHELATOMETRIC TITRATION. Vydra, Frantisek; Vorlicek, Jan; Stulik, Karel (Charles Univ., Prague). Chem. Listy; 63: 35-50(Jan 1969). (In Czech).

Data are presented on the methods of conductometric and impediometric titration using chelates and chelating agents. The scheme of amperometric titration and polarization curves for various phases of titration by EDTA are given for the following materials: iron, aluminum, thallium, copper, indium, gallium, thorium, bismuth, lanthanides, strontium, barium, and alkali metals. (R.V.J.)

28971 COLORIMETRIC DETERMINATION OF URANIUM. Suteu, Al.; Hodisan, T. (Babes-Bolyai-Univ., Cluj). Stud. Cercet. Chim.; 18: 85-98(Jan 1970). (In Rumanian).

Various methods for the colorimetric determination of uranium are reviewed. It is shown that the more sensitive methods include fluorescence and extraction using rodamine B, Arsenazo III, Arsenazo II, dibenzoylmethane, etc. Selective determination was achieved by a combination of dyes and other ions. General procedures of uranium separation by solvent extraction and by complexing are discussed. (R.V.J.)

28972 INFRARED DETERMINATION OF BARIUM, STRONTIUM, AND CALCIUM CARBONATES, SINGLY AND TOGETHER, BY THE PELLET TECHNIQUE. Chasan, David E.; Norwitz, George (Frankford Arsenal, Philadelphia). Appl. Spectrosc.: 25: 226-8(Mar-Apr 1971).

Methods are proposed for the ir determination of barium, strontium, and calcium carbonates, singly or together, by the pellet technique. The sample is weighed into a tarred mortar using a semi-microbalance and is mixed with 300 mg of potassium bromide. The pellet is then formed and the peak heights are determined at the appropriate peak. The measurements for barium, strontium, and calcium carbonates are made at 693 cm^{-1}, 704 cm^{-1} (or 698 cm^{-1}), or 712 cm^{-1}, respectively. The method for the mixed carbonates can be used down to a concentration of 5% of the minor ingredient. Sulfates and nitrates do not interfere with any of the procedures. (auth)

28973 STANDARD METHODS FOR CHEMICAL ANALYSIS OF REACTOR AND COMMERCIAL COLUMBIUM. ASTM E 195-68. Philadelphia; American Society for Testing and Materials (1968). 9p. Available from American Society for Testing and Materials, Philadelphia.

Methods are described for the determination of N, Mo, W, and Fe in commercial Nb. Nitrogen is determined by a distillation and photometric measurement of the yellow complex of ammonia with Nessler reagent. The method is applicable to concentrations of N from 20 to 1000 ppM. Molybdenum and W are determined photometrically using dithiol, and the method is applicable to concentrations from 50 to 1000 ppM. Iron in concentrations from 150 to 1000 ppM is determined photometrically using 1,10-phenanthroline. (B.L.M.)

28974 STANDARD METHODS FOR CHEMICAL ANALYSIS OF CARBON AND GRAPHITE. ASTM C 560-69. Philadelphia; American Society for Testing and Materials (1969). 12p. Available from American Society for Testing and Materials, Philadelphia.

Methods are described for the determination of Si, Fe, Ca, Al, Ti, V, and B in carbon or graphite. The preferred concentration of the sought element in the final solution, the limits of sensitivity, and the precision of the results are tabulated. Si is determined photometrically as the silicomolybdic acid; Fe is determined photometrically as the Fe(II)-ortho-phenanthroline complex; and Ca is precipitated as the oxalate, dissolved, and determined by measuring the decrease in absorbance when added to a dilute $KMnO_4$ solution. Al is determined photometrically using 2-quinizarinsulfonic acid; Ti is determined photometrically by the peroxide colorimetric method; and B is determined by the curcumin-oxalic acid colorimetric method. The interferences are listed for all procedures. (B.L.M.)

28975 STANDARD METHOD OF TEST FOR URANIUM BY CONTROLLED-POTENTIAL COULOMETRY. ASTM E 217-70. Philadelphia; American Society for Testing and Materials (1970). 8p. Available from American Society for Testing and Materials, Philadelphia.

Determination of U by controlled-potential coulometry is carried out at −325 V vs SCE in a solution that is 0.5 M H_2SO_4. Electrolysis is terminated when the current decreases to 50 μA, and the analytical result is computed on the basis of a 2-electron change from U(VI) to U(IV) using Faraday's law. Preliminary electrolytic reduction at 0.75 V eliminates the interferences of most strong oxidants. Copper(II) is reduced along with U(VI) and constitutes an interference, which must be circumvented by coulometric reoxidation of the Cu(Hg) formed. Anion interferences are minimal. The effects of most fission products are small, but Mo interferes seriously and a separation or a medium other than H_2SO_4 is required. Oxygen interferes seriously; and the supporting medium must be O_2 free prior to electrolysis, which must be carried out under a blanket of inert gas. If necessary, U may be separated from interferences by extraction with methyl isobutyl ketone followed by oxidation and dissolution with a bisulfate melt and $HClO_4$. The relative standard deviation of the method is 1%. (B.L.M.)

28976 STANDARD METHOD FOR COLORIMETRIC DETERMINATION OF URANIUM IN AQUEOUS SOLUTIONS. ASTM E 318-69. Philadelphia; American Society for Testing and Materials (1969). 7p. Available from American Society for Testing and Materials, Philadelphia.

Uranium can be determined in aqueous solutions containing 30 to 750 μg/ml by measuring the absorbance of the U-dibenzoylmethane complex at 415 mμ. After oxidation of the U with $KMnO_4$, the U(IV) is extracted with hexone from an aqueous phase salted with an acid-deficient solution of $Al(NO_3)_3$ and tetrapropylammonium nitrate. Color is developed in the hexone phase. Large amounts of Th and Ce(IV) interfere. The precision in a single laboratory was 1.7% RSD. (B.L.M.)

28977 STANDARD METHOD OF TEST FOR THORIUM IN INDUSTRIAL WATER AND INDUSTRIAL WASTE WATER. ASTM D 2333-68. Philadelphia; American Society for Testing and Materials (1968). 5p. Available from American Society for Testing and Materials, Philadelphia.

Thorium was determined spectrophotometrically using 1-(o-arsonophenylazo)-2-naphthol-3,6-disulfonic acid after the Th had been coprecipitated with Ca as the oxalate salts and redissolved. The method is sensitive to $<1 \times 10^{-9}$ g Th/g H_2O. The absorbance of the complex was measured at 545 mμ. Ferric iron is the primary interference and its interference is minimized by adding hydroxylamine hydrochloride and boiling the test solution to reduce the iron. (B.L.M.)

28978 STANDARD METHOD OF TEST FOR URANIUM AND PLUTONIUM CONCENTRATIONS AND ISOTOPIC ABUNDANCES. ASTM E 267-70. Philadelphia; American Society for Testing and Materials (1970). 9p. Available from American Society for Testing and Materials, Philadelphia.

The concentration of Pu and U and their isotopic abundances in solutions of reactor fuels either before or after irradiation was determined by mass spectrometric analysis. A minimum sample containing 50 μg of irradiated U will contain sufficient Pu for measurement. Ion-exchange separations were used to separate Pu and U from fission products and then to separate and purify the Pu and U prior to mass spectrometric analysis. The precision of the method on an interlaboratory basis was 0.7% RSD. (B.L.M.)

28979 STANDARD METHOD OF TEST FOR ATOM PERCENT FISSION IN URANIUM AND PLUTONIUM FUEL ^{148}Nd METHOD. ASTM E 321-69. Philadelphia; American Society for Testing and Materials (1969). 9p. Available from American Society for Testing and Materials, Philadelphia.

Fission product Nd is chemically separated from irradiated U and Pu fuels and determined by isotopic dilution mass spectrometry to measure the burnup of the fuel. The two rare earths adjacent to Nd do not interfere with the procedure, and interferences from other rare earths, either natural or fission product, are removed by an ion-exchange separation. The minimum sample size should be 70 ng of ^{148}Nd. The method is described in detail and can be applied directly to U fuels containing <0.5% initial Pu with 1 to 100 GW day/metric T burnup. The precision of the method, both for a single laboratory and for 8 participating laboratories, is ~1%. (B.L.M.)

28980 STANDARD METHOD OF TEST FOR ATOM PER CENT FISSION IN URANIUM AND PLUTONIUM FUEL (MASS SPECTROMETRIC METHOD). ASTM E 244-69. Philadelphia; American Society for Testing and Materials (1969). 7p. Available from American Society for Testing and Materials, Philadelphia.

A computerized mass spectrometric method is described for the determination of the heavy element at. % fission in irradiated U fuel with an initial Pu content of 0 to 50% from the isotopic analysis of the fuel before and after irradiation. The analysis must be carried out under conditions as nearly identical as possible, and the sample before irradiation must be representative of the fuel. Atomic ratios of the isotopes ^{235}U, ^{236}U, ^{239}Pu, ^{240}Pu, ^{241}Pu, and ^{242}Pu to ^{238}U are measured mass spectrometrically. The at. % fission attributed to fission of ^{235}U, ^{239}Pu, and ^{241}Pu is separately calculated and then summed to obtain the total heavy element at. % fission. (B.L.M.)

Isotope Dilution Procedures

28981 SUBSTOICHIOMETRIC DETERMINATION OF TRACES OF PALLADIUM BY RADIOACTIVE ISOTOPE-DILUTION ANALYSIS. Briscoe, G. B.; Humphries, S. (Univ. of Aston, Birmingham, Eng.). Talanta; 18: 39-49(Jan 1971).

A radioactive isotope-dilution method for the determination of traces of palladium was developed. It is based on the solvent extraction of palladium dithizonate from acid solution by means of a substoichiometric amount of dithizone in carbon tetrachloride. The separation was applied to the determination of traces of palladium in platinum, the rocks W-1 and PCC-1, and a biological material (kale). Amounts of palladium down to 3 ng were determined. (auth) (UK)

Radiometric and Radiochemical Procedures

Refer also to abstracts 29174, 29389, 29390, 29517, and 31613.

28982 DETERMINATION OF THORIUM, URANIUM(VI), AND PLUTONIUM(IV) WITH COBALT(III) HEXAAMMINE CHLORIDE. Ueno, K.; Hoshi, M.; Asano, M. (Japan Atomic Energy Research Inst., Tokai). Radiochem. Radioanal. Lett.; 6: 151-9(3 Apr 1971).

Gravimetric determination methods for thorium and plutonium(IV), and radiometric methods for thorium and uranium(VI) were studied, using cobalt(III) hexaammine chloride as the reagent. Thirty to 120 mg of thorium can be determined with an accuracy of ±1%, 0.6 to 2.5 mg of plutonium(IV) with an accuracy of ±7% by the gravimetric method, and, 0.007 to 1.5 mg of thorium with an accuracy of ±10% and 0.25 to 1.5 mg of uranium(VI) with an accuracy of ±2% by the radiometric method. (auth)

28983 SEPARATION AND DETERMINATION OF ^{137}Cs IN URINE. Everett, R. J.; Mottola, H. A. (Oklahoma State Univ., Stillwater). Anal. Chim. Acta; 54: 309-13(Apr 1971).

A method is described for the analysis of ^{137}Cs in either raw or ashed urine. The method relies on an ammonium molybdophosphate ion exchange and solvent extraction with 4-sec-butyl-2-(α-methylbenzyl)phenol in order to collect and separate ^{137}Cs from interfering activity. The analysis time on 1 liter of urine is ca. 4.5 hr, with only 1 hr of working time. The procedure can be used on raw

XUM

urine if necessary, and requires no addition of cesium carrier or yield corrections. The final residue is suitable for low-level β counting. A 93% recovery of ^{137}Cs is obtained. (auth)

28984 LIQUID SCINTILLATION COUNTING OF RNA: A SIMPLE PROCEDURE FOR EXTRACTION FROM SUCROSE GRADIENTS. Paus, Povel N. (Univ. of Oslo). Anal. Biochem.; 38: 364-73(Dec 1970).

A method is described that permits quantitative extraction of RNA from a range of aqueous solutions used for sedimentation analysis, including cesium salt solutions. The method, which is fast, offers high efficiency even for ^{3}H counting and, with most buffers, stable count rates. This makes double labeling possible without risking biased results. Preliminary experiments showed that the method may have a wider application for the extraction and liquid scintillation counting of macromolecules. (auth)

28985 LIQUID SCINTILLATION COUNTING OF (^{3}H) AND (^{14}C) ON SOLID SUPPORTS: A WARNING. Bransome, E. D. Jr.; Grower, M. F. (Massachusetts Inst. of Tech., Cambridge). Anal. Biochem.; 38: 401-8(Dec 1970).

A decrease in the efficiency of counting a (^{14}C)-labeled molecule small enough to penetrate into the matrix of a solid support was observed. It is accompanied by a disproportionate pulse-height shift. These consequences of "local absorption" were related to the thickness and absorptivity of the solid support, and were most dramatic with (^{3}H)-labeled samples. The relation of (^{14}C) sample channel ratios (CR) to (^{14}C) efficiency was quantitatively different from that of soluble samples but could be used to set up a fairly accurate quench correction curve for single-label counting. The disappearance of most of the (^{3}H) spectrum below the detection threshold prevented any reliable quench correction by means of CR values, and made any assumption of constant efficiency very hazardous. In addition to the nature of the solid support, its geometry in the vial, the size of the sample molecule, and the presence and composition of sample precipitate: all have a significant effect on (^{14}C) and (^{3}H) efficiency. Thus, (^{3}H) counting or (^{3}H) and (^{14}C) counting of samples on solid supports are not reliable unless: (1) Precise standards which exactly reproduce very constant counting conditions are employed. The uniformity needed to avoid significant variations in efficiency is not, in our experience, very easy to achieve. (2) The samples are eluted from the support — the addition of the same compound labeled with another isotope often being necessary. (3) The samples are subjected to oxygen flask combustion, recoveries of (^{3}H) – H_2O and (^{14}C) – CO_2 being virtually quantitative. (auth)

28986 DOUBLE-ISOTOPE DERIVATIVE ASSAY OF SERUM IODOTHYRONINES. II. THYROXINE. Hagen, Garrett A.; Diuguid, Lincoln I.; Kliman, Bernard; Stanbury, John B. (St. Louis Univ. Harvard Medical School, Cambridge, Mass. Massachusetts General Hospital, Boston). Anal. Biochem.; 38: 517-28 (Dec 1970).

An improved method was developed for double isotope derivative assay of total serum T4. In the double isotope derivative assay, tritium-labeled acetic anhydride is used to make a derivative of the unknown T4, which is purified and counted. The new procedure includes greatly shortened and simplified acetylation and purification steps. Also, a resin column method has proved superior to butanol for extracting T4 from serum prior to acetylation. The precision of T4 assay by the double isotope derivative approach compares favorably with that of other methods and may prove useful in thyroid research. (auth)

28987 DETERMINATION OF CALCIUM BY RADIOCHEMICAL REPLACEMENT. Bowen, H. J. M. (Univ. of Reading, Eng.). Analyst; 96: 220-2(Mar 1971).

The determination of calcium ions in solution by radiochemical replacement of silver-110 in labeled solid silver oxalate, cobalt-60 in labeled cobalt oxalate, and manganese-54 in labeled manganese oxalate. The technique can be used to determine 25 to 100 μmole ml^{-1} (100 to 4000 μg ml^{-1}) of calcium, and the lower limit is reduced to 16 μg ml^{-1} by using a 50 per cent methanol solution. Magnesium interferes to only a small extent. Each determination takes less than 5 minutes, and the precision is ±2 per cent. (auth) (UK)

28988 APPARATUS FOR DETERMINING FISSIONABLE AND ABSORBENT MATERIAL IN UNIRRADIATED NUCLEAR FUELS. (to Gesellschaft fuer Kernforschung mbH). British Patent 1,226,310. 24 Mar 1971. Priority date 19 Mar 1969, Germany.

An apparatus is described for the nondestructive, quantitative and/or qualitative determination of unirradiated fissionable materials, such as ^{235}U and ^{239}Pu, by measurement of neutron flux using proton recoil counting tubes filled with methane. The rod-shaped nuclear fuel samples and a number of the neutron detectors are disposed within a heavy moderator block in such a way that the longitudinal axes of the detectors and the samples extend parallel to one another. The detectors are distributed evenly around the circumference and whole length of the samples. (B.L.M.)

28989 NEW METHOD FOR SEPARATION OF AMERICIUM FROM CURIUM AND ASSOCIATED ELEMENTS IN THE ZIRCONIUM PHOSPHATE–NITRIC ACID SYSTEM. Moore, Fletcher L. (Oak Ridge National Lab., Tenn.). Anal. Chem.; 43: 487-9(Mar 1971).

The method is based on the negligible sorbability of americium(V) by zirconium phosphate from dilute nitric acid solutions and the strong sorbability of curium and other actinide elements, lanthanide elements, and cesium. The isotope dilution technique in conjunction with alpha spectrometry is used for an accurate determination of ^{243}Am. (D.P.O.)

28990 ^{14}C IN ALCOHOL. Kasida, Yosihiko (National Inst. of Radiological Sciences, Chiba, Japan). Hakko Kyokaishi; 28: No. 3, 76-83(Mar 1970). (In Japanese).

Since 1963 the concentration of ^{14}C in fermented alcohol has been measured by liquid scintillation counting because alcohol is easily soluble in liquid scintillator. As the alcohol is manufactured by fermentation of starch in sweet potato and of sugar in black syrup or "high-test" molasses, which is fixed from carbon dioxide by anabolism, it reflects the variation of ^{14}C in the biosphere introduced by nuclear weapons tests. The radiocarbon ^{14}C is explained in the viewpoint of nature, natural occurrence, artificial production by nuclear weapons tests, biological effects, and measurement using liquid scintillation counting. (auth) (Japan)

28991 DETERMINATION OF FREE ^{99m}Tc IN LABELED COMPOUNDS BY MEANS OF THIN LAYER CHROMATOGRAPHY. Mitta, A. E. A. (Argentine National Atomic Energy Commission, Buenos Aires); Alvarez, J.; Raban, P. Int. J. Appl. Radiat. Isotop.; 22: 223-5(Mar 1971).

A simple and rapid method, using thin-layer chromatography for determining the radiochemical purity of the most widely used ^{99m}Tc-labeled radiopharmaceuticals is described. The use of a scintillation camera is proposed for a faster radiometric evaluation of chromatograms. Through these procedures, radiochemical purity can be checked within 5 to 30 min of the preparation of the labeled compound. (auth) (UK)

28992 PLUTONIUM DETERMINATION IN SOIL BY LEACHING AND ION-EXCHANGE SEPARATION. Chu, Norton Y. (Atomic Energy Commission, New York). Anal. Chem.; 43: 449-52(Mar 1971).

A method to determine the levels of plutonium in 100-g samples of soil is described. The soil is leached with a mixture of nitric and hydrochloric acids in the presence of ^{236}Pu tracer. Plutonium in the leachate is converted to Pu(IV) with sodium nitrite and absorbed from 8N nitric acid onto Dowex 1–x4 ion exchange resin. Plutonium is removed from the exchanger and electroplated on a platinum disk. The plated disk is counted in an alpha spectrometer. The results obtained by leaching were found to be in good agreement with plutonium measurements of reference soils analyzed by complete solution of the sample. (D.P.O.)

28993 PAPER DISC ESTIMATION OF RADIOACTIVE RNA: STUDIES ON THE PRESENCE AND ELIMINATION OF METABOLICALLY GENERATED ARTIFACTS FROM LABELED PURINE AND PYRIMIDINE PRECURSORS. Yu, Fu-li; Feigelson, Philip (Columbia Univ., New York). Anal. Biochem.; 39: 319-21(Feb 1971).

Conventional usage of the filter-paper disc technique following in vivo hepatic incorporation of certain labeled pyrimidine and purine RNA precursors resulted in the presence of radioactivity on the filter disc in species other than RNA. Thus the filter paper disc technique, conventionally conducted, may be misleading. To eliminate artifacts, it is proposed that replicate filter discs be processed, one group passing through the usual cold TCA washings only, while a parallel group of replicate discs are heated for 20 min at 90°C in 5% trichloroacetic acid (TCA) to remove RNA. True RNA radioactivity is the difference of counts from the cold TCA precipitable material and the radioactivity remaining after hot TCA extraction. (auth)

28994 SIMPLE METHOD FOR COUNTING ^{14}C- AND ^{3}H-PROTEINS IN POLYACRYLAMIDE GELS. Helleiner, C. W.; Wunner, W. H. (Univ. of Glasgow). Anal. Biochem.; 39: 333-8(Feb 1971).

Slices of gels are treated with aqueous NH_4OH on glass fiber discs. Much of the protein diffuses out of the gel. The entire disc, including the remains of the gel slice, is then dried and counted in a toluene–PPO–POPOP scintillant. The principal advantages of this method lie in the simplicity of the equipment and technique and in the low cost of materials required. (D.P.O.)

28995 IMPROVED METHOD FOR HYDROXYPROLINE ANALYSIS IN TISSUE HYDROLYZATES. Switzer, Boyd R.; Summer, George K. (Univ. of North Carolina, Chapel Hill). Anal. Biochem.; 39: 487-91(Feb 1971).

The modifications of the procedures of Juva and Prockop and of Kivirikko, Laitinen, and Prockop have given quite satisfactory analysis of hydroxyproline radioactivity and content from only 1.0 mg of hydrolyzed tissue protein. The increased sensitivity of the modified method permits simultaneous determinations of other cell constituents as, for example, protein and DNA content of the same monolayer culture of fibroblasts, thus allowing for more meaningful studies on the mechanism of collagen biosynthesis in the tissue culture system. (auth)

28996 DETERMINATION AND DEGRADATION OF MICROQUANTITIES OF ACETATE. Schulman, Marvin; Wood, Harland G. (Case Western Reserve Univ., Cleveland). Anal. Biochem.; 39: 505-20(Feb 1971).

A rapid and specific spectrophotometric assay for microquantities of acetate is described. This method involves the conversion of acetate to citrate by CoA transferase, malate dehydrogenase, and citrate synthetase. The assay allows the determination of 5 to 60 nmoles of acetate. Procedures are described for determination of the total acetate present, the ^{14}C-acetate formed from labeled precursors, and the distribution of ^{14}C in the carbons of microquantities of acetate. The quantitative determination of both the total acetate and the ^{14}C-acetate is done by converting the acetate to citrate. Known tritiated acetate is added to the unknown ^{14}C-acetate prior to the enzymic conversion. From the amount of citrate and its ^{14}C and ^{3}H content, both the total acetate and the amount of ^{14}C in the acetate are calculated. The distribution of ^{14}C in the acetate is determined by conversion of the acetate to citrate and subsequent oxidation of the citrate to pentabromoacetone by treatment with $KMnO_4$ and KBr. A rapid semiquantitative assay of the ^{14}C in acetate may be accomplished under some circumstances by oxidation of the sample with $KMnO_4$ followed by ether extraction of the acetate. (auth)

28997 USE OF A MIXTURE OF PROTEINASE-FREE COLLAGENASES FOR THE SPECIFIC ASSAY OF RADIOACTIVE COLLAGEN IN THE PRESENCE OF OTHER PROTEINS. Peterkofsky, Beverly; Diegelmann, Robert (National Cancer Inst., Bethesda, Md.). Biochemistry; 10: 988-94(16 Mar 1971).

An assay procedure was developed in which radioactive collagen may be quantitatively measured even in the presence of large amounts of other proteins. This procedure makes use of bacterial collagenase to cleave the collagen into acid-soluble peptides. Commercially purified collagenase was found to contain at least two noncollagen-degrading proteinase activities, the major one being an SH-containing enzyme and the other containing no essential SH groups. By gel filtration on Sephadex G-200, the latter enzyme was completely removed from the collagenase activity and only trace amounts of the SH-containing enzyme remained. These small amounts of activity could be completely suppressed by the use of N-ethylmaleimide. The procedure used to measure proteolysis is relatively simple and rapid. Radioactive protein is precipitated from a homogenate with trichloroacetic acid after degrading aminoacyl-tRNA with RNase; the precipitate is redissolved and digested with collagenase under optimal conditions for 90 min. Noncollagenous protein is reprecipitated with acid and the radioactivity in peptides derived from collagen which remain in the supernatant solution is measured in a liquid scintillation spectrometer. (auth)

28998 STANDARD METHOD OF TEST FOR ATOM PER CENT FISSION IN URANIUM FUEL (RADIOCHEMICAL METHOD). ASTM E 219-69. Philadelphia; American Society for Testing and Materials (1969). 5p. Available from American Society for Testing and Materials, Philadelphia.

The determination of the U at. % fission that has occurred in U fuel from an analysis of the ^{137}Cs ratio to U ratio after irradiation is described. The method is applicable to high-density, clad U fuels (metal, alloys, or ceramic compounds) in which no separation of U and Cs has occurred. The fuels are best aged for several months after irradiation in order to reduce the 13-day ^{136}Cs activity. The fuel is dissolved and diluted to produce a solution containing a final concentration of U of 100 to 1000 mg U/l. The ^{137}Cs concentration is determined by ASTM method E 320, for Radiochemical Determination of Cesium-137 in Nuclear Fuel Solutions, and the U concentration is determined by ASTM method E 267, for Determination of Uranium and Plutonium Concentrations and Isotopic Abundances, ASTM method E 318, for Colorimetric Determination of Uranium in Aqueous Solutions, or ASTM method E 217, Test For Uranium by Controlled-Potential Coulometry. Calculations are given for correcting the ^{137}Cs concentration for decay during and after irradiation. The accuracy of this method is limited, not only by the experimental errors of the ^{137}Cs and U determinations, but also by the accuracy with which the fission yield and the half-life of ^{137}Cs are known. (B.L.M.)

28999 STANDARD METHOD OF TEST FOR RADIONUCLIDES OF RADIUM IN WATER. ASTM D 2460-70. Philadelphia; American Society for Testing and Materials (1970). 5p. Available from American Society for Testing and Materials, Philadelphia.

A method is described for separating and determining α-emitting Ra isotopes in water at concentrations of ~1 pCi/l. Ra is collected from H_2O by coprecipitation with mixed Ba and Pb sulfates. The precipitate is dissolved in ammoniacal EDTA, and the Ba and Ra sulfates are reprecipitated with acetic acid to separate them from Pb and other radionuclides. The precipitate is dried, weighed to determine chemical yield, and α counted to determine total disintegration rate of Ra isotopes. For a single operator the intrinsic precision of the method is ~5%. (B.L.M.)

29000 STANDARD METHOD OF TEST FOR RADIOACTIVE CESIUM IN WATER. ASTM D 2577-69. Philadelphia; American Society for Testing and Materials (1969). 6p. Available from American Society for Testing and Materials, Philadelphia.

Radioactive Cs in water in concentrations >1 μCi/l is determined by γ counting of a Cs-tetraphenylborate solution in amyl acetate. The method is limited to Cs isotopes of mass 134, 136, 137, and 138. Fission product extraction is prevented by the presence of EDTA in the solution to be extracted. Macro amounts of NH_4^+, Rb^+, K^+, Ag^+, and Na^+ interfere with the determination. After the extraction and measurement of the γ spectrum, the spectrum is resolved into its components by graphical or algebraic methods, and the count rate due to each isotope is obtained. For a single operator, precision of the method is better than ±1%. (B.L.M.)

29001 STANDARD METHODS FOR RADIOCHEMICAL DETERMINATION OF ^{137}Cs IN NUCLEAR FUEL SOLUTIONS. ASTM E 320-70. Philadelphia; American Society for Testing and Materials (1970). 6p. Available from American Society for Testing and Materials, Philadelphia.

Cesium-137 can be determined in solutions resulting from the dissolution of irradiated fuel elements for the determination of burnup by γ spectrometry after precipitation along with an inert Cs carrier as either the perchlorate or chloroplatinate. The elements or solution of elements must be allowed to cool for 130 days to allow for the decay of ^{86}Rb and ^{136}Cs. The presence of ^{134}Cs and ^{136}Cs also contributes a positive bias to the determination, and a computer correction for these is necessary. All radioassays were made with a γ spectrometer capable of better than 10% resolution of the 0.66-MeV ^{137m}Ba γ ray. In an interlaboratory comparison, the RSD was 1.4% for the chloroplatinate separation and 1.7% for the perchlorate separation. (B.L.M.)

29002 STANDARD METHODS FOR ANALYSIS OF ^{32}P. ASTM E 182-62. Philadelphia; American Society for Testing and Materials (1965). 2p. Available from American Society for Testing and Materials, Philadelphia.

Radiochemical purity and the absolute disintegration rate of ^{32}P preparations are determined. Other ASTM methods are referred to for the following determinations: ^{32}P activity by β counting, ^{35}S and other low-energy β contamination by aluminum absorption curve, γ contamination by scintillation counting, and chemical characteristics by chemical tests. The chemical tests include determination of heavy metal contaminants, free acid, total solids, and nonvolatile materials. (B.L.M.)

29003 STANDARD METHOD FOR MEASUREMENT OF ALPHA PARTICLE RADIOACTIVITY OF INDUSTRIAL WATER AND INDUSTRIAL WASTE WATER. ASTM D 1943-66. Philadelphia; American Society for Testing and Materials (1966). 7p. Available from American Society for Testing and Materials, Philadelphia.

Alpha activity for alpha emitters having energies above 3.9 MeV and at activity levels above 0.5 pCi/ml of water can be determined by direct measurement of the activity with a proportional or scintillation counter after the volume of the sample has been reduced by evaporation or some chemical means to yield a minimum weight of the material having a measurable α activity. (B.L.M.)

29004 STANDARD METHOD OF TEST FOR RADIOACTIVE BARIUM IN INDUSTRIAL WATER AND INDUSTRIAL WASTE WATER. ASTM D 2038-68. Philadelphia; American Society for Testing and Materials (1968). 8p. Available from American Society for Testing and Materials, Philadelphia.

XUM

Barium-139 and ^{140}Ba were determined in water at concentrations $>10^{-7}$ Ci/l by repeated precipitations with added Ba carrier as $BaCl_2$ from cold HCl solutions, final precipitation as $BaSO_4$ for determination of chemical yield, and counting of the barium by γ or β counters. Large amounts of stable Ba cause an overestimation of chemical yield. For a single operator, the precision of the method is better than 2% for a random counting error of <1%. (B.L.M.)

29005 STANDARD GENERAL METHODS FOR ANALYSIS OF RADIOISOTOPES. ASTM E 181-62. Philadelphia; American Society for Testing and Materials (1965). 11p. Available from American Society for Testing and Materials, Philadelphia.

Methods are described for the following tests for the analysis of radioisotopes: heavy metal spot test, gross β count, aluminum absorption curve, determination of γ impurities, free acid, total solids, and nonvolatile materials. The presence of heavy metals is indicated by their precipitation with H_2S. Beta particles having a maximum energy of 0.220 MeV or greater are counted, and the method is used primarily for radioisotope products of specific activities that are sufficiently high that the solids left on dried mounts are less than 1 mg/cm^2. The aluminum absorption curve covers the determination of the approximate energies and intensities of β spectra in radioactive sources. The γ-emitting impurities are determined using a γ spectrometer with a NaI(Tl) crystal. The free acid is defined as that acid exclusive of complexes or salts with inherent acid properties and is determined to ~0.5 pH unit by measuring a volume of the solution with a pH meter or pH paper. Total solids are those materials that do not evaporate or ignite at a temperature sufficient to evaporate the mineral acids, HCl and HNO_3, and is determined by weighing the residue after evaporation and drying at 110°C. Nonvolatile matter covers the determination of material that does not evaporate or ignite at a temperature sufficient to convert C to CO or to CO_2 and is determined by weighing the residue after ignition at 600°C. (B.L.M.)

29006 STANDARD METHOD OF TEST FOR RADIOACTIVE MANGANESE IN WATER. ASTM D 2039-69. Philadelphia; American Society for Testing and Materials (1969). 6p. Available from American Society for Testing and Materials, Philadelphia.

Manganese-54 and ^{56}Mn were determined in water at concentrations $>10^{-7}$ Ci/l by precipitating the radioactive Mn with a carrier as MnO_2, reprecipitation as manganese ammonium phosphate for calculation of chemical yield, and counting the final precipitate with a γ counter for ^{54}Mn and ^{56}Mn or with a β particle detector for ^{56}Mn only. Large amounts of Cl^- in the original sample make precipitation difficult, and stable manganese affects the calculation of the chemical yield. For random counting errors of <1%, the precision of the method with a single operator is better than 2%. (B.L.M.)

29007 STANDARD METHODS OF TEST FOR RADIOACTIVE IODINE IN INDUSTRIAL WATER AND INDUSTRIAL WASTE WATER. ASTM D 2334-68. Philadelphia; American Society for Testing and Materials (1968). 11p. Available from American Society for Testing and Materials, Philadelphia.

Three methods described for the determination of radioactive iodine (masses 129, 131, 132, 133, 134, and 135) in industrial water and industrial waste water are: (1) heterogeneous isotopic exchange of iodide with AgI, (2) distillation of elemental iodine into cold CCl_4, and (3) extraction of iodine isotopes into CCl_4. For all methods a complete oxidation-reduction cycle is carried out to ensure the desired chemical form of the iodine, and all methods are completed by the precipitation of iodine as AgI, which is then determined radiometrically. The single operator precision is within 2% when the random counting error is 1%. (B.L.M.)

29008 STANDARD METHOD FOR MEASUREMENT OF GAMMA RADIOACTIVITY OF INDUSTRIAL WATER AND INDUSTRIAL WASTE WATER. ASTM D 1690-61. Philadelphia; American Society for Testing and Materials (1967). 5p. Available from American Society for Testing and Materials, Philadelphia.

A method applicable to the absolute or relative determination of γ emitters in the energy range >0.1 MeV and in the concentration range of 10^{-2} to 10^{-5} μCi/ml of radioactively homogeneous water by scintillation counting is described. (B.L.M.)

29009 STANDARD METHOD FOR MEASUREMENT OF BETA PARTICLE RADIOACTIVITY OF INDUSTRIAL WATER AND INDUSTRIAL WASTE WATER. ASTM D 1890-66. Philadelphia; American Society for Testing and Materials (1966). 9p. Available from American Society for Testing and Materials, Philadelphia.

The method is suitable for either absolute or relative determinations of β emitters in industrial water and industrial waste water and is applicable to β emitters having maximum energies >0.1 MeV and at activity levels >0.5 pCi/ml of radioactively homogeneous water. Either proportional or Geiger–Mueller counters can be used to measure the β activity of the evaporated samples, but the proportional counter is preferable where a wide range of counting rates is encountered due to its shorter resolution time and greater stability. (B.L.M.)

29010 STANDARD METHOD OF TEST FOR ^{59}Fe IN WATER. ASTM D 2461-69. Philadelphia; American Society for Testing and Materials (1969). 5p. Available from American Society for Testing and Materials, Philadelphia.

Radioactive iron in water in concentrations above 0.1 μCi/l was determined by separating the ^{59}Fe from other activities by hydroxide precipitation along with nonradioactive Fe, by liquid–liquid extraction, and ion exchange and by counting with a γ counter or spectrometer or a β detector. Quantities of nonradioactive Fe > 0.2 mg in the sample taken and substances, such as tartrate, that prevent the initial precipitation will interfere with the determination. The method may be used for absolute measurements by calibrating the radiation detector with a standard ^{59}Fe solution or for relative measurements by comparison. For a single operator, the precision is within 3% when the random counting error is 1% or less. (B.L.M.)

Activation Procedures

Refer also to abstracts 29357 and 29391.

29011 (CEA-CONF-1747) FAST ANALYSIS BY 14-MeV NEUTRON ACTIVATION OF FLUORINE DEPOSITS ON THE VEGETATION IN A POLLUTED AREA. Garrec, J.-P.; Fourcy, A. (Commissariat a l'Energie Atomique, Grenoble (France). Centre d'Etudes Nucleaires). Jul 1970. 8p. (In French). (CONF-700951-2). Dep. NTIS (U. S. Sales Only).

From 3. European fluorine chemistry symposium; Aix-en-Provence, France (14 Sep 1970).

A method of detecting fluorine by activation with 14-MeV neutrons and gamma spectrometry is described. This method allows pollutions up to 2000 ppM to be measured. Several nuclear reactions occur when fluorine is irradiated with 14-MeV neutrons. The reaction $^{19}F(n,p)\,^{19}O$ was the most convenient for the determination of fluorine. The 200-keV gamma radiation from ^{19}O was measured (half-life 29sec). The characteristics of the analysis are as following: irradiation time, 1 min; radioactive decay, 30 sec; counting time, 30 sec; analysis, 5 min. The method is rapid and the sampling can be used for other investigations. (France)

29012 (GA-10276) APPLICATIONS OF NEUTRON ACTIVATION ANALYSIS IN SCIENTIFIC CRIME INVESTIGATION. Final Report. Lukens, H. R.; Schlesinger, H. L. (Gulf General Atomic, Inc., San Diego, Calif.). 2 Sep 1970. Contract AT(04-3)-167. 109p. Dep. NTIS.

An eight-year program to explore the usefulness of activation analysis in the field of criminalistics is reviewed. The sampling, activation analysis work, results, and statistical interpretation of results associated with representative population samples of paints, bullet lead, and gunshot residues are described. It was found that paint can be highly characterized by neutron activation analysis (NAA). A review of earlier NAA data regarding paper samples is included. Bullet lead analysis by instrumental NAA was shown to be useful, although to a considerably lesser degree than in the case of paint, paper, or gunshot residues. Recommendations to increase the usefulness of bullet lead comparisons by NAA are given. The probabilities associated with alternative interpretations of the NAA determination of gunshot residue elements in a given case are defined for each combination of a number of specified occupational categories and weapon calibers. The criminalist may now estimate the probabilities that each of alternative interpretations of NAA results in a given case involving one of the foregoing four materials are true or false, and in most instances such probabilities will highly favor one interpretation. (auth)

29013 (RLO-1750-81) WATER TRACING WITH SOLUBLE METAL CHELATES AND NEUTRON ACTIVATION ANALYSIS: A LABORATORY AND FIELD STUDY. Hanson, Peter James (Oregon State Univ., Corvallis. Dept. of Oceanography). 20 Oct 1969. 100p. Dep. NTIS.

Thesis.

Research on the application of soluble, metal chelates for water tracing using thermal neutron activation analysis for tracer determination led to the development of several tracers with promising solution stabilities (conservative behavior) and determination sensitivities. The solution stabilities of the ethylenediaminetetra-

acetic acid (EDTA) and the diethylenetriaminepentaacetic acid (DTPA) chelates of the activable elements Cr, Co, Eu, In, Sb, Sc, and Tb were evaluated in a series of laboratory radiotracer experiments conducted under simulated field conditions. They showed that chelation of metals produces highly conservative solution behavior, DTPA is generally better than EDTA for improving tracer behavior, nonchelated metals are rapidly sorbed onto sediments, and chelation reduces sorption of metals onto sediments. Field tests of EuDTPA, TbDTPA, InDTPA, and Rhodamine B fluorescent dye in a small eastern Washington stream demonstrated that the metal chelates have significantly improved solution stabilities in natural water compared to widely used Rhodamine B. Minimum detection levels in natural waters for the activable tracers were determined to be 0.075 ppB for Eu, 0.10 ppB for Th, and 0.55 ppB for In in comparison to 0.49 ppB for Rhodamine B. Associated determination uncertainties (one standard deviation) amount to ±12% for Eu at 12 ppB, ±12% for Tb at 13 ppB, and ±13% for In at 10 ppB compared to ±7.3% for Rhodamine B at 1 to 10 ppB. Activation procedures are feasible that decrease the minimum detection levels to 0.0015 ppB for Eu, 0.0019 ppB for Tb, and 0.0057 ppB for In in comparison to 0.075 ppB for Rhodamine B. Anion-exchange proved uniquely suited for recovery and concentration of metal-chelate tracers from natural water and as a low background irradiation and counting matrix. A method evaluation and economic analysis clarify the potential application of activable metal chelates for water tracing. (auth)

29014 DETERMINATION OF TRACE AMOUNTS OF GOLD IN NATURAL SWEET WATERS BY NONDESTRUCTIVE ACTIVATION ANALYSIS AFTER PRECONCENTRATION. Schiller, P.; Cook, G. B. (International Atomic Energy Agency, Vienna). Anal. Chim. Acta; 54: 364-8(Apr 1971).

Trace amounts of Au in natural sweet waters were determined by neutron activation and γ spectrometry after preconcentration by coprecipitation with iron(III) hydroxide, lead sulfide, or aluminum hydroxide or by separation with Dowex 1-X8 resin or with flexible polyurethane foam. Of the separation or preconcentration methods investigated, coprecipitation with lead sulfide or absorption on polyurethane foam was most satisfactory. (B.L.M.)

29015 GOLD CONTENT OF NATURAL WATERS IN COLORADO. Gosling, A. W. (Geological Survey, Helena, Mont.); Jenne, E. A.; Chao, T. T. Econ. Geol.; 66: 309-13(Mar-Apr 1971).

Neutron activation analysis of 67 samples of water draining from gold-barren and gold-enriched sedimentary, igneous, and metamorphic rocks of the Colorado Front Range reveals a relatively small range in total gold content (nondetectable to 150 nanograms per liter). "Solute" gold concentrations were generally higher than particulate gold concentrations and both were unrelated to rock or water types. The data suggest the occurrence of a spring flush out of "solute" gold in groundwater discharge during the snow-melt recharge period but indicate that direct hydrogeochemical prospecting for gold is unpromising. (auth)

29016 NEUTRON ACTIVATION ANALYSIS TECHNIQUE FOR NAIL SODIUM CONCENTRATION IN CYSTIC FIBROSIS PATIENTS. Johnson, G. Frank; Thompson, Max F.; Fetteroff, S.; Fasano, A. N. (Barney Children's Medical Center, Dayton, Ohio. Air Force Inst. of Tech., Dayton, Ohio). Pediatrics; 47: 88-93(Jan 1971).

Nail sodium values in mequiv/kg as determined by neutron activation analysis in a variety of normal, hospitalized, and cystic fibrosis children are reported. The elevated sodium values thus determined in cystic fibrosis indicate the usefulness of the method, though they are not in themselves diagnostic. The nails are porous to sodium and reflect the sweat sodium levels. The results are influenced by age, environment of the nail, and other disease conditions. (auth)

29017 PHOTONUCLEAR YIELDS IN BARIUM AND CESIUM WITH 18 ~ 75 MeV BREMSSTRAHLUNG AND THE DETERMINATION OF CESIUM WITH THE INTERNAL-REFERENCE METHOD. Tsai, Hui-tuh (Tohoku Univ., Sendai). Nippon Kagaku Zasshi; 92: 60-4(Jan 1971). (In Japanese).

Yields of the (γ,xnyp) reactions in barium and cesium were studied by irradiating with 18- to 75-MeV bremsstrahlung in order to determine the best conditions for cesium determination with the internal reference method. The radioactivities were measured on the cesium fractions after chemical separation with a lithium-drifted germanium diode. The accuracy of the method was assessed by processing a series of the synthetic mixtures of cesium and barium. When irradiated with 18-MeV bremsstrahlung, ^{136}Cs and ^{132}Cs were produced by the ^{137}Ba(γ,p) and the ^{133}Cs(γ,n) reactions, respectively. A good proportionality was obtained between activity ratios of ^{136}Cs(0.818-MeV) to ^{132}Cs(0.668-MeV) and weight ratios of cesium to barium. An amount of cesium down to about 0.8 μg can be determined with a relative error of within ±2.3% by this method. (auth)

29018 PHOTON ACTIVATION ANALYSIS FOR RUBIDIUM WITH AN INTERNAL-REFERENCE OF CESIUM. Tsai, Hui-tuh (Tohoku Univ., Sendai). Nippon Kagaku Zasshi; 92: 93-5 (Jan 1971). (In Japanese).

The determination of rubidium by activation with 30-MeV bremsstrahlung was studied with cesium as an internal reference element. Gamma activities of ^{84,86}Rb and ^{132}Cs produced by the (γ,n) reactions on the two elements were used for the determination; they were measured by a lithium drifted germanium detector. The accuracy of the method was examined by the use of a series of synthetic cesium–rubidium mixtures of known weight ratios. A good proportionality was observed between the weight ratio of rubidium to cesium and the photopeak-area ratio of ^{84}Rb (0.880-MeV) or ^{86}Rb(1.078-MeV) to ^{132}Cs(0.668-MeV). The sensitivity of this method was found to be about 20 μg of rubidium. (auth)

29019 NEUTRON ACTIVATION DETERMINATION OF Mo IN BIOLOGICAL MATERIALS. Atlavin, A. B.; Veveris, O. E.; Dubinskaya, N. A. (Inst. of Physics, Riga). Latv. PSR Zinat. Akad. Vestis, Fiz. Teh. Zinat. Ser.; No. 6, 3-9(1970). (In Russian).

A neutron activation procedure for the determination of Mo in fish and some other biological materials was developed. This procedure is based on resonance activation, Mo extraction with 8-mercaptoquinoline, and γ spectroscopy. The sensitivity of the method is 2.5 to $4 \cdot 10^{-3}$ ppM. (auth)

29020 COMPARATIVE STUDY OF THE ALUMINUM DETERMINATION IN AMMONIUM ACETATE SOIL EXTRACTS BY SPECTROPHOTOMETRY, ACTIVATION ANALYSIS, AND ATOMIC ABSORPTION. Khera, A. K. (Agricultural Coll. of Norway, Vollebekk); Steinnes, E.; Oeien, A. Acta Agr. Scand.; 20: No. 1, 33-4(1970).

A comparative study on the determination of aluminum in ammonium acetate soil extracts by three different methods based on spectrophotometry, activation analysis, and atomic absorption is presented. There is no significant difference between results obtained by different methods, and good precision is obtained for all methods. The relative merits of each method are briefly discussed. (auth)

29021 POSSIBLE PROBLEM IN DETERMINING OXYGEN IN SILICON BY FAST NEUTRON ACTIVATION ANALYSIS. Nass, H. W. (Union Carbide Corp., Tuxedo, N. Y.). J. Inorg. Nucl. Chem.; 33: 617-20(Mar 1971).

Large amounts of silicon (>0.5 g) in a sample for 14-MeV neutron analysis for oxygen can cause errors due to random coincidence summing of the γ rays from the induced ^{28}Al activity. A method of correcting for this interference is discussed, which allows the analysis of oxygen down to 75 μg in large amounts of silicon. (auth) (UK)

29022 DETERMINATION OF PLATINUM AND PALLADIUM IN GEOLOGICAL MATERIALS BY NEUTRON-ACTIVATION ANALYSIS AFTER FIRE-ASSAY PRECONCENTRATION. Rowe, J. J.; Simon, F. O. (Geological Survey, Washington, D. C.). Talanta; 18: 121-5(Jan 1971).

Fire-assay preconcentration followed by neutron activation analysis permits the determination of as little as 0.5 ppM of platinum and 0.5 ppM of palladium in a 20 g sample. Platinum and palladium are separated with carriers and beta-counted. Results for the platinum and palladium content of seven U.S.G.S. standard rocks are presented. (auth) (UK)

29023 ANALYSIS OF PLATINUM FOR CERTAIN ELEMENTAL IMPURITIES BY NEUTRON ACTIVATION. Abdel-Rassoul, A. A.; El-Shamy, H. K.; Madbouly, R. (Atomic Energy Establishment, Cairo). Talanta; 18: 101-5(Jan 1971).

Silver, ruthenium, cobalt, iron, zinc, cadmium, and mercury were determined in platinum by neutron activation analysis. The scheme developed requires the removal of the platinum matrix by reduction and the sequential separation of the elements by ion-exchange chromatography. The method is suitable for the simultaneous determination (at the ppM level) of these elements in milligram quantities of platinum. (auth) (UK)

29024 ACTIVATION ANALYSIS OF OXYGEN IN PHOSPHORUS WITH FAST NEUTRON. Nakane, Masanori; Ishikawa, Hiroshi; Miyake, Yoshizo (Government Industrial Research Inst., Osaka). Radioisotopes (Tokyo); 20: 7-11(Jan 1971). (In Japanese).

Fast neutron activation analysis of oxygen in phosphorus was investigated. The optimum discriminator level for the measurement of gamma rays from ^{16}N produced by (n,p) reactions was determined to be 4.0 MeV. The effective absorption coefficient for

red phosphorus was determined to be 0.81. The calibration curve made with graphite powder containing glucose showed good linearity in the range of 0 to 50 mg oxygen. An empirical formula of this calibration curve was y = 209.3 x + 190.8, the slope of which showed the sensitivity of the determination. The determination limit of the proposed method was 200 ppM oxygen for red phosphorus. The precision expressed in terms of the coefficient of variation was 3.5 to 1% with the sample containing 1.24 to 19.91 mg of oxygen. (auth)

29025 BORON–POLYETHYLENE IRRADIATION CONTAINERS FOR HIGH ENERGY NEUTRON ACTIVATION ANALYSIS. Jester, W. A.; Prasad, K. N. (Pennsylvania State Univ., University Park). Anal. Chem.; 43: 481-4(Mar 1971).

Two types of boron–polyethylene irradiation containers were constructed and their effects in reducing (n,γ) reactions tested. Polyethylene bricks, one containing 5% boron powder and a second containing 30% boron in the form of boron carbide powder, were used in constructing the rabbits. The results of testing these two rabbits on eight neutron reactions are given and the radiation effects on the boron–polyethylene material are discussed. (D.P.O)

29026 NEUTRON-ACTIVATION ANALYSIS IN THE MINERAL OIL INDUSTRY. I. PRINCIPLES AND TECHNIQUE. II. APPLICATIONS. Rodenbusch, Heinz; Prokop, Reiner. Erdoel Kohle, Erdgas, Petrochem.; 22: 384-8; 463-7(1969). (In German).

Techniques and applications of neutron activation analysis are reviewed with particular reference to the oil industry. Of the 27 elements listed that can be determined in, e.g., crude or refined oils or engine deposits, V, Na, Al, Cl and Zn are among those that can be determined nondestructively in concentrations down to 1 part per 10^9 within 40 min. (52 references.) (Anal. Abstr.)

29027 ON-LINE DATA PROCESSING IN ACTIVATION ANALYSIS. Tominaga, Hiroshi (Japan Atomic Energy Research Inst., Tokyo). Nippon Genshiryoku Gakkaishi; 13: 23-8(Jan 1971). (In Japanese).

The current status of progress in data processing in the field of activation analysis is reviewed. A clear trend is seen towards on-line and real time processing using a small computer and also towards time-sharing with a large computer. A description is given of recent developments in data aquisition and handling systems including programmed pulse height analyzers, and an example is given of a real time activation analysis system. Various computation methods for γ spectra in activation analyses are critically reviewed. (auth)

29028 DIGITAL METHODS OF PHOTOPEAK INTEGRATION IN ACTIVATION ANALYSIS. Baedecker, Philip A. (Univ. of California, Los Angeles). Anal. Chem.; 43: 405-10(Mar 1971).

The precision attainable by several methods of gamma photopeak integration was studied. The "total peak area" method, the methods proposed by Covell, Sterlinski, and Quittner, and some modifications of these methods were considered. A modification by Wasson of the total peak area method is considered to be the most advantageous because of its simplicity and the relatively high precision obtained. A computer routine for analysis of spectral data from nondestructive activation analysis experiments employing a Ge(Li) detector-spectrometer system is described. The routine processses the spectral data, applies appropriate corrections for decay, and provides a readout in concentration units. (auth)

29029 DETERMINATION OF ZINC IN PHARMACEUTICAL PRODUCTS BY NEUTRON ACTIVATION ANALYSIS. Margosis, Michel; Lambert, Joseph P. F. J. Pharm. Sci.; 60: 592-4(Apr 1971).

Nondestructive neutron activation analysis was applied as a rapid, efficient, and specific method for determination of zinc at either low or major concentration levels in various pharmaceutical products in bulk or dosage forms. This technique yielded results that compare well with more conventional methods and offers decided advantages over them. (auth)

29030 IODINE ANALYSIS OF BIOLOGICAL SAMPLES BY NEUTRON ACTIVATION OF ^{127}I, WITH SCINTILLATION COUNTING OF CHERENKOV RADIATION. Hoch, Frederic L.; Kuras, Rosemary A.; Jones, John D. (Univ. of Michigan, Ann Arbor). Anal. Biochem.; 40: 86-94(Mar 1971).

The naturally occurring isotope, ^{127}I, was measured by neutron activation, postirradiation extraction of ^{128}I plus ^{127}I (added carrier), and timed scintillation counting of the aqueous solution utilizing Cherenkov radiation. With extrapolation of the counts to zero time (end of irradiation) and measurement of chemical recovery by weighing of precipitated AgI, there are about 300 cpm above background per nanogram of I, in the range of 0 to 30 ng. The precision for samples of NH_4I is ±2.6% coefficient of variation. The accuracy is good when standards, rat liver mitochondria, or thyroxine solutions are measured both by activation analysis and by a chemical method. The use of Cherenkov radiation simplifies sample preparation, eliminates the need for a γ or β spectrometer, and acts as an energy band-pass. (auth)

29031 LIQUID–LIQUID EXTRACTION BEHAVIOUR OF MERCURY(II) AS CHLORIDE. Tandon, S. N.; Gupta, C. B. (Univ. of Roorkee, India). Talanta; 18: 109-12(Jan 1971).

In studies on neutron-activation determination of mercury, the solvent extraction behaviour of mercury(III) chloride with different organic solvents was determined. The effect of acidity, temperature, concentration of Hg(II), and other anions was studied. Radiochemical separations from ions such as Fe(III), Ga(III), As(III), and Sb(V) can be accomplished. Au(III) and Tl(III) interfere. (auth) (UK)

29032 DETERMINATION OF SCANDIUM, CHROMIUM, IRON, COBALT, ZINC, AND ANTIMONY IN DEPOSITS AND AIRBORNE PARTICULATES BY NEUTRON ACTIVATION ANALYSIS. Bando, Shoji; Imahashi, Tsuyoshi (Japan Atomic Energy Research Inst., Oarai). Jap. Anal.; 20: 49-56(Jan 1971). (In Japanese).

A method of neutron activation analysis was developed for determination of trace amounts of scandium, chromium, iron, cobalt, zinc, and antimony in deposits and airborne particulates. Collected samples in sealed quartz tubes were irradiated for 200 hours in a JRR-2 reactor (thermal neutron flux: 4×10^{13} n/cm^2 · sec) and were analyzed either by the nondestructive method, which used the Ge(Li) detector, or the chemical separation method, which used anion exchange separation followed by extraction with TTA–benzene and DDTC–carbon tetrachloride. The two results were in good agreement. Consequently, the nondestructive method with the Ge(Li) detector was recommended as an efficient means for analyzing many samples of deposits and airborne particulates at a time with high sensitivity. (auth) (Japan)

29033 SIMULTANEOUS DETERMINATION OF CHLORINE, BROMINE, AND IODINE IN SEDIMENTARY ROCKS BY NEUTRON ACTIVATION. Tajima, Eisaku; Akaiwa, Hideo (Gunma Univ., Maebashi, Japan). Radioisotopes (Tokyo); 20: 165-70(Apr 1971). (In Japanese).

A procedure was developed for the activation analysis. The crushed rock samples of 1 g were sealed in polyethylene vials and irradiated in the pneumatic tube of the JRR-2 reactor at a flux of 8×10^{13} n/cm^2/sec for 20 min. Samples and monitors were fused with sodium hydroxide in nickel crucibles in the presence of carriers. The fusion cake was dissolved in water and acidified to about 2M H_2SO_4. Fe^{3+} was added to oxidize I^- to I_2, and I_2 was distilled into sodium sulfite solution. $KMnO_4$ was then added to oxidize Br^- and Cl^- to Br_2 and Cl_2, and these elements were separated from the mother solution by distillation. Chemical yields were measured colorimetrically for iodine and potentiometrically for chlorine and bromine. Yields consistently ranged from 80% to 90%, and time required for chemical separation was about 50 min. (auth)

Inorganic, Organic, and Physical Chemistry

Refer also to abstracts 29174 and 29849.

Chemical Properties

Refer also to abstracts 29445, 31611, and 31612.

29034 (AERE-R-6141) SINGLE-CRYSTAL TARGETS OF RUBIDIUM URANYL NITRATE FOR THE ALIGNED FISSILE NUCLEI EXPERIMENT. Waldron, J. C. (Atomic Energy Research Establishment, Harwell (England)). Sep 1969. 13p. Dep. NTIS (U. S. Sales Only).

The growing of single crystals of rubidium uranyl nitrate and the cutting from them of selected faces that were coated with a thin layer of fissile isotope analog are reported. The crystallographic character of the substance is described. (auth)

29035 (NP-18736) PREPARATION AND PROPERTIES OF A CRYSTALLINE URANIUM(IV)–HYDRAZINE NITRATE COMPOUND. Eschrich, H.; Willeborts, G.; Hansen, P.; Kroebel, R.; Hild, W. (European Company for the Chemical Processing of Irradiated Fuels, Mol (Belgium)). Aug 1970. 47p. (ETR-253). Dep. NTIS (U. S. Sales Only).

A new crystalline compound containing tetravalent uranium,

hydrazine nitrate, nitric acid, and water was prepared. The greyish-green crystals represent a double salt of uranium(IV) nitrate and hydrazinium dinitrate, which may be formulated as $U(NO_3)_4 \cdot 4(N_2H_4 \cdot 2HNO_3) \cdot 2H_2O$ or possibly more correctly as $N_2H_5[U(NO_3)_5] \cdot 3(N_2H_4 \cdot 2HNO_3) \cdot 2H_2O$. Preparation methods and some properties of the new compound are described. (auth)

29036 OXIDATION-REDUCTION POTENTIAL ON PLATINUM ELECTRODE IN SOLUTIONS OF A MIXTURE OF SALTS OF URANIUM(VI) AND URANIUM(IV) AND EQUILIBRIUM CONCENTRATION OF URANIUM(V) IONS IN THE SYSTEM U(VI)–U(V)–U(IV). Stabrovskii, A. I. Elektrokhimiya; 6: 1471-7(Oct 1970). (In Russian).

A study was made of the effect of the acidity of sulfuric acid, nitric acid, and hydrochloric acid solutions of mixtures of salts of uranium(VI) and uranium(IV) on the equilibrium oxidation-reduction potential on a platinum electrode. The value of this potential depends on the acidity of the solutions studied. Polarographic analysis established that when solutions of salts of uranium(VI) and uranium(IV) are mixed, ions of uranium(V) are formed in the solutions of mixtures of these salts. The concentration of these ions depends primarily on the acidity of the solutions. The assumption that there are always ions of uranium(V) present in solutions of mixtures of salts of uranium(VI) and uranium(IV) was experimentally confirmed. The ions of uranium(VI) and uranium(V) determine the potential in the system U(VI)–U(V)–U(IV). The influence of ions of uranium(IV) on the oxidation-reduction potential on a platinum electrode is manifested only in that an increase or decrease in the concentration of these ions causes a corresponding change in the concentration of ions of uranium(V) in the solution. (JPRS)

29037 GASEOUS METAL NITRIDES. IV. THE DISSOCIATION ENERGY OF CERIUM MONONITRIDE. Gingerich, Karl A. (Texas A and M Univ., College Station). J. Chem. Phys.; 54: 3720-2(1 May 1971).

The CeN molecule has been identified in the vapor phase over a Au–Ce–CeS–BN–C mixture, using a combination of Knudsen effusion and mass spectrometric techniques. The third-law enthalpies for the reactions $2CeN(g) = N_2(g) + Ce_2(g)$, $2CeN(g) + Au_2(g) = 2CeAu(g) + N_2(g)$, $2CeN(g) = 2Ce(g) + N_2(g)$, and $2CeN(g) + 2Au(g) = 2CeAu(g) + N_2(g)$ were determined. Combined with published ancillary data, these reaction enthalpies yielded the following thermodynamic properties for gaseous CeN: $CeN(g) = Ce(g) + N(g)$; $D_0^\circ = 123.0 \pm 5.0$ kcal mol^{-1} or 514.6 ± 21 kJ mol^{-1} $2Ce(s) + 0.5\ N_2(g) = CeN(g)$; $\Delta H_{f,298}^\circ = 90.1 \pm 4.0$ kcal mol^{-1} or 377.0 ± 17 kJ mol^{-1}. (auth)

29038 OXIDATION OF NEPTUNIUM(V) BY AQUEOUS NITRIC ACID SOLUTIONS IN THE PRESENCE OF NITROUS ACID. Gourisse, D. (CEN, Fontenay-aux-Roses, France). J. Inorg. Nucl. Chem.; 33: 831-7(Mar 1971). (In French).

The equilibrium, $NpO_2^+ + \frac{1}{2}NO_3^- + \frac{3}{2}H^+ \rightleftharpoons NpO_2^{2+} + \frac{1}{2}HNO_2 + \frac{1}{2}H_2O$, was studied using TBP–30% dodecane under inert atmosphere to avoid disturbances resulting from nitrous acid decomposition. Th reaction is slightly endothermic ($\Delta H \simeq 3.95$ kcal. mole^{-1}). The apparent mass action law constant increases with acidity, this effect resulting from an increase in entropy. At equilibrium, the apparent distribution coefficients of neptunium are poorly affected by temperature variations. The choice of optimal conditions for neptunium extraction depends mainly on the kinetics of oxidation. (auth) (UK)

29039 MASS-SPECTROMETRIC INVESTIGATION OF C_2-EXCHANGE REACTIONS OF LANTHANUM, CERIUM, PRASEODYMIUM, AND NEODYMIUM WITH THEIR DICARBIDES. Filby, E. E.; Ames, L. L. (New Mexico State Univ., Las Cruces). High Temp. Sci.; 3: 41-8(Jan 1971).

The Knudsen-cell mass spectrometric method was used to study the C_2-exchange reactions of the type $M_aC_2(g) + M_bC_2(g) = M_aC_2(g) + M_dC_2(g)$ where M_a and M_b are Ce–La, Ce–Pr, Pr–Nd, and Ce–Nd. The dissociation energies of the gaseous dicarbides were determined from the enthalpies of the exchange reactions coupled with a known value (162 ± 2 Kcal/mole) for the CeC_2 dissociation energy. The dissociation energies were found to be 160 ± 3 Kcal/mole for LaC_2, 151 ± 3 Kcal/mole for PrC_2 and 144 ± 3 Kcal/mole for NdC_2 and are shown to have an approximately constant difference between them and the dissociation energies of the analogous rare earth monoxides. (auth)

Isotope Effects and Exchange

Refer also to abstracts 29153, 29161, 29167, and 29925.

29040 PHOSPHORESCENCE OF SOME DEUTERIUM-SUBSTITUTED PHENYLACETYLENES. Singh, H.; Laposa, J. D. (McMaster Univ., Hamilton, Ont.). J. Lumin.; 3: 287-301(Jan 1971).

Vibrational analyses are presented for the phosphorescence spectra of C_6H_5CCH, C_6H_5CCD, C_6D_5CCH, and C_6D_5CCD in polycrystalline isopentane matrices at 77°K. A relatively long progression in the totally symmetric C–C ring stretching mode is interpreted as indicative of a planar, nonregular-hexagon benzene ring geometry of the lowest triplet state. The variation of the percent polarization of the 0,0 band phosphorescence with excitation into the 0,0 regions of the first two singlet–singlet absorptions signifies that the lowest triplet state of the phenylacetylenes is $^3A_1(^1L_a)$. (auth)

29041 ISOTOPE EFFECT OF ELECTROMIGRATION IN SOME SOLID ALKALI HALIDES. Morimoto, Takeshi; Okada, Isao; Saito, Nobufusa (Tokyo Univ.). Z. Naturforsch.; 26a: 300-7(Feb 1971).

The isotope effect of electromigration in some solid alkali halides was determined in their intrinsic ionic conductivity region. The external cationic mass effect (i.e., relative difference in cationic mobility/relative difference in mass) of lithium fluoride, chloride, bromide, and iodide and potassium chloride was −0.243, −0.207, −0.195, −0.190, and −0.254, respectively, at 750, 540, 470, 370, and 600°C, respectively. No difference of the mass effect was found between polycrystalline and single crystal potassium chloride. When the available data for the mass effect of the solid salts are plotted against the activation energy for electric conductance, there is a tendency for the mass effect to increase as the activation energy increases. (auth)

29042 RELATIVE THERMAL STABILITIES OF COPPER (II) SULFATE PENTAHYDRATE AND BARIUM CHLORIDE DIHYDRATE COMPARED TO THEIR DEUTERIUM OXIDE ANALOGS. Garn, Paul D. (Univ. of Akron, Ohio). pp 921-8 of Thermal Analysis, Vol. 2. /Schwenker, Robert F. Jr. (ed.). New York; Academic Press, Inc. (1969).

From second international conference on thermal analysis; Worcester, Mass. (18 Aug 1968). See CONF-680851.

Study of the literature on hydrated salts and on the effect of isotopic substitution led to a hypothesis that crystalline hydrates would have thermal stabilities different from their deuterium oxide analogs, and that the hydrates might be either more or less stable than their heavy-water counterparts. Although the general isotope effect and heat of solution data would suggest that the heavy-water solvate should be more stable, the two cases tested did not behave in this manner. Barium chloride dihydrate and copper sulfate pentahydrate are more stable, thermally, than their deuterium oxide analogs. (auth)

29043 RATE OF THE REACTION OF ATOMIC HYDROGEN WITH ACETYLENE. II. THE REACTIONS $D + C_2H_2$ AND $H + C_2D_2$. Hoyermann, K.; Wagner, H. Gg.; Wolfrum, J.; Zellner, R. (Univ., Goettingen, Ger.). Ber. Bunsenges. Phys. Chem.; 75: 22-7(Jan 1971). (In German).

The reactions of D and H atoms with C_2H_2 and C_2D_2, respectively, were investigated in an isothermal flow system coupled to an ESR and mass spectrometer. By simultaneously determining the H and D atom concentration using ESR spectroscopy, the rate constants of the isotopic exchange reactions $D + C_2H_2 \rightarrow C_2HD + H$ and $H + C_2D_2 \rightarrow C_2HD + D$ were determined in the temperature range 200 to 465°K and 300 to 470°K, respectively: $k_1 = 3.1 \cdot 10^{13} \exp[(-3700 \pm 200$ cal mol^{-1}/RT)] cm^3/mol sec and $k_3 = 2 \cdot 10^{13} \exp[(-5300 \pm 500$ cal mol^{-1}/RT)] cm^3/mol sec. (auth)

29044 MICROWAVE SPECTRA OF DEUTERATED GLYCOLALDEHYDES. Marstokk, K.-M.; Moellendal, Harald (Univ. of Oslo). J. Mol. Struct.; 7: 101-9(Jan 1971).

The microwave spectra of $CH_2OD–CHO$, $CH_2OH–CDO$, CHDOH–CHO, and CHDOH–CDO were measured and a partial substitution structure of glycolaldehyde calculated. The rotational constants of the parent and the deuterated species were found to be insufficient to yield a complete structure of the molecule. (auth)

29045 ABSOLUTE INTENSITIES AND PRESSURE EFFECTS IN THE INFRARED FUNDAMENTAL BANDS OF METHANE AND ITS DEUTERATED SPECIES. Cowan, Victor Michael. Toronto; Univ. of Toronto (1969). Available from National Library of Canada at Ottawa.

Thesis.

The infrared fundamental bands of methane and its deuterated species were examined in dilute mixtures with helium, at densities from ~100 to ~1000 amagat. There are a total of 24 active fundamentals for CH_4, CH_3D, CH_2D_2, CD_3H, and CD_4, although in some cases only groups of overlapping bands can be observed. For the thirteen separate bands or groups of bands, the density variation of the spectral profiles and the integrated intensities

were studied. The contours were corrected for slit-width effects by an iterative procedure. There is progressive disappearance of the rotational structure with increasing density, until at the highest pressures only broad, almost featureless bands remain. The C–H stretching mode intensities lie in the approximate ratio 4 : 3 : 2 : 1 : 0 for CH_4, CH_3D, CH_2D_2, CD_3H, and CD_4; for the C–D stretching modes, the ratio is 0 : 1 : 2 : 3 : 4. The thirteen observed intensities are interpreted in terms of a two-parameter bond-dipole model for infrared absorption. The best-fit values of the C–H (or C–D) bond dipole and its rate of change with bond length are found to be $\mu_0/r_0 = \pm 0.3167$ debye/Å, $(\partial\mu/\partial r)_0 = \mp 0.6600$ debye/Å. The overall RMS deviation between the best-fit intensities and experiment is 5.5%. The experimental C–H stretching intensities are higher than the corresponding best-fit values, whereas the C–D intensities are lower. This is ascribed to the neglect of mechanical and electrical anharmonicity in the two-parameter model. Values of dispersion half-width are obtained by fitting broadened line spectra to the observed profiles. The broadening coefficients range from 0.036 cm^{-1}/amagat for CH_4 to 0.024 cm^{-1}/amagat for CD_4. The density variation in the profiles is interpreted using a rotational autocorrelation function approach. Calculations are presented of the correlation functions for free spherical and symmetric rotors. The effects of collisions are then calculated in an impact approximation. The models of m- and j-diffusion for rotational motion, developed by Gordon, are generalized to the case where either m- or j-diffusion may occur in a given collision. The results, while quantitatively incorrect, display many of the features of the observed autocorrelation functions. The density variation of Γ with ρ is discussed from the point of view of interference between the free-molecule transition dipole and the moment induced by the overlap interaction in close collisions. (Diss. Abstr. Int., B)

29046 DEUTERIUM ISOTOPE EFFECTS IN THE ATTACHMENT OF $Hg(6^3P_0)$ TO AMMONIA, AND MEASUREMENTS OF THE LIFETIMES OF THE STABILIZED COMPLEXES. Koskikallio, J.; Callear, A. B.; Connor, J. H. (Physical Chemistry Lab., Cambridge, Eng.). Chem. Phys. Lett.; 8: 467-9(1 Mar 1971).

From observations of the decay of the luminescence following the Hg-flash-photosensitized reactions of NH_3 and ND_3, rate coefficients for relaxation of $Hg(6^3P_0)$ were measured in bimolecular collisions and in termolecular collisions chaperoned by N_2 and ammonia. The lifetimes of the stabilized Hg–ammonia complexes were also determined. Marked isotope effects were found both in the bi- and termolecular rate coefficients. (auth)

29047 RESONANCE RAMAN EFFECT IN MnO_4^- WITH 5145 A LASER EXCITATION. Kiefer, W.; Bernstein, H. J. (National Research Council of Canada, Ottawa). Chem. Phys. Lett.; 8: 381-3(1 Mar 1971).

Resonance Raman scattering of the MnO_4^- ion in H_2O and D_2O solutions is reported. Several overtones of the $\nu_1(A_1)$ mode of this ion (T_d symmetry) and combination tones $n\nu_1(A_1) + \nu_3(F_2)$ were observed. From the wavenumbers of the overtones of ν_1 the dissociation energy of the MnO_4^- ion was estimated. (auth)

29048 GENERAL ACID CATALYSIS OF ACETAL HYDROLYSIS. THE HYDROLYSIS OF SUBSTITUTED BENZALDEHYDE DI-TERT-BUTYL ACETALS. Anderson, Edwin; Fife, Thomas H. (Univ. of Southern California, Los Angeles). J. Amer. Chem. Soc.; 93: 1701-4(7 Apr 1971).

The rates of hydrolysis of a series of substituted benzaldehyde di-tert-butyl acetals were measured in water at 25°. A pronounced general acid catalysis is observed in the hydrolysis of these compounds. Steric strain in the ground state which is relieved in the transition state is undoubtedly important in leading to general acid catalysis. The value of ρ for acetic acid catalyzed hydrolysis is −2.0 while that for hydronium ion catalysis is −4.0. The D_2O solvent isotope effects were observed; hydrolysis was much slower in D_2O than in H_2O. A Brønsted plot of log k_{HA} vs. the pK_a of the catalyzing acid in the hydrolysis of benzaldehyde di-tert-butyl acetal has a slope, α, of −0.6. The point for hydronium ion fits on this line with the buffer acids. (auth)

29049 STERIC FACTORS IN THE CATIONIC REARRANGEMENT OF SUBSTITUTED CYCLOBUTANES. Lillien, I.; Handloser, L. (Marshall Univ., Huntington, W. Va.). J. Amer. Chem. Soc.; 93: 1682-93(7 Apr 1971).

The solvolysis and deamination of the cis and trans isomers of 3-methyl- and 3-isopropylcyclobutyl derivatives are discussed and compared. The data support a mechanism which has as its rate-determining step the concerted and stereospecific rearrangement of the cyclobutyl precursor to an intermediate (2-alkylcyclopropyl)-carbinyl ion pair. Differences in solvolytic rates are related to the steric effect of the substituent on the orbital opening and overlap modes involved in this process. The kinetic effect of α-deuterium substitution is normal for both cis- and trans-3-isopropylcyclobutyl solvolysis, and larger for cis. These facts are consistent with a small charge on the 1-carbon of the cyclobutane encountered in a concerted rearrangement, and hindrance to anchimeric assistance in the cis isomer. Differences in isomeric product distribution are ascribed to differences in the behavior of two primary isomeric (2-alkylcyclopropyl)carbinyl intermediates; rationales are suggested. The specificity of the deuterium label position observed in solvolysis and deamination of 1-labeled cyclobutane derivatives supports this sequential genesis of products from the cyclobutanes; further confirmation is provided by solvolysis of the appropriately substituted cyclopropyl compounds. Major product differences are observed in solvolysis vs. deamination of the cis-, but not the trans-cyclobutyl compounds. A secondary cyclopropylalkylcarbinyl intermediate, which results from apparently favored transformation of the cis-(2-alkylcyclopropyl)carbinyl precursor, is implicated as the source of such differences. These product variances appear due to the inability of this secondary cation to escape solvent capture and function as an intermediate in deamination of both isomers, and in trans solvolysis. (auth)

29050 TRANSANNULAR HYDRIDE SHIFTS. MECHANISTIC STUDY IN THE LONGIFOLENE SERIES. Stehelin, Liliane; Lhomme, Jean; Ourisson, Guy (Louis Pasteur Univ., Strasbourg). J. Amer. Chem. Soc.; 93: 1650-7(7 Apr 1971).

A 1 : 5 hydride shift occurs simultaneously with neopentylic rearrangement during the ethanolysis of medium-size ring bromides in the longifolene series. Product analyses and the results of kinetic studies, including kinetic isotope effect studies, indicate the occurrence of two competitive mechanisms with distinct rate-determining steps. When transannular hydride migration predominates, the reaction is accelerated. This is interpreted in terms of σ(C–H) assistance in the rate-determining step of the transannular reactions. (auth)

29051 CHEMICAL EVOLUTION OF A NITROGENASE MODEL. II. MOLYBDATE–CYSTEINE AND RELATED CATALYSTS IN THE REDUCTION OF ACETYLENE TO OLEFINS AND ALKANES. Schrauzer, G. N.; Doemeny, P. A. (Univ. of California, San Diego, La Jolla, Revelle Coll., La Jolla, Calif.). J. Amer. Chem. Soc.; 93: 1608-18(7 Apr 1971).

The catalytic reduction of acetylene to ethylene by molybdenum complexes with sulfur-containing ligands (e.g., cysteine or thioglycerol) and $NaBH_4$ or $Na_2S_2O_4$ as the reducing agent strikingly resembles the enzymatic reduction of acetylene by nitrogen-fixing enzymes. Under these conditions, molybdenum exhibits the highest catalytic activity of all metals. The catalytically active species are presumably Mo(IV)–thiol complexes in which two cis positions are available for the binding of acetylene in the side-on fashion. The kinetic H/D effects on the rate of C_2H_4 and C_2H_6 production are tabulated. Under certain conditions acetylene is also reduced to ethane. In this case the reaction apparently involves binuclear catalytically active species. As in the enzymatic reaction the stereochemical course of the reduction is predominantly cis and is significantly stimulated by biological phosphorylating agents such as ATP. Higher alkynes, e.g., propyne, propargyl alcohol, and 2-butyne are also reduced by the model systems. In the absence of substrate the molybdenum–thiol complexes catalyze hydrogen evolution which is stimulated by ATP, unaffected by CO, and inhibited by acetylene. On the basis of these analogies, we conclude that the reactions of acetylene with nitrogenase occur at a molybdenum-containing binding site of the Mo–Fe protein. Iron, the more abundant metal in nitrogenase, does not seem to participate directly in the binding and the reduction of acetylenic substrates, but may function as an electron-transfer catalyst. (auth)

29052 ZERO-POINT AVERAGE STRUCTURE OF CHLORINE DIOXIDE. A COMPARISON OF ELECTRON-DIFFRACTION AND MICROWAVE RESULTS. Clark, A. H. (Univ. of Manchester, Eng.). J. Mol. Struct.; 7: 485-90(Feb-Mar 1971).

Comparison of the r_α^0 values for the distances $r_{C\cdots O}$ and $r_{O\cdots O}$ with the microwave zero-point average r_z values reveals an excellent consistency between the two sets of results. The e.s.d.'s originally assigned to the electron-diffraction r_a parameters were 0.003 Å, and 0.022 Å, respectively, but the observed deviations of the r_α^0 values from the microwave r_z results are approximately 0.001 Å for both distances making these standard deviations seem somewhat pessimistic. The effects of ^{37}Cl on the microwave spectra and moments of inertia of the molecules are reported. (auth)

29053 DECAY TIMES, INTENSITIES, AND THEIR TEMPERATURE VARIATION OF LUMINESCENCE OF AQUEOUS AND DEUTERATED SOLUTIONS OF EUROPIUM ION. Pant, D. D.; Bhatt, B. C.; Sanwal, D. N. (D.S.B. Government Coll., Naini Tal, India). Indian J. Pure Appl. Phys.; 8: 505-6(Aug 1970).

The decay times and relative intensities of Eu^{3+} luminescence in H_2O and D_2O solutions were carefully studied with a view to resolving the controversy in the results reported by J. L. Kropp and M. W. Windsor [J. chem. Phys., 39(1963), 2769; 42(1965), 1599] and those of P. K. Gallagher [J. chem. Phys., 43(1965), 1742]. The results definitely disagree with those of Gallagher. The dependence of decay times and intensities on H_2O concentration indicates the Stern-Volmer mechanism of quenching. The temperature dependence of these parameters shows a λ-type behaviour for solutions in D_2O-H_2O mixtures. (auth)

29054 HYDROGEN ABSTRACTION FROM METHYL FORMATE BY METHYL RADICALS. Donovan, T. R.; Dorko, W.; Harrison, A. G. (Univ. of Toronto). Can. J. Chem.; 49: 828-32(15 Mar 1971).

The reactions of CH_3 radicals with methyl formate and CD_3 radicals with methyl formate and methyl formate-d were studied. The CH_3 and CD_3 radicals were produced by the photolysis of acetone and acetone-d. The Arrhenius parameters (log A, A in 1 $mole^{-1}$ s^{-1}; E, in kcal $mole^{-1}$) for hydrogen abstraction are given. (auth) (Canada)

29055 INFRARED SPECTRUM OF SOLID AND MATRIX-ISOLATED H_2O_2 AND D_2O_2. Lannon, Joseph A.; Verderame, Frank D.; Anderson, Robert W. Jr. (Pitman-Dunn Research Labs., Philadelphia). J. Chem. Phys.; 54: 2212-23(1 Mar 1971).

The infrared spectrum between 4000 and 200 cm^{-1} of polycrystalline D_2O_2 at −190°C corresponds to that of H_2O_2 indicating that the crystal structure and spiral chain coupling of excitons for each of the six normal modes are the same in D_2O_2 as in H_2O_2. At temperatures near −100°C the crystal spectra of both H_2O_2 and D_2O_2 change with time on CsI and CsBr cold windows. The greatest change observed is that the crystal bands arising from torsion disappear and are replaced by two other bands about 100 cm^{-1} lower in frequency. Also, the exciton bands in the stretching and bending regions lose their fine structure and shift to lower frequency indicating that the peroxides actually dissolve into the salt windows without decomposition at these low temperatures. The spectra of H_2O_2 and D_2O_2 matrix isolated in argon and nitrogen at about 8°K are also reported. Features of these spectra include extraordinarily broad bands in the torsional region, ν_4, in both nitrogen and argon. The relative intensities of the triplet in argon change reversibly with temperature. In argon matrices, spectra of the torsional region indicate that the motion of the peroxide in the cavity is similar to that in the gas phase. The techniques of earlier workers for analysis of hindered internal rotation were applied to calculate energy levels for the matrix-isolated molecule. In argon the triplet in the torsion band is explained in terms of combination sum and difference bands of the internal rotation with translational or librational modes. In a nitrogen matrix, the spectra indicate that the internal rotation is much more hindered. The breadth of the band is explained in terms of a coupling between the hindered internal rotation and translation and/or librational motion as well as combination sum and difference bands with these motions. (auth)

29056 DEUTERIUM EFFECTS ON BINDING OF REDUCED COENZYME ALCOHOL DEHYDROGENASE ISOENZYME EE. Bush, Karen; Mahler, H. R.; Shiner, V. J. Jr. (Indiana Univ., Bloomington). Science; 172: 478-80(30 Apr 1971).

Determination of dissociation constants by two different methods yield the following mean values in 20 millimolar phosphate at pH 7.0 and 25°C: 0.27 micromolar for reduced nicotinamide adenine dinucleotide (NADH); 0.29 micromolar for NADH with deuterium in the nicotinamide 4-B position (B-NADD); and 0.46 micromolar for NADH with deuterium in the nicotinamide 4-A position (A-NADD). These results indicate that dehydrogenases are capable of recognizing and distinguishing the appropriate hydrogen in the coenzyme already in the initial binding reaction. (auth)

29057 KINETICS OF THE $^{15}N/^{14}N$ ISOTOPIC EXCHANGE BETWEEN NITRIC OXIDE AND NITRIC ACID. Axente, D.; Piringer, O. (Inst. of Atomic Physics, Cluj). J. Inorg. Nucl. Chem.; 33: 665-71(Mar 1971).

The kinetics of the isotopic exchange between nitric oxide and nitric acid, the basic reaction of the ^{15}N separation by the Spindel–Taylor method, was measured. The experimental data were obtained by introducing nitric oxide of natural abundance (0.365 percent ^{15}N), at atmospheric pressure into a glass contactor, containing nitric acid (0.2 to 3.2 M) solution labeled with 1.55 percent ^{15}N. The solution was magnetically stirred, at 20°C. The isotopic exchange between nitric oxide and nitric acid being a fast reaction, the influence of the rate of gas diffusion into liquid on the over-all reaction rate, was taken into account. Results indicated that the exchange reaction between nitric oxide and nitric acid is of the second order, related to the nitric acid concentration. The rate constant was determined, and a mechanism for the exchange reaction was proposed, nitrogen dioxide playing the part of a catalyst. On the basis of the rate constant the HETP for a separation column was calculated. (auth) (UK)

29058 DISTRIBUTION OF REACTION PRODUCTS (THEORY). VII. $D^+ + H_2 \rightarrow DH + H^+$ USING AN AB INITIO POTENTIAL-ENERGY SURFACE. Csizmadia, I. G.; Polanyi, J. C.; Roach, A. C.; Wong, W. H. (Univ. of Toronto). Can. J. Chem.; 47: 4097-9(1 Nov 1969).

A three-dimensional classical trajectory calculation was made of the dynamics of the reaction $D^+ + H_2 \rightarrow DH + H^+$. In contrast to earlier trajectory studies the potential-energy surface was obtained ab initio. Consequently, the results have predictive interest. (auth) (Canada)

29059 ISOTOPE EFFECTS IN AUTOXIDATION. X. DERIVATOGRAPHIC AND CONDUCTOMETRIC INVESTIGATION OF DEUTERATED POLYVINYL CHLORIDE. Trauzeddel, R.; Huebner, H. (Zentralinstitut fuer Isotopen- und Strahlentechnik, Leipzig). Isotopenpraxis; 7: 12-14(Jan 1971). (In German).

The difference in the stability of deuterated and ordinary PVC was compared in a wide range of temperature. The measurements were made in a nitrogen and air atmosphere. The HCl elimination is discussed in detail. (auth)

29060 L-AMINO ACID OXIDASE. II. DEUTERIUM ISOTOPE EFFECTS AND THE ACTION MECHANISM FOR THE REDUCTION OF L-AMINO ACID OXIDASE BY L-LEUCINE. Page, David S.; Vanetten, Robert L. (Purdue Univ., Lafayette, Ind.). Biochim. Biophys. Acta; 227: 16-31(Jan 1971).

A study was made of the effect of pH and p^2H upon the rate of reduction of L-amino acid oxidase by L-leucine and by DL-[α-^{2}H]leucine. The reduction process was studied with the system in turnover using a Clark oxygen electrode and also with the anaerobic combination of enzyme and substrate using stopped-flow techniques. A striking pH-dependent deuterium kinetic isotope effect was observed, which is consistent with a change in rate determining step as the pH is changed over the range 6 to 9. A deuterium solvent isotope effect was also observed and shown to be the result both of an upward shift of 0.6 unit in the pK_a of an active site group and of additional effects on the specific rates of the component steps of the reduction process. The experimental results are consistent with the interpretation that a proton transfer step is mediated by a basic group on the enzyme during the reduction reaction. The basic group is tentatively identified as a histidyl residue. The reduction process involves the very rapid formation of a transient, spectrophotometrically distinct intermediate followed by the rapid decay of this intermediate into the fully reduced enzyme, consistent with earlier reports. In addition to the rapid decay, a much slower decay was noted, which may be due to the dissociation of an imidazolium ion in the hindered environment of the active site to form the catalytically active charge form of the enzyme–substrate complex, or to the presence of isoenzymes possessing different catalytic specificities. An action mechanism is presented, which is consistent with the experimental data for the reduction reaction. (auth)

29061 MICROBIAL OXIDATION OF p-DIETHYLBENZENE. Tanabe, Masato; Dehn, Robert L.; Kuo, Mau H. (Stanford Research Inst., Menlo Park, Calif.). Biochemistry; 10: 1087-90 (16 Mar 1971).

A Pseudomonas strain isolated from a fuel storage tank oxidizes p-diethylbenzene exclusively to the monocarboxylic acid, p-ethylphenylacetic acid. Deuterium labeling was used to elucidate the oxidation mechanism. Deuterium labeled p-diethylbenzenes as substrates show an isotope effect of $k_H/k_D = 1.7$. Retention of the deuterium atoms on the α carbon indicates the major pathway of oxidation involves direct terminal oxidation and not dehydrogenation followed by hydration. (auth)

29062 PRESSURE JUMP AND ISOTOPE REPLACEMENT STUDIES OF ACETYLENE HYDROGENATION ON PALLADIUM SURFACE. Inoue, Yasunobu; Yasumori, Iwao (Tokyo Inst. of Tech.). J. Phys. Chem.; 75: 880-7(1 Apr 1971).

The catalytic activity of cold-worked palladium foil for acetylene hydrogenation was examined. From the change in the activity with annealing, the presence of two kinds of active sites were predicted. One was characterized by a high activity of the foil annealed at 200°C (Catalyst L) and another by the low activity of the foil annealed at 800°C (Catalyst H). In order to investigate the kinetic behavior of the reaction on these catalysts, pressure jump and hydrogen–deuterium replacement techniques were applied in addition to the conventional kinetic study. When the hydrogen pressure was jumped up or down, during the hydrogenation on Catalyst H, a transition period of about 1 hr in the rate change appeared

XUM

until the reaction attained a final steady state. Similar relaxation on the rate change due to an isotopic effect was also found when hydrogen was replaced immediately by deuterium. On the other hand, no time lag for the reaction on Catalyst L was observed. Mechanisms for the reaction on these catalysts are developed and it was concluded that the reactive hydrogen in the acetylene hydrogenation was in an absorbed state on Catalyst H and in an adsorbed state on Catalyst L. This conclusion was also supported from the deuterium distributions in ethylene produced. The relaxation phenomenon of the rate can be interpreted on the basis of the role of Catalyst H as the reservoir of absorbed hydrogen. (auth)

29063 STUDIES OF SURFACE REACTIONS OF NO BY ISOTOPE LABELING. II. DEUTERIUM KINETIC ISOTOPE EFFECT IN THE AMMONIA–NITRIC OXIDE REACTION ON A SUPPORTED PLATINUM CATALYST. Otto, K.; Shelef, M.; Kummer, J. T. (Ford Motor Co., Dearborn, Mich.). J. Phys. Chem.; 75: 875-9(1 Apr 1971).

The existence of a kinetic isotope effect was established when substituting ND_3 for NH_3 in the reaction between ammonia and nitric oxide over a supported Pt catalyst at 202.5°C. The ratio of the overall reaction rates at this temperature is $r_{NH_3}/r_{ND_3} \simeq 1.4$. The reaction of NH_3 (or ND_3) with NO is of zero order indicating that the rate-determining step occurs in the adsorbed layer. This step is interpreted as the surface dissociation of ammonia, $(NH_3)_{ads} \rightarrow (NH_2)_{ads} + (H)_{ads}$. (auth)

29064 ION-MOLECULE COLLISION PROCESSES. Mahan, Bruce H. (Univ. of California, Berkeley). Accounts Chem. Res.; 3: 393-401(1970). (UCRL–20316).

Studies are being made of reaction dynamics from the measured product energy and angular distributions. Collisional excitation of molecular vibration, collisional dissociation of molecules, chemical reactions, and isotope effects in low-energy O_2^+–HD collisions are discussed. (M.C.G.)

29065 LATTICE DYNAMICS OF METHANOL: HYDROGEN BONDING AND INFRARED ABSORPTION. Dempster, Andrew B.; Zerbi, Giuseppe (Istituto di Chimica delle Macromolecole del Consiglio, Milan). J. Chem. Phys.: 54: 3600-9(15 Apr 1971).

Mathematical methods of treating lattice dynamics of solids were applied to interpret the infrared spectrum of crystalline CH_3OH and CH_3OD. New spectra were recorded in the near-infrared region for crystalline CH_3OH, CH_3OD, and of mixed crystals at various concentrations. The far-infrared spectrum is also reported. Attempts were made to find spectral evidence of the two crystalline modifications of CH_3OH. A valence force field has been derived by a least squares fitting on the k = 0 modes of both molecules; the assignments of fundamental frequencies are discussed. Based on this derived force field, phonon dispersion curves and one-phonon and two-phonon densities of states have been calculated in the single-chain approximation. These are used in the interpretation of the infrared spectrum. The vibrational spectra of mixed crystals of CH_3OH and CH_3OD reveal unusual features which suggest that the breadth of absorption bands due to the hydrogen-bonded atoms is not a property of a single hydrogen bond but arises from cooperative effects with similar neighbors in the chain. The broadness seems to be a function of the chain length. (auth)

29066 MID- AND FAR-INFRARED SPECTRA OF HF AND DF IN RARE-GAS MATRICES. Mason, M. G.; Von Holle, W. G.; Robinson, D. W. (Johns Hopkins Univ., Baltimore). J. Chem. Phys.; 54: 3491-3503(15 Apr 1971).

The "vibration–rotation" and "pure rotation" spectra of HF and DF in rare-gas matrices near 4°K were studied, and assignments of the features due to the monomeric molecules were made. The perturbations of the purely vibrational levels were used to compute Lennard–Jones parameters for the interaction between the polar molecule and its neighboring atoms. The center of action of the dispersion forces was calculated for HF, and the rotational perturbations were evaluated. The spectral absorption frequencies are rather well reproduced. It was found that the experimental frequency shifts are not consistent with a theory of rotational–translational coupling but that they, and other "anomalous" spectral features, are predicted by considerations of the anisotropies in the rotational potential function. (auth)

29067 VIBRATIONAL ENERGY TRANSFER IN SHOCK-HEATED N_2–HI AND N_2–DI MIXTURES. Breshears, W. D.; Bird, P. F. (Los Alamos Scientific Lab., N. Mex.). J. Chem. Phys.; 54: 2968-74(1 Apr 1971).

The vibrational relaxation of N_2–HI mixtures in the temperature range 1000 to 2700°K and of N_2–DI mixtures in the range 1200 to 2000°K was studied behind incident shock waves by time-resolved measurement of the postshock density gradient using a laser-beam deflection technique. In both systems the vibrational relaxation of N_2 is dominated by vibration–vibration (V–V) energy transfer from the halide gas; contributions due to translation–vibration (T–V) and/or rotation–vibration (R–V) energy transfer are negligible. V–V energy transfer is more efficient in N_2–HI than in H_2–DI collisions, but the difference is much less than predicted by the SSH theory. Results for the effect of N_2 on the relaxation of HI and DI support previous suggestions that R–V energy transfer is the dominant mechanism for vibrational relaxation of the hydrogen halides. (auth)

29068 HYDROGEN REARRANGEMENTS IN THE MASS SPECTRA OF ALKYLBENZENES. Lightner, David A.; Quistad, Gary B.; Irwin, Elizabeth (Univ. of California, Los Angeles). Appl. Spectrosc.; 25: 253-8(Mar-Apr 1971).

By means of extensive deuterium labeling, the γ-carbon has been shown to be the principal site of transferred hydrogen (deuterium) regardless whether the hydrogen (deuterium) is primary, secondary, or tertiary. Although a significant transfer is also observed from the β, δ, ϵ, and more remote (to θ) carbons of the alkyl chain, such transfer is not attended by C–C cleavage (fragmentation) and is interpreted as an exchange between the aromatic ring (ortho-hydrogen atoms) and the alkyl chain hydrogen atoms (deuterium atoms). The data herein also set small upper limits on the formation of m/e 91 ($C_7H_7^+$) from m/e 92 ($C_7H_8^+$) at both high and low ionizing voltages as well as in long and short alkyl chains. (auth)

29069 INFRARED ABSORPTION SPECTRA OF SILICA GEL-$H_2{}^{16}O$, $D_2{}^{16}O$, AND $H_2{}^{18}O$ SYSTEMS. Hino, Masao; Sato, Toshio (Government Industrial Development Lab., Sapporo). Bull. Chem. Soc. Jap.; 44: 33-7(Jan 1971).

Infrared absorption spectra of the systems of silica gel–$H_2{}^{16}O$, $D_2{}^{16}O$, $H_2{}^{18}O$, and some organic vapors were measured in order to assign the bands sensitive to adsorption at 870 and around 950 cm^{-1}. Deuteration of silica gel caused the absorption decrease at 870 cm^{-1} and the appearance of a band at 620 cm^{-1}. The band around 950 cm^{-1} appearing by adsorption not only of water but also of organic vapors showed no shift on deuteration, but shifted toward low frequency side by 25 cm^{-1} on the substitution of ^{16}O of surface silanol groups with ^{18}O. From these facts the bands at 870, 620, and 950 cm^{-1} were assigned to Si–OH bending, Si–OD bending, and Si–O stretching vibrations of surface silanol groups, respectively. The oxygen atom of silanol groups of silica gel was found to exchange with that of adsorbed water molecules even at room temperature for a sample treated at temperature below 300°C. A higher reaction temperature of ca. 200°C was necessary for a sample calcined at 800°C. Mechanism of the oxygen atom exchange reaction was discussed. (auth)

29070 NORMAL COORDINATE TREATMENT AND FORCE CONSTANTS OF ALKANONITRILES. Fujiyama, Tsunetake (Tokyo Univ.). Bull. Chem. Soc. Jap.; 44: 89-93(Jan 1971).

Force constants of the Urey–Bradley type are calculated for a series of alkanonitriles. The calculation covers the mononitriles: CH_3CN, CH_3CH_2CN, $(CH_3)_2CHCN$, $(CH_3)_3CCN$, and the dinitriles: $NCCH_2CN$, $NCCHDCN$, $NCCD_2CN$, trans-$NCCH_2CH_2CN$, gauche-$NCCH_2CH_2CN$. The results show that the force constants can be transferred from molecule to molecule as a group. It is also shown that a group of force constants is characteristic of a corresponding chemical structure or a substituent. (auth)

29071 AVERAGE VALUES OF BOND ANGLES. Kuchitsu, Kozo (Tokyo Univ.). Bull. Chem. Soc. Jap.; 44: 96-9(Jan 1971).

A number of definitions with clear physical significance regarding the "average bond angles" (nonlinear case) are presented. Simple expressions of the average angles in terms of the linear and quadratic mean values of the displacements in the internuclear distances are given. The differences in the various average angles for H_2O, D_2O, CH_4, CD_4 and SO_2 are estimated by means of a normal-coordinate analysis. The differences are shown to be small fractions of one degree. The root-mean-square angles for linear molecules (HCN, DCN, CO_2 and CS_2) are also calculated. (auth)

29072 STRUCTURE OF TRANS ETHYL METHYL ETHER AND THE W FORM OF DIETHYL ETHER. Hayashi, Michiro; Imaishi, Hisae; Ohno, Keiichi; Murata, Hiromu (Hiroshima Univ.). Bull. Chem. Soc. Jap.; 44: 299(Jan 1971).

The observed rotational constants from the microwave spectra of trans ethyl methyl ether and its deuterated and ^{13}C substituted species were compared to the predicted rotational constants in order to obtain structural parameters. Using these structural parameters, the microwave spectra measurements of the W (trans–trans) form of diethyl ether were based on the trial calculation for the rotational constants of four possible molecular forms of diethyl ether. (D.P.O.)

Physical Chemistry

Refer also to abstracts 28924, 28925, 29147, 29154, 29188, 29419, 29421, 29831, 29955, 30668, and 30669.

29073 (CEA-N-1414) DETERMINATION OF EQUATIONS OF STATE FOR GASEOUS HEXAFLUORIDES OF URANIUM, MOLYBDENUM, AND TUNGSTEN. Morizot, Pierre (Commissariat a l'Energie Atomique, Saclay (France). Centre d'Etudes Nucleaires). Feb 1971. 26p. (In French). Dep. NTIS (U. S. Sales Only).

The virial equations of state for UF_6, MoF_6, and WF_6 were determined in the temperature range 40 to 190°C by the constant-volume method. A special corrosion-resisting apparatus was used. The parameters $\sigma, \epsilon/K$ of the 12-6 Lennard–Jones potential were obtained from the experimental results. (France)

29074 (DUN-7221(Vol.1)) NOBLE GAS CONFINEMENT STUDY. VOLUME I. THE DEVELOPMENT OF A LONG-LIVED, HIGH-EXPANSION FOAM FOR ENTRAPPING AIR-BEARING NOBLE GAS. FINAL REPORT, FY-1970. Mecca, J. E.; Jensen, H. F.; Ludwick, J. D. (Douglas United Nuclear, Inc., Richland, Wash.). Feb 1971. Contract AT(45-1)-1857. 85p. Dep. NTIS.

The development of a long-lived foam with many potential uses is one of the benefits realized from the noble gas confinement studies. Under the concept of long-lived, high-expansion foam control, the escaping gases would be passed through a foam generator that would encapsulate the contaminated air. Radioactive decay and slow permeation of the gases through the foam would restrict the final release of the gases to within acceptable radiation control limits. The successful quest for a high-expansion foam (300 to 1 expansion ratio) with the ability to withstand time (120 days or more) without the loss of internal structural integrity is described. The technique developed of blowing the foam with a flooded impingement plate, thus requiring no nozzles or devices prone to plugging, proved to be quite reliable and successful. Facilities and instrumentation are described and test data are presented for bench top tests used to evaluate some 250 foam candidates, and for large scale tests of encapsulation of 5000 cubic feet of mixtures of air and tagged noble gas. The foam development work and techniques employed appear useful for controlling industrial gaseous emission, dust suppression, gas scrubbing of reactor containment vessels and even possibly in agriculture as an insulator for the prevention of frost damage. (auth)

29075 (DUN-7221(Vol.2)) NOBLE GAS CONFINEMENT STUDY. VOLUME II. CRYOGENIC POROUS MEDIA BED. FINAL REPORT, FY-1970. Mecca, J. E.; Ludwick, J. D.; Etheridge, E. L. (Douglas United Nuclear, Inc., Richland, Wash.). Feb 1971. Contract AT(45-1)-1857. 48p. Dep. NTIS.

Trapping rare gases entrained in airstreams on a cryogenic porous medium was investigated. The adsorption bed container was 12 inches in diameter and two feet deep. Activated coconut charcoal was utilized as the adsorber. The bed contained approximately 60 pounds of the purified charcoal. The porous-media bed was constructed of aluminum and designed for an internal pressure of 25 psig. Some tests of the system were carried out. (M.C.G.)

29076 (LF-43, pp 13-17) DEVELOPMENT OF TECHNIQUES FOR GENERATING MONODISPERSE AEROSOLS WITH THE FULWYLER DROPLET GENERATOR. Raabe, O. G.; Newton, G. J. (Lovelace Foundation for Medical Education and Research, Albuquerque, N. Mex.).

In Fission Product Inhalation Program.

The dispersion of monodisperse aerosols using the Fulwyler Droplet Generator is being studied. A high-frequency signal is converted to mechanical vibrations by a piezoelectric crystal coupled to a small, pressurized liquid reservoir. A liquid stream, emitted from the reservoir through a small orifice (≈15 μm) is uniformly disrupted by the ultrasonic vibrations into very uniform droplets of about 20 to 30 μm in diameter. Up to 300,000 droplets per second are generated with less than 1% variation in droplet volume. Monodisperse insoluble particles can be made from droplets containing organic complexes of a chosen metal after heat treatment of the aerosol. The advantages of this method of generating monodisperse aerosols include: greater uniformity of size than obtained by other methods, absence of satellites, and reproducible and accurate electronic control with no moving parts. The technical problems under study include: dispersion and drying of the droplets without coalescence or disintegration, maintenance of dependable operation for long periods, and use of minimum air for dispersion to produce aerosols of high concentration. (auth)

29077 (LF-43, pp 18-24) SOME CHARACTERISTICS OF RUTHENIUM AEROSOLS GENERATED FROM Ru-ORGANIC COMPLEXES AND SUBJECTED TO THERMAL DEGRADATION. Newton, G. J. (Lovelace Foundation for Medical Education and Research, Albuquerque, N. Mex.).

In Fission Product Inhalation Program.

The characteristics of aerosols produced from droplets of a ruthenium chelate after passage through a high-temperature heating column were studied to investigate the nature of oxides of ruthenium as might be formed in nuclear operations or accidents. Ruthenium tetroxide is the volatile species usually incriminated in health physics problems with ruthenium. Aerosols of oxides were produced by heat treatment of droplets of two types: one with ^{14}C as a tracer of the oxalate, and one with ^{103}Ru as a tracer of the ruthenium. The ruthenium aerosols were greatly reduced in concentration by losses to the walls of the system when temperatures around 1000°C were used to form the oxides. The resultant aerosols, however, consisted of very small particles of amorphous ruthenium dioxide. Ruthenium tetroxide, if formed, may have been quickly reduced to the dioxide at high temperature since water vapor was present. The optimum temperature for producing aerosols of ruthenium dioxide that might be suitable for inhalation experiments was found to be between 400 and 700°C. (auth)

29078 (LF-43, pp 25-30) PREPARATION OF AEROSOLS OF THULIUM AND AMERICIUM BY THERMAL DEGRADATION. Boyd, H. A.; Thomas, Randi L. (Lovelace Foundation for Medical Education and Research, Albuquerque, N. Mex.).

In Fission Product Inhalation Program.

The preparation and properties of thulium and americium aerosols produced by thermal degradation of aerosols obtained by nebulization of aqueous suspensions are discussed. The aerosols are described relative to the composition of the suspension and method of stabilization. Tracer studies used to characterize some of the aerosols are reported. (auth)

29079 (LF-43, pp 31-9) PHYSICAL AND CHEMICAL CHARACTERISTICS OF AEROSOLS PRODUCED FROM SOLUTIONS OF POLYVALENT METALLIC NUCLIDES. Kanapilly, G. M.; Raabe, O. G.; Newton, G. J. (Lovelace Foundation for Medical Education and Research, Albuquerque, N. Mex.).

In Fission Product Inhalation Program.

The character of the aerosols produced from solutions of metallic ions is influenced by: the composition of the solution, the droplet sizes, the rate of drying of the droplets, and the rate of heating and cooling when degradation or sintering is involved. The relative effects of these factors were investigated with aqueous solutions of metallic ions of Co, La, Ce, Y, Sb, Al, Zr, and Mo in one or more anionic forms including chloride, lactate, citrate, acetate, EDTA, hydroxide oxalate, acetylacetonate, and tartrate. Production of aerosols consisted of nebulization, drying, degradation at temperatures up to 1150°C, and cooling. Electron microscopic studies and determination of aerodynamic properties were used in physical characterization. The chemical nature of aerosols was studied by tracer techniques and other methods as applicable for specific cases. (auth)

29080 (LF-43, pp 40-51) DISSOLUTION OF SMALL RADIOACTIVE PARTICLES. Kanapilly, G. M.; Raabe, O. G.; Goh, C. H. T.; Chimenti, R. A. (Lovelace Foundation for Medical Education and Research, Albuquerque, N. Mex.).

In Fission Product Inhalation Program.

Experiments using flowing systems to determine the rates of dissolution of aerosol particles collected on filters are described. The effects of the solvent, flow rates, and other variables on the rates of dissolutions of small particles were examined. The rates of dissolution of particles of some of the aerosols used for inhalation exposure were determined and comparisons between biological retentions and the in vitro dissolutions were made. The rates of dissolution were determined for particles of a variety of aerosols including ^{90}Sr in fused clay, $CeCl_3$ (^{144}Ce), CeO_2 (^{144}Ce), and four types of zirconium aerosols ($^{95}Zr-Nb$) particles of varying chemical and physical properties. The rates of dissolution of the different size fractions were found to be inversely related to the particle sizes. All aerosol samples showed higher rates of dissolution in the initial fractions of elution and with further elution the rates approached relatively constant values. (auth)

29081 ADVANCES IN HIGH TEMPERATURE CHEMISTRY. VOLUME 2. Eyring, Leroy (ed.). New York; Academic Press, Inc. (1969). 292p. $16.00.

Six chapters are included; separate abstracts have been prepared for four of them. Discussions of chemical research in streaming thermal plasmas and studies on sublimation mechanisms of solids are also included. (J.G.B.)

XUM

For abstracts of individual chapters see: 29082, 29083, 29987, and 30258

29082 DISSOCIATION ENERGIES AND FREE ENERGY FUNCTIONS OF GASEOUS MONOXIDES. Brewer, Leo (Univ. of California, Berkeley); Rosenblatt, Gerd M. Advan. High Temp. Chem.; 2: 1-83(1969).

Free energy functions were calculated for 66 gaseous diatomic oxides. Data used in the calculations are evaluated. An extensive bibliography is included. (J.G.B.)

29083 MATRIX-ISOLATION TECHNIQUE APPLIED TO HIGH TEMPERATURE MOLECULES. Weltner, W. Jr. (Univ. of Florida, Gainesville). Advan. High Temp. Chem.; 2: 85-105 (1969).

Applications of matrix isolation, a technique for trapping molecules as isolated entities in an inert solid in order to investigate their properties, usually by optical means, are reviewed. The relationship between gas-phase and solid-state spectroscopy is illustrated using studies on the VO molecule. The matrix spectra of $V^{16}O$ and $V^{18}O$ are compared. Vibrational frequencies of metal halide molecules obtained from matrix spectra are tabulated. Electronic state designations for ThO_2, ZrO_2, TaO_2, and WO_2 are tabulated. The orientation of molecules in matrices and applications of matrix isolation to electron paramagnetic resonance spectroscopy are discussed. (J.G.B.)

29084 KINETIC STUDIES OF THE REDUCTION OF CHROMIUM(III) COMPLEXES BY URANIUM(III) IONS. Wang, Robert T.; Espenson, James H. (Ames Lab., Iowa). J. Amer. Chem. Soc.; 93: 1629-33(7 Apr 1971).

Rates were measured for the reduction of a series of Cr(III) $(H_2O)_5X$ complexes by U^{3+}, for X = H_2O, F, Cl, Br, −NCS, N_3, and −SCN. The reactions follow second-order kinetics, with the apparent rate constant markedly dependent upon $[H^+]$, as in the general equation $-d[Cr(III)]/dt = d[U^{4+}]/dt = k' + k'[H^+]^{-1} + k''[H^+]^{-2}$, where different terms are appropriate for different X groups. The mechanism proposed is an inner-sphere electron transfer, in which OH^- plays the role of an especially favorable bridging group. (auth)

29085 PROTON MAGNETIC RESONANCE SHIFTS IN BIS (CYCLOOCTATETRAENYL) URANIUM(IV). Edelstein, N. (Univ. of California, Berkeley); Lamar, G. N.; Mares, F.; Streitwieser, A. Jr. Chem. Phys. Lett.; 8: 399-402(1 Mar 1971).

The measured proton resonance shifts of $U(COT)_2$ were analyzed on the basis of a crystalline field model and magnetic susceptibility data. It is pointed out that in $U(COT)_2$ the orbital and spin angular momenta are coupled antiparallel for the ground state, so that a positive hyperfine coupling constant due to the Fermi contact term will result in an upfield proton resonance shift. The hyperfine coupling constant arising from the Fermi contact term was found to be $A_F = +0.90$ MHz ±25%. (auth)

29086 INFRARED SPECTRA AND GEOMETRIES OF HEAVY METAL HALIDES: $SrCl_2$, $BaCl_2$, $EuCl_2$, EuF_2, $PbCl_2$, AND UCl_2. Hastie, J. W. (National Bureau of Standards, Washington, D. C.); Hauge, R. H.; Margrave, J. L. High Temp. Sci.; 3: 56-72(Jan 1971).

The heavy metal dihalide species $SrCl_2$, $BaCl_2$, $EuCl_2$, EuF_2, $PbCl_2$, and UCl_2, generated under thermodynamic equilibrium conditions, were isolated in matrices of solid Ne, Ar, Kr, and N_2. Methods of production varied from simple Knudsen vaporization for $SrCl_2$, $BaCl_2$, and $PbCl_2$, and decomposition vaporization, such as $EuX_3(s) \rightarrow EuX_2(g) + \frac{1}{2} X_2$, to oxidation vaporization, i.e., $CaCl_2(g) + U(s) \rightarrow UCl_2(g) + Ca(g)$, $Cl_2(g) + U(s) \rightarrow UCl_2(g)$, and $2HCl(g) + U(s) \rightarrow UCl_2(g) + H_2$. Infrared spectra for these matrix-isolated species were obtained (33 to 4000 cm^{-1}) and the symmetric (ν_1) and the antisymmetric (ν_3) vibrations observed in each case. For the chlorides the extreme low-intensity nature of the bending frequency (ν_2), the numerous extraneous low-frequency absorptions associated with lattice modes of the solid matrices, and the ever-present HCl impurities resulted in a less reliable assignment of ν_2 values. In some cases frequency measurement of the various naturally occurring ^{35}Cl, ^{37}Cl isotopic species allowed definite assignments of the stretching frequencies to be made and the following bond angles were calculated: $SrCl_2$(130 ± 8°), $EuCl_2$ (135 ± 8°), and $PbCl_2$(96 ± 3°). Fermi interactions between ν_1 and ν_3 for the unsymmetrical isotopic species were observable in these cases and provided added verification of the frequency assignments. From the relative intensities of ν_1 and ν_3 the following bond angle estimates were made: $BaCl_2$(120 ± 10°), EuF_2 (110 ± 15°), and UCl_2(100 ± 15°). These bond angles were also in accord with a consistent set of force-constant data. (auth)

29087 STRUCTURES OF THE PREDOMINANT HYDROLYSIS PRODUCTS OF URANYL(VI) IN SOLUTION. Aberg, Martha (Royal Inst. of Tech., Stockholm). Acta Chem. Scand.; 24: 2901-15(1970).

X ray scattering from concentrated hydrolyzed and acid solutions of uranyl(VI) chloride was measured. The uranium concentration was kept constant at 3M but the OH:U ratio was varied from 0 to 1.11. The coordination number of the uranyl ion in solution is close to values found in crystal structures. In the hydrolyzed solutions polynuclear complexes are formed in which the U−U distance is 3.86 Å and the uranium atoms are probably joined by double oxygen bridges. The scattering data, the results from emf measurements, and geometrical considerations lead to the conclusion that the predominant polynuclear complexes can contain only two or three uranium atoms. The dinuclear complex has a structure similar to that found for the discrete dinuclear complex $[(UO_2)_2(OH)_2Cl_2(H_2O)_4]$ occurring in crystals of a solid uranyl(VI) hydroxo compound. In the trinuclear complex the uranium atoms form an equilateral or almost equilateral triangle. (auth)

29088 INFRARED STUDIES ON THE COORDINATION INFLUENCE OF THE UO_2^{2+} GROUP ON THE P−O BOND OF TRIPHENYL PHOSPHINE OXIDE. Bandoli, G.; Bortolozzo, G.; Clemente, D. A.; Croatto, U.; Panattoni, C. (Istituto Chimica Generale, Padua). Inorg. Nucl. Chem. Lett.; 7: 401-2(May 1971).

Several uranyl compounds containing the ligand Ph_3PO were studied; these included $UO_2(CH_3COS)_2(C_6H_5)_3PO$, $UO_2(C_6H_5CS_2)_2(C_6H_5)_3PO$, $(UO_2(CH_3COO)_2(C_6H_5)_3PO)_2$, $UO_2((C_2H_5)_2NCS)_2(C_6H_5)_3PO$, $UO_2(CH_3COO)_22$ $(C_6H_5)_3PO$, and $UO_2(NO_3)_22$ $(C_6H_5)_3PO$, the first four of which contain pentacoordinated U and the fifth and sixth hexacoordinated U. From the values of the P−O stretching frequencies in the free ligand compared with the coordinated ligand a mean ir shift of 58 cm^{-1} was found in the pentacoordinated system compared with 45 cm^{-1} in the hexacoordinated system. The lowering of the frequencies can be associated with an increase in the P−O bond distance from 1.46 Å in the free ligand to 1.49 Å in the coordinated ligands. The difference in the ir shifts could be associated with a lowering of force constant, more pronounced with penta coordination than with hexacoordination. There is evidence that the coordination causes appreciable perturbation effects on the P−O localized bond. (UK)

29089 ISOTOPIC EXCHANGE STUDY ON THORIUM PEROXIDE. Hasty, R. A. (Montana State Univ., Bozeman); Boggs, J. E. J. Inorg. Nucl. Chem.; 33: 874-6(Mar 1971).

Thorium peroxychloride was used for an isotopic exchange study with a view to characterizing it in regard to the nature of the peroxide and/or oxide bonding. The dried peroxychloride was subjected to exchange with D_2O containing 1.545% ^{18}O. Data on the number of exchangeable O's found in the peroxychloride are shown tabulated, and varied between 3.0 and 3.2. The results indicated that OH groups, and not oxide groups, are present in the dried peroxychloride. Although this isotopic exchange does not distinguish between peroxy and hydroperoxy groups in nonbridging positions, it confirms the existence of peroxy bridges in the dried peroxychloride. It may also be presumed that the peroxy bridges are present in freshly precipitated peroxychloride. Differences as compared with the peroxynitrate are stated. (UK)

29090 ELECTRON PARAMAGNETIC RESONANCE STUDIES OF CARBON MONOXIDE ADSORBED ON THORIUM OXIDE. Brey, Wallace S. Jr.; Gammage, R. B.; Virmani, Y. P. (Univ. of Florida, Gainesville). J. Phys. Chem.; 75: 895-901(1 Apr 1971).

Adsorption of carbon monoxide on well-outgassed thorium dioxide at room temperature leads to the production of several radical species. Species A, formed first, may be related to the presence of impurities on the surface and has a lifetime of only a few minutes. In a rate process that continues over several days there are produced two interconvertible radicals, B, having an asymmetric g tensor, and C, having an axially symmetric tensor. At higher pressures, the equilibrium between the two radicals is temperature dependent, but pumping out excess CO causes conversion into radical C, as does the presence of water vapor. Following evacuation, the intensity of the signal of C grows slowly over a period of several hundred hours, and thus this species must arise from very tightly bound carbon monoxide. Increasing the temperature causes a sequence of reactions to occur on the surface, in contrast to the behavior of CO on MgO. Species D, stable around 100°C, has some resemblance to species A and may represent nearly neutral or somewhat positive CO. It gives way, at about 200°C, to species E, the spectrum of which indicates that it is CO_2^-. Following heat treatment of the sample at any temperature from 150 to 350°C, a signal of low g value is observed, and its appearance seems to be at the expense of the adsorbed radicals. Finally, at about 500°C, the adsorbate signal gives way to one that is characteristic of carbon. (auth)

29091 PARALLELISM BETWEEN THE REGULARITIES IN THE f-ELECTRON ELEMENTS AND THEIR FREE ION GROUND

TERMS. A DOUBLE–DOUBLE HYPOTHESIS. Fidelis, I. (Inst. of Nuclear Research, Warsaw). Bull. Acad. Pol. Sci., Ser. Sci. Chim.; 18: 681-4(1970).

A striking correlation was found between the full pattern of regularities and the sequence of the free ion ground terms of the f-electron elements with regard to total orbital angular momentum. Parallelisms are given for actinides and lanthanides. (M.C.G.)

29092 COMPLEXES OF URANIUM(V) CHLORIDE WITH NITROGEN DONOR LIGANDS. Paul, Ram Chand; Singh, Gurdev; Singh, Mangal (Panjab Univ., Chandigarh, India). J. Inorg. Nucl. Chem.; 33: 713-20(Mar 1971).

Stable uranium(V) chloride complexes of the general formulae $UCl_5 \cdot 2B$ and $UCl_5 \cdot 3B$ (B = pyridine, quinoline, isoquinoline, α-picoline, and β-picoline) were prepared from uranium(V) chloride solution in thionyl chloride and characterized by measurement of magnetic susceptibilities at temperatures from 86°K to 300°K, electron spin resonance, ir, and reflectance spectra. (auth) (UK)

29093 COORDINATION EFFECTS ON THE SPECTRUM OF URANIUM(IV) IN MOLTEN FLUORIDES. Toth, L. M. (Oak Ridge National Lab., Tenn.). J. Phys. Chem.; 75: 631-6(4 Mar 1971).

The spectrum of U(IV) in molten fluoride solutions (primarily $LiF-BeF_2$ mixtures) exhibits a variation with melt composition, which was attributed to a change in the U(IV) coordination number. An equilibrium between two species $UF_8^{4-} \rightleftharpoons UF_7^{3-} + F^-$ adequately explains the data. The identity of the species in fluoride-rich solvents was established as UF_8^{4-} by comparison of the melt spectra with crystal spectra of known coordination. Although crystal spectra of 7-coordinated U(IV) are more complicated, such a comparison suggests that the species present in fluoride-deficient melts is predominantly UF_7^{3-}. (auth)

29094 BOND LENGTHS IN GAMMA–URANIUM TRIOXIDE. Siegel, S.; Hoekstra, H. R. (Argonne National Lab., Ill.). Inorg. Nucl. Chem. Lett.; 7: 455-9(May 1971).

Reference is made to the powder diffraction studies of Engmann and de Wolff on this topic (Acta Cryst. 16: 993(1963)). An unusual feature of this structure is the 2.06 Å U_1-O_1 bond, which must be considered as a double bond, since no additional U atoms are found at reasonable bonding distances to the O atom. A U–O double bond would be expected to be substantially shorter, and ir data on this oxide indicate a bond length of ~1.76 Å. In view of this unexpected long double bond distance, together with the large errors in O coordinates estimated by the above authors, the $\gamma-UO_3$ structure was re-examined by single crystal methods. Details are given of the experimental work and the data analysis, and bond distances are tabulated. The structure deduced by Engmann and de Wolff, including bond lengths, was substituted. Several questions, however, remain unanswered; the uranyl bond in UO_3 is still about 0.1 Å longer than expected, and the ir stretching frequency is unusually low for a pure uranyl double bond. $\gamma-UO_3$ represents the first instance in which this vibration mode falls below 900 cm^{-1}, and the results might be attributed to the existence of weak bonding forces at distances in excess of 3 Å in the crystal. Other considerations, however, suggest that the length of a pure uranyl bond, and the frequency of its asymmetric stretching mode, are dependent to some extent on the number and identity of the secondary ligands. (UK)

Radiation and Nuclear Chemistry

Refer also to abstract 31633.

29095 RECOMMENDED PRACTICE FOR DETERMINING CHANGES IN CHEMICAL REACTIVITY OF INORGANIC MATERIALS EXPOSED TO HIGH ENERGY RADIATION. ASTM E 183-62. Philadelphia; American Society for Testing and Materials (1965). 4p. Available from American Society for Testing and Materials, Philadelphia.

Two methods are recommended for determining the changes in chemical reactivity of substances exposed to high-energy radiation. These methods are differential thermal analysis or thermogravimetric and derivative thermogravimetric analysis. These methods are based on the continuous measurement of heat evolved or changes in weight accompanying reactions of irradiated substances. When feasible, other measurements that contribute to the correct analysis of the changes are complete chemical, spectrographic, and x-ray analyses as well as density of sample prior to and following irradiation. (B.L.M.)

Radiation Effects

29096 (WERL-HFIL-1) DEVELOPMENT OF POLYIMIDE BONDED SOLID FILM LUBRICANTS. Alvino, W. M.; Rudo, G. E. (Westinghouse Research Labs., Pittsburgh, Pa.). Nov 1968. Contract AT(11-1)-Gen-14. 88p. Dep. NTIS.

The results of work conducted to develop heat and radiation-resistant organically bonded solid film lubricants are described. These solid film lubricants are composed of an organic resin binder (polyimide and amide-imide resins) and several transitional element compounds such as the selenides of tungsten, molybdenum, niobium, and tantalum. The approach, the data and the procedures necessary to mix, apply, and cure these films are outlined. Friction and wear properties of these films at elevated temperatures (550°F) under high loading (15,000 psi) in addition to those parameters affecting the aforementioned properties, such as, resin type, filler and its concentration, film thickness, test surface, radiation, and long term static bonding, are also presented. A polyamide-imide resin designated as AI-131 and loaded with 40 volume or 79 weight percent WSe_2 was found to give the best combination of friction and wear properties under the severe conditions of the test. This composition is unaffected by humidity and gamma radiation and does not bond significantly under conditions of long-time heat and pressure. Coefficients of friction between 0.13 and 0.27 were maintained under test conditions for 3700 sliding motion cycles. Procedures for applying this coating composition onto large metal plate sections using either the draw bar or spray coating technique are also described. (auth)

29097 RADIATION-INDUCED ELECTRICAL CONDUCTANCE IN LIQUID n-HEXANE AND NEOHEXANE. Conrad, Edward Ezra. College Park, Md.; Univ. of Maryland (1970). 94p. University Microfilms Order No. 71-4027.

Thesis.

The decay of radioinduced conductance in liquid n-hexane and neohexane was observed using a high-speed electronic system. The signals were recorded from 10 nsec to 2 msec after a 25 nsec pulse of bremsstrahlung. The radiation was generated by a high intensity flash x-ray source capable of delivering doses to the liquids up to 10^{16} eV · g^{-1}. It was possible to observe the decay of quasifree electrons and to measure their lifetime in n-hexane. In neohexane the lifetime was somewhat shorter than the time resolution of the apparatus (10 nsec). The conductance of the purified materials decayed in a three stage process consisting of: (1) the trapping of the quasifree electrons by shallow traps, (2) the capture of the thermally released electrons by deep traps to form massive anions, and (3) the bimolecular recombination of these anions with the cations. The addition of air decreased the trapping time in both materials. SF_6, when added to neohexane, also decreased the trapping time and eliminated the intermediate decay stage. This was accompanied by an increase in the G-value. Values for the mobilities of the quasifree electrons were determined and are 0.23 $cm^2 \cdot V^{-1} \cdot sec^{-1}$ for n-hexane and a lower limit of 7.0 $cm^2 \cdot V^{-1} \cdot sec^{-1}$ for neohexane. (Diss. Abstr. Int., B)

29098 EFFECT OF RADIATION ON OXYGEN ELECTRODE PERFORMANCE. Zimakov, I. E.; Pletnev, V. P.; Yanchin, V. A.; Chernyshev, A. M.; Spitsyn, V. I. (Inst. of Physical Chemistry, Moscow). Dokl. Akad. Nauk SSSR; 194: 1378-80 (21 Oct 1970). (In Russian).

The influence of nonradioactive Tm_2O_3 and activation by the radioactive isotope ^{170}Tm($T_{\frac{1}{2}}$ = 129 days, $E_{\beta max}$ = 0.970 MeV, and $E_{\gamma max}$ = 0.084 MeV) on the electrochemical properties of oxygen electrodes in oxyhydrogeneous fuel elements was studied. Additions of thulium oxides to the active mass up to 0.25% did not affect the electrochemical behavior of the oxygen electrode, whereas additions of radioactive ^{170}Tm strongly inhibited the polarization of the electrodes. Moreover, with the increase of the specific radioactivity the drop in polarization became even more pronounced. Further studies with radioactive emitter ^{170}Tm additions into the catalyst showed that radiation influenced various physicochemical processes taking place in solids. It was postulated that the observed radiation effects on electrochemical processes are the results of integrated total effects. (R.V.J.)

29099 MELT STRENGTH AND MELT EXTENSIBILITY OF IRRADIATED LINEAR POLYETHYLENE. Tung, Lu Ho; Donald, Harold J.; Caiola, Robert J. (to Dow Chemical Co.). U. S. Patent 3,563,870. 16 Feb 1971. Filed 23 Jan 1969.

In a method for improving the melt strength and melt extensibility of polyethylene, polyethylene having a density ranging from 0.95 to 0.97 and a melt index ranging from 3 to 13 decigrams/min is exposed to a dose of high-energy radiation ranging from 0.05 to 0.15 megarad. After irradiation, the polyethylene is shaped by

extrusion, compression molding, injection molding, or rotational molding into the form of the desired article. (B.L.M.)

29100 MECHANISM OF THE FORMATION OF TREE-SHAPED CHANNELS IN CHARGED-PARTICLE IRRADIATED DIELECTRICS. Deev, Yu. S.; Kruglyi, M. S.; Lyapidevskii, V. K.; Serenkov, V. I. At. Energ. (USSR); 29: 303-4(Oct 1970). (In Russian).

The behavior of poly(methyl methacrylate) exposed to 5-MeV electrons was investigated in order to clarify the origin of tree-shaped cracks in irradiated plastics. Formation of the cracks was accompanied by a characteristic lightning-like sparking, which may be clearly observed in spite of the strong radioinduced luminescence. The simultaneous formation of an electric pulse was also noted. The specimens were exposed in the dark to a 0.1-μA cm^2 electron beam, recording the luminescence through a light guide by means of a photomultiplier. It was found that the electric discharge, which is considered the main cause of the crack formation, also destroys a large amount of the material, as revealed by the gaseous decomposition products. Similar observations with silicate glasses exclude the possibility that the cracks are due to radiation chemical effects. It is proposed that space charges caused by the thermalization of electrons are responsible for all of the observed phenomena. (TTT)

29101 RADIOTHERMOLUMINESCENCE OF CRYSTALLINE AND GLASSY METHANOL. Kroh, J.; Roszak, W.; Czerwik, Z. (Technical Univ., Lodz, Poland). Bull. Acad. Pol. Sci., Ser. Sci. Chim.; 18: 699-704(1970).

The dependence of methanol radiothermoluminescence on the degree of crystallinity of the γ-irradiated matrix and the influence of electron scavengers on the processes resulting in light emission were studied. The radiothermoluminescence of pure, crystalline, deaerated methanol consists of two peaks corresponding to 107 and 140°K. With increasing water concentration these peaks are gradually substituted by a new maximum corresponding to the temperature 100°K. Photobleaching of irradiated samples reduced the radiothermoluminescence very efficiently. The effects of oxygen, carbon tetrachloride, and benzene were studied. (M.C.G.)

29102 BEHAVIOR OF EXTRA ELECTRONS IN THE LIQUIDS METHANE, ETHANE, AND PROPANE. Robinson, M. G.; Fuochi, P. G.; Freeman, G. R. (Univ. of Alberta, Edmonton). Can. J. Chem.; 49: 984-5(15 Mar 1971).

The radioinduced electrical conductances of liquids methane, ethane, and propane were measured. At a field strength of 5 kV/cm the number of ion pairs collected at the electrodes per 100 eV absorbed by the liquid was 1.5 in methane (−160°C), 0.20 in ethane (−90°C), and 0.14 in propane (−90°C). The short-lived conductance transient (k/u overshoot) observed at low field strengths in methane was 40% as large as that in argon. No transient was observable in ethane or propane. The freeness of motion of electrons in liquid methane is nearly as great as that in liquid argon and much greater than that in ethane or propane. (auth) (Canada)

29103 EFFECT OF GAMMA IRRADIATION ON SOME CHEMICAL AND PHYSICAL PROPERTIES OF GLUTEN PROTEINS. Lasztity, R.; Figuli, J. Elelmez. Ipar; 23: 321-5(1969). (In Hungarian).

In the most important physical properties (capacity for absorbing water, extensibility, spreading capacity, organoleptic properties) of dry gluten treated with ionizing rays there is no disadvantageous change up to a dose of 0.18 Mrad. Above 1 Mrad, the important technological properties worsen rapdily, accompanied by unfavorable chemical changes (denaturation, desegregation, change of the N-terminal groups, decrease of mean molecular weight). (auth)

29104 EFFECTS OF IONIZING RADIATION ON PVC. Selker, Alan H. (Weyerhaeuser Co., Longview, Wash.). pp VII.1-17 of Process Radiation in the Plastics Industry, 1969. Pullman, Wash.; Washington State Univ. (1969).

From Conference on process radiation in the plastics industry; Pullman, Wash. (11 Jun 1969). See CONF-690656.

Poly(vinyl chloride) (PVC) is a solid of relatively low penetrability by gases, trapped electrons, trapped free radicals, and trapped ions. It therefore gives a unique opportunity for observation of the formation and decay of these species. It is also extremely versatile as an engineering material for construction and for electrical applications. Hence, there is a practical interest in the properties resulting from exposure of PVC to a radiation field. The mechanism of the breakdown and the cross-linking effects are discussed. Optical and electron spin resonance effects are described, and finally the utility of PVC for electrical applications is briefly discussed. (auth)

29105 SPACE ENVIRONMENT STABILITY PROGRAM IN WHITE PIGMENT COATINGS. Gilligan, J. E.; Zerlaut, G. A. (Illinois Inst. of Tech., Chicago). pp 447-57 of Proceedings of the Institute of Environmental Sciences 17th Annual Technical Meeting and Equipment Exposition, April 26-30, 1971, Los Angeles, California. Mt. Prospect, Ill.; Inst. of Environmental Sciences (1971).

From seventeenth annual meeting and equipment exposition; Los Angeles, Calif. (26 Apr 1971). See CONF-710409.

Results of the in-situ reflectance optical spectroscopy of zinc oxide-based paints and reactively encapsulated (surface-treated) zinc orthotitanate (Zn_2TiO_4) are reported. Optical data were analyzed in conjunction with the results of electron paramagnetic spectroscopy; results of various treatments were evaluated. Experiments with proton and combined proton–uv irradiation indicate that protons affect the optical performance of the zinc oxide-based paints that were tested. (J.G.B.)

Radiation Processes

Refer also to abstract 29735.

29106 MONOMER REACTIVITY RATIOS IN GRAFT COPOLYMERIZATION. Odian, George (Richmond Coll., Staten Island, N. Y.); Kruse, Robert L.; Kho, Jose H. T. J. Polym. Sci., Part A-1; 9: 91-105(Jan 1971).

Monomer reactivity ratios in various radiation- and redox-initiated graft copolymerizations are discussed. The polymers studied were polyethylene, cellulose acetate, poly(vinyl chloride), polytetrafluoroethylene, poly(vinyl alcohol), and poly(methyl methacrylate); the comonomer mixtures were styrene–acrylonitrile, methyl acrylate styrene, acrylonitrile–methyl acrylate, and vinyl acetate–acrylonitrile. The polymer–comonomer mixture systems were so chosen as to permit study of both homogeneous and heterogeneous systems. The homogeneous systems included systems of low and high viscosity. The heterogeneous systems included both polymers swollen by the comonomer mixture and polymers not swollen by the comonomer mixture. None of the homogeneous grafting systems studied showed deviations from the normal copolymerization behavior under a variety of experimental conditions. Monomer reactivity ratios in graft copolymerization were the same as the values in nongraft copolymerization. The heterogeneous systems in which the polymer was swollen by the comonomer mixture yielded grafted copolymer compositions that were the same as those in nongraft copolymerization. The heterogeneous grafting system polytetrafluoroethylene/styrene–acrylonitrile showed deviations from normal copolymerization behavior at low degrees of grafting when the reaction was only on the polymer surface. The behavior became normal at higher degrees of grafting when the system approached that in which the polymer is swollen by the comonomers. In all reaction systems, it was found that the use of radiation to initiate the reaction does not in any way affect the copolymerization behavior of the two monomers in a comonomer pair. (auth)

29107 RADIATION-INDUCED SULFOXIDATION AND SULFOCHLORINATION OF POWDERY POLYETHYLENE PRODUCED BY RADIATION PROCESS. Konishi, Kunio; Yamaguchi, Kouichi; Takehisa, Masaaki (Takasaki Radiation Chemistry Research Establishment, Japan). J. Appl. Polym. Sci.; 15: 257-66(Feb 1971).

Gamma radioinduced sulfoxidation and sulfochlorination of the high specific surface area powdery polyethylene, which was produced by radioinduced polymerization of ethylene at room temperature, were studied and were compared with sulfonation by fuming sulfuric acid. In these reactions the effect of surface area on the chemical reactivity was observed to a certain degree. In gamma radioinduced sulfochlorination, as the reaction proceeds, the ratio of $-SO_2Cl$ to $-Cl$ introduced into the polymer decreases. This can be explained by the difference between the diffusibilities of SO_2 and Cl_2 molecules through sulfochlorinated and/or chlorinated polyethylene. Crystallinity, melting temperature, and density of the sulfochlorinated polymers were measured and are discussed. (auth)

29108 CELLULOSE GRAFT COPOLYMERS. III. EFFECTS OF OXYGEN ON GRAFT COPOLYMERIZATION OF ETHYL ACRYLATE WITH γ-IRRADIATED CELLULOSE. Nakamura, Yoshio; Hinojosa, Oscar; Arthur, Jett C. Jr. (Dept. of Agriculture, New Orleans). J. Appl. Polym. Sci.; 15: 391-401(Feb 1971).

The effects of oxygen on graft copolymerization of ethyl acrylate from methanol–water systems with γ irradiated fibrous cotton cellulose were investigated by electron spin resonance spectroscopy and by the formation of celluose–poly(ethyl acrylate) copolymer. The concentrations of free radicals in cellulose irradiated dry in an atmosphere of nitrogen at 25°C decreased dur-

ing postirradiation storage in nitrogen or oxygen. The concentration of free radicals in the irradiated cellulose, moisture regain of the irradiated cellulose, and formation of cellulose–poly(ethyl acrylate) copolymer decreased with increase in temperature and time of postirradiation storage and to a greater extent when stored in oxygen rather than in nitrogen. From the decrease in moisture regain of irradiated cellulose during postirradiation storage, it was concluded that increased intermolecular bonding occurred in irradiated cellulose during storage in both nitrogen and oxygen atmospheres. When irradiated celluloses, which had been stored in either oxygen or nitrogen, were copolymerized with ethyl acrylate at 60°C, less formation of copolymer was observed than when the copolymerization reactions were conducted at 25°C. It was concluded that there was no evidence for the formation or decomposition of cellulose peroxides during these reactions and that formation of graft copolymer depended primarily on the concentration of free radicals in the irradiated cellulose at the time of copolymerization. (auth)

29109 PROCESS FOR PRODUCING THERMOPLASTIC RESIN FOAM. Shinohara, Yasuo; Takahashi, Toshimasa; Yamaguchi, Kenji (to Toyo Rayon Kabushiki Kaisha). U. S. Patent 3,562,367. 9 Feb 1971. Priority date 27 Feb 1964, Japan.

A continuous process for producing foamed sheets of thermoplastic resins includes melt-blending a resinous composition consisting essentially of homopolymers and copolymers of polyolefins with a chemical foaming agent, which decomposes on heating; forming this mixture into a sheet under heat and pressure such that the foaming agent is not decomposed; applying ionizing radiation to the mixture to effect a partial crosslinking of the resinous composition; and then moving the sheet continuously such that its undersurface floats on the surface of a heated liquid while the sheet is irradiated from above with heat rays to effect foaming of the sheet in three dimensions. The process is applicable to a resinous composition of polyethylene, vinyl acetate–ethylene copolymer with polyethylene, or polyethylene–rubber. (B, L, M.)

29110 THE POLYMORPHISM AND ISOMORPHISM OF POLY(VINYLIDENE FLUORIDE). Doll, Warwick Woodman. Cleveland; Case Western Reserve Univ. (1970). 129p. University Microfilms Order No. 71-1680.

Thesis.

The radiation-initiated solution polymerization of vinylidene fluoride was examined in an effort to determine the effect of polymerization conditions on the head-to-head content of the resulting poly(vinylidene fluoride). No appreciable change was made in the head-to-head content when this new type of polymerization was utilized. However, the polymers that resulted had melting points that were 10 to 15°C higher than the suspension polymerized poly (vinylidene fluoride). An x-ray diffraction study was made on the chain conformation and crystal structure of poly(vinylidene fluoride) phase II. Three chain conformations were considered including two 2_1 helical forms (degenerate (planar) and nondegenerate) and the trans-gauche-trans-gauche' form. The crystal structure determination showed that the trans-gauche-trans-gauche' chain conformation is the correct one. From comparison between observed and calculated intensities, there are two possible space groups, P_{2_1} and P_1, depending upon whether the chains are taken to be antiparallel or parallel to one another. For both cases the reliability indices for the chosen structure are almost identical. A detailed study of high-pressure crystallized poly(vinylidene fluoride) indicated that a mixture of low-melting phase II and high-melting phase I was present rather than a new phase III, as originally suggested. Pressure crystallization at 285°C and 5500 atm resulted in samples that were pure phase I with an increased melting point of 187°C. High-pressure melting behavior obtained for samples of vinylidene fluoride copolymerized with vinyl fluoride, trifluoroethylene, or tetrafluoroethylene indicated that the copolymers had a lower entropy of melting than that of the poly(vinylidene fluoride) homopolymers in the same phase. As the comonomer size increased, the entropy of melting decreased. High-pressure crystallization of copolymers of 91 to 9 mole% vinylidene fluoride–trifluoroethylene and 93 to 7 mole% vinylidene fluoride–tetrafluoroethylene resulted in high melting forms of phase I (planar zigzag). (Diss. Abstr. Int., B.)

29111 EFFECT OF IRRADIATION ON HALOGEN EXCHANGED SILICA–ALUMINA CATALYST. Sano, Masakatsu; Hoshino, Toshio; Yotsuyanagi, Takao; Aomura, Kazuo (Hokkaido Univ., Sapporo). Kogyo Kagaku Zasshi; 74: 1-4(Jan 1971). (In Japanese).

The γ-radioinduced cracking of cumene and isomerization of oxylene over halogenated silica–alumina catalysts were investigated. In both reactions, the activity of the irradiated catalysts was found to increase. However, the surface area, the pore volume, the mean pore diameter, and acid content of the halogenated catalysts did not change upon irradiation. The increases in activity of the halogenated catalyst under irradiation and the electronegativity of the exchanged halogen atom have a good correlation. Results indicate that the increase in activity depends mainly upon the lattice defects produced under irradiation. The larger the electronegativity of the exchanged halogen atoms, the greater the production of the lattice defects. (auth) (Japan)

29112 ELECTRON SPIN RESONANCE STUDY ON PRIMARY PROCESS IN GAMMA-INITIATED SOLID STATE POLYMERIZATION OF TETRAFLUOROETHYLENE BY MEANS OF MATRIX-ISOLATION TECHNIQUE. Nishimura, Hiromichi (Tokyo Univ.); Tabata, Yoneho; Oshima, Keichi; Tamura, Naoyuki. Kogyo Kagaku Zasshi; 73: 2692-8(Dec 1970). (In Japanese).

Tetrafluoroethylene polymerizes with γ irradiation at −196°C in the solid state; ethylene does not. The matrix-isolation technique was used to study the primary process of solid state polymerizations of tetrafluoroethylene and ethylene. Measurements of active species were carried out with an electron spin resonance spectrometer. ESR spectrum of γ-irradiated pure tetrafluoroethylene consists of a broad component at the center and a "wing peak" which was reported by Siegel. This spectrum was assigned to $\sim CF_2\dot{C}F_2$ (the polymer radical). On the other hand, several fragment radicals ($\cdot CF_3$ etc.) were observed in the γ-irradiated tetrafluoroethylene in xenon matrices at a low concentration. This fact suggests that scission of carbon–carbon bond takes place by γ-irradiation of tetrafluoroethylene in xenon matrices. And from these results, the reaction mechanism is discussed. It was also found from the ESR measurement of γ-irradiated ethylene–tetrafluoroethylene system that copolymerization does not take place in the solid-state at −196°C. (auth) (Japan)

29113 THERMAL AND RADIATION INITIATED CONVERSIONS OF TERPHENYL ISOMERS AND THEIR HYDROGENATED DERIVATIVES. Protsidim, P. S.; Lavrovskii, K. P.; Makarov, D. V.; (and others) (Inst. of Petrochemical Synthesis, Moscow). Petrol. Chem. (USSR) (Engl. Transl.); 10: 104-14(1970).

Translated from Neftekhimiya; 10: 376-84(1970).

A study was made of thermal- and radiation-initiated conversions of terphenyl isomers, partially hydrogenated terphenyl isomers (with 30 and 60% hydrogen saturation) and o-, m- and p-tercyclohexyls at 370°C and with an integrated dose range of 0.25 to 6.25×10^{22} eV/g in the radiation field of a nuclear reactor. Under these conditions reactions take place with rupture of all types of bonds characterizing the hydrocarbons studied (C–H, C–C and C ⁻⁻⁻ C rings and C–C bonds between the rings). Radiation-thermal stability decreases in the order: p-terphenyl > m-terphenyl > o-terphenyl for individual terphenyl isomers and their hydrogenated derivatives. A reduction in stability in this order is, apparently, due to the lower (compared with the p-isomer) energy of conjugation as a consequence of additional deformation of m- and o-terphenyls, which is caused by the convergence of phenyl groups and the formation of "overloaded" molecules during hydrogenation of o-terphenyl. (auth) (UK)

29114 RADIATION-CURABLE COMPOSITIONS. Bassemir, Robert W.; Dennis, Richard; Nass, Gerald I. (to Sun Chemical Corp.). U. S. Patent 3,551,235. 29 Dec 1970. Filed 24 Nov 1967.

A radiation-curable solvent-free composition suitable for use as a coating or laminating material is composed of (1) 25 to 95 wt % of a mixture of about 15 to 90 wt % of at least one ester of an ethylenically unsaturated acid and a dihydric alcohol and about 10 to 85 wt % of an aryl sulfonamide–formaldehyde resin and (2) about 5 to 75 wt % of at least one halogenated aromatic, alicyclic, or aliphatic hydrocarbon photoinitiator in which all the halogen atoms are attached directly to the ring in the aromatic or alicyclic compound and to the C chain in the aliphatic compounds. The mixture is cured by exposure to either electron beam radiation or uv light. (B, L, M.)

29115 IRRADIATED POLYETHYLENE. Rainer, William C.; Hitov, Joseph J.; Redding, Edward M.; Sloan, Arthur W.; Stewart, William D. (to W. R. Grace and Co.). U. S. Patent 3,563,869. 16 Feb 1971. Filed 5 Nov 1957.

A process for producing a polyethylene that remains clear and transparent regardless of change in physical form comprises crosslinking by high-energy ionizing radiation (electrons) in the presence of a free radical catalyst selected from the group consisting of peroxy compounds, azo compounds, and poly(nitrosodimethyl terephthalate). (B, L, M.)

29116 METHOD FOR THE RADIATION PRODUCTION OF FILMS FROM UNSATURATED POLYESTER RESINS. Van Gasse, Rene Leopold Eduard (to N.V. Chemische Industrie Synres). U. S. Patent 3,562,125. 9 Feb 1971. Priority date 8 Jul 1966, Netherlands.

XUM

A method is described for the almost complete polymerization of unsaturated polyester resins in a very short time to produce films from such resins. The ratio of equivalence between unsaturated monomer and olefinically unsaturated bonds in the polyester chain ranges between 1.0 and 1.7. Polymerization is effected by radiation with high-energy electrons, the radiant energy being higher than 1×10^8 erg/g/sec. (Offic. Gaz.)

29117 ELECTRON SPIN RESONANCE STUDIES ON RADIATION-INDUCED SOLID STATE POLYMERIZATION OF METHYL METHACRYLATE. Mori, Koichi; Tabata, Yoneho; Oshima, Keichi (Tokyo Univ.). Kogyo Kagaku Zasshi; 73: 2479-81 (Nov 1970). (In Japanese).

Methyl methacrylate monomer was condensed at 77°K on the wall of an ESR capillary from the vapor phase and irradiated with γ rays from a ^{60}Co source at this temperature. It was found from the ESR studies that a 7-line spectrum of the $CH_3-\dot{C}(CH_3)-COOCH_3$ radical, a radical pair with a long tail structure, and a broad singlet spectrum due to trapped electrons exist in the irradiated monomers in the dark. By irradiation with light of longer wavelength than 4,000 Å, the radical pairs were destroyed and the broad singlet spectrum disappeared and moreover the 7-line spectrum was transformed to 5(4)-line spectrum, which was attributed to $R-\dot{C}H_2-C(CH_3)-COOCH_3$ radical. It was evident that methyl methacrylate can be polymerized by light after γ-irradiation, but there was no polymer after the melting of the photo-irradiated monomers; probably the degree of polymerization of polymers obtained may be very low. The mechanism of pair trapping of radicals and the processes of the solid-state polymerization of methyl methacrylate were considered from the experimental results. (auth) (Japan)

29118 ELECTRON SPIN RESONANCE STUDIES ON RADIATION-INDUCED SOLID STATE POLYMERIZATION OF ACRYLONITRILE. Mori, Koichi; Tabata, Yoneho; Oshima, Keichi (Tokyo Univ.). Kogyo Kagaku Zasshi; 73: 2481-7(Nov 1970). (In Japanese).

Needle-like monomer crystals, which were condensed from the vapor monomers on the wall of the ESR capillary were irradiated with γ rays from a ^{60}Co source in the dark at 77°K. If the irradiated monomers are photo-bleached with near-ultraviolet light and then melted rapidly, the yield of polymers is greatly reduced as compared with non-photobleached ones. Moreover, if the γ-irradiated monomers are kept at –120°C for 2 hr, after the photobleaching, the yield of polymers increases considerably in comparison with the rapid melting of the photo-bleached monomers. Therefore, it is evident that post polymerization takes place via both an ionic mechanism and a radical mechanism in the solid state at different temperatures. It was found from the ESR studies that so-called β-crystals obtained by annealing at –120°C can be post-polymerized at 77°K by irradiation with near-ultraviolet light but the chain length of the polymers is not long. The so-called α-crystals obtained by rapid cooling from room temperature to –196°C can be less post-polymerized at the same condition as compared with β-crystals, though at relatively high temperatures, the irradiated α-crystals polymerize very rapidly by a radical mechanism. Molecular weight of polymers obtained from the irradiated α-crystals was greater than that of β-crystals. These differences are attributed to those of aggregation states of monomers between α- and β-forms. (auth) (Japan)

29119 PRODUCTION OF CROSSLINKED POLYMERS. (to Badische Anilin- and Soda-Fabrik Aktiengesellschaft). British Patent 1,226,657. 31 Mar 1971. Priority date 11 Jul 1967, Germany.

A crosslinked polymer was formed by irradiating with high-energy radiation at atmospheric pressure a system containing olefinically unsaturated polymerizable monomers 10 to 90 wt % of which consist of at least one halogen-containing olefinically unsaturated polymerizable ester. The polymerizable ester is an ester of an α,β-olefinically unsaturated polymerizable monocarboxylic acid with a chlorinated and/or brominated monohydric alcohol. (B.L.M.)

29120 ELECTRON-CURABLE PAINT BINDERS. (to Ford Motor Co. Ltd.). British Patent 1,226,282. 24 Mar 1971. Priority date 1 Jul 1968, United States.

An electron-curable paint is made up of a binder almost wholly or of a binder to serve as a vehicle for pigmentary and/or particulate filler material. The binder is a solution in one or more vinyl monomers of a binder resin, which is a vinyl copolymer having pendant from C atoms of the principal C-to-C chain two or more diester side chains and which also contains free hydroxyl groups. Preferably, the principal polymer chain of the binder resin is derived from acrylic acid and/or methacrylic acid and one or more esters of these acids. The paint is applied to a substrate and then cured in place by electron irradiation. (B.L.M.)

29121 PROCESS RADIATION IN THE PLASTICS INDUSTRY, 1969. Sixth Annual Washington State University Pacific Northwest Plastics Short Course Held at Pullman, Washington, June 11–13, 1969. Pullman, Wash.; Washington State University (1969). 170p. $15.00. (CONF-690656).

The conference proceedings are divided into 13 sections. The first section is a background-type paper. Ten sections deal mainly with radiation processes in various industries, chiefly plastics. The 12th section is a recording of a panel discussion entitled Commercial Sources of Radiation—A Frank Confrontation. The last section of the proceedings lists all the conference participants and their addresses. Separate abstracts have been prepared for 7 of the sections. (B.L.M.)

For abstracts of individual papers see: 29104 and 29122–29127.

29122 FUNDAMENTALS OF RADIATION PROCESSING. Stannett, V. T. (North Carolina State Univ., Raleigh). pp II.1-19 of Process Radiation in the Plastics Industry, 1969. Pullman, Wash.; Washington State Univ. (1969).

From Conference on process radiation in the plastics industry; Pullman, Wash. (11 Jun 1969). See CONF-690656.

The elementary concepts of high-energy radiation are reviewed including the types of radiation and the concepts of dose and dose rate. The absorption of radiation and the interaction of radiation with matter are discussed. Attention is given to those types of radiation that are of interest in the radiation processing of high polymers currently or in the near future. Both machine and isotopic sources of radiation are considered, compared, and contrasted. The chemical effects of radiation are discussed first in the area of the primary events such as the formation of ions, radicals, and excited species and then the fate of the active intermediates and the consequences of their reactions. The changes that can be brought about in polymeric materials are described in more practical detail. These are summarized as follows: polymerization of vinyl and other monomers (vapor phase, bulk liquid, emulsion, solution, and solid-state); effects of radiation on high polymers (crosslinking, degradation, other effects); graft polymerization (vapor and liquid phase, techniques available, fundamental considerations); and special radiation processing problems (wood plastics, modification of textile and other fibers, crosslinking of coatings, other possible applications). (auth)

29123 CURING OF COATINGS ON WOOD PRODUCTS BY ELECTRON BEAM. Spencer, Phillip C.; Swanholm, Carl E.; Taylor, Clement R.; VanderBie, William C. (Boise Cascade Corp., Yakima, Wash.). pp IV.1-11 of Process Radiation in the Plastics Industry, 1969. Pullman, Wash.; Washington State Univ. (1969).

From Conference on process radiation in the plastics industry; Pullman, Wash. (11 Jun 1969). See CONF-690656.

Certain aspects of the processing line at the Boise Cascade Corp. pilot plant for curing of coating on wood substrates in addition to an academic comparison of machine-generated electrons for curing versus isotopic curing are discussed. Several advantages of the radiation curing process over conventional curing systems and a comparison of their properties due to specific methods of cure and environmental conditions are also covered. Some discussion is given to future possibilities of radiation curing systems as applied to papers, textiles, metals, and their resultant improved properties. (auth)

29124 CONVERTIBLE POLYMERS FOR RADIATION PROCESSING. Trecker, D. J.; Colomb, H. O. Jr.; Osborn, C. L. (Union Carbide Corp., South Charleston, W. Va.). pp V.1-34 of Process Radiation in the Plastics Industry, 1969. Pullman, Wash.; Washington State Univ. (1969).

From Conference on process radiation in the plastics industry; Pullman, Wash. (11 Jun 1969). See CONF-690656.

A class of polymers containing norbornenyl unsaturation exhibited remarkable crosslinking response to ionizing radiation. These include ethylene copolymers, vinyls, cellulosics, acrylics, and polysiloxanes, which were modified to incorporate the norbornene function either in the polymer backbone or pendant to it. Gel–dose curves were used to illustrate the reactivity of these systems, with 90% insolubility achieved in some cases at doses of ≈1 Mrad. For example, irradiation of a 90–10 ethylene–vinyl 5-norbornene-2-carboxylate copolymer film with 1 MeV electrons provided 90% gel at 0.5 Mrad. This high susceptibility to radiation curing is attributed to the free-radical affinity of the strained norbornenyl double bond, which provides an excellent site for interchain radical addition. Consistent with this interpretation is the high G-value (91) and low kinetic chain length (ca. 2) determined for the crosslinking of ethylene–vinyl 5-norbornene-2-carboxylate at low doses. The linearity of a Charles-by-Pinner

plot of $S + S^{\frac{1}{2}}$ versus 1/(norbornene concentration) illustrates the dependence of crosslinking on norbornenyl content. These polymers are also cured readily by exposure to ultraviolet radiation. The reactivity is credited to both interchain radical addition and interchain cyclodimerization, the latter process predominating when a high triplet energy photosensitizer ($E_T \geq 73$ kcal mole^{-1}) is intermixed with the polymer. Measurements on an 83–17 ethylene–vinyl 5-norbornene-2-carbosylate copolymer film revealed that crosslinking proceeded with an overall quantum yield of 0.51 ± 0.14. (auth)

29125 CHEMONUCLEAR AND RADIATION CHEMICAL PROCESSING FUNDAMENTALS AND PRESENT STATUS OF TECHNOLOGY. Steinberg, Meyer (Brookhaven National Lab., Upton, N. Y.). pp VIII.1-37 of Process Radiation in the Plastics Industry, 1969. Pullman, Wash.; Washington State Univ. (1969).

From Conference on process radiation in the plastics industry; Pullman, Wash. (11 Jun 1969). See CONF-690656.

The worldwide aspects of applied radiation are traced through the historical background and state of art for radiation chemical synthesis. The role of national and international laboratories is reviewed. The fundamentals are given including: a classification of radiation chemical reactors; a definition of terms; quantitative expressions controlling process applications; economic evaluation; characteristic chemical reactions for a given type of radiation reactor; listing of processes that have reached commercial status; and listing of potential processes. The characteristics and development of radiation sources are reviewed. The basics of applied radiation chemistry are reviewed. The chemonuclear or pile radiation processes are reviewed mainly for endothermic reactions. Those of prime interest include the synthesis of ozone from oxygen or air for water treatment purposes; the synthesis of oxides of nitrogen for fixed nitrogen fertilizer market; and the formation of synthesis gas by decomposition of carbon dioxide. Radiation chemical processes, which apply isotopic and machine radiation, are basically exothermic reactions: oxidation; halogenation; polymerization; heterogeneous reactions; production of composite materials; and material modifications. (auth)

29126 PROCESS RADIATION USING ACCELERATOR SOURCES. Schonberg, Russell G. (SHM Nuclear Corp., Sunnyvale, Calif.). pp IX.1-12 of Process Radiation in the Plastics Industry, 1969. Pullman, Wash.; Washington State Univ. (1969).

From Conference on process radiation in the plastics industry; Pullman, Wash. (11 Jun 1969). See CONF-690656.

Present uses of ionizing radiation machine sources are reviewed. Process equipment currently in use is reviewed with a brief background of equipment function. A look into some expected future uses of process radiation is presented with a view toward radiation equipment needs to meet the future uses. Establishment of criteria for machine radiation source design for future needs is presented. Some of the current problems inhibiting growth rate and methods of meeting these problems are discussed. (auth)

29127 ELECTRON BEAM RADIATION APPLICATIONS FOR THE PLASTICS INDUSTRY. Morganstern, Kennard H. (Radiation Dynamics, Inc., Westbury, N. Y.). pp X.1-23 of Process Radiation in the Plastics Industry, 1969. Pullman, Wash.; Washington State Univ. (1969).

From Conference on process radiation in the plastics industry; Pullman, Wash. (11 Jun 1969). See CONF-690656.

Both present and future plastics applications using radiation are discussed, with particular attention to the engineering and cost parameters. The experiences in comparative costs of radiation processes vs conventional processes are considered. Both the initial lower cost of electron beam power and the high efficiency of this radiation enables it to compete favorably with ordinary process techniques on already existing plastic products. (B.L.M.)

29128 IRRADIATION OF PETROLEUM PRODUCTS AND PLASTICS. Yuan, H.-C. (Internationale Atomenergie-Agentur, Vienna). Isotopenpraxis; 7: 1-8(Jan 1971). (In German).

A survey is presented on the state of development and commercial application of radiation processes (polymerization and grafting of plastics, crosslinking of plastics, radiation curing of surface layers, composite materials, modification of textiles, radiation-chemical synthesis of petro-chemical products). Technical and commercial problems of irradiation plants are discussed. (auth)

29129 EFFECT OF γ-IRRADIATION ON CHLORENDIC ACID BASED UNSATURATED POLYESTERS. Gupta, S. K.; Thampy, R. T. (Shri Ram Inst. for Industrial Research, Delhi). Angew. Makromol. Chem.; 15: 147-56(1971).

The effects of gamma irradiation on chlorendic acid based unsaturated polyesters were studied. Four different types of unsaturated polyesters, made by varying the molar ratios of chlorendic acid to isophthalic acid were irradiated with a ^{60}Co source. After irradiation, the chlorine content decreases rapidly as the isophthalate content in the polyester chain increases. As the chlorendic acid content increases, the change in acid value after irradiation decreases. The increase in intrinsic viscosity is quite marked in polyesters of high isophthalate content after gamma irradiation. There is a noticeable decrease in intrinsic viscosity after irradiation of polyesters with a high chlorendic acid content. The effects of gamma irradiation on the percentage of cis and trans forms of these polyesters were studied with the help of infrared spectra. It appears that as the chlorendic acid content increases, gamma radioinduced conversion from trans unsaturation to cis unsaturation increases rapidly. (auth)

29130 RADIATION INDUCED COPOLYMERIZATION OF TETRAFLUOROETHYLENE WITH ETHYLENE IN GAS PHASE. Tabata, Yoneho (Tokyo Univ.); Ito, Wataru. Tokyo Daigaku Kogakubu Fuzoku Sogo Shikenjo Nenpo: 29: 253-9(Sep 1970). (In Japanese).

Radioinduced polymerization of tetrafluoroethylene with ethylene in the gas phase was carried out. Polymerization took place in a low concentration range of tetrafluoroethylene in the monomer mixture. The molar concentration of tetrafluoroethylene in copolymers decreased with conversion percentage and the melting point and decomposition temperature were also influenced profoundly by the conversion percentage. Monomer reactivity ratios were determined as $r_{C_2F_4} = 0.01$, $r_{C_3F_6} = 0.1$. The mechanical properties of polymers obtained in the gas phase were compared with those of liquid–phase polymerization. (auth) (Japan)

29131 RADIATION-INDUCED OXIDATION OF TRICHLOROETHYLENE. Kazanjian, Armen R.; Horrell, David R. (Dow Chemical Co., Golden, Colo.). Contract AT(29-1)-1106. J. Phys. Chem.; 75: 613-16(4 Mar 1971).

The radioinduced oxidation of trichloroethylene was investigated. It was found that a chain reaction is operable, producing extremely high radiation yields. The three major products are dichloroacetyl chloride, phosgene, and trichloroethylene oxide. The effects of dose rate, temperature, and inhibitor on the overall reaction were examined. The reaction was found to continue after the irradiation was stopped. A mechanism is postulated to account for these effects. (auth)

Radiolysis

Refer also to abstracts 29466, 29719, and 29733.

29132 (NYO–3558-24) PROGRESS REPORT, ANNUAL, FEBRUARY 1971. (Roswell Park Memorial Inst., Buffalo, N. Y.). Contract AT(30-1)-3558. 3p. Dep. NTIS.

Research on radiation damage processes at the molecular level is reviewed. (M.C.G.)

29133 THE STUDY OF ORGANIC ANIONS BY A DEFERRED LUMINESCENCE TECHNIQUE: "STIMULATION SPECTRA". Deroulede, A. (Faculte des Sciences, Orsay, France). J. Lumin.; 3: 302-24(Jan 1971).

A technique is described for obtaining "stimulation spectra" of negative species trapped during γ or uv irradiation of organic solids. These spectra correspond to the absorption spectra of the negative species and are due to the liberation of electrons (from traps or from anions) and to their recombination with cations, leading to an emission of light. The spectra thus obtained are not perturbed by the absorption spectra of the positive species present. Depending on the concentration of aromatic solutes, the relative amounts of trapped electrons and anions detected give information on the distance to which free electrons can migrate in the matrix (120 Å in glassy methylcyclohexane (MCH), 320 Å in polycrystalline MCH). Electrons can be transferred reversibly between physical traps and solute molecules by illumination in the respective absorption bands. The solids studied were: solutions of biphenyl in glassy and polycrystalline MCH, 3-methylpentane (3 MP), cyclohexane, and benzene; solutions of styrene, pyrene, naphthalene, durene in glassy MCH or 3 MP, and pure polycrystalline acetone. In ethanol, boric acid, and carbon tetrachloride no stimulation spectra were obtained. (auth)

29134 ESR STUDIES OF THE MECHANISMS FOR RADICAL FORMATION IN IRRADIATED FROZEN SULFURIC ACID SOLUTIONS OF THYMINE. Henriksen, Thormod; Jones, W. Barrie G. (Norsk Hydro's Inst. for Cancer Research, Oslo. Univ., Oslo). Radiat. Res.; 45: 420-33(Feb 1971).

Frozen thymine solutions of H_2SO_4 (0 to 10 mole/liter) were irradiated at 77°K, and the formation of radicals studied by ESR

XUM

techniques. Hydrogen atoms and other unidentified H_2SO_4 radicals seem to be the main ESR products at 77°K. On subsequent warming, large amounts of the 5-thymyl radicals were formed. This formation of thymine radicals reached its maximum in the temperature range from 150 to 190°K, depending somewhat on the physical form of the sample. No direct evidence was found for any of the other thymine radicals known from single crystal studies. Concentration studies showed that the 5-thymyl radicals were formed mainly by indirect mechanisms. While direct addition of radioinduced hydrogen atoms to the 6-position of the thymine ring may take place, such a mechanism must be excluded as the main source for the formation of 5-thymyl radicals in irradiated frozen solutions of sulfuric acid. It is suggested that radioinduced electrons and other solvent radicals may react with thymine to form intermediate thymine radicals. However, the details of these reactions, as well as the subsequent conversion reactions, are not known. (auth)

29135 γ-RADIOLYSIS OF AQUEOUS SOLUTIONS OF 5-BROMO-2'-DEOXYURIDINE IN PRESENCE OF OXYGEN. I. IDENTIFICATION OF PRODUCTS. Kourim, P. (Institut fuer Strahlenchemie, Karlsruhe, Ger.); Bors, W.; Schulte-Frohlinde, D. N. Naturforsch.; 26b: 308-11(Apr 1971). (In German).

The γ radiolysis of 5-bromo-2-deoxyuridine in neutral oxygen-saturated aqueous solutions leads to the following products: hydrogen bromide, hydrogen peroxide, organic peroxides, isodialuric acid deoxyriboside, deoxyuridine, deoxyribosylurea, urea, deoxyribose, and 5-bromouracil. In addition, some unidentified products are formed. The main products are isodialuric acid deoxyriboside and hydrogen bromide. (auth)

29136 γ-RADIOLYSIS OF AQUEOUS SOLUTIONS OF 5-BROMO-2'-DEOXYURIDINE IN PRESENCE OF OXYGEN. II. G-VALUES OF PRODUCTS AND COMPARISON WITH THE RADIOLYSIS OF THE AGLYCONE. Kourim, P. (Institut fuer Strahlenchemie, Karlsruhe, Ger.); Bors, W.; Schulte-Frohlinde, D. Z. Naturforsch.; 26b: 312-14(Apr 1971). (In German).

In the γ radiolysis of 5-bromodeoxyuridine (BUdR) in neutral aqueous O_2-saturated solution OH radicals react both with the base and the sugar moiety of BUdR in an approximately equal amount. At low BUdR concentrations solvated electrons (e_{aq}^-) and H radicals are scavenged by O_2. At high BUdR concentrations e and H radicals react with BUdR. These two species preferentially react with the base, $Br^\ominus$ and isodialuric acid deoxyriboside being the major products. Similarities with the γ radiolysis of 5-bromouracil are discussed. (auth)

29137 MECHANISM FOR THE SOLUBILIZATION OF COLLOIDAL SULFUR BY GAMMA RADIATION. Donaldson, George William. Athens, Ga.; Univ. of Georgia (1970). 209p. University Microfilms Order No. 71-3724.

Thesis.

The mechanism by which colloidal sulfur is solubilized by gamma radiation involves indirect action. The dissolved sulfur in the homogeneous phase undergoes a reaction to produce apparently H_2SO_4. The particles, in turn, dissolve as the system attempts to reestablish equilibrium. This process is described by diffusion kinetics and the rate of decrease of the particle radius per unit time is indicated by: $(dr/dt) = -(D/\rho r)(C_s - C)$. The process can be divided into two stages: (1) a radiolysis step in which dissolved sulfur reacts with reactive species, (2) a recovery stage in which the sulfur in the homogeneous phase tends toward an equilibrium concentration. At the end of the kth radiolysis step of t_1 seconds, the new particle radius is equal to: $r_{kj} = \{r_{jj}^2 - [2DC_s t_1/\rho] + [2D/\rho][(a + bC_{jj})/b^2]\ EXP\ [bt_1] - [2D(a + bC_{jj})/\rho b^2] - [2Dat_1/\rho b]\}^{1/2}$. At the end of the kth recovery step of t_2 seconds, the new particle radius is equal to: $r_{kk} = \{r_{kj}^2 - [2DC_s/\rho k_2] + [2DC_s/\rho k_2]\ EXP(-k_2t_2) + [2DC_{kj}/\rho k_2] - [2DC_{kj}/\rho k_2]\ EXP(-k_2t_2)\}^{1/2}$; where D is the diffusion coefficient for the diffusion of sulfur from the particle sulfur into the homogeneous phase, C_s is saturation concentration of sulfur in an aqueous media, $k_2 = n4\pi rD$, ρ = the density of the sulfur particles (1.80 grams/cc), C_{jj} = the concentration of sulfur in the homogeneous phase at the end of the jth recovery period, C_{kj} = the end of the kth irradiation period, r_{jj} = the particle radius at the end of the jth recovery period, and r_{kj} is the particle radius at the end of the kth irradiation period. Saturated Cl_2 water and Fenton's reagent ($Fe^{+2} + H_2O_2$), a source of OH radicals, react with the sulfur hydrosols at the comparable rates as observed in continually irradiated systems. Scavenging experiments indicate that the OH radical or a precursor to the OH radical oxidizes the dissolved sulfur to SO_4^{2-}. For the irradiated system, the rate of reaction of colloidal sulfur is dependent on the particle concentration, n, ($k_2 = n4\pi rD$) and the intensity of radiation for low dose rates. However, as the intensity is raised above 4.0×10^{15} ev/cc/sec, the rate of reaction becomes independent of the radiation intensity. The process has an activation energy of 14,000 ± 500 calories per mole and is independent of pH. O_2 greatly inhibits the radiolysis reaction. By performing periodic irradiations interspersed with chosen recovery periods, it was possible to determine evidently unique values for D and C_s. D and C_s appear to have values of 2.0×10^{-6} cm²/sec and 2.7×10^{-7} g/cc respectively, where D is the diffusion coefficient of sulfur going into solution and C_s is the saturation concentration of sulfur in water at 25°C. From this mechanistic picture, k_1(the rate constant for the radiolytic reaction of dissolved sulfur) appears to be directly proportional to the dose rate used in the experiments. (For example, at a dose rate of 7.5×10^{15} ev/cc/sec, $k_1 = 0.05\ sec^{-1}$.) As a result, $G(-S_{diss})_{degassed}$ was calculated to be 3.4 and for the oxygenated system, $G(-S_{diss})_{O_2}$ was calculated to be 0.07 molecules/100 ev. (Diss. Abstr. Int., B)

29138 RADIATION INDUCED CHEMILUMINESCENCE OF AQUEOUS FLUORESCEIN DYES. Rodde, Anton Frank. Chicago; Illinois Inst. of Tech. (1970). 109p. University Microfilms Order No. 71-4509.

Thesis.

In the study of the radioinduced chemiluminescence from several fluorescein dyes in aqueous solution, a combined flash photolysis-pulse radiolysis technique distinguishes between possible reactions of the hydrated electron (e_{aq}^-) with either semi-oxidized dye (X) or the hydroxyl dye adduct (SOH·) leading to light emission. Two distinct mechanisms of delayed dye fluorescence are reported. Emission I, which is quenched by the addition of e_{aq}^- or OH scavengers, is shown to proceed from the attack of e_{aq}^- on SOH· yielding the lowest excited dye singlet (S*). Emission II, which is not quenched by OH scavengers, occurs when the dye is pulse irradiated at short delay times following light flash excitation in the visible absorption band of the dye. The emission intensity of process II depends linearly on absorbed dose but quadratically on initial dye triplet yield. From these results and kinetics analysis it is suggested that emission II results from e_{aq}^- attack on a triplet "excimer" yielding S* and the semireduced dye (R). These processes are represented as (I) $e_{aq}^- + SOH\cdot \rightarrow S^* + OH^-$, $S^* \rightarrow S + h\nu$; and (II) $e_{aq}^- + \text{excimer} \rightarrow S^* + R$, $S^* \rightarrow S + h\nu$. (Diss. Abstr. Int., B)

29139 ESR SPECTRUM OF γ-IRRADIATED ADAMANTANE. Bonazzola, L.; Marx, R. (CNRS, Orsay, France). Chem. Phys. Lett.; 8: 413-16(1 Mar 1971).

It was found that the ESR spectrum observed after γ irradiation of solid adamantane is not due to 1- and 2-adamantyl radicals but to a substituted 1-methylcyclohexyl radical resulting from a C–C bond rupture. The reversible thermal changes of the spectrum show that the cyclohexyl ring inter-converts between its two stable configurations with a temperature dependent rate. (auth)

29140 GEMINATE RECOMBINATION OF X-RAY EXCITED CARRIERS IN ORGANIC SOLIDS: POLY-N-VINYLCARBAZOLE. Hughes, R. C. (Sandia Labs., Albuquerque, N. Mex.). Chem. Phys. Lett.; 8: 403-6(1 Mar 1971).

Experimental evidence indicates that the yield of charge carriers in the bulk x-ray excitation of films of poly-N-vinylcarbazole is dominated by geminate (initial) recombination of the electron-hole pairs. This mechanism has been previously verified for high pressure gases and some liquids, but this is the first unambiguous confirmation of geminate carrier recombination in a low mobility solid. The carrier yield versus applied field curve also allows an estimate of about 60Å for the thermalization length of the hot electrons. (auth)

29141 OXYGEN FORMATION IN THE γ-RAY IRRADIATION OF Fe^{2+}–Cu^{2+} SOLUTIONS. Bjergbakke, E.; Hart, Edwin J. (Atomic Energy Commission Research Establishment, Risoe, Denmark. Argonne National Lab., Ill.). Radiat. Res.; 45: 261-73(Feb 1971).

The mechanism of O_2 formation was studied in ^{60}Co γ-irradiated Fe(II) + Cu(II) solutions at 0.01 N $HClO_4$ and at 0.01, 0.08, and 0.80 N H_2SO_4. In the H_2SO_4 system, $G(O_2)$ rises to plateau levels near 0.02 as the $CuSO_4/FeSO_4$ ratio increases. The plateau value diminishes slightly and is displaced toward higher $CuSO_4/FeSO_4$ ratios with increasing acidity. The perchlorate system differs from the sulfate only at high $Cu(ClO_4)/Fe(ClO_4)_2$ ratios where $G(O_2)$ rises to 0.10. The O_2 yield of 0.02 is not derived from "spur" HO_2, OH, H_2O_2 or O_2, although the increase in $G(O_2)$ above this level in the perchlorate system is attributed to H_2O_2. "Spur" O atoms are postulated as the source of O_2 with the yield, $G(O_2) = 0.02$. (auth)

29142 GAMMA RADIOLYSIS OF BRANCHED CHAIN HYDROCARBONS: 2,2-DIMETHYLBUTANE. Castello, Gianrico; Grandi, Francesco; Munari, Stelio (Univ., Genoa). Radiat. Res.; 45: 399-419(Feb 1971).

The gamma radiolysis of liquid 2,2-dimethylbutane was investigated under vacuum as a function of total dose and free radical scavengers. Doses from 0.55×10^{20} to 11.50×10^{20} eV/g were

used. Iodine was used as a scavenger and the alkyl iodides formed were analyzed by gas chromatography with an electron capture detector. It is postulated that the formation of fragmentation products is due to both ionic and radical mechanisms, while the heavy products are formed mainly by recombination of parent free radicals. (auth)

29143 ESR INVESTIGATIONS ON THE REACTION OF THYMINE WITH RADIATION INDUCED ELECTRONS IN ALCOHOLIC MATRICES AT 77°K. Verma, N. C.; Singh, B. B.; Gopal-Ayengar, A. R. (Bhabha Atomic Research Centre, Trombay, India). Stud. Biophys.; 13: 231-6(1969).

Gamma irradiation of thymine in alkaline methanol and ethanol results in the formation of thymine anions at 77°K. On warming to higher temperatures, hydrolysis of anions occurs giving rise to thymyl radicals. The yields of ions and radicals depend on the concentration of the alcohols. (auth)

29144 RADIATION CHEMISTRY OF POLYETHYLENE AND POLY(PROPYLENE OXIDE). Budzol, Melvin. Evanston, Ill.; Northwestern Univ. (1970). 174p. University Microfilms Order No. 71-1808.

Thesis.

The techniques of gel fractionation and ultraviolet and infrared spectroscopy were used to measure some of the chemical changes produced in polyethylene subjected to high-energy radiation while being maintained in the molten state (155°C). Some of the chemical effects produced in isotactic and atactic poly (propylene oxide) irradiated at room temperature were studied by measurement of intrinsic viscosity changes and of extent of gel formation as well as by observation of changes in the infrared spectra of these polymers. Infrared, ultraviolet, and ESR spectroscopy were employed to detect transient species in isotactic and atactic poly (propylene oxide) irradiated at liquid nitrogen temperature. Special irradiation cells were constructed for both the high and the low-temperature irradiations for which an electron beam generator was used as the radiation source. Room temperature irradiations were conducted in a ^{60}Co gamma source. Based on the measured values of the extent of crosslinking and unsaturation changes produced in polyethylene irradiated at 155°C. It was shown that the material balance equation that adequately describes the major chemical events occurring during the radiolysis of polyethylene in the solid state (below 140°C) was inadequate for the molten-state irradiation of polyethylene. Three free radical species trapped in poly (propylene oxide) irradiated at liquid nitrogen temperature were detected and tentatively identified. Various mechanisms for the decay and interconversion of these free radical species are proposed. (Diss. Abstr. Int., B)

29145 RACEMIZATION OF D(–) MANDELIC ACID BY ^{60}Co-γ-IRRADIATION. Ehrl, A. (Gesellschaft fuer Strahlenforschung, Neuherberg, Ger.). Atomkernenergie; 17: 67-17(Feb 1971).

D(–) mandelic acid (10^{-3}M) of the highest purity was dissolved in aerated water and irradiated with ^{60}Co γ radiation. The water used was distilled twice in quartz apparatus. The radiation doses ranged from 30 to 110 krad at the dose rate of 2.78 krad/min. During irradiation the decrease of the initial optical rotation of the D(–) mandelic acid was linear. The following products were found by means of spectropolarimetry and uv absorption spectroscopy: D(–) mandelic acid, L(+) mandelic acid (PhCHOH–COOH), and phenylglyoxylic acid (PhCO–COOH). The formation of these substances can be explained if the mandelic acid radical (PhĊOH–COOH) is regarded as a common intermediate product. This radical results from an attack on the mandelic acid molecule by the radicals primarily produced by radiolysis of water. The stable products, which were analyzed, were finally formed by the recombination of this radical with the water radiolysis products, namely hydrogen atoms (H˙) and hydroxyl radicals (HO˙). As a result of isotropic conditions the recombination of hydrogen atoms with the mandelic acid radical was a random process, producing a racemate mixture of (50%) D(+) mandelic acid and (50%) D(–) mandelic acid. Recombination with hydroxyl radicals however, corresponded to an oxidation of the mandelic acid. The hydrate form of phenylglyoxylic acid (PhC(OH)$_2$–COOH) was the primary result of recombination, and was obviously stabilized by the elimination of water. Phenylglyoxylic acid was produced and measured by uv spectroscopy. (auth)

29146 ESR STUDY OF THE SUGAR RADICAL IN IRRADIATED DEOXYADENOSINE. Alexander, Chester Jr.; Franklin, Carl E. (Univ. of Alabama, University). J. Chem. Phys.; 54: 1909-13(1 Mar 1971).

Single crystals of deoxyadenosine monohydrate grown from H_2O and D_2O solutions were x irradiated and studied by electron spin resonance techniques at room temperature. The results show an isotropic coupling of 7 ± 1.0 G to one β proton and an anisotropic coupling of an α proton with principal values –22.6 ± 0.5 G, –16.4 ± 0.5 G, and –5 ± 0.5 G. The spin density on the carbon atom (C_5'), calculated from the above results, is 0.64. The g-tensor principal values are 2.0029 ± 0.0002, 2.0052 ± 0.0002, and 2.0075 ± 0.0002. These data are consistent with a radical formed in the dexoyribose sugar group as a result of hydrogen abstraction at the C_5' position. (auth)

29147 ELECTRON SPIN RESONANCE (ESR) STUDY OF $\Delta^{10,10'}$-BIANTHRONE AND AN ATTEMPT TO PREPARE CYCLOPROPENYL RADICAL (C_3H_3). Richerzhagen III, Theodore. Seattle; Univ. of Washington (1970). 140p. University Microfilms Order No. 71-1017.

Thesis.

The electron spin resonance (ESR) signal detected in solutions of $\Delta^{10,10'}$-bianthrone (I) were investigated in order to identify the paramagnetic species to determine its relationship to the thermochromism of (I). The spectrum was reduced to coupling constants and these values were verified by computer simulation. It has been found that the ESR signal (1) increases in intensity with increasing temperature, (2) can be detected in a variety of solvents (pyridine, naphthalene, benzene, and others), (3) is detected only in the absence of oxygen, and (4) is not observed if the sample of (I) is prepared and studied in the dark. Thermochromism is observed on heating this same sample in the dark. Illumination of this sample produces the paramagnetic species. Three methods were used in an unsuccessful attempt to prepare the cyclopropenyl radical (C_3H_3˙) in concentration sufficient for detection by ESR. These methods are: (1) gamma irradiation of solid cyclopropene, (2) ultraviolet irradiation of neat solid cyclopropene and cyclopropene dispersed in various organic glasses, and (3) a recently developed method based on the selective hydrogen abstraction shown by the t-butoxyl radical. Modifications are suggested for method (3) which, in principle, would make it possible to prepare the cyclopropenyl radical. (Diss. Abstr. Int., B)

29148 RELEASE OF THE HYDROGEN ATOM IN THYMINE RADIOLYSIS. Drasil, V.; Ryznar, L.; van Duyet, P. (Inst. of Biophysics, Brno). Stud. Biophys.; 20: 147-52(31 May 1970).

Aqueous solutions of tritium-labeled thymine were irradiated with gamma rays of ^{60}Co. The measurements of the radioactivity showed that some products of thymine radiolysis lost tritium bound in the C-6 position. Tritium removed from the pyrimidine molecule can be detected in the redistilled solvent water. The release of hydrogen bound on the sixth carbon atom of thymine into water is most likely connected with the action of OH radicals. This reaction can be observed also in the case of irradiation of macromolecular DNA containing thymine-6-^{3}H. (auth)

29149 PULSE RADIOLYSIS OF AQUEOUS CYANOGEN SOLUTION. Draganic, I. G.; Draganic, Z. D.; Holroyd, R. A. (Brookhaven National Lab., Upton, N. Y.). J. Phys. Chem.; 75: 608-12 (4 Mar 1971).

Pulse radiolysis has been used to study directly radioinduced chemical changes in aqueous solutions of cyanogen. Reaction with the hydrated electron is fast, $k(e^-_{aq} + (CN)_2) = (2.1 \pm 0.2) \times 10^{10}$ M^{-1} sec^{-1}. The absorption spectrum of the cyanogen ion-radical $(CN)_2^-$ shows two maxima at 290 and 440 nm, with respective molar extinction coefficients of 2100 and 360 M^{-1} cm^{-1}. The decay kinetics of the electron adduct show a pseudo-first-order and a second-order process as two consecutive processes; probable reactions are discussed. The reactions of H and OH with cyanogen are slow in dilute solutions, and the rate constants were estimated as $\sim 10^7$ M^{-1} sec^{-1}. The formation of iminoacetonitrile radical N–ĊCNH and oxime radical NC–ĊNOH was considered. (auth)

29150 DEFERRED LUMINESCENCE SPECTRA OF SOME AROMATIC COMPOUNDS IN RIGID ORGANIC MEDIA. Deniau, C.; Deroulede, A.; Kieffer, F.; Rigaut, J. (Faculte des Sciences, Orsay, France). J. Lumin.; 3: 325-50(Jan 1971).

The spectral composition of light emitted when ions trapped during γ-irradiation are made to recombine was studied in rigid matrices containing aromatic solutes: biphenyl, durene, styrene, naphthalene, and pyrene. The recombination of cations with electrons or with anions can be observed separately: the former by optical detrapping of electrons or, in methylcyclohexane (MCH), by warming to the temperature of the first glow peak; the latter by warming to the temperature of the second glow peak in MCH. In all cases, the deferred luminescence consists of the fluorescence and phosphorescence of the solute (with the exception of styrene whose phosphorescence is unknown), and the phosphorescence/fluorescence ratio is enhanced with respect to the ordinary luminescence spectrum. With biphenyl in MCH, all types of deferred luminescence have the same P/F ratio, whereas with durene differences are observed. Also, with durene and styrene, the fluorescence of radicals appears under certain conditions of dose: these radicals are formed respectively by hydrogen abstraction from a methyl group of durene and by hydrogen addition

XUM

to the vinyl group of styrene. With naphthalene and pyrene, excimer fluorescence was observed at high concentrations. It was concluded that radical emission is due to the fact that radicals scavenge electrons and positive charges, the probability of capture of either being different, and that excimer emission results from the neutralization of dimer cations. (auth)

29151 MOESSBAUER STUDY OF PROTON IRRADIATION EFFECTS IN FERROUS SULFATE. Kopcewicz, M.; Kotlicki, A. (Univ., Warsaw). Phys. Status Solidi (b); 44: K127-9 (1 Apr 1971).

$FeSO_4 \cdot 7H_2O$ samples were irradiated with protons at 0.9- to 1.8-MeV energies and 0.05- to 0.8-μA beam currents. The Moessbauer spectra of the irradiated samples are independent of the proton energy but change with current. The quadrupole doublets indicate that dehydration occurs during proton irradiation. A weak line for heavy irradiations indicates the formation of FeS_2. For currents >0.5 μA, lines of Fe_2O_3 appear. The isomer shift is identical with that for a nonirradiated sample, indicating that the electron configuration of the Fe^{2+} ion does not change with irradiation. (D.L.C)

29152 FORMATION OF RADICALS IN IRRADIATED SINGLE CRYSTALS OF SARCOSINE HCl STUDIED BY ESR. Lassmann, G.; Damerau, W. (Institut fuer Biophysik, Berlin). Stud. Biophys.; 17: 27-8(1969). (In German).

X-irradiated single crystals of sarcosine · Hcl and -DCl studied at room temperature showed two different types of radicals. The structure of the shorter living radical fromed by a C–N bond rupture is $\cdot CH_2-$ COOH. The other radical originating from an H abstraction has been identified as $CH_3-\dot{N}H_2-CH-COOH$. (auth)

29153 EPR STUDIES ON TRAPPED SPECIES PRODUCED IN THE GAMMA RADIOLYSIS OF AQUEOUS SUGAR ICES. Zimbrick, J. D.; Myers, L. S. Jr. (Univ. of California, Los Angeles). J. Chem. Phys.; 54: 2899-2909(1 Apr 1971).

The yields, EPR spectral characteristics, and paramagnetic relaxation of trapped electrons (e_T^-) and sugar radicals were studied in ^{60}Co γ-irradiated monosaccharide ices at 77°K. The e_T^- yields in the various ices ranged from 0.95 to 1.8 and were strongly dependent on solute molarity and phase of the ice matrix. In most cases the sugar radical yields were the same as the e_T^- yields. The e_T^- could be bleached with white light to form dielectrons as previously found for e_T^- in alkaline ices. The EPR line shapes, linewidths, and line broadening mechanisms of e_T^- in the sugar ices were similar to the corresponding characteristics of e_T^- in alkaline ice. Spectral studies on the trapped sugar radicals indicated that two groups of radicals were present. The variation of the e_T^- and sugar radical relaxation times with radiation dose was studied in H_2O and D_2O matrices. The results for e_T^- were interpreted as indicating a spatially nonuniform distribution of this species; the spatial nonuniformity is not as great in the D_2O matrix as in the H_2O matrix. The results for the sugar radicals suggested that one group was distributed uniformly, whereas the other group was distributed nonuniformly to the same degree as the e_T^- distribution. (auth)

29154 HEAVY WATER AND ORGANIC FLUIDS AS NEUTRON MODERATOR AND REFLECTOR MATERIALS. Ayres, J. A. (Battelle-Northwest, Richland, Wash.); Trilling, C. A. Nucl. Eng. Des.; 14: 363-89(Feb 1971).

Physical and thermodynamic constants of light and heavy water are compared. Properties of heavy water for use as a reactor coolant are described. Values for density, specific volume, thermal conductivities, viscosity, thermal capacity, specific heat, entropy, enthalpy, vapor pressure, surface tension, heat of vaporization, free energy, and G-values in γ radiolysis are discussed. Properties of some organic materials for possible use as reactor moderators and coolants are given. (91 references) (M.C.G.)

29155 GAS CHROMATOGRAPHIC ANALYSIS OF γ-IRRADIATED ANILINE FOR AMINOAROMATIC PRODUCTS. Knight, J. A. (Georgia Inst. of Tech., Atlanta). J. Chromatogr.; 56: 201-8(7 Apr 1971). (ORO-3519-7).

Gas chromatographic conditions were found for the satisfactory analysis of the isomeric diaminobenzenes, the isomeric aminobiphenyls and diphenylamine, the isomeric aminodiphenylamines, and the isomeric 2,2′-, 2,3′-, and 2,4′-diaminobiphenyls. Satisfactory conditions were found for the analysis of 3,3′-, 3,4′-, and 4,4′-diaminobiphenyl as individual components, but not for the analysis of a mixture containing all three isomers. (auth)

29156 ELECTRONIC SPECTRA OF TRAPPED ELECTRONS IN ORGANIC GLASSES AT 4°K. Hase, Hirotomo; Noda, Masato; Higashimura, Takenobu (Kyoto Univ.). J. Chem. Phys.; 54: 2975-8(1 Apr 1971).

The optical absorption spectra of trapped electrons were observed in γ-irradiated ethanol, ethylene glycol–water, methanol, 10M NaOH, and 2-methyltetrahydrofuran (MTHF) at 4°K. The prominent infrared absorption bands were observed in ethylene glycol–water and ethanol glasses, while the bands in methanol, 10M NaOH, and MTHF glasses were similar in shape, slightly red shifted, to the bands for the radiolysis at 77°K. When the glasses were warmed to 77°K, the bands changed irreversibly into those for the radiolysis at 77°K, reducing the absorption intensity. The spectral changes at the intermediate temperatures between 4°K and 77°K were recorded for ethylene glycol–water and methanol cases. The results are interpreted by the molecular reorientation model proposed in the previous paper [T. Higashimura, M. Noda, T. Warashina, and H. Yoshida, J. Chem. Phys. 53, 1152(1970)]. (auth)

29157 γ RADIOLYSIS OF LIQUIDS AT HIGH PRESSURES. X. THE REACTION H + OH^- AND THE PARTIAL MOLAL VOLUME OF THE HYDRATED ELECTRON. Hentz, Robert R.; Brazier, David W. (Univ. of Notre Dame, Ind.). J. Chem. Phys.; 54: 2777-80(1 Apr 1971).

$G(H_2)$ is independent of pressure over the range 0 to 6.2 kbar in γ radiolysis of the following deaerated aqueous solutions at 23°C: (a) solutions with 0.001M or 0.1M hydroxide, isopropanol at concentrations in the range 9×10^{-4}M to 0.1M, and nitrate at one-fiftieth of the isopropanol concentration; (b) solutions with 0.01M formate, 0.001M nitrate, and 0.01M or 0.1M hydroxide; (c) near-neutral solutions with 0.01M formate and 0.01M or 0.002M benzyl alcohol. From pressure independence of $G(H_2)$ for such solutions and the established pressure independence of the primary yields of water radiolysis, it follows the activation volumes for the reactions of H with hydroxide, isopropanol, formate, and benzyl alcohol are equal. Consequently, $\Delta V_1^{\ddagger} = -5.9$ ml $mole^{-1}$ was obtained for the reaction [1], $H + OH^- \rightarrow H_2O + e_{aq}^-$. Combination of $\Delta V_1^{\ddagger}$ with the previously determined $\Delta V^{\ddagger} = -14.2$ ml $mole^{-1}$ for the back reaction gives ΔV for reaction [1]. From ΔV, with a previous estimate of $\bar{V}(H)$ in the range 5.9 to 10.3 ml $mole^{-1}$, the absolute partial molal volume of e_{aq}^- (based on a value of -5.4 ml $mole^{-1}$ for H^+) was estimated to be in the range -1.7 to 2.7 ml $mole^{-1}$. With an estimated electrostriction contribution of -3 ml $mole^{-1}$, the electron cavity volume was in the range 1 to 6 ml $mole^{-1}$. In effect, such estimates of the electron cavity volume and $\bar{V}(e_{aq}^-)$ are obtained from the pressure dependence of an equilibrium constant. (auth)

29158 PULSE RADIOLYSIS STUDIES. XX. KINETICS OF SOME ADDITION REACTIONS OF GASEOUS HYDROGEN ATOMS BY FAST LYMAN-α ABSORPTION SPECTROPHOTOMETRY. Hikida, T.; Eyre, J. A.; Dorfman, Leon M. (Ohio State Univ., Columbus). J. Chem. Phys.; 54 342?-8(15 Apr 1971).

The pulse radiolysis technique combined with fast Lyman-α absorption spectrophotometry, was used to study the kinetics of several addition reactions of gaseous hydrogen atoms. The following absolute rate constants, at 298°K, were obtained: $H + O_2 + Ar - HO_2 + Ar$, $(5.9 \pm 0.7) \times 10^9 M^{-2} \cdot sec^{-1}$; $H + CO + H_2 = HCO + H_2$, $(4.0 \pm 0.6) \times 10^7 M^{-2} \cdot sec^{-1}$; $H + CO + Ar = HCO + Ar$, $(2.6 \pm 0.4) \times 10^7 M^{-2} \cdot sec^{-1}$; $H + NO + H_2 = HNO + H_2$, $(1.4 \pm 0.2) \times 10^{10} M\ 10^{10} M^{-2} \cdot sec^{-1}$. These results, and our earlier value for k_1 with H_2 as third body, give values of $k_1^{H_2}/k_1^{Ar} = 2.9$ and $k_2^{H_2}/k_2^{Ar} = 1.5$ for the relative third-body efficiencies of hydrogen and argon. The high-pressure limiting rate constant for H-atom addition to ethylene, obtained directly in the high-pressure region, was found to be $H + C_2H_4 = C_2H_5^*$, $(5.5 \pm 0.5) \times 10^8 M^{-1} \cdot sec^{-1}$, with both H_2 and Ar as third body. (auth)

29159 DEGRADATION OF SODIUM ALGINATE BY γ-IRRADIATION AND BY OXIDATIVE-REDUCTIVE DEPOLYMERIZATION. Humphreys, E. R.; Howels, G. R. (Medical Research Council, Harwell, Eng.). Carbohyd. Res.; 16: 65-9(Jan 1971).

Methods are described for preparing degraded sodium alginate by oxidative-reductive depolymerization (ORD) and by γ irradiation. The rate of degradation by ORD was shown to be governed by more than one rate constant, and the degraded products prepared by either method were shown to have gross chemical and biological properties similar to those of a derivative of sodium alginate prepared by hydrolytic degradation. The rate of degradation is discussed in the light of the known structure of alginic acid, and the value of the products as food additives to suppress strontium absorption is assessed. (auth)

29160 EFFECT OF DOSE RATE ON THE RADIATION YIELDS OF RADICALS IN FROZEN ORGANIC MEDIA. Kroh, J.; Wypych, M.; Piekarska, J.; Rybicki, E. (Technical Univ., Lodz, Poland). Bull. Acad. Pol. Sci., Ser. Sci. Chim.; 18: 705-10 (1970).

The effects of dose rate on radiolytic yields from frozen hexane, acetone, and cyclohexene were studied using ^{60}Co γ radiation and

ESR spectra. In all three systems the decrease of dose rate caused an increase in radical yields: from 3.7 to 5.3 for n-hexane, from 2.3 to 5.5 for acetone +10 vol% H_2O, and from 2.6 to 5.0 for cyclohexene. (M.C.G.)

29161 EFFECT OF PHASE ON THE PRIMARY PROCESS OF THE FORMATION OF BUTYL RADICALS IN THE RADIOLYSIS OF SOLID ISOBUTANE-2-d_1. Saitake, Yoshiyuki; Wakayama, Terunobu; Kimura, Toyoaki; (and others) (Nagoya Univ., Japan). Bull. Chem. Soc. Jap.; 44: 301(Jan 1971).

In order to determine whether the phase change affects the primary process of the C–H bond rupture or the isomerization of butyl radicals, the radiolysis of glassy and polycrystalline $(CH_3)_3CD$ was investigated by ESR spectroscopy at 77°K. It was concluded from the spectra that the phase change affects the primary process of C–H bond rupture. (D.P.O.)

29162 ESR STUDY OF RADICALS PRODUCED IN γ-IRRADIATED ALLYL ALCOHOL GLASS AND THEIR PHOTOCHEMICAL REACTION AT 77°K. Noda, Shoji; Torimoto, Keizo; Fueki, Kenji; Kuri, Zen-ichiro (Nagoya Univ., Japan). Bull. Chem. Soc. Jap.; 44: 273-5(Jan 1971).

The ESR spectrum of γ-irradiated allyl alcohol glass and of γ-irradiated triethylamine glass containing allyl alcohol before and after bleaching indicates that the allyl alcohol reacts with a thermal electron dissociatively to produce the allyl radical and the hydroxy anion. The effects of temperature and photolysis on the α-hydroxyallyl radical and the allyl radical in allyl alcohol glass were investigated. (D.P.O.)

29163 POSSIBLE ELECTRON SPIN RESONANCE IDENTIFICATION OF Br^{2-} AND I^{2-} IN γ-IRRADIATED BROMIDE OR IODIDE DOPED BARIUM SULPHATE. Rao, K. V. S.; Symons, M. C. R. (Univ. of Leicester, Eng.). J. Chem. Soc., D; No. 6, 268-70(Mar 1971).

Radical species showing strong hyperfine coupling to one bromide or iodine nucleus detected in γ-irradiated barium sulphate doped with bromide or iodide are identified as the species Br^{2-} and I^{2-}, respectively. (auth) (UK)

Radioisotope Production

Refer also to abstract 31333.

29164 EXTRACTION SEPARATION OF CARRIER-FREE BISMUTH FROM LEAD AND ZINC. Neirinckx, R. D. (South African Council for Scientific and Industrial Research, Pretoria). Anal. Chim. Acta; 54: 357-60(Apr 1971).

Radioactive ^{206}Bi and ^{207}Bi prepared by irradiating a Pb target with deuterons or protons is separated from the Pb and ^{65}Zn produced from the target backing by extraction from 0.2M HNO_3 with an equal volume of 0.3M bis(2-ethylhexyl) phosphate in heptane. Two subsequent washings of the organic phase with equal volumes of 0.20M HNO_3 yielded an organic phase sufficiently pure. The Bi was then back-extracted with 9M HNO_3. (B.L.M.)

29165 THIN-LAYER CHROMATOGRAPHY AS AN AID IN RADIOCHEMISTRY. PART 6. 1. SEPARATION OF Sn, ^{125}Sb, AND ^{125m}Te. 2. SEPARATION OF As, Sb, AND Sn. Seiler, H. (Univ., Basel). Helv. Chim. Acta; 54: 533-7(10 Mar 1971). (In German).

Thin-layer chromatography was applied to the separation of the nuclides of the decay chain: $^{125}Sn \rightarrow {}^{125}Sb \rightarrow {}^{125m}Te$. Different factors influencing the separation were investigated. The method can be used for the carrier-free separation of ^{125m}Te, As, Sb, and Sn were also separated by thin-layer chromatography. (auth)

Recoil Production and Reactions

29166 CHEMICAL EFFECTS ASSOCIATED WITH THE (γ, n) REACTION IN POTASSIUM CHROMATE. Omori, Takashi; Yeh, Yu-chai; Shiokawa, Takanobu (Tohoku Univ., Sendai). Kakuriken Kenkyu Hokoku; 2: 139-46(Dec 1969). (In Japanese).

The initial retention of ^{51}Cr produced by the (γ,n) reaction with an electron linear accelerator is strongly affected by the bremsstrahlung-dose rate and is higher than that observed in the (n,γ) reaction. Even in the solid solution of the potassium chromate in potassium chloride matrix, the initial retention of ^{51}Cr is very high, ~75%. No isotope effect between ^{49}Cr and ^{51}Cr in the initial retention was found. In the thermal annealing reaction, a rapid increase in the retention with heating time was observed, but the pseudo-plateau value is independent of the temperature below 120°C. These observations suggest that radiation annealing during irradiation has a very important role in determining the chemical behavior of the recoil ^{51}Cr atoms. The experimental results can be interpreted reasonably on the "crystal defect" model proposed by Maddock. (auth) (Japan)

29167 ENERGETIC SUBSTITUTION REACTIONS OF TRITIUM ATOMS FROM NUCLEAR RECOIL. Ting, Cheng Teh. Irvine, Calif.; Univ. of Calif. (1970). 156p. University Microfilms Order No. 71-4273.

Thesis.

Several studies were made of the substitution of energetic tritium atoms (from nuclear recoil) for hydrogen in specific hydrocarbons. These hydrocarbons were chosen to permit observation of the secondary decomposition reactions of the energetic tritium-labeled molecules formed. The secondary unimolecular decomposition of both cis- and trans-1,3-dimethylcyclobutane-t to propylene-t was observed over the pressure range from 5 to 70 cm Hg, and in the liquid phase. Decomposition to propylene is least in the liquid phase (12%) and greatest at the lowest pressure (33%), as expected for such secondary reactions. In addition to (2), the decomposition of the excited methylcyclobutane-t formed by the substitution of T-for-CH_3 was also observed experimentally in both gas and liquid phases. In the liquid phase, the yield of methylcyclobutane-t was larger than that of ethylene-t (2.8 vs. 2.3). In the gas phase, however, the yield of methylcyclobutane-t was only 2% as large as the ethylene-t yield, indicating that large excitation energies are regularly formed for such reactions. The observation of no more than trace amounts of the opposite isomer (i.e., cis-1,3-dimethylcyclobutane-t from trans-1,3-dimethylcyclobutane, and vice versa) confirms the unimportance of the Walden inversion mechanism during the primary recoil tritium substitution for hydrogen. The secondary, unimolecular isomerization of methyl isocyanide to acetonitrile was studied in both gas and liquid phases. No measurable amounts of the labeled parent were found in the gas phase, although substantial yields of CH_2TNC are present in the liquid. From the 38 Kcal/mole activation energy, a lower limit of 3 to 4 eV was calculated for excitation energy left in the molecule after the occurrence of the substitution reaction. (Diss. Abstr. Int., B)

29168 HOT-ATOM CHEMISTRY. Matsuura, Tatsuo (Rikkyo Univ., Yokosuka, Japan). Kagaku (Kyoto); 25: 24-36 (Jan 1970). (In Japanese).

Hot-atom chemistry and its recent development are described. The historical development of hot-atom chemistry since Szilard and Chalmers' experiment and the theory are reviewed. Hot-atom chemistry in organic systems is described. The characteristics of hot-atom reactions investigating these reactions by scavenging and moderating methods, the types of hot-atom reactions, and recent topics are considered. The hot-atom chemistry in inorganic systems is described: hot-atom chemistry in oxy-salt systems, recent models of solid-state hot-atom chemistry, hot-atom chemistry of complexes, annealing phenomenon, role of lattice defects in crystals, and other effects. (Japan)

29169 DISTRIBUTION OF RADIONUCLIDES IN SUSPENSIONS OF COLLOIDAL ThO_2 (THOROTRAST). Heyder, J. (Gesellschaft fuer Strahlenforschung, Frankfurt am Main); Kaul, A. Biophysik; 7: 152-6(1971). (In German).

A hypothesis of formation of activity fractions (ion fractions) outside the ThO_2 particles in thorotrast was experimentally confirmed. The hypothesis states that the recoil energy transferred to the atomic nuclei at the moment of their creation inside the ThO_2 particles is sufficient to shoot them out of the particles. The measured activities of the ion fractions of ^{228}Ac and ^{212}Pb were found to be different to the predicted ones. The discrepancies were explained by the effect of adsorption of nuclei of the ion fractions on the surface of the ThO_2 particles. (auth)

29170 ISOMERIC EFFECT IN THE SZILARD–CHALMERS RECOIL OF ^{60m}Co AND ^{60s}Co IN SOME MIXED COMPLEXES OF Cr(III) AND Co(III). Lazzarini, E.; Fantola Lazzarini, A. L. (Politecnico, Milan). J. Inorg. Nucl. Chem.; 33: 631-41(Mar 1971).

Previous investigations on the isomeric effect in the Szilard–Chalmers recoil of ^{60m}Co and ^{60s}Co atoms carried out on pure Co(III) complexes were extended to include six Co(III) and Cr(III) (Co/(Co + Cr) = 0.03–0.05) mixed complexes (solid solution) chosen with ligands which do not promote high backdonation. The primary and the secondary isomeric effects in the Szilard–Chalmers recoil of ^{60m}Co and ^{60s}Co atoms found in pure Co(III) complexes also appear in the mixed crystals. The secondary isomeric effect is strongly dependent on the chemical constitution of the target as is related to the splitting Δ of 3d-orbitals of Cr(III) induced by the ligand field. A physical model for the isomeric effect in Szilard–Chalmers recoil of ^{60m}Co and ^{60s}Co atoms is proposed, which explains present results and those previously obtained for pure Co(III) complexes. (auth) (UK)

XUM

29171 POLYMERIC CHROMIUM(III) COMPLEXES RESULTING FROM THE NEUTRON IRRADIATION OF CRYSTALLINE POTASSIUM CHROMATE. II. EFFECT OF PERIOD OF IRRADIATION ON THE SPECIFIC ACTIVITY AND DISCUSSION OF THE MANNER IN WHICH MONO- AND POLYNUCLEAR RECOIL PRODUCTS ARE FORMED. Guetlich, P.; Froehlich, K.; Odar, S. (Technische Hochschule, Darmstadt, Ger.). J. Inorg. Nucl. Chem.; 33: 621-9(Mar 1971). (In German).

The ^{51}Cr activity distribution and the specific activity of the various mono- and polynuclear recoil products of chromium(III) produced by thermal neutron capture in crystalline K_2CrO_4 were investigated as a function of neutron dose. For all neutron doses under investigation the highest enrichment factors for ^{51}Cr were observed in the fraction of the (presumably) trimeric complex. The enrichment factors for all cationic fractions decreased with increasing neutron dose. A mechanism for the formation of the mono- and polynuclear recoil products as a consequence of the (n,γ) reaction in crystalline K_2CrO_4 is discussed. (auth) (UK)

Radiochemistry

Refer also to abstract 29169

29172 THERMAL ANALYSIS OF PROMETHIUM OXALATE. McNeilly, C. E.; Roberts, F. P. (Battelle-Memorial Inst., Richland, Wash.). Contract AT(45-1)-1830. pp 727-38 of Thermal Analysis. Vol. 2. /Schwenker, Robert F. Jr. (ed.). New York; Academic Press, Inc. (1969).

From second international conference on thermal analysis; Worcester, Mass. (18 Aug 1968). See CONF-680851.

Differential thermal analysis (DTA) and thermogravimetric analysis (TGA) were used to study the decomposition of promethium oxalate. TGA results were quite similar to those for samarium oxalate, as expected; however, the DTA results were almost entirely different, with respect to both types and temperatures of reaction. The starting material was shown by TGA to correspond to the formula $Pm_2(C_2O_4)_3 \cdot 3\,H_2O$. Differential thermal analysis, performed over a one-month period, showed a marked change taking place in the material, presumably due to radiolytic decay of ^{147}Pm to $^{147}Sm + \beta$. Radiation damage due to the beta particles results in the formation of a material with the apparent formula $Pm_2O_2CO_3 \cdot 3\,H_2O$ as determined by TGA. (auth)

29173 CERTIFICATES OF RADIOACTIVITY STANDARDS. Garfinkel, S. B.; Baerg, A. P.; Zigman, P. E. Washington, D. C.; National Academy of Sciences, National Research Council (1966). 11p. Available from National Academy of Sciences, National Research Council, Washington, D. C.

Features of a suitably informative and precise certificate for radioactivity standards are described. Information that should be on the certificate includes: parent nuclide, reference time and date, activity per gram of solution, daughter activity, chemical composition of solution, method of standardization, listing of known radioactive impurities, type of irradiation, chemical and isotopic composition of the target, method and date of chemical purification, estimates of errors in standardization, composition of the stated overall uncertainty, possible systematic errors, and decay characteristics. (M.C.G.)

29174 USERS' GUIDES FOR RADIOACTIVITY STANDARDS. Kahn, B.; Choppin, G. R.; Taylor, J. G. V. Washington, D. C.; National Academy of Sciences, National Research Council (1967). 43p. Available from National Academy of Sciences, National Research Council, Washington, D. C.

Short guides to chemical and counting problems for common standards are given. The guides are prepared separately for these elements: Na, Mg, P, S, Cl, K, Ca, Cr, Fe, Co, Zn, Ga, As, Br, Kr, Sr, Y, Zr, Nb, Ru, Rh, Ag, Sn, Sb, Te, I, Cs, Ba, rare earths, Au, Hg, Tl, Po, Rn, Ra, Th, U, Np, and Am. (M.C.G.)

Separation Processes

Refer also to abstracts 28979, 28999–29001, 29014, 29074, 29075, 29165, 29317, 29393, and 29413.

29175 (BARC–509) SYNTHESES OF PHYLLITIC MINERALS: THEIR UTILISATION IN RADIOACTIVE WASTE TREATMENT. II. FROM MIXED GELS OF SILICA AND ALUMINA IN PRESENCE OF MAGNESIUM ACETATE AND SODIUM ACETATE. Brat, Satya; Balu, K. (Bhabha Atomic Research Centre, Bombay (India)). 1970. 23p. Dep. NTIS (U. S. Sales Only).

Syntheses of phyllitic silicate minerals were carried out using silica gel and mixed gels of silica and alumina in the presence of magnesium acetate and sodium acetate at atmospheric pressure and at a temperature of approximately 100°C. The products obtained were subjected to x-ray evaluations and found to be of an interstratified group of the montmorillonite family. The suitability of the synthetic products for the decontamination of radioactive wastes with CsCl + ^{134}Cs was studied and the products obtained with the initial ingradients SiO_2/Al_2O_3 molecular ratio varying between 2.2 to 2.9 were found to be quite suitable for removal of radioactive cesium from liquid wastes. With the increase in initial ingradients SiO_2/Al_2O_3 molecular ratio beyond 2.9, a decrease in sorption capacity for the removal of cesium ion was observed. (auth)

29176 (BARC–516) RECOVERY OF PROMETHIUM FROM FISSION PRODUCT WASTE. PART III. USE OF MANGANESE DIOXIDE COLUMN ADSORPTION FOLLOWED BY ANION EXCHANGE ELUTION. Shukla, J. P.; Chandrasekharan, E. S.; Rengan, K. (Bhabha Atomic Research Centre, Bombay (India)). 1970. 17p. Dep. NTIS (U. S. Sales Only).

Experiments were carried out to evolve a simple procedure for recovery of ^{147}Pm from nuclear fuel reprocessing wastes. Preliminary purification of Pm from associated fission products is readily accomplished by a MnO_2 column. Final purification of the Pm fraction from other rare earth constituents was achieved by an anion exchanger using 20% 7M HNO_3 – 80% CH_3OH (%v) mixture as the eluant. (auth)

29177 (CEA-R–4090) SEPARATION AND RECOVERY OF PERMANENT GASES BY PREPARATIVE CHROMATOGRAPHY. Dupuis, Marie-Claire; Lutz, Michel; Massimino, Daniel (Commissariat a l'Energie Atomique, Bruyeres-le-Chatel (France). Centre d'Etudes). Jan 1971. 23p. (In French). Dep. NTIS (U. S. Sales Only).

The study and manufacture of a preparative gas chromatograph for the separation and quantitative recovery of the components of a given gas mixture are described. The factors influencing the separation and purity of each component prepared in this way are demonstrated and may be chosen without restriction as a function of the various gas mixtures to be treated. The main applications of the process are: treatment of an Ar mixture containing Kr and Xe traces, treatment of Ar contaminated by tritium, and purification of carbon dioxide labeled with ^{14}C. (auth)

29178 (CEA-R–4102) TOTAL ELEMENTARY SEPARATION OF RARE EARTHS ON CATION EXCHANGE RESINS. Gusmini, Simone; Dubuquoy, Claude (Commissariat a l'Energie Atomique, Bruyeres-le-Chatel (France). Centre d'Etudes). Jan 1971. 25p. (In French). Dep. NTIS (U. S. Sales Only).

Total separation of the rare earths with carrier on a cation resin column was investigated by elution with ammonium lactate and α-hydroxyisobutyrate. The experimental conditions applicable as a function of the analytical reeds and time limits were defined. A lactate concentration gradient is more suitable for fission product rare earths, while a better separation of the yttrium group is obtained with a simultaneous pH and α-hydroxyisobutyrate concentration gradient. The whole rare earth group and yttrium can be treated with α-hydroxyisobutyrate. Technical difficulties involved in the elution that condition the quality of the separation are mentioned. The chemical separation and purification of the rare earth group is discussed. (auth)

29179 (DOCKET-50201–69) WEST VALLEY REPROCESSING PLANT. Environmental Report No. 9, July–December 1970. (Nuclear Fuel Services, Inc., West Valley, N. Y.). Mar 1971. 12p. Dep. NTIS.

Gross radioactivity and concentrations of ^{90}Sr, T, ^{131}I in samples of air, fallout, milk, water, and silt were measured. Airborne particulate activity continued to be less than pre-operational levels. Data are given in graphs. (M.C.G.)

29180 (DOCKET-50201–70) WEST VALLEY REPROCESSING PLANT. Quarterly Report, January 1–March 31, 1971. (Nuclear Fuel Services, Inc., West Valley, N. Y.). 20 Apr 1971. 9p. Dep. NTIS.

Reports on environmental monitoring, low-level liquid effluents, stack effluents, and surveillance tests are reported. Data are given on amounts of gross α, gross β, tritium, ^{90}Sr, ^{129}I, ^{131}I, and ^{85}Kr. (M.C.G.)

29181 (GEPP–85) PRODUCTION OF BULK QUANTITIES OF ULTRAPURE ERBIUM. Parsons, N. H. (General Electric Co., St. Petersburg, Fla. Neutron Devices Dept.). 10 Mar 1971. Contract AT(29-2)-656. 19p. Dep. NTIS.

A vacuum distillation operation is described for the reprocessing of erbium. This distillation method is capable of increasing the purity of commercially available erbium up to 99.96 wt % by mass spectrographic analysis. (auth)

XUM

29182 (RT/CHI-(70)31) DETERMINATION OF EQUILIBRIUM DATA RELATING TO THE CHEMICAL SCHEME OF THE EUREX PROCESS. Baroncelli, F. (Comitato Nazionale per l'Energia Nucleare, Rome (Italy)). 6 Oct 1970. 21p. (In Italian). Dep. NTIS (U. S. Sales Only).

Empirical relationships enabling a rapid calculation of the partition coefficient of UO_2^{2+} between aqueous nitrate solutions and tricaprylammonium nitrate (TCAN) in Solvesso 100 solutions were derived. The influence of the TCAN, aluminum nitrate, nitric acid, and uranium concentrations and temperature on the partition coefficient was evaluated. The range of validity of the empirical relationships was first established. Equilibrium curves related to experimental conditions met in the Eurex process were then calculated. (auth)

29183 (SGAE-SS-6/1969) SOME RESULTS ON THE REMOVAL OF RADIOCESIUM FROM LOW-ACTIVITY WASTE WATER BY COPRECIPITATION WITH FERROCYANIDES. Friedmann, C. (Oesterreichische Studiengesellschaft fuer Atomenergie G.m.b.H., Vienna (Austria)). Apr 1970. 9p. NTIS (U. S. Sales Only).

Coprecipitation of ^{137}Cs with small amounts of cupric and ferric ferrocyanides from actual waste water was investigated. The results indicate that if moderate decontamination factors (30 to 50) suffice, reagent quantities smaller than those now in use at various plants for the treatment of low-activity waste can be employed. (auth) (INIS)

29184 SELECTIVE EXTRACTION OF THORIUM WITH N-BENZYLANILINE IN CHLOROFORM FROM SULPHURIC ACID MEDIA. Khosla, M. M. L. (Defence Lab., Jodhpur, India); Rao, S. P. Anal. Chim. Acta; 54: 315-20(Apr 1971).

N-benzylaniline in chloroform is shown to be a selective extraction reagent for thorium(IV) in 1.5 to 2 M sulfuric acid media. Few cations interfere when ascorbic acid and EDTA are present. Phosphate, oxalate, citrate, tartrate, nitrate, chloride, borate, and arsenate do not interfere, nor do dichromate, chromate, and vanadate after reduction with ascorbic acid. Fluoride can be easily masked with boric acid in dilute sulfuric acid. Uranium (VI) is co-extracted but does not interfere with the EDTA titration of thorium(IV) to a Xylenol Orange end-point. The method is simple and rapid, and effects clean-cut separation. (auth)

29185 EXTRACTION OF EUROPIUM WITH DI(2-ETHYLHEXYL) PHOSPHORIC ACID. Shiokawa, Jiro; Matsumoto, Akira; Takatsuji, Kazuhiko; Morito, Sadaaki; Hirashima, Yoshiyuki (Osaka Univ.). Kogyo Kagaku Zasshi; 74: 14-16(Jan 1971). (In Japanese).

For the purpose of separation of Eu from the lanthanide elements by means of extraction using a 1.0 mole/l solution of di(2-ethylhexyl)phosphoric acid in n-heptane, equilibrium studies of Eu extraction in the range of concentration from 0.01 to 0.16 mole/l were carried out. Distribution coefficients of Eu decreased with increase of both initial HCl concentration (0.0 to 1.0 mole/l) and initial Eu concentration (0.01 to 0.16 mole/l) in the aqueous phase. The value of 0.16 mole/l was an extractable maximum concentration calculated. Under 0.10 mole/l concentration of Eu, Eu was extracted almost quantitatively independent of the HCl concentration. Above that concentration, more Eu was extracted than the calculated values with an increase of both HCl concentration and Eu concentration. When kerosene (bp = 160 to 200°C/760 mmHg) was used as a diluent, distribution coefficients of Eu were slightly raised. (auth) (Japan)

29186 CHROMATOGRAPHIC TECHNIQUES USING LIQUID ANION EXCHANGERS. V. H_2SO_4 SYSTEMS. Brinkman, U. A. Th.; De Vries, G. (Free Reformed Univ., Amsterdam). J. Chromatogr.; 56: 103-9(24 Mar 1971).

Using thin-layer chromatography on silica gel impregnated with Aliquat 336, Alamine 336, Amberlite LA-I, or Primene JM-T, and on nonimpregnated silica gel, the behavior of 25 ions in H_2SO_4 and sulfate salt systems was systematically investigated. The chromatographic data confirm earlier work on liquid–liquid extractions regarding the sorption sequence of the exchangers. A number of successful separations is reported. Two general patterns of dependence of metal extraction on exchanger class exist, viz. the sequence primary < secondary < tertiary ≃ quaternary (the sequence also encountered in monobasic acid systems); and primary > secondary ≃ tertiary ≃ quaternary. In the latter case, the low sorption strength of secondary-quaternary exchangers is attributed to steric effects. (auth)

29187 REVERSED PHASE THIN-LAYER CHROMATOGRAPHIC BEHAVIOR OF THE RARE EARTHS, THORIUM, URANIUM, AND ZIRCONIUM WITH A HIGH MOLECULAR WEIGHT AMINE IN SULFURIC ACID AND AMMONIUM SULFATE SYSTEMS. Shimizu, Tsuneo; Ishikura, Reiko (Gunma Univ., Maebashi, Japan). J. Chromatogr.; 56: 95-102(24 Mar 1971).

Thin-layer plates of silica gel impregnated with a high-molecular-weight amine, Amberlite LA-2, in the sulfate form, were used to investigate systematically the chromatographic behavior of the rare earths, thorium, uranium(VI), and zirconium in sulfuric acid and acid ammonium sulfate media. The R_F values for these metal ions decrease with increasing concentration of the acid and sulfate, in the acid system particularly. An interesting correlation was revealed between the R_F values of the rare earths and the paramagnetic moment of the trivalent rare earths in the high concentration range of the acid and sulfate. An odd-even fluctuation of the R_F values against atomic number was also found for the heavy lanthanides. Differences in the R_F values of the rare earths in acid sulfate media indicate the possibility of good separations of adjacent pairs or groups of the rare earths from each other by selecting an appropriate concentration of sulfate. The rare earths, thorium, uranium(VI), and zirconium can also be separated chromatographically with either 0.5 or 1.0 M sulfuric acid as developing solvent. (auth)

29188 DIFFERENTIAL THERMAL ANALYSIS OF BORIC ACID, BORIC OXIDE, AND POTASSIUM FLUOBORATE. Marano, R. T.; Shuster, E. R. (Nuclear Materials and Equipment Corp., Lewiston, N. Y.). Contract AT(40-1)-3292. pp 709-16 of Thermal Analysis. Vol. 2. /Schwenker, Robert F. Jr. (ed.). New York; Academic Press, Inc. (1969).

From 2. international conference on thermal analysis; Worcester, Mass. (18 Aug 1968). See CONF-680851.

The manufacture of ^{10}B utilizes boric acid or potassium fluoroborate as an intermediate. Studies were made to determine the thermal characteristics of these materials. DTA analyses summaries and thermograms are presented for boric acid, boron oxide, and potassium tetrafluoroborate. The values obtained may be used in assuring uniformity of batch-to-batch quality in production of these boron-10-enriched compounds. (M.C.G.)

29189 PROCESS FOR REPROCESSING IRRADIATED THORIUM- AND URANIUM-CONTAINING NUCLEAR FUELS AND/OR FERTILE MATERIALS. (to Kernforschungsanlage Julich GmbH). British Patent 1,226,718. 31 Mar 1971. Priority date 30 Oct 1968, Germany.

Reprocessing irradiated Th- and U-containing nuclear fuel and/or fertile material includes comminuting the material, treating the comminuted material with a Cl_2(90%)–CO(10%) mixture at a temperature between 900 and 1200°C to form a gaseous chloride mixture, separating the gaseous chloride mixture by fractional condensation into a U-containing fraction and a Th-containing fraction, treating the U-containing fraction so as to form an aqueous U-containing solution, and extracting the U from the solution with an organic quaternary ammonium compound or with a long-chain trialkylamine. Prior to extraction, the U-containing solution may be passed through a column of silica gel or glass with a high silicic acid content or washed with a solution of oxalic acid to remove Pa. Uranium is recovered from the organic extract by washing with a solution containing $MgCl_2$ and HCl to remove unwanted fission products and then with water to recover the U in salt form. (B.L.M.)

29190 ION-EXCHANGE PAPER CHROMATOGRAPHY OF METAL IONS WITH MIXED AQUEOUS-ORGANIC SOLVENTS CONTAINING MINERAL ACID AND A SELECTIVE EXTRACTANT. Sherma, Joseph; Van Lenten, Frank J. (Lafayette Coll., Easton, Pa.). Separ. Sci.; 6: 199-206(Apr 1971).

Mixed solvents containing an organic extractant provide selective separations of metal ions on cation- and anion-exchange papers. The separations of scandium, hafnium plus zirconium, nickel, and thorium from complex mixtures are demonstrated. Various separations in dithizone and dimethyl sulfoxide media are also reported. Results are often the same as those achieved on columns of resin with the same mobile phase. (auth)

29191 SEPARATION OF ^{239}Pu(IV) FROM ^{95}Zr, ^{95}Nb, ^{105}Ru, AND ^{106}Rh BY ANION EXCHANGE RESIN FROM MIXED METHYL ALCOHOL NITRIC ACID SOLUTION. Sherief, M. K.; Grass, F. (Oesterreichische Hochschule, Vienna. Univ., Vienna). Atomkernenergie; 17: 124-6(Mar 1971).

The separation of ^{239}Pu from ^{95}Zr, ^{95}Nb, ^{106}Ru, and ^{106}Rh by anion exchange from 1.5N HNO_3 + 90% methyl alcohol and eluting by 7.5N HNO_3 + 0.01M HF is described. This process has the advantage of increasing the absorbability of ^{239}Pu(IV) from a mixed methyl alcohol–nitric acid system and at the same time decreasing the absorbability of ^{95}Zr, ^{95}Nb, ^{106}Ru, and ^{106}Rh. Thus it is an applicable and feasible method for the concentration of ^{239}Pu(IV), its separation from the waste products of the Purex method, and for recycling of the nuclear fuel after decontamination from the poisoning products. (auth)

XUM

29192 METHOD OF REPROCESSING NUCLEAR FUEL ELEMENTS AND/OR BREEDING ELEMENTS. (to Kernforschungsanlage Juelich GmbH). British Patent 1,226,198. 24 Mar 1971. Priority date 21 Dec 1967, Germany.

A method for reprocessing nuclear fuel elements and/or breeder elements in which the fuel and/or breeding material is present as uranium/thorium mixed oxides or carbides, canned elements or coated particles includes removing the canning or coating, dissolving the fuel and/or breeding material in a pyrosulfate melt, and adding a sufficient amount of a solid alkali metal hydroxide to the melt to precipitate the uranium as the alkali metal uranate mixed with ThO_2. The melt is then filtered and centrifuged to obtain the precipitate which is fluorinated to form the UF_6 for separation by distillation. (B.L.M.)

29193 STUDIES ON ION-EXCHANGE TRANSFER. XIX. PERMSELECTIVITIES OF DIVALENT CATIONS TO SODIUM ION IN CATION EXCHANGE TRANSFER. Dohno, Reizo; Azumi, Takatugu; Takashima, Shiro (Himeji Inst. of Tech., Japan). Nippon Kagaku Zasshi; 92: 136-9(Feb 1971). (In Japanese).

The permselectivities of divalent cations to sodium ion in cation exchange transfer were determined by using hydrochloric acid solution as exchange ion. The logarithm permselectivities against reciprocal concentrations of exchange ion indicated a linear relationship, and the limiting permselectivity coefficients were obtained by extrapolating against hydrochloric acid concentration. These values reveal an increase in the permselectivity of divalent cation in the following order: $Mg^{2+} < Ca^{2+} < Ba^{2+} < Sr^{2+}$, while the order of separation factor: $Mg^{2+} < Ca^{2+} < Sr^{2+} < Ba^{2+}$. The mobility ratios of divalent cation to sodium ion in membrane, which were calculated from the values of separation factor and permselectivity coefficients, increased in the following order: $Mg^{2+} = Ba^{2+} < Ca^{2+} < Sr^{2+}$. These mobility ratios are small in comparison with those ratios in aqueous solution and the transfer of divalent cation in membrane is considerably retarded in comparison with that of sodium ion. (auth)

29194 STUDIES ON THE ABSORPTION OF ^{239}Pu BY ANION EXCHANGE RESIN FROM NITRIC ACID AND MIXED NITRIC ACID METHYL ALCOHOL SYSTEMS. Sherief, M. K.; Grass, F. (Oesterreichische Hochschule, Vienna. Univ., Vienna). Atomkernenergie; 17: 53-4(Feb 1971).

The distribution ratio (K_d) of ^{239}Pu(IV) in nitric acid and mixed nitric acid–methyl alcohol systems was studied. The maximum K_d of ^{239}Pu(IV) was found at 1.5N HNO_3 + 90% methyl alcohol. The relationship between the K_d values and the formation of the ^{239}Pu (IV) hexanitrato complex was explained. (auth)

29195 STUDIES ON THE EXTRACTION AND DETERMINATION OF METAL SALTS WITH ISOBUTYL METHYL KETONE. XIII. EXTRACTION OF THORIUM AND URANIUM. Ichinose, Norio (Tohoku Univ., Sendai). Talanta; 18: 21-6(Jan 1971).

The work deals with the extraction of thorium or uranium from hydrochloric, perchloric, sulfuric, or nitric acid solutions of various concentrations, or from mixed acid solutions, by means of isobutyl methyl ketone. When the extraction is made from 5 to 8M hydrochloric acid that is 10M in lithium chloride or from 7 to 8M hydrochloric acid that is 1M in magnesium chloride, uranium is extracted quantitatively (>99%), whereas thorium is hardly extracted at all. (auth) (UK)

29196 SEPARATION OF BORON ISOTOPES. II. BF_3 SYSTEMS. COMPLEX COMPOUNDS OF BF_3 AND $\beta-\beta'$-DIFLUOROR $\beta-\beta'$-DIETHYLETHER FLUORIDECHLORIDES. Katal'nikov, S. G.; Pisarev, V. E.; Oistach, I. D. Isotopenpraxis; 7: 8-12 (Jan 1971). (In Russian).

An effective method of boron isotope separation is the chemical exchange of BF_3 and its liquid complex compounds. Properties of the complexes and their decomposition products, such as density, viscosity, and mass spectra, were determined to render possible estimation of the influence of these compounds on the isotope separation process. (M.C.G.)

29197 USE OF BOROSILICATE-GLASS RASCHIG RINGS AS A FIXED NEUTRON ABSORBER IN SOLUTIONS OF FISSILE MATERIAL. Hinsdale, Ill.; American Nuclear Sociey (1965). 6p. Available from American Nuclear Society, Hinsdale, Ill.

Recommendations are given on the use of borosilicate-glass raschig rings as a fixed neutron absorber for control of criticality in solutions containing ^{235}U, ^{239}Pu, and ^{233}U, especially in fuel processing plants. The chemical and physical environment, properties of the rings and packed vessels, maintenance inspection procedures, and criticality operating limits are specified. (M.C.G.)

29198 SEPARATION OF URANIUM FROM FISSION PRODUCTS. Ueno, Kaoru; Asano, Masaharu; Kawasaki, Michiko (Japan Atomic Energy Research Inst., Tokai). J. Nucl. Sci. Technol. (Tokyo); 8: 129-32(Mar 1971).

A simple procedure was developed for separating U from fission products and neutron-irradiated Th. The separation is performed with tri-n-butyl phosphate in a system of dodecane with sulfuric acid and aluminum nitrate. Uranium dioxide was irradiated with 20-MeV bremsstrahlung, which produced both ^{237}U and fission products. The target was dissolved in dilute nitric acid and U was extracted into the organic phase. Finally, U in the organic phase was back extracted into an aqueous phase. The γ spectrum and decay curve of the separated U fraction show no radioactive nuclides other than U isotopes and its decay products. This method can also be applied to the preliminary separation of ^{236}U from neutron irradiated Th. The distribution ratios (Kd) for U, Th, and some other elements in the extraction system are also given. (auth)

29199 DISSOLUTION OF STAINLESS STEEL CLAD NUCLEAR FUEL ELEMENTS. Walsh, William J.; Pierce, R. Dean (to United States Atomic Energy Commission). U. S. Patent 3,567,648. 2 Mar 1971. Filed 8 Apr 1969.

The loss by entrainment of nuclear fuel particles in the dissolution of stainless steel cladding of irradiated UO_2 or PuO_2-UO_2 elements with molten zinc can be prevented by mixing a molten salt, such as $CaCl_2-CaF_2$, with the molten zinc to getter any nuclear fuel fines present and enable an essentially complete recovery of nuclear fuel particles. (Offic. Gaz.)

EARTH SCIENCES

Geology and Hydrology

Refer also to abstracts 29240, 29244, and 29266.

29200 (AEC-tr-7227) PARTICLE SIZE SPECTRUM OF THE RADIOACTIVE AEROSOLS IN A URANIUM MINE. Chapuis, Alain; Lopez, Alain; Fontan, Jacques; Billard, Francois; Madelaine, Guy J. Translated by John Harley from J. Aerosol Sci.; 1: 243-53(1970). 12p. Dep. NTIS.

An abstract of this paper, prepared from the original language, appeared as NSA 25: 6430.

29201 (AEC-tr-7228) MEASUREMENT OF THE STATE OF EQUILIBRIUM BETWEEN RADON AND ITS DAUGHTERS IN THE URANIUM MINES. Lopez, Alain; Chapuis, Alain; Fontan, Jacques; Billard, Francois; Madelaine, Guy J. Translated by John Harley from J. Aerosol Sci.; 1: 255-64(1970). 10p. Dep. NTIS.

An abstract of this paper, prepared from the original language, appeared as NSA 25: 6431.

29202 (CEA-tr-R-1978) USE OF DELAYED NEUTRONS FOR DETERMINATION OF URANIUM IN CORE SAMPLES OF BOREHOLES. Igumnov, L. A. Translated from Izv. Vyssh. Ucheb. Zaved., Gorn. Zh.; 9: 3-6(1966). 10p. (In French). Dep. NTIS (U. S. Sales Only).

An abstract of this paper, prepared from the original language, appeared as NSA 20: 41157.

29203 (USGS-474-95) GEOLOGIC AND HYDROLOGIC EFFECTS OF THE HANDLEY EVENT, PAHUTE MESA, NEVADA TEST SITE. Special Studies-83. (Geological Survey, Denver, Colo.). 1971. Contract AT(29-2)-474. 71p. Dep. NTIS.

Surface fractures resulting from the Handley test on March 26, 1970, were the typical radial and concentric fractures associated with the surface collapse area and linear trends associated with the generally north-trending faults. Displacements along faults were observed as much as 8 km distant. A maximum of 60 cm vertical displacement occurred on a fault east of ground zero. A series of fault observation stations permitted determination of the component of fault movement produced by the Handley test along faults which previously had moved during earlier tests. Minor long-term creep was observed along the Boxcar fault prior to the Handley test. Measurements of ground deformation within a few kilometers of Handley ground zero were made by high-accuracy leveling and by Geodimeter distance measurements. Level data reflect subsidence due to cavity collapse and possible compaction out to at least 1.2 km from ground zero, as well as displacements across faults in the manner predicted by elastic theories of faulting. Principal horizontal strains, in general, show contraction radial to ground zero. The ground-water pressure response in aquifers was within a factor of ±2 of the predicted values at the five observation sites. Hole UE20f, 5 km southeast of the explosion site, showed a transient overpressure of 93 m of water (about 9 bars), while the overpressure in Clayton Valley, 115 km to the northwest, was 0.56 m. The water levels in open wells at distances of 50 to 115 km were not disturbed more than 9 cm, but the oscillations were of sufficient frequency to cause surge rates of 127 gallons per minute in a lithium-production well in Clayton Valley. Temporary increases in the turbidity of the well discharges resulted from this surging. In hole UE20f nearly continuous pressure changes indicated that movement of faults very close to that site ended abruptly at 214 minutes postshot. The records obtained at other sites nearby preclude the interpretation that chimney development at the event site caused this pressure response. Slow, transient pressure responses were observed for 2 months after the event at two sites within 7 km to the north. This suggests permanent changes in the porosity of the host rock—some changes apparently occurring weeks after the explosion. (auth)

29204 TRANSPORT OF ^{137}Cs. II. INTERACTION WITH BED SEDIMENTS. Kudo, Akira; Gloyna, Earnest F. (Univ. of Texas, Austin). Water Res.: 5: 71-9(Feb 1971).

The transport of ^{137}Cs in an aqueous environment is described. The interaction phenomena, i.e., uptake and release of ^{137}Cs by sediments, were observed by using a set of flumes each 17 m in length and a model river which was 61 m long. The greatest uptake rate, K_{st}, by bed sediment was 88.7×10^{-4} {[(cpm cm^{-2})/(cpm cm^{-3})]/sec} with a velocity of 0.504 m sec^{-1} (1.65 ft sec^{-1}) and a flow rate of 38.21 sec^{-1} m^{-1} (0.410 cfs ft^{-1}). In this case the sediment transport rate was 117.5 g sec^{-1} m^{-1} (0.0795 lb sec ft^{-1}). The uptake rate increased as the mean velocity in the channel increased. The desorption rate of ^{137}Cs was low, being less than 1 per cent per month for a mean flow velocity of 3.0 cm sec^{-1}. This rate was obtained in a fresh water system where the concentration of total dissolved solids was about 600 mg l^{-1}. (auth) (UK)

29205 STUDIES ON THE NATURAL BACKGROUND RADIATION IN ITALY. Cardinale, A.; Frittelli, L.; Lembo, G.; Gera, F.; Ilari, O. (CSN, Casaccia, Italy. CNEN, Rome). Health Phys.; 20: 285-96(Mar 1971).

The exposure rate due to the γ-ray natural background in some representative areas of Italy was studied by means of a portable high-pressure ionization chamber. In a limited area such study was integrated by a survey on the quality of background radiation, carried out by γ spectrometric measurements. The spectrometric study permitted the determination of the contributions to the total by the individual natural radioactive series and by cosmic rays, while the ionometric method measured the total values of the γ exposure. The measurement areas were chosen on the basis of joint geological and demographical considerations: they are, in fact, representative of the main geological formations, preferentially chosen in the parts of the peninsula characterized by a significant population density. The results of the measurements are therefore indicative of the maximum range of γ exposure to which the Italian population is subjected from natural causes. (auth) (UK)

29206 ESTIMATION OF THE DIFFUSION OF MATERIALS IN CLAYEY GROUNDS. Dolgikh, P. F.; Vladimirov, L. A.; Yudin, F. P. At. Energ. (USSR); 29: 385-7(Nov 1970). (In Russian).

The diffusion-induced spreading of salts in water-resistant clay layers above and below the water table was determined, assuming that other phenomena, such as filtration, chemical interaction, and adsorption play a relatively minor role. The solution of the problem requires an evaluation of the period required for a given diffusing material to reach the permissible mean annual concentration at a given distance from the porous layer of the water table. These diffusion times were calculated for the case of sodium nitrate. The method may be used to calculate diffusion of radioactive materials. As the mean annual permissible concentration of radioactive materials is usually very low, the coefficient α, expressing the ratio of this maximum permissible concentration in the aquifer and the original concentration of the material in the waste effluents was chosen as being 10^{-5}, 10^{-6}, and 10^{-9}; the diffusion coefficients were assumed to be 0.01 and 0.0001 cm^2/day. The results are presented in tabular form without, however, having taken the radioactive decay into account. The method may be used also to calculate the spreading of other materials, even of gases, by diffusion. (TTT)

29207 INVESTIGATIONS ON PROFILE DISTRIBUTION OF ^{90}Sr IN ARABLE SOILS OF LOWER SILESIA. Malysowa, Elzbieta; Bors, Jerzy; Szerszen, Leszek (Coll. of Agriculture, Wroclaw). Rocz. Glebozn.; 19: Suppl. No. 1, 103-12(1968).

The migration of ^{90}Sr in soils under agricultural cultivation in Lower Silesia (Poland) was investigated. Soil profiles were taken, the amount of precipitation measured, and the ^{90}Sr content in samples was determined. It was concluded that: the surface layer is most highly contaminated in all soils; the depth of ^{90}Sr contamination depends primarily on the kind of soil, the more clay and silt the greater the contamination; ^{90}Sr accumulated in the humus horizon of heavy soils; ^{90}Sr is leached into the depth of the profile of light soils; and the migration of ^{90}Sr into the soil profile seems to be independent of pH, of the presence of base cations, or of the quantity of organic C present. (L.C.L.)

29208 GEOCHRONOLOGIC DATA OBTAINED BY THE URANIUM–LEAD METHOD ON SOME SPHENES OF IGNEOUS AND METAMORPHIC ROCKS OF THE SOER-RONDANE MOUNTAINS, ANTARCTICA. Pasteels, Paul. Ann. Soc. Geol. Belg.: 92: 371-5(1970). (In French).

In a medium to high grade metamorphic terrane, sphene from gneisses is dated at 540 m.y. with the U: Pb method. Since cross-cutting granites appear to be 600 Myr old, as indicated by measurements performed on zircon, the question arises whether sphene is subject to post-metamorphic "rejuvenation," as are the micas, or some granite zircon ages are too high in response to presence of incorporated old zircon. The first possibility is favored. (Geophys. Abstr.)

29209 ^{226}Ra IN CONTEMPORARY AND FOSSIL SNOW. Jaworowski, Zbigniew (Central Lab. for Radiological Protection.

XUM

Warsaw); Biltiewicz, Jan; Zylicz, Elzbieta. Health Phys.: 20: 449-50(Apr 1971).

Using an emanation method, 0.3 pCi per g of ^{226}Ra was found in dry, ashed samples of European and Asiatic coal. Using this figure it was calculated that as a result of burning coal throughout the world a concentration corresponding to a fallout rate of 0.3 pCi/m^2 per yr or 0.0004 pCi per l of water is produced. However, from snow samples taken at different distances from a power station in Warsaw ^{226}Ra concentrations of several orders of magnitude greater were found. The time variations of ^{226}Ra concentrations in glacier ice samples were also measured and they were found to have increased a hundred times in the last 80 yr. Since ^{210}Pb is a daughter of ^{226}Ra its use as a natural tracer in atmospheric tracer work is limited. (UK)

29210 DETERMINATION OF THE ABSOLUTE AGE OF LAKE BALKHASH ON THE BASIS OF NONEQUILIBRIUM URANIUM. Chalov, P. I.; Svetlichnaya, N. A.; Tuzova, T. V. (Inst. of Physics and Mathematics, Frunze, USSR). Dokl. Akad. Nauk SSSR; 195: 190-2(1 Nov 1970). (In Russian).

In view of the contradictory results concerning the age of the Balkhash basin it was attempted to determine the absolute age of this lake by examining the isotopic composition, $^{234}U/^{238}U$, of uranium in the bottom deposits and in the water. The water specimens collected from the lake and from rivers emptying into it were analyzed using an α spectrometer to determine the $^{234}U/^{238}U = \gamma$ ratio. It was found that the specimens collected at the Eastern and Western portions of the lake possessed different values of γ. The isotopic composition of uranium in the bottom deposits was found to be uniform; only at the lowest level was there a tendency for γ to decrease toward 1.462. It was concluded that since the formation of the present lake, the hydrographic stem of the basin has not been changed. On the basis of the γ determinations in the deep portion of the Western part of the lake the absolute age was calculated at 37 ± 7 thousands years. This result differs from the absolute age determination of this basin derived from the accumulation of salts. (TTT)

29211 CORRELATIONS BETWEEN THE ^{210}Pb DEPOSIT IN THE ANTARCTIC AND FLUCTUATIONS IN THE EARTH'S MAGNETIC FIELD. Lambert, Gerard; Le Roulley, Jean-Claude; Sanak, Joseph (CNRS, Gif-sur-Yvette, France). Compt. Rend., Ser. B; 272: 177-80(11 Jan 1971). (In French).

Measurement of the ^{210}Pb content along a névé core sample obtained from Antarctica allowed the various layers to be dated. A distinct correlation was observed between fluctuations in the Earth's magnetic activity and the ^{210}Pb content. (auth) (France)

29212 THERMOLUMINESCENT DATING USING FINE GRAINS FROM POTTERY. Zimmerman, D. W. (Oxford Univ.). Archaeometry; 13: 29-52(Feb 1971).

It is stated that ancient pottery can be dated absolutely by the thermoluminescent (TL) method if allowance is made for the fact that the radioactivity within a sherd is non-uniform. The bulk of the α-activity, from the U and Th series, is in the opaque clay matrix, whereas the bulk of the thermoluminescence comes from the less radioactive mineral inclusions, for example quartz and feldspars, and since the range of the α-particles is less than the diameters of the layer inclusions, the archaeologic dose the inclusions have received varies with their size. One method of dealing with this difficulty is known as "fine grain" dating (due to Zimmerman, 1967), the TL measurements being made only on fine grains that have received the full α-dose. This method has the advantage of minimising the effect of the environmental γ-dose from the soil. A detailed description of the technique is given, including several recent modifications. The latter include allowance for the variation of TL efficiency with α-particle energy, and for the effect of ground water on natural dose rate, consideration of the effect of radon emanation on the natural dose rate and radioactivity measurements, and correction for non-linearity of the TL growth curves. The accuracy claimed is to within ±10%. Further development work on the method is indicated. (UK)

29213 DISPERSION STUDIES USING STABLE AND RADIOACTIVE TRACERS IN FRESH WATER STREAMS. Sorensen, J. C. (Univ. of California, Los Angeles); Smith, C. B.; Francisco, V. pp 187-97 of Proceedings of the Institute of Environmental Sciences 17th Annual Technical Meeting and Equipment Exposition, April 26-30, 1971, Los Angeles, California. Mt. Prospect, Ill.; Inst. of Environmental Sciences (1971).

From seventeenth annual meeting and equipment exposition; Los Angeles, Calif. (26 Apr 1971). See CONF-710409.

Several experimental techniques for studying natural streams are described, with emphasis on the use of neutron activation analysis and radioactive tracers for studying the natural behavior of a stream and for tracing the transport and dilution of polluting materials in stream waters. Procedures for radioactive and stable isotope labeling and the desirable properties of both radioactive and stable isotope tracers are discussed. Results of experiments in the Malibu Creek (Calif.) using ^{24}Na as the tracer are presented. Experiments using $^{56}MnCl$ as a stable isotope tracer are proposed. Mathematical models for studying stream kinetic behavior are discussed. It is concluded that radioactive tracer techniques are particularly promising for use in water pollution control studies and that the mathematical models available make it possible to perform theoretical studies of the transport of various materials under varying stream flow conditions. (L.C.L.)

Meteorology

Refer also to abstracts 28990, 29074, 29075, 29179, 29251, and 29444.

29214 (LA-tr-71-7) RADIOACTIVITY DISTRIBUTION OF EMANATION DECAY PRODUCTS BETWEEN AEROSOL PARTICLES OF DETERMINED SIZE RANGES. Flattau, J.; Rutkowska, K. Translated by Alois D. Cernicek (Los Alamos Scientific Lab., N. Mex.), from Pr. Cent. Inst. Ochrony Pracy; 17: No. 52, 45-58(1967). 18p. Dep. NTIS.

An abstract of this paper, prepared from the original language, appeared as NSA 21: 22049.

29215 VERTICAL DISTRIBUTION OF TRITIUM IN WATER VAPOR IN THE LOWER TROPOSPHERE. Bradley, Wayne E.; Stout, Glenn E. (Illinois State Water Survey, Urbana). Tellus: 22: 699-706(1970).

A series of 16 aircraft soundings was made during the summers of 1966 and 1967 to measure the vertical distribution of tritium in water vapor from the surface to an altitude of 5 km. Three types of tritium distributions were found. The Type I soundings showed a generally increasing tritium concentration with increasing height. Type II soundings were characterized by a constant tritium concentration with increasing altitude. On Type III soundings the tritium concentration gradually decreased to approximately 2.4 km and then abruptly increased. These soundings are discussed in terms of the origin of the air masses, evapotranspiration, and the water vapor mixing ratio. (auth) (Sweden)

29216 WORLDWIDE MOVEMENT OF FALLOUT PARTICLES FROM NUCLEAR EXPLOSIONS. Chen, T. S.; Kuroda, P. K. (Univ. of Arkansas, Fayetteville). Health Phys.; 20: 139-41(Mar 1971).

The major peak concentrations of single particles in the ground-level air measured at Fayetteville (94°W, 36°N), Arkansas after the third Chinese nuclear explosion of May 9, 1966 were explained by the calculated air trajectories. The long range air trajectories at 500 mbar were calculated and a positive correlation was found between the variation of meteorological situations and the daily fluctuations of the particle concentration. (auth) (UK)

29217 DETERMINATION OF REMOVAL PARAMETERS OF THE RADON AND THORON DECAY PRODUCTS FROM THE AIR BY AEROSOL PARTICLES AND WATER DROPLETS. Styro, B. I.; Nadolinskaya, I. N. (Inst. of Physics and Mathematics, Vilnyus, USSR). Liet. Fiz. Rinkinys, Liet. TSR Mokslu Akad., Liet. TSR Aukst. Mokyklos; 10: 287-304(1970). In Russian).

A mathematical model for describing the removal of thoron daughter products from the atmosphere by the cloud or fog droplets and aerosol particles is proposed. The set of differential equations describing this theoretical model was solved approximately by the computer. This model was checked assuming that the coefficients of nuclide removal from the air by aerosol particles, ^{1}K, and cloud or fog droplets, ^{2}K, were equal to coefficient of active aerosol removal by droplets ^{3}K. These calculations were made for different values of coefficient ^{3}K; the solutions were shown graphically. Integral curves of the set of differential equations for radon and thoron decay products were analyzed for different values of parameter ^{3}K. The ratio of activities ThB/ThC was investigated graphically. The solution of the set of differential equations for thoron was investigated by the isoclyn method. For every daughter product of thoron the ratio of the concentration of aerosol-bound nuclide to the concentration of nuclid's free atoms was computed. From these results the conclusions concerning expected ratios of removal coefficients were made. The results are compared with those obtained for radon daughter products. (auth)

29218 CORRELATION BETWEEN THE RADIOACTIVITY IN THE AIR AND IN FALLOUT. Gaglione, P. (EURATOM, Ispra, Italy); van der Stricht, E. Minerva Fisiconucl.; 13: 78-85(Jan-Mar 1969). (In French). (CONF-680535-9).

XUM

From fourteenth national conference of the Italian Association for Health Physics and Protection from Radiation; Formia, Italy (29 May 1968).

The results of strontium-90 determinations in air and fallout obtained at the CEN at Mol (Belgium) and at the CCR Establishment of Ispra (Italy) are correlated with the monthly values of the precipitation at these two sites. The data show that the best correlation on a monthly basis between the fallout-to-air activity ratio and the amount of the precipitation is obtained with a linear function. The validity of a similar relation and its possible applications, among which the most important seems to be evaluation of total fallout over extended areas with the simple knowledge of the amount of rainfall and of the air radioactivity are considered. The data sent by the State Members to the Commission of the European Communities are also reported and their analysis indicates that relation found for the Mol and Ispra data is applicable to them also. (auth)

29219 DAILY FLUCTUATIONS OF RADIOACTIVE FALLOUT PARTICLES IN GROUND-LEVEL AIR. Chen, T. S.; Beck, J. N.; Kuroda, P. K. (Univ. of Arkansas, Fayetteville). Tellus: 22: 707-11(1970).

Long-range 500 mb and 300 mb air trajectories were computed in an attempt to interpret the daily variation of the number of fallout particles in the ground-level air observed at Fayetteville (36°N, 94°W), Arkansas, after a nuclear weapon was tested at Lop Nor (40°N, 90°E), China, December 24, 1967. The dates of occurrence of peak concentrations of fallout particles generally coincided with (a) the arrival times of air masses at 500 mb and/or 300 mb after completing a cycle around the world, and (b) the passage of 500 mb troughs at Fayetteville. A significant deviation from the above rule occurred on January 20, 1968, when the highest concentration of fallout particles in air was observed at Fayetteville. According to the computed air trajectories, such a maximum should have occurred 3 days earlier on January 17, 1968. The discrepancy was explained as due to local meteorological conditions; the occurrence of positive vorticity transport at 500 mb followed by the formation of slow-moving cut-off low during January 17 through January 19, 1968. (auth) (Sweden)

29220 ATTEMPT TO TRACE THE MONSOON FLOW USING NATURAL RADON. Rama. Indian J. Meteorol. Geophys.: 19: 167-70(1968).

Measurements of radon concentration in air over the Arabian Sea and the Indian Ocean are reported. They enable an identification of southeast trade winds and of continental air in the monsoon current. (Indian Sci. Abstr.)

29221 INTERHEMISPHERIC DRIFT OF RADIOACTIVE DEBRIS AND TROPICAL CIRCULATION. Saha, Kshudiram (Inst. of Tropical Meteorology, Poona, India). Tellus: 22: 688-98(1970).

Following French nuclear tests on Mururoa Atoll in the south Pacific (test site, 21°S, 138°W) during the northern summers of 1966 to 1968, a high level of surface-air radioactivity was measured at stations in both the hemispheres. In particular, the effect of the 1968 French test was detected in the northern hemisphere up to a latitude of about 50°N. Relevant data for a few stations are presented. Available meteorological data for 1968 are examined to determine the air currents by which radioactive debris from the tests carried out during this year drifted to the northern hemisphere. South Pacific data appear to rule out the possibility that the debris from the test site was transported to the equator and beyond exclusively by the lower-tropospheric trade wind circulation. On the basis of global tropospheric circulation data presented it is suggested that the interhemispheric transport was effected by the trade wind circulation after the debris had been transported by the tropical westerlies to latitudes nearer the equator by lateral diffusion. Available data suggest that the lateral diffusion coefficient of the tropical westerlies of the southern hemisphere may be of the order of 10^6 m^2 sec^{-1} or more. In the west Indian Ocean the trade winds near the equator have strong meridional components, hence when the debris arrives by way of the tropical westerlies it is rapidly transported across the equator by the trade wind circulation. The study appears to support qualitatively earlier work in respect of transequatorial fluxes of air in the lower troposphere in the west Indian Ocean during the summer monsoon season and suggest generally that large transequatorial fluxes should occur in such regions where the intertropical convergence zone (ITCZ) lies well away from the equator in the opposite hemisphere. Meridional motion associated with ITCZ may transport the debris equatorward or poleward depending upon its location within a hemisphere. In case of poleward transport, the debris may arrive at a latitude from where the westerlies can spread it to higher latitudes. (auth) (Sweden)

29222 CRITERIA AND OBJECTIVES FOR THE SURVEILLANCE OF ENVIRONMENTAL RADIOACTIVITY AROUND A NUCLEAR CENTER. De Bortoli, M. C.; Gaglione, P. (CCR-EURATOM, Ispra, Italy). Minerva Fisiconucl.; 13: 215-18(Jul-Sep 1969). (In Italian). (CONF-680535-23).

From fourteenth national conference of the Italian Association for Health Physics and Protection from Radiation; Formia, Italy (29 May 1968).

The principles adopted for the development of the radioactivity monitoring program in the environment of the Euratom Ispra Establishment are outlined. The latest recommendations by the International Commission on Radiological Protection have been considered in the design of the program. The problems arising from the surveillance during the normal operation of the facilities as well as in emergency conditions are discussed along with the relative solutions. (auth)

29223 DEPENDENCE OF NATURAL RADIOACTIVITY OF THE AIR ON THERMAL STRATIFICATION AND WIND VELOCITY. Trippler, K. (Bundesanstalt fuer Bodenforschung, Hanover). Z. Geophys.; 36: 687-96(Dec 1970). (In German).

Measurements of natural radioactivity in the air, temperatures and wind velocities at heights from 0 to 15 m were taken in the countryside far away from any industry. Survey figures for measurements covering a two-month period point to a negative correlation of radioactivity and wind velocity. From the graphic representations of the mean diurnal variations of radioactivity such as apply to a normal and a stable atmosphere a ratio of activity of 1 : 10 can be determined. Mean altitude profiles of radioactivity for different times of day such as occur in a stable atmosphere give an idea of the time variance of the atmospheric turbulence. (auth)

29224 TRACE SUBSTANCES IN RAIN WATER: CONCENTRATION VARIATIONS DURING CONVECTIVE RAINS, AND THEIR INTERPRETATION. Gatz, Donald F.; Dingle, A. Nelson (Univ. of Michigan, Ann Arbor). Tellus: 23: 14-27(1971).

The temporal changes of contaminant concentrations in rainwater samples collected sequentially at a fixed point are dependent upon both the rain scavenging and drop growth processes and the advective effects of the motion field upon the scalar field of concentration variations in the rain cloud. The observations that rainfall intensity and contaminant concentrations are usually negatively correlated, but occasionally for short periods are positively correlated, are explained. Periods of positive correlation appear mainly because of a predominating advective effect, whereas, all drop growth and scavenging processes operate to produce the negative correlation. In the massive storms characterized by Browning (1964) as "SR-storms" and by Newton (1966) as "persistent," an extraordinarily well-organized downdraft is inferred. The strong evaporative effect of this downdraft upon rain in contact with it produces an atypical variation of concentrations in relation to rainfall rates. An example of this is presented. (auth) (Sweden)

29225 VARIATION OF RADON AND THORON CONCENTRATIONS IN RELATION TO THE WIND SPEED. Ikebe, Yukimasa (Nagoya Univ., Japan). J. Meteorol. Soc. Jap.; 48: 461-8(Oct 1970).

The vertical profiles of ^{222}Rn (radon) and ^{220}Rn (thoron) were obtained analytically for different wind conditions with respect to altitude. The theoretical relationships between the concentration of the emanations and wind speed were compared with those obtained by field measurements, and fairly good agreements were obtained. The exhalation rates of ^{222}Rn and ^{220}Rn were also estimated by comparing theoretical relationships with the observed data. The estimated rates were 1.2×10^{-16} $Ci/cm^2 \cdot sec$ for ^{222}Rn and 9.2×10^{-16} $Ci/cm^2 \cdot sec$ for ^{220}Rn. (auth) (Japan)

Mineralogy and Exploration

29226 NOTE ON THE OCCURRENCE OF RADIOACTIVE ALLANITE IN THE BIVANGAON-KANSA AREA, DISTRICT BOLANGIR, ORISSA. Bose, R. N.; Dash, B. R.; Das, L. M. (Geological Survey, Lucknow, India). Proc. Indian Nat. Sci. Acad., Part A; 36: 278-83(Jul 1970).

While conducting systematic geophysical surveys for lead ores in the Saintala area during the season 1966 to 67, the occurrences of allanite at Bivangaon and Kansa were examined. This created further interest and a preliminary survey with a portable Geiger counter was carried out. A short account of this survey and the results of chemical analysis of a few samples are presented. (auth)

29227 STUDY OF THE MINERALIZATION OF RADIOACTIVE ELEMENTS IN SINGHBHUM SHEAR ZONE, BIHAR. Sarkar,

XUM

S. C. (Jadavpur Univ., Calcutta). Proc. Indian Nat. Sci. Acad., Part A; 36: 246-61(Jul 1970).

Some salient aspects of the mineralization of radioactive and the associated elements along the Singhbhum shear zone are discussed. The shear zone in general and the down-dip warps in schistosity and the shear surfaces, in particular, are the loci of mineralization. Ore shoots generally trend towards NNE–NE, subparallel with the dominant lineations in the zone. Rich veins of radioactive minerals and copper sulphides do not generally coincide. Locally, however, there is concentrated mineralization of nickel and molybdenum along with uranium. The ore zone is at places characterized by the development of cherty quartz and oligoclase veins with abundant inclusions of dusty hematite. Radioactive minerals so far recorded and studied are uraninite, pitchblende, xenotime, allanite, autunite, meta-autunite, torbernite, schoepite, meta-schoepite. Details of these as well as other ore minerals associated with them are discussed. The nature of the ore mineralization, the source of the ore materials and the process of their deposition are discussed. A hypogene middle-high temperature hydrothermal origin, with the ore materials essentially derived from an unknown source, is suggested here. (auth)

29228 DEPOSITION OF MOLYBDENUM AND URANIUM ALONG THE MAJOR OCEAN RIDGE SYSTEMS. Turekian, Karl K.; Bertine, Kathe K. (Yale Univ., New Haven). Nature (London); 229: 250-1(22 Jan 1971).

In order to investigate the time varying pattern of the deposition of U and Mo along a ridge site the distribution of these elements with depth in a core raised from the Mid-Atlantic ridge Lamont-Doherty core A 180-74 was studied. The two elements are shown to vary sympathetically with a pronounced enrichment at the depth interval between 40 and 70 cm. It is proposed that most of the sediments with high concentrations of molybdenum and uranium found on seismically active and relatively inactive ocean rises reflect the formation of anaerobic sediments, in part the result of the formation of local ephemeral basins along the ridges and in part the result of the high rate of supply of organic material to the relatively shallow ocean bottoms along the ridge area. (UK)

29229 INFORMATION ON PROSPECTING IN SWEDEN. Gnojek, I.; Duda, V. (Inst. of Applied Geophysics, Prague. Geological Survey, Hamr na Jezere, Czech.). Geol. Pruzkum; 12: 144-7(May 1970). (In Czech).

A comparison of the Czechoslovak scintillation emanometer PMR 03 and the French emanometer EPP 10 is presented. The test and comparison measurements were conducted at 25 localities in various regions of Sweden. Some special methods of ore prospecting are described and information gained from a visit to the Ranstad uranium mine and to the central workshops and laboratories at Malatrask is presented. The devices used in geological surveying are listed and their characteristics are given. They include the British NR 148 A scintillation radiometer, the French SPP 2 NF scintillation radiometer, and the Finnish RDC 212 monitoring beta–gamma radiometer. (NSA of Czech.)

29230 EXPERIENCE IN BETA LOGGING OF ORE WELLS. Davydov, Yu. B. Izv. Vyssh. Ucheb. Zaved., Gorn. Zh.; 10: No. 3, 3-6(1970). (In Russian).

Experiments with probes for determining uranium concentration in unequilibrated uranium ores using beta and gamma measurements in dry holes are described and analyzed. (R.V.J.)

29231 RADIOGRAPHIC STUDY OF URANIUM-CONTAINING PYRITES. Komarov, A. N.; Egorov, V. P. Geol. Rud. Mestorozhd.; 12: 109-12(Jul 1970). (In Russian).

High-sensitivity microradiography based on fragments from induced uranium fission was used for studying hydrothermal uranium sulfide-type uranium deposits in a weakly metamorphic alevrolite agrillite rock. Results of the luminescence analysis showed that the uranium content in pyritic specimens was from 10^{-4} to 10^{-5} and in the ore bearing rock m $\times 10^{-4}$%. Radiography in a synthetic mica irradiated in a reactor neutron flux at 3.5×10^{15} n/cm^2 revealed that ^{235}U fissioned into two fragments one of which produced a track in the mica forming a micro-zone of radioinduced disturbances. Two types of pyrite were found in the veins, uranium-bearing pyrite and uranium-free pyrite. In the uranium-bearing pyrite, uranium was distributed uniformly along the mineral. In 20 to 90% of the minerals, micro-inclusions were found which contained from 10^7 to 10^9 uranium atoms. The rest of uranium had less than 10^7 atoms. (R.V.J.)

29232 POSSIBILITY OF THE ENDOGENOUS ORIGIN OF SOME SECONDARY URANIUM MINERALS. Kotel'nikov, G. N. At. Energ. (USSR); 29: 382-3(Nov 1970). (In Russian).

A uranium deposit consisting of 0.5- to 2-m wide veins filled with white quartz and containing residues of carbonates and barytes was studied to determine the conditions of its mineralization. The studies brought out new facts which contradict the previously accepted infiltration theory concerning their formation and the secondary character of autunite and torbernite minerals. To a depth of 270 m only autunite and torbernite were found without any trace of the classic primary uranium minerals such as uraninite. No autunite and torbernite were found in open cavities and in cracks of granitic rocks as could be expected in case of infiltration. The autunite-torbernite bearing ores always exhibit radioactive equilibrium; no shift of this equilibrium characterizing secondary minerals has been observed. These minerals in quartz bearing veins contain U^{4+} which differentiates them from secondary minerals. Therefore, it is concluded that autunite and torbernite found in these quartz veins are of primary origin. (TTT)

29233 URANIUM PROSPECTING AT SHALLOW AND MEDIUM DEPTHS USING MAGNETOTELLURIC METHODS. Dupis, A. (CNRS, Garchy, France. Univ., Paris). Rev. Geogr. Phys. Geol. Dyn.; 12: 347-60(Sep-Oct 1970). (In French).

The results obtained using magnetotelluric methods to define the paleotopography of the prepermian basements of three sedimentary basins, capable of containing shallow uranium-bearing deposits, are given. The present equipment was originally designed for deep prospecting. Improvements which would make this equipment more suitable for type of prospecting envisaged are suggested. (auth) (France)

29234 URANIUM DEPOSITS AT WESTMORELAND AND ARNHEM LAND. Rade, J. Aust. Mining; 63: No. 2, 62-4(Feb 1971).

Structural trends controlling uranium occurrences in the Westmoreland area on the Northern Territory—Queensland border, and the Darwin–Arnhem Land area in the Northern Territory, are described. The most important trend lies in a north-easterly direction and is associated with north-westerly shear zones in the Arnhem Land area. Uranium mineralization figures from various surveys within these areas are collated. (Australia)

29235 CORRELATION OF URANIUM, THORIUM, AND POTASSIUM WITH AERORADIOACTIVITY IN THE BEREA AREA, VIRGINIA. Neuschel, Sherman K. (Geological Survey, Washington, D. C.); Bunker, Carl M.; Bush, Charles A. Econ. Geol.; 66: 302-8(Mar-Apr 1971).

In the Berea area, a small quartz monzonite pluton intrudes chlorite-actinolite schist and is overlapped by Coastal Plain sand and gravel deposits. A detailed aeroradioactivity survey of the area shows unusually high radioactivity (1,150 counts per second) over the quartz monzonite. A total of 22 auger samples was taken across all formations to a depth of 2 to 3 feet, and radioelement concentrations were determined by gamma-ray spectrometry. There is a general direct correlation of high radioactivity with increase in radioelement concentrations. Abundances of uranium and particularly thorium in the quartz monzonite are two and three times the average for rocks of this type; a comparison is made with other granitic rocks high in uranium and thorium. (auth)

29236 MINERAL REVIEWS: URANIUM. Williams, R. M. (Dept. of Energy, Mines, and Resources, Ottawa). Can. Mining J.; 92: 114-20(Feb 1971).

Uranium continued to be in oversupply in world markets in 1970 and events during the year did little to offer encouragement to Canadian producers for the short term. Forecasts are given for present and planned production and reserves and exploration are reviewed. International developments, sales and outlook as seen by ENEA/IAEA are also discussed. (F.S.A.)

29237 GERMANY AND JAPAN: EXTENSIVE PROGRAMS FOR URANIUM PROSPECTING AND MINING ABROAD. Com. Naz. Energ. Nucl., Notiz.; 17: No. 3, 62-5(Mar 1971). (In Italian).

A review of the current and planned West German and Japanese programs for uranium prospecting abroad is presented. (auth)

29238 ROUBAULTITE $Cu_2(UO_2)_3(OH)_{10\ 5}H_2O$, A NEW MINERAL SPECIES. Cesbron, Fabien (Univ., Paris); Pierrot, Roland; Verbeek, Theodore. Bull. Soc. Fr. Miner. Crist.; 93: 550-4(Sep-Dec 1970). (In French).

Roubaultite, $Cu_2(UO_2)_3(OH)_{10} \cdot 5\ H_2O$, was found in the oxidation zone of the uranium deposit at Shinkolobwe, Katanga, with becquerellite, vandenbrandeite, soddyite, and cuprosklodowskite. The symmetry is triclinic P_1 or $P\bar{1}$ with a = 7.73 Å, b = 6.87 Å, c = 10.87 Å, $\alpha = 86°29'$, $\beta = 134°12'$, $\gamma = 93°10'$, and Z = 1. The strongest lines of the x-ray powder diagram are: 7.74(9)$\bar{1}$01, 6.88(8)010, 5.55(10)100, 3.448(8) 10$\bar{3}$-$\bar{2}$12, 3.226(8)$\bar{1}$21, 3.175(8)$\bar{2}$11. Roubaultite is biaxial (+) with $n'_p = 1.700$, $n'_m = 1.800$, and $n'_g = 1.83$; the study of reflectivities leads to the refractive indices 1.843 and 1.782 for $\lambda = 580$ nm. Crystals present a perfect cleavage (100)

and an imperfect cleavage (010) the calculated specific gravity is 5.02 g/cm^3. The chemical analysis gave: CuO = 13.5%, SeO = 0.3%, UO_3 = 71.6%, H_2O = 14.8%, sum = 100.2%. (auth) (France)

29239 RELATIONS BETWEEN STRUCTURE OF GRANITE MASSIFS AND THE DISTRIBUTION OF URANIUM IN THE MORVAN. Carrat, H. G. (Univ., Nancy). Miner. Deposita; 6: No. 1, 1-22(1971). (In French).

The study of the early but already decisive occurrences of uranium in igneous rocks is discussed. The behavior of this element seems to be different from that of thorium and tin. The mode of uranium variation, similar to that of thorium in volcanic rocks and in quietly evolving granites, is modified by the first fracturing of the granitic systems, with an abruptly increased mobility. Then uranium becomes fixed in early broken and reconsolidated zones in the higher parts of biotite granite systems. It is mainly enriched as a very fine crystallization of uraninite-type minerals, widely scattered in the rock, making up a real preconcentration (presumed age 280 to 300 Myr). At a later date, i.e., since the saalian phase (250 Myr), the main concentration of pitchblende veins took place. This has led to the genetic conclusion that the uranium of the veins could proceed from uraninite previously leached, and then redeposited under the control of both supergene processes and hydrothermal processes of deep seated origin. (auth)

29240 DEPOSITION CONDITIONS OF MOLYBDENUM AND SELENIUM IN EXOGENETIC EPIGENETIC URANIUM DEPOSITS. Lisitsin, A. K. Litol. Polez. Iskop.; No. 5, 27-35(1969). (In Russian).

U contents of ground waters are discussed in terms of E_H-pH diagrams. Mo migrates under exogenic conditions as $[MoO_4]^{2-}$ ions. Deposition as MoS_2 is conditioned by reducing environment and by H_2S produced by sulfate-reducing bacteria. $[SeO_4]^{2-}$, $[SeO_3]^{2-}$, and $[HSeO_3]^-$ are the possible forms of Se transport. By lowering E_H of the ground waters, Se is deposited first, mainly in environments of increased acidity. The deposition of U and Mo is within the fields of FeO stability. MoS_2 is deposited under lower E_H than U oxides. The lack of Se in the reducing geochemical barriers is explained by low Se in the enclosing rocks and ground waters, the lack of Mo by specific conditions required for MoS_2 deposition. (Selenium-Tellurium Abstr.)

Oceanography

Refer also to abstract 29228.

29241 RADIOACTIVITIES IN THE SEA NEAR THE GOTO ISLANDS. Kawai, Hiroshi; Honda, Yoshihide; Morishima, Hiroshige; Kimura, Yuichiro; Koga, Taeko (Kinki Univ., Osaka). Kinki Daigaku Genshiryoku Kenkyusho Nenpo; 7: 9-12(1968). (In Japanese).

With the future possibility of radioactive contamination in the coastal waters of Japan due to ocean nuclear tests and nuclear power facilities, surface seawater, fishes, especially mackerel, planktons and mud were monitored in the sea around the Goto Islands for 7 days in July 1966. For the surface seawater, the activities of ^{90}Sr and ^{137}Cs were below 0.4 and 0.71 pCi/l, respectively; ^{65}Zn and ^{60}Co both below 0.1 pCi/l; and ^{3}H from 32.6 to 65.6 triton units (TU). The ^{90}Sr and ^{137}Cs in mackerel were not different from those in fishes in other areas of Japan in the same year; these activities were higher in the liver than in other organs. (Japan)

Seismology

29242 (NVO-1163-216(Rev.)) OBSERVED SEISMIC DATA HANDLEY EVENT. (Environmental Research Corp., Las Vegas, Nev.). Mar 1971. Contract AT(29-2)-1163. 99p. Dep. NTIS.

The results of the processing of the observed ground motions generated by the Handley event, a contained underground device detonated on Pahute Mesa at the Nevada Test Site are presented. The Handley event yield was approximately the same as the Boxcar and Benham tests. The observed peak resultant vector amplitudes were calculated and plotted versus the slant distance from source to receiver. Regression equations were derived which describe the observed Handley peak resultant vector motions as a function of distance. Pseudo-Relative Velocity spectra with 5% damping were derived from the velocity seismic recordings. Data recorded at 73 instrument locations were processed and are included in the form of graphs and maps. (auth)

29243 (UCRL-50992) APPLICATION OF THE TENSOR CODE TO THE CALCULATION OF RAYLEIGH WAVES. Viecelli, James A. (California Univ., Livermore. Lawrence Radiation Lab.). Jan 1971. 11p. Dep. NTIS.

Analytical methods are used to obtain two- and three-dimensional solutions for the Rayleigh wave generated by a pressure applied to the surface of an elastic half-space. The limitations inherent in the TENSOR finite-difference equation are then explored by comparing the TENSOR solutions with those derived by analytic methods. (auth)

XUM

ENGINEERING

Nuclear Explosions

Refer also to abstracts 29203, 29221, 29242, 29292, 29410, and 29516.

29244 (UCRL–72572) DISTRIBUTION, RESIDENCE TIME, AND INVENTORY OF TRITIUM IN SEDAN CRATER EJECTA. Martin, J. R.; Koranda, J. J. (California Univ., Livermore. Lawrence Radiation Lab.). 10 Nov 1970. 22p. (CONF-701102–18). Dep. NTIS.

From Meeting of the American Nuclear Society; Washington, D. C. (15 Nov 1970).

The field studies reported enabled the derivation of several important parameters for describing the distribution and fate of a specific radionuclide at the site of the largest nuclear crater produced in the Plowshare program. The distribution and postshot movement of radionuclides in earth materials moved by a nuclear explosive appear to be one of the formidable problems facing this technology. Because tritium is very likely to be the most mobile radionuclide present in nuclear crater ejecta, its behavior may reasonably describe the upper limits of movement of radioactivity from ejecta. The movement of other radionuclides in Sedan ejecta, especially those scavenged from the gaseous state, such as ^{137}Cs, has been found to occur in a very limited manner. The derivation of tritium half-distance values in the ejecta field of the Sedan crater is a useful descriptive index of spatial distribution of radioactivity. The use of integrated depth profiles to obtain unit surface activity is a technique that will have wide applicability in radioecology. A reasonable upper limit for tritium residence time may be found in the desert ecosystem where the average rainfall is less than 5 inches/yr. The lower limit may be represented by the tropical rainforest where the rainfall exceeds 100 inches/yr. The residence half-time for tritium in the rainforest ecosystem was found to be 29 ± 1 days compared with the value of 400 ± 40 days (13.2 ± 1.3 months) in the desert ecosystem at Sedan crater. It is very significant that the biological tritium residence time in small mammals living at Sedan crater reflected the residence time for tritium measured in the desert soil. The excellent agreement of this independent measurement of the tritium inventory with that previously obtained by a different method attests to the validity of the techniques described. (auth)

29245 PROCEEDINGS OF THE INSTITUTE OF ENVIRONMENTAL SCIENCES 15th ANNUAL TECHNICAL MEETING AND EQUIPMENT EXPOSITION, APRIL 20–24, 1969, ANAHEIM, CALIFORNIA. Mt. Prospect, Ill.; Institute of Environmental Sciences (1969). 665p. $18.00. (CONF-690454).

Separate abstracts were prepared for 4 of the 106 papers presented. The remaining 102 papers were not within the scope of NSA. (W.H.K.)

For abstracts of individual papers see: 29246, 29247, 29410, and 30509.

29246 NUCLEAR ENVIRONMENT AGAINST WHICH EQUIPMENT MUST BE HARDENED. Davidson, Charles N.; Schneider, William P. (Army CDC Inst. of Nuclear Studies, Fort Bliss, Tex.). pp 301–8 of Proceedings of the Institute of Environmental Sciences 15th Annual Technical Meeting and Equipment Exposition, April 20–24, 1969, Anaheim, California. Mt. Prospect, Ill.; Inst. of Environmental Sciences (1969).

From fifteenth annual technical meeting and equipment exposition; Anaheim, Calif. (20 Apr 1969). See CONF-690454.

The blast, radiation, and thermal effects of nuclear explosions in the atmosphere create special environmental conditions against which ground military equipment must be protected, i.e., hardened. A methodology is presented for determining the characteristics of a specific nuclear environment; the threat to material from specific nuclear environments; criteria for evaluating whether a given piece of equipment is worth hardening; the cost effectiveness of a hardening procedure; and the overall efficiency of a hardening procedure. (L.C.L.)

29247 ANALYTICAL DESCRIPTIONS OF THE NUCLEAR WEAPON ENVIRONMENT AND EFFECTS. Castle, R. T. (Battelle Memorial Inst., Columbus, Ohio). pp 319–22 of Proceedings of the Institute of Environmental Sciences 15th Annual Technical Meeting and Equipment Exposition, April 20–24, 1969, Anaheim, California. Mt. Prospect, Ill.; Inst. of Environmental Sciences (1969).

From fifteenth annual technical meeting and equipment exposition; Anaheim, Calif. (20 Apr 1969). See CONF-690454.

Analytical methods for determining the nuclear weapons environment and its effects are discussed. Due to the many variables involved, i.e., burst height, burst yield, etc., it is important to weapons effects research to develop large and complex computer codes to describe the weapons effects of neutron transport, x-ray transport, x-ray interactions with material, fireball, blast environment, etc. Use of these computer codes is complicated and time consuming. Therefore, it is suggested that many methods are available which can be used in parametric system studies and which have sufficient accuracy and flexibility to give meaningful results. (L.C.L.)

29248 RULISON PROJECT IN RETROSPECT. Haas, Paul (Univ. of Virginia, Charlottesville). Nucl. News; 14: 55-9 (May 1971).

The public safety aspects of the Rulison Project are discussed in terms of the potential hazards to the public, the measures taken by the government-industry sponsors to protect the public, and the objections and questions which have been raised by opponents of the project. (L.C.L.)

Facilities and Equipment

Refer also to abstracts 29269, 29315, 29322, 29779, 29797, 29800, 29921, 30448, 30453, 31571, and 31629.

29249 (AAEC/LIB/Bib-264) HEAT PIPES AND THEIR APPLICATIONS. A Bibliography. Geue, Jean (comp.) ([Australian Atomic Energy Commission Research Establishment, Lucas Heights). Jan 1971. 17p. Dep. NTIS (U. S. Sales Only).

Ninety seven references are listed. They are arranged chronologically by year, covering the period 1964 to 1970, and alphabetically by author within each year. Most references are to general engineering and heat transfer studies, but a percentage involves heat pipes in nuclear systems. Reference is made to an abstract from each article. (Australia)

29250 (BNL–50145(Rev.)) TABULATED DOSE UNIFORMITY RATIO AND MINIMUM DOSE DATA FOR GAMMA IRRADIATOR DESIGN. Rizzo, F. X.; Galanter, L.; Krishnamurthy, K. (Brookhaven National Lab., Upton, N. Y.). Dec 1970. 122p. Dep. NTIS.

Dose uniformity ratios and minimum dose data in cobalt-60 and cesium-137 rectangular source irradiators are tabulated. These data should simplify the task of irradiator design. The tabulated data supplies dose distribution "look-up" information to the irradiator designer, permitting a quick and easy approximation to be made of the performance of most gamma irradiators which utilize rectangular sources and targets. It should find its greatest use in performing estimates for plant and product feasibility studies, cost estimates, and for some preliminary design calculations. The data in the tables are computer calculated values of the uniformity ratios, U (Maximum Dose/Minimum Dose), and the minimum doses in multipass irradiators. Data for two, four and six pass irradiator systems are presented for typical target materials and rectangular plaque sources over a wide range of sizes. Data are presented for both cobalt-60 and cesium-137. To limit the quantity of data, the thickness of the sources and of the absorbers between the source and the target are treated as constants since absorber and source thickness corrections may be easily applied where necessary. Source-to-target air gap was treated as a variable since this correction is considered to be more difficult to perform. The uniformity ratios and the minimum doses which are presented are based upon depth-dose considerations only. That is, it was assumed that the only dose distributions in the irradiator are those in depth and that lateral dose distributions (those occurring in target planes parallel to the plane of the source) were non-existent. (auth)

29251 (ORNL–4654) FUNCTION OF CONDENSING STEAM IN AEROSOL SCRUBBERS. Davis, R. J.; Truitt, J. (Oak Ridge National Lab., Tenn.). Mar 1971. Contract W-7405-eng-26. 161p. Dep. NTIS.

This work was performed to provide information for designing of a particle scrubber which would efficiently and cheaply remove very fine (0.2 to 2 micron) particles from polluted air streams. The basic concept was to grow these fine particles up to a size which could be readily separated in a cyclone or other inertial device. The tiny particles would first be grown by steam conden-

XU

sation, then further grown by turbulent agglomeration. A literature study was made to show that the 0.2 to 2 micron particles do represent a critical air pollution problem area and to show that the scrubber concept is theoretically reasonable. Experiments were done in a simple, vertical pipe, water-cooled condenser into the bottom of which aerosol plus steam was fed. The aerosol concentration and particle size distributions were measured with and without steam addition for a variety of aerosols and steam condensation rates. These experiments demonstrated that growth does occur, even at low water vapor supersaturation, with a variety of particle substances (including hydrophobic, hydrophillic and hygroscopic substances), with a variety of particle sizes, concentrations, and steam condensation rates. Two simple models of patterns of growth by condensation are suggested which are consistent with the observed removal efficiency results; with hydrophobic particles massive growth of a fraction of the particles occurs, with hydrophillic and hygroscopic particles equal growth of all particles occurs. Experiments demonstrated that the removal efficiency of the condenser increased sharply with aerosol velocity and at very high particle number concentration; these qualitatively verified that growth subsequent to condensation can readily occur due to turbulent (or velocity gradient) agglomeration. Observed removal efficiencies were commonly greater than 90%; such efficiencies were observed with a steam consumption rate as low as 19 lbs per 1000 ft^3 of aerosol which corresponds (assuming steam costs $\$0.25/10^6$ Btu) to a cost of $\$0.0047/10^3 ft^3$ of scrubbed aerosol. The results suggest that the concept is valid and should be pursued. (auth)

29252 (RD/B/M-1817) CODE OF DESIGN FOR RESEARCH APPARATUS CONTAINING MOLTEN SODIUM. Stewart, V. J. (Central Electricity Generating Board, Berkeley (England). Berkeley Nuclear Labs.). Oct 1970. 28p. Dep. NTIS (U. S. Sales Only).

This code gives guidance to design engineers on good practice in the design of molten sodium systems and deals specifically with sodium containment, demountable joints, cover gas systems, pressure relief, and other important auxiliaries. There is also a section on heat transfer which includes useful heat transfer correlations. Appendices deal in more detail with thermal stress estimation and a calculation useful in the design of cold traps. (auth) (UK)

29253 GAMMA-IRRADIATION APPARATUS FOR TREATMENT OF ROOT- AND TUBER- CROPS. Srapeniants, R. A.; Voropaev, J. V.; Lurie, L. S.; Khruschev, V. G.; Kaushansky, D. A. Canadian Patent 865,914. 16 Mar 1971.

The apparatus consists of a shielding shell with an irradiation chamber containing a gamma source mounted therein. The chamber is essentially a revolving cylinder open at its ends and inclined toward its discharge end. A labyrinth-type charging mechanism in the form of a screw-type spout is provided at the inlet end of the cylinder with another labyrinth-type discharge mechanism at the outlet end. The cylinder is rotated and the screw-type spouts are vibrated to feed the crops through the cylinder for irradiation by the gamma source. (F.S.A.)

29254 APPARATUS FOR BLENDING PARTICLES. Mattson, Philip T. Jr.; Stevens, Dennis W. (to United States Atomic Energy Commission). U. S. Patent 3,572,405. 23 Mar 1971. Filed 6 Jun 1968.

Particles of at least two groups are fed at predetermined rates of flow to impinge on a deflecting surface means which causes the particles to blend uniformly as they fall into a cavity in which the blended particles are shaped into an article. The particles of the respective groups are blended uniformly even though the particles may be unequal in size and density and the ratio of the respective particles in the article is varied considerably from a one to one ratio. (Official Gazette)

29255 TWO SPECIAL GAMMA-RAY IRRADIATION PLANTS TO PRODUCE MEAN AND ELEVATED EXPOSURE RATES WITHIN THE ^{60}Co GAMMA-RADIATION ENERGY RANGE. Rothe, H.; Hecker, O. (Deutsches Amt fuer Messwesen und Warenpruefung, Berlin). Isotopenpraxis; 6: 390-6(Nov 1970). (In German).

Two gamma-ray irradiation plants are described, which are installed at the German Board for Metrology and Goods Testing. At present, both plants are supplied with ^{60}Co sources. They are used as irradiation sources for the reproduction and transfer of Roentgen units within this energy range. A virtual point radiation source installed in a collimator serves to produce exposure rates from about 0.5 to 4 R/hr. A special irradiation device has been set up to produce exposure rates for the medical field. Having a low total activity of about 2 Ci, it is able to supply a controllable exposure rate ranging between 10 and 30 R/min. (tr-auth)

29256 LARGE STEAM TURBINES FOR NUCLEAR AND CONVENTIONAL POWER STATIONS. Kalderon, D. (English Electric - AEI Turbine Generators Ltd., Rugby, Eng.). J. Sci. Technol. (London); 38: 21-30(1971).

Information is presented on modern steam turbines. Turbine exhaust loading is discussed for a wide variety of different designs for both superheated and saturated cycles, and for high and low rotational speeds. Brief particulars are given of typical machines in the ranges quoted. (UK)

29257 CIRCULATING PUMPS FOR LIQUID-METAL COOLED REACTORS. Stech, P. (Klein, Schanzlin and Becker Pump Co., Rutherford, N. J.): Stipp, H. J. Konstr. Masch., App.- Geraetebau; 22: 205-8(1970). (In German).

A description is given of the function and the construction of circulating pumps for sodium-cycles applied to fast breeder reactors. Specific problems, dependent on material, result from the operational requirements and of these, the problems of cavitation and welding of austenites in liquid metals are dealt with. (INIS)

29258 IRRADIATION HEAD USED IN APPARATUS FOR BEAM THERAPY. Sulkin, A. G.; Kondrashov, V. M. (to Vsesojuzny Nauchno-Issledovatelsky Institut Radiatsionnoi Tekhniki). Canadian Patent 859,837. 29 Dec 1970.

The apparatus includes a protective shield with an exit aperture or window, a rod movable in the shield, a radiation source in the rod, a light source fixed in position in the shield against the exit aperture, and an optical system having a condenser lens and an objective lens arranged in the rod so that the position of its focal point corresponds to that of the expected estimated focus of the radiation source. The optical system is adapted to approach the exit window alternatively with the radiation source to illuminate the surface to be irradiated and then to expose such surface to the irradiation source. (F.S.A.)

29259 AIRCONDITIONING SYSTEM AND ITS AUTOMATIC CONTROL FOR A NUCLEAR POWER STATION. Maeda, Muneharu (Saginomiya Seisakusho Inc., Tokyo). Karyoku Hatsuden; 21: 419-29(Apr 1970). (In Japanese).

To adequately protect personnel and equipment from airborne radioactive contaminants and excessive thermal conditions, the air conditioning and ventilation systems are provided for a nuclear power station. The basic concept is to keep the radioactive concentration in various buildings below the stipulated level by taking in as much air as possible, to keep the pressure in buildings lower than outside atmosphere to prevent radioactive diffusion, to improve habitability for operators, to keep continuous operation with stand-by facilities, and the air conditioning of various safety devices to counteract against reactor accident. The ventilation system is different for each building, and two examples of air supply and exhaust systems in the radioactive waste and turbine buildings are discussed. The air supply system is provided with a temperature regulating system, but, unlike the exhaust system, does not have pressure regulation and filters to prevent outside contamination. One of the most promising heat exchangers for air conditioning systems would be the "Total Heat Exchanger", which is like a Ljungstron air heater, with a horizontal shaft and the heating surface made of asbestos honeycomb. (Japan)

29260 IRRADIATING APPARATUS. Kirkpatrick, William W.; Masefield, John (to Atomic Energy of Canada Ltd.). Canadian Patent 811,240. 22 Apr 1969. Filed 28 Oct 1964.

An irradiation device is described which includes a housing of shielding material defining an irradiating chamber for a sample to be irradiated a plurality of guide tubes within housing said guide tubes being located in a cylindrical array around the chamber a radioactive source in each guide tube and movable by fluid pressure from a position isolated from a sample in the chamber to a working position to irradiate said sample and a series of individually operable fluid-pressure operated assemblies each connected to, an individual guide tube and operable to move, the respective source in said guide tube from the isolated to the working position, and at least one of said fluid pressure-operated assemblies being connected to a plurality of said guide tube. (Canada)

29261 SYSTEM FOR THE AUTOMATIC INDICATION OF IMPURITIES IN SODIUM COOLANTS. Mitropol'skii, A. N.; Pinkhasik, M. S.; Petrenko, A. A.; Tsukerman, I. Kh.; Tarantin, V. D. At. Energ. (USSR); 29: 376-7(Nov 1970). (In Russian).

The impurity content in sodium coolants may be determined by reducing the temperature, thus allowing it to precipitate and to clog a small orifice, through which the sodium circulates. From the temperature at which this occurs the concentration may be cal-

XUM

culated. The system was automated in order to eliminate subjective errors in determining the stoppage of circulation. An expression was derived from the equation for the elementary volume of the liquid metal flowing in the tube and the heat balance equation for the wall and the air to indicate the relation between the air flow rate and the time dependence of the heat transfer agent. On the basis of these dynamic properties, dispersion surveys were plotted; they were approximated by a third-order differential equation with a delayed argument. An algorithm was derived for the control operation on the basis of which the regulator was designed and built. The device had been used with good results on the BR-5 reactor and will be incorporated in the BN-350 reactor, currently under construction. (TTT)

29262 PLANE CROSS-FLOW HEAT EXCHANGERS WITH HEAT GENERATION WITHIN A FLUID STREAM. Di Federico, I. (Univ., Bologna). Nucl. Eng. Des.; 15: 41-53(Mar 1971).

Plane cross flow heat exchangers are examined when the volumetric heat generation rate is constant or depends linearly on the local temperature in the hot fluid stream. The analytical solutions obtained are discussed in both cases with reference to some dimensionless parameters. Temperature distributions and mean exit temperatures of both streams are calculated, and working conditions for the exit hot stream temperature which is equal to or less than the inlet hot fluid temperature are determined. Numerical calculations of mean exit temperature of hot and cold streams and heat exchanger effectiveness are reported. (auth)

29263 COMPARISON OF SAMPLING METHODS FOR AEROSOL PARTICLES FOR ANALYSIS OF PARTICLE SIZE. Melandri, C.; Prodi, V.; Tarroni, G. (CNEN, Bologna). Minerva Fisiconucl.; 13: 185-91(Jul-Sep 1969). (In Italian). (CONF-680535-20).

From fourteenth national conference of the Italian Association for Health Physics and Protection from Radiation; Formia, Italy (29 May 1968).

Particle size has recently been shown as one of the parameters ruling the deposition region in the airways. Submicron particles are particularly relevant from the point of view of inhalation hazards. In this size range, the electron microscope is the reference instrument and still the most widely used. Three sampling techniques particularly suitable to electron microscopy are presented, i.e., thermal precipitation, electrostatic precipitation (point-to-plane E.S.P.) and filtration with very fine pore membrane filters. Thermal precipitators are absolute samplers and the most reliable but sample preparation is long and liable to loss or damage of the sample. E.S.P. and membrane filtration allow a quicker and safer sample preparation but may produce artifacts. Their applicability should therefore be tested in each case. (auth)

Heat Transfer and Fluid Flow

Refer also to abstracts 29249, 29262, 29819, 30029, 30341, 31566, 31587, 31588, 31590, and 31673–31675.

29264 (EUR-4531, pp 821-39) HEAT EXCHANGE BY NATURAL CONVECTION IN POROUS MEDIA. Grossin, R.; Jannot, M.; Micheau, P.; Pirovano, A. (Societe Bertin et Cie, Paris (France)); Klarsfeld, S. (Compagnie de Saint-Gobain, Paris (France)). (In French).

From Second conference on prestressed concrete reactor pressure vessels and their thermal isolation; Brussels, Belgium (18 Nov 1969).

In Second information meeting on prestressed concrete reactor pressure vessels and their thermal isolation.

The transfer of heat associated with the natural convection of a fluid in a homogeneous porous medium was studied. The results of the theoretical study and the experimental verification by optical methods on a porous medium composed of glass wool and an organic liquid are briefly summarized. A final verification of the theory established was made by thermal measurements in operational experiments close to those found in reactors. A complete theory of the natural convection flows and heat transfers in porous media was established. (J.S.R.)

29265 (RD/B/N-1878) FULLY DEVELOPED TURBULENT FLOW THROUGH CONCENTRIC ANNULI. Lawn, C. J.; Elliott, C. J. (Central Electricity Generating Board, Berkeley (England). Berkeley Nuclear Labs.). Feb 1971. 61p. Dep. NTIS (U. S. Sales Only).

Mean velocity and turbulence data are presented for the fully developed flow of air in three radius ratios of concentric annuli. The shear stress distributions were determined by location of the zero-shear position with hot-wires, and by a sliding sleeve technique. This technique, although not entirely satisfactory, proved the reliability of the first method and allowed non-dimensional velocity profiles to be constructed with confidence. These velocity profiles are satisfactorily generated by using an eddy viscosity model and a computer solution. Some of the relevant parameters for more refined calculations, involving the turbulence energy equation, were also evaluated and hypotheses concerning the diffusion of the Reynolds stresses were tested against the data. (auth) (UK)

29266 (SC-ARPIC-1010) EXPERIMENTAL AND ANALYTICAL METHODS FOR THE DETERMINATION OF HEAT AND MASS TRANSFER THROUGH SOIL: A BIBLIOGRAPHY. Elkins, G. H. (comp.) (Sandia Labs., Albuquerque, N. Mex.). Apr 1969. 15p. Dep. NTIS.

A bibliography is presented which lists 128 documents related to the determination of heat and mass transfer through soil. The bibliography was compiled for use in studies related to possible earth impact and burial of aerospace radioisotope thermoelectric generators. (auth)

29267 TRANSVERSE HEAT FLOW IN GASEOUS HYDROGEN ISOTOPES AT LOW TEMPERATURES. Hermans, L. J. F.; Schutte, A.; Knaap, H. F. P.; Beenakker, J. J. M. (Rijksuniversiteit, Leiden). Physica; 51: 319-29(29 Jan 1971).

For gaseous hydrogen isotopes at temperatures between 22 and 110°K, measurements are reported on transverse heat flow, which occurs under the influence of a magnetic field. For HD, the effect is found to be much larger than for H_2 and D_2. The observed strong temperature dependence of the effect is compared with theoretical expressions. Mixtures of para hydrogen with ortho hydrogen as well as mixtures of ortho deuterium with helium have also been investigated. (auth)

29268 BILATERAL APPROACH TO THE ANALYSIS OF TURBULENT FLOW IN AN ANNULUS. Min, T. C.; Hoffman, H. W.; Peebles, F. N. (Univ. of Tennessee, Knoxville. Oak Ridge National Lab., Tenn.). Contract W-7405-eng-2426. Nucl. Eng. Des.; 15: 65-76(Mar 1971).

An approximate solution method for determining local time-mean velocities for fully developed turbulent, axial, upward flow through a concentric annulus is presented. This new treatment employs both the phenomenological approach of von Karman's similarity hypothesis and the statistical aspect of turbulent structure. The statistical microstructural measurements of the Reynolds stresses are incorporated in a proposed universal function. The success of this bilateral approach is attested by the good agreement between predicted and experimental values for the velocity in a developed turbulent flow within an annulus of small radius ratio. With the aid of the universal function, the applicability of the von Karman similarity theory to turbulent shear flow in annuli is demonstrated and, indeed, further appreciated. Possible extension to include turbulent flow through eccentric annuli and multirod channels is indicated. (auth)

29269 PLATE HEAT EXCHANGER. Rylander, Lars (Alfa-Laval AB, Lund, Sweden). Aust. Chem. Process. Eng.; 23: No. 9, 29-32(Sep 1970).

The design and performance of the plate heat exchanger (PHE) are evaluated in terms of its application to the secondary cooling circuits of nuclear power plants. Prerequisites are considered to be minimum space demand, high reliability, no interleakage of media, a safety margin for corrosion and fouling, and a safety margin for the cooling capacity of the heat exchangers. The PHE is considered to fulfill these requirements well. Interleakage is precluded by the design, and little space is taken up compared to a tubular heat exchanger. Applications to the emergency cooling system and service system of light water reactors and to the pressure vessel coolers and service coolers of gas reactors are discussed. (Australia)

29270 THERMAL RADIATION ABSORPTION BY PARTICLE-SEEDED GASES. Williams, J. R.; Partain, W. L.; Shenoy, A. S.; Clement, J. D. (Georgia Inst. of Tech., Atlanta). J. Spacecraft Rockets; 8: 339-46(Apr 1971).

Particle-seeded gases are currently being considered as propellants for gas core nuclear rocket engines and for other applications such as thermal shielding for reentry vehicles and rocket nozzle cooling which require that surfaces be protected from intense thermal radiation. To evaluate radiant heat transfer through a particle-seeded gas, one must know the extinction parameter, the scattering parameter, and the scattering amplitude function of the particles. The extinction parameters of submicron particles dispersed in hydrogen at 1 atm pressure have been measured as a function of wavelength from 1200 to 6800 Å at various temperatures to 2170°K and are approximately 50,000 cm^2/g for carbon, 20,000 cm^2/g for tungsten, and 65,000 cm^2/g for silicon. The extinction parameter of submicron tungsten particles in hy-

XUM

drogen at 12.5 atm showed an increase to nearly 50,000 cm^2/g as the temperature was raised to 2080°K, and at 100 atm it reached approximately 100,000 cm^2/g at 2300°K. The scattering amplitude functions of submicron carbon, tungsten, silicon, tungsten carbide, and silicon carbide dispersed in nitrogen were measured and scattering from these particles was shown to be highly forward, that is, most of the scattered light is scattered at angles <30°. (auth)

Isotope Technology

Refer also to abstracts 29213, 29220, 29250, 29253, 29255, 29266, 29286, 29293, 29294, 29319, 29823, 29938, and 31069.

29271 (CONF-700557-1) HISTORY OF THE COUNTERFLOW GAS CENTRIFUGE. Martin H. Translated from Stroemungsmechanische Vorgaenge in Graszentrifugen, DFVLR-Kolloquium, om 14. Mai 1970, Porz, Wahn, Germany. 3p.

The development of counterflow gas centrifuges in Germany from 1936 to the present is briefly reviewed. (L.C.L.)

29272 ADVANCED PROTOTYPE SYSTEM (APS) FOR SNAP-23A (1 Jul 1970) (Engineering Materials). (Westinghouse Electric Corp., Pittsburgh, Pa. Astronuclear Lab.). (CAPE-2066).

298 drawings.

The Advanced Prototype System (APS), which evolved from the FPMS described in CAPE-2064, consists of the heat source, base assembly, thermoelectric converter, radiator, power converter, and protective cover. The heat source consists of the fuel capsule, a Ta inner diffusion barrier, a U−8 Mo biological shield, an outer diffusion barrier of 0.020 in. thick Ta, a Cu accumulator, and the Inconel 718 heat source jacket. To provide a 20% reduction in wt. and a 10% reduction in height, SrO pellets encapsulated in thin-walled superalloy cans are used. The biological shield is a beveled cylinder with conforming accumulator and jacket. The beveled configuration lowers machining costs. The cylindrical fuel capsule has an operating lifetime of 10 years. It is capable of housing 1117 W of fuel. The base assembly, which supports and insulates the heat source and provides environmental protection, is composed of the support, containment, and Min−K2000 insulation. The hermetic seal and cover gas have been deleted from the insulation system. The containment system, consisting of the outer shell and rain shield, protects the insulation and heat source. The thermoelectric converter is essentially identical to that of the FPMS. A finned Al radiator, located within the protective cover, rejects heat to the atmosphere. A solid-state power conditioner is employed to maintain electrical output at 24 Vdc over the load range of 0 to 83W. It absorbs and dissipates the power which is not used as heat to a finned heat sink. An Al protective cover is attached to the rain shield to protect the APS from physical damage. For details see TID-4100 Suppl. 63. (F.S.)

29273 RADIOISOTOPE PRODUCTION IN ITALY. Rosa, U. (Societa Ricerche Impianti Nucleari, Saluggia, Italy). pp 319-41 of Research Reactor Utilization. Vol. 2. Vienna; International Atomic Energy Agency (1970). (CONF-700204-14).

From IAEA meeting on research reactor utilization; Rome, Italy (2 Feb 1970).

According to the agreement between CEA, CEN and the Nuclear Research Center at Saluggia, Italy, the programme of work of the last center in the field of radioisotope production is devoted to the development of radioactive compounds for medical applications. About 200 curies of ^{131}I have been processed at SORIN, Saluggia in 1969; about 60 curies have been converted into radiopharmaceuticals. All the mercury was converted into organic mercurials for kidney, brain and spleen scanning. The total ^{113m}In and ^{99m}Tc has been converted into more or less complex derivatives and over fifty percent of the ^{125}I has been used for the preparation of labelled reagents for clinical chemistry. Data are also given about some radioactive compounds and reagents prepared at the Nuclear Research Center, Saluggia, for in vivo investigations and for in vitro assay. The radioimmunoassay kits and ^{99m}Tc or ^{113m}In kits supplied in 1969 are also listed. The evolution of the research programme in Italy on the preparation and properties of labelled proteins for metabolic studies is also given. (auth)

29274 PRODUCTION OF RADIONUCLIDES IN AUSTRIA. Sorantin, H. (Oesterreichische Studiengesellschaft fuer Atomenergie GmbH, Vienna). pp 287-318 of Research Reactor Utilization. Vol. 2. Vienna; International Atomic Energy Agency (1970). (CONF-700204-17).

From IAEA meeting on research reactor utilization; Rome, Italy (2 Feb 1970).

After a short theoretical introduction, irradiation facilities of the ASTRA reactor are described and the commercial production of radionuclides in Austria in recent years is reviewed. The kinds of radionuclides produced, the controlling procedures, and the distribution organization are discussed. (INIS)

29275 PRODUCTION OF RADIOISOTOPES IN RESEARCH REACTORS. Bochkarev, V. V.; Levin, V. I. pp 243-86 of Research Reactor Utilization. Vol. 2. Vienna; International Atomic Energy Agency (1970). (CONF-700204-15).

From IAEA meeting on research reactor utilization; Rome, Italy (2 Feb 1970).

The choice of a suitable target and its irradiation conditions and on target preparation and its processing after irradiation are discussed, including the production of the necessary compound or drug. In this connection, most valuable reactions excited by neutrons are discussed, and suitable examples for the primary chemical processing of irradiated targets are given. The principal characteristics of 25 most widely used radioisotopes and of a group of short-lived isotopes, as well as the maximum activities of some isotopes formed as a result of double neutron capture, are listed. The lists of some isotopes formed by reaction (n,γ), of isotope-enriched targets used for radioisotope production, and of genetic radioisotope pairs forming the basis for isotope generators are also given. (INIS)

29276 PROTECTED RADIOISOTOPIC HEAT SOURCE. Anderson, Charles G.; Avona, Vincent L.; Kelly, Donald P. (to United States Atomic Energy Commission). U. S. Patent 3,569,714. 9 Mar 1971. Filed 14 Nov 1969.

A radioisotopic heat source including a container with plurality of closed chambers cooperating to preserve integrity of the contained radioactive heat source against impacts, projectiles, extreme temperatures, and other various environmental conditions pertaining to missiles for carrying the heat source into outer space and landing it on the moon is described. (auth)

29277 MASS-DIFFUSION MERCURY COLUMNS FOR ISOTOPE SEPARATION. Nikolaev, B. I.; Kolokol'tsov, N. A.; Sulaberitsze, G. A.; Tevzadze, G. A.; Chuzhinov, V. A. Isotopenpraxis; 6: 417-21(Nov 1970). (In Russian).

The development of mass-diffusion mercury columns for isotope separation purpose is described. The description refers to a porous diaphragm with optimum diffusion properties rendering the arrangement suitable for continuous operation. The results of the experimental investigation of the separation process in the columns are presented. Neon and argon isotope separation factors were obtained which were superior to those achieved by other authors by 2 or 3 times. The efficiency of the developed equipment is shown for neon isotope separation in a three-stage plant. (tr-auth)

29278 METHOD FOR MEASURING WALL THICKNESS OF ARTICLES USING GASEOUS RADIOACTIVE MATERIAL. Packer, Louis L. (to United Aircraft Corp.). U. S. Patent 3,564,247. 16 Feb 1971. Filed 16 Jun 1966.

A method is described for measuring the wall thickness of hollow turbine blades and turbine vanes by transferring a radioactive gas into the hollow blades or vanes to fill the interior cavity of these articles with the radioactive gas, and then measuring the intensity of the radiation transmitted through the wall of the hollow blade or vane. The intensity of this radiation provides an indication of the thickness of the wall. (Official Gazette)

29279 RADIOACTIVELY-HEATED THERMODYNAMIC ENGINES. Meijer, R. J.; van Witteveen, R. A. J. O. (to N. V. Philips Gloeilampenfabrieken). Canadian Patent 858,666. 15 Dec 1970. Priority date 9 Feb 1966, Netherlands.

A closed heat cycle engine, having a compression space and an expansion space connected by a regenerator, is provided with a heating system constituted by one mass of radioactive isotopes from which heat is supplied to the working medium of the engine. Temperature is adjusted by controlled movement of the isotopes. (F.S.A.)

29280 POWER GENERATION DEVICES WITH ATOMIC ENERGY. DEALING MAINLY WITH ATOMIC ENERGY BATTERIES. Ato, Yasuro (Government Industrial Research Inst., Nagoya, Japan). Kogyo Gijutsu; 11: No. 8, 27-31(Aug 1970). (In Japanese).

The quantity of radioisotopes produced by nuclear reactors and as the result of fuel reprocessing has increased in recent years. Atomic energy batteries utilizing these radioisotopes are attracting world interest. The present situation and future prospects in this field are reviewed. Nuclear batteries consist of the following: the primary type cells using α and β particles; the secondary type cells using p−n junctions, Compton electrons, contact potential difference, and magnetic fields; the tertiary type cell using fluorescence; the thermoelectric cell using Seebeck effect; the thermo-

XUM

electron cell; and dynamic generators using gas turbines. The advantages of nuclear batteries are listed. Applications of these batteries, such as in the U. S. SNAP series, are explained. Future uses are also indicated. (Japan)

29281 SOME REMARKS ON THE SQUARING CRITERIA FOR DIFFUSION CASCADE IN ISOTOPIC ENRICHMENT OF URANIUM. Oliveri, Elio (Univ., Palermo, Italy). Atti Accad. Sci. Lett. Arti Palermo; 28: 45-64(1967-68). (In Italian).

In an industrial separation cascade for uranium, the diffusion process is repeated many times. Since for practical reasons it is necessary to prearrange the obtainable yield, the ideal diffusion coefficient ($0 = \frac{1}{2}$) has to be replaced by the real one which is obtained by setting up a certain number of squared cascades in which the diffusion constant of each step remains constant. On the basis of a schematic representation of one-step casades in which a yield P of gram molecules of uranium with a concentration N_p of ^{235}U are obtained, a differential formula is derived: $dN/ds = [P/L(N_p - N) + mN(1 - N)]$ where $dN/ds = N'_s - N'_{s-1}$, L the cascade constant, P the yield in gram molecules, and N and N' concentration at inflow and outflow. Substituting b for P/Lm one finally obtains the equation

$$m = \log \frac{(N - a_2) \cdot (N_i - a_1)}{(N - a_1) \cdot (N_i - a_2)} = 2m \sqrt{\left(\frac{1 + b}{2}\right)^2 - bN_p} \, (s - s_i)$$

This equation expresses the functional relation between the concentration of the lighter isotope N and the number of steps by which this concentration is attained, where s_i the order of the step, N_i the corresponding concentration and a_1 and a_2 the solution of the equation $N^2 - (1 + b) N + bN_p = 0$. In squaring the diffusion cascades two problems are of interest: the determination of the optimal working conditions for each individual step and the best division of cascades into a certain number of steps. The first problem reduces itself to the finding of the capacity that would reduce q_i and q_j, the respective capacity values to a minimum. The second problem does not lend itself to an analytical solution and, therefore, an approximation method is applied using the serial development of logx as a tool and breaking up the series after the second term. This study of the squaring operation for the diffusion cascade for isotopic uranium enrichment leads, therefore, to an optimization of gradients. Starting with the theoretical exact optimization equation, a theory of approximation is developed which through a second approximation formula allows the anticipation of the optimal conditions of the entire cascade. Thus a criterion is established for the separation of uranium isotope molecules by a squaring procedure in order to obtain the highest enrichment of the lighter isotope. (F.J.W.)

29282 MEASUREMENT OF WORKING TEMPERATURE IN MOTORS BY MEANS OF ^{85}Kr. Ury, J. F. (Forschungsinstitut fuer Automobilbau, Budapest). Isotopenpraxis; 7: 21-7(Jan 1971). (In German).

The so-called krypton method representing a new isotopic-target technique based on radioactive gases embedded in solids has been successfully used in engine research. An attachment has been erected to label metal parts and piston rings with ^{85}Kr by means of ion bombardment. Preliminary tests were performed to determine the thermal properties of kryptonized sheets made of commercially pure aluminum, Nimonic 90, and C-30 carbon steel, for use in measurement of maximum working temperature of piston rings containing radioactive krypton gas in Diesel engines and compressors. Thus, data were obtained for supplying information on the correlations existing between working conditions and piston ring temperatures in Diesel engines as well as on the difference in temperature between the piston rings of different cylinders in compressors. (auth)

29283 RADIONUCLIDES FOR THE INVESTIGATION OF CONCENTRATE CIRCULATION IN CRUDE ZINC AND LEAD OXIDE PRODUCTION. Palige, J.; Michalik, J. (Institut fuer Kernforschung, Warsaw). Isotopenpraxis; 7: 28-30(Jan 1971). (In German).

With regard to the zinc and lead oxide production process, radioactive tracers were used to perform technological investigations aimed at an improvement of technical installations and quality of final products. (auth)

29284 ^{60}Co: BETTING MEGABUCKS ON MEGACURIES. Law, C. A. Nucl. Eng. Int.; 16: 211-14(Mar 1971).

Production of ^{60}Co in Canada, where output from the Pickering reactor is expected to reach 12 to 13 MCi/yr by 1975, is discussed. The work of the AECL and the γ-irradiation facilities offered in the field of radiotherapy, radiography, and industrial irradiation such as sterilization of medical products, food irradiation, and production of materials such as wood-plastic composites, polymer-impregnated concretes, and treated textiles are described. Other uses of ^{60}Co are discussed, and include chemical processing and waste-water treatment, isotopic power sources, and research irradiators. (UK)

29285 DEVELOPMENT OF RADIOISOTOPE-POWERED CARDIAC PACEMAKERS IN THE WORLD. Enomoto, Shigemasa (Japan Atomic Energy Research Inst., Oarai). Genshiryoku Kogyo; 16: No. 12, 38-41(Dec 1970). (In Japanese).

A cardiac pacemaker is an artificial electrical stimulator which is put into the thoracic or abdominal cavity, and corrects cardiac rhythm in case of heart block. The old pacemaker utilized a mercury battery as electric source, and its life span was about 2 years. Therefore, surgical operation was required fairly frequently for exchanging the batteries. Recently, the radioisotope-powered cardiac pacemaker (RPCP) was developed in the U. S., England, and France, and it has a life of 10 years or more. The radioisotope used for RPCP should have long life and high energy flux density, and must not emit radiation having strong penetrating power. At present, only ^{238}Pu is used because it has a half-life of 87.5 years, and emits high energy α-particles but very little γ-radiation. RPCPs developed in U. S., England, and France include 0.15 to 0.4 g of ^{238}Pu, have electric power from 160 to 200 μW, and weigh 100 to 200 g. Dose rate due to radiation is 2 to 5 mR/hr on the surface of the capsule for the ^{238}Pu heat source. Purity of ^{238}Pu is closely related to this radiation leakage because ^{236}Pu mixed in ^{238}Pu is converted into ^{212}Pb, ^{212}Bi, and ^{208}Tl which emit γ-rays. In the U. S., electrolysis was adopted for refining the ^{238}Pu metal. RPCP was actually applied to a man and a woman in England and to two women in France in 1970. (Japan)

Materials Testing

Refer also to abstracts 29391, 29757, 29944, 31664.

29286 (BNWL-1329) DESIGN AND FABRICATION OF A PORTABLE DEVICE FOR NEUTRON RADIOGRAPHY. Cason, J. L. (Battelle-Northwest, Richland, Wash. Pacific Northwest Lab.). Mar 1971. Contract AT(45-1)-1830. 50p. Dep. NTIS.

A research program is being conducted at Battelle-Northwest to determine the usefulness of ^{252}Cf as a source for portable thermal neutron radiography. Emphasis has been in developing a device using ^{252}Cf that could be used for laboratory, hot cell or field radiography. A 268 μgm ^{252}Cf source (NS-1) was obtained from ORNL for experimental testing. This source has a neutron yield of 6.2×10^8 n/sec and was used in an experimental container designed for neutron radiography. A first generation portable device which completely contains the ^{252}Cf has been designed and built and is presently being evaluated. Preliminary work included flux measurements and neutron radiographs. The neutron camera is completely portable and can be used in the laboratory, hot cell or field. The shielding characteristics are such that it can be transported by common carrier per ICC regulations as outlined in 10 Code of Federal regulations. (auth)

29287 (ORNL-4630, pp 145-9) NONDESTRUCTIVE TESTING TECHNIQUES FOR FBR. Harms, W. O.; McClung, R. W. (Oak Ridge National Lab., Tenn.).

In Fuels and materials development program quarterly progress report for period ending September 30, 1970.

New methods, techniques, and equipment for nondestructively evaluating materials for liquid-metal-cooled fast breeder reactors (FBR) are being developed with emphasis on measuring cold work in stainless steel tubing. An eddy-current instrument is being developed to measure both the size and depth of defects and prototype equipment being assembled to model both the instrumentation and purposely flawed specimens. Ultrasonic schlieren techniques are being used to aid the interpretation of results from conventional ultrasonic inspections of welds. A new transducer with multiple sensors is being built for an advanced delta technique. Experimental measurements were made of scattered radiation for different combinations of base and cladding materials. Construction of the prototype low-frequency, high-sensitivity impedance bridge for measuring changes in magnetic permeability related to cold reduction in stainless steel tubing was completed. Extensive calculations were made to determine optimum operating conditions in the presence of potential variations in instrument components and tubing dimensions. Measurements were made on a set of tubes that contained different amounts of cold reduction. (auth)

29288 (ORNL-4630, pp 271-9) NONDESTRUCTIVE TESTING. Harms, W. O.; McClung, R. W. (Oak Ridge National Lab., Tenn.).

In Fuels and materials development program quarterly progress report for period ending September 30, 1970.

New analytical solutions were developed for problems of electromagnetic induction involving multilayered cylindrical con-

XUM

ductors and computer programs were prepared for multilayered planar conductors. Phase shifts were measured on specimens with a large range of electrical resistivities. A polynomial fit of the data was made; the average variation was about 0.24%. New experiments with ultrasonic frequency analysis demonstrated that flaws up to the size of the transmitting source can be identified. Discrimination was also shown in the received spectra between several small reflectors and one large reflector within the same zone. Modification of the electrodischarge machining equipment now allows fabrication of reference notches in fueled materials. Measurements were made with the multichannel analyzer of the scattered and fluorescent radiation for several combinations of materials as a function of changing cladding thickness. The television system for film viewing was demonstrated to be sensitive enough to display a change of 0.005 in film density. A new marker system allows selection, identification, and magnification up to 1000× of specific portions of the video. (auth)

29289 NONDESTRUCTIVE TESTING OF POWER REACTOR COMPONENTS. Latzko, D. G. H. (Univ. of Tech., Delft, Netherlands). Kerntech. Atomprax.; 13: 53-5(Feb 1971).

The first part of this paper underscores the importance of nondestructive testing of nuclear power reactor components for the safety of nuclear power plants. The second part evaluates the economic importance of NDT by comparing the incentives in terms of decreased plant outage to the inspection costs for a typical 800-MW light-water reactor unit. Finally some possible future developments are outlined, with particular reference to the introduction of liquid-metal fast breeder reactors. (auth)

29290 ULTRASONIC IN-SERVICE INSPECTION OF REACTOR PRESSURE VESSELS. Meyer, H.-J. Kerntech. Atomprax.; 13: 56-68(Feb 1971). (In German and English).

In view of the safety requirements for nuclear reactor pressure vessels, nondestructive inspections are to be carried out not only during manufacture but also during the whole operational life of a reactor. Ultrasonic inspection systems and manipulation equipment are described which permit economical inspection of reactor components, at the same time avoiding subjective evaluation and manual probe guidance. Inspection system and manipulation are arranged so that when employing modern electronic components two-dimensional flaws in particular (e.g., cracks) can be traced with a high degree of dependability. (auth)

29291 EXAMINATION OF SPENT FUEL ELEMENTS WITH AN 18-MeV BETATRON. Tucek, J.; Wiechers, R. (Kernforschungszentrum, Karlsruhe, Ger.). Kerntech. Atomprax.; 13: 78-81(Feb 1971). (In German and English).

In the hot cell facility of the Karlsruhe nuclear research center, spent fuel elements are examined radiographically with an 18-MeV materials testing betatron. The special feature of this work is the high activity of the test objects. Selective attenuation of this radiation is achieved by interposing a steel filter between the test specimen and the film. The shape of this filter results in a very even intensity distribution of the betatron radiation. This obviates the need for the lead beam homogenizer installed for this purpose by the manufacturer which, if used, limits the useful beam intensity to about 20% of the original bremsstrahlung intensity. (auth)

29292 NEUTRON RADIOGRAPHY AND ITS APPLICATION POSSIBILITIES. Lausch, W. Kerntech. Atomprax.; 13: 82-8 (Feb 1971). (In German and English).

The most important methods of neutron radiography are discussed. The difference between neutron radiography on the one hand and x-ray and γ-radiography on the other hand is outlined. An attractive neutron source for use in neutron radiography is ^{252}Cf; this source is compared to the Sb–Be source. Neutron radiography should be a good means for monitoring fuel enrichment distributions. This is illustrated for a pin-type fuel element. (auth)

29293 ISOTOPE AND X-RAY RADIOGRAPHY. Becker, E. (Technische Hochschule, Magdeburg, Ger.). (Isotopenpraxis; 6: 381-90(Nov 1970). (In German).

Methods, economics, applications, and general information regarding isotope and x-ray radiography are presented, based on a review of 1966 to 1969 literature on the subject. (L.C.L.)

29294 EXPOSURE PLOTS FOR NEW RADIOGRAPHIC FILMS. Becker, E.; Vorsprach, F. Isotopenpraxis; 6: 424-6(Nov 1970). (In German).

A new x-ray film was produced in Germany for use in industrial radiography. In order for users of the new film to achieve the same image definition as with the old films, a series of graphs is presented. Each graph plots the exposure level versus material thickness for either a range of source-to-film distances for a given photographic density or a range of photographic densities for a given source-to-film distance. Data for both ^{60}Co and ^{192}Ir sources are plotted. (L.C.L.)

29295 NON-DESTRUCTIVE TESTS AT THE CASACCIA CENTER: THERMOGRAPHY APPLICATIONS AND EXPERIMENTS IN COLOR RADIOGRAPHY. De Jaco, L.; Cappabianca, C. (CSN, Casaccia, Italy). Com. Naz. Energ. Nucl., Notiz.: 16: 17-27(Jan 1970). (In Italian).

Basic experiments were carried out to evaluate nondestructive thermographic testing of materials. Infrared emission ranges from wavelength 0.8 to 1000 μm. Knowing the laws of emissivity the surface temperatures of bodies may be determined by means of infrared radiation detectors. Several heat measuring devices are described based on mechanical or electronic scanning, but preference is given to a temperature measuring device using the evaporation of oil. A germanium lens focuses the infrared radiation on a detector consisting of a nitrocellulose membrane of 0.1 μm thick. An absorbing device of black colloidal gold takes up the infrared radiation and converts it into heat which in turn heats the membrane as a function of the intensity of the received radiation. The membrane is attached in the center of a cell and to obtain a thermic picture of the heat emission there are oil vapors on the opposite side of the membrane. The oil condenses on the membrane at various points and in different thicknesses as a function of temperature. By projecting a beam of white light on the oil film one obtains a series of colors produced by the interference of light with various depths of the film. These colors correspond to the different temperatures of the object under examination. The membrane divides the cell in a front and rear half. In the front half is a window of NaCl which allows the infrared rays to strike the membrane. The rear half is covered with a filter paper impregnated with an oil drop for evaporation. The rear part of the cell is externally heated and kept at a pressure of 1 mm Hg. There is also a glass window which allows the observation of the interior of the cell. With this apparatus one has the possibility to photograph the thermic image of a body and to control thermostatic phenomena. Thermographic methods have been used in various phases of reactor research, for instance to determine the sodium level in an irradiation capsule or to obtain oscillographic pictures of heat exchange conditions. The making of thermal phenomena visible has many possibilities for application in industry and medicine. In the chemical industry for instance a continuous close observation of thermic events inside the reaction vessel during chemical reaction would be feasible. (F.J.W.)

29296 RADIATION DEFECTOSCOPY OF CONCRETE AND REINFORCED CONCRETE BY MEANS OF BETATRON BREMSSTRAHLUNG. Vorob'ev, V. A.; Gavkalov, Yu. D. (Tomsk Polytechnic Inst., USSR). Defektoskopiya; No. 1, 124-8(1971). (In Russian).

Basic equations were developed for determining the sensitivity of radiation defectoscopy of concrete and reinforced concrete products. The range of optimum bremsstrahlung energy for testing reinforced concrete construction of various thicknesses was determined and the organization of nondestructive radiation regulated tests in the construction industry is discussed. (R.V.J.)

29297 MECHANICAL (CADWELD) SPLICES IN REINFORCING BARS OF CONCRETE CONTAINMENTS. AEC Safety Guide 10 1971. Washington, D. C.; Atomic Energy Commission (1971). 3p. Available from United States Atomic Energy Commission, Washington, D. C.

A safety guide is presented which describes an acceptable method for the sampling and testing of mechanical splices in reinforcing bars used in concrete containment structures. This testing must be performed to determine whether the splices meet safe design and fabrication standards. (L.C.L.)

29298 MODEL TECHNIQUES FOR PRESTRESSED CONCRETE PRESSURE VESSELS. Proceedings of the Conference, London, 10–11 July 1969. London, Institute of Civil Engineers (1969). 188p. Pound 10. (CONF-690701).

Sixteen papers were presented at this conference. A separate abstract was prepared for each paper. (UK)

For abstracts of individual papers see: 29299–29314.

29299 INSTRUMENTATION TECHNIQUES IN LARGE SCALE CONCRETE MODELS. Hornby, I. W. (Central Electricity Research Lab., Leatherhead, Eng.). Proc. Inst. Civil Eng. (London), 1969; 3-6(1969).

From International Conference on Model Techniques, London, England. See CONF-690701.

Instruments and techniques are described that have been employed at the Central Electricity Research Laboratories for

XUM

short- and long-term measurements in concrete structures and the methods adopted for data logging and subsequent data reduction. Much of the paper deals with the instrumentation for the Oldbury pressure vessel model, but details are given of the recent development of a crack detecting gage. (auth)(UK)

29300 PRACTICE WITH MODEL TECHNIQUES. Bremer, F. (Fried-Krupp GmbH Universalbau, Obering, Ger.). Proc. Inst. Civil Eng. (London), 1969; 7-13(1969).

From International Conference on Model Techniques, London, England. See CONF-690701.

It is concluded that any model practice properly adapted to the objective in view offers a valuable aid for the designer, provided his expectations in respect of the results obtainable are not unreasonably high. It is suggested that there is no need for building large-scale models ad infinitum. Expansion of the knowledge of materials, including their two- and three-dimensional stress behavior and the development of better methods of calculation that also make allowance for the viscous properties of concrete give reason to believe that it will be possible in future to predict the life history of a prestressed concrete vessel with accuracy by a mathematical approach. It is possible to derive the necessary design information exclusively from small-scale or detail models. (auth)(UK)

29301 DEFLECTION MEASUREMENT TECHNIQUES. Brading, K. F.; McKillen, R. R. (Atomic Power Constructions Ltd., Sutton, Eng.). Proc. Inst. Civil Eng. (London), 1969; 15-21(1969).

From International Conference on Model Techniques, London, England. See CONF-690701.

The size and rigidity of concrete pressure vessels present the research worker with some difficulties when attempting to measure deflection. The problem is described and the desirable accuracy quantified; the choice of datum reference frame and its stability is reviewed, together with the accuracy of available deflection gages. Details are given of a displacement transducer developed for model work, and its use in tests on a $\frac{1}{10}$ scale model of the Dungeness 'B' vessel is illustrated. (auth)(UK)

29302 TECHNIQUES FOR RUPTURE TESTING OF PRESTRESSED CONCRETE VESSEL MODELS. Scotto, F. Proc. Inst. Civil Eng. (London), 1969; 23-9(1969).

From International Conference on Model Techniques, London, England. See CONF-690701.

Tests on the 1 : 20 prestressed concrete models of vessels for "high-temperature gas cooled reactors" of the HTGR (English) and THTR (German) type are described along with a couple of simply supported end slabs of the THTR model, prestressed respectively with three systems of straight tendons at 60° and with hooping tendons only. The separate "copper-sealing system" studied for the THTR model to ensure complete tightness up to collapse of the concrete structure and tendons is described in detail. This system is, in fact, essential to avoid the tests in the ultimate condition of the model being invalidated by undue leakages of the pressurizing fluid, and to permit a reliable study of the propagation of concrete cracking as pressure is increased. Detailed information is also given of special "crack detectors" devised by ISMES and developed to detect and follow internal cracks in critical sections of the structure. The reliability and interest of such a type of test and of the relevant results together with economic implications are discussed. (auth)(UK)

29303 INSTRUMENTATION OF FULL-SCALE CONTAINMENT STRUCTURES. Bekowich, R. S. (Bechtel Corp., San Francisco). Proc. Inst. Civil Eng. (London), 1969; 31-6(1969).

From International Conference on Model Techniques, London, England. See CONF-690701.

The instrumentation arrangements and techniques that were utilized to measure the response of several full-scale containment structures during post-tensioning and proof-test pressurization are described. The precautions undertaken to insure reliability of sensors embedded in concrete for long-term measurements are also described. Representative data from sensors embedded for longer than one year are also given. (auth)(UK)

29304 USE OF SIMPLIFIED MODELS FOR THE DESIGN OF END SLABS. Campbell-Allen, D.; Low, E. W. E. (Univ. of Sydney). Proc. Inst. Civil Eng. (London), 1969; 43-51(1969).

From International Conference on Model Techniques, London, England. See CONF-690701.

Models on two scales were used to examine the failure of deep end slabs under pressure. Major variables are depth/diameter ratio and horizontal prestressing force. The determination of the modes of failure was assisted by dissecting specimens which approach failure, and these modes were used as a basis for an analysis of the strength of slabs. The change of scale from model to prototype and its influence on the concrete properties on which failure depends is discussed. (auth)(UK)

29305 SMALL SCALE MODEL PRESTRESSED CONCRETE PRESSURE VESSEL TESTS AT FOULNESS. Davidson, I.; Purdie, A. C. Proc. Inst. Civil Eng. (London), 1969; 53-7(1969).

From International Conference on Model Techniques, London, England. See CONF-690701.

The tests were to investigate two design criteria, that failure must be gradual, and that a minimum ultimate load factor must be achieved. The tests were conducted to determine if overpressure testing correctly simulates a deteriorated vessel at normal pressure. Methods of calculating ultimate pressure to avoid scale model testing of every design are examined along with proportions required to ensure a gradual mode of failure. The models are plain cylinders with flat ends, 36 inches diameter, and they are cast in one continuous pour, using an expanded polystyrene core, which is subsequently removed. Circumferential prestressing is by 24 gage wire which is wrapped on to the outside under controlled tension in a purpose made machine. Longitudinal prestressing is by conventional 7 mm wire. Up to 126 transducers were used to record the response of the models, which were tested with both hydraulic and pneumatic pressures. (auth)(UK)

29306 EXPERIMENTAL INVESTIGATION INTO THE BEHAVIOUR OF PERFORATED END SLABS FOR CONCRETE PRESSURE VESSELS UNDER TEMPERATURE AND EXTERNAL LOAD. Stefanou, G. D. (Imperial Coll. of Science and Tech., London); Yu, C. W.; Gill, S. Proc. Inst. Civil Eng. (London), 1969; 59-67(1969).

From International Conference on Model Techniques, London, England. See CONF-690701.

Results of an investigation are reported on the behavior of perforated circular plates with reinforced holes when subjected to radial in-plane loading and sustained uniform temperature. A method of analysis was used to predict this behavior taking into account elastic effects. For this purpose, a series of experiments was carried out on models of flat circular concrete slabs, some perforated and reinforced with standpipe liners and some unperforated. Information is included on the overall creep and shrinkage strains of a perforated zone; the internal distribution of load between a perforated and unperforated zone; the effect of the thickness of the standpipes and the ratio of pitch-to-diameter on the stiffness of the structure; the elastic response of the concrete before, during, and after heating, and the determination of its elastic constants; the formation of cracks on unloading; and notional material properties for an equivalent homogeneous material which can be considered to replace the perforated zone. (auth)(UK)

29307 MODEL PHILOSOPHY IN RELATION TO PRESTRESSED CONCRETE PRESSURE VESSEL DESIGN PROBLEMS. Langan, D. (Taylor Woodrow Construction Ltd., Whetstone, Eng.). Proc. Inst. Civil Eng. (London), 1969; 69-80 (1969).

From International Conference on Model Techniques, London, England. See CONF-690701.

The representation of thermal loading in model pressure vessels and the problems of simulating boundary conditions for pile cap studies are discussed. The approach of past model work is traced and the likely change of emphasis in further experimental analysis outlined. The usefulness of models in modifying the original design is examined and it is concluded that future models should be used for the better prediction of the short and long term mechanical behavior of concrete in the "mass". (auth)(UK)

29308 PROBLEMS IN ASSESSING THE CORRELATION BETWEEN THE OBSERVED AND PREDICTED BEHAVIOUR OF MODELS. Smith, J. R. (Taylor Woodrow Construction Ltd., Whetstone, Eng.). Proc. Inst. Civil Eng. (London), 1969; 81-9 (1969).

From International Conference on Model Techniques, London, England. See CONF-690701.

Certain aspects of the general field of model analysis applied to prestressed concrete pressure vessels are briefly reviewed, and the main factors which influence the accuracy of correlation between model and prediction are established. These factors are discussed in more detail and, where possible, the likely magnitudes of the errors arising from each are assessed. A numerical assessment of the agreement between typical model and predicted data is then undertaken in an attempt to define reasonable limits for acceptable correlation. The current value of this work to the designer is questioned and future trends are examined. (auth)(UK)

29309 BEHAVIOUR OF THE OLDBURY MODEL VESSEL WITH TIME UNDER THERMAL AND PRESSURE LOADINGS. Hornby, I. W. (Central Electricity Research Labs., Leatherhead, Eng.). Proc. Inst. Civil Eng. (London), 1969; 109-13 (1969).

From International Conference on Model Techniques, London, England. See CONF-690701.

Tests on a model of the Oldbury pressure vessel are described. These tests consisted of loading the model thermally with and without pressure for short periods and thermally with pressure for a more prolonged period. In each loading period the temperature gradients rapidly attained a steady state with the inside of the vessel at 55°C and the outside at approximately 29°C. The major influences affecting creep are discussed and an approximate method for computing the total strain changes that occur with time under a thermal gradient is included. Computed values are compared with strains measured at various positions. The conclusions draw attention to the importance of shrinkage and creep recovery when dealing with a model structure. (auth)(UK)

29310 TWO BUGEY 1/5 MODELS. Launay, P. (Compagnie Industrielle de Travaux (Entreprises Schneider) SA, Paris). Proc. Inst. Civil Eng. (London), 1969; 115-24(1969).

From International Conference on Model Techniques, London, England. See CONF-690701.

The prestressed concrete Bugey reactor vessel has a circular-base cylinder shape and operates at 45 atmospheres and has an upper slab without transverse prestressing including 950 penetrations. The 1/5 scale was chosen for the two models since real concrete and prestressing cables of current unit strength could then be used. One model was used to study the prestressing and pressure in the range of small strains and in cracking and rupture. The second model, after being used to study prestressing and pressure in the range of small strains was used to carry out thermal tests, fatigue tests (pressure and temperature cycles), vibration tests of blower consoles and thermal tests of the upper standpipes unit. Finally, the ultimate possibilities of the structure's strength were tested under high thermal gradient ($\Delta t = 100°C$), followed by a test of pressure to rupture under this same gradient. The tests on the models showed the good correlation between the experimental results and the computations made on electronic computers. Following the model work changes in the definitive design of the BUGEY I vessel were made, for instance reinforcement of the circular prestressing on both sides of blower penetrations and a change to the form of the blower corbels. (UK)

29311 ELASTIC AND ULTIMATE PRESSURE TESTS ON A ONE TENTH SCALE MODEL OF THE DUNGENESS B CONCRETE PRESSURE VESSEL. Brading, K. F. (Atomic Power Constructions Ltd., Sutton, Eng.); McKillen, R. R.; Finigan, A. Proc. Inst. Civil Eng. (London), 1969; 125-34(1969).

From International Conference on Model Techniques, London, England. See CONF-690701.

The design, construction, instrumentation, and testing of a 1/10 scale model of the Dungeness 'B' prestressed concrete pressure vessel are described. Tests were conducted to measure the deflection and strain distribution when subjected to hydraulic pressure at ambient temperature. Initially it was tested by raising the pressure incrementally to the value of proof pressure for the site vessels, and the instrument readings were compared with theoretical predictions. Subsequently the vessel was further pressurised to the maximum value obtainable in order to develop the failure modes. Strain and deflection measurements are presented and the behavior compared with that of a similar vessel to a smaller scale tested previously. (auth)(UK)

29312 TESTING THE ONE TENTH SCALE MODEL OF THE HINKLEY POINT B AND HUNTERSTON B POWER STATION PRESTRESSED CONCRETE PRESSURE VESSELS. Eadie, D. McD.; Bell, D. J. Proc. Inst. Civil Eng. (London), 1969; 135-46 (1969).

From International Conference on Model Techniques, London, England. See CONF-690701.

A 1/10th scale model of the prestressed pressure vessels currently being constructed at the Hinkley Point B and the Hunterston B Power Stations was built and tested to substantiate the ultimate load design analysis. The model was also tested to proof pressure to demonstrate the elastic behavior of the vessel and prove the instrumentation. The model is described with details of the prestressing system, liner and penetrations, instrumentation and construction methods. The test program and results are discussed together with the further investigation carried out during the demolition of the model. (auth)(UK)

29313 COMPARISON OF EXPERIMENTAL RESULTS WITH RESPONSE ANALYSIS FOR A MODEL OF A PRESSURE VESSEL. Rashid, Y. R.; Ople, F. S. Jr.; Chang, T. Y. (Gulf General Atomic Inc., San Diego, Calif.). Proc. Inst. Civil Eng. (London), 1969; 147-57(1969).

From International Conference on Model Techniques, London, England. See CONF-690701.

Experimental data and analytical results are compared for a one-quarter-scale model of a prestressed concrete pressure vessel subjected to an arbitrary test history over a 2-yr period. Tests included sustained prestress, transient and steady-state temperature distributions; short-time and sustained pressures; and pressure overload up to 1500 psig. The response of the model was calculated using a method of analysis that accounts for concrete creep, cable relaxation, cracking, and steel yielding. The method is an application of the finite element method to nonlinear viscoelasticity and is based on a modified superposition principle. A failure surface for the concrete was postulated on the basis of test results which were independent of time and temperature. Strain, displacement, and tendon load change are compared and discussed. (auth)(UK)

29314 SCANDINAVIAN PRESTRESSED CONCRETE PRESSURE VESSEL MODEL PROJECT. Menon, S. K. (Aktiebolaget Atomenergi, Stockholm). Proc. Inst. Civil Eng. (London), 1969; 159-61(1969).

From International Conference on Model Techniques, London, England. See CONF-690701.

A joint initiative was taken by the four Scandinavian countries to design, build and test a model of a prestressed concrete pressure vessel (P.C.P.V.) suitable for water reactors. To make possible the use of P.C.P.V.s for water reactors, certain developments have had to be made to the existing technology of such vessels. This development work has resulted in a design for a removable lid which allows access for refuelling (in the case of LWRs) or service (for LWRs and HWRs, especially integral designs), a thermal insulation system that permits the use of insulations developed mainly for gas-cooled reactor P.C.P.V.s and improved calculation programs for thick-walled vessels. The aims of the model project are to test and demonstrate the designs of the removable lid and the insulation system, to verify the calculation programs and to demonstrate the safety characteristics of the P.C.P.V. (auth)(UK)

Protective Structures

Refer also to abstract 30633.

Radioactive Material Handling

Refer also to abstracts 29259, 29393, 29479, and 31649.

29315 (ANL-7683) SAND-BED FILTRATION OF AEROSOLS: A REVIEW OF PUBLISHED INFORMATION ON THEIR USE IN INDUSTRIAL AND ATOMIC ENERGY FACILITIES. Juvinall, R. A.; Kessie, R. W.; Steindler, M. J. (Argonne National Lab., Ill.). Jun 1970. Contract W-31-109-eng-38. 62p. Dep. NTIS.

The principles of operation, design, cost, and performance of sand-bed filters for removing aerosols from gas streams are reviewed. The sand-bed filters described remove dust from industrial gas and air streams, serve as emergency filtration systems for large nuclear-energy facilities, or remove radioactive aerosols from the off-gas of nuclear-fuel-reprocessing plants or from gas-coolant streams of nuclear reactors. Experience with full-scale sand filters is reported, as well as the results of laboratory-scale investigations. Utilization of sand filters in ventilation systems of protective shelters (for humans) is reviewed in relation to the ability of sand filters to resist the destructive effects of air pressure, shock, high temperature, thermal shock, chemical attack, and moisture. The life and initial cost for sand-bed filters are compared with those for fibrous filters. The effects on filter operation of physical parameters such as the size and shape of sand particles, the composition and thickness of sand layers in a filter, filter design, and the design of bed containment structures are discussed. Filtration mechanisms are described, as are several alternative procedures for regenerating sand filters. The relationship of filter life, collection efficiency, and air-handling capacity to the filter design and operating conditions appropriate for a specific filter application is described. Important variables are aerosol size, composition, and concentration and gas throughput rate. (auth)

29316 (LA-tr-71-12) SOME CRITERIA FOR CHOOSING PRESSES FOR THE COMPACTION OF RADIOACTIVE WASTE. Seyfried, Philippe (Commissariat a l'Energie Atomique, Chusclan (France). Centre de Production de Plutonium de Marcoule). Translated by Anna Vakar (Los Alamos Scientific Lab., N. Mex.), from report CEA-R-3619. 21p. Dep. NTIS.

An abstract of this paper, prepared from the original language, appeared as NSA 23: 16007.

XUM

29317 (ORNL-4522) COMPLETION REPORT: EVALUATION OF THE USE OF PERMSELECTIVE MEMBRANES IN THE NUCLEAR INDUSTRY FOR REMOVING RADIOACTIVE XENON AND KRYPTON FROM VARIOUS OFF-GAS STREAMS. Rainey, R. H.; Carter, W. L.; Blumkin, S. (Oak Ridge National Lab., Tenn.). Apr 1971. Contract W-7405-eng-26. 58p. Dep. NTIS.

The effective permeabilities and separation factors of krypton, xenon, and several other gases were measured using sheets of thin silicone rubber membrane having areas as large as 2 ft^2; the pressure drop across the membrane was varied from 25 to 150 psi. Processes using such membranes were evaluated for removing radioactive noble gases from (1) the off-gas from a plant for recovering used nuclear fuels, (2) a reactor containment building following a nuclear accident, and (3) the cover gas of a liquid metal fast breeder reactor (LMFBR). Radiation exposure of the membrane would not be a limiting factor in the first two applications, but the LMFBR cover gas would have to be stored to allow the short-lived gaseous nuclides to decay before it could be processed in a membrane plant. The costs of removing the noble gases from these systems were estimated. (auth)

29318 MODEL 10 SHIPPING TUBE (2 May 1968) (Engineering Materials). (Richland Operations Office (AEC), Wash.). (CAPE-2074).

1 drawing.

The model 10 container is used in shipping unirradiated fuel elements or non-irradiated fissionable material and is designed and constructed to be in compliance with AEC and the Department of Transportation regulations regarding shipments of radioactive and fissile materials. When the model 10 container is used to ship Pu and U, the material is sealed in an inner containment vessel, using either DOT specification 2R or metal encapsulated in reactor-grade cladding. The container is fabricated from 4 schedule 40 steel pipe. (For details see TID-4100 Suppl. 63) (see also NSA 25: 6516) (F.S.)

29319 RADIOACTIVE SOURCE CAPSULE-HANDLING SYSTEM. Massey, George Robert (to Chevron Research Co.). U. S. Patent 3,564,255. 16 Feb 1971. Filed 25 May 1967.

A capture and sensing system useful in pneumatic transportation of capsules is presented. (Official Gazette)

29320 CONTROL AND MONITORING OF ISOLATED IN DUSTRIAL PRODUCTS WHICH CONTAIN RADIOACTIVE NUCLIDES. Ramos Rodriguez, Eduardo (Junta de Energia Nuclear, Madrid). Energ. Nucl. (Madrid); 14: 419-28(Sep-Oct 1970). (In Spanish).

A summary is presented of a study by R. E. Cunningham on fundamental methods for analyzing the safety and for controlling the use of products and devices which contain radioisotopes and which are available to the public. Since his study concentrated on "isolated" products, products for nuclear study and production were categorically excluded. The "isolated" products are those which individually contain quantities of radioisotopes less than that which would prohibit their use, but which, because of their widespread abundance, create a problem of increased exposure dose to the population. (J.S.R.)

29321 AMERICAN STANDARD: GUIDE FOR DESIGN AND OPERATION OF SHIPPING CONTAINERS FOR IRRADIATED SOLID FUEL FROM NUCLEAR REACTORS. ANSI N 5.3 1964. New York; American Institute of Chemical Engineers (1965). 8p. Available from American National Standards Inst., New York.

A standard guide for the design and operation of containers for shipping irradiated fuel elements from nuclear reactors is presented. (L.C.L.)

29322 FUEL STORAGE FACILITY DESIGN BASIS. AEC Safety Guide 13 1971. Washington, D. C.; Atomic Energy Commission (1971). 3p. Available from United States Atomic Energy Commission, Washington, D. C.

Standards are presented for the design of reactor fuel storage facilities which will assure adequate safety under normal and postulated accident conditions. These systems must be designed to prevent significant reduction in the coolant inventory of the storage facility under accident conditions, and must include appropriate containment, confinement, and filtering systems. (L.C.L.)

Vacuum Engineering

Refer also to abstract 29406.

29323 DECREASE OF THE MIGRATION OF HYDROCARBONS IN AN ULTRAHIGH VACUUM SYSTEM BY MEANS OF A PASSIVE GAS. Kanter, B. Z. (Inst. of Physics of Semiconductors, Novosibirsk, USSR). Instrum. Exp. Tech. (USSR) (Engl. Transl.): No. 4, 1174-5(Jul-Aug 1970).

Translated from Prib. Tekh. Eksp.: No. 4, 186-7(Jul-Aug 1970).

A method of using a passive gas when evacuating a vacuum system by mechanical and diffusion pumps is described. With the use of a passive gas the partial pressure of heavy hydrocarbons in an unheated evacuated ultrahigh vacuum system does not exceed 2×10^{-9} torr. (auth)

INSTRUMENTATION

Radiation Detection Instruments

General Detectors and Monitors

Refer also to abstracts 31064, 31185, 31646, and 31680.

29324 (AEEW-M-970) LOW GAMMA-SENSITIVITY BORON PROPORTIONAL COUNTER. Allen, F. H. (Atomic Energy Establishment, Winfrith (England)). Oct 1970. 20p. Dep. NTIS (U. S. Sales Only).

The design, construction and development of a $^{9}/_{32}$ inch diameter boron proportional counter, with a thermal neutron sensitivity of approximately 3×10^{-5} c/s per unit flux are described. The counter was designed to have a low sensitivity to gamma radiation and to withstand an operating temperature of 200°C.(auth)

29325 (JINR-P13-5707) X-RAY SPECTROMETER WITH COOLED Si(Li)-DETECTOR. Arl't, R. D.; Banifatov, A. E.; Kalinin, A. I.; Petrov, M. M.; Tyvin, L. I. (Joint Inst. for Nuclear Research, Dubna (USSR). Lab. of Nuclear Problems). 1971. 8p. (In Russian). Dep. NTIS (U. S. Sales Only).

The x-ray spectrometer using a Si(Li)-detector and field transistor placed in a chamber-cryostat are described. A resolution of 650 eV was obtained on a 6.4 keV line from ^{57}Co. (auth)

29326 (LA-4445) CALIBRATION OF MOXON-RAE DETECTORS IN THE CURRENT MODE. Ellis, A. N.; Brown, W. K.; Farrell, J. A.; Fullwood, R. R. (Los Alamos Scientific Lab., N. Mex.). Jun 1970. Contract W-7405-eng-36. 15p. Dep. NTIS.

Moxon-Rae type gamma-ray detectors have been used for neutron capture cross-section measurements employing neutrons from an underground nuclear explosion. The efficiency of these detectors has been measured in an experiment on the Physics 8 event. Two detectors were used to view thin strips of gold and ^{238}U mounted on the inside of a spinning drum. The collimated neutron beam was passed through the drum. The drum speed was sufficient to resolve the individual low-energy gold and uranium resonances that appeared as spots of activation on the strips. The spots were located by autoradiographs, cut out, and beta counted. The detector efficiency was determined by comparing the absolute activation in each resonance with the integrated signal recorded from the detectors. The measurement is independent of any knowledge of the neutron flux or of the capture cross sections involved. The measurements have yielded a more precise value of the current mode efficiency than was previously available, and therefore permit more accurate measurements of capture cross sections. (auth)

29327 (NYO-3246-TA-8) RESEARCH ON AVALANCHE TYPE SEMICONDUCTOR RADIATION DETECTORS. Semiannual Report, July-December 1970. Moldofsky, Philip J.; Hewka, Peter V. (General Electric Co., Philadelphia, Pa. Space Div.). Jan 1971. Contract AT(30-1)-3246. 86p. Dep. NTIS.

In the continuing effort toward an in vivo plutonium measurement device using the avalanche detector, the three factors which most strongly affect this low activity counting are detector sensitivity, angular uniformity of sensitivity, and statistics. Two arrays of three detectors each have been constructed. Each three-detector probe has a detector frontal area of 3 cm^2, by far the largest of any probes to date. In addition, with the detectors arranged as a triangular prism, overall efficiency is increased due to a greater total active detector thickness. Angular dependence of sensitivity is also greatly reduced with this array, making possible a more accurate interpretation of measured count rates in terms of actual activity of isotope present in an unknown source-detector geometry. A three-detector probe is now being evaluated. A program to develop fast electronics, matched to the nanosecond time response of the avalanche detector, has been started, beginning with fast video amplifiers developed for the optoelectronics field. The nanosecond charge collection times of such systems will greatly reduce noise due to detector leakage current, thereby increasing detection sensitivity and signal to noise ratio. Preliminary results show that noise reductions of a factor of 30 are attainable with special voltage sensitive amplifiers, using pulse clipping techniques. Collaborations in nuclear medicine and biology continue, with ten active collaborations being carried on at this time. In every case, low level, low energy counting is of primary importance. Radioisotopes employed in the various studies include ^{32}P (eye tumors, malignant melanoma, blood flow, breast tumors), ^{45}Ca (heart muscle), ^{14}C (protein adsorption), ^{125}I (protein adsorption, eye studies), ^{85}Kr (brain blood flow), and ^{69m}Zn (radioisotope washout in eye). Experiments in crystal growth and post-growth processing are continuing, in an effort to achieve a greater degree of avalanche detector gain uniformity. Currently being evaluated are methods of heat treatment, and fast diffusion techniques. Special experimental crystals, such as flat interface Czochralski silicon, are also being studied. Evaluation of production line crystals continues in a search for possible breakthroughs in large scale crystal growth techniques. As part of this program, development of special detector shapes, with emphasis on cylindrical configurations, is continuing. (auth)

29328 (ORNL-TM-3261) PHANTOM FOR THE ADJUSTMENT OF GAMMA-RAY IMAGING DEVICES. Bell, P. R.; Ross, D. A. (Oak Ridge National Lab., Tenn.). May 1971. Contract W-7405-eng-26. 7p. Dep. NTIS.

A test target ("phantom") is described which, when properly loaded with a radionuclide in solution, can be used to assess the performance of a moving-detector scanner or a gamma camera. Since scattered radiation often degrades the quality of the picture delivered by an improperly operated instrument, the phantom intentionally presents a scattering problem as well as problems of target resolution. It also provides special tests for tomographic scanners. An appendix gives instructions for assembly and loading. (auth)

29329 COMPTON DIODES. Gross, Bernard (Laboratoire de Recherches Physiques, Veyrier, Switzerland). Z. Angew. Phys.; 30: 323-31(Jan 1971).

Aspects of the behavior of Compton diodes under steady state and transient conditions are discussed. The advantages of systems with low internal resistance are emphasized. The theory is extended to the high-energy range where the range of the Compton electrons becomes comparable to the thickness of the scatterer. Finally, measurements with the radiation from an 18-MeV Betatron are reported in which the influence of geometrical and material parameters is investigated. (auth)

29330 MATERIALS PROBLEMS IN LITHIUM-DRIFTED GERMANIUM RADIATION DETECTORS. II. Jindal, G. R.; Faust, J. W. Jr. (Pennsylvania State Univ., University Park). J. Appl. Phys.; 42: 2508-15(May 1971).

A description is given of materials problems involved in the preparation of lithium-drifted germanium gamma-ray detectors. A comparison is made of gallium- and indium-doped germanium (both good and bad drifters). Furthermore, heat-treated gallium-doped material is compared with heat-treated material with lithium present. (auth)

29331 TRANSMISSION SURFACE-BARRIER SILICON DETECTORS. Czyzewski, Tomasz; Kaminski, Aleksander; Kobierska, Elzbieta; Marcinkowski, Andrzej (Univ., Warsaw). Nukleonika; 15: 585-91(1970).

A technology of thin transmission surface-barrier silicon detectors has been developed. The detectors obtained have thickness in the range 30 to 5 μ. The detectors were studied with the use of plutonium and thorium alpha sources. (auth)

29332 PRODUCTION OF Si SURFACE-BARRIER SEMICONDUCTOR DETECTORS. Balazs, Arpad. KFKI (Kozp. Fiz. Kut. Intez.) Kozlem.; 18: 165-72(1970). (In Hungarian).

A reliable, and on average 80% efficient method has been developed for the production of surface-barrier type Si semiconductor detectors. The measured values of the detector parameters are resistivity: 2000 Ωcm, sensitive surface: 2 cm^2 reverse current 0.4 μA/100 V, and energy resolution 47 keV/4.7 MeV for α-particles. (auth)

29333 RESEARCH IN NUCLEAR RADIATION SEMICONDUCTOR DETECTORS AND THEIR APPLICATIONS. Coche, Andre (Centro de Investigaciones Nucleares, Strasbourg). Acta Cient.; 3: No. 1, 19-25(Mar 1970). (In Spanish).

Research work done by the Semiconductor Group of the Nuclear Research Center in Strasbourg is summarized. Germanium and silicon detector fabrication and performance are described. Studies have been conducted on mechanisms in metal-semiconductor rectification in metal, on carrier mobilities, internal amplification diodes and ion implantation. First results obtained in the preparation of cadmium telluride, are also given. (auth)

29334 SOLID-STATE CONSTRUCTION FOR DISCHARGE QUENCHING IN GEIGER COUNTERS. Karasik, A. S.; Prokof'ev, O. N. (Scientific-Research Inst. of Radiation Hygiene, Leningrad).

XUM

Instrum. Exp. Tech. (USSR) (Engl. Transl.); No. 4, 1025-7(Jul-Aug 1970).

Translated from Prib. Tekh. Eksp.; No. 4, 61-3(Jul-Aug 1970).

A solid-state construction of a quenching circuit for Geiger counters is described. The device uses a pulse amplifier controlling a chain of dynistors. The chain of dynistors used as a keying element makes it possible to achieve quenching pulses having an amplitude >1 kV, rise time from 0.2 to 0.3 μsec, and length from 10 μsec to 10 msec. (auth)

29335 EFFECT OF CHEMICAL FACTORS ON THE SENSITIVITY OF POLYMERIC DETECTORS. Veprik, Ya. M.; Perelygin, V. P.; Romanenko, V. P.; Tret'yakova, S. P.; Vinogradov, Yu. A. (Joint Inst. for Nuclear Research, Dubna, USSR). Instrum. Exp. Tech. (USSR) (Engl. Transl.); No. 4, 1015-17(Jul-Aug 1970).

Translated from Prib. Tekh. Eksp.; No. 4, 51-3(Jul-Aug 1970).

The effect of chemical factors on the change of sensitivity of nitrocellulose detectors to light charged particles was investigated. It was found that an increase of the content of camphor in nitrocellulose leads to an increase of detector sensitivity. Alpha-particles with an energy to 4.5 MeV were recorded in a detector made from a solution of 7% nitrocellulose and 2.5% camphor. (auth)

29336 SCINTILLATOR FOR RECORDING SLOW NEUTRONS. Markov, Yu. Ya.; Ryazhskaya, O. G. (Physical Inst., Moscow). Instrum. Exp. Tech. (USSR) (Engl. Transl.); No. 4, 1013-14(Jul-Aug 1970).

Translated from Prib. Tekh. Eksp.; No. 4, 50-1(Jul-Aug 1970).

A liquid scintillator for the recording of slow neutrons in large counters, based on white spirit, PPO and POPOP, and gadolinium octoate, with a maximum neutron-recording efficiency of 86% is described. The neutron capture time is 56 ± 2 μsec. The scintillator has been used in a counter 300 liters in volume for studying photonuclear interactions of the muons of cosmic rays in the soil. (auth)

29337 BORON-CONTAINING LIQUID NEUTRON DETECTOR. Kitaev, V. Ya. Instrum. Exp. Tech. (USSR) (Engl. Transl.); No. 4, 1011-12(Jul-Aug 1970).

Translated from Prib. Tekh. Eksp.; No. 4, 48-9(Jul-Aug 1970).

The construction of a boron-containing slow-neutron detector in liquid form using low-noise FÉU-42 photomultipliers is considered. The container of the detector is mounted together with one photomultiplier, the cross-sectional area of the container (80 cm^2) being much greater than that of the photomultiplier photocathode (12 cm^2). From considerations of maximum light collection a cone-shaped form of the container with an average thickness of 2 cm is taken. The operation of the detector is illustrated by the neutron-transmission curve of a copper sample obtained by time-of-flight measurements with a resolution of 7 nsec/m. (auth)

29338 PULSE DELAY TIME IN ^{3}He NEUTRON COUNTERS. Korolev, V. I.; Kamaeva, L. A.; Chaikovskii, V. G.; Shapar, A. V. Instrum. Exp. Tech. (USSR) (Engl. Transl.); No. 4, 1008-10(Jul-Aug 1970).

Translated from Prib. Tekh. Eksp.; No. 4, 46-7(Jul-Aug 1970).

The maximum electrical-pulse delay time has been measured for 19 different ^{3}He neutron counters. The dependences of the effective drift velocity on the average electric field intensity and on the pressure for various gas fillings of the counters have been obtained. (auth)

29339 PHOSWICH FOR NEUTRON DETECTION. Grudskaya, L. E.; Vlasov, V. G.; Poduzhailo, V. G.; Malinovskaya, S. A. (All-Union Scientific-Research Inst. of Single Crystals, Kharkov). Instrum. Exp. Tech. (USSR) (Engl. Transl.); No. 4, 1006-7(Jul-Aug 1970).

Translated from Prib. Tekh. Eksp.; No. 4, 44-5(Jul-Aug 1970).

A composite detector or phoswich is described for detecting neutrons in a background of γ-rays and charged particles with the use of pulse-shape discrimination. The phoswich consists of a liquid scintillator within a plastic scintillation shield. By choosing a liquid scintillator and a plastic which are mutually nonaggressive, one can eliminate the glass container commonly used in phoswich designs. As a result, the resistance of the phoswich to vibration is increased and its spectrometric properties are improved. (auth)

29340 LOW NOISE PREAMPLIFIER EMPLOYING FIELD EFFECT TRANSISTORS. Mitin, A. A.; Sofiev, G. N. (Inst. of Atomic Energy, Moscow). Instrum. Exp. Tech. (USSR) (Engl. Transl.); No. 4, 1039-41(Jul-Aug 1970).

Translated from Prib. Tekh. Eksp.; No. 4, 74-5(Jul-Aug 1970).

A circuit is presented for a low noise preamplifier having a domestic n-channel field effect transistor as the input element. The internal noise of the amplifier at room temperature when disconnected from a detector is less than 1.5 keV (for germanium detectors) in a passband that is limited by the integration and differation time constants to 2 or 3 μsec. The variation of the noise with extraneous input capacity is approximately 0.09 keV/pF. (auth)

29341 TIME-AMPLITUDE CONVERTER FOR THE NANOSECOND RANGE. Basova, B. G.; Kachalin, V. A.; Starostov, B. I. (Scientific-Research Inst. of Atomic Reactors, Melekess, USSR). Instrum. Exp. Tech. (USSR) (Engl. Transl.); No. 4, 1034-8(Jul-Aug 1970).

Translated from Prib. Tekh. Eksp.; No. 4, 69-73(Jul-Aug 1970).

A time-amplitude converter operating in the range from 60 nsec to 1 μsec has been designed and constructed. The device employs the principle of timing by the constant portion of the impulse front, which produces a low (0.2 nsec) displacement of the generator coincidence peak over a 100 to 1 range of generator pulse amplitude. Under operating conditions (FÉU-30, FÉU-63) with plastic scintillators of $\phi 30 \times 30$ mm and $\phi 100 \times 30$ mm for $\gamma-\gamma$ coincidences in ^{60}Co, resolutions of 1.6 were obtained and 2 nsec resolution were obtained for $\alpha-\gamma$ coincidences in ^{244}Cm with a threshold ≈30 keV for γ quanta. (auth)

29342 PULSE SHAPER WITH INDEPENDENT REGULATION OF OUTPUT PULSE DURATION AND DEAD TIME. Grachev, M. I.; Lapshin, V. G.; Rykalin, V. I.; Sen'ko, V. A. (Inst. of High-Energy Physics, Serpukhov, USSR). Instrum. Exp. Tech. (USSR) (Engl. Transl.); No. 4, 1046-8(Jul-Aug 1970).

Translated from Prib. Tekh. Eksp.; No. 4, 79-81(Jul-Aug 1970).

A photomultiplier pulse shaper with independent regulation of output pulse length and dead time, using diodes with charge accumulation, is described. The adjustment range for pulse length and dead time is 7 to 150 nsec. The shaper has three outputs: a logic pulse output producing a triangularly shaped pulse with 7 nsec base, an output which produces a negative square wave pulse of adjustable duration, and an output with a constant-level negative voltage which is switched off for the duration of the output pulse. By connecting this last output to a coincidence circuit, the latter can be transformed into an anticoincidence channel. The maximum repetition rate for output pulses is 100 MHz, and the output signal amplitude is 0.7 V. Input pulse amplitude range is 0.2–40 V, and the shaper can be controlled by external pulses. (auth)

29343 LOW NOISE CHARGE-SENSITIVE PREAMPLIFIER EMPLOYING FIELD EFFECT TRANSISTORS. Pod'yachev, V. N.; Shatunovskii, R. M. Instrum. Exp. Tech. (USSR) (Engl. Transl.); No. 4, 1042-5(Jul-Aug 1970).

Translated from Prib. Tekh. Eksp.; No. 4, 76-8(Jul-Aug 1970).

A circuit is proposed for a preamplifier employing domestic p- and n-channel field effect transistors. A calculation is made of the reduced equivalent noise resistance of the first amplifying device as a function of the noise from the second device and the load resistance. It is shown that it is possible to attain a value of the noise resistance close to the theoretical by striving for the maximum possible gain in the first stage. Experimental temperature relationships are presented for the basic parameters of the field effect transistors as well as experimental and theoretical relationships for the noise resistance as a function of the load resistance. With a preamplifier built out of field effect transistors the noise value (S.N.P.P. Si) obtained at a temperature of approximately 150°K ($\tau_i = \tau_d = 1$ μsec) was 510 eV = 80 eV/pF. On this same preamplifier with a domestic Si detector a resolution of 0.7 keV was obtained for the 14-keV ^{57}Co line and 0.85 keV for the 122- and 136-keV ^{57}Co lines. (auth)

29344 STABILIZATION OF THE GAIN OF A SCINTILLATION COUNTER FOR REGISTERING ^{14}C. Biryulin, Yu. F.; Kolesnikov, N. V. (Physicotechnical Inst., Leningrad). Instrum. Exp. Tech. (USSR) (Engl. Transl.); No. 4, 1069-70(Jul-Aug 1970).

Translated from Prib. Tekh. Eksp.; No. 4, 100-1(Jul-Aug 1970).

The results of stabilization of the amplification channel in the scintillation counter designed for registering a soft β-ray ^{14}C source are described. The light signal from a TKh-4B thyratron was used for reference. The instability was 0.5% in 7 h of operation on adding 3 pulses/min to the background. (auth)

29345 SWITCH FOR READING OUT INFORMATION FROM COUNTERS TO A DIGITAL PRINTER. Rodnov, Yu. V.; Sytin, A. N. Instrum. Exp. Tech. (USSR) (Engl. Transl.); No. 4, 1087-8(Jul-Aug 1970).

Translated from Prib. Tekh. Eksp.; No. 4, 114-16(Jul-Aug 1970).

A 10-position switch is described that is based on a standard decade counter. The switch uses delayed internal feedback for excluding individual branches of the system from interrogation;

a method of noise suppression in the decoder is also proposed. (auth)

29346 FAST TRANSISTOR DC AMPLIFIER. Galkin, I. V.; Gusev, N. F. (Inst. of Atomic Energy, Moscow). Instrum. Exp. Tech. (USSR) (Engl. Transl.): No. 4, 1099-1101(Jul-Aug 1970).

Translated from Prib. Tekh. Eksp.: No. 4, 124-6(Jul-Aug 1970).

The possibility of designing a dc amplifier with straight amplification having a drift $<2 \cdot 10^{-10}$ A/hr and a limiting frequency of ~10 kHz is shown. Silicon KT312V planar transistors operating in a microampere mode with active thermostatic control are used in the first balanced stages. (auth)

29347 PHOTOMULTIPLIER IMPULSE SHAPER WITH STABLE TIME DELAY. Katinov, Yu. V.; Rabin, N. V.; Sutormin, A. I.; Tyapkina, G. N.; Yablonin, K. I. (Inst. of Theoretical and Experimental Physics, Moscow). Instrum. Exp. Tech. (USSR) (Engl. Transl.); No. 4, 1161-3(Jul-Aug 1970).

Translated from Prib. Tekh. Eksp.; No. 4, 174-7(Jul-Aug 1970).

A photomultiplier pulse shaper circuit is described. For an input signal amplitude range of 0.45 to 13.0 V, the change in circuit delay time $\Delta\tau \leq \pm 160$ nsec, the corresponding changes in amplitude and length of the output pulse being no more than 5%. Maximum operating frequency is 50 MHz. Threshold level for shaper operation is 0.4 V. (auth)

29348 IMPROVEMENTS IN OR RELATING TO NUCLEAR RADIATION DETECTORS. Keith, Ronald Leonard Gordon; Wraight, Leonard Arthur (to United Kingdom Atomic Energy Authority). British Patent 1,225,058. 17 Mar 1971. Filed 26 Aug 1968.

Reference is made to "scintillation gamma cameras" of the type described in US Patent 3,011,057 (H.O. Anger), in which a two-dimensional array of photomultiplier tubes is optically coupled to a large area gamma-sensitive scintillator, the tube outputs being combined so that the position of a scintillation occurring as the result of an incident gamma ray can be indicated on a cathode ray tube. For some purposes there is a need for a similar instrument that is sensitive to neutrons, such as in neutron diffraction studies and in neutron radiography, and such an instrument is described. It comprises a neutron-sensitive scintillator, a two-dimensional array of photosensitive devices facing one surface of the scintillator, means for optically coupling the scintillator surface to the photosensitive devices so that a scintillation occurring at any position in the scintillator may be received by each device, and means for combining the outputs of the devices to produce signals characteristic of the scintillation position. The optical means may comprise a solid light guide, which may include a neutron absorber to reduce backscatter of neutrons into the scintillator. The neutron scintillator may be a ZnS plastic phosphor, loaded with LiF. Suitable circuitry is provided for cathode ray tube display or for computer storage, which may include a neutron/gamma discriminator. A neutron collimator may also be provided. (UK)

29349 MEDICAL RADIOISOTOPE SCANNING. Owen, G. M. (University Hospital of Wales, Cardiff); Kirkman, S. Bio-Med. Eng.; 6: 54-61(Feb 1971).

Scanning techniques in nuclear medicine are briefly reviewed with special reference to mechanical (moving-detector) scanners. The use of radiopharmaceuticals (especially technetium-99m), the components and operation of scanning systems, and the display, recording, and processing of count data are discussed. Some applications of gamma cameras and mechanical scanners are outlined and compared. (auth) (UK)

29350 SCINTILLATION SPECTROMETRY OF SOFT X-RAY RADIATION. Al'perovich, V. R.; Komyak, N. I.; Lyskovich, A. B.; Pentsak, G. M. (Special Design Office for X-Ray Apparatus, Leningrad). Instrum. Exp. Tech. (USSR) (Engl. Transl.): No. 4, 1219-21(Jul-Aug 1970).

Translated from Prib. Tekh. Eksp.: No. 4, 223-4(Jul-Aug 1970).

The use of CaI_2 as a scintillation detector for x rays in the energy range from 3.69 (CaK_α) to 23.2 keV (CdK_α) is described. (auth)

29351 VACUUM SORBENT CUT-OFF DEVICE IN THE CRYOSTAT OF A Ge(Li) DETECTOR. Govorov, A. M. (Joint Inst. for Nuclear Research, Dubna, USSR). Instrum. Exp. Tech. (USSR) (Engl. Transl.); No. 4, 1192-3(Jul-Aug 1970).

Translated from Prib. Tekh. Eksp.: No. 4, 202-3(Jul-Aug 1970).

The introduction of a mobile vacuum cut-off in the absorber by maintaining the degree of desorption substantially improves the initial working vacuum of the cryostat (to 2 to $3 \cdot 10^{-7}$) and also increases by more than 10 times the time for which the working conditions are maintained. (auth)

29352 POTENTIAL ALPHA RAY ACTIVITY METER. Schroeder, Gerald L. (to United States Atomic Energy Commission). U. S. Patent 3,555,278. 12 Jan 1971. Filed 18 Dec 1968.

A method and apparatus for measuring the potential alpha ray activity of a gas sample containing a gaseous component such as Rn having solid short-lived daughter products some of which are alpha ray emitters are described. The apparatus collects on a filter the particulate of the solid daughter products over a finite period of time and measures separately the alpha and the beta-gamma activities. The portion of the latter which results in short-lived daughter products producing alpha energy is separated out and added to the alpha activity measured. (auth)

Nuclear Spectroscopic Instrumentation

Refer also to abstracts 31182 and 31208.

29353 (JINR-P13-5708) TIMING WITH Ge(Li)-DETECTOR. Akimov, Yu. K.; Andert, K.; Kalinin, A. I.; Churin, I. N.; Shuravin, V. N. (Joint Inst. for Nuclear Research, Dubna (USSR). Lab. of Nuclear Problems). 1971. 10p. (In Russian). Dep. NTIS (U. S. Sales Only).

The time resolution of 2.2 nsec was obtained in the energy range of 0.07 to 1.33 MeV when γ-quanta from ^{60}Co were detected by the Ge (Li)-detector (the volume being 3 cm^3) and by a scintillation counter. The coincidence curve width at the level 0.1 of its height was 12.5 nsec. The time resolution of 0.9 nsec was obtained for the narrow range of energies. (auth)

29354 (LUNP-7101) ANNLIS: A COMPUTER PROGRAM FOR THE AUTOMATIC ANALYSIS OF GAMMA-RAY SPECTRA. Ekstroem, P.; Mauritzson, I.; Tillman, J. (Lund Univ. (Sweden). Dept. of Physics). Jan 1971. 66p. Dep. NTIS (U. S. Sales Only).

A FORTRAN V code, written for a UNIVAC 1108 computer, for the analysis of gamma-ray spectra from Ge(Li)-detectors is described. The program ANNLIS, automatically locates all peaks in a read-in spectrum, and determines their energies and intensities. Composite peaks are not resolved by the program. The result can be visually checked on a plot from a fast printer. (auth) (Sweden)

29355 (RLO-1388-135) BREIT-WIGNERS VIEWED THROUGH GAUSSIANS. Wilkinson, D. H. (Washington Univ., Seattle). [1971]. 19p. Dep. NTIS.

The frequently-occurring situation is analyzed in which a signal of Breit-Wigner form, as, for example, a particle group from a state in the continuum of an excited nucleus, is detected by a measuring instrument whose resolution function may be represented by a Gaussian, such as a solid-state detector, so that the observed signal is a convolution of the Breit-Wigner and the Gaussian. Tabular, graphical, and analytical answers are given to the questions: What is the form of the convoluted signal? By how much is the peak height lowered by the convolution? How is the Breit-Wigner width Γ to be extracted? What fraction of the area under the convoluted peak lies outside given limits? (auth)

29356 (RT/EL-(70)5) OPTIMIZATION OF ENERGY RESOLUTION IN NUCLEAR SPECTROMETRY MEASUREMENTS WITH GERMANIUM DETECTORS. Coiante, D. (Comitato Nazionale per l'Energia Nucleare, Rome (Italy)). 24 Sep 1970. 52p. (In Italian). Dep. NTIS (U. S. Sales Only).

The usual Ge(Li) detector setup for gamma spectroscopy is described, paying particular attention to the factors that affect line broadening. The optimization of the energy resolution is calculated, and some criteria for choosing the charge preamplifier are given. (auth)

29357 Ge(Li) GAMMA SPECTROMETER. Burmistrov, V. R.; Didorenko, V. A. Izv. Akad. Nauk Kaz. SSR, Ser. Fiz.-Mat.: No. 2, 12-20(Mar-Apr 1970). (In Russian).

Certain stages of the technology of the production of Ge(Li) detectors in Inst. of Nuclear Physics Kazakh SSR are described, in particular the gamma spectrum obtained from mountainous rock using a detector with a volume of 23 cm^3 is cited. This rock was irradiated in a current of 10^{13} neutrons/cm^2 sec from the reactor VVR-K. In the spectrum there is positive detection of a peak corresponding to the energy of the 412-keV gamma line of ^{198}Au. The gold content in this rock is determined to be equal to 3.10^{-7}%. The saturated sensitivity for gold is evaluated as 6.10^{-10} g without the application of radiochemical separation. (tr-auth)

29358 ADAPTATION OF A LONG-LENS BETA-RAY SPECTROMETER FOR THE MEASUREMENT OF SHORT NUCLEAR LIFETIMES. Kownacki, Jan; Bialkowski, Jacek; Moszynski, Marek; Piotrowski, Antoni (Inst. of Nuclear Research, Swierk, Poland). Nukleonika; 15: 649-59(1970).

The long-lens beta-ray spectrometer was designed and adapted to half-life measurements of the nuclear excited states. Plastic scintillator detectors with 56 AVP photomultipliers were used. Satisfactory protection of the photomultipliers from the magnetic field can be achieved by local field compensation using a special set of coils. It is shown that the magnetic spectrometer applied for measurement of nanosecond nuclear lifetimes by the delayed coincidence method gives the possibility of improving the accuracy of the experimental results. The half-lives of the first excited states in ^{139}Ce and ^{147}Sm are presented to illustrate the method described. (auth)

29359 TIME BUNCHING SPECTROMETER USING A BENT ROTATING CRYSTAL. Marx, Dieter (Gesellschaft FUER Kernforschung, Karlsruhe, Ger. Institut Max von Laue-Paul Langevin, Grenoble, France). Atomkernenergie; 17: 199-201(May 1971). (In German).

It is shown that time bunching can be obtained using an ideal, thick, bent rotating crystal and a Bragg angle of 45°. Applications for inelastic neutron scattering experiments are suggested. (auth)

29360 STABILIZED GAMMA-RESONANCE SPECTROMETER. Gol'danskii, V. I.; Dolenko, A. V.; Egiazarov, B. G.; Romashko, V. P.; Shamov, A. I. Instrum. Exp. Tech. (USSR) (Engl. Transl.); No. 4, 1071-4(Jul-Aug 1970).

Translated from Prib. Tekh. Eksp.; No. 4, 101-4(Jul-Aug 1970).

A velocity stabilized γ-resonance spectrometer operating in constant velocity conditions is described. Stabilization of velocity using the absolute magnitude is obtained by comparing the time in which the movable part of the vibrator passes through a given distance which is measured by an optical system with diffraction gratings, and the time is determined from the frequency of a quartz oscillator. The block diagram of the spectrometer and the operational circuit for the velocity stabilization are studied, and the voltage curves at various points of the system are shown. Methods of checking the velocity from the γ-resonance spectrum are described. (auth)

29361 MOESSBAUER SPECTROMETER FOR EXPRESS ANALYSIS. Kamenov, P.; Manushev, D. (Univ., Sofia). Instrum. Exp. Tech. (USSR) (Engl. Transl.); No. 4, 1075-6(Jul-Aug 1970).

Translated from Prib. Tekh. Eksp.; No. 4, 104-6(Jul-Aug 1970).

A Moessbauer spectrometer using a photomultiplier in the current mode is described. The time required to obtain the Moessbauer spectrum is <1 sec for an accuracy comparable with the accuracy of conventional spectrometers whose detectors operate in a pulse mode. (auth)

29362 APPARATUS FOR STUDYING THE DYNAMICS OF CONDENSED SYSTEMS USING A BACK-SCATTERING METHOD. Komarov, V. E.; Kukhto, O. L.; Solov'ev, S. P. (Physicochemical Inst., Moscow). Instrum. Exp. Tech. (USSR) (Engl. Transl.); No. 4, 988-92(Jul-Aug 1970).

Translated from Prib. Tekh. Eksp.; No. 4, 29-33(Jul-Aug 1970).

The parameters and construction of a transit-time device for measuring the spectra of inelastic scattering of neutrons using a back-scattering method are described. To suppress the background of the direct beam, the device includes a mechanical chopper with a two-material rotor and with a shortened packet-collimator. The construction of the chopper, cassettes for the samples, the Be filter, and a unit for controlling the temperature of the sample from ambient to –150°C is detailed. (auth)

29363 COMPUTER-ASSISTED ANALYSIS OF GAMMA-RAY SPECTRA. Atkinson, G. D. Jr.; Whitworth, J. B.; Gage, S. J. (Univ. of Texas, Austin). Comput. Phys. Commun.; 2: 40-6 (Jan 1971).

A computer program to analyze automatically multielement gamma spectra obtained by means of high-resolution detectors is described. Peak energies and net areas are determined, and possible sources of individual gamma rays are given. The spectra cannot contain more than 1024 channels, and the energy calibration curve must be a polynomial of degree 5 or less. The look-up table cannot contain more than 1000 gamma-ray energies, entered in ascending order. Written in FORTRAN for the CDC 6600, the program requires 17000_8 60-bit words of storage. Running times are 5 seconds for compilation and 2 or 3 seconds for handling a 1024-channel spectrum. (R.W.R.)

29364 EFFECT OF AN AUTOMATIC CORRECTION SYSTEM ON SPECTROMETER RESOLUTION. Basova, B. G.; Rabinovich, A. D. (Scientific-Research Inst. of Atomic Reactors, Melekess, USSR). Instrum. Exp. Tech. (USSR) (Engl. Transl.); No. 4, 1028-33(Jul-Aug 1970).

Translated from Prib. Tekh. Eksp.; No. 4, 64-9(Jul-Aug 1970).

The widening and deformation of spectral lines in a spectrometer produced by introducing an automatic correction system is studied. A theoretical evaluation is given and a model for determining the characteristics of an input device with automatic correction system by computer methods is examined. The results are compared with data published earlier. (auth)

29365 AUTOMATIC STABILIZATION OF A DEVICE FOR MEASURING LIFE TIMES IN THE PICOSECOND RANGE. Begzhanov, R. B.; Gladyshev, D. A.; Ikramov, M. Kh. (Inst. of Nuclear Physics, Tashkent). Instrum. Exp. Tech. (USSR) (Engl. Transl.); No. 4, 1054-7(Jul-Aug 1970).

Translated from Prib. Tekh. Eksp.; No. 4, 86-90(Jul-Aug 1970).

A stabilization system is described for a device which measures lifetimes in the picosecond range. The threshold and amplification factor are stabilized. The stabilizing system operates in a periodic manner. A comparison of long-term experiment results with the stabilizing system in operation and disconnected is given. (auth)

29366 SHAPER WITH DOUBLE SHAPING BASED ON DELAY LINES HAVING A MODIFIED NOISE SPECTRUM. Ivanov, V. B.; Shipilov, V. I. Instrum. Exp. Tech. (USSR) (Engl. Transl.); No. 4, 1065-8(Jul-Aug 1970).

Translated from Prib. Tekh. Eksp.; No. 4, 96-9(Jul-Aug 1970).

A shaper is described which is based on two delay lines having a modified noise spectrum. The shaper allows the noise level to be lowered in comparison with that of conventional filters and accurate amplitude measurements to be made at high input loads (up to 10^5 pulses/sec). The degradation of the resolution compared with the results obtained at low loads is at most 0.4 to 0.7 keV. The calibration scale remains constant when the load changes. (auth)

29367 AUTOMATIC AMPLITUDE SPECTROMETER WITH A TRACKING SWEEP. Sorokin, O. M. Instrum. Exp. Tech. (USSR) (Engl. Transl.); No. 4, 1063-4(Jul-Aug 1970).

Translated from Prib. Tekh. Eksp.; No. 4, 94-5(Jul-Aug 1970).

An automatic amplitude spectrometer for obtaining the amplitude spectra of pulses in the microsecond range is described. The scanning of the analyzer "window" is accomplished by a generator which produces a linearly varying voltage; the input of the generator has the amplified voltage corresponding to the rate of change of the differential amplitude distribution signal applied to it in addition to a direct voltage. The resulting tracking sweep allows the details of the amplitude spectra of the pulses to be recorded with good resolution for an overall fast (~15–20 sec) sweep. (auth)

High Energy Physics Instrumentation

29368 (AEC-tr-7099(Pt.2)) CHERENKOV RADIATION IN HIGH-ENERGY PHYSICS. PART II. CHERENKOV COUNTERS: DETERMINATION OF ENERGY AND DIRECTION OF ELEMENTARY PARTICLES. Zrelov, V. P. Translation of Izluchenie Vavilova-Cherenkova i Ego Primenenie v Fizike Vysokikh Energii, Atomizdat, Moscow, 1968. 249p. (TT-70-50003/2). Dep. NTIS.

This monograph describes the principles of operation and design of various Cherenkov counters, which are widely used at intermediate and high energies in cosmic-ray and accelerator experiments. Special emphasis is laid upon counters utilizing the Cherenkov effect in high-intensity beams. This volume mainly deals with single particle counters, which are classified according to threshold and differential counters (having liquid, solid or gaseous radiators), Cherenkov gamma-spectrometers, total-absorption counters, Cherenkov counters for charge determination and counters which indicate the direction of charged particles and photons. The subject matter not only provides a comprehensive survey of the development of Cherenkov counters from quite primitive setups to highly complicated devices, but also comprises the design specifications of Cherenkov counters for a wide range of physical problems. The book is intended for physicists working in the domain of experimental high-energy physics. (202 references) (auth)

29369 (ITEF-753) PROGRAM FOR PROCESSING PHOTOGRAPHS IN A BUBBLE CHAMBER FILLED WITH A HEAVY LIQUID. PART I. Marchenko, N. V.; Marchenko, E. N.; Novikov, A. S.; Spivakovskii, S. I.; Trebukhovskii, Yu. V. (Gosudarstvennyi Komitet po Ispol'zovaniyu Atomnoi Energii SSSR, Moscow. Institut Teoreticheskoi i Eksperimental'noi Fiziki). 1969. 54p. (In Russian). Dep. NTIS (U. S. Sales Only).

Interaction of π^0 mesons and γ quanta or decomposition of neutral particles into π^0 mesons and γ quanta must be studied with a bubble chamber filled with a liquid heavier than liquid hydrogen, such as propane, freon, xenon, etc. In order to take

into account the interactions, slowing-down effects and radiative emissions, a special program which has been developed for such chambers must be used. Such a program was developed for studying the $\pi^- + p \rightarrow n + m\gamma$; $\pi^+ + p \rightarrow \pi^+ + p + m\gamma$; and $\pi^+ + n \rightarrow \pi^+ + n + m\gamma$ reactions with a 120-liter chamber, consisting of an 84-cm high and 36-cm diameter cylinder. The program helped to identify the type of reaction represented in the photographic track, indicating whether it is an incoming particle, a proton, or a γ quantum. The results of the study of the elastic scattering of 20 $\pi^- + p \rightarrow \pi^- + p$ events are presented, indicating the radii of charged particles, their angle of emission and the length of passage. In a study of (e^+e^-) pairs, the mass of the π^0 meson was determined by measuring the $\pi^- + p \rightarrow n + 4\gamma$ reaction. (TTT)

29370 (LAL–1246) HIGH RESOLUTION BEAM HODOSCOPE USING MULTIWIRE PROPORTIONAL CHAMBERS. Merkel, B. (Paris Univ., Orsay (France). Laboratoire de l'Accelerateur Lineaire). Mar 1971. 15p. Dep. NTIS (U. S. Sales Only).

A multiwire proportional chamber with 1 mm spacing and 2.3 mm gap, using 9 μ tungsten wires was built for use as a precise beam hodoscope. An electronegative vapor (freon 13 B 1) was used to restrict the sensitive region to a small volume around the wire. In order to obtain a high detection efficiency for relativistic particles, i.e. a high probability of producing one ion pair in the sensitive volume around the wire, xenon was used as filling gas, with propylene as co-xenon (quencher). An arrangement of four identical chambers, staggered so as to give an effective wire spacing of 0.25 mm, gives a high detection efficiency ($98.8 \pm 0.15\%$ for 400 MeV electrons) together with good spatial resolution. Measurements using a collimated electron beam give a trajectory determination with 0.15 mm accuracy (half width at half maximum). (auth)

29371 (SJC-P–70-4) MUTRON PROJECT (PROPOSAL). (Tokyo Univ. (Japan). Inst. for Nuclear Study). Jul 1970. 86p. (In Japanese and English). Dep. NTIS (U. S. Sales Only).

The purposes of the Mutron project are to investigate the whole processes concerning muons in the energy range from 0.1 to 1 TeV, to confirm anomalous interactions and the qualitative aspects of the interaction between muons and nuclei, and to measure the energy spectrum and the charge ratio of muons. The instrument is composed of a solid iron magnet, a pair-transition meter and a wire spark chamber. Solid angle area is 1 m^2 st. for the magnet, and 10 to 30 m^2 st. for the others. The energy of muons is measurable up to 3 TeV with the magnet, and up to 100 TeV with the pair meter. The production angle of secondary particles and the energy in muon interaction process are measured with the transition meter (so called calorimeter), and the scattering of muons is observed with the wire spark chamber. It is expected that the anomaly of muons is observable in the TeV region by this project. (Japan)

29372 (SJC-T–71-1) OPERATION CHARACTERISTICS OF THE 75 cm HYDROGEN BUBBLE CHAMBER AND THE REFRIGERATOR. 1. Hirabayashi, H.; Ishihara, N.; Kita, I.; Taino, M.; Tateno, H.; Yoshimura, Y. (Tokyo Univ. (Japan). Inst. for Nuclear Study). Jan 1971. 22p. (In Japanese and English). Dep. NTIS (U. S. Sales Only).

A 7.5-cm liquid hydrogen bubble chamber and refrigerator were constructed and test operations have been carried out three times during the test-run time from December 1969 to October 1970 at the Institute for Nuclear Study, University of Tokyo. In the first run, the refrigerator which is the Simple Linde type confirmed that it could afford about 60 liters of liquid hydrogen per hour, or the refrigerating power of about 1000 watts at 25°K. In the later two runs, the bubble chamber was cooled down to about 23°K at the rate of less than 5°K per hour and was filled up with 220 liters of liquid hydrogen. With the expansions of about 0.75% of the total liquid volume which was kept at the temperature of 26.0°K and the pressure of 5.0 kg/cm^2, the tracks of cosmic rays and Compton electrons from cobalt-60 were seen and photographed. Although one must say that the best dynamic equilibrium of the bubble chamber was not attained, several improvements which should be done for the final goal were brought to light and are reported. (auth) (Japan)

29373 Ω SPECTROMETER. Sonderegger, P. (CEA, Saclay, France). J. Phys. (Paris), Colloq.; C5: 116-24(Nov-Dec 1970). (In French).

From Conference on high energy physics; Aix-en-Provence, France (29 Sep 1970). See CONF-700950.

A large magnetic detector using spark chambers is under construction at CERN. Its physics program is being studied. A new outlook on the future uses of proportional chambers is proposed. (France)

29374 SPARK CHAMBER POWER SUPPLY CIRCUIT WITH SEMICONDUCTOR TRIGGER. Iyudin, A. F.; Kurochkin, A. V.; Shermanzon, E. M.; Yurkin, Yu. T. (Moscow Engineering Physics Inst.). Instrum. Exp. Tech. (USSR) (Engl. Transl.): No. 4, 1058-9(Jul-Aug 1970).

Translated from Prib. Tekh. Eksp.: No. 4, 90-1(Jul-Aug 1970).

The circuit of a spark-chamber power supply which utilizes transistors operating in the avalanche mode, dynistors, and a vacuum spark relay is presented. The operational threshold is less than 100 mV. The delay of the high voltage pulse with respect to the input pulse is ~80 nsec. (auth)

29375 OPERATION OF A SPARK CHAMBER AT A HIGH COUNT RATE. Usov, Yu. P.; Anan'in, P. S.; Sterligov, A. G.; Tolmacheva, V. G. (Tomsk Polytechnical Inst., USSR). Instrum. Exp. Tech. (USSR) (Engl. Transl.): No. 4, 1003-5(Jul-Aug 1970).

Translated from Prib. Tekh. Eksp.: No. 4, 42-4(Jul-Aug 1970).

A study is reported on the operation of a spark chamber with an electrode separation of 12 mm during the simultaneous detection of ~10^4 particles. An expression relating the basic characteristics of the spark chamber operation is derived from information about track formation within the chamber. (auth)

29376 HEAT EXCHANGE AND TEMPERATURE CONTROL SYSTEM FOR THE 2-METER LIQUID HYDROGEN BUBBLE CHAMBER. Kiselevich, I. L.; Moskalev, V. I.; Pletnikov, A. A.; (and others) (Inst. for Theoretical and Experimental Physics, Moscow). Instrum. Exp. Tech. (USSR) (Engl. Transl.): No. 4, 999-1002(Jul-Aug 1970).

Translated from Prib. Tekh. Eksp.: No. 4, 38-41(Jul-Aug 1970).

The heat exchange and temperature control system for the ITÉP 2-meter liquid hydrogen bubble chamber is described. The system assures a uniform and constant temperature in the operating volume of the chamber accurate to 0.1°K. (auth)

29377 MEASUREMENT OF THE MOMENTUM OF THE ACCOMPANYING PARTICLES AT SHORT DISTANCES FROM A HIGH-ENERGY NUCLEAR-ACTIVE PARTICLE. Bostandzhyan, N. Kh.; Marikyan, G. A. Instrum. Exp. Tech. (USSR) (Engl. Transl.): No. 4, 996-8(Jul-Aug 1970).

Translated from Prib. Tekh. Eksp.: No. 4, 36-8(Jul-Aug 1970).

The apparatus, which contains an ionization calorimeter and a system of hodoscopic counters, includes an electromagnet whose gaps contain two spark chambers (one above the other) with a working area of 40×80 cm and gaps of 30 cm each. The joint operation of the chambers with the calorimeter allows the momentum spectrum of accompanying particles which pass through the chamber to be determined simultaneously with the energy of the nuclear-active particle recorded by the calorimeter. The photographs obtained show that the maximum value of the measured momenta is ~10 GeV/c. (auth)

29378 SPURIOUS SCATTERING IN NUCLEAR EMULSIONS. Sood, P. M.; Bhatia, V. S. (Panjab Univ., Chandigarh, India). Indian J. Pure Appl. Phys.; 8: 406-8(Jul 1970).

The characteristics of spurious scattering (SS) were investigated for cell lengths 1 to 4 mm up to the 10th order of successive differences, in three regions of an emulsion stack, each region having a different level of SS. It was found that the higher order ratios $R_{1,m}$ [i.e., the ratio of SS in the mth order successive differences to that in the (m – 1)th order successive differences] are different from region to region and cell length to cell length. The variation of SS with cell length is of the power-law type. Further, the study of the causes of SS in emulsions revealed that nonplanarities in pellicle surfaces at the time of their exposure play a major role in producing SS in pellicle emulsions. (auth)

29379 PROGRAM LINKING FSD MEASURING MICROSCOPES WITH A MINSK-2 COMPUTER. Ammosov, V. V.; Gorichev, P. A.; Teplov, E. V.; Shmelev, O. A. (Inst. of High-Energy Physics, Serpukhov, USSR). Instrum. Exp. Tech. (USSR) (Engl. Transl.); No. 4, 1084-6(Jul-Aug 1970).

Translated from Prib. Tekh. Eksp.; No. 4, 112-14(Jul-Aug 1970).

A program for a Minsk-2 computer is described that links the latter with four FSD (flying spot device) measuring microscopes. The program makes it possible to check in real time the order of measurement of bubble-chamber photographs, to ascertain the errors of the operators and of the FSD measuring systems, and to record the measurement results on magnetic tape. The program has been compiled and tested at the Institute of High-Energy Physics. (auth)

29380 CHARGE IDENTIFICATION OF NUCLEAR TRACKS IN PHOTOGRAPHIC EMULSIONS. Gaur, R. K.; Sharma, A. P. (Kurukshetra Univ., India). Indian J. Pure Appl. Phys.; 8: 652-5(Oct 1970).

XUM

Considering the constant spacing model for the distribution of grains in an undeveloped emulsion, a model for the gap and blob formation is proposed. A relation between the probability of development of a grain and the mean-gap-length is derived. The method of determination of charge of the ionizing particle in a nuclear emulsion by measuring mean-gap-length and the probability of development is discussed, and a theoretical expression for the charge of the particle has been obtained as a function of the probability of development (or mean-gap-length) and velocity. This method can yield a good charge resolution for light and medium nuclei of cosmic radiation. (auth)

29381 TRACK WIDTH IN NUCLEAR EMULSIONS. Gaur, R. K.; Sharma, A. P. (Kurukshetra Univ., India). Indian J. Pure Appl. Phys.; 8: 468-72(Aug 1970).

A method for calculating the track profile of multiply charged ions is proposed, considering the emission of secondary electrons perpendicular to the ion's path. The explicit values of the functions showing track width dependence on charge and velocity of the charged particles are obtained on the basis of existing theories. The values of reduced track width calculated on the basis of the theories of P. G. Bizzeti and M. Della Corte [Nuovo Cim., 11 (1959), 317], and R. Katz and J. J. Butts [Phys. Rev., 137 (1965), B198] are compared with the experimentally observed values in order to find the best functional dependence. It is concluded that the theory of Bizzeti and Della Corte gives results which are consistent with the experimentally observed values. (auth)

Radiation Dosimeters

29382 (COO-1105-120) CHARACTERISTICS OF SOME TLD SOLID SYSTEMS. Lin, F. M.; Cameron, J. R. (Wisconsin Univ., Madison. Dept. of Radiology). [nd]. Contract AT(11-1)-1105. 16p. Dep. NTIS.

The performance of three commercial LiF thermoluminescent dosimeters is discussed. LiF embedded in a Teflon matrix (Controls for Radiation Inc.), LiF embedded in a silicon rubber products (Madison Research, Inc.), and extruded LiF (Harshaw Chemical Company) were tested. (W.H.K.)

29383 (JAERI-Memo-4292) CHARACTERISTICS OF PERSONAL MONITORING DOSIMETER. Nishi, Tatsuo; Motizuki, Tamizo; Ashikagaya, Yoshinobu (Japan Atomic Energy Research Inst., Tokyo). Jan 1971. 65p. (In Japanese). Dep. NTIS (U. S. Sales Only).

Characteristics of personal monitoring dosimeters to estimate external exposure doses are described. Dosimeters described are as follows. (1) film badge, (2) pocket dosimeter and alarm meter, (3) film ring and finger dosimeter, (4) glass dosimeter, (5) thermoluminescence dosimeter, and (6) emergency dosimeter. (auth) (Japan)

29384 COMPARISON OF LITHIUM FLUORIDE AND FILM FOR PERSONAL DOSIMETRY OF X- AND GAMMA RADIATIONS. Busuoli, G.; Cavallini, A. (CNEN, Bologna). Minerva Fisiconucl.; 13: 265-70(Oct-Dec 1969).

A comparison between the dose measurements obtained with film dosimeters and LiF powders is made: Tests were carried out on detectors, powders and films, first as exposed when employed in the routine personnel dosimetric service and then as exposed under experimental conditions to known doses at various energies. The experimental results make it clear that both dosimetric methods are satisfactory from the point of view of personnel dosimetry. (auth)

29385 SOLID-STATE DOSIMETRY. Becker, Klaus (Oak Ridge National Lab., Tenn.). CRC Crit. Rev. Radiol. Sci.; 1: 363-433(Aug 1970).

A comprehensive review on solid-state dosimeters including dielectric track detectors, radiophotoluminescent dosimeters, thermoluminescent dosimeters, TSEE (thermally stimulated exoelectron) dosimeters, and miscellaneous solid-state dosimeters is presented. (200 references) (W.H.K.)

29386 LOW DOSE FERROUS SULFATE DOSIMETRY BY DIRECT PHOTON COUNTING. Waggener, Robert G.; Hiatt, Caspar W.; Rogers, Lee F.; Zanca, Peter (Univ. of Texas, San Antonio). Radiat. Res.; 45: 244-51(Feb 1971).

Individual ultraviolet (uv) photons are counted after passage through irradiated and unirradiated ferrous sulfate solution to determine the optical density of the irradiated solution. The lower limit of optical density that may be easily read by the spectrophotometer is approximately 0.15 whereas the lowest optical density that may be read by direct photon counting is approximately 0.0043. Direct photon counting is utilized to extend the lower limit of absorbed dose necessary for ferrous sulfate dosimetry by a factor of approximately 30 to 35 or from 4000 to 120 rads. The reading of the optical density of the irradiated ferrous sulfate solution by direct photon counting is shown to give the same results as the reading by a spectrophotometer within the limits of the spectrophotometer. At the small optical densities considered, experimental random errors may be much larger than the calculated or statistical error and actually determine the lower limit in the measuring range of the method. (auth)

29387 RECENT IMPROVEMENTS IN FLUORO-GLASS DOSIMETER. Yokota, Ryosuke; Muto, Yuhei; Fukuda, Kiyoshi (Tokyo Shibaura Electric Co. Ltd., Kawasaki, Japan). Toshiba Rebyu; 26: 101-5(Jan 1971). (In Japanese).

Higher sensitive, less energy-dependent glasses with less predose have been developed for the fluoro-glass dosimeter; independence on energy in the range of 2 MeV to 30 keV is thereby assured. An exposure dose of 10 mR can be measured more accurately. Another kind of glass, especially fit for β-ray measurement, can also measure β-rays and γ-rays separately. A method of determining the incident energy and its direction has been worked out. Comparison of the glass dosimeter and the film dosimeter reveals definitely that the glass has the better performance. (auth)

29388 ENERGY INDEPENDENT RADIOPHOTOLUMINESCENCE DOSIMETER WITH GOOD FADING STABILITY. Becker, Klaus H. (to United States Atomic Energy Commission). U. S. Patent 3,554,920. 12 Jan 1971. Filed 19 Apr 1968.

A dosimeter having an essentially energy independent response without the use of filters and being substantially stable against fading is provided by a lithium borate glass containing Li, B, and Ag. This glass may be prepared, for example, by melting a mixture of $LiNO_3$, B_2O_3, and $AgPO_3$ in various proportions. The glass also permits sensitive measurements at high temperatures, the measurement of a thermal neutron component in mixed (n, γ) radiation fields, and sensitive measurements at high dose levels such as occur in sterilization and food processing systems. (auth)

Radiometric Instruments

Refer also to abstract 29278.

29389 (ITJ-2/E) SEMICONDUCTOR SYSTEM FOR ANALOG PROCESSING OF SIGNALS OBTAINED FROM RADIOMETRIC CONTROL SET OF THE CALCIUM CONTENT IN THE CEMENT-FEEDING. Korbel, K.; Lacki, E. (Institute of Nuclear Techniques, Krakow (Poland)). 1970. 24p. (In Polish). Dep. NTIS (U. S. Sales Only).

To determine the calcium-content in the cement feeding, being controlled by the radiometric measuring methods, the continuous processing of the results obtained according to the content function $Y(X_1,X_2)$ is desired. The described analog processing system operates on the basis of the slide-rule. The principles of operating of this analog processor as well as its accuracy and thermal stability are discussed. (auth)

29390 (RT/EL-(70)4) HIGH SENSITIVITY BERYLOMETER. Cervellati, R.; Monaci, P.; Sircana, S. (Comitato Nazionale per l'Energia Nucleare, Rome (Italy)). 14 Sep 1970. 31p. Dep. NTIS (U. S. Sales Only).

The industrial applications of beryllium and its high cost have promoted studies on equipments suitable for fast analysis of beryllium ores. The minimum Be content of an ore for being economically exploitable is several hundreds ppm; an instrument for laboratory analysis, aimed at the detection of new beryllium deposits, should have, thus, a sensitivity of a few ppm. An instrument suitable for this program has been made at the C.S.N. Casaccia, CNEN. It is based on the new but rather well known method of the neutron photoproduction. Two ^{124}Sb sources, having a nominal activity of 0.5 Ci each, irradiate a grinded mineral sample up to $\frac{1}{2}$ kg in weight. Six BF_3 tubes, connected in parallel and surrounded by paraffin, detect the neutrons. The parameter K_{Be} results for the present geometry 0.03 cpm/(g · mCi · % Be). The parameter H_{Be} results 3.0 cpm/[g · (mR/hr) · % Be]. The possible definitions of sensitivity are discussed; both are simply related to K_{Be} are proportional to the source activity and are time varying. The background count rate is about 6 cpm. This value determines the minimum detectable mass of Be, which results 3.2 mg for a counting time of half an hour and an activity of 2×75 mCi. Such a mass correspond to a minimum detectable concentration of less than 10 ppm. At the highest activity of 2×700 mCi, the minimum detectable concentration is less than 1 ppm Be. The linearity of the instrument is good in the range

0.5% + 0.005% Be. Aging of the tubes has been observed after several months of operation and has been put in correlation quantitatively with the multiplication factor and the overall gamma irradiation of the tubes. (auth)

29391 MESSVERFAHREN UNTER ANWENDUNG IONISIERENDER STRAHLUNG. (Measuring Methods Using Ionizing Radiation). Hartmann, Werner. Handbuch der Messtechnik in der Betriebskontrolle. Band V. (Handbook of Measuring Techniques for Plant Control. Volume 5). Leipzig; Akademische Verlagsgesellschaft Geest and Portig K.-G. (1969). 1143p. 115,- M.

The book was written for persons involved with industrial measurements, guidance, and control techniques in operations for which ionizing radiation represents an integral part. Treated are: physico-technical bases of radiation application; radiation protection and dosimetry; fine structure analysis with x rays; gross structure testing of material with x rays; investigation of molecular structure through scattering and absorption; determination of ash content of coal by radiation; determination of water content by means of neutrons; ionization gas analysis; activation analysis; K_2O determination; labeling with radioactive nuclides; autoradiography; and measurements of thickness, density, currents, and liquid levels. (H.B.G.)

Miscellaneous Instruments and Components

Refer also to abstracts 29229, 29391, 30026, 30393, and 31571.

29392 (CEA-N-1431) OPTO-ELECTRONIC LINK FOR TRANSMITTING TEMPORAL INFORMATION. Odru, R.; Vacher, J. (Commissariat a l'Energie Atomique, Grenoble (France). Centre d'Etudes Nucleaires). Feb 1971. 8p. (In French). Dep. NTIS (U. S. Sales Only).

An opto-electronic link was effected between an electroluminescent diode and a fast photomultiplier. The combination allows the temporal information associated with time of flight measurements to be obtained in the vicinity of an electrostatic accelerator where very large potential differences exist (~250 kV). Fluctuations in transit time introduced by the link are less than 0.5 ns and the consequent counting losses are very small up to 5 Mc/s. (auth) (France)

29393 (IN-1452) ULTRASONIC LEVEL MONITOR. Boland, T. J.; Thompson, J. B. (Idaho Nuclear Corp., Idaho Falls). Mar 1971. Contract AT(10-1)-1230. 66p. Dep. NTIS.

An ultrasonic level monitor has been developed to monitor the level of radioactive solids waste at the Idaho Chemical Processing Plant. The same basic instrument can also be used to monitor the instantaneous level of the liquid in the pulsed extraction columns at ICPP. A single transducer mounted at or near the top of a containment vessel transmits an ultrasonic signal burst through air to a liquid or solids surface. The large mismatch of acoustic impedance existing at air-liquid or air-solid interfaces results in essentially 100% reflection of the incident ultrasonic wave. The time required for the pulse to make the round trip from the transducer to the reflective surface is a measure of the distance travelled. The design, operation, and performance of the level monitor are presented. (W.H.K.)

29394 (JAERI-Memo-4281) JAERI NUCLEAR INSTRUMENT MODULE SYSTEM 6. (Japan Atomic Energy Research Inst., Tokyo). Jan 1971. 54p. (In Japanese). Dep. NTIS (U. S. Sales Only).

Five kinds of JAERI Nuclear Instrument Modules are described. General descriptions, specifications, circuit descriptions, and performance data for each unit are summarized. These units are MODEL 160 PRE-SCALER, MODEL 161 LINEAR/LOG COUNTRATE METER, MODEL 162 μμ AMMETER, MODEL 163 LINEAR AMPLIFIER, and MODEL 171 DECADE ATTENUATOR. (auth) (Japan)

29395 (JAERI-Memo-4295) JAERI NUCLEAR INSTRUMENT MODULE SYSTEM 7. (Japan Atomic Energy Research Inst., Tokyo). Jan 1971. 70p. (In Japanese). Dep. NTIS (U. S. Sales Only).

Eight kinds of the JAERI Nuclear Instrument Modules are described. General descriptions, specifications, circuits and performance data for each unit are summarized. These units are MODEL 103 and MODEL 104 PORTABLE BIN, MODEL 125 PREAMPLIFIER, MODEL 147 READ-OUT CONTROL, MODEL 155 PULSE SHAPE-TO-HEIGHT CONVERTER, MODEL 165 POWER SUPPLY, and MODEL 176 A and MODEL 176 B MIXER. (auth) (Japan)

29396 (JAERI-Memo-4303) JAERI NUCLEAR INSTRUMENT MODULE SYSTEM 8. (Japan Atomic Energy Research Inst., Tokyo). Jan 1971. 82p. (In Japanese). Dep. NTIS (U. S. Sales Only).

Six kinds of the JAERI Nuclear Instrument Modules are described. General descriptions, specifications, circuit descriptions, and performance data for each unit are summarized. These units are Model 131A multimode amplifier, Model 136A single channel analyzer, Model 140B detector bias supply, Model 144A biased amplifier, Model 148A logic shaper and delay, and Model 152A double delay line amplifier. (auth) (Japan)

29397 n-p JUNCTION PHOTOVOLTAIC DETECTORS IN PbTe PRODUCED BY PROTON BOMBARDMENT. Donnelly, J. P.; Harman, T. C.; Foyt, A. G. (Massachusetts Inst. of Tech., Lexington). Appl. Phys. Lett.; 18: 259-61(15 Mar 1971).

N-p junction photovoltaic detectors in PbTe were fabricated using proton bombardment to create the n-type layer. At 77°K, zero-bias resistance area products of 300 Ω cm^2 were observed for diodes with dimensions as large as 15 mil square. Peak detectivities at 5 μm in reduced background as high as 3.3×10^{11} cm $Hz^{\frac{1}{2}}/W$ were observed. Diode quantum efficiencies were typically greater than 30% at 5 μm. (auth)

29398 AIR SAMPLING INSTRUMENTS. For Evaluation of Atmospheric Contaminants. Cincinnati; American Conference of Governmental Industrial Hygienists (1966). 617p. Available from American Conference on Governmental Industrial Hygienists, Cincinnati.

The principles and usage of air sampling instruments are discussed, and air samplers are classified into groups with a technical discussion of the group followed by individual instrument description. (W.H.K.)

29399 METHODS OF MEASURING VARYING AND PULSED MAGNETIC FIELDS (REVIEW). Babenko, N. S. (Inst. of Nuclear Physics, Novosibirsk, USSR). Instrum. Exp. Tech. (USSR) (Engl. Transl.): No. 4, 963-72(Jul-Aug 1970).

Translated from Prib. Tekh. Eksp.: No. 4, 7-16(Jul-Aug 1970).

Methods of measuring varying and pulsed magnetic fields are reviewed systematically. Particular attention is given to methods of measuring fields up to approximately 10^6 Oe. Six methods are considered: inductive methods; the ferroprobe method; methods using the Hall, Faraday, and Zeeman effects; and the magnetoresistive method. (41 references) (auth)

29400 MASS-SPECTROMETRIC MEASUREMENTS OF THE DIMINUTION OF HYDROGEN IN POLYETHYLENE TARGETS WHICH HAVE BEEN IRRADIATED IN A PROTON SYNCHROTRON. Kukavadze, G. M.; Trebukhovskii, V. V.; Borisov, V. S.; Gol'din, L. L. (Inst. of Theoretical and Experimental Physics, Moscow). Instrum. Exp. Tech. (USSR) (Engl. Transl.): No. 4, 993-5(Jul-Aug 1970).

Translated from Prib. Tekh. Eksp.: No. 4, 33-5(Jul-Aug 1970).

A method is described for measuring the diminution of hydrogen and deuterium in polyethylene films after irradiation with protons using the internal beam of the synchrotron at the Institute of Theoretical and Experimental Physics. A mass-spectrometer with a system for the admission of the gaseous fractions of polyethylene which has been decomposed at high temperature was used as the measuring instrument. The instrument allows measurement of hydrogen content with an accuracy better than 10%. (auth)

29401 TIME-OF-FLIGHT MEASUREMENTS OF THE ELECTRICAL LENGTH OF COAXIAL DELAY CABLES. Pavlovskii, E. S. Instrum. Exp. Tech. (USSR) (Engl. Transl.): No. 4, 1018-19(Jul-Aug 1970).

Translated from Prib. Tekh. Eksp.: No. 4, 53-5(Jul-Aug 1970).

A method is described and results are presented for measurements of the delay times of coaxial cables by comparison with the time of flight of ^{244}Cm alpha particles on a known flight path. The delay times were measured up to 100 nsec with an error ±(0.05-0.12) nsec. (auth)

29402 SEMIAUTOMATIC APPARATUS FOR REGULATING THE NEUTRON DIFFRACTOMETER. Kozorez, A. K.; Skirda, V. I. (Inst. of Nuclear Physics, Ulugbek, USSR). Instrum. Exp. Tech. (USSR) (Engl. Transl.): No. 4, 1052-3(Jul-Aug 1970).

Translated from Prib. Tekh. Eksp.: No. 4, 84-6(Jul-Aug 1970).

A semiautomatic apparatus for regulating the neutron diffractometer is described. The circuit uses binary counters with inverse feedback for scaling by 5 and 25, allowing detector rotation steps of 0.05; 0.1; 0.2; 0.5; 1.0; 2.0; and 4.0°, those most used in taking neutronograms. (auth)

29403 HIGH-ACCURACY VARIABLE TIME DELAY. Shein, Yu. V.; Belov, V. A. Instrum. Exp. Tech. (USSR) (Engl. Transl.): No. 4, 1093-6(Jul-Aug 1970).

Translated from Prib. Tekh. Eksp.; No. 4, 120-3(Jul-Aug 1970).

The electronic circuit of a high-accuracy variable pulse delay is described; this system provides delay times of between 0 and 12.8 μsec in steps of 204.5 nsec to an accuracy of ~0.5%. The output pulses are exactly the same for any given delay time, having an amplitude of ~5 V, a duration of ~100 nsec at a level of 0.5, and a leading edge of ~20 nsec. The maximum operating frequency of the circuit is ~50 kc/sec. (auth)

29404 WIDEBAND FREQUENCY DIVIDER OF A SINUSOIDAL SIGNAL THAT HAS AN ADJUSTABLE DIVISION FACTOR. Uvarov, V. A.; Gusev-Donskoi, V. P. (Radio Engineering Inst., Moscow). Instrum. Exp. Tech. (USSR) (Engl. Transl.); No. 4, 1089-92(Jul-Aug 1970).

Translated from Prib. Tekh. Eksp.; No. 4, 117-20(Jul-Aug 1970).

A frequency divider for a sinusoidal signal is described that has an adjustable division factor and operates in a frequency region of 2.5 to 6.5 Mc. The division factor can be set by the operator or by instruction from a computer, in an interval from 67 to 300 with a step equal to 1. The nonlinear distortion factor of the output voltage of the device is 4%. The divider is used in a system for excitation of betatron oscillations of a proton synchrotron at an energy of 70 GeV. (auth)

29405 POWERFUL PULSE GENERATORS BASED ON AVALANCHE TRANSISTORS. D'yakonov, V. P.; Ali-Zade, D. G. (Azerbaydzhan Inst. of Petroleum and Chemistry, Baku). Instrum. Exp. Tech. (USSR) (Engl. Transl.); No. 4, 1102-4(Jul-Aug 1970).

Translated from Prib. Tekh. Eksp.; No. 4, 126-8(Jul-Aug 1970).

The circuit of a relaxation oscillator based on an avalanche transistor is described. The pulse parameters are given when various types of Soviet transistors are used in the generator. The circuit of a powerful generator using parallel connection of avalanche transistors is described. (auth)

29406 USE OF ZEOLITE PUMPS IN FIELD-EMISSION MICROSCOPY. Kuznetsov, V. A. (Moscow Physicotechnical Inst.). Instrum. Exp. Tech. (USSR) (Engl. Transl.); No. 4, 1190-1(Jul-Aug 1970).

Translated from Prib. Tekh. Eksp.; No. 4, 200-1(Jul-Aug 1970).

Results of mass spectroscopy investigations of the spectrum of residual gases in a sealed field-emission projector with a glass zeolite pump are presented. At a total pressure of residual gases of 10^{-9} torr the partial pressures of the detected gases were the following: Ar, 1.6×10^{-11} torr; N_2, 8×10^{-10} torr; He, 2.8×10^{-9} torr; H_2, 4×10^{-10} torr. The field emission images and volt-ampere characteristics of a tungsten point recorded after 3-h holding of the cleaned point in such a volume did not show any changes. (auth)

29407 OXYGEN DENSITOMETER FOR LIQUID METALS. (to Hitachi Ltd.). British Patent 1,227,089. 31 Mar 1971. Priority date 24 Jul 1968, Japan.

A method for measuring the oxygen concentration in a flowing liquid metal system based on the clogging principle is described. The quantity of oxygen present in the molten metal is calculated by measuring the flow resistance differential between two passageways with a temperature differential. (W.H.K.)

29408 ELECTROSTATIC DEFLECTOR FOR SELECTIVELY AND ADJUSTABLY BENDING A CHARGED PARTICLE BEAM. Larson, James D.; Benjamin, John A. (to United States Atomic Energy Commission). U. S. Patent 3,558,879. 26 Jan 1971. Filed 12 Mar 1968.

An electrostatic deflector consisting of a central plate and a pair of outer plates spaced from and parallel to each other is described. Each plate is provided with a slot for line of sight passage through the deflector and the central plate is charged at a high constant voltage with respect to the outer plate. (auth)

Radiation Effects on Instruments and Instrument Components

Refer also to abstract 29246.

29409 (SC-RR-710188) NEUTRON DAMAGE EFFECTS IN STEP RECOVERY DIODE FREQUENCY MULTIPLIERS. Chaffin, R. J. (Sandia Labs., Albuquerque, N. Mex.). Apr 1971. 45p. Dep. NTIS.

The Step-Recovery Diode (SRD) frequency multiplier has been studied both theoretically and experimentally. The results show that the multiplier is quite susceptible to neutron damage if self-bias is used (which is usually the case), and it is recommended either that the preradiation lifetime should be deliberately shortened or that voltage bias be considered in a radiation environment. The self-bias problem is found to be due to an increase in recombination current brought on by a reduction in minority carrier lifetime with neutron fluence. This study also derives the ultimate failure fluence as a function of multiplier parameters for these multipliers in general. (auth)

29410 LABORATORY SIMULATION FOR TREE STUDIES. Snyder, A. W. (Sandia Labs., Albuquerque, N. Mex.). pp 309-18 of Proceedings of the Institute of Environmental Sciences 15th Annual Technical Meeting and Equipment Exposition, April 20-24, 1969, Anaheim, California. Mt. Prospect, Ill.; Inst. of Environmental Sciences (1969).

From fifteenth annual technical meeting and equipment exposition; Anaheim, Calif. (20 Apr 1969). See CONF-690454.

A summary of the performance which has been achieved with the current designs of laboratory pulse sources of radiation (including megavolt flash x-ray generators, pulse reactors, and dense plasma fusion sources) for TREE (transient radiation effects on electronics) studies in a detonated nuclear weapon environment is presented. Also, a projection of the performance which might be achieved in the near future with some new concepts and with further improvements in the designs of existing sources is given. Intense pulse neutron sources discussed include pulsed fast and thermal reactors, accelerator pulsed fast assemblies of fissile materials, and high energy density plasmas of deuterium and deuterium–tritium gas. Radiation output performance data on Godiva reactor types including the APRF and SPR II; the Super Kukla pulse reactor; TRIGA reactor types including DORF and ACPR; and Pulstar reactors are listed and discussed. (25 references) (W.H.K.)

29411 EFFECTS OF ENERGETIC HEAVY IONS AND RADIATION ON INFRARED COMPONENTS. VanderLind, M. R.; Baroody, E. M. (Battelle Memorial Inst., Columbus, Ohio). pp 418-21 of Proceedings of the Institute of Environmental Sciences 17th Annual Technical Meeting and Equipment Exposition, April 26-30, 1971, Los Angeles, California. Mt. Prospect, Ill.; Inst. of Environmental Sciences (1971).

From seventeenth annual meeting and equipment exposition; Los Angeles, Calif. (26 Apr 1971). See CONF-710409.

The interaction of energetic ions and radiation from a nuclear weapon with infrared detector systems has been investigated. Possible damage mechanisms that may result from these interactions and the effects they may have on component function have been identified. The ion and radiation energies and fluences are those one would expect from an exoatmospheric detonation of a few kiloton nuclear weapon at distances of a few kilometers from the source. Source and separation distances of these magnitudes correspond to ion velocities of about 10^7 to 10^8 cm/sec, energy fluences of about 10^7 ergs/cm^2, and ion fluences of 10^{14}/cm^2. Consideration is given to ion penetration depths, radiation damage processes, energy deposition and sputtering, X-rays from implanted radioactive ions, and surface heating from absorption of fast ions. Disruption of detector performance can result from ionization produced by gamma rays and by knock-on atoms from fast neutrons, and from thermal radiation from surfaces heated by ion bombardment. An attempt has been made to estimate the magnitude of these effects. (auth)

29412 BEHAVIOUR OF CURRENTS GOING THROUGH MOS STRUCTURES UNDER IONIZING RADIATION. Esteve, D.; Buxo, J. (CNRS, Toulouse). Solid-State Electron.; 14: 257-60(Mar 1971).

The measurement conditions and experimental results are given to show the existence of a current that goes through a MOS structure under irradiation. This current was analyzed to test the validity of a model. The experimental values for three physical parameters of the model (the charge density in the space-charge region, the conductivity of the neutral zone of the MOS structure, and the coefficient of the photoemission law of the MOS structure) were obtained. (UK)

LIFE SCIENCES

Biochemistry, Physiology, and Molecular Biology

Basic Processes

Refer also to abstract 29748.

29413 (CONF-691225) REPORTS OF THE SYMPOSIUM ON THE NEW METHOD FOR PRODUCING RADIOACTIVE PREPARATIONS, WARSAW, DECEMBER 9–13, 1969. (Panstwowa Rada do Spraw Pokojowego Wykorzystania Energii Jadrowej, Warsaw (Poland)). 525p. (In Russian).

Fifty reports are included on the technology and new methods of production of radioisotopes and labeled organic compounds in the USSR and other Soviet Republics. The first 20 reports are concerned with the following topics: radioisotopes for biomedical studies; preparation of generators for production of ^{99m}Tc, ^{132}Te, and ^{133}I; separation of ^{103}Rh; labeling of macroaggregates of human serum albumin with ^{131}I; preparation of ^{51}Cr-labeled human serum albumin; and preparation of fluorescent derivatives labeled with ^{197}Hg and ^{203}Hg for diagnosis of infarcted myocarditis. The next five reports are concerned with the following topics: separation of Eu, Nd, Y, and Ru from irradiated reactor fuels of UO_2–Mo; separation of radioisotopes from cyclotron targets; preparation of ^{51}Cr and ^{84}Rb; use of reactor loops for production of ^{125}I; separation of ^{210}Po from irradiated Bi; and preparation of CH_3Br labeled with ^{82}Br. Other topics discussed are: use of tritium, ^{14}C, and ^{35}S for labeling organic compounds; synthesis of complex ethers; preparation of aliphatic acids labeled with ^{14}C; preparation of nitrogen-containing heterocyclic compounds fixed with tritium or deuterium by isotopic exchange; new ceramic sources of ^{137}Cs and ^{90}Sr; and preparation of pure beta sources. (R.V.J.)

29414 RADIOISOTOPES USED TO DETERMINE TUBULAR PASSAGE TIME IN DOG KIDNEYS. Hallwachs, O.; Zum Winkel, K.; Steinhausen, M.; Roel, L. (Univ., Heidelberg). Scand. J. Urol. Nephrol.; 4: 248–51(1970).

The passage time of ^{131}I–hippuran and ^{131}I–insulin was measured with Anger camera scintigraphy after rapid arterial injection of these substances and compared with the results obtained with the Lissamine Green method. Corresponding to the passage time of Lissamine Green through the loops of Henle, there was a decrease in the kidney size in the scintiphotogram. In further agreement with the intravital microscopy, the passage time of the radioactivity was prolonged during hypotension and high intra-pelvic pressure. Similar results were obtained with collimator measurements of ^{125}I–insulin and ^{125}I–hippuran on the renal surface and with simultaneous measurements of the passage time of Lissamine Green. (auth) (Sweden)

29415 IN VITRO LABELLING OF HEPARIN WITH ^{51}Cr. Varga, L.; Antoni, F.; Skalka, M.; Zedginidze, I. (International Atomic Energy Agency, Vienna). Int. J. Appl. Radiat. Isotop.; 22: 165–9(Mar 1971).

A simple and quick method was developed for labelling heparin with ^{51}Cr. The radiochemical purification of the heparin-^{51}Cr complex was made by use of EDTA as the complexing agent. Sephadex G-50 chromatography was used for the separation of EDTA-^{51}Cr and heparin-^{51}Cr. The labelling procedure proved to be mild enough so that the ^{51}Cr-labelled heparin retained its metachromatic staining capacity and its anti-coagulant potency. The ^{51}Cr-heparin was stable at room temperature for 4 weeks and following heat treatment (for 30 min at 100°C). With regard to its properties, ^{51}Cr-labelled heparin should be effective in the studies of the function of heparin in vitro and in vivo and its metabolic pathways. (auth) (UK)

29416 PHARMACOKINETICS OF HALOTHANE IN MAN: A NOVEL APPROACH. Mark, Lester C. (Columbia Univ., New York); Geddes, Ian C.; Scherrer, Jean R.; Dombrowski, Carl S.; Cohn, Stanton H. Int. J. Appl. Radiat. Isotop.; 22: 171–5(Mar 1971).

A unique 54-detector whole-body counter was used to follow the uptake, distribution, and excretion of a single breath of bromine-82-labeled halothane. In a compartmental analysis of the data with the SAAM program, the sum of two exponentials provided an excellent fit. One exponent probably reflects initial uptake and excretion; the second, distribution to viscera. (auth) (UK)

29417 TECHNIQUES FOR LABELLING TSETSE FLIES WITH RADIOISOTOPES. Cuisance, D.; Itard, J. (Institut d'Elevage et de Medecine Veterinaire des Pays Tropicaux, Maisons-Alfort, France). pp 111–30 of Sterility Principle for Insect Control or Eradication. Vienna; International Atomic Energy Agency (1971). (In French).

From Symposium on the sterility principle for insect control or eradication; Athens, Greece (14 Sep 1970). See STI/PUB-265; CONF-700919.

Four radioactive substances injected intravenously into the rabbit, which was used as host, were tested for labeling tsetse flies (Diptera-Muscidae), which are strictly hematophagous and which are the vectors of African trypanosomiasis. The purpose of the tests was to study the dynamics of populations in the field. The radioisotopes studied were: chromium-51, iron-59, cobalt-57 and zinc-65. The iron-59 and chromium-51, in particular, were chosen because of their affinity for the formed elements of blood. Chromium-51 (half-life: 27.8 days) has a biological half-life of 2 to 3 days in the tsetse fly. This radionuclide did not reappear in the progeny. Maximum elimination of the chromium-51 took place on the second and third days after feeding on the labeled rabbit. Iron-59 (half-life: 44.5 days) has a biological half-life of 2 to 3 days in the male tsetse fly, but the counting rate is higher than that for the controls over a period of more than 20 days. The average biological half-life is 24 days in fertilized females; it is dependent on the egg-laying. The radionuclide appears in the progeny; strictly speaking, it is fixed on the nymph, the puparium showing only very slight radioactivity. Cobalt-57 (half-life: 267 days) has a biological half-life of 36 hours in the male tsetse fly and of 3 to 4 days in the female. The radionuclide was not found in the progeny. The radioactivity of the excrement increases very rapidly between the third and seventh days. The quantities of zinc-65 (half-life: 245 days) at disposal were not enough to make a complete study. However, the first results indicate that the duration of labeling in the tsetse fly is at least 15 days after several radioactive meals and that the radioisotope reappears in the progeny. (auth)

Metabolism, Physiology, and Toxicology

Refer also to abstracts 29505, 29524, 29543, 29544, 29581, 29621, 29673, 29674, and 29724.

29418 (BNL–50285) PATHWAYS OF AN ARTIFICIAL ELEMENT IN THE BODY. Brookhaven Lecture Series Number 95. Atkins, Harold L. (Brookhaven National Lab., Upton, N. Y.). 23 Sep 1970. 10p. Dep. NTIS.

Technetium is a man-made element to which the human organism has not been exposed in evolutionary history. Despite this fact the element follows rather precise pathways in the body, localizing primarily in salivary glands, thyroid, and stomach. Technetium-99m can be used as a tracer for technetium pathways in order to study rate and degree of accumulation in these specific sites. Because of favorable physical characteristics technetium-99m is used widely in many nuclear medicine procedures. These physical characteristics are: medium energy gamma emission, essentially no beta particle emission, and a short half-life of six hours. Therefore, large quantities may be administered with low radiation dose to the patient. The problem of availability, despite the short half-life, has been solved by extracting the daughter ^{99m}Tc from its longer-lived parent, molybdenum-99. The degree of accumulation of ^{99m}Tc as pertechnetate in the thyroid in 30 minutes has been as accurate a determination of functional status as the 24-hour radioiodine uptake. Scanning procedures involving the thyroid are more readily performed and interpreted with ^{99m}Tc than with ^{131}I. Incorporation of technetium-99m in a number of different compounds has further enhanced its utility and places it in a most important niche in the field of nuclear medicine. (auth)

29419 (LF–43) FISSION PRODUCT INHALATION PROGRAM. Annual Report, October 1, 1969–September 30, 1970. McClellan, R. O.; Rupprecht, F. C. (eds.) (Lovelace Foundation for Medical Education and Research, Albuquerque, N. Mex.). Nov 1970. Contract AT(29-2)-1013. 328p. Dep. NTIS.

Forty papers are included; separate abstracts were prepared for 31. The remaining nine articles contain information on tissue weight in beagle dogs, blood content of beagle dog tissues, studies on pulmonary function, connective tissue, and lavage, and the effects of virus infection in dogs and man. (E.E.H.)

XUM

For abstracts of individual papers see: 29076–29080, 29420–29438, 29482, 29483, 29514, 29543, 29544, 29622, and 29724.

29420 (LF–43, pp 1-7) ESTIMATION OF THE RELATIVE INHALATION HAZARD OF REACTOR INVENTORY RADIONUCLIDES. Raabe, O. G. (Lovelace Foundation for Medical Education and Research, Albuquerque, N. Mex.).

In Fission Product Inhalation Program.

A simplified approach was used to assess the relative importance of the various radionuclides present in a uranium fueled reactor at operating times of 1 year and 5 years. Release probabilities and solubility probabilities were estimated and combined with organ dose calculations at 7 days and 6000 days to rank the various nuclides with respect to their potential importance if inhalation is the route of entry into the body. This ranking is based upon the multiplication of the reactor inventory values, the relative release probability, the relative solubility probability or its complement for insoluble forms, and the dose to organ of highest dose for the two dosage periods after inhalation deposition of 1 μCi in the lower lung. The results emphasize the importance of ^{131}I, ^{242}Cm, ^{144}Ce–Pr, ^{238}Pu, ^{90}Sr–Y, ^{91}Y, ^{132}Te–I, ^{89}Sr, ^{140}Ba–La, ^{99}Mo, ^{239}Np, ^{239}Pu, ^{95}Zr–Nb, ^{137}Cs–Ba and ^{103}Ru–Rh. (auth)

29421 (LF–43, pp 8-12) PRODUCTION OF RELATIVELY MONODISPERSE AEROSOLS FOR INHALATION EXPERIMENTS BY AEROSOL CENTRIFUGATION. Kotrappa, P. (Lovelace Foundation for Medical Education and Research, Albuquerque, N. Mex.).

In Fission Product Inhalation Program.

Stöber's aerosol spectrometer, based on a spinning spiral duct, was used as an aerosol centrifuge to separate narrow size groups of insoluble aerosols starting with a polydisperse distribution. The samples collected were resuspended in water and aerosolized with a Lovelace nebulizer to produce relatively monodisperse aerosols. Working with near-spherical fused clay particles, aerosols were obtained with geometric standard deviations of less than 1.1 and with number concentrations which would be practical for use in inhalation experiments. A formula for dilution of monodisperse suspensions for aerosolization was used to calculate the maximum number concentration that could be aerosolized from a suspension for a particular nebulizer, to obtain 95% singlets. This method appears to be particularly adaptable for the aerosols of oxides of transuranic elements. Estimated respiratory depositions of the oxides of ^{239}Pu, ^{238}Pu, ^{244}Cm, and ^{241}Am for Beagle dogs breathing the monodisperse aerosols for 1 hour are given for aerodynamic sizes ranging from 0.5 μm to 3.0 μm. (auth)

29422 (LF–43, pp 53-8) RETENTION OF RELATIVELY INSOLUBLE SUBSTANCES FOLLOWING INHALATION. Thomas, R. G. (Lovelace Foundation for Medical Education and Research, Albuquerque, N. Mex.).

In Fission Product Inhalation Program.

The retention of relatively insoluble substances following inhalation appears to follow a pattern which is species dependent. In mice, rats, and dogs following inhalation of labeled fused clay particles, the half-life of loss from the major lung compartment may be approximately 50, 200, or 400 days, respectively. If the process of loss from this compartment, presumed to be alveolar, is solely by dissolution then the different rates of retention may be directly related to surface area-to-mass ratios of the particles deposited. This premise necessitates a prediction that a smaller mass particle size distribution is deposited in the rodent species. A model is described which gives a reasonable fit to the various retention patterns. (auth)

29423 (LF–43, pp 59-65) RELATIVE HAZARDS FOR INHALED ^{95}Zr AND ^{95}Nb PARTICLES FORMED UNDER VARIOUS THERMAL CONDITIONS. Thomas, R. G.; Walker, Sharon A.; McClellan, R. O. (Lovelace Foundation for Medical Education and Research, Albuquerque, N. Mex.).

In Fission Product Inhalation Program.

Inhalation is a common route of potential entry into the body for radionuclides released in nuclear industry accidents. A study with mice exposed via inhalation is reported, which emphasizes the importance of physical-chemical forms (as influenced by heat treatment) of aerosols on their behavior within the body and the subsequent radiation dose. Aerosol droplets containing a near-equilibrium mixture of ^{95}Zr and ^{95}Nb in oxalic acid were passed through a heating column at 100; 250; 600; or 1100°C, respectively, producing particles of various chemical forms to which mice were then exposed (particle size ~1.6 μm activity median aerodynamic diameter). The mice were routinely whole-body counted and measurements were made to determine the ratio of ^{95}Nb and ^{95}Zr in the live animals and in certain organs following sacrifice. At the two highest temperatures, the inhaled and deposited particles were retained tenaciously in the lung and maintained the initial solution ^{95}Nb–^{95}Zr ratio of approximately 1.9. At 100°C, the radionuclides were translocated from lung to skeleton with a ratio of 1.3, indicative of an excess burden of ^{95}Zr. At 250°C, the pattern was similar but less pronounced. The differential patterns of retention resulted in significant differences in radiation dose pattern; at the lowest temperature the highest radiation doses were received by skeleton, lung, and liver, while at the higher temperature the radiation dose was delivered almost exclusively to lung. (auth)

29424 (LF–43, pp 66-70) RETENTION PATTERNS OF ^{124}Sb IN MICE FOLLOWING INHALATION OF PARTICLES FORMED AT DIFFERENT TEMPERATURES. Thomas, R. G.; Walker, Sharon A.; Lucchino, R. C. (Lovelace Foundation for Medical Education and Research, Albuquerque, N. Mex.).

In Fission Product Inhalation Program.

Three studies, in which mice were exposed to aerosols containing ^{124}Sb, were conducted. The inhaled particles were formed by passing droplets, nebulized from a solution of radioantimony in tartaric acid, through a heating column at either 100, 500, or 1100°C. Whole-body retention indicated a rapid early clearance which was greatest with the lowest temperature aerosol, followed by a gradually decreasing rate of loss. Tissue data with the aerosols generated at 500°C and 1100°C showed a 10-fold greater retention in lung than was demonstrated by the data at 100°C. The greater loss from lung at 100°C was reflected in at least a two-fold greater buildup in the skeleton. The data are discussed in terms of present day standards for man. (auth)

29425 (LF–43, pp 71-8) RETENTION OF ^{171}Tm FOLLOWING INHALATION OF OXIDE BY BEAGLE DOGS. Thomas, Randi L.; Kingsley, Barbara L. (Lovelace Foundation for Medical Education and Research, Albuquerque, N. Mex.).

In Fission Product Inhalation Program.

Retention and tissue distribution of ^{171}Tm is being studied in the Beagle dog following inhalation of $^{171}Tm_2O_3$. Initial body burdens were estimated to range from 0.32 to 2.8 mCi per animal. An average of 50% of the initial body burden was excreted during the first two days post-inhalation exposure, with significantly greater amounts of ^{171}Tm detected in the feces than in the urine. Subsequent losses, by fecal and urinary routes, have continued through 130 days of the experiment, leaving about 17% of the initial body burden retained at that time. Dogs have been sacrificed serially and preliminary observations show total lung with 18% of the sacrifice body burden at 128 days after inhalation exposure, skeleton with 63% and liver with 11%. The highest concentrations of radiothulium at 64 days were in lung, femur marrow, the turbinates, ribs, humerus, and femurs, the femur samples showing high ^{171}Tm concentrations both with and without bone marrow. Estimates of cumulative absorbed β dose at 128 days post-inhalation exposure normalized to a 10 kg dog and to an initial lung burden of 1 mCi are 440 rads to lung, 51 rads to skeleton and 19 rads to liver. (auth)

29426 (LF–43, pp 79-81) RETENTION AND DISTRIBUTION OF ^{137}Cs IN THE BEAGLE DOG FOLLOWING INHALATION OF ^{137}Cs IN FUSED MONTMORILLONITE CLAY PARTICLES. Boecker, B. B.; McClellan, R. O.; Scott, J. K. (Lovelace Foundation for Medical Education and Research, Albuquerque, N. Mex.).

In Fission Product Inhalation Program.

To aid in evaluating the retention and distribution of a relatively insoluble radioactive material such as might be released in certain nuclear accidents, 30 dogs were given single, 15-minute exposures to aerosols of fused montmorillonite clay particles containing ^{137}Cs. The AMAD for the aerosols ranged from 1.5 to 2.7 μm among different exposures (σ_g was 1.6 to 1.8). Approximately 60% of the initial body burden was excreted within the first three days, primarily in the feces. At eight days post-inhalation exposure, over 90% of the ^{137}Cs was in the lung and tracheobronchial lymph nodes with some ^{137}Cs found generally distributed throughout the body in tissues such as muscle, liver, kidneys and bone. With time, increasing amounts of ^{137}Cs were found in tracheobronchial lymph nodes such that in the dogs sacrificed at 3 years post-inhalation exposure, 80% of the sacrifice body burden was in lung and 14% in the tracheobronchial lymph nodes. The ^{137}Cs concentration data for lung were fit with a 2-component exponential. The long-term component which represented 70% of the initial lung activity had an effective half-life of 320 days. Observations are continuing on 4 dogs tentatively scheduled for sacrifice at 4 and 5 years post-inhalation exposure. (auth)

29427 (LF–43, pp 82-91) APPLICATION OF A BIOLOGICAL MODEL OF TISSUE DISTRIBUTION AND RETENTION OF INHALED ^{140}La IN BEAGLE DOGS TO AN ANALYSIS OF RADIOLOGICAL HAZARDS TO HUMANS INHALING VARIOUS ISOTOPES OF LANTHANUM. Cuddihy, R. G.; Griffith, W. C. (Lovelace Foundation for Medical Education and Research, Albuquerque, N. Mex.).

In Fission Product Inhalation Program.

XUN

The tissue distribution and retention of ^{140}La in the Beagle dog after inhalation of $LaCl_3$ aerosols was simulated with an analog computer model. This analog model was used to simulate tissue distribution and retention of various other radioactive isotopes of La under conditions of chronic inhalation exposure. From these results, Radiation Concentration Guidelines (RCG) for occupational inhalation exposures were calculated for ^{131}La, ^{132}La, ^{133}La, ^{135}La, ^{137}La, ^{138}La, ^{140}La, ^{141}La, and ^{142}La. The RCG value for ^{140}La was estimated to be 1.6×10^{-7} μCi/cc which is similar to the ICRP recommended level of 2.0×10^{-7} μCi/cc. ^{140}La is the only radioactive isotope of La for which previous exposure guidelines have been reported. (auth)

29428 (LF-43, pp 92-9) TISSUE DISTRIBUTION AND RETENTION OF ^{140}Ba AND ^{140}La IN BEAGLE DOGS AFTER INHALATION OF $BaCl_2$–$LaCl_3$ AEROSOLS. Cuddihy, R. G.; Griffith, W. C. (Lovelace Foundation for Medical Education and Research, Albuquerque, N. Mex.).

In Fission Product Inhalation Program.

The tissue distribution and retention of ^{140}Ba and ^{140}La was studied in Beagle dogs after inhalation of aerosols containing $^{140}BaCl_2$ and $^{140}LaCl_3$. About 60% of the ^{140}La deposited in the respiratory tract was retained in the lung with an effective half-time approaching the physical half-life of ^{140}La and contributing a major radiation dose to lung tissue. The deposited ^{140}Ba was rapidly translocated to the skeleton where radioactive equilibrium with ^{140}La was attained within 15 days post-inhalation exposure and persisted for the 64 day duration of the study. Average beta radiation doses to lung tissue and skeleton of Beagle dogs were estimated to be about 21 and 17 Rad, respectively, for an inhaled initial body burden of 100 μCi of ^{140}Ba and 100 μCi of ^{140}La. (auth)

29429 (LF-43, pp 100-5) RETENTION AND DISTRIBUTION OF ^{244}Cm FOLLOWING INHALATION OF $^{244}CmCl_3$ AND $^{244}CmO_{1.7}$ BY BEAGLE DOGS. Gallegos, A. F.; Boyd, H. A.; Thomas, R. G.; McClellan, R. O. (Lovelace Foundation for Medical Education and Research, Albuquerque, N. Mex.).

In Fission Product Inhalation Program.

Preliminary results on the retention and tissue distribution of ^{244}Cm following inhalation of $^{244}CmCl_3$ and $^{244}CmO_{1.7}$ by Beagle dogs are reported. Fourteen dogs were exposed to a $^{244}CmCl_3$ aerosol (AMAD = 1.5–1.6 μm) and 10 have been serially sacrificed through 64 days post-inhalation exposure. With both forms, the ^{244}Cm was translocated from the lung at a moderately rapid rate such that the liver and skeletal content of ^{244}Cm exceeded that in lung by 8 days post-inhalation exposure. The highest concentrations of ^{244}Cm were observed in lung, liver, tracheobronchial lymph nodes, skeleton, thyroid, and kidney at 16 days post-inhalation exposure. With both forms, approximately 20% of the initial lung burden of ^{244}Cm was excreted in the urine by 16 days post-inhalation exposure. (auth)

29430 (LF-43, pp 123-7) TOXICITY OF INHALED $^{90}SrCl_2$ IN BEAGLE DOGS. IV. Boecker, B. B.; Chiffelle, T. L.; Hobbs, C. H.; Jones, R. K.; McClellan, R. O.; Pickrell, J. A.; Redman, H. C. (Lovelace Foundation for Medical Education and Research, Albuquerque, N. Mex.).

In Fission Product Inhalation Program.

Studies on the metabolism, dosimetry, and effects of inhaled $^{90}SrCl_2$ in the Beagle dog are continuing in an effort to provide a basis for assessing the consequences of inhaling ^{90}Sr such as might be released in certain nuclear accidents. Seventy-two dogs were exposed to aerosols containing ^{90}Sr, resulting in initial body burdens ranging from 2.6 to 280 μCi ^{90}Sr/kg. Forty-eight of these dogs are being maintained for lifetime observation and have been placed in a longevity study consisting of four groups based on their retained ^{90}Sr burden at 14 days post-inhalation. Group means were 1.4, 6.2, 30, and 75 μCi ^{90}Sr/kg. Twenty-four dogs with a 14-day retained ^{90}Sr burden of 31 μCi/kg have been assigned to a sacrifice study. Two of these dogs were sacrificed at 5 days, 2 at 1 month, and 2 at 1 year after inhalation of ^{90}Sr. To date, 25 dogs have died or were euthanized, 6 during the first 31 days after inhalation of ^{90}Sr with severe hematologic dyscrasia, and 19 between 585 and 1787 days after inhalation of ^{90}Sr. The latter group includes 7 with angiosarcomas, 3 with fibrosarcomas, 5 with osteosarcomas, 1 with osteochondrosarcoma, 1 with osteochondrofibrosarcoma, 1 with leukemia, 1 with an epileptic seizure, and 1 with cerebellar hemorrhage. One dog had both an angiosarcoma and an osteosarcoma. The skeletons of these dogs received initial radiation dose rates of 13 to 55 rad/day and cumulative doses to death of 4000 to 22,000 rads. Serial observations are continuing on 45 surviving ^{90}Sr dogs and 22 control dogs. (auth)

29431 (LF-43, pp 128-36) TOXICITY OF INHALED $^{144}CeCl_3$ IN BEAGLE DOGS. IV. Boecker, B. B.; Benjamin, S. A.; Chiffelle, T. L.; Jones, R. K.; Hobbs, C. H.; McClellan, R. O.; Pickrell, J. A.; Redman, H. C. (Lovelace Foundation for Medical Education and Research, Albuquerque, N. Mex.).

In Fission Product Inhalation Program.

Studies on the metabolism, dosimetry, and effects of inhaled $^{144}CeCl_3$ in the Beagle dog are continuing in an effort to provide information that will aid in assessing the biological consequences of inhaling ^{144}Ce such as might be released in certain nuclear accidents. Studies on the tissue distribution of inhaled $^{144}CeCl_3$ indicated that ^{144}Ce deposited in the lung is translocated at a moderately rapid rate to liver and skeleton. The pattern of distribution is such that significant radiation doses are accumulated by all three tissues. Fifty-five dogs that inhaled $^{144}CeCl_3$ and 15 control dogs have been placed in a longevity study and will be observed for their lifespan. These dogs have been placed in 6 groups based on initial ^{144}Ce burden (group means 0, 14, 51, 130, 280, and 480 μCi/kg). These were regrouped on the basis of retained ^{144}Ce at 14 days post-inhalation to yield groups with mean ^{144}Ce content of 0, 5.3, 14, 41, 120, and 230 μCi/kg. Seventeen dogs from the two highest groups have died; 8 at 21 to 44 days post-inhalation with signs attributed to severe bone marrow damage and associated pancytopenia; 2 at 138 and 144 days with radiation pneumonitis; 3 at 309 to 874 days with hepatic necrosis; 1 at 510 days with marrow aplasia; 1 at 375 days with pulmonary fibrosis; and 2 at 799 and 1632 days with neoplasms. One of the last two dogs had an osteosarcoma and the other had a squamous cell carcinoma of the maxilla and a small papillary adenoma of the lung. Serial observations are continuing on the 38 surviving $^{144}CeCl_3$ dogs and 15 control dogs. (auth)

29432 (LF-43, pp 137-9) TOXICITY OF INHALED $^{91}YCl_3$ IN BEAGLE DOGS. IV. Redman, H. C.; Boecker, B. B.; Jones, R. K.; McClellan, R. O.; Pickrell, J. A. (Lovelace Foundation for Medical Education and Research, Albuquerque, N. Mex.).

In Fission Product Inhalation Program.

Studies on the metabolism, dosimetry, and effects of $^{91}YCl_3$ in Beagle dogs are continuing with a view to providing information that will assist in assessing the biological consequences of nuclear accidents in which ^{91}Y or other radionuclides that produce a similar radiation dose pattern may be released. Forty-two dogs with ^{91}Y burdens from 73 to 1300 μCi/kg were placed in four groups with mean initial body burdens of 120, 260, 560, and 920 μCi/kg. For comparison with observed biological effects, these same dogs were regrouped on the basis of retained 14-day body burdens yielding groups with mean values of 30, 58, 140, and 270 μCi/kg. These dogs and 12 control dogs are being maintained for lifetime observation. An additional four dogs with mean initial ^{91}Y burdens of 560 μCi/kg were placed in a sacrifice study. Eleven dogs within the highest exposure groups have died or were euthanized at 17 to 33 days after inhalation of ^{91}Y with changes related to severe bone marrow damage and associated pancytopenia. Two dogs died approximately one year after ^{91}Y inhalation with convulsive seizures that were presumed to be unrelated to the ^{91}Y exposure. Thirty-three dogs that had initial lung burdens of 73 to 660 μCi/kg and all 12 control dogs are surviving at 1100 days or more after inhalation of ^{91}Y. Serial observations are continuing on all surviving dogs. (auth)

29433 (LF-43, pp 140-5) TOXICITY OF INJECTED $^{137}CsCl$ IN THE BEAGLE DOG. III. Redman, H. C.; Boecker, B. B.; Chiffelle, T. L.; Hobbs, C. H.; Jones, R. K.; McClellan, R. O.; Pickrell, J. A.; Rypka, E. W. (Lovelace Foundation for Medical Education and Research, Albuquerque, N. Mex.).

In Fission Product Inhalation Program.

Studies on the metabolism, dosimetry, and effects of intravenously administered $^{137}CsCl$ in the Beagle dog are being conducted to aid in assessing the biological consequences of exposure to ^{137}Cs such as might occur in the event of certain nuclear accidents. The effects of the chronic, relatively uniform whole-body exposure produced by ^{137}Cs are being compared with other diverse radiation dose patterns resulting from inhalation of radioactive aerosols. Sixty-six dogs were entered into the study, 6 with a mean initial ^{137}Cs body burden of 370 μCi/kg, and 12 dogs each with mean initial ^{137}Cs body burdens of 2820, 1940, 1420, 970, and 0 μCi/kg. All six of the highest level dogs died at 19 to 33 days post-injection having cumulative whole-body doses of 950 to 1400 rads. Three dogs in the 2820 μCi/kg level died at 24–27 days post-injection with cumulative whole-body doses of 860–910 rads. One dog in the 2820 μCi/kg level and one dog in the 1940 μCi/kg level died at 77 and 81 days after injection with cumulative whole-body doses of 1300–1400 rads. These early deaths were attributed to severe bone marrow damage which was reflected in an early dose-related pancytopenia. A single control dog died 647 days after being placed on the study with clinico-pathological manifestations of an autoimmune hemolytic anemia. Forty-three ^{137}Cs dogs and 11 controls are surviving at 586 to 840 days after being placed on experiment. The surviving ^{137}Cs dogs had initial body burdens that ranged from 880 to 3000 μCi/kg and received cumulative whole-body doses of 540 to 2200 rads. Serial observations are continuing on all survivors. (auth)

XUM

29434 (LF-43, pp 146-62) TOXICITY OF INHALED ^{90}Y FUSED CLAY IN BEAGLE DOGS. II. Hobbs, C. H.; Barnes, J. E.; Chiffelle, T. L.; Jones, R. K.; Kanapilly, G. M.; Lundgren, D. L.; Mauderly, J. L.; McClellan, R. O.; Pickrell, J. A.; Rypka, E. W. (Lovelace Foundation for Medical Education and Research, Albuquerque, N. Mex.).

In Fission Product Inhalation Program.

Studies on the metabolism, dosimetry, and effects of inhaled ^{90}Y in fused clay in the Beagle dog are being continued with a view to assessing the consequences of inhalation of an energetic beta emitter that has a short effective half-life in the lung. Two major studies being performed are a radiation dose pattern study in which 12 dogs were sacrificed in pairs at 0, 2, 4, 6, 8, and 12 days post-inhalation exposure and a longevity study in which 69 dogs have been exposed to ^{90}Y fused clay to date with initial lung burdens ranging from 80 to 5,200 μCi/kg. The ^{90}Y was retained in lung with a half-life that approximated the physical half-life with only small quantities translocated to tracheobronchial lymph nodes, skeleton, and liver. The infinite radiation doses to lung, tracheobronchial lymph nodes, skeleton, and liver, for an initial lung burden of 1 mCi, were estimated to be 1200, 170, 0.54, and 0.38 rads, respectively, normalized to a 10-kg dog. One mCi deposited in the upper respiratory tract and cleared via the gastrointestinal tract was estimated to result in a dose of 38 rads to the colon. Twenty-one of the 69 longevity dogs have died to date: 6 at 7.5 to 47 days, 12 at 64 to 92 days, and 3 at 117 to 163 days post-inhalation exposure, all with clinico-pathological features consistent with radiation pneumonitis. The cumulative radiation dose to lung for the dogs that have died ranged from 8,400 to 55,000 rads. Forty ^{90}Y exposed dogs and eight control dogs are still surviving at 15 to 373 days post-inhalation exposure. Eight of the ^{90}Y dogs exposed most recently have sufficiently high radiation dose exposures such that it is unlikely that they will survive for long periods of time. The remaining 32 ^{90}Y dogs with cumulative doses to lung of 990 to 6,300 rads and 8 control dogs will be studied for the remainder of their lifespan along with 32 ^{90}Y exposed and four control dogs to be added to the study during the next year. (auth)

29435 (LF-43, pp 163-70) TOXICITY OF INHALED ^{91}Y FUSED CLAY IN BEAGLE DOGS. I. Hobbs, C. H.; Cuddihy, R. G.; Benjamin, S. A.; Jones, R. K.; Kanapilly, G. M.; Mauderly, J. L.; McClellan, R. O.; Pickrell, J. A. (Lovelace Foundation for Medical Education and Research, Albuquerque, N. Mex.).

In Fission Product Inhalation Program.

Studies on the radiological hazards due to inhalation of ^{91}Y in fused clay have been initiated in the Beagle dog to aid in assessing the biological consequences of inhaling a relatively insoluble, high energy β emitter with a short to intermediate effective half-life in the lung. These consist of two parallel studies, a radiation dose pattern study in which 30 dogs were exposed to ^{91}Y entrapped in fused clay and are being serially sacrificed from 0 to 320 days post-exposure, and a longevity study in which 32 dogs have been exposed to ^{91}Y entrapped in fused clay to date with initial lung burdens ranging from 43 to 364 μCi ^{91}Y/kg of body weight. The aerosols ranged in size from 1.6 to 2.3 μm (AMAD). Of the inhaled ^{91}Y 40 to 50% was deposited in the respiratory tract with about 22% deposited in the pulmonary region of the lung. The ^{91}Y deposited in the pulmonary region was retained in the lung with a mean effective half-life of 49 days. The whole-body effective half-life for ^{91}Y was found to be 51 days. Small quantities of ^{91}Y were translocated to the tracheobronchial lymph nodes, liver, and skeleton. The concentration of ^{91}Y in tracheobronchial lymph nodes exceeded that of the lung by 64 days post-exposure. The amount of ^{91}Y excreted in the feces still exceeded that excreted in the urine even after the initial rapid clearance of the upper respiratory tract via the gastrointestinal tract. In the longevity study, to date, 5 dogs have died between 113 and 185 days post-exposure. The cumulative radiation dose to lung at death ranged from 21,000 to 45,000 rads. The surviving dogs with the highest initial lung burdens are presently showing clinical signs typically associated with radiation-induced pulmonary injury. Principal clinical and pathological findings in the dogs that died have been related to pulmonary edema, early fibrosis, and vascular obliterative changes. At this time it appears that 16 dogs with potential cumulative infinite radiation dose to lung of less than 20,000 rads will be long-term survivors. These animals and those that are to be exposed in the future will be observed over their lifespan with particular attention directed toward evaluating ^{91}Y tissue radiation dose distribution and the resulting clinico-pathological effects. (auth)

29436 (LF-43, pp 183-7) TOXICITY OF INHALED ^{144}Ce FUSED CLAY IN BEAGLE DOGS. III. Boecker, B. B.; Chiffelle, T. L.; Hobbs, C. H.; Jones, R. K.; Mauderly, J. L.; McClellan, R. O.; Pickrell, J. A.; Redman, H. C. (Lovelace Foundation for Medical Education and Research, Albuquerque, N. Mex.).

In Fission Product Inhalation Program.

The metabolism, dosimetry, and effects of inhaled ^{144}Ce in fused clay are being investigated in the Beagle dog to aid in assessing the biological consequences of release of ^{144}Ce in a relatively insoluble form such as might occur in certain types of nuclear accidents. Further, the toxicity of inhaled ^{144}Ce fused clay is of broad interest since it may be considered as representative of a group of intermediate-lived beta emitting radionuclides. Two major studies being performed are a metabolism and dosimetry study in which 24 dogs are being serially sacrificed over an extended period of time, and a longevity study with 2 series of dogs; Series I with 15 dogs exposed to aerosols of ^{144}Ce in fused clay to yield initial lung burdens of 88 to 2100 μCi and 3 control dogs exposed to nonradioactive clay and Series II with 48 dogs exposed to date to aerosols of ^{144}Ce in fused clay to yield initial lung burdens of 0.10 to 580 μCi and 6 control dogs exposed to nonradioactive clay. The ^{144}Ce in fused clay is slowly translocated from the lung to tracheobronchial lymph nodes, liver, and skeleton. However, because of the small size of the tracheobronchial lymph nodes they exceed the lung in ^{144}Ce concentration by 100 days post-inhalation. At 768 days post-inhalation exposure, 45% of the retained activity is in lung, 30% in liver, 17% in skeleton, and 4.7% in tracheobronchial lymph nodes. To date, 14 dogs have died or been euthanized at 143 to 410 days after inhalation of ^{144}Ce. The prominent finding has been severe pulmonary fibrosis. The cumulative radiation dose to the lung to time of death has ranged from 18,000 to 110,000 rads. The 49 surviving dogs include dogs with a potential for accumulating radiation exposures to lung of up to 51,000 rads. Serial observations are continuing on all survivors with special attention directed to evaluating ^{144}Ce metabolism and dosimetry, and various clinical, pulmonary function, hematologic, serum chemical, and microbiologic parameters. (auth)

29437 (LF-43, pp 188-96) TOXICITY OF INHALED ^{90}Sr FUSED CLAY IN BEAGLE DOGS. I. Barnes, J. E.; Boecker, B. B.; Hobbs, C. H.; Jones, R. K.; Kanapilly, G. M.; Mauderly, J. L.; McClellan, R. O.; Pickrell, J. A. (Lovelace Foundation for Medical Education and Research, Albuquerque, N. Mex.).

In Fission Product Inhalation Program.

Studies on the metabolism, dosimetry, and effects of inhaled ^{90}Sr fused clay in Beagle dogs have been initiated with a view to obtaining information on the biological consequences of inhaling this important radionuclide in a relatively insoluble form. Moreover, the radiotoxicity of inhaled ^{90}Sr fused clay is of interest as it represents a long-effective half-life beta-emitter which might be deposited in lungs. Two major studies are being performed: a radiation dose pattern study with dogs scheduled for serial sacrifice from 0-2048 days post-inhalation exposure; and a longevity study in which dogs will be observed for their lifespan. Dogs in the radiation dose pattern study have been sacrificed at time intervals of up to 512 days post-inhalation exposure. After an early rapid clearance of ^{90}Sr deposited outside of the lung, the majority of the ^{90}Sr is located in lung. With time, small quantities are translocated to tracheobronchial lymph nodes and skeleton such that by 512 days 89% of the retained activity is in lung, 6.1% in skeleton and 3.2% in tracheobronchial lymph nodes. The effective half-life for ^{90}Sr retention in lung was approximately 370 days. To date, 42 dogs with initial lung burdens of 4.5 to 82 μCi ^{90}Sr/kg body weight and 7 control dogs exposed to non-labelled fused clay have been entered into the longevity study. Thirty-five additional dogs will be added at a later date. No deaths have been observed in dogs followed for up to 240 days post-inhalation exposure, although dogs with the largest amounts of ^{90}Sr initially deposited are showing signs of radiation pneumonitis at this time when they have cumulative radiation doses to lung of 40,000 to 47,000 rads. Serial observations are continuing on all survivors. (auth)

29438 (LF-43, pp 197-204) SOME OBSERVATIONS ON THE TOXICITY OF BETA-EMITTING RADIONUCLIDES INHALED IN FUSED CLAY PARTICLES. McClellan, R. O.; Barnes, J. E.; Boecker, B. B.; Cuddihy, R. G.; Hobbs, C. H.; Jones, R. K.; Redman, H. C. (Lovelace Foundation for Medical Education and Research, Albuquerque, N. Mex.).

In Fission Product Inhalation Program.

The current status of studies in which Beagle dogs have been exposed to aerosols of ^{90}Y, ^{91}Y, ^{144}Ce, and ^{90}Sr in fused clay particles is reviewed. These radionuclides are all avidly retained in the lung with biological retention half-times of about 300 to 400 days and effective half-lives of 64 hours, 49 days, 160 days, and 370 days, respectively. With the passage of time, small quantities of all the radionuclides are translocated to tracheobronchial lymph nodes, and to other tissues depending upon the elemental chemical character of the radionuclide. Beagle dogs have been exposed via inhalation to achieve graded initial lung burdens of each of the radionuclides. Deaths at 7 to 300 days post-inhalation exposure were observed with the survival times and cumulative doses to lung at death being dependent upon the initial dose rate and the rate of de-

XUM

crease of the beta radiation dose rates to lung. The earliest deaths and lowest cumulative doses to lung at death were observed in the dogs that inhaled ^{90}Y fused clay. (auth)

29439 REDUCTION OF PATIENT RADIATION BURDEN IN NUCLEAR MEDICINE THROUGH APPLICATION OF SHORT-LIVED RADIONUCLIDES. Boerner, W. (Medizinische Univ., Wuerzburg, Ger.). Radiologe; 10: 376-81(Sep 1970). (In German).

In nuclear medicine, short-lived radionuclides lead to a significant reduction of radiation burden to the patient. At the present time, these nuclides can be obtained through milking of a cow-system containing a long-lived mother substance; therefore, these nuclides are available far from the production site. Moreover, use of short-lived radioisotopes augments diagnostic accuracy because of the higher activities that can be administered. For various organs, appropriate radioactive substances are discussed and their advantages and limitations are analyzed. (tr-auth)

29440 QUANTITATIVE CHARACTERISTICS OF THE MEANS OF PENETRATION OF ^{90}Sr INTO THE BODIES OF GASTROPOD MOLLUSKS. Nyanishkene, V. M. B.; Polikarpov, G. G. (Inst. of Biology of the Southern Seas, Sevastopol). Radiobiologiya; 10: 928-30(1970). (In Russian).

In experiments with pond snails lasting about one month, it was established that despite the different nature of the distribution of ^{90}Sr concentrations between the shell and the body of the mollusk in the case of different sources of its penetration into the organism (from the water or food—Elodea containing ^{90}Sr), the contribution of ^{90}Sr absorbed from the water medium in the body of the mollusk is an order of magnitude higher, and in the shell two orders of magnitude higher than when this radionuclide is absorbed from food material. (tr-auth)

29441 UPTAKE AND EXCRETION OF RADIOCOBALT BY A FRESHWATER MOLLUSC (UNIO MANCUS VAR. ELONGATULUS). Ravera, Oscar; Merlini, Margaret; Musso, Simone (CCR-EURATOM, Ispra, Italy). Minerva Fisiconucl.; 13: 301-5(Oct-Dec 1969). (In Italian). (CONF-680535-29).

From fourteenth national conference of the Italian Association for Health Physics and Protection from Radiation; Formia, Italy (29 May 1968).

Radioactive cobalt, primarily ^{60}Co is one of the most important isotopes discharged by the Ispra Center into the Creek Novellino, an affluent of Lake Maggiore (Lago Maggiore). Since it is well-known that bivalves (Lamellibranchs) concentrate transition elements to a great extent, the bivalve Unio mancus of Lago Maggiore was chosen for the study of radiocobalt. It is a Lamellibranch with a wide distribution and a high population density in the lake. Studies of radiocobalt uptake and loss were undertaken both in the laboratory and in nature (Creek Novellino). It appears that this Mollusc is able to concentrate measurable amount of radiocobalt even when the activity in the environment is extremely low. The factors involved in these processes are presented and discussed. (auth)

29442 EXCRETION AND RETENTION OF STABLE STRONTIUM IN CHILDREN. Sutton, A. (Medical Research Council Radiobiology Unit, Harwell, Eng.); Sheppherd, H.; Harrison, G. E.; Barltrop, D. Nature (London); 230: 396-7(9 Apr 1971).

In previous work the accumulation of Sr and Ca in children aged 4 to 14 years was studied by giving 100 mg doses of natural Sr, but because the normal dietary intake at these ages is only about 1 mg a day these large doses may have disturbed the balance of Sr in the body and invalidated the conclusions. In the studies reported this problem was overcome by using 5 mg doses of stable Sr enriched in ^{84}Sr, which also avoided giving doses of radioisotopes to the children. Information on Sr turnover could thus be obtained while the subjects consumed a normal diet with a normal content of natural Sr. Radiochemical analyses were made on urine, feces, and venous blood. Change in the rate of urinary excretion of the ^{84}Sr marker with time and the corresponding changes in the plasma concentration of the marker in a boy and in an adult are shown graphically, and the total urinary and fecal outputs of the marker and the derived value for the percentage of marker retained are shown in tabular form. Results confirmed an earlier conclusion that the total excretion of Sr by children aged 4 to 14 years and adults given a single dose is not significantly different, although the relative urinary and fecal excretion differed markedly in the two age groups. Among conclusions reached is that the excretion and retention of Sr are controlled largely by the intake and excretion of Ca. The plasma concentrations and urinary excretion rates of natural Sr and Ca were also measured. It appeared that the renal clearance for Sr and Ca is significantly less in children than in adults. It is significant that the relative renal clearance C_{Sr}/C_{Ca}, or renal discrimination between Sr and Ca, in children was about the same as for adults, and that the plasma concentration of Sr was only slightly higher than in adults. (UK)

29443 QUANTITATIVE ^{6}Li AUTORADIOGRAPHY OF METASTASES OF WALKER-256 CARCINOSARCOMA IN THE PULMONARY TISSUE. Zaichik, V. E.; Krasnoshchekov, G. P.; Letov, V. N.; Ryabukhin, Yu. S. (Inst. of Medical Radiology, Obninsk, USSR). Med. Radiol.; 16: No. 2, 47-51(Feb 1971). (In Russian).

In experiments on 66 Wistar rats with the aid of neutron activation autoradiography on nitrocellulose film, the dynamics of ^{6}Li incorporation into the lungs and metastases of Walker-256 carcinosarcoma were investigated during the first ten hours after injection. Irradiation of samples was carried out in the thermal canal of the BR-5 reactor for a period of 44.5 hours. The ^{6}Li concentration was determined by calculating the tracks on autoradiograms over differentiated areas of the histological section. The ^{6}Li content in metastases during the time interval studied gradually increased, whereas in the lungs it reached the maximum in 4 to 5 hours. The greatest increase of ^{6}Li concentration in metastases in comparison with adjacent areas of the lung (1.8 to 3.5 times) was noted three hours after introduction; the least (1.3 to 2.5 times)—in six hours. A formula for the calculation of ^{6}Li concentration in the samples by the density of tracks on autoradiograms is given. (auth)

29444 INTERCEPTION AND RETENTION OF RADIOACTIVE AEROSOLS BY VEGETATION. Witherspoon, John P. (Oak Ridge National Lab., Tenn.). Atmos. Environ.; 4: 591(1970).

Comments are made on the paper by Chamberlain with this title (Atmos. Environ. 4: 57-58, 1970). It is cautioned that results of such field studies of the retention of aerosols by plants are not directly applicable to retention of particulate fallout where particle diameters may exceed several microns. The equivocal effect of rain is mentioned as an example. The suggested role of the increased shedding of leaf cuticle during active growth and the use of normalized specific activity computations for chronic contamination events are welcomed. (UK)

29445 STUDIES OF REACTIONS OF RADIOISOTOPES OF RARE EARTH ELEMENTS WITH PROTEIN AND AMINO ACIDS. Rogozina, E. M.; Popov, D. K.; Ponikarova, T. M. Zh. Obshch. Khim.; 40: 2466-9(Nov 1970). (In Russian).

Amino acids in organic samples firmly complex rare earth elements, which increases the ability of animals to accumulate radioisotopes of these elements in their organs and tissues. An ion exchange method of investigation was used to study yttrium chelation with pepsin and tripepsin in aqueous solutions. (tr-auth)

29446 CALCIUM AND STRONTIUM METABOLISM AS RELATED TO AGE AND ALGINATES. Gruden, Nevenka; Kosteal, Krista; Buben, Mirka (Inst. for Medical Research and Occupational Hygiene, Zagreb). Arh. Hig. Rada Toksikol.; 21: 27-33 (1970). (In Serbo-Croatian).

The efficiency of alginates in reducing radiostrontium absorption from the intestine was evaluated in 6, 16, and 26 week old male rats. They were fed diets with alginate additives (sodium alginate, Manucol SS/LD/2, 10 g per 100 g of dry food) for 9 days. Calcium-47 and strontium-85 were added to the drinking water of experimental and control animals during the 6th and 7th day of the experiment. After sacrificing the animals on the 9th day, both radioisotopes were determined in dissolved mineralized samples of the carcass and urine. All results are expressed as percentage of the applied dose. The results showed a statistically significant reduction of radiostrontium retention and absorption in animals of all age groups. The radioactive calcium absorption remained unimpaired. The effects of alginates on strontium absorption were more pronounced in younger animals. (auth)

29447 ^{65}Zn IN SERUM PROTEINS IN PERSONS EXPOSED TO ZINC. INVESTIGATION IN VITRO. Stilinovic, L. (Inst. for Medical Research, Zagreb). Arh. Hig. Rada Toksikol.; 21: 23-6(1970).

Blood serum proteins, separated from samples taken from metal workers exposed to zinc oxide fumes, were labeled with ^{65}Zn. Two-dimensional electrochromatographic investigations were made on the samples. It was found that most of the ^{65}Zn was localized in the serum albumin and only a trace amount was associated with the globulins. (E.E.H.)

29448 POTASSIUM CONTENT IN PATIENTS WITH PYELONEPHRITIS (ACCORDING TO DATA OF MEASUREMENT OF THE HUMAN NATURAL RADIOACTIVITY). Karlin, I. D.; Veisman, V. A.; Shcherba, M. M.; Shapiro, E. L. (Leningrad Inst. of Research in Radio-protection). Med. Radiol.; 16: No. 2, 15-18 (Feb 1971). (In Russian).

With the aid of whole-body radiation counters, the total content of potassium in 16 healthy persons and in 52 patients with chronic pyelonephritis was determined by the degree of natural radio-

activity. In patients suffering from chronic pyelonephritis there was a reduced content of total potassium in the body, which intensified with increase in the degree of renal insufficiency. This could be explained by loss of potassium by the kidneys, reduction of the muscular mass of the body, and by augmented catabolism. (auth)

29449 EFFECT OF A MIXTURE OF URANIUM FISSION PRODUCTS ON THE SANITARY CONDITIONS AND HYDROBIONTS OF WEAKLY-MINERALIZED FRESH-WATER BASINS. Gus'kova, V. N.; Bragina, A. N.; Zasedatelev, A. A.; (and others). Gidrobiol. Zh., Akad. Nauk Ukr. SSR; 6: No. 4, 5-11(1970). (In Russian).

Experimental investigations did not establish a considerable negative effect of two mixtures of fission radionuclides in concentrations of 2.0×10^{-7} and 1.0×10^{-5} Ci/l on sanitary conditions and hydrobiants of a reservoir. A concentration of the mixtures of 1.0×10^{-3} Ci/l caused inhibition of biochemical consumption of oxygen and development of fish spawn. A decrease in concentration of mixtures (radionuclides) in water occurred most intensively (by 50 to 60% as compared with the initial one) due to Protococcus algae and duckweed. The lowest values for the accumulation coefficients of the separate isotope mixtures, the concentration being 1.0×10^{-5} Ci/l in water, were found in the muscles of fish. Axis skeleton accumulated mainly ^{89}Sr and ^{140}Ba. (auth)

29450 COMPARATIVE METABOLISM OF RADIONUCLIDES IN MAMMALS. V. RETENTION OF ^{192}Ir IN THE MOUSE, RAT, MONKEY, AND DOG. Furchner, J. E.; Richmond, C. R.; Drake, G. A. (Los Alamos Scientific Lab., N. Mex.). Health Phys., 20: 375-82(Apr 1971).

Mice, rats, monkeys and dogs were contaminated with tracer doses of ^{192}Ir administered via oral, intraperitoneal, and intravenous routes. Distribution and retention as functions of time were determined with 4π liquid scintillation counters. Less than 10% of the oral dose was absorbed. Excretion was predominantly urinary except when ^{192}Ir was given orally. The carcass, which is almost exclusively muscle and bone, was the largest organ pool, but higher concentrations were found in the spleen, kidney and liver. An estimate of the maximum permissible concentration in water (10^{-3} $\mu Ci/cm^3$) was in agreement with the limiting value suggested by the International Commission on Radiation Protection as a guide. (auth) (UK)

29451 PROTRACTED HEPATIC, SPLENIC, AND RENAL RETENTION OF ^{239}Pu IN THE BEAGLE. Stover, Betsy J.; Atherton, David R.; Buster, Dawn S. (Univ. of Utah, Salt Lake City). Contract AT(11-1)-119. Health Phys.; 20: 369-74(Apr 1971).

Retention of plutonium in liver, spleen, and kidneys of beagles injected intravenously with $^{239}Pu(IV)$ in citrate buffer at injected dose levels of 0.016 and 0.048 $\mu Ci/kg$ was measured from young adulthood to death. Dogs at 0.016 $\mu Ci/kg$ suffer no lifeshortening, and those at 0.048 $\mu Ci/kg$, 18%. Hepatic retention is independent of dose level at these and the previously reported level of 0.096 $\mu Ci/kg$, and, thus, at these levels the radiation damage is not sufficiently extensive to result in a significant dose level effect. Sets of hepatic retention equations were calculated and those most appropriate for calculation of radiation dose were designated. Splenic and renal retentions were higher than anticipated from results at higher levels. (auth) (UK)

29452 DISCRIMINATION OF ^{90}Sr WITH RESPECT TO CALCIUM IN FRESHWATER PLANTS. Piskunov, L. I.; Treiger, S. I. (Sverdlovsk Regional Sanitary-Epidemiological Station, USSR). Radiobiologiya; 10: 788-90(1970). (In Russian).

The results of a statistical treatment of the published data of laboratory experiments on the accumulation and discrimination of ^{90}Sr in freshwater plants as a function of the calcium concentration in the water are discussed. The regression equations obtained are discussed. The viewpoint that the discrimination coefficients depend on the calcium concentration in the surrounding water was confirmed. (tr-auth)

29453 STUDIES ON THE POSSIBILITY OF IMPROVING THE SELECTIVE LOCALIZATION OF RADIOPHOSPHORUS IN DIFFERENT TISSUES. Anghileri, Leopoldo J.; Miller, Esther S. (Univ. of Colorado, Denver. Veterans Administration Hospital, Denver). Strahlentherapie; 140: 671-7(Dec 1970).

The distribution of ^{32}P-Cr-alloxantin complex in normal and tumor-bearing mice was compared with that of ^{32}P-orthophosphate. The ^{32}P tag in the chromium complex followed the fate of the total molecule, which differed from that of the ^{32}P-orthophosphate, as shown by the distribution and the analytical fractionation of the phosphorus in different tissues. With an equal dose of this complex in bone or tumor, a lesser radiation dose was delivered in spleen, pancreas, intestines, blood, and nervous tissues than with ^{32}P-orthophosphate. No significant differences of ^{32}P-orthophosphate uptake were found between injections with carrier and without. (auth)

29454 EFFECT OF ISOTOPE DILUTION ON THE BEHAVIOR OF RADIOYTTRIUM IN MAMMALIAN ORGANISM. Seidel, Arnulf; Vladar, Milan; Volf, Vladimir (Kernforschungszentrum, Karlsruhe, Ger.). Strahlentherapie; 140: 717-20(Dec 1970). (In German).

Kinetics, distribution pattern, and binding of ^{88}Y by plasma proteins as influenced by isotopic dilution (in the dose range of 0.01 to 30 μmole Y per animal) were studied in the rat. The results make it likely that Y exists in the blood as chelate as well as colloid, the dispersity and chemical composition of which depends on carrier dosage. (auth)

29455 INCORPORATION AND DISTRIBUTION OF THORON DECAY PRODUCTS FOLLOWING INHALATION BY RATS. Hofmann, Hans Peter (Univ., Giessen, Ger.). Strahlentherapie; 140: 721-30(Dec 1970). (In German).

Examinations were made with regard to retention and distribution of ^{212}Pb, incorporated into carrier aerosols, after inhalation by rats. A compartment model was set up for the resorption of ^{212}Pb in the lung, and the parameters of this model were defined experimentally. The inhalation apparatuses, developed for this purpose, permit work with high ^{212}Pb concentrations without danger. The radiation dose by alpha radiation to single organs in the rats was estimated. Doses of some krad per hour of inhalation can, under the conditions described, be applied to the lung of the rat. (auth)

29456 AVAILABILITY IN THE DOG OF RADIONUCLIDES IN NUCLEAR DEBRIS FROM THE PLOWSHARE EXCAVATION CABRIOLET. Chertok, R. J.; Lake, Suzanne (Univ. of California, Livermore). Health Phys.; 19: 405-9(1970).

The biological availability of radionuclides produced by a nuclear cratering event was studied in the dog. Single doses of nuclear debris obtained from a fallout tray located 1000 ft from Project Cabriolet were given orally to two spayed female beagles, which were then analyzed daily in a whole-body counter with a lithium-drifted germanium detector for the γ-emitting radionuclides. Urine and feces were collected daily and analyzed in the same counting system. The daily analyses were continued until very low levels were reached. For most of the radionuclides detected (^{99}Mo, ^{141}Ce, ^{132}Te, ^{131}I, ^{198}Au, ^{103}Ru, ^{122}Sb, ^{187}W and $^{140}Ba/^{140}La$), the greater part of the dose was eliminated in the feces in the first three days. Little or no ^{141}Ce, ^{198}Au and $^{140}Ba/^{140}La$ was absorbed across the gut wall, as indicated by their very low concentrations in the urine samples. Varying amounts (3 to 12%) of the ingested dose of ^{99}Mo, ^{132}Te, ^{103}Ru and ^{122}Sb were found in the urine. The only radionuclides that were absorbed to any great extent were ^{131}I and ^{187}W (approximately 41% excreted in the urine). (auth)(UK)

Radiation Effects

Refer also to abstracts 29103, 29132, 29553, 29650, 29662–29665, 29713, 29719, and 29720.

29457 CELL. Berdjis, C. C. pp 10-31 of Pathology of Irradiation. /Berdjis, Charles C. (ed.). Baltimore; Williams and Wilkins Co. (1971).

Cellular components and intracellular molecules are directly or indirectly destroyed or modified by radiation. Severe damage or death of cells occurs as a result of these intracellular changes. Cells vary in their ability to survive ionizing radiation. These variations are related to the age, dose, radiosensitivity of the cells, species differences, and time post irradiation. Radioinduced morphological changes produced in the cell include degeneration of the nucleus, disintegration of cytoplasm, increased permeability of cell membranes, increased vacuolization, and production of giant cells. (P.B.M.)

29458 METHOD OF INVESTIGATING THE RADIATION EFFECT ON CHROMATIN DEOXYRIBONUCLEOPROTEIN. Strazhevskaya, N. B.; Troyanovskaya, M. L. (Inst. of Biological Physics, Pushchino, USSR). Radiobiologiya; 10: 808-14(1970). (In Russian).

A sensitive method based on the change in the ability of the complex for phenolic deproteinization is proposed for studying the primary damage to the DNP of chromatin under the influence of ionizing radiation. The effect was evaluated according to the amount of DNA transferred to the phenol–water interface during the process of deproteinization and is expressed in percent of the initial DNA content in the sample. The possibility of removal of the radiation effect as a function of the pH, ionic strength, me-

XUN

chanical influence, and various deproteinizing agents was studied. The method proposed permits the detection of radiation defects in DNP, as well as a change in the state of the complex during the storage of DNP preparations in low ionic strength and of biological material (thymus gland) at low temperature. (tr-auth)

29459 EFFECTS OF DISINTEGRATION OF INCORPORATED ^{3}H AND ^{32}P ON THE PHYSICAL AND BIOLOGICAL PROPERTIES OF DNA. Rosenthal, Peter N.; Fox, Maurice S. (Massachusetts Inst. of Tech., Cambridge). J. Mol. Biol.; 54: 441-63(28 Dec 1970).

Pneumococcal DNA was labeled with high specific activities of ^{32}P- or tritium-labeled pyrimidines and stored at −30°C in a casein hydrolysate medium. The kinetics of inactivation of genetic markers on the labeled DNA was examined using a transformation assay. In addition, the kinetics of DNA strand scission was examined as a function of isotope disintegration. (auth) (UK)

29460 EFFECTS OF TOLUENE AND HIGH ENERGY RADIATION ON UREASE ACTIVITY IN SOIL. Thente, Bo (Lantbrukshoegskolan, Uppsala). Lantbrukshogsk. Ann.; 36: 401-18(1970).

Four cultivated Swedish soils were examined for their urease activity when treated with either toluene or γ radiation. Prolonged incubation showed that the rate of urea decomposition in treated soils was due to urease already existing in the soil. In native soils, a proliferation of microorganisms gave an exponential increase in urease activity after 4 to 10 hours lag phase. Comparative tests of urease activity on air-dried soils treated with toluene or γ radiation showed that the increases and decreases in activity were dependent on the soil. If different doses of radiation were given to the soil, the urease activity in one soil decreased with the dose and in the others increased up to a maximum value and then decreased. With increasing soil water content during radiation the urease activity was decreased. It was also found that the amino-acids glycine, alanine, and tyrosine, which increase their concentration in sterilized soils, may activate the soil urease. It is suggested that the apparently contradictory results obtained in investigations of soil urease activity in native and treated soil might partly be due to a variable sensitivity of microbial cell-walls to toluene and ionizing radiation. (auth) (Sweden)

29461 OSCILLATORY BEHAVIOR OF ENZYMIC REACTIONS: A NEW PHENOMENON. Comorosan, S.; Sandru, D.; Alexandrescu, E. (Fundeni Hospital, Bucharest). Enzymologia; 38: 317-28 (1970).

An unexpected phenomenon is presented wherein when a substrate S of a particular $E_{(S)}$-enzyme is irradiated with very low doses of x rays or uv in such a way as to exclude radio(photo)lysis or chemical transitions and then tested in the respective enzymic reaction, dose dependent oscillations in the activity of the $E_{(S)}$-enzyme are recorded. The oscillatory behavior of enzymic activity induced with low level irradiated substrates proved to be a general effect, obtained repeatedly on a great number of reactions. The effect induced in a chemical substance by low level x rays or uv irradiation (that is the respective quantum "perturbation") may be transmitted to a substrate through an intermolecular transfer of the radiation sensitized reaction type. As the energies involved in the substrate perturbation effects were very low, the possibility of finding this type of effect at the cellular level appears reasonable. In this respect, a relevant proof was obtained by the induction of the substrate perturbation with the energy derived from a biochemical energy generating system. Utilizing nonoverlapping oscillations induced in the activity of two different enzymes E_1 and E_2 sharing the same perturbed S*-substrate, a theoretical flip-flop mechanism was derived. A biochemical flip-flop unit was obtained on an experimental basis. (auth)

29462 RADIATION EFFECTS IN ISOLATED DNA AND THEIR FUNCTIONAL CONSEQUENCES. Abel, H. (Deutsche Akademie der Wissenschaften, Berlin). Stud. Biophys.; 18: 191-6(1969). (In German).

A series of original papers on radiation effects in isolated DNA are illustrated and explained. The relation between radiosensitivity and DNA are discussed as well as consequences of molecular damages in DNA. (auth)

29463 RADIATION EFFECTS IN ISOLATED DNA AND THEIR FUNCTIONAL CONSEQUENCES. II. METHODS OF PREPARATION OF DNA FROM BACILLUS SUBTILIS, CHARACTERIZATION, AND IRRADIATION. Koerner, I. J.; Hartwig, M.; Rakow, A. (Deutsche Adademie der Wissenschaften, Berlin). Stud. Biophys.; 18: 197-204(1969). (In German).

Deoxyribonucleic acid was isolated from Bacillus subtilis and its purity was estimated (RNA content (5): 0; at a protein content of 3% average molecular weight: maximum 38 Mill. D). Molecular weights were estimated by means of rotational viscometry at a maximum shearing stress of 0.012 dyn/cm^2. Irradiation (1 MV x rays, 10^3 and 10^4 rad/min) was monitored by an ionization chamber and calibrated by means of Fricke dosimetry. (auth)

29464 RADIATION EFFECTS IN ISOLATED DNA AND THEIR FUNCTIONAL CONSEQUENCES. III. VISCOMETRIC STUDIES OF X-IRRADIATED BACILLIS SUBTILIS DNA. Hartwig, M. (Deutsche Akademie der Wissenschaften, Berlin). Stud. Biophys.; 18: 205-9(1969). (In German).

Viscometric investigations were used to estimate the breaks in double and single strands of the DNA molecule from Bacillus subtilis after x irradiation in aqueous solution at a concentration of 150 μg/ml. The G-value for the single strand breaks was 0.15. (auth)

29465 RADIATION EFFECTS IN ISOLATED DNA AND THEIR FUNCTIONAL CONSEQUENCES. IV. CROSS-LINKS IN X-IRRADIATED BACILLIS SUBTILIS DNA. Just, S.; Schwarz, K. (Deutsche Akademie der Wissenschaften, Berlin). Stud. Biophys.; 18: 211-18(1969). (In German).

A uv spectroscopic method was used to analyze x radiation damage in Bacillus subtilis DNA. Results agreed with a simple model that considered the influence of intramolecular cross-links, induced by radiation, on the process of thermal denaturation. The probability of radioinduced cross-links was of the same order as the probability of single-strand breaks. In DNA 2 (3% protein) the maximal cross-linked part was 6 times greater than in DNA 1 (6.5% protein). (auth)

29466 RADIATION EFFECTS IN ISOLATED DNA AND THEIR FUNCTIONAL CONSEQUENCES. V. BASE DESTRUCTION AND DENATURATION OF X-IRRADIATED BACILLUS SUBTILIS DNA. Just, S.; Schwarz, K. (Deutsche Akademie der Wissenschaften, Berlin). Stud. Biophys.; 18: 219-26(1969). (In German).

The uv spectroscopic method was used to analyze base damage and denaturation of DNA from Bacillus subtilis in solution after irradiation. Damage was influenced by protein content of the DNA solutions. The G value of base degradation of DNA 1 (6.5% protein) was found to be 0.83 and of DNA 2 (3% protein) 1.28. The ratio of the G values of the degradation of AT base pairs to GC base pairs was 1.67, which was in good agreement with this value found previously by others. (auth)

29467 RADIATION EFFECTS IN ISOLATED DNA AND THEIR FUNCTIONAL CONSEQUENCES. VI. EFFECT OF X-IRRADIATION ON THE TEMPLATE ACTIVITY OF DNA FROM BACILLUS SUBTILIS. Pitra, Ch.; Malz, W. (Deutsche Akademie der Wissenschaften, Berlin). Stud. Biophys.; 18: 227-34(1969). (In German).

In vitro RNA synthesis with native and irradiated DNA was determined as a function of the concentration of DNA, RNA polymerase, and the reaction time. The rate of inhibition after irradiation was the same for all amounts of the DNA and enzyme present in the reaction mixtures. The rate of RNA formed with irradiated and unirradiated DNA as template depended on the reaction time. (auth)

29468 RADIATION EFFECTS IN ISOLATED DNA AND THEIR FUNCTIONAL CONSEQUENCES. VII. INFLUENCE OF X-IRRADIATION ON THE TRANSFORMATION OF THE MARKERS TRY_2 AND HIS_2 OF BACILLUS SUBTILIS. Grunow, R.; Eckart, W. (Deutsche Akademie der Wissenschaften, Berlin). Stud. Biophys.; 18: 235-41(1969). (In German).

The decrease in transformations for the single marker try_2 and his_2 of Bacillus subtilis strain SB25 were investigated after application of different x ray doses. The dose-effect curves showed two parts with different decline. It is suggested that the distribution of the molecular weights of the transforming DNA and/or varied physiological stages of donor cells caused the different transforming activity of tested DNA preparations. (auth)

29469 RADIATION EFFECTS IN ISOLATED DNA AND THEIR FUNCTIONAL CONSEQUENCES. VIII. MODEL CONCEPTION ABOUT INFLUENCE OF RADIATION INDUCED ALTERATIONS IN DNA ON TRANSFORMING ACTIVITY. Grunow, R.; Guenther, K.; Eckart, W.; Schwarz, K. (Deutsche Akademie der Wissenschaften, Berlin). Stud. Biophys.; 18: 243-51(1969). (In German).

The prevention of phenotypic formation of transformants at different stages in the transforming process by radioinduced chemical and structural alterations in extracellular DNA are discussed in relation to the changes that are responsible and the possible mechanisms, such as adsorption and penetration of tf-DNA of and into the recipient cells, pairing of tf-DNA with the recipient chromosome, integration into it, or phenotypic expression of transformed genetical characters. Proceeding from the distribution of molecular weight of tf-DNA fragments used for transformation, the model developed from these concepts considered only the fragments carry-

XUM

ing the markers of interest and the DNA alterations induced by x irradiation such as single and double strand breaks, etc., that proved to be inactivating at the stage of phenotypic expression. (auth)

29470 RADIATION EFFECTS IN ISOLATED DNA AND THEIR FUNCTIONAL CONSEQUENCES. IX. THEORY OF MOLECULAR WEIGHT DISTRIBUTION OF IRRADIATED DNA. Guenther, K. (Deutsche Akademie der Wissenschaften, Berlin). Stud. Biophys.; 18: 253-60(1969). (In German).

For the evaluation of viscosity or sedimentation measurements of irradiated DNA solutions (determination of break numbers), the change of the molecular weight distribution with average break number per molecular weight unit should be known. A calculation yielding the distribution in terms of the initial distribution by an integral transformation was made. The theory was investigated further for a special class of initial distributions for which the viscosity average was also calculated. Methods for the evaluation of experiments are discussed. (auth)

29471 CHANGE OF THE MACROSTRUCTURE OF SPIN-LABELED BOVINE SERUM ALBUMIN UNDER γ IRRADIATION. Yuferov, V. P.; Grigoryan, G. L.; Rozantsev, E. G.; Kalmanson, A. E. (Inst. of Virology, Moscow). Biofizika; 15: 404-7(May-Jun 1970). (In Russian).

Conformation changes in bovine serum albumin under γ irradiation were studied from the relation between isotropic and non-isotropic signals of maleinimide derivatives of 2,2,6,6-tetramethyl-4-aminopipyridine-1-oxyl radical, covalently bonded with protein. After solvent drying of protein irradiated with doses of 10 and 20 MRad only an insignificant increase in the mobility of accepted radical was observed. At a dose of 30 MRad the ESR spectrum of the radical was of isotropic character which pointed to deeper disturbances in protein macrostructure. The increase in radical mobility in irradiated proteins took place at smaller concentrations of urea and dioxane as compared with unirradiated protein. It revealed the presence of local disturbances in protein structures irradiated with the doses of 10 and 20 MRad. (auth)

Immunology

29472 EXPERIMENTAL MODELS FOR EVALUATION OF HOST DEFENSES IN CANCER. Stern, K.; Goldfeder, A. (Univ. of Illinois, Chicago. New York Univ., N. Y.). Israel J. Med. Sci.; 7: 42-51(Jan 1971).

Mice (X/Gf), resistant to induction of tumors by whole-body irradiation, were immunized with sheep red cells four, seven, or 12 days after irradiation, in parallel with mice of the susceptible strains IBA and C57BL/S. Antibody levels were lower in irradiated than in nonirradiated mice of all strains. Changes in immune responses after irradiation did not discriminate between X/Gf mice and mice of the other two strains. On the other hand, splenic phagocytosis of radiolabeled sheep red cells was not affected by the presence of transplanted tumors in X/Gf mice whereas uptake of the radiolabel in the spleens of tumor-bearing C3H/S mice was significantly and consistently depressed. Immunocompetence and specific functions of the reticuloendothelial system may play decisive roles in the defense of the host against development and progression of malignant tumors. (auth)

29473 METABOLISM OF DIFFERENT IMMUNOGLOBULIN CLASSES IN IRRADIATED MICE. V. CONTRIBUTION OF THE GUT TO SERUM IgA LEVELS IN NORMAL AND IRRADIATED MICE. Bazin, H.; Maldague, P.; Schonne, E.; Crabbe, P. A.; Bauldon, H.; Heremans, J. F. (Univ. St. Pierre, Louvain, Belgium). Immunology; 20: 571-96(Apr 1971).

X-irradiation (single dose of 700 R) caused some reduction in the rate of biosynthesis of IgA, only partly accounting for the observed disturbance in the metabolism of IgA. Direct measurements were made on the rate of biosynthesis in vitro of IgA by the isolated small bowel wall of irradiated and normal C_3H mice, and on immunohistological studies and plasma cell counts made on the gut, spleen and lymph nodes of these animals. Irradiated mice continued to excrete approximately normal amounts of IgA into their intestinal contents. The conclusion is that irradiation of the gut causes a rechannelling in the output of IgA synthesized by the plasma cells of the lamina propria, the major part being diverted to the intestinal lumen instead of being fed into the circulating pool of serum IgA. (auth) (UK)

29474 SELECTIVE AND SPECIFIC INHIBITION OF 24 HOUR SKIN REACTIONS IN THE GUINEA-PIG. III. DEPRESSION OF CYTOPHILIC AND HAEMOLYTIC ANTIBODIES BY PRETREATMENT WITH ANTIGEN AND THE EFFECT OF IRRADIATION. Davey, M. Jean; Asherson, G. L.; Stone, S. H. (London Hospital Medical Coll. National Institutes of Health, Bethesda, Md.). Immunology; 20: 513-22(Apr 1971).

Guinea-pigs given 1 mg of alum precipitated bovine γ-globulin prior to immunization with 50 μg bovine γ-globulin (BGG) in Freund's complete adjuvant showed long lasting depressed haemolytic and cytophilic antibody and delayed hypersensitivity. Antibody measured by passive cutaneous anaphylaxis and haemagglutination was either unaffected or raised. Pretreatment with sheep red cells reduced the cytophilic antibody response to sheep red cells in Freund's complete adjuvant. The effect of irradiation followed by alum-precipitated BGG on the immune responses to BGG in Freund's complete adjuvant was studied. 300 R depressed haemolytic and haemagglutinating antibody but had no effect on cytophilic antibody or delayed hypersensitivity. There was no synergy between irradiation and pretreatment with BGG; the depression of immune responses caused by irradiation followed by alum precipitated BGG was no greater than the depression caused by the more effective agent when given alone. (auth) (UK)

29475 CONTRASTING EFFECTS OF CYCLOPHOSPHAMIDE AND RADIATION ON THE IMMUNE RESPONSES OF THE MOUSE. Aisenberg, Alan C.; Murray, Caroline (Harvard Univ., Boston, Massachusetts General Hospital, Boston). J. Exp. Med.; 133: 877-84(1 Apr 1971).

The immunosuppressant cyclophosphamide easily induces specific immunological tolerance in CBA mice, but is unable to produce an immunological defect in adult thymectomized animals. In contrast, lethal (and sublethal) irradiation does not induce tolerance but readily brings out the deficit of thymectomy. Furthermore, bone marrow cells that protect lethally irradiated animals do not prevent drug deaths. This sharp dichotomy indicates that the drug and radiation influence the lymphoid system by different mechanisms. It seems likely that cyclophosphamide action is markedly dependent on rapid cell proliferation, while radiation is not. From this it follows that the cell that must be depleted to expose the immune defect of the thymectomized animal is a nonproliferating lymphoid element with the slow mitotic rate of the marrow stem cell. (auth)

29476 SEPARATION BY POLYACRYLAMIDE GEL ELECTROPHORESIS OF RNA FROM THE SPLEENS OF IMMUNIZED MICE. Majer, Jaroslav; Cohen, Edward P. (Univ. of Chicago). Proc. Soc. Exp. Biol. Med.; 136: 942-5(Mar 1971).

RNA from the spleens of immunized mice was separated by electrophoresis in polyacrylamide gels. Estimates of the molecular weight of various species of RNA were made by this method. Two peaks of special interest were noted. They corresponded to RNA with molecular weights of size approximating the theoretical requirements for messengers for antibody H chains and L chains. Their rate of synthesis, as measured by the incorporation of ^{3}H-uridine, increased after immunization. X irradiation of the mice, before they were injected with antigen, inhibited the appearance of the relevant peaks. They were considered to contain messenger RNA for antibody although undoubtedly contained nonantibody-specifying RNA of similar molecular weight. (auth)

Ecology

Refer also to abstracts 29441, 29449, 31527, and 31645.

29477 FALLOUT ^{54}Mn AND ^{95}Zr IN WATER AND FISHES OF FOUR LAKES IN NORTHERN ITALY. de Bortoli, M. C.; Gaglione, P.; Ravera, O. (EURATOM, Ispra, Italy). Minerva Fisiconucl.; 13: 72-7(Jan-Mar 1969). (CONF-680535-8).

From fourteenth national conference of the Italian Association for Health Physics and Protection from Radiation; Formia, Italy (29 May 1968).

The content of ^{54}Mn and ^{95}Zr (^{95}Zr–^{95}Nb) from fallout was studied in three species of fish (Perca fluviatilis, Scardinius erythrophtalmus, and Lepomis gibbosus) living in four lakes (Monate, Maggiore, Comabbia, and Varese), all of which are in the Ispra area of Northern Italy. The ^{95}Zr–^{95}Nb concentration factor observed for the three species of fishes ranged from 18 to 80. The comparison between the ^{54}Mn and ^{95}Zr–^{95}Nb concentration in the fishes collected from the four lakes showed a very different behavior for the two radionuclides. For example, the highest concentration of ^{95}Zr–^{95}Nb and the lowest of ^{54}Mn was found in the fishes of Lake Varese. In addition, the ^{54}Mn concentration was about the same for the three fish species, whereas the ^{95}Zr–^{95}Nb concentration showed a very large difference among the species. For example, the concentration in Perca was about 25% that of Scardinius. The different behavior of the two nuclides may be the result of many factors, such as the different geochemistry and physico-chemical form and the different role played in the fish metabolism and in the food chain. (E.R.B.)

29478 PRELIMINARY DATA CONCERNING THE USE OF ARTIFICIAL SUBSTRATA FOR THE ECOLOGICAL STUDY OF PERIPHYTON AND FOR THE IDENTIFICATION OF ENVIRONMENTAL RADIOACTIVITY IN A RUNNING-WATER ECOSYSTEM. Zullini, A. (Univ., Milan); Tibaldi, E.; Smedile, E.; Radici, B. Minerva Fisiconucl.; 14: 124-31(Jul-Sep 1970). (In Italian). (CONF-690929-12).

From fifteenth national congress of the Italian Association for Health Physics and Protection Against Radiation; Cagliari, Italy (Sep-Oct 1969).

The plant and animal composition of periphyton in a section of the Po River was studied using various artificial substrates for growing the periphytic forms. The substrate panels (Plexiglas, eternit, glass, slate, PVC, marble, and masonite) were immersed in the river and the subsequent growth of periphyton was analyzed for element concentration, pigment production, and net production rate and the component forms identified by species. The results are discussed within the framework of a broader ecological investigation dealing with food chains in which periphyton plays an important role and the possibility of using the periphytic forms as bio-indicators of environmental radioactivity. The data obtained from the artificial substrate studies confirm this possibility at least in relation to the algal and nematological components of the periphyton. (E.R.B.)

29479 ECOLOGICAL SITE SURVEY AT THE NUCLEAR RESEARCH CENTER OF TRISAIA. Antonelli, A. (CNEN, Rome); Cigna Rossi, L.; Laneri, U.; (and others). Minerva Fisiconucl.; 14: 109-19(Jul-Sep 1970). (In Italian). (CONF-690929-10).

From fifteenth national congress of the Italian Association for Health Physics and Protection Against Radiation; Cagliari, Italy (Sep-Oct 1969).

The results of an ecological survey performed at the site of the Trisaia Reprocessing Plant (along the Sinni river, near the Jonio Sea) before the beginning of hot operations are reported. The main characteristics of the abiotic environment as well as the biological features of the ecosystems involved were examined. On the basis of the data collected and of a socio-ecological survey, two different ways for the discharge of low-activity liquid effluents from the plant are proposed. (auth)

29480 ^{90}Sr IN NORTHERN SWEDEN: RELATIONSHIPS AND ANNUAL VARIATIONS FROM 1961 TO 1969 IN LICHEN, REINDEER, AND MAN. Persson, Bertil R. (Univ. of Lund, Sweden). Health Phys.; 20: 393-402(Apr 1971).

The transport of fallout-^{90}Sr was investigated in the food-chain: lichen-reindeer-man during 1961-1969. The maximum levels which occurred in lichen during 1963-1965 were about 13 nCi/kg dry wt. The ^{90}Sr-level in the lichen-carpet decreased to about 5 nCi/kg dry wt. in 1967-1969. The effective half-time of ^{90}Sr in the lichen-carpet was estimated to be 2.5 ± 0.8 a. The vertical distribution of ^{90}Sr in the lichen-carpet was studied during 1966-1969 and indicates an increased deposition of ^{90}Sr-fallout during 1968-1969. The ^{90}Sr/Ca-ratio was also studied in reindeer-bone and muscle tissues. This ratio increased up to 1965 to about 700 pCi/g in reindeer-meat and to 1000 pCi/g in bone, and then there was a decrease to about 400 pCi/g in both meat and bone in 1969. The seasonal variation of the ^{90}Sr/Ca-ratio in reindeer-meat and bone since 1965 was evaluated from the ^{90}Sr/Ca-ratio in lichen by using a three-compartment model for the Sr-retention in reindeer. The ^{90}Sr/Ca-ratio in the skeleton of adult Swedish Lapps was calculated from the ^{90}Sr/Ca-ratio estimated for diet. The absorbed dose delivered by ^{90}Sr + ^{90}Y during the period 1950-1970 was estimated to be 30 mrad to the endosteum (cells lining bone-surfaces) and 20 mrad to the active bone-marrow. Corresponding absorbed dose values for the whole period 1950-2000 were estimated to be 80 ± 15 mrad to the whole endosteum and 50 ± 10 mrad to the bone-marrow. (auth) (UK)

Genetics and Cytogenetics

Refer also to abstracts 29419, 29468, 29552, 29559, 29718, 29726, and 29751-29753.

29481 (IAEA-R-290-F) THE EVOLUTION OF NEW VARIETIES OF RICE WITH RESPECT TO INCREASED YIELD PER ACRE, RESISTANCE TO DISEASES AND BETTER QUALITY THROUGH THE USE OF RESEARCH ON THE USE OF INDUCED MUTATIONS FOR RICE IMPROVEMENT. Miah, A. J. (International Atomic Energy Agency, Vienna (Austria)). 1970. 9p. NTIS (U. S. Sales Only).

Studies were undertaken to induce useful mutations in rice by means of irradiation and chemical mutagens. Jajai-77 rice proved more radiation resistant than Dokri Basmati. Seed fertility decreased following neutron and gamma irradiation. In the M(2) generation, chlorophyll mutations were studied. In Dokri Basmati they were highest on 1800 R neutron irradiation, with a drop at 1300 R below the value at 1000 R; on gamma irradiation, mutation frequency increased up to 30,000 R and then decreased nonproportionately, at higher doses. In Jajai-77, mutants/1000 M(2) seedlings increased with neutron dose except at 1800 R; on gamma irradiation, mutants increased up to 30,000 R and decreased subsequently. The highest relative frequency in the spectrum of chlorophyll mutations induced by neutron or gamma treatments was found in albina followed by viridis types. The chlorophyll mutation spectrum following treatment with chemical mutagens varied from the spectrum obtained with radiation treatment. Radiation treatments generally produced a higher proportion of albina mutations compared to viridis or xantha types. In general, both chlorophyll and viable mutations increased at lower doses and then decreased at higher doses. Data on chlorophyll mutations were obtained for 370 Basmati (fine grain) and IR-8 (coarse grain), using gamma rays (25 and 35 kR) and chemical mutagens, EMS (ethyl methane sulfonate) and DES (diethyl sulfonate). (INIS)

29482 (LF-43, pp 240-5) PRODUCTION OF CHROMOSOME ABERRATIONS BY ^{241}Am IN THE CHINESE HAMSTER LIVER. Brooks, A. L.; McKay, L. R.; McClellan, R. O. (Lovelace Foundation for Medical Education and Research, Albuquerque, N. Mex.).

In Fission Product Inhalation Program.

Chinese hamsters were injected with activity levels of ^{241}Am decreasing in steps of five from 5×10^{-3} to 8×10^{-6} μCi/g body weight. The hamsters were partially hepatectomized at 4, 13, 40, and 120 days post-injection and were sacrificed 54 hours post-partial hepatectomy. Chromosome damage in the liver cells was assessed by scoring colchicined metaphase cells. The frequency of chromosome aberrations increased with time and the level of activity injected. With the exception of the 5×10^{-3} μCi/g level, there was a linear increase in aberrations with activity injected. The 5×10^{-3} μCi/g level yielded fewer aberrations than expected on the basis of cumulative dose. The abnormalities increased as a linear function of absorbed dose with a coefficient of aberration production of 4.7×10^{-3} aberrations/cell/rad. A radiation dose of 13 rads produced a level of aberrations significantly higher than that found in the controls. (auth)

29483 (LF-43, pp 246-53) RELATIVE BIOLOGICAL EFFECTIVENESS OF ^{241}Am, ^{144}Ce, AND ^{60}Co ON THE PRODUCTION OF METAPHASE CHROMOSOME ABERRATIONS IN THE CHINESE HAMSTER LIVER. Brooks, A. L.; McClellan, R. O.; McKay, L. R. (Lovelace Foundation for Medical Education and Research, Albuquerque, N. Mex.).

In Fission Product Inhalation Program.

Chromosome damage in Chinese hamster liver cells following in vivo alpha (^{241}Am), beta (^{144}Ce), or gamma (^{60}Co) irradiation was compared. The efficiency per rad for producing chromosome aberrations following injection with either ^{144}Ce or ^{241}Am remained relatively constant over the range of dose rates used. Total aberrations increased as a linear function of dose for both internally deposited isotopes with coefficients of 3.3×10^{-4} and 4.7×10^{-3} aberrations/cell/rad for ^{144}Ce and ^{241}Am, respectively. When ^{60}Co acute whole-body gamma exposure data were fit to a linear equation, the coefficient of aberration production was 7.4×10^{-4} aberration/cell/rad. On a rad basis, ^{241}Am was about 14 times as effective as ^{144}Ce in producing chromosome aberrations and about 6 times as effective as single acute whole body ^{60}Co exposure. This agrees with the factor of 10 typically used to relate the effectiveness of alpha and beta radiation for producing biological damage. The exchange type aberrations data were also fit to linear equations with coefficients of 1.8×10^{-4} and 3.4×10^{-3} for ^{144}Ce and ^{241}Am, respectively. The alpha exposure was thus 19 times more effective than beta exposure in producing exchange aberrations. The dose required to produce a significant increase in the frequency of chromosome aberrations as compared to controls was 13 rads for ^{241}Am and 130 rads for ^{144}Ce. (auth)

29484 DEPENDENCE OF CYTOGENETIC DAMAGE ON THE GAMMA RADIATION DOSE RATE. Pyatenko, V. (Inst. of Medical Radiology, Obninsk, USSR). Radiobiologiya; 10: 849-54(1970). (In Russian).

An investigation of the dependence of the frequency of damaged anaphases in pea seedlings on the duration of γ radiation indicated a substantial increase in the effect at a dose rate of 3600 Rad/min, in comparison with 12, 70, and 210 Rad/min. The root tips of the seedlings were fixed at the end of the first cycle of cell division after irradiation. The dose versus effect and time versus effect curves also revealed an increase in the damage with increasing radiation intensity. It is hypothesized that the effect of the dose rate is due to a decrease in the probability of post-radiation re-

XUM

covery of the cells from potential damages to the chromosomes as the γ-ray intensity is increased. (tr-auth)

29485 INFLUENCE OF CHEMICAL SUBSTANCES ON RADIATION DAMAGES TO CHROMOSOMES INDUCED IN DORMANT PEA SEEDS BY GAMMA RAYS AT VARIOUS DOSE RATES. Tsarapkin, L. S.; Tsarapkina, K. A. (Inst. of Medical Radiology, Obninsk, USSR). Radiobiologiya; 10: 844-8(1970). (In Russian).

The influence of soaking in solutions of cysteine, ATP, and EDTA of dormant pea seeds (water content 14 to 18%), irradiated with ^{60}Co at a dose of 15 kRad at rates of 40 and 5000 Rad/min, on the number of cells with chromosome aberrations, was investigated. It was found that cysteine and ATP lowered the degree of cytogenetic damage at 40 Rad/min, while EDTA increased it. At 5000 Rad/min, γ rays possessed lower cytogenetic effectiveness; not one of the chemical influences used affected the number of damaged cells. (tr-auth)

29486 DEPENDENCE OF THE PROTECTIVE EFFECT OF ANOXIA ON THE IRRADIATION DOSE IN THE CASE OF APPEARANCE OF CHROMOSOME ABERRATIONS. Yakovenko, K. N.; Luchnik, N. V. (Inst. of Medical Radiology, Obninsk, USSR). Radiobiologiya; 10: 855-63(1970). (In Russian).

The yield of chromosome aberrations in pea seedlings irradiated with various doses of γ rays in atmospheres of air and argon was studied. Anoxia lowered the yield of aberrations at all the doses investigated. An analysis of the results indicated that the basic mechanism of the oxygen effect consisted of a change in the degree of postradiation recovery. A new method for analysis of the S-shaped dose versus effect curves is proposed. (tr-auth)

29487 MUTAGENIC EFFECT OF FAST NEUTRONS AND X RAYS ON MOUSE SPERMATOGONIA. Pomerantseva, M. D.; Ramaiya, L. K.; Domshlak, M. G. (Inst. of General Genetics, Moscow). Radiobiologiya; 10: 864-73(1970). (In Russian).

An analysis was made of the frequency of appearance of reciprocal translocations and dominant lethal mutations induced by x rays and fast neutrons in mouse spermatogonia. The spermatogonia are genetically less sensitive than postmeiotic cells. The nature of the dose dependence of the yield of mutations in the spermatogonia and in the germ cells at later stages differed. In the dose range in which the yield of mutations in the sperms and spermatids increased linearly with increasing dose, the mutation frequency remained at the same level or decreased in the spermatogonia when the dose was raised above a definite limit. The RBE of fast neutrons was the same at all stages of spermatogenesis, a value of about 4.5. (tr-auth)

29488 EARLY-FLOWERING MUTANTS OF MEDICAGO POLYMORPHA VAR. POLYMORPHA. Brock, R. D. (CSIRO, Canberra, Australia); Andrew, W. D.; Kirchner, R.; Crawford, E. J. Aust. J. Agr. Res.; 22: 215-22(Mar 1971).

Treatment of dry seeds of Medicago polymorpha L. var. polymorpha with 20 kRad gamma rays resulted in a large increase in variation for flowering time. Selection among spaced plants in the M_2 and M_3 generations, primarily for early flowering and secondarily for plant vigor and fertility, resulted in the isolation of mutant lines which flowered from 2 to 3 weeks earlier than the unirradiated controls and which were comparable in vigor with the unirradiated controls. This method of generating variability for plant improvement programs proved to be simple, relatively quick, and economical (c. 1000 plants × 4 generations). It is recommended for more extensive use with self-fertilizing annual species where the primary selection criteria are clear cut and simply measured. (auth)

29489 INFLUENCE OF THE DOSE RATE OF X IRRADIATION ON THE APPEARANCE OF CHROMOSOME ABERRATIONS IN PEA SEEDLINGS. Pyatenko, V. S.; Palyga, G. F.; Tsarapkin, L. S. (Inst. of Medical Radiology, Obninsk, USSR). Radiobiologiya; 10: 780-4(1970). (In Russian).

The effects of dose rate on pea seedlings were studied according to the shape of the dose versus effect and time versus effect curves at various rates of x irradiation, as well as on the basis of an investigation of the dependence of the damage on the duration of exposure. An analysis of the results obtained indicated that the frequency of radiation damages to the chromosomes, determined in these experiments at the anaphase stage, increased with increasing dose rate from 100 to 5000 rad/min. When the dose rate was further increased to 50,000 rad/min, the cytogenetic damage remained at the previous level. (tr-auth)

29490 INITIATION OF CELL DIVISIONS IN ESCHERICHIA COLI K-12 DURING IRRADIATION BY LOW DOSES OF NEUTRONS WITH AN AVERAGE ENERGY OF THE SPECTRUM ABOUT 200 keV. Troitskii, N. A.; Bylinskii, A. F.; Filippovich, A. S. (Inst. of Genetics and Cytology, Minsk). Radiobiologiya; 10: 785-7 (1970). (In Russian).

Prolonged irradiation of nonlysogenic bacteria Escherichia coli suspended in buffer (medium M-9 without glucose), at 20°C with neutrons at doses of the order of hundreds of rad, at which one cell corresponds to no more than one hit, led to an increase in the number of cells capable of forming colonies. In this case the optical density of the suspension did not differ from the control. It is proposed that this effect is due to cleavage of multinuclear cells into smaller ones. The irradiated cells, in contrast to nonirradiated cells, began to reproduce after transfer to full valued medium, bypassing the lag phase. On the basis of an estimate of the effective volume of the process, it is suggested that the initiation of cell divisions is not associated with a direct hit of a neutron in the DNA of the cell. (tr-auth)

29491 INFLUENCE OF THE GAMMA RADIATION DOSE RATE ON THE CYTOGENETIC EFFECT IN THE IRRADIATION OF LETTUCE (LACTUCA SATIVA) SEEDS AND SEEDLINGS. Pap'yan, N. M.; Nevzgodina, L. V. Radiobiologiya; 10: 770-2 (1970). (In Russian).

Air-dried lettuce seeds and seedlings were irradiated with γ rays at various dose rates. It was found that the radiobiological effects depend on the dose and range of dose rates used. (tr-auth)

29492 MALE STERILITY IN PISUM. Klein, H. D. (Univ., Bonn). Nucleus (Chicago); 12: 167-72(Dec 1969).

Four male sterile recessive mutants of Pisum sativum, originating from x ray experiments, were selected and cytogenetically analyzed. All mutants showed, on microscopic examination, rather normal tapetal cells. In all mutants, PMCs were characterized by failure of wall formation at the end of meiosis and by degeneration of the microspores. In mutants 67, 98 A, and 395 microspores remained in tetrad formation and the entire PMC was surrounded by an exine. In 503 separation of the microspores from the tetrads occurred, but no typical pollen wall was formed. Invariably in all mutant types exine lacked pores and a specific surface patterning. Besides failure in wall formation, mutant 98A showed a supernumerary mitotic division following interphase II, but differing from normal mitotic behavior because chromosomes remained undivided. The possible causes of breakdown of microsporogenesis and of pollen abortion are discussed in connection with the significance of callose in the course of meiotic divisions and pollen wall formation. (auth)

29493 CYTOGENETIC EFFECTS OF X RAYS AND CHEMICALS ON TOMATO STUDIES IN M_2 GENERATION. Bose, S.; Saha, A. (Univ. of Calcutta). Nucleus (Chicago); 13: 29-40(Jun 1970).

In the present investigation, studies were made on the M(2) generation in tomato (variety, Best of All), the M(1) generation of which originated from single treatment with distilled water, colchicine (0.2%), and diethyl sulphate (saturated solution), and x ray pre- and post-irradiation (10, 20, 30, and 40 kR) treatment with these chemicals for the same length of time. Chlorophyll mutants and those affecting leaf characters were found. The others were mostly connected with nonfruiting and sterility. The importance of the isolation of stable and true breeding types, especially male sterile ones from later generations, was pointed out. Occurrence of irregularities in guard cell development in plants originating from some of the treatments was recorded. Probable reasons for the non-occurrence of polyploid types have been discussed. While the finding of bridges with fragments has been attributed to inversion, those without fragments have been reasoned to be originating from failure of division of end genes brought about by nucleic acid upset. The importance of the isolation of mutants responsible for meiotic irregularities was stressed. (auth)

29494 INFLUENCE OF pH AND SUCROSE CONCENTRATION ON CYTOLOGICAL EFFECTS OF IRRADIATED AND CONTROL SUCROSE SOLUTIONS. Bradley, Muriel V.; Ross, Sarah T.; Wheelock, Linda H. (Univ. of California, Davis). Nucleus (Chicago); 13: 91-7(Jun 1970).

Primary roots of Vicia faba were treated for 4 hr in irradiated (200 kilorads) and unirradiated 2% or 8% sucrose solutions adjusted with KOH or HCl to series of low pH values immediately before treatment. The pH of each solution was taken again immediately after treatment. Means of the initial and final pH values were plotted against the corresponding percentages of abnormal anaphases scored in squash preparations. Statistical analysis showed that none of the differences in percentages of abnormal anaphases from treatments with irradiated and unirradiated solutions was significant at the 1% level of confidence, whether the sucrose concentration was 2% or 8%. In both irradiated and control 2% sucrose treatments the chromosome aberrations were caused by low pH of the solution in the range of pH 4.0 and below.

XUM

In the 8% sucrose experiments, the relatively high sucrose concentration induced chromosome aberrations in approximately 14% of the anaphases in all treatments with either irradiated or control solutions. No evidence of chromosome aberrations caused by radiomimetic substances in irradiated sucrose solutions was obtained. The difficulties posed by the roots increasing the pH of the solutions during treatments were discussed. (auth)

29495 X-RAY AND DIETHYL SULPHATE INDUCED MUTATION IN RICE (ORYZA SATIVA L.) STUDIES IN THE M_2 GENERATION. Bose, S.; Gupta, D. (Calcutta Univ.). Indian J. Sci. Ind., Sect. A; 4: No. 2, 82-8(1970).

An investigation was made on the M(2) generation of a Boro Paddy (C.B.I.), the M(1) generation of which originated from single treatment with distilled water and diethyl sulphate for 24 hours and pre-and post-irradiation (10 and 20 kR of x rays) treatment with these chemicals for the same length of time. Mutants were observed affecting many characteristics of the plants, such as chlorophyll content, plant height, tillering, and sterility. The importance of the selection of stable and true breeding types from these was emphasized. (auth)

29496 CYTOLOGICAL EFFECTS OF X RAYS, ^{32}P, AND ^{35}S IN M_1 POPULATIONS OF RICE. Basu, A. K.; Basu, Rabindra Krishna (Bose Inst., Calcutta). Nucleus (Chicago); 12: 136-44 (Dec 1969).

Meiotic studies were made in first generation plants grown directly from seeds of three varieties of rice after treatments with x rays ^{32}P, and ^{35}S. Chromosomal abnormalities during first division of meiosis included non-disjunction and early separation of bivalents, laggards, bridges, and fragments. In addition to these, nuclei with one extra chromosome and reciprocal translocation leading to the formation of a ring of four chromosomes were also observed in some of the treated plants. The meiotic abnormalities were common in almost all the treated populations and in general there was no dose-aberration relationship. The M_1 populations had reduced pollen and seed fertility. Seed fertility was affected more than pollen fertility. There was patternless variation in both these characters with increase in radiation dosage. (auth)

29497 CHROMOSOME ABERRATIONS IN SWINE LEUKOCYTES AFTER IN VIVO OR IN VITRO EXPOSURE TO 14 MeV NEUTRONS. McFee, A. F.; Banner, M. W.; Sherrill, Mary N. (Univ. of Tennessee, Oak Ridge. Atomic Energy Commission, Oak Ridge, Tenn.). Contract AT(40-1)-Gen-242. Radiat. Res.; 44: 512-22(Nov 1970).

Chromosome aberration rates were significantly higher among swine leukocytes irradiated with 14-MeV neutrons under in vitro conditions than for those taken just following exposure of the animal. The two methods of irradiation showed similar increases in aberrations with increasing dose levels, which permitted the derivation of formulas for predicting breakage rates at various doses as well as factors for anticipating in vivo breaks based on the in vitro exposure of a blood sample. (auth)

29498 CLINICAL ASPECTS OF INHERITED DISORDERS. Conference Held April 9–10, 1970, Birmingham, Alabama. S. Med. J.; 64: Suppl. No. 1, 1-110(Feb 1971). (CONF-700433).

Twelve article and two panel discussions are included. One article was abstracted separately in NSA. The 11 remaining papers contain information on proceedings. Other topics covered include diagnosis, classification, prevention, and treatment of genetic disorders, prenatal chromosome analysis, and psychological testing of patients with genetic disorders. The two panel discussions are on special problems of the abnormal child and prevention of genetic disease. (E.E.H.)

29499 RADIATION BIOPHYSICAL INVESTIGATIONS IN DROSOPHILA MELANOGASTER. II. INDUCTION OF SEX-LINKED MUTATIONS IN DROSOPHILA MELANOGASTER BY X-RAYS AND NEUTRONS. Ginter, E. K.; Tolkendorf, E.; Haberer, G. (Inst. of Medical Radiology, Obninsk, USSR. Zentralinstitut fuer Kernforschung, Rossendorf, Ger.). Stud. Biophys.; 17: 37-43(1969). (In German).

The effects of neutron and x irradiation on the frequencies of recessive, sex-linked, lethal, and visible mutations induced in spermatozoids of D. melanogaster were compared. It was found that the mutagenic effectiveness of fast neutrons relative to x rays was higher for both the lethal and visible mutations. The linearity of the dose response curves for neutrons and x rays is illustrated. (auth)

29500 TRISOMY ASSOCIATED WITH DIAGNOSTIC X-RAYS. Uchida, Irene A. (McMaster Univ., Hamilton, Ont.). S. Med. J.; 64: Suppl. No. 1, 81-4(Feb 1971).

From Conference on clinical aspects of inherited disorders Birmingham, Ala. (9 Apr 1970).

Information was gathered on the offspring of women who had received abdominal diagnostic x radiation during the years 1956 through 1959. Statistics on their children born both before and after irradiation were correlated to maternal-age matched controls. The observed frequencies of mongoloids were compared with the expected frequencies according to maternal age based on population figures for Manitoba during these years. The frequency of mongoloids in the post-irradiation group was much higher than expected while there was no difference in the controls. These data are compatible with the observations on Drosophila melanogaster in that an increase in nondisjunction apparently results from an increased radiosensitivity that is positively correlated with maternal age. (E.E.H.)

29501 CHROMOSOMAL EXAMINATIONS IN RADIOLOGISTS. Zsebok, Zoltan; Stark, Klara I.; Czeizel, Endre. Magy. Radiol.; 22: 331-43(Dec 1970). (In Hungarian).

Blood samples from 50 radiologists were examined for chromosome mutations due to ionizing radiation. Chromosomal examinations were carried out on 48 hr cultures of venous blood obtained from the bend of the elbow. Preparations suitable for evaluation of the structural chromosomal anomalies were obtained in 34 cases. The rate of the cells showing labile and stable structural chromosomal irregularities was determined in 50–50 cells in each case. The rate of the labile cells in individuals in the control group was 0.8%, signifying always acentric fragments. On the other hand, the rate in the radiologists' group was 6.4%, and this surplus was essentially due to the increase of the dicentric chromosomes. Such chromosomal damage was found in 70.5% of the examined radiologists. The dicentric chromosomes may be considered as the best indicator of the chronic radiation with small doses. The rate of irregularities of the stable chromosomes was not significantly increased in the radiologists. (85 references) (auth)

Health Physics and Safety

Refer also to abstracts 29415 and 29711.

Radioactive Contamination and Decontamination

Refer also to abstracts 28990, 29074, 29075, 29179, and 29480.

29502 (KY–629) ENVIRONMENTAL MONITORING SUMMARY FOR THE PADUCAH PLANT FOR 1970. Davis, K. A. (Paducah Gaseous Diffusion Plant, Ky.). 1 Apr 1971. Contract W-7405-eng-26. 11p. Dep. NTIS.

Results are summarized for outdoor radiation monitoring of air, water, and vegetation in the vicinity of the Paducah Plant for the year of 1970. (auth)

29503 (PROT.-SAN.–8/69) DATA ON ENVIRONMENTAL RADIOACTIVITY COLLECTED IN ITALY, JANUARY–JUNE 1968. (Comitato Nazionale per l'Energia Nucleare, Rome (Italy)). May 1969. 171p. Dep. NTIS (U. S. Sales Only).

Data are presented on the content of fallout radioactivity in environmental and food samples collected in Italy during the first half of 1968. The content of ^{137}Cs in samples of meat, vegetables, milk, surface waters, the content of ^{90}Sr in samples of vegetables, milk, and surface waters, and the gross β activity in samples of the atmosphere and rain water are reported. The results of radiation monitoring studies in the vicinity of nuclear research centers are included. (C.H.)

29504 (PROT.-SAN.–13/69) DATA ON ENVIRONMENTAL RADIOACTIVITY COLLECTED IN ITALY, JULY–DECEMBER 1968. (Comitato Nazionale per l'Energia Nucleare, Rome (Italy)). Dec 1969. 176p. Dep. NTIS (U. S. Sales Only).

Results are reported from fallout monitoring programs in Italy from July to December, 1968. Data are included on the gross β activity in samples of atmosphere, surface waters, and drinking water supplies, and the content of ^{137}Cs and ^{90}Sr in samples of cheese, milk, and vegetables, and the content of ^{90}Sr in drinking water. Results of radiation monitoring studies in the environs of nuclear power stations and nuclear research centers are included. (C.H.)

29505 (SWRHL–39-r) ^{131}I DAIRY COW UPTAKE STUDIES USING A SUBMICROMETER SYNTHETIC DRY AEROSOL (PROJECT SIP). Mason, Benjamin J.; Black, Stuart C.; Barth, Delbert S. (Public Health Service, Las Vegas, Nev. Southwestern Radiological Health Lab.). Mar 1971. 31p. Dep. NTIS.

XUM

The mechanisms associated with the overall transfer of ^{131}I from the environment to cow's milk were studied following the controlled release of a simulated fallout. A ^{131}I-labelled aerosol of submicrometer size was released over a pasture and a corral containing 18 dairy cows. Six of the cows had hay in mangers for their consumption. Another group of six was fed green chop from the contaminated pasture, while the remaining six cows received no other contaminated material. The pasture was contaminated to a level of 1.13 μCi/kg, and cows fed green chop from the pasture secreted a peak level of .07 μCi/liter in milk. The effective half-life of ^{131}I in milk during ingestion of contaminated forage was 5.2 ± 0.85 days which was nearly twice as long as the effective half-lives in previous experiments using aerosols of larger particle size. The effects of feeding practices on the passage of ^{131}I through the atmosphere-forage-cow-milk-man food chain were evaluated. (C.H.)

29506 (SWRHL-97-r) OFF-SITE SURVEILLANCE ACTIVITIES OF THE SOUTHWESTERN RADIOLOGICAL HEALTH LABORATORY FROM JANUARY THROUGH JUNE 1969. (Southwestern Radiological Health Lab., Las Vegas, Nev). Feb 1971. 41p. Dep. NTIS.

During the period January through June 1969, eleven announced nuclear detonations were conducted at the Atomic Energy Commission's Nevada Test Site. None of these events released radioactive material that was detected off-site. One power run of a nuclear reactor rocket engine at the Nuclear Rocket Development Station on June 11, 1969, released gaseous fission products that were detected on one air sampler at the Diablo Highway Maintenance Station on Highway 25. The concentration of ^{131}I, determined from the combined results of the particulate and charcoal filters from this location, was 0.7 pCi/m^3. Some radioactive material from Project Schooner of December 8, 1968, was resuspended from material deposited on and off-site. This material was occasionally found on air samples through March 1969. The maximum gross beta concentration resulting from this re-suspension was 55 pCi/m^3 at Clark Station on January 13, 1969. The principal gamma-emitter identified in this material was ^{181}W. No domestic water or milk samples collected during this period contained fresh fission products. Exposure to the off-site population during this period was well below the safety criteria established by the Atomic Energy Commission. (auth)

29507 MEASUREMENT OF ^{90}Sr AND ^{137}Cs IN POWDERED MILK SAMPLES DURING 1952 TO 1966. Bagliano, G. (CNEN, Rome); Lanzola, E. Minerva Fisiconucl.; 13: 307-12(Oct-Dec 1969). (In Italian). (CONF-680535-30).

From fourteenth national conference of the Italian Association for Health Physics and Protection from Radiation; Formia, Italy (29 May 1968).

Data relative to the ^{90}Sr and ^{137}Cs contamination of samples of powdered milk products in Italy during 1952 to 1966 are reported. A correlation was established with the analogous contamination of fresh milk samples, thus approximating the total milk contamination during 1952 to 1966. (tr-auth)

29508 PRACTICAL CONSIDERATIONS IN THE HOSPITAL TREATMENT OF TWO CASES OF RADIUM CONTAMINATION. Lin, S. (Ospedali Riuniti, Trieste, Italy). Minerva Fisiconucl.; 13: 20-6(Jan-Mar 1969). (In Italian). (CONF-680535-4).

From fourteenth national conference of the Italian Association for Health Physics and Protection from Radiation; Formia, Italy (29 May 1968).

Reference is made to an incident of acute contamination in a refinery following the rupture of a sealed radium source used in the automatic control of the level of catalyst in a catalytic cracking unit. The high radiotoxicity of the contaminant and the possibility of a more extensive contamination of personnel required the rapid establishment within the area of a radioisotope diagnosis and therapy unit, of a radiometric control station, and a decontamination center capable of operating under very unfavorable circumstances. The emergency measures adopted on this occasion, the reconstruction of the level of contamination, and the procedures used in decontamination are also related. (E.R.B.)

29509 STUDIES ON RADIOACTIVITY OF POLISH HONEYS. PART I. Miskiewicz, Wieslawa; Wozniak, Jan. Acta Pol. Pharm.; 27: 587-92(1970). (In Polish).

Total and oxalate beta activity of 17 specimens of honey of various sorts is reported. The measurements were made with Geiger-Müller counters. The relation of the beta activity of honey to its type, origin, region, and total content of mineral constituents was investigated. (auth)

29510 ATTEMPT FOR DEACTIVATION OF MEDICAL DEVICES WITH DETERGENT SOLUTIONS AND VIBRATOR. Zlatanov, St. Voenno Med. Delo; 24: No. 1, 39-44(1969). (In Russian).

The results of the use of Sinpro, a detergent preparation, with or without a sound frequency vibrator to decontaminate stainless steel, plexiglass, and rubber used for the preparation of medical devices are reported. The results demonstrated that the combined application of an aqueous solution of the detergent with a sound frequency vibrator produced good results for compounds of ^{32}P, ^{131}I, and ^{89}Sr. Optimum results were obtained when the combined treatment was used for at least 60 min. (Abstr. Bulg. Sci. Med. Lit.) (TSS)

Dosimetry and Monitoring

Refer also to abstracts 29205, 29219, 29222, 29241, 29383, 29391, 29427, 29448, 29596, 29603, 31174, and 31642.

29511 (AERE-M-1887) CALCULATED QUALITY FACTORS FOR PROTONS IN BODY AND EYE-LENS TISSUES. Dennis, J. A. (Atomic Energy Research Establishment, Harwell (England)). May 1967. 9p. Dep. NTIS (U. S. Sales Only).

Mean values for the Quality Factor and its product with the modifying factor for eye-lens tissue are calculated for application to protons in the energy range 1.0 keV to 30 MeV that are completely absorbed in tissue. Graphs are presented to show QF in body tissue and its product with the eye-lens modifying factor as a function of LET_∞; stopping power of water as a function of proton energy; instantaneous QF values in body tissue and their product with the eye-lens modifying factor as a function of proton energy; and mean QF and MxQF values in body and eye-lens tissues respectively as a function of proton energy. (H.L.W.)

29512 (BRH/DEP-71-4) RADIATION SURVEY OF TELEVISION REPAIR SHOPS IN THE BALTIMORE AREA. Wyatt, John L. Jr.; Moore, Thomas M. (Public Health Service, Rockville, Md. Radiological Health Lab.). Mar 1971. 39p. GPO $0.50.

A pilot study of the x radiation exposure to television service technicians during the course of their work was performed in 70 Baltimore-area television repair shops from March to October 1970. In the first 25 shops, personnel dosimeters were distributed to the service technicians, and radiation exposure rate measurements were made on 58 color television receivers representing 15 different brands. In the remaining shops, no radiation measurements were made on receivers, but dosimeters were distributed to the technicians to enlarge the statistical base for personnel exposure determinations. The survey data indicated that the radiation doses received by the technicians were relatively low. Hence, it was concluded that a national survey does not appear necessary. (auth)

29513 (CONF-710211-1) COMPUTER CALCULATION OF BONE DOSES FOLLOWING ACUTE EXPOSURE TO ^{90}Sr AEROSOLS. Voilleque, Paul G. (Idaho Nuclear Corp., Idaho Falls). 1970. 16p. Dep. NTIS.

From International meeting on bone-seeking radionuclide contaminations and radiation protection; Grenoble, France (1 Feb 1971).

The respiratory tract models of the Task Group on Lung Dynamics of Committee II of the International Commission on Radiological Protection (ICRP) were combined with a three-compartment metabolic model for strontium recommended for acute exposures in ICRP Publication 10 to obtain a dosimetric calculational scheme for acute inhalation exposures to ^{90}Sr. The strontium metabolic model was incorporated into an existing computer code used for acute inhalation β dose calculations. Details of the integration of the two models to determine the β dose absorbed by bones and some computational results are presented. (C.H.)

29514 (LF-43, pp 116-22) DOSE DISTRIBUTION IN THE BEAGLE DOG FROM RADIOGRAPHIC EXPOSURE. Barnes, J. E.; Osborn, L. A. (Lovelace Foundation for Medical Education and Research, Albuquerque, N. Mex.).

In Fission Product Inhalation Program.

The dose distribution in the Beagle dog from radiographic exposures was studied using thermoluminescent dosimetry. Three frozen cadavers were used and the results were compared with those from an Alderson RANDO dog phantom. Data on depth-dose curves, isodose patterns, midline exposure dose, and doses to selected tissues are presented. The maximum midline exposure dose measured for the cadaver was less than 70 mR for the complete radiographic survey. Agreement between the phantom and the cadavers was good except in the cervical spine area. (auth)

XUM

29515 (NP–18794) DOSE CALCULATION FROM THE URINE OF SUBJECTS CONTAMINATED BY IRRADIATED URANIUM. (Electricite de France, Paris). Apr 1968. 38p. (In French). Dep. NTIS (U. S. Sales Only).

Following an accident which occurred during the handling of an irradiated uranium fuel cartridge, four members of the French Electricity staff were contaminated. The urines were analyzed and the ^{137}Cs and ^{89}Sr activities determined. The quantities of Cs and Sr having passed into the blood stream were estimated. Since the contamination was due to the inhalation or ingestion of irradiated uranium powder, the radionuclides responsible were present in the same proportions as in the fuel. The quantities of radionuclides absorbed and the degree of solubility were determined and the radiation doses received by the different organs were expressed as a function of these two factors. (France)

29516 (UCRL–50990) METHODOLOGY FOR COMPUTING POTENTIAL RADIATION DOSE TO MAN FROM NUCLEAR EXCAVATION PROJECTS. Fleming, Edward H. (California Univ., Livermore. Lawrence Radiation Lab.). 11 Jan 1971. 13p. Dep. NTIS.

A step-by-step procedure is presented for computing the radiation dose to man from nuclear excavation projects. The procedure begins with the total amount of each radionuclide produced, considers airborne and deposition concentration vs distance downwind, and includes dose from inhalation, submersion, external gamma radiation, and ingested radioactivity via different food pathways. An estimate of error is provided for each calculational step. (auth)

29517 RAPID AND SIMPLE METHODS FOR THE MEASURING OF β AND γ RADIOACTIVITY IN BIOLOGICAL SAMPLES. Giubileo, M.; Camera, V. (CCR-EURATOM, Ispra, Italy). Minerva Fisiconucl.; 13: 27-31(Jan-Mar 1969). (In Italian). (CONF-680535-5).

From fourteenth national conference of the Italian Association for Health Physics and Protection from Radiation; Formia, Italy (29 May 1968).

The systematic health supervision of workers exposed to radioactive contamination in a nuclear research center is difficult due to the multiplicity of radionuclides in the samples. The medical service of the CCR-Ispra has recently introduced a system that can reveal the presence of β-γ radioactivity in all types of biological samples by means of only three measurements: liquid scintillation counting for β emitters with an energy inferior to 1 MeV, measurement of the Cherenkov effect for betas with an energy above 1 MeV, and γ spectrometry. The time saving is considerable with the preliminary treatment reduced to a minimum, and certain errors due to chemical separations are avoided. The sensitivity is such that contaminations within the maximal permissible limits can be revealed. At the same time the methods are applicable even to accidents involving exposure to radionuclides. The principal advantage is that only two instruments are necessary to satisfy the demands of routine and cases of emergency. After an outline of the criteria adopted for the radiotoxicological surveillance of the personnel, the procedures actually in use in the systematic checks and in case of accident are described. (auth)

29518 STANDARD DEFINITIONS OF TERMS RELATING TO DOSIMETRY. ASTM E 170-63. Philadelphia; American Society for Testing and Materials (1965). 3p. Available from American Society for Testing and Materials, Philadelphia.

Definitions are presented for terms related to radiation dosimetry. These definitions are the same as, or similar to, those recommended by the International Commission on Radiological Units and Measurements (ICRU) as presented in the National Bureau of Standards Handbook 62, but attempt to define some of the terms more exactly. (C.H.)

29519 AMERICAN STANDARD: PRACTICE FOR OCCUPATIONAL RADIATION EXPOSURE RECORDS SYSTEMS. ANSI N 2.2 1966. New York; American Standards Association, Inc. (1966). 10p. Available from American National Standards Inst., New York.

Standards are presented that provide guidance to employers for the generation and retention of records relating to the occupational radiation exposure of personnel. Such records should enable the employer to evaluate the effectiveness of radiation protection programs, demonstrate and facilitate compliance with contractural requirements and applicable government regulations concerning radiation protection, and enable reconstruction for legal or medical purposes of situations and conditions resulting in the radiation exposure and estimations of radiation dose received by personnel. (C.H.)

29520 NOMINAL STANDARD DOSE AND THE RET. Ellis, F. (Churchill Hospital, Oxford). Brit. J. Radiol.; 44: 101-8 (Feb 1971).

Virtual coincidence of isoeffect values for normal tissue (N.S.D.) and Hodgkin's disease (tumor S.D.) is presented, in support of the N.S.D. concept and the Ellis formulae. For most other tumors the tumor effect was incidental to normal tissue tolerance. (auth) (UK)

29521 RADIATION DOSE DISTRIBUTION IN LUNGS OF THOROTRAST PATIENTS. Grillmaier, R.; Muth, H. (Univ. Saarland, Homburg, Ger.). Health Phys.; 20: 409-19(Apr 1971).

The alpha ray doses in lungs from thoron and its decay products depend on the amount of injected Thorotrast and the age of the Thorotrast deposit. They also differ in the various regions of the lung; this is mainly because the different geometrical dimensions of the branches of the bronchial tree determine not only the total amount of radioactivity and the residence time within each branch but also the time available to the thoron decay products to attach themselves to aerosols. The length of the branch, moreover, determines the time available for excretion of the thoron decay products deposited on the mucus layer on lung epithelium. A Thorotrast patient with a deposit of 1 μCi ^{232}Th in the reticuloendothelial system receives, in the 10 yr following injection, 20 rad in the tissue of the terminal bronchii and about 260 rad in those of the trachea. Thirty years after injection these doses are about 80 rad and 1000 rad, respectively. (auth) (UK)

29522 RADIATION BIOPHYSICAL INVESTIGATIONS IN DROSOPHILA MELANOGASTER. I. DETERMINATION OF DOSE RATE COMPONENTS IN INTENSIVE n-γ RADIATION FIELDS FOR RADIOBIOLOGICAL INVESTIGATIONS. Haberer, G.; Regel, K. (Zentralinstitut fuer Kernforschung, Rossendorf, Ger.). Stud. Biophys.; 17: 29-35(1969). (In German).

The dose rate components of neutrons and γ rays produced by the nuclear reaction $^{9}Be(d,n)^{10}B$ at the Cyclotron ZfK Rossendorf were determined by means of two ionization chambers. The separate determination of these dose components was based on the different sensitivities of the chambers for neutrons and γ rays. The neutron dose rates measured with the ionization chambers and with an absolute calibrated dosimeter of the HURST-type, respectively were in good agreement (±20%). The irradiation conditions of Drosophila melanogaster in this radiation field are given. (auth)

29523 INFLUENCE OF ELECTRON SCATTERING CAUSED BY BOUNDARIES OF INHOMOGENEITIES. Manegold, K. (Klinik fuer Strahlentherapie und Nuklearmedizin, Frankfurt am Main). Strahlentherapie; 140: 647-50(Dec 1970). (In German).

During irradiation with high-energy electrons, the diffusion of the electrons influences the dose distribution in cases where there are edges of inhomogeneities in the irradiation field. So-called clubs of diffusion originate at these edges. The direction of such clubs as well as the quantity of dose alterations within sulfur and air inhomogeneities in water were examined. (auth)

29524 DOSIMETRY IN THE BONE MARROW CAVITY OF RAT FEMURS FOLLOWING INCORPORATION OF ^{90}Sr–^{90}Y. Steinbach, Karl Heinz; Weber, Elisabeth (Heiligenberg Institut, Ger.). Strahlentherapie; 140: 667-70(Dec 1970). (In German).

After a single application of 10 μCi ^{90}Sr intravenously in five week old rats, the absorbed dose rate in the femoral medullary canal decreases from (40.3 ± 1.5) Rad/day after two days to (4.2 ± 0.3) Rad/day after 256 days in female animals. During the corresponding period, the absorbed dose rate in the male animals decreased from (39.6 ± 1.7) Rad/day to (3.2 ± 0.3) Rad/day. The influence of the sex of the experimental animals became apparent, in male animals, by an absorbed dose rate which was, on the average, 20% lower. After an incorporation time of 256 days, the absorbed doses were (1800 ± 100) Rad in female and (1400 ± 80) Rad in male animals. (auth)

29525 RADIATION SAFETY OF THE POPULATION IN THE DISTRICT OF AN ATOMIC POWER PLANT. Kozlov, V. M.; Zykova, A. S.; Zhakov, Yu. A.; Yambrovskii, Ya. M. Gig. Sanit.; No. 4, 54-6(Apr 1970). (In Russian).

A study was made on the radiation hazards to the population in the area of the Novovoronezhskaya and Beloyarskaya atomic power plants. It was found that the area surrounding these plants presented no radiation hazards to the population and the land was safe for agricultural purposes. (tr-auth)

Radiation Protection

Refer also to abstract 29658.

XUM

29526 (NP-18790) ANNUAL REPORT TO THE DIRECTOR-GENERAL OF HEALTH FOR THE YEAR ENDED 30 JUNE 1970. (Commonwealth X-Ray and Radium Lab., Melbourne (Australia)). 39p. Dep. NTIS (U. S. Sales Only).

Radiation protection activities of the X-ray and Radium Laboratory of Australia during 1969 are summarized. These included the calibration of ionization chambers used for the dosimetry of x radiation, surveys on the safety of diagnostic x-ray equipment, the calibration of radium and radon sources for therapy, the control of the use of radioisotopes for diagnostic studies, and monitoring of the radiation dose of personnel using radioisotopes and radiation sources, including the maintenance of a film badge service and whole-body γ counter. (C.H.)

29527 (NP-18791) HEALTH PHYSICS PRACTICES AND EXPERIENCES OF ISOTOPE PRODUCERS AND DISTRIBUTORS. (Atomic Industrial Forum, Inc., New York). Sep 1970. 5p. Atomic Industrial Forum, Inc., New York $5.00.

Data are summarized on the health physics practices and regulatory inspections by Federal and State agencies of 26 commercial producers and distributors of radiation sources and radioisotope-labeled chemicals, compounds, and pharmaceuticals in the USA. Methods used for monitoring the radiation dose of personnel are listed and data on the cost of the monitoring programs are included. The effectiveness of the radiation protection programs is indicated by data on the number of inspection citations received during the three-year period from 1967 through 1969. (C.H.)

29528 PROBLEMS OF PROTECTION AROUND A 35 MeV BETATRON. Renzi, R. (Univ., Florence). Minerva Fisiconucl.; 13: 93-104(Jan-Mar 1969). (In Italian). (CONF-680535-11).

From fourteenth national conference of the Italian Association for Health Physics and Protection from Radiation; Formia, Italy (29 May 1968).

All of the results obtained by the detection methods mentioned in the paper lead to the conclusion that at present, the use of the betatron in the practice of medicine still involves technical problems of a particular nature. However, when operating under prescribed conditions, the exposure doses were abundantly below the maximum permissible levels whether for the operators and doctors, or for the patients. (E.R.B.)

29529 PROTECTION OF PERSONNEL WORKING IN A RADIOACTIVE ENVIRONMENT. Busuoli, G. (CNEN, Bologna); Cavallini, A.; Renzi, R. Minerva Fisiconucl.; 13: 131-4(Apr-Jun 1969). (In Italian). (CONF-680535-13).

From fourteenth national conference of the Italian Association for Health Physics and Protection from Radiation; Formia, Italy (29 May 1968).

An assessment of the radiation dose delivered to personnel working at an institute of radiology is presented. In particular, the dose distribution in the body for various types of examinations or treatments was followed. From the experimental results, it can be inferred that, by wearing standard protective clothing, radiation doses can be kept well within the maximum permissible levels. (auth)

29530 RADIATION PROTECTION IN DENTISTRY. Ribbecke, H. Deut. Stomatol.; 19: 56-9(19 Jan 1969). (In German).

Legal regulations and practical aspects of x-ray protection such as distance, position, protective aprons and walls, and diaphragms are discussed. (auth)

Safety Procedures

Refer also to abstract 29320.

29531 (CEA-R-4156) EMOTIVITY PARAMETER IN INDUSTRIAL MEDICINE AND THE SPECIAL CONDITIONS IMPOSED BY RADIOPROTECTION IN THE NUCLEAR INDUSTRY. Bessuges, Jacques (Commissariat a l'Energie Atomique, La Hague (France)). Mar 1971. 40p. (In French). (CONF-700953-1). Dep. NTIS (U. S. Sales Only).

From 11. national meeting on industrial medicine; Nantes, France (9 Sep 1970).

The recording of skin conductivity is a valuable technique for studying emotional behavior, whether it consists of fast variations (psycho-galvanic reflex) or slow variations (emotional tension, vigilance potential). Both phenomena lead to variations in the bioelectric cell mechanisms and homeostatic fluctuations. Recordings have been made on patients during flights in a Breguet aircraft and in compression chambers. A positive correlation between emotional tension and air pressure was found. This technique could be applied to the nuclear industry and might explain the hyperemotivity or drowsiness observed in certain workers working in low pressure chambers, and the hyperemotivity observed in others using glove boxes or wearing diving suits. This method has also been used for drivers. (France)

29532 ASSESSMENT OF THE ECONOMIC EFFECTS OF RADIATION EXPOSURE STANDARDS FOR URANIUM MINERS. FRC A-4 1970. Cambridge, Mass.; Arthur D. Little, Inc. (1970). 365p. Available from Environmental Protection Agency, Rockville, Md.

The economic effects of compliance with the standards proposed by the Interagency Uranium Mining Radiation Review Group of the Federal Radiation Council for the control of radiation exposure of miner personnel on Jan. 1, 1971, or possible alternative dates, are discussed. The economic effects of compliance with each of the three proposed exposure standards on the domestic uranium production industry, on the nuclear power industry, on the electrical power generation industry, on the retail price paid by the home consumer of electricity, and on communities dependent on the domestic uranium production industry are considered. (C.H.)

29533 BACKGROUND MATERIAL FOR THE DEVELOPMENT OF RADIATION PROTECTION STANDARDS. PROTECTIVE ACTION GUIDES FOR ^{89}Sr, ^{90}Sr, AND ^{137}Cs. FRC Report No. 7 1965. Washington, D. C.; Federal Radiation Council (1965). 44p. Available from Environmental Protection Agency, Rockville, Md.

Information is summarized that is pertinent to the development of radiation protection programs for situations involving contamination of the environment by the radionuclides strontium-89, strontium-90, and cesium-137. Two conditions of environmental contamination are examined: an acute localized contaminating event in which prompt action may be necessary to avoid the exposure that would otherwise result; and a widespread, generally increasing, low-level of contamination (from stratospheric fallout) that causes a continuous intake of radioactive materials by large numbers of people for a period of years. Special consideration is given to the situation in the arctic region where, because of unusual ecological conditions and food chains, some population groups are exposed to levels higher than those in other parts of the United States. (C.H.)

29534 AMERICAN STANDARD: RADIATION PROTECTION IN NUCLEAR REACTOR FUEL FABRICATION PLANTS. NATURAL (OR NORMAL) AND ENRICHED URANIUM, THORIUM, AND PLUTONIUM. ANSI N 7.2 1963. New York; American Standards Association, Inc. (1964). 32p. Available from American National Standards Inst., New York.

Standards are presented for the external radiation protection of personnel of nuclear reactor fuel fabrication plants and for control of the accumulation of radioisotopes within their bodies. Separate sections are included for natural uranium, uranium enriched in ^{235}U, plutonium (^{239}Pu), and thorium (^{228}Th and ^{232}Th). (C.H.)

29535 USA STANDARD: RADIATION PROTECTION IN URANIUM MINES AND MILLS (CONCENTRATORS). ANSI N 7.1 1960. New York; United States of America Standards Institute (1961). 25p. Available from American National Standards Inst., New York.

Standards are presented for preventing the overexposure of uranium mine and mill personnel to whole-body external ionizing radiations, ionizing radiation effects on the lining of the respiratory system, and the accumulation of excessive body burdens of radioisotopes. (C.H.)

29536 AMERICAN NATIONAL STANDARD: SUPPLEMENT TO RADIATION PROTECTION IN URANIUM MINES AND MILLS (CONCENTRATORS). ANSI N 7.1a 1969. New York; American National Standards Institute, Inc. (1970). 13p. Available from American National Standards Inst., New York.

Standards for air sampling and analysis to evaluate the effectiveness of methods of control of atmospheric concentrations of ^{222}Rn daughter products (^{218}Po, ^{214}Pb, ^{214}Bi, and ^{214}Po) in uranium mines are presented. The methods are useful for the evaluation of the occupational radiation exposure of underground uranium mine personnel. (C.H.)

29537 X-RAY PROTECTION STANDARDS FOR HOME TELEVISION RECEIVERS. Interim Statement of the National Council on Radiation Protection and Measurements (NCRP). NCRP A-1 1968. Washington, D. C.; National Council on Radiation Protection and Measurements (1968). 4p. Available from NCRP Publications, Washington, D. C.

The 1959 standards for protection of the human population

against x radiation emitted by home television sets are reviewed and certain statements are clarified. (C.H.)

29538 RADIOLOGICAL PROTECTION IN A GENERAL HOSPITAL. Garavaglia, C. (Ospedale Civile de Vimercate, Milan). Minerva Fisiconucl.; 13: 125-30(Apr-Jun 1969). (In Italian). (CONF-680535-12).

From fourteenth national conference of the Italian Association for Health Physics and Protection from Radiation; Formia, Italy (29 May 1968).

The results of the adoption of measures for reducing the exposure dose to patients and personnel in the radiology department of a hospital are studied. The data obtained by means of personnel dosimeters over a period of more than 6 months demonstrated a marked and constant decrease in exposure proportional to the adoption of protective measures. The factors involved in this reduction are analyzed; they include: instruction and training of personnel; use of automatic developing machines and of fixed and portable protective barriers; and adoption of particular radiographic techniques. (tr-auth)

Civil Defense

29539 EXPOSURE TO RADIATION IN AN EMERGENCY. NCRP 29 1962. Chicago; University of Chicago (1962). 91p. Available from NCRP Publications, Washington, D. C.

Standards are presented to help civil defense officials estimate the radiation exposure of human populations in the event of nuclear warfare and during the first few months post-attack. The effects of whole-body irradiation from external sources of γ radiation and injury to the skin caused by β radiation are considered. (C.H.)

Legal Aspects

29540 ALTERATION IN THE URANIUM LAW. Sv. Forfattningssamling: 1019(Dec 1970). (In Swedish).

Alterations in the uranium law concerning compensation to land owners are given. (Sweden)

29541 REGULATIONS ACCORDING TO THE ATOMIC ENERGY LAW CONCERNING THE POSSESSION AND HANDLING OF URANIUM AND THORIUM. Sv. Forfattningssamling: 749 (Dec 1970). (In Swedish).

Regulations for the possession and use of uranium and thorium by individuals and scientific institutions are set forth. Announcement 1959: 608 is superseded. (Sweden)

Medicine

Refer also to abstract 29439.

29542 SURVEY RESULTS OF THE USE OF X RAYS IN THE HEALING ARTS SPECIALTIES IN NORTH DAKOTA, 1964–1968. Kraeger, James A.; Christianson, Gene A. (North Dakota State Dept. of Health, Bismarck). Radiol. Technol.; 42: 161-74(Nov 1970).

The x ray facilities of all healing arts specialties, except dentistry, in North Dakota were surveyed by the State Department of Health to determine the degree of compliance of the x ray facilities with the recommendations published in NBS Handbook 76. An average of 8,529 patients are radiographed per week in the healing arts specialties in North Dakota, for a total of 443,508 patients radiographed per year. Hospitals and multiple-specialty clinics account for 81% of the radiographs. An average of 881 patients receive a fluoroscopic examination each week for a total of 45,812 examinations per year. Of this fluoroscopic workload, 88% are conducted in hospitals and multiple-specialty clinics. Fifty-eight percent of the diagnostic x ray machines were found to be deficient upon initial evaluation. The majority of deficiencies were inadequate collimation and/or inadequate filtration of the useful x ray beam. Major deficiencies resulting in unnecessary genetically significant doses were found to exist in facilities that expose 195,676 persons annually. Forty-nine per cent of the individuals operating x ray equipment in North Dakota are not registered with The American Registry of Radiologic Technologists. Of the non-registered technicians, 76% had less than a year of x-ray training and 74% indicated that aspects of x ray protection were not included in their training. (auth)

Protective Substances

Refer also to abstracts 29419, 29485, 29486, 29609, 29638, 29640, 29643, 29645, 29649, and 29716.

29543 (LF-43, pp 280-5) REMOVAL OF RELATIVELY SOLUBLE ^{144}Ce FROM THE LUNGS OF BEAGLE DOGS: INTRAVENOUS ADMINISTRATION OF A DTPA SOLUTION. Pfleger, R. C.; Muggenburg, B. A.; Cuddihy, R. G.; McClellan, R. O. (Lovelace Foundation for Medical Education and Research, Albuquerque, N. Mex.).

In Fission Product Inhalation Program.

Intravenously administered diethylenetriaminepentaacetic acid (DTPA) was beneficial in removing relatively soluble ^{144}Ce from dogs after an inhalation of a $^{144}CeCl_3$ aerosol; however, the effectiveness depended upon early treatment. In dogs given DTPA one hour after the inhalation exposure, the lung, liver, and skeletal burdens after 28 days were reduced to 36, 32, and 27%, respectively, of the initial lung burden of the exposed untreated control group. DTPA treatment initiated at five days post inhalation of $^{144}CeCl_3$ resulted in a 50% reduction in the lung burden with very little effect on the liver and an apparent mobilization of the ^{144}Ce to the skeleton. The urinary excretion of ^{144}Ce increased to 8 × the control level in the animals treated with DTPA on day 0 but only to 1.9 × in the animal treated on day 5. An animal injected intravenously with sterile isotonic saline one hour after an exposure to a $^{144}CeCl_3$ aerosol had lung, liver, and skeletal burdens and a urinary excretion pattern not significantly different from the exposed untreated control dogs. Comparisons of the data are made to those from a study in which DTPA was added to the fluid used for bronchopulmonary lavage. It is suggested that the effectiveness of DTPA lavage in enhancing the elimination of inhaled $^{144}CeCl_3$ was mediated primarily by absorption of the drug from the lung into the bloodstream. (auth)

29544 (LF-43, pp 286-94) BILATERAL BRONCHOPULMONARY LAVAGE WITH DTPA SOLUTION FOR REMOVING INHALED $^{144}CeCl_3$. Muggenburg, B. A.; Pfleger, R. C.; McClellan, R. O. (Lovelace Foundation for Medical Education and Research, Albuquerque, N. Mex.).

In Fission Product Inhalation Program.

The effectiveness of bilateral bronchopulmonary lavage with diethylenetriaminepentaacetic acid (DTPA) in saline or isotonic saline for removing ^{144}Ce was investigated in Beagle dogs that had inhaled $^{144}CeCl_3$. Five Beagle dogs exposed to the ^{144}Ce aerosol received no lavage treatment and were used as controls. Two dogs were lavaged with DTPA solution on days 0 and 5 after ^{144}Ce exposure, 2 on day 0 only and 2 on day 5 only. Two dogs were lavaged with isotonic saline on days 0 and 5 after exposure to ^{144}Ce. ^{144}Ce was removed in the lavage fluid. More ^{144}Ce was removed on day 0 than on day 5. DTPA treatment enhanced ^{144}Ce excretion in the urine. The effectiveness of bilateral bronchopulmonary lavage treatment with saline or DTPA in saline was compared to unilateral bronchopulmonary lavage with saline or DPTA in saline and use of DTPA intravenously. The most effective treatment was bilateral pulmonary lavage with DTPA on day 0 and 5 after inhalation of $^{144}CeCl_3$ which resulted in a 5 fold reduction in the cumulative radiation dose to lung, liver, and skeleton of the treated dogs as compared to non-treated dogs. (auth)

29545 PROTECTIVE EFFECT OF AN L-CYSTEINE DERIVATIVE, ETHYL-4-CARBOXY-α-PHENYL-2-THIAZOLIDINE ACETATE, ON THE HEMATOPOIETIC DAMAGE CAUSED BY RADIOTHERAPY. Kanda, Kosuke (Fukuoka Red Cross Hospital, Japan). Shinyaku Rinsho; 19: 731-5(May 1970). (In Japanese).

The 2-ethyl ester of 4-carboxy-α-phenyl-2-thiazolidine acetic acid (EPT) shows a radioprotective effect following oral administration, and in this point it differs from other thiol-compounds which are radioprotective only when administered parenterally. EPT was administered to 20 patients with different types of cancers subjected to ^{60}Co γ teletherapy, and to one case of liver cirrhosis, and the changes in hematological finding of these patients was studied. EPT was given by a daily dose of 60 mg from the beginning, or 10 days before, of irradiation. In most cases, the leukopenia caused by irradiation was slight, and in some cases, hemoglobin and red cell count increased. EPT was more effective when administered from seven to 10 days before irradiation, and the effective total dose seemed to be more than 1,000 mg. No side effects of EPT were observed. Its influence upon the radiosensitivity of malignant tumors was not made clear, but the tumor reduction due to irradiation, seen macroscopically or roentgenographically, was not influenced by EPT administration. (Japan)

29546 INVESTIGATION OF THE PARTICIPATION OF CATECHOLAMINE DEPOTS AND α-ADRENORECEPTORS IN THE RADIOPROTECTIVE EFFECT OF HYDROXYPHENYL-ETHANOLAMINES. Kulinskii, V. I. (Ukrainian Inst. for the Advanced Training of Physicians, Kharkov). Radiobiologiya; 10: 887-91 (1970). (In Russian).

Among hydroxyphenylethanolamines, the maximum radioprotective effect was exhibited by noradrenalin; its lower effectiveness at medium doses was due to processes of deposition. A number of

facts namely the decrease (but not removal) of the radioprotective action of adrenalin and noradrenalin by dibenamine only at medium doses, the resistance of the effect of mesaton (phenylephrine) to dibenamine, and the absence of a correlation between the action of dibenamine on the vasoconstrictor and radioprotective effects of hydroxyphenylethanolamines were evidence that the radioprotective action of these substances is realized through adrenoreceptors that differ from the classical ones. (tr-auth)

29547 DIFFERENCE IN THE EFFECTS OF RADIOPROTECTIVE SYMPATHICOMIMETICS ON THE OXYGEN PRESSURE IN THE SPLEEN. Kulinskii, V. I. (Ukrainian Inst. for the Advanced Training of Physicians, Kharkov. Inst. of Developmental Biology, Moscow). Radiobiologiya; 10: 910-13(1970). (In Russian).

The oxygen voltage (pO_2) in the spleens of white mice was determined polarographically after the injection of radioprotective sympathicomimetics and combinations of them with adrenolytics. Adrenalin and isopropylnoradenalin (isoproterenol) substantially lowered pO_2; noradrenaline and mesaton (phenylephrine) did not have any effect or produced only a small decrease. The shifts of pO_2 were not correlated with changes in the peripheral blood flow. The dynamics of pO_2 and the radioprotective effect coincided for adrenalin and isadrine; anaprylin (propanolol) removed this effect of isoproterenol and increased the action of adrenalin, while dibenamine reduced the effect of adrenalin. The absence of a similar correlation for noradrenaline and mesaton led to the assumption of the presence of a nonoxygen mechanism in the radioprotective action of these amines. (tr-auth)

29548 PROTECTIVE INFLUENCE OF ADRENALIN AND ACETYLCHOLINE IN VARIOUS FORMS OF RADIATION SICKNESS OF MICE. Bychkovskaya, N. B.; Strelkov, R. B.; Parasochko, L. A. (Central Scientific Research Roentgenoradiological Inst, Leningrad. Inst. of Experimental Pathology and Therapy, Sukhumi, USSR). Radiobiologiya; 10: 914-16(1970). (In Russian).

The influence of adrenalin in a dose of 2.5 mg/kg and acetylcholine in a dose of 50 mg/kg on the survival and average lifetime of mice irradiated with ^{60}Co γ rays at doses of 700, 800, 900, 1000, 1100, and 1200 R was investigated. By comparing the doses with close effects in the experimental and control groups and calculating the DCF coefficients, it was found that the radioprotective effect of both agents was pronounced in the bone marrow syndrome and negligible in gastrointestinal forms of death. (tr-auth)

29549 EFFECT OF TANDERIL ON RADIATION INDUCED INFLAMMATION. Tatsuno, Ikuro (National Hospital, Kanazawa, Japan). Shinyaku To Rinsho; 19: 810-12(May 1970). (In Japanese).

Tanderil (Oxyphen butazone) (2-phenyl-4-butyl-1-(p-hydroxyphenyl)-3-5-pyrazolidinedione) was administered to 30 patients with different cancers subjected to radiotherapy in order to protect against or treat radiation-induced inflammation. Irradiation was administered using 6 MeV x-rays. Tanderil was administered with a daily dose of 3 or 6 tablets from the beginning of irradiation. The average administration period was 63 days. In suppressing radiation inflammation, Tanderil was remarkably effective in 19 cases, effective in nine cases, and ineffective in two cases. Tanderil was especially effective for protecting against or treating the radiation-induced inflammation of lung, trachea, and upper respiratory tract. Two ineffective cases were radiation pelvic cellulitis following therapy of cervical cancer metastasis and radiation pneumonitis induced by therapy of lung cancer. The continuous administration of Tanderil for a long time did not cause any side effect such as hypersensitivity or leukopenia. (Japan)

29550 EFFECT OF INCREASED ATMOSPHERIC PRESSURE ON THE PROTECTIVE EFFICIENCY OF CERTAIN RADIOPROTECTORS. Sverdlov, A. G.; Martynchik, Yu. F.; Bogatyrev, A. V.; Yarkovets, A. G. (Ioffe Inst. of Physics and Tech., Leningrad). Dokl. Akad. Nauk SSSR; 196: 220-2(1 Jan 1971). (In Russian).

Earlier studies on the protective efficiency of radioprotective agents caused by increased O_2 pressure (P_{O_2}) in the tissues as a result of higher oxygen content in the air or higher atmospheric pressure were further extended by determining the behavior of various classes of chemicals, when the P_{O_2} in the spleen and the muscles of mice was increased. The animals were irradiated by a ^{60}Co source under a pressure of 7 atmospheres at the rate of 9.9 R/min for a total dose of 1000 R; this corresponded to a $DL_{50/30}$. The efficiency of the radioprotectors was determined by the survival rate of the animals. Experiments with mexamine, cystamine, cystaphos, and AET indicated that the protective effectiveness of these agents was the same at the high pressure as at normal pressure, even though the P_{O_2} in the tissues of the animals was greatly increased. Thus, hyperoxia does not decrease the protective effect of these compounds. (TTT)

29551 KINETICS OF THE OXYGEN TENSION IN THE CRITICAL ORGANS UNDER THE INFLUENCE OF MEXAMINE IN COMPARISON WITH ITS RADIOPROTECTIVE EFFECT. Yarmonenko, S. P.; Rampan, Yu. I.; Karochkin, B. B.; (and others) (Inst. of Experimental and Clinical Oncology, Moscow. Inst. of Labor Hygiene and Occupational Diseases, Moscow). Radiobiologiya; 10: 700-5(1970). (In Russian).

The kinetics of oxygen tension (pO_2) in the bone marrow, intestines, and subcutaneous tissue of rats after intraperitoneal injection of various amounts of mexamine qualitatively coincides with the magnitude and duration of the radioprotective effect in the case of γ irradiation of the animals under conditions of a large dose rate (710 R/min). However, a quantitative analysis of the change in pO_2 in individual critical organs in comparison with the dynamics of the death of rats in the case of the bone marrow and intestinal syndromes, as a function of time of injection and amount of mexamine, permitted the presence not only of the hypoxic mechanism, but also of another mechanism of the protective action of the preparation to be assumed. (tr-auth)

29552 DEPENDENCE OF THE PROTECTIVE ACTION OF CYSTEINE ON THE MOISTURE CONTENT OF DORMANT PEA SEEDS. Tsarapkin, L. S. (Inst. of Medical Radiology, Obninsk, USSR). Radiobiologiya; 10: 706-9(1970). (In Russian).

Dormant pea seeds with varous moisture contents were ^{60}Co γ irradiated at a dose of 15 kR and soaked in distilled water or a 0.01 M neutral solution of cysteine. Chromosome aberrations were determined in the anaphases of the root meristem. A decrease in the cytogenetic damage with increasing moisture content of the seeds was observed. The protective action of cysteine was manifested on dormant seeds with a moisture content of 20%. (tr-auth)

29553 INFLUENCE OF RADIOPROTECTIVE AGENTS ON CERTAIN BIOCHEMICAL INDICES CORRELATED WITH THE RADIOSENSITIVITY OF THE ANIMALS. Graevskaya, B. M.; Zolotareva, N. N. (Inst. of Biological Physics, Pushchino, USSR). Radiobiologiya; 10: 750-2(1970). (In Russian).

The influence of radioprotective agents (anoxia, cysteine, cysteamine, and AET) on certain biochemical properties correlated with the radiosensitivity of the animals was investigated. It was established in experiments on mice that radioprotective agents change the investigated biochemical indexes (the activity of tissue and blood proteinases, and the level of catecholamines in the adrenals, glycogen in the liver, and glucose in the peripheral blood) in the same direction in which animals relatively resistant to irradiation differ from more radiosensitive ones. It is suggested that the correlation is determined by the fact that both the investigated indexes and the radiosensitivity of the animals may depend on the level of tissue thiols. (tr-auth)

29554 ESTIMATION OF THE MINIMUM DOSE OF 5-METHOXYTRYPTAMINE INFLUENCING THE ACCUMULATION OF CYSTAMINE IN THE TISSUES AND ITS EXCRETION WITH THE URINE. Mordukhovich, V. V.; Titov, A. V. (Military Medical Academy, Leningrad). Radiobiologiya; 10: 756-8(1970). (In Russian).

The minimum dose of 5-methoxytryptamine affecting the distribution of cystamine in the tissues and its excretion with the urine was 10 mg/kg. In mice and rats this dose lowered the excretion of cystamine with the urine, lowered its content in the kidneys, and increased it in the intestines. (tr-auth)

29555 RADIOPROTECTIVE PROPERTIES OF O-ACYL DERIVATIVES OF SEROTONIN. Gorelova, N. V.; Shashkov, V. S.; Vasin, M. V.; (and others). Radiobiologiya; 10: 758-61 (1970). (In Russian).

It was found in experiments on mice that acylation of the phenolic hydroxyl of serotonin by monocarboxylic acids did not lead to any decrease in the radioprotective activity of the compound. Lengthening the carbon chain of the acyl radical increased the toxicity of the compound. The introduction of carbamoyloxy groups in the 5-position of the indole ring of tryptamine led to a 4 to 7-fold increase in the toxicity and a decrease in the protective effectiveness of the preparation. (tr-auth)

29556 RADIOSENSITIZING EFFECT OF FERROUS IONS. Gaziev, A. I.; Akhmadieva, A. Kh.; Khavaev, A. A.; Skotnikova, O. I. (Inst. of Biophysics, Pushchino, USSR). Radiobiologiya; 10: 761-4(1970). (In Russian).

It was established that Fe^{2+} ions distinctly sensitize cells of Escherichia coli B and rats of the Wistar line to ionizing radiation in the presence of oxygen. It may be assumed that the observed radiosensitizing effect is due to an intensification of the oxygen intoxication during the process of catalysis by Fe^{2+} ions of the free radical reactions in the cell, induced by ionizing radiation. (tr-auth)

XU

29557 NOTE ON THE DEVELOPMENT OF RESISTANCE TO HEAT AND GAMMA RADIATION IN SALMONELLA. Corry, Janet E. L.; Roberts, T. A. (Meat Research Inst., Bristol, Eng.). J. Appl. Bacteriol.; 33: 733-7(Dec 1970).

Repeated heat treatment and subculture increased the heat resistance of one strain of Salmonella typhimurium with no apparent increase in pathogenicity, or significant change in common biochemical characters. Cycling to γ radiation produced similar results. Re-cycled strains contained extremely low proportions of the smooth colonies required for serological and phage typing. (auth) (UK)

29558 EFFECT OF SODIUM CHLORIDE ON THE HEAT AND RADIATION RESISTANCE AND ON THE RECOVERY OF HEATED OR IRRADIATED SPORES OF THE GENUS BACILLUS. Briggs, A.; Yazdany, S. (London Univ.). J. Appl. Bacteriol.; 33: 621-32(Dec 1970).

Increasing concentrations (2, 4, and 8% w/v) of NaCl in the heating medium reduced the heat resistance of spores of Bacillus stearothermophilus but had no effect on the heat or radiation resistances of B. pumilus, B. subtilis, and B. subtilis var. niger or on the radiation resistance of B stearothermophilus. Increasing heat damage rendered all the spores increasingly sensitive to NaCl in the recovery medium. The presence of NaCl during heating reduced the subsequent NaCl sensitivity of B. pumilus, B. subtilis, and B. subtilis var. niger but increased that of B. stearothermophilus. Increasing doses of γ radiation rendered the spores of B. stearothermophilus increasingly sensitive to NaCl in the recovery medium. The effect was less pronounced with B. pumilus, while B. subtilis and B. subtilis var. niger showed little change in their post-irradiation sensitivity to NaCl. The presence of NaCl during γ irradiation had no effect on the subsequent pattern of post-irradiation NaCl sensitivity. (auth)

29559 STUDY ON THE RADIOPROTECTIVE PROPERTY OF THIOUREA AGAINST RADIATION-INDUCED CHROMOSOME DAMAGE. Reddy, S. B. (Karolinska Institutet, Stockholm). Can. J. Genet. Cytol.; 12: 685-8(Dec 1970).

The protective ability of thiourea in five different concentrations ranging from 5×10^{-2} to 1×10^{-5}M was demonstrated on chromosome aberrations in root tips of Allium cepa exposed to 350 R x irradiation. It was found that protection against radioinduced chromosome fragments and anaphase bridges was attained when the germinating seeds were treated with thiourea for 1 hour prior to irradiation. (auth) (Canada)

29560 BONE MARROW TRANSPLANTATION. Congdon, C. C. (Oak Ridge National Lab., Tenn.). Science; 171: 1116-24(19 Mar 1971).

The goals in bone marrow transplantation are its application to the treatment of diseases arising in the blood-forming tissues of man. Techniques for procuring and grafting marrow are of the needle-and-syringe type and are based on the normal physiological processes in which stem cells circulate through blood and other fluids of the mammalian organism. Destruction of bone marrow by irradiation, chemicals, or unknown agencies provides the immediate experimental system for demonstrating the therapeutic value of marrow transplants. Genetic diseases characterized by abnormal marrow function are also modifiable by grafts of blood-forming tissues. Studies with identical twins are critical experiments for showing the clinical value of grafts, even though the transplanted cells cannot be identified by the usual marker techniques. Among the best results seen with marrow grafting is the presumed cure of certain rare hereditary immune-deficiency disorders of children. A major problem in bone marrow transplantation is the immune reaction from cells growing out of the foreign transplant that attack the host (the graft-versus-host reaction). Attempts to use a graft-versus-host response to eliminate tumor cells is a part of the marrow research program. (auth)

29561 RADIATION SURVIVAL: IMPROVED RATES FOLLOWING CHLORTETRACYCLINE ADMINISTRATION. Adamson, Ian Y. R.; Bowden, Drummond H.; Wyatt, John P. (Univ. of Manitoba, Winnipeg). Radiat. Res.; 44: 478-83(Nov 1970).

Oral administration of chlortetracycline to mice before and after 1100 rads whole-body x irradiation resulted in a substantially enhanced survival rate (88%) over nontreated animals. This occurred in spite of severe pancytopenia as illustrated by the depression of marrow DNA and leukocyte values. Antibiotic administration solely in the preirradiation or post-irradiation periods produced a smaller increase in survival (56%). The results are attributed to the control of endogenous and exogenous bacterial infection before and after irradiation rather than a radioprotective effect. (auth)

29562 MODIFICATION OF RADIATION EFFECT ON THE EYE BY TOPICAL APPLICATION OF DIMETHYL SULFOXIDE. Hagemann, Ronald F.; Evans, Titus C.; Riley, Edgar F. (Univ. of Iowa, Iowa City). Radiat. Res.; 44: 368-78(Nov 1970).

Topical ocular application of DMSO prior to head-only irradiation of mice prevented complete cataract formation. While some degree of radiation damage was detected in these lenses, it did not progress to complete lenticular opacity as occurred in the irradiated control animals. The minimum effective DMSO concentration was about 10%. One hundred percent DMSO was effective when applied only one minute prior to exposure. The drug protected against exposures up to 1400 R; 1800 R was lethal. It was not effective when administered following irradiation. The mechanism of DMSO protection may involve hypertonicity to some extent and may involve alteration in epithelial cell metabolism. DMSO, as administered in these experiments, did not result in systemic radioprotection. In the same animals wherein DMSO (in high concentration) protected against radiation cataract, it resulted in radiosensitization of the cornea. This action of DMSO may be due to a nonspecific stress on the irradiated cornea. No corneal lesions were observed in the DMSO treated unirradiated control animals. The reason for the dichotomy between DMSO effect on radiation damage to lens and cornea remains obscure. (auth)

29563 EFFECTS OF OXATHIOLE ON THE CONDITION OF LIVER AND KIDNEYS DURING ^{210}Po INDUCED CHRONIC RADIATION SICKNESS. Mikhailovich, S. M.; Ovdienko, N. I.; Sedov, V. V.; Lebedeva, G. A.; Parfenov, Yu. D. Med. Radiol.; 15: No. 4, 43-51(Apr 1971). (In Russian).

A single injection of 2.5 μCi/kg of Po-210 into dogs resulted in the development of chronic radiation sickness associated with disturbances in the function of the liver and kidneys and leading ultimately to the death of the animal within 9 months of the injection. Treatment with oxathiole promoted remission of the symptoms of radiation sickness in the polonium-affected animals, prevented their death, and led to continuous improvement in the functional state of the liver and kidneys during the 7-yr observation period. Treatment with oxathiole was most effective in doses of 25 or 50 mg/kg. (tr-auth)

29564 INCREASED PROTECTIVE PROPERTY OF SPLEEN CELLS FROM PREIRRADIATED DONORS MEASURED BY TRANSPLANTATION INTO LETHALLY IRRADIATED RECIPIENTS. Kovalchuk, L. V.; Petrov, R. V. (Inst. of Biophysics, Moscow). Stud. Biophys.; 17: 1-4(1969).

A study was made to determine the therapeutic effects of spleen cells from previously irradiated donors after transplantation into lethally irradiated recipients. Mice donors were irradiated with a dose of 600 R 14 days before transplantation. Mice recipients were irradiated with a dose of 1000 R and 24 hrs later received intravenous injections of spleen donor cells in different doses. The results showed that in syngeneic combination the spleen cells of irradiated donors are five to six times more effective than the spleen cells of intact donors. The other mouse strains tested also showed improved survival rates. (E.E.H.)

29565 EFFECTIVENESS OF PRESSOR DRUGS IN BEAGLES EXPOSED TO MIXED GAMMA-NEUTRON RADIATIONS. Davis, Lawrence W.; Brown, James A.; Strike, Thomas A. (Armed Forces Radiobiology Research Inst., Bethesda, Md.). Proc. Soc. Exp. Biol. Med.; 136: 753-9(Mar 1971).

Aortic pressure, right atrial pressure, heart rate, and cardiac output were measured; and mean pressure, stroke volume, and peripheral resistance were calculated in 27 male beagles before and after 5000 or 10,000 rad whole-body doses of mixed gamma-neutron radiations. The response of these beagles to levarterenol, phenylephrine, or metaraminol was also determined before and after irradiation. Irradiation caused a decrease in aortic pressure, cardiac output, and stroke volume and an increase in heart rate. Peripheral resistance increased, but not significantly, in irradiated beagles. Phenylephrine and metaraminol were equally effective before and after the dogs were irradiated, while levarterenol was more effective in irradiated dogs. The results were interpreted as follows: radioinduced hypotension cannot be fully explained by radiation effects on peripheral blood vessels; pressor drugs are effective in irradiated beagles with hypotension, and drug effectiveness is probably decreased only as a terminal event shortly before death; any direct effect of radiation on the heart is of limited significance in whole-body exposure. (auth)

29566 EXPERIMENTAL STUDIES OF RADIATION PROTECTION THROUGH TRYPTAMINE. Sturde, Hans-Carl; Heitmann, Hans-Joachim; Gorschlueter, Klaus (Ruhr Univ., Bochum, Ger.). Strahlentherapie; 140: 745-8(Dec 1970). (In German).

The radioprotective effects of tryptamine are discussed. It was possible to visualize, by means of a very delicate series of experiments in the isolated surviving intestine of guinea-pigs, the radiation protection of different additives of tryptamine in an in vitro application of 8000 R each time. Activity losses of the hista-

XUM

mine solution with augmenting additives of tryptamine (3, 6, 12, 24, 48 μg) can be prevented to an increasing extent, whereas an additive of 1 μg of tryptamine to an aqueous histamine solution (with a concentration of 1 μg/ml) has not yet demonstrated any effect. By adding 96 μg of tryptamine, complete radiation protection was achieved. Radiation doses each time consisted of 8000 R. (auth)

29567 RADIOPROTECTIVE ACTIVITY OF SOME SULPHUR ANALOGUES OF TRYPTOPHOL AND 5-HYDROXYTRYPTAMINE. Deanovic, Z.; Pericic, D.; Supek, Z. (Rudjer Boskovic Inst., Zagreb). Strahlentherapie; 140: 749-52(Dec 1970).

Radioprotective effects of the following substances were tested: 10 analogues of substituted and unsubstituted tryptophol with –SH or –S–S– instead of –OH in the side chain; 5-mercaptotryptamine (serotonin possessing the thio group in position 5); the so-called sulfur analogue of serotonin (SAS) with a sulfur atom instead of nitrogen in the pyrrole ring. Only 5-mercaptotryptamine and SAS showed a significant radioprotective effect against x-irradiation in mice. An attempt was made to correlate the chemical structure and the radioprotective action. (auth)

29568 IN VITRO STUDIES ON RADIOPROTECTIVE EFFECTS OF MELANIN ON MAMMALIAN CELLS. Prevot, H. Jr.; Linden, W. A.; Wehbe, S.; Luegger, A. (Radiologische Univ., Hamburg). Strahlentherapie; 140: 753-6(Dec 1970). (In German).

The hypothesis of radioprotection by melanin on mammalian cells was studied. After administration of melanin, which is absorbed by the cells, the mean lethal dose of 175 Rad could be increased to 250 Rad. These results should permit the conclusion that melanoma cells should have a radiosensitivity according to their melanin content. (auth)

Radiation Sickness and Injuries

29569 SURGICAL TREATMENT OF CHRONIC RADIATION INJURIES OF AXILLA AND SHOULDER. Hirshowitz, Bernard; Mahler, Dan; Goldan, Samuel (Rambam Government Hospital, Haifa, Israel). Plast. Reconst. Surg.; 44: 261-7(Sep 1969).

Six cases are presented of chronic radionecrosis of the axilla and shoulder areas, following post-radical-mastectomy x-radiation therapy. The surgical treatment differed, according to the severity of the radiation damage. Chronic obstructive lymphedema was reduced in three cases by bridge flaps, which facilitated lymph drainage from the upper limb to the trunk. (auth)

Radiodiagnosis

Refer also to abstracts 29016, 29327, 29328, 29348, 29349, 29418, 29501, 29521, 29529, 29538, 29602, 29698, and 29706.

29570 (CONF-691016–(Absts.)) PROCEEDINGS OF SOUTHEASTERN CHAPTER, SOCIETY OF NUCLEAR MEDICINE 10th ANNUAL MEETING, NASHVILLE, TENNESSEE, OCTOBER 23–25, 1969. (Society of Nuclear Medicine, Southeastern Chapter). 35p.

Abstracts of 58 papers presented at this conference are presented that describe the preparation and use of new radioisotope-labeled pharmaceuticals for the scintigraphy of human organs. (C.H.)

29571 (LB/G–2835) NEW POSSIBILITIES IN THE TOPICAL DIAGNOSIS OF CARDIAC INFARCTS. Malek, P.; Vavrejn, B.; Ratusky, J.; Kronrad, L. Translated by E. M. Gillis (Atomic Energy Research Establishment, Harwell (England)), from Radiol. Aust.; 18: No. 1, 57-64(1968). 11p. Dep. NTIS (U. S. Sales Only).

Drugs were developed that possess the ability to collect specifically in damaged striped muscle and in the heart. Particularly favorable results were shown by Brommercurascan and Mercurascan and both were labeled with radioactive mercury (^{203}Hg or ^{197}Hg). These materials allowed a rapid topical diagnosis of myocardial infarction in vivo by means of a positive γ camera scintigram when tested in dogs. (C.H.)

29572 (NIRS-AR-13) ANNUAL REPORT FOR FISCAL 1969. (National Inst. of Radiological Sciences, Chiba (Japan)). Oct 1970. 245p. (In Japanese). Dep. NTIS (U. S. Sales Only).

Research activities during 1969 are reported. Emphasis was placed on the development of methods to determine the internal radiation dose following exposure to Pu and the effects of irradiation on the growth of transplants of hematopoietic organs. Computer facilities were installed for use in radiation dosimetry and a pathogen-free laboratory was constructed for use in studies of radiation injuries. Research and development activities in the fields of biology, chemistry, genetics, physics, pathology, physiology, radiation injuries, and environmental radiation monitoring are summarized. (TSS) (JAPAN)

29573 CLINICAL USES OF RADIOISOTOPES. Burrows, B. A. (Boston Univ.). pp 98-109 of Pathology of Irradiation. /Berdjis, Charles C. (ed.). Baltimore; Williams and Wilkins Co. (1971).

The clinical uses of radioisotopes in nuclear medicine are reviewed. Aspects of function studies, scanning, sample measurements, and therapy are considered. Applications of radioisotopes of chromium, cobalt, iodine, iron, mercury, phosphorus, and technetium are discussed. (P.B.M.)

29574 ATTEMPT TO USE ^{99m}Tc FOR SCINTISCANNING OF SALIVARY GLANDS. Chomicki, O. A.; Wejroch-Kowalska, M. (Postgraduate Medical Education Center, Warsaw. Bielany Hospital, Warsaw). Pol. Med. J.; 9: 1082-6(1970).

Scans of normal salivary glands after oral and/or intravenous administration of 1 to 2 mCi of ^{99m}Tc were obtained. The results were more readable after intravenous administration. Compared with ^{131}I, ^{99m}Tc seems to be the isotope of choice. (auth)

29575 RADIOISOTOPE SCINTISCANNING IN THE DIAGNOSTICS OF GALLBLADDER DISEASES. Toth, Z. (Center of Radiological Protection and Radiobiology, Warsaw). Pol. Med. J.; 9: 1087-92(1970).

The value of radioisotope scintiscanning in the diagnosis of gallbladder diseases was assessed on the basis of examination of 57 patients with the use of ^{131}I-labeled rose bengal. The method is considered to be very useful for detection of gallbladder neoplasms with metastases to the liver. The test is simple and easy and can be done regardless of the condition of the patient. (auth)

29576 FIVE YEAR'S EXPERIENCE WITH ISOTOPIC INVESTIGATIONS OF DISEASED JOINTS. Kolar, J.; Bek, V.; Streda, A.; (and others) (Charles Univ., Prague). Radiol. Diagn.; 11: 501-14(1970).

Investigations of diseases of the joints with radioactive isotopes merit an increased interest in clinical practice. Pathologically increased bone rebuilding can be detected with radioactive bone-seekers; the best results can be obtained with ^{85}Sr. For detection of inflammatory changes in the soft tissues, ^{131}I serum albumin is valuable and other radioactive substances were tested. Reliable results with isotopic investigations of diseased joints could be reached in 90 to 95% of the cases. The clinical material was investigated in 616 patients. The best results can be expected from combined investigations with bone-seekers and substances suitable for investigations of the soft tissues. By this means, the presence and extent, as well as the activity, of the process can be considered. (auth)

29577 NEPHROGRAPHY WITH THE AID OF ^{51}Cr-EDTA AND ^{58}Co-DTPA. Mitrov, G. G.; Salambashev, L. A.; Mushmov, D. D.; Todorov, G. G. (Inst. for Graduate Medical Studies, Sofia). Med. Radiol.; 16: No. 2, 3-7(Feb 1971). (In Russian).

In 10 healthy persons and in 50 patients suffering from different diseases of the kidneys, isotope nephrography was conducted with the aid of ^{131}I-hippuran and ^{51}Cr-EDTA or ^{58}Co DTPA. Comparative data showed that nephrograms with EDTA and DTPA yield valuable additional information in patients suffering from renal diseases with infection of the glomerular apparatus. The wider use of this method is proposed for the purpose of improving the diagnosis of renal diseases. This method is especially indicated in changes of the third phase of the nephrograms with hippuran, without nitrogen retention and without mechanical obstruction to urination. (auth)

29578 INVESTIGATION OF THE KIDNEYS WITH THE AID OF ^{51}Cr-EDTA. Efimov, O. N.; Baichorov, E. O.; Akimtseva, N. I.; Pavlov, B. D. (Inst. of Medical Rabiology, Moscow). Med. Radiol.; 16: No. 2, 7-12(Feb 1971). (In Russian).

A preparation, ^{51}Cr EDTA, is proposed for the investigation of glomerular filtration and scanning of the kidneys. The preparation is stable, inert, and non-toxic: up to 95% of it is eliminated from the organism by the kidneys within the first 24 hours. Clinical and experimental studies of glomerular filtration and scanning of the kidneys were carried out. The technique of investigation is described. Satisfactory correlations of the clearance of ^{51}Cr-EDTA and endogenous creatinine (0.92) and good scanograms of the kidneys were obtained. The radiation dose to the kidneys on introduction of 80 μCi for determining glomerular filtration was about 2 Mrad and after administration of 500 μCi for scanning of the liver was 10 Mrad. (auth)

29579 PILOCARPINE AS A DIAGNOSTIC AID IN THE SCINTILLOGRAPHY OF SIALOPATHIES. Stjernvall, L. (Univ. of

Helsinki); Tarkiainen, E.; Tarkkanen, J. Acta Oto-Laryngol.; 70: 113-25(Aug 1970).

The results are given of scintillography of the salivary glands with various pathological conditions, using ^{131}I and $^{99m}TcO_4^-$ as the active substance, and the parasympathicomimeticum, pilocarpine nitrate, as an agent selectively to interfere with the distribution and movements of radioactivity between various tissue/fluid compartments. The results showed that utilization of pilocarpine nitrate is useful in the evaluation of both the function and the scintillographic appearance of diseases of the salivary glands. Simultaneously the results strongly suggested that a conventional scintillography of the salivary glands, performed alone, does not give sufficient information about the nature and localization of the disease. Instead, the function of the glands must be examined as well. From the viewpoint of the excretory and concentration capacities of the diseased salivary glands, there may be significant differences even between cases belonging to the same clinical group, depending on the prevailing phase of the pathological process. (auth) (Sweden)

29580 RADIOISOTOPE ORGAN IMAGING IN TUMOR DIAGNOSIS AND MANAGEMENT. Sauerbrunn, Bertram J. L. (Veterans Administration Hospital, Washington, D. C.). Amer. Fam. Physician - GP; 3: 86-98(Jan 1971).

A review is presented on scintiscanning and scintiphotography, which provide a unique picture of an organ or lesion. A radioisotope compound is concentrated within an organ by utilizing the physical or chemical characteristics of the compound in conjunction with normal or altered physiologic functions of the organ. In most instances, defects or cold areas in the radioisotope image indicate replacement of normal tissue by a tumor or other abnormality. Bone and brain tumors or hyperfunctioning thyroid nodules, however, show an increased uptake of the radioisotope in the pathologic area, resulting in a hot lesion. (auth)

29581 EXPERIENCES WITH EXPERIMENTAL ISOTOPIC INVESTIGATIONS OF THE JOINTS. Kolar, J.; Bibr, B.; Babicky, A. (Charles Univ., Prague). Radiol. Diagn.; 11: 461-75(1970).

In a series of experiments with female adult Wister rats, the suitability of different radioactive substances for investigations of diseased joints by external counting of their uptakes was studied. Acute, subchronic, and chronic phases of inflammations were investigated. In those forms of joint diseases, where the bone tissue proper has been already damaged, the bone-seekers, mostly ^{85}Sr, are the most suitable radioactive tracers. In acute inflammations with prevalent changes in the soft tissues and without bone damage, the measurements of uptake of ^{131}I -serum albumins offer the best results. Positive findings were established with ^{75}Se, although the curves were of more complex nature. The preferently used forms have been the sodium selenite and selenomethionine. As a new agent for this purpose, ^{132}Te was tested, which is simultaneously deposited in the bones and soft tissues. A very important finding was the presence of a generalized metabolic change of isotopic uptake in joints other than in the ones directly inflammed. The presence of this reaction will make evaluation of the quantitative results of isotopic uptake by comparisons of diseased and healthy joints in the same animal difficult. (auth)

29582 CLINICAL APPLICATIONS OF SERIAL BRAIN SCANNING. Maynard, C. Douglas (Wake Forest Coll., Winston-Salem, N. C.). CRC Crit. Rev. Radiol. Sci.; 1: 525-65(Dec 1970).

The techniques and clinical applications of serial brain scanning are reviewed. Serial brain scanning can be performed in various ways: repeated studies in routine fashion days or weeks apart; multiple exposures taken over a period of minutes or hours; or sequential images obtained at intervals of seconds. Regardless of the approach, the studies are designed to improve the accuracy of detection, to help establish the etiology of a positive scan, or to monitor the course of a disease or the effectiveness of treatment. Much is known about the first of these three methods, and it is recognized as a valuable procedure. Considerably more investigation must be undertaken on the latter two before their true values and limitations can be ascertained. There are 64 citations in the bibliography. (E.R.B.)

29583 ^{113m}In DTPA BRAIN SCANNING IN THE DIAGNOSIS OF EXPANSIVE PROCESSES. Blandino, G.; Bonanno, N.; Conforti, P.; Meduri, M. (Univ., Messina, Italy). Acta Isotop.; 10: 91-102 (15 Dec 1969). (In Italian).

The use of ^{113m}In DTPA in the isotopic diagnosis by means of short-lived compounds has opened new and interesting perspectives. On the basis of 113 cases of ^{113m}In DTPA brain scanning the applications and limits of this new compound in the diagnosis of cerebral tumors were evaluated. DTPA ^{113m}In is to be considered one of the best compounds available for brain scanning since it offers many advantages over ^{99m}Tc. (auth)

29584 PROCEEDINGS OF THE FIRST NORDIC MEETING ON MEDICAL AND BIOLOGICAL ENGINEERING, JANUARY 15-18, 1970, OTANIEMI, FINLAND. Spring, E.; Jauhiainen, T.; Honkavaara, T. (eds.). Helsinki; Finnish Society for Medical and Biological Engineering (1970). 236p. (CONF-700111).

The proceedings consist of 69 abstracts on the following subjects: patient monitoring (12 abstracts), prosthesis (6), thermodilution (4), radiology (6), nucleonics (4), data handling (10), electrophysiology: EMG (6), transducers (7), pacemakers (4), thermography (2), and 6 abstracts on other fields in biomedical engineering, as well as the abstracts of 5 general lectures. (FINLAND)

29585 NUCLEIC ACID SYNTHESIS IN BLADDER TUMORS. Veenema, Ralph J.; Fingerhut, Bruno; Graff, Samuel (Columbia Univ., New York. Francis Delafield Hospital, New York). J. Urol.; 105: 392-6(Mar 1971).

Laboratory and clinical experience with studies of ^{3}H DNA and ^{3}H RNA in bladder tumors and normal urothelium is reviewed. The autoradiographic studies on freshly obtained tissue specimens readily demonstrated the proportion of the cells labeled and, most important with ^{3}H RNA, the position of the granules. A predominantly intranuclear position of the ^{3}H RNA granules appeared to correspond closely with a higher degree of malignancy. In approximately 20% of patients with histologically well-differentiated tumors, the radioautograms differed from the conventional microscopy and showed a high degree of nucleic acid synthesis indicating more active tumors. In vivo and in vitro observations on the laboratory rat bladder tumor model corresponded well with in vitro studies of human bladder tumors. Normal urothelium had a relatively rapid isotope uptake and replicative index in comparison with other forms of tissue. Hyperplasia of the urothelium induced by acetic acid showed extranuclear position of ^{3}H RNA but hyperplasia resulting from a carcinogenic diet regimen in rats showed an intranuclear ^{3}H RNA position. Thio-tepa instillations into rat bladders, started when the rats had received the carcinogenic diet regimen for 4 months, kept the urothelium at the stage of hyperplasia in 15 of 18 rats throughout the entire 9 to 10 months of the carcinogenic diet but the ^{3}H RNA remained intranuclear. External radiotherapy (3,000 to 4,000 rads) to the bladder of 9 rats with bladder tumors caused a shift of ^{3}H RNA to an extranuclear position. Studies of the nucleic acid synthesis in bladder tumors confirmed its value as a research tool as well as selective use in the earlier detection of higher degrees of malignancy. (auth)

29586 PINHOLE SCINTILLATION CAMERA AND ^{99m}Tc PERTECHNETATE IN NORMAL THYROID SCANNING. Pavoni, P. (Univ., Rome); Hurley, P. J.; Strauss, H. W.; Langan, J. K.; Wagner, H. N. Jr. Acta Isotop.; 10: 139-47(15 Dec 1969). (In Italian).

Thyroid scintigram studies were carried out on 31 euthyroid patients by means of a Pho-gamma/III, equipped with a pinhole collimator, and using ^{99m}Tc-pertechnetate. With the right technique and the possibility of administering high doses of the tracer without increasing the amount absorbed by the patient, a high resolution and a good image can be obtained. The method reveals considerable functional dyshomogeneity even within the normal thyroid parenchyma and the data obtained appear to lend support to the hypothesis that modular pathology of the thyroid may be related to a quantitative rather than a qualitative modification. It is suggested that this method may be able to give detailed information on the pathophysiology of the thyroid. (auth)

29587 ANGIOSCINTIPHOTOGRAPHY. Marabini, A.; Franchi, R.; Bistaffa, R. (Ospedale Civile Maggiore, Verona, Italy). Acta Isotop.; 10: 113-30(15 Dec 1969). (In Italian).

A technique for angioscintigraphy using ^{99m}Tc-pertechnetate was evaluated. The application of this technique with γ scintillation camera was demonstrated. It was emphasized that the method is easy to perform and harmless to the patient. (auth)

29588 RADIOACTIVE ISOTOPES AND THERMOGRAPHIC FINDINGS IN BONE LOCALIZATIONS OF SYSTEMIC DISEASES. Macchi, C.; Lovisatti, L.; Conte, G. (Univ., Padua. Ospedale Civile, Padua). Acta Isotop.; 10: 77-90(15 Dec 1969). (In Italian).

The results of scintigraphic (with ^{85}Sr) and thermographic examinations in 14 bone localizations during systemic disease are discussed. The precocity of scintigraphic diagnostics in comparison with radiographic methods are stressed. A possible justification for the negative results of the thermographic examinations is also discussed in detail. (auth)

29589 SCINTIGRAPHIC AND THERMOGRAPHIC DETECTION OF BONE METASTASES. Lovisatti, L.; Macchi, C.; Conte, G.

XUM

(Univ., Padua. Ospedale Civile, Padua). Acta Isotop.: 10: 65-75(15 Dec 1969). (In Italian).

Early diagnosis of skeletal metastasis can be made with the use of radioisotopes much sooner than by means of a mere radiological examination. In the 28 patients who underwent this test using ^{85}Sr, 23 of the 73 suspected localizations, which had proved negative during the radiographic exploration, were confirmed by means of scintigraphic examination and 43 localizations were detected by both methods. In the hope of possibly furthering this contribution to early diagnosis, 17 of the patients also underwent a thermographic examination. None of them, however, showed thermic variation of the localizations, contrary to what was detected for primitive neoplastic lesions of the skeleton. The possible use of this discovery in differential diagnosis between metastatic and primitive lesions is suggested. (auth)

29590 RENAL ADENOCARCINOMA: SCINTIGRAPHIC STUDY OF THE PRIMARY AND METASTATIC AREAS. Malamos, B.; Marketos, S.; Tsigourakos, D.; Korkos, S.; Kesse-Elias, M. (Univ., Atene, Italy). Acta Isotop.: 10: 37-46(15 Dec 1969). (In Italian).

The diagnostic and prognostic significance of various renal scintigraphic patterns was studied in a series of 15 patients operated on for renal carcinoma using Neohydrin-^{197}Hg, ^{198}Au, RISA-^{131}I, ^{99m}Tc, or ^{87m}Sr. The analysis of the results showed that the renal scintigram was abnormal, but not specific, in all cases. There was a relation between the size of the scintigraphic defect and the time of the manifestation of metastases. No correlation between the various patterns of renal scintiscan and the localization of metastases was observed. It was concluded that renal adenocarcinoma scintigraphy seems to be reliable as a pre-operative prognostic criterion. (auth)

29591 SCINTILLATION CAMERA IN THE EVALUATION OF LIVER MORPHOLOGY AND FUNCTION. Ferlin, G.; Ziliotto, D. (Univ., Padua). Acta Isotop.: 10: 23-35(15 Dec 1969).

Indications for the use of the scintillation camera in the study of the liver were evaluated on the basis of the results obtained in 70 normal and abnormal subjects with ^{198}Au colloidal gold (30 cases), ^{99m}Tc-sulfur colloid (20 cases), and ^{131}I-rose bengal (20 cases). Gold-198 colloid at a dose of 150 to 200 μCi yielded satisfactory pictures of the liver with an exposure time of about 5 minutes. Using ^{99m}Tc at a dose of 2 to 3 mCi only 20 to 40 seconds were heeded to obtain images which were usually better than those obtained with the colloidal gold. Employing rose bengal at a dose of 200 μCi a sequence of pictures was obtained at various intervals during an hour with an exposure time of 5 minutes for each image. Usually this sequence showed progressive visualization of the liver, appearance of gall-bladder profile, and excretion of radioactive material in the intestine. The phases of the sequence may appear variably delayed in different hepatic diseases and this may require the taking of further pictures at later intervals. (auth)

29592 EVALUATION OF KIDNEY MORPHOLOGY AND FUNCTION BY MEANS OF THE SCINTILLATION CAMERA. Ziliotto, D.; Ferlin, G.; Austoni, M. (Univ., Padua). Acta Isotop.: 10: 5-21(15 Dec 1969).

The use of the scintillation camera in renal studies allows visualization of the passage of radioactive substances, such as Hippuran-^{131}I, Neohydrin-^{203}Hg, and ^{99m}Tc-pertechnetate, that are excreted by the kidney. On the basis of 150 examinations in 130 patients, the results obtained in normal and nephropathic subjects are presented. The values and disadvantages of the technique are discussed. A general picture is obtained which reproduces renal morphology and yields a functional study of the kidneys. In the nephropathic patients, the picture may appear altered both in the morphology and in the kinetics of the excretion process. It is suggested that the scintillation camera may be advantageously used for subsequent control of the same patient under variable conditions or after therapeutic procedures. (E.E.H.)

29593 GIANT SPLENOMEGALY IN SARCOIDOSIS DEMONSTRATED BY RADIONUCLIDE SCINTIPHOTOGRAPHY. RESPONSE TO CORTICOSTEROID THERAPY. Burt, Robert W.; Kuhl, David E. (Univ. of Pennsylvania, Philadelphia). J. Amer. Med. Ass.; 215: 2110-11(29 Mar 1971).

Although the spleen is frequently involved in sarcoidosis, giant enlargement greater than 1 kg is uncommon. Intravenous administration of ^{99m}Tc-labeled technetium sulfide followed by scintiphotography revealed a massively enlarged spleen studded with multiple round defects. Following therapy with corticosteroids, a reduction in spleen size and the disappearance of parenchymal defects was found by subsequent scintiphotographs. (E.E.H.)

29594 PULMONARY GAS EXCHANGE AFTER RADIOISOTOPE SCANNING OF THE LUNGS. Bjure, J.; Ekstroem-Jodal, B.; Elgefors, B. (Univ. of Goteborg). Scand. J. Resp. Dis.; 51: 242-8(1970).

The pulmonary gas exchange was studied in nine patients with moderate lung disease in the supine position at rest and during exercise before and two hrs after injection of macroaggregated human serum albumin labelled with ^{131}I. Significant decrease of the arterial carbon dioxide tension and significant increase in the alveolo-arterial oxygen tension difference was observed during moderate exercise, indicating an impairment of lung function at the increased load on the pulmonary circulation. Some restriction in the use of this method seems advisable in those patients with lung or heart disease in whom a markedly reduced pulmonary capillary bed can be suspected and in cases with small reserve capacity of the pulmonary capillaries as in infants. (auth)

29595 IMPORTANCE OF THE HEMATOLOGIC EXAMINATIONS IN THE ASSESSMENT OF THE CHRONIC RADIATION LOADS OF THE RADIOLOGISTS. PART III. Mozsa, Szabolcs. Magy. Radiol.; 22: 373-8(Dec 1970). (In Hungarian).

The diagnostical value of the hematologic irregularities observed in the chronic radiation diseases of radiologists is discussed. Alterations of leukocytopoiesis, erythropoiesis, thrombocytopoiesis, and monocytopoiesis, as well as those of the reticulo-histiocyte-system (RHS) are described. The kinetic-morphologic alterations of the bone-marrow are also discussed. A short review of the alterations observed in the plasma is included. (auth)

Radiotherapy

Refer also to abstracts 29258, 29523, 29528, 29652, 29680, 29696, 29705, and 29712.

29596 SYMPOSIUM ON HIGH-ENERGY ELECTRONS, MADRID, SPAIN, 26th TO 28th SEPTEMBER, 1966. PROCEEDINGS. Gil y Gil, C.; Gil Gayarre, C. (comps.). Madrid; General Directorate of Health (1970). 405p. (In several languages). (CONF-660946).

Forty-four papers were presented at this symposium that report clinical results of the use of high-energy electrons for cancer therapy, and the results of related studies on the biological effects of electrons on cultured human cells, and also discuss methods for the dosimetry of electrons. Six of the papers are in French and six are in German. Each paper includes a bibliography. (C.H.)

29597 RADIATION THERAPY IN THE TREATMENT OF CARCINOMA OF THE PROSTATE. Grout, David C.; Grayhack, John T.; Moss, William; Holland, James M. (Northwestern Univ., Evanston, Ill. Passavant Memorial, Evanston, Ill. Veterans Administration Research Hospitals, Chicago). J. Urol.; 105: 411-14(Mar 1971).

Forty-one patients with stage 1, 2, or 3 carcinoma of the prostate were treated initially with ^{60}Co γ radiation. The results of treatment and the complications encountered are discussed. The frequent impressive responses of carcinoma of the prostate to external radiation confirm and support its continued use in selected therapeutic trials. (auth)

29598 RESULTS OF PRIMARY THERAPY OF LARYNGEAL CARCINOMAS WITH CONVENTIONAL X-DEPTH-IRRADIATION OR RADIUM CONTACT IRRADIATION. Seifert, K.; Werner, H.; Arndt, H. J.; Banzhaf, W. (Univ., Kiel). Strahlentherapie; 140: 613-20(Dec 1970). (In German).

Reported are about 277 cases of interior laryngeal carcinoma that were treated primarily by normal x-depth-irradiation or by a radium contact irradiation. Indications are stated in detail after distributing in a code-like manner the following items: age, duration of anamnesis, site of tumor, symptomatology, type of tumor, and extension of tumor. The examined cases represent a negative selection for the tumors of the stages III and IV, partially also for stage II. Taking all stages together, a five-year healing quotient of 49.3% merely by irradiation therapy was attained. On subsequent operative recurrence treatment, this quotient was 55.0%. (auth)

29599 CONTRIBUTION TO INDICATIONS AND METHODS OF IRRADIATION IN CASES OF MALIGNANT SYSTEMIC DISEASES. Schmidt-Hermes, Heinz-Josef; Leetz, Hans-Karl (Univ., Homburg, Ger.). Strahlentherapie; 140: 621-5(Dec 1970). (In German).

A simple and time-saving method for mantle irradiation in malignant systemic diseases is reported. The possibility of an electron pendulum therapy in case of pleural involvement is mentioned. It was concluded that irradiation of the adjoining regions when a lymphosarcoma and a retotheliosarcoma are manifesting is justified. (auth)

29600 RESULTS OF COBALT THERAPY IN INOPERABLE CARCINOMA OF THE LUNG. Ojala, Antti (Univ. of Turku, Finland). Strahlentherapie; 140: 626-9(Dec 1970).

One-hundred-sixty-nine inoperable pulmonary carcinomas were treated with cobalt therapy. The average age of the patients was 61 years. The average tumor dose was 4600 Rad. 83 patients were treated by split-course technique. One-year survival percentage was 31. The results were slightly better in squamous cell carcinoma than in microcellular carcinoma. The better results were achieved by a tumor dose of 4000 to 5000 Rad. The results were not improved by split-course technique. (auth)

29601 X-IRRADIATION OF VERRUCA JUVENILIS WITH SPECIAL EMPHASIS ON ITS PLANTAR FORM. Kautzky, Anton. Strahlentherapie; 140: 630-8(Dec 1970). (In German).

Results of irradiation of verruca juvenilis were satisfactory, also those of its plantar form. Results of short-distance irradiation by means of a 50 kV x-ray tube were also good. Genuine relapses were rare. Super-big warts, especially at the soles of the feet, and a very extended infestation forced the therapeutist to be careful, and did not permit a successful dose. Three times 1,000 R, with one week of interruption each, was sufficient, however, as long as foci did not exceed a diameter of 3 cm. As long as only single, super-small foci were concerned, single doses of 2,500 to 3,000 R could also be applied. (auth)

29602 APPLICATION OF ULTRASOUND-B PICTURE METHODS FOR THE PLANNING OF RADIOTHERAPY. Reisner, K.; Heckrodt, J.; Ay, R. (Univ., Mainz). Strahlentherapie; 140: 639-46(Dec 1970). (In German).

It is possible to produce, without essential stress of the patient, transverse and longitudinal pictures of the abdominal region in scale proportions by means of the ultrasound B-scanning method. These pictures can be photographed by a polaroid camera from the storage picture of the oscillograph tube, be enlarged in a simple way to a scale of 1 : 1 by an episcope, and be used directly for the setting up of irradiation schedules. The procedure is applicable for all tumors of the abdominal space, including gynecological tumors and those of the urinary bladder, furthermore for control of fields and therapy results. Additionally it gives diagnostic information, such as the proof of lymph node enlargement not detectable by lymphangiography. (auth)

29603 SIGNIFICANCE OF GRENZSTRAHLEN FOR RADIATION RESEARCH. III. Becker, Olga. Strahlentherapie; 140: 678-86(Dec 1970). (In German).

Direct and indirect effects of radiation dose absorption must be classified and defined systematically on three planes: the molecular plane, the cellular plane, and the cell complex plane. Furthermore, it is necessary to clearly differentiate the indirect effect of absorption on the skin from the physiological effect which originates from energy absorption in the skin. Another condition for understanding the new problems is a clear conception of the regular weakening of the quantum energy that is transported through space and matter by wave traction. Corpuscular rays, equally the secondary ones that are produced by primary ionization during the photonic conversion, are limited by zero in a range determined by $m/2v^2$. Since skin forms only few millimeters of the surface of the entity, it was possible to effect the absorption for almost the entire quantum energy applied in merely a few millimeters of the surface; this was provoked by the long wave grenz rays as well as by the extremely high decrease of absorption. Opposite facts were found in normal whole-body irradiation, in which a homogenization of the absorptions in all layers was striven for by an extreme induration of the radiation items. In these cases, a minimum of the skin dose was confronting a large body dose. The experiments with skin proved the fact that the destruction represented by epitheliolysis and by radiation ulcers is merely the consequence of the body dose. This indirect effect of destruction is a new phenomenon. (auth)

29604 INVESTIGATIONS CONCERNING THE PROBLEM OF RADIATION-CYTOSTATIC COMBINATION TREATMENT. PART 8. SYNCYTOSTATIC STUDIES WITH ACTINOMYCIN. Ringleb, Dietrich; Kartz, Ludwig; Sippel, Walter (Univ., Giessen, Ger.). Strahlentherapie; 140: 687-92(Dec 1970). (In German).

The effects of a combination of fractionated radiotherapy with actinomycin C were studied on the following mouse systems: testicular weight, growth of the young tail, healing of an ear wound, and reaction of the tail after application of high doses of radiation on part of it. A syncytostatic effect on proliferative tissues was found for the drug as for other chemotherapeutic agents before. The evolution of the radiation reaction was clearly slackened.(auth)

29605 RADIOTHERAPY OF SYNCHRONIZED SKIN TUMORS IN MICE. Ganzer, U.; Nitze, H. R. (Univ., Frankfurt am Main). Strahlentherapie; 140: 711-16(Dec 1970). (In German).

The success of radiotherapy after preceding synchronization was compared with the effect of 5-fluorouracil, combined, and radiotherapy in experiments with mice. The cytostatic and combined treatment did not have an essential therapeutic effect on the autochthonously growing animal tumor. Radiotherapy caused a clearly prolonged survival time. Animals treated by synchronization survived as long as the irradiated ones, and showed the least increase in tumors. Furthermore, it was demonstrated that synchronization had no such additive effect as the usual clinical combination therapy, the effect rather being based on the accumulation of tumor cells in the radiosensitive G_2-phase. (auth)

29606 COMBINED CHEMOTHERAPY AND RADIATION THERAPY OF CANCER. Bardos, Tamas; Ambrus, Gyula (State Univ. of New York, Buffalo. Roswell Park Memorial Inst., Buffalo). Magy. Radiol.; 22: 324-30(Dec 1970). (In Hungarian).

Combined radiation therapy and chemotherapy in comparison to either radiation therapy or cytostatic treatment alone was evaluated in patients with bronchial carcinomas. It was found that the results of the combined treatment not only attains, but even surpasses, the effects of the chemotherapeutic drugs administered alone, or the effects of the radiation by itself although the doses given in the combined treatment were significantly smaller than the doses given separately. The combined treatment is indicated not only because of the better therapeutical results, but also because the side effects may be reduced. (auth)

Radiation Effects on Animals

Refer also to abstract 29560.

29607 (CONF-690940–(Absts.)) EUROPEAN SOCIETY FOR RADIATION BIOLOGY. VIIth Annual Meeting: September 2–6, 1969, Ulm (Donau), Germany. (European Society for Radiation Biology). 156p.

Abstracts of some 150 papers in the field of radiation biology are presented. Emphasis is placed on results of studies on cultured cells. (C.H.)

29608 (NYO–2356-43) STUDIES OF THE EFFECTS OF ULTRAVIOLET RADIATION ON CELL STRUCTURE AND BEHAVIOR. Comprehensive Report, 1967–1970. Freed, Jerome J. (Institute for Cancer Research, Philadelphia, Pa.). 25 Jan 1971. Contract AT(30-1)-2356. 11p. Dep. NTIS.

Radiation studies were continued on cell behavior in relation to underlying cytoplasmic structure and differential activity of genes. For studies on microtubules as determinants of cell behavior, phase contrast time-lapse and electron microscopy were used and a flying spot microscope was developed. Studies on the effects of colchicine on saltatory movement in cells showed that these movements were associated with an aster-like array of cytoplasmic microtubules. Other studies were conducted on amino acid deprivation as a source of chromosome aberrations. Haploid cells of frogs were used for transfer of nuclei from monolayer cultured cells to enucleated eggs to determine effects of variant nuclei in embryonic development. (H.L.W.)

29609 CHANGES IN THE BIOELECTRIC ACTIVITY OF THE NERVE AND MUSCLE TISSUE IN THE FIRST HOURS AFTER X IRRADIATION. Mynchev, N. V. (Military-Medical Academy, Leningrad). Radiobiologiya; 10: 895-8(1970). (In Russian).

Changes in the bioelectric activity and damage to the nerve and muscle tissue after irradiation by x rays, with and without the use of radioprotectors (cystamine, AET), were studied. X irradiation at doses from 9 to 50 kR induced a slowdown of the drop in the emf of damage, a shortening of the latent period, and an increase in the amplitude of the action potential of isolated muscles and nerves. Cystamine and AET, beginning with a concentration of 0.1%, produced an acceleration of the drop in the emf of damage, an increase in the threshold of excitation, and a decrease in the amplitude of the action potential. In the case of irradiation of muscles and nerves in the presence of a radioprotector, a decrease or total disappearance of the effects induced by irradiation was observed. (tr-auth)

29610 RELATIONSHIP BETWEEN THE LEVEL OF ENDOGENOUS SULFHYDRYL GROUPS AND THE NATURE OF THE RADIOSENSITIVITY OF TUMORS. Ismailov, B. I.; Zhemaletdinov, F. G.; Efimov, M. L.; Arkhipova, L. D. (Republican Scientific Research Inst. of Oncology and Radiology, Alma-Ata, USSR). Radiobiologiya; 10: 917-19(1970). (In Russian).

The content of endogenous SH groups in a radioresistant ovarian tumor (OT) and a radiosensitive Pliss lymphosarcoma (PLS) was determined by two methods: biochemically in the entire tumor system (the total amount of protein and nonprotein thiols) and

XUM

cytochemically in the cells (the amount of protein SH groups). The initial level of endogenous thiols determinable in the OT was considerably higher than in the PLS. The radiosensitive tumor, Pliss lymphosarcoma, was characterized by a more pronounced and prolonged postradiation decrease in the level both of total and of protein SH groups. (tr-auth)

29611 SYNCHRONIZATION OF THE MYTOTIC CYCLE OF MAMMALIAN CELLS IN VITRO THROUGH FRACTIONATED X-RAY THERAPY. Linden, W. A.; Prevot, H. Jr.; Schneider, C.; Berg, H.; Luegger, A. (Radiologische Univ., Hamburg. Strahleninstitut, Hamburg). Strahlentherapie; 140: 706-10(Dec 1970). (In German).

Single x irradiation of an exponentially growing culture of L-cells effected, after a weak mitotic interval, an increase of the mitotic index to a maximum factor of 1.65 of the standard values, the irradiation in this case being 50 Rad. Stronger, respectively weaker doses had a lower synchronization effect that could be increased to a considerable extent by multiple rhythmical irradiations of the same single dose. (auth)

Invertebrates

Refer also to abstracts 29499, 29522, 29742, 29743, 29745–29747, and 29751–29756.

29612 SENSITIVITY OF MALE AND FEMALE CODLING MOTHS TO X AND GAMMA RADIATION WITH VARIOUS DOSE RATES. Pristavko, V. P.; Orgel, G. S. (Ukrainian Scientific Research Inst. of Plant Protection, Kiev). Radiobiologiya; 10: 878-81(1970). (In Russian).

The effects of x irradiation (dose rate 48 R/sec) and γ irradiation (dose rate 44, 240, and 308 R/sec) of codling moth pupae on the emergence, lifetime, and reproductive capacity of the moths were studied. The lethal effects of radiations increased with increasing dose rate. The reproductive capacity of the moths was inhibited to a greater extent when female pupae were irradiated. The activity of mating of males after irradiation with doses in the sterilizing range was similar to the activity of normal males in the mating with irradiated females. With decreasing dose rate, the gap between the optimum sterilizing doses that do not inhibit the mating activity and lifetime of the moths and the lethal doses increased. (tr-auth)

29613 TEST WITH DROSOPHILA MELANOGASTER ON SOMATIC RESISTANCE TO X-RAY IRRADIATION. Eeche, Andrievs (Univ. of Stockholm). Hereditas; 66: 71-8(1970).

The somatic resistance to x irradiation was studied in larvae from an isogenic wild type shock of Drosophila melanogaster. In a population, larvae of twelve successive generations were irradiated at the age of 20 ± 4 hours with a dose of 1120 R at an intensity of 80 R per min. Larval resistance to radiation was mainly studied at doses of 1120, 1400, and 1800 R. The data support the conclusion that larvae from series irradiated with 1120 R in earlier generations have greater somatic resistance than larvae from control series. Further tests are being performed to elucidate possible mechanisms which may be responsible for somatic resistance. (auth) (Sweden)

29614 EFFECTS OF GAMMA RAYS ON EGGS OF CULEX PIPIENS FATIGANS, WIED, 1928. de Oliveira, Maria Lindete; de Moraes Rego, Amyrthes; de Azevedo, Zuleide Mota (Univ. Federal de Pernambuco, Recife, Brazil). Bull. Calcutta Sch. Trop. Med.; 17: 12-3(Jan 1969).

Studies were made on the effects of a 990 Ci γ source on the eggs of Culex pipiens fatigans. The percentage of hatching batches of eggs decreased with increasing dose. The average life of larvae born from irradiated eggs decreased rapidly with increased dose. The eggs seemed to have the same sensitivity to γ rays as the directly irradiated larvae. The larvae arising from eggs irradiated with 2400 R did not survive more than 48 hr while directly irradiated larvae survived longer after more than 2000 R. With about 300 to 450 R doses on eggs, the life of hatched larvae increased but those larvae did not reach the pupal stage. (E.E.H.)

29615 POPULATION LONGEVITY IN γ-IRRADIATED COLLEMBOLA. Cavalloro, Raffaele; Delrio, Garino (European Atomic Energy Community, Ispra, Italy). Int. J. Appl. Radiat. Isotop.; 22: 216(Mar 1971).

The radiosensitivity of these primitive Apterygota insects was tested on samples of 1000 individuals of uniform size at a dose rate of 3670 R/min (2480 Ci ^{60}Co) and at a temperature of 22°C. No significant difference in mortality was found between the controls and the irradiated springtails up to 10 days, with doses inferior to 100 krad. After this period, the percentage of mortality increased with increasing doses above 100 krad. (UK)

29616 EFFECT OF ^{60}Co IRRADIATION OF MALE PUPAE OF THE GYPSY MOTH, LYMANTRIA DISPAR L., ON BIOLOGICAL FUNCTIONS OF MALE MOTHS. Maksimovic, M. (Inst. for Plant Protection, Belgrade). pp 15-22 of Sterility Principle for Insect Control or Eradication. Vienna; International Atomic Energy Agency (1971).

From Symposium on the sterility principle for insect control or eradication; Athens, Greece (14 Sep 1970). See STI/PUB-265; CONF-700919.

The effect of irradiating male pupae of the gypsy moth with ^{60}Co was investigated at doses of 30,000 and 40,000 Rad. Certain unfavorable results were noted with male moths. Mortality among irradiated pupae was found to increase proportionally with radiation dose as compared with unirradiated pupae. The age of pupae when irradiated is an important factor. The lowest mortality is obtained by irradiation with 30,000 Rad, when carried out within the last 5 days before emergence. The ability of irradiated males to mate is related to their development as measured by their body length in dry condition. The longer the body, the more the males copulated. Those with body length in dry condition not greater than 7 mm did not copulate at all. The stated radiation doses have a considerable effect on the life span of male moths, as well as on the duration of copulation. Both are shortened as compared with unirradiated males. Sterility induced in males not only makes the eggs obtained on copulation sterile, but also, very probably, affects the female biological functions in mating. The oviposition period and duration of the female life were found to be shortened. Hatchability of eggs is reduced to 43.2%, with male pupal irradiation of 30,000 Rad. In 56.8% eggs, although the caterpillar larva was formed, it did not hatch. The unfavorable effects of overdoses point to the need for investigating lower radiation doses for gypsy moth pupae. (auth)

29617 EFFECT OF GAMMA RADIATION ON THE REPRODUCTIVE ORGANS OF DACUS ZONATUS (SAUNDERS). Huque, Heshamul (Ministry of Agriculture and Works, Karachi, Pakistan). pp 31-6 of Sterility Principle for Insect Control or Eradication. Vienna; International Atomic Energy Agency (1971).

From Symposium on the sterility principle for insect control or eradication; Athens, Greece (14 Sep 1970). See STI/PUB-265; CONF-700919.

The effects of gamma radiation on various life stages of fruit fly Dacus zonatus (Saunders) has been studied in detail to explore the possibilities of its control in the Karachi area by the sterile-male release technique. One aspect of this work, namely the gross changes which take place in the gonads of irradiated male and female flies, is described. The insect material used in these experiments was collected from the local orchards. Pupae from the infested guava fruit (Psidium guajava), 20 to 30 in number, were irradiated 5 to 7 days after pupation and the study was made in adults at various time intervals after emergence. Each test was replicated three times. Haematoxylin and eosin were used as stains and Carnoy's fixative for fixation. The main findings are that the size of both male and female reproductive organs of irradiated insects was reduced. At 5 kR the formation of spermatozoa was completed on the 16th day as against the 12th day with the normal insect. At 8 kR spermatozoids and spermatozoa were not observed even after the 15th day of emergence. At 16 kR necrosis started in the apical region of the testes which could be seen up to mid-region when the dose was increased to 18 kR. The testicular sheath also shrank. (auth)

29618 APPLICATION OF FOUR DIFFERENT DOSES OF GAMMA RADIATION TO ADULT SITOTROGA CEREALELLA (OLIVIER). Aranda Centurion, B. S. (Ministerio de Agricultura y Ganaderia, Asuncion, Paraguay). pp 37-8 of Sterility Principle for Insect Control or Eradication. Vienna; International Atomic Energy Agency (1971). (In Spanish).

From Symposium on the sterility principle for insect control or eradication; Athens, Greece (14 Sep 1970). See STI/PUB-265; CONF-700919.

The work was carried out at the Nuclear Energy Centre for Agriculture at Piracicaba, Brazil. The purpose of the study was to determine the effect of four different gamma radiation doses on adult Sitotroga cerealella Olivier. Doses of 0 (control), 3, 6, 12 and 27 kRad were applied at a rate of 30.2 kRad/h. Use was made of 25 Petri dishes, representing five treatments with five replications. Ten unsexed adult specimens of Sitotroga cerealella Olivier were placed on each Petri dish. The mortality counts took 13 days. The results showed that 6 and 12 kRad gave higher percentage of mortality in shorter time. (auth)

29619 RADIATION PATHOLOGY IN HYLEMYA ANTIQUA (MEIGEN): OUTLINES OF RESEARCH. Theunissen, J. (Inst. for Phytopathological Research, Wageningen, Netherlands). pp 329-40 of Sterility Principle for Insect Control or Eradication. Vienna; International Atomic Energy Agency (1971).

From Symposium on the sterility principle for insect control or eradication; Athens, Greece (14 Sep 1970). See STI/PUB-265; CONF-700919.

The paper contains a discussion on the use of pathological symptoms as a means of determining radiation effects on the gonads of insects. Essential conditions to achieve useful results are: the use of preparations made according to standardized methods, the correct identification of the cell-types concerned, interpretation of the pathological symptoms in terms of physiology and, if possible, quantification of the radiation damage in order to obtain standards which can serve for the comparison of the effects of different treatments. Another part of the paper deals with some general results of histopathological studies on the onion fly. The most favorable sterilizing dose seems to be 3 kR applied to 12–13-day-old pupae. At that stage of development there is generally no sperm as yet present in the testes of the males. The ovaries of females contain only germaria. After irradiation part of the spermatids continue the development to mature, motile and genetically damaged sperm. Other cell-types of the testis show a varied pattern of pathological reactions during the days following irradiation. Irradiation of female pupae results in complete infecundity following failure of the development of the egg chambers. No irradiation damage has been observed in other tissues or organ systems like nervous tissue, the fat body, the intestinal tract or the haemocytes. General features of irradiated testes and ovaria are: reduced dimensions owing to inhibition of the normal development, disappearance of generative cells while somatic elements apparently are not affected and, in testes, a quicker ageing of the whole organ. (auth)

29620 EMBRYOLOGICAL CHANGES IN IRRADIATED EGGS OF TRIATOMA INFESTANS AND SUBSEQUENT DEVELOPMENT. Carcavallo, R. U.; Rewald, E.; Carabajal, C. A. (Direccion de Epidemiologia de la Subsecretaria de Salud Publica de la Provincia, Buenos Aires). pp 503-12 of Sterility Principle for Insect Control or Eradication. Vienna; International Atomic Energy Agency (1971). (In Spanish).

From Symposium on the sterility principle for insect control or eradication; Athens, Greece (14 Sep 1970). See STI/PUB-265; CONF-700919.

The development of a technique for separating the contents of the egg of Triatoma made possible a complete microscopic study of the embryonic structures in the various stages of development, from the earliest until hatching of the first nymphal stage. Using a mixture of chloroform, methyl alcohol and acetic acid in equal parts (a percentual modification of Carnoy's fluid), we obtained three simultaneous effects: spontaneous opening of the operculum, projection of the embryo outside the egg and instantaneous fixation of the cellular structures. A complete study of the structures can be made by subsequent staining with selective dyes and impregnation with silver. A large number of eggs were divided up into four batches, three of which were exposed to different doses of radiation, the fourth serving as a control. In the results obtained using x-rays, the higher the radiation dose and the earlier applied, the greater were the changes. In embryos less than two days old the mean and high doses shown in detail in the tables are lethal: cytological studies revealed profound changes in the nucleus: pyknosis, karyorrhexis and protoplasmic vacuolation. The low doses to young embryos produce less profound changes, but give rise to a physiological weakening of the first-stage nymphs which hatch from them and do not survive to the second stage. The mean doses applied to 6- to 9-day-old eggs cause a delay in the hatching of the first nymph and some slight malformations (semi-atrophy of the tibia and tarsus, malformations of the tergites, etc.), the majority being non-viable as from the second stage. High doses for similar times cause 100% lethality in second stage nymphs owing to an inability to feed from the first alteration. (auth)

Vertebrates

Refer also to abstracts 29419, 29428, 29430–29438, 29446, 29449, 29473–29476, 29482, 29483, 29487, 29497, 29514, 29548, 29550, 29551, 29553, 29555, 29556, 29561, 29562, 29564, 29604, 29724, and 29727.

29621 (COO-119-243) GROWTH DYNAMICS OF OSTEOSARCOMAS IN BEAGLES. Thurman, Gary Boyd (Utah Univ., Salt Lake City. Radiobiology Div.). Jan 1971. Contract AT(11-1)-119. 127p. Dep. NTIS.

An analysis is presented of the growth dynamics, oncogenic skeletal doses and skeletal locations of radiation-induced osteosarcomas in beagles at the University of Utah, Division of Radiobiology as of March, 1970. Two hundred and fifty-six well-documented osteosarcomas have been induced in 201 beagles, each receiving a single intravenous injection of ^{226}Ra (80 tumors), ^{239}Pu (64 tumors), ^{228}Ra (43 tumors), ^{228}Th (56 tumors), ^{90}Sr (8 tumors) or ^{224}Ra (5 tumors). Radiographs of each osteosarcoma were taken during the period of the tumor's growth. The growth dynamics of these osteosarcoma were estimated by measuring the tumor dimensions on as many radiographs as possible. It was clearly evident that the tumor volumes were increasing exponentially with time. Exponential growth constants were calculated for 249 tumors, the corresponding volume doubling times ranged from 4.7 to 60.3 days and averaged 12.4 days. Using individual exponential growth constants, a starting time for each tumor was estimated as the time when the extrapolated tumor's growth curve reached the volume of one cell 10μ ($\mu = 10^{-4}$ cm) in diameter. The accumulated average skeletal dose during the time from injection to tumor starting time was calculated for each tumor and called the oncogenic skeletal dose. It was found that the larger the amount of radionuclide injected, the larger the oncogenic skeletal dose. High incidences of radiation-induced osteosarcomas in the beagles were noted in vertebrae, pelvic bones, humerii, femora and tibiae. Radiation-induced osteosarcomas of the vertebrae and pelvic bones had much higher incidences than the corresponding incidences of naturally-occurring osteosarcomas in dogs. (51 references). (auth)

29622 (LF-43, pp 218-23) CONNECTIVE TISSUE CONSTITUENTS MEASURED ON DOGS EXPOSED TO ^{144}Ce FUSED MONTMORILLONITE CLAY PARTICLES. Pickrell, J. A. (Lovelace Foundation for Medical Education and Research, Albuquerque, N. Mex.).

In Fission Product Inhalation Program.

Previously developed biochemical techniques were utilized in order to more accurately quantitate the relationship between radiation dose delivered to the Beagle dog lung by inhaled ^{144}Ce in fused clay and induced pulmonary fibrosis. Quantities of collagen, elastin, and glucosamine plus X, as well as elastin/collagen, hydroxyproline/hydroxylysine, and hydroxyproline/proline ratios were estimated. Of these connective constituent measurements, the increase in collagen correlated best with increasing cumulative radiation dose. This increase in collagen may represent a reparative process in response to tissue death, interaction on the biosynthetic sequence of collagen, or an effect on related or unrelated metabolic processes. The response of compounds containing glucosamine plus X appeared to parallel and potentially to be related in some way to the collagen response. A variable elastin response was present as indicated by the elastin/collagen ratio and by elastin content. It did not appear to be directly related to radiation dose. The inter-relationships are beginning to provide insight into the mechanism of pulmonary fibrosis induced by inhaling radioactive insoluble particulates. A knowledge of other factors, notably the biosynthesis of these compounds, will be necessary for a more complete understanding of radiation fibrosis. (auth)

29623 GROWTH AND DIFFERENTIATION OF SYNAPTIC STRUCTURES UNDER CIRCUMSTANCES OF DEPRIVATION OF FUNCTION AND OF DISTANT CONNECTIONS. Szentagothai, J.; Hamori, J. (Univ. Medical School, Budapest). Symp. Int. Soc. Cell Biol.; 8: 301-20(1969).

From twelfth international congress of cell biology; Brussels, Belgium (25 Aug 1968). See CONF-680850.

Morphological changes in axonal and dendritic arborizations and in synapses under circumstances of functional deprivation and of interruption or disarrangement of connected neuron systems are discussed on the basis of three experimental models. The first model concerns the development of a peculiar kind of dendritic spine in the synaptic glomeruli of the lateral geniculate body under circumstances of functional deprivation. In the second model a classical type of transneuronal atrophy is studied, the well-known crossed atrophy of the cerebellar cortex that occurs after early cerebral cortical lesions. The analysis in this model is focused on a well-known complex synaptic system of the cerebellar cortex, the glomeruli. Both neuronal arrangement and development of these glomeruli were studied extensively by modern electron microscope techniques, and this synapse might well serve as a model of transneuronal atrophy of synapses in general. In the third model, the experimental situation is reversed as compared to that in the second: the majority of granule neurons are removed by early postnatal x irradiation, and the development of the presynaptic elements—in this case of the mossy fibers—is studied under circumstances in which there is a lack of appropriate postsynaptic elements with which to establish contacts. (auth)

29624 EFFECT OF IRRADIATION ON MAMMALIAN CELLS IN VITRO. Shaw, Edward I. (Univ. of Kansas, Lawrence). pp 32-49 of Pathology of Irradiation. /Berdjis, Charles C. (ed.). Baltimore; Williams and Wilkins Co. (1971).

The effects of irradiation on mammalian cells and their sur-

vival rates were studied. Survival curves of cells were examined and the data showed that the survival of x-irradiated cells was 3% at 400 R and 0.5% at 600 R. (P.B.M.)

29625 EFFECTS OF CONTINUOUS IRRADIATION. Fabrikant, Jacob I. (Johns Hopkins Univ., Baltimore). pp 50-85 of Pathology of Irradiation. /Berdjis, Charles C. (ed.). Baltimore; Williams and Wilkins Co. (1971).

The effects of continuous low-dose γ or x irradiation on mammalian cells were studied. The radiation response of mammalian tissues involves problems of cellular radiosensitivity, organized tissue reaction, and homeostatic mechanisms concerned with the regeneration capacity of the tissues. Cell killing and survival are related to radiosensitivity. The cellular response is dependent on the age of the cell within the cell cycle at the time of irradiation. Continuous irradiation disturbs the integrity of proliferating cell systems. However, regulatory control mechanisms for cell proliferation and differentiation provide effective methods of compensation by changing the patterns of cell population kinetics. (P.B.M.)

29626 SUBLETHAL DAMAGE REPAIR AND ITS ROLE IN THE RADIATION RESPONSE OF CELL RENEWAL SYSTEMS. Elkind, M. M. (Brookhaven National Lab., Upton, N. Y.); Withers, H. R. pp 86-97 of Pathology of Irradiation. /Berdjis, Charles C. (ed.). Baltimore; Williams and Wilkins Co. (1971).

The pathologic effects of ionizing radiation are due to the killing of dividing cells. Observations were given on the effectiveness of sublethal x irradiation in suppressing cell proliferation and the capability of mammalian cells to repair radiation damage. The repair of sublethal damage is reflected in the shape of the survival curve. (P.B.M.)

29627 SOME TOXICITY ASPECTS OF INTERNALLY DEPOSITED ^{239}Pu. Taylor, B. N.; Dougherty, T. F.; Christensen, W. R. (Univ. of Utah, Salt Lake City). pp 110-19 of Pathology of Irradiation. /Berdjis, Charles C. (ed.). Baltimore; Williams and Wilkins Co. (1971).

The toxicity syndrome of plutonium-239 was studied in dogs. Plutonium-239 is retained within the body for prolonged periods and irradiates selected organs and specific tissues within an organ with relatively high energy. Following a single intravenous injection of tetravalent plutonium-239 into dogs, most of the retained radionuclide burden was localized in the skeleton and the liver. The earliest clinically detectable radioinduced change was a drop in the leukocytes of the peripheral blood. The dogs died of liver diseases 400 days following injection. (P.B.M.)

29628 RADIATION EFFECTS IN SKIN. Tessmer, C. F. (Univ. of Texas, Houston. M. D. Anderson Hospital and Tumor Inst., Houston, Tex.). pp 146-170 of Pathology of Irradiation. /Berdjis, Charles C. (ed.). Baltimore; Williams and Wilkins Co. (1971).

The skin responds to ionizing radiation in several recognizable ways and in proportion to the dose. Physical factors that influence the radiation effects on skin are energy transfer, penetration, and the several forms of radiation. Each form and energy level of radiation has a characteristic LET and a recognizable pattern of tissue effect. Following a single whole body x-ray dose of 660 R in rats, the most frequent neoplasm induced was carcinoma of the skin. (P.B.M.)

29629 EFFECTS OF RADIATION ON STRIATED MUSCLE. Zeman, W. (Indiana Univ., Indianapolis); Solomon, M. pp 171-85 of Pathology of Irradiation. /Berdjis, Charles C. (ed.). Baltimore; Williams and Wilkins Co. (1971).

Experiments were performed to show the relative radiosensitivity of striated muscle of rats exposed to therapeutic radiation doses. It was found that under identical conditions of x irradiation, different muscles develop delayed radiation necrosis along different pathogenetic pathways due to the properties of the individual muscles. The properties studied were the arrangement and the length of the muscle fibers. (P.B.M.)

29630 BONE-SEEKING RADIONUCLIDES AND BONES. Jee, W. S. S. (Univ. of Utah, Salt Lake City). pp 186-212 of Pathology of Irradiation. /Berdjis, Charles C. (ed.). Baltimore; Williams and Wilkins Co. (1971).

The early and late radiation damage produced by plutonium, radium, and strontium in bones of dogs was studied. The radionuclides induce loss and damage of marrow cells, sarcomas, and malignant tumors. (P.B.M.)

29631 RADIATION-INDUCED ALTERATIONS IN ODONTOGENESIS AND FORMED TEETH. Kimeldorf, D. J. (Oregon State Univ., Corvallis). pp 278-289 of Pathology of Irradiation. /Berdjis, Charles C. (ed.). Baltimore; Williams and Wilkins Co. (1971).

The tooth provides a model system for the analysis of radiation effects in an organ. Each tooth is an organ containing several types of tissues and a vascular and nerve system. Factors affecting the radiation response are the radiation exposure conditions, the stage of dental development, and the duration of the observation period. X radiation exposure can destroy the tooth bud, arrest growth, discolor teeth, and induce lesions in animals. (P.B.M.)

29632 GASTROINTESTINAL TRACT. Maisin, J. (Univ. of Louvain, Belg.); Maisin, J. R.; Dunjic, A. pp 296-344 of Pathology of Irradiation. /Berdjis, Charles C. (ed.). Baltimore; Williams and Wilkins Co. (1971).

The early destructive changes which appear in the intestinal epithelium, mainly in the intestinal epithelium of the duodenum, after whole body or abdominal doses as low as 80 to 100 rads, are a proof of the radiosensitivity of this part of the digestive tract. The damages seen at higher doses are a function of the dose. The lymphoid nodules and the Payer patches show destruction after doses of 500 to 1,000 rads. A good estimate of the changes in the cellularity of the epithelium of the bowel of the mouse after various doses of whole-body radiation is given by the weight of the intestine following exposure. This depression in the weight of the intestine, which reaches its maximum 2 days after an exposure to sublethal and lethal x ray doses, is correlated with the decrease in length of the stretched small intestine of the mouse 48 hr after a whole body dose of 1,500 rads. (auth)

29633 EFFECTS OF IONIZING RADIATION UPON ENDOCRINE GLANDS. Sommers, S. C. (Lenox Hill Hospital, New York). pp 408-46 of Pathology of Irradiation. /Berdjis, Charles C. (ed.). Baltimore; Williams and Wilkins Co. (1971).

Some of the most important effects of whole body x irradiation are upon the endocrine glands. Rats and rabbits were used to show these effects. The consequent imbalances contributed important knowledge concerning normal endocrine relationships, the pathogenesis, and pathophysiology of structural alterations of these glands and their target organs. Radiation carcinogenesis is a major aspect of pathology of the thyroid, ovary, testis, and pituitary gland. (P.B.M.)

29634 HEMATOPOIETIC CHANGES FOLLOWING IRRADIATION. Proukakis, C.; Lindop, Patricia J. (St. Bartholomew's Hospital, London). pp 447-95 of Pathology of Irradiation. /Berdjis, Charles C. (ed.). Baltimore; Williams and Wilkins Co. (1971).

The effects of x radiation on hematopoietic system of mice were described. Stress was laid on the quantitative aspect of cell killing by irradiation of the hematopoietic stem cells, on which regeneration depends. The early and late effects of irradiation on the hemopoietic system depend on many factors, such as the area and volume of the body exposed, radiation quality and dose rate, the number and pattern of fractions of irradiation given, and biological factors, such as the species and strain, and the age at exposure. (P.B.M.)

29635 LYMPHATIC SYSTEM AND THYMUS. Maisin, J. (Univ., Louvain, Belg.); Maisin, J. R.; Dunjic, A. pp 496-541 of Pathology of Irradiation. /Berdjis, Charles C. (ed.). Baltimore; Williams and Wilkins Co. (1971).

Studies on the x radiosensitivity of the lymphatic system and thymus of rabbits and rats were reviewed. The lymphocytes lose mobility and phagocytic power as a result of radiolesions. The thymus has a high degree of radiosensitivity. The rapid decrease in weight is the result of the primary death of cortical lymphocytes and to a lesser degree to the death of the lymphocytes of the medulla which is more resistant. (P.B.M.)

29636 RADIATION EFFECTS ON THE PULMONARY SYSTEM. van den Brenk, H. A. S. (St. Thomas Hospital, London). pp 569-91 of Pathology of Irradiation. /Berdjis, Charles C. (ed.). Baltimore; Williams and Wilkins Co. (1971).

Attempts to measure radiation reactions in the lungs of mammals in terms of tissue damage and radiosensitivity are complicated by effects that dominate the pathologic picture. Factors that lead to fallacious interpretations of radiosensitivities of lung tissues are obstruction to the air passages, infection, inflammatory reactions, changes in capillary permeability, and hematologic changes. Cell damage and depopulation are the primary effects of radiation and are largely responsible for initiating the pathologic condition termed radiation pneumonitis. (P.B.M.)

29637 COMPARATIVE EVALUATION OF CERTAIN PROCEDURES FOR DETERMINING CHANGES IN DNA OF AN IRRADIATED ORGANISM. Kritskii, G. A.; Abidov, A. A.; Batishchev, A. I.; Aleksandrov, S. V. (Inst. of Biochemistry, Moscow). Radiobiologiya; 10: 803-7(1970). (In Russian).

The influence of x irradiation on certain qualitative and quantita-

tive changes in DNA in the hematogenic system of the rabbit during the period of acute radiation sickness (two days after irradiation) was investigated. A significant disruption of the pyrimidine nucleotide blocks and the accumulation of single thymidylic nucleotide residues in bone marrow DNA was detected at doses of 50 R and above. A significant decrease in the DNA content in whole blood was detected at doses of 5 R and above. (tr-auth)

29638 INFLUENCE OF HISTONES ON CERTAIN ENERGY PROCESSES IN LIVER MITOCHONDRIA OF TOTALLY IRRADIATED ANIMALS. Dovgii, I. E.; Korol, B. A.; Minaev, L. F. (Inst. of Biological Physics, Pushchino, USSR). Radiobiologiya; 10: 836-9(1970). (In Russian).

The influence of total histones on processes of oxidative phosphorylation (OP) in liver mitochondria of nonirradiated and irradiated animals was investigated. It was found that total histones in a concentration of 50 μg stimulate the processes of OP of mitochondria isolated from the livers of nonirradiated animals and inhibit processes of OP of the mitochondria of irradiated animals. Under the action of higher histone concentrations (250 and 500 μg) there was an inhibition of this process in the mitochondria of both nonirradiated and irradiated animals. It was established that histones in a concentration of 50 μg stimulate the succinate oxidase activity, while in a concentration of 250 μg they inhibit it. Total irradiation of the animals at a dose of 400 R caused a disruption of OP in liver mitochondria. (tr-auth)

29639 THE STUDY OF RADIOTOXINS IN THE CASE OF CHRONIC INTAKE OF ^{90}Sr. Vatulina, G. G. (Inst. of Biophysics, Moscow). Radiobiologiya; 10: 840-3(1970). (In Russian).

On examination of rat livers at various periods after the beginning of intake of a chronic amount of ^{90}Sr, products of the oxidation of fats were detected two months after the beginning of intake of the isotope and quinones after 4.5 months in animals of both groups. The appearance of radiotoxins did not depend on the dose and concentration of the isotope introduced (within the range 1 to 4 μCi) and was observed at the same periods in animals of both experimental groups. The accumulation of radiotoxins was abrupt. (tr-auth)

29640 INFLUENCE OF RIBOFLAVIN ON THE ENERGY METABOLISM DURING IRRADIATION. Alferov, A. N. (Kiev Roentgenoradiological and Oncological Scientific Research Inst.). Radiobiologiya; 10: 832-5(1970). (In Russian).

The administration of riboflavin in a concentration of 0.2 mg/kg to rats irradiated at lethal and sublethal doses had a favorable influence on the normalization of respiration and oxidative phosphorylation in liver mitochondria. In the case of local irradiation of rabbit liver, the energy processes in it suffered less than in total irradiation. Riboflavin administered to locally irradiated animals had a more favorable influence on the normalization of energy metabolism in the liver than in the case of lethal and sublethal doses of irradiation. (tr-auth)

29641 DISTURBANCES OF THE DEAMINATION OF CERTAIN NITROGEN COMPOUNDS IN THE LIVER DURING RADIATION SICKNESS. Akopyan, Zh. I.; Gorkin, V. Z.; Kudryashov, Yu. B.; Semina, O. V. (Inst. of Biological and Medical Chemistry, Moscow. Moscow State Univ.). Radiobiologiya; 10: 826-31(1970). (In Russian).

The acute form of radiation sickness was characterized by a decrease in the rate of deamination of biogenic amines (serotonin and tyramine) during their incubation with mitochondria isolated from the livers of irradiated rats. Cadaverine deaminase activity, which is absent in the liver mitochondria of healthy animals, appeared and increased in the liver mitochondria of irradiated rats as radiation sickness developed. In other subcellular fractions of the liver homogenate of irradiated rats, this reaction either was not detected, or it was unchanged during the entire period of radiation sickness. After intraperitoneal injection of oxidized oleic acid into rats, cadaverine deaminase activity was detected in mitochondria isolated from the liver, with a simultaneous decrease in the rate of deamination of tyramine and serotonin. (tr-auth)

29642 REACTION OF THE PITUITARY-ADRENAL SYSTEM OF DOGS TO BRIEF AND PROLONGED IRRADIATION. Shapiro, G. A.; Ostroumova, L. M. (Inst. of Biophysics, Moscow). Radiobiologiya; 10: 923-5(1970).

The influence of brief (300 R, dose rate 570 R/min) and prolonged (800 and 570 R, dose rates 1 and 0.4 R/min, respectively) irradiations on the functional activity of the adrenal cortex and changes in the peripheral blood was studied in experiments on dogs. Doses of 300 and 800 R proved equally effective with respect to the index of lethality ($LD_{35/55}$); a dose of 570 R did not cause death. In contrast to brief irradiation, prolonged irradiation was accompanied by an increase in the glucocorticoid level in the blood during later periods. An inverse relationship between the hormone level and the number of lymphocytes in the peripheral blood was also revealed on a model of prolonged irradiation. (tr-auth)

29643 INFLUENCE OF ETHAPERZINE ON THE INTEROCEPTIVE REFLEXES BEFORE AND AFTER IRRADIATION OF ANIMALS. Lapshin, N. A. (Military-Medical Academy, Leningrad). Radiobiologiya; 10: 920-2(1970). (In Russian).

The influence of ethaperazine (perphenazine) on the interoceptive unconditioned reflexes before and after irradiation was studied in 42 cats (males). It was found that in irradiated and nonirradiated animals, ethaperasinium in a therapeutic dose has no significant influence on the magnitude and nature of the interoceptive reflexes. (tr-auth)

29644 EARLY PATHOMORPHOLOGICAL CHANGES IN THE BRAINS OF ANIMALS DURING WHOLE-BODY IRRADIATION WITH HIGH-ENERGY PROTONS AND FAST NEUTRONS. Gaidamakin, N. A. Radiobiologiya; 10: 892-4(1970). (In Russian).

The pathomorphological changes in the brain during the early periods after irradiation with 120 and 660 MeV protons, in γ and mixed γ-neutron fields at doses from 50 to 1000 R, were studied in mice, rats, and rabbits. Mass destruction of cells of the oligodendroglia and microglia was observed under the ependyma of the anterior horns of the lateral ventricles, in the olfactory lobes and bulbs 6 to 8 hrs after irradiation. At a higher dose of irradiation, decomposition of the glial cells began earlier, it could already be noted after 2 hrs, and ended later, by the end of the first day. At a dose of irradiation less than 100 R, no death of the glial cells was observed. The species of animal and physical peculiarities of radiation had no influence on the nature of the detected pathomorphological changes. (tr-auth)

29645 INFLUENCE OF IRRADIATION AND RADIOPROTECTORS ON THE ACTIVITY OF ALKALINE PHOSPHATASE IN THE MUCOSA OF THE SMALL INTESTINE AND ON ITS SURFACE. Gavrilov, R. I.; Remizova, I. V. (Central Scientific Research Roentgenoradiological Inst., Leningrad). Radiobiologiya; 10: 903-6(1970). (In Russian).

The influence of whole-body x irradiation at doses of 350, 450, 500, and 700 rad on the activity of alkaline phosphatase in rats in a homogenate and on the surface of the mucosa of the proximal and distal segments of the small intestine was studied. In the zone of perimural hydrolysis and in a homogenate of the intestinal mucosa, phase changes in the activity of the enzyme, depending on the irradiation dose and the periods of observations, were noted. The possibility of a decrease in the injurious action of irradiation on enzymatic processes with the aid of radioprotectors was demonstrated. (tr-auth)

29646 EVALUATION OF THE VULNERABILITY OF VARIOUS PORTIONS OF THE GASTROINTESTINAL TRACT OF RATS UNDER THE INFLUENCE OF RADIATION. Fedotova, M. I.; Rozhdestvenskii, L. M. (Inst. of Biophysics, Moscow). Radiobiologiya; 10: 882-6(1970). (In Russian).

The dynamics of the change in the total number of cells in individual portions of the gastrointestinal tract of rats after irradiation at doses of 900, 1200, and 5000 R and the dose versus effect dependence (200 to 5000 R) were determined with the aid of a simple method developed. The aggregate of all the cells of the gastrointestinal tract can be divided into the basic radiosensitive and smaller radioresistant parts. The separate portions of the gastrointestinal tract are similar in radiosensitivity. (tr-auth)

29647 MECHANISM OF THE PROPHYLACTIC INFLUENCE OF UV IRRADIATION OF DUCKLINGS UNDER THE INFLUENCE OF X RAYS. Buturlakin, M. S. (Voronezh State Univ., USSR). Radiobiologiya; 10: 925-7(1970). (In Russian).

The influence of ultraviolet (uv) and x rays on the content of sulfhydryl (SH) groups, determined by the method of amperometric titration, in the blood and livers of ducklings after separate and combined (first uv, then x rays) influences of radiations, was studied. The concentration of SH groups was increased under the influence of uv, decreased under the influence of x rays, and almost unchanged in the case of combined radiations. (tr-auth)

29648 USE OF AN ELECTRONIC PARTICLE COUNTER TO INVESTIGATE CELL POPULATIONS OF THE BONE MARROW AFTER THE INFLUENCE OF RADIATION. Khao, Yu.; Barakina, N. F. (Univ., Liege. Inst. of Developmental Biology, Moscow). Radiobiologiya; 10: 874-7(1970). (In Russian).

A population of so-called X-cells, that appear during the recovery of bone marrow of sublethally irradiated mice, was quantitatively evaluated for the first time with the aid of a cytological technique and the use of an electronic particle counter. It was found that this population is very labile; it appeared on the 10th day after irradiation, on the 12th day it reached a high level, and disappeared

from the bone marrow between the 14th and 16th days. Possibilities of using an electronic counter in the analysis of the change in various cellular forms of the bone marrow after the influence of radiation were demonstrated. (tr-auth)

29649 EFFECT OF SURGICAL TREATMENT ON THE HEALING OF AN EXPERIMENTAL INFECTED WOUND OF THE CORNEA IN RADIATION SICKNESS. Paramei, V. T. Vestn. Oftal'mol.; 1: 68-70(Jan-Feb 1970). (In Russian).

Healing of staphylococcus-infected (strain 209) corneal wounds with and without foreign bodies (75 rabbits, 119 eyes) in radiation sickness (600 R) was studied by applying electrothermometry, bacteriology, and other methods. Antibacterial therapy (levomycetin, iodinol) contributed to the formation of a concreted cicatrix of the cornea in 45 of 49 eyes. In combined medicative and surgical treatment the eyeball could be saved in 25 out of 56 eyes only. Wounds reaching the vitreous body ended with the loss of the eye in all cases owing to enophthalmitis. The character of the eye hyperthermia depended upon the severity of the wound and the method of treatment. The adverse effect of a surgical trauma is to be ascribed to changes in the properties of the eye following radiation injury. (auth)

29650 DNA SYNTHESIS IN DIFFERENTIATING SKELETAL MUSCLE CELLS: INITIATION BY ULTRAVIOLET LIGHT. Stockdale, Frank E. (Stanford Univ., Calif.). Science; 171: 1145-7(19 Mar 1971).

As skeletal muscle cells differentiate, they fail to initiate DNA synthesis. This rigid regulation, which persists even after cells are fully developed, does not extend to repair DNA synthesis, in that uv light initiates DNA synthesis in 99 percent of the muscle nuclei exposed from chick embryos. The rate of repair DNA synthesis in these nuclei, however, drops over 50 percent at the time of cell differentiation. (auth)

29651 PROLONGATION OF SURVIVAL IN LETHALLY IRRADIATED DOGS BY PANCREATIC DUCT LIGATION. Morgenstern, Leon; Patin, C. Snyder; Krohn, Harry L.; Hiatt, Nathan (Cedars-Sinai Medical Center, Los Angeles). Arch. Surg. (Chicago); 101: 586-9(Nov 1970).

Prior pancreatic ductal ligation is a simple and effective experimental method for prolonging survival after a lethal dose of abdominal x-irradiation in dogs. In contrast to the usual average survival time of four days in lethally irradiated controls, survival times up to 153 days were achieved in animals with prior pancreatic ductal ligation. In 13 animals, the average survival time was 33 days. It is theorized that neutralization of intraintestinal proteolytic enzymes to decrease mucosal damage may prove useful clinically in enteropathies of varying etiological patterns. (auth)

29652 RADIATION HEPATITIS IN CHILDREN. Samuels, L. D.; Grosfeld, J. L.; Kartha, M. (Children's Hospital, Columbus, Ohio. Ohio State Univ., Columbus). J. Pediat.; 78: 68-73 (Jan 1971).

The relative radiosensitivity of the human liver, at least in children, was documented in two children. One of them received 2,000 rads total equivalent dose of ^{60}Co radiotherapy for Ewing's sarcoma divided over a 2 week period; severe alteration of liver function and morphology resulted, although no radiation-potentiating chemotherapy was given. A second child, treated for a Wilms' tumor in the right kidney, had clinically and pathologically severe radiation hepatitis after a similar dose of radiotherapy, which followed a course of dactinomycin chemotherapy. The traditional concept of hepatic radioresistance was not supported by these two cases, and it is suggested that critical attention be given to radiotherapy that involves all or part of the liver. (auth)

29653 EFFECT OF X-RAYS ON THE VASCULARIZATION OF THE MOUSE TESTIS. Kochar, Nirmal K.; Harrison, R. G. (Univ. of Liverpool). Fert. Steril.; 22: No. 1, 53-7(Jan 1971).

The testes of mature male mice of the A2G strain were irradiated with a single dose of 1000 R of x rays. The blood vessels of the testes were studied following the injection of India ink at a constant pressure. The blood vessels in normal testes surround the seminiferous tubules. From one to three days after irradiation there was an increase in the blood supply, vessels breached the membrana propria of the tubules, and the tubules at the periphery of the testis became increasingly vascularized. After six days there was a decrease in the blood supply to the testis, but after regeneration at 35 days this increased considerably. The results are discussed in relation to histologic and histochemical changes produced by x rays in the testis. (auth)

29654 EFFECT OF LOW DOSAGE IRRADIATION ON METABOLISM AND FUNCTION OF THE RAT KIDNEY DAMAGED BY ISCHEMIA. Truss, F.; Bargon, G. (Univ., Goettingen, Ger. Radiologische Univ., Goettingen, Ger.). Urologe, Ausg. A; 9: 350-5 (Nov 1970). (In German).

Comparative metabolic and enzymatic-chemical studies were carried out on sections of the cortex of the rat kidney in an attempt to investigate the effects of low dosage irradiation on the kidney damaged by ischemia. The damage by ischemia was produced by clamping the renal pedicle for two hours. Local, fractionated irradiation with 3×200 rads was carried out during the following 48 hours. In the animals with ischemia damage only, all parameters were clearly lowered on the 6th postoperative day but approached normal values three weeks following the operation. In the group of animals treated with irradiation following ischemia no difference from the control group was found on the 6th postoperative day. On the 21st day following the trauma, however, there was no sign of improvement of renal function in this group. Certain parameters indicated worsening of the renal function. The importance of these experiments as applied to human kidneys is discussed, especially in connection with kidney transplantation. (auth)

29655 ERYTHROPOIETIC ACTIVITY OF THE BLOOD IN FRACTIONAL IRRADIATION. Luzanov, V. M.; Muksinova, K. N. (Moscow Inst. of Biophysics). Med. Radiol.; 16: No. 2, 52-6 (Feb 1971). (In Russian).

Male Wistar rats were daily irradiated with a dose of 50 R from a ^{137}Cs γ emitter (12.5 R/min) until total doses of 150, 250, 500, 1000, and 2000 R were reached. The erythropoietic activity of the blood of experimental and control animals was determined on a model of polycythemic rats. The blood erythropoietic activity in irradiated animals increased from the first days of irradiation (total dose of 150 R). With accumulation of the total dose of irradiation the erythropoietic activity gradually increased and in total doses of 1000 to 2000 R exceeded the control values by 7 to 17 times. A correlation between alteration of the erythropoietic activity and myelopoiesis in these animals was noted. The proliferative activity of erythronormoblasts in the bone marrow increased. The shifts of hematopoiesis in prolonged fractional irradiation to a significant measure were due to alteration of the character of humoral regulation. (auth)

29656 THREE TO FIVE DAY LETHALITY IN SHEEP FOLLOWING EXPOSURE TO ^{60}Co γ RADIATION. Alter III, W. A.; Mobley, T. S.; Persing, R. L. (Air Force Weapons Lab., Kirtland AFB, N. Mex.). Health Phys.; 20: 343-5(Mar 1971).

This study was undertaken to determine the dose of radiation sufficient to kill 50% of right unilateral (class B nonuniform) ^{60}Co γ-irradiated sheep within five days (LD 50/5). Death of most animal species within 3 to 5 days postirradiation has been related to severe damage to the mucosa of the intestine, resulting in electrolyte imbalance, fluid loss, malnutrition, and septicemia. By pooling all right unilateral data from current $LD_{50/60}$ studies at this laboratory, an $LD_{50/5}$ for pulsed fission spectrum radiation (PFSR) was determined to be 565 rad midline air exposure with 95% confidence limits of 476 to 832 rad. Comparison of $LD_{50/5}$ doses for PFSR and γ radiation will permit the relative biological effectiveness to be determined for these types of radiation in causing 3 to 5 day postirradiation death. (UK)

29657 DYNAMICS OF THE CHANGE IN THE RESIDUAL INJURY IN THE GASTROINTESTINAL FORM OF DEATH OF MICE AFTER GAMMA IRRADIATION. Kovalev, V. P. (Inst. of Biological Physics, Pushchino, USSR). Radiobiologiya; 10: 764-7(1970). (In Russian).

The dynamics of the recovery of the intact mammalian organism from subiethal γ irradiations in the case of the gastrointestinal form of death was studied. In the dose range of 350 to 500 R, the period of half recovery was less than one day. Within 3 to 4 days the radiation damage was entirely repaired. (tr-auth)

29658 PROTECTION OF DOGS FROM THE EFFECT OF IONIZING RADIATION BY SHIELDING OF A SMALL PORTION OF THE BONE MARROW. Bogatyrev, A. V.; Sverdlov, A. G.; Kavukchyan, T. V. (Ioffe Inst. of Physics and Tech., Leningrad). Radiobiologiya; 10: 766-8(1970). (In Russian).

It was found that shielding of the elbow joint of dogs during x irradiation at doses of 450 and 600 R leads to an increase in the survival rate and a decrease in the severity of radiation sickness. (tr-auth)

29659 RADIOSENSITIVITY OF ROE OF PIKE (ESOX LUCIUS L.) DURING FERTILIZATION AND EARLY CLEAVAGE. Kulikov, N. V. (Inst. of Plant and Animal Ecology, Sverdlovsk, USSR). Radiobiologiya; 10: 768-70(1970). (In Russian).

A sharp change in the radiosensitivity of pike roe during fertilization and early cleavage of the zygote was noted. It is sug-

gested that the first peak of the radiosensitivity corresponds to the stage of approach of the male and female pronuclei, while the following peaks are associated with intermediate phases of the mitotic cycles of the early embryonic mitoses. (tr-auth)

29660 ANTITISSUE ANTIBODIES DURING RADIATION SICKNESS. Alekseeva, O. G. (Inst. of Labor Hygiene and Occupational Diseases, Moscow). Radiobiologiya; 10: 753-5(1970). (In Russian).

The antibodies for homologous thyroglobulin in 406 noninbred white rats were studied by the method of semimicroprecipitation in gel. Among 99 control intact animals, as well as 67 essentially healthy adult rats, subjected to six month internal administration of ^{131}I (6.4 and 12.8 μCi/g) or irradiation (50 and 100 R) or a combined influence, no antibodies were detected. Antibodies were found in 20 to 30% of the essentially healthy rats after 10-day administration of ^{131}I (0.1 μCi/g) and in animals with acute radiation sickness from a single γ irradiation (300 R) or a combined influence; moreover, in one and one and a half-month old rats, antibodies appeared on the 30th day, while in adult rats, they appeared on the 10th day from the beginning of the experiment. (tr-auth)

29661 EGG LAYING OF HENS UNDER THE ACTION OF INCORPORATED ^{131}I. Kirshin, V. A.; Budarkov, V. A.; Frolov, V. P.; Belousov, L. I. (State Veterinary Inst., Kazan). Radiobiologiya; 10: 736-40(1970). (In Russian).

The effects of incorporated ^{131}I on the egg laying of hens were studied. Doses of the isotope equal to 5, 20, and 42.5 mCi per laying hen, in the case of single and fractionated oral introduction, induced a cessation in egg laying. Hens that received 1.2 mCi did not cease their egg laying, but they did not bear fertilized eggs until two weeks after the end of the treatment. During later periods the number of fertilized eggs was comparable with that in the control. The hatching rate of chicks from the eggs of the experimental hens was lower than the control. (tr-auth)

29662 STUDY OF THE BIOSYNTHESIS OF LIVER AND SPLEEN HISTONES OF IRRADIATED ANIMALS. Paskevich, L. V.; Shishkova, G. A.; Paskevich, I. F. (Kharkov Scientific Research Inst. of Medical Radiology). Radiobiologiya; 10: 740-3(1970). (In Russian).

The biosynthesis of liver and spleen histones of white rats 24 hrs after irradiation at a dose of 800 R was studied. It was established by chromatography on carboxymethylcellulose that a substantial activation of biosynthesis of the lysine-rich fraction of the histones takes place in the liver as a result of irradiation. In the spleen, irradiation induced a sharp suppression of the synthesis both of the lysine-rich and of the arginine-rich fractions. In both organs the synthesis of the arginine-rich histone fraction changed less in comparison with the lysine fraction. (tr-auth)

29663 DETERMINATION OF THE ACTIVITY OF THE METHIONINE-METHYL-ACTIVATING ENZYME IN VIVO IN THE LIVERS OF RATS IRRADIATED WITH A LETHAL DOSE OF X RAYS. Voskoboinikov, G. V. (Central Scientific Research Roentgenoradiological Inst., Leningrad). Radiobiologiya; 10: 743-5(1970). (In Russian).

The accumulation of S-adenosylethionine in the tissue of rats after their injection with ethionine was used as an index of the activity of ATP:L-methionine-S-adenosyltransferase, the rate of activation of methionine, and the rate of utilization of ATP in vivo under the conditions of radiation sickness. It was found that the intensity of activation of the amino acid and the rate of utilization of ATP in the livers of rats irradiated at a dose of 1000 R directly before treatment with ethionine, as well as in rats irradiated 24 hrs before the injection, remained at the control level. (tr-auth)

29664 PROTEIN FRACTIONS OF HOMOGENATES AND MITOCHONDRIA OF THE SMALL INTESTINE AND BRAIN OF IRRADIATED ANIMALS. Makhlina, A. M.; Tolchenova, G. A.; Abuzina, T. N. (Leningrad State Univ.). Radiobiologiya; 10: 745-8(1970). (In Russian).

The protein fractions of homogenates and mitochondria of the wall of the small intestine and the brain of rabbits subjected to whole-body x irradiation at a dose of 3 kR were investigated by the method of column chromatography. Together with significant changes in the chromatographic fractions of the proteins of the homogenates and mitochondria of the intestines, no significant changes were detected in the protein fractions of homogenates and mitochondria of the brain 72 hrs after irradiation. (tr-auth)

29665 INFLUENCE OF IRRADIATION OF UNFERTILIZED OVA OF RATS ON THE DYNAMICS OF THE FORMATION OF LDH ISOENZYMES DURING THE PROCESS OF POSTNATAL DEVELOPMENT. Vygovskaya, G. P. (Moscow Technological Inst. of the Meat and Milk Industry). Radiobiologiya; 10: 748-50(1970). (In Russian).

The change in the isoenzymes of lactate dehydrogenase (LDH) in liver, heart, and spleen tissues of baby rats from females and males irradiated at a dose of 400 R during 20 days of postnatal development was investigated. It was found that in the offspring of irradiated males there were no significant changes both in the total activity of LDH and in its isoenzyme composition. In the liver and spleen tissues of baby rats from irradiated females, a delay of the synthesis of the H subunits and, consequently, a drop in the H/M ratio was observed. The total LDH activity in the liver was significantly reduced in all the investigated periods. (tr-auth)

29666 COMPLEX ACTION OF VIBRATION AND X IRRADIATION ON THE DEVELOPMENT AND CONSERVATION OF THE MAZE HABIT IN RATS. Skobeev, E. M. (Inst. of Biological Physics, Pushchino, USSR). Radiobiologiya; 10: 715-19(1970). (In Russian).

Rats were subjected to the influence of a general vertical vibration with a frequency of 70 Hz, amplitude 0.4 mm, duration 15 min, followed by x irradiation at a single dose of 50 R. The interval between the first and second complex exposures was 14 days, and between the second and third, seven days. After the first influence, the number of errors in the maze was insignificantly reduced; the latent period and time of running were shortened. After the second and third influences a certain insignificant deterioration of the indexes of establishment of the maze habit was observed. The latter effect was considered as dominance of the radiation effect. (tr-auth)

29667 SOME PECULIARITIES OF THE ELECTRORETINOGRAM IN DOGS IRRADIATED WITH X RAYS DURING EMBRYOGENESIS. Piontkovskii, I. A.; Arzumanov, Yu. L. (Inst. of Higher Nervous Activity and Neurophysiology, Moscow). Radiobiologiya; 10: 710-14(1970). (In Russian).

The electroretinogram (ERG) was studied in 29 young dogs (18 prenatally irradiated with x rays, 11 intact) during postnatal ontogenesis. An analysis of the data obtained gave a basis for concluding that the ERG in animals subjected to ionizing radiation during embryogenesis was formed with a 2 to 3 day lag. The amplitudes of the "a" and "b" waves were lower than in the control dogs. The synchronization of the firing of the neutrons that generate the "b" wave, according to the index of the slope, was lower for the irradiated than for the intact animals. There was a biological inadequacy of the nuclei of the photoreceptors and bipolar cells, which was confirmed not only by the ERG data, but also by morphological investigations. (tr-auth)

29668 CHANGE IN THE KININ SYSTEM OF THE BLOOD DURING ACUTE RADIATION SICKNESS. Gaponyuk, P. Ya.; Umarkhodzhaev, E. M. (Inst. of Medical Radiology, Obninsk, USSR). Radiobiologiya; 10: 681-4(1970). (In Russian).

Changes in the concentration of kininogen, the kinin-forming activity, and kininase activity of the blood in rats during various periods of acute radiation sickness (irradiation with ^{60}Co at doses of 800 and 900 R, 48 R/sec) were studied. An increase in the kininogen concentration in the blood was detected 3, 7, and 12 days after irradiation. On the third to fourth days after irradiation, against a background of a pronounced gastrointestinal syndrome and the highest death rate peak among the irradiated rats, the kinin-forming activity of the blood was significantly increased, while the kininase activity was lowered. An accumulation of kinins in the irradiated organism three to four days after irradiation and their participation in the pathogenesis of acute radiation sickness is suggested. (tr-auth)

29669 PECULIARITIES OF DAMAGE AND RECOVERY OF IRRADIATED LYMPH NODES IN THE CASE OF SHIELDING OF HALF THE BODY. Pozharisskaya, T. D. (Military Medical Academy, Leningrad). Radiobiologiya; 10: 685-9(1970). (In Russian).

The changes in the lymph nodes of white rats after whole-body and partial-body irradiation were studied. No significant differences in the lymph nodes after whole-body and partial-body irradiation were detected during the period of destruction. The restoration of the cellular composition of the node after partial-body irradiation occurred considerably more rapidly than in the case of whole-body irradiation. From an analysis of the data obtained it was concluded that the acceleration of recovery processes in irradiated nodes in the presence of nonirradiated portions of the body is associated with a repopulation of the destroyed nodes with undamaged lymphocytes from the shielded regions. (tr-auth)

29670 EFFECTS OF IONIZING RADIATION ON THE HORMONAL INDUCTION OF LACTATE DEHYDROGENASE IN THE

XUM

UTERI OF SEXUALLY IMMATURE RATS. Slozhenikina, L. V.; Migushina, V. L.; Kuzin, A. M. (Inst. of Biological Physics, Pushchino, USSR). Radiobiologiya; 10: 643-7(1970). (In Russian).

The effects of ionizing radiation on the induction of lactate dehydrogenase activity by estradiol and its isoenzyme spectrum in the uteri of sexually immature rats were investigated. Resistance of hormonal induction of lactate dehydrogenase in the hormone-dependent organ (the rat uterus) after γ irradiation of the animals at doses of 500 and 1000 R was demonstrated. (tr-auth)

29671 HISTOCHEMICAL CHANGES IN THE MEDULLAR AND CORTICAL TISSUE OF THE ADRENAL GLAD AFTER LOCAL IRRADIATION OF THE HEAD. Tkacheva, G. A. (Inst. of Medical Radiology, Obninsk, USSR). Radiobiologiya; 10: 653-7 (1970). (In Russian).

The histochemical reactions of the cortical and medullar tissues of the adrenal gland were studied in inbred white rats, subjected to local irradiation. The initial effect of irradiation was manifested in a parallel mobilization of the secretory products of the chromaffinic and cortical tissues. A subsequent change in the histochemical reactions indicated an intensive biosynthesis of corticosteroids and catecholamines. The inhibition of the function of the adrenal cortex two weeks after the radiation influence was combined with a high level of secretory activity of the medullar substance. Under such conditions the medullar component was incapable of compensating for the absence of the trophic influence of the pituitary on the adrenal cortex. (tr-auth)

29672 INFLUENCE OF ADRENALECTOMY ON THE POST-RADIATION CHANGES IN DNA SYNTHESIS IN THE LYMPHOID ORGANS OF RATS. Skurikhina, M. M.; Tereshchenko, O. Ya. (Inst. of Biophysics, Moscow). Radiobiologiya; 10: 648-52(1970). (In Russian).

The postradiation change in DNA synthesis in the lymphoid organs of adrenalectomized rats was studied. Using ^{14}C-thymidine as the labeled precursor, its incorporation into the DNA of the spleen and thymus gland of irradiated control and irradiated adrenalectomized rats was measured (dose of irradiation 750 R, γ rays of ^{60}Co, whole-body irradiation). The postradiation decrease in the rate of incorporation of ^{14}C-thymidine into the DNA of the spleen and thymus gland of the control and adrenalectomized rats was determined to a substantial degree by the dilution of the label with endogenous thymidine. Adrenalectomy reduced the postradiation inhibition of DNA synthesis and activated the synthesis of deoxypyrimidines. (tr-auth)

29673 THE ABILITY OF MANGANESE TO PENETRATE THROUGH THE MITOCHONDRIAL MEMBRANES IN THE NORMAL STATE AND AT EARLY PERIOD AFTER THE INFLUENCE OF IONIZING RADIATION. Gorizontova, M. P.; Trebenok, Z. A. (Inst. of Biophysics, Moscow. Inst. of Normal and Pathological Physiology, Moscow). Radiobiologiya; 10: 690-3(1970). (In Russian).

The accumulation of ^{54}Mn by the liver mitochondria of intact and irradiated mice was studied. Two series of experiments were conducted: with the introduction of the isotope in vivo (intraperitoneal injection) and with introduction of the isotope in vitro (into the incubation medium). In both series of experiments an increase in the accumulation of ^{54}Mn by the liver mitochondria of irradiated mice was noted 24 hrs after irradiation. The question of the role of disturbance of the permeability of the mitochondrial membrane in the mechanism of the intensified accumulation of ^{54}Mn by the mitochondria after irradiation is discussed on the basis of the data obtained. (tr-auth)

29674 EFFECTS OF X RAYS ON THE METABOLISM OF CALCIUM IONS IN THE MEMBRANES OF THE SARCOPLASMIC RETICULUM OF PHASE MUSCLE CELLS. Nadareishvili, K. Sh.; Saneblidze, O. I. (Inst. of Physiology, Tbilisi, USSR). Radiobiologiya; 10: 694-9(1970). (In Russian).

The effects of x radiation on the strength, duration, rate of contraction, and relaxation, as well as the effects of addition of ATP during potassium and caffeine contractures were studied on frog sartorius muscles. It was discovered that in the dose range 5 to 30 krad there was a decrease in the rate of contraction and an increase in the rate of relaxation during potassium and caffeine contractures. At doses of 50 krad and more, both the rate of contraction and the rate of relaxation were reduced. An attempt was made to explain these and a number of other facts by a radiation change in the metabolism of calcium ions in the cavities of the sarcoplasmic reticulum. (tr-auth)

29675 HISTOLOGICAL AND ELECTRON MICROSCOPIC INVESTIGATION OF THE CHANGES IN THE STRUCTURE OF THE NEURONS OF THE UPPER CERVICAL SYMPATHETIC GANGLION AFTER X IRRADIATION AT A DOSE OF 1400 R. Ferents, A. I. (Inst. of Microbiology and Virology, Kiev). Radiobiologiya; 10: 658-62(1970). (In Russian).

The changes in the structures of the neurons of the upper cervical sympathetic ganglion of rabbits after whole-body x irradiation at a dose of 1400 R were studied. Hyperimpregnation of the nerve cells, vacuolization of the cytoplasm, nonuniform chromatolysis, hypochromia of the nucleus, as well as swelling of the mitochondria with breakdown of the cristae, dilation of the tubules of the endoplasmic reticulum with partial lysis of the membranes delimiting them, reduction of the fine vesicles of the Golgi apparatus, folding of the nuclear membrane, dilation of its pores and the perinuclear space, and a redistribution of the substance of the karyoplasm were detected by neurohistological and electron microscopic methods. The detected changes are described in the dynamics of the development of acute radiation sickness. (tr-auth)

29676 MECHANISMS OF THE PRIMARY DESTRUCTION OF HEMATOGENIC TISSUE OF MAMMALS UNDER THE INFLUENCE OF IONIZING RADIATION. Barakina, N. F. (Inst. of Developmental Biology, Moscow). Radiobiologiya; 10: 668-71 (1970). (In Russian).

Primary aplasia of the bone marrow at various stages of development in mice was studied quantitatively under the influence of doses of 200, 400, 700, and 1000 R. With increasing radiation dose, the relative role of the delay of cellular reproduction in the destruction of proliferative cells was reduced, whereas the specific role of interphase death increased. In the first stages, the number of cells undergoing maturation was practically unchanged, which can be explained by a delay of their discharge into the peripheral blood leading to the absence of significant changes in the total number of nucleated cells within a broad range of doses. (tr-auth)

29677 RESISTANCE TO REPEATED IRRADIATION OF CELLS BY IMMUNOCOMPETENT AND HEMATOGENIC TISSUE IN MICE. Cheredeev, A. N. (Inst. of Biophysics, Moscow). Radiobiologiya; 10: 663-7(1970). (In Russian).

Studies were made to establish the dose versus effect dependence and to compare the parameters of the dose versus effect curves for immunocompetent and hemopoietic precursors of spleen tissue in normal and irradiated mice. Seven, 14, and 21 days after irradiation at a dose of 500 R, the immunocompetent cells of mice were several times more resistant to the influence of radiation than the cells of nonirradiated mice. By 30 to 60 days after irradiation, the radiosensitivity of the antibody producers approached the normal level. The radiosensitivity of the stem cells of the spleen tissue, both in intact and irradiated mice, proved to be practically the same in any of the investigated periods. The possible mechanisms of the increased radioresistance of the immunocompetent cells are discussed. (tr-auth)

29678 EFFECT OF X-IRRADIATION ON MIGRATION OF AMELOGENIC CELLS IN THE RAT INCISOR. Willhoit, Donald G.; Alexander, John P. (Univ. of North Carolina, Chapel Hill.). Contract AT(40-1)-3554. J. Dent. Res.; 50: 504(Mar-Apr 1971).

The effects of x radiation on the migration rate of amelogenic cells in continuously growing rat incisors was studied as the first step in the characterization of the kinetics of radiation action on this in vivo system. Rats were given single injections of 0.5 μc of tritiated thymidine 1 hr to 12 days following x-ray head exposure. The distance of the first labeled preameloblast from the enamel matrix varied. This indicated that the maturation-differentiation compartment is not decidedly sensitive to irradiation. Thus blockage of the proliferating compartment decreased its size because of maturation depletion. It had virtually disappeared three days post-irradiation. (E.E.H.)

29679 COMBINED EFFECT OF 6-AZAURIDINE AND IRRADIATION IN VIVO AND IN VITRO. VI. NUCLEAR DIAMETERS OF EHRLICH ASCITES CARCINOMA CELLS AFTER REPEATED IRRADIATED AND 6-AzUR APPLICATION. Grozdanovic, J.; Vich, Z.; Truxova, G.; Kratochvil, J. (Health Inst. of Uranium Industry, Pribram, Czech.). Neoplasma; 17: 601-6(1970).

By measuring the nuclear diameters of Ehrlich ascites tumor cells of mice, it was found that repeated x radiation alone or combined with 6-Azauridine, will increase the diameters of the cell nuclei. This result correlates with the results of earlier studies concerning the increase in DNA level in the cells. In passages where 6-Azauridine alone or prior to irradiation was applied, this phenomenon did not occur. Possible reasons for these results are discussed. (E.E.H.)

29680 KINETICS OF THE TUMOUR GROWTH AND TIME FACTOR IN THE RADIOTHERAPY. Dubinin, I.; Karasek, J. (Medical Faculty UJEP, Brno). Neoplasma; 17: 621-4(1970).

On the basis of the exact relationships between tumor proliferation with time and tumor destruction by radiation, analytical expression of the empirical curve of the tumor lethal dose time dependence was derived. (auth)

29681 CHANGES OF PLASMA KININOGEN AND KININ-FORMING ACTIVITY IN IRRADIATED ANIMALS. Gaponiuk, P. Ya.; Umarchodgaev, E. M. (Medical Radiology Inst., Obninsk, USSR). Stud. Biophys.; 17: 13-18(1969).

The concentration of kininogen and kinin-forming activity of plasma was studied at varying times following whole-body ^{60}Co γ irradiation of rats. An increase in plasma kininogen concentration was observed 4, 8, and 13 days after irradiation. On days three and four, an increase in plasma kinin-forming activity was observed, but it was accompanied by pronounced gastrointestinal disturbances and maximum mortality of the irradiated animals. It is presumed that kinins participate in the pathogenesis of x radiation sickness. The possibility of kinin participation in the reaction of blood vessels following irradiation is also suggested. (E.E.H.)

29682 PROCEEDINGS OF A SYMPOSIUM ON CROSS-SPECIES TRANSPLANTATION, BRIGHTON, UTAH, MAY 8-9, 1970. Transplant. Proc.; 2: 431-559(Dec 1970). (CONF-700551).

Eighteen papers are included in this final compilation of the symposium proceedings; one paper was abstracted separately in NSA. The remaining 17 papers contain information on cross-species transplantation in embryonic and neonatal animals, molecular-genetic approaches to animal classification, xenografts of skin in mice, organ transplantation, and the role of antigens in transplantation. (E.E.H.)

For an abstract of an individual paper see: 29683.

29683 RADIATION CHIMERAS. van Bekkum, D. W. (Radiobiological Inst., TNO, Rijswijk, Netherlands). Transplant. Proc.; 2: 479-82(Dec 1970).

From Conference on cross-species transplantation, Salt Lake City, Utah (8 May 1970). See CONF-700551.

The conditions that permit a bone marrow xenograft take, the significance of xenogeneic bone marrow grafting, and the prospects of using bone marrow xenografts in place of allografts for clinical purposes are discussed. At this time, increasing the number of grafted cells and the dose of whole-body irradiation to the recipients are the main approaches in producing xenogeneic bone marrow takes. Attempts have been made to extend this principle of radiation chimerism to organ grafting with limited success. It is expected that banks of HLA typed bone marrow cells, obtained from cadavers, will become an important source for transplants and xenogeneic transplantation will not be necessary. (E.E.H.)

29684 FUNCTION AND MORPHOLOGY OF HYPERTROPHIC RABBIT KIDNEYS FOLLOWING TELECOBALT IRRADIATION WITH 1000 TO 4000 RAD. Bargon, Gerlach; Moench, Helga (Radiologische Univ., Goettingen, Ger.). Strahlentherapie; 140: 693-705(Dec 1970). (In German).

The influence of cobalt-60-gamma irradiation (1000 to 4000 rad) on renal function was examined in experiments with rabbits by delicate nephrological research methods (LAP activity in the urine, determination of the endogenous plasma creatinine, PSP test). The results achieved from the functional tests were compared with results of the morphological examinations that were carried out at the same time. It became evident that the radiation lesion of the kidney was initiated by an increase of permeability of the membrane at the tubular cell and at the glomerular capillary. Seven to 21 days after irradiation, glomerular and tubular functional disturbances and morphological alterations manifested, both of them dose dependent, at the glomerulus and at the tubulus. (auth)

29685 LIPID FRACTION ALTERATIONS IN SERUM AND LIVER OF RATS EXPOSED TO 2000 R LOCAL HEPATIC IRRADIATION: ACTIVITY OF ALKALINE PHOSPHATASE, GOT, AND LIPASES. Gottwald, Gizella; Meszaros, Iren; Bathori, Edit (Medizinisch-Radiologische Forschungsgruppe, Budapest). Strahlentherapie; 140: 731-7(Dec 1970). (In German).

After local rat liver irradiation with 2000 R, the changes of single lipid fractions and of single liver enzymes were examined along with those of the serum. The results justified the supposition that the origin of radiation-induced hyperlipemia is decisively influenced by the liver. The doses used caused only very few alterations in enzyme activity. (auth)

29686 ESTERASE ACTIVITY AND PROTEIN CONTENT OF PLASMA ERYTHROCYTES IN WHOLE-BODY IRRADIATED RATS. Valet, Guenter; Ruhenstroth-Bauer, Gerhard (Max-Planck-Institut fuer Biochemie, Munich). Strahlentherapie; 140: 738-44(Dec 1970). (In German).

The following items of 500 R whole-body irradiated rats (LD 38/30) were examined from day 1 to 18 after irradiation: esterase activity between pH 5.0 to 8.5; protein content; and volume of plasma and erythrocytes. Total plasma, total plasma-protein-content, plasma-protein-concentration, and total plasma-esterase-content decreased after irradiation, whereas the plasma-esterase-concentration temporarily increased beyond the initial values, owing to a more significant loss of non-esterase-active proteins. Volume, protein content, and protein concentration of the erythrocytes altered, during the period of experiments, in a non-measurable manner. Esterase content and esterase concentration continuously decreased to subnormal values. The erythrocyte manifested no obvious reaction to irradiation, if compared to the plasma and to the cells of spleen and liver. (auth)

29687 CAPABILITY FOR LEARNING AND MEMORIZING OF TRAINED QUAILS FOLLOWING HEAD IRRADIATION. Konermann, Gerhard (Univ., Freiburg i. B.). Strahlentherapie; 140: 757-64(Dec 1970). (In German).

Using a double-choice-method with food reward, Japanese quails learned to discriminate plates with black and white or with colored geometrical figures. The acquisition and retention of the discrimination tasks were studied with special regard to the influence of x-irradiation given as head exposure at different dose levels. The irradiations were given either in a single dose immediately after the acquisition of a discrimination task or fractionated after each daily session of trials. As compared with unirradiated controls, acute insults with 200 R as well as with 1000 R were without influence on performance and retention after an interval of three weeks from the learning trials and the x-ray treatment. Also daily insults with 200, 500, and 1000 R after each of the first five sessions of trials did not affect the learning ability itself, but only the performance capacity after the total dose of 5000 R. (auth)

29688 ROLE OF THE FUNCTIONAL STATE OF THE HYPOTHALMUS DURING BIOELECTRICAL REACTIONS OF THE BRAIN CORTEX TO IRRADIATION. Tokhiyan, S. R. Biol. Zh. Arm.; 23: 100(Aug 1970). (In Russian).

In order to test the influence of the hypothalmus on bioelectric reactions of the brain in rabbits, an electrocoagulation of mammalian bodies of the hypothalmus of 23 rabbits was conducted. Six rabbits were maintained as controls. On a background of inhibited bioelectric activity, the cortex registered high frequency flashes of considerable amplitude. The reaction of the brain of irradiated animals with diencephalic pathology was characterized by profound disturbances of the bioelectric activity, reactivity, and assimilability of rhythm, in comparison with nonirradiated controls. (K.S.W.)

Man

Refer also to abstracts 29447, 29498, 29500, 29501, 29516, 29573, 29595, and 29603.

29689 PATHOLOGY OF IRRADIATION. Berdjis, Charles C. (ed.). Baltimore; Williams and Wilkins Company (1971). 719p.

Separate abstracts were prepared for the 26 chapters included. (P.B.M.)

For abstracts of individual chapters see: 29457, 29573, 29624–29636, and 29690–29700.

29690 GENERAL CONSIDERATION. Berdjis, C. C. pp 1-9 of Pathology of Irradiation. /Berdjis, Charles C. (ed.). Baltimore; Williams and Wilkins Co. (1971).

Roentgen rays and radiations from radioactive substances produce physical, chemical, and biological effects. The biologic effects of radiation are due to production of ions within the living cells. In man and animals the reaction to irradiation is dominated by the acute radiation syndrome and its biologic consequences. There are two types of radiation effects, direct and indirect, and three factors influencing radiation effects, individual factors, environmental factors, and physiopathologic factors. (P.B.M.)

29691 RADIATION CARCINOGENESIS: EXPERIMENTAL AND CLINICAL ASPECTS. Rosen, V. J. (Mount Sinai Hospital, Los Angeles); Cole, L. J. pp 120-145 of Pathology of Irradiation. /Berdjis, Charles C. (ed.). Baltimore; Williams and Wilkins Co. (1971).

XUM

The clinical and experimental aspects of carcinogenesis induced by ionizing radiation are reviewed. Radiation may cause neoplasia in man because of its ability to induce somatic mutations. The dose, dose rate, quality, and intensity of the radiation are factors in determining the type of neoplastic response. In radioinduced carcinogenesis the dose response curve is not linear. (P.B.M.)

29692 EFFECTS OF IRRADIATION ON THE NERVOUS SYSTEM. Zeman, W. (Indiana Univ., Indianapolis); Samorajski, T. pp 213-77 of Pathology of Irradiation. /Berdjis, Charles C. (ed.). Baltimore; Williams and Wilkins Co. (1971).

The pathologic effects of ionizing radiation on the human nervous system were studied. Some variables, which govern the effects of x irradiation on the nervous structures, are that different parts of the nervous system react heterogenously to ionizing radiation and that individual and species differences alter the effects of the irradiation. (P.B.M.)

29693 EFFECTS OF IRRADIATION ON SALIVARY GLANDS. Glucksmann, A.; Cherry, C. P. (Strangeways Research Lab., Cambridge, Eng.). pp 290-5 of Pathology of Irradiation. /Berdjis, Charles C. (ed.). Baltimore; Williams and Wilkins Co. (1971).

Ionizing radiation effects on three major salivary glands in mammals and the mucous and serous glands associated with the tongue of man were studied. X irradiation is followed at first by hypersecretion of mucin in the acini, often with inspissation of the mucus and degeneration of the secretory cells. The reserve cells proliferate, form cuboidal and subsequently prickle and parakeratotic cells which transform the ascini into solid squamous formations. Ducts of the mucous and serous glands tend to change their epithelium in places from a columnar to a stratified squamous type, leading to an occlusion of the lumen. (P.B.M.)

29694 LIVER. Lacassagne, A. M. B. (Univ., Paris). pp 345-76 of Pathology of Irradiation. /Berdjis, Charles C. (ed.). Baltimore; Williams and Wilkins Co. (1971).

Studies on the action of ionizing radiations on liver regeneration were carried out in irradiated animals. Hepatic lesions were obtained with γ and x rays. The development of a cirrhosis is evidence of a relative radiosensitivity of the connective tissue that is greater than that of the glandular tissue. The apparition of biliary neotubules was noted following external or internal irradiation. (P.B.M.)

29695 CARDIOVASCULAR SYSTEM. Berdjis, C. C. pp 377-407 of Pathology of Irradiation. /Berdjis, Charles C. (ed.). Baltimore; Williams and Wilkins Co. (1971).

Ionizing radiations produce cardiovascular disorders. Radioinduced changes in the myocardium or vascular system are produced either by direct action or by interference with myocardial metabolic processes and vascular functions. The injurious effects of x radiation to the human heart and vascular structure consist of vascular changes, cardiomyopathy, and myocardial enzyme disturbances. The pathologic picture produced by irradiation is a moderate to severe degree of vasculitis and or myocarditis with edema and degeneration leading to late myocardial fibrosis and vascular sclerosis. The radioinduced cardiovascular damage is dose dependent. (P.B.M.)

29696 LYMPHOID TUMORS AND RADIATION. Maisin, J. (Univ., Louvain, Belg.); Maisin, J. R.; Dunjic, A. pp 542-68 of Pathology of Irradiation. /Berdjis, Charles C. (ed.). Baltimore; Williams and Wilkins Co. (1971).

Human radioinduced leukemia is a rare disease; however, the influence of γ and x radiation on the incidence of human leukemia was thoroughly investigated, mainly among the survivors of the bombings of Hiroshima and Nagasaki, radiologists exposed to repeated small doses of radiation, patients irradiated for chronic arthritis, and children irradiated for thymic hypertrophy. (P.B.M.)

29697 RADIATION PATHOLOGY OF THE GENITOURINARY TRACT. Rosen, B. J. (Mount Sinai Hospital, Los Angeles). pp 592-6 of Pathology of Irradiation. /Berdjis, Charles C. (ed.). Baltimore; Williams and Wilkins Co. (1971).

Most changes in the ureters and bladder of man are associated with high therapeutic doses of ionizing radiation, both from externally applied sources and from radium and radon seed implantations. Effects on the genitourinary tract result from complications of x radiotherapy, especially with the increasing use of supervoltage techniques in treating bladder, rectal, and prostatic neoplasms. The term radiation cystitis covers a multitude of alterations seen in the bladder and ureters as a result of exposure. (P.B.M.)

29698 KIDNEY. Mostofi, F. K. (Armed Forces Inst. of Pathology, Washington, D. C.); Berdjis, C. C. pp 597-635 of Pathology of Irradiation. /Berdjis, Charles C. (ed.). Baltimore; Williams and Wilkins Co. (1971).

Although the kidney was once thought of as radioresistant, it is now known that x radiation causes renal injury and diseases in man. The post irradiation syndrome consists of four parts, sclerosing nephrosis, mild, without nephrosclerosis, sclerosing nephrosis, with mild or severe nephrosclerosis, sclerosing nephrosis, mild or severe, with hypertensive necrotizing vasculitis with no nephrosclerosis, and nephroglomerulosis. This group of radioinduced kidney diseases is commonly designated as chronic radiation nephritis. (P.B.M.)

29699 ACUTE IRRADIATION IN MAN: TREATMENT OF HEMATOLOGIC DISORDERS. Mathe, G.; Amiel, J.-L.; Schwarzenberg, L. (Univ., Paris). pp 636-68 of Pathology of Irradiation. /Berdjis, Charles C. (ed.). Baltimore; Williams and Wilkins Co. (1971).

The effects of acute whole body x irradiation in man can only be studied precisely in patients who are irradiated as part of a therapeutic procedure, for they are the only ones in which the dose received is known accurately. The consequences of whole body external irradiation were observed at high doses in 40 patients. Whole body external irradiation causes profound abnormalities of the cells of the blood and hematopoietic system which can be analyzed by cytologic examination of the blood and hematopoietic organs as well as histologic studies of the hematopoietic tissues. (P.B.M.)

29700 ORGANS OF SPECIAL SENSES. pp 669-89 of Pathology of Irradiation. /Berdjis, Charles C. (ed.). Baltimore; Williams and Wilkins Co. (1971).

Studies were done on the external ionizing radiation effects on the human eye. Age influences the degree of the irradiation effect. The effects of x radiation on adult human retina appear to be mainly on the blood vessels. (P.B.M.)

29701 MULTIPLE BASAL CELL CARCINOMAS ARISING IN RADIATED BURN SCARS. Stone, Nelson H.; Montiel, Milka M. (Northwestern Univ., Evanston, Ill. Chicago Medical School). Plast. Reconstr. Surg.; 46: 506-9(Nov 1970).

A case is reported of a patient who developed seven synchronous basal cell carcinomas near the groins and elbows in burn scars that had been treated many years ago with radiation. A co-carcinogenic etiology (burns plus radiation) is suggested. (auth)

29702 RADIATION INDUCED BONE SARCOMA. Kolar, J.; Palecek, L. (Charles Univ., Prague). Radiol. Diagn.; 11: 485-92(1970).

A case study of an osteogenic sarcoma of the frontal bone is reported, that was induced by combined x ray and radium therapy for malignant retinoblastoma twelve years ago in a girl, irradiated at the age of two years. A summarizing review of other reported cases in the medical literature is given, comprising 75 cases, mostly following irradiation during childhood for malignant retinoblastoma or other tumorous conditions. The latent period was longer than five yrs, and there were no distinct interrelationships between the doses of radiation administered to the patients and the formation of a malignant neoplasm in the underlying skeletal tissue. (auth)

29703 RADIOBIOLOGICAL PRINCIPLES OF RADIATION HYGIENE. Klener, V. Cas. Lek. Cesk.; 109: 986-8(9 Sep 1970). (In Czech).

Valuable information for radiation hygiene may be obtained from radiobiologic studies that follow the frequency of late changes with respect to the dose and its space and time distribution. An analysis of several factors that should be examined during the study of delayed effects of radiation is presented. (auth)

29704 STUDIES ON LYMPHOCYTES DURING EXTRACORPOREAL IRRADIATION OF THE BLOOD IN PATIENTS WITH ACTIVE CIRRHOSIS. Andersen, Vagn; Bjerrum, Ole; Ranek, Leo (Univ. Hospital, Copenhagen). Scand. J. Haematol.; 7: 471-7(Dec 1970).

The lymphocyte concentration in the blood was followed closely in four patients with active cirrhosis who were treated with extracorporeal irradiation of the blood (ECI). A reduction to 25% of the original values was obtained, and three months after treatment the lymphocyte concentration remained below 50% of pretreatment values. This was not significantly different from the results previously obtained in uremic patients although a much more concentrated treatment schedule was employed in the present patients. This shows that the large majority of the recirculating lymphocytes pass through the blood within 3 to 4 days. In vitro stimulation of blood lymphocytes with phytohaemagglutinin showed that in the three patients studied the response per cell did not change significantly during ECI. However, the initially positive transformation response to tuberculin in vitro changed into a negative one during ECI in all cases, indicating that a selective depletion of the tuberculin-sensitive cells of the blood took place during ECI. (auth)

XUM

29705 RADIATION AND LEUKEMIA RATES. Saenger, Eugene L. (Univ. of Cincinnati); Tompkins, Edythalena; Thoma, George E. Science; 171: 1096; 1098(19 Mar 1971).

A reply is given to a criticism by E. B. Lewis, Science 168, 315 (1970) of an article on Incidence of Leukemia Following Treatment of Hyperthyroidism by E. L. Saenger, et al., J. Amer. Med. Ass. 205, 855 (1968). The original article by Saenger stated that the rate of occurrence of leukemia in patients with hyperthyroidism treated with ^{131}I was found to be essentially the same as that of a control group of hyperthyroid patients treated surgically. The study was subsequently cited by Holcomb, Science 167, 853-5 (1970) in support of a statement that there are no studies that show increases in cancer at low (below 50 or 100 rad) doses although there are a few that should have detected it if it had occurred. (P.C.H.)

29706 TREATMENT OF RADIATION-INDUCED CUTANEOUS LESIONS OF THE POPLITEAL REGION WITH SUPRAPATELLAR TUBULAR FLAP. Fontana, P. F.; Longhi, A. (Ospedale Maggiore C. A. Pizzardi, Bologna). Minerva Chir.; 25: 1011-15 (31 Jul 1970). (In Italian).

A case of retracting, sclero-atrophic right popliteal radiodermitis in an 11-yr-old boy subjected to excessively prolonged fluoroscopy in a search for a foreign body at 10 months was successfully managed, with full functional recovery after about 70 days, by means of excision of the damaged parts and the transplant of a contralateral suprapatellar tubular flap. (auth)

29707 CONDITION OF ORGANS AND SYSTEMS FOLLOWING RADIOTHERAPY OF THYROID CANCER. Ivanitskaya, V. I.; Makhonina, M. S.; Shutilova, A. A.; (and others) (Inst. Medical Radiology, Moscow). Med. Radiol.; 15: No. 4, 27-32(Apr 1970). (In Russian).

The use of combined radiotherapy on patients with thyroid cancer did not cause gross organic disturbances in the function of the cardiovascular or nervous systems, liver, or kidneys either immediately following therapy or at a later time. Changes did develop in the organs and systems indicated in patients with hypothyroidism. Radioinduced hematological changes were manifested as leuko- and lymphocytopenia. These were encountered more frequently at remote times following radiotherapy, depending on the radiation dose, and were stable in 27.2% of the patients. Local atrophication and fibrotic changes in the skin of patients were also dose dependent and more frequently followed the use of repeated teletherapy. The use of ^{131}I in combination with teletherapy for the treatment of thyroid cancer improved substantially the long range results and did not initiate gross organic changes or disturbances in the organs and systems indicated. (tr-auth)

29708 EXCRETION OF GLUCOCORTICOIDS AND THEIR METABOLITES IN PERSONS WORKING WITH SOURCES OF IONIZING RADIATION. Kogan, I. A.; Brestovitskaya, I. Ya.; Shreiberg, G. L. (Kahrkov Inst. of Medical Radiology). Med. Radiol.; 16: No. 2, 41-3(Feb 1971). (In Russian).

The fractional content of glucocorticoid metabolites was studied by means of thin-layer chromatography on silica gel in persons working with different sources of ionizing radiation. A total of 92 persons, including 36 persons in the control group, were examined. In accordance with the total dose of irradiation all the examinees were divided into four groups: first group—5 to 30 R, second group—30 to 70 R, third group—70 to 150 R, and fourth group—150 to 400 R. In persons working in conditions of maximum permissible levels the excretion of tetrahydroderivatives did not change. With a significant increase in radiation dose (fourth group) the excretion of cortisol and cortisone sharply declined and their metabolism was disturbed. (auth)

29709 CYTOFLUORIMETRIC INVESTIGATION OF EARLY CHANGES IN THE NUCLEAR NUCLEOPROTEINS IN A CULTURE OF IRRADIATED AMNIOTIC CELLS. Zotikov, A. A. (Inst. of Molecular Biology, Moscow). Radiobiologiya; 10: 672-5(1970). (In Russian).

The change in the state of the nuclear nucleoproteins in cultured human amniotic cells irradiated in vitro was investigated. It was found that soon after irradiation, the intensity of fluorescence of the cell nuclei, fluorochromed with acridine orange, was increased. This effect was detected in the investigation both of living and of fixed cells and depended on the irradiation dose. The initial changes in the desoxyribonucleoprotein, as was found by the cytofluorometry data, were not associated with the change in the amount of DNA. The possible mechanisms of the observed phenomena are discussed. (tr-auth)

29710 RADIOSENSITIVITY OF HUMAN LYMPHOCYTES IN VITRO (IN THE NORMAL STATE AND DURING VIRUS INFECTION). Vasil'ev, I. S.; Filatov, E. P.; Anan'ev, V. A. Radiobiologiya; 10: 676-80(1970). (In Russian).

Experimental material on the sensitivity to γ radiation of lymphocytes of normal donors and donors carrying infectious hepatitis is presented. A higher resistance to irradiation was noted in lymphocytes obtained from virus-carrying donors. (tr-auth)

29711 ANALYSIS OF OCCUPATIONAL DISEASES DUE TO IONIZING RADIATION IN THE HEALTH INSTITUTIONS OF THE NORTH-MORAVIAN REGION. Eisler, L.; Kukacka, R. (Regional Hospital, Ostrava, Czech. Regional Hygienic Station, Ostrava, Czech.). Prakt. Lek.; 49: 592-5(5 Aug 1969). (In Czech).

Based on hospital records, an analysis of occupational diseases due to ionizing radiation was performed for the period 1951 to 1968. A total of 67 injuries (four of which were skin cancers and two myeloid leukemias) were recorded in the period 1951 to 1966. No further cases have been observed since 1966. The decrease of injuries starting in 1960 is explained by hygienic improvements of x-ray installations and by better training of personnel. Further measures for safety in operation of ionizing radiation sources are proposed. (NSA of Czech.)

29712 DENTAL CARIES FROM RADIATION THERAPY. Pansch, James L.; Callaghan, Nathan R.; Appleby, Ralph C. Iowa Dent. J.; 55: 40-1(Jun 1969).

A case of tooth demineralization was observed from radiation of a tumor site in the nasopharynx. Clinically, this case demonstrated radiation of a tumor in the nasopharynx through both parotids and submaxillary glands, xerostomia resulting from partial destruction of these glands, lowered Ph in the oral cavity due to a lack of saliva which decreased its buffering capacity, demineralization of clinical crowns of the teeth due to a lowered Ph, and complete edenulation of patient with uneventful healing. (auth)

Radiation Effects on Plants

Refer also to abstracts 29481, 29484–29486, 29489, 29491–29496, 29552, 29559, 29726, and 29737.

29713 (COO-1793-5) EFFECTS OF ULTRAVIOLET RADIATION ON ALGAE: MECHANISMS OF INACTIVATION AND REPAIR. Annual Progress Report, May 1, 1970–April 30, 1971. Small, Gary D. (South Dakota Univ., Vermillion. Dept. of Biochemistry). Contract AT(11-1)-1793. 4p. Dep. NTIS.

A photoreactivating enzyme was detected in Chlamydomonas reinhardi and Euglena gracilis using the Hemophilus influenzae transformation assay. Photoreactivating enzyme activity was found in extracts of chloroplasts isolated from Euglena. Studies on detection of ultraviolet-induced photoproducts in DNA of algae included development of a method for isolating pyrimidine dimers from enzymic digests of irradiated ^{32}P-labeled DNA. A DNase with a high specificity toward single-stranded DNA was purified for studies on enzymes that may have a role in repair and replication of DNA. (H.L.W.)

29714 DEPENDENCE OF THE RADIOBIOLOGICAL EFFECT ON THE LEVEL OF MINERAL NUTRITION OF THE SUNFLOWER. Riza-Zade, R. R.; Suleimanova, N. L. (Scientific Research Inst. of Agriculture, Baku). Radiobiologiya; 10: 907-9(1970). (In Russian).

In experiments with preplanting irradiation of Armavirskiĭ sunflower seeds, a high degree of variability of the final effect of the action of γ radiation from ^{137}Cs on the level of mineral nutrition was demonstrated. The optimum level of mineral nutrition for the sunflower promotes a substantial increase in the effect of stimulation (at a dose of 2 kR) and a decrease in the effect of inhibition (at a dose of 20 kR) of plants. An unfavorable level of mineral nutrition for the sunflower reduces the effect of the stimulating dose and increases the effect of the inhibiting dose. (tr-auth)

29715 EFFECTS OF RADIATION ON THE ACTIVITY OF AMINO ACLY-tRNA SYNTHETASES AND THE tRNA OF THE COTTON PLANT. Karakuziev, U.; Ibragimov, A. P.; Tulchibaev, M. U. (Inst. of Biochemistry, Tashkent). Radiobiologiya; 10: 815-19(1970). (In Russian).

The change in the activity of certain aminoacyl-tRNA synthetases on the addition of a given amino acid to tRNA and the acceptor activity of the tRNA itself in cotton seedlings, grown from seeds irradiated at doses of 6, 25, and 50 kR, was studied. It was found that both the individual tRNAs and the corresponding enzymes (aminoacyl-tRNA synthetases), as well as the original isoacceptor tRNAs

XUM

have different sensitivities to irradiation. tRNAs were always more radioresistant than the enzymes corresponding to them. Different doses of irradiation had different effects both on tRNA and on the enzyme. Moreover, it was found that for all the investigated isoacceptor tRNAs, the sensitivity to radiation increased with increasing ionic strength of the eluting solution on MAK columns. (tr-auth)

29716 MODIFICATION OF RADIATION DAMAGE TO THE STRUCTURE OF DNA FROM EMBRYOS OF SEEDS WITH THE AID OF HOMOLOGOUS DEOXYRIBONUCLEIC ACID. Nelipovich, P. A.; Tokarskaya, V. I. (Inst. of Biological Physics, Pushchino, USSR). Radiobiologiya; 10: 820-5(1970). (In Russian).

The influence of homologous DNA on the growth and survival of irradiated plants, as well as the restoration of radiation damage to the structure of DNA isolated from seed embryos, induced by homologous deoxyribonucleic acid, was investigated. According to the criterion of survival in the case of swelling of irradiated seeds in preparations of homologous DNA, the effects of recovery came to 46.6% at a dose of 5 kR and 32.5% at a dose of 10 kR. It was found by the method of chromatography on columns with methylated albumin-kieselguhr that treatment of irradiated seeds with DNA promotes restoration of the original polymerization of the molecules of intracellular DNA. The greatest effect of restoration of the structure of endogenous DNA was achieved under the influence of homologous DNA at a concentration of 100 μg/ml on the irradiated seeds. (tr-auth)

29717 DEPENDENCE OF THE RADIOBIOLOGICAL EFFECT ON THE TIME BETWEEN IRRADIATION AND PLANTING OF THE SUNFLOWER. Riza-Zade, R. R.; Suleimanova, N. L. (Scientific Research Inst. of Agriculture, Baku). Radiobiologiya; 10: 772-5 (1970). (In Russian).

It was established in field experiments that a distinct effect of radiation (according to the criteria of growth, development of plants, amount, quality, and structure of yield) in stimulating and inhibiting doses is observed when the seeds are planted no later than 10 days after irradiation. At later periods, a gradual decrease in the effect of radiation was observed with an almost complete removal after 2 yr of storage. (tr-auth)

29718 RADIOBIOLOGICAL CHARACTERISTICS OF YEAST CELLS AND THEIR RELATION TO THE PLOIDY AND THE STATE OF HOMO- AND HETEROZYGOSITY OF THE GENOME. Sokurova, E. N. (Inst. of Medical Radiology, Obninsk, USSR). Radiobiologiya; 10: 720-7(1970). (In Russian).

It was found that haploid strains of yeasts are characterized by exponential survival curves ($n = 1.0$) with D_0 not exceeding 10 kR; they are practically incapable of recovery from radiation damages and die chiefly after one to two divisions. Diploid strains gave survival curves with a shoulder ($n > 1.0$) with D_0 of the order of 15 to 20 kR. All the diploid cells were capable of recovery and died chiefly after several divisions, and in the case of large doses, after one to two divisions. Heterozygous diploids possessed higher radioresistance and higher ability for recovery than homozygous diploids. (tr-auth)

29719 DESTRUCTION OF GAMMA-INDUCED FREE RADICALS IN SEEDS DURING THEIR GERMINATION. Bidzilya, N. I.; Zezina, N. V. (Inst. of Plant Physiology, Kiev). Radiobiologiya; 10: 732-5(1970). (In Russian).

Watercress seeds were irradiated with ^{60}Co γ rays at a dose of 50 krad and placed for swelling and germination in tap water. After definite intervals of time, the number of free radicals (FR) was determined in lyophilized samples. It was found that only 40 to 60 min after the beginning of soaking, the number of γ-radioinduced FR was reduced to the control level. The number of native FR in the nonirradiated seeds was unchanged in this case. After 2 hr of imbibition in both variations of the experiment, the number of FR began to increase, but they differed in nature from the γ-radioinduced FR. Curves of the destruction and increase in FR during the swelling and germination of seeds are cited. (tr-auth)

29720 INVESTIGATION OF THE KINETICS AND MECHANISM OF INACTIVATION OF ENZYMES OF THE FUNGUS BOTRYTIS CINEREA PERS. BY UV RAYS. Zemlyanukhin, A. A.; Chebotarev, L. N. (Voronezh State Univ., USSR). Radiobiologiya; 10: 728-31(1970). (In Russian).

The kinetics of the inactivation of aldolase, glutamic-aspartic and glutamic-alanine transaminases, and tyrosinase in the mycelium of Botrytis cinerea Pers. by low-intensity uv rays was studied. It was found that the changes in the activity of these enzymes induced by radiotoxins arise during the postradiation period. The rate constants of inactivation by the radiotoxins are given. (tr-auth)

29721 SENSITIVITY OF SWEET POTATOES TO IONIZING RADIATION. Gertsuskii, D. F.; Nikishanova, T. I.; Alekseenko, L. B. Kosm. Biol. Med.; 4: No. 3, 87-9(May-Jun 1970). (In Russian).

Young fresh-cut sections of sweet potatoes were subjected to ^{60}Co γ irradiation at doses of 0.5, 1, 2, 5, 8, 10, 15, and 20 krads. Irradiated and control sections were incubated in nutrient solution and, using root formation as a criterion, the growth, development, survival, and harvest biomass were determined. Thus, regarding sensitivity to ionizing radiation, the sweet potato sections rivaled that of potato tubers. The growth and productivity of potatoes were suppressed by 50% following tuber irradiation at doses up to 2 krads, while maximum stimulation was observed in sweet potato sections at 10 krads, at which time the stem length, foliage, and harvest biomass exceeded that of the controls by 140, 105, and 112% respectively. Noticeable suppression occurred only at doses in excess of 20 krads. (tr-auth)

29722 MODIFICATION OF THE SURVIVAL OF IRRADIATED YEAST BY ETHANOL TREATMENT. 1. THE VIABILITY OF CELLS GROWING AFTER γ-IRRADIATION IN THE PRESENCE OF THE ETHANOL. Mosin, A. F. (Inst. of Medical Radiology, Obninsk, USSR). Stud. Biophys.; 17: 19-26(1969). (In Russian).

Experimental results showed that survival of diploid yeast was reduced after γ irradiation on nutrient agar in the presence of 5.5%, 7.5%, or 9% vol/vol ethanol. In the non-irradiated yeast, the ethanol had very little effect on their ability to form macrocolonies. The shape of the survival curves of irradiated yeast grown with ethanol was due to the shape of their shoulders. When the concentration of ethanol was relatively large, the shoulder disappeared. The exponential parts of the survival curves with ethanol were parallel to the controls. The survival of haploid yeast after γ radiation was not affected by the ethanol. It is suggested that the ethanol inhibits recovery processes in yeast and reduces the ability of damaged cells to form macrocolonies. The reduced survival of γ-irradiated yeast at a relatively low concentration of ethanol seemed due to inhibition of recovery processes, and the low survival at relatively large concentrations was the result of complex mechanisms. (auth)

29723 EFFECTS OF THERMAL SHOCK AND X RAYS ON GRAINS OF WHEAT. Atayan, R. R. Biol. Zh. Arm.; 23: No. 8, 61-5(Aug 1970). (In Russian).

Dormant wheat seeds were irradiated with medium hard x rays at doses of 600 R/min. The regime included a thermal shock consisting of a 30 min warmup to 90°C. Such processing does not affect seed germination but inhibits bacterial growth by 30 to 35%. The combined effects of radiation and thermal shock were studied at various doses ranging from 5 to 40 curies. The dose-effect curves show that for doses up to 25 curies, irradiation and post radiation shock are additive quantities. At high radiation doses a protective mechanism becomes operative. (K.S.W.)

Radiation Effects on Microorganisms

Refer also to abstracts 29419, 29490, 29556–29558, 29729, 29732, and 29734.

29724 (LF-43, pp 254-62) EFFECT OF THE INHALATION OF ^{144}Ce IN RELATIVELY INSOLUBLE FORMS ON INFLUENZA VIRUS INFECTION IN MICE. Lundgren, D. L.; Sanchez, A.; Thomas, R. L.; Chiffelle, T. L.; McClellan, R O. (Lovelace Foundation for Medical Education and Research, Albuquerque, N. Mex.).

In Fission Product Inhalation Program.

The effect of β radiation from inhaled ^{144}Ce-fused clay particles or from $^{144}CeO_2$ particles on the course of influenza virus infection in mice was studied. The β radiation absorbed had little or no effect on the hemagglutinin or influenza virus titers in the lungs of mice that inhaled ^{144}Ce when compared with virus inoculated control mice, but appeared to have a slight effect in suppressing hemagglutination inhibiting antibody formation in some mice. An analysis of the differences in lung weights, lung lesions, and mortality between mice inoculated with influenza virus at 4, 8 and 12 weeks after inhalation of ^{144}Ce-fused clay and inoculated control mice showed an increase in all three parameters for irradiated mice at the 8-week period only. A similar analysis of mice inoculated with influenza virus at 8, 12, and 20 weeks after inhaling $^{144}CeO_2$ revealed an increase in mortality at 8 weeks, in all three parameters at 12 weeks and in lung weights and lung lesions at 20 weeks for the irradiated mice. Bacterial contamination of the lungs of mice that had inhaled $^{144}CeO_2$ and control mice reached a peak at day 8, declined and then increased to a second peak at day 14; the contamination occured more frequently in the irradiated mice than in the controls. (auth)

29725 INVESTIGATION OF THE DNAase ACTIVITY OF E. COLI K12 (λ) DURING GAMMA IRRADIATION. Drozhennikov,

V. A.; Guberniev, M. A.; Rybakov, N. I. (Scientific Research Lab. of Experimental Immunobiology, Moscow). Radiobiologiya; 10: 899-902(1970). (In Russian).

The activity of endonuclease I, exonuclease III, and λ-exonuclease of a lysogenic strain of Escherichia coli K12 (λ) under the influence of various doses of γ rays was investigated. It was discovered that the level of activity of endonuclease I and exonuclease III does not increase at doses inducing the maximum degree of induction of vegetative phage. With increasing dose of irradiation, the activity level of these DNAases decreased. When the irradiated cells were incubated under the optimum conditions, the rise in the activity level of the inducible λ-exonuclease increased progressively, reaching a maximum value by the time of lysis of the cells. (tr-auth)

29726 VIRULENCE OF X-VIRUS IN PREPLANTING GAMMA IRRADIATION OF POTATO TUBERS. Anokhin, V. M. (Inst. of Microbiology and Virology, Kiev). Radiobiologiya; 10: 930-3(1970). (In Russian).

The mutagenic effects of γ rays on the X-virus of the potato were studied in vivo. The γ irradiation of tubers infected with the X-virus at doses of 300 and 2000 rad did not increase the frequency of appearance of more virulent strains in the potato plants in comparison with the nonirradiated control. With respect to the characteristic of intensification of symptoms of the disease on differentiator plants, Datura stramonium L., the natural background of mutations of the weakly virulent strain of the X-virus used in the experiments lay within the range of 0.25 to 1.25% of the total number of necrotic spots of Gomphrena globosa L., used for the detection of mutants. (tr-auth)

29727 PROTECTIVE IMMUNITY PRODUCED BY THE INJECTION OF X-IRRADIATED SPOROZOITES OF PLASMODIUM BERGHEI. II. EFFECTS OF RADIATION ON SPOROZOITES. Vanderberg, Jerome P.; Nussenzweig, Ruth S.; Most, Harry; Orton, Colin G. (New York Univ., N. Y.). J. Parasitol.; 54: 1175-80(Dec 1968).

The effects of x radiation on the infectivity and development of sporozoites of Plasmodium berghei were determined. When susceptible mice were injected with x irradiated sporozoites, results showed that the higher the radiation dose, the smaller the percentage of mice that developed patent blood infections. Sporozoites irradiated with more than 10,000 rads failed to produce any blood infections. Small, but apparently mature, exoerythrocytic forms were found in the livers of rats that had been injected with x-irradiated sporozoites. Such forms were more numerous after a low dose of radiation, i.e., 2,000 rads, and were found to persist in the liver for at least 16 days after sporozoite injection. There may be a relationship between the presence of these forms and the protective immunity found in mice inoculated with irradiated sporozoites. (auth)

29728 IRRADIATION OF T2r-BACTERIOPHAGES IN T2-BUFFER IN THE ABSENCE AND PRESENCE OF CYSTEINE BY ROENTGEN RADIATION: INJURY OF THE ABILITY OF ADSORPTION. Tolkendorf, E. (Deutsche Akademie der Wissenschaften, Berlin). Stud. Biophys.; 18: 261-6(1969). (In German).

The adsorption capacity of x-irradiated phages T2r which were suspended in T2-buffer or in the same buffer with addition of cysteine was studied by the adsorption saturation test. The results showed that the adsorption capacity was decreased only at the value of the surviving fraction $<3.5 \cdot 10^{-4}$ or $<2 \cdot 10^{-3}$, respectively. The cause for the inability of the phages to form plaques must therefore be a damage to the injection mechanism or to the DNA. (auth)

Radiosterilization and Radiopreservation

Refer also to abstracts 29557 and 29558.

29729 (IAEA-R-491-F) SCALING-UP OF SALMONELLA RADICIDATION OF FROZEN BONELESS MEATS. Mossel, D. A. A. (International Atomic Energy Agency, Vienna (Austria)). Apr 1970. 25p. NTIS (U. S. Sales Only).

A numerical survey was carried out on Salmonella-contaminated frozen boneless meats manufactured in South America. The Enterobacteriaceae flora and radiation processing values were established for such meats. Subsequent organoleptic analyses were based on four criteria. A technique for direct numerical evaluation of Salmonellae in food was developed. With careful sanitation, particularly during slaughtering and deboning, and subsequent radiation processing with doses of ~0.1 Mrad of γ-radiation, the frozen boneless meat obtained proved organoleptically acceptable. Since two decimal reductions in Enterobacteriaceae count were achieved after processing, the end product was in a virtually Salmonella-free state. (INIS)

29730 (STI/PUB-265) STERILITY PRINCIPLE FOR INSECT CONTROL OR ERADICATION. Proceedings Series. Proceedings of a Symposium Held in Athens, 14-18 September 1970. (International Atomic Energy Agency, Vienna (Austria)). Feb 1971. 553p. (In several languages). (CONF-700919). IAEA $14.00.

Separate abstracts were prepared for 27 papers presented at the conference. An additional 22 papers were presented on various aspects of insect control. (H.L.W.)

For abstracts of individual papers see: 29417, 29616-29620, and 29736-29756.

29731 STUDIES ON INSECT PEST CONTROL USING THE STERILE-MALE TECHNIQUE. 2. ON THE MATING COMPETITION BETWEEN STERILE MALES AND RI LABELING IN ADULT MOTHS. Lee, Chung Choo; Chung, Kyu Hoi (Radiation Research Inst., Seoul). J. Nucl. Sci. (Seoul); 10: No. 2, Part 2, 55-61(1970). (In Korean).

Studies were carried out to obtain data on the use of the sterile male technique for insect pest control. For the sterile inducement of Fall webworm (Hyphantria cunea D.), male pupae (2 to 3 days old) were irradiated to 20 kR to 40 kR of gamma rays. To obtain the mating competition of the sterile males, normal female, normal male, and sterile males were caged together in the ratio of 1:1:0, 1:1:1, 1:1:2, 1:1:3, 1:1:5, and 1:1:8 with the adults and pupae respectively. The obtained results were as follows: The mating competitions in the 1:1:1 were nonsignificant among the groups of 20 kR to 30 kR but increased slightly in the more than 30 kR, in the mating combinations of 1:1:8, the mean of sterile rates was about 83%, according to the increase of mating combinations from 1:1:1 to 1:1:8, the hatching rates approached the theoretical value, and when the mating combinations were composed of the pupae, the results were similar in the case of adult; the hatching rates among the groups of 1:1:8 were higher than that one of adult. (auth)

29732 DEVELOPMENT OF BOTRYTIS CINEREA IN IRRADIATED STRAWBERRIES DURING STORAGE. Barkai-Golan, Rivka (Volcani Inst. of Agricultural Research, Rehovot, Israel); Ben-Yehoshua, S.; Aharoni, N.; Eisenberg, E.; Kahan, R. S. Int. J. Appl. Radiat. Isotop.; 22: 155-8(Mar 1971).

The effect of ^{60}Co γ rays on the keeping quality of three strawberry varieties was studied with naturally infected fruit from the field and with fruit artificially inoculated with spores of Botrytis cinerea. A dose of 100 krad caused a slight reduction of rot incidence in uninoculated fruit stored under suitable conditions for fungal rot development (15°C). This reduction was less noticeable on fruit stored at 0°C and later held at 15°C for shell-life. The same dose reduced decay of artificially inoculated fruit for only 2 days of shelf-life following cold storage. An extension of shelf-life to 4 days enabled fungal recovery and resulted in a considerable rise in rot incidence. A dose of 200 krad was much more effective than 100 krad with both inoculated and noninoculated fruit, in prolonging the incubation period of the fungus in the fruit and in reducing the incidence of decay. The efficiency of a 200-krad dose was still considerable after a prolonged shelf-life of 4 days at room temperature, following cold storage. Neither of the two doses examined caused any visible damage to the stored fruit. (auth) (UK)

29733 INVESTIGATION OF FREE RADICALS IN GAMMA-IRRADIATED FOOD PRODUCTS BY THE METHOD OF ELECTRON PARAMAGNETIC RESONANCE. Povlova, N. I.; Filippov, Yu. M. (All-Union Scientific Research Inst. of Medical Instrument Construction, Moscow. All-Union Scientific Research Inst. of the Canning and Vegetable Drying Industries, Moscow). Radiobiologiya; 10: 776-80(1970). (In Russian).

The free radicals (FR) formed by the γ irradiation of dry and moisture-containing food products were investigated by the EPR method. A dependence of the yield of FR on the irradiation dose, moisture content of the sample, and preliminary heat treatment was demonstrated. When the irradiated products were stored, their FR content decreased. The dependences of the recombination of FR in irradiated and nonirradiated food products on the temperature and time of heat treatment of the samples were determined. (tr-auth)

29734 EFFECT OF IRRADIATION TEMPERATURE IN THE RANGE -196 TO 95C ON THE RESISTANCE OF SPORES OF CLOSTRIDIUM BOTULINUM 33A IN COOKED BEEF. Grecz, N.; Walker, A. A.; Anellis, Abe; Derkowitz, D. (Illinois Inst. of Tech., Chicago. Army Natick Labs., Mass.). Can. J. Microbiol.; 17: 135-42(Feb 1971).

XUM

Cans of ground cooked beef, inoculated with 10^6 or 10^8 spores per can of Clostridium botulinum 33A, were irradiated with ^{60}Co γ rays at a series of 14 temperatures ranging from –196 to 95°C. The higher inoculum level required higher sterilizing doses. The D values, computed on the basis of recoverable C. botulinum, were independent of the inoculum level, and showed that spore resistance progressively decreased with increasing temperature. A statistical analysis of these data disclosed that the change in D values from –196 to 65°C followed equally well a quadratic, exponential, or linear best-fit plot; above 65°C radiation death was much more rapid. An equation was derived from the linear plot to predict D values for any desired temperature between –196 and 65°C. Calculations of E_a and Q_{10} values, based on the linear curve, indicated a very small thermodynamic effect on radiation kill. An Arrhenius analysis of the temperature effect suggested that there was no simple physicochemical mechanism occurring in the inoculated beef pack, which might explain the change in spore kill as a function of temperature. Theoretical commercial radiation processes for beef, based on the 12D concept and strain 33A spores, are presented for several easily controlled irradiation temperatures. (auth) (Canada)

29735 SOME EFFECTS OF HIGH ENERGY RADIATION ON THE KRAFT PULPING OF EUCALYPTS. Crook, F. M.; Nelson, P. F.; Thompson, R. G. (Australian Paper Mfgs. Ltd., Melbourne). Holzforschung; 24: 184-90(Dec 1970).

Kraft cooking of γ-irradiated woods (dose ca 3Mrad) gave dark pulps of low yield. The effects of irradiation were due to chain splitting and consequent peeling of polysaccharides and to condensation of lignin. They were more marked with young Eucalyptus regnans than with overmature woods of the same genus. Water leaching of irradiated chips prior to pulping gave low yield pulps but eliminated the reactions leading to dark colors. Irradiation produced higher free radical concentrations in young E. regnans than in overmature species for a given dose, due to the protective effect of extractives in the latter case. Irradiation had little effect on bisulphite cooking. (auth)

29736 STERILITY PRINCIPLE FOR INSECT CONTROL. HISTORICAL DEVELOPMENT AND RECENT INNOVATIONS. Bushland, R. C. (Dept. of Agriculture, Fargo, N. D.). pp 3-14 of Sterility Principle for Insect Control or Eradication. Vienna; International Atomic Energy Agency (1971).

From Symposium on the sterility principle for insect control or eradication; Athens, Greece (14 Sep 1970). See STI/PUB–265; CONF-700919.

The sterile-male technique of insect control, in the form so well known for its success in the eradication of the screw-worm, Cochliomyia hominivorax (Coquerel), utilizes radiation-induced dominant lethal mutations. Laboratory-reared insects are sterilized by exposure to ionizing radiation and released in overwhelming numbers to compete for mates in a native population. Many species of Diptera tolerate a dose in the range of 5 to 10 krad and can be effectively sterilized in this manner. A similar dose administered to the boll weevil, Anthonomus grandis Boheman, causes so much radiation damage to the midgut that it is necessary to use a chemosterilant with selective action on the gonads to avoid somatic injury. Sterilization of Lepidoptera requires about 50 krad of gamma radiation to induce dominant lethal mutations in all the sperm. Somatic damage from this large dose reduces vigor and mating competitiveness. Aberrations in spermatophore transfer commonly result so the sperm of irradiated males are not competitive. A dose of about 15 krad does not completely sterilize moths, but their chromosomes undergo so many modifications, such as reciprocal translocations, that their F_1 progeny, though active at mating, are almost all sterile. The irradiated adults, since they are treated with only about one-third the sterilizing dose, do not suffer the severe somatic damage associated with complete sterilization and are vigorous and competitive. Further, these males are able to transfer their spermatophores properly so that their sperm are competitive. The sterile-male technique, as practiced to date, requires that insects be reared in the laboratory or be collected in the field, be treated, and then be released to compete for mates in nature. Except for those instances where irradiation causes somatic damage that could be avoided by a chemosterilant with selective action, there is no advantage in using chemical mutagens for insect sterilization. Many female insects mate only once because those females develop a mating avoidance response as a result of a chemical received in the semen. A chemosterilant for males of such species need not be a mutagen but could be a substance with physiological rather than genetic effects since competitive males—but not competitive sperm—are required. If such a chemosterilant were used to sterilize insects in nature, the expense of rearing, treating, and distributing sterile insects would be avoided, and the economic application of the sterile-male technique would be greatly advanced. (auth)

29737 EFFECT OF THE IRRADIATION OF WHEAT GRAINS ON THE DEVELOPMENT AND REPRODUCTION OF SITOPHILUS GRANARIUS L. Bagheri-Zenouz, E. (Univ. of Teheran). pp 23-30 of Sterility Principle for Insect Control or Eradication. Vienna; International Atomic Energy Agency (1971). (In French).

From Symposium on the sterility principle for insect control or eradication; Athens, Greece (14 Sep 1970). See STI/PUB–265; CONF-700919.

The effect of ^{60}Co gamma irradiation of wheat grains on the conditions of development and reproduction of Sitophilus granarius which normally lives off this product was studied. The wheat grains were irradiated with doses of 25, 100, 500 krad and 1 Mrad. In a series of experiments, the fertility and longevity of insects reared on irradiated and on normal wheat were compared. The author also attempted to compare the same data for second generation insects originating with these irradiated media. In experiments on 5 batches of 10 pairs, with 5 replications, the following facts were established with regard to fertility: the average fertility is significantly higher for media irradiated at 100 and 500 krad and 1 Mrad; the difference between the control medium and the medium irradiated at 25 krad is no longer significant. This difference is also found in the case of adults from the second generation reared on the various media. Longevity was found to have increased more significantly in the males than in the females in rearings on irradiated media. This effect is observed at irradiation doses of 25 krad but is greatest for the medium irradiated at 500 krad. The differences in average longevity between the control batch and batches reared on irradiated media, calculated without distinction of sex, remained insignificant. It would seem, therefore, that the irradiation of wheat grains at doses of between 25 krad and 1 Mrad can modify this foodstuff so as to create factors that promote longevity and fertility in adults of Sitophilus granarius. (auth)

29738 MEDITERRANEAN FRUIT FLY SUPPRESSION USING THE STERILITY PRINCIPLE: PROSPECTS AND PROGRAMS. Taylor, E. A. (Dept. of Agriculture, Beltsville, Md.). pp 41-8 of Sterility Principle for Insect Control or Eradication. Vienna; International Atomic Energy Agency (1971).

From Symposium on the sterility principle for insect control or eradication; Athens, Greece (14 Sep 1970). See STI/PUB–265; CONF-700919.

When the sterility principle was used against relatively low populations of two species of tropical fruit flies and integrated with other techniques of population suppression, eradication resulted. Research on the Mediterranean fruit fly, Ceratitis capitata (Wiedemann), has increased several-fold during the past 5 to 10 years, and this extra effort has now resolved some of the problems encountered in the effective use of this insect in integrated suppression programs. This is a brief résumé of the progress and a discussion of some of the problems that still must be resolved. (auth)

29739 STERILE-MALE TECHNIQUE IN THE CONTROL OF THE MEDITERRANEAN FRUIT FLY: PROGRAMS CARRIED OUT IN SPAIN. Mellado, L. (Instituto Nacional de Investigaciones Agronomicas, Madrid). pp 49-54 of Sterility Principle for Insect Control or Eradication. Vienna; International Atomic Energy Agency (1971). (In Spanish).

From Symposium on the sterility principle for insect control or eradication; Athens, Greece (14 Sep 1970). See STI/PUB–265; CONF-700919.

The Instituto Nacional de Investigaciones Agronómicas started in 1965 a program of application of the sterile-male technique for the control of Ceratitis capitata (Wiedemann). Artificial mass rearing was started in Madrid in 1965; at present, the rearing laboratory produces an average of 1 million pupae per day. From 1966 to 1968, field releases of sterile insects (irradiated at a dose of 9 krad) were carried out in the island of Tenerife, over an area of 450 ha. In the first two years no positive results were obtained (partly because of the small number of insects released). In 1968, the total release amounted to 25 million insects; significant differences between the release area (15% infestation) and the control area (70% infestation) were shown. In 1969, field experiments were carried out in a regular plantation (citrus, apricot and peach) in the province of Murcia. 32 million sterile flies were released over an area of 25 ha during the period March–August. Although the release area was not well isolated, the infestation in the area stayed below 1% (except for the last week when there was very little fruit left on the trees), whereas the infestation in the nearby control areas was higher than 60% during the same period. In 1970, experiments are being carried out on irradiation doses (7 krad and 9 krad) and on the problem of punctures caused by sterile females on certain fruit varieties. In conclusion, it has been shown that the sterile-male technique is a fully effective method, when applied to small areas. Experiments on larger areas are being planned for 1971. (auth)

29740 POSSIBILITIES OF INTEGRATED CONTROL OF DACUS OLEAE (GMELIN) BY AUTOCIDAL AND CHEMICAL METHODS. Orphanidis, P. S.; Kalmoukos, P. E. (Institut Phytopathologique Benaki, Athens). pp 55-66 of Sterility Principle for Insect Control or Eradication. Vienna; International Atomic Energy Agency (1971). (In French).

From Symposium on the sterility principle for insect control or eradication; Athens, Greece (14 Sep 1970). See STI/PUB-265; CONF-700919.

The prerequisite for any integrated control of the olive Dacus by autocidal and chemical methods is that satisfactory solutions be found first to a number of questions relating to these techniques. Results of research carried out in the last twelve years (1957 to 1969) on different questions directly or indirectly connected with the integrated control of the olive-tree Dacus by autocidal and chemical methods are summarized. More particularly, the research in question has dealt with the action of chemical sterilants, ionizing radiation, insecticides, attractants and repellants; with questions of toxic residues and other secondary effects; and lastly, with some questions relating to the biology and ecology of the olive fly which are directly connected with the problem of controlling this species by combined methods. (auth)

29741 GENETIC CONTROL OF THE EUROPEAN CHERRY FRUIT FLY, RHAGOLETIS CERASI L. PROGRESS REPORT ON REARING AND STERILIZATION. Haisch, A. (Inst. for Soil Cultivation, Plant Cultivation, and Plant Protection, Munich); Boller, E. F. pp 67-76 of Sterility Principle for Insect Control or Eradication. Vienna; International Atomic Energy Agency (1971).

From Symposium on the sterility principle for insect control or eradication; Athens, Greece (14 Sep 1970). See STI/PUB-265; CONF-700919.

Rhagoletis cerasi L. is a pest insect of economic importance. Efforts to control it by using the sterile-insect release method are being made. An account is given of egg collecting experiments and of the success achieved by using small black wax domes. Rearing tests with larvae have shown that production under laboratory conditions is possible. 22.8 ± 4.8% pupae from 100 larvae could be obtained by feeding with the best diet. This is a promising basis for further experiments. In irradiation experiments the fly has shown a similar sensitivity to that of the Mediterranean fruit fly. The competitiveness of males irradiated with 5 kR is significantly reduced. The egg production of females irradiated with 2 kR or more is low and can be neglected. (auth)

29742 STERILE-INSECT RELEASE METHOD AGAINST RHAGOLETIS CERASI L. PREPARATORY ECOLOGICAL AND BEHAVIORAL STUDIES. Boller, E. F. (Swiss Federal Research Station for Arboriculture, Viticulture, and Horticulture, Waedenswil); Haisch, A.; Prokopy, R. J. pp 77-86 of Sterility Principle for Insect Control or Eradication. Vienna; International Atomic Energy Agency (1971).

From Symposium on the sterility principle for insect control or eradication; Athens, Greece (14 Sep 1970). See STI/PUB-265; CONF-700919.

Investigations concerning ecology and behavior were carried out and are still in progress in order to provide the necessary background information for a successful application of the sterile-insect release method. A long-term quantitative study of the population dynamics has been initiated. This work should facilitate the combination of the method with other means of control such as biotic mortality agents and trapping systems. A study of color-vision and reaction to various shapes of R. cerasi has led to the development of an effective visual throw-away trap that permits dispersion studies and experiments aiming at a strong reduction of the pest population. This fluorescent sticky-board is now in use in Switzerland, West Germany, Austria and the CSSR against R. cerasi and in Italy against Dacus oleae. Olfactory response investigations have been started with a new olfactometer in order to combine visual and chemical stimuli to an optimal trapping system. Releases of marked flies and their recapture with the visual trap revealed a rather small cruising range of the flies (average 200 m, observed maximum 500 m) which is greatly influenced by the density of the fruit trees. Furthermore it was discovered that the orientation of the flies is mainly governed by the shape of the trees and not a host-specific odor. In consequence, as many flies could be recaptured on apple as on cherry trees. These findings suggest the combination of a grid system for release and a "strategic release" in order to account for a heterogeneous distribution of the pest population within the release area. The influence of irradiation and marking procedures on the flight capacity of R. cerasi is being studied by means of a "flight mill" consisting of 10 low-friction rotors and a chart-recorder. The field experiments have been carried out in isolated areas that have been selected as future sites for the first field experiments with the sterile-insect release method. (auth)

29743 GAMMA STERILIZATION OF THE MEDITERRANEAN FRUIT FLY. Hooper, G. H. S. (International Atomic Energy Agency, Vienna). pp 87-95 of Sterility Principle for Insect Control or Eradication. Vienna; International Atomic Energy Agency (1971).

From Symposium on the sterility principle for insect control or eradication; Athens, Greece (14 Sep 1970). See STI/PUB-265; CONF-700919.

The sterility of male C. capitata irradiated in the pupal stage two days before emergence with gamma doses of 1 to 13 krad was investigated. When plotted in arithmetic units the relationship between sterility (expressed as hatch of eggs from crosses of irradiated males and untreated females) and gamma dose is curvilinear. However, if gamma dose is plotted in logarithmic units and percent egg hatch in terms of the angular transformation, a linear relationship is obtained. At 11 krad male sterility was better than 90%. When males were irradiated 1, 2 or 3 days before emergence, the degree of sterility decreased but the competitiveness of the males increased as the time between irradiation and adult emergence decreased. No evidence of recovery of fertility in males irradiated with 5, 7 or 9 krad was found up to 26 days after irradiation. Females were more radiosensitive than males and 3 krad produced infecundity. The fecundity of untreated females was unaffected by matings with irradiated males. (auth)

29744 POSSIBLE USE OF THE STERILE-MALE TECHNIQUE FOR ERADICATION OF THE HORN FLY. Kunz, S. E.; Eschle, J. L. (Dept. of Agriculture, College Station, Tex.). pp 145-56 of Sterility Principle for Insect Control or Eradication. Vienna; International Atomic Energy Agency (1971).

From Symposium on the sterility principle for insect control or eradication; Athens, Greece (14 Sep 1970). See STI/PUB-265; CONF-700919.

The horn fly, Haematobia irritans (Linnaeus), is an obligate, bloodsucking parasite of major importance on cattle in North America. Field studies on the biology and habits of this species have shown that an integrated eradication program utilizing the sterile-male technique might be possible. Mass-rearing procedures have been developed which could at present supply about 350,000 adults/week at a cost of $1 per 1000 flies. Studies are being made to improve the larval rearing media and adult blood diet in an effort to increase reproduction of colony flies, minimize fluctuations in production, and reduce cost. Horn fly pupae can be completely sterilized with 2500 rad from a cobalt-60 source with no apparent reduction in adult emergence or survival. However, sexual competitiveness of the sterile males appears to be reduced, perhaps by as much as 50%. Similar results have been obtained with the chemosterilant tepa. Before a release program can be initiated, a method of producing a more competitive sterile male will need to be developed. In the geographical area studies, there is a period of low adult emergence in the life cycle of the horn fly during which the species would be vulnerable to an eradication attempt. It appears that the sterile-male method would probably be most effective if it were integrated with a chemical control program. The release of sterile, insecticide-resistant flies, the application of late-season chemical control to reduce the overwintering population of normal flies, the introduction of a non-diapausing strain of flies, and the release of a biological control agent, could potentially be used in conjunction with the sterile-male technique. (auth)

29745 STERILITY AND CHAGAS' DISEASE VECTOR CONTROL. Gomez-Nunez, J. C. (Ministerio de Sanidad, Maracay, Venezuela). pp 157-70 of Sterility Principle for Insect Control or Eradication. Vienna; International Atomic Energy Agency (1971).

From Symposium on the sterility principle for insect control or eradication; Athens, Greece (14 Sep 1970). See STI/PUB-265; CONF-700919.

A review is made of results obtained from the application of ionizing radiations and chemosterilants in laboratory studies related to the control of Rhodnius prolixus (Stål) in Venezuela. This vector of Chagas' disease was chosen not only by its local importance but also because its ecological characteristics were considered appropriate for the sterile-male technique. Because of the damage caused by the radiation required for complete sterility the use of both x- and gamma-radiations failed to produce sterile males able to compete with normal ones. However, males exposed to a dose causing 75% sterility had their activity increased and mortality among progeny from normal females, mated with irradiated males, was significantly higher than in

XUM

normal nymphs. These males were tested at varying ratios to normal males in the laboratory and in all cases the initial group fertility reduction was followed by a recovery. Similar tests with chemosterilants produced less undesirable results but recovery of fertility and certain manipulation difficulties indicate that the release of laboratory-treated males in the field would be unfeasible. The same results, though, suggested another approach based on the direct use of chemosterilants within houses infested by vectors of Chagas' disease. Although the work is still at an experimental stage, preliminary results from laboratory studies indicate that chemosterilants placed in a container to prevent human contact could provide an effective control method not only for Rhodnius prolixus but for other house-infesting vectors. (auth)

29746 STUDY, USING THE GAMMA IRRADIATION TECHNIQUE, OF THE MIGRATION AND UTILIZATION OF SPERMATOZOA IN THE BEAN WEEVIL, ACANTHOSCELIDES OBTECTUS (SAY). Huignard, J. (Univ., Tours, France). pp 203-16 of Sterility Principle for Insect Control or Eradication. Vienna; International Atomic Energy Agency (1971). (In French).

From Symposium on the sterility principle for insect control or eradication; Athens, Greece (14 Sep 1970). See STI/PUB-265; CONF-700919.

Males of Acanthoscelides obtectus were irradiated with gamma rays from a cobalt-60 bomb; the dose used was 9000 rad. These males copulate normally, depositing into the copulatory bursa of nonirradiated females a spermatophore containing all the paragonial secretions and spermatozoa which migrate actively towards the spermatheca. The females have a normal fecundity, but their fertility is nil; the embryonic development of the eggs laid stops at a very early stage. The successive use of sterile males and normal males provides a means of studying the migration and utilization of spermatozoa in the same female after two copulations. The spermatozoa deposited during the second copulation, whether by a normal male or by an irradiated male, all migrate into the spermatheca, but they are only partially utilized to fertilize the ovocytes; in all cases the spermatozoa deposited during the first copulation have a predominant role. It is probable that the mixing of the spermatozoa introduced into and stored in the spermatheca after two successive copulations would be only partial, even when egg laying is halted for several days due to the absence of the bean seeds. The use of sterile males in the control of Acanthoscelides obtectus will be effective only if the females encountered are virgin. This would seem to be fairly rare under natural conditions; when the density of insects is high the females mate a few hours after birth. The sterile males will therefore have to be introduced into the contaminated seed store before the adults emerge, but the effectiveness of this method of control may be diminished. (auth)

29747 RESPONSE OF THE FEMALE ARTHROPOD'S REPRODUCTIVE SYSTEM TO RADIATION AND CHEMICAL AGENTS. Grosch, D. S. (North Carolina State Univ., Raleigh). pp 217-28 of Sterility Principle for Insect Control or Eradication. Vienna; International Atomic Energy Agency (1971).

From Symposium on the sterility principle for insect control or eradication; Athens, Greece (14 Sep 1970). See STI/PUB-265; CONF-700919.

An extremely important feature which determines whether a population will survive or collapse in response to a deleterious influence is the maximum number of offspring per female equal to the number of functional eggs produced. Fecundity data can be compared with the Wallace diagram of expectations from induced dominant and recessive mutational contribution to extinction. Females in which ovaries failed to develop, or in which the ovaries have been destroyed may serve as the optimum siphon for sperm from a population's males provided females remain attractive and receptive. Peak vulnerability to destructive agents usually occurs during pre-imaginal development. But in some species where internal transformation lags behind external appearance, the opportunity for complete destruction exists in so-called adults. The alternative situation is one in which the ovaries are fully mature. Two main categories are met here: with oocytes already differentiated to provide for ⅓ or more of the lifetime egg deposit, or with a minor portion of the potential eggs differentiated to oocytes but the major portion as undifferentiated gonial or stem cells. Because of features uniquely suited to such investigations, most of the truly analytical experiments revealing differences in the responses of cell types have been performed in Bracon, but the analysis can be extended to other species. Daily egg production records over an appreciable period are required. The average performance for the most appropriate period of time is plotted. Also plotted is cumulative egg production. Characteristic curves distinguish between agents which cause chromosomal damage (radiations, alkylating agents) and those which interfere with nurse cell function (antimetabolites). A quite different response is obtained with agents which attack somatic tissues (toxic metals, chlorinated hydrocarbons). In conjunction with oviposition studies, information on egg hatchability provides important corroborative evidence. The analysis should not stop with scoring the unhatched eggs. A determination of stage of embryonic death may provide conclusive evidence on mode of action. The failure to complete cleavage and set up a blastoderm can be identified and distinguished from all other types of moribund conditions or stages of death. This feature is characteristic of potent chemosterilants which damage chromosomes. (auth)

29748 IRRADIATION, COMPETITIVENESS, AND THE USE OF RADIOISOTOPES IN STERILE-MALE STUDIES WITH THE ONION FLY, HYLEMYA ANTIQUE (MEIGEN). Noordink, J. Ph. W. (Inst. for Phytopathological Research, Wageningen, Netherlands). pp 323-8 of Sterility Principle for Insect Control or Eradication. Vienna; International Atomic Energy Agency (1971).

From Symposium on the sterility principle for insect control or eradication; Athens, Greece (14 Sep 1970). See STI/PUB-265; CONF-700919.

With a radiation dose of 3 kR proving to cause complete sterility in both male and female onion fly, experiments were carried out with decreased doses. Doses of 0.5 to 2.5 kR resulted in fertility in the males of 50% down to 4%. In females the fecundity dropped to zero at a dose of 2 kR. In competitiveness experiments in which irradiated males were put together in different ratios with normal males and females, it was established that competitiveness of the treated males was not impaired. Removal of all males 10 days after the sexes had been brought together and the subsequent decrease of fertility indicates that the female needs to copulate more than once if she is to produce a maximum quantity of fertile eggs. To study the dispersal of the onion fly, experiments were carried out to label flies with radioisotopes. Because the life cycle is relatively long (6 weeks) ^{22}Na and ^{65}Zn were used besides ^{32}P. Retention of ^{22}Na was low, but ^{32}P as well as ^{65}Zn were very useful. (auth)

29749 GENETIC CONTROL EXPERIMENTS ON THE BEAN WEEVIL, ACANTHOSCELIDES OBTECTUS SAY. Jermy, T. (Research Inst. for Plant Protection, Budapest). pp 349-54 of Sterility Principle for Insect Control or Eradication. Vienna; International Atomic Energy Agency (1971).

From Symposium on the sterility principle for insect control or eradication; Athens, Greece (14 Sep 1970). See STI/PUB-265; CONF-700919.

Papers dealing with experiments on the genetic control of the bean weevil are reviewed, including work on mass rearing, radiation sterilization, population estimation, and competitiveness of sterilized males. Some aspects of the biology of the pest relevant to the use of the genetic control method are also discussed. No field experiments have so far been carried out; however, the data available indicate that the bean weevil is a very good candidate for control by the sterile-release technique in the field, at least in temperate regions. (auth)

29750 FEASIBILITY OF CONTROLLING STORED GRAIN PESTS BY THE STERILE-MALE TECHNIQUE. Pradhan, S.; Chatterji, S. M.; Sethi, G. R.; Bhamburkar, M. W.; Prasad, H. (Indian Agricultural Research Inst., New Delhi). pp 365-71 of Sterility Principle for Insect Control or Eradication. Vienna; International Atomic Energy Agency (1971).

From Symposium on the sterility principle for insect control or eradication; Athens, Greece (14 Sep 1970). See STI/PUB-265; CONF-700919.

Apart from one publication, by Crook and colleagues in 1960, no attempt appears to have been made to evaluate the potentialities of the sterile-male technique against pests of stored grains. This question and reports on the findings of some laboratory experiments conducted at the Division of Entomology, Indian Agriculture Research Institute, New Delhi, are discussed. (auth)

29751 GENETICS OF FACTORS AFFECTING FERTILITY AND OF SEX-RATIO DISTORTIONS IN THE HOUSE FLY. Milani, R. (Univ., Pavia, Italy). pp 381-97 of Sterility Principle for Insect Control or Eradication. Vienna; International Atomic Energy Agency (1971).

From Symposium on the sterility principle for insect control or eradication; Athens, Greece (14 Sep 1970). See STI/PUB-265; CONF-700919.

In amphygonic species fertility properly refers to matings rather than to individuals; the individual contribution to fertility can however be estimated when multiple matings are possible. Fertility of normal house-fly (Musca domestica L.) strains and of mutant stocks differs greatly but the genetic bases of the difference remain undetected. Close inbreeding proverbially reduces fertility; the number of adult flies obtained by single

brother–sister pairs may be halved at each generation. Zygotic losses seem to play an important role in this decrease in fertility and possibly provide tools for genetic manipulations. Heterozygous chromosomal translocations obtained by x-ray treatments cause semisterile conditions, which may prove of great value for devising means of genetic control. Sterility factors affecting gametes or fertilization and cytoplasmic sterility have not so far been discussed for the house fly. Sex determination and sex ratios are controlled by genetic mechanisms which differ between populations. The heterogamety is either chromosomal or genic; in the first case the heterogametic sex is the male, which carries a male-determing Y chromosome, while in the case of genic heterogamety, either sex can be heterogametic, according to the factors involved. Male autosomal determining factors inherited as genes have been recognized and assigned to different linkage groups, but strong evidence exists also for the existence of female-determining factors. By variously recombining the known sex factors, new sexual formulae have been obtained. Some combinations between flies of strains differing in their sex formulae allow the production of F_1 hybrid populations composed of males only. The mass production of male populations would facilitate in various ways control based on the sterility principle. (auth)

29752 SEMISTERILITY FOR INSECT CONTROL. Laven, H.; Jost, E.; Meyer, H.; Selinger, R. (Johannes Gutenberg-Univ., Mainz). pp 415-24 of Sterility Principle for Insect Control or Eradication. Vienna; International Atomic Energy Agency (1971).

From Symposium on the sterility principle for insect control or eradication; Athens, Greece (14 Sep 1970). See STI/PUB-265; CONF-700919.

After the eradication of the screwworm fly from the southeastern United States by the use of radiation-sterilized males, there was and still is great interest and enthusiasm for the sterility approach. Unfortunately, the mutagenic treatment often reduces mating competitiveness. Many field trials have failed and others have only led to satisfactory results by the release of sterilized males in ratios up to 100:1 between sterilized males and normal males. Recent research on the induction of chromosomal translocations has shown that partial sterilization not only has the advantage that the treated insects suffer a less drastic lack of competitiveness, but also that the surviving offspring of the treated insects carry a high percentage of translocations. Translocations in heterozygous condition lead to semisterility of the carriers and are inherited from generation to generation. Data are presented on the correlation between the degree of induced sterility and the percentage of inherited semisterility, on the nature of chromosomal translocations and their mode of inheritance. Several possible ways of using translocations for the control of insect populations are discussed. Further developments of the semisterility mechanisms are indicated. (auth)

29753 CHROMOSOMAL TRANSLOCATIONS AND GENETIC CONTROL OF AEDES AEGYPTI. Rai, K. S.; McDonald, P. T. (Univ. of Notre Dame, Ind.). pp 437-52 of Sterility Principle for Insect Control or Eradication. Vienna; International Atomic Energy Agency (1971).

From Symposium on the sterility principle for insect control or eradication; Athens, Greece (14 Sep 1970). See STI/PUB-265; CONF-700919.

Genetic control mechanisms for insect pests are currently being developed for a number of important species. In view of the environmental contamination that ensues from the use of insecticidal chemicals and the fact that insect populations rapidly become resistant to most insecticides, it is imperative that alternative control methods be developed. In their laboratory, the authors are interested in evaluating the use of chromosomal translocations for genetic control of Aedes aegypti, which transmits diseases such as yellow fever, dengue and haemorrhagic fever. This species is thus one of the most important disease vectors. The authors have recently analyzed two radiation-induced sex-linked reciprocal translocations in this species. One, RT(1:2), involves linkage groups I and II with the original break points 0.3 cross-over unit from the gene for male-determining allele (M) on group 1 and 1.6 units from the wild-type allele of spot abdomen (s^+) on group II. The other translocation, RT(1:3), involves linkage groups I and III with the original break points 0.4 cross-over unit from the wild-type allele of red-eyed gene (re^+) on group 1 and 0.6 unit from the normal allele of black tarsus (blt^+) on group III. Though originally both these translocations involved the male-determining chromosomes, female translocation heterozygotes have been established by appropriate crosses. Furthermore, two types of males heterozygous for each translocation have been constructed. In one type (T_M) the male-determining chromosome is translocated and in the other (T_m) the female-determining chromosome is translocated. In addition, by intercrossing both these translocations, double translocation heterozygous males have been established. Whereas each translocation heterozygote is associated with semisterility, the fertility of double translocation heterozygous males is much lower (7–12% against a multiple marker RED stock). Population dynamics of males heterozygous for each translocation have been tested in sequential generations to evaluate their usefulness for genetic control purposes. Results obtained have demonstrated their potential usefulness. Detailed data from genetic and population studies and computer simulations where different release strategies have been evaluated are presented. In addition, prospects for field testing of the translocation method against an isolated population of Aedes aegypti are discussed. (auth)

29754 RESEARCH ON THE STERILIZATION OF ORYCTES RHINOCEROS L. Hurpin, B. (INRA, Versailles, France). pp 489-501 of Sterility Principle for Insect Control or Eradication. Vienna; International Atomic Energy Agency (1971). (In French).

From Symposium on the sterility principle for insect control or eradication; Athens, Greece(14 Sep 1970). See STI/PUB-265; CONF-700919.

Under a contract from the joint United Nations Special Fund/South Pacific Commission Project on means of controlling Oryctes rhinoceros L. (Coleopt. Scarabaeidae), the study of ways of applying autocidal control procedures to this palm tree pest has been continued. Improved rearing procedures ensure the production of approximately 3000 insects per year, with a yield of the order of 70 fullgrown adults from 100 larvae hatched. These insects were used for research on problems of the biology of reproduction: e.g. rate of ovogenesis, influence of the age of males and females on the time of first mating and on the number of copulations for the same female, action of the number of males and females respectively on the fecundity of the female and on the fertility of the eggs. It was noticed, in particular, that the majority of females were already mated at the time of their emergence from the larval form and showed developing ovocytes. Sterilization of the males is obtained by irradiation of the imagos, the age of the latter being of no great significance. On the other hand, the dose rate of the gamma rays is a factor which must not be ignored, even for doses of as high as 10,000 rad. At that dose a low-rate irradiating facility (50 rad/min) produces only 60% sterilization, while with a dose rate of 500 rad/min sterility is total. The absence of delayed irradiation effects was demonstrated on the basis of larvae exposed to weak doses (2000 rad) and of adults hatching from larvae resulting from the mating of normal females with males irradiated with small doses. The competitiveness of the irradiated males was studied in reared insects and in Oryctes just emerged from larval forms. The ratio of males irradiated at 10,000 rad to normal males must be greater than 10 to have any marked effect on egg fertility. The prospects for applying the procedures to control Oryctes rhinoceros are discussed. (auth)

29755 EFFECT OF GAMMA IRRADIATION OF IMMATURE SUGARCANE BORERS. Walker, D. W.; Quintana-Munoz, V.; Padovani, F. (Puerto Rico Nuclear Center, Mayaguez). pp 513-24 of Sterility Principle for Insect Control or Eradication. Vienna; International Atomic Energy Agency (1971).

From Symposium on the sterility principle for insect control or eradication; Athens, Greece (14 Sep 1970). See STI/PUB-265; CONF-700919.

The effect of gamma radiation was assayed in respect to induced sterility and mortality in the embryonic stage, the five larval stages and the pupal stage of the sugarcane borer Diatraea saccharalis (Fab.) (Lepidoptera: Crambidae). Radiosensitivity was greatest in embryos, followed by the larval stages. Each stage was progressively more radioresistant. Pupal radioresistance was greater, and resistance increased with age within the pupal stage. It is impractical to irradiate any immature stage for producing sterile adults because somatic damage is so severe that only a small proportion of individuals survive to the adult stage. Those few that survived were incapable of mating effectively. (auth)

29756 SOME GAMMA-IRRADIATION EFFECTS ON SURVIVAL, LONGEVITY, AND REPRODUCTION OF ZABROTES SUBFASCIATUS (BOH.). Wiendl, F. M. (Coll. of Agriculture Luiz de Queiroz, Sao Paulo, Brazil). pp 525-30 of Sterility Principle for Insect Control or Eradication. Vienna; International Atomic Energy Agency (1971).

From Symposium on the sterility principle for insect control or eradication; Athens, Greece (14 Sep 1970). See STI/PUB-265; CONF-700919.

Gamma-irradiation effects (from a ^{60}Co source) on Zabrotes subfasciatus (Boh.) (Coleoptera: Bruchidae) were studied to determine efficient doses for controlling the worst pest insect attacking stored beans (Phaseolus vulgaris L.), the largest source of proteins in Brazil. Five dosages were used for the irradiation

XUM

of 0–24-hour eggs: 0.5, 1, 2, 5 and 10 krad; there was no emergence at the 2-krad dosage. Three-day-old larvae (8 days after oviposition) and 2–3-day-old pupae (19–20 days after oviposition) were irradiated with doses of 1, 2, 5, 10 and 20 krad. The larvae irradiated with 5 krad and the pupae irradiated with 20 krad did not emerge into adults. With the low irradiation doses the time elapsing before emergence into adults was greater than that for the control, and adults developing from pupae irradiated at 5 krad were infertile. 1 to 2-day-old adults irradiated with doses of 1, 2, 5, 10 and 20 krad became non-fertile from 10 krad upwards. Irradiated with 14 cumulative doses of 25 krad, there was an increase of 6 days in the longevity with the 25-krad dose, which decreased gradually with the increase of the doses, the adults irradiated with 350 krad living only 24 hours. In order that the results could be compared with confidence the same dose rate was used throughout, namely 19.5 krad/h, with the exception that for the determination of the effect of radiation on the longevity of adults a dose rate of 105 krad/h was used. From the results obtained it was concluded that irradiation of this bruchid is highly effective with relatively low doses, which do not cause side effects on beans, as proved by field and laboratory sprouting, survival, growth and production tests. (auth)

METALS, CERAMICS, AND OTHER MATERIALS

Metals and Alloys

Refer also to abstract 29288.

29757 (ORNL–4630) FUELS AND MATERIALS DEVELOPMENT PROGRAM QUARTERLY PROGRESS REPORT FOR PERIOD ENDING SEPTEMBER 30, 1970. Patriarca, P. (comp.); Rucker, D. J. (ed.) (Oak Ridge National Lab., Tenn.). Mar 1971. Contract W-7405-eng-26. 294p. Dep. NTIS.

Research and development progress is reported in twenty sections. A separate abstract was prepared for each section. (J.R.D.)

For abstracts of individual sections see: 29287, 29288, 29761–29763, 29784–29786, 29822–29825, 29904, 29905, 29922–29924, 29978, 30010, and 30011.

29758 THERMAL ANALYSIS. VOLUME 2. INORGANIC MATERIALS AND PHYSICAL CHEMISTRY. Proceedings of the Second International Conference on Thermal Analysis Held at Worcester, Massachusetts, August 18–23, 1968. Schwenker, Robert F. Jr.; Garn, Paul D. (eds.). New York; Academic Press, Inc. (1969). 835p. (CONF-680851).

The information in the book is presented in fifty-four chapters. A separate abstract was prepared for each of nine chapters. Chapters for which no abstracts were prepared are concerned with aspects of inorganic materials and metallurgy, physical chemistry, minerals, and applied sciences which were not considered in scope for NSA. (J.R.D.)

For abstracts of individual chapters see: 29042, 29172, 29188, 29885, 29919, 29925, 29947, 29981, and 29982.

29759 SYDNEY UNIVERSITY CHEMICAL ENGINEERING ASSOCIATION NEW MATERIALS SYMPOSIUM, SYDNEY, AUGUST 27th, 1970. Sydney; University of Sydney (1970). 131p. (CONF-700804).

Eight papers were presented at the symposium. A separate abstract was prepared for each of three papers. Papers for which no abstracts were prepared are concerned with materials for use in electric and electronic equipment, light weight materials, materials for cryogenic use, and materials for vacuum systems. (J.R.D.)

For abstracts of individual papers see: 29775, 29860, and 29916.

Corrosion and Erosion

29760 (DUN-SA–149) EXAMINATION OF AN INCONEL-600 TUBE FROM N REACTOR STEAM GENERATOR 6A. Kratzer, W. K. (Douglas United Nuclear, Inc., Richland, Wash.). 18 Nov 1970. 18p. Dep. NTIS.

Destructive examination of an Inconel-600 tube removed from N Reactor steam generator 6A showed no damage mechanism that would shorten the design life of the tubes. Intergranular corrosion appears to be progressing in the higher temperature sections of the tubing at a very slow rate as was also observed in the steam generator 4A tubes. (auth)

29761 (ORNL–4630, pp 150–7) SODIUM CORROSION STUDIES. Harms, W. O.; DeVan, J. H. (Oak Ridge National Lab., Tenn.).

In Fuels and materials development program quarterly progress report for period ending September 30, 1970.

The microstructural changes in V and V alloys exposed to Na that contained O at 600°C were evaluated. Unalloyed V and three V–Cr alloys showed grain growth as a result of the exposure at 600°C. Specimens of V–20% Mo also showed grain growth and some indication that cracks formed at grain boundaries during test. Alloys that contained Ti or Zr showed polishing and etching effects that are attributed to internal oxidation. The effect of O in Ta on the penetration of Ta by Na was studied, and the corrosion product formed during penetration was observed by scanning electron microscopy. A bimetallic thermal-convection loop composed of V and type 304 stainless steel and containing V–10% Cr tensile specimens was tested for 3000 hr at a maximum temperature of 710°C. Specimens of V–10% Cr in the loop showed no measurable changes in weight. (auth)

29762 (ORNL–4630, pp 158–62) SODIUM REMOVAL AND CAUSTIC EFFECTS. Harms, W. O.; DeVan, J. H. (Oak Ridge National Lab., Tenn.).

In Fuels and materials development program quarterly progress report for period ending September 30, 1970.

A series of tests to evaluate corrosion effects associated with the cleaning of surfaces exposed to liquid Na were initiated. The tests are concerned with the nature of Na compounds that may result during cleaning and their corrosive action in poorly accessible regions such as a crevice. Related studies are also under way to determine the effects of leakage or spillage of Na on the oxidation of stainless steel at 300 to 600°C. The design requirements for a steam loop that would make it possible to evaluate caustic corrosion and embrittlement effects that arise from Na leaking into steam were investigated. Inconel 625 appeared to be the most promising material for such a loop system. (auth)

29763 (ORNL–4630, pp 280–7) ADVANCED MATERIALS FOR STEAM GENERATORS. Patriarca, P.; Slaughter, G. M. (Oak Ridge National Lab., Tenn.).

In Fuels and materials development program quarterly progress report for period ending September 30, 1970.

Strip specimens of weldments between similar and dissimilar steam-generator alloys were prepared for a comprehensive investigation of chloride-induced stress-corrosion cracking under conditions of static stressing in superheated and saturated steam. Stress-corrosion cracking tests conducted on similar-metal weldments of Types 304 and 410 stainless steel, 18% Cr–18% Ni–2% Si stainless steel, Inconel 600, Inconel 601, Inconel 625, Incoloy 800, and Hastelloy X at 538°C for 25 days in superheated steam (535°C) that contained 0.25 ppM NaCl and 20 ppM O_2 showed no evidence of cracking. Because the loop effluent showed a concentration of 0.25 ppM NaCl while 1 ppM was being injected into the loop, it would appear that the solubility limit of NaCl in superheated steam under the test conditions (900 psi pressure and 538°C) is 0.25 ppM. (auth)

29764 NEW NICKEL-BASE ALLOY SOLVES WELD-ZONE CORROSION PROBLEMS. Leonard, Robert B. (Cabot Corp., Kokomo, Ind.). Metal Progr.; 99: No. 3, 87-8(Mar 1971).

Hastelloy alloy C-276, a nickel-base, corrosion-resistant material containing 16 Cr, 16 Mo, 4 W, and 5 Fe, has excellent ductility and good hot-forming characteristics. It can be joined by standard welding techniques. (auth)

29765 STRESS CORROSION CRACKING OF Ti–8Al–1Mo–1V ALLOY: AQUEOUS AND METHANOL ENVIRONMENTS. Chen, C. M. (Air Force Materials Lab., Wright-Patterson AFB, Ohio); Beck, F. H.; Fontana, M. G. Corrosion; 27: 77-83(Feb 1971).

Stress corrosion cracking of Ti–8Al–1Mo–1V alloy was studied using controlled potential techniques in aqueous and methanol environments with and without halogen ions. The alloy was observed to display susceptible zones in aqueous solutions containing halogen ions, susceptible zones are in the corrosion potential and pitting potential regions. Also, potential zones of anodic and cathodic protection exist. In methanol environments, the alloy displays both potential regions of cathodic protection and anodic susceptibility; the anodic susceptible region is aggravated by the presence of halogen ions. The dependence of cracking susceptibility and immunity to cracking on potential suggests that anodic dissolution, catalytic action of halogen ions, and hydride formation may be important in aqueous solutions; whereas, in methanol solutions, anodic dissolution and halogen ion attack are of primary importance. (auth)

29766 CHARACTERISTICS OF TANTALIDED AND HAFNIDED SAMPLES IN HIGHLY CORROSIVE ELECTROLYTE SOLUTIONS. Danzig, I. F.; Dempsey, R. M.; La Conti, A. B. (General Electric Co., Lynn, Mass.). Corrosion; 27: 55-62(Feb 1971).

An extended feasibility study was made of the use of the metalliding process to the application of highly impervious diffusion coatings on inexpensive conductive metals which normally corrode in acid electrolytes. Tantalum and hafnium, which proved highly corrosion resistant in acid media, are expensive for large scale use in components and cannot be deposited as acid impervious coatings onto inexpensive metals by way of conventional deposition techniques. It was demonstrated that the metalliding process was uniquely suited for the deposition of Ta and Hf as acid resistant diffusion coatings on stainless steel and nickel. The chemical and electrochemical corrosion rates of tantalided and hafnided samples of nickel and AISI Type 316 stainless steel in strong electrolyte solutions were determined. The electrolyte media included sulfuric, nitric, hydrochloric, phosphoric acids, and sodium chloride. Electrolyte concentrations ranged from 5 to 105% by weight and temperatures from 25 to 150°C. The behavior of the metallided samples in the strong electrolyte solutions was found to be related to the nature of the coating which is controlled by the positions of the "iding" ion and major substrate ions in the fluoride or complex fluoride electromotive series, as well as the alloying properties of the "iding" metal

XUM

and substrate. The thermodynamic and alloying properties of nickel and tantalum are such that the plating parameters were optimized to give an alloy coating with a surface which was nearly pure tantalum and impervious to acid. The tantaliding process was explored for applications to acid fuel cell current collectors and electrochemical machining. (auth)

29767 MECHANISM OF THE OXIDATION OF NIOBIUM–ZIRCONIUM ALLOYS. Konev, V. N.; Levina, R. A. Uch. Zap. Ural. Gos. Univ.; No. 96, 114-21(1969). (In Russian).

Oxide film growth kinetics, the oxide composition, and the dependence of oxide morphology on alloy composition and temperature were studied for Zr alloys containing Nb 3.4 to 76.6 at. % in CO_2 at 700 to 1070°C. The oxidation took place by a parabolic law. The use of inert markers showed that the oxidation occurred mainly at the metal/scale boundary, the oxide being basically ZrO_2 for Zr-base alloys and Nb_2O_5 for Nb-base alloys. The outer scale of alloys of intermediate composition contained both oxides. After oxidation for a certain time there was a breakdown of the scale and further oxidation proceeded by the linear law. A mechanism is proposed for the oxidation process. (Referativnyi Zh.)

29768 INFLUENCE OF SOME ALLOYING ELEMENTS ON THE VANADIUM CORROSION OF NICKEL AND NICKEL ALLOYS. Hoch, P. Werkst. Korros.; 21: 630-9(Aug 1970). (In German).

The corrosion of Ni in V_2O_5 melts was increased by all alloying constituents (Fe, Cu, Mo, W) except Cr. Cr produced a definite improvement in the resistance of Ni especially at concentrations >20%. Sulfate ions and alkali sulfates increased corrosion because of the higher solubility of O in this melt and the melting point depression produced. In $NaSO_4$:NaCl mixtures (90:10) the corrosion of Ni–Cr alloys was considerably lower than in the presence of V_2O_5. The effect of Cl is also mentioned. (Metals Abstr.)

29769 OXIDATION KINETICS IN NIOBIUM–ZIRCONIUM ALLOYS. V. Konev, N.; Levina, R. A. Uch. Zap. Ural. Gos. Univ.; No. 96, 106-13(1969). (In Russian).

Determinations of the oxidation kinetics and oxide film compositions are reported for Zr alloys containing Nb 3.4 to 76.6 at. % oxidized in air at 700 to 1000°C. The parabolic constant changed during the course of the oxidation. The oxide composition was close to that expected from the Wagner mechanism. With sufficiently high $6ZrO_2$. NbO_5 contents in the scale, the oxidation rate was reduced. (Referativnyi Zh.

29770 BEHAVIOR OF ZIRCONIUM ALLOYS IN CO_2 AT HIGH TEMPERATURE. Weber, J. (Gebr. Sulzer AG, Winterthur, Switzerland). Schweiz. Arch. Angew. Wiss. Tech.; 36: 278-93(Sep 1970). (In German).

Of the eight alloys studied, the binary combination Zr–Cu with 1.6 and 2.5% copper showed the best corrosion resistance in CO_2 at high temperatures. Around 600°C, the alloy containing 2.5% copper showed definitely superior behavior. Above 550°C, oxygen diffusion assumed great importance by causing brittleness of the metal. For cylindrical samples of the alloy Zr–2.5% Cu at 600°C the following characteristics were determined: oxidation layer after one year, 45 microns; after 2 years, 75 microns; brittle zone after one year, 100 microns; after 2 years, 160 microns. Major difficulties arose from an objective assessment concerning the probability of rupture. (H.B.G.)

29771 EFFECTS OF MECHANICAL STRESS ON THE CORROSION BEHAVIOR OF ZIRCALOY-2. Wiedemann, K. H. (Eidgenoessisches Institut fuer Reaktorforschung, Wuerenlingen, Switzerland). J. Nucl. Mater.; 36: 340-2(Sep 1970). (In German).

Zircaloy sheet samples of 1 mm thickness were stressed up to 10 kp/mm^2 in superheated steam of various temperatures. The following conclusions were reached: rate of corrosion increases with stress; at temperatures above 400°C, the breakway occurs earlier with higher stresses; at 400°C, below the breakaway point, stress exerts no significant influence on corrosion rate; at 350°C, the transition point is not reached even after 1000 to 2000 hours of stress. (H.B.G.)

29772 THERMAL-FLARE STUDY OF THE INTERACTION OF OXYGEN WITH RHENIUM. Ageev, V. N. (Ioffe Inst. of Physics and Tech., Leningrad). Sov. Phys.-Tech. Phys. (Engl. Transl.); 15: 1355-61(Feb 1971).

Translated from Zh. Tekh. Fiz.; 40: 1743-51(Aug 1970).

The thermal-flare method was used with a time-of-flight mass spectrometer to study the desorption of oxygen and rhenium oxides from a Re surface, and to study the formation kinetics of Re oxides. At surface coverages $\theta < 1$, atomic oxygen desorbs in two phases with desorption activation energies of 6.8 ± 0.4 and 3.7 ± 0.1 eV. Rhenium oxides begin to desorb at $\theta > 1$. Three phases are found for the desorption of ReO_3, with desorption activation energies of 3.3 ± 0.1, 2.9 ± 0.1, and 1.4 ± 0.1 eV. At an adsorption temperature T_a = 300°K, the order of the desorption kinetics is $\nu = 2$ for all phases of the ReO_3 desorption. In the T_a range from 900 to 1100°K, there is a transition from $\nu = 2$ to $\nu = 1$ for the high-temperature phase of the ReO_3 desorption. Oxygen diffusion through a layer of rhenium oxides is found, and the diffusion activation energy is measured to be E_d = 0.4 eV. The results obtained are compared with the analogous results for the interaction of oxygen with tungsten. (auth)

29773 CORROSION OF TITANIUM-6A1-4V IN HCl-METHANOL. Takimoto, H. H.; Denault, G. C.; Marsh, P. A. (Aerospace Corp., Los Angeles). SAMPE J.; 6: 65-8(Apr-May 1970).

The dissolution of Ti-6A1-4V in HCl-methanol was investigated. Under the conditions studied, the corrosion rate increased with a higher concentration of HCl, whereas water inhibited corrosion. The presence of cold worked edges in the test specimen also enhanced the rate. Replacement of HCl with NaCl as a catalyst and changing the solvent from methanol to isopropyl alcohol greatly decrease the rate of dissolution of the metal. (auth)

29774 CORROSION OF TUNGSTEN IN BORIC OXIDE AND SODIUM BORATE MELTS. Pecoraro, George Anthony. Troy, N. Y.; Rensselaer Polytechnic Inst. (1970). 278p. University Microfilms Order No. 71-3928.

Thesis.

The corrosion of refractory oxides and the platinum metals by molten glass has been widely studied. The reaction of refractory metals such as molybdenum and tungsten has received much less attention although they are being used to a greater extent in recent years. Tungsten is stronger and more structurally stable than Mo at all temperatures, and therefore might be superior to Mo as a glass-melt refractory or electrode. Because of its potential as a refractory, corrosion studies were conducted to determine kinetics and mechanisms of tungsten corrosion in simple glass melts. The corrosion rate increased with $(O_2)_{melt}$, temperature and time. The dissolved oxygen was the primary corrodant. Other possible sources of corrosion which, in total, had a small effect compared to that of the oxygen were: dissolved water, reduction of Na^+ to Na°, and galvanic corrosion. The physical and chemical characteristics of the corrosion process indicate that mass transport in the melt is the slow step which controls its over-all rate. Either diffusion of oxygen through the melt near the reaction interface to the tungsten-melt boundary, or diffusion of the dissolved tungsten oxide away from the saturated melt adjacent to the metal can be the rate limiting step in the process. Generally, the former was slow when P_{O_2} was less than 0.20 for boric oxide melts and 0.05 for a 10 Na_2O 90 mole % B_2O_3 fusion. When P_{O_2} = 1.0 the oxygen arrives in larger quantities than can be used, so that it no longer is the limiting step: the undissolved W_4O_{11} reaction product on the surface inhibits further chemisorption of oxygen and subsequent corrosion. Under this condition, transport of the dissolved reaction product away from the saturated melt controls the reaction rate by a mechanism characteristic of molecular diffusion. The mechanism of corrosion in B_2O_3 when transport of oxygen is rate limiting is postulated to occur under moving boundary conditions, the details of which are uncertain. Tungsten corrosion in the more fluid sodium borates was postulated to proceed by a convective diffusion mechanism for the condition where diffusion away is rate limiting. Such a process is characterized by a concentration gradient which does not change with time because of conditions resulting from free convection in the melt. Where diffusion of the dissolved tungsten oxide away from the reaction site is the slow step, an analogy can be made to dissolution systems which have been shown to have the same slow step. Mass transport equations derived from dissolution, when used to calculate the theoretical corrosion rate, or to match functional relationships, gave good agreement. (Diss. Abstr. Int., B)

29775 NEW MATERIALS FOR CHEMICAL RESISTANCE. Goggin, Brian (Sybron Pty. Ltd., Australia). pp 9-26 of Sydney University Chemical Engineering Association New Materials Symposium, Sydney, August 27th, 1970. Sydney; Univ. of Sydney (1970).

From Chemical engineering conference; Sydney and Melbourne, Australia (18 Aug 1970). See CONF-700804.

Well known and new materials for chemical resistance applications are discussed. The general characteristics of Ti, Zr, Ta, Hastelloy C-276, Glasteel 3300 and Nucerite are considered with special reference to their chemical resistivity in acid and alkaline environments. Their fabrication, limitations, and applications are also evaluated. (Australia)

29776 CORROSION RESISTANCE OF Mo ALLOYS IN CERTAIN CORROSIVE MEDIA. Ababkov, V. T.; Ginzburg, V. I.;

XUM

Volkov, Yu. K. Sb. Tr. Tsent. Nauch.-Issled. Inst. Chern. Met.; No. 77, 72-6(1970). (In Russian).

The corrosion resistance of Mo alloys in inorganic acids such as H_2SO_4, HCl, H_3PO_4, and gaseous and liquid iodine was studied at high pressures and temperatures. The results showed that the corrosion resistance of Mo alloys in acids was higher than in Ni alloys. The tests revealed a high corrosion resistance of Mo alloys in iodine media. (R.V.J.)

29777 INFLUENCE OF Cr AND Mo ON THE ELECTROCHEMICAL AND CORROSION RESISTANCE OF Ni–Cr–Mo ALLOYS. Andrushova, N. V.; Kazakova, G. V.; Svistunova, T. V.; Chermenskaya, N. F. Sb. Tr. Tsent. Nauch.-Issled. Inst. Chern. Met.; No. 77, 141-5(1970). (In Russian).

Studies of corrosion resistance of Ni–Cr–Mo alloys showed that additions of 25% Cr improved significantly the corrosion resistance of the alloy in 30% H_2SO_4 at 90°C and additions of 5 to 15% Mo improved the corrosion resistance of the alloy in 10% HCl at room temperature. (R.V.J.)

29778 ADVANCES IN CORROSION SCIENCE AND TECHNOLOGY. VOLUME 1. Fontana, Mars G.; Staehle, Roger W. (eds.). New York; Plenum Publishing Corporation (1970). 383p. $22.50.

Information on corrosion technology is presented in five chapters. A separate abstract was prepared for one chapter. Chapters for which no abstracts were prepared are concerned with surface-sensitive mechanical behavior of crystalline inorganic solids, organic corrosion inhibitors, and anodic oxidation of Al. (J.R.D.)

For an abstract of an individual chapter see: 29779.

29779 TECHNIQUES FOR THE MEASUREMENT OF ELECTRODE PROCESSES AT TEMPERATURES ABOVE 100°C. Jones, D. de G.; Masterson, H. G. (Central Electricity Research Labs., Leatherhead, Eng.). pp 1-49 of Advances in Corrosion Science and Technology. Vol. 1. /Fontana, Mars G. (ed.). New York; Plenum Publishing Corp. (1970).

An introductory guide to experimental techniques which were found to be useful in electrochemical studies at temperatures high enough to present extended containment requirements is presented. Developmental progress in these techniques is reviewed by examining the status of pressure vessels and liners, electrode lead sealing, and reference electrodes. Information is included on uses of high-temperature electrochemical techniques. (J.R.D.)

29780 SOME LIMITING FACTORS IN THE USE OF ALLOYS AT HIGH TEMPERATURES. Wallwork, G. R.; Hed, A. Z. (Battelle Memorial Inst., Columbus, Ohio). Oxidation Metals; 3: 171-84(Mar 1971).

Over recent years, research has established some of the more basic principles associated with the complex reactions of gases with alloys at high temperatures. The most suitable alloys are based on Fe, Ni, or Co, protected with SiO_2, Cr_2O_3, or Al_2O_3 scales and the upper limit of temperature at which metals can be used in most engineering operations appears to be about 1200°C. A system of superimposing oxidation data on alloy phase diagrams is outlined that indicates suitable basic compositions for the development of high temperature alloys. The system is called oxide mapping. The principle used is described and its application to the two systems Ni–Cr–Al at 1000°C and Co–Cr–Al at 1100°C is used to illustrate how suitable ternary compositions are selected as the basis of new alloys. (auth)

29781 X-RAY DIFFRACTION INVESTIGATIONS ON INTERNAL OXIDATION ZONES IN SODIUM-CORRODED VANADIUM–TITANIUM ALLOYS. Borgstedt, Hans Ulrich; Schneider, Walter (Kernforschungszentrum, Karlsruhe, Ger.). J. Nucl. Mater.; 37: 114-17(Oct 1970). (In German).

The corrosion phenomena occurring in unalloyed V in V–Ti alloys with 5 to 12% Ti after exposure to flowing Na contaminated with 5 ppM O were investigated. Microhardness measurements showed no embrittlement in the unalloyed V, but the degree of embrittlement increased with Ti concentration. X-ray diffraction studies at the internal oxidation zones showed displacement of the lattice parameter of the matrix and the occurrence of a face centered cubic phase. The pattern of the lattice constants of the matrix modified by oxygen uptake and of the titanium oxide was compared to the elementary lengths of the uncorroded V–Ti mixed crystal. With increasing Ti content the samples show increasing line widths of the cubic interferences connected with strong intensity losses. (J.S.R.)

Preparation and Fabrication

29782 (AAEC/TM–570) REVIEW OF PROCESSES FOR THE PRODUCTION OF HAFNIUM-FREE ZIRCONIUM. Royston, D.; Alfredson, P. G. (Australian Atomic Energy Commission Research Establishment, Lucas Heights). Oct 1970. 24p. Dep. NTIS (U. S. Sales Only).

Industrial processes for the production of hafnium-free zirconium are described in terms of their head-end, zirconium-hafnium separation and zirconium metal forming steps. Possible improvements and alternative processes are outlined. Zirconium-hafnium separation schemes based on selective reduction of the chlorides or distillation and sublimation techniques show the most promise for future development in competition with the established hexone-thiocyanate and TBP-nitric acid solvent extraction schemes. Head-end steps involving direct chlorination of zircon in fluidized beds or caustic fusion and metal production via electrowinning warrant further development. (auth)

29783 (CEA-N–1376) RECENT DEVELOPMENTS IN THE ELECTRODEPOSITION OF METALS IN FUSED SALT MEDIA. Darras, Raymond (Commissariat a l'Energie Atomique, Fontenay-aux-Roses (France). Centre d'Etudes Nucleaires). Jan 1971. 20p. (In French). Dep. NTIS (U. S. Sales Only).

It is now possible to deposit most refractory metals in a coherent and compact form, so that they can be used immediately. The method is based upon the electrolysis of pure alkaline fluoride mixtures, containing a convenient salt of the metal to be deposited. The operation is carried out in an inert atmosphere, at relatively low temperatures, taking advantage of the corresponding eutectics. An alternative method, developed separately, involves diffusion of the deposited metal onto the cathode from the anode. Alloy coatings made in this manner give to the base metals new possibilities especially with regards to fretting, mechanical properties, and high temperature oxidation resistance. Electrolysis of alkaline thiocyanates allows the sulfidation of steel at low temperatures, and has important advantages over classical methods. The three general electrolytic methods described are compared. They give different results due to relatively minor variations in operating conditions, which are nevertheless determining and directly related to the objective aimed in each case. (auth) (France)

29784 (ORNL–4630, pp 96-110) FABRICATION DEVELOPMENT OF FBR CLADDING. Adamson, G. M. Jr.; Martin, W. R. (Oak Ridge National Lab., Tenn.).

In Fuels and materials development program quarterly progress report for period ending September 30, 1970.

Artificial defects are being used to examine the effect of flaws on the mechanical properties of cold-worked Type 316 stainless steel tubing at elevated temperatures. A procedure was developed for producing artificial defects from less than 0.001 to 0.005 in. deep and 0.0001 to 0.0002 in. wide. These defects are an order of magnitude narrower than those used in previous work. Large, artificial flaws reduced both the stress-rupture strength and ductility of 20% cold-worked Type 316 stainless steel at 650°C. (auth)

29785 (ORNL–4630, pp 111-38) WELDING DEVELOPMENT FOR FBR STAINLESS STEEL COMPONENTS. Weir, J. R. Jr.; Slaughter, G. M. (Oak Ridge National Lab., Tenn.).

In Fuels and materials development program quarterly progress report for period ending September 30, 1970.

A test weld was prepared with an experimental flux that proved to have excellent welding characteristics. Test results on mechanical properties showed that submerged-arc welds prepared with low, medium, and high heat inputs have varying stress-rupture properties at lower stresses (longer rupture lives). A program of tensile tests that involves three specimen locations, three solution heat treatments, five aging treatments, and five test temperatures was begun. Gas metal-arc welds were prepared using commercial gas mixtures. Two promising new compositions for shielded metal-arc welds are being investigated; these weld metals, which contain additions of B, P, and Ti, have improved rupture ductility and rupture life. Specimens to which only B was added decreased markedly in strength when they were solution heat treated. An irradiation experiment under way in the Experimental Breeder Reactor-II involves 226 weldment specimens from 13 different welds. In cooperation with WADCO, 320 weldment specimens were prepared for a subsequent irradiation experiment. Studies of the effects of heat treatment revealed highly variable rates of δ-ferrite solution, depending upon time, temperature, composition, and solidification substructure. Agglomeration of carbides at low temperatures and the formation of σ phase were also studied. Results of Strauss tests of weldment composite wafers indicated a critical cooling rate of 150°C/hr in order to avoid sensitization as measured by this test. (auth)

29786 (ORNL–4630, pp 207-25) TUNGSTEN METALLURGY. Patriarca, P.; Schaffhauser, A. C. (Oak Ridge National Lab., Tenn.).

XUM

In Fuels and materials development program quarterly progress report for period ending September 30, 1970.

Tungsten was chemically vapor deposited (CVD) in sheets with low F content for creep testing and welding. Analysis of deposits of W with low Re content prepared with H_2 : (WF_6 + ReF_6) ratios of 1 to 20 showed that the Re content increased with increasing ratio while the deposition rate and efficiency were maximum at the stoichiometric ratio of 3. Since increasing the total gas flow decreased the Re content and increased the overall rate of deposition, it appears that the deposition of Re is more limited by diffusion rate than is the deposition of W. Initial attempts to strengthen CVD W with a dispersion of small TiO_2 particles produced in a flame reactor were not successful. In a program to develop improved welding techniques for W alloys, gas tungsten-arc welding of arc-cast W–25% Re with Mo–50% Re and W–25 at.% Re–30 at.% Mo was completed. The conditions for successful butt welding arc-cast W, W–25% Re, and CVD W sheet with electron-beam and gas tungsten-arc processes are summarized. Data on time to 1% creep for arc-melted W and W–Re alloys is being extended to 1000 hr at 1400 and 2200°C. The high creep strength of CVD W at 1650°C was shown to be reproducible for five different lots of material. Detailed fractographic observations of the nucleation and growth of creep cavities in powder-metallurgy W showed that existing bubbles on grain boundaries are the nucleation sites for creep cavities that grow with time and merge to form cracks at grain boundaries. Additional creep data at 1800 and 2000°C show that the strengthening effect of low-pressure O_2 on the creep properties of W–25% Re is greatest at the higher temperatures and lower stresses. (auth)

29787 (RMI–16) SEMIANNUAL PROGRESS SUMMARY, JULY–DECEMBER 1970. (Reactive Metals, Inc., Ashtabula, Ohio). Feb 1971. Contract AT(30-1)-1405. 29p. Dep. NTIS.

Research efforts devoted to precision extrusion of I and E fuel elements for Hanford are described. In other work the 360-ton Lombard extrusion press was used to extrude tubes and wafers in support of laboratory programs. Results of research are also reported on U thermal expansion anisotropy, U oxidation, U forging, and extrusion processes. The status of programs concerned with reduction of extruded overstock and precision extrusion of Mark 30 sizes is reviewed. (J.R.D.)

29788 (ZJE–69) WELDING OF REACTOR PRESSURE VESSEL OF THE FIRST CZECHOSLOVAK NUCLEAR POWER STATION. Becka, J. (Skoda Concern, Pilsen (Czechoslovakia). Nuclear Power Plants Div.). 1970. 19p. Dep. NTIS (U. S. Sales Only).

The methods of welding e.g., electroslag and arc are described. The properties of the welded joints including chemical composition of the materials and the mechanical properties of weld metal, base material, and welded joint are also described along with the technology of welding. The experience obtained confirms the possibility of the manufacture of the pressure vessels up to the weight of 1000 tons. (auth)

29789 FABRICATING THE REFRACTORY METALS. PART II. METHODS USED TO MAKE PARTS. Mash, Donald R.; Bauer, Dieter W.; Schussler, M. (Fansteel Inc., Baltimore). Metal Progr.; 99: No. 3, 60; 62-4; 66(Mar 1971).

Details are given on the spinning, forming, coating, machining, and welding of refractory metals and alloys. Commercial coating systems for refractory metals of current importance are summarized. Typical brazing filler metals and their service temperatures are listed. (G.M.C.)

29790 WEIGHT WATCHING SPURS ADVANCES IN BERYLLIUM FABRICATION. Metal Progr.; 99: No. 3, 96; 98-100; 102-3(Mar 1971).

Three aerospace programs have spurred several advances in the fabrication and application of beryllium. Adhesive bonding and machining of hot-pressed beryllium blocks were extensively employed to fabricate the Minuteman inertial platform structure. Another Minuteman application was the interstage between the missile's booster and payload. Here a ring-rolled forging made up the basic structure with chemical milling, zinc brazing, drilling, and mechanical fastening as secondary operations. The Agena forward equipment section was fabricated from beryllium cross-rolled sheet. Sheets were cut and creep-formed in internally heated dies. Extruded beryllium tubing was used for the TACSAT I satellite's antennas and machined hot-pressed blocks formed the bearing and power transfer assembly. These applications are covered in detail in this article. (auth)

29791 SINTERING KINETICS OF NICKEL ACTIVATED TUNGSTEN. Ylaesaari, S.; Tikkanen, M. H. (Inst. of Tech., Otaniemi, Finland). Phys. Sintering; 3: 47-54(Jan 1971).

It was shown that Ni activated tungsten most probably sinters by the same basic mechanism as pure tungsten. The activation energy of sintering was lower (28 kcal) than earlier corresponding values, thus demonstrating the necessity of further investigations. Practically all the nickel was situated along the grain boundaries. Approximately 30 wt. % of W was dissolved in this nickel phase. (auth)

29792 WELDING PROBLEMS IN NUCLEAR TECHNOLOGY. Lechtenboehmer, H. Zvaranie; 19: 345-8(Nov 1970). (In Slovak).

Properties are reported of the UTP–068 HH alloyed filler material used in the welding of heavy-duty structures made of unequal materials, such as reactor vessels and other components of nuclear power stations. Some applications of the material are described, e.g., in the welding of a pump casing in the Würgassen nuclear power station, and in the welding of a heat exchanger for the SNR experimental reactor. (INIS)

29793 SINTERING PROCESS OF Ni–P ALLOY COATED TUNGSTEN. Ito, Hiroshi (Nippon Tungsten Co., Ltd., Fukuoka); Mihashi, Yasuo; Tamagusuku, Susumu. J. Jap. Inst. Metals; 35: 6-10(Jan 1971). (In Japanese).

To lower the sintering temperature of tungsten to a technically acceptable level, elements of Group VIII in the periodic system, particularly nickel, were used. In previous experiments, the addition of small amounts of Ni–P alloy to tungsten powder markedly accelerated low-temperature sintering of tungsten compared with nickel addition. To investigate the effects of Ni–P alloy addition to tungsten on low temperature sintering, several experiments, mainly on the diffusion phenomenon, were performed. The liquid phase of Ni–P alloy which occurred at about 900°C accelerated sintering of tungsten. Wetting of Ni–P alloy to tungsten was satisfactory. When nickel coexists with phosphorus, the diffusion rate of nickel to tungsten was markedly large compared with the case devoid of phosphorus. (auth)

29794 BERYLLIUM: PROPERTIES AND FABRICATION. Gelles, S. H.; Ashurst, A. N. DMIC Rev.; 5p(24 Jun 1970).

Recent research on the physical and mechanical properties and fabrication of Be includes: the hydrostatic extrusion drawing of 0.005 in. dia Be wire; warm extrusion of 5-mil Be wire with an ultimate strength of 300,000 lb/in^2 from hot pressed and machined billets; applications of Be in an optical-unit assembly, a telescope housing, an inertial guidance platform, a bearing- and power-transfer assembly, antenna tubes and a bicone antenna support; production of Be sheet with improved ductility by low-temperature rolling coupled with intermediate and postrolling annealing; basic extraction-refining-conversion processes for Be; the direct electrowinning of Be from BeO with several anode materials using a molten salt electrolyte of 56% LiF and 37% BeO; effects of machining, thermal and plating stresses on dimensional stability in Be mirrors; uniaxial tensile properties of commercial vacuum hot pressed Be and cross-rolled Be sheet over a range of strain rates at 72 to 700°F; an etch-pit technique for analysis of fractured Be surfaces; methods of controlling the impurity content and applying heat treatments to hot pressed Be block so as to produce materials with tailored properties; isotropic consolidation of Be; calculated integrated x-ray intensities expected from various crystallographic planes as compared to values measured on randomly packed spherical Be powder; and the corrosion, oxidation and protection of Be in various gaseous environments over a wide range of temperatures and pressures. (Metals Abstr.)

29795 CLADDING TUBES FOR ATOMIC REACTORS ARE PRODUCED AT RAUFOSS. Maskin; 3: No. 9, 30(12 Nov 1970). (In Norwegian).

A/S Raufoss Ammunisjonsfabrikker have in cooperation with the Institutt for Atomenergi built a factory for the production of Zircaloy cladding tubes for nuclear fuel. The production processes and machinery are briefly described. The plant has a projected capacity of 100 tons of cladding tube per year. (INIS)

29796 Zr Hf NEWSLETTER, FEBRUARY 1971. Akron, N. Y.; AMAX Specialty Metals Division (1971). 18p.

A review of developments in the technology of Hf and Zr and their alloys is presented. Information is also included on production of Hf and Zr along with data and information on oxides, borides, carbides, nitrides, and silicides of these elements. 257 references are included. (J.R.D.)

29797 SINTERING OF $PrCo_5$ PERMANENT MAGNETS. Tsui, J.; Strnat, K. (Univ. of Dayton, Ohio). Appl. Phys. Lett.; 18: 107-8(15 Feb 1971).

Permanent magnets were produced by liquid-phase sintering from $PrCo_5$ with a Sm–Co and a Pr–Co alloy as sintering aids. The best values of the energy product achieved with these two additives are 21.1 and 16.6 MGOe; the highest intrinsic coercive forces of different samples are 14,000 and 9470 Oe, respectively. (auth)

XUM

29798 URANIUM ETCHANT AND METHOD. Waldrop, Forrest B.; Bezik, Max J. (to United States Atomic Energy Commission). U. S. Patent 3,573,120. 30 Mar 1971. Filed 6 Sep 1968.

Metallic uranium and U alloys are provided with uniformly etched surfaces for facilitating the reception of adherent protective coatings. The etchant consists of an aqueous solution of either ferric chloride or ferric chloride and nickel chloride. (Official Gazette)

29799 PRODUCTION OF METAL RESISTANT TO NEUTRON IRRADIATION. Levy, Ira S. (to United States Atomic Energy Commission). U. S. Patent 3,573,109. 30 Mar 1971. Filed 24 Apr 1969.

A process is described for producing a metal which is highly resistant to damage by neutron irradiation. Austenitic stainless steels or nickel-base alloys, which also contain suitable carbide-formers such as niobium, titanium, tantalum, or zirconium, are subjected to a series of thermal and mechanical treatments. These treatments include solution heat treatment at a temperature sufficiently high to place in solid solution substantially all the dissolvable carbides; quenching at a controlled rate; plastic deformation at or near room temperature; and plastic deformation at high temperature. (Official Gazette)

29800 LIQUID METAL PURIFIER. Jaross, Robert A. (to United States Atomic Energy Commission). U. S. Patent 3,558,122. 26 Jan 1971. Filed 26 May 1969.

A device for removing oxides from liquid metals consists of a vertically disposed, double-walled tube, an outer shell concentric with and surrounding the double-walled tube, a heat exchanger at the top of the device, a metal oxide collector at the lower end of the device, and a double-walled thermal barrier movable alongside of the metal oxide collector. The device is mounted in the top of a tank containing the liquid metal with the metal oxide collector immersed in the liquid metal. A heat exchange fluid flows upwardly in the double-walled tube, through the heat exchanger, and downwardly in the annulus between the double-walled tube and the outer shell, thereby cooling the metal oxide collector. Metal oxide precipitates on the metal oxide collector and is prevented from redissolving in the liquid metal by moving the thermal barrier to cover part of the metal oxide collector. (Official Gazette)

29801 NUCLEAR FUEL PARTICLES MANUFACTURED FROM A PEROXIDE OF URANIUM. Knotik, K.; Bildstein, H.; Bohnenstingl, J. (Osterreichische Studiengesellschaft fuer Atomenergie, Vienna). Kerntech. Atomprax.; 13: 125-30(Mar 1971). (In English and German).

A method is described for preparing porous uranium dioxide particles starting from a recently developed stable uranium peroxide sol. The description of the manufacturing process is completed by the investigations which were required for optimizing the individual process steps and for testing the products. (auth)

29802 VANADIUM. Rausch, Bernard A. Eng. Mining J.; 172: No. 3, 112-13(Mar 1971).

Production and uses of V during 1970 is reviewed. Prospects for consumption during 1971 are discussed. Information is included on foreign demand, US exports, US imports, supply, sources, stockpile, prices, and outlook. (J.R.D.)

29803 SOLID-STATE ANODIZATION OF ALUMINUM, BERYLLIUM, AND ZIRCONIUM. Miles, J. L. (Arthur D. Little, Inc., Cambridge, Mass.). Proc. Roy. Soc. (London), Ser. A; 321: 503-14 (9 Mar 1971).

Oxide films were grown between aluminum and tin, beryllium and tin, and zirconium and tin. Growth rates were of the order of one atom layer per day and were calculated by measuring the decrease of electron tunnelling currents through the oxide layers. The barrier height, first jump distance, and number of active growth sites were calculated. A reason is suggested for the different growth rates observed for oxides grown in the presence and absence of water vapor. (auth) (UK)

29804 GROWTH OF CADMIUM WHISKERS IN INERT ATMOSPHERES. Kitterman, John Howard. Fort Collins, Colo.; Colorado State Univ. (1970). 231p. University Microfilms Order No. 71-5342.

Thesis.

Quantitative growth rates were determined at a supersaturation of 0.1 for the growth of cadmium whiskers from the vapor in the presence of the inert gases argon and helium. Oxygen was added to argon in a series of tests to determine the effect on whisker growth rates and morphology. The growth rates were found to be radius-dependent in all cases. Growth rates in helium were constant, while growth rates in argon increased inversely with argon pressure to a level of 50 torr argon; below this, the rates decreased and became erratic. In argon, except for the oxygen addition experiments, the growth rates were equal to or above the rates given by the classical linear law for tip impingement only. The growth rates for whiskers in argon are explained on the basis of surface diffusion inhibited by the presence of the inert gas. For helium and argon pressures below 50 torr, possible turbulence accompanied by the heavy condensation rate inhibited surface diffusion. Growth rates with free oxygen additions varied inversely with the oxygen level of the growth system. (Diss. Abstr. Int., B)

29805 MOLYBDENUM. Brackin, Robert B. Eng. Mining J.; 172: No. 3, 119-20(Mar 1971).

Production, uses, and consumption of Mo are reviewed. Information is included on stockpiles, prices, new developments, production of Mo as a by-product, Mo alloying in steel, and usage outlook. (J.R.D.)

29806 BERYLLIUM. Schilling, S. A. Eng. Mining J.; 172: No. 3, 137-8(Mar 1971).

Production and uses of Be are discussed along with market trends. Information is included on supply, demand, and future consumption increases. (J.R.D.)

29807 COLUMBIUM. Buttner, F. H. Eng. Mining J.; 172: No. 3, 90-2(Mar 1971).

The status of Nb production and use is reviewed. Information is included on world production, concentrate prices, demand, price outlook, and new technology. (J.R.D.)

29808 ZIRCONIUM–HAFNIUM. Couch, G. Robert (American Metal Climax, Inc., New York). Eng. Mining J.; 172: No. 3, 102-3(Mar 1971).

The outlook for HF and Zr production, price, and uses during 1971 is discussed. Information is included on supply, import–export, fabrication facilities, and product development. (J.R.D.)

29809 RARE EARTHS. Cannon, Joseph G. (Molybdenum Corp. of America, New York). Eng. Mining J.; 172: No. 3, 105-7 (Mar 1971).

The status and outlook for production and use of rare earths is reviewed. Information is included on supply, demand, applications, and prospects for future development. (J.R.D.)

29810 TANTALUM. Emerson, Mark E. Eng. Mining J.; 172: No. 3, 107-8(Mar 1971).

Production and uses of Ta during 1971 are discussed. Information is included on supply, demand, and prices. (J.R.D.)

29811 URANIUM. Sherman, John T. (Atomic Industrial Forum, Inc., New York). Eng. Mining J.; 172: No. 3, 108-11(Mar 1971).

Discussions of production and uses of U during 1971 are presented. Information is included on purchases of nuclear power plants, fossil fuel supplies, uranium supplies, aspects of power plant siting, exploration of reserves, demand, production and sales, UF_6 conversion, and domestic and foreign developments. (J.R.D.)

29812 THORIUM. Woodmansee, Walter C. Eng. Mining J.; 172: No. 3, 117-18(Mar 1971).

Growth in production and uses of Th is reviewed. Information is included on supply, consumption, prices, legislation and government programs, nuclear developments, and outlook. (J.R.D.)

29813 TUNGSTEN. Ratzker, Menno. Eng. Mining J.; 172: No. 3, 149-50(Mar 1971).

Consumption trends related to W from 1966 to 1970 are reviewed. Discussions of actions by the General Services Administration and their effects on production and sale of Mo are included along with an evaluation of future consumption trends. (J.R.D.)

29814 LOW-PRESSURE, HIGH-TEMPERATURE SILICONIZING OF TUNGSTEN. I. Gelain, C.; Cassuto, A.; Le Goff, P. (CNRS, Nancy). Oxidation Metals; 3: 115-38(Mar 1971).

The study of surface siliconizing of tungsten ribbons by low pressure (10^{-3} to 10^{-6} torr) and high temperature (800 to 1200°C) heterogeneous decomposition of SiH_4 shows a competition between silicon deposition on the surface and its diffusion in the metal. Coatings of W_5Si_3 and WSi_2 are formed which grow parabolically or linearly depending on deposition and temperature conditions; their thickness was determined without destroying the ribbon by measuring the variations of the electrical conductivity with the quantity of silicon introduced. The activation energy of the interdiffusion coefficients, the composition and resistivity of the phases, and the surface parameters corresponding to the surface evolution (monochromatic and total emissive powers) were determined for the different compounds. The decomposition kinetics of SiH_4 were also determined. (auth)

XUM

29815 SOLID STATE BONDING OF NICKEL TO ALUMINA. Calow, C. A.; Porter, I. T. (Atomic Weapons Research Establishment, Aldermaston, Eng.). J. Mater. Sci.; 6: 156-63(Feb 1971).

The effect of sintering atmosphere (argon, hydrogen, and vacuum), sintering temperatures (700 to 1300°C), sintering pressure (½ to 6 tsi) and sintering time (½ to 24 hr) on the room temperature shear bond strength developed between nickel powder compacts and alumina single crystals is described: bond strengths of 3 to 11 × 10^3 psi were developed and are satisfactory for composite strengthening. The spinel, $NiAl_2O_4$, was detected at the nickel/alumina interface. Heat treatment at 1100°C for 300 hr resulted in gross chemical attack, but without degeneration of the bond strength. The variations in shear strength observed are discussed in terms of the nickel grain size and porosity and the differential thermal expansion of the two components. (auth) (UK)

29816 COATING OF NIOBIUM AND NIOBIUM ALLOYS WITH ALUMINUM. PART I. PACK-CEMENTATION COATINGS. Slama, G.; Vignes, A. (Univ., Nancy). J. Less-Common Metals; 23: 375-93(Apr 1971).

Niobium and niobium alloys were coated by pack-cementation. The compound $NbAl_3$ was the main constituent of the coatings. The structures of the coatings (equiaxed-, columnar-, or needle grains) vary according to the structural state of the niobium, either recrystallized or cold-worked (or with the microhardness value of the alloy), the temperature of the heating cycle and the composition of the pack. The mechanical properties of the metal are found to have a strong influence on the structures. If the deformation of the substrate allows the growth stresses arising in the coating to be relaxed, columnar or needle grains are formed, otherwise the structure consists of equiaxed grains. The growth kinetics of the coatings were also studied. (auth)

29817 PREPARATION OF SPECIMENS OF ZIRCONIUM AND ITS ALLOYS FOR METALLOGRAPHIC EXAMINATION. Kashchuk, V. A.; Filippov, F. F. Sb. Nauch. Tr., Tomsk. Inzh.-Stroit. Inst.; 16: 10-14(1969). (In Russian).

Equipment is described for the electrolytic polishing of sections of Zr and Zr modified with Ti, V, Ni, and other transition elements. The conditions chosen are: current density 0.14 to 0.2 A/cm^2; electrolyte temperature 25 to 30°C; polishing time 4 to 5 min; and cathode to anode distance 1.5 to 2.0 cm. Specimens are subsequently etched in a solution containing glycerine 30, HF 10, and HNO_3 20 ml, quickly washed in flowing water, and dried. (Referativnyi Zh.)

Properties Evaluations

Refer also to abstracts 29287, 29965, 29969, 30028, 30672, and 31568.

29818 (AEC-tr-7224) EXPERIMENTS ON WEAR AND FRICTION BETWEEN SUBASSEMBLIES AND GRID SPACERS IN SODIUM. Kleefeldt, K. (Kernforschungszentrum, Karlsruhe (West Germany)). Translation of report KFK-1290. 21p. Dep. NTIS.

An abstract of this paper, prepared from the original language, appeared as NSA 25: 16439.

29819 (EUR-4531, pp 1019-34) THERMAL SHIELDING BY WIRE GAUZE AND METALLIC SHEETS. METALISOL PROCESS. APPLICATION TO THE PRESTRESSED CONCRETE PRESSURE VESSEL OF BUGEY I REACTOR. Delort, G.; Lecourt, Y. (Compagnie des Ateliers et Forges de la Loire, Paris (France)); Soulier (Electricite de France, Clamart). (In French).

From Second conference on prestressed concrete reactor pressure vessels and their thermal isolation; Brussels, Belgium (18 Nov 1969).

In Second information meeting on prestressed concrete reactor pressure vessels and their thermal isolation.

A completely metallic thermal shield, based on the use of wire gauze and metallic sheets of stainless steel and arranged in successive layers, was developed and manufactured commercially under the name of Metalisol. The conditions under which this method of thermal shielding was applied to the Bugey I reactor are reviewed. The original characteristics of the structure are discussed. The application of this type thermal shield to the HTR and BWR reactors is justified. (J.S.R.)

29820 (EUR-4593, pp 519-24) DIFFUSION OF HYDROGEN AND DEUTERIUM THROUGH NIOBIUM. Voelkl, J. (Kernforschungsanlage, Juelich (West Germany). Institut fuer Festkoerperforschung).

From Sixth symposium on fusion technology; Aachen, Germany (22 Sep 1970).

In Proceedings of the 6th symposium on fusion technology.

The permeation rate of hydrogen and deuterium through Nb is estimated under temperature and pressure conditions planned in fusion reactors. For the diffusion coefficient, values determined by a new method were used. The permeation rate turns out to be very high. (auth)

29821 (GEAP-12153) THERMODYNAMIC DATA PROGRAM INVOLVING PLUTONIA AND URANIA AT HIGH TEMPERATURES. Quarterly Report No. 13, August 1-October 31, 1970. Aitken, E. A.; Evans, S. K. (General Electric Co., Pleasanton, Calif. Nucleonics Lab.). Dec 1970. Contract AT(04-3)-189. 7p. Dep. NTIS.

The continuing scope of work related to vaporization of urania, oxygen activity at high temperatures, oxygen redistribution in a temperature gradient, and sodium fuel interactions was presented. Work progress is presented on these tasks. (auth)

29822 (ORNL-4630, pp 139-44) PROPERTIES OF FERRITIC STEEL WELDS. Weir, J. R. Jr.; Slaughter, G. M. (Oak Ridge National Lab., Tenn.).

In Fuels and materials development program quarterly progress report for period ending September 30, 1970.

A literature search is being conducted on the weldability of the ferritic steels of interest. Lehigh restraint specimens of the plain-C steel and the standard 2.25% Cr-1% Mo steel are ready for welding. The low-C version of the 2.25% Cr-1% Mo steel is being researched, but no material is yet on hand. The Nb-stabilized version of the 2.25% Cr-1% Mo steels (Sandvik HT8X6) has received some testing, but this has been limited because of a shortage of material. More Nb-stabilized 2.25% Cr-1% Mo steel is being procured. TIGAMAJIG specimens of the HT8X6 alloy were insensitive to cracking when exposed to a heavy heat input and about 7% strain. Hot-ductility tests of this material by Duffer's Gleeble showed rather remarkable recovery of ductility from the zero-ductility temperature of 1330°C. Tensile tests of this material after thermal excursions by the Duffer's Gleeble show that the Nb-stabilized 2.25% Cr-1% Mo steels require heat treatment after welding. Ductility of this material was poor in the heat-affected zone that resulted from tests on the Duffer's Gleeble. Microprobe studies on precipitates in the microstructure of the Sandvik alloy show them rich in Nb in the proportion of NbC. Further microprobe analysis shows these areas to be low in other carbide formers such as Fe, Cr, and Mo. This indicates that the Nb is successfully tying up the C, as intended. The limited tests thus far on the Nb-stabilized 2.25% Cr-1% Mo steel show that this material possesses fair weldability. (auth)

29823 (ORNL-4630, pp 186-90) CLADDING MATERIALS FOR SPACE ISOTOPIC HEAT SOURCES. Patriarca, P.; Donnelly, R. G. (Oak Ridge National Lab., Tenn.).

In Fuels and materials development program quarterly progress report for period ending September 30, 1970.

Developmental alloys Pt-3% Mo-1.76% Ti and Pt-6% W-1% Hf were found to have tensile strengths superior to that of Pt-30% W and comparable to that of TZM at 1093°C. Studies of oxidation in air showed that the Pt-5% Mo-0.5% Hf and Pt-6% W-1% Hf developmental alloys were somewhat less resistant to oxidation than pure Pt and that the ductilities at room temperature were not affected by oxidation. The annealing temperature for 50% recrystallization in 1 hr for the Pt-Mo-Hf and Pt-W-Hf alloys was estimated to be about 1200°C, a dramatic increase over the 525°C recrystallization temperature of pure Pt. In an effort to develop a strong alloy that resists oxidation and has a melting point above 2000°C, W and Re were added to Pt-Rh. Melting points of about 2060°C were determined, and both alloys are fabricable cold. (auth)

29824 (ORNL-4630, pp 191-206) PHYSICAL AND MECHANICAL METALLURGY OF REFRACTORY ALLOYS. Patriarca, P.; Donnelly, R. G. (Oak Ridge National Lab., Tenn.).

In Fuels and materials development program quarterly progress report for period ending September 30, 1970.

An apparatus was constructed for creep testing alloy T-111 in partial pressures of N_2 comparable to those over UN fuels during operation at 1200 to 1400°C. Microstructures of the developmental, age-hardened alloy Ta-43.5 wt % Zr show uniformly distributed, finely precipitated particles that coarsen upon further aging but remain generally round instead of becoming plate-shaped as previously found with Ta-Hf and Nb-Hf alloys. The hardness of this alloy after aging longer than 10^3 min at 850 to 1150°C decreases from a diamond pyramid hardness of almost 500 dph as quenched to just above 300 dph. The stress-rupture properties of electron-beam and gas tungsten-arc welded Ta-10% W were determined and compared with those for unwelded material. The welds were as strong as unwelded material at low stresses but

XUM

were much weaker at high stresses. Equipment and specimens are being prepared for a study of hot cracking in refractory alloys during welding. Scanning electron microscopy of crack surfaces in TZM and Mo welds revealed indications of a liquid film and porosity at grain boundaries in the weld metal and heat-affected zone. Procedures and fixturing were also developed for welding both T-111 and Mo corrosion loops. The remelt temperature of Ta joints brazed with a Ti–Zr–Be alloy was found to be lower than the initial melting point and tentatively attributed this to enrichment of one phase of the braze alloy with Be, which depresses the melting point. The remelt temperature of a Ti–Zr–Ge alloy was essentially unchanged. The thermal conductivity and electrical resistivity of Ta and Ta–W alloys at low temperatures were measured and used to calculate values for pure Ta and T-111 at high temperatures. The calculated values were within 3% of previous measurements for T-111. (auth)

29825 (ORNL–4630, pp 261-70) JOINING RESEARCH ON NUCLEAR MATERIALS. Weir, J. R. Jr.; Slaughter, G. M. (Oak Ridge National Lab., Tenn.).

In Fuels and materials development program quarterly progress report for period ending September 30, 1970.

Welds were made with experimental Incoloy 800 filler metals in $\frac{1}{2}$-in.-thick fully restrained commercial Incoloy 800 plate. Results of tensile studies at intermediate temperatures (400 to 1000°C) showed that the experimental heats of Inconel 600 did not recover their ductility, which, for most alloys, was impaired at temperatures of 500°C and above. Strength depended upon the alloy content of the individual heat. This difference in strength, however, was negligible at 900°C and above. Experimental heats of stainless steel that contain various amounts of S or C were cold rolled at 0°C. Magne-Gage readings were taken during the initial breakdown of the drop casting. This involved a 31.5% reduction. The Magne-Gage was correlated with standards that contained known volumes of ferrite. The change in quantity of the body-centered cubic phase was predicted from the Magne-Gage correlation. (auth)

29826 (RD/B/N–1889) COLLABORATIVE PROGRAMME ON THE CREEP FATIGUE BEHAVIOUR OF 1 PERCENT Cr–Mo–V. Darlaston, B. J. L. (Central Electricity Generating Board, Berkeley (England). Berkeley Nuclear Labs.). Jan 1971. 15p. Dep. NTIS (U. S. Sales Only).

An informal collaborative programme was set up to examine the creep fatigue behaviour of 1Cr–Mo–V–steel. The programme of work covers uniaxial, biaxial and multiaxial cyclic behaviour of the material. The common objective is to provide a method which can be used to predict satisfactorily the integrity of power plant under thermal fatigue conditions. (auth) (UK)

29827 (RPI–3719-9) PRECIPITATION AND DISPERSION HARDENING IN HCP ALLOYS. Annual Report. Stoloff, Norman S. (Rensselaer Polytechnic Inst, Troy, N. Y.). 1 Mar 1971. Contract AT(30-1)-3719. 20p. Dep. NTIS.

Results of deformation studies on dilute Hf-base alloys are reported. The compositions of the alloys are as follows: Alloy A; O–180 ppM, H–0.8 ppM, and Zr–1.5 ppM. Alloy B; N–17 ppM, O–100 ppM, H–2 ppM, Fe–140 ppM, and Zr–3.6 ppM. Results showed that both oxygen in solution and hydrogen in the form of hydride particles embrittle hafnium. Oxygen promotes transgranular cleavage, while hydrogen produces both grain boundary embrittlement and cracks along hydride particles. It does not appear to be possible to retain significant quantities of hydrogen in solution in hafnium by rapid quenching. Strengthening by hydrogen reaches a plateau at about 2 at. % at 77 and 298°K. The severity of embrittlement by oxygen increases with decreasing temperatures. The effects of hydrogen on ductility at low temperatures, while not as severe, is significant, particularly at 4.2°K. (J.R.D.)

29828 USE OF POROSIMETRY IN THE MEASUREMENT OF PORE SIZE DISTRIBUTION IN POROUS MATERIALS. Rootare, H. M.; Nyce, A. C. Int. J. Powder Met.; 7: 3-11(Jan 1971).

Factors are established which affect accurate information about pore size and shape by mercury porosimetry. These factors include: surface tension of the mercury, contact angle between mercury and the solid, and pore shape factors. (auth)

29829 ASYMMETRIC MECHANICAL PROPERTIES OF MOLYBDENUM–RHENIUM ALLOY SINGLE CRYSTALS. Davidson, D. L. (Southwest Research Inst., San Antonio); Brotzen, F. R. Scr. Met.; 5: 303-7(Apr 1971).

Alloying Re with Mo produces an increased stress asymmetry for a flow on the {112} ⟨111⟩. These results fit the concepts of 3-fold dissociation of the dislocation core on {112} planes, even if the dissociation is insufficient for the creation of an actual stacking fault. (auth)

29830 AGING CHARACTERISTICS OF Cu–Be–Sn ALLOY AND THE EFFECT OF ADDITIONAL ELEMENTS. Amano, Yoshitsugu; Koyama, Koichiro (Himeji Inst. of Tech., Japan). J. Jap. Inst. Metals; 35: 261-8(Mar 1971). (In Japanese).

The aging characteristics and the corrosion resistance of Cu–Be and Cu–Be(1%)–Sn(4.5%) alloys were studied. The transition temperature from the two-stage hardening to the high-temperature age hardening of Cu–Be binary alloys increased with increasing Be content. The ripples of Cu–Be alloys were observed especially clearer under the optical microscope on the process of both the two-stage hardening and the two-step aging. The addition of Sn to Cu–Be(1%) binary alloy improved the age-hardenability. The transition temperature increased with increasing Sn content. The addition of Fe, Co, Ni, Cr, or Ti to Cu–Be(1%)–Sn(4.5%) retarded the discontinuous precipitation at grain boundaries, while the addition of Mn, Zn, or Cd neither retarded nor accelerated. Especially the addition of Co was very effective. By the addition of Sn, the corrosion weight loss of Cu–Be(1%)–Sn systems decreased in 5% HNO_3 solution but increased in 5% HCl solution. The corrosion weight loss of Cu–Be(1%)–Sn(4.5%) increased in 5% HNO_3 solution by the addition of Ti, Mn or Zn. (auth)

29831 HEAT CAPACITY AND DERIVED THERMODYNAMIC FUNCTIONS OF ^{242}Pu FROM 15 TO 373 K. Sandenaw, Thomas A.; Gibney, Robert B. (Los Alamos Scientific Lab., N. Mex.). J. Chem. Thermodyn.; 3: 85-95(Jan 1971).

Heat capacities of ^{242}Pu were determined between 15 and 373°K and values of derived thermodynamic functions were calculated. The curves of C_p against T diverged at about 170°K depending on whether the specimen had been cooled only to about 76°K or whether it had been cooled on down to about 4°K. The divergence was judged as not being a consequence of radiation damage but rather of additional strain caused by anisotropic thermal contraction on cooling to about 4°K. Values of $C_p(T)$, $S^0(T)$, and $-\{G^0(T) - H^0(O)\}/T$ were determined to be 7.86, 13.46, and 7.75 cal mol^{-1} K^{-1}, and $\{H^0(T) - H^0(O)\}$ to be 1701.5 cal mol^{-1}, at T = 298.15 K. The apparent rate of heat generation of the ^{242}Pu metal was determined to be 1.165×10^{-4} W g^{-1} from an intercomparison of results of heat capacity determinations over the temperature range covered. (auth) (UK)

29832 INFLUENCE OF DEFECTS UPON BRITTLE FAILURE OF ELECTROSLAG WELDED JOINTS CAUSED BY RESIDUAL STRESSES. Becka, J. Zvaranie; 19: 294-304(Sep 1970). (In English and Czech).

Values of fracture toughness, components of the spatial residual-stress field, and corresponding specific stress energies are given for individual characteristic zones of an electroslag-welded joint on the CSN 413030.9 modified Ni, Al + Ti steel designed for nuclear reactor pressure vessels. Residual welding stress can initiate brittle cracks even in mild kilned steel at normal temperature. The cracks result from the high value and complexity of the stresses. The critical dimensions of the defect depend on its location and may be smaller than 1 cm. The temperature of brittle crack initiation resulting from residual welding stress alone is 12°C. The critical dimension of the initial defect is 7 mm provided that it is located under the surface of the weld. Heat treatment starting at the austenitizing temperature fully restores the properties of an electroslag-welded joint to those of the base material. (INIS)

29833 INFLUENCE OF HIGH HYDROSTATIC PRESSURE ON THE FLOW STRESS OF PURE IRON AND MOLYBDENUM POLYCRYSTALS. Oguchi, Atsushi; Yoshida, Susumu; Nobuki, Minoru (National Research Inst. for Metals, Tokyo). J. Jap. Inst. Metals; 35: 81-6(Jan 1971). (In Japanese).

The influence of high hydrostatic pressure on the flow stress of zone-refined pure iron, carbon-deoxydized iron, and molybdenum polycrystals was studied at room temperature. Pressurizing tests at a pressure of 12000 kg/cm^2, tensile tests using the differential pressure method between atmospheric pressure and 12000 kg/cm^2, and tensile tests under a constant pressure of 12000 kg/cm^2 were carried out. For zone-refined iron and molybdenum, no pressurizing effects were found on the stress-strain behavior at atmospheric pressure, but a decrease of about 2.4% in flow stress was observed for carbon-deoxydized iron in the region of Lüders deformation after pressurizing. This effect seems to be similar to previous results which were explained by the generation of free dislocations around inclusions of FeO under hydrostatic pressure. According to the results of tensile tests using the differential pressure method, the rate of change of flow stress was about 2.1% for zone-refined iron, 2.8% for carbon-deoxydized iron, and 0.7% for molybdenum in the region of uniform deformation. These rates of change coincide well with those of

XUM

shear modulus of steel and molybdenum under hydrostatic pressure. In the stage of Lüders deformation for iron, the rate of change in flow stress was much greater (5.6 to 5.9%) than that of the shear modulus of steel under the same pressure. Assuming that the difference is due to the activation volume for the thermally activated process which controls the deformation, the activation volume of about 0.2 atomic volume is obtained. The rate of increase of work-hardening under hydrostatic pressure was 1 to 2% for iron in the region of uniform deformation. For molybdenum, it increased from zero strain and became constant (about 3%) at about 20% strain. (auth)

29834 NEW BEARING MATERIALS FOR ULTRAHIGH VACUUM. Hintermann, H. E.; Gass, H. (Laboratoire Suisse de Recherches Horlogeres, Neuchatel, Switzerland). Schweiz. Arch. Angew. Wiss. Tech.; 36: 189-93(Jun 1970). (In German).

The frictional and wear behavior of new ball bearing materials under various environmental conditions, with particular reference to space environments was studied. It is found that, in ultrahigh vacuum, the most suitable material for ball-bearing races is hardenable steel coated with titanium carbide. For ball-bearing spheres, it is sintered aluminum oxide, and for ball-bearing spacers, it is an Ag/10% In or an Ag/40% In alloy, and for less high vacuums polyimide impregnated with 15% MoS_2. (IAA)

29835 EFFECT OF MODIFYING ADDITIONS OF TITANIUM AND NICKEL ON [THE STRUCTURE AND] SOME PROPERTIES OF CAST ZIRCONIUM. Kashchuk, V. A.; Filippov, V. F. Sb. Nauch. Tr., Tomsk. Inzh.- Stroit. Inst.; 16: 15-21(1969). (In Russian).

A study was made of the resistivity, microhardness, and the degree of grain refinement of cast alloys of Zr containing 0.05 to 1.6% Ti or Ni. Ni markedly refined the macro-grain of Zr while Ti had the opposite effect. Similarly Ni increased the microhardness and decreased the resistivity to a larger extent than did Ti. The increase in modifying action by changing from Ti to Ni was associated with an increase in the number of d electrons and the formation in the alloy of a stable state with a more complete localization of the valency electrons in the stable d^{10} configuration. (Referativnyi Zh.)

29336 BERYLLIUM: PROMISE AND PROBLEMS. Clauser, H. R. Iron Age; 206: No. 6, 61-3(6 Aug 1970).

While Be has received qualified acceptance for military and aerospace applications due to its attractive properties, including light weight, high specific stiffness, low atomic number, high melting point, heat sink properties, and dimensional stability, its serious shortcomings, such as brittleness, toxicity, and high cost, make its use for industrial applications questionable. The development history of Be is reviewed briefly and its current status is reported with respect to investmerts in new equipment and research by Be companies and suggestions for expanding its applications. (Metals Abstr.)

29837 INVESTIGATION OF THE DIFFUSION OF HYDROGEN OF HYDRIDES OF ALLOYS. Lileeva, Yu. Ya.; Chertkov, A. A.; Malyuchkov, O. T. Izv. Vyssh. Ucheb. Zaved., Chern. Met.; No. 3, 123-6(1970). (In Russian).

Diffusion of H in Ti–Nb alloys saturated by H was investigated. Hydrides of the alloys containing Nb up to 70.2 at. % were single-phase fcc while in the alloys with Nb contents, up to 94 at. %, there were two phases: bcc of the NbH type and fcc of the TiH_2 type. The activation energy of H diffusion and its dependence on Nb-content were determined by proton magnetic resonance in the temperature range –160 to +250°C. Using a statistical model for free ions, activation energy values were calculated. (Metals Abstr.)

29838 NICKEL UND NICKELLEGIERUNGEN: EIGENSCHAFTEN UND VERHALTEN. (Nickel and Nickel Alloys: Properties and Behavior). Volk, K. E. Berlin; Springer-Verlag (1970). 453p. $23.70.

The uses, physical properties, microstructure, age-hardening behavior, chemical, electrochemical, and catalytic characteristics of nickel and nickel alloys are discussed in detail. (L.C.L.)

29839 PROPERTIES OF CAST NICKEL–CHROMIUM ALLOYS ALLOYED WITH NIOBIUM AND MOLYBDENUM. Nekhendzi, Yu. A.; Ionkina, E. M. Izv. Vyssh. Ucheb. Zaved., Chern. Met.; No. 3, 148-51(1970). (In Russian).

The effects of Nb (2 to 12%) and Mo (5 to 15%) on the microstructure and hardness of Ni–15% Cr alloys at room temperature and at 740°C were investigated. With increasing Nb content the hardness of the alloys increased either gradually, with preservation of the homogeneous solid solution, and/or rapidly, with precipitation of a hardening phase. Mo also increased the hardness of the alloys at toom temperature and at 740°C. In the presence of Mo precipitation hardening started at lower Nb contents. (Metals Abstr.)

29840 ACHIEVEMENT OF HIGH FATIGUE RESISTANCE IN METALS AND ALLOYS. Seventy-Second Annual Meeting, American Society for Testing and Materials, Atlantic City, N. J., 22–27 June 1969. ASTM Special Technical Publication 467. Philadelphia; American Society for Testing and Materials (1970). 303p. $28.75. (ASTM-STP-467; CONF-690650).

Information presented at the symposium is published in papers dealing with cyclic deformation, crack initiation, fracture of ductile metals, strengthening mechanisms, strength of superalloys, crack resistance, surface treatments, stress coining, effects of residual stresses, high temperature rest periods for metals, and effects of compressive self-stresses on metal fatigue. (J.R.D.)

29841 ULTRA-FAST DIFFUSION OF COPPER IN PRASEODYMIUM. Dariel, M. P. (Nuclear Research Centre-Negev, Beer-Sheva, Israel). J. Appl. Phys.; 42: 2251-4(May 1971).

The serial sectioning method has been used to measure the solute diffusivities of copper in praseodymium. In the bcc phase, the diffusivity of copper can be expressed by $D = 5.7 \times 10^{-2}$ exp (–17 800/RT) cm^2/sec, and in the double-hcp phase by $D = 8.4 \times 10^{-2}$ exp (–18 100/RT) cm^2/sec. It is most likely that copper diffuses in praseodymium by means of the combined substitutional–interstitial mechanism, similar to the other noble-metal solutes. Comparison of the present results with the previously measured diffusivities of zinc indicates that the solute diffusivities increase with decreasing solute valence. (auth)

29842 HEAT DISTRIBUTION IN ELECTRON BEAM-MELTED MOLYBDENUM PLATES. Klebanov, G. N.; Troyanov, I. M.; Uglov, A. A. Svar. Proizv.; No. 10, 1-2(Oct 1970). (In Russian).

Temperature measurements were made in the charge zone of electron beam-melted molybdenum alloy plates. The results were correlated with the theory calculated using equations for maximum plate heating by a linear thermal source. It was found that the above equations were sufficiently accurate for calculations of thermal zones in thin molybdenum plates. (INIS)

29843 CALORIMETRIC STUDIES ON CHEMISORPTION OF NITROGEN ON TANTALUM. Yamazaki, Hisashi; Oguri, Takeo; Kanomata, Ichiro (Tokyo Metropolitan Univ.). Jap. J. Appl. Phys.; 10: 304-9(Mar 1971).

Chemisorption behavior of wires and ribbons are studied with Roberts' type adsorption calorimeter. The total saturation coverages are 3.8×10^{14} molecules/cm^2 for both wires and ribbons. Initial values of average sticking probabilities are 0.22 for the wire and 0.20 for the ribbon at room temperature, and average sticking probabilities abruptly decrease at about 1.7×10^{14} molecules/cm^2. Average calorimetric heats also vary with the increase of coverage as 6.7, 6.0 and 5.2 eV for the wire, and 7.3 and 5.4 eV for the ribbon. Properties of the chemisorption states of B_1, B_2, and B_3 are made clear by the multiplex state theory using the above average values. In the B_1-state, the sticking probability is very small i.e. 0.01, and the heat of chemisorption is also small i.e. 5.3 eV. These values for the B_2-state are 0.37 and 6.0 eV. The B_3-state has the largest values of 0.5 and 7.3 eV. The heat of chemisorption of 6.1 eV calorimetrically obtained on an evaporated film is identical with that of the B_2-state. (auth)

29844 INFLUENCE OF BETA-STABILIZERS ON THE STRENGTH AND PLASTICITY OF TITANIUM AT LOW TEMPERATURES. Mikheev, V. S.; Koshelev, P. F.; Nikitin, P. N.; Shnyrev, G. D. (Inst. of Metallurgy, Moscow). Probl. Prochnosti; No. 10, 115-17(1970). (In Russian).

The influence of beta-stabilizing metals (tantalum, vanadium, niobium) on the strength, plasticity, and sensitivity to stress concentration in alpha-solid solution of titanium-based binary alloys, with 2 at. % of the second component, was investigated at temperatures of 20 to –253°C. Attention is paid to the rules governing the change of the mechanical properties of alloys in the multicomponent Ti–Ta–Cr and Ti–Ta–V–Mo systems at low temperatures. (JPRS)

29845 MAGNETIC AND MECHANICAL HARDNESS OF THE INTERMETALLIC COMPOUNDS $SmCo_5$ AND $LaCo_5$. McCurrie, R. A. (Univ. of Bradford, Eng.); Carswell, G. P.; O'Neill, J. B. J. Mater. Sci.; 6: 164-8(Feb 1971).

The magnetisation, coercivity, H_C, and remanence coercivity, H_R, were measured for the intermetallic compounds $SmCo_5$ and $LaCo_5$. The coercivities H_C and H_R for $SmCo_5$ are very much greater than those for $LaCo_5$. The differences in these parameters are much greater than would be expected from a simple theoretical model, so that they cannot be accounted for in terms of differences in the magnetocrystalline anisotropy constants.

XUM

Since the specimens used for the magnetic measurements were produced by mechanical comminution, Knoop hardness measurements were made in an attempt to account for the magnetic behavior in terms of the crystallographic damage and plastic deformation produced during the grinding process. The hardness results show that, within experimental error, the $SmCo_5$ is very nearly isotropic, whereas the $LaCo_5$ is very anisotropic on the {1010} planes with a Knoop hardness of 138 in the ⟨0001⟩ directions and 511 in the ⟨1210⟩. It is concluded that plastic deformation will occur more easily in $LaCo_5$ and that this could, to some extent, explain the comparatively low coercivities. (auth) (UK)

29846 STUDY OF HYDROGEN ADSORPTION ON A (100) TUNGSTEN SURFACE USING A SIMPLE HEED SYSTEM. Leggett, Monica R.; Armstrong, R. A. (National Research Council, Ottawa). Surface Sci.; 24: 404-16(Feb 1971).

The adsorption of hydrogen on tungsten (100) has been studied using HEED and flash desorption. A $c(2 \times 2)$ structure was observed. Microdensitometer traces of the diffraction patterns showed that with increasing hydrogen exposure the intensity of the extra beams increased, reached a maximum value and then the beams split and finally disappeared. All extra beams were broad, those viewed along the (100) azimuth broader than those in the (110). The extra beams can be attributed to scattering from hydrogen atoms adsorbed with a $c(2 \times 2)$ structure in very small square islands on the (100) surface. (auth)

29847 SIMULTANEOUS LEED AND RHEED STUDIES OF THE GROWTH OF ZIRCONIUM ON THE TUNGSTEN (100) SURFACE. Hill, G. E. (Chalmers Univ. of Tech., Goteborg); Marklund, I.; Martinson, J.; Hopkins, B. J. Surface Sci.; 24: 435-50(Feb 1971).

Zirconium was evaporated under ultrahigh vacuum conditions and deposited on atomically clean W(100) surfaces in a combined low energy electron diffraction and reflection high energy electron diffraction apparatus (LEED/RHEED). Both diffraction patterns were used to follow and interpret the two- and three-dimensional growth of zirconium up to an estimated mean coverage of about fifty monolayers. Deposition on substrates at room temperature gave rise to a 1×1 pseudomorphic layer of zirconium with an improving order up to 600°K. Higher temperature annealing of very thin deposits led to a new structure W(100) $(4/3 \times 2) - Zr$, at roughly three-quarter monolayer coverage. Annealing of thicker films gave a return of the 1×1 pseudomorphic growth followed by the development of islands of an abnormal fcc phase of zirconium. The formation of these islands and their removal, at a lower temperature than the pseudomorphic layer, could be readily followed by RHEED although no changes in the LEED pattern were observable. (auth)

29848 FIELD EMISSION AND FIELD ION MICROSCOPE STUDIES OF THE EPITAXIAL GROWTH OF NICKEL ON TUNGSTEN. Smith, G. D. W.; Anderson, J. S. (Oxford Univ.). Surface Sci.; 24: 459-83(Feb 1971).

Single crystals of nickel have been grown on tungsten field emitter tips by vapor deposition in UHV, using substrate temperatures in the range 425 to 700°K, and nickel fluxes of the order of 0.1 to 10 atom layers per minute. The orientation relationship is {111} Ni || {110} W, with ⟨211⟩ Ni || ⟨110⟩ W. The directional misfit is 3.5%. The crystals grow from initial nuclei formed on the {110} step ledges at multilayer coverages. To permit direct FIM study of the crystals, some specimens were grown on nearly perfect, field evaporated tungsten surfaces, held at 500°K. Examination at 78°K, using hydrogen and helium as the imaging gases, gave information regarding the structure, form and degree of perfection of the crystals. An interfacial reaction was observed, which produced considerable disordering at the tungsten surface. The mechanism of this reaction apparently involved the substitutional replacement of tungsten atoms by nickel, in the interface lattice. The implications of these observations with respect to the theory of epitaxial growth are discussed. (auth)

29849 CHEMISORPTION OF NITROGEN AT ACTIVATED SITES ON A POLYCRYSTALLINE TUNGSTEN SURFACE. Winters, Harold F.; Horne, Donald E. (IBM Research Lab., San Jose, Calif.). Surface Sci.; 24: 587-611(Feb 1971).

The exposure of a polycrystalline tungsten surface to atomic nitrogen or bombardment by N_2^+ is shown to enhance chemisorption. Ion bombardment causes the saturation coverage to be increased by about 50% over that found after exposure to the molecular gas. A somewhat greater saturation coverage is obtained by exposure to neutral atomic nitrogen. The additional gas found in these experiments is desorbed at lower temperatures than nitrogen chemisorbed in β sites. These results are interpreted on the basis of chemisorption at endothermic adsorption sites. (auth)

29850 INITIAL GROWTH OF PLATINUM CRYSTALS ON THE TUNGSTEN SURFACE AS OBSERVED BY THE FIELD-ION MICROSCOPE. Sugata, Eizi; Ishii, Sakae; Masui, Katsuhiro (Osaka Univ.). Surface Sci.; 24: 612-24(Feb 1971).

Platinum vapor was deposited on a tungsten surface in ultrahigh vacuum. After the rather irregular spreading of one or two monolayers over the surface, platinum atoms crystallized on some flat planes in a so-called island manner. This may be due to the cohesive tendency of platinum atoms themselves. The temperature of the tungsten (substrate) was kept below about 250°K. The arrangement of atoms in these islands had some relation to the crystallographic planes of the substrate. Stacking and size of the islands were observed using a field-desorption technique. There was no positive evidence of stacking faults in the islands, but a few vacancies were observed. (auth)

29851 DEMONSTRATION BY ANISOTHERMAL CREEP OF A SUPERDUCTILE STRUCTURAL STATE DURING THE RECRYSTALLIZATION OF α URANIUM. Collot, Jean; Cizeron, Georges (Ecole Nationale Superieure des Mines, Paris). Compt. Rend., Ser. C; 272: 520-3(8 Feb 1971). (In French).

A new technique of anisothermal creep at constant load on strongly laminated electrolytically pure uranium showed up a superductility due to the gradual development of a duplex structure during recrystallization. (auth) (France)

29852 EFFECTS OF CHANGES IN VOLUME AND c/a RATIO ON THE PRESSURE DERIVATIVES OF THE ELASTIC MODULI OF H.C.P. Ti AND Zr. Fisher, E. S. (Argonne National Lab., Ill.); Manghnani, M. H. J. Phys. Chem. Solids; 32: 657-67 (Mar 1971).

The hydrostatic pressure derivatives of the single crystal elastic moduli of Ti were measured to 5.5 Kbar. The pressure derivatives are $dC_{11}/dP = 5.01$, $dC_{33}/dP = 4.88$, $dC_{44}/dP = 0.52$, $dC_{66}/dP = 0.45$, $dC_{12} = 4.11$, and $dC_{13}/dP = 4.05$. The positive value for dC_{44}/dP is in sharp contrast to $dC_{44}/dP < 0$ for Zr. This difference is assumed to arise from the difference between $d(c/a)/dP$ in the two hcp crystals and quantitative values of dC_{ij}/dV and $dC_{ij}/d(c/a)$ are calculated. It is then shown that the large differences between the average Grüneisen mode γ_H calculated from dC_{ij}/dP and that obtained from thermal expansion data for both Ti and Zr can be explained by the differences between $d(c/a)/dV$ under hydrostatic pressure and during thermal expansion, respectively. The relatively large negative value for $dC_{44}/d(c/a)$ is quantitatively consistent with Cousins' calculations of the dependence of the electrostatic contribution to C_{44} on the c/a ratio in any hcp metal lattice. (auth) (UK)

29853 OBSERVATION OF AGE HARDENING OF α-ZIRCONIUM AFTER DEFORMATION. De Paula E Silva, Evando; Com-Nougue, Jacques; Beranger, Gerard (Ecole Nationale Superieure des Mines, Paris). Compt. Rend., Ser. C; 272: 180-3(11 Jan 1971). (In French).

The aging treatment of α-zirconium after deformation induces an anomaly in the tensile curve. The effects of aging duration, temperature, and of oxygen content were studied. (auth) (France)

29854 ON THE VARIATION IN THE TEMPERATURE OF RECRYSTALLIZATION OF ZIRCONIUM–OXYGEN SOLID SOLUTIONS AS A FUNCTION OF THE OXYGEN CONCENTRATION. Billion, Marc; Ailloud, Pierre; Renucci, Louis; Langeron, Jean-Paul (CNRS, Vitry-sur-Seine, France). Compt. Rend., Ser. C; 272: 524-6(8 Feb 1971). (In French).

The influence of oxygen on the temperature of recrystallization of strongly laminated zirconium samples was studied. The recrystallization temperature T is shown to vary linearly with the oxygen concentration and the value found for atomic concentrations between 0 and 0.4 at. % is $T = 162 \pm 0.077$°C. (auth)

29855 INFLUENCE OF INTERSTITIAL METALLOID ELEMENTS ON THE INTERGRANULAR EMBRITTLEMENT OF BODY-CENTERED CUBIC METALS. Huntz, Anne-Marie (Ecole Nationale Superieure des Mines, Paris). Metaux (Corros.-Ind.); 46: 25-46(Jan 1971). (In French).

Following a review of the similarity in mechanical properties between refractory metals and iron, the influence of metalloid impurities (carbon, oxygen, nitrogen, sulfur, phosphorus, boron, hydrogen) on the intergranular brittleness of iron is shown, after which the embrittlement of body centered cubic refractory metals is examined. The influence of interstitials (oxygen, carbon, nitrogen, hydrogen) on the intergranular brittleness of molybdenum tungsten, and chromium is discussed. (France)

29856 ELECTROTRANSPORT OF MOLYBDENUM IN Ni–18 AT. PERCENT Mo ALLOY. Kalinovich, D. F.; Kovenskii, I. I.; Smolin, M. D.; Statsenko, V. M. (Inst. of Problems in Materials Science, Kiev). Sov. Phys.-Solid State (Engl. Transl.); 12: 2459-60(Apr 1971).

XUM

Translated from Fiz. Tverd. Tela; 12: 3042-4(Oct 1970).

Thin ^{99}Mo-containing films were deposited on wires of Ni–18 at.% Mo alloy and used in measurements of the diffusion coefficient and velocity of the labeled atoms. The effective charge Z* of Mo was found to range from 13.6 cgs-esu at 950°C to 11.4 at 1350°C, and the diffusion coefficient followed the law $D = 0.45 \exp[-52{,}200/RT]$ cm^2/sec. The temperature dependence of Z* follows the equation $Z^* = Z + b/(T + \rho_0\alpha)$, where $Z = -1.7$ esu, $b = 36{,}900$ deg-cgs-esu, and ρ_0 and α are the temperature-dependence parameters of the electric resistivity of the alloy. The Mo ions migrated toward the cathode, and the effective charge indicated that scattering of holes was the electrotransport mechanism. The sign of Z indicated an acceptor action of Mo toward Ni. (D.L.C.)

29857 STRENGTH AND PLASTICITY OF SUBMICRON TUNGSTEN FIBERS. Fridman, V. Ya. (Inst. of Inorganic Chemistry, Novosibirsk, USSR). Sov. Phys.-Solid State (Engl. Transl.); 12: 2461-2(Apr 1971).

Translated from Fiz. Tverd. Tela; 12: 3044-6(Oct 1970).

A study was made of the tensile breaking strength σ_b and plasticity of W fibers of transverse dimension a ranging from a few microns to several hundredths of a micron. The plot of σ_b vs a showed that, in the 4- to 0.5-μ range, σ_b was practically independent of a, being 200 to 400 kg/mm^2, while below 0.5 μ, σ_b increased rapidly with decreasing a. The strongest sample had $a = 0.1\mu$ and $\sigma_b = 2100$ kg/mm^2, in agreement with Garber et al. The scatter in the data increased with decreasing a. (D.L.C.)

29858 CALCULATION OF THE FORMATION ENERGY AND CONCENTRATION OF VACANCIES IN MOLYBDENUM FROM ENTHALPY MEASUREMENTS. Chekhovskoi, V. Ya.; Petrov, V. A. (Inst. of High Temperatures, Moscow). Sov. Phys.-Solid State (Engl. Transl.); 12: 2473-4(Apr 1971).

Translated from Fiz. Tverd. Tela; 12: 3056-8(Oct 1970).

The calculations were based on careful measurements of the enthalpy and mean specific heat of Mo at 1000 to 2850°K. The energy of formation of vacancies in Mo is found to be U = 42.9 kcal/g-atom, the concentration of vacancies $C = 50.9 \exp(-429 \times 10^2/RT)$, and entropy of vacancy formation 7.8 cal (g-atom)$^{-1}$ deg^{-1}. (D.L.C.)

29859 CATALYTIC PROPERTIES OF RARE-EARTH METALS (Sc, Nd), THEIR HYDRIDES, CARBIDES, AND OXIDES IN THE HIGH-TEMPERATURE PARA-ORTHO HYDROGEN CONVERSION REACTION. Konenko, I. R.; Nadzhm, A.; Tolstopyatova, A. A.; Samsonov, G. V.; Makarenko, G. N. (Inst. of Organic Chemistry, Moscow). Izv. Akad. Nauk SSSR, Ser. Khim.; No. 1, 100-5(Jan 1971). (In Russian).

Rare-earth metals absorb H with the formation of hydrides of various ratios of H/metal. Elemental Sc and Nd and their hydrides, carbides and oxides assume the following sequence: Sc > ScH_2 > ScC > Sc_2O_3; Nd > NdH_3 > NdC_2 > Nd_2O_3 in the order of decreasing specific catalytic activity in the reaction with para-ortho-H conversion at 200°. It is suggested that this order is dependent upon the order of acceptor capacity of the non-metals: H < C < O. The activation energy of this reaction is fairly constant for each series. Relative to their decreasing specific catalytic activity, the subject materials assume the following order: Nd > Y > Sc; NdH_3 > YH_3 > ScH_2; NdC_2 > YC > YC_2 > ScC; Nd_2O_3 > Y_2O_3 > Sc_2O_3. It is suggested that these series are linked with the ionizing potential of the metal. Atoms of each metal are apparently active centers in the reaction with the para-ortho hydrogen conversion. This idea is compatible with the concept of stable electron configurations possessed by catalyst atoms. (tr-auth)

29860 MATERIALS FOR HIGH TEMPERATURE APPLICATIONS. McCartney, E. R. pp 49-55 of Sydney University Chemical Engineering Association New Materials Symposium, Sydney, August 27th, 1970. Sydney; Univ. of Sydney (1970).

From Chemical engineering conference; Sydney and Melbourne, Australia (18 Aug 1970). See CONF-700804.

Materials such as metals, ceramics, and organic polymers are evaluated for use in high temperatures. Properties considered most important include high melting point, inertness, and low volatility. Discussions are included on the use of metals, ceramics, and composites. (J.R.D.)

29861 INTERNAL FRICTION COLD WORK PEAK IN THE NIOBIUM–NITROGEN SYSTEM. Dahlstrom, Norris Alfred. Urbana, Ill., Univ. of Illinois (1970). 78p. University Microfilms Order No. 71-5075.

Thesis.

The internal friction spectrum of undeformed and deformed niobium–nitrogen was studied at about 1 Hz from room temperature to 700°C. The goal of the work was that of elucidating the mechanism of the so-called cold work peak. In particular, questions have been raised from time to time concerning the necessity of externally imposed deformation; this peak has been seen in quench-aged alloys with no external deformation. The latter possibility was examined in considerable detail. Isothermal annealing experiments were performed at 535°C, the approximate temperature of the cold work peak, to follow its development and decay. The internal friction increased rapidly after an incubation time to a maximum value whose height was dependent on the initial amount of nitrogen present. The height then decreased with time. The nature of the precipitates at these various stages was studied by transmission electron microscopy. Wires given treatments similar to the internal friction specimens were jet machined and then electropolished. During the initial stages of nitride precipitation finely dispersed lenticular precipitates less than 500 Å formed; during this stage the cold work peak had not yet developed. During coarsening the peak grew in height and only reached its maximum when the precipitates had increased in size to about 2500 Å and had produced many prismatic dislocation loops and dislocation tangles. Because the precipitates in undeformed samples were able to produce a significant dislocation density, it is concluded that a single dislocation interstitial mechanism causes the so-called cold work peak in both deformed and undeformed aged samples. (Diss. Abstr. Int., B)

29862 SPETSIAL'NYE STALI I SPLAVY. (Special Steels and Alloys). Ababkov, V. T. (ed.). Sbornik Trudov Tsniichm, Vypusk 77. Moscow; Izdatel'stvo Metallurgiya (1970). 248p.

Forty-two articles are included on the properties of high-melting steels and Ni- and Mo-base alloys. The relationship between the dendritic structure of the alloys and their phase diagrams are discussed and data on various stainless steels and corrosion-resistant alloys are analyzed. A separate abstract was prepared for each of four articles of special interest. (R.V.J.)

For abstracts of individual papers see: 29776, 29777, 29863, and 29864.

29863 INFLUENCE OF CARBON ON Mo DUCTILITY. Morgunova, N. N.; Klypin, B. A.; Lastochkin, R. R. Sb. Tr. Tsent. Nauch.-Issled. Inst. Chern. Met.; No. 77, 63-7(1970). (In Russian).

The effects of carbon on the threshold of Mo ductility were studied using vacuum-melted and deformed Mo in a re-crystallized state. Tests with deformed and re-crystallized specimens after 2 hr at 2100°C showed that their cold brittleness was not influenced by 0.02 to 0.29% C with increasing carbon content, the ductility of Mo increased due to the increased number and size of the carbide inclusions at the grain boundaries and formation of almost solid carbide lattices. (R.V.J.)

29864 TEMPERATURE DEPENDENCE OF MECHANICAL PROPERTIES OF CERTAIN Mo AND W ALLOYS. Klypin, B. A.; Morgunova, N. N. Sb. Tr. Tsent. Nauch.-Issled. Inst. Chern. Met.; No. 77, 67-71(1970). (In Russian).

The effects of temperature on the strength, yield, and dimensional stability of deformed Mo and W alloys was studied at temperatures to 2400°C. Pure deformed Mo exhibited the best strength. The highest strength and lowest plasticity were observed in Mo–50% W–0.1% Zr alloys at 2100°C. (R.V.J.)

29865 CURIE–WEISS TEMPERATURE DEPENDENCE OF PARAELASTICITY. Tretkowski, J.; Voelkl, J.; Alefeld, G. (Kernforschungsanlage, Juelich, Ger.). Z. Naturforsch.; 26a: 588-90(Mar 1971).

The elastic properties of a Nb spring loaded with the critical concentration of 34 at. % hydrogen were studied using static Gorsky-effect measurements. Relaxation strength and diffusion coefficients were measured as functions of temperature. The temperature dependence follows a Curie–Weiss law for temperatures $(T - T_c)/T_c \geq 6 \times 10^{-3}$, and there is no singularity in the mobility in the same temperature range. The mean field approximation is valid close to the critical point. (D.L.C.)

29866 DETERMINATION OF LOW SOLUBILITY LIMITS BY MEASUREMENT OF DIFFUSION COEFFICIENTS: APPLICATION TO THE SYSTEM NICKEL–URANIUM. Zanghi, Jean-Pierre; Van Craeynest, Annick; Calais, Daniel (CEN-FAR, Fontenay-aux-Roses, France). J. Nucl. Mater.; 39: 133-44(May 1971). (In French).

A method is described for determining low solubility limits by measuring diffusion coefficients. Coefficients of chemical diffusion at infinite dilution can be measured precisely. A low solubility S_0 can be obtained with the aid of such coefficients by Jost's method. The displacement ϵ of the interface between the two-phase and single-phase zones is followed as a function of time,

relative to the junction plane of a welded couple (element A/A saturated with B + AB precipitate). Here B is the element whose solubility in A is being measured. The following relations apply: $\epsilon = 2\gamma\sqrt{Dt}$, and $S_0/(C_0 - S_0) = \sqrt{\pi}\gamma \exp(\gamma^2)[1 + \text{erf}\,\gamma] = \sqrt{\pi}f(\gamma)$, where C_0 is the concentration of B in the two-phase alloy and γ is a parameter. When $f(\gamma)$ has been tabulated, C_0 determined by chemical analysis, D obtained separately (thin film method), then measurement of ϵ allows one to obtain γ and thus S_0. This method was tested on the Ni–U system. The diffusion coefficients at infinite dilution of uranium in nickel, determined by fissiography, obey an Arrhenius relationship: $D = 1 \exp(-56{,}400/RT)$ cm²/sec. In the same temperature range as used for the diffusion measurements, the solubility of uranium in nickel is in the range 0.70 to 1.35 wt %. The enthalpy of solution was evaluated at 20 kcal/mole, the entropy of vibration at 3.63 cal/°K·mole. (auth)

29867 DIFFUSION AND SOLUBILITY OF PLUTONIUM AND URANIUM IN ALUMINUM. Housseau, Nicole; Van Craeynest, Annick; Calais, Daniel (CEA-CEN, Fontenay-aux-Roses, France). J. Nucl. Mater.; 39: 189-93(May 1971). (In French).

Between 550 and 630°C the diffusion coefficients at infinite dilution of plutonium and of uranium in aluminum are of the order of 10^{-8} cm²/s. The fractional solubilities are 5 to 60×10^{-6} and 5 to 30×10^{-6} respectively. (auth)

29868 CREEP-RUPTURE DATA FOR THE REFRACTORY METALS TO HIGH TEMPERATURES. Conway, J. B.; Flagella, P. N. New York; Gordon and Breach, Science Publishers, Inc. (1971). 794p. (TID-25686).

A compilation of creep-rupture data on refractory metals at temperatures up to 3000°C is presented. The information is presented in chapters on experimental techniques, creep data analysis, rupture data analysis, tungsten and its alloys, rhenium and its alloys, tantalum and its alloys, molybdenum and its alloys, and niobium and its alloys. (J.R.D.)

29869 KINETICS AND MECHANISM OF THE LOW-PRESSURE, HIGH-TEMPERATURE OXIDATION OF TUNGSTEN SILICIDES. III. Gelain, C.; Cassuto, A.; Le Goff, P. (CNRS, Nancy). Oxidation Metals; 3: 153-69(Mar 1971).

Oxidation studies were performed on silicon-coated tungsten which was treated to form various intermetallic compounds on the surface. Two classifications of behavior were noted; a passivated state in which a protective layer of SiO_2 formed at low temperatures and a combustion state in which volatile oxides such as SiO, WO_2, and WO_3 formed. A simple kinetic model was proposed to account for the abrupt transition from one state to the other. The temperature–pressure conditions under which the transition occurs were delineated by a thermodynamic study. The combustion state is characterized by the linear growth of W_5Si_3 on WSi_2 surfaces and by the growth of a solid solution of silicon in tungsten on W_5Si_3 surfaces. The oxygen consumption on W_5Si_3 surfaces followed first-order kinetics with an activation energy of 19 ± 1 kcal/mole. The activation energy for oxygen consumption on the solid solution was the same as for pure tungsten, 28 ± 1 kcal/mole, but the kinetic order of the solid solution was 0.9 compared to 0.7 for pure tungsten. (auth)

29870 NITRIDATION OF Zr AT HIGH TEMPERATURES. Paidassi, Jean; Le Delliou, Raymonde (CEA, Fontenay-aux-Roses, France). Compt. Rend., Ser. C; 272: 249-52(18 Jan 1971). (In French).

The parabolic nitridation of Van Arkel zirconium in very pure nitrogen at atmospheric pressure was studied in the 800 to 1100°C temperature range. At the same time as a layer of zirconium nitride settled on the surface, nitrogen diffused into the underlying metal. The diffusion gradients were determined by microhardness measurements. The thickness of the layer was determined by micrography. The values of the nitrogen diffusion coefficient in zirconium nitride and in the underlying metal were deduced from these measurements as a function of temperature. (auth) (France)

29871 ALLOY SOFTENING IN GROUP VIA METALS ALLOYED WITH RHENIUM. Stephens, J. R.; Witzke, W. R. (Lewis Research Center, Cleveland). J. Less-Common Metals; 23: 325-42(Apr 1971).

An investigation was conducted to determine the effects of temperature and composition on alloy softening in the Group VIA metals Cr, Mo, and W, alloyed with Re. Microhardness measurements were made at homologous temperatures from 0.02 to 0.2 Tm; the range where alloy softening is normally observed in bcc alloys. Rhenium contents ranged from zero up to the maximum solubility of Re in each of the Group VIA metals. Hardness was measured for approximately fourteen alloys from each system at six test temperatures in order adequately to describe alloy softening in Group VIA–Re alloys. Results showed that alloy softening was similar in all three alloy systems, occurring at homologous temperatures less than 0.16 and at Re concentrations less than 16 at. %. The rhenium content required to produce a hardness minimum diminished rapidly in all three systems with increasing test temperature. A sharp temperature dependence of hardness was observed in dilute alloys that exhibited alloy softening. Alloy hardening was observed in concentrated alloys at all temperatures and in dilute alloys at homologous temperatures greater than 0.16. A much lower temperature dependence of hardness was observed for these alloys. (auth)

29872 CORRELATION OF STRENGTH PROPERTIES TO MICROSTRUCTURES IN PRECIPITATION-HARDENED Ti-Nb ALLOYS. Mendiratta, Madan G. New Brunswick, N. J.; Rutgers–The State Univ. (1970). 93p. University Microfilms Order No. 71-3081.

Thesis.

The room temperature tensile properties of a precipitation-hardened Ti–35 wt % Nb alloy were correlated to the microstructures obtained by aging in the ($\alpha + \beta$) phase field. To improve the fracture toughness of this alloy, a bi-modal precipitate microstructure was developed by means of step aging. This bi-modal microstructure consisted of widely spaced, incoherent precipitate particles of the equilibrium α-phase and small, interspersed, coherent precipitate particles of a metastable phase, both types homogeneously distributed throughout the parent β-phase. By controlling favorably with the aid of this microstructure the dislocation–particle interactions, balanced strength properties with a yield stress of 100 KSI and an elongation to fracture of 4% were obtained. The large α particles precipitated by aging at 550°C imparted increased ductility while the smaller particles precipitated from reaging at 400°C conferred a substantial increase in the flow stress. For 35, 41, and 45 wt % Nb alloys aged at low temperatures in the ($\alpha + \beta$) phase field, room temperature tensile properties were measured. It was shown as a function of increasing aging time that the increase in the flow stress as well as in the degree of embrittlement was due to the precipitation of small coherent particles. A combination of transmission electron microscopy and small angle x-rays scattering techniques was utilized to establish the size and distribution of the particles. It was concluded that the experimental tensile behavior, as a function of both the size and the volume fraction of the particles, agreed well with the qualitatively described expected behavior. (Diss. Abstr. Int., B)

29873 CHEMICAL DIFFUSIVITIES OF PLUTONIUM–GALLIUM ALLOYS IN THE EPSILON (b.c.c.) PHASE. Harvey, M. R.; Doyle, J. H.; Rafalski, A. L.; Riefenberg, D. H. (Dow Chemical Co., Golden, Colo.). Contract AT(29-1)-1106. J. Less-Common Metals; 23: 446-50(Apr 1971).

Chemical diffusion data from platinum–0.14 to 3.5 wt % gallium alloys was obtained with the aid of an electron microanalyzer from diffusion couples annealed in the ϵ phase. An increase in Ga concentration resulted in a decrease in the chemical diffusivity. From a comparison of the chemical diffusivities in the ϵ and δ phases it was apparent that diffusion rates for the alloyed ϵ phase were approximately three orders of magnitude higher than for alloyed δ phase. (G.M.C.)

29874 TEMPERATURE DEPENDENCE OF THE FLOW-STRESS OF HEAVILY-DEFORMED DOPED TUNGSTEN. Boser, O. (General Telephone and Electronics Labs. Inc., Bayside, N. Y.). J. Less-Common Metals; 23: 427-35(Apr 1971).

The flow stress of cold-worked, doped tungsten was determined in the temperature range from 77 (liquid nitrogen) to about 800°K. The tungsten specimens were fibrous with a ⟨110⟩ texture in the drawing direction. The measured flow stress was attributed to two components. The temperature independent part is due to a long-range dislocation–dislocation interaction and prevails solely at elevated temperatures. The temperature dependent component was analyzed according to a theory of elastic dipoles interacting in a thermally activated process with dislocations. The Gibbs free activation enthalpy, ΔG_0, and the dipole concentration, C_g, derived from that analysis are $\Delta G_0 = 1.59$ eV and $C_g = 800$ at. ppM, respectively. From these results an activation volume was calculated and compared to the one measured by strain rate changes. The agreement is very good, suggesting that an elastic dipole–dislocation interaction indeed explains the increase of the flow stress with decreasing temperature. The origin of the elastic dipoles cannot be determined unambiguously from this investigation. The elastic dipoles might, however, be due either to impurity atoms in interstitial solution, such as carbon or nitrogen, or to small agglomerates of these impurities. Both possibilities are within the limits of the concentrations found by chemical analysis. (auth)

XUM

29875 ENTHALPY MEASUREMENTS BY DROP CALORIMETRY USING ELECTROMAGNETIC LEVITATION. Chekhovskoi, V. Ya.; Sheindlin, A. E.; Berezin, B. Ya. (Inst. for High Temperatures, Moscow). High Temp. - High Pressures; 2: 301-7(1970).

A method for measuring the enthalpy of chemically active metals is described which employs a block calorimeter in conjunction with electromagnetic levitation of the sample. Measurements of the enthalpy of solid molybdenum in the temperature range 2094 to 2869°K gave results departing over the whole temperature range by no more than ±1.2% from the data recommended in the literature. (auth) (UK)

29876 MEASUREMENT OF THE THERMAL DIFFUSIVITY OF A Pu ALLOY STABILIZED IN THE δ PHASE. Radenac, Antoine; Hocheid, Bernard; Lacoste, Michel; Roy, Claude; Roux, Claude (Centre d'Etudes de Bruyeres-le-Chatel, Montrouge, France). Compt. Rend., Ser. B; 272: 297-9(1 Feb 1971). (In French).

The method using a sustained periodic signal was employed to measure the thermal diffusivity of a Pu alloy containing 6 at. % Gd, stabilized in the δ phase; the temperature range considered was between 30 and 90°C. The value of the diffusivity measured at room temperature (0.040 cm^2/s) is significantly greater for the alloy than for the pure metal. The thermal conductivity of the δ phase obtained from this measurement was compared with that of the α phase. Even though the α phase exhibits low structural symmetry and the δ phase corresponds to an fcc structure, very common in metals, the thermal conductivities are of the same order of magnitude. (auth) (France)

29877 ROLLING WORKABILITY OF PURE TUNGSTEN SINGLE CRYSTALS WITH (110) [001] AND (001) [110] ORIENTATIONS AT ROOM TEMPERATURE TO 200°C. Ohba, Yukio; Tamura, Yoshio; Fujii, Tadayuki (National Research Inst. for Metals, Tokyo). J. Jap. Inst. Metals; 35: 177-82(Mar 1971). (In Japanese).

Pure tungsten single crystals with (110) [001] and (001) [110] orientations were grown by electron-beam zone-melting technique. Rolling deformation on their orientations was studied in the temperature range of room temperature to 200°C. The (001) [110] specimen showed a considerable ductility on rolling above 100°C, but the (110) [001] specimen was fractured in a brittle manner even at 200°C. An abnormal widening which was not observed in pure iron and 3% Si-Fe on rolling at room temperature was found in the (001) [110] specimen at 200°C. In the (110) [001] specimen a crystal is rotated about the [110] axis normal to the rolling direction on rolling. The degree of the crystal rotation to the rolling reduction was found to be small at least up to 50% rolling reduction as compared with the result of 3% Si-Fe. The above phenomena are discussed in relation to the multiplication mechanism of dislocations at a relatively low temperature in tungsten crystals. (auth)

29878 FACTORS AFFECTING THE HIGH TEMPERATURE STRENGTH OF NICKEL-CHROMIUM AND NICKEL-TUNGSTEN ALLOYS. Suto, Hajime; Yamada, Kuniaki (Tohoku Univ., Sendai). J. Jap. Inst. Metals; 35: 231-7(Mar 1971). (In Japanese).

In order to obtain a fundamental knowledge for the study of austenitic heat resisting steels and superalloys, the strengthening factors affecting high temperature creep of nickel-chromium and nickel-tungsten alloys are discussed using Sherby's equation: $\dot{\epsilon}_s = A\gamma^{3.5}(\sigma/E)^5 D$, where $\dot{\epsilon}_s$ is the steady state creep rate, γ is the stacking fault energy, σ is the applied stress, E is Young's modulus, D is a diffusion constant. First of all, the Sherby's equation was ascertained for pure metals. It seems that the most important factor affecting the high temperature strength of nickel-chromium alloys is the decrease of stacking fault energy by the addition of chromium, and that of nickel-tungsten alloys is the decrease of stacking fault energy and of diffusion velocity by tungsten. The contributions of Young's modulus and dislocation locking by solute were also estimated. (auth)

29879 INVESTIGATIONS ON THE VANADIUM-NITROGEN SYSTEMS. SOLUBILITY LIMIT OF NITROGEN, AND PHASE TRANSFORMATION. Hoerz, Gerhard (Max-Planck-Institut fuer Metallforschung, Stuttgart). Z. Metallk.; 62: 208-16(Mar 1971). (In German).

The saturation concentration c_s of nitrogen in the α phase increases from 2.6 at. % at 600°C to 10.8 at. % at 1500°C. β nitride (V_2N-V_3N) is in equilibrium with the α phase at all temperatures in the range of this study. When alloys containing ≧6 at. % N are cooled from 1500 to 100°C within 160 sec, the disordered α phase is transformed by a combination of shear and diffusion. This bainitic transformation yields a twinned lamellar structure. (auth)

29880 SOLID SOLUTION HARDENING OF VA METALS BY NITROGEN AND OXYGEN INTERSTITIALS. Elssner, Gerhard; Hoerz, Gerhard (Max-Planck-Institut fuer Metallforschung, Stuttgart). Z. Metallk.; 62: 217-22(Mar 1971). (In German).

A survey is given of the dependence of the yield stress and Vickers hardness of vanadium, niobium, and tantalum wires with bamboo structure on the oxygen and/or nitrogen content up to 1.2 at. % in solid solution and on the temperature of deformation ranging from −73 to +90°C. In the cases of niobium and tantalum the hardening by nitrogen is considerably more pronounced than by oxygen. With vanadium the effects of both gases are practically the same. The results suggest that the yield stress of VA metals containing interstitial impurities is determined by an athermal and a thermal contribution. (auth)

29881 DIFFUSION IN THE SYSTEM Nb-Pd STUDIED BY MEANS OF ELECTRON-PROBE MICROANALYSIS. Brunsch, Arwed; Steeb, Siegfried (Max-Planck-Institut fuer Metallforschung, Stuttgart). Z. Metallk.; 62: 247-51(Mar 1971). (In German).

Diffusion processes in the Nb-Pd system (700 to 1030°C) were investigated by means of quantitative electron probe microanalysis. At the compositions $NbPd_2$, $NbPd_3$, $NbPd_4$, $NbPd_5$, and $NbPd_6$ intermetallic phases were observed. The equilibrium phase diagram shows the phases Nb_2Pd, $NbPd_2$, and $NbPd_3$ only. From the relation for the thickness of the total diffusion zone $d = k\sqrt{t}$ it can be concluded that volume diffusion predominates in this system. The values of $\log k^2$ as well as the values of $\log D$ versus $1/T$ yield an Arrhenius plot. The partial diffusion coefficients D_{Nb} and D_{Pd} were determined by means of the Darken equations. The temperature dependence of D_{Nb} is greater than that of D_{Pd}. Both coefficients become equal at a certain temperature between 900 and 1030°C. (auth)

Structure and Phase Studies

Refer also to abstract 30002.

29882 (COO-1198-807) ENERGETICS, MORPHOLOGY, CRYSTALLOGRAPHY, AND THEORY OF DISPLACIVE TRANSFORMATIONS IN NEAR-EQUIATOMIC NIOBIUM-RUTHENIUM ALLOYS. Kishore, Bijoy (Illinois Univ., Urbana). Jun 1971. Contract AT(11-1)-1198. 168p. Dep. NTIS.

The displacive phase transformations in the near-equiatomic Nb-Ru alloys were studied using magnetic susceptibility and electrical resistivity measurements, optical metallography and x-ray diffraction. Alloys containing between 41 and 45 at. % Ru undergo a CsCl (β) to face centered tetragonal (β') transformation on cooling to room temperature. Alloys containing more than 46 at. % Ru exhibit a two step CsCl (β) to face centered tetragonal (β') to face centered orthorhombic (β'') transformation on cooling to room temperature. Although the product of each successive transformation consists of stacks of twins (in $\beta' \rightarrow \beta''$, twins within twins), the transformation(s) does not proceed by advance of a sharp planar interface as in many of the first order martensitic transformations resulting in morphologically similar products. Rather, the interphase region consists of a small volume of the crystal over which the parent phase is gradually distorted into the product phase. The associated strain energy is then reduced and the transformation shows no temperature hysteresis nor any thermal history dependence and thus the volume fraction transformed is a single valued function of temperature. The transformation distortions during both $\beta \rightarrow \beta'$ and $\beta' \rightarrow \beta''$ transformations are such that the arrangement of atoms in the $(101)_\beta$ plane approaches that of the hexagonal close packed structure. From the band structure changes associated with such increase in the density of packing of atoms, it could have been stated that such a sequence of structural changes as actually observed is energetically favorable. The model of the transformation thus developed accounts for the variation of transformation temperatures and transformation distortions with Ru content as well as the variation of magnetic susceptibility with temperature and Ru content. (auth)

29883 (SC-T-713021) INTERACTION OF BERYLLIUM WIRE WITH AN ALUMINUM MATRIX. Trottier, Jean-Pierre; Graf, Rene. Translated for Sandia Labs., Albuquerque, N. Mex., from pp 17-27 of AGARD International Symposium on Composite Materials, Paris, 2-3 April 1970. 13p. (CONF-700437-1). Dep. NTIS.

Beryllium wire, both nickel-plated and with the nickel removed, is coated with aluminum by electrolysis. The diffusion phenomena are studied by x-ray diffraction, with a scanning electron microscope and by electron-microprobe analysis, after heat treatments of varying duration at 250, 480, and 600°C. Recrystallization of the wire and matrix is monitored by x-ray. At 250°C, and during short treatments at 480°C, the specimens' structure does not change significantly. (auth)

29884 (UJV-2525-M) INFLUENCE OF INITIAL CONTENT OF THE COOLING RATE FROM THE BETA PHASE TO PREFERRED

XUM

URANIUM ORIENTATION FOLLOWING HEAT TREATMENT. Volf, F.; Slancar, F.; Kraus, V. (Ceskoslovenska Akademie Ved, Rez. Ustav Jaderneho Vyzkumu). Jan 1970. 28p. (In Czech). Dep. NTIS (U. S. Sales Only).

The effect of initial structures and textures and the influence of cooling rate from the beta region on the preferred orientation after heat treatment was investigated for commercial purity grade uranium. Various initial conditions were represented by two groups of fine grained material extruded at high temperatures in the alpha region with different preferred orientations, then by coarse grained material also extruded in the high alpha region and finally by a material which was swaged at lower temperatures after extrusion. The interval of beta treatment conditions was given by water quenching and by cooling rates from 10 to 300°C/sec. More pronounced preferred orientations with negative growth indices in the direction of heat removal were formed during water quenching and after slow cooling, 10°C/sec. Intermediate cooling rates, 50 to 300°C/sec, induced very weak textures, the characteristics of which approach the isotropic condition. Some partial differences were observed in the behavior of the swaged material. However, different initial structures and textures of the extruded uranium did not show any distinct influence on the degree and character of preferred orientation after heat treatment. (auth)

29885 APPLICATION OF DIFFERENTIAL THERMAL ANALYSIS TO THE STUDY OF PHASE EQUILIBRIA IN METAL SYSTEMS. Etter, Don E.; Tucker, Philip A.; Wittenberg, L. J. (Monsanto Research Corp., Miamisburg, Ohio). Contract AT (33-1)-Gen-53. pp 829-50 of Thermal Analysis. Vol. 2. /Schwenker, Robert F. Jr. (ed.). New York; Academic Press, Inc. (1969).

From 2. international conference on thermal analysis; Worcester, Mass. (18 Aug 1968). See CONF-680851.

Differential thermal analysis has been used extensively in the study of phase equilibria of condensed systems because of its ability to detect very small thermal effects. An apparatus employing chromel-alumel thermocouples for use from ambient temperature to 1000°C is described. Detailed interpretations of thermograms are presented for selected compositions of a hypothetical binary phase diagram including congruently and incongruently melting compounds and solid solution, eutectic, and liquidus reactions. The Pu–Cu system is presented as an example of a phase diagram determined by DTA. The stoichiometry of the congruently melting compounds $PuCu_6$ and Pu_4Cu_{17} and the incongruently melting compounds $PuCu_4$ and Pu_2Cu_{11} was established completely by DTA. Eutectic reactions and liquidus temperatures were clearly defined; however, unusual thermal effects were observed because of the "S" shaped liquidus curve. Differential thermal analysis is particularly useful for the rapid determination of the purity of certain metals, since small quantities of impurities influence the melting point and may cause subsolidus reactions. The addition of as little as 0.1 at. % (0.024 wt %) Fe, Co, or Ni to Pu depressed the melting point approximately 15°C and caused additional phase transformations between 407 and 412°C. (auth)

29886 TRANSITION MORPHOLOGY DURING HCP PRECIPITATION FROM BETA-ISOMORPHOUS ALLOYS. Carpenter, R. W.; Liu, C. T. (Oak Ridge National Lab., Tenn.). Scr. Met.; 5: 255-7(Apr 1971).

The α-precipitation morphology of Nb–Hf alloys with 38 and 54 at. % Hf was investigated. Different precipitate morphologies were found when the alloys were aged at temperatures of 600 to 800°C instead of relatively higher temperatures. Because of the similarity of the Nb–Hf system and the Ti–V system, comments are given on 3 papers published previously concerning metastable precipitates observed in Ti–V alloys. The papers were abstracted in NSA as 24: 32444 and 25: 4805 and 4806. (G.M.C.)

29887 REPLY TO TRANSITION MORPHOLOGY DURING HCP PRECIPITATION FROM BETA-ISOMORPHOUS ALLOYS. Narayanan, G. Hari; Archbold, T. F. (Univ. of Washington, Seattle). Scr. Met.; 5: 259-60(Apr 1971).

A rebuttal is given to Carpenter and Liu [Scr. Met., 5: 255-7(1971)] concerning their comments on a paper discussing metastable precipitates in beta–isomorphous titanium alloys (previously published and abstracted in NSA as 25: 4805). (G.M.C.)

29888 ORIGINS OF MICROSTRUCTURES RESULTING FROM PRECIPITATION. Aaronson, H. I.; Aaron, H. B.; Kinsman, K. R. (Ford Motor Co., Dearborn, Mich.). Metallography; 4: 1-42 (Feb 1971).

The nature of the microstructures developed during precipitation is reviewed from a generalized mechanistic point of view. Two fundamental factors are considered to govern the atomic mechanisms, and thus the kinetics and morphology of precipitation: the nature of the site at which nucleation takes place, and the structure of the interphase boundary. Although the details of the operation of these factors are often quite complex, the overall approach to precipitate microstructures which they represent is applicable to precipitation from the solid solutions of a very wide range of alloy systems. (auth)

29889 DISLOCATION ETCH PITS IN ALPHA URANIUM. Somasundaram, R. (Bhabha Atomic Research Centre, Bombay). Trans. Indian Inst. Metals; 23: 109-10(Jun 1970).

Knowledge of density and distribution of dislocations is of great help in understanding the deformation characteristics of metals. Dislocations in a number of metals have been revealed by specialized etching techniques. Attempts have been made to reveal dislocations in uranium by electrolytic etching. The etchants developed are capable of revealing only those dislocations that are decorated by segregated impurities. For greater understanding of the dimensional stability of uranium under thermal cycling and irradiation, it would be preferable to have etchants that reveal dislocations without the diffusion dependent decorating effect. With this in view, uranium was electrolytically etched in a number of electrolytes. After a number of trials, an etchant for revealing dislocations in uranium without the diffusion dependent decorating effect was developed. (auth)

29890 PRECIPITATES WITH UNUSUAL MICROSTRUCTURE IN GRAINS OF Nb–40 Zr–10 Ti ALLOY. Kitada, Masahiro; Doi, Toshio (Hitachi Ltd., Kokubunji, Japan). J. Jap. Inst. Metals; 35: 171-6(Mar 1971). (In Japanese).

Precipitates with unusual microstructure due to the transformation of the β to $\beta' + \beta''$ phases in grains for Nb–40 Zr–10 Ti alloy were investigated by means of optical microscopy, electron (replica) microscopy, and EPMA. In aging isothermally at a temperature between 620 and 850°C after solution treatment, composite-type spherical precipitates were observed in grains, and had an unusual microstructure composed of a nucleus and the two surrounding crystals. The crystals were also composed of inner and outer shells. The inner shell was found to correspond to the Nb-rich phase β'', and the outer shell to the Zr-rich phase β'. The Nb-rich zone was observed in the matrix near the precipitates. In aging at the lower temperature the microstructure was observed to change into more complicated structures than in aging at higher temperature. The phase transformation due to the above-mentioned precipitation attained more than 70% of the whole phase change in the alloy aged at 750°C. (auth)

29891 REVERSION OF METASTABLE PHASES IN Cu–Be ALLOYS. Shiromizu, Ryusuke; Mishima, Yoshitsugu (Tokyo Univ.). J. Jap. Inst. Metals; 35: 183-9(Mar 1971). (In Japanese).

When Cu–Be alloy is aged at low temperatures, the Guinier–Preston (GP) zone is formed at the early stage of aging. At the early stage of high-temperature aging, a streak maximum appears in electron diffraction pattern (γ''). As aging proceeds, the (100) reflection from an intermediate phase γ' appears at the point corresponding to the (110) matrix reflection. The primary purpose of this experiment is to confirm whether complete reversion of metastable γ'' and γ' phase takes place as in the case of the GP zone. By means of hardness measurement and transmission electron microscopic observation, almost complete reversion was observed when the temperature was sufficiently raised. The temperature range T for the respective phases to be stable in Cu–1.79 wt % Be alloy is $T < 510°C$ for γ', $T < 450°C$ for γ'', and $T < 400°C$ for the GP zone. Next, the reversion temperature of γ'' as a function of Be% was examined and metastable phase boundary lines were determined. (auth)

29892 FIBER TEXTURES AND MORPHOLOGY OF DENDRITE IN INGOTS OF ZINC AND Zn–1.5 PERCENT Cd ALLOY. Abe, Hideo; Togano, Kazumasa (Tokyo Univ.). J. Jap. Inst. Metals; 35: 243-50(Mar 1971). (In Japanese).

The fiber textures and the crystallographic shape of dendrite in ingots of zinc and Zn–1.5% Cd alloy solidified under various conditions were investigated. The [0001] simple fiber texture developed near the chilled surface extends over the interior of ingot when the top surface of the melt is chilled. The dendrite observed in the equi-axed grain region is composed of (0001) hexagonal platelets woven by $\langle 10\bar{1}0 \rangle$ dendritic arms and a [0001] stem which connects these platelets. The origin of the [0001] fiber texture near the chilled surface is discussed by considering that the three-dimensional growth of the crystal is achieved by the one-dimensional growth in the [0001] direction plus the two-dimensional growth in the three equivalent $\langle 10\bar{1}0 \rangle$ directions contained in the (0001) plane. (auth)

29893 DIFFUSION INVESTIGATIONS IN THE SYSTEM Pd–Ta BY MEANS OF MICROPROBES. Brunsch, A.; Steeb, S. (Max-

Planck-Institut fuer Metallforschung, Stuttgart). Z. Naturforsch.; 26a: 274-9(Feb 1971). (In German).

Diffusion processes were investigated by means of quantitative electron-probe microanalysis in the system Pd–Ta. The annealing temperature ranged from 700 to 1030°C. In the diffusion zone the phases Pd_7Ta, Pd_3Ta, $Pd_{15}Ta_4$, Pd_5Ta, Pd_6Ta_5, and $Pd_{17}Ta_2$ were observed. The phase diagram only shows the phases PdTa, Pd_2Ta, and Pd_3Ta. From the law $d = k\sqrt{t}$ it can be concluded for the growing process of the total diffusion zone that volume diffusion predominates within this system. The values of $\log k^2$ as well as the values of $\log D$ versus $1/T$ yield an Arrhenius plot. The corresponding values are given in tables for the total diffusion zone as well as for the single phases. The discussion of a scanning-picture shows greater diffusion velocity for the palladium atoms than for the tantalum atoms. (auth)

29894 LEED AND ADSORPTION STUDIES OF BERYLLIUM. Adams, Richard O. (Dow Chemical Co., Golden, Colo.). Contract AT(29-1)-1106. pp 70.1-9 of Structure and Chemistry of Solid Surfaces. /Sonorjai, Gabor A. (ed.). New York: John Wiley and Sons, Inc. (1969). (RFP–1148).

Initial results of low energy electron diffraction (LEED) studies of (0001) surface of beryllium single crystals are given. Two patterns, a 6-spot and a 12-spot, were observed. The 6-spot pattern was assumed to be the pattern attributable to a clean (0001) beryllium surface and the 12-spot due either to oxide layer on the surface or probably to some contamination. From LEED adsorption studies of nitrogen, hydrogen, oxygen, and carbon monoxide it was found that only oxygen and carbon monoxide were adsorbed on beryllium and they formed an amorphous layer. (G.M.C)

29895 SOME RESULTS ON STRUCTURAL AND PHYSICAL CHARACTERISTICS OF UAl_4. Jesse, Andreas (Kernforschungszentrum, Karlsruhe, Ger.). J. Nucl. Mater.; 37: 340-2(Dec 1970). (In German).

The structural and physical properties of UAl_4 prepared by smelting Al and U (67 wt %) at 1550°C under a protective gas after a 500-hr homogenization of the pulverized and thoroughly mixed material under high vacuum are described. A product results with about 84 vol % UAl_4 and the rest Al and UAl_3. The results of the x-ray study of the material are tabulated. The thermal expansion, microhardness, thermal conductivity, specific electrical resistance, and temperature coefficient were also measured and the results are reported. (J.S.R.)

29896 STRUCTURE OF LIQUID CADMIUM–ANTIMONY ALLOYS. Kumar, R.; Sivaramakrishnan, C. S. (National Metallurgical Lab., Jamshedpur, India). J. Mater. Sci.; 6: 48-53(Jan 1971).

The structure of liquid Cd–Sb alloys was determined with the help of the Kumar–Samarin technique of centrifuging liquid metals. Alloys containing 7, 29, 50, 57, and 79 at. % Sb were examined in the range 350 to 650°C. It shows that all alloys except in the vicinity of equi-atomic composition consist of a colloidal dispersion of compound clusters in a random monatomic matrix, and the cluster size depends on composition with minima occurring at the two eutectic compositions. The volume fraction of clusters and their heat of formation were determined. The composition of the compound cluster was deduced as $Cd_{40}Sb_{30}$. Concentration gradient was not established in the equi-atomic alloy during centrifuging. The investigation shows that residual structure can exist far into the liquid state and is not confined to liquids of stoichiometric compound compositions. (auth) (UK)

29897 PRECIPITATION IN THE BERYLLIUM–IRON SYSTEM. Levine, E.; Luetjering, G. (Rutgers–The State Univ., New Brunswick, N. J.). J. Less-Common Metals; 23: 343-57 (Apr 1971).

An investigation was conducted to study the precipitation phenomena in a Be–0.95 wt % Fe alloy and to investigate the mechanism of deformation in this precipitation-hardened system. The alloy quenched from 1050°C and aged at low temperatures (400 to 500°C) gave rise to ordered $Be_{11}Fe$ precipitates partially coherent with the matrix. Nucleation of the precipitates occurred heterogeneously on dislocations and grain boundaries and subsequent growth occurred by a process of coalescence. Two percent compression caused the moving dislocations to bow-out between the precipitated particles. The dislocation density in the vicinity of the particles was much higher than in the surrounding matrix. Ten percent compression resulted in $\{10\bar{1}2\}$ type of twinning. Whereas the moving dislocations by-passed the particles, the twins were able to shear the particles. (auth)

29898 CRYSTAL STRUCTURE OF THE TWO Th_2Fe_7-PHASES. Buschow, K. H. J.; van der Goot, A. S. (Philips Research Labs., Eindhoven, Netherlands). J. Less-Common Metals; 23: 399-402 (Apr 1971).

A new compound was observed in the Th–Fe system: Th_2Fe_7. This compound occurs in two modifications: α–Th_2Fe_7 has the hexagonal Ce_2Ni_7 type of structure. β–Th_2Fe_7 has the rhombohedral Gd_2Co_7 type of structure. (auth)

29899 ALLOTROPIC TRANSFORMATION AND THERMAL EXPANSION OF COBALT BINARY ALLOYS BETWEEN 100 AND 800°C. I. Krajewski, W.; Krueger, J.; Winterhager, J. (Technische Hochschule, Aachen). Cobalt; No. 47, 81-8(Jun 1970).

A dilatometric study of high-purity Co-base terminal solid solutions is reported. The work was to determine the effects of various alloying elements on the allotropic transformation points on heating and cooling, as well as on the coefficient of linear thermal expansion between 100 and 800°C. Results pertaining to the systems of Co with Zr, Nb, Ta, Au, Ni, Pd, Pt, Ti, and V are reported. (Metals Abstr.)

29900 PHASE RELATIONS IN THE SYSTEM BERYLLIUM–ALUMINUM–TITANIUM. Wellner, Peter; Aldinger, Fritz (Max-Planck-Institut fuer Metallforschung, Stuttgart). Z. Metallk.; 62: 228-31(Mar 1971). (In German).

The liquid and solid phase relations of the beryllium–aluminum–titanium system were established by chemical, thermal, microscopic, and x-ray investigations. Forty alloys were annealed at 1200, 1000, and 600°C and the isothermal sections at these temperatures are discussed. An additional isothermal section at 1300°C and several temperature-concentration sections at a constant concentration of one alloying component are described. There are two ternary phases with the approximate compositions TiAlBe and $Ti_5Al_8Be_2$. Preliminary investigations of the solubility range of the ternary phases and of the intermetallic compounds $TiBe_2$ and $TiBe_3$ are discussed. (auth)

Radiation Effects

29901 (CEA-CONF–1693) AMORPHISATION OF A Pd–Si ALLOY BY IRRADIATION WITH FISSION PRODUCTS. Lesueur, Daniel (Commissariat a l'Energie Atomique, Fontenay-aux-Roses (France). Centre d'Etudes Nucleaires). [nd]. 8p. (CONF-700952–1). Dep. NTIS (U. S. Sales Only).

From International conference on metastable alloys; Brela, Yugoslavia (28 Sep 1970).

A Pd–Si alloy (20 at. % Si) obtained in the amorphous state by cooling after melting was studied. The amorphous samples were annealed under vacuum at 800°C for 40 hours. X-ray diffraction diagrams showed the existence of two phases: a face centred cubic solid solution of Si in Pd and an orthorhombic phase Pd_3Si. The samples were irradiated with fast neutrons or fission fragments (^{235}U). The x-ray diffraction lines of the crystal phases disappeared continuously whereas broad rings characteristic of an amorphous structure appeared. No change in structure was observed after irradiation of an amorphous sample. The resistivity ratio of the tempered amorphous state to the crystalline state was found to be 9 at 20°K. Maxima were observed on the resistivity curves of several samples. The sample thickness is an important factor in the profile of the resistivity curves. (France)

29902 (EURFNR–891) ELECTRONIC MICROSCOPE STUDY OF NEEDLE-SHAPED PRECIPITATES IN IRRADIATED AUSTENITIC STEELS. Bisson, Andre; Vouillon, Michel (Commissariat a l'Energie Atomique, Saclay (France). Centre d'Etudes Nucleaires). Translation of French report. 12p. Dep. NTIS.

Work Performed under United States–Euratom Fast Reactor Exchange Program.

Irradiation of 316 austenitic steel by neutrons causes the formation of small precipitates in the {110} planes of the crystal. These are very thin, long tags having the big dimension in the [100] direction. Their thickness is about 50 Å. The nature of these precipitates is still unknown. However, it may be thought from their instability that they are not $M_{23}C_6$. It is important to note that they would be preferential sites for cavities. (auth)

29903 (NYO–3653-5) STUDY OF RADIATION INDUCED DEFECTS IN METALS. Progress Report, December 1, 1969–November 16, 1970. Townsend, John R. (Pittsburgh Univ., Pa.). 17 Nov 1970. Contract AT(30-1)-3653. 14p. Dep. NTIS.

Revision of low temperature irradiation experiment was completed and one run at liquid nitrogen was made. Use of a self-drive system in conjunction with a bridge type of detection permits rapid data acquisition on two samples simultaneously. The single completed run strongly supports the supposition that sample preparation has a large effect upon the pinning process. After a flux of 10^{13} protons/cm^2 the elastic modulus was at its saturation level for a tungsten single crystal, fabricated and mounted so as to minimize cold work. Piezoresistance measurement capabilities were greatly improved by revising the electronics and

the mechanical apparatus. For example, for the O defect in Ta a strain of 10^{-4} is sufficient to give an anelastic piezoresistance signal to noise ratio of 50. The value of the piezoresistivity coefficient for this defect was determined to be $\pi_a = .40 \pm .02$ for a Ta sample containing 0.3 atomic percent oxygen. (auth)

29904 (ORNL-4630, pp 73-95) MECHANICAL PROPERTIES OF ALLOYS IN REACTOR ENVIRONMENTS AND DEVELOPMENT OF FBR CLADDING AND STRUCTURAL ALLOYS. Weir, J. R. Jr.; McCoy, H. E. Jr. (Oak Ridge National Lab., Tenn.).

In Fuels and materials development program quarterly progress report for period ending September 30, 1970.

Measurements of density on Types 304 and 304L stainless steel irradiated at 370 to about 800°C showed that for a given fast-neutron fluence there is a critical temperature above which swelling does not occur and that this temperature increases with increasing fast-neutron fluence. Analysis of results of transmission electron microscopy and density measurements on Type 304 and Ti-modified Type 304 stainless steel irradiated at about 590°C to 2.5 to 3.5×10^{22} neutrons/cm^2 (>0.1 MeV) indicated that for these irradiation conditions the decrease in density is more strongly dependent upon the fluence than it is at a lower irradiation temperature of 460 to 470°C. Tensile tests at or near the irradiation temperature were completed on Type 304 stainless steel irradiated at 450 to 800°C to 1.5 to 3.5×10^{22} neutrons/cm^2 (>0.1 MeV). The observed increase in yield strength and decrease in uniform and total elongation were correlated with microstructures as characterized by transmission electron microscopy. Tensile properties of the modified type 304 stainless steel irradiated at this same temperature and fluence were determined. The strength properties were about the same; the uniform elongation, total elongation, and reduction in area were higher than those of standard Type 304 stainless steel. The creep-rupture properties of Type 304 stainless steel after irradiation were determined at test temperatures of 550, 600, and 704°C. Specimens of Mo, Mo-0.5% Ti, and Mo-50% Re were irradiated at 425°C to fluences of 1.5 to 3.45×10^{22} neutrons/cm^2 (>0.1 MeV). Tensile tests on these materials showed zero or greatly reduced ductility at 400 to 800°C. The microstructures were characterized by transmission electron microscopy. (auth)

29905 (ORNL-4630, pp 239-60) IRRADIATION DAMAGE TO ALUMINUM AND ALUMINUM ALLOYS. Weir, J. R. Jr.; King, R. T. (Oak Ridge National Lab., Tenn.).

In Fuels and materials development program quarterly progress report for period ending September 30, 1970.

Neutron irradiation of solid-solution commercial Al alloys to high fast-neutron fluences at about 50°C caused the formation of voids and swelling. The volume change in Type 8001 Al alloy was proportional to the fluence raised to the 1.02 power and was a negative 5.1% at 2.7×10^{22} neutrons/cm^2 (>0.82 MeV). Changes in mechanical properties were related to the effects of voids, dislocation loops, and impurities produced through transmutation. Irradiation increased the yield strength and ultimate tensile strength at test temperatures as high as 370°C. Although irradiation only slightly reduced ductility at 25°C, it severely reduced the uniform and total plastic strain at 200°C. Irradiation of cold-worked material to 2×10^{22} neutrons/cm^2 (>0.82 MeV) increased the recrystallization temperature to near the melting point. High-purity Al swelled at lower fluences than those required to form voids in commercial alloys; density decreased 7.4% after a nominal exposure to 1×10^{22} neutrons/cm^2 (>0.82 MeV) at about 55°C. The density decrease was not proportional to fluence raised to a constant power over the fluence range of 10^{19} to 10^{22} neutrons/cm^2. Heterogeneous nucleation of voids was observed after irradiations to low neutron fluences, but the voids observed after irradiations to high fluences appeared to be homogeneously distributed. It was inferred from the changes in population with increasing fluence that the nucleation rate for both voids and loops decreased with increasing time. Both the mean and maximum diameters of the voids were proportional to the one-sixth power of time, and voids as large as 2000 Å in diameter were observed after irradiation to the highest fluence. (auth)

29906 (ORNL-TM-3063) EVALUATION OF THE MOLTEN-SALT REACTOR EXPERIMENT HASTELLOY N SURVEILLANCE SPECIMENS: FOURTH GROUP. McCoy, H. E. Jr. (Oak Ridge National Lab., Tenn.). Mar 1971. Contract W-7405-eng-26. 91p. Dep. NTIS.

Two heats of standard Hastelloy N were removed from the core of the MSRE after 22,533 hr at 650°C and exposed to a thermal fluence of 1.5×10^{21} neutrons/cm^2 and a fast fluence >50 keV of 1.1×10^{21} neutrons/cm^2. The mechanical properties have systematically deteriorated with increasing fluence. However, the change in properties is due to the helium produced by the $^{10}B(n,\alpha)^7Li$ transmutation and can be reduced by changes in chemical composition. Some of these modified heats were exposed to the core of the MSRE and show improved resistance to irradiation. The corrosion of the Hastelloy N was largely due to the selective removal of chromium. The rates of removal are much as predicted from the measured diffusion rate of chromium. Other superficial structure modifications were observed, but they likely result from carbide precipitation along slip bands that were formed during machining. (auth)

29907 (ORNL-TM-3299) CYCLOTRON SIMULATION OF NEUTRON-TRANSMUTATION PRODUCED GASES IN REACTOR CLADDING AND STRUCTURAL MATERIALS. King, R. T. (Oak Ridge National Lab., Tenn.). Apr 1971. Contract W-7405-eng-26. 38p. (CONF-690924-3). Dep. NTIS.

From International conference on the use of cyclotrons in chemistry, metallurgy, and biology; Oxford, England (22 Sep 1969).

Cyclotrons were used to simulate the nearly uniform concentrations of helium produced during neutron irradiation of metals by (n,α) reactions. Gas was injected into flat sheet specimens by degrading monoenergetic ion beams with either a stationary or a rotating energy moderator of continually varying thickness. Target specimens were scanned in one and two dimensions, respectively, through these variable energy beams, producing nearly uniform concentrations of gas throughout the specimens. Thermal monitoring and beam current detection systems were employed throughout the bombardments. The effects of cyclotron-injected helium on the mechanical properties of Type 304 stainless steel, a potential cladding material for Liquid Metal Fast Breeder Reactors, were investigated. Helium concentrations ranging from 0.083 to 20.0 atomic ppM severely reduced the ductility of Type 304 stainless steel in both creep and tensile tests over the ranges of strain rate and temperature for which the material fails intergranularly. It was experimentally demonstrated, in agreement with theoretical calculations, that simply passing similar currents of alpha-particles completely through stainless steel does not produce sufficient displacement damage to cause significant changes in ductility. The resistance of a 0.2% Ti-Type 304L stainless steel to helium embrittlement was demonstrated by cyclotron bombardment techniques. The role of helium in low-ductility failures of aluminum reactor components at about 150°C after fast neutron irradiation was also investigated. Tensile data for aluminum alloys containing 5.0 atomic ppM He showed that helium generated by $^{27}Al(n,\alpha)$ reactions may reduce the elevated-temperature ductility of the 1100 and X8001 aluminum alloys, while the properties of the 6061 and 895 SAP alloys were not affected. The gas-injection technique was thus demonstrated to be a useful, relatively inexpensive tool in isolating particular neutron irradiation damage mechanisms. (auth)

29908 NEUTRON IRRADIATION HARDENING OF BORON-DOPED COPPER. Hasegawa, Masayuki; Koiwa, Masahiro; Hirabayashi, Makoto (Tohoku Univ., Sendai). Trans. Jap. Inst. Metals; 12: 39-43(Jan 1971).

The neutron irradiation effect of boron-doped copper, containing 0.08 to 0.9 at. % B, was studied by means of tensile testing, internal friction measurement, and electron microscopy. Thermal neutron fluxes were in the range from 0.36 to 8.9×10^{19} nvt. The increase in proof stress was measured as a function of the concentration of ^4He introduced by the transmutation of ^{10}B, and interpreted to be mainly due to interstitial dislocation loops created secondarily by neutron irradiation. The grain boundary relaxation peak in the internal friction curve was suppressed to a very low level by irradiation and recovered progressively by successive annealing. (auth)

29909 REPORT ON IRRADIATED MATERIALS. Schuele, W. (EURATOM, Ispra, Italy). pp 9-38 of Research Reactor Utilization. Vol. 2. Vienna; International Atomic Energy Agency (1970). (CONF-700204-16).

From IAEA meeting on research reactor utilization; Rome, Italy (2 Feb 1970).

The characteristics of defects in neutron-irradiated materials are emphasized. However, reference is also made to results obtained in irradiations with electrons, alpha particles, etc. After a description of the most important types of point defects produced by irradiation with high-energy particles, some of the properties of point defects in face centered cubic materials are presented. Following the description of the properties of point defects, the influence of radiation on metallurgical processes is discussed. Finally, a brief description of some results of radiation hardening experiments is given. (INIS)

29910 FORMATION OF GOLD NUCLEI ON IONIC CRYSTALS. Postnikov, V. S.; Morgunov, V. N.; Zolotukhin, I. V.; Ievlev, V. M.

XUM

(Voronezh Polytechnic Inst., USSR). Sov. Phys.-Solid State (Engl. Transl.); 12: 2399-2401(Apr 1971).
Translated from Fiz. Tverd. Tela; 12: 2974-6(Oct 1970).

The effect of the ionization by electron bombardment of an atomic beam being condensed on the surface of an ionic crystal on the process of nucleus formation on the latter is considered. The densities of nuclei, formed on simultaneous condensation of irradiated and nonirradiated atomic beams of gold on NaCl, KCl, and KBr crystals, are given. It is shown that charged atoms are more sensitive to defects in the surface layer. This explains the considerably higher density of nuclei obtained from an irradiated atomic beam as compared with ordinary evaporative deposition. (auth)

29911 PHASE TRANSITION ASSOCIATED WITH RADIATION DEFECTS. Khachaturyan, A. G.; Shatalov, G. A. (Inst. of Metallography and Physics of Metals, Moscow). Sov. Phys.-Solid State (Engl. Transl.); 12: 2395-8(Apr 1971).
Translated from Fiz. Tverd. Tela; 12: 2969-73(Oct 1970).

An analysis is made of the ordering of interstitial carbon atoms in the bcc lattice of Fe which has two energetically inequivalent positions: octahedral interstices and radiation-induced vacancies. It is shown that a phase transition occurs in such a system at some definite temperature and concentration of carbon atoms. In this transition the interstitial carbon atoms are transferred spontaneously from one position to another. This phase transition explains the experimentally observed sudden change in the tetragonality of carbon–iron solid solutions. Theoretical estimates of the energy parameters of the ordering process are shown to be in good agreement with the values found experimentally and those deduced from independent theoretical calculations. (auth)

29912 INFLUENCE OF NEUTRON IRRADIATION AT 4°K ON THE SHEAR MODULUS OF COPPER, ALUMINUM, AND PLATINUM. Wenzl, Helmut; Kerscher, Franz; Fischer, Veit; Ehrensperger, Klaus; Papathanassopoulos, Konstantinos (Technische Hochschule, Munich). Z. Naturforsch.; 26a: 489-94 (Mar 1971). (In German).

The change of the shear modulus of pure polycrystalline Al, Cu, and Pt due to reactor neutron irradiation at 4°K has been studied. The shear modulus was determined by measuring the vibrational frequencies of a helical spring in two different modes (between 50 and 300 Hz) together with internal friction and electrical resistance. Large relative decreases of the shear modulus $\Delta G/G$ per molar fraction c of Frenkel defects were found, namely $\Delta G/Gc$ –47, –39, –67 for Al, Cu, and Pt, respectively. The absolute values are much larger than expected from lattice theory. The effects cannot be explained by a relaxation of the defects. (auth)

29913 BEHAVIOUR OF BORON IN STAINLESS STEEL DETECTED BY FISSION TRACK ETCHING METHOD AND EFFECT OF RADIATION ON TENSILE PROPERTIES. Kawasaki, S.; Hishinuma, A.; Nagasaki, R. (Japan Atomic Energy Research Inst., Tokai). J. Nucl. Mater.; 39: 166-74(May 1971).

The behavior of boron and the relation between the boron distribution and the radiation effect of 316 stainless steel were studied. Boron segregates on grain-boundaries in 316 stainless steel during aging in the temperature range 650 to 950°C, and the relation between aging time and temperature for segregation is a nose-type curve. The changes in mechanical properties after irradiation were influenced by the boron distribution in the specimens; ductility losses in specimens in which boron was segregated on grain-boundaries were especially severe. (auth)

29914 VOIDS IN VANADIUM, NIOBIUM, AND MOLYBDENUM BY FAST NEUTRON IRRADIATION AT HIGH TEMPERATURES. Elen, J. D.; Hamburg, G.; Mastenbroek, A. (Reactor Centrum Nederland, Petten, Netherlands). J. Nucl. Mater.; 39: 194-202 (May 1971).

Samples of high purity vanadium, niobium, and molybdenum were irradiated at three constant temperatures in an instrumented capsule. The measured irradiation temperatures, expressed as a fraction of the particular melting temperature, covered the range $0.25 \leq T/T_m \leq 0.47$. The fast neutron fluences for the samples were in the range of 2.2×10^{20} to 5.5×10^{20} n/cm². Using transmission electron microscopy in all samples small voids (mainly cubes) were observed. The logarithmic plot of all counted void densities, over the full range of 5×10^{16}/cc to 1×10^{14}/cc, was found to decrease linearly with increasing T/T_m, regardless of the particular identity of the metal. Voids are larger the higher the irradiation temperature; 25 Å for $T/T_m = 0.25$ and about 120 Å for $T/T_m = 0.47$. The distribution of the voids is influenced by dislocations, interstitial damage, and precipitates. This is discussed in terms of survival of void nuclei, produced in displacement spikes. (auth)

29915 PROTON IRRADIATION EFFECTS IN TYPE 321 STAINLESS STEEL. Keefer, D. W.; Pard, A. G.; Rhodes, C. G.; Kramer, D. (Atomics International, Canoga Park, Calif.). J. Nucl. Mater.; 39: 229-33(May 1971).

A flux of, typically, 9×10^{14} protons/cm²·sec of incident energy 0.75 MeV was used to create voids in 0.0127 mm thick foils of Type 321 stainless steel at 400 and 500°C. Values are reported for displacement rate, number of displacements, void size, void density, and volume increase. In some samples proton irradiation resulted in the transformation of austenite to ferrite. It appeared that excess vacancy concentration present during irradiation of a sample provided sufficiently enhanced diffusion to allow the transformation to occur at 500°C, and, to a lesser extent, at 400°C. (G.M.C.)

29916 NEW MATERIALS IN THE FIELD OF RADIATION. Walker, D. G. (Australian Atomic Energy Research Establishment, Lucas Heights). pp 112-20 of Sydney University Chemical Engineering Association New Materials Symposium, Sydney, August 27th, 1970. Sydney; Univ. of Sydney (1970).
From Chemical engineering conference; Sydney and Melbourne, Australia (18 Aug 1970). See CONF-700804.

The development of materials for application in present and future nuclear power reactors is reviewed, with emphasis on the alloys used as the cladding on nuclear fuel elements. In particular, neutron effects on magnesium, beryllium, and zirconium alloys, and stainless steels are discussed. (Australia)

29917 BERYLLIUM ALLOY FOR NUCLEAR REACTOR. (to Nihon Genshiryoku Kenkyusho). British Patent 1,227,058. 31 Mar 1971. Priority date 10 Mar 1969, Japan.

A Be alloy resistant to ductility loss when exposed to fast neutron fluxes is described. The alloy is composed of Be with additions of 0.01 to 1.0 at. % Cr and 0.02 to 0.3 at. % Ca. The alloy is also resistant to corrosion by moist CO_2. (J.R.D.)

Ceramics and Cermets

Refer also to abstracts 29757 and 29759.

Corrosion and Erosion

29918 (CEA-R–4123) PHYSICAL AND CHEMICAL INTERACTIONS OF WATER ON GRAPHITE. Lafargue, Yves-Paul (Commissariat a l'Energie Atomique, Saclay (France). Centre d'Etudes Nucleaires). Jan 1971. 110p. (In French). Dep. NTIS (U. S. Sales Only).
Thesis. Submitted to Univ. of Paris, France.

At 25°C (total pressure: 1 atm, relative water pressure, x = 0.7) the rate of adsorption on nuclear porous graphite, initially very slow, increases progressively; the phenomenon is limited by the reactivity of the internal surface. These kinetics can be modified by a pretreatment of the solid (measurements at x = 0.4) and by the presence of oxygen traces. The isosteric enthalpy ($\Delta m/m = 1.8 \cdot 10^{-4}$) between 27 and 35°C is 12 kcal/mole. Thermal desorption (by plateau up to 670°C) under an argon pressure of 2.6 or 20 bars depends on water diffusion rate (desorption-fixation competition). Degassing under vacuum demonstrates the existence of twelve types of surface zones. The distribution of these zones governs the reactivity of the sample. The adsorption isobar (p = 18 torrs) shows two stable regions ($\theta < 105$ and $\theta > 300$°C). Oxidation, detected already at room temperature, becomes considerable from 800°C onwards. The various phenomena existing such as physical adsorption, chemisorption, oxidation, always coexist and are interrelated. (auth) (France)

29919 SURFACE AREA EFFECTS ON THE OXIDATION KINETICS OF PYROLYTIC GRAPHITE. Levy, Milton (Army Materials and Mechanics Research Center, Watertown, Mass.). pp 1023-34 of Thermal Analysis. Vol. 2. /Schwenker, Robert F. Jr. (ed.). New York; Academic Press, Inc. (1969).
From 2. international conference on thermal analysis; Worcester, Mass. (18 Aug 1968). See CONF-680851.

The oxidation kinetics of pyrolytic graphite was studied as a function of temperature, air velocity, and surface area. The transition temperature between chemical and diffusion control may be significantly increased or decreased by decreasing or increasing the surface area of pyrolytic graphite. Kinetic theory calculations showed that the maximum reaction rate in the diffusion-controlled region is much greater than the observed rate for specimens having the smallest surface area. (auth)

Preparation and Fabrication

Refer also to abstract 29815.

29920 (LA–4631) CMF-13 RESEARCH ON CARBON AND GRAPHITE. Report No. 15: Summary of Progress, August 1–

October 31, 1970. Smith, Morton C. (Los Alamos Scientific Lab., N. Mex.). Feb 1971. Contract W-7405-eng-36. 30p. Dep. NTIS.

Research is described on carbon and graphite conducted to increase understanding of their properties, to improve raw materials and preparation processes, and to produce predictable finished products. Results of work are reported on Santa Maria coke, Athabasca coke, graphite-carbide composites, binder resins, particle packing, porosity effects on graphite properties, raw materials, manufacturing procedures, and graphite properties. (J.R.D.)

29921 (ORNL–4565) MOUND ASSISTANCE PROGRAM; DEVELOPMENT OF A SOL-GEL PROCESS AND EQUIPMENT FOR THE PRODUCTION OF DENSE $^{238}PuO_2$ MICROSPHERES. Kitts, F. G.; Brooksbank, R. E.; Haire, R. G.; Lloyd, M. H. (Oak Ridge National Lab., Tenn.). Mar 1971. Contract W-7405-eng-26. 112p. Dep. NTIS.

Microspheres of $^{238}PuO_2$, a potentially important isotopic power source, have been produced in kilogram quantities using a plasma torch. The feasibility of producing $^{238}PuO_2$ microspheres by the sol-gel process was investigated. The sol-gel process offers important advantages from the standpoints of product quality, process simplicity, and overall safety. It was found that satisfactory $^{238}PuO_2$ sols could be formed in the laboratory, using the $^{239}PuO_2$ flowsheet, if the feed was carefully prepared and a simple aging step was included. A remotely operated, neutron-shielded facility was constructed to process 200 g of plutonium per day. Successful demonstrations with ^{239}Pu were carried out in this facility and, although those with ^{238}Pu were less satisfactory, valuable experience was gained in preparing $^{238}PuO_2$ sol by remote means. Equipment for the preparation of $^{238}PuO_2$ sols and conversion to dense microspheres was fabricated, installed in a stainless steel enclosure. When difficulties were encountered due to the processing of larger batches of material, electron microscopy was utilized to identify two problem areas: partial hydrolysis of the feed was preventing the formation of highly crystalline plutonium polymer, and degradation of polymer was occurring during evaporation to dryness. The depolymerization process is similar to the simple dissolution of PuO_2 and is a function of time, temperature, and acid concentration. After several equipment improvements, the system proved to be capable of sustained operation; a total of 683 g of ThO_2 was processed in five consecutive runs. It was concluded that $^{238}PuO_2$ sols and high-quality microspheres could be produced in the quantities required. (auth)

29922 (ORNL–4630, pp 3-58) DEVELOPMENT OF FBR OXIDE FUELS. Patriarca, P.; Lotts, A. L.; Cox, C. M. (Oak Ridge National Lab., Tenn.).

In Fuels and materials development program quarterly progress report for period ending September 30, 1970.

About 2.5 kg of microspheres containing $(U,Pu)O_2$ was prepared. Results of economic analyses of the process indicate an advantage of 6 to 8% of the total fabrication cost compared with costs for mechanically blended pellets, coprecipitated pellets, sol-gel pellets, and homogeneous sol-gel Sphere-Pac techniques. Special work on characterization of fuel included determination by metallographic techniques of the distribution of metal content in $(U,Pu)O_2$ pellets made by the sol-gel process, additional development of techniques for analytical sampling for metallic impurities, and investigation of the effect of fission products on O potential. Five encapsulated series I EBR-II fuel pins, all containing Sphere-Pac $(U,Pu)O_2$ fuel, were removed from the EBR-II at the end of run 42. The calculated peak burnup of 6.2% fissions per initial actinide metal atom (FIMA) was achieved. Two of these pins were returned to ORNL, and three will be reinserted in a new subassembly for continued irradiation to a peak burnup of 11.8% FIMA. The entire FMØDEL code for fuel performance was modified to give the capability of load-cycling, steady-state, and limited-transient applications. The code now permits an unlimited number of cycles to be specified and thereby permits exact simulation of the irradiation history of the fuel pin if desired. The current version of the FMØDEL performance code was tested on the published results of several irradiation tests conducted in the EBR-II. The FMØDEL predictions were in reasonable agreement with the postirradiation profilometer traces observed by the experimenters. It was concluded that, while FMØDEL does not consider every physical and chemical phenomenon that can occur, the main sources of cladding strain have been identified and modeled. Additional work with the FMØDEL fuel performance code was directed at interpretation of phenomena of the mechanical interaction of fuel and cladding and the effects of startup rates on the performance of the fuel pins. Other efforts to model LMFBR fuel behavior more accurately were directed toward fuel swelling, release of fission gas, and restructuring. Data on in-reactor grain growth were analyzed and fitted to an equation applicable to fuel-element modeling. (auth)

29923 (ORNL–4630, pp 59-72) DEVELOPMENT OF ADVANCED FBR FUELS. Patriarca, P.; Scott, J. L. (Oak Ridge National Lab., Tenn.).

In Fuels and materials development program quarterly progress report for period ending September 30, 1970.

Several items of equipment that will expand capability and reduce costs are being commissioned in the Interim Plutonium Facility. The precision of the analysis for N content in (U,Pu)N was markedly improved by dissolution in phosphoric acid instead of the more conventional HCl plus HF. Apparent discrepancies in the literature regarding the compatibility of stainless steel with U_2N_3 were explained in terms of uncontrolled variations in the O content of fuel or cladding in different experiments. Preparation of (U,Pu)N test capsules for irradiation tests in the Engineering Test Reactor is 95% complete. (auth)

29924 (ORNL–4630, pp 233-8) DEVELOPMENT OF FUEL ELEMENT FABRICATION. Adamson, G. M. Jr.; Martin, W. R. (Oak Ridge National Lab., Tenn.).

In Fuels and materials development program quarterly progress report for period ending September 30, 1970.

The irradiation experiment planned for insertion into the High Flux Isotope Reactor is being fabricated. The parametric studies of rolling shaped cores to evaluate nonuniform deformation (dogboning) have shown that small, transverse cracks are formed in the cladding over the dogbone region of a shaped core. These cracks are difficult to find after rolling unless the plates are etched. Assistance was provided in evaluating the future of fuel elements irradiated in the Advanced Test Reactor. Work results indicated that the large pimples were likely formed by an interaction of reactor coolant with core materials after the cladding had failed. The cause of cladding failure is unknown. (auth)

29925 IMPACT OF THERMAL ANALYSES ON NUCLEAR AMMONIUM POLYURANATE PREPARATION. Farah, Michael Y.; Zaki, Mourad R.; El-Fekey, Sayed A. (Atomic Energy Establishment, Cairo). pp 1475-88 of Thermal Analysis. Vol. 2. /Schwenker, Robert F. Jr. (ed.). New York; Academic Press, Inc. (1969).

From 2. international conference on thermal analysis; Worcester, Mass. (18 Aug 1968). See CONF-680851.

Results of a study on the controversy pertaining to rigid or tolerant views concerning APU precipitation history and subsequent UO_3 and UO_2 characterization are presented. TGA, DTA, and BET measurements were made as functions of final pH values, aging of powders, nitrates washing, settling, degassing, and comparison with TGA plots for denitrated trioxides. The technological basis for production of a multipurpose metal or ceramic uranium dioxide is thus defined. (auth)

29926 GROWTH OF TRANSITION METAL CARBIDE SINGLE CRYSTALS BY RECRYSTALLIZATION. I. PREPARATION OF FULLY-DENSE TRANSITION METAL CARBIDE. Fleischer, L. R.; Tobin, J. M. (Westinghouse Astronuclear Lab., Pittsburgh). J. Cryst. Growth; 8: 235-42(Mar 1971).

Reactors of liquid Ti, Zr, Hf, V, Nb, and Ta with graphite thimbles were used to produce the transition metal monocarbides. The prepared carbide rods were free of pores, cracks, and inclusions. Carbon concentration gradients were virtually eliminated by extended anneals at high temperatures. The resulting materials were in a highly recovered state with dislocations organized in boundaries or networks. The grain structure was reproducible from a rod of one carbide to other rods of the same carbide, but varied from one carbide to another. The grains of HfC were relatively small and uniform; those of VC were quite large and irregular; the others were intermediate. Ta_2C was prepared by partial carburization of Ta and removal of the outer TaC layer. Efforts to prepare W_2C and WC bodies by this method were unsuccessful. (auth)

29927 GROWTH OF TRANSITION METAL CARBIDE SINGLE CRYSTALS BY RECRYSTALLIZATION. II. TRANSITION METAL CARBIDE RECRYSTALLIZATION AND CRYSTAL GROWTH. Fleischer, L. R.; Tobin, J. M. (Westinghouse Astronuclear Lab., Pittsburgh). J. Cryst. Growth; 8: 243-6(Mar 1971).

Transition metal carbides exhibited recrystallization behavior like that of many common metals. Sufficient strain was developed by deforming these carbides in the 2000 to 2500°C temperature range to induce recrystallization on subsequent annealing at higher temperatures. The recrystallized grain size was a function of the amount of plastic strain. Strain levels near the critical strain encouraged very large grains; single crystals of TiC, ZrC, HfC, NbC, and TaC were prepared by this method. (auth)

XUM

29928 LOW TEMPERATURE METHOD FOR COATING NUCLEAR FUELS WITH MULTIPLE CARBON COATINGS. Beutler, Hans (to United States Atomic Energy Commission). U. S. Patent 3,554,783. 12 Jan 1971. Filed 4 Nov 1968.

A thin, impervious, carbon coating is deposited onto a porous buffer coating in pyrolytically coated fuel microspheres to prevent diffusion of the coating gas into the porous buffer coating during subsequent coating operations. This is accomplished by initiating the deposition at a temperature of about 1500°C and immediately after reducing the deposition temperature to within the range of 1100 to 1300°C to complete deposition of an outer, high density pyrolytic carbon coating. (Official Gazette)

29929 PREPARATION AND COMMINUTION OF HYDROGENATED NIOBIUM. Sasaki, Yasuo; Amano, Muneyuki (National Research Inst. for Metals, Tokyo). J. Jap. Inst. Metals; 35: 77-81(Jan 1971). (In Japanese).

The alloys, containing 3.8, 7.2, and 14.5 at. % hydrogen, were prepared and pulverized with a ball mill. The particle size distribution of the powders was measured by screen analyses, and microscopic observation of the particle shape was carried out. The alloys were brittle enough to be pulverized readily. Cracking and fragmentation of the alloys were enhanced by thermal cycling in the hydrogenation process. With increasing hydrogen content in the alloys, a higher percentage of fine particles was obtained. Particle shape varied with the hydrogen content of the alloys. Rounded or irregular particles were obtained from the lower concentration alloys and acicular or angular particles from the higher concentration alloy. (auth)

29930 SINTERING PROCESS OF ZIRCONIUM DIBORIDE WITH TUNGSTEN. Kislii, P. S.; Kuzenkova, M. A.; Zaverukha, O. V. (Inst. for Materials Development, Kiev). Phys. Sintering; 3: 29-43(Jan 1971).

The existing laws for the sintering of two-phase mixtures of finely dispersed zirconium diboride and tungsten powders were studied and examined. During the sintering process this mixture reacts to form a solid solution of tungsten in zirconium diboride as well as new phases, W_2B (W, Zr) B. It was shown that, under slow heating conditions, new phases were formed even before the isothermal heating, which is accompanied, during the later heating, by sample growth and densification. During the quick heating of the samples, densification takes place in the first 10 minutes of the isothermal heating, without the presence of the diffusion processes in the particle volume and with the slight interaction of zirconium diboride and tungsten in the surface layer. It leads to the conclusion of the existence of mass transfer non-diffusion mechanism in the particle volume in the initial phase of sintering and also to the assumption that the latter was going on by means of plastic deformation in the particle contact zone and in the zone of the activated gliding along the grain boundaries. This was due to dislocation climb parallel to the boundaries during the interaction with vacancies. (auth)

29931 POWDER METALLURGICAL PRODUCTION OF UO_2–PuO_2 STEEL PELLETS. Foehl, C. A.; Ondracek, G. (Kernforschungszentrum, Karlsruhe, Ger.). Atomkernenergie; 17: 158-62(May 1971). (In German).

UO_2–PuO_2-steel cermets are possibly a fuel material for fast neutron high flux reactors. Data are completed concerning the technology of such cermets. The powder characteristic of the UO_2 and steel powder as well as their mixing conditions and densification are considered. It is shown how the density is affected by the oxide content, densification pressure, sintering atmosphere, sintering time, and temperature. (auth)

29932 MANUFACTURE OF STABILIZED SUB-STOICHIOMETRIC OXIDE ATOMIC FUEL MATERIALS. (to Sadem, Societe Anonyme des Entreprises Minieres). British Patent 1,228,654. 15 Apr 1971. Priority date 28 Jun 1968, Germany.

A stabilized substoichiometric UO_2 fuel material is described. A small quantity of Cr, Mo, W or Re up to the solubility limit of the oxide fuel at reactor operating temperatures is added so that a single-phase fuel is obtained. (J.R.D.)

29933 GROWTH OF EuO, EuS, EuSe, AND EuTe SINGLE CRYSTALS. Reed, T. B.; Fahey, R. E. (Massachusetts Inst. of Tech., Lexington). J. Cryst. Growth; 8: 337-40(Apr 1971).

Single crystals of the europium monochalcogenides weighing up to 60 g have been grown from Eu-rich solutions and from stoichiometric melts by using a gradient cooling technique. Since all four compounds have high Eu partial pressures near their melting points, the crystals were grown in weld-sealed tungsten crucibles 1.25 or 2.5 cm in diameter. The oxide was synthesized and grown in the same run. Dried Eu_2O_3 was heated with an excess of Eu metal to about 2200°C, and the solution obtained was directionally frozen from the bottom by cooling to room temperature at 5 to 50°C/hr. The resulting boules were single crystals with total impurities ranging from 250 to 5000 ppM. These crystals were then remelted, either with or without additional Eu metal, and directionally frozen to obtain crystals containing total impurities of about 220 ppM primarily C and Ca. The crystals were also used subsequently for growing crystals doped with Gd or La. The other compounds were synthesized in sealed quartz ampoules by the reaction of Eu metal at about 600°C with vapor of the other element supplied by a reservoir at a lower temperature. Single crystals similar in size and purity to those of the oxide were then grown by the gradient cooling technique. The effect of deviations from stoichiometry on optical and electrical properties is discussed. The melting point of EuO, measured with an optical pyrometer and a W–(W, 26% Re) thermocouple, was 1980 ± 20°C. EuS, EuSe, and EuTe all melt between 2250 and 2500°C. (auth)

29934 LEVITATION MELTING OF URANIUM MONO-CARBIDE. Knights, C. F.; Perkins, R. (Atomic Energy Research Establishment, Harwell, Eng.). J. Nucl. Mater.; 39: 224-5(May 1971).

Uranium monocarbide can be levitation-melted in a simple cylindrical coil associated with a 450 kHz fixed frequency power unit. The 3.6 to 3.7 g sample is melted within 15 sec and held stably above the melting point for not less than 4.5 min. The variation of sample temperature is less than or equal to ±10°C and the absolute temperature is probably within the range 2520 ± 20°C. The behavior is reproducible and the sample is not obscured by the coil. (auth)

29935 HIGH FREQUENCY MELTING OF UO_2–PuO_2. Belieen, R. (BelgoNucleaire, Mol, Belg.); Aerts, L.; Van Lierde, W. Kerntech. Atomprax.; 13: 122-4(Mar 1971).

An attractive system for the preparation of high-density UO_2 and $(U,Pu)O_2$ was developed. The procedure is based on the semiconductor characteristics of these oxides, allowing fusion of uncompacted mixed powders in a high-frequency field inside a solid skin of the same material acting as a crucible. A description of the complete set-up is given. The possibilities of the procedure are illustrated by crushing tests producing powder mixtures having the proper granulometry for fabrication of nuclear fuel elements. (auth)

29936 BORON. Grube, Arthur F. Eng. Mining J.; 172: No. 3, 121-2(Mar 1971).

The growth trends for B compounds and minerals through the 1970's are discussed. Information is included on production, trade, consumption, prices, and future prospects. (J.R.D.)

Properties Evaluations

Refer also to abstracts 29039, 29660, 29828, 29834, 29859, 29870, 30666, 30667, 30684, 30685, 31569, and 31669.

29937 (BMI-X-10274) THERMAL DIFFUSIVITY MEASUREMENTS OF IRRADIATED OXIDE FUELS (LWBR DEVELOPMENT PROGRAM). Matolich, J. Jr.; Storhok, V. W. (Battelle Memorial Inst., Columbus, Ohio). 6 Feb 1970. Contract AT(11-1)-Gen-14; Subcontract 73-14-1251. 52p. Dep. NTIS.

For Bettis Atomic Power Lab., Pittsburgh, Pa.

The effects of irradiation on the thermal conductivity of ThO_2–UO_2 fuels were investigated. It appears that irradiation at a temperature of about 725°C resulted in damage to the lattice that was manifested by a relatively large decrease in thermal diffusivity and thermal conductivity. However, these data are considered to be inconclusive because of the possibility that the presence of large, nonuniformly distributed pores in the specimens influenced the measurements in an unpredictable manner. Irradiation at a temperature of 980°C had no significant effect on thermal conductivity. Apparently any radiation damage to the lattice was annealed out at this temperature in-pile. (auth)

29938 (BNWL-tr-65) SYNTHESIS AND CRYSTALLOGRAPHIC STUDY OF COMPOUNDS OF THE SYSTEM Cs_2O–Al_2O_3–SiO_2. Langlet, Gerard (Commissariat a l'Energie Atomique, Saclay (France). Centre d'Etudes Nucleaires). Translated from report CEA-R-3853. 134p. Dep. NTIS.

The preparation and properties of the system Cs_2O–Al_2O_3–SiO_2 were studied. This compound was studied because of its potential application in cesium-137 radiation sources. The long-term goal of the study was to develop a cesium compound that would have low solubility in water and the usual solvents, high melting or decomposition temperature, high cesium content, high density, and good structural stability. The study indicated that this compound might be suitable for use in radiation sources. (R.C.K.)

29939 (EUR-4531, pp 433-44) POLYGONALLY DIRECTED, WOUND RING STRESS REINFORCEMENTS WITH SEVERAL

INTERMEDIATE FASTNERS FOR ALL STRESS WIRE RINGS (PRISMA SYSTEM). Muehe, L. (Holzmann (Philipp) A. G., Frankfurt am Main (West Germany)). (In German).

From Second conference on prestressed concrete reactor pressure vessels and their thermal isolation; Brussels, Belgium (18 Nov 1969).

In Second information meeting on prestressed concrete reactor pressure vessels and their thermal isolation.

Prestressed concrete pressure vessels with ring-stress reinforcements arranged on the external casing surface are especially desirable when installations as heat exchangers are provided in the vessel wall. A multilayer ring-stress reinforcement with equidistant stress wire arrangement is advantageous in the conservation and inspection of the stressing steel. By use of the construction characteristics of the KA stress method, intermediate fasteners could be built in the form of vise fasteners. The necessary vise force was produced by prestressed screws. A coil machine produces four stress wires simultaneously. The stress force concentrations possible with the ring-stress reinforcements were indicated. (tr-auth)

29940 (EURFNR-820) COMPATIBILITY STUDIES WITH UC OF DIFFERENT STOICHIOMETRIES AND IRON-NICKEL-CHROMIUM ALLOYS AND THE INFLUENCE OF STABILIZERS. Goetzmann, O.; Scherbl, D. (Kernforschungszentrum, Karlsruhe (West Germany). Institut fuer Material- und Festkoerperforschung). Translation of report KFK-1213. 27p. Dep. NTIS.

Work performed under United States-Euratom Fast Reactor Exchange Program.

Compatibility tests were carried out at 900°C on Fe-Ni-Cr-alloys and UC of differing carbon content and with stabilizers added. The carbon contents were 4.1; 4.8, and 5.22 wt %. Chromium and vanadium were used as stabilizers for fuels with the hyperstoichiometric composition and $Cr_{23}C_6$ and VC for the hypostoichiometric composition, respectively. The stabilizer was only mixed into the fuel powder. The mixture was not annealed to reach an equilibrium. No great effect of the stabilizers on the reaction of the hypostoichiometric fuel with the cladding materials was detectable. There was always a strong reaction. The interactions between the stoichiometric and hyperstoichiometric UC and the cladding materials were less than those found with the substoichiometric UC. The stabilizers had a definite effect on the reactions of hyperstoichiometric UC with the cladding materials. (auth)

29941 (INIS-mf-8) DISPERSED-PARTICLE STRENGTHENING IN NICKEL-ZIRCONIA COMPOSITE. Prasad, Y. V. R. K.; Sastry, D. H.; Vasu, K. I. (Department of Atomic Energy, Bombay (India). Chemistry and Metallurgy Committee). 1970. 11p. (CONF-700218-9). NTIS (U. S. Sales Only).

From Symposium on materials science research; Bangalore, India (24 Feb 1970).

The low temperature deformation in zirconia-dispersed (1,2,3, and 4 vol %) nickel was investigated by employing tensile tests and differential-stress creep experiments. At a given strain, the activation volume increases with decreasing volume fraction of the dispersoid. The present results on tensile tests are not in favorable agreement with the Orowan model for initial yielding and the Fisher-Hart-Pry mechanism of strain hardening. It is suggested that the increase in strength and work-hardening rate for the alloys may arise from the high initial dislocation density and its rapid increase with strain. The rate-controlling mechanism for deformation of dispersion-strengthened alloys of zirconia in nickel appears to be the thermally activated intersection of dislocations. (auth) (INIS)

29942 (LA-tr-71-22) HEAT OF FORMATION AND ENTROPY OF FORMATION OF PLUTONIUM CARBIDES. Achacinski, V. V. (Kernforschungszentrum, Karlsruhe (West Germany)). Translated for Los Alamos Scientific Lab., N. Mex., from report KFK-tr-281. 13p. Dep. NTIS.

An abstract of this paper, prepared from the original language, appeared as NSA 23: 39040.

29943 (LA-tr-71-30) ELECTROPHYSICAL PROPERTIES AND NATURE OF THE CHEMICAL BOND IN COMPOUNDS OF BERYLI IUM WITH BORON AND CARBON. Neshpor, V. S.; Samsonov, G. V. Translated by Helen Dahlby (Los Alamos Scientific Lab., N. Mex.), from Izv. Akad. Nauk SSSR, Neorg. Mater.; 7: 50-5(1971). 11p. Dep. NTIS.

Results of investigations show that the resistivity of beryllium borides increases uniformly with increase in the relative content of boron, from the values characteristic for metallic conductors, for the lower borides, to the values characteristic for insulators, for the higher borides of beryllium. The structure and electrophysical properties of the lower borides of beryllium are determined by means of the beryllium bonds, mainly of a metallic type, with a low degree of localization of the s-electrons of beryllium. In these compounds an equilibrium is realized between the electron configurations $(s^2 \rightleftharpoons sp)Be \rightleftharpoons (sp^2 \rightleftharpoons sp^3)B$, which are close in energy and are mutually overlapping, which causes their metallic conductance. The structure and electrophysical properties of the higher borides of beryllium are determined by a motif of the boron bonds of the covalent type. The beryllium atoms in these compounds are electron donors, stabilizing the sp^3-electron configurations of boron and, in their turn, take on stable s^0-configurations. Between the electron configurations of beryllium which are higher on the energy scale and the electron configurations of boron there is an energy gap, which causes their electric insulating properties. With increase in the boron content in beryllium borides, the boron bond strength gradually increases in the structures, the sp^3-electron configurations of the boron atoms and the s^0-configurations of beryllium are stabilized, and the energy difference between them increases. The highest borocarbide of beryllium, BeC_2B_{12}, in structure, hardness, and electrical properties is close to B_4C, which is caused by the opposite effect of the valence electrons of beryllium on the configurations of the valence electrons of boron and carbon. The lowest borocarbide of beryllium, BeC_2B_2, has semimetallic properties, close to the properties of the lower borides of beryllium, and a relatively low hardness, which is caused by the sufficiently strong disturbance of the stable sp^3-configurations of boron by the valence electrons of beryllium. (auth)

29944 (LB/G-2916) ALPHA AUTORADIOGRAPHY OF IRRADIATED NUCLEAR FUEL. Trezza, G. Translated by W. G. Stripp (Atomic Energy Research Establishment, Harwell (England)), from report RT/CHI-(69)2. 17p. Dep. NTIS (U. S. Sales Only).

An abstract of this paper, prepared from the original language, appeared as NSA 23: 36223.

29945 (ORNL-TM-3242) VISCOELASTIC ANALYSIS OF IRRADIATED GRAPHITE WITH VARIABLE CREEP COEFFICIENT. Chang, S. J.; Carpenter, J. A.; Altom, D. W. (Oak Ridge National Lab., Tenn.). May 1971. Contract W-7405-eng-26. 33p. Dep. NTIS.

An addendum to report ORNL-TM-2407 concerning a method of stress analysis for irradiated graphite which may be used for Molten Salt Breeder Reactor (MSBR) core design is presented. To provide a refined analysis, the present method includes the effect of a variable creep coefficient which is caused by the nonuniform temperature distribution. To facilitate a simple formulation, it is assumed that the temperature dependence of the elastic response of the material is approximated to be inversely proportional to the creep rate. It is shown that the problem reduces to the solution of several associated (fictitious) elastic problems which have a common elastic modulus inversely proportional to the creep rate of the irradiated graphite. Numerical examples in the previous report were recalculated based on the present theory. It shows, for large dose values, an improvement to the previous method. A computer program was written for the purpose and can include the previous solution as a special case. (auth)

29946 (SC-T-713023) EFFECT OF BORON ON CERTAIN PHYSICAL CHARACTERISTICS OF SYNTHETIC GRAPHITES. Kotosonov, A. S.; Demin, A. V.; Polozhikhin, A. I.; Nikol'skii, I. F.; Rakcheeva, V. I. Translated by Fredric D. Killebrew (Sandia Labs., Albuquerque, N. Mex.), from Khim. Tverd. Topl.; No. 3, 115-20(1970). 12p. Dep. NTIS.

The effects of boron on the plasticity and structure of the carbon component and on the strength and the electron properties of carbonaceous material produced by thermomechanical treatment (TMT) are discussed. It was established that the deformation of samples during thermochemical treatment and the density and mechanical strength of graphite are increased with elevation in boron content. The structure of borated graphite is characterized by large crystallite dimensions and a smaller interplanar spacing. The electron properties of graphite depend on the amount of boron dissolved in the lattice, replacing part of the carbon atoms. The maximum solubility of boron is limited to one weight percent with respect to the ordered part of the carbon. (auth)

29947 INFLUENCE OF OXIDE ADDITIONS ON THE REDUCTION OF UO_3 AND U_3O_8 AS MEASURED BY DTA AND TG. Berggren, G.; Brown, A. (Aktiebolaget Atomenergi, Studsvik, Sweden). pp 881-91 of Thermal Analysis. Vol. 2. /Schwenker, Robert F. Jr. (ed.). New York; Academic Press, Inc. (1969).

From 2. international conference on thermal analysis; Worcester, Mass. (18 Aug 1968). See CONF-680851.

U_3O_8 and UO_3 powders mixed with various amounts of CeO_2 and PuO_2 have been examined by means of DTA, x-ray diffrac-

tion, and thermogravimetry (TG) in order to study the reduction kinetics. A novel DTA device for use in reducing atmospheres with W/Re thermocouples is described. Simple methods for calculating kinetic parameters from DTA curves have been reviewed and applied. The activation energy for UO_3 and U_3O_8 reduction is not influenced by the oxide additives within the experimental errors (±15%). X-ray diffraction was used to identify intermediate and final products. Comparison with TG was satisfactory. (auth)

29948 YIELD STRENGTH OF DISPERSION HARDENED B.C.C. MATERIALS. Singhal, L. K. (Indian Inst. of Tech., Kanpur). Int. J. Powder Met.; 7: 58-60(Jan 1971).

Dislocation loops produced around dispersed particles were observed. The resulting strengthening is in agreement with theoretical estimates in accord with the Orowan model. (auth)

29949 THERMAL CONDUCTIVITY, ELECTRIC RESISTIVITY, AND SPECIFIC HEAT OF DENSE GRAPHITES. Lutcov, A. I.; Volga, V. I.; Dymov, B. K. (Sojuzelectrod Firm, Moscow). Carbon; 8: 753-60(Dec 1970).

The results of measurements of thermal conductivity, electric resistivity, and heat capacity of graphites with density of 1.9 g/cm^3 and higher in the temperature range 50 to 2500°K are presented. On basis of the modified Debye equation, average crystal parameters for the graphites investigated were calculated. It is concluded that irrespectively of the degree of perfection of the graphite lattice, Umklapp processes markedly affect the thermal conductivity beginning from T = 120 to 140°K. It is shown that the curve of the thermal conductivity vs. temperature at T > 140°K is exponential, the exponent power changing at the excitation of the stiff modes of atomic vibrations. In terms of the experimental data, the thermodynamic functions, enthalpy, thermodynamic potential at 100, 150, 200, 250, 300°K, and at the standard temperature 298.15°K are calculated. The thermodynamic functions of pyrolytic carbon heat-treated at 3000°C are recommended as standards for comparative evaluation of thermodynamic state of various artificial graphites. (auth) (UK)

29950 OXIDATION-RESISTANT COATINGS FOR REFRACTORY METALS. Allen, B. C. DMIC Rev.; 2p(29 Jul 1970).

Recent research on protective coating systems includes work on: Ti-modified chromium silicide coatings for protecting Cr–7Mo–2Ta–0.09C–0.1 Yt alloy; Cr–Yt_2O_3 coating mixtures for protecting high-strength Cr alloys from oxidation and nitridation; nondestructive test methods for coated refractory metals; designs for two Nb alloy structures for space shuttle vehicles, a hot load carrying structure of Nb-752 alloy coated with Cr–Ti–Si and a heat shield and support structure of C–129Y Nb alloy coated with the fused silicides Si–Hf–Cr–Fe and/or Si–Hf–Ta–Cr–Fe; self-sustaining radiative Ta alloy structures coated with fused slurries; and coating systems including a Hf–20Ta cladding or Hf/20Ta/0.25 Si slurry on a Ta–10W alloy and a W/HfO_2 plasma-sprayed composite, an Ir or Ir/Re slurry on W and a pack cementation $MoSi_2$ coating an Mo. A summary report covers the oxidation resistance of high-temperature coatings for superalloys, refractory metals and graphite. (Metals Abstr.)

29951 ENTHALPY OF LANTHANIDE CHLORIDES, BROMIDES, AND IODIDES FROM 298 TO 1300°K: ENTHALPIES OF FUSION AND TRANSITION. Dworkin, A. S.; Bredig, M. A. (Oak Ridge National Lab., Tenn.). High Temp. Sci.; 3: 81-90(Jan 1971).

Enthalpies were measured from room temperature up into the liquid phase with a copper block drop calorimeter for $ScCl_3$, YCl_3, $GdCl_3$, $TbCl_3$, $DyCl_3$, $HoCl_3$, $CeBr_3$, $NdBr_3$, $GdBr_3$, $HoBr_3$, LaI_3, NdI_3, GdI_3, and TbI_3. Enthalpies and entropies of fusion are reported for all of the above and enthalpies and entropies of transition are reported for $TbCl_3$, NdI_3, GdI_3, and TbI_3. Entropies of fusion were found to vary with crystal structure type. The halides with lower entropies of fusion (YCl_3, $DyCl_3$, $HoCl_3$, $GdBr_3$) also had a lower $S_{1300°K} - S_{298°K}$ indicating either a higher degree of order in the liquid or a higher entropy in the solid at room temperature. (auth)

29952 PHASE EQUILIBRIA AND THERMODYNAMIC PROPERTIES IN THE V_nO_{2n-1} SYSTEM. Okinaka, H.; Kosuge, K.; Kachi, S. (Kyoto Univ.). Trans. Jap. Inst. Metals; 12: 44-8(Jan 1971).

The phase equilibria of the V_2O_3–VO_2 system in connection with the oxygen activity were established in the temperature range from 600 to 1200°C. A quenching method was applied to the experiments from 1000 to 1200°C under controlled oxygen atmosphere with the use of a CO_2–H_2 gas mixture. For the temperature range from 600 to 1000°C, a solid electrolyte cell of the type, Pt/adjacent two-phase mixture (V_nO_{2n-1} + $V_{n+1}O_{2(n+1)-1}$)/$(ZrO_2)_{0.85}(CaO)_{0.15}$/$O_2$ (air reference electrode)/Pt, was utilized to measure the oxygen activity. The standard free energy changes of the reactions $(n+1)V_nO_{2n-1} + \frac{1}{2}O_2 \rightleftharpoons nV_{n+1}O_{2(n+1)-1}$ were calculated from the electromotive force developed by the cell. (auth)

29953 EFFECT OF BORON ON SOME PHYSICAL CHARACTERISTICS OF ARTIFICIAL GRAPHITES. Kotosonov, A. S.; Demin, A. V.; Polozhikhin, A. I.; Nikol'skii, I. F.; Rakcheeva, V. I. Khim. Tverd. Topl.; No. 3, 115-20(May-Jun 1970). (In Russian).

The effects of boron (0.01 to 5.0 wt. %) on some physical characteristics of graphite materials based on calcined petroleum coke prepared by the thermomechanical treatment method were studied. An attempt was made to estimate the amount of boron dissolved in the graphite lattice and to establish the interrelationship between the amount of dissolved boron and the total content thereof and certain physical properties of graphite. Specific electric resistivity, magnetic resistance, Hall constant, x-ray diffraction parameters, compression strength, and residual boron content were measured on specimens, as well as relative deformation during thermomechanical treatment. There was found to be an increase in the deformation of specimens during thermomechanical treatment and the density and mechanical strength of the material with an increase in the boron content. The structure of boronized graphite is characterized by increased crystallite size and reduced interlayer distance. The electron properties of the graphite depend mainly on the amount of boron dissolved in the lattice and replacing some of the carbon atoms. From Hall constant data the limiting solubility of boron was found to be limited to 1 percent with respect to the ordered part of carbon. The rest of the boron is localized between the graphite crystallites in the form of carbide compounds. It is assumed that the increased strength of the graphite is due to the carbide phase of boron. (JPRS)

29954 WETTING PROBLEMS IN CONNECTION WITH SINTERING. Tikkanen, M. H.; Ylaesaari, S.; Blomster, K. (Inst. of Tech., Otaniemi, Finland). Phys. Sintering; 3: 1-27(Jan 1971).

It was considered that the wetting phenomenon has a great, and sometimes decisive, significance for sintering of cermets. The conventional way of studying wetting with the help of the classic Young–Dupré wetting equation helps in understanding the nature of the problem, but does not explain the practical problems at high temperatures. The basic reason for this is that wetting at high temperatures is an extremely complex phenomenon, where chemical reactions between the different phases play a decisive part. Considering the scantiness of our knowledge about both liquid and solid metals, and in particular the electronic structure of solid oxides and carbides, the degree of defect structure and other vital properties, it is only natural to be at the very beginning when dealing with the problem of wetting. (auth)

29955 DISSOCIATION ENERGIES OF GASEOUS GADOLINIUM DICARBIDE AND TERBIUM DICARBIDE. Filby, E. E.; Ames, L. L. (New Mexico State Univ., Las Cruces). J. Phys. Chem.; 75: 848-50(18 Mar 1971).

Isomolecular C_2-exchange reactions of the type, $M_aC_2(g) + M_b(g) = M_a(g) + M_bC_2(g)$, were used to determine mass spectrometrically the dissociation energies of GdC_2 and TbC_2. Isomolecular exchange reactions were established between cerium and gadolinium and between gadolinium and terbium. The dissociation energies of GdC_2 and TbC_2 were calculated from the enthalpies of the exchange reactions. The dissociation energy of CeC_2 was used as a reference. The value of 151 ± 3 kcal/mole for GdC_2 was in good agreement with the literature. No data was available for comparison with the determined 150 ± 3 kcal/mole dissociation energy of TbC_2. (G.M.C.)

29956 IMPROVED THERMAL DIFFUSIVITY METHOD APPLIED TO TiB_2, ZrB_2, AND HfB_2 FROM 200 TO 1300°C. Branscomb, T. M.; Hunter, O. Jr. (Iowa State Univ., Ames). J. Appl. Phys.; 42: 2309-15(May 1971).

The thermal diffusivities of dense polycrystalline TiB_2, ZrB_2, and HfB_2 were measured by a laser flash method over the temperature range 200 to 1300°C. An investigation of the effects of radial heat flow was performed and a special sample shape was used to comply with the assumption of one-dimensional heat flow. The values of the diffusivities were found to be described by the empirical equations TiB_2: $\alpha = 0.1290 + [39.26/T(°K)]$ cm^2/sec; ZrB_2: $\alpha = 0.1424 + [81.17/T(°K)]$; and HfB_2: $\alpha = 0.1436 + [35.97/T(°K)]$. Values of thermal conductivity computed from the diffusivity data were found to be described by $\lambda = 0.7867 + [10.30/T(°K)]$W/cm deg for TiB_2, $\lambda = 0.8235 + [108.2/T(°K)]$ for ZrB_2, and $\lambda = 0.7157 + [34.24/T(°K)]$ for HfB_2. (auth)

29957 THERMAL DIFFUSIVITY OF URANIUM AND URANIUM–PLUTONIUM MONOCARBIDES. Wheeler, M. J. (General Electric Co. Ltd., Wembley, Eng.); King, E.; Manford, C.; Hedger, H. J. J. Brit. Nucl. Energy Soc.; 10: 55-64(Jan 1971).

Thermal diffusivity values were determined by a modulated electron beam technique. Results are given for sintered uranium

carbide alloys with and without additions of O or Ni between 500 and 2200°K, arc-cast UC_{1+x} and arc-cast (UPu)C alloys. Additions of 2 wt% O decrease the diffusivity by about 20% at 1200°K, whereas additions of 0.23 wt% Ni increase the diffusivity by about 20%. An inflexion in the diffusivity temperature curve was found for UC_{1-x} at approximately 1900°K: this may be attributed to a change in the vacancy distribution. The diffusivity of hypostoichiometric $(U_{0.9}Pu_{0.1})C$ is close to that of UC_{1-x}. Higher plutonium carbide contents reduce the conductivity to ~70% of that of UC_{1-x} at 40% PuC. (auth) (UK)

29958 A METHOD FOR MEASURING THE THERMAL CONDUCTIVITY OF REFRACTORY MATERIALS WITH A GOOD ELECTRICAL CONDUCTIVITY. Mihailovic, Z.; Naudet, G. (CEA, Saclay, France). Rev. Phys. Appl.; 5: 869-75(Dec 1970). (In French).

An absolute method is described for measuring, at high temperatures (1000 to 2400°C), the value of the thermal conductivity λ of refractory materials with good electrical conductivity. The method is based on the radial temperature difference set up in a noninsulated cylindrical specimen by direct Joule heating. The idea was inspired by a method for measuring the electrical conductivity using the same mode of heating. An exact expression is obtained for λ and the equivalent temperature T_e corresponding to σ, which is measured simultaneously. The method is quicker to set up and yields results more rapidly than classical methods. (France)

29959 CARBIDES: PROPERTIES, PRODUCTION, AND APPLICATIONS. Kosolapova, T. Ya. New York; Plenum Publishing Corporation (1971). 309p. $30.00.

Translation of Karbidy by N. B. Vaughan.

A comprehensive summary of all known metal–carbon systems is presented. Both experimental and theoretical data on carbides is given with respect to: structures, thermodynamic and thermophysical properties, electrophysical and magnetic properties, physicomechanical properties, and chemical properties. Methods of production and various fields of application are discussed. (G.M.C.)

29960 CREEP OF URANIUM AND URANIUM–PLUTONIUM MONOCARBIDES IN COMPRESSION. Killey, N. M. (General Electric Co. Ltd., Wembley, Eng.); King, E.; Hedger, H. J. J. Brit. Nucl. Energy Soc.; 10: 65-72(Jan 1971).

The creep behavior of sintered uranium carbide with and without nickel additions was studied in a vacuum of $>10^{-5}$ torr and compared with previous results for cast UC. The effect of temperature on slightly hypostoichiometric material (4.75 to 4.80 wt % C) over the range 930 to 1200°C is reported, and the effects of both temperature and stress are reported for hyperstoichiometric material (4.84 to 5.4 wt % C) over the ranges 1000 to 1300°C and 16 to 70 MN/m^2. It is evident that the creep behavior of sintered UC can be related to that of cast material of similar composition despite differences of grain size, porosity and strain rate. The deformation of sintered carbide containing ~15% plutonium carbide was studied as a function of carbon equivalent within the range 4.9 to 4.6 wt%. Tests were conducted in a vacuum of 1×10^{-6} torr using nominal stresses in the range 3 to 30 MN/m^2 and temperatures in the range 950 to 1150°C. The deformation is characterized by low activation energies and by large amounts of primary creep, the amount of strain to reach constant rates increasing with decreasing carbon content. (auth) (UK)

29961 ENTHALPIES OF FORMATION OF CERIUM DIOXIDE, CERIUM SESQUICARBIDE, AND CERIUM DICARBIDE. Baker, Floyd B.; Huber, Elmer J. Jr.; Holley, Charles E. Jr.; Krikorian, N. H. (Los Alamos Scientific Lab., N. Mex.). J. Chem. Thermodyn.; 3: 77-83(Jan 1971).

The enthalpies of formation of cerium dioxide, cerium sesquicarbide, and cerium dicarbide were determined by oxygen bomb calorimetry and found to be $\Delta H_f^0(CeO_2, 298.15°K) = -(260.6 \pm 0.2)$ kcal $mole^{-1}$, $\Delta H_f^0(CeC_{1.5}, 298.15°K) = -(21.1 \pm 0.7)$ kcal $mole^{-1}$, and $\Delta H_f^0(CeC_{2.0}, 298.15°K) = -(23.2 \pm 1.3)$ kcal $mole^{-1}$. (auth) (UK)

29962 GRAPHITIZATION OF FREE CARBON PRECIPITATING THROUGH THE REACTION OF UC_2 WITH N_2. Katsura, M.; Yuki, T.; Sano, T.; Sasaki, Y. (Osaka Univ.). J. Nucl. Mater.; 39: 125-32(May 1971).

The degree of graphitization of the carbon formed through the reaction of UC_2 with nitrogen gas was studied as a function of temperature and nitrogen pressure. The degree of graphitization increases with increasing temperature and with decreasing nitrogen pressure. From these results, it might be concluded that the scattering results obtained by the reaction of UC with nitrogen gas is due to the different degree of graphitization of the precipitating carbons. In order to study the equilibrium of the two-phase region of UC–UN solid solution and free carbon, that is, the relation between temperature, nitrogen pressure and the composition of the UC–UN solid solution, it should be necessary to employ the mixture of UN and graphite as the starting material. (auth)

29963 RELEASE OF ^6Li FROM LOW-SINTERED BERYLLIUM OXIDE. Roehrig, H. D.; Hecker, R. (Kernforschungsanlage, Juelich, Ger.). J. Nucl. Mater.; 39: 145-56(May 1971). (In German).

The release behavior of neutron poison ^6Li from low-sintered beryllium oxide was investigated following irradiation by a fast neutron dose ($E > 0.1$ MeV) of $2 \times 10^{20}/cm^2$. Small cylindrical samples from three series characterized by sintering temperatures of 1270, 1300, and 1320°C were available. Release isotherms were measured in a temperature region of 1100 to 1550°C. The strongly anomalous behavior of the curves is quantitatively interpreted as a diffusion process with an overlapping resintering process. The extrapolation to the final structure state leads to an Arrhenius straight line common for all three samples. It is described by $D' = 30 \exp(-71$ kcal/RT Mol) sec^{-1}. As an additional result from the release curves, molar activation energies of 155 or 197 kcal/mole are found for the resintering process which are taken as confirmation for the mentioned interpretation. (auth)

29964 PLUTONIUM DIFFUSION IN HYPERSTOICHIOMETRIC MIXED URANIUM–PLUTONIUM DIOXIDES. Riemer, G.; Scherff, H. L. (EURATOM-CCR, Ispra, Italy). J. Nucl. Mater.; 39: 183-8(May 1971).

The diffusion behavior of plutonium in hyperstoichiometric mixed uranium (15%) plutonium dioxides was investigated as a function of temperature and oxygen/metal ratio. At O/M = 2.10 an activation energy of 86 kcal/mole is found in good agreement with recent results on uranium self-diffusion in UO_{2+x}. At constant temperature (1400°C) and varying O/M ratios the diffusion coefficients are found to increase proportional to x^n, with n being equal to 2.77. The results are discussed in the light of recent theoretical models and experimental results on cation diffusion in uranium dioxide. Comparison is made to earlier results obtained on nearly stoichiometric mixed oxide. (auth)

29965 HIGH TEMPERATURE REACTION BETWEEN URANIUM MONOSULFIDE AND ZIRCONIUM. Yamawaki, M.; Kanno, M.; Mukaibo, T. (Tokyo Univ.). J. Nucl. Mater.; 39: 209-18 (May 1971).

The solid-solid reaction of uranium monosulfide with zirconium was investigated in detail at temperatures ranging from 850 to 1100°C using differential expansion capsules. At all temperatures investigated, three layers were formed between US and unaffected zirconium. The x-ray diffraction study and electron probe microanalysis indicated that the reaction zone was composed of solid solution between uranium and zirconium and a new zirconium subsulfide. Growth of each reaction layer was found to obey a parabolic rate law and its rate was measured. The marker study suggested the location in the zone of reaction where the initial US-zirconium interface existed. (auth)

29966 HEATS OF HYDROLYSIS OF THORIUM CARBIDES. Imai, H.; Honda, T.; Sasaki, Y. (Japan Atomic Energy Research Inst., Ibaraki). J. Nucl. Mater.; 39: 238-40(May 1971).

Heats of hydrolysis of ThC_{1-x} and of ThC_2 were measured with a microcalorimeter, with particular emphasis on thorium monocarbide which was known to have a wide range of composition. The hydrolysis reaction was determined to be exothermic. A grey or white product was formed with evolution of gas upon hydrolysis of thorium carbide at room temperature. X-ray examination indicated that the grey product corresponded to thorium carbide and dioxide and the white material corresponded to $ThO_2 \cdot 2H_2O$. (G.M.C.)

29967 SOME CONSIDERATIONS ON THE THERMAL CONDUCTIVITY OF STOICHIOMETRIC URANIUM DIOXIDE AT HIGH TEMPERATURES. Schmidt, H. E. (European Inst. for Transuranium Elements, Karlsruhe, Ger.). J. Nucl. Mater.; 39: 234-7 (May 1971).

The results of investigations on the thermal conductivity of stoichiometric uranium dioxide at high temperatures indicate a general agreement, with the expected 1/T-behavior below 1200°C, the occurrence of a minimum of about 0.0220 W/cm deg around 1700°C and a subsequent rise to approximately 0.0325 W/cm deg at 2500°C. An analysis of these data indicates that the upswing in thermal conductivity with increasing temperature is mainly due to the observed increase of the heat capacity of uranium dioxide at temperatures above ~1200°C, the two quantities being related by $\lambda = \frac{1}{3} c_v \cdot u \cdot q \cdot \Omega$ with λ: thermal conductivity, c_v: specific heat at constant volume, u: mean velocity of phonon propagation, Ω: phonon mean free path, q: density. Other mechanisms, i.e., electronic and radiative heat transfer, have, if any, only a minor

effect on the thermal conductivity within the temperature range investigated. (auth)

29968 KINETICS AND MECHANISM OF LOW-PRESSURE, HIGH-TEMPERATURE OXIDATION OF SILICON. II. Gelain, C.; Cassuto, A.; Le Goff, P. (CNRS, Nancy). Oxidation Metals; 139-51(Mar 1971).

The reaction of oxygen at low pressures with silicon layers on tungsten ribbons was studied. An abrupt transition was observed between a condition of passivation, in which a thin film of SiO_2 formed at low temperatures, and a steady-state combustion condition at high temperatures. The latter state is characterized by the formation of volatile SiO. The boundary between these two states was defined in terms of the pressure–temperature relation. Oxygen consumption in the combustion state is represented by first-order reaction kinetics with an activation energy of 13 ± 1 kcal/mole. The stability of the two states was defined by a thermodynamic analysis of the SiO_2 layer stability. The oxygen consumption dependence on temperature was described by a kinetic model which involves a consideration of the various elementary steps in the reaction. (auth)

29969 ZIRCONIUM-REFRACTORY ALLOYS. Skelly, H. M.; Dixon, C. F. (Dept. of Energy, Mines, and Resources, Ottawa). J. Less-Common Metals; 23: 415-25(Apr 1971).

Zirconium alloys containing thorium oxide, yttrium oxide, cerium zirconate, or lanthanum oxide were prepared by arc-melting. The refractories apparently dissolved in the molten zirconium and precipitated as a dispersed phase on solidification. High–temperature (650°C) tensile strengths, up to twice that of Zircaloy-2, were observed for arc-melted specimens. The size and distribution of thorium oxide and cerium zirconate particles were shown to vary depending on the heat treatment and, although interparticle spacing, believed to be ideal, was not achieved, particles of a size considered to be fine enough to produce dispersion strengthening were obtained. (auth)

29970 ELASTIC MODULI OF NIOBIUM CARBIDE AND TANTALUM CARBIDE AT HIGH TEMPERATURE. Jun, C. K.; Shaffer, P. T. B. (Carborundum Co., Niagara Falls, N. Y.). J. Less-Common Metals; 23: 367-73(Apr 1971).

The Young's, shear and bulk moduli of polycrystalline $NbC_{0.95}$ and $TaC_{0.99}$ were determined from room temperature to 1500°K by the sonic resonance technique. The Young's and shear moduli decrease linearly with increasing porosity, and also decrease with increasing temperature, in agreement with the Wachtman's empirical equation. The bulk modulus decreases with increasing porosity and with increasing temperature. The Grüneisen constant and Debye temperature of both carbides were determined. The Poisson ratio increases with increasing temperature. (auth)

29971 MICROROENTGENOSPECTRAL INVESTIGATION OF URANOTITANATES. Rakovich, F. I.; Sharkin, O. P.; Tsopova, L. N. Geol. Zh.; 30: No. 4, 119-25(Jul 1970). (In Russian).

X-ray microanalyses and mineralogical studies determined the properties of a complex group of uranium titanates found in the shape of irregular impregnations of acicular, prismatic, and clinoclase crystals in algirite, riebecite, chlorite, titanate, and other minerals. The dimensions of the grains were in millidecimal fractions of a millimeter. Various types of uranium titanates different in their chemical composition and physical constants were found and four groups of uranium titanates were separated. (auth) (INIS)

29972 THERMOPHYSICAL PROPERTIES OF ATJS GRAPHITE AT HIGH TEMPERATURES. Taylor, R. E.; Kimbrough, W. D. (Purdue Univ., Lafayette, Ind.). Carbon; 8: 665-71(Nov 1970).

The spectral emittance (0.65 μ), total hemispherical emittance, electrical resistivity, and thermal conductivity of Grade ATJS Graphite from about 1200 to 2400°K were measured using a multipurpose thermophysical properties apparatus. (auth) (UK)

29973 MECHANICAL BEHAVIOUR OF POLYCRYSTALLINE TaC. Becher, Paul F. (North Carolina State Univ., Raleigh). J. Mater. Sci.; 6: 79-80(Jan 1971).

The behaviour of tantalum carbide subjected to compressive loading was investigated at temperatures above 1200°C in vacuo. The results of the study revealed that ductile behaviour can be accomplished in polycrystalline TaC deformed at strain rates 5×10^{-2} min^{-1} at 1280°C and above. Analyses of the thermomechanical data suggest that deformation occurs in part by dislocation motion controlled by carbon diffusion in contrast to the expected slower diffusing tantalum species; possibly as a result of the effects of chemistry or structural defects (dislocations or grain boundaries). (UK)

29974 RELEASE OF FISSION CESIUM FROM IRRADIATED UO_2 POWDER. Yamagishi, Shigeru; Tanifuji, Takaaki; Fukuda, Takeshi (Japan Atomic Energy Research Inst., Tokai). J. Nucl. Sci. Technol. (Tokyo); 8: 115-21(Mar 1971).

The amount of Cs released from irradiated UO_2 powder in a range of temperature between 820 and 980°C was measured by sweeping with H_2–1% HCl mixture. This mixed gas proved effectively to carry off the released Cs from the UO_2 surface, as verified by observation of the characteristics of CsCl adsorption on UO_2 and desorption therefrom. In addition, the amount of Cs released by knock-out during irradiation was measured. The chemical form of Cs adsorbed on the UO_2 surface after release by knock-out is considered to be elemental. The activation energy for Cs migration in UO_2 is discussed, with account taken of the difference in behavior between single crystals and polycrystals. (auth)

Structure and Phase Studies

Refer also to abstracts 29081, 29879, 29953, and 30272.

29975 (JAERI–1203) PHASE STUDY OF THE SYSTEM UO_2–Dy_2O_3. Uchida, Masaaki; Ichikawa, Michio (Japan Atomic Energy Research Inst., Tokai. Tokai Research Establishment). Jul 1970. 10p. Dep. NTIS (U. S. Sales Only).

The pseudo-binary system UO_2–Dy_2O_3 was prepared by heat-treatment in a helium atmosphere at 1100 to 2100°C, and studied by means of x-ray diffraction and metallography. A fluorite-structure solid solution was formed up to $DyO_{1.5}$ content of 55 to 65 mole %, depending on the temperature. An intermediate phase with bcc structure, different from the so-called C-form DyO_3, was observed, extending to the more uranium-rich region at higher temperature. This phase is considered to be an ordered structure of the fluorite-type solid solution, accompanied by a change of the O/M ratio. Between this and the C-form Dy_2O_3 phase, there exists a broad two-phase region, extending from about 70 to 90 mole % of $DyO_{1.5}$, depending on the temperature. (auth)

29976 (JAERI-Memo–4249) ON THE COLUMNAR GRAIN GROWTH IN THE CENTER LINE HEATED UO_2 PELLET. Ichikawa, Michio; Uchida, Masaaki (Japan Atomic Energy Research Inst., Tokyo). Dec 1970. 23p. (In Japanese). Dep. NTIS (U. S. Sales Only).

Columnar grains grow in sintered UO_2 pellets when heated under a temperature gradient at high temperature. The mechanism of columnar grain growth is believed to be attributed to the migration of lenticular voids up to the central high temperature region. A study was conducted using 95% theoretical density UO_2 pellets, where the heating power and the heating time were taken as parameters, in which it was found that the columnar grain was formed without any trace of lenticular voids. Based on results obtained mainly by ceramography and micro x-ray diffraction, it is concluded that the columnar grain could be formed by the grain growth under a temperature gradient. The driving force for the columnar grain growth was considered to be the thermal stress as well as the decrease in the grain boundary energy. (Japan)

29977 (KFK-1330) PHASE EQUILIBRIA IN THE SYSTEMS UO_2–UO_3–$NdO_{1.5}$ AND NpO_{2+x}–$NdO_{1.5}$. Boroujerdi, Abbasali (Kernforschungszentrum, Karlsruhe (West Germany). Institut fuer Radiochemie). Jan 1971. 49p. (In German). Dep. NTIS (U. S. Sales Only).

The ternary system UO_2–UO_3–$NdO_{1.5}$ at 1250°C was observed to consist of four single-phase regions and three two-phase regions. The single-phase regions include β–U_3O_8 for which solubility of $NdO_{1.5}$ could be detected; and a fluorite phase, $(U,Nd)O_{2\pm x}$, with an uranium valence ranging from +4 to +6. This phase covers a great part of the system. The limiting metal–oxygen compositions in this phase are $MeO_{1.60}$ and $MeO_{2.25}$. A rhombohedral phase was observed which occurs between the limiting compositions $UO_2 \cdot 6NdO_{1.5}$ and $UO_3 \cdot 6NdO_{1.5}$. In the quasibinary system UO_{2+x}–$NdO_{1.5}$ ($p(O_2)$ = 1 atm), the phase width of the fluorite phase $(U,Nd)O_{2\pm x}$ increases with rising temperature. In the quasi-binary system NpO_{2+x}–$NdO_{1.5}$ ($p(O_2)$ = 1 atm) four single-phase regions (two fluorite phases: $F_1 + F_2$, $NpO_3 \cdot 6NdO_{1.5}$ and A–$NdO_{1.5}$) and three two-phase regions were observed. The thermal stability of $(Np_{0.5}, Nd_{0.5})O_{2.00}$ and $NpO_3 \cdot 6NdO_{1.5}$, respectively, is considerably smaller than the stability of the corresponding ternary oxides of uranium. The presence of the actinyl group MeO_2^{n+} (n = 1.2) in the ternary oxides investigated could be excluded by means of ir-spectra. (auth)

29978 (ORNL–4630, pp 163-76) DEVELOPMENT OF FBR NEUTRON-ABSORBER MATERIALS. Adamson, G. M. Jr.; Martin, W. R. (Oak Ridge National Lab., Tenn.).

In Fuels and materials development program quarterly progress report for period ending September 30, 1970.

The problems of unambiguously indexing x-ray powder patterns of unirradiated and irradiated boron carbide were solved using the rhombohedral crystal structure. Transmission electron microscopy of particles of boron carbide was made possible by the development of a new technique for preparing samples for the ion-bombardment milling machine. Particles examined appear to be single crystals with little internal structure. The experiment for the Experimental Breeder Reactor-II was fabricated, assembled, and shipped to the reactor site. (auth)

29979 (SGAE-PH-96/1970) DETERMINATION OF THE DISTRIBUTION OF FISSION PRODUCTS IN FUEL PARTICLE COATINGS BY THE SPUTTERING TECHNIQUE. Betz, G.; Dobrozemsky, R.; Viehboeck, F. P.; Wotke, H. (Oesterreichische Studiengesellschaft fuer Atomenergie G.m.b.H., Vienna (Austria)). May 1970. 15p. NTIS (U. S. Sales Only).

For the retainment of fission products, high-temperature fuel particles normally are coated with pyrolytic carbon and silicon carbide layers. The knowledge of the distribution of the fission products in these coatings for a given history of irradiation is very important for the prediction of the lifetime of fuel particles and for the improvement of the retainment factor. Due to their chemical resistivity and porous structure, the peeling off of the coating layers by chemical or mechanical methods is very difficult and only rough steps of peeling off have been achieved up to now. A new method is investigated: peeling off by sputtering, using an A^+ ion beam of 40 keV energy. The sputtered material is condensed on collecting foils and the fission products are determined by Ge(Li)-γ-spectrometry. The method and the experimental set-up are described and first results on the fission product distribution in PyC and PyC–SiC–PyC coatings are given. (INIS)

29980 COMPOSITION AND PROPERTIES OF THE BINDER METAL IN COBALT BONDED TUNGSTEN-CARBIDE. Ruediger, O.; Hirschfeld, D.; Hoffmann, A.; (and others) (Fried-Krupp GmbH, Essen). Int. J. Powder Met.; 7: 29-38(Jan 1971).

For investigating the composition of the binder phase in WC–CO-alloys, the carbide was removed electrolytically so that the remaining binder could be tested analytically and by x-ray diffraction. It was found that the tungsten content of the binder depended on the carbon content of the alloys, on the grain size of the carbide used, on the cobalt content, and on the sintering and cooling conditions. The tungsten content of the binder increased as the carbon content of the alloys decreased, as the grain size of the carbide increased, as the sintering time increased, and as the Co-content of the alloy decreased. Additional heat treatment for 50 hr at 1250°C followed by water quenching almost eliminated the differences regardless of the initial grain size of the carbide, of the Co-content, and of the sintering time. The W-contents calculated for the binder of binary WC–Co-alloys (free from other phases) from the total carbon contents of the alloys together with the C-values of the corresponding isolates, were in good agreement with the measured W-values for the coarse grained materials. However they differed for the fine grained alloys. In the range of composition used, the tensile strength and the elongation of some melted, forged and heat-treated model alloys of the Co–W–C system were determined. It was found that tensile strength of more than 120 kp/mm^2 at elongations of about 10% can be achieved. (auth)

29981 DTA AND X-RAY ANALYSIS OF RARE EARTH–CHALCOGEN SYSTEMS. Yarembash, E. I. (Kurnakov Inst., Moscow). pp 761-77 of Thermal Analysis. Vol. 2. /Schwenker, Robert F. Jr. (ed.). New York; Academic Press, Inc. (1969).

From 2. international conference on thermal analysis; Worcester, Mass. (18 Aug 1968). See CONF-680851.

RE-chalcogenides of new types Me_4X_7, (Me_4X_9), Me_3X_7, $M3_4Te_{11}$ (Me = La, Ce, Pr, Nd, Sm; X = Se, Te) have been synthesized. Data on the structure of phase diagrams of RE–X systems are indicated. The possibilities of DTA method are discussed. (auth)

29982 USE OF DTA FOR THE DETERMINATION OF THE MONOCLINIC–TETRAGONAL TRANSFORMATION IN ZIRCONIA AND ZIRCONIA-BASED SYSTEMS. Ruh, Robert; Garrett, Harold J. (Air Force Materials Lab., Wright-Patterson Air Force Base, Ohio). pp 851-68 of Thermal Analysis. Vol. 2. /Schwenker, Robert F. Jr. (ed.). New York; Academic Press, Inc. (1969).

From 2. international conference on thermal analysis; Worcester, Mass. (18 Aug 1968). See CONF-680851.

The martensitic monoclinic-tetragonal transformation in zirconia was studied as a function of heating rate using differential thermal analysis. An understanding of the characteristics of martensitic transformations was supplemented by high temperature x-ray diffraction data on ZrO_2 in resolving the DTA results. They revealed basic information about the transformation as well as the general suitability and optimum conditions for its determination by DTA. Having demonstrated its suitability, DTA was then used to determine the transformation in zirconia-based binary systems. (auth)

29983 TRANSMISSION MICROSCOPY OF ION-THINNED BORON CARBIDE. Katz, R. N.; King, A. O. (Army Materials and Mechanics Research Center, Watertown, Mass.). Metallography; 4: 87-9(Feb 1971).

Argon ion-bombardment thinning methods were used to prepare boron carbide for optical and electron transmission microscopy. The transmitted light optical microscopy method did not seem to offer any significant advantage over reflected light microscopy. Transmission electron microscopy, however, revealed a multiplicity of substructural detail in B_4C, many features unobservable with other methods. (G.M.C.)

29984 THERMAL PHASE RELATIONS AND DIELECTRIC PROPERTIES IN THE SYSTEM La_2O_3–ZrO_2–TiO_2. Solacolu, S.; Barbulescu, A. (Polytechnic Inst., Bucharest). Rev. Roum. Chim.; 16: 25-32(Jan 1971). (In French).

Phase relations were determined by differential thermal analysis and x-ray analysis for oxide mixtures prepared by coprecipitation. The results obtained were used to draw the compatibility lines in the system. Dielectric properties were determined for the ceramic bodies obtained by the sintering at 1360° of the masses resulting from the coprecipitated materials calcined at 350° and subjected to a pressure of 4 t/cm^2. Good agreement was found between the dielectric properties and the phase composition of the ceramic masses, corresponding to the compatibility triangles obtained. (tr-auth)

29985 PHASE DIAGRAMS OF THE SYSTEMS OF SAMARIUM, GADOLINIUM, AND DYSPROSIUM OXIDES WITH MAGNESIUM OXIDE. Lopato, L. M.; Ogorodnikova, A. A.; Shevchenko, O. V. (Inst. of Studies of Materials, Kiev). Dopov. Akad. Nauk Ukr. RSR, Ser. B; No. 12, 1106-8(Dec 1970). (In Ukrainian).

According to the method of annealing and tempering and by means of high-temperature DTA, phase diagrams of the systems Sm_2O_3–MgO, Gd_2O_3–MgO, and Dy_2O_3–MgO were plotted within the temperature range of 1500 to 2400°C. The systems studied are of the same type and are characterized by eutectic structure of liquidus-solidus region. Eutectic points are located near the equimolar composition, melting temperatures of eutectics are 2010, 2080, and 2100 ± 20°C for the systems with samarium, gadolinium, and dysprosium oxides, respectively. It is shown that additions of 5 mole% MgO produce a 20 to 50°C decrease in the temperature of polymorphous transformations of rare earth element oxides. (auth)

29986 CRYSTAL STRUCTURE OF Th_3N_4. Bowman, A. L.; Arnold, G. P. (Los Alamos Scientific Lab., N. Mex.). Acta Crystallogr., Sect. B; 27: 243-4(1971).

The crystal structure of Th_3N_4 was determined by neutron diffraction to be rhombohedral, space group $R\bar{3}m$, Th in 1(a) and 2(c), x = 0.2221 (4), N in 2(c) x = 0.1320 (4), and 2(c), x = 0.3766 (5). The hexagonal lattice parameters are a_0 = 3.875 (2), c_0 = 27.39 (4) Å. (auth)

29987 HIGH TEMPERATURE PHASE STUDIES WITH A SOLAR FURNACE. Noguchi, Tetsuo (Government Industrial Research Inst., Nagoya, Japan). Advan. High Temp. Chem.; 2: 235-62(1969).

A description is presented concerning the use of solar furnaces in making temperature and emissivity measurements of oxides. The thermal imaging technique used in determining freezing and melting points is also described. Phase studies of binary oxide systems using these techniques are discussed. (J.R.D.)

29988 PHASE INVESTIGATIONS IN THE U–Cr–N SYSTEM. Spear, Karl E.; Leitnaker, James M. (Oak Ridge National Lab., Tenn.). High Temp. Sci.; 3: 26-8(Jan 1971).

A new ternary phase, $UCrN_{2\pm x}$, was observed and the x-ray diffraction pattern is reported. (auth)

29989 PHASE BEHAVIOR OF THE U–V–N SYSTEM AND PROPERTIES OF UVN_2. Spear, Karl E.; Leitnaker, James M. (Oak Ridge National Lab., Tenn.). High Temp. Sci.; 3: 29-40 (Jan 1971).

The phase behavior of the ternary U–V–N system was investigated by annealing ternary compositions at constant temperatures from 1400 to 2000°C and constant pressures from vacuum to 650 torr N_2. The products were examined by x-ray diffraction techniques and the equilibrium tie lines in the ternary system were established. Qualitative data indicated that ternary solid solubilities were small. A ternary phase UVN_2 was discovered and found to be isomorphous with $UMoC_2$ by X-ray powder diffraction data and intensity calculations. The ternary compound appeared to be stable with respect to decomposition to the binary nitrides over the entire temperature range studied.

XUM

$\Delta H^0_{f,298}$ and S^0_{298} of UVN_2 were calculated to be −129 ± 8 kcal/mole and 23.5 ± 3.0 e.u., respectively. (auth)

29990 ZIRCONIUM–SULFUR SYSTEM AT HIGH TEMPERATURES. Conard, B. R.; Franzen, H. F. (Ames Lab., Iowa). High Temp. Sci.; 3: 49-55(Jan 1971).

The preparation and identification of the solid phases present in the zirconium–sulfur system in the stoichiometry region $0 < S/Zr < 1.5$ are reported. Samples were annealed at temperatures from 1000°C to above the melting points of the solids. Single crystal and powder x-ray diffraction techniques were used to identify the phases present, and combustion and electron microprobe analyses were used to determine chemical compositions in some cases. The existence at high temperatures of several previously reported phases, namely Zr_2S, ZrS_{1-x} ($x > 0$), and $Zr_{1-x}S$($x \geq 0$) was established, and two new phases were found, namely $Zr_{21}S_8$ and Zr_3S_2. Data are reported which permit identification of the solid phases by means of x-ray diffraction techniques. (auth)

29991 STRUCTURE OF CORROSION-RESISTING FILMS FORMED ON TANTALUM AND NIOBIUM IN HIGH-TEMPERATURE DILUTE ACID AQUEOUS SOLUTIONS. Nakayama, Tadayuki; Osaka, Toshiaki (Waseda Univ., Tokyo). J. Jap. Inst. Metals; 35: 35-40(Jan 1971). (In Japanese).

Electron diffraction patterns of oxide films formed on Ta in 2N HNO_3 and Nb in 0.1 N HNO_3 at 200 to 300°C for 1 hr indicated the presence of only the normal rutile-type structure, thought to be TaO_2 and NbO_2, respectively. However, the film formed on Nb in 2N HNO_3 at 200°C for 1 hr gave a diffraction pattern corresponding to a new tetragonal-type structure (T_1-phase). The unit cell dimensions of the T_1-phase were calculated to be a_0 = 8.94 Å, c_0 = 11.9Å, c_0/a_0 = 1.33. Oxide films formed on Ta in 2N H_2SO_4 at 200 to 300°C and on Nb in 0.1N H_2SO_4 at 200°C for 1 hr were also composed of the normal rutile-type crystals. Another tetragonal-type oxide (T_2-phase), however, was formed on Nb in 2N H_2SO_4 at 200 to 300°C for 1 hr, with a_0 = 10.5 Å, c_0 = 5.85 Å, c_0/a_0 = 0.56. The presence of an amorphous film was observed by heating Ta in 2N HCl or Nb in 0.1N HCl at 200 to 300°C for 1 hr. Therefore it is considered that the film acts as a protective barrier under the present experimental conditions. Further, from the above considerations and the fact that the T_1-phase was formed in 0.5N HCl at 200°C, the T_2-phase in 2N HCl at 200°C, and the δ-phase (Nb_2O_5) mainly in 2N HCl at 250°C, it can be deduced that such a phase transition as $NbO_2 \rightarrow T_1$-phase $\rightarrow T_2$-phase $\rightarrow Nb_2O_5$ occurred. (auth)

29992 CRYSTAL STRUCTURES OF $ZrCo_3B_2$ AND $HfCo_3B_2$. Voroshilov, Yu. V.; Kripyakevich, P. I.; Kuz'ma, Yu. B. (Lvov State Univ.). Sov. Phys.-Cryst. (Engl. Transl.); 15: 813-16 (Mar-Apr 1971).

Translated from Kristallografiya; 15: 934-8(Sep-Oct 1970).

The crystal structure of the compound $ZrCo_3B_2$ ("$ZrCo_3B$") has been determined from single-crystal data. The structure is of a new type (space grouping $R3 - C^2_{3i}$, a = 8.418, c = 9.132 Å, c/a = 1.085 a_{rh} = 5.735 Å, α = 129°18′, N = 54, 3 $Zr^{(1)}$ in 3 (a), 6 $Zr^{(2)}$ in 6 (c) with z = 0.3280, 9 $Co^{(1)}$ in 9 (d), 18 $Co^{(2)}$ in 18 (f) with x = 0.1690, y = 0.8340, z = 0.1360, 18 B in 18 (f) with x = 0.072 y = 0.727, z = 0.330) and is a deformed derived structure of the $CeCo_3B_2$ type. The coordination numbers of Zr are 20 and 14, those of Co 14 and 13, and that of B 9; the coordination polyhedron of the boron atom is a deformed trigonal [BCo_6] prism with additional vertices against two side faces (Zr atoms) and against an elongated lateral edge (a B atom forming a dumbbell group with the central atom, δ = 1.697 Å). The parameters of the position of the atoms have been refined by the method of least squares. the final R being 16.8%. $HfCo_3B_2$ (a = 8.38, c = 9.12 Å, c/a = 1.088, a_{rh} = 5.714 Å, α = 131°57′) has the structure of $ZrCo_3B_2$. (auth)

29993 CRYSTAL STRUCTURE OF $CeMg_2Si_2$. Zmii, O. F.; Gladyshevskii, E. I. (Lvov State Univ.). Sov. Phys.-Cryst. (Engl. Transl.); 15: 817-19(Mar-Apr 1971).

Translated from Kristallografiya; 15: 939-41(Sep-Oct 1970).

By x-ray structural analysis the crystal structure of the compound $CeMg_2Si_2$, which is of a new structural type, was determined. The tetragonal unit cell has the dimensions a = 4.250 ± 0.002 Å, c = 5.765 ± 0.002 Å, Z = 1. The atoms occupy the following positions (space group P4/mmm): 1Ce (a)000, 2Mg 2(e)$0\frac{1}{2}z$; 2Si 2(h) $\frac{1}{2}\frac{1}{2}z$; z = 0.223. The structure can be regarded as a stack of double layers of tetragonal antiprisms [$SiCe_4Mg_4$]. In contrast to the $CeAl_2Ga_2$ structure, the layers are not mutally displaced. (auth)

29994 TERNARY SYSTEM Nb_2O_5–NbO_2–TiO_2. Abbattista, Fedele. Atti Accad. Sci. Torino. I. Cl. Sci. Fis., Mat. Natur.; 103: 937-49(Nov-Dec 1969). (In Italian).

The coexistence at 1250°C of phases which appear in the ternary system Nb_2O_5–NbO_2–TiO_2 was investigated. Five complete series of solid solutions were observed between phases which occur in the binary systems Nb_2O_5–TiO_2 and Nb_2O_5–NbO_2. These correspond to the ratios O/Nb + Ti; 2.5 to 2.492, 2.483, 2.478 to 2.467, 2.417, 2.0. Other phases of the two binary systems form limited areas of mixed crystals. In the ternary system ten biphase areas and three triphase areas also occur. From the phase diagram it can be deduced that the alloy Nb–Ti containing 4 to 8 wt% Ti can form during oxidation phenomena at high temperature very effective protective oxide layers, which consist uniquely of two solid solutions in equilibrium without the representative line of the oxide layer composition crossing triphase areas. (tr-auth)

29995 OBSERVATIONS ON THE SYSTEMS Nb_2O_5–TiO_2 AND NbO_2–TiO_2. Abbattista, Fedele. Atti Accad. Sci. Torino. I. Cl. Sci. Fis., Mat. Natur.; 103: 983-91(Nov-Dec 1969). (In Italian).

As a preliminary to the study of the ternary system Nb_2O_5–NbO_2–TiO_2, the two systems Nb_2O_5–TiO_2 and NbO_2–TiO_2 were investigated by studying the ratios of the coexistence of phases occurring at 1250°C. In the first system, in addition to the solid solution of the Nb_2O_5 type which extends up to the ratio Ti + Nb/O = 2.492, other phases appear in which the ratio is 2.483, 2.478 to 2.467, 2.417, and 2.333. In the second system there is a single solid solution field with rutile-type structure from TiO_2 up to all compositions to 85 mole% of NbO_2 after which only the typical superstructure lines typical of NbO_2 appear in the spectrograms. The lattice constants of the rutile type pseudocell vary linearly in all the areas of the system without any appreciable discontinuity. (tr-auth)

29996 MIXED URANIUM AND TRANSITION ELEMENT SULFIDES. Noel, Henri; Padiou, Jean; Prigent, Jacques (Rennes Univ., France). Compt. Rend., Ser. C; 272: 206-8(11 Jan 1971). (In French).

An investigation was made of the US_2–Ms system in which M = Fe, Co, or Ni led to the isolation of some new tetravalent uranium compounds (MUS_3, FeU_2S_5 and MU_6S_{17}) from solid state reactions. The isolation of single crystals in each of these phases allowed the corresponding unit cells and space groups to be determined. (auth)

29997 NUCLEATION AND CRYSTAL GROWTH OF SECONDARY ZIRCONIA DURING THE REACTION OF ZIRCONIUM WITH AIR AT LOW PRESSURE AND AT 810°C. Nierlich, Jean; Paidassi, Jean (CEA, Fontenay-aux-Roses, France). Compt. Rend., Ser. C; 272: 341-4(25 Jan 1971). (In French).

Under the experimental conditions used, only monoclinic zirconia was produced at the zirconium surface and not the nitride. Primary zirconia appeared first and then, after a sufficient period of time, the nucleation and growth of secondary zirconia on top of the primary zirconia was observed. The influence of the partial oxygen pressure (3.10^{-3} to 1.10^{-6} torr) and the reaction duration on this last effect is described. The effect of the nitrogen present in the air on this phenomena was demonstrated by comparing these results with those previously obtained using pure oxygen at low pressure. (auth) (France)

29998 TERNARY SYSTEM UO_3–V_2O_5–Na_2O. Dion, Christian; Leroy, Jean-Marie; Tridot, Gabriel (Ecole Nationale Superieure de Chemie, Lille). Compt. Rend., Ser. C; 272: 392-5(25 Jan 1971). (In French).

Sodium uranivanadates were prepared from solid state reactions by interactions between binary NaU_2O_7–V_2O_5 and UO_3–$NaVO_3$ and by direct synthesis from the UO_3–V_2O_5–Na_2O mixtures. Seven new phases were isolated and identified. (auth) (France)

29999 SLIP SYSTEMS IN VC–TiC ALLOY. Hollox, G. E.; Novak, D. L.; Huntington, R. D.; Slattery, P. W. (Martin Marietta Corp., Baltimore). J. Mater. Sci.; 6: 171-82(Feb 1971).

From the results reported it would appear that a secondary slip system {110} ⟨001⟩ is activated in VC-25% TiC alloys when deformed at high temperatures. Its occurrence has important implications with respect to toughness and ductility of the carbides, particularly at low temperatures. If dislocations having α ⟨001⟩ Burgers vectors are introduced by high temperature deformation as, for example, in some forming process, the intrinsically brittle carbides may be further embrittled, since such dislocations have the highest energy configuration in the cubic lattice and can be considered as crack nuclei lying in {100} cleavage planes. (UK)

30000 CONTRIBUTION TO THE STUDY OF ALPHA TITANIUM–OXYGEN AND ALPHA ZIRCONIUM–OXYGEN SOLID SOLUTIONS. Dubertret, Alain (CNRS, Vitry-sur-Seine, France). Metaux (Corros.-Ind.); 46: 1-24(Jan 1971). (In French).

A review of the knowledge already acquired on the Ti–O and Zr–O equilibrium diagrams is followed by a description of the

methods used to prepare the alloys required for this study. It is shown that solid solutions of oxygen in alpha titanium and alpha zirconium are characterized by the existence of titanium-oxygen and zirconium-oxygen superstructures due to an ordered distribution of oxygen atoms in the octahedral interstitial sites of the compact hexagonal structure of the metallic lattice. The structural study of the alloys Ti–O and Zr–O was undertaken at room temperature by optical microscope observation, the phases present being identified by x-rays. (France)

30001 INVESTIGATION OF SOLID STATE RELATIONSHIPS IN THE SYSTEM U–Te–C. Breeze, E. W.; Brett, N. H.; White, J. (Univ. of Sheffield, Eng.). J. Nucl. Mater.; 39: 157-65(May 1971).

Phase equilibria in the ternary system T–Te–C were investigated in argon and vacuum atmospheres at temperatures between 600 and 1400°C. A ternary diagram showing the solid state compatibility relationships at 1200°C is presented and x-ray data for the compounds U_2TeC_2, U_7Te_{12}, UTe_3, and $UTe_{3.38}$ are given. Compatibility relationship in the quaternary system U–Te–C–O are discussed and a phase diagram for the system is shown. X-ray powder diffraction data for UOTe and the previously unreported compound U_2O_2Te are presented. (auth)

30002 CRYSTAL STRUCTURES OF SEVERAL INTERMETALLIC PHASES OF NEPTUNIUM AND PLUTONIUM ALLOYS WITH ANTIMONY, SELENIUM, AND TELLURIUM. Mitchell, A. W.; Lam, D. J. (Argonne National Lab., Ill.). J. Nucl. Mater.; 39: 219-23(May 1971).

The compounds NpSb, Np_3Se_4, Np_3Te_4, PuSb, PuSb, PuSe, and Pu_3Se_4 were prepared by the isothermal annealing method with a final annealing temperature of 500°C. X-ray diffraction data were obtained on powder samples in a Straumanis-type Debye-Scherrer camera with filtered copper radiation. The x-ray measurements were made immediately after the samples were prepared. Lattice parameters, calculated and observed d-spacings, and the calculated and observed line intensities are reported for these compounds. (G.M.C.)

30003 MUTUAL SOLUBILITY AND PREPARATION OF URANIUM–CERIUM CARBO-NITRIDE. Ihara, S.; Tanaka, K.; Suzuki, M.; Akimoto, Y. (Mitsubishi Metal Mining Co., Ltd., Omiya, Japan). J. Nucl. Mater.; 39: 203-8(May 1971).

Studies were carried out on the pseudo-binary systems of UC–CeN and UN–CeN. Complete miscibility was proved to exist for both systems. Based on this result, the following preparation techniques were developed for mixed carbonitride (U,Ce) (C,N): mixing and reaction of three raw materials, UC, CeN, and UN simultaneously; same procedure but starting with two materials, UC and (U,Ce)N. The variation of the lattice parameter for the MC–MN quasi binary system, where M stands for $(U_{0.8}Ce_{0.2})$, shows positive deviation from Vegard's law whereas that for UC–CeN and UN–CeN deviates to the negative side. (auth)

30004 CRYSTAL STRUCTURE OF CsU_6F_{25}. Brunton, George (Oak Ridge National Lab., Tenn.). Acta Crystallogr., Sect. B; 27: 245(1971).

The complex fluoride CsU_6F_{25} crystallizes with space group $P6_3/mmc$; $a_0 = 8.2424$ (4), $c_0 = 16.412$ (2) Å, Z = 2 and the calculated density = 7.0013 g cm^{-3}. The U^{4+} ion is coordinated by $9F^-$ ions at distances of 2.267 (8) to 2.54 (6) Å and the Cs^+ ion by $12F^-$ at distances of 3.12 (2) and 3.45 (4) Å. The final R value is 0.0685 for 212 reflections >3σ. The reflections were collected with an automated Picker four-circle goniostat. (auth)

30005 HIGH-TEMPERATURE PHASE DIAGRAMS FOR THE SYSTEMS Sc_2O_3–La_2O_3 AND Sc_2O_3–Nd_2O_3. Badie, J-M. (CNRS, Odeillo, France). High Temp. - High Pressures; 2: 309-16(1970). (In French).

Phase diagrams were determined with the aid of the high-temperature x ray diffraction method, for the systems Sc_2O_3–La_2O_3 and Sc_2O_3–Nd_2O_3 up to the vicinity of the fusion temperature. (auth) (UK)

30006 SOLID SOLUTIONS IN THE SYSTEM HAFNIUM DIOXIDE–SILICA. Parfenenkov, V. N.; Grebenshchikov, R. G.; Shevyakov, A. M. (Inst. of Silicate Chemistry, Moscow). Inorg. Mater. (USSR) (Engl. Transl.); 6: 1826-8(Nov 1970).

Translated from Izv. Akad. Nauk SSSR, Neorg. Mater.; 6: 2078-9(Nov 1970).

An investigation of HfO_2-rich portions of the HfO_2–SiO_2 phase system in search of solid solutions is reported. It was found that samples containing 1, 2.5, or 5 mole % SiO_2 were uniform; those with 7.5 or 10 mole % SiO_2 were two-phase. (J.R.D.)

30007 MIXED OXIDES OF Tb–Ce, Tb–Th, AND Tb–Gd. Cola, Mario; Papa, Marcella; Negri, Giulio (Univ., Pavia, Italy). Gazz. Chim. Ital.; 100: 1089-1105(Dec 1970). (In Italian).

Mixed oxides of terbium and cerium, terbium and thorium, and terbium and gadolinium, heated at a constant temperature of 800 and 1200°C in open air and rapidly cooled, were studied by the x-ray powder method. Under these experimental conditions, the mixed oxides of terbium and cerium always gave rise to a monophasic system; at 800°C the system undergoes a transformation from the fluoritic phase of high ceria content to the rombohedral phase (Tb_7O_{12} type) of high terbia content; similarly at 1200°C the fluorite phase transforms to a cubic phase (C-type sesquioxide) of final composition $TbO_{1.65}$. The mixed oxides of terbium and thorium at 1200°C give rise to the fluoritic phase rich in ThO_2 and to the cubic C phase of low thoria content; the monophasic concentration ranges are separated by a wide biphasic region, where both phases are coexisting. The mixed oxides of terbium and gadolinium at 800°C give rise to a monophasic system at all Tb/Gd concentration ratios: the cubic C phase occurs also in mixed oxides of high terbia content, while the rhombohedral phase (Tb_7O_{12} type) can contain only a limited amount of gadolinium. (auth)

30008 PHASE EQUILIBRIUM STUDIES IN ZrO_2-CONTAINING SYSTEMS UNDER CONTROLLED ATMOSPHERIC CONDITIONS. Shultz, Richard Lewis. University Park, Pa.; Pennsylvania State Univ. (1970). 116p. University Microfilms Order No. 71-6359.

Thesis.

Phase equilibrium studies have been carried out in the systems MnO–ZrO_2, FeO–ZrO_2, Mn_3O_4–ZrO_2–SiO_2, MnO–FeO–ZrO_2, CaO–ZrO_2–SiO_2, MgO–ZrO_2–SiO_2, MnO–ZrO_2–SiO_2, and MnO–FeO–ZrO_2–SiO_2 under carefully controlled atmospheric conditions. Primary emphasis was placed on delineating phase relationships in the systems which make up the four-component system MnO–FeO–ZrO_2–SiO_2. The well-known quenching technique was used in most cases. The main features established are described. (Diss. Abstr. Int., B)

Radiation Effects

Refer also to abstracts 29901, 29924, and 31568.

30009 (BMI-1899) EFFECT OF IRRADIATION ON THE CREEP OF URANIUM DIOXIDE. Perrin, James S.; Wilson, William R. D. (Battelle Memorial Inst., Columbus, Ohio). Mar 1971. Contract W-7405-eng-92. 33p. Dep. NTIS.

For Argonne National Lab., Ill.

The in-pile and out-of-pile creep rates of 24.48% enriched UO_2 were measured in the temperature range from 1000 to 1200°C in the stress range from 1500 to 4000 psi at fission rates of 4×10^{12} and 1.2×10^{13} fissions/(cm^3)(sec). The in-pile creep rates are increased with respect to the out-of-pile creep rates, with the amount of enhancement increasing with increasing fission rate. At 1.2×10^{13} fissions/(cm^3)(sec), the in-pile creep rates are greater than the out-of-pile creep rates by approximately a factor of four. Both the out-of-pile and in-pile creep rates are proportional to stress to the first power. The in-pile creep rate is strongly dependent on temperature, and has an activation energy close to that of the out-of-pile creep rate. The present results are compared with results obtained in several other recent investigations. (auth)

30010 (ORNL-4630, pp 179-85) DEVELOPMENT OF URANIUM MONONITRIDE FUELS. Patriarca, P.; Scott, J. L. (Oak Ridge National Lab., Tenn.).

In Fuels and materials development program quarterly progress report for period ending September 30, 1970.

Examination of a fuel pin consisting of UN clad with U–25% Re and irradiated to a burnup of 1.25% heavy-metal atoms at 1300 to 1350°C revealed excellent performance. (auth)

30011 (ORNL-4630, pp 226-9) FAST-NEUTRON IRRADIATION EFFECTS ON ELECTRICAL INSULATORS. Watson, G. M.; Keilholtz, G. W. (Oak Ridge National Lab., Tenn.).

In Fuels and materials development program quarterly progress report for period ending September 30, 1970.

Advanced materials (sapphire Al_2O_3, single-crystal MgO, transparent polycrystalline Y_2O_3, and Si_2ON_2) were irradiated in row 8 of the Experimental Breeder Reactor-II at 400 and 800°C to evaluate their potential usefulness in thermionic converters. Polycrystalline specimens of alumina are now being irradiated in row 7 for comparison with a previous irradiation experiment in row 4, at a higher flux. An irradiation of metal-clad Al_2O_3 specimens in row 8 was completed. Its purpose was to provide results for comparison with those from similar irradiations at comparable fluences in the Engineering Test Reactor, which has a much different neutron energy spectrum. (auth)

30012 ALPHA PARTICLE IRRADIATION DAMAGE IN ThO_2. Douglass, Dana L.; Bronisz, S. E. (Los Alamos Scientific Lab., N. Mex.). J. Amer. Ceram. Soc.; 54: 158-61(Mar 1971).

XUM

The effect of α-particle irradiation (5.5 MeV, total dose ≈10^{15} particles/cm^2) on the microstructure of ThO_2 was studied by transmission electron microscopy. The only as-irradiated damage seen consisted of point defect agglomerations visible as small black spots. Subsequent heating to ≈1500°C in the electron microscope caused the spots to grow into loops 50 to 200 Å in diameter, but no voids, bubbles, or pores were observed. The preferred loop planes were {311}, {110}, and {012}, in that order of frequency. (auth)

30013 RADIATION HARDENING OF ALKALI HALIDES AND MAGNESIUM OXIDE. Reppich, B. (Univ., Erlangen, Ger.). Scr. Met.; 5: 289-93(Apr 1971).

Published results of irradiation experiments on alkali halides and magnesium oxide concerning the defect concentration dependence were reevaluated in order to decide which radiation hardening model describes the real situation better, especially for low defect concentrations. (auth)

30014 STRAIN EFFECTS AND SPALLING IN ALPHA-BOMBARDED ThO_2. Clinard, F. W. Jr.; Douglass, Dana L.; Land, C. C. (Los Alamos Scientific Lab., N. Mex.). J. Amer. Ceram. Soc.; 54: 177-9(Apr 1971).

Samples of bulk polycrystalline ThO_2 were bombarded with 5-MeV α-particles to doses between 9.4×10^{16} and 6.0×10^{17} ions/cm^2. The sample which received the highest dose spalled during bombardment; those receiving lower doses either did not spall or did so only after postirradiation annealing. The spalling was investigated by x-ray analysis and replica and transmission electron microscopy. It is concluded that spalling resulted from severe lattice strains at the interface between damaged and undamaged material and that sintering pores played a part in the fracture process. The role of lattice defects in initiating fracture is discussed. (auth)

30015 IRRADIATION BEHAVIOR OF ISOTROPIC CARBONS. Bokros, J. C.; Stevens, D. W. (Gulf General Atomic Inc., San Diego, Calif.). Carbon; 9: 19-37(Jan 1971).

Comparative dimensional data from irradiation experiments that included both high temperature isotropic (HTI) and low temperature isotropic (LTI) carbons show that at high fluences the volume expansion and accelerations in the dimensional change rates are considerably more pronounced for HTI carbons than for LTI carbons. Alloying LTI carbons with up to 15 wt-% silicon enhances the dimensional stability slightly at ~600°C but has no effect on the behavior in irradiations at higher temperatures. For HTI carbons the effects of the alloying additions are more pronounced. In neither case, however, are the improvements thought to be of practical importance. Data from both multiple irradiations at different temperatures and irradiations in which the temperatures were programmed down during the course of the irradiation show that prior irradiation at high temperature markedly enhances the dimensional changes that occur in subsequent irradiations at lower temperature. The implications of these findings to reactor design are discussed. (auth) (UK)

30016 ESTIMATION OF THE RADIATION RESISTANCE OF BERYLLIUM OXIDE AT VARIOUS TEMPERATURES. Klimenkov, V. I.; Khudyakov, A. V. At. Energ. (USSR); 29: 294-5(Oct 1970). (In Russian).

Irradiation of BeO blocks at temperatures below 100°C results in their breakdown to powder; at elevated temperatures the helium, formed by the (n,α) and (n,2n) reactions which yield ^9Be, forms blisters in the material. In view of this behavior experiments were carried out to determine the range at which BeO has a satisfactory radiation resistance. The low-temperature breakdown of the pressed BeO materials is due to the anisotropy of the coefficient of the thermal expansion. Calculations indicated that at 800°C solid BeO may be able to withstand exposure to a fast neutron flux of more than 10^{22} n/cm^2. The experiments were designed to determine the dependence of pore formation on the temperature and soaking time when heated under laboratory conditions the specimens irradiated at a low temperature, which results in a uniform distribution of helium within the lattice. A temperature-time diagram was plotted on the basis of the results, indicating the temperature range and periods of annealing, at which BeO is stable. It was found that in the 900 to 1000°C range there are few effects which appear at either low or high-temperature irradiation. It is suggested to verify these results by means of direct in-reactor experiments. (TTT)

30017 EFFECTS OF NEUTRON IRRADIATION ON THE PHASE TRANSFORMATIONS OF Li_2O–MgO–Al_2O_3–SiO_2 SYSTEMS. Sirazhiddinov, N. A.; Chubarov, L. B.; Rakhmanbekov, N. Uzb. Khim. Zh.; No. 6, 11-14(1970). (In Russian).

The influence of mixed γ-neutron radiation on the phase transformations crystallized binary cross section glasses of spodumene-spinel and petalite-spinel quaternary system was studied. Water-cooled glass was irradiated with a neutron flux 2×10^{13} n/cm^2sec at specimen temperature not exceeding 40°C. The integral neutron flux was equal to 6.5×10^{18} n/cm^2. X-ray and microscopic studies were made of the crystallization of irradiated and nonirradiated glass at 800 to 1100°C. (R.V.J.)

30018 IRRADIATION-INDUCED CREEP OF URANIUM DIOXIDE. Perrin, J. S. (Battelle Memorial Inst., Columbus, Ohio). Contract W-7405-eng-92. J. Nucl. Mater.; 39: 175-82(May 1971).

The in-pile and out-of-pile creep rates of 24.48% enriched UO_2 were measured in the temperature range 1030 to 1190°C, in the stress range 1700 to 4000 psi, and at fission rates of 4×10^{12} and 1.2×10^{13} fissions/cm^3·sec. The in-pile creep rates are increased with respect to the out-of-pile creep rates, with the amount of enhancement increasing with increasing fission rate. At 1.2×10^{13} fissions/cm^3·sec, the in-pile creep rates are approximately a factor of four greater than the out-of-pile creep rates. Both the out-of-pile and in-pile creep rates are proportional to stress to the first power. The in-pile creep rate is strongly dependent on temperature, and has an activation energy close to the out-of-pile creep rate. The present results are compared to results obtained in several other recent investigations. (auth)

Plastics and Other Materials

Refer also to abstracts 29096, 29109, 29110, 29114, 29116, 29296, 29298–29314, and 31546.

30019 (EUR-4531, pp 27-58) SUMMARY OF A PROGRAM OF RESEARCH AND DEVELOPMENT FOR PRESTRESSED CONCRETE NUCLEAR PRESSURE VESSELS. Whitman, G. D. (Oak Ridge National Lab., Tenn.).

From Second conference on prestressed concrete reactor pressure vessels and their thermal isolation; Brussels, Belgium (18 Nov 1969).

In Second information meeting on prestressed concrete reactor pressure vessels and their thermal isolation.

A review of a prestressed concrete pressure vessel research and development program is presented in which the more significant results are identified. Results of investigations on concrete properties are discussed along with results of moisture distribution experiments, concrete creep tests, temperature tests, and the use of models. (J.R.D.)

30020 (EUR-4531, pp 171-8) I. IRRADIATION OF MORTAR SPECIMENS. Houben, J. A. (Reactor Centrum Nederland, Petten). (In Dutch).

From Second conference on prestressed concrete reactor pressure vessels and their thermal isolation; Brussels, Belgium (18 Nov 1969).

In Second information meeting on prestressed concrete reactor pressure vessels and their thermal isolation.

The apparatus and techniques for the irradiation of mortar specimens in the High Flux Reactor were described. The fast and thermal neutron fluxes on the mortar samples were determined. (J.S.R.)

30021 (EUR-4531, pp 179-83) II. INFLUENCE OF IRRADIATION AND HEATING ON THE STRENGTH OF MORTAR AND CONCRETE. van der Schaaf, C. F. (Bredero N.V., Utrecht (Netherlands)). (In Dutch).

From Second conference on prestressed concrete reactor pressure vessels and their thermal isolation; Brussels, Belgium (18 Nov 1969).

In Second information meeting on prestressed concrete reactor pressure vessels and their thermal isolation.

The effects of radiation on the dynamic modulus of elasticity, the static modulus of elasticity, and the rupture strength of four mortars and four concretes were tested, taking into consideration the effect of heating on these properties. The effects of radiation and thermal treatment on the mortars are tabulated and discussed. (J.S.R.)

30022 (EUR-4531, pp 237-65) EFFECTS OF REACTOR RADIATION ON CONCRETE. Kelly, B. T.; Brocklehurst, J. E.; Mottershead, D.; McNearney, S. (United Kingdom Atomic Energy Authority, Culcheth (England). Reactor Group); Davidson, I. (United Kingdom Atomic Energy Authority, Risley (England). Reactor Group).

From Second conference on prestressed concrete reactor pressure vessels and their thermal isolation; Brussels, Belgium (18 Nov 1969).

In Second information meeting on prestressed concrete reactor pressure vessels and their thermal isolation.

Results of investigations of physical property changes and gas generation in concretes and aggregates exposed to reactor radiation are presented. Results of research on reactor radiation

effects on materials for prestressed concrete pressure vessels are also included. (J.R.D.)

30023 (EUR-4531, pp 267-324) STUDY OF THE PROPERTIES OF CONCRETE AND ESPECIALLY OF CREEP UNDER THE EFFECT OF TEMPERATURE. Ausangee, R.; Boisserie, J. M.; Corbel, J.; Licheron, S.; Lida, M. (Electricite de France, Ecuelles). (In French).

From Second conference on prestressed concrete reactor pressure vessels and their thermal isolation; Brussels, Belgium (18 Nov 1969).

In Second information meeting on prestressed concrete reactor pressure vessels and their thermal isolation.

The creep of one concrete composition with temperature was investigated in preliminary studies using samples of small dimensions. Without stress the samples undergo deformations of contraction or dilation according to the hygrometric degree and the storage temperature. Under the action of a stress, an instantaneous deformation (elastic and plastic) is produced; if the stress is maintained, creep occurs. The effects of water content variations, mechanical characteristics, and the storage conditions on the creep were determined. The effects of temperature were also determined. On the basis of these preliminary test results, the mechanical, rheological, and thermal properties of the concrete in the form of rings under the effect of temperature were studied in greater detail. The tests were carried out concurrently with theoretical calculations. As a result both the experimental studies and the theoretical models were modified to obtain a better fix. The thermal and elastic parameters of the concrete under rapid mechanical or thermal transients could be determined by comparison with the readings of thermometers and extensometers. In the case of a long-term stress, the use of a linear visco-elastic model appears satisfactory. (J.S.R.)

30024 (EUR-4531, pp 373-84) CREEP BEHAVIOR OF PRESTRESSED CONCRETE SLABS WITH REINFORCED HOLES. Irving, J.; Goodall, I. W. (Central Electricity Generating Board, Berkeley (England). Berkeley Nuclear Labs.).

From Second conference on prestressed concrete reactor pressure vessels and their thermal isolation; Brussels, Belgium (18 Nov 1969).

In Second information meeting on prestressed concrete reactor pressure vessels and their thermal isolation.

Results of research are presented which show that considerable changes in stress occur in a heated, reinforced concrete structure. There is a tendency for tensile stresses to be produced in the concrete on cooling and unloading. The structures analyzed are similar to penetrated regions of concrete pressure vessels. A mechanism is described whereby tensile cracking could be caused by cooling during the reactor shut-down cycle. (auth)

30025 (EUR-4531, pp 385-407) FRACTURE BEHAVIOR OF CONCRETE IN A MULTIAXIAL STRESS FIELD. Bremer, F. (Fried-Krupp Universalbau, Essen (West Germany)). (In German).

From Second conference on prestressed concrete reactor pressure vessels and their thermal isolation; Brussels, Belgium (18 Nov 1969).

In Second information meeting on prestressed concrete reactor pressure vessels and their thermal isolation.

The results of a series of studies on the fracture behavior of concrete in two-axial and three-axial stress fields are reported. The results are shown graphically. These results show that in contrast to the view of the classical strength of materials, the average principal stress is the decisive effect on the strength of concrete. In conventional engineering practice, it is usual to calculate with admissible stresses which represent permanent values for given stress states. On the basis of safety and economy, this method is not valid in pressure vessels. The factors that must be considered in safety design are indicated, and methods of calculating the safety of pressure vessels are described. (J.S.R.)

30026 (EUR-4531, pp 409-16) MOISTURE MEASUREMENTS IN MASS CONCRETE. Hornby, I. W. (Central Electricity Generating Board, Leatherhead (England). Research Labs.).

From Second conference on prestressed concrete reactor pressure vessels and their thermal isolation; Brussels, Belgium (18 Nov 1969).

In Second information meeting on prestressed concrete reactor pressure vessels and their thermal isolation.

The design and performance of a moisture gage for large concrete sections is described. Gage operation is based on the electric conductivity of the concrete between two electrodes. Construction of the gage is also described. When the gage is placed in a mass of concrete its moisture content reaches equilibrium with the surrounding concrete. The gage and the mass concrete have the same moisture potential but not necessarily the same moisture content. The temperature and age characteristics of the gages are standardized by comparison with those of sealed gages. (J.R.D.)

30027 (EUR-4531, pp 417-24) STUDY OF BEHAVIOR OF CONCRETE SUBJECTED TO TRIAXIAL STRESSES. Costes, D. (Commissariat a l'Energie Atomique, Saclay (France). Centre d'Etudes Nucleaires). (In French).

From Second conference on prestressed concrete reactor pressure vessels and their thermal isolation; Brussels, Belgium (18 Nov 1969).

In Second information meeting on prestressed concrete reactor pressure vessels and their thermal isolation.

The properties of deformation and of fracture of a concrete in a state of triaxial stress, with the smallest compression being 500 bars and the largest 2000 bars, were studied. Micro-concrete models with 400 kg of cement per m^3 with aggregates of a maximum length of 8 mm were used in the tests, both in the dry state and in the water-saturated state. Typical curves are shown and briefly discussed. (J.S.R.)

30028 (EUR-4531, pp 445-76) TEST OF RING OF PRESTRESSED [CONCRETE] IN HIGH-RESISTANCE SHEET-METAL STEEL. Puyo, A.; Picaut, J. (Bureau d'Etudes A. Coyne et J. Bellier, Paris (France)); Saglio, R.; Rouge, F.; Thome, P.; Bonnin (Commissariat a l'Energie Atomique, Saclay (France). Centre d'Etudes Nucleaires); Dupay, F. (Commissariat a l'Energie Atomique, Chusclan (France). Centre de Production de Plutonium de Marcoule). (In French).

From Second conference on prestressed concrete reactor pressure vessels and their thermal isolation; Brussels, Belgium (18 Nov 1969).

In Second information meeting on prestressed concrete reactor pressure vessels and their thermal isolation.

The use of high-resistant steel hoops for the prestressing of concrete pressure vessels was investigated. Tests were made to become familiar with the problems involved with the placement of the hoops. It was found that the anchoring device based on friction of the last turn is satisfactory. The uniformity of the mounting of the jacks and the equilibrium of the rings during the imposition of the stress were verified along with the behavior of the ring when the steel passes the nominal stress of prestress. The experimental device is described, and the results are given and discussed in detail. The results show that the measurements of the strain gages on the external hoop gives an evaluation of the friction. Effort-deformation curves were deduced from measurements of the strain gages. The validity of the principle was proven by the tests. (J.S.R.)

30029 (EUR-4531, pp 841-81) THERMAL PERFORMANCE OF POROUS INSULANTS IN A HIGH-PRESSURE GAS ENVIRONMENT. Furber, B. N.; Davidson, J. (Nuclear Power Group Ltd., Knutsford (England)).

From Second conference on prestressed concrete reactor pressure vessels and their thermal isolation; Brussels, Belgium (18 Nov 1969).

In Second information meeting on prestressed concrete reactor pressure vessels and their thermal isolation.

Research directed toward establishing the thermal performance of isotropic or near isotropic insulation materials in high-pressure gas systems is described. Factors studied include permeability and heat transfer behavior. An analysis of natural convection data is included along with an analysis of factors affecting insulation performance in reactor environments. (J.R.D.)

30030 (EUR-4531, pp 931-52) PERFORMANCE OF THERMAL INSULATION IMMERSED IN HELIUM. Kinkead, A. N.; Pitchford, B. E. (Atomic Energy Establishment, Winfrith (England)).

From Second conference on prestressed concrete reactor pressure vessels and their thermal isolation; Brussels, Belgium (18 Nov 1969).

In Second information meeting on prestressed concrete reactor pressure vessels and their thermal isolation.

Efforts devoted to testing and evaluating thermal insulation for use on the interior walls of concrete pressure vessels for He cooled reactors are described. A description of the test apparatus is included along with analyses of multi-layer insulation performance in He. (J.R.D.)

30031 (EUR-4531, pp 975-1018) NEW TYPES OF THERMAL-SHIELDING CONCRETES FOR NUCLEAR REACTORS. Dubois, F.; Mauny, P.; Bernard, A.; Elleuch, M. F. (Commissariat a l'Energie Atomique, Saclay (France). Centre d'Etudes Nucleaires). (In French).

From Second conference on prestressed concrete reactor pressure vessels and their thermal isolation; Brussels, Belgium (18 Nov 1969).

XUM

In Second information meeting on prestressed concrete reactor pressure vessels and their thermal isolation.

The characteristics and performance of two thermal-shielding concretes to be used under CO_2 pressure in power reactors were tested and compared with each other. The first concrete with a fused aluminous cement base can be used up to 350°C. It has a low cost and its resistance to rupture by compression is above 100 bars. The thermal conductivity coefficient is less than 0.35 W/m/°C. It can be used in power reactors of the classical graphite–gas type. The second concrete, usable up to 450°C because of the properties of the Super Secar cement, has excellent mechanical characteristics and maintains good performance under neutron flux. It is less satisfactory than the preceding concrete as a thermal insulator however. In spite of its high cost, it can be used for certain applications in reactors operating at high temperature. (J.S.R.)

30032 (GEAP–12148) FISSION GAS RE-SOLUTION RATES: LIMITATION OF FISSION GAS BUBBLE GROWTH BY THE RE-SOLUTION PROCESS. Marlowe, M. O. (General Electric Co., Pleasanton, Calif. Nucleonics Lab.). Nov 1970. Contract AT(04-3)-189. 22p. Dep. NTIS.

The experimental evidence and theoretical analyses of the process of re-solution of fission gas from bubble nuclei in irradiation environments are reviewed. Gas bubble nucleation kinetics are reviewed and it is shown that the model for gas-generation rate-controlled nucleation process is consistent with experimental evidence and the range of uncertainty in the reinjection probability per unit time. The growth of static fission gas bubbles from the nucleation stage in the presence of the re-solution process is considered. It is shown that the parameter (DF/b^2) where D is the gas diffusivity in the fuel, F is the fission rate, and b is the reinjection probability per unit time, must exceed approximately 10^9 cm^{-1} if bubble growth is to occur. That requirement makes intragranular bubble growth at temperatures below the columnar grain growth region and gas release temperature unlikely. It is shown that the present uncertainties in the reinjection probability give uncertainties in the temperature at which bubble growth can occur of the order of 600 to 800°C depending on fission rate. (auth)

30033 PACKING MATERIALS FOR γ-IRRADIATED FOODSTUFFS. Holeckova, L.; Cekalova, B.; Lanzer, O. Prum. Potravin; 21: No. 2, 43-8(Feb 1970). (In Czech).

A total of 7 materials with potential commercial applicability in packing foodstuffs were investigated. Samples of packing foils were irradiated at 16 to 20°C by ^{60}Co γ-rays with doses of 0.5, 1, 3, and 5 Mrad, i.e., in the dose range used for pasteurization and sterilization of food products, at a dose rate of 0.5 Mrad/hr. Twelve various methods were used to investigate post-irradiation effects. The results showed that the most suitable material for packing radiosterilized food was Melinex S-0.015. (INIS)

XUM

PHYSICS (GENERAL)

Astrophysics and Cosmology

Refer also to abstract 30452.

Cosmic Ray Exposure Ages

30034 TRAPPED HELIUM, NEON, AND ARGON IN METEORITES: BOUNDARY CONDITIONS ON THE FORMATION AND EVOLUTION OF THE SOLAR SYSTEM. Black, David Charles. Minneapolis; Univ. of Minnesota (1970). 112p. University Microfilms Order No. 70-20,178.

Thesis.

Studies of meteoritic neon indicate that there are five preferred trapped compositions characterized by trapped $^{20}Ne/^{22}Ne$ ratios of ≥ 14, 12.5, 11.2, 8.2 and ≤ 3.4. Trapped helium and argon, represented by the trapped $^{3}He/^{4}He$ and $^{36}Ar/^{38}Ar$ ratios, respectively, correlate with trapped neon. Plots of $^{3}He/^{4}He$ against $^{20}Ne/^{22}Ne$ show that gas-rich meteorites fall within a zone. The trapped helium–neon structure in gas-rich meteorites appears to result from a multicomponent mixture. Carbonaceous chrondrites also display a correlation between trapped $^{3}He/^{4}He$ and $^{20}Ne/^{22}Ne$ ratios, distinct from that defined by the gas-rich group. Correlation plots of trapped $^{36}Ar/^{38}Ar$ and $^{20}Ne/^{22}Ne$ ratios evidence a topology similar to the helium–neon plot. Gas-rich meteorites fall within a zone, while carbonaceous chrondrites define a separate trend. On the basis of these trends, it appears that four of the five trapped neon compositions are independent components. The component characterized by a trapped $^{20}Ne/^{22}Ne$ value of 11.2 is best understood as a mixture of two of the other trapped components. (TSS) (Diss. Abstr. Int., B)

Stars

Refer also to abstract 30266.

30035 (NBS-SPEC. PUBL–332) SPECTRUM FORMATION IN STARS WITH STEADY-STATE EXTENDED ATMOSPHERES. Proceedings of the International Astronomical Union Colloquium No. 2, Commission 36, Munich, Germany, April 16–19, 1969. Groth, H. G.; Wellmann, P. (National Bureau of Standards, Washington, D. C.). Aug 1970. 332p. (CONF-690446). GPO $1.75.

Commission 36 of the International Astronomical Union sponsored a symposium on Spectrum Formation in Extended Stellar Atmospheres held April 16–19, 1969. The host was the Observatory of the University of Munich. A major problem is the definition of what is meant by an extended stellar atmosphere. There are intuitive notions in the literature, but the question of specific definitions in various kinds of objects was discussed. Questions of what specifically cause the anomalous extent were largely by-passed. Attention focused mainly on the type spectrum to be expected in various situations. The spectral features to be expected in both static and dynamic atmospheres, including and excluding departures from LTE, were discussed. The symposium was divided into four sections: A. Type of problems that exist; B. Theoretical methods for handling non-LTE problems; C. chromospheres and coronae of stars; and D. Summary. This volume contains the formal papers that were presented plus an edited and abridged version of the discussions following each paper. (auth)

30036 (NYO–3962-3) [RESEARCH IN NUCLEAR PHYSICS AND NUCLEOSYNTHESIS]. Annual Progress Report. (Yeshiva Univ., New York. Belfer Graduate School of Science). 1 Feb 1971. Contract AT(30-1)-3962. 18p. Dep. NTIS.

Work on a new liquid drop mass formula, the r-process in supernovae, lithium production in stars, the s-process, chemical evolution of the galaxy, and late stellar evolution is briefly summarized. (W.D.M.)

30037 OVERSHOOTING OF CONVECTIVE CORES IN HELIUM-BURNING HORIZONTAL-BRANCH STARS. Castellani, V. (Univ., Rome); Giannone, P.; Renzini, A. Astrophys. Space Sci.; 10: 340-9(Feb 1971).

In helium-burning horizontal-branch stars, transformation of helium into carbon increases opacity in the convective core. Such a situation can drive an increase of the core-mass extension via the mixing by overshooting. The efficiency of this mechanism is investigated in order to obtain an indication of the time scale for the propagation of the convective boundary. Schwarzschild's criterion is shown to be fulfilled within a few percent at the innermost interface of the core boundary. (auth)

30038 MICROTURBULENCE AND ABUNDANCES IN Am STARS: INFERENCES CONCERNING METALLICISM. Smith, Myron A. (Steward Observatory, Tucson, Ariz. Kitt Peak National Observatory, Tucson, Ariz.). Astron. Astrophys.; 11: 325-44(Apr 1971).

High-dispersion spectra were obtained for sixteen Am stars in three galactic clusters and for four normal standards. A detailed LTE atmosphere curve of growth analysis was made in order to obtain microturbulent parameters and abundances for each star. Examination of the ionization equilibrium of iron confirms that the spectroscopic gravities of Am stars are dwarf-like. The conclusions of Baschek and Reimers (1969) are confirmed that microturbulence exhibits a common maximum in the late A region for both normal and Am stars. This peak agrees precisely with the intersection of the instability strip and the main sequence in the H–R diagram. There is also evidence that microturbulence may be a unique function of T_{eff} along the main sequence. The abundance of iron is enhanced in Am stars by a variable of up to five or more. This enhancement is correlated positively with T_{eff} and inversely with V sin i. The run of abundances in Am stars suggests that the observed peculiarities do not arise through nucleosynthetic processes. In addition, the abundances of the elements relative to iron behave similarly to those of their neighbors in the periodic table. The scatter is surprisingly small except among the deficient elements. The abundance scatter in these latter elements may be accounted for by their correlation with T_{eff} and V sin i. A postulated metallicism index is shown to be anti-correlated with apparent rotation. Moreover, the recent K-line photometry of Henry (1969) implies that some anomalies become more moderate as Am stars evolve off the main sequence. It thus appears that metallicism involves stability, and that the mechanism responsible for it is subject to rotational or convective disruption. No evidence for subgrouping in Am properties is found, either by cluster membership or otherwise. However, various anomalies vary with T_{eff} in various ways and this may account for reported differences between "hot" and "classical" (cool) Am stars. It is suggested that metallicism arises from the operation of a subsurface diffusion process operative between the convective zones due to H I, He I, and He II ionization. The location of the Am domain in the H–R diagram and several other boundary conditions appear to be reasonably explained by such a model. (auth)

30039 OVERSTABLE DAMPING IN A STELLAR SEMI-CONVECTIVE ZONE. Aure, Jean-Luc (Institut d'Astrophysique, Paris). Astron. Astrophys.; 11: 345-50(Apr 1971).

It is shown with a two-zone model and by an asymptotic treatment of the linearized perturbation that the overstability due to the region stratified in mean molecular weight is totally damped by the upper radiative zone in a B star departing from the main sequence. (auth)

30040 CALIBRATION OF THE HERTZSPRUNG–RUSSEL DIAGRAM BY MEANS OF TRIGONOMETRIC PARALLAXES. Jung, J. (Observatoire, Paris). Astron. Astrophys.; 11: 351-8(Apr 1971). (In French).

The principle of maximum likelihood is shown to apply to the determination of the distribution of absolute magnitudes, by means of trigonometric parallax data. The importance of selecting all stars brighter than a given apparent magnitude is stressed. The method developed is applied to class III and V stars, together with the classical method of spectroscopic parallaxes. Both methods agree for the nearer stars, but only the method of maximum likelihood provides reliable estimates for the stars of higher luminosity (essentially class III stars). The results for these stars depend on the procedure used to reduce the relative parallaxes to absolute ones. The calibration resulting from the present investigation is in good agreement with a previous calibration, based on proper motions and radial velocities (Astron. Astrophys., 4: 53(1970)) and confirms the large scatter of the absolute magnitudes found for the G and K giants. (auth)

30041 PHOTOMETRIC INVESTIGATION OF THE DOUBLE CLUSTER h AND χ PERSEI. Vogt, N. (Ruhr-Univ., Bochum, Ger.). Astron. Astrophys.; 11: 359-76(Apr 1971). (In German).

Photometric UBV magnitudes for a total of 11459 stars were determined in an area $60' \times 36'$ containing, and in 8 comparison fields symmetrically surrounding, h and χ Persei. The positions of the comparison fields were chosen so that gradients in extinction and star number density could be dealt with optimally. The reduction of the iris readings to magnitudes followed the theoretical method of Moffat (1969). A new method was applied to elim-

XUM

inate the effects of a variable background density (Moffat and Vogt, 1971). Color–magnitude diagrams were obtained for both clusters by statistical subtraction of the star counts in the comparison fields from those in the cluster area. The influence of variable extinction on the star counts was eliminated by deriving the interstellar extinction as a function of distance for 14 regions within the area containing the clusters and for each of the 8 comparison fields. A method of successive iteration was derived to determine the reddening of late type stars for which no unique reddening solution exists. The statistical color–magnitude diagrams of the clusters led to a new determination of the zero age main sequence. (W.D.M.)

30042 He I LINE PROFILES IN NORMAL B-TYPE SPECTRA. Leckrone, David S. (Goddard Space Flight Center, Greenbelt, Md.). Astron. Astrophys.; 11: 387-406(Apr 1971).

An attempt was made to determine to what extent the profiles of a large number of He I lines, as observed over the entire range of B spectral types, can be matched by theoretical profiles computed in LTE. Detailed profile analyses of as many as 11 He I lines, carried out for the stars 134 Tau (B9 IV), π Cet (B7 V), HR 2154 (B5 IV), ι Her (B3 V), γ Peg (B2 V), HR 1861 (B1 V) and υ Ori (B0 V), are summarized. Original, high dispersion profile data are presented for five of these stars. (W.D.M.)

30043 CV SERPENTIS (THE SOMETIMES ECLIPSING WOLF–RAYET SYSTEM). Cowley, Anne P. (Univ. of Michigan, Ann Arbor); Hiltner, W. A.; Berry, Charles. Astron. Astrophys.; 11: 407-13(Apr 1971).

From spectroscopic observations of CV Ser made in 1970 an improved oribtal period of 29.706 days was determined. It is shown that the deep eclipse observed in 1962 occurred when the Wolf–Rayet component was in conjunction with, but behind, the B star. Orbital elements and masses are derived. The apparent circularity of the orbit and similarity to earlier spectroscopic data suggest that a change in the orbit cannot account for the greatly diminished eclipses. (auth)

30044 EJECTION OF MASS BY RADIATION PRESSURE IN PLANETARY NEBULAE. Finzi, A. (Goddard Space Flight Center, New York); Wolf, R. A. Astron. Astrophys.; 11: 418-30(Apr 1971).

If a star near the end of its evolution still has a substantial hydrogen-rich envelope, then the star must burn or eject the envelope before it becomes a white dwarf. It is suggested that the second thing occurs and that planetary nebulae are formed in this way; partial hydrogen burning should provide the energy needed to eject the hydrogen-rich envelope. It is shown that radiation pressure can cause mass ejection from the highly contracted core of a star of about 1 $M_\odot$, if the luminosity is about 2×10^4 $L_\odot$. Time-independent models were constructed to represent the outflowing, low-mass envelope that surrounds the massive core. The models involve rates of mass ejection in the range from 10^{21} g s^{-1} to 10^{23} g s^{-1}. The velocity at infinity of ejected matter is a few tens of kilometers per second, comparable to the observed expansion velocities of planetary nebulae. (auth)

30045 ZEEMAN OBSERVATIONS OF PECULIAR AND METALLIC-LINE A STARS. van den Heuvel, E. P. J. (Astronomical Inst., Utrecht. Virije Univ., Brussels). Astron. Astrophys.; 11: 461-7(Apr 1971).

Zeeman coudé spectra of thirteen peculiar A stars and one metallic-line A star were studied. The discovery of three new magnetic stars (HR 2977, HR 3082, and HR 3724) and of two new "probably magnetic" stars (HR 4330 and HR 6179) is reported. A preliminary magnetic period of 18.4 days is derived for HD 137949 (33 Librae). It is found that HR 4330 shows large spectrum variations and changes in linewidth in the course of one day. No magnetic fields could be detected with certainty in the rather broad-lined peculiar A stars HR 979 B, HR 2534, HR 5731, and HR 8357 B and in the sharp-lined stars HR 6096 and HR 4751 (the metallic-line star 17 Comae B). The negative result for HR 4751 casts further doubt on the presence of magnetic fields in metallic-line stars. (auth)

30046 ROTATIONAL VELOCITIES OF G AND K GIANTS IN THE HYADES MOVING GROUP. Strittmatter, P. A. (Inst. of Theoretical Astronomy, Cambridge, Eng. Univ. of California, San Diego); Norris, John. Astron. Astrophys.; 11: 477-81 (Apr 1971).

Rotational velocities are presented for Hyades moving group of giants in the spectral range G8-K2. The results confirm Kraft's suggestion, based on the Hyades cluster giants, that these stars rotate less rapidly than would be expected if the stars evolved either (A) maintaining uniform with total angular momentum conserved or (B) conserving the angular momentum of each element. Possible explanations in terms of mass loss or vorticity expulsion are briefly discussed and an observational test is proposed to distinguish between them. (auth)

30047 SEARCH FOR OH EMISSION FROM INFRARED OBJECTS AT 1612 MHz. Paschenko, M (Sternberg Astronomical Inst., Moscow); Slysh, V.; Strukov, I.; (and others). Astron. Astrophys.; 11: 482-4(Apr 1971).

Seventy-three bright infrared stars ($K < 0$) were searched for OH emission at 1612 MHz. Only IRC-20431 (VX Sgr) was found to emit at 1612 MHz. Strong circular polarization was observed at 1667 MHz on this source. (auth)

30048 PERIOD OF γ EQU. Steinitz, Raphael; Pyper, Diane M. (Tel-Aviv Univ., Israel). Astron. Astrophys.; 11: 489-90(Apr 1971).

An analysis of the magnetic variations of γ Equ yielded a period of 1785.7 days (4.9 years). (auth)

30049 NEW HELIUM-WEAK STARS IN THE I ORION ASSOCIATION. Ciatti, F.; Bernacca, P. L. (Univ., Padua). Astron. Astrophys.; 11: 485-8(Apr 1971).

By means of spectroscopic observations at a dispersion of 42 Å/mm at H_γ in the Ia subgroup of the Orion association, five B-type stars with weak helium lines for their colors have been found (HD 35298, 35730, 35881, 36549, 36668). If the term "helium-weak" is more properly used for stars whose helium lines are weak but whose hydrogen lines are normal for the color, then HD 35730 and HD 35881 must be regarded simply as stars with a spectrum–color discrepancy. In addition to helium weaknesses, HD 36668 shows a peculiar spectrum of Si II, Fe II and Ti II lines. (auth)

30050 PROTON–PROTON REACTION AND RELATED REACTIONS IN AN INTENSE MAGNETIC FIELD. Chou, Chih Kang (Goddard Space Flight Center, New York). Astrophys. Space Sci.; 10: 291-308(Feb 1971).

The reaction rates for the proton–proton reaction and the related electron-capture reaction in a strongly magnetized relativistic electron gas of arbitrary degree of degeneracy are computed. The proton–proton reaction rates are unaffected by the presence of the magnetic field for field strengths up to the critical value $H_q = m^2c^3/eh = 4.414 \times 10^{13}$ G. For fields greater than H_q, the proton–proton reaction rates are enhanced linearly with Θ ($\Theta = H/H_q$). The p–e–p reaction is investigated in detail for a wide range of temperatures, densities, and magnetic field strengths that are of interest. The main results are as follows: In the nondegenerate regime the reaction rates are significantly reduced for high temperatures ($T_9 \gtrsim 5$) and low fields ($\Theta \lesssim 1$). For instance, $R_{pep}(H) = 0.04\ R_{pep}(O)$ at $\Theta = 10^{-3}$, $T_9 = 10$. For relatively high fields ($\Theta > 1$) and low temperatures ($T_9 \lesssim 2$), the reaction rates are enhanced approximately linearly with Θ. In the complete degenerate regime the reaction rates are reduced up to one-third of the field-free value for moderate densities ($\rho_6/\mu_e \lesssim 10$). At high densities ($\rho_6/\mu_e \gtrsim 10$) the reaction rates are unaffected by the magnetic field. (auth)

30051 FORMATION OF SUPERHEAVY ELEMENTS IN NATURE. Berlovich, E. E. (Ioffe Inst. of Physics and Tech., Leningrad). Izv. Akad. Nauk SSSR, Ser. Fiz.; 34: 2286-92(Nov 1970). (In Russian).

The possibility of generation of superheavy elements as a result of the fast-neutron capture process during supernova explosions is discussed. The causes limiting the expansion of superheavy elements and the narrow range of mass numbers observable are analyzed. (tr-auth)

30052 WHY PULSARS ARE PULSING. Thum, C. Sterne Weltraum; 9: 199-200(Jul-Aug 1970). (In German).

A model of a neutron star with an oblique axis of rotation is discussed that accounts for the observations obtained about pulsars. The model considered was proposed by Eastlund (1970). The general characteristics of the model are described. The axis of the magnetic field rotates about the rotation axis of the star. The model makes it possible to explain qualitatively the observed very complex polarizations of the pulses. (IAA)

30053 POLARIZATION IN REFLECTION NEBULAE. Zellner III, Benjamin Holmes. Tucson, Ariz.; Univ. of Arizona (1970). 201p. University Microfilms Order No. 70-22,018. Thesis.

Photoelectric measurements of color and polarization in seven reflection nebulae were made between November 1967 and December 1969. Detailed observations were made in NGC 2068, IC 5076, and NGC 7023 with the 154-cm Catalina reflector and the 229-cm Steward reflector. The observations were restricted to one or two regions in each nebula in order to attain higher pre-

cision and wider wavelength coverage than would have been possible in a broader survey. Six filters were used, ranging from 0.33μ to 0.83μ; and probable errors were on the order of ±0.3% in polarization and ±0.03m in color. Smaller amounts of data were obtained in the nebulae Cederblad 201, NGC 2245, IC 4601b, and IC 4603. (TSS) (Diss. Abstr. Int., B)

30054 DENSITY OF THE DUST IN REFLECTION NEBULAE. **Schmidt, Karl-Heinz (Univ., Jena, Ger.). Astron. Nachr.; 292: No. 2, 87-91(1970). (In German).**

The density of the dust in reflection nebulae was investigated taking into consideration searches for reflection nebulae in the Palomar Observatory Sky Survey conducted by Dorschner and Gürtler (1963, 1966) and Van Den Bergh (1966). The Hubble relation of reflection nebulae is discussed. It is found that for such objects with the illuminating star outside of the nebula a lower limit of the dust density is necessary in order to image the nebula on the Palomar Observatory Sky Survey. This limit depends on the absolute magnitude of the illuminating star. (IAA)

30055 ASTRONOMICAL PROPERTIES OF M SUPERGIANTS. **Wawrukiewicz, Anthony S. Rochester, N. Y.; Univ. of Rochester (1970). 115p. University Microfilms Order No. 71-1433. Thesis.**

M supergiants were studied in detail in an effort to determine their usefulness in discussing galactic structure. Distances, which are necessary for any discussion of galactic structure, were calculated in the past using B, V wide-band photometry along with necessary attendant quantities such as the color excess in (B−V). Although these were not ignored in obtaining M-supergiant distances for this thesis, emphasis was placed upon using V,R photometry for them because of their intrinsic redness. All quantities used with the B,V and V,R photometries to obtain distances were rediscussed in the light of new data now available. Because (V−R) is a function of spectral type, it was also necessary to determine spectral types for M supergiants as a function of a narrow-band TiO index at 7100 Å. The wide-band photometry and rederived quantities were then applied to a large number of M supergiants, including many stars of the Warner and Swasey surveys, to obtain distances. The resultant pattern in the galaxy evidenced by these stars strongly suggests that M supergiants are useful as age indicators. For instance, those in the Cygnus and/or Sagittarius arms probably have dispersed into the inter-arm regions due to their being relatively old. Finally, the bright red content of nearby galaxies is discussed. It is concluded that M supergiants almost certainly exist in other galaxies. Thus, accurate distances to these galaxies can be determined which are independent of the Cepheid stars. (Diss. Abstr. Int., B)

30056 VARIABILITY OF THE BRIGHTNESS OF THE BINARY SYSTEM AX MONOCEROTIS. **Magalashvili, N. L.; Kumsishvili, Ia. I. Byull., Abastumanskaya Astrofiz. Observ., Akad. Nauk Gruz. SSR; No. 37, 3-8(1969). (In Russian).**

The results of photoelectric observations of the spectroscopic near-surface region at a temperature of 650°K are described. (IAA)

30057 SUPERNOVA IN NGC 3389. **Chuadze, A. D.; Barblishvili, T. I. Byull., Abastumanskaya Astrofiz. Observ., Akad. Nauk Gruz. SSR; No. 37, 9-12(1969). (In Russian).**

A description is given of observational data for the supernova discovered in the spiral arm of the NGC 3389 galaxy on February 28, 1969. The absolute photovisual magnitude of the supernova at the time of discovery was −18.3, and measurements obtained since that time in the UBV system are tabulated along with the magnitudes of comparison stars. On the basis of the light curve, the supernova is classified as Type I. (IAA)

30058 THREE-COLOR PHOTOGRAPHIC PHOTOMETRY OF ELEVEN RW-AURIGA-TYPE STARS. **Mosidze, L. N. Byull., Abastumanskaya Astrofiz. Observ., Akad. Nauk Gruz. SSR; No. 37, 13-34(1969). (In Russian).**

Results are presented of three-color photometry of eleven RW Auriga-type stars, based on numerous observations carried out during the period from 1960 to 1964. The stars studied include RW Aur, RY Tau, BP Tau, V451 Ori, HK Ori, CO Ori, GW Ori, MH alpha 265-3, SV Cep, BH Cep, and BO Cep. UBV light curves are plotted for these stars, and the H−R diagram for six stars shows that they fall within the known T band. An ultraviolet emission excess is reliably established in the radiation of K spectral class variables. According to the color indices, G spectral class variables in general show a fainter short-wave excess, while in stars of earlier spectral classes this effect is not observed. The results are valuable from the viewpoint of information about physical processes occurring in the atmospheres of RW Aur-type stars and the interstellar absorption in their direction. (IAA)

30059 TWO-DIMENSIONAL QUANTITATIVE SPECTRAL CLASSIFICATION OF F0–G5 STARS ON THE BASIS OF SPECTRA OBTAINED WITH A PRISM IN FRONT OF THE OBJECTIVE. **Shiukashvili, M. A. Byull., Abastumanskaya Astrofiz. Observ., Akad. Nauk Gruz. SSR; No. 37, 43-67(1969). (In Russian).**

Results of studies carried out at the Abastuman observatory on the spectral classification of stars, and a method used for quantitative two-dimensional classification of stars in the F0−G5 spectral class region are described. The observational material was obtained using a 70-cm meniscus telescope with an 8° preobjective prism (dispersion of 166 A/mm near H-gamma). The ratios of central intensities or the depths of specially chosen spectral lines were used as the quantitative characteristics. Reduction curves are based on 81 standard stars. Quantitative spectral classes and absolute magnitudes are listed for 210 stars of the F0−G5 classes. The data confirm the presence of a Hertzsprung gap for relatively faint stars in the F6−G5 interval. (IAA)

30060 CLASSIFICATION OF STARS IN THE NEAR ULTRAVIOLET ON THE BASIS OF MODERATE- AND LOW-DISPERSION SPECTRA. **Dolidze, M. V.; Dzhimsheleishvili, G. N. Byull., Abastumanskaya Astrofiz. Observ., Akad. Nauk Gruz. SSR; No. 37, 68-88(1969). (In Russian).**

Special criteria and the results of spectral classification of relatively bright stars (limiting magnitude of 12) in the near ultraviolet region from 3480 to 3900 A are presented. Results are given for data obtained with 8 and 4° prisms having dispersions of 92 and 400 A/mm, respectively. Tables list the positions and spectral types of the stars, and some preliminary results are included for late F and G and early K type stars with an ultraviolet excess. (IAA)

30061 CERTAIN PROBLEMS OF SPECTRAL CLASSIFICATION AND SPECTROPHOTOMETRY OF LATE SPECTRAL TYPE STARS. **Dzhimsheleishvili, G. N. Byull., Abastumanskaya Astrofiz. Observ., Akad. Nauk Gruz. SSR; No. 37, 89-116(1969). (In Russian).**

A study involving the spectral classification and photometry of the continuous spectrum of weak late-type stars is described. Attention is given to the spectral features in the visual and near-ultraviolet regions of C stars and late stars of equivalent spectral types. Forty new and twenty-four standard stars were classified and reclassified, respectively. It is shown that the ultraviolet anomaly of C stars may be used as a second criterion for the abundance parameter. A blue excess is revealed in CH Cyg. (IAA)

30062 INVESTIGATION OF THE PROBLEM OF THE CONDENSATIONS OF SPECTRA TYPE-A STARS USING THE TRIAL AND ERROR METHOD (MONTE CARLO METHOD). **Kevanishvili, G. T. (Tbilisi State Univ., USSR). Byull., Abastumanskaya Astrofiz. Observ., Akad. Nauk Gruz. SSR; No. 37, 117-40(1969). (In Russian).**

The spatial distribution of about 55,000 type-A stars in the HD catalog was investigated. In several cases, these stars seem to form real condensations, and this conclusion is supported by the application of the Monte Carlo method and Poisson's formula. The condensations are distributed mostly near the Galactic plane. Their angular dimensions vary from 2 to 6° mean dimensions and densities are on the order of those for O and T associations. The condensations mainly contain AO−A2 stars. Condensations fixed in Cyg and Lac are shown to be expanding. (IAA)

30063 BD 61°2565: A STAR WITH PARTICULARLY INTENSE Sr, Eu, AND Cr LINES. **Martin, Nicole; Rebeirot, Edith (CNRS, Marseille). Compt. Rend., Ser. B; 272: 258-60(18 Jan 1971). (In French).**

Photographs of the spectrum of an unusual type of star were studied. Remarks are made on the abnormal intensities of Sr II, Eu II, Cr II, and various rare-earth lines. (France)

30064 OPTICAL STUDES OF CASSIOPEIA A. III. SPECTRA OF THE SUPERNOVA REMNANT. **van den Bergh, Sidney (Univ. of Toronto, Richmond Hill, Ont.). Astrophys. J.; 165: 457-69(1 May 1971).**

The optical remnant of Cas A consists of two components: (1) a system of about 100 fast-moving knots and (2) approximately thirty quasi-stationary flocculi. New spectroscopic observations of both types of objects are reported. These observations are supplemented by earlier data that were generously made available by Minkowski. Intercomparison of radial velocities and proper motions of moving knots yields a very uncertain distance of 2.8 kpc. Such a distance would place Cas A just behind the spine of the Perseus spiral arm. It is suggested that the system of flocculi surrounding Kepler's supernova was formed when a pre-existing circumstellar envelope was engulfed by the expanding shell of the supernova of 1604. The observed overabundance of nitrogen in

XUM

the quasi-stationary flocculi associated with Cas A suggests that these objects were also formed by compression of circumstellar material. The total mass of all quasi-stationary flocculi in Cas A is estimated to be about 5×10^{31} g. (W.D.M.)

30065 CIRCUMSTELLAR SHELLS IN THE YOUNG CLUSTER NGC 2264. Strom, K. M. (State Univ. of New York, Stony Brook); Strom, S. E.; Yost, J. Astrophys. J.; 165: 479-88 (1 May 1971).

Strömgren four-color and Hβ observations of pre-main-sequence A and F stars in the young cluster NGC 2264 suggest that most of these stars are surrounded by circumstellar gas shells. Evidence in support of this suggestion is provided by the apparent Balmer continuum and Hβ emission found for these objects. As the strength of these emission features increases, absorption by circumstellar dust envelopes also appears to increase. This impression is appreciably strengthened by visual and infrared observation of the star Walker 90 (LK Hα 25). This A emission star appears to lie below rather than above the zero-age main sequence in the [V, (B − V)] plane. Its location in the H−R diagram most likely results from an optically thick dust shell having nonselective absorption characteristics at visible wavelengths. The apparently universal presence of dust and gas shells in pre-main-sequence stars renders difficult, if not impossible, interpretations of young cluster H−R diagrams in terms of age spreads and rates of stellar formation. The differences in shell character between early- and late-type pre-main-sequence stars is discussed briefly. (auth)

30066 RELATIVISTIC, SPHERICALLY SYMMETRIC STAR CLUSTERS. V. A RELATIVISTIC VERSION OF PLUMMER'S MODEL. Fackerell, Edward D. (California Inst. of Tech., Pasadena). Astrophys. J.; 165: 489-93(1 May 1971).

An explicit solution is given for a relativistic generalization of Plummer's model of a Newtonian star cluster. This solution is based on Buchdahl's solution for a relativistic fluid sphere resembling the Emden polytrope of index 5. The resultant star cluster has a much greater density contrast (large, diffuse envelope) than relativistic clusters previously analyzed by Ipser. Nevertheless, its stability properties appear to be much the same as for Ipser's compact clusters: Instability against radial perturbations probably sets in when the redshift of a photon emitted from the cluster's center reaches $z \approx 0.55$. (auth)

30067 EXPLOSIVE NUCLEOSYNTHESIS IN HELIUM ZONES. Howard, W. M.; Arnett, W. David; Clayton, Donald D. (Rice Univ., Houston, Tex. Inst. of Theoretical Astronomy, Cambridge, Eng.). Astrophys. J.; 165: 495-507(1 May 1971).

A study by numerical integration is presented of the network of nuclear reactions expected to occur when the helium zones of a star are instantaneously heated and allowed to expand adiabatically. The dependence of the results on nuclear cross-sections, on the peak temperature, and on the time scale of the hydrodynamic expansion are discussed. Of particular interest is the result that the nucleus ^{14}N, constituting about 2% by mass following the earlier operation of the CNO cycle, is substantially converted into ^{15}O, ^{18}F, ^{19}Ne, and ^{21}Ne in ratios close to the solar abundances of ^{15}N, ^{18}O, ^{19}F, and ^{21}Ne. It is very likely that these nuclei are synthesized in such zones. The nucleus ^{22}Ne, on the other hand, is apparently not produced in the explosion in sufficient amounts relative to ^{21}Ne, which indicates that ^{22}Ne is probably synthesized in hydrostatic helium burning and survives the ejection. (auth)

30068 COHERENT EMISSION FROM EXPANDING SUPERNOVA SHELLS. Colgate, Stirling A.; Noerdlinger, Peter D. (New Mexico Inst. of Mining and Tech., Socorro). Astrophys. J.; 165: 509-21(1 May 1971).

When a stellar core of magnetic moment μ undergoes supernova explosion, at some radius r_0 the expanding shell of photons and hot gas may attain a relativistic velocity V, with associated Lorentz factor $\gamma = (1 - V^2/c^2)^{-\frac{1}{2}}$ on the order of 3×10^3 or more. This expanding shell will comb the initial dipole field into a radial configuration, and the associated current sheet will produce a coherent radio emission of power as a function of frequency ν $P(\nu)d\nu = \frac{4}{9}\mu^2 c^{-1} r_0^{-2} \psi(q) d\nu$ ergs, where $q = \pi\nu r_0 c^{-1}\gamma^{-2}$ and the function $\psi(q)$ is unity for $q \ll 1$ and falls to roughly $\frac{1}{3}$ at $q = 1$. The resulting emission in the range of 300 MHz corresponds to an antenna temperature of about 1.5×10^{7}°K for a supernova event per day per steradian at 100 Mpc, dispersed by the galactic and intergalactic electron density. (auth)

30069 DIFFUSE INTERSTELLAR FEATURES IN THE SPECTRUM OF THE MOST HEAVILY REDDENED STAR. Bromage, G. E. (Univ. of Edinburgh). Nature (London); 230: 172-5(19 Mar 1971).

It is stated that the Cygnus OB2 stellar association contains the most heavily reddened early-type star known (star number 12) and a photographic spectrum of this star, at 200 pm (2 Å) resolution, obtained with the Cassegrain spectrographs of the Isaac Newton telescope, is shown and compared with that of star number 10 (BD + 41° 3804) in the same association. The dispersion used was 6nm/mm, and the wavelength range 570 to 675 nm. These spectra show the second strongest diffuse interstellar features in the red so far recorded, only the broad feature near 618 nm seen in supernova spectra being stronger. The computed equivalent widths of the interstellar features, of Hα and of the stellar He I lines, together with central intensities and half-widths for the diffuse features, are tabulated, and the features are discussed in detail. All diffuse interstellar features were of almost equal strength for the two stars, although No. 12 is twice as reddened as No. 10, providing evidence that the diffuse line absorbers cannot be closely associated equally with the various species in the dust population. (UK)

30070 LYMAN-ALPHA EMISSION FROM ARCTURUS. Rottman, G. J.; Moos, H. W.; Barry, J. R. (Johns Hopkins Univ., Baltimore). Astrophys. J.; 165: 661-4(1 May 1971).

The K2 IIIp star Arcturus was observed by a rocket-borne precision-pointing telescope and ultraviolet spectrometer. Only one spectral scan was obtained; it showed a definite enhancement of the H I line at 1216 Å over the geocoronal background. This excess is interpreted as chromospheric Lα emission from Arcturus. (auth)

30071 REDDENING OF ETA CARINAE. Rodgers, A. W. (Australian National Univ., Canberra). Astrophys. J.; 165: 665-7(1 May 1971).

A comparison of infrared and violet line intensities of [S II] indicates no internal reddening in η Car. The anomalous temperature of the [Fe II] lines is discussed. (auth)

30072 DISCOVERY OF CIRCULAR POLARIZATION IN THE WHITE DWARF G99-37. Landstreet, J. D. (Univ. of Western Ontario, London); Angel, J. R. P. Astrophys. J.; 165: L67-70(1 May 1971).

The continuum radiation in a band from 3800 to 6000 Å from the DGp white dwarf G99−37 is found to have circular polarization of 0.63 ± 0.03%. The effect in this band does not appear to be time-variable, although variations of about 0.3% may be present in narrower-wavelength bands. The polarization drops from 0.98% in the ultraviolet to 0.44% in the blue and then rises gradually to a value around 0.8% in the red. A search for linear polarization did not show a definite effect, the measured value in a broad band being p = 0.21 ± 0.13%. A list is given of twenty-four other stars that have been observed for circular polarization with negative results. (auth)

30073 DISCOVERY OF PERIODIC VARIATIONS IN THE CIRCULAR POLARIZATION OF THE WHITE DWARF G195-19. Angel, J. R. P. (Columbia Univ., New York); Landstreet, J. D. Astrophys. J.; 165: L71-5(1 May 1971).

The circular polarization observed in the continuum radiation of the DC white dwarf G195-19 was found to be periodically variable with a period of 1.34 days. In the wavelength band 3800 to 5400 Å, the mean polarization is −0.224% and the amplitude of the variable component is 0.250%. The polarization in other bands is not so strongly modulated. In a broad-wavelength band the star showed no detectable linear polarization (0.09 ± 0.13%) at a time when the circular polarization was close to maximum. (auth)

30074 LUMINOSITY OF THE MAGNETIC WHITE DWARF AC + 70°8247. van Altena, W. F. (Univ. of Chicago, Williams Bay, Wis.). Astrophys. J.; 165: L77-8(1 May 1971).

A new trigonometric parallax for the magnetic white dwarf AC + 70°8247 derived from plates taken with the Yerkes Observatory 40-inch refractor is presented. When averaged with other published values, the final value is $\pi_{abs} = +0\overset{''}{.}081 \pm 0\overset{''}{.}004$ (p.e.) or $M_V = +12.73 \pm 0.11$ (p.e.) mag. The star lies 0.05 ± 0.11 (p.e.) mag below the lower white-dwarf sequence. (auth)

30075 MODELS OF ROTATING STARS. Auchmuty, J. F. G. (State Univ. of New York, Stony Brook); Beals, Richard. Astrophys. J.; 165: L79-82(1 May 1971).

Physically reasonable solutions of the equations for some models of rotating stars can be shown to exist by a variational method. Either angular velocity or angular momentum per unit mass is prescribed, as well as a pressure−density relationship of a certain kind. Allowable pressure−density relationships include those of certain models of polytropes, massive stars, and white dwarfs. (auth)

30076 INFRARED POLARIZATION OF ETA CARINAE AND VY CANIS MAJORIS. Forbes, Fred F. (Univ. of Arizona, Tucson). Astrophys. J.; 165: L83-6(1 May 1971).

Polarization of 6% was observed in the infrared at 1.25 μ for η Car and over 4% at 1.65 μ for VY CMa. The interstellar polarization and the polarization contributed by the nebula associated with VY CMa were separated. There appeared to be a time-dependent variation of the polarization in VY CMa due to the nebula. (auth)

30077 EVIDENCE FOR ^{3}He IN YOUNG OPEN CLUSTERS. Ulrich, Roger K. (Univ. of California, Los Angeles). Astrophys. J.; 165: L95-9(1 May 1971).

Calculations of the pre-main-sequence evolution of stars containing a high abundance of ^{3}He suggest the existence of a ^{3}He main sequence 1 to 2 mag above the normal main sequence. It is proposed that this ^{3}He main sequence can explain some features of the anomalous color-magnitude diagrams of Orion and NGC 2264. The required initial ^{3}He abundances in these cases are $0.002 < N_3/N_4 < 0.004$ and $0.015 < N_3/N_4 < 0.04$, respectively. (auth)

30078 PHOTOELECTRIC MEASUREMENTS OF HIGH-n BALMER LINES IN NGC 7027 AND NGC 7662. Miller, Joseph S. (Univ. of California, Santa Cruz). Astrophys. J.; 165: L101-5(1 May 1971).

Scanner measurements of higher members of the Balmer series in NGC 7027 and NGC 7662 show much better agreement with theory than do older photographic observations. (auth)

30079 NUCLEOSYNTHESIS IN NEUTRON-RICH SUPERNOVA EJECTA. Delano, Michael D. (Yeshiva Univ., New York); Cameron, A. G. W. Astrophys. Space Sci.; 10: 203-26(Feb 1971).

A nuclear reaction network of 903 different strong and electromagnetic reactions linking 107 chemical constituents was used to study the elements synthesized in the neutron-rich material ejected in supernova explosions. A large number of three-body reactions virtually eliminates the usual bottleneck at the A = 5 mass gap. For initially high temperatures and densities, $T = 10^{10}$K and $\rho = 7 \times 10^8$ gm/cm^3, with expansion time scales of 10^{-3} to 10^{-2} sec, three different n to p ratios, $n/p = 4$, $n/p = 3/2$, and $n/p \sim 1$, are considered for the ejected matter. In all three cases, the material synthesized is preponderantly heavy. For the $n/p = 4$ model, the conditions at the charged-particle freeze-out are ideal for the "r-process." The onset of this rapid neutron-capture phase is explicitly shown with a sequence of time-lapse abundance plots. (auth)

30080 NEUTRON-STAR MODELS INCLUDING THE EFFECTS OF HYPERON FORMATION. Cohen, Jeffrey M. (Inst. for Advanced Study, Princeton, N. J.); Cameron, A. G. W. Astrophys. Space Sci.; 10: 227-45(Feb 1971).

A new series of neutron star models was computed. The equation of state used includes the effects of nuclear dissolution, nuclear forces, and the presence of hyperons. The nuclear forces were introduced through use of a generalized form of the Levinger–Simmons V_α and V_γ potentials. The maximum stable masses obtained were 2.28 and 2.37 $M_\odot$, respectively. Details are given of the structure of the outer layers, which are expected to be crystalline. Expressions are given for the angular momentum and rotational energy of a neutron star, and the relevant moment of inertia is tabulated for the models. (auth)

30081 NEUTRINO LUMINOSITY BY THE ORDINARY URCA PROCESS IN AN INTENSE MAGNETIC FIELD. Canuto, V.; Chou, C. K. (Goddard Space Flight Center, New York). Astrophys. Space Sci.; 10: 246-64(Feb 1971).

The neutrino luminosity by the ordinary URCA process in a strongly magnetized electron gas is computed. General formulae are presented for the URCA energy loss rates for an arbitrary degree of degeneracy. Analytic expressions are derived for a completely degenerate, relativistic electron plasma in the special case of neutron–proton conversion. Numerical results are given for more general cases. The main results are as follows: the URCA energy loss rates are drastically reduced for the regime of great degeneracy by a factor up to 10^{-3} for $\Theta \simeq 1$, and $T_9 \lesssim 10$, where $\Theta = H/H_0$, $H_0 = m^2c^3/e\hbar = 4.414 \times 10^{13}$ G. In the nondegenerate regime the neutrino luminosity is enhanced approximately linearly with Θ for the temperature range $1 \lesssim T_9 \lesssim 10$. Possible applications to white dwarfs and neutron stars are briefly discussed. (auth)

30082 ROCHE COORDINATES FOR THE ROTATIONAL PROBLEM. Kopal, Zdenek (Univ. of Manchester, Eng.). Astrophys. Space Sci.; 10: 328-31(Feb 1971).

Curvilinear coordinates in three dimensions associated with the Roche model distorted by centrifugal force alone constitute a Lamé family, of which one (ξ-) coordinate can be defined by equipotential surfaces that are known in closed algebraic form; the other (η) becomes identical with the meridional planes of the rotationally distorted Roche model; while the third (ζ) then follows from the requirements of orthogonality to the others. The explicit form of such coordinates in terms of the polar or cartesian systems has already been established by the author (Astrophys. Space Sci., 8: 149-71(1970)) correctly to quantities of the first order in superficial distortion of the respective Roche model. In the present paper, this latter restriction on accuracy will be removed, and expressions constructed for the ζ-coordinate in the form of infinite series which are exact and converge rapidly for any distortion below that which entails equatorial breakup. (auth)

30083 ECLIPSING SYSTEM OF EPSILON AURIGAE AND ITS POSSIBLE RELEVANCE TO THE FORMATION OF A PLANETARY SYSTEM. Kopal, Zdenek (Univ. of Manchester, Eng.). Astrophys. Space Sci.; 10: 332-9(Feb 1971).

Recent observations of the eclipsing system of ϵ Aurigae converge to a conclusion that its secondary ("invisible") component constitutes a flat disc, some 40 AU across, that is semitransparent, of constant optical depth, and dims light nonselecting without a trace of polarization. Its constituent particles must, therefore, be large in comparison with the wavelength of observation—probably greater, on the average, than 10 μ, with no upper limit imposed by the observations. The mass of this disc appears to be no less than 20 $\odot$ and its mean temperature approximately 500 K. The primary component of ϵ Aurigae is an F21a supergiant, probably less than one million years old; while its less massive (and, consequently, less evolved) companion has not yet reached a stellar stage. The external characteristics of this disc-like companion appear to approximate the properties that have frequently been postulated as prerequisites for the formation of a "planetary system". A hypothesis is put forward that, in the secondary component of ϵ Aurigae, an evolutionary process is taking place that may result in the formation of a planetary system very much more massive than the solar system in the astronomically near future. (auth)

30084 VELOCITY-DEPENDENT NON-LTE SOURCE FUNCTION. II. FINITE LAYERS. Kulander, John L. (Lockheed Palo Alto Research Labs., Palo Alto, Calif.). Astrophys. J.; 165: 543-59(1 May 1971).

The depth variation of the non-LTE line source function for a two-level atom is calculated for various differential velocities qualitatively characteristic of stellar atmospheres. The layers considered are assumed to be uniform in character except for the velocity profiles. The Riccati transformation method is employed in solving the transfer equation. Normally emergent line profiles are presented for a Gaussian absorption coefficient. (auth)

30085 STRONG-CYANOGEN STARS: PHOTOMETRY AND KINEMATICS. Janes, K. A.; McClure, Robert D. (Yale Univ., New Haven). Astrophys. J.; 165: 561-71(1 May 1971).

A group of 185 late G and K giants, selected from the U. S. Naval Observatory Catalog of Photoelectric Observations because they had ultraviolet deficiencies, were observed with the intermediate-band photometric system of the David Dunlap Observatory. A gravity-independent index of cyanogen band strength, δC_m, shows a loose correlation with ultraviolet deficiency for these stars. It was found that approximately 6% of the G and K giants in the solar neighborhood could be classified as strong-cyanogen stars (equivalent to Roman's 4150 stars). A kinematic study shows that the distribution of their space motions differs significantly from that of a random sample of bright giants in the solar neighborhood. In fact, the strong-cyanogen stars appear to be separated into two populations, one consisting of old high-velocity stars and the other apparently associated with young moving groups. Few if any seem to have intermediate age. (auth)

30086 AUTOMATED AND CONVENTIONAL PHOTOMETRY OF THE SHORT-PERIOD VARIABLE STAR 14 AURIGAE. Hudson, Katherine I.; Chiu, Hong-yee; Maran, Stephen P.; Stuart, Frank E.; Vokac, Peter R. (Kitt Peak National Observatory, Tucson, Ariz. Goddard Inst. for Space Studies, New York. Goddard Space Flight Center, Greenbelt, Md.). Astrophys. J.; 165: 573-80(1 May 1971).

Amplitude of the V-light curve of the δ Scuti star 14 Aurigae varied from 0.02 to 0.08 mag on six nights. The changes in amplitude accompanied comparable changes in maximum brightness, whereas changes in minimum brightness were much smaller. The light period is 0.08748d, and the spectroscopic-binary period is 3.788506d. Small variations in color indices, associated with the light variation, resemble those of other δ Scuti stars. The use of

XUM

an automated telescope was effective in obtaining large numbers of routine observations. (auth)

30087 SOLAR-COMPOSITION A STARS IN THE GALATIC HALO. Rodgers, A. W. (Australian National Univ., Canberra). Astrophys. J.; 165: 581-97(1 May 1971).

Spectra and UBV photometry were obtained of the sixty stars identified by Philip and Sanduleak as earlier than A7, $12 < V < 15$, in the region of the South Galactic Pole. Three stars are of type sdB, one is DA, and two are subdwarfs. Of the remainder, nearly half show K-line strengths which are similar to Population I stars; the Balmer-line photometry shows that the majority of these stars have gravities lower than those for main-sequence stars. It is proposed that these stars are accelerated from the galactic disk by means of the Blaauw binary-acceleration mechanism. The weak K-line A stars can be identified with horizontal-branch stars and blue stragglers. The velocity dispersion of the whole sample of A stars is 66 km sec^{-1}. (auth)

30088 BEHAVIOR OF THE ANGULAR VELOCITY NEAR THE SURFACES OF STARS WITH RADIATIVE ENVELOPES. Marks, Dennis W.; Clement, Maurice J. (Univ. of Toronto, Richmond Hill, Ont.). Astrophys. J.; 166: L27-29(15 May 1971).

The combination of radiative viscosity and Jeans's "radiative braking" determines the distribution of angular momentum near the outer boundary of stars without magnetic fields. In the case of slow rotation, it is shown that near the surface of a radiative envelope the angular velocity falls off as the five-thirds power of the radius in any given radial direction. This condition must be satisfied even in the presence of meridian circulation and is imposed for a 10 $M_{\odot}$ star on a time scale of about 1000 years. (auth)

30089 INFRARED STARS: SEARCH FOR 3.5-MILLIMETER RADIATION AND TENTATIVE DETECTION OF VY CANIS MAJORIS. Wilson, W. J. (Aerospace Corp., Los Angeles). Astrophys. J.; 166: L13-16(15 May 1971).

A search was made for 3.5-mm radiation from twelve infrared stars with strong 10-μ radiation. The sources VY CMa and IRC + 10216 were tentatively detected with 3.5-mm fluxes of 0.2 ± 0.07 (1 σ) f.u. and 0.4 ± 0.2 f.u., respectively. The IRC + 10216 result is consistent with a measurement by Kellermann and Pauliny-Toth. If the 3.5-mm radiation comes from an optically thick circumstellar region having the infrared temperature of 600°K, this region would have a linear dimension of ≈100 A.U. (auth)

30090 RADIO OBSERVATIONS OF THE INFRARED OBJECT IRC 19216. Kellermann, K. I.; Pauliny-Toth, I. I. K. (National Radio Astronomy Observatory, Green Bank, W. Va.). Astrophys. J.- 166: L17-18(15 May 1971).

The flux density of the infrared object IRC 10216 was observed at a wavelength of 3.5 mm and found to have a flux density of 0.31 ± 0.10 flux units, in good agreement with the value expected from an extrapolation of the infrared measurements. (auth)

30091 RADIO OBSERVATIONS OF NOVA SCUTI 1970. Herrero, V.; Hjellming, R. M.; Wade, C. M. (National Radio Astronomy Observatory, Green Bank, W. Va.). Astrophys. J.; 166: L19-20(15 May 1971).

Radio emission from Nova Scuti 1970 was measured at wavelengths of 0.35 and 3.7 cm. (auth)

30092 GRAVITATIONAL RADIATION FROM SLOWLY ROTATING, FULLY RELATIVISTIC STARS. Ipser, James R. (California Inst. of Tech., Pasadena). Astrophys. J.; 166: 175-96(15 May 1971).

If pulsars are rotating neutron stars, they might be losing significant amounts of rotational energy by the emission of gravitational radiation. In this connection, it is important to know the rate at which a fully relativistic, rigidly rotating star emits gravitational radiation. Recently developed techniques are used to compute that rate for a relativistic star whose equatorial velocity of rotation is small compared with the velocity of light, and whose deformation from spherical symmetry is small. The deformation is supported by stresses which are anisotropic in general. The analysis yields an emission rate which is identical to that of standard weak-field theory, provided the multipole moments used in the weak-field formula are those which describe the star's Newtonian potential in the near-zone far-field region (gravitational radius $\ll r \ll$ "velocity-of-light circle"). The multipole moments are determined in terms of integrals involving the fully relativistic star's deformation. Also studied are the radiation-reaction forces, whose presence inside the star accompanies the emission of radiation. These forces extract energy and angular momentum from the star at the same rates as the gravitational waves carry them away. (auth)

30093 INTERMEDIATE-AGE CLUSTER IC 4651. Eggen, O. J. (Australian National Univ., Canberra). Astrophys. J.; 166: 87-94(15 May 1971).

Two hundred and ten UBV observations of 102 stars in the region of the open cluster IC 4651 show that it is an intermediate-age cluster with a modulus of 9.5 mag and an ultraviolet excess of +0.06 mag for main-sequence stars with an intrinsic color $B - V = +0.45$ mag. Observations of seven early-type stars in the region show that the cluster reddening is $E(B - V) = +0.15$ mag. The cluster is apparently only slightly older than NGC 752 but is considerably richer and contains more than a dozen red giants. A comparison of the various features of the color-luminosity arrays of this and other old and intermediate-age clusters suggests a significant spread in the ages of the stars within a cluster, which would tend to blur some of the indicators used to measure the mean age and the chemical composition of cluster stars. (auth)

30094 EFFECTIVE TEMPERATURES OF B- AND A-TYPE STARS. Schild, R. (Smithsonian Astrophysical Observatory, Cambridge, Mass.); Peterson, D. M.; Oke, J. B. Astrophys. J.; 166: 95-108(15 May 1971).

A new effective-temperature calibration was derived on the basis of (a) a recent recalibration of the absolute flux of α Lyr, (b) new continuum-flux observations for the bright, hot stars, and (c) new line-blanketed stellar models. With the new data, effective temperatures derived from the slope of the Paschen continuum are in agreement with those from the Balmer discontinuity. Moreover, for Vega, the two continuum indicators and the Hα, Hβ, and Hγ profiles are all in excellent agreement with a model having $T_{eff} = 9650$°K and $\log g = 4.05$. Parameters $T_{eff} = 10200$, $\log g = 4.35$ for Sirius models give satisfactory agreement with the observed continuum fluxes, H-line profiles, and measured angular diameter. (auth)

30095 CALCULATION OF LINEAR, NONADIABATIC PULSATIONS OF STELLAR MODELS. Castor, John I. (Univ. of Colorado, Coulder). Astrophys. J.; 166: 109-29 (15 May 1971).

A computational method for treating linear, nonadiabatic radial pulsations of stellar models is presented. The details of the numerical procedure are given. This procedure also fits easily into the framework of the Henyey method for the calculation of stellar evolution. It was found to be very efficient; in general, less time is required for the stability analysis of a given model than for the construction of the model itself. The method is applied to models of RR Lyrae stars previously treated by Christy, who used the nonlinear method. The agreement is good overall; the growth rates obtained are usually within 50% of Christy's. The differences are that the periods obtained in the present calculations are 2 to 3% longer than Christy's, and instability is found to extend 400°K higher in effective temperature. The first difference can be attributed to Christy's omission of radiation pressure, while the second is possibly due to nonlinearity at Christy's initiation amplitude. A second set of models analyzed was similar to models treated previously by Baker and Kippenhahn. In the present case, however, the models were constructed without convection. Notable differences were found between the present results and those of Baker and Kippenhahn. These were of the luminosity phase lag, the relative contributions of the H and He II ionization zones to the growth rate, and the growth rate at low effective temperature. These differences may all be attributed to the effect of convection. For the phase lag, omission of convection produces better agreement with observations. It is shown that the linear approximation is applicable to much larger amplitudes than was previously thought. This is because the structure within the zone of hydrogen ionization is found to have no effect on the pulsation as a whole, provided the zone of hydrogen ionization is geometrically sufficiently thin. Nonlinear effects then become important only when the relative pressure amplitude approaches unity. This conclusion is valid only if convection is negligible in the models. (auth)

30096 SPECIFICATION OF THE BLUE EDGE OF THE RR LYRAE INSTABILITY STRIP. Iben, Icko Jr. (Massachusetts Inst. of Tech., Cambridge). Astrophys. J.; 166: 131-51(15 May 1971).

The growth rate for small-amplitude pulsations was investigated in the nonadiabatic linear approximation. The effects were explored of including convection, including terms higher than the first in calculating thermodynamic quantities, omitting the contribution of the radiative field to thermodynamic variables, and varying the surface boundary conditions. With regard to the specification of the blue edge of the instability strip, convection and terms higher than the first in partition sums appear to play minimal roles. Insofar as it affects thermodynamic quantities

involved in determining pulsation properties, the radiation field plays an important role. Results are also sensitive to the choice of surface boundary conditions. (auth)

30097 WHY EXPANDING STARS AFTER LEAVING THE MAIN SEQUENCE? Deinzer, W.; Krummheuer, F. (Univ., Goettingen, Ger.). Naturwissenschaften; 57: 392(Aug 1970). (In German).

After consumption of its central hydrogen reserve, stars under radius increase abandon the main sequence of the Hertzsprung–Russell diagram. The reason for leaving the main sequence was sought in the framework of the polytrope theory. Complex polytropes were studied, therefore, in analogy to the known core/shell structure of the post-main-sequence stars. The consideration of the different chemical composition of core and shell gives the desired expansion. The conclusion can be understood with the help of the virial law. This result is illustrated with an example. (J.S.R.)

30098 SPECTROGRAPHIC STUDY OF THE SHELL STAR EW LAC (HD 217 050). I. RADIAL VELOCITIES OF HYDROGEN LINES. Harmanec, P. (Astronomical Inst., Ondrejov, Czech.); Krpata, J.; Hadrava, P. Bull. Astron. Inst. Czech.; 22: 87-91 (1971).

Radial velocities of hydrogen lines based on six Victoria (1965) and four Ondřejov (1968) spectrograms are published. It is shown that no noticeable Balmer progression existed in the times of exposures. (auth)

30099 FORMATION OF A NEUTRON STAR IN A CLOSE BINARY SYSTEM. McCluskey, George E. Jr.; Kondo, Yoji (Manned Spacecraft Center, Houston, Tex.). Astrophys. Space Sci.; 10: 464-70(Mar 1971).

The effects on a close binary system of one component becoming a neutron star as a result of a supernova explosion are discussed. In the case of a Type I supernova, the system can remain bound in many cases of interest. For a Type II supernova, the system will probably be disrupted, although in some cases a remnant of the companion to the supernova may remain in a bound orbit. Consequently, neutron stars formed in Type I supernova explosions may exist in close binary systems. Such systems may be strong x-ray emitters due to mass flow as suggested by Shklovsky. Photons with energies in the 1 to 50-MeV region should also be emitted. (auth)

30100 VARIATION OF THE LIGHT CURVE OF W URSAE MAJORIS. Breinhorst, Robert A. (Univ., Bonn. Kitt Peak National Observatory, Tucson, Ariz.). Astrophys. Space Sci.; 10: 411-30(Mar 1971).

A new set of photoelectric B and V observations of W Ursae Majoris obtained during a period of one week in 1968 is presented. From the measurements it can be concluded that, in general, the light curve in both colors is free from complications. In particular, no systematic brightness differences between consecutive periods can be found. The observations made during total eclipse in two different periods yield flat minima fitting almost perfectly, the mean error of the single measurement being of the order of 0.003m. The duration of the phase of totality is estimated to 0.036 P = 17.3m, thus confirming the value given by Cester and Gridelli. From a plot of the square deviations of the single observations $(\Delta I/I)^2$ from the mean intensity curve vs phase it can be shown that the scattering decreases strongly during primary eclipse, thus indicating that the source producing these fluctuations is essentially confined to the space between the two components. A comparison with earlier photoelectric observations also supports the assumption that the variational behavior of the light curve is caused by a gaseous cloud between the two components rather than by an envelope surrounding the whole system. (auth)

30101 SPECTRUM OF A GASEOUS NEBULA OF PURE HYDROGEN. III. THE BALMER DECREMENT. Gerola, H. (Univ., Buenos Aires); Salem, M.; Panagia, N. Astrophys. Space Sci.; 10: 383-92(Mar 1971).

The Balmer decrement was calculated for a homogeneous, spherical, pure hydrogen nebula, ionized and excited both by radiative and collisional processes. Reabsorption in the Balmer series from sublevels 2s and 2p was taken into account. Calculations were carried out for electron temperatures of 10^4 and 2×10^4 K, electron densities from 10^3 to 10^6 cm^{-3}, and radii from 10^{15} to 10^{17} cm. The results define allowed and forbidden regions in the $\log(H\beta/H\gamma)$ vs $\log(H\alpha/H\beta)$ diagram different from those of previous results obtained by assuming purely radiative or purely collisional ionization and excitation. A brief comparison with observations is presented and discussed. (auth)

30102 HYDROMAGNETIC OSCILLATIONS OF A SELF-GRAVITATING FLUID SPHEROID. Sood, N. K. (Panjab Univ., Chandigarh, India); Trehan, S. K. Astrophys. Space Sci.; 10: 393-401(Mar 1971).

The oscillations of a homogeneous, compressible, self-gravitating fluid spheroid in static equilibrium with a poloidal magnetic field inside and a dipole type field outside were studied using the second-order tensor virial equations. It was found that, for small values of the eccentricity, the equilibrium model is dynamically stable provided the usual criterion of pulsative stability in the absence of a magnetic field ($\gamma > 4/3$) is satisfied. The magnetic field removes the accidental degeneracy of the radial and the nonradial modes of oscillation that exists for $\gamma = 1.6$ in the absence of a magnetic field. (auth)

30103 INDUCED SEMI-CONVECTION IN HELIUM-BURNING HORIZONTAL-BRANCH STARS. II. Castellani, V. (Univ., Rome. Laboratorio di Astrofisica, Frascati, Italy); Giannone, P.; Renzini, A. Astrophys. Space Sci.; 10: 355-62(Mar 1971).

In the evolutionary phase of central helium burning, models of horizontal-branch stars reach a stage at which an intermediate region is unstable against convection. This feature is due to the progressive increase of the core mass by overshooting during the previous evolutionary stages and to the behavior of the radiative temperature gradient at the core boundary. By consideration of the typical time scales of propagation of convection and nuclear burning, a partial mixing (semi-convection) can be induced in a region around the convective core. (auth)

30104 PHOTOMETRIC ELEMENTS OF THE SHORT-PERIOD CEPHEID WZ BOOTIS. Chis, Gheorghe (Astronomical Observatory, Cluj); Lungu, Nicolae. Stud. Cercet. Astron.; 15: 141-5(1970). (1970). (In Rumanian).

The photometric elements of WZ Bootis were determined on the basis of photographic observations made at the Astronomic Observatory of Cluj. The magnitudes of the stars used for comparison are given. For determining the elements, 7 maxima were obtained. By means of the elements the phases were determined, and by means of these, the observations were grouped into 29 normal points by means of which the medium curve was traced. This shows that the star is of the type RR_α Lyrae. (auth)

30105 CONTRIBUTIONS TO THE INTERPRETATION OF THE LIGHT CURVES OF THE CLOSE BINARY SYSTEMS. VI. APPLICATION FOR THE ECLIPSING VARIABLE STAR AI DRACONIS. Ureche, Vasile (Univ., Cluj). Stud. Cercet. Astron.; 15: 187-201(1970).

The method of interpreting the light curves of the close binary systems, developed in previous papers was applied to the eclipsing variable AI Draconis. For this purpose Cester's photoelectric observations were used. The results obtained are given in tabular form. AI Draconis system is semidetached. Using the spectroscopic orbit obtained by Ebbighausen and computing the mass ratio of the light variation between eclipses, the masses and the absolute dimensions of the components were determined. (auth)

30106 EVOLUTION OF CLOSE BINARIES. VIII. TWO EXAMPLES OF MASS EXCHANGE IN CASE AB. Horn, J. (Astronomical Inst., Ondrejov, Czech.). Bull. Astron. Inst. Czech.; 22: 37-41(1971).

Two examples of mass exchange in systems with original mass of the primary 5 $M_\odot$ and with initial mass ratios 0.8 and 0.6 respectively, were investigated. Mass transfer starts near the top of the main-sequence evolution of the primary ($X_c = 0.05$) in both systems. Parameters of the resulted pairs are analogous with the results of mass exchange in usual cases B. They indicate that the obtained systems can hardly be compared with observed close binaries but can more likely account for some peculiar objects. (auth)

30107 UBV PHOTOGRAPHIC PHOTOMETRY IN THE REGION $AR_{1950}: 17^h03^m - 17^h41^m$ $DECL_{1950}: -28.8°$ TO $-33.4°$. II. OPEN STAR CLUSTER TR 28. CATALOGUE OF 76 STARS AND IDENTIFICATION MAP. Antalova, A. (Astronomical Inst., Skalnate Pleso, Czech.). Bull. Astron. Inst. Czech.; 22: 42-6(1971).

Using UBV photographic photometry it was found that Tr 28 is an O star cluster, that forms the nucleus of an O association. The probable distance of Tr 28 is 3 kpc, $A_V = 2.3$m. In the catalog of 76 stars in the vicinity of Tr 28 there are 7 stars belonging to a star cluster denoted by the letter Y. Thirteen members of the O association are given; 17 other members, up to spectral type B3, are given in the catalog. The immediate vicinity of Tr 28 is shown in the identification map and the more remote vicinity is shown in identification map No. 8 in part I (Antalová, 1970). (auth)

XUM

30108 SPECTRAL CLASSIFICATION AND PHOTOMETRY OF STARS IN TWO H II REGIONS. Mayer, P.; Macak, P. (Charles Univ., Prague). Bull. Astron. Inst. Czech.; 22: 46-9(1971).

MK spectral types and UBV photoelectric photometry are given for stars in H II regions IC 417 and IC 1318a. (auth)

30109 TEST OF THE CASSEGRAIN AND COUDE SPECTROGRAPHS OF THE 2-m TELESCOPE AT ONDREJOV BY MEANS OF DETAILED ANALYSIS OF α CYG. Zverko, J. (Astronomical Inst., Skalnate Pleso, Czech.). Bull. Astron. Inst. Czech.; 22: 49-60(1971).

Two spectrograms, obtained by the 2-m telescope at Ondřejov, were used for measuring of the equivalent line-widths in the spectrum of the supergiant α Cyg. The results show the good quality of the spectrograms for both the equivalent line width and the line profile measurings. The mean error of single value of log W_λ is $\sigma = \pm 0.11$. Although there are some systematic deviations between both plates, these may be due to an unequal drawing of the continuum on the intensity tracings. From the contours of the Balmer lines Hγ and Hδ follows the effective temperature $T_{eff} = 9510°$ and surface gravity log g = 1. Turbulent velocities are equal to 17 km/s from Fe II lines and 11 km/s from lines of Ti II. The abundances were determined for several elements by the curve-of-growth method, and the detailed analysis was made for Fe I, Fe II and Ti II. The results are near to the values obtained by other authors. This work made as the test of the cassegrain and coudé spectrographs ability shows the good quality of the plates taken with both spectrographs. (auth)

30110 DIFFERENCE IN MAGNETOHYDRODYNAMIC PROPERTIES OF PHOTOSPHERES OF DWARF AND GIANT STARS OF SPECTRAL TYPES F, G, AND K. Kopecky, M. (Astronomical Inst., Ondrejov, Czech.). Bull. Astron. Inst. Czech.; 21: 310-15(1970).

The accuracy of some properties of the course of electric conductivity in photospheres of stars of spectral types F, G, and K has been improved and the difference of some magnetohydrodynamic parameters such as electric conductivity, Joule dissipation of magnetic fields, velocity of magnetohydrodynamic waves, Reynold's magnetic number, Lundquist's critical number, etc., were studied in photospheres of dwarf and giant stars. Magnetohydrodynamic properties of photospheres of giant and dwarf stars and the characteristic feature of magnetohydrodynamic processes in the photospheres of these stars were determined from the properties of magnetic fields and from macroscopic gas motion in the photospheres of these stars. Differences in the optical models of the photospheres of these stars may esentially influence the difference in magnetohydrodynamic processes in the photospheres of giants and dwarfs only in such cases when properties of magnetic fields and of ordered gas motion are approximately analogous in the photospheres of both the giant and the dwarf. (auth)

30111 EVOLUTION OF CLOSE BINARIES. VII. CASE B OF MASS EXCHANGE IN SYSTEM 7 + 5.6$m_\odot$. Harmanec, P. (Astronomical Inst., Ondrejov, Czech.). Bul. Astron. Inst. Czech.; 21: 316-17(1970).

An example of case B mass exchange in a system with a primary of 7 $M_\odot$ is presented. The resulting system has components with masses 1.13 $M_\odot$ and 11.47 $M_\odot$. Validity of empirical rules suggested by Harmanec (1970) was not confirmed. (auth)

30112 MASS TRANSFER IN CLOSE BINARIES. I. MASS OUTFLOW FROM CONTACT COMPONENTS. Kriz, S. (Astronomical Inst., Ondrejov, Czech.). Bull. Astron. Inst. Czech.; 21: 211-19(1970).

Mass outflow from contact components of close binaries was studied. In components with radiation envelopes the centrifugal force causes the mass ejection even before that particular component attains the Roche limit. Components with convective envelopes lose mass only when expanding over the Roche limit. Mass outflows by a narrow channel in the neighborhood of Lagrange point L_1. An approximate formula for the velocity of this outflow was derived. The velocity is roughly 10 km/sec. (auth)

30113 PHOTOELECTRIC ELEMENTS OF THE ECLIPSING BINARY ST PERSEI. Srivastava, R. K. (Uttar Pradesh State Observatory, Naini Tal, India). Bull. Astron. Inst. Czech.; 21: 219-31(1970).

A revised period for the eclipsing binary ST Persei was obtained to be 2.6483249d. Absolute elements of the system were obtained by using spectroscopic elements given by Blanco and Tollinchi (1957) and photoelectric elements of this work. The primary component was found to lie on the main sequence while the fainter component seems to fall toward the giant branch. The spectral classes now assigned are AoV (primary) and KoIII–IV (secondary). Radiation and color temperatures were also obtained for the fainter component assuming Planck's radiation law. (auth)

30114 ELECTRIC CONDUCTIVITY IN PHOTOSPHERES OF STARS OF SPECTRAL TYPES F, G, AND K. Kopecky, M. (Astronomical Inst., Ondrejov, Czech.). Bull. Astron. Inst. Czech.; 21: 231-7(1970).

The course of electric conductivity with the optical depth τ in photospheres of stars of spectral types K2, G9, G0, and F1 was calculated and is discussed for five different values of gravitational acceleration on the surface of stars. (auth)

30115 OBSERVED SMALL-SCALE STRUCTURE IN PLANETARY NEBULAE. Capriotti, E. R.; Cromwell, R. H.; Williams, R. E. (Univ. of Arizona, Tucson). Astrophys. Lett.; 7: 241-4(Feb 1971).

Direct photographs of several planetary nebulae of relatively large apparent diameter were taken in the light of various emission lines in order to determine the effects of small-scale structure on the ionization. Filaments and condensations showed considerable enhancement with respect to the amorphous gas in the light of [O I] λ6300. The nebulae showed the least structure in Hβ. On the basis of previous theoretical calculations, it is concluded that the regions of relatively strong [O I] and [N II] emission occur within the nebular shell, and are more dense than the surrounding gas. Furthermore, if these regions are to have lifetimes comparable to that of the nebulae, they must have cores of predominantly cold, neutral gas. (auth)

Quasi-Stellar, Radio, and X-Ray Sources

30116 MOTION AND RADIATION OF CHARGED PARTICLES IN STRONG ELECTROMAGNETIC WAVES. I. MOTION IN PLANE AND SPHERICAL WAVES. Gunn, James E. (California Inst. of Tech., Pasadena. Carnegie Institution of Washington, D. C.); Ostriker, Jeremiah P. Astrophys. J.; 165: 523-41 (1 May 1971).

The motion of test particles in strong electromagnetic waves is treated, considering both plane and spherical wave fronts, both with and without radiative reaction. Various limiting cases are discussed. Particles of initially low energy dropped into a strong plane wave are accelerated in the propagation direction up to an energy proportional to B^2; radiative "losses" paradoxically lead to an increase rather than a decrease in the total energy of these particles. In spherical waves, particles injected very close to the source become "phase locked" with the driving wave and are accelerated in the manner described earlier; particles injected further out follow orbits like classical particles in a repulsive inverse-cube force field. Charged particles of arbitrary initial energy will radiate strongly when injected into strong wave fields. The nonlinear inverse Compton ("NIC") radiation so produced depends on particle energy and field-energy density like, and has a spectrum like, synchrotron radiation. The physical processes elaborated here provide channels for converting the rotational kinetic energy of condensed bodies into fast particles and the fields in which these particles can radiate, and it is suggested that these mechanisms are responsible for a wide variety of "nonthermal" astronomical sources. (auth)

30117 OBSERVATIONS OF COMPACT H II REGIONS WITH OPTICAL COUNTERPARTS. Rubin, Robert H. (Univ. of Illinois, Urbana); Turner, Barry E. Astrophys. J.; 165: 471-8(1 May 1971).

Radio and optical measurements were made of the immediate region around the nebula K3-50. The optical spectrum of K3-50 is one of relatively low excitation, which does not permit one to distinguish between an H II region or a low-excitation planetary nebula. However, a very high electron density is indicated. Most of the observational material, and parameters derived from them, are consistent with the hypothesis that K3-50 is a young, compact H II region and not a planetary nebula. Radio data for two other objects, H2-3 and H2-6, previously called planetary nebulae, indicate that these sources are similar in many respects to K3-50. It is believed that these three objects form a class of objects, compact H II regions with optical counterparts, that is intimately related to star formation. If this is true, then additional data may serve to establish an evolutionary sequence. (auth)

30118 PULSAR DISPERSION MEASURES AND THE MEAN AND MEAN-SQUARED INTERSTELLAR ELECTRON DENSITY. Gould, Robert J. (Univ. of California, San Diego, La Jolla). Astrophys. Space Sci.; 10: 265-79(Feb 1971).

Theoretical distributions of pulsar dispersion measures (times

sinb^{II}) are computed for various assumed pulsar spatial distributions above (and below) the galactic plane, assuming a distribution for the ionized gas. The statistics on the twelve high-latitude pulsars lead to the conclusion that the pulsar distribution in z is at least as broad as the distribution of the ionized gas. The value derived for the local mean interstellar electron density in the galactic plane is 0.12 cm^{-3} and is interpreted to be due to a uniform ionized intercloud medium. Interstellar absorption of radio waves at low frequencies and cosmic x rays at low energies are considered with regard to irregularities in the distribution of ionized gas. It is shown that, if the observations are made with a wide-angle receiver, the effective absorption optical depth is $\langle\tau\rangle - \sigma^2/2$ where $\langle\tau\rangle$ is the mean value and σ is the dispersion in τ. This relation assumes $\langle\tau\rangle$ is much larger than σ. Analysis of recent low-frequency radio measurements from a satellite-borne receiver, however, leads to the conclusion that effects of irregularities are large. (auth)

30119 EVIDENCE FOR AN OPTICALLY THICK COMPONENT IN THE GALACTIC RADIO SOURCE SAGITTARIUUS B_2. Hobbs, Robert W.; Modali, Sarma B.; Maran, Stephen P. (Goddard Space Flight Center, Greenbelt, Md.). Astrophys. J.; 165: L87-93 (1 May 1971).

The measured flux density of Sgr B_2 at wavelength 3.55 mm exceeds that predicted by extrapolation of the microwave spectrum and indeed is higher than the observed flux density at wavelength 9.5 mm. This effect may be due to the presence of a compact, optically thick source component. Observations of DR 21 and W3 at 3.55 mm are also discussed. (auth)

30120 OHIO RADIO SOURCES IN CLUSTERS OF GALAXIES. Boeshaar, Patricia C.; Kraus, John D. (Ohio State Univ., Columbus). Astrophys. J.; 165: 445-9(1 May 1971).

Coincidences of radio sources in the Ohio Survey at 1415 MHz with Abell clusters of galaxies were investigated. Sixty coincidences were found within 0.3 cluster radius, compared with eleven expected by chance. (auth)

30121 SEARCH FOR THE REDSHIFTED LINE OF NEUTRAL HYDROGEN IN SELECTED QUASI-STELLAR SOURCES, N GALAXIES, AND SEYFERT GALAXIES. Dent, William A. (Univ. of Massachusetts, Amherst). Astrophys. J.; 165: 451-6(1 May 1971).

An attempt was made to detect the redshifted line of neutral hydrogen in absorption in the quasi-stellar sources 3C 273 and 1510−08, in the N galaxies 3C 120 and 3C 371, and in the Seyfert galaxies NGC 1068 and NGC 1275. A special technique was employed for substantially reducing instrumentally produced spectral features which are a serious problem in searching over wide bandwidths for weak lines superimposed on strong continuum sources. Although no lines were detected, it was possible to estimate upper limits on the column density of H I in these objects. (auth)

30122 ACCELERATION OF CHARGED PARTICLES IN A VARIABLE MAGNETIC FIELD. Bakhareva, M. F.; Lomonosov, V. N.; Tverskoi, B. A. Izv. Akad. Nauk SSSR, Ser. Fiz.; 34: 2313-17(Nov 1970). (In Russian).

Particle acceleration in a homogeneous magnetic field periodically changing with time (Alfven magnetic pumping) was studied. It is shown that with a sufficiently high particle concentration a cyclotron instability appeared that induced particle scattering necessary for effective acceleration. Wave and particle spectra were calculated. It is shown that the effect is capable of explaining the x-ray emission from the Crab nebula and the central pulsar. (tr-auth)

30123 SCINTILLATION OF EXTENDED RADIO SOURCES WHEN THE RECEIVER HAS A FINITE BANDWIDTH. I. Budden, K. G.; Uscinski, B. J. (Cambridge Univ., Eng.). Proc. Roy. Soc. (London), Ser. A; 316: 315-39(5 May 1970).

Many treatments of wave scattering by irregular media take the incident field to be that of a monochromatic plane wave. There are, however, important cases encountered in practice, in particular in radio astronomy, when the incident field is not a plane wave, but is produced by a source of a finite angular size. Moreover, the radiation is not monochromatic, but is received over a continuous band of frequencies. The paper is concerned with fluctuations produced when such a field is scattered by a medium containing weak random irregularities of refractive index. The important statistical properties of these fluctuations are shown to depend on three quantities which are double Fourier integrals with respect to the spatial frequencies present in the scattered field. These functions are assembly averages of products of scattered field components, and are derived by studying the scattering of a wave obliquely incident on a weakly irregular medium. Physical considerations are used to show how a spread of frequencies and angles of arrival, in the incident wave, affect the fluctuations imposed by the medium. The integrands of the Fourier integrals can be used later for the general problem of multiple scatter, but the results in this paper are only for weak single scattering, when the scatterer is either a thin phase changing screen or an extended irregular medium. Formulae are given for the scintillation index, the scintillation visibility, and the spatial autocorrelation function of the fluctuations of received intensity, for some particular cases of source brightness function, receiver bandpass function and autocorrelation function of irregularities in the medium. They are discussed briefly, to illustrate some properties of fluctuations of the scattered field when the incident field is only partially coherent. (auth) (UK)

30124 SCINTILLATION OF EXTENDED RADIO SOURCES WHEN THE RECEIVER HAS A FINITE BANDWIDTH. II. MULTIPLE SCATTER. Budden, K. G.; Uscinski, B. J. (Cambridge Univ., Eng.). Proc. Roy. Soc. (London), Ser A; 321: 15-40 (19 Jan 1971).

The propagation of a radio wave through a very great thickness of weakly scattering medium is studied. An important application is to the interplanetary scintillation of a radio star of finite angular diameter observed with a receiver of finite bandwidth. A previous paper gave the theory and results for a medium whose irregularities are so weak that only single scatter is important. It is now extended to deal with multiple scatter. A partial differential equation is formulated and a series solution is derived which converges when the receiver is in the "near field" for the whole of the scattering medium. A few typical results are given for the scintillation index, scintillation visibility and spatial autocorrelation function of the fluctuations of received intensity, for some particular cases of source brightness function, receiver band-pass function and autocorrelation function of the irregularities in the medium. (auth) (UK)

30125 RELATION BETWEEN THE PROPERTIES OF EXTRAGALACTIC RADIO SOURCES. Richter, G. M. (Zentralinstitut fuer Astrophysik, Potsdam, Ger.). Astron. Nachr.; 292: No. 2, 59-63(1970). (In German).

An empirical relation between the observable properties of radio surface brightness and radio index on the one hand and the intrinsic properties of linear diameter of the radio source, radio luminosity, and optical luminosity on the other hand was found and is shown in a diagram. The relation is strong enough to yield useful distance estimates. In this manner, distances of 8 quasars and 17 unidentified radio sources were obtained. (IAA)

30126 ESTIMATION OF THE ANGULAR DIMENSIONS OF SCINTILLATING RADIO SOURCES ON THE BASIS OF SHIFTS IN HISTOGRAMS OF SCINTILLATION QUASI-PERIODS. Panadzhyan, V. G. Soobshch. Byurakan. Observ., Akad. Nauk Arm. SSR; No. 41, 131-3(1970). (In Russian).

An expression is derived for estimating angular dimensions of scintillating radio sources for the case when interplanetary plasma inhomogeneities can be assumed as a thin phase screen. This expression is valid for a spherically symmetrical Gaussian source model and gives its angular dimensions in terms of the mean quasi-period of the radio source investigated and that of the point source. (IAA)

30127 PULSARS AND NEUTRON STARS. Biermann, Ludwig (Max-Planck-Institut fuer Physik und Astrophysik, Munich). Sterne Weltraum; 9: 220-3(Sep 1970). (In German).

The present state of research in the field of the origin and properties of pulsars is discussed. Following a historical review of the discovery of pulsars, their features observed so far are examined and analyzed. It is suggested that pulsars are rotating neutron stars which, in turn, are superdense supernova remnants. The velocity of rotation of very dense stars is also discussed. Finally, the nature and the properties of ultradense stars, "black holes," are explained. (IAA)

30128 MOLECULES IN INTERSTELLAR SPACE. Lequeux, James (Observatoire de Meudon, Hauts-de-Seine, France). Sci. Progr. Decouverte; No. 3422, 4-12(Jun 1970). (In French).

The significance for galactic physics of the recent discovery of radio-frequency lines from interstellar molecules is discussed. Natural molecular masers abound in interstellar space, yet the presence of certain molecules, which according to present knowledge should not have been there, raises some difficult but also challenging and fascinating problems of physical chemistry. The most curious fact about these interstellar molecules is that their abundance is roughly proportional to the abundance of their constituent atoms in interstellar matter. This suggests their formation through catalysis by dust particles rather than formation through direct combination of individual atoms. This problem will

XUM

surely soon attract the endeavors of many physical chemists. At present, observations of the OH molecule are conducted at Nancay in collaboration with astronomers of the Moscow Sternberg Institute, and a millimeter-wave interferometry project, aimed at the study of interstellar molecules, is being prepared by French radio astronomers. (IAA)

30129 OBSERVATIONS OF QUASI-STELLAR SOURCES AND RADIO GALAXIES AT MILLIMETER WAVELENGTHS. Rather, John Daniel Gray. Berkeley, Calif.; Univ. of California (1970). 161p. University Microfilms Order No. 71-835.

Thesis.

Fluxes of 49 extragalactic objects were measured at wavelengths near 8 millimeters and 1.2 centimeters. A signal-to-noise ratio greater than 4 was attained for 21 of the sources, >3 for 28 sources, and >2 for 35 sources, inclusive. The list of all objects observed included 28 QSO's, 5 Seyfert galaxies, 5 unidentified variable radio sources, 4 BSO's, 3 D galaxies, 1 N galaxy, and 3 miscellaneous objects. BSO 2 was detected with $S/N \geq 2.0$. NGC 1968 may be a variable source in the millimeter range. Spectral indices were compared with results from longer wavelengths. Many of the sources observed tended toward increasingly positive spectral index at millimeter wavelengths. Weaker QSS appeared to have more positive curvature indices than stronger ones. No correlation was found between radio and optical variability in eight sources observed repeatedly for possible flux variations. A possible correlation between radio flux at the point of spectral upturn and optical magnitude was noted, however, for 13 QSS that exhibit the upturn phenomenon. The significance of these findings in the context of source models is discussed. The new data for 3C 273 provided further evidence for the insufficiency of the relativistically expanding source model. A description of the operation of the new 20-foot telescope used in this work is included, together with a discussion of the pointing survey and the overall accuracy of the observations. (Diss. Abstr. Int., B)

30130 QUASARS: MILLISECOND-OF-ARC STRUCTURE REVEALED BY VERY-LONG-BASELINE INTERFEROMETRY. Knight, Curtis A. (Massachusetts Inst. of Tech., Cambridge); Robertson, Douglas S.; Rogers, Alan E. E.; (and others). Science; 172: 52-4(2 Apr 1971).

Observations with the Goldstone–Haystack radio interferometer of the quasars 3C 279 and 3C 273 disclosed the presence of fine structure in their radio emissions. Although the interpretation is not unique, the fringe–amplitude data for quasar 3C 279 are quite consistent with emissions from two points, each contributing equally to the correlated flux. The separation of the two points is estimated to be $(1.55 \pm 0.05) \times 10^{-3}$ arc second, or about 20 light years at the distance of 3×10^9 light years inferred from optical redshift data. The formal uncertainty in the right-ascension component of the separation is about 6×10^{-6} arc second; differential proper motion in this direction at half the speed of light could be discerned within a year. The fringe–amplitude data of quasar 3C 273 allow similar, but less-definitive, interpretations. (auth)

30131 SOLAR-CYCLE THEORY OF PULSARS. Apparao, Krishna M. V.; Chitre, S. M. (Tata Inst. of Fundamental Research, Bombay). Proc. Indian Acad. Sci., Sect. A; 72: 285-91(Dec 1970).

The plausibility of the solar-cycle type of mechanism for pulsar phenomenon is examined. The relevant time scales are found to be within the range of the observed pulsar periods. (auth)

30132 SOFT X RAYS FROM THE CYGNUS LOOP: INTERPRETATION. Tucker, Wallace H. (American Science and Engineering, Inc., Cambridge, Mass.). Science; 172: 372-4 (23 Apr 1971).

Two possible interpretations of the recent soft x-ray observation of the Cygnus Loop are discussed. A synchrotron model requires a magnetic field less than 10^{-6} gauss and electron energies in excess of 10^{14} electron volts. These electrons must either have been reaccelerated or continuously injected into the source for about 50,000 years. The observations are also consistent with the radiation from a hot plasma having the cosmic abundances of the elements. A likely origin for the hot plasma is a blast wave produced by the explosion of a supernova in the interstellar medium. Fitting such a model to the observations implies a kinetic energy release in the explosion of 6×10^{58} ergs for an assumed distance of 770 parsec. (auth)

30133 RECENT MEASUREMENTS OF THE ZEEMAN EFFECT AT 21-CENTIMETER WAVELENGTH. Verschuur, G. L. (National Radio Astronomy Observatory, Green Bank, W. Va.). Astrophys. J.; 165: 651-3(1 May 1971).

The line-of-sight component of the magnetic field in the Taurus dust cloud is less than 3.6 microgauss, and the presence of a strong field in a cloud in the direction of M17 is confirmed. A limit of 11 microgauss is set to the field in a cold H I cloud. (auth)

30134 OBSERVATIONS OF UNRESOLVED GALACTIC X-RAY SOURCES. Hudson, H. S.; Peterson, L. E.; Schwartz, D. A. (Univ. of California, San Diego). Nature (London); 230: 177-9 (19 Mar 1971).

New data are presented on an apparently diffuse x-ray emission from the galactic plane, obtained by the OSO III satellite, and covering the energy range 7.7 to 115 keV. These data are stated to impose important new constraints on theories regarding emission mechanisms; they cover an energy range between two earlier sets of observations at a few keV and 100 MeV. Data on the galactic x-ray and γ-ray diffuse flux are shown in tabular form and discussed. The results are considered in the light of Compton scattering of far-irradiation, Compton scattering of starlight, and the presence of low-luminosity discrete sources. Spectral index limits for the galactic emission suggest that these x rays may come from such sources with effective temperatures of 50 to 80 million K. The observations give a new upper limit of 1.7×10^{-9} W/cm^2 sr for any universal intensity of ir photons, at ~1-mm wavelength, assuming that the local intensity of ~3-GeV electrons is uniform throughout the Galaxy, and the same considerations applied to visible starlight lead to a new upper limit of 3.8×10^{-5} electrons cm^2 sec sr keV for the intensity of ~80 MeV cosmic-ray electrons. It is stated that such x-ray observations represent a new means of exploring the spectrum and spatial distribution of cosmic-ray electrons, and more sensitive experiments should make possible the direct detection of Compton scattered radiation in the submillimetre or microwave spectral rays. (UK)

30135 DETECTION OF THE LINEAR POLARIZATION OF PULSAR MP 0628 AND SOME CHARACTERISTICS OF ITS RADIO EMISSION IN THE METER-WAVELENGTH RANGE. Vitkevich, V. V.; Shitov, Yu. P. (Lebedev Inst. of Physics, Moscow). Dokl. Akad. Nauk SSSR; 195: 53-5(1 Nov 1970). (In Russian).

The waves emitted in the meter-wavelength range by MP 0628, discovered by Vaughan et al., were studied by means of the Pushchino radio telescope and a 12-channel radio receiver. A series of observations were made during the months of November and December 1969 at frequencies of 105 and 86 MHz. The dispersion was found to be 34.36 ± 0.08 pk. cm^{-3}. Variation of the amplitude from channel to channel was attributed to the rotation of the plane of polarization. The level of linear polarization of the emission was found to be high, exceeding 80%. During the observations the angle of polarization of the pulses remained constant within ±30%. The value H of the longitudinal magnetic field of the interstellar medium was found to be $H = 1.6 \times 10^{-6}$ Oersted. (TTT)

30136 OBSERVATIONS OF SOME EXTENDED GALACTIC RADIO SOURCES. Haslam, C. G. T.; Salter, C. J. (Univ. of Manchester, Jodrell Bank, Eng.). Mon. Notic. Roy. Astron. Soc.; 151: 385-95(1971).

A number of the larger angular diameter galactic radio sources in the anticenter quadrant were examined at 408 MHz. Integrated flux densities were computed at this frequency for all but one of the sources, and where sufficient data exist their spectra were investigated. It is shown that one object previously considered to be a supernova remnant, CTB 13, probably does not exist as a discrete source, but represents a section of the low-latitude, disk component of the unresolved background emission. (auth) (UK)

30137 RADIO MAPS OF CONDENSATIONS IN H II REGIONS. Wynn-Williams, C. G. (Mullard Radio Astronomy Observatory, Cambridge, Eng.). Mon. Notic. Roy. Astron. Soc.; 151: 397-420 (1971).

High-resolution maps of the H II regions DR 21, W 49A, and W 3 were made with the Cambridge One-Mile radio telescope at 5 GHz with a half-power beamwidth of 6.5 arc sec. Compact regions are clearly visible with sizes typically in the range 0.1 to 1.0 pc. The peaks of two of the condensations in W 49A are very close to OH emission regions, as is that of G 133.9 + 1.1 in W 3, which has a turnover frequency of 18 GHz. Comparison of radio data with optical isophotes of W 3 indicates a range of at least 12 magnitudes in the obscuration for different parts of the source. The most obscured part contains a group of four condensations one of which has a clear ring structure ½ pc in diameter. By combining data from W 3, W 49, W 58 and DR 21 it is shown that the condensations are probably surrounded by neutral hydrogen and that some, at least, must contain more than one of the earliest type stars known. The time scale of evolution and the connection between H II condensations and subgroups of OB stars in associations is discussed. The discovery of a small continuum radio source close to the W 75(N) OH source is also described. (auth) (UK)

30138 RADIOASTRONOMY AND MICROWAVE SPECTROSCOPY. Davies, R. D. (Univ. of Manchester, Eng.). Phys. Bull. (London); 22: 141-4(Mar 1971).

Following a brief historical introduction the following topics are discussed—cosmic abundance of the elements, the formation of molecules in interstellar space, the radio detection of interstellar molecules, interstellar water vapor, and interstellar formaldehyde. Preliminary observations are included on the inversion spectrum of NH_3 at ~1.25 cm wavelength in the Milky Way, CO emission, HCN detection, cyanoacetylene detection, etc. Some of the molecules, such as OH and formaldehyde, which are close to local thermodynamic equilibrium with their surroundings, will yield important new information concerning such matters as the temperature, density, and velocities of the interstellar medium. Others, such as OH (anomalous) and H_2O may provide interpretations of pumping and emission mechanisms. (UK)

30139 X-RAY PULSATIONS FROM CYGNUS X-1 OBSERVED FROM UHURU. Oda, M.; Gorenstein, P.; Gursky, H.; (and others) (American Science and Engineering, Inc., Cambridge, Mass.). Astrophys. J.; 166: L1-7(15 May 1971).

Large-amplitude x-ray pulsations were observed from Cyg X-1, which occur several times a second with a duration of less than a fraction of a second. The amplitude of the pulsations at times exceeds 25% of the average source intensity. The pulsations do not occur at random. Although the data cannot uniquely determine their period, it was found that the data are consistent with a period of 73 milliseconds. In addition to fine-scale time variations, the average X-ray intensity from the source changes by factors of 2 over times of the order of 10^3 seconds. It is concluded that a pulsating x-ray star has been discovered whose characteristics are quite different from those of NP 0532. (auth)

30140 LINE EMISSION IN THE X-RAY BACKGROUND. Shulman, Seth (Naval Research Lab., Washington, D. C.); Fritz, Gilbert; Meekins, John F.; (and others). Astrophys. J.; 166: L9-12(15 May 1971).

Evidence is presented for a line feature in the 6- to 7-keV region of the diffuse x-ray background spectrum. (auth)

30141 INTERFEROMETER MAP OF THE WATER-VAPOR SOURCES IN W49. Johnston, K. J. (Naval Research Lab., Washington, D. C.); Knowles, S. H.; Sullivan III, W. T.; (and others). Astrophys. J.; 166: L21-26(15 May 1971). 1971).

A map of the water-vapor emission at 22 GHz from W49 was constructed from data taken with a three-station long-baseline interferometer in 1970 June. The source was found to be composed of many individual features, all of which are less than 0.0005″ in size and lie within a circle having an angular diameter of approximately 1.5″. The position of the source is less than 10″ from one of the OH sources in W49. (auth)

30142 ATLAS OF 21-cm LINE PROFILES OF THE OUTER PART OF THE GALAXY IN THE REGION OF THE GALACTIC ANTICENTER. Velden, L. Beitr. Radioastron.; 1: 172-220 (Dec 1970).

The atlas presented contains 1253 H I emission line profiles observed with the 25-m Stockert telescope at fixed positions in the region of the galactic anticenter. The observations are arranged as cross sections of the galactic plane at constant galactic longitude. The line profiles are given as plots of brightness temperature versus radial velocity. Observational program and reduction procedure are discussed. (auth)

30143 KINEMATICS OF H I GASES IN THE GALACTIC ANTICENTER REGION. Velden, L. Beitr. Radioastron.; 1: 221-34(Dec 1970). (In German).

The kinematical properties of the interstellar gas in the anticenter region were investigated. For this purpose, the Gaussian component of 1250 emission line profiles of 21-cm observations in the coordinate range $120° \leq l \leq 240°$ and $-30° \leq b \leq 30°$ were used. (W.D.M.)

30144 REPLY TO: "COMMENTS ON 'ON THE FORMATION OF ENERGY SPECTRA IN SYNCHROTRON SOURCES'" BY E. TADEMARU, C. E. NEWMAN, AND F. C. JONES. Melrose, D. B. (Australian National Univ., Canberra). Astrophys. Space Sci.; 10: 458-63(Mar 1971).

A reply is presented to the objections raised by Tademaru, Newman, and Jones (preceding paper) to an earlier paper by Melrose (1969). (W.D.M.)

30145 STIMULATED COMPTON EFFECT IN VERY COMPACT RADIO SOURCES. Oster, Ludwig (Univ. of Colorado, Boulder); Altschuler, Martin D. Astrophys. Space Sci.; 10: 431-52(Mar 1971).

Expressions for the stimulated Compton effect are derived that are complete to order $\gamma\epsilon/\mu$, where ϵ is the photon energy in the laboratory system, and $\gamma\mu = \gamma m_0 c^2$ is the electron energy. Explicit formulas are given for the energy flow between a relativistic electron and a radiation field that obeys a power law so that the number of photons is proportional to ϵ^{-m-1}. The amount of energy gained by an electron per second is then numerically calculated for conditions suggested by very compact radio sources as functions of the width of the spectrum, the spectral index, and the electron energy. (auth)

30146 COMMENTS ON 'ON THE FORMATION OF ENERGY SPECTRA IN SYNCHROTRON SOURCES' BY DONALD B. MELROSE. Tademaru, E. (Stanford Univ., Calif.); Newman, C. E.; Jones, Frank C. Astrophys. Space Sci.; 10: 453-7(Mar 1971).

It is argued that the stationary energy spectrum given by Melrose (1969) for synchrotron sources resulting from systematic acceleration, energy–space diffusion, and synchrotron losses is unphysical as it requires a constant flow of particles in energy space. The general stationary solution is given. The asymptotic behavior of the time-dependent spectrum is found to depend critically on the boundary conditions; specifically, a stationary flat spectrum does arise for special boundary conditions, but it remains uncertain whether or not the boundary conditions applicable to a real synchrotron source will allow an initially steep spectrum to evolve toward a stationary flat spectrum. (auth)

30147 FLATTENING OF THE X-RAY SPECTRUM OF SCO X-1 AT ENERGIES BEYOND 40 keV. Agrawal, P. C.; Biswas, S.; Gokhale, G. S.; (and others) (Tata Inst. of Fundamental Research, Bombay). Astrophys. Space Sci.; 10: 500-7(Mar 1971).

Measurements of the hard x-ray spectrum of Sco X-1 in the energy interval 20 to 150 keV in three balloon flights from Hyderabad, India are reported. These results show conclusively that the spectrum of Sco X-1 is very flat in the energy interval 40 to 150 keV, and the measured fluxes beyond 60 keV are several orders of magnitude higher than those expected on the basis of an extrapolation of bremsstrahlung spectrum from a thin hot plasma at a temperature corresponding to $kT = 5$ keV, which is applicable for Sco X-1 for energies < 40 keV. The results are compared with those of other investigators of hard x rays from Sco X-1, and the implication of the results is briefly discussed. (auth)

30148 EVOLUTION OF QUASARS. Schmidt, Maarten; Bello, Francis. Sci. Amer.; 224: No. 5, 55-62; 64; 69(May 1971).

Topics discussed include the discovery of quasars, quiet quasars, counting verified quasars, radio-bright quasars, quasar models, and the cosmological hypothesis. (W.D.M.)

30149 MECHANISM FOR PULSAR RADIATION. Apparao, Krishna M. V. (Tata Inst. of Fundamental Research, Bombay). Proc. Indian Acad. Sci., Sect. A: 73: 1-6(Jan 1971).

It is shown that the low-frequency radiation emitted by a magnetic neutron star with the axis of its dipole field at an angle to the rotation axis, is periodic. This low-frequency radiation accelerates electrons and protons to high energies. The synchrotron radiation emitted by the high-energy particles in the ambient magnetic field is shown to be the pulsar radiation. (auth)

30150 SPECTRA OF EMISSION OF EXTRAGALACTIC RADIO SOURCES. Kurilchik, V. N. (Astronomical Inst., Moscow). Astrophys. Lett.; 7: 229-31(Feb 1971).

A statistical study of the spectra of extragalactic radio sources was made. The distribution of the spectral indices exhibits pronounced discrete maxima. It is shown that the power-law energy spectra of the relativistic electrons that originated in the nuclei of galaxies and quasars are in agreement with the Syrovatskii law. $N(E)\,dE \sim E^{-\gamma_0}\,dE \sim E^{-(2+\delta)}\,dE$, for $0 < \delta \leq 0.5$ and $2 < \gamma_0 \leq 2.5$. The features of the radio spectra of the double structures, halo-like structures, and variable components are considered. (auth)

30151 OBSERVATIONS OF VARIABLE RADIO SOURCES AT 2695 MHz. Witzel, A.; Veron, P. (Observatoire, Meudon, France). Astrophys. Lett.; 7: 225-8(Feb 1971).

The results of observations of variable radio sources with the large reflecting telescope of the Nançay radio astronomy station at a frequency of 2695 MHz (λ11 cm) are presented. The reported flux densities are total values, measured in two orthogonal polarization planes. The observations were made between December 1967 and June 1970. (auth)

30152 COMMENTS ON THE EXCITATION AND ABUNDANCE OF INTERSTELLAR SiO BASED ON A SEARCH AT

87 GHz. Dickinson, Dale F. (Smithsonian Astrophysical Observatory, Cambridge, Mass.); Gottlieb, Carl A. Astrophys. Lett.; 7: 205-7(Feb 1971).

A search was made in a number of galactic sources for radiation at 86 846.9 MHz corresponding to the $J = 1 \rightarrow J = 2$ transition for the $X^1\Sigma^+$ state of SiO. Using correlative information from the recent observation of the HCN molecule upper limits were derived for the SiO opacity which were typically ≤ 0.1 (presuming the HCN emission was thermal). This implied a column density for SiO in its lowest rotational state $\leq 10^{12}$ cm^{-2}. (auth)

30153 STUDY OF NGC 604 AT λ21.1 cm IN THE CONTINUUM AND HYDROGEN LINE. Wright, M. C. H. (Cavendish Lab., Cambridge, Eng.). Astrophys. Lett.; 7: 209-12 (Feb 1971).

Radio observations of M33 in both the hydrogen line and 21-cm continuum have led to estimates for the neutral and ionized hydrogen content of NGC 604. The mass and velocity dispersion within the nebula indicate that NGC 604 is dynamically unstable. (auth)

30154 PULSAR ELECTRODYNAMICS. Cohen, Jeffrey M.; Toton, E. T. (Inst. for Advanced Study, Princeton, N. J.). Astrophys. Lett.; 7: 213-15(Feb 1971).

Following the suggestion of Gold that pulsars are rotating magnetic neutron stars, Goldreich and Julian investigated a model with the magnetic dipole axis aligned with the rotation axis. These authors found that, despite the intense surface gravity of the neutron star ($\sim 10^{10}$ times as large as that at the surface of the Sun), the star must possess a dense magnetosphere. On the other hand, Pacini, and Gunn and Ostriker have suggested a mechanism for slowing down the neutron star and accelerating particles to cosmic-ray energies via the electromagnetic radiation from an oblique rotator (a star with magnetic axis not aligned with the rotation axis). All that is missing is a source of particles. Here, it is shown that an oblique rotator must possess a dense magnetosphere which could provide the required particle source. (auth)

30155 OH EMISSION FROM INTERSTELLAR H I CLOUDS. Verschuur, G. L. (National Radio Astronomy Observatory, Green Bank, W. Va.). Astrophys. Lett.; 7: 217-20(Feb 1971).

OH emission has been found in the direction of several interstellar neutral-hydrogen clouds, including an intermediate-velocity cloud and a very cold H I cloud. (auth)

Solar Phenomena

Refer also to abstracts 30308, 30309, and 30802.

30156 (CSIRO-Trans-10424) THE STRUCTURE OF THE CHROMOSPHERE AS SHOWN BY THE FRAUNHOFER LINES H_α AND H_β. Prokof'eva, I. A. Translated by G. Losonci (Australian Atomic Energy Commission Research Establishment, Lucas Heights), from Izv. Gl. Astron. Observ. Pulkove; 21: 155-69(1957). 29p. Dep. NTIS (U. S. Sales Only).

Solar spectra were obtained using the diffraction spectrograph at Pulkova. Nonuniform structure of Fraunhofer lines from location to location was evident from readings with spectrograph split dia. of 164 mm and second-order dispersion in H_α region of 1.02 Å/mm. Chromospheric streams of different densities and radial velocities are considered responsible for the shift of the center of H_α (chromospheric stream profiles are depicted). Undisturbed regions in the lower chromosphere layers are thought to be interspersed with flocculi. (Australia)

30157 (LA-4343(Suppl.)) PARTICLE COLLISIONS IN THE OPPOSING MASS FLOW HYPOTHESIS: A FACET OF THE SUPERNOVA FRAGMENTATION MODEL OF SOLAR SYSTEM FORMATION. Brown, Wilbur K. (Los Alamos Scientific Lab., N. Mex.). Dec 1970. Contract W-7405-eng-36. 9p. Dep. NTIS.

An investigation was made into some of the consequences of the opposing mass-flow hypothesis within the supernova fragmentation model of solar system formation. The results of simple elastic-scattering analysis indicate that, in the particle collisions of the two clashing flows, heavy elements would tend to remain in orbit whereas hydrogen, though still gravitationally bound to the Sun, would be removed from orbit. (auth)

30158 (UCSD-34-P-43-X-9) THE DISTRIBUTION AND ORIGIN OF THE ELEMENTS AND THEIR ISOTOPES IN NATURE. Final Report, 1962-1970. Urey, Harold C. (California Univ., La Jolla, San Diego. Dept. of Chemistry). Contract AT(04-3)-34. 18p. Dep. NTIS.

Lists are given of equipment, personnel, and publications. Research topics are briefly summarized in terms of diamonds in meteorites, stable-isotope variations in meteorites, cosmogenic rare gases and cavities in iron meteorites, ^{81}Kr-Kr dating method, trapped xenon and krypton and the classification of chondrites, solar-type xenon, and Gd isotopic analyses. (W.D.M.)

30159 HIGH-SENSITIVITY SOLAR RADIOSPECTROMETRY AT ARECIBO (PUERTO RICO). Boischot, Andre; De La Noe, Jerome; Du Chaffaut, Maurice; Rosolen, Carlo (Observatoire de Paris, Meudon, France). Compt. Rend., Ser. B; 272: 166-9 (11 Jan 1971). (In French).

High-resolution spectra of the decametric waves emitted by the Sun were obtained using the wide-aperture radiotelescope at Arecibo. The instrumentation is described. The preliminary results obtained are discussed: existence of a discontinuity in the corona at a height of about one solar radius and a new type of burst associated with type III bursts. (France)

30160 SOLAR SOFT X RADIATION. Thomas, Roger Jerry. Ann Arbor, Mich.; Univ. of Michigan (1970). 206p. University Microfilms Order No. 70-21,802.

Thesis.

Data from the University of Michigan's ion chamber photometer aboard OSO-III were used to investigate relationships between solar soft x radiation and phenomena observed at other wavelengths. The Michigan 8- to 12-Å x-ray data are exceptionally well suited for such studies because they cover an interval of more than a year on a nearly continuous basis with excellent time resolution, sensitivity, dynamic range, and stability. X-ray fluxes were determined using the assumption of a 2×10^6 K gray-body spectrum which remains constant with time. Uncertainties in derived fluxes that are caused by this assumption are shown to be small even during x-ray bursts. (TSS) (Diss. Abstr. Int., B)

30161 STUDY OF LOW-ENERGY COSMIC RAYS AT 1 A. U. Kinsey, James Humphreys. College Park, Md.; Univ. of Maryland (1970). 160p. University Microfilms Order No. 70-22,571.

Thesis.

The results from the two scintillator ΔE versus $-\Delta E$ telescopes on IMP-III and IMP-IV and the solid-state telescope on IMP-IV are analyzed, and the resulting proton and alpha particle fluxes are presented. The low-energy flux time histories and energy spectra are shown for the energy interval 18.7 to 81.7 MeV/nucleon from June 1965 to April 1967 and in the interval from 5.2 to 81.7 MeV/nucleon from May 1967 to August 1968. (TSS) (Diss. Abstr. Int., B)

30162 BIENNIAL OSCILLATION, TREE RINGS, AND SUNSPOTS. Schove, D. J. (St. Davids Coll., Kent, Eng.). Weather, (London); 24: 390-7(Oct 1969).

The quasi-biennial oscillation noted in recent years in many weather parameters has had a wavelength of one-fifth of the solar cycle. Analysis of tree-ring data suggests that the wavelength of the "biennial" oscillation shortened in phase with the shortening of the solar cycle. Further careful analysis of the oscillations in the equatorial stratospheric winds and in ozone data suggests that the quasi-biennial oscillation is at its strongest when solar activity is at a maximum and is almost undetectable at solar minima. The two cycles are somehow connected with the solar cycle providing the driving mechanism for the shorter cycle. (Meteorol. Geoastrophys. Abstr.)

30163 MEXICAN SOLAR ECLIPSE. Waldmeier, Max (Eidgenoessische Sternwarte, Zurich). Ster Weltraum; 9: 186-91(Jul-Aug 1970). (In German).

A study of the solar eclipse of March 7, 1 0 in Mexico is described, giving particular attention to work undertaken by the expedition from the Zürich observatory in Switzerland. The general characteristics of the eclipse are briefly reviewed, and the research program conducted is discussed, taking into consideration the equipment used in the investigations. Some photographs obtained of the corona are presented. (IAA)

30164 STUDIES OF PROTON FLUX IN THE RANGE FROM 1.5 TO 50 MeV ON SATELLITES ZOND-4 AND ZOND-5. Konstantinov, B. P.; Bredov, M. M.; Kolchin, A. A.; Lebedev, V. V.; Skrebtsov, G. P. (Ioffe Inst. of Physics and Tech., Leningrad). Izv. Akad. Nauk SSSR, Ser. Fiz.; 34: 2250-4(Nov 1970). (In Russian).

Instrumentation used for measuring proton flux at ranges 1.5 to 10, 30 to 35, and 45 to 50 MeV is described. The measurements were carried out on board Zond-4 and Zond-5. Results are tabulated and analyzed. (tr-auth)

30165 HELIOLATITUDINAL INDEX (HL) OF THE SOLAR ACTIVITY AND THE 11-YEAR VARIATIONS OF COSMIC RAYS. Gushchina, R. T.; Dorman, I. V.; Dorman, L. I.; Pimenov, I. A.

Izv. Akad. Nauk SSSR, Ser. Fiz.; 34: 2426-33(Nov 1970). (In Russian).

A helio-latitudinal index of solar activity was introduced in order to calculate the helio-latitudinal distribution of sunspots and variations of the Earth's helio-latitude. The relationship between the index and variations of the cosmic-ray intensities was analyzed. (tr-auth)

30166 EXTREME-ULTRAVIOLET SPECTRUM OF THE QUIET SUN. Dupree, A. K.; Reeves, E. M. (Harvard Coll. Observatory, Cambridge, Mass.). Astrophys. J.; 165: 599-613 (1 May 1971).

Intensities and identifications of solar emission lines observed at the center of the quiet Sun are presented for the wavelength range 304 to 1394 Å. The spectra were obtained during October 1967 by the Harvard scanning spectrometer on OSO-IV. This instrument has a spatial resolution of 1 arc minute and a spectral resolution of approximately 2 Å. (auth)

30167 TYPE III SOLAR RADIO BURSTS ACCOMPANIED BY SOFT X-RADIATION IN THE ABSENCE OF Hα FLARES. Teske, Richard G. (Univ. of Michigan, Ann Arbor); Soyumer, Tevfik; Hudson, Hugh S. Astrophys. J.; 165: 615-19(1 May 1971).

Several Type-III solar radio bursts which occurred in the absence of reportable flares were observed to be accompanied by weak x radiation detectable at photon energies of between 1.0 and 12.5 keV. The x rays almost invariably preceded the Type-III burst, an observation which suggests that a thermal event precedes the Type-III instability. (auth)

30168 MEAN LIVES AND ABSOLUTE f-VALUES IN NEUTRAL IRON. Klose, Jules Z. (National Bureau of Standards, Washington, D. C.). Astrophys. J.; 165: 637-42(1 May 1971).

Mean lives of three levels in Fe I were determined by using electronic excitation and a method of delayed coincidence. By the use of known relative f-values, absolute f-values were derived from the life-time results for the transitions used in the lifetime measurements. The experimental results are summarized. The error given with each quantity is the standard deviation as determined from the dispersion of the individual measurements. In addition, the experimental results are estimated to contain systematic errors of up to 2%. Both the lifetimes and the f-values are presented in comparison with experimental results of other workers. (auth)

30169 EVIDENCE FROM HARD X RAYS FOR TWO-STAGE PARTICLE ACCELERATION IN A SOLAR FLARE. Frost, K. J.; Dennis, B. R. (Goddard Space Flight Center, Greenbelt, Md.). Astrophys. J.; 165: 655-9(1 May 1971).

A solar x-ray burst that evolves in time through two nonthermal phases is presented. The burst is considered to be bremsstrahlung from electrons accelerated in two stages in the solar atmosphere. In the first stage, acceleration effectively to 100 keV occurs, perhaps by an induced electric field; in the second stage, the acceleration to higher energies could occur by a Fermi mechanism operating in a shock front. (auth)

30170 MEASUREMENTS OF OSCILLATOR STRENGTHS FOR Fe I AND Fe II. Wolnik, S. J.; Berthel, R. O.; Wares, G. W. (Air Force Cambridge Research Labs., Bedford, Mass.). Astrophys. J.; 166: L31-3(15 May 1971).

Absolute gf-values of sixty-eight Fe I and twelve Fe II lines were determined by shock-tube emission spectroscopy. These values extend previous Fe I measurements to include somewhat weaker transitions and an expanded wavelength range (4360 to 6680 Å). Implications regarding recent determinations of iron abundances in the solar photosphere are considered. (auth)

30171 CORRELATIONS BETWEEN THE ^{210}Pb ATMOSPHERIC ABUNDANCE IN TERRE ADELIE AND THE SOLAR ACTIVITY. Lambert, Gerard; Sanak, Joseph; Ardouin, Benedicte (CNRS, Gif-sur-Yvette, France). Compt. Rend., Ser. B; 272: 497-500(22 Feb 1971). (In French).

Atmospheric ^{210}Pb aerosols sampled daily from 1960 to 1968 at the Dumont Durville Station (Terre Adélie) were studied. These 9 years are divided into 31 intervals of unequal duration, whose limits correspond to sharp variations in the monthly average number of sunspots. The correlation between ^{210}Pb abundance (after corrections for the seasonal variations) and the Wolf number was investigated. (France)

30172 SOLAR SPECTRUM FROM λ 7498 TO λ 12016. A TABLE OF MEASURES AND IDENTIFICATIONS. Swensson, J. W.; Benedict, W. S.; Delbouille, L.; Roland, G. Mem. Soc. Roy. Sci. Liege, Vol. Hors Ser.; No. 5, 1-449(1970).

As a result of the nearly 2100 lines attributed to atomic transitions and the nearly 1900 lines assigned to CN, most of the Fraunhofer absorption between λ 7498 and λ 12016 can now be accounted for. A list of the strongest solar lines remaining unidentified (Int. ≥8) is given. It will be noted that few in this grouping are of intensity greater than 15. (auth)

30173 IDENTIFICATION OF NiH IN THE SUNSPOT SPECTRUM. Lambert, D. L. (Univ. of Texas, Austin); Mallia, E. A. Mon. Notic. Roy. Astron. Soc.; 151: 437-47(1971).

Photoelectric scans of the umbral spectrum in the wavelength interval 6200 to 6700 Å were examined and positive identifications established for NiH lines. The band oscillator strengths for the $A^2\Delta - X^2\Delta$ and $B^2\Delta - X^2\Delta$ systems were derived, $f_{00} = 5 \times 10^{-3}$ and 6×10^{-3} respectively, for an adopted dissociation energy of 2.6 eV. It is also shown that the solar isotopic and terrestrial isotopic abundance ratios for ^{58}Ni and ^{60}Ni are probably equal. (auth) (UK)

30174 INNER-SHELL ABSORPTION IN THE SPECTRA OF THE ALKALINE EARTHS. I. MAGNESIUM (Mg I). Newsom. G. H. (Imperial Coll. of Science and Tech., London Ohio State Univ., Columbus. Astrophys. J.; 166: 243-7(15 May 1970).

The absorption spectrum of magnesium vapor in the extreme-ultraviolet region was obtained, and twenty-three previously unknown lines of Mg I were observed near 220 Å. Twenty-one of the lines were classified into five series, involving excitation of an inner-shell 2p electron, and identification of the remaining two lines is suggested. (auth)

30175 OBSERVATIONS OF CHROMOSPHERIC FLARES AT HURBANOVO OBSERVATORY DURING THE YEAR 1969. Knoska, S.; Parajnakova, V. (Slovak Central Observatory, Hurbanovo, Czech.). Bull. Astron. Inst. Czech.; 22: 91-101 (1971).

Observational data are presented on chromospheric flares observed in Hurbanovo in 1969. Data on 255 flares were tabulated, and graphs show the variations of the width of the Hα line measured in the course of the observations of the individual flares. (auth)

30176 NORTH-SOUTH COMPONENT OF THE INTERPLANETARY MAGNETIC FIELD. Coleman, Paul J. Jr.; Rosenberg, Ronald L. (Univ. of California, Los Angeles). J. Geophys. Res.; 76: 2917-26(1 May 1971).

The flights of Mariner 2, 4, and 5 yielded measurements of the interplanetary magnetic field between heliocentric ranges 0.65 and 1.5 AU and between heliographic latitudes 7.5° and −7.5°. An analysis of these measurements indicates that, for a given polarity, the north−south component or more precisely the θ component in a spherical polar coordinate system (r, θ, ϕ), has, in general, a mean value that is significantly different from zero. For an interplanetary field directed outward from the Sun, the mean value of B_θ is negative (northward) above the solar equatorial plane and positive (southward) below it and vice versa for an inward field. Thus, at a point off the equator, the component of B in the $r\theta$ plane is tilted away from the equatorial plane more than the radial from the Sun through that point. The magnitude of the mean value probably depends on both r and θ. By assuming that the radial dependence is a power law in r and the θ dependence is a constant times the latitude $\beta = [(\pi/2) - \theta]$, $B_{\theta S}$ as $(\langle B_{\theta +} \rangle - \langle B_{\theta -} \rangle)/2$ was defined, and from Mariner 4 data $B_{\theta S} \approx -(0.09 \pm 0.03)\beta(r/r_0)^{-(1.8 \pm 0.2)}$ was obtained, where B_θ is in units of 1 γ, β is in degrees, and $r_0 = 1.0$ AU. (auth)

30177 IMPROVED ESTIMATE OF SOLAR NEUTRON FLUX MEASURED IN AN EARLIER EXPERIMENT. Daniel, R. R.; Gokhale, G. S.; Joseph, George; Lavakare, P. J. (Tata Inst. of Fundamental Research, Bombay). J. Geophys. Res.; 76: 3152-3(1 May 1971).

A spark-chamber scintillation counter-detector assembly was flown in a balloon from Hyderabad, India, on April 15, 1966. After evaluating all the data and the results calculated, it was concluded that the enhanced counting rate was due to the emission of energetic neutrons from an active region of the Sun. After a later investigation by Apparao et al., it became clear that the application of the knock-on proton method used in emulsions for deducing the absolute flux of neutrons of energy ≳50 MeV was uncertain because of the increasing contribution of single-pronged stars induced by energetic neutrons. A new evaluation was then made to arrive at a more reliable flux of solar neutrons, which is about 6 times smaller than the previous value. (J.C.W.)

30178 COMPUTER SIMULATION OF THE FORMATION OF PLANETARY SYSTEMS. Dole, Stephen H. (Rand Corp., Santa Monica, Calif.). Icarus; 13: 494-508(Nov 1970).

XUM

One of the many hypotheses about the formation of the solar system postulates that the planets were formed by the aggregation of particulate matter within a cloud of dust and gas surrounding the newly formed Sun. A test of the validity of one version of this hypothesis was obtained in a computerized Monte Carlo simulation of the process. In the model used, nuclei are "injected" into the cloud one at a time, on elliptical orbits. The dimensions of the semimajor axis and the eccentricity of the orbit of each nucleus are determined by using random numbers. As the nuclei orbit within the cloud they grow by aggregation and gradually sweep out dust-free annular lanes. If they grow larger than a specified critical mass they can begin to accumulate gas from the cloud as well. If the orbit of a planet comes inside a certain interaction distance from a planet that was formed earlier, or if the orbits cross one another, the two bodies coalesce to form a single, more massive planet which may then continue to grow by aggregation. The process of injecting nuclei is continued until all the dust has been swept from the system. At this point the run is terminated and the machine output displays the masses and orbital parameters of the planets remaining in the final configuration. Each planetary system produced by using a different random number sequence is unique. However, all the systems so produced share the major regular features of the solar system. The orbital spacings have patterns of regularity suggestive of "Bode's law." The innermost planets are small rocky bodies; the mid-range planets are large gaseous bodies; the outermost planets are generally small. The general pattern of planetary mass distribution is similar to that in the solar system with masses ranging from less than that of Mercury to greater than Jupiter's. (auth)

30179 CONVECTIVE TRANSPORT OF LOW-ENERGY COSMIC RAYS IN THE INTERPLANETARY REGION. Gleeson, L. J. (Monash Univ., Clayton, Australia). Astrophys. Space Sci.; 10: 471-85(Mar 1971).

A complete solution was obtained of the steady-state transport equations, including energy losses, for cosmic rays in the interplanetary region for conditions in which diffusive transport is negligible and convective effects dominate. The region of validity of the solution will, in general, be a shell between heliocentric radii R_1 and R_2 (R_2 may be infinite). The precise range of kinetic energy T and heliocentric radius r in which the solution is valid is not known, but it appears to be applicable in the vicinity of Earth to protons with $T \leq 1$ MeV. For $T \sim 0.5$ MeV near Earth, R_1 may be ~0.5 AU and R_1 will decrease as T, observed near Earth, decreases. The solution is simple in form but quite general; it predicts the differential number density U(r,T) in terms of that observed at radius a (near Earth, say). Thus it may be quite useful in interpreting and coordinating steady-state cosmic-ray observations at $T \sim 1$ MeV. The differential and integral intensities, differential anisotropy, and differential radial gradient at (r, T) also are determined. A simple interpretation of the solution is given in terms of energy losses due to adiabatic deceleration of the particles as they are being convected outward from the Sun. This leads to the useful notion of following a particle in (r,T) as it increases r and decreases T. Particles convected from the outer corona to Earth decrease their kinetic energy by a factor ~500. Following a particle, the Compton–Getting factor remains constant. Particles observed at (a,T) in convective transport have come from nearer the Sun; they may be of solar origin but may also be of galactic origin having penetrated to $r < R_1 < a$ at higher energy. (auth)

30180 RESISTIVE EFFECTS IN THE TURBULENT PHOTOSPHERE AND CHROMOSPHERE. Lerche, I. (Univ. of Chicago). Astrophys. Space Sci.; 10: 486-99(Mar 1971).

The role of finite-resistivity effects in the photosphere and chromosphere was investigated, and it is demonstrated that turbulence in the photospheric conductivity gives rise to a resistive instability, as does the gradient in resistivity between the chromospheric layer of the Sun and the photospheric layer, which latter unstable mode is the well-known tearing mode of Furth, Killeen, and Rosenbluth. In both cases the calculations indicate time scales of the order of seconds or minutes, and it is therefore believed that solar flares and spicules can be produced by finite conductivity instabilities. It is also demonstrated that the finite-resistive diffusion makes it difficult to maintain an initially force-free flux tube in the chromosphere unless the Alfven speed is sufficiently high and/or the flux tube is sufficiently thick. It is also shown that the magnetic fields in the turbulent photosphere become "trapped" by high-conductivity regions and this leads to enhancement of the resistive instabilities. The analysis does not explain the origin of the high-energy particles in solar flares; for this the problem of dynamical acceleration must be investigated. (auth)

30181 DISTRIBUTION OF IONIZATION STAGES OF ARGON UNDER CORONAL CONDITIONS. Lexa, J. (Astronomical Inst., Skalnate Pleso, Czech.). Bull. Astron. Inst. Czech.; 22: 1-11 (1971).

The effectiveness of various ionization and recombination processes under coronal conditions is discussed, in particular, collisional ionization, radiative recombination, and dielectronic recombination. The ionization equilibrium of argon was computed in the electron temperature interval of 2.0 to 4.5×10^6°K, the effect of dielectronic recombination being partly respected. The oscillator strengths, required for determining the dielectronic recombination coefficients, were computed using the Bates–Damgaard method. The results, the relative ionic abundances of ArXI, ArXII, ..., ArXVII, are given. The reliability of the results is discussed, they are compared with House's classical computation (1964) and the possible effect of ArX and ArXVIII ions is discussed. (auth)

30182 SOME REMARKS ON THE SUMMARY OF USE OF EXISTING CORONA MEASUREMENTS. Sykora, J. (Astronomical Inst., Skalnate Pleso, Czech.). Bull. Astron. Inst. Czech.; 22: 12-18(1971).

The green corona data published in Quarterly Bulletin on Solar Activity were used to analyze some discrepancies in the coronal measurements of various corona stations. Some points resulting from the position angle errors, the E–W asymmetry, the instability of the photometric scales, and the threshold of measurements that should be taken into account when using the data of different corona stations are noted. The influence of the differential refraction and the differential extinction on the coronal measurements is analyzed. (auth)

30183 ALIGNMENT OF DUST PARTICLES IN COMET TAILS. Harwit, M. (Astronomical Inst., Prague); Vanysek, V. Bull. Astron. Inst. Czech.; 22: 18-21(1971).

The possibility of dust-particle alignment in comet tails is considered, and it was found that an effect described by Gold (1952) produces significant alignment through bombardment of the grains by solar-wind protons. (auth)

30184 DECREASE OF THE AREA OF INDIVIDUAL LARGE SUNSPOTS NEAR THE CENTRAL MERIDIAN. Pajdusakova, L. (Astronomical Inst., Skalnate Pleso, Czech.). Bull. Astron. Inst. Czech.; 21: 303-7(1970).

It is shown that individual sunspots, except for the smallest ones, show a decrease of their area in the close vicinity to the central meridian. Particularly, the stable and regular spots and individual spots taken from large groups were investigated in this respect. The decrease of their areas may be a real consequence of the negative influence of the Earth on solar activity, or it may be an apparent effect only, relating to the geometrical conditions of observation. (auth)

30185 RUN OF THE DIFFERENCE OF THE MAXIMAL MAGNETIC FIELD STRENGTH OF OPPOSITE POLARITIES IN SUNSPOT GROUPS BEFORE AND AFTER PROTON FLARES. Kuklin, G. V. (Astronomical Inst., Ondrejov, Czech.). Bull. Astron. Inst. Czech.; 21: 307-10(1970).

An attempt was made to obtain typical curves of the run of the difference of the maximal magnetic field strengths of opposite polarities in sunspot groups before and after proton flares. It may be that in the case of recurrent protons in the same sunspot group, for the proton flares separated by 3 days, some regularity of the difference run exists. (auth)

30186 RELATION BETWEEN ELECTRIC CONDUCTIVITY IN SPOT AND PHOTOSPHERE. Kopecky, M. (Astronomical Inst., Ondrejov, Czech.). Bull. Astron. Inst. Czech.; 21: 238-41(1970).

The relation of electric conductivities at the same geometric depths in spot and photosphere substantially depends on the spot model regardless of whether the absolute values of this relation or the change of the latter with geometric depth are concerned. A substantial difference exists between transparent and dense spot models. The same goes for the horizontal gradient of electric conductivity in the spot. (auth)

30187 LIMB FLARES ASSOCIATED WITH SOLAR SOFT X-RAY BURSTS. Pinter, S. (Geophysical Inst., Hurbanovo, Czech.). Bull. Astron. Inst. Czech.; 21: 241-6(1970).

The relations between limb flares and the growth phase of the intensity of solar soft x-ray bursts are considered. The relationship is demonstrated in much detail by two characteristic examples from December 2, 1968, and March 12, 1969. It is shown

that the start of the intensity increase of solar soft x-ray bursts is related to the sudden space expansion of the flare in the H-alpha line. The electron temperature, determined from the observation of the intensity of x rays in two wavelengths, is within the range (3 to 7) × 10^7 °K. (auth)

30188 SECOND OBSERVATION OF Ar XIV OUTSIDE TOTAL ECLIPSE OF THE SUN. Rusin, V. (Astronomical Inst., Skalnate Pleso, Czech.). Bull. Astron. Inst. Czech.; 21: 247-8(1970).

The observation of the big coronal condensation above the eastern limb of the Sun from October 17 to 21, 1969 is described. Besides the emission lines Fe XIV (5303 Å) and Fe X (6374 Å), the two emission lines Ca XV (5694 Å and 5446 Å) and the emission line Ar XIV (4412 Å) were observed October 19 and 20, 1969. (auth)

30189 OBSERVATIONS OF CHROMOSPHERIC FLARES AT ONDREJOV OBSERVATORY DURING THE YEAR 1969. Hrebik, F.; Kvicala, J.; Krivsky, L.; Olmr, J. (Astronomical Inst., Ondrejov, Czech.). Bull. Astron. Inst. Czech.; 21: 249-62(1970).

This paper is a continuation of eleven preceding reports that contained chromospheric flares observed at Ondřejov observatory from 1948 up to the end of 1968 and covers the period of 1969. The data on 264 flares, associated 9400, 808, 536, and 260 MHz events and 27 kHz S.E.A. observed and recorded during 1969 are summarized. The corresponding curves of the Hα line-width changes are plotted. (auth)

Galaxies

30190 PROBLEM OF APPLYING THE MODEL OF A NORMAL LOGARITHMIC SPIRAL TO GALAXIES. Dzigvashvili, R. M.; Borchkhadze, T. M. Byull., Abastumanskaya Astrofiz. Observ., Akad. Nauk Gruz. SSR; No. 37, 141-6(1969). (In Russian).

Characteristic angles (angle between the radius vector and the tangent at a given point of the spiral) for the spirals of six multi-arm galaxies—NGC 1232, 5247, 4303, 4321, 3938, and 3184 were determined. The angles varied over a large interval along the spiral arms; the mean square deviations ranged from 4 to 20°. The deviation of the mean characteristic angle of each arm from the mean angle of the entire galaxy was comparatively small. Attention was given to the use of the normal logarithmic spiral model for estimating the number of arms in the Galaxy. It is shown that the use of the model for this purpose is difficult and yields unreliable results. (IAA)

30191 STUDY OF THE GALACTIC STRUCTURE IN THREE SECTIONS OF THE MILKY WAY IN THE DIRECTION OF CONSTELLATION TAURUS (THE ANTICENTER OF THE GALAXY). Kalandadze, N. B. Byull., Abastumanskaya Astrofiz. Observ., Akad. Nauk Gruz. SSR; No. 38, 3-17(1969). (In Russian).

The results of a study of interstellar absorption and distribution of absorbed matter in three regions of Taurus are presented. The study was made on the basis of data obtained from two-dimensional classification and three-color photography of a group of stars. The spatial distribution of the hot stars suggests their condensation at a distance of 1.5 kps from the Sun and a less-pronounced condensation at 2.5 kps from the Sun. The results of the study are compared with available radio astronomical data. (IAA)

30192 PHYSICAL PROCESSES CONCERNING THE GRAINS OF DUST SURROUNDING STARS: CHARGE AND PHOTOELECTRIC EFFECT. Pecker, Jean-Claude. Compt. Rend., Ser. B; 272: 69-73(4 Jan 1971). (In French).

The combined effect of the aggregation of electrons by grains of interstellar dust and high-energy photons led to an estimation of the charge on these grains; this estimation is dependent upon assumptions made on the photoelectric yield and the radiation field. In any H II region the charge is high, positive, and independent of position. (France)

30193 OBSERVATION OF LINES OF INTERSTELLAR CALCIUM IN THE NORMA CONSTELLATION. Chu-Kit, Marcel (CNRS, Marseille). Compt. Rend., Ser. B; 272: 74-6(4 Jan 1971). (In French).

Studies of the radial velocity of interstellar calcium in the direction of the Norma constellation indicate two velocity maxima of -12 and -49 km/sec and a velocity spread between -60 and -97 km/sec. The first maxima corresponds to the arm of Sagittarius and the second to the arm of Norma. The velocity spread may correspond to a third arm, nearer to the center of the Galaxy and viewed tangentially with respect to the galactic longitude l = 328°. (France)

30194 SPECTROPHOTOMETRY OF THE NUCLEUS OF THE NGC 2655 GALAXY. Andrillat, Yvette (Montpellier Univ., France); Souffrin, Suzy. Compt. Rend., Ser. B; 272: 170-2 (11 Jan 1971). (In French).

A spectrophotometric study of the nucleus of NGC 2655 allowed the equivalent line widths in the emission and absorption processes to be determined. The physical conditions of the emitting gas and the stellar population of the nucleus were then investigated. (France)

30195 THEORETICAL INVESTIGATIONS ABOUT THE INTERSTELLAR DUST. III. DUST FORMATION BY CIRCUMSTELLAR CRUSHING PROCESSES. Dorschner, J. (Univ., Jena, Ger.). Astron. Nachr.; 292: No. 2, 79-85(1970). (In German).

A general equation is discussed for describing circumstellar crushing processes on the basis of concepts considered by Piotrowski (1954). The processes taking place in the "solar system gravel mill" are examined, and a general equation is derived on the basis of a number of assumptions. The general equation contains an equation presented by Piotrowski as a special case. Solutions of the general equation for specific cases are investigated. The results are found to agree with the distribution of particle size of the observed fragments in interplanetary space. (IAA)

30196 THEORETICAL INVESTIGATIONS ABOUT THE INTERSTELLAR DUST. II. OPTICAL PROPERTIES OF SPHERICAL DUST PARTICLES FROM METEORITIC SILICATES AND DIRTY ICE. Dorschner, J. (Univ., Jena, Ger.). Astron. Nachr.; 292: No. 2, 71-8(1970). (In German).

The coefficients of extinction, scattering, and radiation pressure, the scattering functions and the albedo for spherical particles with the index of refraction corresponding to that of meteoritic silicates were studied. The coefficients were obtained on the basis of the Mie theory (1908). The scattering functions were calculated on a computer in accordance with a procedure reported by Chu and Churchill (1955). The obtained values were compared with values of the corresponding parameters for classical dust particles (dirty ice). (IAA)

30197 DIVISION PROCESSES AND INSTABILITY OF SYSTEMS OF GALAXIES. Karachentsev, I. D.; Terebizh, V. Yu. Soobshch. Byurakan. Observ., Akad. Nauk Arm. SSR; No. 41, 99-130(1970). (In Russian).

The role played by division of galactic nuclei during dynamical evolution of systems of galaxies is studied in terms of Ambartsumian's hypothesis. An exact solution of this problem is obtained, and a number of consequences are compared with existing observational data. The existence of instability of the systems of galaxies in terms of model suggested is examined. It is shown that the calculated characteristics of systems of galaxies including radius, population density, distribution of velocity, and amount of crowded double galaxies, and some others are in good agreement with observational data. (IAA)

30198 HIGH-VELOCITY CLOUD COLLISIONS. Chow, Tailow. Rochester, N. Y.; Univ. of Rochester (1970). 102p. University Microfilms Order No. 71-1376.

Thesis.

Since the discovery of the high-velocity neutral hydrogen gases at high galactic latitudes, various possibilities have been considered for their origin and their interpretations. All these interpretations have their difficulties and an attempt is made to critically examine the consequences when high momentum inflowing extragalactic gas clouds collide with galactic gases, the extragalactic gases having initial velocities of perhaps –500 km/sec with respect to the local standard of rest. (Diss. Abstr. Int., B) (TSS)

30199 I Zw 1: A VARIABLE COMPACT GALAXY. Usher, P. C. (Pennsylvania State Univ., University Park); Shen, B. S. P.; Barrett, J. W. Astrophys. J.; 165: 647-50(1 May 1971).

The photometric history of the radio-quiet compact galaxy I Zw 1 (0051 + 12) was investigated on Harvard photographic plates dating back to 1909. The available data indicate that the galaxy is variable and probably undergoes outbursts of about 0.7 mag above a brightness level that is itself variable by about 0.7 mag. (auth)

30200 INTERSTELLAR MOLECULES. Carruthers, George R. (Naval Research Lab., Washington D. C.). Astronaut. Aeronaut.; 9: No. 4, 16-19; 79-80(Apr 1971).

Topics discussed include molecular spectroscopy, optical spectroscopy of interstellar molecules, infrared spectroscopy of interstellar molecules, radio spectroscopy, interstellar molecules

XUM

and star formation, and interstellar molecules and the origin of life. (W.D.M.)

30201 EVIDENCE AND VELOCITY OF A DENSITY WAVE IN THE GALAXY M33. Courtes, G.; Dubout-Crillon, R. (Observatoire, Marseille). Astron. Astrophys.; 11: 468-76(Apr 1971). (In French).

The photographs of the southern arm of M33 taken through interference and colored filters show the most intense and numerous H II regions at the inner edge of the arm and therefore indicate hot stars and a probable maximum of neutral hydrogen. Thus, it may be considered that the front of the spiral arm is located in this inner edge. At the outer edge a maximum in the distribution of brighter stars is observed. These stars are grouped into associations where red supergiants, hot stars, brightest blue supergiants, a few dust clouds, and H II regions are found. An age for the outer edge of the spiral arm due to the expansion of the associations (the age of the front being zero), is estimated as 8×10^6 yr. The difference in age between the front and the outer edge of the spiral arm shows that the circular motion of it is faster than that of the inner edge (the front). Therefore the spiral pattern is a density wave of hydrogen, its rotation velocity Ω_p is small of about +15 km s^{-1} kpc^{-1}. (auth)

30202 ROTATION OF GALAXIES AND THE GRAVITATIONAL INSTABILITY PICTURE. Peebles, P. J. E. (Princeton Univ., N. J.). Astron. Astrophys.; 11: 377-86(Apr 1971).

There is disagreement on whether the simple gravitational instability picture for galaxy formation can account for the observed rotation of galaxies. If not, then of course one must modify or abandon the picture. In an attempt to gain further understanding of this important question, a numerical model for the gravitational separation of protogalaxies in an expanding Universe was studied. The model prediction is a factor of 5 less than an estimate of the angular momentum of the Galaxy. It is not clear whether this discrepancy is real or only a result of the inadequacy of the model and the uncertainty in the Galaxy parameters. For the moment therefore it appears that the instability picture is viable. (auth)

30203 DIAMETER OF H II REGIONS IN THE GALAXY. Georgelin, Y. P. (Observatoire, Marseille). Astron. Astrophys.; 11: 414-17(Apr 1971). (In French).

From new data, the diameters of H II regions in the Galaxy are computed. The histogram of the diameters is very similar to that of M 33 obtained by Sersic (1961). From these data the morphological type of the Galaxy is Sc^-. (auth)

30204 MATTER–ANTIMATTER HYDRODYNAMICS. Omnes, R. (Univ. Paris, Orsay, France). Astron. Astrophys.; 11: 450-60(Apr 1971).

In a preceding paper, the possible importance of dynamical effects generated by matter–antimatter annihilation in the formation of galaxies was suggested. The present work deals with the hydrodynamics of matter and antimatter in contact. Magnetic and gravitational effects are not included. The subject is found to be very rich and intricate. Hydrostatics is studied in detail and it is found that static equilibrium is in general impossible. More evidence is given for the existence of the coalescence effect, which does not amount yet to a rigorous proof. (auth)

30205 ORIENTATION OF RADIO SOURCES AND ELLIPTICAL GALAXIES. Mackay, Craig D. (Mullard Radio Astronomy Observatory, Cambridge, Eng.). Mon. Notic. Roy. Astron. Soc.; 151: 421-5(1971).

A strong correlation was found between the position angle of the major axis of a radio source and the position angle of the major axis of the associated elliptical galaxy. The form of the correlation may suggest that most of these galaxies are oblate ellipsoids with the radio source axis parallel to the plane of the galaxy. (auth) (UK)

30206 GALACTIC EVOLUTION AND NUCLEOSYNTHESIS. Arnett, W. David (Inst. of Theoretical Astronomy, Cambridge, Eng. Rice Univ., Houston, Tex.). Astrophys. J.; 166: 153-73(15 May 1971).

Recent advances in the theory of explosive nucleosynthesis are incorporated into a clearly defined theoretical framework for application to the chemical evolution of the Galaxy. The site of nucleosynthesis is assumed to be exploding stars ($M \gtrsim 10\ M_\odot$). Some aspects of the behavior of elemental (and some observable isotopic) abundances in the range $6 \leq Z \leq 28$ are predicted. Comparison is made with published observational data, and implications for galactic evolution are discussed. Theory and observation agree, but a firm conclusion should await general agreement between observers concerning the reality of the effects found here. Detailed suggestions for new observations and discussions of their significance are presented. (auth)

30207 IS NGC 4569 A MEMBER OF THE VIRGO CLUSTER. Burbidge, E. Margaret; Hodge, Philip M. (Univ. of California, San Diego, La Jolla). Astrophys. J.; 166: 1-5 (15 May 1971).

Measures of the velocity field in the central part of the Sb galaxy NGC 4569 were made. These confirmed that the galaxy has a velocity of approach of −370 km sec^{-1}. Measures of rotation, and estimates of central density obtained from them, were used to determine whether the galaxy, which appears to lie in the Virgo cluster, is at the distance of the other bright galaxies in the Virgo cluster or whether it is closer. It is concluded that it is indeed at a distance of about 15 Mpc. The reasons why it was originally thought to have a redshift of +890 km sec^{-1} were also investigated. (auth)

30208 DUST SCATTERING IN THE FILAMENTS OF M82. Sanders, Robert H.; Balamore, Dilip S. (Columbia Univ., New York). Astrophys. J.; 166: 7-12(15 May 1971).

It is shown that dust scattering and not electron scattering can consistently explain recent observations of high polarization of the narrow H_α line in the filaments of M82. The dust-scattering model implies that the time scale for expulsion of mass from the nucleus of M82 is longer (10^7 years) and the total kinetic energy of the filaments is smaller (4×10^{53} ergs) than had previously been supposed. (auth)

30209 DISTANCE OF THE LOCAL-GROUP GALAXY IC 1613 OBTAINED FROM BAADE'S WORK ON ITS STELLAR CONTENT. Sandage, Allan (Carnegie Institution of Washington, D. C. California Inst. of Tech., Pasadena). Astrophys. J.; 166: 13-35(15 May 1971).

Fifty-nine variables were found by Baade over the face of IC 1613 from a series of plates taken with the 100-inch reflector from 1929 to 1937. Of these, thirty-seven are definite Cepheids ranging in period from 146 days to 2 days, four are probable Cepheids, thirteen are irregular, one is a probable SRc, one is an eclipsing binary, and three are of unknown type. Photometry depends on a photoelectric sequence of thirty-eight stars measured with the 200-inch reflector in the interval $11.6 \leq B \leq 21.7$. Magnitudes of 279 secondary standards used for the variables have been determined relative to the basic sequence. The values are listed. Two interpretations of the period–luminosity relation are given for the Cepheids. The apparent blue modulus is $(m-M)_{AB} = 24.55$ as found from the most recent calibration of the P–L relation. A reddening of $E(B-V) \simeq 0.03$ gives the true modulus as $(m-M)_0 = 24.43$. The integrated absolute magnitude of IC 1613 is $M_B = -14.45$. The brightest blue supergiant is star 22A with $M_B = -7.55$. The brightest red supergiant is the irregular red variable V42 with $M_B = -6.05$, or $M_V \simeq -8.0$ if B = V is assumed to be 2.0. The largest H II region has a linear size of 167 pc. These absolute magnitudes and linear dimensions are much smaller than corresponding values in intrinsically brighter late-type galaxies. The total extent of the Population II component of IC 1613 is 25.0 by 20.3, or 5600 by 4500 pc. The Population I component covers a region only half these dimensions. (auth)

30210 NONLINEAR DENSITY WAVES IN GALAXIES. Vandervoort, Peter O. (Univ. of Chicago). Astrophys. J.; 166: 37-58(15 May 1971).

The dynamics of a nonlinear density wave which is stationary in the sense that it possesses a time-independent structure in a uniformly rotating frame of reference are considered. Waves that prove to be the nonlinear analogues of the waves described by the linear theory of Lin and Shu are investigated in detail. A condition for the occurrence of such waves is that the galaxy must be composed of subsystems of two well-defined types which correspond to the stellar populations of the Galaxy and of similar galaxies. A corollary of this condition is that the spiral pattern of a wave is relatively more open the larger the fraction of the mass of the galaxy in subsystems of the type belonging to Population I. (auth)

30211 CHARGE TRANSFER AND IONIZATION EQUILIBRIUM IN THE INTERSTELLAR MEDIUM. Field, George B. (Univ. of California, Berkeley). Astrophys. J.; 166: 59-64(15 May 1971).

It is shown that charge transfer strongly affects the ionization equilibrium of oxygen in the H I regions of interstellar space. Ion–atom charge transfers at thermal energies ($E \lesssim 1$ eV) are evaluated by using the orbiting approximation of Bahcall and Wolf. The rate coefficients for the reactions $O^+ + H \rightleftharpoons O + H^+$ are evaluated for temperatures between 10^e and 10^{4e}K. The ionization level of oxygen is determined for a range of temperatures and densities. Over the entire range considered, $n(O^+)/n(O) \leq {}^9/_5 n(H^+)/n(H)$, instead of the

value ≈10 n(H^+)/n(H), which would obtain if charge exchange did not occur. (auth)

30212 STRUCTURE IN THE INTERSTELLAR-EXTINCTION CURVE. York, Donald G. (Univ. of Chicago). Astrophys. J.; 166: 65-86(15 May 1971).

A search for structure on the order of 20 to 200 Å in width in extinction curves derived by the use of photographic spectrophotometry reveals that extinction curves for twelve stars differ in shape and do show structure. In general, the broad features are isolated by relatively smooth stretches of the reddening curves, and the wavelengths of the features vary from star to star. The strength of the features is typically 0.02 to 0.04 mag in absorption or emission, measured from the mean reddening curve. To within the limits of the observations, the reddening curve cannot be described as a superposition of many broad features with widths less than 200 Å. The existence of adjacent structural features on the order of 300 to 500 Å is indicated by the observations. The strongest interstellar diffuse features are readily visible at the low dispersions used. New features that appear in more than one extinction curve are found at λλ4725, 5100, 5140, 5420, 5450, 5530, 5725, 5830, 5850, 6235, and 6350. The presence of emission wings on λ4430 and of structure associated with the diffuse features at λλ4760, 4890, 5780, 5797, and 6284 indicates that the diffuse features may not be a set of symmetrically broadened features, such as would be formed by predissociation or autoionization. While definite discrimination between models cannot be made, arguments are presented which favor models involving classical grains with impurities over models involving complex molecules to explain the extinction and the diffuse features. (auth)

30213 POLARIZATION FROM A CIRCULAR DIELECTRIC INFINITE CYLINDER AT OBLIQUE INCIDENCE. Svatos, J. (Charles Univ., Prague). Bull. Astron. Inst. Czech.; 22: 85-6 (1971).

Some Wait's formulae concerning the problem of scattering of a plane wave incident obliquely on an infinite circular cylinder are reexamined and a solution of the polarization efficiency for these dielectric cylinders at oblique incidence is given. (auth)

30214 LIGHT VARIATIONS OF SEYFERT GALAXY 3C 120. Jurkevich, I. (Univ. of Pennsylvania, Philadelphia. General Electric Space Sciences Lab., Valley Forge, Pa.); Usher, P. D.; Shen, B. S. P. Astrophys. Space Sci.; 10: 402-10(Mar 1971).

The fragmentary light-curve of the Seyfert galaxy 3C 120, based on photometry of the best-available Harvard plates of the past 60 yr, was subjected to a periodicity analysis using a method particularly suited to this type of irregularly spaced data. The analysis yields convincing evidence for a period of about 350 d and some indication of a longer period of about 22.5 yr. The observational data often depart appreciably from the light curve synthesized from the two periodic components. In one comparatively well-documented segment (1934–1939), the agreement between observational data and the synthesized model improves if it is assumed that a pair of oppositely directed phase shifts have occurred, disturbing the 350-day period and then causing it to recover. (auth)

30215 NOTE ON THE GRAVITATIONAL THEORY OF SPIRAL ARMS. Basu, B. (Jadavpur Univ., India). Bull. Astron. Inst. Czech.; 22: 30-7(1971).

Spiral arms of the Galaxy are suggested to be the possible manifestations of the density waves produced by gravitational perturbations. The general gas-dynamical equations with perturbation were solved in the spiral form for the galactic disk. Assuming the mass density as given by Oort, the magnitude of the density and potential perturbations were calculated. It is shown that about 50% of the total density of gas and early-type stars responds to the density perturbation while the responding mass of the late-type stars is only about 10%. As this percentage directly depends on the r.m.s. radial velocity of the class of objects, according to the present theory, from the observed fact that O and B stars clearly exhibit spiral pattern while the A stars do not do so, it is suggested that the critical value of the responding mass is probably one-third of the total mass, for spiral pattern to be defined. The perturbation in the velocity of stars is not significant, but that in gas may explain at least a part of the observed velocity dispersion of the gas as given by the 21-cm data. (auth)

30216 ALIGNMENT OF INTERSTELLAR GRAINS BY STARLIGHT. Harwit, M. (Astronomical Inst., Prague). Bull. Astron. Inst. Czech.; 21: 204-11(1970).

The quantized intrinsic angular momentum ħ carried by every photon plays a dominant role in the alignment of interstellar grains. The highly anisotropic starlight acts to orient grains with their angular momentum axes lying in the galactic plane. Similarly, angular momentum imparted to the grains by emitted photons disrupts this orientation and does so at a rate often higher than gas collisions. The rotational Brownian motion set up by these competing processes appears sufficiently anisotropic to explain the observed polarization of starlight. Magnetic alignment may not be necessary at all and might only play a supporting role. Some observational tests to decide this question are suggested. (auth)

30217 NGC 7603, A GALAXY CONNECTED TO A COMPANION OF MUCH LARGER REDSHIFT. Arp, Halton (Carnegie Institution of Washington, D. C. California Inst. of Tech., Pasadena). Astrophys. Lett.; 7: 221-4(Feb 1971).

The galaxy NGC 7603 has a smaller companion galaxy connected to it by a luminous filament. The redshift of NGC 7603 is 8,800 km/sec and the redshift of the companion is 16,900 km/sec. Five spectra show the main galaxy to be of Seyfert type and give accordant redshift measures. Three spectra show K and H absorption lines in the companion and these lines also have consistent redshifts. The direct photographs show that the main galaxy and companion are both peculiar and interacting, so that the chance that they only appear to be connected together by an accident of projection is extremely small. It is concluded that this is a further example of a small companion galaxy that exhibits a redshift intrinsically different from that of the main galaxy. (auth)

30218 MULTIPLE EXPLOSIONS IN RADIO GALAXIES AND HEATING OF THE INTERGALACTIC MEDIUM. Christiansen, Wayne (Univ. of Colorado, Boulder). Astrophys. Lett.; 7: 233-6(Feb 1971).

The statistical determination of radio source lifetimes from radio source counts was re-examined through the hypothesis that giant elliptical galaxies may be capable of undergoing multiple explosions. It is shown that if radio galaxy lifetimes are on the order of 10^6 years, the required explosion rate for all types of strong radio galaxies is rapid enough to heat the intergalactic medium to temperatures between 6×10^4 K and 10^6 K. (auth)

Cosmology

Refer also to abstract 31004.

30219 (CERN-70-31) PHYSICS AND ASTROPHYSICS. Schatzman, E. (European Organization for Nuclear Research, Geneva (Switzerland)). 16 Dec 1970. 110p. Dep. NTIS (U. S. Sales Only).

Lectures are presented on thermodynamics; nonequilibrium; structure and evolution of stars; pulsation, rotation, abundance of the elements, and nucleosynthesis in stars; galaxies and the Universe; and cosmology, gamma rays, strange objects, and abundance of the elements. (W.D.M.)

30220 (P-4494(RAND)) TOPICS IN HIGH ENERGY ASTROPHYSICS BASED ON LECTURES BY PETER GOLDREICH AT THE RAND CORPORATION DURING JUNE–JULY 1969. Gilinsky, V.; Hubbard, H.; Modesitt, G.; Collas, P. (RAND Corp., Santa Monica, Calif.). Nov 1970. 212p.

Lectures were presented on propagation of electromagnetic radiation in the Galaxy, scintillations of radio sources, quasars, synchrotron radiation and inverse Compton scattering, cosmology (Newtonian and relativistic theories), tests of cosmological models with Λ = 0, existence of horizons in cosmology, universal blackbody radiation, nucleosynthesis in the first 1001 seconds, galaxy formation, and pulsar electrodynamics. (W.D.M.)

30221 UNIVERSAL RADIATION AND COSMIC ELECTRONS. Prilutskii, O. F.; Rozental, I. L. Izv. Akad. Nauk SSSR, Ser. Fiz.; 34: 2293-2302(Nov 1970). (In Russian).

Two hypotheses have been suggested for the background radiation which, possibly, was produced by metagalactic radiation. The first hypothesis (called the binary hypothesis) assumed that the radio-background appeared during synchrotron radiation processes but the x-ray and photon background appeared during the inverse cosmic electron Compton effect on the relict radiation. The second hypothesis (synchrotron) stated that all background radiation spectra were the result of the magnetic bremsstrahlung mechanism. Both hypotheses are analyzed and discussed. (R.V.J.)

30222 STATISTICAL ANALYSIS OF GRAVITATIONAL INSTABILITY. Byalko, A. V. (Inst. of Theoretical Physics, Moscow). Zh. Eksp. Teor. Fiz.; 60: 441-50(Feb 1971). (In Russian).

XUM

Density perturbations are considered as a random function of the coordinates. A solution of the Lifshitz equation is obtained for linear perturbations in the region of wave numbers of the order of the Jeans value for all isotropic cosmological models. The perturbation spectra are employed for obtaining the mass distribution of the objects formed. The theoretical formulae are compared with the observed statistics of galaxy masses. It is noted that the Lemaitre model yields good agreement with the experimental data. (auth)

30223 PERTURBATIONS IN AN ANISOTROPIC HOMOGENEOUS UNIVERSE. Doroshkevich, A. G.; Zel'dovich, Ya. B.; Novikov, I. D. (Inst. of Applied Mathematics, Moscow). Zh. Eksp. Teor. Fiz.; 60: 3-8(Jan 1971). (In Russian).

In an anisotropic homogeneous cosmological model the growth of perturbations of matter density is a kinetic effect of the motion of matter in an external field in accordance with the concepts of Lifshits and Khalatnikov (1963) regarding the vacuum stage. By using this result, the law of growth of small perturbations and the general solution for finite perturbations of matter without pressure ($p = 0$) are found. It is shown that in anisotropic models the perturbations grow at a rate from 3 to 5 times greater than that in an isotropic model. For long-wave perturbations in a medium with $P = \epsilon/3$ the increase is 2 or 3 times. The law of variation of the acoustic and gravitational wave amplitudes is also explained. (auth)

30224 ROLE OF QUANTUM FLUCTUATIONS OF A GRAVITATIONAL FIELD IN GENERAL RELATIVITY AND COSMOLOGY. Ginzburg, V. L.; Kirzhnits, D. A.; Lyubushin, A. A. (Lebedev Inst. of Physics, Moscow). Zh. Eksp. Teor. Fiz.; 60: 451-9(Feb 1971). (In Russian).

The role of quantum fluctuations of a gravitational field is discussed from the standpoint of taking them into account in the nonlinear equations of the general theory of relativity. The analysis is carried out for gravitational fields of arbitrary symmetry; however, a direct calculation of the vacuum contribution is performed only for the closed Friedman cosmological model. The result obtained can be summarized as follows. Firstly, it can be asserted that neglection of the Λ term is not justified. Secondly, if suitable (observable) values of the gravitational constant $\kappa = 8\pi k/c^4$ and cosmological constant Λ are employed, the effect of quantum (zero) fluctuations should be extremely small as long as the density of matter is small compared with the characteristic density $\rho_{cr} \sim (c^3\kappa^2\hbar)^{-1} \sim 10^{94}\ g \cdot cm^{-3}$, providing the curvature $a \gg l_f \sim \sqrt{\kappa\hbar c} \sim 10^{-33}$ cm. On the other hand, near a singularity fluctuation, effects may in principle be very considerable. This circumstance may be important for some of the cosmological models being discussed at present. (auth)

30225 SPHERICALLY SYMMETRIC SOLUTIONS OF THE EINSTEIN EQUATIONS FOR A WORLD FILLED WITH RADIATION. Ruzmaikina, T. V.; Ruzmaikin, A. A. (Inst. of Applied Mathematics, Moscow). Zh. Eksp. Teor. Fiz.; 59: 1576-82(Nov 1970). (In Russian).

Spherically symmetric inhomogeneous solutions of the Einstein equations for an expanding universe filled with radiation with an equation of state $p = \epsilon/3$ are considered. A method of solution is employed in the case of small perturbations on the background of the homogeneous and isotropic Friedman model; this method differs from that used by Lifshitz in which a Fourier expansion is applied. The Einstein set in this approximation reduces to a single third-order equation for the density perturbation. By simple substitution this equation can be transformed into a wave equation for propagation of perturbations with a sound velocity $c/\sqrt{3}$. The behavior of local perturbations can be simply investigated on basis of the general solution of the equation. Self-similar solutions with the variable $\xi = r\sqrt{3}/2\sqrt{t}$ are also analyzed. A set of ordinary differential equations for the self-similar solutions is derived. An analytical solution of the set is obtained in the linear approximation and its properties are investigated. (auth)

30226 NEWTONIAN HIERARCHICAL COSMOLOGY. Wertz, James Richard. Austin, Tex.; Univ. of Texas (1970). 148p. University Microfilms Order No. 71-209.

Thesis.

Hierarchical cosmology deals with the question of hierarchical structuring in the matter distribution of the Universe. Thus, galaxies are gathered into clusters that are themselves elements of clusters of clusters, etc., ad infinitum. Although a general relativistic treatment is difficult, considerable information is available from a Newtonian analysis. The density of the Universe is a function both of position and the size of the volume being considered, generally decreasing with increasing radius of the volume under consideration. Only those models for which the density goes to zero as the radius becomes infinite are analyzed. (Observationally, $\rho \propto r^{-1.7}$ in the range $10^{20} < r < 10^{27}$ cm.) Similarly, the Hubble parameter is a function of the order of the cluster involved. Under the assumption of a common origin of clusters, the relative expansion of the Universe may be determined directly from the density–radius relation. For realistic models ("big-bang" hierarchy with $\rho \propto r^{-\theta}$ at present epoch), a Hubble law characteristic of the hierarchy and, at least in principle, subject to observational verification is obtained. (For a reasonable choice of parameters, the result is nearly linear but does not intersect the origin.) A continuous representation for the description of a hierarchical universe is introduced. This permits straightforward analysis of questions regarding the Universe as a whole. General solutions for the evolution of hierarchical models are set forth for both continuous and discrete representations. (To within certain limits which are also set forth, the evolution of the Universe is described by a Friedman equation with distinct scale parameters for each order cluster.) The "big bang" hierarchy is analyzed in some detail, leading to the Hubble Law previously mentioned and the fact that these models have a homogeneous mass distribution at their earliest stages. Their recent history is also analyzed, principally for the discussion of tides, which cause the major distortion from the simple evolutionary picture. A variety of criteria for the instantaneous hierarchical structure are developed that limit the degree of tidal distortion. A model for tidal evolution is presented and analyzed. Methods of approach to a general relativistic treatment and the problem of the propagation of light are presented. Questions of the uniqueness of the present epoch, agreement with the microwave background, and causality are discussed briefly. (Diss. Abstr. Int., B)

30227 INFRARED RADIATION AND COLD MATTER IN UNIVERSE. Bonetti, Alberto. Rend. Semin. Mat. Fis. Milano; 39: 30-5(1969).

The importance of the hitherto little explored far-infrared region extending from 30 μ to millimetric wavelengths is discussed. The study of this so-called infrared gap was made possible by the recent development of bolometric-type sensors such as gallium-doped germanium bolometers. This development, it is pointed out, makes it possible to observe the peculiar structure and distribution of cold matter (cold from a few degrees to a few tens of degrees Kelvin). Cold matter forms a substantial part of matter in the Universe, and from a study of cold matter, it is expected that important contributions will be made toward the solution of such major problems as those of star formation from collapsing diluted matter, complex molecule formation in cold regions, evolution of matter in the dense regions of galactic nuclei and in quasars, and birth and aging of the Universe. (IAA)

30228 ISOTROPY OF THE MICROWAVE BACKGROUND AT 8-MILLIMETER WAVELENGTH. Boughn, S. P.; Fram, D. M.; Partridge, R. B. (Princeton Univ., N. J.). Astrophys. J.; 165: 439-44(1 May 1971).

A preliminary measurement of the isotropy of the cosmic microwave background was made at a relatively short wavelength, 8.6 mm. The measurement was made along the celestial equator. No statistically significant anisotropy was found. (auth)

30229 KINETIC THEORY OF INHOMOGENEOUS ROTATING SELF-GRAVITATING SYSTEMS: ENHANCED COLLISIONAL DIFFUSION AND DISSIPATION. Haggerty, M. J. (Univ. of Texas, Austin). Physica; 51: 477-88(15 Feb 1971).

Kinetic equations are presented for binary interactions in strongly inhomogeneous self-gravitating systems that rotate with uniform angular velocities. The characteristic times for dissipation can be substantially reduced only if a composite-particle approach is taken. (auth)

30230 KINETIC THEORY OF INHOMOGENEOUS ROTATING SELF-GRAVITATING SYSTEMS: LOCAL ENERGY PRODUCTION FROM BINARY INTERACTIONS. Haggerty, M. J.; Severne, G. (Univ. of Texas, Austin. Univ. Libre, Brussels). Physica; 51: 461-76(15 Feb 1971).

A non-Markovian weak-coupling kinetic theory of binary gravitational interactions in a rotating system is presented. Inhomogeneities along the axis of rotation are included. Irreversible increases in local kinetic energy are found, together with a corresponding growth of local correlations. Additional terms of opposite sign can occur when initial correlations or macroscopic inhomogeneities are included. (auth)

30231 NONTHERMAL PRIMEVAL FIREBALL. Peebles, P. J. E. (Princeton Univ., N. J.). Astrophys. Space Sci.; 10: 280-90(Feb 1971).

The possible significance of a large cosmic sub-millimeter

electromagnetic radiation background is considered. It is shown that in some scalar–tensor cosmological models such an effect could be primeval, that is, the result of processes occurring at an epoch earlier than one now can attempt to compute. The radiation background due to electron pair annihilation in a scalar–tensor model also is considered. It is shown that, while this effect could very substantially increase the far-infrared background, it cannot make a spectrum that would be consistent with all the available tentative measurements. (auth)

30232 COSMOLOGICAL MODELS WITH A G-VARIABLE GRAVITATIONAL THEORY. Caloi, V.; Firmani, C. (Instituto Politecnico Nacional, Mexico City). Astrophys. Space Sci.; 10: 309-27(Feb 1971).

A theory of gravitation with variable G is constructed as a modification of Brans–Dicke's theory. The theory is an attempt to include the effect both of matter and radiation on the inertia of a body, according to Mach's principle. "Big Bang" cosmological models are computed and the corresponding primordial chemical compositions are found. (auth)

30233 NONLINEAR CORRECTIONS IN THE LAGRANGIAN DENSITY OF THE GRAVITATIONAL FIELD AND COSMOLOGICAL SOLUTIONS WITHOUT SINGULARITY. Gurovich, V. Ts. (Inst. of Nuclear Physics, Novosibirsk, USSR). Dokl. Akad. Nauk SSSR; 195: 1300-2(21 Dec 1970). (In Russian).

Recent publication of Sakharov's paper on the nonlinear fourfold-curvature additive in the Lagrangian density of the gravitational field stimulated studies on special characteristics of Einstein's equations, aiming at higher-order equations. These fourth-order equations of the Lagrangian density may contain a cosmological solution with continuous transition from shrinking to expansion. The equations of Ruzmaikina et al. were examined to derive an exact cosmological solution concerning the cosmic dust as indicated in Friedman's three models of the Universe. The derivations were solved for $t = -\infty$, 0, and $+\infty$. For $t \sim 0$, when the shrinking changes into expansion, the radius of the Universe passes through a minimum. Calculation of the increase of entropy in the case of the so-called closed model leads to an increase of the period of pulsation. (TTT)

30234 TOPOLOGY OF MODELS OF THE UNIVERSE. Sokolov, D. D. (Moscow State Univ.). Dokl. Akad. Nauk SSSR; 195: 1307-9(21 Dec 1970). (In Russian).

In trying to indicate the potential models of the Universe, an attempt was made to relate Einstein's equations to physical principles which served as the original reference. Using generally applicable physical laws, the principles that delimit the topology of the models of the Universe were identified. Gödel's principles are pointed out as different formulations of the causality principle. The ZN principle of Zel'dovich et al. is indicated in a limit that follows from the CP noninvariance. From their reasoning, limitation of the topology of the models of the Universe was derived as a result of the CP noninvariance. (TTT)

30235 TOTAL ELECTRICAL CHARGE AND MASS OF ELLIPTIC UNIVERSE. Asanov, R. A. (Joint Inst. for Nuclear Research, Dubna, USSR). Teor. Mat. Fiz.; 6: 335-7(Mar 1971). (In Russian).

It is shown that if the space geometry is elliptic, the total electrical charge, momentum, and mass of the Universe are equal to zero. (auth)

30236 FLUCTUATIONS OF 3^0K MICROWAVES AS A RESULT OF THOMSON SCATTERING BY MOVING INTERGALACTIC MATTER. Dautcourt, G. (Zentralinstitut fuer Astrophysik, Babelsberg, Ger.). Monatsber. Deut. Akad. Wiss. Berlin; 12: 453-8(1970). (In German).

A transport equation, completed with respect to the work of Chibisov and Ozernoi, was derived. The angular fluctuations in the 3°K radiation resulting for given turbulence states of intergalactic matter are discussed. (tr-auth)

30237 GRAVITATIONAL KINETIC EQUATIONS. Lerche, I. (Univ. of Chicago). Astrophys. J.; 166: 207-19(15 May 1971).

Equations are derived for the correlations of particles moving under their mutual gravitational attraction. To lowest order in a modification of the Rostoker and Rosenbluth expansion scheme, the equations describe the motion of any one particle in the "average" gravitational field of all the other particles. In next order in the expansion scheme, correlation equations are obtained which describe the evolution of the pair correlation function of two particles and the change in the motion of one particle brought about by the change in the "average" gravitational field. The equations demonstrate that, in general, the particle–particle correlation term is of the same order as the particle–field correlation term. The kinetic equations can be used to discuss the evolution of stellar configurations beyond the independent-particle approximation. (auth)

30238 SOLUTIONS OF ZERILLI'S QUATION FOR EVEN-PARITY GRAVITATIONAL PERTURBATIONS. Fackerell, Edward D. (California Inst. of Tech., Pasadena). Astrophys. J.; 166: 197-206(15 May 1971).

Uniformly valid asymptotic expansions are derived, both in the high-frequency and the low-frequency limits, for the solution of Zerilli's equation for even-parity gravitational perturbations on the Schwarzschild geometry. The high-frequency solutions should prove useful in the analysis of bursts of gravitational radiation, which are emitted during nonspherical gravitational collapse and also during the infall of a particle into a black hole. The low-frequency solutions govern the decay with time of the gravitational-multipole moments of a newly formed, slightly nonspherical, black hole. (auth)

30239 INFRA-RED ASTRONOMICAL BACKGROUND RADIATION. Harwit, M. (Astronomical Inst., Prague). Riv. Nuovo Cim.; 2: 253-77(Apr-Jun 1970).

Techniques for obtaining background measurements at very short (0.8 to 1.1 μm) and longer (1.1 μm) wavelengths are described. The interplanetary, galactic (stellar and interstellar components), and intergalactic backgrounds are considered in detail. The relationship between cosmic rays and the background radiation is discussed. (W.D.M.)

30240 GRAVITATIONAL WAVES AND COSMOLOGY. Bertotti, B. (European Space Research Inst., Frascati, Italy); Cavaliere, A. Nuovo Cim.; 2B: 223-35(11 Apr 1971).

The strong bursts of gravitational waves detected by Weber, if confirmed, suggest the presence in the Galaxy of a relativistic cluster of collapsed bodies that "burns" its own gravitational potential energy and slowly decays into a dead, collapsed object. The possibility of this being a common feature throughout the Universe is discussed, and a simple cosmological model is considered in which the "missing mass" is attributed mainly to gravitational waves and dead, dark galaxies. The production of the former is described by a simple rate equation containing a characteristic frequency α. Using the known value of the Hubble constant H and the present visible mass density it is found when the efficiency of the process is, say, 0.5, $\alpha \approx 8H$, the corresponding gravitational brightness of an average galaxy turns out to agree with Weber's figure (assuming a wide-band spectrum) to within a factor 2. This model features an isotropic cosmological background of gravitational waves, with energy density about 50 times smaller than the energy arriving from the galactic nucleus. (auth)

30241 GRAVITATIONAL INSTABILITY IN AN INHOMOGENEOUS COSMOLOGICAL MODEL. Khiet, Vu Thanh (Univ., Paris). Compt. Rend., Ser. A; 272: 509-12(15 Feb 1971). (In French).

The gravitational instability of a locally nonuniform model of the Universe derived from the generalization of the Shirokov and Fisher model is studied, assuming coordinate conditions different to those of Lifshitz. In the case of a model including matter and radiation, and in the case of the Rosen oscillating model, the time dependence of the growth of a density perturbation is derived. (France)

30242 SCATTERING OF NEUTRINOS BY A LINEARIZED SCHWARZSCHILD METRIC. Lawrence, John K. (Univ. of Vienna). Acta Phys. Austr.; 31: No. 1, 1-7(1970).

The strongest influence exerted on interstellar neutrinos is likely to be gravitation, but many features of interactions of neutrinos with gravitation, such as scattering cross sections, have been treated only qualitatively. The interaction Lagrangian for Fermion fields with the linearized, classical gravitational field is shown to correctly give no scattering for Fermions interacting with the gauge part of the metric. A cross section is given for the scattering of Fermions by a static, linearized Schwarzschild metric in terms of "form factors" expressing the deviation of the interior metric from the exterior form. This cross section is specialized to the case of scattering of unpolarized electrons, and the nonrelativistic limit of this is the Rutherford formula. The cross section is also specialized to the case of scattering of left-handed neutrinos, and the result is the same as the extreme relativistic limit of the unpolarized electron case. (auth)

30243 PERTURBATIONS IN A SPACE OF CONSTANT CURVATURE. Horedt, Gp. (Astronomical Observatory, Cluj). Bull. Astron. Inst. Czech.; 22: 82-4(1971).

XUM

Applying Lifshitz's method, the density and rotational perturbations as well as the propagation of gravitational waves in a space of constant curvature were studied. Seeliger's paradox is not valid. Instability occurs only for density perturbations. The results presented are also applicable to certain parts of a galaxy, cluster, etc., if these are idealized as regions of constant curvature. (auth)

30244 ORIENTATION OF GALAXIES AND MAGNETIC "URFIELD." Reinhardt, Michael (Univ., Bonn). Astrophys. Space Sci.; 10: 363-82(Mar 1971).

Brown's results (1964, 1968) concerning the distribution of orientation angles of spiral galaxies in different areas of the sky are discussed, and a graphical statistical test is applied. The deviations from randomness are found to be significant. It seems difficult to ascribe them to selection effects. It is shown that the observed distributions can be explained if the angular momenta in greater aggregations of galaxies are distributed at random on congruent precession cones with parallel axes. This hypothesis may apply if the following cosmological conditions hold: (i) the matter in the Universe was reheated after the recombination at an epoch, when most of the angular momentum was already transferred to the protogalaxies by tidal interaction, and the angular momenta of the protogalaxies in greater aggregations were predominantly parallel at the epoch of reheating; (ii) the "magnetic" model of the Universe is valid and the "urfield" was uniform at least at the epoch of reheating. Under these assumptions, the "frozen-in" magnetic field will give rise to forces, which—apart from slowing down the rotation of the protogalaxies—will cause precession of their angular momenta around the direction of the "urfield". For a rigid-body approximation the equations of motion are derived and solved numerically. Approximate analytic solutions are also given. The precession period is in the range of 10^4 to 10^8 yr for plausible values of the parameters of the problem. The observed distributions in the four regions of the sky investigated are—via the precession hypothesis—compatible with a direction of the "urfield" indicated by the work of Sofue et al. (1969) and Reinhardt and Thiel (1970) of $l^{II} \approx 280°$, $b^{II} \approx +30°$ to $l^{II} \approx 100°$, $b^{II} \approx -30°$. (auth)

30245 INERTIAL FORCES AS A GRAVITATIONAL EFFECT OF THE EINSTEIN UNIVERSE. Horak, Z. (Technical Univ., Prague). Bull. Astron. Inst. Czech.; 21: 325-6(1970).

Previously (Horák 1970), arguments were given for a complete compatibility of general relativity with Mach's principle. A direct proof of that statement can be obtained from the fact that the field equations actually give the correct formulae for the fictitious forces exerted by the Einstein Universe in noninertial frames. (W.D.M.)

30246 POSSIBLE OBSERVATIONAL TEST TO DETERMINE VARIATIONS OF PLANCK'S CONSTANT ON A COSMIC SCALE. Harwit, M. (Astronomical Inst., Prague). Bull. Astron. Inst. Czech.; 22: 22-9(1971).

The possibility that Planck's constant varies on a cosmic scale has been suggested before, by Dirac (1938) and others. The present paper, however, analyzes the consequence of such a variation, on the ability of interstellar and intergalactic gases to absorb radiation. A number of formal interactions of matter with radiation are postulated for photons characterized by a longitudinal angular momentum component, $\hbar'$ which differs from $\hbar$, i.e., Planck's constant divided by 2π. In some forms of these interactions, the quantum mechanical angular momentum conservation conditions may still be satisfied, provided that the source angular diameter subtends a sufficiently large angle at the absorbing atom. This relation would permit one to set up an observational criterion which determines $(\hbar' - \hbar)/\hbar$ from interstellar absorption line data for extragalactic objects. Similar observations of pulsars might provide interesting information on the dependence of Planck's constant on intense gravitational fields. The limitations placed on this technique are discussed, in general relativistic homogeneous isotropic universes, and it is pointed out that the inability to absorb radiation carrying spin angular momentum $\hbar$ may account for the lack of observed intergalactic absorption. Current estimates of the mass of the Universe could, therefore, be too low if variability of Planck's constant is a significant effect. A final upper bound on $\delta\hbar/\hbar$, based on a line width argument, indicates that this ratio is less than 10^{-5}, at least for 3C 273B, the one object for which sufficient data appears to exist. (auth)

30247 NUCLEI OF GALAXIES AND QUASARS AS INFRARED SOURCES. Bisnovaty-Kogan, G. S.; Sunyaev, R. A. (Inst. of Applied Mathematics, Moscow). Astrophys. Lett.; 7: 237-40 (Feb 1971).

The density of the falling matter near the surface of a neutron star at the regime of critical (saturated) accretion has such a value that the plasma frequency coincides with the frequency of the infrared peak in the spectra of the nuclei of galaxies. A model of the nuclei of galaxies and of quasars is discussed: it deals with frequent supernova explosions, large numbers of neutron stars, and matter accreted by the neutron stars. The large density of gas in the interstellar space supports the critical accretion on the neutron stars. The main part of the energy obtained during accretion radiates at the plasma frequency, which differs little for neutron stars of different masses and, consequently, for different nuclei of galaxies. (auth)

Planetary Phenomena

Refer also to abstracts 30363, 30388, and 30389.

30248 (UCB-34-P-32-PR-5) MASS SPECTROSCOPY RESEARCH. Progress Report. (California Univ., Berkeley. Dept. of Physics). 19 Oct 1970. 17p. Dep. NTIS.

A list of papers published since the last reporting period is given along with brief comments on each of the papers. (W.D.M.)

30249 NEW OUTER-TERRESTRIAL SUBSTANCES. 2. CHEMICAL COMPOSITION OF MOON SAMPLES. Honda, Masatake (Tokyo Univ.). Kagaku (Tokyo); 40: 368-71(Jul 1970). (In Japanese).

Work done on samples of Moon rocks is summarized, and it is concluded that the Fe–Ni material is of meteoritic origin. The formation of igneous rocks is the result of cratering. (TSS) (Japan)

30250 FAR-INFRARED SPECTRUM OF JUPITER. Encrenaz, Th.; Gautier, D.; Vapillon, L.; Verdet, J. P. (Observatoire, Meudon, France). Astron. Astrophys.; 11: 431-49(Apr 1971).

The emission spectrum of Jupiter in the far-infrared, between 10 and 250 cm^{-1}, is computed with high resolution (0.01 cm^{-1} in the ammonia bands) for three atmospheric models. Basic characteristics of these theoretical models are briefly reviewed, and the results of the spectroscopic analysis of H_2 and NH_3 are used for the radiative transfer calculations. The detailed study of the spectra obtained shows how the H_2/He ratio and the thermal Jovian structure can be deduced from far infrared measurements of the Jovian flux. Specifically, these measurements obviously test the existence of an inversion in the Jovian temperature profile. The question of detecting minor components (H_2O, H_2S) in the Jovian atmosphere is also considered. The accuracy necessary for experimental research to collect information needed is shown to be obtained with the equipment available. (auth)

30251 MAGNETIC-FIELD GEOMETRY OF JUPITER AND ITS RELATION TO IO-MODULATED JOVIAN DECAMETRIC RADIO EMISSION. Schatten, Kenneth H.; Ness, Norman F. (Goddard Space Flight Center, Greenbelt, Md.). Astrophys. J.; 165: 621-31(1 May 1971).

Observations of the Io-modulated Jovian decametric radio emission were compared with calculations of the magnetic-field line passing through Io. Calculations of the angle between the Earth and the magnetic-field line near Io and both the northern and southern intersections of that field line with the surface of the planet were undertaken. Four emission sources favorable for synchrotron emission were located by presuming that the angle of intersection between the Earth and the north- (or south-) threaded field was near 90° and that the declination of Io was positive. These four sources correspond closely to the three major observed emission regions and to one region infrequently observed. These calculations imply little distortion of the Jovian magnetic field by Io. This assumption is quite reasonable as the Moon, an object similar in size and density to Io, produces little effect upon the interplanetary magnetic field. A mechanism by which Io could stimulate the emission is presented that is consistent with the calculations conducted. (auth)

Atomic and Molecular Physics

Atomic, Electron, Ion, and Molecular Beams and Their Reactions

Refer also to abstracts 29081, 30659, and 30665.

30252 (EUR-4593, pp 43-9) CONDITIONS FOR THE CONTROL OF BEAM INTENSITY AND CLUSTER SIZE IN HYDROGEN CLUSTER BEAMS. Tay, E. S.; Dawson, P. G. (United Kingdom Atomic Energy Authority, Abingdon (England). Culham Lab.).

From Sixth symposium on fusion technology; Aachen, Germany (22 Sep 1970).

In Proceedings of the 6th symposium on fusion technology.

Experimental results are given of beam intensity and cluster size obtained from three types of nozzles. (auth)

30253 (EUR–4593, pp 51-8) IONIZATION AND ACCELERATION OF HYDROGEN CLUSTERS. Tay, E. S.; Dawson, P. G.; Mosson, G. A. G. (United Kingdom Atomic Energy Authority, Abingdon (England). Culham Lab.).

From Sixth symposium on fusion technology; Aachen, Germany (22 Sep 1970).

In Proceedings of the 6th symposium on fusion technology.

Measurements of the total ionization cross section of hydrogen clusters and the breakup of accelerated cluster ions by molecular impact are described. Important new understandings of the ionization and breakup processes are reported. (auth)

30254 (EUR–4593, pp 59-65) PRODUCTION OF INTENSE RELATIVISTIC ELECTRON BEAMS. Vitkovitsky, Ihor M. (Naval Research Lab., Washington, D. C.).

From Sixth symposium on fusion technology; Aachen, Germany (22 Sep 1970).

In Proceedings of the 6th symposium on fusion technology.

The production of very-high-current relativistic electron beams of interest to thermonuclear fusion experiments is discussed. The scaling laws governing the characteristics of such beams are summarized. These laws were used to determine the methods of producing 20-kJ relativistic beams with electron densities exceeding 10^{13} cm^{-3}. The control of these beams with external magnetic fields was also studied. It provides a method for efficiently injecting a beam into an experimental apparatus. (auth)

30255 (EUR–4593, pp 67-74) ION SOURCE USING A BEAM–PLASMA INTERACTION. Nunogaki, M.; Akimune, H.; Suita, T. (Osaka Univ. (Japan). Dept. of Nuclear Engineering).

From Sixth symposium on fusion technology; Aachen, Germany (22 Sep 1970).

In Proceedings of the 6th symposium on fusion technology.

The design and experimental investigations of a newly developed ion source are described in which a beam–plasma interaction is used for the production of a source plasma. A hollow electron beam brings about a stable and continuous beam–plasma discharge at a hydrogen pressure of the order of 10-mm Hg in a magnetic field. The performance of the source is described. (M.O.W.)

30256 (EUR–4593, pp 75-81) PRODUCTION OF HIGH-CURRENT, HIGH-QUALITY BEAMS OF IONS AND NEUTRAL PARTICLES. Coupland, J. R.; Thompson, E. (United Kingdom Atomic Energy Authority, Abingdon (England). Culham Lab.).

From Sixth symposium on fusion technology; Aachen, Germany (22 Sep 1970).

In Proceedings of the 6th symposium on fusion technology.

Results obtained with a hot cathode constructed arc plasma source and a single-aperture three-electrode accel–decel extraction system are described. The energy range covered is 5 to 25 kV for positive ions and 1.7 to 12.5 kV for neutral beams. Ion currents of the order of 80-mA H_3^+ and 100-mA He^+ at the higher energies were obtained through a 3.8-cm-diameter aperture at a distance of 180 cm from the source. The performance as a neutral injector was evaluated by using the present PHOENIX II injector line. The relationship between experiment and theory and the limitations of this type of source are discussed. (auth)

30257 (EUR–4593, pp 181-6) DESORPTION BY keV PROTONS OF HYDROGEN CONDENSED ON LIQUID-HELIUM-COOLED SURFACES. Erents, S. K.; McCracken, G. M. (United Kingdom Atomic Energy Authority, Abingdon (England). Culham Lab.).

From Sixth symposium on fusion technology; Aachen, Germany (22 Sep 1970).

In Proceedings of the 6th symposium on fusion technology.

Measurements were made of the desorption of solid hydrogen layers, up to 10,000-Å thickness, condensed on copper at temperatures ≥3°K, by 5-keV protons. Yields increase with coverage to a maximum of 50,000 atoms/ion, then subsequently fall as the layer increases above ~1000-Å thickness. (auth)

30258 MOLECULAR BEAMS IN HIGH TEMPERATURE CHEMISTRY. Milne, Thomas A.; Greene, Frank T. (Midwest Research Inst., Kansas City, Mo.). Advan. High Temp. Chem.: 2: 107-50(1969).

Principal features of molecular beam formation from high pressures, the important phenomena accompanying such expansions, and the techniques for production, detection, and identification of such beams are reviewed. Applications involving the sampling of high-temperature systems and the use of these beams as a means of generating and studying cold molecules from hot systems, observing nucleation processes, and obtaining the properties of unusual clusters of molecules and atoms are discussed. (J.G.B.)

30259 MASS SPECTROMETRIC INVESTIGATION OF SURFACE IONIZATION. VIII. DESORPTION OF Th^+, Np^+, AND Pu^+ FROM RHENIUM SURFACES. Smith, David H. (Oak Ridge National Lab., Tenn.). J. Chem. Phys.; 54: 4137-8(1 May 1971).

Desorption energies and interaction frequencies were measured for Th^+, Np^+, and Pu^+ ions on a Re ionizing filament at temperatures up to 2900°K. Mean residence times at 2000 to 2700°K were calculated from the data for these ions and for U^+, using Hertel's data. The times and desorption energies can be correlated with the temperature ranges for routine isotopic analysis. The relative behavior of the ions on Re is compared with that on W. (D.L.C.)

30260 AVERAGE ENERGY OF ELECTRONS SCATTERED INELASTICALLY FROM SOLIDS. Bornshtein, I. M.; Stozharov, V. M. (Leningrad State Pedagogical Inst.). Sov. Phys.-Solid State (Engl. Transl.); 12: 2280-3(Apr 1971).

Translated from Fiz. Tverd. Tela; 12: 2824-8(Oct 1970).

The energy distribution of electrons (primary energy E_p = 0.2-3 keV) scattered inelastically from Be, Ni, and Pb was investigated. The angle of incidence on the target was φ = 0 to 85°. The energy spectra were used to determine the average energies $\bar{E}$ and the average depths of emergence $\bar{d}$ of the inelastically scattered electrons. It was found that $\bar{E}/E_p$ depended on E_p and the dependence was stronger for lower values of the atomic number Z of the target element. In the case of Be, the parameters $\bar{E}$ and $\bar{d}$ also depended on φ; when φ was increased $\bar{E}$ increased, but $\bar{d}$ decreased. (auth)

Atomic and Molecular Properties

Refer also to abstracts 30084, 30168, 30174, 30540, 30671, and 31343.

30261 L-SHELL AUGER AND COSTER–KRONIG ELECTRON SPECTRA. McGuire, Eugene J. (Sandia Labs., Albuquerque, N. Mex.). Phys. Rev., A; 3: 1801-10(Jun 1971).

Individual-term electron transition rates for initial L-shell holes are presented in j–j coupling. Comparison with experimental-term intensities are made for platinum, tellurium, uranium, argon, and krypton. For the latter two elements agreement is poor. Comparison with experiment indicates some prominent peaks in the uranium L_2 Coster–Kronig spectrum are improperly identified. (auth)

30262 LOW-ENERGY LEVEL STRUCTURE OF NEUTRAL CERIUM (Ce I). Martin, W. C. (National Bureau of Standards, Washington, D. C.). Phys. Rev., A; 3: 1810-15(Jun 1971).

The low portion of an extensive level structure derived from analysis of the optical spectrum is reported. Positions, J values, and g_j factors are given for 98 levels, including all 91 levels expected below 10,000 cm^{-1}. A previous report on this analysis showed the ground level to be $4f5d6s^2\ {}^1G_4^?$ and gave the lowest levels of $4f5d^26s$. Comparison of the observed odd-parity levels with calculations by Goldschmidt and Salomon shows that all 86 of the odd levels tabulated here belong to these configurations. All but seven of these odd levels are assigned LS names, although the calculations show that many of them have low LS purities, and a few have strong mixtures of the two configurations. The much simpler system of even levels below 10,000 cm^{-1} includes only the six levels of $4f^26s^2\ {}^3H$ and ${}^3F$, beginning with ${}^3H_4$ at 4762.718 cm^{-1} above the ground-state level. The table of even levels also includes $4f^26s^2\ {}^1G_4$ and the lowest two levels of each of the lowest two terms of $4f^25d6s$, ${}^5I_{4,5}$, and ${}^5K_{5,6}$. (auth)

30263 MEASUREMENT OF THE LEVEL SHIFT IN He^+, n = 3. Mader, D. L.; Leventhal, M.; Lamb, W. E. Jr. (Yale Univ., New Haven). Phys. Rev., A; 3: 1832-48(Jun 1971).

The level shift $\mathcal{F}({}^2S_{\frac{1}{2}}-{}^2P_{\frac{1}{2}})$ and the fine-structure interval $\Delta E - \mathcal{F}({}^2S_{\frac{1}{2}}-{}^2P_{\frac{3}{2}})$ were measured in the n = 3 level of the helium ion He^+ with a microwave-optical technique. Electron bombardment of helium gas produces excited ions. The 1640-Å light from the n = 3 to 2 decay undergoes a decrease when a microwave field induces an S-to-P transition. Extensive data were taken on three transitions as a function of microwave power, helium pressure, and bombarding current in a search for systematic effects. The major effect was a slight shift of the resonance curves with microwave power due to transitions in higher excited states. The high-frequency transitions αc and βd yield $\Delta E - \mathcal{F}$ = 47 844.05 ± 0.48 MHz. Using the Taylor, Parker, and Langenberg value for the fine-structure constant to calculate ΔE, an indirect measurement of $\mathcal{F}$ = 4183.73 ± 0.51 MHz is obtained. Measurements on αe yield a direct value of $\mathcal{F}$ = 4183.17 ± 0.54 MHz, which, combined with the indirect value, yields $\mathcal{F}$ = 4183.45 ± 0.52 MHz, in agreement with the theoretical value of 4184.4 ± 0.5 MHz of Applequist and

XUM

Brodsky. (All uncertainties are expressed as 68% confidence values.) (auth)

30264 STARK AND ZEEMAN EFFECTS ON NEUTRAL-HELIUM LINES. Deutsch, C. (Faculte des Sciences, Paris. CNRS, Bellevue, France); Drawin, H. W.; Herman, L. Phys. Rev., A; 1879-90(Jun 1971).

The effect of a static electromagnetic field on the 2P−nS and 2S−nP He I isolated lines is systematically investigated. Exact expressions are given for the shift of the allowed component, and the behavior of the corresponding transition probability under static perturbation is considered in detail. The usual hydrogenic approximations for the Stark constants are discussed with reference to the most recent values for the oscillator strengths available. They are found to be consistent, especially for the 2^1P-n^1S and 2^1S-n^1P lines with $n \geq 3$, when accurate data are used for the unperturbed excitation energies. The shifts determined with either nondegenerate or degenerate perturbation theory are critically compared, and the greatest difference is found for the magnetic sublevels in the presence of crossed fields. The fourth-order Stark effect is also considered. Calculated shifts are compared with the existing experimental data, and attention is also given to the methods used in plasma spectroscopy for the evaluation of the static Stark effect. (auth)

30265 LIFETIMES OF SOME DOUBLY EXCITED LEVELS IN NEUTRAL HELIUM. Berry, H. G.; Martinson, I.; Curtis, L. J.; Lundin, L. (Research Inst. for Physics, Stockholm). Phys. Rev., A; 1934-7(Jun 1971).

A search was made for radiative transitions from doubly excited levels in He I, using the beam−foil method. The spectra showed the $1s2p\ ^3P-2p^2\ ^3P$ transition at 320.4 Å and some weaker lines, which are also interpreted as transitions from the doubly excited system. Radiative lifetimes were measured for three lines. The value obtained for the $2p^2\ ^3P$ level, 0.080 ± 0.007 nsec, is in agreement with the recent theoretical value of 0.0803 nsec. The possibilities of observing transitions from doubly excited levels in the He I isoelectronic sequence are briefly discussed. (auth)

30266 CALCULATIONS OF VAN DER WAALS BROADENING FOR LINES OF ASTROPHYSICAL INTEREST. Fullerton, Wayne; Cowley, Charles R. (Univ. of Michigan, Ann Arbor). Astrophys. J.; 165: 643-6(1 May 1971).

Van der Waals damping constants are calculated for a number of lines of astrophysical interest by use of a theory that includes higher-order terms in the interaction potential. The relative importance of these higher-order terms is compared for perturbations by hydrogen, helium, and argon. (auth)

30267 X-RAY EMISSION SPECTRA OF VC_x, NbC_x, TaC_x, AND ZrC. Ramqvist, Lars (Axel Johnson Inst. for Industrial Research, Nynaeshamn, Sweden); Ekstig, Boerje; Kaelline, Elisabeth; Noreland, Erik; Manne, Rolf. J. Phys. Chem. Solids; 32: 149-57(Jan 1971).

X-ray emission spectra from VC_x, NbC_x, TaC_x, and ZrC are reported and discussed in conjunction with the corresponding spectra of the pure elements. Comparisons are made with electron spectroscopy measurements, and with earlier reported metal and carbon soft x-ray spectra. In all the investigated carbides the shift measurements and the metal band spectra confirm the positive character of the metal atom. (auth) (UK)

30268 HOW ACCURATE ARE H_β STARK PROFILES. Griem, Hans R. (Univ. of Maryland, College Park). Comments At. Mol. Phys.; 11: 103-5(Aug-Sep 1970).

Two experiments for determining H_β Stark profiles that were performed in almost pure hydrogen plasmas and on microsecond time scales are described. Two arc experiments were performed in argon plasmas having hydrogen admixtures of a few percent. It may be concluded that H_β profile calculations for electron densities of 1×10^{16} to 2×10^{17} cm^{-3} and temperatures of 1 to 2 eV are probably correct within ~5%, excepting the central dip, and that true profiles are more likely to be narrower than calculated profiles. This accuracy is somewhat better than expected from theoretical error estimates and could only be reached by calculations which, among other things, treat the transformation from frequency to wavelength scales more accurately, allow for the interference between different lines, and include quadratic Stark effects in the ion-broadening calculations. The accuracy with which such comparisons can be made deteriorates toward the line wings. (J.C.W.)

30269 WAVE FUNCTIONS FOR He BY ROTATIONAL PROJECTION. Bendazzoli, G. L.; Palmieri, P.; Zauli, C. (Istituto di Chimica Fisica e Spettroscopia, Bologna). Chem. Phys. Lett.; 8: 556-8(15 Mar 1971).

A different-orbitals-for-different-spins wave function, inclusive of a fraction of angular correlation energy, is obtained for the ground state of helium. (auth)

30270 NONADDITIVITY OF INTERMOLECULAR FORCES IN He_3 WITHIN THE SCF LCAO MO APPROXIMATION. Bader, R. F. W.; Novaro, O. A.; Beltran-Lopez, V. (Univ. Nacional Autonoma de Mexico, Mexico City). Chem. Phys. Lett.; 8: 568-70(15 Mar 1971).

The deviation of the interaction energy of the He_3 system from pairwise additivity is calculated by the SCF LCAO MO method. The results are in qualitative agreement with existing perturbation theory calculations but differ considerably in magnitude. (auth)

30271 SECOND-ORDER PERTURBATION THEORY WITH THE CONTACT INTERACTION. Power, J. D.; Pitzer, R. M. (Ohio State Univ., Columbus). Chem. Phys. Lett.; 8: 615-21 (15 Mar 1971).

The second-order energies for the 1s and 2s states of atomic hydrogen perturbed by $r_0/r^2(r + r_0)^2$, the form of the Fermi contact operator derived from the Dirac theory were calculated. This is of interest in the evaluation of both NMR spin−spin coupling constants and of small corrections to the hydrogen-atom hyperfine splitting. The results are compared with those of previous work, which approximated the contact interaction as $\delta(r)/r^2$. (auth)

Positronium, Muonium, and Mesic Atoms and Molecules

30272 POSITRON LIFETIMES IN RARE EARTH OXIDES. Singh, K. P. (Indian Inst. of Tech., Kanpur); Singru, R. M.; Kulkarni, V. G.; Lagu, R. G.; Chandra, G. Phys. Lett.; 34A: 377-8 (19 Apr 1971).
1971).

The data of positron lifetimes with their intensities in La_2O_3, Nd_2O_3, Sm_2O_3, Dy_2O_3, and Yb_2O_3 are presented. A possible origin for the long components τ_2 and τ_4 is suggested. (auth)

Collision Phenomena

30273 (ANL-Trans-879) MEASUREMENT OF THE RADIATIVE LIFETIMES OF $CO_2^+(A^2\Pi_u)$, $CO_2^+(B^2\Sigma_u^+)$, $CH(A^2\Delta)$ AND $CO(C^1\Sigma^+)$ BY PULSED RADIOLYSIS. Le Calve, J.; Bourene, M.; Schmidt, M.; Clerc, M. Translated for Argonne National Lab., Ill., from J. Phys. (Paris); 30: 807-10(1969). 8p. Dep. NTIS.

Gas-phase pulsed radiolysis of CO_2, CH_4, and CO, using a 600-keV 10-joule pulsed electron source, enabled measurement of the radiative lifetime of excited states. The results obtained are $CO_2^+(A^2\Pi_u)$ = 147 ± 10 nsec, $CO_2^+(B^2\Sigma_u^+)$ = 135 ± 10 nsec, $CH(A^2\Delta)$ = 800 ± 100 nsec, and $CO(C^1\Sigma^+)$ = 50 ± 10 nsec. (auth)

30274 (ANL-Trans-881) ABSORPTION OSCILLOGRAM OF $CO_2^+(X^2\Pi_g)$ AND $N_2^+(X^2\Sigma_g^+)$ IONS IN THEIR GROUND STATE PRODUCED BY PULSED RADIOLYSIS OF CO_2 AND N_2. Clerc, Michel; Lesigne, Bernard. Translated for Argonne National Lab., Ill., from J. Chim. Phys.; 67: 701-3(1970). 6p. Dep. NTIS.

An abstract of this paper, prepared from the original language, appeared as NSA 24: 45030.

30275 (JAERI-Memo-4299) DYNAMIC MOLECULAR ORBITALS AND THEIR APPLICATION TO CHARGE EXCHANGE REACTIONS. Ryufuku, Hiroshi (Japan Atomic Energy Research Inst., Tokyo). Jan 1971. 24p. (In Japanese). Dep. NTIS (U. S. Sales Only).

Expressions for the resonance and nonresonance charge-exchange probabilities applicable in collisions between atomic systems are derived theoretically. This is accomplished by means of the PSS method together with "dynamic molecular orbitals." It is shown that in the low-energy limit the present expressions agree with the result derived by the common PSS method and in the high-energy limit with Brinkman and Kramers' formulation using the Born approximation. (auth)

30276 (ORNL-TM-2620) COLLISIONAL IONIZATION BETWEEN CESIUM AND SELECTED MOLECULES. Nalley, S. J.; Compton, R. N.; Schweinler, H. C.; Reinhardt, P. W. (Oak Ridge National Lab., Tenn.). Apr 1971. Contract W-7405-eng-26. 126p. Dep. NTIS.

Thesis. Submitted by S. J. Nalley to Univ. of Tennessee, Knoxville.

An apparatus was designed and assembled, and a method was developed for the observation of low-energy neutral atom−molecule

collisions in the greater-than-thermal energy range. Included in this apparatus were a fast-atom beam source, which utilized the resonance charge-transfer principle to produce a neutral Cs beam from a positive Cs ion beam, a detector for determining the energy of the beam, and a time-of-flight mass spectrometer for identifying the reaction products. The method consisted of directing a neutral Cs beam onto a target gas (pressure $\sim 1 \times 10^{-4}$ torr) in the reaction region of a time-of-flight mass spectrometer and identifying the resultant negative ions from their mass-to-charge ratio. An investigation was then made of the reactants, Cs^* plus NO_2 or N_2O or O_2, to determine the energies at which the negative ions [(Cs + NO_2: NO_2^-, O^-), (Cs + N_2O: N_2O^-, O^-), (Cs + O_2: O_2^-, O^-)] first appeared. An interpretation of the reaction threshold for the production of NO_2^-, N_2O^-, and O_2^- gives lower bounds to the electron affinities for NO_2 (1.94 ± 0.1 eV), N_2O (~0 eV), and O_2 (0.46 ± 0.05 eV). A comparison was made with the theory of the behavior of the relative cross sections for the production of NO_2^-, N_2O^-, and O_2^- in a collision of Cs^* atoms with the parent molecules at energies near threshold. For each collision pair the O^- ion was observed with the limits of experimental error at the minimum energy predicted from the energy and momentum conservation equations. (auth)

30277 (UCRL-20529) HYDROGEN–NITRIC OXIDE SPIN EXCHANGE CROSS SECTION. Dow, Philip (California Univ., Berkeley. Lawrence Radiation Lab.). Mar 1971. Contract W-7405-eng-48. 95p. Dep. NTIS.

Thesis.

The construction of a spectrometer to detect the transition (1.420 GHz) between the hyperfine levels of the hydrogen atom Zeeman-perturbed at zero magnetic field is described. This splitting of the $^2S_{\frac{1}{2}}$ ground state arises from the spin–spin coupling of the proton and the electron. In considering several detection methods, the balanced transmission scheme, in which the sample of hydrogen gas forms one arm of an equivalent null bridge circuit, is found to be far superior to the reflection scheme commonly used in ESR work. Also, the modulation scheme employs a rotating quasi-static magnetic field, instead of the small additional sinusoidal field, in contrast to most ESR spectrometers. The spectrometer is used to investigate the spin-exchange reaction between hydrogen atoms and nitric oxide in a flow system at pressures of about 1 torr. Under these experimental conditions, the residence time of the hydrogen atoms in the radiation field is quite long—of the order of .5 second. This precludes any line-broadening effect due to the finite transit time of hydrogen atoms, but it does result in a line-narrowing effect due to the loss of hydrogen atoms by homogeneous and heterogeneous recombination. Two models of the latter effect are considered, a slug-flow reactor with a concentration gradient of hydrogen atoms and a uniform diffusion-stirred reactor. The H–NO spin-exchange rate constant is not particularly sensitive to the model employed. Although the theoretical line shapes for the two models are different—the second is Lorentzian, whereas the former is not—the data are not sufficiently accurate to distinguish between them. The cross section for the exchange of electron spin between hydrogen and nitric oxide is found to be 2.4×10^{-16} cm^2. This is considerably smaller than the value for hydrogen–hydrogen spin exchange. (auth)

30278 COMPLEX-ANGULAR-MOMENTUM ANALYSIS OF ATOM–ATOM SCATTERING EXPERIMENTS. Remler, E. A. (Coll. of William and Mary, Williamsburg, Va.). Phys. Rev., A; 1949-54(Jun 1971).

S-matrix elements typically encountered in atom–atom scattering may be phenomenologically parametrized using meromorphic functions of complex angular momenta. The contribution to the scattering amplitude of each pole of the S matrix is of such a simple nature (effectively, decaying oscillations for parameters encountered in practice) as to greatly facilitate the deduction of the phase shifts from scattering data. Some of these poles should be close to the true (Regge) poles of the exact S matrix about which much theoretical information is available. There is some discussion outlining how many diverse phenomena such as rainbows, orbiting, and curve crossing can all be parametrized under the same scheme, thus leading to their unified treatment. (auth)

30279 MEASUREMENTS OF INELASTIC ENERGY LOSS IN SINGLE ATOMIC COLLISIONS OF Kr^+ ON Kr AT keV ENERGIES AND LARGE SCATTERING ANGLES. Fastrup, B.; Hermann, G. (Univ. of Aarhus, Denmark). Phys. Rev., A; 1955-8(Jun 1971).

The inelastic energy loss Q was measured for Kr^+–Kr single collisions at incident energies of 20 and 30 keV and scattering angles ranging from 6° to 15°. For distances of closest approach r_0 around 0.385 Å, the inelastic energy-loss distribution is triple peaked, and the differences in energy between the three peaks are independent of r_0. This structure is interpreted as being due to the production of one or two $M_{IV,V}$ vacancies. (auth)

30280 INFINITE-CHANNEL CLOSE-COUPLING APPROXIMATION IN THE SECOND BORN APPROXIMATION. II. TREATMENT OF CHARGE POLARIZATION IN ELASTIC SCATTERING BY USE OF THE T-MATRIX FORMALISM. Bonham, R. A. (Univ. of Hokkaido, Sapporo. Indiana Univ., Bloomington). Phys. Rev., A; 3: 1958-68(Jun 1971).

An operator expansion of the T matrix is shown to lead to an equation for describing charge polarization in elastic scattering similar to that reported previously by use of the infinite-channel close-coupling approximation in the second Born approximation. The resulting equations are used to calculate the charge-polarization corrections for elastic electron scattering from H and He at incident electron energies of 100 eV, 500 eV, and 40 keV over the angular range of 0° to 50°. The results agree well with those of Bromberg and LaBahn and Callaway for elastic scattering from He with an incident electron energy of 500 eV. (auth)

30281 VIBRATIONAL EXCITATION AND COMPOUND STATES IN NO. Spence, D.; Schulz, G. J. (Yale Univ., New Haven). Phys. Rev., A; 1968-76(Jun 1971).

The cross section for elastic scattering by electron impact on NO shows resonances in the energy range 0 to 2 eV. These resonances, with a spacing of about 0.16 eV (ω_e = 0.17 eV), are associated with vibrational levels of NO^-, and there is a near-coincidence in energy between the 4th vibrational state of NO and the 6th vibrational state of NO^-. The width of these resonances increases monotonically from 0.02 to 0.10 eV as the vibrational quantum number of NO^- goes from 1 to 6. The energy dependence of the vibrational cross sections exhibits peaks at the positions of these resonances, and the magnitude of these peaks is measured. The vibrational states of NO^- can decay by the emission of an electron into various vibrational levels of NO. The branching ratio for a few of these decays is measured. A potential-energy diagram of NO^- is drawn, using the experimental evidence. (auth)

30282 DIFFERENTIAL SPIN EXCHANGE AND ELASTIC SCATTERING OF LOW-ENERGY ELECTRONS BY POTASSIUM. Collins, R. E.; Bederson, B.; Goldstein, M. (New York Univ., N. Y.). Phys. Rev., A; 3: 1976-87(Jun 1971).

Results are reported on the elastic scattering of low-energy electrons by potassium. The atomic-beam crossed-beam recoil technique is used, with velocity selection and spin selection and analysis of the atom beam. The results include total, differential, and differential spin-exchange cross sections in the energy range 0.5 to 1.2 eV. Comparison is made with close-coupling, as well as with adiabatic-type, calculations. Additional total cross-section measurements up to 9 eV are also presented. These are significantly smaller and lack the pronounced structure of the early results of Brode. (auth)

30283 BORN WAVE CROSS-SECTION CALCULATIONS FOR COLLISIONAL QUENCHING OF METASTABLE H(2s) BY HELIUM, NEON, ARGON, AND KRYPTON. Levy II, H. (Smithsonian Astrophysical Observatory, Cambridge, Mass. Harvard College Observatory, Cambridge, Mass.). Phys. Rev., A; 3: 1987-91(Jun 1971).

Total quenching cross sections for metastable H(2s) atoms in collisions with helium, neon, argon, and krypton were calculated over the incident-energy range 1.0 keV to 1.6 MeV in the first Born approximation with the added approximation of closure used to describe target excitation. The first-Born-approximation cross sections for helium target atoms are one-third the measured values of Byron, Krotkov, and Medeiros over the incident-energy range 1.0 to 5.0 keV. The first-Born-approximation results for the heavier targets are much larger than experiment, although scaled results based on parameters determined from electron-loss data for H(1s) show fair agreement with recent experiments. The contributions of individual quenching processes are examined, and electron loss dominates for incident energies greater than 4.0 keV. (auth)

30284 VACUUM-ULTRAVIOLET EMISSION FROM PROTON-EXCITED HELIUM GAS. Stewart, T. E.; Hurst, G. S.; Bartell, D. M.; Parks, J. E. (Univ. of Kentucky, Lexington). Phys. Rev., A; 3: 1991-7(Jun 1971).

Vacuum-ultraviolet (vuv) studies were made of the emission from helium gas excited by 4-MeV protons, under conditions where the gas purity was monitored by concomitant total-ionization measurements. The relative intensity of the 584-Å resonance line was studied from 0.01 to 100 torr. Three continua, near 600, 675, and 800 Å, respectively, were investigated from a few torr to 800 torr. The studies of intensity as a function of

XUM

pressure are consistent with the interpretation that the 675-Å continuum is the bound–continuum transition $D^1\Sigma_u^+ \rightarrow X^1\Sigma_g^+$ in the helium diatomic molecule, where the D state is formed by three-body collisions involving the atomic 2^1P state. Some of the 800-Å continuum, as well as the narrow continuum near 600 Å, is produced, most likely, from a similar process involving emission from the $A^1\Sigma_u^+$ molecular state, created from three-body conversion of a 2^1S atomic state. Certain other details are given on the energy pathways following charged-particle excitation of helium gas, and comments are made on some of the recently published emission data for liquid helium. (auth)

30285 EXCHANGE EXCITATION IN HELIUM: EXCITATION FUNCTIONS FOR THE 4^3S, 3^3P, AND 3^3D LEVELS. Kay, R. B.; Showalter, J. G. (American Univ., Washington, D. C.). Phys. Rev., A; 3: 1998-2006(Jun 1971).

Excitation functions and the pressure dependences of the apparent cross sections for the 4^3S, 3^3P, and 3^3D levels are obtained for energies between 50 and 500, 50 and 600, and 50 and 500 eV, respectively, and for pressures in the region 1.0 to 10 μ Hg. The excitation function of the 4^3S is found to be purely monotonically decreasing with energy at a slope of -3.0 ± 0.2. The 3^3D and to a lesser extent the 3^3P excitation functions are composed of two energy dependences, a slow one attributed to mixed F-level cascade, and an initially dominant fast component due to exchange excitation. The fast component falls as $(\text{energy})^{-3.5 \pm 0.2}$ and $(\text{energy})^{-3.7 \pm 0.5}$ for the 3^3P and 3^3D levels, respectively. (auth)

30286 ALGEBRAIC CLOSE-COUPLING CALCULATION OF THE SCATTERING OF ELECTRONS AND POSITRONS BY HYDROGEN. Seiler, G. J.; Oberoi, R. S.; Callaway, J. (Louisiana State Univ., Baton Rouge). Phys. Rev., A; 2006-14(Jun 1971).

The algebraic close-coupling method is applied to slow collisions of electrons and positrons with atomic hydrogen. The wave function is assumed to be of the form appropriate for a 1s–2s–2p close-coupling calculation. The variational method proposed by Nesbet is used to calculate the appropriate phase shifts and cross sections. Excellent agreement with previously published results of Burke, Schey, Smith, and others is obtained for scattering below the n = 2 threshold. Information concerning resonance structure for positrons, and for electrons in the singlet and triplet state, is also obtained. Good results are also obtained above threshold in the 1s–2s and three-state approximations. Problems connected with the choice of asymptotic functions for the open n = 2 channels are discussed. (auth)

30287 ANALYSIS OF SCATTERING AND EXCITATION AMPLITUDES IN POLARIZED ELECTRON–ATOM COLLISIONS. I. ELASTIC SCATTERING ON ONE-ELECTRON ATOMS AND THE EXCITATION PROCESS $^2S_{1/2} \rightarrow {}^2P_{1/2,3/2}$. Kleinpoppen, Hans (Univ. of Colorado, Boulder). Phys. Rev., A; 3: 2015-27(Jun 1971).

Scattering amplitudes are analyzed for the scattering of polarized or unpolarized electrons on polarized or unpolarized atoms (one-electron atoms). The elastic scattering of unpolarized electrons on partially polarized atoms provides the direct and exchange cross sections when the polarizations of the scattered electrons and atoms are observed, respectively. The same quantities can also be obtained from the scattering of partially polarized electrons on unpolarized atoms, while the difference between the phases of the direct and the exchange amplitude can be derived from the spin analysis with polarized electrons and polarized atoms. When the degree of polarization of the colliding particles is known, the intensity of the scattered collision particles determines the interference term of the elastic cross section. The excitation process $^2S_{1/2} \rightarrow {}^2P_{1/2,3/2}$, carried out with any combination of polarized and unpolarized electrons and atoms, has been analyzed in terms of differential and integral excitation amplitudes distinguished in terms of direct, exchange, and interference processes and also in terms related to the excitation of the magnetic substates $m_l = 0$ or ± 1. The analysis of the polarization of the inelastically scattered electrons gives differential excitation amplitudes for the direct, exchange, and interference terms of the excitation cross section without distinguishing between the magnetic substates. Based upon the observations of the intensity and the circular polarization of the emitted line radiation, the analysis of the $^2P_{1/2,3/2} \rightarrow {}^2S_{1/2}$ de-excitation process provides integral excitation amplitudes. Observation of the total intensity of the $^2P_{1/2,3/2} \rightarrow {}^2S_{1/2}$ transition in an excitation process with polarized electrons and polarized atoms enables one to determine interference terms of the excitation cross section. Equal polarization for the exciting electrons and target atoms permits separation of the interference amplitudes for the magnetic substates ($|F_1 - G_1|$ and $|F_0 - G_0|$). Analysis of the circular polarization of the $^2P_{1/2} \rightarrow {}^2S_{1/2}$ transition excited with unpolarized electrons and partially polarized atoms results in partial cross sections describing excitation processes in which the quantum number m_j of the excited state differs from that of the ground state at most in sign. Excitation with polarized electrons and unpolarized atoms should also result in the emission of circular polarized light of the P → S transitions. In this context Farago's proposal for measuring electron-spin polarization by circularly polarized line excitation is discussed as it applied to alkali atoms. Finally, it is pointed out how sets of integral excitation amplitudes determined by collisions, as discussed above, can be used for comparing single-excitation amplitudes with theory. (auth)

30288 FAST-ELECTRON–SLOW-ELECTRON COINCIDENCE STUDY OF VIOLENT Ar^+–Ar COLLISIONS. Thomson, G. M.; Laudieri, P. C.; Smith, W. W.; Russek, A. (Univ. of Connecticut, Storrs). Phys. Rev., A; 3: 2028-34(Jun 1971).

An electron–electron coincidence measurement was made of the energy spectrum of only those slow electrons emitted from violent Ar^+–Ar collisions that produce known-energy fast L → MM Auger electrons. The correlation between the number of ejected slow electrons and the energy of the fast electron is much less than expected from a model based on the generally assumed ordering of the inner-shell (Auger) and outer-shell transitions following inner-shell excitation. Furthermore, details of the spectra show that double Auger (L → MMM) processes do not occur in a large percentage of the events studied. It appears that the branching ratio of outer-shell auto-ionizing transitions to L → MM transitions in argon is smaller than expected, possibly owing to the molecular properties of the Ar^+–Ar collision system. (auth)

30289 ANNIHILATION OF POSITRONS DURING SCATTERING. Fels, Margaret F. (Univ. of California, Los Angeles); Mittleman, Marvin H. Phys. Rev., A; 3: 1827-31(Jun 1971).

The expression for the annihilation rate of positrons in scattering from atoms at an energy above the positronium (Ps) formation threshold is examined. A model describing the physical effects of annihilation is constructed and it is shown that no unexpected terms appear in the annihilation rate even when almost degenerate states of Ps are open channels. A previous calculation of positron–helium scattering is used to calculate the annihilation rate just above the Ps formation threshold where two competing effects complicate the expression. It is concluded that the annihilation rate above threshold comes almost completely from the formation of real Ps. (auth)

30290 COLLISIONS OF AN ATOM AND A HARMONIC OSCILLATOR. Morse, R. I. (Clark Univ., Worcester, Mass.). J. Chem. Phys.; 54: 4138-9(1 May 1971).

A semiclassical approach used by Heidrich, Wilson, and Rapp (J. Chem. Phys., 54: 3885-97(May 1, 1971)) is extended to three dimensions for an exponential replusion. The approach is based on the relationship between the average energy transfer and the transition probabilities for a forced harmonic oscillator. (A.G.W.)

30291 INVESTIGATION OF BACKSCATTERING IN THE D^+–H_2 REACTION SYSTEM. Holliday, M. G.; Muckerman, J. T.; Friedman, L. (Brookhaven National Lab., Upton, N. Y.). J. Chem. Phys.; 54: 3853-6(1 May 1971).

A collision chamber designed for efficient collection of product ions was used to determine the extent of backscattering in the reactions of D^+ and H_2 to form H^+ and HD^+. No significant amount of backscattering in the laboratory system was detected. (auth)

30292 COLLINEAR COLLISIONS OF AN ATOM AND HARMONIC OSCILLATOR. Heidrich, Fred E. (Univ. of California, San Diego, La Jolla); Wilson, Kent R.; Rapp, Donald. J. Chem. Phys.; 54: 3885-97(1 May 1971).

A comparison is made between quantum, semiclassical, and classical treatments of collinear collisions, with exponential repulsive potential, between an atom and a harmonic oscillator. The quantum calculations used for comparison are those of Secrest and Johnson. The semiclassical treatment, called ITFITS, gives analytic transition probabilities in the form of a quantum forced oscillator whose energy transfer is determined separately for each combination of initial and final states by a "refined impulsive" classical approximation symmetrized over initial and final states. Detailed balance is obeyed. The classical treatment is phase averaged, the energy transfer, calculated by numerical integration of the equations of motion, being averaged over the initial phase of the oscillator. The quantum transition probabilities are very well matched for both single and multiple quantum jumps by the semiclassical ITFITS approximation. The quantum average energy transfer is closely approximated both by the semiclassical and classical treatments. It is concluded that, over the range of the quantum data, a semiclassical analysis is quite reasonable for

XUM

transition probabilities and that both semiclassical and classical treatments give an essentially accurate description of average energy partitioning. (auth)

30293 THEORY OF SEMICLASSICAL TRANSITION PROBABILITIES (S MATRIX) FOR INELASTIC AND REACTIVE COLLISIONS. Marcus, R. A. (Univ. of Illinois, Urbana). J. Chem. Phys.; 54: 3965-79(1 May 1971).

The time-independent Schrödinger equation for inelastic collisions is solved directly in the WKB approximation, using action-angle variables and the method of characteristics. A single wave function, consisting of an ingoing and an outgoing term, is thereby derived, describing all collision channels and so avoiding the application of WKB methods to an infinite set of coupled differential equations. An integral is obtained for the S matrix, and asymptotic methods (e.g., steepest descents, stationary phase) are used for its evaluation. The expressions can be calculated using numerical data on classical trajectories or using approximations. To facilitate the latter and to show the connection with approximations in the literature, a canonical perturbation theory is described for the wave phase and amplitude, in a form suited to collisions, and used to relate the theory to those approximations. The topic of collisional selection rules is also considered. The extension of the method employed in the present paper to the direct calculation of differential and total inelastic cross sections, rather than via the S matrix, is briefly described, and the extension to reactive cross sections is also noted. The method can also be used to treat time-dependent problems, and so is not restricted to collisions. These topics and other applications will be described in later papers of this series. (auth)

30294 ANGULAR DISTRIBUTIONS OF PENNING ELECTRONS. Hotop, H.; Niehaus, A. (Univ., Freiburg i. B.). Chem. Phys. Lett.; 8: 497-500(15 Mar 1971).

The intensity of Penning electrons arising from ionization of Ar by a thermal beam of He(2^1S, 2^3S) metastables was measured as a function of the angle θ between metastable-beam and detector directions. The distribution is asymmetric with respect to $\theta = 90°$, favoring large angles, and different for ionization by He(2^1S) and He(2^3S). The results are discussed on the basis of an atomic-orbital picture of the autoionizing system. (auth)

30295 THEORY OF VIBRATIONAL EXCITATION IN THE NEAR CLASSICAL LIMIT. Levine, R. D.; Johnson, B. R. (Ohio State Univ., Columbus). Chem. Phys. Lett.; 8: 501-6(15 Mar 1971).

A theory of vibrational excitation based on the near-classical limit of collision theory is presented. The theory centers attention on the action transferred to the oscillator during the collision. In the correspondence-principle limit, individual transition probabilities can be computed directly. (auth)

30296 ROTATIONAL EXCITATION IN MOLECULAR COLLISIONS: MANY-STATE TEST OF THE STRONG-COUPLING APPROXIMATION. Tsien, T. P.; Pack, R. T. (Brigham Young Univ., Provo, Utah). Chem. Phys. Lett.; 8: 579-81(15 Mar 1971).

A previously discussed strong-coupling approximation for rotationally inelastic molecular collisions is tested on a 16-state model problem and found to give surprisingly accurate results. (auth)

30297 COMPUTATION OF RESONANCE PARAMETERS FOR ELASTIC SCATTERING. Hazi, A. U.; Fels, M. F. (Univ. of California, Los Angeles). Chem. Phys. Lett.; 8: 582-6(15 Mar 1971).

A new method for the calculation of the energy, width, and background phase shift of resonances occurring in elastic scattering is proposed, and its usefulness is demonstrated by applying it to a simple model problem. (auth)

30298 SEMI-EMPIRICAL MODEL FOR PENNING AND ASSOCIATIVE IONIZATION: VELOCITY DEPENDENCE AND BRANCHING RATIOS FOR Ne($^3P_{2,0}$) COLLISIONS WITH Ar, Kr, AND Xe. Micha, D. A.; Tang, S. Y.; Muschlitz, E. E. Jr. (Univ. of Florida, Gainesville). Chem. Phys. Lett.; 8: 587-91 (15 Mar 1971).

A two-state impact-parameter model is developed to provide a comprehensive description of Penning and associative ionization. It is used to fit recent experimental results at low velocities and to predict branching ratios. The model indicates that the interaction leading to ionization is short-ranged. (auth)

30299 CALCULATION OF IONIZATION CROSS SECTIONS OF MOLECULES DUE TO HEAVY-PARTICLE IMPACT ON THE BASIS OF CLASSICAL APPROXIMATION. Tripathi, D. N.; Rai, D. K. (Banaras Hindu Univ., India). Indian J. Pure Appl. Phys.; 8: 612-13(Oct 1970).

The suitability of the classical binary encounter approximation given by M. Gryzinski [Phys. Rev., A138: 305, 322, 336 (1965)] was examined for predicting cross sections for ionization of molecules by impact with protons, deuterons, and He^+ ions. The variation of the ionization cross section with incident energy of the impacting particle shows a similar trend for the six molecules studied, viz., N_2, CO, CO_2, NO, NH_3, and CH_4. Low-energy behavior of the variation of the cross section shows that Gryzinski's approximation is not valid in this region. (auth)

30300 CHARGE EXCHANGE CROSS SECTIONS FOR ELECTRON LOSS FROM B^+, P^+, AND N^+ ON N_2. Moline, R. A. (Bell Telephone Labs., Inc., Murray Hill, N. J.). J. Appl. Phys.; 42: 2471-5(May 1971).

The cross sections for electron loss from singly ionized B, N, and P ions at 100 keV, 200 keV, and 300 keV collisions with N_2 were measured. The cross sections for a singly ionized projectile to become doubly ionized, σ_{12}, are (10^{-16} cm^2 per molecule): σ_{12} (B, 100 keV) = 2.0, σ_{12} (B, 200 keV) = 3.4, σ_{12} (B, 300 keV) = 4.4, σ_{12} (N, 100 keV) = 2.2, σ_{12} (N, 200 keV) = 3.4, σ_{12} (N, 300 keV) = 4.6, σ_{12} (P, 100 keV) = 4.3, σ_{12} (P, 200 keV) = 6.6, and σ_{12} (P, 300 keV) = 8.7. The cross sections for double electron loss were also measured. The observed cross section for $P^+ \rightarrow P^{2+}$ indicates that for a 1% contamination of a 300-keV P^+ ion beam with P^{2+}, the pressure times path length of the beam is 3.5×10^{-6} torr m. (auth)

Atomic Theory

30301 DAMPING OF PLASMA OSCILLATIONS IN ATOMS. Sen, A.; Harris, E. G. (Univ. of Tennessee, Knoxville. Oak Ridge National Lab., Tenn.). Phys. Rev., A; 3: 1815-19(Jun 1971).

The Thomas–Fermi model of the atom is used to calculate the damping of collective oscillations due to the excitation of bound electrons to free states. It is found that in some cases the decay time is much longer than the period of the oscillation. The results indicate that weakly damped plasma oscillations can exist in atoms. (auth)

30302 HYBRID GAUSSIAN-TYPE ORBITAL. A TEST WITH THE HYDROGEN ATOM. Rouse, Robert A. (Univ. of Missouri, St. Louis). J. Chem. Phys.; 54: 4135-6(1 May 1970).

Calculations on the ground state of the hydrogen atom were carried out in order to test the applicability of a different Gaussian-related basis function, $\exp(-\alpha r^2 - \beta r)$. Comparison of the energies obtained with those obtained using other Gaussian-type orbitals indicated that the present orbital can achieve the same accuracy in energy with one-half to one-third the number of terms used with the other orbitals. (A.G.W.)

Cosmic Radiation

Refer also to abstracts 29377, 30161, 30165, 30728, 30792, 30793, 30839, and 31448

30303 (AECL–3856) COSMIC RAY NM-64 NEUTRON MONITOR DATA. XVII. Monthly Graphs, September 1970–December 1970. Steljes, J. F. (Atomic Energy of Canada Ltd., Chalk River (Ontario). Chalk River Nuclear Labs.). Feb 1970. 67p. Dep. NTIS (U. S. Sales Only). AECL $1.50.

Uncorrected and barometer-corrected results from the cosmic-ray stations in Canada using equipment maintained by AECL are given in tabular form for the period from September to December 1970. Normalized graphs are given for the same period. Correction factors for the constant rates of drift of the barometers at each of the four stations are given. Values of barometric coefficients determined on a yearly basis by regression analysis are given for the first time. These may be used for precision work in place of the present constant coefficient of 9.87% per cm Hg. (auth)

30304 SUPERHEAVY NUCLEI IN THE COSMOS. Cherdyntsev, V. V. (Geological Inst., Moscow). Izv. Akad. Nauk SSSR, Ser. Fiz.; 34: 2281-5(Nov 1970). (In Russian).

Data are presented on the existence of superheavy transactinide isotopes in nature. Chemical properties of some substances found in the depths of the Earth's crust were quite similar to osmium. Recent works found a certain similarity of the chemical composition of cosmic rays, solar atmosphere and main-sequence stars, Earth, and meteorites (the standard conditions of nucleogenesis). (tr-auth)

XUM

30305 CHARGE DISTRIBUTION OF HEAVY COSMIC-RAY NUCLEI IN THE REGION $Z \geq 26$. Ivanova, N. S.; Kulikov, V. N.; Gagarin, Yu. F. (Ioffe Inst. of Physics and Tech., Leningrad). Izv. Akad. Nauk SSSR, Ser. Fiz.; 34: 2255-8(Nov 1970). (In Russian).

Charge spectra of primary cosmic rays in the region of large Z were studied with emulsions at 300 km and beyond the Earth's magnetic field. A semi-automatic photometer was used for measuring nuclear charges. Preliminary data are presented on the nuclear flux of the Fe group. Relative contents of nuclei with $Z \geq 30$, ≥ 40, ≥ 50, and ≥ 70 were estimated. (tr-auth)

30306 STUDIES OF THE PRIMARY γ RADIATION WITH $E \geq 200$ MeV MEASURED ON THE SATELLITE BY MEANS OF A SPARK CHAMBER. Volobuev, S. A.; Gal'per, A. M.; Kirillov-Ugryumov, V. G.; (and others). Izv. Akad. Nauk SSSR, Ser. Fiz.; 34: 2259-64(Nov 1970). (In Russian).

Descriptions are given of the instrumentation used and results obtained during measurements of γ quanta with $E \gtrsim 200$ MeV carried out in the satellite Cosmos-264. The primary γ-quantum flux in the direction of the Leo and Virgo constellations was equal to $(4.1 \pm 2.3) \times 10^{-4}$ cm^{-2}sec^{-1}sterad^{-1} (tr-auth)

30307 MEASUREMENTS OF ENERGY SPECTRA OF MULTI-CHARGED NUCLEI ON THE SATELLITE COSMOS-225. Kurnosova, L. V.; Konyakhina, S. S.; Logachev, V. I.; Razorenov, L. A.; Fradkin, M. I. Izv. Akad. Nauk SSSR, Ser. Fiz.; 34: 2265-9(Nov 1970). (In Russian).

Data obtained by Cosmos-225 on the nuclear fluxes with $Z \gtrsim 2$, $Z \gtrsim 6$, and $Z \gtrsim 20$ were used for constructing the energy spectra and hardness spectra (according to the measured latitude) for various groups of nuclei. (tr-auth)

30308 HL INDEX OF THE SOLAR ACTIVITY AND YEARLY VARIATIONS OF COSMIC RAYS. Gushchina, R. T.; Dorman, L. I.; Ilgach, S. F.; Kaminer, N. S.; Pimenov, I. A. Izv. Akad. Nauk SSSR, Ser. Fiz.; 34: 2434-8(Nov 1970). (In Russian).

The relation between the yearly variations of cosmic rays and the yearly variations of the heliolatitudinal index of solar activity was studied. An attempt was made to use the data obtained for estimating the magnitude of the φ_0 parameter. (tr-auth)

30309 ROLE OF HELIOGRAPHIC LATITUDE OF SPOTS IN 11-YEAR MODULATION OF GALACTIC COSMIC RAYS. Stozhkov, Yu. I.; Charakhch'yan, T. N. (Lebedev Inst. of Physics, Moscow. Moscow State Univ.). Izv. Akad. Nauk SSSR, Ser. Fiz.; 34: 2439-44(Nov 1970). (In Russian).

It is shown that the hysteresis phenomenon in cosmic rays is produced mainly by a corresponding hysteresis of the mean heliographic latitude of sunspots, $\bar{\varphi}$. The amplitude of 11-year variations depends significantly on $\bar{\varphi}$, in addition to the number of sunspot groups. (tr-auth)

30310 ENERGY SPECTRA OF 11-YEAR VARIATIONS OF COSMIC-RAY INTENSITIES ON THE RISING SOLAR-ACTIVITY CURVE. Stozhkov, Yu. I.; Charakhch'yan, A. N.; Charakhch'yan, T. N. Izv. Akad. Nauk SSSR, Ser. Fiz.; 34: 2445-50(Nov 1970). (In Russian).

Variations of primary cosmic-ray energy spectra were estimated on the basis of the depth of relative variations observed in cosmic rays over Murmansk and Mirny. It was found that the shape of the spectrum did not vary with solar activity. A considerable hardening of the energy spectrum was observed only during the periods close to minimum solar activity. (tr-auth)

30311 BEHAVIOR OF COSMIC LAYERS IN LOWER IONOSPHERE DURING FORBUSH DECREASES. Velinov, P. I.; Dorman, L. I.; Nesterov, G. T. (Geophysical Inst., Sofia. Inst. of Terrestrial Magnetism, Ionosphere, and Radio Wave Propagation, Moscow). Izv. Akad. Nauk SSSR, Ser. Fiz.; 34: 2451-5(Nov 1970). (In Russian).

Previously it was found that, at an altitude of 50 to 80 km, galactic cosmic rays produce an independent cosmic layer with electron density of the order of 10^3 cm^{-3}. Effects of Forbush-decreases on this cosmic layer were studied using the data on radio-wave absorption, cosmic-ray variations, and geomagnetic activity during April 25 and May 13, 1960. Data obtained from combined measurements of cosmic-ray variations and ionospheric absorption at various points were used for estimating the planetary distributions of geomagnetic thresholds under quiet and perturbed conditions and for comparing with theoretical models of magnetic disturbances. (R.V.J.)

30312 ACCELERATION OF COSMIC RAYS BY MAGNETO-HYDRODYNAMIC DISCONTINUITIES. Alekseev, I. I.; Kropotkin, A. P.; Shabanskii, V. P. Izv. Akad. Nauk SSSR, Ser. Fiz.; 34: 2318-21(Nov 1970). (In Russian).

It is shown that a partial particle reflection takes place during interactions of energetic particles with the front of an MHD discontinuity possessing a different-from-zero normal component of the magnetic field; simultaneously, the particles are accelerated. Such a method of particle acceleration under cosmic conditions was studied theoretically, considering interactions of particles with the converging fronts of oblique shock waves and acceleration of solar protons and electrons at the front of the magnetospheric main shock wave. Data obtained are correlated with experimental data. (tr-auth)

30313 PROBLEMS AND RESULTS OF STUDIES OF COSMIC-RAY VARIATIONS (MODULATION EFFECTS). Dorman, L. I. Izv. Akad. Nauk SSSR, Ser. Fiz.; 34: 2322-37(Nov 1970). (In Russian).

A brief review is given on up-to-date studies of effective galactic cosmic rays (11-year and sporadic variations, the Forbush-decrease, cosmic-ray intensity increase before the Forbush decrease, solar anisotropy of galactic cosmic rays and its variations, microvariations, etc.). Theoretical concepts of the observed phenomena are analyzed. Data obtained on cosmic-ray modulation effects, properties of solar wind and its magnetic field, and propagation of perturbations are discussed. A detailed analysis is given of the 11-year variations and their relation to the various indices of solar activity, in particular to the HL index which was calculated considering heliolatitude distribution of the solar activity. Properties of the solar wind at the boundary of the interstellar gas are evaluated. (tr-auth)

30314 STUDIES OF COSMIC-RAY FLUX IN INTERPLANETARY MEDIA. I. Altukhov, A. M.; Krymskii, G. F.; Kuz'min, A. I.; Transkii, I. A. Izv. Akad. Nauk SSSR, Ser. Fiz.; 34: 2338-50(Nov 1970). (In Russian).

A method for cosmic-ray detection based on the neutron data of the universal network of stations is described. Methods for eliminating the noise due to saturation are discussed. Current behavior during interplanetary disturbances is analyzed. The behavior of currents in the stationary and nonstationary solar-wind structures is also analyzed. (tr-auth)

30315 STUDIES OF COSMIC-RAY FLUX IN INTERPLANETARY MEDIA. II. Altukhov, A. M.; Krymskii, G. F.; Kuz'min, A. I.; Transkii, I. A. Izv. Akad. Nauk SSSR, Ser. Fiz.; 34: 2351-9(Nov 1970). (In Russian).

Equations for cosmic-ray flux were obtained using the approximation of anisotropic diffusion at low-depth modulation. A solution was found for the event in which the solar-wind velocity was not a function of the distance to the Sun and the diffusion coefficient was a power function of the distance. The resolution was applied to the solar-wind model of a conical-shaped high-velocity stream in a slow background. The flux field and the behavior of the flux at the orbit of the Earth were calculated as functions of time. The flux produced by shock waves was studied in the shell approximation. It was found that following western chromospheric flares the flux was directed towards the Sun; in all other cases it was directed away from the Sun. (tr-auth)

30316 COSMIC-RAY INTENSITY INCREASE BEFORE THE FORBUSH DECREASE AND STRONG SHOCK WAVES IN INTERPLANETARY MEDIA. Dorman, L. I.; Kaminer, N. S.; Kobuladze, T. V. Izv. Akad. Nauk SSSR, Ser. Fiz.; 34: 2360-70(Nov 1970). (In Russian).

The increased-intensity effect observed before magnetic storms was analyzed on the basis of data collected by continuous recording of the neutron component of cosmic rays carried out by the global net of stations during 1957–1961. The relationship between the increase and the Forbush-decrease revealed the quantitative dependence of the Forbush-decrease on the parameters of chromospheric flares, rate of the quiet solar wind, etc. Predictions of Forbush effects and amplitudes of geomagnetic storms from the data on the solar and geomagnetic activities are discussed. It was also observed that the Forbush-decrease developed during shock-wave passage through the interplanetary media was also related to parameters of the media. (R.V.J.)

30317 STUDIES OF VH AND VVH NUCLEI OF GALACTIC COSMIC RAYS ACCORDING TO THE TRACKS IN MINERAL METEORITES. Kashkarov, L. L.; Genaeva, L. I.; Malyshev, V. V.; Lavrukhina, A. K. (Inst. of Geochemistry and Analytical Chemistry, Moscow). Izv. Akad. Nauk SSSR, Ser. Fiz.; 34: 2303-7(Nov 1970). (In Russian).

The tracks formed by nuclei of primary cosmic rays with $Z \gtrsim 25$ were studied in the olivine separated from the Ilimaez meteorite. The mean length of track for the VH group was 6.3 μm and for the VVH group, $\gtrsim 20$ μm. The ratio of the VVH/VH fluxes was $(1.6 \text{ to } 2.7) \times 10^{-4}$ for $30 < Z < 40$ and $(0.2 \text{ to } 0.4) \times 10^{-4}$ for $Z > 40$.

The angular distribution of the tracks has a strongly expressed anisotropic character. (tr-auth)

30318 SPECTRUM OF THE FORBUSH DECREASE IN THE REGION OF 3 TO 50 GV. Dorman, L. I.; Sergeev, A. V. Izv. Akad. Nauk SSSR, Ser. Fiz.; 34: 2371-8(Nov 1970). (In Russian).

The Forbush decrease in the neutron component of cosmic rays was recorded by the global network of stations. The relationship between decreased intensity and the hardness of the geomagnetic cut-off was determined. The spectrophotometric method was used in studies of the modulation spectrum at 3 to 50 GV. (tr-auth)

30319 ANTISYMMETRIC DIURNAL AND SEMIDIURNAL VARIATIONS OF COSMIC RAYS. Krivoshapkin, P. A.; Skripin, G. V.; Krymskii, G. F.; Kuz'min, A. I. (Inst. of Space Physics Research and Aeronautics, Vladivostok, USSR). Izv. Akad. Nauk SSSR, Ser. Fiz.; 34: 2379-85(Nov 1970). (In Russian).

Formation of the second spherical harmonic in the cosmic-ray distribution was studied, and the anticipated antisymmetric diurnal (r_1^1) and semidiurnal (r_2^2) variations were calculated for each month at various orientations of the interplanetary magnetic field. Data of neutron monitors of the global network of stations for 1959, 1964, and 1965 were used to find the yearly variations r_1^1 and r_2^2. Experimental data were in agreement with the anticipated data for the mechanism of cosmic-ray screening. (tr-auth)

30320 STUDIES OF INTERPLANETARY SPACE CONDITIONS BY MEANS OF THE THREE-DIMENSIONAL ANISOTROPY OF COSMIC RAYS. Dorman, L. I.; Inozemtseva, O. I. Izv. Akad. Nauk SSSR, Ser. Fiz.; 34: 2386-90(Nov 1970). (In Russian).

Cosmic-ray density gradients in interplanetary space were evaluated using the data on the cosmic-ray neutron component. The model of anisotropic diffusion and experimental data obtained on the solar anisotropy of cosmic rays were used in the study. It was found that, during certain periods following Forbush decreases when a considerable north–south asymmetry effect was observed, the gradient component in the plane perpendicular to the ecliptic plane is different from zero and reaches ~10% per AU for effective particle hardness ~10 GV. (tr-auth)

30321 DIURNAL VARIATION OF COSMIC RAYS AND THE INHOMOGENEITY OF INTERPLANETARY MEDIA. Pankratov, A. K. Izv. Akad. Nauk SSSR, Ser. Fiz.; 34: 2391-5(Nov 1970). (In Russian).

Measurements of 1962 and 1964–1965 were used for determining the diurnal anisotropy of cosmic rays. The diurnal anisotropy was studied as a function of the magnitude of the interplanetary field and the solar-wind velocity. The phase anomalies in the diurnal anisotropy were larger and appeared more often during the Earth immersion into the sector with the field directed away from the Sun than with the field directed towards the Sun. The mean magnitude of anisotropy in the second case was 50% larger than in the first case. (tr-auth)

30322 MODULATION OF GALACTIC COSMIC RAYS AND SOLAR ACTIVITY. Charakhch'yan, A. N.; Charakhch'yan, T. N. Izv. Akad. Nauk SSSR, Ser. Fiz.; 34: 2396-2400(Nov 1970). (In Russian).

The amplitude of 11-year variations of cosmic-ray intensity was determined by the number of sunspot groups and by their mean latitude. The time of restoration of cosmic-ray intensity following sporadic reduction of the number of sunspots was evaluated. Data previously obtained for the velocity of magnetic inhomogeneities of the solar wind in interplanetary space and the modulation sphere radius were confirmed. (tr-auth)

30323 DETERMINATION OF THE MODULATION-REGION BOUNDARIES. Lavrukhina, A. K.; Ustinova, G. K. Izv. Akad. Nauk SSSR, Ser. Fiz.; 34: 2401-7(Nov 1970). (In Russian).

The existence of an effective modulating layer behind the Earths orbit, which reduces by 40% the intensity of galactic cosmic rays with energies of ≥0.2 GeV, was studied by comparing the calculated and observed magnitudes of activities of ^{32}P, ^{51}Cr, ^{46}Sc, ^{45}Ca, ^{54}Mn, and ^{22}Na in stone meteorites. Two possible positions of the modulating layer were indicated as functions of the width of the layer. Diffusion parameters were estimated for both positions. (tr-auth)

30324 SPHERICALLY SYMMETRIC MODEL OF MODULATION OF GALACTIC COSMIC RAYS IN THE PRESENCE OF TWO SOLAR WIND REGIONS WITH ANISOTROPIC AND ISOTROPIC DIFFUSION. Dorman, L. I.; Kobilinski, Z. Izv. Akad. Nauk SSSR, Ser. Fiz.; 34: 2408-14(Nov 1970). (In Russian).

A longitudinal asymmetry of the solar wind intensity as a function of distance from the Sun was studied. A plane problem of isotropic diffusion was resolved in order to determine the cosmic-ray densities in interplanetary space. The asymmetry of the density increased with the increased modulation parameter. In the case of large distances from the Sun, the solution was obtained with a spherically symmetric model. (tr-auth)

30325 MODULATION OF GALACTIC COSMIC RAYS BY THE SOLAR WIND WHOSE ASYMMETRY SLOWLY DECREASES WITH GREATER DISTANCE FROM THE SUN. Dorman, L. I.; Kobilinski, Z. Izv. Akad. Nauk SSSR, Ser. Fiz.; 34: 2415-18(Nov 1970). (In Russian).

Galactic cosmic-ray diffusion into the interplanetary space was calculated with the assumption that the anisotropic diffusion takes place in a region near the Sun and at large distances the conditions in the region became isotropic. (tr-auth)

30326 EFFECTS OF SOLAR-ACTIVITY CYCLE ON THE DEGREE OF IRREGULARITY OF INTERPLANETARY MAGNETIC FIELD. Kuz'min, A. I.; Skripin, G. V.; Filippov, V. A. (Inst. of Space Physics Research and Aeronautics, Vladivostok, USSR). Izv. Akad. Nauk SSSR, Ser. Fiz.; 34: 2419-25(Nov 1970). (In Russian).

Data obtained during 1958 to 1968 using the azimuthal muon telescopes of the Yakutsk underground complex were analyzed. Data on the first and second spherical harmonics of cosmic-ray distribution confirmed softening of the anisotropic energy spectrum with reduced solar activity. Data on the variations of the degree of inhomogeneity of the interplanetary magnetic field with the solar-activity cycle showed that, during the maximum solar activity period, the interplanetary magnetic field is more regular. (tr-auth)

30327 SEARCH FOR ANTIMATTER IN PRIMARY COSMIC RAYS. Greenhill, J. G.; Clarke, A. R.; Elliot, H. (Imperial Coll. of Science and Tech., London). Nature (London): 230: 170-2(19 Mar 1971).

A new method used in a search for antinuclei of charge $Z \geq 6$ in the energy range $5.0 \lesssim E \lesssim 9.0$ GeV/nucleon is reported. This method depends on the fact that the geomagnetic threshold rigidity (R), and therefore the velocity of cosmic rays arriving from the east, is lower for negatively charged primaries than for positive primaries, the difference being greatest in the equatorial zone. The detector used consists of a gas Cherenkov counter combined with two scintillator elements to form a cosmic-ray telescope, which is carried by a balloon. The Cherenkov counter gives a measure of particle velocity, and this, together with the computed threshold rigidity, allows the charge sign in the eastern and western quadrants to be determined. Propylene at 4.8 atm is the filling gas, giving a well-defined velocity threshold for nuclei with mass to charge ratio $A/Z = 2$, corresponding to a magnetic rigidity (Rc) of 18 GV. The associated electronic equipment is described in detail. Two of these telescopes were flown from Kampala (15°N, 32°E). The results set an upper limit to the fraction of antinuclei in the cosmic radiation in the rigidity range 10 to 18 GeV, and the ratio of antinuclei to nuclei ($Z \geq 6$) in the range $10 \leq R \leq 18$ GV was <7.5%. A summary of the present information on fluxes of antiparticles in the primary cosmic rays is shown in diagrammatic form. (UK)

30328 OBSERVATION OF PRIMARY ELECTRONS WITH EMULSION CHAMBER. Nishimura, Jun (Tokyo Univ.); Mikumo, Eiko; Mito, Iwao; Niu, Kiyoshi; Ohta, Itaru. Tokyo Daigaku Uchu Koku Kenkyusho Hokoku; 6: 346-58(Mar 1970). (In Japanese).

The primary electrons above 30 GeV were observed with an emulsion chamber of 25 × 20 cm area. Balloon observation was performed on Sept. 16, 1968, at Haramachi, Fukushima prefecture. The horizontal flight at altitude of 6 gr/cm^2 continued for 380.5 minutes. The electron showers observed in the chamber were classified into those due to electrons, γ rays, and nucleons. The primary electrons above 450 GeV were found only once in the total effective area of 2160 m^2 sec str. The intensity of the primary electrons above 100 GeV was a few times smaller than that observed by Daniel et al. The spectrum from 50 to 300 GeV was found to be approximately $dN/dE = 1.8 \times 10^{-4} \times (100/E)^{3.6 \pm 0.5}/m^2$ sec sterad. The spectrum showed deflection near 50 GeV. The intensity and the position of deflection differ considerably from the data reported by Daniel et al. at the Budapest conference. (Japan)

30329 IS BALL LIGHTNING CAUSED BY ANTIMATTER METEORITES. Ashby, D. E. T. F. (United Kingdom Atomic Energy Authority, Abingdon, Eng.); Whitehead, C. Nature (London); 230: 180-2(19 Mar 1971).

Measurements are reported, made over a period of 12 months, to test the hypothesis that ball lightning may be caused by the annihilation of minute fragments of meteoritic antimatter from the upper atmosphere. Such an hypothesis might explain the un-

XUM

usual properties of ball lightning and, in particular, its ability to enter buildings and aircraft and its estimated energy of 10^5 to 10^6J. The hypothesis depends on the postulate that antimatter can be comparatively stable in the presence of ordinary matter. Annihilation of a speck of antimatter of 5 μm radius and 5×10^{-10} g would liberate 10^5 J, and the ionization produced in the surrounding air by this annihilation could be expected to cause the optical properties attributed to ball lightning. A mechanism is suggested for the concentration of antimatter dust particles by thunderstorms. It is emphasized, however, that these hypotheses are no more than interesting speculations; a detailed analysis of the behavior of antimatter in the presence of ordinary matter is needed. If, however, micron-sized particles of antimatter are annihilated in the vicinity of thunderstorms their presence should be detectable, and experimental means to achieve this are discussed, together with some experimental results, some of which were consistent with annihilation radiation. (UK)

30330 COSMIC-RAY ^{2}H FROM SATELLITE MEASUREMENTS, 1965 to 1969. Hsieh, K. C.; Mason, G. M.; Simpson, J. A. (Univ. of Chicago). Astrophys. J.; 166: 221-33(15 May 1971).

A new measurement of the ^{2}H flux of galactic origin and the ^{2}H/^{4}He ratio in the energy interval 20 to 60 MeV per nucleon was obtained from the University of Chicago experiment on the satellite IMP-5 in 1969. At ~60 MeV per nucleon, $^2H/^4He = (2.1 \pm 0.6) \times 10^{-1}$. This ratio was compared with all other satellite measurements, and it was found that four independent sets of observations over a five year period at this energy yield a ratio $(2.2 \pm 1.0) \times 10^{-1}$. The differential energy spectrum of ^{2}H is much flatter than that measured at the time of the discovery of ^{2}H in 1965, due to the greater uncertainties in background correction in the 1965 measurements. (auth)

30331 TYPE-I VARIATIONS IN EXTENSIVE AIR SHOWERS GENERATED BY PROTONS OR HEAVY NUCLEI AND THEIR EFFECT ON THE DETERMINATION OF THE ENERGY OF THE PRIMARY COSMIC PARTICLE. Capdevielle, Jean-Noel; Dupuy, Jean; Cachon, Andre (Observatoire du Pic du Midi, Bagneres-de-Bigorre, France). Compt. Rend., Ser. B; 272: 493-6(22 Feb 1971). (In French).

The fluctuations of the components in the extensive air showers generated by protons and heavy nuclei were studied at various heights and at sea level using a computer simulation. The probability of primary particles with particular energies (about 10^{15} eV) being associated with an extensive shower of given characteristics was also determined. (France)

30332 DIFFUSE COSMIC X- AND GAMMA RADIATION: THE ISOTROPIC COMPONENT. Silk, Joseph (Princeton Univ., N. J.). Space Sci. Rev.; 11: 671-708(Dec 1970).

Interpretations of the origin of the diffuse x- and γ-ray background must account for the spectrum and the flux, and the spectral predictions of the various theories are discussed. There are only two probable observations of isotropic γ rays, both satellite experiments, by Vette et al. (1970) from 1 to 6 MeV, and by Clark et al. (1968) at ~100 MeV. The former observation was made with omnidirectional detectors; consequently, there is no evidence on the isotropy of the measured γ radiation. Tabulation of the origin of isotropic diffuse x radiation of <1 keV and 1 keV to 1 MeV is given for various experiments listing the mechanism, the evolution and no evolution diffuse or discrete source applying to the mechanism, and the predicted spectral features. The tabulation of the origin of the isotropic diffuse γ radiation includes 1 MeV to 10 MeV and >10 MeV energy range information on the mechanism applying to the evolution and no evolution diffuse or discrete source, and the predicted spectral features (relative to extrapolated x-ray spectrum). 129 references. (J.C.W.)

30333 OPTICAL AND RADIO STUDIES ON EXTENSIVE AIR SHOWERS. Baird, G. A.; Lawless, B.; Slevin, P. J. (University Coll., Dublin). Lett. Nuovo Cim.; 1: 685-9(17 Apr 1971).

The first attempts to study radio pulses at very large zenith angles were made by McBreen et al. (1966) and Charman et al. (1968), both using night-sky Cherenkov systems to detect the showers. The present work confirms the results of McBreen et al. and, more significantly, it is shown that if a radio trigger is used to interrogate a wide-angle optical system, it is possible to establish the presence of a high-energy shower with a fair degree of certainty. (W.D.M.)

30334 COSMIC-RAY MICROVARIATIONS DURING THUNDERSTORM PERTURBATIONS. Attolini, M. R.; Cecchini, S.; Galli, M.; Guidi, I. (CNR, Bologna. Univ., Bologna). Lett. Nuovo Cim.; 1: 716-20(24 Apr 1971).

Cosmic-ray microvariations associated with all the thunderstorms recorded in Bologna during the years 1965 to 1968 are examined. Also, the appearance of these microvariations in the various total ionizing, soft, and hard components are studied, as well as the consistency with a local temperature effect. An attempt is made to find the general characteristics of the phenomenon. (J.F.P.)

Direct Energy Conversion

Refer also to abstract 30453.

30335 COMPARISON OF SOME EXCITATION SCHEMES FOR A JET MHD INDUCTION GENERATOR. Kirillov, Igor R.; Pierson, Edward S. (Univ. of Illinois, Chicago). AIAA (Amer. Inst. Aeronaut. Astronaut.) J.; 9: 570-7(Apr 1971).

An initial analysis of an MHD induction generator operating on a flat, inviscid, pure-liquid jet with the magnetic vector potential specified is presented. The behavior for this model is controlled not by the conventional slips $s = u\alpha/\omega - 1$, where u is the fluid velocity, α the wave number, ω the frequency in rad/sec, and ω/α the velocity of the traveling magnetic field; but by the effective slip $s_e = (u/\omega)[\alpha + x(d\alpha/dx)] - 1$. Numerical and/or analytical solutions for the fluid velocity and powers are obtained for four forms of $\alpha(x)$. The constant α and constant s cases are impractical because of the spatial dependence of the field-fluid interaction. The constant s_e and linear-variation-of-α cases offer the possibility of improved performance with reasonable power densities and the reduction or elimination of viscous losses and ohmic wall losses. This analysis is also applicable to nonjet variable-velocity generators. (auth)

30336 EFFECT OF TEMPERATURE ON THE CRITICAL CURRENT DENSITY ACROSS MHD GENERATOR ELECTRODES MADE OF ZrO_2–Y_2O_3 CERAMICS. Gokhshtein, YA. P.; Safonov, A. A. (Inst. of High Temperatures, Moscow). Dokl. Akad. Nauk SSSR; 195: 109-12(1 Nov 1970). (In Russian).

Passage of direct current through a refractory $ZrO_2-Y_2O_3$ ceramic electrolyzes and destabilizes it, changing the ZrO_2 partially into black zirconium. The mechanism involved was studied by attempting to determine the effect of the temperature on the current density at which no degradation of the material occurs. The temperature dependence of this critical current density was examined on specimens containing ZrO_2 and Y_2O_3 at the ratios of 85:15 and 75:25 wt %, respectively. The apparent porosity of the fired specimens was 25 to 28%, and their density ranged from 4.28 to 4.32 g/cm^2. The tests were carried out in air in a furnace, applying the current and measuring the potential of the electrodes at 1373, 1473, 1573, and 1673°K. It was found that the critical current density is a function of the dimensions and the shape of specimens. As the temperature is increased, the current density decreases. The current is carried to the anode by the mechanism of discharge of oxygen and ions. Passage of a current higher than the critical one creates cracks in the ceramic; they are caused by electrolysis, which destabilizes the cubic solid solution of $ZrO_2-Y_2O_3$. The cracks may be detected by the sudden increase of the resistivity. (TTT)

30337 PROCESS FOR CROSSING BOUNDARY LAYERS IN A MAGNETOHYDRODYNAMIC GENERATOR AND A GENERATOR USING THE PROCESS. Klein, Georges; Sadoune, Joseph (to Compagnie Generale d'Electricite). French Patent 1,592,538. 19 May 1970. Filed 7 Jun 1968. (In French).

A method of crossing the boundary layer appearing in the plasma chamber of a magnetohydrodynamic generator is described, together with the generator developed as a function of this process. The boundary layer to be crossed is pierced by a fine jet of molten metal taken to a suitable temperature, and the following jet is given a velocity sufficient to enable it to pass through this layer under acceptable conditions; it is then possible to establish an electron flux passing from one electrode of the generator to the opposite electrode. In the case of an open-cycle generator the cross section of each jet must be slightly larger than the calculated value in view of the amount of energy that may be dissipated at this point, the corresponding increase serving to compensate the losses of metal due to oxidation and carbonation of the jet. The metals used must have relatively low melting points and vaporize little at temperatures in the range at which a breakthrough of the boundary layer is possible. They must also have a sufficiently low ionization potential in order to facilitate the formation of an arc at the issue of the boundary layer. The alkaline metals may be used: sodium, potassium, cesium, and lithium or a fusible eutectic alloy made up of two alkaline metals. In the special case of a closed-circuit generator where the plasma consists of cesium associated with a

rare gas, the metal chosen is cesium. The intensity of the electron flux passing through the boundary layer decreases linearly when the potential difference applied to the electrodes varies. A suitable electrode consists of a reservoir closed by a lid, containing the liquid metal and ending in an ejection nozzle. The reservoir is made of a ceramic material or a metal. A heating system is placed around the reservoir and a cooling system around the nozzle outlet. In the case of a ceramic reservoir, a metal rod passing through it provides the electrical contact with the mass of molten metal. An anticondensation device consisting of a jet of inert gas, introduced under pressure, inside the ejection nozzle near its outlet, is associated with the electrode. (France)

30338 ANALYSIS OF NONEQUILIBRIUM PLASMAS IN CLOSE-SPACED THERMIONIC CONVERTERS. Shaw, D. T.; Wu, F. T. (State Univ. of New York, Buffalo). J. Appl. Phys.; 42: 2294-2300(May 1971).

The effects of varying interelectrode spacings, current outputs, and cesium pressures on the spatial profiles of the electron temperature and density are determined for an ignited thermionic converter. A new method is introduced for the determination of the boundary conditions of the three transport equations that describe the electron and ion diffusion and the electron energy transport in the interelectrode plasma. Special emphasis is placed on the change of plasma properties as the interelectrode spacing varies from large values to very small values. (auth)

30339 ON ELECTROGASDYNAMIC FLOW IN DUCTS: A LINEAR VOLTAGE GENERATOR. Brunne, M.; Malaczynski, G. Pr. Inst. Masz. Przeply.; No. 46, 121-31(1969). (In German).

The problems of EGD flows in axisymmetric ducts are discussed from the viewpoint of their application as electrogasdynamic voltage generators. General equations used for description of such flows are given and discussed. The Poiseuille flow and radial flow in a variable cross section area duct are considered on the basis of the two-fluid model. Discussed are the conditions which must be satisfied when a stationary flow model is assumed, along with the solutions for the flow in the duct of a linear generator. As a result, the formulation of efficiency of the EGD process is proposed, and the distributions of ion density and field in the generator duct are defined, together with a subsidiary scheme of a linear generator. (App. Mech. Rev.)

30340 OSNOVY TERMOELEKTRONNOGO I MAGNITO-GIDRODINAMICHESKOGO PREOBRAZOVANIYA ENERGII. (Principles of Thermoelectric and Magnetohydrodynamic Conversion of Energy). Aref'ev, K. M.; Paleev, I. I. Moscow; Atomizdat (1970). 216p.

After a thermodynamic treatment of the general subject of gaseous ionization, vacuum and quasi-vacuum types of thermoelectron converters are discussed, followed by the physics of low-temperature plasmas and the operation of the plasma electron converter. Part II deals with the magnetohydrodynamic (MHD) converter, its general principles, and basic vector equations. Plasma conductivity in the MHD converter is discussed, both under conditions of equilibrium ionization and nonequilibrium ionization. Experimental data taken from the operation of MHD converters are presented, with schematic diagrams of closed cycle (inert gas) and open-cycle (combustion products at the working medium) types. Faraday-type MHD converters that operate on current transverse to the plasma flow, and Hall-type MHD converters that operate on the longitudinal Hall current are distinguished. The operation of the most common type of MHD converter is analyzed by vector treatment in some detail. The operational characteristics of four MHD converters are tabulated. Short-duration experiments (5 sec to 15 min) were characterized by voltage 43 to 500 volts and currents 378 to 12,000 amps. Other factors investigated that pertain to MHD converters are velocity effects, other losses, the use of high-conductivity materials in the electromagnet, liquid-metal MHD converters, and commercial MHD converters that operate on alternating current. 244 references. (K.S.W.)

Fluid Physics

30341 (NAL-TN-6) MAGNETOFLUIDDYNAMIC HEAT TRANSFER. Ramamoorthy, P.; Narayana, C. L.; Bose, T. K. (National Aeronautical Lab., Bangalore (India)). Jun 1967. 41p. Dep. NTIS (U. S. Sales Only).

Exact analytical solutions of the heat-transfer problems in magnetofluid-dynamics for the cases of flow through plane parallel channel and between concentric cylinders are presented. The heat-transfer rates at the stagnation point and some useful formulas for the estimation of heat-transfer rates through boundary layers are also discussed. These solutions enable one to understand the phenomenon of the electromagnetic interaction of fluiddynamics of conducting media. (auth)

30342 GENERALIZED MHD COUETTE FLOW WITH HEAT TRANSFER BETWEEN TWO POROUS WALLS UNDER TRANSVERSE MAGNETIC FIELD. Soundalgekar, V. M. Bull. Calcutta Math. Soc.; 59: 185-95(Sep-Dec 1967).

The problem of finding velocity and temperature distributions for the Couette flow of an MHD fluid is solved. The fluid is assumed incompressible with constant properties, however the possibility of wall suction (ingestion) is allowed for. A few numerical results are given. From these it is concluded that the shear stress and heat transfer both decrease with an increasing rate of suction. (App. Mech. Rev.)

30343 MEASUREMENTS IN AN ANNULAR MHD DUCT FOR HIGH HALL-PARAMETER VALUES. Ebert, W. Pr. Inst. Mech. Precyz.; No. 46, 111-20(1969). (In German).

A steady flow (about 120 mps) of argon in an annular (inner radius, 8.3 cm; outer radius, 10 cm; length, 16.4 cm) duct was attained at pressure of the order of 1 Torr. The nonisothermal plasma was flowing from a source (strong glow discharge in the bottom part of the duct) through a magnetic field directed perpendicularly to the flow (radially). Density and temperature of particles in the duct were measured. The measurements may serve as an experimental proof of the Hall phenomenon. Values of the Hall parameter amounting to 30 were achieved. (App. Mech. Rev.)

30344 PLASMA FLOW FOLLOWED BY AN INJECTION OF PLASMA THROUGH ELECTRODES. Shubin, A. P. Zh. Prikl. Mekh. Tekh. Fiz.; No. 6, 26-34(Nov-Dec 1970). (In Russian).

A plane steady-state flow of high-conducting nonviscous plasma in a channel with a proper magnetic field followed by an injection of slanting plasma passing through solid metallic electrodes was studied in the channel of a high-current accelerator. The studies considered the influence of the Hall effect and slow variation of the flow. (R.V.J.)

30345 ELECTROHYDRODYNAMIC FLOW IN A PLANE CHANNEL WITH AXIAL ELECTRODE. Grabovskii, V. I. Zh. Prikl. Mekh. Tekh. Fiz.; No. 6, 35-40(Nov-Dec 1970). (In Russian).

Incompressible flow of nonviscous charged fluid in a plane channel $|x| < \infty$, $|y| \leq h$ with conducting walls was studied with the electrode–emitter of charged particles distributed along the $y = 0$ axis. It was assumed that the motion of the charged particles was steady, and the charge distribution in the emitter can be approximated by the Heaviside unit function. The problem was resolved using linearization of equations according to the parameter of electrohydro interactions. Electric parameters were determined and deformed outlines of the velocity and pressures along the flow region with vortex electrostatic forces were found. (R.V.J.)

30346 TWO-DIMENSIONAL PROBLEM OF ELECTRODYNAMICS OF STEADY-STATE CURRENTS IN NONLINEAR CONDUCTING MEDIA. Rutkevich, I. M. Zh. Prikl. Mekh. Tekh. Fiz.; No. 6, 49-53(Nov-Dec 1970). (In Russian).

A simple two-dimensional problem was resolved for current distribution in nonlinear conducting media over a plane wall consisting of semi-infinite electrodes and insulators. A hodograph was used for obtaining a precise solution for variations of nonlinear conductivity; in formal aspects the numerical solution should be analogous to the gasodynamic problem for plane streamlining. The motion of an isotropic conducting fluid with assigned velocity across a steady-state magnetic field was analyzed. (R.V.J.)

30347 INFLUENCE OF NONCONDUCTING PARTITIONS ON TERMINAL-INDUCED ELECTRIC CURRENTS. Kashkin, Yu. F. Zh. Prikl. Mekh. Tekh. Fiz.; No. 6, 116-21(Nov-Dec 1970). (In Russian).

The influence of grounding of induced electric currents on the total electric and dynamic characteristics of plasma-cluster motion along a rectangular channel of electric discharge tube in a non-homogeneous transverse magnetic field was studied. It was found that an insertion of a long thin nonconducting partition in the region of terminal currents reduced the electric current about two times. In order to prevent the leaking of the axial electric current around the partition, the length of the partition had to exceed six bores of the channel. (R.V.J.)

30348 PREIONIZATION AND VELOCITY EFFECTS IN MHD CHANNELS WITH NONEQUILIBRIUM PLASMAS. Lengyel.

XUM

Lajos L. (Institut fuer Plasmaphysik, Garching, Ger.). AIAA (Amer. Inst. Aeronaut. Astronaut.) J.; 9: 745-7(Apr 1971).

Results of numerical computations pertaining to current and potential distributions in MHD channels are reported. No periodic field distributions were assumed. The computations were performed for a Faraday-type channel with a given finite number of electrode pairs. A two-dimensional approximation is used. The axial current component was assumed to vanish at upstream and downstream "infinities." The constant and uniform magnetic field was intentionally kept low enough to avoid nonconvergent (fluctuating) solutions and results whose interpretation may involve speculation. (M.H.R.)

Geophysics (Upper Atmosphere)

Refer also to abstracts 29211, 30311–30316, 30318, and 30321.

30349 (IPPJ–103) HYDROMAGNETIC MOTION IN THE GEOMAGNETIC TAIL. Sakai, Jun-ichi; Kawamura, Takaichi (Nagoya Univ. (Japan). Inst. of Plasma Physics). Jan 1971. 9p. Dep. NTIS (U. S. Sales Only).

By the presence of the bulk plasma flow in the geomagnetic tail, the typical hydromagnetic waves that are periodic in space along the main magnetic field, have some structures in the direction across the plasma sheet. (auth) (Japan)

30350 (N–70–36812) SUBAURORAL RED ARC AND THE ASSOCIATED IONOSPHERIC PHENOMENA. Chandra, S.; Maier, E. J.; Troy, B. E. Jr.; Rao, B. C. Narasinga (National Aeronautics and Space Administration, Greenbelt, Md. Goddard Space Flight Center). Aug 1970. 18p. (NASA-TM-X-65307; X-621-70-310). NTIS.

The phenomenon of the midlatitude red arc of September 29, 1967 is described from observations of the properties of the ionospheric plasma. The ion and electron temperatures, ion composition and density, and suprathermal electron flux during this period are measured by retarding-potential analyzers near 900 km from OGO 4 and near 2000 km from Explorer 31. These parameters show the following changes in the region L = 2.3 to L = 3.0 during the red-arc period as compared to their values during normal periods: (1) electron and ion temperatures increase to above 4000 K from a normal value of 2000 K at 900 km, while at 2000 km electron temperature increases to above 5000 K from a normal value of 2500 K; (2) at 900 km the ratio of $O^+/(H^+ + He^+)$ changes from 1 to 5 while the total density remains approximately the same; (3) at 2000 km the ion density decreases by a factor of 10 with the composition remaining all H^+; (4) there is no significant increase in the flux of 5- to 10-eV electrons. The relative importance of electric-field heating, magnetospheric conduction, and the changes in the neutral composition in the lower atmosphere are examined in the light of these observations. It is concluded that the SAR ARC is caused by a combination of thermal conduction of energy from the magnetosphere and changes in the neutral composition in the lower atmosphere. (auth) (STAR)

30351 (N–70–40978) TABLES FROM THE PENN STATE MARK 1 IONOSPHERIC MODEL. Nisbet, John S. (Pennsylvania State Univ., University Park. Ionosphere Research Lab.). 20 Aug 1970. 174p. (NASA-CR-113799; SR-362(E)). NTIS.

The models have as variables the latitude and longitude, the day number, the time, and the 2800 MHz (10.7 cm) solar flux. The tables are given for east longitudes of 0, 90, 180, and 270° and latitudes from –60 to +60° in 20° increments. Models are given for the summer and winter solstice and the spring equinox. Values are given of the electron density from 120 to 1250 km, the electron content in 1 cm^2 vertical column from 120 to 1250 km, the F2 peak electron density N_mF_2 in units of $1/cm^3$ and the altitude of the F2 peak in km. Three parameters of midlatitude sporadic E, the percentage probability of observing sporadic E with a critical frequency greater than 0.5 MHz, the average value of the peak electron density when it is observed, and the standard deviation of the lognormal distribution are given. The model is a computer program and the tables presented are representative printouts. (auth) (STAR)

30352 INJECTION OF ENERGETIC ELECTRONS INTO THE INTERNAL MAGNETOSPHERE REGION DURING THE MAGNETIC STORM OF OCTOBER 29–NOVEMBER 4, 1968. Vernov, S. N.; Ivanova, T. A.; Sosnovets, E. N.; (and others). Izv. Akad. Nauk SSSR, Ser. Fiz.; 34: 2270-4(Nov 1970). (In Russian).

Injection of electrons with E > 250, 500, and 800 keV into the gap between radiation belts during the storm of Oct. 29–Nov. 4, 1968, is described. It is shown that after a series of strong substorms the intensity of electrons in the gap (E_e > 250 keV) increased more than two orders of magnitude. In the following series of such perturbations another injection took place and the front of the injected electrons moved closer to the Earth. Electron injections of higher energies at L < 3 were not as effective as at L = 3, and the spectrum was much softer. (tr-auth)

30353 RELATION OF THE ELECTRON FLUX IN THE UPPER ATMOSPHERE TO THE STATE OF THE EARTH MAGNETOSPHERE. Gal'per, A. M.; Dmitrenko, V. V.; Kirillov-Ugryumov, V. G.; Luchkov, B. I.; Shermanzon, E. M. (Moscow Engineering Physics Inst.). Izv. Akad. Nauk SSSR, Ser. Fiz.; 34: 2275-80(Nov 1970). (In Russian).

Measurements of 100- to 1500-MeV electrons at balloon elevations in the atmosphere are described. It is shown that in the radiation belts exist high-energy electrons which spill out into the atmosphere during relatively small magnetic perturbations. The intensity of these electrons at the geomagnetic latitude of 46° was 6×10^{-2} cm^{-2} sec^{-1} $ster^{-1}$ and it diminished one half during 20 to 30 hr from the moment of perturbation. (tr-auth)

30354 RADIAL PROFILE OF THE PROTON BELT. Gubar, Yu. I.; Shabanskii, V. P. Izv. Akad. Nauk SSSR, Ser. Fiz.; 34: 2308-12(Nov 1970). (In Russian).

Distribution of low-energy protons at the equator was studied using data obtained by satellites. It is shown that in 1964 the radial distribution had two maxima, one at r ≈ 2 and the other at r ≈ 3.5. The radiation belts of 1964 and of 1965 were compared, and it was found that the belt shifted. (tr-auth)

30355 SOLAR X-RAY RADIATION AS OBSERVED BY REAL TIME TELEMETRY FROM SOLRAD SATELLITES. Takao, Kazuaki; Tsujii, Tsuneo (Kyoto Univ.). Rep. Ionosphere Space Res. Jap.; 24: 183-91(Sep 1970).

The results of solar x-ray monitoring through the years of 1966 to 1969 observed by real-time telemetry from SOLRAD-8 and SOLRAD-9 satellites are reported. The vague-peaked general solar activity during these years is also revealed in x-ray fluxes. The analysis of the correlation between x-rays and SID's proves that SPA is the most sensitive indicator of ionospheric disturbances caused by soft x-ray bursts. The distribution of x-ray unaccompanied Hα flares indicates the possibility of anisotropic radiation of soft x rays. (auth)

30356 STUDY OF THE ORIGIN OF GEOMAGNETIC PULSATIONS IN EQUATORIAL, LOW, AND MIDDLE LATITUDES. Kato, Yoshio; Morioka, Akira (Tohoku Univ., Sendai). Rep. Ionosphere Space Res. Jap.; 24: 192-206(Sep 1970).

In order to study the origin of the lower-latitude geomagnetic pulsations, the ulf signals are analyzed for data at three representative stations: Huancayo (Peru) for the equator, Maui (Hawaii) for low latitudes, and Onagawa (Japan) for middle latitudes. From these data the characteristics of geomagnetic pulsations with periods longer than 10 seconds are studied, especially amplitude, polarization, phase relation, period range, and power spectrum at each station. After comparison of the observed characteristics with those expected from the two models (ionospheric current model and HM transmission model), it is concluded that an ionospheric current system set up at high latitude by hydromagnetic waves will contribute more to the lower-latitude pulsations than direct transmission of waves through the lower magnetosphere. (auth)

30357 CONVECTIVE BEAM CYCLOTRON INSTABILITY AND DISCRETE VLF EMISSIONS IN THE MAGNETOSPHERE. Matsumoto, Hiroshi; Miyatake, Sadao; Kimura, Iwane (Kyoto Univ.). Rep. Ionosphere Space Res. Jap.; 24: 207-21(Sep 1970).

A theory of generation of discrete vlf emissions is proposed. Briggs' criterion on the instability is applied to the beam-cyclotron instability in the whistler mode, and it is clarified that this cyclotron instability is not of an absolute type as has been thought so far, but of a convective-type. It is proposed that convective beam-cyclotron instability in the whistler mode plays a part of a "moving oscillator" of discrete vlf emissions in the magnetosphere. From consideration of the magnetospheric-plasma inhomogeneity along the geomagnetic field line, frequency–time characteristics as well as intensity of discrete vlf emissions, including those of complex forms such as "inverted hooks" and "oscillatory tones", are well explained by the present theory without any wave condition such as assumed in Helliwell's theory. (auth)

30358 NOTE ON A GENERATION MECHANISM OF BACKGROUND HISS OF POLAR CHORUS. Matsumoto, Hiroshi; Kimura, Iwane (Kyoto Univ.). Rep. Ionosphere Space Res. Jap.; 24: 223-8(Sep 1970).

A possible generation mechanism of the background hiss is proposed. A steady cycle in the magnetosphere is examined in

investigating the characteristics of vlf waves responsible for the precipitation of harder electrons (>40 keV) from the magnetosphere. Kennel and Petschek (1966) had originally presented the steady cycle in the magnetosphere and the vlf waves on the morning side of the magnetosphere related with the instability proposed by Kennel and Petschek are not the midlatitude hiss, but the background hiss of polar chorus. Polar chorus is often accompanied by background hiss that has an upper cutoff frequency around 2 kHz. (J.C.W.)

30359 ELECTRON DENSITY PROFILES FOR QUIET AND DISTURBED TOPSIDE IONOSPHERE AT HIGH LATITUDES. Ondoh, Tadanori (Radio Research Labs., Tokyo). Rep. Ionosphere Space Res. Jap.; 24: 229-36(Sep 1970).

Average electron-density profiles for quiet ($K_p < 1_0$) and disturbed ($K_p > 4_0$) topside ionosphere, at high geomagnetic latitudes above 60°, are shown for a three-hour interval in magnetic local time and for geomagnetically latitudinal sections of 60 to 70° and >70°. Previous studies used an expression $(N_d - N_q)/N_q$ to represent the degree of disturbance, when N_q is the quiet-time electron density and N_d is the disturbed-time electron density. The expression is based on the idea that the disturbed topside ionosphere can be interpreted as an additional state to the quiet-topside ionosphere. The expression often becomes larger than unity for the disturbed topside at high latitudes. The seasonal difference of the disturbed-topside ionosphere has not yet been analyzed in previous studies. Data are used to present analyses for profiles for sunlit months (April–Sept.) in the polar-cap region; profiles for dark months (Oct.–Mar.) in the polar-cap region; and auroral zone profiles (60 to 70°). (J.C.W.)

30360 ROCKET OBSERVATIONS OF ELECTRON DENSITY OF THE DAYTIME IONOSPHERE AT SYOWA STATION, ANTARCTICA. Hirasawa, Takeo (Tokyo Univ.); Nagata, Takesi; Kawaguchi, Sadao; Hirao, Kunio. Rep. Ionosphere Space Res. Jap.; 24: 237-43(Sep 1970).

Two sounding rockets were launched in Feb. 1970 at Syowa Station, Antarctica. The electron-density profile of the polar ionosphere is given. The N(h) profiles show that the ionization density obtained by JA-2 is about 3×10^3 to 2×10^4 electron/cm^3 higher than that obtained by JA-1 in the 78- to 87-km height range. JA-1 rocket was launched in a magnetically quiet condition, and JA-2 during a small positive bay of 40 γ with an ionospheric absorption of 0.5 dB. These facts suggest that the energetic electrons or protons with an energy of about 100 keV was penetrating down to the 70 to 90 km height in the polar ionosphere with a flux of about 10^6 electrons/cm^2/sec to enhance the D- and E-region ionization during the positive-bay event in the daytime. It is also noted that the electron density is larger during the JA-1 rocket descent than during the ascent below 75 km. This indicates that there would exist a horizontal heterogeneity of the ionization in the D layer even at the time of magnetically quiet condition. (J.C.W.)

30361 METEORIC MATERIAL IN THE VICINITY OF THE EARTH. Nazarova, T. N. Cosmic Res. (USSR) (Engl. Transl.); 8: 143-5(Jan-Feb 1970).

Translated from Kosm. Issled.; 8: 154-6(Jan-Feb 1970).

Sporadic meteoritic particles measured in the vicinity of the earth at distances of over 200 km from its surface are shown. Both American and Soviet data are given. (M.O.W.)

30362 TREND OF IONOSPHERIC ABSORPTION DURING SHORTWAVE FADE-OUTS RELATED TO THE TREND OF ENHANCEMENT OF SOLAR X-RAY FLUX. Schwentek, H. (Max-Planck Institut fuer Aeronomie, Lindau, Ger.); Hartmann, G.; Kreplin, R. W. Radio Sci.; 6: 35-40(Jan 1971).

During the period July 1967 to July 1968 about 60 shortwave fadeouts, both weak and strong, were observed at Lindau through simultaneous use of several shortwave paths particularly established for absorption measurements. The frequencies used were 2.50, 2.614, 2.775, and 6.09 MHz; the distance between transmitter and receiver was about 300 km. Moreover, a riometer was used with a corner-reflector antenna directed at the polestar (27.6 MHz). For the quoted shortwave fadeouts the Naval Research Laboratory made available stored data of solar x-ray flux in minute intervals; the data were obtained from satellites OGO 4 and Solrad-9 in the wavelength ranges 0.5 to 3, 1 to 8, 8 to 20, and 44 to 60 Å. The analysis of the various effects shows that there is a very good correlation between the enhancements of solar x-ray flux and ionospheric absorption. The beginning and maximum of the shortwave fadeouts are delayed by 0.5 to 4 minutes in relation to the beginning and maximum of the bursts, with the longer delay corresponding to the shorter wavelength. The end of the effects cannot be determined so definitely; the time differences between bursts and shortwave fadeouts vary between ±7 minutes. Usually, the trend and detail of the shortwave fadeouts very nearly follow the trend of the bursts; thus, bursts may be considered equivalent to shortwave fadeouts. For a number of very clear weaker effects the additional absorption ΔL has been found to be proportional to the additional flux ΔX_E. For a very strong effect after a saturation ΔL increases again. The relative maximums of absorption $\Delta L/L$ during shortwave fadeouts are proportional to the relative enhancement of flux $\Delta X_E/X_E$. (auth)

30363 ORBITAL STATIONS AND STUDY OF THE EARTH FROM SPACE. Petrov, B. N. Vestn. Akad. Nauk SSSR; No. 10, 15-30(Oct 1970). (In Russian).

Creation of orbital stations, operating as a large physics laboratory in space for extended periods with crews working in shifts, offers a new tool for the study of the Earth. These studies could possibly include: physical and geophysical investigation of elementary particles and cosmic rays under conditions of high vacuum; confirmation of the theory of relativity by means of highly accurate clocks; study of the atmosphere on the basis of hydrological and meteorological observations, such as determination of the cloud cover and of regions covered by snow and ice on continents and oceans; astronomical and radioastronomical investigations without interference by atmospheric absorption; and medical and biological studies concerning the effect of weightlessness and other factors on human life processes. The space laboratory could be used for testing new engineering techniques, such as new energy sources, control systems, guidance and life-support systems, extravehicular activity, welding and assembly processes, etc. The laboratory would represent an excellent base for interplanetary trips. (TTT)

30364 OBSERVATION OF THE RADIATION BELTS AND IONOSPHERE OF EARTH BY MEANS OF THE INTERKOSMOS-3 SATELLITE. Vedeshin, L. A.; Pisarenko, N. F. Vestn. Akad. Nauk SSSR; No. 10, 31-6(Oct 1970). (In Russian).

On August 7, 1970, the Interkosmos-3 satellite was launched for studying radiation belts and electromagnetic processes near the Earth at altitudes ranging from 200 to 1300 km. The experiments prepared by Soviet and Czech scientists represented an extension of studies started with the Interkosmos-1 and -2 satellites. They included an investigation of low-frequency electromagnetic oscillations and signals, generated spontaneously in the external ionosphere or passing through it; the laws controlling their propagation; changes in the spectral distribution; and intensity of electromagnetic oscillations generated by plasma in the 0.7- to 12-kHz range under various geophysical conditions. The instruments carried by the satellite included a low-frequency analyzer, an ultrashort-wave transmitter operating in the international wavelength-frequency range near 136 MHz, and an instrument containing electron counters and n–p detectors to study the flux and energy spectrum of the electron and proton components of captured radiation and cosmic rays of solar origin. The information received by telemetering stations in West Germany, Czechoslovakia, and the Soviet Union is under study by Soviet and Czech scientists. (TTT)

30365 THERMALIZATION IN THE EARTH'S BOW SHOCK. Auer, P. L. (Cornell Univ., Ithaca, N. Y.); Kilb, R. W.; Crevier, W. F. J. Geophys. Res.; 76: 2927-39(1 May 1971).

Thermalization processes in the Earth's bow shock are examined with particular emphasis on ion heating. A two-dimensional analysis of the ion–ion streaming instability using the complete electromagnetic dispersion relation with magnetized electrons is presented. For $T_i/T_e \lesssim 0.2$ the peak growth rates are approximately a tenth of the total ion plasma frequency. As the ions are heated above $T_i/T_e \approx 0.2$, the growth rates drop sharply to a fraction of $(m/M)^{1/3}\Omega_e$, where Ω_e is the electron gyrofrequency. For $T_i/T_e \gtrsim 0.6$ the growth rates are comparable to the ion gyrofrequency. It is concluded that ion gyroeffects play a very important role in the ion thermalization process and are the source of the observed secondary peak in the ion-velocity distribution. The ion–ion streaming instability provides only fine-scale diffusion in ion–velocity space. Electron heating to $\beta_e \approx 1$ is shown to be consistent with a c/ω_{pe} length scale for changes in the magnetic field and the operation of the electron–ion drift instability in the leading edge of the Earth's bow shock. (auth)

30366 HYDROMAGNETIC WAVE COUPLING BETWEEN THE SOLAR WIND AND THE PLASMA SHEET. McKenzie, J. F. (European Space Research Inst., Frascati, Italy). J. Geophys. Res.; 76: 2958-66(1 May 1971).

The effects of the wave characteristics and the flow of both the solar wind and the plasma sheet on resonant oscillations of the geomagnetic tail are estimated by employing a simple two-dimensional model of the tail. It is shown that the boundary conditions used in this model allow long-wavelength perturba-

XUM

tions on the surface of the tail to be coupled with waves in the plasma sheet, and that these waves can be driven unstable by the Kelvin-Helmholtz mechanism. For parameters typical of the geomagnetic tail, the period of the unstable antisymmetric modes is approximately 9 min. (auth)

30367 PRIMARY ELECTRON INFLUX TO DAYSIDE AURORAL OVAL. Hoffman, R. A.; Berko, F. W. (Goddard Space Flight Center, Greenbelt, Md.). J. Geophys. Res.; 76: 2967-76(1 May 1971).

Data from the Ogo 4 auroral particles experiment were analyzed to determine properties of the higher-latitude region of electron precipitation in the dayside hemisphere. From 7 months of data a probability map of occurrence of this structured low-energy precipitation was compiled. The highest probabilities are concentrated predominantly between 0500 and 1400 hours magnetic local time, and from 75° to 82½° invariant latitude. There is excellent congruity of these high probabilities of occurrence and the high probability of occurrence of discrete auroral optical emissions, which define the auroral oval in these hours. The soft energy spectrums measured and the estimated total energy influx during typical precipitation events are appropriate for producing the type of aurora observed in these hours. It is concluded that the structured low-energy electron precipitation is the primary energy source for the dayside auroral oval. (auth)

30368 MAGNETOSPHERIC SUBSTORM OF AUGUST 25–26, 1967. Hones, E. W. Jr. (Los Alamos Scientific Lab., N. Mex.); Singer, Sidney; Lanzerotti, L. J.; Pierson, J. D.; Rosenberg, T. J. J. Geophys. Res.; 76: 2977-3009(1 May 1971).

The temporal history of the magnetospheric substorm that began late on August 25, 1967, is examined comprehensively. Features of the substorm that readily identified the occurrence of breakup were preceded for more than 1 hour by causally related magnetosphere-wide phenomena. This period, which is termed the development phase of the substorm, was characterized by a reduction of the thickness of the magnetotail plasma sheet (to $\lesssim 4$ R_E at the rate of ~6 km/sec), the buildup of a partial ring current, and the gradual development of magnetic bays and cosmic-noise absorption at some auroral zone stations. The observed rate of thinning of the plasma sheet is evidence for a dawn-to-dusk electric field of ~1 kV/R_E imposed across the magnetosphere during the period of ~2 hours when the interplanetary magnetic field in the vicinity of Earth was for the most part normal to the ecliptic and pointing southward. Following breakup, increases in the flux of energetic trapped electrons (energies ranging from ~50 keV to ~1 MeV) were detected near local noon. Detailed analysis of measured time dispersions in the E > 400-keV electron data indicated that the electron enhancements were caused by an eastward-drifting cloud of trapped electrons. A satisfactory model of the source, for this event and two others of similar character, incorporated spike-type injection of relativistic electrons in a region of limited longitudinal extent located in the midnight sector. Systematic variations with longitude of the times of onset and maximum intensity of substorm-associated electron precipitation support the belief that such precipitation is derived predominantly from the eastward drifting cloud of trapped electrons. The observations also suggest, however, that dumping of trapped electrons produces weak duskside precipitation during the early expansive phase. Within 30 min after breakup, the plasma sheet reinflated to a total thickness >7 R_E. Upon recovery the plasma-sheet particle density was ~50% of the presubstorm density, but the average energy of the plasma electrons (~3 keV) was approximately twice the initial value; furthermore, the plasma sheet contained a detectable flux of relativistic electrons (>450 keV). (auth)

30369 SATELLITE OBSERVATIONS OF BAND-LIMITED MICROPULSATIONS DURING A MAGNETOSPHERIC SUBSTORM. McPherron, R. L.; Coleman, P. J. Jr. (Univ. of California, Los Angeles). J. Geophys. Res.; 76: 3010-21 (1 May 1971).

Band-limited micropulsations were observed in space by the UCLA fluxgate magnetometer on Ogo 5. Throughout the event the satellite was inbound on the dawn meridian between 7 and 5 R_E just below the magnetic equatorial plane. These pulsations were quasi-sinusoidal, with period 20 sec and rms amplitude of 0.3 γ. Their average polarization was transverse to the main magnetic field, with the major axis azimuthal in the equatorial plane. The average ellipticity was 0.3 and the predominant sense of rotation was right-handed with respect to the main magnetic field. Instantaneously, these parameters were quite variable, with the pulsations occurring in bursts propagating at various angles to the field. During the pulsation event the main field was essentially dipolar; however, the waves were first observed just inside a sharp transition from a region in which the field magnitude had been constant for several Earth radii. No modulation of trapped electrons (E > 50 keV) by the pulsations greater than 4% was observed on the same satellite; however, whistler chorus did appear to consist of quasi-periodic bursts. Simultaneous magnetic-field observations in the auroral zone near the subsatellite point showed that the pulsations were present there with comparable period and amplitude. Furthermore, the ground data reveal that the event occurred in the last phase of a negative bay, i.e., during the recovery phase of a magnetospheric substorm. The characteristics of the pulsations observed in space are similar to the characteristics of Pi1 micropulsations observed on the ground during substorms and lead to identification of these as the same phenomenon. However, a comparison of the characteristics with the predictions of a recent theoretical model purporting to explain the ground observations finds the model seriously deficient. (auth)

30370 COLOR SPECTROGRAMS OF VERY-LOW-FREQUENCY POYNTING FLUX DATA. Gurnett, Donald A.; Mosier, Stephen R.; Anderson, Roger R. (Univ. of Iowa, Iowa City). J. Geophys. Res.; 76: 3022-33(1 May 1971).

A new method is discussed of processing the vlf electric- and magnetic-field data from the Injun 5 satellite to produce color frequency-time spectrograms with the color indicating the Poynting flux direction, up or down the geomagnetic field. The Poynting-flux sensing technique used on Injun 5 employs one electric and one magnetic antenna, both oriented perpendicular to the geomagnetic field and to each other. With this antenna geometry the Poynting-flux direction, up or down the geomagnetic field, can be determined from the cross correlation between the electric- and magnetic-field signals. The technique used to process these signals employs a new type of spectrum analyzer/cross correlator to determine the cross correlation between the electric- and magnetic-field signals as a function of frequency and time. These data can be displayed as a two-color frequency–time spectrogram by using appropriate display techniques. A survey of complex vlf radio-noise phenomena analyzed by using this technique is presented. (auth)

30371 ELECTRON ENERGY SPECTRUM AND STRUCTURE DEDUCED FROM ANALYSIS OF VLF DISCRETE EMISSIONS BY USING THE HELLIWELL CRITERION. Dowden, R. L. (Univ. of Colorado, Boulder). J. Geophys. Res.; 76: 3034-45(1 May 1971).

Helliwell's [1967] theory of vlf discrete emissions is based on cyclotron resonance between energetic streaming electrons and waves in a localized interaction region near the equator. Maximum wave–electron coupling requires that the emission frequency change at a rate determined by the position, relative to the equator, of the interaction region. In general the interaction region drifts along the field line; the drift velocity is determined by equilibrium between the input electron flux and the output radiation. This criterion is used to derive a method to determine the electron stream properties from ground-observed vlf emission spectrograms. This method is applied to the analysis of 75 discrete emissions from a single 3-hour event. Over the range of resonant longitudinal energies scanned by the emissions, 6 to 60 keV, the average energy spectrum was of the form $E^{-2.2}$, in general agreement with satellite measurements in the same region (L = 3.3). The relative stream density, as deduced for this energy spectrum, showed spikes similar to electron microbursts observed in satellites. A further test of Helliwell's requirement for internal consistency, that the interaction drift should never overtake either the emitted wave or the resonant electrons ($-\nu_g < \nu_i < \nu_{||}$), was performed for about a thousand such ν_g, ν_i, $\nu_{||}$ triplets. With four exceptions that were within the probable error, all satisfied this test. (auth)

30372 VLF DISCRETE EMISSIONS DEDUCED FROM HELLIWELL'S THEORY. Dowden, R. L. (Univ. of Colorado, Boulder). J. Geophys. Res.; 76: 3046-54(1 May 1971).

An iterative procedure based on R. A. Helliwell's theory is used to compute frequency-versus-time spectral shapes of vlf discrete emissions for various field-line and electron-stream parameters. A quasi-constant stream produces symmetrical emissions (symmetrical generation about the equator), and superimposed microbursts produce hooks with branching risers. Parameters appropriate to quiet and storm conditions produced the observed characteristics of Q chorus and S chorus, respectively. A general feature of the computed position of the interaction region for constant electron streams of low spectral index is an almost sinusoidal motion of the interaction position about

the equatorial plane. An analytic expression derived for the period of this motion shows that such periodic motion will occur for electron spectral indices less than about 2.4. A mechanism for nondispersed; multiphase periodic emissions is suggested in terms of this periodic drift motion. (auth)

30373 TOPSIDE CURRENT INSTABILITIES. Kindel, J. M.; Kennel, C. F. (Univ. of California, Los Angeles). J. Geophys. Res.; 76: 3055-78(1 May 1971).

Both the electrostatic ion-acoustic and ion-cyclotron waves can be unstable to field-aligned currents comparable to those expected in the auroral zone. However, for a wide range of conditions, the ion-cyclotron wave is unstable to the smaller current. In this paper, both instabilities are studied in single and multi-ion plasmas. Profiles of critical current versus height indicate that, as they flow through the topside ionosphere, field-aligned currents of 10^{9-10} electrons/cm^2 sec (at 200 km) will destablize various ion cyclotron waves. (auth)

30374 MEASUREMENTS OF THE DISTRIBUTION IN ENERGY AND ANGLE OF HIGH-ENERGY NEUTRONS IN THE LOWER ATMOSPHERE. Heidbreder, E.; Pinkau, K.; Reppin, C.; Schoenfelder, V. (Max-Planck-Institut fuer Physik and Astrophysik, Munich). J. Geophys. Res.; 76: 2905-16(1 May 1971).

The energy and angular distribution of high-energy neutrons in the lower atmosphere was measured at ground level in Munich (970 g/cm^2) and at mountain altitude at the Grossglockner (770 g/cm^2) by a novel elastic scattering technique. In the energy range from 80 to 300 MeV, the zenith-angle distribution of the measured neutrons can be approximated up to angles of 60° by a function $P_0 \cos^m \zeta$, where $m = 3.5 \pm 1.2$. The results from both heights were combined in order to improve the statistics. The differential vertical neutron flux between 80 and 300 MeV was found to be $1.54 \times 10^{-3} \times E^{-1.5} \pm 33\%$ (cm^{-2} sec^{-1} MeV^{-1} ster^{-1}) in Munich and $6.25 \times 10^{-3} \times E^{-1.5} \pm 41\%$ (cm^{-2} sec^{-1} MeV^{-1} ster^{-1}) at the Grossglockner. The resulting absorption constant for neutrons in the atmosphere is 150^{+60}_{-40} g/cm^2. (auth)

30375 EXCITATION OF O(^{1}S) ATOMS IN THE DAY AIRGLOW. Feldman, P. D.; Doering, J. P. (Johns Hopkins Univ., Baltimore). J. Geophys. Res.; 76: 3087-94(1 May 1971).

Simultaneous measurements of the differential photoelectron flux, the electron density and temperature, and the intensity of the atomic oxygen green line (λ5577 A; $^1S - {}^1D$) were made between 100 and 300 km with the Sun at a zenith angle of 60°. Dissociative recombination of O_2^+ ions is shown to be the dominant source of O(^{1}S) excitation above 140 km. Photoelectron impact excitation is a minor source except at high altitudes (>240 km) where it contributes about one-half the total excitation. Collisional deactivation of metastable nitrogen molecules in the $A^3E_u^+$ state by atomic oxygen cannot be entirely excluded as a source of O(^{1}S), but the branching ratio into the ^{1}S state must be significantly smaller than unity. (auth)

30376 LOCATION IN THE MAGNETOSPHERE OF FIELD LINES LEADING TO SAR ARCS. Hoch, R. J.; Smith, L. L. (Battelle-Northwest, Richland, Wash.). J. Geophys. Res.; 76: 3079-86(1 May 1971).

Spatial coordinates determined optically from Richland, Washington, for 13 recent SAR arcs are transformed to L intercepts at 400 km. The resulting L values for the SAR arcs are mapped into the magnetic equatorial plane. The locus is found to be a segment of an asymmetric ring. The ring conforms approximately to the expected intercept of the plasmapause in the same plane. Proximity of the SAR-arc field lines to the plasmapause, the electron trough, and the ring current is discussed, and the observed north–south drifts of SAR arcs are reviewed. (auth)

30377 TOPSIDE IONOSPHERE AT SUNRISE. Watt, T. M. (Stanford Research Inst., Menlo Park, Calif.). J. Geophys. Res.; 76: 3095-3105(1 May 1971).

The sunrise behavior of the midlatitude topside ionosphere at low sunspot numbers was examined by using Alouette 1 electron density and plasma scale-height profiles obtained at Stanford University during May and June 1963. Under the assumption that observed variations result from solar control, the data were averaged to form height profiles of plasma scale height and electron density from 450- to 750-km altitude, which vary smoothly with solar-zenith angle χ. The first manifestation of sunrise is a sudden and rapid decrease in plasma scale height, beginning between $\chi = 105°$ and 102° and ending between $\chi = 98°$ and 96°. Electron densities increase rapidly between $\chi = 98$ and 95°. An interpretation of the observations is that the sudden decrease in plasma scale heights is due to an increase in percentage concentration of O^+ ions at all altitudes, due primarily to a thermal expansion of the ionosphere that causes an upward movement of the topside ionization. The velocity of the thermal motion is estimated, and an attempt is made to resolve conflicting evidence from other observations that the topside ionosphere is controlled by either geomagnetic latitude or solar-zenith angle. (auth)

30378 THERMOSPHERIC TEMPERATURE VARIATIONS INFERRED FROM INCOHERENT SCATTER OBSERVATIONS. McClure, J. P. (Univ. of Texas, Dallas). J. Geophys. Res.; 76: 3106-15(1 May 1971).

Radar-based values of the neutral exospheric temperature T_n obtained at 12°S on 127 nights in 1967 and 1968 are presented and discussed. The dominant effect is an annual variation of approximately ±5%, warmer in summer than in winter. Previous radar-based maps of the diurnal temperature bulge show similar seasonal variations of T_n at night. Model atmosphere maps show smaller T_n variations, but since the T_n value of the model is a parameter defining the average distribution of the neutral density, both the radar and model atmosphere maps may be correct. In addition to the annual variation, a semiannual variation and geomagnetic heating effects are also observed. The data indicate that the electron temperature T_e is often less than 20°K above T_n at night, although it appears that $(T_e - T_n)$ may occasionally be 50°K or more. Because of the apparent near equality of T_e, T_i, and T_n, data presented here are suitable for comparison with satellite and other temperature measurements. Agreement is found with an empirical law for T_n based on incoherent scatter at 45°N. Temperatures measured with a retarding potential analyzer (RPA) on Ogo 4 sometimes agree with and sometimes are ~50% higher than nearly overlapping radar temperatures presented here. The Ogo 4 data imply that the ion–neutral heating rate is sometimes much higher than that inferred from radar observations. However, T_i values from the RPA on Ogo 6 are consistent with the radar data presented herein. (auth)

30379 EQUATORIAL ELECTROJET AND THE GRADIENT INSTABILITY. Whitehead, J. D. (ESSA, Boulder, Colo.). J. Geophys. Res.; 76: 3116-26(1 May 1971).

The physics of the equatorial electrojet current is briefly reviewed, and a suitable model is set up to investigate whether it is unstable to the gradient instability. The model allows for the variation of collision frequency with height and an arbitrary electron-density distribution. Approximate solutions that indicate instability are obtained. The electron-density irregularities may be identified with those causing equatorial sporadic-E echoes at hf and non-two-stream irregularities observed at vhf. A tentative explanation of why the vhf echoes can come from two distinct heights is offered. (auth)

30380 DIFFICULTY ASSOCIATED WITH WIND-SHEAR THEORY OF SPORADIC E. Whitehead, J. D. (ESSA, Boulder, Colo.). J. Geophys. Res.; 76: 3127-35(1 May 1971).

It is concluded that the metallic-ion content of the E region is extremely variable in time; this variation is reflected in the variability of sporadic E. However, the production of metallic ions cannot be so variable; therefore the loss rate must be variable. The most efficient loss mechanism is the corkscrew mechanism that transports the metallic ions into the lower E or D region. By switching this mechanism on and off, the metallic-ion content can be changed. Partial reflection of the gravity waves that themselves give the wind shear is suggested as a switching mechanism. There is direct evidence that this does happen. A reversed corkscrew that transports ions upward may sometimes be possible. However, the theory has a major defect in that it predicts most sporadic E where the horizontal component of the Earth's field is least, which is just the opposite of what is observed. (auth)

30381 APPROXIMATE SECOND INVARIANT FOR A DIPOLE FIELD. Schulz, Michael (Aerospace Corp., El Segundo, Calif.). J. Geophys. Res.; 76: 3144-8(1 May 1971).

Mathematically self-consistent analytical approximations to the second invariant and drift frequency in terms of pitch angle and energy are deduced from an existing analytical approximation to the bounce period of a charged particle trapped in the field of a magnetic dipole. The numerical accuracy of the resulting expressions is significantly better than that of the approximations to these functions customarily found in the literature. The results are potentially of interest in simplifying the theories of bimodal diffusion and other dynamical phenomena in the magnetosphere. (auth)

30382 ABSORPTION AT 2.2 MHz IN THE PRESENCE OF A CUSP-TYPE SPORADIC-E LAYER. Purkait, N. N.; Datta,

S. K. (Univ. of Calcutta). J. Geophys. Res.; 76: 3149-51 (1 May 1971).

Absorption of a 2.2-MHz signal in the presence of a cusp-type E_S layer is studied. The magnitude of the absorption is found to be decreased by about 25% of its value for days without any sporadic ionization. The cos χ index of absorption is also increased from a value of 0.72 to 1.2. Detailed analysis of the data shows that the absorption is mostly nondeviative in the presence of cusp-type E_S layer. (auth)

30383 PRINCIPLE OF A SIMPLE MEASURE OF ION TEMPERATURE IN THE IONOSPHERE. Fournier, G. (Office National d'Etudes et de Recherches Aerospatiales, Chatillon-sous-Bagneux, France). J. Geophys. Res.; 76: 3159-61(1 May 1971).

The ion temperature is usually measured with retarding-potential analyzers in space flight. These analyzers give the temperature from the longitudinal distribution of velocities and their accuracy is limited by the work function drift of surfaces. The new method presented explores the transverse distribution of velocities, but it is not clear if the process effectively avoids the spurious effects due to surface pollution. The probe is made of a system with two holes, the collimator, followed by a negatively biased collector that receives the collisionless ion beam selected by the collimator. The current variation with a known angle, between the collimator axis and the spacecraft velocity vector, is related to the Mach number; thus, if the speed is known, it permits the computation of the ion temperature. (J.C.W.)

30384 STUDY OF RANDOM MOVEMENTS OF E- AND F-REGION IRREGULARITIES OVER WALTAIR, INDIA. Sastri, J. Hanumath; Rao, B. Ramachandra (Andhra Univ., Waltair, India). J. Geophys. Res.; 76: 3164-5(1 May 1971).

The results of an investigation on the random movements of E- and F-region irregularities over Waltair during the IQSY period are presented. Pulsed radio-wave soundings in the frequency range of 2.3 to 3.0 and on a fixed frequency of 5.6 MHz were used during the 15 months of testing. Experimental results yielded diurnal and seasonal variations of the random movements. There is a significant variation in random velocity for both regional irregularities with markedly opposite trends for the two regions. (J.C.W.)

30385 D-REGION ATOMIC OXYGEN MEASUREMENT. Henderson, W. R. (National Oceanic and Atmospheric Administration, Boulder, Colo.). J. Geophys. Res.; 76: 3166-7(1 May 1971).

A silver-film sensor was used on a sounding rocket flight to record only atomic oxygen. The relation of the oxidation rate of the surface of the sensor is made to the rate of transport of atomic oxygen to the sensor. This rate of transport to the sensor can then be related to a local concentration by considering the dynamics of the sampling. The atomic oxygen concentration is presented for measurements from 80 to 120 km. (J.C.W.)

30386 PHOTODISSOCIATIVE EXCITATION OF $O(^1D)$ ATOMS IN THE DAY AIRGLOW. Schaeffer, R. C.; Feldman, P. D.; Fastie, W. G. (Johns Hopkins Univ., Baltimore). J. Geophys. Res.; 76: 3168-73(1 May 1971).

An evaluation is made of the contributions to the atomic oxygen dayglow emission at λ6300 A from photodissociation, electron impact, and dissociative recombination. Analysis of the data indicates that the rate of excitation of $O(^1D)$ through dissociation of O_2 in the Schumann–Runge absorption region of solar euv flux is approximately one-third of that expected from the solar flux values of Detwiler et al., and is in good agreement with measurements of Parkinson and Reeves. The measured intensities of λ6300-A emission were $\approx$1.1 kilorayleighs at 100 km. The data are a function of conditions prevailing almost in the middle of a 27-day period from July 13 to Aug. 9, 1968, where the measured fluxes were close to minimum. (J.C.W.)

30387 VACUUM MERGING: A POSSIBLE SOURCE OF THE MAGNETOSPHERIC CROSS-TAIL ELECTRIC FIELD. Dessler, A. J. (Rice Univ., Houston, Tex.). J. Geophys. Res.; 76: 3174-6(1 May 1971).

A magnetic-merging mechanism, referred to as vacuum merging, is restricted to the neutral sheet region immediately behind the Earth where a natural plasma void will tend to form in the solar wind as it flows around the magnetosphere. If the plasma-sheet particle concentration were small, the merging would go at a rapid rate. A simple calculation is presented showing that the merging speed and the cross-tail electric field are inversely proportional to the particle concentration in the plasma sheet. The strength in the electric field derived from the vacuum-merging mechanism is in reasonable accord with the values deduced from experimental data. This suggests that vacuum merging may be the principal source of the cross-tail electric field that drives magnetospheric convection. (J.C.W.)

30388 MAGNETIC OBSERVATIONS OF THE LUNAR CAVITY. Colburn, D. S.; Mihalov, J. D.; Sonett, C. P. (Ames Research Center, Moffett Field, Calif.). J. Geophys. Res.; 76: 2940-57(1 May 1971).

Data from the Ames magnetometer experiment on the lunar orbiter Explorer 35 are examined for a period exceeding 4 months and covering more than 200 orbits. The main features of the diamagnetic cavity disclosed earlier are confirmed. The magnetic signature of the cavity is a variable phenomenon, sometimes vanishing entirely and on rare occasions displaying a decreased field in the interior in contrast to the more common increase. A positive correlation of cavity field increases with Kp and proton thermal speed is consistent with a model based on simple diamagnetism. Exterior small perturbations of the interplanetary field often occur outside the diamagnetic signature. Exterior peak occurrences do not correlate well with cavity signals or any obvious property of the interplanetary field, including magnitude, orientation, and noisiness; however, some control by orientation is not excluded. The peaks tend to occur at a lower proton thermal speed. The general lack of correlation and theoretical considerations indicates a solar-wind–limb interaction as the cause of the external peaks. (auth)

30389 SOLAR WIND INTERACTION WITH MERCURY. Ness, Norman F. (Univ., Rome); Whang, Y. C. J. Geophys. Res.; 76: 3136-43(1 May 1971).

With the exception of its higher density, the planet Mercury is almost equivalent to the Moon in many of its physical properties with respect to the solar-wind interaction with it. At Mercury's heliocentric distance (0.31 to 0.47 AU) the solar-wind properties are characterized by a speed ratio S = 7 to 9, β = 0.3 to 0.5, ϕ = 155 to 165° and $T_\parallel/T_\perp$ = 1.0 to 1.5. A consideration of the motionally induced magnetic field indicates that Mercury, like the Moon, may reveal information about the conductivity of its interior depending on whether or not a bow shock exists. In the absence of such a phenomenon, the plasma and magnetic field in the wake region can be studied by using the guiding-center approach, since the solar-wind ion Larmor radius is very small compared with the planetary radius. The prediction of a plasma cavity downwind from the obstacle and associated perturbation of the interplanetary magnetic field in the wake then follows. Decreases of the magnitude of the field occur inside a Mach cone tangential to the planet but outside the umbral region where a field increase occurs. The axis of the Mercurian Mach cone is aberrated 6 to 11° from the west of the Sun, and the Mach angle itself is about 14 to 19°. These values are about twice those of the lunar wake. Possibly penumbral field increases and stimulated waves upstream and downstream from the wake will also occur. (auth)

30390 AN ANNOTATED BIBLIOGRAPHY ON THE GEGENSCHEIN. Roosen, Robert G. (Goddard Space Flight Center, Greenbelt, Md.). Icarus; 13: 523-39(Nov 1970).

This annotated bibliography contains all references on the Gegenschein that have come to the author's attention during a four-year study (Roosen, 1966, '68, '69 and '70). Position and brightness measurements from individual papers were collected in tabular and graphical form and are presented. The entries were classified as to observations, theories, models, review papers, and other. (auth)

30391 INTERACTION OF HOMOGENEOUS WAVE TURBULENCE AND A MAGNETOHYDRODYNAMIC TANGENTIAL DISCONTINUITY. Tam, Christopher K. W. (Massachusetts Inst. of Tech., Cambridge). J. Plasma Phys.; 5: 265-74(Mar 1971).

The interaction of homogeneous wave turbulence and a magnetohydrodynamic tangential discontinuity was studied. Attention was focused on the turbulent shear stress produced as a result of such an interaction. A magnetohydrodynamic description is used which is believed to be adequate for plasma problems in interplanetary space. As a model for wave turbulence, it is assumed that the turbulent wave field is made up of the seven modes of magnetohydrodynamic waves. They are the entropy waves, the Alfvén waves (two independent modes), the fast and slow waves (each with two independent modes). It was found that, to a first approximation, the turbulent shear stress acting on the surface of discontinuity is linearly proportional to the energy density of the fluctuating magnetic field and to the kinetic energy density of the plasma fluctuations. On applying the present theory to the problem of interaction between the turbulent

XUM

waves in the magnetosheath and the magnetopause, it was found that the turbulent shear stress produced is too weak to produce any large-scale internal magnetospheric convection as was previously contemplated. (auth) (UK)

30392 HYDROMAGNETIC KELVIN–HELMHOLTZ PROBLEM IN A HALL PLASMA. McKenzie, J. F. (European Space Research Inst., Frascati, Italy). J. Plasma Phys.; 5: 275-88(Mar 1971).

The hydromagnetic analogue of the Kelvin–Helmholtz problem is extended to include the effects of the Hall term. In contrast to other results in the literature it is shown that, in the case of incompressible fluids, the stability of a shear plane is unaffected by the introduction of the Hall term. The special case of a hot, unmagnetized fluid on one side of the interface and a cold, magnetized fluid on the other is studied in some detail. In this case it is shown that the presence of the Hall term can have either a stabilizing or a destabilizing effect, depending upon whether the sound speed in the hot fluid is very much greater than the Alfvén speed in the cold fluid or vice versa. (auth) (UK)

30393 RATE OF ORDERED ION MOTION IN THE IONOSPHERE AT 600 km. I. METHOD OF MEASUREMENT. Ponomarev, V. N.; Samborskii, V. S. Kosm. Issled.; 8: 557-62(Jul-Aug 1970). (In Russian).

A method for measuring the ordered rate of ion motion in the ionosphere by means of an ion transducer installed in the satellite Kosmos 184 is described. The design and construction of the transducer are included. (R.V.J.)

30394 RATE OF ORDERED ION MOTION IN THE IONOSPHERE AT 600 km. II. EXPERIMENTAL RESULTS. Ponomarev, V. N. Kosm. Issled.; 8: 563-70(Jul-Aug 1970). (In Russian).

Results are given of the measurement of the ordered ion motion in the ionosphere at 600-km elevation. The data were collected by means of a specially designed ion transducer that was used during Kosmos-184 flight, December 1967. The map of the vertical and horizontal velocity profiles for ion shifts in relation to the satellite orbit and the rate of ion drift in relation to the Earth surface is presented. Data obtained are analyzed in detail. (tr-auth)

30395 STUDIES OF THE AURORAL X RADIATION AT THE CONJUGATE POINTS KERGUELEN–ARCHANGEL. Kambu, F.; Maral, Zh.; Zhulin, I. A.; Kopylov, Yu. M. Kosm. Issled.; 8: 595-602(Jul-Aug 1970). (In Russian).

Data are presented on the auroral x radiation observed at the conjugate points Kerguelen and Archangel. The measurements were taken by high-elevation drift balloons using scintillation detectors with collimators combined with a 128-channel pulse analyzer of 15- to 150-keV energy range. (R.V.J.)

30396 STATISTICAL AND DYNAMIC PRESSURES OF SOLAR WIND ON THE EARTH'S MAGNETOSPHERE. Shevnin, A. D.; Fel'dshtein, Ya. I. Kosm. Issled.; 8: 632-5(Jul-Aug 1970). (In Russian).

Statistical and dynamic pressures of the solar wind on the Earth's magnetosphere are expressed by means of geometric parameters of the magnetosphere. Calculations of solar plasma parameters measured by Mariner-2 during 1962 (which was close to the minimum of the solar activity) revealed a wide range of variations in the solar wind pressure. Thus, for the relatively quiet magnetic field the index, $Q = 1$, $p_\infty = 4.6 \times 10^{-11}$ dyne/cm^2, $p_d = 1.1 \times 10^{-8}$ dyne/cm^2. With rise of magnetic activity within the Q limits (from 0 to 7) the statistical and dynamic solar wind pressures and their relation p_d/p_∞ with the growth $\Delta Q = 1$ correspond to $\Delta p_\infty = 0.61 \times 10^{-11}$ dyne/cm^2, $\Delta p_d = 0.76 \times 10^{-8}$ dyne/cm^2, and $\Delta p_d/p_\infty = 92 + 6Q$. (R.V.J.)

30397 ION FORMATION FUNCTION DURING REACTION OF PROTONS WITH ATMOSPHERE. Osipov, N. K.; Pivovarova, N. B.; Pivovarov, V. G. Kosm. Issled.; 8: 635-6(Jul-Aug 1970). (In Russian).

Geophysical effects of proton flux reactions with the atmosphere observed in the auroral ionosphere are analyzed. The rate of ion formation at various altitudes during proton reactions with the atmosphere is estimated, considering the proton energy and density at infinite altitudes. (R.V.J.)

30398 STABLE MID-LATITUDE RED ARCS: OBSERVATIONS AND THEORY. Nagy, A. F. (Univ. of California, San Diego, La Jolla); Roble, R. G.; Hays, P. B. Space Sci. Rev.; 11: 709-27(Dec 1970).

The stable midlatitude red arcs (SAR-arc) were observed in the night sky by Barbier in 1957 from Haute Province in southern France. They are situated south of the auroral zones and persist throughout the night. Their existence has been confirmed, and a review of the relevant observations and theories is given with the observed features, the ionospheric behavior in the region of an arc, and the various theories for red arc formation. 59 references. (J.C.W.)

30399 ELECTRON AND ION TEMPERATURES IN THE IONOSPHERE. Willmore, A. P. (Physical Research Lab., Ahmedabad, India. Goddard Space Flight Center, Greenbelt, Md.). Space Sci. Rev.; 11: 607-70(Dec 1970).

Many measurements of ionospheric temperature have been made during the last decade and have shown a considerable departure from thermal equilibrium there. Theoretical work has led to a general understanding of the processes that determine the energy balance of the charged particles, and most features of the experimental results are well understood in the F region. The position in the F region where different methods of measurement, known to agree fairly well at greater heights, appear to disagree is less clear, while in the D region no direct observations of charged-particle temperature exist. The theoretical expectation here is that, on account of the rapid exchange of energy among the particles by collisional processes, temperature equality will prevail. (auth)

30400 CONSTITUTION OF MAGNETOSPHERIC STORMS. Iijima, Takesi; Nagata, Takesi (Tokyo Univ.). Ann. Geophys.; 26: 417-26(Apr-Jun 1970).

The constitution of magnetospheric storms and the Earth's magnetic storms in relation to the penetration of the solar wind energy is examined for eight disturbed days by use of magnetic variations, low-energy ion flux (<50 eV), energetic electron flux (>50 keV) on ATS-1 ($r \sim 6.5\ R_E$), magnetic variations in the interplanetary space by IMP-1 and IMP-C, and simultaneous magnetograms on the Earth's surface. The conditions necessary to generate a magnetic storm by an invasion of the solar wind energy into the magnetosphere seem to be an enhancement in the convection of the magnetospheric low-energy plasma, and a growth of an asymmetric belt of energetic plasma; the first phenomenon directly enhances the polar SP, and the second leads to a DR field. In addition, the auroral electrojet (AEJ) is produced by the following processes: the earthward surging of the plasma flow due to the first phenomenon is opposed by the magnetic pressure in the region where the main field is strong, whence inhomogeneities of magnetic field and plasma pressure take place near the night-side inner boundary of the plasma sheet. The asymmetry of the second phenomenon also creates plasma instability. These instabilities cause magnetospheric and auroral flares, which result in high conductive regions in the Earth's polar ionosphere. Then, the electric field of SP due to the first phenomenon, the polarization field due to the second, and the polar high-conductive area become the main causes of the auroral electrojet (AEJ). The storm-time three-dimensional discharge current circuit is formed through the geomagnetic field lines among SP, AEJ, and DR formations. It seems very likely that the plasma convection (SP formation) and the asymmetric belt of energetic plasma (DR formation) are chiefly responsible for the eastward AEJ. (tr-auth) (France)

30401 COMPUTATION OF GEOMAGNETIC L COORDINATES. Schaeffer, R. C. (Univ. of Adelaide). Aust. J. Phys.; 23: 941-6(Dec 1970).

Introduction of a parameter L (a function of the magnitude of the magnetic field, and an integral invariant of the particle motion evaluated between mirror points of the particle trajectory) aids the study of the distribution of geomagnetically trapped charged particles. The application of this parameter to produce more accurate maps of L coordinates computed from the GSFC 12/66 model updated to March 1969 is described. (Australia)

30402 FAST CORRELATION METHOD FOR STUDYING DRIFTING PATTERNS ASSOCIATED WITH IONOSPHERIC IRREGULARITIES. Clark, D. H.; Stevenson, D. J. (Victoria Univ., Wellington, N. Z.). Aust. J. Phys.; 23: 947-9(Dec 1970).

An extension of the full-correlation method of Briggs, Phillips, and Shinn for analysis of drifting patterns associated with ionospheric irregularities is shown. Computer time saving is achieved by using logical procedures to limit calculations of the autocorrelation and cross-correlation functions to the region about a predetermined value of ρ_x, and selecting ρ_x so that linear interpolation could be used to obtain accurate estimates of the delays t_x, τ_x and τ_x^1. Limitations were that some idea of the expected cross-correlation function maximum is required and characteristic velocity is prone to large errors from using $V_c^2 = (V_c^1)^2 - V^2$. (Australia)

XUM

30403 MAGNETIC FIELD PERTURBATIONS IN THE MAGNETOTAIL ASSOCIATED WITH POLAR MAGNETIC SUBSTORMS. Camidge, F. Paul; Rostoker, Gordon (Univ. of Alberta, Edmonton). Can. J. Phys.: 48: 2002-10(1 Sep 1970).

Using data from the IMP-A and IMP-B satellites, it is shown that when a polar magnetic substorm onset is observed at the Earth's surface, there is a pronounced effect in the magnetotail at approximately the same time. This magnetotail perturbation appears as a temporary reduction in the tail field reflecting primarily a reduction in the component of the field pointing along the Sun–Earth line parallel to the neutral sheet. Large perturbations in the component of the magnetic field perpendicular to the ecliptic plane which are observed around 24 R_E suggest that reconnection of magnetic field lines is the physical mechanism responsible for the observed effects. It is suggested that substorms act as a safety valve limiting the size of the magnetotail by periodically bleeding magnetic flux from the tail into the inner dipole configuration. (auth)

30404 POSITIVE IONS IN THE D-REGION. Bates, D. R. (Queen's Univ., Belfast). Comments At. Mol. Phys.; 11: 85-91(Aug-Sep 1970).

The results of measurements, using rocket-borne mass spectrometers, of the ionic composition of the D region are discussed (Narcisi and Bailey, J. Geophys. Res., 70: 3687 (1965)). It had previously been assumed that NO^+, O_2^+, and N_2^+ are the dominant species of positive ions in the D region. Ion–neutral reactions are of great importance. The expected ions are NO^+, O_2^+, and N_2^+, and their abundances are discussed. A metallic ion layer, 10-km thick, with a peak at 95 km (and a minimum above the D region, at 105 km) is observed to contain ions of Na^+, Mg^+, Ca^+, Cr^+, Fe^+, Ni^+. Hydrated protons of H_3O^+, $H_5O_2^+$, and $H_3O^+ \cdot (H_2O)_n$ are the main ions below the sharp transition at 82 km. Ions of S are also present. (J.C.W.)

Low-Temperature Physics and Cryogenic Equipment

Superfluidity

30405 TEMPERATURE DIFFERENCES AND MUTUAL FRICTION IN He II NEAR T_λ. Crooks, Michael J.; Johnson, David L. (Univ. of British Columbia, Vancouver). Can. J. Phys.; 49: 035-9(15 Apr 1971).

Temperatures were measured near the lambda transition at the ends of a cylindrical channel containing He II in the presence of a heat flux through the channel. Two channels of cross sections 1.1 mm^2 and 2.2 mm^2 were used and average temperatures ranged from within 1.0×10^{-2} K of T_λ to within 3×10^{-5} K of T_λ. The results are fitted to a generalized Gorter–Mellink mutual friction expression of the form $\dot{q} = \rho_s ST(S \text{ grad } T/a\rho_n)^{1/m}(T_\lambda - T)^{-\alpha/m}$. (auth) (Canada)

30406 MEASUREMENT OF THE HEAT TRANSPORT BY CONDUCTIVITY OF SUPERFLUID HELIUM IN 4m-LONG PIPES OF 1 TO 10 mm DIAMETER. Passow, C. H.; Aupelt, G.; Bergotz, R.; (and others) (Kernforschungszentrum, Karlsruhe, Ger.). Cryogenics; 11: 143-5(Apr 1971).

The heat conduction in five different 4m-long pipes of a diameter of 1, 3, 5, and 10 mm was measured. The helium was at rest (no mass transport in the pipes). The heat source was distributed along the pipe so that a heat flux of more than 1 W cm^{-2} was obtained at the end of the pipe. The technical stability of the cooling system in a superconducting accelerator was verified. The experimental results were compared with theoretical calculations based on the two-fluid model, and it was shown that heat conduction in technical systems can be calculated sufficiently exactly with this model. The permissible heat flux in the helium seemed to be limited only by the possible temperature gradient. (UK)

30407 ENTHALPY FLUCTUATIONS IN ^{4}He FILMS. Widom, Allan (Northeastern Univ., Boston). Phys. Rev., A; 3: 2042-3(Jun 1971).

The long-range behavior of enthalpy fluctuations in bulk liquid helium at the superfluid λ transition is deduced from the observed specific-heat singularity. In moderately thick films, the specific-heat singularity is rounded into a broad maximum. The growth of this maximum with film thickness is derived, and recent experimental data are discussed. (auth)

30408 THIRD SOUND IN SUPERFLUID HELIUM FILMS OF ARBITRARY THICKNESS. Bergman, David J. (Tel-Aviv Univ., Israel. Soreq Nuclear Research Center, Yavne, Israel). Phys. Rev., A; 3: 2058-66(Jun 1971).

The hydrodynamic equations of a superfluid helium film are solved numerically to yield the dispersion equation of third sound over a wide range of thicknesses, including both unsaturated and saturated films. An analytical approximation to the dispersion equation is found that is good for the entire range where the equations are valid, and which becomes particularly simple in the case of either very thin or very thick films. A clear physical picture is formed of the processes determining the properties of third sound in thick helium films. (auth)

30409 KIRKWOOD SUPERPOSITION APPROXIMATION FOR DILUTE ^{3}He–^{4}He SOLUTIONS. Woo, Chia-wei (Univ. of Illinois, Urbana). Phys. Rev., A; 3: 2141-3(Jun 1971).

The Kirkwood superposition approximation (KSA), which approximates three-particle distribution functions by symmetrical products of two-particle distribution functions, is examined quantitatively for ^{3}He–^{4}He solutions in the zero-concentration limit. Numerical tests are devised for this study, which as a result indicates that errors caused by the KSA are not significant except for quantities involving small differences between large numbers, such as the chemical potential of ^{3}He in solution. This note serves as an appendix to a series of earlier publications on a microscopic theory for dilute ^{3}He–^{4}He solutions. (auth)

Superconductivity

Refer also to abstracts 30557, 30683, and 30949.

30410 (EUR-4593, pp 95-100) LOW-FIELD INSTABILITIES OF HIGH-FIELD COMPOSITE SUPERCONDUCTORS. Martinelli, A. P. (Institut fuer Plasmaphysik, G.m.b.H., Garching (West Germany)).

From Sixth symposium on fusion technology; Aachen, Germany (22 Sep 1970).

In Proceedings of the 6th symposium on fusion technology.

Experimental evidence is given of instabilities at low fields (0 to 20 kOe) in superconductors subjected to flux jumping. Information on the stability of the sample is obtained, both by energizing the sample until it spontaneously quenches and by inducing it to a critical state and superposing short magnetic pulses of various amplitudes. Three different threshold pulse amplitudes are generally observed: one which does not affect the sample, another which causes a partial flux jump, and a third which causes a flux jump followed by normalization of the sample at each preset stationary field and at different values of the impressed transport current. The experimental results show a mechanism of gradual decay of the magnetization currents and their replacement by the transport current and suggest improved material utilization and stability conditions of superconducting coil low-field regions by operating them at transport current densities closer to the critical current densities of the superconductor. (auth)

30411 (EUR-4593, pp 101-6) NORMAL TRANSITIONS OF COMPOSITE SUPERCONDUCTORS INDUCED BY MAGNETIC DISTURBANCES. Martinelli, A. P. (Institut fuer Plasmaphysik, G.m.b.H., Garching (West Germany)).

From Sixth symposium on fusion technology; Aachen, Germany (22 Sep 1970).

In Proceedings of the 6th symposium on fusion technology.

In the course of an investigation for studying the effect of magnetic disturbances externally applied to stabilized superconducting coils (for use in plasma physics) a number of composites (intrinsically stabilized and not) were tested (short and multilayer coil samples) by superposing on them pulsed magnetic fields of fast rise times (5 to 10 μsec) and various amplitudes (up to 10 kOe) and by determining the threshold values which cause sample normalcy. A stationary field (up to 40 kOe) produced by a superconducting coil is also superposed on the sample. The effects of a magnetic disturbance on a superconducting coil are analyzed, viz., high voltage induced in the coil winding and likely to damage it, temperature increase of the composite due to the eddy currents induced by the changing field in the stabilizing copper surrounding the superconducting core, and a pulsed magnetic field that reaches the superconducting core. Limiting criteria are given for the last two effects, which lead to coil instabilities and which should allow coil construction affording improved stability. (auth)

30412 (JINR-P8-5733) INVESTIGATION OF THE RESISTANCE BEHAVIOUR OF SUPERCONDUCTING ALLOY OF Nb + 80% Zr IN THE REGION OF H_{c2}. Khukhareva, I. S.; Goncharov, I. N. (Joint Inst. for Nuclear Research, Dubna (USSR). Lab. of

High Energy). 1971. 16p. (In Russian). Dep. NTIS (U. S. Sales Only).

From the resistance transitions of recrystallized samples in the form of a flat plate the values $H_{c_2}(T)$ and $H_{c_3}(T)$ were determined for the temperature range from 4.2°K to T_c = 8.1°K. The measurement results are compared with the theory. (auth)

30413 (LA-tr-71-26) PREPARATION AND SUPERCONDUCTIVITY OF $CeRu_2$ AND ITS Gd, Mn, Fe, Co, AND Ni-CONTAINING MIXED PHASES. Wilhelm, M.; Hillenbrand, B. Translated for Los Alamos Scientific Lab., N. Mex., from J. Phys. Chem. Solids; 31: 559-65(1970). 14p. Dep. NTIS.

An abstract of this paper, prepared from the original language, appeared as NSA 24: 30287.

30414 (ORNL-tr-2475) PENETRATION OF INDUCTION, ELECTRICAL FIELD, AND LOSSES IN IMPURE TYPE-II SUPERCONDUCTORS HAVING A SURFACE CURRENT. Fournet, G.; Mailfert, A. Translated by R. Gregg Mansfield (Oak Ridge National Lab., Tenn.), from J. Phys. (Paris); 31: 357-67(1970). 22p. Dep. NTIS.

The behavior of hard superconductors in ac magnetic fields is studied. The other works on the same subject used the critical-state model, assuming that the bulk critical current density j depends on the magnetic induction B on each point by the way of a mere algebraic relation; here the critical state model is used in the general form where j is any function of B; a critical surface current is also considered. Rigorous expressions of the electric field at each point are given, and a method of measurement of the critical current densities at low magnetic field is deduced. The behavior of hard superconductors for several critical-state laws is then calculated. Experiments, performed especially with Nb–25% Zr, show a good fit with the theoretical results. Finally, the losses are calculated, and the rigorous theoretical relations obtained for some critical laws show that several expressions given by other works are only approximations. (auth)

30415 QUANTITATIVE CONTROL OF SURFACE PINNING IN A LOW-κ TYPE II ALLOY. Morrison, D. D.; Rose, R. M. (Massachusetts Inst. of Tech., Cambridge). J. Appl. Phys.; 42: 2322-7(May 1971).

Quantitative control of surface pinning in the case of In–2% Bi foils was achieved by pressing diffraction gratings into the foil surfaces. The resulting grooves were effective pinners when they were 8.4ξ or wider and ineffective when 4ξ or narrower; the critical Lorentz force for flux flow was consistent with simple static calculations based on the groove geometry. No pinning occurred for flux flow along the grooves. Near H_{c_2}, the strength of pinning decreased linearly with H, and was essentially constant at lower fields. The J_c(H) peak effect was found to depend on pinner spacing. (auth)

30416 PHASE EQUILIBRIA AND SUPERCONDUCTIVITY IN THE V_3Al–V_3Sn SYSTEM. Alekseevskii, N. E.; Kornilov, I. I.; Matveeva, N. M. (Inst. of Metallurgy, Moscow). Dokl. Akad. Nauk SSSR; 195: 417-20(11 Nov 1970). (In Russian).

The phase diagram and the properties of the vanadium–aluminum system were studied in the 20 to 35 at. % Al range, examining also the V_3Al and V_3Sn alloys that correspond to the stoichiometric composition of the compound V_3X and exhibit a structure similar to that of Cr_3Si. It was found that the heat treatment does not affect the specific resistivity of the annealed and quenched specimens. An increase of the aluminum content resulted in the gradual increase of the resistivity as was to be expected for solid solutions. The microstructure was found to consist of a single phase in the form of solid-solution polyhedra; the x-ray phase study indicated also only a single phase. Thus the V–Al alloys near the V_3Al composition do not change their crystal structure after extended heating and present a solid solution of aluminum in vanadium from the solidus curve to 600°C. The V–Al–Sn system was studied at a constant 75 at. % content of vanadium. The superconductivity of the alloys in the V_3Al–V_3Sn system was attributed to the properties of the V_3Sn compound. The phase equilibrium was not affected by extended heating at 800°C. Alloying of V_3Al with tin leads to the formation of a limited range of solid solutions that do not display superconductivity down to 1.4°K. The tin did not stabilize the compound V_3Al. (TTT)

30417 PHOTOEFFECT IN A SUPERCONDUCTOR IN A WEAK ELECTRIC FIELD. Abramov, L. E.; Slezov, V. V. (Penza State Pedagogical Inst., USSR). Sov. Phys.-Solid State (Engl. Transl.); 12: 2247-8(Apr 1971).

Translated from Fiz. Tverd. Tela; 12: 2785-7(Oct 1970).

The expression derived earlier for the photocurrent is generalized for the case of photoeffect in an external weak uniform electric field. The calculation is carried out using the method of Green's functions. The wave functions for an electron in a metal are found in the quasi-classical approximation. The limiting case of photocurrent at T = 0 near the frequency corresponding to the red boundary of the photocurrent is considered in the absence of an external electric field. (auth)

30418 MAGNETIZATION CURVES FOR TYPE-II SUPERCONDUCTORS WITH SMALL GINZBURG–LANDAU PARAMETERS. Kumpf, U. (Max-Planck-Institut fuer Metallforschung, Stuttgart. Univ., Stuttgart). Phys. Status Solidi (b); 44: 829-43 (1 Apr 1971). (In German).

Magnetization curves of homogeneous lead–thallium single crystals with Ginzburg–Landau parameters $1/\sqrt{2} \leq \kappa \leq 1.8$ (type II superconductors) show at H_{c1} a sudden penetration of the magnetic flux up to an initial induction B_0. This corresponds to the equilibrium distance d_0 in the Shubnikov phase, observed in this material. This behavior may be explained by the assumption of a hitherto unknown, long-range, attractive interaction between flux lines. The investigations of the temperature- and κ-dependence of the initial induction B_0 indicate a region of validity of the Ginzburg–Landau theory. (auth)

30419 SUPERCONDUCTING-STATE PARAMETERS OF ALUMINUM USING OPW FORM FACTORS AT REDUCED VOLUMES. Rajput, J. S. (Banaras Hindu Univ., India). Phys. Status Solidi (b); 44: K69-71(1 Apr 1971).

The important superconducting-state parameters are the phonon interaction parameter, the phonon-mediated attractive electron–electron interaction, the Coulomb pseudopotential, and the renormalization parameter. A method is given for evaluating these parameters at reduced volumes using a model pseudopotential. Results of calculations are given for aluminum. (D.L.C.)

30420 ONSET OF SUPERCONDUCTIVITY IN ONE-DIMENSIONAL SYSTEMS. Tucker, J. R. (Harvard Univ., Cambridge, Mass.); Halperin, B. I. Phys. Rev., B; 3: 3768-82(1 Jun 1971).

Time-dependent Ginzburg–Landau theory is used to investigate the resistive transition in a "one-dimensional" superconductor as a function of temperature and current through the wire. A diagrammatic expansion, in powers of the interaction between fluctuations, is described for the electrical conductivity. The conductivity is then calculated using a Hartree–Fock approximation for the interaction. When large currents flow through the wire, an unstable region is found near the depressed critical temperature, suggesting possible hysteresis effects which may have been observed in recent experiments. (auth)

30421 ELIASHBERG FUNCTION α^2(E)F(E) AND THE STRONG-COUPLING BEHAVIOR OF A DISORDERED SUPERCONDUCTOR. Bergmann, G. (Kernforschungsanlage, Juelich, Ger.). Phys. Rev., B; 3: 3797-3801(1 Jun 1971).

The electron–phonon interaction in a disordered superconductor is calculated. One finds additional electron–phonon processes that do not conserve the lattice momentum and a reduction of the normal and the umklapp processes. The additional electron–phonon processes contribute particularly to processes with low energy transfer, so that the Eliashberg function depends linearly on the energy in the low-energy region. This is in agreement with recent tunneling experiments. The linear part of the Eliashberg function causes the strong-coupling behavior of disordered superconductors. Therefore, the anomalous properties of a disordered superconductor can be explained by the change in the electron–phonon interaction. (auth)

30422 THERMODYNAMIC BEHAVIOR OF TYPE-II SUPERCONDUCTORS WITH SMALL κ NEAR THE LOWER CRITICAL FIELD. Kramer, Lorenz (Rutgers–The State Univ., New Brunswick, N. J.). Phys. Rev., B; 3: 3821-5(1 Jun 1971).

The interaction between well-separated Abrikosov vortices is calculated with the Ginzburg–Landau theory for superconductors with $\kappa < \sqrt{2}$. For $\kappa > 1/\sqrt{2}$, vortices repel each other while for $\kappa < 1/\sqrt{2}$ there is an attraction. Therefore, in the Ginzburg–Landau regime, all type-II superconductors exhibit a λ transition gradually changing into a first-order transition as $\kappa \to 1/\sqrt{2}$. Slightly above H_{c1} a transition from the triangular- to the square-flux-line lattice is found to take place. The variational method used admits more general applications. (auth)

30423 ADDENDUM TO THE THEORY OF ULTRASONIC ATTENUATION IN PURE TWO-BAND SUPERCONDUCTORS IN HIGH FIELDS. Tang, I-Ming (Reed Coll., Portland, Oreg.). Phys. Rev., B; 3: 3960-5(1 Jun 1971).

By modifying the sound-wave dispersion relation for a two-band superconductor, the ultrasonic attenuation coefficient for transverse waves in pure two-band superconductors near H_{c2} is ob-

XUM

tained. An explicit expression for the attenuation is obtained by the use of an "unverified" conjecture used by the author previously to obtain the ultrasonic attenuation of longitudinal waves in pure superconducting niobium near H_{c2}. It is then shown that the Brandt–Pesch–Tewordt method can be applied to pure two-band superconductors near H_{c2} to produce results which are in agreement with those obtained by the use of the unverified conjecture that the effect of the magnetic field on the two energy gaps in a pure two-band superconductor near H_{c2} is similar to that of a uniform current in both bands. (auth)

30424 BULK AND SURFACE NUCLEATION FIELD OF PURE LEAD. Fischer, Gaston (Univ. of Montreal). Solid State Commun.; 9: 379-81(15 Mar 1971).

A recent theory of strong-coupling superconductors by Eilenberger and Ambegaokar is shown to agree well with the experimental slopes at T_c of the critical fields $H_{c2}(T)$ and $H_{c3}(T)$ of pure lead. From the detailed comparison of experiment and theory the authors propose for lead a new "average" Fermi velocity renormalized by electron–phonon interactions. (auth) (UK)

30425 SUPERCONDUCTING-STATE KNIGHT SHIFT IN V_3Au. Ancher, L. J. (Kamerlingh Onnes Laboratorium, Leiden); Poulis, N. J.; Wulffers, L. A. G. M.; Diemer, E. A. P.; Van Reuth, E. C. Physica; 51: 605-19(26 Feb 1971).

The behavior of the ^{51}V resonance in V_3Au and the magnetic susceptibility were measured as a function of temperature. From these measurements it is possible to obtain values for K_s, K_d ($T = 4.2°K$) and K_{orb} of 0.10%, −0.20% and 0.55%, respectively. The temperature dependence of the ^{51}V resonance line in the superconducting state was measured at various magnetic field strengths. The ^{51}V resonance line width and Knight shift are evaluated. In order to interpret the behavior of the Knight shift, a correction for the decreased field in the superconducting state was made. Therefore, the critical field H_{c2} was measured as a function of temperature. The corrected values for ΔH as a function of the field at $T = 0°K$ give rise to a value for K ($T = 0$) of about 0.54% which is in excellent agreement with the value for $K_{orb} = 0.55\%$ obtained from the K(T) versus $\chi(T)$ curve. The ^{51}V resonance line width as a function of temperature shows clearly that the anisotropic Knight shift disappears in the superconducting state when the temperature is decreased to zero. (auth)

30426 MULTIGAP EFFECT ON PHONON STRUCTURE IN TUNNELING EXPERIMENTS. Leger, A.; Klein, J. (Centre National de la Recherche Scientifique, Paris). Phys. Rev., B; 3: 3968-70(1 Jun 1971).

The $\vec{k}$ dependence of the energy-gap function leads to a double gap edge in tunneling characteristics of superconducting thick Pb. Nevertheless, it is shown here experimentally and theoretically that there is no corresponding splitting of the phonon peaks. (auth)

30427 HALL EFFECT IN SUPERCONDUCTING NIOBIUM AND ALLOYS. Gilchrist, J. le G.; Vallier, J.-C. (Centre National de la Recherche Scientifique, Grenoble, France). Phys. Rev., B; 3: 3878-86(1 Jun 1971).

The Hall effect in niobium and some Nb–Ta alloys was studied in the mixed state by calorimetric surface-resistance measurements. In certain conditions the tangent of the Hall angle is given by $(R_+^2 - R_-^2)/(2R_+R_-)$ where R_+, R_- are the surface resistances in right- and left-hand circularly polarized fields. The method of study is critically analyzed and its suitability for studying the mixed state is discussed. It is found that flux pinning causes the magnitude of the Hall angle to be overestimated, which is quite opposite to the influence of pinning on dc Hall-effect measurements. Interpreted like this, the data for moderately pure Nb are consistent with the Hall angle being independent of field in the mixed state. As increasing amounts of Ta are alloyed in, the mixed-state Hall angle becomes smaller compared with the normal state, and for $Nb_{96.8}\,Ta_{3.2}$ it is approximately zero in $0.5\,H_{c2}$. The small and negative Hall angles which have been reported for impure Nb and Nb-rich alloys therefore probably represent the true flux-flow behavior, at least qualitatively, and are not primarily due to pinning. A Ta-rich alloy has a relatively large positive Hall angle as also previously reported by Niessen et al. (auth)

30428 SUPERCONDUCTIVE SUPERCOOLING AND SUPERHEATING OF SMALL CADMIUM SPHERES: SIZE EFFECTS. de la Cruz, Francisco; Maloney, M. David; Cardona, Manuel (Brown Univ., Providence). Phys. Rev., B; 3: 3802-11(1 Jun 1971).

Supercooling and superheating were observed for samples composed of small cadmium spheres of uniform well-defined sizes. The data obtained for large sphere diameters are independent of size and represent, by all indications, ideal bulk properties. The supercooling data for such spheres have been used to obtain the Ginzburg–Landau parameter κ and, in conjunction with BCS expressions, the penetration depth λ and the coherence length ξ_0. The temperature dependence of the supercooling field H_{sc} shows an anomaly for $t \sim 0.8$, very similar to that previously reported for Al and Zn. The superheating field of these "bulk" spheres shows strong effects of the nonlocal electrodynamics below T_c. Spheres of diameters equal to or smaller than 10μ show strong size effects in the supercooling and superheating fields, especially near T_c. The results are examined in the light of existing theories of critical fields for small spheres. A systematic decrease of the critical temperature with sphere size was also observed. It seems related to a decrease in the gap anisotropy, produced by boundary scattering. These results are analyzed in terms of the theory of Markowitz and Kadanoff. (auth)

30429 INTERPHASE BOUNDARY WAVES IN THE INTERMEDIATE STATE OF LEAD. Kushnir, A. J. (Rutgers–The State Univ., New Brunswick, N. J.); McLean, W. L.; Kasdan, A.; Maxfield, B. W. Phys. Rev., B; 3: 3812-20(1 Jun 1971).

The propagation of waves similar to helicon waves was studied in the superconducting intermediate state of lead in polycrystalline samples and in single crystals of varying quality. The theories of Noziéres and Vinen and of Andreev were found to agree well with the results from the highest-quality specimen. The behavior of the other specimens, although resembling in some respects that predicted recently by Maki for impure systems, is probably due to pinning effects. The results in lead are compared with those obtained in earlier work on indium and tin. (auth)

30430 INFLUENCE OF DISLOCATION MOTION ON THE ULTRASONIC-VELOCITY CHANGE IN SUPERCONDUCTING INDIUM. Deaton, B. C. (General Dynamics, Fort Worth, Tex.). Phys. Rev., B; 3: 3782-6(1 Jun 1971).

The change in velocity of compressional sound waves propagating in superconducting and normal indium was measured at 13 MHz as a function of temperature and amplitude of the cw ultrasonic signal. It is found that the velocity of sound is strongly amplitude dependent, especially in the superconducting state. At the highest amplitude utilized, the velocity is observed to have changed by about one part in 10^3. The results can be explained on the basis of a direct interaction between the conduction electrons and oscillating dislocations as proposed by Granato and Lücke and by Kravchenko. (auth)

30431 TUNNELING INTO THE ENERGY BANDS OF THE INTERMEDIATE STATE IN TYPE-I SUPERCONDUCTORS. Kuemmel, Reiner (Univ. of Valle, Cali, Colombia). Phys. Rev., B; 3: 3787-91(1 Jun 1971).

A tunneling experiment is proposed to verify the recently predicted band structure in the excitation spectrum of the laminar intermediate state. The theory shows that the energy bands are reflected by rapid oscillations of the differential tunneling conductance for small voltages of the order of the maximum value of the pair potential. In weak magnetic fields ($H \approx 0.1H_c$) which produce normal regions of some 10^{-2} cm, the distance between two oscillation peaks is of the order of 10^{-5} to 10^{-6} V. (auth)

30432 EXPERIMENTAL TEST OF THE MICROSCOPIC THEORY OF A CURRENT-CARRYING SUPERCONDUCTOR BY MEASUREMENT OF THE ZERO-BIAS CONDUCTIVITY OF TUNNEL JUNCTIONS. Paterno, G.; Ricci, M. V.; Sacchetti, N. (Comitato Nazionale per l'Energia Nucleare, Frascati, Italy). Phys. Rev., B; 3: 3792-6(1 Jun 1971).

The zero-bias conductivity of metal/insulator/superconducting-tin tunneling junctions was measured as a function of the current flowing through the superconductor at various temperatures. Good agreement was found with the microscopic theory by simply adjusting one parameter (the critical current) at an arbitrary temperature. Also, the 0°K critical current density is found to be of the expected order of magnitude. (auth)

30433 SUPERCONDUCTIVITY OF Re–Os, Re–Ru, Ru–Os, AND Re–W hcp ALLOY SYSTEMS AND SLIGHTLY DOPED Re. Chu, C. W. (Bell Telephone Labs., Murray Hill, N. J.); McMillan, W. L.; Luo, H. L. Phys. Rev., B; 3: 3757-62(1 Jun 1971).

The superconducting transition temperature T_c was measured on the hcp Re–Os, Re–Ru, Ru–Os, and Re–W alloy systems and on slightly doped Re. The T_c variation is analyzed and discussed in terms of McMillan's theory. A sharp peak is observed in the slope of the curve for T_c vs Os concentration. This is attributed to the Fermi-surface-topology change of Re due to alloying. A small addition of impurities is observed always to increase the T_c of Re. This is explained in terms of the effects of the band-structure smearing and the Fermi-surface-topology change. By invoking only the second effect near the Fermi level, the unusual im-

purity effect on T_c of slightly doped Tl observed by other workers is accounted for. (auth)

30434 THERMAL CONDUCTIVITY OF SUPERCONDUCTING NIOBIUM. Anderson, A. C.; Satterthwaite, C. B.; Smith, S. C. (Univ. of Illinois, Urbana). Phys. Rev., B; 3: 3762-5(1 Jun 1971).

The thermal conductivity of single-crystal superconducting niobium was measured in the temperature range 0.04 to 4 K. No evidence is found either for thermal transport or for phonon scattering by electrons associated with a second energy gap. (auth)

30435 FERMI-SURFACE TOPOLOGY CHANGES IN In ALLOYS DEDUCED FROM THE BEHAVIOR OF T_c UNDER STRAIN. Overcash, D. R.; Skove, M. J.; Stillwell, E. P. (Clemson Univ., S. C.). Phys. Rev., B; 3: 3765-8(1 Jun 1971).

The effect of dilute alloying on the strain (ϵ) dependence of the superconducting transition temperature T_c of In whiskers was measured. Alloy contents x ranged up to 0.1 at. % Ag, 1.5 at. % Sn, and 3 at. % Cd. The addition of Ag and Sn did not affect $\partial T_c/\partial \epsilon$, but the addition of Cd had a large effect. The initial slope of the T_c -vs-ϵ curve, $(\partial T_c/\partial \epsilon)_{\epsilon=0}$, decreased with increasing Cd content until at 0.9 at. % it was a minimum of 15 mK/%, one-fourth of its value for pure In. As x increased from 0.9 to 2 at. % Cd, $(\partial T_c/\partial \epsilon)_{\epsilon=0}$ increased to almost its value for pure In. The curves T_c vs ϵ were linear in ϵ for $0 \leq x \leq 0.3$ and for $x > 2$ at. %. For $0.3 < x \leq 0.9$ at. % Cd, $\partial^2 T_c/\partial \epsilon^2$ was negative, while for $0.9 < x < 2$ at. % Cd it was positive. For alloys with more than about 2.0 at. % Cd, T_c was linear in ϵ. This behavior is attributed to a change in the topology of the Fermi surface occurring at about 0.9 at. % Cd in In. (auth)

30436 MIXING OF UHF SIGNALS FROM SUPERCONDUCTING TIN FILMS. Churilov, G. E.; Dmitriev, V. M.; Beskorsyi, A. P. (Inst. of Physics and Tech., Kharkov). Ukr. Fiz. Zh. (Russ. Ed.); 15: 1924-6(Nov 1970). (In Russian).

Experimental studies were made of uhf signals on thin superconducting tin films. The intermediate-frequency signal (Ω = 30 MHz) was received directly from the film and was amplified by an intermediate-frequency amplifier. Tin films of ~600-Å thickness and 0.2-mm width were used in the study. The relation of amplitudes of the intermediate-frequency signals to the transporting current, temperature, and the energy ratio was analyzed. Data obtained were in qualitative agreement with the theory for small-magnitude transport currents near the critical temperatures. (R.V.J.)

30437 STABILITY OF SUPERCURRENTS IN FLAT FILMS OF TIN. Meissner, Hans (Stevens Inst. of Tech., Hoboken, N. J.); Tholfsen, Paul. J. Low Temp. Phys.; 4: 141-51(Feb 1971).

Using pulsed 80-nsec-currents, the stability of supercurrents in flat films of tin with compensating current return was investigated. It was found that the voltage along the film rises with time t approximately as $V = b + a[t'/2(t - c)^{\frac{1}{2}}]$, where b represents the (almost instantaneous) flux-flow voltage in a perpendicular field and the time constant t' is an exponentially decreasing function of $J(1 + 420/d)/[1 - (T/T_c)^4][1 - H_\perp/H_{c\perp}]$. Here J is the current density in the film of thickness d in Å, T/T_c is the reduced temperature, and $H_\perp/H_{c\perp}$ is the reduced magnetic field. It is suggested that this instability is of the type investigated by Kramer and by Fink and Presson for currents in a superconducting surface sheath. At lower temperatures a second instability is found which is distinctly different from the one dominant at the higher temperatures. (auth)

30438 ABOUT THE POSSIBILITY OF INCREASING THE SUPERCONDUCTING TRANSITION TEMPERATURE BY THE PHONON MECHANISM. Geilikman, B. T. (Inst. of Atomic Energy, Moscow). J. Low Temp. Phys.; 4: 181-8(Feb 1971).

The equations for the energy gap and for the critical temperature T_c are investigated in the case of superconductors with strong coupling, with regard for the dependence of the interaction constant on the phonon frequency. The effective interaction constant λ, which determines T_c in the Einstein model and delta-function phonon peak model, is calculated, and its dependence on the ordinary interaction constant, phonon frequency and momentum, Fermi momentum, and other parameters is determined. It is shown that the maximum possible value of λ is unity. A solution is found for the critical temperature equation in the case of a delta-function peak and the Einstein model. It is demonstrated that, in the latter case, T_c has a sharp maximum as a function of the electron density. (auth)

30439 MAGNETIZATION BY ROTATION: THE BARNETT EFFECT IN A SUPERCONDUCTOR. Hendricks, J. B.; King, C. A.; Rorschach, H. E. (Rice Univ., Houston, Tex.). J. Low Temp. Phys.; 4: 209-29(Feb 1971).

The magnetic field due to the rotation of a superconductor was measured for a number of hollow and solid tin cylinders of varying purity. The field generated within a hollow cylinder agrees with the predictions of the London theory: $B = -(2mc/e)\omega$. The value of $-2mc/e$ determined from the experiments was 1.17×10^{-7} G-sec, which agrees with the theoretical value of 1.137×10^{-7} G-sec within the experimental error of ±5%. The reversibility of the production of the field was investigated for both hollow and solid cylinders. In the case of the hollow cylinder, effects analogous to flux trapping were observed; if the specimen is cooled below T_c while in rotation, then the "London field" appeared only when the rotation speed was changed. In the case of the solid cylinder, effects analogous to those associated with "frozen-in flux" were observed; the London field appeared reversibly only in those specimens sufficiently pure to exhibit a Meissner effect at fields of the order of 10^{-5} G. In one run a ferrite cylinder was substituted for the superconductor. A Barnett effect was observed: the magnitude of the field generated by rotation was consistent with the permeability measured at audio frequencies by conventional means. A novel heat-transfer effect connected with the rotation of the sample was also observed during the course of measurements on the hollow cylinders. A discussion of the electrodynamics of the rotating superconductor is given in an appendix. (auth)

Equipment and Devices

Refer also to abstract 31040.

30440 (EUR-4593, pp 107-13) INFLUENCE OF NEUTRON IRRADIATION ON BEHAVIOR OF A SUPERCONDUCTOR AND A SUPERCONDUCTING COIL MAGNET. van der Klein, C. A. M.; de Klerk, D. (Leiden Rijksuniversiteit (Netherlands). Kamerlingh Onnes Laboratorium); Elen, J. D. (Reactor Centrum Nederland, Petten).

From Sixth symposium on fusion technology; Aachen, Germany (22 Sep 1970).

In Proceedings of the 6th symposium on fusion technology.

Magnetic investigations were made of the influence of cold rolling and heat treatment and of the influence of neutron irradiation on a Type-II superconductor. The effect of neutron irradiation is similar to the effect of cold working, but only up to H_{c2}. The susceptibility behavior of samples with a dense defect structure can be described by means of surface effects. For samples with a relatively high degree of physical perfection also, bulk effects play an important role. Samples with irradiation damage are not in agreement with the theory based on surface effects but, also, bulk effects are not observed. Nevertheless, the behavior is similar to the behavior of the samples with dense defect structure, but only up to H_{c2}, and for a superconducting coil that is the important region. (auth)

30441 (EUR-4593, pp 117-24) PRESENT STATE OF COSTS FOR LARGE SUPERCONDUCTING MAGNETS AND THEIR FUTURE PROSPECTS. Komarek, P. (Kernforschungsanlage, Juelich (West Germany). Institut fuer Technische Physik).

From Sixth symposium on fusion technology; Aachen, Germany (22 Sep 1970).

In Proceedings of the 6th symposium on fusion technology.

Several factors influence the costs of large superconducting magnets. Dominating are the prices for the superconductive material as a function of the desired field strength; further, the geometrical configuration of the coils and the cryostat established by the application purpose are key factors. The large price reduction of superconductive material during the last five years is reviewed, and possible further reductions are discussed. The costs with regard to plasma reactor magnets are estimated. As an example, the specific costs for the magnets and their cryogenic equipment for three possible reactor configurations with 5000 MW/th power are estimated. Prices between 75/95 DM/kW_{therm} are calculated. (auth)

30442 (NBS-TN-562) A RIGHT ANGLE ^{3}He CRYOSTAT INCORPORATING A HIGH FIELD SUPERCONDUCTING SOLENOID. Marshak, H.; Dove, R. B. (National Bureau of Standards, Washington, D. C.). Dec 1970. 20p. GPO $0.30.

Construction and operation of a novel ^{3}He cryostat, incorporating a large superconducting solenoid mounted at right angles to the cryostat's vertical axis, is described. This new cryostat which is part of the transportable National Bureau of Standards ^{3}He refrigerator, has been successfully used for nuclear orientation studies at the Atomic Energy Research Establishment, Harwell, England. (auth)

30443 SUPERCONDUCTING CAVITY RESONATORS IN THE 10 GHz FREQUENCY BAND. Benacka, S. (Elektrotechnicky

Ustav SAV, Bratislava). Elektrotech. Cas.; 22: 81-92(1971). (In Czech).

High-frequency characteristics of superconductors and metals at low temperatures are described, as well as the experimental results obtained in the Electrotechnical Institute of the Slovak Academy of Sciences in the research on superconducting cylindrical cavity resonators of the TE_{011} type, made from lead of various purities, at the frequency of 9.4 GHz. (auth)

30444 DESIGN OF A SIMPLE CRYOSTAT FOR THERMOLUMINESCENCE MEASUREMENTS ON SOLID-STATE LOW-THERMAL-CONDUCTIVITY SAMPLES. Fleming, R. J.; Legge, C. A.; Ranicar, J. H.; Boronkay, S. (Monash Univ., Clayton, Australia). J. Phys., E (London); 4: 286-8(Apr 1971).

A liquid nitrogen cryostat, suitable for the recording of thermoluminescence glow curves and for the spectral analysis of these curves, is described. The necessity of maintaining isothermal conditions within the samples during both irradiation at 77°K and subsequent heating to 273°K is emphasized. Some results are presented for polyethylene and polystyrene. (auth) (UK)

30445 SUPERCONDUCTING POWER TRANSMISSION. Meyerhoff, R. W. (Union Carbide Corp., Tarrytown, N. Y.). Cryogenics; 11: 91-101(Apr 1971).

The case for and the development of superconducting power lines are presented. After a brief history of superconducting power transmission, studies at present being undertaken in various countries throughout the world are discussed. A final resume outlines problems still to be tackled before superconducting power lines can be put into operation. (auth) (UK)

30446 MICROWAVE DEVICES USING THE PROXIMITY EFFECT BETWEEN SUPERCONDUCTING AND NORMAL METALS. Combet, H. A.; Chouan, Y.; Thepault, E. (Centre National d'-Etudes des Telecommunications, Lannion, France). Cryogenics; 11: 102-6(Apr 1971).

Superconductors coated with normal metals present more strongly temperature or field dependent characteristic lengths (penetration depth, coherence length on the N side ...) than bare superconductors. These properties can be used in "stripline" transmission line structures. Some experimental results obtained with resonant structures at a frequency of 4 GHz, using mainly PbCu, PbSn, or SnAu contacts, are described. The use of the proximity effect in magnetically tunable filter cells or attenuators, and the intrinsic limitations of these devices are discussed. (auth) (UK)

30447 SIMPLE SUPERCONDUCTING CHOPPER AMPLIFIER FOR USE IN MAGNETIC FIELDS. Edwards, G. J. (Michigan State Univ., East Lansing). J. Phys., E (London); 4: 299-300(Apr 1971).

A superconducting chopper amplifier, which is simple to build and can be used adjacent to a 100-kG solenoid, is described. At low fields, the sensitivity of the amplifier is 10^{-11} V, decreasing to 10^{-8} V at 100 kG. (auth) (UK)

30448 SUPERCONDUCTING-WIRE LIQUID HELIUM LEVEL GAUGE. Rozenberg, Ya. I. Instrum. Exp. Tech. (USSR) (Engl. Transl.); No. 4, 1225-6(Jul-Aug 1970).

Translated from Prib. Tekh. Eksp.; No. 4, 228-9(Jul-Aug 1970).

Level gages using a wire of superconducting wire for continuous and discrete measurements of liquid helium levels, and requiring little warmup power, are described. (auth)

Plasma and Thermonuclear Physics

30449 (EUR-4593) PROCEEDINGS OF THE 6th SYMPOSIUM ON FUSION TECHNOLOGY, AACHEN, GERMANY, SEPTEMBER 22-25, 1970. (European Communities, Luxembourg. Commission). 571p. (CONF-700928). EUR $14.00.

Separate abstracts were prepared for 59 papers. Abstracts for the 5 remaining papers appeared previously in NSA; see NSA 25: 7406, 7407, 7408, 7409, and 11919. (M.O.W.)

For abstracts of individual papers see: 29820, 30252-30257, 30410, 30411, 30440, 30441, 30455, 30456, 30474, 30495-30497, and 30554-30595.

30450 (LA-4585) STATUS REPORT OF THE LASL CONTROLLED THERMONUCLEAR RESEARCH PROGRAM FOR 12-MONTH PERIOD ENDING OCTOBER 1970. (Los Alamos Scientific Lab., N. Mex.). Feb 1971. Contract W-7405-eng-36. 86p. Dep. NTIS.

Summaries of research conducted during this report period are given for the following topics: (1) theta pinch, (2) z-pinch, (3) plasma gun program, (4) quadrupole, (5) plasma physics, and (6) plasma simulation. (M.O.W.)

30451 CONTRIBUTIONS TO THE THIRD EUROPEAN CONFERENCE ON CONTROLLED FUSION AND PLASMA PHYSICS AND THE SYMPOSIUM ON BEAM-PLASMA INTERACTIONS, UTRECHT, NETHERLANDS, 23-27 JUNE 1969. Groningen, Netherlands; Wolters-Noordhoff Publishing (1969). 139p. $5.25. (CONF-690619).

The papers included cover the following areas: (1) stellarators and multipoles, (2) open-ended systems, (2) beam-plasma interactions, (4) theory, (5) rotating plasmas and arcs, (6) hf-plasma interactions, (7) pinches and tokamaks, (8) waves, (9) nonlinear phenomena, (10) laser-produced plasmas, (11) high-density plasmas and accelerators, and (12) drift waves. (M.O.W.)

30452 WHAT PROBLEMS OF PHYSICS AND ASTROPHYSICS ARE AT PRESENT ESPECIALLY IMPORTANT AND INTERESTING? Ginzburg, V. L. (Lebedev Inst. of Physics, Moscow). Usp. Fiz. Nauk; 103: 87-119(Jan 1971). (In Russian).

The first problem discussed is controlled thermonuclear synthesis, which involves the fusion of deuterium and tritium. Besides a plasma reactor with magnetic retention of the plasma, it may be possible to heat deuterium to high temperatures with the use of lazers or powerful electron beams. The finding of a high-temperature superconductor may involve the discovery of metallic hydrogen, or the chemical synthesis of a specially tailored conducting organic molecule that would conduct electricity by an exciton mechanism. An interesting problem would be the creation of a metallic exciton liquid in semiconductors at high pressure. In principle, this liquid should show superconductivity. A search for phase transitions of the second order where there is no change in heat or volume change would be of theoretical interest. The conversion is continuous. The discovery of superheavy elements (the far transuranics) would be of great interest, and would require great ingenuity. In the field of microphysics the theory of elementary particles could be improved. A set of characteristics that better characterize elementary particles is required. A better description of quantum space (fundamental length) is required. More clarity could be brought into interactions of particles at high energies and into the violation of CP invariance. In astrophysics we need experimental confirmation of the general theory of relativity, the possible detection of gravitational waves, solutions to the problem of singularity in cosmology, better explanations of quasars, neutron stars, pulsars and the origin of cosmic gamma rays, and of cosmic x rays. (TTT)

30453 ION PROPULSION: TECHNOLOGY AND APPLICATIONS. Brewer, George R. New York; Gordon and Breach, Science Publishers, Inc. (1970). 546p.

A unified treatment is given of the technology of ion propulsion systems. After a discussion of the general performance parameters of the system, its components (ion source, accelerator, power and control subsystems, propellant storage and control subsystems) are described. Life, efficiency, and testing of the system are discussed in later chapters. The final chapters deal with the applications of such systems to satellite control and interplanetary vehicles and with future possibilities. (D.L.C.)

30454 PLASMA PHYSICS INDEX. VOLUME 6, NO. 3, 1971. Bibliography, Author Index, Subject Index. Frankfurt am Main; Zentralstelle fuer Atomkernenergie-Dokumentation (1971). 124p.

A listing is presented of 487 articles on various aspects of plasma physics. (M.O.W.)

Confinement and Heating

30455 (EUR-4593, pp 479-84) PLASMA HEATING BY NEUTRAL INJECTION IN A STELLARATOR REACTOR. Cole, H. C.; Hill, J. W.; Terry, M. J. (United Kingdom Atomic Energy Authority, Abingdon (England). Culham Lab.).

From Sixth symposium on fusion technology; Aachen, Germany (22 Sep 1970).

In Proceedings of the 6th symposium on fusion technology.

The possibility of heating an existing cool plasma to thermonuclear temperatures by injecting a beam of high-energy neutral atoms is outlined. A method of generating such a beam of neutrals is to use a closed electron-drift plasma accelerator, the output from which would be neutralized by charge exchange before injecting into the reactor. The general characteristics obtained with experimental accelerators are presented, and the problems associated with scaling up to the required level are discussed. A tentative design for a 1-MV accelerator is given. (auth)

30456 (EUR–4593, pp 551-6) FREMIX: A HIGH-POWER 8-GHz PLASMA HEATING EXPERIMENT. de Kock, L. C. J. M.; Ornstein, L. Th. M.; Schep, T. J.; Schrader, W. J.; Schram, D. C.; Hugenholtz, C. A. J.; Manintveld, P.; van der Ven, H. W.; Winkel, Th. G. A. (Stichting voor Fundamenteel Onderzoek der Materie, Jutphaas (Netherlands). Instituut voor Plasma-Fysica).

From Sixth symposium on fusion technology; Aachen, Germany (22 Sep 1970).

In Proceedings of the 6th symposium on fusion technology.

A survey was made of the problems encountered in the assembly and the operation of the 40-kW c-w 8-GHz equipment used for the FREMIX experiment. This experiment aims at resonant ion heating in a magnetic bottle at frequencies which are the product of nonlinear mixing of electron cyclotron resonance waves. The problems can be divided into three categories: (1) Requirements for operation of two klystron amplifiers: power supplies with protective equipment, steering circuitry, and cooling water. (2) Waveguide system: arc protection, circulators, and vacuum window. (3) Construction of the plasma chamber; introduction of diagnostic tools: 4-mm interferometry, x-ray detection of escaping particles, and detection of excited radiation and mixing products (1 to 5 MHz; 16 GHz). (auth)

30457 (IPPJ–102) EXPERIMENTS OF PLASMA CONFINEMENT IN JIPP STELLARATOR. I. PRELIMINARY RESULTS USING J x B GUN AND ECRH PLASMA. Miyamoto, Kenro; Mohri, Akihiro; Inoue, Nobuyuki; Fujiwara, Masami; Yatsu, Kiyoshi (Nagoya Univ. (Japan). Inst. of Plasma Physics). Nov 1970. 33p. Dep. NTIS (U. S. Sales Only).

Preliminary results of the experiments on the plasma confinement using J × B type gun and ECRH plasma are described. The diffusion coefficient estimated from the decay times and the plasma radius are inversely proportional to the square of the rotational transform angle ι. The profile of the density distribution is similar to $(r/a_s)^2 J_{-\frac{1}{3}}[1.25(r/a_s)^3]$, which corresponds to the relation $D \propto \iota^{-2} \propto r^{-4}$. The diffusion coefficients estimated from the Bessel distribution are down to $1/7$ to $1/17$ times of the Bohm one. If the foregoing distribution is adopted, the ratios become $1/17$ to $1/40$. The confinement time does not depend appreciably on the property of the magnetic well (and anti-well). The dependence of the confinement time on the magnitude of the magnetic field is apparently linear. (auth) (Japan)

30458 (IPPJ–104) ION HEATING CAUSED BY ION ACOUSTIC WAVES IN AN ION-STREAMING PLASMA. Honzawa, Tadao; Kawai, Yoshinobu (Nagoya Univ. (Japan). Inst. of Plasma Physics). Jan 1971. 20p. Dep. NTIS (U. S. Sales Only).

It is experimentally shown that ion heating occurs because of ion acoustic waves arising from the drift of electrons in an ion-streaming plasma. The drift of electrons is controlled by changing the bias applied to a meshed grid inserted in the plasma. The results of this work indicate that, when the drift velocity of electrons is settled at a proper value, one can observe standing wave-like ion acoustic waves as well as the increase of ion temperature and there is a good correlation between the increase of ion temperature and the amplitudes of the ion waves. Explanation of the mechanism of ion heating is also described. (auth) (Japan)

30459 (MATT–813) PRELIMINARY INVESTIGATION OF OHMICALLY-HEATED PLASMAS IN THE MODEL ST TOKAMAK. Grove, D. J.; Dimock, D. L.; Hinnov, E.; Hosea, J. C.; Johnson, L. C.; Beservey, E. B.; Tolnas, E. L. (Princeton Univ., N. J. Plasma Physics Lab.). Oct 1970. Contract AT(30-1)-1238. 21p. (CONF-701114–2). Dep. NTIS.

From Meeting on division of plasma physics; Washington, D. C. (4 Nov 1970).

Some of the results obtained in the first three months of operation of the Princeton Model ST tokamak are described. The body of the report is the paper submitted to the Fourth European Conference on Controlled Fusion and Plasma Physics (Rome (September, 1970)). Additional figures, which were used in the presentation at Rome and in colloquia at Grenoble and Fontenay-aux-Roses, are given in the Appendix along with complementary comments. (auth)

30460 (MATT-Trans–13) HIGH FREQUENCY HEATING OF A PLASMA. Tolok, V. T. (Akademiya Nauk Ukrainskoi SSR, Kharkov. Fiziko-Tekhnicheskii Institut). Translated for Princeton Univ., N. J. from report NP–15256. 35p. Dep. NTIS.

An abstract of this paper, prepared from the original language, appeared as NSA 19: 41862. (M.O.W.)

30461 (MATT-Trans–79) A STUDY OF THE EFFECT OF THE SHAPE AND MAGNITUDE OF THE DISCHARGE CURRENT PULSE ON PLASMA CONFINEMENT AND HEATING IN THE TOKAMAK-3. Mirnov, S. V. (Gosudarstvennyi Komitet po Ispol'zovaniyu Atomnoi Energii SSSR, Moscow. Institut Atomnoi Energii). Translated for Princeton Univ., N. J. from report IAE–1644. 42p. Dep. NTIS.

The results of measuring the energy and energy lifetime of a plasma as functions of the shape and magnitude of the discharge current pulse are given. As is known, the maximum magnitudes of the energy $E_\perp$ and energy lifetime of a plasma τ_E were reached 2 to 3 milliseconds after the maximum discharge current J in the T-3 device. This paper presents $E_\perp(t)$, $\tau_E(t)$ as functions of the shape of the discharge current pulse and the discharge time. An effort was made to relate the observed relations to the current-density distribution. The internal l_i and external $L_{ext} = 2 \ln b/a$ self-inductances of the plasma column were measured. The magnitude of the "shear" averaged over the radius a was estimated on the basis of the data obtained. Assumptions were made regarding the nature of the processes determining the observed laws. One of the possible assumptions is the assumption of the presence of either a dissipative helical (tearing mode) or overheating instability in the initial discharge stage and while the current is building up. (auth)

30462 (NP–18767) STUDIES OF DIFFUSION OF DENSE DISINTEGRATING PLASMA IN A STELLARATOR. Demirkhanov, R. A.; Baratov, D. G.; Malykh, N. I.; Merezhkin, V. G.; Stotland, M. A.; Ten, Yu.; Khil, Sh. V. (Gosudarstvennyi Komitet po Ispol'zovaniyu Atomnoi Energii SSSR, Sukhumi. Fiziko-Tekhnicheskii Institut). 1970. 13p. (In Russian). Dep. NTIS (U. S. Sales Only).

Disintegration of helium plasma in a two-pass stellarator with magnetic field varying from 6 to 12 kOe was studied under conditions in which the classical diffusion was smaller than the Bohm diffusion and the free electron mean-free-path was considerably shorter than the length of the system. The density and plasma temperature were $\sim 1 \times 10^{14}$ cm^{-3} and 0.6 eV, respectively. Data obtained showed that in the case of recombination, the plasma confinement time (as a function of the magnetic field intensity and the rotational transformation angle) was in good agreement with the hydrodynamic model of classical plasma diffusion in a toroidal helical magnetic field. (tr-auth)

30463 ELIMINATION OF CONE LOSSES IN THE MAGNETOSTATIC MIRROR BY HELP OF MICROWAVES. Golovanivskii, K. S.; Dougar-Jabon, V. D. (Patrice Lumumba Univ., Moscow). Phys. Lett.; 34A: 222-3(8 Mar 1971).

The passing of plasma bunches with the ion longitudinal energy about 1 keV and density $n > 10^{12}$ cm^{-3} through the combined microwave–magnetostatic barrier is experimentally studied. It is shown that cone losses can be removed providing the wave frequency "ω" is equal to the upper hybrid frequency $(\omega = (\omega_c^2 + \omega_p^2)^{1/2})$. (auth)

30464 AXIAL BEHAVIOR AND CONFINEMENT OF PLASMA IN THE MIRROR-FIELD THETA PINCH. Sato, Koichi; Kawakami, Ichiro; Shiina, Shoichi; Ohnishi, Haruyuki (Nihon Univ., Tokyo). J. Phys. Soc. Jap.; 30: 846-56(Mar 1971).

The mechanism of the end loss and the axial behaviors of a mirror θ-pinch plasma are studied. For this purpose, both the mirror and the straight field configurations are used at the first half cycle controlling the reverse bias field. The end loss in the mirror field is found to be decided by the axial motion, which is caused by the axial pressure gradient of the plasma due to the axially inhomogeneous magnetic field. The e-folding time of the decaying plasma at the midplane agrees well with the result of the numerical calculations on the basis of non-steady MHD equations. The relation between the confinement time and the initial conditions of produced plasma is discussed. (auth)

30465 VERIFICATION OF A CLASSICAL, SELF-CONSISTENT THEORY OF PARTICLE LOSS IN A HOT ELECTRON, MAGNETIC MIRROR COMPRESSION EXPERIMENT. Lieberman, M. A.; Lichtenberg, A. J.; Takeshita, T. (Univ. of California, Berkeley). Plasma Phys.; 13: 141-57(Feb 1971).

A careful measurement of the particle decay from a hot electron, magnetic mirror compression experiment ($B_{\theta max} \sim 50$ kG, $n_{e\,max} \sim 5 \times 10^{12}$ cm^{-3}, $kT_e \sim 80$ keV) was performed. The measurement was in good agreement with a classical, self-consistent theory of particle loss, in which a "mirror loss cone" particle distribution is used. The loss rate predicted from a non self-consistent theory (Maxwellian distribution of particles) is approximately three times higher than the measured decay rate. The experiment indicates that the more optimistic estimates of fusion feasibility in open-ended systems are correct, and that parameter regimes exist for hot, mirror-confined plasmas in which the losses are given mainly by classical scattering into the loss cone, unenhanced by the presence of instabilities or turbulence. (auth) (UK)

XUM

30466 DIFFUSION RESULTING FROM NONADIABATIC SCATTERING ON A HELICALLY PERTURBED FIELD IN A TORUS. Moir, R. W.; Lidsky, L. M. (Massachusetts Inst. of Tech., Cambridge). Contract AT(30-1)-3980. Plasma Phys.; 13: 159-71(Feb 1971).

Resonant and nonresonant diffusion of electrons was studied in a toroidal magnetic field with pulsed injection of electrons. Experimental evidence of the theoretical predictions of $B_\perp^{\frac{1}{2}}$ dependence of the diffusion coefficients in strong perturbation fields was obtained. The transition from $B_\perp^2$ to $B_\perp^{\frac{1}{2}}$ behavior for $B_\perp/B_0 <$ 1 per cent where $B_\perp$ is the perturbing and B_0 the uniform magnetic field was observed. Theoretical models based on unperturbed orbit calculations are shown to be invalid for surprisingly small values of $B_\perp/B_0$. Measurements of nonresonant diffusion applicable to dissociation experiments in nonadiabatic traps were conducted. It was found that the diffusion coefficient depends strongly on how nearly resonant the electron is with the perturbed field. For a 50% change in effective perturbation frequency, the diffusion coefficient changes by a factor 1000. Results can be scaled to the problem of nonadiabatic trapping and dissociation of molecular ions. The resulting nonresonant protons would have a lifetime against nonadiabatic scattering 10,000 times longer than the parent molecular ions. (auth) (UK)

30467 ELECTRON HEATING IN LARGE-AMPLITUDE OSCILLATIONS IN A THETA-PINCH. Martone, M.; Segre, S. E. (EURATOM-CNEN, Frascati, Italy). Plasma Phys.; 13: 173-6 (Feb 1971).

The fast-rising magnetic field of a theta pinch, 80 cm in length, was used for the generation of collisionless cylindrical shocks propagating radially inwards in a magnetized, well-ionized hydrogen plasma (Segre et al., 1971). The behavior of the plasma on the axis of the discharge tube after the arrival of the shock wave is reported. (auth) (UK)

30468 MEASUREMENTS ON THE HEATING IN COLLISIONLESS LOW-β TRANSVERSE SHOCK WAVES NEAR THE CRITICAL ALFVEN–MACH NUMBER. Segre, S. E.; Martone, M. (EURATOM-CNEN, Frascati, Italy). Plasma Phys.; 13: 113-18 (Feb 1971).

Collisionless stationary low-β shock waves are produced in the range of Alfvén–Mach number M_A between 3.1 and 4.25. Magnetic probe and Thomson scattering measurements indicate anomalous electron heating at low M_A and the onset of anomalous ion heating at high M_A: the transition occurs between $M_A = 3.1$ and $M_A = 3.3$. No extended "foot" is observed: the magnetic field and temperature transitions remain sharp up to $M_A = 4.25$. (auth) (UK)

30469 EXPERIMENTAL STUDY OF COLLECTIVE PROCESSES AND TURBULENT HEATING OF A PLASMA DURING ANNIHILATION OF OPPOSITE MAGNETIC FIELDS. Babykin, M. V.; Zhuzhunashvili, A. I.; Sobolev, S. S. Zh. Eksp. Teor. Fiz.; 60: 345-55(Jan 1971). (In Russian).

The turbulent state of a plasma and the possibility of turbulent heating in energy dissipation of opposite magnetic fields with a geometry analogous to a θ pinch are investigated. A threshold value of the plasma density that depends on the variable magnetic-field strength is detected in the experiments, below this value instabilities develop. The experimental plasma oscillation spectrum indicates the appearance of both magnetic-field disturbances relative to large-scale instabilities of the whistler-type as well as high-frequency small-scale field fluctuations with a frequency in the vicinity of ω_{pi} and $2\omega_{pi}$ produced as a result of processes involving nonlinear transformation of ion acoustic waves into whistlers. The time of existence of the trapped magnetic field in the plasma is sharply reduced due to development of the instabilities. Emission of 3.2- and 1.6-cm uhf electromagnetic waves from the plasma and also the appearance of fast electrons were observed, indicating that plasma heating occurs. (auth)

30470 STUDY OF TURBULENT HEATING OF A PLASMA BY A LARGE AMPLITUDE WHISTLER. Grigor'eva, L. I.; Sizonenko, V. L.; Smerdov, B. I.; Stepanov, K. N.; Chechkin, V. V. (Physical-Technical Inst., Kharkov). Zh. Eksp. Teor. Fiz.; 60: 605-16 (Feb 1971). (In Russian).

It is shown that when a large-amplitude whistler mode is resonantly excited in a plasma, rapid electron heating occurs. The heating continues for about half of the whistler oscillation period. In this case the whistler amplitude is reduced by several times. With decrease of whistler amplitude a preferential heating of ions is observed. It is shown theoretically that electron heating may be caused by scattering of electrons on turbulent pulsations of magnetized ion-sound oscillations that propagate almost normally to the static magnetic field. Ion and electron heating in low-amplitude rf fields may be explained by a stochastic mechanism that leads to a random change in phase of the magnetized ion-sound oscillations or hydromagnetic turbulent pulsations whose characteristic frequency and growth rate are given. Preferential heating of ions at small amplitudes is due to the effect of inelastic collisions that impede electron heating. (auth)

30471 INITIAL STAGE OF A LIGHT EXPLOSION OF A PARTICLE OF MATTER IN A POWERFUL LIGHT BEAM. Askar'yan, G. A.; Tarasova, N. M. (Lebedev Inst. of Physics, Moscow). Zh. Eksp. Teor. Fiz.; 60: 617-20(Feb 1971). (In Russian).

The initial stage of a light explosion of a small particle of matter in a powerful light beam is considered. The simple model employed yields simple expressions for the time dependence of the plasma-cloud radius, fly-off time, and temperature. This facilitates the choice of optimal conditions as compared to the results of a numerical calculation previously presented. It is shown that, under certain conditions, the radius and expansion velocity increase exponentially in time. Ultra-short pulses in the picosecond range are studied in greater detail. The ranges of optimal and nonoptimal quantities determining the process are estimated. (auth)

30472 INVESTIGATION OF DIFFUSION OF A DENSE DECAYING PLASMA IN A STELLARATOR. Demirkhanov, R. A.; Baratov, D. G.; Malykh, N. I.; (and others) (Sukhumi Physical-Technical Inst., USSR). Zh. Eksp. Teor. Fiz.; 60: 569-78(Feb 1971). (In Russian).

Diffusion of a helium plasma in a double-screw stellarator is investigated experimentally for magnetic-field strengths varying between 6 and 12 kOe. The plasma density and temperature are, respectively, 1×10^{14} cm^{-3} and 0.6 eV. It is shown that the dependence of the plasma-diffusion time on magnetic-field strength and angle of rotational transformation of the lines of force are in agreement with the hydrodynamic model for classical diffusion of a plasma in a toroidal helical magnetic field. (auth)

30473 COMMENTS ON NONLINEAR RESONANT ION HEATING IN A MAGNETOPLASMA. Tulle, P. A. (Univ. of Montreal). Can. J. Phys.; 49: 1072-3(15 Apr 1971).

The calculation of Jayasimha and Thompson (Can. J. Phys., 48: 1894-1905 (1970)) on wave coupling and ion heating is discussed. It is pointed out that the coupled power calculated in the case of a plasma slab is too optimistic because a density profile makes the region of interaction inaccessible. (Canada)

Diagnostics

30474 (EUR-4593, pp 557-66) AUTOMATIC DATA COLLECTION AND PROCESSING AS AN AID TO FUSION RESEARCH. Fullard, K. (United Kingdom Atomic Energy Authority, Abingdon (England). Culham Lab.).

From Sixth symposium on fusion technology; Aachen, Germany (22 Sep 1970).

In Proceedings of the 6th symposium on fusion technology.

A discussion of the need for automatic data processing in fusion research and of available techniques is illustrated by a description of equipment presently being installed on the High-Beta Toroidal Experiment at Culham Laboratory. (auth)

30475 (LA-tr-71-6) PASSIVE DIAGNOSTICS OF A PLASMA FOCUS USING CHARGED PRODUCTS OF THE dd-REACTION. Beliaeva, I. F.; Vikhrev, V. V.; Ivanov, V. D.; Filippov, N. V. Translated by Helen Dahlby (Los Alamos Scientific Lab., N. Mex.), from report IAE-2016. 14p. Dep. NTIS.

In an apparatus of the "noncylindrical z-pinch" type, a method of study using charged products of the d,d reaction was applied. A flux of charged particles carries additional information of the magnitude, direction, and distribution of the magnetic field in comparison with neutron radiation. Special pinhole cameras, provided with nuclear emulsions, were used for recording. The distributions of charged products of d,d reactions obtained in the emulsions are compared with the results of calculations. The maximum value of the magnetic field, $H\varphi$, in the zone of the focus was determined. (auth)

30476 (N-71-10964) DIAGNOSTICS OF A SUPERSONIC PLASMA STREAM USING AN IMMERSED MICROWAVE PROBE. Baker, Frederic A.; Omura, Masayuki; Somes, Austin H. (National Aeronautics and Space Administration, Moffett Field, Calif. Ames Research Center). Nov 1970. 19p. (NASA-TM-X-2132; A-3624). NTIS.

A microwave interferometer to measure electron density and collision-frequency profiles in a supersonic plasma jet is de-

scribed. Unlike most plasma diagnostic interferometers, both the transmitting and receiving horns were immersed in the plasma stream. Advantages and disadvantages of the immersed horn technique are discussed. The measurements were made primarily by a 70-GHz system; another system operating at around 35 GHz was used to check the results at certain points. The measured densities ranged from 10^{12} to 6×10^{13} cm^{-3} and the collision frequency was nominally 10^{10}/sec. Despite the formation of shock waves around the horns, the measured densities compared well with the results obtained from a different microwave measuring technique that is described. (auth) (STAR)

30477 (NP-18765) PROBE METHOD FOR RECORDING IONS PRODUCED BY LASER RADIATION IN POST-LUMINESCENCE DISCHARGE PLASMA. Preprint No. 122. Bakov, I.; Kantor, I.; Kim, A. (Akademiya Nauk SSSR, Moscow. Institut Fiziki). 1970. 16p. (In Russian). Dep. NTIS (U. S. Sales Only).

The mechanism of ion formation produced by laser radiation was studied by a newly developed probe for ion recording. The method permitted recording of probe current variations of the order of 10^{-9} during 10^{-6} sec, which corresponded to a value of the order of 10^{-3} at an ion background density of ~10^{10} cm^{-3}. The method was used for studying multiphoton ionization of atoms in excited metastable states of post-luminescence discharges. The multiphoton ionization of excited atoms essentially establishes the mechanism of the interaction of laser radiation with post-luminescence discharge plasma. (R.V.J.)

30478 (SC-T-713024) TEMPERATURE MEASUREMENTS IN THERMAL PLASMAS OF KNOWN COMPOSITION. Richter, Johannes. Translated for Sandia Labs., Albuquerque, N. Mex., from Z. Astrophys.; 61: 57-66(1965). 12p. Dep. NTIS.

An abstract of this paper, prepared from the original language, appeared as NSA 19: 33485. (M.O.W.)

30479 INVESTIGATION OF EXCITED STATES OF HELIUM ATOMS IN A STATIONARY PIG DISCHARGE. Drawin, H. W. (CEA-CEN, Fontenay-aux-Roses, France); Klan, F.; Ringler, H. Z. Naturforsch.; 26a: 186-97(Feb 1971).

Spectral-line intensities emitted by a quiescent PIG discharge were measured, and the population densities up to a principal quantum number n = 24 were derived from them. The experimentally determined population densities were compared with theoretical ones calculated on the basis of a collisional–radiative model in which one accounts for electron and atom collisions. It is shown that even in the case of different electron and atom temperatures, T_e and T_a, an evaluation of the Boltzmann plot at medium and moderately high quantum numbers always leads to the electron temperature, whereas the Saha–Eggert equation for the same states may yield incorrect electron densities. The theoretical calculations predict an inflection of the slope of the Boltzmann plot from T_e to T_a for very highly excited states. For the plasma parameters under which the PIG discharge was operated ($n_e \cong 2.5 \times 10^{12}$ cm^{-3}, $T_e \cong 1200$°K, $n_0 \cong 1.5 \times 10^{15}$ cm^{-3}, $T_a \cong 300$°K) the change of the slope should become visible for states having principal quantum numbers n > 18. (auth)

30480 DETERMINATION OF THE ROTATION TEMPERATURE OF THE N_2^+ MOLECULE IN A NITROGEN PLASMA BY MEASURING THE INTENSITY RATIO OF TWO ROTATIONAL LINES OF THE λ = 3914 A BAND CORRESPONDING TO THE (0–0) TRANSITION OF THE $B^2\Sigma_u^+ \rightarrow X^2\Sigma_g^+$ SYSTEM. Baronnet, Jean-Marie; Andres, Francoise; Fauchais, Pierre (Limoges Univ., France. Ecole Nationale Superieure de Mecanique et d'Aerotechnique, Poitiers, France). Compt. Rend., Ser. B; 272: 102-5(11 Jan 1971). (In French).

The rotation temperature of N_2^+ in a nitrogen plasma arc was determined from the ratio of the intensities of two rotation lines in (0–0) band of the $B^2\Sigma_u^+ \rightarrow X^2\Sigma_g^+$ system of N_2^+. An accuracy of about 10% was achieved. The radial distribution of the rotation temperature in the jet was determined and compared with that of the electron temperature; it was shown that within the limits of experimental error, local thermodynamic equilibrium was established. (auth) (France)

30481 DETERMINATION OF POPULATION DENSITIES IN A HELIUM PLASMA BY ELECTRON IMPACT SPECTROSCOPY. Boersch, H.; Geiger, J.; Topschowsky, M. (Technische Univ., Berlin). Z. Naturforsch.; 26a: 198-203(Feb 1971). (In German).

The energy spectrum of a narrow electron beam (primary energy 25 keV, energy width 0.08 eV) was measured after having passed a low-voltage helium discharge constricted by a metal capillary. Besides the resonance series that is characteristic for helium atoms in the ground state, electron-energy losses are found due to transitions from excited states. In addition, superelastic collisions occur that are caused by de-excitation processes. Population densities of the atoms in excited states are derived from the intensities in the electron-energy spectrum using the well-known transition probabilities. The result is compared with population densities obtained by means of Saha's equation as well as with those quoted by Drawin. Large discrepancies are found in both cases. (auth)

30482 SPHERICAL PROBE IN A FLOWING PLASMA. Andrews, J. G.; Swift-Hook, D. T. (Central Electricity Generating Board, Southampton, Eng.). J. Phys., A (London); 4: 142-57(Jan 1971).

Ion flow is important in many laboratory discharges, vacuum switches, gas-filled valves, thyratrons, and space satellites. A model is presented for subsonic ion flow past a negative spherical probe immersed in a collisionless ionization-free plasma; a stagnation point develops downstream. Although the floating potential given by previous analyses (which all assume spherical symmetry) is substantially correct, there is some dependence on the ion flow velocity (a few % at M = 0.5). Thus, the change in floating potential can be used to measure ion flow. In general, only slight modification needs to be made to low-pressure probe theories in order to include flow effects. (auth) (UK)

30483 MICROWAVE DIAGNOSTICS OF CONTRACTING RARE-GAS COLUMNS. II. ELECTRON DENSITY PROFILE. Reimann, H.; Heymann, P. (Zentralinstitut fuer Elektronenphysik, Berlin). Beitr. Plasmaphys.; 10: 417-25(1970). (In German).

From the damping of a cylindrical cavity resonator, oscillating at λ ≅ 3.2 cm in the H_{011} mode, constriction of the electron density profile is assessed during the contraction of a noble-gas discharge at medium pressure. A channel model yields equivalent radii of the electron density distribution. Especially at higher values of pR in argon strong constriction is observed, approximately in the same degree as that occurring with intensity of light. (tr-auth)

30484 INTERFEROMETRIC MEASUREMENTS OF TIME-DEPENDENT ELECTRON DENSITY IN THE XENON PINCHED PLASMA LASER. Papayoanou, A.; Gumeiner, I. (Army Electronics Command, Fort Monmouth, N. J.). J. Appl. Phys.; 42: 1914-16(Apr 1971).

Spectroscopic measurements have indicated that laser lines obtained with a xenon "pinch" laser arise from transitions in triply ionized species. Measurements of the time-dependent electron density and of the plasma dynamics indicate that this is indeed the case. (auth)

30485 INVESTIGATION OF PARTICLE STREAMING OUT OF PLASMA. Schmidt, M.; Hinzpeter, G. (Zentralinstitut fuer Elektronenphysik, Greifswald, Ger.). Beitr. Plasmaphys.; 10: 183-98(1970). (In German).

Application of the corpuscular diagnostic method to investigation of particle streaming out of plasma is reviewed. Studies of nonisothermal low-pressure plasmas are emphasized. (129 references.) (J.S.R.)

30486 MICROWAVE DIAGNOSTICS OF CONTRACTED RARE GAS COLUMNS. I. MEASUREMENT OF ELECTRON TEMPERATURE. Heymann, P. Beitr. Plasmaphys.; 9: 491-8(1969). (In German).

The electron temperatures of contracted argon columns were determined by measurement of the incoherent microwave radiation emitted by the plasma. The thermal noise was taken into consideration. The results obtained are compared with the theoretical studies of Wojaczek, and the deviations are discussed. (J.S.R.)

30487 HOLOGRAPHIC INTERFEROMETRY OF LASER-PRODUCED PLASMAS USING PICOSECOND PULSES. Belland, P.; De Michelis, C.; Mattioli, M. (CEN, Fontenay-aux-Roses, France). Opt. Commun.; 3: 7-8(Mar 1971).

Interferograms were obtained using a holographic system illuminated by picosecond pulses. The technique was applied to a picosecond laser-produced plasma, and the total number of electrons present in the plasma was measured to be at least 5×10^{14} for a laser energy of 0.1 joule. (auth)

30488 THERMAL PLASMA FROM A STANDARD INTENSITY SOURCE IN THE WAVELENGTH RANGE 1100 TO 3100 A. Boldt, G. (Max-Planck-Institut fuer Physik und Astrophysik, Munich). Space Sci. Rev.; 11: 728-72(Dec 1970). (In German).

A standard intensity source is described consisting of a thermal argon plasma with small additives of hydrogen, nitrogen, and carbon dioxide. These gases are introduced in such a concentration to produce a series of optically thick spectral lines in the region 1100 to 3100 Å. The intensity in an optically thick line center is

given by the Kirchhoff–Planck function $B_\lambda(T)$ that is determined if the plasma temperature is known. The continuous character of the function allows for interpolation between the spectral lines. At longer wavelengths above 1800 Å only two carbon I lines are found to be optically thick. Here the optically thin argon continuum is calibrated against the carbon I lines and is used as an additional standard emission. By this procedure an absolute intensity scale is constructed at every wavelength between 1100 and 3100 Å. The precision of the absolute intensities depends essentially on the precision of the temperature measurement for the plasma. Four different spectroscopic methods are used for this determination giving a temperature of 12,540 K with an error of ±1 to ±2%. This means an error of ±10 to ±20% for the absolute intensity scale. The internal consistency of the measurements is better than ±2%. A plasma with these properties is produced in a wall-stabilized cascade are burning through a central hole in a stack of refrigerated discs. By an adequate flow pattern of argon, hydrogen, nitrogen, and carbon dioxide an "argon window" is formed through which the radiation of the added gases leaves the arc axially without self-absorption. The arc is burning at a pressure of 1 atm, and a windowless light path to a vacuum spectrograph is formed by a 3 chamber differential pumping stage allowing continuous observation. As a result, the absolute intensities of the optically thick lines observed at high resolution are given. Moreover, the total energy flux of the light source is presented for a lower resolution. In the range 2500 to 3100 Å the absolute scale overlaps the useful range of the carbon arc that is used as an intensity standard in the visible and near ultraviolet. A comparison of the two sources yields a compatibility within the experimental errors of a few percent. (auth)

30489 DIAGNOSTICS FOR HOT-ELECTRON, MAGNETICALLY CONFINED PLASMAS. Lichtenberg, A. J.; Schwartz, M. J.; Lieberman, M. A. (Univ. of California, Berkeley). Plasma Phys.; 13: 89-112(Feb 1971).

Diagnostics were developed for measuring the temperature, density, velocity distribution, axial and radial profiles, and decay rate, of a hot-electron (T_e between 20 and 200 keV) plasma confined in a magnetic mirror field. The diagnostics include the measurement of: (1) the magnitude, spectrum, and spatial distribution of the synchrotron radiation for determining the hot-electron line density, speed distribution, and density profile and angular velocity distribution, respectively; (2) the relative x-ray pulse heights for determining the speed distribution; (3) the relative spatial distribution of visible light for determining the density profile; and (4) microwave cavity frequency shifts for determining the electron number. Comparisons among these diagnostics are made. It is shown that measurements of temperature, density, and axial profile can be considerably in error if the experimental results are compared with Maxwellian velocity distributions, rather than self-consistent, mirror distributions. Theoretical curves of x-ray pulse height distributions and absolute synchrotron radiation spectra are given for self-consistent velocity distributions applicable to a wide range of hot-electron plasmas. (auth) (UK)

30490 SCATTERING FROM MAGNETIC FLUCTUATIONS. Thompson, William B. (Univ. of California, San Diego, La Jolla). J. Plasma Phys.; 5: 225-8(Mar 1971).

Scattering of optical and radio-frequency radiation from electron density fluctuations in a plasma was extensively studied and bids fair to become a useful diagnostic tool. The scattered spectrum, although difficult to observe, contains a great deal of information. The electron density, ion and electron temperatures, the shape of the tail of the electron distribution function, spectral fluctuations in unstable systems, the magnitude and direction of the magnetic field, and the charge to mass ratio of the ions present all seem to be contained in it. Recent observations of Faraday rotation in the optical region imply that fluctuations in the magnetic field strength and direction should give rise to a further scattering which might prove useful in the study of high-β turbulent plasmas. The magnetic effect depends on the ratio Ω/ω where Ω is the gyrofrequency and ω the frequency of the incident radiation, hence is usually rather small; but it is shown to depend also on a factor nl_B^3, where l_B represents a correlation length for magnetic fluctuation, and this need not be small. (auth) (UK)

30491 ANALYTICAL AND EXPERIMENTAL STUDY ON LANDAU DAMPING OF SURFACE WAVE ALONG A PLASMA COLUMN. Ida, Yoshio; Hayashi, Kenichi (Kanazawa Univ., Japan). J. Appl. Phys.; 42: 2423-30(May 1971).

A resonator method is used to demonstrate Landau damping of surface waves along a plasma column. As a method of plasma diagnostics, an open plasma resonator utilizing longitudinal resonance of the surface wave was proposed. This work presents an analysis of anomalous damping in terms of the Q factor observed in the open plasma resonator. In the analysis, the effect of energy absorption by the thermal electrons travelling across the side boundaries of the resonator is accounted for. A method of single-mode excitation that is convenient for experimental determination of the Q factor is also described. The results of Q measurements are compared with the computer solutions; the Landau-damping mechanism responsible for the anomalous damping in the Q factor is examined. (auth)

30492 SPECTROSCOPIC MEASUREMENT OF HIGH TEMPERATURES: A REVIEW. Drawin, H.-W. (CEN, Fontenay-aux-Roses, France). High Temp. - High Pressures; 2: 359-409(1970).

Spectroscopic methods for determining high temperatures are reviewed with particular reference to the temperature measurement of the ionized gases (plasmas) in the state of local thermodynamic equilibrium (LTE plasmas). The general properties of ionized gases are first outlined, and the fundamental thermodynamic laws that can be used as a basis for temperature measurement are given. The conditions for LTE are thoroughly discussed, and the relaxation processes (spatial and temporal) that play an important role in the establishment of LTE are treated in great detail, with reference to numerous recent publications. Molecular, atomic, and ionic states are considered. Finally, the basic relationships for temperature determination are given for methods based on (a) measurement of absolute and relative molecular, atomic, and ionic spectral line intensities; (b) evaluation of intensities originating from continua; (c) line profile measurements; and (d) use of Thompson and Rayleigh scattering. A few of the described methods are also applicable to non-LTE plasmas. (auth) (UK)

30493 OPTICAL MEASUREMENT OF THE VELOCITY DISTRIBUTION OF THE PROTONS IN A HOT PLASMA BEAM. Hess, W. R. (CEN, Grenoble, France). Phys. Lett.; 34A: 367-8(19 Apr 1971).

Charge exchange with excitation from energetic ions reacting with the residual neutral gas was used to measure the velocity distribution of the protons of a hot plasma source. (auth)

30494 METHOD OF DETERMINING THE PLASMA DENSITY BY A CYLINDRICAL PROBE AT MEDIUM PRESSURES. Dote, Toshihiko (Inst. of Physical and Chemical Research, Yamato, Japan). Rikagaku Kenkyusho Hokoku; 46: 122-30(Sep 1970). (In Japanese).

An approximate theory for a cylindrical probe when the mean free path of plasma particles is much smaller than the dimension is discussed. A practical method of determining the plasma density using the theory is also presented. The validity of the theory is checked by comparison with the results obtained by the microwave method. The application of the present method to the measurement for He–Ne laser plasmas in which the gas pressure is higher and the dimension is much smaller is described. (auth) (Japan)

Kinetics (General)

Refer also to abstract 30268.

30495 (EUR-4593, pp 251-6) INVESTIGATION OF THE EROSION PHENOMENON IN HIGH-CURRENT, HIGH-PRESSURE GAS DISCHARGES. Gruber, J. E.; Suess, R. (Institut fuer Plasmaphysik, G.m.b.H., Garching (West Germany)).

From Sixth symposium on fusion technology; Aachen, Germany (22 Sep 1970).

In Proceedings of the 6th symposium on fusion technology.

The erosion measured as the loss of electrode material was determined in different spark gaps with plane parallel electrodes. In the range from 50 to 300 kA and a corresponding total current conduction between 1 and 50 Coulomb per discharge, the erosion in a 1.5-mm gap was found to be nearly two orders of magnitude higher than in a 13-mm gap at atmospheric pressure. The close electrode spacing was found to be responsible for the increased erosion rather than the gas pressure. Erosion values for an oscillatory current are given for aluminum, brass, stainless steel, molybdenum, tungsten, and tungsten–copper alloy. (auth)

30496 (EUR-4593, pp 461-70) INFLUENCE OF WALL MATERIAL ON PLASMA–WALL INTERACTION. Behrisch, R.; Heiland, W. (Institut fuer Plasmaphysik, G.m.b.H., Garching (West Germany).

From Sixth symposium on fusion technology; Aachen, Germany (22 Sep 1970).

In Proceedings of the 6th symposium on fusion technology.

The neutral gas density in the space between the boundary of a

magnetically confined plasma and the first vacuum wall depends on the plasma parameters and the wall material. Idealized assumptions are made to obtain a differential equation for the time development of the neutral gas pressure. On reaching the plasma boundary, the neutral gas is ionized and thereby increases the plasma density or causes contamination of the plasma. Part of the neutral gas is ionized by charge exchange, thus producing fast neutral atoms that impinge on the wall, where various processes are initiated: direct backscattering, collection in the wall material (possibly with bubble formation), desorption, sputtering, and radiation damage. The time development of the neutral gas pressure is mainly governed by the direct backscattering, collection in the wall material, and desorption. The wall material and pretreatment and temperature thereof thus have a major influence on the plasma. For a fusion reactor the first wall material should therefore be such that both helium and hydrogen readily diffuse at the wall temperature expected. (auth)

30497 (EUR–4593, pp 471-7) ON THE INTERACTION OF SPUTTERED WALL MATERIAL WITH FUSION PLASMA. Haas, G. (Institut fuer Plasmaphysik, G.m.b.H., Garching (West Germany)).

From Sixth symposium on fusion technology; Aachen, Germany (22 Sep 1970).

In Proceedings of the 6th symposium on fusion technology.

Most types of fusion reactors have a space with very low density to provide thermal insulation between the hot fusion plasma and the wall. Provided that this vacuum is not produced by itself when the reactor starts up and persists during the entire pulse length, it should be maintained by means of a divertor. Sputtering is induced on the wall by fast neutrals resulting from charge exchange between the residual gas and the plasma. The maximum neutral gas density in this external space before sputtering causes excessive contamination of the plasma was investigated. It was found that a density of up to about 10^{10} cm^{-3} is acceptable. This density, however, cannot be achieved with reasonable technical effort. Therefore, it is proposed that a higher density be allowed and that the gas be as fully ionized as possible. For this purpose it should be sufficient to heat the plasma already formed in the space as a result of photoionization, e.g., electron bombardment or radiofrequencies. (auth)

30498 (N–70-41880) LASER-GENERATED PLASMA AS A SPECTROSCOPIC LIGHT SOURCE. Valero, Francisco P. J.; Goorvitch, David; Ragent, Boris; Fraenkel, Benjamin S. (National Aeronautics and Space Administration, Moffett Field, Calif. Ames Research Center). Oct 1970. 18p. (NASA-TN-D–6048; A–3371). NTIS.

The spectra emitted by laser-generated plasmas were studied in the spectral region from about 40 to 4000 A. The radiating regions of the plasma were spatially resolved using either a stigmatic normal-incidence spectrograph or an astigmatic grazing-incidence spectrograph and crossed-slit apparatus, depending upon the wavelength region. Both emission and absorption spectra were observed for highly ionized atoms. Both line shifts and strong asymmetries were observed. The continuum spectra radiated by the core of the plasma were used to perform absorption experiments in the soft x-ray region. Features of the laser-generated plasma light source that aid in the interpretation of spectra are discussed. The laser-produced plasmas have several unique characteristics that prove to be desirable and convenient for spectroscopic work. (auth) (STAR)

30499 (UUIP–659) STUDIES OF PLASMA DRIFT IN A FXR DISCHARGE. Berg, J. M.; Haendel, S. K. (Uppsala Univ. (Sweden). Inst. of Physics). 1971. 11p. Dep. NTIS (U. S. Sales Only).

Plasma drift in a flash x-ray (FXR) discharge was studied by means of symmetrically placed magnetic probes. The results indicate major changes in position of the discharge column in connection with the pinches. (auth) (Sweden)

30500 ELECTRON BEAMS FOR QUASI-LINEAR AND NON-LINEAR BEAM–PLASMA EXPERIMENTS. Roberson, C.; Gentle, K. W. (Univ. of Texas, Austin). Appl. Phys. Lett.; 18: 115-16(15 Feb 1971).

Electron beams suitable for experimental studies of the nonlinear evolution of the beam–plasma interaction in the quasilinear limit (gentle bump) and in transition to the delta function beam may be obtained by placing a magnetic shield around a simple electron gun. Measurements of the beam energy distribution are presented. (auth)

30501 ELECTROSTATIC BREMSSTRAHLUNG. Melrose, D. B. (Australian National Univ., Canberra). Astrophys. Space Sci.; 10: 197-202(Feb 1971).

Inverse Compton radiation due to scattering of electron plasma waves, called "electrostatic bremsstrahlung" by Colgate (1967), is discussed with the view of resolving a discrepancy that exists between various authors on the mean frequency radiated. (auth)

30502 CLASSICAL DERIVATION OF INVERSE COMPTON RADIATION. Melrose, D. B. (Australian National Univ., Canberra). Astrophys. Space Sci.; 10: 186-96(Feb 1971).

A classical method is used to derive formulas describing inverse Compton radiation in vacuo. It is shown that several expressions, including the power radiated and the rate at which photons are scattered, can be calculated exactly for the case of isotropically distributed unpolarized waves scattered by particles with any energy. (auth)

30503 THRUST FROM ARCJETS WITH SELF-INDUCED MAGNETIC FIELDS. Hassan, H. A. (North Carolina Univ., Raleigh). AIAA (Amer. Inst. Aeronaut. Astronaut.) J.; 9: 578-81(Apr 1971).

Using the quasi one-dimensional magnetohydrodynamic equations, a new formula for the thrust from arcjets with self-induced magnetic fields is derived. The theory takes into consideration the nonlinear interactions between the current and flow field, and thus the resulting thrust formula is not the sum of the various components. If the plasma behaves like a perfect gas, then closed-form expressions for the various performance parameters can be derived. It is shown that the exhaust velocity increases with a decreasing mass flow rate. Moreover, the square of the exhaust velocity, for given arc conditions, is approximately a linear function of the square of the current. The results of the theory are employed to suggest methods for predicting electrode erosion and/or entrainment. (auth)

30504 SLOWING DOWN OF AN INTENSE ELECTRON BEAM IN A DENSE PLASMA. Zakatov, L. P.; Plakhov, A. G. Zh. Eksp. Teor. Fiz.; 60: 588-93(Feb 1971). (In Russian).

Slowing down of an intense monoenergetic electron beam in a dense plasma is investigated under conditions when $\omega_p \gg \omega_H$. The longitudinal and total beam-energy losses are measured experimentally. The mean beam energy on exit from the plasma decreases with growth of beam density. Distribution functions in the beam depending on its initial density are obtained. With increase of beam density a continual transition from a plateau on the distribution function to a distribution with a negative slope ($\partial f/\partial v_z < 0$) is observed. It is assumed that, during the slow stage of relaxation, oscillations are excited that are inclined with respect to the magnetic field. These oscillations are the cause of transformation of longitudinal energy into transverse and of the related rise of the plateau occurring at small energies. (auth)

Kinetics (Experimental)

Refer also to abstracts 29245 and 30255.

30505 (MATT-Trans–83) ELECTRON-ION BEAM INSTABILITY. Nezlin, M. V.; Taktakishvili, M. I.; Trubnikov, A. S. (Gosudarstvennyi Komitet po Ispol'zovaniyu Atomnoi Energii SSSR, Moscow. Institut Atomnoi Energii). Translated for Princeton Univ., N. J. from report IAE–1516. 34p. Dep. NTIS.

An experimental study was made of axially symmetrical electron–ion oscillations of a quasi-neutral electron beam in a longitudinal magnetic field. It was demonstrated that the dispersion properties of the oscillations, their spatial structure and excitation conditions correspond well to the theory of "ordinary" beam electron–ion instability. Excitation of the oscillations is accompanied by ion acceleration to significant energies comparable to the beam electron energies. In contrast to the electron–ion oscillations without axial symmetry and excited as a result of drift-beam instability, the investigated oscillations do not lead to restriction (cutoff) of the beam current. (auth)

30506 (MATT-Trans–84) DRIFT-BEAM INSTABILITY AND ION SOUND IN AN INHOMOGENEOUS PLASMA. Nezlin, M. V.; Taktakishvili, M. I.; Trubnikov, A. S. (Gosudarstvennyi Komitet po Ispol'zovaniyu Atomnoi Energii SSSR, Moscow. Institut Atomnoi Energii). Translated for Princeton Univ., N. J. from report IAE–1515. 36p. Dep. NTIS.

Electron–ion (ion-sound) oscillations without axial symmetry were detected in an electron beam passing through a rarefied gas. It was shown that their spatial structure, dispersion properties, and excitation conditions correspond to the drift beam (ion-sound) instability of an inhomogeneous plasma. (auth)

30507 (NP–18775) SKIN EFFECT IN HIGH-ENERGY Z-DISCHARGES. Dubovoi, L. V.; Fedyakov, V. P.; Fedyakova, V. P. (Scientific Research Inst. of Electro-Physical Apparatus,

Leningrad (USSR)). 1970. 17p. (In Russian). Dep. NTIS (U. S. Sales Only).

Results of experiments with pulsed z discharges, characterized by anomalous plasma conductivity in a skin-layer region are analyzed. It is shown that features of powerful direct discharges, particularly in a case of fast z pinches, are in agreement with the hypothesis of probable excitation of ion-acoustic microinstabilities in current layers of the discharges. (auth)

30508 (NP-18801) EXPERIMENTAL INSTALLATION R-OHM FOR STUDYING HIGH-FREQUENCY FIELD-INTERACTIONS WITH PLASMA. Demirkhanov, R. A.; Kirov, A. G.; Maikurov, V. B.; Rakhel'kin, A. Z.; Savchenko, I. S.; Stotland, M. A. (Gosudarstvennyi Komitet po Ispol'zovaniyu Atomnoi Energii SSSR, Sukhumi. Fiziko-Tekhnicheskii Institut). 1969. 86p. (In Russian). Dep. NTIS (U. S. Sales Only).

Physical concepts introduced into the development and design of the R-Ohm and its construction are described. Calculations of the quasi-constant and high-frequency magnetic fields, the high-frequency system, and parameters of the installations are given in detail. (tr-auth)

30509 INVESTIGATION OF PLASMAS AT VERY HIGH PRESSURE. Soehngen, Erich E.; Bauder, Uwe (Aerospace Research Labs., Wright-Patterson AFB, Ohio). pp 276-80 of Proceedings of the Institute of Environmental Sciences 15th Annual Technical Meeting and Equipment Exposition, April 20-24, 1969, Anaheim, California. Mt. Prospect, Ill.; Inst. of Environmental Sciences (1969).

From fifteenth annual technical meeting and equipment exposition; Anaheim, Calif. (20 Apr 1969). See CONF-690454.

The investigations of plasmas at pressures up to 1000 atm and temperatures in the 10,000°K range are useful for a number of Air Force applications, such as arc heaters, re-entry simulation devices, and high-intensity radiation sources. Of particular interest is the strong increase of the radiation source strength with rising pressure at constant temperature. The Aerospace Research Laboratories of the Air Force have built and tested a medium pressure arc facility for pressures up to 200 atm; a 1000-atm test facility is presently under construction. Wall-stabilized and free-burning arcs have been operated in argon at pressures up to 130 atm and currents up to 200 amps. Measurements of the arc characteristic and the radiation show a strong increase of the electric field strength and the total radiation with increasing pressure. These integral arc data, together with measured temperature distribution across the arc diameter are being used for the determination of the temperature- and pressure-dependent transport properties of the arc gas. (auth)

30510 EXPERIMENTS ON THE RELATION BETWEEN RADIATION AND FLUCTUATION SPECTRUM OF A TURBULENT PLASMA. Bollinger, L. D.; Boehmer, H. (Univ. of Illinois, Urbana). Phys. Rev. Lett.; 26: 535-41(8 Mar 1971).

The experimentally observed radiation from unstable plasma waves generated by the interaction of an electron beam with a plasma is compared with the longitudinal fluctuation spectrum, determined by incoherent microwave scattering. The results are in agreement with a theory by Ichimaru and Starr for the electromagnetic radiation from anisotropic turbulent plasmas. (auth)

30511 EXPERIMENTAL INVESTIGATION OF EFFICIENT SLOWING DOWN OF AN ION BEAM IN A PLASMA DURING ION-ACOUSTIC INSTABILITY. Borisenko, A. G.; Kirichenko, G. S. (Inst. of Nuclear Research, Kiev). Zh. Eksp. Teor. Fiz.; 60: 384-8(Jan 1971). (In Russian).

The interaction between an ion beam and plasma is studied experimentally under conditions when the beam excites ion acoustic instability. It is shown that, when the beam velocities are comparable with the velocity of nonisothermal ion sound, the interaction leads to establishment of an ion-velocity distribution function with a plateau, i.e., to efficient transfer of the ion-beam energy to the plasma. (auth)

30512 EXPERIMENTAL INVESTIGATION OF DESTRUCTION OF METASTABLE HELIUM ATOMS IN A PLASMA AT LOW TEMPERATURES. Fugol, I. Ya.; Grigorashchenko, O. N.; Myshkis, D. A. (Physical-Technical Inst. of Low Temperatures, Kharkov). Zh. Eksp. Teor. Fiz.; 60: 423-40(Jan 1971). (In Russian).

The kinetics of volume destruction of metastable 2^3S He atoms at initial high concentrations (10^{13} to 10^{14} cm^{-3}) is studied experimentally at temperatures between 6 and 300°K and pressures between 3 and 80 mm Hg. The constant $A_2 = 0.35\ cm^3 \cdot sec^{-1} \cdot (mm\ Hg)^{-2}$ for metastable atom destruction in collisions with two normal atoms is measured at room temperature. The constant k for metastable atom collisions is measured at low temperatures, and it is found that $k \sim T^{\frac{1}{2}}$. Conditions for which superelastic collisions with slow electrons are predominant in destruction of the 2^3S He state are elucidated. The constant for this process is calculated, $k_e = 4.5 \cdot 10^{-9}\ cm^3 \cdot sec^{-1}$. From a study of the kinetics, the rate of impact-radiative recombination and the plasma electron temperature could be determined. The major mechanisms of electron heating in a plasma at low temperatures are discussed. (auth)

Kinetics (Theoretical)

Refer also to abstract 30625.

30513 (IPP-1/113) VLASOV DESCRIPTION OF A SUPERCRITICAL MAGNETO-ACOUSTIC COMPRESSION PULSE. Chodura, R.; von Finckenstein, Graf Finck (Institut fuer Plasmaphysik, G.m.b.H., Garching (West Germany)). Dec 1970. 45p. (IPP-6/92). Dep. NTIS (U. S. Sales Only).

The time evolution of a compression pulse driven by a fast-rising magnetic field and propagating perpendicularly to a homogeneous biased magnetic field is investigated numerically. The compression parameters are chosen such that overturning occurs in the pulse (supercritical pulse). The fluid description of the ions then breaks down and is replaced by a Vlasov description. The ion distribution develops a two-stream structure giving rise to a strong broadening of the spatial density profile of the pulse, the occurrence of an upstream "foot" in the magnetic-field profile, and strong heating of the ions. (auth)

30514 (JAERI-Memo-4243) CALCULATION OF THE FLUX OF FAST NEUTRAL PARTICLES FROM A CYLINDRICAL, HIGH-TEMPERATURE PLASMA. Yano, Suykuro (Japan Atomic Energy Research Inst., Tokyo). Dec 1970. 40p. Dep. NTIS (U. S. Sales Only).

Using particle conservation equations for fast hydrogen atoms, slow hydrogen molecules, and charged particles, the fast atomic hydrogen flux produced by charge exchange in a high-temperature plasma was numerically calculated for the average plasma temperatures of 10, 100, and 1000 eV and the neutral gas pressures of 10^{-4} to 10^{-10} torr, assuming the plasma energy does not depend on position. Density of slow hydrogen molecules was assumed to be determined by the pressure of the filling gas for discharge and also by the desorbed gas from the wall by fast-particle impact. The calculated value of atomic hydrogen flux varies over a wide range of 10^4 to 10^{18} atoms $cm^{-2}\ s^{-1}$, depending on the density and energy of the plasma and on the conditions of the wall. The particle loss rate due to charge exchange is considerably large for a low-density plasma with fairly high residual gas pressure, but decreases to quite low values when the plasma density is high. (auth) (Japan)

30515 (N-70-41892) GYROSYNCHROTRON RADIATION AND ITS TRANSFER IN A MAGNETOACTIVE PLASMA. Sakurai, Kunitomo (National Aeronautics and Space Administration, Greenbelt, Md. Goddard Space Flight Center). Sep 1970. 38p. (NASA-TM-X-65352; X-693-70-340). NTIS.

Gyrosynchrotron radiation fields from mildly relativistic electrons in a magnetoactive plasma are asymptotically calculated using the Green tensor and the Fourier transformation. These fields consist of the two components that correspond to the ordinary and extraordinary modes. Taking into account these fields, the emissivities and the absorption coefficients from an arbitrary distribution of electrons are calculated. The transfer of electromagnetic energy takes place along a direction different from that of the wave normal since the radiation fields have a nonvanishing component along the direction of the wave normal. Consideration is given to the problem of radiative transfer in relation to the Stokes parameters. (auth) (STAR)

30516 (N-70-42698) EXPERIMENTAL INVESTIGATION OF SINGLE-PARTICLE BEHAVIOR IN AN AXISYMMETRIC MAGNETIC FIELD. Schertler, Ronald J. (National Aeronautics and Space Administration, Cleveland, Ohio. Lewis Research Center). Oct 1970. 26p. (NASA-TN-D-6047; E-5737). NTIS.

Nonrelativistic particle behavior for single interactions with an axisymmetric mirror magnetic field was experimentally investigated. Measurements were made to determine the fraction of an injected electron beam transmitted through the mirror region as a function of injection angle for a variety of operating conditions. Measurements were carried out for a range of the adiabatic parameter between 0.027 and 0.22. Over this range results showed that, within the experimental error of this investigation, particle behavior remained adiabatic. (auth) (STAR)

30517 (N-71-11428) RESEARCH IN THE THEORY OF MAGNETOHYDRODYNAMIC TURBULENCE. Final Report. Sandri,

Guido (Aeronautical Research Associates of Princeton, Inc., N. J.). Aug 1970. Contract NASw-1778. 88p. (NASA-CR-111804). NTIS.

Research was conducted aimed at understanding the behavior of a plasma when it is unstable and therefore potentially turbulent, but in which collisional effects cannot be neglected. The investigation was prompted by a previous study in which it was shown that the classical kinetic theory, based on adiabatic assumption, fails to give a proper asymptotic characterization of the two-particle correlation function on time scales of the order of the relaxation time of the system. The results of this research demonstrate that the inclusion of three-body collisions damps the peak value of the two-particle correlation, which in leading order, has the form of a wave traveling in the direction of the relative velocity of the particle pair. In addition, it was possible to obtain the kinetic equation to higher order and prove explicitly the H-theorem for the velocity distribution function, including three-body effects. (STAR)

30518 (N-71-11853) PARTICLE FLUX ASSOCIATED WITH STOCHASTIC PROCESSES. Newman, C. E.; Sturrock, P. A.; Tademaru, E. (Stanford Univ., Calif. Inst. for Plasma Research). Aug 1970. Contract F44620-69-C-0008. 9p. (NASA-CR-111402; SU-IPR-386). NTIS.

The Lagrange expansion, which may be used to derive the Fokker–Planck equation, is used to derive the corresponding expression for the flux of particles subject to a stochastic scattering process. The coefficients that occur in this expression are, in general, not the same as the coefficients that occur in the Fokker–Planck equation itself. In the special case that the particle distribution involves only one independent variable, the particle flux is determined by the familiar Fokker–Planck coefficients. Evaluation of particle flux is of special interest in the study of stochastic acceleration. (auth) (STAR)

30519 FORMATION OF A NONEQUILIBRIUM POPULATION IN PLASMA UNDER IONIZATION RESONANCE CONDITIONS. Gudzenko, L. I.; Yakovlenko, S. I. (Inst. of Physics, Moscow). Zh. Eksp. Teor. Fiz.; 59: 1863-71(Nov 1970). (In Russian).

During intense recombination in a dense plasma of complex chemical composition, the resonance reaction of excitation transfer from low-lying levels of one element to high-lying levels of another and also ionization occurring during excitation transfer lead to a significant alteration in the nature of the nonequilibrium population of the levels of the first element. (auth)

30520 NONRESONANT DIFFUSION OF PARTICLES IN STOCHASTIC FIELDS. Biskamp, D. (European Space Research Inst., Frascati, Italy); Pfirsch, D. Z. Naturforsch.; 26a: 181-5(Feb 1971).

A Fokker–Planck equation for the nonresonant scattering of particles by general weakly turbulent electromagnetic fields is derived using a simple quantum-mechanical method. The equation is compared with the corresponding weak-turbulence equation as given in Kadomtsev's book and two applications are discussed. (auth)

30521 ON SETTING UP A THERMODYNAMICALLY COMPLETE EQUATION OF STATE OF AN IMPERFECT PLASMA ON BASIS OF DYNAMIC EXPERIMENTS. Fortov, V. E.; Krasnikov, Yu. G. (Inst. of Physics and Tech., Moscow). Zh. Eksp. Teor. Fiz.; 59: 1645-56(Nov 1970). (In Russian).

A method is considered for writing a thermodynamically complete equation of state of optically dense media (plasma) from experimental results on shock waves. The equation of state is written as E = E (P, V) on the basis of conservation laws in the shock wave front and from results of measurement of shock-compression parameters. This relation is employed for measuring the temperature T = T (P, V) by integration of the differential equation expressing the second law of thermodynamics. The accuracy is estimated by statistical tests with an electron digital computer. The method is verified in the problem of determining the equation of state of a dense cesium plasma whose thermodynamics is described by the Debye theory in the large canonical ensemble. (auth)

30522 LEGENDRE POLYNOMIAL DEVELOPMENT AND GENERAL SPHERICAL SURFACE FUNCTION DEVELOPMENT IN THE BOLTZMANN EQUATION FOR LORENTZ PLASMAS. Winkler, R.; Wilhelm, J.; Schueller, V. (Zentralinstitut fuer Elektronenphysik, Greifswald, Ger.). Beitr. Plasmaphys.: 10: 51-77(1970). (In German).

The correct conversion of the electron Boltzmann equation for Lorentz plasma under bombardment by elastic and inelastic binary collisions (first and second type) with heavy particles is undertaken by application of the Legendre polynomial development for the velocity distribution function of the electron in a partial differential equation system equivalent to the Boltzmann integro-differential equation (hierarchy) for the development of coefficients of electron distributions. The limiting conditions for the applicability of the Legendre polynomial development is discussed, and the tensor moments of the distribution function are calculated in the framework of this development up to any order. The relation of the special development by Legendre polynomials to the general spherical surface function development is investigated, and the Legendre polynomial development is converted into a tensor representation, classified as a special case in the general tensor treatment of the Boltzmann equation with a tensor representation of the spherical surface function development. The tensor Legendre polynomial development and the calculated tensor macroscopic moments can clearly distinguish the special symmetry properties present in this special case in the Lorentz plasma. (tr-auth)

30523 KINETIC THEORY OF FULLY IONIZED PLASMAS. II. KINETIC EQUATIONS. Diener, Gerhard (Technische Univ., Dresden). Beitr. Plasmaphys.; 9: 451-65(1969). (In German).

In order to obtain a kinetic theory for the unstable and weakly inhomogeneous plasma, an expansion of the Bogolyubov laws, which consider plasma oscillations, was proposed in Part I. In accord with this expanded law, the correlation functions are determined as functionals of the single-particle distribution F and the amplitude of the plasma oscillations I. Kinetic equations are obtained for F and I. (tr-auth)

30524 DETERMINATION OF THE RADIAL DISTRIBUTION OF EMISSION AND ABSORPTION COEFFICIENTS AS WELL AS THE TEMPERATURE IN ROTATIONAL-SYMMETRIC PLASMA. Riemann, M. Beitr. Plasmaphys.; 10: 103-13(1970). (In German).

Equations are derived for the determination of the radial distribution of emission and absorption coefficients and the temperature in absorbing rotational-symmetric plasma. Methods for the solution of the equations are discussed. (J.S.R.)

30525 OBSERVATIONS ON THE INFLUENCE OF STEP IONIZATION ON THE DISTRIBUTION FUNCTION AS WELL AS TRANSPORT AND BALANCE VALUES OF ELECTRONS IN NEON LOW-PRESSURE PLASMA AT LOW DEGREES OF IONIZATION. Wilhelm, J.; Winkler, R.; Freitag, H. (Deutsche Akademie der Wissenschaften, Berlin. Zentralinstitut fuer Elektronenphysik, Greifswald, Ger.). Beitr. Plasmaphys.; 10: 171-81(1970). (In German).

On the bases of measurements of the concentration of excited atoms in low-current low-pressure plasma and cross-section values for step ionization determined indirectly from the column theory, preliminary studies were made on the influence of step ionization on the distribution function of the electrons and, as a result of this effect, the influence on the transport and balance coefficients. The electron energy distribution function was calculated by means of the Boltzmann equation in the Lorentz approximation for two selected E/p_0 values and, on the basis of experiments, from the value of the concentration ratio of excited to unexcited neutral atoms. The distribution function obtained was compared with the distribution function obtained, neglecting step ionization. The average energy, mobility, and diffusion coefficients of the electrons are given, and the magnitude of the influence of step ionization on the direct excitation and direct ionization frequency is shown. Corrections are given that can amount, in the transport magnitudes, to 10% and, in the direct-excitation frequencies, up to 50% of the values obtained without consideration of step ionization. (tr-auth)

30526 KINETIC THEORY OF PLASMAS TAKING INTO ACCOUNT TRANSVERSE PLASMA WAVES. Diener, Gerhard (Technische Univ., Dresden). Beitr. Plasmaphys.; 9: 527-34(1969). (In German).

It is shown how a kinetic theory derived previously for particles with Coulomb interaction can be transferred to the treatment of systems consisting of particles and electromagnetic fields. (tr-auth)

30527 EFFECT OF GLASS WALL ON THE DETERMINATION OF PLASMA CONDUCTIVITY BY rf EXTERNAL PROBES. Maiti, J. N.; Basu, J. (Saha Inst. of Nuclear Physics, Calcutta). Jap. J. Appl. Phys.; 10: 533-4(Apr 1971).

A brief theoretical discussion of the problem is given. Percentage corrections for the glass wall were calculated for different parameters. (M.O.W.)

30528 STRUCTURE OF HYDROMAGNETIC SHOCK WAVES. Bickerton, R. J.; Lenamon, L.; Murphy, R. V. W. (United King-

dom Atomic Energy Authority, Abingdon, Eng.). J. Plasma Phys.; 5: 177-97(Mar 1971).

The structure of hydromagnetic shock waves of various types is discussed. The plasma is treated in the two-fluid approximation and collisional transport coefficients are used. This treatment should be valid in a collisional plasma subject to the usual caveat about the use of transport coefficients in situations where the density, temperature, etc., may change significantly over a mean free path. The approach may also have some validity for collisionless shocks if the dissipation mechanisms involve instabilities of sufficiently fine scale and high frequency that they can be described by effective transport coefficients. (auth) (UK)

30529 LONGITUDINAL OSCILLATIONS OF A RELATIVISTIC ELECTRON–ION PLASMA AT ZERO TEMPERATURE. Kosachev, V. V.; Trubnikov, B. A. Zh. Eksp. Teor. Fiz.; 60: 594-604(Feb 1971). (In Russian).

An explicit expression is obtained for the longitudinal dielectric constant $\epsilon(k,\omega)$ of a completely degenerate relativistic electron gas. Low-frequency ion-sound and high-frequency electron oscillations of the plasma are considered in detail. It is shown that relativism affects the plasma parameters but does not significantly alter the character of the oscillation spectrum. (auth)

30530 RESONANT INELASTIC EFFECTS IN A PLASMA LOCATED IN A STRONG FIELD. Podlubnyi, L. I. (Moscow Energy Inst.). Zh. Eksp. Teor. Fiz.; 60: 621-31(Feb 1971). (In Russian).

The rate of energy losses and other kinetic coefficients for a plasma in strong electric and magnetic fields are calculated in the Born approximation by taking into account inelastic collisions between electrons and neutral particles. It is shown that the dependence of the kinetic coefficients on external field strength is of a resonance nature. Resonance oscillations on the energy-losses rate and electrical conductivity are studied with aid of the correlation functions in a strong homogeneous field derived in the Appendix. (auth)

30531 THEORY AND NUMERICAL SOLUTIONS FOR SHEATH GROWTH IN A LOW-PRESSURE PLASMA. Jack, A. G. (Cambridge Univ., Eng.); Sander, K. F.; Varey, R. H. J. Plasma Phys.; 5: 211-24(Mar 1971).

The theory of the development of thick sheaths given in an earlier paper (Sander 1969) is applied to planar sheath growth in practical situations. The results are compared with those resulting from a purely numerical method and from certain approximate equations suggested by other workers in the field. It is concluded that, for practical application, sheath growth is adequately predicted by any of the methods, although calculation of derived quantities by means of the approximate equations needs care. The numerical results in normalised form are presented for certain applied voltage waveforms. (auth) (UK)

30532 HYDRODYNAMICS OF A MAGNETOACTIVE PLASMA IN THE QUASILINEAR APPROXIMATION. Logvinov, V. V.; Machabeli, G. Z. Zh. Eksp. Teor. Fiz.; 60: 579-87(Feb 1971). (In Russian).

Hydrodynamic equations for the first moments are derived from the kinetic equation for the slow distribution function of a magneto-active, spatially homogeneous plasma. The effect of the waves on the directed velocities and temperatures of the various plasma components are taken into account. The distribution functions are taken in a form that permits one to determine the effect of the waves on pressure anisotropy and the currents in a plane perpendicular to a stationary magnetic field H_0. The simplest cases of waves traveling along and across H_0 are considered. Expressions for electron drag and heating are obtained in the high-frequency limit. The role played by Cherenkov and cyclotron resonances in longitudinal propagation of waves is evident from the expressions. For transverse waves moving perpendicular to H_0, expressions are found for the nonlinear drift current excited by a wave perpendicular to the wave vector and magnetic field. Nonlinear effects appearing during propagation of Alfvén and magneto-acoustic waves are briefly discussed in conclusion. (auth)

30533 SOME FEATURES OF THE FIELD OF AN ELECTROMAGNETIC WAVE IN A COLD ANISOTROPIC PLASMA WITH TWO-DIMENSIONAL INHOMOGENEITY. Piliya, A. D.; Fedorov, V. I. (Ioffe Inst. of Physics and Tech., Leningrad). Zh. Eksp. Teor. Fiz.; 60: 389-99(Jan 1971). (In Russian).

In connection with the problem of transformation of electromagnetic waves into plasma waves, the properties of a field in a cold anisotropic plasma with two-dimensional inhomogeneity are considered. It is shown that the peculiarities of the field are related to the singular points of the equation characteristics $\mathrm{div}\, D = 0$, $D_i = \epsilon_{ik} E$, $E = -\nabla\varphi$. The nature of the field singularity depends on the type of singular point of the characteristics (a saddle point leads to a line singularity and a node to a point singularity). (auth)

30534 QUASILINEAR RELAXATION OF AN ULTRARELATIVISTIC ELECTRON BEAM IN A PLASMA. Breizman, B. N.; Ryutov, D. D. (Inst. of Nuclear Physics, Novosibirsk, USSR). Zh. Eksp. Teor. Fiz.; 60: 408-22(Jan 1971). (In Russian).

The kinetic stage of quasi-linear relaxation of an ultrarelativistic electron beam is investigated for both a homogeneous and inhomogeneous plasma. It is shown that, in a homogeneous plasma, the beam liberates about half of its initial energy. Inhomogeneity of the plasma becomes important under the condition that $\mu\Lambda \equiv \Lambda(c/\omega_p L) \times (E/mc^2)(n/n') \gg 1$, where Λ is the Coulomb logarithm, L a characteristic inhomogeneity dimension, c the velocity of light, ω_p the electron plasma frequency, $E \gg mc^2$ the initial electron beam energy, n the plasma concentration and n′ the beam concentration. If the initial angular spread of the beam $\Delta\theta_0$ is large, i.e., $\Delta\theta_0 > (\mu\Lambda)^{-1}$, there will be no relaxation. However, if $\Lambda\theta_0 < (\mu\Lambda)^{-1}$, relaxation will occur, but the beam will liberate only a small part ($\sim(\mu\Lambda)^{-1}$) of its initial energy in the plasma. (auth)

30535 TRANSVERSE ELECTROMAGNETIC FIELD IN A PLASMA. Vezzetti, D. J. (Univ. of Illinois, Chicago). Physica; 52: 1-15(15 Mar 1971).

For a particular class of initial states, a closed equation for the distribution function of the transverse electromagnetic field in a plasma is derived. It is shown that the formal expression for the transverse conductivity of the plasma can be derived, in lowest-order approximation, without the use of external fields. (auth)

30536 VARIABLE STATES OF A HEAVY PLASMA IN RELATION TO TEMPERATURE AND DENSITY. Pritzker, Andreas; Haelg, Walter; Dressler, Kurt (Eidgenoessische Technische Hochschule, Zurich). Z. Angew. Math. Phys.; 22: 54-61(25 Jan 1971). (In German).

Assuming thermodynamic equilibrium, ion and electron densities of a uranium plasma were calculated in the temperature range between 0.5 keV and 50 keV for densities around 10^{23} ions/cm^3 using a simplified Saha equation. The ionization energies are found by extrapolation from known data or by a Slater approximation. The ratios of the partition functions of two successive stages of ionization are set equal to one. A depression of the ionization energies caused by electrostatic interactions is considered. The numerical results include the internal energy of the plasma as a function of temperature. (auth)

30537 EXACT GREEN FUNCTION FOR THE LENARD–BERNSTEIN OPERATOR IN THE PRESENCE OF A STATIC MAGNETIC FIELD. Furutani, Y. (Univ. Paris, Orsay, France). Phys. Lett.; 34A: 357-8(19 Apr 1971).

An exact Green function for the Lenard–Bernstein collision operator in the presence of an external static magnetic field is obtained. (auth)

30538 INTEGRAL EQUATION FOR THE TOTAL CHARGE DENSITY FOR A RELATIVISTIC PLASMA. Lupu, Gh. (Univ., Cluj). Lett. Nuovo Cim.; 1: 469-72(13 Mar 1971).

The Boltzmann–Vlasov equation for a relativistic plasma was used to derive the integral equation for the plasma charge density. The Van Kampen–Case method was used, and it was assumed that the positive ion is smeared out to form a uniform background. Collisions are omitted, and the electron distribution is considered to be but slightly perturbed from a spatially uniform but otherwise arbitrary distribution. (M.O.W.)

30539 PARTIAL PRESSURE OF PLASMA COMPONENTS. Rezikyan, A. M. Izv. Akad. Nauk Arm. SSR, Ser. Fiz.; 5: 294-6(1970). (In Russian).

It is shown that the total of the partial pressures of plasma components is independent of place, if the degree of ionization is limited. (auth)

30540 COLLISIONAL–RADIATIVE VOLUME RECOMBINATION AND IONIZATION COEFFICIENTS FOR QUASI-STATIONARY HELIUM PLASMAS. Drawin, H. W.; Emard, F. (Centre d'Etudes Nucleaires, Fontenay-aux-Roses, France). Z. Phys.; 243: 326-40(1971).

Collisional–radiative recombination and ionization coefficients, α and S, were calculated on the basis of a non-hydrogen-like collisional–radiative model for atomic helium. The singlet and triplet systems were considered as two individual systems cou-

pled to each other through a set of elementary processes for collisions and radiation. Auto-ionization states were not taken into account. Therefore, the computations of the coefficient α were limited to the range $125 \leqq T_e\ [°K] \leqq 64{,}000$. (Above T_e = 64,000°K the auto-ionizing states considerably influence the recombination rates (di-electronic recombination).) The results show that the α- and S-coefficients for helium are more sensitive to radiative trapping than those for hydrogen under comparable absorption conditions. Concerning the α-values: for low electron densities one obtains approximately $\alpha_{helium} \approx 2\ \alpha_{hydrogen}$, whereas at high electron densities one finds approximately $\alpha_{helium} \approx \frac{1}{2}\ \alpha_{hydrogen}$ (to $\frac{1}{10}\ \alpha_{hydrogen}$ at high electron temperatures). Collisional–radiative ionization coefficients for atomic helium have not yet been published in the past. In the present paper one finds for the first time a complete set of S-coefficients for different degrees of radiative trapping. (auth)

Production

Refer also to abstracts 30477, 30553, and 31137.

30541 (IPP–1/114) INVESTIGATIONS ON PREIONIZATION FOR TOROIDAL HIGH-BETA-EXPERIMENTS. Eberhagen, A. (Institut fuer Plasmaphysik, G.m.b.H., Garching (West Germany)). Dec 1970. 26p. Dep. NTIS (U. S. Sales Only).

Preionization is achieved in toroidal geometry by induced azimuthal currents. Favorable breakdown properties down to filling pressures of 3 mTorr D_2 and suitable preionization plasmas were established by application of an rf predischarge and superposition of small magnetic fields with only 10 kV potential difference around the 200-cm-long torus circumference. Detailed studies were performed on the effectiveness of the rf oscillations, e.g., as to their frequency and amplitude, and on the achievement of a stable and clean preionization plasma with only negligible amounts of plasma currents present. (auth)

30542 PLASMA EXPANSION UNDER HEATING BY A CO_2 LASER PULSE. Tomlinson, Richard G. (United Aircraft Research Labs., East Hartford, Conn). Appl. Phys. Lett.; 18: 149-52(15 Feb 1971).

A treatment is presented of the expansion of a gas breakdown plasma produced in argon by the focused radiation from a high-voltage transient-pumped CO_2 laser. With the long pulses attainable from such pulsed CO_2 lasers, a transition is observed in the mechanism of expansion from a radiation-driven detonation to a thermal expansion. The implications of this observation for CO_2 laser heating of plasmas are discussed. (auth)

30543 MODIFIED PIG-TYPE PLASMA SOURCE. Honzawa, Tadao; Aihara, Syuko; Kawai, Yoshinobu (Nagoya Univ., Japan). Kakuyugo Kenkyu: 26: 1-13(Jan 1971). (In Japanese).

An experimental study is described of a plasma source of the modified PIG-type. The source is operated in a magnetic field of moderate intensity, which changes the motion of the electron component. Noiseless plasmas can be obtained with the source under a suitable condition in spite of the operation in a magnetic field. In addition, it is noted that for these plasmas the ion temperature is several times higher than the electron temperature and somewhat controllable. (auth) (Japan)

Stability

Refer also to abstracts 30392, 30505, and 30506.

30544 (IAE–1950) HALL EFFECT IN PLASMA OSCILLATIONS. Igitkhanov, Yu. L.; Kadomtsev, B. B. (Institut Atomnoi Energii, Moscow (USSR)). 1970. 36p. (In Russian). Dep. NTIS (U. S. Sales Only).

Three papers are presented on the case of plasma oscillations where the Hall effect is essential. The first paper considers the arbitrary-amplitude electron oscillations of helical symmetry, neglecting the inertia effect in a conducting medium in a strong magnetic field. It is shown that ordinary helicons are the particular case in a broader set of solutions with frequencies independent of the amplitude. The second paper considers the stability of a low-density pinch when the parameter $\Pi_p = N\ (e^2/m_i c)$ is small compared to unity, and the drift velocity of the electrons exceeds the Alfven phase velocity. In the absence of longitudinal magnetic fields, the pinch proves to be stable, the instability arising as a result of a resonance between the slow helicon and Alfven wave. The finite-amplitude m = 0 mode oscillations in an electron–hole pinch are considered in the third paper. It is shown that the nonlinearity does not stabilize the "sausage" modes in intrinsic semiconductors. In extrinsic semiconductors, it appears that a stabilizing effect due to the plasma drift along the electric field exists. (auth)

30545 THEORY OF TEMPERATURE RELAXATION OF ELECTRON–ION PLASMA IN A HIGH-FREQUENCY ELECTRIC AND CONSTANT MAGNETIC FIELDS. Silin, V. P.; Tikhonchuk, V. T. Zh. Prikl. Mekh. Tekh. Fiz.; No. 6, 41-8(Nov-Dec 1970). (In Russian).

Effective frequency of electron and ion collisions resulting in stabilizing the temperature of plasma in constant magnetic and weak high-frequency electric fields was determined in the case in which hydroscopic radius of electrons was smaller than the Debye screening radius. The relaxation time was determined in a wide range of ratios between the electron and ion temperatures, a wide range of magnetic and electric field strengths, and a wide range of frequencies of the external magnetic field. (R.V.J.)

30546 INSTABILITY OF A FINITE AND HIGH-PRESSURE PLASMA WITH FINITE ELECTRON THERMAL CONDUCTIVITY. Mikhailovskii, A. B.; Tsypin, V. S. Zh. Eksp. Teor. Fiz.; 59: 1694-1701(Nov 1970). (In Russian).

It is shown that an inhomogeneous plasma with a finite ratio of its pressure to that of the magnetic field is unstable with respect to perturbations whose increment depends on the electron thermal conductivity. Such instabilities may develop even for $\nabla T_0 = 0$ (T_0 is the plasma temperature). They are due to density and magnetic-field gradients. A high-pressure almost forceless plasma is also found to be unstable if the pressure gradient is directed along the density gradient. The instabilities investigated may lead to large particle and heat losses in thermonuclear devices. (auth)

30547 STABILITY OF AN ACCELERATED PLASMA SHELL IN THE PRESENCE OF MAGNETIC FIELD. Narasimha Murthy, S. (Indian Inst. of Science, Bangalore, India). J. Indian Inst. Sci.; 52: 151-64(Oct 1970).

The stability of an accelerated cylindrical shell of conducting fluid, in the presence of a magnetic field having axial and azimuthal components, against small wave number axisymmetric disturbances is studied. In the exploding case, it is seen that the system is overstable and the frequency of unbounded oscillations depends on the thickness, the rate of explosion, and the initial magnetic field of the system. Further, one finds that the presence of a volume current distribution reduces the growth rate of instability. In the imploding case pure instability occurs, the growth rate of which increases logarithmically and does not depend on the initial magnetic field but depends on the thickness of the shell and on the rate of collapse. (auth)

30548 STABILITY CONDITION OF FLUTE INSTABILITY IN AN INHOMOGENEOUS PLASMA. Bajwa, G. S.; Srivastava, K. M. (Univ. of Jodhpur, India). Indian J. Pure Appl. Phys.; 8: 585-7(Oct 1970).

The flute instability in a plasma in the presence of a gravitational field, and supported by an inhomogeneous magnetic field with curved lines of force, was investigated. It is shown that the stability is underestimated if the inhomogeneity and curvature of the field are not considered. The analysis was extended for finite Larmor radii of the ions. An instability condition is obtained for controlled fusion research. (auth)

30549 STUDY OF EQUILIBRIUM AND STABILITY OF PLASMA IN HELIOTRON MAGNETIC FIELD. Oshiyama, Hiroshi (Kyoto Univ.). Mem. Fac. Eng., Kyoto Univ.; 32: 427-39(Oct 1970)

Equilibrium and stability problems of plasma in the Heliotron magnetic field are discussed under the assumption that the plasma behaves as a hydromagnetic fluid and its pressure is much less than magnetic pressure. Both plasma pressure and diamagnetic current satisfying the equilibrium conditions are analyzed in the case where the plasma carries only a diamagnetic j_θ current and not a j_z current due to an external electric field. Also, by using the curvilinear coordinate system peculiar to the Heliotron magnetic field, the stability condition for the flute-type instability is discussed according to the energy principle which was investigated by I. B. Bernstein et al. It is concluded that the Heliotron magnetic field provides the equilibrium of plasma inside the separatrix and the plasma in this field is stable against the interchange instability under the proper gradient of plasma pressure. (auth) (Japan)

30550 SUPPRESSION AND ENHANCEMENT OF A DRIFT-TYPE INSTABILITY IN A MAGNETOPLASMA BY A FEEDBACK TECHNIQUE. Keen, B. E.; Aldridge, R. V. (United Kingdom Atomic Energy Authority, Abingdon, Eng.). J. Phys., A (London); 4: 120-41(Jan 1971).

The experimental details and the results obtained are presented

when a feedback system is used to suppress or enhance drift instabilities present in a magnetoplasma. A nonlinear phenomenological theory is developed that predicts how the amplitude and frequency of the instability should change as a function of gain and phase shift in the feedback loop. Comparison of the results with this theory shows good agreement. Further, the effect on the density and temperature profiles when the instability is suppressed was investigated, and from these results a quantitative change in the cross-field diffusion constant is inferred. Also, experiments are reported that show the effects of feeding back distinct azimuthal mode numbers m = 0, ±1, and ±2, as well as the results obtained using more than one separate system. (auth) (UK)

30551 BOUNCE EFFECTS IN THE NEGATIVE MASS INSTABILITY. Launois, D.; Laval, G.; Pellat, R.; Tachon, J. (CEN, Fontenay-aux-Roses, France). Plasma Phys.; 13: 119-30(Feb 1971).

The modified negative mass instability of a plasma in a short mirror magnetic bottle is shown to be strongly affected if one takes into account a finite bounce frequency. The unstable range of density depends on the pitch-angle spreading of the distribution. The case of a large dispersion of the average ion cyclotron frequency is also investigated, and it is found that a rather dilute plasma remains unstable. (auth) (UK)

Thermonuclear Processes

Refer also to abstracts 29410 and 30254.

30552 (BNWL-B-47) HANFORD AS A SITE FOR A CONTROLLED THERMONUCLEAR POWER PLANT PROTOTYPE. Wolkenhauer, W. C. (Battelle-Northwest, Richland, Wash. Pacific Northwest Lab.). Dec 1970. Contract AT(45-1)-1830. 25p. Dep. NTIS.

The following criteria are discussed relative to the Hanford site: (1) land, (2) power, (3) water, (4) potential by-products, (5) unique site capabilities, (6) transportation, (7) manpower, (8) services, and (9) community. (M.O.W.)

30553 (CLM-R-109) LASERS AND THE REACTOR IGNITION PROBLEM. Spalding, I. J. (United Kingdom Atomic Energy Authority, Abingdon (England). Culham Lab.). Nov 1970. 11p. (CONF-701122-2). Dep. NTIS (U. S. Sales Only).

From International conference on laser-produced plasmas; Moscow, USSR (17 Nov 1970).

Some published estimates of the laser energy (W_0) required to heat an inertially confined D–T target in a pulsed-fusion reactor are summarized. Assuming a thermal efficiency of $\frac{1}{3}$ and a laser heating efficiency (target energy/laser pumping energy) of 100%, most of these estimates of W_0 range between 10 and 1000 MJ, depending on the various assumptions which are made about the degree of solid-state target compression, the possibility of target tamping, and the required reactor power gain. Any energy gain due to fusion reactions in material other than the target is omitted in these calculations. These estimates of W_0 are then compared with the maximum fusion outputs that can be handled with and without damage to the structure, and the low permissible cost of replacing damaged components is stressed. The possibility of using nonlinear absorption of repetitively pulsed CO_2 lasers to start up a steady-state stellarator reactor which is fueled by D–T pellet injection and has an output of ~10 GW(E) is then discussed. It is shown that laser energies as low as 80 kJ may be feasible and possible advantages and difficulties of such a hybrid inertial/magnetic confinement approach are outlined. (auth)

30554 (EUR-4593, pp 13-18) MAIN AND HELICAL FIELD WINDINGS ON A TOROIDAL STELLARATOR: PROTO-CLEO. Bayes, D. V.; Millward, P. (United Kingdom Atomic Energy Authority, Abingdon (England). Culham Lab.).

From Sixth symposium on fusion technology; Aachen, Germany (22 Sep 1970).

In Proceedings of the 6th symposium on fusion technology.

PROTO-CLEO is a toroidal stellarator with a main field of 5 kG produced by 30 single-turn coils. The (l = 3) helical winding, which lies inside the vacuum chamber, has 13 field periods around the major circumference, (helix angle $\theta = \frac{13}{3}$). Both windings are supplied by electrolytic capacitor banks. The assembly of the machine is achieved by using demountable joints in the main field coils, allowing the whole coil system to be split for assembly around the vacuum vessel. Accurate alignment of the coils was achieved by using a support structure built from machined castings made of a special nonmagnetic cast iron. The helical winding was built in two halves, each supported by 15 ceramic rings. The positioning of the conductors was achieved by forming them onto a machined toroidal mandrel, between accurately positioned dowel pegs. The support of the conductors was transferred to the ceramic rings with the mandrel still in position, after which it was collapsed and withdrawn, leaving a space–frame of conductors and rings. The joints and current-feed points were designed to give negligible perturbations of the magnetic fields. (auth)

30555 (EUR-4593, pp 19-24) MANUFACTURE AND CONSTRUCTION OF HELICAL WINDING. Hanson, A. W. (United Kingdom Atomic Energy Authority, Abingdon (England). Culham Lab.).

From Sixth symposium on fusion technology; Aachen, Germany (22 Sep 1970).

In Proceedings of the 6th symposium on fusion technology.

The exacting requirements of uniformity of field configuration of many plasma physics machines, coupled with the unconventional winding shapes required, give rise to great problems in obtaining positional accuracy of the winding conductors. This, in addition to the high current densities and high packing factors required, leads to practical engineering problems during construction. A number of general solutions present themselves, such as the use of machined slots for the windings, preshaping of conductors, use of winding mandrels, etc. The winding and insulation requirements of each experiment are, however, very different and the methods used in specific experiments are reviewed. In particular, in STAMP a technique of pretwisting and roll forming of the hollow rectangular section conductor was successfully employed and is fully described. However, difficulties were found with the use of this method for making the ISIS winding and an alternative design was built, using stranded cable. (auth)

30556 (EUR-4593, pp 25-32) STABILITY OF SINGLE-TURN COILS IN PULSED MAGNETIC FIELDS UP TO 1 MG. Andrianov, A. M.; Demichev, V. F.; Eliseev, G. A.; Levit, P. A. ([Gosudarstvennyi Komitet po Ispol'zovaniyu Atomnoi Energii SSSR, Moscow. Institut Atomnoi Energii]).

From Sixth symposium on fusion technology; Aachen, Germany (22 Sep 1970).

In Proceedings of the 6th symposium on fusion technology.

Experiments on the stability of single-turn coils under the action of pulsed magnetic fields as high as 1 MG are described. Copper, beryllium and chromium bronzes, various steels, niobium, molybdenum, tantalum, tungsten and some other metals were used as coil materials. A 58-kJ capacitor bank of low-inductance was used as a current source. Preliminary estimates of the stability of coil materials were based on their dynamical and thermal characteristics. In particular, the impact strength and the critical speed of impact of the materials were taken into account. The stability criteria obtained are in qualitative agreement with the experimental results of the study of the behavior of the materials in strong pulsed magnetic fields. Tantalum is the most stable of all the materials tested. Tantalum coils can be used for repeated production of pulsed magnetic fields as high as 1 MG. Tantalum also shows itself to be the best material for generating stronger fields in short coils. The maximum field of 3.1 MG produced in a tantalum coil was half as much again as that produced in a copper coil. Strong plastic flows and ejection of a melted and vaporized surface material are the principal kinds of coil destruction that limit the strength of the magnetic field. (auth)

30557 (EUR-4593, pp 83-93) RECENT DEVELOPMENTS IN SUPERCONDUCTIVITY AND ITS APPLICATIONS TO FUSION RESEARCH. Hancox, R. (United Kingdom Atomic Energy Authority, Abingdon (England). Culham Lab.).

From Sixth symposium on fusion technology; Aachen, Germany (22 Sep 1970).

In Proceedings of the 6th symposium on fusion technology.

This review deals with several topics. Firstly, some recent improvements in the properties of superconducting materials and their use in magnets are discussed. Secondly, the current applications of superconductors to plasma physics experiments are reviewed. Finally, there are some comments on the problems of a magnetic system for a power reactor. (M.O.W.)

30558 (EUR-4593, pp 133-9) SUPERCONDUCTING LEVITRON. Cornish, D. N. (United Kingdom Atomic Energy Authority, Abingdon (England). Culham Lab.).

From Sixth symposium on fusion technology; Aachen, Germany (22 Sep 1970).

In Proceedings of the 6th symposium on fusion technology.

This machine, being built at Culham for studying stability and confinement of plasmas, is centered around a short-circuited superconducting ring that is levitated on a magnetic field. The ring is 60 cm in mean diameter and carries a total current of 0.5 MA. It must be completely detached from its surroundings and "floats" in a vacuum in which the plasma is produced. The winding must therefore be sealed in a container capable of withstand-

ing the internal pressures generated on warming to room temperature. The levitating field and the vertical field required to confine the plasma will also be produced by superconducting coils. The field geometry required and the lack of space demand high current densities for these windings also. Fine-filament Nb–Ti superconductors will be used and the coils, the largest of which is about 120 cm in diameter, will be fully impregnated in epoxy resin. They will be cooled by high-pressure gas and will operate in low-pressure gas. (auth)

30559 (EUR–4593, pp 141–8) DESIGN AND OPERATION OF A SPHERATOR WITH A LEVITATED, SUPERCONDUCTING RING. Wakefield, K. E. (Princeton Univ., N. J. Plasma Physics Lab.).

From Sixth symposium on fusion technology; Aachen, Germany (22 Sep 1970).

In Proceedings of the 6th symposium on fusion technology.

The essential features of a spherator within which a superconducting ring is continuously levitated are described. The ring, weighing about 110 kg and carrying a total of up to 130,000 ampere turns, is maintained in the midplane of the machine by five feedback control systems whose outputs are derived from optical sensors. The procedures followed in filling the Dewar containing the superconducting coil with liquid helium, sealing it off, energizing the coil, levitating the coil for taking experimental data, and for restoring the system to a safe condition at the conclusion of the experimental run are described. (auth)

30560 (EUR–4593, pp 189–95) NEW CROWBAR SYSTEM FOR THE 2.7-MJ BANK ISAR I AT GARCHING. Klement, G.; Wedler, H. (Institut fuer Plasmaphysik, G.m.b.H., Garching (West Germany)).

From Sixth symposium on fusion technology; Aachen, Germany (22 Sep 1970).

In Proceedings of the 6th symposium on fusion technology.

The linear coil is to be replaced by a toroidal coil as load of the 2.7-MJ bank. The inductance has thus been decreased from 9.5 to 7.4 nH, resulting in an increase of the calculated current ripple from 13.5 to 17.5%. New ferrite decoupled spark gaps with total inductances of 70 nH (Type I) and 35 nH (Type II) were developed. Combined ferrite decoupling and plasma triggering yields a special low-inductance gap (Type III) with small current delay. The triggering methods, the problem of total saturation, and current delay are discussed, and the dependence of the current ripple on the switching time is investigated. (auth)

30561 (EUR–4593, pp 197–203) APPLICATION OF INDUCTIVE ENERGY STORAGE SYSTEMS FOR PRODUCTION OF INTENSE MAGNETIC FIELDS. Salge, J.; Peier, D.; Brilka, R.; Schneider, D. (Technische Universitaet, Brunswick (West Germany)).

From Sixth symposium on fusion technology; Aachen, Germany (22 Sep 1970).

In Proceedings of the 6th symposium on fusion technology.

Starting with some basic considerations concerning the utilization of inductive storage for the generation of intense magnetic fields, circuits for different types of magnetic fields are investigated and discussed. The experiments were conducted on single-stage storage systems. The storage coils were charged by dc power supplies and by condenser banks. The high-magnetic-field coils were performed with multi turns. The highest intensity obtained was about 400 kG, and the investigated pulse length varied between 10^{-6} and 10^{-1} sec. In this connection, some additional experiments were performed concerning the pulse excitation of magnetic-field coils by the ac power system; results are discussed. (auth)

30562 (EUR–4593, pp 205–17) MERITS AND LIMITATIONS OF EXPLOSIVELY DRIVEN CURRENT GENERATORS IN FUSION RESEARCH. Knoepfel, H.; Kroegler, H.; Luppi, R.; Verbeek, R. (Comitato Nazionale per l'Energia Nucleare, Frascati (Italy). Laboratorio Gas Ionizzati).

From sixth symposium on fusion technology; Aachen, Germany (22 Sep 1970).

In Proceedings of the 6th symposium on fusion technology.

The interest of using explosively driven current generators is based mainly on the distinct features of chemical explosives as an energy-storage system, i.e., high-energy density and high power in releasing the energy. Other advantages of these generators in view of different applications are: possibility of shaping the output pulse, both by the intrinsic design of the devices or by using explosively activated switches; low relative weight (which makes them interesting for space applications); and, up to a certain point, moderate costs. On the other hand, the main disadvantage is their partly destructive nature. A detailed and comprehensive discussion on their merits and limitations is given. In particular, an evaluation of the possible operation costs of future explosive generators is given. (auth)

30563 (EUR–4593, pp 219–25) HIGH-CURRENT CAPACITOR BANKS FOR A 2-MJ HIGH BETA TOROIDAL EXPERIMENT (HBTX). Heywood, G. C. H.; Harding, G. E. S.; James, T. E.; Raymond, C. G.; Ward, B. J. (United Kingdom Atomic Energy Authority, Abingdon (England). Culham Lab.).

From sixth symposium on fusion technology; Aachen, Germany (22 Sep 1970).

In Proceedings of the 6th symposium on fusion technology.

This experiment is designed to study a high-beta toroidal plasma confined by a combination of axial and azimuthal fields. In order to optimize the field configuration, which depends on plasma currents, a very flexible fast capacitor bank system was built involving five individual circuits. They include a slow bank of 1 MJ at 8 kV with a risetime of 170 μs and three fast banks totaling 1 MJ at 40 kV with risetimes of about 10 μs. The time of triggering of each bank can be varied over a wide range. The capacitor banks and the triggering system used for the experiment are described. (auth)

30564 (EUR–4593, pp 227–39) DESIGN AND INSTALLATION OF SCYLLAC, A 15-M THETA-PINCH EXPERIMENT. Kemp, E. L.; Boicourt, G. P.; Gribble, R. F.; Hammer, C. F.; Hanks, K. W.; Quinn, W. E.; Sawyer, G. A. (Los Alamos Scientific Lab., N. Mex.).

From sixth symposium on fusion technology; Aachen, Germany (22 Sep 1970).

In Proceedings of the 6th symposium on fusion technology.

Several new components were developed for Scyllac. They included: a 1.85-μF, 60-kV capacitor; reliable, low-inductance coaxial cable; a low-jitter, pressurized, 60-kV spark gap that incorporates a crowbar gap in the assembly; cable cartridge terminations; and a variety of miscellaneous hardware. All component designs were first evaluated as individual components. Then a significant number of them were installed in a prototype system before the design was certified to be used in the Scyllac system. When the Scyllac system components were received they were individually inspected and electrically tested before being installed. The installation is approximately 40% complete and is proceeding on schedule. Some of the unique features of the installed system are discussed. (auth)

30565 (EUR–4593, pp 241–50) HIGH-POWER SPARK GAPS FOR LARGE AND FAST ENERGY STORAGE SYSTEMS. Klement, G.; Wedler, H. (Institut fuer Plasmaphysik, G.m.b.H., Garching (West Germany)).

From sixth symposium on fusion technology; Aachen, Germany (22 Sep 1970).

In Proceedings of the 6th symposium on fusion technology.

Future high-β experiments in which the stored energy will probably be in the region of 50 MJ call for a compactly designed storage system. This will largely depend on the energy stored per circuit. It is shown that this energy is governed by the inductance of the starting switch. The crowbar system is extremely important for the designing of a bank because the confinement time of the plasma is governed by the ripple and the decay time constant of the magnetic field, and both depend on the crowbar switches. As in the case of starting switches, the number of crowbar switches depend on the inductance of the switches. This determines the current load on crowbar gaps. First measurements with a further-developed simultaneously igniting three-electrode gap for crowbarring are described. (auth)

30566 (EUR–4593, pp 259–64) RECENT RESULTS WITH LASER-TRIGGERED SPARK GAPS. Pillsticker, M.; Schmitter, K. H.; Wedler, H. (Institut fuer Plasmaphysik, G.m.b.H., Garching (West Germany)).

From sixth symposium on fusion technology; Aachen, Germany (22 Sep 1970).

In Proceedings of the 6th symposium on fusion technology.

The effects of different parameters on the performance of laser-triggered spark gaps are discussed, and the relevant experiments are reported. (auth)

30567 (EUR–4593, pp 265–71) FAST STORAGE SYSTEM FOR A 500-kV THETA-PINCH EXPERIMENT. Herppich, G.; Suess, R. (Institut fuer Plasmaphysik, G.m.b.H., Garching (West Germany)).

From sixth symposium on fusion technology; Aachen, Germany (22 Sep 1970).

In Proceedings of the 6th symposium on fusion technology.

A 500-kV theta-pinch experiment will be driven by Blumlein-type transmission lines ($Z = 0.58\Omega$) via four feeds. The coil has a diameter of 43 cm and a length of 100 cm. The Blumlein lines are resonance-charged by a capacitor bank of the Marx type. The stored energy is 54 kJ. The lines generate a 125-kV voltage pulse. The current pulse has a risetime constant of 85 nsec and a pulse width of 500 nsec. The corresponding field strength is 5.5 kG.

XUM

The start switches are pressurized multichannel low-inductance spark gaps with four trigger electrodes. The gaps are triggered by pulse generators with a slope about 20 kV/nsec. The inductance of 20 nH is reached by simultaneous triggering of the four gaps. The 1.5-m-wide Blumlein lines are sectioned in 0.5-m-wide lines. Each 43-m-long line has its own spark gap. The lines are in tanks filled with water to avoid corona effects at the edges. The three copper sheets each 0.2-mm thick are insulated with Mylar foils of 2-mm thickness. (auth)

30568 (EUR–4593, pp 273-80) HIGH-POWER SPARK GAP FOR HIGH REPETITION RATES. Kunze, R.-C.; Mueller, G.; Suess, R. (Institut fuer Plasmaphysik, G.m.b.H., Garching (West Germany)).

From sixth symposium on fusion technology; Aachen, Germany (22 Sep 1970).

In Proceedings of the 6th symposium on fusion technology.

A 5-kJ, 30-kV, 40-kHz start and crowbar gap was developed for experiments with collective acceleration. At present, the repetition rate is 1 Hz, further extension to 10-Hz operation being planned. The lifetime is scheduled to be 10^5 discharges. Special attention was paid to high repetition and Coulomb duty. The condition of less than 5% ripple of the crowbar current calls for a decrease of the inductance of the ferrite decoupled crowbar branch. (auth)

30569 (EUR–4593, pp 281-6) PULSE BREAKDOWN OF PLASTIC FOILS IN LIQUIDS. Kunze, R. C.; van Mark, E. (Institut fuer Plasmaphysik, G.m.b.H., Garching (West Germany)).

From sixth symposium on fusion technology; Aachen, Germany (22 Sep 1970).

In Proceedings of the 6th symposium on fusion technology.

Breakdown experiments in plastic foils immersed in liquid impregnation are reported. It was found that with pulse voltages (risetime between 0.2/μsec and 10^3/μsec) the breakdown voltage decreases up to 70% as compared to the dc value depending on plastic material, number and thickness of foils, liquid impregnation, and risetime of the high-voltage pulse. A first tentative explanation for the unexpected breakdown behavior is given. (auth)

30570 (EUR–4593, pp 287-91) VACUUM START AND CLAMP SWITCHES FOR A 20-kJ, 40-kV CAPACITOR UNIT. Zwart, J. W. A.; Verheul, A. (Stichting voor Fundamenteel Onderzoek der Materie, Jutphaas (Netherlands). Instituut voor Plasma-Fysica).

From sixth symposium on fusion technology; Aachen, Germany (22 Sep 1970).

In Proceedings of the 6th symposium on fusion technology.

A combined vacuum start- and clamp-switch was designed for a 40-kV, 20-kJ capacitor unit. The energy is stored in two low-inductance BICC capacitors of 12.5 μF, 40 kV. The switches operate in a range between 40 kV and 200 V. The inductance and the resistance of the switch are 11 nH and 8 mΩ, respectively; the delay is 100 to 200 ns depending on the polarity of the voltage; and the jitter is less than 10 ns. The conducting channel stays in a central position within the switch due to the symmetric current leads; therefore, the estimated lifetime without servicing is 2000 to 5000 discharges at 500-kA peak current. The minimum time between shots is 2 min. (auth)

30571 (EUR–4593, pp 293-9) NEW COMPACT CAPACITIVE ENERGY STORAGE UNIT FOR VOLTAGES ABOVE 100 kV. Kind, D.; Naglik, M. (Technische Universitaet, Brunswick (West Germany)).

From sixth symposium on fusion technology; Aachen, Germany (22 Sep 1970).

In Proceedings of the 6th symposium on fusion technology.

The objective of the project is to design a low-inductance capacitor unit for a total charging voltage as high as 300 kV. Two capacitors are connected in series by means of two starting gaps of a new type. The capacitors are charged symmetrically with reference to ground potential up to a voltage of ±150 kV; their stored energy will then be 3.7 kJ. These versatile capacitors are of the symmetrical coaxial type with a grounded steel housing. They were developed in cooperation with an industrial manufacturer. One of the two terminals is connected to the load coil by a stripline insulated by epoxy resin; the other terminal can be connected to ground by a starting gap. The gap contains several gaps in series–parallel connection, thus gives low inductivity and high-current capability and avoids prefiring. The different parts of the unit are mounted together with the help of high-voltage gaskets made of silicon rubber. It is intended to combine several units of the type described for larger banks. (auth)

30572 (EUR–4593, pp 301-9) INVESTIGATIONS ON HIGH-VOLTAGE GASKETS. Weniger, M. (Technische Universitaet, Brunswick (West Germany)).

From sixth symposium on fusion technology; Aachen, Germany (22 Sep 1970).

In Proceedings of the 6th symposium on fusion technology.

The technique and application of high-voltage connections between detachable parts of a complex setup are discussed. Unavoidable gaps within the dielectric are filled with an elastic insulating material, thus forming a joint with high dielectric strength. The influence of the various parameters on the ac breakdown voltage are determined by a simple testing arrangement. This leads to an empirical formula for the calculation of the different types of high-voltage gaskets. Constructions are shown as examples of applications of high-voltage gaskets of the coaxial forms as radial or axial types. (auth)

30573 (EUR–4593, pp 311-17) LOW-INDUCTANCE, MEGAVOLT MARX GENERATORS. Fitch, R. A.; Wootton, R. E. (Maxwell Labs., Inc., San Diego, Calif.).

From sixth symposium on fusion technology; Aachen, Germany (22 Sep 1970).

In Proceedings of the 6th symposium on fusion technology.

Among the several ways of producing high-voltage pulses the Marx Generator is probably the best known and most widely used, but conventional Marx generators tend to be bulky and slow. Attempts to reduce size and inductance usually compound the difficulty of triggering because interstage capacitances increase. Furthermore, stresses from the erection transients become more severe and reliability suffers. This paper discusses a class of fast Marx-like generators of extremely compact design and describes two operational generators: a 200-kJ, 5.9-MV, 5.3-μH, oil-immersed system and a 100-kJ, 2-MV, 1.6-μH, gas-immersed system. (auth)

30574 (EUR–4593, pp 319-38) PARAMETRIC STUDY OF EXPLODING FOILS AS SWITCHES. Schenk, G. (Comitato Nazionale per l'Energia Nucleare, Frascati (Italy). Laboratorio Gas Ionizzati).

From sixth symposium on fusion technology; Aachen, Germany (22 Sep 1970).

In Proceedings of the 6th symposium on fusion technology.

The effects of the geometric parameters of an exploding foil used as an interrupter for energy transfer from inductive storage to an inductive–resistive load are discussed. In a series of tests using a 40-kJ, 15-kV condenser bank as energy source, insulating plates of 0.5-mm epoxy–fiberglass withstood surface energy dissipation of up to 100 J/cm^2 and, for silicon plates, even higher values. Al_2O_3 gave the best results as surrounding insulator in grain size of 0.177 mm. The characteristic time τ (e.g., current maximum or voltage peak) is proportional to the foil cross section s_0. Calculation and experiment are in agreement. With the time $\tau(S_0)$ thus determined, the foil thickness depends on the maximum permissible energy stress to the insulating surface and on the energy density required for complete vaporization. Finally, the foil length is a function of the requested voltage peak U_R (breakdown voltage of the gap), the foil current $I_s(t)$, and the energy conditions described above. (auth)

30575 (EUR–4593, pp 339-45) DEVELOPMENT OF A HEAVY-CURRENT SWITCHING GAP TRIGGERED WITH LASER. Horii, Kenji; Noguchi, Takuya; Yano, Masaaki (Ministry of International Trade and Industry, Tokyo (Japan). Electrotechnical Lab.).

From sixth symposium on fusion technology; Aachen, Germany (22 Sep 1970).

In Proceedings of the 6th symposium on fusion technology.

Two kinds of laser trigger gaps, of which one electrode was irradiated by the focused laser beam through a hole of the other electrode, were developed. The first is triggered by the precursor plasma wave owing to photo-ionization, and is applicable to the high-voltage parallel starting switch of short delay time. The second is short-circuited by the high-density plasma shock wave from the irradiated electrode, and is applicable to the crowbar switch operating under zero voltage. For the parallel starting switch, the pressurized gaps (1 ~ 3 atmospheric pressure of N_2 gas, gap length 4 mm, maximum working voltage 30 kV) were developed. The laser beam (50 MW peak, 11 ns width) was divided into eight beams with prisms, and used to the parallel running of eight condenser banks (4 μF unit). For the crowbar switch, the pressurized gap (1 ~ 6 atmospheric pressure of N_2 gas, gap length 1.3 mm, maximum working voltage 30 kV) was developed. (auth)

30576 (EUR–4593, pp 347-53) CROWBAR GAP SWITCH WITH TWO TRIGGERING PULSES OF OPPOSITE POLARITIES AND POSSIBILITY OF ACHIEVING MULTIPLE ARC BREAKDOWN. Ikeda, N.; Takeda, S. (Ministry of International Trade and Industry, Tokyo (Japan). Electrotechnical Lab.).

From sixth symposium on fusion technology; Aachen, Germany (22 Sep 1970).

In Proceedings of the 6th symposium on fusion technology.

A crowbar gap switch with a new triggering circuit is reported. The triggering mechanism is that the air gap between the trigger

electrodes inserted in the center of each crowbar gap electrode breaks down at first by the field emission as soon as two pulses of opposite polarities are applied simultaneously to two trigger electrodes, respectively, and then the main discharge path is established. It is found from the superposed oscillogram of the current waveform in the load coil that both time delay and time jitter are very small, and the reliability of operation has become perfect with the auxiliary gaps in trigger circuit. (auth)

30577 (EUR-4593, pp 355-63) TRANSFORMER COUPLED FAST THETA-PINCH DEVICE WITH VARIABLE RISE TIME. Kiyama, Satoru; Ogawa, Kiyoshi (Ministry of International Trade and Industry, Tokyo (Japan). Electrotechnical Lab.).

From sixth symposium on fusion technology; Aachen, Germany (22 Sep 1970).

In Proceedings of the 6th symposium on fusion technology.

In order to investigate the behavior of plasma in the implosion and compression phases and to control the initial conditions of the confinement phase, the θ-pinch device was designed and constructed so as to be able to change the magnetic field rise over a wide range, keeping the maximum magnetic field at a certain value. In this device, a transformer-coupling method and variable inductances were used. The magnetic field rise can be changed from 2×10^9 gauss/sec to 5×10^{10} gauss/sec, and the transmission-line storage of energy was employed in θ preheating to have a preheated fully ionized plasma without diffused magnetic field in it. It thus appears that the very high voltage is generated in the primary circuit at the time of preheating. The special, swinging cascade-type gap switch was devised to withstand this high voltage. The charging voltage of the condenser bank is 80kV, and the total energy is 8 kJ. (auth)

30578 (EUR-4593, pp 365-71) DEVELOPMENT ASPECTS OF FAST METAL-CONTACT SOLID-DIELECTRIC SWITCHES. Skelton, D. E.; Burden, R. A.; Bold, D. (United Kingdom Atomic Energy Authority, Abingdon (England). Culham Lab.).

From sixth symposium on fusion technology; Aachen, Germany (22 Sep 1970).

In Proceedings of the 6th symposium on fusion technology.

The invention and improvement of switches of various types forms a major part of development work in fusion technology. Fast metal-contact solid dielectric clamp switches are required for thermonuclear fusion experiments to achieve a low switch voltage drop and therefore extend the current pulse time appreciably. Recent experimental work on such switches at the Culham Laboratory is summarized. Exploding-foil switches were developed with increased contact width per foil, achieved by optimization of foil geometry and trigger circuit parameters and also with double-sided insulation for operation at higher voltages (~100 kV). An alternative "pinhole with exploding wire" drive system, which permits the production of multiple simultaneous contacts in a single switching plate, was used to make 3-contact and 6-contact switches, having I^2t capabilities of 3.5×10^8 and 1.4×10^9, respectively, without signs of melting. Although most frequently used as clamp switches, some types lend themselves to use as start switches; the problems encountered when used in this mode are considered, and some test results given. A comparison is made with other published switches and various triggering phenomena are described. (auth)

30579 (EUR-4593, pp 373-8) COAXIAL HIGH-POWER TRIGATRON FOR 60 kV. Friedrich, F. J.; Kohlhaas, W.; Stickelmann, C. (Kernforschungsanlage, Juelich (West Germany). Institut fuer Plasmaphysik).

From sixth symposium on fusion technology; Aachen, Germany (22 Sep 1970).

In Proceedings of the 6th symposium on fusion technology.

Due to the availability of capacitors with energy contents as high as 10 kJ, a new switch with increased current capability was developed. This current capability can normally be obtained by paralleling a number of discharge channels, but in the case of a prefire, an excessive current loading occurs in one gap. The switch could be operated for several hundred discharges without any difficulties at 360 kA/150 kHz and was tested for up to 2000 discharges at 100 kA without deterioration. If parallel operation is required from one capacitor, the necessary decoupling length is as low as 0.5 m. (auth)

30580 (EUR-4593, pp 379-84) FAST, SOLID DIELECTRIC, MULTICHANNEL CROWBAR SWITCH. Dokopoulos, P.; Lorbach, F. (Kernforschungsanlage, Juelich (West Germany). Institut fuer Plasmaphysik).

From sixth symposium on fusion technology; Aachen, Germany (22 Sep 1970).

In Proceedings of the 6th symposium on fusion technology.

The flat main electrodes are insulated by two polyester foils with a thin aluminum trigger strip between them. This switch assembly has been used by C. Martin as a start switch for a 30-kV bank. In this switch, triggering is achieved by applying a steep voltage pulse from a Blumlein generator between the trigger electrode and the ground electrode. Both the trigger pulse and the voltage across the switch electrodes combine to breakdown the two foils. Crowbar, however, is impossible without special precautions, because at zero switch voltage the trigger pulse alone has to provide breakdown of both foils. Crowbarring is achieved by the application of the following principles: two polyester foils of different thickness are used, the thicker one placed between the trigger strip and the grounded main electrode; on application of a voltage pulse to the trigger strip, the thinner foil will break down first. This sequence is important in order to avoid a short circuit of the trigger generator. If the internal impedance of the Blumlein generator is small compared to the impedance of the transmission line attached to the switch, the voltage of the trigger electrode is sufficient to puncture the thicker foil too. The total delay time between the application of the trigger pulse and the breakdown of both foils is in the order of a few nanoseconds. 200 parallel discharge channels were achieved with a trigger strip of 50-cm length. The inductance is below 1 nH for a switch with holding 60 kV. (auth)

30581 (EUR-4593, pp 385-92) STUDIES OF SURFACE DISCHARGES ON INSULATING FOILS. Lochter, M. (Kernforschungsanlage, Juelich (West Germany). Institut fuer Plasmaphysik).

From sixth symposium on fusion technology; Aachen, Germany (22 Sep 1970).

In Proceedings of the 6th symposium on fusion technology.

The experimental arrangement described permits the investigation of surface discharges under practical experimental conditions found typically in low-inductance high-voltage systems. The effects of a number of parameters such as voltage, discharge frequency, surface resistance, and surrounding gas on the length of these discharges were determined by time-integrated photographs of Lichtenberg figures. Their propagation velocity was measured by evaluating time-resolved image-converter photographs. The results are presented and discussed. They may be applied to the design of high-voltage components with minimum creepage path for given voltages and discharge frequencies. (auth)

30582 (EUR-4593, pp 393-400) FAST 500-kV ENERGY STORAGE UNIT WITH WATER INSULATION AND SOLID MULTICHANNEL SWITCHING. Dokopoulos, P. (Kernforschungsanlage, Juelich (West Germany). Institut fuer Plasmaphysik).

From sixth symposium on fusion technology; Aachen, Germany (22 Sep 1970).

In Proceedings of the 6th symposium on fusion technology.

The bank unit consists of two 240-kV, 4.5-kJ capacitors in series that are connected to the load and to the switch by means of foil-insulated strip lines. All high-voltage parts are immersed in a tank with a $CuSO_4$-water solution (resistivity = 1 to 10 k$\Omega \cdot$ cm) which tends to prevent field concentration by bleeding off local voltage peaks. Thus, a total creepage path of 30 cm is sufficient to withstand voltages of more than 400 kV. The system is pulse-charged by a Marx generator. The most critical part of this device is the multichannel solid dielectric switch. It works according to the field distortion principle used by C. Martin in his switch for starting a 30-kV bank. In the present work, this switch was developed for a voltage of 400 kV. The triggering was simplified by using the field energy stored in the switch. The switching time is some nanoseconds. Depending upon the applied voltage and upon the rate of rise of the trigger voltage, up to 40 parallel breakdown channels were observed on a length of 15 cm. The inductance of the switching device including the connecting busbars is 10 nH, the major part being due to the connection system. (auth)

30583 (EUR-4593, pp 403-9) TOKAMAK FACILITY OF FONTENAY-AUX-ROSES (TFR). Rebut, P. H.; Huguet, M.; Sledziewski, Z.; Torossian, A. (Commissariat a l'Energie Atomique, Fontenay-aux-Roses (France). Centre d'Etudes Nucleaires).

From sixth symposium on fusion technology; Aachen, Germany (22 Sep 1970).

In Proceedings of the 6th symposium on fusion technology.

A description is given of a Tokamak machine of T3 size energized by a power source using a new alternator (100 MW, 1 sec) giving 150 MJ. The large diameter of the torus is 2 m, the internal diameter of the coil 0.6 m, and the magnetic field 60 kG on the axis. (auth)

30584 (EUR-4593, pp 411-17) TECHNICAL STATUS REPORT ON THE GARCHING TOKAMAK EXPERIMENT "PULSATOR". Knobloch, A.; Klueber, O.; Nuetzel, G. (Institut fuer Plasmaphysik, G.m.b.H., Garching (West Germany)).

XUM

From sixth symposium on fusion technology; Aachen, Germany (22 Sep 1970).

In Proceedings of the 6th symposium on fusion technology.

Pulsator was designed according to experimental scaling relations of the Russian tokamaks and adapted to an existing 14-MJ power supply. Completion of the technical installation is expected in 1971. The characteristic data are: major torus radius 70 cm, plasma radius 12 cm, toroidal magnetic field 28 kG (for q = 1 Kruskal limit), plasma current 300 kA, experimental period 100 msec. Pulsator will include an iron transformer core for 0.42 Vsec at 15 kG in the central part and 0.77 Vsec in the eight return yokes. The maximum loop voltage will be 1 kV. A stainless steel torus with four insulating slots will serve as the vacuum vessel and a main support structure for the pulsed auxiliary windings and the parts of the copper shell. The bellow-shaped liner will be bakeable to temperatures above 400°C. Provisions will be made for additional pulse cleaning. The vacuum system includes both ion getter and turbomolecular pumps. The whole torus with main field, vertical field, and induction windings can be mounted and adjusted outside the transformer core, which has detachable upper return yokes. (auth)

30585 (EUR-4593, pp 419-24) TOROIDAL VERSION OF THE ISAR I THETA-PINCH EXPERIMENT. Breit, E.; Knobloch, A.; Werner, F. (Institut fuer Plasmaphysik, G.m.b.H., Garching (West Germany)).

From sixth symposium on fusion technology; Aachen, Germany (22 Sep 1970).

In Proceedings of the 6th symposium on fusion technology.

The toroidal coil with the dimensions D = 271 cm, d = 22 cm is separated into 48 coil segments, each fed by a collector connecting 18 cables. The collectors, which are coplanar with the torus, are contacted on the peripheral side of the coil. In order to reduce costs and save time it was decided to re-use the installed power cables of the linear arrangement. Owing to the given cable lengths, this means that the collector coil assembly (outer diameter 510 cm) has to be positioned vertically. The toroidal load will be connected so as to ensure symmetric feeding for every possible partial energy operation. (auth)

30586 (EUR-4593, pp 425-30) DESIGN AND CONSTRUCTION OF A HIGH-BETA TOROIDAL EXPERIMENTAL ASSEMBLY (H.B.T.X.). Hucklesby, R. J.; Burden, R. A.; James, T. E. (United Kingdom Atomic Energy Authority, Abingdon (England). Culham Lab.).

From sixth symposium on fusion technology; Aachen, Germany (22 Sep 1970).

In Proceedings of the 6th symposium on fusion technology.

The H.B.T.X. is required to study the confinement of a high-beta plasma by a magnetic field which has high shear produced by plasma currents. The plane is confined by a combination of axial B_z and azimuthal B_θ fields with an initial negative B_z. The assembly consists of a quartz toroidal vacuum vessel 2-m major diameter and 13-cm minor diameter with pumping system. This vessel is supported inside an aluminum alloy shell (the z shell) which has two flanges for supplying the I_z and pre-ionization currents. The I_θ coils surround the I_z shell and are connected as a two-turn coil system. The flanges and coils are fed from 2 MJ of 40-kV (fast) and 8-kV (slow) capacitor banks. The plasma current is 350 kA, the I_θ current 9 MA turns, and the maximum field is 18 kG. A general description is given of the electrical and mechanical design and construction. The two circuits were insulated by a combination of plastic sheets and interleaved plastic mouldings, with a complex silicone rubber moulding at each main flange position. A concrete base supports the assembly. (auth)

30587 (EUR-4593, pp 431-41) DESIGN AND CONSTRUCTION OF "PIACE": AN APPARATUS FOR PLASMA INJECTION AND ADIABATIC COMPRESSION EXPERIMENT. Hirano, K.; Kishimoto, H.; Ushio, M.; Ohi, M.; Ito, H. (Osaka Univ. (Japan). Plasma Physics Lab.).

From sixth symposium on fusion technology; Aachen, Germany (22 Sep 1970).

In Proceedings of the 6th symposium on fusion technology.

PIACE was designed and constructed to study a fast, collisionless, adiabatic compression of hot plasmas. It consists of four theta-compression coils, and two theta-pinch guns attached to both ends of the discharge tube. Four one-turn main-compression coils and the coil of each theta-pinch gun are powered by 60-kV fast capacitor banks. Bias and guide fields are produced by 8-kV slow banks, respectively. All the banks are crowbarred at any desired current phase. Low-pressure gap-decoupled switches are used for crowbar of the fast banks. The total amount of the energy of the fast banks is 162 kJ. The fast banks are composed of 27 independent 6-kJ units in order to be convenient for rearrangement of the capacitor banks. For the full operation of the apparatus, 36 independent trigger pulse systems are used under the control of delay generators. The R-C matching element, a kind of Q spoiler, is mounted on each current collector of the coil to damp the voltage peaking that should give damages to the cables and polyethylene insulators of coils and collectors. As a result, a fast-rising magnetic field of 30 kG was obtained within 1.4 μsec in the main-compression coils. (auth)

30588 (EUR-4593, pp 445-60) DESIGN POSSIBILITIES AND CONSEQUENCES FOR THE CONVENTIONAL PARTS OF FUSION POWER PLANTS. Foerster, S.; Schneider, K. U. (Kernforschungsanlage, Juelich (West Germany). Institut fuer Reaktorentwicklung).

From sixth symposium on fusion technology; Aachen, Germany (22 Sep 1970).

In Proceedings of the 6th symposium on fusion technology.

For operation in a closed helium cycle with gas turbine, turbine inlet temperature of 950°C, and inlet pressure of 90 bar, the proposed quasi-radial reactor heat exchanger for torus-type fusion reactors shows interesting low-mean-volume fraction of cooling structure on the Li-blanket volume of about 5.0%. The structure material (niobium or molybdenum alloy) can be kept at temperatures of 1000°C. With respect to the very expansive mass of structure material in the reactor, the gas turbine cycle without reheat should be preferred to the cycle with reheat. Preferable pressure-expansion ratios in the turbine are to be expected between 3 and 4. As the cost fraction of the complete reactor on the whole, direct plant costs will be about 60%, careful layout of the reactor torus blanket with heat exchanger and magnet as well as high cycle efficiency are required. Efficiencies of about 47% seem to be attainable with the direct cycle without reheat, but should not be lower. For overall plant design, pressure losses in the reactor of 5 to 7.5% and cooling-tube diameters in the reactor of about 1 cm are recommended. The helium/air cooling system, which itself is rather expansive, is very attractive because of its low cost fraction on the direct plant costs. So pollution-free plant operation is possible. It seems that, with a 5000-MW_{th} fusion reactor power plant, electricity-generating costs equal to those expected for HTR-GT power plants (i.e., 1.6 Dpf/kWh) are achievable. The future cost development for coils and reactor structural material, such as niobium, should be observed carefully since these costs are of high influence on the electricity-generation costs. No principal objections for the feasibility of the cycle components are expected. The problems of the reactor technology seem to be much lower than those for economic operation of the fusion plasma. (auth)

30589 (EUR-4593, pp 491-6) FEASIBILITY OF GAS COOLING FOR THE FUSION REACTOR BLANKET. Darvas, J.; Legewie, G. (Kernforschungsanlage, Juelich (West Germany). Institut fuer Reaktorentwicklung).

From sixth symposium on fusion technology; Aachen, Germany (22 Sep 1970).

In Proceedings of the 6th symposium on fusion technology.

Considering the advantages of a gas coolant against liquid metal coolant, in particular the lack of interaction with the magnetic field and the use of gas turbines, the feasibility of He cooling of the CTR blanket was studied. Calculations for He pipes, running parallel to the toroidal vacuum tube, show that relevant figures, such as Nb and Li temperatures, pressure loss and blower power, are within the range of today's technical possibilities, even at high gas-outlet temperature. (auth)

30590 (EUR-4593, pp 497-512) DATA FOR A FUSION REACTOR: SUMMARY OF AN IPP LECTURE SERIES. Knobloch, A. (Institut fuer Plasmaphysik, G.m.b.H., Garching (West Germany)).

From sixth symposium on fusion technology; Aachen, Germany (22 Sep 1970).

In Proceedings of the 6th symposium on fusion technology.

From November 1969 through June 1970 a series of 15 lectures was held, four of them comprising the main results of the Culham conference of 1969, the others reporting results of internal experiments and design considerations and their possible application for fusion reactor design. The main topics up to now were: considerations of existing experimental configurations (high-β stellarator, screw pinch, tokamak), economics and design of fusion reactors (two papers), reactor components (fuel injection with D-T ice, application of an explosive MHD generator, magnet design, blanket and thermodynamic cycle) and wall problems (two papers). The essential information given is reviewed. (auth)

30591 (EUR-4593, pp 513-18) COMPARISON OF DIFFERENT FUSION REACTOR BLANKET SYSTEMS. Daenner, W. (Institut fuer Plasmaphysik, G.m.b.H., Garching (West Germany)).

From sixth symposium on fusion technology; Aachen, Germany (22 Sep 1970).

In Proceedings of the 6th symposium on fusion technology.

XUM

A summary based upon some typical fusion-reactor blanket concepts is given for the neutron effects of typical blanket materials. In comparison with the hypothetical blanket of lithium only, the influence of the vacuum wall and the structural material inside the blanket vessel is pointed out. The effect of adding beryllium as a neutron multiplier is then demonstrated by considering the two main directions of blanket development: (1) the application of a molten salt instead of liquid metal for diminishing the pumping losses; (2) the application of a mixture of liquid lithium and sodium for enlarging the energy deposition inside the blanket region. Finally, the tritium breeding potential is related to those values necessary for achieving an economic fusion reactor. An equation is presented that describes the interdependence between the tritium breeding ratio, the efficiency of the tritium recovery process, fractional burnup, operating time, and tritium doubling time, taking into account the radioactive decay. Introducing values indicated as reasonable by present knowledge, this formula yields a breeding ratio of 1.15 for a tritium doubling time of about 5 years. (auth)

30592 (EUR-4593, pp 525-31) DENSE PLASMA FOCUS AS A NEUTRON SOURCE FOR PULSED MEASUREMENTS IN A BLANKET. Cloth, P.; Conrads, H.; Demmeler, M.; Hecker, R. (Kernforschungsanlage, Juelich (West Germany)).

From sixth symposium on fusion technology; Aachen, Germany (22 Sep 1970).

In Proceedings of the 6th symposium on fusion technology.

A dense plasma focus capable of providing a repetition rate of one neutron flash per second was developed. A low-inductance coaxial condensor bank of 22 μF and an operating voltage of 40 kV are connected to a pair of coaxial electrodes. The use of this source for reactor blanket studies is described. (M.O.W.)

30593 (EUR-4593, pp 533-8) SYSTEM PLANNING FOR A PROTOTYPE FUSION REACTOR. Knobloch, A.; Daenner, W.; Nuetzel, G. (Institut fuer Plasmaphysik, G.m.b.H., Garching (West Germany)).

From sixth symposium on fusion technology; Aachen, Germany (22 Sep 1970).

In Proceedings of the 6th symposium on fusion technology.

Considering the large amount of design data for fusion reactors already available, it was first intended to prepare a detailed planning network for a possible development towards a prototype fusion reactor. But it turned out that even the quantitative problem definitions were far from clear. Thus, the network could not give relevant information on the times involved. In this situation it was felt reasonable to have only a very simple diagram showing two critical paths for the technical realization of a zero-net-power reactor experiment followed by a reactor prototype. One path proceeds from present plasma technology via solution of configuration-independent problems (magnetic field generation, wall, and blanket design), and the other via reactor-oriented plasma physics experiments and subsequent solution of configuration-dependent problems (heating, startup, fuel cycle). Parallel to these activities, economic studies considering the fusion reactor and competing systems must be done. Finally, a correct decision on building a prototype fusion reactor should thus be possible. The design, test, and data evaluation of such prototype reactors would be the last pre-industrial step and a challenging task for fusion technology. (auth)

30594 (EUR-4593, pp 541-4) HIGH-Q CAPACITOR. Baeumler, J.; Kunze, R.-C. (Institut fuer Plasmaphysik, G.m.b.H., Garching (West Germany)).

From sixth symposium on fusion technology; Aachen, Germany (22 Sep 1970).

In Proceedings of the 6th symposium on fusion technology.

A capacitor with a capacitance of 0.1 μF and a maximum operating voltage of 80 kV is described. The dielectric (100-μ polystyrene sheet) and the electrodes (30-μ copper foil) are immersed in oil. The maximum field strength in the dielectric is 50 kV/mm. At frequencies of 1.0 MHz and 2.0 MHz, Q values of 283 and 100, respectively, were measured. The internal inductance of the capacitor is 30 nH and the discharge frequency with short-circuited terminals is 3 MHz. (auth)

30595 (EUR-4593, pp 545-50) HIGH-Q CAPACITORS WITH LIQUID AND GAS IMPREGNATION. Brand, U.; Richter, F.; Cosler, A.; Gresser, H. (Kernforschungsanlage, Juelich (West Germany). Institut fuer Plasmaphysik).

From sixth symposium on fusion technology; Aachen, Germany (22 Sep 1970).

In Proceedings of the 6th symposium on fusion technology.

High-Q capacitors for application in a plasma accelerator operating at a frequency of 1 MHz and peak voltage of 30 kV had to be developed. Investigations on polyethylene(PE) plates and films used as a dielectric were made and resulted in the development of three types of capacitors. The first one is constructed as a plate capacitor using PE plates of 2-mm thickness for the dielectric and carefully rounded 2-mm aluminum plates for electrodes. To prevent sparking on the periphery of the plates, the capacitor is impregnated with a special organic fluid. The capacity is 14 nF, and a Q value higher than 10^3 at 1 MHz was measured. The other two consist of units made from wound PE films and impregnated with SF_6 under 3×10^5 N/m^2 pressure. Loss factors below 10^{-4} at 50 Hz and operating stresses up to 30 kV/mm are realized. (auth)

30596 (JAERI-Memo-4286) REVIEW OF USSR TOKAMAK EXPERIMENTS. Toi, Kazuo; Itoh, Satoshi (Japan Atomic Energy Research Inst., Tokyo). Jan 1971. 108p. (In Japanese). Dep. NTIS (U. S. Sales Only).

The results of USSR Tokamak experiments are reviewed, and classified according to equilibrium, instabilities and oscillations, thermal insulation, and transport phenomena. Several problems of Tokamak plasmas for future study are listed. (auth) (Japan)

30597 (LA-4339-TR) INVESTIGATION OF THE STABILITY OF A TOROIDAL PLASMA RING WITH A HIGH-FREQUENCY CURRENT ALONG THE LONGITUDINAL MAGNETIC FIELD. Vasilevskii, M. A.; Roife, I. M.; Seredenko, E. V. Translated by Anna Vakar (Los Alamos Scientific Lab., N. Mex.), from paper presented at International Symposium on Closed Confinement Systems, Dubna, USSR, September 29-October 3, 1969. 3p. (CONF-690931-5). Dep. NTIS.

Results of an investigation of the stability of a toroidal plasma ring with a high-frequency current in a longitudinal quasi-stationary magnetic field in a chamber with a conducting wall are presented. The results were obtained on "Toloskop". The magnetic field was varied from 0.2 to 6 kOe, and the amplitude of the high-frequency (1.1 Mc) current from 1.5 to 7.5 kA; the concentration of plasma was 10^{14} cm^{-3}. (auth)

30598 (LA-4617) SINGLE-SHOT PULSED MAGNETIC FIELDS FROM INDUCTIVE ENERGY STORES. Hake, Richard R. (Los Alamos Scientific Lab., N. Mex.). Feb 1971. Contract W-7405-eng-36. 44p. Dep. NTIS.

A simplified analysis is presented for the behavior of elemental pulsed-magnetic-field systems employing (a) superconducting magnets as energy stores, (b) superconducting switches with room-temperature shunts as the transfer mode, and (c) nonsuperconducting coils to furnish high-intensity (200 kG) pulsed magnetic fields. Megajoule energy pulses appear feasible, but sufficiently rapid actuation of the necessarily rather large-volume superconducting switches may be troublesome. (auth)

30599 (N-71-10100) HIGH-POWER QUASI-STEADY MPD ACCELERATION. Final Report. Malliaris, A. C.; Libby, D. R.; John, R. R. (Avco Corp., Wilmington, Mass. Avco Systems Div.). May 1970. Contract NAS1-9298. 72p. (NASA-CR-111785; AVSSD-506-70-CR). NTIS.

An investigation of ion-neutral coupling in plasma acceleration is presented. The acceleration of a partially ionized gas by electromagnetic means is considered. Velocities are determined by Doppler-shift measurements of selected spectral lines. Results regarding two different situations are presented from experiments where two basically similar axisymmetric configurations operate under significantly different conditions. In the first case, a large disparity in ion-neutral velocities is observed. In the second case, the said disparity disappears and the common ion-neutral velocities are in good agreement with the center of mass velocity, as determined independently from measurements of motionally induced potentials in the flow. A satisfactory interpretation of the results is obtained when the calculated mean free path for momentum exchange is compared with a typical dimension of the electromagnetic acceleration region. The preparation of a high-power quasi-steady MPD for repetitive operation in the laboratory is also given. Two topics receive particular consideration: (a) generation of desirable mass flow pulses on a repetitive basis and the diagnostics of such pulses by transient probing; and (b) development of a repetitively operating shutter with exposure durations between a few hundred microseconds and a few milliseconds. (auth) (STAR)

30600 (WASH-1172) PROGRESS IN CONTROLLED THERMONUCLEAR RESEARCH. Gould, R. W.; Furth, H. P.; Post, R. F.; Ribe, F. L. (Division of Research (AEC), Washington, D. C.). Dec 1970. 101p. GPO $1.00.

Progress of controlled fusion research is discussed in relation to the following areas: (1) magnetic mirror systems, (2) steady-state toroidal systems, (3) Astron, (4) pulsed high-beta systems, and (5) engineering and environmental aspects of fusion reactors. (M.O.W.)

30601 VACUUM MAGNETIC FIELD AND SURFACE CURRENT DISTRIBUTIONS FOR A SLOTTED CYLINDRICAL SHELL CARRYING AXIAL CURRENT. Ellis, W. R. (United Kingdom Atomic

XUM

Energy Authority, Abingdon, Eng.). J. Phys., D (London); 4: 332-7(Feb 1971).

Exact calculations are presented for the fringing fields inside and outside a hollow partial-cylinder conductor, as used on certain types of plasma pinch machines. The concentration of current density $j_z(\theta)$ at the slot edges is also calculated analytically. (auth) (UK)

30602 EXPERIMENTAL INVESTIGATION OF A WALL JET IN A TORUS. Piekaar, H. W.; Polman, R. W. (FOM-Instituut voor Plasma-Fysica, Jutphaas, Netherlands). Appl. Sci. Res. (The Hague); 23: 393-406(Jan 1971).

Results of an experimental investigation of the velocity profile of a turbulent gas injected in a toroidal configuration are presented. The measurements show surprisingly that it is possible to describe the radial distribution of the azimuthal velocity in terms of a plane wall jet discharging in an external stream. The growth of the inner boundary layer, the width of the jet, and the velocity profile agree with the known experimental data on this subject. A fundamentally different relation was deduced for the decay of the maximum velocity. Up to now Sigalla's formula $U_m/U_j \propto \sqrt{a/x}$ is generally accepted; the data here, based on an essentially extended range of x/a, correlate with the exponential relation $U_m/U_j = \exp[-154(Re_x)^{-0.777}\, x/a]$. (auth)

30603 MAGNETIC SURFACES IN A QUADRUPOLE. Williamson, J. H. (Culham Lab., Abingdon, Eng.). J. Plasma Phys.; 5: 229-38(Mar 1971).

Local imperfections in the magnetic field can alter the topology of the magnetic surfaces, thereby allowing plasma to escape. A modest longitudinal magnetic field will maintain the nested surfaces near the plasma boundary, so that the residual topological changes near the separatrix become unimportant. (auth) (UK)

30604 TEKHNIKA BOL'SHIKH IMPUL'SNYKH TOKOV I MAGNITNYKH POLEI. (Technology of Strong Pulsed Currents and Magnetic Fields). Dashuk, P. N.; Zaients, S. L.; Komel'kov, V. S.; (and others). Moscow; Atomizdat (1970). 472p.

The design, calculations, properties, and construction of powerful condenser banks are described along with their principal elements, including: capacitors, various types of dischargers, (vacuum and high pressure, with solid dielectric), insulated connecting circuits (busbars and cables), and pulsed transformers. Calculational methods for magnetic fields and induction in solenoids and conductors are discussed. The characteristics and behavior of metals in super-strong magnetic fields are analyzed. The techniques used for strong pulsed currents and magnetic fields are considered in relation to high-energy installations for heating and containing plasma. (R.V.J.)

Wave Phenomena

Refer also to abstracts 30491 and 30526.

30605 (NP-18673) FORCED AND FREE OSCILLATIONS. SOME ASPECTS OF LONGITUDINAL PLASMA WAVES. Technical Report No. 70:2. Ljungstroem, Anders (Lund Univ. (Sweden). Dept. of Electrical Engineering). May 1970. 62p. Dep. NTIS (U. S. Sales Only).

Thesis.

The plasma considered consists of a large number of free electrons and a background of positive ions. The state of the plasma is described by a distribution function, which is assumed to satisfy the Boltzmann equation. A solution of the Vlasov equation is constructed using the Fourier transform technique, and its properties are studied. The initial-value problem is solved, and it is shown that van Kampen's solution is equivalent to that one deducted from the Vlasov equation. It is shown that van Kampen's stationary solutions may be regarded as forced oscillations caused by a force field that vanishes in an arbitrarily large region. The behavior of the stationary waves is shown to be, in a sense, unstable. In the second part of the thesis, a new deduction of the solution of the Vlasov equation is presented in connection with a plasma model where it is assumed that every single particle can be followed in the course of its motion, and that a particle initially being in the neighborhood of each electron is characterized by its position (x,v) in phase space when traveling as a free particle. Each electron is also supposed to be closely followed by an ion always in an equilibrium position. The main concept in the analysis is the perturbation of the undisturbed electron coordinate, x, in configuration space. A section on energy balance is also included. (Sweden)

30606 (NP-18807) STUDY OF ABSORPTION OF SHF WAVES BY PLASMA AT UPPER HYBRID FREQUENCIES. Anisimov, A. I.; Vinogradov, N. I.; Golant, V. E.; Pakhomov, L. P. (Akademiya Nauk SSSR, Leningrad. Fiziko-Tekhnicheskii Institut). 1970. 13p. (In Russian). Dep. NTIS (U. S. Sales Only).

The drift velocity and absorption of shf waves by plasma were determined from measurements of spatial distribution of charged particle concentration in a toroidal magnetic field. It was found that the shf absorption by plasma was localized in a relatively narrow region of 1.5 to 2.0 cm. The region of the shf energy absorption coincides with the region of propagation of plasma waves, formed as a result of linear transformation induced externally by electromagnetic waves, and the attenuation length is close to the calculated absorption length of these waves. (tr-auth)

30607 NONLINEAR INTERACTIONS OF ION-ACOUSTIC WAVES AND HELICONS IN PLASMA. Kingsen, A. S. Zh. Prikl. Mekh. Tekh. Fiz.; No. 6, 18-25(Nov-Dec 1970). (In Russian).

Kinetic equations describing tri-plasmon processes of two ion acoustic waves merging into a helicon, and ion acoustic waves scattering on plasma particles with re-emission of helicons were obtained by perturbation theory and statistical normalization along phase oscillations. The rate of Whistler buildup in the turbulent plasma was also estimated on the basis of the nonlinear wave interactions. (R.V.J.)

30608 ELECTROMAGNETIC WAVE PROPAGATION THROUGH SLOWLY VARYING PLASMA. Chakraborty, B. (Jadavpur Univ., Calcutta). J. Math. Phys. (N. Y.); 11: 2570-79(Aug 1970).

The second-order linear inhomogeneous wave equation is solved by the WKB method. Then a sequence of successive substitutions is developed, by the use of which solutions correct up to any higher order are reduced to the WKB solution of an equation like the original equation. This procedure is adopted to study propagation of electromagnetic waves obliquely through slowly but continuously varying plasma layers. The boundary value problems for wave propagation are solved across a plane where N (the equilibrium plasma concentration) is continuous, but its first- and second-order space rates of variation along the normal are discontinuous. The characteristics of the reflected and transmitted fields depend on these derivatives of N such that the reflected wave vanishes in the limit of constant N. The direction of flow of electromagnetic energy is deviated from its straight course in the uniform region. Expressions for relative shift of the wave vector along and perpendicular to the direction in the uniform medium, with respect to the distance of wave advancement in that medium in a given time, are deduced. The deviation of the direction of propagation is slightly more for the field of transverse magnetic (TM) polarization than for the transverse electric (TE) polarization, but both these directions lie in the plane of incidence and are opposite to one another with respect to the direction in the uniform medium, whereby transverse polarizations are meant those with respect to the plane of incidence. Hence, the original wave is split into two waves. Deflection is increased and, consequently, speed of propagation is decreased for the TM field, whereas deflection is decreased and speed of propagation is increased for the TE component, if the wave propagates into a plasma of increasing concentrations; consequently, the TM field will be reflected back earlier than the TE part. This treatment may help in attacking problems of the coupling of different types of plasma waves due to slow variation of equilibrium parameters resulting from more complete sets of equations describing plasma behavior. (auth)

30609 NONSTEADY THIRD HARMONIC GENERATION IN A PLASMA. Tripathi, V. K. (Indian Inst. of Tech., New Delhi). J. Phys., D (London); 4: 164-7(Jan 1971).

The phenomenon of generation of a third harmonic due to the interaction of a microwave with a plasma is investigated in the nonsteady state. The results show that in the limit when time of observation is greater than the period of the wave but much less than the energy relaxation time of electrons, the third harmonic current density may be as much as 20 times the steady-state value for easily obtainable fields. (auth) (UK)

30610 PROPAGATION OF LARGE-AMPLITUDE ELECTRON PLASMA WAVES. Kawai, Yoshinobu; Kondo, Katsumi (Nagoya Univ., Japan). J. Phys. Soc. Jap.; 30: 857-63(Mar 1971).

Electron plasma waves are excited by grids in an argon plasma. The comparison between the experimental results and the theory for an infinite collisionless plasma is made. With increasing wave amplitudes under the condition of $1 < v_{ph}/v_e < 3$, where v_{ph} and v_e are the phase velocity and the thermal velocity, respectively, the enhancement of damping is observed and is found to depend strongly on the phase velocity of the waves. These results are compared with those by Dawson and Shanny. (auth)

30611 ECHOES WITH ION SOUND WAVES. Bachmann, P.; Hinzpeter, G.; Sauer, K; Wallis, G. (Akademie der Wissenschaften, Berlin). Beitr. Plasmaphys.; 10: 321-8(1970). (In German).

Although the experimental and theoretical studies were only preliminary in nature, several principles about the origin and detection of ion-wave echoes could be clarified. The model, without assumption of interactions, described all essential characteristics of spatial echoes; collective interaction caused only insignificant modifications. Pilot measurements at frequencies in the neighborhood of 1 MHz already showed the decline of echo amplitude as predicted by the electron collision–excitation mechanism. Thus, the method offers, for the first time, the possibility to interconnect nonlinear wave effects in plasma with electron transition states in atoms and molecules. (H.B.G.)

30612 PROPAGATION OF ELECTROSTATIC ION WAVES NEAR ION CYCLOTRON HARMONICS. Ohnuma, T.; Miyake, S.; Sato, T.; Watari, T. (Inst. of Plasma Physics, Nagoya Univ.). Phys. Rev. Lett.; 26: 541-3(8 Mar 1971).

The propagation of electrostatic ion waves above the ion cyclotron frequency was studied. Resonance effects and enormous wave damping were observed at frequencies near the ion cyclotron harmonics. (auth)

30613 NONLINEAR WAVE PARTICLE PROCESSES IN AN ELECTROSTATIC WAVE PACKET. Nunn, D. (Imperial Coll. of Science and Tech., London). J. Plasma Phys.; 5: 199-210 (Mar 1971).

The system studied is that of an electrostatic Gaussian wave packet in a cold uniform plasma being excited by a weak resonant beam. To first order in a parameter associated with the weakness of the beam the resonant particle distribution function and resonant particle charge densities are computed. Of particular interest is the nonlinear case where resonant particles suffer several "trapping" oscillations while traversing the wave packet. In this case the resonant particle distribution function becomes very discontinuous in character and increasingly rich in higher harmonies of the packet frequency. The phase average distribution function does not form a plateau, but has its gradient actually reversed. The power input from particles to field is initially of the linear form, but after one trapping oscillation reverses sign and after many trapping periods dies away altogether. These results are of considerable interest in understanding the nonlinear limit of the Landau problem in the case of a narrow band signal. Also, aspects of the time development of the electric field shed light on the triggered emission problem. (auth) (UK)

30614 EFFECT OF SPATIALLY UNIFORM EXTERNAL PERIODIC MAGNETIC FIELD ON WAVE PROPAGATION THROUGH A HOT ELECTRON PLASMA. Das, K. P. (Jalpaiguri Government Engineering Coll., West Bengal, India). J. Plasma Phys.; 5: 151-9(Mar 1971).

Starting from hydrodynamic equations, a dispersion relation is obtained for wave propagation through a hot-electron plasma perpendicular to a spatially uniform external periodic magnetic field, $B_0 \cos \omega_0 t$, and several excitation conditions are deduced. (auth) (UK)

30615 NONLINEAR LANDAU DAMPING OF ELECTROMAGNETIC CYCLOTRON WAVES. Akinrimisi, J.; Sudan, R. N. (Cornell Univ., Ithaca, N. Y.). J. Plasma Phys.; 5: 161-76 (Mar 1971).

The nonlinear scattering of circularly polarized electromagnetic waves is studied. Expressions for matrix elements of interaction are derived and for interacting right-handed circularly polarized waves (whistler waves) the matrix is explicitly calculated for particular velocity distribution functions of electrons. Nonlinear damping rates are computed. It is shown that nonlinear scattering is not in general a dominant process for whistlers in the magnetosphere. (auth) (UK)

30616 ELECTROMAGNETIC ENERGY ABSORPTION AT THE UPPER HYBRID RESONANCE. Baldwin, D. E.; Henderson, D. M.; Ignat, D. W. (Yale Univ., New Haven). J. Appl. Phys.; 42: 2431-40(May 1971).

A method of calculating the bulk response of an inhomogeneous plasma in the zero-temperature approximation is extended to include the presence of a uniform magnetic field where again the process of resonant absorption is of prime importance. Calculations are presented which show the transmission and reflection coefficients of a cylindrical plasma in a parallel-plate waveguide. Experimental results obtained in rectangular waveguides are given to demonstrate the degree to which the zero-temperature models, and the solution of the resultant singular equations may predict physically realizable values for the plasma admittance. (auth)

30617 VERY-LOW-FREQUENCY PLASMA OSCILLATIONS IN A SPHERICAL, MAGNETIZED, COLD-CATHODE DISCHARGE. Schmidt, Pierre; Quinn, Robert G. (Pennsylvania State Univ., University Park). J. Appl. Phys.; 42: 2440-8(May 1971).

Coherent very-low-frequency (vlf) oscillations in the range 0 yo 30 kHz, due to a plasma transport across magnetic field lines, were found in a cold cathode dc discharge, where the cathode is a uniformly magnetized sphere. Similar oscillations are found to occur in coaxial cylindrical discharges with a uniform external magnetic field. The frequency of the oscillations decreases with increasing discharge current, decreasing discharge voltage, background gas pressure, magnetic field strength, ion mass, and increasing diameter of the cathode. The oscillations are rich in harmonics. At the lower frequencies the discharge revolves in the equatorial plane of the cathode. A mixing phenomenon is reported in which sum and difference frequencies are obtained between the signals of the device and an external generator. Using probes as diagnostic tools the maximum of the oscillations was located in the negative glow of the discharge. In addition, it is found that two different modes of oscillation exist, the $m = 0$ mode having no phase difference in the angular direction, and the $m = 1$ mode having a phase difference of 2π in the angular direction. A simple theoretical model, based on the assumption that the frequency of oscillation is proportional to the rotation frequency of the plasma, is developed for the $m = 1$ mode of oscillation. Finally, the use of the device as a sensitive pressure gauge is suggested. (auth)

30618 SPACE-CHARGE WAVES ON PLASMA COLUMNS IN A WEAK MAGNETIC FIELD. Sugai, H.; Sato, N.; Hatta, Y. (Tohoku Univ., Sendai). J. Appl. Phys.; 42: 2421-3(May 1971).

Effects of the thermal motion on the space-charge waves propagating along plasma columns in a weak magnetic field is measured by using a unique experimental method. Good agreement is obtained between the experiment and the theory. (auth)

30619 PROPAGATION OF INTENSE ELECTROMAGNETIC WAVES IN A TWO-COMPONENT PLASMA. Bass, F. G.; Gurevich, Yu. G.; Kvimsadze, M. V. (Inst. of Radio Physics and Electronics, Novosibirsk, USSR. Inst. of Cybernetics, Tbilisi, USSR). Zh. Eksp. Teor. Fiz.; 60: 632-42(Feb 1971). (In Russian).

The effect of an intense electromagnetic wave on plasma concentration and heating of the carriers resulting in variation of the dielectric permeability is studied. The coordinate dependence of the wave amplitude is found for various ratios of the plasma frequencies. (auth)

30620 SHOCK WAVES PROPAGATING ALONG A MAGNETIC FIELD IN A COLLISIONLESS PLASMA. Kurtmullaev, R, Kh.; Masalov, V. L.; Mekler, K. I.; Semenov, V. N. (Inst. of Nuclear Physics, Novosibirsk, USSR). Zh. Eksp. Teor. Fiz.; 60: 400-7 (Jan 1971). (In Russian).

Disturbances excited by a pulsed magnetic piston and propagating along a magnetic field are investigated. Under certain conditions shock waves of the "switch-on-wave" type are formed. The internal structure of the wave front is investigated. (auth)

30621 CORRELATION DAMPING OF LONGITUDINAL PLASMA WAVES IN A NONDEGENERATE MAGNETOPLASMA. Kastelewicz, H. (Deutsche Akademie der Wissenschaften, Berlin). Monatsber. Deut. Akad. Wiss. Berlin; 12: 481-5 (1970). (In German).

The results of a systematic perturbation–theoretical investigation of the damping behavior of longitudinal plasma waves in the presence of a static external magnetic field are reported. The calculations are based on a variant of the temperature-dependent Green function method proposed by du Bois et al. With this variational method it is possible to represent the absorption part of the dielectric constants directly by microscopic dissipation processes of plasmons. These quantum processes are described by "open" graphs. (tr-auth)

30622 MULTIPLE-TIMES TECHNIQUE APPLIED TO THE NEARLY LINEAR PROPAGATION OF A LONG-WAVE PACKET IN A DISPERSIVE PLASMA. Maroli, C. (CNR, Milan. Univ., Milan). Lett. Nuovo Cim.; 1: 295-9(13 Feb 1971).

Mathematical solutions of a system of nonlinear partial differential equations are discussed. A system of equations that describes ion acoustic oscillations, in the limit of massless electrons, is illustrated. The equations for wave packets moving in the same and opposite directions are described. (M.O.W.)

XUM

30623 ELECTROSTATIC OSCILLATIONS IN COLD INHOMOGENEOUS PLASMA. I. DIFFERENTIAL EQUATION APPROACH. Sedlacek, Z. (Inst. of Plasma Physics, Prague). J. Plasma Phys.; 5: 239-63(Mar 1971).

Small-amplitude electrostatic oscillations in a cold plasma with continuously varying density were investigated. The problem is the same as that treated by Barston (1964) but instead of his normal-mode analysis the Laplace transform approach is employed to solve the corresponding initial-value problem. The Green function of the differential equation of the problem shows that there are branch-point singularities on the real axis of the complex frequency-plane, which correspond to the singularities of the Barston eigenmodes and which, asymptotically, give rise to noncollective oscillations with position-dependent frequency and damping proportional to negative powers of time. In addition an infinity of new singularities (simple poles) of the analytic continuation of the Green function into the lower half of the complex frequency-plane were found whose position is independent of the spatial co-ordinate so that they represent collective, exponentially damped modes of plasma oscillations. Thus, although there may be no discrete spectrum, in a more general sense a dispersion relation does exist but must be interpreted in the same way as in the case of Landau damping of hot plasma oscillations. (auth) (UK)

30624 CONSTANT-FREQUENCY OSCILLATIONS IN A BOUNDED THERMALLY PRODUCED PLASMA. Allen, J. E.; Fang, M. T. C.; Fraser, D. A. (Oxford Univ.). Proc. Roy. Soc. (London), Ser. A; 322: 63-72(23 Mar 1971).

Measurements are reported of a constant-frequency oscillation in a current-carrying thermal plasma. A collision-free theory is presented that includes a standing wave in the plasma together with a sheath oscillation. It is postulated that the ion velocity distribution function becomes flattened at $v = \pm\omega/k$, and this gives good agreement between theory and experiment. (auth) (UK)

30625 HIGH-FREQUENCY INSTABILITY AND ANOMALOUS PLASMA RESISTIVITY AT SUPERCRITICAL ELECTRIC FIELDS. Coppi, B. (Massachusetts Inst. of Tech., Cambridge); Dobrowolny, M.; Santini, F. Phys. Lett.; 34A: 395-6(19 Apr 1971).

Excitation of Langmuir waves is shown to occur in a current-carrying plasma when the applied electric field exceeds the runaway critical field. A theoretical model is proposed for the experimentally observed anomalous resistivity in this regime. (auth)

30626 NONLINEAR THEORY OF REFLECTION OF ELECTROMAGNETIC WAVES FROM PLASMA. Demchenko, V. V.; Omel'chenko, A. Ya. (Inst. of Physics and Tech., Kharkov). Ukr. Fiz. Zh. (Russ. Ed.); 15: 2065-71(Dec 1970). (In Russian).

The effect of a hf electromagnetic field on the reflection of obliquely incident waves from a plasma was investigated. Dependences of the wave amplitude on the coordinates as well as equations determining the reflection coefficient and reflected-wave phase shift are obtained in cases of strong and weak nonlinearity of the plasma (nonlinearity is characterized by the ratio of plasma pressure to high-frequency pressure of the wave field). (auth)

30627 EQUILIBRIUM STATES OF INTERACTING WAVES. Stenflo, L. (Inst. of Physics and Tech., Uppsala). Z. Phys.; 243: 341-5(1971).

The nonlinear interaction between three waves (in a plasma) is considered within the well-defined phase description. A new equilibrium state, characterized by comparatively large wave amplitudes, is shown to be possible if the coupling coefficients are influenced by collisional or collective dissipation. (auth)

30628 EFFECT OF EXTERNAL dc ELECTRIC FIELD ON ABSORPTION OF MICROWAVES IN PLASMA. Bhagavat, G. K.; Vanvari, N. (Indian Inst. of Tech., Bombay). Indian J. Pure Appl. Phys.; 8: 383-6(Aug 1970).

Absorption of microwave power in a plasma was investigated using a transmission cavity, excited in the TE_{011} mode, perturbed by the plasma column. The measurements were made in the X-band region using ionized air. The electron density, collision frequency, and frequency of damped oscillations in plasma were determined using the perturbation theory. It was shown that absorption of microwaves increases with an application of dc electric fields along the plasma column. (auth)

Shielding

Refer also to abstracts 31640 and 31671.

30629 (NP-18798) SIMULATION OF AN ELECTRON AVALANCHE IN He USING A MONTE CARLO METHOD. Denes, Jean-Francois (Toulouse Univ. (France)). 5 Feb 1971. 115p. (In French). Dep. NTIS (U. S. Sales Only).

Thesis.

A direct simulation was made of the behavior of electrons in a strong uniform electric field (high E/P values). The results obtained permitted the investigation of the limits to the validity of the classical distribution law for the free paths, the value of the transmission factor, the effect of the initial energy of the electrons and the cathode reflection coefficient. A study of the mean energy in the vicinity of the equilibrium, other macroscopic coefficients, and the ionization probabilities enabled the growth in electron population accompanying the transient phase of the avalanche to be studied. (France)

30630 (ORNL-TM-3318) LOW-ENERGY ELECTRON TRANSPORT WITH THE METHOD OF DISCRETE ORDINATES. Bartine, D. E.; Alsmiller, R. G. Jr.; Mynatt, F. R.; Engle, W. W. Jr.; Barish, J. (Oak Ridge National Lab., Tenn.). 22 Feb 1971. 9p. (CONF-710304-4). Dep. NTIS.

From Symposium on Natural and Manmade Radiation in Space, Las Vegas, Nev.

The one-dimensional discrete ordinates code ANISN was adapted to transport of low-energy (~ a few MeV) electrons. Calculated results obtained with ANISN are compared with experimental data for the transmitted electron energy and angular distributions for 1-MeV electrons normally incident on aluminum slabs of several thicknesses. The calculated and experimental results to date are in good agreement for a thin slab (0.2 of the electron range) but are not in good agreement for thicker slabs (0.6 of the electron range). Calculated results obtained with ANISN are also compared with calculated results obtained using Monte Carlo methods. (auth)

30631 (ORNL-TM-3376) EXPERIMENTAL NUCLEAR CROSS SECTIONS FOR SPACECRAFT SHIELD ANALYSIS. Peelle, R. W. (Oak Ridge National Lab., Tenn.). Apr 1971. 23p. (CONF-710304-9). Dep. NTIS.

From Symposium on natural and manmade radiation in space; Las Vegas, Nev. (1 Mar 1971).

Experiments were performed to validate and to supplement the intranuclear cascade model as a method for estimating cross sections of importance to spacecraft shield design. The experimental situation is inconclusive particularly for neutron-producing reactions, but is relatively sound for reaction cross sections and for proton spectra at several hundred MeV at medium forward angles. Secondary photon contributions are imprecisely known. (auth)

30632 (RT/FI-(70)36) ANALYSIS OF METHODS FOR INTERPRETING BREMSSTRAHLUNG SPECTRA. Fioratti, M. Paganini; Piermattei, S. Ricci (Comitato Nazionale per l'Energia Nucleare, Rome (Italy)). 14 Sep 1970. 21p. (In Italian). Dep. NTIS (U. S. Sales Only).

An analysis is made of the analytical methods for interpreting bremsstrahlung spectra. Owing to the nature of the response matrix, the iterative method is the most adequate one to obtain correct information. (auth)

30633 CALCULATIONS OF WEAPON RADIATION DOSES IN SINGLE-COMPARTMENT ABOVEGROUND CONCRETE STRUCTURES. Mooney, L. G. (Radiation Research Associates, Inc., Fort Worth, Tex.). Nucl. Sci. Eng.; 44: 157-72 (May 1971).

Calculations were performed to determine energy and angle distributions of the fission-product gamma ray, air–ground secondary gamma ray, and neutron fluence incident on structures resulting from the detonation of a representative intermediate-yield thermonuclear weapon 100 m above the ground. These energy and angle distributions were used as input data to the ANISN discrete ordinates code to calculate the penetration of the radiation through various thicknesses of type O–HW1 concrete. The production and transport of concrete capture gamma rays were calculated in tandem with the neutron transport. The penetration results were used to calculate the various radiation components at the center of a simple concrete blockhouse. The inside lengths and widths of the structure varied from 10 to 50 ft and the inside height was fixed at 10 ft. Wall and roof thicknesses varied from 6 to 60 in. The results of the calculations were expressed as structure protection coefficients (dose at the receiver per unit free-field dose). The neutron dose was found to contribute the highest fraction of the total dose for wall and roof thicknesses up to 12 in. For thicknesses of 18 in. and more, the air–ground secondary gamma rays and concrete capture gamma rays were found to dominate, becoming increasingly more important with increasing thickness. The relative magnitude of each component

did not vary significantly with structure size; however, all components were found to decrease with an increase in structure size for a given wall and roof thickness. (auth)

30634 ENGINEERING COMPENDIUM ON RADIATION SHIELDING. VOLUME III. SHIELD DESIGN AND ENGINEERING. Jaeger, R. G. (ed.). New York; Springer-Verlag New York Inc. (1970). 490p.

The following topics are covered: shielding of shipping containers for radiation sources, shielding of fixed storage installations, design and shielding of medical radiation rooms, design and shielding of irradiation facilities, design and shielding of hot cells for research, shielding of electron accelerators, shielding of nucleon accelerators, shielding of irradiated fuel processing and high-level waste storage facilities, shielding of research reactors, shielding of stationary power reactors, and shielding of ship propulsion reactors. (M.H.R.)

30635 DIFFERENTIAL MEASUREMENTS OF FAST-NEUTRON AIR-GROUND INTERFACE EFFECTS. French, R. L.; Mooney, L. G. (Radiation Research Associates, Inc., Fort Worth, Tex.). Nucl. Sci. Eng.; 43: 273-80(Mar 1971).

The effect of the air/ground interface on the scattered fast-neutron dose near the ground was measured at a distance of 1000 ft from a 14-MeV neutron source. The source was the HENRE accelerator operated at a height of 112 ft on the BREN tower at the Nevada Test Site. A horizontal slab of polyethylene 1 ft thick and 5 ft square, with Hurst-type fast-neutron dosimeters mounted on its upper and lower surfaces, separated the neutrons arriving through the upper 2π solid angle from those from the lower 2π. A third detector, mounted on a boom, measured the free-field. The entire assembly was suspended by a hoist system to make measurements at 0.75 to 70 ft above the ground. The scattered dose at the top detector was essentially constant; that at the bottom detector increased by a factor of approximately 2 between 0.75 and 70 ft, and the free-field dose increased by <25% over the same height range. The experiment provided confirmation, both qualitative and quantitative, of the "first-last collision model" of the air/ground interface effect. (auth)

30636 PRECISE MEASUREMENTS OF W, THE MEAN ENERGY REQUIRED FOR ION-PAIR FORMATION IN GASES. I. ALKANES. Stoneham, T. A.; Ethridge, D. R.; Meisels, G. G. (Univ. of Houston, Tex.). J. Chem. Phys.; 54: 4054-9(1 May 1971).

Ionization currents were measured for the complete stopping of ^{63}Ni beta rays in N_2 and in alkane isomers at temperatures from 25 to 200°C and pressures between 400 and 2700 torr. The mean energy expended per ion pair formed, W (beta), was determined from the ratio of ion current in nitrogen to that in the sample at equal electron densities. No dependency of W upon temperature or pressure was observed within the experimental precision of ±0.1%. Using $W(N_2) = 34.6$ eV/ion pair for reference, relative values of W in electron volts/ion pair were found to be 26.94 for methane, 24.18 for ethane, 23.69 for propane, 23.19 for n-butane, 22.82 for n-pentane, 22.62 for n-hexane, 22.47 for n-heptane, 23.52 for 2-methylpropane, 23.07 for 2-methylbutane, 23.42 for 2,2-dimethylpropane, 22.80 for 2-methylpentane, 22.81 for 3-methylpentane, 22.81 for 2,3-dimethylbutane, and 22.88 for 2,2-dimethylbutane. (auth)

30637 MEASUREMENT AND CALCULATION OF DOSE RATE REMOVAL CROSS SECTIONS AND B FACTORS FOR NEUTRONS. Kolb, E.; Tschirf, E. (Oesterreichische Hochschule, Vienna). Acta Phys. Austr.; 29: 160-5(1969). (In German).

The dose rate removal cross section and the buildup factors for neutrons (0.5 to 10 MeV) from a Pu–Be source and 14-MeV neutrons from a neutron generator were experimentally determined for the shielding materials water, oil, and paraffin. The removal cross sections are tabulated, and the buildup factors are given graphically. The experimental arrangement used in the measurements is described. (J.S.R.)

30638 MEASUREMENT OF GAMMA RADIATION CONDUCTION IN A TUBE WITH A CONSTANT CURVATURE. Herre, F. (Gesellschaft fuer Wiederaufarbeitung von Kernbrennstoffen mbH, Leopoldshafen, Ger.); Roesinger, S. Kerntech. Atomprax.; 13: 131-4(Mar 1971). (In English and German).

The exposure rate and gamma spectrum of a ^{60}Co source were measured inside a curved tube embedded in quartz sand and in steel grit. The measurement results obtained make it possible to estimate the radiation level that may be expected on the outside of a shielding at the exit of a curved pipe penetration. (auth)

30639 ANGULAR DISTRIBUTION OF NEUTRONS SCATTERED IN AIR FROM A MONOENERGETIC ISOTROPIC POINT SOURCE. Kokovikhin, V. F.; Kondurushkin, N. A.; Belovintsev, V. Ya.; Barchugov, V. V. This paper was summarized in At. Energ. (USSR); 29: 118(Aug 1970) as paper No. 410/5534. (In Russian).

Computer calculations were made by the Monte Carlo method of the angular distributions of neutrons in an infinite region filled with air. Calculations were made for distances R of 10 to 1100 m from a source and initial energies of 0.8, 2, 5, 10, and 14 MeV with a lower limiting energy of 0.5 MeV. The density of air was assumed to be 1.293×10^{-3} g/cm^3. The composition of air was taken to be 78% (by volume) nitrogen and 21% (by volume) oxygen (the other admixtures were not taken into account). For each energy, 4000 to 10,000 neutron trajectories were followed. In the calculations, allowance was made for all processes of interaction of neutrons with nuclei of nitrogen and oxygen. The results of the calculations for the initial energies $E_0 = 2$, 5, and 14 MeV and various distances are given. (auth)

30640 ANGULAR AND ENERGY DISTRIBUTIONS OF γ RAYS IN LEAD. Kondrat'ev, B. S. This paper was summarized in At. Energ. (USSR); 29: 119(Aug 1970) as paper No. 411/5577. (In Russian).

Calculations were made by the Monte-Carlo method of the angular and energy distributions of scattered γ-rays of a plane monodirectional source behind lead barriers. The density-of-collisions method was used. The absorption and loss of radiation from the barrier were taken into account by the introduction of a statistical weight. The mean free path and the statistical weight of a quantum were calculated. The method of exponential transformation was used for large thicknesses. The method of "Russian roulette" was also used. Calculations were made of the angular and energy distributions of the γ rays for source energies of 1, 4, and 8 MeV and barrier thicknesses of 0.5, 1, 2, 4, 7, and 10 mean free paths. The angular energy distributions behind barriers of thickness more than two mean free paths can be assumed to be stabilized. With increasing angle of departure, the energy spectrum becomes appreciably softer. The angular distributions of the intensity can be approximated by an exponential dependence. The value of the constant Θ_0 of the angular distribution are given. Satisfactory agreement between the data and the experimental and calculated results of other investigations was obtained for barrier thicknesses greater than two mean free paths. For small thicknesses, a certain increase in Θ_0 with decreasing barrier thickness was noted; this was particularly noticeable for a low initial energy. Satisfactory agreement was obtained between the results of the calculations of the angular distributions by the Monte Carlo method and calculations in the single scattering approximation for thicknesses less than two mean free paths. (auth)

30641 EFFICIENCY OF RADIATORS AND ABSORBERS OF CHARGED PARTICLES. Lenchenko, V. M.; Sazonova, E. V.; Sofienko, L. A. This paper was summarized in At. Energ. (USSR); 29: 38-9(Jul 1970) as paper No. 406/5616. (In Russian).

The energy radiated by radiators or absorbed by absorbers of charged particles (α- and β-particles, Compton electrons, photoelectrons, etc.,) is calculated for three different geometries: cylindrical (filamentary), film, and spherical. (auth)

30642 BRAGG-RULE APPLICABILITY TO STOPPING CROSS SECTIONS OF GASES FOR α PARTICLES OF ENERGY 0.3 TO 2.0 MeV. Bourland, P. D.; Powers, D. (Baylor Univ., Waco, Tex.). Phys. Rev., B; 3: 3635-40(1 Jun 1971).

The additivity of atomic stopping cross sections, Bragg's rule, is tested for α particles in the gaseous compounds H_2, N_2, O_2, NH_3, N_2O, CO, CO_2, CH_4, C_2H_2, C_2H_4, C_2H_6, C_3H_6 (propylene), and $(CH_2)_3$ (cyclopropane). Compounds with single and double bonds are found to obey Bragg's rule. Compounds containing triple-bond structure are found to deviate from Bragg's rule by as much as 12.8%, but an empirical triple-bond correction is made to fit all the data of the present experiment. Evidence is seen for a possible physical-state effect. (auth)

30643 GENERAL EXPRESSION FOR THE DENSITY EFFECT FOR THE IONIZATION LOSS OF CHARGED PARTICLES. Sternheimer, R. M.; Peierls, R. F. (Brookhaven National Lab., Upton, N. Y.). Phys. Rev., B; 3: 3681-92(1 Jun 1971).

A simple reformulation is presented of the expression for the density effect correction δ, i.e., the reduction in the ionization loss of fast charged particles due to the dielectric polarization of the medium. The general expression for δ thus obtained is applicable to both condensed materials and gases. Its accuracy is such that the resulting values of the ionization loss dE/dx are expected to have a maximum error of less than 2% throughout the range of momenta where the density effect is important. (auth)

XUM

30644 EXPERIMENTAL EVIDENCE OF HELICITY EFFECT ON THE ENERGY-LOSS STRAGGLING OF ELECTRONS. Braicovich, L. (Politecnico, Milan. Consiglio Nazionale delle Richerche, Milan); De Michelis, B.; Dupasquier, A.; Fasana, A. Phys. Rev., B; 3: 3754-6(1 Jun 1971).

A simple experiment on the polarization straggling effect suggested by Braicovich is presented. A counting-rate asymmetry of the order of 1% is obtained in a magnetized HCR foil. This result provides the first experimental evidence of the above effect. (auth)

30645 CONCRETE RADIATION SHIELDS. ANS-11.13 1971. Hinsdale, Ill.; American Nuclear Society (1971). 63p. Available from American Nuclear Society, Hinsdale, Ill.

Requirements and recommended practices are covered for the construction of concrete radiation shielding structures and for certain elements of design that relate to problems unique to this type of structure. Discussions of aggregates; design of concrete mixtures and forms; placement of concrete; design and installation of penetrations, embedments, metal liners, and penetration plugs; and an outline of testing and quality assurance provisions needed to verify that the desired quality of design and construction has been achieved are included. These standards apply primarily to shielding structures for hot laboratories, radiochemical plants, experimental facilities, and similar applications. (M.H.R.)

Solid-State Physics

30646 (NYO-2150-66) SOLID STATE PHYSICS; MAGNETIC PHENOMENA. Progress Report, January 1, 1970–December 31, 1970. Bowers, R.; Silsbee, R. H. (Cornell Univ., Ithaca, N. Y. Lab. of Atomic and Solid State Physics). Contract AT(30-1)-2150. 15p. Dep. NTIS.

ALKALI METAL HALIDES—impurities in, ionic
MOLECULES—orientational freedom in alkali-metal halides, (E)
POTASSIUM—ultrasound generation by eddy currents in, zero-field efficiency of, (E)
—magnetoresistance and Hall effect of, (E)
TUNGSTEN—Lorentz number for electron–electron scattering in, (E/T)
ULTRASOUND—generation by eddy currents, zero-field efficiency of, (E) (D.L.C.)

30647 APPLYING METHODS OF NUCLEAR PHYSICS TO SOLID STATE RESEARCH. Kamke, Detlef (Ruhr-Univ., Bochum, Ger.). Naturwissenschaften; 57: 337-44(Jul 1970). (In German).

Ways in which nuclear physics methods can be applied to solid-state research are reviewed. New results obtained by the use of infiltration of hydrogen, detection of particle tracks in solids, material analysis, doped semiconductor materials, and fast ions in single crystals are cited to show the wide range of possibilities. (J.S.R.)

Radiation Effects

Refer also to abstract 30444.

30648 (N-70-37028) DEFECT PRODUCTION IN SINGLE CRYSTALS RESULTING FROM ION BOMBARDMENT. Final Status Report, June 1966–December 1969. Shaffer, Lawrence B. (Hiram Coll., Ohio. X-Ray Physics Lab.). 22 May 1970. 66p. (NASA-CR-112875). NTIS.

The application of standard x-ray techniques to the determination of certain thermodynamic properties of cesium gas is discussed, including the experimental techniques and equipment. The design, fabrication, final configuration, and deficiencies of the equipment used in the single-crystal damage studies are described, along with the experimental technique utilized. The results of the investigation are given for silicon, copper, and germanium, and are stated to be generally inconclusive. (STAR)

30649 (NYO-3504-57) DIRECT OBSERVATION OF LONG RANGE MIGRATION OF SELF-INTERSTITIAL ATOMS IN STAGE I OF IRRADIATED PLATINUM. Report No. 1529. Petroff, P.; Seidman, D. N. (Cornell Univ., Ithaca, N. Y.). 2 Mar 1971. Contract AT(30-1)-3504. 9p. Dep. NTIS.

The motion of single self-interstitial atoms (SIAs) in Stage I of irradiated platinum was observed directly by field-ion microscopy. A specimen irradiated at a temperature of 10°K with 20-keV Pt^+ ions was found to contain immobile SIAs in the bulk at this temperature, as determined via pulse-field evaporation experiments. Direct observation of specimens, irradiated with 20- or 30-keV Pt^+ ions, during warming experiments from 10 to 70°K, showed that a flux of SIAs crossed the surface of the specimens between 13 and 25°K. Application of a diffusion model to the data yielded a value of ~0.06 eV for the enthalpy change of migration and a diffusion coefficient of $\sim 0.5 \exp(-0.06\ \text{eV}/kT)\ \text{cm}^2\ \text{sec}^{-1}$ for the SIA. (auth)

30650 ELECTRON MICROSCOPE OBSERVATION OF LATTICE DISORDER IN ION-IMPLANTED SILICON. Bertolotti, M.; Sette, D.; Stagni, L.; Vitali, G. (Univ., Rome. CNR, Rome). Appl. Phys. Lett.; 18: 257-9(15 Mar 1971).

A technique of electron microscope observation of a replica of the chemical etched surface was used to see the disorder produced around the single-ion paths in In-implanted Si. Structures of variable dimensions ranging from about 100 Å up to nearly 600 Å in diameter were observed with a density of about 10^{10} cm^{-2} in a very thin layer in the surface. (auth)

30651 DEFECT FORMATION AND SPUTTERING OF ALKALI HALIDES WITH LOW ENERGY IRRADIATION. Elliott, D. J.; Townsend, P. D. (Univ. of Sussex, Eng.). Phil. Mag.; 23: 249-60(Feb 1971).

Low-energy electron or photon irradiation of alkali halides produces energetic sputtering of surface atoms. Measurements of both the angular ejection pattern and the sputtering efficiencies are reported. The low threshold energy required for sputtering, the ⟨110⟩ nature of the halogen ejection and the dependence on the total rate with both alkali metal and halogen ion dimensions are all consistent with the model of defect formation proposed by Pooley(Proc. Phys. Soc., 87: 245(1966)) and by Hersh(Phys. Rev., 148: 928(1966)). A variety of surface features appear after irradiation, all of which result from regions of different sputtering rate. The regions are the clean alkali halide surface with a normal sputtering rate, dirty surfaces with a zero rate of sputtering and regions of very high rates of sputtering where dislocations intersect the surface. (auth) (UK)

30652 DOSE DEPENDENCE OF SWELLING IN ELECTRON IRRADIATED NICKEL. Norris, D. I. R. (Berkeley Nuclear Labs., Eng.). Phys. Status Solidi (a); 4: K5-8(16 Jan 1971).

Annealed Ni foils were bombarded with 150-kV argon ions to provide nucleation centers and then irradiated in a 1-MV high-voltage electron microscope. The voids produced are cubes with (100) faces, and an individual void may grow or shrink. The dose dependence of the swelling shows a power law dependence with a power of 2.2 ± 0.2 up to 12 displacements/atom, a linear dependence from 12 to 40 displacements/atom, and saturation thereafter. (D.L.C.)

30653 PHOTOCONDUCTIVITY STUDIES OF Li-DOPED SILICON IRRADIATED WITH 1.5 MeV ELECTRONS. Caillot, M.; Cherki, M.; Kalma, A. H. (Ecole Normale Superieure, Paris). Phys. Status Solidi (a); 4: 121-31(16 Jan 1971).

Annealing studies of lithium-doped silicon irradiated with 1.5-MeV electrons at 77°K were performed by means of photoconductivity up to temperatures of ≈730°K. EPR results obtained in conjunction with the photoconductivity studies are also presented. At least four kinds of Li–defect complexes associated with different photoconductivity features appear in O-free silicon and different ones in O-containing silicon. The annealing behavior of these complexes is dependent on the lithium concentration. The recovery of sample properties at room temperature after electron bombardment occurs only in O-free silicon slightly irradiated and containing low Li concentration. (auth)

30654 FORMATION OF COLOR CENTERS IN KCl CRYSTALS BY ULTRASOFT X RAYS. Saar, A. M. E.; Elango, M. A. (Inst. of Physics and Astronomy, Tartu, USSR). Sov. Phys.-Solid State (Engl. Transl.); 12: 2415-17(Apr 1971).

Translated from Fiz. Tverd. Tela; 12: 2993-6(Oct 1970).

An experimental study was made of the mechanisms controlling the formation of color centers in KCl–Na crystals by ultrasoft x rays in the region of the $L_{II,III}$ absorption edges of Cl^- (quantum energy ~200 eV). The thermoluminescence of crystals irradiated at a temperature of 95°K was also measured. The efficiency of formation of H_A centers (thermoluminescence peak at 125°K) did not depend on the number of doubly ionized anions formed in the crystals to within experimental error (±5%). It was concluded that the color centers were formed mainly by low-energy electronic excitations as in the case of crystals irradiated with hard x rays. (auth)

30655 F-CENTER DESTRUCTION MECHANISM IN PROTON TRACKS IN ALKALI HALIDE CRYSTALS. Vaisburd, D. I.; Kravets, A. N.; Melikyom, L. A.; Minaev, S. M. (Tomsk Poly-

technic Inst., USSR). Sov. Phys.-Solid State (Engl. Transl.); 12: 2249-50(Apr 1971).

Translated from Fiz. Tverd. Tela; 12: 2788-90(Oct 1970).

The "pure form" F-center destruction kinetics in proton-irradiated crystals are studied. The three most probable F-center destruction mechanisms in proton tracks in alkali halide crystals are considered: 1) annihilation with interstitial halogen atoms, 2) with excitons, and 3) with holes. Mobile holes are found to make the major contribution to F-center destruction. (auth)

30656 ELECTRON MICROSCOPE STUDY OF RADIATION DAMAGE IN BISMUTH-ION-IMPLANTED CdS. Govind, P. K. (Univ. of Colorado, Boulder); Fraikor, F. J. J. Appl. Phys.; 42: 2476-2507(May 1971).

Electron microscopy was used to study the ion-fluence dependence of structural disorder in CdS single-crystal platelets following 25-keV bismuth implantations at room temperature in the dose range of 7×10^{15} to 3.2×10^{16} ions/cm^2. Bright-field photomicrographs revealed "black spots" ~100 Å in diameter in the CdS microstructure. The contrast behavior of the strain field surrounding these spots indicated that the majority of spots were interstitial clusters or unresolvable interstitial dislocation loops. The electron diffraction patterns did not show any evidence of amorphous zones in the implanted specimens and there was no indication of a second-phase precipitate. (auth)

30657 PHOTOLUMINESCENCE OF ION-IMPLANTED OXYGEN IN ZnTe. Merz, J. L. (Bell Telephone Labs., Inc., Murray Hill, N. J.). J. Appl. Phys.; 42: 2463-71(May 1971).

Photoluminescence from the oxygen isoelectronic trap implanted into ZnTe is investigated for various ion doses and annealing conditions. The characteristic oxygen spectrum is observed after annealing either in zinc vapor or in vacuum. The anticipated isotope shift is observed in the spectrum for samples implanted with ^{18}O without the usual ^{16}O contamination found in conventionally doped samples. In isochronal anneal studies, the intensity of the oxygen luminescence peaks at 300 to 400°C. For samples annealed in Zn vapor, the anneal curves show a slight dip at higher temperatures, whereas for vacuum anneals the curves fall off rapidly. The dose for maximum luminescence is found to be a function of the anneal temperature. Much of the gross lattice damage is annealed at 500°C; at this temperature the luminescence peaks at a dose of ~10^{14} ions/cm^2, corresponding to an implanted concentration of ~2×10^{18}/cm^3. Although reasonable luminescence intensities have been achieved, compared with conventionally doped samples, only ~5% of the light intensity anticipated on the basis of the implant dose is actually observed as emission from the oxygen isoelectronic trap. (auth)

30658 PHOTOCONDUCTIVITY IN p-TYPE SILICON IRRADIATED WITH 1.2-MeV ELECTRONS AT ~15°K. Vajda, Peter; Cheng, L. J. (Atomic Energy of Canada Ltd., Chalk River, Ont.). J. Appl. Phys.; 42: 2453-62(May 1971).

Floating-zone-refined and pulled (oxygen-rich) p-type silicon crystals were irradiated at ~15°K with various doses of 1.2-MeV electrons. For wavelengths from 1.2 to 5.5 μ and temperatures from 23 to 80°K, their photoconductivity spectra were measured before irradiation, after irradiation, and after isochronal anneals up to 400°K. The 3.9-μ photoconductivity band appears immediately after irradiation in all crystals already at low temperatures, giving further evidence that it is due to the divacancy formed directly during irradiation by electrons. Three main annealing stages of the photoconductivity were found: (a) below ~150°K, (b) 160 to 280°K, and (c) 280 to 360°K. Stage (a) is thought to be due to charge redistribution among some levels. A radiation-induced deep level at $E_v + (0.12 \pm 0.02)$ eV anneals out in stage (b) and is thought to be related to the neutral vacancy in some way. The third stage is attributed to the breaking up of vacancy–impurity complexes. The electrical conductivity, measured simultaneously with the photoconductivity, exhibits a large stage (b) and a small stage (c). The annealing behavior of the spectra and the conductivity depends strongly on the measuring temperature. The dependence of the spectra on chopper speed was also investigated. The dependence of $\Delta\sigma$ in the low-temperature range ($\gtrsim$45°K) can be explained by the existence of a shallow α-type trapping level, which is likely the dopant level. (auth)

30659 INELASTIC SURFACE SCATTERING OF NONPENETRATING PARTICLES. Manson, R.; Celli, V. (Univ. of Virginia, Charlottesville). Surface Sci.; 24: 495-514(Feb 1971).

An extension is presented of the authors' earlier work (Phys. Rev. Letters 22(1969) 346; Surface Sci. 19(1970) 67) to include a treatment of one-phonon inelastic scattering of particles which do not penetrate appreciably into the crystal. A full quantum-mechanical treatment of the lattice vibrations is used throughout, and the results are not restricted to small scattered intensities. Calculations are presented for the scattering of helium atoms by a simplified model of the crystal surface. (auth)

30660 STORED ENERGY RELEASE OF SOLID ARGON AFTER REACTOR IRRADIATION AT 4.6°K. Wehr, G.; Boening, K.; Kalus, J.; Vogl, G.; Wenzl, H. (Technische Univ., Munich). J. Phys., C (London); 4: 324-30(1 Mar 1971).

Solid argon was irradiated with neutrons at 4.6°K in the low-temperature irradiation facility of the Munich reactor FRM to produce point defects. After irradiation, the stored energy of the samples was measured with a differential heat flow calorimeter at temperatures increasing at a rate of 0.3°K min^{-1}. By estimating the defect concentration, the enthalpy of formation of Frenkel pairs $E_f^F \simeq 0.5$ eV were obtained. From the observed stored energy recovery spectra and the assumption that the annealing reactions are of second order, two migration enthalpies were obtained: $E_{m_i} = (0.058 \pm 0.006)$ eV, and $E_{m_k} = (0.130 \pm 0.013)$ eV. These enthalpies of migration are tentatively attributed to the migration of interstitials and vacancies, respectively. (auth) (UK)

Physical Properties

30661 (AERE-R-5953) EFFECT OF HIGH PRESSURES AND VARYING TEMPERATURES ON THE RESISTIVITY OF YTTERBIUM. King, E. (Atomic Energy Research Establishment, Harwell (England)). Jan 1969. 28p. Dep. NTIS (U. S. Sales Only).

High-accuracy experimental data are presented to show the effect of pressures up to ~90 kB on the electrical resistivity of ytterbium in the temperature range 77 to 624°K. The effect of purity on the resistance peak height is shown and discussed in terms of the semiconductor behavior of Yb under pressure. A value of ~0.09 eV is deduced for the energy gap. The return to metallic behavior in the bcc phase above ~60 kB and its effect on the electrical resistance are also discussed. (auth)

30662 (COO-1569-76) NUCLEAR ORIENTATION OF ^{142}Pr IN PRASEODYMIUM METAL. Smith, C. H.; Weyhmann, W. (Minnesota Univ., Minneapolis. Tate Lab. of Physics). Feb 1971. Contract AT(11-1)-1569. 73p. Dep. NTIS.

The anisotropy of gamma radiation emitted by ^{142}Pr nuclei in polycrystalline praseodymium was measured in applied fields up to 41.7 kOe and temperatures down to 12 millidegree K. The observed anisotropies were fitted to a model in which an appropriate powder average was taken of the electronic moments measured by Lebech and Rainford by neutron diffraction from a single crystal of praseodymium in applied fields. The Van Vleck moments calculated from the crystal field eigenfunctions and energy splittings of Bleaney do not provide a large enough internal field to cause the observed anisotropies. In order to explain the large orientation observed, the first-forbidden beta decay of ^{142}Pr must be assumed to be almost pure Fermi with zero units of angular momentum usually carried away by the beta–neutrino pair. (auth)

30663 (JINR-P3-5554) SOME NOTES ON THE PROBLEMS OF DETERMINING THE PHASES OF STRUCTURAL AMPLITUDES IN THE NEUTRON DIFFRACTION AND OF THE NEUTRON ACCUMULATION. Shapiro, F. L. (Joint Inst. for Nuclear Research, Dubna (USSR). Lab. of Neutron Physics). 1970. 10p. (In Russian). Dep. NTIS (U. S. Sales Only).

The possibility of determining the phases of structural amplitudes for polarized neutron diffraction on a crystal whose elementary cell contains a paramagnetic center is considered. The question of the limiting neutron density in a neutron trap is discussed. (auth)

30664 (NP-18783) TABLES OF MAGNETIC STRUCTURES DETERMINED BY NEUTRON DIFFRACTION. PART II. TETRAGONAL SYSTEM. Oles, A.; Bombik, A.; Kajzar, F.; Kucab, M.; Sikora, W. (Institute of Nuclear Techniques, Krakow (Poland)). Nov 1970. 68p. (INT-4). Dep. NTIS (U. S. Sales Only).

This part covers compounds and alloys belonging to the tetragonal system at room temperature. The tables contain the chemical symbol of the substance, its space group, crystallographic data, cation distribution, temperatures of magnetic transitions, a brief description of magnetic structure including some figures, magnetic moments and their directions, effective magnetic moments, and references on magnetic additional properties. Magnetic space groups for stoichiometric compounds are indicated. (auth)

XUM

30665 (UH-235-P-9-2) PHOTOELECTRIC EMISSION FROM THIN FILMS IN THE VACUUM ULTRAVIOLET REGION. Annual Progress Report, June 1, 1970–February 28, 1971. Pong, W. (Hawaii Univ., Honolulu. Dept. of Physics and Astronomy). 4 Mar 1971. Contract AT(04-3)-235. 49p. Dep. NTIS.

The emphasis of the research was on the scattering of low-energy photoelectrons in solids. Four reprints are included: attenuation length for photoelectrons in PbTe films, photoemission and fluorescence from MgF_2 films, and collision effects in photoemission from thin films. (D.L.C.)

30666 OPTICAL NONLINEAR SUSCEPTIBILITIES OF BERYLLIUM OXIDE. Jerphagnon, J.; Newkirk, H. W. (Bell Telephone Labs., Murray Hill, N. J.). Appl. Phys. Lett.; 18: 245-7(15 Mar 1971).

The nonlinear coefficients of beryllium oxide measured relative to quartz by the Maker fringe technique are $d_{31}(BeO) = \pm(0.46 \pm 0.03)d_{11}(SiO_2)$ and $d_{33}(BeO) = \pm(0.63 \pm 0.04)d_{11}(SiO_2)$ for a fundamental beam at 1.064μ. A simple model accounting for the value of the ratio $d_{31}(BeO)/d_{33}(BeO)$ is proposed. (auth)

30667 ELECTRONIC PROPERTIES OF NONSTOICHIOMETRIC VANADIUM MONOCARBIDES. Neshpor, V. S.; Ordan'yan, S. S.; Nikitin, V. P.; Skaletskaya, N. A. (Leningrad Technological Inst.). Inorg. Mater. (USSR) (Engl. Transl.); 6: 1716-21(Nov 1970).

Translated from Izv. Akad. Nauk SSSR, Neorg. Mater.; 6: 1954-60(Nov 1970).

Measurements of electric and thermal conductivities, thermo-emf, and Hall coefficient were made on VC_x with x varying from 0.4 to 0.9. The VC_x specimens were analyzed for total and free C, V, N, and O. The measured values are plotted versus x, and the implications for the conductivity mechanism are discussed. VC is a metallic conductor that can be described by a single-band model. The conduction band contains virtual bands of electron d states with high effective mass. The thermal conductivity increases linearly with electric conductivity as a function of x, except for $VC_{0.85}$. (D.L.C.)

30668 ELECTRON STRUCTURE AND THE CHEMICAL BONDS IN VANADIUM PENTOXIDE. Abdullaev, A. A.; Kislovskii, L. D. (Inst. of Crystallography, Moscow). Sov. Phys.-Cryst. (Engl. Transl.); 15: 860-2(Mar-Apr 1971).

Translated from Kristallografiya; 15: 988-91(Sep-Oct 1970).

It is shown that the structural polyhedra surrounding the vanadium should be considered as distorted tetragonal pyramids. The distortion is explained as a result of the interaction between the electron configuration of the vanadium atoms (d^4s) and the electron configurations of the oxygens. The "bond bending" which occurs is confirmed by a model calculation using new data from the infrared spectrum. (auth)

30669 CHEMICAL CONSEQUENCES OF NUCLEAR SPIN. Wheatley, P. J. Amsterdam; North-Holland Publishing Company (1970). 200p. $11.50.

This book attempts to bring together the various areas of physical chemistry in which nuclear spin plays a part: atomic spectroscopy, molecular spectroscopy, nuclear quadrupole coupling, statistical thermodynamics, atomic and molecular beams, neutron diffraction, Moessbauer spectroscopy, ESR, and NMR. The last chapter describes methods for determining nuclear spins. (D.L.C.)

30670 SPIN-WAVE THEORY AND THE TEMPERATURE DEPENDENCE OF THE MAGNETIZATION OF EuO AND $Eu_{0.97}Gd_{0.03}O$ SINGLE CRYSTALS. Samokhvalov, A. A.; Morozov, Yu. N.; Volkenshtein, N. V.; Zotov, T. D.; Karpenko, B. V. (Inst. of Metal Physics, Sverdlovsk, USSR). Sov. Phys.-Solid State (Engl. Transl.); 12: 2312-15(Apr 1971).

Translated from Fiz. Tverd. Tela; 12: 2865-8(Oct 1970).

The temperature dependence of the magnetization of EuO and $Eu_{0.97}Gd_{0.03}O$ single crystals was determined. The experimental results were compared with the conclusions that follow from the spin-wave theory. The exchange parameters J_1 and J_2 were determined for the first and second coordination spheres, respectively. Regions of linear dependence of the magnetization on the square of the temperature were observed at low temperatures. These regions did not satisfy the temperature criteria of the spin-wave theory. Possible causes of the observed temperature dependence were considered. (auth)

30671 X-RAY EMISSION SPECTRA OF MANGANESE BORIDES. Shashkina, T. B. (State Inst. of Teaching, Odessa). Phys. Status Solidi (b); 44: 571-5(1 Apr 1971).

X-ray K_{β_5}-emission spectra from manganese and five borides were obtained under primary and secondary excitation. The investigation of the borides included also measurements of the boron K-emission band of each compound and of pure boron. The resolution for the Mn K-band was 0.2 eV and for the boron K-band 0.1 eV. The structures of the spectra of both components are compared and discussed in view of their concentration dependence. (auth)

30672 HEAT TREATMENT OF 2-81 MOLYBDENUM PERMALLOY POWDER CORES. Pingel, Vernon J. (Western Electric Co., Chicago). Int. J. Powder Met.; 7: 43-54(Jan 1971).

Heat treatments in air were applied to 2-81 molybdenum permalloy to increase the permeability, reduce the magnetic losses, and increase the strength of the high-permeability powder cores made from this alloy. Two critical temperatures for heat treatment at approximately 770 and 1,235°F were recognized. Photomicrographs indicate important metallurgical changes in the magnetic material at these temperatures. This work provides a basis for a better understanding of the metallurgy of the powder particles and indicates process controls beneficial to the manufacture of high-permeability cores. (auth)

30673 DIFFUSION OF Ar, Kr, AND Xe IN CaF_2 INVESTIGATED ON U-DOPED SINGLE CRYSTALS OF CaF_2 AFTER NEUTRON IRRADIATION. Felix, F. W. (Hahn-Meitner Inst., Berlin); Lagerwall, S. Y. T. Phys. Status Solidi (a); 4: 73-9 (16 Jan 1971).

The simultaneous diffusion of Ar, Kr, and Xe in CaF_2 was investigated in the temperature range between 700 and 1300°C. The diffusion coefficients were determined from the release kinetics of radioactive gas atoms produced in the crystal by neutron reactions. The activation energies at high temperatures (≧1000°C) are found to be 3.0, 3.4, and 6 eV for Ar, Kr, and Xe, respectively, and about 6 eV for all atomic species at low temperatures (≦1000°C). The rare gases are thought to migrate as interstitial atoms, and the values 3.0 and 3.4 eV are interpreted as pure jump energies, whereas the value 6 eV can be understood as caused by trapping of the atoms by vacancy clusters. The bonding energy between a rare gas atom and a vacancy cluster is then estimated to 2.5 to 3.0 eV. The data and their interpretation are discussed and compared with the results of channeling and ion-bombardment experiments. (auth)

30674 STUDY OF YTTERBIUM AND YTTERBIUM–BARIUM ALLOYS UNDER HIGH PRESSURE AT LOW TEMPERATURE. Jullien, R.; Jerome, D. (Faculte des Sciences, Orsay, France). J. Phys. Chem. Solids; 32: 257-65(Jan 1971). (In French).

Resistivity measurements were performed under pressure in 99.95% pure Yb and Yb alloys with Ba concentration ranging from 1 to 14.5 at. %. It was found that the fcc phase is stable in the solid solution up to ~20 at. %. From resistivity measurements it was found that alloying with Ba increases the metallic character of Yb. The strong quadratic temperature dependence of the resistivity in pure Yb from 4.2 to 35°K increases with pressure as long as Yb remains a semi-metal (0 to 11 kbar). The negative temperature coefficient observed in the alloys is attributed to a temperature independent mobility governed by the scattering against divalent Ba atoms and to the excitation of the carriers in the small overlap semi-metal. The density vs. pressure for the residual free carriers is obtained from Matthiessen's rule and is in agreement with direct estimation given by the transport properties measurements under pressure. The density of carriers for the alloys was deduced from Nordheim's rule from which predictions about the hypothetical fcc phase of Ba were made. It is suggested that the metallic character of Yb is connected with the strong hybridization between the s–p and d bands near the Fermi level. This fact is in good qualitative agreement with the R.A.P.W. band calculation of Johansen and Mackintosh. (auth) (UK)

30675 MAGNETIC DOMAIN PATTERNS IN SMALL CRYSTAL $SmCo_5$ PARTICLES. Bachman, K.; Bischofberger, A.; Hofer, F. (Brown Boveri Research Center, Baden, Switzerland). J. Mater. Sci.; 6: 169-70(Feb 1971).

Using the magnetic Kerr effect, the magnetic domains on $SmCo_5$ single crystals of 10 to 100 μ were observed. Cone-shaped surface domains of reversed magnetisation appeared in thick crystals but were absent on crystals smaller than about 25 μm. Most domains were on a polycrystalline particle continuous at the grain boundaries. In some instances reverse domains appeared to have been nucleated at a grain boundary. This may explain the low coercive field of polycrystalline $SmCo_5$. (UK)

30676 SPECIFIC HEAT OF CHROMIUM–RICH CHROMIUM–NICKEL AND CHROMIUM–IRON–MOLYBDENUM ALLOYS BETWEEN 1.3 AND 4.2°K. Baum, Neal P.; Schroeder, K. (Syracuse Univ., N. Y.). Phys. Rev., B; 3: 3847-51(1 Jun 1971).

XUM

The specific heats of some chromium-based alloy systems were measured in the temperature range 1.3 to 4.2°K. The alloy systems studied were the binary chromium–nickel with up to 4 at.% nickel and the ternary $Cr_{(0.75-x)}Fe_xMo_{0.25}$ with $0 \leq x < 0.20$. The electronic-specific-heat coefficient of the chromium–nickel system increases slowly with increasing nickel concentration and shows a maximum near 2 at.% Ni. The coefficients of the cubic temperature term in the specific heat of some of the binary alloys are relatively high. This observation was attributed to the effect of antiferromagnetic spin waves. (auth)

30677 INELASTIC NEUTRON SCATTERING SPECTRA FROM LANTHANUM DIHYDRIDE AND LANTHANUM TRIHYDRIDE. Maeland, Arnulf J.; Holmes, Douglas E. (Worcester Polytechnic Inst., Mass.). J. Chem. Phys.; 54: 3979-82(1 May 1971).

The optical hydrogen vibrations in lanthanum dihydride and lanthanum trihydride were investigated by the energy-gain scattering of cold neutrons. The approximate frequency distributions, derived from the observed time-of-flight spectra, show peaks which correlate well with the known crystal structures. In fcc lanthanum trihydride, the optical bands are peaked at 940 and 515 cm^{-1} corresponding to hydrogen vibrating at tetrahedral and octahedral sites, respectively, and in lanthanum dihydride there is a single peak at 825 cm^{-1} due to tetrahedral hydrogen. Other weak peaks were observed and are thought to be due to vibrations of hydrogen atoms dissolved in the metal phase; this phase was identified by x rays in both samples. A large width of the optical levels, a common feature in all metallic hydrides, was also observed for LaH_2 and LaH_3. (auth)

30678 EFFECT OF ATOMIC CORES ON ELECTRON TUNNELLING THROUGH DIELECTRIC LAYERS. Modinos, A.; Theophilou, A. (Univ. of Salford, Eng.). J. Phys., C (London); 4: 338-53(1 Mar 1971).

A theory to account for the effect of the atomic cores on an electron tunnelling through dielectric layers is developed. The theory utilizes the final-stage interaction formalism of the T scattering matrix. It is assumed that the atomic core potentials have a very short range and that they in no way overlap with each other. It is assumed that the core potentials are superimposed on a smooth potential barrier U(x) which varies slowly with position. The effect of atomic core scattering on the transparency of the barrier depends on a parameter corresponding to a single scatterer, defined by $F \equiv 1/4\pi(2m/\hbar^2) \int t(r,r')\, dr\, dr'$ and the geometry of the atomic layers, namely the distance between successive layers as well as the distance between atoms in the same layer. It is assumed that the atomic layers have a periodic structure. A qualitative calculation in relation to field emission from tungsten covered with a few layers of inert-gas atoms suggests that positive values of F lead to an increase, while negative values of F lead to a decrease in the effective work function as obtained from the Fowler–Nordheim equation. Moreover, by an appropriate parametrization of F, assuming that the atomic potential in the first layer can be considerably different from that of subsequent layers, one can explain both the reduction in the effective work for multilayer coverage and the changes in the pre-exponential term in the Fowler–Nordheim equation for monolayer as well as multilayer coverage. (auth) (UK)

30679 MAGNETIC PROPERTIES OF URANIUM SILICIDES. Misiuk, A.; Trzebiatowski, W. (Inst. for Low Temperature and Structure Research, Wroclaw). Bull. Acad. Pol. Sci., Ser. Sci. Chim.; 18: 633-7(1970).

The crystal structures and magnetic susceptibilities of U_3Si, U_3Si_2, USi, U_3Si_5, $USi_{1.88}$, USi_3, and $U_6Si_{11}O$ were determined at 85 to 900°K. U_3Si and USi_3 exhibit a temperature-independent susceptibility, while U_3Si_2 shows only slightly temperature-dependent paramagnetism. $U_6Si_{11}O$ does not obey the Curie–Weiss law and decomposes above 400°C. USi has a ferromagnetic transition at 120°K and obeys the Curie–Weiss law at 140 to 300°K. U_3Si_5 obeys the Curie–Weiss law, whereas $USi_{1.88}$ shows deviations. The structures and their correlation with the magnetic properties are discussed. (D.L.C.)

30680 POLARIZED-NEUTRON STUDY OF THE $Ni_{0.968}V_{0.032}$ ALLOY. Maniawski, F. (Inst. of Nuclear Physics, Krakow); Dobrzynski, L.; Sikorska, D. Physica; 51: 627-9 (26 Feb 1971).

The form factor for polarized-neutron Bragg reflections from a $Ni_{0.968}V_{0.032}$ single crystal lies below that for pure Ni. The magnetic moment on the V impurity sites is positive and is estimated to be $\sim 3\ \mu_B$. Spin-density maps show a change in the total symmetry of the unpaired-electron distribution towards e_g symmetry. (D.L.C.)

30681 FERMI SURFACE. II. D-BLOCK AND F-BLOCK METALS. Cracknell, Arthur P. (Univ. of Dundee, Scotland). Advan. Phys.: 20: 1-141(Jan 1971).

A description of the Fermi surfaces of the d-block and f-block metals is given; these include the metals in groups IB, IIB, IIIA, IVA, VA, VIA, VIIA, and VIII of the periodic table. These blocks of the periodic table include the transition metals, the rare-earth metals (or lanthanide metals), and the actinide metals. The Fermi surfaces of many of these metals are quite complicated, and there is often no very close resemblance to the predictions of the free-electron model. Another important feature is that many of these metals possess magnetically ordered structures over certain temperature ranges. As a result of the magnetic ordering, a large magnetic field arises within the metal and causes an energy separation to appear between the spin-up and spin-down bands so that in the magnetically ordered phase there are quite different Fermi surfaces for the spin-up and spin-down electrons. For most of the d-block and f-block metals Fermiology is still one stage less advanced than for the simple metals and it is still concerned with trying to determine accurately the shape of their Fermi surfaces. (auth) (UK)

30682 ELECTRONIC TRANSPORT IN CALCIA-STABILIZED ZIRCONIA. Heyne, L.; Beekman, N. M. (Philips Research Labs., Eindhoven, Netherlands). Proc. Brit. Ceramic Soc.; 19: 229-63 (Mar 1971).

The limits of electrolytic behaviour of calcia-stabilized zirconia are set by N-type electronic conductivity at low oxygen partial pressures, and by P-type conductivity at high pressures. Data collected from the literature are summarized and used to determine the low-pressure limit as a function of temperature. Comparison with the temperature dependence of the ionic conductivity yields a quantitative expression for the N-type conductivity with an activation energy of 3.7 eV. The P-type conductivity at higher pressures can be determined from oxygen permeation experiments and from direct observation of the oxygen transported by a current. To increase the sensitivity of the latter method, a special differential arrangement was developed. The results, compared with and completed by values from the literature, show that the thermal activation energy for hole conductivity amounts to 1.9 eV. The curves for N- and P-type conductivity together yield the temperature dependence for the intrinsic point from which a thermal band gap can be obtained. The latter value corresponds quite well with a band gap of 5 eV obtained from optical data. From the time dependence of permeation and desorption, values for the concentration and mobility of holes can be obtained separately. The effective hole mobility appears to be very small and strongly dependent on temperature. It is assumed that the majority of the holes introduced by the excess of oxygen in the lattice are bound to some kind of impurity centres. However, the accuracy of the available data is too low to be able to decide for a more specified model. (auth) (UK)

30683 NEUTRON-SCATTERING STUDY OF THE LATTICE DYNAMICAL PHASE TRANSITION IN V_3Si. Shirane, G. (Brookhaven National Lab., Upton, N. Y.); Axe, J. D.; Birgeneau, R. J. Solid State Commun.; 9: 397-400(1 Apr 1971).

Neutron-scattering experiments were carried out on single-crystal V_3Si through the phase transition at 21°K. Previous acoustic measurements revealed drastic softening of some long-wavelength phonons, in particular the transverse acoustic (TA) modes with wavevector $\vec{q} \| [110]$ and polarization vector $\vec{e} \| [1\bar{1}0]$. The present experiment shows that this softening is extended, though in lesser degree, to the major part of the Brillouin zone. In approaching the transition temperature, these phonons become heavily damped while the [100] TA modes remain well defined. It was not possible to prove, or disprove, the existence of soft optic modes associated with the phase transition. (auth) (UK)

30684 ELECTRICAL CONDUCTION AND BLACKENING IN YTTRIA-STABILIZED ZIRCONIA. Casselton, R. E. W. (International Research and Development Co. Ltd., Newcastle-upon-Tyne, Eng.). Proc. Brit. Ceramic Soc.; 19: 265-77(Mar 1971).

Results are presented on the nature and effects of low- and high-field conduction at high temperatures in yttria-stabilized zirconia. Both polycrystalline and single-crystal materials were examined. The conditions under which blackening occurs as a result of current passage are summarized. In polycrystalline material (12 mole % yttria), blackening by passing 3 to 20 A/cm^2 increased the conductivity at 1350°C from 2.6×10^{-1} $ohm^{-1}\ cm^{-1}$ to 3 $ohm^{-1}\ cm^{-1}$. X-ray data showed that this was accompanied by contraction of the lattice. Optical absorption spectra for transparent single crystals indicate that the band edge is near 3000 Å. Current-blackened specimens show pronounced scattering, with a peak near 5850 Å. These results suggest that the optical effects

XUM

are due to the formation of colloidal particles in the size range 10 to 50 millimicrons. Electron-spin-resonance spectra observed in current-blackened single crystals indicate that charged defects are also formed. (auth (UK)

30685 MEASUREMENTS OF TOTAL AC CONDUCTIVITY OF THORIA–YTTRIA SOLID SOLUTIONS AT HIGH OXYGEN PRESSURES. Iqbal, M.; Baker, E. H. (Imperial Coll. of Science and Tech., London). Proc. Brit. Ceramic Soc.; 19: 279-83 (Mar 1971).

The total ac conductivities of solid solutions of thoria and yttria were measured at pressures of oxygen in the range 0.2 to 500 atm and at temperatures in the range 800 to 1100°C. In these pressure and temperature regions, a p-type conductivity is confirmed. At moderate pressures, the latter exhibits a proportionality of $P_{O_2}^{\frac{1}{6}}$ but at the highest pressures for samples low in yttria, the conductivity shows a proportionality to $P_{O_2}^{\frac{1}{4}}$. (auth) (UK)

30686 INVESTIGATIONS OF THE CONDUCTIVITY OF VAPOR DEPOSITED TANTALUM LAYERS WITH ISLAND STRUCTURE. Fromm, Eckehard; Hoefer, Gerhard (Max-Planck-Institut fuer Metallforschung, Stuttgart). Z. Metallk.; 62: 223-7(Mar 1971). (In German).

The electric conductivity of very thin tantalum films with island structure depends on the conditions of film preparation, temperature, the electric field strength, and the pressure of residual gases. If the mass thickness is smaller than 25 Å the film structure can easily be described by only two parameters, i.e., island size and island distance. The specific resistivity and the temperature dependence obtained in experiments with tantalum films are in fair agreement with calculated values from a simple model based on phonon-assisted tunneling of conduction electrons. (auth)

Moessbauer Effects and NMR

Refer also to abstract 29151.

30687 (IAE-1966) EVIDENCE OF DISAPPEARANCE OF THE INELASTIC CHANNEL OF THE NUCLEAR REACTION IN THE NUCLEAR RESONANT SCATTERING OF γ-RAYS IN A PERFECT CRYSTAL. Voitovetskii, V. K.; Korsunskii, I. L.; Novikov, A. I.; Pazhin, Yu. F. (Gosudarstvennyi Komitet po Ispol'zovaniyu Atomnoi Energii SSSR, Moscow. Institut Atomnoi Energii). 1970. 6p. Dep. NTIS (U. S. Sales Only).

The effect of disappearance of the inelastic channel of the nuclear reaction in resonant nuclear scattering of γ-quanta as well as in other mechanisms of wave field formation in a perfect single crystal (nuclear and electron scattering interference, electron scattering) was investigated for a perfect tin single crystal containing ^{119}Sn. (auth)

30688 (RISO-M-1348) MOSSPEC: A PROGRAMME FOR RESOLVING MOESSBAUER SPECTRA. Stone, A. J.; Aagaard, H. J.; Fenger, J. (Danish Atomic Energy Commission, Risoe, Research Establishment). Feb 1971. 42p. Dep. NTIS (U. S. Sales Only).

The program fits a sum of Lorentzian lines to a given Moessbauer spectrum by means of the Gauss nonlinear regression procedure with a facility for constraining any set of parameters or linear combinations of parameters. The results are presented as a table of the fitted parameters, a typewriter plot of the residual deviations with an indication of the fit, and a plot of the measured points and the fitted lines; if desired the results of each iteration can also be printed out. (auth) (Denmark)

30689 (UUIP-733) MOESSBAUER INVESTIGATION OF IRON IN BORON. Waeppling, R.; Haeggstroem, L.; Devanarayanan, S. (Uppsala Univ. (Sweden). Inst. of Physics). Feb 1971. 9p. Dep. NTIS (U. S. Sales Only).

Boron samples containing ~1 at. % iron were investigated. It was indicated that the iron atoms populate three different crystallographic positions. The isomer shifts obtained are far from the "metallic" values expected, indicating large rearrangements of electrons around the iron nuclei. (auth) (Sweden)

30690 GAMMA RAYS EMITTED BY NUCLEI IN CRYSTALS. Aleksandrov, P. A.; Kagan, Yu. Zh. Eksp. Teor. Fiz.; 59: 1733-45(Nov 1970). (In Russian).

Gamma decay of excited nuclei in a crystal consisting of the same nuclei but in the ground state is considered. A solution of the problem pertaining to the nature of the radiation from a thick crystal is obtained on basis of the reciprocity theorem for absorbing media and the solution of the problem of stationary distribution of γ-quanta in an ideal crystal obtained previously; the latter solution is obtained on the assumption of resonant nuclear interaction with a single nucleus in the presence of an external source. It is shown that for certain ranges of angle the dependence of decay γ-quanta absorption on thickness is not exponential but rather a power function; this is due to suppression of inelastic channels of the nuclear reaction. In this case the radiation from a thick crystal will be emitted along the surface of cones whose axis is directed along the reciprocal lattice vector and aperture angle is $90° - \theta_B$ (θ_B is the Bragg angle). The angular distribution of the intensity strongly depends on whether the emitting nucleus is located at a node or interstice. It is shown that the position of the emitting nucleus in a unit cell can be analyzed. (auth)

30691 THEORY OF THE NUCLEAR OVERHAUSER EFFECTS IN MULTISPIN SYSTEMS. II. Tumanov, V. S. Vestn. Mosk. Univ., Ser. III. Fiz. Astron.; 11: 517-22(Sep-Oct 1970). (In Russian).

A nonlinearized expression is derived for relaxation of the terms comprising the equations for the population of levels and corresponding intermolecular relaxations. Intermolecular dipole relaxation transitions for the system of the A_iX_k type are studied, and expressions are obtained for relaxation terms forming equations for longitudinal magnetizations. The probabilities of relaxation transitions are obtained, considering all types of intermolecular dipole relaxation for the A_3X system, and analyses are made of the measurements of the partial Overhauser effect. (For Part I, see NSA 24: 18044.) (tr-auth)

30692 NMR STUDIES OF ^{1}H AND ^{3}He CONTAINED IN GOLD FILMS. Weaver, H. T. (Sandia Labs., Albuquerque, N. Mex.). J. Appl. Phys.; 42: 2356-61(May 1971).

Transient nuclear magnetic resonance (NMR) measurements are presented for ^{1}H and ^{3}He in the systems Au–H and Au–He, respectively. Solute content values of 31 at.% H in Au–H and 18 at.% He in Au–He were obtained by spin counting procedures. Spin-spin relaxation times (T_2) of 30, 24, and 0.008 msec and spin–lattice relaxation times (T_1) of 0.25, 0.18, and 0.37 sec at 300, 77, and 4°K, respectively, were found for ^{1}H in Au–H. For helium, T_1 was found to be 0.7, 0.7, and 53 sec and T_2 was 2, 1.1, and 0.8 msec at the above temperatures. The hydrogen data indicate that high-pressure gas pockets are present within the metal whereas the helium situation is not as straightforward. Data from both systems are analyzed regarding possible placement of the hydrogen and helium in the gold lattice. (auth)

30693 MOESSBAUER-EFFECT OBSERVATIONS OF ^{232}Th FOLLOWING COULOMB EXCITATION. Durkee, P.; Hershkowitz, N. (Univ. of Iowa, Iowa City). Phys. Rev., B; 3: 3607-15 (1 Jun 1971).

Resonant absorption following Coulomb excitation was observed for γ rays from the first excited state of ^{232}Th in Th metal and ThC targets with ThO_2, Th metal, ThN, and ThC_2 absorbers. Most spectra were obtained with targets at 30°K and absorbers at 25°K using 1-μA beams of 6-MeV $^4He^+$ ions. Absorber and target recoilless fractions (f_a and f_s) and zero-thickness absorber linewidth (Γ_0) were determined from a series of measurements of the width (half-width at half-maximum) of absorption spectra versus absorber thickness. These spectra were obtained with Th metal targets and ThO_2 absorbers. It is found that $f_a = 0.35 \pm 0.04$ and $f_s = 0.31 \pm 0.06$, which correspond to a Debye temperature of (121 ± 13)°K. The zero-thickness linewidth Γ_0, uncorrected for target-absorber geometry, was found to be 11.35 ± 0.26 mm/sec. The value of Γ_0, corrected for broadening due to the geometry of the experimental configuration, was estimated to be 9.6 ± 0.4 mm/sec. (auth)

30694 ELECTRON PARAMAGNETIC RESONANCE OF COUPLED SPIN SYSTEMS: $Gd_xZr_{1-x}Zn_2$. Davidov, D.; Dublon, G.; Shaltiel, D. (Hebrew Univ., Jerusalem). Phys. Rev., B; 3: 3651-5(1 Jun 1971).

The electron paramagnetic resonance (EPR) of the coupled spin system $Gd_xZr_{1-x}Zn_2$ was measured as a function of the temperature T and the Gd concentration x. By varying x and T, the relaxation parameters were varied in a systematic way to obtain appreciable variation of both the EPR g shift and linewidth. The variation of the relaxation parameters was correlated with the modified Hasegawa model. This is the first time that such a correlation has been obtained in a nonbottlenecked system. (auth)

30695 COUPLING COEFFICIENTS FOR THE INDIRECT NUCLEAR DIPOLE INTERACTION IN INDIUM BY NUCLEAR QUADRUPOLE RESONANCE. Palmer, J. P.; Hewitt, R. R. (Univ. of California, Riverside). Phys. Rev., B; 3: 3676-81 (1 Jun 1971).

Moment analysis of the NQR spectrum of indium metal is used to measure its isotropic and anisotropic dipolar interactions. The

XUM

coupling coefficients $\tilde{A}$ and $\tilde{B}$ are measured to be 2.46×10^{-46} and 1.55×10^{-46} erg cm^3, respectively. The measurement of the NQR in In–Sn alloys is described and found to be in qualitative agreement with earlier NMR results. (auth)

Theory

Refer also to abstract 30706.

30696 (COO-2103-3) ELECTRONIC BAND STRUCTURE AND PHYSICAL PROPERTIES OF THE ACTINIDE METALS AND THEIR COMPOUNDS. Technical Progress Report. Freeman, A. J. (Northwestern Univ., Evanston, Ill.). [1970]. Contract AT(11-1)-2103. 13p. Dep. NTIS.

The Symmetrized Relativistic Augmented Plane Wave method was used in energy band calculations for fcc and bcc Th, bcc U, fcc Pu, fcc Am, and fcc Cm. The results show that the actinides can be separated into two classes: (1) Th through U which can be considered as tight-binding band states, and (2) Pu and higher actinides, whose band overlaps are much reduced. Graphs of the band calculations are presented. (D.L.C.)

30697 (NP-18822) COMMENT ON "ANOMALOUS ELECTRON–PHONON TRANSPORT PROPERTIES OF IMPURE METALS." Smith, Henrik (Helsinki Univ. (Finland). Research Inst. for Theoretical Physics). Mar 1971. 6p. Dep. NTIS (U. S. Sales Only).

The substantial deviations from additivity of electron–phonon and electron–impurity scattering found by Rice and Bunce (Phys. Rev. B2, 3833 (1970)) are shown to result mainly from an unfortunate choice of trial function in the variational calculation of the resistivity. (auth)

Theoretical Physics

Refer also to abstracts 30122, 30520, 30918, 30941, 30946, 30971, 31019, and 31164.

30698 (CEA-N-1096) STUDY OF THE VARIANCE OF A MONTE CARLO CALCULATION. Lanore, Jeanne-Marie (Commissariat a l'Energie Atomique, Fontenay-aux-Roses (France). Centre d'Etudes Nucleaires). Apr 1969. 12p. (In French). Dep. NTIS (U. S. Sales Only).

One of the big problems with Monte Carlo calculations is estimating the variance of the results. By a large number of short calculations the actual value of the variance is found, and the results are applied to the optimization of a Monte Carlo program. (R.W.R.)

30699 (ITF-70-84-P) MODIFIED WKB METHOD. II. Mentkovskii, Yu. L. (Akademiya Nauk Ukrainskoi SSR, Kiev. Institut Teoreticheskoi Fiziki). 1970. 8p. (In Russian). Dep. NTIS (U. S. Sales Only).

A simple method of constructing the absolutely convergent modified WKB—expansions which are free of complicated matrix calculations is suggested. (auth)

30700 QUANTUM-MECHANICS DEBATE. Phys. Today; 24: No. 4, 36-44(Apr 1971).

A previous article by Bryce DeWitt advocating a view of reality, which pictures a world that continually splits so that each possible result of a measurement is equally "real", is attacked on several points. Six letters are presented that appear to represent the principal viewpoints, along with DeWitt's reply. (M.H.R.)

30701 CAN QUANTUM-STATES BE CONSIDERED AS ENSEMBLES OF DISPERSION-FREE STATES? I. Ochs, W. (Univ., Munich). Z. Naturforsch.; 25a: 1546-55(Nov 1970). (In German).

The problem of whether quantum states can be represented by Gibbsian ensembles of dispersion-free microstates having well-defined values for all observables is considered. Such a statistical representation is shown to be possible if and only if the concept and mathematical representation of observables is modified by abandoning the 1–1 correspondence between observables and operators. A particular representation of quantum states by Gibbsian ensembles is constructed. (auth)

30702 SOME PECULIARITIES OF THE TRANSITION RADIATION. Frank, I. M. (Joint Inst. for Nuclear Research, Dubna, USSR). Acta Phys. Pol.; A38: 655-73(Nov 1970). (In Russian).

An elementary solution is obtained for the transition radiation of charged-particle emissions at arbitrary angles to a vacuum–refractory medium interface. Data obtained are applied to analysis of experimental studies. Special cases are considered in which the plane of the motion (determined by the direction of the velocity and the normal to the interface) and the plane of observation (in which the plane of the beam and of the normal to the surface) are mutually perpendicular; also considered is the case in which these planes coincide and the transitional radiation is observed along the normal to the surface. (R.V.J.)

30703 TIME EVOLUTION OF SYSTEMS WITH AN INFINITE NUMBER OF DEGREES OF FREEDOM. Ruell, David (IHES, Bures-sur-Yvette, France). Acta Univ. Wratislaviensis; No. 99, 132-46(1968).

The time evolution of systems with an infinite number of degrees of freedom is studied from a statistical mechanics point of view. The description, interactions, and statistical mechanics of quantum lattice systems, the evolution of classical continuous systems, systems with bounded velocities, and some previous results are treated. (J.F.P.)

30704 COHERENT STATES AND THE GREEN FUNCTION OF A CHARGED PARTICLE IN VARYING ELECTRIC AND MAGNETIC FIELDS. Malkin, I. A.; Man'ko, V. I. Zh. Eksp. Teor. Fiz.; 59: 1746-54(Nov 1970). (In Russian).

A nonrelativistic charged particle moving in homogeneous varying electric and magnetic fields is considered. Some new motion integrals and an exact solution of the problem are obtained. Coherent states and the Green function are set up; the transition amplitudes between Landau levels are calculated in a closed form. The problem of a variable-frequency oscillator in such fields is solved. Linear adiabatic invariants are discussed. (auth)

30705 METHOD FOR SOLVING THE EQUATION OF IONIZING ELECTRIC FIELDS IN A STATIONARY REGIME. Hausard, Michel (College Scientifique Univ., Pau, France); Royer, Ray; Dupuy, Jean. Compt. Rend., Ser. B; 272: 91-4(11 Jan 1971). (In French).

A method for determining the various functions (potential, field, and charge density) at any point in space in the presence of an ion flux is developed. (auth) (France)

30706 TUNNEL EFFECT IN Al–Al_2O_3–Al JUNCTIONS: INCLUSION OF SHORT-RANGE FORCES. Dubey, P. K. (Indian Inst. of Tech., New Delhi). J. Appl. Phys.; 42: 2534-42(May 1971).

Tunneling in metal/insulator/metal junctions is considered, taking into account the short-range forces due to surface ion cores at the junction interfaces. An approximate formula for the tunnel current is derived and expressed in an analytically tractable form for evaluations of the volt–current characteristics of such junctions at finite temperatures. A detailed comparison with experiments is made, stressing the importance of specifying the junction parameters a priori; the earlier procedure of deducing the parameters is avoided. An order-of-magnitude agreement is generally obtained though some observed characteristic features cannot be explained. It is seen from a comparison of the present barrier model with the earlier image-barrier models that the short-range forces are effective to about 5% in determining the barrier height and are indeed important on quantitative scales. Some criticisms and drawbacks of the theory have also been given. (auth)

30707 WAVES AND PARTICLES. De Broglie, L. (Academie des Sciences, Paris). Phys. Bull. (London); 22: 149-50 (Mar 1971).

An historical survey is presented of the work of Schroedinger, Einstein, Max Born, Andrade Sieva and the present author in this field, and particular mention is made of Schroedinger's concept of "configuration space." It is concluded that the success of this concept, which has enabled many accurate predictions to be made, can only be fully explained by a theory involving the concept of the localization of particles incorporated in a physical wave. (UK)

30708 CONTACT TRANSFORMATION AND SPACE–TIME QUANTIZATION. Matsuo, S. (Kyoto Univ.). Lett. Nuovo Cim.; 1: 391-4(27 Feb 1971).

It is proven that the coordinate transformation $(x,y) \rightarrow (X,Y)$ and its inverse are contact transformations with Y and y as canonical conjugate variables of X and x, respectively. The analogy between the space quantization and the quantum mechanics of a point particle is investigated. (J.F.P.)

30709 THREE-BODY PROBLEM IN QUANTUM MECHANICS. I. CASE OF THREE DIFFERENT NONCHARGED SPINLESS PARTICLES. Olkhovskii, V. S. (Univ., Milan, Univ., Turin, Kiev State Univ.). Lett. Nuovo Cim.; 1: 553-60(27 Mar 1971).

XUM

The following topics are covered: a formulation of the problem, an algebraization of the Schroedinger equation for three-particle bound states, and an algebraization of integral equations for transitions in the continuous spectrum. (M.H.R.)

30710 SCHROEDINGER EQUATION WITH RANDOM POTENTIAL. Pastur, L. A. (Inst. of Physics and Technology of Low Temperatures, Moscow). Teor. Mat. Fiz.; 6: 415-24(Mar 1971). (In Russian).

Ergodic properties of some quantities related to the Schroedinger equation with random potential are studied. It is shown that, for the potential representing a metrical transitive (ergodic) random field with realizations bounded from below, the quantities mentioned go with increase of volume in which the equation is considered to nonrandom limits with probability equal to 1. Independence of these limits on boundary conditions is established. (auth)

30711 COULOMB ENERGY IN TIME-SYMMETRIC ELECTRODYNAMICS. Hughes III, Henry Grady (Rice Univ., Houston. Tex.). Amer. J. Phys.; 39: 570-3(May 1971).

The calculation of the interaction energy between a static charge e, and an arbitrarily moving charge e_2 is of interest for two reasons. First, the quantum-mechanical treatment of the hydrogen atom begins by assuming that the interaction is the Coulomb potential. The Coulomb potential is correct for static charges, but if the motion of e_2 gives rise to additional, motion-dependent terms, then further justification is required. Second, there is an alternative to conventional electrodynamics: the time-symmetric theory developed by Wheeler and Feynman. The different formulations for this are compared by comparing their predictions in special cases. Previously, the retarded field was taken as the field of the moving charge, and it was shown that no motion-dependent terms contribute to the interaction energy. It is shown that this result holds whether one takes retarded fields, advanced fields, or appropriate linear combinations of retarded and advanced fields. It is concluded that the various formulations of the interaction energy all reduce to the Coulomb interaction if one particle is static. (M.H.R.)

30712 GREEN FUNCTIONS OF THE SCHROEDINGER EQUATION FOR THE SIMPLEST SYSTEMS. Bakhrakh, V. L.; Vetchinkin, S. I. (Inst. of Chemical Physics, Moscow). Teor. Mat. Fiz.; 6: 392-402(Mar 1971). (In Russian).

Closed analytical representations of Green functions are considered in cases when the corresponding uniform Schroedinger equation can be reduced to the confluent hypergeometrical equation. This class of problems includes a number of basic quantum mechanical modes. (auth)

30713 RADIATION OF FAST CHARGED PARTICLES IN TRANSVERSE SINUSOIDAL ELECTRIC FIELDS. Korkhmazyan, N. A. (Erevan State Univ.). Izv. Akad. Nauk Arm. SSR, Ser. Fiz.; 5: 287-8(1970). (In Russian).

The formulas for intensity of radiation and number of quanta emitted by fast charged particles on flight through a sinusoidal electric field are obtained. (auth)

30714 PHYSICAL NATURE OF ZONES GENERATING TRANSITION RADIATION. Arakelyan, V. A.; Garibyan, G. M. Izv. Akad. Nauk Arm. SSR, Ser. Fiz.; 5: 250-66(1970). (In Russian).

A physical mechanism giving rise to the occurrence of zones generating transition radiation is discussed. To this effect, a detailed study is made of the process of generation of transition radiation in one and then in two plates. It is shown that the physical cause of occurrence of a zone generating a particular wave is the necessity of separating it either from the particle's field or from the fields of other waves of transition radiation. In a stack built up from a large number of plates the latter mechanism is the principal one. In the case of a two-plate stack the radiation is considered travelling in the direction normal to the motion of the charge due to multiple reflections from the walls of the plates. The radiation generated in thin films of matter with both ordinary and large dielectric constants is also studied. (auth)

PHYSICS (HIGH ENERGY)

Particle Interactions and Properties (Experimental)

30715 REVIEW OF EXPERIMENTAL RESULTS. Wroblewski, A. (Univ., Warsaw). pp I1-57 of Proceedings of the Colloquium on High Multiplicity Hadronic Interactions. /Krzywicki, A. (ed.). Paris; Ecole Polytechnique (1970).

From Colloquium on high multiplicity hadronic interactions; Paris, France (13 May 1970). See CONF-700528.

Recent experimental results on total cross sections, cross sections for inelastic channels, topologic cross sections, multiplicity distributions and momentum distribution of secondary particles are reviewed. (France)

Electromagnetic

Refer also to abstract 30797.

30716 EXPERIMENTAL PROBLEMS IN THE PHOTOPRODUCTION OF SEVERAL HADRONS. Brandt, Siegmund (Univ., Heidelberg). Naturwissenschaften; 57: 370-5(Aug 1970). (In German).

Recent experimental studies on the photoproduction of several hadrons are summarized with emphasis placed on the experimental difficulties encountered. Kinematic analysis of elementary processes, production of photons of known energy, monochromatic annihilation photons, and the inverse Compton effect are considered. (J.S.R.)

30717 STUDY OF ELECTRON-FIELD PAIR PRODUCTION BY PHOTONS NEAR THE THRESHOLD WITH A STREAMER CHAMBER TECHNIQUE. Augerat, J.; Avan, L.; Avan, M.; (and others) (Univ., Clermont, France). Lett. Nuovo Cim.; 1: 500-4(20 Mar 1971).

A preliminary experiment was perform.ed in which pairs and triplets were produced in the gas of a streamer chamber filled with helium, using 2.62 MeV γ-rays from ^{228}Th. The interest in the threshold energy region, the streamer chamber technique, and test results are briefly discussed. (L.B.S.)

30718 ELECTROPRODUCTION OF SINGLE π^+-MESONS ON HYDROGEN. Driver, C. (Deutsches Elektronen-Synchrotron, Hamburg); Heinloth, K.; Hoehne, K.; (and others). Phys. Lett.; 35B: 77-80(26 Apr 1971).

The electroproduction of single π^+-mesons on hydrogen, $e + p \rightarrow e' + \pi^+ + n$, was measured up to values of $|q^2| \leq 0.9$ GeV^2/c^2. The differential cross sections were determined for small momentum transfer to the nucleon over the full azimuthal angle $\phi_{\pi q}$. (auth)

30719 ELECTROPRODUCTION OF SINGLE π^+-MESONS ON HYDROGEN: DETERMINATION OF THE LONGITUDINAL PART OF THE CROSS SECTION. Driver, C. (Deutsches Elektronen-Synchrotron, Hamburg); Heinloth, K.; Hoehne, K.; (and others). Phys. Lett.; 35B: 81-2(26 Apr 1971).

The longitudinal contribution σ_L to the cross section for the electroproduction of π^+-mesons on protons was determined from the measured values of $\frac{1}{2}(\sigma_{||} + \sigma_\perp) + \epsilon\sigma_L$ assuming the ratio $\sigma_{||}/\sigma_\perp \leq 0.1$ for $0.02 \leq |t| \leq 0.15$ (GeV/c)^2, as is known from the photoproduction of π^+-mesons. (auth)

30720 DETERMINATION OF THE ANOMALOUS MAGNETIC MOMENT OF THE FREE ELECTRON FROM MEASUREMENTS MADE ON AN ELECTRON GAS AT 80°K USING A BOLOMETRIC TECHNIQUE. Walls, Fred Lexes. Seattle; Univ. of Washington (1970). 137p. University Microfilms Order No. 71-1038.

Thesis.

A new technique for nondestructively interrogating the internal state of stored ions is developed and demonstrated. In this technique, one monitors the translation temperature of the stored ion gas while the ions are undergoing transitions between suitable energy levels. This scheme presupposes the existence of sufficiently strong relaxation processes connecting the levels in question with the ion motion. Specifically, one might think of electric or magnetic interactions between ions and of the effects of motion through inhomogeneous magnetic and electric fields (Majorana flops). The latter effect will be most pronounced if the (internal) transition frequency ω_i to be detected coincides with a characteristic frequency of the translational periodic motion in the trap, ω_t. However, when $\omega_i \neq \omega_t$ it is still possible to assist the relaxation process by modulating the field gradient at the difference frequency $|\omega_i - \omega_t|$, whereby the oscillating ion sees a sideband frequency ω_i. Other relaxation interactions are conceivable. It is further assumed that collisions between stored ions establish very quickly a thermal distribution of ion translational energies. This makes it possible to cool the ions by coupling their disordered axial motion to a suitably tuned LC circuit which also acts as the thermometer. Using this bolometric technique, the anomalous magnetic moment of the free electron is determined from measurements made on ~10^4 electrons contained in a Penning ion trap at a temperature of 80°K. A temperature increase of the electron gas is observed when the frequency of an inhomogeneous rf transverse magnetic field is swept through the value corresponding to $\omega_s - \omega_c$ where ω_s is the ensemble average of the spin precession frequency and ω_c is the ensemble average of the cyclotron frequency of the electron gas. The magnetic field is calibrated by observing a temperature increase of the electron gas when it is irradiated with a microwave electric field near its cyclotron frequency. The magnetic field can be determined directly in terms of the Bohr magneton with this scheme. The absolute accuracy was 2 parts in 10^7 in the most accurate determination and it appears feasible to extend the accuracy to at least 1 part in 10^8 for sufficiently large homogeneous magnetic fields. The effects of space charge and the trapping fields are analyzed in detail. It is shown that using this scheme it is possible, at least in principle, to measure these contributions directly. The anomalous magnetic moment of the free electron is usually characterized by the "g-2" or anomaly factor "a." The value obtained from this experiment is $a = 1.159580(80) \times 10^{-3}$. This is not sufficiently accurate to resolve the discrepancy between the current theoretical and experimental values for "a." It does however provide the basis from which it should be possible to design and carry out a measurement of "a" to accuracies of several parts in 10^8 or better. Futhermore, the energy range is over 7 orders of magnitude lower than that of the method developed by Crane's group at the University of Michigan. This would be an interesting check of the accepted energy dependence of "a" as well. (Diss. Abstr. Int., B)

30721 COULOMB CORRECTIONS IN THE ANALYSIS OF πN EXPERIMENTAL SCATTERING DATA. Oades, G. C. (Rutherford High Energy Lab., Chilton, Eng.). Springer Tracts Mod. Phys.; 55: 61-72(1970).

From Low energy hadron interactions conference; Karlsruhe, Germany (May 1970). See CONF-700558.

The electromagnetic effects which, in a potential model, would occur when the Coulomb potential is included in addition to the nuclear potential are described. These are the effects which can most easily be included when analyzing the basic scattering data for the $\pi + N$ interactions. The review covers the general form of the scattering amplitude in the simultaneous presence of the nuclear and electromagnetic interactions, various treatments of the πN Coulomb corrections, and the effects of Coulomb corrections on low-energy data. (J.F.P.)

Weak

Refer also to abstract 29371.

30722 (COO-1701-12) LEPTONIC DECAY EXPERIMENTS WITH HYPERONS BEAMS AT NAL. Winston, Roland (Chicago Univ., Ill.). [1970]. 6p. Dep. NTIS.

The feasibility and physics of experiments on leptonic decay using hyperon beams is discussed quantitatively. It is assumed that the hyperons in the beam are unpolarized so that only decays with Λ's in the final state contain polarization information. The beta decays of unpolarized hyperons, decays with Λ's in the final state, decays with muons in the final state, and selected possible experiments are considered. (J.F.P.)

30723 SEARCH FOR $K_S \rightarrow \pi^+\pi^-\pi^0$. Cho, Y. (Carnegie-Mellon Univ., Pittsburgh); Dralle, A.; Canter, J.; (and others). Phys. Rev., D; 3: 1557-61(1 Apr 1971).

A search for K_S decaying into the final state $\pi^+\pi^-\pi^0$ was made by studying the time distribution of 3π decays of neutral K mesons produced in the reaction $K^+d \rightarrow K^0pp$. On the basis of 99 3π events, for the complex parameter $x + iy$, the ratio of the amplitude $K_S \rightarrow 3\pi$ to the amplitude $K_L \rightarrow 3\pi$, $x = 0.47 \pm 0.20$, $y = -0.10^{+0.31}_{-0.32}$ was found. The result is consistent with no K_S decays into $\pi^+\pi^-\pi^0$ and no CP violation. Assuming $x = y = 0$, $\Gamma_L(3\pi) = (2.71 \pm 0.28) \times 10^6$ sec^{-1} was obtained. (auth)

XUM

Strong (Baryon-Induced)

Refer also to abstracts 30840 and 30866.

30724 (CERN-Trans-71-4) SEARCH FOR PARTICLES WITH A FRACTIONAL CHARGE (QUARKS) IN THE 70 GeV ACCELERATOR. Antipov, Yu. M.; Vishnevskii, N. K.; Ech, F. A.; (and others) (Gosudarstvennyi Komitet po Ispol'zovaniyu Atomnoi Energii SSSR, Serpukhov. Institut Fiziki Vysokikh Energii). Translated by B. Hodge from report IFVE-68-72. 17p. Dep. NTIS (U. S. Sales Only).

An experimental search for quarks produced by protons at an energy of 70 GeV on an internal aluminum target is described. Measurements were made on a 50-GeV/sec beam of negative particles extracted from the accelerator at an angle of 0°. Upper limits for the differential and total cross sections for quark production are given. (J.F.P.)

30725 (JINR-P1-5633) ELASTIC pp- AND pd-SCATTERING AT 50 AND 70 GeV. Devenski, P. A.; Zayachki, V. I.; Zlatanov, Z. M.; (and others) (Joint Inst. for Nuclear Research, Dubna (USSR). Lab. of High Energy). 1971. 10p. (In Russian). Dep. NTIS (U. S. Sales Only).

The differential cross sections for elastic pp-scattering at 50 GeV and pd-scattering at 70 GeV in the region of four momentum transfer $(00.1 < |t| < 0.17)$ $(GeV/c)^2$ are determined. The slope parameters are also determined. The following results are obtained: $B_{pp} = (11.06 \pm 0.28)$ $(GeV/c)^2$ and $B_{pd} = (40.7 \pm 0.7)$ $(GeV/c)^{-2}$. (auth)

30726 (JINR-P1-5665) CROSS SECTIONS OF INELASTIC CHANNELS OF REACTIONS IN np-INTERACTIONS AT THE NEUTRON MOMENTUM FROM 2 TO 10 GeV/c. Gasparyan, A. P.; Nikitin, A. V.; Troyan, Yu. A. (Joint Inst. for Nuclear Research, Dubna (USSR). Lab. of High Energy). 1971. 24p. (In Russian). Dep. NTIS (U. S. Sales Only).

A method of separation of the channels of the reactions $np \rightarrow np\,\pi^+\pi^-$ and $np \rightarrow np\,\pi^+\pi^-(m\pi^0)$ m = 1,2 ... is suggested and the cross sections of ten inelastic reactions in np -interactions are obtained. (auth)

30727 (NP-18796) OBSERVATION OF THE d* EFFECT IN THE $\bar{p}d \rightarrow p\bar{p}\pi^+\pi^-n$ REACTION AT 5.55 GeV/c. Braun, H.; Evrard, D.; Fridman, A.; Gerber, J-P.; Kahn, R.; Maurer, G.; Michalon, A.; Schiby, B.; Strub, R.; Voltolini, C. (Centre National de la Recherche Scientifique, Strasbourg (France). Centre de Recherches Nucleaires). [nd]. 11p. Dep. NTIS (U. S. Sales Only).

This experiment is based on 150,000 photographs, taken at the ZGS with the 30 inch bubble chamber. Results are presented from a subsample of $p_s\bar{p}\pi^+\pi^-n$ events in which the protons stopping in the chamber do not exhibit the characteristic nucleon-spectator behavior. The selection procedure for this sample is discussed. A strong low mass $p_s n\pi^+$ enhancement at 2.2 GeV/c^2 is observed. This bump is not considered to be a real resonance and is interpreted as having the same origin as the 2.2 GeV/c^2 $d\pi$ enhancement, observed, for instance in the $\bar{p}d \rightarrow \bar{p}d\pi^+\pi^-$ reaction at the same energy. (France)

30728 NUCLEON-ANTINUCLEON PRODUCTION IN HIGH-ENERGY (>10^{12} eV) HADRON COLLISIONS. Tonwar, S. C.; Naranan, S.; Sreekantan, B. V. (Tata Inst. of Fundamental Research, Bombay). Lett. Nuovo Cim.; 1: 531-7(27 Mar 1971).

Results obtained from a detailed study of the time structure of hadrons in extensive air showers carried out at Ootacamund (altitude 800 g cm^{-2}) are presented. It is shown that in ultra-high-energy (>10^{12} eV) collisions of hadrons there is a comparatively large production of nucleon-antinucleon pairs, implying a rapid increase in the production cross section at energies beyond 100 GeV. (L.B.S.)

30729 BARYON RESONANCES IN COSMIC-RAY INTERACTIONS. Kazuno, M. (Dublin Inst. for Advanced Studies). Lett. Nuovo Cim.; 1: 517-23(20 Mar 1971).

An attempt is made to evaluate the average mass of baryon isobars in cosmic ray interactions observed in nuclear emulsions by means of angular measurements of particles emitted in the most backward direction of the c.m.s. of each jet and with the aid of a kinematic relation of the isobar. The results are compared with theoretical predictions of Hagedorn based on thermodynamic considerations. (L.B.S.)

30730 ISOSPIN INVARIANCE IN THE REACTION $n + p \rightarrow \pi^0 + d$. Wilson, S. S. (Univ. of Michigan, Ann Harbor); Longo, M. J.; Young, K. K.; (and others). Phys. Lett.; 35B: 83-6(26 Apr 1971).

A measurement of the differential cross section for the reaction $n + p \rightarrow d + \pi^0$ was made using a neutron beam with kinetic energies up to 720 MeV. The angle and momentum of the deuterons were measured using an analyzing magnet and wire spark chambers with a magnetostrictive readout. The photons from the decaying π^0 were not detected. The neutron energy was calculated from the measured deuteron angle and momentum. The cross sections are compared to those for the reaction $\pi^+ + d \rightarrow p + p$ as a test of isotopic spin invariance in strong interactions. The symmetry of the cross sections about 90° is also investigated, and an upper limit of about 1% is placed on the real part of the ratio of isospin-violating to isospin-conserving amplitudes. (auth)

30731 FORWARD DIFFERENTIAL CROSS SECTIONS FOR THE REACTION $p + p \rightarrow d + \pi^+$ IN THE RANGE 3.4 TO 12.3 GeV/c. Anderson, H. L. (Univ. of Chicago); Dixit, M. S.; Evans, H. J.; (and others). Phys. Rev., D; 3: 1536-56(1 Apr 1971).

A missing-mass spectrometer, employing optical spark chambers with automatic vidicon readout, was used to measure the forward differential cross section ($\cos\theta_{cm} \approx 0.995$) for the reaction $p + p \rightarrow d + \pi^+$ at closely spaced settings of the incident proton momentum in the range $p_0 = 3.4$ to 12.3 GeV/c. The deuterons from the reaction were identified by time of flight, and their momentum and angle of emission measured by a reconstruction of the spark-chamber tracks. Since the incoming proton momentum was accurately known, the missing mass associated with deuteron production could be deduced. The reaction $p + p \rightarrow d + \pi^+$ was identified by the appearance of a distinct peak corresponding to the pion mass in a missing-mass plot. The data confirm the existence of a prominent peak in the forward cross section at $E_{cm} = 3.0$ GeV and show a hitherto unreported shoulder at $E_{cm} = 3.7$ GeV. This structure, along with the well-known sharp maximum at $E_{cm} = 2.2$ GeV, may be understood on the basis of a one-pion-exchange model as reflecting the behavior of the $T = 3/2$ isobars in pion-nucleon scattering. Above $E_{cm} = 3.9$ GeV, the forward differential cross section decreases monotonically as the −2.5 power of s, the square of the total cm energy. This feature also reflects the behavior of the πp scattering cross section. The structureless upper-energy region can also be accommodated within the framework of Regge theory. The cross section $d\sigma/du$ extrapolated to u = 0 varies as the −3.2 power of s, midway between that expected for the N_α and N_γ trajectories. (auth)

30732 HIGH MULTIPLICITY HADRONIC INTERACTIONS: THE PROBLEM OF DATA PRESENTATION. Krzywicki, A. (Ecole Polytechnique, Paris). pp II-1-21 of Proceedings of the Colloquium on High Multiplicity Hadronic Interactions. /Krzywicki, A. (ed.). Paris; Ecole Polytechnique (1970).

From Colloquium on high multiplicity hadronic interactions; Paris, France (13 May 1970). See CONF-700528.

The essence of the problem of data presentation is to differentiate between dynamics and phase-space effects. Two complementary approaches to the problems are distinguished. In the first, the spectrum of one of the parameters describing the final state is studied and one integrates over all possible configurations of other parameters. The different methods used to calculate the phase space integrals once a particular form of the S-matrix element has been postulated are discussed. The second approach consists in attempting to get more insight into the phase using differential methods of data analysis. Applications, refinements, and generalizations of the Dalitz plot idea are reviewed. (France)

30733 ANGULAR CORRELATIONS IN THE REACTION $p\bar{p} \rightarrow 3\pi^+\,3\pi^-\,(\pi^0)$ AT 3.6 GeV/c. Nellen, Bernd (Univ., Bonn). pp III-47-51 of Proceedings of the Colloquium on High Multiplicity Hadronic Interactions. /Krzywicki, A. (ed.). Paris; Ecole Polytechnique (1970).

From Colloquium on high multiplicity hadronic interactions; Paris, France (13 May 1970). See CONF-700528.

The angular correlations in the reactions (1) $p\bar{p} \rightarrow 3\pi^+\,3\pi^-$ and (2) $p\bar{p} \rightarrow 3\pi^+\,3\pi^-\,\pi^0$ are studied. It is shown that the data are well described when the statistical model prediction is weighted for resonance production and Bose-symmetrization. It is assumed that the angular correlations in reaction (1) can be understood as a consequence of the dynamics of the process. (France)

30734 OBSERVATION OF THE ABC EFFECT AND A STRUCTURE AT 450 MeV IN MESON MISSING-MASS SPECTRA. Banaigs, J. (CEN, Saclay, France); Berger, J.; Duflo, J.; (and others). Nucl. Phys.; B28: 509-27(1971). (In French).

The "ABC" effect was observed in the missing mass spectra of the reactions $dp \rightarrow {}^3He + (MM)^0$ at 3.25, 3.42, 3.59 and 3.76 GeV/c and $dp \rightarrow d + (MM)^+$ at 3.25, 3.59 and 3.76 GeV/c, the latter reaction being interpreted in the impulse approximation as equivalent

to Np → d + (MM) at half incident nucleon momenta. A structure, with its mass near 450 MeV, was also observed in the missing mass spectra of the reaction dp → ^{3}He + (MM)^0. (auth)

Strong (Meson-Induced)

Refer also to abstracts 30806 and 30867.

30735 (CERN/HERA-70-7) COMPILATION OF CROSS SECTIONS. VI. π^- INDUCED REACTIONS. Flaminio, E.; Hansen, J. D.; Morrison, D. R. O.; Tovey, N. (European Organization for Nuclear Research, Geneva (Switzerland)). 23 Oct 1970. 172p. Dep. NTIS (U. S. Sales Only).

A compilation of cross sections of reactions produced by negative pions on targets of protons, neutrons and deuterons is presented. Graphs of the variation of cross section with incident laboratory momentum are plotted. Values for the rate of decrease of cross section with incident momentum are given. (auth)

30736 (JINR-P1-5565) COHERENT INTERACTIONS OF π^--MESONS WITH THE PHOTOEMULSION NUCLEI AT 17 GeV. Azimov, S. A.; Grishin, V. G.; Gulyamov, U. G.; (and others) (Joint Inst. for Nuclear Research, Dubna (USSR). Lab. of High Energy). 1971. 15p. (In Russian). Dep. NTIS (U. S. Sales Only).

A new technique of selection of the coherent interactions is described. Using this technique the paths equal to 53^{+7}_{-5} m and $3.8^{+1.1}_{-0.8}$ km, respectively, were obtained for coherent reactions π^- + nucleus → $\pi^-\pi^-\pi^+$ + nucleus and π^- + nucleus → $\pi^-\pi^-\pi^-\pi^+\pi^+$ + nucleus on the photoemulsion nuclei at 17 GeV. (auth)

30737 EVIDENCE FOR A POSSIBLE BOSON RESONANCE OF MASS 2820 MeV. Sabau, M. (Inst. for Atomic Physics, Bucharest); Uretsky, J. L. Lett. Nuovo Cim.; 1: 514-16(20 Mar 1971).

The possibility of the production of a new four-particle boson resonance $X^+ = (\kappa\bar{\kappa}\pi\pi)^+$ from π^+p interactions at 8.04 GeV/c is studied. Fitting a Breit–Wigner distribution plus phase space gave the following X^+ resonance parameters: $M_x = (2820 \pm 10)$ MeV and $\Gamma = (50 \pm 10)$ MeV. The production cross section for the reaction $\pi^+ + p \rightarrow p + X^+$ was estimated to be 25 ± 10 μb. The t-channel ρ exchange is suggested as a possible production mechanism. (L.B.S.)

30738 FORWARD PRODUCTION OF Δ(1236) IN PION–PROTON SCATTERING AT 4 GeV/c AND A COMPARISON WITH THE QUARK MODEL. Derado, I. (Max-Planck-Institut fuer Physik und Astrophysik, Munich). Lett. Nuovo Cim.; 1: 509-13(20 Mar 1971).

The production of the Δ resonance in the u region greater than -3.0 (GeV/c)^2 is studied from events of the types $\pi^- + p \rightarrow \pi^- + \pi^+ + n$ and $\pi^- + p \rightarrow \pi^- + \pi^0 + p$. The results are compared with quark model predictions and are found to be in reasonable agreement for charged Δ resonances. (L.B.S.)

30739 APPLICATION OF INFORMATION THEORY AT SERPUKHOV ENERGIES. Rotelli, P. (Imperial Coll. of Science and Tech., London). Lett. Nuovo Cim.; 1: 660-4(17 Apr 1971).

It is shown that by comparing results of inelastic charged multiplicities of π^-p scattering at 16 and 60 GeV/c agreement is obtained with a statistical prediction based on the information theory approach. (L.B.S.)

30740 POLARIZATION IN BACKWARD π^+p ELASTIC SCATTERING AT 6 GeV/c. Aoi, H.; Booth, N. E.; Caverzasio, C.; (and others) (CERN, Geneva). Phys. Lett.; 35B: 90-2(26 Apr 1971).

The polarization in backward π^+p elastic scattering was measured at 6 GeV/c over the region $+0.04 \geq u \geq -0.32$ (GeV/c)^2. The results indicate that the polarization is small in the region of the backward peak of dσ/du, but becomes large and negative beyond the dip. This behavior is not predicted by recent models. (auth)

30741 ρ^0, f^0, ω^0 PRODUCTION ON NUCLEI AND PROTONS BY 15, 16 GeV/c π^-. Daugeras, B. (Laboratoire de Accelerateur Lineaire, Orsay, France); Fournier, D.; Grivaz, J. F.; (and others). Nuovo Cim.; 2A: 237-48(1 Mar 1971).

Partial cross sections are presented for ρ^0, f^0, and ω^0 production by 15 and 16 GeV/c π^- in the incoherent reactions $\pi^-A \rightarrow \pi^+\pi^-A'$ and $\pi^-A \rightarrow \pi^+\pi^-\pi^0A'$ on nuclei of C_2F_3Cl in a HLBC. Using these results and a nuclear-interaction model, the production cross sections of these resonances in the corresponding reactions on protons, i.e., $\pi^-p \rightarrow \rho^0n$, $\pi^-p \rightarrow f^0n$ and $\pi^-p \rightarrow \omega^0n$, are calculated as a function of the absorption cross-section of the produced resonance in nuclear matter. Difficulties in separating those reactions from other sources of ρ^0, etc., in nuclear reactions are discussed. (auth)

30742 STUDY OF THE ENERGY DEPENDENCE OF 3-BODY REACTIONS BY USE OF LONGITUDINAL PHASE SPACE PLOTS. Drevermann, H. (Univ., Bonn). pp II-22-7 of Proceedings of the Colloquium on High Multiplicity Hadronic Interactions. /Krzywicki, A. (ed.). Paris; Ecole Polytechnique (1970).

From Colloquium on high multiplicity hadronic interactions; Paris, France (13 May 1970). See CONF-700528.

Three-body reactions are studied by use of longitudinal phase space plots. The experiment distributions in LPS are sufficiently well described by the angle ω in the hexagon. The reaction $\pi^+p \rightarrow \pi^+\pi^0p$ is studied at 5 and 8 GeV/c. The dependence of dδ/dω on incident momentum is studied by use of the parametrization: $(d\delta/d\omega) = C(\omega) \cdot p_{Lab}^{-n(\omega)}$ where $C(\omega)$ depends only on ω, and $n(\omega)$ describes the energy dependence of all the reactions contributing to the same ω-interval. For almost all ω, $n(\omega)$ is between 1 and 1.5. Below ω = 110 deg, where diffraction association is expected, $n(\omega)$ is almost zero. Corresponding distributions for the reaction $\pi^+p \rightarrow \pi^+\pi^+n$ are given. (France)

30743 PROPOSAL OF A PARAMETRISATION FOR HIGH MULTIPLICITIES. (Ecole Polytechnique, Paris. CEA, Saclay, France). pp III-28-34 of Proceedings of the Colloquium on High Multiplicity Hadronic Interactions. /Krzywicki, A. (ed.). Paris; Ecole Polytechnique (1970).

From Colloquium on high multiplicity hadronic interactions; Paris, France (13 May 1970). See CONF-700528.

High multiplicity events were studied in a 9 event/μb exposure of the CERN 2 m HBC to a K^- beam of 3.95 GeV/c. The most abundant channel $K^-p \rightarrow p\,K^-\,\pi^+\,\pi^+\,\pi^-\,\pi^-$ is studied. A new set of parameters, which describes the asymmetries in the Dalitz plot of each system of three particles, is introduced to study the Goldhaber effect. The parameters, together with a certain fraction of resonance production, would give a good description of the experimental results. (France)

30744 CORRELATION EFFECTS. Bellini, G. (Univ., Milan). pp III-35-7 of Proceedings of the Colloquium on High Multiplicity Hadronic Interactions. /Krzywicki, A. (ed.). Paris; Ecole Polytechnique (1970).

From Colloquium on high multiplicity hadronic interactions; Paris, France (13 May 1970). See CONF-700528.

The Goldhaber effect is observed in the reaction $\pi^-p \rightarrow 2\pi^+2\pi^-n$ at 8 and 16 GeV/c, in samples where the resonance production was suppressed. This effect is shown to decrease with increasing average pion energy. The results are consistent with an exponential variation with average pion energy of the parameter $c = (\gamma_{unlike} - \gamma_{like})/(\gamma_{unlike+4})(\gamma_{like+4})$, as found by Czyzewsky and Szeptycka. (France)

30745 ANGULAR CORRELATIONS IN THE REACTION $K^+p \rightarrow K^+p\,2\pi^+2\pi^-$ AT GeV/c. (European Atomic Energy Community, Brussels. European Organization for Nuclear Research, Geneva). pp III-52-3 of Proceedings of the Colloquium on High Multiplicity Hadronic Interactions. /Krzywicki, A. (ed.). Paris; Ecole Polytechnique (1970).

From Colloquium on high multiplicity hadronic interactions; Paris, France (13 May 1970). See CONF-700528.

The six body final state $K^+p\,2\pi^+2\pi^-$ is studied from a hydrogen bubble chamber experiment with incident K^+ mesons of 4.97 GeV/c. Considerable attention has been paid to the study of charge dependent angular correlations between pions. This channel is dominated by the production of the known resonances $K^{*0}(890)$, $N^{*++}(1236)$, and simultaneous $K^{*0}N^{*++}$ production. (France)

30746 TEST OF THE THERMODYNAMICAL MODEL WITH SECONDARY PIONS PRODUCED IN 5 GeV/c π^+p COLLISIONS. pp IV-139-46 of Proceedings of the Colloquium on High Multiplicity Hadronic Interactions. /Krzywicki, A. (ed.). Paris; Ecole Polytechnique (1970).

From Colloquium on high multiplicity hadronic interactions; Paris, France (13 May 1970). See CONF-700528.

A specific test has been performed of Hagedorn's thermodynamical model, using transverse momentum (P_t) distributions of the secondary pions observed in 35573 interactions of π^+p at 5 GeV/c. The agreement between the experimental distributions and the prediction is poor. An excess of events is observed in the medium range of P_t. (France)

30747 DOUBLE-REGGE-POLE DESCRIPTION OF THE REACTION $K^-n \rightarrow K^-\pi^-p$ AT 5.5 GeV/c. Cho, Y. (Argonne National Lab., Ill.); Derrick, M.; Johnson, D.; (and others). Phys. Rev., D; 3: 1561-8(1 Apr 1971).

New data on the reaction $K^-d \rightarrow K^-\pi^-pp_s$ at 5.5 GeV/c are presented. The experimental distributions are analyzed in terms of double-peripheral Regge-pole model. The events were assigned to two dominant diagrams using the Van Hove angle. These dia-

XUM

grams, involving Pomeranchuk and meson exchanges, provide a good description of the reaction without additional form factors of the momentum transfer. (auth)

30748 SINGLE-PION PRODUCTION IN K^+p INTERACTIONS AT 4.6 GeV/c. Fu, C.; MacNaughton, J.; Trilling, G. H. (Univ. of California, Berkeley). Nucl. Phys.; B28: 528-40(1971).

A study of K^+p interactions at 4.6 GeV/c leading to single-pion production is presented. Cross sections for the final states $K\Delta$, $K^*(891)p$, $K^*(1420)p$ are given. Comparison of the results of this study with published K^-p and K^-n data at the same momentum indicates that corresponding K^- cross sections are significantly smaller, but other features such as momentum transfer distributions and density matrix elements are very similar. (auth)

Particle Interactions and Properties (Theoretical)

General

Refer also to abstracts 30914 and 30954.

30749 (CALT-69-297) SCALE INVARIANCE AND THE LIGHT CONE. Fritzsch, Harald (Max-Planck-Institut fuer Physik und Astrophysik, Munich (West Germany). Stanford Linear Accelerator Center, Calif.); Gell-Mann, Murray (California Inst. of Tech., Pasadena). [1971]. Contract AT(11-1)-68. 53p. (CONF-710106-9). Dep. NTIS.

From Conference on fundamental interactions at high energy, Coral Gables, Fla. (20 Jan 1971).

The discussion of scale invariance and the light cone covers the dilation operator and broken scale invariance, light cone commutators and deep inelastic electron scattering, generalized light cone scaling and broken scale invariance, bilocal operators, light cone algebra abstracted from a quark picture, and light cone algebra and deep inelastic scattering. (J.F.P.)

30750 (CERN-71-7) PROCEEDINGS OF THE 1970 CERN SCHOOL OF PHYSICS, LOMA-KOLI, FINLAND, 21 JUNE–5 JULY 1970. (European Organization for Nuclear Research, Geneva (Switzerland)). 16 Feb 1971. 361p. Dep. NTIS (U. S. Sales Only).

There were four lectures included for which separate abstracts were prepared. (J.F.P.)

For abstracts of individual lectures see: 30772, 30803, 30822, and 30823.

30751 (IS-T-426) MODEL ANALYSES OF ELEMENTARY PARTICLE SCATTERING AMPLITUDES. Coleman, Thomas Patrick (Ames Lab., Iowa). Feb 1971. Contract W-7405-eng-82. 83p. Dep. NTIS.

Thesis.

Several models of high energy scattering reactions are examined. First, the s-wave S-matrix of the double δ-function potential barrier does not contain a second-order pole, in contrast to an earlier analysis of the same potential. This suggests that the crossing of resonance levels with the same symmetry does not occur. Second, a model in which the $A_2(1300)$ meson consists of two coupled mesons of the same spin and parity is used to explain the variations of the mass structure of the A_2 in several experiments. The roles of these two mesons in group classifications of elementary particles and in S-matrix theory are discussed. Third, the double-Regge pole models of Berger, of Chan, Kajantie, and Ranft, and of Chan, Loskiewicz, and Allison are compared with data from the reaction $pp \to p\pi^-\Delta^{++}$ at 22 GeV/c. Berger's model is most consistent with the data and with earlier analyses. The relative merits of the three models are discussed. (auth)

30752 (JINR-P2-5691) RELATIVISTIC WAVE FUNCTION AND FORM FACTORS OF THE BOUND SYSTEM. Faustov, R. N. (Joint Inst. for Nuclear Research, Dubna (USSR). Lab. of Theoretical Physics). 1971. 21p. (In Russian). Dep. NTIS (U. S. Sales Only).

An explicitly relativistic invariant three-dimensional formulation of the quasipotential method of Logunov and Tavkhelidze for the system of two particles with arbitrary spins and masses is given. This formalism is used to consider the matrix elements of local operators between the bound states (the form factors of the bound system). The transformation law of the three-dimensional wave functions in the transition from the center of mass system to an arbitrary reference frame is obtained. (auth)

30753 CONFERENCE ON HIGH ENERGY PHYSICS, SEPTEMBER 29–OCTOBER 2, 1970, AIX-EN-PROVENCE, FRANCE. J. Phys. (Paris), Colloq.; C5: 1-189(Nov-Dec 1970). (In French). (CONF-700950).

The nine papers introducing the various sessions were abstracted. (France)

For abstracts of individual papers see: 29373, 30754, 30825, 30826, 30853, 30854, 30925, 31060, and 31061.

30754 VERY HIGH ENERGY HADRON PHENOMENA. Van Hove, L. (European Organization for Nuclear Research, Geneva). J. Phys. (Paris), Colloq.; C5: 125-31(Nov-Dec 1970). (In French).

From Conference on high energy physics; Aix-en-Provence, France (29 Sep 1970). See CONF-700950.

After a few remarks on two-body collisions, general hadronic collisions are analyzed in terms of transverse momenta and scaled-down longitudinal momentum variables. (France)

30755 MULTICLUSTER MODEL FOR VERY-HIGH-ENERGY COLLISIONS. Bassetto, A.; Paccanoni, F. (Univ., Padua. Istituto Nazionale di Fisica Nucleare, Padua). Nuovo Cim.; 2A: 306-20(1 Mar 1971).

With a suitable choice of kinematical variables a multicluster model is studied for very-high-energy processes, improving the agreement of the theoretical predictions with experimental multiplicities of secondaries and mean transverse momenta. The consequences of this model on the forward absorptive part of the elastic amplitude are examined in the energy regions where diffraction dissociation dominates. An example is given where a consistency condition determines the character of the leading singularity responsible for the high-energy behavior of the total cross section. (auth)

30756 ANALYTIC EQUIVALENCE OF WAVE FUNCTIONS AND INVARIANT AMPLITUDES FOR MASSIVE PARTICLES. Yndurain, F. J. (CERN, Geneva). Nuovo Cim.; 2A: 104-8 (1 Mar 1971).

It is shown that 1) any pair of wave functions for a massive particle and 2) any pair of sets of invariant amplitudes without kinematical singularities or zeros, for massive particles, are mutually related by matrices whose components are polynomials in the momenta of the particles and therefore analytically equivalent. (auth)

30757 RESTRICTIONS ON THE ANGULAR MOMENTUM OF t-CHANNEL EXCHANGES FROM s-CHANNEL HELICITY CONSERVATION. Blackmon, M. L.; King, M. J.; Wali, K. C. (Syracuse Univ., N. Y.). Phys. Lett.; 35B: 44-6(26 Apr 1971).

It is shown that there are constraints on the angular momentum of t-channel exchanges due to s-channel helicity conservation in the elastic reactions of $0 + S \to 0 + S$. (auth)

30758 GENERAL FEATURES OF INCLUSIVE REACTIONS FROM DUALITY. Veneziano, G. (Massachusetts Inst. of Tech., Cambridge). Contract AT(30 1)-2098. Lett. Nuovo Cim.; 1: 681-4(17 Apr 1971).

The Harari–Freund conjecture, relating background and pomeron in the case of two-body processes, is generalized to the case of elastic 2n-point functions ($n > 2$). General duality predictions are then obtained for inclusive reactions, using optical-like theorems. (L.B.S.)

30759 ALGEBRAICAL APPROACH TO THE SOLUTION OF ONE-DIMENSIONAL MODEL OF N-INTERACTING PARTICLES. Perelomov, A. M. Teor. Mat. Fiz.; 6: 364-91(Mar 1971). (In Russian).

Algebraical apparatus (i.e. the method of increasing B_p^+ and decreasing B_p ($p = 2, 3, \ldots, N$) operators) is developed for the solution of one-dimensional model studied previously and describing N interacting particles. In this method the determination of the Schroedinger wave function is reduced to the differentiation operation. The explicit formula is obtained for the operators B_p^+ and B_p with $p = 2, 3, 4$. Using this formula one can find all the wave functions in the four-particle case. For the arbitrary particle number the formula is obtained for two new sequences of wave functions depending on three quantum numbers. The operators of higher orders can be calculated by the same method. (auth)

30760 RELATIVISTIC ROTATION OF A $S = \frac{1}{2}$ SPIN IN COLLISIONS OF PARTICLES MOVING ARBITRARILY WITH RESPECT TO THE OBSERVER. Golovin, B. M.; Nikanorov, V. I. (Joint Inst. for Nuclear Research, Dubna, USSR). Zh. Eksp. Teor. Fiz.; 60: 28-31(Jan 1971). (In Russian).

Relativistic rotation of the $S = \frac{1}{2}$ spin of particles involved in a binary reaction is considered by applying Lobachevsky geometry in the case of arbitrary motion of the colliding particles with respect to the observer. It is demonstrated that in the general case relativistic rotation of the spin should not only be taken into account in the final state of the system but in the initial as well. (auth)

30761 IDENTITY OF ELEMENTARY PARTICLES. Lyuboshits, V. L.; Podgoretskii, M. I. (Joint Inst. for Nuclear Research, Dubna, USSR). Zh. Eksp. Teor. Fiz.; 60: 9-18(Jan 1971). (In Russian).

The problem of continuous transition between the properties of identical and nonidentical particle systems is considered. It is shown that the continuous parameter for such a transition is the degree of nonorthogonality of the corresponding superpositions. A logically conceivable scheme is described which is consistent with the experimental facts and in accordance with which particle identity is only approximate. (auth)

30762 PROCEEDINGS OF THE COLLOQUIUM ON HIGH MULTIPLICITY HADRONIC INTERACTIONS. Colloquium Held at Paris, France, May 13-15, 1970. Krzywicki, A.; Lestienne, R.; Salmeron, R.; Sosnowski, R. (eds.). Paris; Ecole Polytechnique (1970). 293p. (CONF-700528).

Twenty five papers were presented and all were abstracted. (France)

For abstracts of individual papers see: 30715, 30732, 30733, 30742-30746, 30763-30768, 30795, 30837-30839, 30866, 30880, 30881, 30899-30901, and 30977.

30763 COMMENT ON THE QUESTION WHETHER THE GGLP EFFECT IS DUE TO B-E SYMMETRIZATION OR NOT. Michejda, L. (Univ., Warsaw). pp III-42-6 of Proceedings of the Colloquium on High Multiplicity Hadronic Interactions. /Krzywicki, A. (ed.). Paris; Ecole Polytechnique (1970).

From Colloquium on high multiplicity hadronic interactions; Paris, France (13 May 1970). See CONF-700528.

The problem of whether the Goldhaber effect is due to Bose-Einstein symmetrization or not is discussed. Tests are proposed for the experimental data and for model calculations. A simple argument shows that interference may induce an enhancement of like pairs emitted under small angles in models where phases do not change rapdily. (France)

30764 STATISTICAL MODELS BASED ON THE FERMI MODEL. Lamb, D. Q. (Univ. of Liverpool. Univ. of Rochester, N. Y.). pp IV-89-134 of Proceedings of the Colloquium on High Multiplicity Hadronic Interactions. /Krzywicki, A. (ed.). Paris; Ecole Polytechnique (1970).

From Colloquium on high multiplicity hadronic interactions; Paris, France (13 May 1970). See CONF-700528.

Several developments of statistical models based on the Fermi model are recalled. An SU_3 invariant model is described and a few of its predictions are given. Several other models (a model with angular momentum, the unitary symmetric model, Reggeized multiperipheral model, quark arrangement model) are discussed and compared. (France)

30765 MULTIPERIPHERALISM. Petersson, Bengt (European Organization for Nuclear Research, Geneva). pp V-1-18 of Proceedings of the Colloquium on High Multiplicity Hadronic Interactions. /Krzywicki, A. (ed.). Paris; Ecole Polytechnique (1970).

From Colloquium on high multiplicity hadronic interactions; Paris, France (13 May 1970). See CONF-700528.

Some applications of multiperipheral models are discussed to illustrate the simplicity of such models. Some general features of multi-particle reactions are shown to be in accordance with these models. The connection with the bootstrap program, where it has been shown that it is possible to generate the Pomeron by summing up such amplitudes, is pointed out. Attempts to go beyond these models to more detailed ones, such as a generalized Veneziano model, are also described. (auth)

30766 STATISTICAL CONCEPTS APPLIED IN STUDYING THE GENERALIZED VENEZIANO MODEL. Koba, Z. (Niels Bohr Inst., Copenhagen). pp V-19-33 of Proceedings of the Colloquium on High Multiplicity Hadronic Interactions. /Krzywicki, A. (ed.). Paris; Ecole Polytechnique (1970).

From Colloquium on high multiplicity hadronic interactions; Paris, France (13 May 1970). See CONF-700528.

Attention is called to three different applications of statistical concepts to the Veneziano n point function, the "Hagedorn temperature," statistical mechanics of an infinite set of harmonic oscillators which describes the level structure of resonances, the "hot line" description of high energy reactions due to Chang, Freund and Nambu. (France)

30767 MASS DEPENDENCE OF MOMENTUM TRANSFER DISTRIBUTIONS IN DIFFRACTION DISSOCIATION. Satz, H. (European Organization for Nuclear Research, Geneva). pp V-34-45D of Proceedings of the Colloquium on High Multiplicity Hadronic Interactions. /Krzywicki, A. (ed.). Paris; Ecole Polytechnique (1970).

From Colloquium on high multiplicity hadronic interactions; Paris, France (13 May 1970). See CONF-700528.

Some aspects of the mass dependence of the momentum transfer slopes in high-energy diffraction dissociation are discussed. In general the slope is expected to decrease with increasing mass, reaching asymptotically one-half the elastic slope. Dips are expected near resonance positions, giving an oscillatory behavior. (France)

30768 REVIEW ON HYPOTHESIS OF LIMITING FRAGMENTATION. Yen, E. (Argonne National Lab., Ill.). pp VI-1-18 of Proceedings of the Colloquium on High Multiplicity Hadronic Interactions. /Krzywicki, A. (ed.). Paris; Ecole Polytechnique (1970).

From Colloquium on high multiplicity hadronic interactions; Paris, France (13 May 1970). See CONF-700528.

The hypothesis of limiting fragmentation of Benecke, Chou, Yang, and Yen is reviewed. The hypothesis is stated and supporting arguments from experiment and theory are presented. Further speculations, including the nonexistence of pionization, are discussed. Feynman's predictions based on a field theory with "partons" are listed. (France)

30769 CONDITION OF THE ASYMPTOTIC EQUALITY OF TOTAL CROSS SECTIONS IN TWO SIMPLE MODELS. Savrin, V. I.; Tyurin, N. E.; Khrustalev, O. A. (Inst. of High-Energy Physics, Serpukhov, USSR). Teor. Mat. Fiz.; 7: 30-4(Apr 1971). (In Russian).

For two simple models of the high-energy hadron interaction the condition of asymptotic equality of the total cross sections is investigated. (auth)

30770 ANALYTIC PROPERTIES OF THE SCALAR VERTEX FUNCTION. Frederiksen, J. S.; Woolcock, W. S. (Australian National Univ., Canberra). Nucl. Phys.; B28: 605-28 (1971).

A single spectral representation of the vertex function F, for the conversion of a scalar particle b into a scalar particle d via interaction with a third scalar particle s, is obtained heuristically by using unitarity to evaluate the contribution to ImF from a state $(a\bar{c})$ with the same internal quantum numbers as $(d\bar{b})$ and then making a one-pole approximation to the amplitude for $d\bar{b} \to a\bar{c}$ and a constant approximation to the vertex function for the vertex (cas). For the case where the masses satisfy the inequality $m_a + m_c \geq m_b + m_d$, the above approximations are shown to give the same result as that obtained from the Feynman parametrization of the vertex function arising from the triangle diagram. Two methods are then used to obtain a spectral representation for the triangle diagram vertex function for all allowed mass configurations, including cases for which the threshold is anomalous. The first is to evaluate the triangle diagram vertex function directly; the second is to continue in m_b^2 and m_d^2 the result for the case $m_a + m_c \geq m_b + m_d$. (auth)

Electromagnetic

Refer also to abstracts 30965 and 30998.

30771 (BNL-tr-410) DIRAC MONOPOLE: INTRODUCTORY PAPER. Bolotovskii, B. M.; Usachev, Yu. D. Translated by S. J. Amoretty (Brookhaven National Lab., Upton, N. Y.), from a collection of papers entitled Dirac Monopole. 47p. Dep. NTIS.

The current theory of magnetic charge is discussed. The discussion also involves the interaction of the magnetic charge with matter. (J.F.P.)

30772 (CERN-71-7, pp 181-283) SELECTED TOPICS IN THE THEORY OF ELECTROMAGNETIC INTERACTIONS. Gerasimov, S. B. (Joint Inst. for Nuclear Research, Dubna (USSR). Lab. of Theoretical Physics).

From Proceedings of the 1970 CERN School of Physics, Loma-Koli, Finland, 21 Jun-5 Jul 1970.

The topics reviewed in electromagnetic interaction theory are gauge invariance and tests of quantum electrodynamics, low-en-

XUM

ergy theorems, dispersion relations, sum rules, the vector meson dominance model and meson photoproduction at high energies, the behavior of form factors in electron–nucleon scattering, lepton pair annihilation into hadrons, and pair production in hadron interactions. (J.F.P.)

30773 (DESY–71/3) ON THE ACCURACY OF THE PHOTON-DIFFERENCE METHOD USED IN HIGH-ENERGY PHOTONUCLEAR EXPERIMENTS. Tesch, K. (Deutsches Elektronen-Synchrotron, Hamburg (West Germany)). Jan 1971. 18p. Dep. NTIS (U. S. Sales Only).

The accuracy in calculating the cross sections per photon, σ_k, from a set of measured cross sections per equivalent γ quantum, σ_q, is discussed. Four commonly used approximations for the bremsstrahlung spectrum and corrections for finite target thicknesses and collimator angles are reviewed. For the calculation of σ_k a simple unfolding method is proposed which is known for solving the Fredholm integral equation of the first kind, and in which the necessary smoothing of the resulting curve is derived from the mean experimental error of σ_q. For some examples of cross sections which may be encountered in photonuclear research above 100 MeV, the mean error of σ_k caused by inaccurate knowledge of the bremsstrahlung spectra, by the unfolding method and by the experimental errors of σ_q is calculated. (auth)

30774 (INSJ–126) NEGATIVE PION PHOTOPRODUCTION OFF NEUTRON AT 180° IN THE ENERGY RANGE BETWEEN 300 AND 1200 MeV. Takasaki, Fumihiko (Tokyo Univ. (Japan). Inst. for Nuclear Study). 20 Jan 1971. 37p. Dep. NTIS (U. S. Sales Only).

Differential cross sections for $\gamma + n \rightarrow \pi^- + p$ were measured at 180° for the energy range between 300 and 1200 MeV. A magnetic spectrometer system was used to detect π^- mesons produced in a liquid deuterium. In order to reduce the energy spread due to the internal nucleon motion in the deuteron, a photon difference method was employed with a step of 50 MeV. The data show large peaks at 730 and 950 MeV. An analysis was made for these resonance structures together with the cross sections for $\gamma + p \rightarrow \pi^+ + n$ at the same region, which were obtained in another part of this experiment. A clear effect of $S_{11}(1525)$ was concluded with the substantial difference of the excitation amplitude between two reactions. $D_{13}(1515)$ and $F_{15}(1690)$ also have small but finite contributions to the helicity 1/2 state. $S_{31}(1630)$ is likely excited but it needs further investigations. Photoexcitation amplitudes of resonances obtained here are in good agreements with quark model predictions. (auth)

30775 (JINR–P2–5522) INVARIANCE OF THE NONRELATIVISTIC WAVE EQUATIONS IN THE PRESENCE OF ELECTROMAGNETIC FIELD. Strel'tsov, V. N. (Joint Inst. for Nuclear Research, Dubna (USSR). Lab. of High Energy). 1970. 9p. (In Russian). Dep. NTIS (U. S. Sales Only).

The problems of the nonrelativistic wave equation invariance for particles with spins 0 and $\frac{1}{2}$ in electromagnetic field are discussed. (auth)

30776 (JINR–P2–5679) NUCLEON COMPTON-EFFECT AND SUM RULES FOR DIPOLE NUCLEON MOMENTUM. Lapidus, L. I.; Musakhanov, M. M. (Joint Inst. for Nuclear Research, Dubna (USSR). Lab. of Nuclear Problems). 1971. 21p. (In Russian). Dep. NTIS (U. S. Sales Only).

The sum rule for the nucleon dipole moment is obtained with the help of the dispersion relation and low-energy theorem for the nucleon compton-effect amplitude without P- and T-invariance conditions. In the general expression for nucleon Compton-effect amplitude the invariant functions $y_i \neq 0$ corresponds to P-invariance violation, $T_{\Gamma_{4i}}, Y_{1,3,7,8}$ violates PT-invariance. For forward scatterings relations and between invariant functions spiral amplitudes with $|m' - m| \neq 2$ are considered. (TSS)

30777 (JINR–P2–5705) POSSIBLE METHOD OF MEASURING THE ELECTROMAGNETIC FORM FACTOR OF THE NEUTRINO. Andryushin, V. I.; Bilenkii, S. M.; Gerstein, S. S. (Joint Inst. for Nuclear Research, Dubna (USSR). Lab. of Theoretical Physics). 1971. 10p. (In Russian). Dep. NTIS (U. S. Sales Only).

A possible method of determining the electromagnetic form factor of neutrino is considered. The method is based on the comparison of the cross sections of the processes induced by electromagnetic interaction of neutrinos and electrons with the nuclei. The calculation of the cross section of excitation of the giant resonance by the neutrino beam of $\lesssim$100 MeV is presented as well as the nucleus fission cross sections. (auth)

30778 NEW INTERPRETATION OF VAIDYA RADIATION. Goodinson, P. A. (Queen Elizabeth Coll., London); Newing, R. A. Int. J. Theor. Phys.; 4: 41-4(1971).

If Vaidya radiation is taken to be a combination of an electromagnetic energy flux together with that of a null fluid it is shown that the singularity in the current density along an axis, which arises in the absence of a null field, is removed. (auth) (UK)

30779 BJORKEN–REGGE ASYMPTOTISM OF ELECTROPRODUCTION STRUCTURE FUNCTIONS IN FIELD-CURRENT THEORY. Etim, E. (Univ., Naples). Nuovo Cim.; 2A: 139-57(1 Mar 1971).

The identity between fields and currents which view electromagnetic interactions through hadron dynamics is investigated and recast in a form which correctly reflects the differences between the photon and the neutral vector mesons. In this new form the model satisfactorily describes the scaling behavior and pomeron dominance of the electroproduction structure functions. (auth)

30780 POLARIZATION OF THE RECOIL PROTONS IN THE ELASTIC ELECTRON–PROTON SCATTERING PROCESS. Guenther, U.; Rodenberg, R. (Technische Hochschule, Aachen). Nuovo Cim.; 2A: 25-38(1 Mar 1971).

The imaginary part of the two-photon-exchange amplitude is estimated in an isobar model and used to calculate the polarization P of the recoil protons in elastic (e,p)-scattering processes. Using the unitarity relation for the imaginary part, the sum over the intermediate states is approximated by a sum over nucleon isobars. The spin summations are performed for arbitrary half-integer spin j isobars to obtain an expression for P where the isobaric transition form factors are the only unknown quantities. Numerical calculations were done for N and N*(1236) contributions only. For $\epsilon^{lab} \approx 550$ MeV and a momentum transfer of about 0.25 $(GeV/c)^2$ the maximum value for P was obtained to be about −0.5%. (auth)

30781 SU_3 MASS DIFFERENCES IN FIFTH INTERACTION AND TADPOLE RESULTS. Goyal, Ashok (Univ. of Pennsylvania, Philadelphia). Nuovo Cim.; 2A: 249-69(1 Mar 1971).

The medium strong mass splittings for pseudoscalar mesons, vector mesons and spin-$\frac{3}{2}$ baryons are examined in the framework of the "fifth interaction" proposed by Ne'eman.' In addition to the resonance contributions from the low-lying states, an expression for the contribution from f_8 Regge exchange in terms of contributions to electromagnetic mass differences from A_2^0 Regge exchange is given. Assuming that the A_2^0 Regge pole gives the correct contribution to the e.m. mass differences, the contribution of the f_8-meson is estimated. In the approximation of neglecting the continuum spectrum, the ratio of tadpole contributions is given by the ratio of coupling constants of the f_8-meson with hadrons. The results of the tadpole model are in agreement with the subtraction scheme of Segrè. It is also found that in the presence of such an SU_3-symmetry-breaking term, the renormalization of the hadronic weak-strangeness-changing vector current vertex, to second order in such a term, is quadratically divergent. (auth)

30782 OVERLAPPING RESONANCE MODEL OF DEEP INELASTIC ELECTRON SCATTERING. Domokos, G.; Kovesi-Domokos, S. (Johns Hopkins Univ., Baltimore). Contract AT(30-1)-4076. Nuovo Cim.; 2A: 270-8(1 Mar 1971).

It is suggested that deep inelastic electron scattering can be understood in terms of overlapping resonance contributions to the amplitude of virtual forward Compton scattering. The resonance contributions are calculated with the help of a semi-empirical model of the hadron spectrum, under the assumption that the virtual resonance photoproduction matrix elements are universal functions of the photon energy divided by the resonance mass squared. An asymptotic expression for the structure function W_2 is derived and compared with experimental data. The prediction of the model agrees well with the experimental results. (auth)

30783 BREAKDOWN OF SCALING INVARIANCE IN THE GENERALIZED BJORKEN LIMIT OF PERTURBATION THEORY. Haberler, P. L. F.; Lipshutz, N. R.; Weaver, O. L. (Duke Univ., Durham, N. C.). Nuovo Cim.; 2A: 295-305(1 Mar 1971).

The cross sections for meson electroproduction are examined in two model field theories. It is found that for the interaction of neutral scalar mesons with nucleons the structure functions exhibit scaling in the generalized Bjorken limit, but that for the case of the charge-independent pseudoscalar-meson-nucleon interaction scaling does not always occur. Comments are made on the origin of this breakdown and on its significance for parton models of deeply inelastic electron–hadron scattering. (auth)

30784 PHOTOPRODUCTION OF N*(1236) RESONANCE AND THE VECTOR DOMINANCE MODEL. Bialas, A. (Jagellonian

Univ., Krakow. Inst. of Nuclear Physics, Krakow); Hoegaasen, H. Nuovo Cim.; 2A: 158-68(1 Mar 1971).

The processes a) $\gamma N \to \pi N^*$ and b) $\pi N \to \rho N^*$ are discussed in the framework of the vector dominance model. The relation between the decay distribution of N^* in the reaction a) and the joint decay distribution in the reaction b) is discussed in detail. It is shown that these reactions might provide i) a new useful test of the vector dominance model and ii) an independent determination of the reference frame in which the transverse vector mesons couple directly to photons. (auth)

30785 COULOMB COUPLINGS AND BORN-TERM ANALYSIS FOR $\gamma N \to \pi^{\pm}\Delta$ REACTIONS. Miah, M. A. W. (Daresbury Nuclear Physics Lab., Eng.). Nuovo Cim.; 2A: 197-208(1 Mar 1971).

The forward photoproduction of $\pi^{\pm}\Delta$ is studied in a Coulomb-coupling approximation. It is shown that the prescription suggested by Dombey for the choice of the Coulomb coupling fails to work in these reactions. A way in which these difficulties may be overcome is suggested and this model succeeds in explaining many features of these reactions rather well. (auth)

30786 ELECTROMAGNETIC FORM FACTORS OF THE PROTON AT SQUARED FOUR-MOMENTUM TRANSFERS BETWEEN 10 AND 50 fm^{-2}. Berger, Ch.; Burkert, V.; Knop, G.; Langenbeck, B.; Rith, K. (Univ., Bonn). Phys. Lett.; 35B: 87-9(26 Apr 1971).

Electron–proton elastic scattering cross sections were measured to determine the proton electromagnetic form factors at squared four-momentum transfers q^2 between 10 and 50 fm^{-2}. At these values of q^2 angular distributions between 25° and 110° and in addition at 25° and 35° cross sections for q^2 from 2 to 20 fm^{-2} were measured using the external electron beam of the Bonn 2.5 GeV electron synchrotron. The results confirm deviations from the scaling law. (auth)

30787 SCALING AND DUALITY IN ELECTRO- AND PHOTOPRODUCTION. Rittenberg, V.; Rubinstein, H. R. (Weizmann Inst. of Science, Rehovot, Israel). Phys. Lett.; 35B: 50-4(26 Apr 1971).

Using new sum rules and a new scaling variable it is shown that scaling holds even for small q^2 and for physical photons. Local duality in electroproduction is also discussed and it is shown that to a good approximation it holds in all directions in the $\nu - q^2$ plane. In particular, the high energy electroproduction structure function curve is constructed from photoproduction data. Thus, a unified, "scale invariant" picture of photon–nucleon total cross sections is presented that adds to the challenge of determining the origin of scaling. (auth)

30788 MODEL OF $\eta \to 3\pi$ AND $K \to 3\pi$ DECAYS. Graves-Morris, P. R. (Univ. of Kent, Canterbury, Eng.). Phys. Lett.; 35B: 55-8(26 Apr 1971).

A Faddeev-like theory of $\eta \to 3\pi$ and $K \to 3\pi$ decays is used to describe the spectra of the pions produced in a model with a constant bare decay vertex and pairwise final state interactions. The data on these decays are shown to be compatible with recent S-wave $\pi-\pi$ scattering lengths. (auth)

30789 COMPARISON OF PION ELECTROPRODUCTION DATA WITH VECTOR MESON DOMINANCE PREDICTIONS. Fraas, H. (Univ., Wuerzburg, Ger.); Schildknecht, D. Phys. Lett.; 35B: 72-6(26 Apr 1971).

Single pion electroproduction results are compared with predictions obtained within the vector meson dominance model. The large longitudinal contribution observed in pion electroproduction is successfully predicted from data on pion photoproduction and on production of vector mesons by pions from nucleons. (auth)

30790 ACTION PRINCIPLE FOR A CLASSICAL CHARGED PARTICLE. Lopez, C. A. (Univ. de Chile, Santiago de Chile). Lett. Nuovo Cim.; 1: 527-30(20 Mar 1971).

It is shown that the action integral for a classical charged particle does not lead to the correct equation of motion. It is also indicated how to obtain a satisfactory action integral by properly handling the infinities that appear in the theory. (L.B.S.)

30791 NONTADPOLE CONTRIBUTION TO THE MASS SPLITTING ($m_K - m_\pi$). Miura, K. (Nihon Medical Coll., Chiba, Japan); Shibazaki, I. Lett. Nuovo Cim.; 1: 568-70(27 Mar 1971).

The nontadpole contribution to the mass splitting $m_K - m_\pi$ is estimated using the soft-pseudoscalar-meson approximation and the chiral SU(3) × SU(3) symmetry. (L.B.S.)

30792 TRANSPARENCY OF EXTRAGALACTIC SPACE TO VERY-HIGH-ENERGY PHOTONS. Bonometto, S. A. (Inst. of Theoretical Astronomy, Cambridge, Eng.). Lett. Nuovo Cim.; 1: 677-80(17 Apr 1971).

The effect of different kinds of background radiation on very-high-energy γ rays, owing to e, μ, and π pair creation, is studied. The actual transparency of the extragalactic space to 10^{18} or 10^{19} eV background photons is one or two orders of magnitude higher than that shown in previous results. (L.B.S.)

30793 LATERAL DISTRIBUTION OF HIGH-ENERGY GAMMA-RAY IN AIR SHOWER. Kasahara, Katsumasa; Koniishi, Eiichi (Waseda Univ., Tokyo). Uchusen Kenkyu; 14: 246-52(Oct 1969). (In Japanese).

Simulation was made for the lateral distribution of high energy γ-rays which are observed in an emulsion chamber. The models adopted for the nuclear interaction were the H-quantum model and the two fire-balls model. The cascade was attributed to $\pi^0 - 2\gamma$ decay. Comparison was made with experimental data. In the lateral distribution of γ-ray family, the simulation with the H-quantum model was in good agreement with experiment. The simulation with the two fire-ball model deviated significantly from experiment. The reason for the discrepancy was discussed. The lateral distribution of the Pb jet accompanying γ-family was also compared with experiment. Agreement of the simulation with experiment was good for both models. It was shown by these simulations that the ECC experiment can contribute to the study of the phenomena proper to an air shower. The present simulation is free from the particular interpretation of experimental data, since it is necessary for the effective utilization of the family. (Japan)

30794 ARGUMENTS FOR A COVARIANT SPIN 3-VECTOR. Ringhofer, K. (Univ., Munich). Acta Phys. Austr.; 31: No. 2, 160-70(Jun 1970).

A Foldy–Wouthuysen type of transformation is given for the Hamilton operator of a Dirac particle with an anomalous magnetic moment in a homogeneous magnetic field. Particle and antiparticle states are decoupled as well as states with different spin directions. This leads to a possible definition of a 3-vector operator for the spin. One obtains essentially one of the spin operators already proposed. Its behavior under Lorentz transformations is extremely simple: it is a covariant pseudovector on the mass shell. (auth)

30795 EMPIRICAL RELATION BETWEEN INELASTIC ELECTRON SCATTERING AND MULTIBODY PION REACTIONS. Deutschmann, M. (Technische Hochschule, Aachen). pp VI-19-24 of Proceedings of the Colloquium on High Multiplicity Hadronic Interactions. /Krzywicki, A. (ed.). Paris; Ecole Polytechnique (1970).

From Colloquium on high multiplicity hadronic interactions; Paris, France (13 May 1970). See CONF-700528.

Starting from the idea that electroproduction of excited nuclear systems and corresponding hadron reactions should be related, a correspondence in experimental data was sought. For this purpose, a reaction which could be assumed to proceed via ρ exchange, namely $\pi^+ p \to \pi^0 + M$, M being the missing mass of the π^0. It is found that with certain assumptions the slope of the differential cross section and, in particular, the dependence of the slope on M is agreement with the so called scaling law of inelastic electron scattering. (France)

30796 VECTOR MESONS IN ELECTROMAGNETIC INTERACTIONS. Gourdin, M. (Faculte des Sciences, Orsay, France). Springer Tracts Mod. Phys.; 55: 192-212(1970).

From Low energy hadron interactions conference; Karlsruhe, Germany (May 1970). See CONF-700558.

The review of vector mesons in electromagnetic interactions covers vector meson dominance model assumptions, electron–positron annihilation into mesons, the validity of the vector meson photon analogy, the difficulties in charged-π meson photoproduction, and photoproduction of vector mesons. Electromagnetic sum rules from storage ring experiments, $\omega - \phi$ mixing, and the strong decay of vector mesons into pseudoscalar mesons are also discussed. (J.F.P.)

30797 COUPLING PARAMETERS OF PSEUDOSCALAR MESON PHOTOPRODUCTION ON NUCLEONS. Pfeil, W.; Schwela, D. (Univ., Bonn). Springer Tracts Mod. Phys.; 55: 213-37(1970).

From Low energy hadron interactions conference; Karlsruhe, Germany (May 1970). See CONF-700558.

In this review the interactions $\gamma + p \to p(n) + \pi^0(\pi^+)$, $\gamma + n \to p + \pi^-$, $\gamma + p \to p + \eta$, and $\gamma + p \to \Lambda(\Sigma^0) + K^+$ are discussed. An investigation of such processes is found to be an important means for the determination of the decay widths for the transitions of

XUM

the excited s-channel nucleon resonances into a nucleon and a photon. Dispersive calculations for the photoproduction of single pions in the region of the first pion–nucleon resonance, isobar model calculations, threshold photoproduction and pion–nucleon scattering lengths, and predictions for the $\gamma N\Delta(1230)$ transition moment are considered. Also discussed are decay half widths of the higher nucleon resonances in π photoproduction below 1.5 GeV, and the photoproduction of η and K mesons. (J.F.P.)

30798 PHOTON–PHOTON COLLISIONS, A NEW AREA OF EXPERIMENTAL INVESTIGATION IN HIGH-ENERGY PHYSICS. Arteaga-Romero, N. (College de France, Paris); Jaccarini, A.; Kessler, P.; Parisi, J. Phys. Rev., D; 3: 1569-79(1 Apr 1971).

It is shown that the conditions of photon–photon collisions at high energy can be almost perfectly reproduced by using the "quasi-real" photon spectra originating from electron–positron colliding beams. It is shown that (a) the problem of background elimination can be properly solved by detecting both the outgoing electron and positron at very small angles with respect to their incident directions; (b) in spite of this very stringent restriction on phase space, and of possible additional restrictions due to experimental conditions, reasonably high counting rates will be achieved with the new electron–positron storage rings (of beam energy 2–3 GeV and of luminosity $\sim 10^{32}$ cm^{-2} sec^{-1}) now planned or under construction; and (c) these counting rates increase with rising beam energy. A number of applications are discussed particle-pair creation (e^-e^+, $\mu^-\mu^+$, $\pi^-\pi^+$, K^-K^+, $p\bar{p}$, ...) or single-particle creation (π^0, η, η'). Angular distributions of particles produced are also shown. (auth)

30799 COMMENTS ON PHOTOPRODUCTION AND THE ELECTROMAGNETIC MOMENTS OF CHARGED ρ MESONS. Glueck, M.; Wagner, S. (Univ., Hamburg). Phys. ReV., D; 3: 1669-70(1 Apr 1971).

The relation of photoproduction to the electromagnetic moments of charged meson is reexamined in the light of recent experiments and new theoretical values for the moments. (auth)

30800 COMMENT ON CALCULATIONS OF THE $K^+ - K^0$ MASS DIFFERENCE. Nussinov, S. (Tel-Aviv Univ., Israel). Phys. Rev., D; 3: 1676-7(1 Apr 1971).

A new consistency check for calculations of the electromagnetic mass difference of strange hadrons which use Cottingham's formula and finite-energy rules is suggested and applied to the K^+–K^0 case. (auth)

30801 ELECTROPRODUCTION OF THE P_{33} RESONANCE. Crawford, R. L. (Univ. of Glasgow). Nucl. Phys.: B28: 573-93(1971).

The fixed t-dispersion relations for pion electroproduction are solved for energies below and in the region of the first resonance by making detailed use of the coupled multipole equations and Watson's theorem. The P_{33} multipoles, $G_{E,M}$ and F_π are evaluated by fitting to experimental data. (auth)

Weak

Refer also to abstracts 30930, 31023, and 31282.

30802 (BNL-tr-418) ON THE POSSIBILITY OF DETERMINING THE OSCILLATION PARAMETERS OF NEUTRINOS. Kocharov, G. E.; Ferberg, B. A. (Akademiya Nauk SSSR, Leningrad. Fiziko-Tekhnicheskii Institut). Translated by S. J. Amoretty (Brookhaven National Lab., Upton, N. Y.), from a Russian report. 14p. Dep. NTIS.

A possible verification of the oscillation hypothesis of Pontecorvo is considered in the experiments on the measurement of the energy spectrum and solar neutrino flux. (auth)

30803 (CERN-71-7, pp 1-40) WEAK INTERACTIONS. Arbuzov, B. A. (Gosudarstvennyi Komitet po Ispol'zovaniyu Atomnoi Energii SSSR, Serpukhov. Institut Fiziki Vysokikh Energii).

From Proceedings of the 1970 CERN School of Physics, Loma-Koli, Finland, 21 Jun–5 Jul 1970.

The topics discussed include the properties of weak leptonic currents, higher orders in weak interaction theory, and the violation of CP invariance. (J.F.P.)

30804 (COO-264-569) ANALYSIS OF SPIN CORRELATIONS IN THE BETA DECAY OF THE LAMBDA HYPERON. Garcia, Augusto (Chicago Univ., Ill. Enrico Fermi Inst. Chicago Univ., Ill. Dept. of Physics). Dec 1970. Contract AT(11-1)-264. 54p. (EFI-70-75). Dep. NTIS.

Recent experimental data on lambda β-decay are analyzed. Integrated expressions for the measured quantities in terms of form factors are given up to second order in the parameter $\beta = (m_\Lambda - m_p)/m_\Lambda$. The sensitivity of these experimental quantities as functions of specific form factors is studied in detail and it is exhibited in a form which is useful for the analysis of present experiments and for the planning of future ones. Within the framework of V-A theory, the possibility is explored that the data require the presence of an induced pseudo-tensor form factor. Qualitative discussions of the q^2 dependence of some form factors and of possible admixtures of scalar and tensor interactions are also given. (auth)

30805 (NP-18777) ON DIVERGENCES OF AMPLITUDES OF WEAK NONLEPTONIC PROCESSES WITH THE PHOTON EMISSION. Geshkenbein, B. V.; Ioffe, B. L. (Gosudarstvennyi Komitet po Ispol'zovaniyu Atomnoi Energii SSSR, Moscow. Institut Teoreticheskoi i Eksperimental'noi Fiziki). 1970. 34p. (In Russian). Dep. NTIS (U. S. Sales Only).

Quadratically divergent terms in the amplitudes of nonleptonic processes with one and two photon emission as well as in the amplitudes with one virtual photon, are studied in the theory with intermediate boson. The following conclusions have been obtained: At the zero anomalous magnetic moment of W-boson: In the strong interaction SU(3) × SU(3) breaking scheme proposed previously, the weak nonleptonic amplitudes with the emission of one or two photons in G order and in the first nonvanishing approximation in e have no quadratically divergent terms. There are serious reasons to suppose that the nonleptonic amplitudes without change of parity and parity violation in Ge^2 order (without photon emission) lead to quadratically divergent expressions which cannot be eliminated by any relation between the Cabibbo angle and the parameters determining the SU(3) × SU(3) breaking. For nonleptonic processes with $|\Delta\rho| = 1$ or $\Delta\rho = 0$, $P = -1$, the result is ambiguous and quadratic divergences are possible to be absent. At nonzero anomalous magnetic moment of the W-boson γ the amplitudes of the weak nonleptonic processes with the virtual photon emission have quadratically divergent terms. Calculations of these terms for the case of $K^+ \to \pi^+e^+e^-$ decay, as compared with the experimental data, imposes restrictions on the cutoff limit $\Lambda < 4\rho\gamma^{-\frac{1}{4}}$. The amplitudes of the nonleptonic processes with one virtual photon in Ge^2 order quadratically diverge. (auth)

30806 (NYO-3668-TA-5) BUBBLE CHAMBER GROUP PROGRESS REPORT, JANUARY 1, 1970–DECEMBER 31, 1970. (State Univ. of New York, Stony Brook. Dept. of Physics). Contract AT(30-1)-3668A. 51p. Dep. NTIS.

The Stony Brook Bubble Chamber group in the preceding year worked in the following areas: A series of measurements on hyperon leptonic decay was completed; finishing a three year comprehensive study of half a million pictures in search for these rare decay modes. The measurements include the partial decay rate of the Λ-hyperon decaying into muon, proton, and anti-neutrino $(1.9 \pm 0.6) \times 10^{-4}$, the partial decay rate $(0.78 \pm 0.08) \times 10^{-3}$ and G_A/G_V value $(0.75^{+\frac{0.3}{0.5}}_{-\frac{0.3}{0.5}})$ for the Λ-hyperon decaying into electron, proton and anti-neutrino, an improved (using twice the number of events) G_A/G_V value for the Σ-hyperon decaying into electron neutron and anti-neutrino $(0.30^{+\frac{0.5}{0.6}}_{-\frac{0.5}{0.6}})$. The last mentioned measurement was done in collaboration with Columbia University Bubble Chamber Group. In high energy interactions the pion multiplicity in an exposure of 9 GeV/c K^- on hydrogen, and two prong events in an exposure of 8.5 GeV/c π^+ on hydrogen were measured. The two prong data were used in conjunction with old Columbia University data of different topologies to obtain single particle momentum distributions in the final state. Two optical spark chamber experiments are now in progress: (a) a measurement of the branching ratio $K_S \to \pi^+ + \pi^-/K_S \to \pi^0 + \pi^0$, (b) a high statistics study of the Λ-hyperon beta decay. Experiment (a) is in the last stage of analysis. Experiment (b) is at the picture taking stage, with all the preliminary tests completed in the last year. (Both experiments are done in collaboration with Paolo Franzini and Columbia University.) (auth)

30807 LOW-ENERGY THEOREMS FOR NUCLEAR WEAK AND ELECTROMAGNETIC CURRENTS. Ohtsubo, Hisao; Fujita, Junichi; Takeda, Gyo (Tokyo Univ.). Progr. Theor. Phys. (Kyoto); 44: 1596-1617(Dec 1970).

Under the assumption of CVC and PCAC, low-energy theorems are derived and explicit formulas are given for the two-body exchange currents. It is shown that the low-energy theorem for the exchange current of vector type leads to the Siegert theorem, and the exchange current of axial-vector type is divided into two parts, one directly related to the nuclear forces and the remainder. The beta decay of the triton is examined in detail, and the former type

of exchange currents alone give a good agreement with experiment. (auth)

30808 WEAK INTERACTIONS. Pietschmann, Herbert (Univ., Vienna); Wess, J. Naturwissenschaften; 57: 365-9 (Aug 1970). (In German).

A brief historical review is given of the development of the theory and understanding of weak interactions. The position of weak interactions in the play of forces in matter, the vector-axial vector theory, lepton phenomena, universality, C−P violation, and the question of higher approximations are considered. (J.S.R.)

30809 DEEP INELASTIC NEUTRINO SCATTERING. Landshoff, P. V.; Polkinghorne, J. C. (Cambridge Univ., Eng.). Phys. Lett.; 34B: 621-4(12 Apr 1971).

Previous data from experiments on the inelastic scattering of high-energy neutrinos on propane and freon are considered in comparison with the predictions of the duality−parton model, which was previously described. (J.F.P.)

30810 INTERMEDIATE W BOSONS, GAUGE FIELDS, AND THE NONLEPTONIC WEAK DECAYS. Tomozawa, Yukio (Univ. of Michigan, Ann Arbor). Ann. Phys. (N. Y.); 62: 554-68(Feb 1971).

Following the analysis of Nishijima and Sato, the chiral symmetric gauge field model is used to compute the s-wave amplitudes of the nonleptonic weak decays. It is pointed out that the weak interaction Lagrangian which has been derived from the assumption of octet W bosons is consistent with experiment. The p-wave amplitudes of the nonleptonic hyperon decay are obtained by using the sum rule that has been derived by the author. The result for both s- and p-wave amplitudes, which is a theoretical prediction with no adjustable parameter, is in fair accord with the experimental data. (auth)

30811 INFLUENCE OF A $\frac{3}{2}$-SPURION ON Σ-DECAY. Zingl, Harald F. K. (Univ., Graz). Acta Phys. Austr.; 31: 89-90(1970).

The effect of a $\frac{3}{2}$-spurion in the $\Sigma \rightarrow N + \pi +$ spurion decay is examined, using the Wigner−Eckert theorem and assuming that the $|\Delta I| = \frac{3}{2}$ transition is possible. It is concluded that a small difference in the triangle equations may be a contribution of a $\frac{3}{2}$-spurion in a $\frac{3}{2}$ final state only. (L.B.S.)

30812 HYPERON BETA DECAY. II. Tung, Wu-ki (Univ. of Chicago). Phys. Rev., D; 3: 1678-9(1 Apr 1971).

To make a previous analysis of hyperon β decay complete, the q^2 spectrum of the decay rate and asymmetry functions are discussed. It is shown that these spectra provide a valuable source of information on the hard-to-measure form factors f_2 and g_2. (auth)

30813 UNITARITY CORRECTIONS TO THE HARD-MESON ANALYSIS OF K_{l3} DECAY. Nutbrown, D. A. (Univ. of Rochester, N. Y.). Phys. Rev., D; 3: 1671-4(1 Apr 1971).

The unitarity correction to the approximation of κ dominance of the scalar, strangeness-changing channel in the hard-meson analysis of K_{l3} decay by Chang and Leung. New ranges are obtained for the possible values of F_K/F_π and $f_+(0)$. In particular, the latter satisfies $f_+(0) < 1$. (auth)

30814 CP VIOLATION AND THE STRONG SELF-INTERACTING INTERMEDIATE-VECTOR-BOSON MODEL. Marshak, R. E.; Yang, Y. W.; Rao, J. S. (Univ. of Rochester, N. Y.). Phys. Rev., D; 3: 1640-50(1 Apr 1971).

The strong cubic intermediate-vector-boson (IVB) model of weak interactions, based on a triplet of strong self-interacting W bosons and treating CP violation as a maximal effect at the semiweak level, is reexamined. It is shown that the basic CP = −1 semiweak interaction must possess an essentially unique structure in order to reproduce the successes of the CP-conserving universal (V,A) current−current theory. The consequences to order g^3 (g is the semiweak coupling constant) of the strong cubic IVB model are worked out in detail. The most incisive test of this model at low energies is the detection of gross CP violation in $\Delta Y = 1$ induced neutral-lepton-current decays of hadrons, in particular, the decays $K^+ \rightarrow \pi^+ l\bar{l}$ and $K^0 \rightarrow \mu\mu$. Under certain conditions, the detection of gross CP violation may be possible in $\Delta Y = 0$ W production by neutrinos on nucleons. (auth)

30815 BETA DECAY OF HYPERONS. Oehme, Reinhard; Winston, Roland; Garcia, Augusto (Univ. of Chicago). Phys. Rev., D; 3: 1618-21(1 Apr 1971).

The formulas for spin and angular correlations in hyperon β decay are brought into forms which can give specific information about the character of possible deviations from the universal SU(3) scheme. The recent experimental results for Λ-particle β decay are discussed qualitatively in terms of the proposed combinations of integrated correlation coefficients. (auth)

30816 DASHEN−WEINSTEIN THEOREM IN K_{l3} DECAY: SOFT-PION CORRECTIONS. Acharya, R.; Brink, L. (Inst. of Theoretical Physics, Goteborg). Phys. Rev., D; 3: 1579-82 (1 Apr 1971).

The Mathur−Okubo sum rule in K_{l3} decay, together with Pagels's model for corrections due to partial conservation of axial-vector current, is invoked to estimate the $O(\epsilon^2)$ corrections to the Dashen−Weinstein theorem for $\xi(0)$. The corrections are found to be small, and $\xi(0) \approx -0.6$ is predicted for $\lambda_+ \approx 0.08$. (auth)

30817 NEW FITS TO THE $|\Delta I| = \frac{1}{2}$ AND LEE−SUGAWARA RELATIONS. Yakimiw, E. (Univ. of Montreal). Can. J. Phys.; 49: 951-5(15 Apr 1971).

The $|\Delta I| = \frac{1}{2}$ sum rule for the nonleptonic Σ decay amplitudes is well satisfied when the newly reported values of the Σ^- decay rate and the Σ_0^+ asymmetry parameters are used. Moreover, the mild disagreement which has existed since 1964 with the Lee−Sugawara relation is shown to disappear when the latest data are used. The $\gamma > 0$ solution of the Σ_0^+ decay seems to be favored. (auth) (Canada)

30818 CROSS SECTIONS FOR SCALAR W-MESON AND VECTOR W-MESON PRODUCTION BY MUONS AND NEUTRINOS. Reiff, J. (Univ. of Utrecht). Nucl. Phys.; B28: 495-503 (1971).

Following a recent proposal, cross sections for scalar W-mesons and vector W-mesons are calculated for different combinations of the masses of these two W-mesons. It is found, for M_S much smaller than M_V and the lab energy not too large, that scalar meson production cannot be neglected in comparison to vector meson production. The scalar neutrino cross sections are only a factor two to five larger than the equivalent muon cross sections. (auth)

30819 ABSENCE OF FORM FACTOR IN e^2 CORRECTIONS TO THE AMPLITUDES OF NEUTRINO AND ELECTRON SCATTERING ON NUCLEONS. Ioffe, B. L. (Inst. for Theoretical and Experimental Physics, Moscow); Sokolov, V. V. Nucl. Phys.; B28: 504-8(1971).

Assuming that the imaginary part of the scattering amplitude of a virtual photon (or a W-boson), with momentum q, on nucleon is independent of the momentum transfer t at $|q^2| \gg |t|$, the e^2 correction to the amplitude of process $\nu N \rightarrow lN$ due to photon exchange between hadrons and lepton is calculated. It is shown that this correction does not contain the form factor of the nucleon at large t. (auth)

30820 MUON−ELECTRON SCATTERING CROSS SECTION TO ORDER α^3. Van Nieuwenhuizen, P. (CERN, Geneva). Nucl. Phys.; B28: 429-54(1971).

The amplitude to order α^2 and cross section to order α^3 for $\mu^\pm e^\pm$ scattering are given in exact analytical form. Bremsstrahlung in the lab system for given maximum photon energy is calculated including recoil. A simple and practical rule to extract infrared divergences is given. Numerical results are tabulated. (auth)

30821 DECAY RATE AND BRANCHING RATIO (π^- ^{3}He)/(ALL π^- MODES) OF $_\Lambda{}^3$H. Ram, B.; Williams, W. (New Mexico State Univ., Las Cruces). Nucl. Phys.; B28: 566-72(1971).

The total decay rate and branching ratio R_3 = (π^- ^{3}He)/(all π^- modes) of $_\Lambda{}^3$H were calculated using spatial wave functions for ^{3}He and $_\Lambda{}^3$H obtained in recent years by Herndon and Tang on the basis of their variational calculations of these systems in terms of NN and ΛN potentials with hard cores. The results are about the same as those previously obtained using wave functions without hardcore distortions. (auth)

Strong (General)

30822 (CERN-71-7, pp 41-180) MODERN DEVELOPMENTS IN HADRON PHYSICS. Donnachie, A. (Manchester Univ. (England), Dept. of Theoretical Physics).

From Proceedings of the 1970 CERN School of Physics, Loma-Koli, Finland, 21 Jun–5 Jul 1970.

The topics considered in this review of hadron physics are scattering amplitudes and cross sections, partial waves and phase shifts, properties of phase shifts and resonance formation, charge in Coulomb scattering and isotopic spin, and relativistic kinematics. Also discussed are meson−baryon scattering, the baryon

XUM

spectrum, boson resonances, the quark model, mass differences, and the 1-excitation model. (J.F.P.)

30823 (CERN-71-7, pp 285-358) DUAL MODELS AND DUAL PHENOMENOLOGY. Kajantie, K. (European Organization for Nuclear Research, Geneva (Switzerland)).

From Proceedings of the 1970 CERN School of Physics, Loma-Koli, Finland, 21 Jun-5 Jul 1970.

The correlation between resonances and Regge poles is investigated, and the consequences of assuming that Regge poles and resonances are alternative ways of expressing the same dynamical information are examined. Dual models are considered including $\pi\pi$ scattering, two-body reactions, duality diagrams, the reaction $\bar{p}n \to \pi^+\pi^-\pi^-$, and three-particle final states. (J.F.P.)

30824 (JINR-P2-5630) GRAPHS FOR STUDYING ISOTOPIC RELATIONS IN REACTIONS WITH PRODUCTION OF THREE PARTICLES AND POSSIBLE POMERANCHUK POLE EXCHANGE. Dumbrais, O. V. (Joint Inst. for Nuclear Research, Dubna (USSR). Lab. of High Energy). 1971. 12p. (In Russian). Dep. NTIS (U. S. Sales Only).

Graphs are applied to the analysis of isotopic relations among cross sections for reactions with production of three particles and possible dominance of Pomeranchuk pole exchange at high energies. More experimental data are required to draw any general conclusions about the validity of this hypothesis. (auth)

30825 DUALITY AND DUAL MODELS. Le Bellac, Michel (Univ., Nice); Treille, Daniel. J. Phys. (Paris), Colloq.; C5: 5-30(Nov-Dec 1970). (In French).

From Conference on high energy physics; Aix-en-Provence, France (29 Sep 1970). See CONF-700950.

The basic hypotheses on duality and their consequences in strong interaction dynamics (exchange degeneracy) are discussed. The dual models (Veneziano) are introduced and their applications to multiparticle reactions reviewed. The recent theoretical developments concerning the unitarization of dual models are considered. (France)

30826 STRONG INTERACTION PHENOMENOLOGY. Salin, Ph. (Univ., Bordeaux). J. Phys. (Paris), Colloq.; C5: 54-87 (Nov-Dec 1970). (In French).

From Conference on high energy physics; Aix-en-Provence, France (29 Sep 1970). See CONF-700950.

Recent developments in strong interaction phenomenology are discussed. Some questions relating to the Pomeron are examined: slope, geometric structure, helicity conservation, the violation of Pomeranchuks theorem. The characteristic properties of Regge cuts and absorption models with weak or strong cuts are discussed. Their predictions are compared with experimental data for two-body or quasi-two-body reactions. (France)

30827 NON-HERMITIAN UNCHARGED FIELD AND EXISTENCE OF QUARKS. Krolikowski, W. (Inst. for Nuclear Research, Warsaw. Univ., Warsaw). Acta Phys. Pol.; A39: 229-31(Feb 1971).

It is pointed out that the non-exotic mesons might be reinterpreted as dipoles and non-exotic baryons as tripoles with respect to a complex-charge. In this way the picture of complex dipoles and tripoles replaces here the picture of bound pairs and triples of quarks. (auth)

30828 BREAKDOWN OF THE POMERANCHUK THEOREM AND THE REGGE DIPOLE WITH FINITE CROSS-SECTION. Sumi, Y. (Dalhousie Univ., Halifax, Nova Scotia). Lett. Nuovo Cim.; 1: 565-7(27 Mar 1971).

The possible breakdown of the Pomeranchuk theorem is suggested from Serpukhov data for meson-nucleon scattering. A model is proposed with a Regge dipole whose trajectory is of the form $\alpha_D(t) = 1 - \alpha_1(-t)^{1/\nu}$ + terms of higher order in t, for $t \leq 0$ with $\nu \geq 2$. The model satisfies not only the condition that the total cross sections for particle-particle scattering $\sigma_T^P(s)$ and for the antiparticle-particle scattering $\sigma_T^A(s)$ tend to different constants, $\sigma_T^P(\infty) \neq \sigma_T^A(\infty)$, but still allows the requirement that the integrated cross section remains constant or becomes smaller as the energy increases. (L.B.S.)

30829 LORENTZ ANALYSIS OF DUAL-RESONANCE MODELS IN OPERATOR FORMALISM. Combes, J. M. (CNRS-CPT, Marseille); Soffer, J. Nuovo Cim.; 2A: 279-94(1 Mar 1971).

Nonspurious resonance states are analyzed with a given spin in a Lorentz-covariant framework; these states are chosen to be those diagonalizing the nonspurious part of propagators. Physical states with spinning particles are then constructed with the help of the symmetric three-resonance vertex; they satisfy the usual gauge conditions and duality properties. These states can then be used to construct Veneziano amplitudes for spinning particles consistent with the scalar-particle model. (auth)

30830 AMPLITUDE FOR N NONSPURIOUS EXCITED PARTICLES IN DUAL RESONANCE MODELS. Campagna, P. (Univ. Turin); Napolitano, E.; Sciuto, S.; Fubini, S. Nuovo Cim.; 2A: 911-28(21 Apr 1971).

A form for a dual resonant amplitude with N nonspurious excited particles is proposed in which both duality and factorization are explicitly exhibited. The expression, obtained by writing the amplitude as an expectation value of a product of N operators covariant under the projective group, enjoys the same properties as the standard N-point generalized Veneziano function for ground-state particles. (auth)

30831 SELF-CONSISTENT METHOD FOR INTERACTIONS MEDIATED BY FIELDS. Bolsterli, M. (Los Alamos Scientific Lab., N. Mex.). Ann. Phys. (N. Y.); 62: 569-81(Feb 1971).

A self-consistent procedure for treating a system of fermions interacting via the exchange of virtual mesons is described. (auth)

30832 ELECTROMAGNETIC AND WEAK CORRECTIONS TO THE SCATTERING OF HIGH-ENERGY HADRONS. Frankfurt, L. L. (Ioffe Inst. of Physics and Tech., Leningrad). JETP Lett. (USSR) (Engl. Transl.); 12: 379-80(20 Dec 1970).

Translated from Zh. Eksp. Teor. Fiz., Pis'ma Red.; 12: 536-8(5 Dec 1970).

It is pointed out that as a consequence of the electromagnetic and weak interactions immobile singularities appear in the partial amplitude of purely hadronic processes, resulting from diagrams with exchange in the t-channel of two photons (two W mesons). It is further pointed out that the absence of reggeization of these particles leads to a growth of the electromagnetic and weak corrections to hadron scattering with increasing energy. (L.B.S.)

30833 $X^0(960)$-MESON -2^- OR 0^-? Ogievetskii, V. I. (Joint Inst. for Nuclear Research, Dubna, USSR); Tybor, W.; Zaslavskii, A. N. Phys. Lett.; 35B: 69-71(26 Apr 1971).

It is shown that the available experimental data are equally consistent with spin-parity 0^- and 2^- of the $X^0(960)$ meson, but 2^- seems to be somewhat preferable. Both spin-parity alternatives, and new experiments to distinguish between them, are discussed. (auth)

30834 REGGE RESIDUES AND SUPERMULTIPLETS. Delbourgo, R.; Rotelli, P. (Imperial Coll. of Science and Tech., London). Phys. Lett.; 35B: 65-8(26 Apr 1971).

Biquark and triquark Regge propagators with constant residues are adopted to describe meson and baryon exchange. This leads to conventional polynomial residues and permits excellent extrapolation from hadron pole to scattering regions (e.g., Δ), as well as automatically providing cross-over points. (auth)

30835 MASS SHIFTS IN SECOND ORDER OF PERTURBATION THEORY IN THE DUAL-RESONANCE MODEL. Scherk, J. (Laboratoire de Physique Theorique et Hautes Energies, Orsay, France). Lett. Nuovo Cim.; 1: 672-6(17 Apr 1971).

It has been shown that the normalization procedure devised for the one-loop planar graphs of the dual-resonance model, while keeping the properties of perturbative unitarity and duality, is highly nonunique in the case of arbitrary intercept as an arbitrary function $g(\omega)$ can be introduced in the integrand defining the counterterm. The problem of calculating the mass shifts and spectrum at order g^2 associated with the counterterm is considered. (L.B.S.)

30836 BACKSCATTERING AT HIGH ENERGIES. Golab-Meyer, Zofia (Inst. of Nuclear Physics, Krakow). Postepy Fiz.; 22: 49-65(1971). (In Polish).

A brief review of the backward scattering (region near 180° scattering angle) problem is given. At first the experimental situation (for some typical examples) is considered and then a theoretical model, such as the one baryon exchange model. Regge pole exchange model, direct channel resonances model, and quark model for backward scattering are presented. (auth)

30837 CORRELATION EFFECTS. Zalewski, Kacper (Inst. of Nuclear Research, Krakow). pp III-1-9 of Proceedings of the Colloquium on High Multiplicity Hadronic Interactions. /Krzywicki, A. (ed.). Paris; Ecole Polytechnique (1970).

From Colloquium on high multiplicity hadronic interactions; Paris, France (13 May 1970). See CONF-700528.

Knowledge on correlation effects is very incomplete because of the large number of parameters involved in many-body final states. Several sources of correlation effects are reviewed.

The statistical model involves no correlations and uncorrelated jet models only those of the final particles with the initial ones. Resonance production and interferences between resonances introduce final state correlations. The effect of Goldhaber, Goldhaber, Lee and Pais between charges and momenta of the pions produced in annihilation processes is discussed. (France)

30838 REMARKS ON THE THERMODYNAMICAL MODEL OF STRONG INTERACTIONS. Hagedorn, R. (European Organization for Nuclear Research, Geneva). pp IV-OBis-88 of Proceedings of the Colloquium on High Multiplicity Hadronic Interactions. /Krzywicki, A. (ed.). Paris; Ecole Polytechnique (1970).

From Colloquium on high multiplicity hadronic interactions; Paris, France (13 May 1970). See CONF-700528.

The thermodynamic model of strong interactions is described with the emphasis on aspects neglected previously and on its relations to other recent developments and proposals in high-energy physics. Resonances and fireballs are identified, leading to a bootstrap which determines the asymptotic exponential form of the hadron mass spectrum. The most striking consequence is the universal highest temperature, $T_0 \sim 160$ MeV. It is shown that the hypothesis that the velocity weight functions of the thermodynamic model be energy-independent is equivalent to the hypothesis of "limiting fragmentation" and to Feynman's parton predictions. The main results of the thermodynamic model are discussed and some examples of detailed results are given. (France)

30839 WHICH INFORMATION ON HIGH ENERGY HADRONIC INTERACTIONS MAY BE OBTAINED FROM THE INVESTIGATION OF COSMIC RAY AIR SHOWERS? Thielheim, K. O. (Univ., Kiel). pp IV-147-51 of Proceedings of the Colloquium on High Multiplicity Hadronic Interactions. /Krzywicki, A. (ed.). Paris; Ecole Polytechnique (1970).

From Colloquium on high multiplicity hadronic interactions; Paris, France (13 May 1970). See CONF-700528.

Theoretical investigations concerning the hadronic and electromagnetic component of cosmic ray air showers are reported, using a combination of the isobar model and the Cocconi–Koester–Perkins model. Results indicate that total cross sections, mean elasticity, mean transverse momenta, and probably the upper range of the energy distribution may be inferred from comparisons of the air shower simulations with experimental work. It should not be possible to infer details of the pionization process. (France)

30840 LOW ENERGY HADRON INTERACTIONS. Compilation of Coupling Constants and Low Energy Parameters. Invited Papers Presented at the Ruhestein-Meeting, Karlsruhe, Germany, May 1970. Hoehler, G. (ed.). Springer Tracts in Modern Physics. Ergebnisse der Exakten Naturwissenschaften, Volume 55. New York; Springer-Verlag New York, Inc. (1970). 294p. $21.50. (CONF-700558).

The conference included 11 papers. Separate abstracts were prepared for each paper. (J.F.P.)

For abstracts of individual papers see: 30721, 30796, 30797, 30841, 30867, 30868, 30882, 30883, and 30902–30904.

30841 COMPILATION OF COUPLING CONSTANTS AND LOW-ENERGY PARAMETERS. Ebel, G. (Kernforschungszentrum, Karlsruhe, Ger. Univ., Karlsruhe, Ger.); Julius, D.; Muellensiefen, A.; (and others). Springer Tracts Mod. Phys.; 55: 239-90(1970).

From Low energy hadron interactions conference; Karlsruhe, Germany (May 1970). See CONF-700558.

A compilation of coupling constants and low-energy parameters is given and covers strong, electromagnetic, weak interactions, and SU(3) comparison. The purpose of this compilation is to facilitate access to the original literature. (J.F.P.)

30842 STRONG INTERACTIONS OF ELEMENTARY PARTICLES. Eden, R. J. (Cambridge Univ., Eng.). Essays Phys.; 1: 1-32(1970).

The properties of elementary particles are first outlined; from those properties it is indicated how they may be classified into groups of particles that have certain properties which are similar in character. These groups are related to symmetries or invariance properties that are satisfied by elementary particles and their interactions. The symmetries are described and it is indicated how they can be studied by means of group theory. The experiments on collision processes are related to S matrix elements or collision amplitude. The range of topics that have to be considered when studying collisions of elementary particles is then outlined, and some aspects of the theory of the S-matrix are indicated. (L.B.S.)

30843 IMPLICATIONS OF LOCAL DUALITY IN A SET OF COUPLED REACTIONS. King, M. J.; Wali, Kameshwar C. (Syracuse Univ., N. Y.). Phys. Rev., D; 3: 1602-10(1 Apr 1971).

This is an extension of the study in an earlier paper on meson-decuplet scattering to two sets of coupled reactions: (1) $PB_{10} \rightarrow PB_{10}$, $PB_{10} \rightarrow PB_8$, $PB_8 \rightarrow PB_8$ and (2) $PV \rightarrow PV$, $PV \rightarrow PP$, $PP \rightarrow PP$. P and V refer to the pseudoscalar-meson octet and vector-meson nonet, respectively, while B_8 and B_{10} correspond to the octet of $J^\pi = 1/2^+$ baryons and decuplet $J^\pi = 3/2^+$ baryons, respectively. Some consequences of local duality are examined and compared with experiment in limited energy regions for the above reactions. The assumption that the imaginary parts of the direct-channel helicity amplitudes vanish in the forward (backward) scattering if the crossed t channel (u channel) is exotic leads to systems of equations relating resonance contributions in the direct channel. The solutions predict certain patterns of particles degenerate in mass but with different SU(3), spin, and parity assignments. In particular, the inclusion of spin considerations yields the result that the particles on leading trajectories must be accompanied by daughters with prescribed ratios of coupling constants between the parent and daughter states. The link between these results and those which follow from a complementary description in terms of Regge residues is discussed. (auth)

30844 QUARK MODEL OF DIFFRACTIVE PROCESSES. Ball, J. S. (Univ. of Utah, Salt Lake City); Zachariasen, F. Phys. Rev., D; 3: 1596-1602(1 Apr 1971).

Numerical results from a previously described model of diffraction scattering with nonshrinking forward peaks are presented, and the model is reformulated in terms of quarks with a view to making it more realistic. (auth)

30845 ISOSPIN STRUCTURE OF THE MULTIPERIPHERAL MODEL AND CHARGE DISTRIBUTIONS. Caneschi, L.; Schwimmer, A. (Stanford Univ., Calif.). Phys. Rev., D; 3: 1588-95 (1 Apr 1971).

Several specific assumptions on the isospin structure of the dominant exchange mechanisms are examined in the framework of the multiperipheral model. The consequent predictions for the charged and neutral particle distributions are compared with the present data. (auth)

30846 NONRELATIVISTIC SEPARABLE-POTENTIAL QUARK MODEL OF THE HADRONS. Mongan, T. R.; Kaufman, Leon. Phys. Rev., D; 3: 1582-7(1 Apr 1971).

A nonrelativistic quark model of the hadrons based on nonlocal separable potentials is presented. The model contains a quark–antiquark force and an effective three-body force among quarks, replacing the two-body forces. For single-parameter potentials in which the strength of the interaction drops sharply as the quark relative momenta increase, reasonable values of the lifetimes and radii of the mesons are found. A baryon wave function useful for dynamical calculations is obtained. The validity of the nonrelativistic approximation for this model is confirmed. (auth)

Strong (Baryon No. = 0)

30847 (JINR–P1-5666) POSSIBILITIES OF THE RESONANCE INTERFEROMETRY. Kopylov, G. I. (Joint Inst. for Nuclear Research, Dubna (USSR). Lab. of High Energy). 1971. 26p. (In Russian). Dep. NTIS (U. S. Sales Only).

When two identical particles are produced in the "resonance-particle" system, it is possible to measure the resonance width in a device of the missing mass spectrometer type by recording identical particles only. An artificial broadening of resonance peaks can be observed in such "interferometer of resonances" that gives the principal possibility of measuring the narrow (of order of several MeV) resonance widths. (auth)

30848 (JINR–P1-5668) INTERFERENCE PHENOMENA IN THE SYSTEM OF TWO RESONANCES. Kopylov, G. I.; Podgoretskii, M. I. (Joint Inst. for Nuclear Research, Dubna (USSR). Lab. of High Energy). 1971. 20p. (In Russian). Dep. NTIS (U. S. Sales Only).

The interference phenomena are considered appearing in the case when among the products of two decaying resonances there are identical particles with close velocities. These effects allow the difference of the resonance lifetimes to be directly measured. (auth)

30849 (JINR–P2-5659) DETERMINATION OF THE BREIT–WIGNER RESONANCE WIDTHS USING THE FOURIER ALGORITHM. Dubovik, V. M.; Markovski, B. L.; Soroko, L. M.; Strizh, T. A. (Joint Inst. for Nuclear Research, Dubna (USSR). Lab. of

Theoretical Physics). 1971. 23p. (In Russian). Dep. NTIS (U. S. Sales Only).

The Fourier algorithm is used to determine the B-W widths in the presence of a Gauss-type experimental broadening. It is shown that in general the widths can be found using the low-frequency region only, where the Fourier transform of the Gauss shape has negligibly small amplitudes. Some model curves (in the absence of noise) illustrate the above-mentioned assertions. The case of an incoherent superposition of the B-W doublet components was investigated. The model curve, which is very close to those of the compound radioactive decay, shows that in the case when the noise is low enough the method is of an extensive use. If the noise level and the difference between Γ_1 and Γ_2 are sufficiently large, one can in practice select the short-lived component only. The influence of the "cut-off" effect and of the discrete character of the experimental data on the results obtained by the method is considered. It is shown that in the presence of a high pedestal under the peaks (which is equivalent to the existence of a great number of background events) the method is not suitable for direct applications. In these cases one has, first of all, to subtract the background. Then the method remains valid if the "cut-off" of the spectrum is large enough. The method is applied to analyze the structure of A_2, K*(1420) and Q resonances using previous data. Summarizing, the following conclusions are obtained: the available experimental data on the A_2 meson are not suitable for extracting widths of the components because of the high pedestal; the K*(1420) is a singlet with Γ = 108 MeV; there is a good evidence that Q is an incoherent doublet with the values given. (auth)

30850 (JINR-P2-5759) ALGEBRAIC REALIZATION OF CHIRAL SYMMETRY FOR MESON SYSTEMS AND THEORY OF YANG-MILLS TYPE. Zupnik, B. M.; Ogievetskii, V. I. (Joint Inst. for Nuclear Research, Dubna (USSR). Lab. of Theoretical Physics). 1971. 22p. (In Russian). Dep. NTIS (U. S. Sales Only).

The applicability of algebraic realizations of $SU_2 \times SU_2$ to mesons with $GP(-1)^J = 1$ is investigated. This question arises due to the peculiar form of pion couplings with the above mesons in the chiral dynamics. A procedure is discussed how to take into account the pion mass. It is shown also that the algebraic realization of chiral symmetry is compatible in principle with a theory based on a nonlinear realization of $SU_2 \times SU_2$ for the massive Yang-Mills fields. A combined application of these approaches to π, σ, ρ and A_1 mesons with zero helicity gives satisfactory relations for masses and decay widths. However this meson family is not large enough to derive consistent results for helicity ± 1. (auth)

30851 (SU-1206-240) INEQUALITIES FOR THE $\pi\pi$ PARTIAL WAVES FROM THE PROPERTIES OF A CLASS OF ORTHOGONAL POLYNOMIALS. Balachandran, A. P. (Syracuse Univ., N. Y. Tata Inst. of Fundamental Research, Bombay (India)); Blackmon, Maurice L. (Syracuse Univ., N. Y. Dept. of Physics). Jan 1971. 38p. (NYO-3399-240). Dep. NTIS.

The $\pi\pi$ partial-wave amplitudes are the projections of the corresponding scattering amplitudes with respect to the Legendre polynomials with appropriate arguments. In the past few years, several inequalities for the $\pi\pi$ partial-wave amplitudes have been obtained by using analyticity and unitarity. It is shown that many of these inequalities may be generalized into inequalities for the projections of the $\pi\pi$ scattering amplitudes with respect to suitable classes of orthogonal polynomials. The generalization yields several new inequalities for the $\pi\pi$ partial waves in the region $0 \leq s \leq 4m_\pi^2$. In particular, such inequalities involving only s-, p- and d-waves are derived. (auth)

30852 LIMITS ON STRENGTH OF INTERACTIONS FROM AXIOMATIC FIELD THEORY. Lukaszuk, Leszek (Inst. for Nuclear Research, Warsaw). Acta Univ. Wratislaviensis; No. 113, 230-45(1969).

The qualitative restrictions imposed upon the strength of strong interactions by unitarity, analyticity and crossing symmetry are considered. The $\pi-\pi$ scattering amplitudes are studied. Absolute upper bounds and axiomatic field theory scattering amplitudes are discussed. (J.F.P.)

30853 RESONANCE SPECTROSCOPY. de Rosny, G. (Ecole Polytechnique, Paris). J. Phys. (Paris), Colloq.; C5: 31-53 (Nov-Dec 1970). (In French).

From Conference on high energy physics; Aix-en-Provence, France (29 Sep 1970). See CONF-700950.

New information obtained on meson and baryon resonances since the Lund Conference (1969) is reviewed. An attempt was made to include as many as possible of the unpublished results submitted at the Kiev Conference (1970). (France)

30854 LOW-ENERGY THEORETICAL MODELS. Froissart, Marcel (CEA, Saclay, France). J. Phys. (Paris), Colloq.; C5: 88-94(Nov-Dec 1970). (In French).

From Conference on high energy physics; Aix-en-Provence, France (29 Sep 1970). See CONF-700950.

The theoretical and experimental work on low energy scattering (GeV range) in the $\pi\pi$, πK, πN and NN channels, given at this conference, are presented. It is indicated that real progress has been made in the experimental accuracy obtainable, as well as in the theoretical predictions. The experimental study of inelastic processes is now easier although the theory has not yet provided an efficient means of calculating the results. (France)

30855 LOCAL DUALITY AND CONSERVED CURRENTS. Truffin, C.; Brout, R.; Englert, F. (Univ. Libre, Brussels). Nuovo Cim.; 2A: 169-96(1 Mar 1971).

Local duality in the presence of exotic channels implies infinite superconvergence. It is shown that when the exotic channel is formed from a pair of (conserved) currents of $SU_2 \times SU_2$ it follows that the use of local duality is a viable approximation to the physics of mesons, and in general is much less good for baryons. The meson spectrum falls necessarily on linear parallel trajectories of fixed quantized intercepts. These latter yield masses for the non-strange mesons in astonishing agreement with experiment (a few percent). With extended assumptions, Veneziano forms for amplitudes emerge and for $\pi\pi$ scattering the assumptions yield the Lovelace-Veneziano formula with no satellites. When the exotic channel is coupled to the unconserved currents of $SU_3 \times SU_3$, local duality is generally internally inconsistent with broken SU_3 (unlike for the coupling to the currents of $SU_2 \times SU_2$) but can be reinstated in the presence of SU_3 symmetry (π, η, K degeneracy). For the exotic channel not coupled to currents at all, even SU_3 symmetry is no guarantee of local duality; all trajectories (ρ, π...) must then be collapsed into one to get internal consistency. The natural suggestion then is that local duality is strongly associated with current conservation. The guiding notion is that the set of one-body meson states forms representations and coupling of these one-body states to the many-body cuts may be neglected in a consistent scheme in the presence of conserved currents. (auth)

30856 CROSSING-SYMMETRIC, REGGE-BEHAVED AMPLITUDES WITH CUTS. Holden, J. P. (Univ. of Rochester, N. Y.). Contract AT(30-1)-875. Nuovo Cim.; 2A: 11-24(1 Mar 1971).

A model is presented which incorporates the features of Regge asymptotic behavior and the particle spectrum, as well as having cuts in the energy plane from threshold. In addition, the amplitude incorporates some external-mass dependence and can accommodate nonlinear trajectories without introducing spurious ancestors at the particle poles. A soft-meson amplitude is derived and automatically satisfies the Adler consistency condition provided only the Regge trajectory is nonnegative at the Adler point. In the low-energy regime the model predicts the scattering lengths as a function of trajectory intercept. For values of the intercept comparable to those determined by the Adler condition in the Veneziano model, the current algebra results are essentially reproduced. The $\pi\pi$ phase shifts are also calculated. (auth)

30857 CONNECTION BETWEEN THE NONEQUILIBRIUM AND THE SOFT-PARTICLE EMISSION MODELS AT VERY HIGH ENERGIES. Giovannini, A. (Univ., Turin. Istituto Nazionale di Fisica Nucleare, Turin). Nuovo Cim.; 2A: 209-16(1 Mar 1971).

The connection between the model proposed by Fujiwara and Kitazoe, assuming the production scattering processes at very high energies to be in a nonequilibrium state, and the soft-particle emission model investigated by Predazzi and the present author under the requirement of charge conservation for the same scattering processes is established. (auth)

30858 ω-MESON IN THE $\rho-\pi$ SYSTEM. Cohen, H. (California State Coll., Los Angeles); Pagnamenta, A.; Taylor, J. G. Nuovo Cim.; 2A: 954-64(21 Apr 1971).

A calculation of an approximated relativistic three-pion amplitude is presented. Using a separable approximation, the three-pion equation is reduced to a two-body equation for $\rho-\pi$ scattering. A search is made for a complex pole in the ω channel. It is found that the usual simple pole form for the ρ propagator gives completely negative results. However, by taking a form of the ρ propagator, as recently used by other investigators, reasonable results are obtained. (auth)

30859 MECHANISM FOR SPLITTING THE A_2-MESON. Moffat, J. W. (Univ. of Toronto). Lett. Nuovo Cim.; 1: 546-8(27 Mar 1971).

A possible mechanism for the splitting of the A_2 meson is investigated. The decay process $A_2 \rightarrow K\bar{K}$ and $K\bar{K}$ scattering are

considered. A model is demonstrated in which a single resonance is split when the phase shift passes close to or through π in the vicinity of the original single-resonance position, and the inelastic scattering is smoothly varying and small in this region. (L.B.S.)

30860 COUPLED-CHANNEL UNITARIZATION OF THE VENEZIANO MODEL AND THE PION FORM FACTOR. Gensini, P. (Univ., Lecce, Italy). Nuovo Cim.; 2A: 829-52(21 Apr 1971).

The K-matrix interpretation of the Veneziano four-point formula is extended to a two-channel model of meson–meson scattering; in this framework the pion electromagnetic form factor is numerically computed from the unitarity equations. Various features of the model are discussed in detail: it is shown to reproduce quite well physical reality, even if some shortcomings cannot be avoided, which however do not affect considerably the predictions on the best known meson–meson processes. In this model's framework a reformulation of Harari conjecture is also proposed, and arguments are presented to support it. (auth)

30861 K_L AND K_S AS SHELL-MODEL EIGENSTATES. II. McVoy, K. W.; Romo, W. J. (Argonne National Lab., Ill.). Ann. Phys. (N. Y.); 62: 544-53(Feb 1971).

The Wigner–Weisskopf mass matrix for the neutral K-meson system has two right and two left eigenstates. The relations of these states to each other, to the eigenstates of the true Hamiltonian, and to the symmetry properties of the system are discussed in detail. The generalization to the case of several overlapping resonances is worked out as well. (auth)

30862 PROOF OF THE EXISTENCE OF FUNCTIONS THAT SATISFY EXACTLY BOTH CROSSING AND UNITARITY. III. SUBTRACTIONS. Atkinson, D. (Imperial Coll. of Science and Tech., London). Nucl. Phys.; B13: 415-36(1969).

A proof is given of the existence of functions that satisfy the Mandelstam representation with an arbitrary, finite number of subtractions, the crossing symmetry appropriate to pion–pion scattering, and the elastic unitarity condition below the four-pion threshold. (auth)

30863 MODEL FOR TWO-PION PRODUCTION IN THE DIFFRACTION APPROACH. Dewey, P.; Humpert, B. (Cavendish Lab., Cambridge, Eng.). Lett. Nuovo Cim.; 1: 651-9(17 Apr 1971).

A general model is constructed for the reaction $V + P \to \pi^+ + \pi^-$ (V = vector particle, P = Pomeron) modifying an off-shell single-current amplitude in the Veneziano approach. The point of view is taken that Veneziano 5-point integrals, treating the current as a Reggeon, are the appropriate mathematical functions to describe photonic reactions, whereas the beta-functions should only be used to parametrize hadronic reactions. An attempt is made to describe the above reaction and its hadronic analog $\rho + P \to \pi^+ + \pi^-$ by making the most simple assumptions such as ρ-meson exchange in the s-channel and π-meson exchange in the t and u channels. (L.B.S.)

30864 π-MESON RADIUS AND ANALYTICAL PROPERTIES OF π-MESON FORM FACTOR. Baluni, V. Z. (Moscow State Univ.). Teor. Mat. Fiz.; 6: 328-34(Mar 1971). (In Russian).

By solving the extremal problem for the functional $\Phi\{F,f\} = \int_{4m_\pi^2}^{\infty} f(t)\,|F_\pi(t)|^2\,dt$ (where f(t) is a given positive function and $F_\pi(t)$ is electromagnetic form-factor with the known analytical properties) the restrictions are obtained on the elementary particle radius and on the corresponding form-factor in space-like region. Taking into account the fact that on the basis of experiments (at Novosibirsk and Orsay) with colliding beams, the π-meson form-factor in the interval $4m_\pi^2 \leq t \lesssim 1$ (GeV)^2 can be approximated by the Breit–Wigner formula and assuming that its modulus at $t \gtrsim 1$ (GeV)^2 does not exceed some constant, for the upper bound of the π-meson radius the values 0.69 ± 0.14 (Novosibirsk) and 0.9 ± 0.06 (Orsay) are obtained. (auth)

30865 DISPERSION CALCULATION OF ISOSCALAR 3π AND $K\bar{K}$ ELECTROMAGNETIC FORM FACTORS. Aubrecht II, Gordon J. (Princeton Univ., N. J.). Phys. Rev., D; 3: 1622-37 (1 Apr 1971).

Using dispersion theory and the assumption that the three-pion cut is well represented by the $\rho\pi$ cut, the I = 0, J = 1 $\rho\pi$ and $K\bar{K}$ scattering amplitudes are calculated from a matrix integral equation, using only right-hand cuts, in an effective-range–type approximation. Subtraction constants are determined by the experimental masses and widths of the isoscalar vector resonances. There are no ghosts (spurious first-sheet poles) in the model. The $\rho\pi$ and $K\bar{K}$ isoscalar form factors are calculated and compared to the available e^+e^- colliding-beam data near the ω and ϕ masses. The isoscalar charge radii are also computed. The agreement of the model with the experimental values is satisfactory. An estimate $\Gamma(\rho \to \pi^0\gamma) \simeq$ keV is obtained (the decay has not yet been observed). (auth)

30866 CONTRIBUTION TO THE LAMB STATISTICAL MODEL SUBJECT. Baubillier, M.; Rivoal, M. pp IV-135-8 of Proceedings of the Colloquium on High Multiplicity Hadronic Interactions. /Krzywicki, A. (ed.). Paris; Ecole Polytechnique (1970).

From Colloquium on high multiplicity hadronic interactions; Paris, France (13 May 1970). See CONF-700528.

A comparison of the data for $\bar{p}p \to K\bar{K}n\pi$ at 2.5 GeV/c with the prediction of the Lamb statistical model is presented. The experimental and predicted final-state cross sections are in good agreement except for the three body final state. The agreement for the resonance cross sections is not so good. The Lamb model may be used in formation $\bar{p}p$ experiments to give the smooth variation of the background when one seeks resonances. (France)

30867 LOW ENERGY PION–PION SCATTERING. Morgan, D. (Rutherford High Energy Lab., Chilton, Eng.); Pisut, J. Springer Tracts Mod. Phys.; 55: 1-42(1970).

From Low energy hadron interactions conference; Karlsruhe, Germany (May 1970). See CONF-700558.

A summary of predictions for $\pi\pi$ scattering from current algebra and the Veneziano model, experimental information from $\pi + N \to \pi + \pi + N$ and related processes, forward dispersion relations, pion–nucleon dispersion relations, and information from $K_{\ell 4}$ decays and $K_2^0 \to 2\pi$ decays are discussed, in this review. (J.F.P.)

30868 ANALYTIC EXTRAPOLATIONS AND THE DETERMINATION OF PION–PION PHASE SHIFTS. Pisut, Jan (CERN, Geneva). Springer Tracts Mod. Phys.; 55: 43-60(1970).

From Low energy hadron interactions conference; Karlsruhe, Germany (May 1970). See CONF-700558.

Analytic extrapolations directly or implicitly involved in obtaining the information on the pion–pion scattering are briefly discussed. A qualitative description is given of ambiguities and instabilities arising in some of the methods. (auth)

Strong (Baryon No. = 1)

Refer also to abstracts 30739, 30746, 30747, and 30977.

30869 (JINR–P1-5706) APPLICATION OF THE PHENOMENOLOGICAL QUASI-TWO-BODY MODEL TO π^-p-INTERACTIONS WITH THE STRANGE PARTICLE PRODUCTION AT p = 4 GeV/c. Grishin, V. G.; Inogamov, Sh. V.; Kuznetsov, A. A.; Melnikova, N. N.; Mikhul, A.; Sabeu, M.; Yuldashev, B. S.; Jancso, G.; Boldea, V.; Felea, S. (Joint Inst. for Nuclear Research, Dubna (USSR). Lab. of High Energy). 1971. 24p. (In Russian). Dep. NTIS (U. S. Sales Only).

It is shown that the main features of π^-p-interactions with the strange particle production at p = 4 GeV/c can be described in the framework of the phenomenological quasi-two-body model of multiple particle production. (auth)

30870 (ORNL-tr-2433) ANGULAR AND ENERGY DISTRIBUTIONS OF PARTICLES PRODUCED IN INELASTIC π–N AND N–N COLLISIONS AT VERY-HIGH ENERGIES. Barashenkov, V. S.; Eliseev, S. M. (Joint Inst. for Nuclear Research, Dubna (USSR). Lab. of Theoretical Physics). Translated for Oak Ridge National Lab., Tenn., from report JINR–P2-5331. 10p. Dep. NTIS.

This item was previously abstracted from the original language and appeared in NSA as 25: 7658.

30871 (UCRL-20250) ENERGY CONTINUATION OF AN ENERGY-INDEPENDENT PION-NUCLEON PHASE-SHIFT ANALYSIS FROM 385 TO 1700 MeV/c. Field, R. D. Jr. (California Univ., Berkeley. Lawrence Radiation Lab.). 10 Feb 1971. Contract W-7405-eng-48. 57p. Dep. NTIS.

Starting from an energy-independent phase-shift analysis carried out at 26 momenta between 385 and 1700 MeV/c, an attempt is made to find the proper energy continuation through these momenta. Several path-finding schemes are compared which are designed to take into consideration both the continuity and the smoothness of the partial-wave amplitudes as viewed on an Argand diagram. While differing in detail, the various methods yield essentially the same results for the important partial waves. These results agree in general with paths found by other methods, but contain some evidence for additional resonances between 1500 and 1700 MeV. (auth)

30872 PION–NUCLEON ELASTIC SCATTERING. Giacomelli, G. (Univ., Bologna. Istituto Nazionale di Fisica Nu-

XUM

cleare, Bologna. CERN, Geneva). Riv. Nuovo Cim.; 2: 297-448(Jul-Sep 1970).

The present phenomenological situation of pion–nucleon elastic scattering is discussed. Topics covered include general considerations, total cross sections, elastic cross sections, charge exchange scattering, polarization measurements, phase-shift analysis, optical models, the statistical model, Regge poles, elastic scattering as the shadow of inelastic processes, mixed models, dispersion relations for the forward scattering amplitude, duality, pion–nucleon resonances from particle exchange, and conservation laws. An extensive list of references is given. (L.B.S.)

30873 WEAK DUALITY AND ENERGY DEPENDENCE OF THE SLOPES OF ELASTIC ANGULAR DISTRIBUTIONS. Hama, Y.; Predazzi, E. (Univ., Sao Paulo, Brazil). Nuovo Cim.; 2A: 929-53(21 Apr 1971).

The problem of shrinking or antishrinking of the forward peak of elastic processes is studied within the framework of a weak-duality scheme. It is shown that, within such a scheme, the energy dependence of the slopes of the various elastic processes can be qualitatively understood. Thus, the result is in agreement with the experimental situation in the sense that K^+p and pp shrink, K^-p and $\bar{p}p$ antishrink and π^+p stay essentially constant. (auth)

30874 EXCHANGE DEGENERACY AND ABSORPTION: πN, KN, AND NN REACTIONS. Drouffe, J. M.; Navelet, H. (Centre d'Etudes Nucleaires-de Saclay, Gif-sur-Yvette, France). Nuovo Cim.; 2A: 39-66(1 Mar 1971).

A Reggeized absorption model is formulated for any two-body reaction involving particles of arbitrary spins, with particular attention on the factorization property. The absorptive correction is enhanced to account for diffractive dissociations. Using this model, a phenomenological analysis of πN, KN, $\bar{K}N$, NN and $N\bar{N}$ reactions is achieved. In order to test the compatibility of the exchange-degeneracy assumption, two independent sets of fits are proposed: one with independent Regge trajectories, the other with degenerate trajectories and residues. In both cases, the agreement with the experimental data is qualitatively good. (auth)

30875 MODEL-INDEPENDENT ANALYSIS OF THE FORWARD π^+p SCATTERING DATA. Dumbrais, O. V.; Queen, N. M. (Joint Inst. for Nuclear Research, Dubna (USSR)). Lett. Nuovo Cim.; 1: 524-6(20 Mar 1971).

An analysis is made of experimental data on forward elastic π^+p scattering, where the dispersion relation for the scattering amplitude is represented in terms of various parameters for the asymptotic behavior. Parameter values predicted by various models are given. (L.B.S.)

30876 MODELS OF $Y_0^*(1405)$ AND LOW-ENERGY $\bar{K}N$ INTERACTIONS. Martin, A. D. (Univ. of Durham, Eng.); Martin, B. R.; Ross, G. G. Phys. Lett.; 35B: 62-4(26 Apr 1971).

Two models have been proposed for the $Y_0^*(1405)$ resonance: (a) as an s-wave virtual bound state of the $\bar{K}N$-$\pi\Sigma$ system, and (b) as a CDD pole arising from high-lying channels. The compatibility of these interpretations with low-energy $\bar{K}N$ scattering data is analyzed, and it is found that the virtual bound state interpretation is strongly favored. (auth)

30877 COMMENTS ON A_2 PRODUCTION. Michael, C.; Ruuskanen, P. V. (CERN, Geneva). Phys. Lett.; 35B: 47-9 (26 Apr 1971).

The analysis of high energy A_2 production data is discussed, including comparisons with ω and f_0 production and possible f_0 – A_2 interference effects. (auth)

30878 FIXED-POLE EFFECTS ON EXCHANGE-DEGENERATE REGGE RESIDUES AND THE CROSS-OVER PHENOMENA. Itabashi, K. (Tohoku Univ., Sendai). Lett. Nuovo Cim.; 1: 665-71(17 Apr 1971).

As a basic symmetry of nature, the very strong exchange degeneracy (VSED) is postulated in which the degenerate vector- and tensor-meson trajectories follow a simple common coupling mechanism. The fixed-pole effects are examined, which yield completely different helicity-flip/nonflip characters of (ω, P') and (ρ, A_2) exchanges, and, at the same time, give rise to appropriate cross-over factors in the Regge residue functions. A new type of parametrization of vector- and tensor-meson trajectory contributions to the scattering amplitude is proposed. In order to examine its adequacy, the $I_t = 1$ part of the πN scattering amplitude is calculated by the Regge eikonal theory. (L.B.S.)

30879 GENERATION OF VECTOR MESONS AND A MODEL OF FACTORIZABLE QUARKS. Kobushkin, A. P. (Inst. of Theoretical Physics, Kiev). Dokl. Akad. Nauk SSSR; 195: 318-20(11 Nov 1970). (In Russian).

The high-energy scattering of hadrons at large angles was explained on the basis of the factorization quark amplitudes. In order to overcome the shortcomings of the theory, it was attempted to include in it the spins of quarks involved in the composition of the scattering hadrons. It was shown for the case of meson–baryon scattering that in certain approximations applicable to small scattering angles, the factorization results are transformed into additivity values. The total cross sections agreed with experimental data, even without any further corrections; at the same time the large-angle scattering correlations were also improved. A previously published technique was applied to $0^- + p \to 1 + 1/2^+$ high-energy processes. The following amplitude was derived for the formation of K*(890) mesons: $T(K^+p \to K^{*+}p) = G^4(\theta)K(\theta)r^2(\theta)$, $T(K^-p \to K^{*-}p) = T(K^-p \to \bar{K}^{*0}N) = 0$, whereby $G(\theta)$ is the scattering amplitude of p and n quarks (antiquarks) at the effective potential created by the system of repelling hadrons; $K(\theta)$ is that of λ quark or antiquark; $r(\theta) = G(\pi - \theta/G(\theta))$; θ is the scattering angle in the center of mass system of the colliding hadrons. (TTT)

30880 PION PAIR ANGLES IN THE REACTION $\pi p \to p5\pi$. Drevermann, H. (Univ., Bonn). pp III-38-41 of Proceedings of the Colloquium on High Multiplicity Hadronic Interactions. /Krzywicki, A. (ed.). Paris; Ecole Polytechnique (1970).

From Colloquium on high multiplicity hadronic interactions; Paris, France (13 May 1970). See CONF-700528.

Pion pair angle distributions are studied in the reaction $\pi p \to p5\pi$ at 5 GeV/c. A difference between the asymmetry parameters A_{++} and A_{--} is found in statistical model calculations accounting for leading pion, Δ_{1236}^{++} production, and leading Δ^{++}. A difference between A_{+-} and $(A_{++} + A_{--})/2$ is due to ρ^0 production and Bose–Einstein symmetrization. The different origins of the two differences is consistent with the experimental data. (France)

30881 SOME TRENDS AND PROBLEMS IN THE STUDY OF HIGH MULTIPLICITY HADRONIC INTERACTIONS. Van Hove, L. (European Organization for Nuclear Research, Geneva). pp VII-O-17 of Proceedings of the Colloquium on High Multiplicity Hadronic Interactions. /Krzywicki, A. (ed.). Paris; Ecole Polytechnique (1970).

From Colloquium on high multiplicity hadronic interactions; Paris, France (13 May 1970). See CONF-700528.

Aspects of high multiplicity hadronic interactions treated in the colloquium are discussed, including the energy dependence of inelastic channel cross sections and correlations between outgoing particles. New results on the longitudinal phase space (LPS) analysis of the reaction $\pi^-p \to 2\pi^-\pi^+p$ at 11 and 16 GeV/c, and on a combined isospin and LPS analysis of π^+p reactions at 5 GeV/c are presented. A few remarks are included on the most significant recent advances: dual amplitudes of the multi-Veneziano type and Pomeron exchange in diffraction dissociation. (France)

30882 KAON–NUCLEON INTERACTIONS BELOW 1 GeV/c. Martin, B. R. (University Coll., London). Springer Tracts Mod. Phys.; 55: 73-141(1970).

From Low energy hadron interactions conference; Karlsruhe, Germany (May 1970). See CONF-700558.

A review of kaon–nucleon interactions below 1 GeV/c is given, with emphasis on direct analyses of KN scattering data, and the phenomenological use of dispersion relations. (auth)

30883 REGGE RESIDUES. Michael, C. (CERN, Geneva). Springer Tracts Mod. Phys.; 55: 174-91(1970).

From Low energy hadron interactions conference; Karlsruhe, Germany (May 1970). See CONF-700558.

A discussion of forward and backward high-energy scattering data particularly two-body and quasi-two-body reactions including exchange degeneracy, Regge cuts, the implications of SU(3), and vector-meson dominance is given in order to determine the quantities which are well defined and well determined in Regge analyses. The ratios of the residue functions of the same trajectory to different amplitudes, that is, either to different external particles or to different spin amplitudes are discussed. Pseudoscalar meson –$1/2^+$ baryon scattering is considered, and numerical values for such pole residues and ratios of pole residues are presented. The F/D mixing parameters for the different couplings are analyzed, and the resulting predictions and tests are discussed. (J.F.P.)

30884 REACTION $\pi^-p \to \eta n$ WITH VENEZIANO TERMS. Huma, Hazhat; Harun-Ar Rashid, A. M. (Univ. of Islamabad, Rawalpindi, Pakistan). Phys. Rev., D; 3: 1611-14(1 Apr 1971).

The Veneziano amplitude for $\pi^-p \to \eta n$ scattering is constructed using suitable combinations of beta-function terms. If certain constraints for the pole structure are imposed, the amplitude

shows agreement and consistency with the experimental data over the whole energy region. The shape of the high-energy $\pi^- p \to \eta n$ differential cross section is reproduced. The decay widths for the $5/2^+$ and $5/2^-$ pion–nucleon resonances are obtained, and Adler's self-consistency condition is also approximately satisfied. (auth)

30885 IS THE POMERANCHUK TERM DECOUPLED FROM THE ORDINARY REGGE TRAJECTORIES? Barry, George W. (Univ. of Chicago). Contract AT(11-1-264. Phys. Rev., D; 3: 1638-40(1 Apr 1971).

If the amplitude for diffraction scattering is independent of the universal slope of the ordinary Regge trajectories, there results a helicity selection rule, which corresponds to s-channel helicity conservation for the diffractive part of $\pi p \to \pi p$ and $\gamma p \to \rho^0 p$, in accordance with experiment. A crucial test of the selection rule is that electroproduced ρ^0's should be transversely polarized at high energy. (auth)

30886 FIELD-THEORETIC MODEL FOR LOW-ENERGY $J = 3/2^+$ K^+p SCATTERING. Redei, L. B. (Univ. of Umea, Sweden). Phys. Rev., D; 3: 1650-4(1 Apr 1971).

Assuming broken SU_3 Yakawa coupling between the octet baryons and pseudoscalar octet mesons, low-energy K^+p scattering is discussed. A broad (Γ = 1000 MeV) resonance in the $J = 3/2^+$ channel with mass 1750 MeV. The phase shift does not reach $\pi/2$ in the resonance region. The calculated cross section is in qualitative agreement with the experimental data near the resonance energy. (auth)

30887 MULTIPLE PION PRODUCTION. Perrin, Robert (Brandeis Univ., Waltham, Mass.). Phys. Rev., D; 3: 1667-9 (1 Apr 1971).

Using a chiral-invariant pion–nucleon Lagrangian, cross sections for the emission of arbitrary numbers of soft pions by hard nucleons are summed. The result is obtained in the form of an exponential factor times the cross section for the process with no soft pions present. (auth)

30888 UNIQUE POINT FOR THE DETERMINATION OF π^+p AMPLITUDES. Sakmar, I. A. (Univ. of Western Ontario, London). Phys. Rev., D; 3: 1675-6(1 Apr 1971).

Full polarization at 2.50 GeV/c at a definite angle near the backward direction makes the determination of π^+p amplitudes possible. (auth)

30889 $K\bar{K}\Pi N\bar{N}$ AMPLITUDE IN A VENEZIANO-TYPE MODEL WITH SPIN. Schmidt, M. G. (Univ., Heidelberg). Z. Phys.; 243: 154-65(1971).

The generalized Veneziano model has been applied previously to the processes ($K\bar{K}\Pi N\bar{N}$) with very impressive results, but in this treatment baryon spin was neglected. A covariant spin and isospin decomposition of the above class of processes is given. Postulating factorization at the lowest meson and baryon poles and using the very stringent duality diagram prescription one is led to a Veneziano type ansatz for the various invariant amplitudes. (auth)

30890 HIGH-ENERGY SINGLE-PARTICLE PRODUCTION ON THE VAN HOVE PLOT. Humble, Stephen (Rutherford High Energy Lab., Chilton, Eng.). Nucl. Phys.; B28: 416-28 (1971).

Several single-particle production processes are analysed on the Van Hove longitudinal phase-space plot in terms of a model which includes both Regge-pole exchanges and their related phases at high subenergies and possible resonance formation at low energies. With this model it is found possible to simultaneously fit the data for reactions corresponding to different charge states over a range of incident pion momentum. The analysis stresses the importance of pion exchange in these reactions at the energies considered. (auth)

30891 SEPARATION OF ISOSPIN $1/2$ AND $3/2$ CONTRIBUTIONS IN SINGLE PION PRODUCTION IN π^+p INTERACTIONS AT 8 AND 16 GeV/c. Boesebeck, K. (Technische Hochschule, Aachen, Ger.); Graessler, H.; Kraus, G.; (and others). Nucl. Phys.; B28: 381-96(1971).

The isospin $I = 1/2$ state of the nucleon pion system in π^+p reactions leading to single pion production was separated from the $I = 3/2$ state. The contribution of the former to the total $\pi\pi N$ cross section is found to decrease much less with increasing energy than that of the latter. This is interpreted in terms of pomeron-exchange (or diffractive) processes responsible for at least 70% of the $I = 1/2$ contribution at 16 GeV/c and 50% of the $\pi\pi N$ cross section. For $I = 1/2$, the (N,π) mass spectrum has a broad unresolved enhancement which reaches its maximum value at ≈1300 MeV, well below the first known $I = 1/2$ isobar. The production characteristics of this low mass ($N\pi$) system are different from those of the $\Delta(1236)$. (auth)

30892 ELASTIC SCATTERING OF A SPIN ZERO AND A SPIN $1/2$ PARTICLE AT u = 0. Hadjioannou, F. T.; Papargyropoulos, P. H. (Univ., Athens). Nucl. Phys.; B28: 397-406(1971).

The elastic scattering of a scalar particle (a pion) off a spin $1/2$ particle (a nucleon) at u = 0 is examined in a model of continuous-spin (E_2 representation) pole exchange and the results are compared with the usual Regge-pole models. An interesting result is that continuous-spin pole exchange at u = 0 gives an asymptotic polarization which, depending on the magnitude of the exchanged spin, is different than zero in contrast to the vanishing polarization expected in any single Regge-pole exchange model or when a u-channel twin-Fermion Regge-pole pair that satisfies Mac–Dowel's reflection symmetry is exchanged. Indeed measurement of this polarization yields information about the value of the second Casimir operator κ_0 characteristic of the mass-zero representation under exchange. The asymptotic unpolarized cross section then gives the residue function. (auth)

Strong (Baryon No. ≥ 2)

30893 (INR-P-1233) EIKONAL MODEL FOR HIGH-ENERGY ELASTIC SCATTERING. Rek, Z. (Institute of Nuclear Research, Warsaw (Poland)). 1970. 26p. Dep. NTIS (U. S. Sales Only).

The elastic processes pp, $\bar{p}p$, $\pi^\pm p$, and $K^\pm p$ are investigated in terms of a model with Regge poles and cuts generated by multiple scattering. The Born term consists of the Pomeron and degenerate meson trajectories contributions. Predictions of the model are in reasonable agreement with the experimental data for total cross sections and the slope parameter of elastic differential cross sections in the energy range from 10 to 70 GeV. The slope of Pomeranchuk trajectory is found to be 0.4 $(GeV/c)^{-2}$. Some troubles of the present form of the model, connected with antishrinkage phenomenon and the shape of ReF/ImF in the forward direction, are discussed together with the possible generalization into the case of broken degeneracy. Some predictions are given about the asymptotic values of total cross sections and their behavior in the high energy region. (auth)

30894 (ITF-70-98-P) RIEMANN METHOD IN THE INVERSE PROBLEM. IV. Gugushvili, E. I. (Akademiya Nauk Ukrainskoi SSR, Kiev. Institut Teoreticheskoi Fiziki). 1970. 10p. (In Russian). Dep. NTIS (U. S. Sales Only).

The generalization of the Gel'fand–Levitan method for the case of the charged particles scattering is carried out. The Riemann method is applied for studying the nuclei $A^a_s(\pi,\rho)$ and $\tilde{A}^a_s(\pi,\rho)$. It allows one to investigate the properties of these nuclei for all l simultaneously. (auth)

30895 (NP-18779) ON THE MANY-BARYON RESONANCES. Kondratyuk, L. A.; Shapiro, I. S. (Gosudarstvennyi Komitet po Ispol'zovaniyu Atomnoi Energii SSSR, Moscow. Institut Teoreticheskoi i Eksperimental'noi Fiziki). 1970. 32p. (In Russian). Dep. NTIS (U. S. Sales Only).

The quasi-nuclear model of many-baryon resonances, which results from Δ-N potential interaction, is formulated. The interaction Δ-N, decay modes and production mechanisms of two- and three-baryon resonances, involving the Δ isobar, are investigated. The experimental data on two-baryon resonances with isospin T = 1 are analyzed. (auth)

30896 (NYO-4032-36) TRITON CALCULATIONS WITH REALISTIC POTENTIALS IN A HARMONIC OSCILLATOR BASIS. Jackson, A. D. (State Univ. of New York, Stony Brook. Dept. of Physics). [1970]. 8p. Dep. NTIS.

Previous techniques using the Reid soft-core potential are used to calculate the binding energy and ground-state wave function of the triton with a relativistic nucleon–nucleon interaction. As an indication that a harmonic oscillator is capable of dealing with such realistic potentials, calculations of deuteron properties for the Reid potential are also performed. (J.F.P.)

30897 BINDING ENERGY OF $^5_\Lambda$He WITH TWO-CHANNEL SEPARABLE POTENTIALS. Chong, K. F. (McMaster Univ., Hamilton, Ont.); Law, J. Can. J. Phys.; 49: 224-9(15 Jan 1971).

By means of the two-channel separable potentials of Nogami and Satoh, which are fitted to the hyperon–nucleon scattering data, the Λ binding energy in $^5_\Lambda$He was calculated using the model of Law and Nguyen. The binding energy is sensitive to the coupling to the Σ channel. The results indicate that it is possible to obtain agreement with the experimental binding energy of $^5_\Lambda$He. (auth) (Canada)

30898 NONRELATIVISTIC HARD-PION PRODUCTION AND CURRENT-FIELD ALGEBRA. Banerjee, M. K.; Levinson, C. A.; Shuster, M. D.; Zollman, D. A. (Univ. of Maryland, College Park). Phys. Rev., C; 3: 509-24(Feb 1971).

The mass dispersion approach of Fubini and Furlan is applied to single-pion production in nucleon–nucleon collisions. The finite-mass correction to the zero-mass limit is exhibited, and it is shown that in a nonrelativistic approximation this correction leads directly to a simple distorted-wave Born approximation for the physical amplitude. The transition operator is determined directly from the nucleon field-chirality equal-time commutation relation and, in the rest frame of the pion, is given by the standard interaction term. (auth)

30899 REMARKS ON BOUNDS, MULTIPLICITY, AND ENERGY DEPENDENCE. Lo, S. Y. (Univ. of Glasgow). pp I59-70 of Proceedings of the Colloquium on High Multiplicity Hadronic Interactions. /Krzywicki, A. (ed.). Paris; Ecole Polytechnique (1970).

From Colloquium on high multiplicity hadronic interactions; Paris, France (13 May 1970). See CONF-700528.

It has been recently observed that the distribution of charge multiplicity from N–N, K–N scatterings obey a remarkably simple Poisson distribution from threshold up to cosmic ray energy. Various physical features of the phenomena of inelastic scattering based purely on the Poisson distribution are considered. The case of the missing neutral pions and bounds on the energy dependence of multipion production are discussed. (France)

30900 SLOPE OF THE MOMENTUM TRANSFER DISTRIBUTION. Eisenberg, Y.; Lyons, L. (Weizmann Inst. of Sciences, Rehovoth, Israel). pp II-28-32 of Proceedings of the Colloquium on High Multiplicity Hadronic Interactions. /Krzywicki, A. (ed.). Paris; Ecole Polytechnique (1970).

From Colloquium on high multiplicity hadronic interactions; Paris, France (13 May 1970). See CONF-700528.

The momentum transfer distribution in a multibody reaction $a + b \to c + \ldots$ can often be fitted for low values of the momentum transfer t_{ac} by $d\sigma/dt \sim \exp(A\, t_{ac})$ provided the mass m_d of the recoil system is kept fixed. For many reactions, A decreases with increasing m_d. Three mechanisms which can produce such an effect are considered: a double peripheral process, two single peripheral processes, and the effect of the propagator. The calculations refer to the reaction $p_1\, p_2 \to N^*\pi p$ at 7 GeV/c but the results can readily be generalized. (France)

30901 LIQUID-DROP MODEL FOR HIGH-ENERGY ELASTIC AND INELASTIC SCATTERING. Cerulus, F. (Univ. Louvain, Belg.). pp III-13-27 of Proceedings of the Colloquium on High Multiplicity Hadronic Interactions. /Krzywicki, A. (ed.). Paris; Ecole Polytechnique (1970).

From Colloquium on high multiplicity hadronic interactions; Paris, France (13 May 1970). See CONF-700528.

The model of Chou and Yang, which pictures the elastic scattering of nuclei at high energy as the effect of mutual absorption of the nuclear "stuff" in the two nuclei, is modified to treat inelastic collisions as well. It is assumed that energy and momentum density taken out of the original beam at any point give rise to incoherent secondary particle production. A description of the pionization process is given. Results are presented assuming gaussian densities and form factors. A connection with the Hagedorn thermodynamic theory is pointed out. (France)

30902 ΛKN COUPLING AND EXTRAPOLATION BELOW THE $\bar{K}N$ THRESHOLD. Martin, A. D. (Univ. of Durham, Eng.). Springer Tracts Mod. Phys.; 55: 142-51(1970).

From Low energy hadron interactions conference; Karlsruhe, Germany (May 1970). See CONF-700558.

First, the problems associated with the determination of the ΛKN coupling constant from forward dispersion relations, are briefly reviewed, in particular, stressing the sensitivity of the sum-rule prediction to the extrapolation of the K^-p amplitudes below threshold. Then an attempt to overcome the problem is described which is based on finite-contour dispersion relations. Finally, the possibility of using the data for K^- absorption on nuclei to check the extrapolation of the K^-p solutions below threshold is discussed. (auth)

30903 NUCLEON–NUCLEON INTERACTIONS BELOW 1 GeV/c. Kramer, G. (Univ., Hamburg). Springer Tracts Mod. Phys.; 55: 152-67(1970).

From Low energy hadron interactions conference; Karlsruhe, Germany (May 1970). See CONF-700558.

A discussion is given of the theory of elastic pp and np scattering in the energy range up to 750 MeV. The study is made from the viewpoint of obtaining information about meson resonances in particular their couplings to the nucleon. The on-shell approaches based on fixed-t and partial-wave dispersion relations and the off-shell frameworks based on relativistic and nonrelativistic wave equations are discussed. (J.F.P.)

30904 COUPLING CONSTANTS FROM PCAC. Pilkuhn, H. (Univ., Karlsruhe, Ger.). Springer Tracts Mod. Phys.; 55: 168-73(1970).

From Low energy hadron interactions conference; Karlsruhe, Germany (May 1970). See CONF-700558.

The discussion of coupling constants from PCAC covers the $\Lambda\Sigma\pi$ coupling constant, the $\Sigma\Sigma\pi$ coupling constant from SU(3) symmetry with pseudovector coupling, and kaon coupling constants. (J.F.P.)

30905 EXPECTATIONS FOR PARTICLE–NUCLEUS CROSS SECTIONS AT VERY HIGH ENERGIES AND THE HADRON MASS SPECTRUM. Trefil, J. S. (Univ. of Virginia, Charlottesville). Phys. Rev., D; 3: 1615-18(1 Apr 1971).

Striking decreases in particle-nucleus total cross sections at high energies are predicted, due to the presence of coherent intermediate resonance contributions. A method of utilizing this effect to probe the high-mass hadron spectrum is outlined. (auth)

30906 LOW-ENERGY KAON–NUCLEUS INTERACTIONS. Wycech, S. (Nuclear Physics Lab., Oxford). Nucl. Phys.; B28: 541-65(1971).

The reaction-matrix method and statistical model of nuclei are used to find the K^- meson interactions within nuclei. The results determine the kaon optical potential and the probabilities of hyperon- and pion production processes. The values calculated for the former are in agreement with the experimental kaonic X-ray intensities while the latter are used to discuss the possible neutron excess at the nuclear surface. To explain the experimental data no necessity is found for an anomalously-large neutron excess at the surface. (auth)

30907 LOWER BOUND ON W^{+-}-MESON PRODUCTION IN HIGH-ENERGY PROTON–PROTON COLLISIONS. Sanda, A. I. (Columbia Univ., New York); Suzuki, Mahiko. Contract F44620-70-C-0028. Phys. Rev., D; 3: 2019-27(1 May 1971).

A lower bound is obtained for differential cross sections of $W^{\pm}$-meson production in high-energy proton-proton collisions. Use is made of a current-algebra sum rule derived from time components of weak currents, and of a Regge argument based on duality. Using additional physical assumptions a lower bound on the sum of the total production cross sections for W^+ and W^- mesons can be calculated. The bound turns out large enough to be of practical significance in future experiments, although it is not applicable to data at presently available energies. (auth)

30908 ASYMPTOTIC BEHAVIOR OF PARTICLE DISTRIBUTIONS IN HADRON COLLISIONS. Abarbanel, Henry D. I. (Princeton Univ., N. J.). Contract AT(30-1)-4159. Phys. Rev., D; 3: 2227-41(1 May 1971).

The distribution functions for the "inclusive" production of N specified particles plus anything else are treated from a J-plane point of view. The variables relevant to the exhibition of the asymptotic behavior of these distributions are chosen during a group-theoretic discussion of the matrix elements involved. After the variables are located in this fashion, a crossed-channel partial-wave analysis is carried out to exploit the SO(1,3) symmetry of the production cross sections, and in the context of this partial-wave structure the multi-Regge asymptotics are presented. Such features as pionization and limiting fragmentation are treated, as are certain phenomena involving the approach to limiting distributions, including the rate of approach and specific dependences on certain variables related to longitudinal momenta. Single- and double-particle production is treated in detail, and then a set of numerical estimates is made for proton-proton collisions with incident lab momenta of about 200 to 500 GeV/c to give an indication where many of the phenomenological results might be tested. A mathematical appendix is provided for those interested in group theory. (auth)

30909 BETHE–SALPETER SOLUTION FOR NUCLEON–NUCLEON SCATTERING WITH PION EXCHANGE IN THE $^1S_0$ AND $^3P_0$ STATES. Gammel, J. L.; Menzel, M. T.; Wortman, W. R. (Los Alamos Scientific Lab., N. Mex.). Phys. Rev., D; 3: 2175-84(1 May 1971).

The Bethe–Salpeter equation is solved for nucleon-nucleon scattering in the ladder approximation with pion exchange for the $^1S_0$ and $^3P_0$ states with no approximations beyond use of a finite mesh. It is found that solutions exist without the need for any cutoff so long as the coupling constant $g^2/4\pi$ is between about −4 and +7 for the $^1S_0$ state and for $g^2/4\pi$ less than about

+4 for the $^3P_0$ state. These results are in qualitative agreement with the predictions of Mandelstam. It is found that the Padé approximant as applied to the coefficients of the iteration solution provides an efficient alternative to the method of matrix inversion for solving the equations for a given mesh. (auth)

30910 SCATTERING AND PAIR PRODUCTION FROM THE DEUTERON AT LARGE MOMENTUM TRANSFERS. Gunion, J. F.; Blankenbecler, R. (Stanford Univ., Calif.). Phys. Rev., D; 3: 2125-7(1 May 1971).

Expressions are derived for Glauber double scattering and pair production via twin scattering from the deuteron at large momentum transfers. In the double-scattering region, it is shown that twin scattering is comparable to the Drell-Söding contribution and can even dominate the process. (auth)

30911 VALIDITY OF A LOCAL APPROXIMATION TO THE ONE-PION-EXCHANGE POTENTIAL FOR THE TWO-NUCLEON SYSTEM. Thompson, Richard H.; Gersten, Alexander; Green, A. E. S. (Univ. of Florida, Gainesville). Phys. Rev., D; 3: 2069-75(1 May 1971).

A nonlocal potential (nonlocal in coordinate space) is considered which has been used to describe the exchange of one pion between two nucleons, and which when used in the first Born approximation, reproduces the relativistic S matrix exactly to order g_π^2, the π-N coupling strength squared. This nonlocal potential is compared with its lowest-order (in powers of ∇/m, where m is the nucleon mass) local approximation. This comparison is made by inserting each of the potentials into the Lippmann–Schwinger (LS) equation and comparing the resulting phase parameters. The form factor of Ueda and Green is used to obtain the required convergence. Results are obtained which show that the local potential is in general not a reliable approximation to the nonlocal potential, even for low energies, when used in conjunction with the LS equation. As a by-product of this research, numerical methods are developed which are applicable to any nonlocal potential. (auth)

30912 RELATIVISTIC CALCULATION OF NUCLEON–NUCLEON PHASE PARAMETERS. Gersten, Alexander (Univ. of Florida, Gainesville. Texas A and M Univ., College Station); Thompson, Richard H.; Green, A. E. S. Phys. Rev., D; 3: 2076-83(1 May 1971).

An approximate Bethe–Salpeter equation is used to calculate the N-N phase parameters. The one-boson-exchange (OBE) hypothesis is invoked to approximate the left-hand singularity. A good fit to the existing data is obtained, and certain phase parameters ($^3D_2$, $^1D_2$, and $^3P_2$), which are not fitted well by existing OBE-potential (OBEP) models, are much improved. The observables are not fitted directly, but rather an approximate procedure suggested by MacGregor et al., is used to minimize the experimental χ^2. Comparisons are made with the nonrelativistic OBEP used in conjunction with the Schrödinger equation. (auth)

Particle Invariance Principles and Symmetries

General

Refer also to abstracts 30945, 30947, 30950, and 30966.

30913 (JINR–P2-5729) METHOD OF CALCULATING THE UNITARY WEIGHTS IN THE THEORY OF MULTIPLE PARTICLE PRODUCTION. Barashenkov, V. S.; Beshtoev, Kh. M. (Joint Inst. for Nuclear Research, Dubna (USSR). Lab. of Nuclear Reactions). 1971. 7p. (In Russian). Dep. NTIS (U. S. Sales Only).

A method of calculating the weights more simple than that discussed previously is suggested. (auth)

30914 (NP–18804) SYMMETRY GROUPS AND CURRENT ALGEBRA. Lectures delivered during the 1969 Summer School held in Mexico City, Mexico. Altarelli, Guido (New York Univ., N. Y. Instituto Politecnico Nacional, Mexico City. Centro de Investigacion y de Estudios Avanzados). [1969]. 157p.

Notes compiled by Rigoberto Garcia, Hector Moreno, and Eduardo Hinojosa.

The lectures on symmetry groups cover group notation, reducible and irreducible representations, continuous groups of transformations, SU(2), reduction of tensor products of irreducible representations in SU(2) and SU(3) generators in various representations. Also discussed are identification of particle states in terms of tensors, physical applications, SU(3), SU(3) generators, correspondence between physical states and tensors of irreducible representations of SU(3), irreducible tensor operators under SU(3), regular representation, and applications of SU(3). Current algebra is treated including the elements of current algebra, the Gell-Mann assumption, the naive quark model, extension of the hypothesis to include space components of current densities, the divergence of the axial current, and applications of PCAC to simple soft pion emission in strong interactions. The emission of a soft pion in the presence of an external perturbation, the Weinberg–Tomozowa formula for scattering lengths, Adler–Weisberger relations, and the Weinberg approach to $\pi + \pi$ scattering lengths are also considered. (J.F.P.)

30915 (NP–18808) SELECTED TOPICS IN DISCRETE SYMMETRIES AND CP-VIOLATION. Beg, M. A. B. (Rockefeller Univ., New York. Instituto Politecnico Nacional, Mexico City. Centro de Investigacion y de Estudios Avanzados). [1969]. 59p.

These lectures on discrete symmetries and CP violation cover charge conjugation, space inversion, time inversion, the CPT theorem the neutral K system, and theories of CP violation. (J.F.P.)

30916 CLASSIFICATION OF THE SPIN–ISOSPIN FUNCTIONS OF THE IDENTICAL-NUCLEON SYSTEM. II. Grama, N. (Max-Planck-Institut fuer Kernphysik, Heidelberg). Lett. Nuovo Cim.; 1: 505-8(20 Mar 1971).

It was previously pointed out that the classification of the spin–isospin functions of n-identical-nucleon system may be reduced to the calculation of the inner product of S-functions. A method is given that provides for the calculation of the inner product of 2-element S-functions {n-q, q} and {n-p, p} for each particular value of q. (L.B.S.)

30917 INHOMOGENEOUS $U_{3,1}$-INVARIANT EXTENSION OF VACUUM EXPECTATION VALUES. Santilli, R. M.; Roman, P. (Boston Univ.). Nuovo Cim.; 2A: 965-1015(21 Apr 1971).

The Minkowski space $M_{3,1}$ is represented in terms of the irreducible symmetric homogeneous space P_0/L_0, where P_0 and L_0 are the identity components of the Poincaré group $P = L \circledS T$ and of the Lorentz group L, respectively. A theorem is proved stating that all irreducible symmetric complex extensions $\underline{M}_{3,1}$ of $M_{3,1}$ are as follows: 1) a complex extension of orthogonal type $\underline{M}_{3,1}^{(1)}$ whose group of all isometries is the group $\underline{P}^{(1)} = \underline{L}^{(1)} \circledS \underline{T}$, where $\underline{L}^{(1)}$ and $\underline{T}$ are the complex extensions of the Lorentz group L and of the translational group T; 2) a complex extension of Hermitian type $\underline{M}_{3,1}^{(2)}$ whose group of all isometries is the group $\underline{P}^{(2)} = \underline{L}^{(2)} \circledS \underline{T} = U_{3,1} \circledS \underline{T}$. The implications of the above theorem for physical quantities depending on points of the Minkowski space are investigated for the case of the $L\uparrow$-invariant (parity-conserving) vacuum expectation values of products of field operators, $W_n(x_1, \ldots, x_n) = w_n(\xi_1, \ldots, \xi_{n-1}) = \langle \varphi_1(x_1) \ldots \varphi_n(x_n) \rangle_0$, $\xi_k = x_k - x_{k+1}$, $k = 1, 2, \ldots, n-1$, satisfying the Wightman axioms. A theorem is proved which states that all the extensions $\underline{w}_n(\xi_1, \eta_1; \ldots; \xi_{n-1}, \eta_{n-1}) = \underline{w}_n'(z_1, \ldots, z_{n-1})$ of the n-point functions w_n to complex 4-vectors $z_k = \xi_k - i\eta_k$, $k = 1, 2, \ldots, n$, which i) are (real) analytic in all the real and imaginary components ξ's and η's of the z's; ii) admit the physical n-point functions in the limit when all the η's go to zero, iii) possess simple groups of complex transformations as global invariance groups; are as follows: 1) the extension $\underline{w}_n^{(1)}(\xi_1, \eta_1; \ldots; \xi_{n-1}, \eta_{n-1})$ of the Bargman–Hall–Wightman theorem which is invariant under the connected component $\underline{P}_+^{(1)}$ of the group $\underline{P}^{(1)}$; 2) a new extension $\underline{w}_n^{(2)}(\xi_1, \eta_1; \ldots; \xi_{n-1}, \eta_{n-1})$ which is invariant under the full inhomogeneous $U_{3,1}$ group $\underline{P}^{(2)}$. The above results are extended to distributions in order to construct $P^{(2)}$ invariant analytic extensions of the $L\uparrow$-invariant vacuum expectation values in the proper sense. The $\underline{w}_n^{(2)}$ extension of parity-violating vacuum expectation values is considered too, and in this case the global invariance group results to be the inhomogeneous unimodular $SU_{3,1}$ group. The proposed procedure could also be applied to include tensorial fields satisfying the Wightman axioms, but the inclusion of spinorial fields requires specific supplementary investigations starting, possibly, from the classification of all the complex extensions of the covering of the Minkowski space. Finally, some features of the $\underline{w}_n^{(2)}$ extension, which might be suitable for possible physical applications, are pointed out. (auth)

30918 SEARCH FOR QUANTUM SYSTEMS WITH A GIVEN SPECTRUM-GENERATING ALGEBRA: DETAILED STUDY OF THE CASE OF $SO_{2,1}$. Cordero, P. (International Centre for Theoretical Physics, Trieste, Italy); Ghirardi, G. C. Nuovo Cim.; 2A: 217-36(1 Mar 1971).

A method is introduced to determine the Hamiltonians $\mathcal{H}$ of the quantum-mechanical systems having a given Lie algebra as their spectrum-generating algebra (SGA). Application of this method to the particular case in which the SGA is assumed to be the Lie

XUM

algebra $SO_{2,1}$ allows under several assumptions the determination of a general solution $\mathcal{H}$, for a system of two spinless particles, having this algebra as its SGA, and possessing both a discrete and a continuous spectrum. Velocity-dependent potentials have been included, the only restrictions imposed on $\mathcal{H}$ being that it be at most quadratic in the momentum, and rotationally and time-reversal invariant. The potential obtained as the general solution contains as an essential part of a term which asymptotically is Coulomb-like and is more general than those which have been obtained previously in the same context. The requirement that the potential be angular-momentum independent reduces the possible Hamiltonian to that of the hydrogen atom, with an extra cubic force, which has already been solved. In the case in which a purely discrete spectrum is allowed, the general answer is not given, but still a sufficiently general Hamiltonian is obtained with $SO_{2,1}$ as its SGA, that includes as a particular case the known harmonic oscillator with an extra cubic force. (auth)

30919 SOME FEATURES OF CHIRAL SYMMETRY BREAKING. Dashen, Roger (Inst. for Advanced Study, Princeton, N. J.). Phys. Rev., D; 3: 1879-89(15 Apr 1971).

Some rather paradoxical features of chiral symmetry breaking are shown to be directly related to the fact that the vacuum is supposed to be degenerate in the limit of exact symmetry. The importance of picking the correct one of the many symmetry-limit vacua is stressed. A peculiar phenomena of spontaneous CP violation appearing alongside SU(3) ⊗ SU(3) breaking is observed. (In the model investigated here, the effect is much too large to be at all related to that seen in weak interactions.) For the $(3,\bar{3}) \oplus (\bar{3},3)$ model of symmetry breaking, it is shown that the rate for $K_S^0 \to 2\pi$ should be suppressed by a factor of [SU(3) ⊗ SU(3) breaking]. This may or may not be a difficulty. A number of other topics in chiral symmetry breaking are discussed briefly. (auth)

30920 SCALE TRANSFORMATIONS AND BROKEN CHIRAL SYMMETRY. Schnitzer, Howard J. (Brandeis Univ., Waltham, Mass.). Contract AT(30-1)-3179 M8. Phys. Rev., D; 3: 1898-1910(15 Apr 1971).

Scale transformations of the SU(2) × SU(2) linear σ model are studied in order to relate the mechanisms which break chiral symmetry and scale invariance. It is shown that the "new improved" stress-energy tensor is finite in this model if it is finite in the symmetric theory. Formal trace identities for one-particle irreducible matrix elements of the trace of the "new improved" tensor are derived and verified in second-order perturbation theory, which implies that the pion and σ have canonical dimension to this order. The trace identities are shown to be "anomalous" in the limit in which the renormalized chiral-symmetric mass tends to zero, which implies that there must be a background contribution to matrix elements of the trace. A numerical estimate, not based entirely on perturbation theory, suggests that this background is fairly large, so that the σ meson does not appear to dominate matrix elements of the trace of the stress-energy tensor. (auth)

30921 ARGUMENTS AGAINST ANOMALOUS DIMENSIONS. Jackiw, R. (Massachusetts Inst. of Tech., Cambridge). Contract AT(30-1)-2098. Phys. Rev., D; 3: 2005-9(15 Apr 1971).

Two-dimensional solvable field theories provide examples of anomalous dimensions and conserved dilatation current, while in four-dimensional calculations anomalous dimensions occur together with strongly broken dilatation invariance. It is shown that the situation in two dimensions arises from peculiar phase-space properties which do not generalize to four dimensions. It appears that two-dimensional physics is not a good "laboratory" for studying scale invariance: Even the free-field theory behaves anomalously. It is argued that at the present time there is no theoretical or experimental evidence for the consistency of anomalous dimensions with conserved or weakly broken scale invariance in physically realistic models. (auth)

30922 COVARIANT DERIVATIVES IN BROKEN NONLINEAR CHIRAL SYMMETRY. Bace, Marjan (Univ. of Rochester, N. Y.). Phys. Rev., D; 3: 1994-5(15 Apr 1971).

If the symmetry breaking in nonlinear Lagrangian theories depends on derivatives of boson fields, then the covariant derivatives $D_\mu\varphi_a$ lose their nice transformation properties. (auth)

30923 FACTORIZABLE CURRENT ALGEBRAS AT ALL MOMENTA. Divakaran, P. P. (Tata Inst. of Fundamental Research, Bombay). Phys. Rev., D; 3: 1755-63(15 Apr 1971).

Factorizable representations (of isospin $\frac{1}{2}$) of the SU_2 algebra of conserved currents on the physical Hilbert space of states having all momenta are studied. Without any constraints on the Schwinger term except those arising from current conservation, it is demonstrated that the currents can be expressed as functions of a set of basic variables, and that their commutation relations, as well as the covariance conditions, can be written in terms of these basic variables themselves and a "symmetric Schwinger operator." The Schwinger operator is itself fairly well determined by the covariance conditions and is such as to make the algebra of fields inconsistent with factorizability. Finally, it is shown that a no-go theorem holds even for representations at finite momenta, making the mass spectrum "unphysical." (auth)

30924 GAUGE FIELDS, THEORY OF CURRENTS, AND VECTOR MESONS. Kimel, I. (Univ. of Chicago). Phys. Rev., D; 3: 2084-94(1 May 1971).

Various forms of the gauge-field model with broken symmetry are studied. It is shown that only symmetry breakings which originate in the kinetic terms lead to models consistent with the algebra of currents, and this requires, in particular, the ω-φ mixing to be of current type. Breaking in the mass terms leads to modifications of the algebra, the consequences of which are analyzed. A nonet symmetry model yielding inverse-mass-squared relations is presented, and Sugawara's theory of currents, in relation to the vector mesons, is also studied. The models treated in the paper are compared with experiment. (auth)

Applications (Electromagnetic and Weak)

Refer also to abstracts 30781 and 30803.

30925 SOME RECENT EXPERIMENTAL RESULTS ON WEAK INTERACTIONS. Darriulat, P. (European Organization for Nuclear Research, Geneva). J. Phys. (Paris), Colloq.; C5: 95-115(Nov-Dec 1970). (In French).

From Conference on high energy physics; Aix-en-Provence, France (29 Sep 1970). See CONF-700950.

The experimental values of the CP violating parameters in the $(K_0-\bar{K}_0)$ system are discussed in view of recently obtained results. A few experiments which, in the past two years, have led to a better understanding of the properties of weak currents are presented. (France)

30926 REMARKS CONCERNING C-INVARIANCE VERIFICATION IN EXPERIMENTS WITH COLLIDING e^+e^- BEAMS. Khoze, V. A. JETP Lett. (USSR) (Engl. Transl.); 12: 384-6(20 Dec 1970).

Translated from Zh. Eksp. Teor. Fiz., Pis'ma Red.; 12: 542-4(5 Dec 1970).

It is pointed out that relations for the differential cross sections for e^+e^- annihilation into hadrons, summed over the polarizations of the final particles, can be used to verify C invariance. (L.B.S.)

30927 BROKEN SCALE INVARIANCE, $U_3 \times U_3$ BREAKING AND HADRON LAGRANGIAN STRUCTURE. Parisi, G.; Testa, M. (Univ., Rome). Lett. Nuovo Cim.; 1: 549-52(27 Mar 1971).

It was previously suggested that broken scale invariance could be treated on the same basis as broken SU(3) × SU(3). A phenomenological Lagrangian approach based on a linear σ-model is used to study the symmetry breaking and the meson mass spectrum. (L.B.S.)

30928 POSSIBLE CP VIOLATION IN $K^\pm \to \pi^\pm\gamma\gamma$. Chen, H. H. (Univ. of California, Irvine); Lee, S. Y. Phys. Rev., D; 3: 2172-5(1 May 1971).

A comparison of the decays $K^\pm \to \pi^\pm\gamma\gamma$ for the 2_γ invariant mass near the π^0 mass may show a relatively large asymmetry which is indicative of CP violation. This is shown in a simple phenomenological analysis of these decays. Model estimates of the magnitude of this effect are also given. (auth)

30929 NATURE OF INTRINSIC BREAKDOWN OF CHIRAL SYMMETRY IN TERMS OF PHYSICAL FIELDS. Papastamatiou, N.; Umezawa, H.; Welling, D. (Univ. of Wisconsin, Milwaukee). Phys. Rev., D; 3: 2267-74(1 May 1971).

A method for considering the intrinsic breakdown of chiral SU(3) × SU(3) symmetry is presented. The method is principally based on the knowledge of the physical masses of the particles whose fields transform linearly under the symmetry group. The exact Hamiltonian of asymptotic fields for the parity couples $(0^+,0^-)$ and $(1^+,1^-)$ is considered, and the nature of the resulting transformations is described. It is shown that the transformation does differ appreciably from the simple $(3,3^*)$ form, which has been recently assumed. It is found that the representations which include subgroups of SU(3) beyond

the singlet and octet are restricted by the physical masses but cannot all simultaneously be made to vanish. It is shown that a universal condition on the fields considered exists, which requires the vanishing of the commutator between the axial charge and the divergence of the SU(3) vector generator for those specific cases in which $\Delta I > 1$ and/or $\Delta Y > 1$. This condition provides mass formulas among the scalar and pseudoscalar particles and among the vector and axial-vector particles which are in good agreement with experiment. (auth)

30930 CABIBBO'S THEORY AND SECOND-ORDER SU(3)-SYMMETRY-BREAKING CORRECTIONS. Koeberle, R. (Univ., Sao Paulo, Brazil). Phys. Rev., D; 3: 2112-16(1 May 1971).

Second-order corrections to the vector and axial-vector baryon currents, arising from partial conservation of axial-vector current and partial conservation of vector current in a field-algebra model, are discussed. It is shown that the amount of symmetry breaking is severely limited if an acceptable fit to leptonic-baryon-decay data is required. This does not seem to be consistent with information obtained from meson data and K^+-nucleon scattering. (auth)

30931 EXPERIMENTAL EVIDENCE FROM PARITY-FORBIDDEN α DECAY FOR THE PRESENCE OF NONCANCELING SEAGULL AND SCHWINGER TERMS IN WEAK (NUCLEON → NUCLEON + VECTOR-MESON) AMPLITUDES. Cheng, Wen-kwei (Stevens Inst. of Tech., Hoboken, N. J.); Fischbach, Ephraim; Primakoff, Henry; Tadic, Dubravko; Trabert, Kenneth. Phys. Rev., D; 3: 2289-92(1 May 1971).

It is shown that the recent observation of the parity-forbidden α decay, $^{16}O(8.87\ MeV) \rightarrow {}^{12}C + {}^{4}He$, requires that the weak parity-violating (nucleon → nucleon + vector-meson) amplitudes be nonzero and thus demands the presence of noncanceling seagull and Schwinger terms in these amplitudes. (auth)

30932 MUON PARITY CONSERVATION AND THE UNIVERSALITY PRINCIPLE. Tsai, S. Y. (Nihon Univ., Tokyo). Lett. Nuovo Cim.; 1: 699-702(24 Apr 1971).

A muon-parity-conserving weak-interaction scheme based exclusively on the principle of universality is proposed. First lepton currents are introduced for the purely leptonic case; then hadron currents are incorporated into the scheme. (J.F.P.)

Applications (Strong)

Refer also to abstract 30730.

30933 CONSISTENCY OF SCALE AND CHIRAL SYMMETRY LIMITS. de Alwis, S. P. (Cambridge Univ., Eng.). Nucl. Phys.; B28: 594-604(1971).

The theories are investigated in which the chiral and scale-invariant limits are realized in the Goldstone fashion with the appearance of an octet of pseudoscalar and one scalar, Goldstone bosons. A relation for the coupling constant is derived from the theory. The question of determining the dimension of the chiral symmetry breaking from both theoretical and phenomenological considerations is discussed. (auth)

30934 SCALE-SYMMETRY BREAKING AND SCALING PROPERTIES OF CURRENTS. Genz, H. (Univ., Karlsruhe, Ger.); Katz, J. Phys. Rev., D; 3: 1860-4(15 Apr 1971).

If δ [the term that breaks scale symmetry and not SU(3) ⊗ SU(3)] is a c number, (or vanishes) all components of the SU(3) ⊗ SU(3) currents have the same dimension $l_0 = l_k = 3$. In other words, $l_0 \neq l_k$ implies that a q number δ is present. Presence of a q number δ thus follows if the Schwinger term in the current commutators is a (finite) c number. The commutators of J_0^a with the scale-symmetry-breaking operators δ, u, and θ_μ^μ are obtained in terms of J_k^a and $\partial^\mu J_\mu^a$. As one of their consequences, continuity of the limit $\delta \rightarrow 0$ implies that $l_k = 3$. (auth)

Field Theories

General

30935 ANOMALOUS WARD IDENTITIES IN RENORMALIZED PERTURBATION THEORY. Slavnov, A. A. (Inst. of Mathematics, Moscow). Teor. Mat. Fiz.; 7: 13-19(Apr 1971). (In Russian).

Ward identities are obtained, connecting the renormalized matrix elements of currents. It is shown that the partial conservation hypothesis does not contradict the gauge invariance. (auth)

30936 RAYLEIGH–JEANS LAW IS INCOMPATIBLE WITH CLASSICAL ELECTRODYNAMICS. Bocchieri, P. (Univ., Pavia, Italy); Loinger, A. Lett. Nuovo Cim.; 1: 709-10(24 Apr 1971).

A general and simple argument is given which shows that the equipartition law cannot hold for the classical radiation in a Hohlraum because a thermodynamic equilibrium, having as a consequence the Rayleigh–Jeans law cannot be reached in a finite time, if initially a finite amount of radiant energy is present. It is concluded that the Rayleigh–Jeans formula is incompatible with classical electromagnetism if it is assumed that classical electrodynamics leads to an equilibrium state in a finite time. (J.F.P.)

Quantum Field Theory

Refer also to abstracts 30703, 30852, 30921, 31016, and 31034.

30937 (JINR–P2-5694) CONSTRUCTION OF NON-LOCAL QUANTUM ELECTRODYNAMICS. Efimov, G. V. (Joint Inst. for Nuclear Research, Dubna (USSR). Lab. of Theoretical Physics). 1971. 30p. (In Russian). Dep. NTIS (U. S. Sales Only).

The perturbation theory of electromagnetic interactions is considered. A hypothesis is proposed that the electromagnetic potential $A_\mu(x)$ is connected with the local fermion current $J_\mu = \bar{\psi}\gamma_\mu\psi(x)$ by a nonlocal form-factor $L_I = e\int\int dxdy A_\mu(x)K(x-y)J_\mu(y)$, where $K(x-y)$ is a nonlocal distribution and its Fourier transform $\tilde{K}(p^2)$ is an entire analytical function. The intermediate regularization procedure is introduced that the S-matrix is finite, unitary, causal, gauge invariant when regularization is moved off. The interaction Lagrangian maintains no infinite counter terms. (auth)

30938 (JINR–P2-5717) QUANTUM FIELD THEORY WITH NON-EUCLIDEAN SPACE OF RELATIVE MOMENTA. Kadyshevskii, V. G. (Joint Inst. for Nuclear Research, Dubna (USSR). Lab. of Theoretical Physics). 1971. 20p. (In Russian). Dep. NTIS (U. S. Sales Only).

The possibility of constructing a quantum field theory in which the relative four-momenta belong to four-space of constant curvature and the total four-momentum possesses all the usual properties and obeys the standard conservation law is discussed. The inverse radius of curvature of the relative momentum space plays the role of the fundamental length. (auth)

30939 (NYO–3829-66) REMARKS ON THE THEORY OF PARTICLES WITH SPIN UP TO ONE IN EXTERNAL FIELDS. Seiler, R. (Pittsburgh Univ., Pa. Dept. of Physics). [1970]. Contract AT(30-1)-3829. 21p. (CONF-710106-7). Dep. NTIS.

From Conference on fundamental interactions at high energy; Coral Gables, Fla. (20 Jan 1971).

The quantum theory of particles with spin zero and one half coupled to external fields is treated. The existence and uniqueness of the time evolution operator and S-matrix is shown for certain couplings and locality of the field. Also considered are explicitly solvable models and the breakdown of perturbation theory. (J.F.P.)

30940 AXIOMATIC APPROACH TO QUANTUM FIELD THEORY AND MANY BODY PROBLEM. VOLUME I B. V Winter School of Theoretical Physics in Karpacz, February 17–March 2, 1968. Acta Univ. Wratislaviensis; No. 99, 1-280 (1968).

There were 13 lectures included. Separate abstracts were prepared for all lectures. (J.F.P.)

For abstracts of individual lectures see: 30703 and 30941–30952.

30941 EQUILIBRIUM STATES OF STATISTICAL MECHANICS. Hugenholtz, N. M. (Univ., Groningen, Ger.). Acta Univ. Wratislaviensis; No. 99, 7-22(1968).

The discussion of equilibrium states of statistical mechanics covers the infinite system, transformations, the equilibrium state, and islands and factor types. (J.F.P.)

30942 SOME TOPICS IN AXIOMATIC NONRENORMALIZABLE FIELD THEORY. Choruzyi, S. S. (Mathematical Inst., Moscow). Acta Univ. Wratislaviensis; No. 99, 23-55(1968).

An axiomatic theory of the Wightman type over the test function space different from the Schwartz space and corresponding to nonrenormalizable interactions is considered. (J.F.P.)

30943 ASYMPTOTIC CONDITION IN THE ZACHARIASEN–THIRRING MODEL. Karkowski, W.; Sznajder, N. (Univ. of Wroclaw). Acta Univ. Wratislaviensis; No. 99, 56-63(1968).

In the Zachariasen–Thirring model considered there are two

XUM

kinds of fields, and the only interaction taken into account is the interaction between the fields. A certain operator is treated. (J.F.P.)

30944 POSITIVE FUNCTIONALS ON THE ALGEBRA OF TEST FUNCTIONS. Lassner, G. (Joint Inst. for Nuclear Research, Dubna, USSR); Uhlmann, A. Acta Univ. Wratislaviensis; No. 99, 64-83(1968).

A quantum field is defined by a positive functional W on a *-algebra R of test functions. Restriction is made to the case of a neutral scalar field. The existence of positive functionals is proven. The *-algebra R, the cone of positive elements, and positive functionals on R are discussed. (J.F.P.)

30945 SYMMETRY OPERATIONS AND SPONTANEOUSLY BROKEN SYMMETRIES IN RELATIVISTIC QUANTUM FIELD THEORY. Reeh, H. (Max-Planck Institut, Munich). Acta Univ. Wratislaviensis; No. 99, 84-131(1968).

The discussion of spontaneously broken symmetries in relativistic quantum field theory treats symmetry operations, one-parameter continuous symmetry operations, spontaneously broken symmetries, properties of symmetry transformations, and connection with global observables. (J.F.P.)

30946 INTRODUCTION TO THE HEISENBERG FERROMAGNET. Streater, R. F. (Imperial Coll. of Science and Tech., London). Acta Univ. Wratislaviensis; No. 99, 145-65(1968).

The Heisenberg model of the ferromagnet illustrates the algebraic approach to statistical mechanics and quantum field theory. A concrete illustration is given showing how a theory involving observables alone as the primary quantities can predict the existence and behavior of particlelike states carrying superselection rules. (J.F.P.)

30947 CONTINUOUS TENSOR PRODUCTS OF GROUP REPRESENTATIONS. Streater, R. F. (Imperial Coll. of Science and Tech., London). Acta Univ. Wratislaviensis; No. 99, 166-82(1968).

The topics discussed include a general definition of continuous tensor products, continuous products of group representations, fields and commutation relations, exponential spaces, local functions of the field operators, and equations of motion. (J.F.P.)

30948 REMARKS ON REPRESENTATIONS OF CANONICAL COMMUTATION RELATIONS. Tarski, Jan (Univ., Paris). Acta Univ. Wratislaviensis; No. 99, 183-201(1968).

In order to determine whether two representations of canonical commutation relations are unitarily equivalent or not an approach based on integration in infinitely many dimensional spaces, that is on functional integration, is used. In this way it is endeavored to clarify the structure of functional integrals as well as of the representations. Separable canonical and certain nonseparable transformations are considered. (J.F.P.)

30949 MATHEMATICAL STRUCTURE OF THE B. C. S. MODEL FOR FINITE TEMPERATURES. Thiring, Walter (Univ., Vienna). Acta Univ. Wratislaviensis; No. 99, 202-18 (1968).

It is proven that the thermal Green functions are correctly described by the Bogoliubov Hamiltonian. It is shown that for Green functions of gauge invariant expressions where no averaging over the phase angle is necessary the B.C.S. Hamiltonian is equivalent to any Bogoliubov Hamiltonian. (J.F.P.)

30950 TCP, SPIN, AND STATISTICS, AND CONSISTENCY PROBLEMS FOR INFINITE-COMPONENT FIELDS. Todorov, I. T. (Joint Inst. for Nuclear Research, Dubna, USSR. Inst. of Physics, Sofia). Acta Univ. Wratislaviensis; No. 99, 219-42 (1968).

This is a review on the problems of TCP, spin and statistics and existence of nontrivial mass-spectrum in a theory of local infinite-component fields. Examples are given of free (local) fields, transforming under irreducible unitary representations of the "index group" SL(2,C) which violate spin and statistics for both integer and half-integer spins. Unitary Fermi fields satisfying the Klein-Gordon equation are constructed for the Majorana representations. For these representations an example is given of a free TCP-noninvariant local field. It is shown at what point the axiomatic proof of TCP and spin and statistics does not work when infinite-component fields are involved. A recent negative result of Grodsky and Streater on the possibility of having an infinite-component local field with nondegenerate mass values is formulated and discussed. (auth)

30951 ATTEMPT TO CONSTRUCT TEST-ALGEBRAS FOR HAAG-ARAKI FIELDS. Uhlmann, Armin (Karl-Marx-Univ., Leipzig). Acta Univ. Wratislaviensis; No. 99, 243-70(1968).

Included in the discussion of test algebras for Haag-Araki fields are the subalgebras of an extension of the algebra of test functions, pre-norms, the Banach algebras, positive linear forms, and elements bounded from below. (J.F.P.)

30952 THEOREM ABOUT COMMUTATOR FUNCTIONS AND ITS APPLICATIONS TO QUANTUM FIELD THEORY. Woronowicz, S. (Univ. of Warsaw). Acta Univ. Wratislaviensis; No. 99, 271-80(1968).

A theorem for the decomposition of a function into solutions of Klein-Gordon equations is presented. As an application an analog of the Heisenberg uncertainty relations is proven in the Haag-Araki theory. Also a simple proof is given of a special case of the Bogoliubov-Vladimirov theorem. (J.F.P.)

30953 AXIOMATIC APPROACH TO QUANTUM FIELD THEORY AND MANY BODY PROBLEM. VOLUME II. RELATED TOPICS. V Winter School of Theoretical Physics in Karpacz, February 17-March 2, 1968. Acta Univ. Wratislaviensis; No. 113, 1-291(1969).

There were eleven lectures included. Separate abstracts were prepared for all lectures. (J.F.P.)

For abstracts of individual lectures see: 30852, 30954-30962, and 31034.

30954 GRADIENT TERMS IN COMMUTATORS OF CURRENTS AND FIELDS. Kaellen, Gunnar (Univ. of Lund, Sweden). Acta Univ. Wratislaviensis; No. 113, 5-68(1969).

Some elementary properties of the vacuum expectation value of a product of two vector fields (or currents) are reviewed. In particular, it is emphasized that the appearance or nonappearance of certain terms involving space derivatives of a δ function in the equal time commutator between the time component and one space component of the field is not in contradiction with the canonical formalism when the coefficient in front of this gradient term is finite. When the coefficient involves a divergent integral as happens, e.g., in electrodynamics, a certain formal contradiction exists but is removed if the theory is considered as a consistent limit of a theory with a cut off. For the particular case of electrodynamics it is further pointed out that the coefficient of the gradient terms is related to the self mass of the photon which has to vanish in a consistent theory. (auth)

30955 APPROACH TO NONRENORMALIZABLE FIELD THEORIES. Filippov, A. T. (Joint Inst. for Nuclear Research, Dubna, USSR). Acta Univ. Wratislaviensis; No. 113, 69-91 (1969).

A brief review of the main results obtained in certain previous work is given. The approach used is essentially self-contained and definitely distinct from other approaches. The scattering on singular potentials as a model for renormalizable and nonrenormalizable theories, a rigorously treated simple approximation in field theory, and one exactly soluble model are considered. (J.F.P.)

30956 NONEQUILIBRIUM STATISTICAL MECHANICS AND QUANTUM FIELD THEORY. George, C. (Univ. Libre, Brussels). Acta Univ. Wratislaviensis; No. 113, 92-144 (1969).

A comprehensive survey is given of the general formalism of the statistical mechanics of irreversible processes, including the transformation theory to a quasi-particle description. The relation with quantum field theory is considered through the application of the standard techniques to a system interacting through a Lee-model Hamiltonian. A way of comparing this method with the usual S-matrix method is also examined. (J.F.P.)

30957 QUANTUM MECHANICAL N-BODY PROBLEM. Hepp, Klaus (Eidgenoessische Technische Hochschule, Zurich). Acta Univ. Wratislaviensis; No. 113, 145-81(1969).

An outline is given of how to prove from first principles, i.e. from the Schroedinger equation for a finite number of interacting particles, the existence of scattering states, the unitarity of the S-matrix, maximal analyticity in the physical region of scattering amplitudes and their cluster decomposition properties. The framework of scattering theory, a time-dependent approach to unitarity, and maximal analyticity are discussed. (J.F.P.)

30958 COMPOSITENESS AND VANISHING OF RENORMALIZATION CONSTANTS. Kaschluhn, F. (Humboldt Univ., Berlin). Acta Univ. Wratislaviensis; No. 113, 182-206(1969).

Compositeness conditions for partial wave two-body scattering amplitudes in the elastic approximation are studied for some simple but nontrivial models. The general relations in the N/D approach and the required field theory, the Zachariasen model in

which different dynamical limits are studied, and the pole model where the left-hand cut is approximated by a pole are treated. (J.F.P.)

30959 SINGULARITIES OF TWO-POINT GREEN FUNCTIONS, TWO-BODY FORCES, AND SOME REMARKS ABOUT THE RENORMALIZATION PROCEDURE. Lukierski, Jerzy (Univ. of Wroclaw) Acta Univ. Wratislaviensis; No. 113, 207-29 (1969).

Some examples are given of noncanonical singularities of the two-point Green functions, and it is emphasized that the standard laws of Coulomb and Yukawa are not valid for very small distances. It follows in particular that the conventional notion of charge and mass is not valid for very small distances. Dispersion relations in coordinate space, canonical and noncanonical singularities on the light cone, the reformulation of the Kaellen–Lehmann spectral representation, and two-body forces at very small distances are considered. No new results are presented. (J.F.P.)

30960 SOLUTION OF THE EQUATION OF EVOLUTION WITH TIME-DEPENDING HAMILTONIAN BY MEANS OF CONTINUOUS BAKER–HAUSSDORF FORMULA. Mielnik, B. (Univ. of Warsaw). Acta Univ. Wratislaviensis; No. 113, 246-8(1969).

The problem of finding explicitly the general term in the development of a solution of the equation of evolution is resolved. (J.F.P.)

30961 SOME REMARKS ON CANONICAL FORMULATION OF FIELD THEORY AND ITS GEOMETRIC STRUCTURE. Sniatycki, Jedrzej (Univ. of Warsaw). Acta Univ. Wratislaviensis; No. 113, 259-67(1969).

An attempt is made to clarify the notions that appear in the Hamiltonian formulation of field theory and in this way to deepen the understanding of what is really required from the theory in the canonical quantization procedure. Nonrelativistic dynamics in Lagrangian form, canonical formulation of the theory, and generalization to field theory are discussed. (J.F.P.)

30962 LOCALIZABLE AND NONLOCALIZABLE THEORIES. Voronov, B. L. (Lebedev Inst. of Physics, Moscow). Acta Univ. Wratislaviensis; No. 113, 268-91(1969).

A brief review is given of the basic ideas and results obtained for the connection between the concepts of spectrality and microcausality for permissible classes of quantum field theory, and the behavior of scattering amplitudes at high energies. (J.F.P.)

30963 QUANTUM MECHANICS AND THE GRAVITATIONAL RED SHIFT. Stoeckli, H. F. (Oxford Univ.). Proc. Cambridge Phil. Soc.; 69: Part 2, 315-18(Mar 1971).

It is shown that the formula for the gravitational red shift predicted by the theory of general relativity can also be derived by classical quantum mechanics combined with relativistic arguments. The agreement between the two derivations is a consequence of the separability of the time-dependent wave function, and of the first-order time differential in the wave equation. (auth) (UK)

30964 PARTICLE-LIKE OBJECTS IN A NONLINEAR FIELD THEORY. Muraskin, M. (Univ. of North Dakota, Grand Forks). Int. J. Theor. Phys.; 4: 49-53(1971).

The field theory introduced previously is further discussed. It is found possible for a component of the field to have a minimum at an arbitrary origin point as a consequence of the field equations. (auth) (UK)

30965 STRUCTURE OF THE FEYNMAN AMPLITUDE AND TESTS OF QUANTUM ELECTRODYNAMICS. Ringhofer, K. (Univ., Munich). Acta Phys. Austr.; 31: No. 1, 67-79(1970).

The two electron-n photon Feynman amplitude (which describes electron or positron Compton-scattering, electron–positron pair annihilation and electron–positron pair production with or without real photon radiative corrections) is expressed by the electron propagator and by Kroll's "intrinsic vertices." This representation of the Feynman amplitude is in accordance with extended gauge invariance (or gauge invariance of the second kind) and shows clearly the one-particle structure, but it is highly redundant if the two fermions are on the mass-shell. A change of the electron propagator can be compensated by a corresponding change of the intrinsic vertices, and a change of the off-shell parts of a certain intrinsic vertex can be compensated by a corresponding change of the higher order intrinsic vertices. Therefore, the on-shell amplitude can be expressed by the simplest possible electron propagator —(1/iq + m) and by simple "on-shell intrinsic vertices." As an immediate application tests of quantum electrodynamics are considered. The aim is to get information on possible modifications of the Feynman graph-rules under the assumption of extended gauge invariance. The analysis shows that at least to the first order of perturbation theory the above mentioned processes do not give information on the electron propagator and the (one- and more-photon) vertices. Only the on-shell intrinsic vertices can be tested. (auth)

30966 EQUATIONS OF MOTION INVARIANT UNDER THE GROUP P(1,n). II. Sokur, L. P.; Fushchich, V. I. (Inst. of Mathematics, Moscow). Teor. Mat. Fiz.; 6: 348-63(Mar 1971). (In Russian).

Equations are deduced which generalize the Dirac equation and are invariant relative to the rotations and translations in the (n + 1)-dimensional Minkowski space. The group-theoretical analysis of the equations obtained is carried out. P, T, and C properties of the equations are studied. (auth)

30967 MATRIX SPACE DYNAMICS TAKING INTO ACCOUNT THIRD-ORDER TERMS IN THE LAGRANGIAN. Baum, I. V.; Gorbatenko, M. V.; Romanov, Yu. A. (Moscow Inst. of Physics). Teor. Mat. Fiz.; 6: 338-47(Mar 1971). (In Russian).

General properties of the matrix space dynamics which were formulated previously are used in order to construct the Lagrangian taking into account the second as well as the third order terms by powers of the magnitude of deviation from the vacuum state. It is proved that all cubic terms in the expressions for physical quantities can be eliminated by means of a suitable invariant transformation. This corresponds to the absence of terms proportional to ψ^3 in the similar expressions of the spinor theory. (auth)

30968 S-MATRIX FOR FIELD THEORY WITH LAGRANGIAN DEPENDING ON DERIVATIVES. Braun, M. A.; Evlashev, Yu. A. (Leningrad State Univ.). Teor. Mat. Fiz.; 6: 318-27(Mar 1971). (In Russian).

The theory of a scalar quantum field with the interaction depending on derivatives is considered. The covariant expression for the S-matrix is obtained in terms of the interaction Lagrangian. The invariance of the theory under the point transformation of the field variables is shown. The modification of these results due to regularization procedure is investigated. (auth)

30969 PHENOMENOLOGICAL LAGRANGIANS IN QUANTUM FIELD THEORY. Il'ichev, N. A.; Prokhorov, L. V. (Leningrad State Univ.). Teor. Mat. Fiz.; 6: 305-17(Mar 1971). (In Russian).

It is shown that it is always possible in quantum field theory to construct such an effective interaction which gives the tree approximation scattering amplitude correct at all energies. Passing to the local interaction is discussed for massless as well as for massive particles. It is shown that there is no local effective interaction for massive particles. (auth)

30970 TRANSFORMATION OF GENERAL COVARIANT OBSERVABLE VALUES. Mitskevich, N. V.; Zakharov, V. N. (Patrice Lumumba Friendship of Nations Univ., Moscow. Moscow State Univ.). Dokl. Akad. Nauk SSSR; 195: 321-4(11 Nov 1970). (In Russian).

Use of Cartesian coordinates in the traditional formulation of the special theory of relativity is a convenient method to find physical observable values; however, the special theory may make use of any kind of coordinates, differing from the general theory of relativity only by the zero value of the space–time curvature. A. L. Zel'manov's concept of the chronometric invariant formalism was selected on the basis that the system of reading does not have to be related to a given coordinate system. The values in the general covariant approach were related to observable values in the readout system. The congruence of the universal readout lines determines the field of the unitary time-like vector and of a spatial metric tensor. The derivations indicated that the transformation laws of observable values in the general law of relativity, and for an arbitrarily moving readout system in the special theory, are a natural generalization of Lorentz's formula. (TTT)

30971 QUANTUM MECHANICS ON GROUP SPACE AND HUGYENS' PRINCIPLE. Dowker, J. S. (Univ. of Manchester, Eng.). Ann. Phys. (N. Y.); 62: 361-82(Feb 1971).

The quantum mechanics of a free particle moving on the Riemannian manifold, M, of a simple Lie group is discussed. It is shown that the quasiclassical approximation is exact and the propagator is calculated directly by two methods, the sum over classical paths and the stationary state methods, which are shown explicitly to be equivalent for the case of SU(n). The results are applied to the manifold ("space–time") which is the direct product of M and the linear time axis. It is shown that Huygens' principle is true only if the dimension of M is odd and then only if the mass occurring in the generalized Klein–Gordon equation equals one sixth of

XUM

the scalar curvature of M. It is suggested that this latter quantity be added in as a quantum potential to give the correct quantum Hamiltonian. (auth)

30972 SEMI-GROUP APPROACH TO QUANTUM FIELD EQUATIONS. Salusti, E. (Istituto Nazionale di Fisica Nucleare, Rome. Univ., Rome); Tesei, A. Nuovo Cim.; 2A: 122-38(1 Mar 1971).

Some field equations suggested by the Thirring and Federbush models in quantum field theory are studied in a two-dimensional space–time. The theory of nonlinear semi-groups is used. The unknowns are functions whose values are bounded operators on a Hilbert space. The existence and uniqueness of the global solution are proved. (auth)

30973 EQUAL-TIME COMMUTATORS AND BJORKEN'S THEOREM: GENERAL RESULTS, AND APPLICATIONS TO SOME FIELD-THEORETICAL MODELS. Collina, R.; Luzzatto, G. (Univ., Genoa. Istituto Nazionale di Fisica Nucleare, Genoa). Nuovo Cim.; 2A: 85-103(1 Mar 1971).

Two different definitions of the equal-time commutator matrix elements are considered. One analyzes the equivalence conditions for the definitions, and one derives an infinite-energy sum rule. The general results are considered for the Lee model: first, the model with a cut-off Λ is examined; next, the limit $\Lambda \to \infty$ is taken (point-source Lee model), and an answer is given to questions related to the meaning of various limit procedures. The directly renormalized version of the point-source Lee model is then analysed in the same context: the results are different, for reasons which are examined. Finally, the zero-energy value of a function relevant for the whole theory is studied. (auth)

30974 QUANTUM ELECTRODYNAMICS MULTIPERIPHERAL MODEL AT INFINITE MOMENTUM. Pardee, W. J. (Univ. of Illinois, Urbana). Phys. Rev., D; 3: 1655-66(1 Apr 1971).

The scattering amplitude for the production of an arbitrary number of electron-positron pairs is calculated in a multiperipheral quantum-electrodynamic model at infinite momentum. When electron and photon masses are neglected, it is possible to obtain a simple form for the partial cross sections. The leading s dependence obtained from direct calculation is in minor disagreement with that found by Cheng and Wu. The number distribution P(n), the average number of pairs produced, the two-particle and one-particle momentum distributions, and the "total" cross section are obtained. The two-particle distribution is expressed in terms of the invariant mass, total longitudinal momentum, and transverse momenta of the pair. The contribution of these processes to the absorptive part of the elastic amplitude is studied for small t. The infinite-energy result is a fixed cut in the complex angular momentum plane. (auth)

30975 ADDITIONAL INVARIANCE OF RELATIVISTIC EQUATIONS OF MOTION. Fushchich, V. I. (Inst. of Mathematics, Moscow). Teor. Mat. Fiz.; 7: 3-12(Apr 1971). (In Russian).

The additional (implicit) symmetry of equations invariant under the full Poincaré group is studied. It is shown that relativistic equations are invariant under the homogeneous de Sitter group O(1,4) (or 2,3)) and the matrix group O(4). (auth)

30976 TRANSFORMATIONS TO A ROTATING FRAME. Suzuki, M. Nature (London) Phys. Sci.; 230: 13(Mar 1971).

The apparent paradox considered previously on transformations to rotating co-ordinates is denied. It is stated that the use of Galilean transformations to define the coordinate system for the rotating frame is perfectly valid. The resulting equations are also valid but must be used and interpreted with caution. The time in these equations is not to be read from standard clocks in the rotating frame but from clocks in the inertial frame. Distances are not to be measured with standard rods, but are to be read off an xyz grid which corresponded to the inertial grid at t = 0. As further proof that no paradox exists one need only calculate the expression for the distance between two points in the rotating frame, as measured by standard rods, directly from the transformation equations. (UK)

30977 PROTON–PROTON AND PION–PROTON INELASTIC COLLISIONS AND ELECTROMAGNETIC FORM FACTORS. Sosnowski, R.; Wojcik, W. (Inst. of Nuclear Research, Warsaw). pp VI-25-44 of Proceedings of the Colloquium on High Multiplicity Hadronic Interactions. /Krzywicki, A. (ed.). Paris; Ecole Polytechnique (1970).

From Colloquium on high multiplicity hadronic interactions; Paris, France (13 May 1970). See CONF-700528.

A model for inelastic collisions is discussed in which Huygen's principle is assumed for each secondary particle, and the amplitude is equal to the Fourier transform of the interaction volume. For a single proton, the Fourier transform is taken equal to the proton form factor. The experimental data on pp and πp inelastic collisions are compared with the predictions of the model. The main features of the angular distributions of secondary particles are well reproduced. (France)

30978 QUANTUM ELECTRODYNAMICS AT SMALL DISTANCES. Pipkin, F. M. (Harvard Univ., Cambridge, Mass.). Essays Phys.; 2: 1-91(1970).

A review is given on the general structure of quantum electrodynamics, the evidence for the validity of the theory, and the prospects for resolving the incompleteness. (L.B.S.)

30979 GROUND STATE OF THE HAMILTONIAN IN THE SIMPLEST MODEL OF QUANTUM FIELD THEORY. Zastavenko, L. G. (Joint Inst. for Nuclear Research, Dubna, USSR). Teor. Mat. Fiz.; 7: 20-9(Apr 1971). (In Russian).

An example of quantum field theory with a degenerate ground state was considered previously. The simplest example of quantum field theory in two-dimensional space-time is investigated in detail from this viewpoint. The absence of nontrivial divergences makes the renormalization unnecessary and so all the considerations become more transparent and reliable. (auth)

30980 REGGEON CALCULUS DERIVED FROM THE EIKONAL MODEL. Cardy, J. L. (Cambridge Univ., Eng.). Nucl. Phys.; B28: 455-76(1971).

A reggeon calculus is derived from a hybrid perturbation-theory model using eikonal techniques. The resulting reggeon coupling functions have a simple form which enables many diagrams of interest to be evaluated explicitly. As an example, the properties of iterated Regge cuts are discussed and evaluated. Another important result is that the physical pomeron is not expected to have factorizable residues. (auth)

30981 EXTENSION OF THE EIKONAL APPROXIMATION IN QUANTUM FIELD THEORY. Cardy, J. L. (Cambridge Univ., Eng.). Nucl. Phys.; B28: 477-94(1971).

The eikonal approximation is extended to arbitrary Feynman diagrams, in a renormalized spinless theory. A set of rules is formulated, which gives the eikonal expression for any given set of diagrams. Features reminiscent of a parton model emerge. (auth)

30982 CONSEQUENCES OF THE ASSUMPTION THAT THE S-MATRIX COMMUTES WITH THE AXIAL CHARGE. Fabricius, K. (Univ., Hamburg). Nucl. Phys.; B28: 629-42(1971).

An attempt is made to derive the consequences of the assumption that the axial charge commutes with the S-matrix. Therefore some properties of the axial charge are first studied in perturbation theory and subsequently in a general manner. As a result of the above assumption the self-consistency condition of Adler and the universality of the two-pion isovector coupling are found. (auth)

30983 PROPER-TIME QUANTUM MECHANICS. II. Johnson, Joseph E. (Univ. of South Carolina, Columbia). Phys. Rev., D; 3: 1735-47(15 Apr 1971).

A previous investigation of a proper-time formulation of quantum mechanics based upon an extension of the Poincaré algebra is continued to include a four-vector position operator. The discrete operations of space and time inversion and particle conjugation are studied as groups of automorphisms which must also be supported by the representations of the extended algebra. Supporting representations and matrix forms of the inversions are studied in the content of a proper-time framework. Representations of the extended algebra are decomposed with respect to their constituent irreducible Poincaré representations, and for unique spin the representations (fields) are connected with those of Weinberg. The basis which exhibits the Poincaré content of a representation is studied, and the transformation to that basis is connected for spin $\frac{1}{2}$ to the Foldy–Wouthuysen transformation. The unique spin-$\frac{1}{2}$ representation of the extended algebra has a decomposition which accommodates the leptons in a very suggestive way. The leptons are distinguished from one another without "internal" quantum numbers. The physical mass spectrum (0, m_e, and m_μ) is both allowed and unexplained. The electromagnetic and weak currents assume a simple form. Certain aspects of the formulation of a proper-time field theory are also discussed. (auth)

30984 TROUBLES WITH STRICT CONFORMAL SYMMETRY. Boulware, David G.; Brown, Lowell S.; Peccei, R. D. (Univ. of Washington, Seattle). Contract AT(45-1)-1388. Phys. Rev., D; 3: 1750-4(15 Apr 1971).

Formal low-energy theorems for matrix elements involving the

stress tensor can be used to derive the differential equations that express scale and conformal invariance. It is shown that these equations, when applied to a single-particle matrix element of two fields, yield an integral representation that violates causality save for the trivial case where it reduces to the tree graphs of a free field. Although it is possible to construct conformally invariant, fully off-mass-shell amplitudes whose restriction to the mass shell yields a nontrivial result, these on-mass-shell amplitudes are not invariant under conformal transformations. This pathological behavior can be traced to an implicit assumption of analyticity when the stress tensor carries off small momenta that is, in general, false. (auth)

30985 QUANTIZATION OF $m^2 < 0$ FIELD EQUATIONS. Schroer, Bert (Univ. of Pittsburgh). Contract AT(30-1)-3829. Phys. Rev., D; 3: 1764-70(15 Apr 1971).

A causal covariant quantum field theory is constructed which corresponds to a classical field with $m^2 < 0$. "Pseudotachyons" or "jelly" states lead to a causal screening of "tachyon" states. (auth)

30986 SELF-CONSISTENT DERIVATION OF MULTIPLE MASS VALUES IN RENORMALIZED FIELD THEORIES. Caianiello, E. R. (CNR, Naples); Marinaro, M.; Scarpetta, G. Nuovo Cim.; 3A: 195-219(1 May 1971).

It is shown that the study of self-consistent renormalized models of the $g\phi^4$ theory, obtained by truncating it without destroying renormalizability, yields a nonlinear equation for the physical mass m_f. Already in the lowest possible approximation two possible and mutually exclusive values for m_f are found. The method is quite general, not limited to the $g\phi^4$ theory and seems well suited to a rigorous computation of mass spectra from field theories. A remarkable consequence of the multivaluedness of m_f is that, although the field equations stay invariant under arbitrary renormalization prescriptions, their solutions do not: renormalization parameters lose their indeterminacy and must be fixed from experiment. (auth)

30987 FEYNMAN-PARAMETER APPROACH TO N-TOWER EXCHANGE IN ϕ^3 THEORY. Hasslacher, B.; Sinclair, D. K. (State Univ. of New York, Stony Brook). Contract AT(30-1)-3668B. Phys. Rev., D; 3: 1770-81(15 Apr 1971).

Feynman-parameter techniques are used to investigate the asymptotic form of N-tower graphs in ϕ^3 theory. A detailed study of the two-tower case in the leading lns approximation agrees with the second-order piece of the eikonal expansion. By using certain assumptions about the N-tower case, an iterative scheme is developed for summing all N-tower exchanges. This generates the eikonal form outside of the framework of momentum-space techniques. Furthermore, only a limited class of structures contribute to the asympotic form: the Mandelstam nests. (auth)

30988 CONSISTENT QUANTIZATION OF THE YANG-MILLS FIELD: NOETHER'S THEOREM AND FACTOR-ORDERING PROBLEMS. Fickler, S. I.; Russo, M. (Aerospace Research Labs., Wright-Patterson AFB, Ohio). Phys. Rev., D; 3: 1782-96(15 Apr 1971).

The problem of obtaining a consistent quantization of the Yang–Mills field is examined by invoking the postulated Lorentz and gauge invariance of this theory. Because of the factor-ordering problems that arise from the nonlinear self-coupling of the theory, the Noether's theorem for these physical symmetries does not trivially follow from the invariance of the action. A set of necessary conditions is formulated for any consistent quantization of a nonlinear, non-Abelian gauge theory. (auth)

30989 HARTREE–FOCK APPROXIMATION IN QUANTUM ELECTRODYNAMICS. Gomberoff, L.; Tolmachev, V. (Univ. de Chile, Santiago). Phys. Rev., D; 3: 1796-1804(15 Apr 1971).

A new approach to the bound-state problem in the frame of quantum electrodynamics is proposed, with special emphasis on the electron–proton bound states. It is an alternative approach to the usual one, which is based on the Bethe–Salpeter equation, and does not contain the ambiguities and unfamiliar features inherent in the Bethe–Salpeter theory. This approach is based on a straightforward generalization to quantum electrodynamics of the well-known Hartree–Fock approximation for the nonrelativistic theory of many-electron atoms. (auth)

30990 NEW PICTURES IN QUANTUM MECHANICS. Perlman, H. S. (Oxford Univ.). Phys. Rev., D; 3: 1851-60(15 Apr 1971).

The familiar concept of a picture defined via restrictions on the effects of translations is extended by the introduction of a new class of what can be called rotation pictures, which are defined via restrictions on the effects of rotations. The behavior of operators and state vectors in these rotation pictures is deduced and the mode of transformation between different rotation pictures elucidated. The utility of the concept is illustrated by the construction of a rotation picture in which all operators behave like scalar operators in Lorentz space. (auth)

30991 DERIVATION OF EQUAL-TIME COMMUTATION RELATIONS IN A SELF-CONSISTENT QUANTUM FIELD THEORY. Rest, J.; Srinivasan, V.; Umezawa, H. (Univ. of Wisconsin, Milwaukee). Phys. Rev., D; 3: 1890-7(15 Apr 1971).

A self-consistent quantum field theory is proposed wherein the field equations for the Heisenberg fields are postulated. The Heisenberg fields are required to be linear combinations of normal products of the physical free fields, and the coefficients of the expansion are determined self-consistently. No a priori knowledge of the equal-time commutation relations among the Heisenberg fields is assumed. Using a solvable model, it is shown that local microscopic causality requires the existence of a bound state. (auth)

30992 CONSERVED CURRENTS, REGGEIZATION, AND MANDELSTAM COUNTING IN SECOND-ORDER PERTURBATION THEORY. Dicus, Duane A.; Teplitz, Vigdor L. (Massachusetts Inst. of Tech., Cambridge). Contract AT(30-1)-2098. Phys. Rev., D; 3: 1910-22(15 Apr 1971).

The spinor pole in second-order spinor-vector and spinor–axial-vector scattering is considered for all possible couplings and it is shown that, except for the vector γ^μ coupling, none of the amplitudes factor is considered. Therefore, only in the case of γ^μ coupling does the spinor lie on a nondegenerate Regge trajectory for all values of the coupling constant. The degeneracy in the case of the axial-vector $\gamma^\mu\gamma_5$ coupling is less than for the remainder of the couplings. The axial-vector pole in pseudoscalar-vector scattering is also considered and it is shown that for one particular pseudoscalar–vector–axial-vector coupling, the sense amplitudes factor. These results are reconciled with the Mandelstam counting procedure, and the effects of gauge invariance and isospin on factorization are investigated. (auth)

30993 LOCALLY GENERATED DILATATION CHARGE IN THE THIRRING MODEL. Lowenstein, J. H.; Schroer, B. (Univ. of Pittsburgh). Contract AT(30-1)-3829. Phys. Rev., D; 3: 1981-8(15 Apr 1971).

By applying a "normal-product quantization" the energy-momentum tensor of the Thirring model is constructed as a local function of the Thirring fields. It is shown that the commutation relation of the dilatation current with the field is anomalous, and that the space integrals converge on a dense set of states to the group generators. The appearance of anomalous dimensions for local products of Thirring fields is discussed in the special case of a bilinear mass interaction. (auth)

30994 INFINITY SUPPRESSION IN GRAVITY-MODIFIED QUANTUM ELECTRODYNAMICS. Isham, C. J.; Salam, Abdus; Strathdee, J. (International Centre for Theoretical Physics, Trieste, Italy). Phys. Rev., D; 3: 1805-17(15 Apr 1971).

Computations of gravity-modified quantum electrodynamics are performed using nonpolynominal Lagrangian field-theory techniques. The inverse of the gravitational constant appears as an effective cutoff mass, and, in particular, it is shown that to order e^2 the electron and photon self-energies are finite. The cutoff can be interpreted as if the electron had an intrinsic radius equal to its Schwarzschild radius. A central feature is the construction of the tensor gravity superpropagator. (auth)

Gravitation and General Relativity

Refer also to abstract 30994.

30995 (JINR-P13-5685) POSSIBLE MEASUREMENT OF THE VELOCITY OF PROPAGATION OF GRAVITATIONAL INTERACTION. Vasil'ev, B. V. (Joint Inst. for Nuclear Research, Dubna (USSR). Lab. of Neutron Physics). 1971. 7p. (In Russian). Dep. NTIS (U. S. Sales Only).

The motion of a test body inside the system of oscillating masses in laboratory conditions is considered. It is shown that at the expense of the gravitational interaction with moving masses the test body acquires acceleration the magnitude of which can be sufficient for measuring the delay of the gravitational interaction and for determination of the velocity of gravitation propagation. (auth)

30996 INERTIAL REFERENCE FRAMES IN EINSTEIN'S THEORY OF GRAVITATION. Audretsch, J. (Univ., Freiburg i. B.). Int. J. Theor. Phys.; 4: 1-9(1971).

XUM

A physical definition of the inertial reference frame (IRF) is given, and the properties of solutions of the Einstein equation (with cosmological constant Λ), which admit an IRF (IRF solutions) are investigated. Their Petrov type is uniquely determined by the viscous stress tensor. Only the types I, D or 0 are possible. The unique vacuum IRF solution is the Minkowski spacetime. The unique IRF solution belonging to a perfect fluid is the Einstein universe. Λ is of special importance. For $\Lambda = 0$, the only physically admissible IRF solution is the Minkowski spacetime. For $\Lambda \neq 0$, only interior solutions with strong restrictions for density and pressure are possible. (auth) (UK)

30997 ENERGY–MOMENTUM–STRESS TENSOR AND GRAVITATIONAL FIELD OF UNIFORMLY ROTATING MASSES. Frehland, Eckart (Univ., Freiburg i. B.). Int. J. Theor. Phys.; 4: 33-40(1971).

Beginning with a general ansatz for the energy-momentum-stress tensor of masses in uniform rotation the energy tensor and the gravitational field of two particular systems are determined uniquely; namely, a thin, rotating, hollow cylinder and a spinning rod (dumb-bell). All calculations are made within the framework of linearised theory, but no restriction is made upon angular velocity, except that given by the velocity of light. (auth) (UK)

30998 CONSERVATION OF e/m IN GENERAL RELATIVITY. Komar, Arthur (Yeshiva Univ., New York). Int. J. Theor. Phys.; 4: 45-7(1971).

It is shown that when classical charged particles move under the influence of their mutual gravitational and electromagnetic forces, the charge-to-mass ratio of each particle remains constant in the particle's instantaneous rest frame, despite the fact that in general the particles are accelerating and therefore presumably radiating energy. (auth) (UK)

30999 NOTE ON THE WEAKENED FIELD EQUATIONS. $R_{ijk} - R_{ikj} = 0$. Swami, S. P. (Univ. of Poona). Indian J. Pure Appl. Math.; 1: 485-91(Oct 1970).

Three solutions of a weakened set of field equations $R_{ijk} - R_{ikj} = 0$ with $R_{ij} \neq 0$ and $R_{ij} \neq \lambda g_{ij}$ are given, and some of the geometrical and dynamical aspects of these solutions are considered. The differential equations of the field for a general spherically symmetric metric which are given are useful for finding more general solutions. (auth)

31000 GRAVITATIONAL FIELD EQUATIONS. Rastall, P. (Univ. of British Columbia, Vancouver). Can. J. Phys.; 49: 678-84(15 Mar 1971).

An earlier, scalar theory of gravitation is assumed to be valid for a class of static gravitational fields. The theory is written in tensor form, and generalized to the case of an arbitrary gravitational field. The interaction between the field and its sources is discussed, and the linearized form of the field equations is derived. Some possible alternative field equations are considered which are compatible with the linearized Einstein equations. (auth) (Canada)

31001 REMARKS ON GUPTA'S QUANTIZATION OF THE WEAK GRAVITATIONAL FIELD. Peet, F. G. (Univ. of British Columbia, Vancouver). Can. J. Phys.; 49: 831-6(1 Apr 1971).

The two quantum theories developed by Gupta for the weak gravitational field are reviewed. A third formalism is given in which it is assumed that there are only ten field variables. A difficulty is encountered when one attempts to construct graviton number operators. A contact transformation of the field variables is used to resolve the difficulty. The expressions obtained for the graviton propagator and the energy, momentum, and spin of the gravitons agree with the results of Gupta. (auth) (Canada)

31002 SPIN-TWO MASSLESS-PARTICLE RADIATION AS A GRAVITATIONAL EFFECT. Good, R. H. Jr. (Ames Lab., Iowa). Ann. Phys. (N. Y.); 62: 590-601(Feb 1971).

The theory for a spin-two massless-particle field interacting with sources is developed, in parallel with Maxwell's theory for photons interacting with charges. In the spin-two case there are two fields E_{ij} and B_{ij} which are symmetric traceless tensors of opposite parity. Whereas a Maxwell source must be a conserved current, the spin-two source is built up in a certain way from a conserved stress-energy–momentum tensor. Polarization effects of the radiation are much the same as for electromagnetic fields; there are plane polarized, circularly polarized, and intermediate cases possible. It is suggested that a nonrelativistic test object detects the radiation through the effect of the E_{ij} field on the object's quadrupole and octupole moments. (auth)

31003 APPROACH TO QUANTIZATION OF GENERAL RELATIVITY. Geroch, Robert (Univ. of Texas, Austin). Ann. Phys. (N. Y.); 62: 582-9(Feb 1971).

A proposal which may lead to a quantum theory of the gravitational field is discussed. The states and operators emerge as certain scalar and vector fields on an infinite-dimensional manifold G of classical solutions of Einstein's equations. It is shown that the formalism essentially reproduces quantum electrodynamics when G is replaced by the space of square-integrable solutions of Maxwell's equations. (auth)

31004 NOTE ON GENERALIZED FIELD EQUATIONS IN GENERAL RELATIVITY. Dadhich, Naresh (Univ. of Poona). Indian J. Pure Appl. Math.; 1: 502-5(Oct 1970).

A system of the generalized field equations proposed previously is further modified by the inclusion of the cosmical constant. A tensor T_{pklm} possessing the same symmetry properties as the curvature tensor R_{pklm} is introduced. The equations were studied for the first time with reference to spherically symmetric metrics and an interesting linear relationship was obtained between the components of T_{pklm} and the curvature components. For the generalized equations the condition for a perfect fluid and the equations defining p and ρ are obtained. The analog of the usual divergence equations for material distribution is also obtained. These results may be of interest with reference to the study of implosion and of distributions of superdense matter. (auth)

31005 GRAVITATIONAL FIELD EQUATIONS. Rastall, Peter (Univ. of British Columbia, Vancouver). Can. J. Phys.; 49: 678-84(15 Mar 1971).

An earlier scalar theory of gravitation is assumed to be valid for a class of static gravitational fields. The theory is written in tensor form and generalized to the case of an arbitrary gravitational field. The interaction between the field and its sources is discussed, and the linearized form of the field equations is derived. Some possible alternative field equations are considered which are compatible with the linearized Einstein equations. (auth)

31006 APPLICATIONS OF THE SPECIAL COORDINATE CONDITIONS IN EINSTEIN GRAVITATIONAL THEORY. Shirokov, M. F. (Moscow Aviation Inst.). Dokl. Akad. Nauk SSSR; 195: 814-17(1 Dec 1970). (In Russian).

Einstein's gravitational equations are characterized by the fact that they are not a complete system as only six coordinate conditions of the 10 are determined. Selection of these conditions depends on the convenience of solution of the problem under consideration; for instance, in astronomical studies, the so-called harmonic coordinates are most widely used. In order to extend this further, a special coordinate condition was developed, using pseudotensors of energy and the gravitational field momentum concepts. Although it appeared at first that because of their nonlinear character these coordinate conditions are difficult to handle, it was found that they satisfy precise solutions, such as Schwarzschild's, Einstein, and Rosen's, and Perez's solutions. Transition to coordinates which satisfy the required conditions may be achieved by simple coordinate transformation. The system allows one to solve Einstein's gravitational equation in the new system of coordinates. Several physical conclusions were drawn from the theoretical considerations. (TTT)

31007 DETECTION OF GRAVITATIONAL WAVES. Weber, Joseph. Sci. Amer.; 224: No. 5, 22-9(May 1971).

Specially designed equipment was set up in two widely separated locations for the detection of gravitational waves. These locations are the University of Maryland and Argonne National Laboratory. It was found that simultaneous increases in the output of detectors at the two sites provided evidence for the existence of bursts of gravitational radiation emanating from the direction of the center of the galaxy. These experiments are described, and some of the explanations of the results obtained are summarized. (J.F.P.)

31008 GRAVITATIONAL FIELD EFFECT ON EMISSION OF RELATIVISTIC CHARGES. Pargamanik, L. E.; Dimanshtein, F. A. (Kharkov State Univ.). Ukr. Fiz. Zh. (Russ. Ed.); 15: 2081-3(Dec 1970). (In Russian).

The strong influence of weak variable gravitation fields on the emission from relativistic charged particles was used in detection and studies of gravitational waves. A mathematical analysis is given of the influence of a plane gravitational wave on the synchrotron emission from charged particles in cyclic accelerators. (R.V.J.)

31009 EQUIVALENCE PRINCIPLE FOR MASSIVE BODIES. IV. PLANETARY BODIES AND MODIFIED EOETVOES-TYPE

EXPERIMENTS. Nordtvedt, Kenneth (Montana State Univ., Bozeman). Phys. Rev., D; 3: 1683-9(15 Apr 1971).

Employing a model of massive bodies as made up of an equilibrium assembly of particles interacting with each other via both gravitational and nongravitational forces, the gravitational-to-inertial-mass ratio (M_g/M_i) is calculated for the massive body. An expression for M_g/M_i is obtained which is in agreement with a previously derived expression valid for pure gravitational systems. Also it is found that a body supported at rest on a massive body (e.g., a laboratory on Earth) is accelerated by an external body (e.g., the Sun) at the same rate as the massive body (e.g., the Earth) in general relativity but not in other gravitational theories such as the scalar-tensor gravitational theories. (auth)

31010 SCALE INVARIANCE OF THE SECOND KIND AND THE BRANS–DICKE SCALAR–TENSOR THEORY. Anderson, James L. (Stevens Inst. of Tech., Hoboken, N. J.). Phys. Rev., D; 3: 1689-91(15 Apr 1971).

Invariance of the Brans–Dicke scalar-tensor theory of gravity under scale transformations of the second kind is discussed. It is shown that the requirement of scale invariance of the second kind leads to the unique value $-\frac{3}{2}$ of the adjustable parameter ω in the Brans–Dicke theory. It is further shown that, in order to obtain a consistent set of equations, matter must be coupled to the scalar-tensor field in such a way that the whole theory can be transformed into the usual Einstein tensor theory. This is accomplished by performing a space–time dependent scale change such that the transformed scalar field is everywhere a constant. (auth)

31011 ELECTROMAGNETIC FIELD AND WAVE PROPAGATION IN GRAVITATION. Mo, Tse Chin; Papas, C. H. (California Inst. of Tech., Pasadena). Phys. Rev., D; 3: 1708-12(15 Apr 1971).

From the physical three-vector Maxwell equations for an electromagnetic (E.M.) field in static gravitation, the artifice of replacing the gravitation by an equivalent medium is examined and modified Debye potentials are found for an E.M. wave in a simple, angularly homogeneous, material medium in a Schwarzschild gravitational field. The fact that these potentials do not obey the generalized scalar wave equation implies that gravitation scatters the vector E.M. wave and a scalar wave differently. Also, the amplitude and eikonal equations are obtained and solved by perturbation for a high-frequency wave in a weak spherical gravitational field. To the order M/r, the state of transverse polarization does not change along a ray path whereas the transverse-field amplitudes are modified by the factor $e^{M/r}$ which strengthens the field near the mass. The longitudinal-field amplitude, on the other hand, is modified by $e^{-M/r}$. These effects, in principle, may provide a further test of classical E.M. theory and general relativity. (auth)

Scattering Theory

Refer also to abstracts 30957, 30958, 30962, 30968, 30980, and 31434.

31012 (COO–264–571) COMPLEX NEGATIVE SIGNATURE TRAJECTORIES AND THE POMERANCHUK THEOREM. Oehme, Reinhard (Chicago Univ., Ill.). Jan 1971. Contract AT(11-1)-264. 14p. (FFI–71–3). Dep. NTIS.

Within the framework of complex angular momentum methods, it is shown that amplitudes which violate the Pomeranchuk theorem require negative signature trajectories which are of the form $\alpha(t) = 1 \pm \text{const.}\sqrt{t} + 0(t)$ near $t = 0$. There must be corresponding positive signature trajectories. The character of the singular surfaces with negative signature is discussed briefly. (auth)

31013 (ITEF–782) INVARIANTS OF THE ROTATION GROUP. Marinov, M. S.; Roginskii, V. I. (Gosudarstvennyi Komitet po Ispol'zovaniyu Atomnoi Energii SSSR, Moscow. Institut Teoreticheskoi i Eksperimental'noi Fiziki). 1970. 39p. (In Russian). Dep. NTIS (U. S. Sales Only).

Any quantity transforming under an irreducible representation of the space rotation group may be realized in three forms: as a multispinor $x_{\alpha_1 \ldots \alpha_{2l}}$; as a 3-tensor $t_{i_1 \ldots i_{2l}}$ (for 2l even) or tensor-spinor $t_{\alpha i_1 \ldots i_{2l}}$ (for 2l odd); as an l-spinor $\psi^{\lambda}_{\frac{1}{2}}$ ($\lambda = -l, \ldots, l$). Only one invariant may be constructed of three quantities of a given type; so the three invariants are equal up to a numerical factor that is found in the work. A number of invariants may be constructed of four quantities, not all of them independent. For applications it is of importance to be able to construct an independent set of invariants of every type, as well as to relate the invariants of different types. This problem is solved for arbitrary angular momenta l_1, l_2, l_3, l_4. (auth)

31014 (JINR–E2–5746) RETARDED PART OF THE TWO-TIME GREEN FUNCTION AND TWO-BODY RELATIVISTIC PROBLEM. Kvinikhidze, A. N.; Stoyanov, D. Ts. (Joint Inst. for Nuclear Research, Dubna (USSR). Lab. of Theoretical Physics). 1971. 17p. Dep. NTIS (U. S. Sales Only).

It is shown that the retarded part of the two-time Green function is sufficient for the complete description of the two-body relativistic system. The quasipotential type equations are obtained for the relativistic scattering amplitude and wave function of two particles with arbitrary spins. (auth)

31015 (MIT–2098–726) DUALITY AND DUAL MODELS. Veneziano, G. (Massachusetts Inst. of Tech., Cambridge. Weizmann Inst. of Science, Rehovoth (Israel). Dept. of Nuclear Physics). [1970]. Contract AT(30-1)-2098. 28p. (CONF-700806–58). Dep. NTIS.

From fifteenth international conference on high energy physics; Kiev, USSR (26 Aug 1970).

A qualitative review of duality over the past two years is given. The general aspects of duality, dual models in the tree approximation, and beyond the tree approximation are discussed. (J.F.P.)

31016 (NYO–1932(2)–192) METHOD FOR COMPUTING SCATTERING MATRIX ELEMENTS IN A CLASS OF NON-RENORMALIZABLE FIELD THEORIES. Christ, N. H. (Columbia Univ., New York. Dept. of Physics). [1971]. 11p. (CONF-710106–8). Dep. NTIS.

From Conference on fundamental interactions at high energy; Coral Gables, Fla. (20 Jan 1971).

A method which can be applied to obtain definite results is discussed which is applicable to a class of nonrenormalizable field theories in which the nonrenormalizable coupling can be written in an exponential form. A theory is considered containing two scalar particles whose interactions are described by the Lagrangian density. (J.F.P.)

31017 OUTLINE OF SCATTERING THEORY FOR ABSORPTIVE POTENTIALS. Bertero, M.; Dillon, G. (Univ., Genoa. Istituto Nazionale di Fisica Nucleare, Genoa. Centro di Matematica e di Fisica Teorica, Genoa). Nuovo Cim.; 2A: 1024-38 (21 Apr 1971).

The time-dependent scattering theory is developed in the case of a complex spherically symmetrical potential. In particular the wave operators and the scattering matrix are obtained. Some pathologies, due to the fact that the Hamiltonian is not self-adjoint, are also discussed and their physical interpretation is attempted in the framework of the optical model. (auth)

31018 SYMMETRY PROPERTIES, TESTS, AND REDUCTION OF THE CROSSING MATRIX. Daboul, Jamil (Temple Univ., Philadelphia). Ann. Phys. (N. Y.); 62: 492-543(Feb 1971).

Symmetry properties of the crossing matrix are derived from general symmetry arguments. These properties can be used to test the known crossing matrices, and to reduce the crossing matrix into two or more submatrices, such that one submatrix connects "symmetry-conserving" amplitudes of the s and t channels with each other, whereas the other submatrix connects only the "symmetry-breaking" amplitudes of the two channels with each other. In addition, the crossing matrices are derived for the crossing of any two particles. Furthermore, in the appendices the exact symmetry relations of the c.m. helicity amplitudes under T, CPT, E_{12}, E_{34}, and E for general reactions are derived using consistent intrinsic phases. (L.B.S.)

31019 WAVE AND SCATTERING OPERATORS FOR SINGLE-CHANNEL SYSTEMS. Pearson, D. B. (Univ. of Hull, Eng.). Nuovo Cim.; 2A: 853-80(21 Apr 1971).

A definition is proposed of integrals of the form $\int_{-\infty}^{\infty} L(\lambda)\, dE_\lambda$, where $L(\lambda)$ is a family of linear operators and $\{E_\lambda\}$ is a resolution of the identity. If we assume the wave and scattering operators of time-dependent scattering theory to exist, these operators can be rigorously expressed, for a wide class of scattering systems, in terms of integrals of the above kind, each integration corresponding to a momentum variable being placed on the energy shell. If the arguments are applied to potential scattering, assuming the potential function to be square-integrable, the familiar expressions for the wave and scattering operators in terms of partial-wave T-matrix elements are rigorously derived. (auth)

31020 COMMUTATORS NEAR THE LIGHT CONE, BJORKEN LIMITS, AND O_4 EXPANSION. STUDY OF LADDER MODELS.

XUM

Gatto, R.; Menotti, P. (CERN, Geneva). Nuovo Cim.; 2A: 881-910(21 Apr 1971).

A method based on O_4 expansion of the t = 0 Compton amplitude is developed to discuss the light-cone behavior of the matrix element of a current commutator. The behavior of the O_4 partial waves at small distances is related to properties of scaling of the Compton amplitude. A number of dynamical situations are discussed, in the frame of a ladder model, exhibiting corresponding structures of light-cone singularities. Both scale-invariant and non-scale-invariant behaviors are obtained. The deep Regge limit is obtained and questions related to the appearance of logarithms and of fractional powers in Wilson's expansion near the light-cone are considered. Logarithms appearing in the perturbation expansion are found in particular cases to sum up to non-integer powers. Equal-time commutators of currents with their derivatives are discussed. (auth)

31021 CONSTRUCTIVE DETERMINATION OF THE S-MATRIX FOR SINGULAR POTENTIALS. Stroffolini, R. (Univ., Ferrara, Italy). Nuovo Cim.; 2A: 793-828(21 Apr 1971).

A constructive method is developed for the determination of the S-matrix for singular potentials. The method is illustrated by giving a detailed application to the case of potentials g/r^q (q even) and its application to potentials with q odd is outlined. A brief discussion is given of the case of finite superposition of these potentials. (auth)

31022 DUALITY DIAGRAMS AND THE POMERON. Delbourgo, R.; Rotelli, P. (Imperial Coll. of Science and Tech., London). Nuovo Cim.; 2A: 67-84(1 Mar 1971).

A model for the pomeron is suggested, based upon an interpretation of all planar quark diagrams. The model involves as a subclass those "legal" diagrams used to generalize the Veneziano model to supermultiplet scattering. In consequence the definition of duality is enlarged and more specifically the Harari-Freund identification of resonances with Regge poles and pomeron with background is modified. (auth)

31023 COVARIANT FORMULATION OF THE SATURATION PROBLEM FOR EQUAL-TIME COMMUTATORS. Dahmen, H. D. (Univ., Heidelberg. Kernforschungszentrum, Karlsruhe, Ger.); Rothe, K. D. Nuovo Cim.; 2A: 1-10(1 Mar 1971).

An approximate saturation of the equal-time commutators taking into account the one-particle intermediate states and related disconnected parts, as well as disconnected parts of two-particle states, leads to an equation which has no solution unless one resorts to a specific, though arbitrary Lorentz frame. The resolution of the problem is found by a careful evaluation of the remaining integral over the higher intermediate states. The equation obtained this way is reformulated, under certain assumptions, as a covariant dispersion relation for weak amplitudes. (auth)

31024 INFINITE-COMPONENT FIELD THEORY AND THE VENEZIANO MODEL. Yang, Ying-chuan (National Tsing Hua Univ., Hsinchu, Taiwan). Lett. Nuovo Cim.; 1: 495-9(20 Mar 1971).

A model of an infinite-dimensional Veneziano amplitude that has the unitary properties is proposed. The Bethe-Salpeter equation is used in a group-theoretic algebraic form, which gives solutions of an infinite discrete series and a continuous supplementary series. A Veneziano amplitude containing an infinite satellite term plus a continuous cut contribution is suggested. A unitary, dynamic equation of the scattering amplitude is obtained. (L.B.S.)

31025 INTEGRAL REPRESENTATIONS OF THE EXPANSIONS OVER WIGNER FUNCTIONS. Ezhela, V. V. (Inst. of High Energy Physics, Serpukhov, USSR). Teor. Mat. Fiz.; 7: 35-44(Apr 1971). (In Russian).

The detailed deduction of integral representations, which relate the series over Wigner functions with the corresponding power series, is given. Some properties of these integral transformations are studied. The analytical continuation problem for the expansions over Wigner functions is reduced to the same problem for power series. (auth)

31026 GENERALIZATIONS OF THE JOST-PAIS THEOREM FOR NONLOCAL POTENTIALS. Singh, Y.; Warke, C. S. (McMaster Univ., Hamilton, Ont.). Can. J. Phys.; 49: 1029-34(15 Apr 1971).

General expressions for the Jost function of a nonlocal central potential in any angular momentum state are derived, and generalized when there is a tensor component in the nonlocal potential. The connection of the Jost function to the Fredholm determinants and are generalizations of the Jost-Pais theorem for the corresponding local case. (auth) (Canada)

31027 ANALYTICITY CONSTRAINTS AND RESIDUE FUNCTIONS OF E_2 POLE EXCHANGE. Hadjioannou, F. T.; Papargyropoulos, P. H. (Univ., Athens). Nucl. Phys.; B28: 407-15(1971).

The analyticity constraints of the spectral functions of the E_2 representation of unequal mass scattering amplitudes at light-like momentum transfers are considered. Using these constraints the number of independent couplings, or residue functions, of the E_2 representation poles are reduced. (auth)

31028 CROSSING-SYMMETRIC EXPANSIONS OF SCATTERING AMPLITUDES, THRESHOLD BEHAVIOR, AND ASYMPTOTICS. Macfadyen, N. W. (Carnegie-Mellon Univ., Pittsburgh); Winternitz, P. Contract AT(30-1)-3829. Phys. Rev., D; 3: 1874-9(15 Apr 1971).

A two-variable, explicitly crossing-symmetric expansion of the scattering amplitude is discussed for the two-body scattering of spinless particles (with arbitrary masses). It converges simultaneously in the physical regions of at least two channels, has the correct threshold behavior, and allows for amplitudes growing asymptotically as arbitrary powers of s and t. The expansion is based on the representation theory of the group 0(2,1) in a basis not corresponding to any subgroup reduction and making use of Lamé functions. (auth)

31029 CHARACTERISTICS OF A REGGE TRAJECTORY WITH A FINITE ASYMPTOTIC PHASE. Sivers, Dennis (Univ. of California, Berkeley). Phys. Rev., D; 3: 2275-82(1 May 1971).

The hypothesis that the width of a resonance on a leading Regge trajectory is proportional to its mass is compared with the alternative that high-spin resonances become very stable. When the width grows with the mass, it is observed that the kinematics allow decay channels to have low orbital angular momentum. The dynamical implications of this observation are discussed. (auth)

31030 ANALYTICITY OF A SCATTERING AMPLITUDE IN AN EXTERNAL-MASS VARIABLE. Sullivan, J. D. (CERN, Geneva. Univ., Rome. Univ. of Illinois, Urbana); Potter, W. T. Nuovo Cim.; 3A: 93-115(1 May 1971).

The analyticity in an external-mass variable of a four-point function is studied by looking at simple perturbation theory diagrams. This analyticity information is required in order to apply models like vector-meson dominance and PCAC to two-body scattering amplitudes. A complex singularity is found on the physical sheet but at high energies it moves far from the physical region. The role of these singularities in nuclear shadowing is briefly discussed. (auth)

31031 REGGE TRAJECTORIES FOR MULTICHANNEL POTENTIAL SCATTERING. Capri, A. Z.; Kreuzer, H. J.; Teshima, R. (Univ. of Alberta, Edmonton). Nuovo Cim.; 3A: 135-57(1 May 1971).

Regge trajectories for nonrelativistic multichannel potential scattering are discussed and trajectories are calculated numerically for two models involving separable potentials. It is found that, for an N-channel problem with bordered interaction, N physical trajectories may occur. One of these trajectories, which results from coupling only, tends to "straighten out" in a Re l vs. E plot as the channel number N is increased. All other trajectories tend to resemble one-channel trajectories. A detailed discussion of the analytic continuations involved is also given. (auth)

31032 FOUR-PARTICLE FADDEEV EQUATIONS WITH A SIMPLE KERNEL. Riordan, F. (Birmingham Univ., Eng.). Nuovo Cim.; 3A: 53-81(1 May 1971).

A set of twelve coupled equations gives the four-particle transition operator. The kernel involves three- and two-particle transition operators only and not convolutions of two-particle transition operators as in other treatments. The four-particle transition operator satisfies two-particle unitarity in each two-particle channel. An extension of the concept of a four-particle resolvent operator is given which may simplify the many-body equations. (auth)

31033 LANDAU SINGULARITIES IN MULTI-REGGE THEORY AND FIXED-ANGLE BEHAVIOUR. Goddard, P.; White, A. R. (Cambridge Univ., Eng.). Nuovo Cim.; 3A: 25-44(1 May 1971).

A study of the implications of the Landau singularity structure in multi-Regge theory is begun. The incorporation of a physical-region pole in the three-Reggeon description of the six-particle amplitude is considered. Triple-Regge limits are found to involve fixed-angle limits of the four-particle amplitudes appear-

XUM

ing in the residue of the pole. It is shown that under certain conditions the presence of the physical-region pole necessitates an "undesirable" set of angular-momentum singularities of the form $l_1 + l_2 + l_3 = \text{const}$. Exponential decrease of the four-particle amplitude at fixed angle is then considered and it is shown that some examples of such behavior including those most favored by experimental results, do not necessitate these singularities. (auth)

31034 ANALYSIS OF PHYSICAL PROCESSES INTO PRIMITIVE PARTS. Rayski, Jerzy (Jagiellonian Univ., Krakow). Acta Univ. Wratislaviensis; No. 113, 249-58(1969).

A program is given for determining whether there exists a nontrivial quantum theory of scattering satisfying the following postulates: invariance with respect to the Poincare group, gauge invariance, microcausality, and unitarity of the scattering matrix. (J.F.P.)

Particle Accelerators

Refer also to abstracts 29126, 29371, 29400, 29404, 29528, 30500, 31008, and 31178.

31035 (BNL–15722) TAMING THE WILD FERRITE: A PROPOSAL FOR STABILIZING THE NEW AGS FERRITE CAVITIES. Rakowsky, G.; Tranis, A. (Brookhaven National Lab., Upton, N. Y.). 11 Mar 1971. 15p. Dep. NTIS.

In the course of developing the new accelerating cavities for the AGS Conversion, it has been necessary to study in detail the nonlinearities inherent in ferrite materials. It has been shown that the dependence of effective permeability on the amplitude of rf flux density, coupled with a high Q, may result in instability of the rf cavity. The new ferrite rings, and in fact, the new prototype cavity of the AGS Conversion Project, exhibit the predicted instability. The theory is reviewed (present data on the characteristics of the new Philips 4L2 ferrite being employed), and the predicted behavior of the new cavities is described. It is shown that the instability can be suppressed by shunting the ferrite cavity with an appropriate damping resistance. Coincidentally, this damping resistance can serve a second useful purpose, namely to level the rf input power and allow a good match to the transmission line over the band of operation. The synthesis of the damping network is presented and a practical realization is proposed. (auth)

31036 (CEAL–1053) SEMI-ANNUAL REPORT FOR THE PERIOD JANUARY 1–JUNE 30, 1970. (Cambridge Electron Accelerator, Mass.). 30 Nov 1970. Contract AT(30-1)-2076. 56p. Dep. NTIS.

Data on accelerator operation for experimenters shows that the total number of delivered prime-user hours and parasite-user hours in the first half of 1970 was 4502. The number of delivered prime-time hours was 2628 compared to 3018 originally scheduled; the delivery factor was 0.87. The 18 experiments that were underway are described. Progress on the development of the colliding beam facility in which electron and positron beams, each with an energy of 3.5 GeV, will collide with an available energy of 7.0 GeV in the center-of-mass system is summarized. By the end of June, stored electron and positron beams had been accumulated with peak currents of 25 and 11 mA respectively. Changeover from cycling mode storage to dc storage was accomplished with an efficiency exceeding 90% at peak beam currents of 3 mA or less. Unacceptable losses still occurred at large beam intensities. (As of November 1970 this loss problem had been cured.) A dc-stored-beam 1/e lifetime of two hours was achieved. Electron beams were switched into the bypass successfully, with a 1/e lifetime of 45 minutes. Construction of the components of the core of the on-line detector was nearly completed and tests with 3-GeV positron beams from the accelerator showed the performance to be in accord with expectations. Progress was made on the design and construction of second-generation detectors. Theoretical studies, design studies of a miniature storage ring for producing light of very high monochromaticity, and the development of equipment for producing a beam of polarized electrons are discussed. Also safety and training programs are outlined, and the major publications are listed. (auth)

31037 (JINR–P9-5669) CALCULATION AND GENERATION OF THE MAGNETIC SYSTEM OF THE MONOENERGETIC CYCLOTRON. Vorozhtsov, S. B.; Zaplatin, N. L. (Joint Inst. for Nuclear Research, Dubna (USSR). Lab. of Nuclear Problems). 1971. 10p. (In Russian). Dep. NTIS (U. S. Sales Only).

The stages of formation of the magnetic field in the model of the accelerator sector electromagnet on a 1:10 scale are given. The configuration of the magnetic circuit was chosen in the process of calculations and experiments. (auth)

31038 (JINR–P9-5677) COHERENT FREQUENCIES OF TRANSVERSE OSCILLATIONS IN THE ELECTRON MODEL OF A RING CYCLOTRON. Kochkin, V. A.; Novikov, D. L.; Onishchenko, L. M. (Joint Inst. for Nuclear Research, Dubna (USSR). Lab. of Nuclear Problems). 1971. 18p. (In Russian). Dep. NTIS (U. S. Sales Only).

The calculated values of the frequencies of transverse oscillations in the beam center are presented for several variants of a magnetic field as well as the results of experimental determination of these frequencies by the resonance knockout method. (auth)

31039 (JINR–P9-5714) SOME PROBLEMS OF CHOOSING AND CALCULATING THE FOCUSING SYSTEM OF 30 MeV LINEAR INDUCTION ACCELERATOR. Vakhrushin, Yu. P.; Ivanova, N. I.; Komarov, O. L.; (and others) (Joint Inst. for Nuclear Research, Dubna (USSR). Lab. of Neutron Physics). 1971. 9p. (In Russian). Dep. NTIS (U. S. Sales Only).

The problem of selecting the focusing system for the 30-MeV linear induction accelerator is considered. Calculations for maintaining the radial dimensions of beam in the accelerator during the working part of the accelerating pulse are presented. A laminar stream of electrons is assumed. (C.E.S.)

31040 (KFK–1316) DEVELOPMENTS IN CRYOGENIC AND SUPERCONDUCTING MAGNETS. Arendt, F.; Brechna, H.; Erb, J.; (and others) (Kernforschungszentrum, Karlsruhe (West Germany). Institut fuer Experimentelle Kernphysik). Nov 1970. 35p. (CONF-701120–3). Dep. NTIS (U. S. Sales Only).

From second national conference on particle accelerators; Moscow, USSR (11 Nov 1970).

The present status of development work on superconducting and cryogenic magnets at the Institut für Experimentelle Kernphysik KFZ Karlsruhe is described. Based on experiments with multifilament conductors it was found that the theoretical prediction using Bean's model is confirmed down to 13 μm filament diameter. Test results of a dc superconducting quadrupole ($\partial B/\partial r = 37.2$ T/m, with a warm aperture diameter of 0.12 m), and design studies with superconducting ac dipole magnets with ferromagnetic return yokes are reported. Present work with pure aluminum tapes indicates that Kohler's rule is not fulfilled at temperatures higher than 4.2°K. Discrepancy from theory is enhanced with purity. The relative magnetoresistance is higher with increased values of RRR. (auth)

31041 (LA–4534) A PROPOSAL FOR EPICS: A HIGH-RESOLUTION PION BEAM AND SPECTROMETER FACILITY FOR NUCLEAR STRUCTURE RESEARCH AT LAMPF. Thiessen, H. A.; Sobottka, S. (Los Alamos Scientific Lab., N. Mex.). Sep 1970. Contract W-7405-eng-36. 43p. Dep. NTIS.

The complete EPICS system consists of a high intensity, high resolution pion beam channel, a particle separator for reducing backgrounds, and two spectrometers. The system may be constructed in two stages. The first stage will consist of the channel, separator, and low momentum spectrometer. At the completion of this stage many of the proposed experiments can be performed including elastic and inelastic pion scattering and the study of those two-particle final state reactions for which one particle can be detected in a total absorption detector such as a sodium iodide counter or a Ge(Li) detector. Addition of a high momentum spectrometer will complete the second stage. This spectrometer will allow the study of reactions having a high momentum particle in the final state, as well as several having two-particle final states. Specifications and performance data are given, and the proposed experimental program is summarized. (W.H.K.)

31042 (LA–4639) QUARTERLY STATUS REPORT ON THE MEDIUM-ENERGY PHYSICS PROGRAM FOR THE PERIOD ENDING JANUARY 31, 1971. (Los Alamos Scientific Lab., N. Mex.). Mar 1971. Contract W-7405-eng-36. 56p. Dep. NTIS.

Research and development progress is summarized. Topics include accelerator structures, rf power systems, accelerator control and instrumentation, accelerator physics, experimental area, LAMPF scheduling and facility construction, and the LAMPF users group. Also, physics research is discussed including the pion-absorption experiment, medical applications of muonic x-rays, the Electron Prototype Accelerator, and multiwire proportional counter development. Publications are listed. (W.H.K.)

31043 (NP–18776) METHODS FOR MONITORING PROTON INCIDENCE ON THE INTERNAL TARGETS OF HIGH-ENERGY ACCELERATORS. Goryachev, Yu. M.; Kanavets, V. P.; Morozov, B. V.; Nikiforov, N. A.; Starostin, A. S. (Gosudarstvennyi Komitet

XUM

po Ispol'zovaniyu Atomnoi Energii SSSR, Moscow. Institut Teoreticheskoi i Eksperimental'noi Fiziki). 1970. 8p. (In Russian). Dep. NTIS (U. S. Sales Only).

Methods of absolute and relative monitoring of protons incident on an internal target of high-energy accelerators are described. The techniques have been developed to investigate absolute and relative production cross-sections for deuterons, protons and pions as functions of the target's mass number, but such techniques can be used to measure the cross-section of any other reaction. (auth)

31044 (NP-18780) EFFECTS OF SYNCHROTRON RADIATION ON THE SLOW EJECTION OF ELECTRONS FROM SYNCHROTRON. Mingalev, B. S.; Sivkov, Yu. P.; Simonyan, Kh. A. (Scientific Research Inst. of Electro-Physical Apparatus, Leningrad (USSR)). 1970. 39p. (In Russian). Dep. NTIS (U. S. Sales Only).

Problems are discussed concerned with the slow ejection of electrons from a synchrotron with the help of a resonant swing of betatron oscillations on non-linear perturbations of a magnetic field. The influence of quantum functions of radiation of high energy electrons on the betatron oscillation swing is taken into account. Conclusions on the selection of optimal current pulse shapes in quadrupole and sextupole lenses, producing magnetic field perturbations are made. (auth)

31045 (NP-18799) SEXTUPOLE LENSES WITH IMPROVED NON-LINEARITY IN SLOW EJECTION SYSTEMS. Gal'chun, A. V.; Sivkov, Yu. P. (Scientific Research Inst. of Electro-Physical Apparatus, Leningrad (USSR)). 1970. 10p. (In Russian). Dep. NTIS (U. S. Sales Only).

Application of sextupole lenses with considerable drop-off of a field on the aperture edge in the slow ejection system has been considered. Calculations have shown, that application of these lenses allows to decrease the swing amplitude and to improve slightly the emittance of the external beam as well as to reduce the total length of lenses on the ring. (auth)

31046 (RHEL/R-213) DYNAMIC POLARIZATION MEASUREMENTS IN POLYHYDRIC ALCOHOLS DOPED WITH THEIR CHROMIUM V COMPLEXES AT APPROX. 1°K AND AT 3 kG MAGNETIC FIELDS. Williams, W. G.; Thomas, J. L. (Rutherford High Energy Lab., Chilton (England)). Jan 1971. 15p. Dep. NTIS (U. S. Sales Only). UK 20p.

The dynamic polarization of proton spins in several alcohols containing their chromium V complexes has been observed at approximately 1°K and 3 kG magnetic fields. The results indicate that it might be possible to use alcohol-chromium V complex mixtures which are richer in free protons than glycol, as materials for a polarized proton target. (auth) (UK)

31047 (SJC-A-71-1) FIELD MEASURING SYSTEM OF DRIFT TUBE QUADRUPOLE MAGNETS. Kobayashi, Masaaki; Tanaka, Jiro; Yamashita, Sukeaki; Baba, Hitoshi (Tokyo Univ. (Japan). Inst. for Nuclear Study). Feb 1971. 25p. Dep. NTIS (U. S. Sales Only).

An apparatus for centering drift tube quadrupole magnets and measuring their harmonic field components is described together with the search coil and its calibration method. Sensitivity within 0.5 μm and reproducibility within ±2 μm can be obtained for the magnetic center location. Harmonic field components in four types of model magnets were measured for different pole shapes. (auth) (Japan)

31048 (SJC-A-71-2) DESIGN OF HIGH-GRADIENT ACCELERATING COLUMN. Fukumoto, S.; Inagaki, S.; Nishikawa, T. (Tokyo Univ. (Japan). Inst. for Nuclear Study). Mar 1971. 19p. Dep. NTIS (U. S. Sales Only).

A vertical model of the high gradient accelerating column is designed. The accelerating electrodes are determined by assuming a cylindrical rectilinear beam of 25 mm diameter. The proton beam is accelerated by 5 gaps and the total gap length is about 18 cm. A 750 keV proton beam of 500 mA is to be extracted if a plane disk of the ion emissive surface is formed. (auth) (Japan)

31049 (TRI-70-4) TECHNIQUES APPLIED TO THE DESIGN OF THE TRIUMF MAGNET POLES. Oraas, S. (TRI-Univ. Meson Facility, Vancouver (British Columbia)). Dec 1970. 54p. Dep. NTIS (U. S. Sales Only).

Techniques used in designing the sector-focused magnet for the TRIUMF cyclotron are presented. An empirical method is given for calculating the magnet pole tip shape required to contain a 500 MeV beam of H^- ions. The method is good only for small changes in the shape. In the test case, the generated pole tip had a spiral angle correct to within ±5°, and a hill angle correct to ±1°. The average field was found to be isochronous to ±70 G. An empirical solution to the problem of finding the field inside the magnet air gap is also given. The magnetic field resulting from a given pole tip contour is calculated at a point on the median surface by finding the perpendicular distance from the point to the edge of the pole and comparing this to an experimentally measured curve of field against distance. Fields generated by this technique have their averages correct to within 70 G and flutter to within 8%. Again, previous knowledge of similar pole tips is assumed. The method and results of calculating the pole edge position tolerances for the latest model magnet are given. The field strengths inside the steel return yoke as obtained from a series of flux measurements are also presented. Finally, it is shown that a simple approximation to the magnetic circuit of the magnet predicts the coil induction required to an accuracy of only 25%. (auth)

31050 (UCRL-20156) SHAKING OF PARTICLE BEAMS TO REMOVE NEUTRALIZING IONS. Peterson, J. M. (California Univ., Berkeley. Lawrence Radiation Lab.). Feb 1971. Contract W-7405-eng-48. 3p. (CONF-710308-9). Dep. NTIS.

From National particle accelerator conference; Chicago, Ill. (1 Mar 1971).

Positive ions produced through ionization of the residual gas by the electron beam in an accelerator or storage ring can be trapped in the potential well of the beam and produce focusing forces on the beam that can shift the betatron frequency onto a resonance or stimulate other beam-dynamics effects. At low beam intensity the ions can be removed by means of the electric field imposed by clearing electrodes; however, at high intensity clearing electrodes can become ineffective when the local field of the beam is greater than that imposed by the electrodes or even harmful because of electromagnetic interaction between the beam and the electrode system. The ions can be removed also by letting them coast to the walls in the interval during an empty gap in the beam, but the length of the necessary gap in many cases is impractical. A new method, called "beam shaking," is proposed for removing the neutralizing ions by inducing increasingly larger amplitudes of ion oscillation about the beam until they are driven to the walls. (auth)

31051 (UCRL-20164) ULTRA-NARROW, HIGH-QUALITY, HIGH-FIELD QUADRUPOLE MAGNET. Avery, Robert T.; Tanabe, Jack T. (California Univ., Berkeley. Lawrence Radiation Lab.). Feb 1971. Contract W-7405-eng-48. 2p. (CONF-710308-13). Dep. NTIS.

From National particle accelerator conference; Chicago, Ill. (1 Mar 1971).

An ultra-narrow, high-quality quadrupole magnet has been designed for use in the Bevatron experimental area. Several magnets have been fabricated and tested. Pertinent dimensions are: aperture = 8.244", core width × height × length = 12" × 24" × 24", overall width × height × length = 13" × 41" × 32" (including adjustable stand, terminals and water manifolds but excluding supply and return piping). This corresponds to a width/aperture ratio of ~1.5 compared to previously reported "narrow" ratios of 2.5 to 3.0 and common ratios of 5 or more. This narrow magnet permits significant improvement in beam target utilization by permitting more beam lines and/or moving closer to the target to achieve greater particle acceptance. In spite of its small size, the magnet can achieve field gradients up to 5000 G/in. The measured field quality generally equals or betters that of full-size quads, which is surprising considering the ultra-narrow width and the simple hyperbolic pole shape. A compact cooling circuit arrangement contributed to achievement of these results within such a small volume. (auth)

31052 (UCRL-20169) PRELIMINARY HARDWARE CONCEPTS FOR A HIGH-ENERGY ELECTRON-RING ACCELERATOR. Faltens, A.; Hartwig, E.; Keefe, D.; Salsig, W. (California Univ., Berkeley. Lawrence Radiation Lab.). Feb 1971. Contract W-7405-eng-48. 4p. (CONF-710308-17). Dep. NTIS.

From National particle accelerator conference; Chicago, Ill. (1 Mar 1971).

Results of the first study of the conceptual design of a collective-effect proton accelerator of substantial energy (65 to 100 GeV) are described. Basic theoretical considerations are outlined and components and their arrangement for a conceptual accelerator are discussed. This first study shows that the promise of the ERA principle to produce remarkably compact accelerators can be achieved by use of single-pulse surge-excited acceleration cavities. The example single-pass machine provides accelerating gradients of 250 MeV/meter overall where conventional synchrotrons yield 40 to 80 MeV/meter. The relaxed tolerances of the surge-excited cavities and their associated components allow great advantage to be taken of mass-production techniques with ensuing low cost (0.24M$/GeV). (auth)

XUM

31053 (UCRL-20174) ERA 4-MeV INJECTOR. Avery, R.; Behrsing, G.; Chupp, W. W.; (and others) (California Univ., Berkeley. Lawrence Radiation Lab.). Feb 1971. Contract W-7405-eng-48. 5p. (CONF-710308-14). Dep. NTIS.

From National particle accelerator conference; Chicago, Ill. (1 Mar 1971).

A pulsed electron accelerator which has been constructed and is now in operation at the Lawrence Radiation Laboratory, Berkeley is described. It was designed specifically for and is used as an injector for ERA (electron ring accelerator) studies. Electron bursts of 1200 amperes and 40 nanoseconds duration can be produced at energies of 1.0 to 4.25 MeV. The present repetition rate is approximately one per second. Acceleration is accomplished by means of ferrite loaded accelerating sections, each of which is capable of maintaining a 250 kV voltage pulse across the accelerating gap for a period of 40 ns. The voltage pulse has a rise time of 12 ns and the total timing jitter is of the order of one nanosecond. Five sections stacked together and operated as a unit function as the electron gun. The gun employs a field emission cathode and is operated at approximately 1 MV. Additional acceleration is achieved by means of an iterated system of accelerator sections and solenoidal magnetic lenses. (auth)

31054 (UCRL-20185) DIGITAL CONTROL OF BEVATRON ACCELERATION CYCLE. Evans, Don M.; Lothrop, Fred H. G. (California Univ., Berkeley. Lawrence Radiation Lab.). Feb 1971. Contract W-7405-eng-48. 5p. (CONF-710308-15). Dep. NTIS.

From National particle accelerator conference; Chicago, Ill. (1 Mar 1971).

Control of the Bevatron acceleration system had been entirely analog until developments in proton extraction techniques required substantial reduction of hum and noise during the acceleration cycle. The decision was made to employ a digital processor to control the acceleration cycle. An algorithm is developed which allows introduction of radial-feedback data into the digital processor and the real-time error signal is combined with arbitrary field dependent functions for transmission to the existing master oscillator. A high common-mode rejection digital system is utilized to enter the resultant control data directly into the master-oscillator environment before conversion into the required analog reference for frequency modulation. A comprehensive hardware "calculator" provides a continuous curve of digital representations to be sent along to the oscillator. The implementation of these facilities and the development of an operator-oriented interface to capitalize upon the flexibilities inherent within a digitally oriented system are described. (auth)

31055 (UCRL-20189) BEVATRON GUIDE FIELD CONTROL. Evans, Don M.; Frias, Robert; Hordos, Barney (California Univ., Berkeley. Lawrence Radiation Lab.). Mar 1971. Contract W-7405-eng-48. 4p. (CONF-710308-16). Dep. NTIS.

From National particle accelerator conference; Chicago, Ill. (1 Mar 1971).

The Bevatron guide field power supply has been under computer control for one year. This facility allows operational parameters to be programmed at operator request in order to provide the desired field profiles commensurate with the current experimental program. With a requirement of one part in fifteen thousand accuracy for resonant extraction, the digital system has been enlarged until a real-time closed-loop control function can meet this specification. A one gauss window for entry into flat-zones is now maintained, while a relative flatness tolerance of $\pm\frac{1}{2}$ gauss is held during the typical 2-sec flat-zone. The structure of a new data-acquisition system is described with emphasis upon the use of a fast magnetic-core memory to gather blocks of data, as well as to hold the necessary digital threshold values to be arithmetically compared with the results of the data gathering facility. Also covered, is the implementation of the system in the detection and ultimate reduction of incipient fault conditions within the guide field power supply. (auth)

31056 (UCRL-20191) NEW BEVATRON POLE-FACE WINDINGS POWER SYSTEM. Jackson, L. T. (California Univ., Berkeley. Lawrence Radiation Lab.). Feb 1971. Contract W-7405-eng-48. 2p. (CONF-710308-8). Dep. NTIS.

From National particle accelerator conference; Chicago, Ill. (1 Mar 1971).

The new power systems which individually drive each of the Bevatron pole-face windings must handle a variety of operating parameters as well as satisfying the stringent specification of $dI/dt \leq 14$ A/sec during flattop. The 19 pole-face windings, which run circumferentially around the machine, each constitutes an active load for their power system, with $\hat{B}$ voltages increasing with radius up to 190 V during rectification on the outermost winding. During flattop there is approximately 10 V pp of predominately 720 and 1440 Hz signals across the winding. The 0.5 Ω windings require up to +30 A during injection and ±100 A during flattop. To satisfy the above requirements, a transistor actuator was chosen utilizing 2N3902 high-voltage transistors. A dc supply with multiple taps on the transformer provides output voltages from 12 V to 270 V to allow matching to each pole-face winding with a voltage higher than the $\hat{B}$ voltage of that winding so the difference appearing across the actuator is correct for transistor operation. On the positive actuator, the difference voltage must be great enough to drive the 30 A peak required through the winding during injection. Characteristic waveshapes for PFW13 positive and negative actuators are presented. (auth)

31057 (UCRL-20197) CRYOGENIC PUMPING SYSTEM PROPOSED FOR THE BEVATRON. Reinath, F. S.; Richter, R. M.; Tanabe, J. T.; Zajec, E. (California Univ., Berkeley. Lawrence Radiation Lab.). Feb 1971. Contract W-7405-eng-48. 4p. (CONF-710308-19). Dep. NTIS.

From National particle accelerator conference; Chicago, Ill. (1 Mar 1971).

A cryogenic pumping system capable of pumping 300,000 l/sec of nitrogen is proposed for the Bevatron to decrease the base pressure from $\sim 2 \times 10^{-6}$ to $\sim 2 \times 10^{-7}$ torr. The Bevatron consists of approximately 10,000 ft^3 of free volume with approximately 15,000 ft^2 of free outgassing area. The magnet pole tips, which consists of ½-in. laminations, add a potential 80,000 ft^2 of outgassing area. The design calls for an approximately 360-ft-long 20°K surface shielded by an 80°K surface strung along the inside perimeter of the Bevatron. Initial design considerations indicate that radiant heat flux from the 80°K surface is a prime design factor which could greatly affect the operating and installation costs of 80°K refrigeration. A two-dimensional Monte Carlo type program was devised and used to optimize designs with maximum nitrogen pumping speed and minimum 80°K shield area to reduce the refrigeration costs. (auth)

31058 (UCRL-20208) NEGATIVE MASS INSTABILITIES IN AN ELECTRON-RING COMPRESSOR. Entis, A. C.; Garren, A. A.; Smith, L. (California Univ., Berkeley. Lawrence Radiation Lab.). Feb 1971. Contract W-7405-eng-48. 5p. (CONF-710308-7). Dep. NTIS.

From National particle accelerator conference; Chicago, Ill. (1 Mar 1971).

Experiments on Compressor 4 at LRL show strong evidence of a negative mass instability which develops immediately after injection and generates such a large energy spread that the achievement of electron densities in the range of interest for trapping and accelerating ions becomes very difficult. Two models for the compressor are explored: a straight ceramic tube coated with a thin metallic layer and a metallic pillbox with lossy walls. The first model accounts for the significant materials seen by the beam, and the second model provides a more realistic representation of the compressor geometry. Results of the study have proven to be a useful indication of the problem by predicting the very rapid growth rates observed above threshold and suggesting that thresholds can be raised substantially by the use of suitable metallic coatings. (W.H.K.)

31059 (UCRL-20611) BERKELEY ERA PROGRAM. Lofgren, Edward J. (California Univ., Berkeley. Lawrence Radiation Lab.). Feb 1971. Contract W-7405-eng-48. 4p. (CONF-710308-18). Dep. NTIS.

From National particle accelerator conference; Chicago, Ill. (1 Mar 1971).

The scope and status of the Berkeley Electron Ring Accelerator (ERA) program are reviewed. (auth)

31060 EXPERIMENTAL PROGRAM FOR THE C.E.R.N. STORAGE RINGS. Vivargent, M. (Paris Univ., Orsay, France. European Organization for Nuclear Research, Geneva). J. Phys. (Paris), Colloq.; C5: 132-64(Nov-Dec 1970). (In French).

From Conference on high energy physics; Aix-en-Provence, France (29 Sep 1970). See CONF-700950.

The I.S.R. experimental program is reviewed. In the various experimental fields, the results concerning the weakest and the highest energies are given as well as the theoretical predictions. (France)

31061 PHYSICAL RESULTS OBTAINED WITH ELECTRON AND POSITRON STORAGE RINGS. Bizot, J. C. (Ecole Normale Superieure, Orsay, France). J. Phys. (Paris), Colloq.; C5: 165-80(Nov-Dec 1970). (In French).

From Conference on high energy physics; Aix-en-Provence, France (29 Sep 1970). See CONF-700950.

XUM

Results obtained with electron positron storage rings during past years are presented. These results concern a test on the validity of quantum electrodynamic and also hadron production, especially vector mesons ρ, ω and ϕ. Experiments with high-luminosity rings, either proposed, or under construction are outlined. (France)

31062 POSSIBILITY OF REDUCING THE INJECTION ENERGY AND INCREASING THE LIMIT CURRENT IN AN ION LINEAR ACCELERATOR. Kapchinskii, I. M.; Teplyakov, V. A. (Inst. of Theoretical and Experimental Physics, Moscow). Instrum. Exp. Tech. (USSR) (Engl. Transl.); No. 4, 973-5(Jul-Aug 1970).

Translated from Prib. Tekh. Eksp.; No. 4, 17-19(Jul-Aug 1970).

In a linear accelerator with spatially uniform strong focusing, an adiabatic change in the synchronous phase and specific acceleration can be achieved depending on the velocity of the particles so that the ion bunches keep their distance and charge density distribution while moving. This enables the intensity limit of the beam to be increased considerably while greatly reducing the injection energy with a high locking factor. (auth)

31063 INVESTIGATION OF THE VERTICAL MOTION OF PARTICLES IN A CYCLOTRON. Krasnov, N. N.; Ognev, A. A.; Ponomarev, A. A. (Inst. of Physics and Power, Obninsk, USSR). Instrum. Exp. Tech. (USSR) (Engl. Transl.); No. 4, 976-8(Jul-Aug 1970).

Translated from Prib. Tekh. Eksp.; No. 4, 19-21(Jul-Aug 1970).

A method is described of processing the experimental data on the vertical motion of ions, obtained using a three-lamellar probe. By measuring the current in each of the three lamellae I_1, I_2, and I_3, and the total current in all three lamellae I_Σ, one can, by constructing the graphs $I_1/I_\Sigma = f(R)$, $I_3/I_\Sigma = f(R)$ and $I_\Sigma = f(R)$, analyze the vertical motion of the beam in the cyclotron and establish the location and reasons for the loss in the beam. From the frequency of the vertical oscillations of the beam, for a known potential difference across the dees and the form of the fall-off of the magnetic field along the radius, one can obtain the average value of the initial phase of lens operation. The work was carried out on the 150-cm cyclotron of the Physics and Power Institute. (auth)

31064 METHODS OF MONITORING PROTON DISCHARGE ONTO THE INTERNAL TARGET OF A HIGH-ENERGY ACCELERATOR. Goryachev, Yu. M.; Kanavets, V. P.; Morozov, B. V.; Nikiforov, N. A.; Starostin, A. S. Instrum. Exp. Tech. (USSR) (Engl. Transl.); No. 4, 979-81(Jul-Aug 1970).

Translated from Prib. Tekh. Eksp.; No. 4, 22-4(Jul-Aug 1970).

Methods of absolute and relative monitoring of protons passing through the internal target of a high-energy accelerator are described. The technique was developed primarily for studies of the relative and absolute cross sections of deuteron, proton, and ion generation in relation to the atomic weight of the targets, but it can also be used to measure the cross sections of arbitrary reactions. Telescope detectors are used. (auth)

31065 SHORTENED CHARGE-EXCHANGE GAS TARGET. Pivovar, L. I.; Levchenko, Yu. Z. (Physicochemical Inst., Kharkov). Instrum. Exp. Tech. (USSR) (Engl. Transl.); No. 4, 986-7(Jul-Aug 1970).

Translated from Prib. Tekh. Eksp.; No. 4, 28-9(Jul-Aug 1970).

A charge-exchange gas target made in the form of a set of thin tubes is described. This arrangement enables the length of the target to be substantially reduced at the expense of an increase in its diffusion resistance. (auth)

31066 IMPULSE GENERATOR FOR FEEDING A LINEAR ACCELERATOR. Borisov, D. G.; Gryzlov, A. I.; Belov, Yu. V. (Scientific-Research Inst. for Electrophysical Apparatus, Leningrad). Instrum. Exp. Tech. (USSR) (Engl. Transl.); No. 4, 1049-51(Jul-Aug 1970).

Translated from Prib. Tekh. Eksp.; No. 4, 82-4(Jul-Aug 1970).

The operation of a generator which produces constant amplitude pulses under load is analyzed. The mode of operation desired is ensured by transfer of the excess charge from the accumulator to the voltage supply point by completing the resonance charge process through a resistor, whose value is determined by the magnitude of the excess charge and the time remaining for return of this charge to the power source. Amplitude stabilization is accomplished by varying the generator efficiency by changing the value of the resistance in the transfer network. (auth)

31067 THYRISTOR VOLTAGE STABILIZER FOR A 40-kV MODULATOR. Kozodaev, A. M.; Lazarev, N. V. (Inst. of Theoretical and Experimental Physics, Moscow). Instrum. Exp. Tech. (USSR) (Engl. Transl.); No. 4, 1060-2(Jul-Aug 1970).

Translated from Prib. Tekh. Eksp.; No. 4, 92-4(Jul-Aug 1970).

A circuit is described for stabilizing the high voltage on a powerful capacitive energy accumulator by using a thyristor breaker connected in the primary winding circuit of the stepup power transformer. The circuit permits charging a 2.8-μF capacitor bank to voltages of 10 to 40 kV with an accuracy of ±0.1%, for either periodic or random discharges of the bank, separated by time intervals greater than 0.7 sec. (auth)

31068 CONTROL SYSTEM OF THE IPCR 160 cm CYCLOTRON. Inoue, Toshihiko; Kohno, Isao; Takeda, Shigeru (Inst. of Physical and Chemical Research, Yamato, Japan). Rikagaku Kenkyusho Hokoku; 46: No. 5, 103-21(Sep 1970). (In Japanese).

The control system of the IPCR 160 cm cyclotron was designed as a central remote control system using DC 48 V, and the cyclotron can be operated by one-man control. Since the cyclotron is operated by adjusting many parts of various instruments, the control circuits were unified to three standard circuits. These standard circuits were separated into several modules to simplify the control line system. For convenience to the operator the indication of operation and trouble was devised using a logic circuit system. Since the cyclotron is a radiation generator, a safety device to prevent the human body from radiation was devised with an interlocking system. (auth) (Japan)

31069 PRODUCTION OF ISOTOPICALLY PURE TARGETS IN ELECTROMAGNETIC MASS SEPARATORS BY ION-BEAM RETARDATION. Wotke, H.; Tortschanoff, T.; Hanganut, M. (Reaktorzentrum, Seibersdorf, Austria). Acta Phys. Austr.; 29: 183-9(1969). (In German).

After a short review of the methods for target preparation inside an electromagnetic isotope separator, the problem of target preparation with the beam retardation technique is specially treated. For building up a monoisotopic layer on a carrier-foil by direct impact of an ion beam, the self-sputtering coefficient has to be <1. The energy-dependence of the self-sputtering coefficient according to the formula of Almén is discussed for the case of ^{102}Pd. It proves that for building up targets, the Pd-ions have to be retarded to energies <300 eV. The experimental setup and the results for ^{63}Cu, ^{102}Pd and ^{157}Gd are described. (auth)

31070 APPARATUS FOR THE AUTOMATIC ACCUMULATION (STORAGE) AND ANALYSIS OF INFORMATION IN EXPERIMENTS WITH THE SYNCHROCYCLOTRON. Medved, S. V.; Moiseeva, V. V.; Sinaev, A. N.; Tsakher, G.-Yu.; Chistov, N. A. (Joint Inst. for Nuclear Research, Dubna, USSR). Instrum. Exp. Tech. (USSR) (Engl. Transl.); No. 4, 1081-3(Jul-Aug 1970).

Translated from Prib. Tekh. Eksp.; No. 4, 109-11(Jul-Aug 1970).

An apparatus forming part of a center for the storage and analysis of information in the Nuclear Problems Laboratory of the Joint Institute for Nuclear Research (JINR) is described. The basis of the center is a set of AI-4096 multidimensional analyzers. The development and realization of new programs of work for these devices have enabled them to be used more and more extensively in experiments with the synchrocyclotron and have thus promoted the automation of the storage, examination, analysis, and extraction of information. The center has two-way communication with a Minsk-22 computer through a buffer storage device. (auth)

31071 LARGE-VOLUME HOMOGENEOUS LOW-FIELD ELECTROMAGNET. Daniels, J. M.; Kiang, A. K. C.; Kirkby, P. (Univ. of Toronto). Can. J. Phys.; 49: 576-81(1 Mar 1971).

An electromagnet is described which generates low fields, typically 10 G, that are homogeneous over a large volume. The magnet is constructed of 12 coils lying on the surface of a sphere 1 m in diameter, and 18 coils lying on the surface of a concentric sphere 1.5 m in diameter. Both the measured and calculated field gradients show that $(\partial H/\partial z)/H < 10^{-3}$ cm^{-1} for distances of 20 cm from the common center of the spheres along the common axis. Measured field gradients across the equator show that $(\partial H/\partial x)/H$ and $(\partial H/\partial y)/H < 2 \times 10^{-4}$ cm^{-1} for distances of 30 cm from the common center. The currents in the coils on the outer sphere are in opposition to those in the coils on the inner sphere, in order to cancel the external magnetic field. This feature allows the magnet to be placed inside a close fitting magnetic shield, without interaction between the magnet and the shield. Design formulas, constructional details, and tests on the completed magnet are given. The magnet was designed to produce a uniform magnetic field over a large volume to contain the University of Toronto polarized helium-3 target. (auth)

31072 NUCLEAR RELAXATION OF ^{3}He GAS ON VARIOUS SOLID SURFACES. Timsit, R. S.; Daniels, J. M.; May, A. D. (Univ. of Toronto). Can. J. Phys.; 49: 560-75(1 Mar 1971).

The nuclear spin–lattice relaxation time of ^{3}He gas in contact with metallic and glass surfaces was measured. The relaxation

XUM

time of the gas in the presence of a glass surface is strongly dependent on both the permeability of the glass to helium and the concentration of paramagnetic impurities in the glass. Two relaxation mechanisms may in this case be distinguished, relaxation due to the diffusion of the gas into the glass and relaxation induced during the adsorption of the helium on the glass surface. A phenomenological model to account for these observations is proposed. The mechanism responsible for the relaxation of ^{3}He on metallic surfaces remains obscure. (auth) (Canada)

31073 POLARIZATIONS PRODUCED AND THE RATES OF POLARIZATION IN THE OPTICAL PUMPING OF 2^3S_1 ^{3}He. Timsit, R. S.; Daniels, J. M. (Univ. of Toronto). Can. J. Phys.; 49: 545-59(1 Mar 1971).

The optical pumping of metastable ^{3}He atoms with circularly polarized resonance radiation from a ^{4}He light source was carried out at several ^{3}He gas pressures and at different pumping light intensities and metastable atom concentrations. The dependence of both the equilibrium nuclear polarization and the pumping time on both the metastable atom density and the intensity of the pumping radiation is in satisfactory agreement with the theoretical predictions of Daniels and Timsit. (auth) (Canada)

31074 DETERMINATION OF THE POLARIZATION OF ^{3}He BY OPTICAL METHODS. Daniels, J. M.; Timsit, R. S. (Univ. of Toronto). Can. J. Phys.; 49: 539-44(1 Mar 1971).

Two methods are described for determining the polarization of 2^3S_1 ^{3}He by measuring the transmission of a test beam through the polarized gas. Satisfactory agreement was obtained between the polarizations measured by these methods, and a new formula for the determination of the polarization of ^{3}He from the intensity of the scattered pumping light. This new formula takes into account the fact that the pumping light is not all parallel to the magnetic field, and that it may not be accurately circularly polarized. (auth) (Canada)

31075 EXPECTED PERFORMANCE OF AN OPTICAL PUMPING LIGHT SOURCE AND THE KINETICS OF OPTICAL PUMPING OF 2^3S_1 ^{3}He. Daniels, J. M.; Timsit, R. S. (Univ. of Toronto). Can. J. Phys.; 49: 525-38(1 Mar 1971).

A practical light source for optical pumping necessarily excites transitions other than those which it is desired should be excited. It is shown that a pumping light source for 2^3S_1 ^{3}He may be characterized by three parameters, which describe the transition rates for $\Delta m = \pm 1$, and 0, transitions under standard conditions. Expressions are derived relating these parameters to the geometry of the light source. The equation which describes the flow of angular momentum into ^{3}He is formulated, using these parameters, the light flux, the lifetime of the metastable atoms, and collisional mixing in the 2^3P states. This equation is solved to give the polarization which may be attained, and the rate at which the polarization is built up. A modification of this equation is also given, which takes into account moderate trapping of resonance radiation. An expression is also derived which relates the polarization of ^{3}He to the intensity of the scattered pumping light. (auth) (Canada)

31076 ^{4}He DISCHARGE LIGHT SOURCE AND OPTICAL SYSTEM FOR THE OPTICAL PUMPING OF 2^3S_1 ^{3}He. Daniels, J. M.; Timsit, R. S.; May, A. D.; Yuen, Virginia L. S. (Univ. of Toronto). Can. J. Phys.; 49: 517-24(1 Mar 1971).

Details are given of the construction and performance of a ^{4}He discharge lamp and optical system for optical pumping of 2^3S_1 ^{3}He. The lamp is made of fused quartz and is water cooled. It is excited by 160 MHz radio-frequency power applied to internal electrodes. The first part of the light gathering system is built into the lamp as an integral part of the cooling jacket. For a radio-frequency input of 600 W, 1.4×10^{17} circularly polarized photons s^{-1} are delivered in a cone of half angle 30° to the specimen to be optically pumped. The width of the 1.083 μ line emitted is about 0.087 cm^{-1}. This lamp has behaved satisfactorily during extensive life tests. (auth) (Canada)

31077 EXPERIMENT TO COMPRESS POLARIZED ^{3}He GAS. Timsit, R. S.; Daniels, J. M.; Dennig, E. I.; Kiang, A. K. C.; May, A. D. (Univ. of Toronto). Can. J. Phys.; 49: 508-16(1 Mar 1971).

Helium-3, polarized by optical pumping of the 2^3S_1 metastable atoms at 1 torr pressure, was compressed to a pressure of 217 torr and it was verified that the gas remains polarized. ^{3}He at 1 torr was polarized and compressed into a storage bulb using a Toepler pump, and this was repeated with successive charges of ^{3}He until the pressure in the storage bulb rose to 217 torr after about 4 h of operation. Some of the gas was returned to the low pressure side of the equipment and its polarization was measured. The polarization attained before each charge was compressed was 0.04; the measured polarization of the returned gas was 0.03. (auth) (Canada)

31078 ACCELERATING STRUCTURES WITH RING COUPLING RESONATORS. Kul'man, V. G.; Mirochnik, E. A.; Pirozhenko, V. M. (Inst. of Radio Engineering, Moscow). Instrum. Exp. Tech. (USSR) (Engl. Transl.); No. 4, 1020-4(Jul-Aug 1970).

Translated from Prib. Tekh. Eksp.; No. 4, 56-61(Jul-Aug 1970).

An accelerating $\pi/2$ standing wave mode structure utilizing ring coupling resonators is described. The calculated and experimentally obtained parameters of the structure are presented, and the technology for designing and building cavities of this type and their tuning are discussed. The accelerating structure may be used for proton linear accelerators which accelerate protons to above 100 MeV. (auth)

31079 FIFTH INTERNATIONAL CYCLOTRON CONFERENCE. Proceedings of a Conference Held at Oxford, 17–20 September 1969. McIlroy, R. W. (ed.). London; Butterworths (1971). 807p. £ 20. (CONF-690921).

Separate abstracts were prepared for 83 of the 87 papers presented. The remaining four papers were previously included in NSA. (W.H.K.)

For abstracts of individual papers see: 31080–31162.

31080 INNOVATIONS IN ISOCHRONOUS CYCLOTRONS. Martin, John A. (Oak Ridge National Lab., Tenn.). pp 3-12 of Fifth International Cyclotron Conference. /McIlroy, R. W. (ed.). London; Butterworths (1971).

From International cyclotron conference; Oxford, England (17 Sep 1969). See CONF-690921.

Since the last International Conference on Isochronous Cyclotrons (1966), three major projects have been approved: the 585 MeV proton cyclotron of the Swiss Institute for Nuclear Research (SIN) to be built at Villigen near Zurich; the 500 MeV H^- cyclotron of the Tri-University Meson Facility (TRIUMF) at Vancouver, British Columbia; and the 200 MeV variable energy cyclotron of the Indiana University. A much smaller but unique project has been successfully brought into operation, the cyclograaff at Duke University which combines a small cyclotron with a tandem accelerator in a way which enhances the desirable characteristics of both. Finally, the most important happening since the last conference has been the renewed interest in accelerators for very heavy ions. In the United States alone, there will be more than ten major proposals. The activities and progress of the past several years are reviewed and some of the important innovations accomplished or foreseen discussed. (auth) (UK)

31081 CYCLO-GRAAFF: CONCEPT AND PRACTICE. Purser, F. O.; Newson, H. W.; Roberson, N. R.; Bilpuch, E. G.; Walter, R. L. (Duke Univ., Durham, N. C.). pp 13-23 of Fifth International Cyclotron Conference. /McIlroy, R. W. (ed.). London; Butterworths (1971).

From International cyclotron conference; Oxford, England (17 Sep 1969). See CONF-690921.

The design aims and performance of the Cyclo-Graaff accelerator are discussed. Energy spread from the 15 MeV injector cyclotron was reduced to 15 keV and reliable operation of the accelerator combination was attained. Output pulse time structure was studied and proven useful as a tune up aid. Indications that the external beam from the cyclotron can be used to provide a feedback signal for further energy spread reduction are presented. (auth) (UK)

31082 INDIANA UNIVERSITY 200 MeV CYCLOTRON PROJECT. Rickey, M. E.; Sampson, M. B.; Bardin, B. M. (Indiana Univ., Bloomington). pp 24-9 of Fifth International Cyclotron Conference. /McIlroy, R. W. (ed.). London; Butterworths (1971).

From International cyclotron conference; Oxford, England (17 Sep 1969). See CONF-690921.

A separated sector cyclotron facility is under construction at Indiana University. The ion source and potential drop pre-accelerator and the first cyclotron stage are being assembled at a temporary location. The design of the final cyclotron stage is nearing completion and its assembly will commence when the building, presently under construction, is occupied late in 1970. The completed accelerator will have variable energy over wide limits and will be capable of isochronous operation with both protons and a large number of heavy ions. (auth) (UK)

31083 PROPOSED MIDWEST TANDEM CYCLOTRON (MTC). Khoe, T. K.; Livingood, J. J.; Ramler, W. J. (Argonne National Lab., Ill.). pp 30-40 of Fifth International Cyclotron Conference. /McIlroy, R. W. (ed.). London; Butterworths (1971).

XUM

From International cyclotron conference; Oxford, England (17 Sep 1969). See CONF-690921.

The proposed accelerator system consists of two major components, a modified TU tandem Van de Graaff and a 6-open-sector cyclotron. For the acceleration of heavy ions to high energies, the tandem must serve as an injector for the cyclotron. Alternatively, the tandem can be used by itself to supply heavy ions of moderate energy, and then by employing a small N = 4 cyclotron as an injector for the N = 6 machine, very high energy light ions can be obtained. Energies in MeV per nucleon and external yields in units of 10^{12} particles per s (shown in parentheses) range from 350 (60) for protons to 10 (0.1) for uranium. The cyclotron is a variable energy N = 6 design with a 3-phase rf system including energy flat topping. The vacuum system is to operate at about 10^{-7} torr to minimize heavy ion charge exchange losses. The design aim for energy resolution is to be better than 1 in 10^3. (auth) (UK)

31084 HEAVY-ION ACCELERATOR FACILITY FEATURING A SEPARATED-SECTOR ISOCHRONOUS CYCLOTRON. Martin, J. A.; Hudson, E. D.; Mosko, S. W.; Howell, L. N.; Mallory, M. L. (Oak Ridge National Lab., Tenn.). pp 41-9 of Fifth International Cyclotron Conference. /McIlroy, R. W. (ed.). London; Butterworths (1971).

From International cyclotron conference; Oxford, England (17 Sep 1969). See CONF-690921.

An isochronous cyclotron of modest size with a model TU tandem Van de Graaff as its injector would have the capability of accelerating the heaviest ions to well above the Coulomb barrier for the heaviest elements. An evaluation of several cyclotron designs has led to an isochronous cyclotron with four separate sectors. As now envisaged the cyclotron will be capable of accelerating heavy ions with a charge-to-mass ratio of 0.15 to an energy of 7.5 MeV/a.m.u. A unique feature of the plan is the use of a source of highly charged ions of the Dubna or LRL type in the terminal of the tandem. For example, to obtain energetic uranium ions, 9+ ions from the terminal ion source are accelerated to 144 MeV (0.605 MeV/a.m.u.), passed through a stripping foil to increase the ion charge to 36+, injected into the cyclotron, and accelerated to 1785 MeV (7.5 MeV/a.m.u.). The cyclotron will also accelerate light particles, for example, protons and α-particles to about 300 MeV, deuterons to 150 MeV, and $^3He^{2+}$ ions to 400 MeV. For this added flexibility a small cyclotron will be provided as the alternate light-ion injector. When the tandem is used separately for experiments requiring its special capabilities, the two cyclotrons can also be used together for independent medium-energy research. When the tandem and large cyclotron are used together for heavy-ion acceleration, the injector cyclotron becomes an independent tool for low-energy nuclear chemistry or isotope production. (auth) (UK)

31085 PROPOSED MICHIGAN STATE UNIVERSITY TRANSURANIC ACCELERATOR FACILITY. Blosser, H.; Gordon, M. M.; Johnson, D. A. (Michigan State Univ., East Lansing). pp 50-7 of Fifth International Cyclotron Conference. /McIlroy, R. W. (ed.). London; Butterworths (1971).

From International cyclotron conference; Oxford, England (17 Sep 1969). See CONF-690921.

The design of a versatile facility for accelerating ions of every element to energies sufficient to produce nuclear reactions on any target is described. The design utilizes a large six-sector ring cyclotron with ~40 kG m average bending capability for the main acceleration. The present MSU cyclotron would be the light ion (p, d, ^{3}He, ^{4}He) injector. A number of possible heavy ion injectors are discussed, the field trimming problem is reviewed and initial studies of resonance transitions are described. (auth) (UK)

31086 STATUS REPORT ON SIN. Willax, H. A. (Swiss Inst. for Nuclear Research, Zurich). pp 58-72 of Fifth International Cyclotron Conference. /McIlroy, R. W. (ed.). London; Butterworths (1971).

From International cyclotron conference; Oxford, England (17 Sep 1969). See CONF-690921.

A two stage isochronous accelerator for proton beams of about 100 μA at more than 500 MeV is under construction at the Swiss Institute for Nuclear Research, Zurich. As previously described it consists of a sector focused isochronous cyclotron for 70 MeV, acting as injector, and an isochronous ring cyclotron. The injector cyclotron will also accelerate d, α, ^{3}He, heavy ions as well as polarized d and p to variable energies. Those beams will be used separately. The design goal for the ring cyclotron has been changed from 520 to about 580 MeV. The status of development of the main machine components is described briefly. Prototypes of a sector magnet, an rf cavity and a vacuum chamber section are under test. Building construction work has started at the site near Villigen. It is expected to begin with the installation of the machines in 1971. (auth) (UK)

31087 TRIUMF PROJECT. Warren, J. B. (Univ. of British Columbia, Vancouver). pp 73-84 of Fifth International Cyclotron Conference. /McIlroy, R. W. (ed.). London; Butterworths (1971).

From International cyclotron conference; Oxford, England (17 Sep 1969). See CONF-690921.

The engineering and construction of the "Tri-University Meson Facility," by a group of four Western Canadian Universities—University of Alberta, Simon Fraser University, University of Victoria, and University of British Columbia—commenced at the end of April 1968. This meson workshop and facility for intermediate energy nuclear physics and chemistry is based on a six-sector A.V.F. cyclotron designed to accelerate 100 μA of H^- ions to an energy of 500 MeV. Virtually the whole beam may be extracted by stripping the two electrons from the negative hydrogen ions by passage through a thin foil so the resulting protons swerve out of the cyclotron. The energy of the extracted protons may be continuously varied from 150 to 500 MeV by altering the radial position of this foil. At the outset two beams will be extracted and fed to separate experimental areas; each will have 100% macroscopic duty factor, a microduty structure of 7 ns every 44 ns corresponding to a phase acceptance of 60°, and an energy resolution of ±650 keV. (auth)

31088 BEAM QUALITY AND EXPECTED ENERGY RESOLUTION FROM THE TRIUMF CYCLOTRON. Richardson, J. Reginald; Craddock, M. K. (Univ. of British Columbia, Vancouver). pp 85-94 of Fifth International Cyclotron Conference. /McIlroy, R. W. (ed.). London; Butterworths (1971).

From International cyclotron conference; Oxford, England (17 Sep 1969). See CONF-690921.

H^- ions accelerated in the TRIUMF isochronous cyclotron will require a minimum of 1250 turns to attain a final energy of 500 MeV. Experience with other cyclotrons indicates that with careful control of imperfections, particularly the first harmonic magnetic field component, the internal beam emittance should be no more than 4π mm mrad at 50 MeV or 1.2π mm mrad at 500 MeV. Multiple scattering at the stripping foil will enlarge this a further 20–70% depending on the foil thickness. The total energy spread in the raw extracted beam at 500 MeV will be ±600 keV. When higher resolution is required, slits will be placed at low energy to limit the radial emittance, enabling 6 μA to be extracted with ±150 keV resolution. With the planned addition of third harmonic to the rf cavity, separated turn acceleration will be possible out to maximum energy with the magnet and rf control technology available today; 30 μA should be obtainable with ±25 keV total energy spread and a ±7° phase spread. A third scheme, using slits at the final radius, can give two high current low resolution beams and a simultaneous low current beam with ±60 keV total spread. (auth) (UK)

31089 FRACTIONAL TURN INJECTOR CYCLOTRON. Smythe, Rodman (Univ. of Colorado, Boulder). pp 95-100 of Fifth International Cyclotron Conference. /McIlroy, R. W. (ed.). London; Butterworths (1971).

From International cyclotron conference; Oxford, England (17 Sep 1969). See CONF-690921.

The emergence of the separated-sector cyclotron with its many desirable characteristics has created a pressing need for an accelerator which is suitably matched to it to serve as an injector. The "fractional turn cyclotron" proposed here meets that need and at the same time avoids the disadvantages of dc injectors as well as the extraction and ion source accessibility problems of conventional cyclotrons. It consists of a cyclotron ion source, a simple magnetic field, and a multi-gap rf accelerating structure. The rf extraction from the ion source together with rf acceleration provide high current beam bunches properly synchronized for injection into the separated-sector cyclotron. The design also permits the use of low energy external ion sources, such as a polarized proton ion source. Preliminary design specifications of a 2 MeV injector for a 60 MeV separated-sector cyclotron are given. (auth) (UK)

31090 BEAM TRANSPORT SYSTEM OPTICS STUDIES FOR THE UNIVERSITY OF MARYLAND CYCLOTRON. Berg, R. E. (Univ. of Maryland, College Park). pp 101-4 of Fifth International Cyclotron Conference. /McIlroy, R. W. (ed.). London; Butterworths (1971).

From International cyclotron conference; Oxford, England (17 Sep 1969). See CONF-690921.

The University of Maryland cyclotron beam transport system is designed about two 90°, 60 in, double focusing analyzing magnets. Magnetic field measurements have now been completed for

XUM

all optical elements. Initial optics studies indicate that high-quality performance of the analyzing magnet system down to energy resolution of approximately 0.01% is achievable. The field is very uniform, allowing scaling of operation up to over 12.5 kG fields and absolute energy calibration to better than 0.04%. Results of calculations to optimize performance of the magnets in their dispersive mode are presented. (auth) (UK)

31091 SQUARE WAVE RF SYSTEM DESIGN FOR THE TRIUMF CYCLOTRON. Erdman, K. L. (Univ. of British Columbia, Vancouver); Prochazka, A.; Fredriksson, O. K.; Thomas, R.; Grundman, W. A. pp 105-10 of Fifth International Cyclotron Conference. /McIlroy, R. W. (ed.). London; Butterworths (1971).

From International cyclotron conference; Oxford, England (17 Sep 1969). See CONF-690921.

The unique features of the rf resonator assembly of the TRIUMF accelerator allow the addition of higher harmonics to the fundamental cavity mode, with a consequent increase in phase acceptance and an order of magnitude decrease in rf frequency stability and magnetic field tolerances in the cyclotron. Only the third harmonic of the fundamental for which the rf cavity changes from a shorted $\frac{1}{4}\lambda$ line to a $\frac{3}{4}\lambda$ line will be used, since the improvement in phase acceptance decreases rapidly with increasing harmonic content. This improvement can be seen by comparing the phase acceptance of the beam with first harmonic acceleration alone (−5° to +55°) to acceptance with the addition of the optimum amount of third harmonic (+45° to −45°). The resonant cavity will be supplied with the requisite 1.5 mW of rf power by means of a resonant transmission line from a final power amplifier consisting of parallel 7560 triodes. With third harmonic excitation of the optimum amount the full width of the energy should be within ±25 keV in an rf phase width of 11°. This corresponds to a microscopic duty factor of 6% with separated turn acceleration. (auth) (UK)

31092 DESIGN OF THE 4000 TON MAGNET FOR THE TRIUMF CYCLOTRON. Auld, E. G.; Oraas, S.; Otter, A. J.; (and others) (Univ. of British Columbia, Vancouver). pp 111-19 of Fifth International Cyclotron Conference. /McIlroy, R. W. (ed.). London; Butterworths (1971).

From International cyclotron conference; Oxford, England (17 Sep 1969). See CONF-690921.

The containment of the accelerated H^- beam in the TRIUMF isochronous cyclotron presents some unique design problems. The electric dissociation of the H^- ion as it travels through a magnetic field requires that the maximum field be limited to 5.76 kG to maintain a relatively low activity level inside the vacuum chamber. This results in an overall magnet diameter of 71 ft. Two scale models were built to aid in the design of the 6-sector magnet; a 1:20 scale model of the whole magnet and a 1:8 scale model of the center region. The models were fabricated in a way that was consistent with the eventual construction of their full-scale counterpart. Computer analysis of the measured fields has confirmed that a focused beam of H^- ions can be isochronously accelerated to 500 MeV with a total beam loss due to H^- stripping of 6.5%. The vertical focusing frequency, ν_z, is well within the design limits of 0.35 ± 0.10. The effects on the magnetic field of the magnet support structure, bolting array and vacuum chamber supports have been measured and have been accounted for to a first order. The main coil is to be made of extruded aluminum plate and will be assembled in six separate sections for convenience in manufacturing and handling and to maintain the exact six-fold symmetry of the magnetic field. The final size description is: 500 MeV radius, 312 in; coil radius, 348 in; outside radius, 426 in; gap, 20.8 in; overall height, 197 in; weight, 4200 tons. (auth) (UK)

31093 DESIGN FEATURES OF THE PRINCETON A.V.F. CYCLOTRON FACILITY. Pollock, R. E. (Princeton Univ., N. J.). pp 120-3 of Fifth International Cyclotron Conference. /McIlroy, R. W. (ed.). London; Butterworths (1971).

From International cyclotron conference; Oxford, England (17 Sep 1969). See CONF-690921.

Recent operating performance is reported and several features in the design of the accelerator, beam line and laboratory of the Princeton A.V.F. Cyclotron are described. Although begun as a close copy of the 56 MeV cyclotron at Michigan State University, a number of modifications were made to the machine, and a somewhat different approach to the laboratory layout and beam transport design was adopted. An rf amplifier, outside the vault shielding, drives the dees through tunable half wave transmission lines. Mode separation is obtained with a simple transmission line coupler. The tuning range was extended by a modification of the dee stem inductance. A magnetic channel in the beam extraction system uses coils and laminated iron foil stacks which avoid saturation while reducing the power demand relative to an air core design. The channel is designed for minimum first harmonic perturbation at the critical radius for the $\nu_R = 1$ resonance and for reduction of the first and second radial derivations of the field on the extraction trajectory. Beam energy analysis is achieved with a 90°, 183 cm radius, flat field magnet made double focusing with discrete quadrupoles. Rotating slits and localized shielding in the beam line will permit external bombardments at the full intensity available from the cyclotron. A high resolution, 15 millisteradian spectrograph is under construction. (auth) (UK)

31094 UCL ISOCHRONOUS CYCLOTRON CONCEPTUAL DESIGN AND STATUS REPORT. Macq, P. (Catholic Univ., Louvain, Belg.); Delphin, P.; Dupuis, A.; Peironet, P. pp 124-5 of Fifth International Cyclotron Conference. /McIlroy, R. W. (ed.). London; Butterworths (1971).

From International cyclotron conference; Oxford, England (17 Sep 1969). See CONF-690921.

The U.C.L. isochronous cyclotron is to be a versatile variable energy and multiparticle accelerator. The main features of the machine are described as they appear after completion of the basic studies and initiation of the procurement of the components. (auth) (UK)

31095 RF SYSTEM FOR A PROPOSED HEAVY ION CYCLOTRON. Mosko, S. W. (Oak Ridge National Lab., Tenn.). pp 126-9 of Fifth International Cyclotron Conference. /McIlroy, R. W. (ed.). London; Butterworths (1971).

From International cyclotron conference; Oxford, England (17 Sep 1969). See CONF-690921.

The separated-sector isochronous cyclotron proposed by the Oak Ridge National Laboratory would accelerate any ion of any element; heavy ions with $q/A \geq 0.15$ would be accelerated to 7.5 MeV/a.m.u. and protons to 300 MeV. Ion orbit frequencies range from 0.5 to 10.0 MHz. The heavy-ion cyclotron is a ring structure of four-sector magnets with four rf cavities placed between them. Two cavities operate on the fundamental rf, variable from 10 to 30 MHz. Two other auxiliary cavities operate on the rf second harmonic; their phase can be adjusted for either "flat-top" or "peaked" modes of ion acceleration. Each cavity is a $\lambda/2$ TEM resonator, with the center conductor protruding axially from both sides of the dee. An array of movable panels provides the 3:1 tuning range. An rf power amplifier on each cavity provides up to 400 kW to produce 250 kV on the fundamental dees, and up to 75 kW for 65 kV on the harmonic dees. A quarter-scale model cavity has been fabricated and the rf system is being optimized. (auth) (UK)

31096 EXTERNAL BEAM HANDLING SYSTEM FOR THE A.V.F. CYCLOTRON OF THE UNIVERSITY OF GRONINGEN. Put, L. W. (Univ., Groningen, Netherlands). pp 130-3 of Fifth International Cyclotron Conference. /McIlroy, R. W. (ed.). London; Butterworths (1971).

From International cyclotron conference; Oxford, England (17 Sep 1969). See CONF-690921.

The layout of the beam handling system for the isochronous cyclotron is described. This system differs in some respects from more or less conventional systems. One of the major parts of the system is the analyzing system, consisting of a 105° magnet with homogeneous field and edge focusing and a quadrupole doublet. It will be shown that by including a quadrupole in the system the attainable momentum resolution can be improved considerably. The expected momentum resolution is 1×10^{-4}. The transmission of the analyzing system is 100% for a monoenergetic beam with phase space areas of 10 mm mRad and 70 mm mRad in the horizontal and vertical plane respectively. The design and positioning of the switching magnet is such that both the nonanalyzed beam and the analyzed beam can be switched into the experimental area, while at least three experimental stations can be reached by both types of beams. (auth) (UK)

31097 GRENOBLE CYCLOTRON PROGRESS REPORT. Ferme, J.; Ripouteau, F.; Belmont, J. L.; Laborie, G.; Goin, G. (Institut des Sciences Nucleaires, Grenoble, France). pp 134-40 of Fifth International Cyclotron Conference. /McIlroy, R. W. (ed.). London; Butterworths (1971).

From International cyclotron conference; Oxford, England (17 Sep 1969). See CONF-690921.

The cyclotron was tested and accepted at 50 MeV proton energy in 1968. It has been used for physics experiments since January 1969. The beam energy is at present limited to 40 MeV proton, because of an accidental short-circuit on the main coils. After the repair, the proton energy could be increased to 60 MeV. The

XUM

polarized proton source and the axial injection are in operation. The results are modest, but are improving. (auth) (UK)

31098 CYCLOTRON AND THE COMPUTER: A LOOK AT THE PRESENT AND THE FUTURE. de Forest, R. A. (Michigan State Univ., East Lansing). pp 141-50 of Fifth International Cyclotron Conference. /McIlroy, R. W. (ed.). London; Butterworths (1971).

From International cyclotron conference; Oxford, England (17 Sep 1969). See CONF-690921.

It is shown that current approaches to computer control are philosophically the same and that there is a second approach which it is hoped will be implemented in the future, since it offers advantages in both cost and flexibility. Some details of computer hardware and software are described because they are of importance to persons making long range decisions. At this time, without sophisticated systems of logging and analysis which future cyclotron control systems will have, it is not possible to forecast in detail the changes computer control will bring to beam quality; however, computer control will dictate more careful attention to the engineering details of beam defining and measuring devices. (auth) (UK)

31099 CONTROL SYSTEM OF THE DUBNA MONOENERGY CYCLOTRON. Denisov, Yu. N.; Lyubenko, A. N.; Shishlyanikov, P. T. (Joint Inst. for Nuclear Research, Dubna, USSR). pp 151-6 of Fifth International Cyclotron Conference. /McIlroy, R. W. (ed.). London; Butterworths (1971).

From International cyclotron conference; Oxford, England (17 Sep 1969). See CONF-690921.

The characteristics of a monoenergy cyclotron and the method of particle extraction accepted in the design of the Dubna monoenergy cyclotron impose specific requirements on the control system of the whole machine, consisting of the electrostatic accelerator-injector, the ring cyclotron and all the parts of the beam transport channels. In order to produce particles of the proper energy at the channel exit it is necessary to control the regime of operation of the electrostatic accelerator and the channel for shaping nanosecond bunches of injected particles, the mode of the injection channel, the cyclotron average magnetic field, the frequency of the accelerating voltage, the radial position of the entrance plate of the electrostatic deflector and the bending magnet, the electrical field intensity in the deflector, the field in the deflecting magnet, the magnetic field in the focusing lenses in the channel employed, the fields in the bending magnets, the magnetic field in and the gap width at the foci of analyzing magnets and the positions of beam stops at collimator exits in the experimental rooms, etc. All these adjustments should be performed in the shortest possible time. To achieve this an automatic control system will be used consisting of a digital programmer for modes and analogue correcting devices. The schematic view of the control system is shown. (auth) (UK)

31100 EXTRACTION FROM MEDIUM AND HIGH ENERGY CYCLOTRONS. Joho, W. (Swiss Inst. for Nuclear Research, Zurich). pp 159-79 of Fifth International Cyclotron Conference. /McIlroy, R. W. (ed.). London; Butterworths (1971).

From International cyclotron conference; Oxford, England (17 Sep 1969). See CONF-690921.

A review of some basic extraction systems is given with emphasis on the properties of nonresonant and resonant extraction. Results are given for extraction efficiency and energy spread of the extracted beam as a function of beam quality and radial focusing frequency. It is shown, that for higher energies, large ring cyclotrons can have extraction efficiencies over 90%. Some formulas for the stability of vertical motion are summarized. (auth) (UK)

31101 MAGNETICALLY SELF-SHAPING SEPTUM FOR BEAM DEFLECTION. Hudson, E. D.; McDaniel, F. E. (Oak Ridge National Lab., Tenn.). pp 180-9 of Fifth International Cyclotron Conference. /McIlroy, R. W. (ed.). London; Butterworths (1971).

From International cyclotron conference; Oxford, England (17 Sep 1969). See CONF-690921.

Septum magnets for deflecting charged particles at $\beta \geq 0.5$ were developed with deflection strength equivalent to that of an electrostatic deflector with a gradient exceeding 200 kV/cm. Composed of thin-current-carrying sheet conductors, they are self-shaping and assume the same radius of curvature as the beam to be deflected when the end-points are properly adjusted. The maximum field reduction obtained is limited mainly by the tensile strength of the septum and by the power that can be removed from the thin sheet conductors. As an example of the design, a one-kilogauss unit for the Oak Ridge Isochronous Cyclotron (ORIC), in which $\beta \leq 0.38$, will operate at 4000 A. The water-cooled septum is 4 cm wide and 0.3 cm thick; the 1-cm section centered in the beam is thinned to 0.075 cm. The radial aperture is 1.8 cm; an equivalent electrostatic deflector would require nearly 200 kV across this gap. A conventional electrostatic septum could also be made to conform to the beam shape; requiring only a few amperes, this could substantially increase the extraction efficiency. (auth) (UK)

31102 RESULTS OF BEAM EXTRACTION AT THE JUELICH 90 MeV DEUTERON AEG ISOCHRONOUS CYCLOTRON. Thimmel, H.; Wucherer, P. (AEG-Telefunken, Frankfurt am Main). pp 190-9 of Fifth International Cyclotron Conference. /McIlroy, R. W. (ed.). London; Butterworths (1971).

From International cyclotron conference; Oxford, England (17 Sep 1969). See CONF-690921.

The acceptance tests of the Juelich isochronous cyclotron have been completed. Beam matching to the beam handling and monochromator systems is achieved by using two iron channels and an additional electrostatic channel. The measured properties of the extracted beam are in good agreement with the precalculated data. (auth) (UK)

31103 EXTRACTION PERFORMANCE OF THE HARWELL VARIABLE ENERGY CYCLOTRON. Jones, E. J.; Howard, K. J. (Atomic Energy Research Establishment, Harwell, Eng.). pp 200-7 of Fifth International Cyclotron Conference. /McIlroy, R. W. (ed.). London; Butterworths (1971).

From International cyclotron conference; Oxford, England (17 Sep 1969). See CONF-690921.

Over 50 different beams ranging from protons to neon ions with 10 to 1 energy coverage have now been developed to meet the demand of users of the Harwell V.E.C. With such a wide spectrum of beams there are naturally variations in their orbital characteristics which in turn are reflected in the extraction performance. For most beams the extraction efficiency is greater than 50%; exceptions are some of the harmonic beams where only about 30% was obtained. It should be pointed out that these figures apply for a simple puller and ion source geometry with no defining slits and a variable orbit operation. Substantial improvements in extraction are obtained by using a defining slit in the central region. For example, 70% efficiency can be achieved routinely on a large number of beams, while 80 to 90% was measured with very careful tuning up of machine parameters. The septum part of the extractor consists of a readily detachable tungsten foil of thickness 0.5 mm with a V-shaped slot to assist power dissipation. The maximum power dissipation is estimated at about 2 kW. Over the past 12 months during which there was extensive running with powers of about 1 kW, it was not necessary to replace the septum. The maximum voltage gradient on the extractor channel is about 120 kV/cm and although difficulty was experienced in voltage holding during the first year of operation, this has now been overcome by hard chromium plating of the copper electrodes. (auth) (UK)

31104 MAGNETIC REGENERATOR. Oh, S. W.; Powell, W. B. (Univ. of Birmingham, Eng.). pp 208-14 of Fifth International Cyclotron Conference. /McIlroy, R. W. (ed.). London; Butterworths (1971).

From International cyclotron conference; Oxford, England (17 Sep 1969). See CONF-690921.

It is common to use regenerators to extract beams from synchrocyclotrons; but their use in AVF cyclotrons is rare. The reasons for this may be partly historical and theoretical; but there are also technical difficulties connected with the narrower gaps in AVF cyclotrons and the need to vary the regenerator strength. A regenerator has been in use on the 40 in radial ridge cyclotron for the past six years. This was initially designed as an electrostatic element, and although it worked (at times very well), over the years it became the most unreliable component in the machine. This was due to occasional but serious breakdown of the 40 to 50 kV positive voltage electrode which could not be eliminated. To overcome this difficulty a magnetic regenerator was constructed. This consists of two small, specially shaped, soft iron components. When operated with an electrostatic regenerator with a small voltage of either polarity, the extraction efficiency and beam quality were found to be satisfactory and the regenerator system was both adjustable in strength and completely reliable. (auth) (UK)

31105 FIRST AND SECOND HARMONIC EXTRACTION. van Nieuwland, J. M. (Philips Research Labs., Eindhoven, Netherlands). pp 215-25 of Fifth International Cyclotron Conference. /McIlroy, R. W. (ed.). London; Butterworths (1971).

From International cyclotron conference; Oxford, England (17 Sep 1969). See CONF-690921.

The orbit separation desired for good beam extraction can be obtained in different ways. The separation is mainly determined

XUM

by the harmonic field disturbances. A simple analytic representation of the motion of the orbit center under the influence of first and second harmonic field components is presented. This description gives a clear and accurate insight into the extraction process. It is also used for numerical calculations with slowly varying field parameters at acceleration. A large gradient of the second harmonic field component can drive the orbit center in a fixed direction, determined by the first and second field harmonics. This effect resembles the operation of regenerative extraction. The method with two independently adjustable harmonics has the advantage of permitting flexible control of the increase of the coherent oscillation amplitude and its radial and azimuthal directions. The numerical calculations are made for the field parameters of a Compact Isochronous Cyclotron. (auth) (UK)

31106 DESIGN STUDIES FOR AN ULTRA-THIN SEPTUM EXTRACTION CHANNEL FOR THE MODIFIED NEVIS SYNCHRO-CYCLOTRON. Ziegler, K.; Martin, E.; Cohen, R. (Columbia Univ., New York). pp 226-8 of Fifth International Cyclotron Conference. /McIlroy, R. W. (ed.). London; Butterworths (1971).

From International cyclotron conference; Oxford, England (17 Sep 1969). See CONF-690921.

Extensive computer studies of different current configurations for a magnetic extraction channel were performed. A configuration was found which gives an average field of 5 kG, and a radially focusing gradient of 1 kG/in. By the use of a thin current sheet perpendicular to the median plane of the synchrocyclotron the step from no field to full channel field can be limited to less than 0.06 in. The distortion of the main magnetic field outside the channel is less than 100 G and subtracting, so it can be compensated by additional iron shims. The total power dissipated in the channel is about 200 kW. (auth) (UK)

31107 RESONANCE FREE OR PRECESSIONAL EXTRACTION: A COMPARISON. Liesem, H. (AEG-Telefunken, Grosswelzheim, Ger.). pp 229-34 of Fifth International Cyclotron Conference. /McIlroy, R. W. (ed.). London; Butterworths (1971).

From International cyclotron conference; Oxford, England (17 Sep 1969). See CONF-690921.

Using the measured four sector field of the AEG Compact Cyclotron, precessional extraction ($\nu_r < 1$) was studied and compared with resonance-free extraction ($\nu_r > 1$). (auth) (UK)

31108 STUDY OF THE REGENERATIVE EXTRACTION SYSTEM IN THE CERN SYNCHROCYCLOTRON. Lindbaeck, S. (CERN, Geneva). pp 235-44 of Fifth International Cyclotron Conference. /McIlroy, R. W. (ed.). London; Butterworths (1971).

From International cyclotron conference; Oxford, England (17 Sep 1969). See CONF-690921.

A study of the present regenerative extraction system is briefly reviewed and a proposal is given for improvements yielding an increase in extraction efficiency from the present 5% to a theoretical maximum of 85%. Possible means of obtaining beams of high and low duty cycle were also studied and are briefly discussed. (auth) (UK)

31109 EXTRACTION OF MULTIPLE BEAMS OF VARIOUS ENERGIES FROM THE TRIUMF NEGATIVE ION ISOCHRONOUS CYCLOTRON. Robertson, L. P. (Univ. of Victoria, B. C.); Auld, E. G.; Mackenzie, G. H.; Otter, A. J. pp 245-9 of Fifth International Cyclotron Conference. /McIlroy, R. W. (ed.). London; Butterworths (1971).

From International cyclotron conference; Oxford, England (17 Sep 1969). See CONF-690921.

Acceleration of negative ions in the TRIUMF accelerator permits extraction of up to six proton beams, each beam independently variable in energy from 150 MeV to 500 MeV. The position of the foil which strips the electrons from the accelerated H^- ions can be chosen so that the extraction trajectories of the various energies intersect at a common crossover point outside the accelerator. Calculations show that thin stripping foils can be designed to handle beam powers equivalent to at least 100 μA of 500 MeV protons. A combination magnet placed at the crossover point directs these beams into a transport system which is designed to be achromatic between the stripping foil and the entrance to the experimental area. Field measurements on the $^1/_{20}$ scale model accelerator magnet were used to determine the optical properties of the extracted beams passing through the fringe field. Stripping foil positions as a function of energy, and transfer matrices for these trajectories were calculated for a number of positions of the crossover point for the two directions of motion of the ions in the accelerator. The components of the transfer matrix vary little with position of the crossover point. For the case that the direction of the orbits in the accelerator is opposite to the pole spiral, there is a smaller variation in the matrix elements with extracted beam energy. (auth) (UK)

31110 CYCLOTRON BEAM SHARING FOR MULTIPLE TARGET IRRADIATIONS. Burton, G. (Hammersmith Hospital, London). pp 250-3 of Fifth International Cyclotron Conference. /McIlroy, R. W. (ed.). London; Butterworths (1971).

From International cyclotron conference; Oxford, England (17 Sep 1969). See CONF-690921.

The possibility of electromagnetic beam switching between three parallel beam lines of the Medical Research Council Cyclotron using a low power high repetition rate pulsed electromagnet and three high power dc septum magnets to give the main deflection into the beam lines is discussed. (auth) (UK)

31111 OPTIMISATION OF THE CYCLOTRON CENTRAL REGION FOR THE NUCLEAR PHYSICS USER. Blosser, H. G. (Michigan State Univ., East Lansing). pp 257-73 of Fifth International Cyclotron Conference. /McIlroy, R. W. (ed.). London; Butterworths (1971).

From International cyclotron conference; Oxford, England (17 Sep 1969). See CONF-690921.

Beam requirements for high quality nuclear physics experiments are reviewed along with features of central region arrangements for preferentially transmitting particles satisfying the requirements. With such a central region, phase widths of 1.5° can be achieved and such phase widths in conjunction with good stabilizing circuits lead to highly monochromatic beams. (External beam energy spread 0.04% FWHM at MSU.) Such systems also give 100% extraction efficiency and high transmission through external analysis systems. (Total transmission of 20% at MSU for 1 in 6000 energy resolution and emittance of less than 1 mm mRad.) (auth) (UK)

31112 SOME FACTORS DETERMINING THE BEAM QUALITY OF A.V.F. CYCLOTRONS. Hagedoorn, H. L. (Technological Univ., Eindhoven, Netherlands); Hazewindus, N.; van Nieuwland, J. M. pp 274-88 of Fifth International Cyclotron Conference. /McIlroy, R. W. (ed.). London; Butterworths (1971).

From International cyclotron conference; Oxford, England (17 Sep 1969). See CONF-690921.

Some factors which have a large influence on the beam properties of A.V.F. cyclotrons are discussed. The connection between injected beam and extracted beam is considered without going into detailed orbit dynamics. This results in a qualitative prediction of the time, energy and geometry structure of the external beam as a function of the injected beam parameters. Remarks on the beam dynamics of the first few turns are given, using a general orbit theory. Some numerical calculations on the axial motion are presented, taking into account space charge effects. (auth) (UK)

31113 EFFECTS OF CENTRAL-REGION CONDITIONS ON TIME STRUCTURE AND QUALITY OF CYCLOTRON BEAMS. Reiser, M. (Univ. of Maryland, College Park). pp 289-304 of Fifth International Cyclotron Conference. /McIlroy, R. W. (ed.). London; Butterworths (1971).

From International cyclotron conference; Oxford, England (17 Sep 1969). See CONF-690921.

Time structure, emittance, particle intensity and energy spread of a cyclotron beam are largely determined by central region conditions and can be defined through choice of orbit geometry and use of defining slits. The fundamental limit of beam equality is given by the intrinsic emittance and phase-space density which the beam would have under dc conditions. In the actual case of rf acceleration, ion intensity and energy gain become a function of phase with respect to the rf voltage and the effective emittance increases due to radial dispersion in the magnetic field. For a fixed energy spread at extraction and hence a given spread of orbit centers, the phase width or microscopic duty factor of the beam is larger the smaller the orbit geometry at injection, i.e., the lower the dee voltage. On the other hand, space-charge effects, short-pulse requirements for time-of-flight experiments, etc., favor high dee voltage and hence a large orbit geometry. The Maryland cyclotron was designed to provide some flexibility between the two extremes, permitting a variation of orbit geometry between 155 turns (single-turn extraction) and 700 turns (multi-turn extraction). (auth) (UK)

31114 LONGITUDINAL SPACE CHARGE EFFECT AND ENERGY RESOLUTION. Gordon, M. M. (Michigan State Univ., East Lansing). pp 305-17 of Fifth International Cyclotron Conference. /McIlroy, R. W. (ed.). London; Butterworths (1971).

From International cyclotron conference; Oxford, England (17 Sep 1969). See CONF-690921.

In the design of isochronous cyclotrons with distinctly separated turns at extraction, calculations of energy resolution are customarily based solely on considerations of the beam phase width, the rf voltage and its resultant wave form. Machines of this type have

XUM

been proposed which aim at 100 μA currents with an energy resolution of 10^{-3} or better, and it appears quite likely that the hitherto neglected longitudinal space charge effect will determine the actual current or energy resolution achievable in such cyclotrons. The present work summarizes an extensive analysis of the longitudinal space charge effect and provides formulas for calculating the resultant energy spread within a turn under certain conditions. (auth) (UK)

31115 HARMONIC OPERATION OF THE HARWELL VARIABLE ENERGY CYCLOTRON. Jones, E. J.; Howard, K. J. (Atomic Energy Research Establishment, Harwell, Eng.). pp 318-24 of Fifth International Cyclotron Conference. /McIlroy, R. W. (ed.). London; Butterworths (1971).

From International cyclotron conference; Oxford, England (17 Sep 1969). See CONF-690921.

The currents accelerated on different harmonic modes were compared and it was found that operation on the seventh harmonic is possible with the existing open center geometry of the Harwell Variable Energy Cyclotron. Using the measured threshold voltage for acceleration, the effective gap factor for the first gap crossing was calculated and compared with theory. (auth) (UK)

31116 CYCLOTRON BEAM PULSER FOR PARTICLE TIME-OF-FLIGHT EXPERIMENTS. Johnson, W. P. (Univ. of Maryland, College Park); Blosser, H. G.; Sigg, P. pp 325-32 of Fifth International Cyclotron Conference. /McIlroy, R. W. (ed.). London; Butterworths (1971).

From International cyclotron conference; Oxford, England (17 Sep 1969). See CONF-690921.

The energy resolution in time-of-flight experiments performed on a cyclotron is limited by the reaction product flight times of approximately 60 ns associated with the beam microstructure. A scheme for eliminating N−1 out of every N micropulses from the external beam has been developed for the Michigan State University Cyclotron. The internal beam is stopped on a collimator on the first one-half turn by applying a dc voltage to a radially deflecting plate located in the dee between the ion source and collimator. A 60 ns wide pulse, synchronized with the dee voltage, but with 1/Nth the repetition rate cancels the dc deflection voltage allowing single micropulses through the collimator. Beam currents of 1 μA time-average were obtained with pulse widths of 0.4 ns at one-tenth the rf repetition rate. By removing a set of phase selecting slits inside the cyclotron, time-average currents of 10 μA were obtained at 10% duty cycle with pulse-widths of approximately 1.5 ns. (auth) (UK)

31117 PHASE–SPACE VOLUME MEASUREMENTS ON THE NUFFIELD 60 IN CYCLOTRON. Ettinger, K. V.; Dealler, J. F. B.; Stewart, F. R. (Univ. of Birmingham, Eng.). pp 333-40 of Fifth International Cyclotron Conference. /McIlroy, R. W. (ed.). London; Butterworths (1971).

From International cyclotron conference; Oxford, England (17 Sep 1969). See CONF-690921.

The Nuffield 60 in cyclotron is a classical machine capable of reliable operation with large beam currents and is often used for work in neutron physics. Time-of-flight techniques which utilize the intrinsically discontinuous nature of the particle beam presuppose very short pulses with well defined and known characteristics. The wave form of the beam current and the relation between the energy of the particles and their time of arrival on the target were investigated. This relation expressed in the form of the phase-space volume had to indicate the most practical method of shortening the length of the beam bunch, if it could be done without undue loss in its intensity. (auth) (UK)

31118 EXTERNAL BEAM MONOCHROMATISATION SYSTEM IN THE 2.4 m ISOCHRONOUS CYCLOTRON AT THE KURCHATOV ATOMIC ENERGY INSTITUTE. Basargin, Yu. G. (Efremov Research Inst., Leningrad); Bogdanova, V. I.; Severgin, Yu. P.; (and others). pp 341-7 of Fifth International Cyclotron Conference. /McIlroy, R. W. (ed.). London; Butterworths (1971).

From International cyclotron conference; Oxford, England (17 Sep 1969). See CONF-690921.

The results of calculations for the external beam monochromatization system for the 2.4 m cyclotron at the Kurchatov Atomic Energy Institute are given. In this system an energy spread compensation of the beam by an rf voltage on the debuncher is used. A special mirror-symmetrical achromatic magnetic system provides a momentum separation of the beam. An improvement of energy spread from ±0.2% to 0.02% is expected. The methods of stabilization and fine control in the system are discussed. (auth) (UK)

31119 EMITTANCE MEASUREMENTS AT THE JUELICH ISOCHRONOUS CYCLOTRON (JULIC). Kuhlmann, W.; Bojowald, J.; Mayer-Boericke, G.; Reich, J. (Institut fuer Kernphysik, Juelich, Ger.). pp 348-56 of Fifth International Cyclotron Conference. /McIlroy, R. W. (ed.). London; Butterworths (1971).

From International cyclotron conference; Oxford, England (17 Sep 1969). See CONF-690921.

The emittance-measuring device (EMA) for the Juelich Isochronous Cyclotron (JULIC) is described. The EMA works on the principle of the two-slit method and operates automatically. Measuring of phase-space areas in radical or vertical direction takes about 2 min. High-power beams of up to 90 MeV deuterons at 20 μA and 180 MeV α-particles at 10 μA may be analyzed. The acceptance is 1250 mm mrad resulting from a position range of 50 mm for both slits. The analysing slits consist of carbon-shielded copper. A preliminary survey of the properties of the external beam is given with respect to phase-space areas for deuterons and protons. The measured emittances for 80% beam intensity are less than 20 mm mrad in both planes if the cyclotron is carefully adjusted. (auth) (UK)

31120 PROPOSED USE OF A STORAGE RING TO IMPROVE THE MICROSCOPIC DUTY FACTOR OF A CYCLOTRON. Wright, Byron T. (Univ. of California, Los Angeles). pp 357-62 of Fifth International Cyclotron Conference. /McIlroy, R. W. (ed.). London; Butterworths (1971).

From International cyclotron conference; Oxford, England (17 Sep 1969). See CONF-690921.

A cyclotron beam is introduced into a storage ring. The revolution periods in the cyclotron and in the storage ring are different and are adjusted so that after several cycles there is a beam circulating in the storage ring at all azimuths. A second harmonic in the storage ring magnetic field causes the beam to drift toward an electrostatic deflector. The drift rate is adjusted so that the beam which is transferred into the storage ring on a given rf cycle will enter the deflector over many revolutions. Beam exists at all azimuths in the storage ring, so some beam is entering the electrostatic deflector at all times. A practical example is described in which a beam which initially has a 10% microscopic duty factor is converted into a beam whose minimum and maximum instantaneous values are 28% and 170% of the time average value. The rms deviation from the average value is less than 10%. (auth) (UK)

31121 PRODUCTION OF MONOCHROMATIC BEAMS USING CYCLOTRON ACCELERATION. Basargin, Yu. G.; Litunovskii, R. N.; Minyaev, O. A. (Efremov Scientific Research Inst., Leningrad). pp 363-9 of Fifth International Cyclotron Conference. /McIlroy, R. W. (ed.). London; Butterworths (1971).

From International cyclotron conference; Oxford, England (17 Sep 1969). See CONF-690921.

Three methods of producing a cyclotron beam with low energy spread are considered. The first method is based on the known proposals for "stabilized" separated-turn cyclotrons. The second utilizes the analyzing properties of the cyclotron magnetic field when extracting the beam at a radius close to the boundary of radial stability. In the third method monochromatization of the external beam by a debuncher is considered. The latter two methods require no high degree of stability of the accelerating voltage amplitude and phase. (auth) (UK)

31122 PECULIARITIES OF CHARGED PARTICLE MOTION IN THE MONOENERGETIC CYCLOTRON. Dmitrievskii, V. P.; Kolga, V. V.; Polumordvinova, N. I. (Joint Inst. for Nuclear Research, Dubna, USSR). pp 370-4 of Fifth International Cyclotron Conference. /McIlroy, R. W. (ed.). London; Butterworths (1971).

From International cyclotron conference; Oxford, England (17 Sep 1969). See CONF-690921.

The heightened requirements for cyclotron beam energy spread (1 in 10^4), as well as the necessity for varying the external beam energy, results in the need to consider a number of additional conditions which are usually neglected in ordinary cyclotrons. These conditions are as follows; equal ion energy gain per turn to an accuracy of 1 in 10^4, isochronism of closed orbits, rigid restrictions for all the processes related to increasing free oscillation amplitudes, external injection with limited beam emittances, and the necessity to take account of the effects of space charge. These considerations were the basis for the development of the Dubna monoenergetic cyclotron. Its parameters are tabulated. A number of calculations were performed to investigate the effects of free oscillations induced by the accelerating electric field at energies close to the injection energy $\nu_p \approx 1$. With these numerical calculations it turned out to be necessary to take into account the shape of the electric field, except when changing the particle momentum. These investigations show that the design and construction of a monoenergetic cyclotron having 1 in 10^4 energy resolution are quite possible from the technical point of view. (UK)

XUM

31123 SPECTROMETRIC ISOCHRONOUS CYCLOTRON. Barit, I. Ya.; Vasil'ev, G. A.; Kanunnikov, V. N.; (and others) (Lebedev Inst. of Physics, Moscow. Efremov Scientific Research Inst., Leningrad). pp 375-9 of Fifth International Cyclotron Conference. /McIlroy, R. W. (ed.). London; Butterworths (1971).

From International cyclotron conference; Oxford, England (17 Sep 1969). See CONF-690921.

The characteristics of a spectrometric isochronous cyclotron for producing beams of protons, deuterons and other particles having a maximum energy of 80 MeV (for protons), average current 100 μA and energy spread 10^{-4} are considered. The indicated values of parameters may be obtained by using a magnet having divided sectors, external injection and introducing the third harmonic of the accelerating field. The principal requirements as regards the magnet system, injector and rf system of such a cyclotron are formulated. Preliminary results of the magnetic field calculations and ion motion during acceleration are presented and discussed. (auth) (UK)

31124 HIGH RESOLUTION NUCLEAR STUDIES USING CYCLOTRON BEAMS. Kashy, E.; Trentelman, G. F.; Jolly, R. K. (Michigan State Univ., East Lansing). pp 380-7 of Fifth International Cyclotron Conference. /McIlroy, R. W. (ed.). London; Butterworths (1971).

From International cyclotron conference; Oxford, England (17 Sep 1969). See CONF-690921.

Various types of nuclear experiments which require high resolution particle beams are described. Examples of the performance of the MSU Cyclotron in providing such beams are given. Proton beam currents of approximately 200 nA for $\Delta E/E = 1/6000$ resolution are easily obtained at $E_P \geq 25$ MeV with internal beam currents of only 3 μA. The role of dispersion matching is discussed and preliminary results using the laboratory broad range magnetic spectrograph are shown. (auth) (UK)

31125 OPERATIONAL EXPERIENCE WITH THE H^- BEAM OF THE MILAN CYCLOTRON. Acerbi, E.; Birattari, C.; Castiglioni, M.; (and others) (Univ., Milan). pp 388-98 of Fifth International Cyclotron Conference. /McIlroy, R. W. (ed.). London; Butterworths (1971).

From International cyclotron conference; Oxford, England (17 Sep 1969). See CONF-690921.

The operation of the Milan cyclotron, used mainly to accelerate H^- ions in the energy range from 20 to 45 MeV is reported. The extracted proton beam, obtained by stripping the H^- ions is determined by the characteristics of the acceleration and extraction processes. In practice one wishes to know how the quality and geometry of the external beam depend on the factors controlling the injection, acceleration, and stripping of the H^- ions. The influence of these factors was therefore investigated, and results are presented on the effects of (i) dynamics of the last orbits before extraction, (ii) positioning of the ion source, (iii) magnetic field tuning, (iv) rf voltage, etc. The experimentally determined limits for the stability of some of the above parameters are indicated. A brief description of the extraction and combination device is given, followed by a discussion of the convenience of using stripping foils of variable inclination, to improve the matching of the extracted beam with the transport system. (auth) (UK)

31126 MULTI-CHANNEL NON-INTERCEPTING PHASE PROBE FOR THE UNIVERSITY OF MARYLAND CYCLOTRON. Bird, J. K.; Berg, R. E. (Univ. of Maryland, College Park). pp 399-402 of Fifth International Cyclotron Conference. /McIlroy, R. W. (ed.). London; Butterworths (1971).

From International cyclotron conference; Oxford, England (17 Sep 1969). See CONF-690921.

The University of Maryland Cyclotron will incorporate a non-intercepting phase probe using sampling techniques which will visually display the amplitude and phase of the beam pulse with respect to the rf voltage at 12 radii. There are no frequency-dependent or tuned circuits, and all controls are remote. Use of two additional identical probes, one of which samples the rf dee voltage, allows time calibration of the system. An rf pick-up probe is used to trigger a series of high-speed monostable multivibrators which provide a phase position control and a linear phase sweep of the sampling pulse of up to 180°. These are followed by two more monos of fixed delay to provide a standard charge to a step recovery diode which produces the sampling pulse. The step recovery diode (HPA 0153) is mounted in the dee immediately below the $1\frac{1}{4}$ in. $\times \frac{1}{4}$ in. pick-up plate which is located $\frac{3}{4}$ in. below the median plane. (auth) (UK)

31127 NON-INTERCEPTING CYCLOTRON BEAM MONITOR. Ettinger, K. V.; Stewart, F. R. (Univ. of Birmingham, Eng.). pp 403-9 of Fifth International Cyclotron Conference. /McIlroy, R. W. (ed.). London; Butterworths (1971).

From International cyclotron conference; Oxford, England (17 Sep 1969). See CONF-690921.

The bunched nature of the cyclotron beam permits its measurements under both pulsed and steady conditions without interception of the particles. A simple monitor which consists of a toroidal current transformer and an amplifier tuned to the cyclotron orbital frequency operates satisfactorily down to currents of less than 5×10^{-7} A. Much higher sensitivity, below 10^{-8} A, was provided by a system using frequency conversion and a synchronous detector, with the reference signal derived from the cyclotron oscillator. Output of the monitor provides a dc signal for the beam intensity indicator and also a video output which permits display of the beam envelope. Calibration of the monitor is accomplished by means of a step-recovery diode pulse generator and a calibrated attenuator. Probes described can also be used for energy measurements by a correlation method which is briefly described. (auth) (UK)

31128 RF SYSTEM OF THE MONOENERGETIC CYCLOTRON. Glazov, A. A.; Kochkin, V. A.; Novikov, D. L.; Onischenko, L. M. (Joint Inst. for Nuclear Research, Dubna, USSR). pp 410-13 of Fifth International Cyclotron Conference. /McIlroy, R. W. (ed.). London; Butterworths (1971).

From International cyclotron conference; Oxford, England (17 Sep 1969). See CONF-690921.

The accelerating system of the Dubna monoenergetic cyclotron (MC) is to provide 200 keV energy gain per revolution per charge for all accelerated particles: p, d, α, ^{3}He, ^{6}Li. Particles are to be accelerated at the maximum of the rf voltage, and the vector of the accelerating electrical field strength is directed along the closed particle orbit at all radii. To increase the working phase region a non-sinusoidal rf accelerating field must be applied (sinusoid with a flat top); this is achieved by using additional dees operating at three times the basic frequency. The scheme and configuration of the accelerating cavities of the rf system are determined, first, by the requirement to provide optimum conditions for acceleration and, second, by the general accelerator arrangements. Consideration of these requirements with the four-sector magnet design resulted in the described scheme for the accelerating systems of the monoenergy cyclotron. (UK)

31129 MAGNETIC SYSTEM OF THE MONOENERGETIC CYCLOTRON. Vorozhtsov, S. B.; Zamolodchikov, B. I.; Zaplatin, N. L. (Joint Inst. for Nuclear Research, Dubna, USSR). pp 414-19 of Fifth International Cyclotron Conference. /McIlroy, R. W. (ed.). London; Butterworths (1971).

From International cyclotron conference; Oxford, England (17 Sep 1969). See CONF-690921.

The requirements imposed on the accelerator magnetic field at working radii of $\Delta r = 54$ to 410 cm are mainly that according to the kind of particles accelerated the average field should be isochronous to an accuracy of $\sim 3 \times 10^{-5}$ and the magnetic field variation dependent on flutter should be larger than 0.6. The required structure of the Thomas type magnetic field can be achieved by means of four identical C-shaped sector electromagnets placed 90° apart. Preliminary calculations showed that the total iron weight of the electromagnets is ~1200 t and the power supply of the windings does not exceed 1.5 MW. An experimental model of the magnetic system was made and magnetic measurements performed by means of a Hall detector whose accuracy was not worse than $\pm 0.15 \pm 0.7$ G. The detector was mounted in the gap by using special equipment which permitted its displacement along the azimuth by 360° and along the radius from 0 to 470 mm with accuracies of ±0.1° and ±0.5 mm, respectively. The azimuthal distribution curves of the magnetic field from the sector electromagnet along azimuths at different radii are shown. To obtain reliable results in analyzing the experimental curves of the magnetic field, detailed measurements in the edge zone of the magnet are needed. The azimuthal measurements were made with an alternative interval along the azimuth. The experimental data were treated by computer. The experimental and calculation studies have shown the possibility of producing the necessary magnetic field for the monoenergetic cyclotron. (UK)

31130 ACCELERATION OF VERY HEAVY IONS BY MEANS OF A TWO-CYCLOTRON FACILITY. Boettger, O. (AEG-Telefunken, Frankfurt am Main); Mueller, R. W. pp 446-52 of Fifth International Cyclotron Conference. /McIlroy, R. W. (ed.). London; Butterworths (1971).

From International cyclotron conference; Oxford, England (17 Sep 1969). See CONF-690921.

Acceleration of very heavy ions (uranium ions up to 9 MeV/nucleon) is discussed in connection with the use of a two-cyclotron

XUM

facility. It is shown that the facility costs are at a minimum when the two cyclotrons are of equal size. The costs rise slowly if the second machine is the smaller one, and they rise rapidly if the first machine is the smaller. The technique of the joint operation of both machines is described, and the problems involved are discussed. (auth) (UK)

31131 HEAVY ION ACCELERATION AT ORIC. Lord, R. S.; Duelli, B. L.; Hudson, E. D.; (and others) (Oak Ridge National Lab., Tenn.). pp 453-8 of Fifth International Cyclotron Conference. /McIlroy, R. W. (ed.). London; Butterworths (1971).
From International cyclotron conference; Oxford, England (17 Sep 1969). See CONF-690921.

Microampere beams of 4+ ions of ^{12}C, ^{16}O, and ^{14}N are now accelerated in the Oak Ridge Isochronous Cyclotron from a heated-filament ion source of conventional dimensions. Small beams of $^{13}C^{4+}$ (from natural carbon) and $^{20}Ne^{5+}$ were also obtained. The intensity of these heavy ion beams is strongly dependent on arc power. A water-cooled copper arc chamber and an insulated anti-cathode are used. Up to 1.5 kW can be dissipated in the arc. Studies of pressure attenuation of the beam show a factor of 2 loss for a path length of 650 m at a pressure of $\sim 3 \times 10^{-6}$ torr. Good pressure is maintained by cryopumping at liquid nitrogen temperature adjacent to the circulating beam. (auth) (UK)

31132 GENERATION AND INJECTION OF HEAVY-IONS INTO CYCLOTRONS. Jenkins, K. D. (Univ. of Maryland, College Park). pp 459-68 of Fifth International Cyclotron Conference. /McIlroy, R. W. (ed.). London; Butterworths (1971).
From International cyclotron conference; Oxford, England (17 Sep 1969). See CONF-690921.

Passing an energetic ion beam through a gas or foil target produces ions of only a few charge states closely grouped about a mean value. The radius of curvature in a magnetic field of an ion at the mean charge is a constant, independent of the ion energy. The interrelationships of the specific ionization in gases and foils with regard to kinetic energy, magnetic rigidity, and cyclotron frequency are discussed with their consequences for injection into a cyclotron. Using a gas or foil stripper to start the acceleration process in a cyclotron results in a fixed energy gain for each type of ion due to the Br dependence. Proposed designs of heavy-ion sources employing the advantages of the constant Br are presented. Ions of all elements, nitrogen through uranium, can be accelerated and stripped of a third to a half of their electrons while being accelerated to energies of over 1 MeV per nucleon. One ion source employs a sectored ring magnet (edge focusing) with a static magnetic field adjustable to a Br of 1300 kG cm. In an acceleration ring chamber with a vacuum 10^{-3} torr, the gas maintains the ion in a charge equilibrium state. A fixed frequency cavity type acceleration gap is used. The acceleration is by the stochastic process with the noise produced by the random change in charge. A second proposed source uses a microtron type magnet. The operation is the inverse of the microtron in that the orbital period of each ion charge state is a multiple of that of a pulsed accelerating voltage. A stripping target at the acceleration gap maintains the ion in a charge equilibrium state. (auth) (UK)

31133 ION SOURCES FOR MULTIPLY CHARGED HEAVY IONS. Bennett, J. R. J. (Rutherford High Energy Lab., Chilton, Eng.). pp 469-79 of Fifth International Cyclotron Conference. /McIlroy, R. W. (ed.). London; Butterworths (1971).
From International cyclotron conference; Oxford, England (17 Sep 1969). See CONF-690921.

A review is given of existing sources of multiply charged heavy ions. Particular emphasis is on cyclotron applications. Most sources are of the P.I.G type and the performance of the various models is compared. New methods were recently suggested for producing high charge states of very heavy particles. Some are based on plasmas used in thermonuclear research. A very brief account is given of a few of these devices. Finally, acceleration and stripping of ions is mentioned for completeness, as it can be a very effective way of producing highly charged ions. (auth) (UK)

31134 C.E.V. INJECTOR ION SOURCE. Ah-Hot, L.; Arianer, J.; Baixas, J.; (and others) (Institut de Physique Nucleaire, Orsay, France). pp 480-6 of Fifth International Cyclotron Conference. /McIlroy, R. W. (ed.). London; Butterworths (1971).
From International cyclotron conference; Oxford, England (17 Sep 1969). See CONF-690921.

The multicharge heavy ion source attached to the cyclotron injector is of the hot-cathode reflex type. The high power arc is pulsed in order to produce highly charged states. The ion source, electric focusing, and magnetic analyzing elements are mounted on a platform brought to a 140 kV dc voltage. Qualitative and quantitative results are presented. (auth) (UK)

31135 HEAVY ION ACCELERATION IN THE IPCR 160 cm CYCLOTRON. Kohno, I.; Miyazawa, Y.; Tonuma, T.; (and others) (Inst. of Physical and Chemical Research, Yamato, Japan). pp 487-98 of Fifth International Cyclotron Conference. /McIlroy, R. W. (ed.). London; Butterworths (1971).
From International cyclotron conference; Oxford, England (17 Sep 1969). See CONF-690921.

In the IPCR 160 cm classical cyclotron the operating ranges of the magnet and rf system are 0.5 to 2 Wb/m^2 and 5 to 12 mHz respectively, and various particles of different mass to charge ratios from protons to Ne^{5+} ions can be accelerated with variable energy. Electron bombarded hot cathode heavy ion sources for this cyclotron were developed to produce C^{4+}, N^{4+}, O^{4+}, N^{5+}, and O^{5+} ions. At present these ions are produced in sufficient quantities under arc powers of 2 to 2.5 kW when N_2, O_2, or CO_2 gas is fed into the source at a flow rate of 1 to 2 cm^3/min. The source life is mainly limited by the erosion of the tungsten cathodes to ~20 h. The attenuation of beam current by charge exchange collisions with residual molecules and the spectra of various ions accelerated in the cyclotron are discussed. C^{4+}, N^{4+}, and O^{4+} ions are accelerated from 39 to 120 MeV, 45 to 100 MeV, and 52 to 100 MeV respectively and used for several experiments. (auth) (UK)

31136 PRODUCTION AND ACCELERATION OF HEAVY IONS IN THE HARWELL VARIABLE ENERGY CYCLOTRON. Bennett, J. R. J. (Rutherford High Energy Lab., Chilton, Eng.). pp 499-507 of Fifth International Cyclotron Conference. /McIlroy, R. W. (ed.). London; Butterworths (1971).
From International cyclotron conference; Oxford, England (17 Sep 1969). See CONF-690921.

The design and performance of the ion source for the Harwell Variable Energy Cyclotron is described. The source is of the Penning Ionization Gauge Type, having solid tantalum or tungsten cathode discs which are heated directly by the discharge. The arc is operated continuously and not pulsed. Preliminary results of laboratory tests of a simple modification to the source to produce multiply charged ions of solid materials are also presented. The source is inserted axially into the cyclotron through a slot in the top pole of the cyclotron magnet and is positioned by a precision mechanism to obtain centered orbits. The source was in regular use in the cyclotron and has produced beams of hydrogen, helium, carbon, nitrogen, oxygen, neon, argon, and krypton ions. Of particular note are the extracted beams of 2 μA of 150 MeV N^{5+} ions, 10 μA of 120 MeV C^{4+} ions and 0.08 μA of 180 MeV C^{5+} ions. Very low energy heavy ion beams were accelerated on fifth and seventh harmonics and currents of the order of one microampere of beam extracted despite the poor geometry at the center of the cyclotron. The cyclotron vacuum is adequate to keep beam loss due to stripping down to a reasonable level, though with some low velocity beams the stripping is severe. (auth) (UK)

31137 SOURCES OF HIGHLY-STRIPPED IONS FOR ION ACCELERATORS. Peacock, N. J.; Pease, R. S. (Culham Lab., Abingdon, Eng.). pp 508-14 of Fifth International Cyclotron Conference. /McIlroy, R. W. (ed.). London; Butterworths (1971).
From International cyclotron conference; Oxford, England (17 Sep 1969). See CONF-690921.

Ions with ionization potentials up to 4 keV are now produced in some high-temperature pulsed-plasma devices. The plasma produced by irradiation of any arbitrary target element by a pulsed, high intensity laser beam is considered. The degree of ionization and the absolute number of ions produced were studied spectroscopically and it is evident that stripping of the ions to charge states of up to +20 can be achieved. This agrees with the calculations of the laser absorption and the plasma dynamic processes in the expanding plasma blob. The effective production rate for the highly stripped ions is 10^{14} s^{-1}. Although extraction of these ions for accelerator purposes is technically difficult, calculations show that currents of 10^{13} ions s^{-1} with charge states between +10 and +20 can be expected from the laser plasma source. (auth) (UK)

31138 HIPAC ION SOURCE: RECENT THEORY AND EXPERIMENTS. Daugherty, J. D.; Eninger, J. E.; Janes, G. S.; Levy, R. H. (Avco Everett Research Lab., Everett, Mass.). Contracts AT(30-1)-3863; AFOSR F44620-69-C-0095. pp 515-29 of Fifth International Cyclotron Conference. /McIlroy, R. W. (ed.). London; Butterworths (1971).
From International cyclotron conference; Oxford, England (17 Sep 1969). See CONF-690921.

The HIPAC Ion Source is a novel device intended to produce very highly stripped heavy ions. The achievement of this objective would permit the acceleration of heavy ions in relatively modest cyclotrons. This ion source is presently conceived as a toroidal vacuum chamber of about 20 cm major radius and 3 cm minor radius. An azimuthal magnetic field contains a cloud of ≈10 keV electrons

XUM

having a density of $10^{11}/cm^3$. This cloud forms a toroidal electrostatic potential well which will trap and contain ions as long as the electron cloud remains stable. The 10 keV kinetic energy of the electrons results in an electron impact ionization flux of $\sim 10^6$ W/cm^2. The effective electron beam power of the source is several hundred megawatts but is wholly reactive. Recent theoretical work produced estimates of the ion source emittance of ~100 mm mrad $(MeV/nucleon)^{\frac{1}{2}}$. Recent experiments achieved electron cloud containment times of 5 ms, which were limited solely by vacuum conditions. Electron densities of $7 \times 10^9/cm^3$ were previously achieved in a 10 cm minor radius experiment, which should scale directly to $\sim 2 \times 10^{10}/cm^3$ in a 3 cm device. Current research is directed to extending containment times to the range of ion source interest (0.1 to 4 s), to increasing the electron density and to demonstration of stripping and extraction of heavy ions. The current status of this research and the prospects for the HIPAC Ion Source are reviewed. (auth) (UK)

31139 SERIES COMBINATION OF A TANDEM AND A CYCLOTRON AND VICE VERSA. Boettger, O.; Mahrt, R. (AEG–Telefunken, Frankfurt am Main). pp 530–6 of Fifth International Cyclotron Conference. /McIlroy, R. W. (ed.). London; Butterworths (1971).

From International cyclotron conference; Oxford, England (17 Sep 1969). See CONF-690921.

The addition of a relatively small cyclotron greatly enlarges the potentialities of a tandem Van de Graaff with respect to the achievable energy of various particles. Light particles are accelerated more suitably with the cyclotron as injector, heavier particles with the reverse arrangement. Consideration of the volume in phase space of interest for the beam transfer from one accelerator to the other is given. Furthermore injection into the cyclotron is discussed for polarized light particles, which necessitate bulky ion sources, as well as for particles pre-accelerated by the tandem. Lastly a new type of buncher is presented, which will be capable of almost ideal bunching. (auth) (UK)

31140 CONCEPTUAL DESIGN OF A TWO-STAGE, TWO-GAP CYCLOTRON. Wright, Byron T.; Igo, G. J.; Richardson, J. R.; Verba, J. W. (Univ. of California, Los Angeles). pp 537–44 of Fifth International Cyclotron Conference. /McIlroy, R. W. (ed.). London; Butterworths (1971).

From International cyclotron conference; Oxford, England (17 Sep 1969). See CONF-690921.

The two-stage, two-gap cyclotron which is described has the following features related to the acceleration of heavy ions: (1) isochronization of all orbits is possible, (2) the radiofrequency may be at or near the optimum harmonic of the ion frequency in each stage, (3) one stripping process is used and the stripping foil is extended to the cyclotron and, (4) a minimum of 9 MeV/amu is obtained after two stages of acceleration. The maximum potential required of the preinjector is 700 keV. The machine also produces 200 MeV protons, 240 MeV deuterons, 170 MeV tritons, and corresponding energies of other light ions. For these a small cyclotron is used to pre-accelerate the ions prior to injection into the second stage. (auth) (UK)

31141 DESIGN SPECIFICATIONS FOR COMPACT CYCLOTRONS. Chaudhri, M. Anwar (Hammersmith Hospital, London); Boettger, O. pp 545–55 of Fifth International Cyclotron Conference. /McIlroy, R. W. (ed.). London; Butterworths (1971).

From International cyclotron conference; Oxford, England (17 Sep 1969). See CONF-690921.

Design specifications for compact cyclotrons were examined from the point of view of their applications in the following fields; radioisotope production, production of neutrons, activation analysis, radiation physics and radiation biology and injection into tandems and low-energy nuclear physics. The maximum energy, internal and external beam intensities, energy resolution, beam quality, and energy and particle variability are fully discussed. Extensive tabulations of calculated isotope yields and neutron output as well as of theoretical detection sensitivities for charged-particle activation from cyclotrons of various sizes are presented. (auth) (UK)

31142 20 MeV COMPACT CYCLOTRON. Dupont, F.; Gremont, B. (Thomson, C.S.F., Orsay, France). pp 556–8 of Fifth International Cyclotron Conference. /McIlroy, R. W. (ed.). London; Butterworths (1971).

From International cyclotron conference; Oxford, England (17 Sep 1969). See CONF-690921.

The isochronous compact cyclotron built by Thomson, C.S.F. is a multi-particle, variable energy accelerator. The energy range is 6 to 19 MeV for protons and α-particles, 5 to 9 MeV for deuterons, and 8 to 25 MeV for helium 3. The main features of this machine are as follows: Very compact magnet (11 tons) with a rather small power consumption (30 kW); rf system operating on the second and fourth harmonic modes within the 25 to 50 Mc/s frequency range; extraction system including an electrostatic deflector, a gradient correcting channel, and a quadrupole; and Zucker type source. The choice of the energy range is a compromise between the increasing price and the field of possible experiments. The 19 MeV maximum energy gives a wide access to: activation analysis (the reaction threshold for deuterons is 8 to 10 MeV); nuclear medicine (the cyclotron is the only way to obtain short-lived isotopes which are more and more used in medical research. A deuteron energy of 9 MeV allows one to obtain a great number of short-lived isotopes); and neutron production: with 19 MeV protons and several tons of microamperes of beam, it is possible to have up to 3 or 4×10^{10} fast neutrons/cm^2/s by choosing the best production reaction. (auth) (UK)

31143 BASIC DESIGN PARAMETERS OF A SMALL SIZE ISOCHRONOUS CYCLOTRON. Alekseev, A. G.; Bogdanov, P. V.; Galaev, A. N.; (and others) (Efremov Scientific Research Inst. of Electrophysical Apparatus, Leningrad). pp 559–63 of Fifth International Cyclotron Conference. /McIlroy, R. W. (ed.). London; Butterworths (1971).

From International cyclotron conference; Oxford, England (17 Sep 1969). See CONF-690921.

The design of a small sector-focusing cyclotron with variable-energy particles is described. The possible energy range is as follows: for protons 4 to 15 MeV, deuterium ions 2 to 10 MeV, doubly-charged ions of helium 3 and helium 4, 5 to 25 MeV and 4 to 20 MeV respectively. The expected intensity of the internal beam is 300 μA, with up to 50 μA extracted. The magnetic structure of the cyclotron is chosen as a result of work on a magnet model which is 1 : 1.5 of full size. By choosing a low operating induction a single trim coil consisting of 4 sections placed at radii according to a definite law may be used to give the required characteristics of magnetic field in the whole range of energy for the different types of particle. (auth) (UK)

31144 AEG COMPACT CYCLOTRON. Hartwig, E. (AEG–Telefunken, Frankfurt am Main). pp 564–72 of Fifth International Cyclotron Conference. /McIlroy, R. W. (ed.). London; Butterworths (1971).

From International cyclotron conference; Oxford, England (17 Sep 1969). See CONF-690921.

A recently developed 43 in cyclotron – maximum energy 22 MeV protons-for application in physics, medicine, and (with some modifications) technology is described. (auth) (UK)

31145 DESIGN AND PERFORMANCE OF A COMPACT MULTI-PARTICLE CYCLOTRON. Fleischer, A. A.; Hendry, G. O.; Smith, C. G.; Tom, J. L.; Wells, D. K. (Cyclotron Corporation, Berkeley, Calif.). pp 573–82 of Fifth International Cyclotron Conference. /McIlroy, R. W. (ed.). London; Butterworths (1971).

From International cyclotron conference; Oxford, England (17 Sep 1969). See CONF-690921.

Two compact cyclotrons were constructed and are now being used for routine production of short-lived isotopes at medical research centers. A third of these cyclotrons, as well as two slightly larger ones, are currently being manufactured in Berkeley, California. The measured external beams of the CS-15 and CS-22 cyclotrons are given. Both the CS-15 and CS-22 use two-dee fundamental acceleration with three-fold magnet symmetry. A small spiral angle is used. Unique design features include a folded rf system to conserve space, copper-plated pole tips and hill iron to eliminate the rf liner, a small cold cathode P.I.G. ion source capable of generating intense ion beams, dee voltage regulation, rf stabilisation, and a focusing magnetic channel, which provides a small spot size at the beam exit port. The design parameters and performance of these cyclotrons are discussed. (auth) (UK)

31146 AXIAL INJECTOR FOR THE HARWELL VARIABLE ENERGY CYCLOTRON. Bennett, J. R. J. (Rutherford High Energy Lab., Chilton, Eng.). pp 602–9 of Fifth International Cyclotron Conference. /McIlroy, R. W. (ed.). London; Butterworths (1971).

From International cyclotron conference; Oxford, England (17 Sep 1969). See CONF-690921.

The design and construction of the axial injector for the Harwell Variable Energy Cyclotron is described. The injector is to replace the conventional ion source at the center of the cyclotron for all ion beams. It is hoped that easier working with heavy ions and in particular ions of non-gaseous elements will result. The ion source is of the Penning Ionization Gauge type and the magnetic field necessary for its operation also serves to analyse the beam into the different charge to mass ratio components. The analysed

XUM

beam is injected into the center of the cyclotron down an axial hole in the top pole of the cyclotron magnet and is focused by magnetic quadrupoles. An electrostatic mirror deflects the beam into the median plane of the cyclotron. Electrodes in the dee and dummy dee concentrate the electric field at the first rf gap to give improved acceleration without intercepting the beam. The injector is at present being commissioned and the first preliminary results of acceleration of protons to 27 MeV and C^{2+} to 22 MeV are given. (auth) (UK)

31147 EXTERNAL INJECTION SYSTEM FOR THE GRONINGEN CYCLOTRON. Dermois, O. C. (Kernfysisch Versneller Instituut, Groningen, Netherlands). pp 620-4 of Fifth International Cyclotron Conference. /McIlroy, R. W. (ed.). London; Butterworths (1971).

From International cyclotron conference; Oxford, England (17 Sep 1969). See CONF-690921.

The injector is described as it will be used in the cyclotron. Calculations on orbits are done mainly with an analog computer. The complete system will be tested in a small magnet and the ions will be accelerated a few turns by an rf field. Details of the beam guiding system consisting of a series of cylindrical magnetic lenses made of permanent magnet ring cores arranged around a vacuum tube are discussed. (auth) (UK)

31148 SOME STUDIES ON THE AXIAL INJECTION SYSTEM FOR A COMPACT CYCLOTRON. Hazewindus, N. (Philips Research Labs., Eindhoven, Netherlands). pp 625-37 of Fifth International Cyclotron Conference. /McIlroy, R. W. (ed.). London; Butterworths (1971).

From International cyclotron conference; Oxford, England (17 Sep 1969). See CONF-690921.

Two problems are discussed: the influence of space charge in the electrostatic lenses of the guiding system of an axial injection system and the design of a bunching system. A calculation of the influence of a two-dimensional Gaussian space charge distribution on linear beam optics is presented. It is shown that quadrupole settings calculated using the space charge distribution agree much better with the experimentally observed settings than those obtained from calculations neglecting space charge. The use of a klystron-type buncher is considered in order to increase the current accepted by the cyclotron. The simple bunching theory, ignoring the finite extent of the incoming beam, is used to obtain preliminary values of modulation voltage and drift space length. It is shown that the modulation does not seriously affect the emittance of the axial injection system nor the acceptance of the cyclotron centre. A detailed quantitative description of debunching effects due to the finite beam size is presented. Debunching effects limit the predicted current increase to a factor of between 2 and 2.5. (auth) (UK)

31149 STATUS REPORT ON THE ALICE PROJECT. Ah-Hot, L.; Baron, E.; Bougarel, M. P.; (and others) (Institut de Physique Nucleaire, Orsay, France). pp 638-45 of Fifth International Cyclotron Conference. /McIlroy, R. W. (ed.). London; Butterworths (1971).

From International cyclotron conference; Oxford, England (17 Sep 1969). See CONF-690921.

The main characteristics of the Orsay project are summarized. The injection of a 1 MeV/amu heavy ion beam into the isochronous cyclotron is discussed. The capabilities of this hybrid machine are shown along with the field of new experiments. The present status and the results of several tests are given. (auth) (UK)

31150 INJECTION AND STRIPPING OF A HEAVY ION BEAM IN THE ORSAY CYCLOTRON. Ah-Hot, L.; Baron, E.; Bourgarel, M. P. (Institut de Physique Nucleaire, Orsay, France). pp 646-57 of Fifth International Cyclotron Conference. /McIlroy, R. W. (ed.). London; Butterworths (1971).

From International cyclotron conference; Oxford, England (17 Sep 1969). See CONF-690921.

The ALICE project consists in injecting a 1 MeV/amu heavy ion beam with a charge to mass ratio $Z_{i}/A \geq 0.1$ into a stripping target located on the appropriate equilibrium orbit in the cyclotron. The problems posed by this injection system are enumerated and the capabilities of the system summarized in graph form showing the ratio of the stripped charge (Z_s) to injected charge (Z_i) as a function of mass number (A) to stripped charges (Z_s). The trajectories of $^{14}N^{2\rightarrow7}$, $^{20}Ne^{2\rightarrow8}$, $^{40}A^{4\rightarrow13}$ in the non-uniform magnetic field of the cyclotron were computed and the requirements to accelerate these ions are given. The difficulties due to the beam having to be guided from the linac to the cyclotron and its emittance having to match the acceptance of the machine are discussed. The rf consideration caused by the linac working on a fixed frequency (25 MHz) while the cyclotron frequency ranges from 5 to 10 MHz according to the charge-to-mass ratio are given. The stripping mechanism is explained. (UK)

31151 DESIGN AND PERFORMANCE OF AN H^- INJECTOR CYCLOTRON. Fleischer, A. A.; Hendry, G. O.; Wells, D. K. (Cyclotron Corp., Berkeley, Calif.). pp 658-65 of Fifth International Cyclotron Conference. /McIlroy, R. W. (ed.). London; Butterworths (1971).

From International cyclotron conference; Oxford, England (17 Sep 1969). See CONF-690921.

Two compact negative hydrogen ion cyclotrons utilizing external ion sources with axial injection were constructed for use as high energy ion sources for tandem Van de Graaff accelerators. Approximately 2.5 mA of H^- ions (or 1.5 mA of D^- ions) are generated externally in an Ehlers ion source, analysed and then axially injected into the cyclotron. The axial injection system includes two pairs of electrostatic quadrupoles and a velocity bunching system to transport the beam to an electrostatic mirror in the central region of the cyclotron. The maximum amount of internal beam appears to be limited by space charge in the electrostatic mirror to approximately 100 μA. The peak-to-peak incoherent radial amplitude of the internal beam is about 2.5 mm. The beam is extracted by a precessional extraction system followed by a focusing magnetic channel in the cyclotron fringe field. The positive deflector electrode requires special electron dumps and shielding to prevent P.I.G. discharges. The best measured external beam has been 40 μA. The full area horizontal and vertical emittances are approximately 12 and 15 mm mrad, respectively, and a minimum energy spread of about 16 keV has been observed. The injection system, central region, and negative ion extraction system of this cyclotron are discussed in detail. (auth) (UK)

31152 H^- ION INJECTION INTO THE CENTRAL REGION OF THE TRIUMF CYCLOTRON. Craddock, M. K. (Univ. of British Columbia, Vancouver); Louis, R. J.; Reiser, M. pp 666-9 of Fifth International Cyclotron Conference. /McIlroy, R. W. (ed.). London; Butterworths (1971).

From International cyclotron conference; Oxford, England (17 Sep 1969). See CONF-690921.

The usual central region design problems are alleviated in the TRIUMF cyclotron by three main features: (1) injection at relatively high energy (300 keV) from an external ion source; (2) strong magnetic axial focusing; and (3) squaring the rf wave with a third harmonic. Numerical studies of the initial orbits in the median plane, based on electric and magnetic fields from model measurements, show that non-linearities in the radial motion are negligible, and that a phase range from $-45°$ to $+25°$ will be centred to within the expected beam width, 0.32 in. For the axial motion, tracking and matching studies using a thick lens approximation to the dee gaps show good acceptance for lagging, but a sharp cut-off at $-5°$ for leading phase ions. This is shifted to $-15°$ by the three-sector narrow pole-gap geometry at the center which provides phase-independent magnetic focusing of $\nu_z = 0.2$. Third harmonic squaring of the rf wave advances the cut-off to $-45°$, at the same time improving the radial phase acceptance. (auth) (UK)

31153 RADIAL INJECTION OF A POLARISED BEAM INTO A CYCLOTRON. Bejsovec, V.; Bem, P.; Karban, O.; Mares, J.; Trejbal, Z. (Nuclear Research Inst., Rez, Czech.). pp 670-2 of Fifth International Cyclotron Conference. /McIlroy, R. W. (ed.). London; Butterworths (1971).

From International cyclotron conference; Oxford, England (17 Sep 1969). See CONF-690921.

A source of polarized ions was constructed at the Nuclear Research Institute of the Czechoslovak Academy of Sciences in Rez. From this source, polarized particles accelerated to 40 keV energy are injected radially into a cyclotron, type U-120. The apparatus consists of two principal parts; the source itself and the injection system. Injection makes use of two successive charge-exchange processes, neutralization of the beam before entering the cyclotron and ionization by a stripping foil placed at the center of the cyclotron. The final testing of the whole device is now in progress. The preliminary figure of the beam intensity after the deflector is 5×10^8 particles/s. This value may be improved by increasing the acceleration efficiency which is particularly sensitive to the position of the stripping foil inside the cyclotron. (auth) (UK)

31154 HARWELL 110 IN SYNCHROCYCLOTRON MODIFICATION SCHEME. Scanlon, J. P. (Atomic Energy Research Establishment, Harwell, Eng.). pp 673-87 of Fifth International

Cyclotron Conference. /McIlroy, R. W. (ed.). London; Butterworths (1971).

From International cyclotron conference; Oxford, England (17 Sep-1969). See CONF-690921.

Modifications to the Harwell synchrocyclotron were made with the objective of increasing the accelerated beam currents, improving the extraction efficiency and broadening the field of use of the machine. The means adopted were to install a 30 kV, high repetition rate rf system operating on three frequency ranges to allow acceleration of protons, deuterons, α-particles and $^3H^{++}$; a calutron ion-source; regenerative beam extraction; and improved neutron time-of-flight facilities. Though there are still some problems regarding acceleration of α-particles and $^3He^{++}$, internal beams up to 10 μA protons and 40 μA deuterons were obtained. The extraction efficiency is low as yet, largely because of poor internal beam quality, the reasons for which are discussed. (auth) (UK)

31155 NEVIS SYNCHROCYCLOTRON CONVERSION PROJECT. Cohen, R. (Columbia Univ., New York); Martin, E.; Rainwater, J.; (and others). pp 699-710 of Fifth International Cyclotron Conference. /McIlroy, R. W. (ed.). London; Butterworths (1971).

From International cyclotron conference; Oxford, England (17 Sep 1969). See CONF-690921.

The status of the Columbia University Nevis Synchrocyclotron Modification Project is presented. The machine will be converted to a three-fold symmetry spiral sector focusing AVF synchrocyclotron, having a long duty factor 550 MeV external proton beam. The time average external beam intensity is expected to be between 5 μA and 40 μA. The accelerating rf must cover the frequency band from ~26.5 MHz to 18.5 MHz. One of the three pairs of sector iron shims will be incorporated in the dee and supported on Al_2O_3 insulators. Tuning will be accomplished by two rotating capacitors with axes directed toward the centre of the magnet. This design permits effective magnetic shielding of the rotor to minimize eddy current losses. The reasons leading to the particular approach of this conversion program are given. (auth) (UK)

31156 SOME PECULIARITIES OF PHASE MOTION IN THE PHASOTRON WITH SPATIAL VARIATION OF MAGNETIC FIELD. Dmitrievskii, V. P.; Zamolodchikov, B. I.; Polumordvinova, N. I.; Kolga, V. V. (Joint Inst. for Nuclear Research, Dubna, USSR). pp 711-18 of Fifth International Cyclotron Conference. /McIlroy, R. W. (ed.). London; Butterworths (1971).

From International cyclotron conference; Oxford, England (17 Sep 1969). See CONF-690921.

Accelerator designs envisaging a considerable increase of beam intensity (20 to 50 times) will be of great significance for the development of nuclear physics in the region below 1 GeV. The conversion of present day synchrocyclotrons into phasotrons with spatial variation of the magnetic field is the most promising direction. A radially increasing magnetic field results in considerable reduction of the required frequency sweep which makes it possible to increase the accelerating voltage amplitude several times and increase the capture time by decreasing the parameter of the "K" phase equation. The choice of the main parameters of such a phasotron is determined to a considerable extent by the investigation of particle motion in the acceleration process. The criteria determining the choice of the law of the average magnetic field along the radius as well as field tolerances along the radius are considered. The tolerances for this field in the area of the first phase oscillation are also treated. It is concluded that phasotrons with the average magnetic field increasing along the radius are characterized by some peculiarities of ion phase motion in the process of acceleration. With a constant value of $\sin \varphi_s$ it is possible to tolerate a considerable (2 to 3 times) increase of $K = -\omega/E.d\omega/dE$ without phase loss in acceleration. It is reasonable to take the law of the average magnetic field, keeping in mind the above peculiarity. When "K" in the central region is taken to be considerably smaller than unity, it is necessary to have some additional tolerance for the magnetic field in this region. (UK)

31157 STATUS REPORT ON THE CERN SYNCHROCYCLOTRON IMPROVEMENT PROGRAMME. pp 719-27 of Fifth International Cyclotron Conference. /McIlroy, R. W. (ed.). London; Butterworths (1971).

From International cyclotron conference; Oxford, England (17 Sep 1969). See CONF-690921.

In order to increase the internal beam current of the CERN SC from its present value of ~1 μA to ~10 μA and to improve its radial quality, the pulse repetition rate will be raised from 54 Hz to ~500 Hz and the dee voltage increased to 30 kV and the present open Penning source will be replaced by a hooded arc source. The principal features and the expected performance of the design are outlined and the modification of extraction and pulse stretching are indicated. (auth) (UK)

31158 PROTON SOURCE FOR THE IMPROVED CERN SYNCHROCYCLOTRON. Galiana, R. (CERN, Geneva). pp 728-35 of Fifth International Cyclotron Conference. /McIlroy, R. W. (ed.). London; Butterworths (1971).

From International cyclotron conference; Oxford, England (17 Sep 1969). See CONF-690921.

The features and performance of the ion source for the improved CERN synchrocyclotron are described together with some aspects of its technological development. The problems of operating the source in the accelerator and of stability are discussed. Finally, a survey of the monobloc construction of the central geometry of the accelerator is given. (auth) (UK)

31159 FACTORS AFFECTING BEAM INTENSITY AND QUALITY IN SYNCHROCYCLOTRONS. Holm, S. (CERN, Geneva). pp 736-48 of Fifth International Cyclotron Conference. /McIlroy, R. W. (ed.). London; Butterworths (1971).

From International cyclotron conference; Oxford, England (17 Sep 1969). See CONF-690921.

Theories for efficiency of capture and focusing at the center of a synchrocyclotron are discussed and compared with model experiments. Good agreement is found between theory and experiment on the influence of basic parameters on beam intensity. Measured current values indicate that the goal of 10 μA can easily be reached in the improved CERN synchrocyclotron. A factor three or four times this value is in fact possible. The anticipated construction of the central region will permit injection in well-centered orbits. Quality deterioration due to the necessary polarization of the dee electrode is avoided by means of a similarly polarized anti-dee at the center. During the first inward phase oscillations a build-up of radial oscillation amplitudes might occur. In the intended dee construction the amplitudes created by the cut-back angles are small. (auth) (UK)

31160 CONVERSION STUDIES FOR THE SREL 600-MeV SYNCHROCYCLOTRON. Reiser, M.; Kim, H.; LeVine, D. (Univ. of Maryland, College Park). pp 749-67 of Fifth International Cyclotron Conference. /McIlroy, R. W. (ed.). London; Butterworths (1971).

From International cyclotron conference; Oxford, England (17 Sep 1969). See CONF-690921.

A study of the feasibility of improving the 600-MeV synchrocyclotron at the Space Radiation Effects Laboratory was carried out at the University of Maryland. To achieve the desired beam currents in the range of 20 to 50 μA a change of the main magnetic field is required as well as an increase of dee voltage and repetition rate. Conversion into an isochronous cyclotron is considered impractical due to severe difficulties in magnetic field design. The ion capture process in various other non-isochronous field shapes of a frequency-modulated conversion scheme was investigated with the aid of a special computer program. Use of a magnetic cone to achieve adequate vertical focusing (ν_z values between 0.1 and 0.15) was found to be feasible without loss of capture efficiency. The computer studies revealed the existence of trapped particles which oscillate about an equilibrium radius throughout the entire fm cycle without returning to the center. A very attractive solution of improving the SREL machine appears to be a magnetic field which is isochronised for deuterons (360 MeV) permitting operation either in a fixed-frequency mode (for deuterons and alphas) or as a fm sector-focused cyclotron for 600-MeV protons. (auth) (UK)

31161 MODIFICATION OF A CONVENTIONAL 37 IN CYCLOTRON. Schecter, L.; Easterday, H. T.; Fessenden, P.; (and others) (Oregon State Univ., Corvallis). pp 768 of Fifth International Cyclotron Conference. /McIlroy, R. W. (ed.). London; Butterworths (1971).

From International cyclotron conference; Oxford, England (17 Sep 1969). See CONF-690921.

The conversion of the 37-inch cyclotron was essentially completed and beam development is well under way. The design includes four-fold AVF symmetry with straight sectors, two 45° in-the-valley dees, central region programming, external-gap shimming and a simple mechanical arrangement for frequency changes. The machine is field limited and the best beam achieved so far consists of 100 μA of protons. The beam energy was measured externally by a rough method to be 17.8 MeV with an energy spread of 80 keV. Electrostatic 90° deflection is employed with a magnetic channel to provide some radial focusing and steering. Extraction efficiencies of up to 40% were measured. (auth) (UK)

XUM

31162 RESONANT PROTON BEAM DEPOLARISATION IN A SYNCHROCYCLOTRON. Besnier, G. (Faculte des Sciences, Rennes-Beaulieu, France). pp 769-74 of Fifth International Cyclotron Conference. /McIlroy, R. W. (ed.). London; Butterworths (1971).

From International cyclotron conference; Oxford, England (17 Sep 1969). See CONF-690921.

The main factors which prevent the conservation of horizontal beam polarization in a synchrocyclotron are pointed out. With a vertically polarized beam, it is found that the horizontal field perturbations should be <5 G in the CERN synchrocyclotron in order to avoid 20% loss in polarization. Phase incompatibilities between the horizontal field and polarization may, however, reduce this figure. (auth) (UK)

PHYSICS (NUCLEAR)

Neutron Interactions with Matter

Refer also to abstracts 29245, 29410, 30663, 30677, 31223, 31647, 31651, and 31661.

31163 (AERE-R-5682) CALCULATION OF DIFFERENTIAL NEUTRON SCATTERING CROSS SECTIONS OF POINT DEFECTS IN A RELAXED LATTICE. Martin, D. G. (Atomic Energy Research Establishment, Harwell (England)). Jan 1968. 17p. Dep. NTIS (U. S. Sales Only).

The long-wavelength neutron scattering cross section of an interstitial in an infinite cubic primitive lattice, with all atoms relaxed as in an elastic continuum, was calculated as a function of angle. Complete accuracy would require an infinite summation over all the atoms in the lattice. Two approximations to this summation were considered: (a) only atoms within a sphere centered at the defect were included in the summation; (b) an attempt to improve approximation (a) was made by assuming that all atoms outside the sphere could be treated as a continuum and that values of the relaxation in this region were very small. The validity of these approximations was tested by varying the radius of the sphere and the value of the constant that defined the magnitude of relaxation. It was found that the results described below were independent of both the value of this constant and the orientation of the lattice with respect to the incident neutron beam. Using approximation (a) an overall fit with curves generated for a very large number of atoms was obtained with the results of calculations employing only 32 atoms; however, a more detailed correlation required many hundreds of atoms. By contrast, using approximation (b), an overall fit was obtained when all the relaxed atoms were considered as a continuum; a very good correlation with calculations involving many thousands of atoms was obtained when only 8 atoms were included as discrete scatterers in the lattice sum. It is concluded that accurate calculations of defect cross sections may be performed quite conveniently using approximation (b). The application of these results to point defects in metals is discussed. (auth)

31164 (CEA-N-825) SEVERAL APPLICATIONS OF A SYSTEM OF WEIGHTING IN MONTE CARLO CALCULATIONS. Lanore, Jeanne-Marie (Commissariat a l'Energie Atomique, Fontenay-aux-Roses (France). Centre d'Etudes Nucleaires). Oct 1967. 19p. (In French). Dep. NTIS (U. S. Sales Only).

In Monte Carlo calculations of neutron passage through various materials one attempts to find a formalism in which the weights of the neutrons take on, at each point of phase space, a value dependent only on their coordinates. This method is applied, always with the assumption of constant cross section, to the following cases: neutrons on ^{12}C in spherical geometry, neutrons passing through two media (Fe and C), and weighting dependent on the neutron direction (utilizing the method of biased probabilities). The calculated neutron spectra are given in each case. (R.W.R.)

31165 (CEX-65.04) RADIATION OUTPUT DESCRIPTION FROM THE T(d,n)^{4}He REACTION IN A LARGE TARGET (1000 cm^2): OPERATION HENRE. Burson, Z. G. (Oak Ridge National Lab., Tenn. EG and G, Inc., Las Vegas, Nev.). Jul 1970. 82p. Dep. NTIS.

Eleven major programs, including about 25 individual projects, obtained successful measurements during Operation HENRE (High Energy Neutron Reactions Experiment). To make maximum use of these data and to allow rigorous comparison with calculations, a thorough description of the radiation output from the targets was required. The target substrate was made of 2.54-cm thick copper, 40 cm in diameter and weighing 20,850 g (46 lb). A depression 1.83 cm deep in the center of this plate provided a 37.5-cm diameter flat area for the deposition of a 1000-cm^2 ErT_2 film. The thick rim of the plate provided a means for easy mounting to the accelerator tube. A deuterium beam of 400 ma at 150 kv produced 10^{13} neutrons/sec over 4π. Calculations of the energy and angular distribution of neutrons emerging from the targets show that in the direction of 0^0 (straight down), 80 percent of the neutrons were in the 13- to 15-MeV region, 5 percent were in the 5- to 13-MeV region, and 15 percent were in the 0- to 5-MeV region. At 88°, the percentages were 67, 22.5, and 10.5, respectively. For the total 4π output, the percentages were 80, 6.5, and 13.6, respectively. The calculated angular distribution of the 13- to 15-MeV component compares well with activation-foil data. Another set of activation-foil data, taken at 0^0 utilizing 14 different reactions, was studied in detail. Forty-seven different trial spectra were chosen to evaluate the sensitivity of these foils to spectral changes. The spectrum giving the best fit was nearly the same as that predicted from calculations. The foil data showed a strong sensitivity to the fraction of "14 MeV" neutrons present, but were nearly insensitive to the shape of the spectrum below the "14 MeV" peak. The results of this study are useful and applicable to all measurements taken during Operation HENRE. (auth)

31166 (CONF-710301-8) NEUTRON FILTERED BEAMS AS STANDARD SOURCES. Simpson, O. D.; Smith, J. R.; Rogers, J. W. (Idaho Nuclear Corp., Idaho Falls). [1970]. 7p. Dep. NTIS.

From 3. conference on neutron cross sections and technology; Knoxville, Tenn. (15 Mar 1971).

High-intensity sources of 2-, 24.5-, and 144-keV neutrons were produced using filtered-beam techniques. The beams of neutrons were produced by placing thick filters of scandium, iron, and silicon into beam holes of the Materials Testing Reactor. Development work has consisted of determining optimum lengths, finding techniques to deal with backgrounds, and making some pilot total-neutron-cross-section measurements. These filtered beams constitute a distinctive set of neutron sources and offer constant, well-collimated neutron beams of high intensity for their energy region. They could be established as standard sources of neutrons for the fast-breeder program, much as the 2200 m/sec values were established for the thermal reactors. While the energy resolution is wider than that of some facilities, there is no instrument capable of resolving all the detailed structure encountered in the keV region. The filtered beams really represent an intermediate case between differential and integral measurements, and will be of additional help in resolving discrepancies between these types of measurements. (auth)

31167 (EUR-4519) TIMOC: A GENERAL PURPOSE MONTE CARLO CODE FOR STATIONARY AND TIME DEPENDENT NEUTRON TRANSPORT. Kschwendt, H.; Rief, H. (European Atomic Energy Community, Ispra (Italy). Joint Nuclear Research Center). 16 Jun 1970. 236p. Dep. NTIS (U. S. Sales Only). EUR FF 33.40.

TIMOC is a Monte Carlo code for the solution of the energy and time dependent (or stationary) neutron transport equation in 3-dimensional geometries. It is written in FORTRAN II and FAP and can be operated on the IBM 7090/95. The program can treat all commonly used scattering kernels, such as: isotropic and anisotropic elastic scattering, level excitation, the evaporation model, the energy transfer matrix model, which includes (n,2n) reactions, absorption and fission. After each collision process the neutron history gets assigned a discrete energy value. The nuclear data input is, however, done by group averaged cross sections, which can be generated for any desired group structure from the ENDF/B library using the CODAC code. The geometry routines of TIMOC are exchangeable. At present the following subroutines are available: periodical multilayered slab-, spherical- and cylindrical lattices, an elaborate 3-dimensional cylindrical geometry which allows all kinds of subdivisions, the very flexible O5R geometry routine, which is able to describe any body or body combinations, with surfaces of the 2nd order. TIMOC can generate the neutron fluxes either resulting from an external source or their fundamental mode distribution by a special source iteration procedure in eigenvalue problems. The sampling of the eigenvalues (multiplication factor, mean production and mean destruction time) is based on the life cycle point of view. The code is equipped with several unusual variance reducing methods which can be applied optionally. In addition, a special feature allows the calculation of small perturbation effects. It is based on the method of similar flight paths and does not depend on the total variance of the considered quantity. (auth)

31168 (INR-1260) FLANGE-AL 4 CODE FOR THE GIER COMPUTER. Arkuszewski, J.; Baran, W.; Kowalska, K. (Institute of Nuclear Research, Warsaw (Poland)). 1971. 36p. (In Polish). Dep. NTIS (U. S. Sales Only).

FLANGE-Al 4 is an ALGOL 4 program for calculation of the scattering kernels and scattering cross sections of polycrystalline moderators for which the scattering law has been previously calculated and put on the magnetic tape by the MINIGASKET code. The program is based on the algorithm of the General Atomic FLANGE code written in FORTRAN. (auth)

31169 (JUL-724-FF) ON THE SCATTERING OF SLOW NEUTRONS BY ORTHOHYDROGEN IN THE CUBIC PHASE. Stockmeyer, R. (Kernforschungsanlage, Juelich (West Ger-

XUM

many). Institut fuer Festkoerperforschung). Jan 1971. 23p. Dep. NTIS (U. S. Sales Only).

The scattering law for slow neutrons scattered by solid orthohydrogen at low temperature in the cubic, orientationally ordered phase was derived. The creation of phonons and angular momentum waves was taken into account. (auth)

31170 (KAPL-Trans-4) NEUTRON THERMALIZATION IN H_2O AT 318°K AND 77°K. Ishmaev, S. N.; Sadikov, I. P.; Chernyshov, A. A. (Gosudarstvennyi Komitet po Ispol'zovaniyu Atomnoi Energii SSSR, Moscow. Institut Atomnoi Energii). Translated by R. E. Slovacek (Knolls Atomic Power Lab., Schenectady, N. Y.), from report IAE-1954, 29p. Dep. NTIS.

The process of neutron thermalization with time in water (T = 318°K) and in ice (T = 77°K) was investigated experimentally by measuring the neutron flux time dependence at several fixed energies. To accomplish this a crystal spectrometer was used together with a fast neutron pulsed source. It is shown that the probe tube for extracting the neutron beam from the water system significantly distorts the measured results. The perturbation effect of the hole is the basic reason for the discrepancy with the theory, which was observed in the previous measurements of the time-dependent neutron spectrum in water. The experimental results obtained for water are in complete agreement with previous theoretical calculations based on the Nelkin model for H_2O. Measurements at two water temperatures show that the process of establishing an equilibrium neutron spectrum in time depends essentially on the medium temperature. Analysis of the experimental results permitted one to determine in water and in ice (at T = 77°K) the zeroth and the first discrete eigenvalue of the time-dependent Boltzmann equation scattering operator. The following values of the neutron thermalization time in water were obtained: 5.8 ± 0.6 μsec (at T = 318°K) and 55.5 ± 1.5 μsec (at T = 77°K). (auth)

31171 (LA-4488) MCNA: A COMPUTER PROGRAM TO SOLVE THE ADJOINT NEUTRON TRANSPORT EQUATION BY COUPLED SAMPLING WITH THE MONTE CARLO METHOD. Carter, Leland L. (Los Alamos Scientific Lab., N. Mex.). Aug 1970. Contract W-7405-eng-36. 50p. Dep. NTIS.

A coupled sampling technique that utilizes the Monte Carlo method of solution was reported previously. This report extends this coupled sampling technique to include nuclear fission and time dependence. In the coupled sampling, specific use is made of sampling from the neutron transport equation to construct a scheme for a near-optimal subsequent sampling from the adjoint neutron transport equation. This procedure may be expected to be advantageous when the phase-space volume contributing to the functional is smaller than the phase-space volume of the neutron source. The computer program MCNA was written to utilize the coupled sampling technique. MCNA uses the same neutron interaction models and cross section library as does the Los Alamos code MCN; MCN solves the transport equation with Monte Carlo. (auth)

31172 (NBS-TN-499) MULTIPLE SCATTERING CORRECTIONS FOR THE ASSOCIATED-PARTICLE NEUTRON TIME-OF-FLIGHT TECHNIQUE. Richardson, Allan C. B. (National Bureau of Standards, Washington, D. C.). Oct 1969. 68p. GPO $0.65.

The computer code MAGGIE, for the calculation of multiple scattering and sample attenuation in neutron differential cross section measurements, is revised and corrected. The particular case of the scattering geometry required by the associated-particle time-of-flight is considered in detail. (auth)

31173 (RPI-328-200) LINEAR ACCELERATOR PROJECT. Annual Technical Report, October 1, 1969–September 30, 1970. (Rensselaer Polytechnic Inst., Troy, N. Y.). Contract AT(30-1)-328. 235p. Dep. NTIS.

CRITICAL ASSEMBLIES—neutron spectra in depleted uranium, analysis of fast
—neutron flux in depleted uranium, fast
—neutron spectra in bulk aluminum, fast
ELECTRON BEAMS—energy determination of, using neutron production monitoring
LINEAR ACCELERATORS—beam energy determination for electron, using neutron production monitoring
LITHIUM-7—neutron total cross section at 125 keV to 2 MeV, (E)
NEUTRONS, FAST—spectra in depleted uranium assembly, analysis of
—flux in depleted uranium assembly
—spectra in bulk aluminum assemblies
NUCLEI—neutron capture by, accuracy of cross section measurements using scintillation tanks
—neutron total cross sections for, effect of nonuniform targets on transmission measurements of
RADIATION DETECTORS, SCINTILLATION—accuracy of liquid tank, for neutron capture cross-section measurements (H.D.R.)

31174 (UCRL-19715) INTENSITY ESTIMATION FOR A NEUTRON BEAM FOR BIOLOGICAL AND MEDICAL APPLICATIONS. Goebel, Klaus; Miller, A. Jerry (California Univ., Berkeley. Lawrence Radiation Lab.). Aug 1970. Contract W-7405-eng-48. 12p. Dep. NTIS.

Fast neutrons of energies in the multi-MeV region are of great interest for biological and medical applications because of their special type of interaction with tissue-like material. The neutron energy is delivered to the tissue by one or several of the following means: recoil protons; recoil heavy particles; nuclear disintegration; and low-energy protons from neutron reactions with nitrogen and γ rays from neutron capture in hydrogen. Intensity estimations for different types of neutron beams, based on averaged and interpolated values from published and unpublished sources are discussed. In making the estimates, realistic values for the distance from neutron source to exposure area were assumed. This assumption is necessary for two reasons: to allow for the installation of sufficient shielding to reduce the background radiations in the irradiation area; and to allow for neutron beam divergence so that reasonably large objects can be irradiated uniformly. (auth)

31175 NEW VARIATIONAL METHOD FOR THE PULSED-NEUTRON PROBLEM. Ahmed, Feroz; Kothari, L. S. (Univ. of Delhi). Nucl. Sci. Eng.; 43: 315-18(Mar 1971).

A new variational method, which permits one to take explicit account of the discontinuities in the values of the transport cross section of crystalline moderators at Bragg energies, is developed to study the pulsed-neutron problem in crystalline moderators. For the trial function, the exact solution of the eigenvalue equation for some suitably chosen large value of buckling, say B_1^2, is taken. It is shown, by considering the case of beryllium, that the present method gives the values of the fundamental-mode decay constant and the corresponding eigenfunction in a sufficiently large range of buckling without having to solve the eigenvalue equation for each buckling separately. The results are discussed for two different values of B_1^2—0.04 and 0.06 cm^{-2}. (auth)

31176 THERMAL NEUTRON SCATTERING FROM SIMPLE LIQUID METALS. Nakahara, Yasuaki (Japan Atomic Energy Research Inst., Tokai). J. Nucl. Sci. Technol.; 8: 1-15(Jan 1971).

A new phenomenological method is proposed for the calculation of double differential scattering cross sections in respect of thermal neutron scattering from simple monatomic liquid metals such as liquid sodium. A general expression for the coherent part of the cross section was obtained from a system of classical Vlasov equations for fully ionized ions and electrons interacting with each other through Coulomb or effective potentials. It is demonstrated that the fine structure seen in the reduced scattering law for liquid sodium measured by Randolph can be consistently explained by means of the method. The quantum effects of electrons were estimated by applying the Balescu equation to electrons, with the result that the effects are not as important as in solid metals. Comparison of the ion–electron model with Nelkin–Ranganathan's neutral atom model reveals a marked improvement over the latter, due mainly to the explicit consideration of charges and of the presence of conduction electrons. The gross structure of the reduced scattering law is largely determined by incoherent scattering. The incoherent part of the scattering law has been calculated in the present work by combining the effective width model and the harmonic lattice model. The overall reduced scattering law is given by a combination of the coherent and incoherent parts. The calculated reduced scattering law for liquid sodium shows excellent qualitative and quantitative agreement with experimental values, except for energy transfers comparable to the energy of thermal motions of ions in liquid sodium. (auth)

31177 METHOD OF THERMAL NEUTRON WAVES FOR DETERMINATION OF DIFFUSION PARAMETERS IN HEAVY MATERIALS. Fleck, Carl M.; Nunwarz, Christine (Oesterreichische Hochschule, Vienna). Acta Phys. Austr.; 29: 166-73(1969). (In German).

The δ-shaped source method was used for the experimental determination of the diffusion parameters of lead. The experimental arrangement is described, and the results are reported graphically. The experimental values for the diffusion coefficient, the lifetime, and the diffusion length were compared with the theoretical values. (J.S.R.)

31178 PULSED NEUTRON SOURCE. Gurtovoi, M. E.; Kukhlenko, A. S.; Leshchenko, B. E.; Strizhak, V. I. (Kiev State Univ.). Instrum. Exp. Tech. (USSR) (Engl. Transl.); No. 4, 982-5(Jul-Aug 1970).

Translated from Prib. Tekh. Eksp.; No. 4, 24-8(Jul-Aug 1970).

A low-voltage pulsed neutron T(d,n) generator intended for the time-of-flight spectrometry of fast neutrons is described. The length of the neutron pulse is no greater than 1 nsec and the current in the pulse is ~3 mA. The repetition period is 140 nsec. Cutting and bunching of the pulses are affected before acceleration. (auth)

31179 IMPROVEMENT TO THE G.G. APPROXIMATION IN NEUTRON SLOWING DOWN THROUGH THE METHOD OF GENERALIZED FUNCTION. Yamamura, Yasunori; Sekiya, Tamotsu (Osaka Univ.). J. Nucl. Sci. Technol. (Tokyo); 8: 80-8(Feb 1971).

The neutron slowing down problem in an infinite homogeneous medium is treated within the G.G. approximation through the theory of generalized function (g.f.). As a test function for defining the g.f.'s, the source importance for the slowing down is chosen. In place of the Taylor expansion of the collision term of slowing down equation in the G.G. method the adjoint collision term of the importance equation is expanded. Solutions obtained with this method clearly reproduce the Placzek wiggles, which do not appear in corresponding solutions by the orthodox G.G. method using the same order of approximation, and the solutions are in very good agreement with the exact Placzek function. (auth)

31180 PRODUCTION OF POLARIZED THERMAL NEUTRONS BY MEANS OF AN IRON–COBALT NEUTRON GUIDE. Berndorfer, Knut (Technische Hochschule, Munich). Z. Phys.; 243: 188-200(1971). (In German).

A neutron guide is described by means of which a polarized neutron beam is obtained with a polarization of 80% and a transmission of 60%. The equipment was built up at the 4 MW research reactor in Munich and has been used for depolarization measurements as well as (n,γ) and (n,β) reactions. (auth)

31181 DEPOLARIZATION OF NEUTRONS TRANSMITTED BY MAGNETIC MATERIALS. Toperverg, B. P. (Ioffe Inst. of Physics and Tech., Leningrad). Sov. Phys.-Solid State (Engl. Transl.); 12: 2445-8(Apr 1971).

Translated from Fiz. Tverd. Tela; 12: 3028-32(Oct 1970).

An analysis is made of changes in the polarization vector of neutrons caused by their transmission through ferromagnets and antiferromagnets. Neutron depolarization is attributed to magnetic fields of fluctuation origin, which arise in magnetic materials because of the thermal motion of atomic spins. Equations are obtained for the depolarization in a ferromagnet magnetized to saturation. The neutron polarization vector is assumed to be initially perpendicular to the external magnetic field. An analysis is made of the neutron depolarization in antiferromagnets as a function of the applied field and it is shown that the depolarization is weak in low fields but it increases strongly on approach to the critical field at which sublattice reversal takes place. (auth)

31182 NEUTRON CHOPPER SYSTEM FOR THE ENERGY RANGE 10^{-4} eV TO 10 eV AT THE LOW FLUX REACTOR BER. Fischer, C. O. (Hahn-Meitner Inst., Berlin). Atomkernenergie; 17: 193-8(May 1971).

For time-of-flight experiments at the low flux Berlin research reactor BER (neutron flux density $\Phi_{max} = 8 \cdot 10^{11}$ cm^{-2} s^{-1}) a chopper system is in operation. As only radial beam tubes with very low cadmium ratios are available, an arrangement different from the conventional Fermi–Chopper was necessary to design. In contrast to a Fermi–Chopper, the described system is characterized by hydrogenous stopping material. In comparison with a previously installed Fermi–Chopper system of the same resolution, the intensity could be increased by the factor 5. Simultaneously the background count rate, with respect to the maximum of the neutron spectrum, was reduced from 10 to 2‰. These improvements allow, in spite of the low intensity of the Berlin reactor, time-of-flight experiments with slow neutrons in the energy range from 1.5×10^{-4} to 10 eV at a time resolution between 2 and 10%. As an illustration of the capability of this system, typical spectra and cross section measurements are presented. (auth)

31183 FINE-SPECTRAL INTERFACE EFFECTS OF RESONANCE SCATTERING UPON MULTIGROUP CROSS SECTION AVERAGING. Meneghetti, D.; Phillips, K. E. (Argonne National Lab., Ill.). J. Nucl. Energy; 24: 509-24(Dec 1970).

Fine-energy neutron spectra are utilized to obtain spatially-dependent coarse-energy multigroup cross sections for simulated core-reflector slab-geometry systems in the energy range containing scattering resonances in many of the diluents of fast reactor materials. Comparisons of both pointwise and subregion fine-group to coarse-group cross section sets are shown. Spatially-dependent coarse-group cross section sets enable accurate interface neutron-leakages to be obtained in the energy range containing resonance scattering. (auth) (UK)

31184 SOLUTION OF SINGLE-SPEED NEUTRON TRANSPORT EQUATION IN MULTILAYER PLANE AND SPHERICALLY SYMMETRIC SYSTEMS. Gorelov, V. P.; Yuferev, V. I. Zh. Vychisl. Mat. i Mat. Fiz.; 11: 129-36(Jan-Feb 1971). (In Russian).

The Keyes eigenfunctions were used to obtain a simple solution of monoenergetic neutron transport equations for multilayer plane and spherically symmetric systems. Isotropic and anisotropic scatterings were analyzed. The equations obtained may be used for determining critical dimensions of reactors with reflectors. (R.V.J.)

Nuclear Properties and Reactions, A≤ 5

Refer also to abstracts 30807, 30896, 31046, 31071–31077, 31238, 31332, 31362, and 31419.

31185 (LYCEN–7085) USE OF SEMICONDUCTOR TELESCOPES FOR DETECTING THE RECOIL NUCLEI IN PROTON-LIGHT NUCLEUS COHERENT SCATTERING AT HIGH ENERGY. Brossard, M.; Combe, J.; Fain, J.; (and others) (Clermont-Ferrand Univ. (France). Faculte des Sciences. Lyon Univ. (France). Institut de Physique Nucleaire). Nov 1970. 15p. (In French). Dep. NTIS (U. S. Sales Only).

The use of semiconductor telescopes in detecting and identifying recoil nuclei in coherent proton–nucleus interactions at 600 MeV is described. Preliminary results obtained with gaseous ^{3}He and ^{4}He targets at a pressure of one atmosphere are presented. A mean precision of 1% was obtained for the four-momentum transfer involved in the elastic interaction. (auth) (France)

31186 (LYCEN–7089) DESCRIPTION OF ELASTIC-SCATTERED PROCESSES WITH THE USE OF NON-LOCAL SEPARABLE POTENTIALS. Pigeon, J.; Barguil, J.; Fayard, C.; Lamot, G.-H.; El Baz, E. (Lyon Univ. (France). Institut de Physique Nucleaire). Dec 1970. 49p. Dep. NTIS (U. S. Sales Only).

Elastic scattering processes are studied using nonlocal separable interactions. An explicit general expression for the transition amplitude is given which includes Coulomb effects and possible excitation of the particles involved. An application of this formalism is presented in which a great improvement to Morgan's results for elastic p–p scattering is made by simply including Coulomb effects at low energy. The elastic nucleon–alpha scattering below 50 MeV and the elastic alpha–alpha scattering below 100 MeV are studied; the results obtained are in very good agreement with experimental data. (auth) (France)

31187 (NP–18741) ^{4}He FINAL STATE INTERACTIONS AND QUASIFREE SCATTERING IN DEUTERON-INDUCED THREE-PARTICLE REACTIONS ON ^{6}Li. Hagelberg, R. (Kernforschungszentrum, Karlsruhe (West Germany). Institut fuer Experimentelle Kernphysik). Dec 1970. 56p. (In German). Dep. NTIS (U. S. Sales Only).

Excited states of ^{4}He were investigated through final-state interactions in the three-particle reactions ^{6}Li(d,α$_1$)^{1}H, ^{6}Li(d,α^{3}He)n, and ^{6}Li(d,αd)D by using 52 MeV deuterons. In measuring the differential cross sections, the detector of the first outgoing particle was kept at a fixed position and the second detector scanned over a range of coplanar angles favouring ^{4}He final-state interactions. The data can be fitted consistently with four isospin T = 0 excited states of ^{4}He at 21.9 MeV, 25.5 MeV, 28.5 MeV, and 31.8 MeV with widths (Γ) of 1.8 MeV, 2.9 MeV, 5.3 MeV, and 5.6 MeV, respectively. The 21.9-MeV and the 25.5-MeV states are particularly strongly excited. From the angular correlation the spin assignment for the latter is confirmed to be 0^+ or 1^+. No evidence is found for a narrow state at 23.9 MeV. The internal consistency of the level parameters for the three different reactions as well as their good agreement with the parameters obtained by experiments using two other entrance channels with the same three decay channels confirm the model of sequential decay. For a certain uniquely favorable range of angles in the ^{6}Li(d,αd)D reaction the dominant process is the quasifree scattering of the deuteron by the α cluster of ^{6}Li. The α-cluster momentum distribution is extracted by means of the plane-wave impulse approximation by using both the energy-sharing and the angular-correlation method.

XUM

Both momentum distributions are in good agreement with those obtained from the (p,αp) and (α,2α) reactions and have the shape expected for quasi-free scattering by an L = 0 α cluster. (auth)

31188 ANALYSIS OF D(p,n)2p REACTION AT 45.5 MeV BY THE FADDEEV FORMALISM WITH COULOMB FORCE. Oryu, Shinsho (Science Univ. of Tokyo, Chiba, Japan). Progr. Theor. Phys. (Kyoto); 44: 1208-31(Nov 1970).

The three-nucleon system with two protons is investigated by the Faddeev equation with the Coulomb force. Two kinds of one-dimensional Fredholm-type integral equations are obtained by reduction of the Faddeev equation. One of the solutions represents a Coulomb distorted three-body amplitude, and the other represents a pure nuclear one. These formalisms are applied to the reaction D(p,n)2p at 45.5 MeV, using the effective range approximation for the two-body amplitudes. A good agreement with experiment was obtained. (auth)

31189 DEUTERON BREAKUP BY 78 MeV ALPHA PARTICLES. Bonbright, Daniel Irving. College Park, Md.; Univ. of Maryland (1970). 165p. University Microfilms Order No. 71-4905.

Thesis.

The $^2H(\alpha,\alpha p)n$ reaction was studied at a bombarding energy of 78.3 MeV. Detection of the alpha and proton in coincidence determined all momenta of the outgoing particles. The angles of detection were chosen to include events where the neutron emerged with very little kinetic energy; data was taken for 17 angle pairs. Cross sectional spectra of the reaction revealed two interesting aspects: large contributions from events in which the neutron could be considered unaffected by the colliding alpha particle, and significant peaks corresponding to an alpha-neutron final state interaction. Both were analyzed using single, "quasi-free," collision theory. The former could be fit quite well if the theory were normalized by a factor of $\sim 1/3$; the latter could be reproduced somewhat by the theory, but a normalization factor of ~20 was required. An investigation of second order corrections to the quasi-free theory revealed the importance of multiple scattering collisions in the reaction. The cross section corresponding to the α−n final state interaction, calculated as a double scattering, was significantly larger than that given by the single collision theory. (Diss. Abstr. Int., B)

31190 MUON CAPTURE IN ^{3}He. Guancial, Edward L. Jr. Buffalo; State Univ. of New York (1970). 95p. University Microfilms Order No. 71-6070.

Thesis.

The partial capture rate for the process $^3He + \mu^- \rightarrow {}^3H + \nu$ is calculated assuming a Universal Fermi Interaction along with the CVC hypothesis. An impulse approximation is applied to this interaction in order to derive an effective Hamiltonian for the above process. The triton wave function used is a solution to the three-body Schroedinger equation for non-local separable two-body potentials and is not the usual variational-type wave-function with adjustable parameters. This solution to the Schroedinger equation includes the effects of the tensor forces so that it is a linear combination of the ^{2}S symmetric state, the mixed symmetry ^{2}S state and the three mixed symmetry ^{4}D states. The calculated capture rate agrees in general with existing work. The ratio of the induced pseudo-scaler and the axial-vector coupling constants, $m_\mu F_P / F_A$, that is deduced from this calculation is somewhat smaller than that suggested by the Goldberger–Treiman relation. Radiative muon capture measurements indicate, although not conclusively, deviations from these numbers toward larger values. Suggestions have been made to explain this discrepancy by including the meson exchange effects or including the other possible types of coupling. It is pointed out here that since the contribution of the D-state apparently decreases the capture rate and consequently the pseudo-scaler coupling constant, it is reasonable to expect that a wave function with a smaller D-state contribution will yield better agreement with experiments. A preliminary calculation and brief discussion of this possibility are also given. (Diss. Abstr. Int., B)

31191 DIFFERENTIAL CROSS SECTIONS FOR D(d,d)D ELASTIC SCATTERING AND THE D(d,3He)n, D(d,t)p REACTIONS BETWEEN 12.5 AND 40.0 MeV. Fegley, Ronald Warne. Davis, Calif.; Univ. of California (1970). 117p. University Microfilms Order No. 71-7929.

Thesis.

A large volume deuterium gas target was bombarded with a deuteron beam. Twelve energies between 12.5 and 40 MeV were used. The differential scattering cross section for D(d,d) was measured using solid state detector telescopes with an average absolute error of 6%. The differential cross sections for the two reactions, D(d,^{3}He)n, and D(d,p)^{3}He, were measured with an absolute error of 10%. Excitation functions have been prepared at 10 degree intervals in the c.m. system, and there is no evidence of a resonance. Charge independence of nuclear forces seems to be supported in the two mirror reactions. The d−d system is discussed, and comparison of the experimental results is made with the recent predictions of a resonating cluster model. (Diss. Abstr. Int., B)

31192 BINDING ENERGY OF THE ALPHA PARTICLE ^{4}He. Omojola, A. F. (Univ. of Lagos, Nigeria). J. Phys., A (London); 4: 217-30(Mar 1971).

The problem of the alpha-particle S and D state binding energies is formulated in coordinate space and is followed by a variational calculation of the trial function (of the form $({}^1S_0 + {}^5D_0)$) contribution to the binding energy of the alpha particle (BE(^{4}He)) using a radial wave function of the form $\exp(-\lambda \sum_{i<j=2}^{5} r_{ij}^2)$. The calculation is based on the nuclear forces given by Omojola (J. Phys. A. 3: 630-652, 1970) taking into account the effect of a "hard core" on BE(^{4}He). It is shown that, by fixing the value of the variation parameter of $^1S_0$ to the well-established value from the high energy e−^{4}He scattering and by using a repulsive core of suitable radius given by Hamada and Johnston (Nucl. Phys. 34: 382-403, 1962), the excessive binding obtained with two-body central potentials may be reduced to reasonable values. The results obtained are compared with those of other authors. (auth) (UK)

31193 MICROSCOPIC CALCULATION FOR n–^{3}H SCATTERING. Hackenbroich, H. H.; Heiss, P. (Univ., Cologne). Z. Phys.; 242: 352-9(1971).

Starting from a nucleon−nucleon soft-core potential, the ^{3}H−n scattering states were calculated in the refined cluster model framework. Phase shifts and angular distributions resulting from these calculations are compared with experiments and agree well. In all states except the $J^\pi = 1^-$ state the coupling of channels is extremely small, but in this state considerable spin-mixing is found. (auth)

31194 DIFFERENTIAL CROSS SECTION OF THE DEUTERON PHOTODISINTEGRATION BETWEEN 20 AND 35 MeV. Tietze, K.; Reich, H.; Trier, J. O. (Physikalisch-Technische Bundesanstalt, Brunswick). Z. Phys.; 242: 328-31(1971). (In German).

The differential cross section of the deuteron photodisintegration was determined in the photon energy range 20 to 35 MeV at the angle of 90 degrees in the laboratory system. The experimental points were fitted in this range by a parabola $d\sigma_D(90°)/d\Omega = 140.6 - 5.41E_\gamma + 0.0621E_\gamma^2$ with E_γ in MeV and $d\sigma_D/d\Omega$ in 10^{-30} cm^2/sr. (auth)

31195 ^{5}Li RESONANCE ABOVE THE ^{3}He-d THRESHOLD. Heiss, P.; Hackenbroich, H. H. (Univ., Cologne). Nucl. Phys.; A162: 530-40(1971).

Starting from a soft-core nucleon−nucleon potential the scattering states of ^{5}Li above the ^{3}He-d threshold are calculated using the refined cluster model. Apart from the well-known $3/2^+$ resonance a quartet of $S = 3/2$, $L = 2$ ^{3}He-d resonances is found. Furthermore $3/2^-$ and $1/2^-$ resonances appear in phase-shift and inelastic parameter curves; they are shown to be due to three-body break-up channels connected with an intermediate α^*-p structure, α^* being the first excited state of the ^{4}He nucleus. (auth)

31196 ANGULAR DISTRIBUTION AND EXCITATION FUNCTION OF THE SINGLET DEUTERON IN THE d(p,d)p REACTION. van der Weerd, J. C.; Canada, T. R.; Fink, C. L.; Cohen, B. L. (Univ. of Pittsburgh). Phys. Rev., C; 3: 66-72(Jan 1971).

The d(p,pn)p reaction has been studied to determine the d(p,d)p angular distribution and excitation function for the proton bombarding energy range 7 to 17 MeV. Protons and neutrons were detected in coincidence at the same angle to enhance the detection of d(p,d)p events. The spectra were fitted using the density-of-states function of Phillips, Griffy, and Biedenharn for the singlet deuteron, and a flat background arising from reactions other than d(p,d)p. Angular distributions were taken at 7, 8, 10, 12, 13.5, 15, and 17 MeV. There was forward peaking at all energies, contrary to calculations on the doublet state in n-d scattering by Aaron, Amado, and Yam. The excitation function shows little structure between 7 and 17 MeV. (auth)

31197 ANALYZING POWER OF THE REACTION ^{3}He(d,p)^{4}He FOR VECTOR-POLARIZED DEUTERONS BETWEEN 2 AND 13 MeV. Klinger, W.; Dusch, F.; Fleischmann, R. (Univ., Erlangen, Ger.). Nucl. Phys.; A166: 253-65(1971).

The analyzing power $A_y(\theta,E)$ of the reaction ^{3}He(d,p)^{4}He was measured with vector-polarized deuterons for 23 energies from 2.23 MeV to 13.0 MeV and at lab. angles between 20° and 160°. Angular distributions of the unpolarized differential cross section σ_0 were also obtained. The angular distributions of σ_0 and of the product $\sigma_0 A_y$ were fitted with Legendre polynomials. The energy de-

XUM

pendence of the Legendre coefficients of the expansion $\sigma_0 A_y$ seems to indicate that more than one energy level of the ^{5}Li compound nucleus is responsible for the broad anomaly in the cross section of the ^{3}He(d,p)^{4}He reaction, observed at an excitation energy of ≈20 MeV in ^{5}Li. From 5 MeV to 13 MeV the reaction ^{3}He(d,p)^{4}He is an excellent analyzer for deuteron vector polarization if tensor polarization effects are taken into account. A comparison of the analyzing power A_y to polarization parameters of the reaction ^{3}He(d,p)^{4}He measured by other authors, indicates that forces such as tensor forces should be included in a theoretical treatment of the reaction. (auth)

31198 ABSOLUTE CALIBRATION OF TENSOR ANALYSING POWERS OF THE ^{3}He(d,p)^{4}He AND THE ^{4}He(d,d)^{4}He REACTIONS. Koenig, V.; Grueebler, W.; Ruh, A.; (and others) (Eidgenoessisces Technische Hochschule, Zurich). Nucl. Phys.; A166: 393-6(1971).

The tensor analyzing power T_{20} of ^{3}He(d,p)^{4}He was calibrated absolutely at $\theta_{lab} = 0°$ and $E_d = 6.49$ and 9.30 MeV with the ^{16}O(d,α_1)-^{14}N* reaction. These measurements were used to calibrate T_{20} and T_{22} in ^{4}He(d,d)^{4}He elastic scattering absolutely at two corresponding energies and $\theta_{lab} = 30°$, 60°, and 75°. (auth)

31199 POLARIZATION MEASUREMENTS AND PHASE SHIFTS FOR p-^{4}He SCATTERING BETWEEN 3 AND 18 MeV. Schwandt, P. (Indiana Univ., Bloomington); Clegg, T. B.; Haeberli, W. Nucl. Phys.; A163: 432-48(1971).

Angular distributions of the polarization in proton elastic scattering from ^{4}He were measured at laboratory energies near 4.6, 6.0, 7.9, 9.9 and 11.9 MeV. A phase-shift analysis of available cross-section and polarization angular distributions between 3.0 and 17.5 MeV was performed. The energy dependence of the phase shifts was represented by an effective-range expansion. The phase shifts determined from this expansion permit calculation of the p-^{4}He polarization with an accuracy of better than ±0.02 in this energy range. (auth)

Nuclear Properties and Reactions, 6≤A≤19

Refer also to abstracts 29363, 31173, 31187, 31238, 31312, 31332, 31333, 31360–31362, 31368, and 31419.

31200 (ANU-P-515) A NOTE ON THE EXTRAPOLATION OF THE ^{12}C + ^{12}C AND ^{12}C + ^{16}O REACTION CROSS SECTIONS TO ASTROPHYSICAL ENERGIES. Nagorcka, B. N.; Symons, G. D.; Zuk, W. M. (Australian National Univ., Canberra. Dept. of Nuclear Physics); Patterson, J. R. (Adelaide Univ. (Australia)). [1971]. 3p. Dep. NTIS (U. S. Sales Only).

A previous extrapolation of the ^{12}C + ^{12}C reaction cross section is re-evaluated in the light of new measurements of the ^{12}C + ^{16}O reactions which suggest that the "quasi-molecular" resonances observed in these reactions do not contribute to the cross sections at the lowest energies. (auth)

31201 (JINR-P4-5614) PROPERTIES OF LIGHT NUCLEI WITH REALISTIC N-N-INTERACTION. Balbutsev, E. B. (Joint Inst. for Nuclear Research, Dubna (USSR). Lab. of Theoretical Physics). 1971. 20p. (In Russian). Dep. NTIS (U. S. Sales Only).

The Brueckner reaction matrix elements for the 2sld and 2plf shells are calculated using the Hamada-Johnston potential. The mistake is revealed in the corresponding calculations by Kuo and Brown. Owing to it, a better agreement with experimental data is obtained in the calculations of the single-particle spectrum of ^{17}O and the binding energies of ^{16}O and ^{40}Ca. The "breathing" energy levels of ^{16}O and ^{40}Ca are calculated. The isotope shifts for the O and Ca isotopes are calculated, the rearrangement effects being taken into account. A good agreement with the experimental value is obtained for ^{40}Ca-^{42}Ca. (auth)

31202 (KFK-1288) PRODUCTION OF NEUTRONS THROUGH IRRADIATION OF THICK BERYLLIUM TARGETS WITH DEUTERONS IN THE ENERGY RANGE FROM 15 TO 55 MeV. Schmidt, K.; Muenzel, H. (Kernforschungszentrum, Karlsruhe (West Germany). Institut fuer Radiochemie) Sep 1970. 20p. (In German). Dep. NTIS (U. S. Sales Only).

The angular and energy distributions of neutrons produced by bombarding thick beryllium targets with 53.8-MeV deuterons are studied. A procedure is described whereby neutron spectra for deuteron energies between 15 and 55 MeV may be determined and the geometrical factors necessary for the determination of the induced activity in irradiated samples may be calculated. (auth)

31203 (LYCEN-7088) SUPERMULTIPLET SCHEME FOR LIGHT NUCLEI. Burdet, Guy; Perrin, Martine (Lyon Univ. (France). Institut de Physique Nucleaire). 10 Dec 1970. 18p. (In French). Dep. NTIS (U. S. Sales Only).

A test of the supermultiplet model for light nuclei is proposed. Two odd-A multiplets are interpolated; there results an even odd-like multiplet for A = 4n. The positions of isobaric analog states with high isospin, and those of the specific states of SU_4 appearing in certain reactions, are studied. It is shown that the values obtained for the ground states of the isobaric multiplets are very different from those deduced from the Garvey-Kelson mass formula. This indicates that much greater binding energies exist for neutron-rich nuclei and even, in some cases, stability against β decay for nuclei lying at the extremes of the multiplet. (auth)

31204 (ORNL-TM-3378) REPORT TO THE AEC NUCLEAR CROSS SECTION ADVISORY COMMITTEE. Good, W. M. (Oak Ridge National Lab., Tenn.). Apr 1971. Contract W-7405-eng-26. 26p. Dep. NTIS.

This memo is a collection of brief reports on recent and not yet generally publicized work at ORNL that is of special interest to the NCSAC. Included are abstracts of relevant ORNL reports, as well as papers that have been only submitted for publication. The memo covers the period of time since the last NCSAC meeting. (auth)

31205 (SAL-16) ELECTRON SCATTERING FROM ^{13}C. Yang, Chien-sheng (Saskatchewan Univ., Saskatoon. Saskatchewan Accelerator Lab.). Apr 1970. 169p.

Thesis.

A 140-MeV electron linear accelerator was used to measure electron scattering by ^{13}C. The experimental results for the elastic and inelastic scattering and theoretical calculations of the inelastic form factors based on various nuclear models are presented. The results of the elastic electron scattering experiment using a $^{13}CH_4$ gas target showed that the ratio of the rms charge radius of the ^{13}C nucleus to that of ^{12}C is .975 ± 2%. This confirms the somewhat surprising finding that the rms charge radius of ^{13}C is smaller than that of ^{12}C. Inelastic electron scattering was studied up to about 20 MeV excitation energy and for momentum transfers ranging from .627 F^{-1} to .935 F^{-1} using both solid and gas targets. Eleven levels at excitation energies of 3.69, 7.55, 8.25, 8.86, 9.50, 11.70, 11.97, 12.32, 13.76, 15.11, and 19.15 MeV were observed. The spectra showed that the normal-parity states are strongly excited, especially the levels at 3.69 MeV ($\frac{3}{2}^-$, $\frac{1}{2}$), 7.55 MeV ($\frac{5}{2}^-$, $\frac{1}{2}$), and 15.11 MeV ($\frac{3}{2}^-$, $\frac{3}{2}$), and special attention was paid to these levels. The wave functions of Boyarkina from the intermediate-coupling shell model and the wave functions of Cohen & Kurath and Goldhammer, Hill, & Nachamkin derived from the effective-interaction calculation are the best wave functions available at this stage for the normal-parity states. These wave functions are used to calculate the form factors for transitions from the ground state ($\frac{1}{2}^-$, $\frac{1}{2}$) to the ($\frac{3}{2}^-$, $\frac{1}{2}$), ($\frac{5}{2}^-$, $\frac{1}{2}$), ($\frac{1}{2}^-$, $\frac{1}{2}$), and ($\frac{3}{2}^-$, $\frac{3}{2}$) excited states. The results of these predictions are compared with the experimental form factors for the three levels mentioned above. These wave functions can only roughly predict the form factors for the 3.69-MeV and 7.55-MeV levels but agree fairly well for the 15.11-MeV level. It may be possible to improve the theoretical predictions by including configurations in the 2s-1d shell. (auth)

31206 (SAL-17) ELASTIC SCATTERING OF ELECTRONS FROM THE OXYGEN ISOTOPES. Singhal, Ravi Prakash (Saskatchewan Univ., Saskatoon. Saskatchewan Accelerator Lab.). Jul 1970. 115p.

Thesis.

Elastic scattering of electrons was used to measure the root-mean-square charge radii of the oxygen isotopes (^{16,17,18}O). The momentum-transfer range covered was from 0.392 F^{-1} to 0.993 F^{-1}, and the oxygen isotopes were in gaseous form. The rms charge radii among isotopes do not follow an $A^{\frac{1}{3}}$ law. Since ^{16}O has a doubly-closed 0p shell, the oxygen isotopes are an interesting case for study because the deviations from an $A^{\frac{1}{3}}$ law are especially marked in the vicinity of doubly-closed shells. The data were analyzed to extract the rms radii of ^{17,18}O relative to ^{16}O. The absolute value of the ^{16}O rms radius was obtained by comparing the electron scattering from ^{16}O with that from the proton. A χ^2 fit was used to obtain the values and the uncertainties in the rms radii. The results show that the rms radius of ^{16}O is bigger than that of ^{17}O. ^{18}O is seen to be larger than ^{16}O, but only by about half the amount required by the $A^{\frac{1}{3}}$ law. The results are $R_m(17)/R_m(16) = 0.995 \pm 0.006$ and $R_m(18)/R_m(16) = 1.020 \pm 0.005$. The absolute value of the rms radius of ^{16}O is in very good agreement with previous measurements. A comparison of the ^{16}O charge distribution is made with the predictions of Hartree-Fock theory. (R.W.R)

XUM

31207 CONTRACTION OF THE DEUTERON CLUSTER IN ^{6}Li. Itonaga, Kazunori; Bando, Hiroharu (Kyoto Univ.). Progr. Theor. Phys. (Kyoto); 44: 1232-41(Nov 1970).

Physical origins of the contraction of the deuteron cluster in ^{6}Li are clarified. Two effects are studied under an adiabatic approximation, namely the effect of the Pauli principle and the effect on the potential field induced by the alpha cluster. These two are found to play an opposite role on contraction and extension of the deuteron cluster. The former has a dominant effect and causes the contracted deuteron cluster in ^{6}Li. (auth)

31208 MEASUREMENT OF THE DOPPLER BROADENING OF GAMMA-RAY ENERGY WITH Ge(Li) DETECTOR. Tojo, Takao (Japan Atomic Energy Research Inst., Tokai). J. Nucl. Sci. Technol.; 8: 48-50(Jan 1971).

The use of a high-resolution Ge(Li) detector in measuring the Doppler broadening of γ-ray energies is discussed. A spectrometer employing a 30 cc Ge(Li) detector was used in measuring the Doppler effect on the ^{12}C 4.43-MeV γ-ray following the ^{9}Be(α,n) reaction and on the ^{7}Li 0.477-MeV γ-ray following the ^{10}B(n,α) reaction. It was found that the contribution of the instrumental line width to the broadening is very small. (J.W.R.)

31209 YIELD OF NEUTRONS FROM THICK TARGETS BOMBARDED BY 11.5- AND 23.5-MeV PROTONS. Daruga, V. K.; Matusevich, E. S. At. Energ. (USSR); 29: 456-8(Dec 1970). (In Russian).

Absolute yields of neutrons from thick targets bombarded by 11.5 and 23.5 MeV protons (molecular hydrogen and atomic hydrogen, respectively) were measured using targets of Li, Be, C, Mg, Al, Ti, Fe, Co, Ni, Cu, Zn, Nb, Cd, Ta, W, Pb, Bi, and U with natural isotopic composition and thickness equal to the track of bombarding protons. The ratios of Y(0°)Y(90°) yield as functions of target nuclei Z are given in a graphic form. (R.V.J.)

31210 STUDY OF DEUTERON STRIPPING REACTION BY COUPLED CHANNEL THEORY. III. NUMERICAL RESULTS WITHOUT NONORTHOGONALITY. Ohmura, Takashi (Nihon Univ., Tokyo); Imanishi, Bunryu; Ichimura, Munetake; Kawai, Mitsuji. Progr. Theor. Phys. (Kyoto); 44: 1242-79(Nov 1970).

The method of coupled channels (CC) for the (d,p) reaction described by the authors [Prog. Theor. Phys. 41 (1969), 391 and 43 (1970), 347] was applied to the calculation of ^{16}O(d,p)^{17}O(2s), ^{12}C(d,p)^{13}C(1p), ^{40}Ca(d,p)^{41}Ca(2p) and (1f) and the related (d,d) and (p,p) processes. Detailed numerical studies were made under the assumption that the deuteron and proton channels were coupled by the interaction kernel with the Gaussian-type n-p interaction, V_{np}. The non-orthogonality term in the kernel was neglected. Comparison was made with the results of DWBA and CWBA (Coulomb wave Born approximation) with the same V_{np} and using the same distorting potentials as in CC. The same potentials were used in the optical model (OPT) calculation of the elastic cross sections which were also compared with the results of CC. Appreciable effect of CC was seen in the elastic as well as (d,p) cross sections. In the latter, CC reduces the cross section at the backward angles. The effect of CC was analyzed in terms of the S-matrix elements in the partial wave representation. For the (d,p) matrix elements, $S^{(L)}_{pl,dl}$, the angular momentum space, (L,l), was found to be divided into three fairly distinct regions: (1) the CWBA region with $l > l_0$ and $L > L_0$ where CWBA = DWBA = CC, (2) the DWBA region with $l > l_0$, $L \leq L_0$ where CWBA $\neq$ DWBA = CC and (3) the internal region with $l \leq l_0$ where CWBA $\neq$ DWBA $\neq$ CC. The numbers l_0 and L_0 correspond to the maximum angular momenta at which the distortion of the proton and deuteron partial waves, respectively, becomes appreciable which is indicated by the first appreciable deviation of the absolute value of the elastic S-matrix element from 1, say less than 0.8. For the elastic S-matrix elements CC reduces the absolute value in most cases of (p,p), as one would intuitively expect, but not always so for (d,d). A detailed study of the effect of CC as a function of the coupling strength, D, was also made. In the internal region the effect of CC was found to be appreciable if D is larger than $\sim 1/3$ of the realistic value, D_0. At $D = D_0$, even the addition of the next order term of the DWB series to DWBA or OPT was found to be inadequate in the internal region. It was found that zero-range approximation is useful in semi-quantitative investigation of CC. (auth)

31211 HIGH-ENERGY ELECTRON SCATTERING FROM ^{6}Li. Li, G. C.; Whitney, R. R.; Yearian, M. R. (Stanford Univ., Calif.). Nucl. Phys.; A162: 583-92(1971).

Elastic electron scattering cross sections have been measured for ^{6}Li at 500 MeV and values of q^2, the momentum transfer squared, up to 13 fm^{-2}. Calculations including nucleon–nucleon correlations predict a diffraction minimum beyond the range of previous measurements for ^{6}Li. The results for ^{6}Li do show a diffraction minimum at $q^2 = 8$ fm^{-2}; they are also compared with a phase-shift calculation using an empirical charge distribution. (auth)

31212 ALPHA-PARTICLE OPTICAL POTENTIAL FROM THE NUCLEAR DENSITY DISTRIBUTION. Bernstein, A. M.; Seidler, W. A. (Massachusetts Inst. of Tech., Cambridge). Phys. Lett.; 34B: 569-71(12 Apr 1971).

The optical potential for α-particle scattering has been related to the nuclear density distribution. The scattering of 104-MeV α particles has been calculated for T = 0 nuclei for which the neutron and proton densities are approximately equal (and known from electron scattering). The model's two parameters were fixed ^{40}Ca, and the cross sections for ^{16}O and ^{28}Si were predicted with good agreement with experiment. These results indicate that density distribution may be obtained for N > Z nuclei. (auth)

31213 CHARGED PARTICLE EMISSION FOLLOWING PION CAPTURE IN NUCLEI. Coulson, Larry Vernon. Charlottesville, Va.; Univ. of Virginia (1970). 130p. University Microfilms Order No. 71-6650.

Thesis.

A beam of negative pions from a 600-MeV synchrocyclotron was stopped in thin targets made of ^{7}Li, ^{12}C, and ^{27}Al. The charged particles emitted following the capture of a pion were identified by radius of curvature in a magnetic spectrometer and by range in a 28 gap range chamber. The energy spectra of the hydrogen isotopes emitted as well as the branching ratios for their production for each target were measured. For charged particles with energies above 20 MeV approximately equal numbers of protons, deuterons, and tritons were observed for the ^{7}Li target. From ^{12}C there were 44% protons, 41% deuterons, and 15% tritons (Diss. Abstr. Int., B)

31214 (^{3}He,^{6}Li) REACTION ON LIGHT NUCLEI. Oh, In Ki. Boulder, Colo.; Univ. of Colorado (1970). 170p. University Microfilms Order No. 71-5919.

Thesis.

The (^{3}He, ^{6}Li) reaction was studied and reasonably described in the framework of DWBA (Distorted Wave Born Approximation) theory as the transfer of a triton to a ^{3}He particle, and the triton reduced widths which were in acceptable agreement with shell model predictions were extracted. The (^{3}He, ^{6}Li) angular distributions on ^{12}C, ^{16}O, ^{19}F, ^{23}Na, and ^{27}Al were measured at a ^{3}He bombarding energy of 40.7 MeV. In addition, data were obtained for the ^{10}B(^{3}He, ^{6}Li)^{7}Be, ^{12}C(^{3}He, ^{6}Li)^{9}B, ^{16}O(^{3}He, ^{6}Li)^{13}N, and ^{19}F (^{3}He, ^{6}Li)^{16}O reactions at 30.0 MeV and for the ^{19}F(^{3}He, ^{6}Li)^{16}O reaction at 22.4 MeV. The use of zero-range DWBA analysis is justified for the (^{3}He, ^{6}Li) reaction because the ^{3}He-t model of the ground state ^{6}Li is an s-state. Zero-range DWBA calculations were performed to fit the experimental angular distributions of the (^{3}He, ^{6}Li) reactions. The calculations were in acceptable agreement with the experimental data. A ^{3}He-t potential of Gaussian form which reproduces low energy ^{3}He-t scattering gives a value of $D_0^2 = 3 \times 10^4$ MeV^2 fm^3 for the interaction strength which appears in the DWBA theory, a square well potential gives a value of $D_0^2 = 4.52 \times 10^4$ MeV^2 fm^3 and a square well with a hard core a value of $D_0^2 = 3.89 \times 10^4$ MeV^2 fm^3. With these values of D_0^2, probabilities for the formation of a ^{6}Li particle from ^{3}He + t were estimated to be about 0.267 for the Gaussian potential, 0.181 for the square well and 0.21 for the hard core by comparison of triton reduced widths predicted by j–j coupling and experimental triton reduced widths obtained by zero-range DWBA analyses of the data. Furthermore, by setting the experimental triton reduced width equal to the theoretical triton reduced width for each target, the probability of finding the particle ^{6}Li being formed from ^{3}He + t was obtained for each target. In addition, differential cross sections were obtained for the elastic scattering of ^{3}He from ^{19}F at 22.4, 30.0, and 40.7 MeV. The experimental angular distributions were fitted with an optical model calculation by using a computer search program. (Diss. Abstr. Int., B)

31215 NEUTRON EMISSION FOLLOWING RADIATIVE PION CAPTURE IN COMPLEX NUCLEI. Lam, Wing-chee. Blacksburg, Va.; Virginia Polytechnic Inst. (1970). 118p. University Microfilms Order No. 71-7911.

Thesis.

An account of a measurement of the neutron energy spectrum from radiative pion capture in carbon, oxygen and calcium is given. The measurement was performed at six n–γ correlation angles for the case of carbon and oxygen, and seven n–γ correlation angles for the case of calcium. The observed energy spectra fall off approximately exponentially between 2 and 30 MeV. Evidence of resonance structure was observed at about 4 MeV in the energy spectra of carbon and oxygen. This is in agreement with a theoretical prediction of the giant multipole excitation model.

The neutron yield versus n−γ correlation angles peaks at 180° for all three nuclei studied. This indicates the quasi-free mechanism also plays an important role in the radiative pion capture process. (Diss. Abstr. Int., B)

31216 NEUTRON ENERGY SPECTRA FOLLOWING RADIATIVE PION ABSORPTION ON ^{16}O AND ^{28}Si NUCLEI. Holland, Michael Myers. Charlottesville, Va.; Univ. of Virginia (1970). 92p. University Microfilms Order No. 70-26,563.
Thesis.

The energy spectra of neutrons emitted following radiative absorption of negative pions on ^{16}O and ^{28}Si nuclei were measured. An approximate relative neutron-gamma-ray detector angle of 80 degrees was employed to emphasize those effects due to the decay of the excitation of isobaric analogs of the giant resonance states of the absorbing nucleus. A total of 1274 and 449 events were observed for ^{16}O and ^{28}Si, respectively, corresponding to neutron and gamma-ray thresholds of 2.5 and 70 MeV, respectively. An energy resolution of 1.6 and 1.3 MeV at 10 MeV was achieved for the ^{16}O and ^{28}Si targets, respectively. Radiative pion capture branching ratios of 1−2%, comparable to earlier measurements, were measured. The neutron energy spectra are compared with existing theoretical calculations. (Diss. Abstr. Int., B)

31217 RADIATIVE PION ABSORPTION IN NUCLEI. Guy, Reed Augustus. Charlottesville, Va.; Univ. of Virginia (1970). 211p University Microfilms Order No. 71-6658.
Thesis.

A small percentage of the time in complex nuclei the absorption of a bound negative pion leads to the emission of a high-energy photon; this is the process known as radiative pion absorption. For light nuclei, it is expected that this process will preferentially excite spin-isospin states in the final nucleus that are the isobaric analogs of states in the giant resonance region of the initial nucleus. With these ideas in mind, several processes involving radiative pion absorption in nuclei are considered. Rescattering corrections, in which the pion is scattered by a nucleon before being radiatively absorbed, are calculated in ^{16}O both in perturbation theory and with an approach based on the actual pion-nucleus scattering length. The particle-hole model is employed and the dominance of spin-isospin states is assumed. The calculation shows that incoherent rescattering effects involving an excited nucleus in the intermediate state are of little importance, and this allows a considerable simplification in the evaluation of the rescattering terms. The relationship between this calculation and analyses based on the use of an optical potential is presented. The process in which the radiative absorption of a bound pion is followed by photon de-excitation of the residual nucleus is then considered. Observation of the energy spectrum of the deexcitation photon provides an indirect means of studying the spin-isospin states. Numerical results are presented for ^{16}O and ^{12}C including angular correlations and energy distributions for the outgoing photon for the case in which the pion is absorbed from the 2P atomic orbit. Finally, radiative pion absorption in heavier nuclei is considered. The validity of the leading term in the pion photoproduction amplitude, which was used in the previous calculations for light nuclei, is investigated in detail for heavier nuclei. The particle-hole model is used for the evaluation of nuclear matrix elements. Results, including distribution of spin-isospin strength among various odd-parity states and contributions of corrections to the leading term, are presented for ^{40}Ca and ^{90}Zr. (Diss. Abstr. Int., B)

31218 DIRECT COMPOUND MECHANISM FOR THE REACTION $^{11}B(p,\alpha)\,2\alpha$. Goulard, G. (Univ. of Laval, Quebec). J. Phys. (Paris); 31: 941-49(Nov-Dec 1970). (In French).

The following reaction is studied $A + B \rightarrow C^* \rightarrow D + E + F$. Two possible mechanisms are proposed: an interaction in the final state (Watson type) or a direct break up of C* into three particles. Calculations are made for several incident energies and compared with the different experimental results and with calculations made using the sequential mechanism. (auth) (France)

31219 NUCLEAR RADII OF ^{12}C, ^{13}C, ^{14}N, AND ^{16}O FROM ELECTRON SCATTERING BETWEEN 30 AND 60 MeV. Bentz, Hans Alfred (Technische Hochschule, Darmstadt, Ger.). Z. Phys.; 243: 138-53(1971). (In German).

Elastic electron scattering cross sections of ^{12}C, ^{14}N, and ^{16}O relative to the proton, and of ^{13}C relative to ^{12}C, have been measured. Using harmonic oscillator wave functions the following rms charge radii R_m were deduced by phaseshift calculations: 2.395(28) fm for ^{12}C, 2.384(47) fm for ^{13}C, 2.492(33) fm for ^{15}N, and 2.666(33) fm for ^{16}O. The ratio $R_m(^{13}C)/R_m(^{12}C)$ is 0.995 ± 0.008. The errors given do not include uncertainties from the model dependence of the evaluation which may be of the same magnitude. (auth)

31220 REACTION $^{7}Li(d,\alpha)^{5}He$ IN THE ENERGY RANGE OF 0.6 TO 2.0 MeV. Friedland, E.; Venter, I. (Univ. of Pretoria). Z. Phys.; 243: 126-31(1971). (In German).

The excitation function of the reaction $^{7}Li(d,\alpha)^{5}He$ has been measured between 0.6 and 2.0 MeV in steps of 50 keV. The two resonances at 0.75 and 1.00 MeV corresponding to the levels at 17.28 and 17.48 MeV of the compound nucleus ^{9}Be were resolved. Angular distribution measurements were performed at 14 different energies mainly near the 1.00 MeV resonance. From the analysis of the data the 17.28-MeV level seems to be a positive-parity state ($^3/_2^+ \rightarrow {}^1/_2^+$) while a negative parity ($^1/_2^-$ or $^5/_2^-$) is indicated for the 17.48-MeV level. This is contrary to the order of parities as given in the literature. (auth)

31221 STUDY OF N-^{6}Li COLLISIONS USING THE WHEELER METHOD. Remaud, Bernard (Univ., Nantes, France). Compt. Rend., Ser. B; 272: 390-3(8 Feb 1971). (In French).

The elastic collision n-^{6}Li is studied using the Wheeler group model for the resonances. The wave function corresponding to the ground state of ^{6}Li, presenting symmetries imposed by the shell model and the Pauli exclusion principle, is verified by calculating the binding energy and rms radius. Three types of force are considered for the energies 3.35, 7.5, and 15 MeV, which correspond to known experimental results. The use of Serber type forces gives the most satisfactory results. (auth) (France)

31222 STUDY OF THE $^{12}C(d,d)$, $^{12}C(d,p_0)$, AND $^{12}C(d,p_1)$ REACTIONS BETWEEN 1.4 AND 2.3 MeV. Allab, M.; Amiel, M.; Amokrane, A.; Beaumevieille, H.; Henni, A.; Lambert, M. (Institut d'Etudes Nucleaires, Algiers). J. Phys. (Paris); 31: 919-27(Nov-Dec 1970). (In French).

The angular distributions associated with the $^{12}C(d,d)^{12}C$, $^{12}C(d,p_0)^{13}C$, and $^{12}C(d,p_1)^{13}C$ reactions were measured for deuteron energies between 1.4 and 2.3 MeV. A differentially pumped gas target was used. The angular distributions and excitation curves of the p_0 and deuteron groups were analyzed with the compound nucleus formalism, which suggested J^π values of 2^+, 1^+, and 2^- for the 11.51 MeV, 11.75 MeV, and 11.85 MeV excitation energy levels of ^{14}N. These characteristics are confirmed by comparing the angular distributions of the p_1 group with the absolute cross sections calculated taking into account the stripping mechanism and the resonant mechanism. (auth) (France)

31223 TESTS OF EVALUATED BERYLLIUM (n,2n) CROSS SECTIONS BY ANALYSIS OF 1.4-eV FLUX IN WATER FOR AN AMERICIUM–BERYLLIUM SOURCE ENCLOSED IN BERYLLIUM SPHERES. Alexander, Roger L.; Fieno, Daniel; Ford, C. Hubbard (Lewis Research Center, Cleveland). Nucl. Sci. Eng.; 44: 95-102(Apr 1971).

The neutron flux distribution at indium resonance energy was measured in water for a strong Am−Be neutron source enclosed by Be spheres. The estimated virgin source spectrum and group-averaged Be(n,2n) cross sections for a 30-group calculation are tabulated. For the Am−Be source in a 1.91-cm-thick Be shell, the computed enhancement is 9.4%, while the experimental number is 7.3 ± 2.0%; for a shell 7.0-cm thick, the corresponding results are 26.3% and 22.8 ± 2.5%. (R.W.R.)

31224 NEUTRON YIELD FROM THE (α,n) REACTION IN THE ISOTOPE ^{18}O. Taherzadeh, Mojtaba (California Inst. of Tech., Pasadena). Nucl. Sci. Eng.; 44: 190-3(May 1971).

The problem of evaluating neutron yield from the (α,n) reaction in oxygen has been the subject of much experimental investigation for many years. However, the computational probe has not been extensive, basically due to lack of required data in the literature. Using a computer program, calculations were made to obtain the number of neutrons emitted when α particles from the ^{238}Pu isotope interact with ^{18}O. Neutron yield (n/α) is calculated specifically for each excited state of the recoil ^{21}Ne isotope. The result is in good agreement with the experimental value. (auth)

31225 SPECTRUM OF FAST DEUTERONS EMITTED IN 670-MeV PROTON INTERACTION WITH CARBON NUCLEI. Azhgirei, L. S.; Krumshtein, Z. V.; Ngo Kuang Zui; Petrukhin, V. I.; Khazins, D. M.; Tsisek, Z. (Joint Inst. for Nuclear Research, Dubna, USSR). Yadern. Fiz.; 13: 6-14(Jan 1971). (In Russian).

The spectrum of deuterons emitted at an angle 6.5° in 670-MeV proton interaction with ^{12}C nuclei was measured using a magnetic spectrometer and a time of flight spectrometer within 700 to 1700 MeV/c. Besides the previously observed deuteron peak due to quasielastic proton scattering on two-nucleon groups inside the nucleus, deuterons produced in the reaction $p + N \rightarrow d + \pi$ in the secondary particle momentum spectrum were absorbed. The differential cross section of the reaction $p + N \rightarrow d + \pi$ on ^{12}C nucleus nucleons that has not been previously observed was found to be

XUM

$d\sigma/d\omega \leq (27.9 \pm 3.2) \times 10^{-27}$ cm^2/sterad. The momentum distribution of deuterons corresponding to this reaction is in qualitative agreement with the calculations performed in terms of the independent-particle model. (auth)

31226 INVESTIGATION OF THE ONE-PARTICLE-HOLE AND PROJECTED HARTREE–FOCK APPROXIMATIONS IN ^{12}C AND ^{16}O. Rowe, D. J. (Univ. of Toronto); Ullah, N.; Wong, S. S. M.; Parikh, J. C.; Castel, B. Phys. Rev., C; 3: 73-8(Jan 1971).

Calculations are performed, in the one-particle-hole and projected Hartree–Fock (PHF) approximations, for the low-lying 2^+ and 3^- excitations in ^{12}C and ^{16}O, respectively. A new expression is derived for static moments of excited states in the random-phase approximation (RPA) and general one-particle-hole approximations. The purpose of this study was to investigate: the practical usefulness of the above approximations for nontrivial realistic problems; the validity of the one-particle-hole and PHF approximations for positive- as well as negative-parity excitations; the ability of the equations of motion and PHF methods to predict static moments of excited states; the magnitude of corrections to the RPA with explicit inclusion of ground-state correlations; and the validity of the inconsistent RPA procedure of including backward amplitudes at the expense of violating the Pauli principle. It is concluded that the one-particle-hole approximation is particularly appropriate for negative-parity excitations and that the PHF approximation is appropriate for positive-parity excitations. (auth)

31227 ISOSPIN NONCONSERVATION IN THE REACTIONS ^{16}O(d,α)^{14}N$^*_{T=1}$ AND ^{12}C(d,α)^{10}B$^*_{T=1}$. Jaenecke, J.; Yang, T. F.; Gray, W. S.; Polichar, R. M. (Univ. of Michigan, Ann Arbor). Phys. Rev., C; 3: 79-83(Jan 1971).

The isospin-nonconserving (d,α) reactions on ^{16}O and ^{12}C leading to the 0^+, T = 1 states at E_x = 2.31 MeV in ^{14}N and E_x = 1.74 MeV in ^{10}B have been studied in the energy intervals of E_d = 14.0 to 18.1 MeV and 26.2 to 29.5 MeV, respectively. Two resonances were observed in the excitation function for the reaction on ^{16}O at E_d = 14.4 and 15.0 MeV followed by a weak tail with little energy dependence. This behavior is similar to that observed earlier for the reaction on ^{12}C in the same energy region. The results for ^{12}C at the higher bombarding energies, in conjunction with arguments related to the properties of highly excited states, appear to favor a direct- or semidirect-reaction mechanism. Consistent with the observed facts are virtual E1 Coulomb excitation of the deuteron or the preferential spin-flip process suggested by Noble. No evidence was found for the two-step process involving isospin-mixed intermediate states, which was also suggested by Noble. (auth)

31228 REACTIONS ^{11}B(p,^{3}He)^{9}Be AND ^{11}B(p,t)^{9}B: IS THERE STRONG ISOSPIN MIXING IN MASS 9? Hardy, J. C. (Univ. of California, Berkeley); Loiseaux, J. M.; Cerny, Joseph; Garvey, Gerald T. Nucl. Phys.; A162: 552-60(1971).

The reactions ^{11}B(p,^{3}He)^{9}Be and ^{11}B(p,t)^{9}B have been studied at 45-MeV proton energy. New T = ½ states have been observed at 15.96 ± 0.04 MeV in ^{9}Be and at 15.29 ± 0.04 MeV and 15.58 ± 0.04 MeV in ^{9}B; and in addition there is a possible state or states at ≈15.13 MeV in ^{9}Be. The results were compared to DWBA calculations with (1p) shell wave functions and there is reasonable agreement for the ground states, lowest $\frac{5}{2}^-$ excited states and the lowest $\frac{3}{2}^-$ (T = ½) analogue states. Several candidates are proposed for a $\frac{3}{2}^-$ (T = ½) state near the analogue state. The results are discussed in terms of isospin mixing in the analogue states, prompted by previously observed deviations of their masses from the quadratic multiplet mass equation. All the experimental evidence indicates that isospin mixing of more than a few percent is extremely unlikely. (auth)

31229 INELASTIC SCATTERING OF ELECTRONS AND E2 TRANSITION IN ^{6}Li. Lodhi, M. A. K. (Texas Technological Coll., Lubbock. Technische Hochschule, Darmstadt, Ger.). Z. Phys.; 242: 364-7(1971).

A simple nucleon–nucleon correlation function was included in the independent-particle shell-model (IPSM) wave functions of ^{6}Li. The reduced transition probability and the nuclear form factor of ^{6}Li as obtained from the inelastic scattering of electrons were calculated using the correlated as well as the uncorrelated wave functions of the ground and the first excited states. The correlated transition probability and the form factor are considerably improved over the uncorrelated ones. The correlated form factor is more consistent with the experimental data than the uncorrelated one. (auth)

31230 CALCULATION OF ODD-PARITY STATES IN ^{12}C AND ^{16}O USING THE SUSSEX MATRIX ELEMENTS. Seaborn, J. B.; Cooper, Benjamin S. (Ames Lab., Iowa). Nucl. Phys.; A166: 221-30(1971).

A calculation of odd-parity states and giant resonance cross sections in ^{12}C and ^{16}O is carried out using the phase-shift matrix elements deduced by the Sussex group. The single-particle energies are calculated from the two-body interactions of a single particle or hole with particles in the core. Thus the only parameter in the calculation is the oscillator length associated with the shell-model basis. Gross features of the giant resonance in these nuclei are well accounted for, but detailed agreement with experimental energies of odd-parity states of other angular momenta is rather poor. (auth)

31231 FINE STRUCTURE OF THE GIANT DIPOLE RESONANCE IN ^{16}O NUCLEUS. Ishkhanov, B. S.; Kapitonov, I. M.; Lazutin, E. V.; (and others) (Moscow State Univ.). Yadern. Fiz.; 12: 892-902(Nov 1970). (In Russian).

The cross section is obtained for the reaction ^{16}O(γ,n)^{15}O at the excitation energies 16 to 25 MeV. 18 resonances are observed in the cross section. The nature of these resonances is discussed, as well as possible reasons of discrepances between the theory and the experiment. (auth)

31232 COMPARISON OF PHOTOPROTONS FROM ^{12}C AND ^{13}C. Shin, Y. M.; Wong, C. F.; Caplan, H. S. (Univ. of Saskatchewan, Saskatoon). Nucl. Phys.; A166: 162-72(1971).

Energy spectra and angular distributions of protons from the electrodisintegration of ^{12}C and ^{13}C, were measured with a magnetic spectrometer and solid-state detectors. The 90° cross sections are in agreement with previous results except for $E_p \leq 5$ MeV in ^{13}C. Fine structure observed in the cross sections of ^{12}C could be attributed to the coupling of the valence neutron to the $J^\pi = 1^-$, T = 1, ^{12}C core giant resonance. Comparison of the cross sections and the angular distributions of photoprotons from ^{12}C and ^{13}C suggests that for the most part the excitation mechanism of ^{12}C is applicable to ^{13}C. The results agree reasonably well with the prediction of the 2p-1h theory. (auth)

31233 ELASTIC AND INELASTIC SCATTERING OF 30 AND 50 MeV POLARIZED AND UNPOLARIZED BEAMS OF PROTONS BY ^{40}Ar AND ^{14}N. Rush, A. A.; Burge, E. J.; Smith, D. A. (King's Coll., London). Nucl. Phys.; A166: 378-92(1971).

Measurements were made of the differential cross sections for the elastic scattering of 49.4 MeV protons by ^{40}Ar and ^{14}N and of 30.4 MeV protons by ^{40}Ar. Inelastic data are also reported for the scattering of 49.4 MeV and 30.4 MeV protons by ^{40}Ar leading to the five excited states at 1.46, 2.53, 2.91, 3.23 and 3.71 MeV. Polarizations for ^{40}Ar elastic scattering, and asymmetries for inelastic scattering leading to the 1.46 MeV state, are reported for incident, proton energies of 49.2 and 30.6 MeV. Simple optical-model fits to the elastic scattering data are given. The inelastic data were analyzed using both distorted-wave and strong-coupling approximations. (auth)

31234 NUCLEUS–NUCLEUS SCATTERING AT HIGH ENERGIES. Muellensiefen, Alfred (Univ., Karlsruhe, Ger.). Nucl. Phys.; B28: 368-80(1971).

The measured electric nuclear form factor is related to the opaqueness model of the nucleus. The calculated differential cross section of the proton scattering on ^{4}He, ^{12}C and ^{16}O at 1 GeV is in reasonable agreement with the experimental data if the total cross section is taken as a free parameter. Using the results of elastic pα scattering good agreement is also obtained with the Glauber theory for $\alpha\alpha$ scattering at about 8 GeV/c per nucleon. The calculations are much more easily handled than those of the Glauber model. They may be considered as an improved optical-limit amplitude. In particular, the correct c.m. motion factor differs from that of Czyż and Maximon for the case of nucleus-nucleus scattering. The dσ/dt for α-^{12}C scattering is calculated and the total cross section for the scattering of ^{4}He on C, N and O estimated from which we obtain the mean free path of ^{4}He in air. (auth)

31235 REMEASUREMENT OF THE NEUTRON POLARIZATION FROM THE ^{7}Li(p,n)^{7}Be REACTION FOR 3 TO 4 MeV PROTONS. Hardekopf, R. A. (Duke Univ., Durham, N. C. Triangle Universities Nuclear Lab., Triangle Park, N. C.); Hollandsworth, C. E.; Walter, R. L.; Joyce, J. M.; Morgan, G. L. Nucl. Phys.; A167: 49-56(1971).

Polarizations of the neutrons emitted at 50° in the reaction ^{7}Li(p,n)^{7}Be were obtained in 50 keV steps for proton energies from 3 to 4 MeV to an accuracy of 0.014 for the n_0 group. The solenoid spin-precession technique was employed to reduce instrumental asymmetries. Scattering through 90° to 110° from gaseous helium enclosed at high pressure in a thin walled cell was used as an analyzer. A search program was used to fit Gaussian functions to the asymmetries for both the n_0 and n_1 groups. At the lowest energies a time-of-flight system was employed to measure the polarization of the n_1 group. A poly-

nomial is fit to the polarization values to provide an accurate calibration of the polarization at 50° lab in the range from 3 to 4 MeV proton energy. (auth)

31236 PROTON POLARIZATION IN $^{16}O(p,p)^{16}O$ AND STATES IN ^{17}F. Prior, R. M.; Corrigan, K. W.; Berners, E. D.; Darden, S. E. (Univ. of Notre Dame, Ind.). Nucl. Phys.; A167: 143-56 (1971).

The proton polarization in $^{16}O(p,p)^{16}O$ has been measured for laboratory energies between 8.5 and 12.7 MeV with the polarized proton beam from the Notre Dame polarized ion source. Measurements were made for 12 or more angles at 28 energies. In addition, excitation functions of polarization were measured at several angles between 10.2 and 12.0 MeV. A phase-shift analysis was made of both the polarization and published cross-section data. The energy dependence of the complex phase shifts yielded assignments of $J^\pi = 3/2^+$, $1/2^-$, $3/2^-$ and $5/2^+$ to the ^{17}F levels at E_x = 8.77, 8.97, 9.27 and 9.91 MeV, respectively. The data above 10.0 MeV confirm the assignments made by Toutenhoofd for the resonances near 10.5 and 12.5 MeV. (auth)

Nuclear Properties and Reactions, $20 \leq A \leq 89$

Refer also to abstracts 29363, 31300, 31312, 31332, 31333, 31360–31362, 31368, 31201, 31203, 31204, 31209, 31210, and 31212–31217.

31237 (IAE–1958) STUDIES OF ANALOG STATES OF T = 2 IN $^{26}Mg(^3He,n)^{26}Si$, $^{46}Ti(^3He,n)^{46}Cr$, AND $^{58}Ni(^3He,n)^{60}Zn$ REACTIONS. Brill, O. D.; Vongai, A. D.; Romanov, V. S.; Faiziev, A. R. (Institut Atomnoi Energii, Moscow (USSR)). 1970. 16p. (In Russian). Dep. NTIS (U. S. Sales Only).

During the reaction (^{3}He,n) on ^{26}Mg, ^{46}Ti, and ^{58}Ni intense excitation was observed of lower T = 2 states in ^{26}Si, ^{46}Cr, and ^{60}Zn at 15.27 ± 0.07, 8.77 ± 0.05, and 7.39 ± 0.125 MeV, respectively. (R.V.J.)

31238 (ITF–70–83–E) DIMENSIONS AND FORM OF THE LIGHT NUCLEI WITH THE SURPLUS OF NEUTRONS. Steshenko, A. I.; Filippov, G. F. (Akademiya Nauk Ukrainskoi SSR, Kiev. Institut Teoreticheskoi Fiziki). 1970. 23p. Dep. NTIS (U. S. Sales Only).

The dimensions and shape of light nuclei with a surplus of neutrons are calculated by the variational method on the one-particle wave functions of the three-dimensional anisotropic harmonic oscillator. The position of the boundary of stability for these nuclei is also estimated. (auth)

31239 (LYCEN–7091) MEAN RECOIL, ISOMER RATIO, AND EXCITATION FUNCTIONS FOR REACTIONS INDUCED BY ALPHA PARTICLES IN RUBIDIUM. Demeyer, A.; Chevarier, Noelle; Chevarier, A.; Tran Minh Duc (Lyon Univ. (France). Institut de Physique Nucleaire). Dec 1970. 29p. (In French). Dep. NTIS (U. S. Sales Only).

Excitation functions of reactions induced in ^{85}Rb by alpha particles are compared to those induced in ^{88}Sr by protons as a test of the independence hypothesis in the decay of the ^{89}Y compound nucleus. Mean-free-path measurements indicated the energy range valid for such a comparison. Information concerning the spin parameter was obtained from analysis of the isomer ratios. The shifted-Fermi-gas and superconductor models were tested. (auth) (France)

31240 (NP–18511) STUDY OF PROTON HOLES IN THE (2s–1d) SHELL FROM THE (d,^{3}He) REACTIONS AND COMPARISON WITH (p,2p) REACTIONS. Arditi, Maryse (Paris Univ., Orsay (France). Faculte des Sciences). 1970. 62p. (In French). Dep. NTIS (U. S. Sales Only).

Thesis.

The (d,^{3}He) reactions with nuclei of (2s–1d) shells from ^{24}Mg to ^{28}Si were studied in order to complete results obtained from (p,2p) experiments using the same nuclei, and to facilitate their interpretation, particularly with regard to anomalous distributions. The high energy of the deuterons (82 MeV) permitted, for the case of ^{24}Mg, the study of the residual nuclear states up to an excitation energy of 11 MeV. Achromatic optics allowed a reduction of beam energy from 350 to 180 keV. The D.W.B.A. was used in the analysis of the results and the determination of the angular distributions, the orbital momentum transferred, and the spectroscopic factors. A transfer l = 1 at weak excitation energies was revealed. The results of the stripping experiments and the absence of l = 3 transfer in the pick-up experiments demonstrated that the effects arose from 1p and not 2p proton holes. The distribution in the (p,2p) reaction was interpreted with these results. Thus, the abnormal distributions were explained by the superposition of two distributions: a distribution corresponding to the removal of a 2s proton having undergone a weak distortion, and the extraction of a 1p proton having undergone a larger distortion. In the same way, certain distributions appear to be due to the superposition of the l = 1 and the l = 2 type distributions. With nuclei of the (2s–1d) shell the study of the l = 1 transfer by the (d,^{3}He) reaction and of all the states attributed to the 1p holes observed by the (p,2p) or (e,e'p) reactions indicated that the 1p shell breaks up into two localized levels with ^{16}O. This shell extends 13, 16 and 20 MeV for the cases of ^{24}Mg, ^{28}Si and ^{32}S. This fact explains the lack of agreement between the two types of experiment. In fact, pick-up experiments allow l = 1 transfer at low energies to be observed, but they cannot excite deeper states; in contrast, the (p,2p) experiments yield an angular distribution which is purely of the l = 1 type, and and for the shallow states the angular distribution arises from the superposition of several diverse shell states. For the ^{40}Ca nucleus the shell appears to regroup, as in the case of ^{16}O, for energies in the region of the deep bindings. This result is similar to that predicted by Hartree–Fock calculations but lacks experimental confirmation. (auth) (France)

31241 (UCRL–20436) BETA-DELAYED PROTONS FROM ^{23}Al. Gough, R. A.; Cerny, Joseph; Sextro, R. G.; Esterl, John E. (California Univ., Berkeley. Lawrence Radiation Lab.). Feb 1971. Contract W-7405-eng-48. 7p. (CONF-710209–1). Dep. NTIS.

From International conference on heavy ion physics; Dubna, USSR (11 Feb 1971).

The $^{24}Mg(p,2n)^{23}Al$ reaction was used to produce the lightest nucleon-stable member of the A = 4n + 3, $T_z = -3/2$ mass series. By using standard particle-identifier techniques, a delayed-proton group at 0.88 ± 0.04 MeV (cm) following the decay of ^{23}Al was observed with a half-life of 0.48 ± 0.06 sec. An energy spectrum of identified protons and excitation functions are shown. (R.W.R.)

31242 (γ,n) CROSS SECTIONS OF ALUMINUM AND PHOSPHORUS. Ishkhanov, B. S.; Kapitonov, I. M.; Lazutin, E. V.; Piskarev, I. M.; Shevchenko, V. G. (Moscow State Univ.). Bull. Acad. Sci. USSR, Phys. Ser. (Engl. Transl.); 33: 1594-7(1969).

Translated from Izv. Akad. Nauk SSSR, Ser. Fiz.; 33: 1742-6 (Oct 1969).

Cross sections for the (γ,n) reaction on ^{27}Al and ^{31}P were measured in 100-keV steps from threshold up to 30 MeV. The cross sections show a complex structure with many maxima. (auth) (TSS)

31243 STRUCTURE OF THE PHOTONEUTRON CROSS SECTIONS OF ^{51}V, ^{52}Cr, AND ^{59}Co IN REGION OF THE GIANT DIPOLE RESONANCE. Goryachev, B. I.; Ishkhanov, B. S.; Kapitonov, I. M.; (and others) (Moscow State Univ.). Bull. Acad. Sci. USSR, Phys. Ser. (Engl. Transl.); 33: 1588-93(1969).

Translated from Izv. Akad. Nauk SSSR, Ser. Fiz.; 33: 1736-41 (Oct 1969).

The total photoneutron cross sections for ^{51}V, ^{52}Cr, and ^{59}Co were measured from threshold up to 30 MeV. The partial cross sections were determined by statistical calculations. The results were compared with the theoretical cross sections. (auth) (TSS)

31244 INELASTIC NEUTRON SCATTERING BY EVEN-N GERMANIUM ISOTOPES NEAR THE THRESHOLD FOR EXCITATION OF THE FIRST LEVELS. Konobeevskii, E. S.; Musaelyan, R. M.; Popov, V. I.; Surkova, I. V.; Shtranikh, I. V. (Lebedev Inst. of Physics, Moscow). Bull. Acad. Sci. USSR, Phys. Ser. (Engl. Transl.); 33: 1604-9(1969).

Translated from Izv. Akad. Nauk SSSR, Ser. Fiz.; 33: 1754-60 (Oct 1969).

Scintillation and Ge(Li) detectors were used to measure the γ spectra following neutron inelastic scattering by ^{70,72,74,76}Ge. Excitation functions were determined for the excitation of the first 2^+ states of all the isotopes. The results are compared with calculations based on the theory of average cross sections and using previously determined neutron strength functions. (auth) (TSS)

31245 HAUSER–FESHBACH METHOD AND INELASTIC SCATTERING OF PROTONS WITH EXCITATION OF LEVELS WITH ENERGIES UP TO 4 MeV IN SOME LIGHT AND MEDIUM-MASS NUCLEI. Antropov, A. E.; Gural'nik, D. L.; Zarubin, P. P.; (and others) (Leningrad State Univ.). Bull. Acad. Sci. USSR, Phys. Ser. (Engl. Transl.); 33: 1585-8(1969).

Translated from Izv. Akad. Nauk SSSR, Ser. Fiz.; 33: 1733-5 (Oct 1969).

The inelastic scattering of 6-MeV protons leading to excitation of levels in ^{26}Mg, ^{29}Si, ^{32}S, ^{58}Ni, and ^{60}Ni was analyzed by the Hauser–Feshbach method. Spin-parity assignments for several levels were determined. (auth) (TSS)

XUM

31246 EXCITED CORE MODEL FOR ^{63}Cu AND ^{65}Cu. Antropov, A. E.; Zarubin, P. P.; Morkelyunas, L. Yu.; (and others). Bull. Acad. Sci. USSR, Phys. Ser. (Engl. Transl.); 33: 1581-5 (1969).

Translated from Izv. Akad. Nauk SSSR, Ser. Fiz.; 33: 1728-32 (Oct 1969).

Data on proton inelastic scattering by ^{63,65}Ca are analyzed in terms of the excited-core model. It is concluded that the excited-core model gives a good description of the low-lying states. (auth) (TSS)

31247 DECAY SCHEME OF ^{86}Y. Arl't, R.; Zaitseva, N. G.; Kratsik, B.; (and others) (Joint Inst. for Nuclear Research, Dubna, USSR). Bull. Acad. Sci. USSR, Phys. Ser. (Engl. Transl.); 33: 1463-75(1969).

Translated from Izv. Akad. Nauk SSSR, Ser. Fiz.; 33: 1594-1606(Oct 1969).

The gamma spectrum of ^{86}Y was studied using Ge(Li) detectors. Eighty-five γ transitions were detected and their energies and intensities measured. The data was used along with conversion electron data to establish internal conversion coefficients. The proposed decay scheme includes 22 levels in ^{86}Sr up to 4994 keV. Several transition multipolarities were determined. The proposed decay scheme is discussed in the framework of model descriptions. (tr-auth)

31248 STUDY OF (p,n) REACTIONS IN ^{53}Cr AND ^{75}As. Wiest, Joseph Ernest. Lexington, Ky.; Univ. of Kentucky (1970). 92p. University Microfilms Order No. 71-4146.

Thesis.

The energy levels of ^{53}Mn and ^{75}Se were studied through the ^{53}Cr(p,n)^{53}Mn and ^{75}As(p,n)^{75}Se reactions by using a time-of-flight method with a pulsed proton beam. Angular distributions and excitation functions of the neutrons from these reactions and an excitation function of protons elastically scattered from ^{53}Cr were measured. Excitation energies of 21 excited states of ^{53}Mn were measured; previously unreported levels were observed at 2687 keV and 3123 keV. Excitation energies of three excited states of ^{75}Se were measured. Measured angular distributions of neutron groups corresponding to 18 energy levels in ^{53}Mn and of neutron groups corresponding to four or more energy levels in ^{75}Se were found to be symmetric about 90°, in agreement with predictions of the statistical-reaction model. A Hauser–Feshbach statistical-model analysis of the present work in conjunction with results from previous experiments suggests the following spin assignments (E_x, J): 2274, $^7/_2$; 2406, $^3/_2$; 2571, ($^7/_2$); 3007, ($^3/_2$, $^5/_2$) in ^{53}Mn and 121, ($^3/_2$, $^5/_2$); 439, ($^3/_2$, $^5/_2$) in ^{75}Se. Calculations suggest that the 296-keV level in ^{75}Se may be a doublet. (Diss. Abstr. Int., B)

31249 GAMMA RAYS FROM ^{64,66,68}Zn(p,γ)^{65,67,69}Ga. Nemashkalo, B. A.; Ekhichev, O. I.; Klyucharev, A. P.; Popov, A. I.; Storizhko, V. E. (Inst. of Physics and Tech., Kharkov). Ukr. Fiz. Zh. (Russ. Ed.); 16: 112-18(Jan 1971). (In Russian).

Gamma spectra from the reaction of ^{64,66,68}Zn(p,γ)^{65,67,69}Ga were studied by means of Ge(Li) detector and coincidence spectrometer at E_p = 2 MeV. Gamma energy and relative intensities were determined. Some γ rays which were previously not reported were observed. The level schemes for ^{65}Ga and ^{67}Ga were proposed. (auth)

31250 SEARCH FOR THE 3446 keV LEVEL IN ^{29}P VIA THE ^{28}Si(p,γ)^{29}P REACTION. Zuk, W. M.; Black, J. L.; Davidson, W. F. (Australian National Univ., Canberra). Aust. J. Phys.; 24: 37-42 (1971).

A search for a resonance in the ^{28}Si(p,γ)^{29}P reaction, corresponding to excitation of the 3446-keV level in ^{29}P, has been carried out utilizing a high-efficiency coincidence system. No resonance was observed, and an upper limit of 0.7×10^{-3} eV has been set on $(2J + 1)\Gamma_\gamma\Gamma_p/\Gamma$, which is seven times lower than previous limits. (auth) (Australia)

31251 ANGULAR CORRELATION STUDIES OF THE ^{42}Ca(α,pγ)^{45}Sc REACTION. Zuk, W. M. (Australian National Univ., Canberra); Symonds, G. D.; Baugh, D. J. Aust. J. Phys.; 24: 13-36 (1971).

The spins and decay modes of levels of ^{45}Sc up to an excitation energy of 1663 keV have been investigated via particle-gamma angular correlation measurements of the reaction ^{42}Ca(α,pγ)^{45}Sc. From data obtained here and in previous experiments, spin and parity assignments were deduced for levels at 376.2 ($^3/_2^-$), 542.8 ($^5/_2^+$), 720.7 ($^5/_2^-$), 974.9 ($^1/_2^+$), 1067.1 ($^3/_2^-$, $^1/_2^-$), 1237.2 ($^{11}/_2^-$), 1302.3 ($^3/_2^+$), 1409.5 ($^5/_2^-$, $^7/_2^-$), 1432.9 ($^3/_2^+$, $^5/_2^+$), 1556 ($^1/_2^-$, $^3/_2^-$), and 1662.8 ($^3/_2^-$) keV. Discrepancies in the decay schemes for the 1067.1, 1302.3, 1432.9, and 1556 keV levels have been resolved. (auth) (Australia)

31252 STUDY OF THE ENERGY LEVELS OF ^{27}Si. Barker, F. C.; Carter, K. W.; Kean, D. C.; Piluso, C. J.; Spear, R. H. (Australian National Univ., Canberra). Aust. J. Phys.; 24: 1-5(1971).

The energy levels of ^{27}Si between 3.5 and 5.5 MeV excitation have been studied by magnetic analysis of the reaction ^{28}Si(^{3}He,α)^{27}Si. The level scheme is compared with that of ^{27}Al in the light of an apparent regularity in the parity dependence of energy differences of corresponding levels in mirror nuclei of the 2s–1d shell. It is concluded that levels in ^{27}Si at 4.459 and 4.487 MeV probably have spins of $^7/_2$ and $^{11}/_2$, not necessarily respectively, and positive parity. (auth) (Australia)

31253 INELASTIC SCATTERING OF PROTONS BY ^{50}Cr, ^{52}Cr, ^{54}Cr, AND ^{64}Zn. Nemashkalo, V. A.; Klyucharev, A. P.; Popov, A. I.; Storizhko, V. E. (Inst. of Physics and Tech., Kharkov). Ukr. Fiz. Zh. (Russ. Ed.); 16: 7-11(Jan 1971). (In Russian).

The (p,p'γ) reaction on ^{50}Cr, ^{52}Cr, ^{54}Cr, and ^{64}Zn was studied at proton energies E_p < 4 MeV, and γ-ray angular distribution was measured for the first excited states. The data are compared with the statistical theory of Hauser and Feshbach. A satisfactory agreement with the theory was observed at proton energies below the Coulomb barrier. (auth)

31254 3 PARTICLE–1 HOLE CONFIGURATIONS AND REALISTIC FORCES. Hammann, T. F. (Institut d'Etudes Nucleaires, Algiers). Phys. Lett.; 34B: 561-2(12 Apr 1971). (In French).

A shell model calculation using realistic forces for the ^{50}Sc nucleus is presented. A separable and nonlocal nucleon–nucleon potential, recently presented and tested in this calculation, leads to the same energy spectrum for ^{50}Sc as the reaction matrix calculated by Kuo–Brown. (auth)

31255 MECHANISM FOR EXTENDING THE ^{20}Ne ROTATIONAL BAND. Pittel, S. (Univ. of Colorado, Boulder). Phys. Lett.; 34B: 555-7(12 Apr 1971).

A mechanism for forming a 10^+ member of the ^{20}Ne rotational band is proposed. It is shown that the $(1d_{5/2}-2s_{1/2})^3-1g_{7/2}$ configuration leads to a 10^+ state in the proper energy region with a large E2 radiative width. (auth)

31256 ISOBARIC ANALOG STATES IN ^{52}Cr FROM (p,γ) AND (p,n) REACTIONS IN ^{51}V. Ahmed, N. (Atomic Energy Centre, Dacca, Pakistan); Rahman, M. A.; Rahman, M.; (and others). Lett. Nuovo Cim.; 1: 327-30(20 Feb 1971).

Proton resonances in ^{52}Cr were studied by the (p,n) and (p,γ) reactions at proton energies of 2 to 3 MeV by using an enriched ^{51}V target. The observed gamma spectrum is shown, and the isobaric analog states in ^{52}Cr are tabulated. (R.W.R.)

31257 DECAY OF ^{75}Br. Dzhelepov, B. S.; Dmitriev, A. G.; Zhukovskii, N. N.; Moskvin, L. N.; Penionzhkevich, Yu. E. (Radium Inst., Leningrad). Bull. Acad. Sci. USSR, Phys. Ser. (Engl. Transl.); 33: 1513-17(1969).

Translated from Izv. Akad. Nauk SSSR, Ser. Fiz.; 33: 1650-4 (Oct 1969).

Twenty-eight γ rays associated with the decay of ^{75}Br were studied using a Ge(Li) detector. The results were used to establish 6 levels in ^{75}Se. (auth) (TSS)

31258 NUCLEAR γ-RAYS FOLLOWING MUON CAPTURE. Backenstoss, G. (CERN, Geneva); Charalambus, S.; Daniel, H.; (and others). Nucl. Phys.; A162: 541-51(1971).

The identification of the nuclear γ-rays that occur when muon capture leads to excited nuclei made it possible to evaluate the distribution of excited nuclei formed after the capture process. Mono-isotopic elements were used as targets, and γ-ray spectra were recorded using Ge(Li) detectors. In most cases the observed γ-rays accounted for a high fraction of the capture process. It could be concluded that the probability of zero neutron emission after muon capture was less than 5% contrary to the findings of Kaplan and the predictions of Singer. The chance of single neutron emission was highest, about 50%, and it dropped with increasing neutron multiplicity. The probability of forming a particular excited state in an isotope was in general about proportional to the spin, and about inversely proportional to the energy of the state. (auth)

31259 ^{76}As DECAY. Funel, Genevieve; Ythier, Christian (Univ., Nice, France). Compt. Rend., Ser. B; 272: 158-61 (11 Jan 1971). (In French).

The γ radiation from ^{76}As was studied using a coaxial Ge(Li) detector; 15 new γ ray emissions were observed, most of them at low energies. A decay scheme is proposed. (auth) (France)

31260 LEVELS IN ^{72}Ge POPULATED BY ^{72}Ga. Rester, A. C. (Vanderbilt Univ., Nashville); Ramayya, A. V.; Hamilton,

J. H.; Krmpotic, D.; Rao, P. Venugopala. Nucl. Phys.; A162: 461-80(1971).

The radioactive decay of ^{72}Ga has been investigated by means of Ge(Li) and Si(Li) detectors. The energies and intensities of 71 γ-rays have been determined from the γ-ray singles spectrum. Extensive $\gamma\gamma$ coincidence experiments were performed with two Ge(Li) detectors coupled to a two-parameter analyzer. Internal conversion electron measurements were performed with a Si(Li) detector system. The electron-γ delayed coincidence experiments were carried out with an anthracene crystal and a 35 cm^3 Ge(Li) detector. These extensive coincidence relationships were used to identify the levels of ^{72}Ge populated by ^{72}Ga with excited states at 691.2, 834.02, 1463.88, 1728.24, 2064.80, 2402.0, 2463.74, 2514.65, 2583.5, 2754.1, 2943.45, 3035.41, 3094.7, 3324.92, 3341.68, 3439.3, 3455.2, 3566.0, 3678.1, 3707.1, 3758.6 and 3815.4 keV. The β^- feedings and the log ft values were calculated from the relative γ-ray intensities. (auth)

31261 DECAY OF ^{72}As TO THE LEVELS OF ^{72}Ge. Rester, A. C. (Vanderbilt Univ., Nashville); Hamilton, J. H.; Ramayya, A. V.; Johnson, Noah R. Nucl. Phys.; A162: 481-96(1971).

The decay of ^{72}As has been investigated in a further study of the properties of the ^{72}Ge levels. Gamma-ray singles and coincidence spectra were measured with two Ge(Li) detectors coupled to a two-parameter analyzer, and internal conversion spectra were measured with a Si(Li) detector. There were 60 transitions observed, and 55 of these were fitted into 27 excited states in ^{72}Ge at 691.2, 834.00, 1463.96, 1728.27, 2064.82, 2402.2, 2463.80, 2514.71, 2755, 2939.90, 2943.5, 3035.74, 3094.2, 3325.0, 3337.7, 3341.8, 3419.5, 3455.28, 3550.7, 3678.1, 3708.6, 3803.7, 3816.1, 3872.0, 3983.8, 3985.8 and 3995.0 keV. Some of the properties of the low-lying levels in ^{72}Ge may be interpreted in terms of a vibrational model. (auth)

31262 ELASTIC SCATTERING OF ALPHA PARTICLES BY ^{36}Ar AT 12.83 TO 17.83 MeV. Wallace, William John. Tallahassee; Florida State Univ. (1970). 146p. University Microfilms Order No. 71-7127.

Thesis.

Forty-six point angular distributions for the scattering of α particles by ^{36}Ar were measured from 12.83 to 17.83 MeV in 20 keV intervals throughout the angular range from 29.0 to 167.8° (c.m.). Optical-model fits to the data smoothed in energy with a Lorentzian weighting function were obtained. The computed cross sections were calculated as the incoherent sum of a direct contribution calculated from the optical model plus a compound elastic term based on Hauser-Feshbach theory and statistical-model considerations. The optical model employed a Woods–Saxon real potential and a surface imaginary potential with a form given by the derivative of a Woods–Saxon function. The real well-radius value of 4.9 F was chosen to be consistent with previous analyses of electron scattering data. A representative set of four angular distributions covering the entire energy range was fitted to obtain a consistent set of the other geometric parameters. Four-parameter fits to the data were then obtained by varying only the real potential strength, U, the surface imaginary absorption strength, W_S, the spin cut-off factor, σ, and the spin-zero level density parameter, ρ. No clear-cut evidence for the existence of discrete, phase-equivalent potential sets was observed. Instead, the analysis favored the single potential U = 182.2 MeV, W_S = 36.4 MeV. No improvement of the fits was obtained with a variety of l-dependent modifications to the imaginary potential; with alternative forms of the optical-model parametrization; or by a coupled equations analysis. The coupled channels calculation determined that the effects of coupling to the first 2^+ excited state at 1.98 MeV are weak and that the inelastic scattering cross section is predominantly compound elastic in nature. Compound elastic effects contribute significantly to the scattering at all energies investigated, particularly at the backward angles. The compound elastic parameters extracted by the fitting analysis were confirmed by fluctuation analysis calculations. (Diss. Abst. Int., B)

31263 STATISTICAL MODEL ANALYSIS OF THE ^{75}As(p,n)^{75}Se REACTION. Pellegrini, Benjamin John. New Orleans; Tulane Univ. (1970). 87p. University Microfilms Order No. 71-8080.

Thesis.

Gamma-rays from proton bombardment of ^{75}As targets were observed with Ge(Li) detectors for proton energies below 3 MeV. Branching ratios, angular distributions and excitation functions were obtained for transitions in ^{75}Se populated through the ^{75}As (p,nγ)^{75}Se reaction. The gamma-ray angular distributions were compared to predictions of the statistical model using a modified version of the computer code TRNRX. Relative neutron cross-sections were obtained and were compared to statistical model predictions computed from the computer code LIANA. The statistical model results were combined with branching ratios and reported log ft values to provide consistent spin-parity assignments for the low-lying levels of ^{75}Se. Multipole mixing ratios were obtained for gamma-ray transitions between levels with unique spin-parity assignments. (Diss. Abstr. Int., B)

31264 (d,p) REACTIONS TO THE GROUND STATES OF ^{41}Ca AND ^{49}Ca. King, K.; McKellar, B. H. J. (Univ. of Sydney). Aust. J. Phys.; 23: 641-50(1970).

Calculations for (d,p) stripping on the doubly magic calcium nuclei ^{40}Ca and ^{48}Ca leading to the ground states of ^{41}Ca and ^{49}Ca were carried out on the basis of the sudden approximation method of deuteron stripping developed by Butler, Hewitt, McKellar, and May. The use of realistic form factors found by Philpott, Pinkston, and Satchler to generate the bound state wave function for the neutron captured by the ^{48}Ca core improves the agreement with experimental proton angular distributions arising from the ^{40}Ca (d,p)^{41}Ca g.s. reaction. For both reactions, good agreement is obtained where incident deuteron energies are above the Coulomb barrier. The spectroscopic factor for the $1f_{\frac{7}{2}}$ ground state of ^{41}Ca is found to be 0.60 ± 0.10 while that of the $2p_{\frac{3}{2}}$ ground state of ^{49}Ca is 0.78. (auth) (Australia)

31265 N MIXING IN THE 2s–1d SHELL. Bird, B. (Univ. of Ottawa). Can. J. Phys.; 49: 302-5(1 Feb 1971).

It is shown that the hexadecapole term as suggested by Turner and Trainor does not give $\frac{5}{2}^+$ for the ground state spin of ^{25}Al and ^{25}Mg when major shell mixing is taken into account. The effect of N mixing in the spheroidal core Nilsson model is examined, both with and without band mixing in the 2s-1d shell. (auth) (Canada)

31266 STUDY OF THE DECAY OF THE 3.696 MeV LEVEL IN ^{25}Al. McCallum, G. J.; Sparks, R. J.; Coote, G. E.; Pohl, K. P. (Dept. of Scientific and Industrial Research, Lower Hutt, New Zealand). Can. J. Phys.; 49: 467-74(15 Feb 1971).

The decay of the 3.696 MeV level in ^{25}Al was studied by means of the ^{24}Mg(p,γ)^{25}Al reaction at the 1.49 MeV resonance. Gamma-ray branching ratios, direct angular distributions, and lifetimes determined by the Doppler shift attenuation method are reported. (auth) (Canada)

31267 CHARGED PARTICLES PRODUCED IN CAPTURE OF NEGATIVE MUONS BY ^{28}Si, ^{32}S, ^{40}Ca, AND ^{64}Cu NUCLEI. Budyashov, Yu. G.; Zinov, V. G.; Konin, A. D.; Mukhin, A. I.; Chatrchyan, A. M. (Joint Inst. for Nuclear Research, Dubna, USSR). Zh. Eksp. Teor. Fiz.; 60: 19-27(Jan 1971). (In Russian).

The masses of charged particles emitted as a result of absorption of negative muons by ^{28}Si, ^{32}S, ^{40}Ca and ^{64}Cu nuclei are identified. Energy spectra and emission probabilities are measured for protons with energies exceeding 15 MeV and deuterons with energies exceeding 18 MeV. The energy spectra spread out to 50 MeV; with decrease of nuclear charge the fraction of deuterons in the total number of charged particles increases. Depending on the nuclear charge the proton emission probability has a maximum in the vicinity of calcium. (auth)

31268 STUDY OF THE NUCLEI ^{61}Cu, ^{64}Cu, ^{67}Ga, AND ^{68}Ga USING THE (p,n) REACTION. Bass, William Thomas. Knoxville, Tenn.; Univ. of Tennessee (1970). 94p. University Microfilms Order No. 71-7607.

Thesis.

Neutron time-of-flight techniques were used to study the (p,n) reaction on the nuclei ^{61}Ni, ^{64}Ni, ^{67}Zn, and ^{68}Zn. The locations of excited states in the residual nuclei up to 3 MeV excitation energy were measured with about 10 keV energy resolution. Some 20 to 70 excited states were identified in the residual nuclei. Level energies were assigned with certainties of 2 keV for low-lying states and 5 to 7 keV for higher (2-3 MeV) states. In general the (p,n) cross sections do not exhibit a strong dependence on the properties of the residual state (spin, parity, shell-model configuration, collectivity, etc.). However a certain quantization of the observed peak areas was found. This feature led to a study of the predicted cross sections for final states of different spins and parities using an evaporation mechanism in a form referred to as the Hauser–Feshbach process. An optical model was used to predict barrier transmission functions for incident and exit channels of the compound nucleus. Transmission functions were only required for partial waves of low l-value at the energies used in the present experiment. The method was more sensitive to the spin of the residual nucleus than to final parity. Therefore, in general, only spin predictions were attempted. Spins were assigned to 10–20 levels in ^{64}Cu, ^{67}Ga, and ^{68}Ga. The results were in good agreement with known data. (Diss. Abstr. Int., B)

31269 PROPERTIES OF ^{35}S AND ^{57}Co NUCLEI FROM ANGULAR CORRELATION AND DOPPLER-SHIFT ATTENUATION MEASUREMENTS. Burton, Kenneth Shrum. Tucson, Ariz.;

XUM

Univ. of Arizona (1970). 107p. University Microfilms Order No. 71-8435.

Thesis.

The particle-gamma-ray coincidence version of the Doppler-shift attenuation method was used to obtain mean lives for states in ^{35}S and ^{57}Co. In addition, the particle-gamma-ray method for angular correlations was used to measure spins and multipole mixing ratios in ^{35}S and ^{57}Co. From the results of these experiments, the spin of the 2.35-MeV level in ^{35}S was found to be $^3/_2$, and a tentative assignment of J = $^1/_2$ was made for the 1.99-MeV level in ^{35}S. The E3/M2 mixing ratio of the 1.99-MeV ($^7/_2^-$) → 0 ($^3/_2^+$) transition was measured as $\delta = 0.11 \pm 0.04$. In ^{57}Co, the following mixing ratios were obtained: $\delta(E2/M1) = -0.27 \pm 0.01$ for the 1.22-MeV ($^5/_2^-$) → 0 ($^7/_2^-$) transition, $\delta(E2/M1) = -0.09 \pm 0.01$ for the 1.68-MeV ($^{11}/_2^-$) → 1.22-MeV ($^5/_2^-$) transition, $\delta(E2/M1) = -0.02 \pm 0.01$ for the 1.89-MeV ($^7/_2^-$) → 1.22-MeV ($^5/_2^-$) transition, and $\delta(E2/M1) = -0.13 \pm 0.02$ for the 2.31-MeV ($^7/_2^-$) → 1.22-MeV ($^5/_2^-$) transition. Branching ratios were obtained for the decay of the ^{35}S, 2.35-MeV level, and for the ^{57}Co, 1.68-MeV and 2.31-MeV levels. Excitation energies of three low-lying levels in ^{35}S were also measured as 1574 ± 1 keV, 1995 ± 1 keV, and 2350 ± 1 keV. From considerations of angular correlation and mean life measurements, spin assignments were made for the 1.68-MeV and 2.31-MeV levels of ^{57}Co. These assignments were J(1.68 MeV) = $^{11}/_2$, and J(2.31 MeV) = $^7/_2$. Using the above results, the reduced transition probabilities for electromagnetic transitions among some of the low-lying levels in ^{35}S and ^{57}Co were obtained. These results were compared with the Weisskopf single-particle estimates, with the predictions of the shell model with configuration mixing, and with the predictions of the unified, vibrational model. (Diss. Abstr. Int., B)

31270 STUDY OF THE ^{57}Fe LOW-ENERGY STATES. Eissa, E. A. (Atomic Energy Establishment, Cairo); Honzatko, J. Z. Phys.; 243: 114-20(1971).

The low-energy states of ^{57}Fe were studied by means of thermal neutron radiative capture. The gamma-ray spectrum below 3 MeV was measured using a Ge(Li) detector of an intrinsic volume 5.4 cm^3. On making use of other experiments beside the good resolution of the Ge(Li) detector it was possible to suggest a decay scheme and to get some valuable information. The transitions from the levels 366.7 keV to the ground and first excited states seem to be pure M1 transitions. An evidence for the existence of a transition from the level 1725.5 keV to the 1018.6 keV with an absolute intensity 2.4% is shown. (auth)

31271 g-FACTOR OF THE 181 keV LEVEL OF ^{99}Tc AND HYPERFINE FIELDS OF Tc IN Fe, Co, Ni. Winkler, H.; Rueter, D.; Gerdau, E.; Braunsfurth, J. (Univ., Hamburg). Z. Phys.; 243: 166-70(1971).

The g-factor of the 181-keV level of ^{99}Tc has been redetermined by the spin rotation method. Measurements with polycrystalline sources of Tc in Fe, Co, and Ni yielded values of the hyperfine fields at the Tc nucleus: g = +1.310 (25); H_{hf}(Tc in Fe) = (-)290(15)kOe; H_{hf}(Tc in Co) = (-) 170(5)kOe; and H_{hf}(Tc in Ni) = −47.8(1.5)kOe. (auth)

31272 ELASTIC ELECTRON SCATTERING ON ^{40}Ar FOR THE DETERMINATION OF THE NUCLEAR rms RADIUS. Schuetz, W.; Frank, H. (Technishce Hochschule, Darmstadt, Ger.). Z. Phys.; 243: 132-7(1971). (In German).

The elastic electron scattering cross section of ^{40}Ar has been measured relative to that of the proton using gas targets. The momentum transfer ranged between 0.28 and 0.50 fm^{-1} (40−60 MeV, 90−120°). From partial wave calculations, an rms charge radius of (3.41 ± 0.04) fm was evaluated. The error includes uncertainties due to the choice of the charge distribution. (auth)

31273 REACTION MECHANISM STUDIES OF SINGLE AND DOUBLE DIFFERENTIAL CROSS SECTIONS FROM THE REACTION $^{24}Mg(\alpha,\alpha',\gamma)^{24}Mg$. McNeilly, Gregory Scott. Tallahassee, Fla.; Florida State Univ. (1970). 146p. University Microfilms Order No. 71-7064.

Thesis.

Alpha-gamma angular correlations (double differential cross sections-DDCS) from the reaction $^{24}Mg(\alpha,\alpha',\gamma)^{24}Mg$ were measured at an incident alpha particle energy of 16.65 MeV. An 800 keV thick target provided energy averaged results. The scattered alpha particles were detected (in the horizontal plane) at 7.5 degree steps from 27.5° to 140° in the laboratory frame of reference. The gamma detector (also in the horizontal plane) was moved through 15 detector positions, thus measuring 15 points defining an alpha-gamma angular correlation for each particle angle, from which DDCS parameters were extracted. DDCS parameters were obtained from the reaction $^{24}Mg(\alpha,\alpha_{1.37},\gamma_{1.37})^{24}Mg$ and from the reaction $^{24}Mg(\alpha,\alpha_{4.12}+\alpha_{4.23},\gamma_{1.37})^{24}Mg$. The DDCS data are expressed in millibarns per square steradian (mb/sr^2). The DDCS data, together with available single differential cross section (SDCS) data from the ground state, the 1.37 MeV state, and the 4.12 MeV state of ^{24}Mg, were analyzed. Theoretical fits to these data were calculated using a DWBA plus Hauser−Feshbach (HF) method, and a coupled-channels (CC) plus HF method. The inelastic levels in ^{24}Mg were treated as rotational excitations of a deformed nucleus. The HF contribution to the cross sections is significant for elastic scattering, and dominates the calculated inelastic SDCS. However, the calculated HF contribution is near zero in the angular region 60°−120° for the anisotropic DDCS parameters. DWBA plus HF fits are in close agreement with CC plus HF fits for the SDCS data, and show slightly less agreement for the DDCS data. (auth)

31274 K-CONVERSION COEFFICIENT OF THE 53.3-keV TRANSITION AND K/L + M-RATIO OF THE 13.34-keV TRANSITION IN ^{73}Ge. Vester, K.-P. (Freie Univ., Berlin). Z. Phys.; 242: 320-7(1971).

The K-conversion coefficient of the 53.3 keV transition in ^{73}Ge was measured by coincidence techniques to be $\alpha_{K_i} = 7.1 \pm 0.6$ indicating very good agreement with theory for M2-radiation. The (K/L + M)-ratio of the 13.34 keV transition to the ground state was determined using the same techniques. The resulting value $(K/L + M)_2 = 0.36 \pm 0.03$ supports the E2-character of this radiation and therefore a spin assignment of $^5/_2$ for the 13.34 keV level. The measured lifetime of this transition ($T_{\frac{1}{2}}$ = (2.95 ± 0.05) μsec) corresponds to a factor of 15 greater than the Weisskopf estimation for a pure E2-transition. A short discussion of a possible transfer of the collectivity of the ^{72}Ge-nucleus to the ^{73}Ge-nucleus is given. (auth)

31275 CONTRIBUTIONS OF DIRECT AND COMPOUND PROCESSES TO THE REACTION $^{40}Ca(d,\alpha)^{38}K$ AT E_d = 5 TO 10 MeV. Kroner, G.; Hofmann, A.; Philipp, G.; Thomas, K. (Univ., Erlangen, Ger.). Z. Phys.; 242: 308-19(1971). (In German).

For the reaction $^{40}Ca(d,\alpha)^{38}K$ differential cross sections for the excitation of the low lying states in ^{38}K were measured at bombarding energies between 5 and 10 MeV. Total cross sections were calculated using the statistical theory. It was found, that in the whole energy region the isotropic background of the angular distributions gives a good estimation of the compound contribution to the reaction cross section. (auth)

31276 ELASTIC SCATTERING AND RADIATIVE CAPTURE OF PROTONS WITH EXCITATION OF ISOBARIC ANALOG STATES. Kolomiets, V. M.; Tsekhmistrenko, Yu. V. (Inst. of Physics, Kiev). Bull. Acad. Sci. USSR, Phys. Ser. (Engl. Transl.); 33: 1597-1603(1969).

Translated from Izv. Akad. Nauk SSSR, Ser. Fiz.; 33: 1747-53 (Oct 1969).

A method for analysis of isobaric analog resonance in (p,p) and (p,γ) reactions at proton energies below the threshold of the charge transfer channel is developed. The method is applied to calculating the positions and decay widths for analog resonances in ^{88}Sr (p,p) and (p,γ) reactions at 6 to 8 MeV. (J.W.R.)

31277 β−γ ANGULAR CORRELATION MEASUREMENTS FOR SOME HIGHLY RETARDED ALLOWED β TRANSITIONS. Subotowicz, M.; Kuranc, J.; Sarzynski, J. (Marie Curie-Sklodowska Univ., Lublin). Bull. Acad. Sci. USSR, Phys. Ser. (Engl. Transl.); 33: 1503-4(1969).

Translated from Izv. Akad. Nauk SSSR, Ser. Fiz.; 33: 1638-9 (Oct 1969).

Beta-gamma angular correlations following the decays of ^{22}Na, ^{110}Ag, ^{134}Cs, and ^{160}Tb using a magnetic spectrometer and a NaI(Tl) detector are given. The measured angular correlation coefficients are listed in tabular form. (J.W.R.)

31278 $^{45}Sc(^3He,d)^{46}Ti$ REACTION. DWBA ANALYSIS OF TRANSITIONS TO STATES BETWEEN 7.6 AND 11.0 MeV. Broman, Lars; Larsson, Curt (Chalmers Univ. of Tech., Goteborg). Z. Phys.; 242: 360-3(1971).

Angular distributions of transitions to 29 states in ^{46}Ti between 7.6 and 11.0 MeV excitation energy from the $^{45}Sc(^3He,d)$ reaction at 15 MeV were compared with DWBA predictions. The results support previously suggested T = 2 states in ^{46}Ti. (auth)

31279 RECOIL-DISTANCE LIFETIME MEASUREMENTS FOR STATES IN ^{30}P. Henson, S. H.; Cochavi, S.; Marmor, M.; Fossan, D. B. (State Univ. of New York, Stony Brook). Phys. Rev., C; 3: 191-8(Jan 1971).

The recoil-distance method has been used with the $^{27}Al(\alpha,n)^{30}P$ reaction to measure the lifetimes of the 1.453- and 1.974-MeV levels in ^{30}P. A mean lifetime of τ = 9.2 ± 0.5 psec was obtained for the 2^+ 1.453-MeV level and τ = 6.8 ± 0.4 psec was obtained for the 3^+ 1.974-MeV level. A Ge(Li) γ spectrum was measured in coincidence with neutrons to identify the ^{30}P transitions. Com-

parisons of the resulting reduced transition probabilities with shell-model calculations have been made. (auth)

31280 INVESTIGATION OF THE REACTION $^{35}Cl(n,\gamma)^{36}Cl$. Fubini, A.; Popa, M.; Prosperi, D.; Terrasi, F. (CNEN, Rome). Nuovo Cim.; 2A: 109-21(1 Mar 1971).

The γ radiation emitted following neutron capture in natural chlorine was studied. About 170 transitions were observed. A neutron separation energy of (8581.5 ± 0.2) keV was found for ^{36}Cl. By applying the Ritz combination principle it was possible to construct a level scheme involving 17 excited states in ^{36}Cl. The multipolarity of the transitions of highest intensity was identified: five M1 + E2 transitions (8580.8, 7791.8, 7415.6, 6979.8, 6628.9 keV) and seven E1 transitions (6620.9, 6113.0, 5716.9, 4946.4, 4617.0, 4441.8, 4083.6 keV) were found. A straightforward calculation of the average radiative strength functions allows the conclusion that in ^{36}Cl M1 transitions are weaker than estimated by schematic studies of heavier nuclei. (auth)

31281 STUDY OF THE REACTION $^{22}Ne(p,p)$, $^{22}Ne(p,p')$, AND THE EXCITED STATES OF ^{23}Na. Rihet, Y.; Beaumevieille, H.; Dumazet, G.; Lambert, M.; Meynadier, C. (Institut d'Etudes Nucleaires, Algiers). Nuovo Cim.; 1A: 483-95(1 Feb 1970). (In French).

With the aid of a gas target with 0.63 μm of nickel foil inserted in front of the target, excitation functions were measured for elastic and inelastic scattering of protons from ^{22}Ne at proton energies from 2.4 to 3.2 MeV in 3 keV steps at eleven laboratory angles from 29 to 165°. The above data are used to obtain information about states in ^{23}Na with a width $\Gamma > 3$ keV. It is suggested that the isobaric analog state of the 9th excited state of ^{23}Ne in ^{23}Na would lie around $E_{ex} = 11.85$ MeV ($E_p = 3.2$ MeV). (auth)

31282 COULOMB PROPAGATOR IN RADIATIVE MUON CAPTURE. Rood, H. P. C. (Univ., Groningen, Netherlands); Yano, A. F. Phys. Lett.; 35B: 59-61(26 Apr 1971).

The effect of the Coulomb field is investigated in the radiative muon capture by ^{40}Ca. (auth)

31283 HIGH-RESOLUTION STUDY OF ^{92}Nb BY (d,t) AND (d,tγ) REACTIONS. Bhatis, T. S.; Daehnick, W. W.; Canada, T. R. Univ. of Pittsburgh). Phys. Rev., C; 3: 1361-9(Mar 1971).

The reaction $^{93}Nb(d,t)^{92}Nb$ has been studied with a deuteron beam of 17 MeV. Reaction tritons were momentum-analyzed by the Enge split-pole spectrograph and detected by position-sensitive counters as well as nuclear emulsions placed along the focal plane of the spectrograph. The experimental energy resolution was ~8 keV full width at half-maximum. Up to 3 MeV in excitation, approximately 50 states of ^{92}Nb have been identified including the 6 previously known low-lying states. Angular distributions for 40 of these triton groups were obtained and l-transfer values for the neutron pickup to the corresponding states in ^{92}Nb were assigned by comparison with distorted-wave calculations. A previous classification of the lowest six positive-parity states as belonging to the $(1g_{\frac{9}{2}}^{\pi}2d_{\frac{5}{2}}^{\nu})$ multiplet is confirmed. As there are ambiguities in the assignment of spins to some members of this multiplet on the basis of spectroscopic strengths alone, the electromagnetic-decay properties of the low-lying positive-parity states of ^{92}Nb have been studied via the $^{93}Nb(d,t\gamma)^{92}Nb$ reaction. On the basis of the resulting decay scheme, spin assignments are made to the previously identified $(1g_{\frac{9}{2}}^{\pi}2d_{\frac{5}{2}}^{\nu})$ multiplet of states. The 286-, 357-, 480-, and 500-keV states are assigned J^{π} values of 3^+, 5^+, 4^+, and 6^+, respectively. (auth)

31284 FIRST-FORBIDDEN UNIQUE β-DECAYS IN THE Sr REGION. Vergados, J. D. (State Univ. of New York, Stony Brook). Nucl. Phys.; A166: 285-96(1971).

First-forbidden unique β-moments were calculated for the following nuclear pairs: $^{88}Rb-^{88}Sr$, $^{89}Sr-^{89}Y$, $^{90}Y-^{90}Zr$, $^{90}Sr-^{90}Y$. It is shown that, although the extreme shell model (without configuration mixing) is inadequate to explain the experimental data, very good agreement with experiment is achieved if one uses realistic shell-model wave functions. (auth)

31285 NUCLEAR VARIATIONAL CALCULATIONS WITH IMPROVED MIXED-DENSITY APPROXIMATION. Pandharipande, V. R. (Niels Bohr Inst., Copenhagen). Nucl. Phys.; A166: 317-29(1971).

The Slater mixing-density approximation is modified so as to retain effects of finite interaction range in the approximate exchange energy. A correction for finite number of particles makes the proposed exchange-energy approximation exact for ^4He and infinite matter. Thomas–Fermi and effective single-particle Hamiltonian calculations are carried out with this approximation in ^{40}Ca and ^{208}Pb. The results of these compare very favorably with those of Hartree–Fock calculations in coordinate space. (auth)

31286 COUPLED-CHANNEL CALCULATIONS OF THE GIANT DIPOLE RESONANCE IN THE ONE PARTICLE–ONE HOLE CONTINUUM APPROXIMATION. II. ^{28}Si. Marangoni, M. Saruis, A. M. (CNEN, Bologna). Nucl. Phys.; A166: 397-412 (1971).

The electric dipole giant resonance of ^{28}Si is calculated in the frame of the one particle–one hole continuum approximation by means of the coupled-channel method. The isospin mixing is taken into account, since the single-particle potentials for protons include a central Coulomb part. The residual interaction is a zero-range force. The results are compared with the experimental data and with previous bound-state calculations. Particular attention is paid to the results on the $^{27}Al(p,\gamma_0)^{28}Si$ angular distributions. (auth)

31287 DECAYS OF ^{56}Co AND ^{66}Ga AND PRECISE GAMMA-RAY INTENSITIES. Camp, David C. (Univ. of California, Livermore); Meredith, Gerald L. Nucl. Phys.; A166: 349-77 (1971).

The intensities of the γ-ray transitions from the decay of 77.3 d ^{56}Co and of 9.5 h ^{66}Ga were carefully determined using a high-resolution Ge(Li) detector, which is the central detector in a Compton suppression and pair spectrometer. This work reports six new γ-transitions observed in the decay of ^{56}Co and ten in ^{66}Ga. The former fit into the known decay scheme, while the latter are consistent with levels known from reaction data. A comparison is made between γ-ray intensities determined in this work and those of past investigations. Adopted weighed averages presented for both ^{56}Co and ^{66}Ga are useful for the efficiency calibration of Ge(Li) detectors up to 5 MeV. The adopted intensities for 14 transitions in ^{56}Co with relative intensities greater than 1% have errors on the order of 1%, while 20 transitions in ^{66}Ga with relative intensities greater than 1% have errors less than 2% with over half of these less than 1%. (auth)

31288 LINEAR POLARIZATION OF THE γ RAYS EMITTED IN THE REACTION $^{46}Ti(p,p'\gamma)$. Gallmann, A.; Guillaume, G.; Davison, N. E.; Wagner, P.; Franck, G. (Laboratoire de Physique Nucleaire et d'Instrumentation Nucleaire, Strasbourg). Nucl. Phys.; A166: 271-84(1971). (In French).

The $^{46}Ti(p,p'\gamma)$ reaction was studied at proton energies of 5.489 and 5.508 MeV. The linear polarization of γ-rays emitted by ^{46}Ti levels below 3.25 MeV was measured using the technique involving a single planar Ge(Li) detector. The spin-parity values 2^+, 3^-, 1^- and 2^+ were assigned to the levels at 2.962, 3.059, 3.168, and 3.236 MeV respectively. Gamma-ray branching and mixing ratios also were obtained. (auth)

31289 DETERMINATION OF THE PARITY OF THE 4.19-MeV LEVEL OF ^{36}S. Jundt, F.; Aslanides, E.; Gallmann, A.; Alburger, D. E. (Laboratoire de Physique Nucleaire et d'Instrumentation Nucleaire, Strasbourg). Nucl. Phys.; A166: 266-70 (1971). (In French).

The linear polarization of the 0.90 and 1.28 MeV γ-rays, deexciting the 4.19 and 4.57 MeV levels of ^{36}S was measured. Together with recently measured mixing ratios and angular correlation coefficients, this measurement fixes the parity of the 4.19 MeV level as odd and confirms the even parity of the 4.57 MeV level. (auth)

31290 ENERGY LEVELS AND GAMMA TRANSITIONS IN ^{70}Ga. Arnell, S. E.; Linusson, H.; Sawa, Z. (Chalmers Univ. of Tech., Goteborg. Research Inst. of Physics, Stockholm). Nucl. Phys.; A166: 241-52(1971).

The energy levels of ^{70}Ga were studied with a magnetic spectrograph by means of (d,p) and (d,t) reactions induced by 12 MeV deuterons. Gamma transitions in ^{70}Ga due to $^{69}Ga(d,p\gamma)$, $^{69}Ga(n,\gamma)$, $^{70}Zn(p,n\gamma)$ and $^{67}Zn(\alpha,p\gamma)$ reactions were investigated with coaxial Ge(Li) spectrometers. Gamma-gamma and proton-gamma coincidence experiments were performed in order to infer the positions of the γ-transitions in the level scheme presented. It is highly probable that the 508 keV level is the first excited state in ^{70}Ga. (auth)

31291 ELASTIC AND INELASTIC PROTON SCATTERING ON ^{33}S, ^{34}S, AND ^{35}Cl. Antropov, A. E.; Zarubin, P. P.; Ioannu, P. D.; (and others). Bull. Acad. Sci. USSR, Phys. Ser. (Engl. Transl.); 33: 1576-80(1969).

Translated from Izv. Akad. Nauk SSSR, Ser. Fiz.; 33: 1721-7 (Oct 1969).

Angular distributions for proton elastic and inelastic scattering from ^{33}S, ^{34}S, and ^{35}Cl at 6 MeV, were measured. Optical-model and DWBA analyses of the data were performed. Some spin assignments for levels in ^{33}S and ^{35}Cl are suggested. (J.W.R.)

31292 $^{40}K(n,\gamma)^{41}K$ REACTION AND THE LEVEL STRUCTURE OF ^{41}K. Beckstrand, D. F.; Shera, E. B. (Los Alamos Scientific Lab., N. Mex.). Phys. Rev., C; 3: 208-18(Jan 1971).

The low-lying level structure of ^{41}K has been studied using the

XUM

thermal-neutron capture reaction $^{40}K(n,\gamma)^{41}K$ on an isotopically separated target of ^{40}K. The γ-ray spectrum from this reaction has been studied in the energy range from 0.1 to 10.1 MeV using a Li-drifted Ge spectrometer system. γ-γ coincidence measurements using Ge(Li) detectors have also been made. Spin and parity assignments for the excited states below 2450 keV are proposed, primarily on the basis of γ-ray branching to levels with established spin and parity values. The proposed level energy [keV(I^π)] values are 0($\frac{3}{2}^+$), 980.4($\frac{1}{2}^+$), 1293.4($\frac{1}{2}^-$), 1559.9($\frac{1}{2}^+$), 1582.0($\frac{5}{2}^+$), 1677.5 ($\frac{5}{2}^+$, $\frac{7}{2}^+$), 1698.1($\frac{5}{2}^+$, $\frac{7}{2}^+$), 2144.1($\frac{5}{2}^+$), 2166.0($\frac{1}{2}^+$, $\frac{3}{2}^+$), 2316.5 ($\frac{5}{2}^+$, $\frac{7}{2}^+$), 2447.9($\frac{1}{2}^+$, $\frac{3}{2}^+$). Additional levels have been observed at 2494.7, 2507.9 2527.9, 2599.8, 2681.5, 2712.2, 2756.5, 2760.7, 3042.1, 3142.1, 3164.5, 3213.4, 3235.6, and 3281.1 keV. These low-lying excited states of ^{41}K are discussed in terms of two-particle one-hole configurations of the form $p(d_{\frac{3}{2}})^{-1}n(f_{\frac{7}{2}})^2$. (auth)

31293 DECAY OF THE FIRST EXCITED STATE AT 13.3 keV IN ^{73}Ge. Raghavan, R. S. (Technische Univ., Munich). Z. Phys.; 243: 441-5(1971).

Singles and coincidence measurements of the 13.3-keV transition of ^{73}Ge are reported. The total and K conversion coefficients of this gamma ray and the half-life of this level have been determined. The results are: $\alpha_T = 1095 \pm 55$; $\alpha_K = 312 \pm 30$; $T_{\frac{1}{2}} = 2.98 \pm 0.05$ μs. (auth)

31294 HYPERFINE STRUCTURE INVESTIGATIONS OF ^{51}Mn AND ^{52m}Mn. Joensson, J. O.; Olsmats, M.; Sanner, L.; Wannberg, B. (Uppsala Univ.). Nucl. Phys.; A166: 306-16(1971).

The atomic-beam magnetic resonance method was used to study the hyperfine structure interaction in ^{51}Mn(45 min) and ^{52m}Mn(21 min). The results are for ^{51}Mn: $I = \frac{5}{2}$, $|a| = 74.835(1)$ MHz, $|b| = 0.024(4)$ MHz (b/a > 0), $|\mu_I| = 3.56(1)$ n.m., $|Q| = 0.50(10)$ b, and for ^{52m}Mn: I = 2, $|a| = 0.200(2)$ MHz, $|\mu_I| = 0.0076$ n.m. The nuclear moments were calculated from the measured h.f.s. coupling constants using the known values of a, b, μ_I and Q for ^{55}Mn. The results are compared with shell-model and Coriolis coupling model calculations. (auth)

31295 ELASTIC SCATTERING OF PROTONS FROM ^{40}Ca AT 21.0, 23.5, 26.3, AND 48.0 MeV. Bray, K. H.; Jayaraman, K. S.; Moss, G. A.; (and others) (Univ. of Manitoba, Winnipeg). Nucl. Phys.; A167: 57-64(1971).

With a sector-focused cyclotron a study has been made of the elastic scattering of protons from ^{40}Ca at energies of 21.0, 23.5, 26.3 and 48.0 MeV. The incident proton energies were chosen to match, as closely as possible, available polarization data. The differential cross sections, measured between 15° and 170°, and available polarization data at nearby energies were analyzed in terms of a conventional optical model. (auth)

31296 $^{22}Ne(p,t)^{22}Ne$ REACTION AT 26.9, 35.1, AND 42.4 MeV. Falk, W. R.; Kulisic, P.; McDonald, A. (Univ. of Manitoba, Winnipeg). Nucl. Phys.; A167: 157-76(1971).

Angular distributions of tritons from the $^{22}Ne(p,t)^{20}Ne$ reaction have been measured at proton bombarding energies of 26.9, 35.1 and 42.4 MeV. All the known energy states up to an excitation energy of 6.72 MeV in ^{20}Ne were excited, including the unnatural parity 2^- level at 4.97 MeV. DWBA calculations have been made using the finite-range two-nucleon transfer code of Nelson and Macefield. Various wave functions describing ^{20}Ne and ^{22}Ne, taken from the work of Arima et al., Wildenthal et al., Kuo and Zuker, were used in calculating the spectroscopic amplitudes for transitions to the various final states in ^{20}Ne. Comparison of the nuclear structure information extracted at the different bombarding energies is emphasized. The sensitivity of the DWBA results to the binding energy of the single-particle states is discussed. (auth)

31297 β-γ (CP) CORRELATION MEASUREMENT IN ^{72}Ga. Behrens, H.; Brodt, F. (Univ., Karlsruhe, Ger. Kernforschungszentrums, Karlsruhe, Ger.). Z. Phys.; 243: 402-8(1971). (In German).

The β-γ circular polarization asymmetry for the β948-γ2202 keV transition in ^{72}Ga has been measured using the polarimeter developed at Karlsruhe. The result of the measurement is $A = -0.203 \pm 0.035$. From this result and γ-γ angular correlation measurements of other authors the spin of the 3036-keV level in ^{72}Ge is deduced to be 2^-. The multipolarity of the 2202-keV γ rays in ^{72}Ge is found to be E1. (auth)

31298 (h,p) REACTIONS ON Cr. I. $^{50}Cr(h,p)^{52}Mn$. Hansen, Ole (Univ. of Pennsylvania, Philadelphia); Mulligan, T. J.; Pullen, D. J. Nucl. Phys.; A167: 1-15(1971).

The reaction $^{50}Cr(^3He, p)^{52}Mn$ has been studied at 16.5-MeV incident energy and with a resolution of ≈15 keV FWHM. Forty-nine transitions were observed up to 5.87 MeV of excitation and proton angular distributions were extracted. The distribution shapes in conjunction with DW calculations are used for assignments of spin and parity of many final states. The data are compared to previous information on ^{52}Mn and two states at 2.929 MeV and 5.491 MeV are assigned as isobaric analogs of the two lowest 0^+ states in ^{52}Cr. The strength of the $0^+ \rightarrow 1^+$ excitations is commented upon. (auth)

Nuclear Properties and Reactions, A ≥ 90

Refer also to abstracts 28980, 28998, 29017, 29018, 29326, 29358, 29363, 30452, 31204, 31209, 31258, 31277, 31284, 31285, 31394, and 31661.

31299 (AWRE-O-89/70) ELASTIC AND INELASTIC SCATTERING OF NEUTRONS IN THE ENERGY RANGE 1.0 TO 5.0 MeV BY NATURAL MOLYBDENUM. Coles, R. E.; Porter, D. (Atomic Weapons Research Establishment, Aldermaston (England)). Dec 1970. 37p. (EANDC(UK)-126-AL). Dep. NTIS (U. S. Sales Only). UK 5s. 6d.

The time-of-flight method was used to study fast neutron elastic and inelastic scattering in the energy range 1.0 to 5.0 MeV by natural molybdenum. Differential cross sections at ten angles from 30 to 135° were measured at 0.5-MeV intervals between 1.5 and 5.0 MeV for elastic scattering, inelastic scattering to groups of levels up to 1600 keV excitation in the target nucleus, and inelastic scattering to a continuum above this 1600-keV level. Excitation functions were derived from 125° yields measured at 0.2-MeV intervals between 1.0 and 3.0 MeV for inelastic scattering to groups of levels up to 1600 keV excitation in the target nucleus. The continuum spectra in the range 2.0 to 5.0 MeV were analyzed in terms of statistical evaporation theory and parameters describing the secondary energy distributions of the continuum scattered neutrons extracted. No attempt was made to compare the data with theoretical predictions. Moreover, above 2.0 MeV incident neutron energy, few experimental data are available with which to make comparisons, although comparisons are made where appropriate to previously evaluated cross sections. (auth)

31300 (CNEA-282) RESONANCE INTEGRALS FOR NEUTRON ACTIVATION OF ^{64}Zn, ^{68}Zn, ^{85}Rb, ^{100}Mo, ^{102}Ru, ^{113}In, ^{123}Sb, AND ^{180}Hf. Ricabarra, M. D.; Turjanski, R.; Ricabarra, G. H. (Comision Nacional de Energia Atomica, Buenos Aires (Argentina)). 1970. 17p. (In Spanish). Dep. NTIS (U. S. Sales Only).

The ratio of resonance integral to thermal activation cross section of the isotopes ^{64}Zn, ^{68}Zn, ^{85}Rb, ^{100}Mo, ^{102}Ru, ^{113}In, ^{123}Sb, and ^{180}Hf relative to gold was determined by measuring cadmium ratios. The standard gold or a secondary standard was mixed uniformly in the samples, and the activities were resolved with a lithium-drifted germanium γ-ray spectrometer. Expressed as Westcott S_0 values, the results were as follows: ^{64}Zn, 2.06 ± 0.03; ^{68}Zn, 3.72 ± 0.14; ^{85}Rb, 18.4 ± 0.6; ^{100}Mo, 21.7 ± 0.8; ^{102}Ru, 3.76 ± 0.03; ^{113}In, 24.7 ± 0.5; ^{123}Sb, 28.3 ± 2.1; and ^{180}Hf, 2.17 ± 0.09. All measurements are relative to $S_0 = 17.7$ for gold. (auth)

31301 (CNEA-283) EXCITATION FUNCTIONS FOR THE NUCLEAR REACTIONS $^{159}Tb(d,p)^{160}Tb$ AND $^{159}Tb(d,4n)^{157}Dy$. Siri, L. Nicola; Nassiff, S. J. (Comision Nacional de Energia Atomica, Buenos Aires (Argentina)). 1970. 9p. (In Spanish). Dep. NTIS (U. S. Sales Only).

Excitation functions for the nuclear reactions (d,p) and (d,4n) on ^{159}Tb were determined by activation. The method of stacked metal foils was employed. The energy of the incident deuteron beam was 27.2 MeV. (tr-auth)

31302 (COO-1167-10) MASS YIELD AND CHARGE DISTRIBUTION IN 450 MeV PROTON FISSION OF ^{238}U. Panontin, John A.; Sugarman, Nathan (Chicago Univ., Ill.). [1970]. 56p. Dep. NTIS.

The independent and/or cumulative cross sections of 26 isotopes of silver, cadmium, indium, tin, and antimony from the fission of ^{238}U with 450-MeV protons were measured. The isotopic yield distribution for these elements are presented along with the charge distribution for five mass chains, 115, 117, 125, 127, and 129. The values of the most probable charge, Zp, for fourteen mass chains were calculated and the variation of A/Zp with A defined for the mass region, 100 to 130. For A values between 100 and 120, A/Zp and the charge distribution width are relatively constant at values of 2.424 ± 0.004 and 2.90 ± 0.10 Z units, respectively. In the mass region, 125 to 129, a width of 3.21 Z units and a slightly higher value of A/Zp, 2.430 ± 0.004, are required to account for the data. A mass yield curve encompassing this region of A was also calculated. (auth)

31303 (INR-1271) CONNECTION OF THE RADIATIVE CAPTURE MECHANISM WITH THE NUCLEAR STRUCTURE (A > 100). Brzosko, Jan S. (Institute of Nuclear Research, Warsaw (Poland)). 1971. 72p. Dep. NTIS (U. S. Sales Only).

The present paper is a summing up of investigations into the nature of anomalous amplification in gamma spectra accompanying nucleon radiative capture. The method and results are presented for measurements of gamma-ray spectra in the reactions: (n,γ): E_n = 0.03 to 1.4 MeV, (p,γ): E_p = 4 MeV, and (γ,γ'): E_γ = about 7 MeV for heavy nuclei (A > 100). The results, in units of cross section (with the exception of the (γ,γ') reaction), are compared with calculations based on the assumption of a direct process and the compound-nucleus model. Whereas in the direct process the measured values differ from the calculated values by three orders, in the case of the compound-nucleus model the agreement is good both quantitatively and qualitatively. This agreement is conditional upon account being taken of a resonance occurring in the probability of gamma-ray emission at a gamma energy of about 6 to 8 MeV. The paper discusses conclusions emerging from available experimental information about this resonance and substantiates the view that the anomalous bump in the gamma-ray spectrum is associated with compound-nucleus decay. (auth)

31304 (JAERI-Memo-4251) MULTI-GROUP CONSTANTS FOR FISSION PRODUCT NUCLIDES. Tone, Tatsuzo; Hasegawa, Akira (Japan Atomic Energy Research Inst., Tokyo). Dec 1970. 208p. (In Japanese). Dep. NTIS (U. S. Sales Only).

Many sets of multi-group constants of (n,γ) reactions for fission products have been produced on the basis of several data sources. Energy ranges covered are 10 MeV to 0.215 eV and 10 MeV to 1 keV. Some typical cross sections and yields including the recent data were reviewed and adopted, in which the weight was placed on UKNDL, Benzi and Reffo's cross section data and Meek and Rider's yield data. The fissionable nuclides covered are ^{239}Pu, ^{235}U, and ^{238}U for fast-neutron fission and ^{239}Pu, ^{235}U and ^{241}Pu for thermal-neutron fission. Both group structures were adopted: 25 groups of ABBN set and 70 groups of JAERI-Fast set. (auth) (Japan)

31305 (JINR-P3-5655) NEUTRON RESONANCES OF THE SAMARIUM ISOTOPES. Karzhavina, E. N.; Popov, A. B. (Joint Inst. for Nuclear Research, Dubna (USSR). Lab. of Neutron Physics). 1971. 28p. (In Russian). Dep. NTIS (U. S. Sales Only).

Neutron transmission and yield of γ rays from neutron capture by Sm samples with different isotopic structure were measured using a neutron spectrometer with the resolution being 6 nsec/m. An isotopic identification was performed; and the resonance parameters for ^{147}Sm and ^{149}Sm in the region up to 400 and 250 eV, respectively, are determined. The values of average distances D between levels and of strength functions S_0 for ^{147}Sm and ^{149}Sm are obtained. (auth)

31306 (JINR-P4-5693) NON-ROTATIONAL STATES OF ODD-MASS NUCLEI IN THE ACTINIDE REGION. Komov, A. L.; Malov, L. A.; Soloviev, V. G. (Joint Inst. for Nuclear Research, Dubna (USSR). Lab. of Theoretical Physics). 1971. 17p. (In Russian). Dep. NTIS (U. S. Sales Only).

The energies and wave functions for non-rotational states of odd-mass nuclei in the actinide region are calculated in the superfluid nuclear model. A rather good agreement of the energies of the low-lying nonrotational states in ^{243}Am, ^{247}Bk, ^{243}Cm, ^{235}Np, ^{239}Np, ^{237}Pu, ^{243}Pu, and ^{239}U was obtained. (auth)

31307 (JINR-P7-5497) PRODUCTION OF THE SPONTANEOUSLY FISSIONABLE ISOMER ^{236}U BY THE RADIATIVE THERMAL NEUTRON CAPTURE. Belov, A. G.; Gangrskii, Yu. P.; Dalkhsuren, B.; Kucher, A. M. (Joint Inst. for Nuclear Research, Dubna (USSR). Lab. of Nuclear Reactions). 1971. 13p. (In Russian). Dep. NTIS (U. S. Sales Only).

The spontaneously fissionable isomer ^{236}U with $T_{\frac{1}{2}}$ = 70 ns was produced by the radiative capture of thermal neutrons. The ratio between the cross section of the reaction leading to the isomer production and ^{235}U fission is about 10^{-4}. Delayed conversion-electron coincidences and the fission fragments were measured. (auth)

31308 (KFK-1248) THEORETICAL STRUCTURE LEVEL AND ABSOLUTE TRANSITION PROBABILITIES IN DEFORMED NUCLEI OF UNEVEN MASS NUMBERS. Weller, F.; Markus, G. (Kernforschungszentrum, Karlsruhe (West Germany). Institut fuer Angewandte Kernphysik). Nov 1970. 24p. (In German). Dep. NTIS (U. S. Sales Only).

The method of the calculations is based on the collective model and extends the usual Coriolis-coupling band-mixing calculations by the inclusion of rotation–vibration interactions and quasi-particle–phonon interactions. The success of the method depends on a careful treatment of the pairing correlations, which have a striking influence. The theoretical level structures of the following nuclei are calculated: ^{163}Dy, ^{165}Er, ^{165}Dy, ^{167}Yb, ^{167}Er, ^{169}Yb, ^{171}Yb, ^{173}Yb, ^{161}Tb, ^{167}Tm, ^{169}Tm, ^{171}Tm, ^{173}Lu, and ^{175}Lu. Allowed and K-forbidden gamma-ray transitions in these nuclei are calculated and compared with the experimental values. In most cases the agreement for M1 is good, while the E1 transitions are about an order of magnitude too fast. (auth)

31309 (LA-DC-11648) EFFECT OF THE MULTIPOLE PAIRING AND PARTICLE-HOLE FIELDS IN THE PARTICLE-VIBRATION COUPLING OF ^{209}Pb: I. Bes, D. R.; Broglia, R. A. (Los Alamos Scientific Lab., N. Mex. Minnesota Univ., Minneapolis, School of Physics and Astronomy). [1970]. Contract W-7405-eng-36. 67p. (COO-1764-108). Dep. NTIS.

The particle–vibration coupling formalism for nuclei around closed shells is studied, and a microscopic description is given. Both particle–hole excitations and excitations that change the number of particles by two (pairing mode) are considered as collective modes of excitation of the closed-shell-system (N_0) ground state. To describe the pairing modes, multipole pairing residual interactions are used. The odd particle is allowed to couple to both types of vibrations. The coupling Hamiltonian is linear in the collective phonons and the particle variables. The effective Hamiltonian is constructed by a perturbative method. Explicit expressions are given for the spectroscopic amplitudes and spectroscopic factors associated with the $(N_0 - 1)$ (t,p) $(N_0 + 1)$ and $(N_0 + 2)$ (p,d) $(N_0 + 1)$ reactions, respectively. The concept of effective transfer operator is used. Special attention is paid to the ^{207}Pb(t,p) and ^{210}Pb(p,d) reactions. (auth)

31310 (LYCEN-7084) DECAY SCHEME OF 1.3 h, ^{174}Ta. Charvet, A.; Do Huu Phuoc; Duffait, R.; Emsallem, A.; Chery, R. (Lyon Univ. (France). Institut de Physique Nucleaire). 19 Nov 1970. 23p. Dep. NTIS (U. S. Sales Only).

The decay of ^{174}Ta ($T_{\frac{1}{2}}$ = 1.3 h) was investigated using Ge(Li) and Si(Li) detectors. Single, coincidence, and sum γ-ray spectra, conversion lines, and $e-\gamma$ coincidence relations were studied. The results are in good agreement with those of earlier investigations on the ground-state and the beta-vibrational bands. Above these bands 14 levels were established having the following energies (in keV), spin values, and parities: 1276.8 (3,4); 1318.9 (2^+); 1394.4 (3,4); 1448.9 (3^-); 1503.3 (4^+); 1659.2 (4^+); 2030.1 (3,4); 2124.5 (3,4); 2145.5 (4^+); 2198.2 (4^-); 2237.3 (5); 2490.5 (3,4); 2590.7 (3,4); and 3023.7 (2). The level scheme accounts for 49 of the 60 well-established transitions in the decay of ^{174}Ta. The Q-value corresponding to the ^{174}Ta → ^{174}Hf decay was found to be 3845 ± 80 keV. The half-life of the first 2^+ level was remeasured and found to be 1.68 ± 0.08 ns. The structures of ^{174}Ta and of the ^{174}Hf levels are discussed in terms of current nuclear models. (auth) (France)

31311 (LYCEN-7092) REACTIONS INDUCED IN GOLD BY DEUTERONS WITH ENERGIES BETWEEN 10 AND 70 MeV. Chevarier, Noelle; Chevarier, A.; Demeyer, A.; Tran Minh Duc (Lyon Univ. (France). Institut de Physique Nucleaire). 23 Dec 1970. 22p. (In French). Dep. NTIS (U. S. Sales Only).

Excitation functions were determined for reactions induced in gold by deuterons with energies up to 70 MeV. Isomer ratios were measured for (d,2n), (d,4n), and (d,p2n) reactions. The (d,xn) excitation functions are interpreted using a statistical model which includes evaporation and precompound emission. The Huizenga–Vandenbosch calculation gives good agreement for isomer ratios with (d,2n) and (d,4n) reactions in the energy range corresponding to compound-nucleus processes. It is shown that, with respect to its isomer ratio and its excitation function, the (d,p2n) reaction is dominantly a transfer reaction. (auth) (France)

31312 (ORNL-4619) GRAPHS FOR THE ANALYSIS OF (1-3) GAMMA–GAMMA DIRECTIONAL CORRELATIONS. Ramayya, A. V.; Hamilton, J. H.; Little, P. E.; Collins, E.; Pinajian, J. J. (Oak Ridge National Lab., Tenn.). Apr 1971. Contract W-7405-eng-26. 62p. Dep. NTIS.

The gamma–gamma directional correlations on the (1–3) cascade with the intermediate transition unobserved can be used to obtain multipolarities of transitions and level spins. The correlation coefficients for a skip cascade depend also on the spins of the intermediate levels and the multipolarity of the unobserved transition as well as the spins of the upper and lower states and multipolarities of the first and third gamma rays. A set of graphs for several of the most useful cases of spins and multipolarities for the (1–3) cascades is given. (R.W.R.)

31313 (ORNL-TM-3179) INCLUSION OF FISSION AND CHARGED-PARTICLE EMISSION IN CALCULATIONS OF NUCLEAR REACTIONS; COMPUTED ENERGIES, ANGLES, AND RANGES OF RECOIL NUCLEI. Hahn, R. L.; Hermann, O. W.

XUM

(Oak Ridge National Lab., Tenn.). 7 Apr 1971. Contract W-7405-eng-26. 53p. Dep. NTIS.

Modifications of the code I4C(EVAP) are discussed that include effects due to competition between particle emission and fission and detailed calculations of the kinetic energies, angles, and recoil ranges of product nuclei. It is demonstrated that the cross section for the evaporation from compound-nucleus c of any particle k, be it neutron or charged particle, can be expressed as $\sigma(c,k,f) = \sigma_c P_k[\Gamma_n/(\Gamma_n + \Gamma_f)]_k$, where σ_c is the compound-nucleus-formation cross section, P_k is the usual probability of emission of k in the absence of fission, and the factor in brackets considers the competition between fission and particle emission. This result is to be contrasted with earlier treatments that took $P_k = 0$ unless particle k was a neutron. The empirical formula of Sikkeland, Ghiorso, and Nurmia [Phys. Rev., 172: 1232(1968)] with its simple dependence upon atomic number Z and neutron number N, is shown to be an appropriate measure of $[\Gamma_n/(\Gamma_n + \Gamma_f)]$ in cases where charged particles as well as neutrons compete with the fission process. To obtain kinetic-energy and angular distributions of product nuclei, the transformation of the velocity of the nucleus from center-of-mass to laboratory system is treated in detail. The range-energy theory of Lindhard, Scharff, and Schioett [Kgl. Danske Videnskab. Selskab. Mat.-Fys. Medd., 33, No. 14 (1963)] is used to calculate ranges of the recoil nuclei. Finally, changes that occur in the input and output of EVAP as a result of the above considerations are described. (auth)

31314 (ORNL-tr-2453) STUDY OF THE SPONTANEOUS FISSION OF ^{252}Cf. Zakharova, V. P.; Korostylev, V. A.; Ryazanov, D. K. (Gosudarstvennyi Komitet po Ispol'zovaniyu Atomnoi Energii SSSR, Moscow. Institut Atomnoi Energii). Translated by S. J. Rimshaw and R. G. Mansfield (Oak Ridge National Lab., Tenn.), from report IAE-2036. 9p. Dep. NTIS.

The distributions of the total kinetic energy of the fission products of ^{252}Cf are given as a function of the ratio of the fission product masses (R). A double ionization chamber with a grid was used in measuring the energy. The spectra of the total kinetic energy of the fission fragments (E_k) corresponding to the symmetrical ($R \approx 1$) and strongly asymmetrical ($R \approx 2$) regions loses the form of single-peak Gaussian distributions. Possible reasons of this phenomenon are discussed. (auth)

31315 (ORO-2434-7) AN EXPERIMENTAL STUDY OF NUCLEAR MODELS. I. DECAY SCHEMES AND NUCLEAR REACTIONS. Progress Report, August 1, 1970–July 31, 1971. Sheline, Raymond K. (Florida State Univ., Tallahassee). Contract AT(40-1)-2434. 30p. Dep. NTIS.

Shell-model states were investigated in the nuclei ^{139}La, ^{140}La, ^{141}Ce, and ^{210}Bi. Levels were studied in the transitional nucleus ^{106}Ru and the deformed nuclei ^{153}Tb, ^{158}Gd, ^{164}Ho, ^{175}Lu, and ^{177}Lu. Theoretical work was done on the neutron–proton interaction in deformed odd–odd nuclei. An infrared study of the trimetallic carbonyls and anisotropic chemical shifts is included. (R.W.R.)

31316 INTERNAL IONIZATION IN β DECAY OF ^{131}I. Vaishnis, P. P.; Kutsentov, L. M.; Fleisher, V. G.; Gusev, Yu. K.; Isupov, V. K. (Ioffe Inst. of Physics and Tech., Leningrad). Bull. Acad. Sci. USSR, Phys. Ser. (Engl. Transl.); 33: 1540-5 (1969).

Translated from Izv. Akad. Nauk SSSR, Ser. Fiz.; 33: 1678-84 (Oct 1969).

The effect of beta endpoint energies on electron shake-off during beta decay was examined. It was found that for heavy atoms the probability of shake-off increases with increasing β endpoint energies. Internal ionization of K-shells and external shells in the β-decay of ^{131}I was studied by measuring x-ray spectra from K-shell ionization and slow electron spectra from outer shell ionization. (TSS) (auth)

31317 MEASUREMENTS OF ANGULAR DISTRIBUTIONS AND ENERGY SPECTRA OF PHOTONEUTRONS FROM LEAD TARGETS BOMBARDED BY HIGH ENERGY ELECTRONS. Kimura, Itsuro; Hayashi, Shu A.; Kobayashi, Katsuhei; Yamamoto, Shuji; Shibata, Toshikazu (Kyoto Univ.). Annu. Rep. Res. Reactor Inst., Kyoto Univ.; 3: 75-83(1970).

The angular distributions of photoneutrons from three spherical lead targets and from five lead slabs, bombarded by high energy electrons from a linear accelerator, were measured by the ^{27}Al(n,p)^{27}Mg, ^{27}Al(n,α)^{24}Na and ^{32}S(n,p)^{32}P reactions. The result shows that the angular distribution of photoneutrons from a lead sphere of 15 cm in diameter is nearly isotropic. For slab targets, the angular distributions become more isotropic with decreasing its thickness. From the absolute yields of photoneutrons determined by measuring the activity of ^{27}Mg, the conversion factor of electrons to neutrons was obtained to be slightly less than 1×10^{-3} n/e. The energy spectrum of photoneutrons from a lead target was measured by the neutron time-of-flight method. By the comparison of the neutron spectra for three different electron energies, it has been found that the direct process increases with increasing electron energy. The obtained nuclear temperatures for 16.5 MeV of electron energy were $T_1 = 0.89$ MeV for $E_n < 4$ MeV and $T_2 = 1.49$ MeV for $E_n > 4$ MeV. These values agree reasonably with the previous works. (auth)

31318 INTERNAL BREMSSTRAHLUNG FOLLOWING β DECAY OF ^{114}In. Korotkov, K. A.; Shumeiko, A. P. (Voronezh State Univ., USSR). Bull. Acad. Sci. USSR, Phys. Ser. (Engl. Transl.); 33: 1536-9(1969).

Translated from Izv. Akad. Nauk SSSR, Ser. Fiz.; 33: 1674-7 (Oct 1969).

A three-crystal Compton spectrometer was used to measure the internal bremsstrahlung spectrum accompanying the decay of ^{114}In. The results were compared with calculations performed according to the theory of Knipp and Uhlenbeck with a Coulomb correction. A satisfactory agreement was found. (J.W.R.)

31319 LIFETIMES OF EXCITED STATES OF ^{140}Ce. Lan'ko, E. V.; Dombrovskaya, G. S.; Shubnyi, Yu. K. (Inst. of Nuclear Physics, Alma-Ata, USSR). Bull. Acad. Sci. USSR, Phys. Ser. (Engl. Transl.); 33: 1550-2(1969).

Translated from Izv. Akad. Nauk SSSR, Ser. Fiz.; 33: 1690-2 (Oct 1969).

Delayed β-γ and γ-γ coincidences in the decay of ^{140}La were measured using scintillation detectors and a multichannel analyzer with time-to-amplitude converter. The lifetimes of the 2083- and 2412-keV levels in ^{140}Ce were determined. (TSS) (auth)

31320 INVESTIGATION OF THE γ RAYS ACCOMPANYING DECAY OF ^{109}In. Didorenko, V. A.; Andreev, Yu. A.; Burmistrov, V. R.; Karetskaya, S. P. (Inst. of Nuclear Physics, Alma-Ata, USSR). Bull. Acad. Sci. USSR, Phys. Ser. (Engl. Transl.); 33: 1546-9(1969).

Translated from Izv. Akad. Nauk SSSR, Ser. Fiz.; 33: 1685-9 (Oct 1969).

The γ spectra of ^{109}In ($T_{\frac{1}{2}} = 4.3$ hr) were measured using Ge(Li) detectors with resolutions of 5 and 10 keV at 511 keV. The results were used in proposing a decay scheme. Spin-parity assignments and transition multipolarities for ^{109}Cd levels are included. (TSS) (auth)

31321 ANGULAR CORRELATION OF THE 345 TO 136 keV CASCADE IN ^{181}Ta. Klyucharev, V. A.; Bozhko, V. P.; Golovchenko, Yu. V. (Physical-Tech. Inst., Kiev). Bull. Acad. Sci. USSR, Phys. Ser. (Engl. Transl.); 33: 1533-5(1969).

Translated from Izv. Akad. Nauk SSSR, Ser. Fiz.; 33: 1671-3 (Oct 1969).

The angular correlation of the 345–136 keV gamma cascade in ^{181}Ta was measured using a time-to-amplitude converter. The difference in half-lives of intermediate states permitted selection of the 345–136 keV cascade from the energetically indistinguishable 133–345 keV cascade. (TSS) (auth)

31322 FOUR-PARTICLE LEVELS OF 4p TYPE IN ^{90}Zr AND OF 3p,n TYPE IN ^{90}Nb. Peker, L. K. Bull. Acad. Sci. USSR, Phys. Ser. (Engl. Transl.); 33: 1572-5(1969).

Translated from Izv. Akad. Nauk SSSR, Ser. Fiz.; 33: 1717-20 (Oct 1969).

Four-particle configurations in ^{90}Zr and ^{90}Nb are suggested. These configurations are of 4p type in ^{90}Zr and 3p-1n type in ^{90}Nb. The suggested levels are compared with the experimental level schemes. (J.W.R.)

31323 INTERPRETATION OF THE ANOMALOUS $I^\pi = 7/2^+$ LEVELS IN NUCLEI WITH Z = 43, 45, 47. Peker, L. K.; Sigalov, V. M. (All-Union Scientific-Research Inst. of Metrology, Leningrad). Bull. Acad. Sci. USSR, Phys. Ser. (Engl. Transl.); 33: 1569-72(1969).

Translated from Izv. Akad. Nauk SSSR, Ser. Fiz.; 33: 1713-16 (Oct 1969).

An explanation is given of the anomalous $I^\pi = 7/2^+$ levels in technetium, rhodium, and silver isotopes which also accounts for the small log ft values for the associated beta transitions. The interpretation is also applicable to other beta transitions in the same mass region with small log ft values. (J.W.R.)

31324 FINE STRUCTURE OF THE ALPHA-PARTICLE SPECTRA OF ^{209}At, ^{210}At, ^{211}At, AND ^{211}Po. Golovkov, N. A.; Guetkh, Sh.; Dzhelepov, B. S.; (and others) (Joint Inst. for Nuclear Research, Dubna, USSR). Bull. Acad. Sci. USSR, Phys. Ser. (Engl. Transl.); 33: 1489-96(1969).

Translated from Izv. Akad. Nauk SSSR, Ser. Fiz.; 33: 1622-30 (Oct 1969).

A large double-focusing magnetic spectrometer was used in studying the fine structure in the alpha spectra of ^{209,210,211}At and ^{211}Po. Alpha groups were found in ^{209}At at 5116 keV, in ^{211}At at

5210 and 5141 keV, and in ^{210}At at 5131, 5386, and 5465 keV (tr-auth)

31325 DECAY OF ^{225}Ac. Dzhelepov, B. S.; Zolotavin, A. V.; Ivanov, R. B.; Mikhailova, M. A.; Sergeev, V. O. Bull. Acad. Sci. USSR, Phys. Ser. (Engl. Transl.); 33: 1475-88(1969).

Translated from Izv. Akad. Nauk SSSR, Ser. Fiz.; 33: 1607-21 (Oct 1969).

A magnetic spectrometer was used to measure the conversion electron spectra following the alpha decay of ^{225}Ac. Internally converted transitions with energies of 17 up to 250 keV were studied and several new transitions were found. The data were used in conjunction with known γ transitions to establish multipolarities for several transitions in ^{221}Fr. The properties of low-lying levels of ^{221}Fr are discussed in terms of the Nilsson scheme for small deformations. (tr-auth)

31326 PHENOMENA OF FISSION OF HEAVY NUCLEI BY HIGH-ENERGY PROTONS. Axmann, Hans-Peter (Univ., Vienna); Barbier, Marcel. Acta Phys. Austr.; 29: 174-82 (1969). (In German).

The effective cross sections of some heavy nuclei (W, Re, Au, Pb, ^{209}Bi, ^{232}Th, Pa, ^{235}U, ^{237}Np, and ^{237}Pu) for fission by high-energy protons in the range 10 MeV $\leq E_p \leq$ 29 GeV were given and the dependence of the fissionability of these nuclei on the parameter Z^2/A was shown. For the reaction ^{238}A(p,f) a comprehensive representation of the mass yields in the same energy range and the individual fragment yields for 170 $\leq E_p \leq$ 680 MeV were presented. (tr-auth)

31327 DETERMINATION OF THE LIFETIMES OF THE 1080-keV LEVEL OF ^{115}In AND THE 1300-keV LEVEL OF ^{111}Cd. Mazitov, B. S.; Zaparov, E. A.; Khusainov, Yu. A. (Inst. of Nuclear Physics, Tashkent). Dokl. Akad. Nauk Uzb. SSR; No. 11, 23-5(1969). (In Russian).

Lifetimes for levels at 1300 keV in ^{111}Cd and 1080 keV in ^{115}In were measured following activation of the ^{111}Cd and ^{115}In isomers. (TSS)

31328 DO THE SUPERHEAVY ELEMENTS ALREADY EXIST? Seaborg, Glenn T. (Atomic Energy Commission, Washington, D. C.). Nucleus (Karachi); 7: 86-125(Jul 1970).

A survey is presented on what has been done and is currently being done toward understanding whether natural processes have created superheavy elements in the cosmos. Attempts at finding superheavy elements in nature are briefly described, and the inherent limitations in this type of research are discussed. The various mechanisms for the natural production of superheavy elements are reviewed. (J.W.R.)

31329 INTERNAL CONVERSION MONOENERGETIC POSITRON SPECTRUM IN ^{157}Gd(n,γ)^{158}Gd REACTION. Beitin, M. R.; Berzin, Ya. Ya.; Prokof'ev, P. T.; Simonova, L. I.; Stolyarov, O. A. (Inst. of Physics, Riga). Latv. PSR Zinat. Akad. Vestis, Fiz. Teh. Zinat. Ser.; No. 5, 124-6(1970). (In Russian).

The internal conversion monoenergetic positron spectrum of ^{158}Gd was investigated using a β-spectrograph in the energy interval 1.5 to 2.9 MeV. 14 positron lines were obtained and their energies calculated. Identification of the positron lines is given. The comparison was made between transition energies calculated on the base of the positron and electron conversion spectra. (tr-auth)

31330 MEASUREMENT OF INTERNAL CONVERSION AND INTERNAL PAIR FORMATION COEFFICIENTS IN LEAD ISOTOPES. Allan, C. J. (Univ. of Manitoba, Winnipeg). Can. J. Phys.; 49: 157-73(15 Jan 1971).

The decays of ^{205}Bi, ^{206}Bi, and ^{207}Bi were studied using Ge(Li) detectors for γ-ray detection and a trochoidal β-ray spectrometer for conversion-electron and internal-pairs detection. Numerous conversion coefficients and internal pair formation coefficients were determined. By using $\gamma-\gamma$ coincidence the positions of the 1844-, 1878-, and 1903-keV transitions in the decay of ^{206}Bi were determined. (auth) (Canada)

31331 ISOMERIC SHIFT OF THE 83 keV TRANSITION IN ^{153}Eu. Ansaldo, E.; Grodzins, L.; Frankel, R. B. (Massachusetts Inst. of Tech., Cambridge). Contract AT(30-1)-2098. Lett. Nuovo Cim.; 1: 336-8(20 Feb 1971).

The change in the mean square charge radius between the ground state and 83-keV first excited state in ^{153}Eu is reported from a measurement of the isomer shift in the Moessbauer spectrum between $EuSO_4$, EuB_6, and Eu_2O_3. Transmission spectra for Eu_2O_3 and $EuSO_4$ are given. The results are $\Delta\langle r^2\rangle$ (83 keV) = $(-2.9 \pm 1.1) \times 10^{-3}$ F^2 and $\Delta\langle r^2\rangle$ (103 keV) = $(-9.8 \pm 2.1) \times 10^{-2}$ F^2. (R.W.R.)

31332 EXPERIMENTAL STUDIES OF GAMMA RAYS FROM NEUTRON REACTIONS. Lundberg, Boerje. Stockholm; Stockholm Univ. (1971). 4p.

Thesis.

Neutron capture processes were used in investigations of the validity of the semi-direct capture mechanism. Monoenergetic neutrons were produced by using the nuclear reactions ^{7}Li(p,n)^{7}Be in the keV region, ^{3}H(p,n)^{3}He in the 1 to 4 MeV region, and ^{2}H(d,n)^{3}He in the neutron energy region of 4.5 to 8.3 MeV. The dissertation is based on experiments presented in 9 earlier published papers and 5 conference papers. (Sweden)

31333 YIELDS OF RADIOACTIVITIES INDUCED BY (γ,n) REACTIONS WITH BREMSSTRAHLUNG UP TO 68 MeV. Saito, Tatsuya (Tohoku Univ., Sendai). Nippon Kagaku Zasshi; 92: 164-8(Feb 1971). (In Japanese).

The (γ,n) yields of 12 target nuclides (^{12}C, ^{14}N, ^{16}O, ^{23}Na, ^{55}Mn, ^{197}Au, ^{59}Co, ^{75}As, ^{89}Y, ^{93}Nb, ^{127}I, and ^{203}Tl) were measured at 10, 13, 16, 30, 45, and 68 MeV bremsstrahlung by observing the induced activities. The energy dependence of the yields was investigated extensively. In the case of heavy nuclides, the yields increased greatly as a function of maximum bombarding energy up to 20 MeV, and increased gradually from 20 to 68 MeV. However, in the case of light nuclides, the yields increased greatly up to 30 MeV, because the neutron separation energies of light nuclides are larger than those of heavy ones, and the bremsstrahlung spectrum covers the giant resonance and so the yields increase gradually from 30 MeV up to 68 MeV. The yields were estimated approximately from the parameter of the giant resonance, that is the peak cross section and the half width, in order to compare with the experimental data. As a result, experimental data on light nuclides and heavy ones are nearly in agreement with the estimated data of Nathans et al., Johns et al. and Montalbetti et al., but those of medium weight ones are relatively lower values. (auth)

31334 MEASUREMENT OF THE DELAYED-NEUTRON FRACTIONS FOR THERMAL FISSION OF ^{235}U, ^{239}Pu, AND ^{233}U. Conant, John F.; Palmedo, Philip F. (Brookhaven National Lab., Upton, N. Y.). Nucl. Sci. Eng.; 44: 173-9(May 1971).

The delayed-neutron fractions for thermal fission of ^{235}U, ^{239}Pu, and ^{233}U were measured and found to be ^{235}U: 0.0065 ± 0.0003; ^{239}Pu: 0.0023 ± 0.0002; and ^{233}U: 0.0027 ± 0.0001. The technique used to perform the measurements was intrinsically simple and involved making only relative measurements. The basic approach was to compare the neutron production rate of a thin fissile sample in a thermal-neutron beam with the delayed-neutron production after an abrupt termination of the beam. The work was greatly enhanced through the use of a modified long counter that was developed at the Los Alamos Scientific Laboratory. The results of this work are in essential agreement with the presently accepted values, which were reported in 1957 and were measured by using a different technique than that used here. (auth)

31335 ^{160}Tb → ^{160}Dy DECAY. Finger, M. (Joint Inst. for Nuclear Research, Dubna, USSR); Galan, P.; Galanova, T. J.; (and others). Czech. J. Phys.; 19: 1017-32(1969).

Gamma-ray spectra in the decay of ^{160}Tb were measured with the aid of two coaxial Ge(Li) spectrometers. Absolute intensities and multipolarities were obtained. Three new transitions of 486.5 keV, 1069 keV, and 1102.5 keV were found and introduced into the decay scheme. The level scheme is discussed from the point of view of the generalized model of the nucleus. Experimental data show the 1264.4 keV level to be a two-quasi-particle state of the pp (411↑ − 523↑) type. The beta-transition from the ground state of ^{160}Tb (p411↑ + n521) to this two-quasi-particle sta · with log ft = 8.00 ± 0.05 is interpreted as Ω-forbidden. (auth)

31336 LEVEL SCHEME FOR ^{178}Hf. Prokof'ev, P. T.; Rezvaya, G. L. Bull. Acad. Sci. USSR, Phys. Ser. (Engl. Transl.); 33: 1518-23(1969).

Translated from Izv. Akad. Nauk SSSR, Ser. Fiz.; 33: 1655-61 (Oct 1969).

A beta spectrometer was used to measure the conversion electron spectra emitted following thermal neutron capture by ^{177}Hf. Seventy transitions with electron energies between 70 and 2000 keV were observed. Multipolarities were determined for several transitions. The data were used in studying the properties of collective levels in ^{178}Hf. (auth) (TSS)

31337 LEVELS IN ^{142}Nd. Arl't, R.; Baier, G.; Muziol, G.; Peker, L. K.; Shtrusnyi, Kh. (Joint Inst. for Nuclear Research, Dubna, USSR). Bull. Acad. Sci. USSR, Phys. Ser. (Engl. Transl.) 33: 1505-9(1969).

Translated from Izv. Akad. Nauk SSSR, Ser. Fiz.; 33: 1640-5 (Oct 1969).

The γ rays following the decay of ^{142}Pm were detected using a Ge(Li) detector. Conversion electrons were studied with a magnetic spectrometer. The data were used along with previous results in proposing a level scheme for ^{142}Nd containing 13 excited states up to 3361 keV. (auth) (TSS)

XUM

31338 EXCITED METASTABLE STATES OF ^{93}Y. Cavallini, Pierre; Schussler, Francois; Moussa, Andre (CEA, Grenoble, France). Compt. Rend., Ser. B; 272: 394-6(8 Feb 1971). (In French).

An isomeric state of ^{93}Y produced by the disintegration of ^{93}Sr was established. The nature (E 3) of the 168.6-keV transition was determined. A partial level scheme of ^{93}Y is proposed and the value of the ^{93}Sr disintegration energy (Q_β = 3 800 ± 100 keV) given. (auth) (France)

31339 STUDY OF THE CONVERSION ELECTRONS OF EXCITED ^{230}Th IN THE ELECTRON CAPTURE DISINTEGRATION OF ^{230}Pa. Briand, Jean-Pierre; Chevallier, Pierre; Touati, Alain; Tavernier, Michel (Univ., Paris). Compt. Rend., Ser. B; 272: 155-7(11 Jan 1971). (In French).

The spectrum of the conversion electrons emitted by ^{230}Pa was studied using a Si–Li junction detector. A large number of lines were identified and the conversion coefficients of most of the transitions accompanying the disintegration were derived. (auth) (France)

31340 DETERMINATION OF THE MULTIPOLAR CHARACTER OF THE PHOTONS ACCOMPANYING ^{125}Sb DECAY. Marsol, Claire; Ardisson, Gerard (Institut d'Etudes Nucleaires, Algiers). Compt. Rend., Ser. B; 272: 61-4(4 Jan 1971). (In French).

Ge(Li) junctions were used to measure the gamma ray spectrum of ^{125}Sb after having separated it from its impurities, tin being the principal impurity. Internal conversion coefficients associated with ^{125}Te transitions were calculated. It was possible to assign multipolarities to the ^{125}Te transitions. (France)

31341 NUCLEAR MATTER RADII IN THE TIN ISOTOPES. Boyd, R. N. (Rutgers–The State Univ., New Brunswick, N. J.); Fenton, J.; Williams, M.; Kruse, T.; Savin, W. Nucl. Phys.; A162: 497-512(1971).

Polarization angular distributions for 16-MeV protons elastically scattered from isotopes of tin have been measured to complement the previously measured 16 MeV proton elastic differential cross-section data of Makofske et al. Standard optical-model analysis of the cross section and polarization data was used to yield nuclear matter rms radii for the isotopes examined. In addition differences between pairs of data sets were examined to determine differences in matter rms radii between pairs of isotopes to an apparent accuracy of better than 0.01 fm. The optical-model analysis combined with existing data on charge radii yielded a separation between neutron and proton rms radius of about 0.5 fm. (auth)

31342 INELASTIC SCATTERING OF DEUTERONS AND α-PARTICLES ON ^{191}Ir AND ^{193}Ir. Noergaard, P.; Bisgard, K. M.; Gregersen, K.; Morgen, P. (Royal Veterinary and Agricultural Univ., Copenhagen. Univ. of Aarhus, Denmark). Nucl. Phys.; A162: 449-60(1971).

Collective states in ^{191}Ir and ^{193}Ir were studied by inelastic scattering of 7.0-MeV and 12.1-MeV deuterons and 16.6-MeV α particles. In each nucleus four members of a ground-state rotational band were seen. States observed at 684 keV (^{191}Ir) and 620 keV (^{193}Ir) are interpreted as being K = K_0 + 2 γ-vibrational states. The K = K_0 – 2 members are represented by the low-lying $\frac{1}{2}^+$ bands which contain also the $\frac{1}{2}^+$ [400] state coupled to the $\frac{3}{2}^+$ [402] ground state bands. Reduced excitation probabilities, rotational parameters and decoupling constants are derived. (auth)

31343 VALENT SHELL STRUCTURE EFFECTS ON THE COEFFICIENTS OF INTERNAL CONVERSION OF γ RADIATION AND ON THE ELECTRON DENSITY IN THE NUCLEAR REGION. Anderson, E. M.; Listengarten, M. A.; Khanonkind, M. A. (Leningrad State Univ. Latvian State Univ., Riga). Izv. Akad. Nauk SSSR, Ser. Fiz.; 34: 850-5(Apr 1970). (In Russian).

The influence of structure changes of the valent shell on internal conversion coefficients was studied using the ^{119}Sn atom with eliminated 5p-electron. The relation between the variations in valent shell configuration, the internal conversion coefficient on the external shells, and electron density near zero $|\psi(0)|^2$ was verified by direct calculations. (R.V.J.)

31344 GAMMA–GAMMA PERTURBED ANGULAR CORRELATIONS IN ^{154}Gd. Suwa, Emiko; Ibi, Tamiko; Iwashita, Takeki (Tokyo Gakugei Univ.). Bull. Tokyo Gakugei Univ., Ser. 4, No. 22, 13-19(Jul 1970). (In Japanese).

Perturbed angular correlation measurements have been carried out on the 1278 keV–123 keV gamma cascade accompanying the decay of ^{154}Eu. Integral attenuation coefficients G_{22} have been measured to be 0.46 ± 0.02 for the polycrystalline Eu_2O_3 powder source and 0.62 ± 0.02 for the sources prepared by dissolving Eu_2O_3 in a solution of 63% HNO_3. The unperturbed angular correlation coefficient A_{22} of the cascade was assumed to be 0.227 ± 0.006 following the time differential measurements of correlation coefficients $A_{22}G_{22}$ performed by Stiening et al. for aqueous solution and molten chloride sources. Electric field gradients have been calculated assuming static electric quadrupole interaction for the polycrystalline source and time dependent electric quadrupole interaction for the liquid source. Discussions are made on the basis of the collective model. (auth) (Japan)

31345 INFLUENCE OF THE MOTTELSON AND VALATIN EFFECT ON ROTATIONAL BANDS OF ASYMMETRICAL NUCLEI. Landi, G. (Istituto Nazionale di Fisica Nucleare, Florence). Nuovo Cim.; 2A: 444-54(21 Mar 1971).

From theoretical and phenomenological considerations, the Mottelson–Valatin effect is introduced in the Davidov and Filippov asymmetrical-rotator model. The effect was studied in nuclei of high-transition regions (^{184,186,188,190}Os, ^{182,184,186,188}Pt, ^{190,192,194,196}Pt and ^{126,128,130,132}Xe). The results are satisfactory for all these nuclei. A phenomenological criterion is established to decide if a nucleus has a stable asymmetry or not. (auth)

31346 NUCLEAR STRUCTURE OF ^{124}Te. Hatsushika, Yoshihiko; Fukushima, Hiromi; Kato, Kuniko; Iwashita, Takeki (Tokyo Gakugei Univ.). Bull. Tokyo Gakugei Univ., Ser. 4, No. 22, 20-7(Jul 1970). (In Japanese).

Gamma-rays from the decay of ^{124}Sb have been measured with a 21 cc Ge(Li) detector. Nuclear spin of the 2295 keV excited state of ^{124}Te has been determined to be 3 by means of gamma–gamma directional correlation measurement. The directional correlation pattern of the 1962 keV–603 keV gamma cascade was found to be consistent with that of spin sequence 3(D)2(Q)0. The excited states of ^{124}Te are discussed on the basis of the collective model. (auth) (Japan)

31347 COLLECTIVE EXCITATIONS IN ^{172}Yb AND ^{172}Lu. Sen, Dilip. Baton Rouge, La.; Louisiana State Univ. (1970). 185p. University Microfilms Order No. 71-6606.
Thesis.

The collective excitations in ^{172}Yb (even-even) and in ^{172}Lu were experimentally investigated and the results compared with the predictions of microscopic and macroscopic theories. To this end, the γ-ray spectra accompanying the electron capture decays of ^{172}Hf–^{172}Lu–^{172}Yb were separately using Ge(Li) and Si(Li) detectors. The measured γ-ray intensities were used, in conjunction with the available conversion electron data, to compute internal conversion coefficients. Multipolarities were determined for most of the transitions in both ^{172}Yb and ^{172}Lu. For ^{172}Yb, a level scheme containing 28 levels was proposed in which 97 of the 128 transitions observed were placed. Log ft values, reduced transition probability ratios and inertial parameters were computed and used to identify rotation bands at 1172 keV (K = 3), 1466 keV (K = 2), 1609 keV (K = 2), 1662 keV (K = 3), 2073 keV (K = 4) and 2174 keV (K = 3). These bands and the ground state band contain 23 of the proposed levels. The five remaining levels at 1640, 1706, 2181, 2213 and 2343 keV were classified only according to spin-parity possibilities. The reduced B(E2) transition probability ratios were computed for interband and intraband transitions and compared with theoretical predictions. The collective or two quasi-particle nature of the two K = 2^+ states observed has been investigated through the determination of the B(E2) ratios. The K = 2^+ states observed at 1466, and 1609 keV compare remarkably well with the energies of 1.4 and 1.7 MeV predicted by microscopic theories. However, both of the states show collective behavior to a large extent. The coupling of each of the two K = 2 bands to the ground state band was computed on the basis of the perturbative band mixing theories. In the study of the electron capture decay of ^{172}Hf to levels of ^{172}Lu, sixteen transitions were observed. For the investigation of the levels in odd-odd ^{172}Lu, delayed coincidence measurements were also performed in order to uniquely determine the cascade relationships of the 24, 44, 67, 70, 81, 114 and 125 keV transitions. The gate pulses arising from 24 keV γ-rays were obtained using a NaI(Tl) x-ray detector and the corresponding coincidence spectra were recorded using a Ge(Li) detector. A level scheme consisting of 10 levels has been proposed for ^{172}Lu, in which twelve of the sixteen transitions observed were placed. Log ft values for electron capture to these states were computed and utilized along with the expected Nilsson states for the last odd proton and odd neutron in order to specify the particle configurations for seven of the ten proposed levels. (Diss. Abstr. Int., B)

31348 EXCITED STATES OF ^{174}Hf FROM THE DECAY OF ^{174}Ta. Gillin, Michael Talbot. Davis, Calif.; Univ. of California (1970). 200p. University Microfilms Order No. 71-7931.
Thesis.

The ^{174}Ta activity was produced via the ^{175}Lu(α,5n)^{174}Ta reaction with 66-MeV alpha particles. After removal of the ^{18}F, the half-lives were deduced by direct measurements. The half-lives of approximately 200 transitions, ranging in energy from 60 to 3000

XUM

keV, were identified using Ge(Li) detectors. Over 95% of these lines were assigned to ^{175}Hf, ^{174}Hf, or ^{173}Lu. The half-life of ^{174}Ta was measured to be 7.15 ± 6.5 minutes. Ge(Li)–NaI coincidence work was done. The conversion electron spectrum was first measured using a 3 mm Si(Li) detector with a cooled FET and then using the same type of detector plus a magnet. The energies and gamma intensities of the 100 transitions attributed to the decay of ^{174}Ta were measured. 32 conversion coefficients were determined. 16 levels with spins and parities are proposed on the basis of gamma intensities, coincidence information, and conversion coefficients. 12 more levels are proposed on the basis of energy sums. Spins and parities for 4 of these levels are suggested. 44 transitions are not placed in the decay scheme. A very strong beta feed to the 4+ level of the ground state rotational band was observed. M1 enhancement in the beta vibrational bands and K-forbidden gamma transitions are discussed. A prediction for the ground state spin and parity of ^{174}Ta is made. (Diss. Abstr. Int., B)

31349 EXPERIMENTAL ELECTROMAGNETIC MATRIX ELEMENTS IN THE NUCLEAR MASS-90 REGION. Cochavi, Saadia. Stony Brook, N. Y.; State Univ. of New York (1970). 118p. University Microfilms Order No. 71-8101.

Thesis.

Experimental matrix elements of low-lying states of nuclei in the mass 90 region were studied. Measurements of the magnetic moment of the 2.761-MeV 8^+ state in ^{92}Mo and lifetimes of low-lying states in ^{92}Mo, ^{92}Nb and ^{92,94}Zr were performed. The magnetic moment of the 8^+ state in ^{92}Mo was measured by a time-differential perturbed angular correlation method, as μ = (11.2 ± 0.6) nm. The 8^+ state was populated via the ^{90}Zr(α,2n)^{92}Mo reaction at E_α = 24 MeV. Lifetimes of low-lying states in ^{92}Mo, ^{92}Nb and ^{92,94}Zr were measured by p–γ, n–γ, γ–γ delayed coincidence techniques. The mean lifetimes were obtained from the logarithmic slopes of the time spectra. For the ^{92}Mo measurements a γ-transition study was done using the ^{90}Zr(α,2n)^{92}Mo and ^{92}Mo(p,p′)^{92}Mo reactions and the 4.4 m ^{92}Tc β^+ activity. The mean-life of 2.527-MeV 5^- state was measured to be τ = 2.24 ± 0.06 nsec using the ^{92}Mo(p,p′) reaction and that of the 2.613-MeV 6^+ state was found to be τ = 2.22 ± 0.07 nsec via γ–γ coincidence following the 4.4 m ^{92}Tc β^+ decay. Transition probabilities for low-lying states in ^{92}Nb were studied using the ^{92}Zr(p,n)^{92}Nb reaction at E_p = 6.3 MeV. A Ge(Li) γ spectrum was measured in coincidence with neutrons to identify low-lying states and their γ transitions. The mean lifetimes of the 0.227 MeV 2^- state and the 0.357-MeV (5^+) state were measured to be τ = 6.2 ± 0.7 μsec and τ = 2.73 ± 0.09 nsec, respectively. The γ-transitions, the lifetimes and upper limits of lifetimes determine the 3^+ and 5^+ members of the ^{92}Nb sextuplet to be at 286 and 357 keV, respectively. The second 0^+ states in ^{92}Zr and ^{94}Zr were excited with the (p,p′) reaction at proton analog resonance energies of 7.90-MeV for ^{92}Zr and 8.12 MeV for ^{94}Zr. Their mean lifetimes are τ = 240 ± 40 psec for the 1.382 MeV 0^+ state in ^{92}Zr and τ = 462 ± 30 psec for the 1.30-MeV 0^+ state in ^{94}Zr. The measured g-factor and E1 and E2 strengths are theoretically interpreted in terms of $\pi(1g_{9/2})$, $\pi(2p_{1/2})$ and $\nu(2d_{5/2})$ shell-model configurations. E2 effective charge information was deduced from the experimental B(E2)'s for a $\nu(2d_{5/2})$ and a $\pi(1g_{9/2})$ in the mass 90 region. (Diss. Abstr. Int., B)

31350 ^{165}Ho FAST NEUTRON CROSS SECTIONS. Meadows, J. (Argonne National Lab., Ill.); Smith, A ; Whalen, J.; Beynon, T. D. Z. Phys.; 243: 171-87(1971).

Total neutron cross sections of ^{165}Ho were measured from 0.1 to 1.5 MeV with resolutions of $\lesssim$2.5 keV. The observed total cross sections varied slowly with energy and displayed no significant structure. Differential neutron elastic and inelastic scattering cross sections were determined at intervals of $\lesssim$50 keV from 0.3 to 1.5 MeV. The inelastic excitation of states in ^{165}Ho at: 98, 214, 371, 460, 517, 586, 712, 824, 995, 1104 and 1143 keV was positively observed with probable identification of several additional states. The observed excited structure and the respective cross sections were correlated with known single-particle and collective states and with excited structure postulated from systematics. The measured cross sections were compared with calculated values based upon spherical and deformed optical-potentials, and compound-nuclear processes. Total cross sections were best described by a spherical potential while the differential elastic angular distributions were better represented by deformed-potential calculations. Resonance interference effects were found small and, at the energies of the present experiments, the contribution of direct processes was not large. (auth)

31351 LEVEL SCHEME OF ^{91}Nb FROM THE REACTION ^{90}Zr(p,γ)^{91}Nb. Rauch, F. (Univ., Frankfurt am Main. Franklin Inst., Swarthmore, Pa.). Z. Phys.; 243: 105-13(1971).

The level scheme of ^{91}Nb has been investigated with the reaction ^{90}Zr(p,γ)^{91}Nb. Proton energies between 3.0 and 7.2 MeV were used. The γ spectra were taken with Ge(Li) detectors. Primary γ transitions to 36 excited states of ^{91}Nb up to 3.8 MeV excitation energy and many secondary γ transitions from the decay of those states were observed, leading to an extension of the known level scheme. The proton binding energy for ^{91}Nb was determined as (5167 ± 5) keV. Eleven γ transitions in ^{90}Zr, part of them new, from the competing reaction ^{90}Zr(p,p′γ) were also observed. (auth)

31352 LOW-LYING STATES OF ^{127}I FROM THE (n,n′γ) REACTION. Barnard, E.; Coetzee, N.; de Villiers, J. A. M.; Reitmann, D.; Van Der Merwe, P. (Atomic Energy Board, Pretoria). Z. Phys.; 243: 121-5(1971).

Using time-of-flight methods to discriminate against neutron-induced backgrounds, a 40 cm^3 Ge(Li) detector was used to observe the γ rays from the ^{127}I(n,n′γ) reaction. Based on these γ-rays, energy level and decay schemes are derived up to an excitation of 1780 keV in ^{127}I. This scheme shows seventeen new levels, while the existence of two levels recently determined in Coulomb excitation studies are confirmed. The level scheme is compared with the intermediate coupling unified model predictions. (auth)

31353 EPITHERMAL MEASUREMENTS OF CAPTURE AND FISSION RESONANCE INTEGRALS IN ^{238}U, ^{233}U, ^{239}Pu, AND ^{241}Pu. Eiland, H. M.; Esch, L. J.; Feiner, F.; Mewherter, J. L. (Knolls Atomic Power Lab., Schenectady, N. Y.). Nucl. Sci. Eng.; 44: 180-9(May 1971).

The resonance integrals for capture and fission and their ratios, α, have been measured for ^{233}U, ^{235}U, ^{239}Pu, and ^{241}Pu. Small samples of high isotopic enrichment were irradiated in a water channel of a swimming pool reactor. The number of captures was determined by mass spectrometry and the number of fissions was determined by ^{137}Cs analysis. A combination of cadmium and rhodium neutron filters was used to provide effective cutoff energies in the 2- to 4-eV range. The measured values of α above 3.0 eV are 0.148 ± 0.006, 0 .615 ± 0.019, 0.723 ± 0.044 and 0.285 ± 0.015 for ^{233}U, ^{235}U, ^{239}Pu, and ^{241}Pu, respectively. The corresponding values calculated from ENDF/B cross sections are 0.162, 0.608, 0.650, and 0.212. (auth)

31354 LEVELS IN ^{158}Gd FROM THE (d,p) REACTION. Shelton, W. N.; Sheline, R. K. (Florida State Univ., Tallahassee). Z. Phys.; 242: 368-80(1971).

The nuclear spectroscopy of ^{158}Gd was investigated by deuteron stripping with magnetic analysis of the resulting protons. Over fifty levels were observed. Comparison is made of observed and theoretical relative cross sections. Two new rotational bands were observed; one band based on the 2+ two-quasiparticle state [521+] – [521–] at 2333.6 keV and a second band based on the 1+ two-quasiparticle state [521+] – [521–] at 2494 keV. The ground state (d,p) Q-value was found to be Q_0 = 5706 ± 5 keV. (auth)

31355 SHELL MODEL STATES OF ^{54}Co$_{27}$. Sankey, Richard Roger. Tallahassee; Florida State Univ. (1970). 121p. University Microfilms Order No. 71-7095.

Thesis.

The decay scheme and low-lying levels of the self-conjugate nucleus ^{54}Co were investigated by means of beta, gamma and neutron spectroscopy. The threshold energies for the reactions ^{54}Fe(p,n)^{54}Co and ^{54}Fe(p,n)^{54m}Co were investigated by bombarding isotopically enriched ^{54}Fe targets. The resulting superallowed (0.191 sec.) and allowed (84.22 sec.) positron activities were observed with a plastic scintillator as a function of beam energy. The superallowed activity threshold was found to be at 9.197 ± 0.008 MeV, and the allowed activity threshold at 9.400 MeV. From these measurements the Q-value and ground state mass were determined. Spins of the isomeric levels were deduced. Total absolute cross sections for the two isomeric levels were measured and found to be in the ratio 20 : 1.0 at an energy of 800 keV above the ground state threshold. The gamma decay of the second excited state to the ground state was observed with a Ge(Li) detector. From the gamma-ray energy, the excitation energy of that state was determined to be 938 ± 3 keV. Neutron and gamma-ray angular distribution for the second excited state of ^{54}Co was measured. From these measurements a spin of 1^+ was deduced for this level. (Diss. Abstr. Int., B)

31356 CROSS SECTIONS FOR DIFFERENT CHANNELS IN HEAVY ION NUCLEAR REACTIONS. Galin, J.; Guerreau, D.; Lefort, M.; Tarrago, X. (Paris Univ., Orsay, France). J. Phys. (Paris); 32: 7-9(Jan 1971).

Estimates were made for the critical value l_c of the orbital angular momentum above which a complete fusion nucleus cannot be formed. The cross sections were measured for all the processes not involving the compound nucleus (inelastic scattering,

XUM

transfer reactions, α particle emission) when Ag targets were bombarded by 86 MeV ^{12}C ions and by 78 and 113 MeV ^{14}N ions. The average value of l_c was found to be between 38 and 45 $\hbar$. The range of angular momenta over which transfer reactions occur is briefly discussed. It is shown that quasi elastic single and multi nucleon transfer reactions are possible only for large values of l, designated l_T. When the bombarding energy is sufficiently high, l_T becomes much greater than l_c. There is a region between l_c and l_T in which a very inelastic mechanism occurs. A fusion prompt scission model is proposed involving the temporary formation of very deformed nuclei. (auth) (France)

31357 ABSOLUTE MEASUREMENT OF THE ENERGY OF ^{253}Es α PARTICLES. Grennberg, Bertil; Rytz, Albrecht; Asaro, Frank (Bureau International des Poids et Mesures, Sevres, France. Univ. of California, Berkeley). Compt. Rend., Ser. B; 272: 283-5(25 Jan 1971). (In French).

An absolute magnetic spectrograph was used to measure the absolute energy of the principal α emission from ^{253}Es. The results obtained are presented. (auth) (France)

31358 GAMMA RADIATION OF ^{226}Ra AND ITS DECAY PRODUCTS. Gromov, K. Ya.; Sabirov, B. M.; Urbanets, Ya. Ya. (Joint Inst. for Nuclear Research, Dubna, USSR). Bull. Acad. Sci. USSR, Phys. Ser. (Engl. Transl.); 33: 1510-12(1969).

Translated from Izv. Akad. Nauk SSSR, Ser. Fiz.; 33: 1646-9 (Oct 1969).

Precise measurements of the energies and intensities of γ rays accompanying the decay of ^{226}Ra were made using Ge(Li) detectors. The results were compared with previous measurements. (J.W.R.)

31359 DOUBLE ELECTRON EJECTION IN THE DECAY OF ^{137}Ba. Ljubicic, A.; Jurcevic, M.; Ilakovac, K.; Hrastnik, B. (Inst. Ruder Boskovic, Zagreb). Phys. Rev., C; 3: 831-6(Feb 1971).

Simultaneous ejection of two electrons in the decay of the 662-keV state of ^{137}Ba was investigated by means of two Si(Li) detectors and a two-dimensional pulse-height analyzer. The KK process was observed, while for the K, L + M + ... processes only an upper limit has been determined. The results obtained are $T_{KK}/T_K = (1.8 \pm 0.5) \times 10^{-4}$ and $T_{K,L+M+ \ldots}/T_K \leq 4.5 \times 10^{-4}$. The comparison of the experimental results with the existing theories indicates that the process proceeds primarily via electronic intermediate states. (auth)

31360 DESCRIPTION OF THE EXCITED PAIRED STATES OF ATOMIC NUCLEI BY THE VARIATIONAL APPROACH. Krutov, V. A.; Fomenko, V. N. Vestn. Leningrad. Univ., No. 10, Fiz., Khim.; No. 2, 69-74(May 1970). (In Russian).

A simple method based on the variational approach is suggested for treating the excited paired states of the pairing Hamiltonian, the trial wave functions being taken in the form of the properly symmetrized Bardeen–Cooper–Schrieffer states. The excitation energies and population probabilities are calculated for the lowest paired excited state for two model systems with the number of pairs p = 4 and p = 16. The results obtained for the excitation energies show satisfactory agreement with the exact calculations (for the system with p = 16 the difference between our results and the exact ones does not exceed 5%), whereas the agreement for the population probabilities proved to be worse. (auth)

31361 PAIR-PRODUCTION CROSS SECTIONS AT 2.75 MeV. Atwater, H. F. (Los Alamos Scientific Lab., N. Mex.). Nucl. Sci. Eng.; 44: 102-4(Apr 1971).

After measurement of the total photon cross section for 22 elements from Be to U, the pair-production cross section was derived by calculation and subtraction of the photoelectric, incoherent, and coherent cross sections. The errors in the result vary from 0.75% to 2.0%. An empirical expression for the pair-production cross section was found to be σ_κ (b) = $-3.95 \times 10^{-3} + 4.78 \times 10^{-4} Z^2$. The results are presented in tabular and graphical form. (R.W.R.)

31362 LACK OF EVIDENCE FOR SHELL EFFECTS IN THE (n,p) AND (n,α) REACTION CROSS SECTIONS AT 14 MeV NEUTRON ENERGY. Qaim, S. M. (Univ., Mainz). Z. Naturforsch.; 25a: 1977-8(Dec 1970).

The systematics of cross sections for (n,p) and (n,α) reactions induced by 14- to 15-MeV neutrons are reinvestigated. No clear evidence for the existence of any proton shell effects in these two reactions is found. (auth)

31363 PROBABILITY OF PRODUCTION OF INTERNAL BREMSSTRAHLUNG ACCOMPANYING β DECAY FROM ^{204}Tl, ^{147}Pm, AND ^{45}Ca. Singh, B.; Al-Dargazelli, Shetha, A. (Univ. of Baghdad). Phys. Rev., C; 3: 364-72(Jan 1971).

The production of internal bremsstrahlung accompanying β decay from radioactive nuclei of ^{204}Tl, ^{147}Pm, and ^{45}Ca has been investigated. The β-active source is fixed to the source holder of an experimental chamber with a good collimating arrangement. The internal bremsstrahlung is detected by a scintillation counter of good resolution and known efficiency, and a differential spectrum is obtained using a single-channel pulse analyzer. After making all necessary corrections, the probability of internal bremsstrahlung/mc^2 per β disintegration is obtained. The experimental probability is compared with the theoretical probabilities calculated from the theories of Knipp, Uhlenbeck, and Bloch; Nilsson; and Lewis and Ford. Discrepancies have been observed between experimental and theoretical results, especially in the case of ^{45}Ca, which has not been investigated previously. The experimental results show a distinct deviation from theoretical predictions. (auth)

31364 LIFETIMES OF GROUND-BAND STATES IN $^{148\ 150\ 152}Sm$. Diamond, R. M.; Stephens, F. S.; Nakai, K.; Nordhagen, R. (Univ. of California, Berkeley). Phys. Rev., C; 3: 344-9(Jan 1971).

The lifetimes of a number of ground-band states in $^{148,150,152}Sm$ have been measured by the recoil-distance Doppler-shift method following Coulomb excitation by backscattered ^{40}Ar projectiles. The measured B(E2) values for ^{152}Sm are larger than the rigid-rotor values; in terms of the mixing or stretching parameter α the present experiments yield $\alpha = (+2.2 \pm 0.7) \times 10^{-3}$. For $^{148,150}Sm$ the measured B(E2) values are near those expected for vibrational nuclei. (auth)

31365 BETA DECAY OF ^{111}Ag. Nagarajan, T.; Ravindranath, M.; Reddy, K. Venkata (Andhra Univ., Waltair, India). Phys. Rev., C; 3: 254-8(Jan 1971).

A new very weak β group 414 ± 10 (0.9%) keV is revealed in addition to the three β groups with end points 1035 ± 2 (92%), 789 (1.1%), and 693 ± 3 (6.0%). The 414-keV β group feeds the 621-keV level of ^{111}Cd introduced by Sastry, Lakshminarayana, and Jnanananda. The large shape deviation (17%) reported by Langer et al. for the 693-keV β group indicated a breakdown of the ξ approximation for this group, whereas correlation experiments and theoretical predictions indicated statistical shape. The present measurement C(W) = k[1 – (0.01 ± 0.06)W] confirms the latter conclusions and is in quantitative agreement with the shell-model predictions of Delabaye, Deutsch, and Lipnik. The characteristics of $\frac{1}{2}^- \rightarrow \frac{1}{2}^+$ and $\frac{1}{2}^- \rightarrow \frac{3}{2}^+$ transitions are just similar to those of ^{99}Mo and a theoretical fit of the outer β group of ^{111}Ag yields $3.2 \leq \Lambda \leq 3.3$ and $1.2 \leq \Lambda_0 \leq 1.4$. (auth)

31366 NEGATIVE-PARITY STATES IN ^{139}Pr. Muthukrishnan, R. (North Texas State Univ., Denton); Kromminga, A. Phys. Rev., C; 3: 229-33(Jan 1971).

In a recent experiment some high-lying negative-parity states in ^{139}Pr have been observed. A shell-model calculation of these states with ^{140}Ce as the closed core is reported. Some further experiments to explore the levels of ^{139}Pr are also suggested. (auth)

31367 INVESTIGATION OF THE TWO-QUASI-PARTICLE ROTATIONAL BAND AT 1172 keV IN ^{172}Yb AND DETERMINATION OF THE g_R FACTOR OF THE 3^+ 3 BAND HEAD. Wagner, H. F.; Lange, J. (Institut fuer Strahlen- und Kernphysik, Bonn). Z. Phys., 242: 292-303(1971).

Investigations of the rotational band based on the 3^+ 3 two quasiparticle state in ^{172}Yb have shown that some of its properties can be well described by the collective model of Bohr and Mottelson. As a result of these investigations the ratio $(g_K - g_R)/Q_0 = -(0.0136 \pm 0.0007)$ was derived. The magnetic g-factor of the band head was also determined by an integral angular correlation measurement perturbed by an external magnetic field. As a result g = 0.201 ± 0.030 was derived. Using this value and the result of $(g_K - g_R)/Q_0$ the g_R-factor of the two quasiparticle state was derived as $g_R = 0.283 \pm 0.018$ which is out of the errors smaller than the g_R-factor of the ground state rotational band. An analysis of the angular correlation experiments gave for the mixing parameter δ of the K-forbidden 1094 keV intraband transition: $\delta = -(3.63)$ in agreement with the results of other authors. (auth)

31368 APPROXIMATE HIGH-ENERGY ALPHA-PARTICLE NUCLEUS COLLISION MODEL. Gabriel, T. A.; Santoro, R. T.; Alsmiller, R. G. Jr. (Oak Ridge National Lab., Tenn.). Nucl. Sci. Eng.; 44: 104-10(Apr 1971).

A model for the prediction of the energy and angular distributions of nucleons from alpha-particle–nucleus collisions, as well as the cross sections for the production of various residual nuclei from alpha-particle–nucleus collisions, is described. It is assumed that these collisions may be simulated by transporting the nucleons of the alpha particles through the nucleus separately and independently, except for their relative spatial location when

XUM

they enter the nucleus. Energy spectra for emergent neutrons and protons are shown for 205-MeV alpha particles on ^{27}Al and ^{109}Ag. Excitation functions are given for the production of various isotopes from alpha particles and protons on ^{12}C, ^{27}Al, and ^{93}Nb. (R.W.R.)

31369 MEASUREMENT OF ANGULAR ANISOTROPY OF γ RADIATION EMITTED WITHIN 10^{-8} TO 10^{-7} sec AFTER THE MOMENT OF ^{235}U FISSION BY SLOW NEUTRONS. Val'skii, G. V.; Pleva, Yu. S.; Petrov, G. A. (Ioffe Inst. of Physics and Tech., Leningrad). Yadern. Fiz.; 12: 913-15(Nov 1970). (In Russian).

Using the method of geometrical separation of retarted radiation, the γ ray angular distribution was measured relative to the direction of the fragment velocity. The isotropy observed—(0.005 ± 0.006) may be a consequence of the angular correlation attenuation under the action of extranuclear fields. (auth)

31370 ELASTIC SCATTERING OF 1.33-MeV PHOTONS FROM LEAD AND URANIUM. Hardie, Gerald; DeVries, Joan S.; Chiang, Chwan-kang (Western Michigan Univ., Kalamazoo). Phys. Rev., C; 3: 1287-93(Mar 1971).

Differential cross sections for the elastic scattering of 1.33-MeV photons from lead and uranium have been measured at angles ranging from 12 to 60°, using a lithium-drifted germanium detector. Available calculations of the various elastic scattering amplitudes are briefly reviewed and an argument is presented to establish the relative phases between the two polarization components of the real scattering amplitudes. Those relative phases and the relative phases among the amplitudes of the various scattering processes permit the addition of the amplitudes to calculate theoretical cross sections. Discrepancies exist between the measured and theoretical cross sections. Suggestions by several authors for resolving these discrepancies are discussed and the need for further theoretical work is indicated. (auth)

31371 ANGULAR DISTRIBUTION OF FISSION FRAGMENTS FROM THE ^{170}Yb COMPOUND NUCLEUS EXCITED TO 107 MeV. Kowalski, L. (Montclair State Coll., Upper Montclair, N. J.); Zebelman, A.; Kandil, A.; Miller, J. M. Phys. Rev., C; 3: 1370-2(Mar 1971).

The angular distribution of the fission products formed in the reaction of 126-MeV ^{12}C ions with ^{158}Gd and 137-MeV ^{16}O ions with ^{154}Sm, both of which give ^{170}Yb compound nuclei at an excitation of 107 MeV, have been measured. It is found that the angular distribution in the ^{12}C-ion entrance channel is proportional to $1/\sin\theta$ from about 25 to 155° in the center-of-mass system, while the corresponding range is about 15 to 165° for the ^{16}O-ion entrance channel. The total fission cross sections are 20 ± 2 and 39 ± 4 mb for the two entrance channels, respectively. (auth)

31372 EXPERIMENTAL STUDY OF ELECTROMAGNETIC MATRIX ELEMENTS IN ^{92}Mo. Cochavi, S.; McDonald, J. M.; Fossan, D. B. (State Univ. of New York, Stony Brook). Phys. Rev., C; 3: 1352-61(Mar 1971).

The magnetic moment of the 2761-keV 8^+ state in ^{92}Mo has been measured as $\mu = (11.2 \pm 0.6)\mu_N$ (g = 1.40 ± 0.07) using the ^{90}Zr(α,2n) ^{92}Mo reaction and a time-differential technique. This result, which is consistent with a $|(lg_{9/2})^2, 8^+\rangle$ wave function, gives evidence for an enhanced g_1. The measurement also yielded a mean lifetime for the 8^+ state of τ = 275 ± 10 nsec. The lifetimes of the 2527-keV 5^- and 2613-keV 6^+ states were measured by p-γ and γ-γ delayed-coincidence methods, respectively. A mean life of τ = 2.24 ± 0.06 nsec was obtained for the 5^- state and the mean life of the 6^+ state was found to be τ = 2.22 ± 0.07 nsec. The observed $B(E2: 8^+ \rightarrow 6^+)$ and $B(E2: 6^+ \rightarrow 4^+)$ are consistent with $(lg_{9/2})^2$ proton configurations for the 4^+, 6^+, and 8^+ states. The lifetimes of the 6^+ and 5^- states imply that the $6^+ \rightarrow 5^-$ and $5^- \rightarrow 4^+$ E1 transitions in ^{92}Mo are hindered relative to the Weisskopf estimates by 2×10^4 and 7×10^4, respectively. These results are consistent with pure proton configurations of $(lg_{9/2})^2$ for the 4^+ and 6^+ states and $(2p_{1/2}, lg_{9/2})$ for the 5^- state. (auth)

31373 THERMAL-NEUTRON FISSION OF ^{242m}Am: MASS AND CHARGE DISTRIBUTION. Wolfsberg, K.; Ford, G. P. (Los Alamos Scientific Lab., N. Mex.). Phys. Rev., C; 3: 1333-7(Mar 1971).

35 chain yields from thermal-neutron-induced fission of ^{242m}Am were measured by a recoil-catcher method, using ^{235}U fission as a standard. Fractional cumulative yields of five krypton and of six xenon nuclides were measured by an emanation method. The results are in agreement with known trends. (auth)

31374 E2/M1 ADMIXTURE OF THE $2' \rightarrow 2$ TRANSITION IN ^{106}Pd. Robinson, R. L.; Milner, W. T.; McGowan, F. K.; Stelson, P. H. (Oak Ridge National Lab., Tenn.). Nucl. Phys.; A166: 141-4(1971).

An angular correlation measurement between two cascade γ-rays from the Coulomb-excited state in ^{108}Pd at 931 keV was used to establish a value of $-(3.1 \pm 0.4)$ for the E2/M1 radiative admixture δ of the $2' \rightarrow 2$, 497 keV γ-ray. From this and earlier information, we determined $B(E2; 2' \rightarrow 2) = (24.8 \pm 5.5) \times 10^{-50}$ e$^2 \cdot$cm^4 and $B(M1; 2' \rightarrow 2) = (4.4 \pm 1.4) \times 10^{-3}$ $(e\hbar/2Mc)^2$. (auth)

31375 DECAYS OF ^{176}Ta, ^{176}Lu, AND ^{176m}Lu TO LEVELS IN ^{176}Hf. Bernthal, F. M.; Rasmussen, J. O. (Univ. of California, Berkeley. Yale Univ., New Haven); Hollander, J. M. Phys. Rev., C; 3: 1294-1326(Mar 1971).

The locations of 48 energy levels in ^{176}Hf have been deduced from γ-ray singles, conversion-electron, and γ-γ coincidence measurements on the EC-β^+ decay of 176 Ta. Over 300 γ-ray transitions have been observed in the ^{176}Ta decay spectrum, and about 140 of these have been definitely assigned to the ^{176}Hf level scheme on the basis of 75 γ-γ coincidence spectra. Spin and parity assignments are proposed for 27 levels besides the ground-state rotational-band members. Less extensive γ-ray singles data from ^{176}Lu and ^{176m}Lu decay have also been obtained; these are found to be consistent with the ^{176}Hf level structure proposed on the basis of ^{176}Ta decay data. Two 0^+ excitations in ^{176}Hf identified at 1150 and 1293 keV are found to display quite different decay properties. Evidence for the existence of a series of low-spin four-quasiparticle states near 3 MeV is cited. The ^{176}Hf level structure is compared with available theoretical calculations, and a preliminary interpretation of several unusual features of the level scheme is presented. (auth)

31376 NUCLEAR SPINS OF ^{125}Cs AND ^{136}Cs, HYPERFINE-STRUCTURE SEPARATION AND NUCLEAR MAGNETIC MOMENT OF ^{125}Cs, ^{127}Cs, AND ^{136}Cs. Dabbousi, Osama B.; Prior, Michael H.; Shugart, Howard A. (Univ. of California, Berkeley). Phys. Rev., C; 3: 1326-32(Mar 1971).

The atomic-beam magnetic-resonance method was used to determine the ground-state nuclear spin, the electronic $^2S_{\frac{1}{2}}$ ground-state hyperfine-structure (hfs) separations $\Delta\nu$, and the nuclear magnetic moments of 45-min ^{125}Cs and 13-day ^{136}Cs. A more accurate value of the hfs separation of 6.2-hr ^{127}Cs was obtained by combining resonances reported previously with those reported in this work. (auth)

31377 MEAN LIFETIMES OF LEVELS IN ^{92}Mo. Youngblood, D. H. (Texas A and M Univ., College Station); Kozub, R. L.; Hill, J. C. Nucl. Phys.; A166: 198-204(1971).

The mean lifetimes of the 1.509 MeV, 2.848 MeV and 3.089 MeV levels in ^{92}Mo were measured by the attenuated Doppler-shift technique. The measurements were analyzed by use of the universal stopping cross sections given by Lindhard, Scharff and Schiøtt. The lifetimes obtained are 430, 350, and 32 ± 18 fs respectively. (auth)

31378 LEVELS OF ^{246}Cm FROM THE β^--DECAY SEQUENCE ^{246}Pu(11 days)^{246m}Am(25 min)^{246}Cm. Multhauf, L. G.; Tirsell, K. G.; Morrow, R. J.; Meyer, R. A. (Univ. of California, Livermore). Phys. Rev., C; 3: 1338-51(Mar 1971).

^{246}Pu produced by multiple neutron capture during an underground explosion was recovered and subjected to extensive chemical separations. γ rays in the decay sequence ^{246}Pu(β^-)^{246m}Am(β^-) ^{246}Cm were investigated by use of several Ge(Li) detectors. In all, 158 γ rays were observed, up to 2.2 MeV. Of these, 114 were ascribed to the decay of ^{246m}Am. A decay scheme was deduced, including 37 levels. Bands in ^{246}Cm have been identified with the following bandhead energies: g.s. $K^\pi = 0^+$; 841.70 keV $K^\pi = 2^-$, octupole; 1078.90 keV $K^\pi = 1^-$, octupole; 1124.42 keV $K^\pi = 2^+$, γ; 1249.81 keV $K^\pi = (0^-$, octupole); 1348.89 keV $K^\pi = 1^-$; 1452.06 keV $K^\pi = (1^+)$; 1593.80 keV $K^\pi = 2^{(-)}$; 1604.31 keV $K^\pi = 1^-$. (auth)

31379 PARTICLE-CORE COUPLING IN THE LEAD REGION. Chalapati Rao, K. V. (Saha Inst. of Nuclear Physcis, Calcutta). Nucl. Phys.; A166: 213-20(1971).

Several nuclei in the neighborhood of ^{208}Pb were studied in terms of the core-particle coupling model. The present studies include the high-lying negative-parity states in ^{209}Pb and positive-parity states in ^{209}Bi, the levels of ^{207}Bi, the low-lying negative-parity states of ^{205}Pb and the high-lying positive-parity states of ^{205}Pb. The results are compared with the results of single-nucleon and double-nucleon transfer reactions. (auth)

31380 CONVERSION ELECTRON PARTICLE PARAMETERS OF E2 TRANSITIONS IN ^{152}Sm AND ^{154}Gd. Holmberg, L.; Stefansson, V.; Eriksson, L.; Pettersson, B. G. (Univ. of Stockholm). Nucl. Phys.; A166: 297-305(1971).

Studies of conversion electron particle parameters of E2 transitions in ^{152}Sm and ^{154}Gd have yielded conflicting results. In some cases large discrepancies with the theoretical values have been reported. In this work the following angular correlations are measured: 965γ-122K, 1408γ-122K, 965γ-122γ, 1408γ-122γ in ^{152}Sm and 873γ-123K, 1274γ-123K, 873γ-123γ, 1274γ-123γ in ^{154}Gd. The K conversion electron particle parameters b_2 for the $2^+ \rightarrow 0^+$ tran-

XUM

sitions of 122 keV and 123 keV are determined directly from the second-order angular correlation coefficients, and derived from the fourth-order particle parameters b_4. Possible sources of systematic errors are discussed in some detail. The results are $b_2(122K) = 1.93 \pm 0.04$; $b_2(123K) = 1.93 \pm 0.08$. The agreement with the theoretical values is good. (auth)

31381 SPIN-PARITY ASSIGNMENTS FOR THE LOW-LYING STATES IN ^{95,97}Tc VIA THE NEUTRON DECAY OF 0^+ AND 2^+ ANALOGUE STATES. Kim, H. J.; Robinson, R. L.; Johnson, C. H. (Oak Ridge National Lab., Tenn.). Nucl. Phys.; A167: 65-72(1971).

Three low-lying excited states in each of the nuclei ^{91}Nb, ^{95}Tc, and ^{97}Tc were observed to be strongly populated by the neutron decay of the 2^+ resonances in the compound nuclei ^{92}Nb, ^{96}Tc and ^{98}Tc. These resonances are the isospin analogs of the first 2^+ states of ^{92}Zr, ^{96}Mo, and ^{98}Mo, respectively. The neutron decay of the ground state analog of ^{98}Mo was also investigated. These decays of the analog resonances were investigated via (p,n) reactions. The resonance energies (lab energy) and widths for the 2^+ resonances are: 4.154 ± 0.010 MeV and 33 ± 2 keV, 3.908 ± 0.010 MeV and 32 ± 2 keV, and 4.330 ± 0.010 MeV and 34 ± 2 keV for the compound nuclei ^{92}Nb, ^{96}Tc, and ^{98}Tc, respectively. The energy and width for the 0^+ resonance for ^{98}Tc are 3.505 ± 0.010 MeV and 25 ± 3 keV. The resonance yields to the individual states are compared to the expected yields based on the optical-model transmission coefficients. From these yields and the shapes of the off-resonance angular distributions, the following spin-parities are assigned: $^3/_2^-$ and $^5/_2^-$ for the 651 and 670 keV states of ^{95}Tc, respectively, and $^3/_2^-$ and $^5/_2^-$ for the 575 and 662 keV states of ^{97}Tc, respectively. (auth)

31382 DECAY OF ^{108}Ag. Johnson, N. D. (Vanderbilt Univ., Nashville); Hamilton, J. H.; Kluk, A. F.; Johnson, Noah R. Z. Phys.; 243: 395-401(1971).

The 2.41 min ground state decay of ^{108}Ag has been studied with a Ge(Li) detector. Twelve transitions are observed of which seven have not been reported previously. Five of the new transitions are placed in the level scheme which includes the second 2^+, 930.4 keV level and a new level at 1539.4 keV in ^{108}Pd. (auth)

31383 ^{208}Pb(p,α)^{205}Tl REACTION AT 16.475 MeV. Hopkins, F. F.; Courtney, W. J.; Coker, W. R.; Moore, C. F.; Richard, P. (Univ. of Texas, Austin). Z. Phys.; 243: 446-51(1971).

The (p,α) reaction was studied on a ^{208}Pb target at 16.475 MeV. Nineteen states were observed in ^{205}Tl, up to 3.6 MeV in excitation. Angular distributions were obtained for five strong proton-hole transitions, and DWBA fits made to determine lj values. Results are compared with previous ^{206}Pb(t,α)^{205}Tl, ^{206}Pb(d,^{3}He)^{205}Tl, ^{205}Tl(p,p′), and ^{205}Tl(n,n′) work. (auth)

31384 DECAY OF ^{106m}Rh. Takahashi, K.; Swindle, D. L.; Kuroda, P. K. (Univ. of Arkansas, Fayetteville). Nucl. Phys.; A167: 183-92(1971).

A radiochemically pure source was used to study the decay characteristics of 2.18 h ^{106m}Rh. A high-resolution Ge(Li) spectrometer and β- and γ-scintillation detectors were used. Thirty-nine γ-rays were assigned to ^{106m}Rh and several coincidence measurements were performed. A decay scheme incorporating 35 of the γ-rays is tentatively proposed. The following energy levels in ^{106}Pd were found to be populated: 511.7, 1127.7, 1227.9, 1557.2, 1932.4, 2041.1, 2076.9, 2085.6, 2305.5, 2352.0, 2365.6, 2557.5 and 2952.7 keV. Spin-parity assignments of the levels are discussed. (auth)

31385 NEUTRON-INDUCED FISSION CROSS SECTION OF ^{242}Pu. Bergen, D. W.; Fullwood, R. R. (Los Alamos Scientific Lab., N. Mex.). Nucl. Phys.; A163: 577-82(1971).

The neutron-induced fission cross section of ^{242}Pu is reported from 50 eV to 5 keV and 0.1 to 3 MeV. Fission widths are given up to 381 eV. The half-height of the fission barrier is determined to be 0.76 MeV. The energy of the second minimum in the fission barrier is determined to be 3.6 MeV. (auth)

31386 GAMMA-RAY ENERGIES AND INTENSITIES IN THE DECAY OF ^{205}Bi. Rupp, T. D.; Vegors, S. H. Jr. (Idaho State Univ., Pocatello). Nucl. Phys.; A163: 545-70(1971).

Gamma rays following the decay of ^{205}Bi were studied using Ge(Li) detectors. The energies and intensities of 96 γ-rays in ^{205}Pb have been determined. Of these 29 have not been previously observed. By comparing these γ-ray intensities with previously measured conversion electron intensities, information on the multipolarity of 40 transitions was obtained. This information, together with $\gamma\gamma$ and electron-γ coincidence data, is used to construct a decay scheme for ^{205}Bi. The following new energy levels are suggested: 1129.9 keV, $^5/_2^-$; 1575.3 keV, $^9/_2^-$; 1705.0 keV, $^{11}/_2^-$; 1758.6 keV, $^{11}/_2^+$; 1965.9 keV, $^7/_2^-$; 2203.7 keV, $^{11}/_2^+$; 2252.3 keV, $^9/_2^+$; 2488.2 keV, $^7/_2^+$; and 2521.7 keV, $^9/_2^-$. The decay scheme proposed here is in substantial agreement with many of the results previously reported. A comparison of this decay scheme with several of the current theories is made. In addition, improved energy values have been obtained for several of the prominent γ-rays in ^{206}Bi. (auth)

31387 REINVESTIGATION OF THE DECAY OF ^{200}Tl. Komppa, T.; Pakkanen, A.; Kantele, J. (Univ. of Jyvaeskylae, Finland). Contract AT(30-1)-905. Nucl. Phys.; A163: 513-22 (1971).

A detailed study of γ-rays and γ-ray cascades from 26.1 h ^{200}Tl has been carried out employing Ge(Li) detectors, an anti-Compton spectrometer and a Ge(Li)–NaI(Tl) coincidence spectrometer. A decay scheme is proposed which incorporates six new excited states in ^{200}Hg. The energies and γ-ray decay branching ratios of some of the levels are compared with values calculated from the model of Covello and Sartoris who describe ^{200}Hg as two proton holes coupled to surface vibrations. (auth)

31388 GAMMA TRANSITION STUDIES OF ^{125}Sb FROM THE DECAY OF 9.7 min ^{125m}Sn. Kawase, Y.; Okano, K.; Uehara, S.; Hayashi, T. (Kyoto Univ., Osaka). Nucl. Phys.; A163: 534-44(1971).

Gamma transitions of ^{125}Sb from the decay of 9.7 min ^{125m}Sn have been studied with Ge(Li) detectors and angular correlation measurements for five cascades have been performed by using a multicounter goniometer. The lifetime of the first excited state has been determined by the $\beta\gamma$ delayed coincidence method as $T_{\frac{1}{2}} = 163 \pm 10$ ps. The internal conversion coefficient of the first to ground state transition has been found to be $\alpha_K = 0.018 \pm 0.005$ by using a Si–Ge(Li) conversion coefficient spectrometer. The value of B(E2) obtained for the 332 keV transition is 0.02 $e^2 \cdot b^2$, which is 1.1 times as large as the single-particle unit. The present experimental results are compared with the intermediate coupling model for ^{125}Sb. (auth)

Nuclear Theory

Refer also to abstracts 30036, 30669, 30777, 30894, 30905, 31315, 31316, and 31362.

31389 (ANU-P-500) FIDEL: AN OPTICAL MODEL SEARCH CODE WITH SPIN-ORBIT TERMS FOR SPIN-$^1/_2$ AND SPIN-1 PARTICLES. Rosalky, D. M. (Australian National Univ., Canberra. Research School of Physical Sciences). [1970]. 11p. Dep. NTIS (U. S. Sales Only).

An optical-model search code, which includes spin-orbit terms in the scattering and absorption potentials, for spin-$^1/_2$ and spin-1 particles was developed for use on the IBM 360/50. The optical-model computation is performed by modified sections of the DWBA code DWUCK. A value of χ^2 is calculated in terms of experimental and calculated values of the differential cross section and the vector polarization and is minimized with respect to specified parameters by subroutine FITTEM. (auth) (Australia)

31390 (ANU-P-507) SANDRA: THE DWBA CODES JULIE AND DWUCK ADAPTED FOR USE ON THE IBM 360/50 COMPUTER. Dallimore, P. J.; Davis, J. R. (Australian National Univ., Canberra. Research School of Physical Sciences). [nd]. 16p. Dep. NTIS (U. S. Sales Only).

The distorted wave Born approximation codes JULIE, developed by Bassel, Drisko and Satchler, and DWUCK, developed by Kunz, were adapted for use on the IBM 360/50 computer at the Australian National University. Minor modifications were made to the program [for example, the ability to read in angles in either the center of mass or laboratory coordinate systems], but the mathematical techniques were left unchanged. (auth) (Australia)

31391 (ANU-P-512) HAUSER: A COMPUTER CODE FOR THE CALCULATION OF COMPOUND NUCLEUS CROSS SECTIONS USING THE HAUSER–FESHBACH THEORY. Dallimore, P. J. (Australian National Univ., Canberra. Research School of Physical Sciences). [1970]. 20p. Dep. NTIS (U. S. Sales Only).

A computer code which calculates compound nucleus cross sections using the theory of Hauser and Feshbach was developed for use on the IBM 360/50 computer at the Australian National University. The program incorporates a level-density description of all possible exit channels and includes the width-fluctuation correction factor. (auth) (Australia)

31392 (BNL-tr-416) SINGLE-PARTICLE STATES OF DEFORMED TRANSURANIUM NUCLEI IN THE SAXON–WOODS POTENTIAL. Gareev, F. A.; I vanova, S. P. (Joint Inst. for

Nuclear Research, Dubna (USSR)). Translated by S. J. Amoretty (Brookhaven National Lab., Upton, N. Y.), from report JINR-P4-5221. 25p. Dep. NTIS.

An abstract of this paper, prepared from the original language, appeared as NSA 25: 5684. (auth)

31393 (COO-1051-34) SOME OBSERVATIONS CONCERNING THE USE OF REALISTIC FORCES IN A MICROSCOPIC DESCRIPTION OF THE INELASTIC SCATTERING OF NUCLEONS FROM NUCLEI AT MEDIUM ENERGIES. Petrovich, Fred L. (Michigan State Univ., East Lansing. Dept. of Physics and Astronomy). 1970. 282p. Dep. NTIS.

Thesis.

Several models for nucleon-nucleus scattering are investigated by direct calculation. All of the interaction models considered are consistent with some portion of the data concerning the free two-nucleon force; hence, the term "realistic forces." It is assumed that the projectile-target interaction is given by (1) a pseudo-potential derived from the impulse approximation, (2) the long range part of the Kallio-Kolltveit potential (K-K force) which is known to be a good approximation to the central part of the shell model reaction matrix, and (3) a Yukawa force derived from effective range theory. The local distorted wave approximation (D.W.A.) is used throughout and no consideration is given to components of the interaction with complicated spin dependence such as the tensor and $\vec{l} \cdot \vec{s}$ parts. Approximations are made to treat the exchange component of the D.W.A. transition amplitude which is nonlocal. Application is made to (p,p') transitions in closed and pseudo-closed shell nuclei. Random phase approximation (R.P.A.) states of the target nuclei. The results obtained with all three interaction models are shown to be in reasonable agreement with experiment, although the Yukawa effective range force appears to be somewhat poorer than the other two at incident energies below 30 MeV. The inclusion of exchange plays an essential part in giving this agreement. Further application is made to transition involving low-lying states in nuclei which possess one or two nucleons outside of a closed shell. The purpose is to study core polarization effects which are known to be important in these transitions. Contributions to (p,p') cross sections due to core polarization are large. The relation between the effect of core polarization on the spectrum and in inelastic proton-nucleus scattering is examined. The microscopic model does not do too badly on the (p,p') cross sections, i.e., mass polarization effects. The experimental data is underestimated somewhat. However, effective charges for corresponding γ-transitions, i.e., charge polarization effects, are badly underestimated. (auth)

31394 (ITF-70-95-E) ABOUT CALCULATING (n,2n) REACTION AMPLITUDE ON HEAVY NUCLEI. II. Ol'khovskii, V. S.; Rekami, E.; Ezhov, S. N. (Akademiya Nauk Ukrainskoi SSR, Kiev. Institut Teoreticheskoi Fiziki). 1970. 11p. Dep. NTIS (U. S. Sales Only).

A method for solving the problem of coherent (n,2n) knock-out on heavy nuclei at low energies is developed in the approximation of infinite-mass nuclei. For this the equations of Faddeev or of Baz et al. are not necessary, due to the lack of 2n bound states. One can start from the Gell-Mann-Goldberger equation, whose nonhomogeneous term gives the T-matrix element in the DWBA. One can expand the total wave function (multiplied by the potential V_{12} between the two neutrons) on a complete discrete set of vectors (e.g., the isotropic three-dimensional harmonic-oscillator eigenfunctions). Then, an infinite system of equations is obtained, which can be approximated to a finite system with any degree of accuracy, as the previous expension can be shown to converge. The problem is thus reduced to solving an algebraic (instead of integral) system. The rescattering contribution is also considered. (auth)

31395 (JINR-P1-5648) PARTICLE INTERFERENCE IN THE PROCESSES INVOLVING EXCITED NUCLEI. Grishin, V. G.; Kopylov, G. I.; Podgoretskii, M. I. (Joint Inst. for Nuclear Research, Dubna (USSR). Lab. of High Energy). 1971. 18p. (In Russian). Dep. NTIS (U. S. Sales Only).

The interference phenomena in nuclear reactions, proceeding through the intermediate isolated excited states, are described. The possibility of determination of the excited state width is discussed. (auth)

31396 (RPI-3947-13) NEUTRON AND GAMMA EMISSION FROM HIGHLY EXCITED STATES AND STATES WITH HIGH SPIN. Annual Progress Report, June 1, 1970-May 31, 1971. Sperber, Daniel (Rensselaer Polytechnic TecInst., Troy, N. Y.). Feb 1971. Contract AT(30-1)-3947. 9p. Dep. NTIS.

Analysis of isomer ratios indicates that the moments of inertia of nuclei at higher excitation have the value of the rigid-body moment of inertia. A method for studying the angular distributions of particles evaporated in nuclear reactions in which states in the continuum decay into a wide range of highly excited states is described. The isomer ratios and fission lifetimes for shape isomers were calculated, with special emphasis on the reaction $^{241}Am(n,\gamma)^{242}Am$. Estimates for the cross section for the synthesis of superheavy elements using the present generation of heavy-ion accelerators were made. References to more detailed accounts of some of this work are given. (R.W.R.)

31397 ANALYSIS OF HIGHLY RETARDED ALLOWED BETA TRANSITIONS. Subotowicz, M. (Marie Curie-Sklodowska Univ., Lublin). Bull. Acad. Sci. USSR, Phys. Ser. (Engl. Transl.); 33: 1496-1502(1969).

Translated from Izv. Akad. Nauk SSSR, Ser. Fiz.; 33: 1631-7 (Oct 1969).

The possibility of contributions of nuclear matrix elements for second-forbidden transitions in highly-retarded allowed beta decay is discussed. Experimental data for a large number of nuclei are examined. (J.W.R.)

31398 SHELL CORRECTION TO THE LIQUID-DROP ENERGY OF A NUCLEUS UNDERGOING FISSION. Marshalkin, V. E.; Volkov, Yu. V. Bull. Acad. Sci. USSR, Phys. Ser. (Engl. Transl.); 33: 1610-12(1969).

Translated from Izv. Akad. Nauk SSSR, Ser. Fiz.; 33: 1761-3 (Oct 1969).

The shell correction to the liquid-drop energy and the deviations of level density from a uniform distribution near the Fermi energy were calculated using the single-particle spectrum of a system containing two ellipsoidal subsystems with a connecting neck. It was found that the shell correction is very sensitive to the shape of the system in the transition region. (auth) (TSS)

31399 SPINS OF THE LOWER LEVELS OF FOUR-PARTICLE $[(jp)^2 I_p^{max}; (jn)^2 I_n^{max}]$ CONFIGURATIONS AND POSSIBLE ISOMERIC STATES IN ^{80}Zr, ^{88}Zr, AND SIMILAR NUCLEI. Peker, L. K. (All-Union Scientific-Research Inst. of Metrology, Leningrad). Bull. Acad. Sci. USSR, Phys. Ser. (Engl. Transl.); 33: 1566-8 (1969).

Translated from Izv. Akad. Nauk SSSR, Ser. Fiz.; 33: 1710-12 (Oct 1969).

Modified Brennan-Bernstein rules are extended to the spins of lower levels of multiplets with four-particle $\{(jp)^2 I_p^{max}, (jn)^2 I_n^{max}\}$ configurations. It is shown that the rules correctly describe the ^{212}Po isomer. The rules are used to predict high-spin isomeric states in A = 80 to 96 nuclei. (J.W.R.)

31400 BORN APPROXIMATION IN THE THEORY OF STRIPPING REACTIONS. Korolev, A. M. (Inst. of Physics, Kiev). Bull. Acad. Sci. USSR, Phys. Ser. (Engl. Transl.); 33: 1561-6 (1969).

Translated from Izv. Akad. Nauk SSSR, Ser. Fiz.; 33: 1703-9 (Oct 1969).

The use of the Born approximation in analyzing (d,p) stripping reactions is examined. The nuclear and Coulomb interactions of the proton with the nucleus are considered. For simplicity only spherical even-even nuclei are considered. Deuteron energies are taken to be larger than or of the order of the Coulomb barrier and the protons are restricted to small escape angles. The method of analysis is compared with the Butler stripping theory. It is found that the Born approximation for stripping on light nuclei gives satisfactory results in the region of the first peak at high deuteron energies, but it does not give good results when the behavior of the neutron and proton wave functions near the nucleus is important. (J.W.R.)

31401 PROBABILITY RATIO FOR K AND L CAPTURE. Zyryanova, L. N.; Suslov, Yu. P. (Leningrad State Univ.). Bull. Acad. Sci. USSR, Phys. Ser. (Engl. Transl.); 33: 1553-6 (1969).

Translated from Izv. Akad. Nauk SSSR, Ser. Fiz.; 33: 1693-7 (Oct 1969).

The method for the calculation of the theoretical probability ratio for K and L capture is described. Calculated probability ratios for Z = 3 through 81 are presented in tabular form. Discrepancies between the calculated and experimental values are discussed. The correction factors which are currently being used in calculating probability ratios are mentioned. (J.W.R.)

31402 EFFECTIVE FORCES WITHIN NUCLEI. Dzhibuti, R. I.; Mamasakhlisov, V. I. (Inst. of Physics, Tbilisi, USSR). Bull. Acad. Sci. USSR, Phys. Ser. (Engl. Transl.); 33: 1557-60 (1969).

Translated from Izv. Akad. Nauk SSSR, Ser. Fiz.; 33: 1698-1702(Oct 1969).

A nonlocal two-nucleon potential which is a modification of the Serber potential was used in analyzing the deuteron free state and neutron-proton pairs in nuclear matter. It was found that the effective potential describes the deuteron binding energy but does

XUM

not give a bound n–p pair in nuclear matter. The potential is repulsive at close range, attractive at distances of r > 1 F, and gives rapid "curing" at large distances. (auth) (TSS)

31403 ENERGY SPECTRA OF PARTICLES OBSERVED IN REACTIONS PROCEEDING VIA A COMPOUND NUCLEUS. Rumyantsev, B. A. (Inst. of Nuclear Physics, Novosibirsk, USSR). JETP Lett. (USSR) (Engl. Transl.); 12: 285-7(20 Oct 1970).

Translated from Zh. Eksp. Teor. Fiz., Pis'ma Red.; 12: 411-13(20 Oct 1970).

An effect is considered that explains qualitatively the difference between the observed spectrum and the evaporation spectrum for reactions proceeding via a compound nucleus. The probabilities of the transitions to different states of the superfluid nucleus are small except for the case of the pair-oscillation phonon. It is found that the energy spectrum of the particles emitted by a compound nucleus should have a maximum in the region $E_f \sim E_i - (\rho\Delta/2)\Delta$ with a width $\Gamma \sim \Delta$, where 2Δ is the energy gap (0.5 to 1.5 MeV in even–even nuclei) and ρ is the density of single-particle levels at the Fermi boundary. These results are in qualitative agreement with the data. (R.W.R.)

31404 ISOTOPIC SHIFTS FOR THE ISOBARIC PAIRS. Tatu, V. S. (Inst. for Atomic Physics, Bucharest). Rev. Roum. Phys.; 15: 1029-34(1970).

Some relations concerning the isotope shifts for the pairs of isobars are deduced. From the ratio of these isotope shifts, some useful information regarding the spectral term energies, the ratio of the variations of mean square radius for the nuclei under consideration, a series of quantities of nuclear interest (for instance, the nuclear compressibility corrections), and so on, may be obtained. (auth)

31405 HYPERSPHERICAL-EXPANSION APPROACH TO NUCLEAR BOUND STATES. III. THE LIMIT OF LARGE A. Calogero, F. (Univ., Rome. Istituto Nazionale di Fisica Nucleare, Rome); Simonov, Yu. A.; Surkov, E. L. Nuovo Cim.; 1A: 739-58(21 Feb 1971).

The hyperspherical-expansion approach to nuclear bound states is shown to behave correctly, even in the first approximation, in the limit of large A (A = nucleon number), provided the (input) nucleon–nucleon potential is of the soft-core saturating kind recently suggested as the most likely candidate for physical relevance. A derivation from first principles of the Weizsäcker formula in the large-A region is provided, including explicit expressions for the computation of its numerical coefficients. This formula provides a rigorous upper bound to the ground-state energy of an assembly of many nucleons (nuclear matter). An expression for the density of nuclear matter, which is convenient for studying the dependence of this quantity upon the Coulomb interaction and upon the difference between the numbers of neutrons and protons, is also obtained. (auth)

31406 STATISTICAL THEORY FOR GAMMA RAY DE-EXCITATIONS OF NUCLEI. Bertram, W. K. (Australian Atomic Energy Commission Research Establishment, Sutherland). Aust. J. Phys.; 24: 7-12(1971).

A statistical method is used to describe the process of γ-ray de-excitations of nuclei in excited states. Expressions are derived for the distribution of multiplicities in γ-ray cascades and for the energy spectrum associated with each γ-ray multiplicity. (auth) (Australia)

31407 POSSIBILITY OF QUASI-ROTATIONAL EXCITATIONS IN SPHERICAL NUCLEI. Rohozinski, S. G. (Univ., Warsaw). Acta Phys. Pol.; A39: 241-3(Feb 1971).

The existence of the ground-state quasirotational band in spherical nuclei is examined. The single j-shell model with the pairing-plus-quadrupole forces is used. The result is negative. (auth)

31408 CORIOLIS ANTI-PAIRING THEORY OF NUCLEAR ROTATIONS. NUCLEAR MEISSNER-EFFECT. Birbrair, B. L. (Ioffe Inst. of Physics and Tech., Leningrad). Phys. Lett.; 34B: 558-60(12 Apr 1971).

It is shown that the ground-state rotational bands of spherical nuclei are formed by a gradual alignment of the angular momenta of valence nucleons along the rotation axis. The predicted spin and excitation energy values of the first rotational state in ^{212}Po nucleus are $J = 16^+$ and E = 2.91 MeV which is in reasonable agreement with the experimental data ($J = (18^+)$, E = 2.93 MeV). (auth)

31409 ASYMMETRIC ROTOR PROBLEM AND THE COLLECTIVE EXCITATIONS OF EVEN NUCLEI. Gai, E. V.; Rabotnov, N. S. (Inst. of Physics and Energetics, Obninsk, USSR). Phys. Lett.; 34B: 563-5(12 Apr 1971).

The perturbation theory series provides an exact solution for the rigid rotor states important in the theory of nuclear excitations. The results are used to analyze the experimental data for even nuclei. (auth)

31410 DETERMINATION OF THE OPTICAL POTENTIALS IN TERMS OF DIFFRACTION-MODEL PARAMETERS. Abul-Magd, A. Y.; El-Nadi, M.; Simbel, M. H. (Cairo Univ.). Phys. Lett.; 34B: 566-8(12 Apr 1971).

Glauber's eikonal approximation is used to derive the optical potentials corresponding to the scattering of strongly absorbed nuclear projectiles from the parameters of the phase shifts determined in the diffraction model analyses. (auth)

31411 ENERGY SPECTRUM AND DEFORMATION OF SOME EVEN–EVEN NUCLEI. Bravin, A. V.; Fedorov, A. D. (Saratov State Univ., USSR). Yadern. Fiz.; 13: 43-7(Jan 1971). (In Russian).

Introduction of the deformation parameter β_0 into the kinetic part of the Hamiltonian makes it possible to find this important parameter directly from the energy spectrum. The softness parameter μ and the deformation parameter β_0 are calculated using the least-square method in the frame of the axial-symmetrical nucleus model. With the values obtained the energy of excited states of the even–even nuclei with the mass number in the region $150 < A < 190$ is calculated and the comparison with the experimental levels is performed. (auth)

31412 STATISTICAL EXPRESSION FOR THE NUCLEAR ENERGY. Tyapin, A. S. Yadern. Fiz.; 13: 32-42(Jan 1971). (In Russian).

On the basis of the statistical nuclear model an expression is obtained for the energy that is correct up to terms of the order of 2 MeV. Relation of constants in the mass formula to those characterizing the nucleon distribution in nuclei is discussed. A model calculation of constants in the mass formula is fulfilled in order to estimate the value of the present corrections to the expression for the nuclear energy obtained on basis of the droplet model. (auth)

31413 STUDY OF THREE-PART NUCLEON–NUCLEON INTERACTION POTENTIALS. Ruehl, Franklin Robert Jr. Los Angeles; Univ. of California (1970). 270p. University Microfilms Order No. 71-4881.

Thesis.

The properties of the light 4-n even–even nuclides ranging from ^{4}He to ^{40}Ca are studied in a variational or simple restricted Hartree–Fock calculation, employing an effective three-part two-body nucleon–nucleon interaction. This interaction consists of a trio of Wigner plus Majorana exchange forces each having Gaussian radial dependence. A rectangular harmonic oscillator basis of states is utilized. Two classes of parameter sets are studied: one generated from fitting the ground state energy and equilibrium harmonic oscillator energy of ^{4}He and the binding energy per nucleon and density of nuclear matter, and one obtained from fitting the ground state energy and harmonic oscillator energy of both ^{4}He and ^{40}Ca. The resulting parameters are used to compute the ground state binding energies and harmonic oscillator energies of seven nuclides, ^{8}Be, ^{12}C, ^{20}Ne, ^{24}Mg, ^{28}Si, ^{32}S, and ^{36}Ar, each treated as being axially symmetric, with two possible configurations for all but ^{8}Be and ^{12}C considered. Moreover, ^{28}Si is also analyzed as a spherically symmetric nuclide. Root mean square radii, intrinsic quadrupole moments, shape parameters, Nilsson deformation constants, and transition probabilities are determined for the axial nuclides. Spectra are generated from the deformed intrinsic ground states by an angular momentum projection technique ideally suited to a Cartesian coordinate system. Additionally, the 4p-4h excited state of ^{16}O and the triaxial states of ^{24}Mg and ^{32}S are studied. A tripartite interaction, composed of a tensor force coupled to a two-part central interaction incorporating a pair of Wigner and Majorana exchange forces with Gaussian radial dependence, is utilized in another variational computation. In order to determine precisely what enhancements are engendered by the addition of the tensor force, the two-part interactions used are ones for which results have previously been obtained. To generate parameter sets of interest, the second-derivative test of a function of two variables is applied to the binding energy equation for the oblate nucleon configuration of the axially symmetric nuclide ^{36}Ar. Parameter sets minimizing the ^{36}Ar binding energy within specified limits of the actual experimental value are then employed to calculate values of the various nuclear quantities studied for the same seven axial nuclides. Comparison with known results from the coupled central interaction is provided throughout this part of the overall investigation. (Diss. Abstr. Int., B)

31414 HEXADECAPOLE DEFORMATION AND ROTATION-PARTICLE COUPLING IN THE RARE EARTH NUCLEI. Davis, Alvie Douglas. Los Angeles; Univ. of California (1970). 228p. University Microfilms Order No. 71-3811.

Thesis.

Calculations of the energy spectra for odd-A nuclei in the rare earth region were made using a rotational model for deformed nuclei. Both pairing and band mixing (or Rotation-Particle Coupling, RPC) were included in detail. A hexadecapole (P_4) deformation was considered in addition to the usual Quadrupole (P_2) deformation. In most cases, this additional hexadecapole deformation proved to be quite necessary to achieve a good fit to the experimental energies. Thirty nuclei in the rare earth region were investigated. Good results were obtained for twenty-seven of them. With the parameters found in achieving a fit to the energy spectrum, reduced transitions rates and spectroscopic factors were calculated. Band mixing (or RPC) made it possible to investigate K-forbidden transitions. In most cases there was good agreement with the experimental values. (Diss. Abstr. Int., B)

31415 REPULSION OF SLOW NEUTRONS BY ATTRACTIVE POTENTIALS. Peshkin, M.; Ringo, G. R. (Argonne National Lab., Ill.). Amer. J. Phys.; 39: 324-7(Mar 1971).

A naive calculation of the scattering of slow neutrons by an attractive square-well potential gives a distribution of scattering amplitudes that agrees rather well with available measured amplitudes for thermal neutrons. (auth)

31416 EFFECTIVE INTERACTION OF NUCLEONS IN INFINITE NUCLEAR MATTER. Balazs, Erzsebet; Kisdi, David (Theoretical Physics Research Group, Budapest). Magy. Fiz. Foly.; 18: 197-227(1970). (In Hungarian).

The effective interaction between 2 point charges in a dielectric is not identical with that prevailing between 2 such charges in vacuum; the dielectric acts as a background and modifies the action of the charges. The same considerations must be kept in mind when examining the interaction between 2 nucleons of a many-nucleon system. If the interaction between the free nucleons is known, the effective interaction may be derived on the basis of the many-body problem. The validity of the derivation is determined by comparing the data obtained with the nucleic density as parameter with the extrapolated results of heavy nuclei experiments. The energy versus nuclear matter density exhibits a minimum, indicating that the nuclear interaction is saturated. The nucleon gas is examined on this basis, defining the interacting systems by means of Goldstone diagrams. It is found that the potential energy is a first or second-order approximation of the Brueckner equations. The numerical solution of these equations by an iteration process is described. (TTT)

31417 FISSIONABILITY OF HEAVY NUCLEI. Lin, I. (Showa-Yakka Coll., Tokyo); Oishi, Kimiya; Ito, Kensai. Progr. Theor. Phys. (Kyoto); 44: 1427-8(Nov 1970).

The fission of heavy nuclei by high-energy protons is treated within the framework of high-energy nuclear reaction theory. A two-step model is used in Monte Carlo calculations in which the collision regions are divided into edge and central parts. Results are presented for ratios of fission cross sections to geometrical cross sections for Z^2/A values of 20 to 40 and proton energies of 500, 750, and 1000 MeV. (J.W.R.)

31418 INELASTIC TRANSITION DENSITIES. Ford, W. F.; Braley, R. C. (Lewis Research Center, Cleveland). Nucl. Phys.; A162: 513-29(1971).

The prediction of nuclear observables often involves the calculation of reduced matrix elements of single-particle operators between initial and final nuclear states. A systematic means of evaluating such matrix elements in terms of the inelastic transition densities $\rho^{if}_{LSJ}(r)$ is developed, which essentially gives the probability for absorption of angular momentum J = L + S by the last nucleon as a function of its distance from the nuclear origin. These densities may be expanded in terms of Gauss–Laguerre functions, thus permitting substantial simplification in the matrix element calculation. A number of examples and useful formulas are presented. (auth)

31419 CALCULATION OF NEUTRON TUNNELLING CROSS SECTIONS. May, R. M.; Nicholls, I. R. (Univ. of Sydney). Aust. J. Phys.; 23: 633-9(1970).

An accurate expression for the matrix element for neutron tunnelling reactions is presented using Hulthen wavefunctions for both initial and final neutron states and a Hulthen form for the neutron-binding potential (previous work is confined to asymptotic neutron wavefunctions and zero-range potentials). This work is applied to the neutron tunnelling reaction $^{14}N(^{14}N,^{13}N)^{15}N$. It is also employed to effect a retrospective justification for the rather empirical approximation used by May and Clayton (1968) in their explanation of the astrophysically interesting reaction $^3He(^3He,2p)^4He$. (auth) (Australia)

31420 GAMMA-RAY LINEAR POLARIZATION AND ANGULAR DISTRIBUTION FORMULAS IN TERMS OF PHASE-DEFINED REDUCED MATRIX ELEMENTS. Taras, P. (Univ. of Montreal). Can. J. Phys.; 49: 328-50(1 Feb 1971).

Gamma-ray linear polarization and angular distribution formulas are presented in terms of the phase-defined reduced matrix elements of Rose and Brink. In particular, the mixing ratios are phase consistently related to reduced matrix elements of interaction multipole operators which are also well defined in phase. The mixing ratios extracted from the measurements of gamma-ray angular distribution and linear polarization can then be compared in both magnitude and sign with the predictions of nuclear models. The full potential of a gamma-ray linear polarization measurement is demonstrated by the discussion of a recent measurement. (auth) (Canada)

31421 INTERACTION OF LOW ENERGY PIONS WITH NUCLEI. Scherk, L. (Univ. of British Columbia, Vancouver). Can. J. Phys.: 49: 306-16(1 Feb 1971).

It is shown that the low energy ($\lesssim$40 MeV) pion-nucleus optical potential, which was previously derived by other authors from a microscopic point of view, has a simple geometric structure which can be understood from the analogous problem of adding electric potentials in a dielectric medium. The optical properties of this potential are dominated by the presence of a short-range local repulsion, which is comparable to the energies of interest, and by a strong momentum dependence in the optical interaction. It is shown that, because momentum-dependent processes are strongly suppressed near the top of the resulting potential barrier and because the nuclear density enters the optical interaction in a transparent manner, such momentum-dependent processes as pion absorption provide an excellent tool for investigating the structure of the nuclear surface. Such processes should finally resolve current inconsistencies in the knowledge of the neutron distribution in the nuclear surface. (auth) (Canada)

31422 SUDDEN MODEL FOR TERNARY FISSION. Facchini, U.; Saetta-Menichella, E. (CISE, Milan. Univ., Milan). Phys. Lett.; 34B: 572-4(12 Apr 1971).

A description is given of the ternary fission mechanism by means of the "sudden model", which has been previously proposed by the authors in the case of binary fission. (auth)

31423 NUCLEAR DENSITY DISTRIBUTION FOR NUCLEUS-NUCLEUS SCATTERING. II. Fliessbach, Torsten (Technische Univ., Munich). Z. Phys.; 242: 287-91(1971).

The effect of the antisymmetrization on the density distribution for nucleus-nucleus scattering was investigated. In contrast to an earlier paper (Fliessbach, Z-Physik, 238: 329(1970)) the motion of the nuclei is now taken into account. For experimentally available energies no pronounced density compression in the overlap region was found. For very high energies a superposition of the densities is justified. (auth)

31424 MICROSCOPIC DESCRIPTION OF STATIC QUADRUPOLE MOMENTS OF 2_1^+ STATES BY TIME-DEPENDENT HF EQUATIONS. Meyer, J. (Technische Univ., Munich). Z. Phys.; 242: 332-41(1971).

Large quadrupole moments of 1-phonon states of spherical nuclei are shown to follow in a simple and direct way from time-dependent HF equations using the self-consistent perturbation expansion. Whereas the first order describes harmonic quadrupole oscillations, anharmonic terms arise in second order. The scattering of quasiparticles by quasi-particle pairs, which is neglected in RPA calculations, but included in this paper, leads to a second order response of the system and is shown to produce a strong enhancement of the quadrupole moments. Explicit results are obtained with a pairing-plus-quadrupole interaction and discussed within a schematic two level model. (auth)

31425 ENERGY LEVEL CALCULATIONS IN DAVYDOV MODEL. Abecasis, S. M. (Laboratorio de Radiaciones, Buenos Aires); Femenia, F. R.; Hernandez, E. S. Comput. Phys. Commun.; 2: 33-9(Jan 1971).

A computer program is described for calculating collective excitations and energy-level ratios with the Davydov model in terms of the parameters α, μ, and γ_0. The program can be used for a wide range of values of α, the restrictions on μ and γ_0 being $8° \leq \gamma_0 \leq 30°$ and $0 \leq \mu \leq 1$. Computations are performed with the energy levels of the ground-state rotational band from I = 0 to 20 (in steps of 2) and those of the anomalous band for I = 2 to 10 (in steps of 1) of the Davydov–Filippov model. The program, in FORTRAN IV, requires 8400 36-bit words of storage. On the Bull

XUM

General Electric 625 a run for one nuclide takes about 8 minutes for compilation and 22 seconds for execution. (R.W.R.)

31426 CALCULATION OF FRACTIONAL PARENTAGE COEFFICIENTS FOR THE (1d–2s)-SHELL NUCLEI WITH THE PROJECTION-OPERATOR METHOD. Gurbanovich, I. S.; Smirnov, Yu. F.; Tolstoi, V. N. (Moscow State Univ.). Czech. J. Phys.; 21: 236-46(1971).

The projection operators for the groups SU_n are used for constructing the noncanonical basis vectors of irreducible representations of these groups as linear combinations of the Gel'fand-Tseitlin canonical basis vectors. The structure of the basis vectors of the irreducible representation of the groups SU_4, SU_3, SU_6 in the case of the reduction $SU_4 \supset SU_2 \times SU_2$, $SU_3 \supset R_3$ and $SU_6 \supset SU_3$, respectively, is discussed. A number of formulas have been obtained for the fractional parentage coefficients for the (1d–2s)-shell nuclei. (auth)

31427 GROUND-STATE ENERGIES OF DOUBLY EVEN NUCLEI. Khanna, K. M. (Dibrugarh Univ., India); Sharma, M. L. Czech. J. Phys.; 21: 223-35(1971).

Ground-state energies of doubly even nuclei which are assumed to be composed of rigid and structureless alpha particles are calculated. The alpha particles are assumed to be interacting through a potential composed of a hard core followed by a square well potential in one set of calculations and a Gaussian potential in another set of calculations. The calculations support the existence of the hard core in the alpha–alpha potential and suggest the existence of the alpha clustering in doubly even light nuclei. From the graph between E_0/N and ρ_α it is found that E_0/N is minimum at $\rho_\alpha = 2.57 \times 10^{37}$ particles cm^{-3}. This means that in the surface region an assembly of alpha particles with $\rho_\alpha = 2.57 \times 10^{37}$ particles cm^{-3} is the most stable one. (auth)

31428 ANGULAR DISTRIBUTION OF PARTICLES EVAPORATED IN NUCLEAR REACTIONS. Liggett, G.; Sperber, D. (Rensselaer Polytechnic Inst., Troy, N. Y.). Phys. Rev., C; 3: 167-71(Jan 1971).

A method for the evaluation of the average angular distribution, over a range of energy, of particles evaporated in succession from a compound nucleus is presented. The method is applied to the analysis of the angular distribution in the reaction $^{56}Fe(\alpha,p)^{59}Co$ and the reaction $^{63}Cu(^{12}C,p)^{74}Se$. The analysis indicated that nuclei at high excitation have rigid moments of inertia. (auth)

31429 SPECTRAL DISTRIBUTIONS IN NUCLEI. French, J. B. (Univ. of Rochester, N. Y. Univ., Mexico City); Ratcliff, K. F. Contracts AT(30-1)-875; AT(30-1)-2098. Phys. Rev., C; 3: 94-117(Jan 1971).

Given a finite many-particle vector space, which may be of large dimensionality, and a Hamiltonian which operates inside it, the general properties of the system are studied by a method of expanding preselected basis states in terms of the Hamiltonian eigenfunctions. The corresponding intensity, considered as a function of the Hamiltonian eigenvalues, is a spectral distribution which may be studied via its energy moments; such distributions averaged over subsets of basis states are considered. The properties of these averaged distributions are discussed, as well as methods for applying them in general studies of complicated systems; methods are given for evaluating the moments in some significant cases. Detailed formal results are given for configuration distributions in the spherical shell model. (auth)

31430 APPLICATIONS OF SPECTRAL DISTRIBUTIONS IN NUCLEAR SPECTROSCOPY. Ratcliff, K. F. (Massachusetts Inst. of Tech., Cambridge). Contract AT(30-1)-2098. Phys. Rev., C; 3: 117-43(Jan 1971).

The energy moments of spectral distributions are used to investigate the structure of spectroscopic calculations. Eigenvalue distributions are used to predict energy spectra, which are compared with the results of matrix diagonalization. The nature of the corresponding eigenvectors is similarly analyzed. The propagation of moments for scalar and configuration distributions is illustrated throughout the sd shell. These scalar moments are then used to estimate the trend in theoretical binding energies for these nuclei and in turn are compared with empirical data. Finally, the dependence of the energy and wave function of the ground state of ^{16}O upon the vector space underlying a theoretical calculation is investigated. The unrenormalized Kuo–Brown matrix elements are employed in this analysis, and the role of multiple particle-hole excitations is discussed. (auth)

31431 NUCLEAR SOFT-CORE POTENTIAL AND COSMIC-RAY PHENOMENA. Canuto, V. (Goddard Space Flight Center, New York). Nuovo Cim.; 2A: 1016-23(21 Apr 1971).

It is shown that the soft-core phenomenological potential for the $^1S_0$ state is well reproduced by the exchange of an isoscalar vector meson in the framework of the nonlocal field theory, originally introduced to interpret the fireball properties in high-energy cosmic-ray collision. (auth)

31432 REALISTIC INTERACTIONS AND EXCHANGE EFFECTS IN MICROSCOPIC DESCRIPTIONS OF ELASTIC AND INELASTIC NUCLEON SCATTERING. Owen, Larry Wayne. Knoxville, Tenn.; Univ. of Tennessee (1970). 156p. University Microfilms Order No. 71-7665.

Thesis.

The effects of exchange in microscopic descriptions of elastic and inelastic nucleon-nucleus scattering are investigated using realistic nucleon-nucleon effective interactions. The interaction in even states of relative motion is taken to be the long-range part of the Hamada–Johnston potential. Possible effects upon the elastic scattering of including a central interaction in singlet-odd states are investigated. The spin-orbit optical potential is calculated using two estimates for the nucleon-nucleon spin-orbit interaction in triplet-odd states. The microscopic model of the real part of the optical potential consists of a direct term which is local, and an exchange term which is nonlocal and different for each partial wave. The ground state wave functions of the target nuclei are assumed to be given by the independent particle model. Oscillator, Woods–Saxon, and Hartree–Fock single-particle functions are used. The scattering induced by these nonlocal potentials is obtained exactly by explicitly solving the integro-differential Schroedinger equations. (The numerical methods used are discussed.) In addition, equivalent local potentials of the Woods–Saxon form are obtained by fitting the scattering from the microscopic potentials. The dependence of the equivalent local potentials upon energy, neutron excess and $Z/A^{\frac{1}{3}}$ is investigated. The "perey effect" for nonlocal potentials is observed. Many important features of phenomenological optical potentials are reproduced with this microscopic model to a surprising degree of accuracy. Exchange effects in the inelastic scattering of protons with the Hamada–Johnston interaction are found to be very important. However, the contributions from interaction with the valence nucleons in nuclei with simple configurations are much smaller than the observed cross sections. Core polarization effects, estimated with a collective model description of the core, are very strong. (Diss. Abstr. Int., B)

31433 ENERGY PARAMETERS IN THE RARE-EARTH NUCLEI. Demirkhanov, R. A.; Dorokhov, V. V. Yadern. Fiz.; 12: 875-84(Nov 1970). (In Russian).

The masses and binding energies of ~330 radioactive nuclei were calculated with the help of Q values for nuclear reactions, α, β, and electron-capture decays and using as a basis stable isotope masses measured by the mass-spectrograph method in the region $133 \leq A \leq 181$. The binding energies of stable and radioactive nuclei are used to determine the energy parameters of nuclei. Numerical values of nuclear parameters are determined, the jump in energy parameters by filling of the neutron shell N = 82 is accurately measured. The possible determination of transition boundaries from spherical to deformed nuclei by means of the analysis of energy parameters of nuclei is shown. (auth)

31434 DEDUCTION OF THE GLAUBER FORMULA FROM THE WATSON THEORY. Tarasov, A. V.; Tseren, Ch. (Joint Inst. for Nuclear Research, Dubna, USSR). Yadern. Fiz.; 12: 978-81(Nov 1970). (In Russian).

A method to deduce the Glauber formula for the scattering of particles on nuclei from the Watson theory of multiple scattering is presented. (auth)

31435 REGULARITIES OF PHOTONUCLEAR REACTIONS AS EFFECTS OF THE FEYNMAN GRAPHS PROPERTIES. Dubovoi, E. I. Yadern. Fiz.; 12: 965-77(Nov 1970). (In Russian).

Properties of the photonuclear reactions, A(γ,y)B, are investigated that are due to the contribution from the Feynman triangle graphs taking into account the final-state interactions. It is shown that the radical EI extrema of the triangle graphs result in a number of irregularities in the excitation function of the A(γ,y)B reaction. Applying the consideration to the (γ,n) reactions it is shown that the contribution from the triangle graphs results in a broad maximum (EII) in the cross section, whose position coincides with that of the giant resonance in light and heavy nuclei (as for intermediate nuclei, the coincidence is not good). The position of the radical extrema EI in the (γ,n) reaction coincides with that of the fine structure of the giant resonance in ^{12}C, ^{16}O, ^{19}F, and ^{208}Pb. (auth)

31436 STATISTICAL ANALYSIS OF SPECTRA OF INELASTICALLY SCATTERED NEUTRONS. Stavinskii, V. S. Yadern. Fiz.; 12: 960-4(Nov 1970). (In Russian).

A method is presented for processing of the evaporation spectra that takes into account a possible deviation of the state equation

from the Fermi-gas model. On the basis of this method an analysis is performed of experimental data on the neutron spectra for the (n, n') reactions. The analysis confirms the effect of the discrete structure of the shell-model spectra on the density of nuclear excitation states that has been predicted in theory. (auth)

31437 DENSITY DISTRIBUTION OF DEFORMED NUCLEUS IN THE MODEL OF INDEPENDENT PARTICLES. Chepurnov, V. A. (Inst. of Atomic Energy, Moscow). Yadern. Fiz.; 12: 949-59(Nov 1970). (In Russian).

It is shown that for the nuclear density the angular distribution of the mean-square radius is the value which characterizes deformation. On the basis of this the deformation and radial parameters of the density distributions of the deformed nucleus with $A \approx 165$ were determined in the independent-particle model with a realistic nuclear potential. The effect of doubling is estimated. The obtained charge distribution for Z = 67 is compared with the experimental one. (auth)

31438 PROJECTION DESCRIPTION OF ROTATIONAL AND QUASIROTATIONAL BANDS IN EVEN-EVEN NUCLEI. Frauendorf, S.; Janssen, D.; Munchow, L. (Central Inst. for Nuclear Research, Rossendorf, Ger.). Yadern. Fiz.; 12: 939-48(Nov 1970). (In Russian).

A two-parameter formula for the energies of the ground band of even-even nuclei is derived using the angular momentum projection method. The overlapping integrals of the "turned over" deformed states are investigated in detail and the possibility of simple parametrization is shown. The two-parameter formula describes equally reasonably the states of deformed nuclei with large angular momentum and the quasi-rotational bands. (auth).

31439 APPLICATION OF THE K-HARMONIC METHOD TO THE CALCULATION OF NUCLEAR PROPERTIES. DESCRIPTION OF DEFORMATIONS AND QUADRUPOLE OSCILLATIONS. Grin, Yu. T. (Inst. of Atomic Energy, Moscow). Yadern. Fiz.; 12: 927-38(Nov 1970). (In Russian).

Equations for simultaneous description of density and quadrupole oscillations and static deformations are obtained using the K-harmonic method. The method proposed enables one to consider the binding energy, the radius and multipole momenta of deformed nuclei and the quadrupole oscillation energy with the help of a unique nucleon-nucleon interaction. (auth)

31440 CALCULATION OF NUCLEAR MATRIX ELEMENTS OF DOUBLE β DECAY. Khodel, V. A. (Inst. of Atomic Energy, Moscow). Yadern. Fiz.; 12: 916-22(Nov 1970). (In Russian).

It is shown that the nuclear matrix element of neutrinoless double β decay has the maximal value if the one particle quantum numbers ν_1 and ν_2 of decaying and producing nucleon pairs, respectively, are close to each other. When ν_1 and ν_2 considerably differ, an additional factor $\sim A^{-\frac{1}{3}}$ appears in the nuclear matrix element. The case of close ν_1 and ν_2 can be calculated without introducing additional constants which characterize the renormalization of nuclear matrix elements of the decay by strong interactions between nucleons of the nucleus. Fluctuations of nuclear matrix elements of the decay are studied. It is shown that these fluctuations may be large even for the neighboring nuclei because of the possible interference of matrix elements of different components of quasi-particle wave functions for the initial and final states. (auth)

31441 BOUNDARY-CONDITION-MODEL T MATRIX. Fuda, Michael G. (State Univ. of New York, Buffalo). Phys. Rev., C; 3: 55-65(Jan 1971).

A number of results on the boundary-condition-model (BCM) T matrix are developed. It is shown that the half-off shell T matrix is unique, but the fully off-shell T matrix is not. Further, it is shown that the ambiguity in the T matrix resides in that part of the complete T matrix which is identifiable as the T matrix for the pure BCM, where by pure BCM is meant no forces outside the boundary-condition radius. Three different formulas for the pure BCM T matrix are presented. The first is derived by using the relations that exist between the half-off-shell T matrix and the fully off-shell T matrix for well-behaved potentials, and is found to be separable. The second is taken from the work of Kim and Tubis. The third is derived from a pseudopotential constructed by Hoenig and Lomon. All three agree exactly half off shell, and satisfy the off-shell unitarity relation. Numerical comparisons are given which show that significant differences can occur in the fully off-shell T matrices. An integral- as well as a differential-equation approach are given for finding the contribution to the BCM T matrix from the forces outside the boundary-condition radius. Separable representations for the BCM T matrix are developed, and their usefulness in carrying out calculations on the three-nucleon system is discussed. (auth)

31442 COMPARISON OF THE R-MATRIX NUCLEAR REACTION THEORIES. Schmittroth, F.; Tobocman, W. (Case Western Reserve Univ., Cleveland). Phys. Rev., C; 3: 1010-19(Mar 1971).

A number of reaction theories are tested and compared by their application to a simple model of s-wave scattering from a two-state nucleus. These theories include the extended R-matrix theory of Garside and Tobocman, the L-operator formalism of Lane and Robson, and variations of the Brown–de Dominicis theory. It is found that the Hüfner–Lemmer version of the Brown–de Dominicis theory gives the best results in the few-level approximation. (auth)

31443 EFFECTIVE ORTHOGONALITY OF CHANNEL WAVE FUNCTIONS AND COUPLED EQUATIONS FOR DIRECT INTERACTIONS. Hahn, Yukap (Univ. of Connecticut, Storrs). Phys. Rev., C; 3: 1432-4(Mar 1971).

An explicit proof is given of the effective orthogonality among the channel wave functions obtained from a set of coupled equations by showing that the nonorthogonal parts of the wave functions are physically redundant, thus providing a rigorous basis for the treatment of nuclear stripping and pickup reactions. An orthogonality-preserving procedure of the coupled-channel method is outlined. (auth)

31444 INTERNAL SCATTERING AMPLITUDES FOR BREMSSTRAHLUNG. Liou, M. K.; Sobel, M. I. (City Univ. of New York, Brooklyn). Phys. Rev., C; 3: 1430-2(Mar 1971).

It is shown that the results obtained by several authors for the internal scattering amplitude for bremsstrahlung can be derived in a unified way from an operator identity. This shows the mathematical connection between these various approaches and their essential equivalence. The approaches of these authors are generalized to the case of momentum-dependent potentials. (auth)

31445 NUCLEAR SURFACE PROPERTIES AND THE NUCLEAR COMPRESSIBILITY IN A STATISTICAL APPROXIMATION. Stocker, W. (Univ., Munich). Nucl. Phys.; A166: 205-12(1971).

The statistical method suggested by Brueckner et al. is applied to the system of semi-infinite nuclear matter to study the nuclear surface properties. The energy density as a function of the density consists of the Thomas–Fermi kinetic part plus a potential part including the second derivative of the density. The condition of minimal surface tension leads to a second-order differential equation for the density. Various forms of the exchange part of the potential energy density and the resulting surface properties are investigated. Especially, the connection between the nuclear compressibility and these quantities is extracted. An approximate estimation of the value of the nuclear compressibility is given. It is shown that the ratio of the nuclear surface tension to the surface thickness is determined by properties of homogeneous nuclear matter. (auth)

31446 HRPA CONTRIBUTIONS TO PHONON–PHONON INTERACTION IN THE ADIABATIC LIMIT. Paar, V. (Univ. of Copenhagen). Nucl. Phys.; A166: 341-8(1971).

In the particle-vibration coupling model the leading order phonon-phonon interaction is given by rectangular and two-triangle diagrams. The contributions from diagrams which appear in the adiabatic limit are calculated for the quadrupole vibrator. In this way, the strengths of quartic and cubic anharmonicities are expressed in terms of an underlying shell-model structure. (auth)

31447 NON-LOCAL POTENTIALS AND THE SINGLE-PARTICLE SHELL MODEL. Grimm, R. C.; McCarthy, I. E.; Storer, R. G. (Flinders Univ. of South Australia, Bedford Park). Nucl. Phys.; A166: 330-40(1971).

Accurate solutions of Schroedinger's equation with a non-local potential are used to investigate the energy dependence of the single-particle shell model. With non-locality the wave functions corresponding to single-particle bound states are not uniquely determined by demanding merely that they reproduce the experimentally observed binding energies. Additional experimental data is required to remove this ambiguity. (auth)

31448 NUCLEAR TRANSMUTATION BY NEGATIVE STOPPED MUONS AND THE ACTIVITY INDUCED BY THE COSMIC-RAY MUONS. Charalambus, S. (CERN, Geneva). Nucl. Phys.; A166: 145-61(1971).

Nuclear transmutation and the involved factors when negative muons are stopped in matter are discussed. Some uncertainties about the atomic capture of muons in compounds and about the neutron emission probability following muon capture still exist. The stopping rate of negative cosmic-ray muons in the atmosphere and in the lithosphere up to large depths is reviewed. The activities of some radioisotopes induced by stopped negative muons in the atmosphere and in the lithosphere are calculated and compared with measurements and other calculations. (auth)

XUM

31449 SYMMETRY PROPERTY OF THE INELASTIC SCATTERING AMPLITUDE IN THE ADIABATIC APPROXIMATION. Sherif, H. (Univ. of Alberta, Edmonton). Can. J. Phys.; 49: 983-90(15 Apr 1971).

A symmetry property of the exact T matrix for the inelastic scattering of particles with arbitrary spin is derived, in the adiabatic limit, using time reversal invariance properties of the elastic scattering amplitude and neglecting interaction terms that involve spins or velocities of the target nucleons. The symmetry property is used to show the equality of the generalized polarization and asymmetry tensors for inelastic scattering and to derive the symmetry properties, with respect to the adiabatic recoil axis, of the angular correlation function and the circular polarization of the deexcitation gamma rays. It is also shown that the nuclear excited state is aligned along the axis normal to the scattering plane. A brief discussion of the symmetry properties of the adiabatic DWBA amplitude is given. When interaction terms involving spins or velocities of the target nucleons are taken into account, it is shown that the inelastic scattering T matrix can be divided into two parts; one that satisfies the above-mentioned symmetry relation, and a second part which has a different symmetry. (auth) (Canada)

31450 COMMENT ON RESONANCE AVERAGING. Moldauer, P. A. (Argonne National Lab., Ill.). Phys. Rev., C; 3: 948-9 (Feb 1971).

A recently proposed definition of the average scattering amplitude is evaluated numerically for a variety of resonance models. The results differ from both the predicted and the physically required values. (auth)

31451 IS THERE A GROUND-STATE DEFORMATION IN NUCLEI NEAR CLOSED SHELLS? Beck, R. (Technische Univ., Munich). Z. Phys.; 243: 409-17(1971).

It is shown that the stability of spherical Hartree–Fock–Bogolyubov (HFB) states against deformation may be completely altered if angular momentum conservation is taken into account exactly, leading to a smooth transition from spherical to deformed nuclei. Furthermore, the close connection between the stability matrix in HFB theory and the RPA matrix is destroyed by angular momentum projection. (auth)

31452 GROUP-THEORETICAL OPERATOR ANALYSIS IN THE ds SHELL. Pluhar, Z. (Technische Univ., Brunswick). Nucl. Phys.; A167: 33-48(1971).

A method is presented for the group-theoretical analysis of operators, using the Racah algebras of classification groups. The method is specialized to one- and two-particle operators acting in the ds shell, analyzed with respect to the Elliott SU(3) classification scheme. The cases of identical and nonidentical nucleons are treated separately. Explicit results are given for Hamiltonians with Kuo effective two-particle interactions. The group-theoretical expansions of the Kuo interactions are found to be dominated by central operators preserving spatial symmetry; the components diagonal in the classification scheme are large. (auth)

31453 FRACTIONAL PARENTAGE AND THE EQUATIONS-OF-MOTION METHOD IN PAIRING THEORY. Mauger, J.; Evans, J. A. (Univ. of Sussex, Brighton, Eng.). Nucl. Phys.; A167: 16-32(1971).

The eigenstates of a pairing Hamiltonian are studied in terms of the linearized equation of motion for a pair of fermions. The conventional treatment is found to lead to spurious states arising from the failure to satisfy the Pauli principle. A new formulation is presented in which this defect is absent. (auth)

XUM

REACTOR TECHNOLOGY

Commercial Power Reactors

Refer also to abstracts 29289, 31577, and 31632.

31454 (EUR–4531, pp 81-94) PRESTRESSED CONCRETE PRESSURE VESSEL OF THE VANDELLOS NUCLEAR POWER PLANT. Arathoon, J. P.; Le Cars, F. (Societe pour l'Industrie Atomique, Paris (France)); Muller, J.; Moreau, Ph. (Enterprises Campenon Bernard S. A., Paris (France)). (In French).

From second conference on prestressed concrete reactor pressure vessels and their thermal isolation; Brussels, Belgium (18 Nov 1969).

In Second information meeting on prestressed concrete reactor pressure vessels and their thermal isolation.

The Vandellos Power Reactor is a natural uranium-fueled gas-cooled graphite-moderated reactor. The specifications placed on the pressure vessel are outlined. The principal characteristics of the structure, the heat exchangers, and design requirements are briefly reviewed. The modifications made to the Vandellos vessel in comparison with the pressure vessel of the reactor at Saint Laurent des Eaux (an almost identical reactor) are described and the justifications for the modifications are given. (J.S.R.)

31455 (EUR–4531, pp 95-128) FIRST RESULTS OF PUTTING INTO SERVICE THE ST. LAURENT I PRESTRESSED CONCRETE PRESSURE VESSEL. Costaz, J. L. (Electricite de France, Paris). (In French).

From second conference on prestressed concrete reactor pressure vessels and their thermal isolation; Brussels, Belgium (18 Nov 1969).

In Second information meeting on prestressed concrete reactor pressure vessels and their thermal isolation.

The performance of the Saint Laurent I prestressed concrete pressure vessel after one year's operation is reported. The vessel was not subjected to any stresses that it would not receive during normal operation. The problems connected with the start-up of the coolant circuit, the cooling of the skin, and the temperature of the external face of the vessel and the means used to compensate for the difficulties found are outlined. Ausculation data on the functioning of the vessel, the thermocouples, dynamometers, pendulums, topography, and the thermal balance are given and evaluated. (J.S.R.)

31456 (EUR–4531, pp 129-44) INTERACTION BETWEEN THE DESIGN AND CONSTRUCTION OF PRESTRESSED CONCRETE PRESSURE VESSELS FOR NUCLEAR REACTORS. Williams, A. J.; Tate, L. A. (British Nuclear Design and Construction Ltd., Whetstone (England)); Burrow, R. E. D. (Taylor Woodrow Construction Ltd., Southall (England)).

From second conference on prestressed concrete reactor pressure vessels and their thermal isolation; Brussels, Belgium (18 Nov 1969).

In Second information meeting on prestressed concrete reactor pressure vessels and their thermal isolation.

Construction problems and procedures associated with the prestressed concrete pressure vessels of the Wylfa Reactors and the Hartlepool Power Reactors are described. The development of the wire-wound vessels is reviewed. Problems relating to the construction of the highly penetrated standpipe region are discussed. (3 references.) (D.C.C.)

31457 (EUR–4531, pp 895-930) STEADINESS OF THERMAL SHIELDING DURING ALTERNATE STRESSES OF AERODYNAMIC ORIGIN. Roure, L. (Societe Bertin et Cie, Paris (France)). (In French).

From second conference on prestressed concrete reactor pressure vessels and their thermal isolation; Brussels, Belgium (18 Nov 1969).

In Second information meeting on prestressed concrete reactor pressure vessels and their thermal isolation.

The Bugey nuclear power plant uses CO_2 as the heat transfer agent. Its unidirectional and permanent flow was not established immediately at the output because of the local section discontinuity. Experience on the instationary phenomena showed that the zone of establishment is the site of perturbations of aerodynamic origin. A general study was undertaken to define the nature and to determine the importance of these phenomena. The effect of these stresses on the mechanical stability of the thermal shield was also studied. The experimental results obtained are summarized and the method of theoretical calculations made are given and justified. The theoretical and experimental results are then collated to determine the origin of the vibrations and the dynamic response of the thermal shield exposed to a periodic stress. (J.S.R.)

31458 DESIGN BASIS FOR THE PROTECTION SYSTEM AND THE ACTUATOR SYSTEMS OF NUCLEAR-FUELED GENERATING STATIONS. ANS-4.1 1970. Hinsdale, Ill.; American Nuclear Society (1970). 32p. Available from American Nuclear Society, Hinsdale, Ill.

The design basis is presented for the protection system and the actuator systems of nuclear power plants. (auth)

31459 MODIFYING BRADWELLS' REACTORS. Elec. Times; 159: 54-6(19 Mar 1971).

Changes needed to minimize the effects of corrosion of mild steel components in the Bradwell reactors, and the remote handling techniques developed for overcoming some of these effects are discussed. A description is given of the fitting of stainless steel sleeves into the tops of the fuel channels. These formed, in effect, a new upper charge pan and were designed to prevent debris falling into the channel and also to retain thermocouple cables. (UK)

31460 NUCLEAR POWER IN THE WEST GERMANY IN THE NEXT DECADE. Schuster, Guenter. Com. Naz. Energ. Nucl., Notiz.; 17: No. 3, 35-48(Mar 1971). (In Italian).

The prospects of nuclear energy in the Seventies are reviewed, with particular regard to Germany's nuclear programs. (auth)

31461 RECENT DEVELOPMENT OF THE NUCLEAR POWER PROGRAM IN WEST GERMANY: THE BRUNSBUETTEL AND PHILIPPSBURG POWER PLANTS. Sansone, Magda. Com. Naz. Energ. Nucl., Notiz.; 17: No. 3, 49-56(Mar 1971). (In Italian).

A review of the major nuclear power plants now in operation, under construction, or design in West Germany and a description of the recently ordered Brunsbüttel and Philippsburg power plants are presented. (auth)

31462 ATOMIC REACTORS AND FUEL SOURCES FOR AUSTRALIA. Baxter, J. P. (Australian Atomic Energy Commission, Lucas Heights). At. Energy Aust.; 13: No. 4, 2-9 (Oct 1970).

The status of nuclear technology in Australia is briefly reviewed and an economic comparison is made between nuclear power generation and conventional electricity production. It is considered that under normal Australian conditions electricity cost from nuclear power is approaching comparison with thermal production costs at and above 500 MW. The reactors under consideration for construction on Australia's first nuclear power station site at Jervis Bay are compared. Attention is paid to the fuel systems involved. Fuel for a natural uranium reactor is obtainable indigenously. Enrichment processes are considered, and the economic possibility of establishing a plant in Australia is thought to be increasing. The place of fast breeder reactors in future developments is outlined and possible consequences of nuclear power production such as agro-industrial complexes incorporating desalination plants are mentioned. (Australia)

Operation and Economics

31463 (DOCKET-1155–113) LA CROSSE BOILING WATER REACTOR. Order Extending Provisional Operating Authorization Expiration Date. (Division of Reactor Licensing (AEC), Washington, D. C.). 28 Apr 1971. 2p. Dep. NTIS.

31464 (DOCKET-50010–85) DRESDEN NUCLEAR POWER STATION, UNIT 1. Examination of the Crack in the 4-Inch Cleanup-Demineralizer Piping. Final Report. (Battelle Memorial Inst., Columbus, Ohio). 29 Mar 1971. 29p. Dep. NTIS. For Commonwealth Edison Co., Chicago, Ill.

31465 (DOCKET-50029–150) YANKEE NUCLEAR POWER STATION. Operation Report No. 123, March 1971. (Yankee Atomic Electric Co., Westboro, Mass.). 22 Apr 1971. 7p. Dep. NTIS.

31466 (DOCKET-50146–72) SAXTON REACTOR. Operating Experience Report, September 1, 1970–February 28, 1971. (Saxton Nuclear Experimental Corp., Pa.). 27 Apr 1971. 50p. Dep. NTIS.

XUM

31467 (DOCKET-50155-81) BIG ROCK POINT NUCLEAR PLANT. Quarterly Operations Report No. 80, January-March 1971. (Consumers Power Co., Jackson, Mich.). 29 Apr 1971. 30p. Dep. NTIS.

31468 (DOCKET-50213-105) CONNECTICUT YANKEE ATOMIC POWER PLANT. Operation Report No. 71-3, March 1971. (Connecticut Yankee Atomic Power Co., Haddam). 26 Apr 1971. Contract AT(30-1)-3250. 13p. (NYO-3250-58). Dep. NTIS.

31469 (DOCKET-50237-147) DRESDEN NUCLEAR POWER STATION, UNIT 2. Semiannual Report, July 1-December 31, 1970. (Commonwealth Edison Co., Chicago, Ill.). 3 Mar 1971. 74p. Dep. NTIS.

31470 (DOCKET-50237-157) DRESDEN NUCLEAR POWER STATION, UNIT 2. Summary Technical Report of Secondary Containment Leak Rate Test, February 25, 1971. (Commonwealth Edison Co., Chicago, Ill.). 27 Apr 1971. 4p. Dep. NTIS.

31471 (DOCKET-50237-158) DRESDEN NUCLEAR POWER STATION, UNIT 2. Solid Waste Activity for Second Half of 1970. (Commonwealth Edison Co., Chicago, Ill.). 3 May 1971. 3p. Dep. NTIS.

Information is presented for solid radioactive waste shipments during August to December 1970. (D.C.C.)

31472 (DOCKET-50237-159) DRESDEN NUCLEAR POWER STATION, UNIT 2. Failure of Diesel Generator to Start Following Automatic Initiation Signal. (Commonwealth Edison Co., Chicago, Ill.). 29 Apr 1971. 2p. Dep. NTIS.

31473 (DOCKET-50237-160) DRESDEN NUCLEAR POWER STATION, UNIT 2. Damage to Seismic Restraints on Core Spray Subsystem. (Commonwealth Edison Co., Chicago, Ill.). 29 Apr 1971. 2p. Dep. NTIS.

31474 (DOCKET-50244-70) ROBERT EMMETT GINNA NUCLEAR POWER PLANT, UNIT NO. 1. Failure of Valves 826 A, 826 B, 826 C, and 826 D to Open. (Rochester Gas and Electric Corp., N. Y.). 29 Apr 1971. 2p. Dep. NTIS.

Failure of the valves 826 A, B, C, and D between the concentrated boric acid tanks and the safety injection pumps to open during a diesel generator load and safeguard sequence test is described. Corrective actions are discussed. (D.C.C.)

31475 (DOCKET-50263-67) MONTICELLO NUCLEAR GENERATING PLANT, UNIT 1. High Pressure Coolant Injection System Outage. (Northern States Power Co., Minneapolis, Minn.). 28 Apr 1971. 2p. Dep. NTIS.

31476 (DOCKET-50263-68) MONTICELLO NUCLEAR GENERATING PLANT, UNIT 1. Abnormal Occurrence Report: Inoperability of the Air Ejector Off-Gas System Radiation Monitors. (Northern States Power Co., Minneapolis, Minn.). 29 Apr 1971. 3p. Dep. NTIS.

31477 (DOCKET-50263-69) MONTICELLO NUCLEAR GENERATING PLANT, UNIT 1. Abnormal Occurrence Report: Safety/Relief Valve Settings Exceeding 1080 PSIG. (Northern States Power Co., Minneapolis, Minn.). 30 Apr 1971. 3p. Dep. NTIS.

31478 (DOCKET-50266-47) POINT BEACH NUCLEAR PLANT, UNIT 1. Abnormal Occurrence Report: Failure of Containment Sump Valves to Open. (Wisconsin Electric Power Co., Milwaukee). 26 Apr 1971. 2p. Dep. NTIS.

31479 (TID-25698) GUNDREMMINGEN NUCLEAR POWER PLANT MONTHLY REPORT, JANUARY 1971. (Kernkraftwerk RWE-Bayernwerk G.m.b.H., Gundremmingen (West Germany)). 19 Feb 1971. 42p. (In German). Dep. NTIS.

The plant was run at full load without restrictions. At the beginning of the month the start-up transformer failed owing to a defective step switch, so that there was no start-up voltage until a stand-by transformer from the RWE grid could be set up. Increased attention was paid to the action-readiness of the emergency diesel during this period. The shipping of depleted fuel elements to Mol continued. At the end of the month the transportation of solid waste to Asse was commenced. A start was also made on the modifications to the access to the controlled area. The activity of the reactor water and waste gas remained at a constant low level. (auth)

31480 NUCLEAR CHARGE AND START-UP OF THE FRENCH REACTOR SL-1, PROTOTYPE OF THE VANDELLOS NUCLEAR POWER PLANT. Palop, M. Perello (Junta de Energia Nuclear, Madrid). Energ. Nucl. (Madrid); 14: 375-89(Sep-Oct 1970). (In Spanish).

The final construction phase and the start-up of the integrated graphite-gas reactor SL-1 are reported. The principal events, both positive and negative, during the period of supply to the grid of the power are summarized. The accident which arrested its progress and created power elevation close to its nominal value is described. (tr-auth)

31481 SELECTION AND TRAINING OF NUCLEAR POWER PERSONNEL. ANSI SC-N18.1 1971. Hinsdale, Ill.; American Nuclear Society (1971). 25p. Available from American Nuclear Society, Hinsdale, Ill.

Criteria for the selection and training of personnel for stationary nuclear power plants are presented. The qualifications, responsibilities, and training of personnel in operating and support organizations appropriate for the safe and efficient operation of nuclear power plants are described. Test, mobile and experimental reactors as well as reactors not subject to Atomic Energy Commission licensing are excluded because of differences in operational practices and contractual requirements. (auth)

Safety and Siting

Refer also to abstract 29525.

31482 (AECL-3740) POWER-REACTOR SITING IN VARIOUS COUNTRIES. Hake, G.; Palmer, J. F. (Atomic Energy of Canada Ltd., Chalk River (Ontario)). Nov 1971. 13p. (CONF-701106-6). Dep. NTIS (U. S. Sales Only). AECL $0.50.

From fifth annual midyear topical symposium on health physics aspects of nuclear facility siting; Idaho Falls, Idaho (3 Nov 1970).

There is a lack of firm definition by any country of the policy by which it finally approves a site. Even so, there appears to be a measure of agreement between countries in deciding: (1) The upper limit of credibility of accidental events to be accommodated by the design. (2) The acceptable level of the hazards to the environment under abnormal or accidental circumstances. (3) The confidence required in the performance of devices for limiting the consequences of abnormal or accidental situations. Interesting problems might arise in siting a station near the border between two countries. The particular case of siting near the Canada-U. S. border is discussed briefly. (11 references.) (auth)

31483 (DOCKET-50003-68) INDIAN POINT STATION, UNIT NO. 1. Facility Design Changes. (Consolidated Edison Co. of New York, Inc., New York). 14 Apr 1971. 2p. Dep. NTIS.

Design modifications described include: installation of two thermocouples in cooling system lines for monitoring thermal cycling; installation of filters in compressed air lines for pneumatically-operated containment isolation valves; and change of overhead electrical feeder lines to underground electrical feeder lines. (D.C.C.)

31484 (DOCKET-50016-110) ENRICO FERMI ATOMIC POWER PLANT, UNIT 1. Change No. 25 to Technical Specifications of Provisional Operating License No. DPR-9. (Division of Reactor Licensing (AEC), Washington, D. C.). 24 Apr 1971. 1p. Dep. NTIS.

Revised experience requirements for the position of Plant Superintendent are presented. Provisions for an Assistant Plant Superintendent are described. (D.C.C.)

31485 (DOCKET-50146-73) SAXTON REACTOR. License No. DPR-4; Technical Specifications Change Request No. 43. (Saxton Nuclear Experimental Corp., Pa.). 29 Apr 1971. 4p. Dep. NTIS.

Revised technical specifications are presented concerning the use of sealed Zircaloy-4 tubes with stainless steel specimens. The tubes are pressurized for 1500 psig or less operation. (D.C.C.)

31486 (DOCKET-50155-80) BIG ROCK POINT NUCLEAR PLANT. Corrective Actions to Starting Failure of Emergency Generator. (Consumers Power Co., Jackson, Mich.). 21 Apr 1971. 3p. Dep. NTIS.

31487 (DOCKET-50171-84) PEACH BOTTOM ATOMIC POWER STATION, UNIT 1. Change No. 14 to Technical Specifications of Provisional Operating License No. DPR-12. (Division of Reactor Licensing (AEC), Washington, D. C.). 23 Apr 1971. 2p. Dep. NTIS.

Authorization for revised fuel loading specifications for the

FPTE and revised surveillance requirements for control rods is presented. (D.C.C.)

31488 (DOCKET-50206-112) SAN ONOFRE NUCLEAR GENERATING STATION, UNIT 1. Provisional Operating License No. DPR-13, Amendment 23. Additional Information in Support of Proposed Change No. 4 to Technical Specifications. (Southern California Edison Co., Los Angeles). 30 Apr 1971. 8p. Dep. NTIS.

Additional information is presented concerning the limiting control rod insertion limit curves for Cycle 2 operation. (D.C.C.)

31489 (DOCKET-50237-156) DRESDEN NUCLEAR POWER STATION, UNIT 2. Special Reports Nos. 10-13 on Topics Requested by AEC. (Commonwealth Edison Co., Chicago, Ill.). 21 Apr 1971. 83p. Dep. NTIS.

Additional information is presented on the following topics: in-service inspection of sensitized stainless steel safe-ends of core spray system; clarification of low pressure injection valve malfunction; torus paint; and core spray water hammer incident. (D.C.C.)

31490 (DOCKET-50237-161) DRESDEN NUCLEAR POWER STATION, UNIT 2. Additional Information Regarding Corrective Action on Standby Liquid Control System. (Commonwealth Edison Co., Chicago, Ill.). 3 May 1971. 2p. Dep. NTIS.

31491 (DOCKET-50245-64) MILLSTONE NUCLEAR POWER STATION, UNIT 1. Establishment of Preoperational Environmental Survey Program. (Millstone Point Co., Wethersfield, Conn.). 16 Oct 1969. 1p. Dep. NTIS.

31492 (DOCKET-50249-65) DRESDEN NUCLEAR POWER STATION, UNIT 3. Facility Operating License No. DPR-25; Correction to Proposed Change No. 2 to Appendix A. (Commonwealth Edison Co., Chicago, Ill.). 26 Apr 1971. 1p. Dep. NTIS.

A correction related to the in-service inspection program technical specifications is presented. (D.C.C.)

31493 (DOCKET-50254-35) QUAD-CITIES STATION, UNITS 1 AND 2. Additional Information on Financial Qualifications. (Commonwealth Edison Co., Chicago, Ill.). 22 Apr 1971. 2p. (DOCKET-50265-32). Dep. NTIS.

31494 (DOCKET-50255-38) PALISADES PLANT. Detailed Statement on the Environmental Considerations. (Division of Reactor Licensing (AEC), Washington, D. C.). 7 Apr 1971. 189p. Dep. NTIS.

Information concerning chemical, radioactive, and thermal discharges from the reactor is presented. The effects of reactor operations on the environment are analyzed. (D.C.C.)

31495 (DOCKET-50263-63) MONTICELLO NUCLEAR GENERATING PLANT, UNIT 1. Design Report: Recirculation System. (General Electric Co., San Jose, Calif. Atomic Power Equipment Dept.). 1 Apr 1970. 50p. Dep. NTIS.

For Northern States Power Co., Minneapolis, Minn.

31496 (DOCKET-50263-64) MONTICELLO NUCLEAR GENERATING PLANT, UNIT 1. Stress Analysis Review Report. (Bechtel Corp., San Francisco, Calif.). 8 Oct 1970. 50p. Dep. NTIS.

For Northern States Power Co., Minneapolis, Minn.

A complete review of the stress analysis for the piping systems inside primary containment is presented. (D.C.C.)

31497 (DOCKET-50263-65) MONTICELLO NUCLEAR GENERATING PLANT, UNIT 1. Stagnant Water or Low Steam Flow in Reactor Coolant System. ([General Electric Co., San Jose, Calif. Atomic Power Equipment Dept.]). 21 Apr 1970. 9p. Dep. NTIS.

For Northern States Power Co., Minneapolis, Minn.

Information is presented concerning modifications to high points in non-flowing parts of the cooling system to vent or otherwise remove trapped gases. (D.C.C.)

31498 (DOCKET-50263-66) MONTICELLO NUCLEAR GENERATING PLANT, UNIT 1. Change No. 1 to Technical Specifications of Provisional Operating License No. DPR-22. (Division of Reactor Licensing (AEC), Washington, D. C.). 28 Apr 1971. 8p. Dep. NTIS.

Revised technical specifications concerning protection factors for personnel respiratory equipment are presented. (D.C.C.)

31499 (DOCKET-50269-17) OCONEE NUCLEAR STATION, UNITS 1, 2, AND 3. Preliminary Safety Analysis Report, Amendment 13 (Includes Final Safety Analysis Report, Rev. 6). (Duke Power Co., Charlotte, N. C.). 26 Jun 1970. 7p. (DOCKET-50270-17; DOCKET-50287-14). Dep. CFSTI.

Additional information is presented concerning seismic analysis of piping systems, reactor vessel material surveillance program, control rod drive test program, and computer codes and methods for coolant loss accident analysis. (D.C.C.)

31500 (DOCKET-50271-50) VERMONT YANKEE NUCLEAR POWER STATION. Preliminary Safety Analysis Report, Amendment 25. (Vermont Yankee Nuclear Power Corp., Rutland). 16 Apr 1971. 10p. Dep. NTIS.

Safety analysis of PuO_2-UO_2 fuel elements in the Vermont Yankee Power Reactor is presented. (D.C.C.)

31501 (DOCKET-50271-51) VERMONT YANKEE NUCLEAR POWER STATION. Preliminary Safety Analysis Report, Amendment 26. (Vermont Yankee Nuclear Power Corp., Rutland). 27 Apr 1971. 57p. Dep. NTIS.

Revised and additional data are presented concerning reactor core vibration testing, plant security, plant operation on single recirculation loop with the equalizer line closed, energy absorbing equipment for piping systems, primary containment system, and abnormal operational transients. (D.C.C.)

31502 (DOCKET-50277-19) PEACH BOTTOM ATOMIC POWER STATION, UNITS 2 AND 3. Preliminary Safety Analysis Report, Amendment 8 (Includes Additions and Revisions to Final Safety Analysis Report). (Philadelphia Electric Co., Pa.). 22 Apr 1971. 400p. (DOCKET-50278-19). Dep. NTIS.

Meteorological and hydrological data for the reactor sites are presented. Environmental radiation survey measurements are listed. Stress testing and fabrication requirements for pressure vessel and piping systems are presented. (D.C.C.)

31503 (DOCKET-50280-39) SURRY POWER STATION, UNITS 1 AND 2. Preliminary Safety Analysis Report, Amendment 21 (Includes Additions and Revisions to Final Safety Analysis Report, Part B). (Virginia Electric and Power Co., Richmond). 3 May 1971. 335p. (DOCKET-50281-39). Dep. NTIS.

Tests and inspection requirements for the pressure vessel and primary cooling system are presented. Revised technical specifications are included. Additional data requested by the Division of Reactor Licensing are also presented. (D.C.C.)

31504 (DOCKET-50309-34) MAINE YANKEE ATOMIC POWER STATION. Preliminary Safety Analysis Report, Amendment 23. (Maine Yankee Atomic Power Co., Westboro, Mass.). 5 May 1971. 133p. Dep. NTIS.

Revised design parameters of the Maine Yankee Power Reactor are presented. Included also are additional data on the reactor requested by the Division of Reactor Licensing. (D.C.C.)

31505 (DOCKET-50312-19) RANCHO SECO NUCLEAR GENERATING STATION, UNIT 1. Preliminary Safety Analysis Report, Amendment 5 (Includes Revised License Application). (Sacramento Municipal Utility District, Calif.). 1 May 1971. 33p. Dep. NTIS.

Financial data on the owners of the Rancho Seco Power Reactor are presented in support of the application for construction permit and operating license. The 1970 Annual Report for the Sacramento Municipal Utility District is included. (D.C.C.)

31506 (DOCKET-50312-20) RANCHO SECO NUCLEAR GENERATING STATION, UNIT 1. Preliminary Safety Analysis Report, Amendment 5 (Includes Final Safety Analysis Report, Vol. 1). (Sacramento Municipal Utility District, Calif.). 1 May 1971. 378p. Dep. NTIS.

Information on Rancho Seco Power Reactor is presented under the following broad topics: site and environment; reactor; and reactor coolant. (D.C.C.)

31507 (DOCKET-50312-21) RANCHO SECO NUCLEAR GENERATING STATION, UNIT 1. Preliminary Safety Analysis Report, Amendment 5 (Includes Final Safety Analysis Report, Vol. 2). (Sacramento Municipal Utility District, Calif.). 1 May 1971. 299p. Dep. NTIS.

Information on Rancho Seco Power Reactor is presented under the following broad topics: structures and containment system; safety features; and instrumentation and controls. (D.C.C.)

31508 (DOCKET-50312-22) RANCHO SECO NUCLEAR GENERATING STATION, UNIT 1. Preliminary Safety Analysis Report, Amendment 5 (Includes Final Safety Analysis Report, Vol. 3). (Sacramento Municipal Utility District, Calif.). 1 May 1971. 324p. Dep. NTIS.

XUM

Information on Rancho Seco Power Reactor is presented under the following broad topics: electrical systems; auxiliary and emergency systems; steam and power conversion system; radioactive waste and radiation protection; conduct of operations; and initial tests and operations. (D.C.C.)

31509 (DOCKET-50312-23) RANCHO SECO NUCLEAR GENERATING STATION, UNIT 1. Preliminary Safety Analysis Report, Amendment 5 (Includes Final Safety Analysis Report, Vol. 4). (Sacramento Municipal Utility District, Calif.). 1 May 1971. 772p. Dep. NTIS.

Information on Rancho Seco Power Reactor is presented under the following broad topics: safety analysis; technical specifications; quality assurance program; and site meteorology, geology, and seismology. (D.C.C.)

31510 (DOCKET-50312-24) RANCHO SECO NUCLEAR GENERATING STATION, UNIT 1. Preliminary Safety Analysis Report, Amendment 5 (Includes Final Safety Analysis Report, Vol. 5). (Sacramento Municipal Utility District, Calif.). 1 May 1971. 187p. Dep. NTIS.

Information on Rancho Seco Power Reactor is presented under the following topics: seismic design bases; turbine generator missiles; tritium management for normal operation; iodine spray removal effectiveness; hydrogen purging; and radiation sources. (D.C.C.)

31511 (DOCKET-50313-26) ARKANSAS NUCLEAR ONE, UNIT 1. Preliminary Safety Analysis Report, Amendment 20 (Includes Revised License Application). (Arkansas Power and Light Co., Little Rock). 19 Apr 1971. 63p. Dep. NTIS.

Financial data on the owners of the Arkansas Nuclear One Power Reactor are given in support of the application for construction permit and operating license. The 1970 Annual Report for the Arkansas Power and Light Company is included. (D.C.C.)

31512 (DOCKET-50313-27) ARKANSAS NUCLEAR ONE, UNIT 1. Preliminary Safety Analysis Report, Amendment 20 (Includes Final Safety Analysis Report, Vol. 1). (Arkansas Power and Light Co., Little Rock). 19 Apr 1971. 400p. Dep. NTIS.

Information on the Arkansas Nuclear One Power Reactor is presented under the following broad topics: site and environment; reactor; reactor coolant system; and structures. (D.C.C.)

31513 (DOCKET-50313-28) ARKANSAS NUCLEAR ONE, UNIT 1. Preliminary Safety Analysis Report, Amendment 20 (Includes Final Safety Analysis Report, Vol. 2). (Arkansas Power and Light Co., Little Rock). 19 Apr 1971. 479p. Dep. NTIS.

Information on the Arkansas Nuclear One Power Reactor is presented under the following broad topics: engineered safeguards; instrumentation and control; electrical systems; auxiliary and emergency systems; steam and power conversion system; radioactive waste and radiation protection; conduct of operations; initial tests and operations; safety analysis; and technical specifications. (D.C.C.)

31514 (DOCKET-50313-29) ARKANSAS NUCLEAR ONE, UNIT 1. Preliminary Safety Analysis Report, Amendment 20 (Includes Final Safety Analysis Report, Vol. 3). (Arkansas Power and Light Co., Little Rock). 19 Apr 1971. 157p. Dep. NTIS.

Information on Arkansas Nuclear One Power Reactor is presented under the following broad topics: piping and equipment design; technical qualifications; meteorology; and structures. (D.C.C.)

31515 (DOCKET-50324-20) BRUNSWICK STEAM ELECTRIC PLANT, UNITS 1 AND 2. Preliminary Safety Analysis Report, Amendment 11. (Carolina Power and Light Co., Raleigh, N. C.). 23 Apr 1971. 2p. (DOCKET-50325-20). Dep. NTIS.

Revised completion dates for the construction permit and operating license applications are presented. (D.C.C.)

31516 (DOCKET-50331-25) DUANE ARNOLD ENERGY CENTER. Environmental Report. (Iowa Electric Light and Power Co., Cedar Rapids). 30 Apr 1971. 249p. Dep. NTIS.

Information concerning chemical, radioactive, and thermal discharges from the reactor is presented. The effects of reactor operations on the environment are analyzed. (D.C.C.)

31517 (DOCKET-50335-18) HUTCHINSON ISLAND PLANT, UNIT NO. 1. Preliminary Safety Analysis Report, Amendment 10. (Florida Power and Light Co.). 27 Apr 1971. 15p. Dep. NTIS.

Additional information is presented on the sizing and testing of diesel generator sets to be used as emergency power supply system. (D.C.C.)

31518 (DOCKET-50344-20) TROJAN NUCLEAR PLANT. Additional Information Requested by AEC. (Portland General Electric Co., Oreg.). 23 Apr 1971. 18p. Dep. NTIS.

31519 (DOCKET-50352-12) LIMERICK GENERATING STATION, UNITS 1 AND 2. Preliminary Safety Analysis Report, Amendment 6. (Philadelphia Electric Co., Pa.). 3 May 1971. 224p. (DOCKET-50353-12). Dep. NTIS.

Hydrological and meteorological data for the reactor site are presented. Information on the radioactive waste systems, dose calculations for accident conditions, and classification of piping systems is included. Additional data on the reactor requested by the Division of Reactor Licensing are also included. (D.C.C.)

31520 (DOCKET-50358-14) WM. H. ZIMMER NUCLEAR POWER STATION, UNIT 1. Preliminary Safety Analysis Report, Amendment 7. (Cincinnati Gas and Electric Co., Ohio. Columbus and Southern Ohio Electric Co., Columbus, Ohio. Dayton Power and Light Co., Ohio). 27 Apr 1971. 456p. Dep. NTIS.

Revised design parameters of the William H. Zimmer Power Reactor Unit 1 are presented. Included also are additional data on the reactor requested by the Division of Reactor Licensing. (D.C.C.)

31521 (DOCKET-50368-9) ARKANSAS NUCLEAR ONE, UNIT 2. Preliminary Safety Analysis Report, Amendment 4. (Arkansas Power and Light Co., Little Rock). 13 Apr 1971. 292p. Dep. NTIS.

Revised design parameters of the Arkansas Nuclear One Power Reactor Unit 2 are presented. Included also are additional data on the reactor requested by the Division of Reactor Licensing. (D.C.C.)

31522 (DOCKET-50369-8) McGUIRE NUCLEAR STATION, UNITS 1 AND 2. Preliminary Safety Analysis Report, Amendment 4. (Duke Power Co., Charlotte, N. C.). 22 Apr 1971. 193p. (DOCKET-50370-7). Dep. NTIS.

Revised design parameters of the McGuire Power Reactor Units 1 and 2 are presented. Included also are additional data on the reactor requested by the Division of Reactor Licensing. (D.C.C.)

31523 (DOCKET-50376-10) AGUIRRE NUCLEAR PLANT, UNIT NO. 1. Preliminary Facility Description and Safety Analysis Report, Amendment 4, Vol. 1. (Puerto Rico Water Resources Authority, San Juan). 4 May 1971. 614p. Dep. NTIS.

Additional information requested by the Division of Reactor Licensing is presented. (D.C.C.)

31524 (DOCKET-50376-11) AGUIRRE NUCLEAR PLANT, UNIT NO. 1. Preliminary Facility Description and Safety Analysis Report, Amendment 4, Vol. 2. (Puerto Rico Water Resources Authority, San Juan). 4 May 1971. 528p. Dep. NTIS.

Revised and additional data on the design parameters and operations aspects of the Aguirre Power Reactor Unit 1 are presented. (D.C.C.)

31525 (NP-18770) STATE ROLE IN THERMAL POWER PLANT SITING. A Report to the State of Washington. Blanc, Gene A. (Reid, Batchelor and Associates, Inc., San Francisco, Calif.). [22 Jun 1970]. 36p.

Recommendations are presented regarding the State of Washington thermal power plant siting policy and procedures. The basic policy provisions are intended to protect the environment and to encourage construction of nuclear power plants. The establishment of a Washington State Power Plant Siting Task Force, site evaluation factors, and long term studies are recommended. (H.D.R.)

31526 (TID-25697) SAFETY GUIDES FOR WATER COOLED NUCLEAR POWER PLANTS. (Division of Reactor Standards (AEC), Washington, D. C.). 2 Nov 1970. 48p. Dep. NTIS.

Guides are presented which are intended to identify specific safety issues that should be considered in the design and in the evaluation of water cooled nuclear power plants and to describe a set of principles and specifications which, if satisfied, will represent an acceptable solution of these issues to the U. S. AEC regulatory staff and the Advisory Committee on Reactor Safeguards. The guides include: (1) Net Positive Suction Head for Emergency Core Cooling and Containment Heat Removal System Pumps; (2) Thermal Shock to Reactor Pressure Vessels; (3) Assumptions Used for Evaluating the Potential Radiological Consequences of a Loss of Coolant Accident for Boiling Water Reactors; (4) Assumptions Used for Evaluating the Potential Radiological Consequences of a Loss of Coolant Accident for Pressurized Water Reactors; (5) Assumptions Used for Evaluating the Potential Ra-

diological Consequences of a Steam Line Break Accident for Boiling Water Reactors; (6) Independence Between Redundant Standby (Onsite) Power Sources and Between Their Distribution Systems; (7) Control of the Combustible Gas Concentrations in Containment Following a Loss of Coolant Accident; (8) Personnel Selection and Training; (9) Selection of Diesel Generator Set Capacity for Standby Power Supplies; (10) Mechanical (Cadweld) Splices in Reinforcing Bars of Concrete Containments; (11) Instrument Lines Penetrating Primary Reactor Containment; (12) Instrumentation for Earthquakes; and (13) Fuel Storage Facility Design Basis. (H.D.R.)

31527 BIOLOGICAL ASPECTS OF THERMAL POLLUTION. I. ENTRAINMENT AND DISCHARGE CANAL EFFECTS. Coutant, Charles C. (Oak Ridge National Lab., Tenn.). CRC Crit. Rev. Radiol. Sci.; 1: 341-81(Nov 1970).

Some thermal effects on fish and other aquatic organisms seen at operating thermal power plants are critically evaluated. The presentation concentrates on two areas of ecological effects in the condenser cooling sequence: (1) the condensers and outlet piping; and (2) the discharge canal. Results of ecological field studies at power plants are emphasized and only those laboratory data which appear directly pertinent to effects observed in the field are examined. 140 references. (H.D.R.)

31528 QUALITY ASSURANCE: A REALISTIC APPRAISAL. Lingafelter, Jack; Naymark, Sherman; Pashos, Thomas (Nuclear Services Corp., San Jose, Calif.). Nucl. News; 14: 40-2 (May 1971).

Quality assurance programs for nuclear power plants are reviewed. Organizational requirements and limitations are discussed. (D.C.C.)

31529 PREDICTION OF DAMAGES IN REACTOR PLANTS. de Jong, Karl-Heinz (Zeitschrift Technische Ueberwachung, Duesseldorf). Tech. Ueberwach.; 10: 403-4(Dec 1969). (In German).

The concept of maximum credible accident appears not quite satisfactory for assessing the safety of a nuclear power plant. Therefore, the Institute for Reactor Safety in Essen proposes a calculable probability for risk. This idea introduces a new philosophy into considerations of reactor safety. (tr-auth)

31530 RISK ESTIMATION MODEL IN RADIATION ACCIDENTS AT THE ATOMIC ENERGY STATION. Bobrovnikov, O. P. (Inst. of Biophysics, Moscow). pp 39-44 of Diffusion des Produits de Fission, Montrouge, France; Societe Francaise de Radioprotection (1970).

From International congress on the diffusion of fission products; Saclay, France (4 Nov 1969). See CONF-691104.

A model for estimating the maximum risk is described based on the analysis of maximum AES radiation discharge (including all possible accidental discharges). Assessment of such a value makes it possible to estimate the real hazard from radiation accidents and to take appropriate measures. At the same time this value can be used in the design of atomic energy facilities and the prediction of radiation conditions in the AES environment. (auth) (France)

31531 NUCLEAR POWER: THE SOCIAL CONFLICT. Tsivoglou, Ernest C. (Georgia Inst. of Tech., Atlanta). Environ. Sci. Technol.; 5: 404-10(May 1971).

The sources of radioactive gaseous and liquid wastes from operation of nuclear power plants are examined. Human exposure routes from release of these wastes to the environment are described. The standard gaseous waste treatment systems of water cooled reactors are described, and the potential radiation hazard from nuclear power plant operation and nuclear fuel reprocessing is discussed. The costs of pollution control in the nuclear power industry are examined. (H.D.R.)

Steam and Power Conversion Systems

Refer also to abstract 31623.

31532 (BAW-10027) ONCE-THROUGH STEAM GENERATOR RESEARCH AND DEVELOPMENT REPORT (NONPROPRIETARY VERSION OF BAW-10002). (Babcock and Wilcox Co., Lynchburg, Va. Power Generation Div.). Apr 1971. 124p. Dep. NTIS.

The original research and development tests and results for the once-through steam generator (OTSG) are presented. Additional information on research and development of the OTSG as requested by the U.S.A.E.C. pursuant to their review of the operating license application for the first nuclear station to utilize OTSG units is summarized. The vibration pluck tests on an as-built OTSG and the test results are described. (auth)

Power Reactor Development

31533 (ANL-7798) REACTOR DEVELOPMENT PROGRAM PROGRESS REPORT, MARCH 1971. (Argonne National Lab., Ill.). Contract W-31-109-eng-38. 147p. Dep. NTIS.

Highlights of project activities for March 1971 are summarized. The EBR-2 operations, fuels and materials studies, and engineering development activities are reported. Long-term high-temperature stability and radiation effects on candidate materials for LMFBR instruments were tested. Activities in the development of sodium sampling and analytical methods are described. LMFBR fuel cycle development concentrated on the demonstration of a continuous fluid-bed denitration process for converting uranium/plutonium nitrate solutions to mixed oxide powders. Various physics experiments were conducted in the ZPPR, ZPR-6, and ZPR-9 assemblies in support of FFTF development. Analytical and experimental LMFBR safety studies are described. Environmental activities included thermal plume dispersion studies and the development of circulation models of Lake Michigan. (H.D.R.)

31534 (WASH-1175) SOVIET POWER REACTORS: 1970. Report of the United States of America Nuclear Power Reactor Delegation Visit to the Union of Soviet Socialist Republics, June 15-July 1, 1970. (Division of Reactor Development and Technology (AEC), Washington, D. C.). Aug 1970. 113p. GPO $1.00.

The U.S. delegation toured U.S.S.R. reactor facilities and research institutions in a reciprocal visit on nuclear power. Detailed descriptions of the reactor disciplines and reactor projects are presented from knowledge gained by discussions with technical staffs and by observations of the facilities involved. The development programs and accomplishments in sodium-cooled fast breeder and water-cooled reactors are described. (H.D.R.)

31535 HTR AND GAS BREEDERS: A COMPARISON. TECHNICAL AND SCIENTIFIC ASPECTS OF THE DEVELOPMENT OF FAST GAS-COOLED REACTORS. della Loggia, V. E. (Atomic Energy Establishment, Winfrith, Eng.). Atomwirt., Atomtech.; 16: 86-9(Feb 1971). (In German).

Because of the fact that gas-cooled fast reactors resemble in many respects high-temperature reactors, the problem arises to which degree high-temperature reactor concepts can be applied to gas breeders. An analysis of cooling medium, fuel elements, and major components leads to the conclusion that a relatively minor developmental effort would be necessary for achieving a gas-cooled high-temperature reactor. Even with restriction to presently existing and established technology, without much further development, a gas breeder appears realistic. Its cost would be comparable to that of a sodium breeder. 8 references. (H.B.G.)

31536 GENERAL SITUATION OF THE DEVELOPMENT OF FAST BREEDERS AND THE PROTOTYPE REACTOR SNR 300. Haefele, Wolf (Gesellschaft fuer Kernforschung mbH, Karlsruhe, Ger.). At. Strom; 17: 40-5(Feb-Mar 1971). (In German).

For Belgium, the Netherlands, Luxembourg, and Germany, the major goal of fast breeder reactor development represents the construction of the sodium-cooled fast breeder reactor SNR 300. With conclusion of experimental and theoretical studies, actual construction should start in April 1972. Under the assumption of a construction time of five years, the SNR 300 should be ready for test operations in 1977. During the past year, two major developments occurred: as proposed by the contractor, a non-spherical concrete building was accepted for containment; because of the higher population density in the previously planned reactor site, the commission for reactor safety raised objections, hence, a new site was selected at Kalkar near Kleve on the lower Rhine river. The status of international development concerning fast breeders is discussed comprehensively. (H.B.G.)

31537 FREEZING EXPERIMENTS ON AUSTENITIC TUBES OF THE MZFR. Witt, K. (Kernkraftwerk-Betriebsgesellschaft mbH, Leopoldshafen, Ger.). Atomwirt., Atomtech.; 16: 229-32 (May 1971). (In German).

For emergency blocking of tubes, formed by austenitic material, freezing of the involved sections proved most efficient for repairs on the Karlsruhe MZFR reactor and on Canadian D_2O reactors. Liquid nitrogen was used as the medium for freezing. To study the process of freezing and the solidity of blocking, operators of the MZFR performed freezing experiments on tubes of various cross sections. Characteristics of the ice block were investigated with respect to temperature, pressure, and stresses. (tr-auth)

31538 PROGRESS OF THE FAST BREEDER PROJECT AT KARLSRUHE. Engelmann, P. (Kernforschungszentrum, Karlsruhe, Ger.). Atomwirt., Atomtech.; 16: 251-5(May 1971). (In German).

XUM

An annual report for the year 1970 presents the work done within the fast breeder project at Karlsruhe. Mainly, studies concerned fundamentals for design and development of sodium-cooled fast breeder reactors with oxide and carbide fuel elements. To this section, more than three-fourths of the budget was devoted; the remainder was distributed between the FR 3 studies and work on gas and steam breeders. (H.B.G.)

31539 300 MW THORIUM HIGH-TEMPERATURE POWER PLANT (THTR). Harder, H. (BBC/Krupp Reaktorbau GmbH, Cologne); Oehme, H.; Schoening, J.; Thurnher, K. Atomwirt., Atomtech.; 16: 238-45(May 1971). (In German).

The 300 MW(e) THTR is designed for the purpose of gaining experience with high-temperature reactors possessing high power. The prototype plant represents a decisive step in the realization of the high-temperature reactor construction concept. Uentrop offers a favorable site for construction and operation. The construction period essentially is determined through application of new techniques, especially concerning the prestressed concrete container, the shutdown system, and the refueling system. Nuclear safety is especially high because of low excess reactivity, low radioactivity content of circuits, and complete integration of the helium primary circuit with the core. Presented are project programming, overall design, reactor components, fuel elements, and safety. (H.B.G.)

31540 PRESENT STATUS AND FUTURE DEVELOPMENT OF THE THTR IN THE FEDERAL REPUBLIC OF GERMANY. Schwarz, D. (Vereinigte Elektrizitaetswerke Westfalen AG, Dortmund, Ger.); Schweiger, F. Atomwirt., Atomtech.; 16: 235-7(May 1971). (In German).

Experience with the AVR experimental power reactor confirmed principally the advantages of this reactor type. Further development will make possible economical electric current production through steam turbines in indirect circuits. Because of the fact that realization of the THTR is not only a question of technical possibilities but also of timing, construction of the THTR 300 was accelerated. (tr-auth)

Kinetics and Dynamics

Refer also to abstracts 31568 and 31657.

31541 (EUR-4497) COSTAX-BOIL: A COMPUTER PROGRAMME OF THE COSTANZA SERIES FOR THE AXIAL DYNAMICS OF BWR AND PWR NUCLEAR REACTORS. Forti, G. (European Atomic Energy Community, Ispra (Italy). Joint Nuclear Research Center). 1970. 58p. Dep. NTIS (U. S. Sales Only). EUR FF 9.45.

Costax-Boil is a FORTRAN programme for transient analysis of BWR in the time domain. It couples the two velocity groups neutron diffusion kinetic calculations (up to 10 delayed neutron groups) in one dimension (axial) with the heat conduction equations in the fuel rods and a two phase flow dynamics calculation for the typical coolant channel. Doppler and void reactivity feedback are accounted for pointwise. A flexible input allows representation of reactivity transients, flow recirculation or inlet enthalpy transients, or an arbitrary mixture of them, including control rod bank movement. No pressure variation is possible in the present version. The programme is intended for the analysis of intermediate accidents or severe operational transients in which a detailed spatial representation is essential. (3 references) (auth)

31542 (EURFNR-813) INHERENT STABILITY OF THE STEAM-COOLED BREEDER. Frisch, W.; Huebschmann, W. (Kernforschungszentrum, Karlsruhe (West Germany)). Translation of report KFK-851. 26p. Dep. NTIS.

Work Performed under United States-Euratom Fast Reactor Exchange Program.

The stability of the uncontrolled steam-cooled fast breeder reactor is investigated theoretically. This reactor permits oscillations of the power and the steam pressure. The possibility of such oscillations depends on the core stability, the delay time for the energy transport from the fuel to the evaporator, and the energy storage capacity of the cycle. The core stability proper depends on the reactivity coefficients and the pin power, among other factors. If the power decreases, the reactor approaches instability. For a given reactor the distance from the stability limit is shown as a function of reactor power and reactivity coefficient ratio. The influence of other parameters, such as those mentioned above and the steam pressure and temperature, on the stability limit is shown. The load dependent stability diagram chosen is compared with the usual stability presentation for full power. (6 references.) (auth)

Control Systems

31543 (AAEC/E-203) FEASIBILITY STUDY OF THE AUTOMATIC CONTROLS FOR A PEBBLE BED REACTOR POWER STATION. Gilbert, C. P.; Ackland, L. B. (Australian Atomic Energy Commission Research Establishment, Lucas Heights). Nov 1970. 116p. Dep. NTIS (U. S. Sales Only).

A conceptual automatic control system proposed for a pebble bed reactor power station was examined to establish its feasibility over a wide range of operating conditions. Frequency response methods, making use of a digital computer, were used to design the various control loops, and the resulting system was examined on an analog computer. The system could be made to work under all conditions, but the response at power levels <30% of full load was so slow that its value in practice would be doubtful. Future systems could be improved by making provision for temperature control of the super-heated steam, and by providing for the adjustment of reactor power directly from incoming load changes. (Australia)

31544 (ORNL-TM-3102) MSBR CONTROL STUDIES: ANALOG SIMULATION PROGRAM. Sides, W. H. Jr. (Oak Ridge National Lab., Tenn.). May 1971. Contract W-7405-eng-26. 29p. Dep. NTIS.

A preliminary investigation was made of the dynamics and possible control schemes for the proposed 1000-MW(e) single-fluid Molten-Salt Breeder Reactor (MSBR). For this purpose an analog computer simulation of the plant was devised. The system, simulation model, and analog computer program are described. For the purposes of the analysis, the MSBR plant consisted of a graphite-moderated circulating-fuel (primary salt) reactor, a shell- and tube heat exchanger for transferring the generated heat to a coolant (secondary salt), a shell-and-tube supercritical steam generator, and a possible control system. The analog simulation of the plant consisted of a lumped-parameter heat transfer model for the core, primary heat exchanger, and steam generator; a two-delayed-neutron-group model of the circulating-fuel nuclear kinetics with temperature reactivity feedbacks; and the external control system. The simulation was carried out on the ORNL Reactor Controls Department analog computer. So that the model would have the maximum dynamic range, the system differential equations were not linearized, and as a result the requisite quantity of equipment required that the model be severly limited spatially to minimize the number of equations. In addition, the pressure in the water side of the steam generator, as well as in the rest of the plant, and the physical properties of the salts and water were taken to be time invariant. The temperature of the feedwater to the steam generators was also held constant. (auth)

31545 (ORNL-TM-3311) SYSTEMATIC PROCEDURE FOR DETERMINING SYSTEM PARAMETERS BY PERFORMANCE INDEX MINIMIZATION. Chang, Sen-I (Oak Ridge National Lab., Tenn.). May 1971. Contract W-7405-eng-26. 97p. Dep. NTIS.

Thesis. Submitted to Univ. of Tennessee, Knoxville.

A study was made of the parameter space approach to determine optimum control system parameters by performance index minimization. The method which was developed can apply to high order multiple-input–multiple-output systems as well as to low order single-input–single-output systems. The controller parameters appearing in a mathematical model of the system are optimized by adjusting them in such a manner as to minimize certain integral measures of the difference between the actual and desired output response. The minimization is performed according to an optimization scheme known as the steepest descent procedure. A computer code was written for the IBM-360 which performs the calculations described above. 19 references. (auth)

Cooling Systems

Refer also to abstracts 29257, 29261, 29315, 29317, and 29407.

31546 (EUR-4531) SECOND INFORMATION MEETING ON PRESTRESSED CONCRETE REACTOR PRESSURE VESSELS AND THEIR THERMAL ISOLATION, BRUSSELS, 18-20 NOVEMBER 1969. (European Communities, Luxembourg. Commission). Sep 1970. 1114p. (In several languages). (CONF-691112). EUR $24.00.

Information is presented on prestressed concrete pressure vessels and thermal insulation for reactors. Separate abstracts are included for 37 of the 41 papers presented. Four papers have been previously abstracted and listed in NSA. (D.C.C.)

For abstracts of individual papers see: 29264, 29819, 29939, 30019–30031, 31454–31457, 31547–31553, 31575–31578, and 31662–31667.

31547 (EUR-4531, pp 477-88) REACTOR PRESSURE VESSEL OF FINISHED SECTIONS. SECTION MODELS FOR TESTING

CONSTRUCTION IMPROVEMENT. Rissler, P. (Siemens A. G., Erlangen (West Germany)). (In German).

From second conference on prestressed concrete reactor pressure vessels and their thermal isolation; Brussels, Belgium (18 Nov 1969).

In Second information meeting on prestressed concrete reactor pressure vessels and their thermal isolation.

Prestressed concrete vessels for water-cooled reactors are subjected to limitations which lead to unusually compact constructions. Simultaneously very concentrated forces occur whose absorption requires full consideration. The section construction arises from these bases. The separate section ring serves for the extensive construction and testing of details caused partially by the construction method and partially by the operation. An improved section form, the supporting behavior of simple spacers, and the construction of a large pipe wall entrance were tested in particular. (tr-auth)

31548 (EUR-4531, pp 507-16) SCANDINAVIAN MODEL PROJECT. I. Menon, Sh. (Aktiebolaget Atomenergi, Stockholm (Sweden)).

From second conference on prestressed concrete reactor pressure vessels and their thermal isolation; Brussels, Belgium (18 Nov 1969).

In Second information meeting on prestressed concrete reactor pressure vessels and their thermal isolation.

A project to build and test a model of a concrete pressure vessel for a 750 MW boiling water reactor is described. Special features of the pressure vessel include: a removable top head, and an insulation system designed to operate in a reactor in a two face coolant. The load from the internal pressure is transmitted by a large number of struts to the cylindrical part of the vessel. These struts are fitted with bolted wedges in order to minimize tolerance problems. The sealing is provided by toroidal seals with bolted flanges. (D.C.C.)

31549 (EUR-4531, pp 527-56) RESULTS OF MODEL INVESTIGATIONS ON MULTIPLE PRESSURE VESSELS. Schrage, H. P. (Fried-Krupp Universalbau, Essen (West Germany)). (In German).

From second conference on prestressed concrete reactor pressure vessels and their thermal isolation; Brussels, Belgium (18 Nov 1969).

In Second information meeting on prestressed concrete reactor pressure vessels and their thermal isolation.

Studies were made to develop the multi-layer construction method for prestressed concrete reactor pressure vessels and to test scale models. The problems in the construction of the model, the equipping of the model for testing purposes, the research techniques, and the test results were reported. The removal of the unbound water in an evacuated system was successful. Friction studies showed the limitations of the exponential friction law. Temperature studies showed that the water gap could be maintained constant at more than 21° Celsius. Function tests of the pressure equilibrium cylinder were satisfactory. Short-term pressure studies were made to compare the theoretical values with the experimental values. The deviations between the two were discussed. Fissure formation and support behavior of the vessel model were determined. (J.S.R.)

31550 (EUR-4531, pp 601-13) PRESSURE VESSELS FOR WATER AND GAS REACTORS. Arathoon, J. P.; Peuchmaur, A. (Societe pour l'Industrie Atomique, Paris (France)). (In French).

From second conference on prestressed concrete reactor pressure vessels and their thermal isolation; Brussels, Belgium (18 Nov 1969).

In Second information meeting on prestressed concrete reactor pressure vessels and their thermal isolation.

The use of prestressed concrete for the pressure vessels of both water and gas reactors was investigated. Experimental studies showed that the construction of a concrete vessel with removable concrete lid, in which the mechanical behavior and the removal are analogous to the metallic vessels currently in use for water reactors, is possible with present techniques. For gas reactors two types of solutions were investigated: one in which the reactor and its heat exchangers are integrated in the same cavity, and one in which the heat exchangers are placed in separate cavities. The tightness covering and the thermal protection are identical for both cases. An economic comparison is made of the two solutions. The prestressed concrete pressure vessels are found to be the best solution for gas reactors although additional studies are needed on the double cavity concept which is economically feasible from the preliminary studies. (J.S.R.)

31551 (EUR-4531, pp 615-45) BWR PRESTRESSED CONCRETE PRESSURE VESSELS. Merot, J. P.; Languille, M. (Societe d'Etudes et d'Equipments d'Entreprises, Paris (France)). (In French).

From second conference on prestressed concrete reactor pressure vessels and their thermal isolation; Brussels, Belgium (18 Nov 1969).

In Second information meeting on prestressed concrete reactor pressure vessels and their thermal isolation.

Studies were made on the adaptation of prestressed concrete to BWR for both the pressure vessel and the safety enclosure. The studies were carried out for a power of 600 MW(e) so that the results could be made with companion studies being made on the use of concrete pressure vessels and metal safety enclosures. The vessel and the safety enclosure together with their auxiliary components were described in detail. The performance was evaluated. The results were compared with those obtained for a metallic safety enclosure with respect to the economics of the two concepts, increased safety, ease of construction, and present technical and technological limitations. (J.S.R.)

31552 (EUR-4531, pp 647-89) STRUCTURAL INTEGRATION OF A PRESTRESSED CONCRETE PRESSURE VESSEL IN A NUCLEAR POWER PLANT AND COMPARISON WITH A STEEL VESSEL INSTALLATION. Mueller, W.; Zeitzschel, G. (Allgemeine Elektricitaets-Gesellschaft, AEG-Telefunken, Frankfurt am Main (West Germany)). (In German).

From second conference on prestressed concrete reactor pressure vessels and their thermal isolation; Brussels, Belgium (18 Nov 1969).

In Second information meeting on prestressed concrete reactor pressure vessels and their thermal isolation.

The construction and performance of the pressure vessel and the pressure reduction system in the prestressed concrete construction were described. The fuel element exchange device was discussed. The reactor building was described in its basic construction and in various peculiarities of the floor plan. A qualitative comparison was made between the two systems. Advantages and disadvantages, resulting from the materials used and the various geometries for the pressure vessel and pressure reduction system, were compared. (tr-auth)

31553 (EUR-4531, pp 797-812) NONLINEAR ANALYSIS OF STRESSES IN THE STRUCTURE OF THE PRESTRESSED CONCRETE PRESSURE VESSEL FOR A FAST REACTOR. Hussain-Khan, M. (Bonnard et Gardel, Ingenieurs-Conseil, Lausanne (Switzerland)); Saugy, B. (Ecole Polytechnique Federale de Lausanne (Switzerland)). (In French).

From second conference on prestressed concrete reactor pressure vessels and their thermal isolation; Brussels, Belgium (18 Nov 1969).

In Second information meeting on prestressed concrete reactor pressure vessels and their thermal isolation.

The results of the nonlinear analysis of the stresses in the structure of a prestressed concrete pressure vessel for a fast reactor are presented. The behavior of this structure during a rapid increase of the pressure at the interior of the reactor and turbine cavities up to the rupture of the structure was examined. The analysis showed the effect of the taking into consideration of the instantaneous nonlinearity of the concrete in the calculation of the stresses of a massive prestressed structure. In the particular case examined of a reactor vessel, a reduction of the stresses in the most stressed element was noted of the order of 10 to 20%. A reduction of their distortion of 20 to 50% was also observed; this latter was a determinant factor of the criterion of their rupture. The presence of cavities in the walls of the vessel leads to concentrations of stresses. However, because of the nonlinear behavior of the concrete, these concentrations are not as unfavorable as the elastic analysis would suggest. The analysis shows that it is possible to follow the behavior of the structure for a rapid increase of the internal pressure up to very high values, allowing the determination of a safety coefficient to rupture. 8 references. (J.S.R.)

31554 (IAEA-126, pp 19-51) STRUCTURAL DESIGN PHILOSOPHY AND CRITERIA FOR CONCRETE REACTOR VESSELS: U. S. PRACTICE. Rockenhauser, W. (International Atomic Energy Agency, Vienna (Austria)). 1970. NTIS (U. S. Sales Only).

Prestressed concrete reactor pressure vessels technology standards have not yet been established. However, efforts are being made in the U. S., as well as in Europe, to write uniform "tentative criteria" or "recommended practices" which could eventually become the codes for design and construction of these vessels. Much of the material presented is drawn from the content of tentative criteria and from the design standards for the first U. S. PCPV, the Ft. St. Vrain reactor. It is followed by a comparison of European and U. S. standards and a brief discussion

XUM

of the relative merits of the various approaches. The basic concrete structure, the post-tensioning system, and the nonprestressed reinforcement are discussed. (auth) (INIS)

31555 (IAEA–126, pp 53-9) CONTRIBUTION FROM THE UNITED KINGDOM. Davidson, I. (International Atomic Energy Agency, Vienna (Austria)). 1970. NTIS (U. S. Sales Only).

The basic philosophy in the UK is to provide adequate pressure relief valves on each PCRV, to design for the working loads, and for a nominal ultimate load factor, to test models, to carry out a pressure test and to monitor each vessel throughout its life. A committee of the British Standards Institution has almost completed the first Code of Practice, in line with the philosophy summarized above. It is hoped to extend the Code to cover Limit State Design. It is suggested that more knowledge about the long term properties of concrete under working conditions would be advantageous, and could be facilitated by international collaboration. (auth) (INIS)

31556 (IAEA–126, pp 61-8) WORK ON REACTOR VESSELS OF PRESTRESSED CONCRETE IN YUGOSLAVIA. Petrovic, B. (International Atomic Energy Agency, Vienna (Austria)). 1970. NTIS (U. S. Sales Only).

The design for a two-wall concrete reactor pressure vessel model has been developed in Yugoslavia. The external vessel is prestressed with steel cables in the usual way. There are no cables in the internal vessel and this vessel is prestressed by a hydraulic system, inserted between the outer and the inner vessels. Calculations show that, for such a vessel conception, economics could be made for about 25 percent in cables and about 40 percent in concrete, using at the same time the same prestressing as for single walled vessels. The model of such a vessel type is under construction in the Institute of the SR Serbia for Testing Materials in Beograd. The results of mathematical analyses of the action of seismic forces are discussed. (auth) (INIS)

31557 (IAEA–126, pp 69-83) PROBLEMS AND PROSPECTS OF PRESTRESSED CONCRETE VESSELS: FRENCH EXPERIENCE UP TO 1970. Costes, D. (International Atomic Energy Agency, Vienna (Austria)). 1970. NTIS (U. S. Sales Only).

After an historical survey of French background in PCPV's, the coordinated program carried out or long term stressing, development of new concretes, heat transfer studies and development of insulation technologies, calculation programmes, measurements on actual vessels, and some design problems is described. Basic and safety problems in nuclear application are discussed. The general safety standard is very high, but the ability to warn before failure due to weakening of some component is not always established. The French official regulation draft for gas reactor PCPV's is summarized, with a personal opinion about the future evolution of that text. The economics for PCPV's is examined. (auth) (INIS)

31558 (IAEA–126, pp 85-97) TEST STAND FOR THE PRESTRESSED CONCRETE VESSEL CONTAINING THE HELIUM LOOP. Komoli, L. H. (International Atomic Energy Agency, Vienna (Austria)). 1970. NTIS (U. S. Sales Only).

The planned large scale PCRV-Model has the following new features: hot liner (300°C), elevated temperature in the concrete vessel wall (up to 120°C) and a heating-cooling system in the wall to maintain temperature at desired level. Preliminary R & D work underway: high temperature insulating concrete, structural concrete and prestressing steel at elevated temperatures, high temperature instrumentation. The vessel is to be erected at the site of the Reactor Center Seibersdorf, Austria, late 1970, to be tested with hot water 1971 (water reactor conditions) and start Helium-tests 1972. Design and erection: Reaktorbau Forschungs- und Baugesellschaft mbH & Co. in collaboration with Oesterreichische Studiengesellschaft fuer Atomenergie Ges.m.b.H. and several Austrian industrial firms. (auth) (INIS)

31559 (IAEA–126, pp 99-114) ULTIMATE DESIGN EXPERIENCE FROM SMALL DIMENSION MODELS TESTING. Scotto, F. (International Atomic Energy Agency, Vienna (Austria)). 1970. NTIS (U. S. Sales Only).

Experience in the field of prestressed concrete pressure vessel models is described. The behavior of the structure as the pressure increases, starting from working condition up to structural collapse, is outlined. The "nearly elastic," the "definitely anelastic" and the collapse limits of the structure are discussed with regard to the concrete, the liner and the cable steel behavior. (auth) (INIS)

31560 (IAEA–126, pp 115-77) REPORT ON THE STARTING OF A COORDINATED WORK PROGRAM FOR PRESTRESSED CONCRETE REACTOR PRESSURE VESSELS IN THE FEDERAL REPUBLIC OF GERMANY. Jaeger, T. A. (International Atomic Energy Agency, Vienna (Austria)). 1970. NTIS (U. S. Sales Only).

An optimum design of a PCPV for gas-cooled or water-cooled power reactor systems can be achieved only if the reactor vessel is not considered as just a construction project, but if it is interpreted as a functional unit incorporated in the specific power reactor system with interrelated functional, safety and economic connections with the system. The concept of a basic program for research development of prestressed concrete reactor pressure vessels in the Federal Republic of Germany, as well as the basic structural design philosophy, criteria and safety of PCPV, are presented. Several special engineering developments for PCPV (e.g. multilayer, prefabricated vessel structures, and prestressing systems) are described. Detailed descriptions of "Joint Development Programmes of Prestressed Concrete Pressure Vessels for BWR" (AEG-Telefunken and Fried. Krupp GmbH), "Prestressing System Developments Using Different Methods," "Computational Methods" and "Instrumentation Assessment Programme" are given in the appendixes. (auth) (INIS)

31561 (IAEA–126, pp 179-212) DESIGN PHILOSOPHY AND CRITERIA OF SAFETY FOR PRESTRESSED CONCRETE PRESSURE VESSELS: PRACTICE IN CZECHOSLOVAKIA. David, M. (International Atomic Energy Agency, Vienna (Austria)). 1970. NTIS (U. S. Sales Only).

The main conclusions and results of about three years' work in Czechoslovakia in development of PCPV's are described with particular reference to the design philosophy and criteria of safety. Development was made for gas-cooled reactors of 500 MW(e) with heat exchangers placed inside the PCPV's. The most difficult problem of the structural design was to find an appropriate method for solving requirements of the fine mesh of penetrations together with extremely high internal working pressure (80 kg/cm^2). Various small scale models of elastic materials in the scale of about 1 : 40 were investigated and methods of measurement of strains and photoelasticity were employed. The program which is proposed for the short model is described and the estimation of cost of PCPV's is discussed in general terms. (auth) (INIS)

31562 (IAEA–126, pp 213-41) SWEDISH DEVELOPMENT ON PRESTRESSED CONCRETE PRESSURE VESSELS FOR WATER REACTORS. Menon, S. (International Atomic Energy Agency, Vienna (Austria)). 1970. NTIS (U. S. Sales Only).

A project to design, build and test a model of a PCPV suitable for water reactors is described. The project is backed by the atomic energy organizations of Denmark, Finland, Norway and Sweden, as well as by utilities and the reactor industry in Sweden. The model, which has dimensions 2 m internal diameter and 4 m internal height, is characterized by its removable top head and its insulation system. The model was hydraulically pressure tested at temperatures of 25°C and 70°C at pressures up to 95 bar. The tests included a 4-week test at 70°C and 85 bar (design pressure). The results were very satisfactory. (auth) (INIS)

31563 HELIUM LEAK TESTS ON REACTOR COMPONENTS. Gollwitzer, S. Atomwirt., Atomtech.; 16: 233-4(May 1971). (In German).

For monitoring the leakage of components in the primary circuit of nuclear power plants, mass spectrometers proved to be most efficient. They permit the detection of leakages as low as 10^{-10} torr liter/sec. Generally, helium served as testing gas. Leakage tests were performed with the vacuum method. To obtain reliable results, the test sample must be handled under special conditions. From a practical standpoint, leakage testing is discussed with respect to premises, regulations, conditions, and economics. (tr-auth)

31564 DESIGN AND MANUFACTURE PROCESS OF LARGE-SIZED REACTOR PRESSURE-VESSEL. Dorner, Heinrich (Siemens AG, Erlangen, Ger.). At. Strom; 17: 56-68(Apr 1971). (In German).

The calculation method for reactor pressure-vessels is explained and the range of stress calculated is compared with the stresses measured at the pressure test. The manufacturing processes are described, and the great importance of close cooperation between engineer and technician for materials during the whole creation process of a reactor pressure-vessel is shown. (auth)

31565 NUCLEAR REACTORS. Coast, Geoffrey; Morgan, Vernon (to United Kingdom Atomic Energy Authority). British Patent 1,226,537. 31 Mar 1971. Filed 27 Oct 1967.

Reference is made to nuclear power stations employing gas-cooled graphite-moderated reactors and gas turbines systems. A serious disadvantage in conventional systems is that the turbine outlet temperature of the gas re-entering the reactor is higher than desirable for graphite structures under continuous reactor operation conditions, and this temperature can only be reduced at a heavy penalty in cycle efficiency. In the system described a bleed duct is provided that by-passes part of the compressor to lead a fraction of the coolant to the graphite structures of the reactor at a temperature lower than that of the remainder flowing to the reactor. This coolant can also be used to cool the pressure vessel wall and its components, in this way leading to savings in the cost of thermal insulation. The bleed duct can tap off from an intermediate point in the compressor at 59°C and a pressure of 1040 psi. It has been calculated that an 8½% bleed would be sufficient to maintain the permanent graphite moderating core structure at the desired temperature. In order to avoid overcooling of the graphite where the coolant enters the moderating structure the coolant channels in this structure should converge in the direction of flow. Some constructional variants of the system are also described. (UK)

31566 DEPOSITING OF RADIOACTIVE PRODUCTS IN PIPES DURING TURBULENT FLOW. THEORETICAL ASPECTS AND EXPERIMENTAL VERIFICATION. Haulet, R.; De Kerdelleau, J.; du Pontavice, Y. (CEA, Saclay, France). pp 159-89 of Diffusion des Produits de Fission. Montrouge, France; Societe Francaise de Radioprotection (1970). (In French).

From International congress on the diffusion of fission products; Saclay, France (4 Nov 1969). See CONF-691104.

The primary coolant circuit of a reactor is contaminated by activation and fission products. The deposition of these products at various points in the pipes depends upon the flow, and thermal characteristics of the circuit. Much theoretical work has been done in assessing the rate of deposition (particularly along the straight sections). Models are considered, which are valid in the turbulent flow region, most commonly met in reactors. With an out-of-pile loop, cooled with CO_2 gas and contaminated by the oxidation of the irradiated uranium, which is canned with magnesium, the deposition of small pieces or sleeves of steel or graphite of the three fission products ^{131}I, ^{132}Te and ^{99}Mo and the uranium activation product ^{239}Np, was studied. When some hypotheses are made on particle granularity, the experimental results are in good agreement with those derived using Davies formula ($x^{\frac{1}{3}}$ law). The validity of this mathematical model for Reynolds numbers between 2,500 and 25,000 and probably beyond is demonstrated. (auth) (France)

31567 DISTRIBUTION OF FISSION PRODUCTS IN A HIGH TEMPERATURE GAS COOLED REACTOR. Rowland, P. R.; Carlyle, M.; Soubelet, G. C. (Atomic Energy Establishment, Winfrith, Eng.). pp 191-204 of Diffusion des Produits de Fission. Montrouge, France; Societe Francaise de Radioprotection (1970).

From International congress on the diffusion of fission products; Saclay, France (4 Nov 1969). See CONF-691104.

Work in progress in the O.E.C.D. Dragon Reactor Project for the measurement of fission products at various points of a gas coolant circuit is described. The release from the Dragon particle fuel is normally low and careful methods are used to obtain accurate results. Two basic techniques are used. Layers of accurately known thickness and superficial area from selected regions of the coolant circuit surface can be removed using an electrolytic method (the electroleach) during shutdown. This is used mainly for measurement of the deposited metallic radioisotopes. It can be operated by remote handling in regions of the reactor which are otherwise inaccessible. Sampling tubes can be inserted directly into the main hot coolant and removed from it while the reactor is operating. Fission products deposit on the sample tube walls or on filters. This is used to measure iodine and, by application of diffusion equations, to analyze the form in which isotopes are transported (e.g. as precursors, as molecules or as particulates). These techniques are supported by measurement of inert gas isotope activities in the coolant. Some of the results obtained so far are analyzed and their implications for reactor maintenance and safety are briefly examined. An important preliminary finding is that a high proportion of the isotopes deposited in the coolant circuit are held in the surface films on the metal components (probably within the oxides). (auth) (France)

Fuels

31568 (EURFNR-823) FAST BREEDER PROJECT: TWO-YEARLY REPORT, 1968-69. (Kernforschungszentrum, Karlsruhe (West Germany)). Translation of report KFK-1269. 378p. Dep. NTIS.

Work performed under United States-Euratom Fast Reactor Exchange Program.

Information on the development of fast breeder reactors is presented under the following headings: fuel design; production and irradiation of fuel rods; material development; corrosion tests and coolant analyses; work on fuel cycle; large physical experiments; reactor theory; safety of fast reactors; development of instrumentation and signal processing for core monitoring; effect of reactor incidents on the environment activity release; Na technology experiments; thermodynamic and hydrodynamic tests in gas and steam; reactor designs; and FR-3 fast high flux test reactor. (D.C.C.)

31569 (ORNL-TM-3388) PERFORMANCE CAPABILITY OF ADVANCED FUELS AND FAST BREEDER REACTORS. Washburn, T. N.; Scott, J. L. (Oak Ridge National Lab., Tenn.). May 1971. Contract W-7405-eng-26. 20p. Dep. NTIS.

The boundary limits of fuel performance are shown on plots of specific power (W/g) against linear power (kW/ft). For $(U,Pu)O_2$ fuels, these boundaries form a triangle with borders of about 100 W/g minimum specific power, about 0.200 in. minimum fuel diameter, and a maximum linear power of about 12 kW/ft for the core average or about 19 kW/ft for the highest rated fuel pin. For (U,Pu)C and (U,Pu)N fuels, the minimum specific power and minimum fuel diameter are the same as for the oxides. However, the higher thermal conductivity of these advanced fuels permits linear powers to about 30 kW/ft core average and about 45 kW/ft for the highest rated pin, when a sodium bond is used between the fuel and cladding to prevent excessive fuel temperatures and to provide space to accommodate fuel swelling. There is substantial economic advantage in operating fuel at these highly rated conditions, but a large amount of development work and irradiation testing must be performed with both the carbides and nitrides to permit an absolute comparison of their worth relative to oxides. 23 references. (auth)

31570 (RT/ING-(70)24) EXPERIMENTAL VIBRATION CHARACTERISTICS OF A B.W.R. FUEL ASSEMBLY. Ferrucci, N.; Pitimada, D. (Comitato Nazionale per l'Energia Nucleare, Rome (Italy)). 21 Oct 1970. 43p. (CONF-700608-35). Dep. NTIS (U. S. Sales Only).

From American nuclear society meeting; Los Angeles, Calif. (29 Jun 1970).

The bending modes of single rods assembled in a B. W. R. fuel assembly are determined testing a model in air. The measured resonances are compared against the modes of the end restrained rod without intermediate spacers. End fixity values of single rods are determined using both static and dynamic methods. 11 references. (auth)

31571 THERMAL SCANNER (5 Jan 1970) (Engineering Materials). (Los Alamos Scientific Lab., N. Mex.). (CAPE-2069).

18 drawings.

This device determines the size and movement of fission product gas bubbles in the bond of a Na-bonded reactor fuel pin. Position of the bubbles in the bond is determined by thermocouples that measure the temperature of the fuel-pin cladding. The scanner consists of a thermocouple rotor assembly, bubble injection apparatus, and an outer section. Details of a fuel pin mockup are included. The mockup has a 10-mil wall, 0350 in. OD stainless-steel cladding, a cylinder of UC, and a 10-mil Na bond. Inside the UC cylinder an electric heater produces heat at ~ the same rate as a fuel pin would in a breeder reactor. The cladding temperatures are measured by 40 thermocouples mounted on a rotor that fits around a fuel pin or the mockup. During measurement each thermocouple measures heat at 11 azimuthal locations. The outer structure, which is fabricated to reduce thermal stresses, is the structural containment of the scanner. (For details see TID-4100 Suppl. 63) (see also NSA 24: 43858) (F.S.)

31572 STUDIES ABOUT ADVANCED FUEL ELEMENTS. Karsten, G. (Kernforschungszentrum, Karlsruhe, Ger.). Atomwirt., Atomtech.; 16: 256-60(May 1971). (In German).

The SATURN 1 code capability is discussed. It will permit various modifications in fuel rods and the development of core designs based on irradiation experiments. The two major concepts for sodium fast breeder reactors, oxide and carbide, are discussed. The present status of development is described for various fuel elements and cladding materials. (H.B.G.)

31573 MEASUREMENTS ON FUEL ELEMENTS FOR POWER REACTORS IN A CRITICAL ASSEMBLY. Mayer, Walter; Andres, Ruprecht; Kilian, Peter (AEG Kernenergieversuchsanlage, Grosswelzheim, Ger.). At. Strom; 17: 69-71(Apr 1971). (In German).

XUM

The critical assembly is serving to control the layout and production of fuel elements for power reactors. A brief description of the plant is given. The experiments made hitherto are compiled. Some representative examples of typical measurements are given. The results of the experiments will contribute to the security and optimization of an economic exploitation of power reactors. It is shown that the starting period may be reduced. (auth)

Auxiliary and Emergency Systems

Refer also to abstracts 31546, 31551, and 31552.

31574 (ANL–7793) INSTRUMENTATION SYSTEMS TO PROTECT LMFBR CORE INTEGRITY. Lipinski, W. C.; Cohn, C. E.; MacFarlane, D. R.; Mulcahey, T. P.; Okrent, D.; Porges, K. G.; Redman, W. C.; van Erp, J. B.; Vonderohe, R. H. (Argonne National Lab., Ill.). Mar 1971. Contract W-31-109-eng-38. 244p. Dep. NTIS.

The role of instrumentation systems in providing protection for cores of future liquid-metal-cooled fast breeder reactors is described. The existing status of instrumentation systems for core protection is reviewed and consideration given to how such systems might be improved, through extension of current technology in the areas of detectors, circuitry, and information processing. Credible types of accidents and malfunctions are considered, in order to establish the time scale required for instrument system response and action. Emphasis is given to the effectiveness of various types of detection systems in providing protection against localized abnormalities. An indication is given of the direction for future developmental activities in order to satisfy the dual requirements of reliability and economy in systems intended to insure fast-reactor safety. 147 references. (auth)

31575 (EUR–4531, pp 953–64) METHODS OF TESTING HTR THERMAL SHIELDING. Naudin, P. (Societe Bertin et Cie, Paris (France)). (In French).

From second conference on prestressed concrete reactor pressure vessels and their thermal isolation; Brussels, Belgium (18 Nov 1969).

In Second information meeting on prestressed concrete reactor pressure vessels and their thermal isolation.

The principal problems to be resolved in the design of thermal shields for the HTR and in the measurement of their efficiency are discussed with a consideration of the most realistic representations of the actual operational stresses. The test equipment consists of a reservoir under pressure with capacity for rapid pressure build-up and decompression, systems of heating, hot fluid circulation, and measurement devices. Each of these components is described in detail. Examples are given of the utilization of the test installation to show the validity and applicability of the test results. (J.S.R.)

31576 (EUR–4531, pp 1035–53) THERMAL SHIELDING BY SCREENS OF CIRCULATING GAS. Freour, A. (Societe pour l'Industrie Atomique, Paris (France)); Wuerdig, P. (Deutsche Babcock und Wilcox A. G., Oberhausen (West Germany)). (In French).

From second conference on prestressed concrete reactor pressure vessels and their thermal isolation; Brussels, Belgium (18 Nov 1969).

In Second information meeting on prestressed concrete reactor pressure vessels and their thermal isolation.

The principal results obtained during performance tests of the gas screen thermal protection system are presented. The tests were made on a normal trap, on a blower trap, on a sky trap, and on a soil trap. The structures of each of these types of thermal shields were described. The results show that the normal trap gives satisfactory results. The blower trap has low thermal losses in the penetration zone but these are much higher along the blower channel. The behavior in the transitory regime is analogous to that of the normal trap. The sky trap has great thermal efficiency. The soil trap has a thermal efficiency analogous to that of the sky trap, but the flux level is much higher and significant variations appear in the transitory regime. A comparison is made between the gas screen thermal protection system and more conventional techniques. (J.S.R.)

31577 (EUR–4531, pp 1063–78) THERMAL SHIELDING OF PRESSURE VESSELS, TANKS, AND ELEMENTS OF NUCLEAR REACTORS BY MEANS OF HONEYCOMB METALLIC STRUCTURES (THERMAL SHIELDING OF FLUID FILMS). Dupont, J. (Sud-Aviation S. A., Suresnes (France)). (In French).

From second conference on prestressed concrete reactor pressure vessels and their thermal isolation; Brussels, Belgium (18 Nov 1969).

In Second information meeting on prestressed concrete reactor pressure vessels and their thermal isolation.

The honeycomb metallic structures proposed for the thermal shielding of the component, tanks, and vessels of nuclear reactors were developed for the thermal insulation of the force tubes of the EL-4 reactor. The performance of these shields at the EL-4 is described. The honeycomb metallic structure solves many problems of thermal insulation. Their validity was experimentally verified for the reactor tank of the Phenix reactor. The application of these structures to gas and water reactors is discussed. (J.S.R.)

31578 (EUR–4531, pp 1085–97) THERMAL SHIELDING FOR WATER REACTORS. Freour, A. (Societe pour l'Industrie Atomique, Paris (France)). (In French).

From second conference on prestressed concrete reactor pressure vessels and their thermal isolation; Brussels, Belgium (18 Nov 1969).

In Second information meeting on prestressed concrete reactor pressure vessels and their thermal isolation.

Two types of thermal shielding for water reactors were examined. In the first type the thermal shielding consisting of metallic sheets is bathed in the medium in the cavity of the pressure vessel, whereas in the second type the metallic sheet thermal shielding is in a gaseous medium. The design and performance of both types are described. The gas shielding design has the complications of the placement of passages in the vessel and of the increase of the number of auxiliary circuits. However it has the necessary safety and good performance. The water design simplifies the installation, but it requires extensive knowledge of the technical characteristics of the metallic sheets in water. (J.S.R.)

31579 (MRR–79) EMERGENCY CORE COOLING. Borsche, D. (Technische Hochschule, Munich (West Germany). Institut fuer Mess- und Regelungstechnik). Jan 1970. 27p. NTIS (U. S. Sales Only).

The problems of emergency cooling after a loss-of-coolant accident caused by tube rupture in the primary coolant system are analyzed. In boiling water reactors two different types of emergency cooling at low pressures are used: core flooding and core spray cooling. A qualitative comparison of the two methods is made. Special problems are discussed. A brief description of the LOCTA–R, TACT–V, NURLOC, ARC-II, MOXY-II, CHEMLOC-II codes is given. (INIS)

31580 STANDARD METHOD FOR MEASUREMENT OF DELAYED NEUTRON-EMITTING FISSION PRODUCTS IN NUCLEAR REACTOR COOLANT WATER DURING REACTOR OPERATION. ASTM D 2470-70. Philadelphia; American Society for Testing and Materials (1970). 7p. Available from American Society for Testing and Materials, Philadelphia.

31581 IMPROVEMENTS IN OR RELATING TO FUELLING ARRANGEMENTS FOR FAST NUCLEAR REACTORS. Barker, Allan (to United Kingdom Atomic Energy Authority). British Patent 1,227,758. 7 Apr 1971. Filed 16 Aug 1967.

The object of the arrangement described is to provide an improved fast reactor refuelling system compared with that used in the Scottish DPFR (Dounreay Prototype Fast Reactor) from both design and cost aspects and with particular application to very large power reactors. An annular store is provided for irradiated and unirradiated fuel elements, submerged in a pool of liquid coolant. The store is concentric with the reactor core and rotatable about the axis of the core, and means are provided for moving fuel elements between store and reactor core. The store is preferably in lateral register with the core, thus saving space. The system for moving fuel elements includes handling means for loading and unloading the store and separate means for moving fuel elements from store to reactor core. The annular store may be suspended from a rotary carriage journaled in a fixed structural part of the reactor installation. The second fuel handling means may comprise a transfer machine mounted eccentrically on a rotatable shield itself mounted eccentrically in or on a second rotatable shield which is disposed concentrically with and above the reactor core. The transfer machine is adapted to contain liquid coolant. The first fuel element handling means may comprise a charge/discharge machine, with buckets containing liquid coolant. (UK)

31582 IMPROVEMENTS IN OR RELATING TO FUEL HANDLING EQUIPMENT FOR NUCLEAR REACTORS. Hyde, John Edgar; Hopkins, Shirley Russell (to United Kingdom Atomic Energy Authority). British Patent 1,227,754. 7 Apr 1971. Filed 21 Jul 1967.

Reference is made in particular to fuel handling equipment for liquid metal (Na) cooled fast reactors. In transfer buckets for fuel sub-assemblies the decay heat is such that the temperature of the Na coolant rises significantly as soon as the bucket is clear of the coolant pool, the spillage of Na from the bucket may occur during the raising operation due to thermal expansion and during the time the bucket is in the transfer flask. The object of the equipment described is to provide means for preventing or reducing the likelihood of such spillage by producing the transfer bucket with syphon means having suitably located inlet and outlet. The highest point of the syphon means is above the level of the inlet and below the top of the bucket. The syphon means in preferably located in a cavity provided by a double-walled upper portion of the bucket, with its inlet extending through the inner wall and its outlet through the outer wall. Perferably four such syphon means are provided, each consisting of a pipe of inverted U-shape contained in the cavity, with four pipes equally spaced there-around. The bucket preferably has an internal ring below the level of the syphon pipe inlets providing lateral location for a fuel sub-assembly, and the lower end of the bucket is preferably shaped to provide support for the lower end of the sub-assembly. (UK)

31583 REACTOR CONTAINMENT SPRAY SYSTEMS. RESEARCH IN THE UNITED STATES. Row, T. H. (Oak Ridge National Lab., Tenn.). pp 205-22 of Diffusion des Produits de Fission. Montrouge, France; Societe Francaise de Radioprotection (1970).

From International congress on the diffusion of fission products; Saclay, France (4 Nov 1969). See CONF-691104.

The Oak Ridge National Laboratory serves as coordinator for the USAEC-sponsored research into the effectiveness of sprays as an engineered safety feature. Research on sprays includes a search for spray solution additives that will enhance the fission product removal; investigation of solution sensitivity to additive concentration, pH, temperature, humidity, and drop size through the use of a single drop suspended in a wind-tunnel; determination of the thermal and radiation stability of solution by following changes in pH and iodine equivalence, the appearance of solids, and the generation of radiolytic H_2; examination of the corrosive nature of spray solutions on typical materials of construction; and engineering scale tests of the removal effectiveness of sprays under simulated accident conditions. Two aqueous solutions have been examined in detail and appear to be acceptable for use in the high temperature and radiation environment expected following the accident. The solutions are: 0.153M NaOH, 3000 ppM B and 0.153M NaOH, 3000 ppM B, 1 wt % $Na_2S_2O_3$. The removal half-time for molecular iodine from a stream air atmosphere (130°C) by 20°C spray solution was consistently less than 1 min for either solution while the removal of methyl iodide is a much slower process. Half-times are 1 hr for the solution containing sodium thiosulfate and 3–4 hr for the base-borate solution. The cleanup of cesium and uranium aerosols by sprays is also favorable with a one hour spray period giving decontamination factors of 90 for cesium and 15 for uranium, in a condensing steam environment. After radiation exposure, the base-borate solution exhibited a change pH from 9.3 to 9.2 and no solid generation. The thiosulfate system showed some degradation. Hydrogen was generated in both aqueous solutions. The corrosion tests of metals and protective coatings by the solutions has indicated that aluminum and copper are the only materials seriously affected and that a number of currently available coatings can be used successfully in containment buildings. (auth) (France)

Operation and Economics

31584 MAXIMIZING THE AVERAGE FUEL BURNUP OVER ENTIRE CORE: A POISON MANAGEMENT OPTIMIZATION PROBLEM FOR MULTIZONE LIGHT-WATER REACTOR CORES. Suzuki, Atsuyuki; Kiyose, Ryohei (Tokyo Univ.). Nucl. Sci. Eng.; 44: 121-34(May 1971).

The problem of optimal control rod withdrawal sequence is formulated for a multizone core model of a nuclear reactor. In particular, the maximum average burnup problem for light-water reactors is investigated to find the governing principles in optimal control rod programming. The optimal solution depends only on end-of-life (EOL) states, and in the optimal state, the control poisons are all withdrawn from the entire core and the power distribution will be as uneven as possible within the constraints on the power peaking factor. We define the core composition, including the control poison, which represents the nuclear performance of each zone and it is taken as an independent control vector. The admissible control is defined such that the control vector satisfies the criticality condition and the constraints of power peaking factor. Some complexities of the other constraints to be considered are resolved by determining the reachable region of the burnup of each zone which is chosen as a state vector. The method described is based on a topological mapping theory, and for illustrative purposes, the results in the case of a two-zone model are shown by using the method. 14 references. (auth)

31585 APPLICATION OF THE METHOD OF REDUCED COSTS TO ESTIMATES OF THE EFFECTIVENESS OF UTILIZATION OF NUCLEAR FUEL. Taliev, A. V.; Kramerov, A. Ya. This paper was summarized in At. Energ. (USSR); 29: 36(Jul 1970) as paper No. 402/5524. (In Russian).

The determination of the fuel component of reduced costs for nuclear power stations is a difficult task, because of the discrete pattern of consumption of nuclear fuel, the transients present in the initial period of operation, and the different time factors affecting losses in the fuel cycle, each component of them depending moreover on the reactor characteristics to be assigned in the reactor design process. With the object of overcoming these difficulties and working out a unified approach, reliance was placed on the method of reduced costs in a generalized form. The specific reduced costs for nuclear fuel are determined from a generalized formula. Concrete computational formulas are derived, on the basis of this general formula and valid assumptions applicable to particular cases. An exact method and an approximate method for calculating the fuel component in the case of a reactor with partial reloading (batch refueling) features are presented. (auth)

31586 STAGE OF ADVANCEMENT IN THE FIELD OF THE EXTERNAL HTGR FUEL CYCLE WITH A Th–U CYCLE. Roth, Bernhard F. (Brown, Boveri/Krupp Reaktorbau GmbH, Mannheim, Ger.). At. Strom; 17: 30-40(Feb-Mar 1971). (In German).

On the grounds of the advanced development of the high-temperature gas-cooled reactor, the problem of the external fuel cycle is rapidly gaining in point. The necessity and economic importance of reprocessing are set forth by an example. The stage of advancement of the fabrication, reprocessing and refabrication of HTGR fuels is described. Furthermore, the difficulties occurring at each of the processing steps as well as the specific costing are dealt with. An outlook on the development of the HTGR fuel cycle is given for the Federal Republic of Germany. 55 references. (auth)

Safety and Siting

Refer also to abstracts 29074, 29075, and 29420.

31587 (CONF-710302–2) MOXY: A DIGITAL COMPUTER CODE FOR COMPUTING CORE HEAT TRANSFER. Evans, D. R. (Idaho Nuclear Corp., Idaho Falls). 29 Mar 1971. 16p. Dep. NTIS.

From Meeting on new development in reactor mathematics and applications; Idaho Falls, Idaho (29 Mar 1971).

MOXY (MOdel X-Y) is one of several computer codes for the evaluation of power reactors during a LOCA. MOXY solves the equations of the X-Y Model (in which an array of rods is represented in x-y coordinates) for a bundle of rods during a LOCA. The code uses a pseudo-three-dimensional model in which axial conduction and radiation are neglected, but in which the energy balance equation for steam traveling axially upward through the rod bundle is solved. Heat transfer by conduction, convection, and radiation and heat generation by metal-water reaction are considered. Presented are the heat transfer models used, the solution techniques for these models, and a brief evaluation of the models in which code results are compared with experimental data from the Fuel Heatup Simulation Tests (FHUST). 11 references. (auth)

31588 (CONF-710302–4) FLOW SIMULATION THROUGH GRAPHICS: A HIGH-SPEED INTERPRETATION OF REACTOR BLOWDOWN CALCULATIONS. Lintner, M. A.; Solbrig, C. W. (Idaho Nuclear Corp., Idaho Falls). [1970]. 28p. Dep. NTIS.

From Meeting on new development in reactor mathematics and applications; Idaho Falls, Idaho (29 Mar 1971).

The various techniques of graphic representation which should be considered when attempting to produce motion pictures portraying fluid motion are discussed. Also, a detailed description of a method used to produce motion picture flow representation in a reactor primary loop is presented. (auth)

31589 (CONF-710302–5) DISTRIBUTION OF SOLID FISSION PRODUCTS IN UO_2. McFadden, J. H.; Baston, V. F.; Yuill, W. A. (Idaho Nuclear Corp., Idaho Falls). [1971]. 8p. Dep. NTIS.

From Meeting on new development in reactor mathematics and applications; Idaho Falls, Idaho (29 Mar 1971).

XUM

The migration of fission products during reactor operation is described by a thermomigration model that has been used successfully to describe noble gas release from fuel pins during normal operation. The basic assumption in the derivation of this model is that the driving force for migration of fission products during reactor operation is a Gibbs-free-energy gradient, which is dependent on temperature and concentration gradients. Examples of forces contributing to the Gibb-free-energy gradient and proportional to the thermal gradient are entropy effects, thermoelectric effects and thermal stresses. 11 references. (auth)

31590 (CONF-710302-6) EFFECTS OF STATE PROPERTIES ON HIGH PRESSURE COMPRESSIBLE HYDRODYNAMICS. Moore, K. V.; Gruen, G. E. (Idaho Nuclear Corp., Idaho Falls). [1970]. 10p. Dep. NTIS.

From Meeting on new development in reactor mathematics and applications; Idaho Falls, Idaho (29 Mar 1971).

The ASME equations of state for water were incorporated into RELAP3 as a trial version called RELAP3/ASME. In comparisons to experimental data, this trial version gives substantial improvement over RELAP3 in predicting subcooled blowdown pressure histories. The standard version of RELAP3 is a computer code for analyzing reactor core and loop thermal hydraulics during blowdown. Continuous calculations from the subcooled portion of the blowdown into the two-phase regime are at least conceptually permitted. The failure of RELAP3 to correctly predict subcooled pressure histories was traced to inaccurate sonic velocities. Water properties are built-in as tables of pressure versus enthalpy and density. Thermodynamic derivative quantities, such as sonic velocity, are implicit within these tables. These tables and any dependence on interpolation schemes were eliminated in RELAP3/ASME by incorporating the 1967 ASME equations of state. Each equation, which is defined for particular ranges of pressure and temperature, uses either pressure and temperature or specific volume and temperature as independent variables. Within RELAP3/ASME, a two-dimensional Taylor series expansion is performed on the ASME equations which transforms the independent variables to specific internal energy and specific volume. (auth)

31591 (CONF-710302-7) MATHEMATICAL TECHNIQUES FOR VIBRATION ANALYSIS OF REACTOR SYSTEMS. Noble, C. (Idaho Nuclear Corp., Idaho Falls). [1970]. 14p. Dep. NTIS.

From Meeting on new development in reactor mathematics and applications; Idaho Falls, Idaho (29 Mar 1971).

The vibration analysis of a nuclear reactor by the finite element method can be divided into three major steps: generating the stiffness and mass matrices, determining the natural frequencies (eigenvalues) and mode shapes (eigenvectors), and solving the uncoupled equations of motion for displacements in normal coordinates. The mathematical techniques used to solve the eigenvalue problem and techniques to solve the differential equations for displacements in normal coordinates are described. The eigenvalue problem is solved by the STRAP-D code, which reduces the dimensions of the stiffness matrix by condensing, and by the STRAP-MS code which reduces the dimensions by modal synthesis. The solution of the equations of motion is accomplished by Laplace transform techniques. (auth)

31592 (CONF-710302-8) NODAL SENSITIVITY IN MODELING A LARGE PRESSURIZED WATER REACTOR SYSTEM FOR A LOSS-OF-COOLANT ACCIDENT. Slater, C. E.; Hentzen, R. D. (Idaho Nuclear Corp., Idaho Falls). [1970]. 35p. Dep. NTIS.

From Meeting on new development in reactor mathematics and applications; Idaho Falls, Idaho (29 Mar 1971).

Computer codes have been developed that attempt to predict the course of a loss-of-coolant accident and the effectiveness of the emergency safety systems. The extent of geometrical description used in digital computer codes for predicting the consequences of a loss-of-coolant accident in a large pressurized water reactor system has evolved from simple codes employing only three control volumes to present generation codes in which the number of control volumes or nodes is limited only by the core storage of the computer. The increased nodal description has frequently resulted in an increase in computation time. In order to avoid extensive computation time for safety analysis calculations, the geometrical description is often reduced by lumping similar system components together into a common control volume. The effect of the number and distribution of control volumes used in describing a large pressurized water reactor system on the solution of the conservation equations of mass, momentum, and energy is analyzed. A version of the RELAP3 code, dimensioned for two-hundred control volumes, was utilized. A large pressurized water reactor system of current design subjected to a loss-of-coolant accident (100% offset shear of inlet piping) was described with several computer models that exhibited wide variation in both the number and distribution of the control volumes. The blowdown behavior calculated by the RELAP3 code using the various models was then compared. The number of variables that could be compared were numerous and led to difficulty in establishing criteria for comparing the effects of nodal description on the solution to the governing equations. In the interest of brevity and because of their importance and sensitivity to small perturbations in pressure, core flow rates and core surface temperatures were chosen as the common variables for comparison among the various models. The study has been divided into two general areas: modeling of components in which no energy is transferred across the boundary and modeling of components in which energy is transferred across the boundary (the core and steam generators). As initially suspected and as later verified by the study, strong coupling was exhibited among the conservation equations when energy was transferred into or from the fluid. The need of adequate nodal description in loss-of-coolant accident analyses is discussed. Some general guidelines for modeling large pressurized water reactors are presented. (auth)

31593 (CONF-710302-9) CORRELATIONS TO PREDICT MAXIMUM PWR CONTAINMENT PRESSURES FOLLOWING A LOSS-OF-COOLANT ACCIDENT. Slaughterbeck, D. C. (Idaho Nuclear Corp., Idaho Falls); Specter, H. (Atomic Energy Commission, Washington, D. C.). [1970]. 16p. Dep. NTIS.

From Meeting on new development in reactor mathematics and applications; Idaho Falls, Idaho (29 Mar 1971).

The correlations developed on the basis of a parametric analysis of a simplified containment model provide a method for prediction of the maximum containment pressures in large PWR containments following a loss-of-coolant accident. The figures provide the framework to account for initial fluid enthalpies, heat transfer to the steam generators during blowdown, and heat absorption in the containment structures. The trend of pressure estimated with the correlations agrees with predictive data from safety analysis reports. 11 references. (auth)

31594 (CONF-710302-10) IDAHO NUCLEAR CODE AUTOMATION: A STANDARDIZED AND MODULARIZED CODE STRUCTURE. Solbrig, C. W.; Ybarrondo, L. J.; Wagner, R. J. (Idaho Nuclear Corp., Idaho Falls). Mar 1971. 26p. Dep. NTIS.

From Meeting on new development in reactor mathematics and applications; Idaho Falls, Idaho (29 Mar 1971).

The Idaho Nuclear Code Automation (INCA) system to be implemented during the course of the Loss-of-Coolant Accident Analysis Program being conducted as part of the Loss-of-Fluid Test (LOFT) program is described. Most of the knowledge, both analytical and experimental, concerning nuclear safety analyses will ultimately reside in computer codes. The value and reliability of this knowledge depend upon the accessibility and ease of use of these codes. Some of the problems encountered in the present generation of nuclear safety codes are (1) difficulty in interfacing codes, (2) inconsistency between codes, (3) long running time to ensure stability, and (4) overemphasis on empirical correlations. A comprehensive plan for developing the third generation of nuclear safety codes with an integrated code automation system that will alleviate these difficulties is presented. 12 references. (auth)

31595 (DOCKET-50231-79) SOUTHWEST EXPERIMENTAL FAST OXIDE REACTOR. Request for Additional Information on Vessel Flange Bolt Stresses. (Division of Reactor Licensing (AEC), Washington, D. C.). 19 Apr 1971. 1p. Dep. NTIS.

31596 (DOCKET-50231-81) SOUTHWEST EXPERIMENTAL FAST OXIDE REACTOR. License No. DR-15; Technical Specifications Proposed Change No. 5. (General Electric Co., Sunnyvale, Calif. [Breeder Reactor Development Operation]). 28 Apr 1971. 8p. Dep. NTIS.

Technical specifications concerning thermal stress limits and inspection requirements for reactor vessel head bolts are presented. (D.C.C.)

31597 (IRS-R-1) SERIES OF GUIDE LINES AND RECOMMENDATIONS AUXILIARY TESTS. RECOMMENDATION ON REGULAR PERIODIC TESTS OF THE SAFETY OF NUCLEAR POWER PLANTS BY INDEPENDENT EXPERTS. (Technischer Ueberwachungs-Verein e. V., Cologne (West Germany). Institut fuer Reaktorsicherheit). Aug 1969. 20p. (In German). Dep. NTIS (U. S. Sales Only).

The regular periodic tests on the safety of nuclear power plants to be performed by independent experts are outlined, indicating the type of testing needed and the frequency of the test. Test recommendations are made for the reactor building,

XUM

the reactor core, reactor protection, reactor control and shutdown, radiation protection, primary coolant system, secondary coolant system, auxiliary circuits and devices, storage and handling of fuel elements, energy and current supply, catastrophic protection devices, and fire protection devices. (J.S.R.)

31598 (WCAP-7401) LOSS-OF-COOLANT ANALYSIS: COMPARISON BETWEEN BLODWN-2 CODE RESULTS AND TEST DATA. Fabic, Stanislav (Westinghouse Electric Corp., Pittsburgh, Pa. PWR Systems Div.). Nov 1969. 128p.

BLODWN-2 Code was written to describe the hydraulic transients within the reactor primary coolant system caused by the loss of coolant through an assumed rupture. Subcooled, transition and two-phase (saturated) blowdown regimes are considered. The code employs the method of characteristics and assumes one-dimensionality of flow and homogeneity of the liquid-vapor mixture. A degree of thermal nonequilibrium is specified through a special manner in which the local velocity of sound in the vapor-liquid mixture is computed. Initial nonuniformities of the liquid temperature distribution can be considered. These were found to be mainly responsible for the observed local pressure undershoots. The ability to consider multiple flow branches and a large number of mesh points (2400) gives the code the required flexibility to represent the various flow passages within the primary coolant system and in the detail necessary for tracking the acoustic decompression waves. These waves are mainly responsible for the loads on the reactor internals, piping and other system components. The various comparisons are presented for test data and BLODWN-2 calculation results. Good comparisons were obtained, starting with the blowdown of a simple pipe and ending with that of a complex primary coolant loop. Analysis of the blowdown of a larger vessel indicated that higher order effects introduced by the multidimensionality of flow and pressure fields cannot be obtained through simple one-dimensional modeling. A synthesis of an equivalent piping network would allow application of the one-dimensional BLODWN-2 program to such cases. Work is presently underway to determine the most suitable method for synthesizing networks that would satisfactorily bring out the effects of multidimensionality. (20 references) (auth)

31599 INTEGRATED MODEL FOR ANALYZING DISRUPTIVE ACCIDENTS IN FAST REACTORS. Sha, William T. (Argonne National Lab., Ill.); Waltar, Alan E. Nucl. Sci. Eng.; 44: 135-56(May 1971).

A two-dimensional (R-Z) integral model for characterizing fast reactor excursions from accident inception through core disassembly is presented. For predisassembly calculations, a Eulerian geometric model is used and multichannel heat-transfer computations are performed. Reactivity feedback due to Doppler broadening, coolant density change and voiding, and fuel movement are taken into account. A Lagrangian coordinate system is used in the disassembly phase, wherein the neutronics balance consists of Doppler broadening and material motion. A unique feature of the model is the ability to accommodate a pointwise Energy-Density-Dependent Equation-of-State according to the local sodium inventory that actually exists at the time of disassembly. By providing a consistent basis for establishing the effective reactivity ramp rate, Doppler coefficient, appropriate Equation-of-State, and temperature distribution at the start of core disassembly, much of the arbitrariness normally associated with large accident analyses can be removed. For most accident analyses, this model predicts a significantly lower energy yield during a superprompt critical nuclear excursion than would be computed by using the conventional modified Bethe-Tait analyses. 76 references. (auth)

31600 UNDERGROUND NUCLEAR POWER PLANTS: ENVIRONMENTAL AND ECONOMIC ASPECTS. Rogers, Franklyn C. (Harza Engineering Co., Chicago). Nucl. News; 14: No. 5, 36-9(May 1971).

Conceptual design parameters and cost factors associated with an underground 1000 MW(e) BWR-type nuclear power plant are presented. (D.C.C.)

31601 ASEISMATIC DESIGN OF EQUIPMENTS FOR NUCLEAR POWER STATION. Ochiai, Kanehiro; Nagayama, Tsutomu (Hitachi Ltd., Ibaraki, Japan). Hitachi Hyoron; 52: 887-91(Oct 1970). (In Japanese).

The components and equipment for nuclear power stations must be designed to withstand earthquake stresses. The principles for aseismatic design of the components and equipment are described. An example of mechanical model for inner structure of a BWR type reactor subjected to the dynamic response analysis and the flow chart of the calculating program is presented. (Japan)

31602 DIFFUSION DES PRODUITS DE FISSION. (Diffusion of Fission Products). International Congress Held at Saclay, France, November 4-6, 1969. Montrouge, France; Societe Francaise de Radioprotection (1970). 549p. (In French and English). (CONF-691104).

Thirty-one papers were presented and all of them were abstracted. They were grouped under the five following categories: models of reactor accidents; release of fission products from nuclear fuels; behavior and trapping of fission products in the primary loops and the containment shells of thermal neutron reactors; behavior and trapping of fission products in the primary loops and the containment shells of fast neutron reactors; radiological consequences of accidents. Abstracts of 4 of the papers appeared in previous issues of NSA. They may be located under CONF-691104 in the Report Number Index. (France)

For abstracts of individual papers see: 31530, 31566, 31567, 31583, 31603-31622, 31638, 31639, and 31642.

31603 NEED FOR CONSISTENCY IN ACCIDENT MODELS. Farmer, F. R. (United Kingdom Atomic Energy Authority, Risley, Eng.). pp 9-11 of Diffusion des Produits de Fission. Montrouge, France; Societe Francaise de Radioprotection (1970).

From International congress on the diffusion of fission products; Saclay, France (4 Nov 1969). See CONF-691104.

Accident models have become progressively embellished and complex. Time sanctifies past assumptions but other new conditions are added as imagination or later discoveries open new possibilities. Apart from this growth in complexity there is a general urge to evaluate conclusions with greater precision and to embark on expensive theoretical and experimental work to do this. A piecemeal growth of safety studies has led, and will continue to lead, to many inconsistencies: to some needless waste of effort and some out of balance in investment in protective measures. There is a need for greater realism and consistency in safety work. This requires the fundamental recognition that some events are more likely than others, and that in order to attach a degree of likeliness to accident models there must be a good understanding of the reactor both as a system and as an assembly of mechanical and electrical components. (auth) (France)

31604 APPRAISAL OF FISSION PRODUCT RELEASE AND RETENTION IN RELATION TO REACTOR SAFETY. Beattie, J. R. (United Kingdom Atomic Energy Authority, Risley, Eng.). pp 13-24 of Diffusion des Produits de Fission. Montrouge, France; Societe Francaise de Radioprotection (1970).

From International congress on the diffusion of fission products; Saclay, France (4 Nov 1969). See CONF-691104.

Prediction of the possible risks to the health and well-being of the population has rightly figured most prominently in accident analyses. In these studies people living in the neighborhood of the reactor are considered both as individuals and as a population group, and the remoter possibility affecting people living even further afield has also been taken into account. These analyses should lead to an improvement in the intrinsic safety of the reactor and to the introduction of relevant and reliable engineered safeguard systems. A rational study of the physical and chemical factors affecting the release of fission products and the possibilities of minimizing or preventing their subsequent release from the reactor building form an important part of these studies. These factors and their importance, relative to one another and in relation to overall reactor safety are discussed in the framework of the probability of occurrence of given types of accident, and of the nature and severity of the hazard to the population. (auth) (France)

31605 STUDIES FOR SAFETY ANALYSIS OF LOSS-OF-COOLANT ACCIDENTS. Fujie, H.; Yamanouchi, A.; Sagawa, N.; Cgasawara, H.; Murata, T. (Hitachi, Ltd., Tokyo). pp 59-77 of Diffusion des Produits de Fission. Montrouge, France; Societe Francaise de Radioprotection (1970).

From International congress on the diffusion of fission products; Saclay, France (4 Nov 1969). See CONF-691104.

In order to establish the method of safety analysis for loss-of-coolant accidents, an engineering test program was conducted using a non-nuclear mode reactor plant. In this program, several factors which affect the amount of fission products released from the reactor plant to the atmosphere were investigated experimentally and analytically. The temperature change of the sheathed heaters (simulated fuel rods) after loss-of-coolant in both the case with and without spray cooling was measured, and a method was obtained for calculating the temperature change of the fuel rods in a loss-of-coolant accident. The flow rates of steam water mixture through the orifices of 10 to 70 mm diameter from the pressure vessel were measured. A theory to predict critical flow rates was obtained. The experimental values agreed with the calculated values. Heat transfer coefficients of the structure in the

container vessel were obtained with measuring devices installed in the model container and the relation between the heat transfer coefficient, the time lapse, and the inner container pressure was obtained. The effects of the spray cooling system to reduce the inner-pressure of the container vessel, were measured using the model container. The relation between the container spray cooling-efficiency and the inner pressure was obtained from the experiments. (auth) (France)

31606 INSTANTANEOUS RELEASE OF SHORT PERIOD FISSION GASES IN FUEL PINS. Chenebault, P. (CEA, Grenoble, France). pp 79-86 of Diffusion des Produits de Fission, Montrouge, France; Societe Francaise de Radioprotection (1970). (In French).

From International congress on the diffusion of fission products; Saclay, France (4 Nov 1969). See CONF-691104.

During irradiation of a UO_2 pin at specific nuclear powers reaching 1600 W/cm^3, the fission gases released were collected and analyzed by γ spectrometry. Over a large moderate power region, the fraction of radioactive rare gases with half lives greater than 14 minutes is inversely proportional to their disintegration constant. (auth) (France)

31607 EXPERIENCES ON THE RELEASE OF IODINE FROM URANIUM DIOXIDE FUEL. Devell, L.; Carlson, F.; Hesboel, R.; Jansson, L.; Svensson, P. (Aktiebolaget Atomenergi, Studsvik, Sweden). pp 87-105 of Diffusion des Produits de Fission, Montrouge, France; Societe Francaise de Radioprotection (1970).

From International congress on the diffusion of fission products; Saclay, France (4 Nov 1969). See CONF-691104.

The significance of the different factors influencing the release of iodine from uranium dioxide fuel is discussed in view of the experiences obtained in the operation of the Swedish reactor and the experiments performed. Comparisons are made between results from out-of-pile measurements of release rate parameters and release data obtained during operation with damaged fuel at the 65 MW(t) Agesta Nuclear Power Station and during the testing of intentionally punctured fuel pins in a pressurized water in-pile loop. The results show lower but not very different release rates for iodine isotopes compared with noble gas isotopes with the same half-lives. Start-up and shutdown bursts of iodine for high rated elements were about one to a few per cent of the fuel inventory. Depending on experimental conditions the main portion of released iodine from pellets heated out-of-pile was either in the form of the element methyl iodide, or particulate. (auth) (France)

31608 EXPERIMENTAL STUDY OF THE EMISSION OF FISSION PRODUCTS DUE TO CLADDING FAILURES PRODUCED DURING A RAPID LOSS OF GASEOUS COOLANT (DERAPEG EXPERIMENT). Aji, M.; Le Go, P.; Lurie, R. (CEA, Saclay, France). pp 107-16 of Diffusion des Produits de Fission, Montrouge, France; Societe Francaise de Radioprotection (1970). (In French).

From International congress on the diffusion of fission products; Saclay, France (4 Nov 1969). See CONF-691104.

The experimental setup consisted of an EL4-type Pegase loop containing a fuel element, exposed to neutron flux, and a 20 m^3 container, which receives carbon dioxide during the loss of coolant. A few runs were carried out with different fuels (12 or 19 rods) and different claddings (stainless steel, beryllium-calcium and zirconium-copper). The rods were 11 mm in diameter and 450 mm long. Each bundle contained 4 to 7 kg of uranium dioxide. A few of them were filled with 15 kg/cm^2 helium to simulate the fission gas pressure. During the loss of coolant the carbon dioxide gas pressure varied exponentially between 60 and 1 kg/cm^2 in a period of 1 second. The maximum temperature reached was 1100°C. Different results were obtained with different fuels; the release rates for rare gases varied between 0.004% (stainless steel cladding) and 0.3% (beryllium calcium cladding). The release rates for ^{131}I and ^{133}I were about 100 times less. These low values might be explained by the low burnup. (auth) (France)

31609 UNINTENTIONAL FISSION PRODUCT RELEASES DURING NORMAL AND HIGH POWER LOAD CONDITIONS IN A BOILING HEAVY WATER TEST REACTOR. Ottersen, U.; Fjellestad, K. (Institutt for Atomenergi, Halden, Norway). pp 117-35 of Diffusion des Produits de Fission, Montrouge, France; Societe Francaise de Radioprotection (1970).

From International congress on the diffusion of fission products; Saclay, France (4 Nov 1969). See CONF-691104.

Fission product releases were studied in the Halden reactor. The experimental program, emphasizing fuel development, resulted in a number of fuel failures with accompanied releases of activity. A considerable proportion of the UO_2 test fuel assemblies operate with center temperatures in the 2,000 to 2,800°C range, and sometimes the cores are molten. In some of these cases, failures have occurred resulting in the release of large quantities of iodines and noble gases to the moderator. Some uranium has also escaped to the moderator. Estimated values for the percentages of iodines and noble gases released are given, and the way of reducing activities to tolerable values before release to the stack is dealt with. The intrusion of moisture through defects seems to be important in connection with the release of iodines. The carryover of iodine from the water to the steam phase observed is high compared with results obtained for other boiling water reactors. The distribution of the various iodine species (I_2, I^-, IO_3^- and organic iodides) between the steam and the moderator was studied. In the reactor the activity ratio of ^{131}I between unit volumes of condensed steam and moderator was in the 20 to 30% range. The concentration of non-volatile γ emitters (^{140}La, Zr, ^{95}Nb, ^{60}Co) in the condensed steam was 1% below that in the moderator. Solvent extraction methods were used to analyze the various iodine species in the steam phase and the moderator. (auth) (France)

31610 ACTIVITIES OF THE SCALBATRAIO CENTRE FOR RESEARCH IN NUCLEAR SAFETY: THE REMOVAL OF IODINE BY SPRAYS AND GENERAL PURPOSES. Guerrini, P. (Univ., Pisa, Italy); Lanza, S.; Mazzini, M.; (and others). pp 223-48 of Diffusion des Produits de Fission, Montrouge, France; Societe Francaise de Radioprotection (1970).

From International congress on the diffusion of fission products; Saclay, France (4 Nov 1969). See CONF-691104.

The main experimental facilities and research programs conducted at the new Scalbatraio Center for Nuclear Safety Research are reported. Emphasis is put on the iodine removal part of the research; the PSICO 10 facility is described, and preliminary results obtained are given. (auth) (France)

31611 TRAPPING OF METHYL IODIDE AT HIGH PRESSURE AND HIGH TEMPERATURE. Taylor, R.; Yuille, W. D. (United Kingdom Atomic Energy Authority, Sellafield, Eng.). pp 249-64 of Diffusion des Produits de Fission, Montrouge, France; Societe Francaise de Radioprotection (1970).

From International congress on the diffusion of fission products; Saclay, France (4 Nov 1969). See CONF-691104.

The trapping of methyl iodide by an impregnated charcoal in $CO_2-CO-CH_4$ atmospheres was investigated at pressures in the range 15 lbf/in.^{2} to 400 lbf/in.^{2} and temperatures from 20 to 300°C. The relative humidity of the gas, at these pressures and temperature, varied between 1% and 100%. The effectiveness of the material is described by a parameter obtained by dividing the product of the decontamination factor and the volume flow rate by the volume of the packed bed. This parameter is appropriate for operation for several hours up to ~230°C but above this temperature desorption becomes appreciable. At high pressures performance is sensitive to water contact below 100°C. For coolants containing 700 vpm water the boundary of the region in which the parameter exceeds 10, passes through 100 lbf/in.^{2} 20°C and 400 lbf/in.^{2} 104°C. Beyond this boundary the performance falls quite sharply. Within the region defined by these limits it is possible to design a trapping plant which is much smaller than would be required for equal performance at atmospheric pressure. (auth) (France)

31612 TRAPPING OF IODINE AND METHYL IODIDE AT HIGH TEMPERATURES. Caron, J. (CECA, Paris); Vandermeersch, J.; Charamathieu, A.; Thal, M. F. pp 285-300 of Diffusion des Produits de Fission, Montrouge, France; Societe Francaise de Radioprotection (1970). (In French).

From International congress on the diffusion of fission products; Saclay, France (4 Nov 1969). See CONF-691104.

An earlier study of iodine and methyl iodide trapping by 5 cm layers of activated coconut or coal carbons had shown that the efficiency at 200°C, after sweeping with the gas for a 4 hour period, was equal to at least 10^4 for nonimpregnated carbons and 10^5 for carbons impregnated with potassium iodide or triethylenediamine. In a further study the gas current was passed through for periods varying up to 7 days. It was then observed that at temperatures above 100°C the elution of iodine compounds increased with temperature. All the carbons showed a large efficiency drop, by at least a factor 100, during the first two days. After 6 days the efficiency at 200°C of impregnated coal carbons recommended for room temperatures falls to below 10. Coconut charcoal, at this temperature, still retains an acceptable efficiency, of the order of 1000 for iodine and 100 for methyl iodide, so long as the pre-test heating time is short, otherwise the charcoal deteriorates, probably by oxidation. Another adsorbent material, was sought which would be more resistant to high temperatures. Alumina and silica gels and molecular sieves were tested. Only 13 X silver exchanged molecular sieves gave a satisfactory efficiency for methyl iodide, in damp air at room temperature and in dry air at 200°C. However, the amount of silver required appears to be prohibitive. Research was therefore continued with

XUM

other impregnating materials. An additional 500 hour test at 350°C under argon gave an efficiency greater than 10^6 for the same 13 X silver exchanged molecular sieves. (auth) (France)

31613 RADIOCHEMICAL DETERMINATION OF BARIUM DIFFUSION COEFFICIENTS IN LIQUID SODIUM. Cooper, M. H.; Taylor, G. R. (Westinghouse Electric Corp., Madison, Pa.). pp 301-14 of Diffusion des Produits de Fission. Montrouge, France; Societe Francaise de Radioprotection (1970).

From International congress on the diffusion of fission products; Saclay, France (4 Nov 1969). See CONF-691104.

Diffusion coefficients for barium in liquid sodium have been determined radiochemically by measuring the concentration of excess ^{137m}Ba sorbed on the surfaces of specimens immersed in static sodium with about 1 mCi of dissolved ^{137}Cs. The experimental procedure consisted of equilibrating the specimen for one hour at constant temperature, withdrawing the specimen from the solution, and measuring the 0.662 MeV gamma emission from ^{137m}Ba (half-life, 2.6 minutes) as a function of time. After about twenty minutes, the gamma production is approximately constant and is due essentially to the ^{137m}Ba in equilibrium with the sorbed ^{137}Cs, since the excess sorbed ^{137m}Ba has decayed to a negligible level. The initial excess sorbed ^{137m}Ba activity is determined by subtracting the equilibrium ^{137m}Ba-^{137}Cs count rate from earlier count rates and graphically extrapolating this differential count to the initial time (i.e., the time at which the specimen was removed from the solution). The barium diffusion coefficients were calculated using Fick's second law and incorporating the production and decay of ^{137m}Ba. The diffusion coefficients for ^{137m}Ba were calculated and the measured excess sorbed ^{137m}Ba concentrations range from 1.90×10^{-6} cm^2/sec at 149°C to 3.9×10^{-5} cm^2/sec at 538°C with an activation energy of 5,230 cal/gm-mole when extrapolated to zero Cs concentration. Mathematical analyses have not yielded a suitable explanation for the observed concentration dependence. (auth) (France)

31614 BEHAVIOR OF BARIUM AND STRONTIUM FISSION PRODUCTS IN LIQUID SODIUM. Clough, W. S. (Atomic Energy Research Establishment, Harwell, Eng.). pp 315-25 of Diffusion des Produits de Fission. Montrouge, France; Societe Francaise de Radioprotection (1970).

From International congress on the diffusion of fission products; Saclay, France (4 Nov 1969). See CONF-691104.

A knowledge of the behavior of fission products in liquid sodium is important in the consideration of both the safety and the economic aspects of fast reactor operation. In normal operation the information can be used to predict the fate of fission products released into the sodium (e.g. plate out on walls or transport to trapping systems). In accident conditions the vapor pressure of the fission product in the sodium may be the rate determining step for its release to the environment. The behavior of the fission product with respect to both transport through liquid sodium and vaporization from the sodium will be mainly controlled by its chemical form. Thermodynamic calculations are presented which indicate that both strontium and barium are likely to be present as the oxide in reactor grade sodium. The volatility of the alkaline earth oxides is expected to be very low in reactor sodium but lack of basic data on their activity coefficients in liquid sodium prevents their vapor pressures from being calculated exactly. An apparatus is described in which the relative volatility of sodium and strontium has been measured at the temperature, concentration and level of sodium purity relevant to fast reactor application. As expected, the volatility of the strontium has been found to be very low at 500°C and escape of the alkaline earth fission products to the gas phase is not likely to present an important hazard in normal operation or accident conditions. Further results are presented which show that strontium is capable of migration in liquid sodium at 500°C and transport of strontium and barium fission products (to cooler sections of the system and cold traps) is to be expected in a fast reactor system. (auth) (France)

31615 OUT-OF-PILE STUDIES ON THE DIFFUSION OF THE CONTAMINATION IN LIQUID SODIUM AND FAST REACTOR CONTAINMENT VESSELS. DESCRIPTION OF EQUIPMENT AND PRELIMINARY RESULTS. Saroul, J. (CEA, Cadarache, France). pp 327-48 of Diffusion des Produits de Fission. Montrouge, France; Societe Francaise de Radioprotection (1970). (In French).

From International congress on the diffusion of fission products; Saclay, France (4 Nov 1969). See CONF-691104.

The principal aims of these out-of-pile experiments are the study of fission product behavior in sodium and argon, and the study of the behavior of the aerosols released by sodium fires and the associated contamination. The Pirana experiment has already provided interesting information on the partition coefficients of iodine, cesium and barium-lanthanum between liquid sodium and argon, and their plate-out on the walls under static conditions. This facility was modified by incorporating a purification circuit and a plugging meter. This loop is described and preliminary results on the diffusion of rare gases (^{85}Kr), under dynamic conditions, are presented. It is envisaged that this research will be continued with the fission products already mentioned. The study of the aerosols and the contamination released from sodium fires is designated the Fanal program and concerns essentially, the release, the transport in buildings and ducts, and the filtration. The experimental equipment is described. It consists of two vessels of 400 liters and 25 m^3 respectively, and a filter testing facility. Some results are given. (auth) (France)

31616 LMFBR AEROSOL RESEARCH AT ATOMICS INTERNATIONAL. Morewitz, H. A.; Silberberg, M. (Atomics International, Canoga Park, Calif.). pp 349-60 of Diffusion des Produits de Fission. Montrouge, France; Societe Francaise de Radioprotection (1970).

From International congress on the diffusion of fission products; Saclay, France (4 Nov 1969). See CONF-691104.

The release and transport of coolant, fuel, and fission product aerosols produced in postulated LMFBR accidents are under investigation at Atomics International. Aerosols produced in both sodium spray and pool fires, as well as those produced from vaporized fuel during the LMFBR design basis accident (DBA), are being studied. The program of research includes experiments in a variety of pressure vessels and theoretical modeling of the various situations. Semi-empirical descriptions of the fallout in the primary containment and subsequent leakage to the secondary have been developed, as well as more exact descriptions of the agglomeration and fallout process. The latter models are based on improved computer aided solutions of the Boltzmann equations formulated for sols. Aerosols of oxidized sodium released from sodium pool fires and sodium spray fires have been studied at concentrations from 2 μgm/cc to 200 μgm/cc. Aerosols from arc vaporized UO_2 have been observed at concentrations of 10^{-4} μgm/cc to 15 μgm/cc. Aerosol mixtures of Na_2O and U_3O_8 have also been investigated. These experiments have been compared to the models, and good agreement obtained over a wide range of parameters. These models may be used as an interim analysis technique while more exact characterization of the details of aerosol behavior is being developed. (auth) (France)

31617 EXPERIMENTS ON THE BEHAVIOR OF NUCLEAR AEROSOLS IN FAST BREEDER REACTOR CONTAINMENT. Schikarski, W.; Wild, H. (Kernforschungszentrum, Karlsruhe, Ger.). pp 361-74 of Diffusion des Produits de Fission. Montrouge, France; Societe Francaise de Radioprotection (1970).

From International congress on the diffusion of fission products; Saclay, France (4 Nov 1969). See CONF-691104.

The consequences of severe accidents in fast breeder reactors largely depend upon the generation and behavior of nuclear aerosols. It is shown that the aerosol model is a useful tool for describing the importance of the various aerosols parameters relevant to the accidental release and transport. The most important parameters are the particle number concentration, the airborne mass concentration, the particle size distribution and their time dependence. The TUNA facility (Teststand fuer die Untersuchung Nuklearer Aerosole) was used for the experimental determination of these parameters. Fast reactor accident conditions are simulated with respect to aerosol generation using the exploding wire technique, and with respect to aerosol behavior by the appropriate choice of atmosphere in the vessel. UO_2 aerosols were used. It was found that the particle number concentration decreased very rapidly during an initial time duration ($\leq$1 hr). After a period of less than two days the decrease in concentration exhibited exponential characteristics with a relatively long half-life. Experiments on the mass concentration revealed a different behavior with respect to time. However, three ranges were also identified with a more stable final range. The predominant processes occurring during the decrease in the aerosol concentration in the vessel were investigated; they are coagulation and sedimentation. An equation describing the particle number concentration as a function of time is derived. An upper limit for the long term aerosol mass concentrations is estimated to be 30 mg/m^3. (auth) (France)

31618 BEHAVIOR OF FISSION PRODUCT AEROSOLS IN RELATION TO THE SAFETY OF SODIUM COOLED FAST BREEDER REACTORS. Stoute, J. R. D.; Van de Vate, J. F. (Reactor Centrum Nederland, Petten, Netherlands). pp 375-94 of Diffusion des Produits de Fission. Montrouge, France; Societe Francaise de Radioprotection (1970).

From International congress on the diffusion of fission products; Saclay, France (4 Nov 1969). See CONF-691104.

The research is aimed at obtaining useful data for the safety evaluation of large sodium cooled fast breeder reactors. The most

XUM

important part of the investigations concerned sodium aerosols, pure or mixed with strontium acid, with nitrogen as the gaseous phase. The decay in the aerosol mass concentration as a function of time was studied. The experimental parameters were the concentrations of oxygen and water vapor in the nitrogen, light exposure, temperature gradients, and thermal convection. Research was also carried out on other aerosols, providing information about the long term stability of aerosols in confined spaces. The following parameters were studied: the volume, height, and internal surface of the aerosol vessel, the initial aerosol concentration and the specific energy of aerosol formation. In every case the aerosols were generated by the exploding wire technique, thus closely simulating accident conditions. The mass concentrations were determined using neutron activated aerosol material and counting the filter loads. Analysis of stereoscopic electronmicrographs of samples obtained from point to plane electrostatic precipitators revealed the dimensions of the primary aerosol particles and the chain-like agglomerates. (auth) (France)

31619 ESTIMATION OF AEROSOL CONCENTRATION IN A NUCLEAR REACTOR CONTAINMENT AFTER AN ACCIDENT. Davis, R. J. (Oak Ridge National Lab., Tenn.). pp 427-46 of Diffusion des Produits de Fission. Montrouge, France; Societe Francaise de Radioprotection (1970).

From International congress on the diffusion of fission products; Saclay, France (4 Nov 1969). See CONF-691104.

A computer code to estimate particle phase concentration vs time in a reactor containment has been devised. Several approximations but no empirical constants are used. The object was to provide a systematic hypothesis to guide experiments and illustrate that concentration vs time could be simply estimated from theory. The calculation uses the self-preserving particle size distribution and presumes three deposition mechanisms are important. The distribution function was derived from a steady state postulate. (auth) (France)

31620 SITE AND SAFEGUARD REQUIREMENTS FOR RADIOIODINE CONTROL. Willis, C. A. (McDonnel Douglas Astronautics Co., Santa Monica, Calif.). pp 447-63 of Diffusion des Produits de Fission. Montrouge, France; Societe Francaise de Radioprotection (1970).

From International congress on the diffusion of fission products; Saclay, France (4 Nov 1969). See CONF-691104.

Equations are developed relating leak rates and cleanup rates to exclusion radius and low-population distance requirements for the control of radioiodine. Only constant leak and cleanup rates are considered but both single and double containment systems are evaluated, with and without stacks. Results are given for a 25% release of the radioiodine from a 10^{-3} MW(t) reactor. (auth) (France)

31621 ESCAPE INTEGRALS, A USEFUL CONCEPT IN REACTOR HAZARD EVALUATION. Alonso, A.; De La Cruz, F. D. (Junta de Energia Nuclear, Madrid). pp 465-76 of Diffusion des Produits de Fission. Montrouge, France; Societe Francaise de Radioprotection (1970).

From International congress on the diffusion of fission products; Saclay, France (4 Nov 1969). See CONF-691104.

By the introduction of the escape integral concept it was possible to develop a practical method to assess the amount of each fission nuclide of interest escaping to the environment in the case of an accident. This assessment is a major element in predicting nuclear reactor hazards. For a given situation the escape integral depends on the physical and chemical properties of the fission nuclide, on the type and characteristics of the reactor containment and its engineered safeguards and on the accident itself. Analytical expressions are given for single and double containment systems incorporating different types of engineered safeguards and for explosion, fire, and slow-meltdown type reactor accidents. A digital computing method to solve the expressions for explosion type accidents with one or two containment barriers is included. This formulation can be easily extended to more than two barriers. Some numerical results, obtained by this method are presented. (auth) (France)

31622 CONSEQUENCES OF ACCIDENTS IN NUCLEAR PLANTS. Candes, P.; Guirlet, J.; Bessis, J. (CEA, Saclay, France). pp 477-88 of Diffusion des Produits de Fission. Montrouge, France; Societe Francaise de Radioprotection (1970). (In French).

From International congress on the diffusion of fission products; Saclay, France (4 Nov 1969). See CONF-691104.

No matter how stringent the precautions securing the containment of radioactive products, the possibility of accidental escape cannot be excluded. Firstly, the working personnel and then the neighboring population to the nuclear plant are exposed to risks. It is necessary to evaluate the consequences of such accidents in order to take steps to avoid the spreading of contamination. A computer program was developed for evaluating the activities due to the fission products, the irradiation conditions, the duration of the irradiation, and the time lag between the occurrence of the accident and the suppression of the radiation being taken into account. A second program using the results of the first allows the estimation of the likely doses to be sustained by workers and the population. External and internal doses are considered, inside and outside the building, and at larger distances beneath the plume; the deposition by the plume is also considered. (auth) (France)

Power Conversion Systems

31623 (GA-10338) STEAM GENERATORS FOR HIGH-TEMPERATURE GAS-COOLED REACTOR PLANTS IN THE U.S.A. Schuetzenduebel, W. G. (Gulf General Atomic, Inc., San Diego, Calif.). 19 Mar 1971. Contract AT(04-3)-633. 135p. Dep. NTIS.

The development of steam generators for gas-cooled high-temperature reactors is described. The development from the existing steam generators operating at the 40 MW(e) plant at Peach Bottom to those developed for the 330 MW(e) plant at Fort St. Vrain is reviewed. Data on the steam generator designs for an 1100 MW(e) commercial HTGR plant and for a 300 MW(e) gas-cooled fast reactor demonstration plant are included. 17 references. (auth)

31624 (JUL-698-RG) MEDEA: MODEL OF A STEAM PLANT. DESCRIPTION OF USE. Hansen, Ulf (Kernforschungsanlage, Juelich (West Germany). Institut fuer Reaktorentwicklung). Sep 1970. 146p. (In German). Dep. NTIS (U. S. Sales Only).

MEDEA calculates the time independent pressure and temperature distribution in a helium-water steam generator. The changing material properties of the fluids with pressure and temperature are treated exactly. The steam generator may consist of economizer, evaporator, superheater and reheater in variable flow patterns. In case of reheating the high-pressure turbine is taken into account. The main control circuits influencing the behavior of the system are simulated. These are water spraying of the hot steam, load dependent control of steam pressure at the HP-turbine inlet and values before LP-turbine to ensure constant pressure in the reheater section. Investigations of hydrodynamic flow stability in single tubes can be performed. The program is written in FORTRAN IV for the IBM 360/75. (auth)

31625 GAS TURBINE PLANTS. (to Sulzer Brothers Ltd.). British Patent 1,228,797. 21 Apr 1971. Priority date 27 Jul 1967, Switzerland.

REACTORS, POWER—power conversion system for, description of carbon dioxide gas turbine (D.C.C.)

Research and Test Reactors

Refer also to abstracts 29362, 29410, 29819, 31182, 31530, 31533, 31568, 31573, and 31622.

31626 (BNWL-576) FFTF OUT-OF-REACTOR CRITICALITY SAFETY: OBJECTIVES AND CRITERIA. Brown, C. L. (Battelle-Northwest, Richland, Wash. Pacific Northwest Lab.). Nov 1967. Contract AT(45-1)-1830. 11p. Dep. NTIS.

The FFTF will be reviewed for criticality safety at each stage of design. Limits and controls will be specified wherever necessary to assure criticality safety. The minimum requirement in all FFTF operations will be that no single action, credible error, or equipment failure be capable of causing accidental criticality. Evaluations will be based on well established criticality safety principles. (auth)

31627 (BNWL-585) RADIOACTIVITY IN FFTF CLOSED LOOPS. Brehm, W. F.; Koehmstedt, P. L.; Kovacevich, E. A.; Shannon, D. W. (Battelle-Northwest, Richland, Wash. Pacific Northwest Lab.). Oct 1967. Contract AT(45-1)-1830. 46p. Dep. NTIS.

Two major Fast Flux Test Facility (FFTF) design requirements are (1) the capability of running closed loop fuel tests to failure and (2) at the same time maintaining a system of high reliability and availability. A quantitative study of the expected levels of deposited radioisotopes in the FFTF system is presented. The study discusses FFTF requirements, describes probable closed loop contamination levels from corrosion products, vented fuel, and failed fuel, relates potential FFTF radiation levels to past sodium reactor experience, and relates closed loop development activities to FFTF needs. 13 references. (H.D.R.)

XUM

31628 (BNWL-586) CALCULATED CRITICAL PARAMETERS FOR FFTF FUEL UNDER MELTDOWN CONDITIONS. Brown, C. L. (Battelle-Northwest, Richland, Wash. Pacific Northwest Lab.). Sep 1967. Contract AT(45-1)-1830. 6p. Dep. NTIS.

In FFTF operations involving irradiated fuel, criticality safety evaluations must take into consideration the possibility of fuel meltdown due to accidental loss of cooling. To provide a basis for these evaluations, critical masses were estimated for unmoderated PuO_2-UO_2, PuC-UC, and PuO_2-SS fuel pins in spherical, cylindrical, and hemispherical geometry. For 30 wt % PuO_2-UO_2, the critical number of undamaged subassemblies is 15. Under meltdown conditions, the critical number would be between 7 and 11 subassemblies, depending on the resultant geometry. (auth)

31629 (BNWL-587) FFTF CRITICALITY SAFETY SYSTEM 71: INERT GAS CELL EXAMINATION FACILITY CONCEPTUAL DESIGN EVALUATION. Brown, C. L. (Battelle-Northwest, Richland, Wash. Pacific Northwest Lab.). Sep 1967. Contract AT(45-1)-1830. 6p. Dep. NTIS.

Criticality safety in System 71 is based on the assumption that the fuel cannot be moderated. The calculated minimum critical number of unmoderated subassemblies side by side is 15; under meltdown conditions, the minimum critical number is seven. It is recommended that unit operations be limited to one, or at the most two, subassemblies; and that storage of subassemblies be in a single-row slab arrangement, with 12 in. between subassemblies in a row and a six-foot spacing to other fissile material. (auth)

31630 (BNWL-630) FFTF PNL: RELIABILITY ASSURANCE PROGRAM PLAN FOR THE FFTF. Albert, W. G. (Battelle-Northwest, Richland, Wash. Pacific Northwest Lab.). Nov 1967. Contract AT(45-1)-1830. 54p. Dep. NTIS.

The PNL Reliability Assurance Program constitutes a formal method for: (1) Providing objective review of FFTF design, testing and supporting activities; and (2) Controlling design and test activities of PNL and PNL contractors to ensure effective implementation of the Reliability Assurance Requirements for the FFTF. A Reliability Assurance Program Plan is presented which defines responsibilities and describes reliability assurance tasks to be performed. The program plan, along with detailed reliability assurance procedures required for implementing tasks described in the plan, will be incorporated into a PNL Reliability Assurance Manual for the FFTF. (auth)

31631 (DOCKET-50231-80) SOUTHWEST EXPERIMENTAL FAST OXIDE REACTOR. Characteristic Curves for the Fast Reactivity Excursion Device Poison Slugs. (General Electric Co., Sunnyvale, Calif. Breeder Reactor Development Operation). 23 Apr 1971. 11p. Dep. NTIS.

31632 (FEI-201) STUDIES OF PHYSICAL CHARACTERISTICS OF THE CRITICAL ASSEMBLY MOCKUP FOR THE BOR-REACTOR. Blyskavka, A. A.; Bondarenko, V. V.; Voropaev, A. I.; (and others) (Gosudarstvennyi Komitet po Ispol'zovaniyu Atomnoi Energii SSSR, Obninsk. Fiziko-Energeticheskii Institut). 1970. 44p. (In Russian). Dep. NTIS (U. S. Sales Only).

31633 (IJS-253) DESCRIPTION OF THE INSTITUTE AND WORKS PERFORMED DURING THE SUMMER OF 1969. Smalc, Andrej (Institut Jozef Stefan, Ljubljana (Yugoslavia)). Mar 1970. 120p. (In Slovenian). Dep. CFSTI (U. S. Sales Only).

Following a general introduction and overview of the work of the Institute and its purpose, the various divisions are discussed in detail —physics, chemistry, biochemistry, mathematics, reactor, radiation safety, and information. The organization is described, with names of individuals in various positions, and publications in journals, books, conference proceedings, and other literature are listed for each section of each division. (TTT)

31634 (SRRC-41/71) REPORT ON SESSION 1969/1970. Wilson, H. W. (Scottish Research Reactor Centre, East Kilbride (Scotland)). Jan 1971. 20p. Dep. NTIS (U. S. Sales Only).

Design modifications and experimental programs for the Scottish Universities Reactor are described. (D.C.C.)

31635 (Y-DR-44) STATIC AND DYNAMIC EXPERIMENTS WITH A REPETITIVELY PULSED BOOSTER. Mihalczo, J. T. (Union Carbide Corp., Oak Ridge, Tenn. Y-12 Plant). 22 Mar 1971. Contract W-7405-eng-26. 56p. Dep. NTIS.

A series of dynamic measurements were performed with a multiplying assembly in which a rotating beryllium reflector (worth 4.8 dollars in reactivity) moved past an unreflected core surface ~60 times/sec at a speed of 264 meters/sec. A pulse of 14.1 MeV neutrons (~1 μsec wide) was injected into the assembly each time the rotating reflector attained a position for which the reactivity of the assembly was maximum. The time distribution of neutrons after injection of the pulse was measured. The maximum prompt neutron multiplication of the assembly, which was reflected with iron on all sides but one and contained 58.6 kg of uranium (enriched to 93.2 wt% in ^{235}U isotope) metal at delayed criticality, was varied by fuel loading changes from 75 to 285. The pulsed assembly, with a maximum prompt neutron multiplication of 285, produced neutron pulses having a width at half maximum of 3.9 μsec and a peak-to-minimum ratio of 12,400. The pulse, when thermalized by a $10.16 \times 10.16 \times 3.81$ cm polyethylene scatterer, was broadened to a width at half maximum of 20.9 μsec with a peak-to-minimum ratio of 1590. The use of cadmium in the scatterer can neither reduce the width of the pulse of neutrons to less than 7 μsec nor increase the peak-to-minimum ratio to more than 7400. The fraction of all neutrons that are in the pulse varied with reactivity and the position of the measurement from 0.77 to 0.85. The number of thermal neutrons leaking from the outer surface of the scatterer was 3.3×10^{-5} n/cm^2-fission. Thus, a repetitively pulsed booster of this type with 1/60 MW-sec of energy in the pulse would produce a leakage fluence of $\sim 1.7 \times 10^{10}$ thermal neutrons/cm^2 per pulse. 17 references. (auth)

31636 CODE OF GOOD PRACTICES FOR THE PERFORMANCE OF CRITICAL EXPERIMENTS. ANS-STD.1 1967. Hinsdale, Ill.; American Nuclear Society (1967). 2p. Available from American Nuclear Society, Hinsdale, Ill.

This Code of Good Practices is for guidance in the performance of critical experiments. It is intended for catholic applicability and is formulated in general terms in order to avoid imposing undue limitations on specific local experiment practices. (auth)

31637 PROPOSED GUIDE FOR THE DESIGN OF A NUCLEAR POOL FACILITY, REVISION 11. ANS 7.20 1966. Hinsdale, Ill.; American Nuclear Society (1966). 3p. Available from American Nuclear Society, Hinsdale, Ill.

Recommendations for the design of a nuclear pool facility are presented. A nuclear pool is defined as a contained body of water for attenuating nuclear radiation from a reactor or cooling and storing radioactive materials or both. The top surface of the water is usually exposed to the atmosphere. This guide is applicable only to the design of light-water filled pools. Particular emphasis is given to design-recommendations developed to cope with the health and safety hazards that will be associated with the radioactive materials in the pool. These hazards shall be considered in the design and construction of a nuclear pool facility. Design features such as piping design, concrete structural design, and welding design, insofar as they pertain to structural strength, are not considered because they are covered by existing standards, codes, and practices, viz., those of ASA, AWS, ASTM, ACI. Where not specifically designated herein applicable parts of the existing standards, codes, and practices shall be used as agreed upon between buyer and seller. Specific recommendations are: piping containing radioactive or potentially radioactive fluids should be designed in accordance with ASA B31.1, Code for Pressure Piping and applicable Special Rulings; valves in these systems should conform to ASA B16.5, Code for Steel Pipe Flanges and Flanged Fittings; and tanks or other fabricated vessels that will contain radioactive or potentially radioactive fluids shall be designed in accordance with the ASME Boiler and Pressure Vessel Code, Section VIII. Where existing standards, codes and practices must be modified because of radiation effects, nuclear hazards, and the need to prevent contamination of the environment, this guide shall apply. This guide does not recommend or endorse any particular design or product or limit in any way the choice of design or construction to conform with the guide. (auth)

31638 ANALYSIS OF THERMAL RELIABILITY OF THE RA REACTOR CORE. Milivojevic, S.; Mitrovic, S. (Boris Kidric Inst. of Nuclear Sciences, Belgrade). pp 25-38 of Diffusion des Produits de Fission. Montrouge, France; Societe Francaise de Radioprotection (1970).

From International congress on the diffusion of fission products; Saclay, France (4 Nov 1969). See CONF-691104.

A method is presented, which allows the behavior of various reactor constants, their fluctuations about mean values, and the probabilities of reaching or exceeding certain limiting values to be determined from statistical data obtained during the operation of the reactor. The method also facilitates the comparison of analytical data with calculated and critical values. The method is used in analyzing the maximum temperature of the fuel cladding of the RA reactor at Vinca. An operating period of two years at a nominal power of 6.5 MW was studied, all the working aspects being considered. The possibility of applying the method to the control and safety procedures of the reactor and improving the results obtained for accident analysis after a certain operating period is discussed. (auth) (France)

XUM

31639 BEHAVIOR OF CERTAIN FISSION PRODUCTS DURING AN ACCIDENT IN THE SILOE REACTOR. Amardeil, P. (CEA, Grenoble, France). pp 137-43 of Diffusion des Produits de Fission, Montrouge, France; Societe Francaise de Radioprotection (1970). (In French).

From International congress on the diffusion of fission products; Saclay, France (4 Nov 1969). See CONF-691104.

On November 7, 1967, an element of the Siloe core partially melted as the result of an accident. This element was of the Si-23 type (aluminum alloy and 93% enriched uranium with aluminum cladding). Samples were taken from the melted and non-melted regions. An analysis was performed to determine the percentages of the radioelements (^{95}Zr, ^{144}Ce, ^{137}Ce, ^{103}Ru, ^{90}Sr and ^{140}Ba + La) lost by the fuel. The results obtained are in general significant but incomplete as the analytical means employed was limited and the integrated flux received by the molten fuel not completely known. Attempts were also made to determine the behavior of fission products present in the water and in the air. (auth) (France)

Rocket and Space Reactors

31640 (ORNL-TM-3368) DESIGN OF ASYMMETRIC 4π SHIELDS FOR SPACE REACTORS. Engle, W. W. Jr.; Childs, R. L.; Mynatt, F. R. (Oak Ridge National Lab., Tenn.). 1 Apr 1971. Contract W-7405-eng-26. 19p. (CONF-710304-7). Dep. NTIS.

From Symposium on natural and manmade radiation in space; Las Vegas, Nev. (1 Mar 1971).

A one-dimensional shield optimization program based on the method of discrete ordinates has been developed and is used to determine material thicknesses used in asymmetric 4π shields for space power reactors. The two-dimensional discrete ordinates program DOT is used to check the design and the information generated in the DOT calculation is used as a guide in shaping the shield which may be considered a first step in two-dimensional shield optimization. 6 references. (auth)

31641 REUSABLE NUCLEAR SHUTTLE: ITS OPERATION, TEST PROGRAM, AND PROBLEM AREAS. Boehmer, Clifford B. (McDonnell Douglas Astronautics Co., Huntington Beach, Calif.). pp 422-7 of Proceedings of the Institute of Environmental Sciences 17th Annual Technical Meeting and Equipment Exposition, April 26-30, 1971, Los Angeles, California. Mt. Prospect, Ill.; Inst. of Environmental Sciences (1971).

From 17. annual meeting and equipment exposition; Los Angeles, Calif. (26 Apr 1971). See CONF-710409.

One of the elements of the integrated program plan for space exploration is the Reusable Nuclear Shuttle (RNS). This vehicle will use the NERVA nuclear engine to provide low-cost transportation to lunar and geosynchronous orbit. Current design and development studies of the RNS have produced two concepts, (1) a single 33-ft-diameter propellant tank and (2) a cluster of 15-ft-diameter modules which would be placed in orbit by the Space Shuttle and assembled in a 260-nmi earth orbit. The design, testing, and safety aspects of the RNS are described. (auth)

31642 NORMAL RUN AND THE ACCIDENT CASE FOR A NUCLEAR ROCKET ENGINE. Bernhardt, D. E.; McBride, J. R. (Public Health Service, Las Vegas, Nev.). pp 45-57 of Diffusion des Produits de Fission, Montrouge, France; Societe Francaise de Radioprotection (1970).

From International congress on the diffusion of fission products; Saclay, France (4 Nov 1969). See CONF-691104.

Project Rover is the U. S. program to develop a nuclear powered rocket for deep space exploration. The reactor for this application is unique in that it is an open cycle hydrogen cooled reactor. The core is composed of fuel elements made up of uranium carbide beads in a graphite matrix. The reactor operates at high power densities with coolant temperature up to 4500°R. The normal radioactive effluent releases are composed of fission products diffusing through the fuel (primarily noble gases and halogens) and small particulate matter from erosion and corrosion of the core. Because of the experimental nature of the reactor and the radioactive effluent releases the tests are conducted at the Nuclear Rocket Development Station, Nevada, in a relatively isolated area. The reactor tests are conducted under the supervision of a safety advisory panel which is supplied with meteorological and dose predictions. There is active monitoring and tracking of the effluent by the Southwestern Radiological Health Laboratory. The dose predictions include both a normal run estimate and a maximum credible accident (MCA) evaluation. The normal run release is based on experience from previous tests and the change in diffusion coefficients of the fission products with the temperature of the core-integral power may be 10^8 MW-sec or more with fission product releases around 1 percent. The accident analysis is based on a controlled drum-roll-out excursion experiment where the reactor was tested to destruction to simulate an MCA—10^4 MW-sec and about 70 percent fission product release. The general population exposures to date have been well below the guidelines set by the Federal Radiation Council. Results from the Phoebus 1B test are used to illustrate the predictions and actual results. (auth) (France)

Marine and Portable Power Reactors

31643 GUIDE FOR THE CLASSIFICATION OF NUCLEAR SHIPS. ABS-01 1962. New York; American Bureau of Shipping (1962). 16p. Available from American Bureau of Shipping, New York.

Information relating to guides for the design and development of nuclear powered merchant ships is presented under the following headings: hull, containment, pressure vessels, nuclear piping and ductwork systems, reactor core and fuel elements, control and instrumentation, standby components, emergency components, spare parts, special nuclear considerations, and surveys. (D.C.C.)

31644 DANGERS OF IONIZING RADIATIONS IN NAVAL NUCLEAR PROPULSION. Cozza, Alberto. Ann. Med. Nav., 72: 409-16(Jul-Aug 1967). (In French).

The possible hazards to crew or the environment from operation of nuclear powered ships are discussed. Although potential accident risks are low, the establishment of international rules for nuclear ships is needed. (H.D.R.)

Production Reactors

31645 (BNWL-1527) EXPERIMENTAL DRIFTS OF JUVENILE SALMONIDS THROUGH EFFLUENT DISCHARGES AT HANFORD. PART II. 1969 DRIFTS AND CONCLUSIONS. Becker, C. D.; Coutant, C. C.; Prentice, E. F. (Battelle-Northwest, Richland, Wash. Pacific Northwest Lab.). Jan 1971. Contract AT(45-1)-1830. 61p. Dep. NTIS.

Field investigations were conducted from March to September, 1968 and 1969 to determine the effect of heated reactor effluents on juvenile salmonids passing through the central Columbia River. The fundamental approach was to drift groups of fish held in live-boxes through areas representing maximum thermal increments while monitoring exposure temperatures and subsequently comparing survival or mortality among test and control groups. Drifts were conducted either through shoreline areas, which received heated water via intragravel seepage from shoreline retention basins (peculiar to the Hanford site), or through midriver effluent plumes that issued from subsurface point discharges. Results of the investigations are presented. 22 references. (auth)

31646 (DUN-SA-136) ON OPERATION OF HALOGEN QUENCHED GEIGER-MUELLER TUBES. Worster, L. D. (Douglas United Nuclear, Inc., Richland, Wash.). 4 Jun 1970. 21p. Dep. NTIS.

The Hanford N Reactor fuel element rupture monitoring system consists of 1004 channels containing halogen quenched GM tubes for continuous monitoring of coolant samples. The system is described, and the modifications performed to correct an extremely high failure rate of the GM tubes are discussed. 8 references. (H.D.R.)

Reactor Theory

Refer also to abstract 31533.

31647 (HEDL-TME-71-40) CROSS SECTION STRUCTURE FACTOR INTERPOLATION SCHEMES. Kidman, R. B. (Hanford Engineering Development Lab., Richland, Wash.). Mar 1971. Contract AT(45-1)-2170. 16p. Dep. NTIS.

To carry out multigroup calculations requires effective group cross sections. One way of obtaining such cross section sets is to multiply infinitely dilute group constants with temperature and composition dependent correction factors (also called structure factors, f-factors, or self-shielding factors). Since only a finite number of reactor compositions can be represented in any table of f-factors, interpolation schemes are used to obtain f-factors for media with intermediate temperatures and/or compositions. The actual structure factor behavior has suggested new interpola-

XU

tion schemes. These new schemes (1DX-M1) are described and some comparisons made with previous interpolation routines. (auth)

31648 (KFKI-70-30-RPT) DETERMINATION OF NEUTRON SPECTRA FROM ACTIVATION DATA BY MEANS OF RFO1 AND RFO7 CODES. Turi, L.; Fisher, A. (Magyar Tudomanyos Akademia Kozponti Fizikai Kutato Intezete, Budapest). [nd]. 18p. (In Russian). Dep. NTIS (U. S. Sales Only).

Two methods for unfolding neutron spectra from activation data are described. Program RF01 can be used only for the case of threshold detectors. Program RF07 has no such restrictions. By using proper foils the spectrum in the whole energy range of reactors can be determined simultaneously. The algorithm of the methods and input/output specifications of the codes are given. (auth)

31649 OPTIMIZATION OF NUCLEAR SYSTEMS BY GEOMETRIC PROGRAMMING. Bouchey, G. D.; Beightler, C. S.; Koen, B. V. (Univ. of Texas, Austin). Nucl. Sci. Eng.; 44: 267-72(May 1971).

The general mathematical relations required for the geometric programming solution of problems in the analysis and optimization of nuclear systems are developed. The method is applied to simplified problems in the field of nuclear engineering. The example problems concern: (1) minimization of the cost of storing and shipping radioactive nuclear fuels; (2) optimization of sampling techniques in the measurement of special nuclear materials; and (3) optimization of reactor core geometry and composition. 12 references. (H.D.R.)

Kinetics

Refer also to abstracts 31173, 31175, 31183, 31545, 31592, 31598, and 31638.

31650 (AEEW-M-1012) PARAMETER FITTINGS OF A NUCLEAR REACTOR MATHEMATICAL MODEL IN THE FREQUENCY DOMAIN WITH ALTERNATIVE FORMS OF WEIGHTING FUNCTION. Cummins, J. D. (Atomic Energy Establishment, Winfrith (England)). Apr 1971. 12p. Dep. NTIS (U. S. Sales Only). UK 7½p.

One aspect of the matching of mathematical models to experimental responses is considered. The integral least squares difference between open loop experimental and model frequency responses is modified by a weighting function, so as to emphasize in the model matching the part of the experimental open loop frequency response in the region of the (−1.0) point on the Nyquist Diagram. The intuitive idea behind this form of weighting function is to obtain a mathematical model which is equivalent to the industrial plant, at least as far as stability in the linear sense is concerned, and also a model which will respond in a similar manner to demand changes and disturbances when the control loop is closed. (auth) (UK)

31651 (ANL-7717) ARC SYSTEM: ONE-DIMENSIONAL TRANSPORT THEORY CAPABILITY, SNARC1D. Bryant, L. T.; Leaf, G. K. (Argonne National Lab., Ill.). Jan 1971. Contract W-31-109-eng-38. 387p. Dep. NTIS.

The modules described are based upon a translation of the transport code SNARG-1D. The computational module NUC003 solves the discrete-ordinate S_N approximation to the one-dimensional multigroup neutron transport equation, using the numerical approximations and solution techniques developed by Bengt Carlson. Module NUI005 processes the input data required for execution of NUC003. Module-dependent input is accepted in the form of a BCD data set and/or a binary data set. Isotropic and linearly anisotropic scattering between energy groups is permitted. Real or adjoint solutions may be calculated for homogeneous or inhomogeneous problems. Standard angular quadrature sets for S_N orders up to 16 are provided for slab and spherical geometry. Alternative angular quadrature schemes may be obtained by supplying appropriate input. Inhomogeneous sources of two types are permitted: volume sources (neutrons per unit volume per sec) and surface sources (neutrons per unit surface area per sec). A rudimentary group-skipping option in which user-specified groups are not recalculated during the iteration processes is provided to accelerate convergence. A P_1 calculation may be performed for specified groups. These two options are mutually exclusive. Three types of searches can be performed to achieve a specified reactivity: (1) Dimension criticality search, in which region boundaries within the reactor may be varied and/or the size (outside dimension) of the reactor may be varied; (2) Concentration search, operating on the volume fractions of the materials modifying, as necessary, each cross section type; or (3) Inverse reactor period (α) search, in which the flux is assumed separable with respect to space and time, with time variation given by exp (αt). Output edits are provided and appropriate output data sets are written. (auth)

31652 (KFK-1353) TREATMENT OF SPACE DEPENDENCE OF THE ENERGETIC RESONANCE SELF SHIELDING AT BOUNDARIES OF HOMOGENEOUS ZONES IN REACTORS. Huschke, H. (Kernforschungszentrum, Karlsruhe (West Germany). Institut fuer Neutronenphysik und Reaktortechnik). Jan 1971. 117p. (In German). Dep. NTIS (U. S. Sales Only).

Thesis. Submitted to Karlsruhe Univ., Ger.

The problem of space dependent resonance self shielding at boundaries is investigated for the case of two half-spaces with different concentration of a resonant material. A formalism is developed which allows a description of this phenomenon, also at boundaries of narrow zones by using the f-factor tables of the existing Karlsruhe group cross section sets. For two assemblies the influence of space dependent resonance self shielding on important reactor parameters is investigated. 21 references. (auth)

31653 (KFK-1361) STRATEGY FOR SPEEDING UP TWO-DIMENSIONAL SN-METHODS WITH THE HELP OF THE COARSE LATTICE TECHNIQUE. Kinnebrock, W. (Kernforschungszentrum, Karlsruhe (West Germany). Institut fuer Neutronenphysik und Reaktortechnik). Jan 1971. 14p. (In German). Dep. NTIS (U. S. Sales Only).

The time of two dimensional SN-calculations can be shortened if the initial flux is prepared by a SN-calculation with less spatial points. Also this initial calculation can be shortened in time in the same way. In this connection there arises the question for a strategy, which influences the global calculation-time in an optimal way. Presented is a statistical interpretation of 120 transport-problems, calculated by the two dimensional SN-code "SNOW" with different strategies. Simultaneously there is developed a theory, describing the calculation-time in dependence of the applied strategy. This theory made it possible to find strategies which save about 60% calculation-time in the mean. 11 references. (auth)

31654 APPLICATION OF ALTERNATING-DIRECTION IMPLICIT METHODS TO THE SPACE-DEPENDENT KINETICS EQUATIONS. Wight, A. L.; Hansen, K. F.; Ferguson, D. R. (Massachusetts Inst. of Tech., Cambridge). Nucl. Sci. Eng.; 44: 239-51(May 1971).

An approximate solution of the multigroup neutron diffusion kinetics equations with delayed neutrons in two-dimensional geometry can be obtained by matrix splitting methods based on an Alternating-Direction Implicit (ADI) scheme. The method is shown to be consistent and numerically stable. An exponential transformation of the semi-discrete equations reduces the truncation error so that the method becomes usable for practical computations. The results of numerical experiments are presented to illustrate the accuracy and stability of the method. These results indicate that another splitting method based on an Alternating-Direction Explicit scheme is slightly superior. 11 references. (auth)

31655 SOME COMMENTS ON PERTURBATION THEORY. Selengut, D. S. (Knolls Atomic Power Lab., Schenectady, N. Y.). Nucl. Sci. Eng.; 44: 272-5(May 1971).

Perturbation expressions for a reactor system are developed regarding the problem as one of finding the difference in some scalar parameter between two arbitrary systems, in which any similar terms are canceled analytically. The results reduce to familiar expressions in the proper limit, but are more general in some respects. (H.D.R.)

31656 SYNTHESIS OF FAST REACTOR SPACE-ENERGY NEUTRON FLUXES. Ombrellaro, P. A. (Argonne National Lab., Ill.). Nucl. Sci. Eng.; 44: 204-20(May 1971).

Spectral synthesis methods, in which the space-energy flux is synthesized from known flux spectra, are applied to one-dimensional, fast reactor static problems. The methods include few-group synthesis models that employ either the same trial spectra in all regions of the reactor model or different trial spectra in different spatial regions. Numerical results demonstrate that the space-energy flux can be adequately represented by these few-group synthesis models; moreover, the spatially dependent spectra agree very well with similar, "exact" flux spectra calculated by direct multigroup methods. Region-integrated reaction rates calculated with the synthesized flux spectra are in good agreement with those calculated with the flux spectra derived from direct methods. 23 references. (auth)

31657 HOROWITZ OPERATORS FOR ORGANIC MODERATORS. Kammerer, Peter (Univ., Karlsruhe, Ger.). Atomkernenergie; 17: 189-91(May 1971).

XUM

The construction of simple 5-parameter scattering operators for organic moderators is performed starting from experimental neutron spectra, which are measured under the conditions of a homogeneous, nearly infinite-medium. These operators retain the same form for all those hydrogeneous organic moderators but with different values of the parameters. They allow an easy analytical treatment of neutron spectra. 5 references. (auth)

31658 MEASUREMENT AND THE CALCULATION OF NEUTRON SPECTRA IN IRON ASSEMBLIES. Kimura, Itsuro; Sekimoto, Hiroshi; Nishihara, Hiroshi; (and others) (Kyoto Univ.). Annu. Rep. Res. Reactor Inst., Kyoto Univ.; 3: 58-74(1970).

The energy spectra of fast neutrons in two iron assemblies (90 cm × 90 cm × 100 cm and 50 cm × 50 cm × 50 cm) have been measured by the time-of-flight method with an electron linear accelerator. The experimental results have been compared with the theoretical spectra calculated by a one dimensional S_n code, with three different cross section data, the YOM set, the ABBN set and the KFK library. It has been found that the YOM set gives the gross shape of neutron spectra most properly, the KFK library gives better information about the fine structure of spectra, but for this case the agreement is not satisfactory enough, especially around 1 MeV. (auth)

Dynamics

Refer also to abstract 31541.

Experimental Applications

Refer also to abstract 31619.

31659 IMPROVED METHOD FOR CALCULATING FOIL PERTURBATION EFFECTS. Newman, Darrell F. (Battelle-Northwest, Richland, Wash.). Nucl. Sci. Eng.; 44: 261-6(May 1971).

A technique in which foil perturbation corrections are calculated for the heterogeneous reactor lattice using transport theory in two dimensions and two energy groups is presented. Results obtained using this approach are compared with results obtained from the more generally used formulas. The experimental configuration chosen for this comparison consisted of a water-moderated lattice of UO_2–2 wt % PuO_2 fuel rods on a 1.0-in. square lattice pitch. Separable fuel elements with 0.005-in.-thick end caps were used to allow placement of ½-in. diam foils of Al–Pu close to the fuel pellets. Reaction rates of Al–Pu were measured relative to corresponding reaction rates in a thermal column. Both bare and cadmium-covered foils were irradiated separately. Subcadmium activities were inferred from the difference of the bare and cadmium-covered activities. 9 references. (auth)

31660 MEASUREMENTS AND CALCULATIONS OF NEUTRON MIGRATION AND ITS ANISOTROPY IN LATTICES OF FUEL RODS AND LIQUID COOLANT. Harris, D. R. (Los Alamos Scientific Lab., N. Mex.); Mitchell, J. A. Nucl. Sci. Eng.; 44: 221-38(May 1971).

In the design of power reactors containing lattices of fuel rods in liquid coolant, it would be useful to employ cell-averaged transport parameters reflecting anisotropic neutron migration when this is significant. Measurements and Monte Carlo calculations of anisotropic neutron migration are described for rod lattices. The well-known flux peaking near thin sources is found to be accompanied by thin source effects on migration areas. Situations of substantial migration anisotropy and thin source effects are delimited. 43 references. (auth)

31661 ANALYSIS OF EXPONENTIAL EXPERIMENTS WITH LATTICES OF PLUTONIUM IN HEAVY WATER. Ozer, Odelli (Brookhaven National Lab., Upton, N. Y.). Nucl. Sci. Eng.; 43: 286-302(Mar 1971).

Some Pu–Al–D_2O lattice experiments are analyzed primarily with ENDF/B data and methods based on asymptotic theory. The effects of varying the ^{239}Pu cross sections in the unresolved-resonance range are calculated. The uncertainties associated with the determination of the radial bucklings are reduced with the use of one-dimensional transport calculations in the radial direction and an assumed exponential dependence in the axial direction. Two-dimensional calculations for a few of the lattices are made to calculate relaxation lengths as well as to determine the applicability of one-dimensional or asymptotic theory methods. (auth)

Reactor Components, Fuels, and Accessories

Refer also to abstracts 28979, 28980, 28988, 28998, 29256, 29290, 29298, 29301–29314, 29757, 29760, 29787, 29788, 29795, 29811, 29904, 29922–29924, 29932, 30010, 30019, 30022, 30030, and 30031.

31662 (EUR-4531, pp 59-71) CONCEPTION OF THE BASIC PROGRAM OF GERMAN RESEARCH AND DEVELOPMENT ON PRESTRESSED CONCRETE REACTOR PRESSURE VESSELS. Jaeger, Thomas A. (Bundesanstalt fuer Materialpruefung, Berlin (West Germany)). (In German).

From second conference on prestressed concrete reactor pressure vessels and their thermal isolation; Brussels, Belgium (18 Nov 1969).

In Second information meeting on prestressed concrete reactor pressure vessels and their thermal isolation.

The German research and development program on prestressed concrete reactor pressure vessels was directed to give a broad applicability of research results with an economic use of this material and to obtain the greatest possible flexibility in the construction development. Research therefore was concentrated on parametric studies, calculation methods, analysis of construction plans, material research, heat insulation, structure testing, and operational monitoring. Each of these is briefly discussed. (J.S.R.)

31663 (EUR-4531, pp 489-505) INDIVIDUAL TENSION COMPONENTS FOR VERTICAL PRESTRESS WITH BREAKING LOADS ABOVE 1500 Mp. Muehe, L. (Holzmann (Philipp) A. G., Frankfurt am Main (West Germany)). (In German).

From second conference on prestressed concrete reactor pressure vessels and their thermal isolation; Brussels, Belgium (18 Nov 1969).

In Second information meeting on prestressed concrete reactor pressure vessels and their thermal isolation.

Deviating from the usual prestressed concrete construction in prestressed concrete pressure vessels at least for the vertical stress, individual tension components with very large fracture load were required. The clamp anchors used in the KA tension method are evidently able to anchor individual tension components with fracture loads over 1500 Mp. With a 1000 Mp test machine accurate fracture tests were made. Deformation and displacement measurements and the determination of the actual efficiency of a clamp anchor described were carried out. A complete tension component for the reactor structure, which uses the clamp anchors studied, was illustrated. It consists of 240 bevel-ribbed oval stress steels of the grade St 154/160, which are held without spacer to a bundle. Because of the selected ribs the distances of the tension steels from each other are sufficiently large to bring about a permanent corrosion protection. For stressing these tension components a hollow piston press was used which works against clamp anchors on the large tension components. (tr-auth)

31664 (EUR-4531, pp 697-734) NONLINEAR ANALYSIS OF PRESSURE VESSELS BEHAVIOR INCLUDING CRACKING. Zienkiewicz, O. C.; Owen, D. R. J.; Phillips, D. V. (Wales Univ., Swansea).

From second conference on prestressed concrete reactor pressure vessels and their thermal isolation; Brussels, Belgium (18 Nov 1969).

In Second information meeting on prestressed concrete reactor pressure vessels and their thermal isolation.

The possibilities offered by the finite element method in solving problems encountered with prestressed concrete reactor vessels are summarized. Many problems of practical interest can be solved provided that, the model chosen represents the structural action of the vessel with sufficient accuracy and that the material behavior can be adequately specified. With this in mind it is hoped that in the future, numerical analysis will focus attention on the properties requiring determination and indicate areas where experiments are in fact of little value. (auth)

31665 (EUR-4531, pp 735-57) DYNAMIC RELAXATIONS AS AN EFFECTIVE METHOD FOR SPATIAL CALCULATIONS ON CONCRETE PRESSURE VESSELS. Schnellenbach, G. (Bochum Univ. (West Germany). Institut fuer Konstruktiven Ingenieurbau). (In German).

From second conference on prestressed concrete reactor pressure vessels and their thermal isolation; Brussels, Belgium (18 Nov 1969).

In Second information meeting on prestressed concrete reactor pressure vessels and their thermal isolation.

A brief description of the dynamic relaxation method for the spatial calculations on concrete pressure vessels is presented. Properties and advantages of this method are described. Dynamic relaxation is an obvious method for the numerical solution of problems of the elasticity theory. The direct formulation of large equilibrium systems and their solution are avoided. The storage needs for the numerical calculation are therefore smaller than in other methods. The stability of the numerical calculation is simple to guarantee. The program for the numerical calculation in complicated spatial cases remains short. The boundary conditions can be simply and accurately fulfilled. This is valid also for curved envelopes as they occur in circular openings. 10 references. (tr-auth)

31666 (EUR-4531, pp 759-76) NUMERICAL CALCULATION METHODS FOR PRESTRESSED CONCRETE REACTOR PRESSURE VESSELS. Brandes, K. (Bundesanstalt fuer Materialpruefung, Berlin (West Germany)). (In German).

From second conference on prestressed concrete reactor pressure vessels and their thermal isolation; Brussels, Belgium (18 Nov 1969).

In Second information meeting on prestressed concrete reactor pressure vessels and their thermal isolation.

On the basis of two computer-oriented methods – dynamic relation and finite element techniques – the advances in the contemporary calculation of reactor pressure vessels were outlined. An arrangement into a larger system of the principles of these types of methods was investigated. On the basis of such principles it appears possible to develop additional methods for the solution of technical problems. Two improvement possibilities were formulated. 49 references. (tr-auth)

31667 (EUR-4531, pp 777-95) THREE-DIMENSIONAL ELASTIC AND ELASTOPLASTIC CALCULATIONS ON REACTOR PRESSURE VESSELS. Argyris, J. H.; Grieger, I. (Stuttgart Univ. (West Germany). Institut fuer Statik und Dynamik der Luft- und Raumfahrtkonstruktionen). (In German).

From second conference on prestressed concrete reactor pressure vessels and their thermal isolation; Brussels, Belgium (18 Nov 1969).

In Second information meeting on prestressed concrete reactor pressure vessels and their thermal isolation.

The application of the matrix displacement method to the three-dimensional elastic and elastoplastic calculation of reactor pressure vessels is described and illustrated with examples. The examples show the generality and strength of the matrix displacement method in the static calculation of three-dimensional linear and non-linear problems of reactor construction. The application of new elements gives better results with simultaneous reduction of calculation time. 32 references. (J.S.R.)

31668 (IRS-T-17) CONFERENCE ON WORK TO DEVELOP STEEL REACTOR PRESSURE VESSELS, JUELICH, GERMANY, 22 APRIL 1968. (Technischer Ueberwachungs-Verein e. V., Cologne (West Germany). Institut fuer Reaktorsicherheit). 1969. 137p. (In German). (CONF-680474).

Reactor pressure vessels, constructed in multilayers, are discussed with respect to: practical experiences on the Saxton reactor, construction and testing, and the development of large size containers. The problems of material, stress resistance, tendencies in the development of reactor pressure containers with the associated problems, behavior of cylindrical and spherical cavities under internal pressure, stress resistance under increasing internal pressure, and development of a specialty steel for nuclear pressure containers are described. (H.B.G.)

31669 (ORNL-4602) EFFECT OF IODINE DECAY HEAT ON CHARCOAL ADSORBERS. Shields, R. P.; Siman-Tov, M. (Oak Ridge National Lab., Tenn.). Apr 1971. Contract W-7405-eng-26. 101p. Dep. NTIS.

A procedure for the thermal analysis of the charcoal adsorber in a reactor containment system has been developed to estimate maximum temperatures which may prevail under accident conditions. A differential equation which relates the charcoal temperature to the heat generation rate, air flow rate, and the heat parameters of air and charcoal has been solved both analytically and numerically. The analytical method assumes a two inch thick slab of charcoal only and is applicable to high flow rates. A computer code has been developed for numerical solution of the equation for the charcoal slab in both one and three-dimensions. The principal considerations have been given to very low flows and for times soon after onset of the accident; conditions which pose the greatest threat to the charcoal. Examples are given of the application of this code to reactor off-gas charcoal adsorbers. 13 references. (auth)

31670 (ORNL-TM-3293) TRANS: A ONE-DIMENSIONAL FORTRAN IV PROGRAM FOR COMPUTING THE TIME RESPONSE OF FUEL RODS TO A LOADING-UNLOADING ENVIRONMENT. Stillman, W. E. (Oak Ridge National Lab., Tenn.). May 1971. Contract W-7405-eng-26. 65p. Dep. NTIS.

The TRANS code is designed to compute transient stresses in cylindrical fuel rods. This version considers the response to thermal and pressure loads in one bilinear material with temperature-dependent properties. Plastic and creep strain increments are computed for load or time increments, respectively, and the resulting stresses determined. The stresses can be evaluated for any time in a general load cycle. (auth)

31671 (ORNL-TM-3367) POPOP4 LIBRARY AND CODES FOR PREPARING SECONDARY GAMMA-RAY PRODUCTION CROSS SECTIONS. Ford III, W. E. (Oak Ridge National Lab., Tenn.). 1 Apr 1971. Contract W-7405-eng-26. 22p. (CONF-710304-8). Dep. NTIS.

From Symposium on natural and manmade radiation in space; Las Vegas, Nev. (1 Mar 1971).

The POPOP4 code for converting secondary γ-radiation yield data to multigroup secondary γ-radiation production cross sections and the POPOP4 library of secondary γ-radiation yield data are described. Recent results in the "testing" of U and Fe data sets from the POPOP4 library are given. The data sets were tested by comparing calculated secondary γ-radiation pulse-height spectra with spectra measured at the ORNL TSR-II reactor. 26 references. (auth)

31672 LEAKAGE-RATE TESTING OF CONTAINMENT STRUCTURES. ANS 7.60 1970. Hinsdale, Ill.; American Nuclear Society (1970). 17p. Available from American Nuclear Society, Hinsdale, Ill.

Uniform methods are described for determining the ability of a reactor container to retain, within the limits of permissible leakage rates, any gases, vapors, liquid, or other fluid materials that would be of a hazardous nature if not contained and which might be present in the containment structure as a result of an energy release, rupture, or leak in the nuclear reactor components or accessories. The need for restriction of leakage from the containment structure is based on the maintenance of public health and safety. The provisions of this standard specify the practices and test requirements for the quantitative determination of leakage rates of containment structures for the housing of operating nuclear reactors. The provisions apply to containment structures for nuclear power, test, research, and training reactors, wherever a gas-tight containment structure is specified as a condition for operation. (auth)

31673 TEMPERATURE FIELDS IN FUEL ELEMENT BUNDLES WITH REGARD TO THE HYPERFINE STRUCTURE OF HEAT SOURCE DENSITY AND AN UNEVEN HEAT TRANSFER BETWEEN FUEL MATERIAL AND CAN. PART II. SUPPLEMENTS TO THE THEORY OF HEAT TRANSFER BETWEEN FUEL AND CAN. DISCUSSION OF NUMERICAL EXAMPLES. Wolf, Lothar; Johannsen, Klaus (Technische Univ., Berlin). Waerme; 74: 122-31(1968). (In German).

Mathematical equations are developed for heat transfer between fissionable material and cladding under elliptical deformation of the cladding. Several numerical examples are discussed and analyzed. Effects of uneven heat transfer between fissionable material and cladding also are discussed with regard to the position of the fissionable material. 7 references. (H.B.G.)

31674 TEMPERATURE FIELDS IN FUEL ELEMENT BUNDLES WITH REGARD TO THE HYPERFINE STRUCTURE OF HEAT SOURCE DENSITY AND AN UNEVEN HEAT TRANSFER BETWEEN FUEL MATERIAL AND CAN. PART I. THEORY. Wolf, Lothar; Johannsen, Klaus (Technische Univ., Berlin). Waerme; 74: 52-60(1968). (In German).

Calculated are temperature fields for single fuel elements regardless of their position within a larger bundle. The intensity of the heat source in the fissionable material may vary radially as well as azimuthally, while heat transfer between fissionable material and cladding may change only azimuthally. Established are general relations for temperature fields within single cylindrical fuel elements, composing the core of a heterogenous reactor. The influence of uneven heat conduction between fissionable material and cladding are approximated by linearization of the coupled problems. 14 references. (H.B.G.)

31675 TEMPERATURE FIELDS IN FUEL ELEMENT BUNDLES WITH VARIABLE-RANGE HEAT TRANSFER BETWEEN FUEL ELEMENT SURFACE AND COOLANT. Wolf, Lothar (Technische Univ., Berlin). Waerme; 75: 169-82(1969). (In German).

XUM

Reviewed are both literature and experimental studies concerning heat transfer under various boundary conditions as existing in complicated cooling channel geometries. By assuming that the coefficient varies azimuthally, heat transfer is treated theoretically between fuel elements and cooling medium. A general mathematical equation is given for radial as well as azimuthal distribution of heat sources which permits calculation of heat transfer from fissionable material to cladding to cooling medium. Variations in temperatures of both fissionable material and cladding are explained by several examples. 38 references. (tr-auth)

31676 GUIDE FOR SPECIFYING CLEANLINESS OF REACTOR SYSTEM COMPONENTS. Hinsdale, Ill.; American Nuclear Society (1965). 3p. Available from American Nuclear Society, Hinsdale, Ill.

Classes of cleanliness are defined and methods for specifying degrees of cleanliness for components to be installed in nuclear systems are described. Examples drawn from industrial experience are cited as typical of applications appropriate to cleanliness classes. These examples should be considered only as guides. This standard does not set cleanliness requirements for particular components. The class of cleanliness and the cleaning procedures and processes used to attain the class of cleanliness shall be subject to the purchaser's approval. (auth)

31677 PROGRAM FOR TESTING BIOLOGICAL SHIELDING IN NUCLEAR REACTOR PLANTS. ANS 6.3 1967. Hinsdale, Ill.; American Nuclear Society (1967). 4p. Available from American Nuclear Society, Hinsdale, Ill.

An operational shield testing program that is to be used in evaluating the installed biological shielding in nuclear plants is described. A general testing procedure is outlined and the necessary radiation measurements and types of radiation-measuring instruments are prescribed. (auth)

31678 IMPROVEMENTS IN FUEL ASSEMBLIES FOR NUCLEAR REACTORS. Andersson, Herbert Olof; Ekwall, Per Anders (to Allmanna Svenska Elektriska Aktiebolaget). British Patent 1,229,018. 21 Apr 1971. Priority date 4 Sep 1967, Sweden.

REACTOR FUEL ELEMENTS—spacers for bundle arranged rod type ceramic, design configurations of (D.C.C.)

31679 COMPACTING NUCLEAR FUEL. Voice, Eric Handley (to United Kingdom Atomic Energy Authority). British Patent 1,226,497. 31 Mar 1971. Filed 27 Mar 1969.

Reference is made to the manufacture of coated particle fuel elements. During compacting of such fuel by direct tamping there is a risk of fracture or other damage to the coating. A method giving a reasonably uniform distribution of particles in their container is desirable. The fuel element described comprises a rigid container for the fuel and other filler material symmetrical about a central axis, and the contents are compacted by centrifugal force engendered by rotation of the container about an axis normal to the central axis. In one arrangement the coated particulate fuel is fed into a funnel that distributes the particules into a number of horizontal conduits axially aligned with corresponding bores in the fuel containers. Voids between the particles are avoided by deformation of the outer coatings on adjacent particles under the centrifugal pressure. The containers may be cylindrical or spherical in shape. (UK)

31680 USE OF A Ge(Li) GAMMA SPECTROMETER IN ORDER TO CONTROL THE ACTIVITY OF THE HEAT-TRANSFER MEDIUM IN NUCLEAR REACTORS. Demidov, A. M.; Kotel'nikov, G. A.; Oskerko, A. A. At. Energ. (USSR); 30: 60-2(Jan 1971). (In Russian).

A one-liter sample was taken for analysis. This sample was concentrated to a volume of about 20 cm^3 by passage through a cation exchanger. The following count rates were obtained for various radioactivities in counts per second-liter (half-life is given in parenthesis): 10,000 to 35,000 for sodium-24 (15 hr); 100 to 3000 for chromium-51 (28 days); 6 to 1000 for manganese-54 (291 days); 500 to 60,000 for manganese-56 (2.6 hr); 5 to 1700 for cobalt-58 (71 days); 5 to 620 for iron-59 (44 days); 20 to 3900 for cobalt-60 (5.25 yr); 4000 for copper-64 (13 hr); 130 for zirconium-95 (63 days); 40 to 5000 for molybdenum-99 (67 hr); 30 to 500 for antimony-122 (2.8 days); 7 to 150 for antimony-124 (60 days); 20 to 7000 for iodine-131 (8 days); 50 to 36,000 for iodine-133 (21 hr); 80 for barium-140 (13 days), and 700 to 10,000 for tungsten-187 (24 hr). The sodium-24 was the result of a (n,alpha) reaction on aluminum-27. The chromium, copper, antimony and tungsten activities were a result of activating stable isotopes of these elements with thermal neutrons. In case of a fuel element rupture, fission product peaks of ^{85m}Kr, ^{140}Ba, ^{131}I, ^{95}Zr, and ^{103}Ru are readily observed. (TTT)

GENERAL

31681† (AERE-M-2184) INTRODUCTION TO LEED AND A DISCUSSION OF SOME TYPICAL LEED EXPERIMENTS. Riviere, J. C. (Atomic Energy Research Establishment, Harwell (England)). Mar 1969. 46p. Dep. NTIS (U. S. Sales Only).

31682 (AERE-R-6719) LMM AUGER SPECTRA OF SOME TRANSITION METALS OF THE FIRST SERIES. Coad, J. P.; Riviere, J. C. (Atomic Energy Research Establishment, Harwell (England)). Jan 1971. 19p. Dep. NTIS (U. S. Sales Only).

31683 (ANL-Trans-880) IR-SPECTROSCOPIC INVESTIGATIONS OF THE CRYSTALLINE TETRAHYDRATE OF HYDROGEN BROMIDE $H_9O_4^+Br^-$. Rudolph, Joachim; Zimmermann, Herbert. Translated for Argonne National Lab., Ill., from Z. Phys. Chem. (Frankfurt); 43: 311-26(1964). 14p. Dep. NTIS.

31684 (BNL-50266) EXPERIMENTAL DATA ON DISPERSION AND DEPOSITION OF TIMOTHY AND CORN POLLEN FROM KNOWN SOURCES. Raynor, Gilbert S.; Hayes, Janet V.; Ogden, Eugene C. (Brookhaven National Lab., Upton, N. Y.). Oct 1970. 32p. Dep. NTIS.

31685 (BNWL-1558) VARIOUS HOLOGRAPHIC SCANNING CONFIGURATIONS FOR UNDER-SODIUM VIEWING. Collins, H. Dale (Battelle-Northwest, Richland, Wash. Pacific Northwest Lab.). Mar 1971. Contract AT(45-1)-1830. 45p. Dep. NTIS.

31686 (BNWL-B-29) INTERRELATIONSHIPS OF GEOLOGIC FORMATIONS AND PROCESSES AFFECTING ECOLOGY AS EXPOSED AT RATTLESNAKE SPRINGS, HANFORD PROJECT. Brown, Randall E. (Battelle-Northwest, Richland, Wash. Pacific Northwest Lab.). May 1970. Contract AT(45-1)-1830. 42p. Dep. NTIS.

31687 (COO-908-34) CHLOROPHYLL ONE-ELECTRON PHOTOCHEMISTRY: FLASH PHOTOLYSIS STUDIES OF THE CHLOROPHYLL-QUINONE REACTION IN ALCOHOL SOLVENTS. White, Robert A.; Tollin, Gordon (Arizona Univ., Tucson. Dept. of Chemistry). 1971. Contract AT(11-1)-908. 51p. Dep. NTIS.

31688 (COO-1041-18) X-RAY SLIT SYSTEM FOR CRYSTALS WITH SMALL ANGLE BOUNDARIES. Eubig, C.; Tomizuka, C. T. (Arizona Univ., Tucson. Dept. of Physics). [nd]. Contract AT(11-1)-1041. 7p. Dep. NTIS.

31689 (COO-1041-19) WIRE-CUTTING TOOL FOR USE WITH A SPARK CUTTER. Eubig, C.; Tomizuka, C. T. (Arizona Univ., Tucson. Dept. of Physics). [nd]. Contract AT(11-1)-41. 7p. Dep. NTIS.

31690 (COO-1569-71) AN NMR AND NUCLEAR RELAXATION STUDY OF SATELLITE LINES IN DILUTE Co-Cr, Co-V, AND Co-Mn ALLOYS. Aslam, J.; Weyhmann, W. (Minnesota Univ., Minneapolis. Tate Lab. of Physics). Mar 1971. Contract AT(11-1)-1569. 77p. Dep. NTIS.

31691 (COO-1750-3) FINAL TECHNICAL REPORT, NOVEMBER 1, 1969-JANUARY 31, 1971. Dougall, Donald K. (Ohio State Univ. Research Foundation, Columbus). Contract AT(11-1)-1750. 29p. Dep. NTIS.

31692 (COO-2048-2) EVALUATION OF THE GERARD-PAPIRNO CHARACTERIZATION OF NOTCH DUCTILITY IN HIGH-STRENGTH AISI 4340 STEEL. Final Technical and Topical Report, Phase I. Firrao, Donato; Spretnak, Joseph W. (Ohio State Univ., Columbus. Dept. of Metallurgical Engineering). 28 Feb 1971. Contract AT(11-1)-2048. 79p. Dep. NTIS.

31693 (COO-2094-4) ICR QUARTERLY REPORT NO. 27. Ashenhurst, Robert L. (Chicago Univ., Ill. Inst. for Computer Research). 1 Nov 1970. Contract AT(11-1)-2094. 123p. Dep. NTIS.

31694 (COO-2118-1) ILI IAC III COMPUTER SYSTEM MANUAL: TAXICRINIC PROCESSOR. VOLUME 1. Report No. 417. Nordmann, Bernard J. Jr. (Illinois Univ., Urbana. Dept. of Computer Science). 24 Nov 1970. Contract AT(11-1)-2118. 272p. Dep. NTIS.

31695 (EGG-1183-2242) ENVIRONMENTAL AIR QUALITY SUPPORT STUDY. Accomplishments through FY70. Nybakken, T. W. (EG and G, Inc., Santa Barbara, Calif.). Jul 1970. 24p. Dep. NTIS.

31696 (IN-1421) MOLECULAR POTENTIAL FUNCTION IN TERMS OF GROUP VALENCE FORCE SYMMETRY COORDINATES. McMurry, H. L. (Idaho Nuclear Corp., Idaho Falls). Apr 1971. Contract AT(10-1)-1230. 35p. Dep. NTIS.

31697 (IS-T-424) EXPERIMENTAL AND THEORETICAL EVALUATION OF THE NITROUS OXIDE-ACETYLENE FLAME AS AN ATOMIZATION CELL FOR FLAME SPECTROSCOPY. Rasmuson, James Orley (Ames Lab., Iowa). Feb 1971. Contract W-7405-eng-82. 119p. Dep. NTIS.
Thesis.

31698 (ITF-70-74) LIGHT ABSORPTION BY THE PAIR OF TRIPLET EXCITONS. Gaididei, Yu. B.; Petrov, E. G. (Akademiya Nauk Ukrainskoi SSR, Kiev. Institut Teoreticheskoi Fiziki). 1970. 20p. (In Russian). Dep. NTIS (U. S. Sales Only).

31699 (LA-4582) SINGLE AND MULTIPLE FIELD ENABLING SYSTEM FOR TELEVISION DISC RECORDING. Calligan III, J. H. (Los Alamos Scientific Lab., N. Mex.). Nov 1970. Contract W-7405-eng-36. 5p. Dep. NTIS.

31700 (LA-4601) STRESS CALCULATIONS IN MAGEE DIFFERENCE FORM. Blewett, Patrick J. (Los Alamos Scientific Lab., N. Mex.). Dec 1970. Contract W-7405-eng-36. 10p. Dep. NTIS.

31701 (LA-4620) EVOLUTION OF COMPUTER SOFTWARE. Wells, Mark B. (Los Alamos Scientific Lab., N. Mex.). Feb 1971. Contract W-7405-eng-36. 11p. Dep. NTIS.

31702 (LA-4627) IMPROVED LIGHT SCATTERING PHOTOMETER FOR AIR FILTRATION SYSTEM STUDIES. Hiebert, R. D.; Stafford, R. G.; Pollat, L. L. (Los Alamos Scientific Lab., N. Mex.). Feb 1971. Contract W-7405-eng-36. 7p. Dep. NTIS.

31703 (LA-4641) LIGHT SCATTERING FROM AEROSOLS. Suydam, B. R. (Los Alamos Scientific Lab., N. Mex.). Feb 1971. Contract W-7405-eng-36. 7p. Dep. NTIS.

31704 (LA-4642) SCATTERING OF LIGHT FROM A STRATIFIED SPHERE. Suydam, B. R. (Los Alamos Scientific Lab., N. Mex.). Feb 1971. Contract W-7405-eng-36. 8p. Dep. NTIS.

31705 (LA-tr-71-33) THIN LAYER CHROMATOGRAPHY: APPLICATION TO ORGANIC COMPOUNDS. Itokawa, Hideji. Translated for Los Alamos Scientific Lab., N. Mex., from Jap. Anal.; 19: 1592-1600(1970). 26p. Dep. NTIS.

31706 (NP-18803) ANNUAL REPORT, YEAR ENDED 31st DECEMBER 1969. (Australian Inst. of Nuclear Science and Engineering, Lucas Heights). 53p. Dep. NTIS (U. S. Sales Only).
Contents include the Institute's activities during the 1969 calender year such as the maintenance of the neutron diffraction research group at Lucas Heights and research support at Australian universities. AINSE research and training grants, fellowships, studentships, and titles of papers presented at the Institute's plasma physics conference, heat transfer and fluid flow conference, and radiation biology conference are listed. Summaries of AINSE projects and publications arising from such projects are given. Financial aspects for 1969 are also included. (Australia)

31707 (NYO-2150-68) STUDY OF THE TRANSVERSE MAGNETORESISTANCE OF POLYCRYSTALLINE POTASSIUM. Taub, H.; Schmidt, R. L.; Maxfield, B. W.; Bowers, R. (Cornell Univ., Ithaca, N. Y. Lab. of Atomic and Solid State Physics). Feb 1971. 74p. Dep. NTIS.

31708 (NYO-2280-32) MUTATION RATES AND MUTATIONAL LOADS IN MAN. Yearly Progress Report of Scientific Activity from September 1, 1969-August 31, 1970. (Pavia Univ. (Italy). Istituto di Genetica). Contract AT(30-1)-2280. 19p. Dep. NTIS.

31709 (NYO-2598-52) LOSS OF ORGANIC AND INORGANIC MATERIALS FROM ABOVE-GROUND PLANT PARTS BY LEACHING. Progress Report, 1970-71. Tukey, H. B. Jr. (Cornell Univ., Ithaca, N. Y. Dept. of Floriculture and Ornamental Horticulture). Contract AT(30-1)-2598. 12p. Dep. NTIS.

XUM

31710 (NYO–3618-10) REGIONAL BLOOD FLOW IN SUBCORTICAL STRUCTURES IN MAN. Technical Progress Report, Sem-Jacobsen, C. W.; Ingvar, David H. (Gaustad Sykehus, Oslo (Norway). EFG Research Lab.). 20 Mar 1971. Contract AT(30-1)-3618. 26p. Dep. NTIS.

31711 (NYO–3699-53) THEORETICAL PHONON PHYSICS. Progress Report, April 1, 1970–March 31, 1971. Krumhansl, J. A. (Cornell Univ., Ithaca, N. Y. Lab. of Atomic and Solid State Physics). Contract AT(30-1)-3699. 12p. Dep. NTIS.

31712 (NYO–3924-9) RADIOISOTOPIC AND VOLUMETRIC STUDIES OF TUMOR GROWTH IN SITU. Annual Progress Report. Dethlefsen, Lyle A. (Pennsylvania Univ., Philadelphia. Dept. of Radiology). Apr 1971. 3p. Dep. NTIS.

31713 (NYO–3924-10) RADIOISOTOPIC AND VOLUMETRIC STUDIES OF TUMOR GROWTH IN SITU. Comprehensive Progress Report, 1967–1971. Dethlefsen, Lyle A. (Pennsylvania Univ., Philadelphia. Dept. of Radiology). Contract AT(30-1)-3924. 6p. Dep. NTIS.

31714 (ORNL-TM-3328) CONCENTRATION AND DESALTING OF PROTEIN SOLUTIONS PROGRAM PROGRESS REPORT FOR THE PERIOD JUNE 1 TO AUGUST 31, 1970. Hancher, C. W.; Ryon, A. D.; Rogers, F. L. (Oak Ridge National Lab., Tenn.). May 1971. Contract W-7405-eng-26. 17p. Dep. NTIS.

31715 (ORNL-tr-2469) ELIMINATION AND METABOLISM OF BENZO(a)PYRENE AFTER INTRATRACHEAL INJECTION. Dehnen, W.; Tomingas, R.; Beck, E. G.; Manojlovic, N.; Kirch, M. Translated by R. Gregg Mansfield (Oak Ridge National Lab., Tenn.), from Z. Krebsforsch.; 75: 14-22(1970). 10p. Dep. NTIS.

31716 (ORO–3291-14) APPLICATION OF ADIABATIC CALORIMETRY TO METAL SYSTEMS. Progress Report, 1969–70. Stansbury, E. E.; Brooks, C. R. (Tennessee Univ., Knoxville. Dept. of Chemical and Metallurgical Engineering). Contract AT-(40-1)-3291. 49p. Dep. NTIS.

31717 (ORO–3634-11) DETECTION OF WEAK HISTOCOMPATIBILITY ANTIGENS ON MOUSE PERITONEAL MACROPHAGES. De Angelis, W. J.; Haughton, G. (North Carolina Univ., Chapel Hill). [1970]. Contract AT(40-1)-3634. 13p. Dep. NTIS.

31718 (ORO–3634-12) DETECTION AND MEASUREMENT OF WEAK HISTOINCOMPATIBILITIES BY TRANSFER OF MOUSE PERITONEAL EXUDATE CELLS. Haughton, G.; De Angelis, W. J.; Cooper, M. Y. (North Carolina Univ., Chapel Hill. Dept. of Bacteriology and Immunology). [1970]. Contract AT(40-1)-3634. 14p. Dep. NTIS.

31719 (ORO–3634-13) SEROLOGICAL DETECTION OF THE MALE LIMITED H–Y ANTIGEN ON PERITONEAL EXUDATE CFLI S. Haughton, G.; Cooper, Margaret Y.; De Angelis, W. J. (North Carolina Univ., Chapel Hill. Dept. of Bacteriology and Immunology). [1970]. Contract AT(40-1)-3634. 13p. Dep. NTIS.

31720 (ORO–3982-10) IN VITRO BIOSYNTHESIS OF PLANT PROTEINS AND NUCLEIC ACIDS. Progress Report, 1970–1971. (Florida Univ., Gainesville. Radiation Biology Lab.). [1971]. Contract AT(40-1)-3982. 14p. Dep. NTIS.

31721 (PRNC–145) LEAST-SQUARE REFINEMENT OF THE X-RAY DATA ON AZURITE, $Cu_3(OH)_2(CO_3)_2$. (Puerto Rico Nuclear Center, Mayaguez). [nd]. Contract AT(40-1)-1833. 10p. Dep. NTIS.

31722 (PRNC–146) CRYSTAL STRUCTURF OF $CoBr_2.6H_2O$ AT ROOM TEMPERATURE BY NEUTRON DIFFRACTION. Kleinberg, Robert (Puerto Rico Nuclear Center, Mayaguez). [1970]. Contract AT(40-1)-1833. 10p. Dep. NTIS.

31723 (RLO–1750-62) SOUND SCATTERING LAYERS OFF THE OREGON COAST. Donaldson, Henry A.; Pearcy, William G. (Oregon State Univ., Corvallis. Dept. of Oceanography). [nd]. 15p. Dep. NTIS.

31724 (RLO–2229-T-1-3) FJORDS AS SEDIMENTARY MICROCOSMS. Hoskin, Charles M.; Burrell, David C. (Alaska Univ., College. Inst. of Marine Science). [1971]. Contract AT(04-3)-310. 25p. Dep. NTIS.

31725 (RPI–3639-16) STUDIES OF GAS-PARTICLE HEAT TRANSFER COEFFICIENTS IN PACKED AND FLUIDIZED BEDS BY FREQUENCY RESPONSE TECHNIQUES. Annual Progress Report, January 1, 1970–February 28, 1971. Littman, Howard (Rensselaer Polytechnic Inst., Troy, N. Y.). Mar 1971. Contract AT(30-1)-3639. 5p. Dep. NTIS.

31726 (SC-DC–713922) EXPERIMENTAL AND THEORETICAL INVESTIGATIONS OF A LIQUID FILM INTERACTING WITH A SUPERSONIC STREAM. Saric, William S. (Sandia Labs., Albuquerque, N. Mex.). [1971]. 11p. Dep. NTIS.

31727 (SC-DC–713982) CAVITATION STUDY OF UNDERWATER TRAJECTORY. (Sandia Labs., Albuquerque, N. Mex.). 1 Apr 1971. 22p. Dep. NTIS.

31728 (SC-DR–70-838) METHODS FOR PREDICTING TURBULENT JET MIXING. Mark, J. L. (Sandia Labs., Albuquerque, N. Mex.). Dec 1970. 41p. Dep. NTIS.

31729 (SC-DR–710211) INTERACTIVE MONITOR FOR A TELEMETRY PLAYBACK SYSTEM. Fienning, W. C. (Sandia Labs., Albuquerque, N. Mex.). Apr 1971. 78p. Dep. NTIS.

31730 (SC-RR–69-761) SOME DYNAMIC MECHANICAL PROPERTIES OF ARMCO 21-6-9 STAINLESS STEEL. Guess, T. R. (Sandia Labs., Albuquerque, N. Mex.). Nov 1969. 38p. Dep. NTIS.

31731 (SC-RR–710071) ANALYSIS OF THE LATERAL MOTION OF A PROJECTILE IN THE GUN TUBE. Perdreauville, Farrell J. (Sandia Labs., Albuquerque, N. Mex.). 19 Mar 1971. 78p. Dep. NTIS.

31732 (SC-T–71-3010) CRITERIA FOR THE DETACHMENT OF A THREE-DIMENSIONAL BOUNDARY LAYER. Bam-Zelikovich, G. M. Translated by Marcel I. Weinreich (Sandia Labs., Albuquerque, N. Mex.), from Izv. Akad. Nauk SSSR, Mekh. Zhidk. Gaza; No. 4, 50-4(1970). 17p. Dep. NTIS.

31733 (SC-T–713025) METHOD AND TECHNIQUE OF SURVEYING DURING PHOTOGRAPHING AND VISUAL OBSERVATION IN A FIELD OF HIGH FREQUENCY CURRENTS. Frantov, G. S.; Mikhalevsky, V. I. Translated by Marcel I. Weinreich (Sandia Labs., Albuquerque, N. Mex.), from Zh. Nauch. Prikl. Fotogr. Kinematogr.; 13: 309-10(1968). 6p. Dep. NTIS.

31734 (SCL-T–69-257) STRUCTURE AND PROPERTIES OF ELECTROLYTICALLY DEPOSITED TIN–LEAD ALLOYS. Riedel, W. Translated by B. J. Hazzard for Sandia Labs., Albuquerque, N. Mex., from Metalloberflaeche; 23: No. 2, 42-6(1969). 17p. Dep. NTIS.

31735 (SCL-T–69-258) NEW BIAXIAL TENSILE TESTER FOR FLAT SPECIMENS. Shiratori, E.; Ikegami, K. Translated by A. Kajikawa for Sandia Labs., Albuquerque, N. Mex., from Zairyo; 16: No. 165, 433-9(1967). 24p. Dep. NTIS.

31736 (SCL-T–710240) INFLUENCE OF STARTING PARAMETERS ON RIPPLE FORMATION IN EXPLOSIVE WELDING OF METALS. Deribas, A. A.; Kudinov, V. M.; Matveenkov, F. I. Translated by A. M. A. Mincer for Sandia Labs., Livermore, Calif., from Fiz. Goreniya Vzryva; No. 4, 561-8(1967). 15p. Dep. NTIS.

31737 (TID–25465) AERODYNAMIC CHARACTERISTICS OF ATMOSPHERIC BOUNDARY LAYERS. Plate, Erich J. (Argonne National Lab., Ill. Karlsruhe Univ. (West Germany)). 1971. 190p. Dep. NTIS.

31738 (TID–25694) CELL RESPONSE TO NUCLEIC ACID PENETRATION. Progress Report, August 1969–September 1970. Stuy, Johan H. (Florida State Univ., Tallahassee). Contract AT(40-1)-3885. 10p. Dep. NTIS.

31739 (TID–25695) DIATOMS IN LAKES AND LAKE SEDIMENTS AS AN INDEX TO ENVIRONMENT. Technical Progress Report, May 1, 1970–January 31, 1971. Wright, H. E. Jr. (Minnesota Univ., Minneapolis). Contract AT(11-1)-2046. 20p. Dep. NTIS.

31740 (UCID–30002) FUNCTION OPTIMIZATION ON A LINE SEGMENT BY GOLDEN SFCTION. Hausman, Robert F. Jr. (California Univ., Livermore. Lawrence Radiation Lab.). 1 Apr 1971. 8p. Dep. NTIS.

31741 (UCLA–12-813) IMPROVED FEEDBACK CONTROL FOR THE NULL-POINT COMPENSATING SYSTEM. Mork, H. M.; Farmer, R. W.; Flygare, K. A. (California Univ., Los Angeles. Lab. of Nuclear Medicine and Radiation Biology). Mar 1971. Contract AT-04-1-GEN-12. 22p. Dep. NTIS.

31742 (UCLA-34-P-91-47) SPIN-LATTICE RELAXATION AND ZEEMAN EFFECTS IN THE TRIPLET STATE OF PYRAZINE-d_4. Hall, L. H. (California Univ., Los Angeles. Dept. of Chemistry). Apr 1971. Contract AT(04-3)-34. 235p. Dep. NTIS.
Thesis.

31743 (UCRL-19648) ELECTRON MICROSCOPY INVESTIGATIONS OF FERROUS MARTENSITES. Thomas, Gareth (California Univ., Berkeley. Lawrence Radiation Lab.). Jan 1971. Contract W-7405-eng-48. 41p. (CONF-700553-1). Dep. NTIS.
From American Institute of Metallurgical Engineering meeting; Las Vegas, Nev. (11 May 1970).

31744 (UCRL-19691) RELAXATION TIME MEASUREMENTS IN FLECTRON PARAMAGNETIC RESONANCE. Chang, James J. (California Univ., Berkeley. Lawrence Radiation Lab.). Feb 1971. Contract W-7405-eng-48. 203p. Dep. NTIS.
Thesis.

31745 (UCRL-20461) KINETICS OF THE REACTION OF CARBON DIOXIDE WITH HYDROXYL ION. Hsu, Chiu-chuan Shirley (California Univ., Berkeley. Lawrence Radiation Lab.). Mar 1971. Contract W-7405-eng-48. 79p. Dep. NTIS.
Thesis.

31746 (UCRL-20524) CRACK GROWTH MECHANISMS IN FIBROUS COMPOSITES. Gerberich, William W. (California Univ., Berkeley. Lawrence Radiation Lab.). Feb 1971. Contract W-7405-eng-48. 114p. Dep. NTIS.
Thesis.

31747 (UCRL-51008) LASER BEAM FILTERING BY SATURABLE DYES. Harrach, R. J.; MacVicar, T. D.; Kachen, G. I.; Steinmetz, L. L. (California Univ., Livermore. Lawrence Radiation Lab.). 4 Feb 1971. Contract W-7405-eng-48. 12p. Dep. NTIS.

31748 (UCRL-51021) ENGINEERING TESTS OF HALON 1301 FIRE EXTINGUISHING SYSTEMS FOR FIELD ASSEMBLY BUILDINGS. Gaskill, James R.; Harder, Charles A.; Nelson, Gary O. (California Univ., Livermore. Lawrence Radiation Lab.). 25 Feb 1971. 26p. Dep. NTIS.

31749 (UCRL-71888(Pt.1)) ICE AGE THEORY ANALYSIS BY COMPUTER MODEL SIMULATION. PART I. MacCracken, m. C. (California Univ., Livermore. Lawrence Radiation Lab.). Jul 1969. 46p. Dep. NTIS.

31750 (UCRL-71888(Pt.2)) ICE AGE THEORY ANALYSIS BY COMPUTER MODEL SIMULATION. PART II. MacCracken, M. C. (California Univ., Livermore. Lawrence Radiation Lab.). Jul 1969. 48p. Dep. NTIS.

31751 (UCRL-72803) TESTS OF ICE AGE THEORIES USING A ZONAL ATMOSPHERIC MODEL. MacCracken, Michael C. (California Univ., Livermore. Lawrence Radiation Lab.). Oct 1970. 60p. Dep. NTIS.

31752 (UCRL-72818(Rev.1)) IDENTIFICATION OF DYNAMIC SYSTEMS FROM EXPERIMENTAL DATA. Hillyer, David F. (California Univ., Livermore. Lawrence Radiation Lab.). 2 Feb 1971. 68p. (CONF-710502-2). Dep. NTIS.
From Experimental stress analysis meeting; Salt Lake City, Utah (18 May 1971).

31753 (UCRL-Trans-10524) MACHINING WITH A PLASMA JET. Spur, G.; Clausen, R.; Herzke, J. Translated by I. M. R. Jones for Univ. of California, Lawrence Radiation Lab., Livermore, from CIRP, Ann. Int. Inst. Prod. Eng. Res.; 18: 81.8-8(1970). 15p. Dep. NTIS.

31754 (UCRL-Trans-10525) ELECTROCHEMICAL OXIDATION OF SULFUR DIOXIDE ON A PLATINUM ELECTRODE. Comtat, Maurice; Mahenc, Jean. Translated by Z. St-Gallay for Univ. of California, Lawrence Radiation Lab., Livermore, from Bull. Soc. Chim. Fr.; No. 11, 3862-9(1969). 36p. Dep. NTIS.

31755 (UCRL-Trans-10526) PROTECTION OF STRAIN GAGES AND SEMICONDUCTOR TRANSDUCERS AGAINST MOISTURE. Andreae, Goetz. Translated by W. G. Stripp for Univ. of California Lawrence Radiation Lab., Livermore, from Zum Problem des Feuchtigkeitsschutzes von Dehnungsmesstreifen und Halbleitergebern. 283p. Dep. NTIS.

31756 (UCSD-34-P-127-8) PRECISION DEEP-SEA TIME RELEASE. Sessions, Meredith H.; Marshall, Phillip M. (California Univ., San Diego. Scripps Institution of Oceanography, La Jolla, Calif.). 3 Mar 1971. Contract AT(04-3)-34. 18p. Dep. NTIS.

31757 (Y-1758) ASPECTS OF THE BRITTLE FRACTURE FAILURE OF A 36-INCH-ID, 30,000-PSI ISOSTAT WITH THREADED CLOSURE. Pohto, H. A. (Union Carbide Corp., Oak Ridge, Tenn. Y-12 Plant). 30 Apr 1971. Contract W-7405-eng-26. 39p. Dep. NTIS.

31758 (Y-1759) ADAPTIVE CONTROL SURVEY. Kahles, John F. (Metcut Research Associates, Inc., Cincinnati, Ohio). 12 May 1971. Contract W-7405-eng-26; Subcontract 65Y-35001V. 113p. Dep. NTIS.
For Union Carbide Corp., Oak Ridge, Tenn. Y-12 Plant.

31759 (Y-1791) PRACTICAL LOW-RANGE MOISTURE GENERATOR. Wolny, R. F. (Union Carbide Corp., Oak Ridge, Tenn. Y-12 Plant). 5 May 1971. Contract W-7405-eng-26. 20p. Dep. NTIS.

31760 CELLULAR DYNAMICS OF THE NEURON. 12th International Congress of Cell Biology, Brussels, Belgium, August 25-31, 1968. Barondes, Samuel H. (ed.). Symposia of International Society for Cell Biology. Volume 8. New York; Academic Press, Inc. (1969). 394p. (CONF-680850).
A separate abstract was prepared for one of the 19 papers appearing in these proceedings. The other papers (not within the scope of NSA) discuss: synthesis and transport of neuroplasm; synthesis, transport, and action of neurotransmitters; functional implications of synaptic ultrastructure; neurobiological studies on Periplaneta; and morphological and biochemical correlates of neuronal plasticity. (E.R.B.)
For an abstract of an individual paper see: 29623.

31761 CODE OF GOOD PRACTICES FOR THE DOCUMENTATION OF DIGITAL COMPUTER PROGRAMS. ANS-STD.2 1967. Hinsdale, Ill.; American Nuclear Society (1967). 3p. Available from American Nuclear Society, Hinsdale, Ill.

31762 PROCEEDINGS OF THE INSTITUTE OF ENVIRONMENTAL SCIENCES 17th ANNUAL TECHNICAL MEETING AND EQUIPMENT EXPOSITION, APRIL 26-30, 1971, LOS ANGELES, CALIFORNIA. Mt. Prospect, Ill.; Institute of Environmental Sciences (1971). 509p. (CONF-710409).
Papers are included on various aspects of environmental management and engineering. A separate abstract was prepared for each of 4 papers concerning radioactive tracer techniques, radiation effects, and nuclear rocket propulsion. (H.D.R.)
For abstracts of individual papers see: 29105, 29213, 29411, and 31641.

31763 RECOMMENDED PROGRAMMING PRACTICES TO FACILITATE THE INTERCHANGE OF DIGITAL COMPUTER PROGRAMS. ANS 10.2 1971. Hinsdale, Ill.; American Nuclear Society (1971). 9p. Available from American Nuclear Society, Hinsdale, Ill.

XUM

CORPORATE AUTHOR INDEX

In the Corporate Author Index, technical report literature is indexed by the organization or institution responsible for issuing the report. Entries are given for all report literature and for published literature for which a corporate author approach is especially desirable, e.g., symposium and conference proceedings.

Each entry under a corporate author gives the publication title and the *NSA* volume and abstract numbers. Report numbers, where applicable, are given in parentheses at the end of the entry.

A

ADELAIDE UNIV. (AUSTRALIA). DEPT. OF PHYSICS.
Extrapolation of $^{12}C + ^{12}C$ and $^{12}C + ^{16}O$ reaction cross sections to astrophysical energies, 25:31200 (ANU-P-515)

AERONAUTICAL RESEARCH ASSOCIATES OF PRINCETON, INC., N. J.
Prog. rpt. on theory of MHD turbulence, final, 8/70, 25:30517 (N-71-11428)

AKADEMIYA NAUK SSSR, LENINGRAD. FIZIKO-TEKHNICHESKII INSTITUT.
Absorption of shf waves by plasma at upper hybrid frequencies, 25:30606 (NP-18807)
Possibility of determining oscillation parameters of neutrinos, 25:30802 (BNL-tr-418)

AKADEMIYA NAUK SSSR, MOSCOW. INSTITUT FIZIKI.
Probe method for recording ions produced by laser radiation in post-luminescence discharge plasma, 25:30477 (NP-18765)

AKADEMIYA NAUK UKRAINSKOI SSR, KHARKOV. FIZIKO-TEKHNICHESKII INSTITUT.
High frequency heating of a plasma, 25:30460 (MATT-Trans-13)

AKADEMIYA NAUK UKRAINSKOI SSR, KIEV. INSTITUT TEORETICHESKOI FIZIKI.
Calculating (n,2n) reaction amplitude on heavy nuclei. II, 25:31394 (ITF-70-95-E)
Dimensions and form of the light nuclei with the surplus of neutrons, 25:31238 (ITF-70-83-E)
Light absorption by the pair of triplet excitons, 25:31698 (ITF-70-74)
Modified WKB method. II, 25:30699 (ITF-70-84-P)
Riemann method in inverse problem. IV, 25:30894 (ITF-70-98-P)

AKTIEBOLAGET ATOMENERGI, STOCKHOLM (SWEDEN).
Scandinavian model project. I, 25:31548 (EUR-4531, pp 507-16)

ALASKA UNIV., COLLEGE. INST. OF MARINE SCIENCE.
Fjords as sedimentary microcosms, 25:31724 (RLO-2229-T-1-3)

ALLGEMEINE ELEKTRICITAETS-GESELLSCHAFT, AEG-TELEFUNKEN, FRANKFURT AM MAIN (WEST GERMANY).
Structural integration of a prestressed concrete pressure vessel in a nuclear power plant and comparison with a steel vessel installation, 25:31552 (EUR-4531, pp 647-89)

AMES LAB., IOWA.
Experimental and theoretical evaluation of the nitrous oxide--acetylene flame as an atomization cell for flame spectroscopy, 25:31697 (IS-T-424)
Model analyses of elementary particle scattering amplitudes, 25:30751 (IS-T-426)

ARGONNE NATIONAL LAB., ILL.
Aerodynamic characteristics of atmospheric boundary layers, 25:31737 (TID-25465)
ARC system: one-dimensional transport theory capability, SNARC1D, 25:31651 (ANL-7717)
Effect of irradiation on the creep of uranium dioxide, 25:30009 (BMI-1899)
Instrumentation systems to protect LMFBR core integrity, 25:31574 (ANL-7793)
Prog. rpt. on reactor development, 3/71, 25:31533 (ANL-7798)
Sand-bed filtration of aerosols: a review of published information on their use in industrial and atomic energy facilities, 25:29315 (ANL-7683)

ARIZONA UNIV., TUCSON. DEPT. OF CHEMISTRY.
Chlorophyll one-electron photochemistry: flash photolysis studies of the chlorophyll--quinone reaction in alcohol solvents, 25:31687 (COO-908-34)

ARIZONA UNIV., TUCSON. DEPT. OF PHYSICS.
Wire-cutting tool for use with a spark cutter, 25:31689 (COO-1041-19)
X-ray slit system for crystals with small angle boundaries, 25:31688 (COO-1041-18)

ARKANSAS POWER AND LIGHT CO., LITTLE ROCK.
Arkansas Nuclear One, Unit 1. Preliminary safety analysis report, Amendment 20 (includes final safety analysis report, Vol. 1), 25:31512 (DOCKET-50313-27)
Arkansas Nuclear One, Unit 1. Preliminary safety analysis report, Amendment 20 (includes revised license application), 25:31511 (DOCKET-50313-26)
Arkansas Nuclear One, Unit 1. Preliminary safety analysis report, Amendment 20 (includes final safety analysis report, Vol. 2), 25:31513 (DOCKET-50313-28)
Arkansas Nuclear One, Unit 1. Preliminary safety analysis report, Amendment 20 (includes final safety analysis report, Vol. 3), 25:31514 (DOCKET-50313-29)
Arkansas Nuclear One, Unit 2. Preliminary safety analysis report, Amendment 4, 25:31521 (DOCKET-50368-9)

ATOMIC ENERGY COMMISSION, WASHINGTON, D. C.
Correlations to predict maximum PWR containment pressures following a loss-of-coolant accident, 25:31593 (CONF-710302-9)

ATOMIC ENERGY ESTABLISHMENT, WINFRITH (ENGLAND).
Low gamma-sensitivity boron proportional counter, 25:29324 (AEEW-M-970)
Parameter fittings of a nuclear reactor mathematical model in the frequency domain with alternative forms of weighting function, 25:31650 (AEEW-M-1012)
Performance of thermal insulation immersed in helium, 25:30030 (EUR-4531, pp 931-52)

ATOMIC ENERGY OF CANADA LTD., CHALK RIVER (ONTARIO).
Power-reactor siting in various countries, 25:31482 (AECL-3740)

ATOMIC ENERGY OF CANADA LTD., CHALK RIVER (ONTARIO). CHALK RIVER NUCLEAR LABS.
Cosmic ray NM-64 neutron monitor data. XVII, 25:30303 (AECL-3856)

ATOMIC ENERGY RESEARCH ESTABLISHMENT, HARWELL (ENGLAND).
Calculated quality factors for protons in body and eye-lens tissues, 25:29511 (AERE-M-1887)
Calculation of differential neutron scattering cross sections of point defects in a relaxed lattice, 25:31163 (AERE-R-5682)
Effect of high pressures and varying temperatures on the resistivity of ytterbium, 25:30661 (AERE-R-5953)
Introduction to LEED and discussion of some typical LEED experiments, 25:31681 (AERE-M-2184)
LMM Auger spectra of some transition metals of first series, 25:31682 (AERE-R-6719)
Single-crystal targets of rubidium uranyl nitrate for the aligned fissile nuclei experiment, 25:29034 (AERE-R-6141)

ATOMIC INDUSTRIAL FORUM, INC., NEW YORK.
Health physics practices and experiences of isotope producers and distributors, 25:29527 (NP-18791)

ATOMIC WEAPONS RESEARCH ESTABLISHMENT, ALDERMASTON (ENGLAND).
Elastic and inelastic scattering of neutrons in the energy range 1.0 to 5.0 MeV by natural Mo, 25:31299 (AWRE-O-89/70)

AUSTRALIAN ATOMIC ENERGY COMMISSION RESEARCH ESTABLISHMENT, LUCAS HEIGHTS.
Feasibility study of the automatic controls for a pebble bed reactor power station, 25:31543 (AAEC/E-203)
Heat pipes and their applications, 25:29249 (AAEC/LIb/Bib-264)
Review of processes for the production of hafnium-free zirconium, 25:29782 (AAEC/TM-570)

AUSTRALIAN INST. OF NUCLEAR SCIENCE AND ENGINEERING, LUCAS HEIGHTS.
Prog. rpt., annual, 1969, 25:31706 (NP-18803)

AUSTRALIAN NATIONAL UNIV., CANBERRA. DEPT. OF NUCLEAR PHYSICS.
Extrapolation of $^{12}C + ^{12}C$ and $^{12}C + ^{16}O$ reaction cross sections to astrophysical energies, 25:31200 (ANU-P-515)

XUM

AUSTRALIAN NATIONAL UNIV., CANBERRA. RESEARCH SCHOOL OF PHYSICAL SCIENCES.
FIDEL: optical model search code with spin-orbit terms for spin-$^1/_2$ and spin-1 particles, 25:31389 (ANU-P-500)
HAUSER: computer code for calculation of compound nucleus cross sections, 25:31391 (ANU-P-512)
SANDRA: DWBA codes JULIE and DWUCK adapted for use on IBM 360/50 computer, 25:31390 (ANU-P-507)
AVCO CORP., WILMINGTON, MASS. AVCO SYSTEMS DIV.
Prog. rpt. on high-power quasi-steady MPD acceleration, final, 5/70, 25:30599 (N-71-10100)

B

BABCOCK AND WILCOX CO., LYNCHBURG, VA. POWER GENERATION DIV.
Once-through steam generator research and development report, 25:31532 (BAW-10027)
BATTELLE MEMORIAL INST., COLUMBUS, OHIO.
Dresden Nuclear Power Station, Unit 1. Examination of the crack in the 4-inch cleanup-demineralizer piping. Final report, 25:31464 (DOCKET-50010-85)
Effect of irradiation on the creep of uranium dioxide, 25:30009 (BMI-1899)
Thermal diffusivity measurements of irradiated oxide fuels (LWBR Development Program), 25:29937 (BMI-X-10274)
BATTELLE-NORTHWEST, RICHLAND, WASH. PACIFIC NORTHWEST LAB.
Calculated critical parameters for fftf fuel under meltdown conditions, 25:31628 (BNWL-586)
Design and fabrication of a portable device for neutron radiography, 25:29286 (BNWL-1329)
Experimental drifts of juvenile salmonids through effluent discharges at Hanford. II, 25:31645 (BNWL-1527)
FFTF criticality safety, 25:31629 (BNWL-587)
FFTF out-of-reactor criticality safety: objectives and criteria, 25:31626 (BNWL-576)
Hanford as a site for a controlled thermonuclear power plant prototype, 25:30552 (BNWL-B-47)
Interrelationships of geologic formations and processes affecting ecology as exposed at Rattlesnake Springs, 25:31686 (BNWL-B-29)
Radioactivity in FFTF closed loops, 25:31627 (BNWL-585)
Reliability assurance program plan for FFTF, 25:31630 (BNWL-630)
Various holographic scanning configurations for under-sodium viewing, 25:31685 (BNWL-1558)
BECHTEL CORP., SAN FRANCISCO, CALIF.
Monticello Nuclear Generating Plant, Unit 1. Stress analysis review report, 25:31496 (DOCKET-50263-64)
BETTIS ATOMIC POWER LAB., PITTSBURGH, PA.
Thermal diffusivity measurements of irradiated oxide fuels (LWBR Development Program), 25:29937 (BMI-X-10274)
BHABHA ATOMIC RESEARCH CENTRE, BOMBAY (INDIA).
Chemical separation and spectrographic determination of trace amounts of rare earth elements in uranium, 25:28915 (BARC-517)
Determination of total hydrogen content of UO_2 pellets, 25:28912 (BARC-500)
Lithium isotopic analysis on recording Fabry--Perot spectrometer, 25:28913 (BARC-508)
Recovery of Pm from fission product waste. III, 25:29176 (BARC-516)
Syntheses of phyllitic minerals: their utilization in radioactive waste treatment. II, 25:29175 (BARC-509)
Water chemistry studies: chemical analysis manual for moderator and coolant water systems, 25:28914 (BARC-515)
BOCHUM UNIV. (WEST GERMANY). INSTITUT FUER KONSTRUKTIVEN INGENIEURBAU.
Dynamic relaxations as an effective method for spatial calculations on concrete pressure vessels, 25:31665 (EUR-4531, pp 735-57)
BONNARD ET GARDEL. INGENIEURS-CONSEIL, LAUSANNE (SWITZERLAND).
Nonlinear analysis of stresses in the structure of the prestressed concrete pressure vessel for a fast reactor, 25:31553 (EUR-4531, pp 797-812)
BREDERO N.V., UTRECHT (NETHERLANDS).
Influence of irradiation and heating on the strength of mortar and concrete, 25:30021 (EUR-4531, pp 179-83)
BRITISH NUCLEAR DESIGN AND CONSTRUCTION LTD., WHETSTONE (ENGLAND).
Interaction between the design and construction of prestressed concrete pressure vessels for nuclear reactors, 25:31456 (EUR-4531, pp 129-44)
BROOKHAVEN NATIONAL LAB., UPTON, N. Y.
Experimental data on dispersion and deposition of timothy and corn pollen from known sources, 25:31684 (BNL-50266)
Pathways of an artificial element in the body, 25:29418 (BNL-50285)
Tabulated dose uniformity ratio and minimum dose data for gamma irradiator design, 25:29250 (BNL-50145(Rev.))
Taming the wild ferrite, 25:31035 (BNL-15722)
BUNDESANSTALT FUER MATERIALPRUEFUNG, BERLIN (WEST GERMANY).
German research and development on prestressed concrete reactor pressure vessels, 25:31662 (EUR-4531, pp 59-71)
Numerical calculation methods for prestressed concrete reactor pressure vessels, 25:31666 (EUR-4531, pp 759-76)
BUREAU D'ETUDES A. COYNE ET J. BELLIER, PARIS (FRANCE).
Test of ring of prestressed concrete in high-resistance sheet-metal steel, 25:30028 (EUR-4531, pp 445-76)

C

CALIFORNIA INST. OF TECH., PASADENA.
Scale invariance and the light cone, 25:30749 (CALT-69-297)
CALIFORNIA UNIV., BERKELEY. DEPT. OF PHYSICS.
Prog. rpt. on mass spectroscopy research, annual, 10/70, 25:30248 (UCB-34-P-32-PR-5)
CALIFORNIA UNIV., BERKELEY. LAWRENCE RADIATION LAB.
Berkeley ERA program, 25:31059 (UCRL-20611)
Beta-delayed protons from ^{23}Al, 25:31241 (UCRL-20436)
Bevatron guide field control, 25:31055 (UCRL-20189)
Crack growth mechanisms in fibrous composites, 25:31746 (UCRL-20524)
Cryogenic pumping system proposed for Bevatron, 25:31057 (UCRL-20197)
Digital control of Bevatron acceleration cycle, 25:31054 (UCRL-20185)
Electron microscopy investigations of ferrous martensites, 25:31743 (UCRL-19648)
Energy continuation of an energy-independent pion-nucleon phase-shift analysis from 385 to 1700 MeV/c, 25:30871 (UCRL-20250)
ERA 4-MeV injector, 25:31053 (UCRL-20174)
Hydrogen--nitric oxide spin exchange cross section, 25:30277 (UCRL-20529)
Intensity estimation for a neutron beam for biological and medical applications, 25:31174 (UCRL-19715)
Kinetics of the reaction of carbon dioxide with hydroxyl ion, 25:31745 (UCRL-20461)
Negative mass instabilities in an electron-ring compressor, 25:31058 (UCRL-20208)
New bevatron pole-face windings power system, 25:31056 (UCRL-20191)
Preliminary hardware concepts for a high-energy electron-ring accelerator, 25:31052 (UCRL-20169)
Relaxation time measurements in electron paramagnetic resonance, 25:31744 (UCRL-19691)
Shaking of particle beams to remove neutralizing ions, 25:31050 (UCRL-20156)
Ultra-narrow, high-quality, high-field quadrupole magnet, 25:31051 (UCRL-20164)
CALIFORNIA UNIV., LA JOLLA, SAN DIEGO. DEPT. OF CHEMISTRY.
Prog. rpt. on distribution and origin of elements and their isotopes in nature, final, 1962--70, 25:30158 (UCSD-34-P-43-X-9)
CALIFORNIA UNIV., LIVERMORE. LAWRENCE RADIATION LAB.
Application of the tensor code to the calculation of rayleigh waves, 25:29243 (UCRL-50992)
Distribution, residence time, and inventory of tritium in Sedan crater ejecta, 25:29244 (UCRL-72572)
Engineering tests of Halon 1301 fire extinguishing systems for field assembly buildings, 25:31748 (UCRL-51021)
Function optimization on a line segment by GOLDEN section, 25:31740 (UCID-30002)
Ice age theory analysis by computer model simulation. I, 25:31749 (UCRL-71888(Pt.1))
Ice age theory analysis by computer model simulation. II, 25:31750 (UCRL-71888(Pt.2))
Identification of dynamic systems from experimental data, 25:31752 (UCRL-72818(Rev.1))
Laser beam filtering by saturable dyes, 25:31747 (UCRL-51008)
Methodology for computing potential radiation dose to man from nuclear excavation projects, 25:29516 (UCRL-50990)
Tests of ice age theories using a zonal atmospheric model, 25:31751 (UCRL-72803)
CALIFORNIA UNIV., LOS ANGELES. DEPT. OF CHEMISTRY.
Spin-lattice relaxation and Zeeman effects in triplet state of pyrazine-d_4, 25:31742 (UCLA-34-P-91-47)
CALIFORNIA UNIV., LOS ANGELES. LAB. OF NUCLEAR MEDICINE AND RADIATION BIOLOGY.
Improved feedback control for Null-point compensating system, 25:31741 (UCLA-12-813)
CALIFORNIA UNIV., SAN DIEGO.
Precision deep-sea time release, 25:31756 (UCSD-34-P-127-8)
CAMBRIDGE ELECTRON ACCELERATOR, MASS.
Prog. rpt. on Cambridge Electron Accelerator, semiannual, 1--6/70, 25:31036 (CEAL-1053)
CAROLINA POWER AND LIGHT CO., RALEIGH, N.C.
Brunswick Steam Electric Plant, Units 1 and 2. Preliminary safety analysis report, Amendment 11, 25:31515 (DOCKET-50324-20)
CENTRAL ELECTRICITY GENERATING BOARD, BERKELEY (ENGLAND). BERKELEY NUCLEAR LABS.
Code of design for research apparatus containing molten sodium, 25:29252 (RD/B/M-1817)
Collaborative program on creep fatigue behavior of 1

percent Cr--Mo--V, 25:29826 (RD/B/N-1889)
Creep behavior of prestressed concrete slabs with reinforced holes, 25:30024 (EUR-4531, pp 373-84)
Fully developed turbulent flow through concentric annuli, 25:29265 (RD/B/N-1878)

CENTRAL ELECTRICITY GENERATING BOARD, LEATHERHEAD (ENGLAND). RESEARCH LABS.
Moisture measurements in mass concrete, 25:30026 (EUR-4531, pp 409-16)

CENTRE NATIONAL DE LA RECHERCHE SCIENTIFIQUE, STRASBOURG (FRANCE). CENTRE DE RECHERCHES NUCLEAIRES.
Observation of d^* effect in anti pd → p anti p π^+ π^-n reaction at 5.55 GeV/c, 25:30727 (NP-18796)

CESKOSLOVENSKA AKADEMIE VED, REZ. USTAV JADERNEHO VYZKUMU.
Influence of initial content of the cooling rate from the beta phase to preferred uranium orientation following heat treatment, 25:29884 (UJV-2525-M)

CHICAGO UNIV., ILL.
Complex negative signature trajectories and Pomeranchuk theorem, 25:31012 (COO-264-571)
Leptonic decay experiments with hyperons beams at NAL, 25:30722 (COO-1701-12)
Mass yield and charge distribution in 450 MeV proton fission of ^{238}U, 25:31302 (COO-1167-10)

CHICAGO UNIV., ILL. DEPT. OF PHYSICS.
Analysis of spin correlations in the beta decay of the lambda hyperon, 25:30804 (COO-264-569)

CHICAGO UNIV., ILL. ENRICO FERMI INST.
Analysis of spin correlations in the beta decay of the lambda hyperon, 25:30804 (COO-264-569)

CHICAGO UNIV., ILL. INST. FOR NUCLEAR STUDIES.
Prog. rpt., 11/70, 25:31693 (COO-2094-4)

CINCINNATI GAS AND ELECTRIC CO., OHIO.
Wm. H. Zimmer Nuclear Power Station, Unit 1. Preliminary safety analysis report, Amendment 7, 25:31520 (DOCKET-50358-14)

CLERMONT-FERRAND UNIV. (FRANCE). FACULTE DES SCIENCES.
Use of semiconductor telescopes for detecting the recoil nuclei in proton-light nucleus coherent scattering at high energy, 25:31185 (LYCEN-7085)

COLUMBIA UNIV., NEW YORK. DEPT. OF PHYSICS.
Method for computing scattering matrix elements in a class of non-renormalizable field theories, 25:31016 (NYO-1932(2)-192)

COLUMBUS AND SOUTHERN OHIO ELECTRIC CO., COLUMBUS, OHIO.
Wm. H. Zimmer Nuclear Power Station, Unit 1. Preliminary safety analysis report, Amendment 7, 25:31520 (DOCKET-50358-14)

COMISION NACIONAL DE ENERGIA ATOMICA, BUENOS AIRES (ARGENTINA).
Excitation functions for the nuclear reactions $^{159}Tb(d,p)^{160}Tb$ and $^{159}Tb(d,4n)^{157}Dy$, 25:31301 (CNEA-283)
Resonance integrals for neutron activation of ^{64}Zn, ^{68}Zn, ^{85}Rb, ^{100}Mo, ^{102}Ru, ^{113}In, ^{123}Sb, and ^{180}Hf, 25:31300 (CNEA-282)

COMITATO NAZIONALE PER L'ENERGIA NUCLEARE, FRASCATI (ITALY). LABORATORIO GAS IONIZZATI.
Merits and limitations of explosively driven current generators in fusion research, 25:30562 (EUR-4593, pp 205-17)
Parametric study of exploding foils as switches, 25:30574 (EUR-4593, pp 319-38)

COMITATO NAZIONALE PER L'ENERGIA NUCLEARE, ROME (ITALY).
Analysis of methods for interpreting bremsstrahlung spectra, 25:30632 (RT/FI-(70)36)
Data on environmental radioactivity collected in Italy, 1--6/68, 25:29503 (PROT.-SAN.-8/69)
Data on environmental radioactivity collected in Italy, 7--12/68, 25:29504 (PROT.-SAN.-13/69)
Equilibrium data relating to Eurex process, 25:29182 (RT/CHI-(70)31)
Experimental vibration characteristics of a B.W.R. fuel assembly, 25:31570 (RT/ING-(70)24)
High sensitivity beryloneter, 25:29390 (RT/EL-(70)4)
Optimization of energy resolution in nuclear spectrometry measurements with germanium detectors, 25:29356 (RT/EL-(70)5)

COMMISSARIAT A L'ENERGIE ATOMIQUE, BRUYERES-LE-CHATEL (FRANCE). CENTRE D'ETUDES.
Separation and recovery of permanent gases by preparative chromatography, 25:29177 (CEA-R-4090)
Study of impurities distribution in a metal (plutonium), 25:28916 (CEA-R-4071)
Total elementary separation of rare earths on cation exchange resins, 25:29178 (CEA-R-4102)

COMMISSARIAT A L'ENERGIE ATOMIQUE, CHUSCLAN (FRANCE). CENTRE DE PRODUCTION DE PLUTONIUM DE MARCOULE.
Some criteria for choosing presses for the compaction of radioactive waste, 25:29316 (LA-tr-71-12)
Test of ring of prestressed concrete in high-resistance sheet-metal steel, 25:30028 (EUR-4531, pp 445-76)

COMMISSARIAT A L'ENERGIE ATOMIQUE, FONTENAY-AUX-ROSES (FRANCE). CENTRE D'ETUDES NUCLEAIRES.
Amorphization of a Pd--Si alloy by irradiation with fission products, 25:29901 (CEA-CONF-1693)
Recent developments in the electrodeposition of metals in fused salt media, 25:29783 (CEA-N-1376)
Several applications of a system of weighting in Monte Carlo calculations, 25:31164 (CEA-N-825)
Study of the variance of a Monte Carlo calculation, 25:30698 (CEA-N-1096)
Tokamak facility of Fontenay-aux-Roses, 25:30583 (EUR-4593, pp 403-9)

COMMISSARIAT A L'ENERGIE ATOMIQUE, GRENOBLE (FRANCE). CENTRE D'ETUDES NUCLEAIRES.
Fast analysis by 14-MeV neutron activation of fluorine deposits on the vegetation in a polluted area, 25:29011 (CEA-CONF-1747)
Opto-electronic link for transmitting temporal information, 25:29392 (CEA-N-1431)

COMMISSARIAT A L'ENERGIE ATOMIQUE, LA HAGUE (FRANCE).
Emotivity parameter in industrial medicine and the special conditions imposed by radioprotection in the nuclear industry, 25:29531 (CEA-R-4156)

COMMISSARIAT A L'ENERGIE ATOMIQUE, SACLAY (FRANCE). CENTRE D'ETUDES NUCLEAIRES.
Determination of equations of state for gaseous hexafluorides of uranium, molybdenum, and tungsten, 25:29073 (CEA-N-1414)
Electronic microscope study of needle-shaped precipitates in irradiated austenitic steels, 25:29902 (EURFNR-891)
New types of thermal-shielding concretes for nuclear reactors, 25:30031 (EUR-4531, pp 975-1018)
Physical and chemical interactions of water on graphite, 25:29918 (CEA-R-4123)
Study of behavior of concrete subjected to triaxial stresses, 25:30027 (EUR-4531, pp 417-24)
Synthesis and crystallographic study of compounds of the system Cs_2O--Al_2O_3--SiO_2, 25:29938 (BNWL-tr-65)
Test of ring of prestressed concrete in high-resistance sheet-metal steel, 25:30028 (EUR-4531, pp 445-76)

COMMISSARIAT A L'ENERGIE ATOMIQUE, VALDUC (FRANCE). CENTRE D'ETUDES.
Study of impurities distribution in a metal (plutonium), 25:28916 (CEA-R-4071)

COMMONWEALTH EDISON CO., CHICAGO, ILL.
Dresden Nuclear Power Station, Unit 1. Examination of the crack in the 4-inch cleanup-demineralizer piping. Final report, 25:31464 (DOCKET-50010-85)
Dresden Nuclear Power Station, Unit 1. Semiannual report, July 1--December 31, 1970, 25:31469 (DOCKET-50237-147)
Dresden Nuclear Power Station, Unit 2. Additional information regarding corrective action on Standby Liquid Control System, 25:31490 (DOCKET-50237-161)
Dresden Nuclear Power Station, Unit 2. Damage to seismic restraints on core spray subsystem, 25:31473 (DOCKET-50237-160)
Dresden Nuclear Power Station, Unit 2. Failure of diesel generator to start following automatic initiation signal, 25:31472 (DOCKET-50237-159)
Dresden Nuclear Power Station, Unit 2. Solid waste activity for second half of 1970, 25:31471 (DOCKET-50237-158)
Dresden Nuclear Power Station, Unit 2. Special reports Nos. 10--13 on topics requested by AEC, 25:31489 (DOCKET-50237-156)
Dresden Nuclear Power Station, Unit 2. Summary technical report of secondary containment leak rate test, February 25, 1971, 25:31470 (DOCKET-50237-157)
Dresden Nuclear Power Station, Unit 3. Facility Operating License No. DPR-25; correction to Proposed Change No. 2 to Appendix A, 25:31492 (DOCKET-50249-65)
Quad-Cities Station, Units 1 and 2. Additional information on financial qualifications, 25:31493 (DOCKET-50254-35)

COMMONWEALTH X-RAY AND RADIUM LAB., MELBOURNE (AUSTRALIA).
Prog. rpt., annual, 6/30/70, 25:29526 (NP-18790)

COMPAGNIE DE SAINT-GOBAIN, PARIS (FRANCE).
Heat exchange by natural convection in porous media, 25:29264 (EUR-4531, pp 821-39)

COMPAGNIE DES ATELIERS ET FORGES DE LA LOIRE, PARIS (FRANCE).
Thermal shielding by wire gauze and metallic sheets, 25:29819 (EUR-4531, pp 1019-34)

CONNECTICUT YANKEE ATOMIC POWER CO., HADDAM.
Connecticut Yankee Atomic Power Plant. Operation report No. 71-3, March 1971, 25:31468 (DOCKET-50213-105)

CONSOLIDATED EDISON CO. OF NEW YORK, INC., NEW YORK.
Indian Point Station, Unit No. 1. Facility design changes, 25:31483 (DOCKET-50003-68)

CONSUMERS POWER CO., JACKSON, MICH.
Big Rock Point Nuclear Plant. Corrective actions to starting failure of emergency generator, 25:31486 (DOCKET-50155-80)
Big Rock Point Nuclear Plant. Quarterly operations report No. 80, January--March 1971, 25:31467 (DOCKET-50155-81)

CORNELL UNIV., ITHACA, N. Y.
Direct observation of long range migration of self-interstitial atoms in Stage I of irradiated platinum, 25:30649 (NYO-3504-57)

CORNELL UNIV., ITHACA, N. Y. DEPT. OF FLORICULTURE AND ORNAMENTAL HORTICULTURE.
Prog. rpt. on loss of organic and inorganic materials from above-ground plant parts by leaching, 1970--71, 25:31709 (NYO-2598-52)

CORNELL UNIV., ITHACA, N. Y. LAB. OF ATOMIC AND SOLID STATE PHYSICS.
Prog. rpt. on solid state physics; magnetic phenomena, 1/--12/70, 25:30646 (NYO-2150-66)
Prog. rpt. on theoretical phonon physics, 4/70--3/71,

XUM

25:31711 (NYO-3699-53)
Study of the transverse magnetoresistance of polycrystalline potassium, 25:31707 (NYO-2150-68)

D

DANISH ATOMIC ENERGY COMMISSION, RISOE. RESEARCH ESTABLISHMENT.
MOSSPEC: program for resolving Moessbauer spectra, 25:30688 (RISO-M-1348)
DAYTON POWER AND LIGHT CO., OHIO.
Wm. H. Zimmer Nuclear Power Station, Unit 1. Preliminary safety analysis report, Amendment 7, 25:31520 (DOCKET-50358-14)
DEPARTMENT OF ATOMIC ENERGY, BOMBAY (INDIA). CHEMISTRY AND METALLURGY COMMITTEE.
Dispersed-particle strengthening in nickel-zirconia composite, 25:29941 (INIS-mf-8)
DEUTSCHE BABCOCK UND WILCOX A.G., OBERHAUSEN (WEST GERMANY).
Thermal shielding by screens of circulating gas, 25:31576 (EUR-4531, pp 1035-53)
DEUTSCHES ELEKTRONEN-SYNCHROTRON, HAMBURG (WEST GERMANY).
Accuracy of photon-difference method used in high-energy photonuclear experiments, 25:30773 (DESY-71/3)
DIVISION OF REACTOR DEVELOPMENT AND TECHNOLOGY (AEC), WASHINGTON, D. C.
Soviet power reactors: 1970, 25:31534 (WASH-1175)
DIVISION OF REACTOR LICENSING (AEC), WASHINGTON, D. C.
Enrico Fermi Atomic Power Plant, Unit 1. Change No. 25 to technical specifications of Provisional Operating License No. DPR-9, 25:31484 (DOCKET-50016-110)
La Crosse Boiling Water Reactor. Order extending provisional operating authorization expiration date, 25:31463 (DOCKET-1155-113)
Monticello Nuclear Generating Plant, Unit 1. Change No. 1 to technical specifications of Provisional Operating License No. DPR-22, 25:31498 (DOCKET-50263-66)
Palisades Plant. Detailed statement on the environmental considerations, 25:31494 (DOCKET-50255-38)
Peach Bottom Atomic Power Station, Unit 1. Change No. 14 to technical specifications of Provisional Operating License No. DPR-12, 25:31487 (DOCKET-50171-84)
Southwest Experimental Fast Oxide Reactor. Request for additional information on vessel flange bolt stresses, 25:31595 (DOCKET-50231-79)
DIVISION OF RESEARCH (AEC), WASHINGTON, D. C.
Progress in controlled thermonuclear research, 25:30600 (WASH-1172)
DIVISION OF SAFETY STANDARDS (AEC), WASHINGTON, D. C.
Safety guides for water cooled nuclear power plants, 25:31526 (TID-25697)
DOUGLAS UNITED NUCLEAR, INC., RICHLAND, WASH.
Examination of an Inconel-600 tube from N Reactor steam generator 6A, 25:29760 (DUN-SA-149)
Operation of halogen quenched Geiger--Mueller tubes, 25:31646 (DUN-SA-136)
Prog. rpt. on noble gas confinement study, final, FY-1970, 25:29074 (DUN-7221(Vol.1))
Prog. rpt. on noble gas confinement study, final, FY-1970, 25:29075 (DUN-7221(Vol.2))
DUKE POWER CO., CHARLOTTE, N.C.
McGuire Nuclear Station, Units 1 and 2. Preliminary safety analysis report, Amendment 4, 25:31522 (DOCKET-50369-8)
Oconee-1, 2, and 3 preliminary safety analysis report, Amend. 13, 25:31499 (DOCKET-50269-17)

E

ECOLE POLYTECHNIQUE, PARIS (FRANCE).
Conference on high multiplicity hadronic interactions, Paris, 5/70, 25:30762
ECOLE POLYTECHNIQUE FEDERALE DE LAUSANNE (SWITZERLAND).
Nonlinear analysis of stresses in the structure of the prestressed concrete pressure vessel for a fast reactor, 25:31553 (EUR-4531, pp 797-812)
EG AND G, INC., LAS VEGAS, NEV.
Radiation output description from the T(d,n)⁴He reaction in a large target (1000 cm²): Operation Henre, 25:31165 (CEX-65.04)
EG AND G, INC., SANTA BARBARA, CALIF.
Environmental air quality support study, 25:31695 (EGG-1183-2242)
ELECTRICITE DE FRANCE, CLAMART.
Thermal shielding by wire gauze and metallic sheets, 25:29819 (EUR-4531, pp 1019-34)
ELECTRICITE DE FRANCE, ECUELLES.
Study of the properties of concrete and especially of creep under the effect of temperature, 25:30023 (EUR-4531, pp 267-324)
ELECTRICITE DE FRANCE, PARIS.
Dose calculation from the urine of subjects contaminated by irradiated uranium, 25:29515 (NP-18794)
First results of putting into service the St. Laurent I prestressed concrete pressure vessel, 25:31455 (EUR-4531, pp 95-128)
ENTERPRISES CAMPENON BERNARD S.A., PARIS (FRANCE).
Prestressed concrete pressure vessel of the Vandellos nuclear power plant, 25:31454 (EUR-4531, pp 81-94)
ENVIRONMENTAL RESEARCH CORP., LAS VEGAS, NEV.
Observed seismic data Handley event, 25:29242 (NVO-1163-216(Rev.))
EUROPEAN ATOMIC ENERGY COMMUNITY, ISPRA (ITALY). JOINT NUCLEAR RESEARCH CENTER.
COSTAX-BOIL: program for axial dynamics of BWR and PWR nuclear reactors, 25:31541 (EUR-4497)
TIMOC: Monte Carlo code for stationary and time dependent neutron transport, 25:31167 (EUR-4519)
EUROPEAN COMMUNITIES, LUXEMBOURG. COMMISSION.
Conference on prestressed concrete reactor pressure vessels and their thermal isolation, Brussels, Belgium, 11/69, 25:31546 (EUR-4531)
Symposium on fusion technology, Aachen, Germany, 9/70, 25:30449 (EUR-4593)
EUROPEAN COMPANY FOR THE CHEMICAL PROCESSING OF IRRADIATED FUELS, MOL (BELGIUM).
Preparation and properties of a crystalline uranium(IV)--hydrazine nitrate compound, 25:29035 (NP-18736)
EUROPEAN ORGANIZATION FOR NUCLEAR RESEARCH, GENEVA (SWITZERLAND).
Compilation of cross sections. VI, 25:30735 (CERN-HERA-70-7)
Dual models and dual phenomenology, 25:30823 (CERN-71-7, pp 285-358)
Physics and astrophysics, 25:30219 (CERN-70-31)
Proceedings of 1970 CERN school of Physics, Loma-Koli, Finland, 6--7/70, 25:30750 (CERN-71-7)
EUROPEAN SOCIETY FOR RADIATION BIOLOGY.
Conference of European Society for Radiation Biology, Ulm, Ger., 9/69, 25:29607 (CONF-690940-(Absts.))

F

FLORIDA POWER AND LIGHT CO.
Hutchinson Island Plant, Unit No. 1. Preliminary safety analysis report, Amendment 10, 25:31517 (DOCKET-50335-18)
FLORIDA STATE UNIV., TALLAHASSEE.
Prog. rpt. on all response to nucleic acid penetration, 8/69--9/70, 25:31738 (TID-25694)
Prog. rpt. on experimental study of nuclear models, 8/70--7/71. I, 25:31315 (ORO-2434-7)
FLORIDA UNIV., GAINESVILLE. RADIATION BIOLOGY LAB.
Prog. rpt. on biosynthesis of plant proteins and nucleic acids, 1970--71, 25:31720 (ORO-3982-10)
FRIED-KRUPP UNIVERSALBAU, ESSEN (WEST GERMANY).
Fracture behavior of concrete in a multiaxial stress field, 25:30025 (EUR-4531, pp 385-407)
Results of model investigations on multiple pressure vessels, 25:31549 (EUR-4531, pp 527-56)

G

GAUSTAD SYKEHUS, OSLO (NORWAY). EEG RESEARCH LAB.
Prog. rpt. on regional blood flow in subcortical structures in man, 3/71, 25:31710 (NYO-3618-10)
GENERAL ELECTRIC CO., PHILADELPHIA, PA. SPACE DIV.
Prog. rpt. on Avalanche type semiconductor radiation detectors, semiannual, 7--12/70, 25:29327 (NYO-3246-TA-8)
GENERAL ELECTRIC CO., PLEASANTON, CALIF. NUCLEONICS LAB.
Fission gas re-solution rates: limitations of fission gas bubble growth by the re-solution process, 25:30032 (GEAP-12148)
Prog. rpt. on thermodynamic data program involving plutonia and uranias at high temperatures, 8--10/70, 25:29821 (GEAP-12153)
GENERAL ELECTRIC CO., ST. PETERSBURG, FLA. NEUTRON DEVICES DEPT.
Production of bulk quantities of ultrapure erbium, 25:29181 (GEPP-85)
GENERAL ELECTRIC CO., SAN JOSE, CALIF. ATOMIC POWER EQUIPMENT DEPT.
Monticello Nuclear Generating Plant, Unit 1. Design report: recirculation system, 25:31495 (DOCKET-50263-63)
Monticello Nuclear Generating Plant, Unit 1. Stagnant water or low steam flow in reactor coolant system, 25:31497 (DOCKET-50263-65)
GENERAL ELECTRIC CO., SUNNYVALE, CALIF. BREEDER REACTOR DEVELOPMENT OPERATION.
Southwest Experimental Fast Oxide Reactor. Characteristic curves for the Fast Reactivity Excursion Device poison slugs, 25:31631 (DOCKET-50231-80)
Southwest Experimental Fast Oxide Reactor. License No. DR-15; technical specifications Proposed Change No. 5, 25:31596 (DOCKET-50231-81)
GEOLOGICAL SURVEY, DENVER, COLO.
Geologic and hydrologic effects of the Handley event, Pahute Mesa, Nevada Test Site, 25:29203 (USGS-474-95)
GOSUDARSTVENNYI KOMITET PO ISPOL'ZOVANIYU ATOMNCI ENERGII SSSR, MOSCOW. INSTITUT ATOMNOI ENERGII.
Drift-beam instability and ion sound in an inhomogeneous plasma, 25:30506 (MATT-Trans-84)
Effect of shape and magnitude of discharge current pulse on plasma confinement and heating in Tokamak-3, 25:30461 (MATT-Trans-79)

XUM

Electron-ion beam instability, 25:30505 (MATT-Trans-83)
Evidence of disappearance of inelastic channel of nuclear reaction in nuclear resonant scattering of γ-rays in perfect crystal, 25:30687 (IAE-1966)
Neutron thermalization in H_2O at 318°K and 77°K, 25:31170 (KAPL-Trans-4)
Stability of single-turn coils in pulsed magnetic fields up to 1 MG, 25:30556 (EUR-4593, pp 25-32)
Study of sponfaneous fission of ^{252}Cf, 25:31314 (ORNL-tr-2453)

GOSUDARSTVENNYI KOMITET PO ISPOL'ZOVANIYU ATOMNOI ENERGII SSSR, MOSCOW. INSTITUT TEORETICHESKOI I EKSPERIMENTAL'NOI FIZIKI.
Divergences of amplitudes of weak nonleptonic processes with photon emission, 25:30805 (NP-18777)
Invariants of the rotation group, 25:31013 (ITEF-782)
Many-baryon resonances, 25:30895 (NP-18779)
Methods for monitoring proton incidence on the internal targets of high-energy accelerators, 25:31043 (NP-18776)
Program for processing photographs in bubble chamber filled with heavy liquid. I, 25:29369 (ITEF-753)

GOSUDARSTVENNYI KOMITET PO ISPOL'ZOVANIYU ATOMNOI ENERGII SSSR, OBNINSK. FIZIKO-ENERGETICHESKII INSTITUT.
Physical characteristics of critical assembly mockup of the BOR-reactor, 25:31632 (FEI-201)

GOSUDARSTVENNYI KOMITET PO ISPOL'ZOVANIYU ATOMNOI ENERGII SSSR, SERPUKHOV. INSTITUT FIZIKI VYSOKIKH ENERGII.
Search for particles with fractional charge in 70 GeV accelerator, 25:30724 (CERN-Trans-71-4)
Weak interactions, 25:30803 (CERN-71-7, pp 1-40)

GOSUDARSTVENNYI KOMITET PO ISPOL'ZOVANIYU ATOMNOI ENERGII SSSR, SUKHUMI. FIZIKO-TEKHNICHESKII INSTITUT.
Experimental installation R-Ohm for studying high-frequency field-interaction with plasma, 25:30508 (NP-18801)
Studies of diffusion of dense disintegrating plasma in a stellarator, 25:30462 (NP-18767)

GULF GENERAL ATOMIC, INC., SAN DIEGO, CALIF.
Prog. rpt. on applications of neutron activation analysis in scientific crime investigation, final, 9/70, 25:29012 (GA-10276)
Steam generators for high-temperature gas-cooled reactor plants in the USA, 25:31623 (GA-10338)

H

HANFORD ENGINEERING DEVELOPMENT LAB., RICHLAND, WASH.
Cross section structure factor interpolation schemes, 25:31647 (HEDL-TME-71-40)

HAWAII UNIV., HONOLULU. DEPT. OF PHYSICS AND ASTRONOMY.
Prog. rpt. on photoelectric emission from thin films in the vacuum ultraviolet region, annual, 6/70--2/71, 25:30665 (UH-235-P-9-2)

HELSINKI UNIV. (FINLAND). RESEARCH INST. FOR THEORETICAL PHYSICS.
Comment on anomalous electron--phonon transport properties of impure metals, 25:30697 (NP-18822)

HIRAM COLL., OHIO. X-RAY PHYSICS LAB.
Defect production in single crystals resulting from ion bombardment, 25:30648 (N-70-37028)

HOLZMANN (PHILIPP) A. G., FRANKFURT AM MAIN (WEST GERMANY).
Individual tension components for vertical prestress with breaking loads above 1500 Mp, 25:31663 (EUR-4531, pp 489-505)
Polygonally directed, wound ring stress reinforcements with several intermediate fastners for all stress wire rings (PRISMA system), 25:29939 (EUR-4531, pp 433-44)

I

IDAHO NUCLEAR CORP., IDAHO FALLS.
Computer calculation of bone doses following acute exposure to ^{90}Sr aerosols, 25:29513 (CONF-710211-1)
Correlations to predict maximum PWR containment pressures following a loss-of-coolant accident, 25:31593 (CONF-710302-9)
Distribution of solid fission products in UO_2, 25:31589 (CONF-710302-5)
Effects of state properties on high pressure compressible hydrodynamics, 25:31590 (CONF-710302-6)
Flow simulation through graphics: a high-speed interpretation of reactor blowdown calculations, 25:31588 (CONF-710302-4)
Idaho nuclear code automation: a standardized and modularized code structure, 25:31594 (CONF-710302-10)
Mathematical techniques for vibration analysis of reactor systems, 25:31591 (CONF-710302-7)
Molecular potential function in terms of group valence force symmetry coordinates, 25:31696 (IN-1421)
MOXY: a digital computer code for computing core heat transfer, 25:31587 (CONF-710302-2)
Neutron filtered beams as standard sources, 25:31166 (CONF-710301-8)
Nodal sensitivity in modeling a large pressurized water reactor system for a loss-of-coolant accident, 25:31592 (CONF-710302-8)
Ultrasonic level monitor, 25:29393 (IN-1452)

ILLINOIS UNIV., URBANA.
Energetics, morphology, crystallography, and theory of displacive transformations in near-equiatomic niobium--ruthenium alloys, 25:29882 (COO-1198-807)

ILLINOIS UNIV., URBANA. DEPT. OF COMPUTER SCIENCE.
Illiac III computer system manual, 25:31694 (COO-2118-1)

INSTITUT ATOMNOI ENERGII, MOSCOW (USSR).
Analogous states of T = 2 in $^{28}Mg(^3He,n)^{28}Si$, $^{48}Ti(^3He,n)^{48}Cr$, and $^{58}Ni(^3He,n)^{60}Zn$ reactions, 25:31237 (IAE-1958)
Hall effect in plasma oscillations, 25:30544 (IAE-1950)

INSTITUT FUER PLASMAPHYSIK, G.M.B.H. GARCHING (WEST GERMANY).
Comparison of different fusion reactor blanket systems, 25:30591 (EUR-4593, pp 513-18)
Data for a fusion reactor: summary of an IPP lecture series, 25:30590 (EUR-4593, pp 497-512)
Erosion in high-current, high-pressure gas discharges, 25:30495 (EUR-4593, pp 251-6)
Fast storage system for a 500-kV theta-pinch experiment, 25:30567 (EUR-4593, pp 265-71)
High-power spark gap for high repetition rates, 25:30568 (EUR-4593, pp 273-80)
High-power spark gaps for large and fast energy storage systems, 25:30565 (EUR-4593, pp 241-50)
High-Q capacitor, 25:30594 (EUR-4593, pp 541-4)
Influence of wall material on plasma--wall interaction, 25:30496 (EUR-4593, pp 461-70)
Interaction of sputtered wall material with fusion plasma, 25:30497 (EUR-4593, pp 471-7)
Investigations on preionization for toroidal high-beta-experiments, 25:30541 (IPP-1/114)
Low-field instabilities of high-field composite superconductors, 25:30410 (EUR-4593, pp 95-100)
New crowbar system for 2.7-MJ bank Isar I at Garching, 25:30560 (EUR-4593, pp 189-95)
Normal transitions of composite superconductors induced by magnetic disturbances, 25:30411 (EUR-4593, pp 101-6)
Pulse breakdown of plastic foils in liquids, 25:30569 (EUR-4593, pp 281-6)
Recent results with laser-triggered spark gaps, 25:30566 (EUR-4593, pp 259-64)
Status report on Garching Tokamak experiment Pulsator, 25:30584 (EUR-4593, pp 411-17)
System planning for a prototype fusion reactor, 25:30593 (EUR-4593, pp 533-8)
Toroidal version of the Isar I theta-pinch experiment, 25:30585 (EUR-4593, pp 419-24)
Vlasov description of a supercritical magneto-acoustic compression pulse, 25:30513 (IPP-1/113)

INSTITUT JOZEF STEFAN, LJUBLJANA (YUGOSLAVIA).
Description of the Institute and works performed during the summer of 1969, 25:31633 (IJS-253)

INSTITUTE FOR CANCER RESEARCH, PHILADELPHIA, PA.
Prog. rpt. on effects of ultraviolet radiation on cell structure and behavior, 1967--1970, 25:29608 (NYO-2356-43)

INSTITUTE OF NUCLEAR RESEARCH, WARSAW (POLAND).
Connection of radiation capture mechanism with the nuclear structure (A > 100), 25:31303 (INR-1271)
Eikonal model for high-energy elastic scattering, 25:30893 (INR-P-1233)
FLANGE-AL 4 code for the Gier computer, 25:31168 (INR-1260)

INSTITUTE OF NUCLEAR TECHNIQUES, KRAKOW (POLAND).
Semiconductor system for analog processing of signals obtained from radiometric control set of the calcium content in the cement-feeding, 25:29389 (ITJ-2/E)
Tables of magnetic structures determined by neutron diffraction. II, 25:30664 (NP-18783)

INSTITUTO POLITECNICO NACIONAL, MEXICO CITY. CENTRO DE INVESTIGACION Y DE ESTUDIOS AVANZADOS.
Selected topics in discrete symmetries and CP-violation, 25:30915 (NP-18808)
Symmetry groups and current algebra, 25:30914 (NP-18804)

INTERNATIONAL ATOMIC ENERGY AGENCY, VIENNA (AUSTRIA).
Conference on sterility principle for insect control or eradication, Athens, 9/70, 25:29730 (STI/PUB-265)
Contribution from the United Kingdom, 25:31555 (IAEA-126, pp 53-9)
Design philosophy and criteria of safety for prestressed concrete pressure vessels: practice in Czechoslovakia, 25:31561 (IAEA-126, pp 179-212)
Evolution of new varieties of rice with respect to increased yield per acre, resistance to diseases and better quality through use of induced mutations, 25:29481 (IAEA-R-290-F)
Problems and prospects of prestressed concrete vessels: French experience up to 1970, 25:31557 (IAEA-126, pp 69-83)
Report on the starting of a coordinated work program for prestressed concrete reactor pressure vessels in the Federal Republic of Germany, 25:31560 (IAEA-126, pp 115-77)
Scaling-up of salmonella radicidation of frozen boneless meats, 25:29729 (IAEA-R-491-F)
Structural design philosophy and criteria for concrete reactor vessels: U. S. practice, 25:31554 (IAEA-126, pp 19-51)
Swedish development on prestressed concrete pressure vessels for water reactors, 25:31562 (IAEA-126, pp 213-41)

XUM

Test stand for the prestressed concrete vessel containing the helium loop, 25:31558 (IAEA-126, pp 85-97)
Ultimate design experience from small dimension models testing, 25:31559 (IAEA-126, pp 99-114)
Work on reactor vessels of prestressed concrete in Yugoslavia, 25:31556 (IAEA-126, pp 61-8)
INTERNATIONAL BUSINESS MACHINES CORP., POUGHKEEPSIE, N. Y.
Determination anomalous magnetic moment of free electron, 25:30720
IOWA ELECTRIC LIGHT AND POWER CO., CEDAR RAPIDS.
Duane Arnold Energy Center. Environmental report, 25:31516 (DOCKET-50331-25)

J

JAPAN ATOMIC ENERGY RESEARCH INST., TOKAI. TOKAI RESEARCH ESTABLISHMENT.
Phase study of the system UO_2--Dy_2O_3, 25:29975 (JAERI-1203)
JAPAN ATOMIC ENERGY RESEARCH INST., TOKYO.
Calculation of flux of fast neutral particles from a cylindrical, high-temperature plasma, 25:30514 (JAERI-Memo-4243)
Characteristics of personal monitoring dosimeter, 25:29383 (JAERI-Memo-4292)
Columnar grain growth in center line heated UO_2 pellet, 25:29976 (JAERI-Memo-4249)
Dynamic molecular orbitals and their application to charge exchange reactions, 25:30275 (JAERI-Memo-4299)
JAERI nuclear instrument module system 6, 25:29394 (JAERI-Memo-4281)
JAERI nuclear instrument module system 7, 25:29395 (JAERI-Memo-4295)
JAERI nuclear instrument module system 8, 25:29396 (JAERI-Memo-4303)
Multi-group constants for fission product nuclides, 25:31304 (JAERI-Memo-4251)
Review of USSR Tokamak experiments, 25:30596 (JAERI-Memo-4286)
JOINT INST. FOR NUCLEAR RESEARCH, DUBNA (USSR).
Single-particle states of deformed transuranium nuclei in Saxon--Woods potential, 25:31392 (BNL-tr-416)
JOINT INST. FOR NUCLEAR RESEARCH, DUBNA (USSR). LAB. OF HIGH ENERGY.
Application of phenomenological quasi-two-body model to π^-p-interactions with strange particle production at p = 4 GeV/c, 25:30869 (JINR-P1-5706)
Coherent interactions of π^--mesons with photoemulsion nuclei at 17 GeV, 25:30736 (JINR-P1-5565)
Cross sections of inelastic channels of reactions in np-interactions at the neutron momentum from 2 to 10 GeV/c, 25:30726 (JINR-P1-5665)
Elastic pp- and pd-scattering at 50 and 70 GeV, 25:30725 (JINR-P1-5633)
Graphs for studying isotopic relations in reactions with production of three particles and possible Pomeranchuk pole exchange, 25:30824 (JINR-P2-5630)
Interference phenomena in the system of two resonances, 25:30848 (JINR-P1-5668)
Invariance of the nonrelativistic wave equations in the presence of electromagnetic field, 25:30775 (JINR-P2-5522)
Particle interference in the processes involving excited nuclei, 25:31395 (JINR-P1-5648)
Possibilities of the resonance interferometry, 25:30847 (JINR-P1-5666)
Resistance behavior of superconducting alloy of Nb + 80 percent Zr in region of H/sub c2/, 25:30412 (JINR-P8-5733)
JOINT INST. FOR NUCLEAR RESEARCH, DUBNA (USSR). LAB. OF NEUTRON PHYSICS.
Choosing and calculating focusing system of 30 MeV linear induction accelerator, 25:31039 (JINR-P9-5714)
Measurement of velocity of propagation of gravitational interaction, 25:30995 (JINR-P13-5685)
Neutron resonances of the samarium isotopes, 25:31305 (JINR-P3-5655)
Problems of determining phases of structural amplitudes in neutron diffraction and of neutron accumulation, 25:30663 (JINR-P3-5554)
JOINT INST. FOR NUCLEAR RESEARCH, DUBNA (USSR). LAB. OF NUCLEAR PROBLEMS.
Calculation and generation of the magnetic system of the monoenergetic cyclotron, 25:31037 (JINR-P9-5669)
Coherent frequencies of transverse oscillations in the electron model of a ring cyclotron, 25:31038 (JINR-P9-5677)
Nucleon Compton-effect and sum rules for dipole nucleon momentum, 25:30776 (JINR-P2-5679)
Timing with Ge(Li)-detector, 25:29353 (JINR-P13-5708)
X-ray spectrometer with cooled Si(Li)-detector, 25:29325 (JINR-P13-5707)
JOINT INST. FOR NUCLEAR RESEARCH, DUBNA (USSR). LAB. OF NUCLEAR REACTIONS.
Method of calculating the unitary weights in the theory of multiple particle production, 25:30913 (JINR-P2-5729)
Production of spontaneously fissionable isomer ^{236}U at radiative thermal neutron capture, 25:31307 (JINR-P7-5497)
JOINT INST. FOR NUCLEAR RESEARCH, DUBNA (USSR). LAB. OF THEORETICAL PHYSICS.
Algebraic realization of chiral symmetry for meson systems and theory of Yang--Mills type, 25:30850 (JINR-P2-5759)
Angular and energy distributions of particles produced in inelastic π^---N and N--N collisions at very-high energies, 25:30870 (ORNL-tr-2433)
Construction of non-local quantum electrodynamics, 25:30937 (JINR-P2-5694)
Determination of Breit--Wigner resonance widths using Fourier algorithm, 25:30849 (JINR-P2-5659)
Method of measuring electromagnetic form factor of neutrino, 25:30777 (JINR-P2-5705)
Non-rotational states of odd-mass nuclei in the actinide region, 25:31306 (JINR-P4-5693)
Properties of light nuclei with realistic N--N-interaction, 25:31201 (JINR-P4-5614)
Quantum field theory with non-euclidean space of relative momenta, 25:30938 (JINR-P2-5717)
Relativistic wave function and form factors of the bound system, 25:30752 (JINR-P2-5691)
Retarded part of two-time Green function and two-body relativistic problem, 25:31014 (JINR-E2-5746)
Selected topics in the theory of electromagnetic interactions, 25:30772 (CERN-71-7, pp 181-283)

K

KARLSRUHE UNIV. (WEST GERMANY).
Aerodynamic characteristics of atmospheric boundary layers, 25:31737 (TID-25465)
Treatment of space dependence of the energetic resonance self shielding at boundaries of homogeneous zones in reactors, 25:31652 (KFK-1353)
KERNFORSCHUNGSANLAGE, JUELICH (WEST GERMANY).
Dense plasma focus as a neutron source for pulsed measurements in a blanket, 25:30592 (EUR-4593, pp 525-31)
KERNFORSCHUNGSANLAGE, JUELICH (WEST GERMANY). INSTITUT FUER FESTKOERPERFORSCHUNG.
Diffusion of hydrogen and deuterium through niobium, 25:29820 (EUR-4593, pp 519-24)
Scattering of slow neutrons by orthohydrogen in cubic phase, 25:31169 (JUL-724-FF)
KERNFORSCHUNGSANLAGE, JUELICH (WEST GERMANY). INSTITUT FUER PLASMAPHYSIK.
Coaxial high-power trigatron for 60 kV, 25:30579 (EUR-4593, pp 373-8)
Fast 500-kV energy storage unit, 25:30582 (EUR-4593, pp 393-400)
Fast, solid dielectric, multichannel crowbar switch, 25:30580 (EUR-4593, pp 379-84)
High-Q capacitors with liquid and gas impregnation, 25:30595 (EUR-4593, pp 545-50)
Studies of surface discharges on insulating foils, 25:30581 (EUR-4593, pp 385-92)
KERNFORSCHUNGSANLAGE, JUELICH (WEST GERMANY). INSTITUT FUER REAKTORENTWICKLUNG.
Design possibilities and consequences for the conventional parts of fusion power plants, 25:30588 (EUR-4593, pp 445-60)
Feasibility of gas cooling for the fusion reactor blanket, 25:30589 (EUR-4593, pp 491-6)
MEDEA: model of a steam plant, 25:31624 (JUL-698-RG)
KERNFORSCHUNGSANLAGE, JUELICH (WEST GERMANY). INSTITUT FUER TECHNISCHE PHYSIK.
Present state of costs for large superconducting magnets and their future prospects, 25:30441 (EUR-4593, pp 117-24)
KERNFORSCHUNGSZENTRUM, KARLSRUHE (WEST GERMANY).
Experiments on wear and friction between subassemblies and grid spacers in sodium, 25:29818 (AEC-tr-7224)
Heat of formation and entropy of formation of plutonium carbides, 25:29942 (LA-tr-71-22)
Inherent stability of the steam-cooled breeder, 25:31542 (EURFNR-813)
Prog. rpt. on fast breeder project, 1968--69, 25:31568 (EURFNR-823)
KERNFORSCHUNGSZENTRUM, KARLSRUHE (WEST GERMANY). INSTITUT FUER ANGEWANDTE KERNPHYSIK.
Theoretical structure level and absolute transition probabilities in deformed nuclei of uneven mass numbers, 25:31308 (KFK-1248)
KERNFORSCHUNGSZENTRUM, KARLSRUHE (WEST GERMANY). INSTITUT FUER EXPERIMENTELLE KERNPHYSIK.
Developments in cryogenic and superconducting magnets, 25:31040 (KFK-1316)
Helium-4 final state interactions and quasifree scattering in deuteron-induced three-particle reactions on ^6Li, 25:31187 (NP-18741)
KERNFORSCHUNGSZENTRUM, KARLSRUHE (WEST GERMANY). INSTITUT FUER MATERIAL UND FESTKOERPERFORSCHUNG.
Compatibility studies with UC of different stoichiometries and iron--nickel--chromium alloys and the influence of stabilizers, 25:29940 (EURFNR-820)
KERNFORSCHUNGSZENTRUM, KARLSRUHE (WEST GERMANY). INSTITUT FUER NEUTRONENPHYSIK UND REAKTORTECHNIK.
Strategy for speeding up two-dimensional SN-methods with help of the coarse lattice technique, 25:31653 (KFK-1361)

Treatment of space dependence of the energetic resonance self shielding at boundaries of homogeneous zones in reactors, 25:31652 (KFK-1353)

KERNFORSCHUNGSZENTRUM, KARLSRUHE (WEST GERMANY). INSTITUT FUER RADIOCHEMIE.
Phase equilibria in the systems UO_2--UO_3--$NdO_{1.5}$ and NpO_{2+x}/--$NdO_{1.5}$, 25:29977 (KFK-1330)
Production of neutrons through irradiation of thick beryllium targets with deuterons in energy range from 15 to 55 MeV, 25:31202 (KFK-1288)

KERNKRAFTWERK RWE-BAYERNWERK G.M.B.H., GUNDREMMINGEN (WEST GERMANY).
Gundremmingen nuclear power plant monthly report, January 1971, 25:31479 (TID-25698)

L

LEIDEN RIJKSUNIVERSITEIT (NETHERLANDS). KAMERLINGH ONNES LABORATORIUM.
Influence of neutron irradiation on behavior of a superconductor and a superconducting coil magnet, 25:30440 (EUR-4593, pp 107-13)

LOS ALAMOS SCIENTIFIC LAB., N. MEX.
Calibration of Moxon--Rae detectors in the current mode, 25:29326 (LA-4445)
Design and installation of Scyllac, 25:30564 (EUR-4593, pp 227-39)
Effect of the multipole pairing and particle-hole fields in the particle-vibration coupling of ^{209}Pb: I, 25:31309 (LA-DC-11648)
EPICS: high-resolution pion beam and spectrometer facility for nuclear structure research, 25:31041 (LA-4534)
Evolution of computer software, 25:31701 (LA-4620)
Improved light scattering photometer for air filtration system studies, 25:31702 (LA-4627)
Light scattering from aerosols, 25:31703 (LA-4641)
MCNA: computer program to solve adjoint neutron transport equation, 25:31171 (LA-4486)
Particle collisions in opposing mass flow hypothesis, 25:30157 (LA-4343(Suppl.))
Prog. rpt. on carbon and graphite, 8--10/70, 25:29920 (LA-4631)
Prog. rpt. on controlled thermonuclear research program, annual, 10/70, 25:30450 (LA-4585)
Prog. rpt. on medium-energy physics program, 1/31/71, 25:31042 (LA-4639)
Scattering of light from a stratified sphere, 25:31704 (LA-4642)
Single and multiple field enabling system for television disc recording, 25:31699 (LA-4582)
Single-shot pulsed magnetic fields from inductive energy stores, 25:30598 (LA-4617)
Stress calculations in MAGEE difference form, 25:31700 (LA-4601)

LOVELACE FOUNDATION FOR MEDICAL EDUCATION AND RESEARCH, ALBUQUERQUE, N. MEX.
Application of a biological model of tissue distribution and retention of inhaled ^{140}La in beagle dogs to an analysis of radiological hazards to humans inhaling various isotopes of lanthanum, 25:29427 (LF-43, pp 82-91)
Bilateral bronchopulmonary lavage with DTPA solution for removing inhaled $^{144}CeCl_3$, 25:29544 (LF-43, pp 286-94)
Connective tissue constituents measured on dogs exposed to ^{144}Ce fused montmorillonite clay particles, 25:29622 (LF-43, pp 218-23)
Development of techniques for generating monodisperse aerosols with the Fulwyler Droplet Generator, 25:29076 (LF-43, pp 13-17)
Dissolution of small radioactive particles, 25:29080 (LF-43, pp 40-51)
Dose distribution in the beagle dog from radiographic exposure, 25:29514 (LF-43, pp 116-22)
Effect of the inhalation of ^{144}Ce in relatively insoluble forms on influenza virus infection in mice, 25:29724 (LF-43, pp 254-62)
Estimation of the relative inhalation hazard of reactor inventory radionuclides, 25:29420 (LF-43, pp 1-7)
Fission Product Inhalation Program. Annual report, October 1, 1969--September 30, 1970, 25:29419 (LF-43)
Physical and chemical characteristics of aerosols produced from solutions of polyvalent metallic nuclides, 25:29079 (LF-43, pp 31-9)
Preparation of aerosols of thulium and americium by thermal degradation, 25:29078 (LF-43, pp 25-30)
Production of chromosome aberrations by ^{241}Am in the Chinese hamster liver, 25:29482 (LF-43, pp 240-5)
Production of relatively monodisperse aerosols for inhalation experiments by aerosol centrifugation, 25:29421 (LF-43, pp 8-12)
Relative biological effectiveness of ^{241}Am, ^{144}Ce, and ^{60}Co on the production of metaphase chromosome aberrations in the Chinese hamster liver, 25:29483 (LF-43, pp 246-53)
Relative hazards for inhaled ^{95}Zr and ^{95}Nb particles formed under various thermal conditions, 25:29423 (LF-43, pp 59-65)
Removal of relatively soluble ^{144}Ce from the lungs of beagle dogs: intravenous administration of a DTPA solution, 25:29543 (LF-43, pp 280-5)
Retention and distribution of ^{137}Cs in the beagle dog following inhalation of ^{137}Cs in fused montmorillonite clay particles, 25:29426 (LF-43, pp 79-81)
Retention and distribution of ^{244}Cm following inhalation of $^{244}CmCl_3$ and $^{244}CmO_{1.7}$ by beagle dogs, 25:29429 (LF-43, pp 100-5)
Retention of ^{171}Tm following inhalation of oxide by beagle dogs, 25:29425 (LF-43, pp 71-8)
Retention of relatively insoluble substances following inhalation, 25:29422 (LF-43, pp 53-8)
Retention patterns of ^{125}Sb in mice following inhalation of particles formed at different temperatures, 25:29424 (LF-43, pp 66-70)
Some characteristics of ruthenium aerosols generated from Ru-organic complexes and subjected to thermal degradation, 25:29077 (LF-43, pp 18-24)
Some observations on the toxicity of beta-emitting radionuclides inhaled in fused clay particles, 25:29438 (LF-43, pp 197-204)
Tissue distribution and retention of ^{140}Ba and ^{140}La in beagle dogs after inhalation of $BaCl_2$--$LaCl_3$ aerosols, 25:29428 (LF-43, pp 92-9)
Toxicity of inhaled ^{144}Ce fused clay in beagle dogs. III, 25:29436 (LF-43, pp 183-7)
Toxicity of inhaled $^{144}CeCl_3$ in beagle dogs. IV, 25:29431 (LF-43, pp 128-36)
Toxicity of inhaled ^{90}Sr fused clay in beagle dogs. I, 25:29437 (LF-43, pp 188-96)
Toxicity of inhaled $^{90}SrCl_2$ in beagle dogs. IV, 25:29430 (LF-43, pp 123-7)
Toxicity of inhaled ^{90}Y fused clay in beagle dogs. II, 25:29434 (LF-43, pp 146-62)
Toxicity of inhaled ^{91}Y fused clay in beagle dogs. I, 25:29435 (LF-43, pp 163-70)
Toxicity of inhaled $^{91}YCl_3$ in beagle dogs. IV, 25:29432 (LF-43, pp 137-9)
Toxicity of injected $^{137}CsCl$ in the beagle dog. III, 25:29433 (LF-43, pp 140-5)

LUND UNIV. (SWEDEN). DEPT. OF ELECTRICAL ENGINEERING.
Forced and free oscillations. some aspects of longitudinal plasma waves. technical report no. 70:2, 25:30605 (NP-18673)

LUND UNIV. (SWEDEN). DEPT. OF PHYSICS.
ANNLIS: computer program for automatic analysis of gamma-ray spectra, 25:29354 (LUNP-7101)

LYON UNIV. (FRANCE). INSTITUT DE PHYSIQUE NUCLEAIRE.
Decay scheme of 1.3 h. ^{174}Ta, 25:31310 (LYCEN-7084)
Description of elastic-scattered processes with the use of non-local separable potentials, 25:31186 (LYCEN-7089)
Mean recoil, isomer ratio, and excitation functions for reactions induced by alpha particles in rubidium, 25:31239 (LYCEN-7091)
Reactions induced in gold by deuterons with energies between 10 and 70 MeV, 25:31311 (LYCEN-7092)
Supermultiplet scheme for light nuclei, 25:31203 (LYCEN-7088)
Use of semiconductor telescopes for detecting the recoil nuclei in proton-light nucleus coherent scattering at high energy, 25:31185 (LYCEN-7085)

M

MAGYAR TUDOMANYOS AKADEMIA KOZPONTI FIZIKAI KUTATO INTEZETE, BUDAPEST.
Determination of neutron spectra from activation data by means of rfol and rfo7 codes, 25:31648 (KFKI-70-33-RPT)

MAINE YANKEE ATOMIC POWER CO., WESTBORO, MASS.
Maine Yankee Atomic Power Station. Preliminary safety analysis report, Amendment 23, 25:31504 (DOCKET-50309-34)

MANCHESTER UNIV. (ENGLAND). DEPT. OF THEORETICAL PHYSICS.
Modern developments in hadron physics, 25:30822 (CERN-71-7, pp 41-180)

MASSACHUSETTS INST. OF TECH., CAMBRIDGE.
Duality and dual models, 25:31015 (MIT-2098-726)

MAX-PLANCK-INSTITUT FUER PHYSIK UND ASTROPHYSIK, MUNICH (WEST GERMANY).
Scale invariance and the light cone, 25:30749 (CALT-69-297)

MAXWELL LABS., INC., SAN DIEGO, CALIF.
Low-inductance, megavolt Marx Generators, 25:30573 (EUR-4593, pp 311-17)

METCUT RESEARCH ASSOCIATES INC., CINCINNATI, OHIO.
Adaptive control survey, 25:31758 (Y-1759)

MICHIGAN STATE UNIV., EAST LANSING. DEPT. OF PHYSICS AND ASTRONOMY.
Use of realistic forces in microscopic description of inelastic scattering of nucleons from nuclei at medium energies, 25:31393 (COO-1051-34)

MILLSTONE POINT CO., WETHERSFIELD, CONN.
Millstone Nuclear Power Station, Unit 1. Establishment of preoperational environmental survey program, 25:31491 (DOCKET-50245-64)

MINISTRY OF INTERNATIONAL TRADE AND INDUSTRY, TOKYO (JAPAN).
Crowbar gap switch with two triggering pulses, 25:30576 (EUR-4593, pp 347-53)
Development of a heavy-current switching gap triggered

XUM

with laser, 25:30575 (EUR-4593, pp 339-45)
Transformer coupled fast theta-pinch device with variable rise time, 25:30577 (EUR-4593, pp 355-63)
MINNESOTA UNIV., MINNEAPOLIS.
Prog. rpt. on diatoms in lakes and lake sediments as index to environment, 5/70--1/71, 25:31739 (TID-25695)
MINNESOTA UNIV., MINNEAPOLIS. SCHOOL OF PHYSICS AND ASTRONOMY.
Effect of the multipole pairing and particle-hole fields in the particle-vibration coupling of ^{209}Pb: I, 25:31309 (LA-DC-11648)
MINNESOTA UNIV., MINNEAPOLIS. TATE LAB. OF PHYSICS.
NMR and nuclear relaxation study of satellite lines in dilute Co--Cr, Co--V, and Co--Mn alloys, 25:31690 (COO-1569-71)
Nuclear orientation of ^{142}Pr in praseodymium metal, 25:30662 (COO-1569-76)

N

NAGOYA UNIV. (JAPAN). INST. OF PLASMA PHYSICS.
Experiments of plasma confinement in JIPP stellarator. I, 25:30457 (IPPJ-102)
Hydromagnetic motion in the geomagnetic tail, 25:30349 (IPPJ-103)
Ion heating caused by ion acoustic waves in an ion-streaming plasma, 25:30458 (IPPJ-104)
NATIONAL AERONAUTICAL LAB., BANGALORE (INDIA).
Magnetofluiddynamic heat transfer, 25:30341 (NAL-TN-6)
NATIONAL AERONAUTICS AND SPACE ADMINISTRATION, CLEVELAND, OHIO. LEWIS RESEARCH CENTER.
Experimental investigation of single-particle behavior in an axisymmetric magnetic field, 25:30516 (N-70-42698)
NATIONAL AERONAUTICS AND SPACE ADMINISTRATION, GREENBELT, MD. GODDARD SPACE FLIGHT CENTER.
Gyrosynchrotron radiation and its transfer in a magnetoactive plasma, 25:30515 (N-70-41892)
Subauroral red arc and the associated ionospheric phenomena, 25:30350 (N-70-36812)
NATIONAL AERONAUTICS AND SPACE ADMINISTRATION, MOFFETT FIELD, CALIF. AMES RESEARCH CENTER.
Diagnostics of a supersonic plasma stream using an immersed microwave probe, 25:30476 (N-71-10964)
Laser-generated plasma as a spectroscopic light source, 25:30498 (N-70-41880)
NATIONAL BUREAU OF STANDARDS, WASHINGTON, D. C.
Conference on spectrum formation in stars with steady-state extended atmospheres, Munich, Ger., 4/69, 25:30035 (NBS-SPEC. PUBL-332)
Multiple scattering corrections for the associated-particle neutron time-of-flight technique, 25:31172 (NBS-TN-499)
Right angle ^{3}He cryostat incorporating a high field superconducting solenoid, 25:30442 (NBS-TN-562)
NATIONAL INST. FOR METALLURGY, JOHANNESBURG (SOUTH AFRICA).
Colorimetric determination of minor quantities of nitrate in uranium compounds, 25:28918 (NIM-951)
NATIONAL INST. OF RADIOLOGICAL SCIENCES, CHIBA (JAPAN).
Prog. rpt., annual, 1969, 25:29572 (NIRS-AR-13)
NAVAL RESEARCH LAB., WASHINGTON, D. C.
Production of intense relativistic electron beams, 25:30254 (EUR-4593, pp 59-65)
NEW YORK UNIV., N. Y.
Symmetry groups and current algebra, 25:30914 (NP-18804)
NORTH CAROLINA UNIV., CHAPEL HILL.
Detection of weak histocompatibility antigens on mouse peritoneal macrophages, 25:31717 (ORO-3634-11)
NORTH CAROLINA UNIV., CHAPEL HILL. DEPT. OF BACTERIOLOGY AND IMMUNOLOGY.
Detection and measurement of weak histoincompatibilities by transfer of mouse peritoneal exudate cells, 25:31718 (ORO-3634-12)
Serological detection of the male limited H--Y antigen on peritoneal exudate cells, 25:31719 (ORO-3634-13)
NORTHERN STATES POWER CO., MINNEAPOLIS, MINN.
Monticello Nuclear Generating Plant, Unit 1. Abnormal occurrence report: safety/relief valve settings exceeding 1080 psig, 25:31477 (DOCKET-50263-69)
Monticello Nuclear Generating Plant, Unit 1. Abnormal occurrence report: inoperability of the air ejector off-gas system radiation monitors, 25:31476 (DOCKET-50263-68)
Monticello Nuclear Generating Plant, Unit 1. Design report: recirculation system, 25:31495 (DOCKET-50263-63)
Monticello Nuclear Generating Plant, Unit 1. High pressure coolant injection system outage, 25:31475 (DOCKET-50263-67)
Monticello Nuclear Generating Plant, Unit 1. Stagnant water or low steam flow in reactor coolant system, 25:31497 (DOCKET-50263-65)
Monticello Nuclear Generating Plant, Unit 1. Stress analysis review report, 25:31496 (DOCKET-50263-64)
NORTHWESTERN UNIV., EVANSTON, ILL.
Prog. rpt. on electronic band structure and physical properties of actinide metals and their compounds, 1970, 25:30696 (COO-2103-3)
NUCLEAR FUEL SERVICES, INC., WEST VALLEY, N.Y.
West Valley Reprocessing Plant. Environmental report No. 9, July--December 1970, 25:29179 (DOCKET-50201-69)
West Valley Reprocessing Plant. Quarterly report, January 1--March 31, 1971, 25:29180 (DOCKET-50201-70)
NUCLEAR POWER GROUP LTD., KNUTSFORD (ENGLAND).
Thermal performance of porous insulants in a high-pressure gas environment, 25:30029 (EUR-4531, pp 841-81)

O

OAK RIDGE NATIONAL LAB., TENN.
Advanced materials for steam generators, 25:29763 (ORNL-4630, pp 280-7)
Cladding materials for space isotopic heat sources, 25:29823 (ORNL-4630, pp 186-90)
Collisional ionization between cesium and selected molecules, 25:30276 (ORNL-TM-2620)
Completion report: evaluation of the use of permselective membranes in the nuclear industry for removing radioactive xenon and krypton from various off-gas streams, 25:29317 (ORNL-4522)
Cyclotron simulation of neutron-transmutation produced gases in reactor cladding and structural materials, 25:29907 (ORNL-TM-3299)
Design of asymmetric 4 π shields for space reactors, 25:31640 (ORNL-TM-3368)
Development of advanced FBR fuels, 25:29923 (ORNL-4630, pp 59-72)
Development of FBR neutron-absorber materials, 25:29978 (ORNL-4630, pp 163-76)
Development of FBR oxide fuels, 25:29922 (ORNL-4630, pp 3-58)
Development of fuel element fabrication, 25:29924 (ORNL-4630, pp 233-8)
Development of uranium mononitride fuels, 25:30010 (ORNL-4630, pp 179-85)
Effect of iodine decay heat on charcoal adsorbers, 25:31669 (ORNL-4602)
Evaluation of the Molten-Salt Reactor Experiment Hastelloy N surveillance specimens: fourth group, 25:29906 (ORNL-TM-3063)
Experimental nuclear cross sections for spacecraft shield analysis, 25:30631 (ORNL-TM-3376)
Fabrication development of FBR cladding, 25:29784 (ORNL-4630, pp 96-110)
Fast-neutron irradiation effects on electrical insulators, 25:30011 (ORNL-4630, pp 226-9)
Function of condensing steam in aerosol scrubbers, 25:29251 (ORNL-4654)
Graphs for analysis of (1-3) gamma--gamma directional correlations, 25:31312 (ORNL-4619)
Inclusion of fission and charged-particle mission in calculations of nuclear reactions, 25:31313 (ORNL-TM-3179)
Irradiation damage to aluminum and aluminum alloys, 25:29905 (ORNL-4630, pp 239-60)
Joining research on nuclear materials, 25:29825 (ORNL-4630, pp 261-70)
Low-energy electron transport with the method of discrete ordinates, 25:30630 (ORNL-TM-3318)
Mechanical properties of alloys in reactor environments and development of FBR cladding and structural alloys, 25:29904 (ORNL-4630, pp 73-95)
Mound assistance program: development of a sol-gel process and equipment for production of dense $^{238}PuO_2$ microspheres, 25:29921 (ORNL-4565)
MSBR control studies: analog simulation program, 25:31544 (ORNL-TM-3102)
Nondestructive testing techniques for FBR, 25:29287 (ORNL-4630, pp 145-9)
Nondestructive testing, 25:29288 (ORNL-4630, pp 271-9)
Performance capability of advanced fuels and fast breeder reactors, 25:31569 (ORNL-TM-3388)
Phantom for the adjustment of gamma-ray imaging devices, 25:29328 (ORNL-TM-3261)
Physical and mechanical metallurgy of refractory alloys, 25:29824 (ORNL-4630, pp 191-206)
POPOP4 library and codes for preparing secondary gamma-ray production cross sections, 25:31671 (ORNL-TM-3367)
Prog. rpt. on concentration and desalting of protein solutions program, 6--8/70, 25:31714 (ORNL-TM-3328)
Prog. rpt. on fuels and materials development, 9/30/70, 25:29757 (ORNL-4630)
Properties of ferritic steel welds, 25:29822 (ORNL-4630, pp 139-44)
Radiation output description from the T(d,n)^{4}He reaction in a large target (1000 cm^{2}): Operation Henre, 25:31165 (CEX-65.04)
Report to the AEC nuclear cross section advisory committee, 25:31204 (ORNL-TM-3378)
Sodium corrosion studies, 25:29761 (ORNL-4630, pp 150-7)
Sodium removal and caustic effects, 25:29762 (ORNL-4630, pp 158-62)
Summary of a program of research and development for prestressed concrete nuclear pressure vessels, 25:30019 (EUR-4531, pp 27-58)
Systematic procedure for determining system parameters by performance index minimization, 25:31545 (ORNL-TM-3311)
TRANS: a one-dimensional FORTRAN IV program for computing the time response of fuel rods to a loading-unloading environment, 25:31670 (ORNL-TM-3293)

Tungsten metallurgy, 25:29786 (ORNL-4630, pp 207-25)
Viscoelastic analysis of irradiated graphite with variable creep coefficient, 25:29945 (ORNL-TM-3242)
Welding development for FBR stainless steel components, 25:29785 (ORNL-4630, pp 111-38)

OESTERREICHISCHE STUDIENGESELLSCHAFT FUER ATOMENERGIE G.M.B.H., VIENNA.
Determination of the distribution of fission products in fuel particle coatings by the sputtering technique, 25:29979 (SGAE-PH-96/1970)
Some results on the removal of radiocesium from low-activity waste water by coprecipitation with ferrocyanides, 25:29183 (SGAE-SS-6/1969)

OHIO STATE UNIV., COLUMBUS. DEPT. OF METALLURGICAL ENGINEERING.
Evaluation of Gerard-Papirno characterization of notch ductility in steel, 25:31692 (COO-2048-2)

OHIO STATE UNIV. RESEARCH FOUNDATION, COLUMBUS.
Prog. rpt., final, 11/69--1/71, 25:31691 (COO-1750-3)

OREGON STATE UNIV., CORVALLIS. DEPT. OF OCEANOGRAPHY.
Sound scattering layers off the Oregon coast, 25:31723 (RLO-1750-62)
Water tracing with soluble metal chelates and neutron activation analysis, 25:29013 (RLO-1750-61)

OSAKA UNIV. (JAPAN). DEPT. OF NUCLEAR ENGINEERING.
Ion source using a beam--plasma interaction, 25:30255 (EUR-4593, pp 67-74)

OSAKA UNIV. (JAPAN). PLASMA PHYSICS LAB.
Design and construction of PIACE, 25:30587 (EUR-4593, pp 431-41)

P

PADUCAH GASEOUS DIFFUSION PLANT, KY.
Environmental monitoring summary for Paducah Plant, 1970, 25:29502 (KY-629)

PANSTWOWA RADA DO SPRAW POKOJOWEGO WYKORZYSTANIA ENERGII JADROWEJ, WARSAW (POLAND).
Conference on the new method for producing radioactive preparations, Warsaw, December 9--13, 1969, 25:29413 (CONF-691225)

PARIS UNIV. (FRANCE).
Physical and chemical interactions of water on graphite, 25:29918 (CEA-R-4123)

PARIS UNIV., ORSAY (FRANCE). FACULTE DES SCIENCES.
Proton holes in (2s--1d) shell from (d,^{3}He) reactions, 25:31240 (NP-18511)

PARIS UNIV., ORSAY (FRANCE). LABORATOIRE DE L'ACCELERATEUR LINEAIRE.
High resolution beam hodoscope using multiwire proportional chambers, 25:29370 (LAL-1246)

PAVIA UNIV. (ITALY). ISTITUTO DI GENETICA.
Prog. rpt. on mutation rates and mutational loads in man, 9/69--8/70, 25:31708 (NYO-2280-32)

PENNSYLVANIA STATE UNIV., UNIVERSITY PARK. IONOSPHERE RESEARCH LAB.
Tables from Penn State Mark 1 ionospheric model, 25:30351 (N-70-40978)

PENNSYLVANIA UNIV., PHILADELPHIA. DEPT. OF RADIOLOGY.
Prog. rpt. on radioisotopic and volumetric studies of tumor growth in situ, 1967--71, 25:31713 (NYO-3924-10)
Prog. rpt. on radioisotopic and volumetric studies of tumor growth in situ, annual, 4/71, 25:31712 (NYO-3924-9)

PHILADELPHIA ELECTRIC CO., PA.
Limerick Generating Station, Units 1 and 2. Preliminary safety analysis report, Amendment 6, 25:31519 (DOCKET-50352-12)
Peach Bottom Atomic Power Station, Units 2 and 3. Preliminary safety analysis report, Amendment 8 (includes additions and revisions to final safety analysis report), 25:31502 (DOCKET-50277-19)

PITTSBURGH UNIV., PA.
Prog. rpt. on radiation induced defects in metals, annual, 12/69--11/70, 25:29903 (NYO-3653-5)

PITTSBURGH UNIV., PA. DEPT. OF PHYSICS.
Theory of particles with spin up to one in external fields, 25:30939 (NYO-3829-66)

PORTLAND GENERAL ELECTRIC CO., OREG.
Trojan Nuclear Plant. Additional information requested by AEC, 25:31518 (DOCKET-50344-20)

PRINCETON UNIV., N. J. PLASMA PHYSICS LAB.
Design and operation of a spherator with a levitated, superconducting ring, 25:30559 (EUR-4593, pp 141-8)
Preliminary investigation of ohmically-heated plasmas in the model ST Tokamak, 25:30459 (MATT-813)

PUBLIC HEALTH SERVICE, LAS VEGAS, NEV. SOUTHWESTERN RADIOLOGICAL HEALTH LAB.
Iodine-131 dairy cow uptake studies using a submicrometer synthetic dry aerosol (Project SIP), 25:29505 (SWRHL-39-r)

PUBLIC HEALTH SERVICE, ROCKVILLE, MD. RADIOLOGICAL HEALTH LAB.
Radiation survey of television repair shops in Baltimore area, 25:29512 (BRH/DEP-71-4)

PUERTO RICO NUCLEAR CENTER, MAYAGUEZ.
Crystal structure of $CoBr_2.6H_2O$ at room temperature by neutron diffraction, 25:31722 (PRNC-146)
Least-square refinement of the x-ray data on Azurite, $Cu_3(OH)_2(CO_3)_2$, 25:31721 (PRNC-145)

PUERTO RICO WATER RESOURCES AUTHORITY, SAN JUAN.
Aguirre Nuclear Plant, Unit No. 1. Preliminary facility description and safety analysis report, Amendment 4, Vol. 1, 25:31523 (DOCKET-50376-10)
Aguirre Nuclear Plant, Unit No. 1. Preliminary facility description and safety analysis report, Amendment 4, Vol. 2, 25:31524 (DOCKET-50376-11)

R

RAND CORP., SANTA MONICA, CALIF.
High energy astrophysics, 25:30220 (P-4494(RAND))

REACTIVE METALS, INC., ASHTABULA, OHIO.
Semiannual progress summary, July--December 1970, 25:29787 (RMI-16)

REACTOR CENTRUM NEDERLAND, PETTEN.
Influence of neutron irradiation on behavior of a superconductor and a superconducting coil magnet, 25:30440 (EUR-4593, pp 107-13)
Irradiation of mortar specimens, 25:30020 (EUR-4531, pp 171-8)

REID, BATCHELOR AND ASSOCIATES, INC., SAN FRANCISCO, CALIF.
State role in thermal power plant siting, 25:31525 (NP-18770)

RENSSELAER POLYTECHNIC INST., TROY, N. Y.
Prog. rpt. on gas-particle heat transfer coefficients in packed and fluidized beds by frequency response techniques, annual, 1/70--2/71, 25:31725 (RPI-3639-16)
Prog. rpt. on linear accelerator project, annual, 10/69--9/70, 25:31173 (RPI-328-200)
Prog. rpt. on neutron and gamma emission from highly excited states and states with high spin, annual, 6/70--5/71, 25:31396 (RPI-3947-13)
Prog. rpt. on precipitation and dispersion hardening in HCP alloys, annual, 3/1/71, 25:29827 (RPI-3719-9)

ROCHESTER GAS AND ELECTRIC CORP., N. Y.
Robert Emmett Ginna Nuclear Power Plant, Unit No. 1. Failure of valves 826 A, 826 B, 826 C, and 826 D to open, 25:31474 (DOCKET-50244-70)

ROCKEFELLER UNIV., NEW YORK.
Selected topics in discrete symmetries and CP-violation, 25:30915 (NP-18808)

ROSWELL PARK MEMORIAL INST., BUFFALO, N. Y.
Prog. rpt., annual, 2/71, 25:29132 (NYO-3558-24)

RUTHERFORD HIGH ENERGY LAB., CHILTON (ENGLAND).
Dynamic polarization measurements in polyhydric alcohols doped with their Cr(V) at approx. 1°K and at 3 kG magnetic fields, 25:31046 (RHEL/R-213)

S

SACRAMENTO MUNICIPAL UTILITY DISTRICT, CALIF.
Rancho Seco Nuclear Generating Station, Unit 1. Preliminary safety analysis report, Amendment 5 (includes final safety analysis report, Vol. 2), 25:31507 (DOCKET-50312-21)
Rancho Seco Nuclear Generating Station, Unit 1. Preliminary safety analysis report, Amendment 5 (includes revised license application), 25:31505 (DOCKET-50312-19)
Rancho Seco Nuclear Generating Station, Unit 1. Preliminary safety analysis report, Amendment 5 (includes final safety analysis report, Vol. 5), 25:31510 (DOCKET-50312-24)
Rancho Seco Nuclear Generating Station, Unit 1. Preliminary safety analysis report, Amendment 5 (includes final safety analysis report, Vol. 1), 25:31506 (DOCKET-50312-20)
Rancho Seco Nuclear Generating Station, Unit 1. Preliminary safety analysis report, Amendment 5 (includes final safety analysis report, Vol. 3), 25:31508 (DOCKET-50312-22)
Rancho Seco Nuclear Generating Station, Unit 1. Preliminary safety analysis report, Amendment 5 (includes final safety analysis report, Vol. 4), 25:31509 (DOCKET-50312-23)

SANDIA LABS., ALBUQUERQUE, N. MEX.
Analysis of the lateral motion of a projectile in the gun tube, 25:31731 (SC-RR-710071)
Bibliography on heat and mass transfer through soil, 25:29266 (SC-ARPIC-1010)
Cavitation study of underwater trajectory, 25:31727 (SC-DC-713982)
Dynamic mechanical properties of Armco 21-6-9 stainless steel, 25:31730 (SC-RR-69-761)
Experimental and theoretical investigations of a liquid film interacting with a supersonic stream, 25:31726 (SC-DC-713922)
Interactive monitor for a telemetry playback system, 25:31729 (SC-DR-710211)
Methods for predicting turbulent jet mixing, 25:31728 (SC-DR-70-838)
Neutron damage effects in step recovery diode frequency multipliers, 25:29409 (SC-RR-710188)

SASKATCHEWAN UNIV., SASKATOON. SASKATCHEWAN ACCELERATOR LAB.
Elastic scattering of electrons from the oxygen isotopes, 25:31206 (SAL-17)
Electron scattering from ^{13}C, 25:31205 (SAL-16)

XUM

SAXTON NUCLEAR EXPERIMENTAL CORP., PA.
Saxton Reactor. License No. DPR-4; technical specifications Change Request No. 43, 25:31485 (DOCKET-50146-73)
Saxton Reactor. Operating experience report, September 1, 1970--February 28, 1971, 25:31466 (DOCKET-50146-72)
SCIENTIFIC RESEARCH INST. OF ELECTRO-PHYSICAL APPARATUS, LENINGRAD (USSR).
Effects of synchrotron radiation on the slow ejection of electrons from synchrotron, 25:31044 (NP-18780)
Sextupole lenses with improved non-linearity in slow ejection systems, 25:31045 (NP-18799)
Skin effect in high-energy Z-discharges, 25:30507 (NP-18775)
SCIENTIFIC SOCIETY OF MECHANICAL ENGINEERS, BUDAPEST (HUNGARY).
Conference on material testing, Budapest, 10/70, 25:28917 (CONF-701044-(Sect.3))
SCOTTISH RESEARCH REACTOR CENTRE, EAST KILBRIDE (SCOTLAND).
Prog. rpt., annual, 1969--70, 25:31634 (SRRC-41/71)
SCRIPPS INSTITUTION OF OCEANOGRAPHY, LA JOLLA, CALIF.
Precision deep-sea time release, 25:31756 (UCSD-34-P-127-8)
SIEMENS A.G., ERLANGEN (WEST GERMANY).
Reactor pressure vessel of finished sections, 25:31547 (EUR-4531, pp 477-88)
SKODA CONCERN, PILSEN (CZECHOSLOVAKIA). NUCLEAR POWER PLANTS DIV.
Welding of reactor pressure vessel of first Czechoslovak nuclear power station, 25:29788 (ZJE-69)
SOCIETE BERTIN ET CIE, PARIS (FRANCE).
Heat exchange by natural convection in porous media, 25:29264 (EUR-4531, pp 821-39)
Methods of testing HTR thermal shielding, 25:31575 (EUR-4531, pp 953-64)
Steadiness of thermal shielding during alternate stresses of aerodynamic origin, 25:31457 (EUR-4531, pp 895-930)
SOCIETE D'ETUDES ET D'EQUIPMENTS D'ENTREPRISES, PARIS (FRANCE).
BWR prestressed concrete pressure vessels, 25:31551 (EUR-4531, pp 615-45)
SOCIETE POUR L'INDUSTRIE ATOMIQUE, PARIS (FRANCE).
Pressure vessels for water and gas reactors, 25:31550 (EUR-4531, pp 601-13)
Prestressed concrete pressure vessel of the Vandellos nuclear power plant, 25:31454 (EUR-4531, pp 81-94)
Thermal shielding by screens of circulating gas, 25:31576 (EUR-4531, pp 1035-53)
Thermal shielding for water reactors, 25:31578 (EUR-4531, pp 1085-97)
SOCIETY OF NUCLEAR MEDICINE. SOUTHEASTERN CHAPTER.
Conference of Southeastern Chapter, Society of Nuclear Medicine, Nashville, Tenn., 10/69, 25:29570 (CONF-691016-(Absts.))
SOUTH DAKOTA UNIV., VERMILLION. DEPT. OF BIOCHEMISTRY.
Prog. rpt. on effects of ultraviolet radiation on algae: mechanisms of inactivation and repair, annual, 5/70--4/71, 25:29713 (COO-1793-5)
SOUTHERN CALIFORNIA EDISON CO., LOS ANGELES.
San Onofre Nuclear Generating Station, Unit 1. Provisional Operating License No. DPR-13, Amendment 23. Additional information in support of Proposed Change No. 4 to technical specifications, 25:31488 (DOCKET-50206-112)
SOUTHWESTERN RADIOLOGICAL HEALTH LAB., LAS VEGAS, NEV.
Off-site surveillance activities of SWRHL, 1--6/69, 25:29506 (SWRHL-97-r)
STANFORD LINEAR ACCELERATOR CENTER, CALIF.
Scale invariance and the light cone, 25:30749 (CALT-69-297)
STANFORD UNIV., CALIF. INST. FOR PLASMA RESEARCH.
Particle flux associated with stochastic processes, 25:30518 (N-71-11853)
STATE UNIV. OF NEW YORK, STONY BROOK. DEPT. OF PHYSICS.
Prog. rpt. of Bubble Chamber Group, 1/70--12/70, 25:30806 (NYO-3668-TA-5)
Triton calculations with realistic potentials in a harmonic oscillator basis, 25:30896 (NYO-4032-36)
STICHTING VOOR FUNDAMENTEEL ONDERZOEK DER MATERIE, JUTPHAAS (NETHERLANDS). INSTITUUT VOOR PLASMA-FYSICA.
FREMIX: a high-power 8-GHz plasma heating experiment, 25:30456 (EUR-4593, pp 551-6)
Vacuum start and clamp switches for a 20-kJ, 40-kv capacitor unit, 25:30570 (EUR-4593, pp 287-91)
STUTTGART UNIV. (WEST GERMANY). INSTITUT FUER STATIK UND DYNAMIK DER LUFT- UND RAUMFAHRTKONSTRUKTIONEN.
Three-dimensional elastic and elastoplastic calculations on reactor pressure vessels, 25:31667 (EUR-4531, pp 777-95)
SUD-AVIATION S.A., SURESNES (FRANCE).
Thermal shielding of pressure vessels, tanks, and elements of nuclear reactors, 25:31577 (EUR-4531, pp 1063-78)
SYRACUSE UNIV., N. Y.
Inequalities for the w w partial waves from the properties of a class of orthogonal polynomials, 25:30851 (SU-1206-240)
SYRACUSE UNIV., N. Y. DEPT. OF PHYSICS.
Inequalities for the w w partial waves from the properties of a class of orthogonal polynomials,

T

TATA INST. OF FUNDAMENTAL RESEARCH, BOMBAY (INDIA).
Inequalities for the w w partial waves from the properties of a class of orthogonal polynomials, 25:30851 (SU-1206-240)
TAYLOR WOODROW CONSTRUCTION LTD., SOUTHALL (ENGLAND).
Interaction between the design and construction of prestressed concrete pressure vessels for nuclear reactors, 25:31456 (EUR-4531, pp 129-44)
TECHNISCHE HOCHSCHULE, MUNICH (WEST GERMANY). INSTITUT FUER MESS- UND REGELUNGSTECHNIK.
Emergency core cooling, 25:31579 (MRR-79)
TECHNISCHE UNIVERSITAET, BRUNSWICK (WEST GERMANY).
Application of inductive energy storage systems for production of intense magnetic fields, 25:30561 (EUR-4593, pp 197-203)
Investigations on high-voltage gaskets, 25:30572 (EUR-4593, pp 301-9)
New compact capacitive energy storage unit for voltages above 100 kV, 25:30571 (EUR-4593, pp 293-9)
TECHNISCHER UEBERWACHUNGS-VEREIN E. V., COLOGNE (WEST GERMANY). INSTITUT FUER REAKTORSICHERHEIT.
Conference on work to develop steel reactor pressure vessels, Juelich, Germany, 4/68, 25:31668 (IRS-T-17)
Series of guid lines and recommendations auxiliary tests, 25:31597 (IRS-R-1)
TENNESSEE UNIV., KNOXVILLE.
Collisional ionization between cesium and selected molecules, 25:30276 (ORNL-TM-2620)
Systematic procedure for determining system parameters by performance index minimization, 25:31545 (ORNL-TM-3311)
TENNESSEE UNIV., KNOXVILLE. DEPT. OF CHEMICAL AND METALLURGICAL ENGINEERING.
Prog. rpt. on application of adiabatic calorimetry of metal systems, 1969--70, 25:31716 (ORO-3291-14)
TOKYO UNIV. (JAPAN). INST. FOR NUCLEAR STUDY.
Design of high-gradient accelerating column, 25:31048 (SJC-A-71-2)
Field measuring system of drift tube quadrupole magnets, 25:31047 (SJC-A-71-1)
Mutron project, 25:29371 (SJC-P-70-4)
Negative pion photoproduction off neutron at 180° in energy range between 300 and 1200 MeV, 25:30774 (INSJ-126)
Operation characteristics of 75 cm hydrogen bubble chamber and the refrigerator. I, 25:29372 (SJC-T-71-1)
TOULOUSE UNIV. (FRANCE).
Simulation of an electron avalanche in He using a Monte Carlo method, 25:30629 (NP-18798)
TRI--UNIV. MESON FACILITY, VANCOUVER (BRITISH COLUMBIA).
Techniques applied to design of TRIUMF magnet poles, 25:31049 (TRI-70-4)

U

UNION CARBIDE CORP., OAK RIDGE, TENN. Y-12 PLANT.
Adaptive control survey, 25:31758 (Y-1759)
Aspects of the brittle fracture failure of a 30-inch-ID, 30,000-psi isostat with threaded closure, 25:31757 (Y-1758)
Practical low-range moisture generator, 25:31759 (Y-1791)
Static and dynamic experiments with a repetitively pulsed booster, 25:31635 (Y-DR-44)
UNITED KINGDOM ATOMIC ENERGY AUTHORITY, ABINGDON (ENGLAND). CULHAM LAB.
Automatic data collection and processing as an aid to fusion research, 25:30474 (EUR-4593, pp 557-66)
Conditions for the control of beam intensity and cluster size in hydrogen cluster beams, 25:30252 (EUR-4593, pp 43-9)
Design and construction of a high-beta toroidal experimental assembly, 25:30586 (EUR-4593, pp 425-30)
Desorption by keV protons of hydrogen condensed on liquid-helium-cooled surfaces, 25:30257 (EUR-4593, pp 181-6)
Development aspects of fast metal-contact solid-dielectric switches, 25:30578 (EUR-4593, pp 365-71)
High-current capacitor banks for a 2-MJ high beta toroidal experiment (HBTX), 25:30563 (EUR-4593, pp 219-25)
Ionization and acceleration of hydrogen clusters, 25:30253 (EUR-4593, pp 51-8)
Lasers and the reactor ignition problem, 25:30553 (CLM-R-109)
Main and helical field windings on a toroidal stellarator: PROTO--CLEO, 25:30554 (EUR-4593, pp 13-18)
Manufacture and construction of helical winding, 25:30555 (EUR-4593, pp 19-24)
Plasma heating by neutral injection in a stellarator reactor, 25:30455 (EUR-4593, pp 479-84)
Production of high-current, high-quality beams of ions and neutral particles, 25:30256 (EUR-4593, pp 75-81)
Recent developments in superconductivity and its applications to fusion research, 25:30557 (EUR-4593,

pp 83-93)
Superconducting Levitron, 25:30558 (EUR-4593, pp 133-9)
UNITED KINGDOM ATOMIC ENERGY AUTHORITY, CULCHETH (ENGLAND). REACTOR GROUP.
Effects of reactor radiation on concrete, 25:30022 (EUR-4531, pp 237-65)
UNITED KINGDOM ATOMIC ENERGY AUTHORITY, RISLEY (ENGLAND). REACTOR GROUP.
Effects of reactor radiation on concrete, 25:30022 (EUR-4531, pp 237-65)
UNITED STATES-EURATOM FAST REACTOR EXCHANGE PROGRAM.
Compatibility studies with UC of different stoichiometries and iron--nickel--chromium alloys and the influence of stabilizers, 25:29940 (EURFNR-820)
Electronic microscope study of needle-shaped precipitates in irradiated austenitic steels, 25:29902 (EURFNR-891)
Inherent stability of the steam-cooled breeder, 25:31542 (EURFNR-813)
Prog. rpt. on fast breeder project, 1968--69, 25:31568 (EURFNR-823)
UPPSALA UNIV. (SWEDEN). INST. OF PHYSICS.
Moessbauer investigation of iron in boron, 25:30689 (UUIP-733)
Plasma drift in FXR discharge, 25:30499 (UUIP-659)
UTAH UNIV., SALT LAKE CITY. RADIOBIOLOGY DIV.
Growth dynamics of osteosarcomas in beagles, 25:29621 (COO-119-243)

V

VERMONT YANKEE NUCLEAR POWER CORP., RUTLAND.
Vermont Yankee Nuclear Power Station. Preliminary safety analysis report, Amendment 25, 25:31500 (DOCKET-50271-50)
Vermont Yankee Nuclear Power Station. Preliminary safety analysis report, Amendment 26, 25:31501 (DOCKET-50271-51)
VIRGINIA ELECTRIC AND POWER CO., RICHMOND.
Surry Power Station, Units 1 and 2. Preliminary safety analysis report, Amendment 21 (includes additions and revisions to final safety analysis report, Part B), 25:31503 (DOCKET-50280-39)

W

WALES UNIV., SWANSEA.
Nonlinear analysis of pressure vessels behavior including cracking, 25:31664 (EUR-4531, pp 697-734)
WASHINGTON UNIV., SEATTLE.
Breit--Wigners viewed through Gaussians, 25:29355 (RLO-1388-135)
WEIZMANN INST. OF SCIENCE, REHOVOTH (ISRAEL). DEPT. OF NUCLEAR PHYSICS.
Duality and dual models, 25:31015 (MIT-2098-726)
WESTINGHOUSE ELECTRIC CORP., PITTSBURGH, PA. PWR SYSTEMS DIV.
Loss-of-coolant analysis: comparison between BLODWN-2 code results and test data, 25:31598 (WCAP-7401)
WESTINGHOUSE RESEARCH LABS., PITTSBURGH, PA.
Development of polyimide bonded solid film lubricants, 25:29096 (WERL-HFIL-1)
WISCONSIN ELECTRIC POWER CO., MILWAUKEE.
Point Beach Nuclear Plant, Unit 1. Abnormal occurrence report: failure of containment sump valves to open, 25:31478 (DOCKET-50266-47)
WISCONSIN UNIV., MADISON. DEPT. OF RADIOLOGY.
Characteristics of some TLD solid systems, 25:29382 (COO-1105-120)

Y

YANKEE ATOMIC ELECTRIC CO., WESTBORO, MASS.
Yankee Nuclear Power Station. Operation report No. 123, March 1971, 25:31465 (DOCKET-50029-150)
YESHIVA UNIV., NEW YORK. BELFER GRADUATE SCHOOL OF SCIENCE.
Prog. rpt. on nuclear physics and nucleosynthesis, annual 2/71, 25:30036 (NYO-3962-3)

Z

ZENTRALSTELLE FUER ATOMKERNENERGIE-DOKUMENTATION, FRANKFURT AM MAIN (WEST GERMANY).
Plasma physics index, Vol. 6, No. 3, 1971, 25:30454

PERSONAL AUTHOR INDEX

Authors' names are indexed in the form appearing in the abstracted publication. Each entry under an author's name gives the publication title and the *NSA* volume and abstract numbers. Report numbers, where applicable, are given in parentheses at the end of the entry.

Because of problems involved in the mechanical preparation of this index, all accent marks are omitted. The following changes in spelling have been introduced to reduce some of the confusion which might result from omitting the accents:

Germanic	ä appears as	ae
Germanic	ö	oe
Germanic	ü	ue
Scandinavian	ø	oe

A

AAGAARD, H. J., MOSSPEC: program for resolving Moessbauer spectra, 25:30688 (RISO-M-1348)
AARON, H. B., Origins of microstructures resulting from precipitation, 25:29888
AARONSON, H. I., Origins of microstructures resulting from precipitation, 25:29888
ABABKOV, V. T., Corrosion resistance of Mo alloys in certain corrosive media, 25:29776
Special steels and alloys, 25:29862
ABARBANEL, Henry D. I., Asymptotic behavior of particle distributions in hadron collisions, 25:30908
ABBATTISTA, Fedele, Observations on systems Nb_2O_5--TiO_2 and NbO_2--TiO_2, 25:29995
Ternary system Nb_2O_5--NbO_2--TiO_2, 25:29994
ABDEL-RASSOUL, A. A., Analysis of platinum for certain elemental impurities by neutron activation, 25:29023
ABDULLAEV, A. A., Electron structure and the chemical bonds in vanadium pentoxide, 25:30668
ABE, Hideo, Fiber textures and morphology of dendrite in ingots of Zn and Zn--1.5 percent Cd alloy, 25:29892
ABECASIS, S. M., Energy level calculations in Davydov model, 25:31425
ABEL, H., Radiation effects in isolated DNA and their functional consequences, 25:29462
ABERG, Martha, Hydrolysis products of uranyl(VI), 25:29087
ABIDOV, A. A., Procedures for determining changes in DNA of irradiated organism, 25:29637
ABRAMOV, L. E., Photoeffect in a superconductor in a weak electric field, 25:30417
ABUL-MAGD, A. Y., Determination of the optical potentials in terms of diffraction-model parameters, 25:31410
ABUZINA, T. N., Protein fractions of intestine and brain of irradiated animals, 25:29664
ACERBI, E., Operational experience with H⁻ beam of Milan cyclotron, 25:31125
ACHACINSKI, V. V., Heat of formation and entropy of formation of plutonium carbides, 25:29942 (LA-tr-71-22)
ACHARYA, R., Dashen--Weinstein theorem in K/sub 13/ decay, 25:30816
ACKLAND, L. B., Feasibility study of the automatic controls for a pebble bed reactor power station, 25:31543 (AAEC/E-203)
ADAM, J., Extractions with long-chain amines. III, 25:28930
ADAMS, Richard O., Leed and adsorption studies of beryllium, 25:29894
ADAMSON, G. M. Jr., Development of FBR neutron-absorber materials, 25:29978 (ORNL-4630, pp 163-76)
Development of fuel element fabrication, 25:29924 (ORNL-4630, pp 233-8)
Fabrication development of FBR cladding, 25:29784 (ORNL-4630, pp 96-110)
ADAMSON, Ian Y. R., Radiation survival: improved rates following chlortetracycline administration, 25:29561
AERTS, L., High frequency melting of UO_2--PuO_2, 25:29935
AGEEV, V. N., Thermal-flare study of the interaction of oxygen with rhenium, 25:29772
AGRAWAL, P. C., Flattening of the x-ray spectrum of Sco X-1, 25:30147
AHARONI, N., Development of Botrytis cinerea in irradiated strawberries, 25:29732
AH-HOT, L., CEV injector ion source, 25:31134
Injection and stripping of heavy ion beam in Orsay cyclotron, 25:31150
Status report on Alice project, 25:31149
AHMAD, S. A., Lithium isotopic analysis on recording Fabry--Perot spectrometer, 25:28913 (BARC-508)
AHMED, Feroz, New variational method for the pulsed-neutron problem, 25:31175
AHMED, N., Isobaric analog states in ^{52}Cr from (p,γ) and (p,n) reactions in ^{51}V, 25:31256
AIHARA, Syuko, Modified PIG-type plasma source, 25:30543
AILLOUD, Pierre, Temperature of recrystallization of Zr--O solid solutions, 25:29854
AISENBERG, Alan C., Contrasting effects of cyclophosphamide and radiation on the immune responses of the mouse, 25:29475
AITKEN, E. A., Prog. rpt. on thermodynamic data program involving plutonia and urania at high temperatures, 8--10/70, 25:29821 (GEAP-12153)
AJI, M., Experimental study of emission of fission products due to cladding failures produced during rapid loss of gaseous coolant, 25:31608
AKAIWA, Hideo, Simultaneous determination of chlorine, bromine, and iodine in sedimentary rocks by neutron activation, 25:29033
AKHMADIEVA, A. Kh., Radiosensitizing effect of ferrous ions, 25:29556
AKIMOTO, Y., Mutual solubility and preparation of uranium--cerium carbo-nitride, 25:30003
AKIMOV, Yu. K., Timing with Ge(Li)-detector, 25:29353 (JINR-P13-5708)
AKIMTSEVA, N. I., Investigation of kidneys with aid of ^{51}Cr-EDTA, 25:29578
AKIMUNE, H., Ion source using a beam--plasma interaction, 25:30255 (EUR-4593, pp 67-74)
AKINRIMISI, J., Nonlinear Landau damping of electromagnetic cyclotron waves, 25:30615
AKOPYAN, Zh. I., Deamination of nitrogen compounds in liver during radiation sickness, 25:29641
ALBERT, W. G., Reliability assurance program plan for FFTF, 25:31630 (BNWL-630)
ALBURGER, D. E., Determination of the parity of the 4.19-MeV level of ^{34}S, 25:31289
AL-DARGAZELLI, Shetha S., Probability of production of internal bremsstrahlung accompanying β decay from ^{204}Tl, ^{147}Pm, and ^{45}Ca, 25:31363
ALDINGER, Fritz, Phase relations in the system beryllium--aluminum--titanium, 25:29900
ALDRIDGE, R. V., Suppression and enhancement of a drift-type instability, 25:30550
ALEFELD, G., Curie--Weiss temperature dependence of paraelasticity, 25:29865
ALEKSANDROV, P. A., Gamma rays emitted by nuclei in crystals, 25:30690
ALEKSANDROV, S. V., Procedures for determining changes in DNA of irradiated organism, 25:29637
ALEKSEENKO, L. B., Sensitivity of sweet potatoes to ionizing radiation, 25:29721
ALEKSEEV, A. G., Basic design parameters of a small size isochronous cyclotron, 25:31143
ALEKSEEV, I. I., Acceleration of cosmic rays by magnetohydrodynamic discontinuities, 25:30312
ALEKSEEVA, O. G., Antitissue antibodies during radiation sickness, 25:29660
ALEKSEEVSKII, N. E., Phase equilibria and superconductivity in the V_3Al--V_3Sn system, 25:30416
ALEXANDER, Chester Jr., ESR study of sugar radical in irradiated deoxyadenosine, 25:29146
ALEXANDER, John P., Effect of x-irradiation on migration of amelogenic cells in the rat incisor, 25:29678
ALEXANDER, Roger L., Tests of evaluated beryllium (n,2n) cross sections by analysis of 1.4-eV flux in water for an americium--beryllium source enclosed in beryllium spheres, 25:31223
ALEXANDRESCU, E., Oscillatory behavior of enzymic reactions, 25:29461
ALFEROV, A. N., Riboflavin effects on energy metabolism during irradiation, 25:29640
ALFREDSON, P. G., Review of processes for the production of

hafnium-free zirconium, 25:29782 (AAEC/TM-570)
ALI-ZADE, D. G., Powerful pulse generators based on avalanche transistors, 25:29405
ALLAB, M., Reactions $^{12}C(d,d)$, $^{12}C(d,p_0)$, and $^{12}C(d,p_1)$, 25:31222
ALLAN, C. J., Internal conversion and internal pair formation coefficients in Pb isotopes, 25:31333
ALLEN, B. C., Oxidation-resistant coatings for refractory metals, 25:29950
ALLEN, F. H., Low gamma-sensitivity boron proportional counter, 25:29324 (AEEW-M-970)
ALLEN, J. E., Constant-frequency oscillations in a bounded thermally produced plasma, 25:30624
ALONSO, A., Escape integrals, a useful concept in reactor hazard evaluation, 25:31621
AL'PEROVICH, V. R., Scintillation spectrometry of soft x-ray radiation, 25:29350
ALSMILLER, R. G. Jr., Approximate high-energy alpha-particle nucleus collision model, 25:31368
Low-energy electron transport with the method of discrete ordinates, 25:30630 (ORNL-TM-3318)
ALTARELLI, Guido, Symmetry groups and current algebra, 25:30914 (NP-18804)
ALTER III, W. A., Lethality in sheep following exposure to ^{60}Co, 25:29656
ALTOM, D. W., Viscoelastic analysis of irradiated graphite with variable creep coefficient, 25:29945 (ORNL-TM-3242)
ALTSCHULER, Martin D., Stimulated Compton effect in very compact radio sources, 25:30145
ALTUKHOV, A. M., Cosmic-ray flux in interplanetary media. II, 25:30315
Cosmic-ray flux in interplanetary media. I, 25:30314
ALVAREZ, J., Determination of free /sup 99m/Tc in labeled compounds by means of thin layer chromatography, 25:28991
ALVINO, W. M., Development of polyimide bonded solid film lubricants, 25:29096 (WERL-HFIL-1)
AMANO, Muneyuki, Preparation and comminution of hydrogenated niobium, 25:29929
AMANO, Yoshitsugu, Aging characteristics of Cu--Be--Sn alloy, 25:29830
AMARDEIL, P., Behavior of certain fission products during an accident in Siloe reactor, 25:31639
AMBRUS, Gyula, Combined chemotherapy and radiation therapy of cancer, 25:29606
AMES, L. L., C_2-exchange reactions of La, Ce, Pr, and Nd with their dicarbides, 25:29039
Dissociation energies of gaseous gadolinium dicarbide and terbium dicarbide, 25:29955
AMIEL, J.-L., Acute irradiation in man: treatment of hematologic disorders, 25:29699
AMIEL, M., Reactions $^{12}C(d,d)$, $^{12}C(d,p_0)$, and $^{12}C(d,p_1)$, 25:31222
AMMOSOV, V. V., Program linking FSD measuring microscopes with a Minsk-2 computer, 25:29379
AMOKRANE, A., Reactions $^{12}C(d,d)$, $^{12}C(d,p_0)$, and $^{12}C(d,p_1)$, 25:31222
ANAN'EV, V. A., Radiosensitivity of human lymphocytes in vitro, 25:29710
ANAN'IN, P. S., Operation of a spark chamber at a high count rate, 25:29375
ANCHER, L. J., Superconducting-state Knight shift in V_3Au, 25:30425
ANDERSEN, Vagn, Extracorporeal irradiation of blood in patients with active cirrhosis, 25:29704
ANDERSON, A. C., Thermal conductivity of superconducting niobium, 25:30434
ANDERSON, Charles G., Protected radioisotopic heat source, 25:29276
ANDERSON, E. M., Valent shell structure effects on coefficients of internal conversion, 25:31343
ANDERSON, Edwin, General acid catalysis of acetal hydrolysis. The hydrolysis of substituted benzaldehyde di-tert-butyl acetals, 25:29048
ANDERSON, H. L., Forward differential cross sections for reaction $p + p \rightarrow d + \pi^+$ in range 3.4 to 12.3 GeV/c, 25:30731
ANDERSON, J. S., Epitaxial growth of Ni on W, 25:29848
ANDERSON, James L., Scale invariance of second kind and Brans--Dicke scalar--tensor theory, 25:31010
ANDERSON, Robert W. Jr., Infrared spectrum of solid and matrix-isolated H_2O_2 and D_2O_2, 25:29655
ANDERSON, Roger R., Color spectrograms of very-low-frequency Poynting flux data, 25:30370
ANDERSSON, Herbert Olof, Improvements in fuel assemblies for nuclear reactors, 25:31678
ANDERT, K., Timing with Ge(Li)-detector, 25:29353 (JINR-P13-5708)
ANDREAE, Goetz, Protection of strain gages and semiconductor transducers against moisture, 25:31755 (UCRL-Trans-10526)
ANDREEV, Yu. A., γ rays accompanying decay of ^{109}In, 25:31320
ANDRES, Francoise, Rotation temperature of N_2^+ molecule, 25:30480
ANDRES, Ruprecht, Measurements on fuel elements for power reactors in a critical assembly, 25:31573
ANDREW, W. D., Early-flowering mutants of Medicago polymorpha var. polymorpha, 25:29488
ANDREWS, J. G., Spherical probe in a flowing plasma, 25:30482
ANDRIANOV, A. M., Stability of single-turn coils in pulsed magnetic fields up to 1 MG, 25:30956 (EUR-4593, pp 25-32)
ANDRILLAT, Yvette, Spectrophotometry of nucleus of NGC 2655 galaxy, 25:30194
ANDRUSHOVA, N. V., Influence of Cr and Mo on electrochemical and corrosion resistance of Ni--Cr--Mo alloys, 25:29777
ANDRYUSHIN, V. I., Method of measuring electromagnetic form factor of neutrino, 25:30777 (JINR-P2-5705)
ANELLIS, Abe, Irradiation resistance of spores of Clostridium botulinum in beef, 25:29734
ANGEL, J. R. P., Discovery of circular polarization in the white dwarf G99--37, 25:30072
Discovery of periodic variations in the circular polarization of the white dwarf G195--19, 25:30073
ANGHILERI, Leopoldo J., Studies on the possibility of improving the selective localization of radiophosphorus in different tissues, 25:29453
ANISIMOV, A. I., Absorption of shf waves by plasma at upper hybrid frequencies, 25:30606 (NP-18807)
ANOKHIN, V. M., Virulence of X-virus in preplanting gamma irradiation of potato tubers, 25:29726
ANSALDO, E., Isomeric shift of the 83 keV transition in ^{153}Eu, 25:31331
ANTALOVA, A., UBV photographic photometry. II, 25:30107
ANTIPOV, Yu. M., Search for particles with fractional charge in 70 GeV accelerator, 25:30724 (CERN-Trans-71-4)
ANTONELLI, A., Ecological site survey at Trisaia, 25:29479
ANTONI, F., Labelling of heparin with ^{51}Cr, 25:29415
ANTROPOV, A. E., Elastic and inelastic proton scattering on ^{33}S, ^{34}S, and ^{35}Cl, 25:31291
Excited core model for ^{63}Cu and ^{65}Cu, 25:31246
Hauser--Feshbach method and inelastic scattering of protons, 25:31245
AOI, H., Polarization in backward π^+p elastic scattering at 6 GeV/c, 25:30740
AOMURA, Kazuo, Effect of irradiation on halogen exchanged silica--alumina catalyst, 25:29111
APPARAO, Krishna M. V., Mechanism for pulsar radiation, 25:30149
Solar-cycle theory of pulsars, 25:30131
APPLEBY, Ralph C., Dental caries from radiation therapy, 25:29712
ARAKELYAN, V. A., Physical nature of zones generating transition radiation, 25:30714
ARANDA CENTURION, B. S., Application of four different doses of gamma radiation to adult Sitotroga cerealella, 25:29618
ARATHOON, J. P., Pressure vessels for water and gas reactors, 25:31550 (EUR-4531, pp 601-13)
Prestressed concrete pressure vessel of the Vandellos nuclear power plant, 25:31454 (EUR-4531, pp 81-94)
ARBUZOV, B. A., Weak interactions, 25:30803 (CERN-71-7, pp 1-40)
ARCHBOLD, T. F., Reply to transition morphology during hcp precipitation from beta-isomorphous alloys, 25:29887
ARDISSON, Gerard, Multipolar character of photons accompanying ^{125}Sb decay, 25:31340
ARDITI, Maryse, Proton holes in (2s--1d) shell from (d,^{3}He) reactions, 25:31240 (NP-16511)
ARDOUIN, Benedicte, Correlations between ^{210}Pb atmospheric abundance in Terre Adelie and solar activity, 25:30171
AREF'EV, K. M., Principles of thermoelectric and magnetohydrodynamic conversion of energy, 25:30340
ARENDT, F., Developments in cryogenic and superconducting magnets, 25:31040 (KFK-1316)
ARGYRIS, J. H., Three-dimensional elastic and elastoplastic calculations on reactor pressure vessels, 25:31667 (EUR-4531, pp 777-95)
ARIANER, J., CEV injector ion source, 25:31134
ARKHIPOVA, L. D., Relationship between level of endogenous sulfhydryl groups and radiosensitivity of tumors, 25:29610
ARKUSZEWSKI, J., FLANGE-AL 4 code for the Gier computer, 25:31168 (INR-1260)
ARL'T, R., Decay scheme of ^{84}Y, 25:31247
Levels in ^{142}Nd, 25:31337
ARL'T, R. D., X-ray spectrometer with cooled Si(Li)-detector, 25:29325 (JINR-P13-5707)
ARMITAGE, Donald Bruce, Determination and distribution of various trace elements in natural waters, 25:28919
ARMSTRONG, R. A., Hydrogen adsorption on (100) W surface using simple HEED system, 25:29846
ARNDT, H. J., Results of primary therapy of laryngeal carcinomas with conventional x-depth-irradiation or radium contact irradiation, 25:29598
ARNELL, S. E., Energy levels and gamma transitions in ^{70}Ga, 25:31290
ARNETT, W. David, Explosive nucleosynthesis in helium zones, 25:30067
Galactic evolution and nucleosynthesis, 25:30206
ARNOLD, G. P., Crystal structure of Th_3N_4, 25:29986
ARP, Halton, NGC 7603, a galaxy connected to a companion of much larger redshift, 25:30217
ARTEAGA-ROMERO, N., Photon--photon collisions, new area of experimental investigation in high-energy physics, 25:30798
ARTHUR, Jett C. Jr., Cellulose graft copolymers. III, 25:29108

ARZUMANOV, Yu. L., Electroretinogram in dogs irradiated during embryogenesis, 25:29667
ASANO, M., Determination of Th, U(VI), and Pu(IV), 25:28982
ASANO, Masaharu, Separation of uranium from fission products, 25:29198
ASANOV, R. A., Total electrical charge and mass of elliptic universe, 25:30235
ASARO, Frank, Energy of ^{253}Es α particles, 25:31357
ASHBY, D. E. T. F., Is ball lightning caused by antimatter meteorites, 25:30329
ASHENHURST, Robert L., Prog. rpt., 11/70, 25:31693 (COO-2094-4)
ASHERSON, G. L., Selective and specific inhibition of 24 hour skin reactions in the guinea-pig. III, 25:29474
ASHIKAGAYA, Yoshinobu, Characteristics of personal monitoring dosimeter, 25:29383 (JAERI-Memo-4292)
ASHURST, A. N., Beryllium: properties and fabrication, 25:29794
ASKAR'YAN, G. A., Initial stage of a light explosion of a particle of matter in a powerful light beam, 25:30471
ASLAM, J., NMR and nuclear relaxation study of satellite lines in dilute Co--Cr, Co--V, and Co--Mn alloys, 25:31690 (COO-1569-71)
ASLANIDES, E., Determination of the parity of the 4.19-MeV level of ^{36}S, 25:31289
ATAYAN, R. R., Effects of thermal shock and x rays on wheat, 25:29723
ATHERTON, David R., Protracted hepatic, splenic, and renal retention of ^{239}Pu in the beagle, 25:29451
ATKINS, Harold L., Pathways of an artificial element in the body, 25:29418 (BNL-50285)
ATKINSON, D., Existence of functions that satisfy exactly both crossing and unitarity. III, 25:30862
ATKINSON, G. D. Jr., Computer-assisted analysis of gamma-ray spectra, 25:29363
ATLAVIN, A. B., Neutron activation determination of Mo in biological materials, 25:29019
ATO, Yasuro, Power generation devices with atomic energy, 25:29280
ATTOLINI, M. R., Cosmic-ray microvariations during thunderstorm perturbations, 25:30334
ATWATER, H. F., Pair-production cross sections at 2.75 MeV, 25:31361
AUBRECHT II, Gordon J., Dispersion calculation of isoscalar 3π and K anti K electromagnetic form factors, 25:30865
AUCHMUTY, J. F. G., Models of rotating stars, 25:30075
AUDRETSCH, J., Inertial reference frames in Einstein's theory of gravitation, 25:30996
AUER, P. L., Thermalization in the Earth's bow shock, 25:30365
AUGERAT, J., Electron-field pair production by photons near threshold with streamer chamber technique, 25:30717
AULD, E. G., Design of 4000 ton magnet for TRIUMF cyclotron, 25:31092
Extraction of multiple beams of various energies from TRIUMF negative ion isochronous cyclotron, 25:31109
AUPELT, G., Measurement of heat transport by conductivity of superfluid helium in pipes, 25:30406
AURE, Jean-Luc, Overstable damping in a stellar semi-convective zone, 25:30039
AUSANGEE, R., Study of the properties of concrete and especially of creep under the effect of temperature, 25:30023 (EUR-4531, pp 267-324)
AUSTONI, M., Evaluation of kidney morphology and function by means of the scintillation camera, 25:29592
AVAN, L., Electron-field pair production by photons near threshold with streamer chamber technique, 25:30717
AVAN, M., Electron-field pair production by photons near threshold with streamer chamber technique, 25:30717
AVERY, R., ERA 4-MeV injector, 25:31053 (UCRL-20174)
AVERY, Robert T., Ultra-narrow, high-quality, high-field quadrupole magnet, 25:31051 (UCRL-20164)
AVONA, Vincent L., Protected radioisotopic heat source, 25:29276
AXE, J. D., Lattice dynamical phase transition in V_3Si, 25:30683
AXENTE, D., Kinetics of $^{15}N/^{14}N$ isotopic exchange between nitric oxide and nitric acid, 25:29057
AXMANN, Hans-Peter, Phenomena of fission of heavy nuclei by high-energy protons, 25:31326
AY, R., Application of ultrasound-B picture methods for the planning of radiotherapy, 25:29602
AYRES, J. A., Heavy water and organic fluids as neutron moderator and reflector materials, 25:29154
AZHGIREI, L. S., Spectrum of fast deuterons emitted in 670-MeV proton interaction with carbon nuclei, 25:31225
AZIMOV, S. A., Coherent interactions of π⁻-mesons with photoemulsion nuclei at 17 GeV, 25:30736 (JINR-P1-5565)
AZUMI, Takatugu, Studies on ion-exchange transfer. XIX, 25:29193

B

BABA, Hitoshi, Field measuring system of drift tube quadrupole magnets, 25:31047 (SJC-A-71-1)
BABENKO, N. S., Methods of measuring varying and pulsed magnetic fields, 25:29399
BABICKY, A., Experiences with experimental isotopic investigations of the joints, 25:29581
BABYKIN, M. V., Collective processes and turbulent heating of a plasma, 25:30469
BACE, Marjan, Covariant derivatives in broken nonlinear chiral symmetry, 25:30922
BACHMAN, K., Magnetic domain patterns in small crystal $SmCo_5$ particles, 25:30675
BACHMANN, P., Echoes with ion sound waves, 25:30611
BACKENSTOSS, G., Nuclear γ-rays following muon capture, 25:31258
BADER, R. F. W., Nonadditivity of intermolecular forces in He_3 within SCF LCAO MO approximation, 25:30270
BADIE, J-M., High-temperature phase diagrams for the systems Sc_2O_3--La_2O_3 and Sc_2O_3--Nd_2O_3, 25:30005
BAEDECKER, Philip A., Digital methods of photopeak integration in activation analysis, 25:29028
BAERG, A. P., Certificates of radioactivity standards, 25:29173
BAEUMLER, J., High-Q capacitor, 25:30594 (EUR-4593, pp 541-4)
BAGHERI-ZENOUZ, E., Effect of the irradiation of wheat grains on the development and reproduction of Sitophilus granarius L, 25:29737
BAGLIANO, G., Strontium-90 and ^{137}Cs in milk during 1952 to 1966, 25:29507
BAICHOROV, E. O., Investigation of kidneys with aid of ^{51}Cr-EDTA, 25:29578
BAIER, G., Levels in ^{142}Nd, 25:31337
BAIRD, G. A., Optical and radio studies on extensive air showers, 25:30333
BAIXAS, J., CEV injector ion source, 25:31134
BAJWA, G. S., Stability condition of flute instability in an inhomogeneous plasma, 25:30548
BAKER, E. H., ac conductivity of thoria--yttria solid solutions, 25:30685
BAKER, Floyd B., Enthalpies of formation of cerium dioxide, cerium sesquicarbide, and cerium dicarbide, 25:29961
BAKER, Frederic A., Diagnostics of a supersonic plasma stream using an immersed microwave probe, 25:30476 (N-71-10964)
BAKHAREVA, M. F., Acceleration of charged particles in a variable magnetic field, 25:30122
BAKHRAKH, V. L., Green functions of Schroedinger equation for simplest systems, 25:30712
BAKOV, I., Probe method for recording ions produced by laser radiation in post-luminescence discharge plasma, 25:30477 (NP-18765)
BALACHANDRAN, A. P., Inequalities for the π π partial waves from the properties of a class of orthogonal polynomials, 25:30851 (SU-1206-240)
BALAMORE, Dilip S., Dust scattering in the filaments of M82, 25:30208
BALAZS, Arpad, Production of Si surface-barrier semiconductor detectors, 25:29332
BALAZS, Erzsebet, Effective interaction of nucleons in infinite nuclear matter, 25:31416
BALBUTSEV, E. B., Properties of light nuclei with realistic N--N-interaction, 25:31201 (JINR-P4-5614)
BALDWIN, D. E., Electromagnetic energy absorption at the upper hybrid resonance, 25:30616
BALL, J. S., Quark model of diffractive processes, 25:30844
BALU, K., Syntheses of phyllitic minerals: their utilization in radioactive waste treatment. II, 25:29175 (BARC-509)
BALUNI, V. Z., Pi-meson radius and analytical properties of π-meson form factor, 25:30864
BAM-ZELIKOVICH, G. M., Criteria for the detachment of a three-dimensional boundary layer, 25:31732 (SC-T-713010)
BANAIGS, J., ABC effect and a structure at 450 MeV in meson missing-mass spectra, 25:30734
BANDO, Hiroharu, Contraction of deuteron cluster in ^{6}Li, 25:31207
BANDO, Shoji, Determination of Sc, Cr, Fe, Co, Zn, and Sb in deposits and airborne particulates by neutron activation analysis, 25:29032
BANDOLI, G., Infrared studies on coordination influence of UO_2^{2+} group on P--O bond of triphenyl phosphine oxide, 25:29088
BANERJEE, M. K., Nonrelativistic hard-pion production and current-field algebra, 25:30898
BANIFATOV, A. E., X-ray spectrometer with cooled Si(Li)-detector, 25:29325 (JINR-P13-5707)
BANNER, M. W., Chromosome aberrations in swine leukocytes after in vivo or in vitro exposure to 14 MeV neutrons, 25:29497
BANZHAF, W., Results of primary therapy of laryngeal carcinomas with conventional x-depth-irradiation or radium contact irradiation, 25:29598
BARAKINA, N. F., Destruction of hematogenic tissue of mammals under ionizing radiation, 25:29676
Use of electronic particle counter to investigate cell populations of bone marrow after irradiation, 25:29648
BARAN, W., FLANGE-AL 4 code for the Gier computer, 25:31168 (INR-1260)
BARASHENKOV, V. S., Angular and energy distributions of particles produced in inelastic π--N and N--N collisions at very-high energies, 25:30870 (ORNL-tr-2433)
Method of calculating the unitary weights in the theory of multiple particle production, 25:30913 (JINR-P2-

5729)
BARATOV, D. G., Diffusion of a dense decaying plasma in a stellarator, 25:30472
Studies of diffusion of dense disintegrating plasma in a stellarator, 25:30462 (NP-18767)
BARBIER, Marcel, Phenomena of fission of heavy nuclei by high-energy protons, 25:31326
BARBLISHVILI, T. I., Supernova in NGC 3389, 25:30057
BARBULESCU, A., Thermal phase relations and dielectric properties in system La_2O_3--ZrO_2--TiO_2, 25:29984
BARCHUGOV, V. V., Angular distribution of neutrons scattered in air, 25:30639
BARDIN, B. M., Indiana Univ. 200 MeV cyclotron project, 25:31082
BARDOS, Tamas, Combined chemotherapy and radiation therapy of cancer, 25:29606
BARGON, G., Effect of low dosage irradiation on metabolism and function of the rat kidney damaged by ischemia, 25:29654
BARGON, Gerlach, Function and morphology of hypertrophic rabbit kidneys following telecobalt irradiation with 1000 to 4000 rad, 25:29684
BARGUIL, J., Description of elastic-scattered processes with the use of non-local separable potentials, 25:31186 (LYCEN-7089)
BARISH, J., Low-energy electron transport with the method of discrete ordinates, 25:30630 (ORNL-TM-3318)
BARIT, I. Ya., Spectrometric isochronous cyclotron, 25:31123
BARKAI-GOLAN, Rivka, Development of Botrytis cinerea in irradiated strawberries, 25:29732
BARKER, Allan, Improvements in or relating to fuelling arrangements for fast nuclear reactors, 25:31581
BARKER, F. C., Energy levels of ^{27}Si, 25:31252
BARLTROP, D., Excretion and retention of stable strontium in children, 25:29442
BARNARD, E., Low-lying states of ^{127}I, 25:31352
BARNES, J. E., Dose distribution in the beagle dog from radiographic exposure, 25:29514 (LF-43, pp 116-22)
Some observations on the toxicity of beta-emitting radionuclides inhaled in fused clay particles, 25:29438 (LF-43, pp 197-204)
Toxicity of inhaled ^{90}Sr fused clay in beagle dogs. I, 25:29437 (LF-43, pp 188-96)
Toxicity of inhaled ^{90}Y fused clay in beagle dogs. II, 25:29434 (LF-43, pp 146-62)
BARON, E., Injection and stripping of heavy ion beam in Orsay cyclotron, 25:31150
Status report on Alice project, 25:31149
BARONCELLI, F., Equilibrium data relating to Eurex process, 25:29182 (RT/CHI-(70)31)
BARONDES, Samuel H., Conference on cellular dynamics of the neuron, Brussels, 8/68, 25:31760
BARONNET, Jean-Marie, Rotation temperature of N_2^+ molecule, 25:30480
BARODDY, E. M., Effects of energetic heavy ions and radiation on infrared components, 25:29411
BARRETT, J. W., I Zw 1: a variable compact galaxy, 25:30199
BARRY, George W., Pomeranchuk term decoupled from ordinary Regge trajectories, 25:30885
BARRY, J. R., Lyman-alpha emission from Arcturus, 25:30070
BARTELL, D. M., Vacuum-ultraviolet emission from proton-excited helium gas, 25:30284
BARTH, Delbert S., Iodine-131 dairy cow uptake studies using a submicrometer synthetic dry aerosol (Project SIP), 25:29505 (SWRHL-39-r)
BARTINE, D. E., Low-energy electron transport with the method of discrete ordinates, 25:30630 (ORNL-TM-3318)
BASARGIN, Yu. G., External beam monochromatization system in 2.4 m isochronous cyclotron at Kurchatov Atomic Energy Inst, 25:31118
Production of monochromatic beams using cyclotron acceleration, 25:31121
BASOVA, B. G., Effect of an automatic correction system on spectrometer resolution, 25:29364
Time--amplitude converter for the nanosecond range, 25:29341
BASS, F. G., Propagation of intense electromagnetic waves in a two-component plasma, 25:30619
BASS, William Thomas, Study of the nuclei ^{61}Cu, ^{64}Cu, ^{67}Ga, and ^{68}Ga using the (p,n) reaction, 25:31268
BASSEMIR, Robert W., Radiation-curable compositions, 25:29114
BASSETTO, A., Multicluster model for very-high-energy collisions, 25:30755
BASTON, V. F., Distribution of solid fission products in UO_2, 25:31589 (CONF-710302-5)
BASU, A. K., Cytological effects of x rays, ^{32}P, and ^{35}S in rice, 25:29496
BASU, B., Gravitational theory of spiral arms, 25:30215
BASU, J., Effect of glass wall on the determination of plasma conductivity by rf external probes, 25:30527
BASU, Rabindra Krishna, Cytological effects of x rays, ^{32}P, and ^{35}S in rice, 25:29496
BATES, D. R., Positive ions in D-region, 25:30404
BATHORI, Edit, Lipid fraction alterations in serum and liver of rats exposed to 2000 r local hepatic irradiation, 25:29685
BATISHCHEV, A. I., Procedures for determining changes in DNA of irradiated organism, 25:29637
BAUBILLIER, M., Contribution to Lamb statistical model subject, 25:30866
BAUDER, Uwe, Investigation of plasmas at very high pressure, 25:30509
BAUER, Dieter W., Fabricating the refractory metals. Part II. Methods used to make parts, 25:29789
BAUGH, D. J., Angular correlation of $^{42}Ca(\alpha,p\gamma)^{45}Sc$, 25:31251
BAULDON, H., Metabolism of different immunoglobulin classes in irradiated mice. V, 25:29473
BAUM, I. V., Matrix space dynamics taking into account third-order terms in Lagrangian, 25:30967
BAUM, Neal P., Specific heat of chromium--rich chromium--nickel and chromium--iron--molybdenum alloys between 1.3 and 4.2°K, 25:30676
BAUMANN, Elizabeth W., Sensitivity of the fluoride-selective electrode below the micromolar-range, 25:28923
BAXTER, J. P., Atomic reactors and fuel sources for Australia, 25:31462
BAYES, D. V., Main and helical field windings on a toroidal stellarator: PROTO--CLEO, 25:30554 (EUR-4593, pp 13-18)
BAZIN, H., Metabolism of different immunoglobulin classes in irradiated mice. V, 25:29473
BEALS, Richard, Models of rotating stars, 25:30075
BEATTIE, J. R., Appraisal of fission product release and retention in relation to reactor safety, 25:31604
BEAUMEVIEILLE, H., Reaction $^{22}Ne(p,p)$, $^{22}Ne(p,p')$, and excited states of ^{23}Na, 25:31281
Reactions $^{12}C(d,d)$, $^{12}C(d,p_0)$, and $^{12}C(d,p_1)$, 25:31222
BECHER, Paul F., Mechanical behavior of polycrystalline TaC, 25:29973
BECK, E. G., Elimination and metabolism of benzo(a)pyrene after intratracheal injection, 25:31715 (ORNL-tr-2469)
BECK, F. H., Stress corrosion cracking of Ti--8Al--1Mo--1V alloy: aqueous and methanol environments, 25:29765
BECK, J. N., Daily fluctuations of radioactive fallout particles in ground-level air, 25:29219
BECK, R., Is there a ground-state deformation in nuclei near closed shells, 25:31451
BECKA, J., Influence of defects upon brittle failure of electroslag welded joints caused by residual stresses, 25:29832
Welding of reactor pressure vessel of first Czechoslovak nuclear power station, 25:29788 (ZJE-69)
BECKER, C. D., Experimental drifts of juvenile salmonids through effluent discharges at Hanford. II, 25:31645 (BNWL-1527)
BECKER, E., Exposure plots for new radiographic films, 25:29294
Isotope and x-ray radiography, 25:29293
BECKER, Klaus, Solid-state dosimetry, 25:29385
BECKER, Klaus H., Energy independent radiophotoluminescence dosimeter with good fading stability, 25:29388
BECKER, Olga, Significance of Grenzstrahlen for radiation research. III, 25:29603
BECKSTRAND, D. F., Reaction $^{40}K(n,\gamma)^{41}K$ and the level structure of ^{41}K, 25:31292
BEDERSON, B., Differential spin exchange and elastic scattering of low-energy electrons by potassium, 25:30282
BEEKMAN, N. M., Electronic transport in calcia-stabilized zirconia, 25:30682
BEG, M. A. B., Selected topics in discrete symmetries and CP-violation, 25:30915 (NP-18808)
BEGZHANOV, R. B., Automatic stabilization of a device for measuring life times in the picosecond range, 25:29365
BEHRENS, H., β--γ correlation measurement in ^{72}Ga, 25:31297
BEHRISCH, R., Influence of wall material on plasma--wall interaction, 25:30496 (EUR-4593, pp 461-70)
BEHRSING, G., ERA 4-MeV injector, 25:31053 (UCRL-20174)
BEIGHTLER, C. S., Optimization of nuclear systems by geometric programming, 25:31649
BEITIN, M. R., Internal conversion monoenergetic positron spectrum in $^{157}Gd(n,\gamma)^{158}Gd$ reaction, 25:31329
BEJSOVEC, V., Radial injection of a polarised beam into a cyclotron, 25:31153
BEK, V., Five year's experience with isotopic investigations of diseased joints, 25:29576
BEKOWICH, R. S., Instrumentation of full-scale containment structures, 25:29303
BELIAEVA, I. F., Passive diagnostics of a plasma focus using charged products of the dd-reaction, 25:30475 (LA-tr-71-6)
BELIEEN, R., High frequency melting of UO_2--PuO_2, 25:29935
BELL, D. J., Testing one tenth scale model of Hinkley Point B and Hunterston B Power Station prestressed concrete pressure vessels, 25:29312
BELL, P. R., Phantom for the adjustment of gamma-ray imaging devices, 25:29328 (ORNL-TM-3261)
BELLAND, P., Holographic interferometry of laser-produced plasmas using picosecond pulses, 25:30487
BELLINI, G., Correlation effects, 25:30744
BELLO, Francis, Evolution of quasars, 25:30148
BELMONT, J. L., Grenoble cyclotron progress report, 25:31097
BELOUSOV, L. I., Egg laying of hens under action of incorporated ^{131}I, 25:29661
BELOV, A. G., Production of spontaneously fissionable isomer ^{234}U at radiative thermal neutron capture,

XUM

25:31307 (JINR-P7-5497)
BELOV, V. A., High-accuracy variable time delay, 25:29403
BELOV, Yu. V., Impulse generator for feeding a linear accelerator, 25:31066
BELOVINTSEV, V. Ya., Angular distribution of neutrons scattered in air, 25:30639
BELTRAN-LOPEZ, V., Nonadditivity of intermolecular forces in He_2 within SCF LCAO MO approximation, 25:30270
BEM, P., Radial injection of a polarised beam into a cyclotron, 25:31153
BENACKA, S., Superconducting cavity resonators in 10 GHz frequency band, 25:30443
BENDAZZOLI, G. L., Wave functions for He by rotational projection, 25:30269
BENEDICT, W. S., Solar spectrum from lambda 7498 to lambda 12016, 25:30172
BENJAMIN, John A., Electrostatic deflector for selectively and adjustably bending a charged particle beam, 25:29408
BENJAMIN, S. A., Toxicity of inhaled $^{144}CeCl_3$ in beagle dogs. IV, 25:29431 (LF-43, pp 128-36)
Toxicity of inhaled ^{91}Y fused clay in beagle dogs. I, 25:29435 (LF-43, pp 163-70)
BENNAKKER, J. J. J., Transverse heat flow in gaseous hydrogen isotopes at low temperatures, 25:29267
BENNETT, J. R. J., Axial injector for Harwell variable energy cyclotron, 25:31146
Ion sources for multiply charged heavy ions, 25:31133
Production and acceleration of heavy ions in Harwell variable energy cyclotron, 25:31136
BENTZ, Hans Alfred, Nuclear radii of ^{12}C, ^{13}C, ^{14}N, and ^{16}O, 25:31219
BEN-YEHOSHUA, S., Development of Botrytis cinerea in irradiated strawberries, 25:29732
BERANGER, Gerard, Observation of age hardening of α-zirconium after deformation, 25:29853
BERDJIS, C. C., Cardiovascular system, 25:29695
Cell, 25:29457
General consideration, 25:29690
Kidney, 25:29698
BERDJIS, Charles C., Pathology of irradiation, 25:29689
BEREZIN, B. Ya., Enthalpy measurements by drop calorimetry using electromagnetic levitation, 25:29875
BERG, H., Synchronization of the mytotic cycle of mammalian cells in vitro through fractionated x-ray therapy, 25:29611
BERG, J. M., Plasma drift in FXR discharge, 25:30499 (UUIP-659)
BERG, R. E., Beam transport system optics studies for Univ. of Maryland cyclotron, 25:31090
Multi-channel non-intercepting phase probe for Univ. of Maryland cyclotron, 25:31126
BERGEN, D. W., Neutron-induced fission cross section of ^{240}Pu, 25:31385
BERGER, Ch., Electromagnetic form factors of the proton, 25:30786
BERGER, J., ABC effect and a structure at 450 MeV in meson missing-mass spectra, 25:30734
BERGGREN, G., Influence of oxide additions on the reduction of UO_3 and U_3O_8 as measured by DTA and TG, 25:29947
BERGMAN, David J., Third sound in superfluid helium films of arbitrary thickness, 25:30408
BERGMANN, G., Eliashberg function $\alpha^2(E)F(E)$ and the strong-coupling behavior of a disordered superconductor, 25:30421
BERGOTZ, R., Measurement of heat transport by conductivity of superfluid helium in pipes, 25:30406
BERKO, F. W., Primary electron influx to dayside auroral oval, 25:30367
BERLOVICH, E. E., Formation of superheavy elements in nature, 25:30051
BERNACCA, P. L., New helium-weak stars in the I Orion association, 25:30049
BERNARD, A., New types of thermal-shielding concretes for nuclear reactors, 25:30031 (EUR-4531, pp 975-1018)
BERNDORFER, Knut, Production of polarized thermal neutrons by means of an iron--cobalt neutron guide, 25:31180
BERNERS, E. D., Proton polarization in $^{16}O(p,p)^{16}O$ and states in ^{17}F, 25:31236
BERNHARDT, D. E., Normal run and the accident case for a nuclear rocket engine, 25:31642
BERNSTEIN, A. M., Alpha-particle optical potential from the nuclear density distribution, 25:31212
BERNSTEIN, H. J., Resonance Raman effect in MnO_4^- with 5145 A laser excitation, 25:29047
BERNTHAL, F. M., Decays of ^{176}Ta, ^{176}Lu, and /sup 176m/Lu to levels in ^{176}Hf, 25:31375
BERRY, Charles, CV Serpentis, 25:30043
BERRY, H. G., Lifetimes of some doubly excited levels in neutral helium, 25:30265
BERTERO, M., Outline of scattering theory for absorptive potentials, 25:31017
BERTHEL, R. O., Measurements of oscillator strengths for Fe I and Fe II, 25:30170
BERTINE, Kathe K., Deposition of molybdenum and uranium along the major ocean ridge systems, 25:29228
BERTOLOTTI, M., Electron microscope observation of lattice disorder in ion-implanted silicon, 25:30650
BERTOTTI, B., Gravitational waves and cosmology, 25:30240
BERTRAM, W. K., Statistical theory for gamma ray de-excitations, 25:31406
BERZIN, Ya. Ya., Internal conversion monoenergetic positron spectrum in $^{157}Gd(n,\gamma)^{158}Gd$ reaction, 25:31329
BES, D. R., Effect of the multipole pairing and particle-hole fields in the particle-vibration coupling of ^{209}Pb: I, 25:31309 (LA-DC-11648)
BESERVEY, E. B., Preliminary investigation of ohmically-heated plasmas in the model ST Tokamak, 25:30459 (MATT-813)
BESHTOEV, Kh. M., Method of calculating the unitary weights in the theory of multiple particle production, 25:30913 (JINR-P2-5729)
BESKORSYI, A. P., Mixing of uhf signals from superconducting tin films, 25:30436
BESNIER, G., Resonant proton beam depolarisation in a synchrocyclotron, 25:31162
BESSIS, J., Consequences of accidents in nuclear plants, 25:31622
BESSUGES, Jacques, Emotivity parameter in industrial medicine and the special conditions imposed by radioprotection in the nuclear industry, 25:29531 (CEA-R-4156)
BETZ, G., Determination of the distribution of fission products in fuel particle coatings by the sputtering technique, 25:29979 (SGAE-PH-96/1970)
BEUTLER, Hans, Low temperature method for coating nuclear fuels with multiple carbon coatings, 25:29928
BEYNON, T. D., Holmium-165 fast neutron cross sections, 25:31350
BEZIK, Max J., Uranium etchant and method, 25:29798
BHAGAVAT, G. K., Effect of external dc electric field on absorption of microwaves in plasma, 25:30628
BHAMBURKAR, M. W., Feasibility of controlling stored grain pests by the sterile-male technique, 25:29750
BHAT, R. K., Determination of total hydrogen content of UO_2 pellets, 25:28912 (BARC-500)
BHATIA, T. S., High-resolution study of ^{92}Nb by (d,t) and (d,t γ) reactions, 25:31283
BHATIA, V. S., Spurious scattering in nuclear emulsions, 25:29378
BHATT, B. C., Decay times, intensities, and their temperature variation of luminescence of aqueous and deuterated solutions of Eu ion, 25:29053
BIALAS, A., Photoproduction of N*(1236) resonance and vector dominance model, 25:30784
BIALKOWSKI, Jacek, Adaptation of a long-lens beta-ray spectrometer for the measurement of short nuclear lifetimes, 25:29358
BIBR, B., Experiences with experimental isotopic investigations of the joints, 25:29581
BICKERTON, R. J., Structure of hydromagnetic shock waves, 25:30528
BIDZILYA, N. I., Gamma-induced free radicals in seeds, 25:29719
BIERMANN, Ludwig, Pulsars and neutron stars, 25:30127
BILDSTEIN, H., Nuclear fuel particles manufactured from a peroxide of uranium, 25:29801
BILENKII, S. M., Method of measuring electromagnetic form factor of neutrino, 25:30777 (JINR-P2-5705)
BILLARD, Francois, Measurement of the state of equilibrium between radon and its daughters in the uranium mines, 25:29201 (AEC-tr-7228)
Particle size spectrum of the radioactive aerosols in a uranium mine, 25:29200 (AEC-tr-7227)
BILLION, Marc, Temperature of recrystallization of Zr--O solid solutions, 25:29854
BILLON, Jean-Pierre, Study of impurities distribution in a metal (plutonium), 25:28916 (CEA-R-4071)
BILPUCH, E. G., Cyclo--Graaff: concept and practice, 25:31081
BILTIEWICZ, Jan, Radium-226 in contemporary and fossil snow, 25:29209
BIRATTARI, C., Operational experience with H- beam of Milan cyclotron, 25:31125
BIRBRAIR, B. L., Coriolis anti-pairing theory of nuclear rotations, 25:31408
BIRD, B., N mixing in the 2s--1d shell, 25:31265
BIRD, J. K., Multi-channel non-intercepting phase probe for Univ. of Maryland cyclotron, 25:31126
BIRD, P. F., Vibrational energy transfer in shock-heated N_2--HI and N_2--DI mixtures, 25:29067
BIRGENEAU, R. J., Lattice dynamical phase transition in V_3Si, 25:30683
BIRYULIN, Yu. F., Stabilization of gain of a scintillation counter for registering ^{14}C, 25:29344
BISCHOFBERGER, A., Magnetic domain patterns in small crystal $SmCo_5$ particles, 25:30675
BISGARD, K. M., Inelastic scattering of deuterons and α-particles on ^{191}Ir and ^{193}Ir, 25:31342
BISKAMP, D., Nonresonant diffusion of particles in stochastic fields, 25:30520
BISNOVATY-KOGAN, G. S., Nuclei of galaxies and quasars as infrared sources, 25:30247
BISSON, Andre, Electronic microscope study of needle-shaped precipitates in irradiated austenitic steels, 25:29902 (EURFNR-891)
BISTAFFA, R., Angioscintiphotography, 25:29587
BISWAS, S., Flattening of the x-ray spectrum of Sco X-1, 25:30147
BIZOT, J. C., Physical results obtained with electron and positron storage rings, 25:31061
BJERGBAKKE, E., Oxygen formation in the γ-ray irradiation of Fe^{2+}--Cu^{2+} solutions, 25:29141

BJERRUM, Ole, Extracorporeal irradiation of blood in patients with active cirrhosis, 25:29704
BJURE, J., Pulmonary gas exchange after radioisotope scanning, 25:29594
BLACK, David Charles, Trapped He, Ne, and Ar in meteorites, 25:30034
BLACK, J. L., Search for 3446 keV level in ^{29}P, 25:31250
BLACK, Stuart C., Iodine-131 dairy cow uptake studies using a submicrometer synthetic dry aerosol (Project SIP), 25:29505 (SWRHL-39-r)
BLACKMON, M. L., Restrictions on the angular momentum of t-channel exchanges from s-channel helicity conservation, 25:30757
BLACKMON, Maurice L., Inequalities for the π π partial waves from the properties of a class of orthogonal polynomials, 25:30851 (SU-1206-240)
BLANC, Gene A., State role in thermal power plant siting, 25:31525 (NP-18770)
BLANDINO, G., Indium-113m DTPA brain scanning in diagnosis of expansive processes, 25:29583
BLANKENBECLER, R., Scattering and pair production from the deuteron at large momentum transfers, 25:30910
BLEWETT, Patrick J., Stress calculations in MAGEE difference form, 25:31700 (LA-4601)
BLOMSTER, K., Wetting problems in connection with sintering, 25:29954
BLOSSER, H., Proposed Michigan State Univ. transuranic accelerator facility, 25:31085
BLOSSER, H. G., Cyclotron beam pulser for particle time-of-flight experiments, 25:31116
Optimisation of the cyclotron central region for the nuclear physics user, 25:31111
BLUMKIN, S., Completion report: evaluation of the use of permselective membranes in the nuclear industry for removing radioactive xenon and krypton from various off-gas streams, 25:29317 (ORNL-4522)
BLYSKAVKA, A. A., Physical characteristics of critical assembly mockup of the BOR-reactor, 25:31632 (FEI-201)
BOBROVNIKOV, O. P., Risk estimation model in radiation accidents at Atomic Energy Station, 25:31530
BOCCHIERI, P., Rayleigh-Jeans law is incompatible with classical electrodynamics, 25:30936
BOCHKAREV, V. V., Production of radioisotopes in research reactors, 25:29275
BOECKER, B. B., Retention and distribution of ^{137}Cs in the beagle dog following inhalation of ^{137}Cs in fused montmorillonite clay particles, 25:29426 (LF-43, pp 79-81)
Some observations on the toxicity of beta-emitting radionuclides inhaled in fused clay particles, 25:29438 (LF-43, pp 197-204)
Toxicity of inhaled ^{144}Ce fused clay in beagle dogs. III, 25:29436 (LF-43, pp 183-7)
Toxicity of inhaled $^{144}CeCl_3$ in beagle dogs. IV, 25:29431 (LF-43, pp 128-36)
Toxicity of inhaled ^{90}Sr fused clay in beagle dogs. I, 25:29437 (LF-43, pp 188-96)
Toxicity of inhaled $^{90}SrCl_2$ in beagle dogs. IV, 25:29430 (LF-43, pp 123-7)
Toxicity of inhaled $^{91}YCl_3$ in beagle dogs. IV, 25:29432 (LF-43, pp 137-9)
Toxicity of injected ^{137}CsCl in the beagle dog. III, 25:29433 (LF-43, pp 140-5)
BOEHMER, Clifford B., Reusable nuclear shuttle, 25:31641
BOEHMER, H., Relation between radiation and fluctuation spectrum of turbulent plasma, 25:30510
BOENING, K., Stored energy release of solid argon after reactor irradiation at 4.6°K, 25:30660
BOERNER, W., Reduction of patient radiation burden in nuclear medicine through application of short-lived radionuclides, 25:29439
BOERSCH, H., Determination of population densities in a helium plasma by electron impact spectroscopy, 25:30481
BOESEBECK, K., Single pion production in π⁺p interactions at 8 and 16 GeV/c, 25:30891
BOESHAAR, Patricia C., Ohio radio sources in clusters of galaxies, 25:30120
BOETTGER, O., Acceleration of very heavy ions by means of a two-cyclotron facility, 25:31130
Design specifications for compact cyclotrons, 25:31141
Series combination of tandem and cyclotron, 25:31139
BOGATYREV, A. V., Protection of dogs from ionizing radiation by shielding bone marrow, 25:29658
Protective efficiency of radioprotectors, 25:29550
BOGDANOV, P. V., Basic design parameters of a small size isochronous cyclotron, 25:31143
BOGDANOVA, V. I., External beam monochromatization system in 2.4 m isochronous cyclotron at Kurchatov Atomic Energy Inst, 25:31118
BOGGS, J. E., Isotopic exchange study on thorium peroxide, 25:29089
BOHNENSTINGL, J., Nuclear fuel particles manufactured from a peroxide of uranium, 25:29801
BOICOURT, G. P., Design and installation of Scyllac, 25:30564 (EUR-4593, pp 227-39)
BOISCHOT, Andre, High-sensitivity solar radiospectrometry at Arecibo, 25:30159
BOISSERIE, J. M., Study of the properties of concrete and especially of creep under the effect of temperature, 25:30023 (EUR-4531, pp 267-324)
BOJOWALD, J., Emittance measurements at Juelich isochronous cyclotron, 25:31119
BOKROS, J. C., Irradiation behavior of isotropic carbons, 25:30015
BOLAND, T. J., Ultrasonic level monitor, 25:29393 (IN-1452)
BOLD, D., Development aspects of fast metal-contact solid-dielectric switches, 25:30578 (EUR-4593, pp 365-71)
BOLDEA, V., Application of phenomenological quasi-two-body model to π⁻p-interactions with strange particle production at p = 4 GeV/c, 25:30869 (JINR-P1-5706)
BOLDT, G., Thermal plasma from a standard intensity source in wavelength range 1100 to 3100 A, 25:30486
BOLLER, E. F., Genetic control of Rhagoletis cerasi, 25:29741
Sterile-insect release method against Rhagoletis cerasi, 25:29742
BOLLINGER, L. D., Relation between radiation and fluctuation spectrum of turbulent plasma, 25:30510
BOLOTOVSKII, B. M., Dirac monopole: introductory paper, 25:30771 (BNL-tr-410)
BOLSTERLI, M., Self-consistent method for interactions mediated by fields, 25:30831
BOMBIK, A., Tables of magnetic structures determined by neutron diffraction. II, 25:30664 (NP-18783)
BONANNO, N., Indium-113m DTPA brain scanning in diagnosis of expansive processes, 25:29583
BONAZZOLA, L., ESR spectrum of γ-irradiated adamantane, 25:29139
BONBRIGHT, Daniel Irving, Deuteron breakup by 78 MeV alpha particles, 25:31189
BONDARENKO, V. V., Physical characteristics of critical assembly mockup of the BOR-reactor, 25:31632 (FEI-201)
BONETTI, Alberto, Infrared radiation and cold matter in universe, 25:30227
BONHAM, R. A., Infinite-channel close-coupling approximation in the second Born approximation. II, 25:30280
BONNIN, Test of ring of prestressed concrete in high-resistance sheet-metal steel, 25:30028 (EUR-4531, pp 445-76)
BONOMETTO, S. A., Transparency of extragalactic space to very-high-energy photons, 25:30792
BOOTH, N. E., Polarization in backward π⁺p elastic scattering at 6 GeV/c, 25:30740
BORCHKHADZE, T. M., Problem of applying the model of a normal logarithmic spiral to galaxies, 25:30190
BORGSTEDT, Hans Ulrich, X-ray diffraction investigations on internal oxidation zones in sodium-corroded vanadium--titanium alloys, 25:29781
BORISENKO, A. G., Slowing down of an ion beam in a plasma during ion-acoustic instability, 25:30511
BORISOV, D. G., Impulse generator for feeding a linear accelerator, 25:31066
BORISOV, V. S., Mass-spectrometric measurements of the diminution of hydrogen in polyethylene targets which have been irradiated in a proton synchrotron, 25:29400
BORNSHTEIN, I. M., Average energy of electrons scattered inelastically from solids, 25:30260
BORONKAY, S., Simple cryostat for thermoluminescence measurements, 25:30444
BOROUJERDI, Abbasali, Phase equilibria in the systems UO_2--UO_3--$NdO_{1.5}$ and $NpO/2+x/$--$NdO_{1.5}$, 25:29977 (KFK-1330)
BORS, Jerzy, Profile distribution of ^{90}Sr in soils of Lower Silesia, 25:29207
BORS, W., Gamma-radiolysis of aqueous solutions of 5-bromo-2'-deoxyuridine in presence of O. I, 25:29135
Gamma-radiolysis of aqueous solutions of 5-bromo-2'-deoxyuridine in presence of O. II, 25:29136
BORTOLOZZO, G., Infrared studies on coordination influence of UO_2^{2+} group on P--O bond of triphenyl phosphine oxide, 25:29088
BOSE, R. N., Occurrence of radioactive allanite, 25:29226
BOSE, S., Cytogenetic effects of x rays and chemicals on tomato, 25:29493
X-ray and diethyl sulfate induced mutation in rice, 25:29495
BOSE, T. K., Magnetofluiddynamic heat transfer, 25:30341 (NAL-TN-6)
BOSER, O., Temperature dependence of the flow-stress of heavily-deformed doped tungsten, 25:29874
BOSTANDZHYAN, N. Kh., Measurement of the momentum of the accompanying particles at short distances from a high-energy nuclear-active particle, 25:29377
BOUCHEY, G. D., Optimization of nuclear systems by geometric programming, 25:31649
BOUGAREL, M. P., Status report on Alice project, 25:31149
BOUGHN, S. P., Isotropy of the microwave background at 8-millimeter wavelength, 25:30228
BOULWARE, David G., Strict conformal symmetry, 25:30984
BOURENE, M., Measurement of radiative lifetimes of $CO_2^+(A^2\Pi_1/sub\ u/)$, $CO_2^+(B^2\Sigma/sub\ u/^+)$, $CH(A^2\Delta)$ and $CO(C^1\Sigma^+)$ by pulsed radiolysis, 25:30273 (ANL-Trans-879)
BOURGAREL, M. P., Injection and stripping of heavy ion beam in Orsay cyclotron, 25:31150
BOURLAND, P. D., Bragg-rule applicability to stopping cross sections of gases for α particles of energy 0.3 to 2.0 MeV, 25:30642
BOWDEN, Drummond H., Radiation survival: improved rates following chlortetracycline administration, 25:29561
BOWEN, H. J. M., Determination of calcium by radiochemical

XUM

replacement, 25:28987
BOWERS, R., Prog. rpt. on solid state physics; magnetic phenomena, 1/--12/70, 25:30646 (NYO-2150-66)
Study of the transverse magnetoresistance of polycrystalline potassium, 25:31767 (NYO-2150-68)
BOWMAN, A. L., Crystal structure of Th_3N_4, 25:29986
BOYD, H. A., Preparation of aerosols of thulium and americium by thermal degradation, 25:29078 (LF-43, pp 25-30)
Retention and distribution of ^{244}Cm following inhalation of $^{244}CmCl_3$ and $^{244}CmO_1$, by beagle dogs, 25:29429 (LF-43, pp 100-5)
BOYD, R. N., Nuclear matter radii in the tin isotopes, 25:31341
BOZHKO, V. P., Angular correlation of 345 to 136 keV cascade in ^{181}Ta, 25:31321
BRACKIN, Robert B., Molybdenum, 25:29805
BRADING, K. F., Deflection measurement techniques, 25:29301
Elastic and ultimate pressure tests on one tenth scale model of Dungeness B concrete pressure vessel, 25:29311
BRADLEY, Muriel V., Cytological effects of irradiated sucrose, 25:29494
BRADLEY, Wayne E., Vertical distribution of tritium in water vapor in the lower troposphere, 25:29215
BRAGINA, A. N., Effect of a mixture of uranium fission products on the sanitary conditions and hydrobionts of weakly-mineralized fresh-water basins, 25:29449
BRAICOVICH, L., Experimental evidence of helicity effect on the energy-loss straggling of electrons, 25:30644
BRALEY, R. C., Inelastic transition densities, 25:31418
BRAND, U., High-Q capacitors with liquid and gas impregnation, 25:30595 (EUR-4593, pp 545-50)
BRANDES, K., Numerical calculation methods for prestressed concrete reactor pressure vessels, 25:31666 (EUR-4531, pp 759-76)
BRANDT, Siegmund, Experimental problems in the photoproduction of several hadrons, 25:30716
BRANSCOMB, T. M., Improved thermal diffusivity method applied to TiB_2, ZrB_2, and HfB_2 from 200 to 1300°C, 25:29956
BRANSOME, E. D. Jr., Liquid scintillation counting of (^3H) and (^{14}C) on solid supports: a warning, 25:28985
BRAT, Satya, Syntheses of phyllitic minerals: their utilization in radioactive waste treatment. II, 25:29175 (BARC-509)
BRAUN, H., Observation of d^* effect in anti pd + p anti p π^+ π^-n reaction at 5.55 GeV/c, 25:30727 (NP-18796)
BRAUN, M. A., S-matrix for field theory with Lagrangian depending on derivatives, 25:30968
BRAUNSFURTH, J., g-factor of the 181 keV level of ^{99}Tc, 25:31271
BRAVIN, A. V., Energy spectrum and deformation of some even--even nuclei, 25:31411
BRAY, K. H., Elastic scattering of protons from ^{40}Ca at 21.0, 23.5, 26.3, and 48.0 MeV, 25:31295
BRAZIER, David W., γ radiolysis of liquids at high pressures. X, 25:29157
BRECHNA, H., Developments in cryogenic and superconducting magnets, 25:31040 (KFK-1316)
BREDIG, M. A., Enthalpy of La chlorides, bromides, and iodides from 298 to 1300°K, 25:29951
BREDOV, M. M., Proton flux from 1.5 to 50 MeV on satellites Zond-4 and Zond-5, 25:30164
BREEZE, E. W., Solid state relationships in the system U--Te--C, 25:30001
BREHM, W. F., Radioactivity in FFTF closed loops, 25:31627 (BNWL-585)
BREINHORST, Robert A., Variation of the light curve of W Ursae Majoris, 25:30100
BREIT, E., Toroidal version of the Isar I theta-pinch experiment, 25:30585 (EUR-4593, pp 419-24)
BREIZMAN, B. N., Quasilinear relaxation of an ultrarelativistic electron beam in a plasma, 25:30534
BREMER, F., Fracture behavior of concrete in a multiaxial stress field, 25:30025 (EUR-4531, pp 385-407)
Practice with model techniques, 25:29300
BRESHEARS, W. D., Vibrational energy transfer in shock-heated N_2--HI and N_2--DI mixtures, 25:29067
BRESTOVITSKAYA, I. Ya., Excretion of glucocorticoids and their metabolites in persons working with sources of ionizing radiation, 25:29706
BRETT, N. H., Solid state relationships in the system U--Te--C, 25:30001
BREWER, George R., Ion propulsion, 25:30453
BREWER, Leo, Dissociation energies and free energy functions of gaseous monoxides, 25:29082
BREWER, Peter G., Analytical methods in oceanography. I. Inorganic methods, 25:28921
BREY, Wallace S. Jr., Electron paramagnetic resonance studies of carbon monoxide adsorbed on thorium oxide, 25:29090
BRIAND, Jean-Pierre, Electron capture disintegration of ^{230}Pa, 25:31339
BRIGGS, A., Heat and radiation resistance and recovery of spores of Bacillus, 25:29558
BRILKA, R., Application of inductive energy storage systems for production of intense magnetic fields, 25:30561 (EUR-4593, pp 197-203)
BRILL, O. D., Analogous states of T = 2 in $^{26}Mg(^3He,n)^{28}Si$, $^{46}Ti(^3He,n)^{48}Cr$, and $^{58}Ni(^3He,n)^{60}Zn$ reactions, 25:31237 (IAE-1958)
BRINK, L., Dashen--Weinstein theorem in K/sub 13/ decay, 25:30816
BRINKMAN, U. A. Th., Chromatographic techniques using liquid anion exchangers. V, 25:29186
BRISCOE, G. B., Substoichiometric determination of traces of palladium by radioactive isotope-dilution analysis, 25:28981
BROCK, R. D., Early-flowering mutants of Medicago polymorpha var. polymorpha, 25:29488
BROCKLEHURST, J. E., Effects of reactor radiation on concrete, 25:30022 (EUR-4531, pp 237-65)
BRODT, F., β--γ correlation measurement in ^{72}Ga, 25:31297
BROGLIA, R. A., Effect of the multipole pairing and particle-hole fields in the particle-vibration coupling of ^{209}Pb: I, 25:31309 (LA-DC-11648)
BROMAGE, G. E., Diffuse interstellar features in the spectrum of the most heavily reddened star, 25:30069
BROMAN, Lars, Reaction $^{45}Sc(^3He,d)^{46}Ti$, 25:31278
BRONISZ, S. E., Alpha particle irradiation damage in ThO_2, 25:30012
BROOKS, A. L., Production of chromosome aberrations by ^{241}Am in the Chinese hamster liver, 25:29482 (LF-43, pp 240-5)
Relative biological effectiveness of ^{241}Am, ^{144}Ce, and ^{60}Co on the production of metaphase chromosome aberrations in the Chinese hamster liver, 25:29483 (LF-43, pp 246-53)
BROOKS, C. R., Prog. rpt. on application of adiabatic calorimetry of metal systems, 1969--70, 25:31716 (ORO-3291-14)
BROOKSBANK, R. E., Mound assistance program: development of a sol-gel process and equipment for production of dense $^{238}PuO_2$ microspheres, 25:29921 (ORNL-4565)
BROSCHE, D., Emergency core cooling, 25:31579 (MRR-79)
BROSSARD, M., Use of semiconductor telescopes for detecting the recoil nuclei in proton-light nucleus coherent scattering at high energy, 25:31185 (LYCEN-7085)
BROTZEN, F. R., Asymmetric mechanical properties of molybdenum--rhenium alloy single crystals, 25:29829
BROUT, R., Local duality and conserved currents, 25:30855
BROWN, A., Influence of oxide additions on the reduction of UO_3 and U_3O_8 as measured by DTA and TG, 25:29947
BROWN, C. L., Calculated critical parameters for fftf fuel under meltdown conditions, 25:31628 (BNWL-586)
FFTF criticality safety, 25:31629 (BNWL-587)
FFTF out-of-reactor criticality safety: objectives and criteria, 25:31626 (BNWL-576)
BROWN, James A., Effectiveness of pressor drugs in beagles exposed to mixed gamma-neutron radiations, 25:29565
BROWN, Lowell S., Strict conformal symmetry, 25:30984
BROWN, Randall E., Interrelationships of geologic formations and processes affecting ecology as exposed at Rattlesnake Springs, 25:31686 (BNWL-B-29)
BROWN, W. K., Calibration of Moxon--Rae detectors in the current mode, 25:29326 (LA-4445)
BROWN, Wilbur K., Particle collisions in opposing mass flow hypothesis, 25:30157 (LA-4343(Suppl.))
BRUNNE, M., Electrogasdynamic flow in ducts, 25:30339
BRUNSCH, A., Diffusion investigations in system Pd--Ta, 25:29893
BRUNSCH, Arwed, Diffusion in system Nb--Pd, 25:29881
BRUNTON, George, Crystal structure of CsU_6F_{22}, 25:30004
BRYANT, L. T., ARC system: one-dimensional transport theory capability, SNARC1D, 25:31651 (ANL-7717)
BRZOSKO, Jan S., Connection of radiation capture mechanism with the nuclear structure (A > 100), 25:31303 (INR-1271)
BUBEN, Mirka, Calcium and strontium metabolism as related to age and alginates, 25:29446
BUDARKOV, V. A., Egg laying of hens under action of incorporated ^{131}I, 25:29661
BUDDEN, K. G., Scintillation of extended radio sources when receiver has finite bandwidth. I, 25:30123
Scintillation of extended radio sources when receiver has finite bandwidth. II, 25:30124
BUDYASHOV, Yu. G., Charged particles produced in capture of negative muons by ^{28}Si, ^{32}S, ^{40}Ca, and ^{64}Cu nuclei, 25:31267
BUDZOL, Melvin, Radiation chemistry of polyethylene and poly(propylene oxide), 25:29144
BUFFEREAU, Michel, Study of impurities distribution in a metal (plutonium), 25:28516 (CEA-R-4071)
BUKETOV, E. A., Colorimetric determination of tellurium with sodium pyrosulfite, 25:28931
BUNKER, Carl M., Correlation of uranium, thorium, and potassium with aeroradioactivity in the Berea area, Virginia, 25:29235
BURBIDGE, E. Margaret, Is NGC 4569 a member of the Virgo cluster, 25:30207
BURDEN, R. A., Design and construction of a high-beta toroidal experimental assembly, 25:30586 (EUR-4593, pp 425-30)
Development aspects of fast metal-contact solid-dielectric switches, 25:30578 (EUR-4593, pp 365-71)
BURDET, Guy, Supermultiplet scheme for light nuclei, 25:31203 (LYCEN-7088)
BURGE, E. J., Elastic and inelastic scattering of 30 and 50 MeV polarized and unpolarized beams of protons by ^{40}Ar and ^{14}N, 25:31233
BURKERT, V., Electromagnetic form factors of the proton,

25:30786
BURMISTROV, V. R., Ge(Li) gamma spectrometer, 25:29357
γ rays accompanying decay of ^{109}In, 25:31320
BURRELL, David C., Fjords as sedimentary microcosms, 25:31724 (RLO-2229-T-1-3)
BURROW, R. E. D., Interaction between the design and construction of prestressed concrete pressure vessels for nuclear reactors, 25:31456 (EUR-4531, pp 129-44)
BURROWS, B. A., Clinical uses of radioisotopes, 25:29573
BURSON, Z. G., Radiation output description from the T(d,n)^{4}He reaction in a large target (1000 cm^2): Operation Henre, 25:31165 (CEX-65.04)
BURT, Robert W., Giant splenomegaly in sarcoidosis demonstrated by radionuclide scintiphotography, 25:29593
BURTON, G., Cyclotron beam sharing for multiple target irradiations, 25:31110
BURTON, Kenneth Shrum, Properties of ^{35}S and ^{57}Co nuclei, 25:31269
BUSCHOW, K. H. J., Crystal structure of two Th_2Fe_7-phases, 25:29898
BUSH, Charles A., Correlation of uranium, thorium, and potassium with aeroradioactivity in the Berea area, Virginia, 25:29235
BUSH, Karen, Deuterium effects on binding of reduced coenzyme alcohol dehydrogenase isoenzyme EE, 25:29056
BUSHLAND, R. C., Sterility principle for insect control. historical development and recent innovations, 25:29736
BUSTER, Dawn S., Protracted hepatic, splenic, and renal retention of ^{239}Pu in the beagle, 25:29451
BUSUOLI, G., Personal dosimetry of x- and gamma radiations, 25:29384
Protection of personnel in radioactive environment, 25:29529
BUTTNER, F. H., Columbium, 25:29807
BUTURLAKIN, M. S., Prophylactic influence of uv irradiation of ducklings under influence of x rays, 25:29647
BUXO, J., Behaviour of current MOS, 25:29412
BYALKO, A. V., Statistical analysis of gravitational instability, 25:30222
BYCHKOVSKAYA, N. B., Protective influence of adrenalin and acetylcholine in radiation sickness of mice, 25:29548
BYLINSKII, A. F., Cell division in Escherichia Coli during irradiation by neutrons of 200 keV, 25:29490

C

CACHON, Andre, Type-I variations in extensive air showers, 25:30331
CAIANIELLO, E. R., Self-consistent derivation of multiple mass values in renormalized field theories, 25:30986
CAILLOT, M., Photoconductivity studies of Li-doped Si irradiated with 1.5 MeV electrons, 25:30653
CAIOLA, Robert J., Melt strength and melt extensibility of irradiated linear polyethylene, 25:29099
CALAIS, Daniel, Determination of low solubility limits by measurement of diffusion coefficients, 25:29866
Diffusion and solubility of plutonium and uranium in aluminum, 25:29867
CALLAGHAN, Nathan R., Dental caries from radiation therapy, 25:29712
CALLAWAY, J., Algebraic close-coupling calculation of the scattering of electrons and positrons by hydrogen, 25:30286
CALLEAR, A. B., Deuterium isotope effects in attachment of Hg(6^3P_0) to ammonia, 25:29046
CALLIGAN III, J. H., Single and multiple field enabling system for television disc recording, 25:31699 (LA-4582)
CALOGERO, F., Hyperspherical-expansion approach to nuclear bound states. III, 25:31405
CALOI, V., Cosmological models with a G-variable gravitational theory, 25:30232
CALOW, C. A., Solid state bonding of nickel to alumina, 25:29815
CAMERA, V., Measuring of β and γ radioactivity in biological samples, 25:29517
CAMERON, A. G. W., Neutron-star models including the effects of hyperon formation, 25:30080
Nucleosynthesis in neutron-rich supernova ejecta, 25:30079
CAMERON, J. R., Characteristics of some TLD solid systems, 25:29382 (COO-1105-120)
CAMIDGE, F. Paul, Magnetic field perturbations in the magnetotail associated with polar magnetic substorms, 25:30403
CAMP, David C., Decays of ^{56}Co and ^{66}Ga, 25:31287
CAMPAGNA, P., Amplitude for N nonspurious excited particles in dual resonance models, 25:30830
CAMPBELL-ALLEN, D., Use of simplified models for the design of end slabs, 25:29304
CANADA, T. R., Angular distribution and excitation function of singlet deuteron in d(p,d)p reaction, 25:31196
High-resolution study of ^{92}Nb by (d,t) and (d,t γ) reactions, 25:31283
CANDES, P., Consequences of accidents in nuclear plants, 25:31622
CANESCHI, L., Isospin structure of the multiperipheral model and charge distributions, 25:30845
CANNON, Joseph G., Rare earths, 25:29809
CANTER, J., Search for K/sub S/ → $\pi^+\pi^-\pi^0$, 25:30723
CANUTO, V., Neutrino luminosity by the ordinary URCA process, 25:30081
Nuclear soft-core potential and cosmic-ray phenomena, 25:31431
CAPDEVIELLE, Jean-Noel, Type-I variations in extensive air showers, 25:30331
CAPLAN, H. S., Photoprotons from ^{12}C and ^{13}C, 25:31232
CAPPABIANCA, C., Non-destructive tests, 25:29295
CAPRI, A. Z., Regge trajectories for multichannel potential scattering, 25:31031
CAPRIOTTI, E. R., Observed small-scale structure in planetary nebulae, 25:30115
CARABAJAL, C. A., Embryological changes in irradiated eggs of Triatoma infestans, 25:29620
CARCAVALLO, R. U., Embryological changes in irradiated eggs of Triatoma infestans, 25:29620
CARDINALE, A., Studies on natural background radiation in Italy, 25:29205
CARDONA, Manuel, Superconductive supercooling and superheating of small cadmium spheres: size effects, 25:30428
CARDY, J. L., Extension of the eikonal approximation in quantum field theory, 25:30981
Reggeon calculus derived from the eikonal model, 25:30980
CARLSON, F., Experiences on the release of iodine from uranium dioxide fuel, 25:31607
CARLYLE, M., Distribution of fission products in a high temperature gas cooled reactor, 25:31567
CARON, J., Trapping of iodine and methyl iodide at high temperatures, 25:31612
CARPENTER, J. A., Viscoelastic analysis of irradiated graphite with variable creep coefficient, 25:29945 (ORNL-TM-3242)
CARPENTER, R. W., Transition morphology during hcp precipitation from beta-isomorphous alloys, 25:29886
CARRAT, H. G., Relations between structure of granite massifs and the distribution of uranium in the Morvan, 25:29239
CARRUTHERS, George R., Interstellar molecules, 25:30200
CARSWELL, G. P., Magnetic and mechanical hardness of $SmCo_5$ and $LaCo_5$, 25:29845
CARTER, K. W., Energy levels of ^{27}Si, 25:31252
CARTER, Leland L., MCNA: computer program to solve adjoint neutron transport equation, 25:31171 (LA-4488)
CARTER, W. L., Completion report: evaluation of the use of permselective membranes in the nuclear industry for removing radioactive xenon and krypton from various off-gas streams, 25:29317 (ORNL-4522)
CASON, J. L., Design and fabrication of a portable device for neutron radiography, 25:29286 (BNWL-1329)
CASSELTON, R. E. W., Electrical conduction and blackening in yttria-stabilized zirconia, 25:30684
CASSUTO, A., Kinetics and mechanism of low-pressure, high-temperature oxidation of Si. II, 25:29968
Kinetics and mechanism of low-pressure, high-temperature oxidation of W silicides. III, 25:29869
Low-pressure, high-temperature siliconizing of W. I, 25:29814
CASTEL, B., One-particle-hole and projected Hartree--Fock approximations in ^{12}C and ^{14}O, 25:31226
CASTELLANI, V., Induced semi-convection in He-burning horizontal-branch stars. II, 25:30103
Overshooting of convective cores in helium-burning horizontal-branch stars, 25:30037
CASTELLO, Gianrico, Gamma radiolysis of branched chain hydrocarbons: 2,2-dimethylbutane, 25:29142
CASTIGLIONI, M., Operational experience with H$^-$ beam of Milan cyclotron, 25:31125
CASTLE, R. T., Analytical descriptions of the nuclear weapon environment and effects, 25:29247
CASTOR, John I., Calculation of linear, nonadiabatic pulsations of stellar models, 25:30095
CAVALIERE, A., Gravitational waves and cosmology, 25:30240
CAVALLINI, A., Personal dosimetry of x- and gamma radiations, 25:29384
Protection of personnel in radioactive environment, 25:29529
CAVALLINI, Pierre, Excited metastable states of ^{93}Y, 25:31338
CAVALLORO, Raffaele, Population longevity in γ-irradiated Collembola, 25:29615
CAVERZASIO, C., Polarization in backward π$^+$p elastic scattering at 6 GeV/c, 25:30740
CECCHINI, S., Cosmic-ray microvariations during thunderstorm perturbations, 25:30334
CEKALOVA, B., Packing materials for γ-irradiated foodstuffs, 25:30033
CELLI, V., Inelastic surface scattering of nonpenetrating particles, 25:30659
CERNY, Joseph, Beta-delayed protons from ^{23}Al, 25:31241 (UCRL-20436)
Reactions ^{11}B(p,^{3}He)^{9}Be and ^{11}B(p,t)^{9}B, 25:31228
CERULUS, F., Liquid-drop model for high-energy elastic and inelastic scattering, 25:30901
CERVELLATI, R., High sensitivity berylometer, 25:29390 (RT/EL-(70)4)
CESBRON, Fabien, Roubaultite $Cu_2(UO_2)_3(OH)_{10}\cdot 4H_2O$, a new mineral species, 25:29238
CHAFFIN, R. J., Neutron damage effects in step recovery

diode frequency multipliers, 25:29409 (SC-RR-710188)
CHAIKOVSKII, V. G., Pulse delay time in ^{3}He neutron counters, 25:29338
CHAKRABORTY, B., Electromagnetic wave propagation through slowly varying plasma, 25:30608
CHALAPATI RAO, K. V., Particle-core coupling in the lead region, 25:31379
CHALOV, P. I., Determination of absolute age of Lake Balkhash on the basis of nonequilibrium U, 25:29210
CHANDRA, G., Positron lifetimes in rare earth oxides, 25:30272
CHANDRA, S., Subauroral red arc and the associated ionospheric phenomena, 25:30350 (N-70-36812)
CHANDRASEKHARAN, E. S., Recovery of Pm from fission product waste. III, 25:29176 (BARC-516)
CHANG, James J., Relaxation time measurements in electron paramagnetic resonance, 25:31744 (UCRL-19691)
CHANG, S. J., Viscoelastic analysis of irradiated graphite with variable creep coefficient, 25:29945 (ORNL-TM-3242)
CHANG, Sen-I, Systematic procedure for determining system parameters by performance index minimization, 25:31545 (ORNL-TM-3311)
CHANG, T. Y., Comparison of experimental results with response analysis for a model of a pressure vessel, 25:29313
CHAO, T. T., Gold content of natural waters in Colorado, 25:29015
CHAPUIS, Alain, Measurement of the state of equilibrium between radon and its daughters in the uranium mines, 25:29201 (AEC-tr-7228)
Particle size spectrum of the radioactive aerosols in a uranium mine, 25:29200 (AEC-tr-7227)
CHARAKHCH'YAN, A. N., Energy spectra of 11-year variations of cosmic-ray intensities on the rising solar-activity curve, 25:30310
Modulation of galactic cosmic rays and solar activity, 25:30322
CHARAKHCH'YAN, T. N., Energy spectra of 11-year variations of cosmic-ray intensities on the rising solar-activity curve, 25:30310
Modulation of galactic cosmic rays and solar activity, 25:30322
Role of heliographic latitude of spots in 11-year modulation of galactic cosmic rays, 25:30309
CHARALAMBUS, S., Nuclear γ-rays following muon capture, 25:31258
Nuclear transmutation by negative stopped muons and the activity induced by the cosmic-ray muons, 25:31448
CHARAMATHIEU, A., Trapping of iodine and methyl iodide at high temperatures, 25:31612
CHARVET, A., Decay scheme of 1.3 h. ^{179}Ta, 25:31310 (LYCEN-7084)
CHASAN, David E., Infrared determination of barium, strontium, and calcium carbonates, singly and together, by the pellet technique, 25:28972
CHATRCHYAN, A. M., Charged particles produced in capture of negative muons by ^{28}Si, ^{32}S, ^{40}Ca, and ^{64}Cu nuclei, 25:31267
CHATTERJI, S. M., Feasibility of controlling stored grain pests by the sterile-male technique, 25:29750
CHAUDHRI, M. Anwar, Design specifications for compact cyclotrons, 25:31141
CHEBOTAREV, L. N., Inactivation of enzymes of Botrytis cinerea by uv rays, 25:29720
CHECHKIN, V. V., Turbulent heating of a plasma by a large amplitude whistler, 25:30470
CHEKHOVSKOI, V. Ya., Enthalpy measurements by drop calorimetry using electromagnetic levitation, 25:29875
Formation energy and concentration of vacancies in Mo, 25:29858
CHEN, C. M., Stress corrosion cracking of Ti--8Al--1Mo--1V alloy: aqueous and methanol environments, 25:29765
CHEN, H. H., Possible CP violation in $K^{+-} \to \pi^{+-}\gamma\gamma$, 25:30928
CHEN, T. S., Daily fluctuations of radioactive fallout particles in ground-level air, 25:29219
Worldwide movement of fallout particles from nuclear explosions, 25:29216
CHENEBAULT, P., Instantaneous release of short period fission gases in fuel pins, 25:31606
CHENG, L. J., Photoconductivity in p-type silicon irradiated with 1.2-MeV electrons at approximately 15°K, 25:30658
CHENG, Wen-kwei, Presence of noncanceling seagull and Schwinger terms in weak (nucleon + nucleon + vector-meson) amplitudes, 25:30931
CHEPURNOV, V. A., Density distribution of deformed nucleus in the model of independent particles, 25:31437
CHERDYNTSEV, V. V., Superheavy nuclei in the cosmos, 25:30304
CHEREDEEV, A. N., Resistance to irradiation by immunocompetent and hematogenic tissue in mice, 25:29677
CHERKI, M., Photoconductivity studies of Li-doped Si irradiated with 1.5 MeV electrons, 25:30653
CHERMENSKAYA, N. F., Influence of Cr and Mo on electrochemical and corrosion resistance of Ni--Cr--Mo alloys, 25:29777
CHERNYSHEV, A. M., Effect of radiation on oxygen electrode performance, 25:29098
CHERNYSHOV, A. A., Neutron thermalization in H_2C at 318°K and 77°K, 25:31170 (KAPL-Trans-4)
CHERRY, C. P., Effects of irradiation on salivary glands, 25:29693
CHERTKOV, A. A., Investigation of the diffusion of hydrogen of hydrides of alloys, 25:29837
CHERTOK, R. J., Availability in the dog of radionuclides in nuclear debris from Plowshare excavation Cabriolet, 25:29456
CHERY, R., Decay scheme of 1.3 h. ^{179}Ta, 25:31310 (LYCEN-7084)
CHEVALLIER, Pierre, Electron capture disintegration of ^{230}Pa, 25:31339
CHEVARIER, A., Mean recoil, isomer ratio, and excitation functions for reactions induced by alpha particles in rubidium, 25:31239 (LYCEN-7091)
Reactions induced in gold by deuterons with energies between 10 and 70 MeV, 25:31311 (LYCEN-7092)
CHEVARIER, Noelle, Mean recoil, isomer ratio, and excitation functions for reactions induced by alpha particles in rubidium, 25:31239 (LYCEN-7091)
Reactions induced in gold by deuterons with energies between 10 and 70 MeV, 25:31311 (LYCEN-7092)
CHIANG, Chwan-kang, Elastic scattering of 1.33-MeV photons from lead and uranium, 25:31370
CHIFFELLE, T. L., Effect of the inhalation of ^{144}Ce in relatively insoluble forms on influenza virus infection in mice, 25:29724 (LF-43, pp 254-62)
Toxicity of inhaled ^{144}Ce fused clay in beagle dogs. III, 25:29436 (LF-43, pp 183-7)
Toxicity of inhaled $^{144}CeCl_3$ in beagle dogs. IV, 25:29431 (LF-43, pp 128-36)
Toxicity of inhaled $^{90}SrCl_2$ in beagle dogs. IV, 25:29430 (LF-43, pp 123-7)
Toxicity of inhaled ^{90}Y fused clay in beagle dogs. II, 25:29434 (LF-43, pp 146-62)
Toxicity of injected ^{137}CsCl in the beagle dog. III, 25:29433 (LF-43, pp 140-5)
CHILDS, R. L., Design of asymmetric 4 π shields for space reactors, 25:31640 (ORNL-TM-3368)
CHIMENTI, R. A., Dissolution of small radioactive particles, 25:29080 (LF-43, pp 40-51)
CHIS, Gheorghe, Photometric elements of short-period cepheid WZ Bootis, 25:30104
CHISTOV, N. A., Apparatus for the automatic accumulation (storage) and analysis of information in experiments with the synchrocyclotron, 25:31070
CHITRE, S. M., Solar-cycle theory of pulsars, 25:30131
CHIU, Hong-yee, Automated and conventional photometry of the short-period variable star 14 Aurigae, 25:30086
CHO, Y., Double-Regge-pole description of reaction K⁻n → K⁻π⁻p at 5.5 GeV/c, 25:30747
Search for K/sub S/ → π⁺π⁻π⁰, 25:30723
CHODURA, R., Vlasov description of a supercritical magneto-acoustic compression pulse, 25:30513 (IPP-1/113)
CHOMICKI, O. A., Attempt to use /sup 99m/Tc for scintiscanning of salivary glands, 25:29574
CHONG, K. F., Binding energy of /sub Λ/^{5}He with two-channel separable potentials, 25:30897
CHOPPIN, G. R., Users' guides for radioactivity standards, 25:29174
CHORUZYI, S. S., Some topics in axiomatic nonrenormalizable field theory, 25:30942
CHOU, C. K., Neutrino luminosity by the ordinary URCA process, 25:30081
CHOU, Chih Kang, Proton--proton reaction and related reactions in an intense magnetic field, 25:30050
CHOUAN, Y., Microwave devices using the proximity effect between superconducting and normal metals, 25:30446
CHOW, Tai-low, High-velocity cloud collisions, 25:30198
CHRIST, N. H., Method for computing scattering matrix elements in a class of non-renormalizable field theories, 25:31016 (NYO-1932(2)-192)
CHRISTENSEN, W. R., Some toxicity aspects of internally deposited ^{239}Pu, 25:29627
CHRISTIAN, Gary D., Potentiometric studies with an ion permselective membrane, 25:28956
CHRISTIANSEN, Wayne, Multiple explosions in radio galaxies and heating of the intergalactic medium, 25:30218
CHRISTIANSON, Gene A., X rays in healing arts in North Dakota, 1964--1968, 25:29542
CHU, C. W., Superconductivity of Re--Os, Re--Ru, Ru--Os, and Re--W hcp alloy systems and slightly doped Re, 25:30433
CHU, Norton Y., Plutonium determination in soil by leaching and ion-exchange separation, 25:28992
CHUADZE, A. D., Supernova in NGC 3389, 25:30057
CHUBAROV, L. B., Effects of neutron irradiation on phase transformations of Li_2O--MgO--Al_2O_3--SiO_2 systems, 25:30017
CHU-KIT, Marcel, Observation of interstellar calcium in Norma constellation, 25:30193
CHUNG, Kyu Hoi, Insect pest control using sterile-male technique. II, 25:29731
CHUPP, W. W., ERA 4-MeV injector, 25:31053 (UCRL-20174)
CHURILOV, G. E., Mixing of uhf signals from superconducting tin film-, 25:30436
CHURIN, I. N., Timing with Ge(Li)-detector, 25:29353 (JINR-P13-5708)
CHUZHINOV, V. A., Mass-diffusion mercury columns for isotope separation, 25:29277
CIATTI, F., New helium-weak stars in the I Orion

association, 25:30049
CIGNA ROSSI, L., Ecological site survey at Trisaia, 25:29479
CIZERON, Georges, Demonstration by anisothermal creep of superductile structural state during recrystallization of α U, 25:29851
CLARK, A. H., Zero-point average structure of Cl dioxide, 25:29052
CLARK, D. H., Fast correlation method for studying drifting patterns associated with ionospheric irregularities, 25:30402
CLARKE, A. R., Search for antimatter in primary cosmic rays, 25:30327
CLAUSEN, R., Machining with a plasma jet, 25:31753 (UCRL-Trans-10524)
CLAUSER, H. R., Beryllium: promise and problems, 25:29836
CLAYTON, Donald D., Explosive nucleosynthesis in helium zones, 25:30067
CLEGG, T. B., Polarization measurements and phase shifts for p-^{4}He scattering, 25:31199
CLEMENT, J. D., Thermal radiation absorption by particle-seeded gases, 25:29270
CLEMENT, Maurice J., Behavior of the angular velocity near the surfaces of stars with radiative envelopes, 25:30088
CLEMENTE, D. A., Infrared studies on coordination influence of UO_2^{2+} group on P--O bond of triphenyl phosphine oxide, 25:29088
CLERC, M., Measurement of radiative lifetimes of $CO_2^+(A^2PI/sub\ u/)$, $CO_2^+(B^2\Sigma/sub\ u/^+)$, $CH(A^2\Delta)$ and $CO(C^1\Sigma^+)$ by pulsed radiolysis, 25:30273 (ANL-Trans-879)
CLERC, Michel, Absorption oscillogram of $CO_2^+(X^2PI/sub\ g/)$ and $N_2^+(X^2\Sigma/sub\ g/^+)$ ions in their ground state produced by pulsed radiolysis of CO_2 and N_2, 25:30274 (ANL-Trans-881)
CLINARD, F. W. Jr., Strain effects and spalling in alpha-bombarded ThO_2, 25:30014
CLOTH, P., Dense plasma focus as a neutron source for pulsed measurements in a blanket, 25:30592 (EUR-4593, pp 525-31)
CLOUGH, W. S., Behavior of barium and strontium fission products in liquid sodium, 25:31614
COAD, J. P., LMM Auger spectra of some transition metals of first series, 25:31682 (AERE-R-6719)
COAST, Geoffrey, Nuclear reactors, 25:31565
COCHAVI, S., Experimental study of electromagnetic matrix elements in ^{92}Mo, 25:31372
Recoil-distance lifetime measurements for states in ^{30}P, 25:31279
COCHAVI, Saadia, Experimental electromagnetic matrix elements in the nuclear mass-90 region, 25:31349
COCHE, Andre, Semiconductor detectors, 25:29333
COETZEE, N., Low-lying states of ^{127}I, 25:31352
COHEN, B. L., Angular distribution and excitation function of singlet deuteron in d(p,d)p reaction, 25:31196
COHEN, Edward P., Separation by polyacrylamide gel electrophoresis of RNA from the spleens of immunized mice, 25:29476
COHEN, H., Omega-meson in rho--π system, 25:30858
COHEN, Jeffrey M., Neutron-star models including the effects of hyperon formation, 25:30080
Pulsar electrodynamics, 25:30154
COHEN, R., Design studies for an ultra-thin septum extraction channel for modified NEVIS synchrocyclotron, 25:31106
Nevis synchrocyclotron conversion project, 25:31155
COHN, C. E., Instrumentation systems to protect LMFBR core integrity, 25:31574 (ANL-7793)
COHN, Stanton H., Pharmacokinetics of halothane in man, 25:29416
COIANTE, D., Optimization of energy resolution in nuclear spectrometry measurements with germanium detectors, 25:29356 (RT/EL-(70)5)
COKER, W. R., Reaction ^{208}Pb(p,α)^{205}Tl at 16.475 MeV, 25:31383
COLA, Mario, Mixed oxides of Tb--Ce, Tb--Th, and Tb--Gd, 25:30007
COLBURN, D. S., Magnetic observations of the lunar cavity, 25:30388
COLE, H. C., Plasma heating by neutral injection in a stellarator reactor, 25:30455 (EUR-4593, pp 479-84)
COLE, L. J., Radiation carcinogenesis: experimental and clinical aspects, 25:29691
COLEMAN, P. J. Jr., Satellite observations of band-limited micropulsations during a magnetospheric substorm, 25:30369
COLEMAN, Paul J. Jr., North--south component of the interplantary magnetic field, 25:30176
COLEMAN, Thomas Patrick, Model analyses of elementary particle scattering amplitudes, 25:30751 (IS-T-426)
COLES, R. E., Elastic and inelastic scattering of neutrons in the energy range 1.0 to 5.0 MeV by natural Mo, 25:31299 (AWRE-O-89/70)
COLGATE, Stirling A., Coherent emission from expanding supernova shells, 25:30068
COLLAS, P., High energy astrophysics, 25:30220 (P-4494(RAND))
COLLINA, R., Equal-time commutators and Bjorken's theorem, 25:30973
COLLINS, E., Graphs for analysis of (1-3) gamma--gamma directional correlations, 25:31312 (ORNL-4619)
COLLINS, H. Dale, Various holographic scanning configurations for under-sodium viewing, 25:31685 (BNWL-1558)
COLLINS, R. E., Differential spin exchange and elastic scattering of low-energy electrons by potassium, 25:30282
COLLOT, Jean, Demonstration by anisothermal creep of superductile structural state during recrystallization of α U, 25:29851
COLOMB, H. O. Jr., Convertible polymers for radiation processing, 25:29124
COMBE, J., Use of semiconductor telescopes for detecting the recoil nuclei in proton-light nucleus coherent scattering at high energy, 25:31185 (LYCEN-7085)
COMBES, J. M., Lorentz analysis of dual-resonance models in operator formalism, 25:30829
COMBET, H. A., Microwave devices using the proximity effect between superconducting and normal metals, 25:30446
COM-NOUGUE, Jacques, Observation of age hardening of α-zirconium after deformation, 25:29853
COMOROSAN, S., Oscillatory behavior of enzymic reactions, 25:29461
COMPTON, R. N., Collisional ionization between cesium and selected molecules, 25:30276 (ORNL-TM-2620)
COMTAT, Maurice, Electrochemical oxidation of sulfur dioxide on a platinum electrode, 25:31754 (UCRL-Trans-10525)
CONANT, John F., Measurement of delayed-neutron fractions for thermal fission of ^{235}U, ^{239}Pu, and ^{233}U, 25:31334
CONARD, B. R., Zirconium--sulfur system at high temperatures, 25:29990
CONFORTI, P., Indium-113m DTPA brain scanning in diagnosis of expansive processes, 25:29583
CONGDON, C. C., Bone marrow transplantation, 25:29560
CONNOR, J. H., Deuterium isotope effects in attachment of $Hg(6^3P_0)$ to ammonia, 25:29046
CONRAD, Edward Ezra, Radiation-induced electrical conductance in liquid n-hexane and neohexane, 25:29097
CONRADS, H., Dense plasma focus as a neutron source for pulsed measurements in a blanket, 25:30592 (EUR-4593, pp 525-31)
CONTE, G., Radioactive isotopes and thermographic findings in bone localizations of systemic diseases, 25:29588
Scintigraphic and thermographic detection of bone metastases, 25:29589
CONWAY, J. B., Creep-rupture data for the refractory metals to high temperatures, 25:29868
COOK, G. B., Determination of trace amounts of gold in natural sweet waters by nondestructive activation analysis after preconcentration, 25:29014
COOPER, Benjamin S., Calculation of odd-parity states in ^{12}C and ^{16}O, 25:31230
COOPER, M. H., Radiochemical determination of barium diffusion coefficients in liquid sodium, 25:31613
COOPER, M. Y., Detection and measurement of weak histoincompatibilities by transfer of mouse peritoneal exudate cells, 25:31718 (ORO-3634-12)
COOPER, Margaret Y., Serological detection of the male limited H--Y antigen on peritoneal exudate cells, 25:31719 (ORO-3634-13)
COOTE, G. E., Decay of 3.696 MeV level in ^{28}Al, 25:31266
COPPI, B., High-frequency instability and anomalous plasma resistivity at supercritical electric fields, 25:30625
CORBEL, J., Study of the properties of concrete and especially of creep under the effect of temperature, 25:30023 (EUR-4531, pp 267-324)
CORDERO, P., Search for quantum systems with given spectrum-generating algebra, 25:30918
CORNISH, D. N., Superconducting Levitron, 25:30558 (EUR-4593, pp 133-9)
CORRIGAN, K. W., Proton polarization in ^{16}O(p,p)^{16}O and states in ^{17}F, 25:31236
CORRY, Janet E. L., Resistance to heat and γ radiation in Salmonella, 25:29557
COSLER, A., High-Q capacitors with liquid and gas impregnation, 25:30595 (EUR-4593, pp 545-50)
COSTAZ, J. L., First results of putting into service the St. Laurent I prestressed concrete pressure vessel, 25:31455 (EUR-4531, pp 95-128)
COSTES, D., Problems and prospects of prestressed concrete vessels: French experience up to 1970, 25:31557 (IAEA-126, pp 69-83)
Study of behavior of concrete subjected to triaxial stresses, 25:30027 (EUR-4531, pp 417-24)
COUCH, G. Robert, Zirconium--hafnium, 25:29808
COULSON, Larry Vernon, Charged particle emission following pion capture in nuclei, 25:31213
COUPLAND, J. R., Production of high-current, high-quality beams of ions and neutral particles, 25:30256 (EUR-4593, pp 75-81)
COURTES, G., Evidence and velocity of a density wave in the galaxy M33, 25:30201
COURTNEY, W. J., Reaction ^{208}Pb(p,α)^{205}Tl at 16.475 MeV, 25:31383
COUTANT, C. C., Experimental drifts of juvenile salmonids through effluent discharges at Hanford. II, 25:31645 (BNWL-1527)
COUTANT, Charles C., Biological aspects of thermal pollution. I. Entrainment and discharge canal effects, 25:31527
COWAN, Victor Michael, Absolute intensities and pressure

effects in the infrared fundamental bands of methane and its deuterated species, 25:29045
COWLEY, Anne P., CV Serpentis, 25:30043
COWLEY, Charles R., Calculations of Van Der Waals broadening for lines of astrophysical interest, 25:30266
COX, C. M., Development of FBR oxide fuels, 25:29922 (ORNL-4630, pp 3-58)
COZZA, Alberto, Dangers of ionizing radiations in naval nuclear propulsion, 25:31644
CRABBE, P. A., Metabolism of different immunoglobulin classes in irradiated mice. V, 25:29473
CRACKNELL, Arthur P., Fermi surface. II, 25:30681
CRADDOCK, M. K., Beam quality and expected energy resolution from TRIUMF cyclotron, 25:31088
H⁻ ion injection into central region of TRIUMF cyclotron, 25:31152
CRAWFORD, E. J., Early-flowering mutants of Medicago polymorpha var. polymorpha, 25:29488
CRAWFORD, R. L., Electroproduction of P_{33} resonance, 25:30801
CREVIER, W. F., Thermalization in the Earth's bow shock, 25:30365
CROATTO, U., Infrared studies on coordination influence of UO_2^{2+} group on P--O bond of triphenyl phosphine oxide, 25:29088
CROMWELL, R. H., Observed small-scale structure in planetary nebulae, 25:30115
CROOK, F. M., Effects of high energy radiation on pulping of Eucalypts, 25:29735
CROOKS, Michael J., Temperature differences and mutual friction in He II near T/sub lambda/, 25:30405
CSIZMADIA, I. G., Distribution of reaction products (theory). VII, 25:29058
CUDDIHY, R. G., Application of a biological model of tissue distribution and retention of inhaled ^{140}La in beagle dogs to an analysis of radiological hazards to humans inhaling various isotopes of lanthanum, 25:29427 (LF-43, pp 82-91)
Removal of relatively soluble ^{144}Ce from the lungs of beagle dogs: intravenous administration of a DTPA solution, 25:29543 (LF-43, pp 280-5)
Some observations on the toxicity of beta-emitting radionuclides inhaled in fused clay particles, 25:29438 (LF-43, pp 197-204)
Tissue distribution and retention of ^{140}Ba and ^{140}La in beagle dogs after inhalation of $BaCl_2$--$LaCl_3$ aerosols, 25:29428 (LF-43, pp 92-9)
Toxicity of inhaled ^{91}Y fused clay in beagle dogs. I, 25:29435 (LF-43, pp 163-70)
CUISANCE, D., Techniques for labelling tsetse flies with radioisotopes, 25:29417
CUMMINS, J. D., Parameter fittings of a nuclear reactor mathematical model in the frequency domain with alternative forms of weighting function, 25:31650 (AEEW-M-1012)
CURTIS, L. J., Lifetimes of some doubly excited levels in neutral helium, 25:30265
CZEIZEL, Endre, Chromosomal examinations in radiologists, 25:29501
CZERWIK, Z., Radiothermoluminescence of crystalline and glassy methanol, 25:29101
CZYZEWSKI, Tomasz, Transmission surface-barrier silicon detectors, 25:29331

D

DABBOUSI, Osama B., Nuclear spins of ^{125}Cs and ^{136}Cs, hyperfine-structure separation and nuclear magnetic moment of ^{125}Cs, ^{127}Cs, and ^{136}Cs, 25:31376
DABOUL, Jamil, Symmetry properties, tests, and reduction of crossing matrix, 25:31018
DADHICH, Naresh, Generalized field equations in general relativity, 25:31004
DAEHNICK, W. W., High-resolution study of ^{92}Nb by (d,t) and (d,t γ) reactions, 25:31283
DAENNER, W., Comparison of different fusion reactor blanket systems, 25:30591 (EUR-4593, pp 513-18)
System planning for a prototype fusion reactor, 25:30593 (EUR-4593, pp 533-8)
DAHLSTROM, Norris Alfred, Internal friction cold work peak in the niobium--nitrogen system, 25:29861
DAHMEN, H. D., Covariant formulation of the saturation problem for equal-time commutators, 25:31023
DALKHSUREN, B., Production of spontaneously fissionable isomer ^{236}U at radiative thermal neutron capture, 25:31307 (JINR-P7-5497)
DALLIMORE, P. J., HAUSER: computer code for calculation of compound nucleus cross sections, 25:31391 (ANU-P-512)
SANDRA: DWBA codes JULIE and DWUCK adapted for use on IBM 360/50 computer, 25:31390 (ANU-P-507)
DAMERAU, W., Formation of radicals in irradiated single crystals of sarcosine.HCl studies by ESR, 25:29152
DANIEL, H., Nuclear γ-rays following muon capture, 25:31258
DANIEL, R. R., Improved estimate of solar neutron flux measured in an earlier experiment, 25:30177
DANIELS, J. M., Determination of polarization of ^{3}He by optical methods, 25:31074
Experiment to compress polarized ^{3}He gas, 25:31077
Helium-4 discharge light source and system for optical pumping of 2^3S_1 ^{3}He, 25:31076
Large-volume homogeneous low-field electromagnet, 25:31071
Nuclear relaxation of ^{3}He gas on various solid surfaces, 25:31072
Performance of optical pumping light source and kinetics of pumping of 2^3S_1 ^{3}He, 25:31075
Polarizations produced and rates of polarization in optical pumping of 2^3S_1 ^{3}He, 25:31073
DANZIG, I. F., Characteristics of tantalided and hafnided samples in highly corrosive electrolyte solutions, 25:29766
DARDEN, S. E., Proton polarization in ^{18}O(p,p)^{18}O and states in ^{19}F, 25:31236
DARIEL, M. P., Ultra-fast diffusion of copper in praseodymium, 25:29841
DARLASTON, B. J. L., Collaborative program on creep fatigue behavior of 1 percent Cr--Mo--V, 25:29826 (RD/B/N-1889)
DARRAS, Raymond, Recent developments in the electrodeposition of metals in fused salt media, 25:29783 (CEA-N-1376)
DARRIULAT, P., Some recent experimental results on weak interactions, 25:30925
DARUGA, V. K., Yield of neutrons from thick targets bombarded by 11.5- and 23.5-MeV protons, 25:31209
DARVAS, J., Feasibility of gas cooling for the fusion reactor blanket, 25:30589 (EUR-4593, pp 491-6)
DAS, K. P., Effect of magnetic field on wave propagation through hot electron plasma, 25:30614
DAS, L. M., Occurrence of radioactive allanite, 25:29226
DASH, B. R., Occurrence of radioactive allanite, 25:29226
DASHEN, Roger, Chiral symmetry breaking, 25:30919
DASHUK, P. N., Technology of strong pulsed currents and magnetic fields, 25:30604
DATTA, S. K., Absorption at 2.2 MHz in the presence of a cusp-type sporadic-E layer, 25:30382
DAUGERAS, B., Production (rho^0, f^0, ω^0) on nuclei and protons by 15, 16 Gev/c π$^-$, 25:30741
DAUGHERTY, J. D., HIPAC ion source, 25:31138
DAUTCOURT, G., Fluctuations of 3^{0}K microwaves as result of Thomson scattering by moving intergalactic matter, 25:30236
DAVEY, M. Jean, Selective and specific inhibition of 24 hour skin reactions in the guinea-pig. III, 25:29474
DAVID, M., Design philosophy and criteria of safety for prestressed concrete pressure vessels: practice in Czechoslovakia, 25:31561 (IAEA-126, pp 179-212)
DAVIDOV, D., Electron paramagnetic resonance of coupled spin systems: Gd/sub x/ Zr/sub 1-x/Zn_2, 25:30694
DAVIDSON, Charles N., Nuclear environment against which equipment must be hardened, 25:29246
DAVIDSON, D. L., Asymmetric mechanical properties of molybdenum--rhenium alloy single crystals, 25:29829
DAVIDSON, I., Contribution from the United Kingdom, 25:31555 (IAEA-126, pp 53-9)
Effects of reactor radiation on concrete, 25:30022 (EUR-4531, pp 237-65)
Small scale model prestressed concrete pressure vessel tests at Foulness, 25:29305
DAVIDSON, J., Thermal performance of porous insulants in a high-pressure gas environment, 25:30029 (EUR-4531, pp 841-81)
DAVIDSON, W. F., Search for 3446 keV level in ^{29}P, 25:31250
DAVIES, R. D., Radioastronomy and microwave spectroscopy, 25:30138
DAVIS, Alvie Douglas, Hexadecapole deformation and rotation-particle coupling in the rare earth nuclei, 25:31414
DAVIS, J. R., SANDRA: DWBA codes JULIE and DWUCK adapted for use on IBM 360/50 computer, 25:31390 (ANU-P-507)
DAVIS, K. A., Environmental monitoring summary for Paducah Plant, 1970, 25:29502 (KY-629)
DAVIS, Lawrence W., Effectiveness of pressor drugs in beagles exposed to mixed gamma-neutron radiations, 25:29565
DAVIS, R. J., Estimation of aerosol concentration in a nuclear reactor containment after an accident, 25:31619
Function of condensing steam in aerosol scrubbers, 25:29251 (ORNL-4654)
DAVIS, Warren F., Comparison of modified Kjeldahl and vacuum fusion technique for determination of N in Ta alloys, 25:28937
DAVISON, N. E., Linear polarization of the γ rays emitted in the reaction ^{46}Ti(p,p'γ), 25:31288
DAVYDOV, Yu. B., Experience in beta logging of ore wells, 25:29230
DAWSON, P. G., Conditions for the control of beam intensity and cluster size in hydrogen cluster beams, 25:30252 (EUR-4593, pp 43-9)
Ionization and acceleration of hydrogen clusters, 25:30253 (EUR-4593, pp 51-8)
DEALLER, J. F. B., Phase--space volume measurements on Nuffield 60 in cyclotron, 25:31117
DE ALWIS, S. P., Consistency of scale and chiral symmetry limits, 25:30933
DE ANGELIS, W. J., Detection and measurement of weak histoincompatibilities by transfer of mouse peritoneal exudate cells, 25:31718 (ORO-3634-12)

Detection of weak histocompatibility antigens on mouse peritoneal macrophages, 25:31717 (ORO-3634-11)
Serological detection of the male limited H--Y antigen on peritoneal exudate cells, 25:31719 (ORO-3634-13)
DEANOVIC, Z., Radioprotective activity of some sulphur analogues of tryptophol and 5-hydroxytryptamine, 25:29567
DEATON, B. C., Influence of dislocation motion on the ultrasonic-velocity change in superconducting indium, 25:30430
DE AZEVEDO, Zuleide Mota, Effects of gamma rays on eggs of Culex pipiens fatigans, Wied, 1928, 25:29614
DE BORTOLI, M. C., Fallout ^{54}Mn and ^{95}Zr in water and fishes of lakes in northern Italy, 25:29477
Surveillance of environmental radioactivity around a nuclear center, 25:29222
DE BROGLIE, L., Waves and particles, 25:30767
DEEV, Yu. S., Mechanism of the formation of tree-shaped channels in charged-particle irradiated dielectrics, 25:29100
DE FOREST, R. A., Cyclotron and computer, 25:31098
DEHN, Robert L., Microbial oxidation of p-diethylbenzene, 25:29061
DEHNEN, W., Elimination and metabolism of benzo(a)pyrene after intratracheal injection, 25:31715 (ORNL-tr-2469)
DEINZER, W., Why expanding stars after leaving the main sequence, 25:30097
DE JACO, L., Non-destructive tests, 25:29295
DE JONG, Karl-Heinz, Prediction of damages in reactor plants, 25:31529
DE KERDELLEAU, J., Depositing of radioactive products in pipes during turbulent flow, 25:31566
DE KLERK, D., Influence of neutron irradiation on behavior of a superconductor and a superconducting coil magnet, 25:30440 (EUR-4593, pp 107-13)
DE KOCK, L. C. J. M., FREMIX: a high-power 8-GHz plasma heating experiment, 25:30456 (EUR-4593, pp 551-6)
DE LA CRUZ, F. D., Escape integrals, a useful concept in reactor hazard evaluation, 25:31621
DE LA CRUZ, Francisco, Superconductive supercooling and superheating of small cadmium spheres: size effects, 25:30428
DELANO, Michael D., Nucleosynthesis in neutron-rich supernova ejecta, 25:30079
DE LA NOE, Jerome, High-sensitivity solar radiospectrometry at Arecibo, 25:30159
DELBOUILLE, L., Solar spectrum from lambda 7498 to lambda 12016, 25:30172
DELBOURGO, R., Duality diagrams and the Pomeron, 25:31022
Regge residues and supermultiplets, 25:30834
DELLA LOGGIA, V. E., HTR and gas breeders: a comparison, 25:31535
DELORT, G., Thermal shielding by wire gauze and metallic sheets, 25:29819 (EUR-4531, pp 1019-34)
DELPHIN, P., UCL isochronous cyclotron conceptual design and status report, 25:31094
DELRIO, Garino, Population longevity in γ-irradiated Collembola, 25:29615
DEMCHENKO, V. V., Nonlinear theory of reflection of electromagnetic waves from plasma, 25:30626
DEMEYER, A., Mean recoil, isomer ratio, and excitation functions for reactions induced by alpha particles in rubidium, 25:31239 (LYCEN-7091)
Reactions induced in gold by deuterons with energies between 10 and 70 MeV, 25:31311 (LYCEN-7092)
DE MICHELIS, B., Experimental evidence of helicity effect on the energy-loss straggling of electrons, 25:30644
DE MICHELIS, C., Holographic interferometry of laser-produced plasmas using picosecond pulses, 25:30487
DEMICHEV, V. F., Stability of single-turn coils in pulsed magnetic fields up to 1 MG, 25:30556 (EUR-4593, pp 25-32)
DEMIDOV, A. M., Use of gamma spectrometer to control activity of heat-transfer medium in reactors, 25:31680
DEMIN, A. V., Effect of boron on certain physical characteristics of synthetic graphites, 25:29946 (SC-T-713023)
Effect of boron on some physical characteristics of artificial graphites, 25:29953
DEMIRKHANOV, R. A., Diffusion of a dense decaying plasma in a stellarator, 25:30472
Energy parameters in the rare-earth nuclei, 25:31433
Experimental installation R-Ohm for studying high-frequency field-interaction with plasma, 25:30508 (NP-18801)
Studies of diffusion of dense disintegrating plasma in a stellarator, 25:30462 (NP-18767)
DEMMELER, M., Dense plasma focus as a neutron source for pulsed measurements in a blanket, 25:30592 (EUR-4593, pp 525-31)
DE MORAES REGO, Amyrthes, Effects of gamma rays on eggs of Culex pipiens fatigans, Wied, 1928, 25:29614
DEMPSEY, R. M., Characteristics of tantalided and hafnided samples in highly corrosive electrolyte solutions, 25:29766
DEMPSTER, Andrew B., Lattice dynamics of methanol: hydrogen bonding and infrared absorption, 25:29065
DENAULT, G. C., Corrosion of Ti-6A-4V in HCl-methanol, 25:29773
DENES, Jean-Francois, Simulation of an electron avalanche in He using a Monte Carlo method, 25:30629 (NP-18798)
DENIAU, C., Deferred luminescence spectra of some aromatic compounds in rigid organic media, 25:29150
DENIAUD, Suzanne, Study of impurities distribution in a metal (plutonium), 25:28916 (CEA-R-4071)
DENISOV, Yu. N., Control system of Dubna monoenergy cyclotron, 25:31099
DENNIG, E. I., Experiment to compress polarized ^{3}He gas, 25:31077
DENNIS, B. R., Evidence from hard x rays for two-stage particle acceleration in a solar flare, 25:30169
DENNIS, J. A., Calculated quality factors for protons in body and eye-lens tissues, 25:29511 (AERE-M-1887)
DENNIS, Richard, Radiation-curable compositions, 25:29114
DENT, William A., Search for the redshifted line of neutral hydrogen in selected quasi-stellar sources, N galaxies, and Seyfert galaxies, 25:30121
DE OLIVEIRA, Maria Lindete, Effects of gamma rays on eggs of Culex pipiens fatigans, Wied, 1928, 25:29614
DE PAULA E SILVA, Evando, Observation of age hardening of α-zirconium after deformation, 25:29853
DERADO, I., Forward production of Δ(1236) in pion--proton scattering at 4 GeV/c, 25:30738
DERIBAS, A. A., Influence of starting parameters on ripple formation in explosive welding of metals, 25:31736 (SCL-T-710240)
DERKOWITZ, D., Irradiation resistance of spores of Clostridium botulinum in beef, 25:29734
DERMOIS, D. C., External injection system for Groningen cyclotron, 25:31147
DE ROSNY, G., Resonance spectroscopy, 25:30853
DEROULEDE, A., Deferred luminescence spectra of some aromatic compounds in rigid organic media, 25:29150
Study of organic anions by a deferred luminescence technique, 25:29133
DERRICK, M., Double-Regge-pole description of reaction K⁻n → K⁻π⁻p at 5.5 GeV/c, 25:30747
DESSLER, A. J., Vacuum merging: a possible source of the magnetospheric cross-tail electric field, 25:30387
DETHLEFSEN, Lyle A., Prog. rpt. on radioisotopic and volumetric studies of tumor growth in situ, 1967--71, 25:31713 (NYO-3924-10)
Prog. rpt. on radioisotopic and volumetric studies of tumor growth in situ, annual, 4/71, 25:31712 (NYO-3924-9)
DEUTSCH, C., Stark and Zeeman effects on neutral-He lines, 25:30264
DEUTSCHMANN, M., Empirical relation between inelastic electron scattering and multibody pion reactions, 25:30795
DEVAN, J. H., Sodium corrosion studies, 25:29761 (ORNL-4630, pp 150-7)
Sodium removal and caustic effects, 25:29762 (ORNL-4630, pp 158-62)
DEVANARAYANAN, S., Moessbauer investigation of iron in boron, 25:30689 (UUIP-733)
DEVELL, L., Experiences on the release of iodine from uranium dioxide fuel, 25:31607
DEVENSKI, P. A., Elastic pp- and pd-scattering at 50 and 70 GeV, 25:30725 (JINR-P1-5633)
DE VILLIERS, J. A. M., Low-lying states of ^{127}I, 25:31352
DE VRIES, G., Chromatographic techniques using liquid anion exchangers. V, 25:29186
DEVRIES, Joan S., Elastic scattering of 1.33-MeV photons from lead and uranium, 25:31370
DEWEY, P., Model for two-pion production in the diffraction approach, 25:30863
DIAMOND, R. M., Lifetimes of ground-band states in ^{148,150} ^{152}Sm, 25:31364
DICKINSON, Dale F., Excitation and abundance of interstellar SiO, 25:30152
DICUS, Duane A., Conserved currents, Reggeization, and Mandelstam counting in second-order perturbation theory, 25:30992
DIDORENKO, V. A., Ge(Li) gamma spectrometer, 25:29357
γ rays accompanying decay of ^{109}In, 25:31320
DIEGELMANN, Robert, Use of a mixture of proteinase-free collagenases for the specific assay of radioactive collagen in the presence of other proteins, 25:28997
DIEMER, E. A. P., Superconducting-state Knight shift in V_3Au, 25:30425
DIENER, Gerhard, Kinetic theory of fully ionized plasmas. II, 25:30523
Kinetic theory of plasmas taking into account transverse plasma waves, 25:30526
DI FEDERICO, I., Plane cross-flow heat exchangers with heat generation within a fluid stream, 25:29262
DILLON, G., Outline of scattering theory for absorptive potentials, 25:31017
DIMANSHTEIN, F. A., Gravitational field effect on emission of relativistic charges, 25:31008
DIMOCK, D. L., Preliminary investigation of ohmically-heated plasmas in the model ST Tokamak, 25:30459 (MATT-813)
DINGLE, A. Nelson, Trace substances in rain water, 25:29224
DION, Christian, Ternary system UO_3--V_2O_5--Na_2O, 25:29998
DIUGUID, Lincoln I., Double-isotope derivative assay of serum iodothyronines. II. Thyroxine, 25:28986
DIVAKARAN, P. P., Factorizable current algebras at all momenta, 25:30923
DIXIT, M. S., Forward differential cross sections for reaction p + p → d + π⁺ in range 3.4 to 12.3 GeV/c,

25:30731
DIXON, C. F., Zirconium-refractory alloys, 25:29969
DMITRENKO, V. V., Relation of electron flux in upper atmosphere to state of Earth magnetosphere, 25:30353
DMITRIEV, A. G., Decay of ^{75}Br, 25:31257
DMITRIEV, V. M., Mixing of uhf signals from superconducting tin films, 25:30436
DMITRIEVSKII, V. P., Charged particle motion in monoenergetic cyclotron, 25:31122
Phase motion in the phasotron with spatial variation of magnetic field, 25:31156
DMITROVIC, M., Spectrographic determination of impurities in vanadium pentoxide and high purity lead, 25:28947
DOBROWOLNY, M., High-frequency instability and anomalous plasma resistivity at supercritical electric fields, 25:30625
DOBROZEMSKY, R., Determination of the distribution of fission products in fuel particle coatings by the sputtering technique, 25:29979 (SGAE-PH-96/1970)
DOBRZYNSKI, L., Polarized-neutron study of the $Ni_{0.968}V_{0.032}$ alloy, 25:30680
DOEMENY, P. A., Chemical evolution of a nitrogenase model. II. Molybdate--cysteine and related catalysts in the reduction of acetylene to olefins and alkanes, 25:29051
DOERING, J. P., Excitation of O(^{1}S) atoms in the day airglow, 25:30375
DOHNO, Reizo, Studies on ion-exchange transfer. XIX, 25:29193
DO HUU PHUOC, Decay scheme of 1.3 h. ^{179}Ta, 25:31310 (LYCEN-7084)
DOI, Toshio, Precipitates with unusual microstructure in grains of Nb--40 Zr--10 Ti alloy, 25:29890
DOKOPOULOS, P., Fast 500-kV energy storage unit, 25:30582 (EUR-4593, pp 393-400)
Fast, solid dielectric, multichannel crowbar switch, 25:30580 (EUR-4593, pp 379-84)
DOLE, Stephen H., Computer simulation of the formation of planetary systems, 25:30178
DOLENKO, A. V., Stabilized gamma-resonance spectrometer, 25:29360
DOLGIKH, P. F., Estimation of the diffusion of materials in clayey grounds, 25:29206
DOLIDZE, M. V., Classification of stars in the near ultraviolet, 25:30060
DOLL, Warwick Woodman, Polymorphism and isomorphism of poly(vinylidene fluoride), 25:29110
DOMBROVSKAYA, G. S., Lifetimes of excited states of ^{140}Ce, 25:31319
DOMBROWSKI, Carl S., Pharmacokinetics of halothane in man, 25:29416
DOMOKOS, G., Overlapping resonance model of deep inelastic electron scattering, 25:30782
DOMSHLAK, M. G., Mutagenic effect of fast neutrons and x rays on mouse spermatogonia, 25:29487
DONALD, Harold J., Melt strength and melt extensibility of irradiated linear polyethylene, 25:29099
DONALDSON, George William, Mechanism for the solubilization of colloidal sulfur by gamma radiation, 25:29137
DONALDSON, Henry A., Sound scattering layers off the Oregon coast, 25:31723 (RLO-1750-62)
DONNACHIE, A., Modern developments in hadron physics, 25:30822 (CERN-71-7, pp 41-180)
DONNELLY, J. P., Junction (n--p) photovoltaic detectors in PbTe produced by proton bombardment, 25:29397
DONNELLY, R. G., Cladding materials for space isotopic heat sources, 25:29823 (ORNL-4630, pp 186-90)
Physical and mechanical metallurgy of refractory alloys, 25:29824 (ORNL-4630, pp 191-206)
DONOVAN, T. R., Hydrogen abstraction from methyl formate by methyl radicals, 25:29054
DORFMAN, Leon M., Pulse radiolysis studies. XX, 25:29158
DORKO, W., Hydrogen abstraction from methyl formate by methyl radicals, 25:29054
DORMAN, I. V., Heliolatitudinal index (HL) of solar activity and 11-year variations of cosmic rays, 25:30165
DORMAN, L. I., Behavior of cosmic layers in lower ionosphere during Forbush decreases, 25:30311
Cosmic-ray increase before Forbush decrease, 25:30316
Cosmic-ray variations, 25:30313
Heliolatitudinal index (HL) of solar activity and 11-year variations of cosmic rays, 25:30165
HL index of solar activity and yearly variations of cosmic rays, 25:30308
Interplanetary space conditions by three-dimensional anisotropy of cosmic rays, 25:30320
Modulation of galactic cosmic rays by solar wind, 25:30325
Spectrum of Forbush decrease in region 3 to 50 GV, 25:30318
Spherically symmetric model of modulation of galactic cosmic rays, 25:30324
DORNER, Heinrich, Design and manufacture process of large-sized reactor pressure-vessel, 25:31564
DOROKHOV, V. V., Energy parameters in the rare-earth nuclei, 25:31433
DOROSHKEVICH, A. G., Perturbations in an anisotropic homogeneous universe, 25:30223
DORSCHNER, J., Theoretical investigations about the interstellar dust. II, 25:30196
Theoretical investigations about the interstellar dust. III, 25:30195
DOTE, Toshihiko, Determining plasma density by cylindrical probe at medium pressures, 25:30494
DOUGALL, Donald K., Prog. rpt., final, 11/69--1/71, 25:31691 (COO-1750-3)
DOUGAR-JABON, V. D., Elimination of cone losses in the magnetostatic mirror by help of microwaves, 25:30463
DOUGHERTY, T. F., Some toxicity aspects of internally deposited ^{239}Pu, 25:29627
DOUGLASS, Dana L., Alpha particle irradiation damage in ThO_2, 25:30012
Strain effects and spalling in alpha-bombarded ThO_2, 25:30014
DOVE, R. B., Right angle ^{3}He cryostat incorporating a high field superconducting solenoid, 25:30442 (NBS-TN-562)
DOVGII, I. E., Effects of histones on energy processes in liver mitochondria of irradiated animals, 25:29638
DOW, Philip, Hydrogen--nitric oxide spin exchange cross section, 25:30277 (UCRL-20529)
DOWDEN, R. L., Electron energy spectrum and structure deduced from analysis of vif discrete emissions, 25:30371
vif discrete emissions deduced from Helliwell's theory, 25:30372
DOWKER, J. S., Quantum mechanics on group space and Huygens' principle, 25:30971
DOYLE, J. H., Chemical diffusivities of Pu--Ga alloys in epsilon (bcc) phase, 25:29873
DRAGANIC, I. G., Pulse radiolysis of aqueous cyanogen solution, 25:29149
DRAGANIC, Z. D., Pulse radiolysis of aqueous cyanogen solution, 25:29149
DRAKE, G. A., Comparative metabolism of radionuclides in mammals. V, 25:29450
DRALLE, A., Search for K/sub S/ + $\pi^+\pi^-\pi^0$, 25:30723
DRASIL, V., Release of the hydrogen atom in thymine radiolysis, 25:29148
DRAWIN, H. W., Excited states of He atoms in stationary PIG discharge, 25:30479
Recombination and ionization coefficients for quasi-stationary He plasmas, 25:30540
Stark and Zeeman effects on neutral-He lines, 25:30264
DRAWIN, H.-W., Spectroscopic measurement of high temperatures, 25:30492
DRESSLER, Kurt, Variable states of a heavy plasma in relation to temperature and density, 25:30536
DREVERMANN, H., Energy dependence of 3-body reactions by use of longitudinal phase space plots, 25:30742
Pion pair angles in reaction $\pi p \to p2\pi$, 25:30880
DRIVER, C., Electroproduction of single π^+-mesons on H, 25:30719
Electroproduction of single π^+-mesons on H, 25:30718
DROUFFE, J. M., Exchange degeneracy and absorption: πN, KN, and NN reactions, 25:30874
DROZHENNIKOV, V. A., DNAase activity of E. coli K12 (lambda) during gamma irradiation, 25:29725
DUBERTRET, Alain, Contribution to study of alpha Ti--O and alpha Zr--O solid solutions, 25:30000
DUBEY, P. K., Tunnel effect in Al--Al_2O_3--Al junctions: inclusion of short-range forces, 25:30706
DUBININ, I., Kinetics of the tumour growth and time factor in the radiotherapy, 25:29680
DUBINSKAYA, N. A., Neutron activation determination of Mo in biological materials, 25:29019
DUBLON, G., Electron paramagnetic resonance of coupled spin systems: Gd/sub x/ Zr/sub 1-x/Zn_2, 25:30694
DUBOIS, F., New types of thermal-shielding concretes for nuclear reactors, 25:30031 (EUR-4531, pp 975-1018)
DUBOUT-CRILLON, R., Evidence and velocity of a density wave in the galaxy M33, 25:30201
DUBOVIK, V. M., Determination of Breit--Wigner resonance widths using Fourier algorithm, 25:30849 (JINR-P2-5659)
DUBOVOI, E. I., Regularities of photonuclear reactions as effects of the Feynman graphs properties, 25:31435
DUBOVOI, L. V., Skin effect in high-energy Z-discharges, 25:30507 (NP-18775)
DUBUQUOY, Claude, Total elementary separation of rare earths on cation exchange resins, 25:29178 (CEA-R-4102)
DU CHAFFAUT, Maurice, High-sensitivity solar radiospectrometry at Arecibo, 25:30159
DUDA, V., Information on prospecting in Sweden, 25:29229
DUELLI, B. L., Heavy ion acceleration at ORIC, 25:31131
DUFFAIT, R., Decay scheme of 1.3 h. ^{179}Ta, 25:31310 (LYCEN-7084)
DUFLO, J., ABC effect and a structure at 450 MeV in meson missing-mass spectra, 25:30734
DUMAZET, G., Reaction ^{22}Ne(p,p), ^{22}Ne(p,p'), and excited states of ^{23}Na, 25:31281
DUMBRAIS, O. V., Graphs for studying isotopic relations in reactions with production of three particles and possible Pomeranchuk pole exchange, 25:30824 (JINR-P2-5630)
Model-independent analysis of forward π^+-p scattering data, 25:30875
DUNJIC, A., Gastrointestinal tract, 25:29632
Lymphatic system and thymus, 25:29635
Lymphoid-tumors and radiation, 25:29696
DUPASQUIER, A., Experimental evidence of helicity effect on the energy-loss straggling of electrons, 25:30644

DUPAY, F., Test of ring of prestressed concrete in high-resistance sheet-metal steel, 25:30028 (EUR-4531, pp 445-76)
DUPIS, A., Uranium prospecting at shallow and medium depths using magnetotelluric methods, 25:29233
DUPONT, F., 20 MeV compact cyclotron, 25:31142
DUPONT, J., Thermal shielding of pressure vessels, tanks, and elements of nuclear reactors, 25:31577 (EUR-4531, pp 1063-78)
DU PONTAVICE, Y., Depositing of radioactive products in pipes during turbulent flow, 25:31566
DUPREE, A. K., Extreme-ultraviolet spectrum of the quiet Sun, 25:30166
DUPUIS, A., UCL isochronous cyclotron conceptual design and status report, 25:31094
DUPUIS, Marie-Claire, Separation and recovery of permanent gases by preparative chromatography, 25:29177 (CEA-R-4090)
DUPUY, Jean, Method for solving the equation of ionized electric fields in a stationary regime, 25:30705
Type-I variations in extensive air showers, 25:30331
DURKEE, P., Moessbauer-effect observations of ^{232}Th following Coulomb excitation, 25:30693
DUSCH, F., Analyzing power of the reaction ^{3}He(d,p)^{4}He, 25:31197
DWORKIN, A. S., Enthalpy of La chlorides, bromides, and iodides from 298 to 1300°K, 25:29951
D'YAKONOV, V. P., Powerful pulse generators based on avalanche transistors, 25:29405
DYMOV, B. K., Thermal conductivity, electric resistivity, and specific heat of dense graphites, 25:29949
DZHELEPOV, B. S., Alpha spectra of ^{209}At, ^{210}At, ^{211}At, and ^{211}Po, 25:31324
Decay of ^{225}Ac, 25:31325
Decay of ^{75}Br, 25:31257
DZHIBUTI, R. I., Effective forces within nuclei, 25:31402
DZHIMSHELEISHVILI, G. N., Certain problems of spectral classification and spectrophotometry of late spectral type stars, 25:30061
Classification of stars in the near ultraviolet, 25:30060
DZIGVASHVILI, R. M., Problem of applying the model of a normal logarithmic spiral to galaxies, 25:30190

E

EADIE, D. McD, Testing one tenth scale model of Hinkley Point B and Hunterston B Power Station prestressed concrete pressure vessels, 25:29312
EASTERDAY, H. T., Modification of a conventional 37 in cyclotron, 25:31161
EBEL, G., Compilation of coupling constants and low-energy parameters, 25:30841
EBERHAGEN, A., Investigations on preionization for toroidal high-beta-experiments, 25:30541 (IPP-1/114)
EBERT, W., Measurements in annular MHD duct for high Hall-parameter values, 25:30343
ECH, F. A., Search for particles with fractional charge in 70 GeV accelerator, 25:30724 (CERN-Trans-71-4)
ECKART, W., Radiation effects in isolated DNA and their functional consequences. VIII, 25:29469
Radiation effects in isolated DNA and their functional consequences. VII, 25:29468
EDELSTEIN, N., Proton magnetic resonance shifts in bis(cyclooctatetraenyl) U(IV), 25:29085
EDEN, R. J., Strong interactions of elementary particles, 25:30842
EDWARDS, G. J., Superconducting chopper amplifier for use in magnetic fields, 25:30447
EECHE, Andrievs, Drosophila melanogaster somatic resistance to x-ray irradiation, 25:29613
EFIMOV, G. V., Construction of non-local quantum electrodynamics, 25:30937 (JINR-P2-5694)
EFIMOV, M. L., Relationship between level of endogenous sulfhydryl groups and radiosensitivity of tumors, 25:29610
EFIMOV, O. N., Investigation of kidneys with aid of ^{51}Cr-EDTA, 25:29578
EGGEN, O. J., Intermediate-age cluster IC 4651, 25:30093
EGIAZAROV, B. G., Stabilized gamma-resonance spectrometer, 25:29360
EGOROV, V. P., Radiographic study of uranium-containing pyrites, 25:29231
EHRENSPERGER, Klaus, Influence of neutron irradiation at 4°K on shear modulus of Cu, Al, and Pt, 25:29912
EHRL, A., Racemization of D(-) mandelic acid by ^{60}Co-γ-irradiation, 25:29145
EILAND, H. M., Epithermal measurements of capture and fission resonance integrals in ^{235}U, ^{233}U, ^{239}Pu, and ^{241}Pu, 25:31353
EISENBERG, E., Development of Botrytis cinerea in irradiated strawberries, 25:29732
EISENBERG, Y., Slope of the momentum transfer distribution, 25:30900
EISLER, L., Analysis of occupational diseases due to ionizing radiation in the health institutions of the North-Moravian region, 25:29711
EISSA, E. A., Iron-57 low-energy states, 25:31270
EKHICHEV, O. I., Gamma rays from ^{64} ^{66} ^{68}Zn(p,γ)^{65} ^{67} ^{69}Ga, 25:31249
EKSTIG, Boerje, X-ray emission spectra of VC/sub x/, NbC/sub x/, TaC/sub x/, and ZrC, 25:30267
EKSTROEM, P., ANNLIS: computer program for automatic analysis of gamma-ray spectra, 25:29354 (LUNP-7101)
EKSTROEM-JODAL, B., Pulmonary gas exchange after radioisotope scanning, 25:29594
EKWALL, Per Anders, Improvements in fuel assemblies for nuclear reactors, 25:31678
ELANGO, M. A., Formation of color centers in KCl crystals by ultrasoft x rays, 25:30654
EL BAZ, E., Description of elastic-scattered processes with the use of non-local separable potentials, 25:31186 (LYCEN-7089)
ELEN, J. D., Influence of neutron irradiation on behavior of a superconductor and a superconducting coil magnet, 25:30440 (EUR-4593, pp 107-13)
Voids in V, Nb, and Mo by fast neutron irradiation at high temperatures, 25:29914
EL-FEKEY, Sayed A., Impact of thermal analyses on nuclear ammonium polyuranate preparation, 25:29925
ELGEFORS, B., Pulmonary gas exchange after radioisotope scanning, 25:29594
ELISEEV, G. A., Stability of single-turn coils in pulsed magnetic fields up to 1 MG, 25:30556 (EUR-4593, pp 25-32)
ELISEEV, S. M., Angular and energy distributions of particles produced in inelastic π--N and N--N collisions at very-high energies, 25:30870 (ORNL-tr-2433)
ELKIND, M. M., Sublethal damage repair and its role in the radiation response of cell renewal systems, 25:29626
ELKINS, G. H., Bibliography on heat and mass transfer through soil, 25:29266 (SC-ARPIC-1010)
ELLEUCH, M. F., New types of thermal-shielding concretes for nuclear reactors, 25:30031 (EUR-4531, pp 975-1018)
ELLIOT, H., Search for antimatter in primary cosmic rays, 25:30327
ELLIOTT, C. J., Fully developed turbulent flow through concentric annuli, 25:29265 (RD/B/N-1878)
ELLIOTT, D. J., Defect formation and sputtering of alkali halides with low energy irradiation, 25:30651
ELLIS, A. N., Calibration of Moxon--Rae detectors in the current mode, 25:29326 (LA-4445)
ELLIS, F., Nominal standard dose and RET, 25:29520
ELLIS, W. R., Vacuum magnetic field and surface current distributions for a slotted cylindrical shell carrying axial current, 25:30601
EL-NADI, M., Determination of the optical potentials in terms of diffraction-model parameters, 25:31410
EL-SHAMY, H. K., Analysis of platinum for certain elemental impurities by neutron activation, 25:29023
ELSSNER, Gerhard, Solid solution hardening of VA metals by N and O interstitials, 25:29880
EMARD, F., Recombination and ionization coefficients for quasi-stationary He plasmas, 25:30540
EMERSON, Mark E., Tantalum, 25:29810
EMSALLEM, A., Decay scheme of 1.3 h. ^{174}Ta, 25:31310 (LYCEN-7084)
ENCRENAZ, Th., Far-infrared spectrum of Jupiter, 25:30250
ENGELMANN, P., Progress of fast breeder project at Karisruhe, 25:31538
ENGLE, W. W. Jr., Design of asymmetric 4 π shields for space reactors, 25:31640 (ORNL-TM-3368)
Low-energy electron transport with the method of discrete ordinates, 25:30630 (ORNL-TM-3318)
ENGLERT, F., Local duality and conserved currents, 25:30855
ENINGER, J. E., HIPAC ion source, 25:31138
ENOMOTO, Shigemasa, Development of radioisotope-powered cardiac pacemakers in the world, 25:29285
ENTIS, A. C., Negative mass instabilities in an electron-ring compressor, 25:31058 (UCRL-20208)
ERB, J., Developments in cryogenic and superconducting magnets, 25:31040 (KFK-1316)
ERDEY, L., Spectrochemical analysis of hard metals by a rotating disc solution technique, 25:28944
ERDMAN, K. L., Square wave rf system design for TRIUMF cyclotron, 25:31091
ERENTS, S. K., Desorption by keV protons of hydrogen condensed on liquid-helium-cooled surfaces, 25:30257 (EUR-4593, pp 181-6)
ERIKSSON, L., Conversion electron particle parameters of E2 transitions in ^{152}Sm and ^{154}Gd, 25:31360
ERMAKOV, A. N., Organic reagents in the analytical chemistry of Zr, 25:28969
ESCH, L. J., Epithermal measurements of capture and fission resonance integrals in ^{235}U, ^{233}U, ^{239}Pu, and ^{241}Pu, 25:31353
ESCHLE, J. L., Possible use of the sterile-male technique for eradication of the horn fly, 25:29744
ESCHRICH, H., Preparation and properties of a crystalline uranium(IV)--hydrazine nitrate compound, 25:29035 (NP-18736)
ESPENSON, James H., Kinetic studies of the reduction of chromium(III) complexes by uranium(III) ions, 25:29084
ESTERL, John E., Beta-delayed protons from ^{23}Al, 25:31241 (UCRL-20436)
ESTEVE, D., Behaviour of current MOS, 25:29412
ETHERIDGE, E. L., Prog. rpt. on noble gas confinement study, final, FY-1970, 25:29075 (DUN-7221(Vol.2))
ETHRIDGE, D. R., Precise measurements of W, the mean energy required for ion-pair formation in gases. I.

XUM

Alkanes, 25:30636
ETIM, E., Bjorken--Regge asymptotism of electroproduction structure functions in field-current theory, 25:30779
ETTER, Don E., Application of differential thermal analysis to the study of phase equilibria in metal systems, 25:29885
ETTINGER, K. V., Non-intercepting cyclotron beam monitor, 25:31127
Phase--space volume measurements on Nuffield 60 in cyclotron, 25:31117
EUBIG, C., Wire-cutting tool for use with a spark cutter, 25:31689 (COO-1041-19)
X-ray slit system for crystals with small angle boundaries, 25:31688 (COO-1041-18)
EVANS, D. R., MOXY: a digital computer code for computing core heat transfer, 25:31587 (CONF-710302-2)
EVANS, Don M., Bevatron guide field control, 25:31055 (UCRL-20189)
Digital control of Bevatron acceleration cycle, 25:31054 (UCRL-20185)
EVANS, H. J., Forward differential cross sections for reaction p + p + d + π^+ in range 3.4 to 12.3 GeV/c, 25:30731
EVANS, J. A., Fractional parentage and the equations-of-motion method in pairing theory, 25:31453
EVANS, S. K., Prog. rpt. on thermodynamic data program involving plutonia and urania at high temperatures, 8--10/70, 25:29821 (GEAP-12153)
EVANS, Titus C., Modification of radiation effect on the eye by topical application of dimethyl sulfoxide, 25:29562
EVERETT, R. J., Separation and determination of ^{137}Cs in urine, 25:28983
EVLASHEV, Yu. A., S-matrix for field theory with Lagrangian depending on derivatives, 25:30968
EVRARD, D., Observation of d^* effect in anti pd + p anti p π^+ π^-n reaction at 5.55 GeV/c, 25:30727 (NP-18796)
EYRE, J. A., Pulse radiolysis studies. XX, 25:29158
EYRING, Leroy, Advances in high temperature chemistry. Volume 2, 25:29081
EZHELA, V. V., Integral representations of expansions over Wigner functions, 25:31025
EZHOV, S. N., Calculating (n,2n) reaction amplitude on heavy nuclei. II, 25:31394 (ITF-70-95-E)

F

FABIC, Stanislav, Loss-of-coolant analysis: comparison between BLODWN-2 code results and test data, 25:31598 (WCAP-7401)
FABRICIUS, K., Consequences of assumption that S-matrix commutes with axial charge, 25:30982
FABRIKANT, Jacob I., Effects of continuous irradiation, 25:29625
FACCHINI, U., Sudden model for ternary fission, 25:31422
FACKERELL, Edward D., Relativistic, spherically symmetric star clusters. V, 25:30066
Solutions of Zerilli's equation for even-parity gravitational perturbations, 25:30238
FAFURINA, E. N., Spectral isotopic analysis of elements in middle part of Mendeleev Periodic Table, 25:28952
FAHEY, R. E., Growth of EuO, EuS, EuSe, and EuTe single crystals, 25:29933
FAIN, J., Use of semiconductor telescopes for detecting the recoil nuclei in proton-light nucleus coherent scattering at high energy, 25:31185 (LYCEN-7085)
FAIZIEV, A. R., Analogous states of T = 2 in $^{28}Mg(^3He,n)^{28}Si$, $^{56}Ti(^3He,n)^{56}Cr$, and $^{58}Ni(^3He,n)^{60}Zn$ reactions, 25:31237 (IAE-1958)
FALK, W. R., Reaction $^{22}Ne(p,t)^{20}Ne$ at 26.9, 35.1, and 42.4 MeV, 25:31296
FALTENS, A., Preliminary hardware concepts for a high-energy electron-ring accelerator, 25:31052 (UCRL-20169)
FANG, M. T. C., Constant-frequency oscillations in a bounded thermally produced plasma, 25:30624
FANTOLA LAZZARINI, A. L., Isomeric effect in Szilard--Chalmers recoil of /sup 60m/Co and /sup 60g/Co in some mixed complexes of Cr(III) and Co(III), 25:29170
FARAH, Michael Y., Impact of thermal analyses on nuclear ammonium polyuranate preparation, 25:29925
FARMER, F. R., Need for consistency in accident models, 25:31603
FARMER, R. W., Improved feedback control for Null-point compensating system, 25:31741 (UCLA-12-813)
FARRELL, J. A., Calibration of Moxon--Rae detectors in the current mode, 25:29326 (LA-4445)
FASANA, A., Experimental evidence of helicity effect on the energy-loss straggling of electrons, 25:30644
FASANO, A. N., Neutron activation analysis technique for nail sodium concentration in cystic fibrosis patients, 25:29016
FASTIE, W. G., Photodissociative excitation of O(^{1}D) atoms in the day airglow, 25:30386
FASTRUP, B., Inelastic energy loss in single atomic collisions of Kr^+ on Kr at keV energies, 25:30279
FAUCHAIS, Pierre, Rotation temperature of N_2^+ molecule, 25:30480
FAUST, J. W. Jr., Materials problems in lithium-drifted Ge radiation detectors. II, 25:29330
FAUSTOV, R. N., Relativistic wave function and form factors of the bound system, 25:30752 (JINR-P2-5691)
FAYARD, C., Description of elastic-scattered processes with the use of non-local separable potentials, 25:31186 (LYCEN-7089)
FEDOROV, A. D., Energy spectrum and deformation of some even--even nuclei, 25:31411
FEDOROV, V. I., Field of an electromagnetic wave in a cold anisotropic plasma, 25:30533
FEDOTOVA, M. I., Vulnerability of gastrointestinal tract of rats under influence of radiation, 25:29646
FEDYAKOV, V. P., Skin effect in high-energy Z-discharges, 25:30507 (NP-18775)
FEDYAKOVA, V. P., Skin effect in high-energy Z-discharges, 25:30507 (NP-18775)
FEGLEY, Ronald Warne, Differential cross sections for D(d,d)D elastic scattering and the D(d,3He)n, D(d,t)p reactions between 12.5 and 40.0 MeV, 25:31191
FEIGELSON, Philip, Paper disc estimation of radioactive RNA: studies on the presence and elimination of metabolically generated artifacts from labeled purine and pyrimidine precursors, 25:28993
FEINER, F., Epithermal measurements of capture and fission resonance integrals in ^{235}U, ^{233}U, ^{239}Pu, and ^{241}Pu, 25:31353
FELDMAN, P. D., Excitation of O(^{1}S) atoms in the day airglow, 25:30375
Photodissociative excitation of O(^{1}D) atoms in the day airglow, 25:30386
FEL'DSHTEIN, Ya. I., Statistical and dynamic pressures of solar wind on the Earth's magnetosphere, 25:30396
FELEA, S., Application of phenomenological quasi-two-body model to π^-p-interactions with strange particle production at p = 4 GeV/c, 25:30869 (JINR-P1-5706)
FELIX, F. W., Diffusion of Ar, Kr, and Xe in CaF_2 investigated on U-doped CaF_2, 25:30673
FELS, M. F., Computation of resonance parameters for elastic scattering, 25:30297
FELS, Margaret F., Annihilation of positrons during scattering, 25:30289
FEMENIA, F. R., Energy level calculations in Davydov model, 25:31425
FENGER, J., MOSSPEC: program for resolving Mcessbauer spectra, 25:30688 (RISO-M-1348)
FENTON, J., Nuclear matter radii in the tin isotopes, 25:31341
FERBERG, B. A., Possibility of determining oscillation parameters of neutrinos, 25:30802 (BNL-tr-418)
FERENTS, A. I., Structure of neurons of sympathetic ganglion after x irradiation, 25:29675
FERGUSON, D. R., Application of alternating-direction implicit methods to the space-dependent kinetics equations, 25:31654
FERLIN, G., Evaluation of kidney morphology and function by means of the scintillation camera, 25:29592
Scintillation camera in the evaluation of liver morphology and function, 25:29591
FERME, J., Grenoble cyclotron progress report, 25:31097
FERRUCCI, N., Experimental vibration characteristics of a B.W.R. fuel assembly, 25:31570 (RT/ING-(70)24)
FESSENDEN, P., Modification of a conventional 37 in cyclotron, 25:31161
FETTEROFF, S., Neutron activation analysis technique for nail sodium concentration in cystic fibrosis patients, 25:29016
FICKLER, S. I., Consistent quantization of Yang--Mills field, 25:30988
FIDELIS, I., Parallelism between the regularities in f-electron elements and their free ion ground terms, 25:29091
FIELD, George B., Charge transfer and ionization equilibrium in the interstellar medium, 25:30211
FIELD, R. D. Jr., Energy continuation of an energy-independent pion-nucleon phase-shift analysis from 385 to 1700 MeV/c, 25:30871 (UCRL-20250)
FIENNING, W. C., Interactive monitor for a telemetry playback system, 25:31729 (SC-DR-710211)
FIEND, Daniel, Tests of evaluated beryllium (n,2n) cross sections by analysis of 1.4-eV flux in water for an americium--beryllium source enclosed in beryllium spheres, 25:31223
FIFE, Thomas H., General acid catalysis of acetal hydrolysis. The hydrolysis of substituted benzaldehyde di-tert-butyl acetals, 25:29048
FIGULI, J., Effect of gamma irradiation on some chemical and physical properties of gluten proteins, 25:29103
FILATOV, E. P., Radiosensitivity of human lymphocytes in vitro, 25:29710
FILBY, E. E., C_2-exchange reactions of La, Ce, Pr, and Nd with their dicarbides, 25:29039
Dissociation energies of gaseous gadolinium dicarbide and terbium dicarbide, 25:29955
FILER, T. D., Fluorometric determination of submicrogram quantities of zirconium, 25:28963
FILIPPOV, A. T., Approach to nonrenormalizable field theories, 25:30955
FILIPPOV, F. F., Preparation of specimens of zirconium and its alloys for metallographic examination, 25:29817
FILIPPOV, G. F., Dimensions and form of the light nuclei with the surplus of neutrons, 25:31238 (ITF-70-83-E)
FILIPPOV, N. V., Passive diagnostics of a plasma focus using charged products of the dd-reaction, 25:30475

XUM

(LA-tr-71-6)
FILIPPOV, V. A., Effects of solar-activity cycle on irregularity of interplanetary magnetic field, 25:30326
FILIPPOV, V. F., Effect of modifying additions of Ti and Ni on [the structure and] some properties of cast Zr, 25:29835
FILIPPOV, Yu. M., Free radicals in γ-irradiated food by EPR, 25:29733
FILIPPOVICH, A. S., Cell division in Escherichia Coli during irradiation by neutrons of 200 keV, 25:29490
FINDEISEN, Berndt, Suitability of vitreous carbon as a mortar material for spectrochemical analysis, 25:28938
FINGER, M., Decay ^{160}Tb + ^{160}Dy, 25:31335
FINGERHUT, Bruno, Nucleic acid synthesis in bladder tumors, 25:29585
FINIGAN, A., Elastic and ultimate pressure tests on one tenth scale model of Dungeness B concrete pressure vessel, 25:29311
FINK, C. L., Angular distribution and excitation function of singlet deuteron in d(p,d)p reaction, 25:31196
FINZI, A., Ejection of mass by radiation pressure in planetary nebulae, 25:30044
FIORATTI, M. Paganini, Analysis of methods for interpreting bremsstrahlung spectra, 25:30632 (RT/FI-(70)36)
FIRMANI, C., Cosmological models with a G-variable gravitational theory, 25:30232
FIRRAO, Donato, Evaluation of Gerard-Papirno characterization of notch ductility in steel, 25:31692 (COO-2048-2)
FISCHBACH, Ephraim, Presence of noncanceling seagull and Schwinger terms in weak (nucleon + nucleon + vector-meson) amplitudes, 25:30931
FISCHER, C. O., Neutron chopper system for energy range 10^{-4} eV to 10 eV, 25:31182
FISCHER, Gaston, Bulk and surface nucleation field of pure lead, 25:30424
FISCHER, Veit, Influence of neutron irradiation at 4°K on shear modulus of Cu, Al, and Pt, 25:29912
FISHER, A., Determination of neutron spectra from activation data by means of rfo1 and rfo7 codes, 25:31648 (KFKI-70-30-RPT)
FISHER, E. S., Elastic moduli of hcp Ti and Zr, 25:29852
FISHER, R. P., Optimization of experimental conditions for spectrofluorimetric determination of europium, samarium, and terbium as their hexafluoroacetylacetone-trioctylphosphine oxide complexes, 25:28954
FITCH, R. A., Low-inductance, megavolt Marx Generators, 25:30573 (EUR-4593, pp 311-17)
FJELLESTAD, K., Unintentional fission product releases during normal and high power load conditions in a boiling heavy water test reactor, 25:31609
FLAGELLA, P. N., Creep-rupture data for the refractory metals to high temperatures, 25:29868
FLAMINIO, E., Compilation of cross sections. VI, 25:30735 (CERN-HERA-70-7)
FLATTAU, J., Radioactivity distribution of emanation decay products between aerosol particles of determined size ranges, 25:29214 (LA-tr-71-7)
FLECK, Carl M., Method of thermal neutron waves for determination of diffusion parameters in heavy materials, 25:31177
FLEISCHER, A. A., Design and performance of a compact multi-particle cyclotron, 25:31145
Design and performance of H⁻ injector cyclotron, 25:31151
FLEISCHER, L. R., Growth of transition metal carbide single crystals by recrystallization. I, 25:29926
Growth of transition metal carbide single crystals by recrystallization. II, 25:29927
FLEISCHMANN, R., Analyzing power of the reaction ^{3}He(d,p)^{4}He, 25:31197
FLEISHER, V. G., Internal ionization in β decay of ^{131}I, 25:31316
FLEMING, Edward H., Methodology for computing potential radiation dose to man from nuclear excavation projects, 25:29516 (UCRL-50990)
FLEMING, R. J., Simple cryostat for thermoluminescence measurements, 25:30444
FLIESSBACH, Torsten, Nuclear density distribution for nucleus--nucleus scattering. II, 25:31423
FLYGARE, K. A., Improved feedback control for Null-point compensating system, 25:31741 (UCLA-12-813)
FOEHL, C. A., Powder metallurgical production of UO_2--PuO_2 steel pellets, 25:29931
FOERSTER, S., Design possibilities and consequences for the conventional parts of fusion power plants, 25:30588 (EUR-4593, pp 445-60)
FOMENKO, V. N., Description of the excited paired states of atomic nuclei by the variational approach, 25:31360
FONTAN, Jacques, Measurement of the state of equilibrium between radon and its daughters in the uranium mines, 25:29201 (AEC-tr-7228)
Particle size spectrum of the radioactive aerosols in a uranium mine, 25:29200 (AEC-tr-7227)
FONTANA, M. G., Stress corrosion cracking of Ti--8Al--1Mo--1V alloy: aqueous and methanol environments, 25:29765
FONTANA, Mars G., Advances in corrosion science and technology. I, 25:29778
FONTANA, P. F., Treatment of radiation-induced cutaneous lesions, 25:29706
FORBES, Fred F., Infrared polarization of eta Carinae and VY Canis Majoris, 25:30076
FORD, C. Hubbard, Tests of evaluated beryllium (n,2n) cross sections by analysis of 1.4-eV flux in water for an americium--beryllium source enclosed in beryllium spheres, 25:31223
FORD, G. P., Thermal-neutron fission of /sup 242m/Am: Mass and charge distribution, 25:31373
FORD, W. F., Inelastic transition densities, 25:31418
FORD III, W. E., POPOP4 library and codes for preparing secondary gamma-ray production cross sections, 25:31671 (ORNL-TM-3367)
FORTI, G., COSTAX-BOIL: program for axial dynamics of BWR and PWR nuclear reactors, 25:31541 (EUR-4497)
FORTOV, V. E., Thermodynamically complete equation of state of imperfect plasma, 25:30521
FOSSAN, D. B., Experimental study of electromagnetic matrix elements in ^{92}Mo, 25:31372
Recoil-distance lifetime measurements for states in ^{30}P, 25:31279
FOURCY, A., Fast analysis by 14-MeV neutron activation of fluorine deposits on the vegetation in a polluted area, 25:29011 (CEA-CONF-1747)
FOURNET, G., Penetration of induction, electrical field, and losses in impure Type-II superconductors having a surface current, 25:30414 (ORNL-tr-2475)
FOURNIER, D., Production (rho^0, f^0, ω^0) on nuclei and protons by 15, 16 Gev/c π⁻, 25:30741
FOURNIER, G., Principle of a simple measure of ion temperature in the ionosphere, 25:30383
FOX, Maurice S., Effects of incorporated ^{3}H and ^{32}P on DNA, 25:29459
FOYT, A. G., Junction (n--p) photovoltaic detectors in PbTe produced by proton bombardment, 25:29397
FRAAS, H., Comparison of pion electroproduction data with vector meson dominance predictions, 25:30789
FRADKIN, M. I., Measurements of energy spectra of multicharged nuclei, 25:30307
FRAENKEL, Benjamin S., Laser-generated plasma as a spectroscopic light source, 25:30498 (N-70-41880)
FRAIKOR, F. J., Electron microscope study of radiation damage in bismuth-ion-implanted CdS, 25:30656
FRAM, D. M., Isotropy of the microwave background at 8-millimeter wavelength, 25:30228
FRANCHI, R., Angioscintiphotography, 25:29587
FRANCISCO, V., Dispersion studies using stable and radioactive tracers in fresh water streams, 25:29213
FRANCK, G., Linear polarization of the γ rays emitted in the reaction ^{46}Ti(p,p'γ), 25:31288
FRANK, H., Elastic electron scattering on ^{40}Ar, 25:31272
FRANK, I. M., Peculiarities of transition radiation, 25:30702
FRANKEL, R. B., Isomeric shift of the 83 keV transition in ^{153}Eu, 25:31331
FRANKFURT, L. L., Electromagnetic and weak corrections to the scattering of high-energy hadrons, 25:30832
FRANKLIN, Carl E., ESR study of sugar radical in irradiated deoxyadenosine, 25:29146
FRANTOV, G. S., Method and technique of surveying during photographing and visual observation in a field of high frequency currents, 25:31733 (SC-T-713025)
FRANZEN, H. F., Zirconium--sulfur system at high temperatures, 25:29990
FRASER, D. A., Constant-frequency oscillations in a bounded thermally produced plasma, 25:30624
FRAUENDORF, S., Projection description of rotational and quasirotational bands in even--even nuclei, 25:31438
FREDERIKSEN, J. S., Analytic properties of the scalar vertex function, 25:30770
FREDRIKSSON, D. K., Square wave rf system design for TRIUMF cyclotron, 25:31091
FREED, Jerome J., Prog. rpt. on effects of ultraviolet radiation on cell structure and behavior, 1967--1970, 25:29608 (NYO-2356-43)
FREEMAN, A. J., Prog. rpt. on electronic band structure and physical properties of actinide metals and their compounds, 1970, 25:30696 (COO-2103-3)
FREEMAN, G. R., Behavior of extra electrons in the liquids methane, ethane, and propane, 25:29102
FREHLAND, Eckart, Energy--momentum--stress tensor and gravitational field of uniformly rotating masses, 25:30997
FREITAG, H., Observations on the influence of step ionization on the distribution function as well as transport and balance values of electrons in neon low-pressure plasma at low degrees of ionization, 25:30525
FRENCH, J. B., Spectral distributions in nuclei, 25:31429
FRENCH, R. L., Differential measurements of fast-neutron air-ground interface effects, 25:30635
FREOUR, A., Thermal shielding by screens of circulating gas, 25:31576 (EUR-4531, pp 1035-53)
Thermal shielding for water reactors, 25:31578 (EUR-4531, pp 1085-97)
FRIAS, Robert, Bevatron guide field control, 25:31055 (UCRL-20189)
FRIDMAN, A., Observation of d* effect in anti pd + p anti p π⁺ π⁻n reaction at 5.55 GeV/c, 25:30727 (NP-18796)
FRIDMAN, V. Ya., Strength and plasticity of submicron tungsten fibers, 25:29857
FRIEDLAND, E., Reaction ^{7}Li(d,α)^{5}He in range of 0.6 to 2.0 MeV, 25:31220
FRIEDMAN, L., Investigation of backscattering in D⁺--H_2

XUM

reaction system, 25:30291
FRIEDMANN, C., Some results on the removal of radiocesium from low-activity waste water by coprecipitation with ferrocyanides, 25:29183 (SGAE-SS-6/1969)
FRIEDRICH, F. J., Coaxial high-power trigatron for 60 kV, 25:30579 (EUR-4593, pp 373-8)
FRISCH, W., Inherent stability of the steam-cooled breeder, 25:31542 (EURFNR-813)
FRITTELLI, L., Studies on natural background radiation in Italy, 25:29205
FRITZ, Gilbert, Line emission in the x-ray background, 25:30140
FRITZSCH, Harald, Scale invariance and the light cone, 25:30749 (CALT-69-297)
FROEHLICH, K., Polymeric chromium(III) complexes resulting from neutron irradiation of crystalline K chromate. II, 25:29171
FROISSART, Marcel, Low-energy theoretical models, 25:30854
FROLOV, V. P., Egg laying of hens under action of incorporated ^{131}I, 25:29661
FROMM, Eckehard, Investigations of the conductivity of vapor deposited tantalum layers with island structure, 25:30686
FROST, K. J., Evidence from hard x rays for two-stage particle acceleration in a solar flare, 25:30169
FU, C., Single-pion production in K+p interactions at 4.6 GeV/c, 25:30748
FUBINI, A., Investigation of reaction $^{35}Cl(n,\gamma)^{36}Cl$, 25:31280
FUBINI, S., Amplitude for N nonspurious excited particles in dual resonance models, 25:30830
FUDA, Michael G., Boundary-condition-model T matrix, 25:31441
FUEKI, Kenji, Radicals produced in γ-irradiated allyl alcohol glass, 25:29162
FUGOL, I. Ya., Experimental investigation of destruction of metastable helium atoms in a plasma at low temperatures, 25:30512
FUJIE, H., Studies for safety analysis of loss-of-coolant accidents, 25:31605
FUJII, Tadayuki, Rolling workability of pure W single crystals, 25:29877
FUJITA, Jun-Ichi, Low-energy theorems for nuclear weak and electromagnetic currents, 25:30807
FUJIWARA, Masami, Experiments of plasma confinement in JIPP stellarator. I, 25:30457 (IPPJ-102)
FUJIYAMA, Tsunetake, Normal coordinate treatment and force constants of alkanonitriles, 25:29070
FUKUDA, Kiyoshi, Recent improvements in fluoro-glass dosimeter, 25:29387
FUKUDA, Takeshi, Release of fission Cs from irradiated UO_2 powder, 25:29974
FUKUMOTO, S., Design of high-gradient accelerating column, 25:31048 (SJC-A-71-2)
FUKUSHIMA, Hiromi, Nuclear structure of ^{126}Te, 25:31346
FULLARD, K., Automatic data collection and processing as an aid to fusion research, 25:30474 (EUR-4593, pp 557-66)
FULLERTON, Wayne, Calculations of Van Der Waals broadening for lines of astrophysical interest, 25:30266
FULLWOOD, R. R., Calibration of Moxon--Rae detectors in the current mode, 25:29326 (LA-4445)
Neutron-induced fission cross section of ^{242}Pu, 25:31385
FUNEL, Genevieve, Arsenic-76 decay, 25:31259
FUOCHI, P. G., Behavior of extra electrons in the liquids methane, ethane, and propane, 25:29102
FURBER, B. N., Thermal performance of porous insulants in a high-pressure gas environment, 25:30029 (EUR-4531, pp 841-81)
FURCHNER, J. E., Comparative metabolism of radionuclides in mammals. V, 25:29450
FURTH, H. P., Progress in controlled thermonuclear research, 25:30600 (WASH-1172)
FURUTANI, Y., Exact Green function for Lenard--Bernstein operator, 25:30537
FUSHCHICH, V. I., Additional invariance of relativistic equations of motion, 25:30975
Equations of motion invariant under group P(1,n). II, 25:30966

G

GABRIEL, T. A., Approximate high-energy alpha-particle nucleus collision model, 25:31368
GADDY, R. H., Emission spectrochemical determination of tantalum in curium oxide, 25:28964
GAFFNEY, Thomas E., Ion specific detection of internal standards labelled with stable isotopes, 25:28967
GAGARIN, Yu. F., Charge distribution of heavy cosmic-ray nuclei in region Z greater than or equal to 26, 25:30305
GAGE, S. J., Computer-assisted analysis of gamma-ray spectra, 25:29363
GAGLIONE, P., Fallout ^{54}Mn and ^{95}Zr in water and fishes of lakes in northern Italy, 25:29477
Radioactivity in air and fallout, 25:29218
Surveillance of environmental radioactivity around a nuclear center, 25:29222
GAI, E. V., Asymmetric rotor problem and the collective excitations of even nuclei, 25:31409
GAIDAMAKIN, N. A., Pathomorphological changes in brains of animals during whole body irradiation, 25:29644
GAIDIDEI, Yu. B., Light absorption by the pair of triplet excitons, 25:31698 (ITF-70-74)
GALAEV, A. N., Basic design parameters of a small size isochronous cyclotron, 25:31143
GALAN, P., Decay ^{160}Tb + ^{160}Dy, 25:31335
GALANOVA, T. J., Decay ^{160}Tb + ^{160}Dy, 25:31335
GALANTER, L., Tabulated dose uniformity ratio and minimum dose data for gamma irradiator design, 25:29250 (BNL-50145(Rev.))
GAL'CHUN, A. V., Sextupole lenses with improved non-linearity in slow ejection systems, 25:31045 (NP-18799)
GALIANA, R., Proton source for improved CERN synchrocyclotron, 25:31158
GALIN, J., Cross sections for heavy ion nuclear reactions, 25:31356
GALKIN, I. V., Fast transistor dc amplifier, 25:29346
GALLEGOS, A. F., Retention and distribution of ^{244}Cm following inhalation of $^{244}CmCl_3$ and $^{244}CmO_{1.7}$ by beagle dogs, 25:29429 (LF-43, pp 100-5)
GALLI, M., Cosmic-ray microvariations during thunderstorm perturbations, 25:30334
GALLMANN, A., Determination of the parity of the 4.19-MeV level of ^{36}S, 25:31289
Linear polarization of the γ rays emitted in the reaction $^{46}Ti(p,p'\gamma)$, 25:31288
GAL'PER, A. M., Primary γ radiation with E greater than or equal to MeV, 25:30306
Relation of electron flux in upper atmosphere to state of Earth magnetosphere, 25:30353
GAMMAGE, R. B., Electron paramagnetic resonance studies of carbon monoxide adsorbed on thorium oxide, 25:29090
GAMMEL, J. L., Bethe--Salpeter solution for nucleon--nucleon scattering with pion exchange, 25:30909
GANGRSKII, Yu. P., Production of spontaneously fissionable isomer ^{236}U at radiative thermal neutron capture, 25:31307 (JINR-P7-5497)
GANZER, U., Radiotherapy of synchronized skin tumors in mice, 25:29605
GAPONIUK, P. Ya., Changes of plasma kininogen and kinin-forming activity in irradiated animals, 25:29681
GAPONYUK, P. Ya., Change in kinin system of blood during acute radiation sickness, 25:29668
GARAVAGLIA, C., Radiological protection in a general hospital, 25:29538
GARCIA, Augusto, Analysis of spin correlations in the beta decay of the lambda hyperon, 25:30804 (COO-264-569)
Beta decay of hyperons, 25:30815
GAREEV, F. A., Single-particle states of deformed transuranium nuclei in Saxon--Woods potential, 25:31392 (BNL-tr-416)
GARFINKEL, S. B., Certificates of radioactivity standards, 25:29173
GARIBYAN, G. M., Physical nature of zones generating transition radiation, 25:30714
GARN, Paul D., Conference on thermal analysis, Worcester, Mass., 8/68. II, 25:29758
Relative thermal stabilities of copper(II) sulfate pentahydrate and barium chloride dihydrate compared to their deuterium oxide analogs, 25:29042
GARREC, J.-P., Fast analysis by 14-MeV neutron activation of fluorine deposits on the vegetation in a polluted area, 25:29011 (CEA-CONF-1747)
GARREN, A. A., Negative mass instabilities in an electron-ring compressor, 25:31058 (UCRL-20208)
GARRETT, Harold J., Use of DTA for the determination of the monoclinic--tetragonal transformation in zirconia and zirconia-based systems, 25:29982
GARVEY, Gerald T., Reactions $^{11}B(p,^3He)^9Be$ and $^{11}B(p,t)^9B$, 25:31228
GASKILL, James R., Engineering tests of Halon 1301 fire extinguishing systems for field assembly buildings, 25:31748 (UCRL-51021)
GASPARYAN, A. P., Cross sections of inelastic channels of reactions in np-interactions at the neutron momentum from 2 to 10 GeV/c, 25:30726 (JINR-P1-5665)
GASS, H., New bearing materials for ultrahigh vacuum, 25:29834
GATTO, R., Commutators near light cone, Bjorken limits, and O_4 expansion, 25:31020
GATZ, Donald F., Trace substances in rain water, 25:29224
GAUR, R. K., Charge identification of nuclear tracks in photographic emulsions, 25:29380
Track width in nuclear emulsions, 25:29381
GAUTIER, D., Far-infrared spectrum of Jupiter, 25:30250
GAVKALOV, Yu. D., Radiation defectoscopy of concrete and reinforced concrete by means of betatron stremsstrahlung, 25:29296
GAVRILOV, R. I., Influence of irradiation and radioprotectors on activity of alkaline phosphatase in mucosa of small intestine, 25:29645
GAZIEV, A. I., Radiosensitizing effect of ferrous ions, 25:29556
GEDDES, Ian C., Pharmacokinetics of halothane in man, 25:29416
GEIGER, J., Determination of population densities in a helium plasma by electron impact spectroscopy, 25:30481
GEILIKMAN, B. T., Increasing superconducting transition temperature by phonon mechanism, 25:30438
GEISSLER, C., Sample preparation for precision carbon

isotopic analysis, 25:28968
GELAIN, C., Kinetics and mechanism of low-pressure, high-temperature oxidation of Si. II, 25:29968
Kinetics and mechanism of low-pressure, high-temperature oxidation of W silicides. III, 25:29869
Low-pressure, high-temperature siliconizing of W. I, 25:29814
GELLES, S. H., Beryllium: properties and fabrication, 25:29794
GELL-MANN, Murray, Scale invariance and the light cone, 25:30749 (CALT-69-297)
GENAEVA, L. I., Studies of VH and VVH nuclei in mineral meteorites, 25:30317
GENSINI, P., Coupled-channel unitarization of Veneziano model and pion form factor, 25:30860
GENTLE, K. W., Electron beams for quasi-linear and nonlinear beam--plasma experiments, 25:30500
GENZ, H., Scale-symmetry breaking and scaling properties of currents, 25:30934
GEORGE, C., Nonequilibrium statistical mechanics and quantum field theory, 25:30956
GEORGELIN, Y. P., Diameter of H II regions in the Galaxy, 25:30203
GERA, F., Studies on natural background radiation in Italy, 25:29205
GERASIMOV, S. B., Selected topics in the theory of electromagnetic interactions, 25:30772 (CERN-71-7, pp 181-283)
GERBER, J-P., Observation of d* effect in anti pd + p anti p π^+ π^-n reaction at 5.55 GeV/c, 25:30727 (NP-18796)
GERBERICH, William W., Crack growth mechanisms in fibrous composites, 25:31746 (UCRL-20524)
GERDAU, E., g-factor of the 181 keV level of ^{99}Tc, 25:31271
GEROCH, Robert, Approach to quantization of general relativity, 25:31003
GEROLA, H., Spectrum of a gaseous nebula of pure H. III, 25:30101
GERSTEIN, S. S., Method of measuring electromagnetic form factor of neutrino, 25:30777 (JINR-P2-5705)
GERSTEN, Alexander, Relativistic calculation of nucleon--nucleon phase parameters, 25:30912
Validity of a local approximation to the one-pion-exchange potential for the two-nucleon system, 25:30911
GERTSUSKII, D. F., Sensitivity of sweet potatoes to ionizing radiation, 25:29721
GESHKENBEIN, B. V., Divergences of amplitudes of weak nonleptonic processes with photon emission, 25:30805 (NP-18777)
GEUE, Jean, Heat pipes and their applications, 25:29249 (AAEC/LIB/Bib-264)
GHIRARDI, G. C., Search for quantum systems with given spectrum-generating algebra, 25:30918
GIACOMELLI, G., Pion--nucleon elastic scattering, 25:30872
GIANNONE, P., Induced semi-convection in He-burning horizontal-branch stars. II, 25:30103
Overshooting of convective cores in helium-burning horizontal-branch stars, 25:30037
GIBNEY, Robert B., Heat capacity and derived thermodynamic functions of ^{242}Pu from 15 to 373K, 25:29831
GILBERT, C. P., Feasibility study of the automatic controls for a pebble bed reactor power station, 25:31543 (AAEC/E-203)
GILCHRIST, J. le G., Hall effect in superconducting niobium and alloys, 25:30427
GIL GAYARRE, C., Conference on high-energy electrons, Madrid, 9/66, 25:29596
GILINSKY, V., High energy astrophysics, 25:30220 (P-4494(RAND))
GILL, S., Behavior of perforated end slabs for concrete pressure vessels, 25:29306
GILLIGAN, J. E., Space environment stability program in white pigment coatings, 25:29105
GILLIN, Michael Talbot, Excited states of ^{176}Hf from the decay of ^{176}Ta, 25:31348
GIL Y GIL, C., Conference on high-energy electrons, Madrid, 9/66, 25:29596
GINGERICH, Karl A., Gaseous metal nitrides. IV. The dissociation energy of cerium mononitride, 25:29037
GINTER, E. K., Radiation biophysical investigations in Drosophila melanogaster. II, 25:29499
GINZBURG, V. I., Corrosion resistance of Mo alloys in certain corrosive media, 25:29776
GINZBURG, V. L., Role of quantum fluctuations of a gravitational field in general relativity and cosmology, 25:30224
What problems of physics and astrophysics are at present especially important and interesting, 25:30452
GIOVANNINI, A., Nonequilibrium and soft-particle emission models, 25:30857
GIUBILEO, M., Measuring of β and γ radioactivity in biological samples, 25:29517
GLADYSHEV, D. A., Automatic stabilization of a device for measuring life times in the picosecond range, 25:29365
GLADYSHEVSKII, E. I., Crystal structure of $CeMg_2Si_2$, 25:29993
GLAZOV, A. A., Rf system of the monoenergetic cyclotron, 25:31128
GLEESON, L. J., Convective transport of low-energy cosmic rays in the interplanetary region, 25:30179
GLOYNA, Earnest F., Transport of ^{137}Cs. II, 25:29204
GLUCKSMANN, A., Effects of irradiation on salivary glands, 25:29693
GLUECK, M., Photoproduction and electromagnetic moments of charged rho mesons, 25:30799
GNOJEK, I., Information on prospecting in Sweden, 25:29229
GODDARD, P., Landau singularities in multi-Regge theory and fixed-angle behavior, 25:31033
GOEBEL, Klaus, Intensity estimation for a neutron beam for biological and medical applications, 25:31174 (UCRL-19715)
GOETZMANN, O., Compatibility studies with UC of different stoichiometries and iron--nickel--chromium alloys and the influence of stabilizers, 25:29940 (EURFNR-826)
GOGGIN, Brian, New materials for chemical resistance, 25:29775
GOH, C. H. T., Dissolution of small radioactive particles, 25:29080 (LF-43, pp 40-51)
GOIN, G., Grenoble cyclotron progress report, 25:31097
GOKHALE, A. S., Water chemistry studies: chemical analysis manual for moderator and coolant water systems, 25:28914 (BARC-515)
GOKHALE, G. S., Flattening of the x-ray spectrum of Sco X-1, 25:30147
Improved estimate of solar neutron flux measured in an earlier experiment, 25:30177
GOKHSHTEIN, Ya. P., Critical current density across MHD generator electrodes made of ZrO_2--Y_2O_3 ceramics, 25:30336
GOLAB-MEYER, Zofia, Backscattering at high energies, 25:30836
GOLANT, V. E., Absorption of shf waves by plasma at upper hybrid frequencies, 25:30606 (NP-18807)
GOLDAN, Samuel, Surgical treatment of chronic radiation injuries of axilla and shoulder, 25:29569
GOL'DANSKII, V. I., Stabilized gamma-resonance spectrometer, 25:29360
GOLDFEDER, A., Experimental models for evaluation of host defenses in cancer, 25:29472
GOL'DIN, L. L., Mass-spectrometric measurements of the diminution of hydrogen in polyethylene targets which have been irradiated in a proton synchrotron, 25:29400
GOLDSTEIN, M., Differential spin exchange and elastic scattering of low-energy electrons by potassium, 25:30282
GOLLWITZER, S., Helium leak tests on reactor components, 25:31563
GOLOVANIVSKII, K. S., Elimination of cone losses in the magnetostatic mirror by help of microwaves, 25:30463
GOLOVCHENKO, Yu. V., Angular correlation of 345 to 136 keV cascade in ^{181}Ta, 25:31321
GOLOVIN, B. M., Relativistic rotation of a $S = 1/2$ spin in collisions of particles moving arbitrarily with respect to the observer, 25:30760
GOLOVKOV, N. A., Alpha spectra of ^{209}At, ^{210}At, ^{211}At, and ^{211}Po, 25:31324
GOMBEROFF, L., Hartree--Fock approximation in quantum electrodynamics, 25:30989
GOMEZ-NUNEZ, J. C., Sterility and chagas' disease vector control, 25:29745
GONCHAROV, I. N., Resistance behavior of superconducting alloy of Nb + 80 percent Zr in region of H/sub c2/, 25:30412 (JINR-P8-5733)
GOOD, R. H. Jr., Spin-two massless-particle radiation as a gravitational effect, 25:31002
GOOD, W. M., Report to the AEC nuclear cross section advisory committee, 25:31204 (ORNL-TM-3378)
GOODALL, I. W., Creep behavior of prestressed concrete slabs with reinforced holes, 25:30024 (EUR-4531, pp 373-84)
GOODINSON, P. A., New interpretation of Vaidya radiation, 25:30778
GOORVITCH, David, Laser-generated plasma as a spectroscopic light source, 25:30498 (N-70-41880)
GOPAL-AYENGAR, A. R., Reaction to thymine with radiation induced electrons in alcoholic matrices at 77°K, 25:29143
GORBATENKO, M. V., Matrix space dynamics taking into account third-order terms in Lagrangian, 25:30967
GORDON, M. M., Longitudinal space charge effect and energy resolution, 25:31114
Proposed Michigan State Univ. transuranic accelerator facility, 25:31085
GORELOV, V. P., Solution of single-speed neutron transport equation in multilayer plane and spherically symmetric systems, 25:31184
GORELOVA, N. V., Radioprotective properties of o-acyl derivatives of serotonin, 25:29555
GORENSHTEIN, L. I., Diantipyrinylmethane pyrocatecholate complex of molybdenum and its analytical application, 25:28926
GORENSTEIN, P., X-ray pulsations from Cygnus X-1 observed from Uhuru, 25:30139
GORICHEV, P. A., Program linking FSD measuring microscopes with a Minsk-2 computer, 25:29379
GORIZONTOVA, M. P., Manganese penetration of mitochondrial membranes after influence of ionizing radiation, 25:29673
GORKIN, V. Z., Deamination of nitrogen compounds in liver during radiation sickness, 25:29641
GOROKHOVA, L. G., Colorimetric determination of tellurium with sodium pyrosulfite, 25:28931

XUM

GORSCHLUETER, Klaus, Experimental studies of radiation protection through tryptamine, 25:29566
GORYACHEV, B. I., Structure of photoneutron cross sections of ^{51}V, ^{52}Cr, and ^{59}Co, 25:31243
GORYACHEV, Yu. M., Methods for monitoring proton incidence on the internal targets of high-energy accelerators, 25:31043 (NP-18776)
Methods of monitoring proton discharge onto the internal target of a high-energy accelerator, 25:31064
GOSLING, A. W., Gold content of natural waters in Colorado, 25:29015
GOTO, Hidehiro, Rapid determination of hydrogen in metals by the argon gas carrier fusion-gas chromatographic method, 25:28936
GOTTLIEB, Carl A., Excitation and abundance of interstellar SiO, 25:30152
GOTTWALD, Gizella, Lipid fraction alterations in serum and liver of rats exposed to 2000 r local hepatic irradiation, 25:29685
GOUGH, R. A., Beta-delayed protons from ^{23}Al, 25:31241 (UCRL-20436)
GOULARD, G., Direct compound mechanism for reaction $^{11}B(p,\alpha)2\alpha$, 25:31218
GOULD, R. W., Progress in controlled thermonuclear research, 25:30600 (WASH-1172)
GOULD, Robert J., Pulsar dispersion measures and the mean and mean-squared interstellar electron density, 25:30118
GOURDIN, M., Vector mesons in electromagnetic interactions, 25:30796
GOURISSE, D., Oxidation of Np(V) by aqueous nitric acid solutions in presence of nitrous acid, 25:29036
GOVIND, P. K., Electron microscope study of radiation damage in bismuth-ion-implanted CdS, 25:30656
GOVOROV, A. M., Vacuum sorbent cut-off device in cryostat of a Ge(Li) detector, 25:29351
GOYAL, Ashok, SU_3 mass differences in fifth interaction and tadpole results, 25:30781
GRAAB, Judson W., Comparison of modified Kjeldahl and vacuum fusion technique for determination of N in Ta alloys, 25:28937
GRABOVSKII, V. I., Electrohydrodynamic flow in a plane channel with axial electrode, 25:30345
GRACHEV, M. I., Pulse shaper with independent regulation of output pulse duration and dead time, 25:29342
GRAESSLER, H., Single pion production in π^+p interactions at 8 and 16 GeV/c, 25:30891
GRAEVSKAYA, B. M., Influence of radioprotective agents correlated with radiosensitivity of animals, 25:29553
GRAF, Rene, Interaction of beryllium wire with an aluminum matrix, 25:29883 (SC-T-713021)
GRAFF, Samuel, Nucleic acid synthesis in bladder tumors, 25:29585
GRAMA, N., Classification of spin-isospin functions of identical-nucleon system. II, 25:30916
GRANDI, Francesco, Gamma radiolysis of branched chain hydrocarbons: 2,2-dimethylbutane, 25:29142
GRASS, F., Separation of ^{239}Pu(IV) from ^{95}Zr, ^{95}Nb, ^{106}Ru, and ^{106}Rh by anion exchange resin from mixed methyl alcohol nitric acid solution, 25:29191
Studies on absorption of ^{239}Pu by anion exchange resin from nitric acid and mixed nitric acid methyl alcohol systems, 25:29194
GRAVES-MORRIS, P. R., Model of eta + 3π and K + 3π decays, 25:30788
GRAY, W. S., Isospin nonconservation in reactions $^{16}O(d,\alpha)^{14}N^*$/sub 0$^+$, T = 1/ and $^{12}C(d,\alpha)^{10}B^*$/sub 0$^+$, T = 1/, 25:31227
GRAYHACK, John T., Radiation therapy in the treatment of carcinoma of the prostate, 25:29597
GREBENSHCHIKOV, R. G., Solid solutions in the system hafnium dioxide--silica, 25:30006
GRECZ, N., Irradiation resistance of spores of Clostridium botulinum in beef, 25:29734
GREEN, A. E. S., Relativistic calculation of nucleon--nucleon phase parameters, 25:30912
Validity of a local approximation to the one-pion-exchange potential for the two-nucleon system, 25:30911
GREENE, Frank T., Molecular beams in high temperature chemistry, 25:30258
GREENHILL, J. G., Search for antimatter in primary cosmic rays, 25:30327
GREGERSEN, K., Inelastic scattering of deuterons and α-particles on ^{191}Ir and ^{193}Ir, 25:31342
GREMONT, B., 20 MeV compact cyclotron, 25:31142
GRENNBERG, Bertil, Energy of ^{253}Es α particles, 25:31357
GRESSER, H., High-Q capacitors with liquid and gas impregnation, 25:30595 (EUR-4593, pp 545-50)
GRIBBLE, R. F., Design and installation of Scyllac, 25:30564 (EUR-4593, pp 227-39)
GRIEGER, I., Three-dimensional elastic and elastoplastic calculations on reactor pressure vessels, 25:31667 (EUR-4531, pp 777-95)
GRIEM, Hans R., How accurate are H/sub β/ Stark profiles, 25:30268
GRIFFITH, W. C., Application of a biological model of tissue distribution and retention of inhaled ^{140}La in beagle dogs to an analysis of radiological hazards to humans inhaling various isotopes of lanthanum, 25:29427 (LF-43, pp 82-91)
Tissue distribution and retention of ^{140}Ba and ^{140}La in beagle dogs after inhalation of $BaCl_2$--$LaCl_3$ aerosols, 25:29428 (LF-43, pp 92-9)
GRIGORASHCHENKO, O. N., Experimental investigation of destruction of metastable helium atoms in a plasma at low temperatures, 25:30512
GRIGOR'EVA, L. I., Turbulent heating of a plasma by a large amplitude whistler, 25:30470
GRIGORYAN, G. L., Macrostructure of bovine serum albumin under γ irradiation, 25:29471
GRILLMAIER, R., Radiation dose distribution in lungs of Thorotrast patients, 25:29521
GRIMM, R. C., Non-local potentials and the single-particle shell model, 25:31447
GRIN, Yu. T., Application of the K-harmonic method to the calculation of nuclear properties, 25:31439
GRISHIN, V. G., Application of phenomenological quasi-two-body model to π^-p-interactions with strange particle production at p = 4 GeV/c, 25:30869 (JINR-P1-5706)
Coherent interactions of π^--mesons with photoemulsion nuclei at 17 GeV, 25:30736 (JINR-P1-5565)
Particle interference in the processes involving excited nuclei, 25:31395 (JINR-P1-5648)
GRIVAZ, J. F., Production (rho^0, f^0, ω^0) on nuclei and protons by 15, 16 Gev/c π^-, 25:30741
GRODZINS, L., Isomeric shift of the 83 keV transition in ^{153}Eu, 25:31331
GROMAKOVA, Z. I., Colorimetric determination of tellurium with sodium pyrosulfite, 25:28931
GROMOV, K. Ya., Gamma radiation of ^{226}Ra and its decay products, 25:31358
GROSCH, D. S., Response of the female arthropod's reproductive system to radiation and chemical agents, 25:29747
GROSFELD, J. L., Radiation hepatitis in children, 25:29652
GROSS, Bernard, Compton diodes, 25:29329
GROSSIN, R., Heat exchange by natural convection in porous media, 25:29264 (EUR-4531, pp 821-39)
GROTH, H. G., Conference on spectrum formation in stars with steady-state extended atmospheres, Munich, Ger., 4/69, 25:30035 (NBS-SPEC. PUBL-332)
GROUT, David C., Radiation therapy in the treatment of carcinoma of the prostate, 25:29597
GROVE, D. J., Preliminary investigation of ohmically-heated plasmas in the model ST Tokamak, 25:30459 (MATT-813)
GROWER, M. F., Liquid scintillation counting of (^3H) and (^{14}C) on solid supports: a warning, 25:28985
GROZDANOVIC, J., Combined effect of 6-Azauridine and irradiation in vivo and in vitro. VI, 25:29679
GRUBE, Arthur F., Boron, 25:29936
GRUBER, J. E., Erosion in high-current, high-pressure gas discharges, 25:30495 (EUR-4593, pp 251-6)
GRUDEN, Nevenka, Calcium and strontium metabolism as related to age and alginates, 25:29446
GRUDSKAYA, L. E., Phoswich for neutron detection, 25:29339
GRUEEBLER, W., Absolute calibration of tensor analysing powers of the $^3He(d,p)^4He$ and the $^4He(d,d)^4He$ reactions, 25:31198
GRUEN, G. E., Effects of state properties on high pressure compressible hydrodynamics, 25:31590 (CONF-710302-6)
GRUNDMAN, W. A., Square wave rf system design for TRIUMF cyclotron, 25:31091
GRUNOW, R., Radiation effects in isolated DNA and their functional consequences. VIII, 25:29469
Radiation effects in isolated DNA and their functional consequences. VII, 25:29468
GRYZLOV, A. I., Impulse generator for feeding a linear accelerator, 25:31066
GUANCIAL, Edward L. Jr., Muon capture in ^3He, 25:31190
GUBAR, Yu. I., Radial profile of the proton belt, 25:30354
GUBERNIEV, M. A., DNAase activity of E. coli K12 (lambda) during gamma irradiation, 25:29725
GUDZENKO, L. I., Formation of a nonequilibrium population in plasma under ionization resonance conditions, 25:30519
GUENTHER, K., Radiation effects in isolated DNA and their functional consequences. VIII, 25:29469
Radiation effects in isolated DNA and their functional consequences. IX, 25:29470
GUENTHER, U., Polarization of the recoil protons in the elastic electron--proton scattering process, 25:30780
GUERREAU, D., Cross sections for heavy ion nuclear reactions, 25:31356
GUERRINI, P., Activities of Scalbatraio center for research in nuclear safety, 25:31610
GUESS, T. R., Dynamic mechanical properties of Armco 21-6-9 stainless steel, 25:31730 (SC-RR-69-761)
GUETKH, Sh., Alpha spectra of ^{209}At, ^{210}At, ^{211}At, and ^{211}Po, 25:31324
GUETLICH, P., Polymeric chromium(III) complexes resulting from neutron irradiation of crystalline K chromate. II, 25:29171
GUGUSHVILI, E. I., Riemann method in inverse problem. IV, 25:30894 (ITF-70-98-P)
GUIDI, I., Cosmic-ray microvariations during thunderstorm perturbations, 25:30334
GUILLAUME, G., Linear polarization of the γ rays emitted in the reaction $^{46}Ti(p,p'\gamma)$, 25:31288
GUIRLET, J., Consequences of accidents in nuclear plants, 25:31622
GULYAMOV, U. G., Coherent interactions of π^--mesons with photoemulsion nuclei at 17 GeV, 25:30736 (JINR-P1-

XUM

5565)
GUMEINER, I., Time-dependent electron density in Xe pinched plasma laser, 25:30484
GUNION, J. F., Scattering and pair production from the deuteron at large momentum transfers, 25:30910
GUNJI, Katsubumi, Improvement in isotopic ratio measurement of uranium, 25:28927
GUNN, James E., Motion and radiation of charged particles in strong electromagnetic waves. I, 25:30116
GUPTA, C. B., Liquid--liquid extraction behavior of mercury(II) as chloride, 25:29031
GUPTA, D., X-ray and diethyl sulfate induced mutation in rice, 25:29495
GUPTA, S. K., Effect of γ-irradiation on chlorendic acid based unsaturated polyesters, 25:29129
GURAL'NIK, D. L., Hauser--Feshbach method and inelastic scattering of protons, 25:31245
GURBANOVICH, I. S., Fractional parentage coefficients for (1d--2s)-shell nuclei, 25:31426
GUREVICH, Yu. G., Propagation of intense electromagnetic waves in a two-component plasma, 25:30619
GURNETT, Donald A., Color spectrograms of very-low-frequency Poynting flux data, 25:30370
GUROVICH, V. Ts., Nonlinear corrections in Lagrangian density of gravitational field and cosmological solutions without singularity, 25:30233
GURSKY, H., X-ray pulsations from Cygnus X-1 observed from Uhuru, 25:30139
GURTOVOI, M. E., Pulsed neutron source, 25:31178
GUSEV, N. F., Fast transistor dc amplifier, 25:29346
GUSEV, Yu. K., Internal ionization in β decay of ^{131}I, 25:31316
GUSEV-DONSKOI, V. P., Wideband frequency divider of a sinusoidal signal that has an adjustable division factor, 25:29404
GUSHCHINA, R. T., Heliolatitudinal Index (HL) of solar activity and 11-year variations of cosmic rays, 25:30165
HL index of solar activity and yearly variations of cosmic rays, 25:30308
GUS'KOVA, V. N., Effect of a mixture of uranium fission products on the sanitary conditions and hydrobionts of weakly-mineralized fresh-water basins, 25:29449
GUSMINI, Simone, Total elementary separation of rare earths on cation exchange resins, 25:29178 (CEA-R-4102)
GUY, Reed Augustus, Radiative pion absorption in nuclei, 25:31217

H

HAAS, G., Interaction of sputtered wall material with fusion plasma, 25:30497 (EUR-4593, pp 471-7)
HAAS, Paul, Rulison Project in retrospect, 25:29248
HABERER, G., Radiation biophysical investigations in Drosophila melanogaster. I, 25:29522
Radiation biophysical investigations in Drosophila melanogaster. II, 25:29499
HABERLER, P. L. F., Breakdown of scaling invariance in generalized Bjorken limit of perturbation theory, 25:30783
HACKENBROICH, H. H., Lithium-5 resonances above ^{3}He-d threshold, 25:31195
Microscopic calculation for n--^{3}H scattering, 25:31193
HADJIOANNOU, F. T., Analyticity constraints and residue functions of E_2 pole exchange, 25:31027
Elastic scattering of a spin zero and a spin 1/2 particle at u = 0, 25:30892
HADRAVA, P., Spectrographic study of EW LAC. I, 25:30098
HAEBERLI, W., Polarization measurements and phase shifts for p-^{4}He scattering, 25:31199
HAEFELE, Wolf, Development of fast breeders and prototype reactor SNR 300, 25:31536
HAEGGSTROEM, L., Moessbauer investigation of iron in boron, 25:30689 (UUIP-733)
HAELG, Walter, Variable states of a heavy plasma in relation to temperature and density, 25:30536
HAENDEL, S. K., Plasma drift in FXR discharge, 25:30499 (UUIP-659)
HAGEDOORN, H. L., Beam quality of AVF cyclotrons, 25:31112
HAGEDORN, R., Thermodynamical model of strong interactions, 25:30838
HAGELBERG, R., Helium-4 final state interactions and quasifree scattering in deuteron-induced three-particle reactions on ^{6}Li, 25:31187 (NP-18741)
HAGEMANN, Ronald F., Modification of radiation effect on the eye by topical application of dimethyl sulfoxide, 25:29562
HAGEN, Garrett A., Double-isotope derivative assay of serum iodothyronines. II. Thyroxine, 25:28986
HAGGERTY, M. J., Kinetic theory of inhomogeneous rotating self-gravitating systems: local energy production from binary interactions, 25:30230
Kinetic theory of inhomogeneous rotating self-gravitating systems: enhanced collisional diffusion and dissipation, 25:30229
HAHN, R. L., Inclusion of fission and charged-particle emission in calculations of nuclear reactions, 25:31313 (ORNL-TM-3179)
HAHN, Yukap, Effective orthogonality of channel wave functions and coupled equations for direct interactions, 25:31443
HAIRE, R. G., Mound assistance program: development of a sol-gel process and equipment for production of dense $^{238}PuO_2$ microspheres, 25:29921 (ORNL-4565)
HAISCH, A., Genetic control of Rhagoletis cerasi, 25:29741
Sterile-insect release method against Rhagoletis cerasi, 25:29742
HAKE, G., Power-reactor siting in various countries, 25:31482 (AECL-3740)
HAKE, Richard R., Single-shot pulsed magnetic fields from inductive energy stores, 25:30598 (LA-4617)
HALL, L. H., Spin-lattice relaxation and Zeeman effects in triplet state of pyrazine-d_4, 25:31742 (UCLA-34-P-91-47)
HALLWACHS, D., Radioisotopes to determine tubular passage time in dog kidneys, 25:29414
HALPERIN, B. I., Onset of superconductivity in one-dimensional systems, 25:30420
HAMA, Y., Weak duality and energy dependence of the slopes of elastic angular distributions, 25:30873
HAMBURG, G., Voids in V, Nb, and Mo by fast neutron irradiation at high temperatures, 25:29914
HAMILTON, J. H., Decay of ^{108}Ag, 25:31382
Decay of ^{72}As to the levels of ^{72}Ge, 25:31261
Graphs for analysis of (1-3) gamma--gamma directional correlations, 25:31312 (ORNL-4619)
Levels in ^{72}Ge populated by ^{72}Ga, 25:31260
HAMMANN, T. F., 3 particle--1 hole configurations and realistic forces, 25:31254
HAMMAR, Carl-Gustaf, Ion specific detection of internal standards labelled with stable isotopes, 25:28967
HAMMER, C. F., Design and installation of Scyllac, 25:30564 (EUR-4593, pp 227-39)
HAMORI, J., Growth and differentiation of synaptic structures under circumstances of deprivation of function and of distant connections, 25:29623
HANCHER, C. W., Prog. rpt. on concentration and desalting of protein solutions program, 6--8/70, 25:31714 (ORNL-TM-3328)
HANCOX, R., Recent developments in superconductivity and its applications to fusion research, 25:30557 (EUR-4593, pp 83-93)
HANDLOSER, L., Steric factors in the cationic rearrangement of substituted cyclobutanes, 25:29049
HANGANUT, M., Production of isotopically pure targets in electromagnetic mass separators by ion-beam retardation, 25:31069
HANKS, K. W., Design and installation of Scyllac, 25:30564 (EUR-4593, pp 227-39)
HANSEN, J. D., Compilation of cross sections. VI, 25:30735 (CERN-HERA-70-7)
HANSEN, K. F., Application of alternating-direction implicit methods to the space-dependent kinetics equations, 25:31654
HANSEN, Ole, Reactions (h,p) on Cr. I, 25:31298
HANSEN, P., Preparation and properties of a crystalline uranium(IV)--hydrazine nitrate compound, 25:29035 (NP-18736)
HANSEN, Ulf, MEDEA: model of a steam plant, 25:31624 (JUL-698-RG)
HANSON, A. W., Manufacture and construction of helical winding, 25:30555 (EUR-4593, pp 19-24)
HANSON, Peter James, Water tracing with soluble metal chelates and neutron activation analysis, 25:29013 (RLO-1750-81)
HARDEKOPF, R. A., Neutron polarization from ^{7}Li(p,n)^{7}Be reaction for 3 to 4 MeV protons, 25:31235
HARDER, Charles A., Engineering tests of Halon 1301 fire extinguishing systems for field assembly buildings, 25:31748 (UCRL-51021)
HARDER, H., 300 MW thorium high-temperature power plant (THTR), 25:31539
HARDIE, Gerald, Elastic scattering of 1.33-MeV photons from lead and uranium, 25:31370
HARDING, G. E. S., High-current capacitor banks for a 2-MJ high beta toroidal experiment (HBTX), 25:30563 (EUR-4593, pp 219-25)
HARDY, J. C., Reactions ^{11}B(p,^{3}He)^{9}Be and ^{11}B(p,t)^{9}B, 25:31228
HARMAN, T. C., Junction (n--p) photovoltaic detectors in PbTe produced by proton bombardment, 25:29397
HARMANEC, P., Evolution of close binaries. VII, 25:30111
Spectrographic study of EW LAC. I, 25:30098
HARMS, W. O., Nondestructive testing techniques for FBR, 25:29287 (ORNL-4630, pp 145-9)
Nondestructive testing, 25:29288 (ORNL-4630, pp 271-9)
Sodium corrosion studies, 25:29761 (ORNL-4630, pp 150-7)
Sodium removal and caustic effects, 25:29762 (ORNL-4630, pp 158-62)
HARRACH, R. J., Laser beam filtering by saturable dyes, 25:31747 (UCRL-51008)
HARRIS, D. R., Measurements and calculations of neutron migration and its anisotropy in lattices of fuel rods and liquid coolant, 25:31660
HARRIS, E. G., Damping of plasma oscillations in atoms, 25:30301
HARRISON, A. G., Hydrogen abstraction from methyl formate by methyl radicals, 25:29054
HARRISON, G. E., Excretion and retention of stable strontium in children, 25:29442
HARRISON, R. G., Effect of x-rays on the vascularization of the mouse testis, 25:29653

XUM

HART, Edwin J., Oxygen formation in the γ-ray irradiation of Fe^{2+}--Cu^{2+} solutions, 25:29141
HARTMANN, G., Ionospheric absorption during shortwave fadeouts related to enhancement of solar x-ray flux, 25:30362
HARTMANN, Werner, Measuring methods using ionizing radiation, 25:29391
HARTWIG, E., AEG compact cyclotron, 25:31144
Preliminary hardware concepts for a high-energy electron-ring accelerator, 25:31052 (UCRL-20169)
HARTWIG, M., Radiation effects in isolated DNA and their functional consequences. II, 25:29463
Radiation effects in isolated DNA and their functional consequences. III, 25:29464
HARUN-AR RASHID, A. M., Reaction $\pi^- p \to \eta n$ with Veneziano terms, 25:30884
HARVEY, M. R., Chemical diffusivities of Pu--Ga alloys in epsilon (bcc) phase, 25:29873
HARWIT, M., Alignment of dust particles in comet tails, 25:30183
Alignment of interstellar grains by starlight, 25:30216
Infra-red astronomical background radiation, 25:30239
Test to determine variations of Planck's constant on cosmic scale, 25:30246
HASE, Hirotomo, Electronic spectra of trapped electrons in organic glasses at 4°K, 25:29156
HASEGAWA, Akira, Multi-group constants for fission product nuclides, 25:31304 (JAERI-Memo-4251)
HASEGAWA, Masayuki, Neutron irradiation hardening of boron-doped copper, 25:29908
HASLAM, C. G. T., Observations of some extended galactic radio sources, 25:30136
HASSAN, H. A., Thrust from arcjets with self-induced magnetic fields, 25:30503
HASSLACHER, B., Feynman-parameter approach to N-tower exchange in phi^3 theory, 25:30987
HASTIE, J. W., Infrared spectra and geometries of $SrCl_2$, $BaCl_2$, $EuCl_2$, EuF_2, $PbCl_2$, and UCl_2, 25:29086
HASTY, R. A., Isotopic exchange study on thorium peroxide, 25:29089
HATSUSHIKA, Yoshihiko, Nuclear structure of ^{124}Te, 25:31346
HATTA, Y., Space-charge waves on plasma columns in a weak magnetic field, 25:30618
HAUGE, R. H., Infrared spectra and geometries of $SrCl_2$, $BaCl_2$, $EuCl_2$, EuF_2, $PbCl_2$, and UCl_2, 25:29086
HAUGHTON, G., Detection and measurement of weak histoincompatibilities by transfer of mouse peritoneal exudate cells, 25:31718 (ORO-3634-12)
Detection of weak histocompatibility antigens on mouse peritoneal macrophages, 25:31717 (ORO-3634-11)
Serological detection of the male limited H--Y antigen on peritoneal exudate cells, 25:31719 (ORO-3634-13)
HAULET, R., Depositing of radioactive products in pipes during turbulent flow, 25:31566
HAUSARD, Michel, Method for solving the equation of ionized electric fields in a stationary regime, 25:30705
HAUSMAN, Robert F. Jr., Function optimization on a line segment by GOLDEN section, 25:31740 (UCID-30002)
HAYASHI, Kenichi, Landau damping of surface wave along a plasma column, 25:30491
HAYASHI, Michiro, Structure of trans ethyl methyl ether and the W form of diethyl ether, 25:29072
HAYASHI, Shu A., Measurements of angular distributions and energy spectra of photoneutrons from lead targets bombarded by high energy electrons, 25:31317
HAYASHI, T., Gamma transition studies of ^{125}Sb, 25:31388
HAYES, Janet V., Experimental data on dispersion and deposition of timothy and corn pollen from known sources, 25:31684 (BNL-50266)
HAYS, P. B., Stable mid-latitude red arcs: observations and theory, 25:30398
HAZEWINDUS, N., Axial injection system for compact cyclotron, 25:31148
Beam quality of AVF cyclotrons, 25:31112
HAZI, A. U., Computation of resonance parameters for elastic scattering, 25:30297
HECKER, O., Irradiation plants to produce exposure rates within ^{60}Co gamma-radiation energy range, 25:29255
HECKER, R., Dense plasma focus as a neutron source for pulsed measurements in a blanket, 25:30592 (EUR-4593, pp 525-31)
Release of ^6Li from low-sintered Be oxide, 25:29963
HECKRODT, J., Application of ultrasound-B picture methods for the planning of radiotherapy, 25:29602
HED, A. Z., Some limiting factors in the use of alloys at high temperatures, 25:29780
HEDGER, H. J., Creep of uranium and uranium--plutonium monocarbides in compression, 25:29960
Thermal diffusivity of uranium and uranium--plutonium monocarbides, 25:29957
HEIDBREDER, E., Measurements of the distribution in energy and angle of high-energy neutrons in the lower atmosphere, 25:30374
HEIDRICH, Fred E., Collinear collisions of an atom and harmonic oscillator, 25:30292
HEILAND, W., Influence of wall material on plasma--wall interaction, 25:30496 (EUR-4593, pp 461-70)
HEINLOTH, K., Electroproduction of single π^+-mesons on H, 25:30718
Electroproduction of single π^+-mesons on H, 25:30719
HEISS, P., Lithium-5 resonances above ^3He-d threshold, 25:31195
Microscopic calculation for n--^3H scattering, 25:31193
HEITMANN, Hans-Joachim, Experimental studies of radiation protection through tryptamine, 25:29566
HELLEINER, C. W., Simple method for counting ^{14}C- and ^3H-proteins in polyacrylamide gels, 25:28994
HENDERSON, D. M., Electromagnetic energy absorption at the upper hybrid resonance, 25:30616
HENDERSON, W. R., D-region atomic oxygen measurement, 25:30385
HENDRICKS, J. B., Magnetization by rotation: Barnett effect in a superconductor, 25:30439
HENDRY, G. D., Design and performance of a compact multi-particle cyclotron, 25:31145
Design and performance of H^- injector cyclotron, 25:31151
HENNI, A., Reactions $^{12}C(d,d)$, $^{12}C(d,p_0)$, and $^{12}C(d,p_1)$, 25:31222
HENRIKSEN, Thormod, ESR studies of the mechanisms for radical formation in irradiated frozen sulfuric acid solutions of thymine, 25:29134
HENSON, S. H., Recoil-distance lifetime measurements for states in ^{30}P, 25:31279
HENTZ, Robert R., γ radiolysis of liquids at high pressures. X, 25:29157
HENTZEN, R. D., Nodal sensitivity in modeling a large pressurized water reactor system for a loss-of-coolant accident, 25:31592 (CONF-710302-8)
HEPP, Klaus, Quantum mechanical N-body problem, 25:30957
HEREMANS, J. F., Metabolism of different immunoglobulin classes in irradiated mice. V, 25:29473
HERMAN, L., Stark and Zeeman effects on neutral-He lines, 25:30264
HERMANN, G., Inelastic energy loss in single atomic collisions of Kr^+ on Kr at keV energies, 25:30279
HERMANN, O. W., Inclusion of fission and charged-particle mission in calculations of nuclear reactions, 25:31313 (ORNL-TM-3179)
HERMANS, L. J. F., Transverse heat flow in gaseous hydrogen isotopes at low temperatures, 25:29267
HERNANDEZ, E. S., Energy level calculations in Davydov model, 25:31425
HERPPICH, G., Fast storage system for a 500-kV theta-pinch experiment, 25:30567 (EUR-4593, pp 265-71)
HERRE, F., Measurement of gamma radiation conduction in a tube with a constant curvature, 25:30638
HERRERO, V., Radio observations of Nova Scuti 1970, 25:30091
HERSHKOWITZ, N., Moessbauer-effect observations of ^{232}Th following Coulomb excitation, 25:30693
HERZKE, J., Machining with a plasma jet, 25:31753 (UCRL-Trans-10524)
HESBOEL, R., Experiences on the release of iodine from uranium dioxide fuel, 25:31607
HESS, W. R., Velocity distribution of protons in a hot plasma beam, 25:30493
HEWITT, R. R., Coupling coefficients for the indirect nuclear dipole interaction in indium by nuclear quadrupole resonance, 25:30695
HEWKA, Peter V., Prog. rpt. on Avalanche type semiconductor radiation detectors, semiannual, 7--12/70, 25:29327 (NYO-3246-TA-8)
HEYDER, J., Distribution of radionuclides in suspensions of colloidal ThO_2, 25:29169
HEYMANN, P., Microwave diagnostics of contracted rare gas columns. I, 25:30486
Microwave diagnostics of contracting rare-gas columns. II, 25:30483
HEYNE, L., Electronic transport in calcia-stabilized zirconia, 25:30682
HEYWOOD, G. C. H., High-current capacitor banks for a 2-MJ high beta toroidal experiment (HBTX), 25:30563 (EUR-4593, pp 219-25)
HIATT, Caspar W., Low dose ferrous sulfate dosimetry by direct photon counting, 25:29386
HIATT, Nathan, Survival in lethally irradiated dogs, 25:29651
HIEBERT, R. D., Improved light scattering photometer for air filtration system studies, 25:31702 (LA-4627)
HIGASHIMURA, Takenobu, Electronic spectra of trapped electrons in organic glasses at 4°K, 25:29156
HIKIDA, T., Pulse radiolysis studies. XX, 25:29158
HILD, W., Preparation and properties of a crystalline uranium(IV)--hydrazine nitrate compound, 25:29035 (NP-18736)
HILL, G. E., Simultaneous LEED and RHEED studies of growth of Zr on W (100) surface, 25:29847
HILL, J. C., Mean lifetimes of levels in ^{92}Mo, 25:31377
HILL, J. W., Plasma heating by neutral injection in a stellarator reactor, 25:30455 (EUR-4593, pp 479-84)
HILLENBRAND, B., Preparation and superconductivity of $CeRu_2$, and its Gd, Mn, Fe, Co, and Ni-containing mixed phases, 25:30413 (LA-tr-71-26)
HILLYER, David F., Identification of dynamic systems from experimental data, 25:31752 (UCRL-72818(Rev.1))
HILTNER, W. A., CV Serpentis, 25:30043
HINNOV, E., Preliminary investigation of ohmically-heated plasmas in the model ST Tokamak, 25:30459 (MATT-813)
HINO, Masao, Infrared absorption spectra of silica gel-$H_2{}^{16}O$, $D_2{}^{16}O$, and $H_2{}^{18}O$ systems, 25:29069
HINOJOSA, Oscar, Cellulose graft copolymers. III,

XUM

25:29108
HINTERMANN, H. E., New bearing materials for ultrahigh vacuum, 25:29834
HINZPETER, G., Echoes with ion sound waves, 25:30611
Investigation of particle streaming out of plasma, 25:30485
HIRABAYASHI, H., Operation characteristics of 75 cm hydrogen bubble chamber and the refrigerator. I, 25:29372 (SJC-T-71-1)
HIRABAYASHI, Makoto, Neutron irradiation hardening of boron-doped copper, 25:29908
HIRANO, K., Design and construction of PIACE, 25:30587 (EUR-4593, pp 431-41)
HIRAO, Kunio, Rocket observations of electron density of daytime ionosphere, 25:30360
HIRASAWA, Takeo, Rocket observations of electron density of daytime ionosphere, 25:30360
HIRASHIMA, Yoshiyuki, Extraction of Eu with di(2-ethylhexyl) phosphoric acid, 25:29185
HIRSCHFELD, D., Composition and properties of the binder metal in cobalt bonded tungsten-carbide, 25:29980
HIRSHOWITZ, Bernard, Surgical treatment of chronic radiation injuries of axilla and shoulder, 25:29569
HISHINUMA, A., Behaviour of boron in stainless steel detected by fission track etching method and effect of radiation on tensile properties, 25:29913
HITOV, Joseph J., Irradiated polyethylene, 25:29115
HJELLMING, R. M., Radio observations of Nova Scuti 1970, 25:30091
HOBBS, C. H., Some observations on the toxicity of beta-emitting radionuclides inhaled in fused clay particles, 25:29438 (LF-43, pp 197-204)
Toxicity of inhaled ^{144}Ce fused clay in beagle dogs. III, 25:29436 (LF-43, pp 183-7)
Toxicity of inhaled $^{144}CeCl_3$ in beagle dogs. IV, 25:29431 (LF-43, pp 128-36)
Toxicity of inhaled ^{90}Sr fused clay in beagle dogs. I, 25:29437 (LF-43, pp 188-96)
Toxicity of inhaled $^{90}SrCl_2$ in beagle dogs. IV, 25:29430 (LF-43, pp 123-7)
Toxicity of inhaled ^{90}Y fused clay in beagle dogs. II, 25:29434 (LF-43, pp 146-62)
Toxicity of inhaled ^{91}Y fused clay in beagle dogs. I, 25:29435 (LF-43, pp 163-70)
Toxicity of injected ^{137}CsCl in the beagle dog. III, 25:29433 (LF-43, pp 140-5)
HOBBS, Robert W., Evidence for an optically thick component in the galactic radio source Sagittarius B_2, 25:30119
HOCH, Frederic L., Iodine analysis of biological samples by neutron activation of ^{127}I, with scintillation counting of Cherenkov radiation, 25:29030
HOCH, P., Influence of some alloying elements on the vanadium corrosion of nickel and nickel alloys, 25:29768
HOCH, R. J., Location in the magnetosphere of field lines leading to SAR arcs, 25:30376
HOCHEID, Bernard, Thermal diffusivity of Pu alloy stabilized delta phase, 25:29876
HODGE, Philip M., Is NGC 4569 a member of the Virgo cluster, 25:30207
HODISAN, T., Colorimetric determination of uranium, 25:28971
HOEFER, Gerhard, Investigations of the conductivity of vapor deposited tantalum layers with island structure, 25:30686
HOEGAASEN, H., Photoproduction of N*(1236) resonance and vector dominance model, 25:30784
HOEHLER, G., Conference on low energy hadron interactions, Karlsruhe, Ger., 5/70, 25:30840
HOEHNE, K., Electroproduction of single π^+-mesons on H, 25:30719
Electroproduction of single π^+-mesons on H, 25:30718
HOEKSTRA, H. R., Bond lengths in gamma--uranium trioxide, 25:29094
HOERZ, Gerhard, Investigations on V--N systems, 25:29879
Solid solution hardening of VA metals by N and O interstitials, 25:29880
HOFER, F., Magnetic domain patterns in small crystal $SmCo_5$ particles, 25:30675
HOFFMAN, H. W., Bilateral approach to the analysis of turbulent flow in an annulus, 25:29268
HOFFMAN, R. A., Primary electron influx to dayside auroral oval, 25:30367
HOFFMANN, A., Composition and properties of the binder metal in cobalt bonded tungsten-carbide, 25:29980
HOFMANN, A., Direct and compound processes to the reaction $^{40}Ca(d,\alpha)^{38}K$ at E/sub d/ = 5 to 10 MeV, 25:31275
HOFMANN, Hans Peter, Incorporation and distribution of thoron decay products following inhalation by rats, 25:29455
HOLDEN, J. P., Crossing-symmetric, Regge-behaved amplitudes with cuts, 25:30856
HOLECKOVA, L., Packing materials for γ-irradiated foodstuffs, 25:30033
HOLLAND, James M., Radiation therapy in the treatment of carcinoma of the prostate, 25:29597
HOLLAND, Michael Myers, Neutron energy spectra following radiative pion absorption on ^{16}O and ^{28}Si nuclei, 25:31216
HOLLANDER, J. M., Decays of ^{176}Ta, ^{176}Lu, and /sup 176m/Lu to levels in ^{176}Hf, 25:31375
HOLLANDSWORTH, C. E., Neutron polarization from $^7Li(p,n)^7Be$ reaction for 3 to 4 MeV protons, 25:31235
HOLLEY, Charles E. Jr., Enthalpies of formation of cerium dioxide, cerium sesquicarbide, and cerium dicarbide, 25:29961
HOLLIDAY, M. G., Investigation of backscattering in D^+--H_2 reaction system, 25:30291
HOLLOX, G. E., Slip systems in VC--TiC alloys, 25:29999
HOLM, S., Factors affecting beam intensity and quality in synchrocyclotrons, 25:31159
HOLMBERG, L., Conversion electron particle parameters of E2 transitions in ^{152}Sm and ^{156}Gd, 25:31380
HOLMES, Douglas E., Inelastic neutron scattering spectra from lanthanum dihydride and lanthanum trihydride, 25:30677
HOLMSTEDT, Bo, Ion specific detection of internal standards labelled with stable isotopes, 25:28967
HOLROYD, R. A., Pulse radiolysis of aqueous cyanogen solution, 25:29149
HONDA, Masatake, New outer-terrestrial substances. II, 25:30249
HONDA, T., Heats of hydrolysis of thorium carbides, 25:29966
HONDA, Yoshihide, Radioactivities in sea near the Goto Islands, 25:29241
HONES, E. W. Jr., Magnetospheric substorm of August 25--26, 1967, 25:30368
HONKAVAARA, T., Proceedings of the first Nordic meeting on medical and biological engineering, Otaniemi, Finland, 1/70, 25:29584
HONZATKO, J., Iron-57 low-energy states, 25:31270
HONZAWA, Tadao, Ion heating caused by ion acoustic waves in an ion-streaming plasma, 25:30458 (IPPJ-104)
Modified PIG-type plasma source, 25:30543
HOOPER, G. H. S., Gamma sterilization of the Mediterranean fruit fly, 25:29743
HOPKINS, B. J., Simultaneous LEED and RHEED studies of growth of Zr on W (100) surface, 25:29847
HOPKINS, F. F., Reaction $^{208}Pb(p,\alpha)^{205}Tl$ at 16.475 MeV, 25:31383
HOPKINS, Shirley Russell, Improvements in or relating to fuel handling equipment for nuclear reactors, 25:31582
HORAK, Z., Inertial forces as gravitational effect of Einstein Universe, 25:30245
HORDOS, Barney, Bevatron guide field control, 25:31055 (UCRL-20189)
HOREDT, Gp., Perturbations in a space of constant curvature, 25:30243
HORII, Kenji, Development of a heavy-current switching gap triggered with laser, 25:30575 (EUR-4593, pp 339-45)
HORN, J., Evolution of close binaries. VIII, 25:30106
HORNBY, I. W., Behavior of Oldbury model vessel with time under thermal and pressure loadings, 25:29309
Instrumentation techniques in large scale concrete models, 25:29299
Moisture measurements in mass concrete, 25:30026 (EUR-4531, pp 409-16)
HORNE, Donald E., Chemisorption of nitrogen at activated sites on a polycrystalline tungsten surface, 25:29849
HORRELL, David R., Radiation-induced oxidation of trichloroethylene, 25:29131
HOSEA, J. C., Preliminary investigation of ohmically-heated plasmas in the model ST Tokamak, 25:30459 (MATT-813)
HOSHI, M., Determination of Th, U(VI), and Pu(IV), 25:28982
HOSHINO, Toshio, Effect of irradiation on halogen exchanged silica--alumina catalyst, 25:29111
HOSKIN, Charles M., Fjords as sedimentary microcosms, 25:31724 (RLO-2229-T-1-3)
HOSOYA, Minoru, Rapid determination of hydrogen in metals by the argon gas carrier fusion-gas chromatographic method, 25:28936
HOTOP, H., Angular distributions of Penning electrons, 25:30294
HOUBEN, J. A., Irradiation of mortar specimens, 25:30020 (EUR-4531, pp 171-8)
HOUSSEAU, Nicole, Diffusion and solubility of plutonium and uranium in aluminum, 25:29867
HOWARD, K. J., Extraction performance of Harwell variable energy cyclotron, 25:31103
Harmonic operation of Harwell variable energy cyclotron, 25:31115
HOWARD, W. M., Explosive nucleosynthesis in helium zones, 25:30067
HOWELL, L. N., Heavy-ion accelerator facility featuring a separated-sector isochronous cyclotron, 25:31084
HOWELLS, G. R., Degradation of Na alginate by γ-irradiation and by oxidative-reductive depolymerization, 25:29159
HOYERMANN, K., Rate of the reaction of atomic hydrogen with acetylene. II, 25:29043
HRASTNIK, B., Double electron ejection in decay of ^{137}Ba, 25:31359
HREBIK, F., Observations of chromospheric flares at Ondrejov, 25:30189
HSIEH, K. C., Cosmic-ray ^{2}H from satellite measurements, 1965 to 1969, 25:30330
HSU, Chiu-chuan Shirley, Kinetics of the reaction of carbon dioxide with hydroxyl ion, 25:31745 (UCRL-20461)
HUBBARD, H., High energy astrophysics, 25:30220 (P-4494(RAND))
HUBER, Elmer J. Jr., Enthalpies of formation of cerium dioxide, cerium sesquicarbide, and cerium dicarbide,

XUM

25:29961
HUCKLESBY, R. J., Design and construction of a high-beta toroidal experimental assembly, 25:30586 (EUR-4593, pp 425-30)
HUDSON, E. D., Heavy ion acceleration at ORIC, 25:31131
Heavy-ion accelerator facility featuring a separated-sector isochronous cyclotron, 25:31084
Magnetically self-shaping septum for beam deflection, 25:31101
HUDSON, H. S., Observations of unresolved galactic x-ray sources, 25:30134
HUDSON, Hugh S., Type III solar radio bursts accompanied by soft x-radiation in the absence of Hα flares, 25:30167
HUDSON, Katherine I., Automated and conventional photometry of the short-period variable star 14 Aurigae, 25:30086
HUEBNER, H., Isotope effects in autoxidation. X, 25:29059
HUEBSCHMANN, W., Inherent stability of the steam-cooled breeder, 25:31542 (EURFNR-813)
HUGENHOLTZ, C. A. J., FREMIX: a high-power 8-GHz plasma heating experiment, 25:30456 (EUR-4593, pp 551-6)
HUGENHOLTZ, N. M., Equilibrium states of statistical mechanics, 25:30941
HUGHES, R. C., Geminate recombination of x-ray excited carriers in organic solids, 25:29140
HUGHES III, Henry Grady, Coulomb energy in time-symmetric electrodynamics, 25:30711
HUGUET, M., Tokamak facility of Fontenay-aux-Roses, 25:30583 (EUR-4593, pp 403-9)
HUIGNARD, J., Study, using the gamma irradiation technique, of the migration and utilization of spermatozoa in the bean weevil, 25:29746
HUMA, Nazhat, Reaction π⁻p → etan with Veneziano terms, 25:30884
HUMBLE, Stephen, High-energy single-particle production on Van Hove plot, 25:30890
HUMPERT, B., Model for two-pion production in the diffraction approach, 25:30863
HUMPHREYS, E. R., Degradation of Na alginate by γ-irradiation and by oxidative-reductive depolymerization, 25:29159
HUMPHRIES, S., Substoichiometric determination of traces of palladium by radioactive isotope-dilution analysis, 25:28981
HUNTER, D. Jr., Improved thermal diffusivity method applied to TiB_2, ZrB_2, and HfB_2 from 200 to 1300°C, 25:29956
HUNTINGTON, R. D., Slip systems in VC--TiC alloys, 25:29999
HUNTZ, Anne-Marie, Intergranular embrittlement of bcc metals, 25:29855
HUQUE, Heshamul, Effect of gamma radiation on the reproductive organs of Dacus zonatus, 25:29617
HURLEY, P. J., Pinhole scintillation camera and /sup 99m/Tc-pertechnetate in normal thyroid scanning, 25:29586
HURPIN, B., Sterilization of Oryctes rhinoceros, 25:29754
HURST, G. S., Vacuum-ultraviolet emission from proton-excited helium gas, 25:30284
HUSAIN, Khadim, Quantitative cation exchange separation of zirconium and hafnium in formic acid media, 25:28955
HUSCHKE, H., Treatment of space dependence of the energetic resonance self shielding at boundaries of homogeneous zones in reactors, 25:31652 (KFK-1353)
HUSSAIN-KHAN, M., Nonlinear analysis of stresses in the structure of the prestressed concrete pressure vessel for a fast reactor, 25:31553 (EUR-4531, pp 797-812)
HYDE, John Edgar, Improvements in or relating to fuel handling equipment for nuclear reactors, 25:31582

I

IBEN, Icko Jr., Specification of the blue edge of the RR Lyrae instability strip, 25:30096
IBI, Tamiko, Gamma--gamma perturbed angular correlations in ^{156}Gd, 25:31344
IBRAGIMOV, A. P., Radiation effects on amino acyl-tRNA synthetases and tRNA of cotton plant, 25:29715
ICHIKAWA, Michio, Columnar grain growth in center line heated UO_2 pellet, 25:29976 (JAERI-Memo-4249)
Phase study of the system UO_2--Dy_2O_3, 25:29975 (JAERI-1203)
ICHINOSE, Norio, Studies on extraction and determination of metal salts with isobutyl methyl ketone. XIII, 25:29195
IDA, Yoshio, Landau damping of surface wave along a plasma column, 25:30491
IEVLEV, V. M., Formation of gold nuclei on ionic crystals, 25:29910
IGITKHANOV, Yu. L., Hall effect in plasma oscillations, 25:30544 (IAE-1950)
IGNAT, D. W., Electromagnetic energy absorption at the upper hybrid resonance, 25:30616
IGO, G. J., Conceptual design of two-stage, two-gap cyclotron, 25:31140
IGUMNOV, L. A., Use of delayed neutrons for determination of uranium in core samples of boreholes, 25:29202 (CEA-tr-R-1978)
IHARA, S., Mutual solubility and preparation of uranium--cerium carbo-nitride, 25:30003
IIJIMA, Takesi, Constitution of magnetospheric storms, 25:30400
IKEBE, Yukimasa, Variation of radon and thoron concentrations in relation to the wind speed, 25:29225
IKEDA, N., Crowbar gap switch with two triggering pulses, 25:30576 (EUR-4593, pp 347-53)
IKEGAMI, K., New biaxial tensile tester for flat specimens, 25:31735 (SCL-T-69-258)
IKRAMOV, M. Kh., Automatic stabilization of a device for measuring life times in the picosecond range, 25:29365
ILAKOVAC, K., Double electron ejection in decay of ^{137}Ba, 25:31359
ILARI, O., Studies on natural background radiation in Italy, 25:29205
ILGACH, S. F., HL index of solar activity and yearly variations of cosmic rays, 25:30308
IL'ICHEV, N. A., Phenomenological lagrangians in quantum field theory, 25:30969
IMAHASHI, Tsuyoshi, Determination of Sc, Cr, Fe, Co, Zn, and Sb in deposits and airborne particulates by neutron activation analysis, 25:29032
IMAI, H., Heats of hydrolysis of thorium carbides, 25:29966
IMAISHI, Hisae, Structure of trans ethyl methyl ether and the W form of diethyl ether, 25:29072
INAGAKI, S., Design of high-gradient accelerating column, 25:31048 (SJC-A-71-2)
INGVAR, David H., Prog. rpt. on regional blood flow in subcortical structures in man, 3/71, 25:31710 (NYO-3618-10)
INOGAMOV, Sh. V., Application of phenomenological quasi-two-body model to π⁻p-interactions with strange particle production at p = 4 GeV/c, 25:30869 (JINR-P1-5706)
INOUE, Nobuyuki, Experiments of plasma confinement in JIPP stellarator. I, 25:30457 (IPPJ-102)
INOUE, Toshihiko, Control system of IPCR 160 cm cyclotron, 25:31068
INOUE, Yasunobu, Pressure jump and isotope replacement studies of acetylene hydrogenation on palladium surface, 25:29062
INOZEMTSEVA, O. I., Interplanetary space conditions by three-dimensional anisotropy of cosmic rays, 25:30320
IOANNU, P. D., Elastic and inelastic proton scattering on ^{32}S, ^{34}S, and ^{35}Cl, 25:31291
IOFFE, B. L., Absence of form factor in e^2 corrections to amplitudes of neutrino and electron scattering on nucleons, 25:30819
Divergences of amplitudes of weak nonleptonic processes with photon emission, 25:30805 (NP-18777)
IONKINA, E. M., Properties of cast nickel--chromium alloys alloyed with niobium and molybdenum, 25:29839
IPSER, James R., Gravitational radiation from slowly rotating, fully relativistic stars, 25:30092
IQBAL, M., ac conductivity of thoria--yttria solid solutions, 25:30685
IRVING, J., Creep behavior of prestressed concrete slabs with reinforced holes, 25:30024 (EUR-4531, pp 373-84)
IRWIN, Elizabeth, Hydrogen rearrangements in the mass spectra of alkylbenzenes, 25:29068
ISHAM, C. J., Infinity suppression in gravity-modified quantum electrodynamics, 25:30994
ISHIHARA, N., Operation characteristics of 75 cm hydrogen bubble chamber and the refrigerator. I, 25:29372 (SJC-T-71-1)
ISHII, Sakae, Growth of Pt crystals on W surface, 25:29850
ISHIKAWA, Hiroshi, Activation analysis of oxygen in phosphorus with fast neutron, 25:29024
ISHIKURA, Reiko, Reversed phase thin-layer chromatographic behavior of rare earths, Th, U, and Zr with a high molecular weight amine in sulfuric acid and ammonium sulfate systems, 25:29187
ISHKHANOV, B. S., (γ,n) cross sections of Al and P, 25:31242
Fine structure of the giant dipole resonance in ^{16}O nucleus, 25:31231
Structure of photoneutron cross sections of ^{51}V, ^{52}Cr, and ^{59}Co, 25:31243
ISHMAEV, S. N., Neutron thermalization in H_2O at 318°K and 77°K, 25:31170 (KAPL-Trans-4)
ISMAILOV, B. I., Relationship between level of endogenous sulfhydryl groups and radiosensitivity of tumors, 25:29610
ISUPOV, V. K., Internal ionization in β decay of ^{131}I, 25:31316
ITABASHI, K., Fixed-pole effects on exchange-degenerate Regge residues and cross-over phenomena, 25:30878
ITARD, J., Techniques for labelling tsetse flies with radioisotopes, 25:29417
ITO, H., Design and construction of PIACE, 25:30587 (EUR-4593, pp 431-41)
ITO, Hiroshi, Sintering process of Ni--P alloy coated W, 25:29793
ITO, Kensai, Fissionability of heavy nuclei, 25:31417
ITO, Wataru, Radioinduced copolymerization of tetrafluoroethylene with ethylene in gas phase, 25:29130
ITOH, Akio, Determination of the compositions of thin film compounds by using the electron-probe x-ray microanalyzer. I, 25:28966
ITOH, Satoshi, Review of USSR Tokamak experiments, 25:30596 (JAERI-Memo-4286)
ITOKAWA, Hideji, Thin layer chromatography: application to

XUM

organic compounds, 25:31705 (LA-tr-71-33)
ITONAGA, Kazunori, Contraction of deuteron cluster in ^{6}Li, 25:31207
IVANITSKAYA, V. I., Organs and systems following radiotherapy of thyroid cancer, 25:29707
IVANOV, R. B., Decay of ^{225}Ac, 25:31325
IVANOV, V. B., Shaper with double shaping based on delay lines having a modified noise spectrum, 25:29366
IVANOV, V. D., Passive diagnostics of a plasma focus using charged products of the dd-reaction, 25:30475 (LA-tr-71-6)
IVANOVA, N. I., Choosing and calculating focusing system of 30 MeV linear induction accelerator, 25:31039 (JINR-P9-5714)
IVANOVA, N. S., Charge distribution of heavy cosmic-ray nuclei in region Z greater than or equal to 26, 25:30305
IVANOVA, S. P., Single-particle states of deformed transuranium nuclei in Saxon--Woods potential, 25:31392 (BNL-tr-416)
IVANOVA, T. A., Injection of energetic electrons into magnetosphere during magnetic storm, 25:30352
IVANOVA, Z. I., Use of cupferron for the potentiometric determination of thorium and cerium when present together, 25:28958
IWASHITA, Takeki, Gamma--gamma perturbed angular correlations in ^{154}Gd, 25:31344
Nuclear structure of ^{124}Te, 25:31346
IYUDIN, A. F., Spark chamber power supply circuit with semiconductor trigger, 25:29374

J

JACCARINI, A., Photon--photon collisions, new area of experimental investigation in high-energy physics, 25:30798
JACK, A. G., Sheath growth in a low-pressure plasma, 25:30531
JACKIW, R., Arguments against anomalous dimensions, 25:30921
JACKSON, A. D., Triton calculations with realistic potentials in a harmonic oscillator basis, 25:30896 (NYO-4032-36)
JACKSON, L. T., New bevatron pole-face windings power system, 25:31056 (UCRL-20191)
JAEGER, R. G., Engineering compendium on radiation shielding. III, 25:30634
JAEGER, T. A., Report on the starting of a coordinated work program for prestressed concrete reactor pressure vessels in the Federal Republic of Germany, 25:31560 (IAEA-126, pp 115-77)
JAEGER, Thomas A., German research and development on prestressed concrete reactor pressure vessels, 25:31662 (EUR-4531, pp 59-71)
JAENECKE, J., Isospin nonconservation in reactions ^{16}O(d,α)^{14}N*/sub 0+, T = 1/ and ^{12}C(d,α)^{10}B*/sub 0+, T = 1/, 25:31227
JAMES, T. E., Design and construction of a high-beta toroidal experimental assembly, 25:30586 (EUR-4593, pp 425-30)
High-current capacitor banks for a 2-MJ high beta toroidal experiment (HBTX), 25:30563 (EUR-4593, pp 219-25)
JANCSO, G., Application of phenomenological quasi-two-body model to π^-p-interactions with strange particle production at p = 4 GeV/c, 25:30869 (JINR-P1-5706)
JANES, G. S., HIPAC ion source, 25:31138
JANES, K. A., Strong-cyanogen stars: photometry and kinematics, 25:30085
JANNOT, M., Heat exchange by natural convection in porous media, 25:29264 (EUR-4531, pp 821-39)
JANSSEN, D., Projection description of rotational and quasirotational bands in even--even nuclei, 25:31438
JANSSON, L., Experiences on the release of iodine from uranium dioxide fuel, 25:31607
JAROSS, Robert A., Liquid metal purifier, 25:29800
JAUHIAINEN, T., Proceedings of the first Nordic meeting on medical and biological engineering, Otaniemi, Finland, 1/70, 25:29584
JAWOROWSKI, Zbigniew, Radium-226 in contemporary and fossil snow, 25:29209
JAYARAMAN, K. S., Elastic scattering of protons from ^{40}Ca at 21.0, 23.5, 26.3, and 48.0 MeV, 25:31295
JEE, W. S. S., Bone-seeking radionuclides and bones, 25:29630
JENKINS, K. D., Generation and injection of heavy-ions into cyclotrons, 25:31132
JENNE, E. A., Gold content of natural waters in Colorado, 25:29015
JENSEN, H. F., Prog. rpt. on noble gas confinement study, final, FY-1970, 25:29074 (DUN-7221(Vol.1))
JERMY, T., Genetic control experiments on the bean weevil, 25:29749
JEROME, D., Study of ytterbium and ytterbium--barium alloys under high pressure at low temperature, 25:30674
JERPHAGNON, J., Optical nonlinear susceptibilities of beryllium oxide, 25:30666
JESSE, Andreas, Structural and physical characteristics of UAl$_4$, 25:29895
JESTER, W. A., Boron--polyethylene irradiation containers for high energy neutron activation analysis, 25:29025
JINDAL, G. R., Materials problems in lithium-drifted Ge radiation detectors. II, 25:29330
JOENSSON, J. O., Hyperfine structure investigations of ^{51}Mn and /sup 52m/Mn, 25:31294
JOHANNSEN, Klaus, Temperature fields in fuel element bundles. I, 25:31674
Temperature fields in fuel element bundles. II, 25:31673
JOHN, R. R., Prog. rpt. on high-power quasi-steady MPD acceleration, final, 5/70, 25:30599 (N-71-10100)
JOHNSON, B. R., Theory of vibrational excitation in the near classical limit, 25:30295
JOHNSON, C. H., Spin-parity assignments for low-lying states in ^{95} ^{97}Tc, 25:31381
JOHNSON, D., Double-Regge-pole description of reaction K-n + K-π-p at 5.5 GeV/c, 25:30747
JOHNSON, D. A., Proposed Michigan State Univ. transuranic accelerator facility, 25:31085
JOHNSON, David L., Temperature differences and mutual friction in He II near T/sub lambda/, 25:30405
JOHNSON, G. Frank, Neutron activation analysis technique for nail sodium concentration in cystic fibrosis patients, 25:29016
JOHNSON, Joseph E., Proper-time quantum mechanics. II, 25:30983
JOHNSON, L. C., Preliminary investigation of ohmically-heated plasmas in the model ST Tokamak, 25:30459 (MATT-813)
JOHNSON, N. D., Decay of ^{108}Ag, 25:31382
JOHNSON, Noah R., Decay of ^{108}Ag, 25:31382
Decay of ^{72}As to the levels of ^{72}Ge, 25:31261
JOHNSON, W. P., Cyclotron beam pulser for particle time-of-flight experiments, 25:31116
JOHNSTON, K. J., Interferometer map of the water-vapor sources in W49, 25:30141
JOHO, W., Extraction from medium and high energy cyclotrons, 25:31100
JOLLY, R. K., High resolution nuclear studies using cyclotron beams, 25:31124
JONES, D. de G., Techniques for the measurement of electrode processes at temperatures above 100°C, 25:29779
JONES, E. J., Extraction performance of Harwell variable energy cyclotron, 25:31103
Harmonic operation of Harwell variable energy cyclotron, 25:31115
JONES, Frank C., Formation of energy spectra in synchrotron sources, 25:30146
JONES, John D., Iodine analysis of biological samples by neutron activation of ^{127}I, with scintillation counting of Cherenkov radiation, 25:29030
JONES, R. K., Some observations on the toxicity of beta-emitting radionuclides inhaled in fused clay particles, 25:29438 (LF-43, pp 197-204)
Toxicity of inhaled ^{144}Ce fused clay in beagle dogs. III, 25:29436 (LF-43, pp 183-7)
Toxicity of inhaled ^{144}CeCl$_3$ in beagle dogs. IV, 25:29431 (LF-43, pp 128-36)
Toxicity of inhaled ^{90}Sr fused clay in beagle dogs. I, 25:29437 (LF-43, pp 188-96)
Toxicity of inhaled ^{90}SrCl$_2$ in beagle dogs. IV, 25:29430 (LF-43, pp 123-7)
Toxicity of inhaled ^{90}Y fused clay in beagle dogs. II, 25:29434 (LF-43, pp 146-62)
Toxicity of inhaled ^{91}Y fused clay in beagle dogs. I, 25:29435 (LF-43, pp 163-70)
Toxicity of inhaled ^{91}YCl$_3$ in beagle dogs. IV, 25:29432 (LF-43, pp 137-9)
Toxicity of injected ^{137}CsCl in the beagle dog. III, 25:29433 (LF-43, pp 140-5)
JONES, W. Barrie G., ESR studies of the mechanisms for radical formation in irradiated frozen sulfuric acid solutions of thymine, 25:29134
JOSEPH, George, Improved estimate of solar neutron flux measured in an earlier experiment, 25:30177
JOSHI, B. D., Chemical separation and spectrographic determination of trace amounts of rare earth elements in uranium, 25:28915 (BARC-517)
JOST, E., Semisterility for insect control, 25:29752
JOYCE, J. M., Neutron polarization from ^{7}Li(p,n)^{7}Be reaction for 3 to 4 MeV protons, 25:31235
JULIUS, D., Compilation of coupling constants and low-energy parameters, 25:30841
JULLIEN, R., Study of ytterbium and ytterbium--barium alloys under high pressure at low temperature, 25:30674
JUN, C. K., Elastic moduli of niobium carbide and tantalum carbide at high temperature, 25:29970
JUNDT, F., Determination of the parity of the 4.19-MeV level of ^{36}S, 25:31289
JUNG, J., Calibration of the Hertzsprung--Russel diagram, 25:30040
JURCEVIC, M., Double electron ejection in decay of ^{137}Ba, 25:31359
JURKEVICH, I., Light variations of Seyfert galaxy 3C 120, 25:30214
JUST, S., Radiation effects in isolated DNA and their functional consequences. IV, 25:29465
Radiation effects in isolated DNA and their functional consequences. V, 25:29466
JUVINALL, R. A., Sand-bed filtration of aerosols: a review

of published information on their use in industrial and atomic energy facilities, 25:29315 (ANL-7683)

K

KACHALIN, V. A., Time--amplitude converter for the nanosecond range, 25:29341
KACHEN, G. I., Laser beam filtering by saturable dyes, 25:31747 (UCRL-51008)
KACHI, S., Phase equilibria and thermodynamic properties in V/sub n/O/sub 2n-1/ system, 25:29952
KADOMTSEV, B. B., Hall effect in plasma oscillations, 25:30544 (IAE-1950)
KADYSHEVSKII, V. G., Quantum field theory with non-euclidean space of relative momenta, 25:30938 (JINR-P2-5717)
KAELLEN, Gunnar, Gradient terms in commutators of currents and fields, 25:30954
KAELLNE, Elisabeth, X-ray emission spectra of VC/sub x/, NbC/sub x/, TaC/sub x/, and ZrC, 25:30267
KAGAN, Yu., Gamma rays emitted by nuclei in crystals, 25:30690
KAHAN, R. S., Development of Botrytis cinerea in irradiated strawberries, 25:29732
KAHLES, John F., Adaptive control survey, 25:31758 (Y-1759)
KAHN, B., Users' guides for radioactivity standards, 25:29174
KAHN, R., Observation of d* effect in anti pd + p anti p $\pi^+\pi^-$n reaction at 5.55 GeV/c, 25:30727 (NP-18796)
KAJANTIE, K., Dual models and dual phenomenology, 25:30823 (CERN-71-7, pp 285-358)
KAJZAR, F., Tables of magnetic structures determined by neutron diffraction. II, 25:30664 (NP-18783)
KALANDADZE, N. B., Galactic structure in three sections of the Milky Way, 25:30191
KALDERON, D., Large steam turbines for nuclear and conventional power stations, 25:29256
KALININ, A. I., Timing with Ge(Li)-detector, 25:29353 (JINR-P13-5708)
X-ray spectrometer with cooled Si(Li)-detector, 25:29325 (JINR-P13-5707)
KALINOVICH, D. F., Electrotransport of Mo in Ni--18 at. percent Mo alloy, 25:29856
KALMA, A. H., Photoconductivity studies of Li-doped Si irradiated with 1.5 MeV electrons, 25:30653
KALMANSON, A. E., Macrostructure of bovine serum albumin under γ irradiation, 25:29471
KALMOUKOS, P. E., Possibilities of integrated control of Dacus oleae, 25:29740
KALUS, J., Stored energy release of solid argon after reactor irradiation at 4.6°K, 25:30660
KAMAEVA, L. A., Pulse delay time in ^{3}He neutron counters, 25:29338
KAMBU, F., Studies of the auroral x radiation at conjugate points Kerguelen--Archangel, 25:30395
KAMENOV, P., Moessbauer spectrometer for express analysis, 25:29361
KAMINER, N. S., Cosmic-ray increase before Forbush decrease, 25:30316
HL index of solar activity and yearly variations of cosmic rays, 25:30308
KAMINSKI, Aleksander, Transmission surface-barrier silicon detectors, 25:29331
KAMKE, Detlef, Applying methods of nuclear physics to solid state research, 25:30647
KAMMERER, Peter, Horowitz operators for organic moderators, 25:31657
KANAPILLY, G. M., Dissolution of small radioactive particles, 25:29080 (LF-43, pp 40-51)
Physical and chemical characteristics of aerosols produced from solutions of polyvalent metallic nuclides, 25:29079 (LF-43, pp 31-9)
Toxicity of inhaled ^{90}Sr fused clay in beagle dogs. I, 25:29437 (LF-43, pp 188-96)
Toxicity of inhaled ^{90}Y fused clay in beagle dogs. II, 25:29434 (LF-43, pp 146-62)
Toxicity of inhaled ^{91}Y fused clay in beagle dogs. I, 25:29435 (LF-43, pp 163-70)
KANAVETS, V. P., Methods for monitoring proton incidence on the internal targets of high-energy accelerators, 25:31043 (NP-18776)
Methods of monitoring proton discharge onto the internal target of a high-energy accelerator, 25:31064
KANDA, Kosuke, Protective effect of an L-cysteine derivative on hematopoietic damage caused by radiotheraphy, 25:29545
KANDIL, A., Angular distribution of fission fragments from the ^{170}Yb compound nucleus excited to 107 MeV, 25:31371
KANEKO, Keiji, Emission spectrographic determination of rare earth elements in lanthanum, 25:28965
KANNO, M., High temperature reaction between uranium monosulfide and zirconium, 25:29965
KANOMATA, Ichiro, Calorimetric studies on chemisorption of nitrogen on tantalum, 25:29843
KANTELE, J., Decay of ^{200}Tl, 25:31387
KANTER, B. Z., Decrease of the migration of hydrocarbons in an ultrahigh vacuum system by means of a passive gas, 25:29323
KANTOR, I., Probe method for recording ions produced by laser radiation in post-luminescence discharge plasma, 25:30477 (NP-18765)
KANTOR, T., Spectrochemical analysis of hard metals by a rotating disc solution technique, 25:28944
KANUNNIKOV, V. N., Spectrometric isochronous cyclotron, 25:31123
KAPCHINSKII, I. M., Possibility of reducing the injection energy and increasing the limit current in an ion linear accelerator, 25:31062
KAPITONOV, I. M., (γ,n) cross sections of Al and P, 25:31242
Fine structure of the giant dipole resonance in ^{16}O nucleus, 25:31231
Structure of photoneutron cross sections of ^{51}V, ^{52}Cr, and ^{59}Co, 25:31243
KARACHENTSEV, I. D., Division processes and instability of systems of galaxies, 25:30197
KARAKUZIEV, U., Radiation effects on amino acyl-tRNA synthetases and tRNA of cotton plant, 25:29715
KARASEK, J., Kinetics of the tumour growth and time factor in the radiotherapy, 25:29680
KARASIK, A. S., Solid-state construction for discharge quenching in Geiger counters, 25:29334
KARBAN, O., Radial injection of a polarised beam into a cyclotron, 25:31153
KARETSKAYA, S. P., γ rays accompanying decay of ^{109}In, 25:31320
KARKOWSKI, W., Asymptotic condition in the Zachariasen-Thirring, 25:30943
KARLIN, I. D., Potassium content in patients with pyelonephritis, 25:29448
KARNIK, S. G., Determination of total hydrogen content of UO_2 pellets, 25:28912 (BARC-500)
KAROCHKIN, B. B., Oxygen tension in critical organs under influence of mexamine in comparison with radioprotective effect, 25:29551
KARPENKO, B. V., Magnetization of EuO and $Eu_{0.7}Gd_{0.3}O$ single crystals, 25:30670
KARSTEN, G., Studies about advanced fuel elements, 25:31572
KARTHA, M., Radiation hepatitis in children, 25:29652
KARTZ, Ludwig, Investigations concerning the problem of radiation-cytostatic combination treatment. VIII, 25:29604
KARZHAVINA, E. N., Neutron resonances of the samarium isotopes, 25:31305 (JINR-P3-5655)
KASAHARA, Katsumasa, Lateral distribution of high-energy gamma-ray in air shower, 25:30793
KASCHLUHN, F., Compositeness and vanishing of renormalization constants, 25:30558
KASDAN, A., Interphase boundary waves in the intermediate state of lead, 25:30429
KASHCHUK, V. A., Effect of modifying additions of Ti and Ni on [the structure and] some properties of cast Zr, 25:29835
Preparation of specimens of zirconium and its alloys for metallographic examination, 25:29817
KASHKAROV, L. L., Studies of VH and VVH nuclei in mineral meteorites, 25:30317
KASHKIN, Yu. F., Influence of nonconducting partitions on terminal-induced electric currents, 25:30347
KASHY, E., High resolution nuclear studies using cyclotron beams, 25:31124
KASIDA, Yoshiko, Carbon-14 in alcohol, 25:28990
KASTELEWICZ, H., Correlation damping of longitudinal plasma waves in a nondegenerate magnetoplasma, 25:30621
KATAL'NIKOV, S. G., Separation of boron isotopes. II, 25:29196
KATINOV, Yu. V., Photomultiplier impulse shaper with stable time delay, 25:29347
KATO, Kuniko, Nuclear structure of ^{124}Te, 25:31346
KATO, Yoshio, Study of origin of geomagnetic pulsations in equatorial, low, and middle latitudes, 25:30356
KATSURA, M., Graphitization of free C precipitating through reaction of UC_2 with N_2, 25:29962
KATZ, J., Scale-symmetry breaking and scaling properties of currents, 25:30934
KATZ, R. N., Transmission microscopy of ion-thinned boron carbide, 25:29983
KAUFMAN, Leon, Nonrelativistic separable-potential quark model of the hadrons, 25:30646
KAUL, A., Distribution of radionuclides in suspensions of colloidal ThO_2, 25:29169
KAUSHANSKY, D. A., Gamma-irradiation apparatus for treatment of root- and tuber- crops, 25:29253
KAUTZKY, Anton, X-irradiation of verruca juvenilis with special emphasis on its plantar form, 25:29601
KAVUKCHYAN, T. V., Protection of dogs from ionizing radiation by shielding bone marrow, 25:29658
KAWAGUCHI, Sadao, Rocket observations of electron density of daytime ionosphere, 25:30360
KAWAI, Hiroshi, Radioactivities in sea near the Goto Islands, 25:29241
KAWAI, Yoshinobu, Ion heating caused by ion acoustic waves in an ion-streaming plasma, 25:30458 (IPPJ-104)
Modified PIG-type plasma source, 25:30543
Propagation of large-amplitude electron plasma waves, 25:30610
KAWAKAMI, Ichiro, Axial behavior and confinement of plasma in the mirror-field theta pinch, 25:30464
KAWAMURA, Takaichi, Hydromagnetic motion in the geomagnetic

tail, 25:30349 (IPPJ-103)
KAWASAKI, Michiko, Separation of uranium from fission products, 25:29198
KAWASAKI, S., Behaviour of boron in stainless steel detected by fission track etching method and effect of radiation on tensile properties, 25:29913
KAWASE, Y., Gamma transition studies of ^{125}Sb, 25:31388
KAY, R. B., Exchange excitation in He, 25:30285
KAZAKOVA, G. V., Influence of Cr and Mo on electrocnemical and corrosion resistance of Ni--Cr--Mo alloys, 25:29777
KAZANJIAN, Armen R., Radiation-induced oxidation of trichloroethylene, 25:29131
KAZUNO, M., Baryon resonances in cosmic-ray interactions, 25:30729
KEAN, D. C., Energy levels of ^{27}Si, 25:31252
KEBULADZE, T. V., Cosmic-ray increase before Forbush decrease, 25:30316
KEEFE, D., Preliminary hardware concepts for a high-energy electron-ring accelerator, 25:31052 (UCRL-20169)
KEEFER, D. W., Proton irradiation effects in type 321 stainless steel, 25:29915
KEEN, B. E., Suppression and enhancement of a drift-type instability, 25:30550
KEILHOLTZ, G. W., Fast-neutron irradiation effects on electrical insulators, 25:30011 (ORNL-4630, pp 226-9)
KEITH, Ronald Leonard Gordon, Improvements in or relating to nuclear radiation detectors, 25:29348
KELLERMANN, K. I., Radio observations of the infrared object IRC 10216, 25:30090
KELLY, B. T., Effects of reactor radiation on concrete, 25:30022 (EUR-4531, pp 237-65)
KELLY, Donald P., Protected radioisotopic heat source, 25:29276
KEMP, E. L., Design and installation of Scyllac, 25:30564 (EUR-4593, pp 227-39)
KENNEL, C. F., Topside current instabilities, 25:30373
KERSCHER, Franz, Influence of neutron irradiation at 4°K on shear modulus of Cu, Al, and Pt, 25:29912
KESSE-ELIAS, M., Renal adenocarcincma: scintigraphic study of primary and metastatic areas, 25:29590
KESSIE, R. W., Sand-bed filtration of aerosols: a review of published information on their use in industrial and atomic energy facilities, 25:29315 (ANL-7683)
KESSLER, P., Photon--photon collisions, new area of experimental investigation in high-energy physics, 25:30798
KEVANISHVILI, G. T., Condensations of spectral type-A stars, 25:30062
KHACHATURYAN, A. G., Phase transition associated with radiation defects, 25:29911
KHANNA, K. M., Ground-state energies of doubly even nuclei, 25:31427
KHANONKIND, M. A., Valent shell structure effects on coefficients of internal conversion, 25:31343
KHAO, Yu., Use of electronic particle counter to investigate cell populations of bone marrow after irradiation, 25:29648
KHAVAEV, A. A., Radiosensitizing effect of ferrous ions, 25:29556
KHAZINS, D. M., Spectrum of fast deuterons emitted in 670-MeV proton interaction with carbon nuclei, 25:31225
KHERA, A. K., Comparative study on Al determination in ammonium acetate soil extracts by spectrophotometry, activation analysis, and atomic absorption, 25:29020
KHIET, Vu Thanh, Gravitational instability in an inhomogeneous cosmological model, 25:30241
KHIL, Sh. V., Studies of diffusion of dense disintegrating plasma in a stellarator, 25:30462 (NP-18767)
KHLOPINA, T. N., Spectral isotopic analysis of elements in middle part of Mendeleev Periodic Table, 25:28952
KHO, Jose H. T., Monomer reactivity ratios in graft copolymerization, 25:29106
KHODEL, V. A., Calculation of nuclear matrix elements of double β decay, 25:31440
KHOE, T. K., Proposed Midwest tandem cyclotron (MTC), 25:31083
KHOSLA, M. M. L., Selective extraction of Th with N-benzylaniline in chloroform from sulphuric acid media, 25:29184
KHOZE, V. A., C-invariance verification in experiments with colliding e$^+$e$^-$ beams, 25:30926
KHRUSCHEV, V. G., Gamma-irradiation apparatus for treatment of root- and tuber- crops, 25:29253
KHRUSTALEV, O. A., Condition of the asymptotic equality of total cross sections in two simple models, 25:30769
KHUDYAKOV, A. V., Estimation of the radiation resistance of beryllium oxide at various temperatures, 25:30016
KHUKHAREVA, I. S., Resistance behavior of superconducting alloy of Nb + 80 percent Zr in region of H/sub c2/, 25:30412 (JINR-P8-5733)
KHUSAINOV, Yu. A., Lifetimes of 1080-keV level of ^{115}In and 1300-keV level of ^{111}Cd, 25:31327
KHVOSTOVA, V. P., Spectrophotometric determination of small amounts of ruthenium and osmium in minerals and industrial samples, 25:28960
KIANG, A. K. C., Experiment to compress polarized ^{3}He gas, 25:31077
  Large-volume homogeneous low-field electromagnet, 25:31071
KIDMAN, R. B., Cross section structure factor interpolation schemes, 25:31647 (HEDL-TME-71-40)
KIEFER, W., Resonance Raman effect in MnO_4^- with 5145 A laser excitation, 25:29047
KIEFFER, F., Deferred luminescence spectra of some aromatic compounds in rigid organic media, 25:29150
KILB, R. W., Thermalization in the Earth's bow shock, 25:30365
KILIAN, Peter, Measurements on fuel elements for power reactors in a critical assembly, 25:31573
KILLEY, N. M., Creep of uranium and uranium--plutonium monocarbides in compression, 25:29960
KIM, A., Probe method for recording ions produced by laser radiation in post-luminescence discharge plasma, 25:30477 (NP-18765)
KIM, H., Conversion studies for SREL 600-MeV synchrocyclotron, 25:31160
KIM, H. J., Spin-parity assignments for low-lying states in ^{95} ^{97}Tc, 25:31381
KIMBROUGH, W. D., Thermophysical properties of ATJS graphite at high temperatures, 25:29972
KIMEL, I., Gauge fields, theory of currents, and vector mesons, 25:30924
KIMELDORF, D. J., Radiation-induced alterations in odontogenesis and formed teeth, 25:29631
KIMURA, Itsuro, Measurement and the calculation of neutron spectra in iron assemblies, 25:31658
  Measurements of angular distributions and energy spectra of photoneutrons from lead targets bombarded by high energy electrons, 25:31317
KIMURA, Iwane, Convective beam cyclotron instability and discrete vlf emissions in the magnetosphere, 25:30357
  Note on a generation mechanism of background hiss of polar chorus, 25:30358
KIMURA, Toyoaki, Effect of phase on primary process of formation of butyl radicals in radiolysis of solid isobutane-2-d_1, 25:29161
KIMURA, Yuichiro, Radioactivities in sea near the Goto Islands, 25:29241
KIND, D., New compact capacitive energy storage unit for voltages above 100 kV, 25:30571 (EUR-4593, pp 293-9)
KINDEL, J. M., Topside current instabilities, 25:30373
KING, A. D., Transmission microscopy of ion-thinned boron carbide, 25:29983
KING, C. A., Magnetization by rotation: Barnett effect in a superconductor, 25:30439
KING, E., Creep of uranium and uranium--plutonium monocarbides in compression, 25:29960
  Effect of high pressures and varying temperatures on the resistivity of ytterbium, 25:30661 (AERE-R-5953)
  Thermal diffusivity of uranium and uranium--plutonium monocarbides, 25:29957
KING, K., Reactions (d,p) to the ground states of ^{41}Ca and ^{49}Ca, 25:31264
KING, M. J., Implications of local duality in a set of coupled reactions, 25:30843
  Restrictions on the angular momentum of t-channel exchanges from s-channel helicity conservation, 25:30757
KING, R. H., Colorimetric determination of minor quantities of nitrate in uranium compounds, 25:28918 (NIM-951)
KING, R. T., Cyclotron simulation of neutron-transmutation produced gases in reactor cladding and structural materials, 25:29907 (ORNL-TM-3299)
  Irradiation damage to aluminum and aluminum alloys, 25:29905 (ORNL-4630, pp 239-60)
KINGSEN, A. S., Nonlinear interactions of ion-acoustic waves and helicons in plasma, 25:30607
KINGSLEY, Barbara L., Retention of ^{171}Tm following inhalation of oxide by beagle dogs, 25:29425 (LF-43, pp 71-8)
KINKEAD, A. N., Performance of thermal insulation immersed in helium, 25:30030 (EUR-4531, pp 931-52)
KINNEBROCK, W., Strategy for speeding up two-dimensional SN-methods with help of the coarse lattice technique, 25:31653 (KFK-1361)
KINSEY, James Humphreys, Low-energy cosmic rays at 1 A. U, 25:30161
KINSMAN, K. R., Origins of microstructures resulting from precipitation, 25:29888
KIRCH, M., Elimination and metabolism of benzo(a)pyrene after intratracheal injection, 25:31715 (ORNL-tr-2469)
KIRCHNER, R., Early-flowering mutants of Medicago polymorpha var. polymorpha, 25:29488
KIRICHENKO, G. S., Slowing down of an ion beam in a plasma during ion-acoustic instability, 25:30511
KIRILLOV, Igor R., Comparison of some excitation schemes for a jet MHD induction generator, 25:30335
KIRILLOV-UGRYUMOV, V. G., Primary γ radiation with E greater than or equal to MeV, 25:30306
  Relation of electron flux in upper atmosphere to state of Earth magnetosphere, 25:30353
KIRKBRIGHT, G. F., Dewar tube sample cell assembly for low-temperature fluorimetry, 25:28925
KIRKBY, P., Large-volume homogeneous low-field electromagnet, 25:31071
KIRKMAN, S., Medical radioisotope scanning, 25:29349
KIRKPATRICK, William W., Irradiated apparatus, 25:29260
KIROV, A. G., Experimental installation R-Ohm for studying high-frequency field-interaction with plasma, 25:30508 (NP-18801)
KIRSHIN, V. A., Egg laying of hens under action of incorporated ^{131}I, 25:29661

KIRZHNITS, D. A., Role of quantum fluctuations of a gravitational field in general relativity and cosmology, 25:30224
KISDI, David, Effective interaction of nucleons in infinite nuclear matter, 25:31416
KISELEVICH, I. L., Heat exchange and temperature control system for the 2-meter liquid hydrogen bubble chamber, 25:29376
KISHIMOTO, H., Design and construction of PIACE, 25:30587 (EUR-4593, pp 431-41)
KISHORE, Bijoy, Energetics, morphology, crystallography, and theory of displacive transformations in near-equiatomic niobium--ruthenium alloys, 25:29882 (COO-1198-807)
KISLII, P. S., Sintering process of zirconium diboride with tungsten, 25:29930
KISLOVSKII, L. D., Electron structure and the chemical bonds in vanadium pentoxide, 25:30668
KITA, I., Operation characteristics of 75 cm hydrogen bubble chamber and the refrigerator. I, 25:29372 (SJC-T-71-1)
KITADA, Masahiro, Precipitates with unusual microstructure in grains of Nb--40 Zr--10 Ti alloy, 25:29890
KITAEV, V. Ya., Boron-containing liquid neutron detector, 25:29337
KITTERMAN, John Howard, Growth of cadmium whiskers in inert atmospheres, 25:29804
KITTS, F. G., Mound assistance program: development of a sol-gel process and equipment for production of dense $^{238}PuO_2$ microspheres, 25:29921 (ORNL-4565)
KIYAMA, Satoru, Transformer coupled fast theta-pinch device with variable rise time, 25:30577 (EUR-4593, pp 355-63)
KIYOSE, Ryohei, Maximizing the average fuel burnup over entire core: a poison management optimization problem for multizone light-water reactor cores, 25:31584
KLAN, F., Excited states of He atoms in stationary PIG discharge, 25:30479
KLARSFELD, S., Heat exchange by natural convection in porous media, 25:29264 (EUR-4531, pp 821-39)
KLEBANOV, G. N., Heat distribution in electron beam-melted molybdenum plates, 25:29842
KLEEFELDT, K., Experiments on wear and friction between subassemblies and grid spacers in sodium, 25:29818 (AEC-tr-7224)
KLEIN, Georges, Process for crossing boundary layers in a magnetohydrodynamic generator and a generator using the process, 25:30337
KLEIN, H. D., Male sterility in Pisum, 25:29492
KLEIN, J., Multigap effect on phonon structure in tunneling experiments, 25:30426
KLEINBERG, Robert, Crystal structure of $CoBr_2.6H_2O$ at room temperature by neutron diffraction, 25:31722 (PRNC-146)
KLEINPOPPEN, Hans, Analysis of scattering and excitation amplitudes in polarized electron--atom collisions. I, 25:30287
KLEMENT, G., High-power spark gaps for large and fast energy storage systems, 25:30565 (EUR-4593, pp 241-50)
New crowbar system for 2.7-MJ bank Isar I at Garching, 25:30560 (EUR-4593, pp 189-95)
KLENER, V., Radiobiological principles of radiation hygiene, 25:29703
KLIMAN, Bernard, Double-isotope derivative assay of serum iodothyronines. II. Thyroxine, 25:28986
KLIMENKOV, V. I., Estimation of the radiation resistance of beryllium oxide at various temperatures, 25:30016
KLINGER, W., Analyzing power of the reaction $^3He(d,p)^4He$, 25:31197
KLOSE, Jules Z., Mean lives and absolute f-values in neutral iron, 25:30168
KLUEBER, D., Status report on Garching Tokamak experiment Pulsator, 25:30584 (EUR-4593, pp 411-17)
KLUK, A. F., Decay of ^{108}Ag, 25:31382
KLYPIN, B. A., Influence of carbon on Mo ductility, 25:29863
Temperature dependence of mechanical properties of certain Mo and W alloys, 25:29864
KLYUCHAREV, A. P., Gamma rays from $^{64,66,68}Zn(p,\gamma)^{65,67,69}Ga$, 25:31249
Inelastic scattering of protons by ^{50}Cr, ^{52}Cr, ^{54}Cr, and ^{64}Zn, 25:31253
KLYUCHAREV, V. A., Angular correlation of 345 to 136 keV cascade in ^{181}Ta, 25:31321
KNAAP, H. F. P., Transverse heat flow in gaseous hydrogen isotopes at low temperatures, 25:29267
KNIGHT, Curtis A., Quasars: millisecond-of-arc structure revealed by very-long-baseline interferometry, 25:30130
KNIGHT, J. A., Gas chromatographic analysis of γ-irradiated aniline for aminoaromatic products, 25:29155
KNIGHTS, C. F., Levitation melting of uranium mono-carbide, 25:29934
KNOBLOCH, A., Data for a fusion reactor: summary of an IPP lecture series, 25:30590 (EUR-4593, pp 497-512)
Status report on Garching Tokamak experiment Pulsator, 25:30584 (EUR-4593, pp 411-17)
System planning for a prototype fusion reactor, 25:30593 (EUR-4593, pp 533-8)
Toroidal version of the Isar I theta-pinch experiment, 25:30585 (EUR-4593, pp 419-24)
KNOEPFEL, H., Merits and limitations of explosively driven current generators in fusion research, 25:30562 (EUR-4593, pp 205-17)
KNOP, G., Electromagnetic form factors of the proton, 25:30786
KNOSKA, S., Observations of chromospheric flares at Hurbanovo, 25:30175
KNOTIK, K., Nuclear fuel particles manufactured from a peroxide of uranium, 25:29801
KNOWLES, S. H., Interferometer map of the water-vapor sources in W49, 25:30141
KOBA, Z., Statistical concepts applied in studying generalized Veneziano model, 25:30766
KOBAYASHI, Katsuhei, Measurements of angular distributions and energy spectra of photoneutrons from lead targets bombarded by high energy electrons, 25:31317
KOBAYASHI, Masaaki, Field measuring system of drift tube quadrupole magnets, 25:31047 (SJC-A-71-1)
KOBIERSKA, Elzbieta, Transmission surface-barrier silicon detectors, 25:29331
KOBILINSKI, Z., Modulation of galactic cosmic rays by solar wind, 25:30325
Spherically symmetric model of modulation of galactic cosmic rays, 25:30324
KOBUSHKIN, A. P., Generation of vector mesons and a model of factorizable quarks, 25:30879
KOCHAR, Nirmal K., Effect of x-rays on the vascularization of the mouse testis, 25:29653
KOCHAROV, G. E., Possibility of determining oscillation parameters of neutrinos, 25:30802 (BNL-tr-418)
KOCHKIN, V. A., Coherent frequencies of transverse oscillations in the electron model of a ring cyclotron, 25:31038 (JINR-P9-5677)
Rf system of the monoenergetic cyclotron, 25:31128
KOEBERLE, R., Cabibbo's theory and second-order SU(3)-symmetry-breaking corrections, 25:30930
KOEHMSTEDT, P. L., Radioactivity in FFTF closed loops, 25:31627 (BNWL-585)
KOEN, B. V., Optimization of nuclear systems by geometric programming, 25:31649
KOENIG, V., Absolute calibration of tensor analysing powers of the $^3He(d,p)^4He$ and the $^4He(d,d)^4He$ reactions, 25:31198
KOERNER, I. J., Radiation effects in isolated DNA and their functional consequences. II, 25:29463
KOGA, Taeko, Radioactivities in sea near the Goto Islands, 25:29241
KOGAN, I. A., Excretion of glucocorticoids and their metabolites in persons working with sources of ionizing radiation, 25:29708
KOHLHAAS, W., Coaxial high-power trigatron for 60 kV, 25:30579 (EUR-4593, pp 373-8)
KOHNO, I., Heavy ion acceleration in IPCR 160 cm cyclotron, 25:31135
KOHNO, Isao, Control system of IPCR 160 cm cyclotron, 25:31068
KOIWA, Masahiro, Neutron irradiation hardening of boron-doped copper, 25:29908
KOKOVIKHIN, V. F., Angular distribution of neutrons scattered in air, 25:30639
KOLAR, J., Experiences with experimental isotopic investigations of the joints, 25:29581
Five year's experience with isotopic investigations of diseased joints, 25:29576
Radiation induced bone sarcoma, 25:29702
KOLB, E., Measurement and calculation of dose rate removal cross sections and B factors for neutrons, 25:30637
KOLCHIN, A. A., Proton flux from 1.5 to 50 MeV on satellites Zond-4 and Zond-5, 25:30164
KOLESNIKOV, N. V., Stabilization of gain of a scintillation counter for registering ^{14}C, 25:29344
KOLGA, V. V., Charged particle motion in monoenergetic cyclotron, 25:31122
Phase motion in the phasotron with spatial variation of magnetic field, 25:31156
KOLLER, L., Problems in the quantitative spectral analysis of rare earth metal traces. II, 25:28946
KOLOKOL'TSOV, N. A., Mass-diffusion mercury columns for isotope separation, 25:29277
KOLOMIETS, V. M., Elastic scattering and radiative capture of protons, 25:31276
KOMAR, Arthur, Conservation of e/m in general relativity, 25:30998
KOMAREK, P., Present state of costs for large superconducting magnets and their future prospects, 25:30441 (EUR-4593, pp 117-24)
KOMAROV, A. N., Radiographic study of uranium-containing pyrites, 25:29231
KOMAROV, D. L., Choosing and calculating focusing system of 30 MeV linear induction accelerator, 25:31039 (JINR-P9-5714)
KOMAROV, V. E., Apparatus for studying the dynamics of condensed systems using a back-scattering method, 25:29362
KOMEL'KOV, V. S., Technology of strong pulsed currents and magnetic fields, 25:30604
KOMOLI, L. H., Test stand for the prestressed concrete vessel containing the helium loop, 25:31558 (IAEA-126, pp 85-97)
KOMORI, Takuji, Improvement in isotopic ratio measurement of uranium, 25:28927
KOMOV, A. L., Non-rotational states of odd-mass nuclei in

XUM

the actinide region, 25:31306 (JINR-P4-5693)
KOMPPA, T., Decay of ^{200}Tl, 25:31387
KOMYAK, N. I., Scintillation spectrometry of soft x-ray radiation, 25:29350
KONDO, Katsumi, Propagation of large-amplitude electron plasma waves, 25:30610
KONDO, Yoji, Formation of a neutron star in a close binary system, 25:30099
KONDRASHOV, V. M., Irradiation head for beam therapy, 25:29258
KONDRAT'EV, B. S., Angular and energy distributions of γ rays in lead, 25:30640
KONDRATYUK, L. A., Many-baryon resonances, 25:30895 (NP-18779)
KONDURUSHKIN, N. A., Angular distribution of neutrons scattered in air, 25:30639
KONENKO, I. R., Properties of rare-earth metals (Sc, Nd), their hydrides, carbides, and oxides, 25:29859
KONERMANN, Gerhard, Capability for learning and memorizing of trained quails following head irradiation, 25:29687
KONEV, N., Oxidation kinetics of Nb--Zr alloys. V, 25:29769
KONEV, V. N., Mechanism of oxidation of Nb--Zr alloys, 25:29767
KONIN, A. D., Charged particles produced in capture of negative muons by ^{28}Si, ^{32}S, ^{40}Ca, and ^{64}Cu nuclei, 25:31267
KONISHI, Eiichi, Lateral distribution of high-energy gamma-ray in air shower, 25:30793
KONISHI, Kunio, Radiation-induced sulfoxidation and sulfochlorination of powdery polyethylene produced by radiation process, 25:29107
KONOBEEVSKII, E. S., Inelastic neutron scattering by even-N Ge isotopes, 25:31244
KONSTANTINOV, B. P., Proton flux from 1.5 to 50 MeV on satellites Zond-4 and Zond-5, 25:30164
KONYAKHINA, S. S., Measurements of energy spectra of multicharged nuclei, 25:30307
KOPAL, Zdenek, Eclipsing system of epsilon Aurigae, 25:30083
Roche coordinates for the rotational problem, 25:30082
KOPCEWICZ, M., Moessbauer study of proton irradiation effects in ferrous sulfate, 25:29151
KOPECKY, M., Difference in magnetohydrodynamic properties of photospheres of dwarf and giant stars of spectral types F, G, and K, 25:30110
Electric conductivity in photospheres of stars of spectral types F, G, and K, 25:30114
Relation between electric conductivity in spot and photosphere, 25:30186
KOPYLOV, G. I., Interference phenomena in the system of two resonances, 25:30848 (JINR-P1-5668)
Particle interference in the processes involving excited nuclei, 25:31395 (JINR-P1-5648)
Possibilities of the resonance interferometry, 25:30847 (JINR-P1-5666)
KOPYLOV, Yu. M., Studies of the auroral x radiation at conjugate points Kerguelen--Archangel, 25:30396
KORANDA, J. J., Distribution, residence time, and inventory of tritium in Sedan crater ejecta, 25:29244 (UCRL-72572)
KORBEL, K., Semiconductor system for analog processing of signals obtained from radiometric control set of the calcium content in the cement-feeding, 25:29389 (ITJ-2/E)
KORKHMAZYAN, N. A., Radiation of fast charged particles in transverse sinusoidal electric fields, 25:30715
KORKOS, S., Renal adenocarcinoma: scintigraphic study of primary and metastatic areas, 25:29590
KORNILOV, I. I., Phase equilibria and superconductivity in the V_3Al--V_3Sn system, 25:30416
KOROL, B. A., Effects of histones on energy processes in liver mitochondria of irradiated animals, 25:29638
KOROLEV, A. M., Born approximation in the theory of stripping reactions, 25:31400
KOROLEV, V. I., Pulse delay time in ^{3}He neutron counters, 25:29338
KOROSTYLEV, V. A., Study of spontaneous fission of ^{252}Cf, 25:31314 (ORNL-tr-2453)
KOROTKOV, K. A., Internal bremsstrahlung following β decay of ^{114}In, 25:31318
KORSUNSKII, I. L., Evidence of disappearance of inelastic channel of nuclear reaction in nuclear resonant scattering of γ-rays in perfect crystal, 25:30687 (IAE-1966)
KOSACHEV, V. V., Longitudinal oscillations of a relativistic electron--ion plasma at zero temperature, 25:30529
KOSHELEV, P. F., Influence of beta-stabilizers on the strength and plasticity of titanium at low temperatures, 25:29844
KOSKIKALLIO, J., Deuterium isotope effects in attachment of Hg(6^3P_0) to ammonia, 25:29046
KOSOLAPOVA, T. Ya., Carbides, 25:29959
KOSTEAL, Krista, Calcium and strontium metabolism as related to age and alginates, 25:29446
KOSUGE, K., Phase equilibria and thermodynamic properties in V/sub n/O/sub 2n-1/ system, 25:29952
KOTEL'NIKOV, G. A., Use of gamma spectrometer to control activity of heat-transfer medium in reactors, 25:31680
KOTEL'NIKOV, G. N., Possibility of the endogenous origin of some secondary uranium minerals, 25:29232
KOTHARI, L. S., New variational method for the pulsed-neutron problem, 25:31175
KOTLICKI, A., Moessbauer study of proton irradiation effects in ferrous sulfate, 25:29151
KOTOSONOV, A. S., Effect of boron on certain physical characteristics of synthetic graphites, 25:29946 (SC-T-713623)
Effect of boron on some physical characteristics of artificial graphites, 25:29953
KOTRAPPA, P., Production of relatively monodisperse aerosols for inhalation experiments by aerosol centrifugation, 25:29421 (LF-43, pp 6-12)
KOURIM, P., Gamma-radiolysis of aqueous solutions of 5-bromo-2'-deoxyuridine in presence of O. I, 25:29135
Gamma-radiolysis of aqueous solutions of 5-bromo-2'-deoxyuridine in presence of O. II, 25:29136
KOVACEVICH, E. A., Radioactivity in FFTF closed loops, 25:31627 (BNWL-585)
KOVALCHUK, L. V., Increased protective property of spleen cells from preirradiated donors measured by transplantation into lethally irradiated recipients, 25:29564
KOVALENKO, P. N., Use of cupferron for the potentiometric determination of thorium and cerium when present together, 25:28958
KOVALEV, V. P., Residual injury in gastrointestinal death of mice after gamma irradiation, 25:29657
KOVENSKII, I. I., Electrotransport of Mo in Ni--18 at. percent Mo alloy, 25:29856
KOVESI-DOMOKOS, S., Overlapping resonance model of deep inelastic electron scattering, 25:30782
KOWALSKA, K., FLANGE-AL 4 code for the Gier computer, 25:31168 (INR-1260)
KOWALSKI, L., Angular distribution of fission fragments from the ^{170}Yb compound nucleus excited to 107 MeV, 25:31371
KOWNACKI, Jan, Adaptation of a long-lens beta-ray spectrometer for the measurement of short nuclear lifetimes, 25:29358
KOYAMA, Koichiro, Aging characteristics of Cu--Be--Sn alloy, 25:29830
KOZODAEV, A. M., Thyristor voltage stabilizer for a 40-kV modulator, 25:31067
KOZOREZ, A. K., Semiautomatic apparatus for regulating the neutron diffractometer, 25:29402
KOZUB, R. L., Mean lifetimes of levels in ^{92}Mo, 25:31377
KRAEGER, James A., X rays in healing arts in North Dakota, 1964--1968, 25:29542
KRAJEWSKI, W., Allotropic transformation and thermal expansion of Co binary alloys between 100 and 800°C. I, 25:29899
KRAMER, D., Proton irradiation effects in type 321 stainless steel, 25:29915
KRAMER, G., Nucleon--nucleon interactions below 1 GeV/c, 25:30903
KRAMER, Lorenz, Thermodynamic behavior of Type-II superconductors with small kappa near the lower critical field, 25:30422
KRAMEROV, A. Ya., Application of the method of reduced costs to estimates of the effectiveness of utilization of nuclear fuel, 25:31585
KRASNIKOV, Yu. G., Thermodynamically complete equation of state of imperfect plasma, 25:30521
KRASNOBAEVA, N., Direct spectral determination of rhenium in molybdenum and copper concentrates, 25:28945
KRASNOSHCHEKOV, G. P., Quantitative ^{6}Li autoradiography of metastases of Walker-256 carcinosarcoma in pulmonary tissue, 25:29443
KRASNOV, N. N., Vertical motion of particles in cyclotron, 25:31063
KRATOCHVIL, J., Combined effect of 6-Azauridine and irradiation in vivo and in vitro. VI, 25:29679
KRATSIK, B., Decay scheme of ^{88}Y, 25:31247
KRATZER, W. K., Examination of an Inconel-600 tube from N Reactor steam generator 6A, 25:29760 (DUN-SA-149)
KRAUS, G., Single pion production in π⁺p interactions at 8 and 16 GeV/c, 25:30891
KRAUS, John D., Ohio radio sources in clusters of galaxies, 25:30120
KRAUS, V., Influence of initial content of the cooling rate from the beta phase to preferred uranium orientation following heat treatment, 25:29884 (UJV-2525-M)
KRAVETS, A. N., F-center destruction mechanism in proton tracks in alkali halide crystals, 25:30655
KREPLIN, R. W., Ionospheric absorption during shortwave fade-outs related to enhancement of solar x-ray flux, 25:30362
KREUZER, H. J., Regge trajectories for multichannel potential scattering, 25:31031
KRIKORIAN, N. H., Enthalpies of formation of cerium dioxide, cerium sesquicarbide, and cerium dicarbide, 25:29961
KRIPYAKEVICH, P. I., Crystal structures of $ZrCo_3B_2$ and $HfCo_3B_2$, 25:29992
KRISHNAMOORTHY, T. S., Determination of total hydrogen content of UD_2 pellets, 25:28912 (BARC-500)
KRISHNAMURTHY, K., Tabulated dose uniformity ratio and minimum dose data for gamma irradiator design, 25:29250 (BNL-50145(Rev.))
KRITSKII, G. A., Procedures for determining changes in DNA of irradiated organism, 25:29637

KRIVOSHAPKIN, P. A., Antisymmetric diurnal and semidiurnal variations of cosmic rays, 25:30319
KRIVSKY, L., Observations of chromospheric flares at Ondrejov, 25:30189
KRIZ, S., Mass transfer in close binaries. I, 25:30112
KRMPOTIC, D., Levels in ^{72}Ge populated by ^{72}Ga, 25:31260
KROEBEL, R., Preparation and properties of a crystalline uranium(IV)--hydrazine nitrate compound, 25:29035 (NP-18736)
KROEGLER, H., Merits and limitations of explosively driven current generators in fusion research, 25:30562 (EUR-4593, pp 205-17)
KROH, J., Effect of dose rate on the radiation yields of radicals in frozen organic media, 25:29160
Radiothermoluminescence of crystalline and glassy methanol, 25:29101
KROHN, Harry L., Survival in lethally irradiated dogs, 25:29651
KROLIKOWSKI, W., Non-Hermitian uncharged field and existence of quarks, 25:30827
KROMMINGA, A., Negative-parity states in ^{139}Pr, 25:31366
KRONER, G., Direct and compound processes to the reaction ^{40}Ca(d,α)^{38}K at E/sub d/ = 5 to 10 MeV, 25:31275
KRONRAD, L., New possibilities in the topical diagnosis of cardiac infarcts, 25:29571 (LB/G-2835)
KROPOTKIN, A. P., Acceleration of cosmic rays by magnetohydrodynamic discontinuities, 25:30312
KRPATA, J., Spectrographic study of EW LAC. I, 25:30098
KRUEGER, J., Allotropic transformation and thermal expansion of Co binary alloys between 100 and 800°C. I, 25:29899
KRUGLYI, M. S., Mechanism of the formation of tree-shaped channels in charged-particle irradiated dielectrics, 25:29100
KRUMHANSL, J. A., Prog. rpt. on theoretical phonon physics, 4/70--3/71, 25:31711 (NYO-3699-53)
KRUMMHEUER, F., Why expanding stars after leaving the main sequence, 25:30097
KRUMSHTEIN, Z. V., Spectrum of fast deuterons emitted in 670-MeV proton interaction with carbon nuclei, 25:31225
KRUSE, Robert L., Monomer reactivity ratios in graft copolymerization, 25:29106
KRUSE, T., Nuclear matter radii in the tin isotopes, 25:31341
KRUTOV, V. A., Description of the excited paired states of atomic nuclei by the variational approach, 25:31360
KRYMSKII, G. F., Antisymmetric diurnal and semidiurnal variations of cosmic rays, 25:30319
Cosmic-ray flux in interplanetary media. II, 25:30315
Cosmic-ray flux in interplanetary media. I, 25:30314
KRZYWICKI, A., Conference on high multiplicity hadronic interactions, Paris, 5/70, 25:30762
High multiplicity hadronic interactions, 25:30732
KSCHWENDT, H., TIMOC: Monte Carlo code for stationary and time dependent neutron transport, 25:31167 (EUR-4519)
KUCAB, M., Tables of magnetic structures determined by neutron diffraction. II, 25:30664 (NP-18783)
KUCHER, A. M., Production of spontaneously fissionable isomer ^{234}U at radiative thermal neutron capture, 25:31307 (JINR-P7-5497)
KUCHITSU, Kozo, Average values of bond angles, 25:29071
KUDINOV, V. M., Influence of starting parameters on ripple formation in explosive welding of metals, 25:31736 (SCL-T-710240)
KUDO, Akira, Transport of ^{137}Cs. II, 25:29204
KUDRYASHOV, Yu. B., Deamination of nitrogen compounds in liver during radiation sickness, 25:29641
KUEMMEL, Reiner, Tunneling into the energy bands of the intermediate state in Type-I superconductors, 25:30431
KUHL, David E., Giant splenomegaly in sarcoidosis demonstrated by radionuclide scintiphotography, 25:29593
KUHLMANN, W., Emittance measurements at Juelich isochronous cyclotron, 25:31119
KUKACKA, R., Analysis of occupational diseases due to ionizing radiation in the health institutions of the North-Moravian region, 25:29711
KUKAVADZE, G. M., Mass-spectrometric measurements of the diminution of hydrogen in polyethylene targets which have been irradiated in a proton synchrotron, 25:29400
KUKHLENKO, A. S., Pulsed neutron source, 25:31178
KUKHTO, O. L., Apparatus for studying the dynamics of condensed systems using a back-scattering method, 25:29362
KUKLIN, G. V., Run of the difference of the maximal magnetic field strength of opposite polarities in sunspot groups before and after proton flares, 25:30185
KULANDER, John L., Velocity-dependent non-LTE source function. II, 25:30084
KULIKOV, N. V., Radiosensitivity of roe of pike Esox lucius, 25:29659
KULIKOV, V. N., Charge distribution of heavy cosmic-ray nuclei in region Z greater than or equal to 26, 25:30305
KULINSKII, V. I., Effects of radioprotective sympathicomimetics on oxygen pressure in the spleen, 25:29547
Participation of catecholamine depots and alpha-adrenoreceptors in radioprotective effect of hydroxyphenylethanolamines, 25:29546
KULISIC, P., Reaction ^{22}Ne(p,t)^{20}Ne at 26.9, 35.1, and 42.4 MeV, 25:31296
KULKARNI, V. G., Positron lifetimes in rare earth oxides, 25:30272
KUL'MAN, V. G., Accelerating structures with ring coupling resonators, 25:31078
KUMAR, R., Structure of liquid cadmium--antimony alloys, 25:29896
KUMMER, J. T., Studies of surface reactions of NO by isotope labeling. II. Deuterium kinetic isotope effect in the ammonia--nitric oxide reaction on a supported platinum catalyst, 25:29063
KUMPF, U., Magnetization curves for Type-II superconductors with small Ginzburg--Landau parameters, 25:30418
KUMSISHVILI, Ia. I., Brightness of binary system AX Monocerotis, 25:30056
KUNZ, S. E., Possible use of the sterile-male technique for eradication of the horn fly, 25:29744
KUNZE, R. C., Pulse breakdown of plastic foils in liquids, 25:30569 (EUR-4593, pp 281-6)
KUNZE, R.-C., High-power spark gap for high repetition rates, 25:30568 (EUR-4593, pp 273-80)
High-Q capacitor, 25:30594 (EUR-4593, pp 541-4)
KUO, Mau H., Microbial oxidation of p-diethylbenzene, 25:29061
KURANC, J., β--γ angular correlation measurements, 25:31277
KURAS, Rosemary A., Iodine analysis of biological samples by neutron activation of ^{127}I, with scintillation counting of Cherenkov radiation, 25:29030
KURI, Zen-ichiro, Radicals produced in γ-irradiated allyl alcohol glass, 25:29162
KURILCHIK, V. N., Spectra of emission of extragalactic radio sources, 25:30150
KURNOSOVA, L. V., Measurements of energy spectra of multicharged nuclei, 25:30307
KUROCHKIN, A. V., Spark chamber power supply circuit with semiconductor trigger, 25:29374
KURODA, P. K., Daily fluctuations of radioactive fallout particles in ground-level air, 25:29219
Decay of /sup 106m/Rh, 25:31384
Worldwide movement of fallout particles from nuclear explosions, 25:29216
KURTMULLAEV, R. Kh., Shock waves propagating along a magnetic field in a collisionless plasma, 25:30620
KUSHNIR, A. J., Interphase boundary waves in the intermediate state of lead, 25:30429
KUTSENTOV, L. M., Internal ionization in β decay of ^{131}I, 25:31316
KUZENKOVA, M. A., Sintering process of zirconium diboride with tungsten, 25:29930
KUZIN, A. M., Effects of ionizing radiation on lactate dehydrogenase in rats, 25:29670
KUZ'MA, Yu. B., Crystal structures of $ZrCo_3B_2$ and $HfCo_3B_2$, 25:29992
KUZ'MIN, A. I., Antisymmetric diurnal and semidiurnal variations of cosmic rays, 25:30319
Cosmic-ray flux in interplanetary media. II, 25:30315
Cosmic-ray flux in interplanetary media. I, 25:30314
Effects of solar-activity cycle on irregularity of interplanetary magnetic field, 25:30326
KUZNETSOV, A. A., Application of phenomenological quasi-two-body model to π-p-interactions with strange particle production at p = 4 GeV/c, 25:30869 (JINR-P1-5706)
KUZNETSOV, V. A., Use of zeolite pumps in field-emission microscopy, 25:29406
KVICALA, J., Observations of chromospheric flares at Ondrejov, 25:30189
KVIMSADZE, M. V., Propagation of intense electromagnetic waves in a two-component plasma, 25:30619
KVINIKHIDZE, A. N., Retarded part of two-time Green function and two-body relativistic problem, 25:31014 (JINR-E2-5746)

L

LABORIE, G., Grenoble cyclotron progress report, 25:31097
LACASSAGNE, A. M. B., Liver, 25:29694
LACKI, E., Semiconductor system for analog processing of signals obtained from radiometric control set of the calcium content in the cement-feeding, 25:29389 (ITJ-2/E)
LA CONTI, A. B., Characteristics of tantalided and hafnided samples in highly corrosive electrolyte solutions, 25:29766
LACOSTE, Michel, Thermal diffusivity of Pu alloy stabilized delta phase, 25:29876
LAFARGUE, Yves-Paul, Physical and chemical interactions of water on graphite, 25:29918 (CEA-R-4123)
LAGERWALL, S. Y. T., Diffusion of Ar, Kr, and Xe in CaF_2 investigated on U-doped CaF_2, 25:30673
LAGU, R. G., Positron lifetimes in rare earth oxides, 25:30272
LAKE, Suzanne, Availability in the dog of radionuclides in nuclear debris from Plowshare excavation Cabriolet, 25:29456
LAL, Sudarshan, Potentiometric studies with an ion permselective membrane, 25:28956
LAM, D. J., Crystal structures of several intermetallic

phases of Np and Pu alloys with Sb, Se, and Te, 25:30002
LAM, Wing-chee, Neutron emission following radiative pion capture in complex nuclei, 25:31215
LAMAR, G. N., Proton magnetic resonance shifts in bis(cyclooctatetraenyl) U(IV), 25:29085
LAMB, D. Q., Statistical models based on Fermi model, 25:30764
LAMB, W. E. Jr., Measurement of level shift in He^+, n = 3, 25:30263
LAMBERT, D. L., Identification of NiH in sunspot spectrum, 25:30173
LAMBERT, Gerard, Correlations between ^{210}Pb atmospheric abundance in Terre Adelie and solar activity, 25:30171
Correlations between ^{210}Pb deposit in Antarctic and fluctuations in Earth's magnetic field, 25:29211
LAMBERT, Joseph P. F., Determination of zinc in pharmaceutical products by neutron activation analysis, 25:29029
LAMBERT, M., Reaction $^{22}Ne(p,p)$, $^{22}Ne(p,p')$, and excited states of ^{23}Na, 25:31281
Reactions $^{12}C(d,d)$, $^{12}C(d,p_0)$, and $^{12}C(d,p_1)$, 25:31222
LAMOT, G.-H., Description of elastic-scattered processes with the use of non-local separable potentials, 25:31186 (LYCEN-7089)
LAND, C. C., Strain effects and spalling in alpha-bombarded ThO_2, 25:30014
LANDI, G., Influence of Mottelson and Valatin effect on rotational bands of asymmetrical nuclei, 25:31345
LANDSHOFF, P. V., Deep inelastic neutrino scattering, 25:30809
LANDSTREET, J. D., Discovery of circular polarization in the white dwarf G99--37, 25:30072
Discovery of periodic variations in the circular polarization of the white dwarf G195--19, 25:30073
LANERI, U., Ecological site survey at Trisaia, 25:29479
LANGAN, D., Model philosophy in relation to prestressed concrete pressure vessel design problems, 25:29307
LANGAN, J. K., Pinhole scintillation camera and /sup 99m/Tc-pertechnetate in normal thyroid scanning, 25:29586
LANGE, J., Two-quasi-particle rotational band at 1172 keV in ^{172}Yb, 25:31367
LANGENBECK, B., Electromagnetic form factors of the proton, 25:30786
LANGERON, Jean-Paul, Temperature of recrystallization of Zr--O solid solutions, 25:29854
LANGLET, Gerard, Synthesis and crystallographic study of compounds of the system Cs_2O--Al_2O_3--SiO_2, 25:29938 (BNWL-tr-65)
LANGUILLE, M., BWR prestressed concrete pressure vessels, 25:31551 (EUR-4531, pp 615-45)
LAN'KO, E. V., Lifetimes of excited states of ^{140}Ce, 25:31319
LANNON, Joseph A., Infrared spectrum of solid and matrix-isolated H_2O_2 and D_2O_2, 25:29055
LANORE, Jeanne-Marie, Several applications of a system of weighting in Monte Carlo calculations, 25:31164 (CEA-N-825)
Study of the variance of a Monte Carlo calculation, 25:30698 (CEA-N-1096)
LANZA, S., Activities of Scalbatraio center for research in nuclear safety, 25:31610
LANZER, D., Packing materials for γ-irradiated foodstuffs, 25:30033
LANZEROTTI, L. J., Magnetospheric substorm of August 25--26, 1967, 25:30368
LANZOLA, E., Strontium-90 and ^{137}Cs in milk during 1952 to 1966, 25:29507
LAPIDUS, L. I., Nucleon Compton-effect and sum rules for dipole nucleon momentum, 25:30776 (JINR-P2-5679)
LAPOSA, J. D., Phosphorescence of some deuterium-substituted phenylacetylenes, 25:29040
LAPSHIN, N. A., Influence of ethaperzine on the interoceptive reflexes before and after irradiation of animals, 25:29643
LAPSHIN, V. G., Pulse shaper with independent regulation of output pulse duration and dead time, 25:29342
LARSON, James D., Electrostatic deflector for selectively and adjustably bending a charged particle beam, 25:29408
LARSSON, Curt, Reaction $^{45}Sc(^3He,d)^{46}Ti$, 25:31278
LASSMANN, G., Formation of radicals in irradiated single crystals of sarcosine.HCl studies by ESR, 25:29152
LASSNER, G., Positive functionals on the algebra of test functions, 25:30944
LASTOCHKIN, R. R., Influence of carbon on Mo ductility, 25:29863
LASZTITY, R., Effect of gamma irradiation on some chemical and physical properties of gluten proteins, 25:29103
LATZKO, D. G. H., Nondestructive testing of power reactor components, 25:29289
LAUDIERI, P. C., Fast-electron--slow-electron coincidence study of violent Ar+--Ar collisions, 25:30288
LAUNAY, P., Two Bugey 1/5 models, 25:29310
LAUNOIS, D., Bounce effects in the negative mass instability, 25:30551
LAUSCH, W., Neutron radiography and its application possibilities, 25:29292
LAVAKARE, P. J., Improved estimate of solar neutron flux measured in an earlier experiment, 25:30177
LAVAL, G., Bounce effects in the negative mass instability, 25:30551
LAVEN, H., Semisterility for insect control, 25:29752
LAVROVSKII, K. P., Thermal and radiation initiated conversions of terphenyl isomers and their hydrogenated derivatives, 25:29113
LAVRUKHINA, A. K., Determination of the modulation-region boundaries, 25:30323
Studies of VH and VVH nuclei in mineral meteorites, 25:30317
LAW, C. A., Cobalt-60: betting megabucks on megacuries, 25:29284
LAW, J., Binding energy of /sub Λ/^{5}He with two-channel separable potentials, 25:30897
LAWLESS, B., Optical and radio studies on extensive air showers, 25:30333
LAWN, C. J., Fully developed turbulent flow through concentric annuli, 25:29265 (RD/B/N-1878)
LAWRENCE, John K., Scattering of neutrinos by linearized Schwarzschild metric, 25:30242
LAZAREV, N. V., Thyristor voltage stabilizer for a 40-kV modulator, 25:31067
LAZUTIN, E. V., (γ,n) cross sections of Al and P, 25:31242
Fine structure of the giant dipole resonance in ^{16}O nucleus, 25:31231
LAZZARINI, E., Isomeric effect in Szilard--Chalmers recoil of /sup 60m/Co and /sup 60g/Co in some mixed complexes of Cr(III) and Co(III), 25:29170
LEAF, G. K., ARC system: one-dimensional transport theory capability, SNARC1D, 25:31651 (ANL-7717)
LEBEDEV, V. V., Proton flux from 1.5 to 50 MeV on satellites Zond-4 and Zond-5, 25:30164
LEBEDEVA, G. A., Effects of oxethiole on condition of liver and kidneys during ^{210}Po-induced chronic radiation sickness, 25:29563
LE BELLAC, Michel, Duality and dual models, 25:30825
LE CALVE, J., Measurement of radiative lifetimes of $CO_2^+(A^2PI/sub\ u/)$, $CO_2^+(B^2\Sigma/sub\ u/^+)$, $CH(A^2\Delta)$ and $CO(C^1\Sigma^+)$ by pulsed radiolysis, 25:30273 (ANL-Trans-879)
LE CARS, F., Prestressed concrete pressure vessel of the Vandellos nuclear power plant, 25:31454 (EUR-4531, pp 81-94)
LECHTENBOEHMER, H., Welding problems in nuclear technology, 25:29792
LECKRONE, David S., He I line profiles in normal B-type spectra, 25:30042
LECOURT, Y., Thermal shielding by wire gauze and metallic sheets, 25:29619 (EUR-4531, pp 1019-34)
LE DELLIOU, Raymonde, Nitridation of Zr at high temperatures, 25:29870
LEE, Chung Choo, Insect pest control using sterile-male technique. II, 25:29731
LEE, S. Y., Possible CP violation in $K^{+-} \to \pi^{+-}\gamma\gamma$, 25:30928
LEETZ, Hans-Karl, Contribution to indications and methods of irradiation in cases of malignant systemic diseases, 25:29599
LEFORT, M., Cross sections for heavy ion nuclear reactions, 25:31356
LEGER, A., Multigap effect on phonon structure in tunneling experiments, 25:30426
LEGEWIE, G., Feasibility of gas cooling for the fusion reactor blanket, 25:30589 (EUR-4533, pp 491-6)
LEGGE, C. A., Simple cryostat for thermoluminescence measurements, 25:30444
LEGGETT, Monica R., Hydrogen adsorption on (100) W surface using simple HEED system, 25:29846
LE GO, P., Experimental study of emission of fission products due to cladding failures produced during rapid loss of gaseous coolant, 25:31608
LE GOFF, P., Kinetics and mechanism of low-pressure, high-temperature oxidation of Si. II, 25:29968
Kinetics and mechanism of low-pressure, high-temperature oxidation of W silicides. III, 25:29869
Low-pressure, high-temperature siliconizing of W. I, 25:29814
LEITNAKER, James M., Phase behavior of U--V--N system and properties of UVN_2, 25:29989
Phase investigations in U--Cr--N system, 25:29988
LEMAN, E. P., Effect of multiply scattered γ-radiation in the x-ray radiometric method, 25:28939
LEMBO, G., Studies on natural background radiation in Italy, 25:29205
LENAMON, L., Structure of hydromagnetic shock waves, 25:30528
LENCHENKO, V. M., Efficiency of radiators and absorbers of charged particles, 25:30641
LENGYEL, Lajos L., Preionization and velocity effects in MHD channels with nonequilibrium plasmas, 25:30348
LEONARD, Robert B., New nickel-base alloy solves weld-zone corrosion problems, 25:29764
LEQUEUX, James, Molecules in interstellar space, 25:30128
LERCHE, I., Gravitational kinetic equations, 25:30237
Resistive effects in the turbulent photosphere and chromosphere, 25:30180
LE ROULLEY, Jean-Claude, Correlations between ^{210}Pb deposit in Antarctic and fluctuations in Earth's magnetic field, 25:29211
LEROY, Jean-Marie, Ternary system UO_3--V_2O_5--Na_2O, 25:29998
LESHCHENKO, B. E., Pulsed neutron source, 25:31178
LESIGNE, Bernard, Absorption oscillogram of $CO_2^+(X^2PI/sub$

g/) and N_2^+(X²Σ/sub g/⁺) ions in their ground state produced by pulsed radiolysis of CO_2 and N_2, 25:30274 (ANL-Trans-881)
LESTIENNE, R., Conference on high multiplicity hadronic interactions, Paris, 5/70, 25:30762
LESUEUR, Daniel, Amorphization of a Pd--Si alloy by irradiation with fission products, 25:29901 (CEA-CONF-1693)
LETOV, V. N., Quantitative ^{6}Li autoradiography of metastases of Walker-256 carcinosarcoma in pulmonary tissue, 25:29443
LEVCHENKO, Yu. Z., Shortened charge-exchange gas target, 25:31065
LEVENTHAL, M., Measurement of level shift in He^+, n = 3, 25:30263
LEVIN, V. I., Production of radioisotopes in research reactors, 25:29275
LEVINA, R. A., Mechanism of oxidation of Nb--Zr alloys, 25:29767
Oxidation kinetics of Nb--Zr alloys. V, 25:29769
LEVINE, D., Conversion studies for SREL 600-MeV synchrocyclotron, 25:31160
LEVINE, E., Precipitation in the beryllium--iron system, 25:29897
LEVINE, R. D., Theory of vibrational excitation in the near classical limit, 25:30295
LEVINSON, C. A., Nonrelativistic hard-pion production and current-field algebra, 25:30898
LEVIT, P. A., Stability of single-turn coils in pulsed magnetic fields up to 1 MG, 25:30556 (EUR-4593, pp 25-32)
LEVY, Ira S., Production of metal resistant to neutron irradiation, 25:29799
LEVY, Milton, Surface area effects on the oxidation kinetics of pyrolytic graphite, 25:29919
LEVY, R. H., HIPAC ion source, 25:31138
LEVY II, H., Born wave cross-section calculations for collisional quenching of metastable H(2s), 25:30283
LEXA, J., Distribution of ionization stages of argon under coronal conditions, 25:30181
LHOMME, Jean, Transannular hydride shifts. Mechanistic study in the longifolene series, 25:29050
LI, G. C., High-energy electron scattering from ^{6}Li, 25:31211
LIBBY, D. R., Prog. rpt. on high-power quasi-steady MPD acceleration, final, 5/70, 25:30599 (N-71-10100)
LICHERON, S., Study of the properties of concrete and especially of creep under the effect of temperature, 25:30023 (EUR-4531, pp 267-324)
LICHTENBERG, A. J., Diagnostics for hot-electron, magnetically confined plasmas, 25:30489
Verification of classical, self-consistent theory of particle loss in hot electron, magnetic mirror compression experiment, 25:30465
LIDA, M., Study of the properties of concrete and especially of creep under the effect of temperature, 25:30023 (EUR-4531, pp 267-324)
LIDSKY, L. M., Diffusion resulting from nonadiabatic scattering on a helically perturbed field in a torus, 25:30466
LIEBERMAN, M. A., Diagnostics for hot-electron, magnetically confined plasmas, 25:30489
Verification of classical, self-consistent theory of particle loss in hot electron, magnetic mirror compression experiment, 25:30465
LIESEM, H., Resonance free or precessional extraction, 25:31107
LIGGETT, G., Angular distribution of particles evaporated in nuclear reactions, 25:31428
LIGHTNER, David A., Hydrogen rearrangements in the mass spectra of alkylbenzenes, 25:29068
LILEEVA, Yu. Ya., Investigation of the diffusion of hydrogen of hydrides of alloys, 25:29837
LILLIEN, I., Steric factors in the cationic rearrangement of substituted cyclobutanes, 25:29049
LIN, F. M., Characteristics of some TLD solid systems, 25:29382 (COO-1105-120)
LIN, I., Fissionability of heavy nuclei, 25:31417
LIN, S., Treatment of two cases of radium contamination, 25:29508
LINDBAECK, S., Regenerative extraction system in CERN synchrocyclotron, 25:31108
LINDEN, W. A., In vitro studies on radioprotective effects of melanin on mammalian cells, 25:29568
Synchronization of the mytotic cycle of mammalian cells in vitro through fractionated x-ray therapy, 25:29611
LINDOP, Patricia J., Hematopoietic changes following irradiation, 25:29634
LINGAFELTER, Jack, Quality assurance: a realistic appraisal, 25:31528
LINTNER, M. A., Flow simulation through graphics: a high-speed interpretation of reactor blowdown calculations, 25:31588 (CONF-710302-4)
LINUSSON, H., Energy levels and gamma transitions in ^{70}Ga, 25:31290
LIOU, M. K., Internal scattering amplitudes for bremsstrahlung, 25:31444
LIPINSKI, W. C., Instrumentation systems to protect LMFBR core integrity, 25:31574 (ANL-7793)
LIPSHUTZ, N. R., Breakdown of scaling invariance in generalized Bjorken limit of perturbation theory, 25:30783
LISITSIN, A. K., Deposition conditions of molybdenum and selenium in exogenetic epigenetic uranium deposits, 25:29240
LISTENGARTEN, M. A., Valent shell structure effects on coefficients of internal conversion, 25:31343
LITTLE, P. E., Graphs for analysis of (1-3) gamma--gamma directional correlations, 25:31312 (ORNL-4619)
LITTMAN, Howard, Prog. rpt. on gas-particle heat transfer coefficients in packed and fluidized beds by frequency response techniques, annual, 1/70--2/71, 25:31725 (RPI-3639-16)
LITUNOVSKII, R. N., Production of monochromatic beams using cyclotron acceleration, 25:31121
LIU, C. T., Transition morphology during hcp precipitation from beta-isomorphous alloys, 25:29886
LIVINGOOD, J. J., Proposed Midwest tandem cyclotron (MTC), 25:31083
LJUBICIC, A., Double electron ejection in decay of ^{137}Ba, 25:31359
LJUNGSTROEM, Anders, Forced and free oscillations. some aspects of longitudinal plasma waves. technical report no. 70:2, 25:30606 (NP-18673)
LLOYD, M. H., Mound assistance program: development of a sol-gel process and equipment for production of dense $^{238}PuO_2$ microspheres, 25:29921 (ORNL-4565)
LO, S. Y., Bounds, multiplicity, and energy dependence, 25:30899
LOCHTER, M., Studies of surface discharges on insulating foils, 25:30581 (EUR-4593, pp 385-92)
LODHI, M. A. K., Inelastic scattering of electrons and E2 transition in ^{6}Li, 25:31229
LOFGREN, Edward J., Berkeley ERA program, 25:31059 (UCRL-20611)
LOGACHEV, V. I., Measurements of energy spectra of multicharged nuclei, 25:30307
LOGVINOV, V. V., Hydrodynamics of a magnetoactive plasma in the quasilinear approximation, 25:30532
LOINGER, A., Rayleigh-Jeans law is incompatible with classical electrodynamics, 25:30936
LOISEAUX, J. M., Reactions $^{11}B(p,^3He)^9Be$ and $^{11}B(p,t)^9B$, 25:31228
LOMONOSOV, V. N., Acceleration of charged particles in a variable magnetic field, 25:30122
LONGHI, A., Treatment of radiation-induced cutaneous lesions, 25:29706
LONGO, M. J., Isospin invariance in reaction n + p → π^0 + d, 25:30730
LOPATO, L. M., Phase diagrams of systems of Sm, Gd, and Dy oxides with Mg oxide, 25:29985
LOPEZ, Alain, Measurement of the state of equilibrium between radon and its daughters in the uranium mines, 25:29201 (AEC-tr-7228)
Particle size spectrum of the radioactive aerosols in a uranium mine, 25:29200 (AEC-tr-7227)
LOPEZ, C. A., Action principle for a classical charged particle, 25:30790
LORBACH, F., Fast, solid dielectric, multichannel crowbar switch, 25:30580 (EUR-4593, pp 379-84)
LORD, R. S., Heavy ion acceleration at ORIC, 25:31131
LOTHROP, Fred H. G., Digital control of Bevatron acceleration cycle, 25:31054 (UCRL-20185)
LOTTS, A. L., Development of FBR oxide fuels, 25:29922 (ORNL-4630, pp 3-58)
LOUIS, R. J., H^- ion injection into central region of TRIUMF cyclotron, 25:31152
LOVISATTI, L., Radioactive isotopes and thermographic findings in bone localizations of systemic diseases, 25:29588
Scintigraphic and thermographic detection of bone metastases, 25:29589
LOW, E. W. E., Use of simplified models for the design of end slabs, 25:29304
LOWENSTEIN, J. H., Locally generated dilatation charge in Thirring model, 25:30993
LUCCHINO, R. C., Retention patterns of ^{124}Sb in mice following inhalation of particles ormed at different temperatures, 25:29424 (LF-43, pp 66-70)
LUCHKOV, B. I., Relation of electron flux in upper atmosphere to state of Earth magnetosphere, 25:30353
LUCHNIK, N. V., Protective effect of anoxia on irradiation dose in case of chromosome aberrations, 25:29486
LUDWICK, J. D., Prog. rpt. on noble gas confinement study, final, FY-1970, 25:29074 (DUN-7221(Vol.1))
Prog. rpt. on noble gas confinement study, final, FY-1970, 25:29075 (DUN-7221(Vol.2))
LUEGGER, A., In vitro studies on radioprotective effects of melanin on mammalian cells, 25:29568
Synchronization of the mytotic cycle of mammalian cells in vitro through fractionated x-ray therapy, 25:29611
LUETJERING, G., Precipitation in the beryllium--iron system, 25:29897
LUKASZUK, Leszek, Limits on strength of interactions from axiomatic field theory, 25:30852
LUKENS, H. R., Prog. rpt. on applications of neutron activation analysis in scientific crime investigation, final, 9/70, 25:29012 (GA-10276)
LUKIERSKI, Jerzy, Singularities of two-point Green functions, 25:30959
LUND, Walter, Stability constants of the Mo(VI) complexes of DTPA and TTHA, 25:28920
LUNDBERG, Boerje, Experimental studies of gamma rays from

neutron reactions, 25:31332
LUNDGREN, D. L., Effect of the inhalation of ^{144}Ce in relatively insoluble forms on influenza virus infection in mice, 25:29724 (LF-43, pp 254-62)
Toxicity of inhaled ^{90}Y fused clay in beagle dogs. II, 25:29434 (LF-43, pp 146-62)
LUNDIN, L., Lifetimes of some doubly excited levels in neutral helium, 25:30265
LUNGU, Nicolae, Photometric elements of short-period cepheid WZ Bootis, 25:30104
LUO, H. L., Superconductivity of Re--Os, Re--Ru, Ru--Os, and Re--W hcp alloy systems and slightly doped Re, 25:30433
LUPPI, R., Merits and limitations of explosively driven current generators in fusion research, 25:30562 (EUR-4593, pp 205-17)
LUPU, Gh., Integral equation for the total charge density for a relativistic plasma, 25:30538
LURIE, L. S., Gamma-irradiation apparatus for treatment of root- and tuber- crops, 25:29253
LURIE, R., Experimental study of emission of fission products due to cladding failures produced during rapid loss of gaseous coolant, 25:31608
LUTCOV, A. I., Thermal conductivity, electric resistivity, and specific heat of dense graphites, 25:29949
LUTZ, Michel, Separation and recovery of permanent gases by preparative chromatography, 25:29177 (CEA-R-4090)
LUZANOV, V. M., Erythropoietic activity of the blood in fractional irradiation, 25:29655
LUZZATTO, G., Equal-time commutators and Bjorken's theorem, 25:30973
LYAPIDEVSKII, V. K., Mechanism of the formation of tree-shaped channels in charged-particle irradiated dielectrics, 25:29100
LYONS, L., Slope of the momentum transfer distribution, 25:30900
LYSKOVICH, A. B., Scintillation spectrometry of soft x-ray radiation, 25:29350
LYUBENKO, A. N., Control system of Dubna monoenergy cyclotron, 25:31099
LYUBOSHITS, V. L., Identity of elementary particles, 25:30761
LYUBUSHIN, A. A., Role of quantum fluctuations of a gravitational field in general relativity and cosmology, 25:30224

M

MAASS, I., Sample preparation for precision carbon isotopic analysis, 25:28968
MACAK, P., Spectral classification and photometry of stars in two H II regions, 25:30108
MACCHI, C., Radioactive isotopes and thermographic findings in bone localizations of systemic diseases, 25:29588
Scintigraphic and thermographic detection of bone metastases, 25:29589
MACCRACKEN, M. C., Ice age theory analysis by computer model simulation. I, 25:31749 (UCRL-71888(Pt.1))
Ice age theory analysis by computer model simulation. II, 25:31750 (UCRL-71888(Pt.2))
MACCRACKEN, Michael C., Tests of ice age theories using a zonal atmospheric model, 25:31751 (UCRL-72803)
MACFADYEN, N. W., Crossing-symmetric expansions of scattering amplitudes, threshold behavior, and asymptotics, 25:31028
MACFARLANE, D. R., Instrumentation systems to protect LMFBR core integrity, 25:31574 (ANL-7793)
MACHABELI, G. Z., Hydrodynamics of a magnetoactive plasma in the quasilinear approximation, 25:30532
MACKAY, Craig D., Orientation of radio sources and elliptical galaxies, 25:30205
MACKENZIE, G. H., Extraction of multiple beams of various energies from TRIUMF negative ion isochronous cyclotron, 25:31109
MACNAUGHTON, J., Single-pion production in K$^+$p interactions at 4.6 GeV/c, 25:30748
MACQ, P., UCL isochronous cyclotron conceptual design and status report, 25:31094
MACVICAR, T. D., Laser beam filtering by saturable dyes, 25:31747 (UCRL-51008)
MADBOULY, R., Analysis of platinum for certain elemental impurities by neutron activation, 25:29023
MADELAINE, Guy J., Measurement of the state of equilibrium between radon and its daughters in the uranium mines, 25:29201 (AEC-tr-7228)
Particle size spectrum of the radioactive aerosols in a uranium mine, 25:29200 (AEC-tr-7227)
MADER, D. L., Measurement of level shift in He$^+$, n = 3, 25:30263
MAEDA, Muneharu, Airconditioning system and its automatic control for a nuclear power station, 25:29259
MAELAND, Arnulf J., Inelastic neutron scattering spectra from lanthanum dihydride and lanthanum trihydride, 25:30677
MAGALASHVILI, N. L., Brightness of binary system AX Monocerotis, 25:30056
MAGYAR, B., Accuracy and applicability of x-ray fluorescence for determination of the concentration of the elements phosphorus to uranium in solution, 25:28962
MAHAN, Bruce H., Ion-molecule collision processes, 25:29064
MAHENC, Jean, Electrochemical oxidation of sulfur dioxide on a platinum electrode, 25:31754 (UCRL-Trans-10525)
MAHLER, Dan, Surgical treatment of chronic radiation injuries of axilla and shoulder, 25:29569
MAHLER, H. R., Deuterium effects on binding of reduced coenzyme alcohol dehydrogenase isoenzyme EE, 25:29056
MAHRT, R., Series combination of tandem and cyclotron, 25:31139
MAIER, E. J., Subauroral red arc and the associated ionospheric phenomena, 25:30350 (N-70-36812)
MAIKUROV, V. B., Experimental installation R-Ohm for studying high-frequency field-interaction with plasma, 25:30508 (NP-18801)
MAILFERT, A., Penetration of induction, electrical field, and losses in impure Type-II superconductors having a surface current, 25:30414 (ORNL-tr-2475)
MAISIN, J., Gastrointestinal tract, 25:29632
Lymphatic system and thymus, 25:29635
Lymphoid tumors and radiation, 25:29696
MAISIN, J. R., Gastrointestinal tract, 25:29632
Lymphatic system and thymus, 25:29635
Lymphoid tumors and radiation, 25:29696
MAITI, J. N., Effect of glass wall on the determination of plasma conductivity by rf external probes, 25:30527
MAJER, Jaroslav, Separation by polyacrylamide gel electrophoresis of RNA from the spleens of immunized mice, 25:29476
MAKARENKO, G. N., Properties of rare-earth metals (Sc, Nd), their hydrides, carbides, and oxides, 25:29859
MAKAROV, D. V., Thermal and radiation initiated conversions of terphenyl isomers and their hydrogenated derivatives, 25:29113
MAKHLINA, A. M., Protein fractions of intestine and brain of irradiated animals, 25:29664
MAKHMETOV, M., Determination of arsenic and tellurium in gaseous media, 25:28959
Determination of Se, Te, Au, and Ag in Cu electrolysis slimes, 25:28933
MAKHONINA, M. S., Organs and systems following radiotherapy of thyroid cancer, 25:29707
MAKSIMOVIC, M., Effect of ^{60}Co irradiation of male pupae of the gypsy moth, 25:29616
MAKSIMYCHEVA, Z. T., Fluorescence determination of copper, 25:28928
MALACZYNSKI, G., Electrogasdynamic flow in ducts, 25:30339
MALAMOS, B., Renal adenocarcinoma: scintigraphic study of primary and metastatic areas, 25:29590
MALDAGUE, P., Metabolism of different immunoglobulin classes in irradiated mice. V, 25:29473
MALEK, P., New possibilities in the topical diagnosis of cardiac infarcts, 25:29571 (LB/G-2836)
MALINOVSKAYA, S. A., Phoswich for neutron detection, 25:29339
MALKIN, I. A., Coherent states and Green function of charged particle in varying electric and magnetic fields, 25:30704
MALLIA, E. A., Identification of NiH in sunspot spectrum, 25:30173
MALLIARIS, A. C., Prog. rpt. on high-power quasi-steady MPD acceleration, final, 5/70, 25:30599 (N-71-10100)
MALLORY, M. L., Heavy-ion accelerator facility featuring a separated-sector isochronous cyclotron, 25:31084
MALONEY, M. David, Superconductive supercooling and superheating of small cadmium spheres: size effects, 25:30428
MALOV, L. A., Non-rotational states of odd-mass nuclei in the actinide region, 25:31306 (JINR-P4-5693)
MALYKH, N. I., Diffusion of a dense decaying plasma in a stellarator, 25:30472
Studies of diffusion of dense disintegrating plasma in a stellarator, 25:30462 (NP-18767)
MALYSHEV, V. V., Studies of VH and VVH nuclei in mineral meteorites, 25:30317
MALYSOWA, Elzbieta, Profile distribution of ^{90}Sr in soils of Lower Silesia, 25:29207
MALYUCHKOV, O. T., Investigation of the diffusion of hydrogen of hydrides of alloys, 25:29837
MALZ, W., Radiation effects in isolated DNA and their functional consequences. VI, 25:29467
MAMASAKHLISOV, V. I., Effective forces within nuclei, 25:31402
MANEGOLD, K., Influence of electron scattering caused by boundaries of inhomogenieties, 25:29523
MANFORD, C., Thermal diffusivity of uranium and uranium--plutonium monocarbides, 25:29957
MANGHNANI, M. H., Elastic moduli of hcp Ti and Zr, 25:29852
MANIAWSKI, F., Polarized-neutron study of the $Ni_{0.968}V_{0.032}$ alloy, 25:30680
MANINTVELD, P., FREMIX: a high-power 8-GHz plasma heating experiment, 25:30456 (EUR-4593, pp 551-6)
MAN'KO, V. I., Coherent states and Green function of charged particle in varying electric and magnetic fields, 25:30704
MANNE, Rolf, X-ray emission spectra of VC/sub x/, NbC/sub x/, TaC/sub x/, and ZrC, 25:30267
MANOJLOVIC, N., Elimination and metabolism of benzo(a)pyrene after intratracheal injection, 25:31715 (ORNL-tr-2469)
MANSON, R., Inelastic surface scattering of nonpenetrating

particles, 25:30659
MANUSHEV, D., Moessbauer spectrometer for express analysis, 25:29361
MARABINI, A., Angioscintiphotography, 25:29587
MARAL, Zh., Studies of the auroral x radiation at conjugate points Kerguelen--Archangel, 25:30395
MARAN, Stephen P., Automated and conventional photometry of the short-period variable star 14 Aurigae, 25:30086
Evidence for an optically thick component in the galactic radio source Sagittarius B_2, 25:30119
MARANGONI, M., Coupled-channel calculations of the giant dipole resonance in the one particle--one hole continuum approximation. II, 25:31286
MARANO, R. T., Differential thermal analysis of boric acid, boric oxide, and potassium fluoborate, 25:29186
MARCHENKO, E. N., Program for processing photographs in bubble chamber filled with heavy liquid. I, 25:29369 (ITEF-753)
MARCHENKO, N. V., Program for processing photographs in bubble chamber filled with heavy liquid. I, 25:29369 (ITEF-753)
MARCINKOWSKI, Andrzej, Transmission surface-barrier silicon detectors, 25:29331
MARCUS, R. A., Semiclassical transition probabilities for inelastic and reactive collisions, 25:30293
MARENKOV, O. S., Effect of multiply scattered γ-radiation in the x-ray radiometric method, 25:28939
MARES, F., Proton magnetic resonance shifts in bis(cyclooctatetraenyl) U(IV), 25:29085
MARES, J., Radial injection of a polarised beam into a cyclotron, 25:31153
MARGOSIS, Michel, Determination of zinc in pharmaceutical products by neutron activation analysis, 25:29029
MARGRAVE, J. L., Infrared spectra and geometries of $SrCl_2$, $BaCl_2$, $EuCl_2$, EuF_2, $PbCl_2$, and UCl_2, 25:29086
MARIKYAN, G. A., Measurement of the momentum of the accompanying particles at short distances from a high-energy nuclear-active particle, 25:29377
MARINARO, M., Self-consistent derivation of multiple mass values in renormalized field theories, 25:30986
MARINOV, M. S., Invariants of the rotation group, 25:31013 (ITEF-782)
MARK, J. L., Methods for predicting turbulent jet mixing, 25:31728 (SC-DR-70-838)
MARK, Lester C., Pharmacokinetics of halothane in man, 25:29416
MARKETOS, S., Renal adenocarcinoma: scintigraphic study of primary and metastatic areas, 25:29590
MARKLUND, I., Simultaneous LEED and RHEED studies of growth of Zr on W (100) surface, 25:29847
MARKOV, Yu. Ya., Scintillator for recording slow neutrons, 25:29336
MARKOVSKI, B. L., Determination of Breit--Wigner resonance widths using Fourier algorithm, 25:30849 (JINR-P2-5659)
MARKS, Dennis W., Behavior of the angular velocity near the surfaces of stars with radiative envelopes, 25:30088
MARKUS, G., Theoretical structure level and absolute transition probabilities in deformed nuclei of uneven mass numbers, 25:31308 (KFK-1248)
MARLOWE, M. O., Fission gas re-solution rates: limitations of fission gas bubble growth by the re-solution process, 25:30032 (GEAP-12148)
MARMOR, M., Recoil-distance lifetime measurements for states in ^{30}P, 25:31279
MAROLI, C., Multiple-times technique applied to the nearly linear propagation of a long-wave packet in a dispersive plasma, 25:30622
MARSH, P. A., Corrosion of Ti-6A-4V in HCl-methanol, 25:29773
MARSHAK, H., Right angle ^3He cryostat incorporating a high field superconducting solenoid, 25:30442 (NBS-TN-562)
MARSHAK, R. E., CP violation and strong self-interacting intermediate-vector-boson model, 25:30814
MARSHALKIN, V. E., Shell correction to liquid-drop energy, 25:31398
MARSHALL, Phillip M., Precision deep-sea time release, 25:31756 (UCSD-34-P-127-8)
MARSOL, Claire, Multipolar character of photons accompanying ^{125}Sb decay, 25:31340
MARSTOKK, K.-M., Microwave spectra of deuterated glycolaldehydes, 25:29044
MARTIN, A. D., Coupling (AKN) and extrapolation below the anti KN threshold, 25:30902
Models of $Y_0^*(1405)$ and low-energy anti KN interactions, 25:30876
MARTIN, B. R., Kaon--nucleon interactions below 1 GeV/c, 25:30882
Models of $Y_0^*(1405)$ and low-energy anti KN interactions, 25:30876
MARTIN, D. G., Calculation of differential neutron scattering cross sections of point defects in a relaxed lattice, 25:31163 (AERE-R-5682)
MARTIN, E., Design studies for an ultra-thin septum extraction channel for modified NEVIS synchrocyclotron, 25:31106
Nevis synchrocyclotron conversion project, 25:31155
MARTIN, J. A., Heavy-ion accelerator facility featuring a separated-sector isochronous cyclotron, 25:31064
MARTIN, J. R., Distribution, residence time, and inventory of tritium in Sedan crater ejecta, 25:29244 (UCRL-72572)
MARTIN, John A., Innovations in isochronous cyclotrons, 25:31080
MARTIN, Nicole, BD 61°2565: a star with particularly intense Sr, Eu, and Cr lines, 25:30063
MARTIN, W. C., Low-energy level structure of neutral Ce, 25:30262
MARTIN, W. R., Development of FBR neutron-absorber materials, 25:29978 (ORNL-4630, pp 163-76)
Development of fuel element fabrication, 25:29924 (ORNL-4630, pp 233-8)
Fabrication development of FBR cladding, 25:29784 (ORNL-4630, pp 96-110)
MARTINELLI, A. P., Low-field instabilities of high-field composite superconductors, 25:30410 (EUR-4593, pp 95-100)
Normal transitions of composite superconductors induced by magnetic disturbances, 25:30411 (EUR-4593, pp 101-6)
MARTIN H., History of the counter-flow gas centrifuge, 25:29271 (CONF-700557-1)
MARTINSON, I., Lifetimes of some doubly excited levels in neutral helium, 25:30265
MARTINSON, J., Simultaneous LEED and RHEED studies of growth of Zr on W (100) surface, 25:29847
MARTONE, M., Electron heating in large-amplitude oscillations in a theta-pinch, 25:30467
Measurements on heating in collisionless low-β transverse shock waves near critical Alfven--Mach number, 25:30468
MARTYNCHIK, Yu. F., Protective efficiency of radioprotectors, 25:29550
MARX, Dieter, Time bunching spectrometer using a bent rotating crystal, 25:29359
MARX, R., ESR spectrum of γ-irradiated adamantane, 25:29139
MASALOV, V. L., Shock waves propagating along a magnetic field in a collisionless plasma, 25:30620
MASEFIELD, John, Irradiated apparatus, 25:29260
MASH, Donald R., Fabricating the refractory metals. Part II. Metnods used to make parts, 25:29789
MASON, Benjamin J., Iodine-131 dairy cow uptake studies using a submicrometer synthetic dry aerosol (Project SIP), 25:29505 (SWRHL-39-r)
MASON, G. M., Cosmic-ray ^2H from satellite measurements, 1965 to 1969, 25:30330
MASON, M. G., Mid- and far-infrared spectra of HF and DF in rare-gas matrices, 25:29066
MASSEY, George Robert, Radioactive source capsule-handling system, 25:29319
MASSIMINO, Daniel, Separation and recovery of permanent gases by preparative chromatography, 25:29177 (CEA-R-4090)
MASTENBROEK, A., Voids in V, Nb, and Mo by fast neutron irradiation at high temperatures, 25:29914
MASTERSON, H. G., Techniques for the measurement of electrode processes at temperatures above 100°C, 25:29779
MASUI, Katsuhiro, Growth of Pt crystals on W surface, 25:29850
MATHE, G., Acute irradiation in man: treatment of hematologic disorders, 25:29699
MATHUR, P. K., Water chemistry studies: chemical analysis manual for moderator and coolant water systems, 25:28914 (BARC-515)
MATOLICH, J. Jr., Thermal diffusivity measurements of irradiated oxide fuels (LWBR Development Program), 25:29937 (BMI-X-10274)
MATSUBARA, Tadao, X-ray excited optical luminescence analysis of trace rare earths in high-purity yttrium and gadolinium oxides, 25:28961
MATSUI, Hiroshi, X-ray excited optical luminescence analysis of trace rare earths in high-purity yttrium and gadolinium oxides, 25:28961
MATSUMOTO, Akira, Extraction of Eu with di(2-ethylhexyl) phosphoric acid, 25:29185
MATSUMOTO, Hiroshi, Convective beam cyclotron instability and discrete vlf emissions in the magnetosphere, 25:30357
Note on a generation mechanism of background hiss of polar chorus, 25:30358
MATSUO, S., Contact transformation and space--time quantization, 25:30708
MATSUURA, Tatsuo, Hot-atom chemistry, 25:29168
MATTIOLI, M., Holographic interferometry of laser-produced plasmas using picosecond pulses, 25:30487
MATTSON, Philip T. Jr., Apparatus for blending particles, 25:29254
MATUSEVICH, E. S., Yield of neutrons from thick targets bombarded by 11.5- and 23.5-MeV protons, 25:31209
MATVEENKOV, F. I., Influence of starting parameters on ripple formation in explosive welding of metals, 25:31736 (SCL-T-71024C)
MATVEEVA, N. M., Phase equilibria and superconductivity in the V_3Al--V_3Sn system, 25:30416
MAUDERLY, J. L., Toxicity of inhaled ^{144}Ce fused clay in beagle dogs. III, 25:29436 (LF-43, pp 183-7)
Toxicity of inhaled ^{90}Sr fused clay in beagle dogs. I, 25:29437 (LF-43, pp 188-96)
Toxicity of inhaled ^{90}Y fused clay in beagle dogs. II, 25:29434 (LF-43, pp 146-62)
Toxicity of inhaled ^{91}Y fused clay in beagle dogs. I,

25:29435 (LF-43, pp 163-70)
MAUGER, J., Fractional parentage and the equations-of-motion method in pairing theory, 25:31453
MAUNY, P., New types of thermal-shielding concretes for nuclear reactors, 25:30031 (EUR-4531, pp 975-1018)
MAURER, G., Observation of d* effect in anti pd → p anti p π+ π−n reaction at 5.55 GeV/c, 25:30727 (NP-18796)
MAURITZSON, I., ANNLIS: computer program for automatic analysis of gamma-ray spectra, 25:29354 (LUNP-7101)
MAXFIELD, B. W., Interphase boundary waves in the intermediate state of lead, 25:30429
Study of the transverse magnetoresistance of polycrystalline potassium, 25:31767 (NYO-2150-68)
MAY, A. D., Experiment to compress polarized ^{3}He gas, 25:31077
Helium-4 discharge light source and system for optical pumping of 2^3S_1 ^{3}He, 25:31076
Nuclear relaxation of ^{3}He gas on various solid surfaces, 25:31072
MAY, R. M., Neutron tunnelling cross sections, 25:31419
MAYER, P., Spectral classification and photometry of stars in two H II regions, 25:30108
MAYER, Walter, Measurements on fuel elements for power reactors in a critical assembly, 25:31573
MAYER-BOERICKE, G., Emittance measurements at Juelich isochronous cyclotron, 25:31119
MAYNARD, C. Douglas, Clinical applications of serial brain scanning, 25:29582
MAYNE, P. J., Dewar tube sample cell assembly for low-temperature fluorimetry, 25:28925
MAZITOV, B. S., Lifetimes of 1080-keV level of ^{115}In and 1300-keV level of ^{111}Cd, 25:31327
MAZZINI, M., Activities of Scalbatraio center for research in nuclear safety, 25:31610
MCBRIDE, J. R., Normal run and the accident case for a nuclear rocket engine, 25:31642
MCCALLUM, G. J., Decay of 3.696 MeV level in ^{28}Al, 25:31266
MCCARTHY, I. E., Non-local potentials and the single-particle shell model, 25:31447
MCCARTNEY, E. R., Materials for high temperature applications, 25:29860
MCCLELLAN, R. O., Bilateral bronchopulmonary lavage with DTPA solution for removing inhaled ^{144}CeCl$_3$, 25:29544 (LF-43, pp 286-94)
Effect of the inhalation of ^{144}Ce in relatively insoluble forms on influenza virus infection in mice, 25:29724 (LF-43, pp 254-62)
Fission Product Inhalation Program. Annual report, October 1, 1969--September 30, 1970, 25:29419 (LF-43)
Production of chromosome aberrations by ^{241}Am in the Chinese hamster liver, 25:29482 (LF-43, pp 240-5)
Relative biological effectiveness of ^{241}Am, ^{144}Ce, and ^{60}Co on the production of metaphase chromosome aberrations in the Chinese hamster liver, 25:29483 (LF-43, pp 246-53)
Relative hazards for inhaled ^{95}Zr and ^{95}Nb particles formed under various thermal conditions, 25:29423 (LF-43, pp 59-65)
Removal of relatively soluble ^{144}Ce from the lungs of beagle dogs: intravenous administration of a DTPA solution, 25:29543 (LF-43, pp 280-5)
Retention and distribution of ^{137}Cs in the beagle dog following inhalation of ^{137}Cs in fused montmorillonite clay particles, 25:29426 (LF-43, pp 79-81)
Retention and distribution of ^{244}Cm following inhalation of ^{244}CmCl$_3$ and ^{244}CmO$_{1.7}$ by beagle dogs, 25:29429 (LF-43, pp 100-5)
Some observations on the toxicity of beta-emitting radionuclides inhaled in fused clay particles, 25:29438 (LF-43, pp 197-204)
Toxicity of inhaled ^{144}Ce fused clay in beagle dogs. III, 25:29436 (LF-43, pp 183-7)
Toxicity of inhaled ^{144}CeCl$_3$ in beagle dogs. IV, 25:29431 (LF-43, pp 128-36)
Toxicity of inhaled ^{90}Sr fused clay in beagle dogs. I, 25:29437 (LF-43, pp 188-96)
Toxicity of inhaled ^{90}SrCl$_2$ in beagle dogs. IV, 25:29430 (LF-43, pp 123-7)
Toxicity of inhaled ^{90}Y fused clay in beagle dogs. II, 25:29434 (LF-43, pp 146-62)
Toxicity of inhaled ^{91}Y fused clay in beagle dogs. I, 25:29435 (LF-43, pp 163-70)
Toxicity of inhaled ^{91}YCl$_3$ in beagle dogs. IV, 25:29432 (LF-43, pp 137-9)
Toxicity of injected ^{137}CsCl in the beagle dog. III, 25:29433 (LF-43, pp 140-5)
MCCLUNG, R. W., Nondestructive testing techniques for FBR, 25:29287 (ORNL-4630, pp 145-9)
Nondestructive testing, 25:29288 (ORNL-4630, pp 271-9)
MCCLURE, J. P., Thermospheric temperature variations inferred from incoherent scatter observations, 25:30378
MCCLURE, Robert D., Strong-cyanogen stars: photometry and kinematics, 25:30085
MCCLUSKEY, George E. Jr., Formation of a neutron star in a close binary system, 25:30099
MCCOY, H. E. Jr., Evaluation of the Molten-Salt Reactor Experiment Hastelloy N surveillance specimens: fourth group, 25:29906 (ORNL-TM-3063)
Mechanical properties of alloys in reactor environments and development of FBR cladding and structural alloys, 25:29904 (ORNL-4630, pp 73-95)
MCCRACKEN, G. M., Desorption by keV protons of hydrogen condensed on liquid-helium-cooled surfaces, 25:30257 (EUR-4593, pp 181-6)
MCCURRIE, R. A., Magnetic and mechanical hardness of SmCo$_5$ and LaCo$_5$, 25:29845
MCDANIEL, F. E., Magnetically self-shaping septum for beam deflection, 25:31101
MCDONALD, A., Reaction ^{22}Ne(p,t)^{20}Ne at 26.9, 35.1, and 42.4 MeV, 25:31296
MCDONALD, J. M., Experimental study of electromagnetic matrix elements in ^{92}Mo, 25:31372
MCDONALD, P. T., Chromosomal translocations and genetic control of Aedes aegypti, 25:29753
MCFADDEN, J. H., Distribution of solid fission products in UO_2, 25:31589 (CONF-710302-5)
MCFEE, A. F., Chromosome aberrations in swine leukocytes after in vivo or in vitro exposure to 14 MeV neutrons, 25:29497
MCGOWAN, F. K., E2/M1 admixture of the 2' → 2 transition in ^{108}Pd, 25:31374
MCGUIRE, Eugene J., L-shell Auger and Coster--Kronig electron spectra, 25:30261
MCILROY, R. W., Fifth international cyclotron conference, Oxford, 9/69, 25:31079
MCKAY, L. R., Production of chromosome aberrations by ^{241}Am in the Chinese hamster liver, 25:29482 (LF-43, pp 240-5)
Relative biological effectiveness of ^{241}Am, ^{144}Ce, and ^{60}Co on the production of metaphase chromosome aberrations in the Chinese hamster liver, 25:29483 (LF-43, pp 246-53)
MCKELLAR, B. H. J., Reactions (d,p) to the ground states of ^{41}Ca and ^{49}Ca, 25:31264
MCKENZIE, J. F., Hydromagnetic Kelvin--Helmholtz problem in Hall plasma, 25:30392
Hydromagnetic wave coupling between the solar wind and the plasma sheet, 25:30366
MCKILLEN, R. R., Deflection measurement techniques, 25:29301
Elastic and ultimate pressure tests on one tenth scale model of Dungeness B concrete pressure vessel, 25:29311
MCLEAN, W. L., Interphase boundary waves in the intermediate state of lead, 25:30429
MCMAHON, Robert E., Ion specific detection of internal standards labelled with stable isotopes, 25:28967
MCMILLAN, W. L., Superconductivity of Re--Os, Re--Ru, Ru--Os, and Re--W hcp alloy systems and slightly doped Re, 25:30433
MCMURRY, H. L., Molecular potential function in terms of group valence force symmetry coordinates, 25:31696 (IN-1421)
MCNEARNEY, S., Effects of reactor radiation on concrete, 25:30022 (EUR-4531, pp 237-65)
MCNEILLY, C. E., Thermal analysis of promethium oxalate, 25:29172
MCNEILLY, Gregory Scott, Reaction ^{24}Mg(α,α'γ)^{24}Mg, 25:31273
MCPHERRON, R. L., Satellite observations of band-limited micropulsations during a magnetospheric substorm, 25:30369
MCVOY, K. W., K/sub L/ and K/sub S/ as shell-model eigenstates. II, 25:30861
MEADOWS, J., Holmium-165 fast neutron cross sections, 25:31350
MECCA, J. E., Prog. rpt. on noble gas confinement study, final, FY-1970, 25:29074 (DUN-7221(Vol.1))
Prog. rpt. on noble gas confinement study, final, FY-1970, 25:29075 (DUN-7221(Vol.2))
MEDURI, M., Indium-113m DTPA brain scanning in diagnosis of expansive processes, 25:29583
MEDVED, S. V., Apparatus for the automatic accumulation (storage) and analysis of information in experiments with the synchrocyclotron, 25:31070
MEEKINS, John F., Line emission in the x-ray background, 25:30140
MEIJER, R. J., Radioactively-heated thermodynamic engines, 25:29279
MEISELS, G. G., Precise measurements of W, the mean energy required for ion-pair formation in gases. I. Alkanes, 25:30636
MEISSNER, Hans, Stability of supercurrents in flat films of tin, 25:30437
MEKLER, K. I., Shock waves propagating along a magnetic field in a collisionless plasma, 25:30620
MELANDRI, C., Sampling methods for aerosol particles, 25:29263
MELIKYOM, L. A., F-center destruction mechanism in proton tracks in alkali halide crystals, 25:30655
MELLADO, L., Sterile-male technique in the control of the Mediterranean fruit fly, 25:29739
MELNIKOVA, N. N., Application of phenomenological quasi-two-body model to π−p-interactions with strange particle production at p = 4 GeV/c, 25:30869 (JINR-P1-5706)
MELROSE, D. B., Classical derivation of inverse Compton radiation, 25:30502
Electrostatic bremsstrahlung, 25:30501
Formation of energy spectra in synchrotron sources, 25:30144

MENDIRATTA, Madan G., Correlation of strength properties to microstructures in precipitation-hardened Ti--Nb alloys, 25:29872
MENEGHETTI, D., Effects of resonance scattering upon multigroup cross section averaging, 25:31183
MENON, S., Swedish development on prestressed concrete pressure vessels for water reactors, 25:31562 (IAEA-126, pp 213-41)
MENON, S. K., Scandinavian prestressed concrete pressure vessel model project, 25:29314
MENON, Sh., Scandinavian model project. I, 25:31548 (EUR-4531, pp 507-16)
MENOTTI, P., Commutators near light cone, Bjorken limits, and D_4 expansion, 25:31020
MENTKOVSKII, Yu. L., Modified WKB method. II, 25:30699 (ITF-70-84-P)
MENZEL, M. T., Bethe--Salpeter solution for nucleon--nucleon scattering with pion exchange, 25:30909
MERCEA, Judith, Interferometric determination of small quantities of D_2O and H_2O, 25:28929
MEREDITH, Gerald L., Decays of ^{56}Co and ^{66}Ga, 25:31287
MEREZHKIN, V. G., Studies of diffusion of dense disintegrating plasma in a stellarator, 25:30462 (NP-18767)
MERKEL, B., High resolution beam hodoscope using multiwire proportional chambers, 25:29370 (LAL-1246)
MERKLE, Emery J., Comparison of modified Kjeldahl and vacuum fusion technique for determination of N in Ta alloys, 25:28937
MERLINI, Margaret, Uptake and excretion of radiocobalt by a freshwater mollusc, 25:29441
MEROT, J. P., BWR prestressed concrete pressure vessels, 25:31551 (EUR-4531, pp 615-45)
MERZ, J. L., Photoluminescence of ion-implanted oxygen in ZnTe, 25:30657
MESZAROS, Iren, Lipid fraction alterations in serum and liver of rats exposed to 2000 r local hepatic irradiation, 25:29685
MEWHERTER, J. L., Epithermal measurements of capture and fission resonance integrals in ^{235}U, ^{233}U, ^{239}Pu, and ^{241}Pu, 25:31353
MEYER, H., Semisterility for insect control, 25:29752
MEYER, H.-J., Ultrasonic in-service inspection of reactor pressure vessels, 25:29290
MEYER, J., Description of static quadrupole moments of 2_1^+ states by HF equations, 25:31424
MEYER, R. A., Levels of ^{246}Cm from the β--decay sequence ^{246}Pu(11 days) /sup 246m/Am(25 min)^{246}Cm, 25:31378
MEYERHOFF, R. W., Superconducting power transmission, 25:30445
MEYNADIER, C., Reaction ^{22}Ne(p,p), ^{22}Ne(p,p'), and excited states of ^{23}Na, 25:31281
MIAH, A. J., Evolution of new varieties of rice with respect to increased yield per acre, resistance to diseases and better quality through use of induced mutations, 25:29481 (IAEA-R-290-F)
MIAH, M. A. W., Coulomb couplings and Born-term analysis for γN → π⁺Δ reactions, 25:30785
MICHA, D. A., Semi-empirical model for Penning and associative ionization, 25:30298
MICHAEL, C., A_2 production, 25:30877
Regge residues, 25:30883
MICHALIK, J., Radionuclides for the investigation of concentrate circulation in crude zinc and lead oxide production, 25:29283
MICHALON, A., Observation of d* effect in anti pd → p anti p π⁺ π⁻n reaction at 5.55 GeV/c, 25:30727 (NP-18796)
MICHEAU, P., Heat exchange by natural convection in porous media, 25:29264 (EUR-4531, pp 821-39)
MICHEJDA, L., Comment on question whether GGLP effect is due to B--E symmetrization or not, 25:30763
MIELNIK, B., Solution of the equation of evolution with time-depending Hamiltonian, 25:30960
MIGUSHINA, V. L., Effects of ionizing radiation on lactate dehydrogenase in rats, 25:29670
MIHAILOVIC, Z., Measuring thermal conductivity of refractory materials, 25:29958
MIHALCZO, J. T., Static and dynamic experiments with a repetitively pulsed booster, 25:31635 (Y-DR-44)
MIHALOV, J. D., Magnetic observations of the lunar cavity, 25:30388
MIHASHI, Yasuo, Sintering process of Ni--P alloy coated W, 25:29793
MIKHAILOVA, M. A., Decay of ^{225}Ac, 25:31325
MIKHAILOVICH, S. M., Effects of oxathiole on condition of liver and kidneys during ^{210}Po-induced chronic radiation sickness, 25:29563
MIKHAILOVSKII, A. B., Instability of a finite and high-pressure plasma with finite electron thermal conductivity, 25:30546
MIKHALEVSKY, V. I., Method and technique of surveying during photographing and visual observation in a field of high frequency currents, 25:31733 (SC-T-713025)
MIKHEEV, V. S., Influence of beta-stabilizers on the strength and plasticity of titanium at low temperatures, 25:29844
MIKHUL, A., Application of phenomenological quasi-two-body model to π⁻p-interactions with strange particle production at p = 4 GeV/c, 25:30869 (JINR-P1-5706)
MIKUMO, Eiko, Observation of primary electrons with emulsion chamber, 25:30328
MILANI, R., Genetics of factors affecting fertility and of sex-ratio distortions in the house fly, 25:29751
MILES, J. L., Solid-state anodization of Al, Be, and Zr, 25:29803
MILIVOJEVIC, S., Analysis of thermal reliability of RA reactor core, 25:31638
MILLER, A. Jerry, Intensity estimation for a neutron beam for biological and medical applications, 25:31174 (UCRL-19715)
MILLER, Esther S., Studies on the possibility of improving the selective localization of radiophosphorus in different tissues, 25:29453
MILLER, J. M., Angular distribution of fission fragments from the ^{170}Yb compound nucleus excited to 107 MeV, 25:31371
MILLER, Joseph S., Photoelectric measurements of high-n Balmer lines in NGC 7027 and NGC 7662, 25:30078
MILLWARD, P., Main and helical field windings on a toroidal stellarator: PROTO--CLEO, 25:30554 (EUR-4593, pp 13-18)
MILNE, Thomas A., Molecular beams in high temperature chemistry, 25:30258
MILNER, W. T., E2/M1 admixture of the 2' → 2 transition in ^{108}Pd, 25:31374
MIN, T. C., Bilateral approach to the analysis of turbulent flow in an annulus, 25:29268
MINAEV, L. F., Effects of histones on energy processes in liver mitochondria of irradiated animals, 25:29638
MINAEV, S. M., F-center destruction mechanism in proton tracks in alkali halide crystals, 25:30655
MINGALEV, B. S., Effects of synchrotron radiation on the slow ejection of electrons from synchrotron, 25:31044 (NP-18780)
MINYAEV, O. A., Production of monochromatic beams using cyclotron acceleration, 25:31121
MIRNOV, S. V., Effect of shape and magnitude of discharge current pulse on plasma confinement and heating in Tokamak-3, 25:30461 (MATT-Trans-79)
MIROCHNIK, E. A., Accelerating structures with ring coupling resonators, 25:31078
MISAWA, Shunji, Determination of the compositions of thin film compounds by using the electron-probe x-ray microanalyzer. I, 25:28966
MISHIMA, Yoshitsugu, Reversion of metastable phases in Cu--Be alloys, 25:29891
MISIUK, A., Magnetic properties of uranium silicides, 25:30679
MISKIEWICZ, Wieslawa, Studies on radioactivity of Polish honeys. I, 25:29509
MITCHELL, A. W., Crystal structures of several intermetallic phases of Np and Pu alloys with Sb, Se, and Te, 25:30002
MITCHELL, J. A., Measurements and calculations of neutron migration and its anisotropy in lattices of fuel rods and liquid coolant, 25:31660
MITIN, A. A., Low noise preamplifier employing field effect transistors, 25:29340
MITO, Iwao, Observation of primary electrons with emulsion chamber, 25:30328
MITOV, V. N., Effect of multiply scattered γ-radiation in the x-ray radiometric method, 25:28939
X-ray radiometric determination of Pb in samples with a ^{75}Se source, 25:28940
MITROPOL'SKII, A. N., System for the automatic indication of impurities in sodium coolants, 25:29261
MITROV, G. G., Nephrography with aid of ^{51}Cr-EDTA and ^{58}Co-DTPA, 25:29577
MITROVIC, S., Analysis of thermal reliability of RA reactor core, 25:31638
MITSKEVICH, N. V., Transformation of general covariant observable values, 25:30970
MITTA, A. E. A., Determination of free /sup 99m/Tc in labeled compounds by means of thin layer chromatography, 25:28991
MITTLEMAN, Marvin H., Annihilation of positrons during scattering, 25:30289
MIURA, K., Nontadpole contribution to mass splitting (m/sub K/--m/sub π/), 25:30791
MIYAKE, S., Propagation of electrostatic ion waves near ion cyclotron harmonics, 25:30612
MIYAKE, Yoshizo, Activation analysis of oxygen in phosphorus with fast neutron, 25:29024
MIYAMOTO, Kenro, Experiments of plasma confinement in JIPP stellarator. I, 25:30457 (IPPJ-102)
MIYATAKE, Sadao, Convective beam cyclotron instability and discrete vlf emissions in the magnetosphere, 25:30357
MIYAZAWA, Y., Heavy ion acceleration in IPCR 160 cm cyclotron, 25:31135
MO, Tse Chin, Electromagnetic field and wave propagation in gravitation, 25:31011
MOBLEY, T. S., Lethality in sheep following exposure to ^{60}Co, 25:29656
MODALI, Sarma B., Evidence for an optically thick component in the galactic radio source Sagittarius B_2, 25:30119
MODESITT, G., High energy astrophysics, 25:30220 (P-4494(RAND))
MODINOS, A., Effect of atomic cores on electron tunnelling through dielectric layers, 25:30678
MOELLENDAL, Harald, Microwave spectra of deuterated glycolaldehydes, 25:29044
MOENCH, Helga, Function and morphology of hypertrophic rabbit kidneys following telecobalt irradiation with

1000 to 4000 rad, 25:29684
MOFFAT, J. W., Mechanism for splitting the A_2-meson, 25:30859
MOHRI, Akihiro, Experiments of plasma confinement in JIPP stellarator. I, 25:30457 (IPPJ-102)
MOIR, R. W., Diffusion resulting from nonadiabatic scattering on a helically perturbed field in a torus, 25:30466
MOISEEVA, V. V., Apparatus for the automatic accumulation (storage) and analysis of information in experiments with the synchrocyclotron, 25:31070
MOLDAUER, P. A., Comment on resonance averaging, 25:31450
MOLDOFSKY, Philip J., Prog. rpt. on Avalanche type semiconductor radiation detectors, semiannual, 7--12/70, 25:29327 (NYO-3246-TA-8)
MOLINE, R. A., Charge exchange cross sections for electron loss from B^+, P^+, and N^+ on N_2, 25:30300
MONACI, P., High sensitivity beryllometer, 25:29390 (RT/EL-(70)4)
MONGAN, T. R., Nonrelativistic separable-potential quark model of the hadrons, 25:30846
MONTIEL, Milka M., Multiple basal cell carcinomas arising in radiated burn scars, 25:29701
MOONEY, L. G., Calculations of weapon radiation doses in single-compartment aboveground concrete structures, 25:30633
Differential measurements of fast-neutron air-ground interface effects, 25:30635
MOORE, C. F., Reaction $^{208}Pb(p,\alpha)^{205}Tl$ at 16.475 MeV, 25:31383
MOORE, Fletcher L., New method for separation of americium from curium and associated elements in the zirconium phosphate--nitric acid system, 25:28989
MOORE, K. V., Effects of state properties on high pressure compressible hydrodynamics, 25:31590 (CONF-710302-6)
MOORE, Thomas M., Radiation survey of television repair shops in Baltimore area, 25:29512 (BRH/DEP-71-4)
MOOS, H. W., Lyman-alpha emission from Arcturus, 25:30070
MORDUKHOVICH, V. V., Minimum dose of 5-methoxytryptamine influencing the accumulation of cystamine in tissues and its excretion with urine, 25:29554
MOREAU, Ph., Prestressed concrete pressure vessel of the Vandellos nuclear power plant, 25:31454 (EUR-4531, pp 81-94)
MOREWITZ, H. A., LMFBR aerosol research at Atomics International, 25:31616
MORGAN, D., Low energy pion--pion scattering, 25:30867
MORGAN, G. L., Neutron polarization from $^7Li(p,n)^7Be$ reaction for 3 to 4 MeV protons, 25:31235
MORGAN, Vernon, Nuclear reactors, 25:31565
MORGANSTERN, Kennard H., Electron beam radiation applications for the plastics industry, 25:29127
MORGEN, P., Inelastic scattering of deuterons and α-particles on ^{191}Ir and ^{193}Ir, 25:31342
MORGENSTERN, Leon, Survival in lethally irradiated dogs, 25:29651
MORGUNOV, V. N., Formation of gold nuclei on ionic crystals, 25:29910
MORGUNOVA, N. N., Influence of carbon on Mo ductility, 25:29863
Temperature dependence of mechanical properties of certain Mo and W alloys, 25:29864
MORI, Koichi, Electron spin resonance studies on radiation-induced solid state polymerization of methyl methacrylate, 25:29117
Electron spin resonance studies on radiation-induced solid state polymerization of acrylonitrile, 25:29118
MORIMOTO, Takeshi, Isotope effect of electromigration in some solid alkali halides, 25:29041
MORIOKA, Akira, Study of origin of geomagnetic pulsations in equatorial, low, and middle latitudes, 25:30356
MORISHIMA, Hiroshige, Radioactivities in sea near the Goto Islands, 25:29241
MORITO, Sadaaki, Extraction of Eu with di(2-ethylhexyl) phosphoric acid, 25:29185
MORIZOT, Pierre, Determination of equations of state for gaseous hexafluorides of uranium, molybdenum, and tungsten, 25:29073 (CEA-N-1414)
MORK, H. M., Improved feedback control for Null-point compensating system, 25:31741 (UCLA-12-813)
MORKELYUNAS, L. Yu., Excited core model for ^{63}Cu and ^{65}Cu, 25:31246
MOROZOV, B. V., Methods for monitoring proton incidence on the internal targets of high-energy accelerators, 25:31043 (NP-18776)
Methods of monitoring proton discharge onto the internal target of a high-energy accelerator, 25:31064
MOROZOV, Yu. N., Magnetization of EuO and $Eu_{0.97}Gd_{0.03}O$ single crystals, 25:30670
MORRISON, D. D., Quantitative control of surface pinning in a low-kappa Type II alloy, 25:30415
MORRISON, D. R. O., Compilation of cross sections. VI, 25:30735 (CERN-HERA-70-7)
MORROW, R. J., Levels of ^{246}Cm from the β^--decay sequence ^{246}Pu(11 days) /sup 246m/Am(25 min)^{246}Cm, 25:31378
MORSE, R. I., Collisions of an atom and a harmonic oscillator, 25:30290
MOSIDZE, L. N., Photometry of RW-Auriga-type stars, 25:30058
MOSIER, Stephen R., Color spectrograms of very-low-frequency Poynting flux data, 25:30370
MOSIN, A. F., Modification of survival of irradiated yeast by ethanol treatment. I, 25:29722
MOSKALEV, V. I., Heat exchange and temperature control system for the 2-meter liquid hydrogen bubble chamber, 25:29376
MOSKO, S. W., Heavy-ion accelerator facility featuring a separated-sector isochronous cyclotron, 25:31084
Rf system for a proposed heavy ion cyclotron, 25:31095
MOSKVIN, L. N., Decay of ^{75}Br, 25:31257
MOSS, G. A., Elastic scattering of protons from ^{40}Ca at 21.0, 23.5, 26.3, and 48.0 MeV, 25:31295
MOSS, William, Radiation therapy in the treatment of carcinoma of the prostate, 25:29597
MOSSEL, D. A. A., Scaling-up of salmonella radicidation of frozen boneless meats, 25:29729 (IAEA-R-491-F)
MOSSON, G. A. G., Ionization and acceleration of hydrogen clusters, 25:30253 (EUR-4593, pp 51-8)
MOST, Harry, Immunity produced by the injection of x-irradiated sporozoites of Plasmodium berghei. II, 25:29727
MOSTOFI, F. K., Kidney, 25:29698
MOSZYNSKI, Marek, Adaptation of a long-lens beta-ray spectrometer for the measurement of short nuclear lifetimes, 25:29358
MOTIZUKI, Tamizo, Characteristics of personal monitoring dosimeter, 25:29383 (JAERI-Memo-4292)
MOTTERSHEAD, D., Effects of reactor radiation on concrete, 25:30022 (EUR-4531, pp 237-65)
MOTTOLA, H. A., Separation and determination of ^{137}Cs in urine, 25:28983
MOUSSA, Andre, Excited metastable states of ^{93}Y, 25:31338
MOZSA, Szabolcs, Hematologic examinations in assessment of chronic radiation loads of radiologists. III, 25:29595
MUCKERMAN, J. T., Investigation of backscattering in D^+--H_2 reaction system, 25:30291
MUEHE, L., Individual tension components for vertical prestress with breaking loads above 1500 Mp, 25:31663 (EUR-4531, pp 489-505)
Polygonally directed, wound ring stress reinforcements with several intermediate fastners for all stress wire rings (PRISMA system), 25:29939 (EUR-4531, pp 433-44)
MUELLENSIEFEN, A., Compilation of coupling constants and low-energy parameters, 25:30841
MUELLENSIEFEN, Alfred, Nucleus--nucleus scattering at high energies, 25:31234
MUELLER, G., High-power spark gap for high repetition rates, 25:30568 (EUR-4593, pp 273-80)
MUELLER, R. W., Acceleration of very heavy ions by means of a two-cyclotron facility, 25:31130
MUELLER, W., Structural integration of a prestressed concrete pressure vessel in a nuclear power plant and comparison with a steel vessel installation, 25:31552 (EUR-4531, pp 647-89)
MUENZEL, H., Production of neutrons through irradiation of thick beryllium targets with deuterons in energy range from 15 to 55 MeV, 25:31202 (KFK-1288)
MUGGENBURG, B. A., Bilateral bronchopulmonary lavage with DTPA solution for removing inhaled $^{144}CeCl_3$, 25:29544 (LF-43, pp 286-94)
Removal of relatively soluble ^{144}Ce from the lungs of beagle dogs: intravenous administration of a DTPA solution, 25:29543 (LF-43, pp 280-5)
MUKAIBO, T., High temperature reaction between uranium monosulfide and zirconium, 25:29965
MUKHIN, A. I., Charged particles produced in capture of negative muons by ^{28}Si, ^{32}S, ^{40}Ca, and ^{64}Cu nuclei, 25:31267
MUKSINOVA, K. N., Erythropoietic activity of the blood in fractional irradiation, 25:29655
MULCAHEY, T. P., Instrumentation systems to protect LMFBR core integrity, 25:31574 (ANL-7795)
MULLER, J., Prestressed concrete pressure vessel of the Vandellos nuclear power plant, 25:31454 (EUR-4531, pp 81-94)
MULLIGAN, T. J., Reactions (h,p) on Cr. I, 25:31298
MULTHAUF, L. G., Levels of ^{246}Cm from the β^--decay sequence ^{246}Pu(11 days) /sup 246m/Am(25 min)^{246}Cm, 25:31378
MUNARI, Stelio, Gamma radiolysis of branched chain hydrocarbons: 2,2-dimethylbutane, 25:29142
MUNCHOW, L., Projection description of rotational and quasirotational bands in even--even nuclei, 25:31438
MURASKIN, M., Particle-like objects in a nonlinear field theory, 25:30964
MURATA, Hiromu, Structure of trans ethyl methyl ether and the W form of diethyl ether, 25:29072
MURATA, T., Studies for safety analysis of loss-of-coolant accidents, 25:31605
MURPHY, R. V. W., Structure of hydromagnetic shock waves, 25:30528
MURRAY, Caroline, Contrasting effects of cyclophosphamide and radiation on the immune responses of the mouse, 25:29475
MUSAELYAN, R. M., Inelastic neutron scattering by even-N Ge isotopes, 25:31244
MUSAKHANOV, M. M., Nucleon Compton-effect and sum rules for dipole nucleon momentum, 25:30776 (JINR-P2-5679)
MUSCHLITZ, E. E. Jr., Semi-empirical model for Penning and associative ionization, 25:30298
MUSHMOV, D. D., Nephrography with aid of ^{51}Cr-EDTA and ^{58}Co-DTPA, 25:29577
MUSSO, Simone, Uptake and excretion of radiocobalt by a

XUM

freshwater mollusc, 25:29441
MUSTAFIN, I. S., Organic re gents in analytical chemistry of Zr and Hf. VI, 25:28932
MUTH, H., Radiation dose distribution in lungs of Thorotrast patients, 25:29521
MUTHUKRISHNAN, R., Negative-parity states in ^{139}Pr, 25:31366
MUTO, Yuhei, Recent improvements in fluoro-glass dosimeter, 25:29387
MUZIOL, G., Levels in ^{142}Nd, 25:31337
MYERS, L. S. Jr., Trapped species produced in the gamma radiolysis of aqueous sugar ices, 25:29153
MYNATT, F. R., Design of asymmetric 4 π shields for space reactors, 25:31640 (ORNL-TM-3368)
Low-energy electron transport with the method of discrete ordinates, 25:30630 (ORNL-TM-3318)
MYNCHEV, N. V., Bioelectric activity of nerve and muscle tissue in first hours after x irradiation, 25:29609
MYSHKIS, D. A., Experimental investigation of destruction of metastable helium atoms in a plasma at low temperatures, 25:30512

N

NADAREISHVILI, K. Sh., Effects of x rays on metabolism of calcium ions in muscle cells, 25:29674
NADOLINSKAYA, I. N., Removal parameters of radon and thoron decay products from air, 25:29217
NADZHM, A., Properties of rare-earth metals (Sc, Nd), their hydrides, carbides, and oxides, 25:29859
NAGARAJAN, T., Beta decay of ^{111}Ag, 25:31365
NAGASAKI, R., Behaviour of boron in stainless steel detected by fission track etching method and effect of radiation on tensile properties, 25:29913
NAGATA, Takesi, Constitution of magnetospheric storms, 25:30400
Rocket observations of electron density of daytime ionosphere, 25:30360
NAGAYAMA, Tsutomu, Aseismatic design of equipments for nuclear power station, 25:31601
NAGLIK, M., New compact capacitive energy storage unit for voltages above 100 kV, 25:30571 (EUR-4593, pp 293-9)
NAGORCKA, B. N., Extrapolation of ^{12}C + ^{12}C and ^{12}C + ^{16}O reaction cross sections to astrophysical energies, 25:31200 (ANU-P-515)
NAGY, A. F., Stable mid-latitude red arcs: observations and theory, 25:30398
NAKAHARA, Yasuaki, Thermal neutron scattering from simple liquid metals, 25:31176
NAKAI, K., Lifetimes of ground-band states in ^{148} ^{150} ^{152}Sm, 25:31364
NAKAMURA, Yoshio, Cellulose graft copolymers. III, 25:29108
NAKANE, Masanori, Activation analysis of oxygen in phosphorus with fast neutron, 25:29024
NAKAYAMA, Tadayuki, Structure of corrosion-resisting films formed on tantalum and niobium in high-temperature dilute acid aqueous solutions, 25:29991
NALLEY, S. J., Collisional ionization between cesium and selected molecules, 25:30276 (ORNL-TM-2620)
NAPOLITANO, E., Amplitude for N nonspurious excited particles in dual resonance models, 25:30830
NARANAN, S., Nucleon--antinucleon production in high-energy (> 10^{12} eV) hadron collisions, 25:30728
NARASIMHA MURTHY, S., Stability of an accelerated plasma shell in the presence of magnetic field, 25:30547
NARAYANA, C. L., Magnetofluiddynamic heat transfer, 25:30341 (NAL-TN-6)
NARAYANAN, G. Hari, Reply to transition morphology during hcp precipitation from beta-isomorphous alloys, 25:29887
NASS, Gerald I., Radiation-curable compositions, 25:29114
NASS, H. W., Possible problem in determining oxygen in silicon by fast neutron activation analysis, 25:29021
NASSIFF, S. J., Excitation functions for the nuclear reactions ^{159}Tb(d,p)^{160}Tb and ^{159}Tb(d,4n)^{157}Dy, 25:31301 (CNEA-283)
NAUDET, G., Measuring thermal conductivity of refractory materials, 25:29958
NAUDIN, P., Methods of testing HTR thermal shielding, 25:31575 (EUR-4531, pp 953-64)
NAVELET, H., Exchange degeneracy and absorption: πN, KN, and NN reactions, 25:30874
NAYMARK, Sherman, Quality assurance: a realistic appraisal, 25:31528
NAZAROVA, T. N., Meteoric material in vicinity of Earth, 25:30361
NEDYALKOVA, N., Direct spectral determination of rhenium in molybdenum and copper concentrates, 25:28965
NEGRI, Giulio, Mixed oxides of Tb--Ce, Tb--Th, and Tb--Gd, 25:30007
NEIRINCKX, R. D., Extraction separation of carrier-free Bi from Pb and Zn, 25:29164
NEKHENDZI, Yu. A., Properties of cast nickel--chromium alloys alloyed with niobium and molybdenum, 25:29839
NELIPOVICH, P. A., Modification of radiation damage to structure of DNA from embryos of seeds with homologous DNA, 25:29716
NELLEN, Bernd, Angular correlations in reaction p anti p $\rightarrow$ $3\pi^+$ $3\pi^-$ (π^0) at 3.6 GeV/c, 25:30733
NELSON, Gary O., Engineering tests of Halon 1301 fire extinguishing systems for field assembly buildings, 25:31748 (UCRL-51021)
NELSON, P. F., Effects of high energy radiation on pulping of Eucalypts, 25:29735
NEMASHKALO, B. A., Gamma rays from ^{64} ^{66} ^{68}Zn(p,γ)^{65} ^{67} ^{69}Ga, 25:31249
NEMASHKALO, V. A., Inelastic scattering of protons by ^{50}Cr, ^{52}Cr, ^{54}Cr, and ^{64}Zn, 25:31253
NESHPOR, V. S., Electronic properties of nonstoichiometric vanadium monocarbides, 25:30667
Electrophysical properties and nature of the chemical bond in compounds of beryllium with boron and carbon, 25:29943 (LA-tr-71-30)
NESS, Norman F., Magnetic-field geometry of Jupiter, 25:30251
Solar wind interaction with Mercury, 25:30389
NESTEROV, G. T., Behavior of cosmic layers in lower ionosphere during Forbush decreases, 25:30311
NEUSCHEL, Sherman K., Correlation of uranium, thorium, and potassium with aeroradioactivity in the Berea area, Virginia, 25:29235
NEVZGODINA, L. V., Cytogenetic effect in irradiation of lettuce, 25:29491
NEWING, R. A., New interpretation of Vaidya radiation, 25:30778
NEWKIRK, H. W., Optical nonlinear susceptibilities of beryllium oxide, 25:30666
NEWMAN, C. E., Formation of energy spectra in synchrotron sources, 25:30146
Particle flux associated with stochastic processes, 25:30518 (N-71-11853)
NEWMAN, Darrell F., Improved method for calculating foil perturbation effects, 25:31659
NEWSOM, G. H., Inner-shell absorption in the spectra of the alkaline earths. I, 25:30174
NEWSON, H. W., Cyclo--Graaff: concept and practice, 25:31081
NEWTON, G. J., Development of techniques for generating monodisperse aerosols with the Fulwyler Droplet Generator, 25:29076 (LF-43, pp 13-17)
Physical and chemical characteristics of aerosols produced from solutions of polyvalent metallic nuclides, 25:29079 (LF-43, pp 31-9)
Some characteristics of ruthenium aerosols generated from Ru-organic complexes and subjected to thermal degradation, 25:29077 (LF-43, pp 18-24)
NEZLIN, M. V., Drift-beam instability and ion sound in an inhomogeneous plasma, 25:30506 (MATT-Trans-84)
Electron-ion beam instability, 25:30505 (MATT-Trans-83)
NGO KUANG ZUI, Spectrum of fast deuterons emitted in 670-MeV proton interaction with carbon nuclei, 25:31225
NICHOLLS, I. R., Neutron tunnelling cross sections, 25:31419
NIEHAUS, A., Angular distributions of Penning electrons, 25:30294
NIERLICH, Jean, Nucleation and crystal growth of secondary zirconia during reaction of Zr with air at low pressure and at 810°C, 25:29997
NIKANOROV, V. I., Relativistic rotation of a S = $^1/_2$ spin in collisions of particles moving arbitrarily with respect to the observer, 25:30760
NIKIFOROV, N. A., Methods for monitoring proton incidence on the internal targets of high-energy accelerators, 25:31043 (NP-18776)
Methods of monitoring proton discharge onto the internal target of a high-energy accelerator, 25:31064
NIKISHANOVA, T. I., Sensitivity of sweet potatoes to ionizing radiation, 25:29721
NIKITIN, A. V., Cross sections of inelastic channels of reactions in np-interactions at the neutron momentum from 2 to 10 GeV/c, 25:30726 (JINR-P1-5665)
NIKITIN, P. N., Influence of beta-stabilizers on the strength and plasticity of titanium at low temperatures, 25:29844
NIKITIN, V. P., Electronic properties of nonstoichiometric vanadium monocarbides, 25:30667
NIKOLAEV, B. I., Mass-diffusion mercury columns for isotope separation, 25:29277
NIKOL'SKII, I. F., Effect of boron on certain physical characteristics of synthetic graphites, 25:29946 (SC-T-713023)
Effect of boron on some physical characteristics of artificial graphites, 25:29953
NISBET, John S., Tables from Penn State Mark 1 ionospheric model, 25:30351 (N-70-40978)
NISHI, Tatsuo, Characteristics of personal monitoring dosimeter, 25:29383 (JAERI-Memo-4292)
NISHIHARA, Hiroshi, Measurement and the calculation of neutron spectra in iron assemblies, 25:31658
NISHIKAWA, T., Design of high-gradient accelerating column, 25:31048 (SJC-A-71-2)
NISHIMURA, Hiromichi, Gamma-initiated solid state polymerization of tetrafluoroethylene, 25:29112
NISHIMURA, Jun, Observation of primary electrons with emulsion chamber, 25:30328
NITZE, H. R., Radiotherapy of synchronized skin tumors in mice, 25:29605
NIU, Kiyoshi, Observation of primary electrons with emulsion chamber, 25:30326
NOBLE, C., Mathematical techniques for vibration analysis of reactor systems, 25:31591 (CONF-710302-7)

NOBUKI, Minoru, Influence of high hydrostatic pressure on the flow stress of pure iron and molybdenum polycrystals, 25:29833
NODA, Masato, Electronic spectra of trapped electrons in organic glasses at 4°K, 25:29156
NODA, Shoji, Radicals produced in γ-irradiated allyl alcohol glass, 25:29162
NOEL, Henri, Mixed uranium and transition element sulfides, 25:29996
NOERDLINGER, Peter D., Coherent emission from expanding supernova shells, 25:30068
NOERGAARD, P., Inelastic scattering of deuterons and α-particles on ^{191}Ir and ^{193}Ir, 25:31342
NOGUCHI, Takuya, Development of a heavy-current switching gap triggered with laser, 25:30575 (EUR-4593, pp 339-45)
NOGUCHI, Tetsuo, High temperature phase studies with a solar furnace, 25:29987
NOORDINK, J. Ph. W., Irradiation, competitiveness, and the use of radioisotopes in sterile-male studies with the onion fly, 25:29748
NORDHAGEN, R., Lifetimes of ground-band states in ^{148} ^{150} ^{152}Sm, 25:31364
NORDMANN, Bernard J. Jr., Illiac III computer system manual, 25:31694 (COO-2118-1)
NORDTVEDT, Kenneth, Equivalence principle for massive bodies. IV, 25:31009
NORELAND, Erik, X-ray emission spectra of VC/sub x/, NbC/sub x/, TaC/sub x/, and ZrC, 25:30267
NORRIS, D. I. R., Dose dependence of swelling in electron irradiated nickel, 25:30652
NORRIS, John, Rotational velocities of G and K giants in Hyades moving group, 25:30046
NORWITZ, George, Infrared determination of barium, strontium, and calcium carbonates, singly and together, by the pellet technique, 25:28972
NOVAK, D. L., Slip systems in VC--TiC alloys, 25:29999
NOVARO, O. A., Nonadditivity of intermolecular forces in He_3 within SCF LCAO MO approximation, 25:30270
NOVIKOV, A. I., Evidence of disappearance of inelastic channel of nuclear reaction in nuclear resonant scattering of γ-rays in perfect crystal, 25:30687 (IAE-1966)
NOVIKOV, A. S., Program for processing photographs in bubble chamber filled with heavy liquid. I, 25:29369 (ITEF-753)
NOVIKOV, D. L., Coherent frequencies of transverse oscillations in the electron model of a ring cyclotron, 25:31038 (JINR-P9-5677)
Rf system of the monoenergetic cyclotron, 25:31128
NOVIKOV, I. D., Perturbations in an anisotropic homogeneous universe, 25:30223
NUETZEL, G., Status report on Garching Tokamak experiment Pulsator, 25:30584 (EUR-4593, pp 411-17)
System planning for a prototype fusion reactor, 25:30593 (EUR-4593, pp 533-8)
NUNN, D., Nonlinear wave particle processes in an electrostatic wave packet, 25:30613
NUNOGAKI, M., Ion source using a beam--plasma interaction, 25:30255 (EUR-4593, pp 67-74)
NUNWARZ, Christine, Method of thermal neutron waves for determination of diffusion parameters in heavy materials, 25:31177
NUSSENZWEIG, Ruth S., Immunity produced by the injection of x-irradiated sporozoites of Plasmodium berghei. II, 25:29727
NUSSINOV, S., Calculations of $K^+ - K^0$ mass difference, 25:30800
NUTBROWN, D. A., Unitarity corrections to hard-meson analysis of K/sub l3/ decay, 25:30813
NYANISHKENE, V. M. B., Penetration of ^{90}Sr into bodies of gastropod mollusks, 25:29440
NYBAKKEN, T. W., Environmental air quality support study, 25:31695 (EGG-1183-2242)
NYCE, A. C., Use of porosimetry in the measurement of pore size distribution in porous materials, 25:29828

O

OADES, G. C., Coulomb corrections in the analysis of πN experimental scattering data, 25:30721
OBEROI, R. S., Algebraic close-coupling calculation of the scattering of electrons and positrons by hydrogen, 25:30286
OCHIAI, Kanehiro, Aseismatic design of equipments for nuclear power station, 25:31601
OCHKUR, A. P., Effect of multiply scattered γ-radiation in the x-ray radiometric method, 25:28939
OCHS, W., Can quantum-states be considered as ensembles of dispersion-free states. I, 25:30701
ODA, M., X-ray pulsations from Cygnus X-1 observed from Uhuru, 25:30139
ODAR, S., Polymeric chromium(III) complexes resulting from neutron irradiation of crystalline K chromate. II, 25:29171
ODIAN, George, Monomer reactivity ratios in graft copolymerization, 25:29106
ODRU, R., Opto-electronic link for transmitting temporal information, 25:29392 (CEA-N-1431)
OEHME, H., 300 MW thorium high-temperature power plant (THTR), 25:31539
OEHME, Reinhard, Beta decay of hyperons, 25:30815
Complex negative signature trajectories and Pomeranchuk theorem, 25:31012 (COO-264-571)
OEIEN, A., Comparative study on Al determination in ammonium acetate soil extracts by spectrophotometry, activation analysis, and atomic absorption, 25:29020
OGASAWARA, H., Studies for safety analysis of loss-of-coolant accidents, 25:31605
OGAWA, Kiyoshi, Transformer coupled fast theta-pinch device with variable rise time, 25:30577 (EUR-4593, pp 355-63)
OGDEN, Eugene C., Experimental data on dispersion and deposition of timothy and corn pollen from known sources, 25:31684 (BNL-50266)
OGIEVETSKII, V. I., Algebraic realization of chiral symmetry for meson systems and theory of Yang--Mills type, 25:30850 (JINR-P2-5759)
X^0(960)-meson -2- or 0-, 25:30833
OGNEV, A. A., Vertical motion of particles in cyclotron, 25:31063
OGORODNIKOVA, A. A., Phase diagrams of systems of Sm, Gd, and Dy oxides with Mg oxide, 25:29985
OGUCHI, Atsushi, Influence of high hydrostatic pressure on the flow stress of pure iron and molybdenum polycrystals, 25:29833
OGURI, Takeo, Calorimetric studies on chemisorption of nitrogen on tantalum, 25:29843
OH, In ki., Reaction (^{3}He,^{6}Li) on light nuclei, 25:31214
OH, S. W., Magnetic regenerator, 25:31104
OHBA, Yukio, Rolling workability of pure W single crystals, 25:29877
OHI, M., Design and construction of PIACE, 25:30587 (EUR-4593, pp 431-41)
OHMURA, Takashi, Study of deuteron stripping reaction by coupled channel theory. III, 25:31210
OHNISHI, Haruyuki, Axial behavior and confinement of plasma in the mirror-field theta pinch, 25:30464
OHNO, Keiichi, Structure of trans ethyl methyl ether and the W form of diethyl ether, 25:29072
OHNUMA, T., Propagation of electrostatic ion waves near ion cyclotron harmonics, 25:30612
OHTA, Itaru, Observation of primary electrons with emulsion chamber, 25:30328
OHTSUBO, Hisao, Low-energy theorems for nuclear weak and electromagnetic currents, 25:30807
OISHI, Kimiya, Fissionability of heavy nuclei, 25:31417
OISTACH, I. D., Separation of boron isotopes. II, 25:29196
OJALA, Antti, Results of cobalt therapy in inoperable carcinoma of the lung, 25:29600
OKADA, Isao, Isotope effect of electromigration in some solid alkali halides, 25:29041
OKANO, K., Gamma transition studies of ^{125}Sb, 25:31388
OKE, J. B., Effective temperatures of B- and A-type stars, 25:30094
OKINAKA, H., Phase equilibria and thermodynamic properties in V/sub n/O/sub 2n-1/ system, 25:29952
OKRENT, D., Instrumentation systems to protect LMFBR core integrity, 25:31574 (ANL-7793)
OLES, A., Tables of magnetic structures determined by neutron diffraction. II, 25:30664 (NP-18783)
OLIVERI, Elio, Squaring criteria for diffusion cascade in isotopic enrichment of U, 25:29281
OL'KHOVSKII, V. S., Calculating (n,2n) reaction amplitude on heavy nuclei. II, 25:31394 (ITF-70-95-E)
Three-body problem in quantum mechanics. I, 25:30709
OLMR, J., Observations of chromospheric flares at Ondrejov, 25:30189
OLSMATS, M., Hyperfine structure investigations of ^{51}Mn and /sup 52m/Mn, 25:31294
OMBRELLARO, P. A., Synthesis of fast reactor space-energy neutron fluxes, 25:31656
OMEL'CHENKO, A. Ya., Nonlinear theory of reflection of electromagnetic waves from plasma, 25:30626
OMNES, R., Matter--antimatter hydrodynamics, 25:30204
OMOJOLA, A. F., Binding energy of the alpha particle, 25:31192
OMORI, Takashi, Chemical effects associated with (γ,n) reaction in potassium chromate, 25:29166
OMURA, Masayuki, Diagnostics of a supersonic plasma stream using an immersed microwave probe, 25:30476 (N-71-10964)
ONDOH, Tadanori, Electron density profiles for quiet and disturbed topside ionosphere at high latitudes, 25:30359
ONDRACEK, G., Powder metallurgical production of UO_2--PuO_2 steel pellets, 25:29931
O'NEILL, J. B., Magnetic and mechanical hardness of $SmCo_5$ and $LaCo_5$, 25:29845
ONISCHENKO, L. M., Rf system of the monoenergetic cyclotron, 25:31128
ONISHCHENKO, L. M., Coherent frequencies of transverse oscillations in the electron model of a ring cyclotron, 25:31038 (JINR-P9-5677)
OPLE, F. S. Jr., Comparison of experimental results with response analysis for a model of a pressure vessel, 25:29313
ORAAS, S., Design of 4000 ton magnet for TRIUMF cyclotron, 25:31092
Techniques applied to design of TRIUMF magnet poles, 25:31049 (TRI-70-4)

XUM

ORDAN'YAN, S. S., Electronic properties of nonstoichiometric vanadium monocarbides, 25:30667
ORGEL, G. S., Sensitivity of codling moths to x and gamma radiation, 25:29612
ORNSTEIN, L. Th. M., FREMIX: a high-power 8-GHz plasma heating experiment, 25:30456 (EUR-4593, pp 551-6)
ORPHANIDIS, P. S., Possibilities of integrated control of Dacus oleae, 25:29740
ORTON, Colin G., Immunity produced by the injection of x-irradiated sporozoites of Plasmodium berghei. II, 25:29727
ORYU, Shinsho, Analysis of D(p,n)2p reaction at 45.5 MeV, 25:31188
OSAKA, Toshiaki, Structure of corrosion-resisting films formed on tantalum and niobium in high-temperature dilute acid aqueous solutions, 25:29991
OSBORN, C. L., Convertible polymers for radiation processing, 25:29124
OSBORN, L. A., Dose distribution in the beagle dog from radiographic exposure, 25:29514 (LF-43, pp 116-22)
OSHIMA, Keiichi, Electron spin resonance studies on radiation-induced solid state polymerization of methyl methacryiate, 25:29117
Electron spin resonance studies on radiation-induced solid state polymerization of acrylonitrile, 25:29118
Gamma-initiated solid state polymerization of tetrafluoroethylene, 25:29112
OSHIYAMA, Hiroshi, Equilibrium and stability of plasma in Heliotron magnetic field, 25:30549
OSIPOV, N. K., Ion formation function during reaction of protons with atmosphere, 25:30397
OSKERKO, A. A., Use of gamma spectrometer to control activity of heat-transfer medium in reactors, 25:31680
OSTER, Ludwig, Stimulated Compton effect in very compact radio sources, 25:30145
OSTRIKER, Jeremiah P., Motion and radiation of charged particles in strong electromagnetic waves. I, 25:30116
OSTROUMOVA, L. M., Reaction of pituitary-adrenal system of dogs to irradiation, 25:29642
OTOMO, Makoto, Spectrophotometric determination of U(VI), 25:28934
OTTER, A. J., Design of 4000 ton magnet for TRIUMF cyclotron, 25:31092
Extraction of multiple beams of various energies from TRIUMF negative ion isochronous cyclotron, 25:31109
OTTERSEN, U., Unintentional fission product releases during normal and high power load conditions in a boiling heavy water test reactor, 25:31609
OTTO, K., Studies of surface reactions of NO by isotope labeling. II. Deuterium kinetic isotope effect in the ammonia--nitric oxide reaction on a supported platinum catalyst, 25:29063
OURISSON, Guy, Transannular hydride shifts. Mechanistic study in the longifolene series, 25:29050
OVDIENKO, N. I., Effects of oxathiole on condition of liver and kidneys during ^{210}Po-induced chronic radiation sickness, 25:29563
OVERCASH, D. R., Fermi-surface topology changes in In alloys deduced from the behavior of T/sub c/ under strain, 25:30435
OWEN, D. R. J., Nonlinear analysis of pressure vessels behavior including cracking, 25:31664 (EUR-4531, pp 697-734)
OWEN, G. M., Medical radioisotope scanning, 25:29349
OWEN, Larry Wayne, Realistic interactions and exchange effects in microscopic descriptions of elastic and inelastic nucleon scattering, 25:31432
OZER, Odelli, Analysis of exponential experiments with lattices of plutonium in heavy water, 25:31661

P

PAAR, V., HRPA contributions to phonon--phonon interaction in the adiabatic limit, 25:31446
PACCANONI, F., Multicluster model for very-high-energy collisions, 25:30755
PACK, R. T., Rotational excitation in molecular collisions, 25:30296
PACKER, Louis L., Method for measuring wall thickness of articles using gaseous radioactive material, 25:29278
PADIOU, Jean, Mixed uranium and transition element sulfides, 25:29996
PADOVANI, F., Effect of gamma irradiation of immature sugarcane borers, 25:29755
PAGE, David S., L-amino acid oxidase. II, 25:29060
PAGNAMENTA, A., Omega-meson in rho--w system, 25:30858
PAIDASSI, Jean, Nitridation of Zr at high temperatures, 25:29870
Nucleation and crystal growth of secondary zirconia during reaction of Zr with air at low pressure and at 810°C, 25:29997
PAJDUSAKOVA, L., Decrease of the area of individual large sunspots near the central meridian, 25:30184
PAKALNS, P., Spectrophotometric determination of Si by a standard addition procedure, 25:28924
PAKHOMOV, L. P., Absorption of shf waves by plasma at upper hybrid frequencies, 25:30606 (NP-16807)
PAKKANEN, A., Decay of ^{200}Tl, 25:31387
PAKSY, L., Use of the medium method of two standards taken from uniformly normalized calibration curves in spectrometric steel analysis. I, 25:28950
PALECEK, L., Radiation induced bone sarcoma, 25:29702
PALEEV, I. I., Principles of thermoelectric and magnetohydrodynamic conversion of energy, 25:30340
PALIGE, J., Radionuclides for the investigation of concentrate circulation in crude zinc and lead oxide production, 25:29283
PALMEDO, Philip F., Measurement of delayed-neutron fractions for thermal fission of ^{235}U, ^{239}Pu, and ^{233}U, 25:31334
PALMER, J. F., Power-reactor siting in various countries, 25:31482 (AECL-3740)
PALMER, J. P., Coupling coefficients for the indirect nuclear dipole interaction in indium by nuclear quadrupole resonance, 25:30695
PALMIERI, P., Wave functions for He by rotational projection, 25:30269
PALOP, M. Perello, Nuclear charge and start-up of French Reactor SL-1, 25:31480
PALYGA, G. F., Influence of x irradiation on chromosome aberrations in pea seedlings, 25:29489
PANADZHYAN, V. G., Estimation of angular dimensions of scintillating radio sources, 25:30126
PANAGIA, N., Spectrum of a gaseous nebula of pure H. III, 25:30101
PANATTONI, C., Infrared studies on coordination influence of UO_2^{2+} group on P--O bond of triphenyl phosphine oxide, 25:29088
PANDHARIPANDE, V. R., Nuclear variational calculations with improved mixed-density approximation, 25:31285
PANKRATOV, A. K., Diurnal variation of cosmic rays and the inhomogeneity of interplanetary media, 25:30321
PANONTIN, John A., Mass yield and charge distribution in 450 MeV proton fission of ^{238}U, 25:31302 (COO-1167-10)
PANSCH, James L., Dental caries from radiation therapy, 25:29712
PANT, D. D., Decay times, intensities, and their temperature variation of luminescence of aqueous and deuterated solutions of Eu ion, 25:29053
PAPA, Marcella, Mixed oxides of Tb--Ce, Tb--Th, and Tb--Gd, 25:30007
PAPARGYROPOULOS, P. H., Analyticity constraints and residue functions of E_2 pole exchange, 25:31027
Elastic scattering of a spin zero and a spin 1/2 particle at u = 0, 25:30892
PAPAS, C. H., Electromagnetic field and wave propagation in gravitation, 25:31011
PAPASTAMATIOU, N., Nature of intrinsic breakdown of chiral symmetry in terms of physical fields, 25:30929
PAPATHANASSOPOULOS, Konstantinos, Influence of neutron irradiation at 4°K on shear modulus of Cu, Al, and Pt, 25:29912
PAPAYOANOU, A., Time-dependent electron density in Xe pinched plasma laser, 25:30484
PAPP, L., Development of drilled electrodes of synthetic materials and their use for determination of rare earth oxide traces in rare earths, 25:28948
PAP'YAN, N. M., Cytogenetic effect in irradiation of lettuce, 25:29491
PARAJNAKOVA, V., Observations of chromospheric flares at Hurbanovo, 25:30175
PARAMEI, V. T., Effect of surgical treatment on healing of cornea in radiation sickness, 25:29649
PARASOCHKO, L. A., Protective influence of adrenalin and acetylcholine in radiation sickness of mice, 25:29548
PARD, A. G., Proton irradiation effects in type 321 stainless steel, 25:29915
PARDEE, W. J., Quantum electrodynamics multiperipheral model at infinite momentum, 25:30974
PARFENENKOV, V. N., Solid solutions in the system hafnium dioxide--silica, 25:30006
PARFENOV, Yu. D., Effects of oxathiole on condition of liver and kidneys during ^{210}Po-induced chronic radiation sickness, 25:29563
PARGAMANIK, L. E., Gravitational field effect on emission of relativistic charges, 25:31008
PARIKH, J. C., One-particle-hole and projected Hartree--Fock approximations in ^{12}C and ^{16}O, 25:31226
PARISI, G., Broken scale invariance, U_3 x U_3 breaking and hadron Lagrangian structure, 25:30927
PARISI, J., Photon--photon collisions, new area of experimental investigation in high-energy physics, 25:30798
PARKS, J. E., Vacuum-ultraviolet emission from proton-excited helium gas, 25:30284
PARSONS, N. H., Production of bulk quantities of ultrapure erbium, 25:29181 (GEPP-85)
PARTAIN, W. L., Thermal radiation absorption by particle-seeded gases, 25:29270
PARTRIDGE, R. B., Isotropy of the microwave background at 8-millimeter wavelength, 25:30228
PASCHENKO, M., OH emission from infrared objects at 1612 MHz, 25:30047
PASHOS, Thomas, Quality assurance: a realistic appraisal, 25:31528
PASKEVICH, I. F., Biosynthesis of liver and spleen histones of irradiated animals, 25:29662
PASKEVICH, L. V., Biosynthesis of liver and spleen histones of irradiated animals, 25:29662
PASSOW, C. H., Measurement of heat transport by conductivity of superfluid helium in pipes, 25:30406

PASTEELS, Paul, Geochronologic data obtained by the U--Pb method on some sphenes of igneous and metamorphic rocks of the Soer-Rondane Mountains, Antartica, 25:29208
PASTUR, L. A., Schroedinger equation with random potential, 25:30710
PATEL, B. M., Chem.cal separation and spectrographic determination of trace amounts of rare earth elements in uranium, 25:28915 (BARC-517)
PATERNO, G., Experimental test of microscopic theory of a current-carrying superconductor, 25:30432
PATIN, C. Snyder, Survival in lethally irradiated dogs, 25:29651
PATRIARCA, P., Advanced materials for steam generators, 25:29763 (ORNL-4630, pp 280-7)
Cladding materials for space isotopic heat sources, 25:29823 (ORNL-4630, pp 186-90)
Development of advanced FBR fuels, 25:29923 (ORNL-4630, pp 59-72)
Development of FBR oxide fuels, 25:29922 (ORNL-4630, pp 3-58)
Development of uranium mononitride fuels, 25:30010 (ORNL-4630, pp 179-85)
Physical and mechanical metallurgy of refractory alloys, 25:29824 (ORNL-4630, pp 191-206)
Prog. rpt. on fuels and materials development, 9/30/70, 25:29757 (ORNL-4630)
Tungsten metallurgy, 25:29786 (ORNL-4630, pp 207-25)
PATTERSON, J. R., Extrapolation of $^{12}C + ^{12}C$ and $^{12}C + ^{16}O$ reaction cross sections to astrophysical energies, 25:31200 (ANU-P-515)
PAUL, Ram Chand, Complexes of uranium(V) chloride with N donor ligands, 25:29092
PAULINY-TOTH, I. I. K., Radio observations of the infrared object IRC 10216, 25:30090
PAUS, Povel N., Liquid scintillation counting of RNA: a simple procedure for extraction from sucrose gradients, 25:28984
PAVLOV, B. D., Investigation of kidneys with aid of ^{51}Cr-EDTA, 25:29578
PAVLOVSKII, E. S., Time-of-flight measurements of the electrical length of coaxial delay cables, 25:29401
PAVONI, P., Pinhole scintillation camera and /sup 99m/Tc-pertechnetate in normal thyroid scanning, 25:29586
PAZHIN, Yu. F., Evidence of disappearance of inelastic channel of nuclear reaction in nuclear resonant scattering of γ-rays in perfect crystal, 25:30687 (IAE-1966)
PEACOCK, N. J., Sources of highly-stripped ions for ion accelerators, 25:31137
PEARCY, William G., Sound scattering layers off the Oregon coast, 25:31723 (RLO-1750-62)
PEARSON, D. B., Wave and scattering operators for single-channel systems, 25:31019
PEASE, R. S., Sources of highly-stripped ions for ion accelerators, 25:31137
PECCEI, R. D., Strict conformal symmetry, 25:30984
PECKER, Jean-Claude, Physical processes concerning the grains of dust surrounding stars: charge and photoelectric effect, 25:30192
PECORARO, George Anthony, Corrosion of tungsten in boric oxide and sodium borate melts, 25:29774
PEEBLES, F. N., Bilateral approach to the analysis of turbulent flow in an annulus, 25:29268
PEEBLES, P. J. E., Nonthermal primeval fireball, 25:30231
Rotation of galaxies and the gravitational instability picture, 25:30202
PEELLE, R. W., Experimental nuclear cross sections for spacecraft shield analysis, 25:30631 (ORNL-TM-3376)
PEET, F. G., Gupta's quantization of weak gravitational field, 25:31001
PEIER, D., Application of inductive energy storage systems for production of intense magnetic fields, 25:30561 (EUR-4593, pp 197-203)
PEIERLS, R. F., General expression for the density effect for the ionization loss of charged particles, 25:30643
PEIRONET, P., UCL isochronous cyclotron conceptual design and status report, 25:31094
PEKER, L. K., Four-particle levels in ^{90}Zr and ^{90}Nb, 25:31322
Interpretation of anomalous I/sup π/ = 7/2$^+$ levels in nuclei with Z = 43, 45, 47, 25:31323
Isomeric states in ^{88}Zr, ^{88}Zr, and similar nuclei, 25:31399
Levels in ^{142}Nd, 25:31337
PELLAT, R., Bounce effects in the negative mass instability, 25:30551
PELLEGRINI, Benjamin John, Statistical model analysis of the $^{75}As(p,n)^{75}Se$ reaction, 25:31263
PENIONZHKEVICH, Yu. E., Decay of ^{75}Br, 25:31257
PENTSAK, G. M., Scintillation spectrometry of soft x-ray radiation, 25:29350
PERDREAUVILLE, Farrell J., Analysis of the lateral motion of a projectile in the gun tube, 25:31731 (SC-RR-710071)
PERELOMOV, A. M., Algebraical approach to solution of one-dimensional model of N-interacting particles, 25:30759
PERELYGIN, V. P., Effect of chemical factors on the sensitivity of polymeric detectors, 25:29335
PERICIC, D., Radioprotective activity of some sulphur analogues of tryptophol and 5-hydroxytryptamine, 25:29567
PERKINS, R., Levitation melting of uranium mono-carbide, 25:29934
PERLMAN, H. S., New pictures in quantum mechanics, 25:30990
PERRIN, J. S., Irradiation-induced creep of uranium dioxide, 25:30018
PERRIN, James S., Effect of irradiation on the creep of uranium dioxide, 25:30009 (BMI-1899)
PERRIN, Martine, Supermultiplet scheme for light nuclei, 25:31203 (LYCEN-7088)
PERRIN, Robert, Multiple pion production, 25:30887
PERSING, R. L., Lethality in sheep following exposure to ^{60}Co, 25:29656
PERSSON, Bertil R., Strontium-90 in Northern Sweden, 25:29480
PESHKIN, M., Repulsion of slow neutrons by attractive potentials, 25:31415
PETER, L., Spectral analytical determination of tellurium traces in cast iron, 25:28943
PETERKOFSKY, Beverly, Use of a mixture of proteinase-free collagenases for the specific assay of radioactive collagen in the presence of other proteins, 25:28997
PETERSON, D. M., Effective temperatures of B- and A-type stars, 25:30094
PETERSON, J. M., Shaking of particle beams to remove neutralizing ions, 25:31050 (UCRL-20156)
PETERSON, L. E., Observations of unresolved galactic x-ray sources, 25:30134
PETERSSON, Bengt, Multiperipheralism, 25:30765
PETRENKO, A. A., System for the automatic indication of impurities in sodium coolants, 25:29261
PETROFF, P., Direct observation of long range migration of self-interstitial atoms in Stage I of irradiated platinum, 25:30649 (NYO-3504-57)
PETROV, B. N., Orbital stations and study of the Earth from space, 25:30363
PETROV, E. G., Light absorption by the pair of triplet excitons, 25:31698 (ITF-70-74)
PETROV, G. A., Angular anisotropy of γ radiation emitted after ^{235}U fission by slow neutrons, 25:31369
PETROV, M. M., X-ray spectrometer with cooled Si(Li)-detector, 25:29325 (JINR-P13-5707)
PETROV, R. V., Increased protective property of spleen cells from preirradiated donors measured by transplantation into lethally irradiated recipients, 25:29564
PETROV, V. A., Formation energy and concentration of vacancies in Mo, 25:29858
PETROVIC, B., Work on reactor vessels of prestressed concrete in Yugoslavia, 25:31556 (IAEA-126, pp 61-8)
PETROVICH, Fred L., Use of realistic forces in microscopic description of inelastic scattering of nucleons from nuclei at medium energies, 25:31393 (COO-1051-34)
PETRUKHIN, V. I., Spectrum of fast deuterons emitted in 670-MeV proton interaction with carbon nuclei, 25:31225
PETTERSSON, B. G., Conversion electron particle parameters of E2 transitions in ^{152}Sm and ^{154}Gd, 25:31380
PEUCHMAUR, A., Pressure vessels for water and gas reactors, 25:31550 (EUR-4531, pp 601-13)
PFEIL, W., Coupling parameters of pseudoscalar meson photoproduction on nucleons, 25:30797
PFIRSCH, D., Nonresonant diffusion of particles in stochastic fields, 25:30520
PFLEGER, R. C., Bilateral bronchopulmonary lavage with DTPA solution for removing inhaled $^{144}CeCl_3$, 25:29544 (LF-43, pp 286-94)
Removal of relatively soluble ^{144}Ce from the lungs of beagle dogs: intravenous administration of a DTPA solution, 25:29543 (LF-43, pp 280-5)
PHILIPP, G., Direct and compound processes to the reaction $^{40}Ca(d,\alpha)^{38}K$ at E/sub d/ = 5 to 10 MeV, 25:31275
PHILLIPS, D. V., Nonlinear analysis of pressure vessels behavior including cracking, 25:31664 (EUR-4531, pp 697-734)
PHILLIPS, K. E., Effects of resonance scattering upon multigroup cross section averaging, 25:31183
PHIPPS, Alan M., Separation of perrhenate, molybdate, and selenite ions on silica gel, 25:28953
PICAUT, J., Test of ring of prestressed concrete in high-resistance sheet-metal steel, 25:30028 (EUR-4531, pp 445-76)
PICKRELL, J. A., Connective tissue constituents measured on dogs exposed to ^{144}Ce fused montmorillonite clay particles, 25:29622 (LF-43, pp 218-23)
Toxicity of inhaled ^{144}Ce fused clay in beagle dogs. III, 25:29436 (LF-43, pp 183-7)
Toxicity of inhaled $^{144}CeCl_3$ in beagle dogs. IV, 25:29431 (LF-43, pp 128-36)
Toxicity of inhaled ^{90}Sr fused clay in beagle dogs. I, 25:29437 (LF-43, pp 188-96)
Toxicity of inhaled $^{90}SrCl_2$ in beagle dogs. IV, 25:29430 (LF-43, pp 123-7)
Toxicity of inhaled ^{90}Y fused clay in beagle dogs. II, 25:29434 (LF-43, pp 146-62)
Toxicity of inhaled ^{91}Y fused clay in beagle dogs. I, 25:29435 (LF-43, pp 163-70)
Toxicity of inhaled $^{91}YCl_3$ in beagle dogs. IV, 25:29432 (LF-43, pp 137-9)
Toxicity of injected $^{137}CsCl$ in the beagle dog. III, 25:29433 (LF-43, pp 140-5)
PIEKAAR, H. W., Experimental investigation of a wall jet in

XUM

a torus, 25:30602
PIEKARSKA, J., Effect of dose rate on the radiation yields of radicals in frozen organic media, 25:29160
PIERCE, R. Dean, Dissolution of stainless steel clad nuclear fuel elements, 25:29199
PIERMATTEI, S. Ricci, Analysis of methods for interpreting bremsstrahlung spectra, 25:30632 (RT/FI-(70)36)
PIERROT, Roland, Roubaultite $Cu_2(UO_2)_3(OH)_{10}\cdot 5H_2O$, a new mineral species, 25:29238
PIERSON, Edward S., Comparison of some excitation schemes for a jet MHD induction generator, 25:30335
PIERSON, J. D., Magnetospheric substorm of August 25--26, 1967, 25:30368
PIETSCHMANN, Herbert, Weak interactions, 25:30808
PIGEON, J., Description of elastic-scattered processes with the use of non-local separable potentials, 25:31186 (LYCEN-7089)
PILIYA, A. D., Field of an electromagnetic wave in a cold anisotropic plasma, 25:30533
PILKUHN, H., Coupling constants from PCAC, 25:30904
PILLSTICKER, M., Recent results with laser-triggered spark gaps, 25:30566 (EUR-4593, pp 259-64)
PILUSO, C. J., Energy levels of ^{27}Si, 25:31252
PIMENOV, I. A., Heliolatitudinal index (HL) of solar activity and 11-year variations of cosmic rays, 25:30165
HL index of solar activity and yearly variations of cosmic rays, 25:30308
PINAJIAN, J. J., Graphs for analysis of (1-3) gamma--gamma directional correlations, 25:31312 (ORNL-4619)
PINGEL, Vernon J., Heat treatment of 2-81 molybdenum permalloy powder cores, 25:30672
PINKAU, K., Measurements of the distribution in energy and angle of high-energy neutrons in the lower atmosphere, 25:30374
PINKHASIK, M. S., System for the automatic indication of impurities in sodium coolants, 25:29261
PINTER, S., Limb flares associated with solar soft x-ray bursts, 25:30187
PIONTKOVSKII, I. A., Electroretinogram in dogs irradiated during embryogenesis, 25:29667
PIOTROWSKI, Antoni, Adaptation of a long-lens beta-ray spectrometer for the measurement of short nuclear lifetimes, 25:29358
PIPKIN, F. M., Quantum electrodynamics at small distances, 25:30978
PIRINGER, O., Kinetics of $^{15}N/^{14}N$ isotopic exchange between nitric oxide and nitric acid, 25:29087
PIROVANO, A., Heat exchange by natural convection in porous media, 25:29264 (EUR-4531, pp 821-39)
PIROZHENKO, V. M., Accelerating structures with ring coupling resonators, 25:31078
PISARENKO, N. F., Observation of radiation belts and ionosphere by Interkosmos-3 satellite, 25:30364
PISAREV, V. E., Separation of boron isotopes. II, 25:29196
PISKAREV, I. M., (γ,n) cross sections of Al and P, 25:31242
PISKUNOV, L. I., Discrimination of ^{90}Sr with respect to Ca in freshwater plants, 25:29452
PISUT, J., Low energy pion--pion scattering, 25:30867
PISUT, Jan, Analytic extrapolations and the determination of pion--pion phase shifts, 25:30868
PITCHFORD, B. E., Performance of thermal insulation immersed in helium, 25:30030 (EUR-4531, pp 931-52)
PITIMADA, D., Experimental vibration characteristics of a B.W.R. fuel assembly, 25:31570 (RT/ING-(70)24)
PITRA, Ch., Radiation effects in isolated DNA and their functional consequences. VI, 25:29467
PITTEL, S., Mechanism for extending the ^{20}Ne rotational band, 25:31255
PITZER, R. M., Second-order perturbation theory with the contact interaction, 25:30271
PIVOVAR, L. I., Shortened charge-exchange gas target, 25:31065
PIVOVAROV, V. G., Ion formation function during reaction of protons with atmosphere, 25:30397
PIVOVAROVA, N. B., Ion formation function during reaction of protons with atmosphere, 25:30397
PLAKHOV, A. G., Slowing down of an intense electron beam in a dense plasma, 25:30504
PLATE, Erich J., Aerodynamic characteristics of atmospheric boundary layers, 25:31737 (TID-25465)
PLETNEV, V. P., Effect of radiation on oxygen electrode performance, 25:29098
PLETNIKOV, A. A., Heat exchange and temperature control system for the 2-meter liquid hydrogen bubble chamber, 25:29376
PLEVA, Yu. S., Angular anisotropy of γ radiation emitted after ^{235}U fission by slow neutrons, 25:31369
PLUHAR, Z., Group-theoretical operator analysis in the ds shell, 25:31452
PODGORETSKII, M. I., Identity of elementary particles, 25:30761
Interference phenomena in the system of two resonances, 25:30848 (JINR-P1-5668)
Particle interference in the processes involving excited nuclei, 25:31395 (JINR-P1-5648)
PODLUBNYI, L. I., Resonant inelastic effects in a plasma located in a strong field, 25:30530
PODUZHAILO, V. G., Phoswich for neutron detection, 25:29339
POD'YACHEV, V. N., Low noise charge-sensitive preamplifier employing field effect transistors, 25:29343
POHL, K. P., Decay of 3.696 MeV level in ^{28}Al, 25:31266
POHTO, H. A., Aspects of the brittle fracture failure of a 30-inch-ID, 30,000-psi isostat with threaded closure, 25:31757 (Y-1758)
POLANYI, J. C., Distribution of reaction products (theory). VII, 25:29058
POLICHAR, R. M., Isospin nonconservation in reactions $^{14}O(d,\alpha)^{14}N^*$/sub 0+, T = 1/ and $^{12}C(d,\alpha)^{10}B^*$/sub 0+, T = 1/, 25:31227
POLIKARPOV, G. G., Penetration of ^{90}Sr into bodies of gastropod mollusks, 25:29440
POLKINGHORNE, J. C., Deep inelastic neutrino scattering, 25:30809
POLLAT, L. L., Improved light scattering photometer for air filtration system studies, 25:31702 (LA-4627)
POLLOCK, R. E., Design features of Princeton AVF cyclotron facility, 25:31093
POLMAN, R. W., Experimental investigation of a wall jet in a torus, 25:30602
POLOZHIKHIN, A. I., Effect of boron on certain physical characteristics of synthetic graphites, 25:29946 (SC-T-713023)
Effect of boron on some physical characteristics of artificial graphites, 25:29953
POLUKAROV, A. N., Determination of arsenic and tellurium in gaseous media, 25:28959
Determination of Se, Te, Au, and Ag in Cu electrolysis slimes, 25:28933
POLUMORDVINOVA, N. I., Charged particle motion in monoenergetic cyclotron, 25:31122
Phase motion in the phasotron with spatial variation of magnetic field, 25:31156
POLYANSKII, V. A., Spectral isotopic analysis of elements in middle part of Mendeleev Periodic Table, 25:28952
POMERANTSEVA, M. D., Mutagenic effect of fast neutrons and x rays on mouse spermatogonia, 25:29487
PONG, W., Prog. rpt. on photoelectric emission from thin films in the vacuum ultraviolet region, annual, 6/70--2/71, 25:30665 (UH-235-P-9-2)
PONIKAROVA, T. M., Studies of reactions of radioisotopes of rare earth elements with protein and amino acids, 25:29445
PONOMAREV, A. A., Vertical motion of particles in cyclotron, 25:31063
PONOMAREV, V. N., Rate of ordered ion motion in the ionosphere at 600 km. I, 25:30393
Rate of ordered ion motion in the ionosphere at 600 km. I, 25:30394
POPA, M., Investigation of reaction $^{35}Cl(n,\gamma)^{36}Cl$, 25:31280
POPOV, A. B., Neutron resonances of the samarium isotopes, 25:31305 (JINR-P3-5655)
POPOV, A. I., Gamma rays from ^{64} ^{66} $^{68}Zn(p,\gamma)^{65}$ ^{67} ^{69}Ga, 25:31249
Inelastic scattering of protons by ^{50}Cr, ^{52}Cr, ^{54}Cr, and ^{64}Zn, 25:31253
POPOV, D. K., Studies of reactions of radioisotopes of rare earth elements with protein and amino acids, 25:29445
POPOV, V. I., Inelastic neutron scattering by even-N Ge isotopes, 25:31244
PORGES, K, G., Instrumentation systems to protect LMFBR core integrity, 25:31574 (ANL-7793)
PORTER, D., Elastic and inelastic scattering of neutrons in the energy range 1.0 to 5.0 MeV by natural Mo, 25:31299 (AWRE-O-89/70)
PORTER, I. T., Solid state bonding of nickel to alumina, 25:29815
POST, R. F., Progress in controlled thermonuclear research, 25:30600 (WASH-1172)
POSTNIKOV, V. S., Formation of gold nuclei on ionic crystals, 25:29910
POTTER, W. T., Analyticity of a scattering amplitude in an external-mass variable, 25:31030
POULIS, N. J., Superconducting-state Knight shift in V_3Au, 25:30425
POVLOVA, N. I., Free radicals in γ-irradiated food by EPR, 25:29733
POWELL, W. B., Magnetic regenerator, 25:31104
POWER, J. D., Second-order perturbation theory with the contact interaction, 25:30271
POWERS, D., Bragg-rule applicability to stopping cross sections of gases for α particles of energy 0.3 to 2.0 MeV, 25:30642
POYARKOVA, I. F., Use of cupferron for the potentiometric determination of thorium and cerium when present together, 25:28958
POZHARISSKAYA, T. D., Recovery of irradiated lymph nodes in case of partial-body shielding, 25:29669
PRADHAN, S., Feasibility of controlling stored grain pests by the sterile-male technique, 25:29750
PRASAD, H., Feasibility of controlling stored grain pests by the sterile-male technique, 25:29750
PRASAD, K. N., Boron--polyethylene irradiation containers for high energy neutron activation analysis, 25:29025
PRASAD, Y. V. R. K., Dispersed-particle strengthening in nickel-zirconia composite, 25:29941 (INIS-mf-8)
PREDAZZI, E., Weak duality and energy dependence of the slopes of elastic angular distributions, 25:30873
PRENTICE, E. F., Experimental drifts of juvenile salmonids

through effluent discharges at Hanford. II, 25:31645 (BNWL-1527)
PREVOT, H. Jr., In vitro studies on radioprotective effects of melanin on mammalian cells, 25:29568
Synchronization of the mytotic cycle of mammalian cells in vitro through fractionated x-ray therapy, 25:29611
PRIBIL, R., Extractions with long-chain amines. III, 25:28930
PRIGENT, Jacques, Mixed uranium and transition element sulfides, 25:29996
PRILUTSKII, O. F., Universal radiation and cosmic electrons, 25:30221
PRIMAKOFF, Henry, Presence of noncanceling seagull and Schwinger terms in weak (nucleon + nucleon + vector-meson) amplitudes, 25:30931
PRIOR, Michael H., Nuclear spins of ^{125}Cs and ^{134}Cs, hyperfine-structure separation and nuclear magnetic moment of ^{125}Cs, ^{127}Cs, and ^{136}Cs, 25:31376
PRIOR, R. M., Proton polarization in ^{16}O(p,p)^{16}O and states in ^{17}F, 25:31236
PRISTAVKO, V. P., Sensitivity of codling moths to x and gamma radiation, 25:29612
PRITZKER, Andreas, Variable states of a heavy plasma in relation to temperature and density, 25:30536
PROCHAZKA, A., Square wave rf system design for TRIUMF cyclotron, 25:31091
PRODI, V., Sampling methods for aerosol particles, 25:29263
PROKHOROV, L. V., Phenomenological lagrangians in quantum field theory, 25:30969
PROKOF'EV, O. N., Solid-state construction for discharge quenching in Geiger counters, 25:29334
PROKOF'EV, P. T., Internal conversion monoenergetic positron spectrum in ^{157}Gd(n,γ)^{158}Gd reaction, 25:31329
Level scheme for ^{178}Hf, 25:31336
PROKOF'EVA, I. A., Structure of the chromosphere as shown by Fraunhofer lines H/sub α/ and H/sub β/, 25:30156 (CSIRO-Trans-10424)
PROKOP, Reiner, Neutron-activation analysis in mineral oil industry. I and II, 25:29026
PROKOPY, R. J., Sterile-insect release method against Rhagoletis cerasi, 25:29742
PROSPERI, D., Investigation of reaction ^{35}Cl(n,γ)^{36}Cl, 25:31280
PROTSIDIM, P. S., Thermal and radiation initiated conversions of terphenyl isomers and their hydrogenated derivatives, 25:29113
PROUKAKIS, C., Hematopoietic changes following irradiation, 25:29634
PULLEN, D. J., Reactions (h,p) on Cr. I, 25:31298
PURDIE, A. C., Small scale model prestressed concrete pressure vessel tests at Fouiness, 25:29305
PURKAIT, N. N., Absorption at 2.2 MHz in the presence of a cusp-type sporadic-E layer, 25:30382
PURSER, F. D., Cyclo--Graaff: concept and practice, 25:31081
PUT, L. W., External beam handling system for AVF cyclotron of the Univ. of Groningen, 25:31096
PUYO, A., Test of ring of prestressed concrete in high-resistance sheet-metal steel, 25:30028 (EUR-4531, pp 445-76)
PYATENKO, V. S., Dependence of cytogenetic damage on the gamma radiation dose, 25:29484
Influence of x irradiation on chromosome aberrations in pea seedlings, 25:29489
PYPER, Diane M., Period of γ Equ, 25:30048

Q

QAIM, S. M., Shell effects in (n,p) and (n,α) reaction cross sections at 14 MeV, 25:31362
QUEEN, N. M., Model-independent analysis of forward π⁺-p scattering data, 25:30875
QUINN, Robert G., Vlf plasma oscillations in spherical, magnetized, cold-cathode discharge, 25:30617
QUINN, W. E., Design and installation of Scyllac, 25:30564 (EUR-4593, pp 227-39)
QUINTANA-MUNOZ, V., Effect of gamma irradiation of immature sugarcane borers, 25:29755
QUISTAD, Gary B., Hydrogen rearrangements in the mass spectra of alkylbenzenes, 25:29068
QURESHI, Mohsin, Quantitative cation exchange separation of zirconium and hafnium in formic acid media, 25:28955

R

RAABE, O. G., Development of techniques for generating monodisperse aerosols with the Fulwyler Droplet Generator, 25:29076 (LF-43, pp 13-17)
Dissolution of small radioactive particles, 25:29080 (LF-43, pp 40-51)
Estimation of the relative inhalation hazard of reactor inventory radionuclides, 25:29420 (LF-43, pp 1-7)
Physical and chemical characteristics of aerosols produced from solutions of polyvalent metallic nuclides, 25:29079 (LF-43, pp 31-9)
RABAN, P., Determination of free /sup 99m/Tc in labeled compounds by means of thin layer chromatography, 25:28991
RABIN, N. V., Photomultiplier impulse shaper with stable time delay, 25:29347
RABINOVICH, A. D., Effect of an automatic correction system on spectrometer resolution, 25:29364
RABOTNOV, N. S., Asymmetric rotor problem and the collective excitations of even nuclei, 25:31409
RADE, J., Uranium deposits at Westmoreland and Arnhem Land, 25:29234
RADENAC, Antoine, Thermal diffusivity of Pu alloy stabilized delta phase, 25:29876
RADICI, B., Ecological study of periphyton and identification of environmental radioactivity in a running-water ecosystem, 25:29478
RAFALSKI, A. L., Chemical diffusivities of Pu--Ga alloys in epsilon (bcc) phase, 25:29873
RAGENT, Boris, Laser-generated plasma as a spectroscopic light source, 25:30498 (N-70-41880)
RAGHAVAN, R. S., Decay of first excited state at 13.3 keV in ^{73}Ge, 25:31293
RAHMAN, M., Isobaric analog states in ^{52}Cr from (p,γ) and (p,n) reactions in ^{51}V, 25:31256
RAHMAN, M. A., Isobaric analog states in ^{52}Cr from (p,γ) and (p,n) reactions in ^{51}V, 25:31256
RAI, D. K., Ionization cross sections of molecules due to heavy-particle impact, 25:30299
RAI, K. S., Chromosomal translocations and genetic control of Aedes aegypti, 25:29753
RAINER, William C., Irradiated polyethylene, 25:29115
RAINEY, R. H., Completion report: evaluation of the use of permselective membranes in the nuclear industry for removing radioactive xenon and krypton from various off-gas streams, 25:29317 (ORNL-4522)
RAINWATER, J., Nevis synchrocyclotron conversion project, 25:31155
RAJPUT, J. S., Superconducting-state parameters of Al, 25:30419
RAKCHEEVA, V. I., Effect of boron on certain physical characteristics of synthetic graphites, 25:29946 (SC-T-713023)
Effect of boron on some physical characteristics of artificial graphites, 25:29953
RAKHEL'KIN, A. Z., Experimental installation R-Ohm for studying high-frequency field-interaction with plasma, 25:30508 (NP-18801)
RAKHMANBEKOV, N., Effects of neutron irradiation on phase transformations of Li_2O--MgO--Al_2O_3--SiO_2 systems, 25:30017
RAKOVICH, F. I., Microroentgenospectral investigation of uranotitanates, 25:29971
RAKOW, A., Radiation effects in isolated DNA and their functional consequences. II, 25:29463
RAKOWSKY, G., Taming the wild ferrite, 25:31035 (BNL-15722)
RAM, B., Decay rate and branching ratio (π⁻³He)/(all π⁻ modes) of /sub Λ/³H, 25:30821
RAMA, Attempt to trace the monsoon flow using natural radon, 25:29220
RAMAIYA, L. K., Mutagenic effect of fast neutrons and x rays on mouse spermatogonia, 25:29487
RAMAMOORTHY, P., Magnetofluiddynamic heat transfer, 25:30341 (NAL-TN-6)
RAMAYYA, A. V., Decay of ^{72}As to the levels of ^{72}Ge, 25:31261
Graphs for analysis of (1-3) gamma--gamma directional correlations, 25:31312 (ORNL-4619)
Levels in ^{72}Ge populated by ^{72}Ga, 25:31260
RAMLER, W. J., Proposed Midwest tandem cyclotron (MTC), 25:31063
RAMOS RODRIGUEZ, Eduardo, Control and monitoring of isolated industrial products which contain radioactive nuclides, 25:29320
RAMPAN, Yu. I., Oxygen tension in critical organs under influence of mexamine in comparison with radioprotective effect, 25:29551
RAMQVIST, Lars, X-ray emission spectra of VC/sub x/, NbC/sub x/, TaC/sub x/, and ZrC, 25:30267
RANEK, Leo, Extracorporeal irradiation of blood in patients with active cirrhosis, 25:29704
RANICAR, J. H., Simple cryostat for thermoluminescence measurements, 25:30444
RAO, B. C. Narasinga, Subauroral red arc and the associated ionospheric phenomena, 25:30350 (N-70-36812)
RAO, B. Ramachandra, Study of random movements of E- and F-region irregularities over Waltair, India, 25:30384
RAO, J. S., CP violation and strong self-interacting intermediate-vector-boson model, 25:30814
RAO, K. V. S., Possible electron spin resonance identification of Br^{2-} and I^{2-} in γ-irradiated bromide or iodide doped Ba sulfate, 25:29163
RAO, P. Venugopala, Levels in ^{72}Ge populated by ^{72}Ga, 25:31260
RAO, S. P., Selective extraction of Th with N-benzylaniline in chloroform from sulphuric acid media, 25:29184
RAPP, Donald, Collinear collisions of an atom and harmonic oscillator, 25:30292
RASHID, Y. R., Comparison of experimental results with response analysis for a model of a pressure vessel, 25:29313
RASMUSON, James Orley, Experimental and theoretical evaluation of the nitrous oxide--acetylene flame as an atomization cell for flame spectroscopy, 25:31697 (IS-

XUM

T-424)
RASMUSSEN, J. O., Decays of ^{176}Ta, ^{176}Lu, and /sup 176m/Lu to levels in ^{176}Hf, 25:31375
RASTALL, P., Gravitational field equations, 25:31000
RASTALL, Peter, Gravitational field equations, 25:31005
RATCLIFF, K. F., Applications of spectral distributions in nuclear spectroscopy, 25:31430
Spectral distributions in nuclei, 25:31429
RATHER, John Daniel Gray, Observations of quasi-stellar sources and radio galaxies at millimeter wavelengths, 25:30129
RATUSKY, J., New possibilities in the topical diagnosis of cardiac infarcts, 25:29571 (LB/G-2835)
RATZKER, Menno, Tungsten, 25:29813
RAUCH, F., Level scheme of ^{91}Nb, 25:31351
RAUSCH, Bernard A., Vanadium, 25:29802
RAVERA, O., Fallout ^{54}Mn and ^{95}Zr in water and fishes of lakes in northern Italy, 25:29477
RAVERA, Oscar, Uptake and excretion of radiocobalt by a freshwater mollusc, 25:29441
RAVINDRANATH, M., Beta decay of ^{111}Ag, 25:31365
RAYMOND, C. G., High-current capacitor banks for a 2-MJ high beta toroidal experiment (HBTX), 25:30563 (EUR-4593, pp 219-25)
RAYNOR, Gilbert S., Experimental data on dispersion and deposition of timothy and corn pollen from known sources, 25:31684 (BNL-50266)
RAYSKI, Jerzy, Analysis of physical processes into primitive parts, 25:31034
RAZORENOV, L. A., Measurements of energy spectra of multicharged nuclei, 25:30307
REBEIROT, Edith, BD 61°2565: a star with particularly intense Sr, Eu, and Cr lines, 25:30063
REBUT, P. H., Tokamak facility of Fontenay-aux-Roses, 25:30583 (EUR-4593, pp 403-9)
REDDING, Edward M., Irradiated polyethylene, 25:29115
REDDY, K. Venkata, Beta decay of ^{111}Ag, 25:31365
REDDY, S. B., Radioprotective property of thiourea against chromosome damage, 25:29559
REDEI, L. B., Field-theoretic model for low-energy J = $^{3}/_{2}^{+}$ K^{+}p scattering, 25:30886
REDMAN, H. C., Some observations on the toxicity of beta-emitting radionuclides inhaled in fused clay particles, 25:29438 (LF-43, pp 197-204)
Toxicity of inhaled ^{144}Ce fused clay in beagle dogs. III, 25:29436 (LF-43, pp 183-7)
Toxicity of inhaled $^{144}CeCl_3$ in beagle dogs. IV, 25:29431 (LF-43, pp 128-36)
Toxicity of inhaled $^{90}SrCl_2$ in beagle dogs. IV, 25:29430 (LF-43, pp 123-7)
Toxicity of inhaled $^{91}YCl_3$ in beagle dogs. IV, 25:29432 (LF-43, pp 137-9)
Toxicity of injected ^{137}CsCl in the beagle dog. III, 25:29433 (LF-43, pp 140-5)
REDMAN, W. C., Instrumentation systems to protect LMFBR core integrity, 25:31574 (ANL-7793)
REED, T. B., Growth of EuO, EuS, EuSe, and EuTe single crystals, 25:29933
REEH, H., Symmetry operations and spontaneously broken symmetries in relativistic quantum field theory, 25:30945
REEVES, E. M., Extreme-ultraviolet spectrum of the quiet Sun, 25:30166
REGEL, K., Radiation biophysical investigations in Drosophila melanogaster. I, 25:29522
REICH, H., Differential cross section of deuteron photodisintegration between 20 and 35 MeV, 25:31194
REICH, J., Emittance measurements at Juelich isochronous cyclotron, 25:31119
REIFF, J., Cross sections for scalar W-meson and vector W-meson production by muons and neutrinos, 25:30818
REIMANN, H., Microwave diagnostics of contracting rare-gas columns. II, 25:30483
REINATH, F. S., Cryogenic pumping system proposed for Bevatron, 25:31057 (UCRL-20197)
REINHARDT, Michael, Orientation of galaxies and a magnetic 'urfield', 25:30244
REINHARDT, P. W., Collisional ionization between cesium and selected molecules, 25:30276 (ORNL-TM-2620)
REISER, M., Conversion studies for SREL 600-MeV synchrocyclotron, 25:31160
Effects of central-region conditions on time structure and quality of cyclotron beams, 25:31113
H^{-} ion injection into central region of TRIUMF cyclotron, 25:31152
REISNER, K., Application of ultrasound-B picture methods for the planning of radiotherapy, 25:29602
REITMANN, D., Low-lying states of ^{127}I, 25:31352
REK, Z., Eikonal model for high-energy elastic scattering, 25:30893 (INR-P-1233)
REKAMI, E., Calculating (n,2n) reaction amplitude on heavy nuclei. II, 25:31394 (ITF-76-9s-E)
REMAUD, Bernard, Study of n-^{6}Li collisions, 25:31221
REMIZOVA, I. V., Influence of irradiation and radioprotectors on activity of alkaline phosphatase in mucosa of small intestine, 25:29645
REMLER, E. A., Complex-angular-momentum analysis of atom--atom scattering experiments, 25:30278
RENGAN, K., Recovery of Pm from fission product waste. III, 25:29176 (BARC-516)
RENUCCI, Louis, Temperature of recrystallization of Zr--O solid solutions, 25:29854
RENZI, R., Protection around a betatron, 25:29528
Protection of personnel in radioactive environment, 25:29529
RENZINI, A., Induced semi-convection in He-burning horizontal-branch stars. II, 25:30103
Overshooting of convective cores in helium-burning horizontal-branch stars, 25:30037
REPPICH, B., Radiation hardening of alkali halides and magnesium oxide, 25:30013
REPPIN, C., Measurements of the distribution in energy and angle of high-energy neutrons in the lower atmosphere, 25:30374
REST, J., Equal-time commutation relations in self-consistent quantum field theory, 25:30991
RESTER, A. C., Decay of ^{72}As to the levels of ^{72}Ge, 25:31261
Levels in ^{72}Ge populated by ^{72}Ga, 25:31260
REWALD, E., Embryological changes in irradiated eggs of Triatoma infestans, 25:29620
REZIKYAN, A. M., Partial pressure of plasma components, 25:30539
REZVAYA, G. L., Level scheme for ^{176}Hf, 25:31336
RHODES, C. G., Proton irradiation effects in type 321 stainless steel, 25:29915
RIBBECKE, H., Radiation protection in dentistry, 25:29530
RIBE, F. L., Progress in controlled thermonuclear research, 25:30600 (WASH-1172)
RICABARRA, G. H., Resonance integrals for neutron activation of ^{64}Zn, ^{68}Zn, ^{85}Rb, ^{100}Mo, ^{102}Ru, ^{113}In, ^{123}Sb, and ^{180}Hf, 25:31300 (CNEA-282)
RICABARRA, M. D., Resonance integrals for neutron activation of ^{64}Zn, ^{68}Zn, ^{85}Rb, ^{100}Mo, ^{102}Ru, ^{113}In, ^{123}Sb, and ^{180}Hf, 25:31300 (CNEA-282)
RICCI, M. V., Experimental test of microscopic theory of a current-carrying superconductor, 25:30432
RICHARD, P., Reaction ^{208}Pb(p,α)^{205}Tl at 16.475 MeV, 25:31383
RICHARDSON, Allan C. B., Multiple scattering corrections for the associated-particle neutron time-of-flight technique, 25:31172 (NBS-TN-499)
RICHARDSON, J. R., Conceptual design of two-stage, two-gap cyclotron, 25:31140
RICHARDSON, J. Reginald, Beam quality and expected energy resolution from TRIUMF cyclotron, 25:31088
RICHERZHAGEN III, Theodore, ESR study of A/sup 10 10'/-bianthrone and attempt to prepare cyclopropenyl radical, 25:29147
RICHMOND, C. R., Comparative metabolism of radionuclides in mammals. V, 25:29450
RICHTER, F., High-Q capacitors with liquid and gas impregnation, 25:30595 (EUR-4593, pp 545-50)
RICHTER, G. M., Relation between the properties of extra-galactic radio sources, 25:30125
RICHTER, Johannes, Temperature measurements in thermal plasmas of known composition, 25:30478 (SC-T-713024)
RICHTER, R. M., Cryogenic pumping system proposed for Bevatron, 25:31057 (UCRL-20197)
RICKEY, M. E., Indiana Univ. 200 MeV cyclotron project, 25:31082
RIEDEL, W., Structure and properties of electrolytically deposited tin--lead alloys, 25:31734 (SCL-T-69-257)
RIEF, H., TIMOC: Monte Carlo code for stationary and time dependent neutron transport, 25:31167 (EUR-4519)
RIEFENBERG, D. H., Chemical diffusivities of Pu--Ga alloys in epsilon (bcc) phase, 25:29873
RIEMANN, M., Radial distribution of emission and absorption coefficients in rotational-symmetric plasma, 25:30524
RIEMER, G., Plutonium diffusion in hyperstoichiometric mixed uranium--plutonium dioxides, 25:29964
RIGAUT, J., Deferred luminescence spectra of some aromatic compounds in rigid organic media, 25:29150
RIHET, Y., Reaction ^{22}Ne(p,p), ^{22}Ne(p,p'), and excited states of ^{23}Na, 25:31281
RILEY, Edgar F., Modification of radiation effect on the eye by topical application of dimethyl sulfoxide, 25:29562
RINGHOFER, K., Arguments for a covariant spin 3-vector, 25:30794
Structure of Feynman amplitude and tests of quantum electrodynamics, 25:30965
RINGLEB, Dietrich, Investigations concerning the problem of radiation-cytostatic combination treatment. VIII, 25:29604
RINGLER, H., Excited states of He atoms in stationary PIG discharge, 25:30479
RINGO, G. R., Repulsion of slow neutrons by attractive potentials, 25:31415
RIORDAN, F., Four-particle Faddeev equations with simple kernel, 25:31032
RIPOUTEAU, F., Grenoble cyclotron progress report, 25:31097
RISSLER, P., Reactor pressure vessel of finished sections, 25:31547 (EUR-4531, pp 477-88)
RITH, K., Electromagnetic form factors of the proton, 25:30786
RITTENBERG, V., Scaling and duality in electro- and photoproduction, 25:30787
RIVIERE, J. C., Introduction to LEED and discussion of some typical LEED experiments, 25:31681 (AERE-M-2184)
LMM Auger spectra of some transition metals of first series, 25:31682 (AERE-R-6719)

RIVOAL, M., Contribution to Lamb statistical model subject, 25:30866
RIZA-ZADE, R. R., Radiobiological effect on mineral nutrition of the sunflower, 25:29714
Radiobiological effect on time between irradiation and planting of sunflower, 25:29717
RIZZO, F. X., Tabulated dose uniformity ratio and minimum dose data for gamma irradiator design, 25:29250 (BNL-50145(Rev.))
ROACH, A. C., Distribution of reaction products (theory). VII, 25:29058
ROBERSON, C., Electron beams for quasi-linear and nonlinear beam--plasma experiments, 25:30500
ROBERSON, N. R., Cyclo--Graaff: concept and practice, 25:31081
ROBERTS, F. P., Thermal analysis of promethium oxalate, 25:29172
ROBERTS, T. A., Resistance to heat and γ radiation in Salmonella, 25:29557
ROBERTSON, Douglas S., Quasars: millisecond-of-arc structure revealed by very-long-baseline interferometry, 25:30130
ROBERTSON, L. P., Extraction of multiple beams of various energies from TRIUMF negative ion isochronous cyclotron, 25:31109
ROBINSON, D. W., Mid- and far-infrared spectra of HF and DF in rare-gas matrices, 25:29066
ROBINSON, M. G., Behavior of extra electrons in the liquids methane, ethane, and propane, 25:29102
ROBINSON, R. L., E2/M1 admixture of the 2' → 2 transition in ^{108}Pd, 25:31374
Spin-parity assignments for low-lying states in ^{95} ^{97}Tc, 25:31381
ROBLE, R. G., Stable mid-latitude red arcs: observations and theory, 25:30398
ROCKENHAUSER, W., Structural design philosophy and criteria for concrete reactor vessels: U. S. practice, 25:31554 (IAEA-126, pp 19-51)
RODDE, Anton Frank, Radiation induced chemiluminescence of aqueous fluorescein dyes, 25:29138
RODENBERG, R., Polarization of the recoil protons in the elastic electron--proton scattering process, 25:30780
RODENBUSCH, Heinz, Neutron-activation analysis in mineral oil industry. I and II, 25:29026
RODGERS, A. W., Reddening of eta Carinae, 25:30071
Solar-composition A stars in the galactic halo, 25:30087
RODNOV, Yu. V., Switch for reading out information from counters to a digital printer, 25:29345
ROEHRIG, H. D., Release of ^{6}Li from low-sintered Be oxide, 25:29963
ROEL, L., Radioisotopes to determine tubular passage time in dog kidneys, 25:29414
ROESINGER, S., Measurement of gamma radiation conduction in a tube with a constant curvature, 25:30638
ROGERS, Alan E. E., Quasars: millisecond-of-arc structure revealed by very-long-baseline interferometry, 25:30130
ROGERS, F. L., Prog. rpt. on concentration and desalting of protein solutions program, 6--8/70, 25:31714 (ORNL-TM-3328)
ROGERS, Franklyn C., Underground nuclear power plants: environmental and economic aspects, 25:31600
ROGERS, J. W., Neutron filtered beams as standard sources, 25:31166 (CONF-710301-8)
ROGERS, Lee F., Low dose ferrous sulfate dosimetry by direct photon counting, 25:29386
ROGINSKII, V. I., Invariants of the rotation group, 25:31013 (ITEF-782)
ROGOZINA, E. M., Studies of reactions of radioisotopes of rare earth elements with protein and amino acids, 25:29445
ROHOZINSKI, S. G., Possibility of quasi-rotational excitations in spherical nuclei, 25:31407
ROIFE, I. M., Stability of toroidal plasma ring with hf current along longitudinal magnetic field, 25:30597 (LA-4339-TR)
ROLAND, G., Solar spectrum from lambda 7498 to lambda 12016, 25:30172
ROMAN, P., Inhomogeneous $U_{3,1}$-invariant extension of vacuum expectation values, 25:30917
ROMANENKO, V. P., Effect of chemical factors on the sensitivity of polymeric detectors, 25:29335
ROMANOV, V. S., Analogous states of T = 2 in ^{26}Mg(^{3}He,n)^{28}Si, ^{46}Ti(^{3}He,n)^{48}Cr, and ^{58}Ni(^{3}He,n)^{60}Zn reactions, 25:31237 (IAE-1958)
ROMANOV, Yu. A., Matrix space dynamics taking into account third-order terms in Lagrangian, 25:30967
ROMASHKO, V. P., Stabilized gamma-resonance spectrometer, 25:29360
ROMO, W. J., K/sub L/ and K/sub S/ as shell-model eigenstates. II, 25:30861
ROOD, H. P. C., Coulomb propagator in radiative muon capture, 25:31282
ROOSEN, Robert G., An annotated bibliography on Gegenschein, 25:30390
RODTARE, H. M., Use of porosimetry in the measurement of pore size distribution in porous materials, 25:29828
RORSCHACH, H. E., Magnetization by rotation: Barnett effect in a superconductor, 25:30439
ROSA, U., Radioisotope production in Italy, 25:29273
ROSALKY, D. M., FIDEL: optical model search code with spin-orbit terms for spin-$^{1}/_{2}$ and spin-1 particles, 25:31389 (ANU-P-500)
ROSE, R. M., Quantitative control of surface pinning in a low-kappa Type II alloy, 25:30415
ROSEN, B. J., Radiation pathology of the genitourinary tract, 25:29697
ROSEN, V. J., Radiation carcinogenesis: experimental and clinical aspects, 25:29691
ROSENBERG, Ronald L., North--south component of the interplantary magnetic field, 25:30176
ROSENBERG, T. J., Magnetospheric substorm of August 25--26, 1967, 25:30368
ROSENBLATT, Gerd M., Dissociation energies and free energy functions of gaseous monoxides, 25:29082
ROSENTHAL, Peter N., Effects of incorporated ^{3}H and ^{32}P on DNA, 25:29459
ROSOLEN, Carlo, High-sensitivity solar radiospectrometry at Arecibo, 25:30159
ROSS, D. A., Phantom for the adjustment of gamma-ray imaging devices, 25:29328 (ORNL-TM-3261)
ROSS, G. G., Models of Y_0^*(1405) and low-energy anti KN interactions, 25:30876
ROSS, Sarah T., Cytological effects of irradiated sucrose, 25:29494
ROSTOKER, Gordon, Magnetic field perturbations in the magnetotail associated with polar magnetic substorms, 25:30403
ROSZAK, W., Radiothermoluminescence of crystalline and glassy methanol, 25:29101
ROTELLI, P., Application of information theory at Serpukhov energies, 25:30739
Duality diagrams and the Pomeron, 25:31022
Regge residues and supermultiplets, 25:30834
ROTH, Bernhard F., Stage of advancement in field of external HTGR fuel cycle with Th--U cycle, 25:31586
ROTHE, H., Irradiation plants to produce exposure rates within ^{60}Co gamma-radiation energy range, 25:29255
ROTHE, K. D., Covariant formulation of the saturation problem for equal-time commutators, 25:31023
ROTTMAN, G. J., Lyman-alpha emission from Arcturus, 25:30070
ROUGE, F., Test of ring of prestressed concrete in high-resistance sheet-metal steel, 25:30028 (EUR-4531, pp 445-76)
ROURE, L., Steadiness of thermal shielding during alternate stresses of aerodynamic origin, 25:31457 (EUR-4531, pp 895-930)
ROUSE, Robert A., Hybrid Gaussian-type orbital, 25:30302
ROUX, Claude, Thermal diffusivity of Pu alloy stabilized delta phase, 25:29876
ROW, T. H., Reactor containment spray systems, 25:31583
ROWE, D. J., One-particle-hole and projected Hartree--Fock approximations in ^{12}C and ^{16}O, 25:31226
ROWE, J. J., Determination of platinum and palladium in geological materials by neutron-activation analysis after fire-assay preconcentration, 25:29022
ROWLAND, P. R., Distribution of fission products in a high temperature gas cooled reactor, 25:31567
ROY, Claude, Thermal diffusivity of Pu alloy stabilized delta phase, 25:29876
ROYER, Ray, Method for solving the equation of ionized electric fields in a stationary regime, 25:30705
ROYSTON, D., Review of processes for the production of hafnium-free zirconium, 25:29782 (AAEC/TM-570)
ROZANTSEV, E. G., Macrostructure of bovine serum albumin under γ irradiation, 25:29471
ROZENBERG, Ya. I., Superconducting-wire liquid helium level gauge, 25:30448
ROZENTAL, I. L., Universal radiation and cosmic electrons, 25:30221
ROZHDESTVENSKII, L. M., Vulnerability of gastrointestinal tract of rats under influence of radiation, 25:29646
RUBIN, Robert H., Observations of compact H II regions with optical counterparts, 25:30117
RUBINSTEIN, H. R., Scaling and duality in electro- and photoproduction, 25:30787
RUCKER, D. J., Prog. rpt. on fuels and materials development, 9/30/70, 25:29757 (ORNL-4630)
RUDD, G. E., Development of polyimide bonded solid film lubricants, 25:29096 (WERL-HFIL-1)
RUDOLPH, Joachim, IR-spectroscopic investigations of crystalline tetrahydrate of hydrogen bromide $H_5O_4^+Br^-$, 25:31683 (ANL-Trans-880)
RUEDIGER, D., Composition and properties of the binder metal in cobalt bonded tungsten-carbide, 25:29980
RUEHL, Franklin Robert Jr., Study of three-part nucleon--nucleon interaction potentials, 25:31413
RUELL, David, Time evolution of systems with an infinite number of degrees of freedom, 25:30703
RUETER, D., g-factor of the 181 keV level of ^{99}Tc, 25:31271
RUH, A., Absolute calibration of tensor analysing powers of the ^{3}He(d,p)^{4}He and the ^{4}He(d,d)^{4}He reactions, 25:31198
RUH, Robert, Use of DTA for the determination of the monoclinic--tetragonal transformation in zirconia and zirconia-based systems, 25:29982
RUHENSTROTH-BAUER, Gerhard, Esterase activity and protein content of plasma erythrocytes in whole-body irradiated rats, 25:29686
RUMYANTSEV, B. A., Energy spectra of particles observed in reactions proceeding via a compound nucleus, 25:31403

RUPP, T. D., Gamma-ray energies and intensities in decay of ^{205}Bi, 25:31386
RUPPRECHT, F. C., Fission Product Inhalation Program. Annual report, October 1, 1969--September 30, 1970, 25:29419 (LF-43)
RUSH, A. A., Elastic and inelastic scattering of 30 and 50 MeV polarized and unpolarized beams of protons by ^{40}Ar and ^{14}N, 25:31233
RUSIN, V., Second observation of Ar XIV outside total eclipse of Sun, 25:30188
RUSSEK, A., Fast-electron--slow-electron coincidence study of violent Ar$^+$--Ar collisions, 25:30288
RUSSO, M., Consistent quantization of Yang--Mills field, 25:30988
RUTKEVICH, I. M., Two-dimensional problem of electrodynamics of steady-state currents in nonlinear conducting media, 25:30346
RUTKOWSKA, K., Radioactivity distribution of emanation decay products between aerosol particles of determined size ranges, 25:29214 (LA-tr-71-7)
RUUSKANEN, P. V., A_2 production, 25:30877
RUZMAIKIN, A. A., Spherically symmetric solutions of Einstein equations for world filled with radiation, 25:30225
RUZMAIKINA, T. V., Spherically symmetric solutions of Einstein equations for world filled with radiation, 25:30225
RYABUKHIN, Yu. S., Quantitative ^{6}Li autoradiography of metastases of Walker-256 carcinosarcoma in pulmonary tissue, 25:29443
RYAZANOV, D. K., Study of spontaneous fission of ^{252}Cf, 25:31314 (ORNL-tr-2453)
RYAZHSKAYA, O. G., Scintillator for recording slow neutrons, 25:29336
RYBAKOV, N. I., DNAase activity of E. coli K12 (lambda) during gamma irradiation, 25:29725
RYBICKI, E., Effect of dose rate on the radiation yields of radicals in frozen organic media, 25:29160
RYKALIN, V. I., Pulse shaper with independent regulation of output pulse duration and dead time, 25:29342
RYLANDER, Lars, Plate heat exchanger, 25:29269
RYON, A. D., Prog. rpt. on concentration and desalting of protein solutions program, 6--8/70, 25:31714 (ORNL-TM-3328)
RYPKA, E. W., Toxicity of inhaled ^{90}Y fused clay in beagle dogs. II, 25:29434 (LF-43, pp 146-62)
Toxicity of injected ^{137}CsCl in the beagle dog. III, 25:29433 (LF-43, pp 140-5)
RYTZ, Albrecht, Energy of ^{253}Es α particles, 25:31357
RYUFUKU, Hiroshi, Dynamic molecular orbitals and their application to charge exchange reactions, 25:30275 (JAERI-Memo-4299)
RYUTOV, D. D., Quasilinear relaxation of an ultrarelativistic electron beam in a plasma, 25:30534
RYZNAR, L., Release of the hydrogen atom in thymine radiolysis, 25:29148

S

SAAR, A. M. E., Formation of color centers in KCl crystals by ultrasoft x rays, 25:30654
SABAU, M., Evidence for possible boson resonance of mass 2820 MeV, 25:30737
SABEU, M., Application of phenomenological quasi-two-body model to π^-p-interactions with strange particle production at p = 4 GeV/c, 25:30869 (JINR-P1-5706)
SABIROV, B. M., Gamma radiation of ^{226}Ra and its decay products, 25:31358
SACCHETTI, N., Experimental test of microscopic theory of a current-carrying superconductor, 25:30432
SADIKOV, I. P., Neutron thermalization in H_2O at 316°K and 770°K, 25:31170 (KAPL-Trans-4)
SADOUNE, Joseph, Process for crossing boundary layers in a magnetohydrodynamic generator and a generator using the process, 25:30337
SAENGER, Eugene L., Radiation and leukemia rates, 25:29705
SAETTA-MENICHELLA, E., Sudden model for ternary fission, 25:31422
SAFONOV, A. A., Critical current density across MHD generator electrodes made of ZrO_2--Y_2O_3 ceramics, 25:30336
SAGAWA, N., Studies for safety analysis of loss-of-coolant accidents, 25:31605
SAGLIO, R., Test of ring of prestressed concrete in high-resistance sheet-metal steel, 25:30028 (EUR-4551, pp 445-76)
SAHA, A., Cytogenetic effects of x rays and chemicals on tomato, 25:29493
SAHA, Kshudiram, Interhemispheric drift of radioactive debris and tropical circulation, 25:29221
SAITAKE, Yoshiyuki, Effect of phase on primary process of formation of butyl radicals in radiolysis of solid isobutane-2-d_1, 25:29161
SAITO, Nobufusa, Isotope effect of electromigration in some solid alkali halides, 25:29041
SAITO, Tatsuya, Yields of radioactivities induced by (γ,n) reactions with bremsstrahlung up to 68 MeV, 25:31333
SAKAI, Jun-ichi, Hydromagnetic motion in the geomagnetic tail, 25:30349 (IPPJ-103)
SAKMAR, I. A., Unique point for determination of π^+p amplitudes, 25:30888
SAKSENA, G. D., Lithium isotopic analysis on recording Fabry--Perot spectrometer, 25:28913 (BARC-508)
SAKURAI, Kunitomo, Gyrosynchrotron radiation and its transfer in a magnetoactive plasma, 25:30515 (N-70-41892)
SALAM, Abdus, Infinity suppression in gravity-modified quantum electrodynamics, 25:30994
SALAMBASHEV, L. A., Nephrography with aid of ^{51}Cr-EDTA and ^{58}Co-DTPA, 25:29577
SALEM, M., Spectrum of a gaseous nebula of pure H. III, 25:30101
SALGE, J., Application of inductive energy storage systems for production of intense magnetic fields, 25:30561 (EUR-4593, pp 197-203)
SALIN, Ph., Strong interaction phenomenology, 25:30826
SALMERON, R., Conference on nigh multiplicity hadronic interactions, Paris, 5/70, 25:30762
SALSIG, W., Preliminary hardware concepts for a high-energy electron-ring accelerator, 25:31052 (UCRL-20169)
SALTER, C. J., Observations of some extended galactic radio sources, 25:30136
SALUSTI, E., Semi-group approach to quantum field equations, 25:30972
SAMBORSKII, V. S., Rate of ordered ion motion in the ionosphere at 600 km. I, 25:30393
SAMOKHVALOV, A. A., Magnetization of EuO and $Eu_{0.97}Gd_{0.03}O$ single crystals, 25:30670
SAMORAJSKI, T., Effects of irradiation on the nervous system, 25:29692
SAMPSON, M. B., Indiana Univ. 200 MeV cyclotron project, 25:31082
SAMSONOV, G. V., Electrophysical properties and nature of the chemical bond in compounds of beryllium with boron and carbon, 25:29943 (LA-tr-71-30)
Properties of rare-earth metals (Sc, Nd), their hydrides, carbides, and oxides, 25:29859
SAMUELS, L. D., Radiation hepatitis in children, 25:29652
SANAK, Joseph, Correlations between ^{210}Pb atmospheric abundance in Terre Adelie and solar activity, 25:30171
Correlations between ^{210}Pb deposit in Antarctic and fluctuations in Earth's magnetic field, 25:29211
SANCHEZ, A., Effect of the inhalation of ^{144}Ce in relatively insoluble forms on influenza virus infection in mice, 25:29724 (LF-43, pp 254-62)
SANDA, A. I., Lower bound on W$^+$--meson production in high-energy proton--proton collisions, 25:30907
SANDAGE, Allan, Distance of the local-group galaxy IC 1613 obtained from Baade's work on its stellar content, 25:30209
SANDENAW, Thomas A., Heat capacity and derived thermodynamic functions of ^{242}Pu from 15 to 373K, 25:29831
SANDER, K. F., Sheath growth in a low-pressure plasma, 25:30531
SANDERS, Robert H., Dust scattering in the filaments of M82, 25:30208
SANDRI, Guido, Prog. rpt. on theory of MHD turbulence, final, 8/70, 25:30517 (N-71-11428)
SANDRU, D., Oscillatory behavior of enzymic reactions, 25:29461
SANEBLIDZE, O. I., Effects of x rays on metabolism of calcium ions in muscle cells, 25:29674
SANKEY, Richard Roger, Shell model states of $^{58}Co_{27}$, 25:31355
SANNER, L., Hyperfine structure investigations of ^{51}Mn and /sup 52m/Mn, 25:31294
SANO, Masakatsu, Effect of irradiation on halogen exchanged silica--alumina catalyst, 25:29111
SANO, T., Graphitization of free C precipitating through reaction of UC_2 with N_2, 25:29962
SANSONE, Magda, Recent development of the nuclear power program in West Germany, 25:31461
SANTILLI, R. M., Inhomogeneous $U_{3,1}$-invariant extension of vacuum expectation values, 25:30917
SANTINI, F., High-frequency instability and anomalous plasma resistivity at supercritical electric fields, 25:30625
SANTORO, R. T., Approximate high-energy alpha-particle nucleus collision model, 25:31368
SANWAL, D. N., Decay times, intensities, and their temperature variation of luminescence of aqueous and deuterated solutions of Eu ion, 25:29053
SARIC, William S., Experimental and theoretical investigations of a liquid film interacting with a supersonic stream, 25:31726 (SC-DC-713922)
SARKAR, S. C., Mineralization of radioactive elements in Singhbhum shear zone, Bihar, 25:29227
SAROUL, J., Out-of-pile studies on diffusion of contamination in liquid Na and fast reactor containment vessels, 25:31615
SARUIS, A. M., Coupled-channel calculations of the giant dipole resonance in the one particle--one hole continuum approximation. II, 25:31286
SARZYNSKI, J., β--γ angular correlation measurements, 25:31277
SASAKI, Y., Graphitization of free C precipitating through reaction of UC_2 with N_2, 25:29962
Heats of hydrolysis of thorium carbides, 25:29966
SASAKI, Yasuo, Preparation and comminution of hydrogenated niobium, 25:29929
SASTRI, J. Hanumath, Study of random movements of E- and F-

region irregularities over Waltair, India, 25:30384
SASTRY, D. H., Dispersed-particle strengthening in nickel-zirconia composite, 25:29941 (INIS-mf-8)
SATO, Koichi, Axial behavior and confinement of plasma in the mirror-field theta pinch, 25:30464
SATO, Matsuji, X-ray excited optical luminescence analysis of trace rare earths in high-purity yttrium and gadolinium oxides, 25:28961
SATO, N., Space-charge waves on plasma columns in a weak magnetic field, 25:30618
SATO, T., Propagation of electrostatic ion waves near ion cyclotron harmonics, 25:30612
SATO, Toshio, Infrared absorption spectra of silica gel-$H_2{}^{16}O$, $D_2{}^{16}O$, and $H_2{}^{18}O$ systems, 25:29069
SATTERTHWAITE, C. B., Thermal conductivity of superconducting niobium, 25:30434
SATZ, H., Mass dependence of momentum transfer distributions in diffraction dissociation, 25:30767
SAUER, K., Echoes with ion sound waves, 25:30611
SAUERBRUNN, Bertram J. L., Radioisotope organ imaging in tumor diagnosis and management, 25:29580
SAUGY, B., Nonlinear analysis of stresses in the structure of the prestressed concrete pressure vessel for a fast reactor, 25:31553 (EUR-4531, pp 797-812)
SAVCHENKO, I. S., Experimental installation R-Ohm for studying high-frequency field-interaction with plasma, 25:30508 (NP-18801)
SAVIN, W., Nuclear matter radii in the tin isotopes, 25:31341
SAVRIN, V. I., Condition of the asymptotic equality of total cross sections in two simple models, 25:30769
SAWA, Z., Energy levels and gamma transitions in ^{70}Ga, 25:31290
SAWYER, G. A., Design and installation of Scyllac, 25:30564 (EUR-4593, pp 227-39)
SAZONOVA, E. V., Efficiency of radiators and absorbers of charged particles, 25:30641
SCANLON, J. P., Harwell 110 in synchrocyclotron modification scheme, 25:31154
SCARPETTA, G., Self-consistent derivation of multiple mass values in renormalized field theories, 25:30986
SCHAEFFER, R. C., Computation of geomagnetic L coordinates, 25:30491
Photodissociative excitation of O(^{1}D) atoms in the day airglow, 25:30386
SCHAFFHAUSER, A. C., Tungsten metallurgy, 25:29785 (ORNL-4630, pp 207-25)
SCHATTEN, Kenneth H., Magnetic-field geometry of Jupiter, 25:30251
SCHATZMAN, E., Physics and astrophysics, 25:30219 (CERN-70-31)
SCHECTER, L., Modification of a conventional 37 in cyclotron, 25:31161
SCHENK, G., Parametric study of exploding foils as switches, 25:30574 (EUR-4593, pp 319-38)
SCHEP, T. J., FREMIX: a high-power 8-GHz plasma heating experiment, 25:30456 (EUR-4593, pp 551-6)
SCHERBL, D., Compatibility studies with UC of different stoichiometries and iron--nickel--chromium alloys and the influence of stabilizers, 25:29940 (EURFNR-820)
SCHERFF, H. L., Plutonium diffusion in hyperstoichiometric mixed uranium--plutonium dioxides, 25:29964
SCHERK, J., Mass shifts in second order of perturbation theory in the dual-resonance model, 25:30835
SCHERK, L., Interaction of pions with nuclei, 25:31421
SCHERRER, Jean R., Pharmacokinetics of halothane in man, 25:29416
SCHERTLER, Ronald J., Experimental investigation of single-particle behavior in an axisymmetric magnetic field, 25:30516 (N-70-42698)
SCHIBY, B., Observation of d* effect in anti pd → p anti p $\pi^+ \pi^-$n reaction at 5.55 GeV/c, 25:30727 (NP-18796)
SCHIKARSKI, W., Experiments on the behavior of nuclear aerosols in fast breeder reactor containment, 25:31617
SCHILD, R., Effective temperatures of B- and A-type stars, 25:30094
SCHILDKNECHT, D., Comparison of pion electroproduction data with vector meson dominance predictions, 25:30789
SCHILLER, P., Determination of trace amounts of gold in natural sweet waters by nondestructive activation analysis after preconcentration, 25:29014
SCHILLING, S. A., Beryllium, 25:29806
SCHLESINGER, H. L., Prog. rpt. on applications of neutron activation analysis in scientific crime investigation, final, 9/70, 25:29012 (GA-10276)
SCHMIDT, H. E., Some considerations on the thermal conductivity of stoichiometric uranium dioxide at high temperatures, 25:29967
SCHMIDT, K., Production of neutrons through irradiation of thick beryllium targets with deuterons in energy range from 15 to 55 MeV, 25:31202 (KFK-1288)
SCHMIDT, Karl-Heinz, Density of the dust in reflection nebulae, 25:30054
SCHMIDT, M., Investigation of particle streaming out of plasma, 25:30485
Measurement of radiative lifetimes of $CO_2{}^+(A^2\Pi_i/sub\ u/)$, $CO_2{}^+(B^2\Sigma/sub\ u/^+)$, $CH(A^2\Delta)$ and $CO(C^1\Sigma^+)$ by pulsed radiolysis, 25:30273 (ANL-Trans-879)
SCHMIDT, M. G., K anti K II N anti N amplitude in a Veneziano-type model with spin, 25:30889
SCHMIDT, Maarten, Evolution of quasars, 25:30148
SCHMIDT, Pierre, Vlf plasma oscillations in spherical, magnetized, cold-cathode discharge, 25:30617
SCHMIDT, R. L., Study of the transverse magnetoresistance of polycrystalline potassium, 25:31707 (NYC-2160-68)
SCHMIDT-HERMES, Heinz-Josef, Contribution to indications and methods of irradiation in cases of malignant systemic diseases, 25:29599
SCHMITTER, K. H., Recent results with laser-triggered spark gaps, 25:30566 (EUR-4593, pp 259-64)
SCHMITTROTH, F., Comparison of the R-matrix nuclear reaction theories, 25:31442
SCHNEIDER, C., Synchronization of the mytotic cycle of mammalian cells in vitro through fractionated x-ray therapy, 25:29611
SCHNEIDER, D., Application of inductive energy storage systems for production of intense magnetic fields, 25:30561 (EUR-4593, pp 197-203)
SCHNEIDER, K. U., Design possibilities and consequences for the conventional parts of fusion power plants, 25:30588 (EUR-4593, pp 445-60)
SCHNEIDER, Walter, X-ray diffraction investigations on internal oxidation zones in sodium-corroded vanadium--titanium alloys, 25:29781
SCHNEIDER, William P., Nuclear environment against which equipment must be hardened, 25:29246
SCHNELLENBACH, G., Dynamic relaxations as an effective method for spatial calculations on concrete pressure vessels, 25:31665 (EUR-4531, pp 735-57)
SCHNITZER, Howard J., Scale transformations and broken chiral symmetry, 25:30920
SCHOENFELDER, V., Measurements of the distribution in energy and angle of high-energy neutrons in the lower atmosphere, 25:30374
SCHOENING, J., 300 MW thorium high-temperature power plant (THTR), 25:31539
SCHONBERG, Russell G., Process radiation using accelerator sources, 25:29126
SCHONNE, E., Metabolism of different immunoglobulin classes in irradiated mice. V, 25:29473
SCHOVE, D. J., Biennial oscillation, tree rings, and sunspots, 25:30162
SCHRADER, W. J., FREMIX: a high-power 8-GHz plasma heating experiment, 25:30456 (EUR-4593, pp 551-6)
SCHRAGE, H. P., Results of model investigations on multiple pressure vessels, 25:31549 (EUR-4531, pp 527-56)
SCHRAM, D. C., FREMIX: a high-power 8-GHz plasma heating experiment, 25:30456 (EUR-4593, pp 551-6)
SCHRAUZER, G. N., Chemical evolution of a nitrogenase model. II. Molybdate--cysteine and related catalysts in the reduction of acetylene to olefins and alkanes, 25:29051
SCHROEDER, Gerald L., Potential alpha ray activity meter, 25:29352
SCHROEDER, K., Specific heat of chromium--rich chromium--nickel and chromium--iron--molybdenum alloys between 1.3 and 4.2°K, 25:30676
SCHROER, B., Locally generated dilatation charge in Thirring model, 25:30990
SCHROER, Bert, Quantization of $m^2 < 0$ field equations, 25:30985
SCHUELE, W., Report on irradiated materials, 25:29909
SCHUELLER, V., Legendre polynomical development in Boltzmann equation for Lorentz plasmas, 25:30522
SCHUETZ, W., Elastic electron scattering on ^{40}Ar, 25:31272
SCHUETZENDUEBEL, W. G., Steam generators for high-temperature gas-cooled reactor plants in the USA, 25:31623 (GA-10338)
SCHUFFENHAUER, Werner, Suitability of vitreous carbon as a mortar material for spectrochemical analysis, 25:28938
SCHULMAN, Marvin, Determination and degradation of microquantities of acetate, 25:28996
SCHULTE-FROHLINDE, D., Gamma-radiolysis of aqueous solutions of 5-bromo-2'-deoxyuridine in presence of O. I, 25:29135
Gamma-radiolysis of aqueous solutions of 5-bromo-2'-deoxyuridine in presence of O. II, 25:29136
SCHULZ, G. J., Vibrational excitation and compound states in NO, 25:30281
SCHULZ, Michael, Approximate second invariant for a dipole field, 25:30381
SCHUSSLER, Francois, Excited metastable states of ^{93}Y, 25:31338
SCHUSSLER, M., Fabricating the refractory metals. Part II. Methods used to make parts, 25:29789
SCHUSTER, Guenter, Nuclear power in West Germany in next decade, 25:31460
SCHUTTE, A., Transverse heat flow in gaseous hydrogen isotopes at low temperatures, 25:29267
SCHWANDT, P., Polarization measurements and phase shifts for p-^{4}He scattering, 25:31199
SCHWARTZ, D. A., Observations of unresolved galactic x-ray sources, 25:30134
SCHWARTZ, M. J., Diagnostics for hot-electron, magnetically confined plasmas, 25:30489
SCHWARZ, D., Present status and future development of THTR in Federal Republic of Germany, 25:31540
SCHWARZ, K., Radiation effects in isolated DNA and their functional consequences. V, 25:29466
Radiation effects in isolated DNA and their functional consequences. IV, 25:29465
Radiation effects in isolated DNA and their functional consequences. VIII, 25:29469

XUM

SCHWARZENBERG, L., Acute irradiation in man: treatment of hematologic disorders, 25:29699
SCHWEIGER, F., Present status and future development of THTR in Federal Republic of Germany, 25:31540
SCHWEINLER, H. C., Collisional ionization between cesium and selected molecules, 25:30276 (ORNL-TM-2620)
SCHWELA, D., Coupling parameters of pseudoscalar meson photoproduction on nucleons, 25:30797
SCHWENKER, Robert F. Jr., Conference on thermal analysis, Worcester, Mass., 8/68. II, 25:29758
SCHWENTEK, H., Ionospheric absorption during shortwave fade-outs related to enhancement of solar x-ray flux, 25:30362
SCHWIMMER, A., Isospin structure of the multiperipheral model and charge distributions, 25:30845
SCIUTO, S., Amplitude for N nonspurious excited particles in dual resonance models, 25:30830
SCOTT, J. K., Retention and distribution of ^{137}Cs in the beagle dog following inhalation of ^{137}Cs in fused montmorillonite clay particles, 25:29426 (LF-43, pp 79-81)
SCOTT, J. L., Development of advanced FBR fuels, 25:29923 (ORNL-4630, pp 59-72)
Development of uranium mononitride fuels, 25:30010 (ORNL-4630, pp 179-85)
Performance capability of advanced fuels and fast breeder reactors, 25:31569 (ORNL-TM-3388)
SCOTTO, F., Techniques for rupture testing of prestressed concrete vessel models, 25:29302
Ultimate design experience from small dimension models testing, 25:31559 (IAEA-126, pp 99-114)
SEABORG, Glenn T., Do the superheavy elements already exist, 25:31328
SEABORN, J. B., Calculation of odd-parity states in ^{12}C and ^{16}O, 25:31230
SEDLACEK, Z., Electrostatic oscillations in cold inhomogeneous plasma. I, 25:30623
SEDOV, V. V., Effects of oxathiole on condition of liver and kidneys during ^{210}Po-induced chronic radiation sickness, 25:29563
SEGRE, S. E., Electron heating in large-amplitude oscillations in a theta-pinch, 25:30467
Measurements on heating in collisionless low-β transverse shock waves near critical Alfven--Mach number, 25:30468
SEIDEL, Arnulf, Effect of isotope dilution on the behavior of radioyttrium in mammalian organism, 25:29454
SEIDLER, W. A., Alpha-particle optical potential from the nuclear density distribution, 25:31212
SEIDMAN, D. N., Direct observation of long range migration of self-interstitial atoms in Stage I of irradiated platinum, 25:30649 (NYO-3504-57)
SEIFERT, K., Results of primary therapy of laryngeal carcinomas with conventional x-depth-irradiation or radium contact irradiation, 25:29598
SEILER, G. J., Algebraic close-coupling calculation of the scattering of electrons and positrons by hydrogen, 25:30286
SEILER, H., Thin-layer chromatography as an aid in radiochemistry. VI, 25:29165
SEILER, R., Theory of particles with spin up to one in external fields, 25:30939 (NYO-3829-66)
SEKIMOTO, Hiroshi, Measurement and the calculation of neutron spectra in iron assemblies, 25:31658
SEKIYA, Tamotsu, Improvement to GG approximation in neutron slowing down, 25:31179
SELENGUT, D. S., Some comments on perturbation theory, 25:31655
SELINGER, R., Semisterility for insect control, 25:29752
SELKER, Alan H., Effects of ionizing radiation on PVC, 25:29104
SEMENOV, V. N., Shock waves propagating along a magnetic field in a collisionless plasma, 25:30620
SEMINA, O. V., Deamination of nitrogen compounds in liver during radiation sickness, 25:29641
SEM-JACOBSEN, C. W., Prog. rpt. on regional blood flow in subcortical structures in man, 3/71, 25:31710 (NYO-3618-10)
SEN, A., Damping of plasma oscillations in atoms, 25:30301
SEN, Dilip, Collective excitations in ^{172}Yb and ^{172}Lu, 25:31347
SEN'KO, V. A., Pulse shaper with independent regulation of output pulse duration and dead time, 25:29342
SEREDENKO, E. V., Stability of toroidal plasma ring with hf current along longitudinal magnetic field, 25:30597 (LA-4339-TR)
SERENKOV, V. I., Mechanism of the formation of tree-shaped channels in charged-particle irradiated dielectrics, 25:29100
SERGEEV, A. V., Spectrum of Forbush decrease in region 3 to 50 GV, 25:30318
SERGEEV, V. O., Decay of ^{225}Ac, 25:31325
SESSIONS, Meredith H., Precision deep-sea time release, 25:31756 (UCSD-34-P-127-8)
SETHI, G. R., Feasibility of controlling stored grain pests by the sterile-male technique, 25:29750
SETTE, D., Electron microscope observation of lattice disorder in ion-implanted silicon, 25:30650
SEVERGIN, Yu. P., External beam monochromatization system in 2.4 m isochronous cyclotron at Kurchatov Atomic Energy Inst, 25:31118
SEVERNE, G., Kinetic theory of inhomogeneous rotating self-gravitating systems: local energy production from binary interactions, 25:30230
SEXTRO, R. G., Beta-delayed protons from ^{23}Al, 25:31241 (UCRL-20436)
SEYFRIED, Philippe, Some criteria for choosing presses for the compaction of radioactive waste, 25:29316 (LA-tr-71-12)
SHA, William T., Integrated model for analyzing disruptive accidents in fast reactors, 25:31599
SHABANSKII, V. P., Acceleration of cosmic rays by magnetohydrodynamic discontinuities, 25:30312
Radial profile of the proton belt, 25:30354
SHAFFER, Lawrence B., Defect production in single crystals resulting from ion bombardment, 25:30648 (N-70-37028)
SHAFFER, P. T. B., Elastic moduli of niobium carbide and tantalum carbide at high temperature, 25:29970
SHALTIEL, D., Electron paramagnetic resonance of coupled spin systems: Gd/sub x/ Zr/sub 1-x/Zn$_2$, 25:30694
SHAMOV, A. I., Stabilized gamma-resonance spectrometer, 25:29360
SHANNON, D. W., Radioactivity in FFTF closed loops, 25:31627 (BNWL-585)
SHAPAR, A. V., Pulse delay time in ^{3}He neutron counters, 25:29338
SHAPIRO, E. L., Potassium content in patients with pyelonephritis, 25:29448
SHAPIRO, F. L., Problems of determining phases of structural amplitudes in neutron diffraction and of neutron accumulation, 25:30663 (JINR-P3-5554)
SHAPIRO, G. A., Reaction of pituitary-adrenal system of dogs to irradiation, 25:29642
SHAPIRO, I. S., Many-baryon resonances, 25:30895 (NP-18779)
SHARKIN, O. P., Microroentgenospectral investigation of uranotitanates, 25:29971
SHARMA, A. P., Charge identification of nuclear tracks in photographic emulsions, 25:29380
Track width in nuclear emulsions, 25:29381
SHARMA, M. L., Ground-state energies of doubly even nuclei, 25:31427
SHASHKINA, T. B., X-ray emission spectra of manganese borides, 25:30671
SHASHKOV, V. S., Radioprotective properties of o-acyl derivatives of serotonin, 25:29555
SHATALOV, G. A., Phase transition associated with radiation defects, 25:29911
SHATUNOVSKII, R. M., Low noise charge-sensitive preamplifier employing field effect transistors, 25:29343
SHAW, D. T., Analysis of nonequilibrium plasmas in close-spaced thermionic converters, 25:30338
SHAW, Edward I., Effect of irradiation on mammalian cells in vitro, 25:29624
SHCHERBA, M. M., Potassium content in patients with pyelonephritis, 25:29448
SHCHUKINA, V. S., Organic reagents in analytical chemistry of Zr and Hf. VI, 25:28932
SHEIN, Yu. V., High-accuracy variable time delay, 25:29403
SHEINDLIN, A. E., Enthalpy measurements by drop calorimetry using electromagnetic levitation, 25:29875
SHELEF, M., Studies of surface reactions of NO by isotope labeling. II. Deuterium kinetic isotope effect in the ammonia--nitric oxide reaction on a supported platinum catalyst, 25:29063
SHELINE, R. K., Levels in ^{158}Gd from the (d,p) reaction, 25:31354
SHELINE, Raymond K., Prog. rpt. on experimental study of nuclear models, 8/70--7/71. I, 25:31315 (ORO-2434-7)
SHELTON, W. N., Levels in ^{158}Gd from the (d,p) reaction, 25:31354
SHEN, B. S. P., I Zw 1: a variable compact galaxy, 25:30199
Light variations of Seyfert galaxy 3C 120, 25:30214
SHENOY, A. S., Thermal radiation absorption by particle-seeded gases, 25:29270
SHEPPHERD, H., Excretion and retention of stable strontium in children, 25:29442
SHERA, E. B., Reaction ^{40}K(n,γ)^{41}K and the level structure of ^{41}K, 25:31292
SHERIEF, M. K., Separation of ^{239}Pu(IV) from ^{95}Zr, ^{95}Nb, ^{106}Ru, and ^{106}Rh by anion exchange resin from mixed methyl alcohol nitric acid solution, 25:29191
Studies on absorption of ^{239}Pu by anion exchange resin from nitric acid and mixed nitric acid methyl alcohol systems, 25:29194
SHERIF, H., Symmetry property of the inelastic scattering amplitude in the adiabatic approximation, 25:31449
SHERMA, Joseph, Ion-exchange paper chromatography of metal ions with mixed aqueous-organic solvents containing mineral acid and a selective extractant, 25:29190
SHERMAN, John T., Uranium, 25:29811
SHERMANZON, E. M., Relation of electron flux in upper atmosphere to state of Earth magnetosphere, 25:30353
Spark chamber power supply circuit with semiconductor trigger, 25:29374
SHERRILL, Mary N., Chromosome aberrations in swine leukocytes after in vivo or in vitro exposure to 14 MeV neutrons, 25:29497
SHEVCHENKO, O. V., Phase diagrams of systems of Sm, Gd, and Dy oxides with Mg oxide, 25:29985
SHEVCHENKO, V. G., (γ,n) cross sections of Al and P,

XUM

25:31242
SHEVNIN, A. D., Statistical and dynamic pressures of solar wind on the Earth's magnetosphere, 25:30396
SHEVYAKOV, A. M., Solid solutions in the system hafnium dioxide--silica, 25:30006
SHIBATA, Toshikazu, Measurements of angular distributions and energy spectra of photoneutrons from lead targets bombarded by high energy electrons, 25:31317
SHIBAZAKI, I., Nontadpole contribution to mass splitting (m/sub K/--m/sub π/), 25:30791
SHIELDS, R. P., Effect of iodine decay heat on charcoal adsorbers, 25:31669 (ORNL-4602)
SHIINA, Shoichi, Axial behavior and confinement of plasma in the mirror-field theta pinch, 25:30464
SHIMIZU, Tsuneo, Reversed phase thin-layer chromatographic behavior of rare earths, Th, U, and Zr with a high molecular weight amine in sulfuric acid and ammonium sulfate systems, 25:29187
SHIN, Y. M., Photoprotons from ^{12}C and ^{13}C, 25:31232
SHINER, V. J. Jr., Deuterium effects on binding of reduced coenzyme alcohol dehydrogenase isoenzyme EE, 25:29056
SHINOHARA, Yasuo, Process for producing thermoplastic resin foam, 25:29109
SHIOKAWA, Jiro, Extraction of Eu with di(2-ethylhexyl) phosphoric acid, 25:29185
SHIOKAWA, Takanobu, Chemical effects associated with (γ,n) reaction in potassium chromate, 25:29166
SHIPILOV, V. I., Shaper with double shaping based on delay lines having a modified noise spectrum, 25:29366
SHIRANE, G., Lattice dynamical phase transition in V_3Si, 25:30683
SHIRATORI, E., New biaxial tensile tester for flat specimens, 25:31735 (SCL-T-69-258)
SHIROKOV, M. F., Applications of special coordinate conditions in Einstein gravitational theory, 25:31006
SHIROMIZU, Ryusuke, Reversion of metastable phases in Cu--Be alloys, 25:29891
SHISHKOVA, G. A., Biosynthesis of liver and spleen histones of irradiated animals, 25:29662
SHISHLYANIKOV, P. T., Control system of Dubna monoenergy cyclotron, 25:31099
SHITOV, Yu. P., Linear polarization of pulsar NP 0628 and radio emission in meter-wavelength range, 25:30135
SHIUKASHVILI, M. A., Spectral classification of F0--G5 stars, 25:30059
SHLENSKAYA, V. I., Spectrophotometric determination of small amounts of ruthenium and osmium in minerals and industrial samples, 25:28960
SHMELEV, O. A., Program linking FSD measuring microscopes with a Minsk-2 computer, 25:29379
SHNYREV, G. D., Influence of beta-stabilizers on the strength and plasticity of titanium at low temperatures, 25:29844
SHOWALTER, J. G., Exchange excitation in He, 25:30285
SHREIBERG, G. L., Excretion of glucocorticoids and their metabolites in persons working with sources of ionizing radiation, 25:29708
SHTRANIKH, I. V., Inelastic neutron scattering by even-N Ge isotopes, 25:31244
SHTRUSNYI, Kh., Levels in ^{142}Nd, 25:31337
SHUBIN, A. P., Plasma flow followed by an injection of plasma through electrodes, 25:30344
SHUBNYI, Yu. K., Lifetimes of excited states of ^{140}Ce, 25:31319
SHUGART, Howard A., Nuclear spins of ^{125}Cs and ^{136}Cs, hyperfine-structure separation and nuclear magnetic moment of ^{125}Cs, ^{127}Cs, and ^{136}Cs, 25:31376
SHUKLA, J. P., Recovery of Pm from fission product waste. III, 25:29176 (BARC-516)
SHULMAN, Seth, Line emission in the x-ray background, 25:30140
SHULTZ, Richard Lewis, Phase equilibrium studies in ZrO_2 systems, 25:30008
SHUMEIKO, A. P., Internal bremsstrahlung following β decay of ^{114}In, 25:31318
SHURAVIN, V. N., Timing with Ge(Li)-detector, 25:29353 (JINR-P13-5706)
SHUSTER, E. R., Differential thermal analysis of boric acid, boric oxide, and potassium fluoborate, 25:29188
SHUSTER, M. D., Nonrelativistic hard-pion production and current-field algebra, 25:30898
SHUTILOVA, A. A., Organs and systems following radiotherapy of thyroid cancer, 25:29707
SIDES, W. H. Jr., MSBR control studies: analog simulation program, 25:31544 (ORNL-TM-3102)
SIEGEL, S., Bond lengths in gamma--uranium trioxide, 25:29094
SIGALOV, V. M., Interpretation of anomalous I/sup π/ = 7/2+ levels in nuclei with Z = 43, 45, 47, 25:31323
SIGG, P., Cyclotron beam pulser for particle time-of-flight experiments, 25:31116
SIKORA, W., Tables of magnetic structures determined by neutron diffraction. II, 25:30664 (NP-18783)
SIKORSKA, D., Polarized-neutron study of the $Ni_{0.968}V_{0.032}$ alloy, 25:30680
SILBERBERG, M., LMFBR aerosol research at Atomics International, 25:31616
SILIN, V. P., Temperature relaxation of plasma in hf electric and constant magnetic fields, 25:30545
SILK, Joseph, Diffuse cosmic x- and gamma radiation, 25:30332
SILSBEE, R. H., Prog. rpt. on solid state physics; magnetic phenomena, 1/--12/70, 25:30646 (NYO-2150-66)
SIMAN-TOV, M., Effect of iodine decay heat on charcoal adsorbers, 25:31669 (ORNL-4602)
SIMBEL, M. H., Determination of the optical potentials in terms of diffraction-model parameters, 25:31410
SIMON, F. O., Determination of platinum and palladium in geological materials by neutron-activation analysis after fire-assay preconcentration, 25:29022
SIMONOV, Yu. A., Hyperspherical-expansion approach to nuclear bound states. III, 25:31405
SIMONOVA, L. I., Internal conversion monoenergetic positron spectrum in $^{157}Gd(n,\gamma)^{158}Gd$ reaction, 25:31329
SIMONYAN, Kh. A., Effects of synchrotron radiation on the slow ejection of electrons from synchrotron, 25:31044 (NP-18780)
SIMPSON, J. A., Cosmic-ray ^2H from satellite measurements, 1965 to 1969, 25:30330
SIMPSON, O. D., Neutron filtered beams as standard sources, 25:31166 (CONF-710301-8)
SINAEV, A. N., Apparatus for the automatic accumulation (storage) and analysis of information in experiments with the synchrocyclotron, 25:31070
SINCLAIR, D. K., Feynman-parameter approach to N-tower exchange in phi^3 theory, 25:30987
SINGER, Sidney, Magnetospheric substorm of August 25--26, 1967, 25:30368
SINGH, B., Probability of production of internal bremsstrahlung accompanying β decay from ^{204}Tl, ^{147}Pm, and ^{45}Ca, 25:31363
SINGH, B. B., Reaction to thymine with radiation induced electrons in alcoholic matrices at 77°K, 25:29143
SINGH, Gurdev, Complexes of uranium(V) chloride with N donor ligands, 25:29092
SINGH, H., Phosphorescence of some deuterium-substituted phenylacetylenes, 25:29040
SINGH, K. P., Positron lifetimes in rare earth oxides, 25:30272
SINGH, Mangal, Complexes of uranium(V) chloride with N donor ligands, 25:29092
SINGH, Y., Generalizations of Jost--Pais theorem for nonlocal potentials, 25:31026
SINGHAL, L. K., Yield strength of dispersion hardened BCC materials, 25:29948
SINGHAL, Ravi Prakash, Elastic scattering of electrons from the oxygen isotopes, 25:31206 (SAL-17)
SINGRU, R. M., Positron lifetimes in rare earth oxides, 25:30272
SIPPEL, Walter, Investigations concerning the problem of radiation-cytostatic combination treatment. VIII, 25:29604
SIRAZHIDDINOV, N. A., Effects of neutron irradiation on phase transformations of Li_2O--MgO--Al_2O_3--SiO_2 systems, 25:30017
SIRCANA, S., High sensitivity berylometer, 25:29390 (RT/EL-(70)4)
SIRI, L. Nicola, Excitation functions for the nuclear reactions $^{159}Tb(d,p)^{160}Tb$ and $^{159}Tb(d,4n)^{157}Dy$, 25:31301 (CNEA-283)
SIVARAMAKRISHNAN, C. S., Structure of liquid cadmium--antimony alloys, 25:29896
SIVERS, Dennis, Characteristics of Regge trajectory with finite asymptotic phase, 25:31029
SIVKOV, Yu. P., Effects of synchrotron radiation on the slow ejection of electrons from synchrotron, 25:31044 (NP-18780)
Sextupole lenses with improved non-linearity in slow ejection systems, 25:31045 (NP-18759)
SIZONENKO, V. L., Turbulent heating of a plasma by a large amplitude whistler, 25:30470
SKALETSKAYA, N. A., Electronic properties of nonstoichiometric vanadium monocarbides, 25:30667
SKALKA, M., Labelling of heparin with ^{51}Cr, 25:29415
SKELLY, H. M., Zirconium-refractory alloys, 25:29969
SKELTON, D. E., Development aspects of fast metal-contact solid-dielectric switches, 25:30578 (EUR-4593, pp 365-71)
SKIRDA, V. I., Semiautomatic apparatus for regulating the neutron diffractometer, 25:29402
SKOBEEV, E. M., Action of vibration and x irradiation on maze habit in rats, 25:29666
SKOTNIKOVA, O. I., Radiosensitizing effect of ferrous ions, 25:29556
SKOVE, M. J., Fermi-surface topology changes in In alloys deduced from the behavior of T/sub c/ under strain, 25:30435
SKREBTSOV, G. P., Proton flux from 1.5 to 50 MeV on satellites Zond-4 and Zond-5, 25:30164
SKRIPIN, G. V., Antisymmetric diurnal and semidiurnal variations of cosmic rays, 25:30319
Effects of solar-activity cycle on irregularity of interplanetary magnetic field, 25:30326
SKURIKHINA, M. M., Postradiation changes in DNA synthesis in lymphoid organs of rats, 25:29672
SLAMA, G., Coating of Nb and Nb alloys with Al. I, 25:29816
SLANCAR, F., Influence of initial content of the cooling rate from the beta phase to preferred uranium orientation following heat treatment, 25:29884 (UJV-2525-M)
SLATER, C. E., Nodal sensitivity in modeling a large pressurized water reactor system for a loss-of-coolant

XUM

accident, 25:31592 (CONF-710302-8)
SLATTERY, P. W., Slip systems in VC--TiC alloys, 25:29999
SLAUGHTER, G. M., Advanced materials for steam generators, 25:29763 (ORNL-4630, pp 280-7)
Joining research on nuclear materials, 25:29825 (ORNL-4630, pp 261-70)
Properties of ferritic steel welds, 25:29822 (ORNL-4630, pp 139-44)
Welding development for FBR stainless steel components, 25:29785 (ORNL-4630, pp 111-38)
SLAUGHTERBECK, D. C., Correlations to predict maximum PWR containment pressures following a loss-of-coolant accident, 25:31593 (CONF-710302-9)
SLAVNOV, A. A., Anomalous ward identities in renormalized perturbation theory, 25:30935
SLEDZIEWSKI, Z., Tokamak facility of Fontenay-aux-Roses, 25:30583 (EUR-4593, pp 403-9)
SLEVIN, P. J., Optical and radio studies on extensive air showers, 25:30333
SLEZOV, V. V., Photoeffect in a superconductor in a weak electric field, 25:30417
SLOAN, Arthur W., Irradiated polyethylene, 25:29115
SLOZHENIKINA, L. V., Effects of ionizing radiation on lactate dehydrogenase in rats, 25:29670
SLYSH, V., OH emission from infrared objects at 1612 MHz, 25:30047
SMALC, Andrej, Description of the Institute and works performed during the summer of 1969, 25:31633 (IJS-253)
SMALL, Gary D., Prog. rpt. on effects of ultraviolet radiation on algae: mechanisms of inactivation and repair, annual, 5/70--4/71, 25:29713 (COO-1793-5)
SMEDILE, E., Ecological study of periphyton and identification of environmental radioactivity in a running-water ecosystem, 25:29478
SMERDOV, B. I., Turbulent heating of a plasma by a large amplitude whistler, 25:30470
SMIRNOV, Yu. F., Fractional parentage coefficients for (1d--2s)-shell nuclei, 25:31426
SMITH, A., Holmium-165 fast neutron cross sections, 25:31350
SMITH, C. B., Dispersion studies using stable and radioactive tracers in fresh water streams, 25:29213
SMITH, C. G., Design and performance of a compact multi-particle cyclotron, 25:31145
SMITH, C. H., Nuclear orientation of ^{142}Pr in praseodymium metal, 25:30662 (COO-1569-76)
SMITH, D. A., Elastic and inelastic scattering of 30 and 50 MeV polarized and unpolarized beams of protons by ^{40}Ar and ^{14}N, 25:31233
SMITH, David H., Mass spectrometric investigation of surface ionization. VIII, 25:30259
SMITH, G. D. W., Epitaxial growth of Ni on W, 25:29848
SMITH, Henrik, Comment on anomalous electron--phonon transport properties of impure metals, 25:30697 (NP-18822)
SMITH, J. R., Neutron filtered beams as standard sources, 25:31166 (CONF-710301-8)
Problems in assessing the correlation between the observed and predicted behaviour of models, 25:29308
SMITH, L., Negative mass instabilities in an electron-ring compressor, 25:31058 (UCRL-20208)
SMITH, L. L., Location in the magnetosphere of field lines leading to SAR arcs, 25:30376
SMITH, Morton C., Prog. rpt. on carbon and graphite, 8--10/70, 25:29920 (LA-4631)
SMITH, Myron A., Microturbulence and abundances in Am stars, 25:30038
SMITH, S. C., Thermal conductivity of superconducting niobium, 25:30434
SMITH, W. W., Fast-electron--slow-electron coincidence study of violent Ar^+--Ar collisions, 25:30288
SMOLIN, M. D., Electrotransport of Mo in Ni--18 at. percent Mo alloy, 25:29856
SMYTHE, Rodman, Fractional turn injector cyclotron, 25:31089
SNIATYCKI, Jedrzej, Some remarks on canonical formulation of field theory and its geometric structure, 25:30961
SNYDER, A. W., Laboratory simulation for TREE studies, 25:29410
SOBEL, M. I., Internal scattering amplitudes for bremsstrahlung, 25:31444
SOBOLEV, S. S., Collective processes and turbulent heating of a plasma, 25:30469
SOBOTTKA, S., EPICS: high-resolution pion beam and spectrometer facility for nuclear structure research, 25:31041 (LA-4534)
SOEHNGEN, Erich E., Investigation of plasmas at very high pressure, 25:30509
SOFFER, J., Lorentz analysis of dual-resonance models in operator formalism, 25:30829
SOFIENKO, L. A., Efficiency of radiators and absorbers of charged particles, 25:30641
SOFIEV, G. N., Low noise preamplifier employing field effect transistors, 25:29340
SOKOLOV, D. D., Topology of models of Universe, 25:30234
SOKOLOV, V. V., Absence of form factor in e^2 corrections to amplitudes of neutrino and electron scattering on nucleons, 25:30819
SOKUR, L. P., Equations of motion invariant under group P(1,n). II, 25:30966
SOKUROVA, E. N., Radiobiological characteristics of yeast cells, 25:29718
SOLACOLU, S., Thermal phase relations and dielectric properties in system La_2O_3--ZrO_2--TiO_2, 25:29984
SOLBRIG, C. W., Flow simulation through graphics: a high-speed interpretation of reactor blowdown calculations, 25:31588 (CONF-710302-4)
Idaho nuclear code automation: a standardized and modularized code structure, 25:31594 (CONF-710302-10)
SOLOMON, M., Effects of radiation on striated muscle, 25:29629
SOLOV'EV, S. P., Apparatus for studying the dynamics of condensed systems using a back-scattering method, 25:29362
SOLOVIEV, V. G., Non-rotational states of odd-mass nuclei in the actinide region, 25:31306 (JINR-P4-5693)
SOMASUNDARAM, R., Dislocation etch pits in alpha uranium, 25:29889
SOMES, Austin H., Diagnostics of a supersonic plasma stream using an immersed microwave probe, 25:30476 (N-71-10964)
SOMMERS, S. C., Effects of ionizing radiation upon endocrine glands, 25:29633
SONDEREGGER, P., Q spectrometer, 25:29373
SONETT, C. P., Magnetic observations of the lunar cavity, 25:30388
SOOD, N. K., Hydromagnetic oscillations of a self-gravitating fluid spheroid, 25:30102
SOOD, P. M., Spurious scattering in nuclear emulsions, 25:29378
SORANTIN, H., Production of radionuclides in Austria, 25:29274
SORENSEN, J. C., Dispersion studies using stable and radioactive tracers in fresh water streams, 25:29213
SOROKIN, O. M., Automatic amplitude spectrometer with a tracking sweep, 25:29367
SOROKO, L. M., Determination of Breit--Wigner resonance widths using Fourier algorithm, 25:30849 (JINR-P2-5659)
SOSNOVETS, E. N., Injection of energetic electrons into magnetosphere during magnetic storm, 25:30352
SOSNOWSKI, R., Conference on high multiplicity hadronic interactions, Paris, 5/70, 25:30762
Proton--proton and pion--proton inelastic collisions and electromagnetic form factors, 25:30977
SOUBELET, G. C., Distribution of fission products in a high temperature gas cooled reactor, 25:31567
SOUFFRIN, Suzy, Spectrophotometry of nucleus of NGC 2655 galaxy, 25:30194
SOULIER, Thermal shielding by wire gauze and metallic sheets, 25:29819 (EUR-4531, pp 1019-34)
SOUNDALGEKAR, V. M., Generalized MHD Couette flow with heat transfer between two porous walls under transverse magnetic field, 25:30342
SOYUMER, Tevfik, Type III solar radio bursts accompanied by soft x-radiation in the absence of Hα flares, 25:30167
SPALDING, I. J., Lasers and the reactor ignition problem, 25:30553 (CLM-R-109)
SPARKS, R. J., Decay of 3.696 MeV level in ^{25}Al, 25:31266
SPEAR, Karl E., Phase behavior of U--V--N system and properties of UVN_2, 25:29989
Phase investigations in U--Cr--N system, 25:29988
SPEAR, R. H., Energy levels of ^{27}Si, 25:31252
SPECTER, H., Correlations to predict maximum PWR containment pressures following a loss-of-coolant accident, 25:31593 (CONF-710302-9)
SPENCE, D., Vibrational excitation and compound states in NO, 25:30281
SPENCER, Derek W., Analytical methods in oceanography. I. Inorganic methods, 25:28921
SPENCER, Phillip C., Curing of coatings on wood products by electron beam, 25:29123
SPERBER, D., Angular distribution of particles evaporated in nuclear reactions, 25:31428
SPERBER, Daniel, Prog. rpt. on neutron and gamma emission from highly excited states and states with high spin, annual, 6/70--5/71, 25:31396 (RPI-3947-13)
SPITSYN, V. I., Effect of radiation on oxygen electrode performance, 25:29098
SPIVAKOVSKII, S. I., Program for processing photographs in bubble chamber filled with heavy liquid. I, 25:29369 (ITEF-753)
SPRETNAK, Joseph W., Evaluation of Gerard-Papirno characterization of notch ductility in steel, 25:31692 (COO-2048-2)
SPRING, E., Proceedings of the first Nordic meeting on medical and biological engineering, Otaniemi, Finland, 1/70, 25:29584
SPUR, G., Machining with a plasma jet, 25:31753 (UCRL-Trans-10524)
SRAPENIANTS, R. A., Gamma-irradiation apparatus for treatment of root- and tuber- crops, 25:29253
SREEKANTAN, B. V., Nucleon--antinucleon production in high-energy (> 10^{12} eV) hadron collisions, 25:30728
SRINIVASAN, V., Equal-time commutation relations in self-consistent quantum field theory, 25:30991
SRIVASTAVA, K. M., Stability condition of flute instability in an inhomogeneous plasma, 25:30548
SRIVASTAVA, R. K., Photoelectric elements of eclipsing binary ST Persei, 25:30113
STABROVSKII, A. I., Oxidation-reduction potential in solutions of salts of U and equilibrium concentration

XUM

of U ions, 25:29036
STAEHLE, Roger W., Advances in corrosion science and technology. I, 25:29778
STAFFORD, R. G., Improved light scattering photometer for air filtration system studies, 25:31702 (LA-4627)
STAGNI, L., Electron microscope observation of lattice disorder in ion-implanted silicon, 25:30650
STANBURY, John B., Double-isotope derivative assay of serum iodothyronines. II. Thyroxine, 25:28986
STANNETT, V. T., Fundamentals of radiation processing, 25:29122
STANSBURY, E. E., Prog. rpt. on application of adiabatic calorimetry of metal systems, 1969--70, 25:31716 (ORO-3291-14)
STARK, Klara I., Chromosomal examinations in radiologists, 25:29501
STAROSTIN, A. S., Methods for monitoring proton incidence on the internal targets of high-energy accelerators, 25:31043 (NP-18776)
Methods of monitoring proton discharge onto the internal target of a high-energy accelerator, 25:31064
STAROSTOV, B. I., Time--amplitude converter for the nanosecond range, 25:29341
STATSENKO, V. M., Electrotransport of Mo in Ni--18 at. percent Mo alloy, 25:29856
STAVINSKII, V. S., Statistical analysis of spectra of inelastically scattered neutrons, 25:31436
STECH, P., Circulating pumps for liquid-metal cooled reactors, 25:29257
STEEB, S., Diffusion investigations in system Pd--Ta, 25:29893
STEEB, Siegfried, Diffusion in system Nb--Pd, 25:29881
STEELE, T. W., Colorimetric determination of minor quantities of nitrate in uranium compounds, 25:28918 (NIM-951)
STEFANOU, G. D., Behavior of perforated end slabs for concrete pressure vessels, 25:29306
STEFANSSON, V., Conversion electron particle parameters of E2 transitions in ^{152}Sm and ^{156}Gd, 25:31380
STEHELIN, Liliane, Transannular hydride shifts. Mechanistic study in the longifolene series, 25:29050
STEINBACH, Karl Heinz, Dosimetry in bone marrow cavity of rat femurs following incorporation of ^{90}Sr--^{90}Y, 25:29524
STEINBERG, Meyer, Chemonuclear and radiation chemical processing fundamentals and present status of technology, 25:29125
STEINDLER, M. J., Sand-bed filtration of aerosols: a review of published information on their use in industrial and atomic energy facilities, 25:29315 (ANL-7683)
STEINHAUSEN, M., Radioisotopes to determine tubular passage time in dog kidneys, 25:29414
STEINITZ, Raphael, Period of γ Equ, 25:30048
STEINMETZ, L. L., Laser beam filtering by saturable dyes, 25:31747 (UCRL-51008)
STEINNES, E., Comparative study on Al determination in ammonium acetate soil extracts by spectrophotometry, activation analysis, and atomic absorption, 25:29020
STELJES, J. F., Cosmic ray NM-64 neutron monitor data. XVII, 25:30303 (AECL-3856)
STELSON, P. H., E2/M1 admixture of the 2' → 2 transition in ^{108}Pd, 25:31374
STENFLO, L., Equilibrium states of interacting waves, 25:30627
STEPANOV, K. N., Turbulent heating of a plasma by a large amplitude whistler, 25:30470
STEPHENS, F. S., Lifetimes of ground-band states in ^{148} ^{150} ^{152}Sm, 25:31364
STEPHENS, J. R., Alloy softening in Group VIA metals alloyed with Re, 25:29871
STEPHENSON, Donald A., Multivariable analysis of quantitative x-ray emission data. The system zirconium oxide--aluminum oxide--silicon oxide-calcium oxide--cerium oxide, 25:28957
STERLIGOV, A. G., Operation of a spark chamber at a high count rate, 25:29375
STERN, K., Experimental models for evaluation of host defenses in cancer, 25:29472
STERNHEIMER, R. M., General expression for the density effect for the ionization loss of charged particles, 25:30643
STESHENKO, A. I., Dimensions and form of the light nuclei with the surplus of neutrons, 25:31238 (ITF-70-83-E)
STEVENS, D. W., Irradiation behavior of isotropic carbons, 25:30015
STEVENS, Dennis W., Apparatus for blending particles, 25:29254
STEVENSON, D. J., Fast correlation method for studying drifting patterns associated with ionospheric irregularities, 25:30402
STEWART, F. R., Non-intercepting cyclotron beam monitor, 25:31127
Phase--space volume measurements on Nuffield 60 in cyclotron, 25:31117
STEWART, T. E., Vacuum-ultraviolet emission from proton-excited helium gas, 25:30284
STEWART, V. J., Code of design for research apparatus containing molten sodium, 25:29252 (RD/B/M-1817)
STEWART, William D., Irradiated polyethylene, 25:29115
STICKELMANN, C., Coaxial high-power trigatron for 60 kV, 25:30579 (EUR-4593, pp 373-8)
STILINOVIC, L., Fate of ^{65}Zn in human serum proteins, 25:29447
STILLMAN, W. E., TRANS: a one-dimensional FORTRAN IV program for computing the time response of fuel rods to a loading-unloading environment, 25:31670 (ORNL-TM-3293)
STILLWELL, E. P., Fermi-surface topology changes in In alloys deduced from the behavior of T/sub c/ under strain, 25:30435
STIPP, H. J., Circulating pumps for liquid-metal cooled reactors, 25:29257
STJERNVALL, L., Pilocarpine in scintillography of sialopathies, 25:29579
STOCH, H., Colorimetric determination of minor quantities of nitrate in uranium compounds, 25:28918 (NIM-951)
STOCKDALE, Frank E., DNA synthesis in differentiating skeletal muscle cells, 25:29650
STOCKER, W., Nuclear surface properties and the nuclear compressibility in a statistical approximation, 25:31445
STOCKMEYER, R., Scattering of slow neutrons by orthohydrogen in cubic phase, 25:31169 (JUL-724-FF)
STOECKLI, H. F., Quantum mechanics and the gravitational red shift, 25:30963
STOLOFF, Norman S., Prog. rpt. on precipitation and dispersion hardening in HCP alloys, annual, 3/1/71, 25:29827 (RPI-3719-9)
STOLYAROV, O. A., Internal conversion monoenergetic positron spectrum in ^{157}Gd(n,γ)^{158}Gd reaction, 25:31329
STONE, A. J., MOSSPEC: program for resolving Moessbauer spectra, 25:30688 (RISO-M-1348)
STONE, Nelson H., Multiple basal cell carcinomas arising in radiated burn scars, 25:29701
STONE, S. H., Selective and specific inhibition of 24 hour skin reactions in the guinea-pig. III, 25:29474
STONEHAM, T. A., Precise measurements of W, the mean energy required for ion-pair formation in gases. I. Alkanes, 25:30636
STORER, R. G., Non-local potentials and the single-particle shell model, 25:31447
STORHOK, V. W., Thermal diffusivity measurements of irradiated oxide fuels (LWBR Development Program), 25:29937 (BMI-X-10274)
STORIZHKO, V. E., Gamma rays from ^{64} ^{66} ^{68}Zn(p,γ)^{65} ^{67} ^{69}Ga, 25:31249
Inelastic scattering of protons by ^{50}Cr, ^{52}Cr, ^{54}Cr, and ^{64}Zn, 25:31253
STOTLAND, M. A., Experimental installation R-Ohm for studying high-frequency field-interaction with plasma, 25:30508 (NP-18801)
Studies of diffusion of dense disintegrating plasma in a stellarator, 25:30462 (NP-18767)
STOUT, Glenn E., Vertical distribution of tritium in water vapor in the lower troposphere, 25:29215
STOUTE, J. R. D., Behavior of fission product aerosols in relation to the safety of sodium cooled fast breeder reactors, 25:31618
STOVER, Betsy J., Protracted hepatic, splenic, and renal retention of ^{239}Pu in the beagle, 25:29451
STOYANOV, D. Ts., Retarded part of two-time Green function and two-body relativistic problem, 25:31014 (JINR-E2-5746)
STOZHAROV, V. M., Average energy of electrons scattered inelastically from solids, 25:30260
STOZHKOV, Yu. I., Energy spectra of 11-year variations of cosmic-ray intensities on the rising solar-activity curve, 25:30310
Role of heliographic latitude of spots in 11-year modulation of galactic cosmic rays, 25:30309
STRATHDEE, J., Infinity suppression in gravity-modified quantum electrodynamics, 25:30994
STRAUSS, H. W., Pinhole scintillation camera and /sup 99m/Tc-pertechnetate in normal thyroid scanning, 25:29586
STRAZHEVSKAYA, N. B., Radiation effect on chromatin deoxyribonucleoprotein, 25:29458
STREATER, R. F., Continuous tensor products of group representations, 25:30947
Introduction to the Heisenberg ferromagnet, 25:30946
STREDA, A., Five year's experience with isotopic investigations of diseased joints, 25:29576
STREITWIESER, A. Jr., Proton magnetic resonance shifts in bis(cyclooctatetraenyl) U(IV), 25:29085
STRELKOV, R. B., Protective influence of adrenalin and acetylcholine in radiation sickness of mice, 25:29548
STREL'TSOV, V. N., Invariance of the nonrelativistic wave equations in the presence of electromagnetic field, 25:30775 (JINR-P2-5522)
STRIKE, Thomas A., Effectiveness of pressor drugs in beagles exposed to mixed gamma-neutron radiations, 25:29565
STRITTMATTER, P. A., Rotational velocities of G and K giants in Hyades moving group, 25:30046
STRIZH, T. A., Determination of Breit--Wigner resonance widths using Fourier algorithm, 25:30849 (JINR-P2-5659)
STRIZHAK, V. I., Pulsed neutron source, 25:31178
STRNAT, K., Sintering of $PrCo_5$ permanent magnets, 25:29797
STROFFOLINI, R., S-matrix for singular potentials, 25:31021

XUM

STROM, K. M., Circumstellar shells in the young cluster NGC 2264, 25:30065
STROM, S. E., Circumstellar shells in the young cluster NGC 2264, 25:30065
STRUB, R., Observation of d* effect in anti pd + p anti p π^+ π^-n reaction at 5.55 GeV/c, 25:30727 (NP-18796)
STRUKOV, I., OH emission from infrared objects at 1612 MHz, 25:30047
STUART, Frank E., Automated and conventional photometry of the short-period variable star 14 Aurigae, 25:30086
STULIK, Karel, Amperometric, conductometric, chelatometric titration, 25:28970
STURDE, Hans-Carl, Experimental studies of radiation protection through tryptamine, 25:29566
STURROCK, P. A., Particle flux associated with stochastic processes, 25:30518 (N-71-11853)
STUY, Johan H., Prog. rpt. on all response to nucleic acid penetration, 8/69--9/70, 25:31738 (TID-25694)
STYRO, B. I., Removal parameters of radon and thoron decay products from air, 25:29217
SUBOTOWICZ, M., β--γ angular correlation measurements, 25:31277
Highly retarded allowed beta transitions, 25:31397
SUDAN, R. N., Nonlinear Landau damping of electromagnetic cyclotron waves, 25:30615
SUESS, R., Erosion in high-current, high-pressure gas discharges, 25:30495 (EUR-4593, pp 251-6)
Fast storage system for a 500-kV theta-pinch experiment, 25:30567 (EUR-4593, pp 265-71)
High-power spark gap for high repetition rates, 25:30568 (EUR-4593, pp 273-80)
SUGAI, H., Space-charge waves on plasma columns in a weak magnetic field, 25:30618
SUGARMAN, Nathan, Mass yield and charge distribution in 450 MeV proton fission of ^{238}U, 25:31302 (COO-1167-10)
SUGATA, Eizi, Growth of Pt crystals on W surface, 25:29850
SUITA, T., Ion source using a beam--plasma interaction, 25:30255 (EUR-4593, pp 67-74)
SULABERITSZE, G. A., Mass-diffusion mercury columns for isotope separation, 25:29277
SULEIMANOVA, N. L., Radiobiological effect on mineral nutrition of the sunflower, 25:29714
Radiobiological effect on time between irradiation and planting of sunflower, 25:29717
SULKIN, A. G., Irradiation head for beam therapy, 25:29258
SULLIVAN, J. D., Analyticity of a scattering amplitude in an external-mass variable, 25:31030
SULLIVAN III, W. T., Interferometer map of the water-vapor sources in W49, 25:30141
SUMI, Y., Breakdown of Pomeranchuk theorem and Regge dipole with finite cross-section, 25:30828
SUMMER, George K., Improved method for hydroxyproline analysis in tissue hydrolyzates, 25:28995
SUNYAEV, R. A., Nuclei of galaxies and quasars as infrared sources, 25:30247
SUPEK, Z., Radioprotective activity of some sulphur analogues of tryptophol and 5-hydroxytryptamine, 25:29567
SURKOV, E. L., Hyperspherical-expansion approach to nuclear bound states. III, 25:31405
SURKOVA, I. V., Inelastic neutron scattering by even-N Ge isotopes, 25:31244
SUSLOV, Yu. P., Probability ratio for K and L capture, 25:31401
SUTEU, Al., Colorimetric determination of uranium, 25:28971
SUTO, Hajime, Factors affecting the high temperature strength of Ni--Cr and Ni--W alloys, 25:29878
SUTORMIN, A. I., Photomultiplier impulse shaper with stable time delay, 25:29347
SUTTON, A., Excretion and retention of stable strontium in children, 25:29442
SUWA, Emiko, Gamma--gamma perturbed angular correlations in ^{154}Gd, 25:31344
SUYDAM, B. R., Light scattering from aerosols, 25:31703 (LA-4641)
Scattering of light from a stratified sphere, 25:31704 (LA-4642)
SUZUKI, Atsuyuki, Maximizing the average fuel burnup over entire core: a poison management optimization problem for multizone light-water reactor cores, 25:31584
SUZUKI, M., Mutual solubility and preparation of uranium--cerium carbo-nitride, 25:30003
Transformations to a rotating frame, 25:30976
SUZUKI, Mahiko, Lower bound on W*--meson production in high-energy proton--proton collisions, 25:30907
SVATOS, J., Polarization from a circular dielectric infinite cylinder at oblique incidence, 25:30213
SVENSSON, P., Experiences on the release of iodine from uranium dioxide fuel, 25:31607
SVERDLOV, A. G., Protection of dogs from ionizing radiation by shielding bone marrow, 25:29658
Protective efficiency of radioprotectors, 25:29650
SVETLICHNAYA, N. A., Determination of absolute age of Lake Balkhash on the basis of nonequilibrium U, 25:29210
SVISTUNOVA, T. V., Influence of Cr and Mo on electrochemical and corrosion resistance of Ni--Cr--Mo alloys, 25:29777
SWAMI, S. P., Weakened field equations, 25:30999
SWANHOLM, Carl E., Curing of coatings on wood products by electron beam, 25:29123
SWENSSON, J. W., Solar spectrum from lambda 7498 to lambda 12016, 25:30172
SWIFT-HOOK, D. T., Spherical probe in a flowing plasma, 25:30482
SWINDLE, D. L., Decay of /sup 106m/Rh, 25:31384
SWITZER, Boyd R., Improved method for hydroxyproline analysis in tissue hydrolyzates, 25:28995
SYKORA, J., Use of existing corona measurements, 25:30182
SYMONS, G. D., Angular correlation of ^{42}Ca(α,pγ)^{45}Sc, 25:31251
Extrapolation of ^{12}C + ^{12}C and ^{12}C + ^{16}O reaction cross sections to astrophysical energies, 25:31260 (ANU-P-515)
SYMONS, M. C. R., Possible electron spin resonance identification of Br^{2-} and I^{2-} in γ-irradiated bromide or iodide doped Ba sulfate, 25:29163
SYTIN, A. N., Switch for reading out information from counters to a digital printer, 25:29345
SZABO, Zs., Spectrochemical analysis of hard metals by a rotating disc solution technique, 25:28944
SZARVAS, P., Development of drilled electrodes of synthetic materials and their use for determination of rare earth oxide traces in rare earths, 25:28948
SZENTAGOTHAI, J., Growth and differentiation of synaptic structures under circumstances of deprivation of function and of distant connections, 25:29623
SZERSZEN, Leszek, Profile distribution of ^{90}Sr in soils of Lower Silesia, 25:29207
SZILVASSY-VAMOS, Zs., Investigation of the detection limits of iodine with the hollow cathode lamp, 25:28951
SZNAJDER, N., Asymptotic condition in the Zachariasen-Thirring, 25:30943
SZOPORY, B., Spectral analytical determination of tellurium traces in cast iron, 25:28943

T

TABATA, Yoneho, Electron spin resonance studies on radiation-induced solid state polymerization of methyl methacrylate, 25:29117
Electron spin resonance studies on radiation-induced solid state polymerization of acrylonitrile, 25:29118
Gamma-initiated solid state polymerization of tetrafluoroethylene, 25:29112
Radioinduced copolymerization of tetrafluoroethylene with ethylene in gas phase, 25:29130
TACHON, J., Bounce effects in the negative mass instability, 25:30551
TADEMARU, E., Formation of energy spectra in synchrotron sources, 25:30146
Particle flux associated with stochastic processes, 25:30518 (N-71-11853)
TADIC, Dubravko, Presence of noncanceling seagull and Schwinger terms in weak (nucleon + nucleon + vector-meson) amplitudes, 25:30931
TAHERZADEH, Mojtaba, Neutron yield from the (α,n) reaction in the isotope ^{18}O, 25:31224
TAINO, M., Operation characteristics of 75 cm hydrogen bubble chamber and the refrigerator. I, 25:29372 (SJC-T-71-1)
TAJIMA, Eisaku, Simultaneous determination of chlorine, bromine, and iodine in sedimentary rocks by neutron activation, 25:29033
TAKAHASHI, K., Decay of /sup 106m/Rh, 25:31384
TAKAHASHI, Toshimasa, Process for producing thermoplastic resin foam, 25:29109
TAKAO, Kazuaki, Solar x-ray radiation as observed by real time telemetry from Solrad satellites, 25:30355
TAKASAKI, Fumihiko, Negative pion photoproduction off neutron at 180° in energy range between 300 and 1200 MeV, 25:30774 (INSJ-126)
TAKASHIMA, Shiro, Studies on ion-exchange transfer. XIX, 25:29193
TAKATSUJI, Kazuhiko, Extraction of Eu with di(2-ethylhexyl) phosphoric acid, 25:29185
TAKEDA, Gyo, Low-energy theorems for nuclear weak and electromagnetic currents, 25:30807
TAKEDA, S., Crowbar gap switch with two triggering pulses, 25:30576 (EUR-4593, pp 347-53)
TAKEDA, Shigeru, Control system of IPCR 160 cm cyclotron, 25:31068
TAKEHISA, Masaaki, Radiation-induced sulfoxidation and sulfochlorination of powdery polyethylene produced by radiation process, 25:29107
TAKESHITA, T., Verification of classical, self-consistent theory of particle loss in hot electron, magnetic mirror compression experiment, 25:30465
TAKIMOTO, H. H., Corrosion of Ti-6A-4V in HCl-methanol, 25:29773
TAKTAKISHVILI, M. I., Drift-beam instability and ion sound in an inhomogeneous plasma, 25:30506 (MATT-Trans-84)
Electron-ion beam instability, 25:30505 (MATT-Trans-83)
TALIEV, A. V., Application of the method of reduced costs to estimates of the effectiveness of utilization of nuclear fuel, 25:31585
TALIPOV, Sh. T., Fluorescence determination of copper, 25:28928
TAM, Christopher K. W., Interaction of homogeneous wave turbulence and MHD tangential discontinuity, 25:30391
TAMAGUSUKU, Susumu, Sintering process of Ni--P alloy coated W, 25:29793

XUM

TAMURA, Kimiko, Improvement in isotopic ratio measurement of uranium, 25:28927
TAMURA, Naoyuki, Gamma-initiated solid state polymerization of tetrafluoroethylene, 25:29112
TAMURA, Syuzo, Improvement in isotopic ratio measurement of uranium, 25:28927
TAMURA, Yoshio, Rolling workability of pure W single crystals, 25:29877
TANABE, J. T., Cryogenic pumping system proposed for Bevatron, 25:31057 (UCRL-20197)
TANABE, Jack T., Ultra-narrow, high-quality, high-field quadrupole magnet, 25:31051 (UCRL-20164)
TANABE, Masato, Microbial oxidation of p-diethylbenzene, 25:29061
TANAKA, Jiro, Field measuring system of drift tube quadrupole magnets, 25:31047 (SJC-A-71-1)
TANAKA, K., Mutual solubility and preparation of uranium--cerium carbo-nitride, 25:30003
TANANAIKO, M. M., Diantipyrinylmethane pyrocatecholate complex of molybdenum and its analytical application, 25:28926
TANDON, S. N., Liquid--liquid extraction behavior of mercury(II) as chloride, 25:29031
TANG, I-Ming, Addendum to the theory of ultrasonic attenuation in pure two-band superconductors in high fields, 25:30423
TANG, S. Y., Semi-empirical model for Penning and associative ionization, 25:30298
TANIFUJI, Takaaki, Release of fission Cs from irradiated UO_2 powder, 25:29974
TARANTIN, V. D., System for the automatic indication of impurities in sodium coolants, 25:29261
TARAS, P., Gamma-ray linear polarization and angular distribution formulas, 25:31420
TARASOV, A. V., Deduction of the Glauber formula from the Watson theory, 25:31434
TARASOVA, N. M., Initial stage of a light explosion of a particle of matter in a powerful light beam, 25:30471
TARKIAINEN, E., Pilocarpine in scintillography of sialopathies, 25:29579
TARKKANEN, J., Pilocarpine in scintillography of sialopathies, 25:29579
TARRAGO, X., Cross sections for heavy ion nuclear reactions, 25:31356
TARRONI, G., Sampling methods for aerosol particles, 25:29263
TARSKI, Jan, Remarks on representations of canonical commutation relations, 25:30948
TATE, L. A., Interaction between the design and construction of prestressed concrete pressure vessels for nuclear reactors, 25:31456 (EUR-4531, pp 129-44)
TATENO, H., Operation characteristics of 75 cm hydrogen bubble chamber and the refrigerator. I, 25:29372 (SJC-T-71-1)
TATSUNO, Ikuro, Effect of Tanderil on radiation induced inflammation, 25:29549
TATU, V. S., Isotopic shifts for the isobaric pairs, 25:31404
TAUB, H., Study of the transverse magnetoresistance of polycrystalline potassium, 25:31707 (NYO-2150-68)
TAVERNIER, Michel, Electron capture disintegration of ^{230}Pa, 25:31339
TAY, E. S., Conditions for the control of beam intensity and cluster size in hydrogen cluster beams, 25:30252 (EUR-4593, pp 43-9)
  Ionization and acceleration of hydrogen clusters, 25:30253 (EUR-4593, pp 51-8)
TAYLOR, B. N., Some toxicity aspects of internally deposited ^{239}Pu, 25:29627
TAYLOR, Clement R., Curing of coatings on wood products by electron beam, 25:29123
TAYLOR, E. A., Mediterranean fruit fly suppression using the sterility principle: prospects and programs, 25:29738
TAYLOR, G. R., Radiochemical determination of barium diffusion coefficients in liquid sodium, 25:31613
TAYLOR, J. G., Omega-meson in rho--w system, 25:30858
TAYLOR, J. G. V., Users' guides for radioactivity standards, 25:29174
TAYLOR, R., Trapping of methyl iodide at high pressure and high temperature, 25:31611
TAYLOR, R. E., Thermophysical properties of ATJS graphite at high temperatures, 25:29972
TEN, Yu., Studies of diffusion of dense disintegrating plasma in a stellarator, 25:30462 (NP-18767)
TEPLITZ, Vigdor L., Conserved currents, Reggeization, and Mandelstam counting in second-order perturbation theory, 25:30992
TEPLOV, E. V., Program linking FSD measuring microscopes with a Minsk-2 computer, 25:29379
TEPLYAKOV, V. A., Possibility of reducing the injection energy and increasing the limit current in an ion linear accelerator, 25:31052
TEREBIZH, V. Yu., Division processes and instability of systems of galaxies, 25:30197
TERESHCHENKO, O. Ya., Postradiation changes in DNA synthesis in lymphoid organs of rats, 25:29672
TERRASI, F., Investigation of reaction $^{35}Cl(n,\gamma)^{36}Cl$, 25:31280
TERRY, M. J., Plasma heating by neutral injection in a stellarator reactor, 25:30455 (EUR-4593, pp 479-84)
TESCH, K., Accuracy of photon-difference method used in high-energy photonuclear experiments, 25:30773 (DESY-71/3)
TESEI, A., Semi-group approach to quantum field equations, 25:30972
TESHIMA, R., Regge trajectories for multichannel potential scattering, 25:31031
TESKE, Richard G., Type III solar radio bursts accompanied by soft x-radiation in the absence of Hα flares, 25:30167
TESSMER, C. F., Radiation effects in skin, 25:29628
TESTA, M., Broken scale invariance, $U_3 \times U_3$ breaking and hadron Lagrangian structure, 25:30927
TEVZADZE, G. A., Mass-diffusion mercury columns for isotope separation, 25:29277
THAL, M. F., Trapping of iodine and methyl iodide at high temperatures, 25:31612
THAMPY, R. T., Effect of γ-irradiation on chlorendic acid based unsaturated polyesters, 25:29129
THENTE, Bo, Effects of toluene and radiation on urease in soil, 25:29460
THEOPHILOU, A., Effect of atomic cores on electron tunnelling through dielectric layers, 25:30678
THEPAULT, E., Microwave devices using the proximity effect between superconducting and normal metals, 25:30446
THEUNISSEN, J., Radiation pathology in Hylemya antiqua, 25:29619
THIELHEIM, K. O., Information on high energy hadronic interactions from cosmic ray air showers, 25:30839
THIESSEN, H. A., EPICS: high-resolution pion beam and spectrometer facility for nuclear structure research, 25:31041 (LA-4534)
THIMMEL, H., Beam extraction at Juelich 90 MeV deuteron AEG isochronous cyclotron, 25:31102
THIRING, Walter, Mathematical structure of the BCS model for finite temperatures, 25:30949
THOLFSEN, Paul, Stability of supercurrents in flat films of tin, 25:30437
THOMA, George E., Radiation and leukemia rates, 25:29705
THOMAS, Gareth, Electron microscopy investigations of ferrous martensites, 25:31743 (UCRL-19648)
THOMAS, J. L., Dynamic polarization measurements in polyhydric alcohols doped with their Cr(V) at approx. 1°K and at 3 kG magnetic fields, 25:31046 (RHEL/R-213)
THOMAS, K., Direct and compound processes to the reaction $^{40}Ca(d,\alpha)^{38}K$ at E/sub d/ = 5 to 10 MeV, 25:31275
THOMAS, R., Square wave rf system design for TRIUMF cyclotron, 25:31091
THOMAS, R. G., Relative hazards for inhaled ^{95}Zr and ^{95}Nb particles formed under various thermal conditions, 25:29423 (LF-43, pp 59-65)
  Retention and distribution of ^{244}Cm following inhalation of $^{244}CmCl_3$ and $^{244}CmO_1$ ₇ by beagle dogs, 25:29429 (LF-43, pp 100-5)
  Retention of relatively insoluble substances following inhalation, 25:29422 (LF-43, pp 53-8)
  Retention patterns of ^{125}Sb in mice following inhalation of particles formed at different temperatures, 25:29424 (LF-43, pp 66-70)
THOMAS, R. L., Effect of the inhalation of ^{144}Ce in relatively insoluble forms on influenza virus infection in mice, 25:29724 (LF-43, pp 254-62)
THOMAS, Randi L., Preparation of aerosols of thulium and americium by thermal degradation, 25:29078 (LF-43, pp 25-30)
  Retention of ^{171}Tm following inhalation of oxide by beagle dogs, 25:29425 (LF-43, pp 71-8)
THOMAS, Roger Jerry, Solar soft x radiation, 25:30160
THOME, P., Test of ring of prestressed concrete in high-resistance sheet-metal steel, 25:30028 (EUR-4531, pp 445-76)
THOMPSON, E., Production of high-current, high-quality beams of ions and neutral particles, 25:30256 (EUR-4593, pp 75-81)
THOMPSON, J. B., Ultrasonic level monitor, 25:29393 (IN-1452)
THOMPSON, Max F., Neutron activation analysis technique for nail sodium concentration in cystic fibrosis patients, 25:29016
THOMPSON, R. G., Effects of high energy radiation on pulping of Eucalypts, 25:29735
THOMPSON, Richard H., Relativistic calculation of nucleon--nucleon phase parameters, 25:30912
  Validity of a local approximation to the one-pion-exchange potential for the two-nucleon system, 25:30911
THOMPSON, William B., Scattering from magnetic fluctuations, 25:30490
THOMSON, G. M., Fast-electron--slow-electron coincidence study of violent Ar^+--Ar collisions, 25:30288
THUM, C., Why pulsars are pulsing, 25:30052
THURMAN, Gary Boyd, Growth dynamics of osteosarcomas in beagles, 25:29621 (COO-119-243)
THURNHER, K., 300 MW thorium high-temperature power plant (THTR), 25:31539
TIBALDI, E., Ecological study of periphyton and identification of environmental radioactivity in a running-water ecosystem, 25:29478
TIETZE, K., Differential cross section of deuteron photodisintegration between 20 and 35 MeV, 25:31194
TIKHONCHUK, V. T., Temperature relaxation of plasma in hf electric and constant magnetic fields, 25:30545

XUM

TIKKANEN, M. H., Sintering kinetics of nickel activated tungsten, 25:29791
Wetting problems in connection with sintering, 25:29954
TILLMAN, J., ANNLIS: computer program for automatic analysis of gamma-ray spectra, 25:29354 (LUNP-7101)
TIMSIT, R. S., Determination of polarization of ^{3}He by optical methods, 25:31074
Experiment to compress polarized ^{3}He gas, 25:31077
Helium-4 discharge light source and system for optical pumping of 2^3S_1 ^{3}He, 25:31076
Nuclear relaxation of ^{3}He gas on various solid surfaces, 25:31072
Performance of optical pumping light source and kinetics of pumping of 2^3S_1 ^{3}He, 25:31075
Polarizations produced and rates of polarization in optical pumping of 2^3S_1 ^{3}He, 25:31073
TING, Cheng Teh, Energetic substitution reactions of tritium atoms from nuclear recoil, 25:29167
TIRSELL, K. G., Levels of ^{246}Cm from the β^--decay sequence ^{246}Pu(11 days) /sup 246m/Am(25 min)^{246}Cm, 25:31378
TITOV, A. V., Minimum dose of 5-methoxytryptamine influencing the accumulation of cystamine in tissues and its excretion with urine, 25:29554
TKACHEVA, G. A., Changes in adrenal glad after irradiation of head, 25:29671
TLALKA, R., Experience with spectral analysis of nuclear materials with the laser microprobe, 25:28949
TOBIN, J. M., Growth of transition metal carbide single crystals by recrystallization. II, 25:29927
Growth of transition metal carbide single crystals by recrystallization. I, 25:29926
TOBOCMAN, W., Comparison of the R-matrix nuclear reaction theories, 25:31442
TODOROV, G. G., Nephrography with aid of ^{51}Cr-EDTA and ^{58}Co-DTPA, 25:29577
TODOROV, I. T., TCP, spin, and statistics, and consistency problems for infinite-component fields, 25:30950
TOGANO, Kazumasa, Fiber textures and morphology of dendrite in ingots of Zn and Zn--1.5 percent Cd alloy, 25:29892
TOI, Kazuo, Review of USSR Tokamak experiments, 25:30596 (JAERI-Memo-4286)
TOJO, Takao, Measurement of Doppler broadening of gamma-ray energy, 25:31208
TOKARSKAYA, V. I., Modification of radiation damage to structure of DNA from embryos of seeds with homologous DNA, 25:29716
TOKHIYAN, S. R., Bioelectrical reactions of the brain cortex to irradiation, 25:29688
TOLCHENOVA, G. A., Protein fractions of intestine and brain of irradiated animals, 25:29664
TOLKENDORF, E., Irradiation of T2r-bacteriophages in T2-buffer in the absence and presence of cysteine by roentgen radiation, 25:29728
Radiation biophysical investigations in Drosophila melanogaster. II, 25:29499
TOLLIN, Gordon, Chlorophyll one-electron photochemistry: flash photolysis studies of the chlorophyll--quinone reaction in alcohol solvents, 25:31687 (COO-908-34)
TOLMACHEV, V., Hartree--Fock approximation in quantum electrodynamics, 25:30989
TOLMACHEVA, V. G., Operation of a spark chamber at a high count rate, 25:29375
TOLNAS, E. L., Preliminary investigation of ohmically-heated plasmas in the model ST Tokamak, 25:30459 (MATT-813)
TOLOK, V. T., High frequency heating of a plasma, 25:30460 (MATT-Trans-13)
TOLSTOI, V. N., Fractional parentage coefficients for (1d--2s)-shell nuclei, 25:31426
TOLSTOPYATOVA, A. A., Properties of rare-earth metals (Sc, Nd), their hydrides, carbides, and oxides, 25:29859
TOM, J. L., Design and performance of a compact multi-particle cyclotron, 25:31145
TOMINAGA, Hiroshi, On-line data processing in activation analysis, 25:29027
TOMINGAS, R., Elimination and metabolism of benzo(a)pyrene after intratracheal injection, 25:31715 (ORNL-tr-2469)
TOMIZUKA, C. T., Wire-cutting tool for use with a spark cutter, 25:31689 (COO-1041-19)
X-ray slit system for crystals with small angle boundaries, 25:31688 (COO-1041-18)
TOMLINSON, Richard G., Plasma expansion under heating by a CO_2 laser pulse, 25:30542
TOMOZAWA, Yukio, Intermediate W bosons, gauge fields, and the nonleptonic weak decays, 25:30810
TOMPKINS, Edythalena, Radiation and leukemia rates, 25:29705
TONE, Tatsuzo, Multi-group constants for fission product nuclides, 25:31304 (JAERI-Memo-4251)
TONUMA, T., Heavy ion acceleration in IPCR 160 cm cyclotron, 25:31135
TONWAR, S. C., Nucleon--antinucleon production in high-energy (> 10^{12} eV) hadron collisions, 25:30728
TOPERVERG, B. P., Depolarization of neutrons transmitted by magnetic materials, 25:31181
TOPSCHOWSKY, M., Determination of population densities in a helium plasma by electron impact spectroscopy, 25:30481
TORIMOTO, Keizo, Radicals produced in γ-irradiated allyl alcohol glass, 25:29162
TOROSSIAN, A., Tokamak facility of Fontenay-aux-Roses, 25:30583 (EUR-4593, pp 403-9)
TORTSCHANOFF, T., Production of isotopically pure targets in electromagnetic mass separators by ion-beam retardation, 25:31069
TOTH, L. M., Coordination effects on the spectrum of uranium(IV) in molten fluorides, 25:29093
TOTH, M., Problems in the quantitative spectral analysis of rare earth metal traces. II, 25:28946
TOTH, Z., Radioisotope scintiscanning in the diagnostics of gallbladder diseases, 25:29575
TOTON, E. T., Pulsar electrodynamics, 25:30154
TOUATI, Alain, Electron capture disintegration of ^{230}Pa, 25:31339
TOVEY, N., Compilation of cross sections. VI, 25:30735 (CERN-HERA-70-7)
TOWNSEND, John R., Prog. rpt. on radiation induced defects in metals, annual, 12/69--11/70, 25:29903 (NYO-3653-5)
TOWNSEND, P. D., Defect formation and sputtering of alkali halides with low energy irradiation, 25:30651
TRABERT, Kenneth, Presence of noncanceling seagull and Schwinger terms in weak (nucleon + nucleon + vector-meson) amplitudes, 25:30931
TRANIS, A., Taming the wild ferrite, 25:31035 (BNL-15722)
TRAN MINH DUC, Mean recoil, isomer ratio, and excitation functions for reactions induced by alpha particles in rubidium, 25:31239 (LYCEN-7091)
Reactions induced in gold by deuterons with energies between 10 and 70 MeV, 25:31311 (LYCEN-7092)
TRANSKII, I. A., Cosmic-ray flux in interplanetary media. I, 25:30314
Cosmic-ray flux in interplanetary media. II, 25:30315
TRAUZEDDEL, R., Isotope effects in autoxidation. X, 25:29059
TREBENOK, Z. A., Manganese penetration of mitochondrial membranes after influence of ionizing radiation, 25:29673
TREBUKHOVSKII, V. V., Mass-spectrometric measurements of the diminution of hydrogen in polyethylene targets which have been irradiated in a proton synchrotron, 25:29400
TREBUKHOVSKII, Yu. V., Program for processing photographs in bubble chamber filled with heavy liquid. I, 25:29369 (ITEF-753)
TRECKER, D. J., Convertible polymers for radiation processing, 25:29124
TREFIL, J. S., Expectations for particle--nucleus cross sections at very high energies and the hadron mass spectrum, 25:30905
TREHAN, S. K., Hydromagnetic oscillations of a self-gravitating fluid spheroid, 25:30102
TREIGER, S. I., Discrimination of ^{90}Sr with respect to Ca in freshwater plants, 25:29452
TREILLE, Daniel, Duality and dual models, 25:30825
TREJBAL, Z., Radial injection of a polarised beam into a cyclotron, 25:31153
TRENTELMAN, G. F., High resolution nuclear studies using cyclotron beams, 25:31124
TRETKOWSKI, J., Curie--Weiss temperature dependence of paraelasticity, 25:29865
TRET'YAKOVA, S. P., Effect of chemical factors on the sensitivity of polymeric detectors, 25:29335
TREZZA, G., Alpha autoradiography of irradiated nuclear fuel, 25:29944 (LB/G-2916)
TRIDOT, Gabriel, Ternary system UO_3--V_2O_5--Na_2O, 25:29998
TRIER, J. D., Differential cross section of deuteron photodisintegration between 20 and 35 MeV, 25:31194
TRILLING, C. A., Heavy water and organic fluids as neutron moderator and reflector materials, 25:29154
TRILLING, G. H., Single-pion production in K$^+$p interactions at 4.6 GeV/c, 25:30748
TRIPATHI, D. N., Ionization cross sections of molecules due to heavy-particle impact, 25:30299
TRIPATHI, V. K., Nonsteady third harmonic generation in a plasma, 25:30609
TRIPKOVIC, M., Spectrographic determination of impurities in vanadium pentoxide and high purity lead, 25:28947
TRIPPLER, K., Dependence of natural radioactivity of the air on thermal stratification and wind velocity, 25:29223
TROITSKII, N. A., Cell division in Escherichia Coli during irradiation by neutrons of 200 keV, 25:29490
TROTTIER, Jean-Pierre, Interaction of beryllium wire with an aluminum matrix, 25:29883 (SC-T-713021)
TROY, B. E. Jr., Subauroral red arc and the associated ionospheric phenomena, 25:30350 (N-70-36812)
TROYAN, Yu. A., Cross sections of inelastic channels of reactions in np-interactions at the neutron momentum from 2 to 10 GeV/c, 25:30726 (JINR-P1-5665)
TROYANOV, I. M., Heat distribution in electron beam-melted molybdenum plates, 25:29842
TROYANOVSKAYA, M. L., Radiation effect on chromatin deoxyribonucleoprotein, 25:29458
TRUBNIKOV, A. S., Drift-beam instability and ion sound in an inhomogeneous plasma, 25:30506 (MATT-Trans-84)
Electron-ion beam instability, 25:30505 (MATT-Trans-83)
TRUBNIKOV, B. A., Longitudinal oscillations of a relativistic electron--ion plasma at zero temperature, 25:30529
TRUFFIN, C., Local duality and conserved currents, 25:30855
TRUITT, J., Function of condensing steam in aerosol scrubbers, 25:29251 (ORNL-4654)

XUM

TRUSS, F., Effect of low dosage irradiation on metabolism and function of the rat kidney damaged by ischeria, 25:29654

TRUXOVA, G., Combined effect of 6-Azauridine and irradiation in vivo and in vitro. VI, 25:29679

TRZEBIATOWSKI, W., Magnetic properties of uranium silicides, 25:30679

TSAI, Hui-tuh, Photon activation analysis for rubidium with an internal-reference of cesium, 25:29018

Photonuclear yields in Be and Cs with 18 approximately 75 MeV bremsstrahlung, 25:29017

TSAI, S. Y., Muon parity conservation and the universality principle, 25:30932

TSAKHER, G.-Yu., Apparatus for the automatic accumulation (storage) and analysis of information in experiments with the synchrocyclotron, 25:31070

TSARAPKIN, L. S., Influence of chemical substances on radiation damages to chromosomes in dormant pea seeds, 25:29485

Influence of x irradiation on chromosome aberrations in pea seedlings, 25:29489

Protective action of cysteine on moisture content of pea seeds, 25:29552

TSARAPKINA, K. A., Influence of chemical substances on radiation damages to chromosomes in dormant pea seeds, 25:29485

TSCHIRF, E., Measurement and calculation of dose rate removal cross sections and B factors for neutrons, 25:30637

TSEKHMISTRENKO, Yu. V., Elastic scattering and radiative capture of protons, 25:31276

TSEREN, Ch., Deduction of the Glauber formula from the Watson theory, 25:31434

TSIEN, T. P., Rotational excitation in molecular collisions, 25:30296

TSIGOURAKOS, D., Renal adenocarcinoma: scintigraphic study of primary and metastatic areas, 25:29590

TSISEK, Z., Spectrum of fast deuterons emitted in 670-MeV proton interaction with carbon nuclei, 25:31225

TSIVOGLOU, Ernest C., Nuclear power: the social conflict, 25:31531

TSOPOVA, L. N., Microroentgenospectral investigation of uranotitanates, 25:29971

TSUI, J., Sintering of $PrCo_5$ permanent magnets, 25:29797

TSUJII, Tsuneo, Solar x-ray radiation as observed by real time telemetry from Solrad satellites, 25:30355

TSUKERMAN, I. Kh., System for the automatic indication of impurities in sodium coolants, 25:29261

TSYPIN, V. S., Instability of a finite and high-pressure plasma with finite electron thermal conductivity, 25:30546

TUCEK, J., Examination of spent fuel elements, 25:29291

TUCKER, J. R., Onset of superconductivity in one-dimensional systems, 25:30420

TUCKER, Philip A., Application of differential thermal analysis to the study of phase equilibria in metal systems, 25:29885

TUCKER, Wallace H., Soft x rays from the Cygnus Loop, 25:30132

TUICHIBAEV, M. U., Radiation effects on amino acyl-tRNA synthetases and tRNA of cotton plant, 25:29715

TUKEY, H. B. Jr., Prog. rpt. on loss of organic and inorganic materials from above-ground plant parts by leaching, 1970--71, 25:31709 (NYO-2598-52)

TULLE, P. A., Comments on nonlinear resonant ion heating in a magnetoplasma, 25:30473

TUMANOV, V. S., Theory of nuclear Overhauser effects in multispin systems. II, 25:30691

TUNG, Lu Ho, Melt strength and melt extensibility of irradiated linear polyethylene, 25:29099

TUNG, Wu-ki, Hyperon beta decay. II, 25:30812

TUREKIAN, Karl K., Deposition of molybdenum and uranium along the major ocean ridge systems, 25:29228

TURI, L., Determination of neutron spectra from activation data by means of rfo1 and rfo7 codes, 25:31648 (KFKI-70-30-RPT)

TURJANSKI, R., Resonance integrals for neutron activation of ^{64}Zn, ^{68}Zn, ^{85}Rb, ^{100}Mo, ^{102}Ru, ^{113}In, ^{123}Sb, and ^{180}Hf, 25:31300 (CNEA-282)

TURKIN, Yu. I., Spectral isotopic analysis of elements in middle part of Mendeleev Periodic Table, 25:28952

TURNER, Barry E., Observations of compact H II regions with optical counterparts, 25:30117

TUZOVA, T. V., Determination of absolute age of Lake Balkhash on the basis of nonequilibrium U, 25:29210

TVERSKOI, B. A., Acceleration of charged particles in a variable magnetic field, 25:30122

TYAPIN, A. S., Statistical expression for the nuclear energy, 25:31412

TYAPKINA, G. N., Photomultiplier impulse shaper with stable time delay, 25:29347

TYBOR, W., $X^0(960)$-meson -2- or 0-, 25:30833

TYURIN, N. E., Condition of the asymptotic equality of total cross sections in two simple models, 25:30769

TYVIN, L. I., X-ray spectrometer with cooled Si(Li)-detector, 25:29325 (JINR-P13-5707)

U

UCHIDA, Irene A., Trisomy associated with diagnostic x-rays, 25:29500

UCHIDA, Masaaki, Columnar grain growth in center line heated UO_2 pellet, 25:29976 (JAERI-Memo-4249)

Phase study of the system UO_2--Dy_2O_3, 25:29975 (JAERI-1203)

UEHARA, S., Gamma transition studies of ^{125}Sb, 25:31388

UENO, K., Determination of Th, U(VI), and Pu(IV), 25:28982

UENO, Kaoru, Separation of uranium from fission products, 25:29198

UGLOV, A. A., Heat distribution in electron beam-melted molybdenum plates, 25:29842

UHLMANN, A., Positive functionals on the algebra of test functions, 25:30944

UHLMANN, Armin, Attempt to construct test-algebras for Haag--Araki fields, 25:30951

ULLAH, N., One-particle-hole and projected Hartree--Fock approximations in ^{12}C and ^{16}O, 25:31226

ULRICH, Roger K., Evidence for ^3He in young open clusters, 25:30077

UMARCHODGAEV, E. M., Changes of plasma kininogen and kinin-forming activity in irradiated animals, 25:29681

UMARKHODZHAEV, E. M., Change in kinin system of blood during acute radiation sickness, 25:29668

UMEZAWA, H., Equal-time commutation relations in self-consistent quantum field theory, 25:30991

Nature of intrinsic breakdown of chiral symmetry in terms of physical fields, 25:30929

URBANETS, Ya. Ya., Gamma radiation of ^{226}Ra and its decay products, 25:31358

URECHE, Vasile, Interpretation of light curves of close binary systems. VI, 25:30105

URETSKY, J. L., Evidence for possible boson resonance of mass 2820 MeV, 25:30737

UREY, Harold C., Prog. rpt. on distribution and origin of elements and their isotopes in nature, final, 1962--70, 25:30158 (UCSD-34-P-43-X-9)

URY, J. F., Measurement of working temperature in motors by means of ^{85}Kr, 25:29282

USACHEV, Yu. D., Dirac monopole: introductory paper, 25:30771 (BNL-tr-410)

USCINSKI, B. J., Scintillation of extended radio sources when receiver has finite bandwidth. II, 25:30124

Scintillation of extended radio sources when receiver has finite bandwidth. I, 25:30123

USHER, P. C., I Zw 1: a variable compact galaxy, 25:30199

USHER, P. D., Light variations of Seyfert galaxy 3C 120, 25:30214

USHIO, M., Design and construction of PIACE, 25:30587 (EUR-4593, pp 431-41)

USOV, Yu. P., Operation of a spark chamber at a high count rate, 25:29375

USTINOVA, G. K., Determination of the modulation-region boundaries, 25:30323

UVAROV, V. A., Wideband frequency divider of a sinusoidal signal that has an adjustable division factor, 25:29404

V

VACHER, J., Opto-electronic link for transmitting temporal information, 25:29392 (CEA-N-1431)

VAISBURD, D. I., F-center destruction mechanism in proton tracks in alkali halide crystals, 25:30655

VAISHNIS, P. P., Internal ionization in β decay of ^{131}I, 25:31316

VAJDA, Peter, Photoconductivity in p-type silicon irradiated with 1.2-MeV electrons at approximately 15°K, 25:30658

VAKHRUSHIN, Yu. P., Choosing and calculating focusing system of 30 MeV linear induction accelerator, 25:31039 (JINR-P9-5714)

VALERO, Francisco P. J., Laser-generated plasma as a spectroscopic light source, 25:30498 (N-70-41880)

VALET, Guenter, Esterase activity and protein content of plasma erythrocytes in whole-body irradiated rats, 25:29686

VALLIER, J.-C., Hall effect in superconducting niobium and alloys, 25:30427

VAL'SKII, G. V., Angular anisotropy of γ radiation emitted after ^{235}U fission by slow neutrons, 25:31369

VAN ALTENA, W. F., Luminosity of the magnetic white dwarf AC + 70°8247, 25:30074

VAN BEKKUM, D. W., Radiation chimeras, 25:29683

VAN CRAEYNEST, Annick, Determination of low solubility limits by measurement of diffusion coefficients, 25:29866

Diffusion and solubility of plutonium and uranium in aluminum, 25:29867

VAN DEN BERGH, Sidney, Optical studies of Cassiopeia A. III, 25:30064

VAN DEN BRENK, H. A. S., Radiation effects on the pulmonary system, 25:29636

VAN DEN HEUVEL, E. P. J., Zeeman observations of peculiar and metallic-line A stars, 25:30045

VANDERBERG, Jerome P., Immunity produced by the injection of x-irradiated sporozoites of Plasmodium berghei. II, 25:29727

VANDERBIE, William C., Curing of coatings on wood products by electron beam, 25:29123

VAN DER GOOT, A. S., Crystal structure of two Th_2Fe_7-phases, 25:29898

XUM

VAN DER KLEIN, C. A. M., Influence of neutron irradiation on behavior of a superconductor and a superconducting coil magnet, 25:30440 (EUR-4593, pp 107-13)
VANDERLIND, M. R., Effects of energetic heavy ions and radiation on infrared components, 25:29411
VANDERMEERSCH, J., Trapping of iodine and methyl iodide at high temperatures, 25:31612
VAN DER MERWE, P., Low-lying states of ^{127}I, 25:31352
VAN DER SCHAAF, C. F., Influence of irradiation and heating on the strength of mortar and concrete, 25:30021 (EUR-4531, pp 179-83)
VAN DER STRICHT, E., Radioactivity in air and fallout, 25:29218
VAN DER VEN, H. W., FREMIX: a high-power 8-GHz plasma heating experiment, 25:30456 (EUR-4593, pp 551-6)
VANDERVOORT, Peter O., Nonlinear density waves in galaxies, 25:30210
VAN DER WEERD, J. C., Angular distribution and excitation function of singlet deuteron in d(p,d)p reaction, 25:31196
VAN DE VATE, J. F., Behavior of fission product aerosols in relation to the safety of sodium cooled fast breeder reactors, 25:31618
VAN DUYET, P., Release of the hydrogen atom in thymine radiolysis, 25:29148
VAN ERP, J. B., Instrumentation systems to protect LMFBR core integrity, 25:31574 (ANL-7793)
VANETTEN, Robert L., L-amino acid oxidase. II, 25:29060
VAN GASSE, Rene Leopold Eduard, Method for the radiation production of films from unsaturated polyester resins, 25:29116
VAN HOVE, L., Some trends and problems in the study of high multiplicity hadronic interactions, 25:30881
Very high energy hadron phenomena, 25:30754
VAN LENTEN, Frank J., Ion-exchange paper chromatography of metal ions with mixed aqueous-organic solvents containing mineral acid and a selective extractant, 25:29190
VAN LIERDE, W., High frequency melting of UO_2--PuO_2, 25:29935
VAN MARK, E., Pulse breakdown of plastic foils in liquids, 25:30569 (EUR-4593, pp 281-6)
VAN NIEUWENHUIZEN, P., Muon--electron scattering cross section to order α^3, 25:30820
VAN NIEUWLAND, J. M., Beam quality of AVF cyclotrons, 25:31112
First and second harmonic extraction, 25:31105
VAN REUTH, E. C., Superconducting-state Knight shift in V_3Au, 25:30425
VANVARI, N., Effect of external dc electric field on absorption of microwaves in plasma, 25:30628
VAN WITTEVEEN, R. A. J. O., Radioactively-heated thermodynamic engines, 25:29279
VANYSEK, V., Alignment of dust particles in comet tails, 25:30183
VAPILLON, L., Far-infrared spectrum of Jupiter, 25:30250
VAREY, R. H., Sheath growth in a low-pressure plasma, 25:30531
VARGA, L., Labelling of heparin with ^{51}Cr, 25:29415
VARGA, Stefan, Radionuclide x-ray fluorescence analysis. III, 25:28922
Radionuclide x-ray-fluorescence analysis. I, 25:28935
VASIL'EV, B. V., Measurement of velocity of propagation of gravitational interaction, 25:30995 (JINR-P13-5685)
VASIL'EV, G. A., Spectrometric isochronous cyclotron, 25:31123
VASIL'EV, I. S., Radiosensitivity of human lymphocytes in vitro, 25:29710
VASILEVSKII, M. A., Stability of toroidal plasma ring with hf current along longitudinal magnetic field, 25:30597 (LA-4339-TR)
VASIN, M. V., Radioprotective properties of o-acyl derivatives of serotonin, 25:29555
VASU, K. I., Dispersed-particle strengthening in nickel-zirconia composite, 25:29941 (INIS-mf-8)
VATULINA, G. G., Radiotoxins in case of chronic intake of ^{90}Sr, 25:29639
VAVREJN, B., New possibilities in the topical diagnosis of cardiac infarcts, 25:29571 (LB/G-2835)
VEDESHIN, L. A., Observation of radiation belts and ionosphere by Interkosmos-3 satellite, 25:30364
VEENEMA, Ralph J., Nucleic acid synthesis in bladder tumors, 25:29585
VEGORS, S. H. Jr., Gamma-ray energies and intensities in decay of ^{205}Bi, 25:31386
VEISMAN, V. A., Potassium content in patients with pyelonephritis, 25:29448
VELDEN, L., Atlas of 21-cm line profiles of outer part of Galaxy in region of galactic anticenter, 25:30142
Kinematics of H I gases in galactic anticenter region, 25:30143
VELINOV, P. I., Behavior of cosmic layers in lower ionosphere during Forbush decreases, 25:30311
VENEZIANO, G., Duality and dual models, 25:31015 (MIT-2098-726)
General features of inclusive reactions from duality, 25:30758
VENKATESWARLU, Ch., Determination of total hydrogen content of UO_2 pellets, 25:28912 (BARC-500)
VENKATESWARLU, K. S., Water chemistry studies: chemical analysis manual for moderator and coolant water systems, 25:28914 (BARC-515)
VENTER, I., Reaction $^7Li(d,\alpha)^5He$ in range of 0.6 to 2.0 MeV, 25:31220
VEPRIK, Ya. M., Effect of chemical factors on the sensitivity of polymeric detectors, 25:29335
VERBA, J. W., Conceptual design of two-stage, two-gap cyclotron, 25:31140
VERBEEK, R., Merits and limitations of explosively driven current generators in fusion research, 25:30562 (EUR-4593, pp 205-17)
VERBEEK, Theodore, Roubaultite $Cu_2(UO_2)_3(OH)_{10}\cdot 8H_2O$, a new mineral species, 25:29238
VERDERAME, Frank D., Infrared spectrum of solid and matrix-isolated H_2O_2 and D_2O_2, 25:29055
VERDET, J. P., Far-infrared spectrum of Jupiter, 25:30250
VERGADOS, J. D., First-forbidden unique β-decays in the Sr region, 25:31284
VERHEUL, A., Vacuum start and clamp switches for a 20-kJ, 40-kV capacitor unit, 25:30570 (EUR-4593, pp 287-91)
VERMA, N. C., Reaction to thymine with radiation induced electrons in alcoholic matrices at 77°K, 25:29143
VERNOV, S. N., Injection of energetic electrons into magnetosphere during magnetic storm, 25:30352
VERON, P., Observations of variable radio sources at 2695 MHz, 25:30151
VERSCHUUR, G. L., OH emission from interstellar H I clouds, 25:30155
Recent measurements of the Zeeman effect at 21-centimeter wavelength, 25:30133
VESTER, K.-P., K-conversion coefficient of 53.3-keV transition in ^{73}Ge, 25:31274
VETCHINKIN, S. I., Green functions of Schroedinger equation for simplest systems, 25:30712
VEVERIS, O. E., Neutron activation determination of Mo in biological materials, 25:29019
VEZZETTI, D. J., Transverse electromagnetic field in a plasma, 25:30535
VICH, Z., Combined effect of 6-Azauridine and irradiation in vivo and in vitro. VI, 25:29679
VIECELLI, James A., Application of the tensor code to the calculation of rayleigh waves, 25:29243 (UCRL-50992)
VIEHBOECK, F. P., Determination of the distribution of fission products in fuel particle coatings by the sputtering technique, 25:29979 (SGAE-PH-96/1970)
VIGNES, A., Coating of Nb and Nb alloys with Al. I, 25:29816
VIKHREV, V. V., Passive diagnostics of a plasma focus using charged products of the dd-reaction, 25:30475 (LA-tr-71-6)
VINOGRADOV, N. I., Absorption of shf waves by plasma at upper hybrid frequencies, 25:30606 (NP-18807)
VINOGRADOV, Yu. A., Effect of chemical factors on the sensitivity of polymeric detectors, 25:29335
VIRMANI, Y. P., Electron paramagnetic resonance studies of carbon monoxide adsorbed on thorium oxide, 25:29090
VISHNEVSKII, N. K., Search for particles with fractional charge in 70 GeV accelerator, 25:30724 (CERN-Trans-71-4)
VITALI, G., Electron microscope observation of lattice disorder in ion-implanted silicon, 25:30650
VITKEVICH, V. V., Linear polarization of pulsar MP 0628 and radio emission in meter-wavelength range, 25:30135
VITKOVITSKY, Ihor M., Production of intense relativistic electron beams, 25:30254 (EUR-4593, pp 59-65)
VIVARGENT, M., Experimental program for CERN storage rings, 25:31060
VLADAR, Milan, Effect of isotope dilution on the behavior of radioyttrium in mammalian organism, 25:29454
VLADIMIROV, L. A., Estimation of the diffusion of materials in clayey grounds, 25:29206
VLASOV, V. G., Phoswich for neutron detection, 25:29339
VOELKL, J., Curie--Weiss temperature dependence of paraelasticity, 25:29865
Diffusion of hydrogen and deuterium through niobium, 25:29820 (EUR-4593, pp 519-24)
VOGL, G., Stored energy release of solid argon after reactor irradiation at 4.6°K, 25:30660
VOGT, N., Photometric investigation of the double cluster h and chi Persei, 25:30041
VOICE, Eric Handley, Compacting nuclear fuel, 25:31679
VOILLEQUE, Paul G., Computer calculation of bone doses following acute exposure to ^{90}Sr aerosols, 25:29513 (CONF-710211-1)
VOITOVETSKII, V. K., Evidence of disappearance of inelastic channel of nuclear reaction in nuclear resonant scattering of γ-rays in perfect crystal, 25:30687 (IAE-1966)
VOKAC, Peter R., Automated and conventional photometry of the short-period variable star 14 Aurigae, 25:30086
VOLF, F., Influence of initial content of the cooling rate from the beta phase to preferred uranium orientation following heat treatment, 25:29884 (UJV-2525-M)
VOLF, Vladimir, Effect of isotope dilution on the behavior of radioyttrium in mammalian organism, 25:29454
VOLGA, V. I., Thermal conductivity, electric resistivity, and specific heat of dense graphites, 25:29949
VOLK, K. E., Nickel and nickel alloys, 25:29838
VOLKENSHTEIN, N. V., Magnetization of EuO and $Eu_{0.97}Gd_{0.03}O$ single crystals, 25:30670
VOLKOV, Yu. K., Corrosion resistance of Mo alloys in certain corrosive media, 25:29776
VOLKOV, Yu. V., Shell correction to liquid-drop energy,

XUM

25:31398
VOLOBUEV, S. A., Primary γ radiation with E greater than or equal to MeV, 25:30306
VOLTOLINI, C., Observation of d* effect in anti pd → p anti p π+ π−n reaction at 5.55 GeV/c, 25:30727 (NP-18796)
VONDEROHE, R. H., Instrumentation systems to protect LMFBR core integrity, 25:31574 (ANL-7793)
VON FINCKENSTEIN, Graf Finck, Vlasov description of a supercritical magneto-acoustic compression pulse, 25:30513 (IPP-1/113)
VONGAI, A. D., Analogous states of T = 2 in ^{26}Mg(^{3}He,n)^{28}Si, ^{48}Ti(^{3}He,n)^{48}Cr, and ^{58}Ni(^{3}He,n)^{60}Zn reactions, 25:31237 (IAE-1958)
VON HOLLE, W. G., Mid- and far-infrared spectra of HF and DF in rare-gas matrices, 25:29066
VORLICEK, Jan, Amperometric, conductometric, chelatometric titration, 25:28970
VOROB'EV, V. A., Radiation defectoscopy of concrete and reinforced concrete by means of betatron stremsstrahlung, 25:29296
VORONOV, B. L., Localizable and nonlocalizable theories, 25:30962
VOROPAEV, A. I., Physical characteristics of critical assembly mockup of the BOR-reactor, 25:31632 (FEI-201)
VOROPAEV, J. V., Gamma-irradiation apparatus for treatment of root- and tuber- crops, 25:29253
VOROSHILOV, Yu. V., Crystal structures of $ZrCo_3B_2$ and $HfCo_3B_2$, 25:29992
VOROZHTSOV, S. B., Calculation and generation of the magnetic system of the monoenergetic cyclotron, 25:31037 (JINR-P9-5669)
Magnetic system of the monoenergetic cyclotron, 25:31129
VORSPRACH, F., Exposure plots for new radiographic films, 25:29294
VOSKOBOINIKOV, G. V., Activity of methionine-methyl-activating enzyme in livers of rats irradiated with x rays, 25:29663
VOUILLON, Michel, Electronic microscope study of needle-shaped precipitates in irradiated austenitic steels, 25:29902 (EURFNR-891)
VYDRA, Frantisek, Amperometric, conductometric, chelatometric titration, 25:28970
VYGOVSKAYA, G. P., Influence of irradiation of ova of rats on formation of LDH isoenzymes, 25:29665

W

WADE, C. M., Radio observations of Nova Scuti 1970, 25:30091
WAEPPLING, R., Moessbauer investigation of iron in coron, 25:30689 (UUIP-733)
WAGGENER, Robert G., Low dose ferrous sulfate dosimetry by direct photon counting, 25:29386
WAGNER, H. F., Two-quasi-particle rotational band at 1172 keV in ^{172}Yb, 25:31367
WAGNER, H. Gg., Rate of the reaction of atomic hydrogen with acetylene. II, 25:29043
WAGNER, H. N. Jr., Pinhole scintillation camera and /sup 99m/Tc-pertechnetate in normal thyroid scanning, 25:29586
WAGNER, P., Linear polarization of the γ rays emitted in the reaction ^{46}Ti(p,p'γ), 25:31288
WAGNER, R. J., Idaho nuclear code automation: a standardized and modularized code structure, 25:31594 (CONF-710302-10)
WAGNER, S., Photoproduction and electromagnetic moments of charged rho mesons, 25:30799
WAKAYAMA, Terunobu, Effect of phase on primary process of formation of butyl radicals in radiolysis of solid isobutane-2-d_{11}, 25:29161
WAKEFIELD, K. E., Design and operation of a spherator with a levitated, superconducting ring, 25:30559 (EUR-4593, pp 141-8)
WALDMEIER, Max, Mexican solar eclipse, 25:30163
WALDRON, J. C., Single-crystal targets of rubidium uranyl nitrate for the aligned fissile nuclei experiment, 25:29034 (AERE-R-6141)
WALDROP, Forrest B., Uranium etchant and method, 25:29798
WALI, K. C., Restrictions on the angular momentum of t-channel exchanges from s-channel helicity conservation, 25:30757
WALI, Kameshwar C., Implications of local duality in a set of coupled reactions, 25:30843
WALKER, A. A., Irradiation resistance of spores of Clostridium botulinum in beef, 25:29734
WALKER, D. G., New materials in the field of radiation, 25:29916
WALKER, D. W., Effect of gamma irradiation of immature sugarcane borers, 25:29755
WALKER, Sharon A., Relative hazards for inhaled ^{95}Zr and ^{95}Nb particles formed under various thermal conditions, 25:29423 (LF-43, pp 59-65)
Retention patterns of ^{125}Sb in mice following inhalation of particles formed at different temperatures, 25:29424 (LF-43, pp 66-70)
WALLACE, William John, Elastic scattering of alpha particles by ^{36}Ar at 12.83 to 17.83 MeV, 25:31262
WALLIS, G., Echoes with ion sound waves, 25:30611
WALLS, Fred Lexes, Determination anomalous magnetic moment of free electron, 25:30720
WALLWORK, G. R., Some limiting factors in the use of alloys at high temperatures, 25:29780
WALSH, William J., Dissolution of stainless steel clad nuclear fuel elements, 25:29199
WALTAR, Alan E., Integrated model for analyzing disruptive accidents in fast reactors, 25:31599
WALTER, R. L., Cyclo--Graaff: concept and practice, 25:31081
Neutron polarization from ^{7}Li(p,n)^{7}Be reaction for 3 to 4 MeV protons, 25:31235
WANG, Robert T., Kinetic studies of the reduction of chromium(III) complexes by uranium(III) ions, 25:29084
WANNBERG, B., Hyperfine structure investigations of ^{51}Mn and /sup 52m/Mn, 25:31294
WARD, B. J., High-current capacitor banks for a 2-MJ high beta toroidal experiment (HBTX), 25:30563 (EUR-4593, pp 219-25)
WARES, G. W., Measurements of oscillator strengths for Fe I and Fe II, 25:30170
WARKE, C. S., Generalizations of Jost--Pais theorem for nonlocal potentials, 25:31026
WARREN, J. B., TRIUMF project, 25:31087
WASHBURN, T. N., Performance capability of advanced fuels and fast breeder reactors, 25:31569 (ORNL-TM-3388)
WATARI, T., Propagation of electrostatic ion waves near ion cyclotron harmonics, 25:30612
WATSON, G. M., Fast-neutron irradiation effects on electrical insulators, 25:30011 (ORNL-4630, pp 226-9)
WATT, T. M., Topside ionosphere at sunrise, 25:30377
WAWRUKIEWICZ, Anthony S., Astronomical properties of M supergiants, 25:30055
WEAVER, H. T., NMR studies of ^{1}H and ^{3}He contained in gold films, 25:30692
WEAVER, O. L., Breakdown of scaling invariance in generalized Bjorken limit of perturbation theory, 25:30783
WEBER, Elisabeth, Dosimetry in bone marrow cavity of rat femurs following incorporation of ^{90}Sr--^{90}Y, 25:29524
WEBER, J., Behavior of Zr alloys in CO_2, 25:29770
WEBER, Joseph, Detection of gravitational waves, 25:31007
WEDLER, H., High-power spark gaps for large and fast energy storage systems, 25:30565 (EUR-4593, pp 241-50)
New crowbar system for 2.7-MJ bank Isar I at Garching, 25:30560 (EUR-4593, pp 189-95)
Recent results with laser-triggered spark gaps, 25:30566 (EUR-4593, pp 259-64)
WEHBE, S., In vitro studies on radioprotective effects of melanin on mammalian cells, 25:29568
WEHR, G., Stored energy release of solid argon after reactor irradiation at 4.6°K, 25:30660
WEIR, J. R. Jr., Irradiation damage to aluminum and aluminum alloys, 25:29905 (ORNL-4630, pp 239-60)
Joining research on nuclear materials, 25:29825 (ORNL-4630, pp 261-70)
Mechanical properties of alloys in reactor environments and development of FBR cladding and structural alloys, 25:29904 (ORNL-4630, pp 73-95)
Properties of ferritic steel welds, 25:29822 (ORNL-4630, pp 139-44)
Welding development for FBR stainless steel components, 25:29785 (ORNL-4630, pp 111-38)
WEJROCH-KOWALSKA, M., Attempt to use /sup 99m/Tc for scintiscanning of salivary glands, 25:29574
WELLER, F., Theoretical structure level and absolute transition probabilities in deformed nuclei of uneven mass numbers, 25:31308 (KFK-1248)
WELLING, D., Nature of intrinsic breakdown of chiral symmetry in terms of physical fields, 25:30929
WELLMANN, P., Conference on spectrum formation in stars with steady-state extended atmospheres, Munich, Ger., 4/69, 25:30035 (NBS-SPEC. PUBL-332)
WELLNER, Peter, Phase relations in the system beryllium--aluminum--titanium, 25:29900
WELLS, D. K., Design and performance of a compact multi-particle cyclotron, 25:31145
Design and performance of H⁻ injector cyclotron, 25:31151
WELLS, Mark B., Evolution of computer software, 25:31701 (LA-4620)
WELTNER, W. Jr., Matrix-isolation technique applied to high temperature molecules, 25:29083
WENIGER, M., Investigations on high-voltage gaskets, 25:30572 (EUR-4593, pp 301-9)
WENZL, H., Stored energy release of solid argon after reactor irradiation at 4.6°K, 25:30660
WENZL, Helmut, Influence of neutron irradiation at 4°K on shear modulus of Cu, Al, and Pt, 25:29912
WERNER, F., Toroidal version of the Isar I theta-pinch experiment, 25:30585 (EUR-4593, pp 419-24)
WERNER, H., Results of primary therapy of laryngeal carcinomas with conventional x-depth-irradiation or radium contact irradiation, 25:29598
WERTZ, James Richard, Newtonian hierarchical cosmology, 25:30226
WESS, J., Weak interactions, 25:30808
WEST, T. S., Dewar tube sample cell assembly for low-temperature fluorimetry, 25:28925
WEYHMANN, W., NMR and nuclear relaxation study of satellite lines in dilute Co--Cr, Co--V, and Co--Mn alloys, 25:31690 (COO-1569-71)
Nuclear orientation of ^{142}Pr in praseodymium metal, 25:30662 (COO-1569-76)

XUM

WHALEN, J., Holmium-165 fast neutron cross sections, 25:31350
WHANG, Y. C., Solar wind interaction with Mercury, 25:30389
WHEATLEY, P. J., Chemical consequences of nuclear spin, 25:30669
WHEELER, M. J., Thermal diffusivity of uranium and uranium--plutonium monocarbides, 25:29957
WHEELOCK, Linda H., Cytological effects of irradiated sucrose, 25:29494
WHITE, A. R., Landau singularities in multi-Regge theory and fixed-angle behavior, 25:31033
WHITE, J., Solid state relationships in the system U--Te--C, 25:30001
WHITE, Robert A., Chlorophyll one-electron photochemistry: flash photolysis studies of the chlorophyll--quinone reaction in alcohol solvents, 25:31687 (COO-908-34)
WHITEHEAD, C., Is ball lightning caused by antimatter meteorites, 25:30329
WHITEHEAD, J. D., Difficulty associated with wind-shear theory of sporadic E, 25:30380
Equatorial electrojet and the gradient instability, 25:30379
WHITMAN, G. D., Summary of a program of research and development for prestressed concrete nuclear pressure vessels, 25:30019 (EUR-4531, pp 27-58)
WHITNEY, R. R., High-energy electron scattering from ^{6}Li, 25:31211
WHITWORTH, J. B., Computer-assisted analysis of gamma-ray spectra, 25:29363
WIDOM, Allan, Enthalpy fluctuations in ^{4}He films, 25:30407
WIECHERS, R., Examination of spent fuel elements, 25:29291
WIEDEMANN, K. H., Effects of mechanical stress on corrosion behavior of Zircaloy-2, 25:29771
WIENDL, F. M., Some gamma-irradiation effects on Zabrotes subfasciatus, 25:29756
WIEST, Joseph Ernest, Reactions (p,n) in ^{53}Cr and ^{75}As, 25:31248
WIGHT, A. L., Application of alternating-direction implicit methods to the space-dependent kinetics equations, 25:31654
WILD, H., Experiments on the behavior of nuclear aerosols in fast breeder reactor containment, 25:31617
WILHELM, J., Legendre polynomical development in Boltzmann equation for Lorentz plasmas, 25:30522
Observations on the influence of step ionization on the distribution function as well as transport and balance values of electrons in neon low-pressure plasma at low degrees of ionization, 25:30525
WILHELM, M., Preparation and superconductivity of $CeRu_2$, and its Gd, Mn, Fe, Co, and Ni-containing mixed phases, 25:30413 (LA-tr-71-26)
WILKINSON, D. H., Breit--Wigners viewed through Gaussians, 25:29355 (RLO-1388-135)
WILLAX, H. A., Status report on SIN, 25:31086
WILLEBORTS, G., Preparation and properties of a crystalline uranium(IV)--hydrazine nitrate compound, 25:29035 (NP-18736)
WILLHOIT, Donald G., Effect of x-irradiation on migration of amelogenic cells in the rat incisor, 25:29678
WILLIAMS, A. J., Interaction between the design and construction of prestressed concrete pressure vessels for nuclear reactors, 25:31456 (EUR-4531, pp 129-44)
WILLIAMS, J. R., Thermal radiation absorption by particle-seeded gases, 25:29270
WILLIAMS, M., Nuclear matter radii in the tin isotopes, 25:31341
WILLIAMS, R. E., Observed small-scale structure in planetary nebulae, 25:30115
WILLIAMS, R. M., Mineral reviews: uranium, 25:29236
WILLIAMS, W., Decay rate and branching ratio (π^--^{3}He)/(all π^- modes) of /sub Λ/^{3}H, 25:30821
WILLIAMS, W. G., Dynamic polarization measurements in polyhydric alcohols doped with their Cr(V) at approx. 1°K and at 3 kG magnetic fields, 25:31046 (RHEL/R-213)
WILLIAMSON, J. H., Magnetic surfaces in a quadrupole, 25:30603
WILLIS, C. A., Site and safeguard requirements for radioiodine control, 25:31620
WILLMORE, A. P., Electron and ion temperatures in the ionosphere, 25:30399
WILSON, H. W., Prog. rpt., annual, 1969--70, 25:31634 (SRRC-41/71)
WILSON, Kent R., Collinear collisions of an atom and harmonic oscillator, 25:30292
WILSON, S. S., Isospin invariance in reaction n + p → π^0 + d, 25:30730
WILSON, W. J., Infrared stars, 25:30089
WILSON, William R. D., Effect of irradiation on the creep of uranium dioxide, 25:30009 (BMI-1899)
WINEFORDNER, J. D., Optimization of experimental conditions for spectrofluorimetric determination of europium, samarium, and terbium as their hexafluoroacetylacetone-trioctylphosphine oxide complexes, 25:28954
WINKEL, Th. G. A., FREMIX: a high-power 8-GHz plasma heating experiment, 25:30456 (EUR-4593, pp 551-6)
WINKLER, H., g-factor of the 181 keV level of ^{99}Tc, 25:31271
WINKLER, R., Legendre polynomical development in Boltzmann equation for Lorentz plasmas, 25:30522
Observations on the influence of step ionization on the distribution function as well as transport and balance values of electrons in neon low-pressure plasma at low degrees of ionization, 25:30525
WINSTON, Roland, Beta decay of hyperons, 25:30815
Leptonic decay experiments with hyperons beams at NAL, 25:30722 (COO-1701-12)
WINTERHAGER, J., Allotropic transformation and thermal expansion of Co binary alloys between 100 and 800°C. I, 25:29899
WINTERNITZ, P., Crossing-symmetric expansions of scattering amplitudes, threshold behavior, and asymptotics, 25:31028
WINTERS, Harold F., Chemisorption of nitrogen at activated sites on a polycrystalline tungsten surface, 25:29849
WITHERS, H. R., Sublethal damage repair and its role in the radiation response of cell renewal systems, 25:29626
WITHERSPOON, John P., Interception and retention of radioactive aerosols by vegetation, 25:29444
WITT, K., Freezing experiments on austenitic tubes of MZFR, 25:31537
WITTENBERG, L. J., Application of differential thermal analysis to the study of phase equilibria in metal systems, 25:29885
WITZEL, A., Observations of variable radio sources at 2695 MHz, 25:30151
WITZKE, W. R., Alloy softening in Group VIA metals alloyed with Re, 25:29871
WOJCIK, W., Proton--proton and pion--proton inelastic collisions and electromagnetic form factors, 25:30977
WOLF, Lothar, Temperature fields in fuel element bundles. II, 25:31673
Temperature fields in fuel element bundles. I, 25:31674
Temperature fields in fuel element bundles with variable-range heat transfer between fuel element surface and coolant, 25:31675
WOLF, R. A., Ejection of mass by radiation pressure in planetary nebulae, 25:30044
WOLFRUM, J., Rate of the reaction of atomic hydrogen with acetylene. II, 25:29043
WOLFSBERG, K., Thermal-neutron fission of /sup 242m/Am: Mass and charge distribution, 25:31373
WOLKENHAUER, W. C., Hanford as a site for a controlled thermonuclear power plant prototype, 25:30552 (BNWL-B-47)
WOLNIK, S. J., Measurements of oscillator strengths for Fe I and Fe II, 25:30170
WOLNY, R. F., Practical low-range moisture generator, 25:31759 (Y-1791)
WONG, C. F., Photoprotons from ^{12}C and ^{13}C, 25:31232
WONG, S. S. M., One-particle-hole and projected Hartree--Fock approximations in ^{12}C and ^{16}O, 25:31226
WONG, W. H., Distribution of reaction products (theory). VII, 25:29058
WOO, Chia-wei, Kirkwood superposition approximation for dilute ^{3}He--^{4}He solutions, 25:30409
WOOD, Harland G., Determination and degradation of microquantities of acetate, 25:28996
WOODMANSEE, Walter C., Thorium, 25:29812
WOOLCOCK, W. S., Analytic properties of the scalar vertex function, 25:30770
WOOTTON, R. E., Low-inductance, megavolt Marx Generators, 25:30573 (EUR-4593, pp 311-17)
WORONOWICZ, S., Theorem about commutator functions and its applications to quantum field theory, 25:30952
WORSTER, L. D., Operation of halogen quenched Geiger--Mueller tubes, 25:31646 (DUN-SA-136)
WORTHINGTON, James Brian, Application of kinetics for quantitative chemical analysis of mixtures, 25:28941
WORTMAN, W. R., Bethe--Salpeter solution for nucleon--nucleon scattering with pion exchange, 25:30909
WOTKE, H., Determination of the distribution of fission products in fuel particle coatings by the sputtering technique, 25:29979 (SGAE-PH-96/1970)
Production of isotopically pure targets in electromagnetic mass separators by ion-beam retardation, 25:31069
WOZNIAK, Jan, Studies on radioactivity of Polish honeys. I, 25:29509
WRAIGHT, Leonard Arthur, Improvements in or relating to nuclear radiation detectors, 25:29348
WRIGHT, Byron T., Conceptual design of two-stage, two-gap cyclotron, 25:31140
Proposed use of a storage ring to improve the microscopic duty factor of a cyclotron, 25:31120
WRIGHT, H. E. Jr., Prog. rpt. on diatoms in lakes and lake sediments as index to environment, 5/70--1/71, 25:31739 (TID-25695)
WRIGHT, M. C. H., Study of NGC 604 at lambda21.1 cm, 25:30153
WROBLEWSKI, A., Review of experimental results, 25:30715
WU, F. T., Analysis of nonequilibrium plasmas in close-spaced thermionic converters, 25:30338
WUCHERER, P., Beam extraction at Juelich 90 MeV deuteron AEG isochronous cyclotron, 25:31102
WUERDIG, P., Thermal shielding by screens of circulating gas, 25:31576 (EUR-4531, pp 1035-53)
WULFFERS, L. A. G. M., Superconducting-state Knight shift in V_3Au, 25:30425
WUNNER, W. H., Simple method for counting ^{14}C- and ^{3}H-proteins in polyacrylamide gels, 25:28994
WYATT, John L. Jr., Radiation survey of television repair

shops in Baltimore area, 25:29512 (BRH/DEP-71-4)
WYATT, John P., Radiation survival: improved rates following chlortetracycline administration, 25:29561
WYCECH, S., Low-energy kaon--nucleus interactions, 25:30906
WYNN-WILLIAMS, C. G., Radio maps of condensations in H II regions, 25:30137
WYPYCH, M., Effect of dose rate on the radiation yields of radicals in frozen organic media, 25:29160

Y

YABLONIN, K. I., Photomultiplier impulse shaper with stable time delay, 25:29347
YAKIMIW, E., Fits to the absolute value ΔI = 1/2 and Lee--Sugawara relations, 25:30817
YAKOVENKO, K. N., Protective effect of anoxia on irradiation dose in case of chromosome aberrations, 25:29486
YAKOVLENKO, S. I., Formation of a nonequilibrium population in plasma under ionization resonance conditions, 25:30519
YAMADA, Kuniaki, Factors affecting the high temperature strength of Ni--Cr and Ni--W alloys, 25:29878
YAMAGISHI, Shigeru, Release of fission Cs from irradiated UO_2 powder, 25:29974
YAMAGUCHI, Kenji, Process for producing thermoplastic resin foam, 25:29109
YAMAGUCHI, Kouichi, Radiation-induced sulfoxidation and sulfochlorination of powdery polyethylene produced by radiation process, 25:29107
YAMAMOTO, Shuji, Measurements of angular distributions and energy spectra of photoneutrons from lead targets bombarded by high energy electrons, 25:31317
YAMAMURA, Yasunori, Improvement to GG approximation in neutron slowing down, 25:31179
YAMANOUCHI, A., Studies for safety analysis of loss-of-coolant accidents, 25:31605
YAMASHITA, Sukeaki, Field measuring system of drift tube quadrupole magnets, 25:31047 (SJC-A-71-1)
YAMAWAKI, M., High temperature reaction between uranium monosulfide and zirconium, 25:29965
YAMAZAKI, Hisashi, Calorimetric studies on chemisorption of nitrogen on tantalum, 25:29843
YANCHIN, V. A., Effect of radiation on oxygen electrode performance, 25:29098
YANG, Chien-sheng, Electron scattering from ^{13}C, 25:31205 (SAL-16)
YANG, T. F., Isospin nonconservation in reactions $^{16}O(d,\alpha)^{14}N^{*}$/sub 0+, T = 1/ and $^{12}C(d,\alpha)^{10}B^{*}$/sub 0+, T = 1/, 25:31227
YANG, Y. W., CP violation and strong self-interacting intermediate-vector-boson model, 25:30814
YANG, Ying-chuan, Infinite-component field theory and Veneziano model, 25:31024
YAND, A. F., Coulomb propagator in radiative muon capture, 25:31282
YANO, Masaaki, Development of a heavy-current switching gap triggered with laser, 25:30575 (EUR-4593, pp 339-45)
YANO, Suykuro, Calculation of flux of fast neutral particles from a cylindrical, high-temperature plasma, 25:30514 (JAERI-Memo-4243)
YANSHEVSKII, Yu. P., Effect of multiply scattered γ-radiation in the x-ray radiometric method, 25:28939
YAREMBASH, E. I., DTA and x-ray analysis of rare-earth--chalcogen systems, 25:29981
YARKOVETS, A. G., Protective efficiency of radioprotectors, 25:29550
YARMONENKO, S. P., Oxygen tension in critical organs under influence of mexamine in comparison with radioprotective effect, 25:29551
YASUMORI, Iwao, Pressure jump and isotope replacement studies of acetylene hydrogenation on palladium surface, 25:29062
YATSU, Kiyoshi, Experiments of plasma confinement in JIPP stellarator. I, 25:30457 (IPPJ-102)
YAZDANY, S., Heat and radiation resistance and recovery of spores of Bacillus, 25:29558
YBARRONDO, L. J., Idaho nuclear code automation: a standardized and modularized code structure, 25:31594 (CONF-710302-10)
YEARIAN, M. R., High-energy electron scattering from ^{6}Li, 25:31211
YEH, Yu-chai, Chemical effects associated with (γ,n) reaction in potassium chromate, 25:29166
YEN, E., Hypothesis of limiting fragmentation, 25:30768
YLAESAARI, S., Sintering kinetics of nickel activated tungsten, 25:29791
Wetting problems in connection with sintering, 25:29954
YNDURAIN, F. J., Analytic equivalence of wave functions and invariant amplitudes for massive particles, 25:30756
YOKOTA, Ryosuke, Recent improvements in fluoro-glass dosimeter, 25:29387
YORK, Donald G., Structure in the interstellar-extinction curve, 25:30212
YOSHIDA, Susumu, Influence of high hydrostatic pressure on the flow stress of pure iron and molybdenum polycrystals, 25:29833
YOSHIMURA, Y., Operation characteristics of 75 cm hydrogen bubble chamber and the refrigerator. I, 25:29372 (SJC-T-71-1)
YOST, J., Circumstellar shells in the young cluster NGC 2264, 25:30065
YOTSUYANAGI, Takao, Effect of irradiation on halogen exchanged silica--alumina catalyst, 25:29111
YOUNG, K. K., Isospin invariance in reaction n + p → π^{0} + d, 25:30730
YOUNGBLOOD, D. H., Mean lifetimes of levels in ^{92}Mo, 25:31377
YTHIER, Christian, Arsenic-76 decay, 25:31259
YU, C. W., Behavior of perforated end slabs for concrete pressure vessels, 25:29306
YU, Fu-li, Paper disc estimation of radioactive RNA: studies on the presence and elimination of metabolically generated artifacts from labeled purine and pyrimidine precursors, 25:28993
YUAN, H.-C., Irradiation of petroleum products and plastics, 25:29128
YUDIN, F. P., Estimation of the diffusion of materials in clayey grounds, 25:29206
YUEN, Virginia L. S., Helium-4 discharge light source and system for optical pumping of $2^{3}S_{1}$ ^{3}He, 25:31076
YUFEREV, V. I., Solution of single-speed neutron transport equation in multilayer plane and spherically symmetric systems, 25:31184
YUFEROV, V. P., Macrostructure of bovine serum albumin under γ irradiation, 25:29471
YUILL, W. A., Distribution of solid fission products in UO_2, 25:31589 (CONF-710302-5)
YUILLE, W. D., Trapping of methyl iodide at high pressure and high temperature, 25:31611
YUKI, T., Graphitization of free C precipitating through reaction of UC_2 with N_2, 25:29962
YULDASHEV, B. S., Application of phenomenological quasi-two-body model to π-p-interactions with strange particle production at p = 4 GeV/c, 25:30869 (JINR-P1-5706)
YURKIN, Yu. T., Spark chamber power supply circuit with semiconductor trigger, 25:29374

Z

ZACHARIASEN, F., Quark model of diffractive processes, 25:30844
ZAICHIK, V. E., Quantitative ^{6}Li autoradiography of metastases of Walker-256 carcinosarcoma in pulmonary tissue, 25:29443
ZAIENTS, S. L., Technology of strong pulsed currents and magnetic fields, 25:30604
ZAITSEVA, N. G., Decay scheme of ^{86}Y, 25:31247
ZAJEC, E., Cryogenic pumping system proposed for Bevatron, 25:31057 (UCRL-20197)
ZAKATOV, L. P., Slowing down of an intense electron beam in a dense plasma, 25:30504
ZAKHAROV, V. N., Transformation of general covariant observable values, 25:30970
ZAKHAROVA, V. P., Study of spontaneous fission of ^{252}Cf, 25:31314 (ORNL-tr-2453)
ZAKI, Mourad R., Impact of thermal analyses on nuclear ammonium polyuranate preparation, 25:29925
ZALEWSKI, Kacper, Correlation effects, 25:30837
ZAMOLODCHIKOV, B. I., Magnetic system of the monoenergetic cyclotron, 25:31129
Phase motion in the phasotron with spatial variation of magnetic field, 25:31156
ZANCA, Peter, Low dose ferrous sulfate dosimetry by direct photon counting, 25:29386
ZANGHI, Jean-Pierre, Determination of low solubility limits by measurement of diffusion coefficients, 25:29866
ZAPAROV, E. A., Lifetimes of 1080-keV level of ^{113}In and 1300-keV level of ^{111}Cd, 25:31327
ZAPLATIN, N. L., Calculation and generation of the magnetic system of the monoenergetic cyclotron, 25:31037 (JINR-P9-5669)
Magnetic system of the monoenergetic cyclotron, 25:31129
ZARUBIN, P. P., Elastic and inelastic proton scattering on ^{32}S, ^{34}S, and ^{35}Cl, 25:31291
Excited core model for ^{63}Cu and ^{65}Cu, 25:31246
Hauser--Feshbach method and inelastic scattering of protons, 25:31245
ZASEDATELEV, A. A., Effect of a mixture of uranium fission products on the sanitary conditions and hydrobionts of weakly-mineralized fresh-water basins, 25:29449
ZASLAVSKII, A. N., $X^{0}(960)$-meson -2- or 0-, 25:30833
ZASTAVENKO, L. G., Ground state of Hamiltonian in simplest model of quantum field theory, 25:30979
ZAULI, C., Wave functions for He by rotational projection, 25:30269
ZAVERUKHA, O. V., Sintering process of zirconium diboride with tungsten, 25:29930
ZAYACHKI, V. I., Elastic pp- and pd-scattering at 50 and 70 GeV, 25:30725 (JINR-P1-5633)
ZEBELMAN, A., Angular distribution of fission fragments from the ^{170}Yb compound nucleus excited to 107 MeV, 25:31371
ZEDGINIDZE, I., Labelling of heparin with ^{51}Cr, 25:29415
ZEITZSCHEL, G., Structural integration of a prestressed concrete pressure vessel in a nuclear power plant and comparison with a steel vessel installation, 25:31552 (EUR-4531, pp 647-89)
ZEL'DOVICH, Ya. B., Perturbations in an anisotropic

XUM

homogeneous universe, 25:30223
ZELLNER, R., Rate of the reaction of atomic hydrogen with acetylene. II, 25:29043
ZELLNER III, Benjamin Holmes, Polarization in reflection nebulae, 25:30053
ZEL'TSER, L. E., Fluorescence determination of copper, 25:28928
ZEMAN, W., Effects of irradiation on the nervous system, 25:29692
Effects of radiation on striated muscle, 25:29629
ZEMLYANUKHIN, A. A., Inactivation of enzymes of Botrytis cinerea by uv rays, 25:29720
ZERBI, Giuseppe, Lattice dynamics of methanol: hydrogen bonding and infrared absorption, 25:29065
ZERLAUT, G. A., Space environment stability program in white pigment coatings, 25:29105
ZEZINA, N. V., Gamma-induced free radicals in seeds, 25:29719
ZHEMALETDINOV, F. G., Relationship between level of endogenous sulfhydryl groups and radiosensitivity of tumors, 25:29610
ZHIDIK, L. G., Diantipyrinylmethane pyrocatecholate complex of molybdenum and its analytical application, 25:28926
ZHIGLINSKII, A. G., Spectral isotopic analysis of elements in middle part of Mendeleev Periodic Table, 25:28952
ZHUKOVSKII, N. N., Decay of ^{75}Br, 25:31257
ZHULIN, I. A., Studies of the auroral x radiation at conjugate points Kerguelen--Archangel, 25:30395
ZHUZHUNASHVILI, A. I., Collective processes and turbulent heating of a plasma, 25:30469
ZIEGLER, K., Design studies for an ultra-thin septum extraction channel for modified NEVIS synchrocyclotron, 25:31106
ZIENKIEWICZ, O. C., Nonlinear analysis of pressure vessels behavior including cracking, 25:31664 (EUR-4531, pp 697-734)
ZIGMAN, P. E., Certificates of radioactivity standards, 25:29173
ZILIOTTO, D., Evaluation of kidney morphology and function by means of the scintillation camera, 25:29592
Scintillation camera in the evaluation of liver morphology and function, 25:29591
ZIMAKOV, I. E., Effect of radiation on oxygen electrode performance, 25:29098
ZIMBRICK, J. D., Trapped species produced in the gamma radiolysis of aqueous sugar ices, 25:29153
ZIMMER, K., Problems in the quantitative spectral analysis of rare earth metal traces. II, 25:28946
ZIMMERMAN, D. W., Thermoluminescent dating using fine grains from pottery, 25:29212
ZIMMERMANN, Herbert, IR-spectroscopic investigations of crystalline tetrahydrate of hydrogen bromide $H_9O_4^+Br^-$ 25:31683 (ANL-Trans-880)
ZINGL, Harald F. K., Influence of a 3/2-spurion on Σ-decay, 25:30811
ZINOV, V. G., Charged particles produced in capture of negative muons by ^{28}Si, ^{32}S, ^{40}Ca, and ^{64}Cu nuclei, 25:31267
ZLATANOV, St., Attempt for deactivation of medical devices with detergent solutions and vibrator, 25:29510
ZLATANOV, Z. M., Elastic pp- and pd-scattering at 50 and 70 GeV, 25:30725 (JINR-P1-5633)
ZMII, O. F., Crystal structure of $CeMg_2Si_2$, 25:29993
ZOLLMAN, D. A., Nonrelativistic hard-pion production and current-field algebra, 25:30898
ZOLOTAREVA, N. N., Influence of radioprotective agents correlated with radiosensitivity of animals, 25:29553
ZOLOTAVIN, A. V., Decay of ^{225}Ac, 25:31325
ZOLOTUKHIN, I. V., Formation of gold nuclei on ionic crystals, 25:29910
ZOTIKOV, A. A., Changes in nucleoproteins in irradiated amniotic cells, 25:29709
ZOTOV, T. D., Magnetization of EuO and $Eu_{0.97}Gd_{0.03}O$ single crystals, 25:30670
ZRELOV, V. P., Cherenkov radiation in high-energy physics. II, 25:29368 (AEC-tr-7099(Pt.2))
ZSEBOK, Zoltan, Chromosomal examinations in radiologists, 25:29501
ZUK, W. M., Angular correlation of ^{42}Ca(α,pγ)^{45}Sc, 25:31251
Extrapolation of ^{12}C + ^{12}C and ^{12}C + ^{16}O reaction cross sections to astrophysical energies, 25:31200 (ANU-P-515)
Search for 3446 keV level in ^{29}P, 25:31250
ZULLINI, A., Ecological study of periphyton and identification of environmental radioactivity in a running-water ecosystem, 25:29478
ZUM WINKEL, K., Radioisotopes to determine tubular passage time in dog kidneys, 25:29414
ZUPNIK, B. M., Algebraic realization of chiral symmetry for meson systems and theory of Yang--Mills type, 25:30850 (JINR-P2-5759)
ZVERKO, J., Test of spectrographs 2-m telescope by detailed analysis of α Cyg, 25:30109
ZWART, J. W. A., Vacuum start and clamp switches for a 20-kJ, 40-kV capacitor unit, 25:30570 (EUR-4593, pp 287-91)
ZYLICZ, Elzbieta, Radium-226 in contemporary and fossil snow, 25:29209
ZYRYANOVA, L. N., Probability ratio for K and L capture, 25:31401

SUBJECT INDEX

Cross references are included in cumulative subject indexes and in *Subject Headings Used by the USAEC Division of Technical Information* (USAEC report TID-5001).

The reader is also referred to *Guide to Abstracting and Indexing for Nuclear Science Abstracts* (USAEC report TID-4576).

Most headings in the subject index are specific materials, things, and processes. The headings are followed by modifiers that describe the properties of, or processes applied to, the headings.

All index entries cite *NSA* volume and abstract numbers; volume number precedes the colon and the abstract number follows it. The designation (R) following the abstract number indicates a progress report; (P) indicates a patent; and (T) indicates a translation. Abstracts for reports other than progress reports carry no letter designation. Report numbers, where applicable, are included in parentheses after the abstract number of the citation. Published literature (journal article or book) can be identified by the absence of a report number.

Ideas presented in the original literature, rather than key words, have been indexed. The indexers have selected what seemed the most probable and logical place to look for typical information. Since it is not always possible to anticipate where a user would look for information, the cumulative indexes include numerous cross references. Consideration of synonymous or closely related terms will prove valuable.

Information is indexed for the greatest use to the greatest number of users. This requires that a topic be indexed to headings that most specifically describe it and not ordinarily to the headings that describe its ultimate use or to the general class headings that include the specific headings. For example, information on boiler design for the Fermi Fast Breeder Reactor would be indexed under the headings BOILERS and FERMI FAST BREEDER REACTOR but not necessarily under the headings REACTORS, FAST or REACTORS, BREEDER.

General or broad headings are reserved for general summaries, reviews, comprehensive reports, and similar literature.

Subject Heading Styles

Generally, the direct form of subject entry is used rather than inverted headings; e.g., AMINO ACIDS rather than ACIDS, AMINO; HELIUM ISOTOPES He-4 rather than HELIUM—ISOTOPES He-4 or HELIUM—He-4 ISOTOPES. Note, however, that in some cases parenthetic modifying terms or inverted headings such as NEUTRONS, FAST, are used where the alphabetical arrangement of a direct entry would cause information to be scattered. In addition, organic compounds are usually entered in the index in the inverted form to facilitate grouping like or related compounds with the parent compounds; e.g., BENZENE, BROMO- rather than BROMOBENZENE. In general, the nomenclature used is that of the subject indexes to *Chemical Abstracts*.

Alphabetization

Subject headings are alphabetized word by word. Parenthetic qualifiers, numbers, and Greek letters within subject headings are disregarded in alphabetizing unless there are two or more headings that are otherwise identical, in which case the qualifier, numerical progression, or spelled names for the Greek letters determine the order.

Examples:

M-Capture
  see ELECTRON CAPTURE
MAGNESIUM
MAGNESIUM ALLOYS AND SYSTEMS
MANGANESE FLUORIDES
MANGANESE FLUORIDES MnF_2
MESONS
MESONS (π)
MESONS (ρ)
1-PENTANOL
2-PENTANOL

Modifying Phrases

The modifiers appearing under a subject heading are written specifically to show the relation between the item being indexed and the heading. The modifier therefore contains a maximum of useful information. Although the modifier begins with the word judged to be of greatest use to the greatest number of users, there is still need for the searcher to consider all modifiers under the heading(s) of interest.

Modifiers usually form meaningful phrases when combined with the subject heading. Some are intended to be read following the subject heading, e.g., the entry HYDROGEN—sorption by charcoal should be read "hydrogen sorption by charcoal." As a result of placing the important word first, however, many modifiers must be rearranged for smooth reading, e.g., FORMALDEHYDE—yields in radiolysis of ethyl ether, effects of deuterium on, should be read "effects of deuterium on formaldehyde yields in radiolysis of ethyl ether" and URANIUM—crystal structure of, effect of cooling rate on allotropic transformations in, should be read "effect of cooling rate on allotropic transformations in crystal structure of uranium."

Special characters are added to modifiers in the fields of physics and reactor technology; if the modifier does not establish the experimental or theoretical character of a reference, a symbol (E), (T), or (E/T) is placed immediately after the modifying phrase and before the abstract number.

XUM

Physical States and Configurations of Materials

The specific physical state, if other than normal, or the geometric configuration of the material is included in the modifying phrase; e.g., information on liquid metals is indexed under the specific metal with "liquid" in the modifier and carbon crucibles is indexed under CARBON with "crucibles" appropriately placed in the modifier. The information on carbon crucibles is also indexed under CRUCIBLES.

Nomenclature of Inorganic Compounds

Inorganic compounds are indexed to subject headings in the direct form. Cations are listed in the order of increasing valence for polycationic salts of varying valence and in alphabetic order for polycationic salts in which all cations have the same valence; e.g., SODIUM ALUMINUM SILICATES and POTASSIUM SODIUM SULFATES. If more than one anionic species is presented in a compound, the anions are arranged alphabetically, e.g., BERYLLIUM FLUORIDE HYDROXIDES.

Nomenclature of Organic Compounds

Organic compounds are indexed by subject headings based on the indexes to *Chemical Abstracts* except in the area of enzymes, in which specific enzymes, named according to the 1964 recommendations of the International Union of Biochemistry, are used. In many cases nonproprietary names for drugs are used as subject headings, and cross references are made from the systematic chemical names. Subject headings for hormones appear in the inverted style at HORMONES.

Nomenclature of Life Sciences

Subject headings for plants are names of phyla with one exception: members of the Phylum Tracheophyta are indexed under class or subclass names. Scientific names (genus and species) are used as the initial, or file, word in the modifying phrase. Scientific names are omitted only when the name is not available in the literature or cannot be found in available references.

Subject headings for animals are the names of phyla with the following exceptions: (1) members of Phylum Arthropoda and Phylum Chordata are indexed under appropriate class name, and (2) common names are used for members of Class Mammalia.

Subject headings are entered for various classes of commodities, and specific products are identified in the file-word position of the modifier. In the following examples, approved subject headings are capitalized and typical modifier file words are listed in lower case.

Example 1	Example 2
CEREALS	MEATS
bread	beef
flour	fish
oats	mutton
rice	pork
rye	poultry
wheat	seafood

Diseases, pathological conditions, and in vitro studies of atypical cells and tissues are indexed under subject headings for the organism affected, under the appropriate anatomical structure of physiological phenomenon affected, and under the appropriate disease heading. Subject headings for diseases (defined as any deviation from the norm) are DISEASES; DISEASES, INFECTIOUS; DISEASES, NEOPLASTIC; DISEASES, PHYSIOLOGICAL; DISEASES, PLANT; and DISEASES, TRAUMATIC.

Diseases of mixed etiology are treated in the following manner: neoplastic diseases that are also classified as infectious or physiological are indexed under DISEASES, NEOPLASTIC; diseases in which a microorganism is the etiologic agent are classified under DISEASES, INFECTIOUS; physiological anomalies that are neither neoplastic nor infectious are indexed under DISEASES, PHYSIOLOGICAL; the acute radiation syndrome, nonspecific radiation injuries, trauma, and wounds or incisions inflicted mechanically are indexed under DISEASES, TRAUMATIC.

Specific diseases or pathological conditions are named in the file-word position of the modifier, in the author's terminology, and are set off from the remainder of the modifier by commas. Neoplasms are designated as benign or malignant in the file-word position when more specific information is not available.

Multicomponent Alloys and Other Systems

Multicomponent alloys and systems, except well-known trade names, are indexed under a subject heading for each component in the form "element systems" for nonmetals or "element alloys and systems" for metals. The modifier begins with element symbols for each component arranged alphabetically. In addition, if significance is placed on the base metal of the alloy, this is indicated by adding "-base" to the element symbol.

Example: A 1.5C, 12Cr, 0.25V, 0.8Mo, bal Fe alloy is indexed as

```
CARBON SYSTEMS
  C--Cr--Fe-base--Mo--V, ...
CHROMIUM ALLOYS AND SYSTEMS
  C--Cr--Fe-base--Mo--V,...
IRON ALLOYS AND SYSTEMS
  C--Cr--Fe-base--Mo--V, ...
MOLYBDENUM ALLOYS AND SYSTEMS
  C--Cr--Fe-base--Mo--V, ...
VANADIUM ALLOYS AND SYSTEMS
  C--Cr--Fe-base--Mo--V, ...
```

Well-known alloys, such as ZIRCALOY-2, are indexed under the trade name; cross references from each component of the alloy to the trade name appear in cumulative indexes.

Multicomponent systems in which nonmetallic elements are present in large percentage and which are commonly referred to as systems or mixtures are indexed in a manner similar to alloys.

Example: A tungsten–silicon preparation is indexed as

```
TUNGSTEN ALLOYS AND SYSTEMS
  Si--W, ...
SILICON SYSTEMS
  Si--W, ...
```

Multicompound systems and mixtures of inorganic compounds are indexed under the subject heading for each component compound; the modifiers begin with an alphabetical listing of compound formulas.

Example: A lead titanate–lead zirconate mixture is indexed as

```
LEAD TITANATES
  PbTiO3--PbZrO3
LEAD ZIRCONATES
  PbTiO3--PbZrO3
```

A mixed system of compounds and elements is indexed by a combined form of the preceding conventions; e.g., a dispersion of copper and alumina would be indexed as

ALUMINUM OXIDES
  Al_2O_3--Cu, ...
COPPER ALLOYS AND SYSTEMS
  Al_2O_3—Cu, ...

Mixtures of organic compounds are indexed under subject headings for each component of the mixture; the modifiers begin with an alphabetical listing of compound names.

Example:

ACETIC ACID
  acetic acid--BF_3, ...
BORON FLUORIDES
  acetic acid--BF_3, ...

Example:

BENZENE, CHLORO-
  bromophenol--chlorobenzene, ...
PHENOL, BROMO-
  bromophenol--chlorobenzene, ...

If modifiers for alloys and systems are included with other modifiers under the same subject heading, they are filed last.

Example:

CARBON SYSTEMS
  deposition on nuclear fuel particles
  molecular structure of
  neutron total cross section for
  sorptive properties for xenon
  Young's modulus for
  Al--C--Cr, superconductivity in
  B--C, phase studies for
  C--U--Zr, fabrication and physical properties of

Nomenclature of High Energy Physics

Information on particle-particle events is indexed under subject headings for the specific particles involved. The modifier file word *interactions* is followed by the specific interaction written in symbolic form. Particle nomenclature and symbols follow that of Rosenfeld, et al. *Data on Particles and Resonant States,* UCRL-8030 (latest revision). For consistency the incident particle is always written first. The mass (in MeV) of a resonance state is included in parentheses after the symbol to avoid ambiguity. Hyperfragments are indicated in modifiers as in the following examples: Λ-He^5, Σ-H^3, $\Lambda\Lambda$-Be^{10}. The superscript on the right indicates the total number of baryons in the composite system.

Examples:

MESONS (π^-)
  interactions $\pi^- + p \rightarrow \Lambda + K^+ + \pi^-$ at 6 GeV/c in hydrogen bubble chamber, ΛK(1700) enhancement in, (E)
BARYONS, RESONANCE (N*)
  production of $\Delta^{++}(1236)$ and $\Delta^0(1236)$ from $K^- + p \rightarrow K^- + p + \pi^+ + \pi^-$ interactions at 2.63 and 2.70 GeV/c, (E)
HYPERFRAGMENTS
  binding energy of $\Lambda\Lambda$-He^6, three-body o—Λ—Λ model for

Subject headings are also provided for specific models and theories.

Examples:

ELEMENTARY PARTICLE MODELS (TRIPLET)
  hadron total cross sections in quark, numerical analysis of
CURRENT ALGEBRA
  PCAC hypothesis for A_1 and rho dominance in $\pi \rightarrow e + \nu + \gamma$ decay
REGGE POLE THEORY
  predictions for polarization in $K^- + p \rightarrow$ anti $K^0 + n$, $\pi^- + p \rightarrow \pi^0 + n$, and $\pi^- + p \rightarrow$ eta + n interactions at high energies
SYMMETRY GROUPS
  SU(2) × SU(4) intermediate-coupling model for nucleon and hyperon isobars

Nomenclature of Reactor Technology

Subject headings for reactors are of three types:

(1) Specific reactors, e.g., ARGONNE RESEARCH REACTOR, SAXTON POWER REACTOR

(2) Reactors having a common physics or engineering characteristic, e.g., REACTORS, FAST; REACTORS, ORGANIC-COOLED; REACTORS, PRESSURIZED-WATER

(3) Reactors having a common purpose, e.g., REACTORS, POWER; REACTORS, RESEARCH

Information on specific reactors, type (1), is indexed under the one specific subject heading. Information on classes or types of reactors, types (2) (characteristics) and (3) (purpose), is indexed under all applicable headings. For example, information on a heavy-water-moderated organic-cooled power reactor is indexed under REACTORS, HEAVY WATER-MODERATED; REACTORS, ORGANIC-COOLED; and REACTORS, POWER.

Subject headings exist for selected reactor components, e.g., REACTOR FUEL ELEMENTS. When applicable, headings for components are indexed even though they may have been included in a modifier under a type (1) or (2) heading. The materials in reactor components are indexed when the information is peculiar to the material.

Modifier file words under reactor headings are of two primary types: one type expresses reactor characteristics, e.g., reactivity; the other, components, e.g., control rod. If no subject heading appears for a reactor component, the heading REACTORS is used, and the component is used as the modifier file word.

XUM

A

ACCELERATOR TUBES
design of highrgradient, 25:31048 (SJC-A-71-2)
ACCELERATORS
beam shaking method for removing neutralizing ions in, 25:31050 (UCRL-20156)
description of 1.2-kA, 4-MeV electron, for beam injection in electron-ring accelerator, 25:31053 (UCRL-20174)
synchrotron emission from charged particles in cyclic, gravitational plane wave effects on, (T), 25:31008
uses in industrial radiation processes, 25:29126
ACCIDENTS
radium release, at Italian refinery, hospital facilities for treatment of victims following, 25:29508
ACETATES
determination of microquantities of, spectrophotometric, 25:28996
ACETIC ACID,
[(CARBOXYMETHYLIMINO)BIS(ETHYLENENITRILO)]TETRA-
complexes with molybdenum(VI), potentiometric titration studies on stability constants of, 25:28920
effectiveness for removal of cerium-144 from beagle dogs following inhalation as chloride, 25:29543 (LF-43, pp 280-5)
effectiveness for removal of inhaled cerium-144 chloride from beagle dog lungs in combination with bronchopulmonary lavage, 25:29544 (LF-43, pp 286-94)
evaluation of cobalt-58-labeled, for human nephrography, 25:29577
use of metastable Indium-113-labeled, for radiodiagnosis of human brain tumors, 25:29583
ACETIC ACID,
[ETHYLENEBIS[[(CARBOXYMETHYL)IMINO]ETHYLENENITRILO]]TETRA-
complexes with molybdenum(VI), potentiometric titration studies on stability constants of, 25:28920
ACETIC ACID, (ETHYLENEDINITRILO)TETRA-
effects on chromosome aberrations in γ-irradiated pea seeds, 25:29485
evaluation of chromium-51-labeled, for human nephrography, 25:29577
use of chromium-51-labeled, for kidney scanning, 25:29578
ACETIC ACID, VINYL ESTER
acrylonitrile--vinyl acetate, radioinduced polymerization on polymers, γ, 25:29106
polyethylene--poly(vinyl acetate), radioinduced preparation of foamed sheets of, 25:29109(P)
ACETONE
radiolysis of frozen, effects of dose rate on yields from γ, 25:29160
ACETYLCHOLINE
radioprotective effects of, on survival of mice, γ, 25:29548
ACETYLENE
alpha-particle stopping cross sections in gaseous, test of Bragg's rule for, 25:30642
ACIDS
analysis for copper by fluorescence method, 25:28928
corrosive effects on refractory alloys and metals, evaluation of, 25:29775
determination of free, in phosphorus-32 preparations, ASTM method for, 25:29002
determination of free, in radioisotope solutions, ASTM method for, 25:29005
ACRYLIC ACID, ETHYL ESTER
radiation effects on subsequent polymerization of, with cellulose, effects of oxygen on γ, 25:29108
ACRYLONITRILE
radioinduced solid-state polymerization of, ESR studies of effects of uv radiation on γ, 25:29118
acrylonitrile--methyl methacrylate, radioinduced polymerization on polymers, γ, 25:29106
acrylonitrile--styrene, radioinduced polymerization on polymers, γ, 25:29106
acrylonitrile--vinyl acetate, radioinduced polymerization on polymers, γ, 25:29106
ACTINIDES
Fermi surfaces of, review, 25:30681
quantum number and regularities in f-electron, parallelism between, 25:29091
ACTINIUM ISOTOPES Ac-225
alpha decay of, conversion electron spectra from, (E), 25:31325
ACTINIUM ISOTOPES Ac-228
radioisotopes from distribution of recoil ions of, outside thorium oxide particles in thorotrast, 25:29169
ACTIVATION ANALYSIS
book: Measuring Methods Using Ionizing Radiation, 25:29391
data processing in, review on on-line, 25:29027
equipment for neutron, design and performance of boron--polyethylene rabbits, 25:29025
methods and uses of neutron, in mineral oil industry, review on, 25:29026
photopeak integration in, digital methods of, 25:29028
sensitivity for use in criminalistics, 25:29012(R) (GA-10276)
ADAMANTANE
radiolysis of solid, ESR spectral studies on radicals produced by γ, 25:29139
ADENOSINE, 2'-DEOXY-
radiolysis of single crystals of, ESR study of sugar radicals from, x, 25:29146
ADENOSINE 5'-TRIPHOSPHATE
effects on chromosome aberrations in γ-irradiated pea seeds, 25:29485
ADRENAL GLANDS
radiation effects on activity of dog, acute and chronic, 25:29642
radiation effects on histochemistry of cortical and medullar tissues in rat, partial-body x, 25:29671
AEROSOLS
effects on scavenging of radon decay products from atmosphere, mathematical model for describing, 25:29217
light scattering from, 25:31703 (LA-4641)
production and properties of, research on, 25:29419(R) (LF-43)
production of monodisperse, using Fulwyler Droplet Generator, 25:29076 (LF-43, pp 13-17)
radioactivity in, effects of particle size on distribution of, 25:29214(T) (LA-tr-71-7)
release during liquid metal cooled reactor accidents, mathematical analysis of, 25:31616
release from liquid sodium cooled fast breeder reactors, analysis of accident, 25:31618
release from liquid sodium fires, review of experiments on, 25:31615
release in fast breeder reactor containment systems, analysis of accident, 25:31617
release in reactor containment systems, analysis of accident, 25:31619
removal from gas streams, performance of sand-bed filters for, 25:29315 (ANL-7683)
retention of radioactive, by plants in comparison to retention of particulate fallout, effects of particle size on, 25:29444
sampling for particle size analysis, comparison of methods for, 25:29263
size distribution of radioactive, in air in uranium mines, (E), 25:29200(T) (AEC-tr-7227)
solubility of radioactive particles of, 25:29080 (LF-43, pp 40-51)
transport during liquid metal cooled reactor accidents, mathematical analysis of, 25:31616
transport from liquid sodium fires, review of experiments on, 25:31615
transport in fast breeder reactor containment systems, analysis of accident, 25:31617
AET
radioprotective effects of, on biochemical properties correlated with radiosensitivity in mice, 25:29553
radioprotective effects of, on bioelectric activity in muscle and nerve tissues, x, 25:29609
radioprotective effects on muscles and spleen of mice, effects of increased atmospheric pressure on γ, 25:29550
AGE
effects on irradiated cells, 25:29457
AGUIRRE POWER REACTOR, UNIT 1
design parameters of, requested additional information on, 25:31523 (DOCKET-50376-10)
design parameters of, revised and additional data on, 25:31524 (DOCKET-50376-11)
operations aspects of, requested additional information on, 25:31523 (DOCKET-50376-10)
operations aspects of, revised and additional data on, 25:31524 (DOCKET-50376-11)
AIR
aerosols in uranium mines, size distribution of radioactive, 25:29200(T) (AEC-tr-7227)
flow through concentric annuli, mean velocity and turbulence of fully developed, 25:29265 (RD/B/N-1878)
injection into toroidal geometries, adial distribution of tangential, (E), 25:30602
neutron scattering at air-ground interface, differential measurements of fast-, (E), 25:30635
neutron scattering by, angular distribution of, 25:30639
particle removal from polluted, performance of condensing steam aerosol scrubber for, 25:29251 (ORNL-4654)
radiation monitoring in uranium mines, methods for, 25:29536
reactions of flowing, with pyrolytic graphite, effects of air velocity, surface area, and temperature on, 25:29919
reactions with niobium--zirconium alloys at 700 to 1000°C, oxide film composition and kinetics of oxidation, 25:29769
reactions with zirconium at low pressure and 810°C, study of nucleation and crystal growth of zirconium oxide from, 25:29997
sampling methods for, in uranium mines, 25:29536
AIR SAMPLERS
book: Air Sampling Instruments, 25:29398
design for monitoring airborne alpha sources, 25:29352(P)
AIRGLOW
oxygen 5577-A green-line emission at 100 to 300 km in day ionosphere, mechanism of atomic, (E), 25:30375

oxygen emission at 6300 A from photodissociative excitation, daytime, (E), 25:30386
ALANINE AMINOTRANSFERASE
radioinduced inactivation of, in mycelium of Botrytis cinerea, uv, 25:29720
ALASKA
sediment deposition and transportation patterns of Queen Inlet at Glacier Bay, 25:31724 (RLO-2229-T-1-3)
ALBUMINS
radiation effects on macrostructure of bovine serum, γ, 25:29471
zinc-65 uptake by, in human blood serum, 25:29447
ALCOHOLS
proton polarization in polyhydric, doped with chromium complexes, dynamic, 25:31046 (RHEL/R-213)
ALGAE
content of periphyton component of running-water ecosystem, performance of artificial substrates for determining, 25:29478
ALGINIC ACID
sodium salt, decomposition by oxidative-reductive depolymerization, 25:29159
sodium salt, effects on calcium-47 and strontium-85 metabolism in rats, 25:29446
sodium salt, radiolysis of, kinetics of, 25:29159
ALGORITHMS
formulation of geometric programming method for optimization of nuclear systems, 25:31649
ALKALI METAL CHLORIDES
analysis for copper by fluorescence method, 25:28928
ALKALI METAL HALIDES
impurities in, ionic, 25:30646(R) (NYO-2150-66)
radioinduced defect formation and sputtering in, electron, 25:30651
radioinduced defect formation and sputtering in, photon, 25:30651
radioinduced hardening of, model for effects of defect concentration on, 25:30013
ALKALI METAL HYDROXIDES
corrosive effects on refractory alloys and metals, evaluation of, 25:29775
ALKALI METALS
determination by amperometric, chelatometric, and conductometric titrations, 25:28970
ALKALINE PHOSPHATASE
radiation effects on activity of, in small intestine of rats, effects of radioprotectors on x, 25:29645
ALKANES
beta-particle reactions with gaseous, pressure and temperature dependence of mean energy for ion-pair formation in, (E), 25:30636
ALLANITES
occurrence in Bivangaon and Kansa areas of India, 25:29226
ALLOXANTIN
complexes with chromium, distribution of phosphorus-32-labeled, in tissues of normal or tumor bearing mice in comparison with phosphorus-32-labeled orthophosphate, 25:29453
ALLOYS
book: Achievement of High Fatigue Resistance in Metals and Alloys, 25:29840
conference on new, Sydney, Australia, Aug. 27, 1970, 25:29759
corrosion of nonferrous, high-temperature electrochemical methods for studies of, 25:29779
microstructure of, generalized mechanistic discussion of effects of precipitation on, 25:29888
ALLYL ALCOHOL
radiolysis of glass, ESR study of radicals produced by γ, 25:29162
ALPHA PARTICLES
dose distribution in lungs of man following injection of Thorotrast, 25:29521
dose to rat lungs following inhalation of lead-212-labeled aerosols, 25:29455
effects on bones of dogs, pathological, 25:29630
effects on chromosomes in Chinese hamster liver cells, RBE for americium-241, 25:29483 (LF-43, pp 246-53)
effects on microstructure of metals, 25:29909
effects on microstructure of thorium dioxide at 5.5 MeV, 25:30012
effects on spallation and strain in polycrystalline thorium dioxide at 5 MeV, 25:30014
effects on urinary tract of man, pathological, 25:29697
flux of 5.2- to 81.7-MeV solar and primary cosmic, (E), 25:30161
reactions (α,2n), (α,3n), (α,4n), and (α,αn) with rubidium-85 at 15 to 54 MeV, excitation functions, isomer ratios, and mean recoil distances for, (E/T), 25:31239 (LYCEN-7091)
reactions (α,αp) with deuterium at 78 MeV, analysis using quasi-free collision theory, (E/T), 25:31189
reactions (α,n) with oxygen-18, neutron yield from, (T), 25:31224
reactions (α,p) with calcium-42, p-γ angular correlations in, (E), 25:31251
reactions (α,p) with iron-56, calculation of angular distributions for, (T), 25:31428
reactions (α,pγ) with zinc-67 at 14 MeV, γ spectra from, (E), 25:31290
reactions with aluminum-27 and silver-108 at 205 MeV, neutron and proton spectra from, (T), 25:31368
reactions with aluminum-27, carbon-12, and niobium-93 at 0.2 to 0.9 GeV, excitation functions for, (T), 25:31368
scattering by argon-36 at 12.8 to 17.8 MeV, analysis using optical model and compound elastic contribution, 25:31262
scattering by helium-4 at 0 to 100 MeV, calculation of phase shifts using nonlocal separable potentials for elastic, (T), 25:31186 (LYCEN-7089)
scattering by helium-4, carbon-12, nitrogen-14, and oxygen-16, at 1 GeV per nucleon, absorption cross sections for, 25:31234
scattering by iridium-191, -193 at 16.6 MeV, differential cross sections for inelastic, (E), 25:31342
scattering by magnesium-24 at 16.7 MeV, reaction mechanism study of α--γ angular correlations from, (E), 25:31215
scattering by nickel-64 and lead-208, calculation of optical potentials in terms of diffraction-model parameters, (T), 25:31410
scattering by oxygen-16, silicon-28, and calcium-40 at 104 MeV, differential cross sections for, (T), 25:31212
scattering by palladium-108 at 10.1 MeV, γ--γ angular correlations from inelastic, (E), 25:31374
spectra of 5.2- to 81.7-MeV solar and primary cosmic, (E), 25:30161
stopping cross sections in gases, test of Bragg rule for, 25:30642
ALPHA SOURCES
determination in industrial water or waste by radiometry, ASTM method for, 25:29003
monitoring in environmental samples at West Valley Processing Plant, 1971, 25:29180 (DOCKET-50201-70)
monitoring of airborne, air sampler for, 25:29352(P)
ALUMINUM
analysis for hydrogen by carrier gas fusion--gas chromatographic methods, 25:28936
analysis for silicon as molybdosilicate complex, spectrophotometric method for, 25:28924
anodization of, oxide growth rate in solid-state, 25:29803
determination by amperometric, chelatometric, and conductometric titrations, 25:28970
determination in ammonium acetate extracts of soils by neutron activation, atomic absorption, and spectrophotometry, comparative study on, 25:29020
determination in carbon using 2-quinizarin sulfonic acid, ASTM method for photometric, 25:28974
determination in crude or refined oils or engine deposits by neutron activation and γ spectrometry, 25:29026
determination in high-purity water for reactor cooling and moderating, 25:28914 (BARC-515)
determination in plutonium by absorption spectrophotometry and spectrography, 25:28916 (CEA-R-4071)
determination of trace amounts of, in vanadium, spectrographic, 25:28947
determination using ion permselective membrane, potentiometric, 25:28956
diffusion of plutonium and uranium in, at 550 to 630°C, 25:29867
effects on fluorometric determination of zirconium, 25:28963
electron transport through slabs of, ANISN calculations for 1-MeV, 25:30630 (ORNL-TM-3318)
electron tunneling in junctions with alumina, analysis of, 25:30706
microstructure of pack-cementation coatings of, on niobium, niobium--titanium alloys, and niobium--tungsten alloys, effects of metal mechanical properties on, 25:29816
properties of aerosols produced from aqueous solutions of, 25:29079 (LF-43, pp 31-9)
proton reactions at 70 GeV, upper limits for differential and total cross sections for quark production in, (E), 25:30724(T) (CERN-Trans-71-4)
radiation effects on shear modulus of, at 4°K, neutron, 25:29912
radiation effects on swelling and voids in, high-flux neutron, 25:29905 (ORNL-4630, pp 239-60)
separation from aqueous solutions by thin-layer chromatography using liquid anion exchangers, 25:29186
solvent properties for plutonium and uranium at 550 to 630°C, 25:29867
superconducting-state parameters at reduced volumes, calculations, 25:30419
ALUMINUM ALLOYS AND SYSTEMS
radiation effects on mechanical properties of, use of cyclotron-injected helium for simulation of neutron, 25:29907 (ORNL-TM-3299)
radiation effects on properties of Types 8001 and 1100, fast neutron, 25:29905 (ORNL-4630, pp 239-60)
Al--Be--Ti, phase diagrams at 600 to 1300°C, isothermal, 25:29900
Al--Co--Cr, oxidation resistance at 1100°C, mapping method for selection of optimum, 25:29780
Al--Cr--Ni, oxidation resistance at 1000°C, mapping method for selection of optimum, 25:29780
Al--Mo--Ti-base--V, corrosion cracking in aqueous and

methanol solutions with and without halogen ions, stress, 25:29765
Al--Ni--steel--Ti, failure of electroslag welded joints on, effect of residual welding stress on brittle, 25:29832
Al--Sn--V, phase equilibria and superconductivity in intermetallic V_3LAl--V_3Sn, 25:30416
Al--Ti-base--V, corrosion by hydrochloric acid--methanol and sodium chloride--isopropanol, 25:29773
Al--U, crystal structure of UAl_4, 25:29895
Al--U, properties of UAl_4, electric, mechanical, and thermal, 25:29895
Al--U, radiation effects on aluminum-clad fuel plates of, in-pile, 25:29924 (ORNL-4630, pp 233-8)

ALUMINUM ISOTOPES Al-23
proton decay of, energy spectra and excitation functions for beta-delayed, (E), 25:31241 (UCRL-20436)

ALUMINUM ISOTOPES Al-25
energy level at 3.696 MeV from magnesium-24 (p,γ) reactions, lifetime and branching ratios for, (E), 25:31266
energy levels of, calculation including shell mixing effects, (T), 25:31265

ALUMINUM ISOTOPES Al-27
alpha reactions at 0.2 to 0.9 GeV, excitation functions for, (T), 25:31368
alpha reactions at 205 MeV, neutron and proton spectra from, (T), 25:31368
deuteron elastic scattering at 82 MeV, optical-model analysis of, (E), 25:31240 (NP-18511)
deuteron reactions (d,He-3) at 82 MeV, DWBA analysis of differential cross sections for, (E/T), 25:31240 (NP-18511)
energy levels from silicon-28 (d,He-3) reactions, l-transfer, spectroscopic factors, and spin-parity assignments for, (E/T), 25:31240 (NP-18511)
helium-3 reactions (He-3,Li-6) at 40.7 MeV, DWBA analysis of, (E/T), 25:31214
meson (π^-) capture by proton, deuteron, and triton spectra from, (E), 25:31213
photon reactions (γ,n) up to 30 MeV, cross section for, (E), 25:31242
proton reactions at 11.5 and 23.5 MeV using thick targets, neutron yield from, (E), 25:31209

ALUMINUM OXIDES
analysis of, properties of vitreous carbon as mortar for spectrochemical, 25:28938
bonding of monocrystalline, to nickel powder compacts, effects of sintering atmosphere, pressure, temperature, and time on, 25:29815
electron tunneling in junctions with aluminum, analysis of, 25:30706
properties of sintered, for use as ball bearing spheres in ultrahigh vacuum, 25:29834
radiation effects on dielectric properties of insulators of, fast neutron, 25:30011 (ORNL-4630, pp 226-9)
thermodynamic properties of gaseous diatomic, free energy functions for, 25:29082
Al_2O_3--CaO--CeO_2--SiO_2--ZrO_2, analysis of, x-ray-emission, 25:28957
Al_2O_3--Cs_2O--SiO_2, preparation and properties of, for use as radiation source, 25:29938(T) (BNWL-tr-65)
Al_2O_3--Li_2O--MgO--SiO_2, radiation effects on phase transformations in, neutron, 25:30017
Al_2O_3--SiO_2, radiation effects on catalytic properties of halogenated, in cracking of cumene and isomerization of o-xylene, γ, 25:29111

AMERICIUM
electron band structure calculations for fcc, 25:30696(R) (COO-2103-3)
production and properties of aerosols of, 25:29078 (LF-43, pp 25-30)
separation from berkelium, curium, californium, europium, plutonium, and uranium by ion exchange in zirconium phosphate--nitric acid system, 25:28989

AMERICIUM ISOTOPES
radioactivity standards of, users' guides for, 25:29174

AMERICIUM ISOTOPES Am-241
content in beagle dog lungs following inhalation as oxide, 25:29421 (LF-43, pp 8-12)
effects on chromosomes in Chinese hamster liver cells, internal aberrant, 25:29482 (LF-43, pp 240-5)
production of monodisperse aerosols of, centrifugation method for, 25:29421 (LF-43, pp 8-12)

AMERICIUM ISOTOPES Am-242
neutron fission of metastable, charge and mass distribution of thermal, (E), 25:31373

AMERICIUM ISOTOPES Am-243
determination by ion exchange, isotope dilution, and α spectroscopy, 25:28989
energy levels of, superfluid-model calculations of energies and wave functions of nonrotational, (T), 25:31306 (JINR-P4-5693)

AMERICIUM ISOTOPES Am-246
beta decay of metastable, gamma spectra from, (E), 25:31378

AMIDE POLYMERS
properties as binder for radiation-resistant solid film lubricants, 25:29096 (WERL-HFIL-1)

AMINO ACIDS
effects on uptake of radioactive rare earth isotopes by animals, 25:29445

AMMONIA
abundance in Jovian atmosphere, (T), 25:30250
alpha-particle stopping cross sections in gaseous, test of Bragg's rule for, 25:30642
complexes with cobalt chloride, uses in gravimetric and radiometric determinations of plutonium, thorium, and uranium, 25:28982
ion reactions with, binary-encounter calculation of ionization cross sections for, 25:30299

AMMONIUM COMPOUNDS
effects on radiometric determination of cesium isotopes in water, after extraction as tetraphenylborates, 25:29000

AMMONIUM URANATES
uranium oxide precipitation from, reaction kinetics of, 25:29925

AMPHIBIA
Rana pipiens, effects of variant nuclei of haploid cells of, on embryonic development, 25:29608(R) (NYO-2356-43)
Rana sp., radiation effects on sartorius muscles in, in relation to calcium metabolism x, 25:29674

AMPLIFIERS
description of superconducting chopper, for use in magnetic fields, 25:30447
design of fast transistor dc, 25:29346

ANGIOSPERMIDAE
Allium cepa, radioinduced chromosome aberrations in, protective effects of thiourea against x, 25:29559
Barbarea sp., radioinduced free radical production in seeds of, effects of imbibition and germination on γ, 25:29719
Gossypium sp., radiation effects on activity of aminoacyl-tRNA synthetases and tRNA in, 25:29715
Helianthus sp., radiation effects on seeds of, effects of storage time on, 25:29717
Helianthus sp., radiation effects on, effects of mineral nutrition level on γ, 25:29714
Ipomoea batatas, radiosensitivity of tubers of, effects of growth and productivity on γ, 25:29721
Latuca sativa, radiation effects on cytogenetics of seedlings and seeds of, effects of dose rate on γ, 25:29491
Lemna sp., effects on content of uranium fission products in fresh water, 25:29449
Lycopersicum esculentum, radioinduced mutations in seeds of, M(2) characteristics following combined effects of colchicine or diethyl sulfate and x, 25:29493
Medicago polymorpha, radioinduced mutations in, for early flowering and improved vigor, effects of seed exposure on, 25:29488
Oryza sativa, radiation effects on chromosomes and pollen and seed fertility of M(1) generation of, β and x, 25:29496
Oryza sativa, radioinduced mutations in seeds of, M(2) characteristics following combined effects of diethyl sulfate and x, 25:29495
Oryza sp., mutation induction in, comparison of γ and neutron radiation and ethyl methanesulfonate or diethylsulfonate, 25:29481 (IAEA-R-290-F)
Oryza sp., radioinduced chlorophyll mutations in, effects of dose on γ and neutron, 25:29481 (IAEA-R-290-F)
Pisum sativa, radioinduced mutations in, cytology of male sterile recessive x, 25:29492
Pisum sativum, radioinduced chromosome aberrations in seedlings of, effects of dose rate on x, 25:29489
Pisum sp., radiation effects on chromosome aberrations in seeds of, effects of ATP, cysteine, and EDTA on γ, 25:29485
Pisum sp., radiation effects on chromosome aberrations in seedlings of, protective effects of anoxia against γ, 25:29486
Pisum sp., radiation effects on mitosis in seedlings of, effects of dose on γ, 25:29484
Pisum sp., radioinduced chromosome aberrations in dormant seeds of, effects of moisture content on protective effects of cysteine against γ, 25:29552
Solanum sp., radiation effects on tubers of, infected with x-virus, mutagenic γ, 25:29726
synthesis of arginine in, enzyme reactions for, 25:31691(R) (COO-1750-3)
Triticum sp., radiation effects on germination of seeds of, effects of thermal shock on x, 25:29723
Triticum sp., radiation effects on grains of, effects of, on development and reproduction of grain weevils, γ, 25:29737
Vicia paba, radioinduced chromosome aberrations in roots of, by exposure in sucrose solutions, effects of acidity on γ, 25:29494

ANILINE
radiolysis of, gas chromatographic analysis of products from γ, 25:29155

ANIMALS
bone marrow transplantation in irradiated, review on xenographic, 25:29683
conference on radiation effects on, abstracts of papers from, 25:29607 (CONF-690940-(Absts.))
radiation effects on oxidative phosphorylation in liver mitochondria of, effects of histones on whole-body, 25:29638

XU

radiation effects on salivary glands of, x, 25:29693
radioinduced cirrhosis and lesions in liver of, γ and x, 25:29694
radioinduced damage and loss of lung cells of, 25:29636
radioinduced damage to cells of, γ and x, 25:29690
radioinduced myocarditis in heart of, x, 25:29695
radioisotope uptake by, effects of amino acids and proteins on rare earth, 25:29445
radiosensitivity of gastrointestinal tract of, x, 25:29632

ANOXIA
radioprotective effects of, on biochemical properties correlated with radiosensitivity in mice, 25:29553
radioprotective effects of, on chromosome aberrations in pea seedlings, effects of dose on γ, 25:29486

ANTARCTIC REGION
sphene from Soer-Rondane Mountains of, lead/uranium ages of, 25:29208

2-ANTHRACENESULFONIC ACID, 9,10-DIHYDRO-3,4-DIHYDROXY-9,10-DIOXO-
uses in spectrophotometric determination of uranium, 25:28934

ANTIBIOTICS
effects of iodinol on staphylococcus-infected wounds in cornea of irradiated rabbits, 25:29649

ANTIBODIES
radiation effects on production of homologous thyroglobulin, in rats, γ and/or iodine-131, 25:29660
radioinduced depression of hemagglutinating and hemolytic, in guinea pigs, 25:29474

ANTIFERROMAGNETIC MATERIALS
neutron transmission through, analysis of depolarization in, (T), 25:31181

ANTIGENS
detection of male limited H--Y, on peritoneal exudate cells, serological, 25:31719 (ORO-3634-13)
histocompatibility of, detection and measurement by transfer of mouse peritoneal exudate cells of, 25:31718 (ORO-3634-12)
histocompatibility on mouse peritoneal macrophages, detection of weak, 25:31717 (ORO-3634-11)

ANTIMONY
determination for water flow tracing by neutron activation, 25:29013 (RLO-1750-81)
determination in deposits and airborne particles by neutron activation and scintillation counting, 25:29032
determination of trace amounts of, in vanadium, spectrographic, 25:28947
effects on fluorometric determination of zirconium, 25:28963
properties of aerosols produced from aqueous solutions of, 25:29079 (LF-43, pp 31-9)
separation from arsenic and tin by thin-layer chromatography, 25:29165
separation from mercury by solvent extraction, 25:29031
separation from tellurium and tin by thin-layer chromatography, 25:29165

ANTIMONY ALLOYS AND SYSTEMS
Cd--Sb, atomic structure of liquid, at 350 to 653°C, Kumar--Samarin centrifugation method for studying, 25:29896
Np--Sb, crystal structure of NpSb, 25:30002
Pu--Sb, crystal structure of PuSb, 25:30002

ANTIMONY ISOTOPES
production in proton fission of uranium-238 at 450 MeV, mass yield and charge distribution for, (E), 25:31302 (COO-1167-10)

ANTIMONY ISOTOPES Sb-122
metabolism in beagle dogs following ingestion of nuclear debris from Project Cabriolet, 25:29456

ANTIMONY ISOTOPES Sb-123
neutron activation resonance integrals for, measured relative to gold-197, (E), 25:31300 (CNEA-282)

ANTIMONY ISOTOPES Sb-124
beta decay of, γ spectra from, (E), 25:31346
distribution and retention in mice following inhalation of heat treated aerosols, 25:29424 (LF-43, pp 66-70)

ANTIMONY ISOTOPES Sb-125
beta decay of, γ spectra from, (E), 25:31340
energy levels from tin-125m decay, spins and parities of, (E), 25:31388

ANTIMONY OXIDES
thermodynamic properties of gaseous diatomic, free energy functions for, 25:29082

ANTINEOPLASTIC DRUGS
effects on human bronchial carcinomas, combined effects of radiotherapy and, 25:29606

ARABIAN SEA
meteorological conditions of atmosphere over, natural radon tracer studies of, 25:29220

ARCHAEOLOGICAL SPECIMENS
age of ancient, fine grain luminescence measurements for estimation of, 25:29212

ARGININE
synthesis in plants, enzyme reactions for, 25:31691(R) (COO-1750-3)

ARGON
argon-ion reactions with, electron--electron coincidence study of, 25:30288
diffusion in neutron-irradiated uranium-doped calcium fluoride single crystals, 25:30673
effects of inert atmosphere of, on growth rate of cadmium whiskers, 25:29804
effects on van der waals line broadening in astrophysical spectra, (T), 25:30266
energy-level transitions in, electron spectra from Coster--Kronig and L-shell Auger, (T), 25:30261
fission product behavior in, (E/T), 25:31615
helium-metastable-atom reactions at thermal energies with, angular distribution of electrons from Penning ionization in, (E), 25:30294
hydrogen-metastable-atom reactions at 1.0 keV to 1.6 MeV with, Born-wave calculations of total quenching cross sections for, 25:30283
neon-metastable-atom reactions with, two-state impact-parameter model for associative and Penning ionization in, 25:30298
plasma motion along rectangular channel in magnetic field, effect of short circuit on ionized, (E), 25:30347
plasma of, expansion of carbon-dioxide laser-induced, (E), 25:30542
plasma of, HB Stark broadening profiles in spectral, (E/T), 25:30268
plasma of, large-amplitude electron wave propagation in collisionless, (E/T), 25:30610
plasma of, microwave diagnostics in positive column, (E), 25:30483
plasma of, microwave diagnostics of contracted column, 25:30486
plasma of, spectra in carbon dioxide-, hydrogen-, and nitrogen-seeded, from standard intensity source at 1100 to 3100 A, (E), 25:30488
plasma of, temperature measurements in arcs, 25:30478(T) (SC-T-713024)
radioinduced defects in solid, release of energy stored in 4.6°K neutron, 25:30660
separation from off-gas streams, evaluation of thin silicone rubber membranes for, 25:29317 (ORNL-4522)
separation of krypton, tritium, and xenon from, design of gas chromatograph for, 25:29177 (CEA-R-4090)

ARGON IONS
ionization stages in corona, distribution of, (E/T), 25:30181
reactions with argon atoms, electron--electron coincidence study of, 25:30288
spectral lines due to Ar XIV, solar, (E), 25:30188

ARGON ISOTOPES
abundance in meteorites, (E), 25:30034
separation by mass-diffusion mercury columns, equipment and method for, 25:29277

ARGON ISOTOPES Ar-36
alpha elastic scattering at 12.8 to 17.8 MeV, analysis using optical model and compound elastic contribution, (E/T), 25:31262

ARGON ISOTOPES Ar-40
electron elastic scattering 40 to 60 MeV, cross section for, (E), 25:31272
nuclear radius from electron elastic scattering, (E), 25:31272
proton elastic and inelastic scattering at 30.4 and 49.4 MeV using polarized and unpolarized beams, differential cross sections for, (E), 25:31233

ARGON SYSTEMS
Ar--CO, reactions with radiolytic hydrogen atoms, kinetics of, 25:29158
Ar--O, reactions with radiolytic hydrogen atoms, kinetics of, 25:29158

ARKANSAS NUCLEAR ONE POWER REACTOR
buildings and structures for, final safety analysis of, 25:31512 (DOCKET-50313-27)
buildings and structures for, final safety analysis of, 25:31514 (DOCKET-50313-29)
control systems for, final safety analysis of, 25:31513 (DOCKET-50313-28)
cooling system for, final safety analysis of, 25:31512 (DOCKET-50313-27)
electrical systems for, final safety analysis of, 25:31513 (DOCKET-50313-28)
emergency and auxiliary systems for, final safety analysis of, 25:31513 (DOCKET-50313-28)
engineered safeguards for, final safety analysis of, 25:31513 (DOCKET-50313-28)
instrumentation for, final safety analysis of, 25:31513 (DOCKET-50313-28)
operations aspects of, final safety analysis of, 25:31513 (DOCKET-50313-28)
owners of, financial statements of, 25:31511 (DOCKET-50313-26)
owners of, technical qualifications of, 25:31514 (DOCKET-50313-29)
piping systems for, final safety analysis of, 25:31514 (DOCKET-50313-29)
radiation protection systems for, final safety analysis of, 25:31513 (DOCKET-50313-28)
radioactive waste disposal system for, final safety analysis of, 25:31513 (DOCKET-50313-28)
site for, final safety analysis of, 25:31512 (DOCKET-50313-27)
site for, meteorological data on, 25:31514 (DOCKET-50313-29)
steam and power conversion systems for, final safety

analysis of, 25:31513 (DOCKET-50313-28)
technical specifications for, 25:31513 (DOCKET-50313-28)
ARKANSAS NUCLEAR ONE POWER REACTOR, UNIT 2
design parameters of, revised and additional data on, 25:31521 (DOCKET-50368-9)
operations aspects of, revised and additional data on, 25:31521 (DOCKET-50368-9)
ARSENATES
effects on separation of thorium(IV) from sulfuric acid solutions by extraction using N-phenylbenzylamine in chloroform, 25:29184
ARSENIC
determination by x-ray fluorescence, sensitivity of, 25:28962
determination in gaseous media by hypophosphite dichromate method, 25:28959
determination of trace amounts of, in vanadium, spectrographic, 25:28947
reactions of trivalent, with cerium(IV), catalytic effects of ruthenium on, 25:28941
separation from antimony and tin by thin-layer chromatography, 25:29165
separation from mercury by solvent extraction, 25:29031
ARSENIC ISOTOPES
radioactivity standards of, users' guides for, 25:29174
ARSENIC ISOTOPES As-72
beta decay of, gamma spectra and log ft for, (E), 25:31261
ARSENIC ISOTOPES As-75
photon reactions (γ,n) at 10 to 68 MeV, yields of radioactivities from, (E), 25:31333
proton reactions (p,n) below 3 MeV, statistical model analysis of, (E), 25:31263
proton reactions (p,n) with, Hauser--Feshbach analysis of angular distributions and excitation functions for, (E/T), 25:31248
ARSENIC ISOTOPES As-76
beta decay of, γ spectra from, (T), 25:31259
ARSENIC OXIDES
thermodynamic properties of gaseous diatomic, free energy functions for, 25:29082
ASPARAGINE-KETOACID AMINOTRANSFERASE
radioinduced inactivation of, in mycelium of Botrytis cinerea, uv, 25:29720
ASTATINE ISOTOPES At-209
alpha decay off, fine structure in α spectra from, (E), 25:31324
ASTATINE ISOTOPES At-210
alpha decay off, fine structure in α spectra from, (E), 25:31324
ASTATINE ISOTOPES At-211
alpha decay off, fine structure in α spectra from, (E), 25:31324
ASTROPHYSICS
research problems in, (T), 25:30452
ATLANTIC OCEAN
molybdenum content and distribution from cores of Mid-Atlantic Ridge in, measurement of, 25:29228
uranium content and distribution from cores of Mid-Atlantic Ridge in, measurement of, 25:29228
ATMOSPHERE
boundary layers of, aerodynamic characteristics of, 25:31737 (TID-25465)
composition in lower, effect on occurrence of subauroral red arc at mid-latitude, (E), 25:30350 (N-70-36812)
contamination of, proposal for worldwide system of surveillance and monitoring of, 25:31695 (EGG-1183-2242)
electron intensity in, from radiation belt losses, 100- to 500-MeV, (E), 25:30353
fallout transport in, following 1966 to 1968 French nuclear explosions on Mururoa Atoll, measurement of interhemispheric, 25:29221
fallout transport in, following May 1966 Chinese nuclear explosion, calculation of worldwide, 25:29216
meson.(μ⁻) stopping rate in, 25:31448
neutron energy and angular distribution at ground-level and mountain altitudes in, 80 to 300 MeV, (E), 25:30374
neutron transport in, from nuclear explosions, method for calculation of, 25:29247
radiation monitoring in ground-level, at Fayetteville, Ark. following Dec. 1967 Chinese nuclear explosion, 25:29219
radioactivity in surface to 15 m height, relation between thermal stratification, wind velocity, and natural, (E), 25:29223
radioactivity monitoring, West Valley Processing Plant, 1970, 25:29179 (DOCKET-50201-69)
radon content of, over Arabian and Indian Seas, tracer studies of monsoon currents using natural, 25:29220
radon-220 and -222 distribution in, effects of wind velocity on vertical, (E/T), 25:29225
radon-220 decay product scavenging from, by aerosol particles and water droplets, mathematical model for describing, 25:29217
reaction with solar protons, relation of altitude-dependent ion formation during auroral, (E/T), 25:30397
research on Earth, from orbiting space station, (T), 25:30363
strontium-90 content of, in relation to fallout, effects of rainfall intensity on, 25:29218
x ray transport in, from nuclear explosions, method for calculation of, 25:29247
ATOMIC BEAMS
intensity and cluster sizes of hydrogen, control of, 25:30252 (EUR-4593, pp 43-9)
ATOMIC ENERGY, LEGAL ASPECTS
legislation on uranium law for compensation to land owners in Sweden, 25:29540
regulations for handling and possession of thorium and uranium in Sweden, 25:29541
regulations for x-ray protection in dentistry, 25:29530
ATOMS
electron elastic scattering by, T-matrix formalism for treatment of charge polarization in, 25:30280
electron reactions with one-electron, polarization in analysis of elastic scattering and excitation amplitudes for, 25:30287
plasma oscillations in, damping of, (T), 25:30301
positron scattering above positronium-formation threshold by, annihilation rate in, (T), 25:30289
reactions with diatomic molecules, strong-coupling approximation for rotational excitation in, 25:30296
reactions with diatomic molecules, vibrational excitation in near-classical limit for, (T), 25:30295
reactions with harmonic oscillators, comparison of classical, semiclassical, and quantum treatments of, 25:30292
reactions with harmonic oscillators, semiclassical treatment in three dimensions, 25:30290
scattering by atoms, analysis using S matrices, 25:30278
spectral-line source function for two-level, depth variation of non-LTE, (T), 25:30084
wave functions for, hybrid Gaussian-type, 25:30302
AURORAE
red-arc occurrence in sub-, associated with ionospheric phenomena, Sept. 29, 1967, (E), 25:30350 (N-70-36812)
AURORAL ZONE
electrojets in, relation of magnetospheric magnetic storm generation with production processes of, (E), 25:30400
electron flux into dayside oval, properties of region of low-energy primary, (E), 25:30367
electron-density profiles in disturbed- and quiet-topside ionosphere at 60 to 70 degrees latitude, (E), 25:30359
red arc south of, stable midlatitude SAR-, (E), 25:30398
..d arcs in, relation of plasmapause, ring current, and electron trough to magnetospheric field lines leading to SAR, (E/T), 25:30376
x-radiation intensity in, observations at conjugate points Kerguelen--Archangel of, (E), 25:30395
AUSTRALIA
nuclear power plant development in, 25:31462
radiation protection programs for medical personnel and patients during 1969, 25:29526(R) (NP-18790)
uranium deposits in Northern Territory, geology and mineralization of, 25:29234
AUSTRIA
radioisotope production in research reactors in, review of, 25:29274
AUTORADIOGRAPHY
book: Measuring Methods Using Ionizing Radiation, 25:29391
method for testing irradiated fuels using nitrocellulose sheets, 25:29944(T) (LB/G-2916)
AVES
Anas sp., radiation effects on content of sulfhydryl groups in tissues of, uv and/or x, 25:29647
Coturnix c. japonica, radiation effects on learning and memorizing behavior in, effects of dose on x, 25:29687
Gallus sp., radiation effects on egg production by, following ingestion of iodine-131, 25:29661
AVR REACTOR
operation of, evaluation of, 25:31540
6-AZAURIDINE
effects on nuclear diameter of x-irradiated Ehrlich ascites tumor cells in mice, in vitro, 25:29679

B

BACTERIOPHAGES
radiation effects on adsorption capacity of T2r, combined effects of cysteine and x, 25:29728
BALLISTICS
balloting problems in, 25:31731 (SC-RR-710071)
BARIUM
determination as carbonate alone and with strontium and calcium carbonates by pellet technique, in spectroscopic, 25:28972
determination by amperometric, chelatometric, and conductometric titrations, 25:28970
determination in ores, x-ray radiometric method using selenium-75 source for, 25:28940
determination using ion permselective membrane, potentiometric, 25:28956
diffusion coefficients in liquid sodium, radiochemical determination of, (E/T), 25:31613
effects on fluorometric determination of zirconium, 25:28963
photon reactions (γ,xnyp) at 18 to 75 MeV, photonuclear yields from, 25:29017

separation from other alkaline earths by ion exchange, 25:29193
transport of fission product, in liquid sodium, (E/T), 25:31614
BARIUM ALLOYS AND SYSTEMS
Ba--Yb-base, electric conductivity of, effects of pressure and temperature on, 25:30674
BARIUM CHLORIDES
molecular structure of, 25:29086
spectra in matrices of solid nitrogen or rare gases, ir, 25:29086
BARIUM ISOTOPES
radioactivity standards of, users' guides for, 25:29174
BARIUM ISOTOPES Ba-137
energy level of, analysis of double internal conversion in decay of 662-keV, (E), 25:31359
BARIUM ISOTOPES Ba-139
determination in water by precipitation and radiometry, ASTM method for, 25:29004
BARIUM ISOTOPES Ba-140
accumulation in skeleton of fish, 25:29449
determination in water by precipitation and radiometry, ASTM method for, 25:29004
distribution and retention in beagle dogs following inhalation as chloride, 25:29428 (LF-43, pp 92-9)
metabolism in beagle dogs following ingestion of nuclear debris from Project Cabriolet, 25:29456
BARIUM OXIDES
thermodynamic properties of gaseous diatomic, free energy functions for, 25:29082
BARIUM SULFATES
radiolysis of bromide- or iodide-doped, ESR studies on γ, 25:29163
BARYONS
decay of, Cabibbo theory and SU(3)--symmetry breaking corrections for leptonic, 25:30930
exchange in Regge pole theory, triquark and biquark propagators with constant residues for, 25:30834
interactions with mesons, scale symmetry breaking for scattering length from, 25:30933
interactions with pseudoscalar mesons at high energies, Regge residues for forward and backward, (T), 25:30883
mass splittings in fifth interactions, SU(3) symmetry breaking for medium-strong, 25:30781
model for nonexotic, nonhermitian uncharged field for complex tripole, 25:30827
BARYONS, RESONANCE
decay of many-baryon, quasi-nuclear model for modes of, (T), 25:30895 (NP-18779)
decay of, lifetime difference determination from interference phenomena in system of two resonances in, (T), 25:30848 (JINR-P1-5668)
decay of, width determination from resonance interferometry of, (T), 25:30847 (JINR-P1-5666)
interactions Δ + N, quasi-nuclear model for many-baryon resonance production in potential, (T), 25:30895 (NP-18779)
lifetime difference determination from decay of, interference phenomena in system of two resonances for, (T), 25:30848 (JINR-P1-5668)
production in cosmic-ray interactions, determination of mass of isobars in, 25:30729
production of many-baryon, from Δ + N interactions, quasi-nuclear model for, (T), 25:30895 (NP-18779)
spectroscopy of, review of, 25:30853
width from decay resonance interferometry of, (T), 25:30847 (JINR-P1-5666)
BARYONS, RESONANCE (N*)
decay $N^* \rightarrow N + \gamma$, coupling parameters for pseudoscalar meson production in γ + N interactions for determination of widths of, (E/T), 25:30797
production in $K^+ + p \rightarrow K + N + \pi$ interactions at 4.6 GeV/c, (E), 25:30748
production in π + N interactions at 385 to 1700 MeV/c, energy continuation of energy-independent phase shift analysis for structure for, (T), 25:30871 (UCRL-20250)
production of Δ(1236) in e + N interactions, fixed-t dispersion relations for, 25:30801
production of Δ(1236) in $\pi^- + p \rightarrow \pi^- + \pi^+(\pi^0) + n(p)$ interactions, quark model predictions for forward, (E/T), 25:30738
production of Δ^{++} (1236) in $K^+ + p \rightarrow K^+ + p + 2\pi^+ + 2\pi^-$ interactions at 4.97 GeV/c in hydrogen bubble chamber, (E), 25:30745
production of N^{*++} simultaneously with K^{0*} in $K^+ + p \rightarrow K^+ + p + 2\pi^+ + 2\pi^-$ interactions at 4.97 GeV/c in hydrogen bubble chamber, (E), 25:30745
BARYONS, RESONANCE (Y*)
models as CDD pole and bound state of K-N system, 25:30876
BAUXITE
analysis for rare earths, selection of line pairs for spectroscopic, 25:28946
BEARINGS
materials for ball, for use in ultrahigh vacuum, 25:29834
BEHAVIOR
radiation effects on interoceptive reflex, in cats, effects of perphenazine on, 25:29643
radiation effects on quail learning and memory, effects of dose on x, 25:29687
radiation effects on rat maze habit, combined effects of vibrations and x, 25:29666
BENZENE
effects on radiothermoluminescence of crystalline and glassy methanol, 25:29101
neutron scattering in, Horowitz operators for, (T), 25:31657
BENZENE, 1,2,4,5-TETRAMETHYL-
radiolysis of rigid matrices of methylcyclohexane containing, deferred luminescence spectra following γ, 25:29150
radiolysis of solutions of, in glassy and polycrystalline solvents, stimulation spectra by deferred luminescence technique of anions trapped during γ and uv, 25:29133
BENZENEARSONIC ACID, o-[(2-HYDROXY-3,6-DISULFO-1-NAPHTHYL)AZO]-
use in spectrophotometric determination of thorium in industrial water, ASTM method for, 25:28977
BENZO[a]PYRENE
metabolism after intratracheal injection in mice, 25:31715(T) (ORNL-tr-2469)
BENZYL ALCOHOL
benzyl alcohol--sodium formate, radiolysis of deaerated aqueous solutions of, at 23°C, effects of pressure on yields of hydrogen from γ, 25:29157
BENZYLAMINE, N-PHENYL-
solvent properties of chloroform solutions of, for thorium(IV) from sulfuric acid solutions, 25:29184
BERKELIUM
separation from americium and curium by ion exchange in zirconium phosphate--nitric acid system, 25:28989
BERKELIUM ISOTOPES Bk-247
energy levels of, superfluid-model calculations of energies and wave functions of nonrotational, (T), 25:31306 (JINR-P4-5693)
BERYLLIUM
anodization of, oxide growth rate in solid-state, 25:29803
crystal structure of phases in aluminum and nickel coated wires of, after heating at 250 to 600°C, 25:29883(T) (SC-T-713021)
crystal structure of reaction phases in aluminum coated wires of, after heating at 250 to 600°C, 25:29883(T) (SC-T-713021)
determination in beryllium ores, instrument based on photoproduction of neutrons for, 25:29390 (RT/EL-(70)4)
electron inelastic scattering at 0.2 to 3 keV from, energy spectra from, (E), 25:30260
fabrication of, advances in methods for, 25:29790
fabrication of, research on methods for, 25:29794
microstructure of (0001) surface of, LEED study of, 25:29894
production and uses in US during 1970 and 1971, review on, 25:29806
properties and uses of, past and current status of, 25:29836
properties of, research on mechanical and physical, 25:29794
separation from aqueous solutions by thin-layer chromatography using liquid anion exchangers, 25:29186
sorptive properties for carbon monoxide, hydrogen, nitrogen, and oxygen, 25:29894
BERYLLIUM ALLOYS AND SYSTEMS
radiation effects on fuel cladding of, neutron, 25:29916
Al--Be--Ti, phase diagrams at 600 to 1300°C, isothermal, 25:29900
Be--Cu, aging characteristics of, effects of composition on, 25:29830
Be--Cu-base, phase studies of metastable phase reversion in, at 280 to 600°C, 25:29891
Be--Cu-base--Sn, aging characteristics of, effects of tin content on, 25:29830
Be--Cu-base--Sn, corrosion by nitric or sulfuric acids, effects of manganese, titanium, or zinc additions on, 25:29830
Be--Ti--Zr, melting temperature of brazements of, 25:29824 (ORNL-4630, pp 191-206)
Be-base--Ca--Cr, corrosion resistance of dilute to moist carbon dioxide, effects of calcium and chromium content on, 25:29917(P)
Be-base--Ca--Cr, radiation effects on ductility of dilute, relations of calcium and chromium content with fast neutron, 25:29917(P)
Be-base--Fe, defect structure in, effects of deformation on, 25:29897
Be-base--Fe, precipitation behavior in quenched and aged, 25:29897
BERYLLIUM BORIDES
properties of, chemical and physical, 25:29943(T) (LA-tr-71-30)
BERYLLIUM CARBIDES
properties of, chemical and physical, 25:29943(T) (LA-tr-71-30)
BERYLLIUM FLUORIDES
BeF_2--LiF, spectra of tetravalent uranium in molten, 25:29093
BERYLLIUM ISOTOPES Be-9
deuteron reactions (d,n) at 15 to 55 MeV, angular distributions and spectra from, (E), 25:31202 (KFK-1288)
energy levels at 17.28 and 17.48 MeV from lithium-7 (d,α)

XUM

reactions, (E), 25:31220
energy levels from boron-11 (p,He-3) reactions, spins, parities, isospins, and angular momenta of, (E), 25:31228
neutron reactions (n,2n) at 1.4 eV, cross sections and spectra from, (E), 25:31223
neutron thermalization in, variational method for pulsed-, (T), 25:31175
proton reactions at 11.5 and 23.5 MeV using thick targets, neutron yield from, (E), 25:31209
BERYLLIUM ORES
analysis for beryllium, instrument based on photoproduction of neutrons for, 25:29390 (RT/BL-(70)4)
BERYLLIUM OXIDES
diffusion of lithium-6 from irradiated low-sintered, at 1100 to 1550°C, 25:29963
optical spontaneous polarization of, 25:30666
optical suceptibility of, nonlinear, 25:30666
radiation effects on stability of, relations of temperature with fast neutron, 25:30016
thermodynamic properties of gaseous diatomic, free energy functions for, 25:29082
BETA DECAY
internal ionization in, effect of β endpoint energies on, (T), 25:31316
matrix elements of neutrinoless double, (T), 25:31440
properties of highly-retarded allowed, contribution of second-forbidden matrix elements to, (T), 25:31397
BETA PARTICLES
content of air samples from Project Schooner during 1969, 25:29506 (SWRHL-97-r)
detection in biological samples, methods for mixed γ-ray and, 25:29517
dose to beagle dog lungs following inhalation of insoluble radioisotopes, 25:29438 (LF-43, pp 197-204)
dose to beagle dog lungs following inhalation of insoluble strontium-90, 25:29437 (LF-43, pp 188-96)
dose to beagle dog lungs following inhalation of insoluble cerium-144, 25:29436 (LF-43, pp 183-7)
dose to beagle dogs following intravenous administration of cesium-137 chloride, 25:29433 (LF-43, pp 140-5)
dose to beagle dogs, inhaled cerium-144 chloride, 25:29431 (LF-43, pp 128-36)
dose to beagle dogs, inhaled yttrium-91 chloride, 25:29432 (LF-43, pp 137-9)
dose to bones and lungs of beagle dogs following inhalation of barium-140 and lanthanum-140, 25:29428 (LF-43, pp 92-9)
dose to bones in man from inhaled strontium-90 aerosols, computer method for estimating, 25:29513 (CONF-710211-1)
dose to bones of beagle dogs, inhaled strontium-90 chloride, 25:29430 (LF-43, pp 123-7)
dose to human skin from fallout radioisotopes, methods for estimation of, 25:29539
dose to liver, lungs, and skeleton in beagle dogs following inhalation of thulium-171 oxide, 25:29425 (LF-43, pp 71-8)
dose to lungs of beagle dogs following inhalation of insoluble yttrium-91, 25:29435 (LF-43, pp 163-70)
dose to tissues in beagle dogs following inhalation of insoluble yttrium-90, 25:29434 (LF-43, pp 146-62)
dose to tissues in man following intake of powders of irradiated uranium fuel elements, use of radiometric determination of cesium-137 and strontium-89 in urine for estimation of, 25:29515 (NP-18794)
effects on beagle dog lungs following inhalation of strontium-90 in fused clay particles, 25:29437 (LF-43, pp 188-96)
effects on beagle dogs following intravenous administration of cesium-137 chloride, 25:29433 (LF-43, pp 140-5)
effects on biological and physical properties of pneumococcal DNA following disintegration of incorporated phosphorus-32 or tritium, 25:29459
effects on bones of dogs, pathological, 25:29630
effects on chromosomes and pollen and seed fertility of M(1) generation of rice, 25:29496
effects on chromosomes in Chinese hamster liver cells, for cerium-144, 25:29483 (LF-43, pp 246-53)
effects on content of connective tissue constituents in beagle dog lungs following inhalation of insoluble cerium-144, 25:29622 (LF-43, pp 218-23)
effects on oxygen electrode performance from added thulium-170, 25:29098
effects on susceptibility of mice to influenza virus infection following inhalation of insoluble cerium-144, 25:29724 (LF-43, pp 254-62)
reactions with gaseous alkanes, pressure and temperature dependence of mean energy for ion-pair formation in, (E), 25:30636
BETA SOURCES
activity in Polish honey in relation to mineral content, origin, region, and type, 25:29509
determination in industrial water and wastes, ASTM method for, 25:29009
determination in phosphorus-32 preparations, ASTM method for, 25:29002
determination in radioisotope mixtures, ASTM method for, 25:29005
monitoring in environment of West Valley Processing Plant, 25:29179 (DOCKET-50201-69)
monitoring in environmental samples at West Valley Processing Plant, 1971, 25:29180 (DOCKET-50201-70)
BETA SPECTROMETERS
design of magnetic, for measurement of short nuclear lifetimes, 25:29358
BETATRONS
experimental facilities for 35 MeV, for therapy, 25:29528
radiation monitoring around 35 MeV, during use for therapy, 25:29528
BEVATRON
control system for guide field power supply for, computer-based, 25:31055 (UCRL-20189)
control system for, development of digital, 25:31054 (UCRL-20185)
power system for pole-face windings for, 25:31056 (UCRL-20191)
vacuum system proposal for, cryogenic pumping, 25:31057 (UCRL-20197)
BIANTHRONE
spectra of, ESR, 25:29147
BIBLIOGRAPHIES
on analytical and experimental methods for determining heat and mass transfer through soils, 25:29266 (SC-ARPIC-1010)
on clinical applications of serial brain scanning, 25:29582
on gegenschein, (T), 25:30390
on hafnium and zirconium, 25:29756
on heat pipes, 25:29249 (AAEC/LIB/Bib-264)
on plasma physics, 25:30454
BIG ROCK POINT POWER REACTOR
emergency power supply for, modifications to design parameters and starting procedures for diesel generator, 25:31486 (DOCKET-50155-80)
operations history for January to March 1971, 25:31467 (DOCKET-50155-81)
BINDING ENERGY
calculations for A = 130 to 180 nuclei, 25:31433
statistical expression for, (T), 25:31412
BIOLOGICAL MATERIALS
analysis for carbon-14-labeled proline and hydroxyproline, 25:28995
analysis for iodine-127 by neutron activation and scintillation counting of Cherenkov radiation, 25:29030
analysis for molybdenum by neutron activation and radiochemical separation, 25:29019
analysis for radioisotope contamination, radiometric, 25:29517
analysis for trace amounts of palladium by isotope dilution, 25:28981
neutron dose rate in, 25:31174 (UCRL-19715)
BIPHENYL
radiolysis of rigid matrices of methylcyclohexane containing, deferred luminescence spectra following γ, 25:29150
radiolysis of solutions of, in glassy and polycrystalline solvents, deferred luminescence technique for obtaining stimulation spectra following γ and uv, 25:29133
BISMUTH
determination by amperometric, chelatometric, and conductometric titrations, 25:28970
effects on colorimetric determination of molybdenum, 25:28930
effects on fluorometric determination of zirconium, 25:28963
separation from aqueous solutions by thin-layer chromatography using liquid anion exchangers, 25:29186
BISMUTH ALLOYS AND SYSTEMS
Bi--In-base, surface pinning in, quantitative control of, 25:30415
BISMUTH IONS
implantation in cadmium sulfide at 25 keV, electron microscopic study of radiation damage from, 25:30656
BISMUTH ISOTOPES Bi-205
beta decay of, gamma spectra and log ft from, (E), 25:31386
BISMUTH ISOTOPES Bi-206
energy-level transitions in, (E), 25:31330
separation of carrier-free, from deuteron- or proton-irradiated lead by solvent extraction using bis(2-ethylhexyl) phosphate, 25:29164
BISMUTH ISOTOPES Bi-207
energy levels of, calculation using particle--core coupling model, (T), 25:31379
separation of carrier-free, from deuteron- or proton-irradiated lead by solvent extraction using bis(2-ethylhexyl) phosphate, 25:29164
BISMUTH ISOTOPES Bi-209
energy levels of, calculation using particle--core coupling model, (T), 25:31379
meson reactions (μ⁻,xn) by, gamma spectra from, (E), 25:31258
proton fission at 10 MeV to 29 GeV, cross section for, 25:31326
proton reactions at 11.5 and 23.5 MeV using thick targets, neutron yield from, (E), 25:31209
BISMUTH ISOTOPES Bi-214
determination in uranium air samples, radiometric,

25:29536
BISMUTH OXIDES
thermodynamic properties of gaseous diatomic, free energy functions for, 25:29082
BLACK BODY RADIATION
cosmic background, lecture n, (T), 25:30220 (P-4494(RAND))
BLACK HOLES
gravitational-radiation emission from, (T), 25:30238
properties of invisible companion of epsilon Aurigae, (E/T), 25:30083
properties of, (T), 25:30127
BLADDER
radiodiagnosis of tumor stage in human, tritium tracer studies on DNA and RNA synthesis for use in, 25:29585
BLOOD
flow in cortical structures in man, research progress on regional, 25:31710(R) (NYO-3618-10)
radiation dose to, in normal and tumor-bearing mice following administration of phosphorus-32-labeled chromium alloxantin and orthophosphate, 25:29453
radiation effects on content of sulfhydryl groups in, of ducklings, uv and/or x, 25:29647
radiation effects on DNA content of rabbit, x, 25:29637
radiation effects on erythropoietic activity in rat, fractionated γ, 25:29655
radiation effects on glucocorticoid level in, of dogs, acute and chronic, 25:29642
radiation effects on human, for diagnosis of radiation injuries in radiologists, 25:29595
radiation effects on human, whole-body x, 25:29699
radioinduced changes in, of hypothyroid patients following therapy for thyroid cancer, combined iodine-131 and teletherapy, 25:29707
scanning of circulation of, in human organs, scintigraphy method for, 25:29587
BLOOD CELLS
radioinduced chromosome aberrations in human, chronic, 25:29501
BLOOD PLASMA
radiation effects on content of kininogens and kinin-forming activity in rat, lethal, whole-body γ, 25:29681
radiation effects on esterase activity and protein content in rat, whole-body x, 25:29686
BLOOD SERUM
analysis for thyroxine by double isotope derivative method, 25:28986
zinc-65 uptake by albumins and globulins in human, 25:29447
BLOOD VESSELS
radiation effects on human eye, effects of age on x, 25:29700
radiation effects on, in mouse testes, x, 25:29653
BLUE STELLAR OBJECTS
radio flux from four, (E), 25:30129
BOILERS
development in U.S. of high temperature gas cooled power reactor, review of, 25:31623 (GA-10338)
development of once-through steam generator, review of test results on, 25:31532 (BAW-10027)
materials for, corrosion testing plans for dissimilar metal-couple welds in, 25:29763 (ORNL-4630, pp 280-7)
pressure distribution in helium--water, MEDEA code for time independent, 25:31624 (JUL-698-RG)
temperature distribtuion in helium--water, MEDEA code for time independent, 25:31624 (JUL-698-RG)
BONE MARROW
effects of transplants of, on stem cell repopulation in x-irradiated mammals, review on, 25:29560
radiation dose to, in normal and tumor-bearing mice following administration of phosphorus-32-labeled chromium alloxantin and orthophosphate, 25:29453
radiation effects on DNA breakdown in rabbit, x, 25:29637
radiation effects on hematogenic tissue in mouse, mechanisms of, 25:29676
radiation effects on rat, oxygen tension kinetics during protective effects of mexamine against γ, 25:29551
transplantation in irradiated animals, review on xenographic, 25:29683
BONES
antimony-124 retention in mouse, following inhalation of heat treated aerosols, 25:29424 (LF-43, pp 66-70)
barium-140 retention in beagle dog, following inhalation as chloride, 25:29428 (LF-43, pp 92-9)
cerium-144 content in beagle dog, following inhalation as chloride, 25:29431 (LF-43, pp 128-36)
cerium-144 content in beagle dog, following inhalation, insoluble, 25:29436 (LF-43, pp 183-7)
cerium-144 removal from beagle dog, following inhalation as chloride, effectiveness of intravenous administration of DTPA for, 25:29543 (LF-43, pp 280-5)
curium-244 content in beagle dog, following inhalation as chloride or oxide, 25:29429 (LF-43, pp 100-5)
radiation dose to beagle dog, following inhalation of cerium-144 chloride, β and γ, 25:29431 (LF-43, pp 128-36)
radiation dose to beagle dog, following inhalation of insoluble yttrium-90, 25:29434 (LF-43, pp 146-62)
radiation dose to beagle dog, following inhalation of strontium-90, 25:29430 (LF-43, pp 123-7)
radiation dose to, in man, following acute inhalation of strontium-90 aerosols, method for calculation of, 25:29513 (CONF-710211-1)
radiation dose to, in normal and tumor-bearing mice following administration of phosphorus-32-labeled chromium alloxantin and orthophosphate, 25:29453
radioinduced osteogenic sarcomas in human, following childhood therapy for malignant retinoblastomas, combined effects of radium and x, 25:29702
radioinduced sarcomas and tumors in dog, plutonium, radium, and strontium, α, β, and γ, 25:29630
radioinduced sarcomas in, of beagles following intravenous injection of plutonium-239, radium-224, radium-226, radium-228, strontium-90, and thorium-228, growth dynamics of, 25:29621 (COO-119-243)
radioisotope retention in mouse, following inhalation of heat treated aerosols, 25:29423 (LF-43, pp 59-65)
radioisotope uptake in articular, of rats for diagnosis of diseased joints, iodine-131, mercury-203, selenium-75, strontium-85, or tellurium-132, 25:29581
radiotherapy for Ewing's tumors in human, development of hepatitis following γ, 25:29652
scanning of human, for diagnosis of osteoarticular diseases, effectiveness of iodine-131-labeled RISA and strontium-85, 25:29576
scanning of human, for diagnosis of tumors, effectiveness of scintigraphy and radioisotope, 25:29580
scintigraphy of human, for diagnosis of metastases, combined thermography and strontium-85, 25:29589
scintigraphy of human, for diagnosis of systemic neoplastic diseases, comparison of radiography and thermography with strontium-85, 25:29588
strontium-90 content in beagle dog, following inhalation of fused clay particles, 25:29437 (LF-43, pp 188-96)
thulium-171 retention in beagle dog, following inhalation as oxide, 25:29425 (LF-43, pp 71-8)
yttrium-91 content in beagle dog, following inhalation, insoluble, 25:29435 (LF-43, pp 163-70)
BOR-60 REACTOR
mockup of, physics measurements for critical assembly, 25:31632 (FEI-201)
BORATES
effects on separation of thorium(IV) from sulfuric acid solutions by extraction using N-phenylbenzylamine in chloroform, 25:29184
production and uses of, review on, 25:29936
BORIC ACID
determination in high-purity water for reactor cooling and moderating, 25:28914 (BARC-515)
production of boron-10-enriched, differential thermal analysis for quality control in, 25:29188
BORIDES
production and uses of, review on, 25:29936
BORON
determination in carbon using curcumin-oxalic acid, ASTM method for colorimetric, 25:28974
distribution in Type 316 stainless steel, effects of aging at 650 to 950°C on, 25:29913
effects of distribution of, on tensile properties of irradiated Type 316 stainless steel, 25:29913
effects of interstitial impurity of, on mechanical properties of iron, 25:29855
effects on electric, magnetic, mechanical, and structural properties of graphite, 25:29953
effects on fluorometric determination of zirconium, 25:28963
effects on mechanical properties of synthetic graphite, 25:29946(T) (SC-T-713023)
production and uses of, review on, 25:29936
x-ray emission spectra of, K-band, 25:30671
boron--polyethylene, properties as irradiation containers for high-energy neutron activation analysis, 25:29025
BORON CARBIDES
microstructure of commercial Norbide 325F, data tabulation on, 25:29978 (ORNL-4630, pp 163-76)
microstructure of ion-thinned, optical and electron transmission microscopy study of, 25:29983
radiation effects on, in-pile, 25:29978 (ORNL-4630, pp 163-76)
BORON FLUORIDES
boron isotope exchange between complexed and noncomplexed, 25:29196
BORON IONS
reactions with nitrogen molecules at 10, 200, and 300 keV, cross sections for single and double electron loss in, (E), 25:30300
BORON ISOTOPES
separation by exchange between boron trifluoride and its complexes with organic ligands, 25:29196
BORON ISOTOPES B-9
energy levels from boron-11 (p,t) reactions, spins, parities, isospins, and angular momenta of, (E), 25:31228
BORON ISOTOPES B-10
energy levels from carbon-12 (d,α) reactions, isospin nonconservation in, (E), 25:31227
helium-3 reactions (He-3,Li-6) at 30 MeV, DWBA analysis of, (E/T), 25:31214
BORON ISOTOPES B-11
proton reactions (p,α)2α with, analysis for reaction mechanism in, (T), 25:31218

XUM

proton reactions (p,He-3) and (p,t) at 45 MeV, angular distributions for, (E), 25:31228
BORON OXIDES
corrosive effects of melts of, on tungsten, mechanisms and kinetics of, 25:29774
production of boron-10-enriched, differential thermal analysis for quality control in, 25:29188
thermodynamic properties of gaseous diatomic, free energy functions for, 25:29082
BORON SYSTEMS
B--Co--Hf, crystal structure of $HfCo_3B_2$, 25:29992
B--Co--Zr, crystal structure of $ZrCo_3B_2$, 25:29992
BOSONS
coupling of spin-0 to external quantum fields, (T), 25:30939 (NYO-3829-66)
production of intermediate-scalar and -vector, in μ + N and ν + N interactions, 25:30818
symmetry breaking from covariant derivatives of fields of, chiral, 25:30922
wave equation invariance of spin-0, in electromagnetic field, nonrelativistic, (T), 25:30775 (JINR-P2-5522)
BOSONS, INTERMEDIATE-VECTOR
production of scalar and, in μ + N and ν + N interactions, 25:30818
production of W^+ and W^- in p + p interactions at high energies, lower bound on differential cross section for, 25:30907
theory for $K^+ \rightarrow \pi^+ + e^+ + e^-$ decay with virtual photon emission, divergences of amplitudes in, (T), 25:30805 (NP-18777)
theory for nonleptonic weak interactions with photon emission, divergences of amplitudes in, (T), 25:30805 (NP-18777)
theory for strong self-interacting, CP violation in, 25:30814
BRADWELL REACTORS
cooling system for, minimization of mild steel corrosion in, 25:31459
fuel element channels for, fitting of stainless steel sleeves in, 25:31459
BRAIN
radiation dose to, in normal and tumor-bearing mice following administration of phosphorus-32-labeled chromium alloxantin and orthophosphate, 25:29453
radiation effects on bioelectrical activity in rabbit, effects of hypothalmus on, 25:29688
radiation effects on pathomorphology of mouse, rabbit, and rat, γ, mixed γ--neutron, and proton, 25:29644
radiation effects on protein fractions of mitochondria and tissue homogenates of rabbit, x, 25:29664
radioisotope scanning of, review of clinical applications of, 25:29582
scanning of human, for diagnosis of tumors, effectiveness of scintigraphy and radioisotope, 25:29560
scanning of human, for diagnosis of tumors, use of metastable Indium-113m-labeled DTPA for, 25:29583
BREMSSTRAHLUNG
internal scattering amplitudes for, (T), 25:31444
reactions (γ,n) with aluminum-27 and phosphorus-31 up to 30 MeV, cross sections for, (E), 25:31242
reactions (γ,n) with deuterium at 20 to 35 MeV, cross sections for, (E), 25:31194
reactions (γ,n) with nuclei at 10 to 68 MeV, yields of radioactivities from, (E), 25:31333
reactions (γ,n) with oxygen-16 in giant resonance region, cross section for, (E), 25:31231
reactions (γ,n) with rubidium and cesium at 30 MeV, 25:29018
reactions (γ,xn) with chromium-52, cobalt-59, and vanadium-51 up to 30 MeV, total cross sections for, (E), 25:31243
reactions (γ,xnyp) with barium and cesium, photonuclear yields in, 25:29017
reactions in spherical and slab lead targets, photoneutron spectra, 25:31317
spectra of, analysis of methods for interpreting, 25:30632 (RT/FI-(70)36)
BRITTANY POWER REACTOR (EL-4)
thermal insulation for, performance of honeycomb metal, 25:31577 (EUR-4531, pp 1063-78)
BROMINE
determination by x-ray fluorescence, sensitivity of, 25:28962
determination in sedimentary rocks by neutron activation, 25:29033
determination using ion permselective membrane, potentiometric, 25:28956
BROMINE ISOTOPES Br-75
beta and electron-capture decay of, γ spectra from, (E), 25:31257
BROMINE ISOTOPES Br-82
use as tracer in conjunction with whole-body counter for study of halothane pharmacokinetics in man, 25:29416
use for labeling organic compounds, 25:29413 (CONF-691225)
BROMINE ISOTOPES Br-87
monitoring in water cooled reactor coolant, delayed neutron method for, 25:31580
BROMINE OXIDES
thermodynamic properties of gaseous diatomic, free energy functions for, 25:29082
BROOKHAVEN ALTERNATING-GRADIENT SYNCHROTRON (AGS)
accelerating cavities for converted, stabilization of ferrite, 25:31035 (BNL-15722)
BRUNSBUETTEL POWER REACTOR
design parameters of, 25:31461
BRUNSWICK POWER REACTOR, UNIT 1
construction of, application for permit for revised completion dates for, 25:31515 (DOCKET-50324-20)
operation of, license application for revised completion dates for, 25:31515 (DOCKET-50324-20)
BRUNSWICK POWER REACTOR, UNIT 2
construction of, application for permit for revised completion dates for, 25:31515 (DOCKET-50324-20)
operation of, license application for revised completion dates for, 25:31515 (DOCKET-50324-20)
BUBBLES
growth and nucleation of fission gas, by re-solution process, model for describing limitations of, (T), 25:30032 (GEAP-12148)
movement in liquid sodium bond of reactor fuel elements, scanning apparatus for, 25:31571
BUGEY REACTORS (EDF-5)
pressure vessel for, testing of one-fifth scale model of prestressed concrete, 25:29310
thermal insulation for, effects of thermal stresses on mechanical stability of, 25:31457 (EUR-4531, pp 895-930)
thermal shielding for, design and performance of layered stainless steel-wire gauze, 25:29819 (EUR-4531, pp 1019-34)
BUTANE, 2,2-DIMETHYL-
radioinduced electric conductivity in, x, 25:29097
radiolysis of liquid, effects of dose and iodine scavenging on yields from γ, 25:29142

C

CACTINOMYCIN
effects on tail growth and testicular weight in irradiated mice, 25:29604
CADMIUM
determination of trace amounts of, in platinum by neutron activation following separation by ion exchange chromatography, 25:29023
preparation of whiskers of, by vapor solidification in inert atmospheres of argon and helium, 25:29804
proton reactions at 11.5 and 23.5 MeV using thick targets, neutron yield from, (E), 25:31209
separation from aqueous solutions by thin-layer chromatography using liquid anion exchangers, 25:29186
superconducting supercooling and superheating of small spheres of, size effects in, 25:30428
CADMIUM ALLOYS AND SYSTEMS
Cd--In-base, superconducting transition temperature under strain in, (E), 25:30435
Cd--Sb, atomic structure of liquid, at 350 to 650°C, Kumar--Samarin centrifugation method for studying, 25:29896
Cd--Zn-base, morphology of dendrite and fiber textures in ingots of, 25:29892
CADMIUM ISOTOPES
production in proton fission of uranium-238 at 450 MeV, mass yield and charge distribution for, (E), 25:31302 (COO-1167-16)
CADMIUM ISOTOPES Cd-109
energy-level scheme from indium-109 decay, (E), 25:31320
CADMIUM ISOTOPES Cd-111
energy level at 1300 keV, lifetime of, 25:31327
CADMIUM OXIDES
thermodynamic properties of gaseous diatomic, free energy functions for, 25:29082
CADMIUM SULFIDES
optical spontaneous polarization of, 25:30666
radiation damage in single-crystal platelets of, electron microscopic study of 25-keV bismuth-ion, 25:30656
CALCIUM
abundance in Norma arm of Milky Way, (E), 25:30193
determination as carbonate alone and with strontium and barium carbonates by pellet technique, in spectroscopic, 25:28972
determination in carbon using permanganate, ASTM method for colorimetric, 25:28974
determination in concretes, analog processor for radiometric, 25:29389 (ITJ-2/E)
determination in plutonium by absorption spectrophotometry and spectrography, 25:28916 (CEA-R-4071)
determination in presence of other metals, spectrographic, 25:28944
determination using cobalt oxalate, manganese oxalate, or silver oxalate by radiometric method, 25:28987
determination using ion permselective membrane, potentiometric, 25:28956
effects on strontium-90 accumulation in freshwater plants, discrimination coefficient for, 25:29452
meson (π^-) capture by, neutron spectra from radiative, (E), 25:31273
radiation effects on metabolism of, in frog sartorius muscles, x, 25:29674
separation from other alkaline earths by ion exchange, 25:29193

XUM

CALCIUM ALLOYS AND SYSTEMS
- Be-base--Ca--Cr, corrosion resistance of dilute to moist carbon dioxide, effects of calcium and chromium content on, 25:29917(P)
- Be-base--Ca--Cr, radiation effects on ductility of dilute, relations of calcium and chromium content with fast neutron, 25:29917(P)

CALCIUM CHLORIDES
- $CaCl_2$--CaF_2--Zn, solvent properties for stainless steel cladding of reactor fuels, 25:29199(P)

CALCIUM FLUORIDES
- diffusion of argon, krypton, and xenon in neutron-irradiated uranium-doped single crystals of, at 700 to 1300°C, 25:30673
- $CaCl_2$--CaF_2--Zn, solvent properties for stainless steel cladding of reactor fuels, 25:29199(P)

CALCIUM IONS
- abundance of positive, in ionospheric D region, (E/T), 25:30404
- effects on proton-induced destruction of F centers in sodium chloride crystals, 25:30655
- spectral lines due to, solar, (E), 25:30188

CALCIUM ISOTOPES
- radioactivity standards of, users' guides for, 25:29174

CALCIUM ISOTOPES Ca-40
- alpha scattering at 104 MeV, differential cross sections for, (T), 25:31212
- binding energy and single-particle separation energies of, variational calculation using improved mixed-density approximation, 25:31285
- binding energy of, Brueckner calculation of, (T), 25:31201 (JINR-P4-5614)
- deuteron reactions (d,α) at 5 to 10 MeV, analysis for reaction mechanism in, (E), 25:31275
- deuteron reactions (d,p) with, analysis using BHMM theory, 25:31264
- deuteron reactions (d,p) with, analysis using coupled channel theory, 25:31210
- energy levels of, Brueckner calculation of, (T), 25:31201 (JINR-P4-5614)
- meson (μ^-) capture by, charged-particle masses and energy spectra from, (E), 25:31267
- meson (μ^-) capture by, effect of Coulomb field in radiative, 25:31282
- meson (π^-) capture by, analysis using particle-hole model, (T), 25:31217
- proton elastic scattering at 21.0 to 48.0 MeV, differential cross sections for, (E), 25:31295

CALCIUM ISOTOPES Ca-42
- alpha reactions (α,p) with, p-γ angular corelations from, (E), 25:31251

CALCIUM ISOTOPES Ca-43
- energy-level transitions from scandium-45 (μ^-,2n) reactions, (E), 25:31258

CALCIUM ISOTOPES Ca-44
- energy-level transitions from scandium-45 (μ^-,n) reactions, (E), 25:31258

CALCIUM ISOTOPES Ca-45
- beta decay of, probability for production of internal bremsstrahlung in, (E), 25:31363

CALCIUM ISOTOPES Ca-47
- metabolism in rats, effects of dietary alginates on, 25:29446

CALCIUM ISOTOPES Ca-48
- deuteron reactions (d,p) with, analysis using BHMM theory, 25:31264

CALCIUM OXIDES
- thermodynamic properties of gaseous diatomic, free energy functions for, 25:29082
- Al_2O_3--CaO--CeO_2--SiO_2--ZrO_2, analysis of, x-ray-emission, 25:28957
- CaO--SiO_2--ZrO_2, phase studies of, 25:30008

CALIFORNIUM
- separation from americium and curium by ion exchange in zirconium phosphate--nitric acid system, 25:28989

CALIFORNIUM ISOTOPES Cf-252
- fission of, energy spectra of fragments from spontaneous, (E), 25:31314(T) (ORNL-tr-2453)
- performance and uses of, as neutron source for radiography, 25:29286 (BNWL-1329)

CALORIMETRY
- research progress on applications of adiabatic, to metal systems, 25:31716(R) (ORO-3291-14)

CAMBRIDGE SYNCHROTRON
- development and operation, Jan. 1--June 30, 1970, 25:31036(R) (CEAL-1053)
- research at, Jan. 1--June 30, 1970, 25:31036(R) (CEAL-1053)

CARBAZOLE, 9-VINYL-
- polymers, radiolysis of films of, geminate recombination of charge carriers produced by x, 25:29140

CARBIDES
- book: Carbides: Properties, Production, and Applications, 25:29959

CARBON
- analysis for aluminum, boron, calcium, iron, silicon, titanium, and vanadium, ASTM method for, 25:28974
- deposition of multiple layers of pyrolytic, on fuel microspheres at 1100 to 1500°C, method for, 25:29928(P)
- determination in low-alloy steel, two-standard method for spectrometric, 25:28950
- dispersion of submicron particles of, in hydrogen, effects on radiant heat transfer, 25:29270
- dispersion of submicron particles of, in nitrogen, measurement of scattering amplitude functions for, 25:29270
- effects of interstitial impurity of, on mechanical properties of iron, 25:29855
- effects on ductility of molybdenum, 25:29863
- fission product distribution in coatings of pyrolytic, sputtering and gamma spectrometry methods for determination of, 25:29979 (SGAE-PH-96/1970)
- fission product distribution in layered coating of silicon carbide and pyrolytic, sputtering and gamma spectrometry methods for determination of, 25:29979 (SGAE-PH-96/1970)
- graphitization of, formed from reactions of nitrogen and uranium dicarbide at 800 to 1400°C, effects of nitrogen pressure on, 25:29962
- meson (π^-) capture by, neutron spectra from radiative, (E), 25:31273
- properties of vitreous, as mortar material for spectrochemical analyses, 25:28938
- proton reactions at 11.5 and 23.5 MeV using thick targets, neutron yield from, (E), 25:31209
- radiation effects on dimensional stability of high- and low-temperature isotropic, relations of irradiation temperature with in-pile, 25:30015
- radioinduced ordering of interstitial, in iron, (T), 25:29911

CARBON DIOXIDES
- alpha-particle stopping cross sections in gaseous, test of Bragg's rule for, 25:30642
- corrosive effects of moist, on beryllium-base--calcium--chromium alloys, 25:29917(P)
- corrosive effects on zirconium-base alloys at 500 to 650°C, 25:29770
- electron reactions at 60 keV with, photon emission and absorption by ions produced in, (E), 25:30274(T) (ANL-Trans-881)
- electron reactions at 600 keV with, radiative lifetimes of excited products from, (E), 25:30273(T) (ANL-Trans-879)
- ion reactions with, binary-encounter calculation of ionization cross sections for, 25:30299
- reaction with hydroxyl ion, kinetics of, 25:31745 (UCRL-20461)
- reactions with niobium--zirconium alloys at 700 to 1070°C, kinetics and mechanism of oxidation, 25:29767
- separation of impurities from carbon-14-labeled, design of gas chromatograph for, 25:29177 (CEA-R-4090)

CARBON ISOTOPES
- determination in carbonates and hydrocarbons, sample preparation for mass spectrometric, 25:28968

CARBON ISOTOPES C-12
- abundance in meteorites, (E), 25:30158(R) (UCSD-34-P-43-X-9)
- alpha reactions at 0.2 to 0.9 GeV, excitation functions for, (T), 25:31368
- alpha scattering at 1 GeV per nucleon, absorption cross sections for, 25:31234
- carbon-12 reactions below 4 MeV, extrapolated cross section for, 25:31200 (ANU-P-515)
- deuteron elastic scattering at 1.4 to 2.3 MeV, angular distributions for, (E), 25:31222
- deuteron reactions (d,α) at 26.2 and 29.5 MeV, isospin nonconservation in, (E), 25:31227
- deuteron reactions (d,p) at 1.4 to 2.3 MeV, angular distributions for, (E), 25:31222
- deuteron reactions (d,p) with, analysis using coupled channel theory, 25:31210
- electron elastic scattering at 30 to 60 MeV cross sections for, (E), 25:31219
- electron reactions (e,ep) at 43 MeV, proton spectra and angular distributions for, (E), 25:31232
- energy levels of, calculations using Sussex matrix elements for odd-parity, 25:31230
- energy levels of, one-particle-hole and projected Hartree-Fock approximations for, (T), 25:31226
- energy-level transition in, Doppler broadening of 4.43-MeV, (E), 25:31208
- helium-3 reactions (He-3,Li-6) at 30 MeV, DWBA analysis of, (E/T), 25:31214
- helium-3 reactions (He-3,Li-6) at 40.7 MeV, DWBA analysis of, (E/T), 25:31214
- meson (π^-) capture by proton, deuteron, and triton spectra from, (E), 25:31213
- meson (π^-) capture by, analysis using particle-hole model, (T), 25:31217
- neutron attenuation in, Monte Carlo calculations of, (T), 25:31164 (CEA-N-825)
- nuclear radius from electron elastic scattering, (E), 25:31219
- photon reactions (γ,n) at 10 to 68 MeV, yields of radioactivities from, (E), 25:31333
- proton reactions at 670 MeV deuteron spectrum and differential cross sections for, (E), 25:31225
- proton scattering at 1 GeV, nuclear opaqueness model for differential cross sections for, 25:31234
- reactions (C-12,f) with gadolinium-158 at 126 MeV, angular distribution of fission products from, (E), 25:31371

XUM

reactions (C-12,p) with copper-63, calculation of angular distributions for, (T), 25:31428
reactions with silver at 86 MeV, angular momentum effects on mechanisms of, (E), 25:31356

CARBON ISOTOPES C-13
abundance in meteorites, (E), 25:30158(R) (UCSD-34-P-43-X-9)
effects on the microwave spectra of trans ethyl methyl ether, 25:29072
electron elastic scattering at 30 to 60 MeV cross sections for, (E), 25:31219
electron reactions (e,ep) at 43 MeV, proton spectra and angular distributions for, (E), 25:31232
energy levels from electron elastic and inelastic scattering, form factors for, (E/T), 25:31205 (SAL-16)
nuclear charge radius of, relative to carbon-12, (E/T), 25:31205 (SAL-16)
nuclear radius from electron elastic scattering, (E), 25:31219

CARBON ISOTOPES C-14
activity measurements of, gain stabilization of liquid scintillation detector for, 25:29344
content in biosphere, from natural occurrence and nuclear weapons tests, 25:28990
determination in fermented alcohol by liquid scintillation counting, 25:28990
determination in labeled proteins in polyacrylamide gels by liquid scintillation counting, 25:28994
determination in labeled RNA by paper disc estimation, 25:28993
determination in proline from biological tissue by liquid scintillation counting, 25:28995
determination of acetate-incorporated, by liquid scintillation spectrometry, 25:28996
determination of collagen-incorporated, 25:28997
determination on solid supports by liquid scintillation counting, 25:28985
use for labeling organic compounds, 25:29413 (CONF-691225)

CARBON MONOXIDES
alpha-particle stopping cross sections in gaseous, test of Bragg's rule for, 25:30642
electron reactions at 600 keV with, radiative lifetimes of excited products from, (E), 25:30273(T) (ANL-Trans-879)
ion reactions with, binary-encounter calculation of ionization cross sections for, 25:30299
reactions with radiolytic hydrogen atoms, kinetics of, 25:29158
sorption by thorium dioxide, EPR studies of, 25:29090
sorption on beryllium surface, 25:29894
thermodynamic properties of gaseous, free energy functions for, 25:29082
Ar--CO, reactions with radiolytic hydrogen atoms, kinetics of, 25:29158

CARBON SYSTEMS
C--Co--W, tensile properties of, effects of composition on, 25:29980
C--O--Te--U, phase diagram at 1200°C, 25:30001
C--Te--U, phase diagram at 1200°C, 25:30001

CARBON TETRACHLORIDE
effects on radiothermoluminescence of crystalline and glassy methanol, 25:29101

CARBONATES
analysis for carbon isotopes, sample preparation for mass spectrometric, 25:28968

CARDIAC PACEMAKERS
development of implantable, review of worldwide, 25:29285

CAST IRON
analysis for trace amounts of tellurium, spectrochemical, 25:28943

CATS
radiation effects on interoceptive reflexes in, effects of perphenazine on, 25:29643

CATTLE
iodine-131 uptake by, following fallout deposition, effects of feeding practices on, 25:29505 (SWRHL-39-r)

CAVITIES
formation by underwater trajectory, methods for studying, 25:31727 (SC-DC-713982)

CAVITY RESONATORS
design of ring coupling, for proton linac, 25:31078
performance of superconducting, in 10-GHz frequency band, (E), 25:30443
stabilization of ferrite, for Brookhaven AGS conversion, 25:31035 (BNL-15722)

CELL DIVISION
radiation effects on Escherichia coli, neutron, 25:29490

CELL MEMBRANES
radioinduced permeability in, effects of age and dose on, 25:29457

CELLS
book: Cellular Dynamics of the Neuron, 25:31760
conference on dynamics of nerve, 25:31760
nucleic acid penetration in, research on, 25:31738(R) (TID-25694)
radiation effects on animal and human, γ and x, 25:29690
radiation effects on behavior and structure of, uv, 25:29608(R) (NYO-2356-43)
radiation effects on immunocompetence of mouse spleen, effects of dose on, 25:29677
radiation effects on migration rate of amelogenic, in rat incisor, 25:29678
radiation effects on nuclear diameter of mouse Ehrlich ascites tumor, combined in vitro effects of 6-azauridine and x, 25:29679
radiation effects on populations of x-, in mouse bone marrow, use of electronic particle counter for evaluating, 25:29648
radiation effects on structure of nerve, of upper cervical sympathetic ganglion of rabbits, whole-body x, 25:29675
radioinduced damage in cytoplasm, membranes, and nucleus of, 25:29457
radioinduced deletion of granular nerve, in neonatal cats in relation to subsequent development of presynaptic elements, x, 25:29623
radioinduced mutations in mouse germ, effects of dose on fast neutron and x, 25:29487
radiosensitivity of melanoma, in mice, effects of melanin content on x, 25:29568

CELLS, CULTURED
conference on radiation effects on, abstracts of papers from, 25:29607 (CONF-690940-(Absts.))
radiation effects on growth of mammalian, mechanisms of repair following x, 25:29626
radiation effects on mammalian, survival curves for x, 25:29624
radiation effects on nucleoproteins in human amniotic, cytofluorimetry studies on, 25:29709
radiation effects on, electrons, 25:29596
radiosensitivity of mammalian, effects of age on γ and x, 25:29625

CELLS, L
radiation effects on mitosis in, fractionated x, 25:29611

CELLULOSE
radiation effects on subsequent polymerization of, with ethyl acrylate, ESR studies on γ, 25:29108

CELLULOSE ACETATES
radioinduced polymerization of monomer pairs on, γ, 25:29106

CEMENTS
analysis for calcium, analog processor for radiometric, 25:29389 (ITJ-2/E)
performance of asbestos, as artificial substrate for analysis of periphyton in running-water ecosystem, 25:29478

CERAMIC MATERIALS
properties for use at high temperatures, 25:29860

CERIUM
determination in lanthanum by emission spectrography, 25:28965
determination in presence of thorium using cupferron, potentiometric, 25:28958
energy-level structure of, 25:30262
properties of aerosols produced from aqueous solutions of, 25:29079 (LF-43, pp 31-9)
reactions of tetravalent, with arsenic(III), catalytic effects off ruthenium on, 25:28941
reactions with rare earth carbides, thermodynamics of, 25:29039
separation from aqueous solutions by thin-layer chromatography using liquid anion exchangers, 25:29186

CERIUM ALLOYS AND SYSTEMS
Ce--Co--Ru, preparation and superconductivity of, (E), 25:30413(T) (LA-tr-71-26)
Ce--Fe--Ru, preparation and superconductivity of, (E), 25:30413(T) (LA-tr-71-26)
Ce--Gd--Ru, preparation and superconductivity of, (E), 25:30413(T) (LA-tr-71-26)
Ce--Mg--Si, crystal structure of $CeMg_2Si_2$, 25:29993
Ce--Mn--Ru, preparation and superconductivity of, (E), 25:30413(T) (LA-tr-71-26)
Ce--Ni--Ru, preparation and superconductivity of, (E), 25:30413(T) (LA-tr-71-26)
Ce--Ru, preparation and superconductivity of intermetallic $CeRu_2$, (E), 25:30413(T) (LA-tr-71-26)

CERIUM BROMIDES
thermodynamic properties at 298 to 1300°K, 25:29951

CERIUM CARBIDES
enthalpy of formation of CeC_2 and Ce_2C_3, 25:29961
reactions with rare earths, thermodynamics of, 25:29039

CERIUM CHLORIDES
solubility of aerosol particles of cerium-144-labeled, 25:29080 (LF-43, pp 40-51)

CERIUM ISOTOPES Ce-140
energy levels at 2083 and 2412 keV, lifetime for, (E), 25:31319

CERIUM ISOTOPES Ce-141
metabolism in beagle dogs following ingestion of nuclear debris from Project Cabriolet, 25:29456

CERIUM ISOTOPES Ce-144
distribution and retention in beagle dogs following inhalation, toxicity studies on insoluble, 25:29438 (LF-43, pp 197-204)
effects on beagle dogs following inhalation as chloride, toxic, 25:29431 (LF-43, pp 128-36)
effects on beagle dogs following inhalation of insoluble, 25:29436 (LF-43, pp 183-7)
effects on connective tissue constituents in beagle dog lungs following inhalation of fused clay particles,

25:29622 (LF-43, pp 218-23)
metabolism in beagle dogs following inhalation as chloride, 25:29431 (LF-43, pp 128-36)
metabolism in beagle dogs following inhalation, insoluble, 25:29436 (LF-43, pp 183-7)
removal from beagle dog lungs following inhalation as chloride, effectiveness of bilateral bronchopulmonary lavage with DTPA for, 25:29544 (LF-43, pp 286-94)
removal from beagle dogs following inhalation as chloride, effectiveness of intravenous administration of DTPA for, 25:29543 (LF-43, pp 280-5)

CERIUM NITRIDES
thermodynamic properties of gaseous CeN, 25:29037
CeN--UC, crystal lattice parameters for, relations with composition, 25:30003
CeN--UC--UN, crystal lattice parameters for $U_{0.8}Ce_{0.2}C$--$U_{0.8}Ce_{0.2}N$, relations with composition, 25:30003
CeN--UC--UN, preparation of $U_{0.8}Ce_{0.2}C$--$U_{0.8}Ce_{0.2}N$, methods for, 25:30003
CeN--UN, crystal lattice parameters for, relations with composition, 25:30003

CERIUM OXIDES
effects on reduction of uranium oxides in powder mixtures, 25:29947
enthalpy of formation of CeO_2, 25:29961
solubility of aerosol particles of cerium-144-labeled, 25:29080 (LF-43, pp 40-51)
thermodynamic properties of gaseous diatomic, free energy functions for, 25:29082
Al_2O_3--CaO--CeO_2--SiO_2--ZrO_2, analysis of, x-ray-emission, 25:28957
CeO_2--Tb_2O_3, phase studies at 800 to 1200°C, 25:30007

CERIUM ZIRCONATES
$Ce_2Zr_2O_7$--Zr-base, microstructure of arc-melted and heat treated, 25:29969
$Ce_2Zr_2O_7$--Zr-base, tensile properties at 650°C, 25:29969

CERMETS
corrosion resistance of Nucerite, to acid and alkali environments, 25:29775
wetting of metal--metal carbide and metal--metal oxide, relations with sintering, 25:29954

CESIUM
determination by bremsstrahlung activation using internal reference method, 25:29017
determination of trace amounts of, in seawater, review on methods for, 25:28921
determination using ion permselective membrane, potentiometric, 25:28956
diffusion from irradiated uranium dioxide powder at 820 to 980°C, 25:29974
photon reactions (γ,n) at 30 MeV, 25:29018
photon reactions (γ,xnyp) at 18 to 75 MeV, photonuclear yields from, 25:29017
plasma of, thermodynamically complete equation of state for, (T), 25:30521
properties of gaseous, x-ray equipment for determination of thermodynamic, 25:30648 (N-70-37028)
reactions with nitrogen oxide and oxygen molecules up to 30 eV, charge exchange in, (E), 25:30276 (ORNL-TM-2620)
separation from liquid wastes by sorption on phyllitic silicate minerals, 25:29175 (BARC-509)
use as internal reference element in rubidium determination by bremsstrahlung activation, 25:29018

CESIUM ISOTOPES
determination of radioactive, in water after extraction as tetraphenylborates, radiometric, 25:29000
radioactivity standards of, users' guides for, 25:29174

CESIUM ISOTOPES Cs-125
hyperfine structure, (E), 25:31376
nuclear magnetic moment, (E), 25:31376
nuclear spin, (E), 25:31376

CESIUM ISOTOPES Cs-127
hyperfine structure, (E), 25:31376
nuclear magnetic moment, (E), 25:31376

CESIUM ISOTOPES Cs-134
beta decay of, β--γ angular correlations from, (E), 25:31277

CESIUM ISOTOPES Cs-136
hyperfine structure, (E), 25:31376
nuclear magnetic moment, (E), 25:31376
nuclear spin, (E), 25:31376

CESIUM ISOTOPES Cs-137
content in fish and seawater near Goto Islands, Japan, measurements during July 1966, 25:29241
content of fresh and powdered milk in Italy during 1952 to 1966, fallout, 25:29507
determination in irradiated fuel solutions as measure of burnup by chemical separation and γ spectrometry, ASTM method for, 25:29001
determination in urine by ion exchange, solvent extraction, and β counting, 25:28983
determination in urine of man following intake of powders of irradiated uranium fuels, radiometric, 25:29515 (NP-18794)
determination of ratio of, to uranium in irradiated fuels for calculation of atom percent fission of uranium, ASTM method for, 25:28998
distribution and retention in beagle dogs following inhalation of insoluble, 25:29426 (LF-43, pp 73-81)
distribution in environment following acute release and release in fallout, standards for protection against, 25:29533
effects on beagle dogs following intravenous administration as chloride, toxic, 25:29433 (LF-43, pp 140-5)
separation from low-level liquid wastes by coprecipitation with ferrocyanides, 25:29183 (SGAE-SS-6/1969)
transport through river bed sediments, model river studies of mechanisms of, 25:29204

CESIUM OXIDES
thermodynamic properties of gaseous diatomic, free energy functions for, 25:29082
Al_2O_3--Cs_2O--SiO_2, preparation and properties of, for use as radiation source, 25:29938(T) (BNWL-tr-65)

CESIUM URANIUM FLUORIDES
crystal structure of CsU_6F_{35}, 25:30004

CHALCOGENIDES
crystal structure and phases in rare earth, differential thermal analysis and x-ray studies of, 25:29981

CHARCOAL
filters of, effects of iodine decay heat on performance limits of, 25:31669 (ORNL-4602)
properties of activated coconut, for trapping rare gas fission products in cryogenic beds, 25:29075(R) (DUN-7221(Vol.2))
sorptive properties for iodine and methyl iodide at high temperatures of activated, (E), 25:31612
sorptive properties for methyl iodide at high temperatures and pressures of activated, (E), 25:31611

CHARGED PARTICLES
absorbers of, efficiency of cylindrical, film, and spherical, (T), 25:30641
acceleration in variable magnetic fields, (T), 25:30122
detection and charge identification in nuclear emulsions, 25:29380
detection of light, effect of chemical factors on sensitivity of polymeric track detectors for, 25:29335
diffusion in weakly turbulent stochastic fields, Fokker--Planck equation for, nonresonant, (T), 25:30520
distribution of trapped, computation of geomagnetic L coordinates for studying, (T), 25:30401
energy and equatorial pitch angle of magnetic-dipole-field-trapped, relation to second invariant and drift frequency, (T), 25:30381
interactions with one or two dielectric plates, mechanism of generation of transition radiation from, (T), 25:30714
interactions with vacuum--refractory medium interface, transition radiation from, (T), 25:30702
ionization loss of fast, equation for density effect correction for, 25:30643
motion in axisymmetric magnetic mirror fields, single-particle, (T), 25:30516 (N-70-42698)
motion in electromagnetic fields, singularity in Vaidya radiation from, (T), 25:30778
motion in general relativity theory, conservation of e/m ratio for, (T), 25:30998
motion in homogeneous varying electric and magnetic fields, coherent states and Green function of nonrelativistic, (T), 25:30704
motion in sinusoidal electric fields, radiations from fast, (T), 25:30713
motion of, action integral for equation of, 25:30790
motion of, in strong plane and spherical electromagnetic waves, (T), 25:30116
origin of, in neutron stars, magnetospheric, (T), 25:30154
radiation emision from, moving in strong electromagnetic fields, (T), 25:30116
radiators of, efficiency of cylindrical, film, and spherical, (T), 25:30641
scattering by nuclei, Riemann method in inverse problem for, (T), 25:30894 (ITF-70-98-P)
synchrotron emission from relativistic, gravitation wave detection from gravitational field effects on, (T), 25:31008
synchrotron emission in cyclic accelerators, gravitational plane wave effects on, (T), 25:31008

CHEMICAL REACTIONS
kinetic differences for quantitative analysis of mixtures, 25:28941

CHERENKOV RADIATION
book: Cherenkov Radiation in High-Energy Physics. Part II. Cherenkov Counters: Determination of Energy and Direction of Elementary Particles, 25:29368(T) (AEC-tr-7099(Pt.2))
emission from extensive air showers, (E), 25:30333

CHIMERAS
radiation, in animals, review on xenogeneic bone marrow transplants, in formation of, 25:29683

CHLORAMPHENICOL
effects on staphylococcus-infected wounds in cornea of irradiated rabbits, 25:29649

CHLORIDES
determination in high-purity water for reactor cooling and moderating, 25:28914 (BARC-515)
effects on separation of thorium(IV) from sulfuric acid solutions by extraction using N-phenylbenzylamine in chloroform, 25:29184

CHLORINE
determination by x-ray fluorescence, sensitivity of,

XUM

25:28962
determination in crude or refined oils or engine deposits by neutron activation and γ spectrometry, 25:29026
determination in sedimentary rocks by neutron activation, 25:29033
determination using ion permselective membrane, potentiometric, 25:28956
CHLORINE ISOTOPES
radioactivity standards of, users' guides for, 25:29174
CHLORINE ISOTOPES Cl-35
energy levels from proton inelastic scattering, spin assignments for, (E), 25:31291
neutron capture by, gamma spectra from thermal, (E), 25:31280
proton elastic and inelastic scattering at 6 MeV, angular distributions for, (E), 25:31291
CHLORINE ISOTOPES Cl-36
energy levels from chlorine-35 thermal neutron capture, (E), 25:31280
CHLORINE ISOTOPES Cl-37
effects on microwave spectra and zero-point average structure of chlorine dioxide, 25:29052
CHLORINE OXIDES
thermodynamic properties of gaseous diatomic, free energy functions for, 25:29082
CHLOROPHYLL
reaction with quinone in alcohol solvents, flash photolysis studies of, 25:31687 (COO-908-34)
CHLOROPHYTA
Chlamydomonas reinhardi, radiation effects on DNA of, role of photoreactivating enzymes in repair of uv, 25:29713(R) (COO-1793-5)
Euglena gracilis, radiation effects on DNA of, role of photoreactivating enzymes in repair of uv, 25:29713(R) (COO-1793-5)
Protococcus, effects on content of uranium fission products in fresh water, 25:29449
CHLORTETRACYCLINE
radioprotective effects on mice, 25:29561
CHROMATES
effects on separation of thorium(IV) from sulfuric acid solutions by extraction using N-phenylbenzylamine in chloroform, 25:29184
CHROMATIN
radiation effects on DNP of, effects of acidity, deproteinizing agents, and ionic strength on, 25:29458
CHROMATOGRAPHY
efficiency of ion-exchange paper, with mixed aqueous--organic solvents, 25:29190
use of thin-layer, for organic compounds, 25:31705(T) (LA-tr-71-33)
CHROMIUM
brittleness of, effects of interstitial impurities on intergranular, 25:29855
complexes with cobalt and organic ligands, radiation effects on, isomeric effects on recoil of cobalt-60 from neutron, 25:29170
detection in spectra of BD 61°2565, (E), 25:30063
determination for water flow tracing by neutron activation, 25:29013 (RLO-1750-81)
determination in deposits and airborne particles by neutron activation and scintillation counting, 25:29032
determination in high-purity water for reactor cooling and moderating, 25:28914 (BARC-515)
determination in low-alloy steel, two-standard method for spectrometric, 25:28950
determination in plutonium by absorption spectrophotometry and spectrography, 25:28916 (CEA-R-4071)
determination in presence of other metals, spectrographic, 25:28944
determination of trace amounts of, in vanadium, spectrographic, 25:28947
effects of additions of, on stability of uranium dioxide fuels, 25:29932(P)
effects on corrosion of nickel alloys by vanadium pentoxide melts, 25:29768
effects on fluorometric determination of zirconium, 25:28963
CHROMIUM ALLOYS AND SYSTEMS
Al--Co--Cr, oxidation resistance at 1100°C, mapping method for selection of optimum, 25:29780
Al--Cr--Ni, oxidation resistance at 1000°C, mapping method for selection of optimum, 25:29780
Be-base--Ca--Cr, corrosion resistance of dilute to moist carbon dioxide, effects of calcium and chromium content on, 25:29917(P)
Be-base--Ca--Cr, radiation effects on ductility of dilute, relations of calcium and chromium content with fast neutron, 25:29917(P)
Co-Cr, NMR and nuclear relaxation study of satellite lines in dilute, 25:31690 (COO-1569-71)
Cr--Fe--Ni, compatibility with nonstoichiometric and stoichiometric uranium carbide at 900°C, effects of stabilizers on, 25:29940(T) (EURFNR-820)
Cr--Mo--Ni, corrosion by hydrochloric and sulfuric acids, effects of chromium and molybdenum on, 25:29777
Cr--Mo--steel, properties at high temperatures, ductile and tensile, 25:29822 (ORNL-4630, pp 139-44)
Cr--Mo--steel--U, creep fatigue of, method for prediction of, 25:29826 (RD/B/N-1885)
Cr--N--U, crystal lattice parameters of UCrN/sub 2+-x/, 25:29988
Cr--N--U, phase diagram at 1600°C, tentative, 25:29988
Cr--Ni, radiation effects on mechanical properties of, fast neutron, 25:31568(T) (EURFNR-823)
Cr--Ni-base, hardness at 27 and 740°C, effects of molybdenum and niobium on, 25:29839
Cr--Ni-base, microstructure at 27 and 740°C, effects of molybdenum and niobium on, 25:29839
Cr--Ni-base, strength of, effects of stacking fault energy on high-temperature, 25:29878
Cr--Pt--W, tensile properties of intermetallic compounds of, at 1290°C, 25:29823 (ORNL-4630, pp 186-90)
Cr--Ti--V-base, compatibility with sodium at 600°C, effects of oxygen on, 25:29761 (ORNL-4630, pp 150-7)
Cr--UO_2, radiation effects on mechanical properties of cermets of, fast neutron, 25:31568(T) (EURFNR-823)
Cr--V-base, compatibility with sodium at 600°C, effects of oxygen on, 25:29761 (ORNL-4630, pp 150-7)
Cr-base--Fe--Mo, thermal capacity of Cr/sub 3-x/Fe/sub x/Mo at 1.3 to 4.2°K, 25:30676
Cr-base--Ni, thermal capacity at 1.3 to 4.2°K, 25:30676
Cr-base--Re, hardness at 77 to 430°K, effects of rhenium content on, 25:29871
CHROMIUM BROMIDES
reduction of hydrated, by trivalent uranium, kinetics of, 25:29084
CHROMIUM CHLORIDES
complexes with ammonia, reduction of hydrated, by trivalent uranium, kinetics of, 25:29084
reduction of hydrated, by trivalent uranium, kinetics of, 25:29084
CHROMIUM FLUORIDES
reduction of hydrated, by trivalent uranium, kinetics of, 25:29084
CHROMIUM IONS
abundance of positive, in ionospheric D region, (E/T), 25:30404
CHROMIUM ISOTOPES
effectiveness for radiodiagnosis or radiotherapy in man, 25:29573
radioactivity standards of, users' guides for, 25:29174
CHROMIUM ISOTOPES Cr-48
energy level at 8.77 MeV from titanium-46 (He-3,n) reactions, T = 2 analog, (E), 25:31237 (IAE-1958)
CHROMIUM ISOTOPES Cr-50
helium-3 reactions (He-3,p) at 16.5 MeV, angular distributions and Q for, (E), 25:31298
proton inelastic scattering up to 4 MeV, gamma angular distributions for, (E), 25:31253
CHROMIUM ISOTOPES Cr-51
distribution of recoil, in neutron-irradiated potassium chromate crystals, effects of dose on, 25:29171
evaluation of EDTA-incorporated, for human nephrography, 25:29577
preparation of heparin-incorporated, in vitro for use in metabolism studies, radiochemical method for, 25:29415
reactions of recoils of, in solid solutions of potassium chloride--potassium chromate, chemical effects in, 25:29166
uptake by spleen in tumorous mice, 25:29472
uptake by tsetse flies following ingestion of labeled blood of rabbits, 25:29417
use for labeling human serum albumin, 25:29413 (CONF-691225)
use of EDTA incorporated, for kidney scanning, 25:29578
CHROMIUM ISOTOPES Cr-52
energy levels from proton resonances in vanadium-51, isobaric analog, (E), 25:31256
energy-level transitions from meson (μ^-) reactions with manganese-55, (E), 25:31258
photon reactions (γ,xn) up to 30 MeV, total cross section for, (E), 25:31243
proton inelastic scattering up to 4 MeV, gamma angular distributions for, (E), 25:31253
CHROMIUM ISOTOPES Cr-53
energy-level transitions from meson (μ^-) reactions with manganese-55, (E), 25:31258
proton elastic scattering by, excitation functions for, (E), 25:31248
proton reactions (p,n) with, Hauser--Feshbach analysis of angular distributions and excitation functions for, (E/T), 25:31248
CHROMIUM ISOTOPES Cr-54
energy-level transitions from meson (μ^-) reactions with manganese-55, (E), 25:31258
proton inelastic scattering up to 4 MeV, gamma angular distributions for, (E), 25:31253
CHROMIUM NITRIDES
reduction of hydrated, by trivalent uranium, kinetics of, 25:29084
CHROMIUM OXIDES
thermodynamic properties of gaseous diatomic, free energy functions for, 25:29082
CHROMIUM PERCHLORATES
reduction of hydrated, by trivalent uranium, kinetics of, 25:29084
CHROMIUM THIOCYANATES
reduction of hydrated, by trivalent uranium, kinetics of, 25:29084

CHROMOSOMES
aberrations induced in, by amino acid deprivation, 25:29608(R) (NYO-2356-43)
radioinduced aberrations in human blood cell, chronic, 25:29501
radioinduced aberrations in, of bean roots exposed in sucrose solutions, effects of acidity on γ, 25:29494
radioinduced aberrations in, of children following maternal diagnostic exposure, x, 25:29500
radioinduced aberrations in, of dormant pea seeds, effects of moisture content on protective effects of cysteine against γ, 25:29552
radioinduced aberrations in, of onions, protective effects of thiourea against x, 25:29559
radioinduced aberrations in, of rice seeds, cytology of β and x, 25:29496
radioinduced aberrations of, in Chinese hamster liver cells, comparison of RBE of americium-241 α, cerium-144 β and cobalt-60 γ, 25:29483 (LF-43, pp 246-53)
radioinduced aberrations of, in Chinese hamster liver cells, effects of dose on internal americium-241, 25:29482 (LF-43, pp 240-5)
radioinduced aberrations of, in pea seedlings, effects of dose rate on x, 25:29489
radioinduced aberrations of, in pea seedlings, protective effects of anoxia against γ, 25:29486
radioinduced aberrations of, in pea seeds, effects of ATP, cysteine, and EDTA on γ, 25:29485
radioinduced aberrations of, in swine leukocytes in vitro or in vivo, 14-MeV neutron, 25:29497
radioinduced reciprocal translocations of, in mouse spermatogonia, fast neutron and x, 25:29487
radioinduced translocations in, of house flies, x, 25:29751
radioinduced translocations in, of insects, role in eradication by sterile male technique, 25:29752
radioinduced translocations in, of yellow fever mosquito, effects of, on genetic control of populations, 25:29753
CHROMOSPHERE
resistive effects in turbulent, finite, (T), 25:30180
structure of, as shown by Fraunhofer lines, (E), 25:30156(T) (CSIRO-Trans-10424)
CIRCULATORY SYSTEM
radiation effects on human, following therapy for thyroid cancer, combined iodine-131 and teletherapy, 25:29707
CITRATES
effects on separation of thorium(IV) from sulfuric acid solutions by extraction using N-phenylbenzylamine in chloroform, 25:29184
CIVILIAN DEFENSE
standards for estimation of radiation exposure to human populations in nuclear warfare emergency situation, 25:29539
CLAYS
radioactive material content and diffusion in, method for calculation of, 25:29206
solubility of aerosol particles of strontium-90-labeled fused, 25:29080 (LF-43, pp 40-51)
CLEANING
standards for reactor components, 25:31676
COATINGS
radioinduced curing of, composed of polyesters--aryl sulfonamide--formaldehyde resins containing halogenated photoinitiators, 25:29114(P)
research on oxidation-resistant, for refractory alloys, 25:29950
COAXIAL CABLES
time calibration of delay line, 25:29401
COBALT
complexes with chromium and organic ligands, radiation effects on, isomeric effects on recoil of cobalt-60 from neutron, 25:29170
complexes, radiation effects on, isomeric effects on recoil of cobalt-60 from neutron, 25:29170
determination by x-ray fluorescence, sensitivity of, 25:28962
determination for water flow tracing by neutron activation, 25:29013 (RLO-1750-81)
determination in deposits and airborne particles by neutron activation and scintillation counting, 25:29032
determination in natural waters by solvent extraction and x-ray fluorescence spectroscopy, 25:28919
determination in presence of other metals, spectrographic, 25:28944
determination of trace amounts of, in platinum by neutron activation following separation by ion exchange chromatography, 25:29023
effects on fluorometric determination of zirconium, 25:28963
hyperfine fields of technetium in, (E), 25:31271
properties of aerosols produced from aqueous solutions of, 25:29079 (LF-43, pp 31-9)
separation from aqueous solutions by thin-layer chromatography using liquid anion exchangers, 25:29186
COBALT ALLOYS AND SYSTEMS
Al--Co--Cr, oxidation resistance at 1100°C, mapping method for selection of optimum, 25:29780
Au--Co-base, thermal expansion at 100 to 800°C, 25:29899
Au--Co-base, transformation temperatures of, allotropic, 25:29899
B--Co--Hf, crystal structure of $HfCo_3B_2$, 25:29992
B--Co--Zr, crystal structure of $ZrCo_3B_2$, 25:29992
C--Co--W, tensile properties of, effects of composition on, 25:29980
Ce--Co--Ru, preparation and superconductivity of, (E), 25:30413(T) (LA-tr-71-26)
Co--La, hardness of intermetallic $LaCo_5$, measurement of magnetic and mechanical, 25:29845
Co--Pr, sintering and magnetic properties of $PrCo_5$ permanent magnets, 25:29797
Co--Sm, hardness of intermetallic $SmCo_5$, measurement of magnetic and mechanical, 25:29845
Co--Sm, magnetic properties of intermetallic $SmCo_5$ crystals, 25:30675
Co--WC, binder composition in, effects of composition, carbide grain size, and heat treatments on, 25:29980
Co-base--Nb, thermal expansion at 100 to 800°C, 25:29899
Co-base--Nb, transformation temperatures of, allotropic, 25:29899
Co-base--Ni, thermal expansion at 100 to 800°C, 25:29899
Co-base--Ni, transformation temperatures of, allotropic, 25:29899
Co-base--Pd, thermal expansion at 100 to 800°C, 25:29899
Co-base--Pd, transformation temperatures of, allotropic, 25:29899
Co-base--Pt, thermal expansion at 100 to 800°C, 25:29899
Co-base--Pt, transformation temperatures of, allotropic, 25:29899
Co-base--Ta, thermal expansion at 100 to 800°C, 25:29899
Co-base--Ta, transformation temperatures of, allotropic, 25:29899
Co-base--Ti, thermal expansion at 100 to 800°C, 25:29899
Co-base--Ti, transformation temperatures of, allotropic, 25:29899
Co-base--V, thermal expansion at 100 to 800°C, 25:29899
Co-base--V, transformation temperatures of, allotropic, 25:29899
Co-base--Zr, thermal expansion at 100 to 800°C, 25:29899
Co-base--Zr, transformation temperatures of, allotropic, 25:29899
Co-Cr, NMR and nuclear relaxation study of satellite lines in dilute, 25:31690 (COO-1569-71)
Co-Mn, NMR and nuclear relaxation study of satellite lines in dilute, 25:31690 (COO-1569-71)
Co-V, NMR and nuclear relaxation study of satellite lines in dilute, 25:31690 (COO-1569-71)
COBALT BROMIDES
crystal structure of hydrated, neutron diffraction study of, 25:31722 (PRNC-146)
COBALT CHLORIDES
complexes with ammonia, uses in gravimetric and radiometric determinations of plutonium, thorium, and uranium, 25:28982
COBALT ISOTOPES
effectiveness for radiodiagnosis or radiotherapy in man, 25:29573
radioactivity standards of, users' guides for, 25:29174
COBALT ISOTOPES Co-54
beta decay of, β^+ spectra from, (E), 25:31355
energy levels from iron-54 (p,n) reactions, (E), 25:31355
COBALT ISOTOPES Co-56
beta and electron-capture decay of, precise γ-ray intensities from, (E), 25:31287
COBALT ISOTOPES Co-57
energy levels of, lifetimes, spin assignments, and transition probabilities for, (E), 25:31269
energy-level transitions in, multipole mixing ratios for, (E), 25:31269
uptake by tsetse flies following ingestion of labeled blood of rabbits, 25:29417
COBALT ISOTOPES Co-58
evaluation of DTPA-incorporated, for human nephrography, 25:29577
COBALT ISOTOPES Co-59
meson reactions (μ^-,xn) by, gamma spectra from, (E), 25:31258
photon reactions (γ,n) at 10 to 68 MeV, yields of radioactivities from, (E), 25:31333
photon reactions (γ,xn) up to 30 MeV, total cross section for, (E), 25:31243
proton reactions at 11.5 and 23.5 MeV using thick targets, neutron yield from, (E), 25:31209
COBALT ISOTOPES Co-60
content in seawater near Goto Islands, Japan, measurements during July 1966, 25:29241
production and uses in Canada, review of, 25:29284
reactions of recoil isomers of, in neutron-irradiated cobalt complexes, 25:29170
uptake and excretion by freshwater clams in Lake Maggiore, concentration factors for, 25:29441
use as source in industrial radiography, data on x-ray film exposure levels for, 25:29294
COBALT OXIDES
thermodynamic properties of gaseous diatomic, free energy functions for, 25:29082
COBALT SULFIDES
CoS--US_2, crystal structure of single crystals of, 25:29996
COINCIDENCE CIRCUITS
design for measuring nuclear lifetimes in picosecond

XUM

range, 25:29365
COKE
physical properties of Athabasca, for use in graphite, 25:29920(R) (LA-4631)
properties of Santa Maria, for use in bonded graphites, 25:29920(R) (LA-4631)
COLCHICINE
effects on tomato seeds, M(2) characteristics following combined mutagenic x radiation and, 25:29493
COLLAGEN
determination of radioactive, in presence of other proteins, liquid scintillation spectrometric, 25:28997
radiation effects on content of, in beagle dog lungs following inhalation of insoluble cerium-144, relation of pulmonary fibrosis to β and γ, 25:29622 (LF-43, pp 218-23)
COLLISION PROCESSES
charge-exchange probabilities in atomic, calculation using dynamic molecular orbitals, 25:30275 (JAERI-Memo-4299)
S-matrix in atomic inelastic, calculation using WKB approximation, 25:30293
COLUMBIA RIVER
salmon populations in, effects of thermal discharges on young, 25:31645 (BNWL-1527)
COMETS
dust-particle alignment in tails of, by solar-wind protons, (T), 25:30183
COMPOSITE MATERIALS
conference on new, Sydney, Australia, Aug. 27, 1970, 25:29759
crack growth mechanisms in fibrous, 25:31746 (UCRL-20524)
properties for use at high temperatures,, 25:29860
COMPOSITE PARTICLES
compositeness conditions for partial-wave two-body scattering amplitudes, (T), 25:30958
COMPTON EFFECT
derivation of inverse, classical, (T), 25:30502
lecture on inverse, in astrophysics, (T), 25:30220 (P-4496(RAND))
radiation frequency for inverse, ''electrostatic bremsstrahlung'', (T), 25:30501
stimulation of, in very compact radio sources, (T), 25:30145
COMPUTER PROGRAMS
ANNLIS, for automatic analysis of gamma-ray spectra in FORTRAN IV for UNIVAC 1108, 25:29354 (LUNP-7101)
BLODWN-2, for coolant loss accident analysis for pressurized water reactors, 25:31598 (WCAP-7401)
COSTAX-BOIL, for boiling and pressurized water reactor axial dynamics, FORTRAN H for IBM 360/65, 25:31541 (EUR-4497)
development for calculations of radiation dose to man in vicinity of nuclear excavation projects, 25:29516 (UCRL-50990)
documentation of digital, standards for, 25:31761
energy levels in Davydov model, in FORTRAN IV for Bull G E 625, 25:31425
FIDEL, for optical-model analysis of scattering of spin-1/2 and spin-1 particles, for IBM 360, 25:31389 (ANU-P-500)
FLANGE-AL 4, for calculation of neutron scattering kernels and cross sections, 25:31168 (INR-1260)
FMODEL, for calculation of fuel performance under irradiation, 25:29922 (ORNL-4630, pp 3-58)
for analysis of spectral data from nondestructive activation analysis, 25:29028
for linking FSD microscopes with Minsk-2 computer for processing bubble chamber photographs, 25:29379
for processing photographs in heavy-liquid bubble chamber, for M-20 computer, 25:29369 (ITEF-753)
GOLDEN, for function optimization on line segment using golden section, 25:31740 (UCID-30002)
HAUSER, for calculating compound-nucleus cross sections by Hauser--Feshbach theory, for IBM 360, 25:31391 (ANU-P-512)
I4C (EVAP), for calculation of nuclear-reaction cross sections including charged-particle emission and fission, for IBM 360, 25:31313 (ORNL-TM-3179)
interchange of digital, recommended programming practices to facilitate, 25:31763
MAGGIE, for calculation of multiple scattering and sample attenuation in neutron differential cross section measurements (revised), in FORTRAN V for UNIVAC 1108, 25:31172 (NBS-TN-499)
MARK I, for model of ionosphere, tables from Penn State, 25:30351 (N-70-40978)
MCNA, for adjoint neutron transport equation, in FORTRAN IV for CDC 6600 and CDC 7600, 25:31171 (LA-4486)
MEDEA, for calculating the time independent pressure and temperature distribution in a helium--water steam generator, FORTRAN IV for IBM 360/75, 25:31624 (JUL-698-RG)
MOSSPEC, for resolving Moessbauer spectra, FORTRAN, 25:30688 (RISO-M-1348)
NAA, for analysis of multielement gamma spectra, in FORTRAN for CDC 6600, 25:29363
SANDRA, adaptation of DWUCK and JULIE for DWBA calculations, for IBM 360, 25:31390 (ANU-P-507)
SNARC1D, for solution of one-dimensional multi-group neutron transport equation, FORTRAN for IBM 360, 25:31651 (ANL-7717)
TENSOR, for calculating Rayleigh surface wave phenomena, for CDC 7600, 25:29243 (UCRL-50952)
TIMOC, for stationary and time-dependent neutron transport equation, in FORTRAN II and FAP for IBM 7090/95, 25:31167 (EUR-4519)
TRANS, for stress transients in cylinder shaped fuel rods, FORTRAN 4, 25:31670 (ORNL-TM-3293)
VATCRP, for viscoelastic analysis of irradiated graphite with variable creep coefficient, FORTRAN, 25:29945 (ORNL-TM-3242)
COMPUTERS
ILLIAC III Computer System Manual: Taxicrinic Processor, 25:31694 (COO-2118-1)
programming practices to facilitate interchange of digital computer programs, recommended, 25:31763
research at University of Chicago, November 1970, 25:31693(R) (COO-2094-4)
software development, evolution of, 25:31701 (LA-4620)
CONCRETES
book: Concrete Radiation Shields, 25:30645
creep of prestressed slabs of, effects of reinforced openings on, 25:30024 (EUR-4531, pp 373-84)
deflection in model pressure vessels of, methods for measuring, 25:29301
deformation and fracture under triaxial stress at 500 to 2000 bars pressure, 25:30027 (EUR-4531, pp 417-24)
development for pressure vessels, conference on, 25:31546 (EUR-4531)
fabrication of steel ring-wire reinforced prestressed reactor pressure vessels of, 25:29939 (EUR-4531, pp 433-44)
fracture in multiaxial stress fields, analysis of factors affecting, 25:30025 (EUR-4531, pp 385-407)
moisture content of, performance of electric conductivity gage for measuring, 25:30026 (EUR-4531, pp 409-16)
performance of prestressed pressure vessels of, correlation with model test results, 25:29308
performance of, prestressed pressure vessels of, models for prediction of, 25:29300
prestressed pressure vessels of, use of models in design of, 25:29307
prestressing of reactor pressure vessels of, using steel hoops, 25:30028 (EUR-4531, pp 445-76)
properties of aluminous and Super Secar-type, for thermal shielding in carbon dioxide-cooled reactors, 25:30031 (EUR-4531, pp 975-1018)
properties of prestressed, for use in reactor pressure vessels, 25:30019 (EUR-4531, pp 27-58)
properties of, effects of composition, storage conditions, and temperature on mechanical and thermal, 25:30023 (EUR-4531, pp 267-324)
radiation effects on mechanical and physical properties of, in-pile, 25:30022 (EUR-4531, pp 237-65)
radiation effects on tensile properties of, relations of temperature with neutron, 25:30021 (EUR-4531, pp 179-83)
stress behavior of prestressed reactor pressure vessels of, nonlinear analysis of, 25:31664 (EUR-4531, pp 697-734)
testing of models of prestressed pressure vessels of, methods for, 25:29314
testing of one-fifth scale models of prestressed pressure vessels of, 25:29310
testing of one-fourth scale models of prestressed pressure vessels of, under pressure and thermal loads, 25:29313
testing of one-tenth scale models of prestressed pressure vessels of, 25:29311
testing of one-tenth scale models of prestressed pressure vessels of, 25:29312
testing of pressure vessel end slabs of prestressed, under external load and thermal stress, 25:29306
testing of pressure vessels of, instrumentation and methods for, 25:29299
testing of prestressed pressure vessels of models for, 25:29298
testing of prestressed pressure vessels of, methods for model, 25:29302
testing of prestressed pressure vessels of, under pressure and thermal loads, 25:29309
testing of prestressed pressure vessels of, using small-scale models, 25:29305
testing of prestressed pressure vessels of, using models, 25:29314
testing of prestressed reactor containment structures of, instrumentation for, 25:29303
testing of reinforced and unreinforced, use of betatron bremsstrahlung in defectoscopy method for, 25:29296
testing to failure of prestressed pressure vessel end slabs of, using models, 25:29304
CONNECTICUT YANKEE POWER REACTOR
operations history for March 1971, 25:31468 (DOCKET-50213-105)
CONNECTIVE TISSUE
radiation effects on content of constituents of, in beagle dog lungs following inhalation of insoluble cerium-144, 25:29622 (LF-43, pp 218-23)
CONSTANTS AND CONVERSION FACTORS
variation of Planck's constant on cosmic scale, (T), 25:30246

CONVECTION
heat transfer in porous media by natural, model for, 25:29264 (EUR-4531, pp 821-39)
COPPER
analysis for hydrogen by carrier gas fusion--gas chromatographic methods, 25:28936
defect production by ion bombardment of single-crystal, design and performance of equipment for, 25:30648 (N-70-37028)
determination by amperometric, chelatometric, and conductometric titrations, 25:28970
determination by x-ray fluorescence, sensitivity of, 25:28962
determination in high-purity water for reactor cooling and moderating, 25:28914 (BARC-515)
determination in low-alloy steel, two-standard method for spectrometric, 25:28950
determination in natural waters by solvent extraction and x-ray fluorescence spectroscopy, 25:28919
determination in plutonium by absorption spectrophotometry and spectrography, 25:28916 (CEA-R-4071)
determination using hydrogen peroxide and 1-(2-hydroxyproply)-anabasine, fluorometric, 25:28928
determination using ion permselective membrane, potentiometric, 25:28956
diffusion in praseodymium, 25:29841
effects of divalent, on determination of uranium by controlled-potential coulometry, 25:28975
effects on corrosion of nickel alloys by vanadium pentoxide melts, 25:29768
effects on fluorometric determination of zirconium, 25:28963
isotopic composition of, spectral determination of, (E), 25:28952
proton reactions at 11.5 and 23.5 MeV using thick targets, neutron yield from, (E), 25:31209
radiation effects on shear modulus of, at 4°K, neutron, 25:29912
radioinduced hardening of boron-doped, thermal neutron, 25:29908
separation from aqueous solutions by thin-layer chromatography using liquid anion exchangers, 25:29186
COPPER ALLOYS AND SYSTEMS
Be--Cu, aging characteristics of, effects of composition on, 25:29830
Be--Cu-base, phase studies of metastable phase reversion in, at 280 to 600°C, 25:29891
Be--Cu-base--Sn, aging characteristics of, effects of tin content on, 25:29830
Be--Cu-base--Sn, corrosion by nitric or sulfuric acids, effects of manganese, titanium, or zinc additions on, 25:29830
Cu--Mo--Zr-base, corrosion by carbon dioxide at 600 to 650°C, 25:29770
Cu--Pu, phase studies of, using differential thermal analysis, 25:29885
Cu--W--Zr-base, corrosion by carbon dioxide at 500 to 650°C, 25:29770
Cu--Zr-base, corrosion by carbon dioxide at 500 to 650°C, 25:29770
COPPER ISOTOPES Cu-61
energy levels from nickel-61 (p,n) reactions, spin assignments for, (E), 25:31268
COPPER ISOTOPES Cu-63
carbon-12 reactions (C-12,p) with, calculation of angular distributions for, (T), 25:31428
energy levels from proton inelastic scattering, excited-core description for, (T), 25:31246
COPPER ISOTOPES Cu-64
energy levels from nickel-64 (p,n) reactions, spin assignments for, (E), 25:31268
meson (μ^-) capture by, charged-particle masses and energy spectra from, (E), 25:31267
COPPER ISOTOPES Cu-65
energy levels from proton inelastic scattering, excited-core description for, (T), 25:31246
COPPER MINERALS
structure of azurite, least-square refinement of x-ray data on, 25:31721 (PRNC-145)
COPPER ORES
analysis of concentrates of, for rhenium, direct spectroscopic, 25:28945
analysis of electrolysis slimes of, for gold, selenium, silver, and tellurium, 25:28933
COPPER OXIDES
thermodynamic properties of gaseous diatomic, free energy functions for, 25:29082
COPPER PERCHLORATES
spectra of $Cu(H_2O)_6^{2+}$ obtained from aqueous solutions of, EPR, 25:31744 (UCRL-19691)
$Cu(ClO_4)_2$--$Fe(ClO_4)_2$, radiolysis of aqueous solutions of, mechanism of oxygen formation in γ, 25:29141
COPPER SULFATES
corrosive effects of boiling, on stainless steel weldments, 25:29785 (ORNL-4630, pp 111-38)
$CuSO_4$--$FeSO_4$, radiolysis of aqueous solutions of, mechanism of oxygen formation in γ, 25:29141
CORROSION
book: Advances in Corrosion Science and Technology. Volume 1, 25:29778
mechanisms of, high-temperature electrochemical methods for studies of, 25:29779
CORROSION LOOPS
design for testing steam generator materials, 25:29763 (ORNL-4630, pp 280-7)
COSMIC PARTICLES
acceleration by magnetohydrodynamic discontinuities, (T), 25:30312
charge distribution of heavy primaries of Z greater than or equal to 26, (E), 25:30305
detection of heavy and very-heavy primary, in meteorites, (E), 25:30317
energies of primary, associated with extensive air showers, (E), 25:30331
flux and spectra of low-energy, (E), 25:30161
Forbush decrease of neutron component in region 3 to 50 GV, 25:30318
interactions at very high energies, multicluster model for, 25:30755
measurement of deuterium/helium-4 ratio of primary, 25:30330
meson (μ^-) stopping rate in atmosphere, 25:31448
monitoring of neutrons at Canadian stations during Sept.--Dec., 1970, (E), 25:30303 (AECL-3856)
spectra of primary electrons above 30 GeV, (E), 25:30328
spectra of primary electrons, (E), 25:30134
spectra of primary nuclei, (E), 25:30307
transport in interplanetary space of low-energy primary, convective, (T), 25:30179
COSMIC RADIATION
anisotropy of, three-dimensional, (E/T), 25:30320
background microwave, fluctuations from Thomson scattering by moving intergalactic matter, (T), 25:30236
background microwave, isotropy at 8 mm, (E), 25:30228
background radio and photon, origin of, (T), 25:30221
detection of antimatter in primary, (E), 25:30327
effects on ionization layer in lower ionosphere, behavior during Forbush decreases, (E), 25:30311
effects on lunar surface materials, (E), 25:30249
flux of 200-MeV gamma rays in direction of Leo and Virgo, (E), 25:30306
flux of primary, in interplanetary space, (T), 25:30315
flux of primary, in interplanetary space, (T), 25:30314
intensity increases preceding Forbush decreases, (E/T), 25:30316
intensity variations of, antisymmetric diurnal and semidiurnal, (E/T), 25:30319
intensity variations of, diurnal, (E/T), 25:30321
intensity variations of, effect of sunspot distribution on 11-year, (T), 25:30309
intensity variations of, energy spectra of primary 11-year, effects of solar activity on, (E), 25:30310
intensity variations of, relation of 11-year cycle of, to sunspot distribution, (E/T), 25:30165
intensity variations of, relation of yearly, to sunspot distribution, (E), 25:30308
intensity variations, relation of sunspot groups to 11-year, (E/T), 25:30322
modulation of primary, (E/T), 25:30322
modulation of primary, by solar activity, (T), 25:30313
modulation of primary, by solar wind with anisotropic and isotropic diffusion, (T), 25:30324
modulation of primary, by solar wind with slowly decreasing asymmetry away from Sun, (T), 25:30325
modulation of primary, zone of, from meteorite analysis, (E/T), 25:30323
photon transparency in extragalactic space, 25:30792
relation of primary, to infrared background, (T), 25:30239
spectra of isotropic x-ray background and gamma radiation in, diffuse origin and discrete source of, (E/T), 25:30332
variations during thunderstorm perturbations, micro-, (E), 25:30334
COSMIC RADIO SOURCES
angular dimensions of scintillating, (T), 25:30126
association of Ohio survey, with Abell clusters of galaxies, (E), 25:30120
Compton effect in very compact, stimulated, (T), 25:30145
distances to 17 extragalactic, (T), 25:30125
energy spectra in synchrotron, formation of, (T), 25:30144
energy spectra in synchrotron, formation of, (T), 25:30146
flux densities and spectra of extended galactic, (E), 25:30136
flux densities at 3.5 mm of Sgr B_2, DR 21, and W3, (E), 25:30119
flux densities of variable, at 2695 MHz measured in two polarization planes, 25:30151
flux from extragalactic, (E), 25:30129
lifetimes from source counts, (T), 25:30218
orientation of, relation to orientation of associated elliptical galaxies, (E), 25:30205
properties of extragalactic, relation between, (T), 25:30125
radiation mechanism for nonthermal, (T), 25:30116
scintillation of extended, (E/T), 25:30124
scintillation of extended, (E/T), 25:30123
scintillations of, (T), 25:30220 (P-4494(RAND))

XUM

silicon oxide in, abundance of, 25:30152
spectra and spectral distribution of extragalactic, emission, (E), 25:30150
water-vapor radio emission at 22 GHz from W49, (E), 25:30141
COSMIC RAY TELESCOPES
use in detection of antimatter in primary cosmic radiation, (E), 25:30327
COSMIC SHOWERS
baryon resonance production in, determination of mass of isobars in, 25:30729
Cherenkov light pulses from extensive, (E), 25:30333
composition of extensive, (E), 25:30331
electromagnetic components of EAS, isobar model for, (T), 25:30839
hadron interactions above 10^{12} eV in EAS, cross section for nucleon--antinucleon pair production in, (E), 25:30728
hadronic components of EAS, isobar model for, (T), 25:30839
particle momentum measurements in, hodoscope shower detector for, 25:29377
photon lateral distribution in air, H-quantum and two-fireball models for, (T), 25:30793
radio pulses from extensive, (E), 25:30333
COSMIC X-RAY SOURCES
Cyg X-1, detection x-ray pulsations from, (E), 25:30139
observations of unresolved galactic, (E), 25:30134
Sco X-1, flattening of x-ray spectrum above 40 keV, (E), 25:30147
COSMOLOGY
collisional diffusion and dissipation in inhomogeneous rotating self-gravitating systems, (T), 25:30229
compositions in big-bang, chemical, (T), 25:30232
cosmological constant modification of system of generalized field equations in general relativity theory, 25:31004
Einstein equations for radiation-filled Universe, spherically symmetric solutions for, (T), 25:30225
element abundances in, (T), 25:30219 (CERN-70-31)
energy production from binary interactions in inhomogeneous rotating self-gravitating systems, (T), 25:30230
fluctuations of gravitational field in, role of quantum, (T), 25:30224
gravitational instability in, statistical analysis of, (T), 25:30222
gravitational-wave background in, (T), 25:30240
hierarchical, Newtonian, (T), 25:30226
horizons in, existence of, (T), 25:30220 (P-4494(RAND))
inertial forces as gravitational effect of Einstein Universe, (T), 25:30245
infrared background, significance of, (T), 25:30231
matter-density perturbations in, (T), 25:30223
model for, gravitational instability in inhomogeneous, (T), 25:30241
models of, solutions without singularity for, (T), 25:30233
models with $\Lambda = 0$, tests of, (T), 25:30220 (P-4494(RAND))
models with variable gravitational constant, (T), 25:30232
orientation angles of galaxies, distribution of, (T), 25:30244
perturbations in space of constant curvature, density and rotational, (T), 25:30243
theories of, Newtonian and relativistic, 25:30220 (P-4494(RAND))
CRAB NEBULA
x-ray emission from, (T), 25:30122
CREEP
book: Creep-Rupture Data for the Refractory Metals to High Temperatures, 25:29868
CRITICAL ASSEMBLIES
critical measurements on power reactor fuel elements in, zero-power, 25:31573
kinetics characteristics of repetitively pulsed booster with rotating reflector, (E), 25:31635 (Y-DR-44)
neutron flux in depleted uranium, fast, 25:31173(R) (RPI-328-200)
neutron spectra in bulk aluminum, fast, 25:31173(R) (RPI-328-200)
neutron spectra in depleted uranium, analysis of fast, 25:31173(R) (RPI-328-200)
operation of ZPR-6, ZPR-9, and ZPPR, during March 1971, 25:31533(R) (ANL-7798)
operation of, standards for, 25:31636
physics measurements for BOR-60 mockup, 25:31632 (FEI-201)
CRITICALITY
experiments in, standards for, 25:31636
CROSS SECTIONS
calculation of nuclear, for spacecraft shield analysis, 25:30631 (ORNL-TM-3376)
CRYOSTATS
design of liquid-nitrogen, for thermoluminescence measurements on polymers, 25:30444
fabrication and operation of right angle helium-3, with high-field superconducting solenoid, 25:30442 (NBS-TN-562)
CRYSTALS
gamma-ray emission by nuclei in, thickness dependence of, (T), 25:30690
light absorption in molecular, 25:31698 (ITF-70-74)
neutron diffraction on paramagnetic center-containing, structural amplitudes in polarized, (T), 25:30663 (JINR-P3-5554)
neutron scattering cross section for point defects in relaxed lattice, calculation of long-wavelength, (T), 25:31163 (AERE-R-5682)
structure of, with small angle boundaries, x-ray slit system for studying, 25:31688 (COO-1041-18)
surface scattering of nonpenetrating particles by, theory of inelastic, 25:30659
CUMENE
radioinduced cracking over halogenated alumina--silica catalyst, γ, 25:29111
CURIUM
electron band structure calculations for fcc, 25:30696(R) (COO-2103-3)
separation from americium and associated elements by ion exchange in zirconium phosphate--nitric acid system, 25:28989
CURIUM ISOTOPES Cm-243
energy levels of, superfluid-model calculations of energies and wave functions of nonrotational, (T), 25:31306 (JINR-P4-5693)
CURIUM ISOTOPES Cm-244
content in beagle dog lungs following inhalation as oxide, 25:29421 (LF-43, pp 8-12)
distribution and retention in beagle dogs following inhalation as chloride or oxide, 25:29429 (LF-43, pp 100-5)
production of monodisperse aerosols of, centrifugation method for, 25:29421 (LF-43, pp 8-12)
CURIUM ISOTOPES Cm-246
beta decay of, gamma spectra from, (E), 25:31378
CURIUM OXIDES
analysis for tantalum by emission spectroscopy, 25:28964
CURRENT ALGEBRA
commutators near light cone, Bjorken limits and O(4) expansion of, 25:31020
current commutators in, review of gradient terms in, 25:30954
current--field algebra for hard-pion production in nonrelativistic N + N → N + N + π interactions, 25:30898
equal-time commutators in, covariant dispersion representation for saturation of, 25:31023
interactions of particles in, lectures on, 25:30914 (NP-16804)
PCAC hypothesis for hadron coupling constants, 25:30904
SU(2) X SU(2) chiral, for meson systems realizations of, 25:30850 (JINR-P2-5759)
SU(2) x SU(2), scale transformations of linear sigma model in, 25:30920
SU(2), factorizable representations of, 25:30923
SU(3) x SU(3), scaling property of, 25:30934
symmetry breaking in gauge field models and Sugawara theory of currents, 25:30924
CUTTING TOOLS
development of wire, for use with spark cutter, 25:31689 (COO-1041-19)
CYANOGEN
abundance in late G and K giant stars, (E), 25:30085
radiolysis of aqueous solutions of, electron pulse, 25:29149
CYCLOHEXENE
radiolysis of frozen, effects of dose rate on yields from γ, 25:29160
CYCLOOCTATETRAENE
complexes with uranium, proton magnetic resonance shifts in, 25:29085
CYCLOPHOSPHAMIDE
effects on immune responses in mice, comparison of mechanism of x radiation and, 25:29475
CYCLOPROPANE
alpha-particle stopping cross sections in gaseous, test of Bragg's rule for, 25:30642
CYCLOPROPENE
radiolysis of solid, yields of cyclopropenyl radical from γ and uv, 25:29147
CYCLOTRONS
beam deflection septum magnets for, magnetically self-shaping, 25:31101
beam duty factor of, proposed use of storage ring for improving microscopic, 25:31120
beam emittance measurements at Juelich isochronous, 25:31119
beam energy resolution of isochronous, longitudinal space charge effect on, 25:31114
beam energy spread from isochronous, for injection in tandem Van de Graaff accelerator, 25:31081
beam energy spread in, methods for minimizing, 25:31121
beam extraction from isochronous, first and second harmonic method for, 25:31105
beam extraction methods for, comparison of resonance-free and precessional, 25:31107
beam extraction system for Harwell variable-energy, performance of, 25:31103
beam extraction system for Juelich 90-MeV deuteron isochronous, 25:31102
beam extraction system for Univ. of Birmingham

XUM

isochronous, magnetic regenerator for, 25:31104
beam extraction systems for medium- and high-energy, review of, 25:31100
beam handling system for Univ. of Groningen isochronous, 25:31096
beam injection and stripping in ALICE isochronous, heavy-ion, 25:31150
beam injection in compact, design of bunching system for, 25:31148
beam injection system for compact, effects of space charge in electrostatic lenses of axial, 25:31148
beam injection system for Groningen AVF, axial, 25:31147
beam injection system for U-120, radial polarized, 25:31153
beam injector for Harwell variable energy, axial, 25:31146
beam injector for separated-sector, development of fractional turn cyclotron, 25:31089
beam monitor for, non-intercepting, 25:31127
beam monochromator system for Kurchatov 2.4-meter isochronous, 25:31118
beam optimization in central region of, 25:31111
beam oscillations in electron model of ring, coherent frequencies of transverse, 25:31038 (JINR-P9-5677)
beam parameters of MSU, for high-resolution nuclear studies, 25:31124
beam phase probe for Univ. of Maryland, multichannel non-intercepting, 25:31126
beam phase-space volume measurements on Nuffield 60-in, 25:31117
beam properties in AVF, factors affecting, 25:31112
beam properties of, effects of central region conditions on, 25:31113
beam pulser for MSU, for time-of-flight experiments, 25:31116
beam sharing for multiple target irradiations, 25:31110
beam transport system for Univ. of Maryland isochronous, 25:31090
charged-particle motion in monoenergetic, 25:31122
conference on, Oxford, Sept. 1969, 25:31079
control system for Dubna monoenergy, proposed automatic, 25:31099
control system for IPCR 160-cm, 25:31068
control systems for, status of computer-based, 25:31098
description of AEG 43-inch compact, 25:31144
description of proposed Midwest tandem, for heavy ions, 25:31083
description of series combination of tandem Van de Graaff with, 25:31139
design and performance for H^- beam injection in tandem Van de Graaff accelerator, 25:31151
design and performance of compact multiparticle, 25:31145
design concepts for double, for acceleration of heavy ions, 25:31130
design concepts of two-stage two-gap, for heavy ions, 25:31140
design of Belgium isochronous, conceptual, 25:31094
design of compact 20-MeV isochronous, 25:31142
design parameters of small isochronous, 25:31143
design proposal for Michigan State Univ. separated-sector, for heavy ions, 25:31085
design proposal for separated-sector isochronous, with Van de Graaff injector for heavy ions, 25:31084
design specifications for compact, 25:31141
design study for isochronous, for nuclear spectroscopy studies, 25:31123
development of ALICE isochronous, for heavy ions, 25:31149
development of fractional turn, for injection in separated-sector cyclotrons, 25:31089
development of Indiana Univ. isochronous, 25:31082
development of isochronous, review on, 25:31080
development of SIN ring, for heavy ions, 25:31086
experimental facility for Princeton isochronous, design features of, 25:31093
ion source and injection in, heavy, 25:31132
ion source for Harwell variable energy, design and performance of PIG heavy, 25:31136
ion source for, hot-cathode reflex-type heavy, 25:31134
ion sources for, review on heavy, 25:31133
magnet poles for TRIUMF, design of, 25:31049 (TRI-70-4)
magnet system for monoenergetic, design of, 25:31037 (JINR-P9-5669)
magnetic system for Dubna monoenergetic, 25:31129
operating parameters of Dubna monoenergetic, 25:31122
operation and performance of Grenoble, 25:31097
operation of Harwell variable energy, harmonic, 25:31115
operation of Milan, for acceleration of H^- beams, 25:31125
particle motion in, vertical, (E/T), 25:31063
performance of 37-inch AVF, 25:31161
performance of IPCR 160-cm, for heavy ion acceleration, 25:31135
radiofrequency system for proposed ORNL separated sector, for heavy ions, 25:31095
radiofrequency system of Dubna monoenergetic, 25:31128

CYLINDERS
gravitational field from energy--momentum--stress tensor for uniformly rotating, 25:30997

CYSTAMINE
distribution in intestines and kidneys of mice and rats, effects of 5-methoxytryptamine on, 25:29554
excretion in urine of mice and rats, effects of 5-methoxytryptamine on, 25:29554
radioprotective effects of, on bioelectric activity in muscle and nerve tissues, x, 25:29609
radioprotective effects on muscles and spleen of mice, effects of increased atmospheric pressure on γ, 25:29550

CYSTEAMINE
radioprotective effects of, on biochemical properties correlated with radiosensitivity in mice, 25:29553

CYSTEINE
effects on adsorption capacity of x-irradiated T2r bacteriophages, 25:29728
effects on chromosome aberrations in γ-irradiated pea seeds, 25:29485
radioprotective effects of, on biochemical properties correlated with radiosensitivity in mice, 25:29553
radioprotective effects of, on dormant pea seeds, effects of moisture content on γ, 25:29552

CYTOPLASM
radiation effects on structure of, in relation to cell behavior, uv, 25:29606(R) (NYO-2356-43)
radioinduced damage in, effects of age and dose on, 25:29457

D

DATA ACQUISITION SYSTEMS
description of, for JINR synchrocyclotron, 25:31070

DATA PROCESSING SYSTEMS
development of on-line, for activation analysis, 25:29027

DATA RECORDING SYSTEMS
standards for occupational radiation exposure of personnel, 25:29519

DATA TABULATIONS
coupling constants and low-energy parameters for electromagnetic, strong, and weak interactions, 25:30841
cross sections for π^- + p, π^- + n, and π^- + d interactions, 25:30735 (CERN-HERA-70-7)
magnetic structures of tetragonal materials, determined by neutron diffraction, 25:30664 (NP-18783)
neutron cross sections and multigroup constants for (n,γ) reactions with fission products, (E), 25:31304 (JAERI-Memo-4251)

DEER
strontium-90 content of reindeer in Sweden during 1961 to 1969, 25:29480

DELAY LINES
time calibration of coaxial, 25:29401

DEOXYRIBONUCLEASE
radiation effects on activity of endonuclease I, exonuclease III, and lambda-exonuclease in Escherichia coli, effects of dose on γ, 25:29725

DETERGENTS
effectiveness for decontamination of medical equipment in combination with sound frequency vibrator, 25:29510

DEUTERIUM
alpha reactions (α,αp) at 78 MeV, analysis using quasi-free collision theory, (E/T), 25:31189
deuteron elastic scattering at 12.5 to 40 MeV, differential cross sections for, (E), 25:31191
deuteron reactions (d,He-3) and (d,t) at 12.5 to 40 MeV, differential cross sections for, (E), 25:31191
diffusion through niobium, in fusion reactor conditions, 25:29820 (EUR-4593, pp 519-24)
effects in ammonia--nitric oxide reaction on a supported platinum catalyst, 25:29063
effects on acetylene hydrogenation on palladium surface, 25:29062
effects on autoxidation of poly(vinyl chloride), 25:29059
effects on binding of reduced coenzyme alcohol dehydrogenase isoenzyme EE, 25:29056
effects on bond angles of hydrogen cyanide, methane, and water, 25:29071
effects on collision reactions between hydrogen molecules and oxygen ions O_2^+, 25:29064
effects on distribution of trapped electrons and sugar radicals in γ-radiolysis products of aqueous monosaccharide ices at 77°K, 25:29153
effects on ESR spectra of γ-irradiated solid isobutane, 25:29161
effects on force constants of alkenonitriles, 25:29070
effects on hydrogen abstraction from methyl formate by methyl radicals, 25:29054
effects on infrared absorption spectra of silica gel--water systems, 25:29069
effects on ir spectra of crystalline methanol, 25:29065
effects on ir spectra of hydrofluoric acid in argon, krypton, or xenon at 4°K, 25:29066
effects on ir spectra of methane, 25:29045
effects on kinetics of decay of photolyzed ammonia--mercury complexes, 25:29046
effects on kinetics of hydride shifts in longifolenes, 25:29050
effects on kinetics of hydrolysis of substituted benzaldehyde di-tert-butyl acetals, 25:29048

XUM

effects on kinetics of reduction of acetylene to ethylene by molybdenum(IV)--thiol complexes, 25:29051
effects on kinetics of solvolysis of substituted cyclobutanes, 25:29049
effects on luminescences of aqueous solutions of europium ions, 25:29053
effects on microbial oxidation of p-diethylbenzene, 25:29061
effects on microwave spectra of glycolaldehydes, 25:29044
effects on phosphorescence of phenylacetylenes, 25:29040
effects on rate of reduction of L-amino acid oxidase, effects of pH on, 25:29060
effects on spectra of permanganate ion, 25:29047
effects on the microwave spectra of trans ethyl methyl ether, 25:29072
effects on thermal stability of barium chloride dihydrate and copper sulfate pentahydrate, 25:29042
effects on vibrational energy transfer in shock-heated hydrogen iodide--nitrogen mixtures, 25:29067
exchange with hydrogen in aetylene, rate constants of, 25:29043
exchange with hydrogen in alkylbenzenes, mass spectra of, 25:29068
flux in primary cosmic radiation, (E), 25:30330
photodisintegration at 20 to 35 MeV, cross section for, (E), 25:31194
plasma of, charged-particle analysis from d,d reactions in dense focus discharge, (E), 25:30475(T) (LA-tr-71-6)
plasma of, preionization for toroidal high-β experiments, 25:30541 (IPP-1/114)
proton reactions (p,d)p at 7 to 17 MeV, angular distribution and excitation function of the singlet deuteron in, (E), 25:31196
proton reactions (p,n) at 45.5 MeV, analysis using Faddeev method with Coulomb force, (T), 25:31188
uses in labeled compounds as internal standards for mass spectrometry, 25:28967
DEUTERIUM IONS
reactions with hydrogen molecules, 25:29058
DEUTERIUM PEROXIDES
spectra of solid and matrix-isolated, ir, 25:29055
DEUTERONS
interactions anti p + d + p + anti p + π^+ + π^- + n at 5.55 GeV/c in deuterium bubble chamber, d* effect in, (E), 25:30727 (NP-18796)
interactions d + p + ^{3}He + missing mass at 3.25 to 3.76 GeV/c, ABC effect and 450 MeV structure in, 25:30734
interactions d + p + d + missing mass at 3.25 to 3.76 GeV/c, ABC effect and 450 MeV structure in, 25:30734
interactions K^+ + d + K^0 + p + p, search for K^0 + π^+ + π^- + π^0 decay from, (E), 25:30723
interactions π^- + d, compilation of cross sections for, 25:30735 (CERN-HERA-70-7)
interactions with elementary particles at large momentum transfers, Glauber double scattering and pair production from, 25:30910
reactions (d,4n) with terbium-159 at 19.9 to 27.2 MeV, excitation functions and gamma spectra from, (E), 25:31301 (CNEA-283)
reactions (d,α) with calcium-40 at 5 to 10 MeV, analysis for reaction mechanism in, (E), 25:31275
reactions (d,α) with carbon-12 at 26.2 and 29.5 MeV, isospin nonconservation in, (E), 25:31227
reactions (d,α) with lithium-7 at 0.6 to 2.0 MeV, excitation function and angular distributions for, (E), 25:31220
reactions (d,α) with oxygen-16 at 14.0 to 18.1 MeV, isospin nonconservation in, (E), 25:31227
reactions (d,αt), (d,αHe-3), and (d,αd) with lithium-6 at 52 MeV, spectra from, (E), 25:31187 (NP-18741)
reactions (d,He-3) and (d,t) with deuterium at 12.5 to 40 MeV, differential cross sections for, (E), 25:31191
reactions (d,He-3) with aluminum-27, magnesium-24, silicon-28, and sodium-23 at 82 MeV, DWBA analysis of differential cross sections for, (E/T), 25:31240 (NP-18511)
reactions (d,n) with beryllium-9 at 15 to 55 MeV, angular distributions and spectra from, (E), 25:31202 (KFK-1288)
reactions (d,p) with calcium-140, carbon-12, and oxygen-16, analysis using coupled channel theory, 25:31210
reactions (d,p) with calcium-40 and -48, analysis using BHMM theory, 25:31264
reactions (d,p) with carbon-12 at 1.4 to 2.3 MeV, angular distributions for, (E), 25:31222
reactions (d,p) with gadolinium-157 at 12 MeV, proton spectra from, (E), 25:31354
reactions (d,p) with gallium-69 at 12.1 MeV, proton spectra from, (E), 25:31290
reactions (d,p) with helium-3 at 2.2 to 13 MeV using vector-polarized beams, analyzing power and angular distributions for, (E), 25:31197
reactions (d,p) with helium-3 at 6.5 and 9.3 MeV using polarized beams, tensor analyzing power for, (E), 25:31198
reactions (d,p) with nuclei, use of Born approximation for analysis of, (T), 25:31400
reactions (d,p) with terbium-159 at 6.9 to 27.2 MeV, excitation functions and gamma spectra from, (E), 25:31301 (CNEA-283)
reactions (d,p), (d,p2n), and (d,xn) with gold-197 at 10 to 70 MeV, excitation functions and isomer ratios for, (E), 25:31311 (LYCEN-7092)
reactions (d,pγ) with gallium-69 at 7 MeV, γ spectra from, (E), 25:31290
reactions (d,t) with gallium-71 at 12.1 MeV, triton spectra from, (E), 25:31290
reactions (d,t) with niobium-93 at 17 MeV, triton spectra and angular distributions for, (E), 25:31283
reactions with molecules, binary-encounter calculation of ionization cross sections for, 25:30299
scattering by aluminum-27, magnesium-24, and silicon-28 at 82 MeV, optical-model analysis of, (E), 25:31240 (NP-18511)
scattering by carbon-12 at 1.4 to 2.3 MeV, angular distributions for elastic, (E), 25:31222
scattering by deuterium at 12.5 to 40 MeV, differential cross sections for elastic, (E), 25:31191
scattering by helium-3, lithium-5 resonances in, (T), 25:31195
scattering by helium-4 at 7 and 9.7 MeV using polarized beams, tensor analyzing power for elastic, (E), 25:31198
scattering by hydrogen molecules, backscattering in, (E), 25:30291
scattering by iridium-191, -193 at 7.0 and 12.1 MeV, differential cross sections for inelastic, (E), 25:31342
DIAMONDS
occurrence in meteorites, (E), 25:30158(R) (UCSD-34-P-43-X-9)
DIBENZYLAMINE, N-(2-CHLOROETHYL)-
effects on adrenalin effects on oxygen pressure in mouse spleen, 25:29547
hydrochloride, effects on radioprotective mechanism of hydroxyphenylethanolamines, 25:29546
DICHROMATES
determination using ion permselective membrane, potentiometric, 25:28956
effects on separation of thorium(IV) from sulfuric acid solutions by extraction using N-phenylbenzylamine in chloroform, 25:29184
DIELECTRIC FILMS
electron tunneling through, theory of effect of atomic cores on, 25:30676
DIELECTRICS
electric discharges on foils of, in capacitor banks, 25:30581 (EUR-4593, pp 385-92)
DIET
effects of irradiated, on development and reproduction of grain weevils, 25:29737
DIFFERENTIAL THERMAL ANALYSIS
book: Thermal Analysis. Volume 2. Inorganic Materials and Physical Chemistry, 25:29758
DIODES
radiation damage effects in step recovery diode frequency multipliers, neutron, 25:29409 (SC-RR-710188)
o-DIPHENOL OXIDASE
radioinduced inactivation of, in mycelium of Botrytis cinerea, uv, 25:29720
DISEASES
radiodiagnosis of human kidney, evaluation of cobalt-58-labeled DTPA, chromium-51-labeled EDTA, and iodine-131-labeled hippuran for, 25:29577
DISEASES, INFECTIOUS
Chagas' disease, radiation control of insect vectors of, in comparison to control by chemosterilants, 25:29745
parasitemia, development in mice following infection with x-irradiated Plasmodium berghei sporozoites, 25:29727
pyelonephritis, effects on potassium content in man, use of whole-body counters for studying, 25:29448
DISEASES, NEOPLASTIC
adenocarcinomas, radiodiagnosis of metastatic and primary, in human kidneys, evaluation of scintigraphic methods for, 25:29590
cancer, radioinduced, in skin of man, occupational, 25:29711
carcinomas, radioinduced basal cell, in man following therapy for burns, long-term, 25:29701
carcinomas, radioinduced, in man, 25:29691
carcinomas, radioinduced, on skin of rats, x, 25:29628
carcinomas, radiotherapy of human bronchial, combined effects of chemo- and, 25:29606
carcinomas, radiotherapy of human inoperable pulmonary and squamous cell, effectiveness of cobalt-60 γ, 25:29600
carcinomas, radiotherapy of human laryngeal, using radium or x radiation, 25:29598
carcinomas, radiotherapy of human prostate gland, γ, 25:29597
carcinosarcomas, lithium-6 content in metastases of, in rat lungs, autoradiographic study on, 25:29443
carcinosarcomas, radiotherapy for Wilms', in children, development of hepatitis following γ, 25:29652
Hodgkin's disease, radiotherapy in man, correlation between nominal standard tissue and tumor dose and RET, 25:29520
leukemia, radiation effects on development of, in man following iodine-131 therapy for hyperthyroidism, comparison of surgical treatment with, 25:29705
leukemia, radioinduced in beagle dogs following

XUM

inhalation of strontium-90 chloride, β, 25:29430 (LF-43, pp 123-7)
leukemia, radioinduced, in man following atomic bombings or radiotherapy for arthritis or thymic hypertrophy, γ and x, 25:29696
leukemia, radioinduced, in man, occupational, 25:29711
lymphosarcomas, radiosensitivity of Pliss, relation between level of endogenous sulfhydryl groups and, 25:29610
lymphosarcomas, radiotherapy of human, effectiveness of electron pendulum irradiation or mantle irradiation for, 25:29599
malignant, radiodiagnosis in human gall bladder by scanning, effectiveness of iodine-131-labeled rose bengal for, 25:29575
malignant, radiodiagnosis of human joint, effectiveness of strontium-85, 25:29576
malignant, radioinduced in beagle dogs following inhalation of cerium-144 chloride, 25:29431 (LF-43, pp 128-36)
malignant, radiotherapy of human breast, development of radionecrosis in axilla and shoulder following x, 25:29569
malignant, radiotherapy of human thyroid, condition of organs and systems following, 25:29707
melanomas, radiosensitivity of mouse, effects of melanin on x, 25:29568
metastases, radiodiagnosis of human bone, combined thermography and strontium-85 scintigraphy for, 25:29589
osteosarcomas, radioinduced, in dogs following intravenous injection of plutonium-239, radium-224, radium-226, radium-228, strontium-90, and thorium-228, 25:29621 (COO-119-243)
radiodiagnosis of systemic, in human bones, comparison of radiography, scintigraphy, and thermography for, 25:29588
radiotherapy, use of high-energy electrons for, 25:29596
retinosarcomas, radiotherapy of childhood, review of development of osteosarcomas following, 25:29702
retotheliosarcomas, radiotherapy of human, effectiveness of electron pendulum irradiation or mantle irradiation for, 25:29599
sarcomas, radioinduced osteogenic, in man following childhood therapy for malignant retinoblastoma, combined effects of radium and x, 25:29702
sarcomas, radioinduced, in beagle dogs following inhalation of strontium-90 chloride, β, 25:29430 (LF-43, pp 123-7)
sarcomas, radioinduced, in bones of dogs, plutonium, radium, and strontium, α, β, and γ, 25:29630
sarcomas, radiotherapy of Ewing's, in children, development of hepatitis following γ, 25:29652
tumors, effects on splenic phagocytosis of chromium-51-labeled sheep erythrocytes in mice, 25:29472
tumors, growth in situ, radioisotopic and volumetric studies of, 25:31712(R) (NYO-3924-9)
tumors, growth in situ, radioisotropic and volumetric studies of, 25:31713(R) (NYO-3924-10)
tumors, radiation dose to malignant, during therapy, correlation between RET, nominal standard tissue dose, and, 25:29520
tumors, radiation effects on nuclear diameter of cells of mouse Ehrlich ascites, combined effects of 6-azauridine and x, 25:29679
tumors, radiodiagnosis of human brain, use of metastable Indium-113m-labeled DTPA for, 25:29583
tumors, radiodiagnosis of human effectiveness of radioisotope scanning and scintigraphy for, 25:29580
tumors, radiodiagnosis of malignant stage of human bladder, tritium tracer studies on DNA and RNA synthesis for use in, 25:29585
tumors, radioinduced, in bones of dogs, plutonium, radium, and strontium, α, β, and γ, 25:29630
tumors, radiosensitivity of ovarian, relation between level of endogenous sulfhydryl groups and, 25:29610
tumors, radiotherapy of human bladder, use of ultrasound scanning for planning, 25:29602
tumors, radiotherapy of human gynecological, use of ultrasound scanning for planning, 25:29602
tumors, radiotherapy of human nasopharynx, demineralization of teeth following, 25:29712
tumors, radiotherapy of synchronized mouse skin, effects of 5-fluorouracil on, 25:29605
tumors, radiotherapy of, model for time dependent lethal, 25:29680

DISEASES, PHYSIOLOGICAL
arthritis, radiotherapy in man, development of leukemia following γ and x, 25:29696
cerebellar hemorrhage, radioinduced in beagle dogs following inhalation of strontium-90 chloride, β, 25:29430 (LF-43, pp 123-7)
cirrhosis, radiation effects on lymphocytes in blood, of patients with, extracorporeal, 25:29704
cirrhosis, radioinduced, in liver of animals and man, γ and x, 25:29694
cirrhosis, radioinduced, in liver of animals and man, γ and x, 25:29694
cystitis, radioinduced, in man following therapy, alpha, gamma, and x, 25:29697
dermatitis, radioinduced, in man following excessive fluoroscopy, effectiveness of surgical treatment for x, 25:29706
Down's syndrome, radiation effects on incidence of, in children following maternal diagnostic exposure, x, 25:29500
epilepsy, radioinduced in beagle dogs following inhalation of strontium-90 chloride, β, 25:29430 (LF-43, pp 123-7)
fibrosis, radioinduced pulmonary, in beagle dogs following inhalation of insoluble cerium-144, β and γ, 25:29436 (LF-43, pp 183-7)
fibrosis, radioinduced pulmonary, in beagle dogs following inhalation of insoluble cerium-144, mechanisms of, 25:29622 (LF-43, pp 218-23)
hepatitis, radioinduced, in children following therapy for Ewing's or Wilms' tumors, γ, 25:29652
hyperlipemia, radioinduced in rats following liver exposure, 25:29685
hyperthyroidism, radiotherapy of human, comparison of leukemia development following surgical treatment or iodine-131, 25:29705
inflammations, radiodiagnosis of human joint, effectiveness of iodine-131-labeled RISA for, 25:29576
inflammations, radiodiagnosis of joint, in rats, use of iodine-131, mercury-203, selenium-75, strontium-85, or tellurium-132 uptake in bones and tissues for, 25:29581
myocarditis, radioinduced, in hearts of animals and man, x, 25:29695
necrosis, radioinduced, in beagle dog liver following inhalation of cerium-144 chloride, 25:29431 (LF-43, pp 128-36)
necrosis, radioinduced, in human axilla and shoulder area following post mastectomy therapy, surgical treatment of x, 25:29569
nephritis, radioinduced, in kidneys of man following therapy, x, 25:29698
pancytopenia, radioinduced, in beagle dogs following inhalation of cerium-144 chloride, 25:29431 (LF-43, pp 128-36)
pneumonitis, radioinduced, in beagle dog lungs following inhalation of insoluble strontium-90, β, 25:29437 (LF-43, pp 188-96)
pneumonitis, radioinduced, in beagle dogs following inhalation of insoluble yttrium-90, 25:29434 (LF-43, pp 146-62)
pneumonitis, radioinduced, in beagle dogs following inhalation of cerium-144 chloride, 25:29431 (LF-43, pp 128-36)
sarcoidosis, radiodiagnosis of splenomegaly in human case of, use of technetium-99m-labeled technetium sulfide for, 25:29593
thymic hypertrophy, radiotherapy in man, development of leukemia following γ and x, 25:29696
verruca juvenilis, radiotherapy of human, effectiveness of x, 25:29601

DISEASES, TRAUMATIC
burns, radiotherapy of human, development of basal cell carcinomas following, 25:29701
radiation injuries, hematological examination for diagnosis of, in radiologists, 25:29595
radiation sickness, protective effects of acetylcholine and adrenalin against bone marrow syndrome and gastrointestinal phase of, in mice, γ, 25:29548
radiation sickness, protective effects of elbow joint shielding against, in dogs, 25:29658
radiation sickness, treatment in dogs, effectiveness of oxathiole for, 25:29563

DISPERSION RELATIONS
formulation for saturation of equal-time commutators, covariant, 25:31023
interactions N + N → N + N + π, hard-pion production in nonrelativistic, 25:30898

DOGS
cerium-144 metabolism in beagle, following inhalation as chloride, 25:29431 (LF-43, pp 128-36)
cerium-144 metabolism in beagle, following inhalation of fused clay particles, 25:29436 (LF-43, pp 183-7)
cerium-144 removal from beagle, following inhalation as chloride, effectiveness of intravenous administration of DTPA for, 25:29543 (LF-43, pp 280-5)
cerium-144 removal from lungs of beagle, following inhalation as chloride, effectiveness of bilateral bronchopulmonary lavage with DTPA for, 25:29644 (LF-43, pp 286-94)
cesium-137 distribution and retention in beagle, following inhalation, insoluble, 25:29426 (LF-43, pp 79-81)
clearance of iodine-125- and iodine-131-labeled hippuran and inulin from kidneys of, comparison of Lissamine Green method with, 25:29414
curium-244 distribution and retention in beagle, following inhalation as chloride or oxide, 25:29429 (LF-43, pp 100-5)
iridium-192 metabolism in, following intraperitoneal, intravenous, and oral administration, 25:29450
lanthanum-140 distribution and retention in beagle, following chronic inhalation as chloride, model for, 25:29427 (LF-43, pp 82-91)
plutonium-239 retention in kidneys, liver, and spleen of beagle, following intravenous injection, effects of dose on, 25:29451

XUM

radiation dose distribution in beagle, from radiographic exposure, x, 25:29514 (LF-43, pp 116-22)
radiation dose to beagle, following inhalation of insoluble yttrium-90, β, 25:29434 (LF-43, pp 146-62)
radiation dose to beagle, following inhalation of cerium-144 chloride, β and γ, 25:29431 (LF-43, pp 128-36)
radiation dose to beagle, following intravenous administration of cesium-137 chloride, β and γ, 25:29433 (LF-43, pp 140-5)
radiation dose to lungs of beagle, following inhalation of insoluble cerium-144, relation of induced pulmonary fibrosis to, 25:29622 (LF-43, pp 218-23)
radiation effects on adrenal cortex and peripheral blood in, effects of dose on, 25:29642
radiation effects on beagle, following inhalation of insoluble yttrium-91, 25:29435 (LF-43, pp 163-70)
radiation effects on beagle, following inhalation of yttrium-91 chloride, 25:29432 (LF-43, pp 137-9)
radiation effects on electroretinographic patterns in, exposed in utero during embryogenesis, x, 25:29667
radiation effects on heart of beagle, protective effects of metaraminol, norepinephrine, and phenylephrine on lethal, whole-body, mixed γ and neutron, 25:29565
radiation effects on kidneys and liver of, following injection, protective effects of oxathiole against chronic polonium-210, 25:29563
radiation effects on leukocytes in, plutonium-239 alpha and gamma, 25:29627
radiation effects on survival of beagle, following inhalation of insoluble cerium-144, strontium-90, yttrium-90, or yttrium-91, 25:29438 (LF-43, pp 197-204)
radiation effects on survival of, effects of pancreatic duct ligation on lethal x, 25:29651
radiation effects on survival of, protective effects of elbow joint shielding against x, 25:29658
radioinduced diseases in beagle, following inhalation of cerium-144 chloride, β and γ, 25:29431 (LF-43, pp 128-36)
radioinduced osteosarcomas in beagle, following intravenous injection of plutonium-239, radium-224, radium-226, radium-228, strontium-90, and thorium-228, growth dynamics of, 25:29621 (COO-119-243)
radioinduced sarcomas and tumors in bones of, plutonium, radium, and strontium α, β, and γ, 25:29630
radioisotope content in lungs of beagle, following inhalation as oxides, 25:29421 (LF-43, pp 8-12)
radioisotope distribution and retention in beagle, following inhalation in fused clay particles, 25:29438 (LF-43, pp 197-204)
radioisotope distribution and retention in beagle, following inhalation of soluble barium-140 and lanthanum-140, 25:29428 (LF-43, pp 92-9)
radioisotope distribution and retention in, following inhalation, in fused clay particles, model for insoluble, 25:29422 (LF-43, pp 53-8)
radioisotope metabolism in Beagle, following ingestion of nuclear debris from Project Cabriolet, 25:29456
strontium-90 distribution and retention in beagle, following inhalation, insoluble, 25:29437 (LF-43, pp 188-96)
strontium-90 metabolism in beagle, following inhalation as chloride, 25:29430 (LF-43, pp 123-7)
thulium-171 distribution and retention in beagle, following inhalation as oxide, 25:29425 (LF-43, pp 71-8)
yttium-91 metabolism in beagle, following inhalation as chloride, 25:29432 (LF-43, pp 137-9)
yttrium-90 effects on beagle, following inhalation of insoluble, 25:29434 (LF-43, pp 146-62)

DRESDEN POWER REACTOR, UNIT 1
piping system for, examination of crack in cleanup-demineralizer, 25:31464 (DOCKET-50010-85)

DRESDEN POWER REACTOR, UNIT 2
containment structure for, point maintenance for, 25:31489 (DOCKET-50237-156)
containment system for, leak rate testing of secondary, 25:31470 (DOCKET-50237-157)
control system for, concentration and volume requirements for standby liquid, 25:31490 (DOCKET-50237-161)
cooling system for, in-service inspection of sensitized stainless steel components of, 25:31489 (DOCKET-50237-156)
cooling system for, water hammer damage and corrective maintenance for, 25:31489 (DOCKET-50237-156)
emergency core cooling system for, water hammer damage to seismic restraints for, 25:31473 (DOCKET-50237-160)
operations history for July to December 1970, 25:31469 (DOCKET-50237-147)
operations incident of April 19, 1971, failure of diesel generator to start on automatic initiation signal, 25:31472 (DOCKET-50237-159)
protection systems for, modification of low pressure injection system valve, 25:31489 (DOCKET-50237-156)
radioactive waste from, shipments during August to December 1970 of solid, 25:31471 (DOCKET-50237-158)

DRESDEN POWER REACTOR, UNIT 3
inspection program for, technical specification correction for inservice, 25:31492 (DOCKET-50249-65)

DRUGS
analysis of radio-, by thin-layer chromatography and scintillation camera, 25:28991

DUANE ARNOLD POWER REACTOR
effluents from, effects on environment of chemical, radioactive, and thermal, 25:31516 (DOCKET-50331-25)

DUNGENESS B REACTORS
pressure vessel for, testing of one-tenth scale model of prestressed concrete, 25:29311

DUSTS
alignment in comet tails by solar-wind protons, (T), 25:30183
alignment of interstellar, by starlight, (T), 25:30216
analysis for antimony, chromium, cobalt, iron, scandium, and zinc by neutron activation, 25:29032
electric charge on grains of interstellar, (T), 25:30192

DYES
radioinduced chemiluminescence of aqueous solutions of fluorescein, 25:29138
radiolysis of aqueous solutions of fluorescein-type, combined electron pulse and photon, 25:29138

DYSPROSIUM
determination in lanthanum by emission spectrography, 25:28965

DYSPROSIUM CHLORIDES
thermodynamic properties at 298 to 1300°K, 25:29951

DYSPROSIUM ISOTOPES Dy-160
energy-level scheme from terbium-160 decay, (E), 25:31335

DYSPROSIUM OXIDES
positron lifetimes in, 25:30272
Dy_2O_3--MgO, phase diagram at 1500 to 2400°C, 25:29985
Dy_2O_3--UO_2, phase studies of, 25:29975 (JAERI-1203)

E

ECONOMICS
impact of compliance with radiation exposure standards for uranium mine personnel on, of electric power generation industry and uranium mining industry, 25:29532

ECOSYSTEMS
periphyton component of running-water, as indicator of environmental radioactivity, performance of artificial substrates for analysis of, 25:29478
survey in vicinity of Trisaia Reprocessing Plant to determine methods for disposal of low-activity liquid radioactive wastes, 25:29479

EDDY CURRENT TESTING
equipment and method for measurement of defects in reactor materials, 25:29287 (ORNL-4630, pp 145-9)
method for reactor materials, 25:29288 (ORNL-4630, pp 271-9)

EGGS
radiation effects on development of, of reduviid bugs, effects of dose on x, 25:29620
radiation effects on hatchability of mosquito, effects of dose on γ, 25:29614
radiation effects on production of, by hens following ingestion of iodine-131, 25:29661

EINSTEINIUM ISOTOPES Es-253
alpha decay of, α energy for, (E), 25:31357

ELASTIN
radiation effects on content of, in beagle dog lungs following inhalation of insoluble cerium-144, relation of pulmonary fibrosis to β and γ, 25:29622 (LF-43, pp 218-23)

ELECTRIC ARCS
plasma jets from MPD, thrust of, 25:30503
plasma temperature measurement in argon, spectroscopic, 25:30478(T) (SC-T-713024)
pressure effects on electric field and radiation characteristics of, 130-atm, (E), 25:30509

ELECTRIC CAPACITORS
design of banks of, for 2-MJ high-beta toroidal plasma experiment, 25:30563 (EUR-4593, pp 219-25)
design of banks of, for fusion research, 25:30582 (EUR-4593, pp 393-400)
design of high-Q, for plasma experiments, 25:30595 (EUR-4593, pp 545-50)
design of high-Q, with liquid and gas impregnation, 25:30594 (EUR-4593, pp 541-4)
design of unit for above 100-kV range, 25:30571 (EUR-4593, pp 293-9)
insulator foils for banks of, surface discharges on, 25:30581 (EUR-4593, pp 385-92)
switches for 20-kJ, 40-kV, vacuum start and clamp, 25:30570 (EUR-4593, pp 287-91)
switches for fast energy-storage systems, high-power spark-gap, 25:30565 (EUR-4593, pp 241-50)
switches for, design of solid dielectric multichannel crowbar, 25:30580 (EUR-4593, pp 379-84)
switches for, performance of exploding-foil, 25:30574 (EUR-4593, pp 319-38)

ELECTRIC DISCHARGE
design of high-power spark gaps for high repetition rates, 25:30568 (EUR-4593, pp 273-80)
electrode erosion in high-current and high-pressure, 25:30495 (EUR-4593, pp 251-6)
helium excitation in stationary PIG, population densities from, (E/T), 25:30479
oscillations in spherical magnetized cold-cathode, vlf,

XUM

(E), 25:30617
performance of laser-triggered spark gaps, 25:30566 (EUR-4593, pp 259-64)
plasma diagnostics in positive column, microwave, (E), 25:30483
plasma production in modified PIG-type, 25:30543
switch for high-voltage, development off laser-triggered spark gap, 25:30575 (EUR-4593, pp 339-45)
switches for high voltage, crowbar gap with two triggering pulses, 25:30576 (EUR-4593, pp 347-53)
ELECTRIC FIELDS
charged-particle motion in homogeneous varying, coherent states and Green function of nonrelativistic, (T), 25:30704
charged-particle motion in sinuscidal, radiations from fast, (T), 25:30713
plasma relaxation in hf, electron-ion, (T), 25:30545
production in magnetosphere, vacuum-merging mechanism of convection-driven cross-tail, (E/T), 25:30387
properties in presence of ion flux, (T), 25:30705
ELECTRIC GENERATORS
design and performance of explosive-driven, for fusion research, 25:30562 (EUR-4593, pp 205-17)
ELECTRIC INSULATORS
performance of plastic foils in liquids, 25:30569 (EUR-4593, pp 281-6)
ELECTRIC POWER
transmission of, using superconductors, 25:30445
ELECTRIC PROBES
performance for ion current measurements in laser-produced plasma, 25:30477 (NP-18765)
performance of cylindrical, for plasma density measurement at medium pressures, 25:30494
performance of spherical, for plasma jet diagnostics, 25:30482
ELECTRODES
design of reference, for electrochemical studies at high pressures and temperatures, 25:29779
erosion in high-current and high-pressure discharges, 25:30495 (EUR-4593, pp 251-6)
performance of oxygen, effects of thulium oxide on, 25:29098
radiation effects on performance of oxygen, thulium-170 β and γ, 25:29098
ELECTRODYNAMICS
Coulomb energy in time-symmetric, 25:30711
currents in nonlinear conducting media, two-dimensional problem of steady-state, (T), 25:30346
Rayleigh--Jeans law incompatibility with classical, 25:30936
ELECTROHYDRODYNAMIC GENERATORS
gas flow in ducts of linear voltage, 25:30339
ELECTROJETS
current in equatorial, model to investigate gradient instability in, (E/T), 25:30379
production processes of auroral, relation to magnetospheric magnetic storm generation, (E), 25:30400
ELECTROMAGNETIC FIELDS
charged-particle diffusion in weakly turbulent, Fokker--Planck equation for, (T), 25:30520
charged-particle motion in, singularity in Vaidya radiation from, (T), 25:30778
Maxwell equations for, in static gravitation, 25:31011
particle nonrelativistic wave equation invariance in, spin-0 and -1/2, (T), 25:30775 (JINR-P2-5522)
properties in cold anisotropic plasma with two-dimensional inhomogeneity, (T), 25:30533
ELECTROMAGNETIC LENSES
design of ultra-narrow, high-quality, high-field quadrupole, 25:31051 (UCRL-20164)
magnetic field measuring system for drift tube quadrupole, search coil, 25:31047 (SJC-A-71-1)
performance of dc superconducting quadrupole, 25:31040 (KFK-1316)
ELECTROMAGNETIC WAVES
absorption by plasma at upper hybrid resonance, (T), 25:30616
absorption by plasma at upper hybrid resonance, shf, (E/T), 25:30606 (NP-18807)
charged-particle motion and radiation in strong, (T), 25:30116
damping in plasma, nonlinear Landau, (T), 25:30615
emission from expanding supernova shells, coherent, (T), 25:30068
instabilities in ion-cyclotron, above field-aligned single and multi-ion ionospheric F-layer, (T), 25:30373
interaction of helicon and ion acoustic waves in plasma, nonlinear, (T), 25:30607
propagation in ionosphere at 200 to 1300 km, Interkosmos-3 study of lf, (E), 25:30364
propagation in static gravitation field, 25:31011
propagation in the Galaxy, (T), 25:30220 (P-4494(RAND))
propagation of intense, in two-component plasma, (T), 25:30619
propagation through slowly varying plasma, WKB solution of, (T), 25:30608
reflection from plasma, nonlinear theory of oblique incident, (T), 25:30626
scattering from magnetic fluctuations in plasma, diagnostic use of optical, 25:30490
ELECTRON BEAMS
energy determination of, using neutron production monitoring, 25:31173(K) (RPI-328-200)
interactions with dense plasma, intense monoenergetic, (E/T), 25:30504
interactions with inhomogeneous plasma, electron--ion oscillations from, (E), 25:30506(T) (MATT-Trans-84)
interactions with magnetoplasma, electron--ion oscillations from, (E), 25:30505(T) (MATT-Trans-83)
interactions with plasma, ion emission from, (E), 25:30255 (EUR-4593, pp 67-74)
interactions with plasma, radiations from unstable waves in, (E), 25:30510
production for studying quasi-linear and nonlinear beam--plasma interactions, 25:30500
production of intense relativistic, for fusion experiments, 25:30254 (EUR-4593, pp 59-65)
relaxation of ultrarelativistic, in homogeneous and inhomogeneous plasma, quasi-linear, (T), 25:30534
ELECTRON CAPTURE
probability ratios for K and L, (T), 25:31401
ELECTRON GAS
oscillations of degenerate relativistic, longitudinal, (T), 25:30529
ELECTRON PAIRS
annihilation of, tests of quantum electrodynamics from structure of Feynman amplitude for, (T), 25:30965
photoproduction in nuclear fields at 2.75 MeV, cross sections for, (E/T), 25:31361
production in quantum electrodynamics multiperipheral model at infinite momentum, 25:30974
production of, tests of quantum electrodynamics from structure of Feynman amplitude for, (T), 25:30965
ELECTRON PARAMAGNETIC RESONANCE
book: Chemical Consequences of Nuclear Spin, 25:30669
ELECTRON-RING ACCELERATORS
beam instabilities in ring compressor in, negative mass, 25:31058 (UCRL-20208)
design concepts for high-energy proton, preliminary, 25:31052 (UCRL-20169)
electron beam injector for, 1.2-kA, 4-MeV, 25:31053 (UCRL-20174)
research at Berkeley, status of, 25:31059 (UCRL-20611)
ELECTRON SOURCES
design of gun for studying quasi-linear and nonlinear beam--plasma interactions, 25:30500
ELECTRONIC EQUIPMENT
radiation effects on, nuclear explosion radiation simulators for studying transient, 25:29410
ELECTRONIC FILTERS
design of double delay line, for shaping pulses from semiconductor detectors, 25:29366
ELECTRONS
acceleration in solar flares, two-stage, (E/T), 25:30169
conference on use of high-energy, for therapy of neoplasms, 25:29596
coupling to protons, Hartree--Fock approximation in quantum electrodynamics for bound state of, 25:30989
dosimetry of high-energy, for therapy, methods for, 25:29596
dosimetry of high-energy, problems of inhomogeneities in, 25:29523
effects of pulsed, in combination with photons on chemiluminescence of aqueous solutions of fluorescein dyes, 25:29138
effects of pulsed, on aqueous cyanogen solutions, 25:29149
effects of pulsed, on hydrogen molecules, production of hydrogen atoms by, 25:29158
effects on condensation of gold nuclei from atomic beam on ionic crystals, 25:29910
effects on crosslinking of polyethylenes in presence of free radical catalysts, 25:29115(P)
effects on cultured mammalian cells, biological, 25:29596
effects on curing of coatings composed of polyesters--aryl sulfonamide--formaldehyde resins containing halogenated photoinitiators, 25:29114(P)
effects on curing of coatings on wood, 25:29123
effects on curing of paint binders, 25:29120(P)
effects on formation of defects and sputtering in alkali halides, 25:30651
effects on lithium-doped silicon at 1.5 MeV, ESR and photoconductivity study of annealing of, 25:30653
effects on lymphosarcomas and retotheliosarcomas in man, pendulum method for therapeutic, 25:29599
effects on microstructure of metals, 25:29909
effects on nickel, dose dependence of swelling, 25:30652
effects on p-type silicon at 1.2 MeV and 15°K, photoconductivity study of annealing of defects induced in, 25:30658
effects on poly(methyl methacrylates), mechanisms of formation of tree-shaped cracks from, 25:29100
effects on polyethylene and poly(propylene oxide), 25:29144
effects on polymerization in plastics industry, review on, 25:29127
effects on polymerization of unsaturated polyester resins, 25:29116(P)
effects on polymers containing norbornenyl unsaturation,

XUM

yields of products from, 25:29124
emission from thin films, research program on vacuum-uv photo-, 25:30665(R) (UH-235-P-9-2)
energy loss in magnetized HCR foil of helical, polarization straggling effect in, 25:30644
energy spectra and structure deduced from magnetospheric vlf discrete emissions, Helliwell criterion for, (E/T), 25:30371
flux into dayside auroral oval, properties of region of low-energy primary, (E), 25:30367
injection into region between radiation belts, (E), 25:30352
interactions e + N, absence of form factor in e^2 corrections to amplitudes of, 25:30819
interactions e + N, empirical relation of $\pi^+ + p + \pi^0$ + missing mass interactions with inelastic, (T), 25:30795
interactions e + N, fixed-t dispersion relations for P_{33} resonance production in, (T), 25:30801
interactions e + N, overlapping resonance model of deep inelastic, 25:30782
interactions e + N, scaling and duality in, 25:30787
interactions e + N, vector meson dominance predictions for single π production in, (T), 25:30789
interactions e + p + e' + π^+ + n, differential cross sections for, (E), 25:30718
interactions e + p + e' + π^+ + n, longitudinal part of cross section for, (E/T), 25:30719
interactions e + p, electromagnetic form factor of proton from cross sections from elastic, (E), 25:30786
interactions e + p, isobar model calculations of polarization of recoil protons in elastic, (T), 25:30780
interactions e + p, structure functions and cross sections for meson production in, 25:30783
interactions $e^+ + e^-$ + hadrons, experimental verification of C invariance in, 25:30926
interactions $\mu^- + e^-$, radiative corrections to, 25:30820
interactions of, tests of quantum electrodynamics from structure of Feynman amplitude for Compton, (T), 25:30965
interactions with phonons and impurities in metals, deviations from additivity in theory of scattering, 25:30697 (NP-18822)
magnetic moment of free, bolometric measurements of anomalous, 25:30720
precipitation of 100- to 500-MeV magnetically trapped, into atmosphere, (E), 25:30353
reactions (e,ep) with carbon-12 and -13 at 43 MeV, proton spectra and angular distributions for, (E), 25:31232
reactions with carbon dioxide and nitrogen molecules at 600 keV, photon emission and absorption by ions produced in, (E), 25:30274(T) (ANL-Trans-881)
reactions with carbon dioxide, carbon monoxide, and methane at 600 keV, radiative lifetimes of excited products from, (E), 25:30273(T) (ANL-Trans-879)
reactions with helium at 50 to 600 eV, cross sections and pressure dependence of exchange excitation of 4^3S, 3^3P, and 3^3D levels in, (E), 25:30285
reactions with nitric oxide at 0 to 2 eV, electron attachment and vibrational excitation in, (E), 25:30281
reactions with one-electron atoms, polarization in analysis of elastic scattering and excitation amplitudes for, 25:30287
reactions with potassium at 0.5 to 1.2 eV, differential cross sections for elastic scattering and spin exchange in, (E), 25:30282
scattering by argon-40 at 40 to 60 MeV, cross section for, (E), 25:31272
scattering by atoms, T-matrix formalism for treatment of charge polarization in elastic, 25:30280
scattering by carbon-12, -13, nitrogen-14, and oxygen-16 at 30 to 60 MeV, cross sections for, (E), 25:31219
scattering by helium and hydrogen atoms at 100 eV, 500 eV, and 40 keV, charge-polarization corrections in elastic, (T), 25:30280
scattering by hydrogen atoms, algebraic cross-coupling calculation of, 25:30286
scattering by lithium-6 at 200 and 500 MeV, differential cross sections for elastic and inelastic, (E), 25:31211
scattering by lithium-6, form factors for inelastic, (T), 25:31229
scattering by nuclei, theory of elastic, 25:31206 (SAL-17)
scattering by potassium at 0.5 to 9 eV, total cross sections for elastic, (E), 25:30262
scattering from beryllium, nickel, and lead at 0.2 to 3 keV, energy spectra from inelastic, (E), 25:30260
spectra of primary cosmic, (E), 25:30134
spectra of primary cosmic, above 30 GeV, (E), 25:30328
transport in aluminum slabs at 1 MeV, ANISN calculations for, 25:30630 (ORNL-TM-3318)
tunneling in aluminum/alumina/aluminum junctions, analysis of, 25:30706
tunneling through dielectric layers, theory of effect of atomic cores on, 25:30678
yields of trapped, from γ radiolysis of aqueous monosaccharide ices at 77°K, EPR studies on, 25:29153
yields of trapped, from γ radiolysis of organic glasses at 4 to 77°K, ESR studies on, 25:29156

ELECTROSTATIC ANALYZERS
design of, 25:29408(P)

ELEMENTARY PARTICLE MODELS
direct-channel resonance, review of backward interactions at high energies, 25:30836
dual resonance, amplitude for N nonspurious excited particles in, 25:30830
dual resonance, Lorentz analysis of nonspurious resonance states in, 25:30829
dual resonance, mass shifts in second order of perturbation theory in, 25:30835
dual, lectures on strong interactions in, 25:30823 (CERN-71-7, pp 285-358)
dual, review of, 25:31015 (MIT-2098-726)
duality--parton, for deep inelastic ν + N interactions at high energies in freon and propane, 25:30809
eikonal, for elastic strong interactions at high energies, 25:30893 (INR-P-1233)
eikonal, reggeon calculus from, 25:30980
H-quantum, for photon lateral distribution in air showers, 25:30793
isobar, for hadronic and electromagnetic components of cosmic EAS, 25:30839
Lamb statistical, cross sections of anti p + p + K + anti K + mν interactions at 2.5 GeV/c in, 25:30866
Lee, Bjorken theorem and equivalence principle for equal-time commutators in, 25:30973
multicluster, for interactions at very high energies, 25:30755
multiperipheral, charged and neutral particle distributions from isospin structure, 25:30845
multiperipheral, particle interactions in, 25:30765
nonequilibrium for multiparticle production, 25:30857
one-baryon exchange, review of backward interactions at high energies in, 25:30836
quasi-nuclear, for many-baryon resonance production in Δ + N interactions, 25:30895 (NP-18779)
Reggeized multiperipheral, hadron interactions in, 25:30764
soft-particle emission, for multiparticle production, 25:30857
statistical, asymmetry parameters for π pair angle distributions in π + p + p + 5π interactions at 5 GeV/c in, 25:30880
statistical, hadron interactions in, 25:30764
thermodynamic, test in momentum distributions of secondary π produced in π^+ + p interactions at 5 GeV/c, 25:30746
thermodynamic,strong interactions in, 25:30838
two-fireball, for photon lateral distribution in air showers, 25:30793
Veneziano, amplitude of three-body hadron production in K + N, N + N, and π + N interactions with spin in, 25:30889
Veneziano, coupled-channel unitarization of, 25:30860
Veneziano, model for pomeron from duality diagrams in, 25:31022
Veneziano, particle interactions in generalized, 25:30765
Veneziano, review of multiparticle interactions in, 25:30825
Veneziano, statistical concepts for n-point function for interactions in, 25:30766

ELEMENTARY PARTICLE MODELS (TRIPLET)
amplitudes of K*(890) and K*(890) production in K + p + K(890) + p interactions at high energies in factorizable quark, 25:30879
diffractive scattering in quark, 25:30844
formulation of nonrelativistic separable-potential quark, for hadrons, 25:30846
hadron interactions in quark arrangement, 25:30764
interactions at high energies in quark, review of backward, 25:30836
interactions ν + N at high energies in, in freon and propane in duality--quark, deep inelastic, 25:30809

ELEMENTARY PARTICLES
angular momentum for, invariants of rotation group for arbitrary, (T), 25:31013 (ITEF-782)
book: Cherenkov Radiation in High-Energy Physics. Part II. Cherenkov Counters: Determination of Energy and Direction of Elementary Particles, 25:29368(T) (AEC-tr-7099(Pt.2))
characteristics of, (T), 25:30452
conference on, (T), 25:30753
coupling of spin-0 and -$^1/_2$, to external quantum fields, (T), 25:30939 (NYO-3829-66)
electromagnetic interactions of, compilation of coupling constants and low-energy parameters for, (E), 25:30841
electromagnetic interactions of, lectures on, (T), 25:30772 (CERN-71-7, pp 181-283)
electromagnetic interactions of, review of role of vector mesons in, (T), 25:30796
electromagnetic interactions of, scaling behavior and pomeron dominance of structure functions for, 25:30779
form factors of system of two particles with arbitrary spins and masses, quasipotential method for, (T), 25:30752 (JINR-P2-5691)
identity of, approximate, (T), 25:30761
interactions at high energies, mass dependence of momentum transfer distributions in diffraction dissociation in, (T), 25:30767

interactions at high energies, model analyses of amplitudes of, (T), 25:30751 (IS-T-426)
interactions at high energies, review of particle models for backward (E/T), 25:30836
interactions at very high energies, multicluster model for, 25:30755
interactions in multiperipheral model, charged and neutral particle structure from, 25:30845
interactions of arbitrary-spin, retarded part of two-time Green function for relativistic amplitude and wave function of two-body, (T), 25:31014 (JINR-E2-5746)
interactions of spin-zero and spin-$^1/_2$, continuous-spin pole exchange in, 25:30892
interactions of unequal-mass, analyticity constraints and residue functions of E_2 pole exchange for, 25:31027
interactions of, algebraic approach to solution of one-dimensional model of n-body, (T), 25:30759
interactions of, analytic properties of scalar vertex function for, 25:30770
interactions of, Bose--Einstein symmetrization for Goldhaber effect in, (T), 25:30763
interactions of, constraints on angular momentum of t-channel exchanges from s-channel helicity conservation in elastic, 25:30757
interactions of, correlation effects for many-body final states in, (T), 25:30837
interactions of, general duality predictions for inclusive, 25:30758
interactions of, generalized Veneziano model for, (T), 25:30765
interactions of, lectures on CP violation in, (T), 25:30915 (NP-18808)
interactions of, lectures on current algebra for, (T), 25:30914 (NP-18804)
interactions of, model with Regge dipole for breakdown of Pomeranchuk theorem for, 25:30828
interactions of, multiperipheral models for, (T), 25:30765
interactions of, relativistic rotation of S = $^1/_2$ spin in two-body, (T), 25:30760
interactions of, review of cross sections and multiplicity and momentum distributions for, (E), 25:30715
interactions of, review of hypothesis of limiting fragmentation for, (T), 25:30768
interactions of, review of Veneziano model for multiparticle, (T), 25:30825
interactions of, statistical concepts for n-point function in Veneziano model for, (T), 25:30766
interactions with deuterons at large momentum transfers, Glauber double scattering and pair production from, 25:30910
invariance principles for, lectures on, (T), 25:30915 (NP-18808)
lectures on, 25:30750 (CERN-71-7)
mass formulas from SU(3) x SU(3) chiral symmetry breaking, 25:30929
production of, method for calculating unitary weights for multiple, (T), 25:30913 (JINR-P2-5729)
reactions with nuclei at very high energies, hadron spectrum from cross sections for, 25:30905
research at New York Univ., Dec. 1969 to Jan. 1971, (E), 25:30806(R) (NYO-3668-TA-5)
strong interactions at high energies, electromagnetic and weak corrections to, 25:30832
strong interactions of, compilation of coupling constants and low-energy parameters for, (E), 25:30841
strong interactions of, duality hypotheses for exchange degeneracy in, (T), 25:30825
strong interactions of, graphs for isotopic relations for Pomeranchuk pole exchange in three-body hadron production in, (T), 25:30824 (JINR-P2-5630)
strong interactions of, lectures on dual models and phenomenology for, (T), 25:30823 (CERN-71-7, pp 285-358)
strong interactions of, phenomenology of, (T), 25:30826
strong interactions of, review on, 25:30842
strong interactions of, thermodynamic model for, (T), 25:30838
symmetry for, lectures on SU(2) and SU(3), (T), 25:30914 (NP-18804)
wave functions and invariant amplitudes for massive, analytic equivalence of, 25:30756
wave functions of system of two particles with arbitrary spins and masses, quasipotential method for relativistic, (T), 25:30752 (JINR-P2-5691)
weak interactions of, compilation of coupling constants and low-energy parameters for, (E), 25:30841
weak interactions of, CP violation in strong self-interacting intermediate-vector-boson model of, 25:30814
weak interactions of, lectures on CP violation in, (T), 25:30803 (CERN-71-7, pp 1-40)
weak interactions of, lectures on, (T), 25:30803 (CERN-71-7, pp 1-40)
weak interactions of, review of, (T), 25:30808
weak interactions of, universality principle for muon parity conservation in, (T), 25:30932
weak interactions with photon emission, W boson theory for divergences of amplitudes of nonleptonic, (T), 25:30805 (NP-18777)

ELEMENTARY PARTICLES (TRIPLET)
production of quarks in proton reactions with aluminum at 70 GeV, upper limits for differential and total cross sections for, (E), 25:30724(T) (CERN-Trans-71-4)

ELEMENTS
abundance in atmosphere of α Cyg, (E), 25:30109
abundance of 6 < Z > 28, in explosive nucleosynthesis, (T), 25:30206
abundances of, cosmological, (T), 25:30219 (CERN-70-31)
cosmic abundance of, (E), 25:30138
determination of trace amounts of, in seawater, review on methods for, 25:28921

EMBRYOS
radiation effects on initiation of unscheduled DNA synthesis in muscle differentiating cells of chick, in vitro uv, 25:29650
radiation effects on structures of developing, of reduviid bugs, effects of dose on x, 25:29620
radiosensitivity of, of sugarcane borers in comparison to larvae and pupae, γ, 25:29755

ENDOCRINE GLANDS
radiation effects on rabbit and rat, x, 25:29633

ENGINES
design of closed-cycle thermodynamic, with radioisotope heat source, 25:29279(P)

ENVIRONMENT
conference on, 1969 Institute of Environmental Sciences, April 20 to 24, 1969, Anaheim, Calif, 25:29245
conference on, April 26 to 30, 1971, Los Angeles, 25:31762
radioisotope transport in, standards for protection against acute localized and worldwide fallout cesium-137, strontium-89, and strontium-90, 25:29533

ENZYMES
radiation effects on activity of, in rat liver and serum, local x, 25:29685
radiation effects on oscillatory behavior of reactions of, uv and x, 25:29461
role of photoreactivating, in repair of uv-radioinduced damage to DNA of green algae, 25:29713(R) (COO-1793-5)

ERBIUM
purification of bulk quantities of, by vacuum distillation, 25:29181 (GEPP-85)

ERYTHROCYTES
radiation effects on esterase activity and protein content in rat, whole-body x, 25:29686

ERYTHROPOIESIS
radiation effects on, in blood of rats, fractionated γ, 25:29655

ESTERS
polymers, radiation effects on structure of chlorendic acid-containing, γ, 25:29129
polymers, radioinduced production of films from unsaturated, 25:29116(P)
radioinduced crosslinking of halogen-containing olefinically unsaturated, 25:29119(P)

ETHANE
alpha-particle stopping cross sections in gaseous, test of Bragg's rule for, 25:30642
radiation effects on electric conductivity of liquid, pulsed x, 25:29102

ETHANE, 2-BROMO-2-CHLORO-1,1,1-TRIFLUORO-
pharmacokinetics in man, use of bromine-82 tracer and whole-body counter for study of, 25:29416

ETHANESULFONIC ACID
effects on induction of chlorophyll mutations in, comparison of γ and neutron radiation and, 25:29481 (IAEA-R-290-F)

ETHANOL
effects on survival of γ-irradiated diploid and haploid yeasts, 25:29722
radiolysis of glasses of, at 4 to 77°K, ESR studies on trapped electrons produced by γ, 25:29156

ETHIONINE
effects on activity of methionine adenosyltransferase in liver of x-irradiated rats, 25:29663

ETHYL SULFATES
effects on rice seeds, M(2) characteristics following combined mutagenic effects of x radiation and, 25:29495
effects on tomato seeds, M(2) characteristics following combined mutagenic x radiation and, 25:29493

ETHYLENE
alpha-particle stopping cross sections in gaseous, test of Bragg's rule for, 25:30642
radioinduced polymerization with tetrafluoroethylene, 25:29130
ethylene--tetrafluoroethylene, radioinduced polymerization of solid at -196°C, ESR studies on γ, 25:29112

ETHYLENE, CHLORO-, POLYMERS
performance as artifical substrate for analysis of periphyton component of running-water ecosystems, 25:29478
radiation effects on, review on, 25:29104
radioinduced polymerization of monomer pairs on, γ, 25:29106

ETHYLENE, 1,1-DIFLUORO-
radioinduced polymerization of, 25:29110
1,1-difluoroethylene--tetrafluoroethylene, radioinduced polymerization of, 25:29110
1,1-difluoroethylene--trifluoroethylene, radioinduced

XUM

polymerization of, 25:29110
ETHYLENE, DIFLUORO-, POLYMERS
properties of crystallized, 25:29110
ETHYLENE GLYCOL
radiolysis of glasses of aqueous, at 4 to 77°K, ESR studies on trapped electrons produced by γ, 25:29156
ETHYLENE POLYMERS
analysis of synchrotron targets of, for deuterium and hydrogen diminution, mass-spectrometric, 25:29400
neutron scattering in, Horowitz operators for, (T), 25:31657
radiation chemistry of molten, 25:29144
radiation effects on melt strength and extensibility of, 25:29099(P)
radioinduced crosslinking in presence of free radical catalysts, electron, 25:29115(P)
radioinduced polymerization of monomer pairs on, γ, 25:29106
radioinduced preparation of foamed sheets of, 25:29109(P)
radioinduced sulfoxidation and sulfochlorination of powder of, γ, 25:29107
radioinduced thermoluminescence of, cryostat measurements of, 25:30444
boron--polyethylene, properties as irradiation containers for high-energy neutron activation analysis, 25:29025
polyethylene--poly(vinyl acetate), radioinduced preparation of foamed sheets of, 25:29109(P)
polyethylene--rubber, radioinduced preparation of foamed sheets of, 25:29109(P)
ETHYLENE, TETRAFLUORO-
radioinduced polymerization of solid, at -196°C, ESR studies on γ, 25:29112
radioinduced polymerization with ethylene, 25:29130
1,1-difluoroethylene--tetrafluoroethylene, radioinduced polymerization of, 25:29113
ethylene--tetrafluoroethylene, radioinduced polymerization of solid at -196°C, ESR studies on γ, 25:29112
ETHYLENE, TETRAFLUORO-, POLYMERS
radioinduced polymerization of monomer pairs on, γ, 25:29106
ETHYLENE, TRICHLORO-
radioinduced oxidation of, γ, 25:29131
ETHYLENE, TRIFLUORO-
1,1-difluoroethylene--trifluoroethylene, radioinduced polymerization of, 25:29110
EUMYCOTA
Botrytis cinerea, radiation effects on development of, in stored strawberries, effects of dose and storage temperature on γ, 25:29732
Botrytis cinerea, radioinduced inactivation of aldolase, glutamic-aspartic and glutamin-alanine transaminase and tyrosinase in mycelium of, uv, 25:29720
yeasts, radiation effects on survival of diploid and haploid, effects of ethanol on γ, 25:29722
yeasts, radiosensitivity of, effects of ploidy and hetero- or homozygosity of genome on, 25:29718
EUROPIUM
detection in spectra of BD 61°2565, (E), 25:30063
determination as hexafluoroacetylacetone--trioctylphosphine oxide complex, spectrofluorometric, 25:28954
determination as impurities in gadolinium and yttrium oxides by x-ray luminescence methods, 25:28961
determination for water flow tracing by neutron activation, 25:29013 (RLO-1750-81)
determination in bauxite, selection of line pairs for spectroscopic, 25:28946
determination in lanthanum by emission spectrography, 25:28965
isotopic composition of, spectral determination of, (E), 25:28952
separation from americium and curium by ion exchange in zirconium phosphate--nitric acid system, 25:28989
separation from other rare earths by ion exchange, 25:29178 (CEA-R-4102)
separation from rare earths by solvent extraction using bis(2-ethylhexyl) phosphate, 25:29185
EUROPIUM CHLORIDES
molecular structure of, 25:29086
spectra in matrices of solid nitrogen or rare gases, ir, 25:29086
EUROPIUM FLUORIDES
molecular structure of, 25:29086
spectra in matrices of solid nitrogen or rare gases, ir, 25:29086
EUROPIUM ISOTOPES
separation of fission-product, from irradiated fuels of Mo--UO_2, 25:29413 (CONF-691225)
EUROPIUM ISOTOPES Eu-152
beta and electron-capture decay of, γ--γ and γ-conversion electron angular correlations from, (E), 25:31380
EUROPIUM ISOTOPES Eu-153
energy levels of, mean square charge radius relative to ground state for, (E), 25:31331
energy-level transitions in, isomer shifts for, (E), 25:31331
EUROPIUM ISOTOPES Eu-154
beta decay of, γ--γ and γ-conversion electron angular correlations from, (E), 25:31380
beta decay of, perturbed γ--γ angular correlations from, (E), 25:31344
EUROPIUM OXIDES
dependence magnetization of single crystal of, temperature dependents of, (E/T), 25:30670
growth of large EuO single crystals, 25:29933
EuO-base--GdO, magnetization of single crystal of, temperature dependence of, (E/T), 25:30670
EUROPIUM SELENIDES
growth of large EuSe single crystals, 25:29933
EUROPIUM SULFIDES
growth of large EuS single crystals, 25:29933
EUROPIUM TELLURIDES
growth of large EuTe single crystals, 25:29933
EXHAUST SYSTEMS
design and operation of nuclear power plant, 25:29259
EXOSKELETONS
strontium-90 distribution in, snail, effects of sorption from food or water on, 25:29440
EXOSPHERE
effect of subauroral red arc on, at 900 to 2000 km, (E), 25:30350 (N-70-36812)
EXPERIMENTAL BREEDER REACTOR-II
operation during March 1971, 25:31533(R) (ANL-7798)
EXPONENTIAL PILES
neutron spectra in iron assemblies, analysis of cross section sets for fast, (E/T), 25:31658
physics parameters of plutonium--aluminum-heavy water lattices, effects of various cross section sets on analysis of, (E/T), 25:31661
EYES
proton dose to lens of human, calculation of quality factors for, 25:29511 (AERE-M-1887)
radiation effects on blood vessels of human, effects of age on x, 25:29700
radiation effects on electroretinographic patterns of dog, exposed in utero during embryogenesis, x, 25:29667
radioinduced anomalies in cornea and lens of, in mice, protective effects of dimethyl sulfoxide against x, 25:29562
radioinduced injuries in cornea of rabbit, healing effects of drugs and surgery on, 25:29649

F

FALLOUT
monitoring at Fayetteville, Ark. following May 1966 Chinese nuclear explosion, 25:29216
monitoring in environment of West Valley Processing Plant, 25:29179 (DOCKET-50201-69)
monitoring in ground-level atmosphere at Fayetteville, Ark. following Dec. 1967 Chinese nuclear explosion, 25:29219
monitoring in Italy during 1968, 25:29503 (PROT.-SAN.-8/69)
monitoring in Italy during 1968, 25:29504 (PROT.-SAN.-13/69)
radiation dose to human populations from fresh, methods for estimation of, 25:29539
radioactivity in, effects of particle size on distribution of, 25:29214(T) (LA-tr-71-7)
retention of particulate, by plants in comparison to retention of radioactive aerosols, effects of particle size on, 25:29444
strontium-90 content of, in relation to atmosphere, effects of rainfall intensity on, 25:29218
transport from 1966 to 1968 French nuclear explosions on Mururoa Atoll, measurement of interhemispheric, 25:29221
transport of May 1966 Chinese nuclear explosion-produced, calculation of worldwide, 25:29216
FAST FLUX TEST FACILITY
coolant loops for, radioisotope deposition levels in closed, (E/T), 25:31627 (BNWL-585)
criticality safety of, design objectives and criteria for, 25:31626 (BNWL-576)
design of, reliability assurance program plan for, 25:31630 (BNWL-630)
development during March 1971, 25:31533(R) (ANL-7798)
fuel elements for, criticality safety of inert gas cell examination facility for, (T), 25:31629 (BNWL-587)
fuel meltdown in, calculated critical masses and configurations for, (T), 25:31628 (BNWL-586)
FATS
radiation effects on accumulation of oxidation products of, in rat liver, chronic strontium-90 β, 25:29639
FECES
yttrium-91 excretion in beagle dog, following inhalation, insoluble, 25:29435 (LF-43, pp 163-70)
FEDERAL REPUBLIC OF GERMANY
nuclear power development in, prospects for, 25:31460
uranium prospecting and mining in, programs for, 25:29237
FERMI FAST BREEDER REACTOR
personnel for, revised qualifications for operation, 25:31484 (DOCKET-50016-110)
FERMIONS
coupling of spin-$^1/_2$ to external quantum fields, (T), 25:30939 (NYO-3829-66)
interactions mediated by virtual meson exchange, self-

XUM

consistent method for, 25:30831
interactions of, relativistic rotation of S = 1/2 spin in two-body, (T), 25:30760
motion in homogeneous magnetic field, covariant spin 3-vector operator for, (T), 25:30794
wave equation invariance of spin-1/2, in electromagnetic field, nonrelativistic, (T), 25:30775 (JINR-P2-5522)
FERROMAGNETIC MATERIALS
neutron transmission through, analysis of depolarization in, (T), 25:31181
FIELD EMISSION MICROSCOPES
vacuum pumps for, performance of zeolite, 25:29406
FILMS
photoemission from thin, research program on vacuum-uv, 25:30665(R) (UH-235-P-9-2)
FILTERS
performance limits of charcoal, effects of iodine decay heat on, 25:31669 (ORNL-4602)
performance of sand-bed, for removing aerosols from gas streams, 25:29315 (ANL-7683)
FIRES
extinguishing systems for field assembly buildings, engineering tests of Halon 1301, 25:31748 (UCRL-51021)
FISSION
shell-structure effects in, corrections for, (T), 25:31398
sudden model for ternary, (T), 25:31422
theory of high-energy proton induced, 25:31417
FISSION PRODUCTS
behavior in liquid sodium and argon, (E/T), 25:31615
behavior in liquid sodium, (E/T), 25:31614
deposition in carbon dioxide cooled reactor cooling systems during turbulent flow, (E/T), 25:31566
detection of gaseous, in air samples at Nevada Test Site following power run of nuclear reactor rocket engine during 1969, 25:29506 (SWRHL-97-r)
distribution in cooling systems of nigh temperature gas cooled reactors, 25:31567
distribution in operating reactor fuel pins, thermomigration model for, (T), 25:31589 (CONF-710302-5)
distribution in pyrolytic carbon and layered pyrolytic carbon silicon carbide coatings, sputtering and gamma spectrometry methods for determination of, 25:29979 (SGAE-PH-96/1970)
effects of uranium, on hydrobionts and sanitation of fresh-water basins, 25:29449
effects on amorphous structure of palladium--silicon alloys, 25:29901 (CEA-CONF-1693)
effects on man following inhalation of reactor accident released, estimation of, 25:29420 (LF-43, pp 1-7)
effects on radiometric determination of cesium isotopes in water, after extraction as tetraphenylborates, 25:29000
growth and nucleation of bubbles of gaseous, by re-solution process, model for describing limitations of, 25:30032 (GEAP-12148)
inhalation by mammals, research on, 25:29419(R) (LF-43)
neutron reactions (n,γ) at 0.215 eV to 10 MeV with, cross sections and multigroup constants for, (E), 25:31304 (JAERI-Memo-4251)
release during reactor accidents, analysis of hazards from, 25:31622
release during reactor accidents, analysis of maximum radiation hazards from, 25:31530
release during reactor operation, conference on characteristics and consequences of, 25:31602
release from failed reactor fuel elements during gas coolant loss accidents, (E), 25:31608
release from reactors, escape integral concept analysis for accident, 25:31621
release from reactors, safety analysis of, 25:31604
release from rocket reactor ground tests, analysis of normal operation and accident condition, 25:31642
release in sodium cooled fast breeder reactor accidents, analysis of, 25:31618
release in water cooled reactor coolant loss accidents, factors affecting magnitude of, (E/T), 25:31605
release of gaseous, during short period irradiation of uranium oxide (UO_2) fuel pins, (E), 25:31606
separation from uranium and thorium in sulfuric acid by solvent extraction using TBP in dodecane, 25:29198
trapping of rare gas, development of long-lived, high-expansion plastic foam for, 25:29074(R) (DUN-7221(Vol.1))
trapping of rare gas, in cryogenic porous media bed with charcoal adsorber, 25:29075(R) (DUN-7221(Vol.2))
FISSIONABLE MATERIAL
determination in plutonium- and uranium-containing fuels by mass spectrometry, ASTM computerized method for, 25:28980
determination in unirradiated fuels by neutron flux measurements, apparatus for nondestructive, 25:28988(P)
shipping of, design of BNW Model 10 container for, 25:29318
FLUID FLOW
detachment of laminar and turbulent boundary layers during three-dimensional, 25:31732(T) (SC-T-713010)
magnetohydrodynamic Couette, with heat transfer between porous walls under transverse magnetic field, 25:30342
magnetohydrodynamic, heat transfer for, through plane parallel channels and between concentric cylinders, (T), 25:30341 (NAL-TN-6)
magnetohydrodynamic, motion of isotropic conducting, across steady-state magnetic field, (T), 25:30346
mixing of turbulent jet, method for predicting, 25:31728 (SC-DR-70-838)
velocity of fully developed turbulent, through concentric annulus, bilateral method for determining local time-mean, 25:29268
FLUORIDE VOLATILITY PROCESSES
development for reprocessing fuel or breeding elements, 25:29192(P)
FLUORIDES
determination in high-purity water for reactor cooling and moderating, 25:28914 (BARC-515)
determination of free, using lanthanum fluoride electrode, 25:28923
effects on separation of thorium(IV) from sulfuric acid solutions by extraction using N-phenylbenzylamine in chloroform, 25:29184
FLUORINE
determination in deposits on plants by neutron activation, 25:29011 (CEA-CONF-1747)
determination using ion permselective membrane, potentiometric, 25:28956
effects on fluorometric determination of zirconium, 25:28963
FLUORINE ISOTOPES F-17
energy levels from proton elastic scattering by oxygen-16, spins and parities of resonance, (E), 25:31236
FLUORINE ISOTOPES F-18
production in stars by explosive nucleosynthesis in helium zones, (T), 25:30067
FLUORINE ISOTOPES F-19
helium-3 elastic scattering at 22.4, 30, and 40.7 MeV, differential cross sections for, (E), 25:31214
helium-3 reactions (He-3,Li-6) at 22.4 MeV, DWBA analysis of, 25:31214
helium-3 reactions (He-3,Li-6) at 30 MeV, DWBA analysis of, (E/T), 25:31214
helium-3 reactions (He-3,Li-6) at 40.7 MeV, DWBA analysis of, (E/T), 25:31214
production in stars by explosive nucleosynthesis in helium zones, (T), 25:30067
FLUOROMETRY
sample cell for, at liquid nitrogen temperatures, 25:28925
FOAMS
production of long-lived, high-expansion plastic, for trapping rare gas fission products, 25:29074(R) (DUN-7221(Vol.1))
FOILS
performance of exploding, as switch for capacitors, 25:30574 (EUR-4593, pp 319-38)
FOOD
packaging of radiosterilized, evaluation of materials for, 25:30033
radioactivity of Polish honey in relation to mineral content, origin, region, and type, β, 25:29509
radiolysis of, EPR spectral studies on effects of dose, moisture content, and temperature on free radicals produced by γ, 25:29733
FOOD CHAINS
iodine-131 transport through atmosphere-forage-cow-milk-man, mechanisms for, 25:29505 (SWRHL-39-r)
strontium-90 content of, in Sweden during 1961 to 1969, 25:29480
FORBUSH DECREASES
cosmic-ray intensity increases preceding, (E/T), 25:30316
effects on cosmic layer in lower ionosphere, (E), 25:30311
spectra of, in region 3 to 50 GV, (E), 25:30318
FORENSIC SCIENCE
activation analysis uses in, review of research on, 25:29012(R) (GA-10276)
FORT ST. VRAIN POWER REACTOR, UNIT 1
steam generators for, development and fabrication of, 25:31623 (GA-10338)
FRANCE
uranium deposits in Morvan Mountains of, relation with structure of granite massifs, 25:29239
FRANCIUM ISOTOPES Fr-221
energy-level scheme from actinium-225 decay, (E), 25:31325
FREE RADICALS
radioinduced in Eucalyptus wood, γ, 25:29735
radioinduced production in sarcosine deuteriochloride and hydrochloride monocrystals, ESR spectral studies on x, 25:29152
radioinduced production in watercress seeds, effects of imbibition and germination on γ, 25:29719
radioinduced production of, in food products, EPR spectral studies on effects of dose, moisture content, and temperature on γ, 25:29733
yields of trapped sugar, from γ radiolysis of aqueous monosaccharide ices at 77°K, EPR studies on, 25:29153
FREQUENCY CONVERTERS
design of wideband, for excitation of betatron oscillations in proton synchrotron, 25:29404

XUM

FRUCTOSEDIPHOSPHATE ALDOLASE
radioinduced inactivation of, in mycelium of Botrytis cinerea, uv, 25:29720
FRUITS
strawberries, radiation effects on development of Botrytis cinerea in stored, effects of dose and storage temperature on γ, 25:29732
strawberries, radiation processing of Botrytis-contaminated, effects of dose and storage temperature on shelf life following cobalt-60 γ, 25:29732
FUEL CAPSULES
materials for radioisotope heat source, development and testing of refractory, 25:29823 (ORNL-4630, pp 186-90)
FURAN, TETRAHYDRO-
radiolysis of glasses of, at 4 to 77°K, ESR studies on trapped electrons produced by γ, 25:29156
FURFURYL ALCOHOL
properties of resins of, for use as graphite binder, 25:29920(R) (LA-4631)
FURNACES
design of induction, for use in fuel compatibility testing, 25:29923 (ORNL-4630, pp 59-72)
design of solar, for use in oxide phase studies, 25:29987

G

GADOLINIUM
determination in bauxite, selection of line pairs for spectroscopic, 25:28946
determination in lanthanum by emission spectrography, 25:28965
separation from other rare earths by ion exchange, 25:29178 (CEA-R-4102)
GADOLINIUM ALLOYS AND SYSTEMS
Ce--Gd--Ru, preparation and superconductivity of, (E), 25:30413(T) (LA-tr-71-26)
Gd--Pu-base, thermal conductivity of delta phase of, at 30 to 90°C, 25:29876
Gd--Zn--Zr, electron paramagnetic resonance of coupled-spin Gd/sub x/Zr/sub 1-x/Zn_2, variations in, (E/T), 25:30694
GADOLINIUM BROMIDES
thermodynamic properties at 298 to 1300°K, 25:29951
GADOLINIUM CARBIDES
dissociation energy of gaseous GdC_2, use of isomolecular carbon-exchange reactions for determination of, 25:29955
GADOLINIUM CHLORIDES
thermodynamic properties at 298 to 1300°K, 25:29951
GADOLINIUM IODIDES
thermodynamic properties at 298 to 1300°K, 25:29951
GADOLINIUM ISOTOPES
abundance in meteorites, (E), 25:30158(R) (UCSD-34-P-43-X-9)
GADOLINIUM ISOTOPES Gd-154
energy-level transitions from europium-154 decay, conversion electron particle parameters for, (E), 25:31380
energy-level transitions in, (E), 25:31344
GADOLINIUM ISOTOPES Gd-157
deuteron reactions (d,p) at 12 MeV, proton spectra from, (E), 25:31354
neutron capture with internal pair production, conversion positron spectra from thermal, (E), 25:31329
GADOLINIUM ISOTOPES Gd-158
carbon-12 fission at 126 MeV, angular distribution of fission products from ytterbium-170 compound nucleus in, (E), 25:31371
energy levels from gadolinium-157 (d,p) reactions, (E), 25:31354
energy-level transitions from gadolinium-157 neutron capture, internal conversion positron spectra from, (E), 25:31329
GADOLINIUM OXIDES
analysis for rare earth impurities by x-ray luminescence methods, 25:28961
thermodynamic properties of gaseous diatomic, free energy functions for, 25:29082
EuO-base--GdO, magnetization of single crystal of, temperature dependence of, (E/T), 25:30670
Gd_2O_3--MgO, phase diagram at 1500 to 2400°C, 25:29985
Gd_2O_3--Tb_2O_3, phase studies at 800 to 1200°C, 25:30007
GAGES AND METERS
design for measuring dimensions of extruded uranium cores, 25:29787(R) (RMI-16)
GALAXIES
angular momentum and magnetic "urfield", (T), 25:30244
density wave in M33, velocity of, (E), 25:30201
density waves in spiral, nonlinear, (T), 25:30210
distance of IC 1613, (E), 25:30209
distance of NGC 4569, (E), 25:30207
division processes in systems of, (T), 25:30197
dust scattering in filaments of M82, (E/T), 25:30208
evolution of, explosive nucleosynthesis in chemical, (T), 25:30206
formation of, (T), 25:30220 (P-4494(RAND))
formation of, matter--antimatter hydrodynamics in, (T), 25:30204
gravitational-wave emission from dead dark, (T), 25:30240
infrared emission from nuclei of, model featuring matter accretion by neutron stars, (T), 25:30247
instability of systems of, (T), 25:30197
luminosity variations in I Zwl, (E), 25:30199
mass expulsion from nucleus of M82, (E/T), 25:30208
masses of, 25:30222
model of normal logarithmic spiral for, (E/T), 25:30190
orientation of elliptical, relation to orientation of associated radio sources, (E), 25:30205
orientation of, (T), 25:30244
photometry of supernova in spiral arm of NGC 3389, (E), 25:30057
properties of, (T), 25:30219 (CERN-70-31)
radio sources associated with clusters of, Ohio survey, (E), 25:30120
rotation of, and gravitational instability, (T), 25:30202
spectra of 3C 120 and 3C 371, search for redshifted line of neutral hydrogen in, (E), 25:30121
spectral redshift of small companion, associated with NGC 7603, (E), 25:30217
spectrophotometry of the nucleus of NGC 2655, (E), 25:30194
stellar population of the nucleus of NGC 2655, (E), 25:30194
structure of, gravitational theory of spiral, (T), 25:30215
velocity field in central part of NGC 4569, (E), 25:30207
GALL BLADDER
scanning of human, for diagnosis of malignant diseases, effectiveness of iodine-131-labeled rose bengal for, 25:29575
GALLIUM
determination by amperometric, chelatometric, and conductometric titrations, 25:28970
determination in plutonium by absorption spectrophotometry and spectrography, 25:28916 (CEA-R-4071)
effects on fluorometric determination of zirconium, 25:28963
separation from aqueous solutions by thin-layer chromatography using liquid anion exchangers, 25:29186
separation from mercury by solvent extraction, 25:29031
GALLIUM ALLOYS AND SYSTEMS
Ga--Pu-base, diffusion in epsilon phase of, compared with delta phase, chemical, 25:29873
GALLIUM ISOTOPES
radioactivity standards of, users' guides for, 25:29174
GALLIUM ISOTOPES Ga-65
energy levels from zinc-64 (p,γ) reactions, (E), 25:31249
GALLIUM ISOTOPES Ga-66
beta and electron-capture decay of, precise γ-ray intensities from, (E), 25:31287
GALLIUM ISOTOPES Ga-67
energy levels from zinc-66 (p,γ) reactions, (E), 25:31249
energy levels from zinc-67 (p,n) reactions, spin assignments for, (E), 25:31268
GALLIUM ISOTOPES Ga-68
energy levels from zinc-68 (p,n) reactions, spin assignments for, (E), 25:31268
GALLIUM ISOTOPES Ga-69
deuteron reactions (d,p) at 12.1 MeV, proton spectra from, (E), 25:31290
deuteron reactions (d,pγ) at 7 MeV, γ spectra from, (E), 25:31290
energy levels from zinc-68 (p,γ) reactions, (E), 25:31249
neutron spectra by, γ spectra from thermal, (E), 25:31290
GALLIUM ISOTOPES Ga-70
energy levels of, spin assignments for, (E), 25:31290
GALLIUM ISOTOPES Ga-71
deuteron reactions (d,t) at 12.1 MeV, triton spectra from, (E), 25:31290
GALLIUM ISOTOPES Ga-72
beta decay of, β--γ circular polarization in, (E), 25:31297
beta decay of, gamma spectra and log ft for, (E), 25:31260
GALLIUM OXIDES
thermodynamic properties of gaseous diatomic, free energy functions for, 25:29082
GAMMA CAMERAS
performance of, review of, 25:29349
testing of, phantom for, 25:29328 (ORNL-TM-3261)
GAMMA DECAY
statistical theory of nuclear, 25:31406
GAMMA RADIATION
angular distribution and polarization formulas for, formulation using phase-defined reduced matrix elements, 25:31420
detection in biological samples, methods for mixed β and, 25:29517
distribution in lead, (T), 25:30640
Doppler broadening of, measurement using lithium-drifted germanium detectors, 25:31208
dose to beagle dog lungs following inhalation of insoluble cerium-144, 25:29436 (LF-43, pp 183-7)

XUM

dose to beagle dogs following intravenous administration of cesium-137 chloride, 25:29433 (LF-43, pp 140-5)
dose to beagle dogs, inhaled cerium-144 chloride, 25:29431 (LF-43, pp 128-36)
dose to beagle dogs, inhaled yttrium-91 chloride, 25:29432 (LF-43, pp 137-9)
dose to liver, lungs, and skeleton in beagle dogs following inhalation of thulium-171 oxide, 25:29425 (LF-43, pp 71-8)
dose to lungs of beagle dogs following inhalation of insoluble yttrium-91, 25:29435 (LF-43, pp 163-70)
dose to man during nuclear attack, methods for estimation of, 25:29539
dose to man in vicinity of nuclear excavation projects, computer method for calculation of external, 25:29516 (UCRL-50990)
dose to tissues in man following intake of powders of irradiated uranium fuels, use of radiometric determination of cesium-137 in urine for estimation of, 25:29515 (NP-18794)
doses in single-compartment aboveground concrete structures from thermonuclear explosion 100 m above ground, (T), 25:30633
dosimetry for radiobiological studies on Drosophila, 25:29522
effect on reproductive capacity of rhinoceros beetles, effects of dose on, 25:29754
effectiveness for insect population control using sterile male technique, 25:29731
effectiveness for therapy of inoperable pulmonary or squamous cell carcinomas in man, effects of split-course method on cobalt-60, 25:29600
effects of dose on reproduction and survival of gypsy moths following exposure of male pupae, 25:29616
effects on 2,2-dimethylbutane, effects of dose and iodine scavenging on, 25:29142
effects on alfalfa seeds for early flowering and improved vigor, mutagenic, 25:29488
effects on allyl alcohol glass, ESR study of radicals produced by, 25:29162
effects on aniline, gas chromatographic analysis of products from, 25:29155
effects on aqueous monosaccharide ices at 77°K, spectral studies on trapped electrons and sugar radicals produced by, 25:29153
effects on aqueous solutions of 5-bromo-2'-deoxyuridine in presence of oxygen, yields from, 25:29135
effects on aqueous solutions of 5-bromo-2'-deoxyuridine in presence of oxygen, yields from, 25:29136
effects on beagle dogs following intravenous administration of cesium-137 chloride, 25:29433 (LF-43, pp 140-5)
effects on biochemistry, heat-sensitivity, pathogenicity, and subsequent radiosensitivity of Salmonella typhimurium, 25:29557
effects on bones of dogs, pathological, 25:29630
effects on bromide- or iodide-doped barium sulfate, 25:29163
effects on carcinoma in human prostate gland, therapeutic, 25:29597
effects on cells of animals and man, review of damaging, 25:29690
effects on chemical and physical properties of gluten proteins, 25:29103
effects on chromosomes in bean roots exposed in sucrose solutions, effects of acidity cytotoxic effects of, on chromosomes of Vicia on aberrant, 25:29494
effects on chromosomes in Chinese hamster liver cells, RBE for cobalt-60, 25:29483 (LF-43, pp 246-53)
effects on chromosomes in pea seedlings, protective effects of anoxia against aberrant, 25:29486
effects on chromosomes in pea seeds, effects of ATP, cysteine, and EDTA on aberrant, 25:29485
effects on chromosomes of dormant pea seeds, effects of moisture content on protective effects of cysteimine against aberrant, 25:29552
effects on condensation of gold nuclei from atomic beam on ionic crystals, 25:29910
effects on content of connective tissue constituents in beagle dog lungs following inhalation of insoluble cerium-144, 25:29622 (LF-43, pp 218-23)
effects on content of kininogen and kinin-forming activity in rat blood plasma, lethal, whole-body, 25:29681
effects on copper(II) and iron(II) in perchloric and sulfuric acids, 25:29141
effects on cracking of cumene and isomerization of o-xylene catalyzed by halogenated alumina--silica, 25:29111
effects on D(-) mandelic acid, 25:29145
effects on deaerated aqueous solutions of benzyl alcohol, 2-propanol, sodium formate, sodium hydroxide, and/or sodium nitrate, effects of pressure on hydrogen yields from, 25:29157
effects on development of Botrytis cinerea in stored strawberries, effects of dose and storage temperature on cobalt-60, 25:29732
effects on DNA synthesis in lymphoid tissues in rats, effects of adrenalectomy on subsequent whole-body, 25:29672
effects on DNAase activity in Escherichia coli, effects of dose on, 25:29725
effects on electronics, simulators for studying transient nuclear explosion, 25:29410
effects on embryos, larvae, and pupae of sugarcane borers, 25:29755
effects on erythropoietic activity in rat blood, effects of dose fractionation on, 25:29655
effects on estradiol-induced lactate dehydrogenase activity in uterus of immature rats, inhibitory, 25:29670
effects on food products, EPR spectral studies on effects of dose, moisture content, and temperature on free radicals produced by, 25:29733
effects on free radical production in watercress seeds, effects of imbibition and germination on, 25:29719
effects on frozen acetone, cyclohexene, and hexane, effects of dose rates on yields from, 25:29160
effects on gastrointestinal tract in mice, dynamics of recovery following sublethal, 25:29657
effects on glasses of aqueous ethylene glycol, ethanol, methanol, sodium hydroxide, or tetrahydrofuran, at 4 to 77°K, ESR studies on trapped electrons produced by, 25:29156
effects on gonads of Dacus (fruit fly), effects of dose and pupal exposure on, 25:29617
effects on hatchability and survival of mosquito eggs and larvae, 25:29614
effects on heart of beagle dogs, protective effects of metaraminol, norepinephrine, and phenylephrine on lethal, whole-body, mixed neutron and, 25:29565
effects on heat-treated Bacillus spores, effects of NaCl content of heating medium on, 25:29558
effects on heavy water and water, yields from, 25:29154
effects on homologous thyroglobulin antibody production in rats, combined effects of iodine-131 and, 25:29660
effects on human lymphocytes of normal and hepatitis-infected donors, in vitro, 25:29710
effects on induction of chlorophyll mutations in rice, comparison of neutron and, 25:29481 (IAEA-R-290-F)
effects on intestinal mucosa of sheep, unilateral lethal cobalt-60 and pulsed mixed fission neutron and, 25:29656
effects on kininase and kininogen activity in blood of rats, 25:29668
effects on lettuce seedlings and seeds, effects of dose rate on cytogenetic, 25:29491
effects on lifetime and reproductive capacity of codling moth pupae, effects of dose rates on, 25:29612
effects on liver in human children following therapy for Ewing's or Wilms' tumors, 25:29652
effects on liver of animals and man, pathological, 25:29694
effects on longevity, reproduction, and survival of bean weevils, effects of dose on, 25:29756
effects on macrostructure of bovine serum albumin, 25:29471
effects on mammalian cells, effects of age on damaging, 25:29625
effects on man following radiotherapy, leukemogenic, 25:29696
effects on man, protective effects of ethyl ester of 2-thiazolidineacetic acid, 4-carboxy-α-phenyl against therapeutic doses of, 25:29545
effects on materials for packaging radiosterilized foods, (E), 25:30033
effects on mice, protective effects of spleen cell transplants from irradiated donors against lethal, 25:29564
effects on mitosis in pea seedlings, effects of dose on, 25:29484
effects on mortality among populations of springtail insects, effects of dose on cobalt-60, 25:29615
effects on muscles and spleen of mice, effects of increased atmospheric pressure on protective effects of AET, cystamine, cystaphos, and mexamine against, 25:29550
effects on organic solids, stimulation spectra of trapped anions from, 25:29133
effects on organoleptic properties and survival of Salmonella in frozen meats, 25:29729 (IAEA-R-491-F)
effects on oxidation of trichloroethylene, 25:29131
effects on oxygen electrode performance from added thulium-170, 25:29098
effects on pathomorphology of mouse, rabbit, and rat brain in mixed fast neutron and proton fields, whole-body, 25:29644
effects on permeability units containing thin silicone rubber membranes, 25:29317 (ORNL-4522)
effects on poly(propylene oxide), 25:29144
effects on polymerization of monomer pairs on polymers, 25:29106
effects on polymerization of solid ethylene--tetrafluoroethylene or tetrafluoroethylene at -196°C, ESR studies on, 25:29112
effects on pulping of Eucalyptus wood by sterilization, 25:29735
effects on renal function and morphology in rabbits, methods for studying, 25:29684
effects on reproductive capacity of cherry fruit fly, 25:29741
effects on reproductive capacity of female and male Mediterranean fruit flies, effects of dose and pupal

XUM

exposure on, 25:29743
effects on reproductive capacity of female arthropods, 25:29747
effects on reproductive capacity of horn flies, effects of pupal exposure on, 25:29744
effects on reproductive capacity of reduviid bug vectors of Chagas' disease in comparison to effects of chemosterilants, 25:29745
effects on sensitivity of Bacillus spores to NaCl in recovery medium, effects of dose and NaCl content of medium during exposure on, 25:29558
effects on shelf life of Botrytis-contaminated strawberries, effects of dose and storage temperature on cobalt-60, 25:29732
effects on sodium alginate, 25:29159
effects on solid adamantane, ESR spectral studies on radicals produced by, 25:29139
effects on solid cyclopropene, 25:29147
effects on solid film lubricants, 25:29096 (WERL-HFIL-1)
effects on solid isobutane, ESR spectra of products from, 25:29161
effects on solid-state polymerization of acrylonitrile, ESR studies on, 25:29118
effects on solid-state polymerization of methyl methacrylate, ESR studies on, 25:29117
effects on solubilization of colloidal sulfur, effects of free radical scavengers and oxygen on, 25:29137
effects on some aromatic compounds in rigid organic media, deferred luminescence spectra following, 25:29150
effects on spermatozoa of bean weevils, 25:29746
effects on structure of chlorendic acid-containing polyesters, 25:29129
effects on subsequent polymerization of cellulose with ethyl acrylate, 25:29108
effects on sulfoxidation and sulfochlorination of polyethylene powder, 25:29107
effects on sunflower seeds, effects of mineral nutrition on, 25:29714
effects on survival of Clostridium botulinum spores in beef, effects of temperature on, 25:29734
effects on survival of diploid and haploid yeasts, effects of ethanol on, 25:29722
effects on survival of mice, protective effects of acetylcholine and adrenalin against, 25:29548
effects on survival of sheep, LD-50/5 dose for unilateral cobalt-60, 25:29656
effects on survival of sheep, RBE for LD-50/5 dose for unilateral pulsed mixed fission neutron and, 25:29656
effects on survival of Sitotroga cerealella (grain moth), effects of dose on, 25:29618
effects on sweet potatoes tubers, effects of growth and productivity on, 25:29721
effects on thermoluminescence of crystalline and glassy methanol, 25:29101
effects on thymine in ethanol or methanol solution at 77°K, 25:29143
effects on thymine, mechanism for release of hydrogen atom in, 25:29148
effects on urease activity in soils, comparison of toluene and, 25:29460
effects on urinary tract of man, pathological, 25:29697
effects on wheat grains, effects of, on development of and reproduction of grain weevils, 25:29737
effects on x-virus in potato tubers, mutagenic, 25:29726
emission by nuclei in crystals, thickness dependence of, (T), 25:30690
flux of greater than or equal to 200-MeV, in direction of Leo and Virgo, (E), 25:30306
origin of cosmic diffuse, isotropic, (E/T), 25:30332
penetration in curved tube, spectrum of, 25:30638
production cross sections for secondary, POPOP 4 computer program calculation of, (E/T), 25:31671 (ORNL-TM-3367)
production in Universe, (T), 25:30219 (CERN-70-31)
reactions with nuclei at 2.75 MeV, pair-production cross sections for, (E/T), 25:31361
scattering by iodine-127, lead, and mercury at 6.1 to 7.1 MeV, gamma spectra from inelastic, (E/T), 25:31303 (INR-1271)

GAMMA SOURCES
determination in industrial water or waste water by scintillation counting, ASTM method for, 25:29008
determination in phosphorus-32 preparations, ASTM method for, 25:29002
determination in radioisotope mixtures, ASTM method for, 25:29005
development of intense pulsed, for simulating nuclear explosions for studying transient radiation effects on electronics, 25:29410

GAMMA SPECTROMETERS
data analysis of lithium-drifted germanium, computer program for automatic, 25:29354 (LUNP-7101)
fabrication of lithium-drifted germanium, for gold assay by activation analysis, 25:29357
performance of lithium-drifted germanium, for activity determination in reactor coolants, 25:31680
resolution of lithium-drifted germanium, optimization of, 25:29356 (RT/EL-(70)5)

GAMMA SPECTROSCOPY
data analysis in, computer program for, (T), 25:29363

GAS CENTRIFUGES
development of counterflow, in Germany, review of, 25:29271(T) (CONF-700557-1)

GAS FLOW
characterization of supersonic, at liquid layer interface, 25:31726 (SC-DC-713922)
electrohydrodynamic, in generator ducts, 25:30339
magnetohydrodynamic channel, preionization and velocity effects in, 25:30348
magnetohydrodynamic steady duct, for high Hall-parameter values, (E), 25:30343
magnetohydrodynamic, through channel with magnetic field followed by injection through electrodes, effects of Hall effect on steady-state, (T), 25:30344
magnetohydrodynamics, through rectangular channel in magnetic field, effect of short circuit on, (E), 25:30347

GASEOUS DIFFUSION PROCESS
cascades for, calculation of optimized squared-off, 25:29281

GASES
analysis for tellurium and arsenic, 25:28959
heat transfer through particle-seeded, evaluation of radiant, (E), 25:29270
injection into toroidal geometries, radial distribution of tangential, (E), 25:30602
radiation absorption by interstellar and intergalactic, effects of variable Planck's constant on, 25:30246
use of radioactive, in method for measuring thickness of hollow turbine blades, 25:29278(P)

GASTROINTESTINAL TRACT
radioinduced injuries in mouse, dynamics of recovery following γ, 25:29657
radiosensitivity of animal, x, 25:29632
radiosensitivity of rat, 25:29646

GENETICS
conference on clinical aspects of inherited disorders, Birmingham, Ala., April 9-10, 1970, 25:29498

GEOMAGNETIC FIELDS
fluctuations in, correlation with lead-210 deposits in Antarctica, (E), 25:29211
pulsations in, origin mechanisms of equatorial, low-, and mid-latitude, (E/T), 25:30356
radio-wave propagation along magnetospheric, color spectrograms of vlf Poynting flux measurements of, (E), 25:30370

GERMANIUM
defect production by ion bombardment of single-crystal, design and performance of equipment for, 25:30648 (N-70-37028)
effects on fluorometric determination of zirconium, 25:28963
microstructures of gallium- and indium-doped lithium-drifted, used in detector fabrication, 25:29330

GERMANIUM ALLOYS AND SYSTEMS
Ge--Ti--Zr, melting temperature of brazements of, 25:29824 (ORNL-4630, pp 191-206)

GERMANIUM ISOTOPES Ge-70
neutron inelastic scattering by, excitation functions for 2^+ levels in fast, (E), 25:31244

GERMANIUM ISOTOPES Ge-72
energy level at 3.036 MeV from gallium-72 decay, spin and parity of, (E), 25:31297
energy levels from arsenic-72 decay, spins and transition probability for, (E), 25:31261
energy levels from gallium-72 decay, spins and parities of, (E), 25:31260
neutron inelastic scattering by, excitation functions for 2^+ levels in fast, (E), 25:31244

GERMANIUM ISOTOPES Ge-73
energy level at 13.3 keV, gamma decay, total and K-conversion coefficients, and half-life of, (E), 25:31293
energy level at 13.34 keV from arsenic-73 decay, lifetime and spin assignment for, (E), 25:31274
energy-level transition from arsenic-73 decay, K-conversion coefficient of 53.3-keV, (E), 25:31274

GERMANIUM ISOTOPES Ge-74
neutron inelastic scattering by, excitation functions for 2^+ levels in fast, (E), 25:31244

GERMANIUM ISOTOPES Ge-76
neutron inelastic scattering by, excitation functions for 2^+ levels in fast, (E), 25:31244

GERMANIUM OXIDES
thermodynamic properties of gaseous diatomic, free energy functions for, 25:29082

GLACIERS
occurrence of continental, computer model studies of theories for, 25:31750 (UCRL-71888(Pt.2))
occurrence of, computer model studies of theories for, 25:31749 (UCRL-71888(Pt.1))
occurrence of, use of zonal atmospheric model for testing theories of, 25:31751 (UCRL-72803)

GLASS
performance as artifical substrate for analysis of periphyton component of running-water ecosystems, 25:29478

GLASS WOOL
heat transfer from organic liquids to, effects of porosity on, 25:29264 (EUR-4531, pp 821-39)

GLOBULINS
radiation effects on immune reactions to bovine gamma, in guinea pigs, 25:29474

zinc-65 uptake by, in human blood serum, 25:29447
GLOVE BOXES
design for use in fuel compatibility testing, 25:29923 (ORNL-4630, pp 59-72)
GLUCOSE, 2-AMINO-2-DEOXY-
radiation effects on content of, in beagle dog lungs following inhalation of insoluble cerium-144, relation of pulmonary fibrosis to β and γ, 25:29622 (LF-43, pp 218-23)
GLUTEN
radiation effects on chemical and physical properties of, γ, 25:29103
GOLD
determination in copper electrolysis slimes, gravimetric and iodometric, 25:28933
determination in rocks, lithium-drifted germanium gamma spectrometer for activation, 25:29357
determination in water by neutron activation, 25:29015
determination in water by neutron activation and γ spectrometry after preconcentration, 25:29014
effects on fluorometric determination of zirconium, 25:28963
radiation effects on nuclei condensation of atomic beam of, on ionic crystals, 25:29910
GOLD ALLOYS AND SYSTEMS
Au--Co-base, thermal expansion at 100 to 800°C, 25:29899
Au--Co-base, transformation temperatures of, allotropic, 25:29899
Au--H, nuclear magnetic resonance study of sputtered films of, 25:30692
Au--He-3, nuclear magnetic resonance study of sputtered films of, 25:30692
Au--V, superconducting-state Knight shift in intermetallic V_3Au, 25:30425
GOLD ISOTOPES
radioactivity standards of, users' guides for, 25:29174
GOLD ISOTOPES Au-197
deuteron reactions (d,p), (d,p2n), and (d,xn) at 10 to 70 MeV, excitation functions and isomer ratios for, (E), 25:31311 (LYCEN-7092)
neutron capture by, calibration of Moxon--Rae detector for measurement of cross section for, 25:29326 (LA-4445)
photon reactions (γ,n) at 10 to 68 MeV, yields of radioactivities from, (E), 25:31333
proton fission at 10 MeV to 29 GeV, cross section for, 25:31326
GOLD ISOTOPES Au-198
metabolism in beagle dogs following ingestion of nuclear debris from Project Cabriolet, 25:29456
use for radiodiagnosis of metastatic and primary adenocarcinomas in human kidneys, 25:29590
use of colloidal, for scintigraphy of human liver for function and morphology, 25:29591
GOLD OXIDES
thermodynamic properties of gaseous diatomic, free energy functions for, 25:29082
GONADS
radiation damage to, of onion flies, 25:29619
radiation effects on, of Dacus (fruit fly), effects of dose and pupal exposure on γ, 25:29617
GRANITES
structure of Morvan Mountains, France, relations with uranium distribution, 25:29239
GRAPHITE
creep and dimensional stability of irradiated, computer program for viscoelastic analysis of, 25:29945 (ORNL-TM-3242)
crystal structure of Poco-type, 25:29920(R) (LA-4631)
mechanical properties of synthetic, effects of boron on, 25:29946(T) (SC-T-713023)
mechanical properties of, effects of porosity on, 25:29920(R) (LA-4631)
oxidation of pyrolytic, by flowing air, effects of air velocity, surface area, and temperature on, 25:29919
properties of ATJS, at 1200 to 2400°K, electric, physical, and thermal, 25:29972
properties of bonded and molded, prepared from Athabasca and Santa Maria coke flours, 25:29920(R) (LA-4631)
properties of dense, at 50 to 2500°K, electric and thermal, 25:29949
properties of extruded, incorporating furfuryl alcohol resin binders, 25:29920(R) (LA-4631)
properties of, effects of boron additions on electric, magnetic, mechanical, and structural, 25:29953
reactions with liquid hafnium, niobium, tantalum, titanium, vanadium, and zirconium to prepare corresponding monocarbides, 25:29926
reactions with water, effects of temperature on chemical and physical, 25:29918 (CEA-R-4123)
stability of extruded, effects of baking and curing atmosphere and temperature on, 25:29920(R) (LA-4631)
graphite--ZrC, properties of composites of, mechanical and physical, 25:29920(R) (LA-4631)
GRAVITATION
Brans--Dicke scalar--tensor theory of, scale invariance of, 25:31010
collisional diffusion and dissipation in inhomogeneous rotating self-gravitating systems, (T), 25:30229
constant of, cosmological models with variable, (T), 25:30232
coupling to matter in quantum electrodynamics, suppression of infinities by, 25:30994
effects on galactic spiral structure, (T), 25:30215
Einstein equations in, special coordinate conditions for, 25:31006
Einstein theory of, inertial reference frames in, (T), 25:30996
energy production from binary interactions in inhomogeneous rotating self-gravitating systems, (T), 25:30230
field equations for, generalization of, 25:31005
field equations in, 25:31000
field equations in, solutions of weakened set of, 25:30999
instability due to, in inhomogeneous cosmological model, (T), 25:30241
instability in galaxies, (T), 25:30202
interactions in, measurement of velocity of propagation of, (E/T), 25:30995 (JINR-P13-5685)
propagation of, measurement of velocity of, (E/T), 25:30995 (JINR-P13-5685)
GRAVITATIONAL COLLAPSE
emission of gravitational radiation during nonspherical, (T), 25:30238
GRAVITATIONAL FIELDS
effects of intense, on Planck's constant, (T), 25:30246
effects on synchrotron emission from charged particles in cyclic accelerators, (T), 25:31008
effects on synchrotron emission from relativistic charged particles for detection of gravitational waves, (T), 25:31008
fluctuations of, significance in relativity and cosmology of quantum, (T), 25:30224
Lagrangian density of, nonlinear corrections in, (T), 25:30233
masses in, energy--momentum--stress tensor for uniformly rotating rod-shaped and cylindrical, 25:30997
neutrino scattering by linearized Schwarzschild metric, (T), 25:30242
oscillations of fluid spheroids containing, hydromagnetic, (T), 25:30102
quantization of weak, (T), 25:31001
spectral red shift in, quantum mechanics for, (T), 25:30963
stellar motions in, (T), 25:30237
GRAVITATIONAL RADIATION
detection by spin-two massless particle radiation, 25:31002
detection of, (E), 25:31007
detection of, gravitational field effects on synchrotron emission from relativistic charged particles for, (T), 25:31008
effects on synchrotron emission from charged particles in cyclic accelerators, (T), 25:31008
emission during nonspherical gravitational collapse, (T), 25:30238
emission from dead dark galaxies, (T), 25:30240
emission from slowly rotating fully relativistic stars, (T), 25:30092
graviton Lagrangian and superpropagator, 25:30994
propagation in space of constant curvature, effects of density perturbations on, (T), 25:30243
GRENOBLE REACTORS (SILOE)
fuel element meltdown in, release and transport of fission products from, (E), 25:31639
GROUND
deformation and fracture of Nevada Test Site, effects of Handley event underground nuclear explosion on, 25:29203 (USGS-474-95)
motion from Handley event underground nuclear explosion, data tabulation on peak resultant vector, 25:29242 (NVO-1163-216(Rev.))
neutron scattering at air-ground interface, differential measurements of fast-, (E), 25:30635
GROUND WATERS
levels and pressures of Nevada Test Site, effects of Handley event underground nuclear explosion on, 25:29203 (USGS-474-95)
uranium content of, effects on deposition of molybdenum and selenium in near-surface uranium deposits, 25:29240
GROUP THEORY
group-theoretical operator analysis in the ds shell, 25:31452
Lie group, particle motion in Riemann manifold of, 25:30971
Poincare group in, additional invariance of relativistic equations of motion under full, 25:30975
representations of quantized fields in, continuous tensor products of, 25:30947
rotation group in, arbitrary angular momentum from invariants of, 25:31013 (ITEF-782)
semigroups for field equations in quantum field theory, 25:30972
unitary weights for multiple particle production in, method for calculating, 25:30913 (JINR-P2-5729)
GUINEA PIGS
radiation effects on immune reactions to bovine gamma globulin in Freund's adjuvant, 25:29474
radiation effects on isolated intestines in, protective effects of tryptamine against x, 25:29566

XUM

GUNDREMMINGEN POWER REACTOR
coolant chemistry measurements during January 1971, 25:31479 (TID-25698)
maintenance during January 1971, 25:31479 (TID-25698)
operations during January 1971, 25:31479 (TID-25698)
GYPSUMS
analysis for lead and oxygen, radiometric x-ray method for, 25:28939

H

HI REGIONS
collisions of high-velocity galactic and extragalactic, (T), 25:30198
distribution in anticenter region of Milky Way, (E), 25:30142
ionization equilibrium of oxygen in, (T), 25:30211
kinematics of, in the galactic anticenter region, (E), 25:30143
magnetic fields in, measurements of Zeeman splitting of 21-cm lines from, 25:30133
radio emission from hydroxyl in, at 1665 and 1667 MHz, (E), 25:30155
HII REGIONS
condensations in, radio maps of, (E), 25:30137
diameters of, in Milky Way, (E), 25:30203
distribution in M33, (E), 25:30201
electric charge on dust grains in, (T), 25:30192
optical and radio observations of KJ-50, H2-3, and H2-6, (E), 25:30117
spectral types of stars in IC 417 and IC 1318a, (E), 25:30108
HADRONS
interactions and properties of, review of, 25:30822 (CERN-71-7, pp 41-180)
interactions at high energies in cosmic EAS, isobar model for, (T), 25:30839
interactions at high energies, asymptotic behavior of particle distributions in, 25:30908
interactions at high energies, electromagnetic and weak corrections to strong, 25:30832
interactions at high energies, mass dependence of momentum transfer distributions in diffraction dissociation in, (T), 25:30767
interactions at low energies, conference on, (E/T), 25:30840
interactions at very high energies, transverse momenta and scaled-down longitudinal momentum variables for, (T), 25:30754
interactions in extensive air showers above 10^{12} eV, cross section for nucleon--antinucleon pair production in, (E), 25:30728
interactions of, asymptotic equality of total cross sections in two simple models for, (T), 25:30769
interactions of, Bose--Einstein symmetrization for Goldhaber effect in, (T), 25:30763
interactions of, conference on high-multiplicity, (E/T), 25:30762
interactions of, correlation effects for many-body final states in, (T), 25:30837
interactions of, data presentation for high-multiplicity, (E), 25:30732
interactions of, generalized Veneziano model for, (T), 25:30765
interactions of, implications of local duality in set of coupled, 25:30843
interactions of, light cone for scale invariance for, (T), 25:30749 (CALT-69-297)
interactions of, multiperipheral models for, (T), 25:30765
interactions of, review of cross sections and multiplicity and momentum distributions for, (E), 25:30715
interactions of, review of hypothesis of limiting fragmentation for, (T), 25:30768
interactions of, statistical concepts for n-point function in Veneziano model for, (T), 25:30766
interactions of, statistical models based on Fermi model for, (T), 25:30764
interactions of, trends and problems in high-multiplicity, (T), 25:30881
interactions with hadrons, compilation of coupling constants and low-energy parameters for, (E), 25:30841
interactions with hadrons, duality hypotheses for exchange degeneracy in, (T), 25:30825
interactions with hadrons, graphs for isotopic relations for Pomeranchuk pole exchange in three-body hadron production in, (T), 25:30824 (JINR-P2-5630)
interactions with hadrons, lectures on dual models and phenomenology for, (T), 25:30823 (CERN-71-7, pp 285-358)
interactions with hadrons, phenomenology of, (T), 25:30826
interactions with hadrons, thermodynamic model for, (T), 25:30838
model of, nonrelativistic separable-potential quark, 25:30846
production in γ + p, review of multiple, (E), 25:30716
production in strong interactions, graphs for isotopic relations for Pomeranchuk pole exchange in three-body, (T), 25:30824 (JINR-P2-5630)
HAFNIUM
deposition on substrates from alkaline fluoride mixtures containing salts of, method for electro-, 25:29783 (CEA-N-1376)
effects on fluorometric determination of zirconium, 25:28963
production and uses during 1971, review on, 25:29808
production and uses of, newsletter on, 25:29796
reactions with graphite thimbles to prepare hafnium monocarbide, 25:29926
separation from aqueous solutions by thin-layer chromatography using liquid anion exchangers, 25:29186
separation from other metals by ion-exchange paper chromatography, 25:29190
separation from zirconium by ion exchange in formic acid media, 25:28955
separation from zirconium, review of methods for, 25:29782 (AAEC/TM-570)
HAFNIUM ALLOYS AND SYSTEMS
production and uses of, newsletter on, 25:29796
properties of, newsletter on, 25:29796
B--Co--Hf, crystal structure of $HfCo_3B_2$, 25:29992
Fe--H--Hf-base--N--O--Zr, ductility and tensile properties of dilute, effects of composition on, 25:29827(R) (RPI-3719-9)
H--Hf-base--O--Zr, ductility and tensile properties of dilute, effects of composition on, 25:29827(R) (RPI-3719-9)
Hf--Nb, precipitation morphology of, effects of aging temperature on a-, 25:29886
Hf--Pt-base, tensile properties at 1290°C, 25:29823 (ORNL-4630, pp 186-90)
Hf--Pt-base--W, tensile properties at 25 to 1290°C, 25:29823 (ORNL-4630, pp 186-90)
HAFNIUM BORIDES
thermal conductivity of HfB_2 at 200 to 1300°C, 25:29956
uses of, newsletter on, 25:29796
HAFNIUM CARBIDES
preparation of HfC, by reactions of liquid hafnium with graphite thimbles, 25:29926
preparation of monocrystalline monocarbide, recrystallization method for, 25:29927
uses of, newsletter on, 25:29796
HAFNIUM ISOTOPES Hf-172
electron-capture decay of, γ spectra from, (E), 25:31347
HAFNIUM ISOTOPES Hf-174
energy levels from tantalum-174 beta and electron-capture decay, lifetimes and spin--parity assignments for, (E), 25:31310 (LYCEN-7084)
energy levels from tantalum-174 decay, lifetimes and spin--parity assignments for, (E), 25:31348
energy-level transitions from tantalum-174 beta and electron-capture decay, conversion coefficients, intensities, and multipolarities for, (E), 25:31310 (LYCEN-7084)
HAFNIUM ISOTOPES Hf-176
energy levels from tantalum-176 and lutetium-176 decay, spins and parities of, (E), 25:31375
HAFNIUM ISOTOPES Hf-177
neutron capture by, conversion electron spectra from thermal, (E), 25:31336
HAFNIUM ISOTOPES Hf-178
energy-level scheme from hafnium-177 thermal neutron capture, (E), 25:31336
HAFNIUM ISOTOPES Hf-180
neutron activation resonance integrals for, measured relative to gold-197, (E), 25:31300 (CNEA-282)
HAFNIUM NITRIDES
uses of, newsletter on, 25:29796
HAFNIUM OXIDES
thermodynamic properties of gaseous diatomic, free energy functions for, 25:29082
HfO_2--SiO_2, solid solutions of, occurrence of hafnium oxide-rich, 25:30006
HAFNIUM SILICIDES
uses of, newsletter on, 25:29796
HALDEN BOILING REACTOR
fuel element failures in, release and transport of fission products from, (E), 25:31609
HALIDES
corrosive effects of aqueous solution of, on aluminum--molybdenum--titanium--vanadium alloy, 25:29765
HAMSTERS
radioinduced chromosome aberrations in liver cells of Chinese, comparison of RBE of α, β, and γ, 25:29483 (LF-43, pp 246-53)
radioinduced chromosome aberrations in liver cells of Chinese, internal americium-241, 25:29482 (LF-43, pp 240-5)
HANDLING AND STORAGE
equipment for radioactive material, design standards for pool facility for, 25:31637
HANFORD PRODUCTION REACTORS
thermal effluents from, effects on young salmon in Columbia River, 25:31645 (BNWL-1527)
HANFORD PRODUCTION REACTORS (N)
fuel element failure monitoring system for, operation of Geiger--Mueller tubes in, (E), 25:31646 (DUN-SA-136)
steam generator for, corrosion of Inconel 600 tubes in, 25:29760 (DUN-SA-149)

XUM

HARTLEPOOL POWER REACTORS
pressure vessels for, design and construction of prestressed concrete, 25:31456 (EUR-4531, pp 129-44)
HASTELLOY C
corrosion resistance of as-welded Type 276, 25:29764
corrosion resistance of Type-276, to acid and alkali environments, evaluation of, 25:29775
fabrication and ductility of Type 276, 25:29764
HASTELLOY N
radiation effects on corrosion and mechanical properties of, evaluation of pile neutron, 25:29906 (ORNL-TM-3063)
HASTELLOY X
corrosion of similar-metal welds in, by steam, 25:29763 (ORNL-4630, pp 280-7)
radiation effects on mechanical properties of, fast neutron, 25:31568(T) (EURFNR-823)
HEART
diagnosis of myocardial infarction in, use of gamma camera scintigraphy of mercury-197- or mercury-203-labeled Brommercurascan or Mercurascan for, 25:29571(T) (LB/G-2835)
radiation effects on activity and isoenzyme composition of lactate dehydrogenase in, of neonatal rats following parental exposure, 25:29665
radioinduced myocarditis in animal and human, x, 25:29695
HEAT
effects on biochemistry, pathogenicity, and subsequent heat-sensitivity of Salmonella typhimurium, 25:29557
effects on γ-radiosensitivity of Bacillus spores, effects of NaCl content of heating medium on, 25:29558
effects on sensitivity of Bacillus spores to NaCl in recovery medium, effects of NaCl content of heating medium on, 25:29558
sensitivity of Bacillus spores, effects of NaCl content of heating medium on, 25:29558
HEAT EXCHANGERS
design and performance of plate, for secondary cooling system of nuclear power plants, 25:29269
heat transfer and temperature distribution in plane cross flow, with heat generation in one fluid, method for calculation of, 25:29262
HEAT PIPES
bibliography on, 25:29249 (AAEC/LIB/Bib-264)
HEAT-RESISTING ALLOYS AND METALS
coatings for, research on oxidation-resistant, 25:29950
fabrication of, description of methods for, 25:29789
properties for use at high temperatures, evaluation of refractory and superalloy, 25:29860
HEAT SOURCES
design of protected, for intact lunar landing, 25:29276(P)
HEAT TRANSFER
calculation method between fuel material and cladding in deformed rods, (T), 25:31673
calculation method for uneven thermal conductivity between fuel material and cladding, (T), 25:31674
calculation method for uneven, between fuel element surface and coolant, (T), 25:31675
measurement of gas-particle, coefficients in packed and fluidized beds by frequency response methods, 25:31725(R) (RPI-3639-16)
HEAT TRANSFER SYSTEMS
design parameters for testing high temperature gas cooled reactor thermal insulation, 25:31575 (EUR-4531, pp 953-64)
HEATED EFFLUENTS
ecological effects of thermal power plant, from condenser cooling water discharges, (E), 25:31527
effects on young salmon in Columbia River, 25:31645 (BNWL-1527)
plume dispersion in Lake Michigan, (E/T), 25:31533(R) (ANL-7798)
HELIUM
abundance in B-type stars, (E), 25:30042
abundance in Jovian atmosphere, (T), 25:30250
abundance in stars in I Orion association, (E), 25:30049
burning in horizontal-branch stars, effect on convective cores, (T), 25:30037
burning in horizontal-branch stars, induced semi-convection in, (T), 25:30103
burning in stars, explosive, (T), 25:30067
effects of inert atmosphere of, on growth rate of cadmium whiskers, 25:29804
effects on multi-layer metallic foil thermal insulation, at reactor temperatures, 25:30030 (EUR-4531, pp 931-52)
effects on van der waals line broadening in astrophysical spectra, (T), 25:30266
electron avalanche in, simulation using Monte Carlo method, 25:30629 (NP-18798)
electron elastic scattering at 100 eV, 500 eV, and 40 keV by, charge-polarization corrections in, (T), 25:30280
electron reactions at 50 to 600 eV with, cross sections and pressure dependence of exchange excitation of 4^3S, 3^3P, and 3^3D levels in, (E), 25:30285
energy levels of, beam--foil measurements of lifetimes of doubly excited, 25:30265
hydrogen-metastable-atom reactions at 1.0 keV to 1.6 MeV with, Born-wave calculations of total quenching cross sections for, 25:30283
interactions between atoms in triatomic, SCF LCAO MO calculation of nonadditive part of, 25:30270
metastable atoms of, heating from destruction of, in low-temperature plasma, (E), 25:30512
nucleosynthesis of, in first 1001 seconds, (T), 25:30220 (P-4494(RAND))
photon reactions at 2.62 MeV in streamer chamber, pair and triplet production from, (E), 25:30717
plasma of, collisional--radiative recombination and ionization coefficients for quasi-stationary, (T), 25:30540
plasma of, determination of excited population densities by electron impact spectroscopy in, (E), 25:30481
plasma of, diffusion in stellarator of dense decaying, (E), 25:30472
plasma of, excitation in stationary PIG discharge, population densities from, (E/T), 25:30479
proton reactions at 4 MeV with gaseous, vacuum-ultraviolet emission following excitation in, (E), 25:30284
reactions with argon at thermal energies of metastable atoms of, angular distribution of electrons from Penning ionization in, (E), 25:30294
scattering of ^4He atoms at silicon surface of atoms of, calculations, 25:30659
spectra of, Stark and Zeeman effects on, 25:30264
wave functions for ground-state, using different spins for different orbitals, 25:30269
HELIUM IONS
effects of cyclotron-injected, on mechanical properties of aluminum alloys, SAP alloy, and stainless steels, 25:29907 (ORNL-TM-3299)
energy levels of He^+, intervals between n = 3, (E), 25:30263
production in hot cathode constricted arcs, for plasma injection experiments, 25:30256 (EUR-4593, pp 75-81)
reactions with molecules, binary-encounter calculation of ionization cross sections for, 25:30299
HELIUM ISOTOPES
abundance in meteorites, (E), 25:30034
HELIUM ISOTOPES He-3
abundance in Orion and NGC 2264 clusters, (E), 25:30077
deuteron reactions (d,p) at 2.2 to 13 MeV using vector-polarized beams, analyzing power and angular distributions for, (E), 25:31197
deuteron reactions (d,p) at 6.5 and 9.3 MeV using polarized beams, tensor analyzing power for, (E), 25:31198
deuteron scattering by, lithium-5 resonances in, (T), 25:31195
helium-3 reactions (He-3,2p) with, analysis of neutron tunneling effect in, (T), 25:31419
meson (μ^-) capture by, analysis using universal Fermi interaction and CVC theory, (T), 25:31190
proton elastic scattering cross sections at 600 MeV, (E), 25:31185 (LYCEN-7085)
reactions (He-3,d) with scandium-45 at 15, 25:31278
reactions (He-3,Li-6) with aluminum-27, carbon-12, fluorine-19, oxygen-16, and sodium-23 at 40.7 MeV, DWBA analysis of, 25:31214
reactions (He-3,Li-6) with boron-10, carbon-12, fluorine-19, and oxygen-16 at 30 MeV, DWBA analysis of, (E/T), 25:31214
reactions (He-3,Li-6) with fluorine-19 at 22.4 MeV, DWBA analysis of, (E/T), 25:31214
reactions (He-3,n) with magnesium-26, nickel-58, and titanium-46 at 13.2 MeV, neutron spectra and angular distributions for, (E), 25:31237 (IAE-1958)
reactions (He-3p) with chromium-50 at 16.5 MeV, angular distributions and Q for, (E), 25:31298
scattering by fluorine-19 at 22.4, 30, and 40.7 MeV, differential cross sections for elastic, 25:31214
targets of, at 217 torr, design of compressed polarized, 25:31077
targets of, design of large-volume homogeneous-field magnet for polarized, 25:31071
targets of, helium-4 discharge light source and optical system for optical pumping of polarized, 25:31076
targets of, kinetics of optical pumping of polarized, 25:31075
targets of, measurement of spin--lattice relaxation time on solid surfaces for design of polarized, 25:31072
targets of, optical methods for measuring polarization of, 25:31074
targets of, rates of polarization in optically pumped polarized, 25:31073
Au--He-3, nuclear magnetic resonance study of sputtered films of, 25:30692
He-3--He-4, Kirkwood superposition approximation for dilute solutions, (T), 25:30409
HELIUM ISOTOPES He-4
alpha elastic scattering at 0 to 100 MeV, calculation of phase shifts using nonlocal separable potentials for, (T), 25:31186 (LYCEN-7089)
alpha scattering at 8 GeV/c per nucleon, cross sections for, 25:31234
binding energy of, variational calculation using hard-core potential, (T), 25:31192
deuteron elastic scattering at 7 and 9.7 MeV using polarized beams, tensor analyzing power for, (E), 25:31198

XUM

energy levels from lithium-6 (d,at), (d,αHe-3), and (d,αd) reactions, spin--parity assignments and widths for, (E), 25:31187 (NP-18741)
enthalpy fluctuations in superfluid films, (T), 25:30407
flux in primary cosmic radiation, (E), 25:30330
heat transport by conductivity in superfluid, in pipes, (E), 25:30406
neutron elastic scattering at 1 to 34 MeV, calculation of cross-section and polarization angular distributions using nonlocal separable potentials for, (T), 25:31186 (LYCEN-7089)
proton elastic scattering at 2 to 50 MeV, calculation of cross-section and polarization angular distributions and phase shifts using nonlocal separable potentials for, (T), 25:31186 (LYCEN-7089)
proton elastic scattering at 4.6 to 11.9 MeV, phase shifts and polarization in, (E), 25:31199
proton scattering at 1 GeV, nuclear opaqueness model for differential cross sections for, 25:31234
temperature differences and mutual friction in liquid II, near lambda point, 25:30405
third sound in superfluid films of arbitrary thickness, (T), 25:30408
He-3--He-4, Kirkwood superposition approximation for dilute solutions, (T), 25:30409
HEMATOPOIESIS
radiation effects on, in bone marrow of mice, mechanisms of, 25:29676
HEMATOPOIETIC SYSTEM
radiation effects on human, whole-body x, 25:29699
radiation effects on mouse, effects of dose and dose rate on x, 25:29634
radiosensitivity of mouse spleen, effects of dose on, 25:29677
HEPARIN
preparation of chromium-51-labeled, in vitro for use in metabolism studies, radiochemical method for, 25:29415
HEXANE
radioinduced electric conductivity in, x, 25:29097
radiolysis of frozen, effects of dose rate on yields from γ, 25:29160
HIGH-ENERGY PHYSICS
conference on, (T), 25:30753
lectures on, 25:30750 (CERN-71-7)
research at New York Univ., Dec. 1969 to Jan. 1971, (E), 25:30806(R) (NYO-3668-TA-5)
HIGH-TEMPERATURE GAS-COOLED REACTOR EXPERIMENT
cooling systems of, distribution of fission products in, (E), 25:31567
HINKLEY POINT 1 REACTORS
pressure vessel for, testing prestressed concrete models of, 25:29312
HIPPURIC ACID, o-IODO-
clearance of iodine-125- and iodine-131-labeled, from kidneys of dogs, comparison of Lissamine Green method with, 25:29414
sodium salt, evaluation of iodine-131-labeled, for human nephrography, 25:29577
HIROSHIMA
leukemia incidence in human population exposed to atomic bombing of, 25:29696
HISTONES
effects on oxidative phosphorylation in liver mitochondria of irradiated animals, 25:29638
radiation effects on synthesis of, in liver and spleen of rats, 25:29662
HODOSCOPES
design of high-resolution beam, using multiwire proportional detectors, 25:29370 (LAL-1246)
design of shower detector, for momentum measurement of cosmic shower particles, 25:29377
HOLMIUM BROMIDES
thermodynamic properties at 298 to 1300°K, 25:29951
HOLMIUM CHLORIDES
thermodynamic properties at 298 to 1300°K, 25:29951
HOLMIUM ISOTOPES Ho-165
energy levels from neutron inelastic scattering, (E), 25:31350
neutron elastic and inelastic scattering at 0.3 to 1.5 MeV, differential cross sections for, (E), 25:31350
neutron total cross sections at 0.1 to 1.5 MeV, (E), 25:31350
HORMONES, ADRENAL
cortisol, radiation effects on human excretion of, occupational, 25:29708
cortisone, radiation effects on human excretion of, occupational, 25:29708
epinephrine, effects on oxygen pressure in mouse spleen, effects of propranolol and dibenamine on, 25:29547
epinephrine, radioprotective effects of, effects of N-(2-chloroethyl)dibenzylamine hydrochloride on, 25:29546
epinephrine, radioprotective effects of, on survival of mice, γ, 25:29548
norepinephrine, effects on oxygen pressure in mouse spleen, 25:29547
norepinephrine, radioprotective effects of, effects of N-(2-chloroethyl)dibenzylamine hydrochloride on, 25:29546
norepinephrine, radioprotective effects of, on beagle dog hearts, lethal, whole-body mixed γ and neutron, 25:29565
radiation effects on level of, in blood of dogs, 25:29642
HORMONES, SEX
estradiol, effects on lactate dehydrogenase activity in γ-irradiated rats, 25:29670
HORMONES, THYROID
thyroxine, determination in serum by double isotope derivative method, 25:28986
HOSPITALS
facilities for treatment of radium-contaminated personnel following accidental release at Italian refinery, 25:29508
radiation protection in radiology department of general, program for, 25:29538
HOT CELLS
design with inert gas environment, 25:31629 (BNWL-587)
HUNTERSTON REACTORS
pressure vessel for, testing prestressed concrete models of, 25:29312
HUTCHINSON ISLAND POWER REACTOR, UNIT 1
emergency power supply for, sizing and testing of diesel generator, 25:31517 (DOCKET-50335-18)
HYDRAULIC PRESSES
design and operation of, for compaction of low-level radioactive waste, 25:29316(T) (LA-tr-71-12)
HYDRAZINE
nitrate, compounds with uranium nitrates, preparation and properties of hydrated, 25:29035 (NP-18736)
HYDROBROMIC ACID
spectra of crystalline tetrahydrate of, ir, 25:31683(T) (ANL-Trans-880)
yields from γ radiolysis of aqueous solutions of 5-bromo-2'-deoxyuridine in presence of oxygen, 25:29136
yields from γ radiolysis of aqueous solutions of 5-bromo-2'-deoxyuridine in presence of oxygen, 25:29135
HYDROCARBONS
analysis for carbon isotopes, sample preparation for mass spectrometric, 25:28968
reactions with recoil tritium atoms, yields of labeled products from, 25:29167
HYDROCHLORIC ACID
corrosive effects on chromium--molybdenum--nickel alloys, effects of molybdenum content on, 25:29777
corrosive effects on hafnided and tantalided nickel and Type 316 stainless steel at 60°C, 25:29766
corrosive effects on molybdenum alloys, relations with concentration, pressure, and temperature, 25:29776
effects on oxidation-reduction potential of solutions of salts of tetravalent and hexavalent uranium, 25:29036
separation of thorium and uranium from aqueous solutions of, by solvent extraction using 4-methyl-2-pentanone, effects of lithium chloride or magnesium chloride on, 25:29195
HCl--methanol, corrosive effects on aluminum--titanium--vanadium alloy, 25:29773
HYDROFLUORIC ACID
analysis for free fluoride using lanthanum fluoride electrode, 25:28923
HYDROGEN
abundance in Jovian atmosphere, (T), 25:30250
abundance of neutral and ionized, in NGC 604, (E), 25:30153
alpha-particle stopping cross sections in gaseous, test of Bragg's rule for, 25:30642
atomic beams of, control of intensity and cluster size of, 25:30252 (EUR-4593, pp 43-9)
determination in metals by carrier gas fusion--gas chromatographic methods, 25:28936
determination in uranium dioxide pellets, 25:28912 (BARC-500)
determination using ion permselective membrane, potentiometric, 25:28956
deuteron backscattering by molecular, (E), 25:30291
diffusion in niobium--titanium alloys at -160 to +250°C, activation energy of, 25:29837
diffusion through niobium, in fusion reactor conditions, 25:29820 (EUR-4593, pp 519-24)
distribution of neutral, around H II regions, (E), 25:30137
effects of interstitial impurity of, on mechanical properties of iron and refractory metals, 25:29855
effects on van der waals line broadening in astrophysical spectra, (T), 25:30266
electron elastic scattering at 100 eV, 500 eV, and 40 keV by atomic, charge-polarization corrections in, (T), 25:30280
electron scattering by atomic, algebraic close-coupling calculation of, 25:30286
energy of 1s and 2s states of atomic, second-order perturbation-theory treatment of contact interaction in, 25:30271
heat transfer in, containing dispersed submicron particle of carbon, silicon, or tungsten, extinction parameters for evaluation of radiant, 25:29270
ionization and acceleration of molecular, for injection and confinement experiments, 25:30253 (EUR-4593, pp 51-8)
neutron scattering law for solid ortho-, at low energies, (T), 25:31169 (JUL-724-FF)
plasma of, electron heating by large-amplitude oscillations in theta pinch, (E), 25:30467
plasma of, Hβ Stark broadening profiles in spectral,

(E/T), 25:30268
positron scattering by atomic, algebraic close-coupling calculation of, 25:30286
production of atomic beams of, for plasma injection experiments, 25:30256 (EUR-4593, pp 75-81)
proton elastic scattering at 0 to 25 MeV, calculation of phase shifts using nonlocal separable potentials for, (T), 25:31186 (LYCEN-7089)
proton reactions with adsorbed layers of, on copper, desorption yields from 5-keV, (E), 25:30257 (EUR-4593, pp 181-6)
radiolysis of molecular, production of hydrogen atoms by electron pulse, 25:29158
reactions of molecular, with deuterium ions, 25:29058
reactions of radiolytic atoms of, with argon and oxygen or carbon monoxide, or nitric oxide, kinetics of, 25:29158
reactions with nitric oxide of atomic, spin-exchange cross sections for, (E), 25:30277 (UCRL-20529)
reactions with rare gases at 1.0 keV to 1.6 MeV of metastable atoms of, Born-wave calculations of total quenching cross sections for, 25:30283
sorption by tungsten crystal surfaces, high-energy electron diffraction studies of, 25:29846
sorption on beryllium surface, 25:29894
spectra of nebulae consisting of pure, Balmer decrement in, (T), 25:30101
spectra of neutral, redshifted line in quasars, N galaxies, and Seyfert galaxies, (E), 25:30121
wave functions for ground-state atomic, accuracy of hybrid Gaussian-type, 25:30302
yields from γ radiolysis of deaerated aqueous solutions of benzyl alcohol, 2-propanol, sodium formate, sodium hydroxide, and/or sodium nitrate, effects of pressure on, 25:29157

HYDROGEN IONS (H_2^+)
acceleration system for injection and confinement experiments, 25:30253 (EUR-4593, pp 51-8)
production in hot cathode constricted arcs, for plasma injection experiments, 25:30256 (EUR-4593, pp 75-81)

HYDROGEN IONS (H_3^+)
production in hot cathode constricted arcs, for plasma injection experiments, 25:30256 (EUR-4593, pp 75-81)

HYDROGEN ISOTOPES
heat transfer in gaseous, at 22 to 110°K, effects of magnetic fields on transverse, (E), 25:29267

HYDROGEN OXIDES H_2O
abundance of hydrated ionized, in ionospheric D region, (E/T), 25:30404

HYDROGEN PEROXIDES
spectra of solid and matrix-isolated, ir, 25:29055
yields from γ radiolysis of aqueous solutions of 5-bromo-2'-deoxyuridine in presence of oxygen, 25:29135

HYDROGEN SULFIDES
abundance in Jovian atmosphere, (T), 25:30250

HYDROGEN SYSTEMS
Au--H, nuclear magnetic resonance study of sputtered films of, 25:30692
Fe--H--Hf-base--N--O--Zr, ductility and tensile properties of dilute, effects of composition on, 25:29827(R) (RPI-3719-9)
H--Hf-base--O--Zr, ductility and tensile properties of dilute, effects of composition on, 25:29827(R) (RPI-3719-9)
H--Nb, elastic properties of, Gorsky-effect study of Curie--Weiss temperature dependence of, 25:29865
H--Nb-base, particle size distribution in, effects of composition and thermal cycling on, 25:29929
H--Nb-base, preparation of powdered, using ball mill, 25:29929

HYDROLASES
radiation effects on activity of, in rat plasma erythrocytes, whole-body x, 25:29686
radiation effects on content of cadaverine deaminase in liver mitochondria of rats, 25:29641

HYDROMAGNETIC WAVES
coupling between solar wind and plasma sheet, effect on magnetotail resonant oscillations, (T), 25:30366
propagation through lower magnetosphere, effect on lower-latitude pulsations, (E/T), 25:30356

HYDROXIDES
determination using ion permselective membrane, potentiometric, 25:28956

HYDROXYL (HO)
detection in H I regions from 1665- and 1667-MHz emissions, 25:30155
radio emission from, associated with infrared stars, (E), 25:30047
thermodynamic properties of gaseous diatomic, free energy functions for, 25:29082

HYPERFRAGMENTS
decay Λ-$H^3 \rightarrow \pi^- + {}^3He$, branching ratio and rate of (T), 25:30821
hypheron (Λ) binding energy in Λ-He^5, calculation using two-channel separable potentials for, (T), 25:30897

HYPERONS
decay of, angular and spin correlations in beta, (T), 25:30815
decay of, chiral-symmetric gauge field model for s-wave and p-wave amplitudes of nonleptonic, 25:30810
decay of, physics and feasibility of experiments using hyperon beams for study of leptonic, (E), 25:30722 (COO-1701-12)
decay of, q^2 spectrum and asymmetry functions for beta, 25:30812
formation in neutron stars, (T), 25:30080

HYPERONS (Λ)
coupling constant for $\Lambda\Sigma\pi$, PCAC hypothesis for, (T), 25:30904
coupling constants for $N\Lambda K$, PCAC hypothesis for, (T), 25:30904
coupling of ΛKN, review of forward dispersion relations for, (T), 25:30902
decay $\Lambda \rightarrow p + e + \text{anti } \nu$, spin correlations and form factors in, 25:30804 (COO-264-569)
decay $\Lambda \rightarrow p + e^- + \text{anti } \nu$, angular and spin correlations in, (T), 25:30815

HYPERONS (Σ)
coupling constant for $\Lambda\Sigma\pi$, PCAC hypothesis for, (T), 25:30904
coupling constant for $\Sigma\Sigma\pi$, PCAC hypothesis and SU(3) symmetry with pseudovector coupling for, (T), 25:30904
coupling constants for $N\Sigma K$, PCAC hypothesis for, (T), 25:30904
decay of, Lee--Sugawara relations from $\Delta I = 1/2$ sum rule for amplitudes of nonleptonic, (T), 25:30817
decay $\Sigma \rightarrow N + \pi$ + spurion, effect of 3/2 spurion on, 25:30811

I

ICE
optical properties of interstellar particles of dirty, (T), 25:30196

IMMUNE REACTIONS
development in mice following infection by x-irradiated Plasmodium berghei sporozoites, 25:29727
radiation effects on mouse spleen, x, 25:29476
radiation effects on mouse, comparison of cyclophosphamide with x, 25:29475
radiation effects on, in mice, x, 25:29472
radioinduced depression in guinea pigs, synergistic effects of bovine gamma globulin on, 25:29474

IMMUNOGLOBULINS
radiation effects on content of intestinal lumen and serum of mice, x, 25:29473

IMPEDANCE BRIDGES
design for use with eddy current method for measuring cold work in stainless steel, 25:29287 (ORNL-4630, pp 145-9)

INCOLOY 800
corrosion of similar-metal welds in, by steam, 25:29763 (ORNL-4630, pp 280-7)
radiation effects on mechanical properties of, fast neutron, 25:31568(T) (EURFNR-823)

INCONEL 600
corrosion of Hanford N Reactor steam generator tubes of, 25:29760 (DUN-SA-149)
corrosion of similar-metal welds in, by steam, 25:29763 (ORNL-4630, pp 280-7)
ductility at 400 to 1000°C, effects of manganese, phosphorus, and sulfur contents on, 25:29825 (ORNL-4630, pp 261-70)
radiation effects on mechanical properties of, fast neutron, 25:31568(T) (EURFNR-823)

INCONEL 601
corrosion of similar-metal welds in, by steam, 25:29763 (ORNL-4630, pp 280-7)

INCONEL 625
corrosion of similar-metal welds in, by steam, 25:29763 (ORNL-4630, pp 280-7)
properties for use in caustic-resistant steam corrosion loops, 25:29762 (ORNL-4630, pp 158-62)

INDIA
allanite deposits in Bivangaon and Kansa areas of, occurrence of, 25:29226
uranium deposits in Singhbhum shear zone at Bihar, mineralization of, 25:29227

INDIAN OCEAN
meteorological conditions of atmosphere over, natural radon tracer studies of, 25:29220

INDIAN POINT POWER REACTOR, UNIT 1
containment system for, installation of filters in compressed air lines for isolation valves of, 25:31483 (DOCKET-50003-68)
cooling system for, installation of thermocouples in, 25:31483 (DOCKET-50003-68)
electrical feeder lines for, change to underground, 25:31483 (DOCKET-50003-68)

INDIUM
determination by amperometric, chelatometric, and conductometric titrations, 25:28970
determination for water flow tracing by neutron activation, 25:29013 (RLO-1750-81)
effects on fluorometric determination of zirconium, 25:28963
nuclear dipole interactions in, quadrupole resonance study of, 25:30695
separation from aqueous solutions by thin-layer chromatography using liquid anion exchangers, 25:29186
ultrasonic-velocity change in superconducting, effect of dislocation motion of, (E), 25:30430

INDIUM ALLOYS AND SYSTEMS
Ag--In-base, superconducting transition temperature under strain in, (E), 25:30435
Ag-base--In, properties for use as ball bearing spacers in ultrahigh vacuum, 25:29834
Bi--In-base, surface pinning in, quantitative control of, 25:30415
Cd--In-base, superconducting transition temperature under strain in, (E), 25:30435
In--Sn, nuclear quadrupole resonance spectrum of, 25:30695
In-base--Sn, superconducting transition temperature under strain in, (E), 25:30435
INDIUM IONS
implantation in silicon at 30 keV, electron microscopic observation of lattice disorder induced in, 25:30650
INDIUM ISOTOPES
production in proton fission of uranium-238 at 450 MeV, mass yield and charge distribution for, (E), 25:31302 (COO-1167-10)
INDIUM ISOTOPES In-109
beta and electron-capture decay of, γ spectra from, (E), 25:31320
INDIUM ISOTOPES In-113
neutron activation resonance integrals for, measured relative to gold-197, (E), 25:31300 (CNEA-282)
use of DTPA-incorporated metastable, for radiodiagnosis of human brain tumors, 25:29583
INDIUM ISOTOPES In-114
beta decay of, internal bremsstrahlung spectra from, (E), 25:31318
INDIUM ISOTOPES In-115
energy level at 1300 keV, lifetime of, 25:31327
proton reactions (p,γ) at 4 MeV, gamma spectra from, (E/T), 25:31303 (INR-1271)
INDIUM OXIDES
thermodynamic properties of gaseous diatomic, free energy functions for, 25:29082
INDOLE, 3-(2-AMINOETHYL)-5-METHOXY-
effects on cystamine distribution and excretion in intestines, kidneys, and urine of mice and rats minimum dose for, 25:29554
radioprotective effects of, on bone marrow, intestines, and subcutaneous tissues in rats in relation to kinetics of oxygen tension, γ, 25:29551
radioprotective effects on muscles and spleen of mice, effects of increased atmospheric pressure on γ, 25:29550
INDUSTRIAL MANAGEMENT
method for measurement of emotional stability of personnel using electric conductivity of skin, 25:29531 (CEA-R-4156)
INFRARED RADIATION
cosmic background, contributions of interplanetary, interstellar, and intergalactic sources to, (T), 25:30239
cosmic background, origin of, (T), 25:30231
cosmic background, techniques for observing, (T), 25:30239
emission from cold matter in Universe, (T), 25:30227
emission from nuclei of galaxies and quasars, (T), 25:30247
INFRARED SPECTROMETERS
radiation effects on, nuclear explosion, 25:29411
INORGANIC COMPOUNDS
conference on thermal analysis of, Worcester, Mass., Aug. 18 to 23, 1968, 25:29758
radiation effects on chemical reactivity of, ASTM method for determining, 25:29095
INSECTA
Acanthoscelides obtectus, eradication of, study of sterile male technique for, 25:29746
Acanthoscelides obtectus, eradication of, use of sterile male technique for, 25:29749
Acanthoscelides obtectus, mass rearing for genetic control of, 25:29749
Aedes aegypti, radioinduced translocations in chromosomes of, effects of, on genetic control of populations of, 25:29753
Bracon sp., reproductive capacity of female, effects of chemosterilants, γ and x radiation on, 25:29747
Carpocapsa pomonella, radiation effects on lifetime and reproductive capacity of, effects of dose rates on γ and x, 25:29612
Ceratitis capitata, eradication of, in Spain, effectiveness of sterile male technique for, 25:29739
Ceratitis capitata, eradication of, review of research programs on use of sterile male technique for, 25:29738
Ceratitis capitata, radiation effects on reproductive capacity of female and male, effects of dose and pupal exposure on, 25:29743
control of grain pest, review of sterile male technique for, 25:29750
Culex pipiens, radiation effects on hatchability and survival of eggs and larvae of, γ, 25:29614
Dacus oleae, control of, in Greece, use of ionizing radiation in combination with insecticides, attractants, and repellants for, 25:29740
Dacus zonatus, radiation effects on gonads of, effects of dose and pupal exposure on γ, 25:29617
Diatraea saccharalis, radiosensitivity of embryos, larvae, and pupae of, γ, 25:29755
Drosophila melanogaster, radiation dose to, in γ fields, ionization chamber measurements on γ and neutron, 25:29522
Drosophila melanogaster, radioinduced sex-linked, lethal, and visible mutations in sperm of, comparison of fast neutron and x, 25:29499
Drosophila melanogaster, radiosensitivity of successive generations of larvae of, effects of dose on x, 25:29613
eradication of, effectiveness of sterile male technique for, 25:29752
Glossina sp., labeling of, by feeding labeled rabbit blood, 25:29417
Haematobia irritans, eradication of, use of γ radiation sterile male technique for, 25:29744
Hylemya antiqua, control of, study of sterile male technique for, 25:29748
Hylemya antiqua, radiation damage to gonads of, pathology of, 25:29619
Hyphantria cunea, control of, use of radiosterilized male technique for, 25:29731
Hyphantria cunea, radiosterilization of male, effects on mating competition of, 25:29731
Lymantria dispar, radiation effects of dose on reproduction and survival of adult, following exposure of male pupae, γ, 25:29616
Musca domestica, control of, use of sterile male technique for, 25:29751
Musca domestica, sex ratio distortions of, genetics of, 25:29751
Oryctes rhinoceros, control of, use of sterile male technique for, 25:29754
radiosensitivity of Collembola, in relation to population mortality, effects of dose on γ, 25:29615
radiosterilization of, conference on methods for, 25:29730 (STI/PUB-265)
radiosterilization of, review of, for sterile male technique of eradication, 25:29736
Rhagoletis cerasi, development of trapping system for, using chemical and visual stimuli, 25:29742
Rhagoletis cerasi, eradication of, preparatory behavioral and ecological studies for use of sterile-insect technique for, 25:29742
Rhagoletis cerasi, eradication of, use of γ radiation sterile insect release technique for, 25:29741
Rhodnius prolixus, radiosterilization of, for control of Chagas' disease, comparison of, with chemosterilization, γ and x, 25:29745
Sitophilus granarius, development in wheat, effects of γ irradiation of wheat grains on, 25:29737
Sitotroga cerealella, radiation effects on survival of, effects of dose on γ, 25:29618
Triatoma infestans, radiation effects on structures of developing embryos of, effects of dose on x, 25:29620
Zabrotes subfasciatus, radiation effects on longevity, reproduction, and survival of, effects of dose on γ, 25:29756
INSECTICIDES
effects on reproductive capacity of female arthropods, 25:29747
effects on reproductive capacity of reduviid bug vectors of Chagas' disease in comparison to effects of γ and x radiation, 25:29745
use for control of olive fruit fly in Greece in combination with ionizing radiation, 25:29740
INSTRUMENTS
specifications for JAERI modular, 25:29396 (JAERI-Memo-4303)
specifications for JAERI modular, 25:29395 (JAERI-Memo-4295)
specifications for JAERI modular, 25:29394 (JAERI-Memo-4281)
INTERSTELLAR MATERIAL
alignment of grains of, by starlight, (T), 25:30216
calcium abundance in Norma, (E), 25:30193
charge transfer and ionization equilibrium in, (T), 25:30211
distribution of, in galactic anticenter direction, (E), 25:30191
dust formation by circumstellar crushing processes, (T), 25:30195
electric charge on grains of, (T), 25:30192
molecules in, abundance and formation of, (T), 25:30128
molecules in, spectroscopy of, (E/T), 25:30200
optical properties of spherical dust particles, (T), 25:30196
polarization of starlight by circular dielectric infinite cylinders, (T), 25:30213
reddening of star No. 12 in Cygnus OB2, (E), 25:30069
spectroscopy of, molecular, 25:30138
INTESTINES
cystamine in mouse and rat, effects of 5-methoxytryptamine on, 25:29554
radiation dose to, in normal and tumor-bearing mice following administration of phosphorus-32-labeled chromium alloxantin and orthophosphate, 25:29453
radiation effects on alkaline phosphatase activity in mucosa of small, in rats, effects of radioprotectors on x, 25:29645
radiation effects on content of immunoglobulins in lumen

and serum of mouse, x, 25:29473
radiation effects on isolated guinea pig, protective effects of tryptamine against x, 25:29566
radiation effects on mucosa of sheep, unilateral lethal cobalt-60 γ and pulsed mixed fission neutron and γ, 25:29656
radiation effects on protein fractions of mitochondria and tissue homogenates in rabbit, x, 25:29664
radiation effects on rat, oxygen tension kinetics during protective effects of mexamine against γ, 25:29551

INULIN
clearance of iodine-125- and iodine-131-labeled, from kidneys of dogs, comparison of Lissamine Green method with, 25:29414

INVARIANCE PRINCIPLES
C invariance in $e^+ + e^-$ → hadrons interactions, experimental verification of, 25:30926
C, P, and T properties of equations of motion invariant under group P(1,n) in Minkowski space, 25:30966
CP violation in K^0 - anti K^0 system, review of parameters for, (E), 25:30925
CP violation in particle interactions, lectures on, (T), 25:30915 (NP-18808)
CP violation in strong self-interacting intermediate vector boson model, 25:30814
CP violation in weak interactions, lectures on, (T), 25:30803 (CERN-71-7, pp 1-40)
CPT invariance for local infinite-component fields, review of, 25:30950
isospin invariance in n + p → π^0 + d interactions at threshold to 720 MeV, test of, (E), 25:30730
parity conservation in weak interactions, universality principle for muon, (T), 25:30932
scale invariance breakdon in generalized Bjorken limit of perturbation theory, 25:30783
scale invariance for hadron interactions, light cone for, 25:30749 (CALT-69-297)
scale invariance in SU(2) x SU(2) linear sigma model, 25:30920
scale invariance in two-dimensional field theories, 25:30921
scale invariance of Brans--Dicke scalar--tensor theory, 25:31010
scale invariance, meson mass spectra for breaking of, 25:30927
scale invariant and chiral symmetry limits, sigmaπN coupling from, 25:30933
scale symmetry breaking and scaling properties of currents, 25:30934
theory for K^0, lectures on, 25:30915 (NP-18808)
theory for, lectures on, 25:30915 (NP-18808)

IODINE
corrosive effects of gaseous and liquid, on molybdenum alloys, 25:29776
determination by x-ray fluorescence, sensitivity of, 25:28962
determination in sedimentary rocks by neutron activation, 25:29033
determination of, hollow-cathode lamp for spectroscopic, 25:28951
determination using ion permselective membrane, potentiometric, 25:28956
effects on yields from γ radiolysis of 2,2-dimethylbutane, 25:29142
release from defected uranium oxide (UO_2) fuel pins, during reactor operation, (E), 25:31607
removal from reactor containment, effectiveness of spray systems for, (E), 25:31610
sorption by activated carbon at high temperatures, (E), 25:31612

IODINE ISOTOPES
decay heat effects on charcoal filters, 25:31669 (ORNL-4602)
determination of radioactive, in industrial water by chemical separation and radiometry, ASTM method for, 25:29007
effectiveness for radiodiagnosis or radiotherapy in man, 25:29573
radioactivity standards of, users' guides for, 25:29174

IODINE ISOTOPES I-125
clearance of inulin and hippuran-incorporated, from dog kidneys, comparison of Lissamine Green method with, 25:29414
production of, using reactor loops, 25:29413 (CONF-691225)

IODINE ISOTOPES I-127
determination in biological samples by neutron activation and scintillation counting of Cherenkov radiation, 25:29030
energy levels from neutron inelastic scattering, low-lying, (E), 25:31352
meson reactions (μ^-,xn) by, gamma spectra from, (E), 25:31258
neutron inelastic scattering by, gamma spectra from, (E), 25:31352
photon inelastic scattering at 6.1 to 7.1 MeV, gamma spectra from, (E/T), 25:31303 (INR-1271)
photon reactions (γ,n) at 10 to 68 MeV, yields of radioactivities from, (E), 25:31333

IODINE ISOTOPES I-129
monitoring in environmental samples at West Valley Processing Plant, 1971, 25:29180 (DOCKET-50201-70)

IODINE ISOTOPES I-131
beta decay of, internal ionization in, (E), 25:31316
clearance of inulin and hippuran-incorporated, from dog kidneys, comparison of Lissamine Green method with, 25:29414
content in environment of West Valley Processing Plant, 25:29179 (DOCKET-50201-69)
content of air samples at Nevada Test Site during 1969, 25:29506 (SWRHL-97-r)
content of fallout, in cow milk, effects of feeding practices on, 25:29505 (SWRHL-39-r)
determination in serum thyroxine by liquid scintillation counting, 25:28986
effectiveness for scanning of human salivary glands, effects of pilocarpine nitrate on, 25:29579
effectiveness for scanning of human salivary glands, comparison of technetium-99m with, 25:29574
effectiveness of rose bengal-incorporated, for diagnosis of human malignant gall bladder diseases, 25:29575
effects on cardiovascular system, kidneys, liver, and nervous system of patients following therapy for thyroid cancer, combined teletherapy and, 25:29707
effects on egg production by hens following ingestion, inhibitory, 25:29661
effects on homologous thyroglobulin antibody production in rats, combined effects of γ radiation and, 25:29660
effects on leukemia development in man following therapy for hyperthyroidism, comparison of surgical treatment and, 25:29705
evaluation of hippuran-incorporated, for human nephrography, 25:29577
metabolism in beagle dogs following ingestion of nuclear debris from Project Cabriolet, 25:29456
monitoring in environmental samples at West Valley Processing Plant, 1971, 25:29180 (DOCKET-50201-70)
release from reactors, safety analysis of fission product, 25:31620
removal from medical equipment, effectiveness of detergent solution combined with sound frequency vibrator for, 25:29510
uptake of RISA-incorporated, in tissues of rats for diagnosis of diseased joints, 25:29581
use for labeling macroaggregated human serum albumin, 25:29413 (CONF-691225)
use of hippuran-incorporated, for scintigraphy of human kidneys for function and morphology, 25:29592
use of macroaggregated human serum albumin-incorporated, for diagnosis of pulmonary blood flow, measurement of gas exchange following, 25:29594
use of RISA-incorporated, for diagnosis of osteoarticular diseases in human bones, 25:29576
use of RISA-incorporated, for radiodiagnosis of metastatic and primary adenocarcinomas in human kidneys, 25:29590
use of rose bengal-incorporated, for scintigraphy of human liver for function and morphology, 25:29591

IODINE ISOTOPES I-133
production of, development of generators for, 25:29413 (CONF-691225)

IODINE ISOTOPES I-137
monitoring in water cooled reactor coolant, delayed neutron method for, 25:31580

IODINE OXIDES
thermodynamic properties of gaseous diatomic, free energy functions for, 25:29082

ION-ACOUSTIC WAVES
instabilities above single and multi-ion ionospheric F-layer plasma, field-aligned, (T), 25:30373
interaction with helicon in plasma, nonlinear, (T), 25:30607

ION BEAMS
effects on copper, germanium, and silicon single crystals, equipment for investigating, 25:30648 (N-70-37028)
interactions with plasma, efficient transfer of energy during, (E), 25:30511

ION SOURCES
description of heavy-ion hot-cathode reflex, for cyclotrons, 25:31134
design and performance of beam--plasma system, 25:30255 (EUR-4593, pp 67-74)
design and performance of PIG heavy, for Harwell variable energy cyclotron, 25:31136
development of heavy, for cyclotrons, 25:31132
development of heavy, review on, 25:31133
development of HIPAC, for production of highly-stripped heavy ions, 25:31138
development of laser plasma, for production of highly-stripped ions, 25:31137
performance of hot cathode constricted arc, for hydrogen and helium ions, 25:30256 (EUR-4593, pp 75-81)

IONOSPHERE
absorption during shortwave fadeouts, correlation to enhancement of solar x-ray flux, (E), 25:30362
current system at high latitude, effect on lower-latitude pulsations, (E/T), 25:30356
D region, abundance of positive ions in, mechanism of, (E/T), 25:30404
D region, atomic oxygen concentration from 80 to 120 km, silver-film sensor method for, (E), 25:30385

XUM

D region, electron-density profile of daytime polar, (E), 25:30360
disturbances in, correlation to soft solar x-ray bursts, 1966 to 1969, (E), 25:30355
E region, electron-density profile of daytime polar, (E), 25:30360
E region, irregularities over Waltair, India, motion of seasonal-dependent random, (E), 25:30384
electromagnetic processes at 200 to 1300 km in, Interkosmos-3 study of If, (E), 25:30364
electron and ion temperature variations in, solar cycle- and magnetic storm-associated latitude-dependent, (E/T), 25:30399
electron-density profiles in disturbed- and quiet-topside ionosphere at >70 degrees latitude, (E), 25:30359
F region, field-aligned instabilities in single and multi-ion plasma above, ion-acoustic and ion-cyclotron, (T), 25:30373
F region, irregularities over Waltair, India, motion of seasonal-dependent random, (E), 25:30384
instability in equatorial, model to investigate gradient, (E/T), 25:30379
ion motion at 600 km in, satellite-borne transducer for measurements of, (E), 25:30393
ion motion at 600 km in, satellite-borne transducer measurements of, (E), 25:30394
ion temperature in, measuring method and probe for, (E/T), 25:30383
ionization layer due to cosmic radiation in lower, behavior during Forbush decreases, (E), 25:30311
irregularities in, fast-correlation method for studying drift pattern-associated, (T), 25:30402
model of, tables from Penn State MARK I computer, 25:30351 (N-70-40978)
oxygen 5577-A green-line emission in day airglow, mechanism of atomic, (E), 25:30375
properties of midlatitude topside, at low sunspot numbers, sunrise, (E), 25:30377
red arc south of auroral zone in, stable midlatitude SAR-, (E), 25:30398
research on Earth, from orbiting space station, (T), 25:30363
sporadic E, correlation of cusp-type, with radio absorption changes measured at 2.2 MHz, (E), 25:30382
sporadic E, wind-shear theory of, switching mechanism of gravity waves-associated, (T), 25:30380

IONS
flux effects on electric fields, (T), 25:30705
reactions with molecules, binary-encounter calculation of ionization cross sections for, 25:30299
temperature of ionospheric, measuring method and probe for, (E/T), 25:30383

IRIDIUM ISOTOPES Ir-191
alpha inelastic scattering at 16.6 MeV differential cross sections for, (E), 25:31342
deuteron inelastic scattering at 7.0 and 12.1 MeV, differential cross sections for, (E), 25:31342
energy levels from deuteron and alpha inelastic scattering, spins and parities of, (E), 25:31342

IRIDIUM ISOTOPES Ir-192
metabolism in dogs, mice, monkeys, and rats following intraperitoneal, intravenous, and oral administration, 25:29450
use as source in industrial radiography, data on x-ray film exposure levels for, 25:29294

IRIDIUM ISOTOPES Ir-193
alpha inelastic scattering at 16.6 MeV differential cross sections for, (E), 25:31342
deuteron inelastic scattering at 7.0 and 12.1 MeV, differential cross sections for, (E), 25:31342
energy levels from deuteron and alpha inelastic scattering, spins and parities of, (E), 25:31342

IRIDIUM OXIDES
thermodynamic properties of gaseous diatomic, free energy functions for, 25:29082

IRON
abundance in Am stars, (E/T), 25:30038
abundance in atmosphere of α Cyg, (E), 25:30109
abundance in photosphere, (E), 25:30170
analysis of high-purity, for impurities by spectrography, 25:28947
determination by amperometric, chelatometric, and conductometric titrations, 25:28970
determination in carbon using o-phenanthroline, ASTM method for colorimetric, 25:28974
determination in deposits and airborne particles by neutron activation and scintillation counting, 25:29032
determination in high-purity water for reactor cooling and moderating, 25:28914 (BARC-515)
determination in natural waters by solvent extraction and x-ray fluorescence spectroscopy, 25:28919
determination in niobium photometrically using 1,10-phenanthroline, 25:28973
determination in plutonium by absorption spectrophotometry and spectrography, 25:28916 (CEA-R-4071)
determination in presence of other metals, spectrographic, 25:28944
determination of trace amounts of, in platinum by neutron activation following separation by ion exchange chromatography, 25:29023
determination of trace amounts of, in vanadium, spectrographic, 25:28947
effects on corrosion of nickel alloys by vanadium pentoxide melts, 25:29768
energy levels in neutral, mean lives and absolute f-values for, (E), 25:30168
flow stress of polycrystalline, effects of hydrostatic pressure on, 25:29833
hyperfine fields of technetium in, (E), 25:31271
mechanical properties of, effects of interstitial metalloid impurities on, 25:29855
neutron attenuation in, Monte Carlo calculations of, (T), 25:31164 (CEA-N-825)
proton reactions at 11.5 and 23.5 MeV using thick targets, neutron yield from, (E), 25:31209
separation from aqueous solutions by thin-layer chromatography using liquid anion exchangers, 25:29186
separation from mercury by solvent extraction, 25:29031
spectral lines of, oscillator strengths for, (E), 25:30170

IRON ALLOYS AND SYSTEMS
corrosion of, high-temperature methods for studies of, 25:29779
Be-base--Fe, defect structure in, effects of deformation on, 25:29897
Be-base--Fe, precipitation behavior in quenched and aged, 25:29897
Ce--Fe--Ru, preparation and superconductivity of, (E), 25:30413(T) (LA-tr-71-26)
Cr--Fe--Ni, compatibility with nonstoichiometric and stoichiometric uranium carbide at 900°C, effects of stabilizers on, 25:29940(T) (EURFNR-826)
Cr-base--Fe--Mo, thermal capacity of Cr/sub 3-x/Fe/sub x/Mo at 1.3 to 4.2°K, 25:30676
Fe--H--Hf-base--N--O--Zr, ductility and tensile properties of dilute, effects of composition on, 25:29827(R) (RPI-3719-9)
Fe--Mo--Ni-base, properties of 2-81 permalloy, effects of heat treatments in production process on magnetic and tensile, 25:30672
Fe--Th, crystal structure of α- and β-Th_2Fe_7, 25:29898
Fe-base--ThO_2, yield strength of dispersion-hardened bcc, 25:29948

IRON BORIDES
iron-57 Moessbauer spectra in boron-rich $FeB_{7.4}$ and FeB_{110}, 25:30689 (UUIP-733)

IRON CHLORIDES $FeCl_3$
properties of aqueous, for etching uranium and uranium alloys, 25:29798(P)

IRON IONS
abundance of positive, in ionospheric D region, (E/T), 25:30404
effects on radiosensitivity of Escherichia coli and rats in presence of oxygen, 25:29556
spectral lines due to, solar, (E), 25:30188
spectral lines of, oscillator strengths for, (E), 25:30170

IRON ISOTOPES
effectiveness for radiodiagnosis or radiotherapy in man, 25:29573
radioactivity standards of, users' guides for, 25:29174

IRON ISOTOPES Fe-55
energy-level transitions from meson (μ^-) reactions with cobalt-59, (E), 25:31258

IRON ISOTOPES Fe-56
alpha reactions (α,p) with calculation of angular distributions for, (T), 25:31428
energy levels from cobalt-56 decay, spin--parity assignments for, (E), 25:31287
energy-level transitions from meson (μ^-) reactions with cobalt-59, (E), 25:31258
neutron capture by, gamma spectra from thermal, (E), 25:31270

IRON ISOTOPES Fe-57
energy levels and transitions from neutron capture by iron-56, (E), 25:31270
energy-level transitions from meson (μ^-) reactions with cobalt-59, (E), 25:31258
Moessbauer spectra in boron, 25:30689 (UUIP-733)

IRON ISOTOPES Fe-58
energy-level transitions from meson (μ^-) reactions with cobalt-59, (E), 25:31258

IRON ISOTOPES Fe-59
determination in water, ASTM method for radiometric, 25:29010
uptake by tsetse flies following ingestion of labeled blood of rabbits, 25:29417

IRON OXIDES
thermodynamic properties of gaseous diatomic, free energy functions for, 25:29082

IRON OXIDES FeO
FeO--MnO--SiO_2--ZrO_2, phase studies of, 25:30008
FeO--MnO--ZrO_2, phase studies of, 25:30008
FeO--ZrO_2, phase studies of, 25:30008

IRON PERCHLORATES
$Cu(ClO_4)_2$--$Fe(ClO_4)_2$, radiolysis of aqueous solutions of, mechanism of oxygen formation in γ, 25:29141

IRON SULFATES
$CuSO_4$--$FeSO_4$, radiolysis of aqueous solutions of, mechanism of oxygen formation in γ, 25:29141

IRON SULFATES $FeSO_4$
radiolysis of heptahydrate of, Moessbauer study of proton, 25:29151
IRON SULFIDES
FeS--US_2, crystal structure of single crystals of, 25:29996
IRRADIATION FACILITIES
description of Canadian, for industrial, medical, and research uses, 25:29284
description of cobalt-60 gamma, for producing controlled exposure rates for medical use, 25:29255
design and operation of, with fluid-controlled positioning of sample and source, 25:29260(P)
design of gamma, data tabulation on dose uniformity ratio and minimum dose for, 25:29250 (BNL-50145(Rev.))
design of gamma, for processing root and tuber crops, 25:29253(P)
development for chemical industry, 25:29128
irradiation head for beam therapy-type, design and operation of, 25:29258(P)
ISODIALURIC ACID
deoxyriboside, yields from γ radiolysis of aqueous solutions of 5-bromo-2'-deoxyuridine in presence of oxygen, 25:29136
deoxyriboside, yields from γ radiolysis of aqueous solutions of 5-bromo-2'-deoxyuridine in presence of oxygen, 25:29135
ISOPROTERENOL
effects on oxygen pressure in mouse spleen, 25:29547
ISOQUINOLINE
complexes with uranium(V) chloride, properties of, 25:29092
ISOTOPES
spectral lines of Z = 10 to 78, calculation of resolution of, (T), 25:28952
ITALY
fallout monitoring during 1968, 25:29503 (PROT.-SAN.-8/69)
radiation monitoring at Ispra, development of program for environmental, 25:29222
radiation monitoring in vicinity of nuclear research centers during 1968, 25:29503 (PROT.-SAN.-8/69)
radiation monitoring of environment in, during 1968, 25:29504 (PROT.-SAN.-13/69)
radioactivity in environment of, measurement of natural gamma, 25:29205
radioisotope content of fresh and powdered milk in, during 1952 to 1966, fallout cesium-137 and strontium-90, 25:29507
radioisotope production in, for medical uses, 25:29273
radioisotopes content of fish and water from lakes of northern, fallout manganese-54 and zirconium-95--niobium-95, 25:29477

J

JAPAN
prospecting and mining of, review of programs for, 25:29237
research activities at National Institute of Radiological Sciences during 1969, 25:29572(R) (NIRS-AR-13)
JOINTS
sampling and testing of Cadweld-type spliced, in reinforcing bars in concrete containment structures, safety standards for, 25:29297
JUPITER (PLANET)
atmosphere of, composition of, (T), 25:30250
infrared spectra of, (T), 25:30250
magnetic-field geometry of, relation to Io-modulated radio emission, (E), 25:30251
radio emission from, magnetic-field effects on Io-modulated, (E), 25:30251

K

KIDNEYS
clearance of iodine-125- and iodine-131-labeled hippuran and inulin from dog, comparison of Lissamine Green method with, 25:29414
curium-244 content in beagle dog, following inhalation as chloride or oxide, 25:29429 (LF-43, pp 100-5)
cystamine in mouse and rat, effects of 5-methoxytryptamine on, 25:29554
plutonium-239 retention in, of beagles, 25:29451
radiation dose to human, during chromium-51 scanning, 25:29578
radiation dose to, in normal and tumor-bearing mice following administration of phosphorus-32-labeled chromium alloxantin and orthophosphate, 25:29483
radiation effects on function and morphology of rabbit, methods for studying γ, 25:29684
radiation effects on function of, in dogs following injection, protective effects of oxathiole against chronic polonium-210, 25:29563
radiation effects on human, following therapy for thyroid cancer, combined iodine-131 and teletherapy, 25:29707
radiation effects on ischemia damaged, in rats, fractionated low-dose, 25:29654
radiodiagnosis of diseases of human, evaluation of chromium-51, cobalt-58, and iodine-131 for, 25:29577
radioinduced nephritis in, of man following therapy, x, 25:29698
radiotherapy for Wilms' tumors in human, development of hepatitis following γ, 25:29652
scanning of human, use of chromium-51-labeled EDTA for, 25:29578
scintigraphy of human, for function and morphology, evaluation of, 25:29592
scintigraphy of human, for radiodiagnosis of metastatic and primary adenocarcinomas, 25:29590
KININS
radiation effects on accumulation of, in rat blood, γ, 25:29668
radiation effects on activity and content of, in rat-blood plasma, lethal, whole-body γ, 25:29681
KRYPTON
diffusion in neutron-irradiated uranium-doped calcium fluoride single crystals, 25:30673
energy-level transitions in, electron spectra from Coster--Kronig and L-shell Auger, (T), 25:30261
hydrogen-metastable-atom reactions at 1.0 keV to 1.6 MeV with, Born-wave calculations of total quenching cross sections for, 25:30283
krypton-ion reactions at 20 to 30 keV and scattering angles of 6 to 15° with, energy losses in, (E), 25:30279
neon-metastable-atom reactions with, two-state impact-parameter model for associative and Penning ionization in, 25:30298
separation from off-gas streams, evaluation of thin silicone rubber membranes for, 25:29317 (ORNL-4522)
separation of trace amounts of, from argon, design of gas chromatograph for, 25:29177 (CEA-R-4090)
KRYPTON IONS
reactions with krypton at 20 and 30 keV and scatering angles of 6 to 15°, energy losses in, (E), 25:30279
KRYPTON ISOTOPES
trapping in meteorites, 25:30168(R) (UCSD-34-P-43-X-9)
KRYPTON ISOTOPES Kr-81
abundance in meteorites, (E), 25:30158(R) (UCSD-34-P-43-X-9)
KRYPTON ISOTOPES Kr-85
monitoring in environmental samples at West Valley Processing Plant, 1971, 25:29180 (DOCKET-50201-70)
use for measuring working temperature of piston rings in Diesel engine, method for, 25:29282

L

LA CROSSE BOILING-WATER REACTOR
operation of, extended authorization expiration date for, 25:31463 (DOCKET-1155-113)
LABORATORY EQUIPMENT
design for liquid sodium research, standards for, 25:29252 (RD/B/M-1817)
LACTATE DEHYDROGENASE
radiation effects on activity and isoenzyme composition of, in heart, liver, and spleen of neonatal rats following parental exposure, 25:29665
radioinduced inhibition of estradiol-induced, in immature rats, γ, 25:29670
LAKES
age of Balkhash, in USSR, uranium-234/-238 method for estimation of, 25:29210
diatom content in, as index to environment, 25:31739(R) (TID-25695)
radioisotope content of fish and water from, in northern Italy, fallout manganese-54 and zirconium-95--niobium-95, 25:29477
LANTHANUM
analysis for rare earths by emission spectrography, 25:28965
determination in bauxite, selection of line pairs for spectroscopic, 25:28946
determination using ion permselective membrane, potentiometric, 25:28956
effects on fluorometric determination of zirconium, 25:28963
properties of aerosols produced from aqueous solutions of, 25:29079 (LF-43, pp 31-9)
reactions with rare earth carbides, thermodynamics of, 25:29039
LANTHANUM ALLOYS AND SYSTEMS
Co--La, hardness of intermetallic $LaCo_5$, measurement of magnetic and mechanical, 25:29845
LANTHANUM CARBIDES
reactions with rare earths, thermodynamics of, 25:29039
LANTHANUM FLUORIDES
analysis for free fluoride using lanthanum fluoride electrode, 25:28923
LANTHANUM HYDRIDES
hydrogen vibrations in LaH_2 and LaH_3, neutron inelastic scattering study of, 25:30677
LANTHANUM IODIDES
thermodynamic properties at 298 to 1300°K, 25:29951
LANTHANUM ISOTOPES
effects on man following inhalation, model for estimation of, 25:29427 (LF-43, pp 82-91)
LANTHANUM ISOTOPES La-140
distribution and retention in beagle dogs following

XUM

chronic inhalation as chloride, model for, 25:29427 (LF-43, pp 82-91)
distribution and retention in beagle dogs following inhalation as chloride, 25:29428 (LF-43, pp 92-9)
metabolism in beagle dogs following ingestion of nuclear debris from Project Cabriolet, 25:29456
LANTHANUM OXIDES
positron lifetimes in, 25:30272
thermodynamic properties of gaseous diatomic, free energy functions for, 25:29082
La_2O_3--Sc_2O_3, phase diagram of, 25:30065
La_2O_3--TiO_2--ZrO_2, dielectric properties of, 25:29984
La_2O_3--TiO_2--ZrO_2, phase diagram of, 25:29984
La_2O_3--Zr-base, tensile properties at 650°C, 25:29969
LARVAE
radiation effects on survival of mosquito, γ, 25:29614
radiosensitivity of successive generations of Drosophila melanogaster, effects of dose on x, 25:29613
radiosensitivity of, of sugarcane borers in comparison to embryos and pupae, γ, 25:29755
LASER RADIATION
filtering by saturable dyes, 25:31747 (UCRL-51006)
interactions with plasma, probe method for ion measurements from, 25:30477 (NP-18765)
LASERS
evaluation for spectral analysis of nuclear materials, 25:28949
use for startup of deuterium--tritium fueled thermonuclear reactors, 25:30553 (CLM-R-109)
LEAD
determination in alabaster, radiometric x-ray method for, 25:28939
determination in ores, x-ray radiometric method using selenium-75 source for, 25:28940
determination using ion permselective membrane, potentiometric, 25:28956
electron inelastic scattering at 0.2 to 3 keV from, energy spectra from, (E), 25:30260
gamma distribution in, angular and energy, (T), 25:30640
neutron diffusion parameters for, (E), 25:31177
nucleation field of pure superconducting, bulk and surface, 25:30424
phonon structure in tunneling in thick superconducting, multigap effect on, 25:30426
photon elastic scattering at 1.33 MeV, differential cross sections for, (E), 25:31370
photon inelastic scattering at 6.1 to 7.1 MeV, gamma spectra from, (E/T), 25:31303 (INR-1271)
photon reactions in spherical and slab targets, photoneutron spectra and angular distributions from, 25:31317
proton fission at 10 MeV to 29 GeV, cross section for, 25:31326
proton reactions at 11.5 and 23.5 MeV using thick targets, neutron yield from, (E), 25:31209
proximity effect in superconducting, coated with normal metals, 25:30446
separation of bismuth-206 and bismuth-207 from deuteron- or proton-irradiated, by solvent extraction using bis(2-ethylhexyl) phosphate, 25:29164
wave propagation in superconducting intermediate state of, interphase boundary, 25:30429
LEAD ALLOYS AND SYSTEMS
Pb--Sn, structure and properties of electrolytically deposited, 25:31734(T) (SCL-T-69-257)
Pb--Tl, magnetization curves of superconducting single crystals of, with small Ginzburg--Landau parameter, (E/T), 25:30418
LEAD CHLORIDES
molecular structure of, 25:29086
spectra in matrices of solid nitrogen or rare gases, ir, 25:29086
LEAD IONS
effects on proton-induced destruction of F centers in sodium chloride crystals, 25:30655
LEAD ISOTOPES Pb-205
energy levels from bismuth-205 decay, spins and parities of, (E), 25:31386
energy levels of, calculation using particle--core coupling model, (T), 25:31379
energy-level transitions in, internal conversion and internal pair formation coefficients for, (E), 25:31330
LEAD ISOTOPES Pb-206
energy-level transitions from meson (μ⁻) reactions with bismuth-209, (E), 25:31258
energy-level transitions in, internal conversion and internal pair formation coefficients for, (E), 25:31330
LEAD ISOTOPES Pb-207
energy-level transitions from meson (μ⁻) reactions with bismuth-209, (E), 25:31258
energy-level transitions in, internal conversion and internal pair formation coefficients for, (E), 25:31330
neutron resonance parameters at 3 to 700 keV for, (E), 25:31204 (ORNL-TM-3378)
LEAD ISOTOPES Pb-208
alpha scattering by, calculation of optical potentials in terms of diffraction-model parameters, (T), 25:31410
binding energy and single-particle separation energies of, variational calculation using improved mixed-density approximation, 25:31285
energy-level transitions from meson (μ⁻) reactions with bismuth-209, (E), 25:31258
proton reactions (p,α) at 16.475 MeV, alpha spectra and angular distributions from, (E), 25:31383
LEAD ISOTOPES Pb-209
energy levels from lead-207 (t,p) and lead-210 (p,d) reactions, effects of multipole pairing and particle--hole fields in particle--vibration coupling of, (T), 25:31309 (LA-DC-11648)
energy levels of, calculation using particle--core coupling model, (T), 25:31379
LEAD ISOTOPES Pb-210
abundance in atmosphere, relation to solar activity, (E), 25:30171
content in Antarctic neve samples, correlation with magnetic-field fluctuations, (E), 25:29211
LEAD ISOTOPES Pb-212
distribution and retention of aerosols-incorporated, in rat lungs following inhalation, 25:29455
radioisotopes from distribution of recoil ions of, outside thorium oxide particles in thorotrast, 25:29169
LEAD ISOTOPES Pb-214
determination in uranium air samples, radiometric, 25:29536
LEAD OXIDES
production of, radioactive tracer methods for improving processes for, 25:29283
thermodynamic properties of gaseous diatomic, free energy functions for, 25:29082
LEAD TELLURIDES
radioinduced p--n junctions in, 200-keV proton, 25:29397
LEUKOCYTES
radiation effects on, in dogs, plutonium-239, 25:29627
radioinduced chromosome aberrations in swine, 14-MeV neutron, 25:29497
LEVEL INDICATORS
design of superconducting wire, for liquid helium, 25:30448
development of ultrasonic, for solid radioactive wastes, 25:29393 (IN-1452)
LICHENS
strontium-90 content of, in Sweden during 1961 to 1969, 25:29480
LIGASES
radiation effects on activity of aminoacyl-tRNA, in cotton plants, 25:29715
LIGHT
alignment of interstellar grains by, (T), 25:30216
scattering from magnetic fluctuations in plasma, diagnostic use of optical, 25:30490
scattering from stratified sphere, 25:31704 (LA-4642)
LIGHT SOURCES
design and performance of helium-4 discharge, for optically pumped polarized helium-3 targets, 25:31076
performance for optical pumping of polarized helium-3 targets, 25:31075
performance of laser-produced plasma, for spectroscopy, 25:30498 (N-70-41880)
LIGHTNING
origin of ball, in annihilation of antimatter meteorites, (T), 25:30329
LIMERICK POWER REACTOR, UNIT 1
accidents in, radiation dose calculations for, 25:31519 (DOCKET-50352-12)
design parameters of, requested additional information on, 25:31519 (DOCKET-50352-12)
operations aspects of, requested additional information on, 25:31519 (DOCKET-50352-12)
piping systems for, classification of, 25:31519 (DOCKET-50352-12)
radioactive waste systems for, safety analysis of, 25:31519 (DOCKET-50352-12)
site for, hydrological and meteorological data for, 25:31519 (DOCKET-50352-12)
LIMERICK POWER REACTOR, UNIT 2
accidents in, radiation dose calculations for, 25:31519 (DOCKET-50352-12)
design parameters of, requested additional information on, 25:31519 (DOCKET-50352-12)
operations aspects of, requested additional information on, 25:31519 (DOCKET-50352-12)
piping systems for, classification of, 25:31519 (DOCKET-50352-12)
radioactive waste systems for, safety analysis of, 25:31519 (DOCKET-50352-12)
site for, hydrological and meteorological data for, 25:31519 (DOCKET-50352-12)
LIMESTONE
performance as artifical substrate for analysis of periphyton component of running-water ecosystems, 25:29478
LINEAR ACCELERATORS
beam current limit in ion, possibility of reducing injection energy to increase, 25:31062
beam energy determination for electron, using neutron production monitoring, 25:31173(R) (RPI-328-200)
beam focusing system for 30-MeV induction, 25:31039 (JINR-P9-5714)
cavity resonators for proton, design of ring coupling,,

25:31078
power supply for 25-MeV proton, thyristor voltage stabilizer for 40-kV modulator for, 25:31067
power supply for, operation of pulse generator, 25:31066
LIPIDS
radiation effects on rat liver and serum, local x, 25:29685
LIQUID FLOW
electrohydrodynamic, of incompressible nonviscous charged fluid in plane channel, velocity and pressure of, (T), 25:30345
LIQUID METAL FAST BREEDER REACTOR
accidents in, release and transport of aerosols produced in, (E/T), 25:31616
cover gas for, evaluation of permselective membranes for removing rare gases from, 25:29317 (ORNL-4522)
development during March 1971, 25:31533(R) (ANL-7798)
fuel cycle development for, (E), 25:31533(R) (ANL-7798)
fuels for, performance limits for plutonium oxide (PuO_2)--uranium oxide (UO_2), plutonium carbide (PuC)--uranium carbide (UC), and plutonium nitride (PuN)--uranium nitride (UN), 25:31569 (ORNL-TM-3388)
instrumentation for, equipment and requirements of core protection, 25:31574 (ANL-7793)
instrumentation for, high temperature and radiation effects on, (E), 25:31533(R) (ANL-7798)
physics studies on, (E/T), 25:31533(R) (ANL-7798)
safety studies on, (E/T), 25:31533(R) (ANL-7798)
LITHIUM
analysis of, using recording Fabry--Perot spectrometer, isotopic, 25:28913 (BARC-508)
production in stars, 25:30036(R) (NYO-3962-3)
proton reactions at 11.5 and 23.5 MeV using thick targets, neutron yield from, (E), 25:31209
LITHIUM FLUORIDES
BeF_2--LiF, spectra of tetravalent uranium in molten, 25:29093
LiF--KF--NaF, properties of refractory metal salt incorporating, for use as bath in metal electrodeposition, 25:29783 (CEA-N-1376)
LITHIUM ISOTOPES
determination in lithium samples using recording Fabry--Perot spectrometer, 25:28913 (BARC-508)
LITHIUM ISOTOPES Li-5
energy levels from He-3--d scattering, spins and parities of, (T), 25:31195
LITHIUM ISOTOPES Li-6
cluster model description of, contraction of deuteron in α--α, (T), 25:31207
content in metastases of carcinosarcomas in rat lungs, autoradiographic studies on, 25:29443
deuteron reactions (d,αt), (d,αHe-3), and (d,αd) at 52 MeV, spectra from, (E), 25:31187 (NP-18741)
diffusion from irradiated low-sintered beryllium oxide at 1100 to 1550°C, 25:29963
effects on electromigration in solid lithium bromide, chloride, fluoride, and iodide, 25:29041
electron elastic and inelastic scattering at 200 and 500 MeV, differential cross sections for, (E), 25:31211
electron inelastic scattering by, form factors for, (T), 25:31229
energy levels from electron inelastic scattering, E2 transition probabilities for, (T), 25:31229
neutron elastic scattering at fast energies, analysis using Wheeler group model, 25:31221
nuclear radius from electron elastic and inelastic scattering, (E), 25:31211
LITHIUM ISOTOPES Li-7
deuteron reactions (d,α) at 0.6 to 2.0 MeV, excitation function and angular distributions for, (E), 25:31220
energy-level transition in, Doppler broadening of 0.477-MeV, (E), 25:31208
meson (π^-) capture by proton, deuteron, and triton spectra from, (E), 25:31213
neutron total cross section at 125 keV to 2 MeV, (E), 25:31173(R) (RPI-328-200)
proton reactions at 3 to 4 MeV, neutron polarization in, (E), 25:31235
LITHIUM OXIDES
thermodynamic properties of gaseous diatomic, free energy functions for, 25:29082
Al_2O_3--Li_2O--MgO--SiO_2, radiation effects on phase transformations in, neutron, 25:30017
LIVER
cerium-144 content in beagle dog, following inhalation as chloride, 25:29431 (LF-43, pp 128-36)
cerium-144 content in beagle dog, following inhalation, insoluble, 25:29436 (LF-43, pp 183-7)
cerium-144 removal from beagle dog, following inhalation as chloride, effectiveness of intravenous administration of DTPA for, 25:29543 (LF-43, pp 280-5)
cesium-137 distribution and retention in beagle dog, following inhalation on fused clay particles, 25:29426 (LF-43, pp 79-81)
curium-244 content in beagle dog, following inhalation as chloride or oxide, 25:29429 (LF-43, pp 100-5)
plutonium-239 retention in, of beagles, 25:29451
radiation dose to beagle dog, following inhalation of cerium-144 chloride, β and γ, 25:29431 (LF-43, pp 128-36)
radiation dose to beagle dog, following inhalation of insoluble yttrium-90, 25:29434 (LF-43, pp 146-62)
radiation dose to, during kidney scanning using chromium-51, 25:29578
radiation dose to, in normal and tumor-bearing mice following administration of phosphorus-32-labeled chromium alloxantin and orthophosphate, 25:29453
radiation effects on activity and isoenzyme composition of lactate dehydrogenase in, of neonatal rats following parental exposure, 25:29665
radiation effects on activity of methionine adenosyltransferase in rat, effects of ethionine on lethal x, 25:29663
radiation effects on cadaverine deaminase activity and deamination of serotonin and tyramine in mitochondria of rat, 25:29641
radiation effects on content of sulfhydryl groups in, of ducklings, uv and/or x, 25:29647
radiation effects on enzyme activity and lipid fractions in rat, local x, 25:29685
radiation effects on function of, in dogs following injection, protective effects of oxathiole against chronic polonium-210, 25:29563
radiation effects on human, following therapy for thyroid cancer, combined iodine-131 and teletherapy, 25:29707
radiation effects on radiotoxin production in rat, strontium-90 β, 25:29639
radiation effects on synthesis of histones in rat, 25:29662
radioinduced chromosome aberrations in Chinese hamster, on internal americium-241, 25:29482 (LF-43, pp 240-5)
radioinduced chromosome aberrations in Chinese hamster, comparison of RBE of americium-241, cerium-144, and cobalt-60 γ, 25:29483 (LF-43, pp 246-53)
radioinduced cirrhosis and lesions in animal and human, γ and x, 25:29694
radioisotope retention in mouse, following inhalation of heat treated aerosols, 25:29423 (LF-43, pp 59-65)
radiosensitivity in human children during therapy for malignant tumors, γ, 25:29652
scintigraphy of human, for function and morphology, evaluation of, 25:29591
thulium-171 retention in beagle dog, following inhalation as oxide, 25:29425 (LF-43, pp 71-8)
yttrium-91 content in beagle dog, following inhalation, insoluble, 25:29435 (LF-43, pp 163-70)
LOOPS
design for liquid sodium research, standards for, 25:29252 (RD/B/M-1817)
LOS ALAMOS MESON PHYSICS FACILITY
development, Nov. 1970--Jan. 1971, 25:31042(R) (LA-4639)
experimental facility for, proposal for high-resolution pion beam and spectrometer, 25:31041 (LA-4534)
research program, Nov. 1970--Jan. 1971, 25:31042(R) (LA-4639)
LUBRICANTS
friction and wear properties of polyimide-bonded solid film, 25:29096 (WERL-HFIL-1)
radiation stability of polyimide-bonded solid film, 25:29096 (WERL-HFIL-1)
testing for extrusion of fuel elements, 25:29787(R) (RMI-16)
LUNAR MATERIALS
composition of, (E), 25:30249
mass spectroscopy of, (E), 25:30248(R) (UCB-34-P-32-PR-5)
LUNGS
antimony-124 retention in mouse, following inhalation of heat treated aerosols, 25:29424 (LF-43, pp 66-70)
cerium-144 content in beagle dog, following inhalation as chloride, 25:29431 (LF-43, pp 128-36)
cerium-144 content in beagle dog, following inhalation, insoluble, 25:29436 (LF-43, pp 183-7)
cerium-144 removal from beagle dog, following inhalation as chloride, effectiveness of bilateral bronchopulmonary lavage with DTPA for, 25:29544 (LF-43, pp 286-94)
cerium-144 removal from beagle dog, following inhalation as chloride, effectiveness of intravenous administration of DTPA for, 25:29543 (LF-43, pp 280-5)
cesium-137 retention in beagle dog, following inhalation of insoluble, 25:29426 (LF-43, pp 79-81)
curium-244 content in beagle dog, following inhalation as chloride or oxide, 25:29429 (LF-43, pp 100-5)
lanthanum-140 retention in beagle dog, following inhalation as chloride, 25:29428 (LF-43, pp 92-9)
lithium-6 content in, of rats with Walker-256 carcinosarcoma, autoradiographic study on, 25:29443
radiation dose distribution in, of man following injection of Thorotrast, α, 25:29521
radiation dose to beagle dog, following inhalation of insoluble strontium-90, β, 25:29437 (LF-43, pp 188-96)
radiation dose to beagle dog, following inhalation of insoluble cerium-144, relation of induced pulmonary fibrosis to, 25:29622 (LF-43, pp 218-23)
radiation dose to beagle dog, following inhalation of insoluble yttrium-90, 25:29434 (LF-43, pp 146-62)
radiation dose to beagle dog, following inhalation of insoluble radioisotopes, β, 25:29438 (LF-43, pp 197-204)
radiation dose to beagle dog, following inhalation of insoluble cerium-144, β and γ, 25:29436 (LF-43, pp 183-7)

XUM

radiation dose to beagle dog, following inhalation of, yttrium-91, β and γ, 25:29435 (LF-43, pp 163-70)
radiation dose to beagle dog, following inhalation of cerium-144 chloride, β and γ, 25:29431 (LF-43, pp 128-36)
radiation dose to rat, following inhalation of lead-212-labeled aerosols, α, 25:29455
radiation dose to, in normal and tumor-bearing mice following administration of phosphorus-32-labeled chromium alloxantin and orthophosphate, 25:29453
radiation effects on, of influenza virus infected mice following inhalation of insoluble cerium-144, β, 25:29724 (LF-43, pp 254-62)
radioinduced damage and loss of cells of animal, 25:29636
radioisotope content in beagle dog, following inhalation as oxides, 25:29421 (LF-43, pp 8-12)
radioisotope retention in mouse, following inhalation of heat treated aerosols, 25:29423 (LF-43, pp 59-65)
radiotherapy of bronchial carcinomas in human, combined effects of chemo- and, 25:29606
scanning of human, for diagnosis of blood flow, measurement of gas exchange following iodine-131, 25:29594
strontium-90 content in beagle dog, following inhalation of fused clay particles, 25:29437 (LF-43, pp 168-96)
thulium-171 retention in beagle dog, following inhalation as oxide, 25:29425 (LF-43, pp 71-8)
yttrium-91 content in beagle dog, following inhalation, insoluble, 25:29435 (LF-43, pp 163-70)

LUTETIUM
separation from other rare earths by ion exchange, 25:29178 (CEA-R-4102)

LUTETIUM ISOTOPES Lu-172
electron-capture decay of, γ spectra from, (E), 25:31347
energy levels and transitions from hafnium-172 decay, properties of collective, (E), 25:31347

LUTETIUM ISOTOPES Lu-176
beta and electron-capture decay of, gamma and conversion electron spectra from, (E), 25:31375

LYMPH NODES
cerium-144 content in beagle dog, following inhalation, insoluble, 25:29436 (LF-43, pp 183-7)
cesium-137 retention in dog tracheobronchial, following inhalation of insoluble, 25:29426 (LF-43, pp 79-81)
curium-244 content in beagle dog, following inhalation as chloride or oxide, 25:29429 (LF-43, pp 100-5)
radiation dose to beagle dog, following inhalation of insoluble yttrium-90, 25:29434 (LF-43, pp 146-62)
radiation effects on rat, comparison of recovery from partial- and whole-body, 25:29669
strontium-90 content in beagle dog, following inhalation of fused clay particles, 25:29437 (LF-43, pp 168-96)
yttrium-91 content in beagle dog, following inhalation, insoluble, 25:29435 (LF-43, pp 163-70)

LYMPH SYSTEM
radiosensitivity of rabbit and rat, x, 25:29635

LYMPHOCYTES
radiation effects on content of, in blood of dogs, 25:29642
radiation effects on count and reactivity of, in blood of patients with cirrhosis, extracorporeal, 25:29704
radiosensitivity of human, from normal and infected donors, in vitro γ, 25:29710

LYSINE, HYDROXY-
radiation effects on content of, in beagle dog lungs following inhalation of insoluble cerium-144, relation of pulmonary fibrosis to β and γ, 25:29622 (LF-43, pp 218-23)

M

MC GUIRE POWER REACTOR, UNIT 1
design parameters of, revised and additional data on, 25:31522 (DOCKET-50369-8)
operations aspects of, revised and additional data on, 25:31522 (DOCKET-50369-8)

MC GUIRE POWER REACTOR, UNIT 2
design parameters of, revised and additional data on, 25:31522 (DOCKET-50369-8)
operations aspects of, revised and additional data on, 25:31522 (DOCKET-50369-8)

MACHINING
processes of, adaptive control survey of, 25:31758 (Y-1759)

MAGNESIUM
determination in plutonium by absorption spectrophotometry, mass spectrometry, and spectrography, 25:28916 (CEA-R-4071)
determination in presence of other metals, spectrographic, 25:28944
determination using ion permselective membrane, potentiometric, 25:28956
proton reactions at 11.5 and 23.5 MeV using thick targets, neutron yield from, (E), 25:31209
separation from aqueous solutions by thin-layer chromatography using liquid anion exchangers, 25:29186
separation from other alkaline earths by ion exchange, 25:29193
spectra of, inner-shell absorption in, (E), 25:30174

MAGNESIUM ALLOYS AND SYSTEMS
radiation effects on fuel cladding of, neutron, 25:29916
Ce--Mg--Si, crystal structure of $CeMg_2Si_2$, 25:29993

MAGNESIUM IONS
abundance of positive, in ionospheric D region, (E/T), 25:30404

MAGNESIUM ISOTOPES
radioactivity standards of, users' guides for, 25:29174

MAGNESIUM ISOTOPES Mg-24
alpha inelastic scattering at 16.7 MeV, reaction mechanism study of α--γ angular correlations from, (E), 25:31215
deuteron elastic scattering at 82 MeV, optical-model analysis of, (E), 25:31240 (NP-18511)
deuteron reactions (d,He-3) at 82 MeV, DWBA analysis of differential cross sections and spectra from, (E/T), 25:31240 (NP-18511)
proton reactions (p,γ) at 1.49 MeV, γ-ray angular distributions for, (E), 25:31266

MAGNESIUM ISOTOPES Mg-25
energy levels of, calculation including shell mixing effects, (T), 25:31265

MAGNESIUM ISOTOPES Mg-26
energy fuels from aluminum-27 (d,He-3) reactions, l-transfer, spectroscopic factors, and spin-parity assignments for, (E/T), 25:31240 (NP-18511)
energy levels from proton inelastic scattering, spin-parity assignments for, (E), 25:31245
helium-3 reactions (He-3,n) at 13.2 MeV, neutron spectra and angular distributions for, (E), 25:31237 (IAE-1958)

MAGNESIUM OXIDES
radiation effects on dielectric properties of insulators of, fast neutron, 25:30011 (ORNL-4630, pp 226-9)
radioinduced hardening of, model for effects of defect concentration on, 25:30013
thermodynamic properties of gaseous diatomic, free energy functions for, 25:29082
Al_2O_3--Li_2O--MgO--SiO_2, radiation effects on phase transformations in, neutron, 25:30017
Dy_2O_3--MgO, phase diagram at 1500 to 2400°C, 25:29985
Gd_2O_3--MgO, phase diagram at 1500 to 2400°C, 25:29985
MgO--SiO_2--ZrO_2, phase studies of, 25:30008
MgO--Sm_2O_3, phase diagram at 1500 to 2400°C, 25:29985

MAGNESIUM PERCHLORATES
use of tetrahydrate of, as practical low-range moisture generator, 25:31759 (Y-1791)

MAGNET COILS
book: Technology of Strong Pulsed Currents and Magnetic Fields, 25:30604
design of helical, manufacture and construction of, 25:30555 (EUR-4593, pp 19-24)
development of superconducting, review of, 25:30557 (EUR-4593, pp 83-93)
performance of single-shot pulsed superconducting, 25:30598 (LA-4617)
properties of superconducting, effects of neutron irradiation on, 25:30440 (EUR-4593, pp 107-13)
stability of single-turn, in pulsed fields up to 1 MG, 25:30556 (EUR-4593, pp 25-32)

MAGNETIC FIELDS
activity of, effect on day and night temperature of thermosphere, (E), 25:30378
book: Technology of Strong Pulsed Currents and Magnetic Fields, 25:30604
charged-particle acceleration in variable, (T), 25:30122
charged-particle motion in homogeneous varying, coherent states and Green function of nonrelativistic, (T), 25:30704
charged-particle trapping in dipole, second invariant and drift frequency for approximate pitch angle-dependences of, 25:30381
control of high-rise-time, for theta-pinch device, transformer-coupled and variable-inductance method for, 25:30577 (EUR-4593, pp 355-63)
detection in peculiar and metallic-line A stars, (E), 25:30045
distribution in primordial universe, (T), 25:30244
effects of interplanetary, on diurnal variation of cosmic rays, (E/T), 25:30321
effects on transverse heat transfer in gaseous hydrogen isotopes at 22 to 110°K, 25:29267
fermion motion in homogeneous, covariant spin 3-vector operator for, (T), 25:30794
intensity variations of interplanetary, solar-cycle effects on, (E/T), 25:30326
measurement of varying and pulsed, review on, 25:29399
perturbations of north--south component of interplanetary, (E/T), 25:30176
plasma relaxation in constant, electron-ion, (T), 25:30545
production of intense, inductive energy storage systems for, 25:30561 (EUR-4593, pp 197-203)
proton--proton interactions in intense, (T), 25:30050
shock-wave propagation along, in collisionless plasma, (E/T), 25:30620
solar-wind interaction with lunar limb, creation of diamagnetic cavity on antisolar side of moon from, (E/T), 25:30388
strength of interstellar, from MP 0628 data, (E), 25:30135

MAGNETIC MATERIALS
electron energy loss in magnetized HCR foil, polarization straggling effect in helical, 25:30644
magnetic structures from neutron diffraction of tetragonal, tables, 25:30664 (NP-18783)
MAGNETIC MIRROR MACHINES
developmental progress of, 25:30600 (WASH-1172)
plasma diagnostics in, method evaluation for, 25:30489
plasma equilibrium and stability in Heliotron, (T), 25:30549
plasma instabilities in, bounce effects on negative mass, (T), 25:30551
plasma losses in compression experiment, self-consistent theory for, (E/T), 25:30465
MAGNETIC MIRRORS
charged-particle motion in axisymmetric, single-particle, (T), 25:30516 (N-70-42698)
plasma confinement in magnetostatic, with helping microwaves, (E), 25:30463
plasma end losses in combined theta pinch, (T), 25:30464
MAGNETIC MONOPOLES
interactions with matter, (T), 25:30771(T) (BNL-tr-410)
theory for Dirac, 25:30771(T) (BNL-tr-410)
MAGNETIC STORMS
development of polar substorms, effect on magnetotail magnetic field perturbations, (E), 25:30403
effect on ionospheric electron and ion temperature variations, (E/T), 25:30399
electron injection into magnetosphere during Oct.-Nov. 1968, (E), 25:30352
generation of, by solar wind penetration into magnetosphere, (E), 25:30400
pulsations during magnetospheric substorms, Ogo-5 observations of band-limited Pil micro-, (E), 25:30369
temporal history of Aug. 25 to 26, 1967 magnetospheric substorm, extensive relationships of, (E/T), 25:30368
MAGNETOHYDRODYNAMIC GENERATORS
book: Principles of Thermoelectric and Magnetohydrodynamic Conversion of Energy. In Russian, 25:30340
boundary layers in, process for crossing, 25:30337(P)
electrode decomposition in, effect of temperature on critical density from, 25:30336
excitation scheme comparisons for jet induction, (T), 25:30335
MAGNETOMETERS
development for varying and pulsed magnetic fields, review on, 25:29399
MAGNETOPAUSE
plasma instabilities in, hydromagnetic analog of Kelvin--Helmholtz problem including Hall effects, 25:30392
MAGNETOSPHERE
electric-field in, vacuum-merging mechanism of convection-driven cross-tail, (E/T), 25:30387
electron injection into, during magnetic storm of Oct.-Nov. 1968, (E), 25:30352
emission of vlf waves in morning-side, generation of background hiss of polar chorus from, (E/T), 25:30358
field lines in, leading to SAR red arcs, relation to plasmapause, ring current, and electron trough locations, (E/T), 25:30376
hydromagnetic-wave coupling between solar wind and plasma sheet in, effect on magnetotail resonant oscillations, (T), 25:30366
hydromagnetic-wave propagation through lower, effect on lower-latitude pulsations, (E/T), 25:30356
ion instability in bow shock thermalization, (E/T), 25:30365
magnetic storm on June 8, 1968 in, Ogo-5 observations of band-limited Pil micropulsations during substorm, (E), 25:30369
magnetic-substorm phenomena of Aug. 25 to 26, 1967, extensive relationships of, (E/T), 25:30368
radio-wave emission for given field-line and electron-stream parameters, spectral shapes of vlf discrete, (E/T), 25:30372
radio-wave emission from, whistler-mode convective beam-cyclotron instability generation mechanism of vlf, (T), 25:30357
radio-wave emission in, Helliwell criterion for electron energy spectra and structure deduced from vlf discrete, (E/T), 25:30371
radio-wave propagation along field lines in, color spectrograms of vlf Poynting flux measurements of, (E), 25:30370
solar wind penetration into, generating magnetic storms, (E), 25:30400
solar-wind pressure on, (E/T), 25:30396
thermal conduction in, effect on occurrence of subauroral red arc at mid-latitude, (E), 25:30350 (N-70-36812)
wave turbulence in, tangential discontinuities in, 25:30391
MAGNETOTAIL
magnetic field perturbations in, associated with polar magnetic substorm onset, (E), 25:30403
oscillations in, effect of hydromagnetic-wave coupling between solar wind and plasma sheet on resonant, (T), 25:30366
plasma motion in, hydromagnetic waves in, 25:30349 (IPPJ-103)
MAGNETS
cost factors for large superconducting, present status of, 25:30441 (EUR-4593, pp 117-24)
design of large-volume homogeneous low-field, for polarized helium-3 target, 25:31071
development of superconducting and cryogenic, 25:31040 (KFK-1316)
properties of 2-81 permalloy powder cores of, effects of heat treatment on, 25:30672
sintering and properties of $PrCo_5$ permanent, 25:29797
MAINE YANKEE POWER REACTOR
design parameters of, revised and additional data on, 25:31504 (DOCKET-50309-34)
operations aspects of, revised and additional data on, 25:31504 (DOCKET-50309-34)
MAMMALIA
fission product inhalation by, research on, 25:29419(R) (LF-43)
MAN
halothane pharmacokinetics in, use of bromine-82 tracer and whole-body counter for study of, 25:29416
potassium content in, with pyelonephritis, whole-body counting of, 25:29448
radiation distribution in lungs of, following injection of Thorotrast, α, 25:29521
radiation dose to bones of, following acute inhalation of strontium-90 aerosols, method for estimation using biological models with computer calculations for β, 25:29513 (CONF-710211-1)
radiation dose to tissues in, from inhalation of lanthanum isotopes, model for estimation of, 25:29427 (LF-43, pp 82-91)
radiation dose to, during emergency exposure, standards for estimation of, 25:29539
radiation dose to, following inhalation or ingestion of powders of irradiated uranium fuels, use of radiometric determination of cesium-137 and strontium-89 in urine for estimation of, 25:29515 (NP-18794)
radiation dose to, in vicinity of nuclear excavation projects, method for measurement using computer calculations of external gamma, fission product yields, and fission product dispersion and intake, 25:29516 (UCRL-50990)
radiation effects on blood and hematopoietic system of, whole-body x, 25:29699
radiation effects on incidence of mongoloid children of, following maternal diagnostic exposure, x, 25:29500
radiation effects on lymphocytes in, with cirrhosis, extracorporeal, 25:29704
radiation effects on nervous system in, x, 25:29692
radiation effects on nucleoproteins in cultured amniotic cells of, cytofluorimetry studies on, 25:29709
radiation effects on organs and systems following combined iodine-131 and teletherapy of thyroid gland, 25:29707
radiation effects on salivary glands of, x, 25:29693
radiation effects on stem cells in, developments in bone marrow transplants for treatment of, 25:29560
radiation effects on tooth demineralization in, following therapy for nasopharynx tumors, 25:29712
radiation hazards to, during use of 35 MeV betatron for therapy, design specifications and shielding for protection against, 25:29528
radiation hazards to, from inhalation of radioisotopes from reactor accident release, estimation of relative, 25:29420 (LF-43, pp 1-7)
radiation hazards to, from Project Rulison, review of controversy concerning, 25:29248
radiation protection of, during radiography in general hospital, program for, 25:29538
radiation protection programs for, during diagnosis and therapy of diseases in Australia, 25:29526(R) (NP-18790)
radioinduced basal cell carcinomas in, following therapy for burns, long-term, 25:29701
radioinduced carcinomas in, effects of dose and dose rate on, 25:29691
radioinduced cirrhosis and lesions in liver of, γ and x, 25:29694
radioinduced cystitis in urinary tract of, radium and radon alpha, gamma, and x, 25:29697
radioinduced damage to cells of, γ and x, 25:29690
radioinduced dermatitis in, following excessive fluoroscopy, x, 25:29706
radioinduced hepatitis following therapy for Ewing's or Wilms' tumors in children of, γ, 25:29652
radioinduced leukemia in, following radiotherapy of arthritis and thymic hypertrophy, γ and x, 25:29696
radioinduced myocarditis in heart of, x, 25:29695
radioinduced necrosis in human axilla and shoulder following post mastectomy therapy, surgical treatment of x, 25:29569
radioinduced nephritis in kidneys of, following therapy, x, 25:29698
radioprotective effects of ethyl ester of 2-thiazolidineacetic acid, 4-carboxy-α-phenyl on, during therapy, γ, 25:29545
radioprotective effects of oxygen butazone on, during therapy, x, 25:29549
radiosensitivity of lymphocytes of, effects of infectious hepatitis in donor on in vitro γ, 25:29710
radiotherapy of bladder or gynecological tumors in, use of ultrasound scanning for planning, 25:29602

XUM

radiotherapy of bronchial carcinomas in, combined effects of chemo- and, 25:29606
radiotherapy of carcinomas in prostate gland of, γ, 25:29597
radiotherapy of Hodgkin's disease in, correlation between nominal standard tissue dose and RET during, 25:29520
radiotherapy of hyperthyroidism in, comparison of leukemia development following surgical treatment or iodine-131, 25:29705
radiotherapy of inoperable pulmonary or squamous cell carcinomas in, effectiveness of cobalt-60 γ, 25:29600
radiotherapy of laryngeal carcinomas in, using radium or x radiation, 25:29598
radiotherapy of lymphosarcomas and retotheliosarcomas in, effectiveness of electron pendulum irradiation or mantle irradiation for, 25:29599
radiotherapy of verruca juvenilis in, effectiveness of x, 25:29601
strontium excretion and retention by children and adult, strontium-84 tracer study of, 25:29442
strontium-90 content of, in Sweden during 1961 to 1969, 25:29480

MANDELIC ACID
radioinduced racemization of D(-), γ, 25:29145
radiolysis of D(-), identification of products from γ, 25:29145

MANGANESE
determination by x-ray fluorescence, sensitivity of, 25:28962
determination in low-alloy steel, two-standard method for spectrometric, 25:28950
determination in natural waters by solvent extraction and x-ray fluorescence spectroscopy, 25:28919
determination in presence of other metals, spectrographic, 25:28944
determination of trace amounts of, in vanadium, spectrographic, 25:28947
effects on corrosion of beryllium--copper--tin alloys by nitric acid, 25:29830
effects on ductility of Inconel 600 at 400 to 1000°C, 25:29825 (ORNL-4630, pp 261-70)
separation from aqueous solutions by thin-layer chromatography using liquid anion exchangers, 25:29186
x-ray emission spectra of, K-band, 25:30671

MANGANESE ALLOYS AND SYSTEMS
Ce--Mn--Ru, preparation and superconductivity of, (E), 25:30413(T) (LA-tr-71-26)
Co-Mn, NMR and nuclear relaxation study of satellite lines in dilute, 25:31690 (COO-1569-71)

MANGANESE BORIDES
x-ray emission spectra of Mn_4B, Mn_2B, MnB, Mn_3B_4, and MnB_2, K-band, 25:30671

MANGANESE ISOTOPES Mn-51
nuclear electric and magnetic moments and hyperfine structure constants of, (E), 25:31294

MANGANESE ISOTOPES Mn-52
energy levels from chromium-50 (He-3,p) reactions, spins, parities, isospin, and angular momenta for, (E), 25:31298
nuclear magnetic moments, spin, and hyperfine structure constants of isomeric, (E), 25:31294

MANGANESE ISOTOPES Mn-53
energy levels from chromium-53 (p,n) reactions, spin assignments for, (E), 25:31248

MANGANESE ISOTOPES Mn-54
content of fish and water from lakes of northern Italy, fallout, 25:29477
determination in water by precipitation and γ spectrometry, ASTM method for, 25:29006
uptake by liver mitochondria in irradiated mice, 25:29673

MANGANESE ISOTOPES Mn-55
meson reactions (μ^-,xn) by, gamma spectra from, (E), 25:31258
photon reactions (γ,n) at 10 to 68 MeV, yields of radioactivities from, (E), 25:31333

MANGANESE ISOTOPES Mn-56
determination in water by precipitation and γ or β spectrometry, ASTM method for, 25:29006

MANGANESE OXIDES
thermodynamic properties of gaseous diatomic, free energy functions for, 25:29082
FeO--MnO--SiO_2--ZrO_2, phase studies of, 25:30008
FeO--MnO--ZrO_2, phase studies of, 25:30008
Mn_3O_4--SiO_2--ZrO_2, phase studies of, 25:30008
MnO--SiO_2--ZrO_2, phase studies of, 25:30008
MnO--ZrO_2, phase studies of, 25:30008

MANY BODY PROBLEM
hyperspherical-expansion approach to, (T), 25:31405

MARTENSITE
electron metallography of ferrous, 25:31743 (UCRL-19648)
radioinduced phase transition in, effects on tetragonality, (T), 25:29911

MASS LAW
derivation from first principles of Weizsaecker formula for heavy nuclei, (T), 25:31405

MASS SPECTROGRAPHY
research in, (E), 25:30248(R) (UCB-34-P-32-PR-5)
standards in, uses of compounds labeled with stable isotopes as, 25:28967

MATERIALS TESTING
method for nonlinear analysis of pressure vessel stress response, 25:31664 (EUR-4531, pp 697-734)

MATERIALS TESTING, DESTRUCTIVE
method for mechanical splices in reinforcing bars in concrete containment structures, safety standards for, 25:29297

MATERIALS TESTING, NONDESTRUCTIVE
bubble detection in liquid sodium bonded, engineering drawings for equipment for, 25:31571
methods for power reactor components, economics and importance of, 25:29289

MATTER
density perturbations in anisotropic homogeneous Universe, (T), 25:30223
distribution in Universe, Newtonian hierarchical, (T), 25:30226
distribution of cold, in Universe, (T), 25:30227
distribution of superdense, cosmological constant modification of system of generalized field equations in general relativity theory for study of, (T), 25:31004
hydrodynamics of mixture of antimatter and, (T), 25:30204
infrared emission from cold, in Universe, (T), 25:30227
intergalactic, effects on fluctuations of cosmic microwave background, (T), 25:30236

MATTER, ANTI-
annihilation of meteorites containing, as source of ball lightning, (T), 25:30329
detection in primary cosmic radiation, (E), 25:30327
hydrodynamics of mixture of matter and, (T), 25:30204

MEATS
beef, radiation processing of, effects of temperature on survival of Clostridium botulinum spores following, 25:29734
radiation processing of frozen, organoleptic properties and salmonella survival following γ, 25:29729 (IAEA-R-491-F)

MECHANICS
algebraic theory for statistical, Heisenberg ferromagnet in, 25:30946
equilibrium states in statistical, 25:30941
formalism for statistical, relation with quantum field theory, 25:30956
structural analysis using lumped-mass models, dynamic, 25:31752 (UCRL-72818(Rev.1))
time evolution of systems with infinite number of degrees of freedom in statistical, 25:30703

MEDICAL PERSONNEL
compliance with safety rules for use of x-ray equipment in North Dakota, survey of, 25:29542
radiation injuries to radiological, hematological examinations for diagnosis of, 25:29595
radiation protection programs for, in Australia, 25:29526(R) (NP-18790)
radioinduced chromosome aberrations in blood cells of radiological, chronic, 25:29501

MEDICAL SUPPLIES
decontamination using detergent solution and sound frequency vibrator, 25:29510

MEDICINE
conference on clinical aspects of inherited disorders, Birmingham, Ala., April 9-10, 1970, 25:29498
conference on engineering developments for, abstracts of papers from, 25:29584
conference on nuclear, abstracts of papers from, 25:29570 (CONF-691016-(Absts.))
radiation protection in dental, regulations and practical aspects of x, 25:29530
radioisotope uses in, evaluation of short-lived, 25:29439

MELANIN
radioprotective effects of, on melanoma cells in mice, x, 25:29568

MEMBRANE FILTERS
performance of permselective, for removal of rare gases from off-gas streams, 25:29317 (ORNL-4522)

MEMBRANES
properties of ion permselective, for potentiometric studies, 25:28956

MERCAPTO GROUP
content of tumors, relation between radiosensitivity and, 25:29610
radiation effects on content of, in tissues of ducklings, uv and/or x, 25:29647

MERCHANT VESSELS
design requirements of nuclear powered, guides for, 25:31643
hazards to crew in nuclear powered, review of possible, 25:31644
operations aspects of nuclear powered, guides for, 25:31643

MERCURY
determination by neutron activation, solvent extraction separations for, 25:29031
determination of trace amounts of, in platinum by neutron activation following separation by ion exchange chromatography, 25:29023
effects on colorimetric determination of molybdenum, 25:28930
photon inelastic scattering at 6.1 to 7.1 MeV, gamma spectra from, (E/T), 25:31303 (INR-1271)

separation from antimony, arsenic, gallium, and iron by solvent extraction, 25:29031
MERCURY (PLANET)
solar-wind interactions with, interior conductivity studies from, (E/T), 25:30389
MERCURY ISOTOPES
effectiveness for radiodiagnosis or radiotherapy in man, 25:29573
radioactivity standards of, users' guides for, 25:29174
MERCURY ISOTOPES Hg-197
use for diagnosis of myocarditis, 25:29413 (CONF-691225)
use of Brommercurascan- or Mercurascan-incorporated, for scintigraphy of heart for diagnosis of myocardial infarction in, 25:29571(T) (LB/G-2835)
use of Neohydrin-incorporated, for radiodiagnosis of metastatic and primary adenocarcinomas in human kidneys, 25:29590
MERCURY ISOTOPES Hg-200
energy levels from thallium-200 decay, spins and parities of, (E), 25:31387
MERCURY ISOTOPES Hg-203
uptake in bones and tissues of rats for diagnosis of joint diseases, 25:29561
use for diagnosis of myocarditis, 25:29413 (CONF-691225)
use of Brommercurascan- or Mercurascan-incorporated, for scintigraphy of heart for diagnosis of myocardial infarction in, 25:29571(T) (LB/G-2835)
use of neohydrin-incorporated, for scintigraphy of human kidneys for function and morphology, 25:29592
MERCURY OXIDES
thermodynamic properties of gaseous diatomic, free energy functions for, 25:29082
MESONS
electroproduction of, scale invariance breakdown in generalized Bjorken limit, 25:30783
exchange in Regge pole theory, triquark and biquark propagators with constant residues for, 25:30834
exchange of virtual, in fermion interactions, self-consistent method for, 25:30831
interactions and properties of, relation between local duality and conserved currents for, 25:30855
interactions with $^1/_2{}^+$ baryons at high energies, Regge residues for forward and backward, (T), 25:30883
interactions with baryons, scale symmetry breaking for scattering length for, 25:30933
interactions with mesons, two-channel unitarized Veneziano model, 25:30860
mass splittings in fifth interaction, S(3) symmetry breaking for medium-strong, 25:30781
model for nonexotic nonhermitian uncharged field for complex dipole, 25:30827
role of vector, in electromagnetic interactions, (T), 25:30796
symmetry for systems of, algebraic realization of chiral SU(2) X SU(2), (T), 25:30850 (JINR-P2-5759)
MESONS (eta)
decay eta → 3π, Faddeev-like theory for π spectra in, 25:30788
production in γ + p → p + eta interactions, review of coupling parameters for, (E/T), 25:30797
MESONS (K)
coupling constants for NAK, PCAC hypothesis for, (T), 25:30904
coupling constants for NΣK, PCAC hypothesis for, (T), 25:30904
coupling of ΛKN, review of forward dispersion relations for, (T), 25:30902
decay K → 3π, Faddeev-like theory for π spectra in, 25:30788
decay K → π + l + ν, soft-pion corrections to Dashen--Weinstein theorem for form factor in, 25:30816
decay K → π + l + ν, unitarity correction to hard-meson analysis of, 25:30813
interactions K + N, exchange degeneracy in Reggeized absorption model for, 25:30874
interactions K + N, Poisson distribution for bounds, multiplicity, and energy dependence of inelastic, (T), 25:30899
interactions K + N, Veneziano model with spin for amplitude of three-body hadron production in, (T), 25:30889
interactions N + N below 1 GeV/c, direct data analyses and phenomenological dispersion relations, (T), 25:30882
interactions π + K in GeV range, low-energy models for, (T), 25:30854
mass splitting (K - π), nontadpole contribution to, 25:30791
reactions with nuclei at low energies, reaction-matrix method and statistical model of, 25:30906
MESONS (K⁻)
absorption in nuclei at rest, extrapolation of K⁻ + p interactions below threshold from, (T), 25:30902
decay K⁻ → π⁻ + γ + γ, CP violation in, 25:30928
interactions K⁺ + K⁻, dispersion calculation of scattering amplitude and form factor for, 25:30865
interactions K⁻ + n → K⁻ + π⁻ + p at 5.5 GeV/c, double-Regge-pole analysis, (E/T), 25:30747
interactions K⁻ + N → π + Σ, models of Σ(1405) as CDD pole and bound state of, 25:30876
interactions K⁻ + p → K⁻ + p at high energies, eikonal model for, (T), 25:30893 (INR-P-1233)
interactions K⁻ + p → K⁻(890) + p at high energies, factorizable quark model for amplitude of, (T), 25:30879
interactions K⁻ + p + p → K⁻ + 2π⁺ + 2π⁻ at 3.95 GeV/c in hydrogen bubble chamber, parametrization for, (E), 25:30743
interactions K⁻ + p below threshold, ΛKN coupling and K⁻ absorption in nuclei at rest for extrapolation of, (T), 25:30902
interactions K⁻ + p, weak duality for slopes of angular distributions of elastic, 25:30873
MESONS (K⁰)
CP violation in K⁰ - anti K⁰ system, review of parameters for, (E), 25:30925
decay K⁰ → 2π, chiral symmetric gauge field model for, 25:30810
decay K⁰ → π⁺ + π⁻ + π⁰ from K⁺ + d → K⁰ + p + p interactions, (E), 25:30723
decay $K_2{}^0$ → 2π, chiral symmetry breaking for, 25:30919
invariance principles for, lectures on, 25:30915 (NP-18808)
mass difference (K⁺ - K⁰) consistency test using Cottingham formula and finite-energy sum rules for, 25:30800
mass matrix for $K_1{}^0$ - $K_2{}^0$ system, shell-model eigenstates of, 25:30861
MESONS (anti K⁰)
CP violation in K⁰ - anti K⁰ system, review of parameters for, (E), 25:30925
MESONS (K⁺)
decay K⁺ → π⁺ + e⁺ + e⁻ with virtual photon emission, W boson theory for divergences of amplitudes of, (T), 25:30805 (NP-18777)
decay K⁺ → π⁺ + γ + γ, CP violation in, 25:30928
interactions K⁺ + d → K⁰ + p + p, search for K⁰ → π⁺ + π⁻ + π⁰ decay from, (E), 25:30723
interactions K⁺ + K⁻, dispersion calculation of scattering amplitude and form factor for, 25:30865
interactions K⁺ + p → K + N + π at 4.6 GeV/c, cross sections for Δ, K*(891), and K*(1420) production in, (E), 25:30748
interactions K⁺ + p → K⁺ + p at high energies, eikonal model for, (T), 25:30893 (INR-P-1233)
interactions K⁺ + p → K*(890) + p at high energies, factorizable quark model for amplitude of, (T), 25:30879
interactions K⁺ + p at low energies, field-theoretic model of, 25:30886
interactions K⁺ + p → K⁺ + p + 2π⁺ + 2π⁻ at 4.97 GeV/c in hydrogen bubble chamber, π⁺ angular correlations and resonance production in, (E), 25:30745
interactions K⁺ + p, weak duality for slopes of angular distributions of elastic, 25:30873
mass difference (K⁺ - K⁰) consistency test using Cottingham formula and finite-energy sum rules for, 25:30800
production in γ + p → Λ(I⁰) + K⁺ interactions, review of coupling parameters for, (E/T), 25:30797
MESONS (μ)
interactions μ + N → ν + W + N, cross sections for scalar and vector W-meson production in, 25:30818
interactions of, universality principle for muon parity conservation in, (T), 25:30932
properties of, proposed experimental facility at Tokyo proton synchrotron for studying, 25:29371 (SJC-P-70-4)
MESONS (μ⁻)
capture by calcium-40, copper-64, sulfur-32, and silicon-28, charged-particle masses and energy spectra from, (E), 25:31267
capture by calcium-40, effect of Coulomb field in radiative, 25:31282
capture by helium-3, analysis using universal Fermi interaction and CVC theory, (T), 25:31190
interactions μ + e⁺, cross sections to order α^3 for, 25:30820
interactions μ⁻ + e⁻, radiative corrections to, 25:30820
reactions (μ⁻,xn) with scandium-45, manganese-55, cobalt-59, niobium-93, iodine-127, and bismuth-209, gamma spectra from, (E), 25:31258
reactions with nuclei in matter, (T), 25:31448
MESONS (μ⁺)
interactions μ⁻ + e⁺, radiative corrections to, 25:30820
interactions μ⁺ + e⁺, radiative corrections to, 25:30820
MESONS (ω)
theory as bound state of rho--π system, two-body Bethe--Salpeter amplitude for, 25:30858
MESONS (π)
coupling constant for AIπ, PCAC hypothesis for, (T), 25:30904
coupling constant for IIπ, PCAC hypothesis and SU(3) symmetry with pseudovector coupling for, (T), 25:30904
exchange in N + N interactions, local approximation to potential for, 25:30911
form factor for, functional and Breit--Wigner formula for analytical properties of, (T), 25:30864
form factor from unitarized Veneziano model, electromagnetic, 25:30860
interactions π + K in GeV range, low-energy models for, (T), 25:30854
interactions π + N at 385 to 1700 MeV/c, energy continuation of energy-independent phase shift analysis

XUM

for resonance-like structure in, (T), 25:30871 (UCRL-20250)
interactions π + N at very high energies, angular and energy distributions of particles produced in, (T), 25:30870(T) (ORNL-tr-2433)
interactions π + N in GeV range, low-energy models for, (T), 25:30854
interactions π + N, continuous-spin pole exchange for elastic, 25:30892
interactions π + N, cross sections for multiple soft-π production in, 25:30887
interactions π + N, exchange degeneracy in Reggeized absorption model for, 25:30874
interactions π + N, fixed-pole effects on exchange-degenerate Regge residues, 25:30878
interactions π + N, review of Coulomb corrections in analysis of, (E/T), 25:30721
interactions π + N, review of elastic, 25:30872
interactions π + N, Veneziano model with spin for amplitude of three-body hadron production in, (T), 25:30889
interactions π + p → p + 5π at 5 GeV/c, statistical model for asymmetry parameters for π pair angular distributions in, (T), 25:30880
interactions π + p → π + p, s-channel helicity conservation for diffraction part of, (T), 25:30885
interactions π + p, proton electromagnetic form factor for inelastic, (T), 25:30977
interactions π + π → π + π + m(π), relation between nonequilibrium shower model and soft-pion emission model for, 25:30857
interactions π + π → π + π, Veneziano amplitude for, 25:30855
interactions π + π at low energies, review of, (E/T), 25:30867
interactions π + π in GeV range, low-energy models for, (T), 25:30854
interactions π + π, axiomatic field theory for limits of strength of, (T), 25:30852
interactions π + π, existence of functions exactly satisfying crossing and unitarity subtractions for, (T), 25:30862
interactions π + π, properties of class of orthogonal polynomials for inequalities for partial waves of, (T), 25:30851 (SU-1206-240)
interactions π + π, review of analytic extrapolations and phase shifts for, (T), 25:30868
interactions π + π, scattering lengths and phase shifts for, 25:30856
interactions rho + π, dispersion calculation of scattering amplitude and form factor for, 25:30865
interactions rho + π, two-body Bethe--Salpeter amplitude for ω bound state of, 25:30858
interactions with nuclei, properties of optical potential for, (T), 25:31421
mass splitting (K - π), nontadpole contribution to, 25:30791
production in e + N interactions, vector meson dominance predictions for, (T), 25:30789
production in photon and rho resonance interactions with pomerons, model for, 25:30863
production in π⁺ + p interactions at 5 GeV/c, test of thermodynamic model in momentum distributions from, (E), 25:30746
production of hard, in N + N → N + N + π nonrelativistic interactions, dispersion relations and current--field algebra for, (T), 25:30898
production of soft, chiral-invariant Lagrangian for cross sections of multiple, 25:30887
radius of, functional and Breit--Wigner formula for upper limit of, (T), 25:30864
symmetry for, algebraic realization of chiral SU(2) X SU(2), (T), 25:30850 (JINR-P2-5759)

MESONS (π⁻)
capture by aluminum-27, carbon-12, and lithium-7, proton, deuteron, and triton spectra from, (E), 25:31213
capture by calcium, carbon, and oxygen, neutron spectra from radiative, (E), 25:31273
capture by calcium-40, carbon-12, oxygen-16, and zirconium-90, analysis using particle-hole model, (T), 25:31217
capture by oxygen-16 and silicon-28, neutron spectra from radiative, (E), 25:31216
capture by oxygen-16, rescattering effects in radiative, (T), 25:31217
interaction π⁻ + p → eta + n differential cross section from Veneziano amplitude for, 25:30884
interactions π⁻ + d, compilation of cross sections for, 25:30735 (CERN-HERA-70-7)
interactions π⁻ + n, compilation of cross sections for, 25:30735 (CERN-HERA-70-7)
interactions π⁻ + p → 2 π⁺ + 2π⁻ + n at 8 and 16 GeV/c, correlation effects in, (E), 25:30744
interactions π⁻ + p → 2π⁻ + π⁺ + p at 11 and 16 GeV/c, longitudinal phase space analysis of, (T), 25:30881
interactions π⁻ + p → A_2^- + p, analysis of A_2 production in, (E/T), 25:30877
interactions π⁻ + p → f⁰ + n at 15 and 16 GeV/c in heavy liquid bubble chamber, cross sections for, (E), 25:30741
interactions π⁻ + p → ω⁰ + n at 15 and 16 GeV/c in heavy liquid bubble chamber, cross sections for, (E), 25:30741
interactions π⁻ + p → π⁻ + p at high energies, eikonal model for, (T), 25:30893 (INR-P-1233)
interactions π⁻ + p → π⁻ + π⁺(π⁰) + n(p), quark model predictions for forward production of Δ(1236) in, (E/T), 25:30738
interactions π⁻ + p → rho⁰ + n at 15 d 16 GeV/c in heavy liquid bubble chamber, cross sections for, (E), 25:30741
interactions π⁻ + p at 16 and 60 GeV/c, inelastic charged multiplicities from, (E/T), 25:30739
interactions π⁻ + p at 4 GeV/c, phenomenological quasi-two-body model for strange particle product in, (T), 25:30869 (JINR-P1-5706)
interactions π⁻ + p at 8 GeV/c, Van Hove phase-space plots for analysis of single-particle production in, 25:30890
interactions π⁻ + p, compilation of cross sections for, 25:30735 (CERN-HERA-70-7)
interactions π⁻ + p, model-independent analysis of forward elastic, 25:30875
interactions π⁻ + p, weak duality for slopes of angular distributions of elastic, 25:30873
production in γ + n → p + π⁻ interactions, review of coupling parameters for, (E/T), 25:30797
production in K⁺ + p → K⁺ + p + 2π⁺ + 2π⁻ interactions at 4.97 GeV/c in hydrogen bubble chamber, angular correlations for, (E), 25:30745
production of π⁺--π⁻ pairs in π + p → p + 5π interactions at 5 GeV/c, statistical model for asymmetry parameters for angle distributions for, (T), 25:30880
reactions with nuclei at 15 and 16 GeV/c, cross sections for rho⁰, f⁰, ad ω⁰ production in, (E), 25:30741
reactions with nuclei at 17 GeV in emulsions, selection technique for coherent, (E), 25:30736 (JINR-P1-5565)

MESONS (π⁰)
production in γ + p → p + π⁰ interactions, review of coupling parameters for, (E/T), 25:30797

MESONS (π⁺)
interactions π⁺ + p → A_2^+ + p, analysis of A_2 production in, (E/T), 25:30877
interactions π⁺ + p → p + (K anti Kππ)⁺ at 8.04 GeV/c, evidence for K anti Kππ(2820) production in, (E/T), 25:30737
interactions π⁺ + p → π + π + N at 8 and 16 GeV/c, separation of isospin-1/2 and -3/2 contributions to, 25:30891
interactions π⁺ + p → π⁰ + missing mass, empirical relation of inelastic e + N interactions with, (T), 25:30795
interactions π⁺ + p → π⁺ + p at high energies, eikonal model for, (T), 25:30893 (INR-P-1233)
interactions π⁺ + p → π⁺ + π⁰(π⁺) + p(n) at 5 and 8 GeV/c, longitudinal phase plots for study of energy dependence of, (E), 25:30742
interactions π⁺ + p at 2.50 GeV/c, polarization at definite angle for determination of, 25:30888
interactions π⁺ + p at 5 GeV/c, isospin and longitudinal phase space analysis of, (T), 25:30881
interactions π⁺ + p at 5 GeV/c, test of thermodynamic model in momentum distributions of secondary π produced in, (E), 25:30746
interactions π⁺ + p at 6 GeV/c, polarization in backward elastic, (E), 25:30740
interactions π⁺ + p at 8 GeV/c, Van Hove phase-space plots for analysis of single-particle production in, 25:30890
interactions π⁺ + p, model-independent analysis of forward elastic, 25:30875
interactions π⁺ + p, weak duality for slopes of angular distributions of elastic, 25:30873
production in e + p → e' + π⁺ + n interactions, differential cross sections for, (E), 25:30718
production in e + p → e' + π⁺ + n interactions, longitudinal part of cross section for, (E/T), 25:30719
production in γ + p → n + π⁺ interactions, review of coupling parameters for, (E/T), 25:30797
production in K⁺ + p → K⁺ + p + 2π⁺ + 2π⁻ interactions at 4.97 GeV/c in hydrogen bubble chamber, angular correlations for, (E), 25:30745
production of π⁺--π⁻ pairs in π + p → p + 5π interactions at 5 GeV/c, statistical model for asymmetry parameters for angle distributions for, (T), 25:30880

MESONS (rho)
interactions rho + π, dispersion calculation of scattering amplitude and form factor for, 25:30865
interactions rho + π, two-body Bethe--Salpeter amplitude for ω bound state of, 25:30858
interactions with pomerons, model for 2π production in, 25:30863
production in γ + N → Δ + rho⁺(rho⁻) interactions, relation of electromagnetic moments of charged rho to, 25:30799
production in γ + n → p + rho⁻ interactions, relation of electromagnetic moments of charged rho to, 25:30799
symmetry for, algebraic realization of chiral SU(2) X SU(2), (T), 25:30850 (JINR-P2-5759)

MESONS (X⁰)
parity and spin of, 25:30833

MESONS, RESONANCE
coupling of sigmaππ from scale and chiral symmetry, 25:30933
coupling to nucleons from on- and off-shell methods for n + p → n + p and p + p → p + p interactions below 750 MeV/c, (T), 25:30903
decay of, lifetime difference determination from interference phenomena in system of two resonances in, (T), 25:30848 (JINR-P1-5668)
decay of, width determination from resonance interferometry of, (T), 25:30847 (JINR-P1-5666)
lifetime difference determination from decay of, interference phenomena in system of two resonances for, (T), 25:30848 (JINR-P1-5668)
mass structure of A_2, model for, (T), 25:30751 (IS-T-426)
production of A_2 in π + p interactions, f^0--A_2 interference in, (E/T), 25:30877
production of ABC and 450 MeV structure in d + p interactions at 3.25 to 3.76 GeV/c, 25:30734
production of K anti Kππ(2820), and $π^+$ + p interactions at 8.04 GeV/c, (E/T), 25:30737
production of K*(891) and K*(1420) in K^+ + p → K + N + π interactions at 4.6 GeV/c, (E), 25:30748
production of K^{0*} (890) in K^+ + p → K^+ + p + $2π^+$ + $2π^-$ interactions at 4.97 GeV/c in hydrogen bubble chamber, (E), 25:30745
production of K^{0*} simultaneously with N^{*++} in K^+ + p → K^+ + p + $2π^+$ + $2π^-$ interactions at 4.97 GeV/c in hydrogen bubble chamber, (E), 25:30745
spectroscopy of, review of, 25:30853
splitting of A_2, mechanism for, 25:30859
symmetry for A_1 and sigma, algebraic realization of chiral SU(2) X SU(2), (T), 25:30850 (JINR-P2-5759)
width from decay resonance interferometry of, (T), 25:30847 (JINR-P1-5666)
widths of K(1420) and Q, Fourier algorithm for determination of Breit--Wigner, (T), 25:30849 (JINR-P2-5659)
METALLURGICAL EQUIPMENT
design for removing oxides from liquid metals, 25:29800(P)
METALS
abundance in Am stars, (E/T), 25:30038
analysis of liquid, for oxygen, apparatus for, 25:29407(P)
book: Achievement of High Fatigue Resistance in Metals and Alloys, 25:29840
determination of heavy, in phosphorus-32 preparations, ASTM method for, 25:29002
determination of heavy, in radioisotope mixtures, ASTM method for, 25:29005
electron--phonon and --impurity scattering in impure, deviations from additivity in theory of, 25:30697 (NP-18822)
Fermi surfaces of d-block and f-block, review, 25:30681
neutron scattering in liquid, ion-electron model for thermal, (T), 25:31176
oxide removal from liquid, design of equipment for, 25:29800(P)
radiation effects on microstructure of, alpha particle, electron, and neutron, 25:29909
welding of, effects of starting parameters on ripple formation in explosive, 25:31736(T) (SCL-T-710240)
METARAMINOL
norepinephrine, radioprotective effects of, on beagle dog hearts, lethal, whole-body mixed γ and neutron, 25:29565
METEORITES
antimatter in, as source of ball lightning, (T), 25:30329
carbon isotopes in, (E), 25:30158(R) (UCSD-34-P-43-X-9)
classification of chondrites, 25:30158(R) (UCSD-34-P-43-X-9)
cosmic-ray exposure ages from krypton-81 abundance, (E), 25:30158(R) (UCSD-34-P-43-X-9)
cosmic-ray induced radioactivities in stone, determination of cosmic-ray modulation regions from, (E/T), 25:30323
diamonds in, (E), 25:30158(R) (UCSD-34-P-43-X-9)
gadolinium isotopes in, (E), 25:30158(R) (UCSD-34-P-43-X-9)
isotopic ratios in, argon, helium, and neon, (E), 25:30034
mass spectroscopy of, (E), 25:30248(R) (UCB-34-P-32-PR-5)
particle tracks in, due to primary cosmic nuclei with Z greater than or equal to 25, (E), 25:30317
rare gases in iron, cosmogenic, (E), 25:30158(R) (UCSD-34-P-43-X-9)
xenon isotopes in Pesyanoe, (E), 25:30158(R) (UCSD-34-P-43-X-9)
METEOROIDS
detection near earth, flux of, 25:30361
METEOROLOGY
weather parameters, solar cycle effects on, (E), 25:30162
METHACRYLIC ACID, METHYL ESTER
radioinduced polymerization of solid, ESR studies on effects of uv radiation on γ, 25:29117
acrylonitrile--methyl methacrylate, radioinduced polymerization on polymers, γ, 25:29106
methyl methacrylate--styrene, radioinduced polymerization on polymers, γ, 25:29106
METHACRYLIC ACID, METHYL ESTER, POLYMERS
performance as artifical substrate for analysis of periphyton component of running-water ecosystems, 25:29478
radiation effects on, mechanisms of formation of tree-shaped cracks from electron, 25:29100
radioinduced polymerization of monomer pairs on, γ, 25:29106
METHANE
alpha-particle stopping cross sections in gaseous, test of Bragg's rule for, 25:30642
electron reactions at 600 keV with, radiative lifetimes of excited products from, (E), 25:30273(T) (ANL-Trans-879)
ion reactions with, binary-encounter calculation of ionization cross sections for, 25:30299
radiation effects on electric conductivity of liquid, pulsed x, 25:29102
METHANE, IODO-
sorption by activated carbon at high temperatures and pressures, (E), 25:31611
sorption by activated carbon at high temperatures, (E), 25:31612
METHANESULFONIC ACID
effects on induction of chlorophyll mutations in, comparison of γ and neutron radiation and, 25:29481 (IAEA-R-290-F)
METHANOL
corrosive effects of halogen- and nonhalogen-containing solutions of, on aluminum--molybdenum--titanium--vanadium alloy, 25:29765
radioinduced thermoluminescence of crystalline and glassy, effects of benzene, carbon tetrachloride, oxygen, and water on γ, 25:29101
radiolysis of glasses of, at 4 to 77°K, ESR studies on trapped electrons produced by γ, 25:29156
HCl--methanol, corrosive effects on aluminum--titanium--vanadium alloy, 25:29773
METHIONINE ADENOSYLTRANSFERASE
radiation effects on activity of, in rat liver, effects of ethionine on lethal x, 25:29663
METHYL ISOCYANIDE
reactions with recoil tritium atoms, isomerization reaction mechanisms of, 25:29167
METHYL SULFOXIDE
radioprotective effects on cornea and lens of eyes in mice, 25:29562
MICE
antimony-124 distribution and retention in, following inhalation of heat treated aerosols, 25:29424 (LF-43, pp 65-70)
cystamine distribution in intestines and kidneys of, effects of 5-methoxytryptamine on, 25:29554
cystamine excretion in urine of, effects of 5-methoxytryptamine on, 25:29554
immune reactions to infection by x-irradiated Plasmodium berghei sporozoites, 25:29727
iridium-192 metabolism in, following intraperitoneal, intravenous, and oral administration, 25:29450
oxygen pressure in spleen of, comparison of effects of radioprotective sympathomimetics on, 25:29547
radiation dose distribution in tissues of normal or tumor bearing, following administration of phosphorus-32-labeled chromium alloxantin or orthophosphate, 25:29453
radiation effects on all populations of bone marrow in, use of electronic particle counter for evaluating, 25:29648
radiation effects on antigen-initiated RNA synthesis in spleen of, polyacrylamide gel electrophoresis studies on, 25:29476
radiation effects on blood vessels in testes of, x, 25:29653
radiation effects on content of immunoglobulins in intestinal lumen and serum of, x, 25:29473
radiation effects on cornea and lens of eyes of, protective effects of dimethyl sulfoxide against x, 25:29562
radiation effects on hematogenic tissue in bone marrow of, mechanisms of, 25:29676
radiation effects on hematopoietic system of, effects of dose and dose rate on x, 25:29634
radiation effects on immune responses in, comparison of mechanism of cyclophosphamide and x, 25:29475
radiation effects on immune responses in, effects of strain on x, 25:29472
radiation effects on melanoma cells in, protective effects of melanin against x, 25:29568
radiation effects on muscles and spleen of, effects of increased atmospheric pressure on protective effects of AET, cystamine, cystaphos, and mexamine against γ, 25:29550
radiation effects on pathomorphology of brain of, γ, mixed γ--neutron, and proton, 25:29644
radiation effects on permeability of mitochondrial membrane of, to manganese-54 mechanisms for, 25:29673
radiation effects on spermatogonia in, mutagenic fast neutron and x, 25:29487
radiation effects on survival of, protective effects of

XUM

acetylcholine and adrenalin against γ, 25:29548
radiation effects on survival of, protective effects of chlortetracycline against x, 25:29561
radiation effects on susceptibility of, to influenza virus infection following inhalation of insoluble cerium-144, β, 25:29724 (LF-43, pp 254-62)
radiation effects on synchronized skin tumors in, combined effects of 5-fluorouracil and, 25:29605
radiation effects on testicular weight and tail growth in, combined effects of actinomycin C on, 25:29604
radiation effects on, protective effect of sulfur analogs of serotonin and tryptophol against, 25:29567
radiation effects on, protective effects of o-acyl derivatives of serotonin against, 25:29555
radiation effects on, protective effects of spleen cell transplants from irradiated donors against lethal γ, 25:29564
radioinduced injuries in gastrointestinal tract of, dynamics of recovery following γ, 25:29657
radioisotope distribution and retention in, following inhalation of heat treated aerosols, 25:29423 (LF-43, pp 59-65)
radioisotope distribution and retention in, following inhalation, in fused clay particles, model for insoluble, 25:29422 (LF-43, pp 53-8)
radiosensitivity of hemopoietic and immunocompetent cells in spleen of, effects of dose on, 25:29677
radiosensitivity of, protective effects of AET, anoxia, cysteamine, and cysteine on biochemical properties correlated with, 25:29553

MICHIGAN, LAKE
thermal plume dispersion in, (E/T), 25:31533(R) (ANL-7798)

MICROWAVE EQUIPMENT
description of, using proximity effect between superconducting and normal metals, 25:30446

MICROWAVES
absorption by plasma, effect of external dc electric fields on, (T), 25:30628
cosmic background, fluctuations as results of Thomson scattering by moving intergalactic matter, (T), 25:30236
cosmic background, isotropy at 8 mm, (E), 25:30228
cosmic background, origin of, (T), 25:30221
emission of 3.5-mm, from IRC + 10216, (E), 25:30090
emission of 3.5-mm, from VY CMa and IRC + 10216, (E), 25:30089
interactions with plasma, third harmonic generation in, (T), 25:30609
use for electron temperature measurement in contracted argon columns, 25:30486
use for plasma jet diagnostics, electron density and collision frequency, (E), 25:30476 (N-71-10964)

MILK
iodine-131 content of cow, following fallout deposition, effects of feeding practices on, 25:29505 (SWRHL-39-r)
radiation monitoring of off-site, following nuclear explosions at Nevada Test Site during 1969, 25:29506 (SWRHL-97-r)
radioactivity monitoring, West Valley Processing Plant, 1970, 25:29179 (DOCKET-50201-69)
radioisotope content of fresh and powdered, in Italy during 1952 to 1966, fallout cesium-137 and strontium-90, 25:29507

MILKY WAY
angular momentum in, (T), 25:30202
arms of, number of, (E/T), 25:30190
calcium abundance in Norma arm of, (E), 25:30193
charge transfer and ionization equilibrium in interstellar medium, (T), 25:30211
electromagnetic-wave propagation in, (T), 25:30220 (P-4494(RAND))
electron densities in interstellar space from pulsar dispersions, (T), 25:30118
evolution of, chemical, (T), 25:30036(R) (NYO-3962-3)
H II region diameters in, (E), 25:30203
hydrogen distribution in anticenter region of, neutral, (E), 25:30142
hydrogen kinematics in anticenter region, neutral, (E), 25:30143
morphological type for, (E), 25:30203
properties of interstellar medium in, (E), 25:30138
stellar extinction curves in, (E), 25:30212
structure of, gravitational theory of spiral, (T), 25:30215
structure of, in three sections in anticenter direction, (E), 25:30191
x-ray background in plane of, (E), 25:30134

MILLSTONE POINT POWER REACTOR, UNIT 1
site for, preoperational environmental radiation survey program for, 25:31491 (DOCKET-50245-64)

MINERALS
analysis for ruthenium and osmium, spectrophotometric, 25:28960

MINES
aerosols in air of uranium, size distribution of radioactive, (E), 25:29200(T) (AEC-tr-7227)
radon and radon decay products in French uranium, methods for measuring, 25:29201(T) (AEC-tr-7228)

MITOCHONDRIA
radiation effects on cadaverine deaminase activity and deamination of serotonin and tyramine in rat liver, 25:29641
radiation effects on oxidative phosphorylation and respiration in rat liver, effects of riboflavin on, 25:29640
radiation effects on oxidative phosphorylation in animal liver, effects of histones on, 25:29638
radiation effects on permeability of membranes of rat liver, to manganese-54, mechanisms of, 25:29673
radiation effects on protein fractions of, in brain and small intestine in rabbits, x, 25:29664

MITOSIS
radiation effects on frequency of, in pea seedlings, effects of dose on, 25:29484
radiation effects on L-cell, fractionated x, 25:29611
radiosensitivity of pike roe during, 25:29659

MIXERS
design and operation of, for uniform blending of dissimilar dry particles, 25:29254(P)

MOESSBAUER EFFECT
book: Chemical Consequences of Nuclear Spin, 25:30669
gamma emission by nuclei in crystals, thickness dependence of, (T), 25:30690
inelastic channel disappearance in nuclear reaction of gamma resonant scattering in perfect tin-119 single crystal, 25:30687 (IAE-1966)
spectra resolution, computer program for, 25:30688 (RISO-M-1348)

MOESSBAUER SPECTROMETERS
design of velocity-stabilized, 25:29360
design using photomultiplier in current mode, 25:29361

MOISTURE GAGES
performance of concrete, using electric conductivity measurements, 25:30026 (EUR-4531, pp 409-16)

MOLECULAR BEAMS
production and properties of, at high pressure and temperature, 25:30258

MOLECULES
abundance in interstellar space, (T), 25:30128
atom reactions with diatomic, comparison of classical, semiclassical, and quantum treatments of, 25:30292
atom reactions with diatomic, semiclassical treatment in three dimensions, 25:30290
atom reactions with diatomic, strong-coupling approximation for rotational excitation in, 25:30296
atom reactions with diatomic, vibrational excitation in near-classical limit for, (T), 25:30295
formation in interstellar space, (E), 25:30138
formation in interstellar space, (T), 25:30128
ion reactions with, binary-encounter calculation of ionization cross sections for, 25:30299
orientational freedom in alkali-metal halides, (E), 25:30646(R) (NYO-2150-66)
spectroscopy of interstellar, (E), 25:30138
spectroscopy of interstellar, (E/T), 25:30200
vibrational potential functions of, method for choosing coordinates for calculating, 25:31696 (IN-1421)
wave functions for, use of dynamic orbitals in calculation of collisional charge-exchange probabilities, 25:30275 (JAERI-Memo-4299)

MOLLUSCA
Physa sp., strontium-90 distribution in body and shell of, effects of sorption from food or water source on, 25:29440
Unio mancus, cobalt-60 uptake and excretion by, in Lake Maggiore, concentration factors for, 25:29441

MOLTEN SALT BREEDER REACTOR
control system for 1000 MW(e) single fluid, analog computer simulation of, 25:31544 (ORNL-TM-3102)

MOLYBDATES
complexes with silicon, effects of various acids and salts on formation of, 25:28924

MOLYBDENUM
book: Creep-Rupture Data for the Refractory Metals to High Temperatures, 25:29868
brittleness of, effects of interstitial impurities on intergranular, 25:29855
complexes with DTPA and TTHA, potentiometric titration studies on stability constants of, 25:28920
content and distribution in ocean sediments from Mid-Atlantic Ridge, measurement of, 25:29228
deposition from ground waters to near-surface uranium deposits, effects of ground water and soil conditions on, 25:29240
deposition on substrates from alkaline fluoride mixtures containing salts of, methods for electro-, 25:29783 (CEA-N-1376)
determination as complex with diantipyryl hydrochloride and pyrochatechol, photometric, 25:28926
determination as thioglycollate complex by solvent extraction using trioctylamine and colorimetry, 25:28930
determination in low-alloy steel, two-standard method for spectrometric, 25:28950
determination in niobium photometrically using dithiol, 25:28973
determination in plutonium by absorption spectrophotometry and spectrography, 25:28916 (CEA-R-4071)
determination of trace amounts of, in fish and other biological materials by neutron activation and

XUM

radiochemical separation, 25:29019
determination of trace amounts of, in seawater, review on methods for, 25:28921
determination of trace amounts of, in vanadium, spectrographic, 25:28947
ductility of, effects of carbon on, 25:29863
effects of additions of, on stability of uranium dioxide fuels, 25:29932(P)
effects on corrosion of nickel alloys by vanadium pentoxide melts, 25:29768
effects on determination of uranium by controlled-potential coulometry, 25:28975
effects on fluorometric determination of zirconium, 25:28963
electromigration in nickel--molybdenum alloy at 900 to 1350°C, 25:29856
enthalpy of solid, at 2094 to 2869°K, drop calorimetry with electromagnetic levitation method for measurement of, 25:29875
flow stress of polycrystalline, effects of hydrostatic pressure on, 25:29833
neutron elastic and inelastic scattering at 1.0 to 5.0 MeV, differential cross sections and excitation functions for, (E), 25:31299 (AWRE-O-89/70)
production and uses of, review on, 25:29805
properties of aerosols produced from aqueous solutions of, 25:29079 (LF-43, pp 31-9)
radiation effects on microstructure of, fast neutron, 25:29904 (ORNL-4630, pp 73-95)
radiation effects on void formation in, relations of irradiation temperature with fast neutron, 25:29914
separation from aqueous solutions by thin-layer chromatography using liquid anion exchangers, 25:29186
separation from rhenium and selenium as molybdate on silica gel chromatographs, 25:28953
temperature distribution in electron beam-melted plates of, 25:29842
vacancy formation energy and content in, from enthalpy and specific heat measurements at 1000 to 2850°K, 25:29858
welding for fabrication of corrosion loops, 25:29824 (ORNL-4630, pp 191-206)
welding to TZM alloy, mechanisms of cracking during, 25:29824 (ORNL-4630, pp 191-206)

MOLYBDENUM ALLOYS AND SYSTEMS
analysis for rhenium, chromatographic, 25:28953
book: Creep-Rupture Data for the Refractory Metals to High Temperatures, 25:29868
book: Special Steels and Alloys (In Russian), 25:29862
corrosion by iodine and mineral acids, effects of pressure and temperature on, 25:29776
effects on hardness and microstructure of chromium--nickel alloys at 27 and 740°C, 25:29839
mechanical properties to 2400°C, 25:29864
Al--Mo--Ti-base--V, corrosion cracking in aqueous and methanol solutions with and without halogen ions, stress, 25:29765
Cr--Mo--Ni, corrosion by hydrochloric and sulfuric acids, effects of chromium and molybdenum on, 25:29777
Cr--Mo--steel, properties at high temperatures, ductile and tensile, 25:29822 (ORNL-4630, pp 139-44)
Cr--Mo--steel--U, creep fatigue of, method for prediction of, 25:29826 (RD/B/N-1889)
Cr-base--Fe--Mo, thermal capacity of Cr/sub 3-x/Fe/sub x/Mo at 1.3 to 4.2°K, 25:30676
Cu--Mo--Zr-base, corrosion by carbon dioxide at 500 to 650°C, 25:29770
Fe--Mo--Ni-base, properties of 2-81 permalloy, effects of heat treatments in production process on magnetic and tensile, 25:30672
Mo--Ni-base, electromigration of molybdenum in, at 950 to 1350°C, 25:29856
Mo--Pt-base, tensile properties at 25 to 1093°C, 25:29823 (ORNL-4630, pp 186-90)
Mo--Pt-base--Ti, tensile properties at 25 to 1290°C, 25:29823 (ORNL-4630, pp 186-90)
Mo--Re, radiation effects on microstructure of, fast neutron, 25:29904 (ORNL-4630, pp 73-95)
Mo--Re--W, fabrication of irradiation capsules of, welding methods for, 25:30010 (ORNL-4630, pp 179-85)
Mo--UO_2, radiation effects on mechanical properties of cermets of, fast neutron, 25:31568(T) (EURFNR-823)
Mo--UO_2, separation of fission products from irradiated fuels of, 25:29413 (CONF-691225)
Mo--V-base, compatibility with sodium at 600°C, effects of oxygen on, 25:29761 (ORNL-4630, pp 150-7)
Mo--W--Zr, mechanical properties at 2100°C, 25:29864
Mo--Zr-base, corrosion by carbon dioxide at 500 to 650°C, 25:29770
Mo-base--Re, hardness at 77 to 576°K, effects of rhenium content on, 25:29871
Mo-base--Re, mechanical properties of monocrystalline, asymmetric, 25:29829
Mo-base--Ti, radiation effects on microstructure of, fast neutron, 25:29904 (ORNL-4630, pp 73-95)

MOLYBDENUM FLUORIDES
equations of state for, at 40 to 190°C, 25:29073 (CEA-N-1414)

MOLYBDENUM ISOTOPES Mo-92
energy level at 2.761 MeV, nuclear magnetic moment of, (E), 25:31349
energy levels at 1509, 2848, and 3089 keV from alpha inelastic scattering, lifetimes of, (E), 25:31377
energy levels from zirconium-90 (α,2n) reactions, lifetimes and electromagnetic matrix elements for, (E), 25:31372
energy levels of, lifetimes of low-lying, (E), 25:31349

MOLYBDENUM ISOTOPES Mo-95
proton reactions (p,n) at 3.5 to 4.4 MeV, angular distributions for, (E), 25:31381

MOLYBDENUM ISOTOPES Mo-97
proton reactions (p,n) at 3.5 to 4.4 MeV, angular distributions for, (E), 25:31381

MOLYBDENUM ISOTOPES Mo-99
metabolism in beagle dogs following ingestion of nuclear debris from Project Cabriolet, 25:29456

MOLYBDENUM ISOTOPES Mo-100
neutron activation resonance integrals for, measured relative to gold-197, (E), 25:31300 (CNEA-282)

MOLYBDENUM ORES
analysis of concentrates of, for rhenium, direct spectroscopic, 25:28945

MOLYBDENUM OXIDES
thermodynamic properties of gaseous diatomic, free energy functions for, 25:29082

MOLYBDENUM SELENIDES
properties of polyimide-bonded, as solid film lubricants, 25:29096 (WERL-HFIL-1)

MONKEYS
iridium-192 metabolism in, following intraperitoneal, intravenous, and oral administration, 25:29450

MONOSACCHARIDES
radiolysis of aqueous ices of, at 77°K, spectral studies on trapped electrons and sugar radicals produced by γ, 25:29153

MONTE CARLO METHOD
variance estimation in, methods for, (T), 25:30698 (CEA-N-1096)
weighting in, applications of method for, (T), 25:31164 (CEA-N-825)

MONTICELLO POWER REACTOR, UNIT 1
cooling system for, design report for recirculation, 25:31495 (DOCKET-50263-63)
cooling system for, modifications for venting trapped gases in high points of, 25:31497 (DOCKET-50263-65)
operations incident of April 20, 1971, incorrect piping connections for air ejector off-gas system radiation monitors, 25:31477 (DOCKET-50263-69)
operations incident of April 22, 1971, cooling system safety relief valves setpoints above 1080 psig, 25:31476 (DOCKET-50263-66)
operations incident of April 22, 1971, extended maintenance for high pressure coolant injection system, 25:31475 (DOCKET-50263-67)
personnel for, revised protection factors for respiratory equipment for, 25:31498 (DOCKET-50263-66)
piping systems for, stress analysis for, 25:31496 (DOCKET-50263-64)

MONZONITES
thorium content of Berea area, Va. quartz, correlation with aeroradioactivity measurements, 25:29235
uranium content of Berea area, Va. quartz, correlation with aeroradioactivity measurements, 25:29235

MOON
cavity creation on antisolar side of, solar wind-lunar limb interaction-produced, (E/T), 25:30388

MORTARS
radiation effects on tensile properties of, relations of temperature with neutron, 25:30021 (EUR-4531, pp 179-83)
radiation effects on, equipment and methods for studies of in-pile, 25:30020 (EUR-4531, pp 171-8)

MUSCLES
cesium-137 distribution and retention in beagle dog, following inhalation on fused clay particles, 25:29426 (LF-43, pp 79-81)
radiation dose to, in normal and tumor-bearing mice following administration of phosphorus-32-labeled chromium alloxantin and orthophosphate, 25:29453
radiation effects on bioelectric activity of, protective effects of AET and cystamine against, x, 25:29609
radiation effects on initiation of unscheduled DNA synthesis in differentiating cells of chick embryo, in vitro uv, 25:29650
radiation effects on sartorius, in frogs in relation to calcium metabolism, x, 25:29674
radioisotope content of fish, 25:29449
radiosensitivity of rat striated, x, 25:29629

MUTATIONS
radioinduced chlorophyll, in rice, effects of dose on γ and neutron, 25:29481 (IAEA-R-290-F)
radioinduced dominant lethal, in insects, role in eradication by sterile male technique, 25:29736
radioinduced sex-linked, lethal, and visible, in Drosophila sperm, comparison of fast neutron and x, 25:29499
radioinduced, in alfalfa for early flowering and improved vigor, γ, 25:29488
radioinduced, in mouse spermatogonia, fast neutron and x, 25:29487
radioinduced, in pea seeds, cytology of male sterile recessive x, 25:29492
radioinduced, in rice seeds for studies on M(2)

XUM

generation, combined effects of diethyl sulfate and x, 25:29495
radioinduced, in tomato seeds, M(2) characteristics following combined effects of colchicine or diethyl sulfate and x, 25:29493
radioinduced, in X-virus in potato tubers, virulence of γ, 25:29726
rates and loads in man, research progress on, 25:31708(R) (NYO-2280-32)
MZFR (SIEMENS REACTOR)
maintenance of, freeze blocking of tubes in, (E), 25:31537
moderator tubes in, freeze blocking of, (E), 25:31537

N

NAGASAKI
leukemia incidence in human population exposed to atomic bombing of, 25:29696
NAILS
analysis for sodium in human children as indicator of cystic fibrosis by neutron activation, 25:29016
NAPHTHALENE
radiolysis of rigid matrices of methylcyclohexane containing, deferred luminescence spectra following γ, 25:29150
radiolysis of solutions of, in glassy and polycrystalline solvents, deferred luminescence technique for obtaining stimulation spectra following γ and uv, 25:29133
NAPHTHALENE, 1-(CHLOROMETHYL)-8-METHYL-
neutron cross sections for, effects on analysis of plutonium lattice experiments of various, (E/T), 25:31661
NATURAL BACKGROUND RADIATION
content in atmosphere to 15 m height, effects of thermal stratification and wind velocity on, 25:29223
measurement of gamma, in Italian environment, 25:29205
NATURAL GAS
production stimulation by Project Rulison, public safety aspects of, 25:29248
NATURAL WATERS
flow tracing of, using activable metal chelates and neutron activation analysis, 25:29013 (RLO-1756-81)
radioactivity monitoring, West Valley Processing Plant, 1970, 25:29179 (DOCKET-50201-69)
NEBULAE
colors in reflection, (E), 25:30053
dust density in reflection, (E/T), 25:30054
hydrogen abundance in NGC 604, neutral and ionized, (E), 25:30153
light polarization in reflection, (E), 25:30053
spectra of pure hydrogen, Balmer decrement in, (T), 25:30101
x-ray emission from Cygnus Loop, interpretation of, (E), 25:30132
NEMATODA
content of periphyton component of running-water ecosystem, performance of artificial substrates for determining, 25:29478
NEODYMIUM
catalytic properties of, in high-temperature para-ortho conversion reaction, 25:29859
determination in bauxite, selection of line pairs for spectroscopic, 25:28946
determination in lanthanum by emission spectrography, 25:28965
reactions with rare earth carbides, thermodynamics of, 25:29039
separation from other rare earths by ion exchange, 25:29178 (CEA-R-4102)
NEODYMIUM BROMIDES
thermodynamic properties at 298 to 1300°K, 25:29951
NEODYMIUM CARBIDES
catalytic properties of, in high-temperature para-ortho conversion reaction, 25:29859
reactions with rare earths, thermodynamics of, 25:29039
NEODYMIUM HYDRIDES
catalytic properties of, in high-temperature para-ortho conversion reaction, 25:29859
NEODYMIUM IODIDES
thermodynamic properties at 298 to 1300°K, 25:29951
NEODYMIUM ISOTOPES
separation of fission-product, from irradiated fuels of Mo--UO_2, 25:29413 (CONF-691225)
NEODYMIUM ISOTOPES Nd-142
energy-level scheme from promethium-142 decay, (E), 25:31337
NEODYMIUM ISOTOPES Nd-148
determination in plutonium or uranium fuels as measure of burnup by chemical separation and mass spectrometry, ASTM method for, 25:28979
NEODYMIUM OXIDES
catalytic properties of, in high-temperature para-ortho conversion reaction, 25:29859
NdO--NpO_2, phase equilibria in nonstoichiometric, at 1250°C, 25:29977 (KFK-1330)
positron lifetimes in, 25:30272
Nd_2O_3--Sc_2O_3, phase diagram of, 25:30005
NdO--UO_2--UO_3, phase equilibria at 1250°C in, 25:29977 (KFK-1330)
NEON
hydrogen-metastable-atom reactions at 1.0 keV to 1.6 MeV with, Born-wave calculations of total quenching cross sections for, 25:30283
isotopic composition of, spectral determination of, (E), 25:28952
plasma of, effect of step ionization on ion distribution function for low-pressure, (T), 25:30525
reactions with argon, krypton, and xenon of metastable atoms of, two-state impact-parameter model for associative and Penning ionization in, 25:30298
NEON ISOTOPES
abundance in meteorites, (E), 25:30034
separation by mass-diffusion mercury columns, equipment and method for, 25:29277
NEON ISOTOPES Ne-19
production in stars by explosive nucleosynthesis in helium zones, (T), 25:30067
NEON ISOTOPES Ne-20
energy levels from neon-22 (p,t) reactions, spins, parities, and angular momenta of, (E), 25:31296
energy levels of, mechanism for extending the rotational band in, (T), 25:31255
NEON ISOTOPES Ne-21
production in stars by explosive nucleosynthesis in helium zones, (T), 25:30067
NEON ISOTOPES Ne-22
energy levels from sodium-23 (d,He-3) reactions, l-transfer, spectroscopic factors, and spin--parity assignments for, (E/T), 25:31240 (NP-18511)
production in stars by explosive nucleosynthesis in helium zones, (T), 25:30067
proton elastic and inelastic scattering at 2.4 to 3.2 MeV, angular distributions, excitation functions, and spectra from, (E), 25:31281
proton reactions (p,t) at 26.9 to 42.4 MeV, angular distributions for, (E), 25:31296
NEPTUNIUM
oxidation by aqueous nitric acid solutions in presence of nitrous acid, 25:29038
NEPTUNIUM ALLOYS AND SYSTEMS
Np--Sb, crystal structure of NpSb, 25:30002
Np--Se, crystal structure of Np_3Se_4, 25:30002
Np--Te, crystal structure of Np_3Te_4, 25:30002
NEPTUNIUM IONS
desorption from rhenium surfaces, energy and residence time of, 25:30259
NEPTUNIUM ISOTOPES
radioactivity standards of, users' guides for, 25:29174
NEPTUNIUM ISOTOPES Np-235
energy levels of, superfluid-model calculations of energies and wave functions of nonrotational, (T), 25:31306 (JINR-P4-5693)
NEPTUNIUM ISOTOPES Np-237
deposition on rubidium uranyl nitrate single crystals, 25:29034 (AERE-R-6141)
proton fission at 10 MeV to 29 GeV, cross section for, 25:31326
NEPTUNIUM ISOTOPES Np-239
energy levels of, superfluid-model calculations of energies and wave functions of nonrotational, (T), 25:31306 (JINR-P4-5693)
NEPTUNIUM OXIDES
NdO--NpO_2, phase equilibria in nonstoichiometric, at 1250°C, 25:29977 (KFK-1330)
NERVES
radiation effects on bioelectric activity of, protective effects of AET and cystamine against, x, 25:29609
NERVOUS SYSTEM
book: Cellular Dynamics of the Neuron, 25:31760
conference on cellular dynamics in, 25:31760
development of presynaptic elements in, of x-irradiated neonatal cats, 25:29623
differentiation of synaptic structures in, under conditions of deprivation of function and of distant connections, 25:29623
radiation dose to, in normal and tumor-bearing mice following administration of phosphorus-32-labeled chromium alloxantin and orthophosphate, 25:29453
radiation effects on human, following therapy for thyroid cancer, combined iodine-131 and teletherapy, 25:29707
radiation effects on human, x, 25:29692
NEUTRINOS
emission from white dwarfs and neutron stars, (T), 25:30081
energy spectra of solar, verification of oscillation hypothesis from, (E/T), 25:30802(T) (BNL-tr-418)
flux of solar, verification of oscillation hypothesis from, (E/T), 25:30802(T) (BNL-tr-418)
form factor of, method based on cross sections of electron and neutrino reactions with nuclei for determining electromagnetic, (E/T), 25:30777 (JINR-P2-5705)
interactions $\nu + N \rightarrow \mu + W + N$, cross sections for scalar and vector W-meson production in, 25:30818
interactions $\nu + N$ at high energies in freon and propane, duality--parton model for deep inelastic, (T), 25:30809
interactions $\nu + N$, absence of form factor in e^2 corrections to amplitudes of, 25:30819
oscillation parameters of, solar neutrino energy spectra and flux for verification of hypothesis for, (E/T),

25:30802(T) (BNL-tr-418)
reactions (ν,f) with nuclei at 100 MeV, determination of neutrino electromagnetic form factor from cross section for, (E/T), 25:30777 (JINR-P2-5705)
reactions with nuclei at 100 MeV, determination of neutrino electromagnetic form factor from cross section for giant resonance excitation in, (E/T), 25:30777 (JINR-P2-5705)
scattering by linearized Schwarzschild metric, (T), 25:30242
NEUTRINOS (ANTI ν)
scattering by linearized Schwarzschild metric, (T), 25:30242
NEUTRON CHOPPERS
design and performance for range from 10^{-4} to 10 eV, 25:31182
NEUTRON CROSS SECTIONS
calculations for fast neutron spectra in iron assemblies, comparison of data sets for, (E/T), 25:31658
data sets of, interpolation schemes for structure factors for, 25:31647 (HEDL-TME-71-40)
measurements of differential, computer program for calculating multiple scattering and sample attenuation in, (E), 25:31172 (NBS-TN-499)
multigroup constants for (n,γ), for fission products, (E), 25:31304 (JAERI-Memo-4251)
NEUTRON DIFFRACTOMETERS
control system for, semiautomatic, 25:29402
NEUTRON SOURCES
design for producing polarized thermal neutrons, (E), 25:31180
design of accelerator--target T(d,n) pulsed, 25:31178
development of high-intensity 2-, 24.5-, and 144-keV, using thick scandium, iron, and silicon filters in reactor beam holes, 25:31166 (CONF-710301-8)
development of intense pulsed, for simulating nuclear explosions for studying transient radiation effects on electronics, 25:29410
intensity estimations for (p,n) and (d,n) type, for biological and medical applications, 25:31174 (UCRL-19715)
performance of portable californium-252, for radiography, 25:29286 (BNWL-1329)
performance of T(d,n), used in operation HENRE, (E), 25:31165 (CEX-65.04)
use of dense plasma focus, for fusion blanket studies, 25:30592 (EUR-4593, pp 525-31)
NEUTRON SPECTROMETERS
design of time-of-flight, for neutron inelastic scattering studies, 25:29362
operation of time bunching, using bent rotating crystal, 25:29359
NEUTRON STARS
formation in close-binary systems, (T), 25:30099
matter accretion by, in nuclei of galaxies and quasars, (T), 25:30247
model for, oblique-rotator, (T), 25:30052
models of, including effects of hyperon formation, (T), 25:30080
neutrino luminosity by URCA process in intense magnetic fields of, (T), 25:30081
properties and origin of, (T), 25:30127
proton--proton interactions in, (T), 25:30050
radiation emission mechanism for, (T), 25:30149
NEUTRONS
angular distribution at ground-level and mountain altitudes of atmospheric, from 80 to 300 MeV, (E), 25:30374
attenuation in carbon and iron, Monte Carlo calculations of, (T), 25:31164 (CEA-N-825)
attenuation in cross section measurements, computer program for calculation of sample, (E), 25:31172 (NBS-TN-499)
capture by A = 115 to 238 nuclei at 30 to 1400 keV, cross sections, excitation functions, and gamma spectra from, (E/T), 25:31303 (INR-1271)
capture by gold-197 and uranium-238, calibration of Moxon--Rae detector for cross section measurements of, 25:29326 (LA-4445)
capture by nuclei, accuracy of cross section measurements using scintillation tanks, 25:31173(R) (RPI-328-200)
capture by nuclei, semidirect capture-analysis of gamma spectra from, (E/T), 25:31332
coupling to meson resonances from on- and off-shell methods for n + p → n + p and p + p → p + p interactions below 750 MeV/c, (T), 25:30903
detection of, liquid--plastic phoswich scintillation detector for, 25:29339
detection of, pulse delay time in helium-3-filled ionization detectors for, 25:29338
diffraction on crystal containing paramagnetic center of polarized, structural amplitudes in, (T), 25:30663 (JINR-P3-5554)
dose rate removal cross sections and buildup factors, (E/T), 25:30637
doses in single-compartment aboveground concrete structures from thermonuclear explosion 100 m above ground, (T), 25:30633
dosimetry for radiobiological studies on Drosophila in γ fields, 25:29522
effects of high fluxes of, on properties of aluminum, 25:29905 (ORNL-4630, pp 239-60)
effects on cell division in Escherichia coli, 25:29490
effects on cobalt complexes, isomeric effects on recoil of cobalt-60 from, 25:29170
effects on electronics, simulators for studying transient nuclear explosion, 25:29410
effects on heart of beagle dogs, protective effects of mataraminol, norepinephrine, and phenylephrine on lethal, whole-body, mixed γ and, 25:29565
effects on induction of chlorophyll mutations in rice, comparison of γ radiation and, 25:29481 (IAEA-R-290-F)
effects on mechanical properties of aluminum alloys, SAP alloy, and stainless steels, use of cyclotron-injected helium for simulation of, 25:29907 (ORNL-TM-3299)
effects on microstructure of metals, 25:29909
effects on microstructure of Type 316 stainless steel, electron microscope study of, 25:29902(T) (EURFNR-891)
effects on phase transformations in oxides of aluminum, lithium, magnesium, and silicon, 25:30017
effects on properties of alloys and metals for use as fuel cladding, 25:29916
effects on shear modulus of aluminum, copper, and platinum at 4°K, 25:29912
effects on solid argon at 4.6°K, release of energy stored in, 25:30660
effects on step recovery diode frequency multipliers, 25:29409 (SC-RR-710188)
effects on tensile properties of concrete and mortar, relations with temperature, 25:30021 (EUR-4531, pp 179-83)
emission from active solar region, improved measurements of energetic, (E/T), 25:30177
energy spectra at ground-level and mountain altitudes of atmospheric, from 80 to 300 MeV, (E), 25:30374
flux in two-dimensional geometry during rapid reactor transients, alternating-direction implicit methods for analysis of, 25:31654
flux monitoring of, boron-coated proportional detector with low gamma sensitivity for in-core, 25:29324 (AEEW-M-970)
flux shape in plutonium lattice experiments, asymptotic theory methods for analysis of, (E/T), 25:31661
flux spectra in fast reactors, variational spectral synthesis methods for space-energy, 25:31656
interactions γ + n → p + π⁻, review of coupling parameters for, (E/T), 25:30797
interactions γ + n → p + rho⁻, relation of electromagnetic moments of charged rho to, 25:30799
interactions γ + n → π⁻ + p at 300 to 1200 MeV, differential cross sections for, (E), 25:30774 (INSJ-126)
interactions K⁻ + n → K⁻ + π⁻ + p at 5.5 GeV/c, double-Regge-pole analysis, (E/T), 25:30747
interactions n + p → n + p + π⁺ + π⁻ + mπ⁰ at 2 to 10 GeV/c, method for separation from channels of n + p → n + p + π⁺ + π⁻ interactions, (E), 25:30726 (JINR-P1-5665)
interactions n + p → n + p + π⁺ + π⁻ at 2 to 10 GeV/c, method for separation from channels of n + p → n + p + π⁺ + π⁻ + mπ⁰ interactions, (E), 25:30726 (JINR-P1-5665)
interactions n + p → n + p below 750 MeV/c, review of meson resonance coupling to nucleons from on- and off-shell methods for, (T), 25:30903
interactions n + p → π⁰ + d at threshold to 720 MeV, test of isospin invariance in, (E), 25:30730
interactions n + p at 2 to 10 GeV/c, cross sections of inelastic, (E), 25:30726 (JINR-P1-5665)
interactions π⁻ + n, compilation of cross sections for, 25:30735 (CERN-HERA-70-7)
leakage at core--reflector interfaces, effects on multigroup cross section averaging, 25:31183
monitoring of cosmic, at Canadian stations during Sept.--Dec., 1970, (E), 25:30303 (AECL-3856)
reaction rates in heterogeneous reactor lattices, foil perturbation effects on, (E/T), 25:31659
reactions (n,2n) with heavy nuclei at low energies, T-matrix method for calculating, (T), 25:31394 (ITF-70-95-E)
reactions (n,f) with uranium-235, angular anisotropy of γ rays from slow, (E), 25:31369
reactions (n,γ) with fission products at 0.215 eV to 10 MeV, cross sections and multigroup constants for, (E), 25:31304 (JAERI-Memo-4251)
reactions with nuclei, effect of nonuniform targets on transmission measurements of total cross sections for, 25:31173(R) (RPI-328-200)
reactions with plutonium--aluminum lattices in heavy water, buckling, eigenvalues, plutonium-239 and -240 resonance integrals, and spectra from, (E/T), 25:31661
reactions with samarium-147 and -149, resonance parameters for, (E), 25:31305 (JINR-P3-5655)
scattering by air, angular distribution of, 25:30639
scattering by nuclei at low energies, analysis using attractive square-well potential, (E), 25:31415
scattering by nuclei, statistical analysis of inelastic, (T), 25:31436
scattering by point defects in relaxed lattice, calculation of cross sections for, (T), 25:31163 (AERE-R-5682)
scattering by tritium, microscopic analysis using soft-core potential, (T), 25:31193

XUM

scattering from lanthanum dihydride and trihydride, inelastic, 25:30677
scattering in cross section measurements, computer program for calculating multiple, (E), 25:31172 (NBS-TN-499)
scattering in organic moderators, Horowitz operators for, (T), 25:31657
scattering kernels and cross sections for polycrystalline moderators, computer program for calculation of, 25:31168 (INR-1260)
scattering law for solid orthohydrogen at low energies, (T), 25:31169 (JUL-724-FF)
slowdown in infinite homogeneous medium, improved Goertzel-Greuling approximation for, (T), 25:31179
spectra in reactors, activation data unfolding by RF01 and RF07 codes for determination of, (T), 25:31648 (KFKI-70-30-RPT)
thermalization in crystalline moderators, variational method for pulsed-neutron, (T), 25:31175
thermalization in water at 318 and 77°K, (E), 25:31170(T) (KAPL-Trans-4)
transmission through ferromagnets and antiferromagnets, analysis of depolarization in, (T), 25:31181
transport equation for, computer program using coupled sampling with Monte Carlo method for adjoint, (T), 25:31171 (LA-4488)
transport equation for, general purpose Monte Carlo code for stationary and time-dependent, 25:31167 (EUR-4519)
transport equation for, SNARCID code for solution of one-dimensional multi-group, 25:31651 (ANL-7717)
transport in atmosphere, analytical method for describing, 25:29247
transport in lattices of fuel rods and liquid coolant, anisotropic, (E/T), 25:31660
transport in multilayer plane and spherically symmetric systems, solutions of equations for, (E), 25:31184

NEUTRONS, DELAYED
use for determination of uranium in borehole samples, 25:29202(T) (CEA-tr-R-1978)

NEUTRONS, EPITHERMAL
capture-to-fission ratio for uranium-233, -235 and plutonium-239, -241, (E), 25:31353
flux distributions in water for Am--Be sources enclosed in beryllium spheres, (E/T), 25:31223
reactions (n,2n) with beryllium-9 at 1.4 eV, cross sections and spectra from, (E), 25:31223

NEUTRONS, FAST
dose rate in biological materials, 25:31174 (UCRL-19715)
effects on chromosomes in swine leukocytes, aberrant, 25:29497
effects on density and mechanical properties of Type 304 stainless steel, relations with temperature, 25:29904 (ORNL-4630, pp 73-95)
effects on ductility of dilute beryllium-base--calcium--chromium alloys, 25:29917(P)
effects on frequency of sex-linked, lethal, and visible mutations in Drosophila sperm, 25:29499
effects on mechanical properties of fast breeder reactor fuels and metal alloys, 25:31568(T) (EURFNR-823)
effects on microstructure of refractory metal and alloys, 25:29904 (ORNL-4630, pp 73-95)
effects on mutations and translocations in mouse spermatogonia, 25:29487
effects on pathomorphology of mouse, rabbit, and rat brain in mixed γ and proton fields, whole-body, 25:29644
effects on properties of electric insulators, 25:30011 (ORNL-4630, pp 226-9)
effects on properties of Types 8001 and 1100 aluminum alloys, 25:29905 (ORNL-4630, pp 239-60)
effects on stability of beryllium oxide, relations with temperature, 25:30016
effects on void formation in molybdenum, niobium, and vanadium, relations with irradiation temperature, 25:29914
flux in depleted uranium assembly, 25:31173(R) (RPI-328-200)
reactions (n,p) and (n,α) with nuclei at 14 MeV, shell efects in cross sections for, (E), 25:31362
reactions with holmium-165 at 0.1 to 1.5 MeV, total cross sections for, (E), 25:31350
reactions with lithium-7 at 125 keV to 2 MeV, total cross section for, (E), 25:31173(R) (RPI-328-200)
scattering at air-ground interface, differential measurements of, (E), 25:30635
scattering by germanium-70, -72, -74, and -76, excitation functions for 2+ levels in, (E), 25:31244
scattering by helium-4 at 1 to 34 MeV, calculation of cross-section and polarization angular distributions using nonlocal separable potentials for elastic, (T), 25:31186 (LYCEN-7089)
scattering by holmium-165 at 0.3 to 1.5 MeV, differential cross sections for elastic and inelastic, (E), 25:31350
scattering by iodine-127, gamma spectra from, (E), 25:31352
scattering by lithium-6, analysis using Wheeler group model, 25:31221
scattering by molybdenum at 1.0 to 5.0 MeV, differential cross sections and excitation functions for elastic and inelastic, (E), 25:31299 (AWRE-O-89/70)
spectra in bulk aluminum assemblies, 25:31173(R) (RPI-328-200)
spectra in depleted uranium assembly, analysis of, 25:31173(R) (RPI-328-200)
spectra in iron assemblies of, analysis of cross section sets for, (E/T), 25:31658

NEUTRONS, FISSION
effects on intestinal mucosa of sheep, unilateral lethal pulsed mixed γ and, 25:29656
effects on survival of sheep, RBE for LD-50/5 dose for unilateral pulsed mixed γ and, 25:29656

NEUTRONS, INTERMEDIATE
reactions (n,f) with plutonium-242 at 50 eV to 5 keV, cross section and fission width for, (E), 25:31385

NEUTRONS, PILE
effects on corrosion and mechanical properties of Hastelloy N, evaluation of, 25:29906 (ORNL-TM-3063)
effects on creep of 24.48 percent enriched uranium dioxide at 1000 to 1200°C and 1500 to 4000 psi stress, 25:30009 (BMI-1893)
effects on mortar, equipment and methods for studying, 25:30020 (EUR-4531, pp 171-8)
effects on properties of concrete, 25:30022 (EUR-4531, pp 237-65)

NEUTRONS, THERMAL
capture by chlorine-35, gamma spectra from, (E), 25:31280
capture by gadolinium-157 with internal pair production, conversion positron spectra from, (T), 25:31329
capture by gallium-69, γ spectra from, (E), 25:31290
capture by hafnium-177, conversion electron spectra from, (E), 25:31336
capture by iron-56, gamma spectra from, (E), 25:31270
capture by potassium-30, gamma spectra from, (E), 25:31292
capture by uranium-235, cross section for production of isomeric uranium-236 relative to fission for, (E), 25:31307 (JINR-P7-5497)
detection of, design and performance of boron-containing liquid scintillation detector for, 25:29337
detection of, large liquid scintillation detector for, 25:29336
diffusion in lead, parameters for, (E), 25:31177
effects on hardening of boron-doped copper, 25:29908
effects on potassium chromate crystals, distribution of recoil chromium-51 from, 25:29171
effects on tensile properties of Type 316 stainless steel, relations with boron distribution, 25:29913
production of polarized beams of, (E), 25:31180
reactions (n,f) with americium-242m, charge and mass distribution in, (E), 25:31373
reactions (n,f) with uranium-233, -235 and plutonium-239, delayed neutron fractions in, (E), 25:31334
scattering in liquid metals, ion-electron model for, (T), 25:31176
scattering law for liquid sodium, calculation using ion-electron model, (T), 25:31176

NEVADA TEST SITE
geology and hydrology of, effects of Handley event underground nuclear explosion on, 25:29203 (USGS-474-95)
monitoring activities following nuclear explosions at, during 1969, off-site, 25:29506 (SWRHL-97-r)

NICKEL
bonding of powder compacts of, to monocrystalline aluminum dioxide, effects of sintering atmosphere, pressure, temperature, and time on, 25:29815
book: Nickel and Nickel Alloys: Properties and Behavior (In German), 25:29838
corrosion of hafnided and tantalided, by acid and sodium chloride solutions at 25 to 150°C, 25:29766
deposition on tungsten crystal surfaces, microscopic studies of vapor, 25:29848
determination by x-ray fluorescence, sensitivity of, 25:28962
determination in high-purity water for reactor cooling and moderating, 25:28914 (BARC-515)
determination in low-alloy steel, two-standard method for spectrometric, 25:28950
determination in natural waters by solvent extraction and x-ray fluorescence spectroscopy, 25:28919
determination in plutonium by absorption spectrophotometry and spectrography, 25:28916 (CEA-R-4071)
determination in presence of other metals, spectrographic, 25:28944
determination of trace amounts of, in vanadium, spectrographic, 25:28947
determination using ion permselective membrane, potentiometric, 25:28956
effects on creep of sintered uranium monocarbide in vacuum, 25:29960
effects on electric conductivity, grain refinement, and microhardness of zirconium, 25:29835
effects on fluorometric determination of zirconium, 25:28963
effects on sintering of tungsten, 25:29791
effects on thermal diffusivity of sintered uranium monocarbide at 500 to 2200°K, 25:29957
electron inelastic scattering at 0.2 to 3 keV from, energy spectra from, (E), 25:30260
hyperfine fields of technetium in, (E), 25:31271

proton reactions at 11.5 and 23.5 MeV using thick targets, neutron yield from, (E), 25:31209
radioinduced swelling in, dose dependence of electron-microscopic, 25:30652
separation from aqueous solutions by thin-layer chromatography using liquid anion exchangers, 25:29186
separation from other metals by ion-exchange paper chromatography, 25:29190
solvent properties for uranium at low limits at 975 to 1075°C, measurement of diffusion coefficients for determination of, 25:29866

NICKEL ALLOYS AND SYSTEMS
book: Nickel and Nickel Alloys: Properties and Behavior (In German), 25:29838
corrosion by vanadium pentoxide melts, effects of chromium, copper, iron, molybdenum, and tungsten additions on, 25:29768
Al--Cr--Ni, oxidation resistance at 1000°C, mapping method for selection of optimum, 25:29780
Al--Ni--steel--Ti, failure of electroslag welded joints on, effect of residual welding stress on brittle, 25:29832
Ce--Ni--Ru, preparation and superconductivity of, (E), 25:30413(T) (LA-tr-71-26)
Co-base--Ni, thermal expansion at 100 to 800°C, 25:29899
Co-base--Ni, transformation temperatures of, allotropic, 25:29899
Cr--Fe--Ni, compatibility with nonstoichiometric and stoichiometric uranium carbide at 900°C, effects of stabilizers on, 25:29940(T) (EURFNR-820)
Cr--Mo--Ni, corrosion by hydrochloric and sulfuric acids, effects of chromium and molybdenum on, 25:29777
Cr--Ni, radiation effects on mechanical properties of, fast neutron, 25:31568(T) (EURFNR-823)
Cr--Ni-base, hardness at 27 and 740°C, effects of molybdenum and niobium on, 25:29839
Cr--Ni-base, microstructure at 27 and 740°C, effects of molybdenum and niobium on, 25:29839
Cr--Ni-base, strength of, effects of stacking fault energy on high-temperature, 25:29878
Cr-base--Ni, thermal capacity at 1.3 to 4.2°K, 25:30676
Fe--Mo--Ni-base, properties of 2-81 permalloy, effects of heat treatments in production process on magnetic and tensile, 25:30672
Mo--Ni-base, electromigration of molybdenum in, at 950 to 1350°C, 25:29856
Ni--P, effects on low-temperature sintering of tungsten, 25:29793
Ni--Si, analysis for silicon as molybdosilicate complex, spectrophotometric method for, 25:28924
Ni--Zr-base, polishing for metallographic examination, electrolytic, 25:29817
Ni--ZrO_2, deformation of dispersion-strengthened, low-temperature, 25:29941 (INIS-mf-8)
Ni-base--W, strength of, effects of diffusion velocity and stacking fault energy on high-temperature, 25:29878
Ni-based--V, polarized-neutron study of $Ni_{0.968}V_{0.032}$, 25:30680

NICKEL CHLORIDES
properties of aqueous, for etching uranium and uranium alloys, 25:29798(P)

NICKEL HYDRIDES
detection in sunspot spectra, (E), 25:30173

NICKEL IONS
abundance of positive, in ionospheric D region, (E/T), 25:30404

NICKEL ISOTOPES Ni-58
abundance of, solar and terrestrial, (E), 25:30173
energy levels from proton inelastic scattering, spin-parity assignments for, (E), 25:31245
helium-3 reactions (He-3,n) at 13.2 MeV, neutron spectra and angular distributions for, (E), 25:31237 (IAE-1958)

NICKEL ISOTOPES Ni-60
abundance of, solar and terrestrial, (E), 25:30173
energy levels from proton inelastic scattering, spin-parity assignments for, (E), 25:31245

NICKEL ISOTOPES Ni-61
proton reactions (p,n) with, cross sections for, (E), 25:31268

NICKEL ISOTOPES Ni-64
alpha scattering by, calculation of optical potentials in terms of diffraction-model parameters, (T), 25:31410
proton reactions (p,n) with, cross sections for, (E), 25:31268

NICKEL OXIDES
thermodynamic properties of gaseous diatomic, free energy functions for, 25:29082

NICKEL SULFIDES
NiS--US_2, crystal structure of single crystals of, 25:29996

NIOBIUM
analysis of commercial, for iron, molybdenum, nitrogen, and tungsten, ASTM method for, 25:28973
book: Creep-Rupture Data for the Refractory Metals to High Temperatures, 25:29868
coating with aluminum at 700 to 1200°C, pack-cementation method for, 25:29816
deposition on substrates from alkaline fluoride mixtures containing salts of, methods for electro-, 25:29783 (CEA-N-1376)
determination in presence of other metals, spectrographic, 25:28944
determination of trace amounts of, in seawater, review on methods for, 25:28921
deuterium diffusion through, in fusion reactor conditions, 25:29820 (EUR-4593, pp 519-24)
effects of beta-stabilizer, on mechanical properties of titanium alloys at -253 to +20°C, 25:29844
effects on fluorometric determination of zirconium, 25:28963
effects on hardness and microstructure of chromium--nickel alloys at 27 and 740°C, 25:29839
Hall effect in superconducting, (E), 25:30427
hardness and yield stress of wires of, effects of deformation temperature and nitrogen and oxygen interstitial content on, 25:29880
hydrogen diffusion through, in fusion reactor conditions, 25:29820 (EUR-4593, pp 519-24)
oxide films on, crystal structure of corrosion-resisting, 25:29991
production and uses of, review on, 25:29807
properties for use as carbide-former in neutron damage-resistant stainless steel, 25:29799(P)
radiation effects on void formation in, relations of irradiation temperature with fast neutron, 25:29914
reactions with graphite thimbles to prepare niobium monocarbide, 25:29926
separation from plutonium by anion exchange from mixed methanol--nitric acid solutions, 25:29191
thermal conductivity of superconducting, (E), 25:30434

NIOBIUM ALLOYS AND SYSTEMS
book: Creep-Rupture Data for the Refractory Metals to High Temperatures, 25:29868
Co-base--Nb, thermal expansion at 100 to 800°C, 25:29899
Co-base--Nb, transformation temperatures of, allotropic, 25:29899
H--Nb, elastic properties of, Gorsky-effect study of Curie--Weiss temperature dependence of, 25:29865
H--Nb-base, particle size distribution in, effects of composition and thermal cycling on, 25:29929
H--Nb-base, preparation of powdered, using ball mill, 25:29929
Hf--Nb, precipitation morphology of, effects of aging temperature on α-, 25:29886
N--Nb, internal friction at 23 to 700°C and 1 Hz, mechanisms of cold work peaks in, 25:29861
Nb--Pd, diffusion processes at 700 to 1030°C, quantitative electron probe microanalysis study of, 25:29881
Nb--Ru, phase transformation in near-equiatomic, crystallography, kinetics, and theory of displacive, 25:29882 (COO-1198-807)
Nb--Ta, Hall effect in superconducting, (E), 25:30427
Nb--Ti-base, tensile properties of precipitation-hardened, relation of microstructure with room temperature, 25:29872
Nb--Zr, oxidation by air at 700 to 1000°C, oxide film composition and kinetics of, 25:29769
Nb--Zr, oxidation by carbon dioxide at 700 to 1070°C, kinetics and mechanism of, 25:29767
Nb--Zr-base, resistance behavior of superconducting near H/sub c2/, (E/T), 25:30412 (JINR-P8-5733)
Nb-base--Ti, coating with aluminum at 900 to 1200°C, pack-cementation method for, 25:29816
Nb-base--Ti, diffusion of hydrogen in, at -160 to +250°C, activation energy of, 25:29837
Nb-base--Ti--Zr, microstructure of precipitates in, effects of aging at 620 to 850°C, 25:29890
Nb-base--W, coating with aluminum at 900 to 1100°C, pack-cementation method for, 25:29816
Nb-base--Zr, superconducting properties of, 25:30414(T) (ORNL-tr-2475)

NIOBIUM CARBIDES
elastic properties of polycrystalline $NbC_{0.99}$, at 300 to 1500°K, sonic resonance method for determination of, 25:29970
preparation of monocrystalline monocarbide, recrystallization method for, 25:29927
preparation of NbC, by reactions of liquid niobium with graphite thimbles, 25:29926
x-ray emission spectra of NbC/sub x/, 25:30267

NIOBIUM HYDRIDES
analysis for hydrogen by carrier gas fusion--gas chromatographic methods, 25:28936

NIOBIUM ISOTOPES Nb-90
energy levels of, four-particle, (T), 25:31322

NIOBIUM ISOTOPES Nb-91
energy levels from zirconium-90 (p,γ) reactions, (E), 25:31351
proton binding energy for, (E), 25:31351

NIOBIUM ISOTOPES Nb-92
energy levels from niobium-93 (d,t) reactions, spins and parities of, (E), 25:31283
energy levels from zirconium-91 (p,n) reactions, width of isobaric analog, (E), 25:31381
energy levels of, lifetimes of low-lying, (E), 25:31349

NIOBIUM ISOTOPES Nb-93
alpha reactions at 0.2 to 0.9 GeV, excitation functions for, (T), 25:31368
deuteron reactions (d,t) at 17 MeV, triton spectra and angular distributions for, (E), 25:31283

XUM

meson reactions (μ^-,xn) by, gamma spectra from, (E), 25:31258
photon reactions (γ,n) at 10 to 68 MeV, yields of radioactivities from, (E), 25:31333
proton reactions 0.2 to 0.9 GeV, excitation functions for, (T), 25:31368
proton reactions at 11.5 and 23.5 MeV using thick targets, neutron yield from, (E), 25:31209
NIOBIUM ISOTOPES Nb-95
distribution and retention in mice following inhalation of heat treated aerosols of, 25:29423 (LF-43, pp 59-65)
NIOBIUM OXIDES
crystal structure of corrosion-resisting films of, formed on niobium in dilute acid solutions at 200 to 300°C, 25:29991
thermodynamic properties of gaseous diatomic, free energy functions for, 25:29082
Nb_2O_5--TiO_2, phase studies at 1250°C, 25:29995
NbO_2--Nb_2O_5--TiO_2, phase studies at 1250°C, 25:29994
NbO_2--TiO_2, phase studies at 1250°C, 25:29995
NIOBIUM SELENIDES
properties of polyimide-bonded, as solid film lubricants, 25:29096 (WERL-HFIL-1)
NITRATES
determination in high-purity water for reactor cooling and moderating, 25:28914 (BARC-515)
determination in uranium compounds, colorimetric, 25:28918 (NIM-951)
determination using ion permselective membrane, potentiometric, 25:28956
effects on separation of thorium(IV) from sulfuric acid solutions by extraction using N-phenylbenzylamine in chloroform, 25:29184
NITRIC ACID
corrosive effects on beryllium--copper--tin alloys, relations of manganese, titanium, or zinc additions with, 25:29830
corrosive effects on tantalided nickel and Type 316 stainless steel at 60 to 123°C, 25:29766
effects on oxidation-reduction potential of solutions of salts of tetravalent and hexavalent uranium, 25:29036
nitrogen-15 exchange with nitrogen-14 between nitric oxide and, kinetics of, 25:29057
reactions of aqueous solutions of, with neptunium in presence of nitrous acid, oxidation, 25:29038
separation of thorium and uranium from aqueous solutions of, by solvent extraction using 4-methyl-2-pentanone, effects of lithium chloride or magnesium chloride on, 25:29195
use as pickle solution for uranium, criticality control in, 25:29787(R) (RMI-16)
NITROCELLULOSE
use for alpha autoradiography of irradiated fuels, 25:29944(T) (LB/G-2916)
NITROGEN
abundance in Cas A, (E), 25:30064
alpha-particle stopping cross sections in gaseous, test of Bragg's rule for, 25:30642
boron-ion reactions at 100, 200, and 300 keV with molecular, cross sections for single and double electron loss in, (E), 25:30300
determination in niobium by distillation and photometry of ammonia complex with Nessler reagent, 25:28973
determination in tantalum alloys by modified Kjeldahl and vacuum fusion method, 25:28937
determination in thin films of, tantalum nitrides, titanium nitrides, or zirconium nitrides by electron-probe x-ray micro method, 25:28966
determination of trace amounts of, in seawater, review on methods for, 25:28921
diffusion in zirconium and zirconium nitride at 800 to 1100°C, 25:29870
effects of interstitial impurity of, on mechanical properties of iron and refractory metals, 25:29855
effects on hardness and yield stress of niobium, tantalum, and vanadium wires, relations with deformation temperature and oxygen content, 25:29880
electron reactions at 600 keV with molecular, photon emission and absorption by ions produced in, (E), 25:30274(T) (ANL-Trans-881)
heat transfer in, containing dispersed submicron particles, scattering amplitude functions for evaluation of radiant, 25:29270
ion reactions with molecular, binary-encounter calculation of ionization cross sections for, 25:30299
nitrogen-ion (N^+) reactions at 100, 200, and 300 keV with molecular, cross sections for single and double electron loss in, (E), 25:30300
phosphorus-ion reactions at 100, 200, and 300 keV with molecular, cross sections for single and double electron loss in, (E), 25:30300
plasma of, rotation temperature of molecular ionized nitrogen in arcs of, (E), 25:30480
reactions with uranium dicarbide at 800 to 1400°C, effects of nitrogen pressure on graphitization of carbon formed from, 25:29962
reactions with zirconium at 800 to 1100°C, 25:29870
separation from off-gas streams, evaluation of thin silicone rubber membranes for, 25:29317 (ORNL-4522)
solubility in vanadium at 600 to 1500°C, 25:29879
sorption at activated sites on polycrystalline tungsten, kinetics of chemi-, 25:29849
sorption by tantalum, calorimetric study of chemical, 25:29843
sorption on beryllium surface, 25:29894
NITROGEN IONS (N^+)
reactions with nitrogen molecules at 10, 200, and 300 keV, cross sections for single and double electron loss in, (E), 25:30300
NITROGEN IONS (N_2^+)
abundance in ionospheric D region, (E/T), 25:30404
rotation temperature of, in nitrogen plasma arc, (E), 25:30480
NITROGEN ISOTOPES N-14
alpha scattering at 1 GeV per nucleon, absorption cross sections for, 25:31234
conversion into oxygen-15, fluorine-18, neon-21, and neon-19 in explosive nucleosynthesis, (T), 25:30067
electron elastic scattering at 30 to 60 MeV cross sections for, (E), 25:31219
energy levels from carbon-12 deuteron resonances, spin-parity assignments for, (E), 25:31222
energy levels from oxygen-16 (d,α) reactions, isospin nonconservation in, (E), 25:31227
exchange with nitrogen-15 between nitric acid and nitric oxide, kinetics of, 25:29057
nitrogen-14 reactions (N-14, N-13) with, analysis of neutron tunneling effect in, (T), 25:31419
nuclear radius from electron elastic scattering, (E), 25:31219
photon reactions (γ,n) at 10 to 68 MeV, yields of radioactivities from, (E), 25:31333
proton elastic scattering at 49.4 MeV, differential cross sections for, (E), 25:31233
NITROGEN ISOTOPES N-15
exchange with nitrogen-14 between nitric acid and nitric oxide, kinetics of, 25:29057
production in stars by explosive nucleosynthesis in helium zones, (T), 25:30067
uses in labeled compounds as internal standards for mass spectrometry, 25:28967
NITROGEN OXIDES
abundance of positive ionized, in ionospheric D region, E/T), 25:30404
reactions with radiolytic hydrogen atoms, kinetics of, 25:29158
NITROGEN OXIDES NO
electron reactions at 0 to 2 eV with, electron attachment and vibrational excitation in, (E), 25:30281
ion reactions with, binary-encounter calculation of ionization cross sections for, 25:30299
nitrogen-15 exchange with nitrogen-14 between nitric acid and, kinetics of, 25:29057
reactions with hydrogen atoms, spin-exchange cross sections for, (E), 25:30277 (UCRL-20529)
thermodynamic properties of gaseous, free energy functions for, 25:29082
NITROGEN OXIDES NO_2 OR N_2O_4
cesium-atom reactions up to 30 eV with, charge exchange in, (E), 25:30276 (ORNL-TM-2620)
NITROGEN OXIDES N_2O
alpha-particle stopping cross sections in gaseous, test of Bragg's rule for, 25:30642
cesium-atom reactions up to 30 eV with, charge exchange in, (E), 25:30276 (ORNL-TM-2620)
NITROGEN SYSTEMS
Cr--N--U, crystal lattice parameters of UCrN/sub 2+-x/, 25:29988
Cr--N--U, phase diagram at 1600°C, tentative, 25:29988
Fe--H--Hf-base--N--O--Zr, ductility and tensile properties of dilute, effects of composition on, 25:29827(R) (RPI-3719-9)
N--Nb, internal friction at 23 to 700°C and 1 Hz, mechanisms of cold work peaks in, 25:29861
N--U--V, crystal lattice parameters of UVN_2, 25:29989
N--U--V, phase diagram at 1400 to 2000°C, 25:29989
N--U--V, thermodynamic properties of UVN_2, 25:29989
N--V-base, phase transformation of α solid solution of, effects of cooling on, 25:29879
NORBORNENYL COMPOUNDS
polymers, radioinduced crosslinking of, yields of products from electron, 25:29124
NOVAE
radio observations of Scuti 1970, at 0.35 and 3.7 cm, 25:30091
NUCLEAR AUXILIARY POWER SYSTEMS
shielding for space vehicle, optimum design parameters of asymmetric 4π, 25:31640 (ORNL-TM-3368)
NUCLEAR BATTERIES
development and uses of radioisotope-fueled, review of, 25:29280
NUCLEAR CHEMISTRY
development programs in Yugoslavia during 1969, 25:31633 (IJS-253)
NUCLEAR ELECTRIC MOMENTS
calculation of states quadrupole, of first 2^+ states using time-dependent Hartree--Fock equations, 25:31424
NUCLEAR EMULSIONS
meson (π^-) reactions with nuclei at 17 GeV in, selection technique for coherent, (E), 25:30736 (JINR-P1-5565)
particle track width in, method for calculation of multiply charged, 25:29381

XUM

particle tracks in, characteristics of spurious scattering in, 25:29378
particle tracks in, charge identification of, 25:29380
NUCLEAR ENGINEERING
research at Australian Inst. of Nuclear Science and Engineering, 1969, 25:31706(R) (NP-18803)
NUCLEAR EXPLOSIONS
monitoring activities following, at Nevada Test Site during 1969, off-site, 25:29506 (SWRHL-97-r)
NUCLEAR EXPLOSIONS, ATMOSPHERIC
effects on environment, analytical method for describing, 25:29247
effects on ground-based military equipment, methodology for evaluating environmental, 25:29246
fallout from 1966 to 1968 French, on Mururoa Atoll, measurement of interhemispheric transport of, 25:29221
fallout from Dec. 1967 Chinese, monitoring in ground-level atmosphere at Fayetteville, Ark, 25:29219
fallout monitoring from May 1966 Chinese, at Fayetteville, Ark, 25:29216
fallout transport from May 1966 Chinese, calculation of worldwide, 25:29216
NUCLEAR EXPLOSIONS, UNDERGROUND
effects of Handley evnt, on geology and hydrology of Nevada Test Site, 25:29203 (USGS-474-95)
ground motion from Handley event, data tabulation on peak resultant vector, 25:29242 (NVO-1163-216(Rev.))
radiation dose to man in vicinity of, computer method for calculation of, 25:29516 (UCRL-50990)
NUCLEAR MAGNETIC RESONANCE
book: Chemical Consequences of Nuclear Spin, 25:30669
NUCLEAR MATERIALS MANAGEMENT
sampling techniques for, geometric programming method for optimization of, 25:31649
NUCLEAR MATTER
density of, hyperspherical-expansion expression for, (T), 25:31405
ground-state energy of, (T), 25:31405
nucleon interactions in infinite, effective, (T), 25:31416
NUCLEAR MODELS
alpha cluster, for calculation ground-state energies of even--even nuclei, 25:31427
Davydov, computer program for calculating energy levels in, (T), 25:31425
optical, computer search program with spin-orbit terms for spin-1/2 and spin-1 particles, (T), 25:31369 (ANU-P-500)
optical, determination of potentials in terms of diffraction-model parameters, (T), 25:31410
particle-vibration coupling, HRPA contributions to phonon--phonon interaction in, (T), 25:31446
shell, ground-state deformation in nuclei near closed shells in, 25:31451
shell, group-theoretical operator analysis in the ds shell, 25:31452
shell, nonlocal potential for single-particle, (T), 25:31447
NUCLEAR ORIENTATION
theory of nuclear Overhauser effect in multispin systems, 25:30691
NUCLEAR PHYSICS
development programs in Yugoslavia during 1969, 25:31633 (IJS-253)
research at Australian Inst. of Nuclear Science and Engineering, 1969, 25:31706(R) (NP-18803)
research at Florida State Univ., August 1, 1970 to July 31, 1971, (E/T), 25:31315(R) (ORO-2434-7)
research at ORNL relating to nuclear cross sections, January--April, 1971, (E), 25:31204 (ORNL-TM-3378)
research at Rensselaer Polytechnic Inst., June 1970 to May 1971, (T), 25:31396(R) (RPI-3947-13)
use in solid-state research, review, 25:30647
NUCLEAR POWER PLANTS
air conditioning system for, operation and performance of, 25:29259
components and equipment for, earthquake resistant design requirements for, 25:31601
cooling systems for, design and performance of plate heat exchanger for secondary, 25:29269
development in Australia, 25:31462
development in Germany, prospects for, 25:31460
personnel for, standards for selecting and training, 25:31481
quality assurance programs for, organizational limitations and requirements for, 25:31528
radiation hazards to human population and soils in environs of Soviet Union, 25:29525
radioactive effluents from, sources and control of, 25:31531
safety of, risk probability method for evaluation of, 25:31529
safety tests for, list of periodic auxiliary, 25:31597 (IRS-R-1)
sales in US during 1970, 25:29811
siting of, policies for, 25:31482 (AECL-3740)
siting of, role of Washington State in setting criteria for, 25:31525 (NP-18770)
thermal effluents from, ecological effects of, (E), 25:31527
NUCLEAR QUADRUPOLE RESONANCE
book: Chemical Consequences of Nuclear Spin, 25:30669
NUCLEAR REACTIONS
angular distribution of particles evaporated from the compound nucleus in, (T), 25:31428
cross sections for (n,p) and (n,α) at 14 MeV, shell effects in, (E), 25:31362
cross sections for compound-nucleus formation in, computer program using Hauser--Feshbach theory for calculating, (T), 25:31391 (ANU-P-512)
cross sections including charged-particle emission and fission, computer program for calculating, (T), 25:31313 (ORNL-TM-3179)
interference effects in, with intermediate resonances, (T), 25:31395 (JINR-P1-5648)
mechanisms of heavy-ion induced, angular momentum effects on, (T), 25:31356
neutron tunneling mechanism for, matrix elements for, (T), 25:31419
resonance averaging in, (T), 25:31450
spectra from compound-nucleus, explanation of differences between observed and evaporation, (T), 25:31403
theory of, comparison of R-matrix, 25:31442
NUCLEAR REACTIONS (DIRECT)
channel wave functions and coupled equations for, effective orthogonality of, (T), 25:31443
cross sections for, computer program for DWBA calculations of, (T), 25:31390 (ANU-P-507)
NUCLEAR SPIN
book: Chemical Consequences of Nuclear Spin, 25:30669
calculation for four-particle states using extended Brennan--Bernstein rules, (T), 25:31399
NUCLEAR STRUCTURE
calculation for deformed nuclei using K-harmonics method, (T), 25:31439
calculation of inelastic transition densities, 25:31418
calculations for rare earth region using hexadecapole deformation and rotation--particle coupling, (T), 25:31414
calculations for rotational bands in even--even nuclei using angular momentum projection method, 25:31438
calculations for transuranium region using Woods--Saxon potential, 25:31392(T) (BNL-tr-416)
NUCLEAR THEORY
applications of spectral distributions in nuclear spectroscopy, 25:31430
asymmetric rotor problem and the collective excitation of even nuclei, 25:31409
boundary-condition-model T matrix in, 25:31441
calculation of fractional parentage coefficients for (1d-2s)-shell nuclei with the projection-operator method, 25:31426
calculation of inelastic transition densities, 25:31418
Coriolis anti-pairing theory of nuclear rotations, 25:31408
determination of optical potentials in terms of diffraction-model parameters, 25:31410
energy spectrum and deformation of even--even nuclei, 25:31411
fractional parentage and the equations-of-motion method in pairing theory, 25:31453
ground-state deformation in nuclei near closed shells, 25:31451
group-theoretical operator analysis in the ds shell, 25:31452
nuclear surface properties in, analysis using Brueckner method, 25:31445
nucleon--nucleon potential in, effective nonlocal, 25:31402
nucleon--nucleon potential, exchange of isoscalar vector meson in nonlocal field theory for, 25:31431
possibility of quasi-rotational excitations in spherical nuclei, 25:31407
spectral distributions in nuclei, 25:31429
statistical of gamma de-excitation, 25:31406
NUCLEAR WEAPONS
radiation dose to human populations following detonation of, standards for estimation of, 25:29539
NUCLEI
binding energies and masses of A = 130 to 180, 25:31433
binding energy and nuclear properties of light, calculations using three-part nucleon--nucleon potentials, (T), 25:31413
binding energy of, statistical expression for, (T), 25:31412
bound states of, hyperspherical-expansion calculations of, (T), 25:31405
charge distribution of cosmic primary heavy, of Z greater than or equal to 26, (E), 25:30305
charged-particle scattering by, Riemann method in inverse problem for, (T), 25:30894 (ITF-70-98-P)
detection of heavy and very-heavy, from particle tracks in meteorites, (E), 25:30317
deuteron reactions (d,p) with, use of Born approximation for analysis of, (T), 25:31400
echo-resonance parameters for Z = 47 to 92, from radiative-capture measurements, (E/T), 25:31303 (INR-1271)
electron elastic scattering by, theory of, 25:31206 (SAL-17)
energy levels in Davydov model, computer program for calculating, (T), 25:31425

XUM

energy levels of even--even, alpha-cluster calculation of ground-state energies for, (T), 25:31427
energy levels of light, predictions of supermultiplet model of highrisospin isobaric analog, (T), 25:31203 (LYCEN-7088)
energy levels of, coincidence system for measuring picosecond lifetimes of, 25:29365
energy levels of, magnetic beta spectrometer for short lifetime measurements of, 25:29358
energy levels of, variational calculation of energies and population probabilities for paired, (T), 25:31360
energy spectrum and deformation of even--even, (T), 25:31411
energy-level transition densities in, (T), 25:31418
energy-level transitions in, graphs for analysis of (1--3) gamma--gamma directional correlations in, (T), 25:31312 (ORNL-4619)
energy-level transitions in, phase-defined reduced matrix element for multipole mining ratios of, 25:31420
energy-level transitions in, statistical theory of gamma de-excitation, (T), 25:31406
excitation of rotational states in even, collective, (E), 25:31409
excitations in spherical, possibility of quasi-rotational, (T), 25:31407
fractional parentage coefficients for (1d-2s)-shell, calculation using the projection-operator method, (T), 25:31426
isotope shifts for isobaric pairs of, nuclear properties from, (T), 25:31404
mass formula for, liquid droplet, (T), 25:30036(R) (NYO-3962-3)
meson (K) reactions at low energies, reaction-matrix method and statistical model of, 25:30906
meson (K^-) absorption at rest, extrapolation of $K^- + p$ interactions below threshold from, (T), 25:30902
meson (μ^-) reactions in matter, (T), 25:31448
meson (π) interactions with, properties of optical potential for, (T), 25:31421
meson (π^-) reactions at 15 and 16 GeV/c, cross sections for rho^0, f^0, and ω^0 production in, (E), 25:30741
meson (π^-) reactions at 17 GeV in emulsions, selection technique for coherent, (E), 25:30736 (JINR-P1-5565)
neutrino fission at 100 MeV, determination of neutrino electromagnetic form factor from cross section for, (E/T), 25:30777 (JINR-P2-5705)
neutrino reactions at 100 MeV, determination of electromagnetic form factor of neutrino from cross section for giant resonance excitation from, (E/T), 25:30777 (JINR-P2-5705)
neutron capture at 30 to 1400 keV by A = 115 to 238, cross sections, excitation functions, and gamma spectra from, (E/T), 25:31303 (INR-1271)
neutron capture by, accuracy of cross section measurements using scintillation tanks, 25:31173(R) (RPI-328-200)
neutron capture by, semidirect capture analysis of gamma spectra from, (E/T), 25:31332
neutron inelastic scattering by, statistical analysis of, (T), 25:31436
neutron reactions (n,2n) at low energies with heavy, T-matrix method for calculating, (T), 25:31394 (ITF-70-95-E)
neutron reactions (n,p) and (n,α) at 14 MeV, shell effects in cross sections for, (E), 25:31362
neutron scattering at low energies, analysis using attractive square-well potential, (T), 25:31415
neutron total cross sections for, effect of nonuniform targets on transmission measurements of, 25:31173(R) (RPI-328-200)
nucleon density of deformed, calculation using independent-particle model, 25:31437
nucleon elastic and inelastic scattering by, realistic interactions for exchange effects in microscopic descriptions of, (T), 25:31432
nucleon inelastic scattering at medium energies, microscopic analysis using realistic potentials, 25:31393 (COO-1051-34)
nucleon radiative capture by, compound-nucleus model of, (T), 25:31303 (INR-1271)
particle reactions at very high energies, hadron spectrum from cross sections for, 25:30905
photon reactions at 2.75 MeV, pair production cross sections for, (E/T), 25:31361
photon reactions with, accuracy of photon-diffference method for calculation of cross sections in, 25:30773 (DESY-71/3)
photon reactions with, analysis using Feynman diagrams, (T), 25:31435
proton elastic scattering with isobaric analog excitation, method for analysis of, (T), 25:31276
proton fission at 500, 750, and 1000 MeV, analysis using nuclear reaction theory, 25:31417
proton reactions (p,γ) with isobaric analog excitation, method for analysis of, (T), 25:31276
quadrupole moments of neutron-rich A = 4 to 40, variational calculation of, (T), 25:31238 (ITF-70-83-E)
radii of neutron-rich A = 4 to 40, variational calculation of, (T), 25:31238 (ITF-70-83-E)
rotational states of spherical, Coriolis anti-pairing theory of, (T), 25:31408
scattering by nuclei at high energies, liquid drop model for elastic and inelastic, (T), 25:30901
scattering by nuclei, effect of antisymmetrization on density distribution for, (T), 25:31423
spectra of primary cosmic, (E), 25:30307
spectral distributions in, (T), 25:31429

NUCLEIC ACID
biosynthesis of plant, in vitro, 25:31720(R) (ORO-3982-10)

NUCLEIC ACID, DEOXYRIBO-
effects of homologous, of structure of irradiated DNA of seed embryos, 25:29716
radiation effects on Bacillus subtilis, x, 25:29463
radiation effects on biological and physical properties of pneumococcal, following disintegration of incorporated phosphorus-32 or tritium, β, 25:29459
radiation effects on initiation of unscheduled synthesis of, in muscle cells of chick embryos, in vitro uv, 25:29650
radiation effects on isolated, 25:29462
radiation effects on molecular weight distribution of solutions of, 25:29470
radiation effects on structure of seed embryo, effects of homologous DNA on repair of, 25:29716
radiation effects on synthesis of, in lymphoid tissues of rats, effects of adrenalectomy on subsequent inhibitory whole-body γ, 25:29672
radiation effects on template activity of Bacillus subtilis, RNA synthesis following x, 25:29467
radiation effects on transformation of his_2 and try_2 markers in Bacillus subtilis, x, 25:29468
radiation effects on, in rabbit hematopoietic system, effects of dose on x, 25:29637
radiation effects on, of green algae, role of photoreactivating enzymes in repair of uv, 25:29713(R) (COO-1793-5)
radioinduced base degradation and denaturation of Bacillus subtilis, x, 25:29466
radioinduced chemical and structural changes in transforming, mechanisms for phenotypic expression following x, 25:29469
radioinduced cross links in Bacillus subtilis, x, 25:29465
radioinduced double and single strand breaks in Bacillus subtilis, viscometric studies on x, 25:29464
synthesis in human bladder tumors for diagnosis of malignant stages, tritium tracer studies on, 25:29585

NUCLEIC ACID, RIBO-
analysis for tritium by extraction and scintillation counting, 25:28984
determination of radioisotope-labeled, by paper disc technique, elimination of metabolically generated artifacts from labeled base precursors in, 25:28993
radiation effects on activity of transfer, in, 25:29715
radiation effects on synthesis of Bacillus subtilis, as function of DNA template activity, 25:29467
radiation effects on synthesis of, in immunized mouse spleen, polyacrylamide gel electrophoresis studies on x, 25:29476
use of intranuclear tritium-labeled, in human bladder tumors for diagnosis of malignant stage, 25:29585

NUCLEOGENESIS
explosive, in chemical evolution of galaxies, (T), 25:30206
explosive, in helium zones, (T), 25:30067
helium production in primordial, (T), 25:30220 (P-4494(RAND))
of superheavy elements in supernovae, (T), 25:30051
reaction networks for 107 chemical constituents in supernova ejecta, (T), 25:30079

NUCLEONS
coupling constants for NAK, PCAC hypothesis for, (T), 25:30904
coupling constants for NIK, PCAC hypothesis for, (T), 25:30904
coupling of AKN, review of forward dispersion relations for, (T), 25:30902
decay N + N + vector meson, evidence from parity-forbidden α decay for noncanceling seagull and Schwinger terms in, 25:30931
dipole moment of, nucleon Compton-effect amplitude for sum rules for, (T), 25:30776 (JINR-P2-5679)
interactions Δ + N, quasi-nuclear model for many-baryon resonance production in potential, (T), 25:30895 (NP-18779)
interactions e + N, absence of form factor in e^2 corrections to amplitudes of, 25:30819
interactions e + N, empirical relation of $\pi^+ + p \rightarrow \pi^0 +$ missing mass interactions with inelastic, (T), 25:30795
interactions e + N, fixed-t dispersion relations for P_{33} resonance production in, (T), 25:30801
interactions e + N, overlapping resonance model of deep inelastic, 25:30782
interactions e + N, scaling and duality in, 25:30787
interactions e + N, vector meson dominance predictions for single π production in, (T), 25:30789
interactions γ + N + Δ + rho$^+$(rho$^-$), relation of electromagnetic moments of charged rho to, 25:30799
interactions γ + N + γ + N, sum rules for nucleon dipole moment from Compton-effect amplitude of, (T), 25:30776

(JINR-P2-5679)
interactions γ + N → π + N*, vector dominance model for, 25:30784
interactions γ + N → π+(π−) + Δ Coulomb couplings and Born-term analysis for, 25:30785
interactions γ + N, differential cross sections for π production in, (T), 25:30801
interactions γ + N, scaling and duality in, 25:30787
interactions K + N, exchange degeneracy in Reggeized absorption model for, 25:30874
interactions K + N, Poisson distribution for bounds, multiplicity, and energy dependence of inelastic, (T), 25:30899
interactions K + N, Veneziano model with spin for amplitude of three-body hadron production in, (T), 25:30889
interactions K⁻ + N → π + Σ, models of Σ(1405) as CDD pole and bound state of, 25:30876
interactions μ + N → ν + W + N, cross sections for scalar and vector W-meson production in, 25:30818
interactions N + N → N + N + π, dispersion relations and current--field algebra for hard-pion production in nonrelativistic, (T), 25:30898
interactions N + N at very high energies, angular and energy distributions of particles produced in, (T), 25:30870(T) (ORNL-tr-2433)
interactions N + N below 1 GeV/c, direct data analyses and phenomenological dispersion relations, (T), 25:30882
interactions N + N in GeV range, low-energy models for, (T), 25:30854
interactions N + N in infinite nuclear matter, effective potential for, (T), 25:31416
interactions N + N in ladder approximation with π exchange, Bethe--Salpeter equation for, 25:30909
interactions N + N, approximate Bethe--Salpeter equation for calculation of phase parameters for, 25:30912
interactions N + N, exchange degeneracy in Reggeized absorption model for, 25:30874
interactions N + N, local approximation to one-pion-exchange potential for, 25:30911
interactions N + N, Poisson distribution for bounds, multiplicity, and energy dependence of inelastic, (T), 25:30899
interactions N + N, Veneziano model with spin for amplitude of three-body hadron production in, (T), 25:30889
interactions ν + N → μ + W + N, cross sections for scalar and vector W-meson production in, 25:30818
interactions ν + N at high energies in freon and propane, duality--parton model for deep inelastic, (T), 25:30809
interactions ν + N, absence of form factor in e² corrections to amplitudes of, 25:30819
interactions π + N → rho + N*, vector dominance model for, 25:30784
interactions π + N at 385 to 1700 MeV/c, energy continuation of energy-independent phase shift analysis for resonance-like structure in, (T), 25:30871 (UCRL-20250)
interactions π + N at very high energies, angular and energy distributions of particles produced in, (T), 25:30870(T) (ORNL-tr-2433)
interactions π + N in GeV range, low-energy models for, (T), 25:30854
interactions π + N, continuous-spin pole exchange for elastic, 25:30892
interactions π + N, cross sections for multiple soft-π production in, 25:30887
interactions π + N, exchange degeneracy in Reggeized absorption model for, 25:30874
interactions π + N, fixed-pole effects on exchange-degenerate Regge residues, 25:30878
interactions π + N, review of Coulomb corrections in analysis of, (E/T), 25:30721
interactions π + N, review of elastic, 25:30872
interactions π + N, Veneziano model with spin for amplitude of three-body hadron production in, (T), 25:30889
production of N--anti N pairs from hadron interactions in extensive air showers above 10^{12} eV, cross sections for, (E), 25:30728
scattering by nuclei, realistic interactions for exchange effects in microscopic descriptions of elastic and inelastic, (T), 25:31432
scattering inelastically by nuclei, microscopic analysis using realistic potentials, 25:31393 (COO-1051-34)
spin--isospin functions of system of n-identical, classification of, 25:30916

NUCLEONS (anti N)
detection in primary cosmic radiation, (E), 25:30327
production of N--anti N pairs from hadron interactions in extensive air showers above 10^{12} eV, cross sections for, (E), 25:30728

NUCLEOPROTEINS
radiation effects on, in cultured human amniotic cells, cytofluorimetry studies on, 25:29709

NUCLEOPROTEINS, DEOXYRIBO-
radiation effects on chromatin, phenolic deproteinization method for studying, 25:29458

NUTRIENTS
role in γ radiobiological effects on γ-radiation effects on sunflower seeds, 25:29714

O

OCEANOGRAPHY
instrumentation for, precision deep-sea time release, 25:31756 (UCSD-34-P-127-6)

OCONEE POWER REACTOR, UNIT 1
control rod drives for, test program for, 25:31499 (DOCKET-50269-17)
coolant loss accident for, computer programs for analysis of, 25:31499 (DOCKET-50269-17)
piping systems for, information on earthquake resistant analysis of, 25:31499 (DOCKET-50269-17)
pressure vessel for, material surveillance program for, 25:31499 (DOCKET-50269-17)

OCONEE POWER REACTOR, UNIT 2
control rod drives for, test program for, 25:31499 (DOCKET-50269-17)
coolant loss accident for, computer programs for analysis of, 25:31499 (DOCKET-50269-17)
piping systems for, information on earthquake resistant analysis of, 25:31499 (DOCKET-50269-17)
pressure vessel for, material surveillance program for, 25:31499 (DOCKET-50269-17)

OCONEE POWER REACTOR, UNIT 3
control rod drives for, test program for, 25:31499 (DOCKET-50269-17)
coolant loss accident for, computer programs for analysis of, 25:31499 (DOCKET-50269-17)
piping systems for, information on earthquake resistant analysis of, 25:31499 (DOCKET-50269-17)
pressure vessel for, material surveillance program for, 25:31499 (DOCKET-50269-17)

OILS
neutron dose rate removal cross sections and buildup factors for, (E/T), 25:30637

OLDBURY REACTORS
pressure vessel for, testing under pressure and thermal loads of prestressed concrete, 25:29309

OLEIC ACID
effects on cadaverine deaminase activity in liver mitochondria of irradiated rats, 25:29641

OOCYTES
radiation effects on, of insects, γ and x, 25:29747

ORDNANCE MATERIEL
protection of ground-based, against environmental effects of atmospheric nuclear explosions, evaluation of methods for, 25:29246

ORES
analysis for barium and lead, x-ray radiometric method using selenium-75 source for, 25:28940

ORGANIC COMPOUNDS
heat transfer to glass wool from liquid, effects of porosity on, 25:29264 (EUR-4531, pp 821-39)

ORGANS
scanning of human, angioscintigraphy method for, 25:29587

ORNL ISOCHRONOUS CYCLOTRON
beam deflection septum magnets for, magnetically self-shaping, 25:31101
performance for acceleration of heavy ions, 25:31131

OSMIUM
determination in minerals and industrial samples, spectrophotometric, 25:28960
determination in presence of ruthenium without separation, 25:28941

OSMIUM ALLOYS AND SYSTEMS
Os--Re, superconductivity of hcp, (E), 25:30433
Os--Ru, superconductivity of hcp, (E), 25:30433

OSMIUM ISOTOPES Os-184
energy levels of, calculation including Mottelson--Valatin effect, (T), 25:31345

OSMIUM ISOTOPES Os-186
energy levels of, calculation including Mottelson--Valatin effect, (T), 25:31345

OSMIUM ISOTOPES Os-188
energy levels of, calculation including Mottelson--Valatin effect, (T), 25:31345

OSMIUM ISOTOPES Os-190
energy levels of, calculation including Mottelson--Valatin effect, (T), 25:31345

OSMIUM OXIDES
thermodynamic properties of gaseous diatomic, free energy functions for, 25:29082

OSTEICHTHYES
egg development of, effects of uranium fission products on, 25:29449
Esox lucius, radiosensitivity of roe of, during fertilization and early cleavage, 25:29659
radiation monitoring of Japanese coastal, near Goto Islands, July 1966, 25:29241
radioisotope content of skeleton and muscles of, 25:29449
radioisotope content of, from lakes of northern Italy, fallout manganese-54 and zirconium-95--niobium-95, 25:29477
Salmo, survival rate in Columbia River thermal effluents, 25:31645 (BNWL-1527)

XUM

OXALATES
determination using ion permselective membrane, potentiometric, 25:28956
effects on separation of thorium(IV) from sulfuric acid solutions by extraction using N-phenylbenzylamine in chloroform, 25:29184
1,3-OXATHIOLE
radioprotective effects of, on kidneys and liver in dogs injected with polonium-210, 25:29563
OXIDES
phase studies of metal, using solar furnace, 25:29987
removal from liquid metals, design of equipment for, 25:29800(P)
OXYGEN
abundance of ionospheric D-region atomic, silver-film sensor method for, (E), 25:30385
activity in vanadium dioxide--vanadium oxide system at 600 to 1200°C, equilibrium, 25:29952
alpha-particle stopping cross sections in gaseous, test of Bragg's rule for, 25:30642
cesium-atom reactions up to 30 eV with molecular, charge exchange in, (E), 25:30276 (ORNL-TM-2620)
consumption by hydrobionts, effects of uranium fission products on biochemical, 25:29449
determination in alabaster, radiometric x-ray method for, 25:28939
determination in high-purity water for reactor cooling and moderating, 25:28914 (BARC-515)
determination in liquid metals, apparatus for, 25:29407(P)
determination in phosphorus by fast neutron activation, 25:29024
determination in silicon by 14-MeV neutron activation, 25:29021
effects of interstitial impurity of, on mechanical properties of iron and refractory metals, 25:29855
effects on age hardening of deformed α-zirconium, 25:29853
effects on determination of uranium by controlled-potential coulometry, 25:28975
effects on hardness and yield stress of niobium, tantalum, and vanadium wires, relations with deformation temperature and nitrogen content, 25:29880
effects on polymerization of ethyl acrylate with γ-irradiated cellulose, 25:29108
effects on radiosensitivity of Escherichia coli and rats in presence of ferrous ions, 25:29556
effects on radiothermoluminescence of crystalline and glassy methanol, 25:29101
effects on sodium reactions with refractory metals at high temperatures, 25:29761 (ORNL-4630, pp 156-7)
effects on thermal diffusivity of sintered uranium monocarbide at 500 to 2200°K, 25:29957
emission of forbidden atomic OI ($^1D--^3P$) 6300-A, SAR red-arc, (E), 25:30398
meson (π⁻) capture by, neutron spectra from radiative, (E), 25:31273
pressure in mouse spleen, effects of radioprotective sympathomimetics on, 25:29547
reactions with polycrystalline rhenium surfaces, thermal-flare studies of, 25:29772
reactions with silicon coatings on tungsten ribbons at 700 to 1200°C and low pressures, kinetics and mechanism of oxidation, 25:29568
reactions with silicon-coated tungsten at 600 to 1600°C and low pressure, kinetics and mechanism of oxidation, 25:29869
separation from off-gas streams, evaluation of thin silicone rubber membranes for, 25:29317 (ORNL-4522)
sorption on beryllium surface, 25:29894
spectra of atomic, at 100 to 300 km in day ionosphere, excitation of 5577-A green-line, (E), 25:30375
spectra of daytime airglow of atomic, photodissociative excitation of, (E), 25:30386
tension in tissues of γ-irradiated rats, effects of mexamine on kinetics of, 25:29551
tension in tissues of rats, effects of mexamine on kinetic of, 25:29551
yields from radiolysis of copper(II) and iron(II) in perchloric and sulfuric acids, 25:29141
OXYGEN FLUORIDES
thermodynamic properties of gaseous diatomic, free-energy functions for, 25:29082
OXYGEN IONS
implantation into zinc telluride, photoluminescence study of, 25:30657
OXYGEN IONS (O^+)
abundance in ionospheric D region, (E/T), 25:30404
OXYGEN ISOTOPES O-15
production in stars by explosive nucleosynthesis in helium zones, (T), 25:30067
OXYGEN ISOTOPES O-16
alpha decay of excited, evidence of noncanceling seagull and Schwinger terms in weak parity-violating amplitude from, 25:30931
alpha scattering at 1 GeV per nucleon, absorption cross sections for, 25:31234
alpha scattering at 104 MeV, differential cross sections for, (T), 25:31212
binding energy of, Brueckner calculation of, (T), 25:31201 (JINR-P4-5614)
deuteron reactions (d,α) at 14.0 to 18.1 MeV, isospin, 25:31227
deuteron reactions (d,p) with, analysis using coupled channel theory, 25:31210
electron elastic scattering at 30 to 60 MeV cross sections for, (E), 25:31219
energy levels of, Brueckner calculation of, (T), 25:31201 (JINR-P4-5614)
energy levels of, calculations using Sussex matrix elements for odd-parity, 25:31230
energy levels of, one-particle-hole and projected Hartree-Fock approximations for, (T), 25:31226
helium-3 reactions (He-3,Li-6) at 30 MeV, DWBA analysis of, (E/T), 25:31214
helium-3 reactions (He-3,Li-6) at 40.7 MeV, DWBA analysis of, (E/T), 25:31214
meson (π⁻) capture by, analysis using particle-hole model, (T), 25:31217
meson (π⁻) capture by, neutron spectra from radiative, (E), 25:31216
meson (π⁻) capture by, rescattering effects in radiative, (T), 25:31217
nuclear radii and form factors from electron elastic scattering at 44 to 121 MeV, (E/T), 25:31206 (SAL-17)
nuclear radius from electron elastic scattering, (E), 25:31219
photon reactions (γ,n) at 10 to 68 MeV, yields of radioactivities from, (E), 25:31333
photon reactions (γ,n) in giant resonance region, cross section for, (E), 25:31231
proton elastic scattering at 8.5 to 12.7 MeV, polarization in, (E), 25:31236
proton scattering at 1 GeV, nuclear opaqueness model for differential cross sections for, 25:31234
reactions (O-16,f) with samarium-154 at 137 MeV, angular distribution of fission products from, (E), 25:31371
OXYGEN ISOTOPES O-17
energy levels of, Brueckner calculation of, (T), 25:31201 (JINR-P4-5614)
nuclear radii and form factors from electron elastic scattering at 44 to 121 MeV, (E/T), 25:31206 (SAL-17)
OXYGEN ISOTOPES O-18
alpha reactions (α,n) with, neutron yield from, (T), 25:31224
effects on infrared absorption spectra of silica gel--water system, 25:29069
effects on matrix spectra of vanadium oxide, 25:29083
exchange between thorium oxychloride and heavy water, 25:29089
nuclear radii and form factors from electron elastic scattering at 44 to 121 MeV, (E/T), 25:31206 (SAL-17)
production in stars by explosive nucleosynthesis in helium zones, (T), 25:30067
OXYGEN SYSTEMS
Ar--O, reactions with radiolytic hydrogen atoms, kinetics of, 25:29158
C--O--Te--U, phase diagram at 1200°C, 25:30001
Fe--H--Hf-base--N--O--Zr, ductility and tensile properties of dilute, effects of composition on, 25:29827(R) (RPI-3719-9)
H--Hf-base--O--Zr, ductility and tensile properties of dilute, effects of composition on, 25:29827(R) (RPI-3719-9)
O--Ti, crystal structure of solid solutions of alpha, 25:30000
O--U--Y, crystal lattice parameters of solid solutions of, 25:29922 (ORNL-4630, pp 3-58)
O--Zr, crystal structure of solid solutions of alpha, 25:30000
O--Zr, crystallization of solid solutions of, effects of oxygen content on temperature of, 25:29854

P

PACIFIC OCEAN
sound scattering layers off Oregon coast, 25:31723 (RLO-1750-62)
PACKAGING
radiation effects on materials for radiosterilized food, gamma, 25:30033
PADUCAH AREA (Ky.)
radiation monitoring of environment of, during 1970, 25:29502 (KY-629)
PAINTS
radiation effects on curing polymerizable binders for, electron, 25:29120(P)
radiation effects on properties of zinc oxide-base, proton and uv, 25:29105
PALISADES POWER REACTOR
effluents from, effects on environment of chemical, radioactive, and thermal, 25:31494 (DOCKET-50255-38)
PALLADIUM
determination of trace amounts of, in biological materials, platinum, and rocks by isotope dilution, 25:28981
determination of trace amounts of, in standard rocks by neutron activation following fire-assay concentration, 25:29022
effects on fluorescence determination of copper, 25:28928

PALLADIUM ALLOYS AND SYSTEMS
Co-base--Pd, thermal expansion at 100 to 800°C, 25:29899
Co-base--Pd, transformation temperatures of, allotropic, 25:29899
Co-base--Pt, thermal expansion at 100 to 800°C, 25:29899
Co-base--Pt, transformation temperatures of, allotropic, 25:29899
Nb--Pd, diffusion processes at 700 to 1030°C, quantitative electron probe microanalysis study of, 25:29881
Pd--Ta, diffusion processes at 700 to 1030°C, electron-microprobe study of, 25:29893
Pd-base--Si, radiation effects on amorphous structure of, fission products, 25:29901 (CEA-CONF-1693)
PALLADIUM ISOTOPES Pd-103
separation of rhodium-103 from, by ion exchange, 25:29413 (CONF-691225)
PALLADIUM ISOTOPES Pd-106
energy levels from rhodium-106m decay, spins and parities of, (E), 25:31384
PALLADIUM ISOTOPES Pd-108
alpha inelastic scattering at 10.1 MeV, γ--γ angular correlations from, (E), 25:31374
energy levels from silver-108 decay, spins and parities of, (E>, 25:31382
energy-level transition from Coulomb excitation, multipole mixing ratio of 497 keV, (E), 25:31374
PALLADIUM OXIDES
thermodynamic properties of gaseous diatomic, free energy functions for, 25:29082
PANCREAS
effects of duct ligation of, on survival of x-irradiated dogs, 25:29651
radiation dose to, in normal and tumor-bearing mice following administration of phosphorus-32-labeled chromium alloxantin and orthophosphate, 25:29453
PARAFFIN
neutron dose rate removal cross sections and buildup factors for, (E/T), 25:30637
PARTICLE TRACKS
analysis of bubble chamber, program for linking FSD microscopes with Minsk-2 computer for analysis of, 25:29379
analysis of heavy-liquid bubble chamber, computer program for, 25:29369 (ITEF-753)
charge identification of nuclear emulsion, 25:29380
PARTICLES
content in rainwater, effects of rainfall intensity on, (E), 25:29224
mixing of dissimilar dry, design and operation of equipment for, 25:29254(P)
removal of very fine, from polluted air streams, performance of condensing steam aerosol scrubber for, (E), 25:29251 (ORNL-4654)
PATHOLOGY
book: Pathology of Irradiation, 25:29689
PEACH BOTTOM POWER REACTOR, UNIT 1
control rods for, revised surveillance requirements for, 25:31487 (DOCKET-50171-84)
fuel elements for, revised loading specifications for FPTE, 25:31487 (DOCKET-50171-84)
steam generators for, development and performance of, 25:31623 (GA-10338)
PEACH BOTTOM POWER REACTOR, UNIT 2
piping systems for, fabrication and stress testing of, 25:31502 (DOCKET-50277-19)
pressure vessel for, fabrication and stress testing of, 25:31502 (DOCKET-50277-19)
site for, environmental radiation survey for, 25:31502 (DOCKET-50277-19)
site for, hydrological and meteorological data for, 25:31502 (DOCKET-50277-19)
PEACH BOTTOM POWER REACTOR, UNIT 3
piping systems for, fabrication and stress testing of, 25:31502 (DOCKET-50277-19)
pressure vessel for, fabrication and stress testing of, 25:31502 (DOCKET-50277-19)
site for, environmental radiation survey for, 25:31502 (DOCKET-50277-19)
site for, hydrological and meteorological data for, 25:31502 (DOCKET-50277-19)
2-PENTANONE, 4-METHYL-
solvent properties for separation of thorium and uranium from hydrochloric, nitric, perchloric, or sulfuric acid solutions, effects of lithium chloride or magnesium chloride on, 25:29195
PERCHLORIC ACID
separation of thorium and uranium from aqueous solutions of, by solvent extraction using 4-methyl-2-pentanone, effects of lithium chloride or magnesium chloride on, 25:29195
PERMANGANATES
determination using ion permselective membrane, potentiometric, 25:28956
PERPHENAZINE
effects on unconditioned reflexes in irradiated cats, 25:29643
PERSONNEL
emotional stability of nuclear industry, method of measurement using electric conductivity of skin, 25:29531 (CEA-R-4156)
protection of radiography, effectiveness of protective clothing for, 25:29529
radiation dose to color television equipment repair, x, 25:29512 (BRH/DEP-71-4)
radiation effects on glucocorticoid excretion by, 25:29708
radiation effects on, evaluation of studies on delayed, 25:29703
radiation exposure record systems for, standards for, 25:29519
radiation protection standards for uranium mine and mill, 25:29536
radiation protection standards for uranium mine and mill, 25:29535
radiation protection standards for uranium mine, economic impact of compliance with, 25:29532
radiation protection standards for, of nuclear reactor fuel fabrication plants, 25:29534
radioactive contamination of nuclear, at Ispra, methods for measurement of mixed β and γ, 25:29517
radioinduced malignancies in, in Czechoslovakia, methods for protection against, 25:29711
training of nuclear power plant, standards for, 25:31481
treatment of radium-contaminated, following accidental release at Italian refinery, hospital facilities for, 25:29508
PERTURBATION THEORY
axial charge in, 25:30982
scale invariance breakdown in generalized Bjorken limit of, 25:30783
scattering amplitudes in second-order, conserved currents, Reggeization, and Mandelstam counting in, 25:30992
Ward identities in renormalized, anomalous, 25:30935
PETROLEUM
radiation processing of, 25:29128
PHANTOMS
design for adjustment of gamma-ray imaging devices, 25:29328 (ORNL-TM-3261)
PHARMACEUTICALS
analysis for zinc by neutron activation and γ spectroscopy, 25:29029
preparation of radio-, in Italy, review of, 25:29273
PHENOL, 4-sec-BUTYL-2-(α-METHYLBENZYL)-
solvent properties for cesium from urine after ammonium molybdophosphate ion exchange, 25:28983
PHENYLEPHRINE
effects on oxygen pressure in mouse spleen, 25:29547
norepinephrine, radioprotective effects of, on beagle dog hearts, lethal, whole-body mixed γ and neutron, 25:29565
radioprotective effects of, effects of N-(2-chloroethyl)dibenzylamine hydrochloride on, 25:29546
PHILIPPSBURG POWER REACTOR
design parameters of, 25:31461
PHONONS
interactions with electrons in impure metals, deviations from additivity in theory of scattering, 25:30697 (NP-18822)
PHOSPHATES
effects on separation of thorium(IV) from sulfuric acid solutions by extraction using N-phenylbenzylamine in chloroform, 25:29184
PHOSPHINE OXIDE, TRIPHENYL-
complexes with uranyl compounds, phosphorus--oxygen bonding in, effects of coordination on, 25:29088
PHOSPHORIC ACID
corrosive effects on molybdenum alloys, relations with concentration, pressure, and temperature, 25:29776
corrosive effects on tantalided nickel and Type 316 stainless steel at 150°C, 25:29766
distribution of phosphorus-32-labeled, in tissues of normal or tumor bearing mice in comparison with phosphorus-32-labeled chromium alloxantin, 25:29453
PHOSPHORIC ACID, BIS(2-ETHYLHEXYL) ESTER
solvent properties for bismuth-206 and bismuth-207 from deuteron- or proton-irradiated lead, 25:29164
PHOSPHORIC ACID, TRIBUTYL ESTER
solvent properties for fission products, thorium, and uranium, 25:29198
PHOSPHOROTHIOIC ACID, S-(2-AMINOETHYL) ESTER
radioprotective effects on muscles and spleen of mice, effects of increased atmospheric pressure on γ, 25:29550
PHOSPHORUS
analysis for oxygen by fast neutron activation, 25:29024
determination in low-alloy steel, two-standard method for spectrometric, 25:28950
effects of interstitial impurity of, on mechanical properties of iron, 25:29855
effects on ductility of Inconel 600 at 400 to 1000°C, 25:29825 (ORNL-4630, pp 261-70)
effects on fluorometric determination of zirconium, 25:28963
PHOSPHORUS IONS
reactions with nitrogen molecules at 10, 200, and 300 keV, cross sections for single and double electron loss in, (E), 25:30300
PHOSPHORUS ISOTOPES
effectiveness for radiodiagnosis or radiotherapy in man, 25:29573
radioactivity standards of, users' guides for, 25:29174

XUM

PHOSPHORUS ISOTOPES P-29
energy level at 3.446 MeV from the silicon-28 (p,γ) reaction, search for, (E), 25:31250
PHOSPHORUS ISOTOPES P-30
energy levels from aluminum-27 (α,n) reactions, lifetimes of, (E), 25:31279
PHOSPHORUS ISOTOPES P-31
photon reactions (γ,n) up to 30 MeV, cross section for, (E), 25:31242
PHOSPHORUS ISOTOPES P-32
analysis for radioactive and other impurities, ASTM method for, 25:29002
effects on biological and physical properties of pneumococcal DNA following incorporation, β, 25:29459
effects on chromosomes and pollen and seed fertility of M(1) generation of rice, 25:29496
removal from medical equipment, effectiveness of detergent solution combined with sound frequency vibrator for, 25:29510
uptake of chromium alloxantin-incorporated, by tissues of normal or tumor-bearing mice in comparison with phosphorus-32-labeled orthophosphate, 25:29453
use as tracer for determining distribution of onion flies, 25:29748
PHOSPHORUS OXIDES
thermodynamic properties of gaseous diatomic, free energy functions for, 25:29082
PHOSPHORUS SYSTEMS
Ni--P, effects on low-temperature sintering of tungsten, 25:29793
PHOSPHORYLATION
radiation effects on oxidative, in animal liver mitochondria, effects of histones on, 25:29638
radiation effects on oxidative, in rat liver mitochondria, effects of riboflavin on, 25:29640
PHOTOELECTRIC CELLS
fabrication and performance of n--p junctions in lead telluride, 25:29397
PHOTOELECTRIC EFFECT
electron emision from thin films in vacuum uv region, research program on, 25:30665(R) (UH-235-P-9-2)
PHOTOGRAPHIC FILM
performance of x-ray, for industrial radiography, 25:29294
PHOTOGRAPHY
method in field of high frequency currents, 25:31733(T) (SC-T-713025)
PHOTOMETERS
design of light scattering, for air filtration system studies, 25:31702 (LA-4627)
PHOTOMULTIPLIER TUBES
pulse shaper for scintillation detector, design of, 25:29342
pulse shaper for, design and performance of, 25:29347
PHOTONS
distribution in air showers, H-quantum and two-fireball models for lateral, (T), 25:30793
effects in combination with pulsed electrons on chemiluminescence of aqueous solutions of fluorescein dyes, 25:29138
effects on formation of defects and sputtering in alkali halides, 25:30651
emission in weak interactions, W boson theory for divergences of amplitudes of, (T), 25:30805 (NP-18777)
interactions γ + γ at high energies, use of electron--positron colliding beam for experimental study of, 25:30798
interactions γ + N → Δ + rho⁺(rho⁻), relation of electromagnetic moments of charged rho to, 25:30799
interactions γ + N → γ + N, sum rules for nucleon dipole moment from Compton-effect amplitude of, (T), 25:30776 (JINR-P2-5679)
interactions γ + n → p + π⁻, review of coupling parameters for, (E/T), 25:30797
interactions γ + n → p + rho⁻, relation of electromagnetic moments of charged rho to, 25:30799
interactions γ + N → π + N*, vector dominance model for, 25:30784
interactions γ + n → π⁻ + p at 300 to 1200 MeV, differential cross sections for, (E), 25:30774 (INSJ-126)
interactions γ + N → π⁺(π⁻) + Δ Coulomb couplings and Born-term analysis for, 25:30785
interactions γ + N, differential cross sections for π production in, (T), 25:30801
interactions γ + N, scaling and duality in, 25:30787
interactions γ + p → Λ(Σ⁰) + K⁺, review of coupling parameters for, (E/T), 25:30797
interactions γ + p → p + eta, review of coupling parameters for, (E/T), 25:30797
interactions γ + p → p(n) + π⁰(π⁺), review of coupling parameters for, (E/T), 25:30797
interactions γ + p → π⁺ + p at 300 to 1200 MeV, resonance structures in, (E), 25:30774 (INSJ-126)
interactions γ + p → rho⁰ + p, s-channel helicity conservation for diffractive part of, (T), 25:30885
interactions γ + p, review of production of several hadrons in, (E), 25:30716
interactions π + N → rho + N*, vector dominance model for, 25:30784
interactions with background radiation at very high energies in extragalactic space, e, μ, and π pair creation in, 25:30792
interactions with pomerons, model for 2π production in, 25:30863
polarization by circular dielectric infinite cylinders in interstellar space, (T), 25:30213
reactions with helium at 2.62 MeV in streamer chamber, pair and triplet production from, (E), 25:30717
reactions with nuclei, accuracy of photon-difference method for calculation of cross sections in, 25:30773 (DESY-71/3)
reactions with nuclei, analysis using Feynman diagrams, (T), 25:31435
scattering by lead and uranium at 1.33 MeV, differential cross sections for elastic, (E), 25:31370
scattering of, derivation of inverse Compton effect, (T), 25:30502
PHOTOSPHERE
electric conductivity in, relation to sunspots, (T), 25:30186
iron abundance in, (E), 25:30170
resistive effects in turbulent, finite, (T), 25:30180
PHYSICAL CHEMISTRY
book: Chemical Consequences of Nuclear Spin, 25:30669
PHYSICS
research progress on theoretical phonon, 25:31711(R) (NYO-3699-53)
2-PICOLINE
complexes with uranium(V) chloride, properties of, 25:29092
3-PICOLINE
complexes with uranium(V) chloride, properties of, 25:29092
PILOCARPINE
nitrate, effects on iodine-131 and technetium-99m scanning of human salivary glands, 25:29579
PINCH DEVICES
current density at slot edges of, surface, (T), 25:30601
design and construction of PIACE, for injection and adiabatic compression, 25:30587 (EUR-4593, pp 431-41)
design of Scyllac, 25:30564 (EUR-4593, pp 227-39)
design of toroidal ISAR I, 25:30585 (EUR-4593, pp 419-24)
design of transformer-coupled fast theta-, with variable rise time, 25:30577 (EUR-4593, pp 355-63)
electron heating by large-amplitude oscillations in theta-, (E), 25:30467
magnetic field calculations for fringe fields of, vacuum, (T), 25:30601
plasma diagnostics in Scylla, research on, (E/T), 25:30450(R) (LA-4585)
plasma end losses in combined magnetic mirror and theta, (T), 25:30464
plasma intabilities in Scylla, research on, (E/T), 25:30450(R) (LA-4585)
power supplies for 500-kV theta, design of, 25:30567 (EUR-4593, pp 265-71)
power supplies for ISAR I, crowbar system for, 25:30560 (EUR-4593, pp 189-95)
research at LASL during Nov. 1969--Oct. 1970, 25:30450(R) (LA-4585)
PINCH EFFECT
oscillations in electron--hole, finite-amplitude m = 0, 25:30544 (IAE-1950)
skin effect in high-energy z, (E), 25:30507 (NP-18775)
stability of low-density, 25:30544 (IAE-1950)
PIPES
helium II in cylindrical, temperature differences and mutual friction near lambda point in, 25:30405
PISTON ENGINES
temperature of piston rings in Diesel, krypton-85 tracer method for measurement of working, 25:29282
PITUITARY GLAND
radiation effects on activity of dog, acute and chronic, 25:29642
PLANETARY NEBULAE
mass ejection by radiation pressure in, (T), 25:30044
spectra in, Hβ, O I, and N II, (E), 25:30115
spectra of NGC 7027 and NGC 7662, high-n Balmer lines in, (E), 25:30078
structure in, effects on ionization of small-scale, (E), 25:30115
PLANETS
formation in epsilon Aurigae eclipsing binary, (E/T), 25:30083
formation of systems of, computer simulation of, (T), 25:30178
mass ratio for, gravitational-to-inertial, 25:31009
PLANTS
analysis of deposits on, for fluorine by neutron activation, 25:29011 (CEA-CONF-1747)
organic and inorganic material loss from above-ground, by leaching, 25:31709(R) (NYO-2598-52)
photosynthesis, respiration, and transpiration of, improved feedback control for Null-Point compensating system for measurement of, 25:31741 (UCLA-12-813)
radiation effects on growth and survival of, effects of homologous DNA on, 25:29716
radioactive aerosol retention by, in comparison to retention of particulate fallout, effects of particle size on, 25:29444
strontium-90 accumulation in freshwater, in relation to

calcium content of water, discrimination coefficient for, 25:29452
PLASMA
acceleration of cylindrical shell in presence of magnetic field, stability of, (T), 25:30547
atom emission from high temperature, flux of, (T), 25:30514 (JAERI-Memo-4243)
bibliography on, 25:30454
book: Advances in High Temperature Chemistry, 25:29081
book: Technology of Strong Pulsed Currents and Magnetic Fields, 25:30604
boundary layer interactions with vacuum walls, wall material effects on, 25:30496 (EUR-4593, pp 461-70)
boundary sheath growth in low-pressure, (T), 25:30531
charged-particle diffusion in weakly turbulent stochastic fields, Fokker--Planck equation for, (T), 25:30520
charged-particle motion in axisymmetric magnetic mirror fields, single-particle, (T), 25:30516 (N-70-42698)
collisions in, particle flux associated with stochastic processes in, (T), 25:30518 (N-71-11853)
conductivity in supercritical electric fields, anomalous, (T), 25:30625
conference on, 25:30451
conference on fusion technology, 6th, Aachen, Germany, 9/70, 25:30449 (EUR-4593)
confinement and heating in Tokamak T-3, (E), 25:30461(T) (MATT-Trans-79)
confinement in l = 3 stellarators, source and electron cyclotron resonance heating effects on, (E), 25:30457 (IPPJ-102)
confinement in magnetic mirror compression experiment, self-consistent theory for particle loss in, (E/T), 25:30465
confinement in magnetostatic mirrors with helping microwaves, cone losses in, (E), 25:30463
confinement in mirror theta pinches, end losses, (T), 25:30464
diagnostics in Scylla devices, research on, (E/T), 25:30450(R) (LA-4585)
diagnostics in thermal argon, from standard intensity source at 1100 to 3100 A, carbon dioxide-, hydrogen-, and nitrogen-seeded, (E), 25:30488
diagnostics of argon arc, thermodynamics, (E), 25:30478(T) (SC-T-713024)
diagnostics of contracted argon column, microwave, 25:30486
diagnostics of helium, determination of excited population densities by electron impact spectroscopy, (E), 25:30481
diagnostics of helium, excitation in stationary PIG discharge, population densities from, (E/T), 25:30479
diagnostics of high-temperature, review of spectroscopic, 25:30492
diagnostics of hot, optical spectra measurements for proton velocity distribution, 25:30493
diagnostics of hot-electron mirror-confined, performance evaluation for, 25:30489
diagnostics of Landau damping of surface waves resonator method for, in column, (E), 25:30491
diagnostics of laser-produced, probe method for, 25:30477 (NP-18765)
diagnostics of laser-produced, using holographic interferometry, 25:30487
diagnostics of nitrogen, comparison of rotation temperature of N_2^+, (E), 25:30480
diagnostics of positive column, microwave, (E), 25:30483
diagnostics of xenon pinch, interferometric, 25:30484
diagnostics of, automatic data collection and processing at HBTX for, 25:30474 (EUR-4593, pp 557-66)
diagnostics of, corpuscular method for streaming particles, 25:30485
diagnostics using cylindrical probes at medium pressures, density, 25:30494
diagnostics using external rf probes, effect of glass wall on conductivity, (T), 25:30527
diagnostics using light scattering from magnetic fluctuations, 25:30490
diffusion in flash x-ray discharge tubes, 25:30499 (UUIP-659)
diffusion in stellarators, recombination effects on, (E/T), 25:30462 (NP-18767)
diffusion of decaying helium in stellarator, across magnetic fields, (E/T), 25:30472
diffusion of electrons in toroidal magnetic fields, effects of nonadiabatic scattering on, 25:30466
electromagnetic field in cold anisotropic, with two-dimensional inhomogeneity, (T), 25:30533
electromagnetic-wave propagation in two-component intense, effects on density and heating, (T), 25:30619
electron beam interactions with inhomogeneous, electron--ion oscillations from, (E), 25:30506(T) (MATT-Trans-84)
electron beam interactions with magnetized, electron--ion oscillations from, (E), 25:30505(T) (MATT-Trans-83)
electron beam interactions with, ion emission from, (E), 25:30255 (EUR-4593, pp 67-74)
electron beam interactions with, radiations from unstable waves in, (E), 25:30510
electron beams for research in, production of intense, 25:30254 (EUR-4593, pp 59-65)
electron--ion recombination and ionization coefficients for quasi-stationary helium, (T), 25:30540
electron-beam interactions with dense, intense monoenergetic, (E/T), 25:30504
electron-beam quasi-linear relaxation in inhomogeneous and homogeneous, ultrarelativistic, (T), 25:30534
equilibrium and stability in Heliotron magnetic fields, (T), 25:30549
explosion of small particle in powerful light beam, initial time-dependent parameters of light, (T), 25:30471
flow in annular MHD duct at high Hall-parameter values, (E), 25:30343
flow in MHD channels, preionization and velocity effects in nonequilibrium, 25:30348
flow through channel with magnetic field followed by injection through electrodes, effects of Hall effect on steady-state, (T), 25:30344
heating and confinement in Tokamak T-3, (E), 25:30461(T) (MATT-Trans-79)
heating at electron cyclotron resonance, high-power 8-GHz, 25:30456 (EUR-4593, pp 551-6)
heating by collisionless low-β shock waves, near critical Alfven--Mach number, (E), 25:30468
heating by external hf electromagnetic fields, (E), 25:30460(T) (MATT-Trans-13)
heating by ion acoustic waves in ion-streaming, ion, (E), 25:30458 (IPPJ-104)
heating by large-amplitude oscillations in theta-pinch, electron, (E), 25:30467
heating by large-amplitude whistler excitation in, turbulent, (T), 25:30470
heating by lasers and electron beams, (T), 25:30452
heating by neutral injection into stellarators, 25:30455 (EUR-4593, pp 479-84)
heating during annihilation of opposite magnetic fields, turbulent, (E), 25:30469
heating in model ST tokamak, ohmic, (E), 25:30459 (MATT-813)
heating of magnetized, nonlinear resonant, (T), 25:30473
helium metastable atom destruction in low-temperature, kinetics of and heating effects of, (E), 25:30512
injection into quadrupole magnetic fields, trapping in, (E), 25:30450(R) (LA-4585)
interactions with hf fields, R-Qhm installation for studying, 25:30508 (NP-18801)
interactions with sputtered wall materials, (T), 25:30497 (EUR-4593, pp 471-7)
ion beam interaction with, efficient transfer of energy during, (E), 25:30511
ion distribution function for low-pressure neon, effects of step ionization on, (T), 25:30525
ion recombination in dense, effect of ionization resonance on nonequilibrium population during, (T), 25:30519
ionization and volume recombination coefficients for quasi-stationary helium, (T), 25:30540
ionization of deuterium, in toroidal high-β experiments, 25:30541 (IPP-1/114)
ionization of uranium, relation to temperature and density, (T), 25:30536
kinetic theory for transverse waves in, 25:30526
kinetic theory of fully ionized, correlation functions for, 25:30523
kinetic theory of Lorentz, Legendre polynomial development for, (T), 25:30522
kinetic theory of magneto-active, in quasi-linear approximation, (T), 25:30532
kinetic theory of, exact Green function for Lenard--Bernstein operator in magnetic fields, 25:30537
kinetics in strong magnetic and electric fields, Born approximation calculation of, (T), 25:30530
kinetics of imperfect, thermodynamically complete equation of state for, (T), 25:30521
kinetics of relativistic, integral equation for total charge density, (T), 25:30538
kinetics of, particle flux from stochastic scattering processes in, (T), 25:30518 (N-71-11853)
kinetics of, transverse electromagnetic fields in, (T), 25:30535
magnetic fields, collective effects during annihilation of opposite, (E), 25:30469
oscillations in bounded current-carrying thermal, constant-frequency, (E), 25:30624
oscillations in cold inhomogeneous, small-amplitude electrostatic, (T), 25:30623
oscillations in spherical magnetized cold-cathode discharges, vlf, (E), 25:30617
oscillations in, helical electron, 25:30544 (IAE-1950)
oscillations in, studies of Hall effect in, 25:30544 (IAE-1950)
oscillations of degenerate relativistic, longitudinal, (T), 25:30529
pinch effect in, skin effect in high-energy z, (E), 25:30507 (NP-18775)
pinch effect in, Vlasov theory for supercritical magneto-acoustic compression pulse, 25:30513 (IPP-1/113)
pressure of components of, partial, (T), 25:30539
production and expansion of argon, by carbon-dioxide laser pulse heating, (E), 25:30542
production by laser irradiation, probe method for ion measurements from, 25:30477 (NP-18765)
production by laser-irradiation of targets, ion emission

XUM

from, 25:31137
production in modified PIG discharges, 25:30543
properties at pressures up to 130 atm, arc and radiation, (E), 25:30509
radiations from high-temperature, flux of fast neutral, (T), 25:30514 (JAERI-Memo-4243)
radiations from magneto-, gyrosynchrotron, 25:30515 (N-70-41892)
radiations from unstable waves in electron-beam excited, (E), 25:30510
research at LASL during Nov. 1969--Oct. 1970, 25:30450(R) (LA-4585)
research progress on controlled fusion, summary of, 25:30600 (WASH-1172)
shock wave structure in, hydromagnetic, (T), 25:30528
shock-wave propagation in collisionless, along magnetic-field lines, (E/T), 25:30620
spectra in argon and hydrogen, Hβ Stark broadening profiles in, (E/T), 25:30268
spectra of rotational-symmetric, radial distribution of emission and absorption coefficients for, (T), 25:30524
stability and equilibrium in Heliotron magnetic fields, (T), 25:30549
stability in Scylla devices, research on, (E/T), 25:30450(R) (LA-4585)
stability in short magnetic mirrors, bounce effects in negative mass, (T), 25:30551
stability of accelerated shell of, in magnetic fields, (T), 25:30547
stability of finite and high-pressure, with finite electron thermal conductivity, (T), 25:30546
stability of, hydromagnetic analog of Kelvin--Helmholtz problem including Hall effects, 25:30392
stabilization of drift instabilities in magnetized, using feedback technique, 25:30550
stabilization of flute instability in inhomogeneous, criteria for, (T), 25:30548
temperature relaxation of electron-ion, in hf electric and constant magnetic fields, (T), 25:30545
turbulence in, theory for magnetohydrodynamic, 25:30517(R) (N-71-11428)
use of laser-produced, as spectroscopic light source, 25:30498 (N-70-41880)
wave absorption at upper hybrid resonance, electromagnetic, (T), 25:30616
wave absorption at upper hybrid resonance, shf, (E/T), 25:30606 (NP-18807)
wave absorption by, effect of external dc electric fields on microwave, (T), 25:30628
wave damping along column of, resonator method for measuring Landau, (E), 25:30491
wave damping in nondegenerate magneto-, correlation, (T), 25:30621
wave damping in, nonlinear Landau, (T), 25:30615
wave echoes in, properties of ion acoustic, (E/T), 25:30611
wave excitation by supercritical electric fields, hf, (T), 25:30625
wave interactions in, equilibrium states of three nonlinear, (T), 25:30627
wave interactions in, ion acoustic and helicon nonlinear, (T), 25:30607
wave interactions with, third harmonic generation in microwave, (T), 25:30609
wave propagation above ion cyclotron frequency, electrostatic ion, (E), 25:30612
wave propagation along column of weakly magnetized, space-charge, (E/T), 25:30618
wave propagation in cold, nonlinear processes in electrostatic, (T), 25:30613
wave propagation in collisionless argon, large-amplitude electron, (E/T), 25:30610
wave propagation in dispersive, multiple-time technique for nearly linear, 25:30622
wave propagation in hot electron, effect of spatially uniform external periodic magnetic field on, (T), 25:30614
wave propagation in, kinetic theeory of transverse, 25:30526
wave propagation in, kinetic theory of longitudinal forced and free, 25:30605 (NP-18673)
wave propagation through slowly varying, WKB solution of electromagnetic, (T), 25:30608
wave reflection from, nonlinear theory of oblique incident electromagnetic, (T), 25:30626
x-ray emission from hot, in Cygnus Loop, (E), 25:30132

PLASMA ACCELERATORS
ion--neutral coupling in high-power MPD, 25:30599(R) (N-71-10100)
jet diagnostics in dense focus, using charged particle from d,d reactions in, (E), 25:30475(T) (LA-tr-71-6)
jet thrust from MPD arc, with self-induced magnetic fields, 25:30503
use of dense focus, for fusion blanket studies, 25:30592 (EUR-4593, pp 525-31)

PLASMA JETS
diagnostics in dense focus discharge, using charged particles from d,d reactions in, (E), 25:30475(T) (LA-tr-71-6)
diagnostics using immersed microwave probes, (E), 25:30476 (N-71-10564)
diagnostics using spherical probes, ion flow, 25:30482
use in production of circular-cylindrical surfaces on lathe, 25:31753(T) (UCRL-Trans-10524)

PLASMAPAUSE
relation of location of, to magnetospheric field lines leading to SAR arcs, (E/T), 25:30376

PLASTICS
conference on process radiation in plastics industry, Pullman, Washington, June 11-13, 1969, 25:29121
performance of liquid-impregnated foils of, for electric insulation, 25:30569 (EUR-4593, pp 281-6)
radiation processing of, 25:29128
radiation production of, review on electron, 25:29127

PLATINUM
analysis for trace amounts of palladium by isotope dilution, 25:28981
analysis for trace impurities by neutron activation following separation by ion exchange chromatography, 25:29023
deposition on tungsten surfaces, mechanisms of vapor, 25:29850
determination of trace amounts of, in standard rocks by neutron activation following fire-assay concentration, 25:29022
energy-level transitions in, electron spectra from Coster--Kronig and L-shell Auger, (T), 25:30261
radiation effects on shear modulus of, at 4°K, neutron, 25:29912
radioinduced self-interstitial atoms in, long-range migration in Stage I annealing of 20- and 30-keV platinum-ion, 25:30649 (NYO-3504-57)

PLATINUM ALLOYS AND SYSTEMS
Cr--Pt--W, tensile properties of intermetallic compounds of, at 1290°C, 25:29823 (ORNL-4630, pp 186-90)
Hf--Pt-base, tensile properties at 1290°C, 25:29823 (ORNL-4630, pp 186-90)
Hf--Pt-base--W, tensile properties at 25 to 1290°C, 25:29823 (ORNL-4630, pp 186-90)
Mo--Pt-base, tensile properties at 25 to 1093°C, 25:29823 (ORNL-4630, pp 186-90)
Mo--Pt-base--Ti, tensile properties at 25 to 1290°C, 25:29823 (ORNL-4630, pp 186-90)
Pt-base--Rh, tensile properties at 1093 to 1290°C, 25:29823 (ORNL-4630, pp 186-90)

PLATINUM IONS
effects on platinum at 20 and 30 keV, long-range migration of self-interstitial atoms in Stage I annealing of, 25:30649 (NYO-3504-57)

PLATINUM ISOTOPES Pt-182
energy levels of, calculation including Mottelson--Valatin effect, (T), 25:31345

PLATINUM ISOTOPES Pt-184
energy levels of, calculation including Mottelson--Valatin effect, (T), 25:31345

PLATINUM ISOTOPES Pt-186
energy levels of, calculation including Mottelson--Valatin effect, (T), 25:31345

PLATINUM ISOTOPES Pt-188
energy levels of, calculation including Mottelson--Valatin effect, (T), 25:31345

PLATINUM ISOTOPES Pt-190
energy levels of, calculation including Mottelson--Valatin effect, (T), 25:31345

PLATINUM ISOTOPES Pt-192
energy levels of, calculation including Mottelson--Valatin effect, (T), 25:31345

PLATINUM ISOTOPES Pt-194
energy levels of, calculation including Mottelson--Valatin effect, (T), 25:31345

PLATINUM ISOTOPES Pt-196
energy levels of, calculation including Mottelson--Valatin effect, (T), 25:31345

PLATINUM OXIDES
thermodynamic properties of gaseous diatomic, free energy functions for, 25:29082

PLOWSHARE PROJECT
crater ejecta from Sedan event in, measurement of tritium distribution and transport in, 25:29244 (UCRL-72572)
public safety aspects of Project Rulison in, review of controversy concerning, 25:29248
radioisotope availability in dogs from Project Cabriolet, metabolism studies on, 25:29456

PLUTONIUM
analysis for impurities by mass spectrometry, spectrography, and spectrophotometry, 25:28916 (CEA-R-4071)
composition of, differential thermal analysis studies of, 25:29885
determination by gravimetric method using cobalt hexaammine chloride, 25:28982
determination in reactor fuels by ion-exchange separation and mass spectrometry, ASTM method for, 25:28978
determination in soil by leaching, ion exchange separation, and alpha counting, 25:28992
determination in vivo, development of avalanche silicon detectors for low-level, 25:29327(R) (NYO-3246-TA-8)
diffusion in aluminum at 550 to 630°C, 25:29867
diffusion in hyperstoichiometric plutonium dioxide--uranium dioxide at 1250 to 1500°C, effects of oxygen/metal ratio on, 25:29964
electron band structure calculations for fcc,

25:30696(R) (COO-2103-3)
separation from americium and curium by ion exchange in zirconium phosphate--nitric acid system, 25:28989
separation from niobium, rhodium, ruthenium, and zirconium by anion exchange from mixed methanol--nitric acid solution, 25:29191
separation from nitric acid and mixed nitric acid--methanol systems by ion exchange, 25:29194
shipping of, design of BNW Model 10 container for, 25:29318
solubility in aluminum at 550 to 630°C, 25:29867
PLUTONIUM ALLOYS AND SYSTEMS
Cu--Pu, phase studies of, using differential thermal analysis, 25:29885
Ga--Pu-base, diffusion in epsilon phase of, compared with delta phase, chemical, 25:29873
Gd--Pu-base, thermal conductivity of delta phase of, at 30 to 90°C, 25:29876
Pu--Sb, crystal structure of PuSb, 25:30002
Pu--Se, crystal structure of PuSe and Pu_3Se_4, 25:30002
PLUTONIUM CARBIDES
entropy of, 25:29942(T) (LA-tr-71-22)
formation of, heat of, 25:29942(T) (LA-tr-71-22)
PuC--UC, creep behavior of sintered, in vacuum at 950 to 1150°C, effects of stress on, 25:29960
PuC--UC, specific power limits in liquid metal cooled fast breeder reactors, 25:31569 (ORNL-TM-3388)
PuC--UC, swelling during irradiation in liquid metal cooled fast breeder reactors, limits for, 25:31569 (ORNL-TM-3388)
PuC--UC, thermal diffusivity of arc-cast, at 500 to 2200°K, 25:29957
PLUTONIUM IONS
desorption from rhenium surfaces, energy and residence time of, 25:30259
PLUTONIUM ISOTOPES Pu-237
energy levels of, superfluid-model calculations of energies and wave functions of nonrotational, (T), 25:31306 (JINR-P4-5693)
proton fission at 10 MeV to 29 GeV, cross section for, 25:31326
PLUTONIUM ISOTOPES Pu-238
content in beagle dog lungs following inhalation as oxide, 25:29421 (LF-43, pp 8-12)
production of monodisperse aerosols of, centrifugation method for, 25:29421 (LF-43, pp 8-12)
use as heat source for heaters in lunar-landing vehicles, 25:29276(P)
use as heat source in implantable cardiac pacemakers, review of worldwide developments in, 25:29285
PLUTONIUM ISOTOPES Pu-239
content in beagle dog lungs following inhalation as oxide, 25:29421 (LF-43, pp 8-12)
criticality control in solutions of, borosilicate-glass raschig rings as fixed neutron absorber for, 25:29197
determination in unirradiated fuels by neutron flux measurements, apparatus for nondestructive, 25:28988(P)
distribution of injected tetravalent, in dogs, 25:29627
effects on leukocytes in dogs, lethal, 25:29627
neoplastic effects of, on bones of dogs, calculation of accumulated skeletal dose following intravenous injection and tumor growth dynamics of, 25:29621 (COO-119-243)
neutron capture-to-fission ratio for, epithermal, (E), 25:31353
neutron fission of, delayed neutron fractions in thermal, (E), 25:31334
osteosarcomas induced in beagles following intravenous injection of, calculation of dose and tumor growth dynamics of, 25:29621 (COO-119-243)
production of monodisperse aerosols of, centrifugation method for, 25:29421 (LF-43, pp 8-12)
retention in kidneys, liver, and spleen of beagles following intravenous injection, effects of dose on, 25:29451
separation from Purex Process wastes by anion exchange, 25:29191
PLUTONIUM ISOTOPES Pu-241
neutron capture-to-fission ratio for, epithermal, (E), 25:31353
PLUTONIUM ISOTOPES Pu-242
neutron fission at 50 eV to 5 keV, cross section and fission width for, (E), 25:31385
thermal capacity at 15 to 373°K, 25:29831
thermodynamic properties of, 25:29831
PLUTONIUM ISOTOPES Pu-243
energy levels of, superfluid-model calculations of energies and wave functions of nonrotational, (T), 25:31306 (JINR-P4-5693)
PLUTONIUM ISOTOPES Pu-246
energy levels from beta decay of americium-246m, spins and parities of, (E), 25:31378
PLUTONIUM NITRIDES
PuN--UN, compatibility with stainless steel, literature survey on, 25:29923 (ORNL-4630, pp 59-72)
PuN--UN, preparation of fuels of, equipment and methods for, 25:29923 (ORNL-4630, pp 59-72)
PuN--UN, properties and stability of fuels of, 25:29923 (ORNL-4630, pp 59-72)
PuN--UN, specific power limits in liquid metal cooled fast breeder reactors, 25:31569 (ORNL-TM-3388)
PuN--UN, swelling during irradiation in liquid metal cooled fast breeder reactors, 25:31569 (ORNL-TM-3388)
PLUTONIUM OXIDES PuO_2
effects on reduction of uranium oxides in powder mixtures, 25:29947
production of dense microspheres of plutonium-238-enriched, development of sol-gel equipment and method for, 25:29921 (ORNL-4565)
PuO_2--stainless steel--UO_2, fabrication of pellets of, powder metallurgical, 25:29931
PuO_2--UO_2, composition and properties of sphere-pac fuels of, 25:29922 (ORNL-4630, pp 3-58)
PuO_2--UO_2, diffusion of plutonium in hyperstoichiometric, at 1250 to 1500°C, effects of oxygen/metal ratio on, 25:29964
PuO_2--UO_2, fabrication of sphere-pac fuels of, 25:29922 (ORNL-4630, pp 3-58)
PuO_2--UO_2, preparation of high-density, high-frequency melting method for, 25:29935
PuO_2--UO_2, radiation effects on clad sphere-pac fuel pins of, in-pile, 25:29922 (ORNL-4630, pp 3-58)
PuO_2--UO_2, radiation effects on mechanical properties of, fast neutron, 25:31568(T) (EURFNR-823)
PuO_2--UO_2, segregation in, analysis of mechanisms for, (T), 25:29821(R) (GEAP-12153)
PuO_2--UO_2, specific power limits in liquid metal cooled fast breeder reactors, 25:31569 (ORNL-TM-3388)
PuO_2--UO_2, swelling during irradiation in liquid metal cooled fast breeder reactors, limits for, 25:31569 (ORNL-TM-3388)
PuO_2--UO_2, uranium activity in solid solutions of, transpiration method for studying, 25:29821(R) (GEAP-12153)
PNEUMATIC SYSTEMS
design and operation of, for transport of radiation source capsules, 25:29319(P)
POINT BEACH POWER REACTOR, UNIT 1
operations incident of April 16, 1971, failure of containment sump valves to open, 25:31478 (DOCKET-50266-47)
POLLEN
dispersion and deposition of timothy and corn, 25:31684 (BNL-50266)
POLONIUM ISOTOPES
radioactivity standards of, users' guides for, 25:29174
POLONIUM ISOTOPES Po-210
effects on kidneys and liver of dogs following injection, protective effects of oxathiole against chronic, 25:29563
separation from irradiated bismuth, 25:29413 (CONF-691225)
POLONIUM ISOTOPES Po-211
alpha decay off, fine structure in α spectra from, (E), 25:31324
POLONIUM ISOTOPES Po-214
determination in uranium air samples, radiometric, 25:29536
POLONIUM ISOTOPES Po-218
determination in uranium air samples, radiometric, 25:29536
POLYMERIZATION
radioinduced, review on methods for, 25:29122
POPULATIONS
control of genetics of, of bean weevils, 25:29749
radiation hazards to human, in nuclear power reactor environments in Soviet Union, 25:29525
radiation hazards to, from radioisotopes contained in commercially available industrial products, methods for controlling and monitoring, 25:29320
standards for radiation protection of human, from x radiation emitted by home television receivers, 25:29537
POROUS MATERIALS
pore size distribution in, mercury porosimetry method for measurement of, 25:29828
POSITRONS
interactions $e^+ + e^- \rightarrow$ hadrons, experimental verification of C invariance in, 25:30926
interactions $\mu + e^+$, cross sections to order α^2 for, 25:30820
interactions $\mu^- + e^+$, radiative corrections to, 25:30820
interactions $\mu^+ + e^+$, radiative corrections to, 25:30820
interactions of, tests of quantum electrodynamics from structure of Feynman amplitude for Compton, (T), 25:30965
lifetimes in rare earth oxides, 25:30272
scattering by atoms above positronium-formation threshold, annihilation rate in, (T), 25:30289
scattering by hydrogen atoms, algebraic cross-coupling calculation of, 25:30286
POTASSIUM
content in Berea area, Va. quartz monzonite, correlation with aeroradioactivity measurements, 25:29235
content in patients with pyelonephritis, use of whole-body radiation counters for measuring, 25:29448
determination in plutonium by absorption spectrophotometry and mass spectrometry, 25:28916 (CEA-R-4071)
determination using ion permselective membrane, potentiometric, 25:28956
effects on radiometric determination of cesium isotopes

XUM

in water, after extraction as tetraphenylborates, 25:29000
electron elastic scattering at 0.5 to 9 eV by, total cross sections for, (E), 25:30282
electron reactions at 0.5 to 1.2 eV with, differential cross sections for elastic scattering and spin exchange in, (E), 25:30282
magnetoresistance and Hall effect of, 25:30646(R) (NYO-2150-66)
magnetoresistance of polycrystalline, transverse, 25:31707 (NYO-2150-68)
ultrasound generation by eddy currents in, zero-field efficiency of, (E), 25:30646(R) (NYO-2150-66)
POTASSIUM ACID FLUORIDES
analysis for silicon as molybdosilicate complex, spectrophotometric method for, 25:28924
POTASSIUM BROMIDES
gold nuclei condensation from atomic beam on crystals of, effects of radiation on, 25:29910
POTASSIUM CHLORIDES
gold nuclei condensation from atomic beam on crystals of, effects of radiation on, 25:29910
radioinduced color centers in crystals of sodium-doped, mechanism of formation of ultrasoft x-, 25:30654
KCl--$KCrO_4$, reactions of solid solutions of, with recoil chromium-51, chemical effects in, 25:29166
POTASSIUM CHROMATES
radiation effects on crystals of, distribution of recoil chromium-51 from neutron, 25:29171
KCl--$KCrO_4$, reactions of solid solutions of, with recoil chromium-51, chemical effects in, 25:29166
POTASSIUM FLUORIDES
LiF--KF--NaF, properties of refractory metal salt incorporating, for use as bath in metal electrodeposition, 25:29783 (CEA-N-1376)
POTASSIUM FLUOROBORATES
production of boron-10-enriched, differential thermal analysis for quality control in, 25:29188
POTASSIUM ISOTOPES
radioactivity standards of, users' guides for, 25:29174
POTASSIUM ISOTOPES K-40
neutron capture by, gamma spectra from thermal, (E), 25:31292
POTASSIUM ISOTOPES K-41
effects on electromigration in solid potassium chloride, 25:29041
energy levels from potassium-40 thermal neutron capture, spins and parities of, (E), 25:31292
POTASSIUM OXIDES
thermodynamic properties of gaseous diatomic, free energy functions for, 25:29082
POTASSIUM SULFATES
corrosive effects of aqueous solutions of, on aluminum--molybdenum--titanium--vanadium alloy, 25:29765
POWER PLANTS
site selection for thermonuclear, prospects of Hanford, Wash, 25:30552 (BNWL-B-47)
POWER SUPPLIES
design of capacitor banks for fusion research, 25:30582 (EUR-4593, pp 393-400)
development of inductive energy storage systems for intense magnetic field production, 25:30561 (EUR-4593, pp 197-203)
PRASEODYMIUM
determination as impurities in gadolinium and yttrium oxides by x-ray luminescence methods, 25:28961
determination in lanthanum by emission spectrography, 25:28965
diffusion of copper in, 25:29841
praseodymium-142 nuclear orientation in, from anisotropy of gamma emission, 25:30662 (COO-1569-76)
reactions with rare earth carbides, thermodynamics of, 25:29039
separation from other rare earths by ion exchange, 25:29178 (CEA-R-4102)
PRASEODYMIUM ALLOYS AND SYSTEMS
Co--Pr, sintering and magnetic properties of $PrCo_5$ permanent magnets, 25:29797
PRASEODYMIUM CARBIDES
reactions with rare earths, thermodynamics of, 25:29039
PRASEODYMIUM ISOTOPES Pr-139
energy levels of, Shell-model calculation of negative-parity, (T), 25:31366
PRASEODYMIUM ISOTOPES Pr-142
nuclear orientation in praseodymium metal, fron anisotropy of gamma emission, 25:30662 (COO-1569-76)
PREAMPLIFIERS
design of low noise, using field effect transistors for semiconductor detectors, 25:29340
design of low-noise charge-sensitive, using field effect transistors for semiconductor detectors, 25:29343
PRESSURE VESSELS
conference on models techniques for prestressed, London, July 10 to 11, 1969, 25:29298
construction of laminated steel, for power reactors, 25:31668 (IRS-T-17)
construction of large-scale test model prestressed concrete, planning for, 25:31558 (IAEA-126, pp 85-97)
construction of prestressed concrete reactor, test model analysis for multi-layer, 25:31549 (EUR-4531, pp 527-56)
construction of prestressed concrete, for gas cooled graphite moderated power reactors, 25:31456 (EUR-4531, pp 129-44)
construction of prestressed concrete, for power reactors, 25:31552 (EUR-4531, pp 647-89)
construction procedures for water cooled reactor prestressed concrete, section models for testing, 25:31547 (EUR-4531, pp 477-88)
creep in prestressed concrete reactor, effects of reinforced openings on, 25:30024 (EUR-4531, pp 373-84)
deflection in concrete models of, methods for measuring, 25:29301
design criteria for reactor prestressed concrete, review of U.S, 25:31554 (IAEA-126, pp 19-51)
design for electrochemical studies at high pressures and temperatures, 25:29779
design of concrete reactor, for use in multiaxial stress fields, 25:30025 (EUR-4531, pp 385-407)
design of prestressed concrete reactor, uses of models in, 25:29307
design of prestressed concrete, for gas cooled graphite moderated power reactors, 25:31456 (EUR-4531, pp 129-44)
design of prestressed concrete, or 600 MW(e) water reactors, 25:31551 (EUR-4531, pp 615-45)
design of reactor, stress calculations for, 25:31564
design of steel ring-wire reinforced prestressed concrete reactor, 25:29939 (EUR-4531, pp 433-44)
design parameters of prestressed concrete, for gas cooled graphite moderated power reactors, 25:31454 (EUR-4531, pp 81-94)
design parameters of prestressed concrete, for gas cocled and water cooled reactors, 25:31550 (EUR-4531, pp 601-13)
development in Germany of prestressed concrete reactor, 25:31662 (EUR-4531, pp 59-71)
development in Sweden of prestressed concrete, for boiling water power reactors, 25:31548 (EUR-4531, pp 507-16)
development of laminated steel, for power reactors, 25:31668 (IRS-T-17)
development of prestressed concrete reactor, conference on, 25:31546 (EUR-4531)
development of prestressed concrete reactor, review of, 25:30019 (EUR-4531, pp 27-58)
development of reactor prestressed concrete, in Czechoslovakia, 25:31561 (IAEA-126, pp 179-212)
development of reactor prestressed concrete, in Germany, 25:31560 (IAEA-126, pp 115-77)
development of reactor prestressed concrete, in Sweden, 25:31562 (IAEA-126, pp 213-41)
development of reactor prestressed concrete, in United Kingdom, 25:31555 (IAEA-126, pp 53-9)
development of reactor prestressed concrete, in Yugoslavia, 25:31556 (IAEA-126, pp 61-8)
development of reactor prestressed concrete, review in France of, 25:31557 (IAEA-126, pp 69-83)
development of reactor prestressed concrete, scale model testing for, 25:31559 (IAEA-126, pp 99-114)
elasticity of reactor, matrix displacement method for three dimensional calculations of, 25:31667 (EUR-4531, pp 777-95)
end slabs for prestressed concrete, pressure testing to failure of, 25:29304
end slabs for prestressed concrete, testing under external load and thermal stress of, 25:29306
fabrication of steel reactor, welding methods for, 25:29788 (ZJE-69)
fabrication processes for reactor, 25:31564
failure of 30-inch-ID, brittle fracture, 25:31757 (Y-1758)
inspection of reactor, ultrasonic equipment and method for in-service, 25:29290
performance of prestressed concrete, correlation with model test results, 25:29308
performance of prestressed concrete, for 600 MW(e) boiling water reactors, 25:31551 (EUR-4531, pp 615-45)
performance of prestressed concrete, for gas cooled graphite moderated power reactors, 25:31455 (EUR-4531, pp 95-128)
performance of prestressed concrete, for power reactors, 25:31552 (EUR-4531, pp 647-89)
performance of prestressed concrete, models for prediction of, 25:29300
prestressing of concrete reactor, using steel hoops, 25:30028 (EUR-4531, pp 445-76)
radiation effects on prestressed concrete reactor, in-pile, 25:30022 (EUR-4531, pp 237-65)
stress analysis of prestressed concrete reactor, dynamic relaxation method for, 25:31665 (EUR-4531, pp 735-57)
stress analysis of prestressed concrete reactor, numerical calculations methods for, 25:31666 (EUR-4531, pp 759-76)
stress analysis of prestressed concrete, for fast reactors, 25:31553 (EUR-4531, pp 797-812)
stress limits for clamp anchors of prestressed concrete reactor, measurement of vertical, 25:31663 (EUR-4531, pp 489-505)
stress response of prestressed concrete reactor, nonlinear analysis of, 25:31664 (EUR-4531, pp 697-734)
testing of concrete, instrumentation and methods for, 25:29299

testing of one-fifth scale models of prestressed concrete, 25:29310
testing of one-fourth scale models of prestressed concrete, under pressure and thermal loads, 25:29313
testing of one-tenth scale models of prestressed concrete, 25:29312
testing of one-tenth scale models of prestressed concrete, 25:29311
testing of prestressed concrete models of, methods for, 25:29302
testing of prestressed concrete, under pressure and thermal loads, 25:29309
testing of prestressed concrete, using models, 25:29314
testing of prestressed concrete, using small-scale models, 25:29305
thermal insulation for helium-cooled reactor, performance evaluation of, 25:30030 (EUR-4531, pp 931-52)

PROLINE
radiation effects on content of, in beagle dog lungs following inhalation of insoluble cerium-144, relation of pulmonary fibrosis to β and γ, 25:29622 (LF-43, pp 218-23)

PROLINE, HYDROXY-
radiation effects on content of, in beagle dog lungs following inhalation of insoluble cerium-144, relation of pulmonary fibrosis to β and γ, 25:29622 (LF-43, pp 218-23)

PROMETHIUM
separation from fuel reprocessing wastes by sorption on manganese dioxide followed by anion exchange elution, 25:29176 (BARC-516)

PROMETHIUM ISOTOPES Pm-142
beta decay of, γ and conversion electron spectra from, (E), 25:31337

PROMETHIUM ISOTOPES Pm-147
beta decay in promethium oxalate, differential thermal analysis of chemical effects of, 25:29172
beta decay of, probability for production of internal bremsstrahlung in, (E), 25:31363

PROMETHIUM OXALATES
promethium-147 beta decay in, differential thermal analysis of chemical effects of, 25:29172

PROPANE
radiation effects on electric conductivity of liquid, pulsed x, 25:29102

PROPANE, 2-METHYL-
radiolysis of polycrystalline and glassy, ESR spectra of butyl radicals from γ, 25:29161

1,3-PROPANEDIONE, 1,3-DIPHENYL-
use as colorimetric reagent for uranium, ASTM method based on, 25:28976

2-PROPANOL
Na_2NO_3--2-propanol--sodium formate, radiolysis of deaerated aqueous solutions of, at 23°C, effects of pressure on yields of hydrogen from γ, 25:29157
Na_2NO_3--NaOH--2-propanol, radiolysis of deaerated aqueous solutions of, at 23°C, effect of pressure on yields of hydrogen from γ, 25:29157
NaCl--2-propanol, corrosive effects on aluminum--titanium--vanadium alloy, 25:29773

PROPENE
alpha-particle stopping cross sections in gaseous, test of Bragg's rule for, 25:30642

PROPRANOLOL
effects on radioprotective sympathomimetic effects on oxygen pressure in mouse spleen, 25:29547

PROPULSION
book: Ion Propulsion, 25:30453

PROPYLENE OXIDE
polymers, radiation chemistry of isotactic and atactic, at room and low temperature, 25:29144

PROSPECTING
equipment and methods for uranium, in Sweden, evaluation of radiometric, 25:29229
methods for shallow and medium depth uranium deposits, development of magnetotelluric, 25:29233

PROSTATE GLAND
radiotherapy of carcinomas of human, γ, 25:29597

PROTACTINIUM
proton fission at 10 MeV to 29 GeV, cross section for, 25:31326

PROTACTINIUM ISOTOPES Pa-230
electron-capture decay of, conversion electron spectra from, (E), 25:31339

PROTECTIVE CLOTHING
effectiveness for protection of radiography personnel, 25:29529

PROTEINS
analysis for carbon-14 and tritium in polyacrylamide gels by liquid scintillation counting, 25:28994
analysis for radioactive collagen, 25:28997
biosynthesis of plant, in vitro, 25:31720(R) (ORO-3982-10)
concentration and desalting of solutions of, research progress on, 25:31714(R) (ORNL-TM-3328)
effects on uptake of radioactive rare earth isotopes by animals, 25:29445
preparation and properties of labeled, for metabolic studies, Italian research program on, 25:29273
radiation effects on content of, in rat plasma erythrocytes, whole-body x, 25:29686
radiation effects on fractions of, in mitochondria and tissue homogenates in brain and small intestine of rabbits, x, 25:29664
yttrium-88 distribution and retention in rat plasma, effects of dilution on, 25:29454

PROTON BEAMS
monitoring on internal accelerator targets, telescope detector system for, 25:31064
monitoring on internal target of high-energy accelerators, methods for, 25:31043 (NP-18776)
production in hot cathode constricted arcs, for plasma injection experiments, 25:30256 (EUR-4593, pp 75-81)

PROTON SOURCES
design and performance of hot-cathode, for modified CERN synchrocyclotron, 25:31158

PROTONS
coupling to electrons, Hartree--Fock approximation in quantum electrodynamics for bound state of, 25:30989
dust-particle alignment in comet tails by solar-wind, (T), 25:30183
effects on elastic modulus of monocrystalline tungsten at 10 MeV and 77°K, 25:29903(R) (NYO-3653-5)
effects on ferrous sulfate heptahydrate, Moessbauer study of, 25:29151
effects on lead telluride at 200-keV, n--p photoelectric diodes produced by, 25:29397
effects on microstructure of Type 321 stainless steel at 0.75 MeV and 400 and 500°C, 25:29915
effects on pathomorphology of mouse, rabbit, and rat brain in mixed γ and γ--neutron fields, whole-body, 25:29644
effects on properties of zinc oxide-base paints, 25:29105
effects on sodium chloride crystals at 3.5 MeV, F-center destruction in, 25:30655
flux of 1.5- to 50-MeV solar, measured by Zond-4 and Zond-5, (E), 25:30164
flux of 5.2- to 81.7-MeV solar and primary cosmic, (E), 25:30161
form factor in p + p and π + p inelastic interactions, electromagnetic, (T), 25:30977
form factors from elastic e + p interactions, electromagnetic, (E), 25:30786
interacions p + p → d + π^+ at 3.4 to 12.3 GeV/c, forward differential cross sections for, (E), 25:30731
interaction π^- + p → eta + n differential cross section from Veneziano amplitude for, 25:30884
interactions anti p + p → $3\pi^+ + 3\pi^-$ ($+\pi^0$) at 3.6 GeV/c, angular correlations in, (E), 25:30733
interactions anti p + p → anti p + p at high energies, eikonal model for, (T), 25:30893 (INR-P-1233)
interactions anti p + p → K + anti K + mπ at 2.5 GeV/c, Lamb statistical model for cross sections of, (E/T), 25:30866
interactions anti p + p, weak duality for slopes of angular distributions of elastic, 25:30873
interactions d + p → ^{3}He + missing mass at 3.25 to 3.76 GeV/c, ABC effect and 450 MeV structure in, 25:30734
interactions d + p → d + missing mass at 3.25 to 3.76 GeV/c, ABC effect and 450 MeV structure in, 25:30734
interactions e + p → e^1 + π^+ + n, differential cross sections for, (E), 25:30718
interactions e + p → e^1 + π^+ + n, longitudinal part of cross section for, (E/T), 25:30719
interactions e + p, isobar model calculations of polarization of recoil protons in elastic, (T), 25:30780
interactions e + p, structure functions and cross sections for meson production in, 25:30783
interactions γ + p → Λ(Σ^0) + K^+, review of coupling parameters for, (E/T), 25:30797
interactions γ + p → p + eta, review of coupling parameters for, (E/T), 25:30797
interactions γ + p → p(n) + π^0(π^+), review of coupling parameters for, (E/T), 25:30797
interactions γ + p → π^+ + p at 300 to 1200 MeV, resonance structures in, (E), 25:30774 (INSJ-126)
interactions γ + p → rho^0 + p, s-channel helicity conservation for diffractive part of, (T), 25:30885
interactions γ + p, review of production of several hadrons in, (E), 25:30716
interactions K^+ + p → K + N + π at 4.6 GeV/c, cross sections for Δ, K*(891), and K*(1420) production in, (E), 25:30748
interactions K^+ + p → K^+ + p at high energies, eikonal model for, (T), 25:30893 (INR-P-1233)
interactions K^- + p → K^- + p at high energies, eikonal model for, (T), 25:30893 (INR-P-1233)
interactions K^+ + p → K*(890) + p at high energies, factorizable quark model for amplitude of, (T), 25:30879
interactions K^- + p → K-(890) + p at high energies, factorizable quark model for amplitude of, (T), 25:30879
interactions K^- + p → p + K^- + $2\pi^+$ + $2\pi^-$ at 3.95 GeV/c in hydrogen bubble chamber, parametrization for, (E), 25:30743
interactions K^+ + p at low energies, field-theoretic model of, 25:30886
interactions K^- + p below threshold, ΛKN coupling and K^- absorption in nuclei at rest for extrapolation of, (T), 25:30902

XUM

interactions $K^+ + p \rightarrow K^+ + p + 2\pi^+ + 2\pi^-$ at 4.97 GeV/c in hydrogen bubble chamber, π^+ angular correlations and resonance production in, (E), 25:30745
interactions $K^+ + p$, weak duality for slopes of angular distribution of elastic, 25:30873
interactions $K^- + p$, weak duality for slopes of angular distributions of elastic, 25:30873
interactions $n + p \rightarrow n + p + \pi^+ + \pi^- + m\pi^0$ at 2 to 10 GeV/c, method for separation from channels of $n + p \rightarrow n + p + \pi^+ + \pi^-$ interactions, (E), 25:30726 (JINR-P1-5665)
interactions $n + p \rightarrow n + p + \pi^+ + \pi^-$ at 2 to 10 GeV/c, method for separation from channels of $n + p \rightarrow n + p + \pi^+ + \pi^- + m\pi^0$ interactions, (E), 25:30726 (JINR-P1-5665)
interactions $n + p \rightarrow n + p$ below 750 MeV/c, review of meson resonance coupling to nucleons from on- and off-shell methods for, (T), 25:30903
interactions $n + p \rightarrow \pi^0 + d$ at threshold to 720 MeV, test of isospin invariance in, (E), 25:30730
interactions $n + p$ at 2 to 10 GeV/c, cross sections of inelastic, (E), 25:30726 (JINR-P1-5665)
interactions $p + d \rightarrow p + d$ at 70 GeV, differential cross sections and slope parameters for, (E), 25:30725 (JINR-P1-5633)
interactions $p + p \rightarrow N^* + \pi + p$ at 7 GeV/c, slope of momentum transfer distribution for, (T), 25:30900
interactions $p + p \rightarrow p + p$ at 50 GeV, differential cross sections and slope parameters for, (E), 25:30725 (JINR-P1-5633)
interactions $p + p \rightarrow p + p$ at high energies, eikonal model for, (T), 25:30893 (INR-P-1233)
interactions $p + p \rightarrow p + p$ below 750 MeV/c, review of meson resonance coupling to nucleons from on- and off-shell methods for, (T), 25:30903
interactions $p + p$ at 200 to 500 GeV/c, asymptotic behavior of particle distributions in, 25:30908
interactions $p + p$ at high energies, lower bound on differential cross section for W^+ and W^- production in, 25:30907
interactions $p + p$, proton electromagnetic form factor for inelastic, (T), 25:30977
interactions $p + p$, weak duality for slopes of angular distributions of elastic, 25:30873
interactions $\pi + p \rightarrow p + p + 5\pi$ at 5 GeV/c, statistical model for asymmetry parameters for π pair angular distributions in, (T), 25:30880
interactions $\pi + p \rightarrow \pi + p$, s-channel helicity conservation for diffraction part of, (T), 25:30885
interactions $\pi + p$, proton electromagnetic form factor for inelastic, (T), 25:30977
interactions $\pi^- + p \rightarrow 2\pi^+ + 2\pi^- + n$ at 8 and 16 GeV/c, correlation effects in, (E), 25:30744
interactions $\pi^- + p \rightarrow 2\pi^- + \pi^+ + p$ at 11 and 16 GeV/c, longitudinal phase space analysis of, (T), 25:30881
interactions $\pi^- + p \rightarrow A_2^- + p$, analysis of A_2 production in, (E/T), 25:30877
interactions $\pi^+ + p \rightarrow A_2^+ + p$, analysis of A_2 production in, (E/T), 25:30877
interactions $\pi^- + p \rightarrow f^0 + n$ at 15 and 16 GeV/c in heavy liquid bubble chamber, cross sections for, (E), 25:30741
interactions $\pi^- + p \rightarrow \omega^0 + n$ at 15 and 16 GeV/c in heavy liquid bubble chamber, cross sections for, (E), 25:30741
interactions $\pi^+ + p \rightarrow p + (K \text{ anti } K\pi)^+$ at 8.04 GeV/c, evidence for K anti Kπ(2820) production in, (E/T), 25:30737
interactions $\pi^+ + p \rightarrow \pi + \pi + N$ at 8 and 16 GeV/c, separation of isospin-$^1/_2$ and -$^3/_2$ contributions to, 25:30891
interactions $\pi^+ + p \rightarrow \pi^0 +$ missing mass, empirical relation of inelastic e + N interactions with, (T), 25:30795
interactions $\pi^+ + p \rightarrow \pi^+ + p$ at high energies, eikonal model for, (T), 25:30893 (INR-P-1233)
interactions $\pi^- + p \rightarrow \pi^- + p$ at high energies, eikonal model for, (T), 25:30893 (INR-P-1233)
interactions $\pi^+ + p \rightarrow \pi^+ + \pi^0(\pi^+) + p(n)$ at 5 and 8 GeV/c, longitudinal phase plots for study of energy dependence of, (E), 25:30742
interactions $\pi^- + p \rightarrow \pi^- + \pi^+(\pi^0) + n(p)$, quark model predictions for forward production of $\Delta(1236)$ in, (E/T), 25:30738
interactions $\pi^- + p \rightarrow rho^0 + n$ at 15 d 16 GeV/c in heavy liquid bubble chamber, cross sections for, (E), 25:30741
interactions $\pi^- + p$ at 16 and 60 GeV/c, inelastic charged multiplicities from, (E/T), 25:30739
interactions $\pi^+ + p$ at 2.50 GeV/c, polarization at definite angle for determination of, 25:30888
interactions $\pi^- + p$ at 4 GeV/c, phenomenological quasi-two-body model for strange particle product in, (T), 25:30869 (JINR-P1-5706)
interactions $\pi^+ + p$ at 5 GeV/c, isospin and longitudinal phase space analysis of, (T), 25:30881
interactions $\pi^+ + p$ at 5 GeV/c, test of thermodynamic model in momentum distributions of secondary π produced in, (E), 25:30746
interactions $\pi^+ + p$ at 6 GeV/c, polarization in backward elastic, (E), 25:30740
interactions $\pi^+ + p$ at 8 GeV/c, Van Hove phase-space plots for analysis of single-particle production in, 25:30890
interactions $\pi^- + p$ at 8 GeV/c, Van Hove phase-space plots for analysis of single-particle production in, 25:30890
interactions $\pi^- + p$, compilation of cross sections for, 25:30735 (CERN-HERA-70-7)
interactions $\pi^+ + p$, model-independent analysis of forward elastic, 25:30875
interactions $\pi^- + p$, model-independent analysis of forward elastic, 25:30875
interactions $\pi^+ + p$, weak duality for slopes of angular distributions of elastic, 25:30873
interactions $\pi^- + p$, weak duality for slopes of angular distributions of elastic, 25:30873
interactions with protons in intense magnetic fields, (T), 25:30050
polarization in polyhydric alcohols doped with chromium complexes, dynamic, 25:31046 (RHEL/R-213)
quality factors for, in body and eye-lens tissues, calculation of, 25:29511 (AERE-M-1887)
reactions (p,α) with lead-208 at 16.475 MeV, alpha spectra and angular distributions from, (E), 25:31383
reactions (p,α)2α with boron-11, analysis for reaction mechanism in, (T), 25:31218
reactions (p,d)p at 7 to 17 MeV, angular distribution and excitation function of the singlet deuteron in, (E), 25:31196
reactions (p,f) with nuclei at 500, 750, and 1000 MeV, analysis using nuclear reaction theory, 25:31417
reactions (p,f) with uranium-238 at 450 MeV, mass yield and charge distribution from, (E), 25:31302 (COO-1167-10)
reactions (p,f) with Z = 74 to 94 nuclei, cross sections for, 25:31326
reactions (p,γ) with indium-115 and silver at 4 MeV, gamma spectra from, (E/T), 25:31303 (INR-1271)
reactions (p,γ) with magnesium-24 at 1.49 MeV, γ-ray angular distributions for, (E), 25:31266
reactions (p,γ) with nuclei with isobaric analog excitation, method for analysis of, (T), 25:31276
reactions (p,γ) with silicon-28 at 725 keV, gamma spectra from, (E), 25:31250
reactions (p,γ) with vanadium-51 at 0.8 to 3.0 MeV, excitation functions for, (E), 25:31256
reactions (p,γ) with zirconium-90 at 3.0 to 7.2 MeV, gamma spectra from, (E), 25:31351
reactions (p,He-3) and (p,t) with boron-11 at 45 MeV, angular distributions for, (E), 25:31228
reactions (p,n) with arsenic-75 and chromium-53, Hauser--Feshbach analysis of angular distributions and excitation functions for, (E/T), 25:31248
reactions (p,n) with arsenic-75 below 3 MeV, statistical model analysis of, (E), 25:31263
reactions (p,n) with deuterium at 45.5 MeV, analysis using Faddeev method with Coulomb force, (T), 25:31188
reactions (p,n) with lithium-7 at 3 to 4 MeV, neutron polarization in, (E), 25:31235
reactions (p,n) with nickel-61, nickel-64, zinc-67, and zinc-68, cross sections for, (E), 25:31268
reactions (p,nγ) with zinc-70 at 1.4 to 4 MeV, γ spectra from, (E), 25:31290
reactions (p,t) with neon-22 at 26.9 to 42.4 MeV, angular distributions for, (E), 25:31296
reactions with adsorbed hydrogen layers on copper at 5 keV, desorption yields from, (E), 25:30257 (EUR-4593, pp 181-6)
reactions with aluminum at 70 GeV, upper limits for differential and total cross sections for quark production in, (E), 25:30724(T) (CERN-Trans-71-4)
reactions with auroral atmosphere, relation to altitude-dependent ion formation, (E/T), 25:30397
reactions with carbon-12 at 670 MeV, deuteron spectrum and differential cross sections for, (E), 25:31225
reactions with helium gas at 4 MeV, vacuum-ultraviolet emission following excitation in, (E), 25:30284
reactions with molecules, binary-encounter calculation of ionization cross sections for, 25:30299
reactions with niobium-93 at 0.2 to 0.9 GeV, excitation functions for, (T), 25:31368
reactions with Z = 3 to 92 nuclei using thick targets, neutron yields from, (E), 25:31209
scattering by calcium-40 at 21.0 to 48.0 MeV, differential cross sections for, (E), 25:31295
scattering by carbon-12 at 1 GeV, nuclear opaqueness model for differential cross sections for, (E/T), 25:31234
scattering by chlorine-35, sulfur-33, and sulfur-34 at 6 MeV, angular distributions for elastic and inelastic, (E), 25:31291
scattering by chromium-50, -52, -54 and zinc-64 up to 4 MeV, gamma angular distributions for, (E), 25:31253
scattering by chromium-53, excitation functions for elastic, (E), 25:31248
scattering by helium-3 at 600 MeV, cross sections for elastic, (E), 25:31185 (LYCEN-7085)
scattering by helium-4 at 1 GeV, nuclear opaqueness model for differential cross sections for, (E/T), 25:31234
scattering by helium-4 at 2 to 50 MeV, calculation of cross-section and polarization angular distributions and phase shifts using nonlocal separable potentials

for elastic, (T), 25:31186 (LYCEN-7089)
scattering by helium-4 at 4.6 to 11.9 MeV, phase shifts and polarization in elastic, (E), 25:31199
scattering by hydrogen at 0 to 25 MeV, calculation of phase shifts using nonlocal separable potentials for elastic, (T), 25:31186 (LYCEN-7089)
scattering by neon-22 at 2.4 to 3.2 MeV, angular distributions, excitation functions, and spectra from elastic and inelastic, (E), 25:31281
scattering by nitrogen-14 at 49.4 MeV, differential cross sections for elastic, (E), 25:31233
scattering by nuclei with isobaric analog excitation, method for analysis of elastic, (T), 25:31276
scattering by oxygen-16 at 1 GeV, nuclear opaqueness model for differential cross sections for, (E/T), 25:31234
scattering by oxygen-16 at 8.5 to 12.7 MeV, polarization in elastic, (E), 25:31236
scattering by tin-116, -118, -120, and -124 at 16.00 MeV, polarizaion angular distribution for elastic, (E), 25:31341
scattering by titanium-46 near 5.5 MeV, γ linear polarization from inelastic, (E), 25:31288
scattering of argon-40 at 30.4 and 49.4 using polarized and unpolarized beams, differential cross sections for elastic and inelastic, 25:31233
spectra of 5.2- to 81.7-MeV solar and primary cosmic, (E), 25:30161

PROTONS (anti p)
interactions anti p + d → p + anti p + π^+ + π^- + n at 5.55 GeV/c in deuterium bubble chamber, d* effect in, (E), 25:30727 (NP-18796)
interactions anti p + p → $3\pi^+$ + $3\pi^-$ ($+\pi^0$) at 3.6 GeV/c, angular correlations in, (E), 25:30733
interactions anti p + p → anti p + p at high energies, eikonal model for, (T), 25:30893 (INR-P-1233)
interactions anti p + p → K + anti K + mπ at 2.5 GeV/c, Lamb statistical model for cross sections of, (E/T), 25:30866
interactions anti p + p, weak duality for slopes of angular distributions of elastic, 25:30873

PROTOZOA
Plasmodium berghei, radiation effects on development and infectivity of sporozoites of, x, 25:29727

PULSARS
charged-particle resource in, magnetospheric, (T), 25:30154
dispersion measures for, (T), 25:30118
electrodynamics of, (T), 25:30154
electrodynamics of, Goldreich--Julian model for, 25:30220 (P-4494(RAND))
gravitational radiation emission from, (T), 25:30092
model for, featuring solar-cycle type mechanism, (T), 25:30131
model for, oblique-rotator, (T), 25:30052
MP 0628, linear polarization of, (E), 25:30135
properties and origin of, (T), 25:30127
pulse emission mechanism for, (T), 25:30149

PULSE ANALYZERS
description of automatic, with tracking sweep, 25:29367

PULSE CONVERTERS
design and performance of time-to-amplitude, for nanosecond range, 25:29341

PULSE GENERATORS (ELECTRONICS)
design and performance of low-inductance megavolt Marx, 25:30573 (EUR-4593, pp 311-17)
design of relaxation oscillator, based on avalanche transistors, 25:29405
operation of linac power, 25:31066

PULSE SHAPERS
design and performance for scintillation detectors, 25:29347
design for photomultiplier tube with independent regulation of output pulse duration and dead time, 25:29342
design of low-noise double delay line, for semiconductor detectors, 25:29366

PUMPS (LIQUID METAL)
design and operation of, for circulating sodium coolant in fast breeder reactors, 25:29257

PUPAE
radiation effects on lifetime and reproductive capacity of codling moth, effects of dose on γ and x, 25:29612
radiation effects on male, of gypsy moths, effects of dose on reproduction and survival of adults, γ, 25:29616
radiosensitivity of, of sugarcane borers in comparison to embryos and larvae, γ, 25:29755

PUREX PROCESS
waste from, recovery of plutonium-239 from, 25:29191

PYRAZINE
spin-lattice relaxation and Zeeman effects in triplet state of deuterated, 25:31742 (UCLA-34-P-91-47)

3,5-PYRAZOLIDINEDIONE, 4-BUTYL-1-(p-HYDROXYPHENYL)-2-PHENYL-
radioprotective effects of, on human patients during therapy, x, 25:29549

PYRENE
radiolysis of rigid matrices of methylcyclohexane containing, deferred luminescence spectra following γ, 25:29150
radiolysis of solutions of, in glassy and polycrystalline solvents, deferred luminescence technique for obtaining stimulation spectra following γ and uv, 25:29133

PYRIDINE
complexes with uranium(V) chloride, properties of, 25:29092

PYRITES
uranium content of, radiographic measurements of, 25:29231

PYROMETERS
design for measuring temperatures on extruded metal surfaces, 25:29787(R) (RMI-16)

Q

QUAD CITIES POWER REACTOR, UNIT 1
owners of, financial statements of, 25:31493 (DOCKET-50254-35)

QUAD CITIES POWER REACTOR, UNIT 2
owners of, financial statements of, 25:31493 (DOCKET-50254-35)

QUANTUM ELECTRODYNAMICS
commutators of fields in, review of gradient terms in, 25:30954
formulation of nonlocal, 25:30937 (JINR-P2-5694)
graviton Lagrangian and superpropagator in, 25:30994
Hartree--Fock approximation for bound-state problem in, 25:30989
infinity suppression in gravity-modified, 25:30994
multiperipheral model at infinite momentum in, 25:30974
review on, 25:30978
tests of, structure of two-electron--n-photon Feynman amplitude for, 25:30965

QUANTUM FIELD THEORY
algebraic theory for, Heisenberg ferromagnet in, 25:30946
boson fields in, nonlinear chiral symmetry breaking from covariant derivatives of, 25:30922
commutation relations for Heisenberg fields in, derivation of equal-time, 25:30991
commutation relations in, representations of canonical, 25:30948
commutator functions for, theorem for, 25:30952
commutators of fields in, review of gradient terms in, 25:30954
compositeness conditions for partial-wave two-body scattering amplitudes in, 25:30958
conformed symmetry in, low-energy theorems for, 25:30984
eikonal approximation for Feynman diagrams in, 25:30981
eikonal model for reggeon calculus in, 25:30980
evolution equation with time-dependent Hamiltonian in, continuous Baker--Haussdorf formula for solution of, 25:30960
field equations in Thirring and Federbush models of, nonlinear semigroups for, 25:30972
field equations in, quantization of $m^2 < 0$, 25:30985
fields in, review of CPT, spin, statistics, and consistency problems for local infinite-component, 25:30950
fields in, test algebras for Haag--Araki, 25:30951
formulation of, geometric structure of canonical, 25:30961
formulation with non-Euclidean space of relative momenta, 25:30938 (JINR-P2-5717)
functionals on algebra of test functions in, positive, 25:30944
Green functions in, review of two-body forces and renormalization for singularities of two-point, 25:30959
group representations of quantized fields in, continuous tensor products of, 25:30947
interactions π + π in axiomatic, limits of strength of, 25:30852
Lagrangians in, phenomenological, 25:30969
lectures on axiomatic, 25:30953
lectures on axiomatic, 25:30940
Lee model in, Bjorken theorem and equivalence principle for equal-time commutators in, 25:30973
mass values in renormalized, self-consistent derivation of multiple, 25:30986
matrix space dynamics with third-order terms in Lagrangian for, 25:30967
model for finite temperatures in, mathematical structure of B.C.S, 25:30949
model of, asymptotic condition in Zachariasen--Thirring, 25:30943
model of, ground state of Hamiltonian in simplest, 25:30979
N-tower exchanges in phi^3, Feynman-parameter method for, 25:30987
particle coupling to external fields in, spin-0 and $-1/2$, 25:30939 (NYO-3829-66)
quantization of weak gravitational field in, 25:31001
renormalization constants for partial-wave two-body scattering amplitudes in, vanishing of, 25:30958
S-matrix and axial charge in, 25:30982
S-matrix elements in class of nonrenormalizable, method for computing, 25:31016 (NYO-1932(2)-192)
S-matrix for, Lagrangian depending on derivatives for, 25:30968
scale dimensions in two-dimensional models of, anomalous,

XUM

25:30921
scattering amplitudes in, compositeness and vanishing of renormalization constants for partial-wave two-body, 25:30958
scattering amplitudes in, n-body problem for, 25:30957
scattering in, existence of nontrivial theory of, 25:31034
statistical mechanics for, nonequilibrium, 25:30956
statistical mechanics in, equilibrium states of, 25:30941
symmetries in relativistic, spontaneously broken, 25:30945
theory for nonlinear, particle-like objects in, 25:30964
theory for nonrenormalizable, review of, 25:30955
theory for Wightman-type axiomatic nonrenormalizable, 25:30942
theory for, review of localizable and nonlocalizable, 25:30962
Thirring model in, locally generated dilation charge in, 25:30993
time evolution of systems with infinite number of degrees of freedom in, 25:30703
Yang--Mills field, Noether theorem and factor-ordering problems in quantization, 25:30988
QUANTUM MECHANICS
Coulomb energy in time-symmetric electrodynamics, 25:30711
debate on reality in, (T), 25:30700
formulation of, extension of Poincare algebra for proper-time, 25:30983
Hamiltonian with SO(4,2) spectrum-generating algebra, 25:30918
history of, waves and particles in, 25:30707
particle motion in Riemann manifold of Lie group, 25:30971
representation of quantum states by Gibbsian ensembles, 25:30701
rotation pictures in, behavior of operators and state vectors in, 25:30990
Schroedinger equation for simplest systems in, closed analytical representations of Green functions of, 25:30712
Schroedinger equation with random potential, 25:30710
space--time quantization analogy with point particle in, contact transformation for, 25:30708
three-body problem in, different noncharged spinless particles in, 25:30709
wave operators for single-channel systems, 25:31019
WKB expansions in, method for constructing absolutely convergent modified, 25:30699 (ITF-70-84-P)
QUASARS
distances to eight, (T), 25:30125
evolution of, review on, (T), 25:30148
infrared emission from nuclei of, model featuring matter accretion by neutron stars, (T), 25:30247
luminosities and spectral shifts of, (T), 25:30220 (P-4494(RAND))
radio flux from 28, (E), 25:30129
spectra of 3C 273 and 1510-08, search for redshifted line of neutral hydrogen in, (E), 25:30121
structure of 3C 273 and 3C 279 revealed by long-baseline interferometry, (E), 25:30130
QUENCHING CIRCUITS
design of solid-state, for G--M detectors, 25:29334
QUINOLINE
complexes with uranium(V) chloride, properties of, 25:29092
QUINONES
radiation effects on production of, in rat liver, chronic strontium-90 β, 25:29639
reactions with chlorophyll in alcohol solvents, flash photolysis studies of, 25:31687 (COO-908-34)

R

RABBITS
radiation effects on bioelectrical activity in brain of, effects of hypothalmus on, 25:29688
radiation effects on DNA in hematopoietic system in, x, 25:29637
radiation effects on endocrine glands of, x, 25:29633
radiation effects on eyes of, healing effects of drugs and surgery on infected corneal wounds following, 25:29649
radiation effects on pathomorphology of brain of, γ, mixed γ--neutron, and proton, 25:29644
radiation effects on renal function and morphology in, methods for studying γ, 25:29684
radiation effects on structure of neurons of upper cervical sympathetic ganglion of, whole-body x, 25:29675
radiosensitivity of lymphatic system and thymus of, x, 25:29635
RADIATION
book: Pathology of Irradiation, 25:29689
dose to man in vicinity of nuclear excavation projects, computer method for calculating, 25:29516 (UCRL-50990)
dose to radiography personnel, effectiveness of protective clothing for reducing, 25:29529
effects on activity and isoenzyme composition of lactate dehydrogenase in heart, liver, and spleen of neonatal rats following parental exposure, 25:29665
effects on activity of aminoacyl-tRNA synthetases and TRNA in cotton plants, 25:29715
effects on adrenal-pituitary system in dogs, acute and chronic, 25:29642
effects on bioelectrical activity in rabbit brain, 25:29688
effects on cardiovascular system, kidneys, liver, and nervous system of patients following therapy for thyroid cancer, combined iodine-131 and teletherapy, 25:29707
effects on cell populations of mouse bone marrow, use of electronic particle counter for evaluating, 25:29648
effects on chromosomes in human blood cells, aberrant chronic, 25:29501
effects on cornea of rabbits, healing effects of drugs and surgery on staphylococcus-infected wounds following, 25:29649
effects on count and reactivity of lymphocytes in blood of patients with cirrhosis, extracorporeal, 25:29704
effects on crosslinking of halogen-containing olefinically unsaturated esters, 25:29119(P)
effects on currents through MOS structures, 25:29412
effects on demineralization of teeth following therapy for nasopharynx tumors in man, 25:29712
effects on development of basal cell carcinomas in man following therapy for burns, long-term, 25:29701
effects on development of osteogenic sarcomas in man following childhood therapy for malignant retinoblastomas, combined radium and, 25:29702
effects on DNP of chromatin, phenolic deproteinization method for studying, 25:29458
effects on Escherichia coli and rats, effects of ferrous ions in presence of oxygen on, 25:29556
effects on flight capacity of cherry fruit fly, 25:29742
effects on gastrointestinal tract of rats, effects of dose on, 25:29646
effects on glucocorticoid metabolism in man, effects of dose on occupational, 25:29708
effects on gonads of onion flies, pathological, 25:29619
effects on growth of tumors, model for time dependent lethal, 25:29680
effects on hematogenic tissue in bone marrow of mice, mechanisms of inhibitory, 25:29676
effects on hemopoietic and immunocompetent cells in spleen of mice, effects of dose on, 25:29677
effects on immune reactions to bovine gamma globulin in Freund's adjuvant in guinea pigs, 25:29474
effects on infrared detectors, nuclear explosion, 25:29411
effects on interoceptive reflexes in cats, effects of perphenazine on, 25:29643
effects on intracellular components of cells, damaging, 25:29457
effects on ischemia damaged kidneys in rats, fractionated low-dose, 25:29654
effects on isolated DNA, 25:29462
effects on lung cells of animals, pathological, 25:29636
effects on lymph nodes of rats, comparison of recovery from partial- and whole-body, 25:29669
effects on lymphosarcomas and retotheliosarcomas in man, mantle method for therapeutic, 25:29599
effects on man, effects of dose and dose rate on carcinogenic, 25:29691
effects on man, evaluation of studies on delayed, 25:29703
effects on melt strength and extensibility of polyethylenes, 25:29099(P)
effects on mice, protective effects of AET, anoxia, cysteamine, and cysteine on biochemical properties correlated with, 25:29553
effects on mice, protective effects of o-acyl derivatives of serotonin against, 25:29555
effects on molecular weight distribution of DNA solutions, 25:29470
effects on nucleoproteins in cultured human amniotic cells, cytofluorimetric studies on, 25:29709
effects on ordering of interstitial carbon atoms in iron, (T), 25:29911
effects on oxidative phosphorylation and respiration in rat liver mitochrondria, effects of riboflavin on lethal, 25:29640
effects on oxidative phosphorylation in animal liver mitochondria, effects of histones on whole-body, 25:29638
effects on permeability of mitochondrial membrane of mice to manganese-54 mechanisms for, 25:29673
effects on personnel, evaluation of occupational, 25:29711
effects on pike roe during fertilization and early cleavage, 25:29659
effects on poly(vinyl chloride), review on, 25:29104
effects on polymerization, review on, 25:29122
effects on polymers at 77°K, thermoluminescence, 25:30444
effects on preparation of foamed thermoplastic sheets, 25:29109(P)
effects on processes at molecular level, 25:29132(R) (NYO-3558-24)
effects on reproductive capacity of grain insects, 25:29750

effects on reproductive capacity of Mediterranean fruit fly, review of research programs on, 25:29738
effects on reproductive capacity of Mediterranean fruit fly in Spain, 25:29739
effects on reproductive capacity of onion flies, 25:29748
effects on skin, ulcerogenic whole-body, 25:29603
effects on stem cells in mammals, developments in bone marrow transplants for treatment of, 25:29560
effects on structure of DNA of seed embryos, effects of homologous DNA on, repair of, 25:29716
effects on sunflower seeds, effects of storage time on, 25:29717
effects on synchronized skin tumors in mice, combined effects of 5-fluorouracil and, 25:29605
effects on synthesis of histones in liver and spleen of rats, 25:29662
effects on tail growth and testicular weight in mice, combined effects of actinomycin C on fractionated, 25:29604
effects on yeasts, effects of ploidy and hetero- or homozygosity of genome on recovery from lethal, 25:29718
exposure record systems for personnel, standards for, 25:29519
translocations induced in chromosomes of yellow fever mosquito by, effects of, on genetic control of populations, 25:29753
translocations induced in insect chromosomes by, role in eradication by sterile male technique, 25:29752
use of ionizing, for control of olive fruit fly in Greece in combination with insecticides, attractants, and repellants, 25:29740

RADIATION CHEMISTRY
changes in chemical reactivity of irradiated inorganic materials, ASTM method for determining, 25:29095
conference on process radiation in plastics industry, Pullman, Washington, June 11-13, 1969, 25:29121
molecular processes in, 25:29132(R) (NYO-3558-24)
processes in industrial, review on, 25:29125
processes in industrial, using accelerators, 25:29126

RADIATION DETECTORS
behavior of Compton diodes, 25:29329
design of telescope, for monitoring of proton beams on internal accelerator target, 25:31064
readout to digital printer, commutator switch for automatic, 25:29345
resolution-function of, Breit--Wigner signals as seen by Gaussian, (T), 25:29355 (RLO-1388-135)

RADIATION DETECTORS, BUBBLE CHAMBER
operation of INS 75-cm liquid hydrogen, 25:29372 (SJC-T-71-1)
particle tracks in heavy-liquid, computer program for analysis of, 25:29369 (ITEF-753)
particle tracks in, program for linking FSD microscopes with Minsk-2 computer for analysis of, 25:29379
temperature control and heat exchange system for ITEP 2-meter hydrogen, 25:29376

RADIATION DETECTORS, CHERENKOV
book: Cherenkov Radiation in High-Energy Physics. Part II. Cherenkov Counters: Determination of Energy and Direction of Elementary Particles, 25:29368(T) (AEC-tr-7099(Pt.2))

RADIATION DETECTORS, DIELECTRIC TRACK
development for dosimetry, review on, 25:29385
sensitivity of polymeric, effect of chemical factors on, 25:29335

RADIATION DETECTORS, GEIGER-MUELLER
operation of halogen quenched, in reactor fuel element failure monitoring system, (E), 25:31646 (DUN-SA-136)
quenching circuit for, design of solid-state, 25:29334

RADIATION DETECTORS, IONIZATION CHAMBER
characteristics for personnel monitoring, 25:29383 (JAERI-Memo-4292)
pulse delay time in helium-3-filled, for neutron detection, 25:29338

RADIATION DETECTORS, PROPORTIONAL
design of boron-coated, with low gamma sensitivity for in-core neutron flux monitoring, 25:29324 (AEEW-M-970)
design of multiwire, for use as precise beam hodoscope, 25:29370 (LAL-1246)
uses in high-energy physics, 25:29373

RADIATION DETECTORS, SCINTILLATION
accuracy of liquid tank, for neutron capture cross-section measurements, 25:31173(R) (RPI-328-200)
design and performance of boron-containing liquid, for thermal neutron detection, 25:29337
design of liquid--plastic phoswich, for neutron detection, 25:29339
development of calcium iodide, for soft x-ray spectroscopy, 25:29350
gain stabilization of liquid, for carbon-14 beta detection, 25:29344
pulse analyzer for, description of automatic, 25:29367
pulse shaper for, design and performance of, 25:29347
pulse shaper for, design of, 25:29342
scintillator for large liquid, for thermal neutron detection, 25:29336

RADIATION DETECTORS, SEMICONDUCTOR
development and research on, 25:29333
performance of telescope, for detecting nuclei from proton scattering on light nuclei, 25:31185 (LYCEN-7085)
preamplifier for, design of, 25:29343
preamplifier for, design of, 25:29340
pulse shaper for, low-noise double delay line, 25:29366

RADIATION DETECTORS, SEMICONDUCTOR (GERMANIUM)
cryostat for lithium-drifted, vacuum sorbent cut-off device for, 25:29351
development of lithium-drifted, for gold assay by activation analysis, 25:29357
performance of lithium-drifted, for measurement of Doppler broadening of γ-rays, 25:31208
preparation of lithium-drifted, study of gallium- and indium-doped materials used in, 25:29330
resolution of lithium-drifted, for gamma spectroscopy, optimization of, 25:29356 (RT/EL-(70)5)
time resolution of lithium-drifted, 25:29353 (JINR-P13-5708)

RADIATION DETECTORS, SEMICONDUCTOR (SILICON)
calibration of Moxon--Rae, in current mode for neutron capture cross section measurements, 25:29326 (LA-4445)
development of avalanche, for low-level in vivo measurement of plutonium, 25:29327(R) (NYO-3246-TA-8)
fabrication of surface-barrier, 25:29332
performance of lithium-drifted, for x-ray spectroscopy, 25:29325 (JINR-P13-5707)
preparation and performance of transmission surface-barrier, for telescope detectors, 25:29331

RADIATION DETECTORS, SPARK CHAMBER
operation at high count rate, 25:29375
power supply circuit for, 25:29374

RADIATION DOSE
data tabulation on dose uniformity ratio and minimum, for design of gamma irradiators, 25:29250 (BNL-50145(Rev.))
distribution in high-energy electron therapy, problems of inhomogeneities in measuring, 25:29523
distribution in skin in relation to whole-body exposure, 25:29603
distribution in tissues of normal and tumor bearing mice, following administration of phosphorus-32, comparison of phosphorus-32-labeled alloxantin and phosphorus-32-labeled orthophosphate, 25:29453
estimation for human populations in emergency situations, methods for external β and γ, 25:29539
nominal standard, to human tissues and tumors, correlation between RET and, 25:29520

RADIATION DOSIMETERS
development of solid-state, review on, 25:29385

RADIATION DOSIMETERS, CHEMICAL
readout of ferrous sulfate, direct photon counting method for low-dose, 25:29366

RADIATION DOSIMETERS, EXOELECTRON
development of, review on, 25:29385

RADIATION DOSIMETERS, LUMINESCENT
development of high-sensitivity energy-independent glass, 25:29387

RADIATION DOSIMETERS, PHOTOGRAPHIC FILM
characteristics for personnel monitoring, 25:29383 (JAERI-Memo-4292)
performance in comparison to lithium fluoride powder for personnel dosimetry, 25:29384

RADIATION DOSIMETERS, PHOTOLUMINESCENT
characteristics for personnel monitoring, 25:29383 (JAERI-Memo-4292)
development of, review on, 25:29385
preparation of energy-independent doped lithium borate glass, 25:29388(P)

RADIATION DOSIMETERS, THERMOLUMINESCENT
characteristics for personnel monitoring, 25:29383 (JAERI-Memo-4292)
development of, review on, 25:29385
performance of commercial lithium fluoride, 25:29382 (COO-1105-120)
performance of lithium fluoride, in comparison with photographic film for personnel dosimetry, 25:29384

RADIATION DOSIMETRY
book: Measuring Methods Using Ionizing Radiation, 25:29391
terminology, standard definitions of, 25:29518

RADIATION MONITORING
procedures for rocket reactor ground tests, 25:31642
program for Ispra environs, development of, 25:29222
programs at Paducah (Ky.) Gaseous Diffusion Plant during 1970, 25:29502 (KY-629)

RADIATION PROTECTION
methods for protecting population against radioactivity in commercially available industrial products, 25:29320
program in radiology department of general hospital, 25:29538
programs for medical personnel and patients in Australia during 1969, 25:29526(R) (NP-18790)
programs of commercial producers of radiation sources and radioisotope-labeled compounds in USA, evaluation of, 25:29527 (NP-18791)
regulations for dentistry, 25:29530
standards for personnel in uranium mines, 25:29536
standards for personnel of nuclear reactor fuel fabrication plants, 25:29534
standards for personnel of uranium mines and mills, 25:29535

XUM

standards for x-rays emitted by home television receivers, 25:29537
standards, for protection of environment against acute localized and worldwide contamination by cesium-137, strontium-89, and strontium-90, 25:29533
RADIATION SOURCES
radiation protection programs of commercial producers of, in USA, evaluation of, 25:29527 (NP-18791)
transport of encapsulated, design and operation of pneumatic system for, 25:29319(P)
RADIATION STANDARDS AND UNITS
terminology for dosimetry, standards for, 25:29518
RADIATION TARGETS
design of shortened charge-exchange gas, 25:31065
deuterium diminution in proton synchrotron polyethylene, mass-spectrometric measurements of, 25:29400
development of dynamic polarized proton, using polyhydric alcohols doped with chromium complexes, 25:31046 (RHEL/R-213)
development of large-volume polarized helium-3, 25:31071
development of polarized helium-3, 25:31077
development of polarized helium-3, 25:31072
development of polarized helium-3, 25:31076
development of polarized helium-3, 25:31075
hydrogen diminution in proton synchrotron polyethylene, mass-spectrometric measurements of, 25:29400
polarization of helium-3, methods for measuring, 25:31074
polarization rates in helium-3, 25:31073
preparation and processing for radioisotope production, 25:29275
production of isotopically pure, in electromagnetic mass separators by ion-beam retardation, 25:31069
RADIO GALAXIES
explosions in giant elliptical, multiple, (T), 25:30218
flux from four, (E), 25:30129
RADIO WAVES
absorption in interstellar space, (T), 25:30118
effect of shortwave fadeouts on trend of ionospheric absorption to solar x-ray flux, (E), 25:30362
emission for given field-line and electron-stream parameters, spectral shapes of magnetospheric vlf discrete, (E/T), 25:30372
emission of magnetospheric vlf discrete, Helliwell criterion for electron energy spectra and structure deduced from, (E/T), 25:30371
emission of magnetospheric vlf, whistler-mode convective beam-cyclotron instability generation mechanism of, (T), 25:30357
emission of pulses from extensive air showers, (E), 25:30333
generation of background hiss of polar chorus, from morning-side magnetospheric vlf waves, (E/T), 25:30358
propagation along field lines in magnetosphere, color spectrograms of vlf Poynting flux measurements of, (E), 25:30370
RADIOACTIVE MATERIALS
content and diffusion in clay soils, method for calculation of, 25:29206
RADIOACTIVE WASTE
cesium-137 separation from low-level liquid, by coprecipitation with ferrocyanides, 25:29183 (SGAE-SS-6/1969)
compaction of low-level solid, criteria for hydraulic presses for, 25:29316(T) (LA-tr-71-12)
disposal of low-activity liquid, at Trisaia Reprocessing Plant, ecological survey to determine methods for, 25:29479
level monitor for solid, development of ultrasonic, 25:29393 (IN-1452)
processing of, use of phyllitic silicate minerals in, 25:29175 (BARC-509)
release from nuclear power plants, sources and control of, 25:31531
separation of promethium from fuel reprocessing, by sorption on manganese dioxide followed by anion exchange elution, 25:29176 (BARC-516)
RADIOACTIVITY
content in atmosphere and fallout at Mol and Ispra, effects of rainfall intensity on, 25:29218
distribution in fallout, effects of aerosol particle size on, 25:29214(T) (LA-tr-71-7)
standards of, certificates of, 25:29173
RADIOBIOLOGY
conference on engineering developments for, abstracts of papers from, 25:29584
conference on, abstract of papers from, 25:29607 (CONF-690940-(Absts.))
molecular processes in, 25:29132(R) (NYO-3558-24)
RADIOCHEMICAL PROCESSING PLANTS
criticality control in, use of borosilicate-glass raschig rings as neutron absorber for, 25:29197
off-gas streams from, evaluation of permselective silicone rubber membranes for removing rare gases from, 25:29317 (ORNL-4522)
off-gases from, performance of sand-bed filters for removing radioactive aerosols from, 25:29315 (ANL-7683)
radiation protection standards for personnel of, 25:29534
site survey for Trisaia, to determine methods for disposal of low-activity liquid wastes, 25:29479
RADIOCHEMISTRY
developments of industrial, 25:29128
radiation monitoring of research centers for, in Italy during 1968, 25:29504 (PROT.-SAN.-13/69)
RADIOGRAPHY, BIOMEDICAL
effectiveness for diagnosis of systemic neoplastic diseases in human bones, comparison of strontium-85 scintigraphy and thermography with, 25:29588
protection of patients and personnel during, hospital program for, 25:29538
RADIOGRAPHY, INDUSTRIAL
book: Measuring Methods Using Ionizing Radiation, 25:29391
development of radioisotope and x-ray, review of 1966 to 1969 literature on, 25:29293
equipment for thermal neutron, development of portable, 25:29286 (BNWL-1329)
films for, exposure plots for x-ray, 25:29294
method for spent fuel elements using 18-MeV betatron, 25:29291
methods and sources for neutron, for nondestructive testing of materials and fuel enrichment distribution control, 25:29292
RADIOISOTOPE SCANNERS
performance of, review of, 25:29349
testing of, phantom for, 25:29328 (ORNL-TM-3261)
RADIOISOTOPE SCANNING
applications of serial brain, review of clinical, 25:29582
conference on, abstracts of papers from, 25:29570 (CONF-691016-(Absts.))
effectiveness for diagnosis and therapeutic evaluation of tumors in patients, 25:29580
review of methods for thyroid gland, 25:29573
RADIOISOTOPES
analysis of, ASTM method for, 25:29005
content in commercially available industrial products, methods for controlling and monitoring radiation hazards to population from, 25:29320
determination of trace amounts of, in seawater, review on methods for, 25:28921
distribution and retention in dogs, mice, and rats following inhalation in fused clay particles, model for insoluble, 25:29422 (LF-43, pp 53-8)
effects on cells of animals and man, review of damaging, 25:29690
production in ASTRA research reactor in Austria, review of, 25:29274
production in Italy for medical uses, review of, 25:29273
production in research reactors, target preparation and processing for, 25:29275
production of, conference on new methods for, 25:29413 (CONF-691225)
properties of research reactor-produced, summary of, 25:29275
radiation protection programs of commercial producers of compounds labeled with, in USA, evaluation of, 25:29527 (NP-18791)
separation from target materials, 25:29413 (CONF-691225)
standards of, users' guides for, 25:29174
use as heat source in thermodynamic engine, 25:29279(P)
use for diagnosis of human diseases, development and performance of scanning and stationary detectors for, review of, 25:29349
use for tracer applications in medicine, evaluation of short-lived, 25:29439
uses as excitation sources in x-ray fluorescence analysis, 25:28922
RADIOLOGY
research activities at National Institute of Radiological Sciences, Japan, during 1969, 25:29572(R) (NIRS-AR-13)
RADIOMETRIC TESTING
book: Measuring Methods Using Ionizing Radiation, 25:29391
method for fuel cladding thickness measurements, 25:29287 (ORNL-4630, pp 145-9)
method for reactor materials, 25:29288 (ORNL-4630, pp 271-9)
RADIOPROTECTIVE COMPOUNDS
effects on alkaline phosphatase activity in small intestine of x-irradiated rats,, 25:29645
hydroxyphenylethanolamines, role of catecholamine depots and α-adrenoreceptors in mechanism of, 25:29546
RADIOSTERILIZATION
eradication of insects by, review of, 25:29736
RADIOTHERAPY
conference on use of high-energy electrons for, 25:29596
dose distribution in high-energy electron, problems of inhomogeneities in measuring, 25:29523
equipment for beam-type, design and operation of irradiation head for, 25:29258(P)
review of radioisotopes for, 25:29573
RADIUM
effectiveness for therapy of laryngeal carcinomas, 25:29598
effects on development of osteogenic sarcomas in man following childhood therapy for malignant retinoblastomas, combined x and, 25:29702
RADIUM ISOTOPES
determination of α-emitting, in water by precipitation

and α counting, ASTM method for, 25:28999
radioactivity standards of, users' guides for, 25:29174
RADIUM ISOTOPES Ra-224
neoplastic effects of, on bones of dogs, calculation of accumulated skeletal dose following intravenous injection and tumor growth dynamics of, 25:29621 (COO-119-243)
osteosarcomas induced in beagles following intravenous injection of, calculation of dose and tumor growth dynamics of, 25:29621 (COO-119-243)
radioisotopes from distribution of recoil ions of, outside thorium oxide particles in thorotrast, 25:29169
RADIUM ISOTOPES Ra-226
alpha decay of, γ energies and intensities from, (E), 25:31358
content in contemporary and fossil snow, effects of coal burning power stations on, 25:29209
neoplastic effects of, on bones of dogs, calculation of accumulated skeletal dose following intravenous injection and tumor growth dynamics of, 25:29621 (COO-119-243)
osteosarcomas induced in beagles following intravenous injection of, calculation of dose and tumor growth dynamics of, 25:29621 (COO-119-243)
RADIUM ISOTOPES Ra-228
neoplastic effects of, on bones of dogs, calculation of accumulated skeletal dose following intravenous injection and tumor growth dynamics of, 25:29621 (COO-119-243)
osteosarcomas induced in beagles following intravenous injection of, calculation of dose and tumor growth dynamics of, 25:29621 (COO-119-243)
radioisotopes from distribution of recoil ions of, outside thorium oxide particles in thorotrast, 25:29169
RADON
content ratio to radon decay products in French uranium mines, methods for measuring, 25:29201(T) (AEC-tr-7228)
use of natural, for tracing monsoon currents in atmosphere over Arabian and Indian Seas, (E), 25:29220
RADON ISOTOPES
radioactivity standards of, users' guides for, 25:29174
RADON ISOTOPES Rn-220
distribution in atmosphere, effects of wind velocity on vertical, (E/T), 25:29225
scavenging from atmosphere by aerosol particles and water droplets, methematical model for describing, 25:29217
RADON ISOTOPES Rn-222
determination in uranium air samples, radiometric, 25:29536
distribution in atmosphere, effects of wind velocity on vertical, (E/T), 25:29225
monitoring of airborne, air sampler for, 25:29352(P)
RAINWATER
effects of droplets of, on scavenging of radon decay products from atmosphere, mathematical model for describing, 25:29217
effects on strontium-90 content of atmosphere and fallout, 25:29218
particle content of, effects of rainfall intensity on, (E), 25:29224
RANCHO SECO POWER REACTOR
buildings and structures for, design bases for earthquake resistant, 25:31510 (DOCKET-50312-24)
buildings and structures for, final safety analysis of, 25:31507 (DOCKET-50312-21)
containment system for, final safety analysis of, 25:31507 (DOCKET-50312-21)
containment system for, performance of iodine spray removal, 25:31510 (DOCKET-50312-24)
control system for, final safety analysis of, 25:31507 (DOCKET-50312-21)
cooling system for, final safety analysis of, 25:31506 (DOCKET-50312-20)
emergency and auxiliary systems for, final safety analysis of, 25:31508 (DOCKET-50312-22)
engineered safeguards for, final safety analysis of, 25:31507 (DOCKET-50312-21)
instrumentation for, final safety analysis of, 25:31507 (DOCKET-50312-21)
operations aspects of, final safety analysis of, 25:31508 (DOCKET-50312-22)
owners of, financial statements of, 25:31505 (DOCKET-50312-19)
quality assurance program for, 25:31509 (DOCKET-50312-23)
radiation protection system for, final safety analysis of, 25:31508 (DOCKET-50312-22)
radiation sources for, final safety analysis of, 25:31510 (DOCKET-50312-24)
radioactive effluents from, tritium management for normal operation, 25:31510 (DOCKET-50312-24)
radioactive waste disposal system for, final safety analysis of, 25:31508 (DOCKET-50312-22)
site for, final safety analysis of, 25:31506 (DOCKET-50312-20)
site for, geological, meteorological, and seismological data for, 25:31509 (DOCKET-50312-23)
steam and power conversion systems for, final safety analysis of, 25:31508 (DOCKET-50312-22)
technical specifications for, 25:31509 (DOCKET-50312-23)
testing of, final safety analysis of initial, 25:31508 (DOCKET-50312-22)
turbines for, safety analysis of missiles in, 25:31510 (DOCKET-50312-24)
RARE EARTH ISOTOPES
radioactivity standards of, users' guides for, 25:29174
uptake of radioactive, in organs and tissues of animals, effects of amino acids and proteins on, 25:29445
RARE EARTH OXIDES
analysis for impurities, electrode development for spectroscopic, 25:28948
determination in rare earths, electrode development for spectroscopic, 25:28948
RARE EARTH SELENIDES
crystal structure and phases in, differential thermal analysis and x-ray studies of, 25:29981
RARE EARTH SULFIDES
crystal structure and phases in, differential thermal analysis and x-ray studies of, 25:29981
RARE EARTH TELLURIDES
crystal structure and phases in, differential thermal analysis and x-ray studies of, 25:29981
RARE EARTHS
analysis for hydrogen by carrier gas fusion--gas chromatographic methods, 25:28936
analysis for rare earth oxides, electrode development for spectroscopic, 25:28948
complexes with amino acids and proteins, role in radioisotope uptake by animals of, 25:29445
detection in spectra of BD 61°2565, (E), 25:30063
determination as impurities in gadolinium and yttrium oxides by x-ray luminescence methods, 25:28961
determination by amperometric, chelatometric, and conductometric titrations, 25:28970
determination in bauxite, selection of line pairs for spectroscopic, 25:28946
determination of mixtures of, using ligand exchange reactions, data reduction system for, 25:28941
determination of trace amounts of, in seawater, review on methods for, 25:28921
determination of trace amounts of, in uranium and thorium by carrier distillation spectrography, 25:28915 (BARC-517)
energy levels of Z = 65 to 71, lifetimes and spin--parity assignments for, (T), 25:31308 (KFK-1248)
energy-level transitions in Z = 65 to 71, hindrance factors and multipolarities for, (T), 25:31308 (KFK-1248)
Fermi surfaces of, review, 25:30681
production and uses of, review on, 25:29809
quantum number and regularities in f-electron, parallelism between, 25:29091
separation by reversed-phase thin-layer chromatography, 25:29187
separation from thorium, uranium, and zirconium by thin-layer chromatography, 25:29187
separation of europium from, by solvent extraction using bis(2-ethylhexyl) phosphate, 25:29185
RARE GASES
determination of trace amounts of, in seawater, review on methods for, 25:28921
separation from off-gas streams, evaluation of thin silicone rubber membranes for, 25:29317 (ORNL-4522)
trapping in cavities in iron meteorites, (E), 25:30158(R) (UCSD-34-P-43-X-9)
trapping in cryogenic porous media bed with charcoal adsorber, 25:29075(R) (DUN-7221(Vol.2))
trapping in long-lived, high-expansion plastic foam, 25:29074(R) (DUN-7221(Vol.1))
RATS
cystamine distribution in intestines and kidneys of, effects of 5-methoxytryptamine on, 25:29554
cystamine excretion in urine of, effects of 5-methoxytryptamine on, 25:29554
iridium-192 metabolism in, following intraperitoneal, intravenous, and oral administration, 25:29450
lithium-6 content in metastases of carcinosarcoma in lungs of, autoradiographic studies on, 25:29443
radiation dose to lungs in, following inhalation of lead-212-labeled aerosols, α, 25:29455
radiation effects on activity and isoenzyme composition of lactate dehydrogenase in heart, liver, and spleen of neonatal following parental exposure, 25:29665
radiation effects on activity of methionine adenosyltransferase in liver of, effects of ethionine on lethal x, 25:29663
radiation effects on alkaline phosphatase activity in small intestine of, radioprotective effects of compounds on x, 25:29645
radiation effects on bone marrow, intestines, and subcutaneous tissues of, oxygen tension kinetics during protective effects of mexamine against γ, 25:29651
radiation effects on cadaverine deaminase activity and deamination of nitrogen compounds in liver of, 25:29641
radiation effects on content of kininogens and kinin-forming activity in plasma of, lethal, whole-body γ, 25:29681
radiation effects on DNA synthesis in lymphoid tissues of, effects of adrenalectomy on subsequent inhibitory

XUM

whole-body γ, 25:29672
radiation effects on endocrine glands of, x, 25:29633
radiation effects on energy metabolism in liver mitochondria of, effects of riboflavin on partial and whole-body, 25:29640
radiation effects on enzyme activity and lipid fractions in liver and serum in, local x, 25:29685
radiation effects on erythropoietic activity in blood of, fractionated γ, 25:29655
radiation effects on esterase activity and protein content in plasma erythrocytes in, whole-body x, 25:29686
radiation effects on histochemistry of cortical and medullar tissues in adrenal glands of, partial-body x, 25:29671
radiation effects on homologous thyroglobulin antibody production in, combined effects of γ and/or iodine-131, 25:29660
radiation effects on ischemia damaged kidneys in, fractionated low-dose, 25:29654
radiation effects on kininase and kininogen activity in blood of, γ, 25:29668
radiation effects on lymph nodes of, comparison of recovery from partial- and whole-body, 25:29669
radiation effects on maze habit in, combined effects of vibrations and x, 25:29666
radiation effects on migration of amelogenic cells in incisors of, 25:29678
radiation effects on pathomorphology of brain of, γ, mixed γ--neutron, and proton, 25:29644
radiation effects on radiotoxin production in liver of, strontium-90 β, 25:29639
radiation effects on synthesis of histones in liver and spleen of, 25:29662
radioinduced carcinomas in skin of, x, 25:29628
radioinduced inhibition of estradiol-induced lactate dehydrogenase activity in uterus of immature, γ, 25:29670
radioisotope distribution and retention in, following inhalation, in fused clay particles, model for insoluble, 25:29422 (LF-43, pp 53-8)
radioisotope metabolism in, effects of dietary alginates on calcium-47 and strontium-85, 25:29446
radiosensitivity of gastrointestinal tract of, 25:29646
radiosensitivity of lymphatic system and thymus of, x, 25:29635
radiosensitivity of striated muscles in, x, 25:29629
radiosensitivity of, effects of ferrous ions in presence of oxygen on, 25:29556
strontium-90 distribution in the femoral medullary canal in, following intravenous injection, effects of sex on, 25:29524
yttrium-88 distribution and retention in protein plasma in, effects of dilution on, 25:29454

REACTIVITY
variations in reactor systems, perturbation theory expressions for small, 25:31655

REACTOR CONTAINMENT STRUCTURES
construction of prestressed concrete, for power reactors, 25:31552 (EUR-4531, pp 647-89)
design of prestressed concrete, for 600 MW(e) boiling water reactors, 25:31551 (EUR-4531, pp 615-45)
performance of prestresed concrete, for 600 MW(e) boiling water reactors, 25:31551 (EUR-4531, pp 615-45)
performance of prestressed concrete, for power reactors, 25:31552 (EUR-4531, pp 647-89)
pressures in pressurized water, following coolant loss accidents, (T), 25:31593 (CONF-710302-9)
rare gas removal from, following nuclear accident, evaluation of permselective membranes for, 25:29317 (ORNL-4522)
testing of prestressed concrete, instrumentation for, 25:29303
testing of, standards for leak rate, 25:31672

REACTOR CONTAINMENT SYSTEMS
filters for, effects of iodine decay heat on performance limits of charcoal, 25:31669 (ORNL-4602)
fission product release and transport in, analysis of accident, 25:31617
spray systems for, iodine removal by, (E), 25:31610
spray systems for, review of U. S. research on, 25:31583

REACTOR CONTROL SYSTEMS
design of optimum, performance index minimization of parameter space method for, (E/T), 25:31545 (ORNL-TM-3311)
design of power, standards for, 25:31458
development of single fluid molten salt breeder reactor, analog computer program for, 25:31544 (ORNL-TM-3102)
performance requirements of automatic, for pebble bed power reactors, 25:31543 (AAEC/E-203)

REACTOR COOLANTS
properties of organic, review on, 25:29154
sampling of, use of γ spectrometer for, 25:31680

REACTOR EXPERIMENTAL FACILITIES
design of time-of-flight system for neutron inelastic scattering studies, 25:29362

REACTOR FUEL ELEMENTS
cladding for, development of materials for, 25:29916
cladding for, radiation testing of aluminum and aluminum alloy, 25:29905 (ORNL-4630, pp 239-60)
cladding of, equipment for detection of bubbles in liquid sodium bond of, 25:31571
cladding tubes for, equipment and methods for production of Zircaloy, 25:29795
critical measurements on, zero-power, 25:31573
development of stainless steel clad mixed oxide, (E/T), 25:31533(R) (ANL-7798)
development of uranium oxide (UO_2) and uranium carbide (UC), for sodium cooled fast breeder reactors, 25:31572
extrusion of internally- and externally-cooled, development of precision methods for, 25:29787(R) (RMI-16)
fabrication for research reactors, development of methods for, 25:29924 (ORNL-4630, pp 233-8)
failure during gas coolant loss accidents, fission product release from, (E), 25:31608
failure of, trapping of rare gases released in, 25:29074(R) (DUN-7221(Vol.1))
failure of, trapping of rare gases released in, 25:29075(R) (DUN-7221(Vol.2))
fission product distribution in operating pin type, thermomigration model for, (T), 25:31589 (CONF-710302-5)
fission product release from uranium oxide (UO_2), during short period irradiation, (E), 25:31606
friction and wear between spacer grids and rod-type, in sodium at 680°C, 25:29818(T) (AEC-tr-7224)
heat transfer between coolant and surface of, calculation method for uneven, 25:31675
heat transfer between fuel material and cladding of, calculation method for uneven, (T), 25:31674
heat transfer in bundle arranged rod type, effects of cladding deformation on, (T), 25:31673
iodine release from defected uranium oxide (UO_2), during reactor operation, (E), 25:31607
irradiation testing of plutonium oxide (PuO_2)--uranium oxide (UO_2), uranium oxide (UO_2), uranium oxide (UO_2) cermets, uranium carbide (UC), and uranium nitride (UN), 25:31568(T) (EURFNR-823)
mockup of pin type, with liquid sodium bond, 25:31571
shipping of irradiated, standards for design and operation of containers for, 25:29321
shipping of unirradiated, design of BNW Model 10 container for, 25:29318
spacers for bundles of rod type ceramic, design configurations of, 25:31678(P)
spacers for liquid metal cooled rod type, effects on heat transfer and fluid flow of, 25:31568(T) (EURFNR-823)
stress transients in cylinder shaped rod, computer program calculation of, 25:31670 (ORNL-TM-3293)
temperature distribution in clad rod, effect of uneven heat transfer between fuel material and cladding on, (T), 25:31674
temperature distribution in rod, effects of cladding deformation on, (T), 25:31673
temperature distribution in rod, effects of uneven surface and coolant on, (T), 25:31675
testing of spent, use of 18-MeV betatron for nondestructive, 25:29291
vibration characteristics of water cooled parallel rod, effects of end restraint and spacer configurations on, (E), 25:31570 (RT/ING-(70)24)

REACTOR FUELS
analysis for plutonium and uranium by ion-exchange separation and mass spectrometry, ASTM method for, 25:28978
analysis of plutonium- and uranium-containing, for fissionable materials by mass spectrometry, ASTM computerized method for, 25:28980
analysis of unirradiated, for fissionable materials by neutron flux measurements, apparatus for nondestructive, 25:28988(P)
burnup in multizone light-water reactor cores, optimal control rod programming for maximum average, (T), 25:31584
burnup measurement on, by analysis for cesium-137 by radiochemical separation and γ spectrometry, ASTM method for, 25:29001
burnup measurements on, by analysis for neodymium-148 by chemical separation and mass spectrometry, ASTM method for, 25:28979
coating of microspheres of, with multiple pyrolytic carbon layers at 1100 to 1500°C, deposition method for, 25:29928(P)
compacting of coated particle, method for use of centrifugal force for, 25:31679(P)
cycle costs for batch refueling in power reactors, method for calculation of, 25:31585
cycle development for mixed oxide fast, 25:31533(R) (ANL-7798)
cycle for fast breeder, chemical processing requirements for, 25:31568(T) (EURFNR-823)
cycles for HTGR-type thorium--uranium, development of, 25:31586
deformation of aluminum-clad ceramic, mechanisms of nonuniform, 25:29924 (ORNL-4630, pp 233-8)
development of mixed oxide fast, during March 1971, 25:31533(R) (ANL-7798)
development of, program for research, 25:29757(R) (ORNL-4630)
dissolution of irradiated, stainless steel-clad, 25:29199(P)

performance limits for plutonium oxide (PuO_2)--uranium oxide (UO_2), plutonium carbide (PuC)--uranium carbide (UC), and plutonium nitride (PuN)--uranium nitride (UN), in liquid metal cooled fast breeder reactors, 25:31569 (ORNL-TM-3388)
plutonium fission in, ASTM method of determining percentage of, 25:28980
reprocessing of irradiated ceramic, dissolution and fluorination process fo., 25:29192(P)
reprocessing of irradiated thorium- and uranium-containing, by fractional condensation of chlorides and solvent extraction, 25:29189(P)
reprocessing of, equilibrium data for Eurex process for, 25:29182 (RT/CHI-(70)31)
reprocessing of, use of borosilicate-glass raschig rings as neutron absorber for criticality control in, 25:29197
shipping and storage of radioactive, geometric programming method for minimization of cost of, 25:31649
storage facilities for, standards for the design of, 25:29322
testing of irradiated, use of cellulose nitrate in alpha autoradiographic, 25:29944(T) (LB/G-2916)
uranium fission in, ASTM method for determination of percent, 25:28998
uranium fission in, ASTM method for determining percentage of, 25:28980

REACTOR LOADING MACHINES
design of liquid sodium cooled fast, 25:31581(P)

REACTOR SAFETY
blowdown pressure calculations for water cooled reactors, effects of equations of state variables on subcooled, (T), 25:31590 (CONF-710302-6)
coolant loss accident analysis in water cooled reactors, integrated computer code automation system for, (T), 25:31594 (CONF-710302-10)
coolant loss accidents in pressurized water reactors, nodal sensitivity in modeling, 25:31592 (CONF-710302-8)
coolant loss accidents in pressurized water reactors, computer program analysis of, (E/T), 25:31598 (WCAP-7401)
coolant loss accidents in pressurized water reactors, calculation of maximum pressure in containment structure during, (T), 25:31593 (CONF-710302-9)
coolant loss accidents in water cooled reactor, MOXY code for calculation of core heat transfer during, (T), 25:31587 (CONF-710302-2)
coolant loss accidents in water cooled reactors, finite element techniques for vibration analysis of, (T), 25:31591 (CONF-710302-7)
coolant loss accidents in water cooled reactors, high speed graphic simulation of blowdown during, (T), 25:31588 (CONF-710302-4)
core disassembly accidents in fast reactors, two-dimensional integral model of, 25:31599
fission product release characteristics and consequences, conference on, 25:31602
guides for water cooled nuclear power plants, 25:31526 (TID-25697)
risk probability method for assessment of, 25:31529

REACTOR SAFETY EXPERIMENTS
operation of TREAT, during March 1971, 25:31533(R) (ANL-7798)

REACTOR SIMULATORS
modeling coolant loss accidents in pressurized water reactors, nodal sensitivity in, 25:31592 (CONF-710302-8)
use of analog computer, for development of 1000 MW(e) single fluid molten salt breeder reactor control system, 25:31544 (ORNL-TM-3102)

REACTORS
accident models for, development of consistency in, 25:31603
accidents in, analysis of aerosol release for, 25:31619
accidents in, fission product escape integral concept analysis of radiation hazards for, 25:31621
components for, cleaning standards for, 25:31676
core composition and configuration in, geometric programming method for optimization of, 25:31649
fission product release from, relative inhalation hazards to man from, 25:29420 (LF-43, pp 1-7)
fission product release from, safety analysis of, 25:31620
materials for, research programs on development of, 25:29757(R) (ORNL-4630)
neutron flux in two-dimensional geometry during fast transients, alternating-direction implicit methods for analysis of, 25:31654
neutron leakage at core--reflector interfaces, effects on multigroup cross section averaging, 25:31183
neutron migration in lattices of fuel rods and liquid coolant, anisotropic, (E/T), 25:31660
neutron spectra in, activation data unfolding by RF01 and RF07 codes for determination of, (T), 25:31648 (KFKI-70-30-RPT)
neutron thermalization in crystalline moderators in, variational method for pulsed-, (T), 25:31175
operation of, statisticel analysis of limiting conditions for, (T), 25:31638
physics calculations for, coarse lattice technique for shortening two-dimensional SN-method, 25:31653 (KFK-1361)
physics calculations for, interpolation schemes for neutron cross section structure factors for, 25:31647 (HEDL-TME-71-40)
physics parameters of, effects of space dependent resonance self-shielding at zone boundaries on, (T), 25:31652 (KFK-1353)
pressure vessels for, conference on development of prestressed concrete, 25:31546 (EUR-4531)
pressure vessels for, development in Germany of prestressed concrete, 25:31662 (EUR-4531, pp 59-71)
pressure vessels for, review of development of prestressed concrete, 25:30019 (EUR-4531, pp 27-58)
pressure vessels for, vertical stress limits for clamp anchors of prestressed concrete, 25:31663 (EUR-4531, pp 489-505)
radioactive effluents from, safety analysis of, 25:31604
reactivity variations in, perturbation theory expressions for small, 25:31655
shielding for, standards for testing biological, 25:31677
shielding requirements for, computer program for calculation of secondary γ radiation, (E/T), 25:31671 (ORNL-TM-3367)
stability of, parameter fitting of model calculations in frequency domain with weighting function for, (E/T), 25:31650 (AEEW-M-1012)
thermal insulation for, conference in development of, 25:31546 (EUR-4531)
thermal insulation for, performance of circulating gas screen, 25:31576 (EUR-4531, pp 1035-53)

REACTORS, BOILING
components for, earthquake resistant design requirements for, 25:31601
containment structures for 600 MW(e), design and performance of prestressed concrete, 25:31551 (EUR-4531, pp 615-45)
coolant loss accidents in, guide for evaluation of radiological consequences from, 25:31526 (TID-25697)
cost analysis for underground 1000 MW(e), 25:31600
design parameters for underground 1000 MW(e), conceptual, 25:31600
dynamics of, computer program analysis of axial, 25:31541 (EUR-4497)
emergency core cooling systems for, comparison of flooding and spray, 25:31579 (MRR-79)
pressure vessel for 750 MW, test model development in Sweden for prestressed concrete, 25:31548 (EUR-4531, pp 507-16)
pressure vessels for 600 MW(e), design and performance of prestressed concrete, 25:31551 (EUR-4531, pp 615-45)
steam line rupture in, guide for evaluation of radiological consequences from, 25:31526 (TID-25697)

REACTORS, BREEDER
accidents in fast, analysis of aerosol release for, 25:31617
accidents in liquid sodium cooled fast, analysis of sodium combustion, 25:31568(T) (EURFNR-823)
accidents in liquid sodium cooled fast, analysis of aerosol release for, 25:31618
development in Europe, status of, 25:31536
development in Germany during 1970, 25:31538
development in U.S.S.R., review of, 25:31534 (WASH-1175)
development of gas cooled fast, technical and economic aspects of, 25:31535
fuel cladding for liquid sodium cooled fast, corrosion and compatibility of metal alloy, 25:31568(T) (EURFNR-823)
fuel cycle for liquid sodium cooled fast, chemical processing requirements for, 25:31568(T) (EURFNR-823)
fuel element assemblies for liquid sodium cooled fast, effects of spacer configurations on heat transfer and fluid flow in, 25:31568(T) (EURFNR-823)
fuel element for, temperature scanner for bubbles in sodium bond, 25:31571
fuel elements for liquid sodium cooled fast, irradiation testing of plutonium oxide (PuO_2)--uranium oxide (UO_2), uranium oxide (UO_2), uranium oxide (UO_2) cermets, uranium carbide (UC), and uranium nitride (UN), 25:31568(T) (EURFNR-823)
fuel elements for sodium cooled, development of uranium oxide (UO_2) and uranium carbide (UC), 25:31572
physics measurements for liquid sodium cooled fast, effects of core loading and configuration on, 25:31568(T) (EURFNR-823)
stability of steam cooled fast, calculation of inherent, 25:31542(T) (EURFNR-813)

REACTORS, CANDU-TYPE
maintenance of, freeze blocking of tubes in, (E), 25:31537
moderator tubes in, freeze blocking of, (E), 25:31537

REACTORS, FAST
accidents in breeder, analysis of aerosol release for, 25:31617
accidents in liquid metal cooled breeder, analysis of sodium combustion, 25:31568(T) (EURFNR-823)
accidents in liquid sodium cooled breeder, analysis of aerosol release for, 25:31618
coolant combustion in sodium cooled, aerosol release and transport from, (E/T), 25:31615

XUM

design calculations for, SNARC1D code in ARC system for, 25:31651 (ANL-7717)
development in Europe, status of, 25:31536
development in Germany during 1970, 25:31538
development in U.S.S.R., review of, 25:31534 (WASH-1175)
development of gas cooled breeder, technical and economic aspects of, 25:31535
excursions in, two-dimensional integral model for analysis of superprompt critical, 25:31599
fuel cladding for liquid sodium cooled breeder, corrosion and compatibility of metal alloy, 25:31568(T) (EURFNR-823)
fuel cycle for liquid sodium cooled breeder, chemical processing requirements for, 25:31568(T) (EURFNR-823)
fuel element assemblies for liquid sodium cooled breeder, effects of spacer configurations on heat transfer and fluid flow in, 25:31568(T) (EURFNR-823)
fuel element transfer bucket for liquid sodium cooled, description of spill resistant, 25:31582(P)
fuel elements for liquid sodium cooled breeder, irradiation testing of plutonium oxide (PuO_2)--uranium oxide (UO_2), uranium oxide (UO_2), uranium oxide (UO_2) cermets, uranium carbide (UC), and uranium nitride (UN), 25:31568(T) (EURFNR-823)
fuel elements for sodium cooled, development of uranium oxide (UO_2) and uranium carbide (UC), 25:31572
loading machine for liquid sodium cooled, 25:31581(P)
neutron flux spectra in, variational spectral synthesis methods for space-energy, 25:31656
physics measurements for liquid sodium cooled breeder, effects of core loading and configuration on, 25:31568(T) (EURFNR-823)
pressure vessels for, stress analysis of prestressed concrete, 25:31553 (EUR-4531, pp 797-812)
stability of steam cooled breeder, calculation of inherent, 25:31542(T) (EURFNR-813)

REACTORS, GAS-COOLED
cooling streams for, performance of sand-bed filters for removing radioactive aerosols from, 25:29315 (ANL-7683)
cooling system for moderator and pressure vessel of graphite moderated, description of bleed duct by-pass, 25:31565(P)
cooling systems of, activation and fission product deposition during turbulent flow in, (E/T), 25:31566
development of high temperature fast breeder, technical and economic aspects of, 25:31535
fuel cycles for high temperature, development of thorium--uranium, 25:31586
fuel element failures in, fission product release from, (E), 25:31608
power conversion system for, description of carbon dioxide gas turbine, 25:31625(P)
pressure vessels for, design parameters of prestressed concrete, 25:31550 (EUR-4531, pp 601-13)
pressure vessels for, testing methods for prestressed concrete, 25:29302
steam generators for high temperature power, development in U.S. of, 25:31623 (GA-10338)
steam generators for, MEDEA code for pressure and temperature distribution in helium--water, 25:31624 (JUL-698-RG)
thermal insulation for high temperature, heat transfer systems and equipment for testing, 25:31575 (EUR-4531, pp 953-64)
thermal insulation for, high-pressure performance of, 25:30029 (EUR-4531, pp 841-81)
thermal insulation for, performance of honeycomb metal, 25:31577 (EUR-4531, pp 1063-78)
thermal shielding for, properties of aluminous and Super Secar-type concretes for, 25:30031 (EUR-4531, pp 975-1018)

REACTORS, GERMANY
development of fast breeders during 1970, 25:31538

REACTORS, GRAPHITE-MODERATED
cooling system for moderator and pressure vessel of gas cooled, description of bleed duct by-pass, 25:31565(P)

REACTORS, HETEROGENEOUS
neutron reaction rates in, method for calculation of foil perturbation effects on, (E/T), 25:31659

REACTORS, LIQUID METAL-COOLED
accidents in fast breeder, analysis of aerosol release for, 25:31618
accidents in fast breeder, analysis of sodium combustion, 25:31568(T) (EURFNR-823)
coolant combustion in sodium cooled, aerosol release and transport from, (E/T), 25:31615
cooling systems for sodium-cooled fast breeder, design and operation of pumps for, 25:29257
cooling systems for sodium-cooled, design and operation of system for automatically monitoring impurities in, 25:29261
development in Germany during 1970, 25:31538
fuel cladding for fast breeder, corrosion and compatibility of metal alloy, 25:31568(T) (EURFNR-823)
fuel cycle for fast breeder, chemical processing requirements for, 25:31568(T) (EURFNR-823)
fuel element assemblies for fast breeder, effects of spacer configurations on heat transfer and fluid flow in, 25:31568(T) (EURFNR-823)
fuel element transfer bucket for fast, description of spill resistant, 25:31582(P)
fuel elements for fast breeder, irradiation testing of plutonium oxide (PuO_2)--uranium oxides (UC_2), uranium oxide (UO_2), uranium oxide (UO_2) cermets, uranium carbide (UC), and uranium nitride (UN), 25:31568(T) (EURFNR-823)
fuel elements for sodium cooled, development of uranium oxide (UO_2) and uranium carbide (UC), 25:31572
loading machine for fast, 25:31581(P)
physics measurements for fast breeder, effects of core loading and configuration on, 25:31568(T) (EURFNR-823)

REACTORS, MARITIME
accidents in, potential hazards from, 25:31644
design requirements of, guides for, 25:31643
operations aspects of, guides for, 25:31643

REACTORS, ORGANIC-MODERATED
neutron spectra in, Horowitz operators for, (T), 25:31657

REACTORS, PEBBLE-BED
control system for power, performance requirements of automatic, 25:31543 (AAEC/E-203)

REACTORS, POWER
accidents in, analysis of maximum radiation hazards for, 25:31530
accidents in, analysis of radiation hazards for, 25:31622
components for, economics and importance of nondestructive testing of, 25:29289
containment structures for 600 MW(e) boiling water, design and performance of prestressed concrete, 25:31551 (EUR-4531, pp 615-45)
containment structures for, construction and performance of prestressed concrete, 25:31552 (EUR-4531, pp 647-89)
control system for pebble bed, performance requirements of automatic, 25:31543 (AAEC/E-203)
control systems for, design basis standards for, 25:31458
cooling systems for, helium leak testing procedures for, 25:31563
cost analysis for underground 1000 MW(e) boiling, 25:31600
design parameters for underground 1000 MW(e) boiling, conceptual, 25:31600
development in U.S.S.R., review of, 25:31534 (WASH-1175)
development of liquid metal cooled fast breeder, in Germany during 1970, 25:31538
fuel cycle costs for batch refueling in, method for calculation of, 25:31585
fuel elements for, zero-power critical measurements on, 25:31573
power conversion system for, description of carbon dioxide gas turbine, 25:31625(P)
pressure vessel for 750 MW boiling water, test model development in Sweden for prestressed concrete, 25:31548 (EUR-4531, pp 507-16)
pressure vessels for 600 MW(e) boiling water, design and performance of prestressed concrete, 25:31551 (EUR-4531, pp 615-45)
pressure vessels for, construction and performance of prestressed concrete, 25:31552 (EUR-4531, pp 647-89)
pressure vessels for, design and fabrication of, 25:31564
pressure vessels for, development and construction of laminated steel, 25:31668 (IRS-T-17)
pressure vessels for, development in Czechoslovakia of prestressed concrete, 25:31561 (IAEA-126, pp 179-212)
pressure vessels for, development in France of prestressed concrete, 25:31557 (IAEA-126, pp 69-83)
pressure vessels for, development in Germany of prestressed concrete, 25:31560 (IAEA-126, pp 115-77)
pressure vessels for, development in Sweden of prestressed concrete, 25:31562 (IAEA-126, pp 213-41)
pressure vessels for, development in U.K. of prestressed concrete, 25:31555 (IAEA-126, pp 53-9)
pressure vessels for, development in Yugoslavia of prestressed concrete, 25:31556 (IAEA-126, pp 61-8)
pressure vessels for, dynamic relaxation method for stress analysis of prestressed concrete, 25:31665 (EUR-4531, pp 735-57)
pressure vessels for, matrix displacement method for three dimensional elastic and elastoplastic calculations of, 25:31667 (EUR-4531, pp 777-95)
pressure vessels for, nonlinear analysis of stress response of prestressed concrete, 25:31664 (EUR-4531, pp 697-734)
pressure vessels for, numerical calculations methods for stress analysis of prestressed concrete, 25:31666 (EUR-4531, pp 759-76)
pressure vessels for, planning for large-scale test model of prestressed concrete, 25:31558 (IAEA-126, pp 85-97)
pressure vessels for, scale model tests on prestressed concrete, 25:31559 (IAEA-126, pp 99-114)
pressure vessels for, test model analysis for multi-layer construction of prestressed concrete, 25:31549 (EUR-4531, pp 527-56)
pressure vessels for, U.S. design criteria for prestressed concrete, 25:31554 (IAEA-126, pp 19-51)
protection systems for, design basis standards for, 25:31458
radiation monitoring of environment of, in Italy during 1968, 25:29504 (PRUT.-SAN.-13/69)

XUM

safety guides for water cooled, 25:31526 (TID-25697)
steam generators for high temperature gas cooled, development in U.S. of, 25:31623 (GA-10338)
steam generators for, MEDEA code for pressure and temperature distribution in helium--water, 25:31624 (JUL-698-RG)

REACTORS, PRESSURIZED-WATER
coolant loss accident in, nodal sensitivity in modeling, 25:31592 (CONF-710302-8)
coolant loss accidents in, computer program analysis of, (E/T), 25:31598 (WCAP-7401)
coolant loss accidents in, correlations for prediction of maximum containment pressures following, (T), 25:31593 (CONF-710302-9)
coolant loss accidents in, guide for evaluation of radiological consequences from, 25:31526 (TID-25697)
dynamics of, computer program analysis of axial, 25:31541 (EUR-4497)
steam generators for, development and testing of once-through, 25:31532 (BAW-10027)

REACTORS, RESEARCH
accidents in, analysis of maximum radiation hazards for, 25:31530
accidents in, analysis of radiation hazards for, 25:31622
core for RA (Vinca), statistical analysis of thermal limits for, (T), 25:31638
design modifications for FR-3, during 1968 and 1969, 25:31568(T) (EURFNR-823)
design modifications for Scottish Universities Reactor, during 1969 to 1970, 25:31634(R) (SRRC-41/71)
operations for FR-3, during 1968 and 1969, 25:31568(T) (EURFNR-823)
operations for Scottish Universities Reactor, during 1969 to 1970, 25:31634(R) (SRRC-41/71)
operations in Yugoslavia of TRIGA Mark 2, during 1969, 25:31633 (IJS-253)
radioisotope production in ASTRA, review of, 25:29274
radioisotope production in, target preparation and processing for, 25:29275

REACTORS, SUPERHEATING
stability of steam cooled fast breeder, calculation of inherent, 25:31542(T) (EURFNR-813)

REACTORS, SWIMMING-POOL
design of, standards for, 25:31637

REACTORS, U.S.S.R.
development of power, review of, 25:31534 (WASH-1175)

REACTORS, WATER-COOLED
blowdown in, high-speed graphic simulation of, (T), 25:31588 (CONF-710302-4)
blowdown pressure calculations for, effects of equations of state variables on subcooled, (T), 25:31590 (CONF-710302-6)
containment heat removal pumps for, guide for net positive suction head of, 25:31526 (TID-25697)
containment spray systems for, review of U. S. research on, 25:31583
containment structures for, guide for Cadweld splices in reinforcing bars of, 25:31526 (TID-25697)
containment structures for, guide for instrument line penetrations of, 25:31526 (TID-25697)
coolant in, delayed neutron emitting fission product monitoring method for, 25:31580
coolant loss accidents in, factors affecting fission product release from, (E/T), 25:31605
coolant loss accidents in, finite element techniques for vibration analysis of, (T), 25:31591 (CONF-710302-7)
coolant loss accidents in, guide for control of combustible gas concentrations following, 25:31526 (TID-25697)
coolant loss accidents in, integrated computer code automation system for analysis of, 25:31594 (CONF-710302-10)
coolant loss accidents in, MCXY code for computing core heat transfer during, (T), 25:31587 (CONF-710302-2)
development in U.S.S.R., review of, 25:31534 (WASH-1175)
emergency core cooling system pumps for, guide for net positive suction head of, 25:31526 (TID-25697)
fuel burnup in multizone, optimal control rod programming for maximum average, (T), 25:31584
fuel element storage facility for, guide for design basis of, 25:31526 (TID-25697)
personnel for, guide for selection and training of, 25:31526 (TID-25697)
power supplies for, guide for diesel generator set capacity for, 25:31526 (TID-25697)
power supplies for, guide for redundant standby, 25:31526 (TID-25697)
pressure vessel for, testing of models of prestressed concrete, 25:29314
pressure vessels for, design parameters of prestressed concrete, 25:31550 (EUR-4531, pp 601-13)
pressure vessels for, development in Sweden of prestressed concrete, 25:31562 (IAEA-126, pp 213-41)
pressure vessels for, guide for analysis of thermal shock effects on, 25:31526 (TID-25697)
pressure vessels for, section models for testing construction procedures for prestressed concrete, 25:31547 (EUR-4531, pp 477-88)
safety guides for, 25:31526 (TID-25697)
seismic response of, guide for instrumentation for determination of, 25:31526 (TID-25697)
thermal insulation for, performance of gas and water cooled metal plates for, 25:31578 (EUR-4531, pp 1085-97)
thermal insulation for, performance of honeycomb metal, 25:31577 (EUR-4531, pp 1063-78)

RECOILS
reactions in organic and inorganic systems, review on, 25:29168

REFRACTORY MATERIALS
thermal conductivity of electrically-conducting, at 1000 to 2400°C, absolute method for measuring, 25:29958

REGGE POLE THEORY
baryon and meson exchange in, triquark and biquark propagators with constant residues for, 25:30834
cuts in absorption models in, 25:30826
double-pole model for amplitudes of interactions at high energies in, 25:30751 (IS-T-426)
dual models for strong interactions in, lectures on, 25:30823 (CERN-71-7, pp 285-358)
dual models in, review of, 25:31015 (MIT-2098-726)
dual models in, review of unitarization of, 25:30825
duality hypotheses for exchange degeneracy in strong interactions in, 25:30825
duality in, review of, 25:31015 (MIT-2098-726)
duality--parton model for deep inelastic $\nu + N$ interactions at high energies in freon and propane in, 25:30809
eikonal model for elastic strong interactions at high energies in, 25:30893 (INR-P-1233)
exchange-degenerate residues for meson--baryon and baryon--baryon interactions, 25:30878
multiperipheral model for hadron interactions in, 25:30764
pole exchange model for backward interactions at high energies in, review of, 25:30836
Pomeranchuk pole exchange in three-body hadron production in strong interactions, graphs for isotopic relations for, 25:30824 (JINR-P2-5630)
Pomeranchuk theorem in, violation of, 25:30826
Pomeranchuk theorem violation in, complex negative-signature trajectories for amplitudes with, 25:31012 (COO-264-571)
pomeron dominance of electroproduction structure functions, 25:30779
Pomeron in, 25:30826
pomeron model from duality diagrams in Veneziano model, 25:31022
reggeon calculus from hybrid perturbation-theory model using eikonal technique, 25:30980
residues for pseudoscalar meson forward and backward interactions with $^1/_2{}^+$ baryons at high energies in, 25:30883
scattering amplitude in multi-, Landau singularity and fixed-angle behavior of, 25:31033
trajectories for amplitudes with Pomeranchuk theorem violation in, complex negative-signature, 25:31012 (COO-264-571)
trajectories for multi-channel potential scattering, 25:31031
trajectory with finite asymptotic phase, characteristics of, 25:31029

RELATIVE BIOLOGICAL EFFECTIVENESS
comparison for α, β, and γ radiation for induction of chromosome aberrations in Chinese hamster liver cells, 25:29483 (LF-43, pp 246-53)

RELATIVISTIC STAR CLUSTERS
gravitational-wave emission from, (T), 25:30240
model of, solution of Plummer's, (T), 25:30066
stability of, (T), 25:30066

RELATIVITY THEORY
charged-particle motion in general, conservation of e/m ratio for, 25:30998
coordinate transformations to rotating reference frame in special, 25:30876
equations of motion in, additional invariance of, 25:30975
equivalence principle for massive bodies in general, 25:31009
field equations in general, cosmological constant modification of system of generalized, 25:31004
field equations in general, solutions of weakened set of, 25:30999
fluctuations of gravitational field in general, role of quantum, (T), 25:30224
gravitation in general, inertial reference frames in Einstein theory of, 25:30996
gravitational red shift in general, quantum mechanics for, 25:30963
Minkowski space in, equations of motion invariant under group P(1,n) in, 25:30966
observable values in special, transformation of general covariant, (T), 25:30970
quantization of general, 25:31003

REMOTE-HANDLING EQUIPMENT
fuel element spill resistant transfer bucket, for liquid sodium cooled fast reactors, 25:31582(P)

REPRODUCTION
radiation effects on, of gypsy moths, effects of dose and pupal exposure on γ, 25:29616
radiation effects on, of rhinoceros beetles, effects of dose on γ, 25:29754

XUM

RESINS
radioinduced polymerization of unsaturated polyester, electron, 25:29116(P)
RESPIRATION
radiation effects on, in rat liver mitochondria, effects of riboflavin on, 25:29640
RHENIUM
book: Creep-Rupture Data for the Refractory Metals to High Temperatures, 25:29868
determination in copper and molybdenum concentrates, direct spectroscopic, 25:28945
determination in molybdenum and tungsten alloys, chromatographic, 25:28953
effects of additions of, on stability of uranium dioxide fuels, 25:29932(P)
proton fission at 10 MeV to 29 GeV, cross section for, 25:31326
reactions with oxygen, thermal-flare studies of surface, 25:29772
separation from aqueous solutions by thin-layer chromatography using liquid anion exchangers, 25:29186
separation from molybdenum and selenium as perrhenate on silica gel chromatographs, 25:28953
sorptive properties for actinide ions, desorption energies and residence times, 25:30259
superconducting transition temperature of slightly doped, (E), 25:30433
RHENIUM ALLOYS AND SYSTEMS
book: Creep-Rupture Data for the Refractory Metals to High Temperatures, 25:29868
Cr-base--Re, hardness at 77 to 430°K, effects of rhenium content on, 25:29871
Mo--Re, radiation effects on microstructure of, fast neutron, 25:29904 (ORNL-4630, pp 73-95)
Mo--Re--W, fabrication of irradiation capsules of, welding methods for, 25:30010 (ORNL-4630, pp 179-85)
Mo-base--Re, hardness at 77 to 576°K, effects of rhenium content on, 25:29871
Mo-base--Re, mechanical properties of monocrystalline, asymmetric, 25:29829
Os--Re, superconductivity of hcp, (E), 25:30433
Re--Ru, superconductivity of hcp, (E), 25:30433
Re--W, creep under stress, effects of oxygen at high temperature on, 25:29786 (ORNL-4630, pp 207-25)
Re--W, superconductivity of hcp, (E), 25:30433
Re--W, welding of, effects of filler metal and methods on, 25:29786 (ORNL-4630, pp 207-25)
Re--W-base, hardness at 77 to 730°K, effects of rhenium content on, 25:29871
RHENIUM OXIDES
thermodynamic properties of gaseous diatomic, free energy functions for, 25:29082
RHODIUM
separation from plutonium by anion exchange from mixed methanol--nitric acid solutions, 25:29191
RHODIUM ALLOYS AND SYSTEMS
Pt-base--Rh, tensile properties at 1093 to 1290°C, 25:29823 (ORNL-4630, pp 186-90)
RHODIUM ISOTOPES Rh-103
separation from palladium-103 by ion exchange, 25:29413 (CONF-691225)
RHODIUM ISOTOPES Rh-105
energy level of, description of anomalous 7/2+, (T), 25:31323
RHODIUM ISOTOPES Rh-106
beta decay of metastable, beta and gamma spectra, Q, and log ft of, (E), 25:31384
RHODIUM ISOTOPES Rh-107
energy level of, description of anomalous 7/2+, (T), 25:31323
RHODIUM OXIDES
thermodynamic properties of gaseous diatomic, free energy functions for, 25:29082
RICHLAND AREA (WASH.)
ecology as exposed at Rattlesnake Springs, interrelationships of geologic formations and processes affecting, 25:31686 (BNWL-B-29)
RING CURRENT
disturbance in, effect of magnetospheric magnetic storm generation on, (E), 25:30400
relation of location of, to magnetospheric field lines leading to SAR arcs, (E/T), 25:30376
ROBERT E. GINNA POWER REACTOR, UNIT 1
operations incident of April 22, 1971, failure of concentrated boric acid tanks valves to open, 25:31474 (DOCKET-50244-70)
ROCKET REACTORS (NERVA)
operation of reusable nuclear shuttle concept, development program for, 25:31641
safety of reusable shuttle concept, development program for, 25:31641
ROCKS
analysis for trace amounts of palladium by isotope dilution, 25:28981
analysis of sedimentary, for bromine, chlorine, and iodine by neutron activation, 25:29033
analysis of standard, for palladium and platinum by neutron activation following fire-assay concentration, 25:29022
RODS
gravitational field from energy--momentum--stress tensor for uniformly rotating, 25:30997
ROVER REACTORS
radioactive effluents from, analysis of normal operation and accident condition ground tests, 25:31642
RUBBER
polyethylene--rubber, radioinduced preparation of foamed sheets of, 25:29109(P)
RUBIDIUM
determination by bremsstrahlung activation, 25:29018
determination using ion permselective membrane, potentiometric, 25:28956
effects on radiometric determination of cesium isotopes in water, after extraction as tetraphenylborates, 25:29000
isotopic composition of, spectral determination of, (E), 25:28952
photon reactions (γ,n) at 30 MeV, 25:29018
RUBIDIUM ISOTOPES Rb-84
preparation of, new method for, 25:29413 (CONF-691225)
RUBIDIUM ISOTOPES Rb-85
alpha reactions (α,2n), (α,3n), (α,4n), and (α,αn) at 15 to 54 MeV, excitation functions, isomer ratios, and mean recoil distances for, (E/T), 25:31239 (LYCEN-7091)
neutron activation resonance integrals for, measured relative to gold-197, (E), 25:31300 (CNEA-282)
RUBIDIUM ISOTOPES Rb-88
beta decay of, shell-model analysis of first-forbidden unique, (T), 25:31284
RUBIDIUM OXIDES
thermodynamic properties of gaseous diatomic, free energy functions for, 25:29082
RUBIDIUM URANYL NITRATES
coating single crystals of, with fissile isotopes, 25:29034 (AERE-R-6141)
preparation of single crystals of, 25:29034 (AERE-R-6141)
RUPTURE
book: Creep-Rupture Data for the Refractory Metals to High Temperatures, 25:29868
RUTHENIUM
determination in minerals and industrial samples, spectrophotometric, 25:28960
determination in presence of osmium without separation, kinetic differences between catalyzed reactions for, 25:28941
determination of trace amounts of, in platinum by neutron activation following separation by ion exchange chromatography, 25:29023
effects on reactions of arsenic(III) with cerium(IV), 25:28941
separation from plutonium by anion exchange from mixed methanol--nitric acid solutions, 25:29191
RUTHENIUM ALLOYS AND SYSTEMS
Ce--Co--Ru, preparation and superconductivity of, (E), 25:30413(T) (LA-tr-71-26)
Ce--Fe--Ru, preparation and superconductivity of, (E), 25:30413(T) (LA-tr-71-26)
Ce--Gd--Ru, preparation and superconductivity of, (E), 25:30413(T) (LA-tr-71-26)
Ce--Mn--Ru, preparation and superconductivity of, (E), 25:30413(T) (LA-tr-71-26)
Ce--Ni--Ru, preparation and superconductivity of, (E), 25:30413(T) (LA-tr-71-26)
Ce--Ru, preparation and superconductivity of intermetallic $CeRu_2$, (E), 25:30413(T) (LA-tr-71-26)
Nb--Ru, phase transformation in near-equiatomic, crystallography, kinetics, and theory of displacive, 25:29882 (COO-1198-807)
Os--Ru, superconductivity of hcp, (E), 25:30433
Re--Ru, superconductivity of hcp, (E), 25:30433
RUTHENIUM ISOTOPES
separation of fission-product, from irradiated fuels of Mo--UO_2, 25:29413 (CONF-691225)
RUTHENIUM ISOTOPES Ru-102
neutron activation resonance integrals for, measured relative to gold-197, (E), 25:31300 (CNEA-282)
RUTHENIUM ISOTOPES Ru-103
metabolism in beagle dogs following ingestion of nuclear debris from Project Cabriolet, 25:29456
RUTHENIUM OXIDES
production and properties of aerosols of, 25:29077 (LF-43, pp 18-24)
thermodynamic properties of gaseous diatomic, free energy functions for, 25:29082

S

S-MATRIX
commutator for axial charge, consequences of, 25:30982
elements of, in class of nonrenormalizable field theories, method for computing, 25:31016 (NYO-1932(2)-192)
field theory with Lagrangian depending on derivatives for, 25:30968
representation for singular potentials, 25:31021
unitarity of, quantum mechanical n-body problem for, 25:30957
SAINT LAURENT-DES-EAUX REACTOR (EL-4)
core for, configuration and composition of initial,

25:31480
pressure vessel for, performance of prestressed concrete, 25:31455 (EUR-4531, pp 95-128)
startup of, summary of initial, 25:31480
SALIVARY GLANDS
radiation effects on animal and human, x, 25:29693
scanning of human, comparison of effectiveness of technetium-99m and iodine-131, 25:29574
scanning of human, effects of pilocarpine nitrate on iodine-131 and technetium-99m, 25:29579
technetium-99m localization in human, 25:29418 (BNL-50285)
SAMARIUM
determination as hexafluoroacetylacetone--trioctylphosphine oxide complex, spectrofluorometric, 25:28954
determination in lanthanum by emission spectrography, 25:28965
separation from other rare earths by ion exchange, 25:29178 (CEA-R-4102)
SAMARIUM ALLOYS AND SYSTEMS
Co--Sm, hardness of intermetallic $SmCo_5$, measurement of magnetic and mechanical, 25:29845
Co--Sm, magnetic properties of intermetallic $SmCo_5$ crystals, 25:30675
SAMARIUM ISOTOPES Sm-147
neutron resonance parameters up to 400 eV, (E), 25:31305 (JINR-P3-5655)
SAMARIUM ISOTOPES Sm-148
energy levels from Coulomb excitation, lifetimes of ground-band, (E), 25:31364
SAMARIUM ISOTOPES Sm-149
neutron resonane parameters up to 250 eV, (E), 25:31305 (JINR-P3-5655)
SAMARIUM ISOTOPES Sm-150
energy levels from Coulomb excitation, lifetimes of ground-band, (E), 25:31364
SAMARIUM ISOTOPES Sm-152
energy levels from Coulomb excitation, lifetimes of ground-band, (E), 25:31364
energy-level transitions from europium-152 decay, conversion electron particle parameters for, (E), 25:31380
SAMARIUM ISOTOPES Sm-154
oxygen-16 fission at 137 MeV, angular distribution of fission products from ytterbium-170 compound nucleus in, (E), 25:31371
SAMARIUM OXIDES
positron lifetimes in, 25:30272
MgO--Sm_2O_3, phase diagram at 1500 to 2400°C, 25:29985
SAMPLING
methods for aerosol, for particle size analysis, comparison of electrostatic precipitation, filtration, and thermal precipitation, 25:29263
SAN ONOFRE POWER REACTOR, UNIT 1
control rods for, insertion limit conditions for Cycle 2 operation of, 25:31488 (DOCKET-50206-112)
SAP (SINTERED ALUMINUM POWDERS)
radiation effects on mechanical properties of, use of cyclotron-injected helium for simulation of neutron, 25:29907 (ORNL-TM-3299)
SARCOSINE
deuteriochloride, radiolysis of monocrystals of, ESR spectral studies on free radicals produced by x, 25:29152
hydrochloride, radiolysis of monocrystals of, ESR spectral studies on free radicals produced by x, 25:29152
SATELLITES
propulsion of, book on ion, 25:30453
SAXTON POWER REACTOR
operations history for September 1970 to February 1971, 25:31466 (DOCKET-50146-72)
pressure vessel for, design and performance of steel, 25:31668 (IRS-T-17)
radiation target cans for, technical specifications for pressurized Zircaloy 4 tubes with stainless steel specimens for, 25:31485 (DOCKET-50146-73)
SCANDIUM
catalytic properties of, in high-temperature para-ortho conversion reaction, 25:29859
determination for water flow tracing by neutron activation, 25:29013 (RLO-1750-81)
determination in deposits and airborne particles by neutron activation and scintillation counting, 25:29032
determination of trace amounts of, in seawater, review on methods for, 25:28921
effects on fluorometric determination of zirconium, 25:28963
separation from aqueous solutions by thin-layer chromatography using liquid anion exchangers, 25:29186
separation from other metals by ion-exchange paper chromatography, 25:29190
SCANDIUM CARBIDES
catalytic properties of, in high-temperature para-ortho conversion reaction, 25:29859
SCANDIUM CHLORIDES
thermodynamic properties at 298 to 1300°K, 25:29951
SCANDIUM HYDRIDES
catalytic properties of, in high-temperature para-ortho conversion reaction, 25:29859
SCANDIUM ISOTOPES Sc-45
energy levels from calcium-42, (α,p) reactions, spins and parities of, (E), 25:31251
helium-3 reactions (He-3,d) at 15 MeV, DWBA analysis of angular distributions for, (E), 25:31278
meson reactions (μ^-,xn) by, gamma spectra from, (E), 25:31258
SCANDIUM ISOTOPES Sc-50
energy levels of, shell-model calculation using realistic forces for 3 particle-1 hole, (T), 25:31254
SCANDIUM OXIDES
catalytic properties of, in high-temperature para-ortho conversion reaction, 25:29859
thermodynamic properties of gaseous diatomic, free energy functions for, 25:29082
La_2O_3--Sc_2O_3, phase diagram of, 25:30005
Nd_2O_3--Sc_2O_3, phase diagram of, 25:30005
Sc_2O_3--ZrO_2, crystal transformation in, differential thermal analysis studies of monoclinic-tetragonal, 25:29982
SCATTERING
amplitudes of Compton, O(4) expansion of current commutators near light cone for, 25:31020
amplitudes of high-energy, review of localizable and nonlocalizable quantum field theory for, 25:30962
amplitudes of two-body arbitrary-spin-particle, retarded part of two-time Green function for relativistic, 25:31014 (JINR-E2-5746)
amplitudes of unequal-mass, analyticity constraints and residue functions of E_2 pole exchange for, 25:31027
amplitudes of, analyticity in external-mass variable of, 25:31030
amplitudes of, compositeness and vanishing of renormalization constants for partial-wave two-body, 25:30958
amplitudes of, covariant dispersion relation for weak, 25:31023
amplitudes of, integral representations of expansions over Wigner functions for, 25:31025
amplitudes of, quantum mechanical n-body problem for, 25:30957
amplitudes of, symmetry properties from crossing matrix for, 25:31018
amplitudes of, two-variable crossing-symmetric expansion of, 25:31028
amplitudes of, unitary property for infinite-dimensional Veneziano, 25:31024
amplitudes with cuts in Regge model, crossing-symmetric, 25:30856
amplitudes with Pomeranchuk theorem violation, complex negative-signature trajectories for, 25:31012 (COO-264-571)
angular momentum in, invariants of rotation group for arbitrary, 25:31013 (ITEF-782)
Glauber formula for nuclear, deduction from Watson theory, (T), 25:31434
operators for single-channel systems, 25:31019
optical potentials of nuclear, in terms of diffraction-model parameters, (T), 25:31410
potential, generalizations of Jost--Pais theorem for nonlocal, 25:31026
potential, Regge trajectories for multichannel, 25:31031
potentials in optical model, time-dependent theory for absorptive, 25:31017
resonance averaging in nuclear, (T), 25:31450
resonances in elastic, calculation of background phase shifts, energies, and widths of, 25:30297
S-matrix in inelastic, calculation using WKB approximation, 25:30293
symmetry property of the amplitude of inelastic in the adiabatic approximation, 25:31449
theory of, existence of nontrivial quantum, 25:31034
transition operator for, Faddeev equations for four-particle, 25:31032
wave function for two-body arbitrary-spin-particle, retarded part of two-time Green function for relativistic, 25:31014 (JINR-E2-5746)
SCHIZOMYCOTA
Bacillus sp, sensitivity of heat-treated spores of, to NaCl in recovery medium, effects of NaCl content of heating medium on, 25:29558
Bacillus sp., radiation effects on sensitivity of spores of, to NACl in recovery medium, effects of dose and NaCl content of medium during exposure on γ, 25:29558
Bacillus sp., radiosensitivity of heat-treated spores of, effects of NaCl content of heating medium on γ, 25:29558
Bacillus sp., sensitivity of spores of, to heat, effects of NaCl content of heating medium on, 25:29558
Bacillus subtilis, radiation effects on DNA from, x, 25:29463
Bacillus subtilis, radiation effects on template activity of DNA from, RNA synthesis following x, 25:29467
Bacillus subtilis, radioinduced base degradation and denaturation of DNA from, x, 25:29466
Bacillus subtilis, radioinduced cross links in DNA from, x, 25:29465
Bacillus subtilis, radioinduced double and single strand breaks in DNA of, viscometric studies on x, 25:29464
Bacillus subtilis, radioinduced transformation of his_2

XUM

and try$_2$ markers in DNA from, x, 25:29468
Clostridium botulinum, radiosensitivity of spores of, in beef, effects of temperature on γ, 25:29734
Escherichia coli K12 lambda, radiation effects on DNAase activity in, γ, 25:29725
Escherichia coli, radiation effects on cell divisions in, neutron, 25:29490
Escherichia coli, radiosensitivity of, effects of ferrous ions in presence of oxygen on, 25:29556
Salmonella sp., radiation effects on survival of, in frozen meats, organoleptic properties following γ, 25:29729 (IAEA-R-491-F)
Salmonella typhimurium, biochemistry of heat-treated, 25:29557
Salmonella typhimurium, pathogenicity of heat-treated, 25:29557
Salmonella typhimurium, radiation effects on biochemistry, heat-sensitivity, pathogenicity, and subsequent radiosensitivity of, γ, 25:29557
Salmonella typhimurium, sensitivity of heat-treated, to subsequent heating, 25:29557

SCINTILLATION CAMERAS
design of Anger-type neutron, 25:29348(P)

SCRUBBERS
design and performance of condensing steam, for removing five particles from air streams, 25:29251 (ORNL-4654)

SEALS AND GLANDS
design for electrode leads through high-pressure autoclaves, 25:29779
performance of high-voltage, for fusion research, 25:30572 (EUR-4593, pp 301-9)

SEAWATER
analysis for cobalt, copper, iron, manganese, nickel, and uranium by solvent extraction and x-ray fluorescence spectroscopy, 25:28919
analysis for trace elements and radioisotopes, review on methods for, 25:28921
radiation monitoring of Japanese coastal, near Goto Islands, July 1966, 25:29241

SEDIMENTARY DEPOSITS
diatom content in, as index to environment, 25:31739(R) (TID-25695)

SEED
radiation effects on lettuce, effects of dose rate on γ, 25:29491
radiation effects on structure of DNA of, effects of homologous DNA on repair of, 25:29716
radiation effects on sunflower, effects of storage time before planting on latent, 25:29717
radioinduced chromosome aberration in dormant pea, effects of moisture content on protective effects of cysteine against γ, 25:29552
radioinduced free radicals in watercress, effects of imbibition and germination on γ, 25:29719

SEEDLINGS
radiation effects on lettuce, effects of dose rate on γ, 25:29491

SEISMIC WAVES
characteristics of Rayleigh-type, use of TENSOR code for calculation of, 25:29243 (UCRL-50992)
propagation from Handley event underground nucleear explosion, instrument emplacement and performance for measuring, 25:29242 (NVO-1163-216(Rev.))

SELENIUM
deposition from ground waters to near-surface uranium deposits, effects of ground water and soil conditions on, 25:29240
determination by x-ray fluorescence, sensitivity of, 25:28962
determination in copper electrolysis slimes, iodometric, 25:28933
effects on fluorometric determination of zirconium, 25:28963
separation from rhenium and molybdenum as selenite on silica gel chromatographs, 25:28953

SELENIUM ISOTOPES Se-75
energy levels from arsenic-75 (p,n) reactions, spin assignments for, (E), 25:31248
energy levels from arsenic-75 (p,n) reactions, spin-parity assignments for, (E), 25:31263
energy levels from bromine-75 decay, (E), 25:31257
energy-level transitions from arsenic-75 decay, multipole mixing ratios for, (E), 25:31263
uptake in bones and tissues of rats for diagnosis of joint diseases, 25:29581

SELENIUM ISOTOPES Se-76
energy levels from arsenic-76 decay, (E), 25:31259

SELENIUM OXIDES
thermodynamic properties of gaseous diatomic, free energy functions for, 25:29082

SELENIUM SYSTEMS
Np--Se, crystal structure of Np_2Se_4, 25:30002
Pu--Se, crystal structure of PuSe and Pu_2Se_4, 25:30002

SEMICONDUCTOR JUNCTIONS
radiation effects on currents through MOS structures, 25:29412

SEPARATION PROCESSES
development for separating hafnium from zirconium, rev.ew on, 25:29782 (AAEC/TM-570)

SEROTONIN
deamination in liver of radiation effects on deamination of, in rat liver, 25:29641
radioprotective effects of o-acyl derivatives of, on mice, 25:29555
radioprotective effects of sulfur analogs of, on mice, x, 25:29567

SEWAGE
analysis for alpha emitters by radiometry, ASTM method for, 25:29003
analysis for beta emitters by proportional counting, ASTM method for, 25:29009
analysis for γ emitters by scintillation counting, ASTM method for, 25:29008
analysis for radioactive barium by precipitation and radiometry, ASTM method for, 25:29004
analysis for radioactive iodine by cnemical separation and radiometry, ASTM method for, 25:29007
analysis for thorium spectrophotometrically using o-[2-hydroxy-3,6-disulfo-1-naphthyl]azo]benzenearsonic acid, ASTM method for, 25:28977
distribution and transport in streams, tracer methods for studying, (E/T), 25:29213

SEX
effects on strontium-90 distribution in femoral medullary canal in rats following intravenous injection, 25:29524

SEYFERT GALAXIES
light variations of 3C 120, (E), 25:30214
radio flux from five, (E), 25:30129
spectra of NGC 1068 and NGC 1275, search for redshifted line of neutral hydrogen in, (E), 25:30121
spectral redshift of NGC 7603, relation to smaller companion galaxy, (E), 25:30217

SHEEP
radiation effects on intestinal mucosa of, unilateral lethal cobalt-60 γ and pulsed mixed fission neutron and γ, 25:29656
radiation effects on survival of, LD-50/5 dose for unilateral cobalt-60 γ, 25:29656
radiation effects on survival of, RBE for LD-50/5 dose for unilateral pulsed mixed fission neutron/gamma, 25:29656

SHIELDED CONTAINERS
design and operation of, for shipping irradiated fuel elements, standards for, 25:29321
design of BNW Model 10, engineering drawings for, 25:29318

SHIELDING
book: Engineering Compendium on Radiation Shielding. Vol. III. Shield Design and Engineering, 25:30634
cross sections for spacecraft, intranuclear cascade model for, 25:30631 (ORNL-TM-3376)
design for 35 MeV betatron used in therapy, 25:29528
design parameters of asymmetric 4π, 25:31640 (ORNL-TM-3368)
testing of reactor biological, standards for, 25:31677

SHIELDING MATERIALS
book: Concrete Radiation Shields, 25:30645

SHIPPING
container for fuel elements and fissionable materials, design of, 25:29318

SHOCK WAVES
interactions with plasma near critical Alfven--Mach number, electron heating in collisionless, (E), 25:30468
propagation along magnetic field in collisionless plasma, (E/T), 25:30620
propagation in interplanetary space, (E/T), 25:30316
structure of hydromagnetic, two-fluid approximation for, (T), 25:30528

SILANE
decomposition at 800 to 1200°C and low pressure to siliconize surface of tungsten ribbons, study of heterogeneous, 25:29814

SILICATES
preparation of phyllitic mineral, for use in decontamination of radioactive wastes, 25:29175 (BARC-509)

SILICON
analysis for oxygen by 14-MeV neutron activation, 25:29021
complexes with molybdates, effects of various acids and salts on formation of, 25:28924
defect production by ion bombardment of single-crystal, design and performance of equipment for, 25:30648 (N-70-37028)
determination in carbon as molybdenum blue complex, ASTM method for colorimetric, 25:28974
determination in low-alloy steel, two-standard method for spectrometric, 25:28950
determination in various materials as molybdosilicate complex, spectrophotometric method for, 25:28924
dispersion of submicron particles of, in hydrogen, effects on radiant heat transfer, 25:29270
dispersion of submicron particles of, in nitrogen, measurement of scattering amplitude functions for, 25:29270
effects on fluorometric determination of zirconium, 25:28963
helium-4 atom scattering at surfaces of, calculations, 25:30659
ion-implantation-induced lattice disorder in, electron

XUM

microscopic observation of 30-keV indium, 25:30650
oxidation of coating of, at 700 to 1200°C and low pressures, kinetics and mechanism of, 25:29968
radioinduced defects in lithium-doped n-type, ESR and photoconductivity study of annealing of 1.5-MeV electron, 25:30653
radioinduced defects in p-type, photoconductivity study of annealing of 1.2-MeV electron, 25:30658

SILICON CARBIDES
dispersion of submicron particles of, in nitrogen, measurement of scattering amplitude functions for, 25:29270
fission product distribution in layered coating of pyrolytic carbon and, sputtering and gamma spectrometry methods for determination of, 25:29979 (SGAE-PH-96/1970)

SILICON ISOTOPES Si-27
energy levels from silicon-28 (He-3,α) reactions, spins and parities of, (E), 25:31252

SILICON ISOTOPES Si-28
alpha scattering at 104 MeV, differential cross sections for, (T), 25:31212
deuteron elastic scattering at 82 MeV, optical-model analysis of, (E), 25:31240 (NP-18511)
deuteron reactions (d,He-3) at 82 MeV, DWBA analysis of differential cross sections for, (E/T), 25:31240 (NP-18511)
energy level at 15.27 MeV from magnesium-26 (He-3,n) reactions, T = 2 analog, (E), 25:31237 (IAE-1958)
energy levels of, coupled-channel calculation in 1p--1h continuum approximation for giant resonance, (T), 25:31286
meson (μ^-) capture by, charged-particle masses and energy spectra from, (E), 25:31267
meson (π^-) capture by, neutron spectra from radiative, (E), 25:31216
proton reactions (p,γ) at 725 keV, gamma spectra from, (E), 25:31250

SILICON ISOTOPES Si-29
energy levels from proton inelastic scattering, spin-parity assignments for, (E), 25:31245

SILICON OXIDES
abundance in cosmic radio sources, (E), 25:30152
analysis of, properties of vitreous carbon as mortar for spectrochemical, 25:28938
thermodynamic properties of gaseous diatomic, free energy functions for, 25:29082
Al_2O_3--CaO--CeO_2--SiO_2--ZrO_2, analysis of, x-ray-emission, 25:28957
Al_2O_3--Cs_2O--SiO_2, preparation and properties of, for use as radiation source, 25:29938(T) (BNWL-tr-65)
Al_2O_3--Li_2O--MgO--SiO_2, radiation effects on phase transformations in, neutron, 25:30017
Al_2O_3--SiO_2, radiation effects on catalytic properties of halogenated, in cracking of cumene and isomerization of o-xylene, γ, 25:29111
CaO--SiO_2--ZrO_2, phase studies of, 25:30008
FeO--MnO--SiO_2--ZrO_2, phase studies of, 25:30008
HfO_2--SiO_2, solid solutions of, occurrence of hafnium oxide-rich, 25:30006
MgO--SiO_2--ZrO_2, phase studies of, 25:30008
Mn_3O_4--SiO_2--ZrO_2, phase studies of, 25:30008
MnO--SiO_2--ZrO_2, phase studies of, 25:30008

SILICON OXYNITRIDES
radiation effects on dielectric properties of insulators of, fast neutron, 25:30011 (ORNL-4630, pp 226-9)

SILICON SYSTEMS
Ce--Mg--Si, crystal structure of $CeMg_2Si_2$, 25:29993
Ni--Si, analysis for silicon as molybdosilicate complex, spectrophotometric method for, 25:28924
Pd-base--Si, radiation effects on amorphous structure of, fission products, 25:29901 (CEA-CONF-1693)
Si--U, analysis for silicon as molybdosilicate complex, spectrophotometric method for, 25:28924

SILICONE RUBBERS
permeability of membranes of, to rare gases, 25:29317 (ORNL-4522)
radiation effects on stability of thin membranes of, in off-gas streams, 25:29317 (ORNL-4522)

SILTS
age of Lake Balkhash, USSR, uranium-234/-238 method for estimation of, 25:29210
analysis for antimony, chromium, cobalt, iron, scandium, and zinc by neutron activation, 25:29032
cesium-137 transport through river bed, model river studies of mechanisms of, 25:29204
molybdenum content and distribution in, from Mid-Atlantic Ridge, measurement of, 25:29228
radioactivity monitoring, West Valley Processing Plant, 1970, 25:29179 (DOCKET-50201-69)
uranium content and distribution in ocean, from Mid-Atlantic Ridge, measurement of, 25:29228

SILVER
carbon-12 reactions at 86 MeV, angular momentum effects on mechanism of, (E), 25:31356
determination in copper electrolysis slimes, gravimetric or titrimetric, 25:28933
determination of trace amounts of, in platinum by neutron activation following separation by ion exchange chromatography, 25:29023
determination of trace amounts of, in vanadium, spectrographic, 25:28947
determination using ion permselective membrane, potentiometric, 25:28956
effects on fluorometric determination of zirconium, 25:28963
effects on radiometric determination of cesium isotopes in water, after extraction as tetraphenylborates, 25:29000
nitrogen-14 reactions at 78 and 113 MeV, angular momentum effects on mechanisms of, (E), 25:31356
proton reactions (p,γ) at 4 MeV, gamma spectra from, (E/T), 25:31303 (INR-1271)

SILVER ALLOYS AND SYSTEMS
Ag--In-base, superconducting transition temperature under strain in, (E), 25:30435
Ag-base--In, properties for use as ball bearing spacers in ultrahigh vacuum, 25:29834

SILVER ISOTOPES
production in proton fission of uranium-238 at 450 MeV, mass yield and charge distribution for, (E), 25:31302 (COO-1167-10)

SILVER ISOTOPES Ag-107
energy level of, description of anomalous 7/2+, (T), 25:31323

SILVER ISOTOPES Ag-108
alpha reactions at 205 MeV, neutron and proton spectra from, (T), 25:31368
beta and electron-capture decay of, gamma spectra from, (E), 25:31382

SILVER ISOTOPES Ag-109
energy level of, description of anomalous 7/2+, (T), 25:31323

SILVER ISOTOPES Ag-110
beta decay of, β--γ angular correlations from, (E), 25:31277

SILVER ISOTOPES Ag-111
beta decay scheme, (T), 25:31365

SILVER OXIDES
thermodynamic properties of gaseous diatomic, free energy functions for, 25:29082

SKELETAL SYSTEM
radioisotope accumulation in fish, barium-140 and strontium-89, 25:29449

SKIN
electric conductivity of human, relation to emotional stability, 25:29531 (CEA-R-4156)
radiation dose distribution in, in relation to whole-body exposure, 25:29603
radiation effects on human, following therapy for thyroid cancer, dose dependent teletherapy, 25:29707
radiation effects on synchronized tumors on mouse, combined effects of 5-fluorouracil and, 25:29605
radioinduced basal cell carcinomas on human, following therapy for burns, long-term, 25:29701
radioinduced carcinomas on rat, x, 25:29628

SLAGS
analysis of copper electrolyte, for tellurium, colorimetric, 25:28931

SLATE
performance as artifical substrate for analysis of periphyton component of running-water ecosystems, 25:29478

SNOW
radium-226 content of contemporary and fossil, effects of coal burning power stations on, 25:29209

SODIUM
acoustic imaging in liquid, holographic scanning configurations for, 25:31685 (BNWL-1558)
analysis of liquid, for oxygen, apparatus for, 25:29407(P)
chemistry of liquid, in reactor cooling systems, (E), 25:31533(R) (ANL-7798)
cleaning from surfaces, relations with corrosion, 25:29762 (ORNL-4630, pp 158-62)
combustion of liquid, in fast breeder reactor environment, 25:31568(T) (EURFNR-823)
compatibility with refractory metals and alloys at 600°C, effects of oxygen on, 25:29761 (ORNL-4630, pp 150-7)
corrosive effects of oxygen-contaminated, on titanium--vanadium alloys and vanadium, 25:29781
corrosive effects on austenitic steels of liquid, 25:31568(T) (EURFNR-823)
determination in crude or refined oils or engine deposits by neutron activation and γ spectrometry, 25:29026
determination in nails of cystic fibrosis patients by neutron activation, 25:29016
determination in plutonium by mass spectrometry, 25:28916 (CEA-R-4071)
determination using ion permselective membrane, potentiometric, 25:28956
diffusion coefficients for barium in liquid, radiochemical determination of, (E/T), 25:31613
effects on friction and wear between fuel rods and spacer grids at 680°C, 25:29818(T) (AEC-tr-7224)
effects on radiometric determination of cesium isotopes in water, after extraction as tetraphenylborates, 25:29000
fission product behavior in liquid, (E/T), 25:31614
fission product behavior in, (E/T), 25:31615
handling of liquid, at high temperatures, design standards for equipment for, 25:29252 (RD/B/M-1817)
impurities in reactor coolant, design and operation of

XUM

system for automatically monitoring, 25:29261
neutron scattering law for liquid, calculation using ion-electron model, 25:31176
pump for liquid, in fast breeder reactor coolant systems, design and operation of, 25:29257
SODIUM BORATES
corrosive effects of melts of, on tungsten, mechanisms and kinetics of, 25:29774
SODIUM CHLORIDES
corrosive effects on hafnided and tantalided nickel and Type 316 stainless steel at 25 to 60°C, 25:29766
effects on γ-radiosensitivity and heat-sensitivity of Bacillus spores, 25:29558
gold nuclei condensation from atomic beam on crystals of, effects of radiation on, 25:29910
radioinduced F-center destruction in crystals of, mechanism of 3.5-MeV proton, 25:30655
sensitivity of γ-irradiated Bacillus spores in recovery medium, effects of NaCl content of exposure medium and radiation dose on, 25:29558
sensitivity of heat-treated Bacillus spores following transfer into recovery medium, effects of NaCl content of heating medium on, 25:29558
NaCl--2-propanol, corrosive effects on aluminum--titanium--vanadium alloy, 25:29773
SODIUM FLUORIDES
LiF--KF--NaF, properties of refractory metal salt incorporating, for use as bath in metal electrodeposition, 25:29783 (CEA-N-1376)
SODIUM FORMATES
benzyl alcohol--sodium formate, radiolysis of deaerated aqueous solutions of, at 23°C, effects of pressure on yields of hydrogen from γ, 25:29157
Na_2NO_3--2-propanol--sodium formate, radiolysis of deaerated aqueous solutions of, at 23°C, effects of pressure on yields of hydrogen from γ, 25:29157
SODIUM HYDROXIDES
radiolysis of glasses of, at 4 to 77°K, ESR studies on trapped electrons produced by γ, 25:29156
Na_2NO_3--NaOH--2-propanol, radiolysis of deaerated aqueous solutions of, at 23°C, effect of pressure on yields of hydrogen from γ, 25:29157
SODIUM IONS
abundance of positive, in ionospheric D region, (E/T), 25:30404
SODIUM ISOTOPES
radioactivity standards of, users' guides for, 25:29174
SODIUM ISOTOPES Na-22
beta decay of, β--γ angular correlations from, (E), 25:31277
use as tracer for determining distribution of onion flies, 25:29748
SODIUM ISOTOPES Na-23
deuteron reactions (d,He-3) at 82 MeV, DWBA analysis of differential cross sections for, (E/T), 25:31240 (NP-18511)
energy levels from magnesium-24 (D,He-3) reactions, l-transfer, spectroscopic factors, and spin-parity assignments for, (E/T), 25:31240 (NP-18511)
energy levels from proton resonances in neon-22, resonance parameters and spin--parity assignments for, (E), 25:31281
helium-3 reactions (He-3,Li-6) at 40.7 MeV, DWBA analysis of, (E/T), 25:31214
photon reactions (γ,n) at 10 to 68 MeV, yields of radioactivities from, (E), 25:31333
SODIUM ISOTOPES Na-24
use as tracer for studying distribution and transport of pollutants in streams, (E), 25:29213
SODIUM NITRATES
Na_2NO_3--2-propanol--sodium formate, radiolysis of deaerated aqueous solutions of, at 23°C, effects of pressure on yields of hydrogen from γ, 25:29157
Na_2NO_3--NaOH--2-propanol, radiolysis of deaerated aqueous solutions of, at 23°C, effect of pressure on yields of hydrogen from γ, 25:29157
SODIUM OXIDES
thermodynamic properties of gaseous diatomic, free energy functions for, 25:29082
Na_2O--UO_3--V_2O_5, phase studies of, 25:29998
SOILS
analysis for plutonium by leaching, ion exchange separation, and alpha counting, 25:28992
analysis of ammonium acetate extracts of, for aluminum by neutron activation, atomic absorption, and spectrophotometry, comparative study on, 25:29020
heat and mass transfer through, bibliography on analytical and experimental methods for determining, 25:29266 (SC-ARPIC-1010)
radiation effects on urease activity in, comparison of toluene and γ, 25:29460
radiation hazards to, in nuclear power reactor environments in Soviet Union, 25:29525
strontium-90 distribution and transport in arable, of Lower Silesia, measurement of, 25:29207
tritium distribution and transport in, ejected by Sedan event, measurement of, 25:29244 (UCRL-72572)
SOL-GEL PROCESS
equipment and process development for, for production of dense plutonium-238 dioxide microspheres, 25:29921 (ORNL-4565)
SOLAR ACTIVE REGIONS
magnetic-field strengths in, relation to proton flares, (E), 25:30185
SOLAR CORONA
argon ionization stages in, distribution of, (E/T), 25:30181
observations at various stations, errors in, (E), 25:30182
photography during eclipse of Mar. 7, 1970, (E), 25:30163
radio discontinuity in, at 1 solar radius, (E), 25:30159
SOLAR DISTURBANCES
effects of cycle of, on interplanetary magnetic field, (E/T), 25:30326
SOLAR FLARES
effects on magnetic-field strengths in sunspot groups, (E), 25:30185
electron acceleration in, two-stage, (E/T), 25:30169
observations of chromospheric, at Ondrejov during 1969, (E), 25:30189
observations on chromospheric, at Hurbanovo during 1969, (E), 25:30175
production by finite conductivity instabilities, (T), 25:30180
relation of limb, to x-ray bursts, (E), 25:30187
x-ray bursts associated with, soft, (E), 25:30160
x-ray emission during, hard, (E/T), 25:30169
SOLAR PARTICLES
acceleration at magnetosphere bow shock, (T), 25:30312
flux and spectra of low-energy, (E), 25:30161
proton fluxes at 1.5 to 50 MeV measured by Zond-4 and Zond-5, (E), 25:30164
transport in interplanetary space of low-energy, convective, (T), 25:30179
SOLAR RADIATION
enhancement of x-ray, effect on ionospheric absorption during shortwave fadeouts, (E), 25:30362
monitoring of x, Solrad-8 and -9 real-time telementry from 1966 to 1969, (E), 25:30355
SOLAR RADIO BURSTS
detection of new type, associated with Type III bursts, (E), 25:30159
x radiation associated with Type-III, soft, (E), 25:30167
SOLAR SPICULES
production by finite conductivity instabilities, (T), 25:30180
SOLAR SYSTEM
cosmic-ray anisotropy in, three-dimensional, (E/T), 25:30320
cosmic-ray modulation by, zone of, from meteorite analysis, 25:30323
dust formation by circumsolar crushing processes, (T), 25:30195
formation and evolution of, boundary conditions on, (E), 25:30034
formation of planets in, computer simulation of, (T), 25:30178
formation of, supernova fragmentation model of, (T), 25:30157 (LA-4343(Suppl.))
SOLAR WIND
cosmic-ray modulation by, primary, (T), 25:30313
cosmic-ray modulation by, primary, (T), 25:30314
cosmic-ray modulation by, primary, (T), 25:30315
cosmic-ray modulation by, with anisotropic and isotropic diffusion, primary, (T), 25:30324
cosmic-ray modulation by, with slowly decreasing asymmetry away from Sun, primary, (T), 25:30325
dust-particle alignment in comet tails by protons in, (T), 25:30183
effects on diurnal variation of cosmic rays, (E/T), 25:30321
effects on lunar surface materials, (E), 25:30249
hydromagnetic-wave coupling with plasma sheet, effect on magnetotail resonant oscillations, (T), 25:30366
interaction with lunar limb, creation of diamagnetic cavity on antisolar side of moon from, (E/T), 25:30388
interactions with Mercury, interior conductivity studies from, (E/T), 25:30389
modulation of primary cosmic radiation by, (E/T), 25:30322
penetration into magnetosphere, generation of magnetic storm from, (E), 25:30400
plasma instabilities in, hydromagnetic analog of Kelvin--Helmholtz problem including Hall effects, 25:30392
pressure effects on magnetosphere, dynamic and statistical, (E/T), 25:30396
SOLAR X-RAY BURSTS
characteristics of soft, (E), 25:30160
relation to limb flares, (E), 25:30187
SOLID STATE PHYSICS
experiments in, introduction and discussion of LEED, 25:31681 (AERE-M-2184)
research in, nuclear physics methods use in, review, 25:30647
SOLIDS
book: Advances in High Temperature Chemistry, 25:29081
determination in phosphorus-32 preparations, ASTM method for, 25:29002
determination in radioisotope mixtures, ASTM method for, 25:29005

XUM

SOLVENT EXTRACTION PROCESSES
equilibrium data for Eurex, 25:29182 (RT/CHI-(70)31)
SOUND GENERATORS
performance for decontamination of medical equipment in combination with detergent solution, 25:29510
SOUTHWEST EXPERIMENTAL FAST OXIDE REACTOR
experimental facilities for, reactivity worth of control slug for FRED, 25:31631 (DOCKET-50231-80)
pressure vessel for, request for additional information on flange bolt stresses for, 25:31595 (DOCKET-50231-79)
pressure vessel for, thermal stress limits and inspection requirements for head bolts of, 25:31596 (DOCKET-50231-81)
SOVIET UNION
sediments from Lake Balkhash in, uranium-234/-238 ages of, 25:29210
SPACE
gravitational-wave propagation in constant curvature, (T), 25:30243
heating of intergalactic, (T), 25:30218
magnetic fields in interplanetary, north--south component of, (E/T), 25:30176
SPACE VEHICLES
development of reusable nuclear shuttle concept, design and test program for, 25:31641
heaters for lunar-landing, design of plutonium-238-fueled heat sources for, 25:29276(P)
operation and uses of orbiting space stations, Earth study from, (T), 25:30363
propulsion of, book on ion, 25:30453
shielding for nuclear powered, optimum design parameters of asymmetric 4π, 25:31640 (ORNL-TM-3368)
SPAIN
radiation control of Mediterranean fruit fly in, 25:29739
SPECTRA
line broadening in astrophysical, effects of Ar, H, and He perturbers on van der Waals, (T), 25:30266
SPECTROMETERS
development of large magnetic spark chamber omega, 25:29373
resolution of nuclear, effect of automatic correction system on, 25:29364
SPECTROSCOPY
applications of spectral distributions in nuclear, (T), 25:31430
atomization cell for flame, experimental and theoretical evaluation of acetylene--nitrous oxide flame as, 25:31697 (IS-T-424)
conference on, Section III, 5th Congress on Materials Testing, Budapest, Oct. 19-24, 1970, 25:28917 (CONF-701044-(Sect.3))
distributions in nuclear, (T), 25:31429
line shapes as seen through detectors with Gaussian resolution functions, Breit--Wigner, (T), 25:29355 (RLO-1388-135)
mortar materials for, properties of vitreous carbon as, 25:28938
SPERM
radiation effects on, of bean weevils, γ, 25:29746
SPERMATOGENESIS
radiation effects on, of Dacus (fruit fly), effects of dose and pupal exposure on γ, 25:29617
SPERMATOGONIA
radioinduced mutations and reciprocal translocations in mouse, fast neutron and x, 25:29487
SPHENE
age of Soer-Rondane Mountains, Antarctica, lead/uranium method for estimation of, 25:29208
SPINAL CORD
radiation effects on structure of neurons of upper cervical sympathetic ganglion in rabbit, whole-body x, 25:29675
SPLEEN
chromium-51 uptake by, in tumorous mice, effects of strain on, 25:29472
oxygen pressure in mouse, effects of radioprotective sympathomimetics on, 25:29547
plutonium-239 retention in, of beagles, 25:29451
radiation dose to, in normal and tumor-bearing mice following administration of phosphorus-32-labeled chromium alloxantin and orthophosphate, 25:29453
radiation effects on activity and isoenzyme composition of lactate dehydrogenase in, of neonatal rats following parental exposure, 25:29665
radiation effects on RNA synthesis in immunized mouse, polyacrylamide gel electrophoresis studies on x, 25:29476
radiation effects on synthesis of histones in rat, 25:29662
radioprotective effects of cell transplants of, from irradiated donors on recipient mice, γ, 25:29564
radiosensitivity of hemopoietic and immunocompetent cells in mouse, effects of dose on, 25:29677
scanning for diagnosis of splenomegaly in sarcoidosis patients, use of technetium-99m-labeled technetium sulfide for, 25:29593
SPORES
radiation effects on sensitivity of Bacillus, to NaCl in recovery medium, effects of dose and NaCl content of medium during exposure on γ, 25:29558
radiosensitivity of heat-treated Bacillus, effects of NaCl content of heating medium on γ, 25:29558
sensitivity of Bacillus, to heat, effects of NaCl content of heating medium on, 25:29558
sensitivity of heat-treated Bacillus, to NaCl in recovery medium, effects of NaCl content of heating medium on, 25:29558
STAINLESS STEEL
analysis for hydrogen by carrier gas fusion--gas chromatographic methods, 25:28936
boron distribution in Type 316, effects of aging at 650 to 950°C on, 25:29913
compatibility with plutonium nitride--uranium nitride, literature survey on, 25:29923 (ORNL-4630, pp 59-72)
composition and fabricability of Type 216, 25:29784 (ORNL-4630, pp 96-110)
corrosion of hafnided and tantalided Type 316, by acid and sodium chloride solutions at 25 to 150°C, 25:29766
corrosion of similar-metal welds in Types 304 and 410, by steam, 25:29763 (ORNL-4630, pp 280-7)
corrosion of weldments of, by boiling aqueous copper sulfate, 25:29785 (ORNL-4630, pp 111-38)
deformation of tubes of Type 316, eddy current method for measurement of, 25:29287 (ORNL-4630, pp 145-9)
dissolution of fuel claddings of, in liquid zinc--molten halide systems, 25:29199(P)
fabrication of thermal insulation of, layered with wire gauze, 25:29819 (EUR-4531, pp 1019-34)
fabrication of tubes of, Type 316 by planetary swaging, 25:29784 (ORNL-4630, pp 96-110)
mechanical properties of Armco 21-6-9, 25:31730 (SC-RR-69-761)
mechanical properties of submerged-arc welds on Type 304, at 370 to 650°C, 25:29785 (ORNL-4630, pp 111-38)
mechanical properties of tubes of cold-worked Type 316, effects of artificially-induced defects on, 25:29784 (ORNL-4630, pp 96-110)
microstructure of austenitic, relations of weldability with second phases in, 25:29825 (ORNL-4630, pp 261-70)
microstructure of welds on austenitic, effects of heat treatments on, 25:29785 (ORNL-4630, pp 111-38)
production of neutron damage-resistant, by addition of niobium, tantalum, titanium, or zirconium for carbide formation, 25:29799(P)
radiation effects on density and swelling of Type 304, fast neutron, 25:29904 (ORNL-4630, pp 73-95)
radiation effects on fuel cladding of, neutron, 25:29916
radiation effects on mechanical properties of Type 304, relations of titanium modification with fast neutron, 25:29904 (ORNL-4630, pp 73-95)
radiation effects on mechanical properties of Type 304 and titanium-containing Type 304L, use of cyclotron-injected helium for simulation of neutron, 25:29907 (ORNL-TM-3259)
radiation effects on microstructure of Type 316, electron microscope study of neutron, 25:29902(T) (EURFNR-891)
radiation effects on microstructure of Type 321, at 400 and 500°C, 0.75-MeV proton, 25:29915
radiation effects on tensile properties of Type 316, relations of boron distribution with thermal neutron, 25:29913
weld filler metals for, development and testing of, 25:29785 (ORNL-4630, pp 111-38)
PuO_2--stainless steel--UO_2, fabrication of pellets of, powder metallurgical, 25:29931
STANDARDS
Analysis of Phosphorus-32, ASTM E 182-62, 25:29002
Analysis of Radioisotopes, ASTM E 181-62, 25:29005
borosilicate-glass raschig rings as fixed neutron absorber in solutions of fissile material, 25:29197
certificates of radioactivity, 25:29173
Chemical Analysis of Carbon and Graphite, ASTM C 560-69, 25:28974
Chemical Analysis of Commercial Columbium, ASTM E 195-68, 25:28973
cleaning of reactor components, ANS 7.4 1965, 25:31676
Colorimetric Determination of Uranium in Aqueous Solutions, ASTM E 318-69, 25:28976
computer program documentation, digital, 25:31761
computer program interchange, recommended programming practices to facilitate digital, 25:31763
critical assemblies operation, ANS-STD.1 1967, 25:31636
criticality experiments, ANS-STD.1 1967, 25:31636
definitions of terms related to radiation dosimetry, ASTM E 170-63, 25:29518
Determining Changes in Chemical Reactivity of Inorganic Materials Exposed To High Energy Radiation, ASTM E 183-62, 25:29095
fission product monitoring method for water cooled reactors, ASTM D2470-70, 25:31580
for estimation of radiation exposure of human populations in emergency situations, NCRP 29 (1962), 25:29539
for occupational radiation exposure records systems for personnel, ANSI N 2.2 (1966), 25:29519
for radiation exposure of uranium miners, economic impact of compliance with, FRC A-4 (1970), 25:29532
fuel storage facility design basis, AEC Safety Guide 13 1971, 25:29322
guide for design and operation of shipping containers for irradiated fuel elements from nuclear reactors, ANSI N 5.3 1964, 25:29321

XUM

Measurement of Alpha Particle Radioactivity of Industrial Water and Industrial Waste Water, ASTM D 1943-66, 25:29003
Measurement of Beta Particle Radioactivity of Industrial Water and Industrial Waste Water, ASTM D 1890-66, 25:29009
Measurement of Gamma Radioctivity of Industrial Water and Industrial Waste Water, ASTM D 1690-61, 25:29008
mechanical (Cadwell) splices in reinforcing bars of concrete containments, AEC Safety Guide 10 1971, 25:29297
nuclear powered merchant vessel design and operation, ABS-01 1962, 25:31643
personnel selection and training for nuclear power plants, ANSI SC-N 18.1 1971, 25:31481
power reactor control systems and protection systems design, ANS 4.1 1970, 25:31458
radiation protection in nuclear reactor fuel fabrication plants, ANSI N 7.2 (1963), 25:29534
radiation protection in uranium mines and mills in USA, ANSI N 7.1 (1960), 25:29535
radiation protection in uranium mines and mills in USA, ANSI N 7.1a (1969), 25:29536
radiation protection, background material for the development of protective action guides for environmental cesium-137, strontium-89, and strontium-90, FRC Report No. 7, 1965, 25:29533
radioactive materials pool storage facility design, ANS 7.20 1966, 25:31637
radioactivity, users' guides for, 25:29174
Radiochemical Determination of Cesium-137 in Nuclear Fuel Solutions, ASTM E 320-70, 25:29001
reactor biological shielding tests, ANS 6.3 1967, 25:31677
reactor containment structure leak rate testing, ANS 7.60 1970, 25:31672
swimming-pool reactor design, ANS 7.20 1966, 25:31637
Test for Atom Percent Fission in Uranium and Plutonium Fuel, Neodymium-148 Method, ASTM E 321-69, 25:28979
Test for Atom Percent Fission in Uranium and Plutonium Fuel (Mass Spectrometric Method), ASTM E 244-69, 25:28980
Test for Atom Percent Fission in Uranium Fuels (Radiochemical Method), ASTM E 219-69, 25:28998
Test for Iron-59 in Water, ASTM D 2461-69, 25:29010
Test for Radioactive Barium in Industrial Water and Industrial Waste Water, ASTM D 2038-68, 25:29004
Test for Radioactive Cesium in Water, ASTM D 2577-69, 25:29000
Test for Radioactive Iodine in Industrial Water and Industrial Waste Water, ASTM D 2334-68, 25:29007
Test for Radioactive Manganese in Water, ASTM D 2039-69, 25:29006
Test for Radionuclides of Radium in Water, ASTM Method D 2460-70, 25:28999
Test for Thorium in Industrial Water and Industrial Waste Water, ASTM D 2333-68, 25:28977
Test for Uranium and Plutonium Concentrations and Isotopic Abundance, ASTM E 267-70, 25:28978
Test for Uranium by Controlled-Potential Coulometry, ASTM E 217-70, 25:28975
x-ray protection standards for home television receivers, NCRP A-1 (1968), 25:29537

STAR CLUSTERS
color-magnitude relations for h and chi Persei, (E), 25:30041
distance of TR 28, (E), 25:30107
helium-3 abundance in Orion and NGC 2264, (E), 25:30077
photometry of h and chi Persei, three-color, (E), 25:30041
photometry of TR 28, (E), 25:30107
spectra of helium-weak stars in I Orion association, (E), 25:30049
stars in Hyades moving group, rotational velocities of G and K giant, (E), 25:30046
stars in IC 4651, photometry of 102, (E), 25:30093
stars in NGC 2264, circumstellar shells in pre-main-sequence A and F, (E), 25:30065

STARS
angular momentum of G and K giant, in Hyades moving group, (E), 25:30046
angular velocities near surfaces of, with radiative envelopes, (T), 25:30088
atmospheres of, conference at Munich, April 1969, on extended, 25:30035 (NBS-SPEC. PUBL-332)
atmospheres of, velocity-dependent non-LTE source function in, (T), 25:30084
brightness variations in AX Monocerotis, (E), 25:30056
conference on spectrum formation in, with steady-state extended atmospheres, Munich, 4/69, 25:30035 (NBS-SPEC. PUBL-332)
convective cores in helium-burning horizontal-branch, overshooting of, (T), 25:30037
cyanogen abundance in late G and K giant, (E), 25:30085
damping in semi-convective zones in B, overstable, (T), 25:30039
distribution in IC 1613, (E), 25:30209
distribution in M33, (E), 25:30201
distribution in nucleus of NGC 2655, (E), 25:30194
distribution of A-type, (E), 25:30062
distribution of hot, in anticenter direction, (E), 25:30191
electric conductivity in photospheres of F, G, and K, (T), 25:30114
evolution and structure of, (T), .25:30219 (CERN-70-31)
evolution of central, of planetary nebulae, (T), 25:30044
evolution of, containing an overabundance of helium-3, (E), 25:30077
evolution of, late, (T), 25:30036(R) (NYO-3962-3)
evolution of, specification of blue edge of RR Lyrae instability strip in, (T), 25:30096
expansion of, upon leaving the main sequence, (T), 25:30097
extinction curves for, structure in interstellar, (E), 25:30212
formation from compact H II regions, (E), 25:30117
gravitational kinetic equations for, (T), 25:30237
gravitational radiation emission from slowly rotating fully relativistic, (T), 25:30092
helium abundance in B-type, (E), 25:30042
helium burning in horizontal-branch, induced semi-convection in, (T), 25:30103
infrared polarization of eta Car and VY CMa, (E), 25:30076
iron abundance in Am, (E/T), 25:30038
light curve for AI Dra, (E), 25:30105
light curve of W U Ma, variation of, (E), 25:30100
light polarization in white-dwarf G195-19, periodic variations in circular, (E), 25:30073
light polarization in white-dwarf G99-37, circular, (E), 25:30072
lithium production in, (T), 25:30036(R) (NYO-3962-3)
luminosities of, calibration of H--R diagram by trigonometric parallaxes, (E/T), 25:30040
luminosity of magnetic white-dwarf AC + 70°8247, (E), 25:30074
magnetic fields in peculiar and metallic-line A, (E), 25:30045
magnitudes for K and G giant, absolute, (E/T), 25:30040
magnitudes of, in reflection nebulae, (E/T), 25:30054
mass exchange in close binary, (T), 25:30111
mass exchange in close-binary, (T), 25:30106
mass flow in close binary, (T), 25:30112
mass of CV Ser, (E), 25:30043
metal abundances in Am, (E/T), 25:30038
microwave emission from IRC + 10216 infrared, 3.5-mm, (E), 25:30090
microwave emission rom VY CMa and IRC + 10216 infrared, 3.5-mm, 25:30089
models for, linear nonadiabatic pulsations of, (T), 25:30095
neutrino luminosity by URCA process in white-dwarf, (T), 25:30081
neutron-star formation in close-binary, (T), 25:30099
nucleosynthesis in helium zones, explosive, (T), 25:30067
nucleosynthesis in, (T), 25:30219 (CERN-70-31)
observations of pre-main-sequence A and F, in cluster NGC 2264, circumstellar shells from, 25:30065
orbital period for CV Ser, (E), 25:30043
oscillations of self-gravitating fluid spheroid, hydromagnetic, (T), 25:30102
period of γ Equ, magnetic, (E), 25:30048
period--luminosity relation for Cepheids in IC 1613, (E), 25:30209
photoelectric elements of ST Persei, (E), 25:30113
photometric elements of WZ Bootis, (E), 25:30104
photometry of 102, in open cluster IC 4651, (E), 25:30093
photometry of 11 RW-Aur type, UBV, (E), 25:30058
photometry of late G and K giant, (E), 25:30085
photometry of short-period variable 14 Aurigae, (E), 25:30086
photospheres of F, G, and K dwarf and giant, magnetohydrodynamic properties of, (E/T), 25:30110
planetary system formation in epsilon Aurigae, (E/T), 25:30083
pressure--density relations for massive and white-dwarf, (T), 25:30075
properties of M-supergiant, (E/T), 25:30055
proton--proton interactions in intense magnetic fields of white-dwarf, (T), 25:30050
pulsation and rotation in, (T), 25:30219 (CERN-70-31)
radio emission from OH of infrared, at 1612 MHz, (E), 25:30047
rotating, models for, (T), 25:30075
rotation of, Roche coordinates for problem of, (T), 25:30082
spectra of 60 A-type, in region of South Galactic Pole, (E), 25:30087
spectra of α Cyg, (E), 25:30109
spectra of B-type, helium line profiles in, (E), 25:30042
spectra of BD 61°2565, (E), 25:30063
spectra of eta Car, absence of reddening in, from observation of S II and Fe II lines, 25:30071
spectra of EW Lac, radial velocities of hydrogen lines in, (E), 25:30098
spectra of heavily reddened Cygnus OB2 No. 12, (E), 25:30069
spectra of helium-weak, in I Orion association, (E), 25:30049

XUM

spectral classification and spectrophotometry of late-type, (E), 25:30061
spectral classification for relatively bright, in near ultraviolet, (E), 25:30060
spectral classification of 210 F0-G5, (E), 25:30059
spectral classification of, in IC 417 and IC 1318a, (E), 25:30108
supernovae effects in close-binary, (T), 25:30099
temperatures in ST Persei, radiation and color, (E), 25:30113
temperatures of B and A, effective, (E), 25:30094
turbulence in Am, micro-, (E/T), 25:30038
ultraviolet emission from Arcturus, Lyman-α, (E), 25:30070
velocities of G and K giant, in Hyades moving group, rotational, 25:30046

STATISTICS
algebraic theory for statistical mechanics, Heisenberg ferromagnet in, 25:30946
equilibrium states in statistical mechanics, 25:30941
formalism for statistical mechanics, relation with quantum field theory, 25:30956
time evolution of systems with infinite number of degrees of freedom in statistical mechanics, 25:30703

STEAM
corrosive effects of superheated, on Zircaloy-2 at 350 to 550°C, effects of mechanical stress on, 25:29771
corrosive effects on similar-metal welds in heat-resisting boiler materials, 25:29763 (ORNL-4630, pp 280-7)
use of condensing, in aerosol scrubbers, (E), 25:29251 (ORNL-4654)

STEAM POWER PLANTS
thermal effluents from, ecological effects of, (E), 25:31527

STEEL
analysis for silicon as molybdosilicate complex, spectrophotometric method for, 25:28924
analysis of low-alloy, two-standard method for spectrometric, 25:28950
analysis of, use of laser microprobe in spectral, 25:28949
book: Special Steels and Alloys (In Russian), 25:29862
corrosion by liquid sodium of austenitic, 25:31568(T) (EURFNR-823)
corrosion of channel of, use of stainless steel sleeves for minimization of, 25:31459
corrosion of, high-temperature methods for studies of, 25:29779
corrosion resistance of glass-coated, to acid and alkali environments, 25:29775
ductility in high-stength AISI 4340, Gerard--Papirno characterization of notch, 25:31692 (COO-2048-2)
fabrication of reactor pressure vessels of, welding methods for, 25:29788 (ZJE-69)
mechanical properties of pressure vessel, 25:31668 (IRS-T-17)
properties for use in concrete reactor pressure vessel prestressing hoops, 25:30028 (EUR-4531, pp 445-76)
properties of ferritic, for use in steam generators, 25:29822 (ORNL-4630, pp 139-44)
properties of titanium carbide-coated hardenable, for use as ball bearing races in ultrahigh vacuum, 25:29834
use of wires of, for reinforcing prestressed concrete reactor pressure vessels, 25:29939 (EUR-4531, pp 433-44)
Al--Ni--steel--Ti, failure of electroslag welded joints on, effect of residual welding stress on brittle, 25:29832
Cr--Mo--steel, properties at high temperatures, ductile and tensile, 25:29822 (ORNL-4630, pp 139-44)
Cr--Mo--steel--U, creep fatigue of, method for prediction of, 25:29826 (RD/B/N-1889)

STELLARATORS
design and operation of spherator with levitated superconducting ring, 25:30559 (EUR-4593, pp 141-8)
magnets for toroidal PROTO--CLEO, design of main and helical, 25:30554 (EUR-4593, pp 13-18)
plasma confinement in l = 3, source and electron cyclotron resonance heating effects on, (E), 25:30457 (IPPJ-102)
plasma diffusion in, recombination effects on, (E/T), 25:30462 (NP-18767)
plasma heating by neutral injection, 25:30455 (EUR-4593, pp 479-84)
startup of deuterium--tritium fueled, laser use for, 25:30553 (CLM-R-109)

STOMACH
technetium-99m localization in human, 25:29418 (BNL-50285)

STORAGE RINGS
beam shaking method for removing neutralizing ions in, 25:31050 (UCRL-20156)
development of Cambridge $e^+ - e^-$ colliding beam, 25:31036(R) (CEAL-1053)
experimental program for CERN, 25:31060
experimental programs for electron--positron, 25:31061
experimental programs for high-luminosity, 25:31061
use for improving microscopic duty factor of cyclotron, proposed, 25:31120

STRAIN GAGES
moisture protection of, 25:31755(T) (UCRL-Trans-10526)

STRANGE PARTICLES
production in π^- + p interactions at 4 GeV/c, phenomenological quasi-two-body model for, (T), 25:30869 (JINR-P1-5706)

STREAMS
pollution by sewage disposal, tracer methods for studying, (E/T), 25:29213

STRESS
calculations for extension of two-dimensional Lagrangian hydrodynamics code (MAGEE), 25:31700 (LA-4601)

STRONTIUM
detection in spectra of BD 61°2565, (E), 25:30063
determination as carbonate alone and with barium and calcium carbonates by pellet technique, in spectroscopic, 25:28972
determination by amperometric, chelatometric, and conductometric titrations, 25:28970
determination using ion permselective membrane, potentiometric, 25:28956
effects on fluorometric determination of zirconium, 25:28963
excretion and retention by children in comparison to adults, strontium-84 tracer study of, 25:29442
separation from other alkaline earths by ion exchange, 25:29193
transport of fission product, in liquid sodium, (E/T), 25:31614

STRONTIUM CHLORIDES
molecular structure of, 25:29086
spectra in matrices of solid nitrogen or rare gases, ir, 25:29086

STRONTIUM ISOTOPES Sr-84
use as tracer for determining strontium excretion and retention by children and adults, 25:29442

STRONTIUM ISOTOPES Sr-85
metabolism in rats, effects of age and dietary alginates on, 25:29446
uptake in tissues of rats for diagnosis of joint diseases, 25:29581
use for diagnosis of osteoarticular diseases in human bones, 25:29576
use for scintigraphy of human bones for diagnosis of metastases, combined thermography and, 25:29589
use for scintigraphy of human bones for diagnosis of systemic neoplastic diseases, comparison of radiography and thermography with, 25:29588

STRONTIUM ISOTOPES Sr-86
energy-level scheme from yttrium-86 decay, (E), 25:31247

STRONTIUM ISOTOPES Sr-87
use of metastable, for radiodiagnosis of metastatic and primary adenocarcinomas in human kidneys, 25:29590

STRONTIUM ISOTOPES Sr-89
accumulation in skeleton of fish, 25:29449
beta decay of, shell-model analysis of first-forbidden unique, (T), 25:31284
determination in urine of man following intake of powders of irradiated uranium fuels, radiometric, 25:29515 (NP-18794)
distribution in environment following acute release and release in fallout, standards for protection against, 25:29533
removal from medical equipment, effectiveness of detergent solution combined with sound frequency vibrator for, 25:29510

STRONTIUM ISOTOPES Sr-90
beta decay of, shell-model analysis of first-forbidden unique, (T), 25:31284
content in atmosphere and fallout, effects of rainfall intensity on correlation between, (E), 25:29218
content in environment of West Valley Processing Plant, 25:29179 (DOCKET-50201-69)
content in fish and seawater near Goto Islands, Japan, measurements during July 1966, 25:29241
content of fresh and powdered milk in Italy during 1952 to 1966, fallout, 25:29507
content of lichen--reindeer--man food chain in Sweden during 1961 to 1969, 25:29480
distribution and retention in beagle dogs following inhalation, toxicity studies on insoluble, 25:29438 (LF-43, pp 197-204)
distribution and retention in beagle dogs following inhalation of fused clay particles, 25:29437 (LF-43, pp 188-96)
distribution and transport in arable soils of Lower Silesia, measurement of, 25:29207
distribution in environment following acute release and release in fallout, standards for protection against, 25:29533
distribution in femoral medullary canal in rats following intravenous injection, effects of sex on, 25:29524
distribution in snails, effects of sorption from food or water source on, 25:29440
effects on beagle dogs following inhalation as chloride, toxic, 25:29430 (LF-43, pp 123-7)
effects on radiotoxin production in rat liver, chronic, 25:29639
metabolism in beagle dogs following inhalation as chloride, 25:29430 (LF-43, pp 123-7)
monitoring in environmental samples at West Valley Processing Plant, 1971, 25:29180 (DOCKET-50201-70)

XUM

neoplastic effects of, on bones of dogs, calculation of accumulated skeletal dose following intravenous injection and tumor growth dynamics of, 25:29621 (COO-119-243)
osteosarcomas induced in beagles following intravenous injection of, calculation of dose and tumor growth dynamics of, 25:29621 (COO-119-243)
radiation dose to human bones following acute inhalation of aerosols of, methods for estimation of β, 25:29513 (CONF-710211-1)
uptake by freshwater plants in relation to calcium content of water, discrimination coefficient for, 25:29452

STRONTIUM ISOTOPES Sr-93
beta decay of, Q value for, (E), 25:31338

STRONTIUM OXIDES
thermodynamic properties of gaseous diatomic, free energy functions for, 25:29082

STRUCTURES
radiation doses in single-compartment aboveground concrete, calculations of weapon, 25:30633

STYRENE
radiolysis of rigid matrices of methylcyclohexane containing, deferred luminescence spectra following γ, 25:29150
radiolysis of solutions of, in glassy and polycrystalline solvents, deferred luminescence technique for obtaining stimulation spectra following γ and uv, 25:29133
acrylonitrile--styrene, radioinduced polymerization on polymers, γ, 25:29106
methyl methacrylate--styrene, radioinduced polymerization on polymers, γ, 25:29106

STYRENE POLYMERS
radioinduced thermoluminescence of, cryostat measurements of, 25:30444

SULFATES
determination using ion permselective membrane, potentiometric, 25:28956

SULFUR
determination by x-ray fluorescence, sensitivity of, 25:28962
determination in low-alloy steel, two-standard method for spectrometric, 25:28950
effects of interstitial impurity of, on mechanical properties of iron, 25:29855
effects on ductility of Inconel 600 at 400 to 1000°C, 25:29825 (ORNL-4630, pp 261-70)
radiation effects on solubilization of colloidal, mechanism of γ, 25:29137

SULFUR DIOXIDES
oxidation on platinum electrode, electrochemical, 25:31754(T) (UCRL-Trans-10525)

SULFUR ISOTOPES
radioactivity standards of, users' guides for, 25:29174

SULFUR ISOTOPES S-32
energy levels from proton inelastic scattering, spin-parity assignments for, (E), 25:31245
meson (μ⁻) capture by, charged-particle masses and energy spectra from, (E), 25:31267

SULFUR ISOTOPES S-33
energy levels from proton inelastic scattering, spin assignments for, (E), 25:31291
proton elastic and inelastic scattering at 6 MeV, angular distributions for, (E), 25:31291

SULFUR ISOTOPES S-34
proton elastic and inelastic scattering at 6 MeV, angular distributions for, (E), 25:31291
triton reactions (t,p) at 3.1 MeV, γ linear polarization from, (E), 25:31289

SULFUR ISOTOPES S-35
determination in phosphorus-32 preparations, ASTM method for, 25:29002
effects on chromosomes and pollen and seed fertility of M(1) generation of rice, 25:29496
energy levels of, lifetimes, spin assignments, and transition probabilities for, (E), 25:31269
energy-level transitions in, multipole mixing ratios for, (E), 25:31269
use for labeling organic compounds, 25:29413 (CONF-691225)

SULFUR ISOTOPES S-36
energy levels at 4.19 and 4.57 MeV from sulfur-34 (t,p) reactions, parity assignments for, (E), 25:31289

SULFUR OXIDES
thermodynamic properties of gaseous diatomic, free energy functions for, 25:29082

SULFUR SYSTEMS
S--Zr, crystal lattice parameters of compounds of, 25:29990
S--Zr, phase studies at high temperatures, 25:29990

SULFURIC ACID
corrosive effects on beryllium--copper--tin alloys, 25:29830
corrosive effects on chromium--molybdenum--nickel alloys, effects of chromium content on, 25:29777
corrosive effects on hafnided and tantalided nickel and Type 316 stainless steel at 25 to 120°C, 25:29766
corrosive effects on molybdenum alloys, relations with concentration, pressure, and temperature, 25:29776
effects on oxidation-reduction potential of solutions of salts of tetravalent and hexavalent uranium, 25:29036
separation of thorium and uranium from aqueous solutions of, by solvent extraction using 4-methyl-2-pentanone, effects of lithium chloride or magnesium chloride on, 25:29195

SUN
activity of, effects on energy spectra of 11-year variations of primary cosmic radiation, (E), 25:30310
eclipse of Mar. 7, 1970, (E), 25:30163
effect of cycle of, on day and night temperature of thermosphere, (E), 25:30378
effect of cycle of, on ionospheric electron and ion temperature variations, (E/T), 25:30399
infrared spectra of, between 7498 and 12016 A, (E), 25:30172
neutrino energy spectra and flux from, verification of oscillation hypothesis for, (E/T), 25:30802(T) (BNL-tr-418)
neutron emission from active region of, improved measurements of energetic, (E/T), 25:30177
spectra at decametric wavelengths, (E), 25:30159
spectra of quiet, extreme-ultraviolet, (E), 25:30166

SUNSPOTS
area decrease of, near the central meridian, (E), 25:30184
distribution of, effects on 11-year variations of cosmic radiation, (T), 25:30309
distribution of, helio-latitudinal index for, and relation to cosmic-ray 11-year variations, (E/T), 25:30165
distribution of, helio-latitudinal index for, and relation to cosmic-ray yearly intensity variations, (E), 25:30308
effect of low activity of, on topside midlatitude ionosphere at sunrise, (E), 25:30377
effects of cycle of, on weather parameters, (E), 25:30162
electric conductivity in, relation to photosphere, (T), 25:30186
relation to lead-210 abundance in atmosphere, (E), 25:30171
relation to modulation of primary cosmic radiation, (E/T), 25:30322
spectra of, detection of nickel hydride in, (E), 25:30173

SUPERCONDUCTIVITY
model for finite temperatures in, mathematical structure of B.C.S, 25:30949

SUPERCONDUCTORS
electric conductivity of tunnel junctions, test of microscopic theory by zero-bias, (E), 25:30432
Eliashberg function and strong-coupling behavior of disordered, 25:30421
magnetization by rotation of, Barnett effect, 25:30439
photoeffect in weak electric field, Green's function development of equations for current in, 25:30417
properties of impure Type-II, with surface current, 25:30414(T) (ORNL-tr-2475)
properties of, effects of neutron irradiation on, 25:30440 (EUR-4593, pp 107-13)
resistive transition in one-dimensional, (T), 25:30420
search for high-temperature, (T), 25:30452
stability of high-field composite, in low fields, (E), 25:30410 (EUR-4593, pp 95-100)
thermodynamic behavior of Type-II, with small kappa near lower critical field, (T), 25:30422
transition temperature increase by phonon mechanism in, (T), 25:30438
transitions of composite, induced by magnetic disturbances, normal, (E), 25:30411 (EUR-4593, pp 101-6)
tunneling into energy bands of intermediate state in Type-I, (E), 25:30431
ultrasonic attenuation theory for pure two-band, in high fields, 25:30423

SUPERNOVA REMNANTS
CTB 13, radio flux density of, (E), 25:30136
spectroscopy of Cas A, (E), 25:30064

SUPERNOVAE
classification of, in spiral arm of NGC 3389, (E), 25:30057
effects in close-binary systems, (T), 25:30099
electromagnetic-wave emission from expanding shells of, coherent, (T), 25:30068
element nucleosynthesis in, superheavy, (T), 25:30051
fragmentation model for solar system formation, (T), 25:30157 (LA-4343(Suppl.))
neutron capture processes in, rapid, (T), 25:30036(R) (NYO-3962-3)
nucleosynthesis in neutron-rich ejecta from, (T), 25:30079
particle collisions in opposing mass flow hypothesis of, 25:30157 (LA-4343(Suppl.))

SURRY POWER REACTOR, UNIT 1
cooling system for, inspection and testing requirements for, 25:31503 (DOCKET-50280-39)
design parameters of, requested additional information on, 25:31503 (DOCKET-50280-39)
operations aspects of, requested additional information on, 25:31503 (DOCKET-50280-39)
pressure vessel for, inspection and testing requirements for, 25:31503 (DOCKET-50280-39)
technical specifications for, revised, 25:31503 (DOCKET-

XUM

50280-39)
SURRY POWER REACTOR, UNIT 2
cooling system for, inspection and testing requirements for, 25:31503 (DOCKET-50280-39)
design parameters of, requested additional information on, 25:31503 (DOCKET-50280-39)
operations aspects of, requested additional information on, 25:31503 (DOCKET-50280-39)
pressure vessel for, inspection and testing requirements for, 25:31503 (DOCKET-50280-39)
technical specifications for, revised, 25:31503 (DOCKET-50280-39)
SWEDEN
strontium-90 content of lichen--reindeer--man fod chain during 1961 to 1969, 25:29480
uranium prospecting in, radiometric methods for, 25:29229
SWINE
radioinduced chromosome aberrations in leukocytes of, 14-MeV neutron, 25:29497
SWITCHES
design of coaxial high-power trigatron, 25:30579 (EUR-4593, pp 373-8)
design of commutator, for automatic readout of detectors to digital printer, 25:29345
design of crowbar gap, with two triggering pulses, 25:30576 (EUR-4593, pp 347-53)
design of crowbar system or 2.7-MJ bank ISAR I, 25:30560 (EUR-4593, pp 189-95)
design of fast, solid dielectric, multichannel crowbar, 25:30580 (EUR-4593, pp 379-84)
design of high-power spark gap, for fast energy-storage systems, 25:30565 (EUR-4593, pp 241-50)
design of high-power spark gaps for high repetition rates, 25:30568 (EUR-4593, pp 273-80)
design of vacuum start and clamp, for 20-kJ, 40-kV capacitors, 25:30570 (EUR-4593, pp 287-91)
development of fast metal-contact solid-dielectric, 25:30578 (EUR-4593, pp 365-71)
development of laser-triggered spark gaps, 25:30575 (EUR-4593, pp 339-45)
performance of exploding-foil, for use with capacitors, 25:30574 (EUR-4593, pp 319-38)
SYMMETRY GROUPS
breaking in gauge field models and Sugawara theory of current, 25:30924
breaking of chiral, covariant derivatives of boson fields for, 25:30922
broken, in relativistic quantum field theory, spontaneously, 25:30945
O(1,4), relativistic equations of motion additional invariance under, 25:30975
O(2,3), relativistic equations of motion under, additional invariance of, 25:30975
O(4), relativistic equations of motion under, additional invariance of, 25:30975
P(1,n), equations of motion invariant under, in Minkowski space, 25:30966
SU(2) x SU(2) chiral, relation of scale invariance to broken, 25:30920
SU(2) X SU(2), relation between local duality and conserved currents in, 25:30855
SU(2), theory for, lectures on, 25:30914 (NP-18804)
SU(3) x SU(3) breaking for physical fields, nature of intrinsic chiral, 25:30929
SU(3) x SU(3) chiral, breaking of, 25:30919
SU(3) x SU(3) chiral, sigmaww coupling from broken scale and, 25:30933
U(3) X U(3) breaking, meson mass spectra for broken scale invariance and, 25:30927
U(3,1), invariant extension of vacuum expectation values in inhomogeneous, 25:30917
SYMMETRY GROUPS SU(3)
breaking of, for baryon leptonic decay, 25:30930
coupling constant for ΣΣw from, 25:30904
model based on Fermi model for hadron interactions in, invariant statistical, 25:30764
theory for, lectures on, 25:30914 (NP-18804)
SYMPATHOMIMETICS
effects on oxygen pressure in spleens of mice, comparison of radioprotective, 25:29547
SYNCHROCYCLOTRONS
beam capture and focusing at center of, 25:31159
beam depolarization in, resonant proton, 25:31162
beam extraction system for CERN, regenerative, 25:31108
beam extraction system for modified Columbia Univ., ultra-thin septum magnet for, 25:31106
beam phase motion in, with spatial variation of magnetic field, 25:31156
design conversion study for Univ. of Maryland 600-MeV, 25:31160
design modifications of CERN, 25:31157
design modifications of Harwell 110-inch, 25:31154
development of Columbia Univ. AVF, 25:31155
experimental facility for JINR, automatic data accumulation and storage system for, 25:31070
ion source for improved CERN, hot-cathode proton, 25:31158
SYNCHROTRON RADIATION
emission from charged particles in cyclic accelerators, gravitational plane wave effects on, (T), 25:31008
lecture on, in astrophysics, (T), 25:30220 (P-4494(RAND))
spectra of, in cosmic radio sources, (T), 25:30144
spectra of, in cosmic radio sources, (T), 25:30146
SYNCHROTRONS
beam extraction from electron, effects of synchrotron radiation on slow, 25:31044 (NP-18780)
beam extraction system for ITEP proton, use of sextupole lenses in slow, 25:31045 (NP-18799)
betatron oscillations in proton, wideband frequency divider for excitation of, 25:29404
experimental facility for Tokyo proton, for studying muons, 25:29371 (SJC-P-70-4)
target analysis system for deuterium and hydrogen diminution, mass-spectrometric, 25:29400
SYSTEMS FOR NUCLEAR AUXILIARY POWER (SNAP-23)
thermoelectric converter for 23A, design of advanced prototype, 25:29272
SZILARD-CHALMERS REACTIONS
theory and characteristics of, review on, 25:29168

T

T-111 (TANTALUM ALLOY)
analysis for nitrogen by modified Kjeldahl and vacuum fusion method, 25:28937
mechanical properties at high temperatures, effects of nitrogen interstitials on, 25:29824 (ORNL-4630, pp 191-206)
welding for fabrication of corrosion loops, 25:29824 (ORNL-4630, pp 191-206)
T-222 (TANTALUM ALLOY)
analysis for nitrogen by modified Kjeldahl and vacuum fusion method, 25:28937
TANTALUM
book: Creep-Rupture Data for the Refractory Metals to High Temperatures, 25:29868
corrosion by sodium at 600°C, effects of oxygen on, 25:29761 (ORNL-4630, pp 150-7)
corrosion resistance to acid and alkali environments, evaluation of, 25:29775
deposition on substrates from alkaline fluoride mixtures containing salts of, methods for electro-, 25:29783 (CEA-N-1376)
determination in curium oxide, emission spectrochemical, 25:28964
determination in presence of other metals, spectrographic, 25:28944
determination in thin films of tantalum nitrides by electron-probe x-ray micro method, 25:28966
effects of beta-stabilizer, on mechanical properties of titanium alloys at -253 to +20°C, 25:29844
effects on fluorometric determination of zirconium, 25:28963
electric conductivity of island-structured thin films of, effects of electric field strength, preparation, residual gas pressure, and temperature on, 25:30686
hardness and yield stress of wires of, effects of deformation temperature and nitrogen and oxygen interstitial content on, 25:29880
oxide films on, crystal structure of corrosion-resisting, 25:29991
piezoelectric properties of oxygen-containing, improved mechanical stress system for measurement of, 25:29903(R) (NYO-3653-5)
production and uses during 1971, review on, 25:29810
properties for use as carbide-former in neutron damage-resistant stainless steel, 25:29799(P)
properties of, electric and thermal, 25:29824 (ORNL-4630, pp 191-206)
proton reactions at 11.5 and 23.5 MeV using thick targets, neutron yield from, (E), 25:31209
reactions with graphite thimbles to prepare tantalum carbides, 25:29926
sorptive properties for nitrogen, calorimetric study of chemical, 25:29843
TANTALUM ALLOYS AND SYSTEMS
book: Creep-Rupture Data for the Refractory Metals to High Temperatures, 25:29868
Co-base--Ta, thermal expansion at 100 to 800°C, 25:29899
Co-base--Ta, transformation temperatures of, allotropic, 25:29899
Nb--Ta, Hall effect in superconducting, (E), 25:30427
Pd--Ta, diffusion processses at 700 to 1030°C, electron-microprobe study of, 25:29893
Ta--W, properties of, electric and thermal, 25:29824 (ORNL-4630, pp 191-206)
Ta--Zr, hardness of, effects of aging on, 25:29824 (ORNL-4630, pp 191-206)
Ta-base--W, stress rupture of welds of, at 1200 to 1650°C, 25:29824 (ORNL-4630, pp 191-206)
TANTALUM BORIDES
properties of powdered, characterization of, 25:29978 (ORNL-4630, pp 163-76)
TANTALUM CARBIDES
elastic properties of polycrystalline $TaC_{0.99}$, at 300 to 1500°K, sonic resonance method for determination of, 25:29970
mechanical properties of polycrystalline, above 1200°C in vacuum, effects of compressive loading on, 25:29973
preparation of monocrystalline monocarbide,

XUM

recrystallization method for, 25:29927
preparation of TaC and Ta_2C, by reactions of liquid tantalum with graphite thimbles, 25:29926
x-ray emission spectra of TaC/sub x/, 25:30267
TANTALUM HYDRIDES
analysis for hydrogen by carrier gas fusion--gas chromatographic methods, 25:28936
TANTALUM ISOTOPES Ta-174
beta and electron-capture decay of, branching ratios, electron and gamma spectra, log-ft values, and Q values for, (E), 25:31310 (LYCEN-7084)
beta decay of, half-life and conversion electron and γ spectra for, (E), 25:31348
TANTALUM ISOTOPES Ta-176
beta and electron-capture decay of, gamma and conversion electron spectra from, (E), 25:31375
TANTALUM ISOTOPES Ta-181
isomeric transition in, angular correlation of 345 to 136 keV cascade from, (E), 25:31321
TANTALUM NITRIDES
analysis of thin films of, by electron-probe x-ray micro method, 25:28966
TANTALUM OXIDES
crystal structure of corrosion-resisting films of, formed on tantalum in dilute acid solutions at 200 to 300°C, 25:29991
properties and structure of, matrix isolation method for studying, 25:29083
thermodynamic properties of gaseous diatomic, free energy functions for, 25:29082
TANTALUM SELENIDES
properties of polyimide-bonded, as solid film lubricants, 25:29096 (WERL-HFIL-1)
TARTRATES
effects on separation of thorium(IV) from sulfuric acid solutions by extraction using N-phenylbenzylamine in chloroform, 25:29184
TECHNETIUM
hyperfine fields of, in iron, cobalt, and nickel, (E), 25:31271
TECHNETIUM ISOTOPES
effectiveness for radiodiagnosis or radiotherapy in man, 25:29573
TECHNETIUM ISOTOPES Tc-95
energy levels from molybdenum-95 (p,n) reactions, spins and parities of, (E), 25:31381
TECHNETIUM ISOTOPES Tc-96
energy levels from molybdenum-95 (p,n) reactions, width of isobaric analog, (E), 25:31381
TECHNETIUM ISOTOPES Tc-97
energy levels from molybdenum-97 (p,n) reactions, spins and parities of, (E), 25:31381
TECHNETIUM ISOTOPES Tc-98
energy levels from molybdenum-97 (p,n) reactions, width of isobaric analog, (E), 25:31381
TECHNETIUM ISOTOPES Tc-99
determination of free metastable, in labeled compounds by thin-layer chromatography and scintillation cameras, 25:28991
effectiveness of metastable, for scanning human salivary glands, comparison of iodine-131 with, 25:29574
effectiveness of metastable, for scanning of human salivary glands, effects of pilocarpine nitrate on, 25:29579
energy level at 181 keV, g-factor for, (E), 25:31271
localization of metastable, in human salivary glands, stomach, and thyroid, 25:29418 (BNL-50285)
physical properties of metastable, in relation to use in nuclear medicine, 25:29418 (BNL-50285)
production of metastable, development of generators for, 25:29413 (CONF-691225)
use of metastable, for radiodiagnosis of metastatic and primary adenocarcinomas in human kidneys, 25:29590
use of pertechnetate-incorporated metastable, for scintigraphy of human kidneys for function and morphology, 25:29592
use of pertechnetate-incorporated metastable, for angioscintigraphy of human organs, 25:29587
use of pertechnetate-incorporated metastable, for scintigraphy of human thyroid gland, 25:29586
use of sulfur colloid-incorporated metastable, for scintigraphy of human liver for function and morphology, 25:29591
use of technetium sulfide-incorporated metastable, for diagnosis of splenomegaly in sarcoidosis patients, 25:29593
TEETH
radiation effects on color and growth of animal, effects of age on x, 25:29631
radiation effects on migration rate of amelogenic cells in rat incisor, 25:29678
radioinduced demineralization of human, following therapy for nasopharynx tumors, 25:29712
TELEMETERING SYSTEMS
design of opto-electronic, for transmission of timing signals, 25:29392 (CEA-N-1431)
monitor for, interactive, 25:31729 (SC-DR-710211)
TELEVISION EQUIPMENT
development of closed-circuit, for evaluation of radiographs, 25:29288 (ORNL-4630, pp 271-9)
programming video disc recorder, single and multiple field enabling system for, 25:31699 (LA-4582)
radiation dose to personnel repairing color, x, 25:29512 (BRH/DEP-71-4)
radiation protection standards for home receivers, x, 25:29537
TELLURIUM
determination in copper electrolysis slimes, iodometric, 25:28933
determination in gaseous media, iodometric, 25:28959
determination of trace amounts of, in cast iron, spectrochemical, 25:28943
determination using sodium pyrosulfite, colorimetric, 25:28931
energy-level transitions in, electron spectra from Coster--Kronig and L-shell Auger, (T), 25:30261
separation from antimony and tin by thin-layer chromatography, 25:29165
TELLURIUM ISOTOPES Te-123
energy-level transitions from meson (μ^-) reactions with iodine-127, (E), 25:31258
TELLURIUM ISOTOPES Te-124
energy levels from antimony-124 decay, (E), 25:31346
energy-level transitions from meson (μ^-) reactions with iodine-127, (E), 25:31258
TELLURIUM ISOTOPES Te-125
energy-level transitions from antimony-125 decay, conversion coefficients and multipolarities for, (E), 25:31340
energy-level transitions from meson (μ^-) reactions with iodine-127, (E), 25:31258
preparation of carrier-free isomeric, by thin-layer chromatography, 25:29165
TELLURIUM ISOTOPES Te-126
energy-level transitions from meson (μ^-) reactions with iodine-127, (E), 25:31258
TELLURIUM ISOTOPES Te-132
metabolism in beagle dogs following ingestion of nuclear debris from Project Cabriolet, 25:29456
production of, development of generators for, 25:29413 (CONF-691225)
uptake in bones and tissues of rats for diagnosis of joint diseases, 25:29581
TELLURIUM OXIDES
thermodynamic properties of gaseous diatomic, free energy functions for, 25:29082
TELLURIUM SYSTEMS
C--O--Te--U, phase diagram at 1200°C, 25:30001
C--Te--U, phase diagram at 1200°C, 25:30001
Np--Te, crystal structure of Np_3Te_4, 25:30002
TEMPERATURE
effects of near-surface atmospheric, on natural radioactivity in atmosphere to 15 m height, (E), 25:29223
measurement of working, of piston rings in Diesel engine, krypton-85 tracer method for, 25:29282
TENSILE PROPERTIES
measurement of flat specimens, biaxial tester for, 25:31735(T) (SCL-T-69-258)
TERBIUM
determination as hexafluoroacetylacetone--trioctylphosphine oxide complex, spectrofluorometric, 25:28954
determination as impurities in gadolinium and yttrium oxides by x-ray luminescence methods, 25:28961
determination for water flow tracing by neutron activation, 25:29013 (RLO-1750-81)
separation from other rare earths by ion exchange, 25:29178 (CEA-R-4102)
TERBIUM CARBIDES
dissociation energy of gaseous TbC_2, use of isomolecular carbon-exchange reactions for determination of, 25:29955
TERBIUM CHLORIDES
thermodynamic properties at 298 to 1300°K, 25:29951
TERBIUM IODIDES
thermodynamic properties at 298 to 1300°K, 25:29951
TERBIUM ISOTOPES Tb-159
deuteron reactions (d,4n) at 19.9 to 27.2 MeV, excitation functions and gamma spectra from, (E), 25:31301 (CNEA-283)
deuteron reactions (d,p) at 6.9 to 27.2 MeV, excitation functions and gamma spectra from, (E), 25:31301 (CNEA-283)
TERBIUM ISOTOPES Tb-160
beta decay of, β--γ angular correlations from, (E), 25:31277
beta decay of, γ spectra from, (E), 25:31335
TERBIUM OXIDES
CeO_2--Tb_2O_3, phase studies at 800 to 1200°C, 25:30007
Gd_2O_3--Tb_2O_3, phase studies at 800 to 1200°C, 25:30007
Tb_2O_3--ThO_2, phase studies at 800 to 1200°C, 25:30007
TERPHENYL
pyrolysis of hydrogenated and normal, effects of isomeric state on, 25:29113
radioinduced conversion of isomers and hydrogenated isomers of, 25:29113
radiolysis of hydrogenated and normal, effects of isomeric state on, 25:29113
TESTES
radiation effects on weight of mouse combined effects of actinomycin C on, 25:29604
radioinduced vascularization of mouse, x, 25:29653

XUM

TEXTILES
radiation processing of, 25:29128
THALLIUM
determination by amperometric, chelatometric, and conductometric titrations, 25:28970
determination using ion permselective membrane, potentiometric, 25:28956
effects on fluorometric determination of zirconium, 25:28963
THALLIUM ALLOYS AND SYSTEMS
Pb--Tl, magnetization curves of superconducting single crystals of, with small Ginzburg--Landau parameter, (E/T), 25:30418
THALLIUM ISOTOPES
radioactivity standards of, users' guides for, 25:29174
THALLIUM ISOTOPES Tl-200
beta decay of, gamma spectra and log ft from, (E), 25:31387
THALLIUM ISOTOPES Tl-203
photon reactions (γ,n) at 10 to 68 MeV, yields of radioactivities from, (E), 25:31333
THALLIUM ISOTOPES Tl-204
beta decay of, probability for production of internal bremsstrahlung in, (E), 25:31363
THALLIUM ISOTOPES Tl-205
energy levels from lead-208 (p,α) reactions, spins and parities of, (E), 25:31383
THALLIUM OXIDES
thermodynamic properties of gaseous diatomic, free energy functions for, 25:29082
THERMAL INSULATION
development of reactor, conference on, 25:31546 (EUR-4531)
performance in high-pressure gas environments, factors affecting, 25:30029 (EUR-4531, pp 841-81)
performance of circulating gas screen, for reactors, 25:31576 (EUR-4531, pp 1035-53)
performance of gas and water cooled metal plates, for water cooled reactors, 25:31578 (EUR-4531, pp 1085-97)
performance of honeycomb metal, for gas cooled and water cooled reactors, 25:31577 (EUR-4531, pp 1063-78)
performance of multi-layer metallic foil-type, in helium coolant, 25:30030 (EUR-4531, pp 931-52)
stability of gas cooled reactor, effects of thermal stresses on mechanical, 25:31457 (EUR-4531, pp 895-930)
testing of high temperature gas cooled reactor, heat transfer systems and equipment for, 25:31575 (EUR-4531, pp 953-64)
THERMAL RADIATION SHIELDING
performance of layered stainless steel-wire gauze, for Bugey I reactor, 25:29819 (EUR-4531, pp 1019-34)
THERMAL SHOCK
effects on germination of wheat seeds, effects of x radiation on, 25:29723
THERMAL TRANSFER TESTING
method for nuclear industry, description of, 25:29295
THERMIONIC CONVERTERS
plasma analysis in close-spaced, boundary conditions for electron and ion diffusion and transport for, (T), 25:30338
THERMOELECTRIC CONVERTERS
book: Principles of Thermoelectric and Magnetohydrodynamic Conversion of Energy. In Russian, 25:30340
burial of radioisotope-fueled earth-impacted, methods for determining heat and mass transfer in soils following, 25:29266 (SC-ARPIC-1010)
components for SNAP-23A advanced prototype, engineering drawings for design of, 25:29272
THERMOLUMINESCENCE
measurements for fine grains from pottery, age estimation method using, 25:29212
THERMONUCLEAR REACTORS
blanket systems for, comparison of, 25:30591 (EUR-4593, pp 513-18)
conference on fusion technology, 6th, Aachen, Germany, 9/70, 25:30449 (EUR-4593)
coolant for, feasibility of gas, 25:30589 (EUR-4593, pp 491-6)
design and construction of HBTX, 25:30586 (EUR-4593, pp 425-30)
design of prototype, system planning for, 25:30593 (EUR-4593, pp 533-8)
design of superconducting levitron, 25:30558 (EUR-4593, pp 133-9)
development of, review of, 25:30590 (EUR-4593, pp 497-512)
developmental progress of, 25:30600 (WASH-1172)
engineering and economic aspects of toroidal, 25:30588 (EUR-4593, pp 445-60)
gas injection into toroidal, radial distribution of tangential, (E), 25:30602
magnetic surfaces in quadrupoles, 25:30603
magnets for, review of technology of superconducting, 25:30557 (EUR-4593, pp 83-93)
problems of, (T), 25:30452
site selection for, prospects of Hanford, Wash, 25:30552 (BNWL-B-47)
sputtering of wall materials in, plasma interactions with, (T), 25:30497 (EUR-4593, pp 471-7)
stability of toroidal plasma ring with hf currents along longitudinal magnetic field, 25:30597(T) (LA-4339-TR)
THERMONUCLEAR WEAPONS
radiation doses to structures from, detonated 100 m above ground, γ and neutron, (T), 25:30633
THERMOSPHERE
electromagnetic processes at 200 to 1300 km in, Interkosmos-3 study of if, (E), 25:30364
temperature of, effects of seasonal variations, magnetic activity, and solar cycle on day and nighttime, (E), 25:30378
2-THIAZOLIDINEACETIC ACID, 4-CARBOXY-α-PHENYL-, 2-ETHYL ESTER
radioprotective effects of, on human patients during therapy, γ, 25:29545
THICKNESS GAGES
development of radiometric, for measuring thickness of hollow turbine blades, 25:29278(P)
THIOCYANATES
determination using ion permselective membrane, potentiometric, 25:28956
THORIUM
analysis for trace amounts of rare earth by carrier distillation spectrography, 25:28915 (BARC-517)
content in Berea area, Va. quartz monzonite, correlation with aeroradioactivity measurements, 25:29235
determination by amperometric, chelatometric, and conductometric titrations, 25:28970
determination by gravimetric and radiometric methods using cobalt hexaammine chloride, 25:28982
determination in industrial water and waste spectrophotometrically using o-[(2-hydroxy-3,6-disulfo-1-naphthyl)azo]benzenearsonic acid, ASTM method for, 25:28977
determination in presence of cerium using cupferron, potentiometric, 25:28958
effects on determination of palladium in biological materials, platinum, and rocks by isotope dilution, 25:28981
effects on fluorometric determination of zirconium, 25:28963
electron band structure calculations for fcc and bcc, 25:30696(R) (COO-2103-3)
handling and possession of, in Sweden, regulations for, 25:29541
production and uses of, review on, 25:29812
separation from aqueous solutions by thin-layer chromatography using liquid anion exchangers, 25:29186
separation from hydrochloric, nitric, perchloric, or sulfuric acid solutions by solvent extraction using 4-methyl-2-pentanone, effects of lithium chloride or magnesium chloride on, 25:29195
separation from other metals by ion-exchange paper chromatography, 25:29190
separation from rare earths, uranium, and zirconium by thin-layer chromatography, 25:29187
separation from sulfuric acid media by solvent extraction using N-phenylbenzylamine in chloroform, 25:29184
separation of neutron-irradiated, from uranium and fission products in sulfuric acid by solvent extraction using TBP in dodecane, 25:29198
thorium-232 Moessbauer effect in, following Coulomb excitation, 25:30693
THORIUM ALLOYS AND SYSTEMS
Fe--Th, crystal structure of α- and β-Th_2Fe_7, 25:29898
Th--Zr-base, microstructure of swaged, 25:29969
Th--Zr-base, tensile properties at 650°C, 25:29969
Th--Zr-base--ZrO_2, tensile properties at 650°C, 25:29969
THORIUM CARBIDES
hydrolysis of ThC/sub 1-x/ and ThC_2, microcalorimeter method for measurement of heats of, 25:29966
thorium-232 Moessbauer effect in ThC_2, following Coulomb excitation, 25:30693
ThC_2--UC_2, reprocessing of fuels of dissolution and fluorination process for, 25:29192(P)
THORIUM FLUORIDES
analysis for free fluoride using lanthanum fluoride electrode, 25:28923
THORIUM HIGH-TEMPERATURE REACTOR
design parameters of, summary of, 25:31539
development of, status of, 25:31540
THORIUM IONS
desorption from rhenium surfaces, energy and residence time of, 25:30259
THORIUM ISOTOPES
radioactivity standards of, users' guides for, 25:29174
THORIUM ISOTOPES Th-228
alpha decay in thorotrast, distribution of recoils from, 25:29169
neoplastic effects of, on bones of dogs, calculation of accumulated skeletal dose following intravenous injection and tumor growth dynamics of, 25:29621 (COO-119-243)
osteosarcomas induced in beagles following intravenous injection of, calculation of dose and tumor growth dynamics of, 25:29621 (COO-119-243)
THORIUM ISOTOPES Th-230
energy-level transitions from protactinium-230 decay, conversion coefficients for, (E), 25:31339
THORIUM ISOTOPES Th-232
alpha decay in thorotrast, distribution of recoils from, 25:29169

XUM

Moessbauer effect in thorium, thoria, thorium nitride, and thorium carbide following Coulomb excitation, 25:30693
proton fission at 10 MeV to 29 GeV, cross section for, 25:31326
THORIUM NITRIDES
crystal structure of Th_3N_4, 25:29986
thorium-232 Moessbauer effect in, following Coulomb excitation, 25:30693
THORIUM OXIDES
thermodynamic properties of gaseous diatomic, free energy functions for, 25:29082
Tb_2O_3--ThO_2, phase studies at 800 to 1200°C, 25:30007
THORIUM OXIDES ThO_2
analysis of, use of laser microprobe in spectral, 25:28949
distribution in lungs of man, effects of age on, 25:29521
electric conductivity of, effects of high oxygen pressures on ac, 25:30685
properties and structure of, matrix isolation method for studying, 25:29083
radiation effects on microstructure of, 5.5-MeV alpha particle, 25:30012
radiation effects on spallation and strain in polycrystalline, 5-MeV alpha particle, 25:30014
sorptive properties for carbon monoxide, EPR studies of, 25:29090
thorium-228 and thorium-232 decay in colloidal solutions of, distribution of recoil, 25:29169
thorium-232 Moessbauer effect in, following Coulomb excitation, 25:30693
Fe-base--ThO_2, yield strength of dispersion-hardened bcc, 25:29948
ThO_2--UO_2, radiation effects on thermal conductivity of, relations of burnup level with in-pile, 25:29937 (BMI-X-10274)
ThO_2--UO_2, reprocessing of fuels of, dissolution and fluorination process for, 25:29192(P)
ThO_2--Zr-base, microstructure of arc-melted and swaged, 25:29969
ThO_2--Zr-base, tensile properties at 650°C, 25:29969
ThO_2-base--Y_2O_3, electric conductivity of solid solutions, effects of high oxygen pressures on ac, 25:30685
THORIUM OXYCHLORIDES
oxygen-18 exchange between heavy water and, 25:29089
THORIUM PEROXIDES
structure of, isotope exchange studies on, 25:29089
THULIUM
production and properties of aerosols of, 25:29078 (LF-43, pp 25-30)
separation from other rare earths by ion exchange, 25:29178 (CEA-R-4102)
THULIUM ISOTOPES Tm-171
distribution and retention in beagle dogs following inhalation as oxide, 25:29425 (LF-43, pp 71-8)
THULIUM OXIDES
effects on oxygen electrode performance, 25:29096
THYMINE
radiolysis of ethanol or methanol solutions of, at 77°K, yields of ions and radicals from x, 25:29143
radiolysis of frozen sulfuric acid solutions of, ESR studies on radical formation in x, 25:29134
radiolysis of, mechanism for release of hydrogen atom in γ, 25:29148
THYMUS GLAND
radiosensitivity of rabbit and rat, x, 25:29635
THYROGLOBULIN
radiation effects on production of antibodies of, in rats, γ and/or iodine-131, 25:29660
THYROID GLAND
curium-244 content in beagle dog, following inhalation as chloride or oxide, 25:29429 (LF-43, pp 100-5)
scanning of human, effectiveness of technetium-99m in comparison to iodine-131, 25:29418 (BNL-50285)
scanning of human, for diagnosis of tumors, effectiveness of scintigraphy and radioisotope, 25:29580
scintigraphy of human, for function studies, use of technetium-99m-labeled pertechnetate and pinhole scintillation camera for, 25:29586
technetium-99m localization in human, 25:29418 (BNL-50285)
TIMING CIRCUITS
design of high-accuracy variable time delay, 25:29403
TIN
current stability in flat superconducting films, 25:30437
effects on fluorometric determination of zirconium, 25:28963
magnetization by rotation of superconducting, 25:30439
proximity effect in superconducting, coated with normal metals, 25:30446
separation from antimony and arsenic by thin-layer chromatography, 25:29165
separation from antimony and tellurium by thin-layer chromatography, 25:29165
ultra-high-frequency signal mixing from superconducting films of, (E), 25:30436
TIN ALLOYS AND SYSTEMS
Al--Sn--V, phase equilibria and superconductivity in intermetallic V_3LAl--V_3Sn, 25:30416
Be--Cu-base--Sn, aging characteristics of, effects of tin content on, 25:29830
Be--Cu-base--Sn, corrosion by nitric or sulfuric acids, effects of manganese, titanium, or zinc additions on, 25:29830
In--Sn, nuclear quadrupole resonance spectrum of, 25:30695
In-base--Sn, superconducting transition temperature under strain in, (E), 25:30435
Pb--Sn, structure and properties of electrolytically deposited, 25:31734(T) (SCL-T-69-257)
TIN ISOTOPES
production in proton fission of uranium-238 at 450 MeV, mass yield and charge distribution for, (E), 25:31302 (COO-1167-10)
TIN ISOTOPES Sn-116
nuclear radii from proton elastic scattering, (E), 25:31341
proton elastic scattering at 1600 MeV, polarization angular distribution for, (E), 25:31341
TIN ISOTOPES Sn-118
nuclear radii from proton elastic scattering, (E), 25:31341
proton elastic scattering at 1600 MeV, polarization angular distribution for, (E), 25:31341
TIN ISOTOPES Sn-119
internal conversion in, effects of valent shell structure on, 25:31343
Moessbauer spectrum in perfect tin single crystal, disappearance of inelastic channel in nuclear reaction of, 25:30687 (IAE-1966)
TIN ISOTOPES Sn-120
nuclear radii from proton elastic scattering, (E), 25:31341
proton elastic scattering at 1600 MeV, polarization angular distribution for, (E), 25:31341
TIN ISOTOPES Sn-124
nuclear radii from proton elastic scattering, (E), 25:31341
proton elastic scattering at 1600 MeV, polarization angular distribution for, (E), 25:31341
TIN ISOTOPES Sn-125
beta decay of metastable, gamma transitions and log ft in, (E), 25:31388
TIN OXIDES
thermodynamic properties of gaseous diatomic, free energy functions for, 25:29082
TISSUE HOMOGENATES
radiation effects on protein fractions of, in brain and small intestine in rabbits, x, 25:29664
TISSUES
analysis for molybdenum by neutron activation and radiochemical separation, 25:29019
proton dose to human, calculation of quality factors for, 25:29511 (AERE-M-1887)
radiation dose to human, during therapy of malignant tumors, correlation between RET, tumor dose, and nominal standard, 25:29520
radiation effects on DNA synthesis in rat lymphoid, effects of adrenalectomy on subsequent inhibitory whole-body γ, 25:29672
radiation effects on subcutaneous, oxygen tension kinetics during protective effects of mexamine against γ, 25:29551
radioisotope uptake in, of rats for diagnosis of joint diseases, iodine-131, mercury-203, selenium-75, strontium-85, or tellurium-132, 25:29581
TITANIUM
abundance in atmosphere of α Cyg, (E), 25:30109
analysis of sponge of, for silicon as molybdosilicate complex, spectrophotometric method for, 25:28924
corrosion resistance to acid and alkali environments, evaluation of, 25:29775
determination in carbon using peroxide, ASTM method for colorimetric, 25:28974
determination in presence of other metals, spectrographic, 25:28944
determination in thin films of titanium nitrides by electron-probe x-ray micro method, 25:28966
effects on corrosion of beryllium--copper--tin alloys by nitric acid, 25:29830
effects on electric conductivity, grain refinement, and microhardness of zirconium, 25:29835
effects on fluorometric determination of zirconium, 25:28963
elastic properties of monocrystalline, effects of lattice parameters and volume change on pressure derivatives of, 25:29852
properties for use as carbide-former in neutron damage-resistant stainless steel, 25:29799(P)
proton reactions at 11.5 and 23.5 MeV using thick targets, neutron yield from, (E), 25:31209
reactions with graphite thimbles to prepare titanium monocarbide, 25:29926
separation from aqueous solutions by thin-layer chromatography using liquid anion exchangers, 25:29186
TITANIUM ALLOYS AND SYSTEMS
mechanical properties at -253 to +20°C, effects of beta-stabilizer niobium, tantalum, and vanadium on, 25:29844

XUM

precipitation in β-isomorphous, metastable, 25:29887
Al--Be--Ti, phase diagrams at 600 to 1300°C, isothermal, 25:29900
Al--Mo--Ti-base--V, corrosion cracking in aqueous and methanol solutions with and without halogen ions, stress, 25:29765
Al--Ni--steel--Ti, failure of electroslag welded joints on, effect of residual welding stress on brittle, 25:29832
Al--Ti-base--V, corrosion by hydrochloric acid--methanol and sodium chloride--isopropanol, 25:29773
Be--Ti--Zr, melting temperature of brazements of, 25:29824 (ORNL-4630, pp 191-206)
Co-base--Ti, thermal expansion at 100 to 800°C, 25:29899
Co-base--Ti, transformation temperatures of, allotropic, 25:29899
Cr--Ti--V-base, compatibility with sodium at 600°C, effects of oxygen on, 25:29761 (ORNL-4630, pp 150-7)
Ge--Ti--Zr, melting temperature of brazements of, 25:29824 (ORNL-4630, pp 191-206)
Mo--Pt-base--Ti, tensile properties at 25 to 1290°C, 25:29823 (ORNL-4630, pp 186-90)
Mo-base--Ti, radiation effects on microstructure of, fast neutron, 25:29904 (ORNL-4630, pp 73-95)
Nb--Ti-base, tensile properties of precipitation-hardened, relation of microstructure with room temperature, 25:29872
Nb-base--Ti, coating with aluminum at 900 to 1200°C, pack-cementation method for, 25:29816
Nb-base--Ti, diffusion of hydrogen in, at -160 to +250°C, activation energy of, 25:29837
Nb-base--Ti--Zr, microstructure of precipitates in, effects of aging at 620 to 850°C, 25:29890
O--Ti, crystal structure of solid solutions of alpha, 25:30000
Ti--V, precipitation in β-isomorphorous, comments on metastable, 25:29886
Ti--V-base, compatibility with sodium at 600°C, effects of oxygen on, 25:29761 (ORNL-4630, pp 150-7)
Ti--V-base, corrosion by oxygen-contaminated sodium, 25:29781
Ti--V-base, crystal structure of internal oxidation zones in sodium-corroded, 25:29781
Ti--Zr-base, polishing for metallographic examination, electrolytic, 25:29817

TITANIUM BORIDES
thermal conductivity of TiB_2 at 200 to 1300°C, 25:29956

TITANIUM CARBIDES
preparation of monocrystalline monocarbide, recrystallization method for, 25:29927
preparation of TiC, by reactions of liquid titanium with graphite thimbles, 25:29926
TiC--VC, slip mechanisms in, 25:29999

TITANIUM ISOTOPES Ti-46
energy levels from proton inelastic scattering, spin--parity assignments for, (E), 25:31288
energy-level transitions from proton inelastic scattering, γ mixing and branching ratios for, (E), 25:31288
helium-3 reactions (He-3,n) at 13.2 MeV, neutron spectra and angular distributions for, (E), 25:31237 (IAE-1958)
proton inelastic scattering near 5.5 MeV, γ linear polarization from, (E), 25:31288

TITANIUM NITRIDES
analysis of thin films of, by electron-probe x-ray micro method, 25:28966

TITANIUM OXIDES
thermodynamic properties of gaseous diatomic, free energy functions for, 25:29082
La_2O_3--TiO_2--ZrO_2, dielectric properties of, 25:29984
La_2O_3--TiO_2--ZrO_2, phase diagram of, 25:29984
Nb_2O_5--TiO_2, phase studies at 1250°C, 25:29995
NbO_2--Nb_2O_5--TiO_2, phase studies at 1250°C, 25:29994
NbO_2--TiO_2, phase studies at 1250°C, 25:29995

TOKAMAK DEVICES
design of Garching Pulsator, 25:30584 (EUR-4593, pp 411-17)
development at Fontenay-aux-Roses, 25:30583 (EUR-4593, pp 403-9)
development in USSR, review of, 25:30596 (JAERI-Memo-4286)
plasma confinement and heating in T-3, (E), 25:30461(T) (MATT-Trans-79)

TOKAMAK MODEL ST
plasma heating in, ohmic, (E), 25:30459 (MATT-813)

TOLUENE
effects on urease activity in soils, comparison of γ radiation and, 25:29460

TOXINS
radiation effects on production of, in rat liver, chronic strontium-90 β, 25:29639

TRACER TECHNIQUES
book: Measuring Methods Using Ionizing Radiation, 25:29391
development of radioactive, for improving lead and zinc oxide production processes, 25:29283
evaluation of radioactive and stable isotope, for water pollution control studies, 25:29213

TRANSACTINIDE ELEMENTS
discovery of heavy, (T), 25:30452
existence of superheavy, survey of research on, 25:31328
existence of, in Universe, (T), 25:30304
nucleosynthesis in supernovae, (T), 25:30051

TRANSDUCERS
design of satellite-borne, for determination of ionospheric ion motion at 600 km, (E), 25:30393
moisture protection of semiconductor, 25:31755(T) (UCRL-Trans-10526)

TRANSITION METALS
Fermi surfaces of, review, 25:30681
spectra of, LMM Auger, 25:31682 (AERE-R-6719)

TRANSITION RADIATION
emission from vacuum--refractory media interface, spectra of, (T), 25:30702
generation of, in one and two dielectric plates, mechanism of, (T), 25:30714

TRANSPLANTS
conference on cross-species, Brighton, Utah, May 8-9, 1970, 25:29682

TRANSURANIUM ELEMENTS
energy levels of, calculation using Woods--Saxon potential, (T), 25:31392(T) (BNL-tr-416)

TRITIUM
content in environment of West Valley Processing Plant, 25:29179 (DOCKET-50201-69)
content in seawater near Goto Islands, Japan, measurements during July 1966, 25:29241
determination in labeled proteins in polyacrylamide gels by liquid scintillation counting, 25:28994
determination in labeled RNA by paper disc estimation, 25:28993
determination in RNA by separation and liquid scintillation counting, 25:28984
determination in serum thyroxine by liquid scintillation counting, 25:28986
determination on solid supports by liquid scintillation counting, 25:28985
distribution and transport in Sedan crater ejecta, measurement of, 25:29244 (UCRL-72572)
distribution in water vapor in lower troposphere, airborne measurements of vertical, 25:29215
effects on biological and physical properties of pneumococcal DNA following incorporation, β, 25:29459
monitoring in environmental samples at West Valley Processing Plant, 1971, 25:29180 (DOCKET-50201-70)
neutron scattering by, microscopic analysis using soft-core potential, (T), 25:31193
reactions of recoil atoms of, in isomerization of methyl isocyanide to acetonitrile, 25:29167
reactions of recoil atoms of, with hydrocarbons, yields of labeled products from, 25:29167
separation from argon, design of gas chromatograph for, 25:29177 (CEA-R-4090)
use for labeling organic compounds, 25:29413 (CONF-691225)
use in determining microquantities of acetate by isotope dilution and scintillation counting, 25:28996
use of thymidine-incorporated, for labeling amelogenic cells in incisors of rats following x irradiation, 25:29678

TRITONS
binding energy of, realistic potentials in harmonic oscillator basis for calculating, (T), 25:30896 (NYO-4032-36)
decay of, low-energy theorems for nuclear, weak, and electromagnetic currents in beta, (T), 25:30807
reactions (t,p) with sulfur-34 at 3.1 MeV, γ linear polarization from, (E), 25:31289
wave function for, realistic potentials in harmonic oscillator basis for calculating groundstate, (T), 25:30896 (NYO-4032-36)

TRI-UNIVERSITY MESON FACILITY (TRIUMF)
cyclotron for, beam quality and expected energy resolution from, 25:31088
cyclotron for, description of, 25:31087
cyclotron for, design of 4000 ton magnet for, 25:31092
cyclotron for, design of sector-focused magnet poles for, 25:31049 (TRI-70-4)
cyclotron for, extraction of multiple beams of various energies from, 25:31109
cyclotron for, H^- ion injection in, 25:31152
cyclotron for, square wave rf system design for, 25:31091

TROJAN POWER REACTOR, UNIT 1
design parameters of, requested additional information on, 25:31518 (DOCKET-50344-20)
operations aspects of, requested additional information on, 25:31518 (DOCKET-50344-20)

TROPOSPHERE
tritium distribution in water vapor in lower, airborne measurements of vertical, 25:29215

TRYPTAMINE
radioprotective effects of, on isolated intestines in guinea pigs, x, 25:29566

TRYPTOPHOL
radioprotective effects of, sulfur analogs of, on mice, x, 25:29567

TUBES
gamma-ray penetration in curved, spectrum of, 25:30638

TUNGSTEN
book: Creep-Rupture Data for the Refractory Metals to High Temperatures, 25:29868

XUM

brittleness of, effects of interstitial impurities on intergranular, 25:29855
coating of atomically clean crystal surfaces of, with zirconium, electron diffraction studies of mechanisms of, 25:29847
coating of crystal surfaces of, with nickel, microscopic studies of, 25:29848
coating with platinum, mechanisms of vapor, 25:29850
corrosion by boric oxide and sodium borate melts, mechanisms and kinetics of, 25:29774
creep of high-purity chemical vapor deposited, at 1200 to 2200°C, 25:29786 (ORNL-4630, pp 207-25)
crystal orientations of monocrystalline, at 25 to 200°C, effects of rolling deformation on, 25:29877
deposition on substrates from alkaline fluoride mixtures containing salts of, method for electro-, 25:29783 (CEA-N-1376)
determination in low-alloy steel, two-standard method for spectrometric, 25:28950
determination in niobium photometrically using dithiol, 25:28973
determination in presence of other metals, spectrographic, 25:28944
dispersion of submicron particles of, in hydrogen, effects on radiant heat transfer, 25:29270
dispersion of submicron particles of, in nitrogen, measurement of scattering amplitude functions for, 25:29270
effects of additions of, on stability of uranium dioxide fuels, 25:29932(P)
effects on colorimetric determination of molybdenum, 25:28930
effects on corrosion of nickel alloys by vanadium pentoxide melts, 25:29768
effects on fluorometric determination of zirconium, 25:28963
flow stress of cold-worked doped, at 77 to 800°K, 25:29874
Lorentz number for electron--electron scattering in, (E/T), 25:30646(R) (NYO-2150-66)
mechanical properties of monocrystalline, at 25 to 200°C, effects of rolling on, 25:29877
microstructure of powder metallurgy, at high temperatures, 25:29786 (ORNL-4630, pp 207-25)
oxidation of silicon-coated, at 600 to 1600°C and low pressures, kinetics and mechanism of, 25:29869
plasticity and strength of submicron fibers of, effects of transverse dimension on, 25:29857
preparation of high-purity, by chemical vapor deposition from tungsten hexafluoride, 25:29786 (ORNL-4630, pp 207-25)
production and uses in US during 1966 to 1970, review on, 25:29813
proton fission at 10 MeV to 29 GeV, cross section for, 25:31326
proton reactions at 11.5 and 23.5 MeV using thick targets, neutron yield from, (E), 25:31209
radiation effects on elastic modulus of monocrystalline, at 77°K, 10-MeV proton, 25:29903(R) (NYO-3653-5)
siliconizing of surface of ribbons of, by heterogeneous decomposition of silane at 800 to 1200°C and low pressure, 25:29814
sintering of nickel-activated, kinetics of, 25:29791
sintering of powdered mixture of zirconium diboride and, mechanism of, 25:29930
sintering of, effects of nickel--phosphorus alloy on low-temperature, 25:29793
sorptive properties at activated polycrystal sites for nitrogen, kinetics of chemi-, 25:29849
sorptive properties of crystal surfaces of, for hydrogen, high-energy electron diffraction studies of, 25:29846

TUNGSTEN ALLOYS AND SYSTEMS
analysis for rhenium, chromatographic, 25:28953
book: Creep-Rupture Data for the Refractory Metals to High Temperatures, 25:29868
book: Special Steels and Alloys (In Russian), 25:29862
mechanical properties to 2400°C, 25:29864
C--Co--W, tensile properties of, effects of composition on, 25:29980
Cr--Pt--W, tensile properties of intermetallic compounds of, at 1290°C, 25:29823 (ORNL-4630, pp 186-90)
Cu--W--Zr-base, corrosion by carbon dioxide at 500 to 650°C, 25:29770
Hf--Pt-base--W, tensile properties at 25 to 1290°C, 25:29823 (ORNL-4630, pp 186-90)
Mo--Re--W, fabrication of irradiation capsules of, welding methods for, 25:30010 (ORNL-4630, pp 179-85)
Mo--W--Zr, mechanical properties at 2100°C, 25:29864
Nb-base--W, coating with aluminum at 900 to 1100°C, pack-cementation method for, 25:29816
Ni-base--W, strength of, effects of diffusion velocity and stacking fault energy on high-temperature, 25:29878
Re--W, creep under stress, effects of oxygen at high temperature on, 25:29786 (ORNL-4630, pp 207-25)
Re--W, superconductivity of hcp, (E), 25:30433
Re--W, welding of, effects of filler metal and methods on, 25:29786 (ORNL-4630, pp 207-25)
Re--W-base, hardness at 77 to 730°K, effects of rhenium content on, 25:29871
Ta--W, properties of, electric and thermal, 25:29824 (ORNL-4630, pp 191-206)
Ta-base--W, stress rupture of welds of, at 1200 to 1650°C, 25:29824 (ORNL-4630, pp 191-206)
W--Zr-base, corrosion by carbon dioxide at 500 to 650°C, 25:29770

TUNGSTEN CARBIDES
dispersion of submicron particles of, in nitrogen, measurement of scattering amplitude functions for, 25:29270
Co--WC, binder composition in, effects of composition, carbide grain size, and heat treatments on, 25:29980

TUNGSTEN FLUORIDES
equations of state for, at 40 to 190°C, 25:29073 (CEA-N-1414)

TUNGSTEN ISOTOPES W-181
content of air samples from Project Schooner during 1969, 25:29506 (SWRHL-97-r)

TUNGSTEN ISOTOPES W-187
metabolism in beagle dogs following ingestion of nuclear debris from Project Cabriolet, 25:29456

TUNGSTEN OXIDES
properties and structure of, matrix isolation method for studying, 25:29083
thermodynamic properties of gaseous diatomic, free energy functions for, 25:29082

TUNGSTEN SELENIDES
properties of polyimide-bonded, as solid film lubricants, 25:29096 (WERL-HFIL-1)

TURBINE BLADES
thickness of hollow, method using radioactive gas for measuring, 25:29278(P)

TURBINES
design and performance of large, for saturated and superheated steam cycles for conventional and nuclear power stations, 25:29256

TYRAMINE
deamination in liver of radiation effects on deamination of, in rat liver, 25:29641

TZM (MOLYBDENUM ALLOY)
tensile properties at 1093 to 1290°C, 25:29823 (ORNL-4630, pp 186-90)
welding to molybdenum, mechanisms of cracking during, 25:29824 (ORNL-4630, pp 191-206)

U

ULTRASONIC TESTING
equipment and method for in-service inspection of reactor pressure vessels, 25:29250
method for evaluation of welds in reactor materials, 25:29287 (ORNL-4630, pp 145-9)
method for reactor materials, 25:29288 (ORNL-4630, pp 271-9)

ULTRASOUND
generation by eddy currents, zero-field efficiency of, (E), 25:30646(R) (NYO-2150-66)
method for abdominal scanning in man prior to radiotherapy of bladder and gynecological tumors, 25:29602

ULTRAVIOLET RADIATION
effects on activity of aldolase, glutamic-aspartic and glutamic-alanine transaminase, and tyrosinase in mycelium of Botrytis cinerea, 25:29720
effects on content of sulfhydryl groups in tissues of ducklings, 25:29647
effects on curing of coatings composed of polyesters--aryl sulfonamide--formaldehyde resins containing halogenated photoinitiators, 25:29114(P)
effects on cytoplasmic structure in relation to cell behavior, 25:29608(R) (NYO-2356-43)
effects on DNA of green algae, role of photoreactivating enzymes in repair of, 25:29713(R) (COO-1793-5)
effects on initiation of unscheduled DNA synthesis in muscle cells of chick embryos, in vitro, 25:29650
effects on organic solids, stimulation spectra of trapped anions from, 25:29133
effects on oscillatory behavior of enzymatic reactions, 25:29461
effects on post-polymerization of γ-irradiated crystalline acrylonitrile, ESR studies on, 25:29118
effects on properties of zinc oxide-base paints, 25:29105
effects on radicals produced in γ radiolysis of allyl alcohol glass, 25:29162
effects on solid cyclopropene and cyclopropene dispersed in organic glasses, 25:29147

UNDERGROUND STRUCTURES
cost analysis of 1000 MW(e) boiling power reactor, conceptual, 25:31600
design parameters of 1000 MW(e) boiling power reactor, conceptual, 25:31600

UNITED STATES
regulatory inspection of commercial producers of radiation sources and radioisotope-labeled compounds in, evaluation of, 25:29527 (NP-18791)

UNIVERSE
distribution of cold matter in, (T), 25:30227
Einstein equations for radiation-filled, spherically symmetric solutions for, (T), 25:30225
electric charge of elliptical, total, (T), 25:30235
gravitational effect of Einstein, inertial forces as,

XUM

(T), 25:30245
infrared emission from cold matter in, (T), 25:30227
mass of elliptical, (T), 25:30235
mass of, effects of variable Planck's constant on, (T), 25:30246
matter distribution in, Newtonian hierarchical, (T), 25:30226
models of, topological, (T), 25:30234
momentum in elliptical, (T), 25:30235
perturbations of matter density in anisotropic homogeneous, (T), 25:30223
pulsations of, in closed models, (T), 25:30233
URACIL, 5-BROMO-
yields from γ radiolysis of aqueous solutions of 5-bromo-2'-deoxyuridine in presence of oxygen, 25:29135
URACIL, 5-FLUORO-
effects on radiosensitivity of skin tumors in mice, 25:29605
URANIUM
activity coefficient in plutonium dioxide--uranium dioxide solid solutions, transpiration method for studying, 25:29821(R) (GEAP-12153)
analysis for trace amounts of rare earth by carrier distillation spectrography, 25:28915 (BARC-517)
anodization prior to extrusion, method for, 25:29787(R) (RMI-16)
complexes with cyclooctatetraene, proton magnetic resonance shifts in, 25:29085
compounds, analysis for nitrates, colorimetric, 25:28918 (NIM-951)
compounds, oxidation-reduction potential of acid solutions of tetravalent and hexavalent, effects on acidity on, 25:29036
content and distribution in ocean sediments from Mid-Atlantic Ridge, measurement of, 25:29228
content in Berea area, Va. quartz monzonite, correlation with aeroradioactivity measurements, 25:29235
content in ground waters, effects on deposition of molybdenum and selenium in near-surface uranium deposits, 25:29240
content in pyrites, radiographic measurements of, 25:29231
content of pentavalent, in U(IV)--U(V)--U(VI), electrochemical determination of equilibrium, 25:29036
crystal preferred orientation after heat treatment, effects of cooling rate and initial structure and texture on, 25:29884 (UJV-2525-M)
determination as complex with Alizarin Red in diphenylguanidinium salt by solvent extraction and spectrophotometry, 25:28934
determination by controlled-potential coulometry, ASTM method for, 25:28975
determination by radiometric method using cobalt hexaammine chloride, 25:28982
determination colorimetrically using dibenzoylmethane, ASTM method for, 25:28976
determination in borehole samples using delayed neutrons, 25:29202(T) (CEA-tr-R-1978)
determination in natural waters by solvent extraction and x-ray fluorescence spectroscopy, 25:28919
determination in reactor fuels by ion-exchange separation and mass spectrometry, ASTM method for, 25:28978
determination of ratio of, to cesium-137 in irradiated fuels for calculation of atom percent fission, ASTM method for, 25:28998
determination of, evaluation of various colorimetric methods for, 25:28971
diffusion in aluminum at 550 to 630°C, 25:29867
dimensional variations of extruded, effects of thermal anisotropy on, 25:29787(R) (RMI-16)
dislocation etch pits in α-, development of etchant for revealing, 25:29889
ductility during crystallization of alpha anisothermal creep method for studies of, 25:29851
effects of hexavalent, on separation of thorium(IV) from sulfuric acid solutions by extraction using N-phenylbenzylamine in chloroform, 25:29184
effects on determination of palladium in biological materials, platinum, and rocks by isotope dilution, 25:28981
effects on fluorometric determination of zirconium, 25:28963
electron band structure calculations for bcc, 25:30696(R) (COO-2103-3)
energy-level transitions in, electron spectra from Coster--Kronig and L-shell Auger, (T), 25:30261
enrichment using counterflow gas centrifuges, review of German developments in, 25:29271(T) (CONF-700557-1)
etching of, properties of aqueous ferric chloride and nickel chloride for, 25:29798(P)
extrusion of, equipment and methods for, 25:29787(R) (RMI-16)
handling and possession of, in Sweden, regulations for, 25:29541
photon elastic scattering at 1.33 MeV, differential cross sections for, (E), 25:31370
plasma of, relation of ionization to temperature and density, (T), 25:30536
production and uses during 1971, review on, 25:29811
production in Canada, predictions of present and planned, 25:29236
proton reactions at 11.5 and 23.5 MeV using thick targets, neutron yield from, (E), 25:31209
radiation exposure standards for personnel mining, economic impact of compliance with, 25:29532
radiation monitoring of air in mines for, methods for, 25:29536
radiation protection standards for personnel of mines and mills, 25:29535
reactions of trivalent, with chromium complexes, kinetics of reduction, 25:29084
separation as uranyl from nitrate solutions by solvent extraction using trioctyl ammonium nitrate, 25:29182 (RT/CHI-(70)31)
separation from americium and curium by ion exchange in zirconium phosphate--nitric acid system, 25:28989
separation from aqueous solutions by thin-layer chromatography using liquid anion exchangers, 25:29186
separation from fission products and thorium in sulfuric acid by solvent extraction using TBP in dodecane, 25:29198
separation from hydrochloric, nitric, perchloric, or sulfuric acid solutions by solvent extraction using 4-methyl-2-pentanone, effects of lithium chloride or magnesium chloride on, 25:29195
separation from irradiated fuels containing thorium/uranium mixed carbides or oxides, dissolution and fluorination process for, 25:29192(P)
separation from rare earths, thorium, and zirconium by thin-layer chromatography, 25:29187
separation from spent fuels by fractional condensation of chlorides and solvent extraction, 25:29189(P)
shipping of, design of BNW Model 10 container for, 25:29318
solubility in aluminum at 550 to 630°C, 25:29867
solubility limits in nickel at 975 to 1075°C, measurement of diffusion coefficients for determination of low, 25:29866
spectra of tetravalent, in molten fluorides, 25:29093
URANIUM ALLOYS AND SYSTEMS
etching of, properties of aqueous ferric chloride and nickel chloride for, 25:29798(P)
Al--U, crystal structure of UAl_4, 25:29895
Al--U, properties of UAl_4, electric, mechanical, and thermal, 25:29895
Al--U, radiation effects on aluminum-clad fuel plates of, in-pile, 25:29924 (ORNL-4630, pp 233-8)
C--O--Te--U, phase diagram at 1200°C, 25:30001
C--Te--U, phase diagram at 1200°C, 25:30001
Cr--N--U, crystal lattice parameters of UCrN/sub 2+-x/, 25:29988
Cr--N--U, phase diagram at 1600°C, tentative, 25:29988
N--U--V, crystal lattice parameters of UVN_2, 25:29989
N--U--V, phase diagram at 1400 to 2000°C, 25:29989
N--U--V, thermodynamic properties of UVN_2, 25:29989
O--U--Y, crystal lattice parameters of solid solutions of, 25:29922 (ORNL-4630, pp 3-58)
Si--U, analysis for silicon as molybdosilicate complex, spectrophotometric method for, 25:28924
URANIUM CARBIDES
compatibility of nonstoichiometric and stoichiometric, with chromium--iron--nickel cladding alloys at 900°C, effects of stabilizers on, 25:29940(T) (EURFNR-820)
creep behavior of sintered hyper- and hypostoichiometric, in vacuum at 930 to 1300°C, effects of nickel and stress on, 25:29960
melting of UC, with 450 kHz power unit, levitation, 25:29934
radiation effects on mechanical properties of, fast neutron, 25:31568(T) (EURFNR-823)
reactions of UC_2, with nitrogen at 800 to 1400°C, effects of nitrogen pressure on graphitization of carbon formed from, 25:29962
thermal diffusivity of arc-cast nonstoichiometric, at 500 to 2200°K, 25:29957
thermal diffusivity of sintered, at 500 to 2200°K, effects of nickel and oxygen on, 25:29957
CeN--UC, crystal lattice parameters for, relations with composition, 25:30003
CeN--UC--UN, crystal lattice parameters for $U_{0.8}Ce_{0.2}C$--$U_{0.8}Ce_{0.2}N$, relations with composition, 25:30003
CeN--UC--UN, preparation of $U_{0.8}Ce_{0.2}C$--$U_{0.8}Ce_{0.2}N$, methods for, 25:30003
PuC--UC, creep behavior of sintered, in vacuum at 950 to 1150°C, effects of stress on, 25:29960
PuC--UC, specific power limits in liquid metal cooled fast breeder reactors, 25:31569 (ORNL-TM-3388)
PuC--UC, swelling during irradiation in liquid metal cooled fast breeder reactors, limits for, 25:31569 (ORNL-TM-3388)
PuC--UC, thermal diffusivity of arc-cast, at 500 to 2200°K, 25:29957
ThC_2--UC_2, reprocessing of fuels of dissolution and fluorination process for, 25:29192(P)
URANIUM CHLORIDES
molecular structure of, 25:29086
spectra in matrices of solid nitrogen or rare gases, ir, 25:29086
URANIUM CHLORIDES UCl_5
complexes with isoquinoline, 2-picoline, 3-picoline, pyridine, or quinoline, properties of, 25:29092
URANIUM DEPOSITS
distribution in Morvan Mountains, France, relations with

structure of granite massifs, 25:29239
exploration for Canadian, review of methods for, 25:29236
geology and mineralization of Northern Territory, Australia, 25:29234
mineralization of quartz vein-contained, 25:29232
mineralization of Singhbhum shear zone, Bihar, India, 25:29227
prospecting and mining of, review of programs for, 25:29237
prospecting for shallow and medium depth, magnetotelluric methods for, 25:29233
prospecting for Swedish, performance of radiometric equipment and methods for, 25:29229
uranium content and distribution in, beta and gamma well logging method for determination of, 25:29230

URANIUM FLUORIDES UF_6
equations of state for, at 40 to 190°C, 25:29073 (CEA-N-1414)

URANIUM ISOTOPES
radioactivity standards of, users' guides for, 25:29174

URANIUM ISOTOPES U-233
criticality control in solutions of, borosilicate-glass raschig rings as fixed neutron absorber for, 25:29197
deposition on rubidium uranyl nitrate single crystals, 25:29034 (AERE-R-6141)
neutron capture-to-fission ratio for, epithermal, (E), 25:31353
neutron fission of, delayed neutron fractions in thermal, (E), 25:31334

URANIUM ISOTOPES U-234
content ratio to uranium-238 in Lake Balkhash, USSR bottom sediments, use in age estimation, 25:29210

URANIUM ISOTOPES U-235
abundance relative to uranium-238, developments in mass spectrometric method for measurement of, 25:28927
criticality control in solutions of, borosilicate-glass raschig rings as fixed neutron absorber for, 25:29197
deposition on rubidium uranyl nitrate single crystals, 25:29034 (AERE-R-6141)
determination in unirradiated fuels by neutron flux measurements, apparatus for nondestructive, 25:28988(P)
neutron capture by, cross section for isomeric uranium-236 production relative to fission for thermal, (E), 25:31307 (JINR-P7-5497)
neutron capture-to-fission ratio for, epithermal, (E), 25:31353
neutron fission of, angular anisotropy of γ rays from slow, (E), 25:31369
neutron fission of, delayed neutron fractions in thermal, (E), 25:31334
proton fission at 10 MeV to 29 GeV, cross section for, 25:31326

URANIUM ISOTOPES U-238
abundance relative to uranium-235, developments in mass spectrometric method for measurement of, 25:28927
content ratio to uranium-234 in Lake Balkhash, USSR bottom sediments, use in age estimation, 25:29210
neutron capture by, calibration of Moxon--Rae detector for measurement of cross section for, 25:29326 (LA-4445)
proton fission at 450 MeV, mass yield and charge distribution from, (E), 25:31302 (COO-1167-10)

URANIUM ISOTOPES U-239
energy levels of, superfluid-model calculations of energies and wave functions of nonrotational, (T), 25:31306 (JINR-P4-5693)

URANIUM MINERALS
crystal structure of $Cu_2(UO_2)_3(OH)_{10} \cdot 5H_2O$, 25:29238
properties of $Cu_2(UO_2)_3(OH)_{10} \cdot 5H_2O$, chemical and physical, 25:29238

URANIUM NITRATES
compounds with hydrazine nitrate, preparation and properties of hydrated, 25:29035 (NP-18736)

URANIUM NITRIDES
development of fuels of, for space reactors, 25:30010 (ORNL-4630, pp 179-85)
radiation effects on clad fuels of, for space reactors, in-pile, 25:30010 (ORNL-4630, pp 179-85)
radiation effects on mechanical properties of, fast neutron, 25:31568(T) (EURFNR-823)
CeN--UC--UN, crystal lattice parameters for $U_{0.8}Ce_{0.2}C$--$U_{0.8}Ce_{0.2}N$, relations with composition, 25:30003
CeN--UC--UN, preparation of $U_{0.8}Ce_{0.2}C$--$U_{0.8}Ce_{0.2}N$, methods for, 25:30003
CeN--UN, crystal lattice parameters for, relations with composition, 25:30003
PuN--UN, compatibility with stainless steel, literature survey on, 25:29923 (ORNL-4630, pp 59-72)
PuN--UN, preparation of fuels of, equipment and methods for, 25:29923 (ORNL-4630, pp 59-72)
PuN--UN, properties and stability of fuels of, 25:29923 (ORNL-4630, pp 59-72)
PuN--UN, specific power limits in liquid metal cooled fast breeder reactors, 25:31569 (ORNL-TM-3388)
PuN--UN, swelling during irradiation in liquid metal cooled fast breeder reactors, 25:31569 (ORNL-TM-3388)

URANIUM OXIDE SILICIDES
magnetic susceptibility of $U_6Si_{11}O$, temperature dependence of, 25:30679

URANIUM OXIDES UO
thermodynamic properties of gaseous, free energy functions for, 25:29082

URANIUM OXIDES UO_2
analysis of pellets of, for hydrogen, 25:28912 (BARC-500)
analysis of, use of laser microprobe in spectral, 25:28949
diffusion of cesium from irradiated powdered, at 820 to 980°C, 25:29974
grain growth in center of heated pellets of, mechanisms of columnar, 25:29976 (JAERI-Memo-4249)
preparation by precipitation from ammonium uranates, 25:29925
preparation of high-density, high-frequency melting method for, 25:29935
preparation of porous particles of, from peroxide sols, 25:29801
preparation of stabilized substoichiometric fuels of, method for, 25:29932(P)
radiation effects on creep of 24.48 percent enriched, at 1000 to 1200°C and 1500 to 4000 psi stress, pile neutron, 25:30009 (BMI-1899)
radiation effects on mechanical properties of, fast neutron, 25:31568(T) (EURFNR-823)
radioinduced creep of enriched, at 1030 to 1190°C, comparison of out-of-pile creep with in-pile, 25:30018
thermal conductivity of stoichiometric, above 1200°C, relations of heat capacity with, 25:29967
Cr--UO_2, radiation effects on mechanical properties of cermets of, fast neutron, 25:31568(T) (EURFNR-823)
Dy_2O_3--UO_2, phase studies of, 25:29975 (JAERI-1203)
Mo--UO_2, radiation effects on mechanical properties of cermets of, fast neutron, 25:31568(T) (EURFNR-823)
Mo--UO_2, separation of fission products from irradiated fuels of, 25:29413 (CONF-691225)
NdO_2--UO_2--UO_3, phase equilibria at 1250°C in, 25:29977 (KFK-1330)
PuO_2--stainless steel--UO_2, fabrication of pellets of, powder metallurgical, 25:29931
PuO_2--UO_2, composition and properties of sphere-pac fuels of, 25:29922 (ORNL-4630, pp 3-58)
PuO_2--UO_2, diffusion of plutonium in hyperstoichiometric, at 1250 to 1500°C, effects of oxygen/metal ratio on, 25:29964
PuO_2--UO_2, fabrication of sphere-pac fuels of, 25:29922 (ORNL-4630, pp 3-58)
PuO_2--UO_2, preparation of high-density, high-frequency melting method for, 25:29935
PuO_2--UO_2, radiation effects on clad sphere-pac fuel pins of, in-pile, 25:29922 (ORNL-4630, pp 3-58)
PuO_2--UO_2, radiation effects on mechanical properties of, fast neutron, 25:31568(T) (EURFNR-823)
PuO_2--UO_2, segregation in, analysis of mechanisms for, (T), 25:29821(R) (GEAP-12153)
PuO_2--UO_2, specific power limits in liquid metal cooled fast breeder reactors, 25:31569 (ORNL-TM-3388)
PuO_2--UO_2, swelling during irradiation in liquid metal cooled fast breeder reactors, limits for, 25:31569 (ORNL-TM-3388)
PuO_2--UO_2, uranium activity in solid solutions of, transpiration method for studying, 25:29821(R) (GEAP-12153)
ThO_2--UO_2, radiation effects on thermal conductivity of, relations of burnup level with in-pile, 25:29937 (BMI-X-10274)
ThO_2--UO_2, reprocessing of fuels of, dissolution and fluorination process for, 25:29192(P)

URANIUM OXIDES UO_3
oxygen--uranium bond lengths in γ, 25:29094
preparation by precipitation from ammonium uranates, 25:29925
reduction of, effects of cerium oxide and plutonium oxide additions on, 25:29947
Na_2O--UO_3--V_2O_5, phase studies of, 25:29998
NdO_2--UO_2--UO_3, phase equilibria at 1250°C in, 25:29977 (KFK-1330)

URANIUM OXIDES U_3O_8
analysis of, use of laser microprobe in spectral, 25:28949
reduction of, effects of cerium oxide and plutonium oxide additions on, 25:29947

URANIUM PEROXIDES
conversion of sol to porous dioxide particle kernels, 25:29801

URANIUM RESERVES
estimates of worldwide, 25:29811
estimation of Canadian, 25:29236

URANIUM SILICIDES
magnetic susceptibility of U_3Si, U_3Si_2, USi, USi_5, $USi_{1.88}$, and USi_3, temperature dependence of, 25:30679

URANIUM SULFIDES
reactions with zirconium at 850 to 1100°C, use of differential expansion capsules for studying solid-state, 25:29965
CoS--US_2, crystal structure of single crystals of, 25:29996
FeS--US_2, crystal structure of single crystals of, 25:29996
NiS--US_2, crystal structure of single crystals of, 25:29996

XUM

URANIUM TITANATES
properties of, x-ray microanalysis of chemical and physical, 25:29971
URANYL CHLORIDES
hydrolysis of, x-ray scattering studies on structures of products from, 25:29087
URANYL COMPOUNDS
complexes with triphenylphosphine oxide, phosphorus--oxygen bonding in, effects of coordination on, 25:29088
effects on fluorescence determination of copper, 25:28928
fluorescence in 6 M hydrochloric acid at liquid nitrogen temperatures, 25:28925
URANYL IONS
bond values in γ-uranium trioxide, 25:29094
UREA
yields from γ radiolysis of aqueous solutions of 5-bromo-2'-deoxyuridine in presence of oxygen, 25:29135
UREA, THIO-
radioprotective effects of, on chromosome aberrations in onions, x, 25:29559
UREASE
radiation effects on activity of, in soils, comparison of toluene and γ, 25:29460
URIDINE, 5-BROMO-2'-DEOXY-
radiolysis of aqueous solutions of, in presence of oxygen, yields from, 25:29136
radiolysis of aqueous solutions of, in presence of oxygen, yields from γ, 25:29135
URIDINE, 2'-DEOXY-
yields from γ radiolysis of aqueous solutions of 5-bromo-2'-deoxyuridine in presence of oxygen, 25:29135
URINARY TRACT
radioinduced cystitis in human, radium, and radon alpha, gamma, and x, 25:29697
URINE
analysis for cesium-137 and strontium-89, 25:29515 (NP-18794)
analysis for cesium-137 by ion exchange, solvent extraction, and β counting, 25:28983
cerium-144 excretion in beagle dog, following inhalation as chloride, effects of bronchopulmonary lavage with DTPA on, 25:29544 (LF-43, pp 286-94)
cerium-144 excretion in beagle dog, following inhalation as chloride, effects of intravenous administration of DTPA on, 25:29543 (LF-43, pp 280-5)
curium-244 excretion in beagle dog, following inhalation as chloride or oxide, 25:29429 (LF-43, pp 100-5)
excretion of cystamine in mouse and rat, effects of 5-methoxytryptamine on, 25:29554
yttrium-91 excretion in beagle dog, following inhalation, insoluble, 25:29435 (LF-43, pp 163-70)

V

VACUUM PUMPS
performance of zeolite, for field emission microscopes, 25:29406
VACUUM SYSTEMS
evacuation of ultrahigh, using passive gas for reducing migration of hydrocarbons, 25:29323
VAN ALLEN RADIATION BELTS
charged-particle distribution in, computation of geomagnetic L coordinates for studying, (T), 25:30401
properties of, Interkosmos-3 study of, (E), 25:30364
proton belt of, radial profile of, (E), 25:30354
VAN DE GRAAFF ACCELERATORS
beam injection in tandem, isochronous cyclotron energy spread for, 25:31081
beam injection system for tandem, design and performance of cyclotron for H^-, 25:31151
description of series combination of cyclotron with tandem, 25:31139
VANADATES
effects on separation of thorium(IV) from sulfuric acid solutions by extraction using N-phenylbenzylamine in chloroform, 25:29184
VANADIUM
analysis for impurities, spectrographic, 25:28947
corrosion by oxygen-contaminated sodium, 25:29781
crystal structure of internal oxidation zones in sodium-corroded, 25:29781
determination in carbon as 3,3-dimethylnaphthidine complex, ASTM method for colorimetric, 25:28974
determination in crude or refined oils or engine deposits by neutron activation and γ spectrometry, 25:29026
determination in low-alloy steel, two-standard method for spectrometric, 25:28950
effects of beta-stabilizer, on mechanical properties of titanium alloys at -253 to +20°C, 25:29844
effects on fluorometric determination of zirconium, 25:28963
hardness and yield stress of wires of, effects of deformation temperature and nitrogen and oxygen interstitial content on, 25:29880
production and uses in US during 1970 and 1971, review on, 25:29802
radiation effects on void formation in, relations of irradiation temperature with fast neutron, 25:29914
reactions with graphite thimbles to prepare vanadium monocarbide, 25:29926
separation from aqueous solutions by thin-layer chromatography using liquid anion exchangers, 25:29186
solvent properties for nitrogen at 600 to 1500°C, 25:29879
VANADIUM ALLOYS AND SYSTEMS
Al--Mo--Ti-base--V, corrosion cracking in aqueous and methanol solutions with and without halogen ions, stress, 25:29765
Al--Sn--V, phase equilibria and superconductivity in intermetallic V_3LAl--V_3Sn, 25:30416
Al--Ti-base--V, corrosion by hydrochloric acid--methanol and sodium chloride--isopropanol, 25:29773
Au--V, superconducting-state Knight shift in intermetallic V_3Au, 25:30425
Co-base--V, thermal expansion at 100 to 800°C, 25:29899
Co-base--V, transformation temperatures of, allotropic, 25:29899
Co-V, NMR and nuclear relaxation study of satellite lines in dilute, 25:31690 (COO-1565-71)
Cr--Mo--steel--U, creep fatigue of, method for prediction of, 25:29826 (RD/B/N-1885)
Cr--Ti--V-base, compatibility with sodium at 600°C, effects of oxygen on, 25:29761 (ORNL-4630, pp 150-7)
Cr--V-base, compatibility with sodium at 600°C, effects of oxygen on, 25:29761 (ORNL-4630, pp 150-7)
Mo--V-base, compatibility with sodium at 600°C, effects of oxygen on, 25:29761 (ORNL-4630, pp 150-7)
N--U--V, crystal lattice parameters of UVN_2, 25:29989
N--U--V, phase diagram at 1400 to 2000°C, 25:29989
N--U--V, thermodynamic properties of UVN_2, 25:29989
N--V-base, phase transformation of α solid solution of, effects of cooling on, 25:29879
Ni-based--V, polarized-neutron study of $Ni_{0.944}V_{0.032}$, 25:30680
Ti--V, precipitation in β-isomorphorous, comments on metastable, 25:29886
Ti--V-base, compatibility with sodium at 600°C, effects of oxygen on, 25:29761 (ORNL-4630, pp 150-7)
Ti--V-base, corrosion by oxygen-contaminated sodium, 25:29781
Ti--V-base, crystal structure of internal oxidation zones in sodium-corroded, 25:29781
V--Zr-base, polishing for metallographic examination, electrolytic, 25:29817
V-base--Zr, compatibility with sodium at 600°C, effects of oxygen on, 25:29761 (ORNL-4630, pp 150-7)
VANADIUM CARBIDES
electronic properties of nonstoichiometric VC, 25:30667
preparation of VC, by reactions of liquid vanadium with graphite thimbles, 25:29926
x-ray emission spectra of VC/sub x/, 25:30267
TiC--VC, slip mechanisms in, 25:29599
VANADIUM HYDRIDES
analysis for hydrogen by carrier gas fusion--gas chromatographic methods, 25:28936
VANADIUM ISOTOPES V-51
photon reactions (γ,xn) up to 30 MeV, total cross section for, (E), 25:31243
proton reactions (p,γ) at 0.8 to 3.0 MeV, excitation functions for, (E), 25:31256
VANADIUM OXIDES
corrosive effects of melts of V_2O_5, on nickel alloys, relations with chromium, copper, iron, molybdenum, and tungsten additions, 25:29768
electron structure and chemical bonds in V_2O_5, 25:30668
properties and structure of, matrix isolation method for studying, 25:29083
thermodynamic properties of gaseous diatomic, free energy functions for, 25:29082
Na_2O--UO_3--V_2O_5, phase studies of, 25:29998
VO_2--V_2O_3, oxygen activity in, at 600 to 1200°C, equilibrium, 25:29952
VO_2--V_2O_3, thermodynamic properties at 600 to 1200°C, 25:29952
VANADIUM SILICIDES
phase transition in V_3Si single crystals, neutron-scattering study of lattice-dynamical, 25:30683
VANADYL PERCHLORATES
spectra of $VO(H_2O)_5^{2+}$, obtained from aqueous solutions of, EPR, 25:31744 (UCRL-19691)
VANDELLOS POWER REACTOR
pressure vessel for, design parameters of prestressed concrete, 25:31484 (EUR-4531, pp 81-94)
VANSTAR-7
compatibility with sodium at 600°C, effects of oxygen on, 25:29761 (ORNL-4630, pp 150-7)
VANSTAR-8
compatibility with sodium at 600°C, effects of oxygen on, 25:29761 (ORNL-4630, pp 150-7)
VANSTAR-9
compatibility with sodium at 600°C, effects of oxygen on, 25:29761 (ORNL-4630, pp 150-7)
VENTILATION
equipment and methods for nuclear power plant, 25:29259
VERMONT YANKEE POWER REACTOR
containment system for, safety analysis of primary, 25:31501 (DOCKET-50271-51)
core for, vibration testing of, 25:31501 (DOCKET-50271-51)
fuel elements for, safety analysis of plutonium

XUM

oxide(PuO_2)--uranium oxide(UO_2), 25:31500 (DOCKET-50271-50)
operation of, safety analysis of single recirculation loop with closed equalizer line, 25:31501 (DOCKET-50271-51)
operation of, safety analysis of transients during, 25:31501 (DOCKET-50271-51)
piping systems for, energy absorbing equipment for, 25:31501 (DOCKET-50271-51)
security procedures for, 25:31501 (DOCKET-50271-51)
VIBRATIONS
analysis in water cooled reactors, finite element techniques for, 25:31591 (CONF-710302-7)
characteristics in liquid cooled parallel rods, effects of end restraint and spacer configurations on, 25:31570 (RT/ING-(70)24)
effects on maze habit in rats, combined effects of x radiation and, 25:29666
VINYL ALCOHOL POLYMERS
radioinduced polymerization of monomer pairs on, γ, 25:29106
VINYL COMPOUNDS
radiation curing of binders of, electron, 25:29120(P)
VIRGINIA
thorium deposits in Berea area of, correlation of aeroradioactivity and geological data on, 25:29235
uranium deposits in Berea area of, correlation of aeroradioactivity and geological data on, 25:29235
VIRUSES
hepatitis, effects on γ radiosensitivity of human lymphocytes, in vitro, 25:29710
influenza, radiation effects on infectivity of, in mice following inhalation of insoluble cerium-144, 25:29724 (LF-43, pp 254-62)
radiation effects on x-, in potato tubers, γ, 25:29726
VITAMIN B GROUP
riboflavin, effects on energy metabolism in liver mitochondria of irradiated rats, 25:29640
VOLTAGE REGULATORS
design of thyristor, for 40-kV modulator for proton linac, 25:31067

W

WASHINGTON
nuclear power plant siting in, recommendations for, 25:31525 (NP-18770)
WATER
abundance in Jovian atmosphere, (T), 25:30250
analysis for alpha emitters by radiometry, ASTM method for, 25:29003
analysis for α-emitting radium isotopes by precipitation and α counting, ASTM method for, 25:28999
analysis for beta emitters by proportional counting, ASTM method for, 25:29009
analysis for cobalt, copper, iron, manganese, nickel, and uranium by solvent extraction and x-ray fluorescence spectroscopy, 25:28919
analysis for copper by fluorescence method, 25:28928
analysis for gold by neutron activation, 25:29015
analysis for gold by neutron activation and γ spectrometry after preconcentration, 25:29014
analysis for γ emitters by scintillation counting, ASTM method for, 25:29008
analysis for heavy water, interferometric, 25:28929
analysis for iron-59, ASTM method for radiometric, 25:29010
analysis for isotopic purity by ir spectral studies, sample input system for apparatus for, 25:28942(P)
analysis for manganese-54 and manganese-56 by precipitation and radiometry, ASTM method for, 25:29006
analysis for radioactive barium by precipitation and radiometry, ASTM method for, 25:29004
analysis for radioactive cesium isotopes after extraction as tetraphenylborates, radiometric, 25:29000
analysis for radioactive iodine by chemical separation and radiometry, ASTM method for, 25:29007
analysis for thorium spectrophotometrically using o-[2-hydroxy-3,6-disulfo-1-naphthyl)azo]benzenearsonic acid, ASTM method for, 25:28977
analysis of high-purity, for reactor cooling and moderating, 25:28914 (BARC-515)
determination in heavy water, interferometric, 25:28929
effects on radiothermoluminescence of crystalline and glassy methanol, 25:29101
neutron dose rate removal cross sections and buildup factors for, (E/T), 25:30637
neutron thermalization at 318 and 77°K, (E), 25:31170(T) (KAPL-Trans-4)
radiation monitoring of off-site, following nuclear explosions at Nevada Test Site during 1969, 25:29506 (SWRHL-97-r)
radiolysis of, yields from γ, 25:29154
reactions with graphite, effects of temperature on chemical and physical, 25:29918 (CEA-R-4123)
stopping power of, as function of proton energy, 25:29511 (AERE-M-1887)
WATER-d_2
analysis for water, interferometric, 25:28929
determination in water, interferometric, 25:28929
effects on luminescences of aqueous solutions of europium ions, 25:29053
effects on thermal stability of barium chloride dihydrate and copper sulfate pentahydrate, 25:29042
properties of, review on, 25:29154
radiolysis of, yields from γ, 25:29154
WATER VAPOR
radio emission from, in W49, at 22 GHz, (E), 25:30141
tritium distribution in lower troposphere, airborne measurements of vertical, 25:29215
WEISWEILER POWER REACTOR
development of, status of, 25:31536
WELDING
filler materials for use in nuclear technology, properties of alloyed, 25:29792
WELL LOGGING
method for beta and gamma, for determining uranium content and distribution in ore bodies, 25:29230
WEST VALLEY PROCESSING PLANT
environmental monitoring at, 1971, 25:29180 (DOCKET-50201-70)
radioactivity monitoring in environment of, July-Dec., 1970, 25:29179 (DOCKET-50201-69)
WHISTLERS
excitation in plasma, turbulent electron heating by large-amplitude, (T), 25:30470
production in turbulent plasma by nonlinear interaction of helicon and ion acoustic waves, 25:30607
WHOLE-BODY COUNTERS
performance of 54-channel, in conjunction with bromine-82 tracer for study of halothane pharmacokinetics in man, 25:29416
WILLIAM H. ZIMMER POWER REACTOR, UNIT 1
design parameters of, revised and additional data on, 25:31520 (DOCKET-50358-14)
operations aspects of, revised and additional data on, 25:31520 (DOCKET-50358-14)
WIND
effects of near-surface, on natural radioactivity in atmosphere to 15 m height, (E), 25:29223
effects on vertical distribution of radon-220 and radon-222 in atmosphere, (E/T), 25:29225
WOOD
performance of masonite, as artificial substrate for analysis of periphyton in running-water ecosystem, 25:29478
radiation effects on bisulfite and Kraft pulping of Eucalyptus, by sterilization, γ, 25:29735
radioinduced curing of coatings on, electron, 25:29123
WYLFA REACTORS
pressure vessels for, design and construction of prestressed concrete, 25:31456 (EUR-4531, pp 129-44)

X

X RADIATION
absorption of cosmic, in interstellar space, (T), 25:30118
cosmic background, line feature at 6 to 7 keV in, (E), 25:30140
cosmic background, observations in galactic plane, (E), 25:30134
cosmic background, origin of, (T), 25:30221
dose distribution in beagle dogs from radiographic exposure, 25:29514 (LF-43, pp 116-22)
dose to color television repair personnel, 25:29512 (BRH/DEP-71-4)
effectiveness for therapy of laryngeal carcinomas, 25:29598
effectiveness for therapy of verruca juvenilis, effects of dose on, 25:29601
effects of nuclear weapon-produced, on materials, analytical method for describing, 25:29247
effects of pulsed, on electric conductivity of liquid ethane, methane, and propane, 25:29102
effects of ultrasoft, on sodium-doped potassium chloride crystals, 25:30654
effects on activity of methionine adenosyltransferase in liver of rats, effects of ethionine on lethal, 25:29663
effects on adsorption capacity of T2r bacteriophages, combined effects of cysteine and, 25:29728
effects on alkaline phosphatase activity in small intestine of rats, effects of dose on whole-body, 25:29645
effects on antigen-initiated RNA synthesis in mouse spleen, polyacrylamide gel electrophoresis studies on, 25:29476
effects on axilla and shoulder in man following post mastectomy therapy, surgical treatment of, 25:29569
effects on base structure and denaturation of DNA from Bacillus subtilis, 25:29466
effects on bioelectric activity of muscle and nerve tissues, radioprotective effects of AET and cystamine against, 25:29609
effects on blood and hematopoietic system in man, pathological, 25:29699
effects on blood vessels in human eyes, pathological, 25:29700

XUM

effects on blood vessels in mouse testes, 25:29653
effects on cells of animals and man, review of damaging, 25:29690
effects on chromosomes and pollen and seed fertility of M(1) generation of rice, 25:29496
effects on chromosomes in onion root tips, protective effects of thiourea against aberrant, 25:29559
effects on chromosomes in pea seedlings, effects of dose rate on aberrant, 25:29489
effects on content of immunoglobulins in intestinal lumen and serum of mice, 25:29473
effects on content of sulfhydryl groups in tissues of ducklings, 25:29647
effects on cross links in DNA from Bacillus subtilis, 25:29465
effects on deletion of granule neurons in neonatal cats in relation to subsequent development of presynaptic elements, 25:29623
effects on development and infectivity of Plasmodium berghei sporozoites, 25:29727
effects on development of cutaneous lesions in man following excessive fluoroscopy, 25:29706
effects on DNA from Bacillus subtilis, 25:29463
effects on DNA in hematopoietic system in rabbits, 25:29637
effects on double and single strand breaks in DNA of Bacillus subtilis, viscometric studies on, 25:29464
effects on electric conductivity of 2,2-dimethylbutane and hexane, 25:29097
effects on electroretinographic patterns in dogs exposed in utero during embryogenesis, 25:29667
effects on endocrine glands of rabbits and rats, pathological, 25:29633
effects on esterase activity and protein content in plasma erythrocytes in rats, whole-body, 25:29686
effects on eyes of mice, protective effects of dimethyl sulfoxide against, 25:29562
effects on frequency of sex-linked, lethal, and visible mutations in Drosophila sperm, 25:29499
effects on frozen sulfuric acid solutions of thymine, ESR studies on, 25:29134
effects on gastrointestinal tract of animals, damaging, 25:29632
effects on germination of wheat seeds, effects of thermal shock on, 25:29723
effects on growth of mammalian cells, damaging, 25:29626
effects on heart of animals and man, pathological, 25:29695
effects on hematopoietic system of mice, pathological, 25:29634
effects on histochemistry of cortical and medullar tissues in adrenal gland of rats, partial-body, 25:29671
effects on human nervous system, pathological, 25:29692
effects on immune responses in mice, comparison of mechanism of cyclophosphamide and, 25:29475
effects on immune responses to sheep erythrocytes in mice, 25:29472
effects on incidence of mongoloid children following maternal diagnostic exposure, 25:29500
effects on isolated intestines in guinea pigs, protective effects of tryptamine against, 25:29566
effects on kidneys of man, pathological, 25:29696
effects on learning and memorizing behavior in quails, effects of dose on, 25:29687
effects on lifetime and reproductive capacity of codling moth pupae, effects of dose rates on, 25:29612
effects on lipid fractions and liver and serum enzymes in rats, local, 25:29685
effects on liver of animals and man, pathological, 25:29694
effects on lymphatic system and thymus of rabbits and rats, pathological, 25:29635
effects on mammalian cells, effects of age on damaging, 25:29625
effects on mammalian cells, lethal, 25:29624
effects on man following radiotherapy, leukemogenic, 25:29696
effects on man, protective effects of oxygen butazone against therapeutic doses of, 25:29549
effects on maze habit in rats, combined effects of vibrations and, 25:29666
effects on melanoma cells in mice, protective effects of melanin against, 25:29568
effects on mice, protective effects of chlortetracyline against, 25:29561
effects on mice, protective effects of sulfur analogs of serotonin and tryptophol against, 25:29567
effects on migration rate of amelogenic cells in rat incisor, 25:29678
effects on mitosis in L-cells, fractionated, 25:29611
effects on mucous, salivary, and serous glands in animals and man, damaging, 25:29693
effects on nuclear diameter of Ehrlich ascites tumor cells in mice, combined in vitro effects of 6-azauridine and, 25:29679
effects on oscillatory behavior of enzymatic reactions, 25:29461
effects on pea seeds, cytology of male sterile recessive mutagenic, 25:29492
effects on poly(9-vinylcarbazole), films, geminate recombination of charge carriers produced by, 25:29140
effects on protein fractions of mitochondria and tissue homogenates in brain and small intestine in rabbits, whole-body, 25:29664
effects on reproductive capacity of female arthropods, 25:29747
effects on reproductive capacity of reduviid bug vectors of Chagas' disease in comparison to effects of chemosterilants, 25:29745
effects on rice seeds, M(2) characteristics following combined mutagenic effects of diethyl sulfate and, 25:29495
effects on sarcosine deuteriochloride and hydrochloride monocrystals, ESR spectral studies on free radicals produced by, 25:29152
effects on sartorius muscles in frogs in relation to calcium metabolism, 25:29674
effects on skin of rats, carcinogenic, 25:29628
effects on spermatogonia in mice, effects of dose on mutagenic, 25:29487
effects on striated muscles of rats, pathological, 25:29629
effects on structure of neurons of upper cervical sympathetic ganglion of rabbits, whole-body, 25:29675
effects on structures of developing embryos of reduviid bugs, effects of dose on, 25:29620
effects on successive generations of Drosophila melanogaster larvae, effects of dose on, 25:29613
effects on sugar radicals in deoxyadenosine single crystals, 25:29146
effects on survival of dogs, effects of pancreatic duct ligation on lethal, 25:29651
effects on survival of dogs, protective effects of elbow joint shielding against, 25:29658
effects on teeth of animals, damaging, 25:29631
effects on template activity of DNA from Bacillus subtilis, RNA synthesis following, 25:29467
effects on tomato seeds, M(2) characteristics following combined mutagenic effects of colchicine or diethyl sulfate and, 25:29493
effects on transformation of his_2 and try_2 markers in Bacillus subtilis, effects of DNA on, 25:29468
effects on transforming DNA, mechanisms for phenotypic expression following, 25:29469
effects on urinary tract of man, pathological, 25:29697
emission from Crab Nebula, (T), 25:30122
emission from hot plasma in Cygnus Loop, (E), 25:30132
emission of hard, during solar flares, (E/T), 25:30169
emission of soft, from Sun, (E), 25:30160
emission of soft, in conjunction with Type-III radio bursts, (E), 25:30167
hazards to patients and personnel during radiography in general hospital, program for protection against, 25:29538
monitoring of solar, Solrad-8 and -9 real-time telemetry from 1966 to 1969, (E), 25:30355
origin of cosmic diffuse, isotropic, (E/T), 25:30332
translocations induced in chromosomes of house flies by, 25:29751
transport in atmosphere, analytical method for describing, 25:29247

X-RAY-DIFFRACTION ANALYSIS
book: Measuring Methods Using Ionizing Radiation, 25:29391

X-RAY EMISSION ANALYSIS
method using radioisotopes, effects of multiply scattered γ radiation on, 25:28939
statistics for handling quantitative data from, 25:28957

X-RAY EQUIPMENT
plasma drift in flash x-ray tubes, 25:30499 (UUIP-659)
safety of medical, in North Dakota, survey of, 25:29542

X-RAY FLUORESCENCE ANALYSIS
method for, using radioisotopes, review on, 25:28935
radioisotope uses in, 25:28922
sensitivity for elements A = 15 through 92, 25:28962

X-RAY SOURCES
development of intense pulsed, for simulating nuclear explosions for studying transient radiation effects on electronics, 25:29410

X-RAY SPECTROMETERS
design and performance of lithium-drifted silicon, 25:29325 (JINR-P13-5707)
development of calcium iodide scintillation low-level, 25:29350

XENON
diffusion in neutron-irradiated uranium-doped calcium fluoride single crystals, 25:30673
neon-metastable-atom reactions with, two-state impact-parameter model for associative and Penning ionization in, 25:30298
plasma of, interferometric measurements of electron density in discharge, 25:30484
separation from off-gas streams, evaluation of thin silicone rubber membranes for, 25:29317 (ORNL-4522)
separation of trace amounts of, from argon, design of gas chromatograph for, 25:29177 (CEA-R-4090)

XENON ISOTOPES
abundance in Pesyanoe meteorite, (E), 25:30158(R) (UCSD-34-P-43-X-9)
trapping in meteorites, 25:30158(R) (UCSD-34-P-43-X-9)

XENON ISOTOPES Xe-126
energy levels of, calculation including Mottelson--

XUM

Valatin effect, (T), 25:31345
XENON ISOTOPES Xe-128
energy levels of, calculation including Mottelson--Valatin effect, (T), 25:31345
XENON ISOTOPES Xe-130
energy levels of, calculation including Mottelson--Valatin effect, (T), 25:31345
XENON ISOTOPES Xe-132
energy levels of, calculation including Mottelson--Valatin effect, (T), 25:31345
o-XYLENE
radioinduced isomerization over halogenated alumina--silica catalyst, γ, 25:29111

Y

YANKEE POWER REACTOR
operations history for March 1971, 25:31465 (DOCKET-50029-150)
YTTERBIUM
electric conductivity of, effects of pressure and temperature on, (E/T), 25:30661 (AERE-R-5953)
electric conductivity of, effects of pressure and temperature on, 25:30674
YTTERBIUM ALLOYS AND SYSTEMS
Ba--Yb-base, electric conductivity of, effects of pressure and temperature on, 25:30674
YTTERBIUM ISOTOPES Yb-172
energy levels and transistion from lutetium-172 decay, properties of collective, 25:31347
energy levels near 1172 keV, g-factors for, (E), 25:31367
YTTERBIUM OXIDES
positron lifetimes in, 25:30272
YTTRIUM
determination in lanthanum by emission spectrography, 25:28965
effects on fluorometric determination of zirconium, 25:28963
properties of aerosols produced from aqueous solutions of, 25:29079 (LF-43, pp 31-9)
separation from aqueous solutions by thin-layer chromatography using liquid anion exchangers, 25:29186
separation from other rare earths by ion exchange, 25:29178 (CEA-R-4102)
YTTRIUM ALLOYS AND SYSTEMS
O--U--Y, crystal lattice parameters of solid solutions of, 25:29922 (ORNL-4630, pp 3-58)
YTTRIUM CHLORIDES
thermodynamic properties at 298 to 1300°K, 25:29951
YTTRIUM ISOTOPES
separation of fission-product, from irradiated fuels of Mo--UO_2, 25:29413 (CONF-691225)
YTTRIUM ISOTOPES Y-86
beta and electron-capture decay of, γ spectra from, (E), 25:31247
YTTRIUM ISOTOPES Y-88
distribution and retention in plasma proteins in rats, effects of dilution on, 25:29454
YTTRIUM ISOTOPES Y-89
energy levels from strontium-88 proton resonances, widths for isobaric analog, (T), 25:31276
photon reactions (γ,n) at 10 to 68 MeV, yields of radioactivities from, (E), 25:31333
YTTRIUM ISOTOPES Y-90
beta decay of, shell-model analysis of first-forbidden unique, (T), 25:31284
distribution and retention in beagle dogs following inhalation, toxicity studies on insoluble, 25:29438 (LF-43, pp 197-204)
effects on beagle dogs following inhalation of insoluble, 25:29434 (LF-43, pp 146-62)
YTTRIUM ISOTOPES Y-91
distribution and retention in beagle dogs following inhalation of fused clay particles, 25:29435 (LF-43, pp 163-70)
distribution and retention in beagle dogs following inhalation, toxicity studies on insoluble, 25:29438 (LF-43, pp 197-204)
effects on beagle dogs following inhalation as chloride, toxic, 25:29432 (LF-43, pp 137-9)
effects on beagle dogs following inhalation of fused clay particles, clinical and pathological, 25:29435 (LF-43, pp 163-70)
metabolism in beagle dogs following inhalation as chloride, 25:29432 (LF-43, pp 137-9)
YTTRIUM ISOTOPES Y-93
energy levels from strontium-93 decay, (E), 25:31338
isomeric transition in, (E), 25:31338
YTTRIUM OXIDES
analysis for rare earth impurities by x-ray luminescence methods, 25:28961
radiation effects on dielectric properties of insulators of, fast neutron, 25:30011 (ORNL-4630, pp 226-9)
thermodynamic properties of gaseous diatomic, free energy functions for, 25:29082
ThO_2-base--Y_2O_3, electric conductivity of solid solutions, effects of high oxygen pressures on ac, 25:30685
Y_2O_3--Zr-base, tensile properties at 650°C, 25:29969
Y_2O_3--ZrO_2, crystal transformation in, differential thermal analysis studies of monoclinic-tetragonal, 25:29982
YUGOSLAVIA
nuclear chemistry and physics research and development programs in, review of 1969, 25:31633 (IJS-253)

Z

ZINC
determination by x-ray fluorescence, sensitivity of, 25:28962
determination in crude or refined oils or engine deposits by neutron activation and γ spectrometry, 25:29026
determination in deposits and airborne particles by neutron activation and scintillation counting, 25:29032
determination in pharmaceuticals by neutron activation and γ spectroscopy, 25:29029
determination of trace amounts of, in platinum by neutron activation following separation by ion exchange chromatography, 25:29023
determination of trace amounts of, in vanadium, spectrographic, 25:28947
determination using ion permselective membrane, potentiometric, 25:28956
effects on corrosion of beryllium--copper--tin alloys by nitric acid, 25:29830
morphology of dendrite and fiber textures in ingots of, 25:29892
proton reactions at 11.5 and 23.5 MeV using thick targets, neutron yield from, (E), 25:31209
separation from aqueous solutions by thin-layer chromatography using liquid anion exchangers, 25:29186
ZINC ALLOYS AND SYSTEMS
$CaCl_2$--CaF_2--Zn, solvent properties for stainless steel cladding of reactor fuels, 25:29199(P)
Cd--Zn-base, morphology of dendrite and fiber textures in ingots of, 25:29892
Gd--Zn--Zr, electron paramagnetic resonance of coupled-spin Gd/sub x/Zr/sub 1-x/Zn_2, variations in, (E/T), 25:30694
ZINC ISOTOPES
radioactivity standards of, users' guides for, 25:29174
ZINC ISOTOPES Zn-60
energy level at 7.39 MeV from nickel-58 (He-3,n) reactions, T = 2 analog, (E), 25:31237 (IAE-1958)
ZINC ISOTOPES Zn-64
neutron activation resonance integrals for, measured relative to gold-197, (E), 25:31300 (CNEA-282)
proton inelastic scattering up to 4 MeV, gamma angular distributions for, (E), 25:31253
proton reactions (p,γ) at 2 MeV, gamma spectra from, (E), 25:31249
ZINC ISOTOPES Zn-65
content in seawater near Goto Islands, Japan, measurements during July 1966, 25:29241
uptake by albumins and globulins in human blod serum, 25:29447
uptake by tsetse flies following ingestion of labeled blood of rabbits, 25:29417
use as tracer for determining distribution of onion flies, 25:29748
ZINC ISOTOPES Zn-66
energy levels from gallium-66 decay, spin--parity assignments for, (E), 25:31287
proton reactions (p,γ) at 2 MeV, gamma spectra from, (E), 25:31249
ZINC ISOTOPES Zn-67
alpha reactions (α,pγ) at 14 MeV, γ spectra from, (E), 25:31290
proton reactions (p,n) with, cross sections for, (E), 25:31268
ZINC ISOTOPES Zn-68
neutron activation resonance integrals for, measured relative to gold-197, (E), 25:31300 (CNEA-282)
proton reactions (p,γ) at 2 MeV, gamma spectra from, (E), 25:31249
proton reactions (p,n) with, cross sections for, (E), 25:31268
ZINC ISOTOPES Zn-70
proton reactions (p,nγ) at 1.4 to 4 MeV, γ spectra from, (E), 25:31290
ZINC OXIDES
optical spontaneous polarization of, 25:30666
production of, radioactive tracer methods for improving processes for, 25:29283
radiation effects on properties of paints of, proton and uv, 25:29105
thermodynamic properties of gaseous diatomic, free energy functions for, 25:29082
ZINC TELLURIDES
oxygen-ion implants in, photoluminescence study of, 25:30657
ZINC TITANATES
radiation effects on properties of paints of, proton and uv, 25:29105
ZIRCALOY
production of reactor cladding tubes of, equipment and methods for, 25:29795

ZIRCALOY-2
corrosion by superheated steam at 350 to 550°C, effects of mechanical stress on, 25:29771
tensile properties at 650°C, 25:29969
ZIRCONIUM
anodization of, oxide growth rate in solid-state, 25:29803
book: Organic Reagents in Analytical Chemistry of Zirconium, in Russian, 25:28969
corrosion resistance to acid and alkali environments, evaluation of, 25:29775
deposition on atomically clean tungsten crystal surfaces, electron diffraction studies of mechanisms of, 25:29847
deposition on substrates from alkaline fluoride mixtures containing salts of, methods for electro-, 25:29783 (CEA-N-1376)
determination in high-purity water for reactor cooling and moderating, 25:28914 (BARC-515)
determination in thin films of zirconium nitrides by electron-probe x-ray micro method, 25:28966
determination in zirconium alloys using zirconium, spectrophotometric, 25:28932
determination of submicrogram quantities of, fluorometric, 25:28963
determination of trace amounts of, in seawater, review on methods for, 25:28921
diffusion of nitrogen in, at 800 to 1100°C, 25:29870
elastic properties of monocrystalline, effects of lattice parameters and volume change on pressure derivatives of, 25:29852
grain refinement of, effects of nickel and titanium on, 25:29835
hardening of deformed α-, effects of aging duration, oxygen content, and temperature on age, 25:29853
nitridation at 800 to 1100°C, 25:29870
polishing for metallographic examination, electrolytic, 25:29817
production and uses during 1971, review on, 25:29808
production of hafnium-free, review of methods for, 25:29782 (AAEC/TM-570)
properties for use as carbide-former in neutron damage-resistant stainless steel, 25:29799(P)
properties of aerosols produced from aqueous solutions of, 25:29079 (LF-43, pp 31-9)
properties of, effects of nickel and titanium on electric and mechanical, 25:29835
reactions with air at low pressure and 810°C, study of nucleation and crystal growth of zirconium oxide from, 25:29997
reactions with graphite thimbles to prepare zirconium monocarbide, 25:29926
reactions with uranium monosulfide at 850 to 1100°C, use of differential expansion capsules for studying solid-state, 25:29965
separation from aqueous solutions by thin-layer chromatography using liquid anion exchangers, 25:29186
separation from other metals by ion-exchange paper chromatography, 25:29190
separation from plutonium by anion exchange from mixed methanol--nitric acid solutions, 25:29191
separation from rare earths, thorium, and uranium by thin-layer chromatography, 25:29187
separation from zirconium by ion exchange in formic acid media, 25:28955
solubility of aerosol particles of zirconium-95-labeled, 25:29080 (LF-43, pp 40-51)
tensile properties at 650°C, 25:29969
ZIRCONIUM ALLOYS AND SYSTEMS
analysis for zirconium, spectrophotometric, 25:28932
analysis of, use of laser microprobe in spectral, 25:28949
production and uses of, newsletter on, 25:29796
properties of, newsletter on, 25:29796
radiation effects on fuel cladding of, neutron, 25:29916
B--Co--Zr, crystal structure of $ZrCo_3B_2$, 25:29992
Be--Ti--Zr, melting temperature of brazements of, 25:29824 (ORNL-4630, pp 191-206)
$Ce_2Zr_2O_7$--Zr-base, microstructure of arc-melted and heat treated, 25:29969
$Ce_2Zr_2O_7$--Zr-base, tensile properties at 650°C, 25:29969
Co-base--Zr, thermal expansion at 100 to 800°C, 25:29899
Co-base--Zr, transformation temperatures of, allotropic, 25:29899
Cu--Mo--Zr-base, corrosion by carbon dioxide at 500 to 650°C, 25:29770
Cu--W--Zr-base, corrosion by carbon dioxide at 500 to 650°C, 25:29770
Cu--Zr-base, corrosion by carbon dioxide at 500 to 650°C, 25:29770
Fe--H--Hf-base--N--O--Zr, ductility and tensile properties of dilute, effects of composition on, 25:29827(R) (RPI-3719-9)
Gd--Zn--Zr, electron paramagnetic resonance of coupled-spin Gd/sub x/Zr/sub 1-x/Zn_2, variations in, (E/T), 25:30694
Ge--Ti--Zr, melting temperature of brazements of, 25:29824 (ORNL-4630, pp 191-206)
H--Hf-base--O--Zr, ductility and tensile properties of dilute, effects of composition on, 25:29827(R) (RPI-3719-9)
La_2O_3--Zr-base, tensile properties at 650°C, 25:29969
Mo--W--Zr, mechanical properties at 2100°C, 25:29864
Mo--Zr-base, corrosion by carbon dioxide at 500 to 650°C, 25:29770
Nb--Zr, oxidation by air at 700 to 1000°C, oxide film composition and kinetics of, 25:29769
Nb--Zr, oxidation by carbon dioxide at 700 to 1070°C, kinetics and mechanism of, 25:29767
Nb--Zr-base, resistance behavior of superconducting near H/sub c2/, (E/T), 25:30412 (JINR-P8-5733)
Nb-base--Ti--Zr, microstructure of precipitates in, effects of aging at 620 to 850°C, 25:29890
Nb-base--Zr, superconducting properties of, 25:30414(T) (ORNL-tr-2475)
Ni--Zr-base, polishing for metallographic examination, electrolytic, 25:29817
O--Zr, crystal structure of solid solutions of alpha, 25:30000
O--Zr, crystallization of solid solutions of, effects of oxygen content on temperature of, 25:29854
S--Zr, crystal lattice parameters of compounds of, 25:29990
S--Zr, phase studies at high temperatures, 25:29990
Ta--Zr, hardness of, effects of aging on, 25:29824 (ORNL-4630, pp 191-206)
Th--Zr-base, microstructure of swaged, 25:29969
Th--Zr-base, tensile properties at 650°C, 25:29969
Th--Zr-base--ZrO_2, tensile properties at 650°C, 25:29969
ThO_2--Zr-base, microstructure of arc-melted and swaged, 25:29969
ThO_2--Zr-base, tensile properties at 650°C, 25:29969
Ti--Zr-base, polishing for metallographic examination, electrolytic, 25:29817
V--Zr-base, polishing for metallographic examination, electrolytic, 25:29817
V-base--Zr, compatibility with sodium at 600°C, effects of oxygen on, 25:29761 (ORNL-4630, pp 150-7)
W--Zr-base, corrosion by carbon dioxide at 500 to 650°C, 25:29770
Y_2O_3--Zr-base, tensile properties at 650°C, 25:29969
Zr-base--ZrO_2, tensile properties at 650°C, 25:29969
ZIRCONIUM BORIDES
sintering of powdered mixture of tungsten and, mechanism of, 25:29930
thermal conductivity of ZrB_2 at 200 to 1300°C, 25:29956
uses of, newsletter on, 25:29796
ZIRCONIUM CARBIDES
preparation of monocrystalline monocarbide, recrystallization method for, 25:29927
preparation of ZrC, by reactions of liquid zirconium with graphite thimbles, 25:29926
uses of, newsletter on, 25:29796
x-ray emission spectra of ZrC, 25:30267
graphite--ZrC, properties of composites of, mechanical and physical, 25:29920(R) (LA-4631)
ZIRCONIUM FLUORIDES
analysis for free fluoride using lanthanum fluoride electrode, 25:28923
ZIRCONIUM HYDRIDES
analysis for hydrogen by carrier gas fusion--gas chromatographic methods, 25:28936
ZIRCONIUM ISOTOPES Zr-90
energy levels of, four-particle, (T), 25:31322
energy-level transitions from meson (μ^-) reactions with niobium-93, (E), 25:31258
meson (π^-) capture by, analysis using particle-hole model, (T), 25:31217
proton reactions (p,γ) at 3.0 to 7.2 MeV, gamma spectra from, (E), 25:31351
ZIRCONIUM ISOTOPES Zr-91
energy-level transitions from meson (μ^-) reactions with niobium-93, (E), 25:31258
proton reactions (p,n) at 3.5 to 4.4 MeV, angular distributions for, (E), 25:31381
ZIRCONIUM ISOTOPES Zr-92
energy levels of, lifetimes of low-lying, (E), 25:31349
energy-level transitions from meson (μ^-) reactions with niobium-93, (E), 25:31258
ZIRCONIUM ISOTOPES Zr-93
energy-level transitions from meson (μ^-) reactions with niobium-93, (E), 25:31258
ZIRCONIUM ISOTOPES Zr-94
energy levels of, lifetimes of low-lying, (E), 25:31349
ZIRCONIUM ISOTOPES Zr-95
content of fish and water from lakes of northern Italy, fallout, 25:29477
distribution and retention in mice following inhalation of heat treated aerosols of, 25:29423 (LF-43, pp 59-65)
ZIRCONIUM NITRIDES
analysis of thin films of, by electron-probe x-ray micro method, 25:28966
diffusion of nitrogen in, at 800 to 1100°C, 25:29870
uses of, newsletter on, 25:29796
ZIRCONIUM OXIDES
analysis of, properties of vitreous carbon as mortar for spectrochemical, 25:28938
crystal transformation in, differential thermal analysis studies of monoclinic-tetragonal, 25:29982
crystallization from reactions of zirconium with air at low pressure and 810°C, 25:29997
electric conduction in yttria-stabilized, effects of

XUM

blackening on, 25:30684
electronic transport in calcia-stabilized, N- and P-type, 25:30682
properties and structure of, matrix isolation method for studying, 25:29083
thermal conductivity of calcium oxide and yttrium oxide-doped, at high temperatures, absolute method for measuring, 25:29958
thermodynamic properties of gaseous diatomic, free energy functions for, 25:29082
uses of, newsletter on, 25:29796
Al_2O_3--CaO--CeO_2--SiO_2--ZrO_2, analysis of, x-ray-emission, 25:28957
CaO--SiO_2--ZrO_2, phase studies of, 25:30008
FeO--MnO--SiO_2--ZrO_2, phase studies of, 25:30008
FeO--MnO--ZrO_2, phase studies of, 25:30008
FeO--ZrO_2, phase studies of, 25:30008
La_2O_3--TiO_2--ZrO_2, dielectric properties of, 25:29984
La_2O_3--TiO_2--ZrO_2, phase diagram of, 25:29984
MgO--SiO_2--ZrO_2, phase studies of, 25:30008
Mn_3O_4--SiO_2--ZrO_2, phase studies of, 25:30008
MnO--SiO_2--ZrO_2, phase studies of, 25:30008
MnO--ZrO_2, phase studies of, 25:30008
Ni--ZrO_2, deformation of dispersion-strengthened, low-temperature, 25:29941 (INIS-mf-8)
Sc_2O_3--ZrO_2, crystal transformation in, differential thermal analysis studies of monoclinic-tetragonal, 25:29982
Th--Zr-base--ZrO_2, tensile properties at 650°C, 25:29969
Y_2O_3--ZrO_2, crystal transformation in, differential thermal analysis studies of monoclinic-tetragonal, 25:29982
Zr-base--ZrO_2, tensile properties at 650°C, 25:29969

ZIRCONIUM SILICIDES
uses of, newsletter on, 25:29796

ZODIACAL LIGHT
bibliography on gegenschein, (T), 25:30390

REPORT NUMBER INDEX

Reports, conference papers and proceedings, numbered translations, and patents are included in this index. Each item is listed by report number; this is followed by the abstract number and a brief notation regarding public availability. The index entries show which reports are on file in the institutions listed on the back of the front cover (Dep.), which reports have been published in open-literature journals (journal citation), and which reports can be purchased (source and price). Whenever a report is identified by more than one number, the availability is given under the primary number, and a cross reference is given under the secondary report number.

The report number codes apply to USAEC reports unless designated otherwise. Non-USAEC reports are identified by parenthetical notes after the report codes; e.g., (non-AEC), (British), (Canadian), (French). The note (Misc.) identifies the codes used for both USAEC and non-USAEC reports. Patents are listed under the heading "PATENTS"; the country of origin is included in parentheses.

A comprehensive list of both USAEC and non-USAEC report codes is contained in the latest revision of TID-85, *Report Number Series Used by the Division of Technical Information in Cataloging Reports.* This information is also included in the Cumulative Report Number Index (issued annually).

Availability of USAEC Reports

All USAEC Reports abstracted in *Nuclear Science Abstracts* are available through one or more of the following sources:

(1) University and public libraries in the United States. A list of these organizations appears on the inside front cover of each issue of *NSA*.

(2) NCR Microcard Editions in Microcard and micronegative form. Orders and inquiries should be sent to: Order Processing Department, 365 South Oak Street, West Salem, Wisconsin 54669.

(3) National Technical Information Service, U. S. Department of Commerce, Springfield, Virginia 22151.

(4) Superintendent of Documents, U. S. Government Printing Office, Washington, D. C. 20402.

(5) National Cash Register Co., P. O. Box 3111, Oak Ridge, Tenn. 37830, in micronegative form. Purchase details available on request.

Availability of Non-USAEC Reports

U. S. Reports. Reports of U. S. Government agencies are available to the public from the National Technical Information Service (NTIS). If specific availability is not shown, inquiries may be directed to NTIS.

Non-U. S. Reports. Reports of atomic energy organizations of other countries are available from NTIS for U. S. sale only. Specific availability in the country of origin is shown, when known, at the report number entry. Otherwise, inquiries should be made to the organizations listed below:

AUSTRALIA

Australian Atomic Energy Commission Research Establishment. Available upon request from the Library, Australian Atomic Research Establishment, Private Mail Bag, Sutherland, New South Wales, Australia.

BELGIUM

Centre d'Etude de l'Energie Nucléaire. Available upon request to individuals and organizations from the Centre d'Etude de l'Energie Nucléaire (C.E.N.), Studiecentrum voor Kernenergie (S.C.K.), Technical Information Dept., MOL-DONK (Belgium).

CERN

CERN European Organization for Nuclear Research. Available without charge from CERN European Organization for Nuclear Research, Geneva 23, Switzerland. Copies are deposited in libraries throughout the world.

FRANCE

Commissariat à l'Energie Atomique. Inquiries for reports numbered 1-2199 should be addressed to Service Central de Documentation du C.E.A., Centre d'Etudes Nucléaires de Saclay, Boîte postale n° 2, 91. GIF-sur-YVETTE, FRANCE. Reports numbered 2200 and above are available from La Documentation Française, 31 quai Voltaire, 75, PARIS (7e), FRANCE.

Service Central de Protection contre les Rayonnements Ionisants. Copies are available from Ministère de la Santé Publique, Service Central de Protection contre les Rayonnements Ionisants, B.P. n° 78 Le Vesinet (France) Telex 25667.

GERMANY

Deutsches Elektronen-Synchrotron DESY. Copies are available from Deutsches Elektronen-Synchrotron DESY, Dokumentation, 2000 Hamburg 52, Notkestieg 1, Germany.

Gesellschaft für Kernforschung mbH (KFK). Copies are available from Gesellschaft für Kernforschung mbH, 75 Karlsruhe, Postfach 947, Germany. Copies are also deposited in many national nuclear centers in the world.

Kernforschungsanlage. Copies may be ordered from Zentralbibliothek der Kernforschungsanlage Jülich, Jülich, Bundesrepublik Deutschland.

Hahn-Meitner-Institute für Kernforschung. Available without charge from Hahn-Meitner-Institute für Kernforschung Ber-

XUM

lin, Bibliothek, Glienicker Strasse 100, 1 Berlin 39, Germany. Copies are deposited in many national nuclear centers in the world.

Johann-Wolfgang-Goethe Universität, Frankfurt Am Main, Institut für Kernphysik, (IKF). Copies are available from Gmelin Institut, 40–42 Varrentrappstrasse, Frankfurt (Main), West Germany.

ISRAEL

Israel Atomic Energy Commission. Available without charge from Israel Atomic Energy Commission, Soreq Nuclear Research Centre, Yavne, Israel.

ITALY

Centro Informazioni Studi Esperienze (CISE). For sale at CISE Press Office, Casella Postale 3986, Milano, Italy. Copies are deposited in the libraries of various nuclear centers in Italy and abroad.

Comitato Nazionale per l'Energia Nucleare. Copies are available from Comitato Nazionale per l'Energia Nucleare, Divisione Affari Internazionali e Studi Economici, Ufficio Pubblicazioni, Via Belisario, 15, Roma, Italy.

JAPAN

Japan Atomic Energy Research Institute (JAERI). Available from the Staff Supply Cooperative of Japan Atomic Energy Research Institute (JAERI), Tokai-mura, Naka-gun, Ibaraki-ken, Japan. Copies are deposited in depositories in Tokyo, Nagoya, and Osaka.

Nagoya University. Copies are available from Research Information Center, Institute of Plasma Physics, Nagoya University, Nagoya, Japan.

University of Tokyo. Available free of charge from Institute for Nuclear Study, University of Tokyo, Tanashi-Machi, Kitatama-gun, Tokyo, Japan.

NETHERLANDS

Reactor Centrum Nederland. For sale by Reactor Centrum Nederland, 112 Scheveningseweg, 's-Gravenhage, The Netherlands. Copies are deposited in university libraries in Holland and in many national nuclear centers in the world.

NEW ZEALAND

Institute of Nuclear Sciences. Copies are available from Librarian, N. Z. Institute of Nuclear Sciences, D.S.I.R., Private Bag, Lower Hutt, New Zealand. Copies are deposited in other countries.

PAKISTAN

Atomic Energy Center. Copies are available from Atomic Energy Center, P. O. Box 658, Lahore, (West Pakistan).

POLAND

Reports of the Polish nuclear institutes are published by the Nuclear Energy Information Center of the Government Commissioner for Use of Nuclear Energy. Copies are available free of charge from Nuclear Energy Information Center, Palace of Culture and Science, Warsaw, Poland.

SPAIN

Junta de Energia Nuclear. "JEN" reports are available without charge from Servicio de Documentation, Junta de Energia Nuclear, Ciudad Universitaria, Madrid (3), España.

SWITZERLAND

Eidgenössisches Institut für Reaktorforschung. "EIR" reports are available from Eidgenössisches Institut für Reaktorforschung, c/o Bibliothek, 5303 Würenlingen/Switzerland.

TURKEY

Turkish Atomic Energy Commission. Copies are available free of charge from T.A.E.C., Çekmece Nuclear Research Center, P. O. Box 1, Airport, Istanbul, Turkey.

Conferences

Published conference proceedings as well as individual unpublished papers from conferences are included in this index. A CONF number is assigned to the conference if published proceedings are received and also if only a single paper is received. The base number used is year-month-sequence. Thus, the number CONF-650101 indicates that the conference was held in 1965, in January, and that this was the first January 1965 conference so received. This number would be assigned to complete published proceedings. If individual papers are received, the base number is extended to include a paper number, e.g., CONF-650101-1. As additional papers are received, they will be assigned consecutive numbers in the series, CONF-650101-1, CONF-650101-2, etc. This numbering system ensures that all papers received from a conference will be associated with that conference in this index.

If published proceedings are received after the receipt of individual papers, the complete proceedings will be abstracted and the abstract number will appear in this index with the base CONF number.

Abbreviations Used in Availability Column

AECL	Reports of the Atomic Energy of Canada Limited are for sale by the Scientific Document Distribution Office, Atomic Energy of Canada Limited, Chalk River, Ontario, Canada.
CFSTI	See NTIS
DENM	Reports of the Atomic Energy Commission Research Establishment, Riso, are available on exchange from the Library, Danish Atomic Energy Commission, Risö, Roskilde, Denmark. Also for sale at the price shown from Jul. Gjellerup, Booksellers, 87 Sölvgade, Kobenhavn K., Denmark. Reports of Danatom are available on loan from Research Establishment, Risö, Roskilde, Denmark. Copies are available from Danatom, Aurehojvej 2, Hellerup, Denmark.
Dep.	AEC reports so designated are maintained in the organizations listed on the inside front cover of *NSA*. Prior to July 1, 1965, reports were deposited either in printed copy form or in microform. After that time, all reports have been in the form of micronegatives. Reports from other countries so designated are available in the United States at the organizations listed on the inside front cover of *NSA*.

DTIE Available from the U. S. Atomic Energy Commission, Division of Technical Information Extension, P. O. Box 62, Oak Ridge, Tennessee 37830. (Conference papers are available on loan only.)

EM Blueprints of AEC engineering drawings are available from NTIS, U. S. Department of Commerce, Springfield, Virginia 22151. Current prices of the CAPE-packages may be obtained from this address. TID-4100, available from the Division of Technical Information Extension, P. O. Box 62, Oak Ridge, Tennessee 37830, contains information on all the CAPE-packages for sale.

EUR For sale by Centrale de vente des publications des Communautés européennes 37, rue Glesener-Luxembourg.

GPO For sale by the Superintendent of Documents, Government Printing Office, Washington, D. C. 20402.

IAEA Available from the International Atomic Energy Agency, Vienna, Austria, and from its sales agencies in various countries throughout the world. A list of these agencies is found in each STI/DOC and STI/PUB publication.

NORW Reports from Forsvarets Forskningsinstitutt are available from Norwegian Defense Research Establishment, Library, P. O. Box 25, Kjeller, Norway.
"KR" reports are available on an exchange basis from the Library, Institutt for Atomenergi, Box 40, Kjeller, Norway.
Reports of the Norwegian Reactor School are available from the Library, Institutt for Atomenergi, P. O. Box 40, Kjeller, Norway.

NRC For sale by the National Research Council of Canada, Ottawa, Ontario, Canada.

NTIS For sale by the National Technical Information Service (NTIS), U. S. Department of Commerce, Springfield, Virginia 22151 at the following prices for eye legible copy:

1–300 pages	$3.00
301–600 pages	$6.00
601–900 pages	$9.00

Documents over 900 pages have special prices which may be obtained from NTIS. Microfiche copy of each separately bound document can be purchased for $0.95.
Reports issued by organizations outside the United States will be sold by NTIS *only to purchasers within the United States.*
Purchasers outside the United States may acquire such reports from the sources described elsewhere in these columns.

OECD Available from O. E. C. D., Publications 2, rue, André-Pascal, 75 Paris 16^{e}, France, and from its sales agencies in various countries throughout the world. A list of these agencies is found in each OECD publication.

SWED "AE" reports are for sale from Aktiebolaget Atomenergi, Library Section, Box 43041, Stockholm 43, Sweden. Microcopy of these reports is available from the International Documentation Center, Turnba, Sweden.
Reports of the VDDIT-series may be obtained from Aktiebolaget Atomenergi, Information Office, Scientific and Technical Information, Box 43041, Stockholm 43, Sweden.
Other series are not generally available to the public. Organizations in the Atomic Energy field may obtain copies from Aktiebolaget Atomenergi.

UK United Kingdom Atomic Energy Authority reports generally may be purchased from Her Majesty's Stationery Office, P. O. Box 569, London S.E.1. Copies of many UKAEA reports (particularly earlier ones) may be purchased in microcopy form from Micro Methods Ltd., East Ardsley, Wakefield, Yorkshire, England. Copies of UKAEA reports are deposited with the National Lending Library for Science and Technology and 10 public libraries in England; with the USAEC and (through USAEC) with NTIS; and in most national nuclear centers throughout the world. In the USA, UKAEA reports are available on a subscription basis, by subject category, from UNIPUB, Inc., P. O. Box 433, New York, N. Y. 10016, USA.

UN Mail orders should be directed to the Sales Section, Room 1059, United Nations Headquarters, New York, New York 10017.

ZAED Available from Zentralstelle für Atomkernenergie Dokumentation, 6000 Frankfurt/Main 90, P. O. Box 901069, Westendstr. 21, West Germany

XUM

Report No.	Abstract No.	Availability
A-	(Misc.)	
3371	25-30498	See N-70-41880
3624	25-30476	See N-71-10964
AAEC/E-	(Australian)	
203	25-31543	Dep. NTIS (U. S. Sales Only), 116p.
AAEC/LIB/Bib-	(Australian)	
264	25-29249	Dep. NTIS (U. S. Sales Only), 17p.
AAEC/TM-	(Australian)	
570	25-29782	Dep. NTIS (U. S. Sales Only), 24p.
AEC-tr-		
7099(Pt.2)	25-29368	Dep. NTIS
7224	25-29818	Dep. NTIS
7227	25-29200	Dep. NTIS
7228	25-29201	Dep. NTIS
AECL-	(Canadian)	
3740	25-31482	Dep. NTIS (U. S. Sales Only). AECL $0.50, 13p.
3856	25-30303	Dep. NTIS (U. S. Sales Only). AECL $1.50, 67p.
AEEW-M-	(British)	
970	25-29324	Dep. NTIS (U. S. Sales Only), 20p.
1012	25-31650	Dep. NTIS (U. S. Sales Only). UK 7½p, 12p.
AERE-M-	(British)	
1887	25-29511	Dep. NTIS (U. S. Sales Only), 9p.
2184	25-31681	Dep. NTIS (U. S. Sales Only), 46p.
AERE-R-	(British)	
5682	25-31163	Dep. NTIS (U. S. Sales Only), 17p.
5953	25-30661	Dep. NTIS (U. S. Sales Only), 28p.
6141	25-29034	Dep. NTIS (U. S. Sales Only), 13p.
6719	25-31682	Dep. NTIS (U. S. Sales Only), 19p.
ANL-		
7683	25-29315	Dep. NTIS, 62p.
7717	25-31651	Dep. NTIS, 387p.
7793	25-31574	Dep. NTIS, 244p.
7798	25-31533	Dep. NTIS, 147p.
ANL-Trans-		
879	25-30273	Dep. NTIS
880	25-31683	Dep. NTIS
881	25-30274	Dep. NTIS
ANU-P-	(Australian)	
500	25-31389	Dep. NTIS (U. S. Sales Only), 11p.
507	25-31390	Dep. NTIS (U. S. Sales Only), 16p.
512	25-31391	Dep. NTIS (U. S. Sales Only), 20p.
515	25-31200	Dep. NTIS (U. S. Sales Only), 3p.
ASTM-STP-	(Non-AEC)	
467	25-29840	Philadelphia; American Society for Testing and Materials (1970). 303p. $28.75
AVSSD-	(Non-AEC)	
506-70-CR	25-30599	See N-71-10100
AWRE-O-	(British)	
89/70	25-31299	Dep. NTIS (U. S. Sales Only). UK 5s. 6d, 37p.
BARC-	(Non-AEC)	
500	25-28912	Dep. NTIS (U. S. Sales Only), 12p.
508	25-28913	Dep. NTIS (U. S. Sales Only), 26p.
509	25-29175	Dep. NTIS (U. S. Sales Only), 23p.
515	25-28914	Dep. NTIS (U. S. Sales Only), 31p.
516	25-29176	Dep. NTIS (U. S. Sales Only), 17p.
517	25-28915	Dep. NTIS (U. S. Sales Only), 34p.
BAW-	(Misc.)	
10027	25-31532	Dep. NTIS, 124p.
BMI-	(Misc.)	
1899	25-30009	Dep. NTIS, 33p.
BMI-X-		
10274	25-29937	Dep. NTIS, 52p.
BNL-		
15722	25-31035	Dep. NTIS, 15p.
50145(Rev.)	25-29250	Dep. NTIS, 122p.
50266	25-31684	Dep. NTIS, 32p.
50285	25-29418	Dep. NTIS, 10p.
BNL-tr-		
410	25-30771	Dep. NTIS
416	25-31392	Dep. NTIS
418	25-30802	Dep. NTIS
BNWL-		
576	25-31626	Dep. NTIS, 11p.
585	25-31627	Dep. NTIS, 46p.
586	25-31628	Dep. NTIS, 6p.
587	25-31629	Dep. NTIS, 6p.
630	25-31630	Dep. NTIS, 54p.
1329	25-29286	Dep. NTIS, 50p.
1527	25-31645	Dep. NTIS, 61p.
1558	25-31685	Dep. NTIS, 45p.
BNWL-B-		
29	25-31686	Dep. NTIS, 42p.
47	25-30552	Dep. NTIS, 25p.
BNWL-tr-		
65	25-29938	Dep. NTIS
BRH/DEP-	(Non-AEC)	
71-4	25-29512	GPO $0.50
CALT-		
69-297	25-30749	Dep. NTIS, 53p.
CAPE-		
2066	25-29272	EM
2069	25-31571	EM
2074	25-29318	EM
CEA-CONF-	(French)	
1693	25-29901	Dep. NTIS (U. S. Sales Only), 8p.
1747	25-29011	Dep. NTIS (U. S. Sales Only), 8p.
CEA-N-	(French)	
825	25-31164	Dep. NTIS (U. S. Sales Only), 19p.
1096	25-30698	Dep. NTIS (U. S. Sales Only), 12p.
1376	25-29783	Dep. NTIS (U. S. Sales Only), 20p.
1414	25-29073	Dep. NTIS (U. S. Sales Only), 26p.
1431	25-29392	Dep. NTIS (U. S. Sales Only), 8p.
CEA-R-	(French)	
3619	25-29316	For translation see LA-tr-71-12
3853	25-29938	For translation see BNWL-tr-65
4071	25-28916	Dep. NTIS (U. S. Sales Only), 59p.
4090	25-29177	Dep. NTIS (U. S. Sales Only), 23p.
4102	25-29178	Dep. NTIS (U. S. Sales Only), 25p.
4123	25-29918	Dep. NTIS (U. S. Sales Only), 110p.
4156	25-29531	Dep. NTIS (U. S. Sales Only), 40p.
CEA-tr-R-	(French)	
1978	25-29202	Dep. NTIS (U. S. Sales Only)
CEAL-		
1053	25-31036	Dep. NTIS, 56p.
CERN-	(European Organization for Nuclear Research)	
70-31	25-30219	Dep. NTIS (U. S. Sales Only), 110p.
71-7	25-30750	Dep. NTIS (U. S. Sales Only), 361p.
CERN-HERA-	(European Organization for Nuclear Research)	
70-7	25-30735	Dep. NTIS (U. S. Sales Only), 172p.
CERN-Trans-	(European Organization for Nuclear Research)	
71-4	25-30724	Dep. NTIS (U. S. Sales Only)
CEX-		
65.04	25-31165	Dep. NTIS, 82p.
CLM-R-	(British)	
109	25-30553	Dep. NTIS (U. S. Sales Only), 11p.
CNEA-	(Argentinean)	
282	25-31300	Dep. NTIS (U. S. Sales Only), 17p.
283	25-31301	Dep. NTIS (U. S. Sales Only), 9p.
CONF-660946-	(Symposium on High-Energy Electrons, Madrid, Spain, Sept. 26-28, 1966)	
	25-29596	Madrid; General Directorate of Health (1970). 405p
CONF-680474-	(Conference on Work to Develop Steel Reactor Pressure Vessels, Julich, Germany, Apr. 22, 1968)	
	25-31668	See IRS-T-17
CONF-680535-	(14th National Conference of the Italian Association for Health Physics and Protection from Radiation, Formia, Italy, May 29-31, 1968)	
4	25-29508	Minerva Fisiconucl.; 13: 20-6(Jan-Mar 1969)
5	25-29517	Minerva Fisiconucl.; 13: 27-31(Jan-Mar 1969)
8	25-29477	Minerva Fisiconucl.; 13: 72-7(Jan-Mar 1969)
9	25-29218	Minerva Fisiconucl.; 13: 78-85(Jan-Mar 1969)
11	25-29528	Minerva Fisiconucl.; 13: 93-104(Jan-Mar 1969)
12	25-29538	Minerva Fisiconucl.; 13: 125-30(Apr-Jun 1969)
13	25-29529	Minerva Fisiconucl.; 13: 131-4(Apr-Jun 1969)
20	25-29263	Minerva Fisiconucl.; 13: 185-91(Jul-Sep 1969)

XUM

Report No.	Abstract No.	Availability
23	25-29222	Minerva Fisiconucl.; 13: 215-18(Jul-Sep 1969)
29	25-29441	Minerva Fisiconucl.; 13: 331-5(Oct-Dec 1969)
30	25-29507	Minerva Fisiconucl.; 13: 307-12(Oct-Dec 1969)
CONF-680850-		(12th International Congress of Cell Biology, Brussels, Belgium, Aug. 25-31, 1968)
	25-31760	New York; Academic Press, Inc. (1969). 394p
CONF-680851-		(2nd International Conference on Thermal Analysis, Worcester, Mass., Aug. 18-23, 1968)
	25-29758	New York; Academic Press, Inc. (1969). 835p
CONF-690446-		(International Astronomical Union Colloquium No. 2, Commission 36, Munich, Germany, Apr. 16-19, 1969)
	25-30035	See NBS-SPEC. PUBL-332
CONF-690454-		(15th Annual Technical Meeting and Equipment Exposition, Anaheim, Calif., Apr. 20-24, 1969)
	25-29245	Mt. Prospect, Ill.; Institute of Environmental Sciences (1969). 665p. $18.00
CONF-690619-		(3rd Conference on Controlled Fusion and Plasma Physics, Utrecht, Netherlands, June, 1969)
	25-30451	Groningen, Netherlands; Wolters-Noordhoff Publishing (1969). 139p. $5.25
CONF-690650-		(Conference on Achievement of High Fatigue Resistance in Metals and Alloys, Atlantic City, N.J., June 22-27, 1969)
	25-29840	Philadelphia; American Society for Testing and Materials (1970). 303p. $28.75
CONF-690656-		(Conference on Process Radiation in the Plastics Industry, Pullman, Wash., June 11-13, 1969)
	25-29121	Pullman, Wash.; Washington State University (1969). 170p. $15.00
CONF-690701-		(International Conference on Model Techniques, London, England, July 10-12, 1969)
	25-29298	London; Institute of Civil Engineers (1969). 188p. Pound 10
CONF-690921-		(5th International Cyclotron Conference, Oxford, England, Sept. 17-20, 1969)
	25-31079	London; Butterworths (1971). 807p. Pound 20
CONF-690924-		(International Conference on the Use of Cyclotrons in Chemistry, Metallurgy and Biology, Oxford, England, Sept. 22-23, 1969)
3	25-29907	See ORNL-TM-3299
CONF-690929-		(15th National Congress of the Italian Association for Health Physics and Protection Against Radiation, Cagliari, Italy, Sept. 29-Oct. 3, 1969)
10	25-29479	Minerva Fisiconucl.; 14: 199-19(Jul-Sep 1970)
12	25-29478	Minerva Fisiconucl.; 14: 124-31(Jul-Sep 1970)
CONF-690931-		(International Symposium on Closed Confinement Systems, Dubna, U.S.S.R., Sept. 29-Oct. 3, 1969)
5	25-30597	See LA-4339-TR
CONF-690940-		(7th Annual Meeting of the European Society for Radiation Biology, Ulm, Germany, Sept. 2-6, 1969)
(Absts.)	25-29607	
CONF-691016-		(10th Annual Meeting Southeastern Chapter Society of Nuclear Medicine, Nashville, Tenn., Oct. 23-25, 1969)
(Absts.)	25-29570	
CONF-691104-		(International Congress on the Diffusion of Fission Products, Saclay, France, Nov. 4-6, 1969)
	25-31602	Montrouge, France; Societe Francaise de Radioprotection (1970). 549p
CONF-691112-		(2nd Conference on Prestressed Concrete Reactor Pressure Vessels and Their Thermal Isolation, Brussels, Belgium, Nov. 18-20, 1969)
	25-31546	See EUR-4531
CONF-691225-		(Symposium on the New Methods for Producing Radioactive Preparations, Warsaw, Poland, Dec. 9-13, 1969)
	25-29413	
CONF-700111-		(1st Nordic Meeting on Medical and Biological Engineering, Otaniemi, Finland, Jan. 15-18, 1970)
	25-29584	Helsinki; Finnish Society for Medical and Biological Engineering (1970). 236p
CONF-700204-		(IAEA Meeting on Research Reaction Utilization, Rome, Italy, Feb. 2-6, 1970)
14	25-29273	pp 319-41 of Research Reactor Utilization. Vol. 2. Vienna; International Atomic Energy Agency (1970)
15	25-29275	pp 243-86 of Research Reactor Utilization. Vol. 2. Vienna; International Atomic Energy Agency (1970)
16	25-29909	pp 9-38 of Research Reactor Utilization. Vol. 2. Vienna; International Atomic Energy Agency (1970)
17	25-29274	pp 287-318 of Research Reactor Utilization. Vol. 2. Vienna; International Atomic Energy Agency (1970)
CONF-700218-		(Symposium on Materials Science Research, Bangalore, India, Feb. 24, 1970)
9	25-29941	See INIS-mf-8
CONF-700433-		(Conference on Clinical Aspects of Inherited Disorders, Birmingham, Ala., Apr. 9-10, 1970)
	25-29498	S. Med. J.; 64: Suppl. No. 1, 1-110(Feb 1971)
CONF-700437-		(International Symposium on Composite Materials, Paris, France, Apr. 2-3, 1970)
1	25-29883	See SC-T-713021
CONF-700528-		(Colloquium on High Multiplicity Hadronic Interactions, Paris, France, May 1970)
	25-30762	Paris; Ecole Polytechnique (1970). 293p
CONF-700551-		(Conference on Cross-Species Transplantation, Salt Lake City, Utah, May 8-9, 1970)
	25-29682	Transplant. Proc.; 2: 431-559(Dec 1970)
CONF-700553-		(American Institute of Metallurgical Engineering Meeting, Las Vegas, Nev., May 11-14, 1970)
1	25-31743	See UCRL-19648
CONF-700557-		(Meeting on Mechanical Flow Processes in Gas Centrifuges, Porz-Wahn, Germany, May 14, 1970)
1	25-29271	
CONF-700558-		(Low Energy Hadron Interactions Conference, Karlsruhe, Germany, May, 1970)
	25-30840	New York; Springer-Verlag New York, Inc. (1970). 294p. $21.50
CONF-700608-		(American Nuclear Society Meeting, Los Angeles, Calif., June 29-July 2, 1970)
35	25-31570	See RT/ING-(70)24
CONF-700804-		(Chemical Engineering Conference, Sydney and Melbourne, Australia, Aug. 18-26, 1970)
	25-29759	Sydney; University of Sydney (1970). 131p
CONF-700806-		(15th International Conference on High Energy Physics, Kiev, U.S.S.R., Aug. 26-Sept. 4, 1970)
58	25-31015	See MIT-2098-726
CONF-700919-		(Symposium on the Sterility Principle for Insect Control or Eradication, Athens, Greece, Sept. 14-18, 1970)
	25-29730	See STI/PUB-265
CONF-700928-		(6th Symposium on Fusion Technology, Aachen, Germany, Sept. 22-26, 1970)
	25-30449	See EUR-4593
CONF-700950-		(Conference on High Energy Physics, Aix-en-Provence, France, Sept. 29-Oct. 2, 1970)
	25-30753	J. Phys. (Paris), Colloq.; C5: 1-189(Nov-Dec 1970)

XUM

Report No.	Abstract No.	Availability
CONF-700951-		(3rd European Fluorine Chemistry Symposium, Aix-en-Provence, France, Sept. 14-17, 1970)
2	25-29011	See CEA-CONF-1747
CONF-700952-		(International Conference on Metastable Alloys, Brela, Yugoslavia, Sept. 28-30, 1970)
1	25-29901	See CEA-CONF-1693
CONF-700953-		(11th National Meeting on Industrial Medicine, Nantes, France, Sept. 9-13, 1970)
1	25-29531	See CEA-R-4156
CONF-701044-		(5th Congress on Material Testing, Budapest, Hungary, Oct. 19-24, 1970)
(Sect.3)	25-28917	
CONF-701102-		(Meeting of the American Nuclear Society, Washington, D.C., Nov. 15-19, 1970)
18	25-29244	See UCRL-72572
CONF-701106-		(5th Annual Midyear Topical Symposium on Health Physics Aspects of Nuclear Facility Siting, Idaho Falls, Idaho, Nov. 3-6, 1970)
6	25-31482	See AECL-3740
CONF-701114-		(Meeting on Division of Plasma Physics, Washington, D.C., Nov. 4-7, 1970)
2	25-30459	See MATT-813
CONF-701120-		(2nd National Conference on Particle Accelerators, Moscow, U.S.S.R., Nov. 11-18, 1970)
3	25-31040	See KFK-1316
CONF-701122-		(International Conference on Laser-Produced Plasmas, Moscow, U.S.S.R., Nov. 17-21, 1970)
2	25-30553	See CLM-R-109
CONF-710106-		(Conference on Fundamental Interactions at High Energy, Coral Gables, Fla., Jan. 20-22, 1971)
7	25-30939	See NYO-3829-66
8	25-31016	See NYO-1932(2)-192
9	25-30749	See CALT-69-297
CONF-710209-		(International Conference on Heavy Ion Physics, Dubna, U.S.S.R., Feb. 11-17, 1971)
1	25-31241	See UCRL-20436
CONF-710211-		(International Meeting on Bone-Seeking Radionuclide Contaminations and Radiation Protection, Grenoble, France, Feb. 1-5, 1971)
1	25-29513	Dep. NTIS, 16p.
CONF-710301-		(3rd Conference on Neutron Cross Sections and Technology, Knoxville, Tenn., Mar. 15-17, 1971)
8	25-31166	Dep. NTIS, 7p.
CONF-710302-		(Meeting on New Development in Reactor Mathematics and Applications, Idaho Falls, Idaho, Mar. 29-31, 1971)
2	25-31587	Dep. NTIS, 16p.
4	25-31588	Dep. NTIS, 28p.
5	25-31589	Dep. NTIS, 8p.
6	25-31590	Dep. NTIS, 10p.
7	25-31591	Dep. NTIS, 14p.
8	25-31592	Dep. NTIS, 35p.
9	25-31593	Dep. NTIS, 16p.
10	25-31594	Dep. NTIS, 26p.
CONF-710304-		(Symposium on Natural and Manmade Radiation in Space, Las Vegas, Nev., Mar. 1-5, 1971)
4	25-30630	See ORNL-TM-3318
7	25-31640	See ORNL-TM-3368
8	25-31671	See ORNL-TM-3367
9	25-30631	See ORNL-TM-3376
CONF-710308-		(National Particle Accelerator Conference, Chicago, Ill., Mar. 1-3, 1971)
7	25-31058	See UCRL-20208
8	25-31056	See UCRL-20191
9	25-31050	See UCRL-20156
13	25-31051	See UCRL-20164
14	25-31053	See UCRL-20174
15	25-31054	See UCRL-20185
16	25-31055	See UCRL-20189
17	25-31052	See UCRL-20169
18	25-31059	See UCRL-20611
19	25-31057	See UCRL-20197
CONF-710409-		(17th Annual Meeting and Equipment Exposition, Los Angeles, Calif., Apr. 26-30, 1971)
	25-31762	Mt. Prospect, Ill.; Institute of Environmental Sciences (1971). 509p
CONF-710502-		(Experimental Stress Analysis Meeting, Salt Lake City, Utah, May 18-21, 1971)
2	25-31752	See UCRL-72818(Rev.1)
COO-		
119-243	25-29621	Dep. NTIS, 127p.
264-569	25-30804	Dep. NTIS, 54p.
264-571	25-31012	Dep. NTIS, 14p.
908-34	25-31687	Dep. NTIS, 51p.
1041-18	25-31688	Dep. NTIS, 7p.
1041-19	25-31689	Dep. NTIS, 7p.
1051-34	25-31393	Dep. NTIS, 282p.
1105-120	25-29382	Dep. NTIS, 16p.
1167-10	25-31302	Dep. NTIS, 56p.
1198-807	25-29882	Dep. NTIS, 168p.
1569-71	25-31690	Dep. NTIS, 77p.
1569-76	25-30662	Dep. NTIS, 73p.
1701-12	25-30722	Dep. NTIS, 6p.
1750-3	25-31691	Dep. NTIS, 29p.
1764-108	25-31309	See LA-DC-11648
1793-5	25-29713	Dep. NTIS, 4p.
2048-2	25-31692	Dep. NTIS, 79p.
2094-4	25-31693	Dep. NTIS, 123p.
2103-3	25-30696	Dep. NTIS, 13p.
2118-1	25-31694	Dep. NTIS, 272p.
CSIRO-Trans-		(Australian)
10424	25-30156	Dep. NTIS (U. S. Sales Only)
DESY-		(German)
71/3	25-30773	Dep. NTIS (U. S. Sales Only), 18p.
DOCKET-1155-		(LaCrosse Boiling Water Reactor) (AEC)
113	25-31463	Dep. NTIS, 2p.
DOCKET-50003-		(Indian Point Station; See Also DOCKET-50247, DOCKET-50286) (Non-AEC)
68	25-31483	Dep. NTIS, 2p.
DOCKET-50010-		(Dresden Nuclear Power Station; See also DOCKET-50237 and DOCKET-50249) (Non-AEC)
85	25-31464	Dep. NTIS, 29p.
DOCKET-50016-		(Enrico Fermi Atomic Power Plant) (Non-AEC)
110	25-31484	Dep. NTIS, 1p.
DOCKET-50029-		(Yankee Atomic Electric Co.) (Non-AEC)
150	25-31465	Dep. NTIS, 7p.
DOCKET-50146-		(Saxton Nuclear Experimental Corporation) (Non-AEC)
72	25-31466	Dep. NTIS, 50p.
73	25-31485	Dep. NTIS, 4p.
DOCKET-50155-		(Big Rock Point Reactor) (Misc.)
80	25-31486	Dep. NTIS, 3p.
81	25-31467	Dep. NTIS, 30p.
DOCKET-50171-		(Peach Bottom Atomic Power Station; See also DOCKET-50277 and DOCKET-50278) (Non-AEC)
84	25-31487	Dep. NTIS, 2p.
DOCKET-50201-		(West Valley Reprocessing Plant--Formerly Spent Fuel Processing Plant) (Misc.)
69	25-29179	Dep. NTIS, 12p.
70	25-29180	Dep. NTIS, 9p.
DOCKET-50206-		(San Onofre Nuclear Generating Station) (Misc.)
112	25-31488	Dep. NTIS, 8p.
DOCKET-50213-		(Connecticut Yankee Atomic Power Plant) (Misc.)
105	25-31468	Dep. NTIS, 13p.
DOCKET-50231-		(Southwest Experimental Fast Oxide Reactor) (Non-AEC)
79	25-31595	Dep. NTIS, 1p.
80	25-31631	Dep. NTIS, 11p.
81	25-31596	Dep. NTIS, 8p.
DOCKET-50237-		(Dresden Nuclear Power Station, See also DOCKET-50249) (Non-AEC)
147	25-31469	Dep. NTIS, 74p.
156	25-31489	Dep. NTIS, 83p.
157	25-31470	Dep. NTIS, 4p.
158	25-31471	Dep. NTIS, 3p.
159	25-31472	Dep. NTIS, 2p.
160	25-31473	Dep. NTIS, 2p.
161	25-31490	Dep. NTIS, 2p.
DOCKET-50244-		(Robert Emmett Ginna Nuclear Power Plant, Formerly Brookwood Nuclear Station) (Non-AEC)
70	25-31474	Dep. NTIS, 2p.

XUM

Report No.	Abstract No.	Availability
DOCKET-50245-	(Millstone Point Nuclear Power Station) (Non-AEC)	
64	25-31491	Dep. NTIS, 1p.
DOCKET-50249-	(Dresden Nuclear Power Station; See also DOCKET-50237) (Non-AEC)	
65	25-31492	Dep. NTIS, 1p.
DOCKET-50254-	(Quad-Cities Station; See also DOCKET-50265) (Non-AEC)	
35	25-31493	Dep. NTIS, 2p.
DOCKET-50255-	(Palisades Plant) (Non-AEC)	
38	25-31494	Dep. NTIS, 189p.
DOCKET-50263-	(Monticello Nuclear Generating Plant) (Non-AEC)	
63	25-31495	Dep. NTIS, 50p.
64	25-31496	Dep. NTIS, 50p.
65	25-31497	Dep. NTIS, 9p.
66	25-31498	Dep. NTIS, 8p.
67	25-31475	Dep. NTIS, 2p.
68	25-31476	Dep. NTIS, 3p.
69	25-31477	Dep. NTIS, 3p.
DOCKET-50265-	(Quad-Cities Station; See also DOCKET-50254) (Non-AEC)	
32	25-31493	See DOCKET-50254-35
DOCKET-50266-	(Point Beach Nuclear Plant) (Non-AEC)	
47	25-31478	Dep. NTIS, 2p.
DOCKET-50269-	(Oconee Nuclear Station, See also DOCKET-50270, and DOCKET-50287) (Non-AEC)	
17	25-31499	Dep. CFSTI, 7p.
DOCKET-50270-	(Oconee Nuclear Station, See also DOCKET-50269, and DOCKET-50287) (Non-AEC)	
17	25-31499	See DOCKET-50269-17
DOCKET-50271-	(Vermont Yankee Nuclear Power Station) (Non-AEC)	
50	25-31500	Dep. NTIS, 10p.
51	25-31501	Dep. NTIS, 57p.
DOCKET-50277-	(Peach Bottom Atomic Power Station; See also DOCKET-50171 and DOCKET-50278) (Non-AEC)	
19	25-31502	Dep. NTIS, 400p.
DOCKET-50278-	(Peach Bottom Atomic Power Station; See also DOCKET-50171 and DOCKET-50277) (Non-AEC)	
19	25-31502	See DOCKET-50277-19
DOCKET-50280-	(Surry Power Station, See also DOCKET-50281) (Non-AEC)	
39	25-31503	Dep. NTIS, 335p.
DOCKET-50281-	(Surry Power Station, See also DOCKET-50280) (Non-AEC)	
39	25-31503	See DOCKET-50280-39
DOCKET-50287-	(Oconee Nuclear Station; see also DOCKET-50269 and DOCKET-50270) (Non-AEC)	
14	25-31499	See DOCKET-50269-17
DOCKET-50309-	(Maine Yankee Atomic Power Company) (Non-AEC)	
34	25-31504	Dep. NTIS, 133p.
DOCKET-50312-	(Rancho Seco Nuclear Generating Station) (Non-AEC)	
19	25-31505	Dep. NTIS, 33p.
20	25-31506	Dep. NTIS, 378p.
21	25-31507	Dep. NTIS, 299p.
22	25-31508	Dep. NTIS, 324p.
23	25-31509	Dep. NTIS, 772p.
24	25-31510	Dep. NTIS, 187p.
DOCKET-50313-	(Russellville Nuclear Unit) (Non-AEC)	
26	25-31511	Dep. NTIS, 63p.
27	25-31512	Dep. NTIS, 400p.
28	25-31513	Dep. NTIS, 479p.
29	25-31514	Dep. NTIS, 157p.
DOCKET-50324-	(Brunswick Steam Electric Plant, Units 1 and 2, See also DOCKET-50325) (Non-AEC)	
20	25-31515	Dep. NTIS, 2p.
DOCKET-50325-	(Brunswick Steam Electric Plant, Units 1 and 2, See also DOCKET-50324) (Non-AEC)	
20	25-31515	See DOCKET-50324-20
DOCKET-50331-	(Daune Arnold Energy Center) (Non-AEC)	
25	25-31516	Dep. NTIS, 249p.
DOCKET-50335-	(Hutchinson Island Plant) (Non-AEC)	
18	25-31517	Dep. NTIS, 15p.
DOCKET-50344-	(Trojan Nuclear Plant) (Non-AEC)	
20	25-31518	Dep. NTIS, 18p.
DOCKET-50352-	(Limerick Generating Station) (See also DOCKET-50353) (Non-AEC)	
12	25-31519	Dep. NTIS, 224p.
DOCKET-50353-	(Limerick Generating Station) (See also DOCKET-50352) (Non-AEC)	
12	25-31519	See DOCKET-50352-12
DOCKET-50358-	(Wm. H. Zimmer Nuclear Power Station, Units 1 and 2) (See also DOCKET-50359) (Non-AEC)	
14	25-31520	Dep. NTIS, 456p.
DOCKET-50368-	(Arkansas Nuclear One) (Non-AEC) (Unit 2)	
9	25-31521	Dep. NTIS, 292p.
DOCKET-50369-	(McGuire Nuclear Station) (See also DOCKET-50370) (Non-AEC) (Units 1 and 2)	
8	25-31522	Dep. NTIS, 193p.
DOCKET-50370-	(McGuire Nuclear Station) (See also DOCKET-50369) (Non-AEC) (Units 1 and 2)	
7	25-31522	See DOCKET-50369-8
DOCKET-50376-	(Aguirre Nuclear Plant) (Non-AEC)	
10	25-31523	Dep. NTIS, 614p.
11	25-31524	Dep. NTIS, 528p.
DUN-		
7221(Vol.1)	25-29074	Dep. NTIS, 85p.
7221(Vol.2)	25-29075	Dep. NTIS, 48p.
DUN-SA-		
136	25-31646	Dep. NTIS, 21p.
149	25-29760	Dep. NTIS, 18p.
E-	(Misc.)	
5737	25-30516	See N-70-42698
EANDC(UK)-	(European-American Nuclear Data Committee)	
126-AL	25-31299	See AWRE-O-89/70
EFI-		
70-75	25-30804	See COO-264-569
71-3	25-31012	See COO-264-571
EGG-		
1183-2242	25-31695	Dep. NTIS, 24p.
ETR-	(Belgian)	
253	25-29035	See NP-18736
EUR-	(European Atomic Energy Community)	
4497	25-31541	Dep. NTIS (U. S. Sales Only). EUR FF 9.45, 58p.
4519	25-31167	Dep. NTIS (U. S. Sales Only). EUR FF 33.40µ 236p.
4531	25-31546	EUR $24.00
4593	25-30449	EUR $14.00
EURFNR-	(European Atomic Energy Community)	
813	25-31542	Dep. NTIS
820	25-29940	Dep. NTIS
823	25-31568	Dep. NTIS
891	25-29902	Dep. NTIS
FEI-	(Russian)	
201	25-31632	Dep. NTIS (U. S. Sales Only), 44p.
GA-	(Misc.)	
10276	25-29012	Dep. NTIS, 109p.
10338	25-31623	Dep. NTIS, 135p.
GEAP-	(Misc.)	
12148	25-30032	Dep. NTIS, 22p.
12153	25-29821	Dep. NTIS, 7p.
GEPP-		
85	25-29181	Dep. NTIS, 19p.
HEDL-TME-		
71-40	25-31647	Dep. NTIS, 16p.
IAE-	(Russian)	
1515	25-30506	For translation see MATT-Trans-84
1516	25-30505	For translation see MATT-Trans-83
1644	25-30461	For translation see MATT-Trans-79
1950	25-30544	Dep. NTIS (U. S. Sales Only), 36p.
1954	25-31170	For translation see KAPL-Trans-4
1958	25-31237	Dep. NTIS (U. S. Sales Only), 16p.
1966	25-30687	Dep. NTIS (U. S. Sales Only), 6p.
2016	25-30475	For translation see LA-tr-71-6
2036	25-31314	For translation see ORNL-tr-2453
IAEA-R-	(International Atomic Energy Agency)	
290-F	25-29481	NTIS (U. S. Sales Only), 9p.
491-F	25-29729	NTIS (U. S. Sales Only), 25p.
IFVE-	(Russian)	
68-72	25-30724	For translation see CERN-Trans-71-4
IJS-	(Yugoslavian)	

XUM

Report No.	Abstract No.	Availability
253	25-31633	Dep. CFSTI (U. S. Sales Only), 120p.
IN-		
1421	25-31696	Dep. NTIS, 35p.
1452	25-29393	Dep. NTIS, 66p.
INIS-mf-	(International Atomic Energy Agency)	
8	25-29941	NTIS (U. S. Sales Only), 11p.
INR-	(Non-AEC)	
1260	25-31168	Dep. NTIS (U. S. Sales Only), 36p.
1271	25-31303	Dep. NTIS (U. S. Sales Only), 72p.
INR-P-	(Polish)	
1233	25-30893	Dep. NTIS (U. S. Sales Only), 26p.
INSJ-	(Japanese)	
126	25-30774	Dep. NTIS (U. S. Sales Only), 37p.
INT-	(Misc.)	
4	25-30664	See NP-18783
IPP-	(Non-AEC)	
1/113	25-30513	Dep. NTIS (U. S. Sales Only), 45p.
1/114	25-30541	Dep. NTIS (U. S. Sales Only), 26p.
6/92	25-30513	See IPP-1/113
IPPJ-	(Japanese)	
102	25-30457	Dep. NTIS (U. S. Sales Only), 33p.
103	25-30349	Dep. NTIS (U. S. Sales Only), 9p.
104	25-30458	Dep. NTIS (U. S. Sales Only), 20p.
IRS-R-	(West German)	
1	25-31597	Dep. NTIS (U. S. Sales Only), 20p.
IRS-T-	(West German)	
17	25-31668	
IS-T-		
424	25-31697	Dep. NTIS, 119p.
426	25-30751	Dep. NTIS, 83p.
ITEF-	(Russian)	
753	25-29369	Dep. NTIS (U. S. Sales Only), 54p.
782	25-31013	Dep. NTIS (U. S. Sales Only), 39p.
ITF-	(Russian)	
70-74	25-31698	Dep. NTIS (U. S. Sales Only), 20p.
70-83-E	25-31238	Dep. NTIS (U. S. Sales Only), 23p.
70-84-P	25-30699	Dep. NTIS (U. S. Sales Only), 8p.
70-95-E	25-31394	Dep. NTIS (U. S. Sales Only), 11p.
70-98-P	25-30894	Dep. NTIS (U. S. Sales Only), 10p.
ITJ-	(Polish)	
2/E	25-29389	Dep. NTIS (U. S. Sales Only), 24p.
JAERI-	(Japanese)	
1203	25-29975	Dep. NTIS (U. S. Sales Only), 10p.
JAERI-Memo-	(Japanese)	
4243	25-30514	Dep. NTIS (U. S. Sales Only), 40p.
4249	25-29976	Dep. NTIS (U. S. Sales Only), 23p.
4251	25-31304	Dep. NTIS (U. S. Sales Only), 208p.
4281	25-29394	Dep. NTIS (U. S. Sales Only), 54p.
4286	25-30596	Dep. NTIS (U. S. Sales Only), 108p.
4292	25-29383	Dep. NTIS (U. S. Sales Only), 65p.
4295	25-29395	Dep. NTIS (U. S. Sales Only), 70p.
4299	25-30275	Dep. NTIS (U. S. Sales Only), 24p.
4303	25-29396	Dep. NTIS (U. S. Sales Only), 82p.
JINR-	(Russian)	
E2-5746	25-31014	Dep. NTIS (U. S. Sales Only), 17p.
P1-5565	25-30736	Dep. NTIS (U. S. Sales Only), 15p.
P1-5633	25-30725	Dep. NTIS (U. S. Sales Only), 10p.
P1-5648	25-31395	Dep. NTIS (U. S. Sales Only), 18p.
P1-5665	25-30726	Dep. NTIS (U. S. Sales Only), 24p.
P1-5666	25-30847	Dep. NTIS (U. S. Sales Only), 26p.
P1-5668	25-30848	Dep. NTIS (U. S. Sales Only), 20p.
P1-5706	25-30869	Dep. NTIS (U. S. Sales Only), 24p.
P2-5331	25-30870	For translation see ORNL-tr-2433
P2-5522	25-30775	Dep. NTIS (U. S. Sales Only), 9p.
P2-5630	25-30824	Dep. NTIS (U. S. Sales Only), 12p.
P2-5659	25-30849	Dep. NTIS (U. S. Sales Only), 23p.
P2-5679	25-30776	Dep. NTIS (U. S. Sales Only), 21p.
P2-5691	25-30752	Dep. NTIS (U. S. Sales Only), 21p.
P2-5694	25-30937	Dep. NTIS (U. S. Sales Only), 30p.
P2-5705	25-30777	Dep. NTIS (U. S. Sales Only), 10p.
P2-5717	25-30938	Dep. NTIS (U. S. Sales Only), 20p.
P2-5729	25-30913	Dep. NTIS (U. S. Sales Only), 7p.
P2-5759	25-30850	Dep. NTIS (U. S. Sales Only), 22p.
P3-5554	25-30663	Dep. NTIS (U. S. Sales Only), 10p.
P3-5655	25-31305	Dep. NTIS (U. S. Sales Only), 28p.
P4-5221	25-31392	For translation see BNL-tr-416
P4-5614	25-31201	Dep. NTIS (U. S. Sales Only), 20p.
P4-5693	25-31306	Dep. NTIS (U. S. Sales Only), 17p.
P7-5497	25-31307	Dep. NTIS (U. S. Sales Only), 13p.
P8-5733	25-30412	Dep. NTIS (U. S. Sales Only), 16p.
P9-5669	25-31037	Dep. NTIS (U. S. Sales Only), 10p.
P9-5677	25-31038	Dep. NTIS (U. S. Sales Only), 18p.
P9-5714	25-31039	Dep. NTIS (U. S. Sales Only), 9p.
P13-5685	25-30995	Dep. NTIS (U. S. Sales Only), 7p.
P13-5707	25-29325	Dep. NTIS (U. S. Sales Only), 8p.
P13-5708	25-29353	Dep. NTIS (U. S. Sales Only), 10p.
JUL-	(German)	
698-RG	25-31624	Dep. NTIS (U. S. Sales Only), 146p.
724-FF	25-31169	Dep. NTIS (U. S. Sales Only), 23p.
KAPL-Trans-		
4	25-31170	Dep. NTIS
KFK-	(German)	
851	25-31542	For translation see EURFNR-813
1213	25-29940	For translation see EURFNR-820
1248	25-31308	Dep. NTIS (U. S. Sales Only), 24p.
1269	25-31568	For translation see EURFNR-823
1288	25-31202	Dep. NTIS (U. S. Sales Only), 20p.
1290	25-29818	For translation see AEC-tr-7224
1316	25-31040	Dep. NTIS (U. S. Sales Only), 35p.
1330	25-29977	Dep. NTIS (U. S. Sales Only), 49p.
1353	25-31652	Dep. NTIS (U. S. Sales Only), 117p.
1361	25-31653	Dep. NTIS (U. S. Sales Only), 14p.
KFK-tr-	(German)	
281	25-29942	For translation see LA-tr-71-22
KFKI-	(Hungarian)	
70-30-RPT	25-31648	Dep. NTIS (U. S. Sales Only), 18p.
KY-		
629	25-29502	Dep. NTIS, 11p.
LA-		
4339-TR	25-30597	Dep. NTIS
4343(Suppl.)	25-30157	Dep. NTIS, 9p.
4445	25-29326	Dep. NTIS, 15p.
4488	25-31171	Dep. NTIS, 50p.
4534	25-31041	Dep. NTIS, 43p.
4562	25-31699	Dep. NTIS, 5p.
4585	25-30450	Dep. NTIS, 86p.
4601	25-31700	Dep. NTIS, 10p.
4617	25-30598	Dep. NTIS, 44p.
4620	25-31701	Dep. NTIS, 11p.
4627	25-31702	Dep. NTIS, 7p.
4631	25-29920	Dep. NTIS, 30p.
4639	25-31042	Dep. NTIS, 56p.
4641	25-31703	Dep. NTIS, 7p.
4642	25-31704	Dep. NTIS, 8p.
LA-DC-		
11648	25-31309	Dep. NTIS, 67p.
LA-tr-		
71-6	25-30475	Dep. NTIS
71-7	25-29214	Dep. NTIS
71-12	25-29316	Dep. NTIS
71-22	25-29942	Dep. NTIS
71-26	25-30413	Dep. NTIS
71-30	25-29943	Dep. NTIS
71-33	25-31705	Dep. NTIS
LAL-	(French)	
1246	25-29370	Dep. NTIS (U. S. Sales Only), 15p.
LB/G-	(British)	
2835	25-29571	Dep. NTIS (U. S. Sales Only)
2916	25-29944	Dep. NTIS (U. S. Sales Only)
LF-	(Misc.)	
43	25-29419	Dep. NTIS, 328p.
LUNP-	(Swedish)	
7101	25-29354	Dep. NTIS (U. S. Sales Only), 66p.
LYCEN-	(French)	
7084	25-31310	Dep. NTIS (U. S. Sales Only), 23p.
7085	25-31185	Dep. NTIS (U. S. Sales Only), 15p.
7088	25-31203	Dep. NTIS (U. S. Sales Only), 18p.
7089	25-31186	Dep. NTIS (U. S. Sales Only), 49p.
7091	25-31239	Dep. NTIS (U. S. Sales Only), 29p.
7092	25-31311	Dep. NTIS (U. S. Sales Only), 22p.
MATT-		
813	25-30459	Dep. NTIS, 21p.
MATT-Trans-		
13	25-30460	Dep. NTIS
79	25-30461	Dep. NTIS
83	25-30505	Dep. NTIS
84	25-30506	Dep. NTIS
MIT-	(Misc.)	
2098-726	25-31015	Dep. NTIS, 28p.
MRR-	(West German)	
79	25-31579	NTIS (U. S. Sales Only), 27p.
N-	(Misc.)	
70-36812	25-30350	NTIS, 18p.

XUM

Report No.	Abstract No.	Availability
70-37028	25-30648	NTIS, 66p.
70-40978	25-30351	NTIS, 174p.
70-41880	25-30498	NTIS, 18p.
70-41892	25-30515	NTIS, 38p.
70-42698	25-30516	NTIS, 26p.
71-10100	25-30599	NTIS, 72p.
71-10964	25-30476	NTIS, 19p.
71-11428	25-30517	NTIS, 88p.
71-11853	25-30518	NTIS, 9p.
NAL-TN-	(Indian)	
6	25-30341	Dep. NTIS (U. S. Sales Only), 41p.
NASA-CR-	(Misc.)	
10100	25-30599	See N-71-10100
111402	25-30518	See N-71-11853
111804	25-30517	See N-71-11428
112875	25-30648	See N-70-37028
113799	25-30351	See N-70-40978
NASA-TM-X-	(Misc.)	
2132	25-30476	See N-71-10964
65307	25-30350	See N-70-36812
65352	25-30515	See N-70-41892
NASA-TN-D-	(Misc.)	
6047	25-30516	See N-70-42698
6048	25-30498	See N-70-41880
NBS-SPEC. PUBL-	(Non-AEC)	
332	25-30035	GPO $1.75
NBS-TN-	(Misc.)	
499	25-31172	GPO $0.65
562	25-30442	GPO $0.30
NIM-	(Non-AEC)	
951	25-28918	Dep. NTIS (U. S. Sales Only), 3p.
NIRS-AR-	(Japanese)	
13	25-29572	Dep. NTIS (U. S. Sales Only), 245p.
NP-	(AEC File No. for Non-AEC Reports)	
15256	25-30460	For translation see MATT-Trans-13
18511	25-31240	Dep. NTIS (U. S. Sales Only), 62p.
18673	25-30605	Dep. NTIS (U. S. Sales Only), 62p.
18736	25-29035	Dep. NTIS (U. S. Sales Only), 47p.
18741	25-31187	Dep. NTIS (U. S. Sales Only), 56p.
18765	25-30477	Dep. NTIS (U. S. Sales Only), 16p.
18767	25-30462	Dep. NTIS (U. S. Sales Only), 13p.
18770	25-31525	
18775	25-30507	Dep. NTIS (U. S. Sales Only), 17p.
18776	25-31043	Dep. NTIS (U. S. Sales Only), 8p.
18777	25-30805	Dep. NTIS (U. S. Sales Only), 34p.
18779	25-30895	Dep. NTIS (U. S. Sales Only), 32p.
18780	25-31044	Dep. NTIS (U. S. Sales Only), 39p.
18783	25-30664	Dep. NTIS (U. S. Sales Only), 68p.
18790	25-29526	Dep. NTIS (U. S. Sales Only), 39p.
18791	25-29527	Atomic Industrial Forum, Inc., New York $5.00
18794	25-29515	Dep. NTIS (U. S. Sales Only), 38p.
18796	25-30727	Dep. NTIS (U. S. Sales Only), 11p.
18798	25-30629	Dep. NTIS (U. S. Sales Only), 115p.
18799	25-31045	Dep. NTIS (U. S. Sales Only), 10p.
18801	25-30508	Dep. NTIS (U. S. Sales Only), 86p.
18803	25-31706	Dep. NTIS (U. S. Sales Only), 53p.
18804	25-30914	
18807	25-30606	Dep. NTIS (U. S. Sales Only), 13p.
18808	25-30915	
18822	25-30697	Dep. NTIS (U. S. Sales Only), 6p.
NVO-		
1163-216 (Rev.)	25-29242	Dep. NTIS, 99p.
NYO-		
1932(2)-192	25-31016	Dep. NTIS, 11p.
2150-66	25-30646	Dep. NTIS, 15p.
2150-68	25-31707	Dep. NTIS, 74p.
2280-32	25-31708	Dep. NTIS, 19p.
2356-43	25-29608	Dep. NTIS, 11p.
2598-52	25-31709	Dep. NTIS, 12p.
3246-TA-8	25-29327	Dep. NTIS, 86p.
3250-58	25-31468	See DOCKET-50213-105
3399-240	25-30851	See SU-1206-240
3504-57	25-30649	Dep. NTIS, 9p.
3558-24	25-29132	Dep. NTIS, 3p.
3618-10	25-31710	Dep. NTIS, 26p.
3653-5	25-29903	Dep. NTIS, 14p.
3668-TA-5	25-30806	Dep. NTIS, 51p.
3699-53	25-31711	Dep. NTIS, 12p.
3829-66	25-30939	Dep. NTIS, 21p.
3924-9	25-31712	Dep. NTIS, 3p.
3924-10	25-31713	Dep. NTIS, 6p.
3962-3	25-30036	Dep. NTIS, 18p.
4032-36	25-30896	Dep. NTIS, 8p.
ORNL-		
4522	25-29317	Dep. NTIS, 58p.
4565	25-29921	Dep. NTIS, 112p.
4602	25-31669	Dep. NTIS, 101p.
4619	25-31312	Dep. NTIS, 62p.
4630	25-29757	Dep. NTIS, 294p.
4654	25-29251	Dep. NTIS, 161p.
ORNL-TM-		
2620	25-30276	Dep. NTIS, 126p.
3063	25-29906	Dep. NTIS, 91p.
3102	25-31544	Dep. NTIS, 29p.
3179	25-31313	Dep. NTIS, 53p.
3242	25-29945	Dep. NTIS, 33p.
3261	25-29328	Dep. NTIS, 7p.
3293	25-31670	Dep. NTIS, 65p.
3299	25-29907	Dep. NTIS, 38p.
3311	25-31545	Dep. NTIS, 97p.
3318	25-30630	Dep. NTIS, 9p.
3328	25-31714	Dep. NTIS, 17p.
3367	25-31671	Dep. NTIS, 22p.
3368	25-31640	Dep. NTIS, 19p.
3376	25-30631	Dep. NTIS, 23p.
3378	25-31204	Dep. NTIS, 26p.
3388	25-31569	Dep. NTIS, 20p.
ORNL-tr-		
2433	25-30870	Dep. NTIS
2453	25-31314	Dep. NTIS
2469	25-31715	Dep. NTIS
2475	25-30414	Dep. NTIS
ORO-		
2434-7	25-31315	Dep. NTIS, 30p.
3291-14	25-31716	Dep. NTIS, 49p.
3519-7	25-29155	J. Chromatogr.; 56: 201-8(7 Apr 1971)
3634-11	25-31717	Dep. NTIS, 13p.
3634-12	25-31718	Dep. NTIS, 14p.
3634-13	25-31719	Dep. NTIS, 13p.
3982-10	25-31720	Dep. NTIS, 14p.
P-	(Misc.)	
4494(RAND)	25-30220	
PATENTS	(British)	
1,225,058	25-29348	
1,226,198	25-29192	
1,226,282	25-29120	
1,226,310	25-28988	
1,226,497	25-31679	
1,226,537	25-31565	
1,226,657	25-29119	
1,226,718	25-29189	
1,226,823	25-28942	
1,227,058	25-29917	
1,227,089	25-29407	
1,227,754	25-31582	
1,227,758	25-31581	
1,228,654	25-29932	
1,228,797	25-31625	
1,229,018	25-31678	
PATENTS	(Canadian)	
811,240	25-29260	
858,666	25-29279	
859,837	25-29258	
865,914	25-29253	
PATENTS	(French)	
1,592,538	25-30337	
PATENTS	(U. S.)	
3,551,235	25-29114	
3,554,783	25-29928	
3,554,920	25-29388	
3,555,278	25-29352	
3,558,122	25-29800	
3,558,879	25-29408	
3,562,125	25-29116	
3,562,367	25-29109	
3,563,869	25-29115	
3,563,870	25-29099	
3,564,247	25-29278	
3,564,255	25-29319	
3,567,648	25-29199	
3,569,714	25-29276	
3,572,405	25-29254	
3,573,109	25-29799	
3,573,120	25-29798	
PRNC-		
145	25-31721	Dep. NTIS, 10p.
146	25-31722	Dep. NTIS, 10p.
PROT.-SAN.-	(Italian)	
8/69	25-29503	Dep. NTIS (U. S. Sales Only), 171p.
13/69	25-29504	Dep. NTIS (U. S. Sales Only), 176p.
RD/B/M-	(British)	
1817	25-29252	Dep. NTIS (U. S. Sales Only), 28p.
RD/B/N-	(British)	

XUM

Report No.	Abstract No.	Availability
1878	25-29265	Dep. NTIS (U. S. Sales Only), 61p.
1889	25-29826	Dep. NTIS (U. S. Sales Only), 15p.
RFP-		
1148	25-29894	pp 70.1-9 of Structure and Chemistry of Solid Surfaces. /Sonorjai, Gabor A. (ed.). New York; John Wiley and Sons, Inc. (1969)
RHEL/R-	(British)	
213	25-31046	Dep. NTIS (U. S. Sales Only). UK 20p, 15p.
RISO-M-	(Danish)	
1348	25-30688	Dep. NTIS (U. S. Sales Only), 42p.
RLO-		
1388-135	25-29355	Dep. NTIS, 19p.
1750-62	25-31723	Dep. NTIS, 15p.
1750-81	25-29013	Dep. NTIS, 100p.
2229-T-1-3	25-31724	Dep. NTIS, 25p.
RMI-	(Misc.)	
16	25-29787	Dep. NTIS, 29p.
RPI-	(Misc.)	
328-200	25-31173	Dep. NTIS, 235p.
3639-16	25-31725	Dep. NTIS, 5p.
3719-9	25-29827	Dep. NTIS, 20p.
3947-13	25-31396	Dep. NTIS, 9p.
RT/CHI-	(Italian)	
(69)2	25-29944	For translation see LB/G-2916
(70)31	25-29182	Dep. NTIS (U. S. Sales Only), 21p.
RT/EL-	(Italian)	
(70)4	25-29390	Dep. NTIS (U. S. Sales Only), 31p.
(70)5	25-29356	Dep. NTIS (U. S. Sales Only), 52p.
RT/FI-	(Italian)	
(70)36	25-30632	Dep. NTIS (U. S. Sales Only), 21p.
RT/ING-	(Italian)	
(70)24	25-31570	Dep. NTIS (U. S. Sales Only), 43p.
SAL-	(Canadian)	
16	25-31205	
17	25-31206	
SC-ARPIC-		
1010	25-29266	Dep. NTIS, 15p.
SC-DC-		
713922	25-31726	Dep. NTIS, 11p.
713982	25-31727	Dep. NTIS, 22p.
SC-DR-		
70-838	25-31728	Dep. NTIS, 41p.
710211	25-31729	Dep. NTIS, 78p.
SC-RR-		
69-761	25-31730	Dep. NTIS, 38p.
710071	25-31731	Dep. NTIS, 78p.
710188	25-29409	Dep. NTIS, 45p.
SC-T-		
713010	25-31732	Dep. NTIS
713021	25-29883	Dep. NTIS
713023	25-29946	Dep. NTIS
713024	25-30478	Dep. NTIS
713025	25-31733	Dep. NTIS
SCL-T-		
69-257	25-31734	Dep. NTIS
69-258	25-31735	Dep. NTIS
710240	25-31736	Dep. NTIS
SGAE-PH-	(Austrian)	
96/1970	25-29979	NTIS (U. S. Sales Only), 15p.
SGAE-SS-	(Austrian)	
6/1969	25-29183	NTIS (U. S. Sales Only), 9p.
SJC-A-	(Non-AEC)	
71-1	25-31047	Dep. NTIS (U. S. Sales Only), 25p.
71-2	25-31048	Dep. NTIS (U. S. Sales Only), 19p.
SJC-P-	(Japanese)	
70-4	25-29371	Dep. NTIS (U. S. Sales Only), 86p.
SJC-T-	(Japanese)	
71-1	25-29372	Dep. NTIS (U. S. Sales Only), 22p.
SR-	(Misc.)	
362(E)	25-30351	See N-70-40978
SRRC-	(Misc.)	
41/71	25-31634	Dep. NTIS (U. S. Sales Only), 20p.

Report No.	Abstract No.	Availability
STI/PUB-	(International Atomic Energy Agency)	
265	25-29730	IAEA $14.00
SU-	(Misc.)	
1206-240	25-30851	Dep. NTIS, 38p.
SU-IPR-		
386	25-30518	See N-71-11853
SWRHL-		
39-r	25-29505	Dep. NTIS, 31p.
97-r	25-29506	Dep. NTIS, 41p.
TID-		
25465	25-31737	Dep. NTIS, 190p.
25686	25-29868	New York; Gordon and Breach, Science Publishers, Inc. (1971). 794p
25694	25-31738	Dep. NTIS, 10p.
25695	25-31739	Dep. NTIS, 20p.
25697	25-31526	Dep. NTIS, 48p.
25698	25-31479	Dep. NTIS, 42p.
TRI-	(British Columbia)	
70-4	25-31049	Dep. NTIS (U. S. Sales Only), 54p.
TT-	(Misc.)	
70-50003/2	25-29368	See AEC-tr-7099(Pt.2)
UCB-		
34-P-32-PR-5	25-30248	Dep. NTIS, 17p.
UCID-		
30002	25-31740	Dep. NTIS, 8p.
UCLA-		
12-813	25-31741	Dep. NTIS, 22p.
34-P-91-47	25-31742	Dep. NTIS, 235p.
UCRL-		
19648	25-31743	Dep. NTIS, 41p.
19691	25-31744	Dep. NTIS, 203p.
19715	25-31174	Dep. NTIS, 12p.
20156	25-31050	Dep. NTIS, 3p.
20164	25-31051	Dep. NTIS, 2p.
20169	25-31052	Dep. NTIS, 4p.
20174	25-31053	Dep. NTIS, 5p.
20185	25-31054	Dep. NTIS, 5p.
20189	25-31055	Dep. NTIS, 4p.
20191	25-31056	Dep. NTIS, 2p.
20197	25-31057	Dep. NTIS, 4p.
20208	25-31058	Dep. NTIS, 5p.
20250	25-30871	Dep. NTIS, 57p.
20316	25-29064	Accounts Chem. Res.; 3: 393-401(1970)
20436	25-31241	Dep. NTIS, 7p.
20461	25-31745	Dep. NTIS, 79p.
20524	25-31746	Dep. NTIS, 114p.
20529	25-30277	Dep. NTIS, 95p.
20611	25-31059	Dep. NTIS, 4p.
50990	25-29516	Dep. NTIS, 13p.
50992	25-29243	Dep. NTIS, 11p.
51008	25-31747	Dep. NTIS, 12p.
51021	25-31748	Dep. NTIS, 26p.
71888(Pt.1)	25-31749	Dep. NTIS, 46p.
71888(Pt.2)	25-31750	Dep. NTIS, 48p.
72572	25-29244	Dep. NTIS, 22p.
72803	25-31751	Dep. NTIS, 60p.
72818(Rev. 1)	25-31752	Dep. NTIS, 68p.
UCRL-Trans-		
10524	25-31753	Dep. NTIS
10525	25-31754	Dep. NTIS
10526	25-31755	Dep. NTIS
UCSD-		
34-P-127-8	25-31756	Dep. NTIS, 18p.
34-P-43-X-9	25-30158	Dep. NTIS, 18p.
UH-		
235-P-9-2	25-30665	Dep. NTIS, 49p.
UJV-	(Czechoslovakian)	
2525-M	25-29884	Dep. NTIS (U. S. Sales Only), 28p.
USGS-		
474-95	25-29203	Dep. NTIS, 71p.
UUIP-	(Swedish)	
659	25-30499	Dep. NTIS (U. S. Sales Only), 11p.
733	25-30689	Dep. NTIS (U. S. Sales Only), 9p.
WASH-		
1172	25-30600	GPO $1.00
1175	25-31534	GPO $1.00
WCAP-	(Misc.)	
7401	25-31598	
WERL-HFIL-		

XUM

Report No.	Abstract No.	Availability
1	25-29096	Dep. NTIS, 88p.
X-	(Misc.)	
621-70-310	25-30350	See N-70-36812
693-70-340	25-30515	See N-70-41892
Y-		
1758	25-31757	Dep. NTIS, 39p.
1759	25-31758	Dep. NTIS, 115p.

Report No.	Abstract No.	Availability
1791	25-31759	Dep. NTIS, 20p.
Y-DR-		
44	25-31635	Dep. NTIS, 56p.
ZJE-	(Czechslovakian)	
69	25-29788	Dep. NTIS (U. S. Sales Only), 19p.

XUM

Appendix I
JOURNAL LIST

This list of journals supplements the listing which appeared as Appendix II in Volume 25, Number 1. The journals are arranged alphabetically by abbreviation. An additional supplement will be included in number 19 of this volume.

The title abbreviations are based on the National Clearinghouse for Periodical Title Word Abbreviations, *Word Abbreviation List* published by the Standards Committee Z-39 of the American National Standards Institute.

TID-4579 (5th Ed.) *Serial Titles Cited in Nuclear Science Abstracts* lists the titles and abbreviations of the journals regularly scanned for *NSA* as well as those from which an occasional item is taken. This publication is available from the National Technical Information Service (NTIS), U. S. Department of Commerce, Springfield, Virginia, 22151, for $6.00 for full size or reproduction copy and $0.95 for microfiche copy.

A

Acta Agr. Scand.
Acta Agriculturae Scandinavica (Sweden)

Acta Fac. Rerum Natur. Univ. Comenianae, Phys.
Acta Facultatis Rerum Naturalium Universitatis Comenianae, Physica (Czechoslovakia)

Acta Math. (Uppsala)
Acta Mathematica (Uppsala) (Sweden)

Acta Neurol. (Naples)
Acta Neurologica (Naples) (Italy)

Acta Pathol. Microbiol. Scand., Sect. A
Acta Pathologica et Microbiologica Scandinavica, Section A. Pathology (Denmark)

Acta Pathol. Microbiol. Scand., Sect. A, Suppl.
Acta Pathologica et Microbiologica Scandinavica, Section A. Pathology, Supplementum (Formerly Acta Pathologica et Microbiologica Scandinavica, Supplementum) (Denmark)

Acta Pathol. Microbiol. Scand., Sect. B
Acta Pathologica et Microbiologica Scandinavica, Section B. Microbiology and Immunology (Denmark)

Acta Polytech. (Prague), IV
Acta Polytechnica (Prague), Rada IV. Technicko-Teoreticka (Czechoslovakia)

Acta Univ. Upsal., Abstr. Uppsala Diss. Med.
Acta Universitatis Upsaliensis, Abstracts of Uppsala Dissertations in Medicine (Sweden)

Acta Univ. Wratislaviensis
Acta Universitatis Wratislaviensis (Poland)

Acta Vet. (Brno)
Acta Veterinaria (Brno) (Czechoslovakia)

Actinides Lanthanides Rev.
Actinides and Lanthanides Reviews (Netherlands)
Supersedes Actinides Reviews

Advan. High Temp. Chem.
Advances in High Temperature Chemistry (U.S.)

Advan. Hum. Genet.
Advances in Human Genetics (U. S.)

Advan. Mater. Res.
Advances in Materials Research (U. S.)

Advan. Microbial Physiol.
Advances in Microbial Physiology (England)

Advan. Oto-Rhino-Laryngol.
Advances in Oto-Rhino-Laryngology (Switzerland)
Supersedes Bibliotheca Oto-Rhino-Laryngologica

AGARD Conf. Proc.
AGARD Conference Proceedings (France)

Agents Actions
Agents and Actions (Switzerland)

Agrochimica
Agrochimica (Italy)

AMDEL (Aust. Miner. Develop. Lab.) Bull.
AMDEL (Australian Mineral Development Laboratories) Bulletin (Australia)

Amer. Fam. Physician - GP
American Family Physician - GP (U. S.)
Supersedes GP, Journal of the American Academy of General Practice

Angew. Bot.
Angewandte Botanik (West Germany)

Ann. Gastroenterol. Hepatol.
Annales de Gastroenterologie et d'Hepatologie (France)

Ann. Limnol.
Annales de Limnologie (France)

Ann. Med. Interne
Annales de Medecine Interne (France)
Supersedes Bull. Mem. Soc. Med. Hop. Paris

Ann. Meteorol.
Annalen der Meteorologie (West Germany)

Ann. Soc. Geol. Belg.
Annales de la Societe Geologique de Belgique (Belgium)

XUM

Annu. Bull., Int. Dairy Fed.
Annual Bulletin, International Dairy Federation (Belgium)

Apidologie
Apidologie (France)
Supersedes Annales de l'Abeille

Arch. De Vecchi Anat. Patol. Med. Clin.
Archivio De Vecchi Anatomia Patological e la Medicina Clinic (Italy)

Argonne Rev.
Argonne Reviews (U. S.)
Supersedes Argonne National Laboratory Reviews

At. Energy Law Rep.
Atomic Energy Law Reports (U. S.)

Atherosclerosis
Atherosclerosis (Netherlands)
Supersedes Journal of Atherosclerosis Research

Aust. Chem. Eng.
Australian Chemical Engineering (Australia)

Aust. Chem. Process. Eng.
Australian Chemicel Processing and Engineering (Australia)

Aust. Fish.
Australian Fisheries (Australia)

Aust. Food Mfr. Distrib.
Australian Food Manufacturer and Distributor (Australia)

Aust. J. Bot.
Australian Journal of Botany (Australia)

Aust. J. Soil Res.
Australian Journal of Soil Research (Australia)

Aust. J. Statist.
Australian Journal of Statistics (Australia)

Aust. N. Z. J. Med.
Australian and New Zealand Journal of Medicine (Australia)
Supersedes Australasian Annals of Medicine

Australas. J. Pharm., Sci. Suppl.
Australasian Journal of Pharmacy, Science Supplement (Australia)

B

Beitr. Pathol.
Beitraege zur Pathologie (West Germany)
Supersedes Beitraege zur Pathologischen Anatomie und zur Allgemeinen Pathologie

Beitr. Radioastron.
Beitraege zur Radiostronomie (West Germany)

Betontech. Ber.
Betontechnische Berichte (West Germany)

Biol. Listy
Biologicke Listy (Czechoslovakia)

Biomed. Sci. Instrum.
Biomedical Sciences Instrumentation (U.S.)

Bol. Estud. Med. Biol.
Boletin de Estudios Medicos y Biologicos (Mexico)

Brit. J. Occup. Saf.
British Journal of Occupational Safety (England)

Brot Gebaeck
Brot und Gebaeck (West Germany)

Bul. Inst. Politeh. Brasov, Ser. B
Buletinul Institutului Politehnic din Brasov, Seria B. Economie Forestiera (Romania)

Bull. Inst. Int. Froid
Bulletin de l'Institut International du Froid (France)

Bull., Int. Union Cancer
Bulletin, International Union Against Cancer (Switzerland)

Bul. Stiint. Univ. Craiova
Buletinul Stiintific al Universitatii Craiova (Romania)

Bygg
Bygg (Norway)

Byull., Abastumanskaya Astrofiz. Observ., Akad. Nauk Gruz. SSR
Byulleten, Abastumanskaya Astrofizicheskaya Observatoriya, Akademiya Nauk Gruzinskoi SSR (Georgian S.S.R.)

Byull. Gl. Bot. Sada
Byulleten Glavnogo Botanicheskogo Sada (U.S.S.R.)

C

Calif. Agr.
California Agriculture (U. S.)

Californium-252 Progr.
Californium-252 Progress (U. S.)

Can. Inst. Food Technol. J.
Canadian Institute of Food Technology Journal (Canada)

Carbohyd. Res.
Carbohydrate Research (Netherlands)

Cesk. Pediat.
Ceskoslovenska Pediatrie (Czechoslovakia)

Cesk. Zdrav.
Ceskoslovenske Zdravotnictvi (Czechoslovakia)

Chem. N. Z.
Chemistry in New Zealand (New Zealand)
Supersedes Journal of the New Zealand Institute of Chemistry

Chem. Scr.
Chemica Scripta (Sweden)
Supersedes Arkiv for Kemi

Chest (Chicago)
Chest (Chicago) (U. S.)
Supersedes Diseases of the Chest

Chirurgie
Chirurgie (France)
Supersedes Memoires de l'Academie de Chirurgie

Chitaniumu Jirukoniumu
Chitaniumu Jirukoniumu (Titanium, Zirconium) (Japan)

Chutanzo
Chutanzo (Casting and Forging) (Japan)

Ciel Terre
Ciel et Terre (Belgium)

Civil Eng. Trans., Inst. Eng., Aust.
Civil Engineering Transactions, Institution of Engineers, The, Australia (Australia)

XUM

Combust. Sci. Technol.
Combustion Science and Technology (U. S.-England)

Commun. Dublin Inst. Advan. Stud., Ser. A
Communications of the Dublin Institute for Advanced Studies, Series A (Ireland)

Composits
Composits (England)

Constructeur
Constructeur, De (Absorbed Constructiematerialen) (Netherlands)

Current (N. Y.)
Current (New York) (U. S.)

Curr. Notes Int. Aff.
Current Notes on International Affairs (Australia)

D

Dai-4-Ki Kenkyu
Dai-4-Ki Kenkyu (Quaternary Research) (Japan)

Denshi Tsushin Gakkai Ronbunshi, C
Denshi Tsushin Gakkai Ronbunshi, C (Japan)

Deut. Gewaesserk. Mitt.
Deutsche Gewaesserkundliche Mitteilungen (West Germany)

Develop. Appl. Spectrosc.
Developments in Applied Spectroscopy (U. S.)

Diastema
Diastema (South Africa)

E

East. Metals Rev.
Eastern Metals Review (India)

Eclogae Geol. Helv.
Eclogae Geologicae Helvetiae (Switzerland)

ELDO/ESRO Sci. Tech. Rev.
ELDO/ESRO Scientific and Technical Review (France)

Electro
Electro (Norway)
Supersedes Elektroteknisk Tidsskrift

Electromedica
Electromedica (West Germany)

Electromyography
Electromyography (Belgium)

Elektronika
Elektronika (Formerly Przeglad Elektroniki) (Poland)

Elektrotehnika (Zagreb)
Elektrotehnika (Zagreb) (Yugoslavia)

Energomashinostroenie
Energomashinostroenie (U.S.S.R.)

Erzmetall
Erzmetall (West Germany)
Supersedes Z. Erzbergbau Metallhuettenw.

Eur. J. Clin. Invest.
European Journal of Clinical Investigation (West Germany)
Supersedes Archiv fuer Klinische Medizin

Eur. Potato J.
European Potato Journal (Netherlands)

F

Farbe Lack
Farbe und Lack (West Germany)

Farm. Obz.
Farmaceuticky Obzor (Czechoslovakia)

Faserforsch. Textiltech.
Faserforschung und Textiltechnik (East Germany)

Fields Quanta
Fields and Quanta (England)

Finska Lakaresallsk. Handl.
Finska Lakaresallskapets Handlingar (Finland)

Fiziol. Biokhim. Kul't. Rast.
Fiziologiya i Biokhimiya Kul'turnykh Rastenii (Ukrainian S. S. R.)

Fiz.-Khim. Mekh. Mater.
Fiziko-Khimicheskaya Mekhanika Materialov (Ukrainian S.S.R.)
Issued in English translation as Soviet Materials Science

Fonderia Ital.
Fonderia Italiana (Italy)

Food Ind. J.
Food Industries Journal (India)

Forsch. Geb. Ingenieurw.
Forschung auf dem Gebiete des Ingenieurwesens (West Germany)

Forsk. Framsteg
Forskning och Framsteg (Sweden)

Fortune
Fortune (U.S.)

Frequenz
Frequenz (West Germany)

Fukushima Igaku Zasshi
Fukushima Igaku Zasshi (Fukushima Medical Journal) (Japan)

Funtai Kogaku
Funtai Kogaku (Powder Engineering) (Japan)

G

Ganka
Ganka (Ophthalmology) (Japan)

Gas- Wasserfach, Wasser - Abwasser
Gas- und Wasserfach, Wasser - Abwasser (West Germany)
Continues in part Gas- und Wasserfach, Das

Geofiz. Sb.
Geofizicheskii Sbornik (Ukrainian S.S.R.)

Geol. Pruzkum
Geologicky Pruzkum (Czechoslovakia)

Geol. Zh. (Russ. Ed.)
Geologicheskii Zhurnal (Russian Edition) (Ukrainian S.S.R.)

G. Psichiat. Neuropatol.
Giornale di Psichiatria e di Neuropatologia (Italy)

XUM

Gradbeni Vestn.
Gradbeni Vestnik (Yugoslavia)

Gynecol. Invest.
Gynecologic Investigation (Switzerland)
Supersedes Gynaecologia

H

Heizung-Lueftung-Haustech.
Heizung-Lueftung-Haustechnik (West Germany)

Helgolaender Wiss. Meeresunters.
Helgolaender Wissenschaftliche Meeresuntersuchungen (West Germany)

Hoshasen Kagaku
Hoshasen Kagaku (Japan)

HSMHA Health Rep. (U.S.)
HSMHA (Health Services and Mental Health Administration) Health Reports (U. S.)
Supersedes Public Health Reports (U. S.)

Husipar
Husipar (Hungary)

I

Iden
Iden (Heredity) (Japan)

Ig. Mod.
Igiene Moderna (Italy)

Indian J. Hort.
Indian Journal of Horticulture (India)

Indian J. Math.
Indian Journal of Mathematics (Indian)

Indian J. Pure Appl. Math.
Indian Journal of Pure and Applied Mathematics (India)

Indian J. Sci. Ind.
Indian Journal of Science and Industry (India)

Indian J. Sci. Ind., Sect. A
Indian Journal of Science and Industry, Section A. Agricultural Sciences (India)

Indian Miner.
Indian Minerals (India)

Industriekurier
Industriekurier (West Germany)

Infec. Immunity
Infection and Immunity (U. S.)

Ingenieursblad
Ingenieursblad (Belgium)

Int. J. Magn.
International Journal of Magnetism (England - U. S.)

Ionos. Issled.
Ionosfernye Issledovaniya (U.S.S.R.)

Irrig. Power
Irrigation and Power (India)

Isotope Ind. Landwirt.
Isotope in Industrie und Landwirtschaft (Austria)

Izv. Akad. Nauk Kirg. SSR
Izvestiya Akademii Nauk Kirgizskoi SSR (Kirgiz S.S.R.)

Izv. Akad. Nauk SSSR, Mekh. Tverd. Tela
Izvestiya Akademii Nauk SSSR, Mekhanika Tverdogo Tela (U.S.S.R.)

Izv. Akad. Nauk Turkm. SSR, Ser. Biol. Nauk
Izvestiya Akademiya Nauk Turkmenskoi SSR, Seriya

J

J. Aust. Entomol. Soc.
Journal of the Australian Entomological Society (Australia)

J. Brit. Astron. Ass.
Journal of the British Astronomical Association (England)

J. Cryst. Mol. Struct.
Journal of Crystal and Molecular Structure (England)

J. Helminthol.
Journal of Helminthology (England)

J. Inst. Nucl. Eng.
Journal of the Institution of Nuclear Engineers (England)
Supersedes Nuclear Energy

J. Lumin.
Journal of Luminescence (Netherlands)

J. Med. (Basel)
Journal of Medicine (Basel) (Switzerland)
Supersedes Medicina Experimentalis

J. Med. Microbiol.
Journal of Medical Microbiology (Scotland)

J. Membrane Biol.
Journal of Membrane Biology (U. S.)

J. Norw. Med. Ass.
Journal of the Norwegian Medical Association (Norway)

J. Oil Colour Chem. Ass.
Journal of the Oil and Colour Chemists' Association (England)

J. Phys., F (London)
Journal of Physics, F (London). Metal Physics (England)

J. Polym. Sci., Part D
Journal of Polymer Science, Part D Macromolecular Reviews (U.S.)

J. Range Manage.
Journal of Range Management (U. S.)

J. Roy. Coll. Surg. Ireland
Journal of the Royal College of Surgeons in Ireland (Ireland)

J. Therm. Anal.
Journal of Thermal Analysis (England)

J. Univ. Poona
Journal of the University of Poona (India)

K

Kaijo Hoan Daigakko Kenkyu Hokoku, Dai-2-Bu
Kaijo Hoan Daigakko Kenkyu Hokoku, Dai-2-Bu (Journal of Maritime Safety Academy, Part 2) (Japan)

XUM

Kansai Ika Daigaku Zasshi
Kansai Ika Daigaku Zasshi (The Journal of the Kansai Medical School) (Japan)

Kaut. Gummi Kunstst.
Kautschuk und Gummi Kunststoffe (West Germany)

Kazan. Med. Zh.
Kazanskii Meditsinskii Zhurnal (U.S.S.R.)

Khim. Drev.
Khimiya Drevesiny (Latvian S.S.R.)

Kratk. Soobshch. Fiz.
Kratkie Soobshcheniya po Fizike (U.S.S.R.)

Kyushu Ketsueki Kenkyu Dokokaishi
Kyushu Ketsueki Kenkyu Dokokaishi (Journal of Kyushu Hematological Society) (Japan)

L

Lantbrukshogsk. Ann.
Lantbrukshogskolans Annaler (Sweden)

Lek. Zpr.
Lekarske Zpravy (Czechoslovakia)

M

Mada
Mada (Israel)

Manuscr. Math.
Manuscripta Mathematica (West Germany)

Maroc Med.
Maroc Medical (Morocco)

Mar. Pollut. Bull.
Marine Pollution Bulletin (England)

Maschinenmarkt
Maschinenmarkt (West Germany)

Mecan. Mater. Elec.
Mecanique Materiaux Electricite (France)
Supersedes Mecanique Electricite

Metallgesellschaft
Metallgesellschaft (West Germany)

Metallges., Mitt. Arbeitsbereich
Metallgesellschaft, Mitteilungen aus dem Arbeitsbereich (West Germany)

Methods Comput. Phys.
Methods in Computational Physics (U. S.)

Methods Exp. Phys.
Methods of Experimental Physics (U.S.)

Microvasc. Res.
Microvascular Research (U. S. - England)

Minerva Oftalmol.
Minerva Oftalmologica (Italy)

Munkavedelem
Munkavedelem (Hungary)

N

Nat. Saf. News
National Safety News (U. S.)

Natuurwetensch. Tijdschr. (Ghent)
Natuurwetenschappelijk Tijdschrift (Ghent) (Belgium)

Nauch. Tr. Vissh. Med. Inst., Sofia
Nauchni Trudove na Visshiya Meditsinski Institut, Sofia (Bulgaria)

Neuropharmacology
Neuropharmacology (England)
Supersedes International Journal of Neuropharmacology

New Sci. Sci. J.
New Scientist and Science Journal (England)
Formerly issued separately as New Scientist and Science Journal

Nitrogen
Nitrogen (England)

Nucl. Active
Nuclear Active (South Africa)

Nucl. Technol.
Nuclear Technology (U. S.)
Supersedes Nuclear Applications and Technology

Nutr. Metab.
Nutrition and Metabolism (Switzerland)
Supersedes Nutritio et Dieta

N. Y. Times Mag.
New York Times Magazine (U.S.)

O

Occup. Health Nurs.
Occupational Health Nursing (U. S.)

Oceans
Oceans (U. S.)

Ohio Rep.
Ohio Report (U.S.)

Organometal. Chem. Rev., Sect. A
Organometallic Chemistry Reviews, Section A. Subject Reviews (Netherlands)
Supersedes in part Organometallic Chemistry Reviews

Osp. Ital. Chir.
Ospedali d'Italia Chirurgia (Italy)

Osp. Magg.
Ospedale Maggiore (Italy)

P

Period. Polytech., Mech. Eng.
Periodica Polytechnica, Mechanical Engineering (Hungary)
Supersedes Periodica Polytechnica, Engineering

Pharmacol. Res. Commun.
Pharmacological Research Communication (England)

Physiol. Chem. Phys.
Physiological Chemistry and Physics (U. S.)

Phys. Rep.
Physics Reports. A Review Section of Physics Letters (Section C) (Netherlands)

XUM

Postepy Astronaut.
Postepy Astronautyki (Poland)

Powder Met. Int.
Powder Metallurgy International (West Germany)

Prakt. Lek.
Prakticky Lekar (Czechoslovakia)

Probl. Arktiki Antarktiki
Problemy Arktiki i Antarktiki (U.S.S.R.)

Probl. Kosm. Phys.
Probleme der Kosmichen Physik (West Germany)

Probl. Metalloved. Fiz. Metal.
Problemy Metalovedeniya i Fiziki Metallov (U.S.S.R.)

Probl. Sov. Geol.
Problemy Sovetskoi Geologii (U.S.S.R.)

Proc. Aust. Soc. Anim. Prod.
Proceedings of the Australian Society of Animal Production (Australia)

Proc. Indian Nat. Sci. Acad., Part A
Proceedings of the Indian National Science Academy, Part A. Physical Sciences (Formerly Proceedings of the National Institute of Sciences of India, Part A) (India)

Proc. Indian Nat. Sci. Acad., Part B
Proceedings of the Indian National Science Academy, Part B. Biological Sciences (Formerly Proceedings of the National Institute of Sciences of India, Part B) (India)

Proc., Inst. Teknol. Bandung
Proceedings, Institut Teknologi Bandung (Indonesia)

Proc. Roy. Soc. Med., Suppl.
Proceedings of the Royal Society of Medicine, Supplement (England)

Progr. Nucl. Acid Res. Mol. Biol.
Progress in Nucleic Acid Research and Molecular Biology (Formerly Progress in Nucleic Acid Research) (U. S.)

Punjab Med. J.
Punjab Medical Journal (India)

R

Reakts. Metody Issled. Org. Soedin.
Reakstii i Metody Issledovaniya Organicheskikh Soedinenii (U.S.S.R.)

Recent Progr. Hormone Res.
Recent Progress in Hormone Research (U.S.)

Recherche (Paris)
Recherche, La (Paris) (France)
Supersedes Atomes (Paris)

Rev. Agroquim. Tecnol. Aliment.
Revista de Agroquimica y Tecnologia de Alimentos (Spain)

Rev. Biol. Med. Nucl.
Revista de Biologia y Medicina Nuclear (Uruguay)

Rev. Fr. Allergol.
Revue Francaise d'Allergologie (France)
Supersedes Revue Francaise d'Allergie

Rev. Med. (Tirgu-Mures)
Revista Medicala (Tirgu-Mures) (Romania)

Rev. Mex. Fis., Supl. Reactor
Revista Mexicana de Fisica, Suplemento del Reactor (Mexico)

Rev. Venez. Sanid. Asistencia Soc.
Revista Venezolana de Sanidad y Asistencia Social (Venezuela)

Riv. Sper. Freniat. Med. Leg. Alienazioni Ment.
Rivista Sperimentale di Freniatria e Medicina Legale delle Alienazioni Mentali (Italy)

S

Safety (London)
Safety (London) (England)

SAMPE J.
SAMPE (Society of Aerospace Material and Process Engineers) Journal (U.S.)

Sb. Nauch. Tr., Magnitogorsk. Gornomet. Inst.
Sbornik Nauchnykh Trudov, Magnitogorskii Gornometallurgicheskii Institut (U.S.S.R.)

Sb. Nauch. Tr., Tomsk. Inzh.-Stroit. Inst.
Sbornik Nauchnykh Trudov, Tomskii Inzhenerno-Stroitel'nyi Institut (U.S.S.R.)

Schweiz. Bauztg.
Schweizerische Bauzeitung (Switzerland)

Search
Search. Science, Technology and Society (Australia)
Supersedes Australian Journal of Science

Seibutsu Kagaku
Seibutsu Kagaku (Biological Science) (Japan)

Semin. Nucl. Med.
Seminars in Nuclear Medicine (U.S.)

Showa Igakkai Zasshi
Showa Igakkai Zasshi (The Journal of the Showa Medical Association) (Japan)

Shoyakugaku Zasshi
Shoyakugaku Zasshi (Journal of Pharmacognosy) (Japan)

Soobshch. Byurakan. Observ., Akad. Nauk Arm. SSR
Soobshcheniya Byurakanskoi Observatorii, Akademiya Nauk Armyanskoi SSR (Armenian S.S.R.)

Spec. Publ., Geol. Soc. Aust.
Special Publication, Geological Society of Australia (Australia)

SPIE Semin. Proc.
SPIE (Society of Photo-Optical Instrumentation Engineers) Seminar Proceedings (U.S.)

Springer Tracts Mod. Phys.
Springer Tracts in Modern Physics. Ergebnisse der Exakten Naturwissenschaften (West Germany)

Stahlbau
Stahlbau (West Germany)

Strength Mater. (USSR) (Engl. Transl.)
Strength of Materials (USSR) (English Translation of Problemy Prochnosti) (U. S.)

Stud. Cercet. Met.
Studii si Cercetari de Metalurgie (Romania)

Sumitomo Search
Sumitomo Search (Japan)

XUM

Symp. Zool. Soc. London
Symposia of the Zoological Society of London and The Malacological Society of London (England)

Synthesis
Synthesis (West Germany)

T

Tekniikka
Tekniikka (Finland)
Supersedes Teknillinen Aikakuslehti

Teplofiz. Teplotekh.
Teplofizika i Teplotekhnika (Ukrainian S.S.R.)

Termoproch. Mater. Konstr. Elem.
Termoprochnost Materialov i Konstruktivnykh Elementov (U.S.S.R.)

Tien Wen Hsueh Pao
Tien Wen Hsueh Pao (Journal of Astronomy) (China)

TNO Nieuws
TNO Nieuws (Netherlands)

Tokyo Toritsu Eisei Kenkyusho Nempo
Tokyo Toritsu Eisei Kenkyusho Nempo (Annual Report of Tokyo Metropolitan Labs. for Medical Science) (Japan)

Tool. Prod.
Tooling and Production (U. S.)

Trans. Amer. Foundrymen's Soc.
Transactions of the American Foundrymen's Society (U.S.)

Trans. Soc. Advan. Electrochem. Sci. Technol.
Transactions of the Society for Advancement of Electrochemical Science and Technology (India)

Tr. Gidrometeorol. Nauch.-Issled. Tsent. SSSR
Trudy Gidrometeorologicheskogo Nauchno-Issledovatel'skogo Tsentra SSSR (U.S.S.R.)

Tr. Inst. Fiz. Zemli, Akad. Nauk SSSR
Trudy Instituta Fiziki Zemli, Akademiya Nauk SSSR (U.S.S.R.)

Tr. Mosk. Obshchest. Ispyt. Prir.
Trudy Moskovskogo Obshchestva Ispytatelei Prirody (U.S.S.R.)

Tr. 1 [Pervogo] Mosk. Med. Inst.
Trudy 1 [Pervogo] Moskovskogo Meditsinskogo Instituta (U.S.S.R.)

Tr. Tbilis. Gos. Univ.
Trudy Tbilisskogo Gosudarstvennogo Universiteta (Georgian S.S.R.)

U

Uch. Zap. Leningrad. Gos. Univ., Ser. Fiz. Nauk
Uchenye Zapiski Leningradskogo Gosudarstvennogo Universiteta, Seriya Fizicheskikh Nauk (U.S.S.R.)

Uch. Zap. Ural. Gos. Univ.
Uchenye Zapiski Ural'skogo Gosudarstvennogo Universiteta (U.S.S.R.)

Urologe, Ausg. A
Urologe, Der, Ausgabe A (West Germany)
Supersedes in part Urologe, Der

V

Vestn. Khar'kov. Politekh. Inst.
Vestnik Khar'kovskogo Politekhnicheskogo Instituta (Ukrainian S.S.R.)

Vestn. Min. Zdrav.
Vestnik Ministerstva Zdravotnictvi (Czechoslovakia)

Vigyan Pragati
Vigyan Pragati (India)

Vod. Hospod., B
Vodni Hospodarstvi, B (Czechoslovakia)

Vop. Magmat. Metamorfiz.
Voprosy Magmatizma i Metamorfizma (U.S.S.R.)

W

Wasser, Luft Betr.
Wasser, Luft und Betrieb (West Germany)

Weather (London)
Weather (London) (England)

Werkstatt Betr.
Werkstatt und Betrieb (West Germany)

Z

Zairyo Kagaku
Zairyo Kagaku (Japan)

Z. Tierphysiol. Tierernaehr. Futtermittelk.
Zeitschrift fuer Tierphysiologie Tierernaehrung und Futtermittelkunde (West Germany)

Z. Wasser- Abwasserforsch.
Zeitschrift fuer Wasser- und Abwasserforschung (West Germany)

Z. Wirt. Fertigung
Zeitschrift fuer Wirtschaftliche Fertigung (West Germany)

☆U. S. Government Printing Office: 1971—436-215/29

XUM

UNITED STATES
ATOMIC ENERGY COMMISSION
P. O. BOX 62
OAK RIDGE, TENNESSEE 37830

OFFICIAL BUSINESS

POSTAGE AND FEES PAID
U. S. ATOMIC ENERGY COMMISSION

POSTAGE AND FEES PAID
U.S. GOVERNMENT PRINTING OFFICE

UN'
GOVERNME

PUBL
W

UNIVERSITY MICROFILMS
SERIAL PUBLICATIONS
300 NORTH ZEEB ROAD
ANN ARBOR MICHIGAN

40106

1

AEC SYMPOSIUM SERIES

Available from the National Technical Information Service, U. S. Department of Commerce, Springfield, Virginia 22151

1 **Progress in Medical Radioisotope Scanning** (TID-7673), Oak Ridge Institute of Nuclear Studies, 1963, $6.00

2 **Reactor Kinetics and Control** (TID-7662), The University of Arizona, 1964, $6.00

3 **Dynamic Clinical Studies with Radioisotopes** (TID-7678), Oak Ridge Institute of Nuclear Studies, 1964, $6.00

4 **Noise Analysis in Nuclear Systems** (TID-7679), University of Florida, 1964, $6.00

5 **Radioactive Fallout from Nuclear Weapons Tests** (CONF-765), U. S. Atomic Energy Commission, 1965, $6.00

6 **Radioactive Pharmaceuticals** (CONF-651111), Oak Ridge Institute of Nuclear Studies, 1966, $6.00

7 **Neutron Dynamics and Control** (CONF-650413), The University of Arizona, 1966, $6.00

8 **Luminescence Dosimetry** (CONF-650637), Stanford University, 1967, $6.00

9 **Neutron Noise, Waves, and Pulse Propagation** (CONF-660206), University of Florida, 1967, $6.00

10 **Use of Computers in Analysis of Experimental Data and the Control of Nuclear Facilities** (CONF-660527), Argonne National Laboratory, 1967, $6.00

11 **Compartments, Pools, and Spaces in Medical Physiology** (CONF-661010), Oak Ridge Associated Universities, 1967, $6.00

12 **Thorium Fuel Cycle** (CONF-660524), Oak Ridge National Laboratory, 1968, $6.00

13 **Radioisotopes in Medicine: In Vitro Studies** (CONF-671111), Oak Ridge Associated Universities, 1968, $6.00

14 **Abundant Nuclear Energy** (CONF-680810), Oak Ridge Associated Universities, 1969, $6.00

15 **Fast Burst Reactors** (CONF-690102), The University of New Mexico, 1969, $9.00

16 **Biological Implications of the Nuclear Age** (CONF-690303), Lawrence Radiation Laboratory, 1969, $6.00

17 **Radiation Biology of the Fetal and Juvenile Mammal** (CONF-690501), Pacific Northwest Laboratory, 1969, $9.00

18 **Inhalation Carcinogenesis** (CONF-691001), Oak Ridge National Laboratory, 1970, $6.00

19 **Myeloproliferative Disorders of Animals and Man** (CONF-680529), Pacific Northwest Laboratory, 1970, $9.00

20 **Medical Radionuclides: Radiation Dose and Effects** (CONF-691212), Oak Ridge Associated Universities, 1970, $6.00

21 **Morphology of Experimental Respiratory Carcinogenesis** (CONF-700501), Oak Ridge National Laboratory, 1970, $6.00

22 **Precipitation Scavenging (1970)** (CONF-700601), Pacific Northwest Laboratory, 1970, $6.00

XUM

XUM